BIRLA CENTRAL LIBRARY
PILANI (Rajasthan)

Class No. 621-384
Book No. Z 482 E
Accession No. 55224

ELECTRONICS MANUAL FOR RADIO ENGINEERS

ELECTRONICS MANUAL FOR RADIO ENGINEERS

Copyright, 1949, by the McGraw-Hill Book Company, Inc. Printed in the United States of America. All rights reserved. This book, or parts thereof, may not be reproduced in any form without permission of the publishers.

ELECTRONICS MANUAL FOR RADIO ENGINEERS

BY VIN ZELUFF AND JOHN MARKUS
ASSOCIATE EDITORS OF *ELECTRONICS*

FIRST EDITION

McGRAW-HILL BOOK COMPANY, INC.
NEW YORK • TORONTO • LONDON • 1949

BOOKS by JOHN MARKUS and VIN ZELUFF

ELECTRONICS FOR ENGINEERS

WHAT ELECTRONICS DOES

HANDBOOK OF INDUSTRIAL ELECTRONIC CIRCUITS

ELECTRONICS MANUAL FOR RADIO ENGINEERS

PREFACE

Monthly magazines are not exactly convenient for reference—even in bound volumes—after they have accumulated for a few years. Needed articles get more and more elusive as time passes and titles are forgotten. Often, the hunter gives up after going through individual issues one by one—a truly time-consuming process.

In an earnest attempt to solve one aspect of this problem for the readers of one McGraw-Hill publication —*Electronics*—we brought out "Electronics for Engineers" several years ago. The response from all types of electronic engineers to this collection of electronic design articles confirmed the statement by Keith Henney in its preface that "one article alone, available when needed, can justify a place for this book on an engineer's desk."

This second book has been prepared to solve the same problem for engineers in the radio broadcasting, communication, manufacturing and research fields. The 289 articles that it brings together for quick reference are the all-time-great radio articles published in *Electronics* during 1940-1948. The emphasis throughout is on the practical circuit information needed by practicing engineers, the mathematical foundations needed by radio design engineers and researchers, and the measuring and operating techniques needed by radio operators, technicians and maintenance men for putting radio equipment into use and keeping it at peak efficiency. Here too are articles for radio production men, covering such vital cost-cutting topics as quality control, inspection procedures and production-floor test equipment.

The contents of this book are logically arranged in sixteen chapters according to the major interests of those in the radio field: Antennas; Audio; Circuit Theory; Components; D-C Amplifiers; Filters; Ionosphere; Measurements; Microwaves; Power Supplies; Production; Receivers; Television; Transmission Lines; Transmitters; and Tubes. A desired article can be located quickly in any of four ways: (1) by flipping through the appropriate chapter; (2) by scanning the article titles listed for that chapter in the table of contents; (3) by using the subject index at the back of the book, which is so completely cross-indexed that success is generally achieved on the first try even when the article title is not known; (4) by using the author index at the back of the book, if the name of the author is remembered.

With the significant work of other engineers in one handy reference volume, it becomes practical and economical to start a problem where others left off rather than from scratch. Hours and even days of searching through technical literature can be saved, and the need for duplicative laboratory research and experimentation can be reduced to a minimum.

Since this volume encompasses the war years when research and practical development in the radio field were at an all-time high, engineers in other countries will find here the practical answer to missing copies resulting from war damage or limited wartime circulation of *Electronics*.

The engineer authors whose works appear in this volume deserve congratulations for their permanent contributions to the art and industry of radio.

VIN ZELUFF and JOHN MARKUS
Associate Editors, *Electronics*

New York, N.Y.
April, 1949

CONTENTS

Preface v

I. ANTENNAS

Effect of Feed on Pattern of Wire Antennas
Aug. 1947 D. C. Cleckner 1
Antenna Power Divider
July 1944 Earle Travis 4
Phasing Networks for Broadcast Arrays
June 1944 C. Russell Cox 5
Phase Monitor for Broadcast Arrays
Dec. 1947 B. C. O'Brien and F. L. Sherwood 9
Adjustment of Directional Antennas
Apr. 1943 William S. Duttera 11
Multi-Wire Dipole Antennas
Jan. 1940 John D. Kraus 14
Low-Impedance Loop Antenna for Broadcast Receivers
Sept. 1946 L. O. Vladimir 16
F-M and Television Receiving Antennas
Nov. 1948 George P. Kearse 20
F-M Antenna Coupler
Aug. 1945 John P. Taylor 21
Triplex Antenna for Television and F-M
July 1947 L. J. Wolf 23
Cooperative Two-Station Antenna System
Nov. 1946 Lindsay McManus 26
Clip-on Antenna Meter
Sept. 1946 27
Slotted-Cylinder Antenna
Feb. 1947 E. C. Jordan and W. E. Miller 28
Remote Indicating Antenna Ammeter
Jan. 1946 C. R. Cox 31
Transport Aircraft Antenna Characteristics
Dec. 1947 E. F. Kiernan 32
Aircraft Antenna Pattern Plotter
May 1947 O. H. Schmitt and W. P. Peyser 34
Cavity Aircraft Antenna
Jan. 1947 H. Kees and F. Gehres 37
Artificial Antenna
Nov. 1945 Sidney Wald 39
Microwave Antenna Beam Evaluator
Aug. 1947 H. LeCaine and M. Katchky 44

II. AUDIO

Crystal Pickup Compensation Circuits
Nov. 1945 B. B. Bauer 49
Automatic Gain Control and Limiting Amplifier
Sept. 1947 W. M. Jurek and J. H. Guenther 53
Dynamic Suppression of Phonograph Record Noise
Dec. 1946 H. H. Scott 57
Dynamic Noise Suppressor
Dec. 1947 H. H. Scott 60
Audio Noise Reduction Circuits
Dec. 1947 Harry F. Olson 66
Background Noise Suppressor
June 1947 71
Audio Mixer Design
June 1945 Richard W. Crane 72
Automatic Fader
Oct. 1945 Dan Hunter 74
Volume Expander Design
Dec. 1945 Robert W. Ehrlich 75
Surgeless Volume Expander
Sept. 1946 A. Nelson Butz, Jr. 79
Three-Band Variable Equalizer
Jan. 1947 L. D. Grignon 80
Automatic Audio Phase Reverser
Nov. 1947 Alvin H. Smith 83
Low-Distortion Crossover Network
Nov. 1948 Paul W. Klipsch 85
Technique for Distortion Analysis
June 1948 Samuel Sabaroff 87
Beat-Frequency Tone Generator with R-C Tuning
May 1948 J. W. Whitehead 91
Design of Loudspeaker Dividing Networks
Feb. 1948 Earl R. Schuler 92
Simple Harmonic Wave Analyzer
Dec. 1942 R. F. Thomson 94
Wow Meter for Turntable Testing
Mar. 1948 G. L. Sansbury and E. W. Pappenfus 97
Microphone Calibrator
Nov. 1948 D. H. Bastin 100
Thermistor-Regulated Low-Frequency Oscillator
Oct. 1946 Lawrence Fleming 103
Volume Compressor for Radio Stations
Dec. 1943 George Q. Herrick 106
Frequency Response of Magnetic Recording
Aug. 1947 Otto Kornei 107
Reverberation Time Nomographs
Apr. 1947 R. C. Coile 112
Voice-Operated Electronic Relay
June 1945 Carl J. Quirk 113
Instrument for Intermodulation Measurements
Mar. 1948 George Daniel 115
Intermodulation Testing
July 1946 John K. Hilliard 116
Phase-Shift Oscillator Design Charts
Nov. 1943 Walter W. Kunde 121
Telephone Recording
Aug. 1947 K. L. MacIlvain 123

III. CIRCUIT THEORY

Cathode Follower Circuits
Nov. 1943 Walther Richter 125
Graphical Solutions for Cathode Followers
Jan. 1947 Herbert L. Krauss 131
Analysis of Cathode Follower
Nov. 1945 137
Cathode Follower of Very Low Output Resistance
Nov. 1946 139
Bandwidth vs. Noise in Communication Systems
Jan. 1948 140

Wideband Phase Shift Networks
Dec. 1946 R. B. Dome 144
Stabilised Negative Impedances
July 1946 E. L. Ginzton 148
Constant-Current Circuits
Nov. 1946 O. T. Fundingsland and G. J. Wheeler 170
Design of Phantastron Time Delay Circuits
Apr. 1948 R. N. Close and M. T. Lebenbaum 174
Self-Switching R-F Amplifier
June 1947 H. M. Wagner and J. F. Herrick 182
Frequency Control for Low-Impedance Oscillator Tanks
June 1947 V. M. Albers 186
Conversion from Series to Parallel Impedance
Oct. 1945 Gershon J. Wheeler 187
Graphical Determination of Percent Harmonic Distortion
July 1948 Robert W. Buchheim 188
Optimum Conditions for an R-C Oscillator
Feb. 1948 H. A. Whale 189
Pulse-Modulated Oscillator
Mar. 1947 Allan Easton 191
Equivalent Series and Parallel Impedances
June 1945 R. L. Peek, Jr. 197
Design Curves for Parallel-T Network
July 1948 Dawkins Espy 197
Cathode-Coupled Half-Shot Multivibrator
Sept. 1947 Robert K. F. Scal 199
Voltmeter Loading
Nov. 1947 R. E. Lafferty 201
Reactance Networks with Resistance Terminations
Jan. 1943 E. S. Purington 203
Cathode Follower Nomograph
May 1947 Melvin B. Kline 209
Cathode Follower Nomograph for Pentodes
June 1947 Melvin B. Kline 210
Cathode Follower Impedance Nomograph
July 1947 Melvin B. Kline 211
DB Gain-Loss Calculator
Feb. 1947 Lloyd A. Lohr 212
Impedance Nomograph
Sept. 1946 Gershon J. Wheeler 213
Impedance-Admittance Conversion Chart
Jan. 1946 Robert C. Paine 213
Theoretical Signal-to-Noise Ratios
June 1946 J. Ernest Smith 214
Two-Terminal Oscillator
May 1946 Murray G. Crosby 218

IV. COMPONENTS

Frequency Stability of Tuned Circuits
Feb. 1944 G. V. Eltgroth 221
R-F Inductance Meter
Sept. 1947 Harold A. Wheeler 224
Temperature Coefficients in Electronic Circuits
Jan. 1948 Chester I. Soucy 227
Mutual Inductance of Concentric Coils
Nov. 1946 Thomas C. Blow 232
Resonance in Mica Capacitors
Mar. 1944 A. P. Green and C. T. McComb 233
High-Q Iron-Cored Inductor Calculations
Aug. 1945 Stephen L. Javna 234
Measuring Coil Characteristics Without an Impedance Bridge
May 1943 H. D. Brailsford 239
Crystal Rectifiers
July 1946 W. E. Stephens 243

V. D-C AMPLIFIERS

Survey of D-C Amplifiers
Aug. 1945 Maurice Artzt 251
D-C Amplifier Design Techniques
Mar. 1944 Edward L. Ginzton 257
Bridge-Balanced Amplifiers
May 1948 Y. P. Yu 262
D-C Amplifier for Low-Level Signals
Oct. 1947 C. B. Aiken and W. C. Welz 265
A Stable D-C Amplifier
July 1944 G. Robt. Mezger 271
A D-C Amplifier of High-Current, Low-Impedance Output
Aug. 1945 Lawrence Fleming 276
Gas-Tube Coupling for D-C Amplifiers
Oct. 1946 F. Iannone and H. Baller 278
High-Gain D-C Amplifier
Oct. 1947 W. G. Shepard 280
Stabilized D-C Amplifier with High Sensitivity
June 1947 H. S. Anker 281
Cathode Follower Coupling in D-C Amplifiers
Aug. 1946 Y. P. Yu 283

VI. FILTERS

Resistance-Capacitance Filter Chart
Nov. 1945 Ernest Frank 289
High and Low-Pass Filter Design
Feb. 1945 C. J. Merchant 291
R-C Bandpass Filter Design
Apr. 1947 Jack L. Bowers 292
The Effect of Incidental Dissipation in Filters
Oct. 1946 E. A. Guillemin 295
Filters for Electronic Equipment
July 1945 Gershon J. Wheeler 301
Pi Networks as Coupled Tank Circuits
Aug. 1944 Frederic D. Schottland 301
Single-Sideband Crystal Filters
Oct. 1948 Paul K. Taylor 306
Phase-Shifter Nomograph
May 1946 Raymond E. Lafferty 311
The Swinging Filter
June 1943 Robert M. Hanson 312
Transient Delay Line
Apr. 1946 John M. Lester 317

VII. IONOSPHERE

Propagation of Very Short Waves
Jan. 1948 Donald E. Kerr 321
2-MC Sky-Wave Transmission
May 1946 J. A. Pierce 331
Ionosphere Measuring Equipment
July 1946 P. G. Sulzer 340
Ionosphere Equipment for Field Use
May 1947 Glenn H. Musselman 345
Recording Sky-Wave Signals
Nov. 1947 Wilbert B. Smith 348
Measurement of VHF Bursts
Jan. 1945 352

VIII. MEASUREMENTS

R-F Bridge for Broadcast Stations
Apr. 1948 F. Schumann and C. Duke 354
FCC Frequency Measurement Techniques
June 1947 Alfred K. Robinson 357
Components of UHF Field Meters
Nov. 1946 Eduard Karplus 359
Design of F-M Signal Generator
Nov. 1946 D. M. Hill and M. G. Crosby 365
Wide-Range Sweeping Oscillator
Aug. 1947 370
VHF Impedance Measurements
Dec. 1945 D. Stanley Henry 374
Wide-Range Signal Generator with Automatic Amplitude Control
May 1945 Howard T. Sterling 377
High-Accuracy Signal Generator
Dec. 1947 J. J. Bann 378
Direct-Coupled R-F Amplifier
Dec. 1948 Earle Travis 379
Power Measurements at Very High Frequencies
Oct. 1945 William Maron 379

Frequency-Scanning VHF Impedance Meter
June 1948 Lester L. Libby . . . 381
Calibrating Laboratory Standards Against WWV
Feb. 1947 Gardner P. Wilson . . . 384
Checking UHF Oscillator Stability
Dec. 1945 L. E. Pinney . . . 385
VHF Transmitter Power Measurements
Feb. 1947 Leonard R. Malling . . . 386
Static for Radio Receiver Tests
June 1947 J. C. R. Licklider and E. B. Newman . . . 387
Noise Generator for Receiver Measurements
July 1948 Peter G. Sulzer . . . 390
Noise Meter
Feb. 1944 . . . 393
Oscilloscope for Pulse Studies
Dec. 1944 H. Atwood, Jr. and R. P. Owen . . . 394
Direct-Coupled Oscilloscope
July 1948 J. H. Reyner . . . 398
Cathode-Ray Q Meter
Nov. 1945 Rudolf Feldt . . . 403
Time-Base Calibration
Sept. 1945 Walter W. Ludman . . . 404
Pulse Transmission in Amplifiers
Oct. 1946 Arthur E. Newlon . . . 407
Electronic Switch for the Production of Pulses
Apr. 1947 C. R. Smitley and R. E. Graber 413
Stable Voltmeter
Mar. 1947 R. W. Gilbert . . . 416
Pulse Response of Diode Voltmeters
Jan. 1946 Allan Easton . . . 419
High-Frequency Crystal Voltmeter
Mar. 1948 B. F. Tyson . . . 423
Measuring Complex Components
Feb. 1947 George E. Pihl . . . 424
Impedance Measurements
Feb. 1947 . . . 427
Grid-Dip Oscillator
July 1948 . . . 428
Phase Meter
June 1948 E. O. Vandeven . . . 428
Construction of Shielded Room in VHF Field
Apr. 1948 Cecil C. Pine . . . 430
Radiation from R-F Heating Generators
May 1946 Arthur G. Swan . . . 432
Measuring and Monitoring Broadcast Frequencies
July 1946 Larry S. Cole . . . 433
Measuring Pulse Characteristics
Feb. 1946 Allan Easton . . . 434
Measurement of Velocity of Propagation in Cable
July 1946 B. Kramer and F. Stolte . . . 439
High-Resistance D-C Voltmeter
Mar. 1946 D. L. Waidelich . . . 441
Measuring Mutual Inductance and Capacitance
Aug. 1946 A. W. Simon . . . 444
Carrier-Frequency Voltmeter
Dec. 1948 A. W. Simon . . . 445

IX. MICROWAVES

Engineering Approach to Waveguides
May 1946 Theodore Moreno . . . 447
Waveguide Data
Jan. 1947 Leonard E. Sherbin . . . 452
Minimum Attenuation in Waveguides
Jan. 1946 Edwin N. Phillips . . . 455
Circular Waveguide Fields
Feb. 1945 George R. Cooper . . . 458
Apertures in Cavities
Dec. 1948 J. H. Owen Harries . . . 462
Cavity Oscillator Circuits
Feb. 1946 A. M. Gurewitsch . . . 466
Waveguide Transmission Systems
June 1946 Theodore Moreno . . . 469
Coaxial Butterfly Circuits
Apr. 1946 Ervin E. Gross, Jr. . . . 474
Simplified Microwave AFC
Nov. 1947 F. A. Jenks . . . 479
Impedance Measurements at VHF
July 1947 E. G. Hills . . . 489
UHF Impedance Measurements
June 1945 N. Marchand and R. Chapman . . . 494
Comparator for Coaxial Line Adjustments
Apr. 1947 O. M. Woodward, Jr. . . . 497
SHF Heterodyne Frequency Meter
Apr. 1947 Carson D. Jeffries . . . 501
Direct-Reading Wavemeter Design
Mar. 1948 G. E. Feiker and H. R. Meahl . . . 504
Buzzer Signal Generator for 3,000 Mc
Oct. 1946 . . . 508
Improving Stability of UHF Oscillators
May 1947 Carl A. Helber . . . 509
Variable-Frequency Oscillator for 25 Centimeters
Jan. 1945 . . . 512
Stabilizing Frequency of Reflex Oscillators
Feb. 1948 George G. Bruck . . . 514
3-CM Continuous-Range Oscillator
Dec. 1947 Irving M. Gottlieb . . . 515
Bolometer Amplifier
Feb. 1948 D. D. King, J. Taylor and W. H. Faulkner, Jr. . . . 517
Piston Attenuator
Feb. 1948 Raymond E. Laffety . . . 519
Standing Wave Meter
Jan. 1947 Heinz E. Kallmann . . . 520

X. POWER SUPPLIES

Analysis of Full-Wave Rectifier and Capacitive-Input Filter
Sept. 1947 D. L. Waidelich . . . 524
Thermionic Rectifier Circuits
Feb. 1944 Richard C. Hitchcock . . . 528
Voltage-Regulated Power Supplies
July 1948 P. Koontz and E. Dilatush . . . 532
Multi-voltage Regulated Power Supplies
Sept. 1946 J. R. Mentzer . . . 537
Versatile Power Supply
June 1948 William B. Miller . . . 539
Power Supply for Microwave Equipment
Feb. 1947 Oliver Hoag . . . 540
Filter Ripple Chart
Mar. 1948 C. K. Hooper . . . 544
Automatic Control of Battery Charging
May 1947 E. L. Deeter and A. C. Plautz . . . 545
Voltage-Stabilized Bias Supply for Power Tubes
Sept. 1943 . . . 546
A Variable-Frequency Electronic Generator
Sept. 1943 Dana A. Griffin . . . 547

XI. PRODUCTION

Sensitivity Limits in Radio Manufacturing
Nov. 1945 A. S. Blatterman . . . 550
Quality Engineering in Tube Manufacture
Nov. 1944 Eugene Goddess . . . 553
Shrinkage Analysis in Tube Manufacture
Dec. 1944 Eugene Goddess . . . 556
Quality Control in Tube Manufacture
Jan. 1945 Eugene Goddess . . . 558
Central Signal Generator for Production Testing
July 1947 Fred Miller . . . 562
Automatic Limit Bridge for Production Testing
Jan. 1948 R. D. Campbell and E. J. Totah . . . 567
Direct-Indicating Comparison Bridge for Production Testing
Dec. 1945 . . . 570
Frequency Meter for Use by Factory Personnel
May 1945 W. R. Strauss . . . 571
Pulse-Type Tester for High-Power Tubes
Feb. 1947 E. C. Easton and E. L. Chaffee . . . 572
High-Speed Resistor Reader
Feb. 1948 A. W. Daubendick . . . 575
Overvoltage Testing of Capacitors
June 1947 R. J. Hopkins . . . 577

Curve-Tracer for Acoustic Devices
Dec. 1945 R. K. Hellmann . . . 579
Tube-Seasoning Timer
Feb. 1946 M. Silverman . . . 583
Soldering Litz Ends
Mar. 1947 Emerick Toth . . . 583
Concentricity Tester for Enamel Film on Wire
Apr. 1943 Elmer F. Hansen . . . 584
B-H Curve Tracer for Lamination Samples
Nov. 1943 Robert Adler . . . 585

XII. RECEIVERS

Adjustable-Bandwidth F-M Discriminator
Sept. 1947 W. G. Tuller and T. P. Cheatham, Jr. . . . 590
Single-Stage F-M Detector
Oct. 1946 William E. Bradley . . . 593
Nonlinear Limiter
May 1947 Edmund R. Brill . . . 596
F-M and A-M Receiver for Comparison Tests
July 1946 William F. Frankart . . . 597
Synchronized Oscillators as F-M Receiver Limiters
Aug. 1944 C. W. Carnahan and H. P. Kalmus . . . 598
Squelch Circuits for F-M Receivers
Apr. 1948 C. W. Carnahan . . . 604
Superregenerative Detection Theory
Sept. 1948 William E. Bradley . . . 606
Superregenerator Design
Sept. 1948 A. Hazeltine, D. Richman and B. D. Loughlin 609
Single-Sideband Converter
July 1948 . . . 612
Superregenerative Detector Selectivity
Mar. 1946 Allan Easton . . . 613
Superregenerative Circuit Applications
Feb. 1948 Harry Stockman . . . 617
Wideband I-F Amplifiers
Apr. 1947 Matthew T. Lebenbaum . . . 620
AGC-Noise Considerations in Receiver Design
May 1945 John B. Moore . . . 624
Noise and Output Limiters
Nov. 1946 Emerick Toth . . . 627
Simplified Single-Sideband Reception
May 1948 Oswald G. Villard, Jr. . . . 639
Single-Signal Single-Sideband Adaptor
July 1948 E. W. Rosentreter . . . 643
Tracking Permeability-Tuned Circuits
Sept. 1948 A. W. Simon . . . 645
Tracking the Permeability-Tuned Circuits
Nov. 1947 A. W. Simon . . . 646
Permeability Tuning of Broadcast Receivers
Aug. 1947 L. O. Vladimir . . . 647
Method of Plotting Tracking Error
Jan. 1947 E. B. Menzies . . . 652
VHF Receiver Measurements
June 1948 H. Gordon and L. George . . . 653
High-Level Detector
May 1946 J. C. Rankin . . . 654
Directly Coupled Phase Inverter
Mar. 1948 E. Johnson . . . 655
Noise-Free Code Reception
June 1947 D. L. Hings . . . 656
Mixer Frequency Charts
Aug. 1946 R. S. Badessa . . . 659
Beat-Frequency Interference Chart
Apr. 1946 Don Barton . . . 660
Reduction of Heterodyne Interference
Dec. 1945 H. W. Belles . . . 661
Surge Protection of Pilot and Heater Circuits
Aug. 1947 Ralph P. Glover . . . 662
Use of Shunt Diode for Supplying Bias Voltage
Sept. 1945 Howard T. Sterling . . . 664
Diode Contact Potential for Negative Bias
Oct. 1947 Howard T. Sterling . . . 665
Remote Tuning with Reactance Tubes
Aug. 1945 H. B. Bard, Jr. . . . 667
Continuously Variable Radio Remote Control
Nov. 1946 David W. Moore, Jr. . . . 669
Radio Control Circuit
June 1947 . . . 672

XIII. TELEVISION

Carrier-Difference Reception of Television Sound
Jan. 1947 R. B. Dome . . . 673
Timing Action of the Blocking Oscillator
Oct. 1945 Emanuel Last . . . 676
Design Factors for Intercarrier Television Sound
July 1948 Stuart W. Seeley . . . 678
Stagger-Tuned Amplifier Design
May 1948 Henry Wallman . . . 682
Multivibrator Design by Graphic Methods
June 1948 A. E. Abbot . . . 685
Low-Frequency Compensation for Amplifiers
Feb. 1948 Kurt Schlesinger . . . 688
Clipping and Clamping Circuits
July 1947 Norman W. Mather . . . 691
Square-Wave Differentiating Circuit Analysis
Aug. 1945 G. P. Ohman . . . 694
Current Oscillator for Television Sweep
Sept. 1946 George Clifford Sziklai . . . 698
Iron-Core Components in Pulse Amplifiers
Aug. 1943 Reuben Lee . . . 702
Square-Wave Response
Aug. 1947 A. J. Baracket . . . 708
Multivibrator Circuits
Oct. 1946 Norman W. Mather . . . 709
Linear Sweep Circuits
Dec. 1946 Robert P. Owen . . . 711
Pulsed Rectifiers for Television Receivers
Aug. 1947 I. G. Maloff . . . 713
Transient Video Analyzer
June 1946 Clement Moritz . . . 714
Test Oscilloscope for Television
Nov. 1946 A. H. Brolly and W. R. Brock . . . 720
Television Synchronizing Signal Generator
Oct. 1948 A. J. Baracket . . . 722
Counter Circuits for Television
May 1948 A. Easton and P. H. Odessey 728
Television Receiver Laboratory
Mar. 1948 Frank R. Norton . . . 732
Television Resolution Chart
Dec. 1947 . . . 735
Television Service Areas
Oct. 1948 John H. Battison . . . 738
Photometry in Television Engineering
July 1948 D. W. Epstein . . . 739
Simplified Television System
June 1947 R. E. Barrett and M. M. Goodman . . . 743

XIV. TRANSMISSION LINES

Design of Transmission Line Tank Circuits
May 1947 Walter C. Hollis . . . 748
Characteristic Impedance of Balanced Lines
July 1946 Peter J. Sutro . . . 753
Vectorial Treatment of Transmission Lines
Dec. 1945 J. P. Shanklin . . . 754
Mismatch Loss Chart for Transmission Lines
Jan. 1948 J. M. Hollywood . . . 757
Transmission Lines as Tuning Elements
Oct. 1945 H. E. Newell, Jr. . . . 758
High-Frequency Cable Design
Feb. 1948 K. H. Zimmermann . . . 760

XV. TRANSMITTERS

F-M Transmitter Performance Measurements
Feb. 1948 H. P. Thomas and L. M. Leeds . . . 764
Hum-Reducing Circuit
Jan. 1947 Alvin H. Smith . . . 767

Wide-Deviation Reactance Modulator
Apr. 1948 HARRY D. HELFRICH, JR. . . . 768
Extending Linear Range of Reactance Modulators
May 1948 FRITZ BRUNNER . . . 770
Stability of Crystal Oscillators
May 1947 A. J. ZINK, JR. . . . 771
Transmitter Breakdown Alarm
Feb. 1944 W. K. ANGUS . . . 774
Wide-Angle Phase Modulator
Feb. 1947 H. K. BRADFORD . . . 775
Cascade Phase-Shift Modulator
Dec. 1946 M. MARKS . . . 779
Serrasoid F-M Modulator
Oct. 1948 J. R. DAY . . . 785
F-M Service Areas
June 1948 JOHN H. BATTISON . . . 789
Overmodulation Without Sideband Splatter
Jan. 1947 OSWALD G. VILLARD, JR. . . . 790
Bridging Amplifier for F-M Monitoring
Jan. 1946 GEORGE E. BEGGS, JR. . . . 796
Low-Impedance Reactances for VHF
May 1948 E. K. STODOLA and H. LISMAN . . . 799
UHF Repeater Station
June 1944 MAURICE E. KENNEDY . . . 802
F-M Short-Range Carrier System
Dec. 1947 E. H. B. BARTELINK and E. DASKAM . . . 805
Quick Neutralizing Tests
Aug. 1944 JOSEPH ZELLE . . . 810
Simplified Carrier-Failure and Tone Alarm System
Mar. 1943 JOSEPH HEROLD . . . 811
Frequency Deviation Measurement of F-M Transmitters
Oct. 1941 L. N. HOLLAND and L. J. GIACOLETTO . . . 812
Using Phone Line for Remote Indication of Overmodulation
July 1943 ALVIN LEEMAN . . . 814
Speech Scrambling Methods
Oct. 1943 WILLIAM W. ROBERTS . . . 815
Automatic Control Circuits for Broadcast Transmitters
Nov. 1943 W. R. SLOAT . . . 821
Foolproof Cuing System for Broadcast Stations
Feb. 1943 JOSEPH ZELLE . . . 825
Grounded-Grid Power Amplifiers
Apr. 1946 E. E. SPITZER . . . 826

XVI. TUBES

Filament and Heater Characteristics
July 1944 CECIL E. HALLER . . . 830
Graphical Determination of Operating Point of Self-Biased Tube
Feb. 1944 ARTHUR SCHACH . . . 835
Tube Failures in Eniac
Oct. 1947 F. ROBERT MICHAEL . . . 837
Producing Tube Curves on an Oscilloscope
Nov. 1947 HENRY E. WEBKING . . . 840
Disk-Seal Tubes
Feb. 1945 E. D. MCARTHUR . . . 844
Klystron Oscillators
Nov. 1944 A. E. HARRISON . . . 849
Testing Cathode-Ray Screens
Feb. 1948 J. C. TELLIER and J. F. FISHER . . . 856
Photographing Patterns on Cathode-Ray Tubes
Feb. 1944 RUDOLPH FELDT . . . 861
Noise in Gas Tubes
Mar. 1947 J. D. COBINE and C. J. GALLAGHER . . . 869
Simple Test Set for Mercury Vapor Rectifiers
Apr. 1943 M. J. WEINER . . . 872

INDEX . . . 873

ANTENNAS

Effect of Feed on Pattern of Wire Antennas

Measured radiation patterns for straight wire antennas of various lengths from a half wavelength to three wavelengths and fed at various points are presented herewith. They show that feed point affects the number, orientation, and magnitude of the lobes

By D. C. CLECKNER

RADIATION PATTERNS of wire antennas one-half wavelength or longer are dependent on the position of feed used to excite the antenna. There has been considerable confusion in published handbooks as to just how a certain length antenna is fed to get the desired pattern. This investigation was made to determine the effects of the position of feed upon the pattern of wire antennas.

No attempt will be made to explain the results except to state that the current distribution differs appreciably from a sinusoidal distribution for certain off-center feeds.

Because the pattern of a single fed wire antenna is independent of the impedance match between it and the receiver or transmitter, it was not necessary to have a perfect impedance match between the antenna and the detector. However, the receiver had a coaxial feed and, therefore, a balance to unbalance transformer had to be used. In order to preserve the balance, it was necessary to have a partial impedance match. In the case of high impedance feeds (end feeds or feeds an even number of half wavelengths from the end) a quarter wave sec-

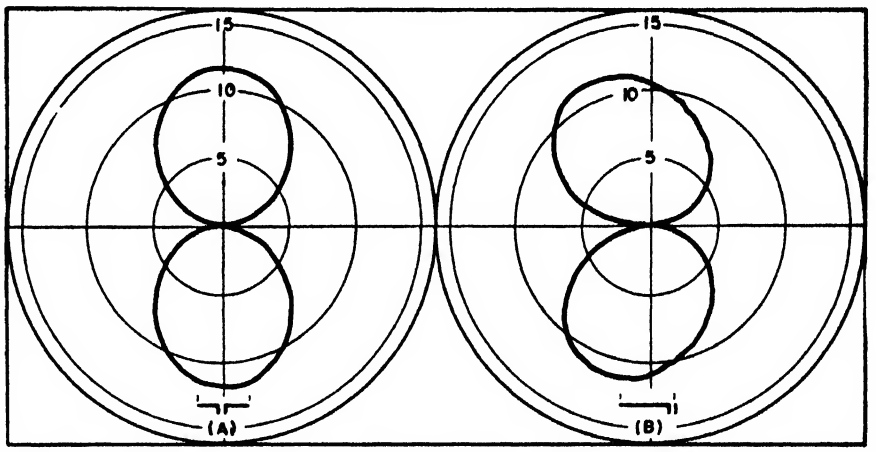

FIG. 1—Radiation from a half-wavelength antenna. Antenna outline with each pattern shows feed point; outline marked off in half wavelengths

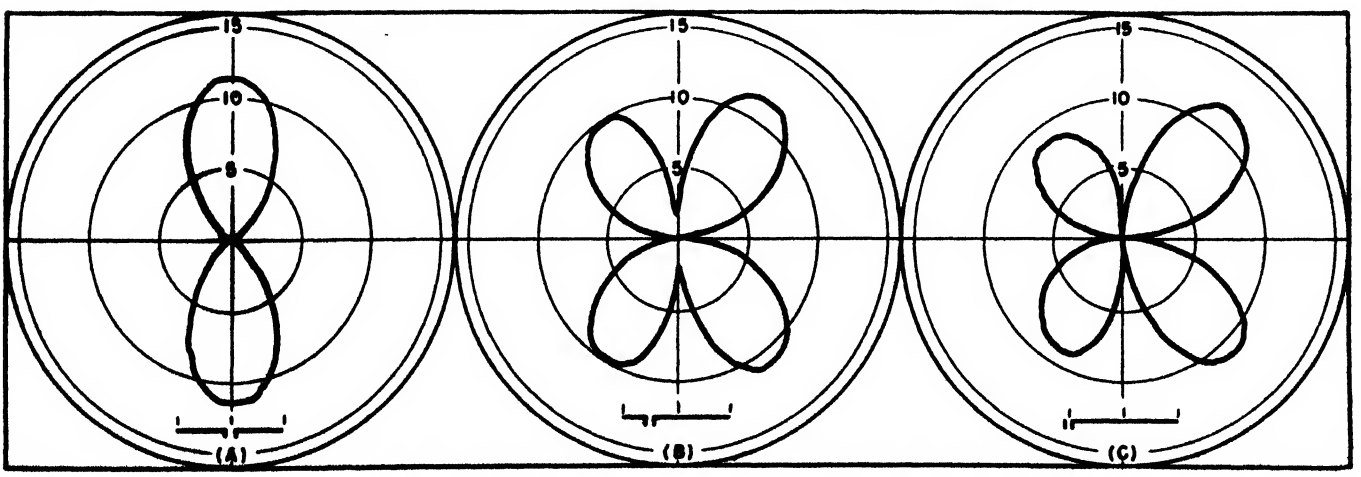

FIG. 2—Shape of field strength pattern of an antenna one-wavelength long depends on the location of the feed point

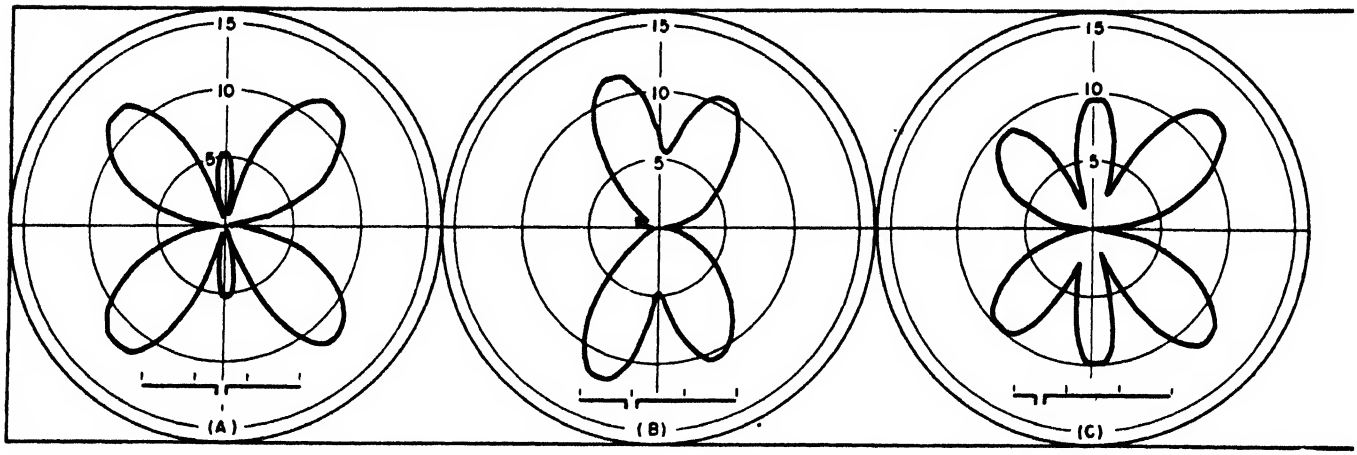

FIG. 3—Field strength patterns of a one and one-half wavelength antenna for four different feed positions

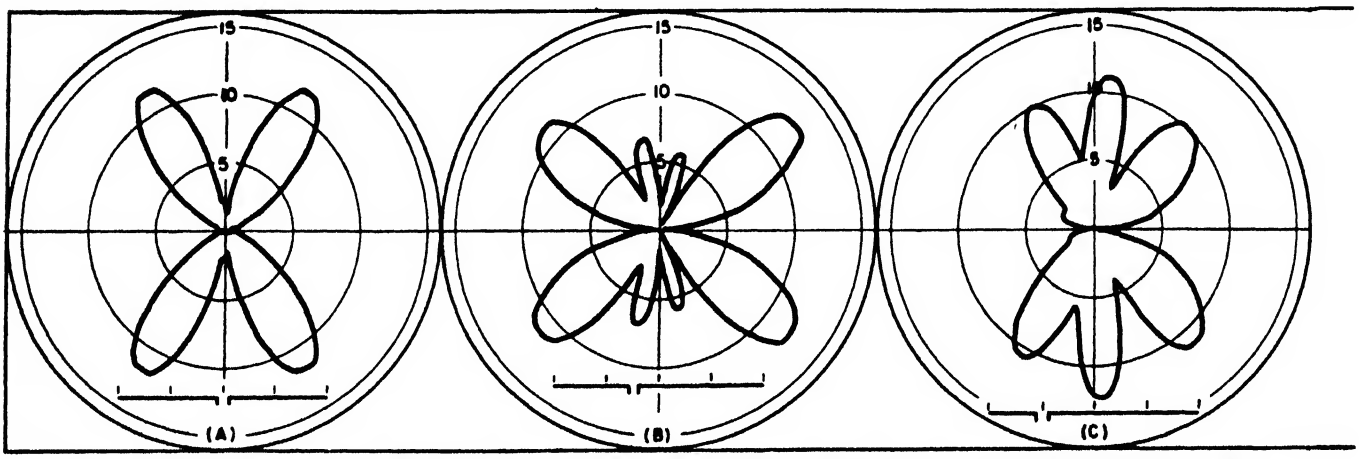

FIG. 4—Radiation patterns of a two-wavelength antenna showing effect of moving feed position from center to one end

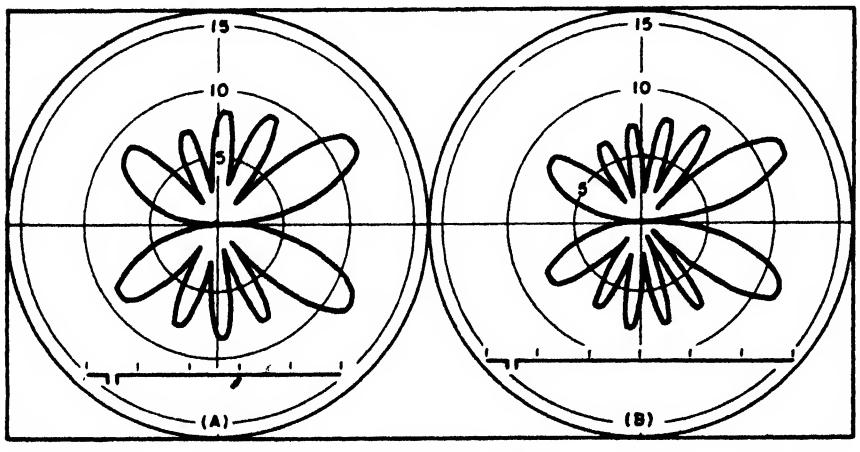

FIG. 5—Radiation from long wire antennas

tion of parallel wire transmission line was inserted between the antenna and the balancing unit.

The field strength patterns that are shown in the accompanying figures were measured by using scale models of the antennas at 10 and 20 cm. This method of measuring field strength patterns was used by the Antenna Laboratory of the Ohio State University Research Foundation during World War II for the determination of aircraft antenna characteristics.

The equipment used to measure these patterns consisted of an electro-magnetic transmitting horn, a rotating table upon which a hollow vertical plywood shaft was fastened, the antenna to be measured being mounted on top of the shaft and supported by polystyrene rods when necessary. The antenna to be measured was then a receiving antenna. A Littelfuse bolometer was used as the detector. The patterns were continuously recorded by means of a selsyn system between the rotating table and shaft and the recording table. A concentric line lighthouse tube oscillator and a 10 cm two-cavity klystron were used as transmitting sources.

Measurements

The patterns of the half wavelength antenna shown in Figure 1 were taken using first a balanced

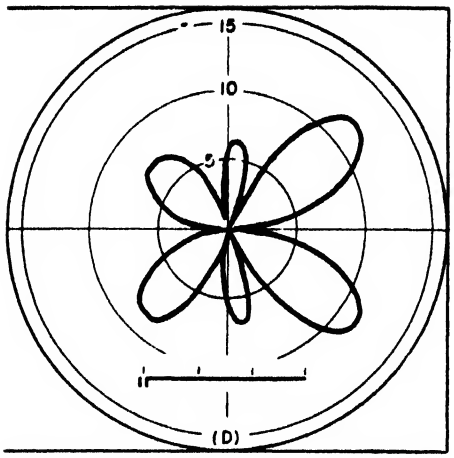

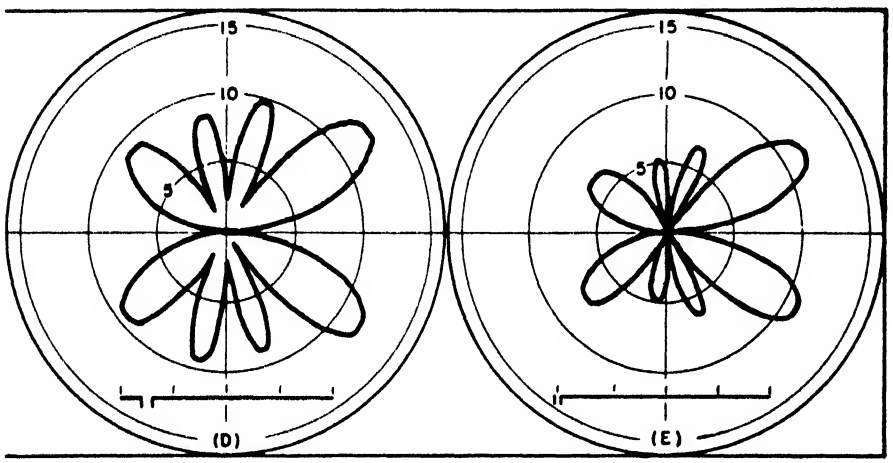

current feed at the center of the half wavelength and then a voltage feed at the end of the half wavelength wire. (Each diagram has an illustration of its antenna, marked in half wavelengths.) It was apparent that the current distribution on the half wavelength antenna is not sinusoidal when it was end fed. With end feeding the lobes are displaced 15 to 20 degrees from their position when the half wavelength wire was center fed.

Full-Wave Antenna

The full wavelength antenna was measured using a balanced voltage feed at the center of the antenna. The two half-wavelength portions of the antenna then have in-phase antenna currents flowing on them. The pattern obtained using this feed point is shown in Fig. 2A. The feed point was moved one-quarter wavelength off center and fed with a balanced current feed. The pattern (Fig. 2B) was nearly that which is usually published for a full wavelength antenna. However, the two lobes of energy on the same side of the wire are not equal in amplitude, but were present at about the published angle of 54 degrees. The minimum differed in amplitude from those obtained when the same length was end fed. When the full wavelength wire was end fed with a voltage feed, the lobes on both sides of the wire closest to the fed end of the antenna were reduced in amplitude even more than when the feed point was a quarter wavelength from the end of the wire, as seen in Fig. 2C.

Effect of Feed Point

A one and one-half wavelength wire was measured for center feed, Fig. 3A, one-quarter wavelength off center, Fig. 3B, one-half wavelength off center, Fig. 3C, and end fed, Fig. 3D. It is interesting to note the differences in amplitude of the broadside lobes and that the position of the large lobes off the free end of the end fed wire are slightly closer than the corresponding lobes for other feed points.

A two wavelength wire was measured using a balanced voltage feed at the center, (Fig. 4A), a current feed one-quarter wavelength off center (Fig. 4B), a voltage feed a half wavelength off center (Fig. 4C), a current feed three-quarters wavelength off center (Fig. 4D), and end fed with a voltage type feed (Fig. 4E). Different distributions must be present on the antenna for different feeds and the current distributions apparently are not sinusoidal even for the balanced center feed since the broadside minima are not complete. The pattern with the feed one-quarter wavelength off center (Fig. 4B), indicates that current distributions on each half of the wire were not identical let alone sinusoidal. When the wire was fed one-half wavelength off center (Fig. 4C), the minima were not complete and of different values due to the unbalanced current distribution along the antenna.

Off-Center Feed

When the wire was fed three-quarters wavelength off center (Fig. 4D), the current distribution was again different from that when the antenna was end fed (Fig. 4E), as it was for the same types of feeds using the three-half wavelengths antenna (Fig. 3). The large lobes off the free end of the wire were again closer to the wire when the two-wavelength antenna was fed three-quarter wavelength off center, (Fig. 4D), than when the wire was fed one-quarter wavelength from the end (Fig. 4E).

Also shown in Figure 5 are the patterns of longer wires, namely, two and one-half wavelengths and three wavelengths long. Time did not permit further measurements. The minima were not complete as was shown before for similar type feeds used on shorter lengths of wire. Similar effects of non-sinusoidal current distributions were present when unterminated rhombic and V antennas were measured.

This investigation was prompted by discussion between C. H. Page and G. H. Brown at the I.R.E. 1947 Winter Convention in New York City, of the effect of the diameter of the antenna on the pattern when various positions of feeds are used.

Antenna Power Divider

Chart facilitates finding correct values of L and C for any desired division of currents in a two-element broadcast array, with constant phase shift and constant resistive input

By EARLE TRAVIS

A SIMPLE power divider for a two-element broadcast antenna array can be built from the basic circuit shown in Fig. 1. Here resistors R represent actual measured values of characteristic impedance for the two transmission lines and must be equal, while L and C are variable and allow for any power division desired. As long as the correct relationships are maintained, the input impedance will be resistive and of a constant value, and most important, the phase shift between lines will remain constant. This means that the operator can vary tower current without having to change phasing adjustments.

The required relationships are that $X_L X_C$ always be equal to R^2 and that Z_B/Z_A always be equal to the current ratio K, which is equal to the square root of the power ratio.

By means of the chart in Fig. 2 it is possible to observe these relationships automatically and find quickly the values of X_L and X_C for any current ratio desired. The chart gives the cosine value for each series circuit. From this, the angle and its tangent can be found in a trig table, and the reactance value of each branch computed from $X_A = R \tan A$ and $X_B = R \tan B$. Knowing the operating frequency, L and C are computed from $L = X_L/2\pi f$ and $C = 1/2\pi f X_B$.

Conclusion

Usually it is best to let cosine B be negative so that branch B is capacitive. This allows for smaller units, but the capacitor must withstand fairly high voltage. In the case of high power it might be better to let cosine B be positive so its circuit is inductive. This will call for larger units, but the capacitor will not have to withstand such high voltage.

Example: Operating frequency is 1000 kc, current ratio is 3/1 and R is 230 ohms. For a current ratio of 3/1, the chart gives a value of 0.950 for cos A, and a trig table is then used to find tan $A = 0.3284$. Similarly, cos $B = 0.312$ and tan $B = 3.044$. Substituting in $X_A = R \tan A$, $X_A = 230 \times 0.3284 = 75.51$ ohms. Similarly, $X_B = 230 \times 3.044 = 700$ ohms. Allowing X_B to be capacitive, $C = 1/6.28 \times 1{,}000{,}000 \times 700 = 227.5$ $\mu\mu$f. X_A is then inductive, and $L = 75.51/6.28 \times 1{,}000{,}000 = 12$ μh. The alternate solution with X_A capacitive and X_B inductive gives $C = 0.0021$ μf and $L = 111.4$ μh.

The vector diagrams in Fig. 3 cover three different current ratios. Note that when the two current vectors are added in each case, their sum is always the same and is along the reference axis. This shows that the input of this power-dividing network is always resistive and of constant value.

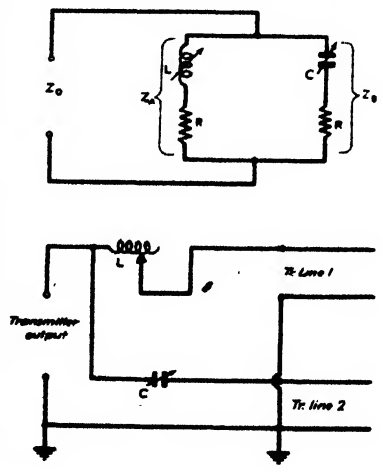

FIG. 1—Basic power-dividing circuit (above, with transmission lines represented by R), and actual circuit

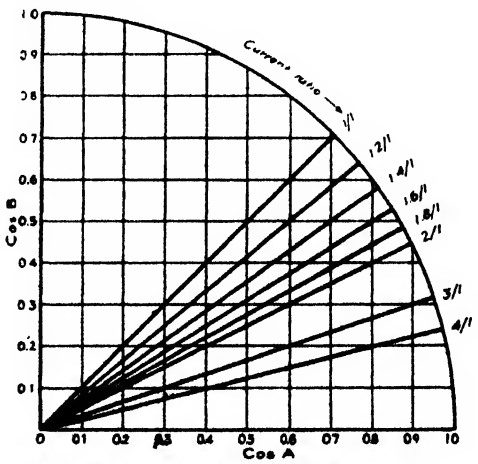

FIG. 2—Cosine values for finding L and C are at intersection of curve with line for desired current ratio

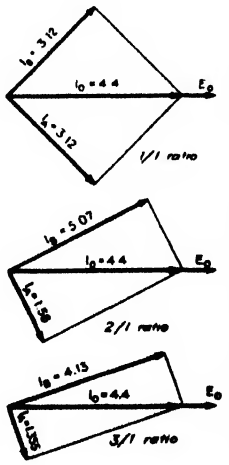

FIG. 3—Vector diagrams showing that input of circuit is always constant and resistive

Phasing Networks for Broadcast Arrays

Graphical methods are applied to the design of phase-shifting and impedance-matching networks required to distribute power properly in directional antennas. Compared to conventional network analysis the vector method results in economy of circuit components and simplified design procedure

By C. R. COX

VECTOR synthesis is a convenient mathematical tool which is very helpful to the designer of r-f phase-shifting and impedance-matching networks for the directional arrays used by many broadcast stations. Not only does this combination graphical and mechanical technique afford a clear understanding of the operation of a-c circuits, but it can also be used to synthesize network designs which display great simplicity when compared to circuits determined by ordinary methods. Problems in the design of phasing networks for directional antenna arrays are particularly susceptible to solution by vector methods.

Principles of Vector Synthesis

In general, the synthesis of a network by vector manipulation usually reduces to the following problem: Given a pair of vectors I_1 and E_1, representing the current through and the voltage across an impedance, it is required to establish a circuit which will transform I_1 and E_1 into another pair of vectors, I_2 and E_2. The latter pair of vectors is usually specified by the conditions of the problem.†

When the input and output impedances R_1 and R_2 between which the network must operate are known, the two currents are related by a simple law which equates input and output powers:

$$I_1^2 R_1 = I_2^2 R_2$$

† If the circuit is free from dissipation, the second pair of vectors is subject to the restriction.

$$\tfrac{1}{2}(E_2 I_2^* + E_1 I_1) = \tfrac{1}{2}(E_2 I_2^* + E_2^* I_2)$$

in which the asterisk (*) denotes the conjugate function. This equation states that the network must neither create nor destroy power.

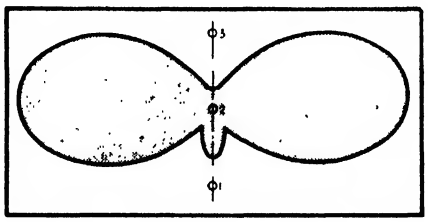

FIG. 1—Desired radiation pattern, which can be produced by the antenna array of Fig. 2

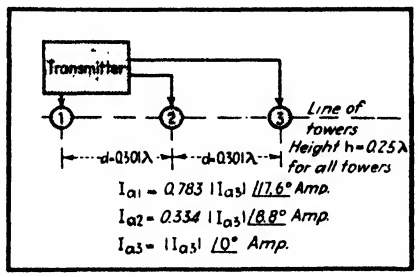

FIG. 2—Antenna array required to produce the radiation pattern of Fig. 1

The method of designing a network by vector synthesis may be most easily outlined by means of a specific example. To illustrate the general method, let it be required to design phasing networks suitable for providing currents of the desired magnitude and phase to three vertical radiators, in order to produce the radiation pattern shown in Fig. 1.

An analysis of this radiation pattern reveals that the towers must be 0.25 λ high, separated by a distance 0.301 λ, and fed with currents whose magnitudes and relative phases are as given in Fig. 2. A block diagram showing the elements of a suitable system of networks to produce the desired radiation pattern is shown in Fig. 3.

The problem at hand is now to design, by methods of vector syn-

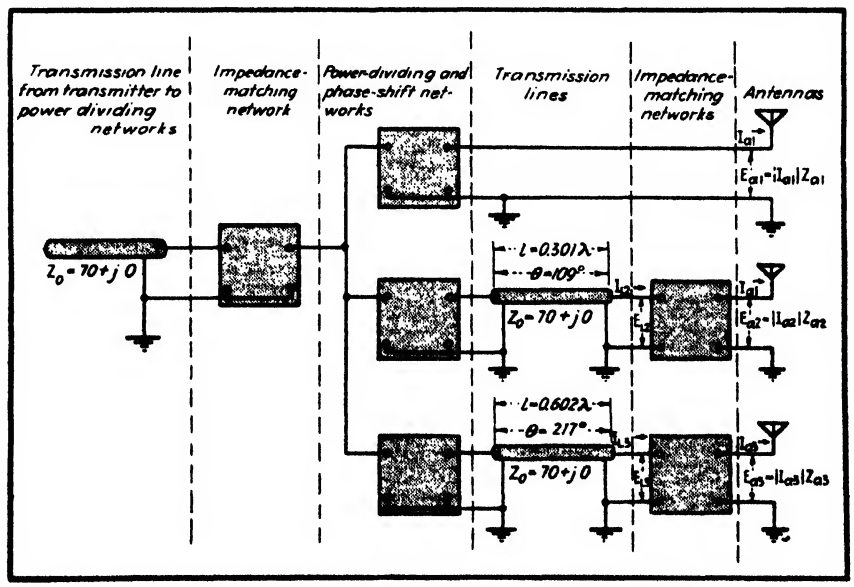

FIG. 3—Block diagram of system of networks and transmission lines for feeding antennas with the currents and voltages necessary to produce directional radiation pattern

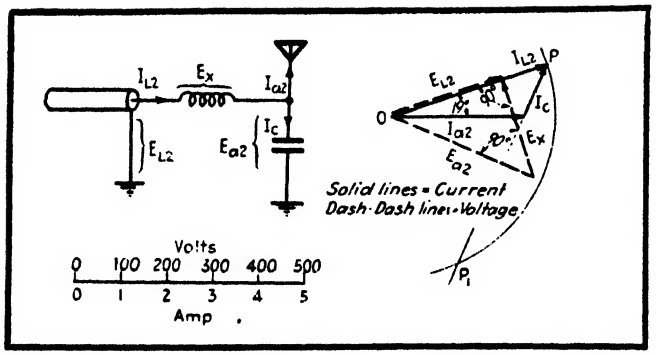

FIG. 4—L-type network for matching impedance of transmission line to impedance of antenna 2, with vector diagram from which design of the network is derived

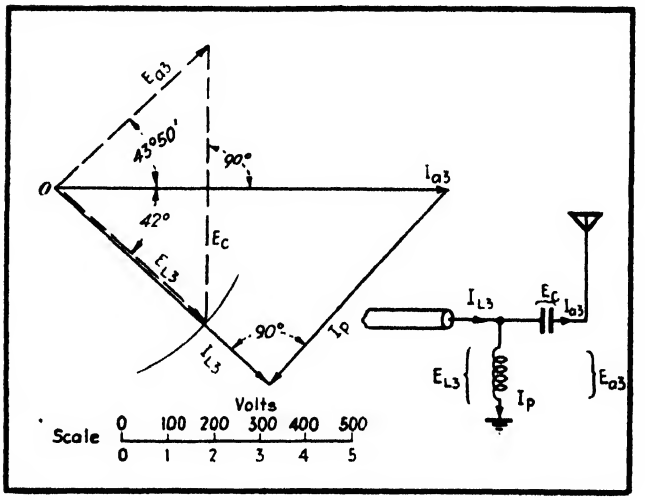

FIG. 5 (*RIGHT*)—Impedance-matching network of the L-type for matching antenna 3 to a 70-ohm transmission line. Vector diagram illustrates method of designing this circuit

thesis, impedance-matching networks between the transmission lines and the antennas, power-dividing and phase-shift networks, and the impedance-matching circuit which connects the transmission line from the transmitter to the three power-dividing and phase-shift networks. (It should be noted from Fig. 2 that antenna 1 is located at the transmitter and consequently does not require a transmission line, as do the other two antennas.)

To design a feed system for the array of Fig. 3, it is necessary to start at the antennas and work back through each network and transmission line toward the transmitter. The conditions of the problem yield the following information regarding antenna currents, impedances, and powers:

$I_{a1} = 6.7/17.6°$ amperes
$I_{a2} = 2.86/8.8°$ amperes
$I_{a3} = 8.56/0°$ amperes
$Z_{a1} = 28.7 + j39 = 48.4/53.67°$ ohms
$Z_{a2} = 108 - j45 = 117/-22.63°$
$Z_{a3} = 38.5 + j37 = 53.5/43.83°$
$P_{a1} = 1290$ watts
$P_{a2} = 890$ watts
$P_{a3} = 2820$ watts

where I_{a1}, I_{a2}, and I_{a3} are currents in antennas 1, 2, and 3 respectively, and the angles represent phases relative to that of I_{a3}. The quantities Z_{a1}, Z_{a2}, and Z_{a3} are the impedances of antennas 1, 2, and 3, respectively, and P_{a1}, P_{a2}, and P_{a3} are the powers in antennas 1, 2, and 3, respectively.

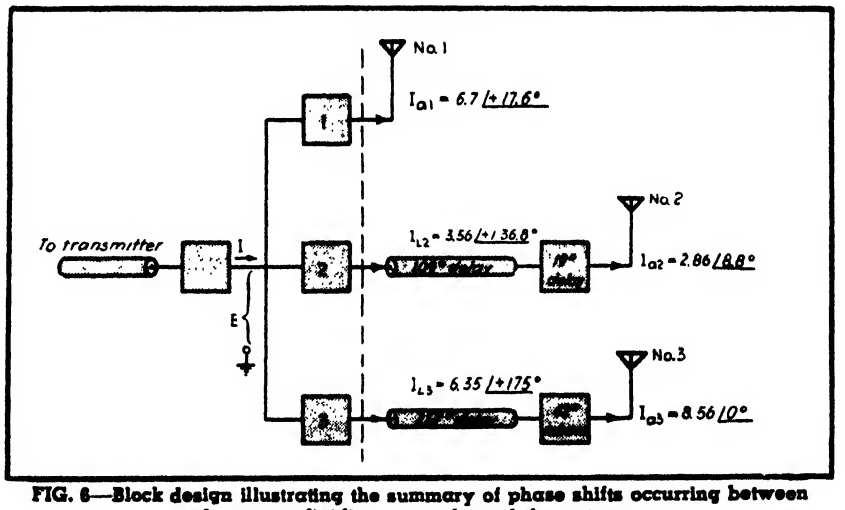

FIG. 6—Block design illustrating the summary of phase shifts occurring between the power-dividing networks and the antenna

From this data the voltage applied to the antennas and the currents in the transmission lines (whose impedance is $Z_o = 70 + j0$) can be determined as follows:

$E_{a1} = |I_{a1}|\,Z_{a1} = 6.7 \times 48.4/53.67° = 324/53.67°$ volts
$E_{a2} = |I_{a2}|\,Z_{a2} = 2.86 \times 117/-22.63° = 335/-22.63°$ volts
$E_{a3} = |I_{a3}|\,Z_{a3} = 8.56 \times 53.5/43.83° = 458/43.83°$ volts

$I_{L2} = \sqrt{P_{a2}/Z_o} = \sqrt{890/70} = 3.56$ amp.
$I_{L3} = \sqrt{P_{a3}/Z_o} = \sqrt{2820/70} = 6.35$ amp.
$E_{L2} = Z_o I_{L2} = 70 \times 3.56 = 250$ volts
$E_{L3} = Z_o I_{L3} = 70 \times 6.35 = 444$ volts

where E_{a1}, E_{a2}, and E_{a3} are the voltages applied to antennas 1, 2, and 3 respectively and the phase angle of each voltage is referred to the corresponding antenna current as a reference, I_{L2} and I_{L3} are the magnitudes of the currents in the transmission lines feeding antennas 2 and 3, and E_{L2} and E_{L3} are the magnitudes of the voltages across these transmission lines. With this data, the impedance-matching networks between the transmission lines and the antennas can now be designed.

Design of Network for Matching Impedances

The sketch in Fig. 4 illustrates the synthesis of a network for matching the line impedance of $Z_o = 70\angle 0°$ ohms to the center antenna impedance of $117\ \angle -22.63°$ ohms. We begin by drawing a vector of length 2.86 units to represent the antenna current I_{a2}. This vector can be drawn in any convenient direction but since it is used

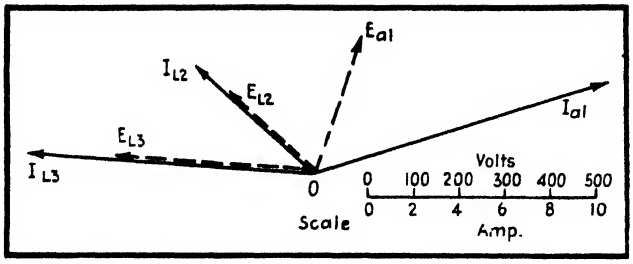

FIG. 7—Vector diagram of voltages and currents which must be produced by phase-shifting and power-dividing networks

FIG. 9—Vector diagram for input circuits →

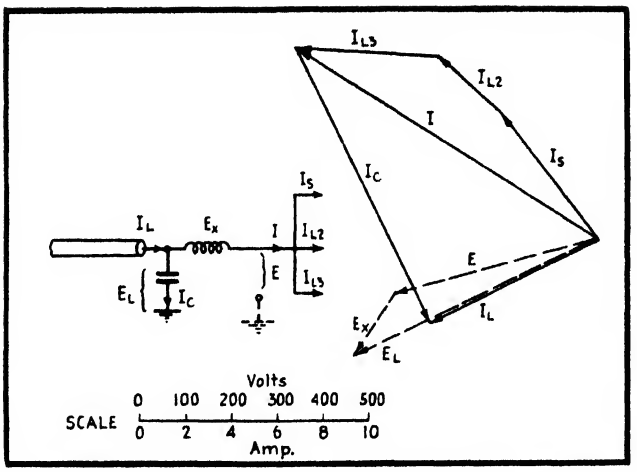

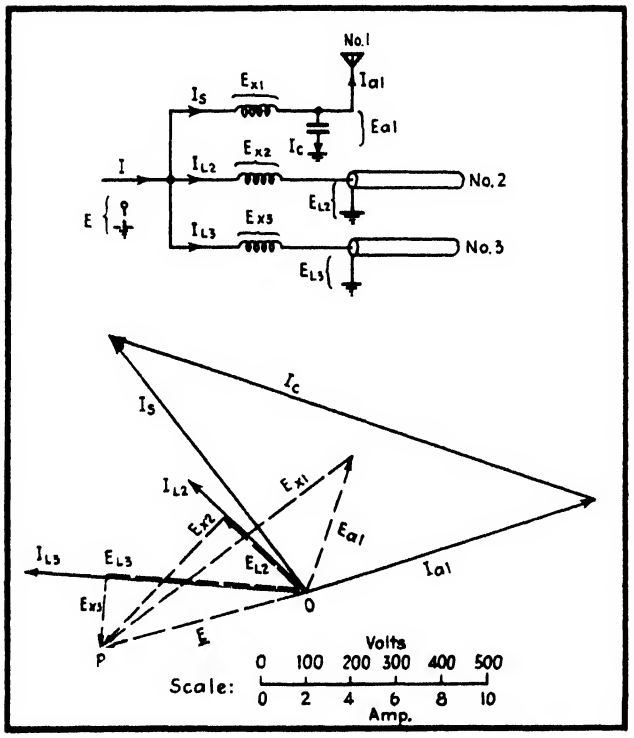

FIG. 8—Synthesis of phasing and power-dividing networks

FIG. 10—Alternative design of phasing networks →

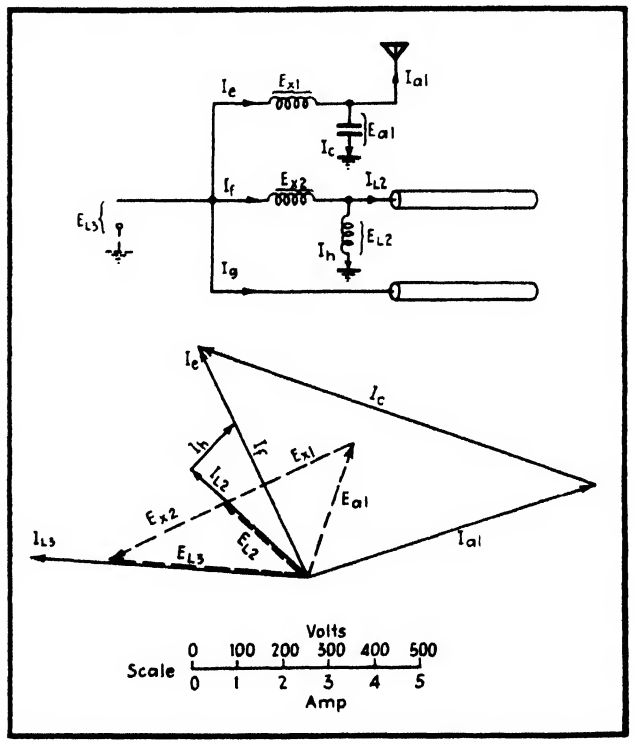

as the reference vector, it will be drawn along the x-axis. To some suitable voltage scale, the vector for the antenna voltage E_{a2}, at an angle of −22.63° with respect to I_{a2}, can also be drawn.

An L network of the type shown will give the impedance transformation. For such a network, Kirchhoff's law for branching currents must be satisfied, i.e., $I_{L2} = I_{a2} + I_c$, where I_c is the current through the capacitor. Therefore the tips of I_{L2} and I_c must coincide at some point P which lies on a circle of radius $I_{L2} = 3.56$, drawn from 0 (zero) as a center. Since the current through a reactance forms a 90-deg angle with the voltage across it, we may lay out I_c at right angles to E_{a2}, and the intersection of I_c with the circle locates the point P.

The potential E_{L2} must equal the sum of E_x and E_{a2}. Therefore, the tail of E_x must lie on the tip of E_{a2}, and the direction of E_x is normal to the current I_{L2} through the inductance. The magnitude of E_x is determined by the point of intersection with I_{L2}, and the voltage triangle is completed by drawing E_{L2} from 0 (zero) to the point of intersection of E_x with current I_{L2}.

Because I_c leads E_{a2} by 90 deg, the parallel reactance must be that due to a capacitance. Similarly, since E_x leads I_{L2} by 90 deg, the series reactance must be that due to an inductance. The magnitudes of the required reactances are obtained by dividing the length of a vector representing voltage across a reactance by the length of the corresponding current vector, i.e.,

$X_L = E_x/I_{L2}$, and $X_c = E_{a2}/I_c$.

The network of Fig. 4 is a delay network because I_{a2} lags behind I_{L2}. Had we chosen to extend I_c in the opposite direction, intersecting the circle at P_1, a phase-advance network would have been obtained.

Choice of Configuration

The choice between the phase-advance and the phase-delay configuration is purely a matter of convenience. Any impedance transformation problem may be solved by either network. However, in designing the matching circuit for antenna 3 we choose the phase-advance network because this choice happens to simplify design of the phasing networks. We begin the construction of the vector diagram for antenna 3 (Fig. 5) by drawing vectors I_{a3} and E_{a3}. The series capacitor introduces a voltage E_c which adds to E_{a3}, but in a direction normal to I_{a3}. Then, a circle of radius E_{L3} locates the tip of E_c, and the vector I_{L3}, whose length is known, is drawn through the point of intersection. The vector I_x, drawn normal to and lagging I_{L3}, completes the construction.

Phasing Networks

A summary of the phase shifts in the lines and antenna tuning units is given in Fig. 6. Each of the two transmission lines introduces a delay (in degrees) of $\theta = 360\ l/\lambda$, where l is the length of the line and λ is the wavelength. For $\lambda = 0.301$ the delay is 109 deg, and for $\lambda = 0.602$ the delay is 217 deg. The apparatus to the left of the dotted line in Fig. 6 is required to divide the transmitter power into three parts and distribute it among the three antennas with the required phase angles and amplitudes. Figure 7 represents the three voltages and currents leaving the phasing apparatus at the dotted lines of Fig. 6.

The remaining problem is that of selecting a voltage vector E which can be rotated and transformed by means of three separate reactance networks to produce E_{a1}, E_{L2}, and E_{L3}. An important point is that the vector E may be of any magnitude and of any phase, and we may therefore select E to suit our own convenience. Referring to Fig. 8 we see that reactances in series with transmission lines 2 and 3 produce voltage vectors E_{x2} and E_{x3} which intersect at P. The vector E, drawn from 0 (zero) to P, is then a convenient vector to represent the input voltage.

Since the antenna current I_{a1} is far removed in direction from E, it is necessary to obtain somehow a new current I, that is at least within 90 deg. of E. This is accomplished by introducing a parallel capacitance across antenna I_a, producing the current I_c leading E_{a1} by 90 deg. An inductance in series with I_a introduces a voltage vector E_{x1}, drawn from the tip of E_{a1} by 90 deg. An inductance in I_a perpendicular to E_{x1} we have satisfied all the conditions of the problem.

Input Circuit

An input circuit, to provide a load impedance of $70 + j0$ ohms for the transmitter, is illustrated in Fig. 9. The total current I is obtained by adding vectorially the three branch currents I_a, I_{L2} and I_{L3}. By adding a series inductance to produce E_x, and a parallel capacitance to produce I_c, the voltage and current triangles are all properly completed.

Alternative Solution

In an earlier paragraph, it was stated that any voltage vector E (Fig. 8) could be selected when designing the phasing networks. Suppose, for instance, that antenna 3 is thought to be the dominant element in the array and that we wish to do all the tuning in the networks feeding antennas 1 and 2. Then, E_{L3} is the input voltage, as shown in Fig. 10. The design in this case follows the same principles established in previous examples.

Completed simplified system of networks designed by vector synthesis, and equivalent system of networks designed by conventional methods

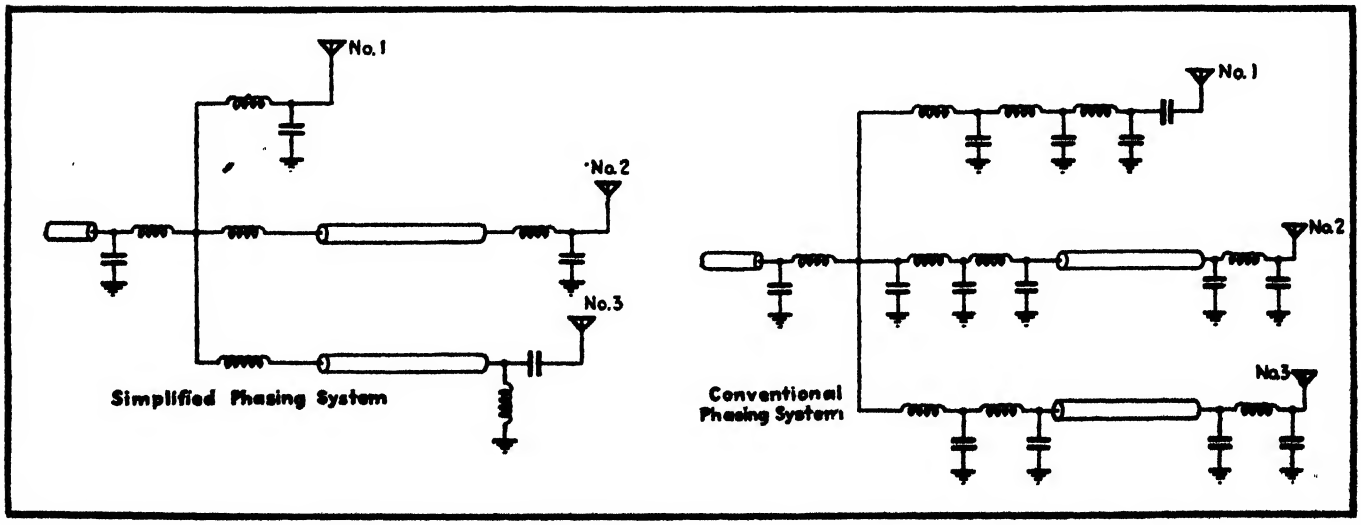

Phase Monitor for Broadcast Arrays

The phase angle between any two directional antenna towers can be checked in thirty seconds to within a degree of the design value for the array, by a device that is mechanically simple to construct, easy to check or use. It requires no power supply and contains no components whose drift or age affects the calibration

By BERNARD C. O'BRIEN and FRANCIS L. SHERWOOD

Directional broadcast antennas are becoming more and more complicated and require an accurate means of measuring the phase and magnitude of the individual tower currents, if the radiated pattern is to be maintained. The phase monitor described here is fundamentally simple and stable and will indicate phase relations between r-f currents in any desired number of towers, within one half of one degree. Readings may be made of either the large or small angle between two currents, and no ambiguity can exist as to the quadrant involved.

The phase monitor is the result of a few experiments with an r-f bridge and some flexible plastic dielectric coaxial line. At approximately 90 degrees from the top of each of our towers, we had installed a large rectangular one-turn shielded loop. Energy picked up by the loop was fed to the transmitter house by three ⅛-inch coaxial lines. Considerable care was taken to make these lines of equal length, in order that each sample of current should experience the same delay in traveling from the towers to the phase monitor.

The principle of operation of the monitor is illustrated in Fig. 1. Two tower sampling currents, between which the phase angle is to be determined, are selected by switches S_A and S_B. A phase delay is introduced in the current chosen by switch S_B, by cutting in and out predetermined lengths of coaxial line, using switches S_1 through S_{11}. Thus, the current from S_B is delayed sufficiently to bring it into phase with that from S_A. The currents leaving the phase delay lines flow through r-f milliammeters and terminating resistors R_A and R_B, to ground. A portion of the voltage drops across R_A and R_B is fed through potentiometers R_2 and capacitors C_1 to a germanium rectifier, X.

When the two r-f voltages leaving potentiometers R_2 are equal in magnitude and exactly in phase, no voltage appears across X, and no current flows through it. When these conditions do not exist, the rectifier current is indicated by the d-c flowing through the two r-f chokes and the galvanometer G, a 0-1 d-c milliammeter. The two r-f milliammeters are in the circuit simply to indicate relative tower currents and have no function in measuring phase relations.

In operation, the switches S_A and S_B are set to the desired position, and potentiometers R_2 are advanced simultaneously, until meter G gives a substantial indication. Delay is then added to channel B, by switches S_1 through S_{11} and both potentiometers R_2 are progressively advanced, until a zero reading is obtained on meter G. The switches S_1 to S_{11} that have been brought into the circuit are then totaled to indicate the amount of phase delay that has been introduced. Maximum accuracy is obtained when one or the other of potentiometers R_2 are advanced to the maximum position. In this manner readings may be duplicated to within 0.5 degree or better.

Sufficient delay line is available to carry a current through a complete

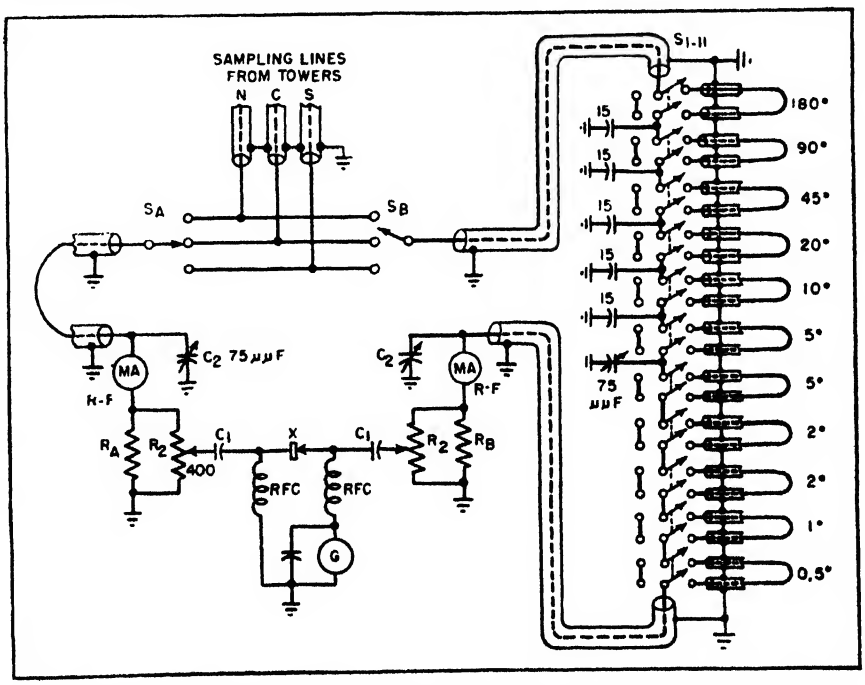

FIG. 1—Schematic diagram of the phase monitor with coaxial-cable phasing sections and switching arrangement at right

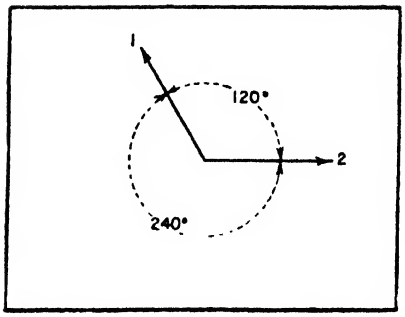

FIG. 2—Vector diagram showing how to measure angle from either tower

360-degree circle. Thus, each phase measurement can be checked by first measuring the smaller angle between two currents by delaying the leading current and next by delaying the lagging current to determine the larger angle which should complete the 360 degrees. As shown in Fig. 2, it is possible to delay the No. 1 current 120 degrees to meet the No. 2 current, or to delay the No. 2 current by 240 degrees to coincide with the No. 1 current. Each pair of measurements made in this way adds to 360 degrees to make the procedure self-checking. Three or more currents can also be checked to total to 360 degrees, a procedure that inspires a good deal of confidence in the readings taken, provided the total comes out right.

Checking Monitor Calibration

It is possible to check the phase delay network itself for any slight variations, simply by putting both switches S_A and S_B on the same source and obtaining a balance with zero degrees and 360 degrees of delay line. This method has been used repeatedly in an effort to detect any tendency of the coaxial sections to change characteristics. So far, no drifting has been observed, within the 0.5-degree accuracy of the monitor.

With a little practice a single phase reading may be made in about thirty seconds. The instrument is always ready for use, as it requires no warming up period or calibrating adjustments. Modulation does not affect the measurements, since the signal is completely canceled for exact balance.

The indicating meter used is a large scale 0-1 milliammeter. A 0.5-degree error at balance is indicated by a needle deflection of about $\frac{1}{16}$ inch on the large scale. More sensitivity can be obtained by substituting a microammeter, or by using an audio amplifier and speaker in place of the meter. A 0.25-degree coaxial section and switch may also be added, for finer readings.

Building a Delay Line

For the coaxial delay line a flexible low-loss plastic dielectric line was used, of about $\frac{1}{4}$ inch outside diameter having an outer coating of rubber. A 175-foot unterminated piece was connected to an r-f bridge and was trimmed to exactly 90 degrees by observing when the bridge indicated a short circuit on our frequency of 1460 kc. The 90-degree section was found to be exactly 106 feet indicating a velocity of 63 percent of that in free space. The characteristic impedance of the line was next determined by locating a nonreactive resistor that gave the same bridge indication when measured either alone or through the 90-degree section of line. The value of this resistor turned out to be 62.5 ohms.

The input impedance at the monitor terminals was next measured and adjusted. It is important that each termination be equal and nonreactive, and constant for all delay combinations; otherwise slight phase shifts will be introduced at this point, with resulting error in measurements. With the bridge connected directly to the r-f milliammeter input post, R_A and R_B were adjusted to give a termination of exactly 62.5 ohms. The remaining

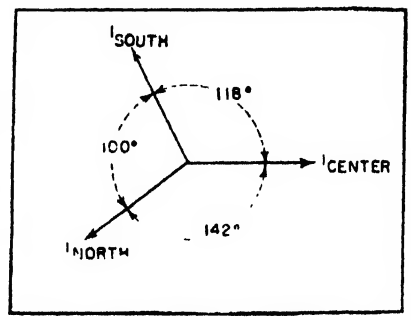

FIG 3—Vector diagram showing actual phase relations of WHEC three-tower array

inductive reactance due to wiring was cancelled by adjusting C_2, 75-micromicrofarad variable capacitors. The wiring from input terminals to S_A and S_B was made as short and symmetrical as possible, in order to minimize reactances at the line terminations.

Inductive reactances due to wiring between switches S_1 to S_{11} were canceled by adding shunt capacitances at various points along the switch row. After some trial and error, the combination of capacitors shown held the input impedance to channel B at 62.5 + j 0 ohms for all settings of the phase delay network.

Adjusting for Zero

The length of the coaxial line between S_A and its associated r-f milliammeter was adjusted to give a delay exactly equal to that between S_B and its r-f meter, when all phase delay switches S_1 through S_{11} were turned off. This was done by feeding both S_A and S_B from the same source and trimming the channel A coaxial line to obtain a zero galvanometer indication, with no delay introduced in channel B.

A specimen phase reading on WHEC's tower currents gives the data presented in Fig. 3 and corresponds exactly to values assigned in the original design for the required directional characteristics of the array.

# of Directional Antennas

A method of measuring resistance and reactance values at radio frequencies with an ordinary 3-inch cathode-ray oscilloscope while full power is being fed to the broadcast antenna. Width and height measurements of an elliptical pattern give the required constants

By WILLIAM S. DUTTERA

IN the alignment of directional antennas there arise two types of problems. The first is that of securing the proper phase relations and amplitude relations between the various antenna currents. The second is that of tuning each antenna to match its transmission line, so no standing waves exist on the line.

The methods of arriving at proper phasing and current ratios are as varied as the number of engineers engaged in tuning directional antennas. It is not proposed to discuss this subject here, but instead to deal with the second part of the problem. Specifically, this involves determining the resistance and reactance which each transmission line sees at its antenna. The engineer wants to know if the line is "working" into too high or too low resistance, how much reactance is present and whether this reactance is inductive or capacitive.

In some cases, particularly with antennas less than about 120 degrees high, it is possible to calculate the line termination networks with reasonable accuracy by a combination of ordinary measurements and proper application of circuit theory. With high antennas having distorted current distribution, or with a combination of high and low antennas, accurate calculations are not possible. It has heretofore been necessary in these cases to obtain final circuit adjustment by what almost becomes a trial and error method.

It must be noted that it is impossible to measure, by normal methods, the impedance of an antenna as a working part of a directional system. The measurement must necessarily be made without disturbing the system, under the condition of partial or full power. It is in this manner that the cathode-ray tube measurements to be described are made.

FIG. 1—Standard method of measuring the resistance and reactance of a load at power frequencies, using ordinary meters

Method Used in 60-cycle Circuits

In 60-cycle single-phase power circuits the load impedance can be found with meters measuring volts, amperes and power factor, connected as shown in Fig. 1. In brief, one current flowing in the power factor meter is proportional to the phase and magnitude of the load current, and the other current is proportional to the phase and magnitude of the load voltage. The resultant action of the fields of these two currents upon a vane produces a displacement of the vane. A pointer attached to the vane indicates directly the phase angle between load current and voltage.

With E, I and the phase angle ϕ known, the resistance R and X are obtained from the following basic formulas:

$$R = \frac{E}{I}\cos\phi \qquad X = \frac{E}{I}\sin\phi$$

Cathode-ray Tube Method

In the r-f version of the procedure for determining load impedance, a cathode-ray tube is substituted for the voltmeter, ammeter, and power factor meter, as shown in Fig. 2. In this case it is simpler to use voltages instead of currents. A cathode-ray tube with electrostatic deflecting plates is chosen. A voltage proportional to the amplitude and phase of the load voltage is taken from voltage divider C_2R_2 and applied to horizontal deflecting plates C and D. A voltage proportional to the amplitude and phase of the line current is secured from a well-shielded trans-

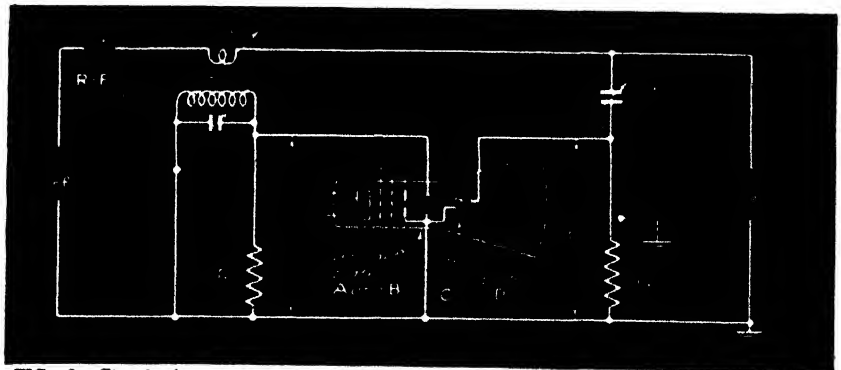

FIG. 2—Circuit for measuring the resistance and reactance of a load at radio frequencies under operating conditions. The cathode-ray tube may be part of an ordinary three-inch cathode-ray oscilloscope

Multi-Wire Dipole Antennas

High-frequency antennas to which transmission lines of high impedance (of the order of 500 ohms) may be directly coupled, without the use of matching transformers, and which use several wires in the dipole, are here described

By JOHN D. KRAUS

THE single-wire half-wave doublet is a common form of short-wave antenna. When operated at its fundamental frequency there is a maximum of current, or current loop, at the center of the antenna and a minimum of current at the ends. The resistance, as measured at the current loop point of this antenna, is about 70 ohms when the antenna is in free space. Thus, a transmission line connecting a transmitter to the current loop point of a single-wire half-wave doublet should have a characteristic impedance of about 70 ohms if a minimum of reflection on the line is desired.

A line of this relatively low characteristic impedance may be convenient in some cases. In other cases, a higher impedance line may be preferable. Such lines, having a characteristic impedance of 300 to 600 ohms and constructed of parallel open wires, are commonly used in short-wave practice. To terminate such an open wire line at the current loop point of a single-wire half-wave doublet with a minimum of reflection requires the use of some type of matching transformer. Quarterwave transformers, building-out sections, and delta matching systems are often used for this purpose.

This article describes a number of new antennas of the multi-wire type[1]. Three of the multi-wire doublets discussed are one-half wavelength long and a number of other types both longer and shorter than a half-wave are also treated. Several of these antennas have terminal resistances which are suitable for the direct connection of an open wire transmission line. For this reason they may be more convenient in certain cases in place of a single-wire doublet which requires some form of matching transformer. The transmission line terminals of all of the types described are located at a current loop point. Lindenblad[2] has recently described a folded antenna, which might be called a 2-wire quarter-wave doublet, in which the terminals are located at a current node.

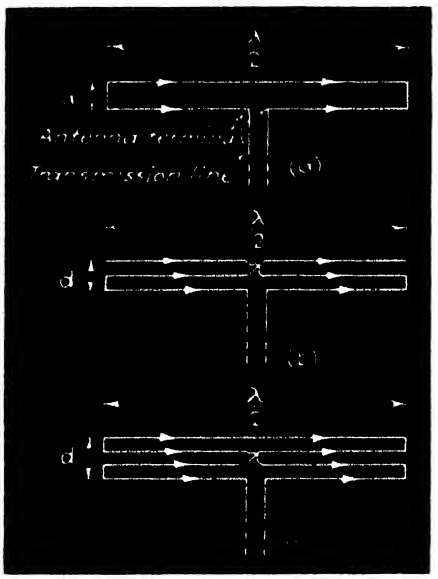

Fig. 1—Two, three and four wire half-wave antennas. The instantaneous currents are in phase with each other and their directions are indicated by the arrows

Multi-Wave Half-Wave Doublets

Figure 1 shows multi-wire half-wave antennas employing two, three, and four parallel in-phase wires. The current distribution at a given instant is indicated by the arrows on the wires. The two-wire half-wave doublet at *a* consists of two parallel closely-spaced half-wave wires connected together at the ends. Very small spacing *d* between the wires of the order of 0.01 wavelength can be used. With the antenna in free space the feed point radiation resistance is about 350 ohms. Thus, it is practical to connect an open wire transmission line of this characteristic impedance directly to the terminals of the antenna and no matching transformer is required.

By using a larger number of parallel in-phase half-wave wires the feed point resistance can be further increased. Thus, Figs. 1b and 1c show three- and four-wire half-wave doublets which have terminal resistances of approximately 875 and 1500 ohms respectively. It is not practical to build open wire lines of sufficiently high characteristic im-

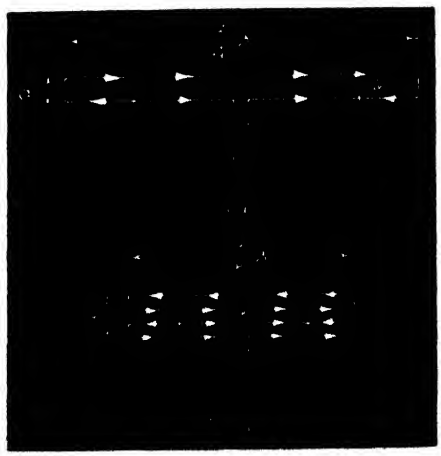

Fig. 2—Two wire, three-quarter wave antenna (terminal resistance 450 ohms) and four-wire, three-eighths wave antenna (terminal resistance 230 ohms)

[1] J. D. Kraus, Multi-Wire Doublet Antennas, *Radio*, No. 239, p. 24, May 1939; also *Radio*, No. 240, p. 21, June 1939.

[2] N. E. Lindenblad, Television Transmitting Antenna for Empire State Building, *RCA Review*, vol. 3, no. 4, p. 400, April 1939.

pedance to directly match these three- and four-wire doublets. However, these doublets can be applied to beam antenna systems where an increased feed point resistance is desired. Several beam antenna systems using multi-wire doublets have recently been described.[3]

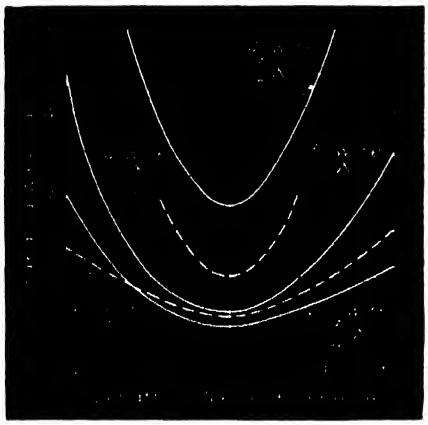

Fig. 3—The length of the antenna becomes more critical as the number of wires is increased. Also, the standing wave ratio increases

Although the feed point resistance of the multi-wire doublets is much higher than for the single-wire half-wave doublet, the radiation characteristics of both types are very similar.

Additional Types

Another type of multi-wire antenna called a two-wire three-quarter wave doublet is shown in Fig. 2a. This antenna is approximately three-quarters wavelength long overall. The resistance at the terminals is about 450 ohms with the antenna in free space and thus, a 450-ohm open-wire line can be directly connected to the terminals of this antenna.

Figure 2b shows a four-wire three-eighths wave doublet. This antenna has four parallel wires and is three-eighths of a wavelength long overall. The terminal resistance is about 230 ohms when the antenna is in free space.

Tests were made on the multi-wire antennas described to determine the effect of antenna length and frequency on the impedance match of the antenna to the transmission line. The standing waves on the transmission line were used as an indication of the condition of match.

The measured variation in the standing wave ratio versus length of the antenna for the multi-wire antennas described is given in Fig. 3. The lengths are plotted in terms of the optimum length, that is, the length resulting in the smallest terminal reactance. The antennas

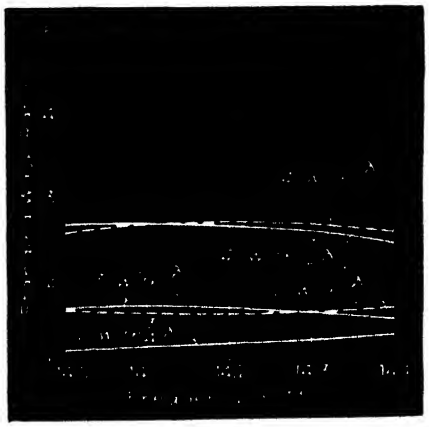

Fig. 4—The standing wave ratio is quite constant over the operating range from 14.0 to 14.4 Mc. A 570 ohm line was used

were tested in a horizontal position. A frequency of about fourteen Mc was used and the frequency, height above ground and spacing between the wires were maintained constant. A 570-ohm transmission line was used in each case and was connected directly to the antenna terminals. The optimum lengths expressed in wavelengths for the various antennas were found to be approximately as follows: Two-wire half-wave, 0.49 λ; three-wire, 0.46 λ; four-wire, 0.47 λ; two-wire three-quarter wave, 0.71 λ; and four-wire three-eighths wave, 0.38 λ.

Using these optimum lengths, the variation of standing wave ratio with frequency was measured. The results are shown in Fig. 4. A 570-ohm line was directly connected to the antenna terminals in each case. Some mismatch is to be expected for certain of the antennas such as the four-wire doublets. However, it is significant that over the frequency range measured (amateur 14.0 to 14.4 Mc band) the standing wave ratios remained very constant.

In the frequency test all of the antennas were suspended in a horizontal position and at a height of about 25 feet above ground except the four-wire half-wave which was about 30 feet above ground. The height of an antenna above ground has, of course, an important effect on its terminal resistance and reactance.

The antennas were constructed of number twelve (B. & S. gauge) wire and the overall spacing d was of the order of 0.015 wavelength or less. Thus, for example, the two-wire half-wave doublet designed for 14 Mc was 34 feet long and had a wire spacing of one foot.

Three-Eighths Wave Vertical

Although the multi-wire antennas described may be used in either a horizontal or a vertical position, a

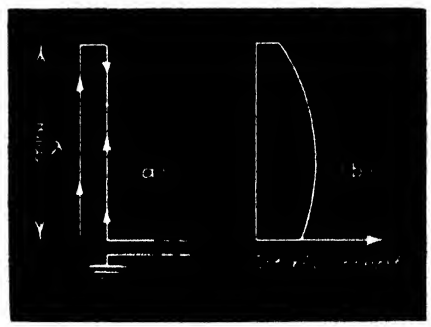

Fig. 5—A three-eighths wave vertical antenna working against ground and its total current distribution

purely vertical type can be constructed by using one-half of the two-wire three-quarter wave antenna and working it against ground. The arrangement for such an antenna is shown in Fig. 5a. The total current distribution (vector sum of currents in both wires) is given in Fig. 5b. The terminal resistance of the antenna is about 250 ohms. An interesting property of this antenna is that due to the multi-wire construction, a current distribution is produced which is similar to that of a vertical top-loaded single-conductor antenna.

[3] J. D. Kraus and H. E. Taylor, Compact-H Beam Antenna, *Radio*, no. 242, p. 34, Oct. 1939; also J. D. Kraus, Twin-3 Flat-Top Beam Antenna, *Radio*, no. 243, Nov. 1939.

Low-Impedance Loop Antenna for Broadcast Receivers

Using a large low-impedance loop antenna improves pickup over that of a smaller high-impedance loop. Design of transformer for optimum coupling of low-impedance loop to grid of first stage is described. Curves give conditions for maximum gain

By L. O. VLADIMIR

LOW-IMPEDANCE LOOP antennas have been used for some time in direction finders, and just prior to the war were beginning to find favor in home receivers. They are of particular value in large console models where advantage can be taken of available area to install efficient antennas.

In addition, low-impedance loop antennas are stable. That is, their inductance will ordinarily not change with age and humidity as much as will that of high-impedance loops. Placement of leads from loop to receiver is not as critical for low-impedance loops as for high-impedance loops. Also, the low-impedance loop is easier to manufacture than the high-impedance loop because its inductance need not be adjusted to within such narrow limits; normal manufacturing variations can be compensated with the antenna trimmer. Of course the coupling transformer must be closely adjusted, but this is standard procedure in coil manufacture.

Coupling Transformer

The heart of the low-impedance loop antenna is the step-up transformer that couples the loop to the grid of the r-f or mixer tube. The characteristic of this circuit is given by the expression, derived in Appendix I

$$Gain = kQ_s(L_{EQ}/L_L)^{1/2} \times [m(1 + m - mk^2)/(1 + m)]^{1/2} \times (1 + m + 2mk^2)^{-1} \quad (1)$$

in which the significance of the terms is shown in Fig. 1 and Table I.

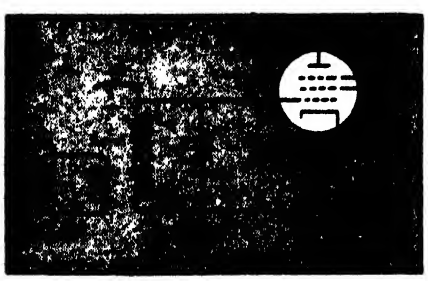

FIG. 1—Low-impedance loop antenna is coupled by step-up transformer to input of first stage

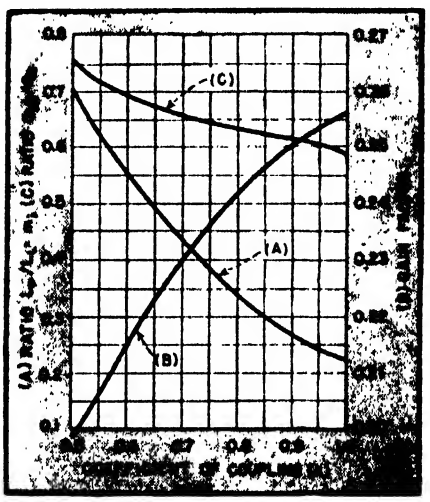

FIG. 2—Curve (A): Inductance ratio as a function of coupling coefficient for maximum gain. Curve (B): Gain factor as a function of coupling coefficient for optimum inductance ratio. Curve (C): Ratio of Q's for optimum inductance ratio varies with coupling coefficient

In the schematic diagram of Fig. 1, the inductance L_L is the loop, which can or cannot be center-tapped. Neither case will affect the results because capacitance coupling between primary and secondary windings is very small compared to inductive coupling.

Equation 1 will be analysed to determine the optimum design of the coupling transformer and to compare merits of the low-impedance loop to those of the high-impedance loop.

Optimum Gain

Of primary interest in determining maximum gain of the coupling transformer is the magnitude of the quantity m in Eq. 1. Because the values L_{EQ}, L_L and Q_s are roughly fixed by other design considerations, we specifically wish to substitute various values of k in Eq. 1 to find what value m must be for maximum gain. While the maximum point could be found by differentiating this equation, the resultant derivative is a sixth order equation and extremely difficult to handle. Accordingly the information was obtained graphically and is shown by curve (A) in Fig. 2.

Knowing the realizable coefficient of coupling which we can obtain in our transformer design, we can find m directly. From this value of m and the loop inductance L_L we can find the required primary inductance L_P. Inasmuch as the quantity L_{EQ} is fixed by tuning considerations, only the quantity

$$k[m(1 + m - mk^2)/(1 + m)]^{1/2} \times (1 + m + 2mk^2)^{-1}$$

of Eq. 1 can be varied freely. Call this quantity the *gain factor* and plot it against k as shown by curve (B) in Fig. 2.

Obviously k should be as large as possible for maximum gain, but the difference in performance between a coil having a k of 85 percent and one having a k of 95 percent hardly justifies extraordinary or costly pre-

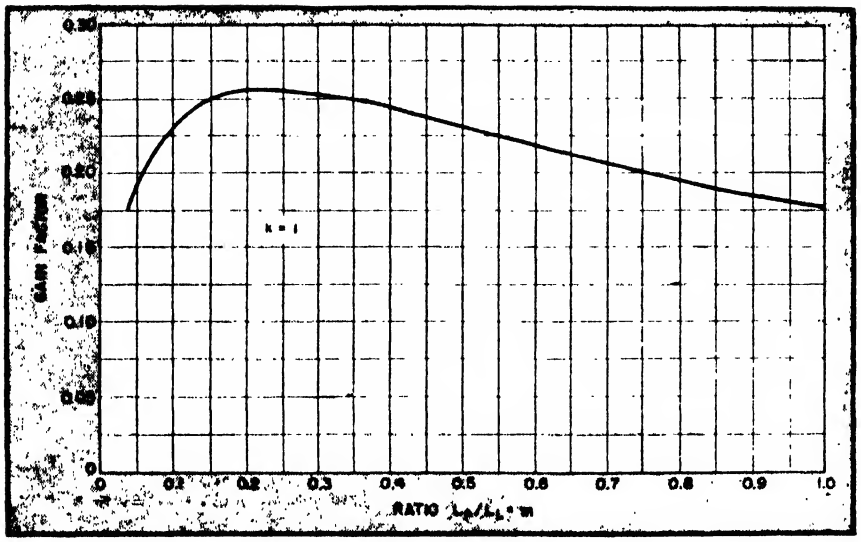

FIG. 3—Gain factor as a function of inductance ratio for constant coupling coefficient shows a broad maximum

cautions to obtain the higher coupling coefficient. Small powdered-iron core coils normally can be made with a k of 85 percent. Such a design is usually satisfactory from both cost and performance standpoints. The addition of powdered-iron cups surrounding the coils may bring k to over 90 percent, but the additional cost is considerable. If a coil is designed without powdered-iron, the coupling coefficient usually obtainable hardly justifies the degradation in performance.

The curve of gain factor as a function of m, allowing k to remain constant, shows the maximum to be rather broad as illustrated in Fig. 3. Thus with k fixed at unity, m can have any value from 0.17 to 0.3 without noticeable loss in gain. Curves for other values of k can be plotted.

Conductor Size

It is usually of interest to estimate the overall total Q of the coil in the circuit. The ratio of this value Q_{tu} to Q_s is plotted as curve (C) in Fig. 2 against coupling coefficient. This ratio holds for values of m to give maximum gain as shown in curve (A) in Fig. 2, and the assumptions are the same as were made in the calculations for that curve, namely that Q_L equals Q_P and the total primary quality (i.e., of L_L and L_P combined) equals one-half Q_s.

The choice of conductor size for L_L, L_P, and L_s is the determining factor in fixing selectivity and must therefore be carefully considered by the designer. When an iron core is used, the secondary can be properly wound with 5/41, 7/41, or 10/44 sse litz wire, and excellent secondary quality thus obtained. Either the loop antenna is constructed of heavy copper wire (No. 10 B&S gage or larger) or it may be made of flat copper ribbon. Such copper ribbon should usually be at least 0.01-inch thick to give satisfactory loop quality. A fairly typical large console loop constructed of ⅝-inch wide flat copper ribbon 0.01-inch thick showed Q measurements of 100 at 600 kc and 175 at 1,400 kc, before the chassis was mounted in the cabinet.

The choice of conductor for the primary winding of the transformer is more difficult. A tabulation of quality obtained in a nine-turn solenoid such as would be used for the primary winding, wound on a 0.43-inch outside diameter Bakelite form through which was placed a ⅜-inch diameter iron core, is given in Table II.

From this table it would appear that No. 28 F. (single coat of vinylacetal insulation) solid wire is a good conductor to use. However, there are other factors which must be taken into account. The primary winding being closely associated with the secondary, in order to obtain close coupling, causes a pronounced loss in quality due to eddy currents induced in the primary conductor.

Due to the high cost of 20/44 or 30/44 litz wire, a suitable compromise may often be found in some such size as 10/41 litz. It should be noted that conductor cross-sectional area is of importance in determining inductor quality as well as the multistranding. Thus 10/41 litz will give better quality than 10/44, and 7/41 litz is usually preferable to 10/44 litz for the same reason, at least as far as the primary winding is concerned.

We now have sufficient information to compare mathematically the performance of a low-impedance loop

Table I—Symbols Used in Text

- A : Area in square meters of loop antenna (Eq. 2)
- α : Algebraic factor, introduced in Appendix II, $\alpha = (1 + m)/m$, see m
- E : Potential; E_L induced into loop antenna, E_g developed across grid of first tube
- k : Coefficient of coupling between transformer windings, see M
- L : Inductance; L_L of loop antenna, L_P of transformer primary, L_s of transformer secondary, L_{sg} as given in Eq. 5
- λ : Wavelength in meters (Eq. 2)
- M : Mutual inductance between transformer windings: $M = k(L_P L_s)^{1/2}$
- m : Ratio of transformer primary inductance to loop antenna inductance, $m = L_P/L_L$, introduced in Appendix I, value for maximum gain given in Fig. 2
- N : Number of turns in loop antenna (Eq. 2)
- Q : Quality; Q_L of loop antenna, Q_P of transformer primary, Q_s of transformer secondary, Q_{sg} as given in Eq. 4
- R : Resistance; R_L of loop antenna, R_P of transformer primary, R_s of transformer secondary, R_{sg} as given in Eq. 6
- V : Voltage picked up by loop in a field of one volt per meter (Eq. 2)

For quantities not listed here, see Fig. 1, 4, and 5.

with that of a high-impedance loop. In designing a receiver it was decided to change from an average-sized high-impedance loop mounted underneath the shelf of a console to a low-impedance loop mounted on a frame within the console cabinet. The frame was swiveled to allow some adjustment of position, but was only slightly smaller in area than the inside of the console.

Voltage pickup of a high-impedance loop in a field of one volt per meter is given by[1]

$$V = 2\pi NA/\lambda \qquad (2)$$

The figure of merit of the loop is equal to Eq. 2 multiplied by the loop quality Q_L.

The high-impedance loop which had been used had an inductance of 200 μh (as determined by tracking considerations). Dimensions were 10.5 by 8.5 inches, and there were 19 turns. At 1,000 kc, 300 meters, the figure of merit, Eq. 2 times Q_L, equals 2.77.

In the case of the low-impedance loop, the voltage pickup is obtained by Eq. 2 as before, but the figure of merit is this expression multiplied by the gain of the coupling transformer given by Eq. 1. This gain is derived from known constants of the coupling transformer and the loop inductance. For this case where the equivalent inductance must remain 200 μh because we will use the same tuning gang, and the antenna inductance will equal 8.4 μh (the inductance of a two-turn loop whose dimensions are 21 by 30 inches), the gain is given by $Q_s(L_{sq}/L_L)^{\frac{1}{2}}$ times the gain factor. For a k of 85 percent from curve (B) in Fig. 2 the gain factor is 0.246, and because Q_s of the coil under consideration is 140 at 1,000 kc, the gain is 168. The figure of merit, Eq. 2 times this gain, equals 2.87.

Thus we have improved the figure of merit of the pickup system although we had to increase the area from 0.058 square meters to 0.408 square meters to do so. It is to be noted that a number of refinements such as spacing between turns of the loop and space factor[2] have been neglected, but results check reasonably well with measurement.

Table II—Quality of Coil Obtained With Different Wires

Wire Type	Frequency in kc		
	1,400	1,000	600
7/41 litz	65	45	35
10/41 litz	73	52	40
20/44 litz	80	53	42
30/44 litz	100	73	57
No. 34 F.	45	32	25
No. 28 F.	67	52	45

Appendix I

The equivalent circuit of Fig. 1 is as shown in Fig. 4A.[3] We are to find the ratio of E_o to E_L, the gain of the network. Let us lump R_L plus R_p and R_s into one equivalent resistance R_{sq} which we shall place in the secondary circuit as in Fig. 4B.

By Thévenin's theorem we can write

$$E_{AB} = \frac{\omega M E_L}{\omega(L_L + L_P - M + M)} = \frac{M E_L}{L_L + L_P}$$

At resonance

$$I_C = \frac{ME_L/(L_L + L_P)}{R_{sq}} = \frac{ME_L}{(L_L + L_P)R_{sq}}$$

And

$$E_o = \frac{1}{\omega C} \times \frac{ME_L}{(L_L + L_P)R_{sq}}$$

Because at resonance the total inductive reactance as seen at the grid of the tube is equal to the capacitive reactance, we can replace $1/\omega C$ with ωL_{sq}, which is the combined reactances of L_s, L_P, and L_L when connected as shown. Thus

$$E_o = \omega L_{sq} \times \frac{ME_L}{(L_L + L_P)R_{sq}}$$

But $\omega L_{sq}/R_{sq} = Q_{sq}$, and because $M = k(L_P L_s)^{\frac{1}{2}}$ we can write

$$\frac{E_o}{E_L} = \frac{MQ_{sq}}{L_L + L_P}$$

or

$$Gain = \frac{k(L_P L_s)^{\frac{1}{2}} Q_{sq}}{L_L + L_P}$$

Although this expression gives the gain of the coupling transformer, it does not clearly indicate the manner in which the transformer constants affect its gain. To convert this equation into a more informative form we proceed as follows:

The primary inductance will always be dependent on the inductance of the antenna loop, so let us choose some arbitrary constant which will be the ratio of these inductances. In fact, it is the value of this ratio which gives maximum gain which we wish to find. Therefore, define $L_P = mL_L$, then

$$Gain = kQ_{sq}\sqrt{\frac{L_s}{L_L}} \times \frac{\sqrt{m}}{1+m} \qquad (3)$$

This equation is quite valid, but the equivalent quality is not directly known, although it can be measured by connecting a Q-meter across the secondary winding with the primary winding connected to the antenna loop. Also it will not be the value of the secondary inductance which will be known when a design is calculated, but the value of the equivalent inductance, because that is fixed by the value of the tuning capacitance and the required tuning range. Therefore this equation will be modified to an expression in terms of the equivalent inductance and the quality of the secondary coil alone, for

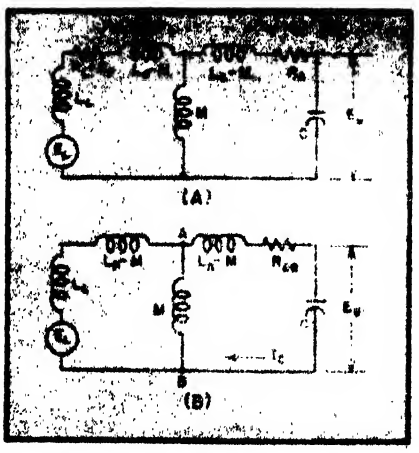

FIG. 4—(A) Equivalent circuit of Fig. 1 can be further simplified to that at (B)

DERIVATION of Eq. 1, upon which the transformer design depends, is based on simple circuit theory. However, because the steps of the derivation indicate the function of the circuit and the limitations of the final design equation, the derivation is given. As will be recognized, the results are applicable to transformer couplings used in other applications than that considered here.

these are the quantities which are usually known.

In Appendix II the equivalent inductance is found to be

$$L_{sq} = L_s \frac{1 + m - mk^2}{1 + m}$$

In Appendix III the equivalent resistance is found to be

$$R_{sq} = R_s \frac{1 + m + 2mk^2}{1 + m}$$

From these results, and because $Q_{sq} = \omega L_{sq}/R_{sq}$ and $Q_s = \omega L_s/R_s$ the equivalent quality is

$$Q_{sq} = Q_s \frac{1 + m - mk^2}{1 + m + 2mk^2} \qquad (4)$$

Substituting into Eq. 3 this expression for the equivalent quality and writing L_s in terms of L_{sq}, we obtain the design equation

$$Gain = kQ_s(L_{sq}/L_L)^{1/2} \times [m(1 + m - mk^2)/(1 + m)]^{1/2} \times (1 + m + 2mk^2)^{-1}$$

Appendix II

To determine the equivalent inductance of the coupling transformer and loop antenna we write from Fig. 4B the inductance to the left of points A-B as

$$\frac{(L_L + L_P - M)M}{L_L + L_P - M + M}$$

This quantity can be simplified using the previously defined relation that $L_P = mL_L$, and by defining $(1 + m)/m = \alpha$, and using the relation $M = k(L_PL_s)^{\frac{1}{2}}$ to the expression

$$\frac{\alpha k(L_PL_s)^{1/2} - k^2L_s}{\alpha}$$

The inductance to the right of points A-B in Fig. 4B is likewise simplified to the expression

$$L_s - k(L_PL_s)^{\frac{1}{2}}$$

Note that the mutual inductance between points A and B has been considered as a parallel branch of the inductance to the left of A-B. The total equivalent inductance across the tuning capacitance is the sum of these two inductances, thus

$$L_{sq} = \frac{\alpha k(L_PL_s)^{1/2} - k^2L_s}{\alpha} + L_s - k(L_PL_s)^{1/2} = \frac{L_s(\alpha - k^2)}{\alpha}$$

Substituting the expression in m for which α stands gives

$$L_{sq} = L_s \frac{1 + m - mk^2}{1 + m} \qquad (5)$$

Appendix III

Likewise, to determine the equivalent resistance of the coupling transformer and loop antenna we simplify the circuit of Fig. 4A to that of Fig. 5A. This simplification is done by considering such a circuit as that at Fig. 5B which we wish to replace with an equivalent series circuit. The impedance seen to the left of terminals C-D is

$$\frac{j\omega L_D(R_C + j\omega L_C)}{R_C + j\omega L_C + j\omega L_D}$$

The real terms are the only ones of interest at present because we wish to find an equivalent resistance for R_L. Call this equivalent resistance R_C', then

$$R_C' = (R_C\omega^2L_D^2)/(R_C^2 + \omega^2L_C^2 + 2\omega^2L_CL_D + \omega^2L_D^2)$$

In the denominator, the R_C^2 term is small compared with the other terms, therefore the expression can be simplified to

$$R_C' = R_C\left(\frac{L_D}{L_C + L_D}\right)^2$$

Because the circuits under discussion have reasonably high quality ($Q > 40$), the inductances can be combined without regard to their resistances. Therefore we can replace the circuit shown in Fig. 5B with the equivalent series circuit shown in Fig. 5C. In this manner we obtain the circuit of Fig. 5A.

Assume that Q_L equals Q_P, then $R_L = R_P/m$ and total primary resistance is $R_P + R_P/m$ or $R_P(1 + m)/m$, which is the primary resistance of the circuit shown in Fig. 4A. The equivalent primary resistance for the circuit of Fig. 5A is

$$R_P \frac{1 + m}{m}\left(\frac{M}{L_L + L_P}\right)^2$$

Let us call this expression R_P', and use the previously given relations $(1 + m)m = \alpha$, $mL_L = L_P$, and $M = k(L_PL_s)^{\frac{1}{2}}$ to simplify it to

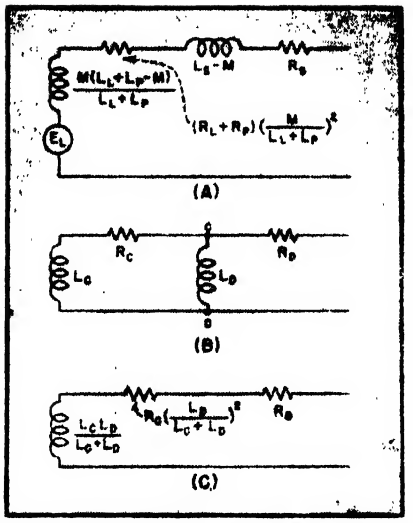

FIG. 5—Equivalent resistance is found from circuit at (A), which is derived from that at Fig. 4A by steps shown here at (B) and (C)

$$R_P' = R_P(k^2L_s/\alpha L_P)$$

Let us also assume that the combined quality of the loop and primary inductances is one half the quality of the secondary inductance. On the average this condition usually exists. The combined quality of loop and primary inductance will be designated by Q_P'; then $2Q_P' = Q_s$, or $2\omega L_P/R_P = \omega L_s/R_s$, so that we have $R_P = 2L_PR_s/L_s$, which when substituted into the foregoing gives

$$R_P' = \frac{2L_PR_s}{L_s} \times \frac{k^2L_s}{\alpha L_P}$$

If we add R_s to this value we obtain the total equivalent resistance which we were seeking, thus

$$R_{sq} = R_P' + R_s = \frac{R_s(2k^2 + \alpha)}{\alpha}$$

Substituting the expression in m for which α stands gives

$$R_{sq} = R_s \frac{1 + m + 2mk^2}{1 + m} \qquad (6)$$

References

(1) Terman, F. E., "Radio Engineers' Handbook", McGraw-Hill Book Co., Inc., New York 1943, p 813, Eq. 40.

(2) Taylor, P. B., Theory of Loop Antenna with Leakage between Turns, *Proc. I. R. E.*, Dec. 1937, p 1574.

(3) Everitt, W. L., "Communication Engineering", McGraw-Hill Book Co., Inc., Chapter VII.

(4) Bachman, W. S., Loop-Antenna Coupling-Transformer Design *Proc. I. R. E.*, Dec. 1945.

F-M and Television Receiving Antennas

By GEORGE P. KEARSE

Type of Antenna; Length in Feet $A = \frac{468}{f_{mc}}$ $B = \frac{492}{f_{mc}}$ $C = \frac{246}{f_{mc}}$	Approximate Terminal Impedance in Ohms	Radiation Pattern: Electric, in Line with Radiator	Radiation Pattern: Magnetic, Right Angles to Radiator	Gain over Dipole: Power	Gain over Dipole: Decibels	Recommended Feed Line, Application and Remarks
DIPOLE PLAIN FOLDED 	72 — — 390	Figure of eight, bidirectional broadside to elements	Circular	Unity	Zero	PLAIN—75-ohm coaxial. FOLDED—300-ohm twin-lead. Use of twin-lead to feed plain dipole gives broadband operation but extreme loss in gain; not recommended General two-direction coverage for receiving in areas of moderate signal strength. Folded dipole slightly more broadbanded than plain. If 300-ohm twin-lead is used as radiator, do not shorten length A for propagation factor
DIPOLE AND REFLECTOR PLAIN FOLDED 	60 — — 250	Uni-directional broadside to radiator	Half of figure of eight	2 to 2½ times	3 to 4 db	PLAIN—50-ohm or 75-ohm coaxial; 75-ohm cable is more broadbanded. FOLDED—300-ohm twin-lead Single-direction coverage, high front-to-back ratio and high gain. Recommended for use in areas of low signal strength and where single-direction radiation pattern is desired. Folded radiator slightly increases bandwidth. If array is to be used over narrow band, calculate length B at lowest frequency desired. Reducing C to 0.15 λ (in air) gives higher gain but lowers impedance and reduces bandwidth
DIPOLE, REFLECTOR, AND DIRECTOR PLAIN FOLDED 	20 to 30 80 to 120	Uni-directional broadside to radiator	Half of figure of eight	2½ to 4 times	4 to 6 db	PLAIN—50-ohm coaxial. If better impedance match is desired, use quarter-wave matching transformer; impedance of transformer should be square root of product of line and antenna impedances. FOLDED—75-ohm coaxial or 95-ohm twin coaxial Single-direction coverage, high front-to-back ratio and high gain. Very frequency-sensitive. Narrow bandwidth. Recommended for use in areas of very low signal strength and for one frequency only. Spacing is λ/4; reducing C to 0.15λ for reflector and 0.1λ for director (in air) increases gain but reduces impedance to 8 to 10 ohms for plain and 30 to 40 ohms for folded dipole
STACKED DIPOLES PLAIN FOLDED 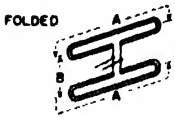	35 to 40 150	Figure of eight, bidirectional broadside to elements	Figure of eight, bidirectional broadside to elements	2 to 2½ times	3 to 4 db	PLAIN—50-ohm coaxial. FOLDED—150-ohm twin-lead. Quarter-wave matching transformer may be used for 300-ohm twin-lead if desired, but will be frequency-sensitive High-gain array for use in areas of low signal strength and where two-direction coverage is needed. Useful over moderate frequency band. Value of B may be reduced to λ/8 (in air) if desired, with a reduction in gain
STACKED DIPOLES AND REFLECTORS PLAIN FOLDED 	25 to 30 100 to 120	Uni-directional broadside to elements	Uni-directional broadside to elements	4 to 5 times	6 to 7 db	PLAIN—50-ohm coaxial cable. Quarter-wave matching transformer may be used for better impedance match but will be frequency-sensitive. FOLDED—95-ohm twin coaxial cable or 150-ohm twin-lead High-gain array for use in areas of low signal strength and where single-direction coverage is desired. Useful over relatively narrow band. Value of C may be reduced to 0.15λ (in air) with an increase in gain. Value of impedance will be lower and array will be more frequency-sensitive. Value of D may be reduced to λ/8 (in air) if desired, with a reduction in gain
TURNSTILE PLAIN 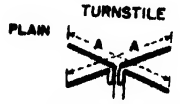 FOLDED 	35 to 40 150	Circular. Radiation pattern changes with frequency	Figure of eight	0.7 of a dipole	−1½ db	PLAIN—50-ohm coaxial cable FOLDED—150-ohm twin-lead Omnidirectional coverage for use in areas of high signal strength. Low gain. Very frequency-sensitive; radiation pattern approximates dipole pattern rotated 45° from axis of either dipole when operated off frequency. With this array, two dipoles are connected together with a quarter-wave phasing section of 75-ohm coaxial cable for plain dipoles and 300-ohm twin-lead for folded dipoles. Length of phasing section must be corrected for propagation constant of line used

F-M Antenna Coupler

An f-m antenna at the top of a base-insulated tower used as an a-m radiator is fed through a concentric line without short-circuiting the tower. The coupling unit which accomplishes this is described in detail

By JOHN P. TAYLOR

WHEN an f-m antenna is mounted on a tower which is used as an a-m antenna it is necessary to provide an f-m coupling unit at the base of the tower. If the tower is of the insulated type, this coupling unit has two functions. The first of these functions is to pass the f-m feed line around the tower insulator without short-circuiting the latter at the a-m frequency. The second function of the coupling unit is to prevent r-f energy at the a-m frequency from passing back down the f-m feed line into the f-m transmitter and causing crosstalk at the f-m frequency. If the a-m tower is of the grounded type only the latter function is involved.

Various circuits suitable for use in f-m coupling units have been proposed. In a particular case, the circuit used depends largely upon the size and availability of the required components. This, in turn, depends chiefly upon the voltage across the tower insulator at the a-m frequency. Thus it is not possible to design an f-m coupling unit which will satisfactorily meet the requirements of all installations, any more than it would be possible to develop a universal a-m coupling unit. However, the fundamental problem is the same in all cases, and some useful ideas on the best method of solving it can be obtained by studying typical installations. One of these, the f-m coupling unit at WBRL, Baton Rouge, will be described here.

The f-m antenna of WBRL[1] is mounted on the top of a 500-ft insulated, self-supporting tower which is the central tower of the three-tower directive antenna array

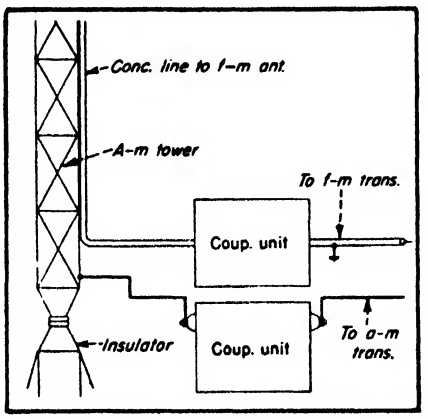

FIG. 1—To avoid short-circuiting the base-insulated a-m tower and to prevent a-m power from feeding back into the f-m transmitter an f-m coupling unit is used. In this instance it is mounted adjacent to an a-m coupling unit at the base of the tower

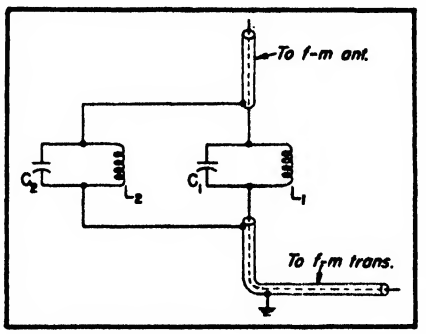

FIG. 2—Breaking the concentric f-m antenna feeder and inserting circuits resonant at the a-m frequency provides isolation at the a-m frequency

of a-m station WJBO. The latter operates at 5 kw on a frequency of 1180 kc. At this frequency the tower is approximately a half wavelength high. Thus for daytime operation (non-directive) when power is fed to this one tower only, the base impedance is quite high. The f-m coupling unit must operate satisfactorily for this condition, as well as for the condition of nighttime operation (directional) when all three towers are used.

The Coupling Problem

The f-m coupling unit is located adjacent to the a-m coupling unit at the base of the tower, as shown in Fig. 1. The line from the f-m coupling unit back to the f-m transmitter in the station building is a concentric line with its outer conductor grounded. If the outer conductor of the part of the f-m line running from the f-m coupling unit to the tower were also grounded, the tower insulator would be short-circuited. The first step, therefore, is to break both the outer and inner conductors of the concentric line and insert blocking circuits as shown in Fig. 2. Here, L_1 and C_1 form a parallel-resonant circuit tuned to present a very high impedance at the a-m frequency. Components L_2 and C_2 perform a similar function.

At the f-m frequency, the blocking circuits have a lower but not entirely negligible value of impedance which it is desirable to bypass. To do this, concentric lines S_1 and S_2 are connected across these circuits as shown in Fig. 3. These open-ended lines present extremely low-impedances at their near ends when tuned to ¼-wavelength at the f-m frequency and therefore, provide the required bypassing. Insofar as the a-m frequency is concerned, lines S_1 and S_2 simply represent small capacitances in parallel with C_1 and C_2 and can be lumped in with these in the tuning operation.

Only one more element is needed

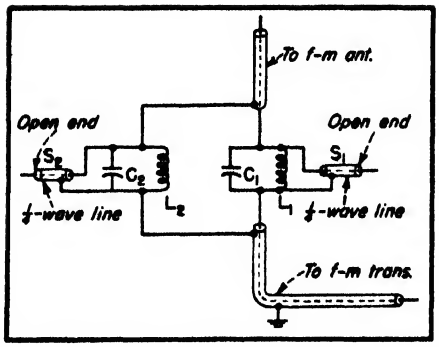

FIG. 3—Open-ended concentric lines S_1 and S_2 provide a low-impedance path for the f-m power

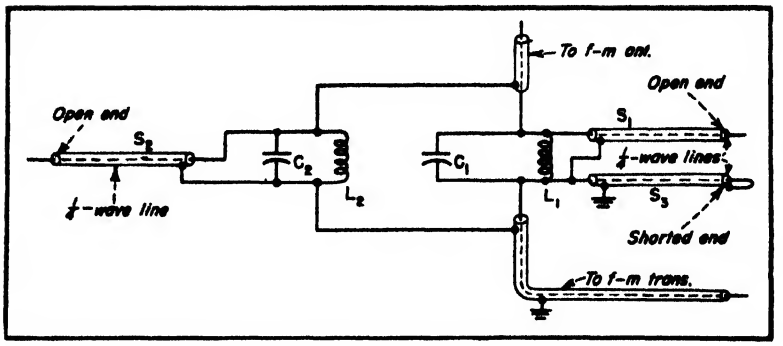

FIG. 4—In the final f-m coupler circuit quarter wave length line S_3 is added in order to effectively ground the lower end of circuit C_1L_1 with respect to a-m power. This line is shorted at its far end

to complete the f-m coupling arrangement, namely, the addition of a grounding line S_3, as shown in Fig. 4. This is a quarter-wavelength of concentric line shorted at the far end. Such a line presents an infinite impedance at the near end. Thus, when the outer conductor of line S_3 is grounded and the inner conductor connected to the bottom of L_1C_1 there is no short-circuit with respect to f-m transmission. At the a-m frequency, however, this length of concentric line is relatively very short and, therefore, the bottom of L_1C_1 is effectively grounded at a-m frequency. This makes the blocking action of the circuit L_1C_1 much more effective.

Construction of the Coupling Unit

The components of the f-m coupling circuit are grouped on a baseboard which is approximately 1½-ft wide and 6-ft long. This assembly is mounted on the wall inside a doghouse adjacent to the a-m coupling unit.

The ⅛-inch concentric line from the f-m transmitter, which is located in the transmitter house some 300 ft away crosses the ceiling of the doghouse at an angle and enters the f-m coupling unit at the top. The ⅛-inch concentric line to the f-m antenna leaves the unit on the right side near the top and passes out of the doghouse through a glass bowl insulator. This insulator is the same type as that through which passes the ⅛-inch copper pipe that forms the a-m antenna feed line.

Outside, f-m and a-m lines run side by side to the lowest brace of the tower. At tower, the pipe which forms the a-m line is solidly attached, while the f-m line continues on up the side of the tower.

Capacitors C_1 and C_2 are Type 77 Faradons. Inductances L_1 and L_2 consist of 53 turns of No. 12 solid wire, tapped every second turn. The three quarter-wave lines extend down along the baseboard. Since the outer conductors of two of these (S_2 and S_3) are grounded anyway, these two are mounted directly on the board. The third (S_1) is above ground, hence is mounted on insulators.

Tuning of the coupling circuits is a two-step process, since adjustments must be found that permit the network to operate as required at both the a-m and f-m frequencies. Since the length of the lines S_1 and S_2 affects the a-m tuning as well as the f-m tuning, whereas the settings of L_1C_1 and L_2C_2 affect the a-m tuning only, it is necessary to make the f-m adjustment first.

The procedure in tuning for the f-m frequency is as follows: A 10-watt crystal-controlled r-f generator operating at the f-m frequency is connected to the input of the network where the line from the f-m transmitter normally connects. A 70-ohm load in series with an r-f milliameter is connected to the output of the network, where the line to the antenna is normally connected. The lengths of the lines S_1 and S_2 are then varied until placing a direct short across the near end of either of these lines produces no change in the output-meter reading. The length of line S_2 is next varied until connecting or disconnecting this line from the network has no effect on the meter reading. In other words, all three lines are adjusted so that they act like quarter-wave lines electrically even though they are physically somewhat shorter than a quarter-wave due to end effects and the lumped capacitance of the end seals. With the adjustments thus made, the f-m energy passes through the coupling network without power loss and without causing reflections on the line.

The procedure in tuning for the a-m frequency is as follows: First, the two parallel circuits L_1C_1 and L_2C_2 are adjusted approximately to resonance at the a-m frequency, using a low power oscillator as a driving source. Second, the network is disconnected from the concentric-line section feeding the antenna. The a-m transmitter is turned on, the a-m coupling circuit tuned and the a-m antenna current noted. Third, the outer conductor of the concentric line section running up the tower is reconnected and the change in the a-m antenna-meter reading noted. By slight readjustment of the tap on L_2, a point is found at which making and breaking the connection to the outer conductor of the line has no effect on the reading of the a-m antenna meter. Fourth, the inner conductor of the concentric line running

up the tower is reconnected to the network and L_1 is adjusted until connecting and reconnecting has no effect on the a-m meter reading. When this is achieved the f-m line has no effect on a-m operations.

As a final check on the operation of the WBRL coupling unit, two types of field tests were made. The field intensity of the a-m station, WJBO, was carefully measured, using an RCA 308-A Field Intensity Meter, at several points—both with and without the f-m network connected to the tower. No difference could be noted. Also, extended observations of both the a-m and f-m signals were made, with high modulation and low modulation levels, using a high-quality receiver. No trace of cross-talk or cross-modulation was noted.

REFERENCES

(1) Taylor, John P., A Square-Loop F-M Antenna. ELECTRONICS, 18, p. 96–100, March, 1945.

Triplex Antenna for Television and F-M

Method of using a single four-bay Superturnstile antenna for simultaneous operation of an f-m transmitter and visual and aural transmitters of a television station, with power gain of 6.4 for f-m and 5 for television. Coupling between transmitters is negligible

By L. J. WOLF

THE TELEVISION and f-m transmitters of the National Broadcasting Company radio stations WNBW and WRC-FM at Washington operate simultaneously into the same Superturnstile antenna system. This results in a considerable saving in the size of the antenna and in the cost of the supporting tower. The full power gain of the antenna is realized for each service, hence no increase in transmitter power is required for this kind of antenna operation.

The quadrature feed to the Superturnstile antenna makes possible the simultaneous or diplex operation of the visual and aural signals from the television transmitter into the antenna. The Superturnstile antenna has an input impedance characteristic which is sufficiently broad for the f-m transmitter to be readily coupled in through a triplexing arrangement.

Superturnstile Radiator Theory

The turnstile type of antenna consists of crossed pairs of radiators, each being approximately a half-wave in length. The pairs are mounted at 90 degrees as in Fig. 1 and fed in quadrature with currents that are equal in magnitude but 90 degrees apart in phase.

The field in any direction from either of the radiators is approximately proportional to sin A, where A is the angle from the radiator. Thus, the maximum radiation from radiator E-W is transmitted in the north and south directions (where sin A is unity), while no field is transmitted from radiator N-S. Similarly, maximum radiation from radiator N-S is transmitted in the east and west directions, while none is transmitted east or west from radiator E-W.

In the northeast direction, the transmitted field is the resultant of radiation from both sets of radiators. Here sin A is 0.707 for each; these are added in 90 degrees quadrature since the currents are in quadrature, so the resultant is unity. For 30 degrees and 60 degrees the values added in quadrature are 0.5 and 0.866, again giving unity. Similarly, for other angles and other quadrants the radiated field is also close to unity.

The basic Superturnstile radiator consists of an open framework of steel rods and tubes, with dimensions as shown in Fig. 2. Two of these radiators mounted at right angles on a tubular supporting steel pole form a radiating system that has a pattern and gain equivalent to two parallel dipoles spaced a half wavelength apart.

A pair of Superturnstile radiators may be considered as a large plane surface containing a slot. Figure 3 shows a flat conductor of large area, with a rectangular

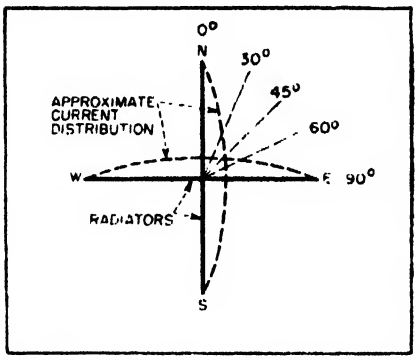

FIG. 1—Horizontal plane through radiators connected in turnstile arrangement

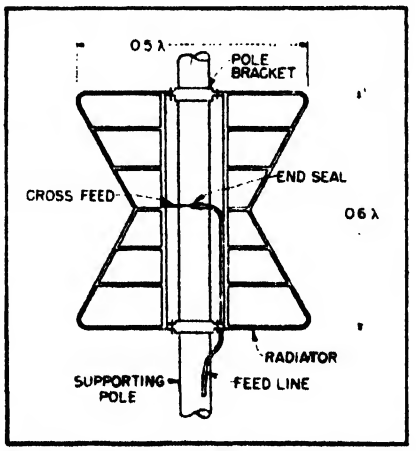

FIG. 2—One pair of Superturnstile radiators mounted on steel pole. Other pair is at right angles to these, using same pole brackets

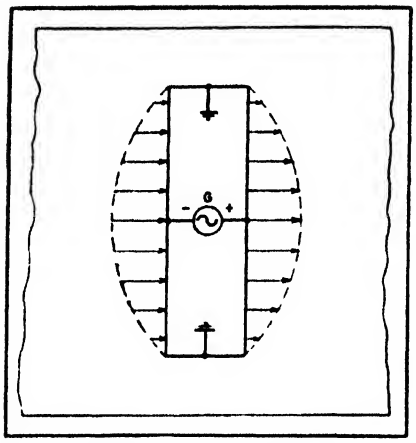

FIG. 3—Currents and voltages in the region of half-wave slot in large conducting plane simulating Superturnstile

slot approximately a half-wave long. A generator *G* applies a-c voltage having an instantaneous polarity (as shown by the plus and minus signs) to the two terminals. Set up along the sides of the slot, a voltage will have a magnitude as represented by the distance of the dotted lines from the sides of the slot. The ends of the slot will be at ground potential. Currents will flow in the plane surface with a magnitude and instantaneous direction at the sides of the slot approximately as shown by the arrows. These currents will flow on both sides of the plane surface and will radiate equally on each side. This condition will be unaffected by openings in the plane surface as long as these openings are small compared with a wavelength.

Radiator Feed

The radiators (Fig. 2) are mounted so that contact to the supporting pole is made at places of zero potential, hence are attached directly without the necessity of any sort of insulator. The feedline for a pair of radiators is brought from the pole onto the radiator over one of the two connecting brackets. At the center of the radiator, the feedline is brought around the pole, half way to the other radiator. The inner conductor connects to the other radiator through a cross-connection strap. Thus, with the outer conductor of the feedline connected to one radiator, and the inner conductor to the other radiator, a balanced feed results. The only insulation needed is that of the end seal on the end of the feedline.

The antenna described has four identical Superturnstile radiator sections. With these, the television power gain is approximately 5, and the f-m power gain is approximately 6.4 as compared to that of a half-wave dipole (without allowance for transmission line loss). The f-m gain is higher because the height in wavelengths is greater for frequency modulation than it is at the television frequency.

Transmission Line

The transmission line between transmitter room and antenna consists of a pair of 3⅛-inch, 51½-ohm coaxial lines designed with conductors and insulators in accordance with RMA recommendations. Special design precautions have been taken to make certain that the lengths of line can be coupled in a satisfactory manner, and to eliminate electrical discontinuities at elbows and connections.

The 20-foot lengths of line are supplied with flanges brazed in place. These flanges are bolted together to join sections of line at installation, using O ring gaskets to keep the line pressure-tight. Differential expansion between the steel tower and the copper outer conductor of the transmission line is provided for by means of spring-hung tower brackets, which permit the line to expand and contract vertically. The line is secured at the top of the tower so that the expansion occurs entirely at the bottom of the tower. Differential expansion of the inner conductor with respect to the outer conductor is allowed for at each flanged connection; the inner conductor connector is of the push-type which allows the inner conductors to slide a slight amount as required.

Electrical discontinuities are minimized as far as possible at bends by providing elbows with a radius which is large compared to the line diameter.

Inasmuch as the E-W and N-S radiators of the antenna are fed in quadrature, the two transmission lines must be kept alike, so that the two lines will maintain at the antenna the correct phase relationship set up at the transmitter. This is accomplished by making the two lines identical as regards lengths of line sections and placement of elbows. The quadrature phase relationship is introduced at the diplexer by making one line 90 degrees longer than the other.

Pressurization of the transmission lines is maintained by an automatic dehydrator which keeps a small positive pressure of dry air on the line at all times.

The diplexing unit consists of a Wheatstone bridge type of network which provides a means of feeding the visual and aural energy of the television transmitter into the antenna without detrimental cross-coupling effects.

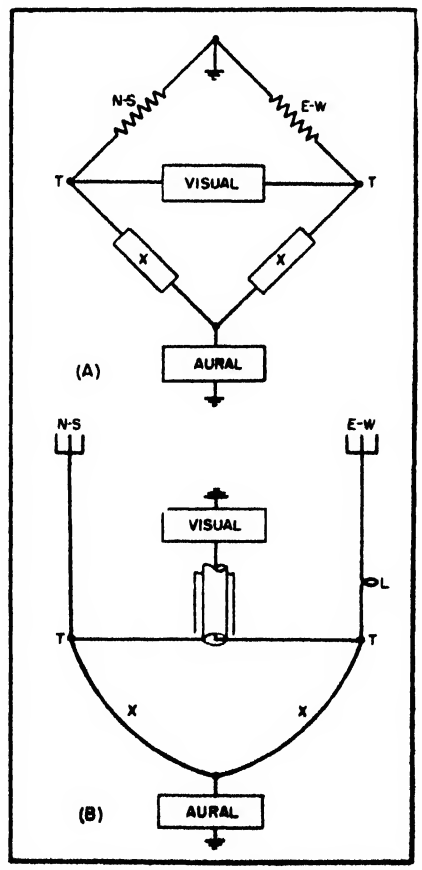

FIG. 4—Fundamental bridge-type diplexing circuit, (A) and practical application (B) to visual-aural diplexing system of television transmitter. Circuit lines represent inner conductors of coaxial lines

Diplexer

In the fundamental diplexing circuit of Fig. 4A, the resistors represent the loads due to the radiators N-S and E-W respectively. The visual power amplifier feeds push-pull to terminals *T*. The aural power amplifiers feeds via a single-ended line through reactances *X* to terminals *T*. The two transmitter sources are uncoupled from each other as long as the two loads and the two reactances are equal respectively. Thus, no cross-feed between transmitter sources will exist, even for modulation sideband components which are nearly identical in frequency.

The physical realization of the bridge circuit is indicated in Fig. 4B. Each connection line represents the inner conductor of a coaxial transmission line. The outer conductors are not shown except for the cylindrical balun sleeve on the connection to the visual transmitter. The visual transmitter feed is single-ended, hence is changed to a double-ended feed by means of this balun. The visual feed is push-pull at terminals *T*, whereas the aural feed is push-push at these same terminals. Loop *L* represents the extra quarter-wavelength of line that provides the quadrature feed of the E-W radiators with respect to the N-S radiators.

Elements *X* are transmission lines which are each a quarter-wave long at the midvisual frequency, which totals a half-wave in length. This length of a half-wave on terminals *T* shunts a high impedance across the visual input circuit. Conversely, terminals *T* are at the same potential with reference to each other at the aural frequency, hence no aural power can couple into the visual transmitter input.

This bridge-type circuit is particularly useful for coupling the visual and aural power amplifiers since the transmitter frequencies are quite close together. The reactance of the circuit elements changes very little from one frequency to the other, hence has no serious detuning effect on either power amplifier

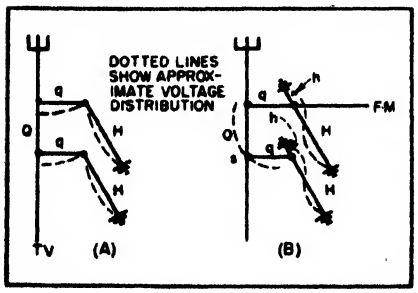

FIG. 5—Fundamental circuit of triplexer (A) showing use of two frequency-selective tuned elements, and method of adding stub elements (B) for coupling an f-m transmitter. Circuit lines represent inner conductors of coaxial lines, and ground symbol indicates shorting plug in line

Triplexing System

The triplexing unit allows the power from the f-m transmitter to be coupled onto the line to the antenna, with the correct phase relationships, without cross-coupling to the television transmitter. Since the television and f-m frequencies are separated by a greater percentage than are television visual and aural frequencies, frequency-selective circuits are used in the triplexer.

Figure 5 illustrates the fundamental triplexing circuits used. The television transmitter *TV* feeds the antenna load directly as in Fig. 5A, with two half-wave circuits *H*, connected to the main line through two quarter-wave circuits *q* which are separated a quarter-wave apart along the main line. Each branch (consisting of an *H* and a *q* in series) is three-quarter-wave long, hence presents a high impedance to the main line. The characteristic impedance of these branch line elements is chosen so that this high impedance is presented to the main line over a band which is at least six megacycles wide.

The circuits associated with the f-m transmitter are added as in Fig. 5B. Circuits *H* are extended by stub sections *h*. The lower *h* stub is adjusted so that the combination of reactances presents a low impedance, or short-circuit at terminal *S* at the frequency of transmitter *F-M*. The upper *h* stub is adjusted so that the input impedance, looking to the antenna from *F-M*, is also matched at the f-m frequency. The voltage magnitudes under this condition are represented by the dotted lines.

Combined Diplex and Triplex System

In the complete system as used at stations WNBW and WRC-FM, a four-section Superturnstile antenna is used as shown diagrammatically in Fig. 6. The E-W and N-S radiators are fed from junction boxes *JB*. The feedlines from the junction boxes are all the same length, so the radiators will all be fed in phase. Each junction box assembly contains a series line transformer, to match the 51½-ohm transmission line to the impedance of the four feedlines in parallel.

The twin transmission lines going down the tower are equal in length between the junction boxes and the triplexer so the phase relationship between lines, as established at the transmitter, will be maintained at the antenna. The lines are carefully installed so that the elbows in the two lines are equally spaced from the triplexer.

The triplexer is located in the transmitter room, with the two transmission lines passing through it to the diplexer. The internal cir-

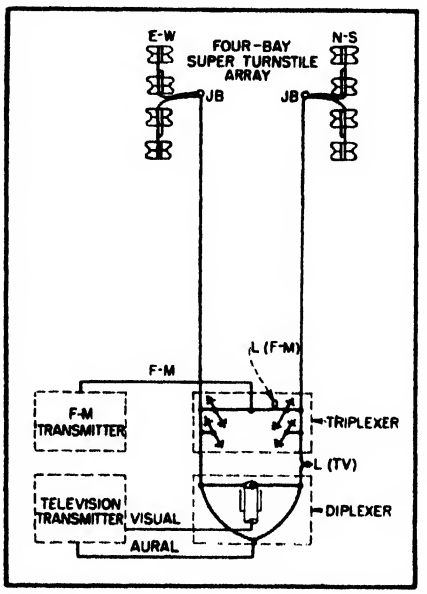

FIG. 6—Complete triplexing system, with N-S and E-W radiators shown separately to clarify connections. Circuit lines are inner conductors of coaxial lines

cuit of the triplexer consists of matched pairs of transmission line elements.

The f-m feed into the triplexer divides as shown, with one side going through a phasing loop. This loop is a quarter-wavelength at the f-m frequency and provides the correct quadrature phase required to give a circular pattern from the turnstile antenna. Only the f-m feed is through this loop; the quadrature loop for television is separate. This arrangement provides a convenient method of maintaining the correct quadrature feeds for the two systems, even though the frequencies are different.

The diplexer terminates the two separate antenna transmission lines. One line between triplexer and diplexer is made a quarter-wave longer than the other at the television frequency. This quadrature length is separate from the f-m loop, hence sets the correct phase relationship for television independently of the f-m requirement.

The diplexer contains the visual input circuit, consisting of a single-ended circuit with a balun to convert to double-ended feed. The balun is suitably compensated to be broad-band so that it does not introduce any appreciable discontinuity over the television channel. The aural input circuit is single-ended and connects to a point where no visual voltage exists, so there is negligible coupling between visual and aural power amplifiers.

Acknowledgement is made to the members of the Television Broadcast Antenna Group of RCA Victor Division, who not only designed this equipment but also made it work, and to the engineers of the Radio Facilities Group of the National Broadcasting Company, who bore the brunt of getting the first equipment installed.

Cooperative Two-Station Antenna System

By LINDSAY McMANUS

A BROADCAST STATION that is probably unique has just been completed by Canadian Marconi Company at Sherbrooke, Quebec. It is, in fact, a combination of two stations—CHLT and CKTS.

CHLT has been operated by the French-language daily newspaper, *La Tribune*, on 1,240 kc. An associated English-language weekly paper, the *Sherbrooke Telegraph* has now taken over this station and the call letters have been changed to CKTS. The *La Tribune*, still retaining its call letters—CHLT—has expanded to 1,000 watts and moved along the dial to 900 kc.

The original CHLT studio has been dispensed with and modern combined studios have been constructed for the two stations. Each station has its own control room facing the main studio with a master control room in between. Local programs and remote pickups are fed through the master control room and thence to either or both transmitters via the separate control rooms.

When CHLT was assigned its new frequency, it was with the provision that two other stations on the same frequency be protected at night. Daytime operation could be at 1,000 watts, omnidirectional, but it was necessary to change to directional operation at sunset.

Common Antenna System

It was desirable to use the existing transmitter building for the two transmitters, having them and their associated audio and monitoring equipment in the same room, and to use the same antenna system for both stations. These plans presented problems in meeting all requirements and regulations and particularly to avoid any interaction or cross modulation throughout the entire audio and radio frequency circuits. Adequate shielding of audio components and lines would take care of this section, but r-f interaction between the two transmitters in the same room and using a common antenna could not be so easily avoided.

A new ground system for a two-tower array was put in and a new 196-foot guyed tower was erected. The existing tower of the same height was moved to a new location to form the directional array. The towers were spaced 120 degrees apart at 900 kc, and it was decided that the desired directional pattern could be obtained by a phase difference of plus 141 degrees with a 1.3 to 1 current ratio in the towers. During the entire process of installing the new ground system, new antenna and shifting of the existing antenna, the transmitter on 1,240 kc continued daily operation without interruption.

Precise measurements were made of the self and mutual impedances of the new array and from these measurements the operating impedances were calculated. Impedances of the various units and tower lighting transformers were measured and included in the calculations and the network component

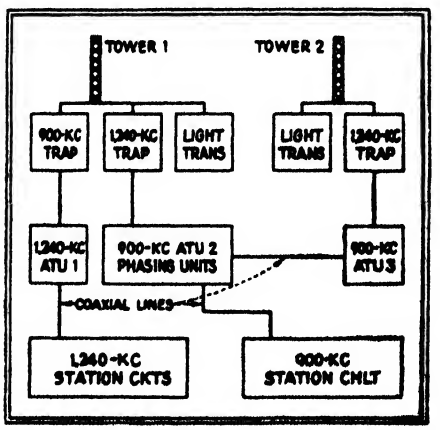

Fig. 1—Two transmitters on different frequencies feed one antenna system

values were set up. Three conditions had to be satisfied simultaneously for the directional pattern; proper matching to coaxial lines, correct current ratio between the towers and the desired electrical separation between the currents. Any one improper condition would throw the others out.

For instance, the self impedance of tower 2 changed radically when the phase difference between towers changed and if the phase difference were not correct the current ratio could not be obtained and the coaxial lines would also be mismatched. Only by precise measurements and careful setting up of the tuning unit components by r-f bridge method could the system be properly adjusted. The final arrangement of the various units is shown in Fig. 1.

Circuit Arrangement

Tower 1 is used during the daytime for both transmitters. CKTS, the 1,240-kc, 250-watt station is fed to this tower through a coaxial gas-filled line, a 1,240-kc antenna tuning unit (ATU1 in diagram) and a rejector unit. The rejector unit is resonated at 900 kc to prevent feedback into the 1,240-kc line from the 900-kc circuit. CHLT, the 900-kc, 1,000-watt station, is fed to the same tower by a coaxial gas-filled line, a 900-kc antenna tuning unit (ATU2), and a rejector unit which is resonated at 1,240 kc to prevent this frequency from feeding back into the 900-kc circuit. Tower 2 also has a 1,240-kc rejector unit and the tower is detuned during the daytime to prevent radiation.

At sunset, a changeover is made at the control unit on the desk at the transmitter building and tower 2 is brought into the 900-kc circuit. This is accomplished by two relays at Tower 1 which change taps on ATU2, disconnect the detuning circuit of tower 2, and also put this tower in the circuit through a phasing unit. The phasing unit matches this junction to the coaxial line running to tower 2, where antenna tuning unit ATU3 matches the line to the tower through the 1,240-kc rejector unit.

Power Division

In the 900-kc circuit at tower 1, phase changes through the antenna tuning and phasing units cancel each other. The 120-degree coaxial line between towers causes a phase shift of −130 degrees and ATU3 is tuned to shift the phase another −89 degrees. This provides the total of −219 or +141 degrees phase difference required.

The setting of the 1.3 to 1 current ratio between the towers is accomplished at the junction of ATU2 and the phasing unit at tower 1. From the calculated directional operating resistances of the towers, the power required in each tower for correct current was found. The necessary power division to produce these currents is made at the junction by matching ATU2 to tower 1 and the phasing unit to the inter-tower coaxial line so that their parallel input impedances correctly divide the power and also match the surge impedance of the coaxial line to the transmitter.

Operation

In changing from one-tower omnidirectional operation to two-tower directional, the shift is made at sunset in approximately one second during a station break for identification. The tuning units at the towers are so adjusted that the coaxial line impedances at the transmitter for the two modes of operation are identical and no transmitter adjustment or retuning is necessary.

As a visual check on the shape of the night pattern, two field indicators have been installed. These consist of small receivers, containing a diode rectifier and d-c amplifier, set up in the field about 400 feet from the towers, one on each side of a low signal zone. The units are mounted on posts and are powered by a 110-volt a-c line. The output of each unit is taken by cable to d-c microammeters in the control unit on the desk at the transmitter building. Changes in the reading of the meters outside of a predetermined operating tolerance indicate to the operator that the pattern shape has altered. Cables also carry the antenna currents to remote meters in the desk control unit and provide a constant check on the currents in the towers for both transmitters.

To uncover any signs of interaction between the two stations, various tests were carried out. It was found that any switching on or off of one transmitter in no way affected the meter readings or field intensity of the other. Either carrier, fully modulated, did not affect the unmodulated carrier of the other transmitter and no signs of cross modulation could be detected with both stations fully modulated with individual or similar programs.

Clip-on Antenna Meter

IN THE LOS ANGELES repair and installation shops of the Highway Patrol, California Department of Motor Vehicles, senior radio technician H. A. Holcomb has put together a useful antenna meter for a quick check on the output of 30-watt Motorola transmitters, of which the patrol uses almost 450.

Illustrated herewith, the unit comprises a small piece of Lucite sheet with a model 507 Weston thermogalvanometer, two large battery clips and a 50 $\mu\mu$f mica capacitor. The current-squared meter has a resistance of 5.2 ohms and its readings are used arbitrarily.

The meter is connected in series with the capacitor, which is placed between the instrument and the upper clip. The unit is simply clipped onto the whip antenna with the lower clip in contact with the compression nut at the bottom of

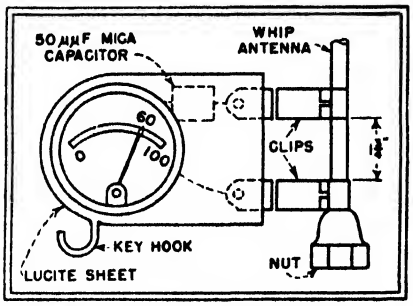

Essential elements of the clip-on antenna meter. The key hook was found to be the most essential item

the whip. A reading of 60 on the scale is taken to indicate a normally operating transmitter. A midscale value was chosen by manipulation of the distance between the two clips. A spacing of 1¾-inch worked out correctly for the particular combination of units.

The same unit is used for determining the output of 6-watt motorcycle transmitters whose power is too low to actuate the meter in its standard form. A special clip lead is attached to the meter side of the capacitor and clipped to the antenna at a point determined by its extreme length to produce a similar reading on the instrument.

The last, and perhaps most important feature of the unit is the small hook at the lower left. On this hook the serviceman places the ignition keys of the radio car to prevent it from being driven away with the tester still attached to the antenna.

Slotted-Cylinder Antenna

Simple mechanical construction, easily obtained vertical directivity, and horizontal polarization make the slotted-cylinder antenna ideal for f-m and television transmission and reception. Directivity and impedance characteristics for designing arrays are presented

By E. G. JORDAN and W. E. MILLER

SLOT ANTENNAS have been successfully used on high speed aircraft to establish electric currents on outside surfaces of the metallic airplane structure and so make the aircraft itself the radiator. Examination of the characteristics of slot radiators shows that they possess properties that make them useful in many other applications as well.

In such applications a particularly useful form of the radiator is a slot cut lengthwise in a long, narrow, hollow cylinder. The first reference in the literature to this form of radiator appeared several years ago[1]. It proposed the use of a slit cylinder to guide or radiate electromagnetic waves. Slot radiators of one form or another have already found commercial application in frequency modulation[2] and television[3].

It is the purpose of this article to discuss some general properties of slot-in-cylinder radiators and to present radiation patterns and impedance curves that should enable engineers to determine the suitability of these antennas for applications in which they may be interested.

Figure 1 shows the vertical and horizontal radiation patterns of a three-quarter wavelength slot cut in a vertical cylinder. For comparison, the vertical pattern of a half-wave dipole is also shown. For equal lengths, the vertical slot and vertical dipole have practically the same vertical radiation patterns. Length of the cylinder itself has no noticeable effect on the pattern. It must be long enough to accommodate the slot, but can be any convenient length longer. The horizontal pattern of the vertical slot-in-cylinder is dependent upon the diameter of the cylinder. In general, radiated field intensity is greater on the side on which the slot is located than it is on the opposite side of the cylinder. However, for cylinder diameters of about one-tenth wavelength or less, radiation in the horizontal plane is essentially uniform.

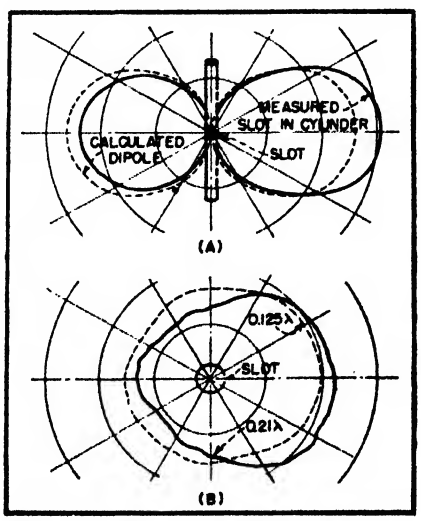

FIG. 1—(A) Vertical radiation pattern of a three-quarter wavelength slot antenna compared to that of a half wavelength dipole, and (B) horizontal radiation pattern of slot antenna in a vertical cylinder of 0.21 wavelength diameter

The radiation pattern of a slot in a narrow cylinder is almost the same as that of the corresponding length dipole, but with one important difference: the electric field produced by a vertical dipole is vertically polarized whereas that produced by a vertical slot is horizontally polarized. Because horizontal polarization is used for both frequency modulation and television, the slot-in-cylinder possesses considerable advantage over

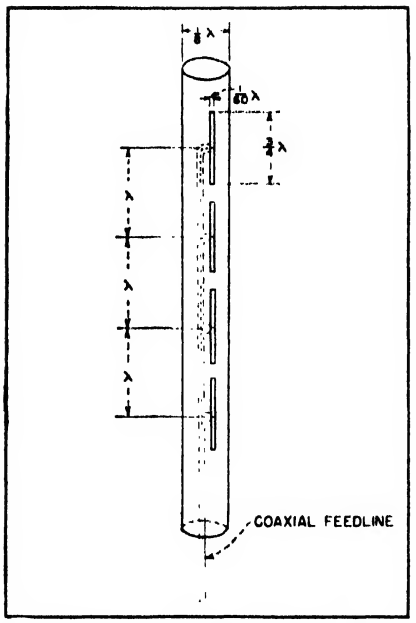

FIG. 2—Vertical directivity can be increased by stacking slots. Mechanical construction is simple. Slots are fed from a transmission line inside the slotted cylinder

the ordinary dipole in these applications. A vertical slot has the desired vertical directivity with nearly uniform radiation in the horizontal plane and, in addition, has the correct polarization for f-m and television broadcasting.

When greater vertical directivity is desired, it can be obtained by stacking slots vertically as illustrated in Fig. 2. Because each unit of the array (that is, each slot) has considerable vertical directivity by itself and therefore radiation from any one element does not interact to a considerable extent with that from other elements, it is possible to space the units a wavelength apart without producing unduly large secondary lobes. Directivity of any array is proportional to its overall length; so when large spacing between units is permissible it is possible to have a long, and hence a highly directive, array without requiring an excessive number of units, simplifying feeding problems. The array of Fig. 2 has four slots, each three-quarters of a wavelength long, and spaced one wavelength center-to-center. When longer slots are used, larger vertical separations are permissible.

In Fig. 3 there are shown the measured vertical and horizontal patterns of the four-element array. Vertical directivity is very sharp and it is seen that most of the power is radiated within a few degrees of the horizontal. The excellent agreement between measured and theoretical patterns indicates that predicted gains can be closely attained in practice. In Fig. 3B there is also shown the relative field intensity in the horizontal direction produced by a pair of horizontal crossed half-wave dipoles fed with the same power as the four-slot array. Figure 4 shows the directed power gain of the slotted-cylinder array as a function of the number of three-quarter wavelength slots, spaced one wavelength apart. The gain shown is referred to that of a single half-wave dipole. The gain over a pair

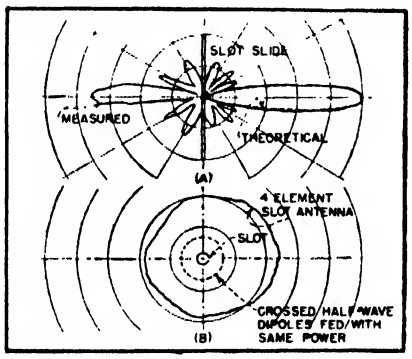

FIG. 3—(A) vertical, and (B) horizontal radiation patterns of slotted-cylinder array shown in Fig. 2

of crossed dipoles (as would be required to produce a uniform horizontal pattern with horizontal polarization) would be double that shown. The values given in Fig. 4 represent the average gain in the horizontal direction. For a one-eighth wavelength diameter cylinder, the horizontal pattern is not uniform and the actual gain is a little greater on the slot side of the cylinder and a little less on the side opposite the slots.

In order to feed the slotted-cylinder antenna properly, it is necessary to know something of its impedance characteristics and how these characteristics vary with slot length and width, and cylinder diameter. Figure 5 shows resistance and reactance of a slotted cylinder as measured at the center of the slot. Impedance is shown as a function of slot length for various ratios of antenna diameter to wavelength. As cylinder diameter in wavelengths is made progressively smaller, the length of the slot required for resonance becomes very large, and there is a certain critical diameter below which resonance cannot be obtained at any slot length. For the particular slot width used in this case, this critical diameter appears to be about 0.11 wavelength. It will be noticed that the resonant length (that is, the length for zero reactance) is very long for narrow diameter cylinders, but becomes smaller as the cylinder diameter increases. For larger diameter cylinders, second resonance points appear at slot lengths roughly double that for the first resonance. Resistance at this second resonant point is comparatively low, being of the order of 40 ohms, while at the first resonant point it ranges between 300 and 1,000 ohms. The effect of greater slot width is to increase the length of slot required for resonance for a given cylinder diameter.

Explanation of Operation

There are two rather simple physical pictures which can be used to explain the operation of the slot-in-cylinder antenna. The first con-

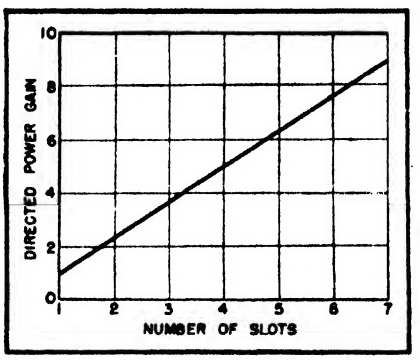

FIG. 4—Concentration of power in the vertical plane, relative to that from a dipole, for an array similar to that of Fig. 2

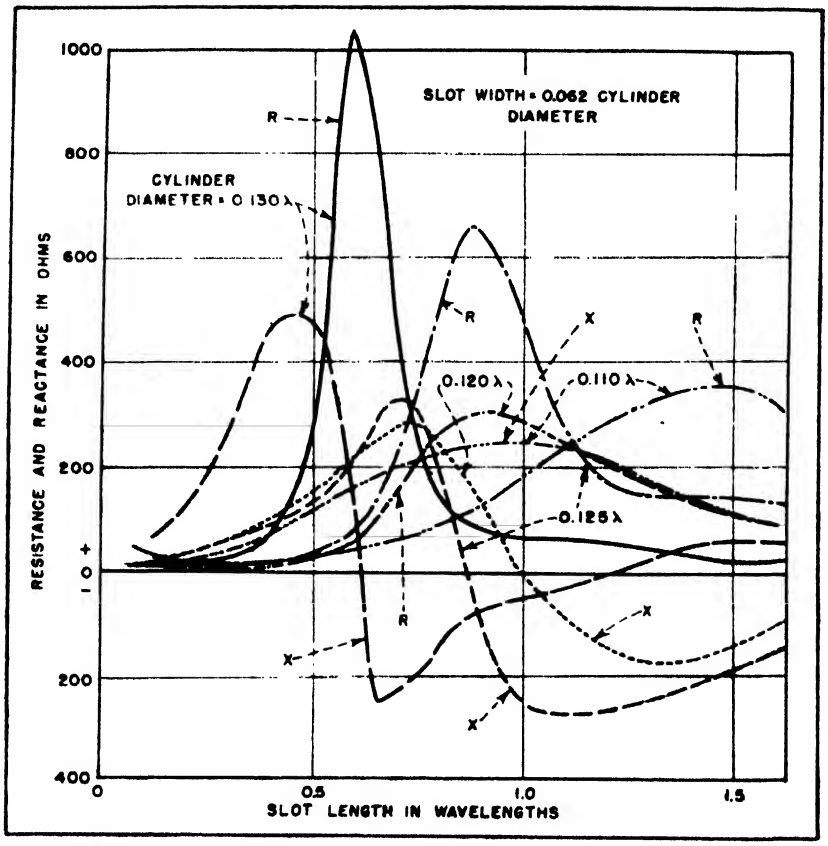

FIG. 5—For a slot representing a fixed fraction of the cylinder diameter, resonant impedance increases and resonant slot length approaches a half wavelength as cylinder diameter is increased

siders the edges of the slot as constituting a parallel-wire transmission line which is shorted at both ends.

A voltage is applied across the transmission line (usually, but not necessarily, at the middle) and standing waves of voltage and current are set up along the line. Because of the close spacing between the edges of the slot, transmission line currents would not be expected to radiate appreciably. However, the slot transmission line has connected to it the remainder of the cylinder which has a twofold effect.

In the first place, the voltage across the slot causes currents to flow around the outside of the cylinder and these currents flowing in the circular path radiate appreciable amounts of power, the diameter of the path being a significant fraction of a wavelength. In addition, the cylinder acts as an inductive reactance shunted across the slot transmission line, and so modifies the phase velocity and hence the wavelength along the line. From transmission line theory it is known that inductive shunt loading will increase both phase velocity and wavelength, and so increase the line length required for resonance. If the loading is too great (that is, if shunt inductive reactance is too low) wave motion along the line ceases and the loaded line acts as an attenuating network.

This simple picture serves to explain most of the characteristics of the impedance curves for narrow cylinders. For larger diameter cylinders it is necessary to resort to waveguide theory for the second physical picture. The inside of the cylinder is a degenerate cylindrical waveguide.

Within a waveguide the phase velocity and wavelength are always greater than the corresponding free-space quantities and the ratio of wavelength in the guide to free-space wavelength becomes very large as the diameter of the cylinder decreases to the cutoff diameter. For completely closed cylindrical waveguides the cutoff diameter for the dominant mode is 0.586 times the wavelength, but when the cylinder has a slot in it, with the excitation applied across the slot, the cutoff diameter is very much less than this value. In this latter case the capacitance of the slot reduces the required diameter of guide in much the same way as the length of a transmission line section required for resonance is reduced by capacitive loading of the load to which it is connected. It is apparent that the greater the capacitive loading (that is, the narrower the slot) the smaller will be the cutoff diameter of the cylinder.

With slot widths used in making the measurements shown, cutoff diameter was of the order of one-tenth wavelength. With narrower slots, or slots the sides of which overlap, cutoff diameter can be reduced to one-thirtieth of a wavelength or less.

Figure 6 shows the electric field intensity across the slot, measured for several cylinder diameters. For large diameters the distribution of electric intensity along the slot is closely sinusoidal with the distance between nodal points only slightly greater than the free-space half wavelength. However, as the cutoff diameter is approached the distance between nodal points becomes relatively larger, attenuation within the guide increases and the distribution changes from sinusoidal to exponential. Figure 7 gives the ratio of wavelength in the guide to wavelength in free space for various cylinder diameters. From the curve or the field distributions on Fig. 6 one can determine the maximum slot length which can be used to give a single lobe in the radiation pattern. Figure 8 shows slot length required for first resonance as a function of cylinder diameter.

Methods of Feed

The slotted-cylinder antenna can be fed by either coaxial or parallel-wire transmission lines running up the inside of the cylinder. Both of these methods were used in obtaining the measurements shown. Choice between a single or double coaxial line or parallel-wire line feed depends upon convenience and impedance-matching possibilities.

The impedance around the second resonant point is low, indicating coaxial-line feed in this region of operation. At the first resonant point the impedance is high and parallel-wire feed inside the cylinder is preferable. However, lower impedances can be obtained by feeding the slot off-center. With an array of slots at one wavelength spacing, slot impedances are effectively in parallel and for a four-slot array operating at the first resonance, the input impedance of the transmission line is of the order of 100 ohms.

It is evident from the discussion on theory of operation that large variations in impedance can be obtained by adjusting the effective capacitance across the slot. The effective slot capacitance will depend primarily on slot width, but will also depend somewhat on the thickness of the cylinder wall. For impedance curves shown, a cylinder wall thickness of approximately 1.5 percent of the cylinder diameter was used.

Bandwidth measurements on the slotted-cylinder antenna indicate bandwidths at the first resonance of between four and eight percent (between frequencies at which the standing-wave ratio on the feed line was two to one). The bandwidths around the second resonance points were not measured, but a study of the impedance curves indicates that they should be considerably wider than at the first resonance points.

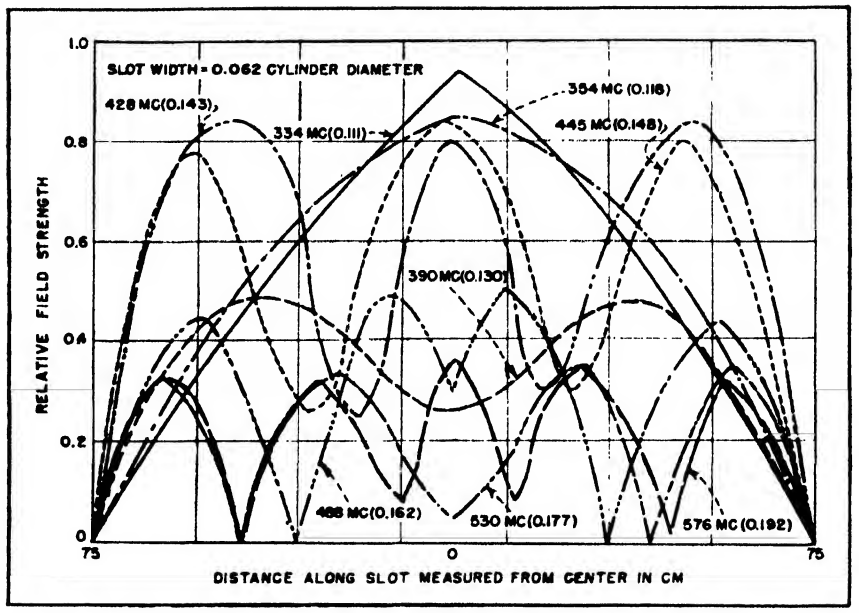

FIG. 6—Field strength distribution along a 150-cm slot varies with frequency because of the change in velocity of propagation along the radiator. Numbers in parentheses indicate cylinder diameter in wavelengths

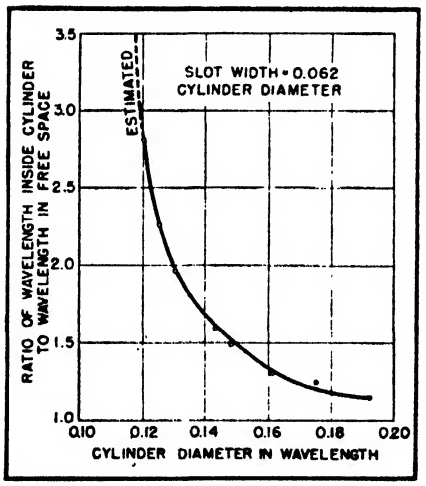

FIG. 7—Resonance phenomena presented in Fig. 5 and 6 can be summarized as a curve of ratio of inside to free-space wavelengths

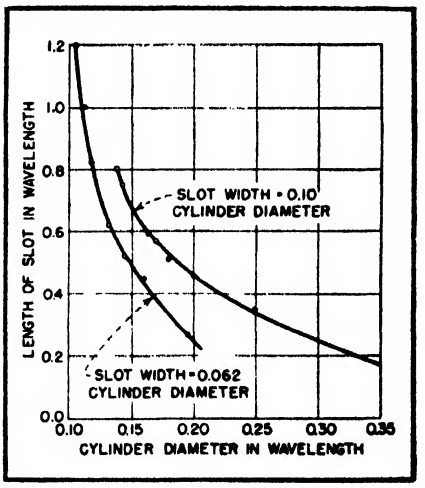

FIG. 8—Design of slotted-cylinder antenna involves choosing cylinder diameter and slot width that give reasonable slot length at the operating frequency

(1) Blumlein, A. D., High Frequency Electrical Conductor or Radiator, U. S. Patent No. 2,236,770, April 15, 1941.
(2) Alford, A., Antenna for F-M Station WGHF, *Communications*, p 22, February 1946.
(3) Color Television on Ultrahigh Frequencies, ELECTRONICS, p 109, April 1946.

Remote Indicating Antenna Ammeter

By C. R. COX

ONE OF THE FCC REQUIREMENTS relating to broadcast station operation is that the magnitude of the antenna current be recorded in a log book at intervals of one-half hour. Since in the majority of standard broadcast installations the antenna is located at a distance of several hundred feet or more

from the transmitter, some means of indicating the antenna current at the transmitter is highly desirable. To fill this purpose, the type 708 remote indicating antenna ammeter was developed by Andrew Company engineers.

In designing the instrument, it was thought desirable to avoid the use of thermocouples, because of their susceptibility to lightning damage. While the occasional loss of a thermocouple due to lightning presents no problem to the owner of a broadcast station, the time spent in shutdown, while thermocouples are being replaced, is very serious and expensive because it means loss of revenue to the station. Accordingly, the ammeter was designed on entirely electronic principles, and contains no thermocouples. In several instances, remote ammeters of this type have withstood without damage a direct stroke on the tower, while in other instances the remote ammeter has been burned to a crisp by lightning, but no loss of broadcasting time resulted.

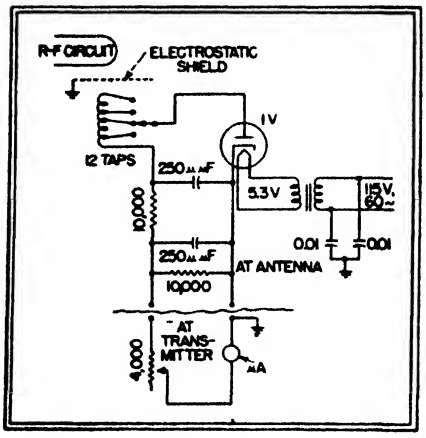

Circuit of electronic antenna ammeter for reading antenna current at the transmitter

In the circuit shown, a current transformer with a primary consisting of a heavy copper rod and an electrostatically shielded secondary feeds a 1-V diode rectifier tube which actuates a d-c microammeter. The microammeter is calibrated in r-f amperes and provides an approximately linear calibration because the diode load resistance is made large in comparison to the tube impedance. An instrument of this type is not absolute and must be adjusted to agree with the regular thermocouple ammeter. FCC regulations provide that this adjustment must be made once a week. When not in use for calibrating purposes, the thermocouple may be switched out of the circuit.

The time constant in the rectifier circuit is such that the instrument is essentially peak reading but this is much smaller than the period corresponding to the highest modulation frequency. Thus, the indication of the meter remains constant with amplitude modulation, provided there is no carrier shift. In contrast, the reading of a thermocouple ammeter increases with modulation.

Transport Aircraft Antenna Characteristics

Method of measuring the characteristics of aircraft antennas with a *Q* meter. Results of measurements on several types of aircraft transmitting antennas are presented

By E. F. KIERNAN

THIS discussion will be confined to methods and data taken from representative domestic transport aircraft equipped with antennas permanently attached above the fuselage.

Two methods may be used for obtaining antenna data. One involves an r-f bridge upon which values of resistance and reactance can be read directly. The bridges available at present are not particularly adapted to aircraft antenna measurements.

Q Meter Measurements

The other measuring method utilizes the *Q* meter, the data from which requires considerable computation to yield the desired constants. The data presented herein

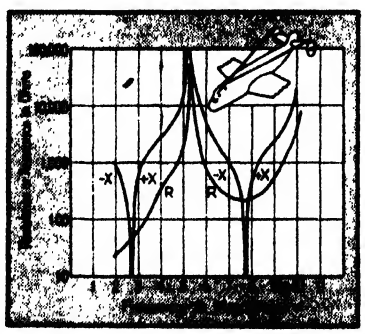

Impedance characteristic of the Douglas DC-4 V antenna

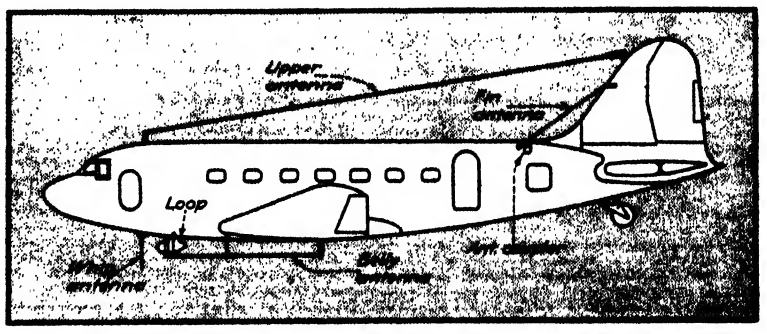

FIG. 1—Profile of Douglas DC-3, showing the various types of antennas used for communication and navigation purposes

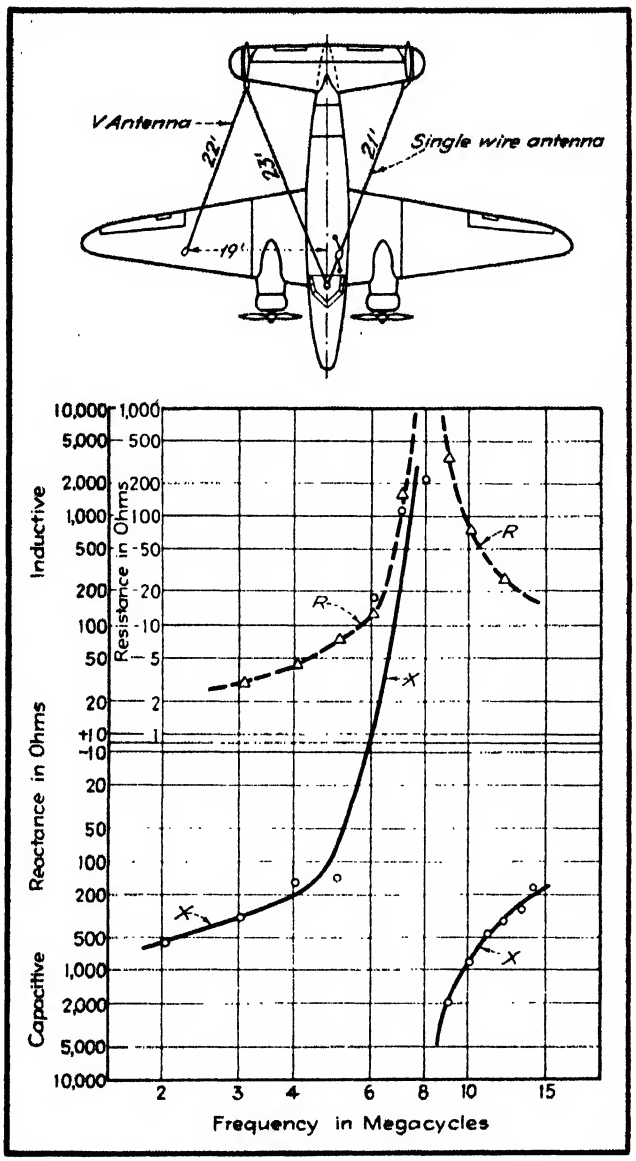

Position and characteristics of V antenna on Lockheed 14 transport. The reactive component of antenna impedance changes sign as the antenna passes through resonance

is based on Q meter measurements.

A Q meter consists essentially of a calibrated variable-frequency oscillator capable of inserting a known voltage in series with a resonant circuit, and a vacuum-tube voltmeter which measures the voltage across the resonant circuit. Then $Q = E/e$, where e is the inserted voltage and E is the voltage read by the v-t voltmeter. By maintaining e constant the v-t voltmeter can be calibrated directly in Q values. In the commercial instrument the components are housed in a cabinet including an a-c power supply, terminals, and a calibrated low-loss variable capacitor. Any suitable coil may be connected across the terminals to form, together with this calibrated capacitor, a tuned circuit. The impedance to be measured is inserted in the tuned circuit either in series or in parallel with the coil.

Two sets of readings are necessary: one to determine the impedance and Q of the coil, and one to determine the impedance and Q of the coil and unknown impedance together. Calculations are then made to determine the impedance and Q of the unknown impedance alone.

Measuring Aircraft Antenna

Precautions are necessary when applying the Q meter to aircraft antenna measurements. The plane should be as far from metallic structures as practical. Grounding wires, such as are used during gas tank filling operations, should be disconnected to minimize the earth's effect on the antenna. For the same reason it is undesirable to use an a-c power line on the Q meter. A rotary converter supplied from the plane battery or a battery cart is required.

A number of coils are needed depending upon the frequency spectrum over which measurements are to be made. Several low-loss fixed capacitors may be needed to supplement the variable capacitor in the Q meter and to place in series with the antenna when the Q readings fall below those conveniently made on the Q meter. In these cases it is necessary to make additional calculations to obtain the antenna reactance. It is necessary to exercise care in adjusting the Q meter when the antenna is in the vicinity of half-wave resonance, because the reactance and resistance values change rapidly in this region.

Table I gives data concerning the top antenna on a Douglas DC-3, shown in Fig. 1. The data in the first seven columns was taken in the field; that in the last five was computed.

The readings C_1 and Q_1 are taken with the antenna disconnected from the Q meter; C_2 and Q_2 with the antenna connected. In the columns labelled C added, P indicates a parallel connection, and S a series connection. It should be noted that when using a series capacitor, if the value of $C_1 - C_2$ becomes larger than the series added capacitance, the antenna has become inductive. This also holds true when C_2 becomes larger than C_1. The formulas used in conjunction with the data are as follows:

$$Q_A = \frac{(C_1 - C_2)\,Q_1\,Q_2}{C_1\,(Q_1 - Q_2)}$$

$X_A = 1.59 \times 10^6 / fC_A$

$R_A = X_A / Q_A$

$C_A = C_1 - C_2$

$$C_A = \frac{(C_1 - C_2)C_s}{C_s + (C_1 - C_2)} \text{ (series capacitor)}$$

Q_A = antenna Q

X_A = antenna reactance in ohms

R_A = antenna resistance (effective), ohms

f = frequency in kilocycles

C_A = antenna capacitance in $\mu\mu f$

C_s = series capacitance in $\mu\mu f$

C_1 and C_2 = reading of variable capacitor in Q meter, in $\mu\mu f$

The quantity $(C_1 - C_2)$ is always taken as positive.

TABLE I. DATA ON DC-3 TOP ANTENNA

Freq. in kc	C_1	C added	C_2	C added	Q_1	Q_2	$C_1 - C_2$	$Q_1 - Q_2$	Q_A	X_A	R_A
2500	443	p141	290	p141	315	120	153	195	50.8	−j416	8.06
3000	406	....	233	....	347	157	173	190	122.0	−j310	2.6
3500	297	....	82	....	372	76	215	296	69.2	−j210	3.03
4000	226.5	....	130	s141	392	147	96.5	245	100.	−j130	4.1
5000	145	....	92.5	s50	424	148	52.5	276	84.	+j30	7.14
6000	210	....	194	s15	224	189	16	35	92.3	+j110	17.4
7000	155	....	134	s15	233	107	21	126	26.8	+j430	41.0
8000	381	p105	390.5	p105	141	89	9.5	52	4.72	+j2100	445.
9000	377	....	370	....	145	85	7.0	60	3.81	−j2520	663.
10000	305	....	286	....	152	76	19.0	76	9.5	−j810	87.
11000	252	....	227.5	s105	160	83	24.5	77	17.1	−j450	32.9
12000	213	....	188	s50	168	92	25.0	76	23.8	−j260	22.

Aircraft Antenna Practice

It has become general practice to connect the aircraft antenna in series with the lumped C and L in the output circuit. Such an arrangement does away with coupling elements and allows a higher transfer efficiency. By providing a group of selectable fixed capacitors and a continuously variable inductor it is possible to reach resonance over a wide range of antenna constants. The system fails, however, at half-wave resonance where a slight change in the physical capacitance of the antenna may reflect a greatly magnified reactive component into the circuit. The simplest solution is to change the length of the antenna so as to shift the half-wave resonant condition away from the working frequency. The radiation efficiency of this extended tank circuit becomes very low when the antenna is a small fraction of a quarter-wavelength. This condition is not encountered on domestic air transports operating between 3000 and 6000 kc, but occurs on planes built for foreign service where bands between 300 and 600 kc are used. The short antenna becomes so highly reactive that voltages up to 30,000 volts may build up. Trailing antennas are then needed.

Dummy Aircraft Antenna

In addition to determining antenna characteristics at the various frequencies, an application of measurements such as these is in the design of dummy antennas. Such antennas are very useful when it is desired to bench-check transmitters under load conditions simulating those imposed by the aircraft antennas.

Aircraft Antenna Pattern Plotter

Technical details of technique in which an aircraft, its antennas, and the signal wavelength are reduced in identical ratio and microwave techniques utilized to obtain as many as 40 complete radiation patterns per hour

By OTTO H. SCHMITT and WILLIAM P. PEYSER

PRACTICAL aircraft antennas are never designed solely from theoretical first principles. In the frequency ranges where aircraft dimensions are comparable with radio wavelengths it is extremely difficult to predict accurately the radiation pattern which a particular antenna installation will exhibit because the entire aircraft is actively a part of the antenna system. Only experimental measurements, therefore, will conclusively establish the actual performance of a new antenna or the effectiveness of a familiar antenna in a new location.

In the day of slow aircraft with antennas draped about the exterior of the plane it was feasible, although terribly expensive, to flight-test an antenna and rearrange it until satisfactory results were obtained. The advent of high airspeed has required enclosure of antennas in the general streamlined structure of the aircraft. It is, therefore, imperative that the position and size of all antennas be established while the aircraft is still on the drafting board and, consequently, before flight tests can possibly be made.

A mockup of the aircraft could obviously be used for test purposes, but it would have to be suspended well above the ground to simulate flight conditions, and would be clumsy to maneuver. Modern mi-

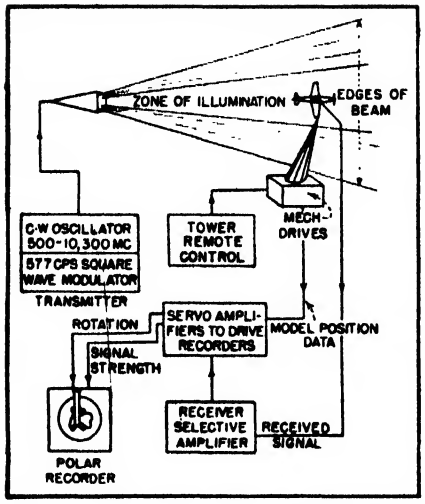

FIG. 1—Block diagram of complete system for measuring aircraft antenna radiation patterns in miniature

crowave techniques, however, make it possible to conduct the experimental measurements in miniature.

Scale-Model Tests

By reducing the aircraft, its antennas, and the wavelength of the radio signals in identical ratio all the geometrical properties of the full-scale system are preserved, and it becomes possible to make measurements on aircraft models no larger than those used as toys. Thus, for example, an aircraft 30 meters in wingspread with an antenna 30 cm high working with 3-meter (100-mc) signals can be perfectly represented by a model 1 meter in wingspread with an antenna 1 cm high if 10-cm (3,000-mc) radiation is used.

With available test frequencies between 500 mc and 10,300 mc and with usable model size between 5 feet and somewhat above 1 foot, we can ordinarily model operating frequencies from below 5 mc to above 500 mc, using small models at the lower frequencies and larger models for the higher frequencies.

Fortunately, an antenna has identical directional characteristics whether used for receiving or transmitting. Thus it is necessary to measure only one characteristic to establish both. It is convenient to use the model antenna as the receiving antenna in all cases, thereby eliminating the necessity of housing the transmitter in the model plane or feeding a microwave signal to it by cable.[1] The problem thus resolves itself into one of providing a suitable model aircraft and antenna, providing a radio-frequency field to illuminate it, and providing means to rotate the model and record automatically the received signal as a function of rotation.

Complete System

The general arrangement of the complete pattern-measuring system is shown diagrammatically in Fig. 1. Continuous-wave transmitters, square-wave modulated at an audio rate, produce any desired radio frequency between 500 and 10,300 mc. Two separate oscillators, each with its own power supply, are employed to cover continuously this entire frequency range. They share a common modulator, and all primary a-c power is drawn from an a-c regulator which is followed by electronic regulators in all d-c circuits to give high stability. Square-wave modulation with 50-percent duty cycle at precisely 577 cps is provided by the modulator unit.

A 2C39 oilcan triode in a grid-separation coaxial-cavity oscillator circuit is used in the transmitter, which covers the 500-2,760 mc range. Tuning is expedited by means of prepared charts specifying the values of cathode and plate line adjustment. Final tuning is, of course, done against a wavemeter. This low-frequency transmitter produces from 50 watts (at its lowest frequency) to at least 5 watts (at its highest frequency), and it is usually throttled down to prevent excessive field strength at the model.

Overlapping the above range and reaching from 2,660 to 10,300 mc, the klystron transmitter uses very highly regulated power supplies for reflector, grid, and accelerator voltages. Five reflex klystrons of the 2K series cover the entire band and are mounted permanently in individual readily-interchangeable plug-in units.

The functioning klystron, a blower, an r-f impedance-matching transformer, and safety devices are mounted in a small remote unit which can be located close to the transmitting radiator, to which it can be connected by a few inches of coaxial cable.

The klystron can be controlled from the transmitter once it is tuned. An output indicator provides an indication both at the remote klystron and at the operating position for use in tuning. In addition, a tunable crystal probe is provided to permit continuous monitoring of the antenna output.

Radiator Family Used

In pattern-measuring work a beam of radiation of angular width just sufficient to illuminate the model uniformly, but not wide enough to cause much reflection from nearby floors or other objects, is required. To meet this condition a family of five radiators, each covering about an octave in frequency, has been developed. These, within their ranges, give nearly uniform angular coverage of 5 to 8 degrees in both H and E planes and have little cross-polarization. The two radiators for the three low-frequency ranges (500-1,000, 1,000-1,800, and 1,750-3,150 mc) are parabolas with wide-band exciters. Interchangeable exciters permit double use of one parabola.

Two pyramidal horns cover the ranges 3,100-5,700 and 5,650-10,300 mc. The horns are fed by tapered-ridge wide-band waveguide exciters which maintain about 2:1 standing wave ratio to 50 ohms over their ranges. Dielectric correctors placed at the mouths of the horns improve their patterns.

All of the radiators fit interchangeably into a single mount. Provision is made to rotate the radiators quickly from vertical to horizontal polarization.

Tower and Models

Airplane models for this system are built precisely to scale (in the patternmaker's fashion, of light, easily worked woods, balsa, sugar pine, spruce, and mahogany) and are hollowed out to house tuning units and to save weight. Models

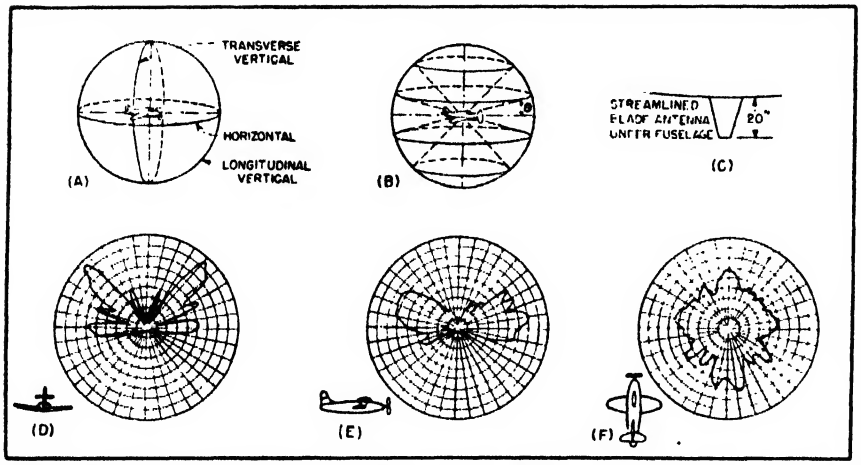

FIG. 2—Principal plane patterns are shown at (A), conical radiation pattern planes at (B), streamlined blade antenna used in tests at (C), and principal plane patterns for streamlined blade antenna at (D, E, and F)

are flame-sprayed first with aluminum and then with copper to provide a highly conductive, easily solderable surface without greatly increasing weight. A skilled model maker requires about one working week to produce a typical model. Once made, a model is usually employed in testing a variety of antennas or one antenna in several positions until a satisfactory location is found. Patches on the model to cover old antenna test locations are readily made with thin sheet copper and solder.

The tower upon which the model is mounted for tests is built of dry spruce strips with thin mahogany bulkheads, braced with tensioned lacings of Fiberglas cord. The Fiberglas cord has elastic constants comparable with those of piano wire so that the resultant tower is extremely rigid, though light in weight and without metal. Wood and lacing are impregnated with a plastic. Mechanical power for rotation of the model is transferred to the tower head by a dielectric torque tube; the model is driven by means of spiral bevel dielectric gears supported in dielectric ball bearings. A draw-in collet arrangement permits quick and secure attachment of models.

The tower is tilted 15 degrees off the vertical to permit the model to rotate about itself rather than about the tower, thus decreasing the width of radio beam required. The tower provides for three independent powered motions of the model. The whole tower moves back and forth on a trestle and it rotates about a vertical axis. In addition, the model can be rotated about its own mounting axis.

Bolometer-Type Detector

Contained in the airplane model is the r-f portion of the receiving system. It consists of an impedance-matching unit which may be of the single or double stub variety, and a bolometer (or a crystal) to demodulate the r-f signal. A detachable tuning tool which can reach into the interior of the model is used to tune the stubs.

The actual detector usually employed in this work is a bolometer which may be either a specially designed Wollaston wire unit or a common instrument Littelfuse of 5 or 10 ma rating. The bolometer is kept at a temperature not far below burnout by a constant d-c biasing current. As modulated r-f reaches the fuse its very fine wire heats and cools in response to the individual modulation cycles, and consequently changes in resistance. These changes in resistance in a current-carrying circuit are equivalent to an audio-frequency voltage input at modulation frequency.

The audio signal is led by a doubly shielded cable to a high-gain audio amplifier located in the receiver rack. The position of this cable in the field of radiation must be carefully chosen, especially at the lower r-f frequencies, to minimize the disturbance introduced in the field.

Audio Amplifier

The audio amplifier has a very high gain (154 db) and low input noise level. Such characteristics are necessary because the klystrons used are low r-f output power devices, delivering only 0.25 to 1 watt to the transmitting radiator. Low noise level is achieved by sharp tuning of the amplifier to 577 cps. Amplifier bandwidth is 6 cps, which permits reasonably rapid response, yet allows an equivalent background audio noise level at the bolometer of 1/40 microvolt or less, only a little above resistance noise level. Surprisingly enough, this low-level audio-frequency signal can be sent without preamplification over a conventional doubly-shielded microphone cable more than 100 feet long.

Bolometer resistance varies linearly in response to temperature change, which in turn is proportional to power input, not to voltage. In recording patterns in terms of power this is an advantage, for the bolometer amplifier yields this information automatically.

To obtain recorder output in terms of antenna voltage instead of power, the square root of the received signal—instead of the received signal itself—must be plotted. The high-gain audio amplifier incorporates a special square-root section to accomplish extraction of this square root through introduction of nonlinear feedback. This section of the amplifier may be switched in or out at will.

A single well-regulated power pack feeds rectified power to the entire high-gain amplifier and the bolometer. Despite high gain and the presence of sharply tuned bandpass circuits the amplifier has no tendency to oscillate. This stability results mainly from the very low power supply impedance (about 5 ohms) and from good decoupling and shielding. Filament heating with a-c is used throughout.

The polar recorder developed for use with the system permits automatic plotting of the audio amplifier output voltage as radial distance against angular position of the aircraft model given by synchro or selsyn generators in the tower base. Two separate high-speed servo motor systems position the turntable and pen respectively. Switching equipment connects the turntable servo to any chosen tower motion.

The recording pen is driven by a servo motor of exceptionally low inertia, writing on polar charts in accordance with the signal from the high-gain amplifier. A precision potentiometer followup system equipped with rate circuits for high-speed deadbeat operation ensures accurate pen positioning.

A pinhole showing a light at the exact center of the turntable aids in centering the polar charts, which are specially printed on tracing paper to permit easy reproduction. A scribed radial line on the turntable surface is lined up with the zero axis of the paper and the paper is clipped to the steel surface with small Alnico rosette magnets.

The airplane model, complete with scale model antenna and bolometer circuit, is mounted on the tower head in the uniform radiation field produced by the proper radiator. The model is rotated and the received signal is recorded on the polar recorder, plotting signal strength against angular position of the model with respect to the source of the radio field.

The angles of elevation and azimuth used in recording antenna patterns represent one pair of the many possible coordinates by means of which the field about an aircraft can be described. In these coordinates the type of patterns shown in Fig. 2A are known as principal plane patterns, and those shown in Fig. 2B are known as conical patterns. Samples of principal plane patterns for the streamlined blade antenna of Fig. 2C are shown at D, E, and F.

Conical patterns are taken by allowing the elevation angle (tower rotation) to assume successive values 5 to 10 degrees apart, each time rotating the model airplane 360 degrees about its mounting axis. A typical family of patterns will include the three principal plane patterns and nineteen conical patterns. Since the horizontal principal plane is included among the conical patterns, however, the family total is twenty-one patterns for any one antenna at one frequency and one polarization.

Once the model is mounted on the tower and the transmitting and receiving systems have been tuned, actual pattern measurements proceed rapidly. Forty-two patterns, representing complete data for an antenna at one frequency and for both polarizations, have often been secured in one hour.

The authors wish to acknowledge the able assistance of the following men, now or formerly with Airborne Instruments Laboratory, in the development of this aircraft antenna radiation pattern measuring system: Roger E. Avery, Wesley A. Fails, Winfield E. Fromm, R. A. Isberg, George W. Smith, and Gerard D. Sullivan.

Reference

(1) Ohio State University Research Foundation Reports 100-3, 100-4, 759-21, 126-33, and 759-34. Development of the rapid semi-automatic equipment was made at the request of the U. S. Navy, using basic operating principles derived from methods established by G. Sinclair and his coworkers at O.S.U. Research Foundation.

Bibliography

(1) Ohio State University Research Foundation Reports 100-3, 100-4, 759-21, -26, -33 and -34.
(2) W. E. Kock, Metal Free Antennas, *Communications*, February 1946, page 63.
(3) Radio Research Laboratory Report 411-213.
(4) Radiation Laboratory Report 601-4.
(5) National Research Center of Canada, "Automatic Antenna Pattern Recorder."
(6) Naval Research Laboratory, Rocket Sonde Research Section. "An Airborne Antenna Pattern Recorder for Airborne Antennas."
(7) Airborne Instruments Laboratory, Inc., Report 105-1.

Cavity Aircraft Antenna

A small, shunt-excited receiving element placed within a cavity which can be recessed into the body of an airplane performs well in 75-mc marker-beacon service and nearly eliminates wind resistance and precipitation static

By HARVEY KEES and FAY GEHRES

HIGH-SPEED modern aircraft have complicated the problem of airborne receiving antenna design. Conventional open-wire aerials are not acceptable on many new airplanes because of their wind resistance and the accompanying precipitation static. The purpose of this article is to describe a recessed or "cavity" antenna designed to minimize wind resistance, and to give an account of some of the problems involved in its development.

The antenna, Fig. 1, has very little drag, as can be seen from the photograph of Fig. 2, showing it on the belly of a DC-3 airplane. It was designed primarily for 75-megacycle marker beacon reception, and is intended as a replacement for conventional open-wire half-wave antennas six feet long.

The antenna is essentially a

shunt-excited element 9 inches long, mounted in a cavity 3 inches deep by 6 inches wide and 10 inches long. The element is tuned to quarter-wave resonance by an adjustable top-loading capacitor.

Flights in Douglas and Beechcraft airplanes over the Evansville, Terre Haute and Indianapolis *Z*-markers show the antenna will deliver 3 to 6 millivolts to a 50-ohm load at 1,000 feet. Maximums of 55 to 85 millivolts were observed across a 50-ohm load at 1,000 feet over the four Indianapolis fan markers.

FIG. 2—The antenna recessed into the belly of a DC-3 airplane

Development

At the start of the cavity antenna development it was arbitrarily decided to try a cavity 18 inches long, 12 inches wide and 4 inches deep. A number of different element sizes and shapes were tested in this cavity, until finally a first experimental design was adopted, having an antenna element 16 inches long and 4 inches wide.

It was desired to use the antenna with a 50-ohm concentric transmission line to the receiver, but it was found that the series impedance at the base of the antenna element was in the order of only a few ohms. Shunt connection to the element proved to be a good means of obtaining the required impedance match.

Figure 3 shows two means of connecting a 50-ohm transmission line to the antenna element. The upper diagram shows a conventional shunt-feed system at the base of the antenna, while the lower diagram shows a shunt-feed connection at the top end of the antenna. Both systems give the same electrical results.

Ground tests indicated that the experimental antenna had 0.9 times the voltage gain of a half-wave dipole. In flight this experimental antenna performed so well that it appeared desirable to attempt a smaller design, and the antenna pictured here was finally obtained. A comparison of the experimental and final-design antennas is interesting.

The volume of the final model cavity is approximately one-fifth that of the experimental model. The bandwidth to the three-to-one standing-wave ratio points for the latter was approximately 440 kilocycles compared with 120 kilocycles for the former. Selectivity curves for the two antennas are given in Fig. 4. The sensitivity of the larger experimental model was twice that of the final design.

The selectivity curves indicate that the Q of both antennas is very high. It is so high for the final antenna that air dielectric capacitors have to be used for top loading, and a capacitor of this type with a large minimum capacitance is employed to obtain bandspread tuning.

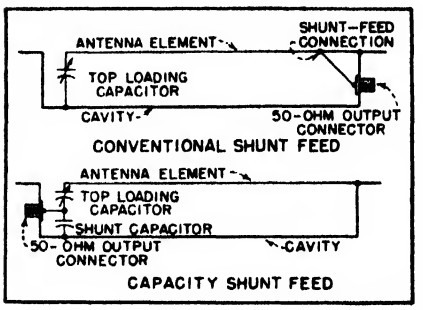

FIG. 3—Two methods of matching a 50-ohm concentric line to a quarter-wavelength receiving element. The system shown in the lower diagram was used

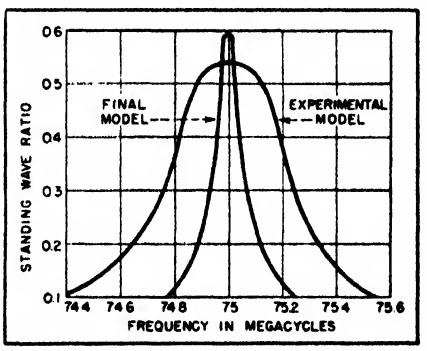

FIG. 4—Selectivity curves for an early experimental model cavity antenna using a fairly large element and the final compact design

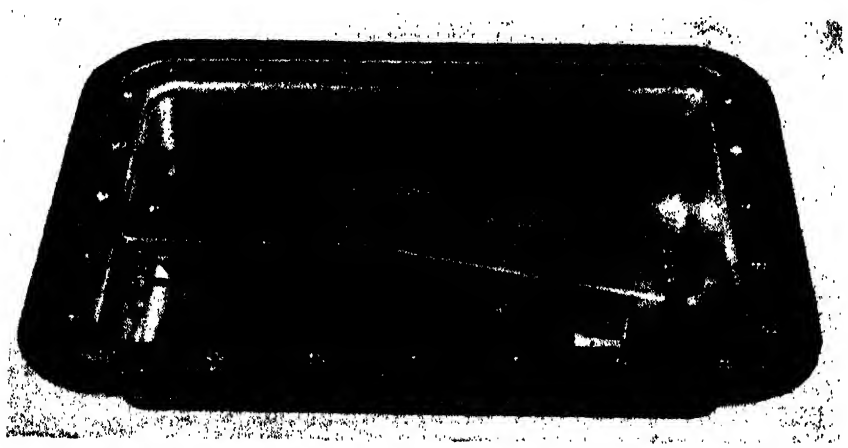

FIG. 1—The final antenna design for 75-mc marker-beacon service

Performance

Temperature tests on early models showed a frequency drift of approximately 200 kilocycles over a temperature cycle of 100 F to —50 F. This drift was reduced to within 25 kilocycles at 75 megacycles by installation of a bimetallic rotor plate on the top-loading capacitor.

Some care in the mechanical design of the cavity antenna is necessary to obtain sufficient stability. However, shake table, temperature,

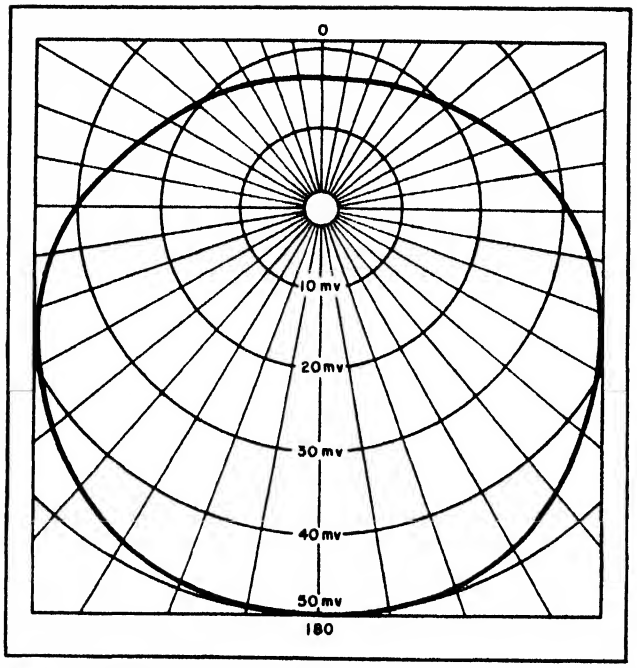

FIG. 5—Pattern of the final design at right angles to the line of flight. The line of flight is into the printed page

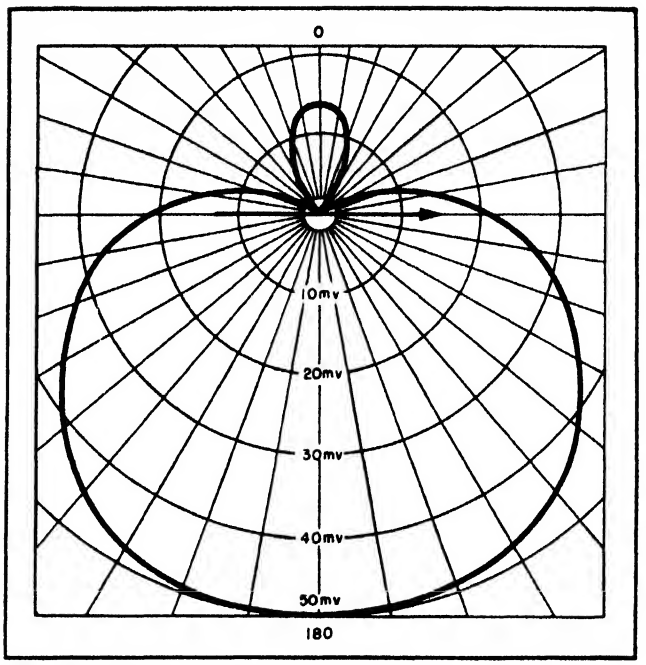

FIG. 6—Pattern of the final design in the line of flight. Line of flight indicated by the arrow

and humidity tests indicate that adequate stability can be obtained without great difficulty.

The bent antenna element in the cavity was adopted to reduce the effects of rain and other extraneous material on the face of the antenna. With the design shown, the output is reduced approximately one db when a heavy stream of water from a garden hose is directed across the face.

Figures 5 and 6 show the directional characteristics of the final antenna, mounted on a 4 by 8-foot ground plane.

Theoretical considerations indicate that cavity antennas act somewhat like corner-reflectors in which some of the gain is cancelled by resistance losses. It appears that the main price paid for a reduction in physical size is a decrease in bandwidth. A general conclusion to be drawn probably is that where large bandwidths are not required, the physical size of most conventional antenna systems can be reduced appreciably—to the point where resistance losses become important.

Artificial Antenna

Design of a two-terminal, lumped-constant network that simulates, within a specified frequency band, the impedance variations of a single-wire antenna. The resulting artificial antenna can be used for tuning transmitters and for power measurements

By SIDNEY WALD

ARTIFICIAL ANTENNAS are necessary for testing variable-frequency radio equipment under conditions closely approximating those encountered in service. It is impractical to use an actual antenna in laboratory tests because radiated energy must be kept at a minimum, and it is usually inconvenient to precisely duplicate an antenna which is used in a special application such as on aircraft.

Although artificial antennas are used for both transmitters and receivers, the complexity of the antenna matching problem is not the same for both classes of equipment. This difference arises mainly because most receiver antenna circuits are untuned while transmitter output circuits, to deliver maximum power to the radiator, must be closely adjusted at each frequency. Because of the greater relative importance of the latter problem, this paper will concern itself with transmitting rather than receiving antennas.

Need for a greatly improved artificial antenna for transmitters

became apparent during the author's experience in the design and testing of aircraft communication transmitters in the medium to high-frequency band. Types of dummy load in wide use for this purpose,

TABLE I—MINIMUM REQUIRED DATA FOR ARTIFICIAL ANTENNA DESIGN

(1) Reactance and resistance at the lower frequency limit.

(2) Quarter-wavelength frequency and resistance.

(3) Resistance at some critical frequency between upper frequency limit and quarter-wavelength frequency.

(4) Resistance at the upper frequency limit.

(5) Half-wavelength frequency. (If this frequency is not known, it can be assumed to be approximately 1.67 times the quarter-wavelength frequency. This constant is empirical and was selected as an average during a study of many fixed, single-wire antennas.)

while perfectly satisfactory for use at a single frequency, resulted in much loss of time and were excessively bulky when applied to equipment having a frequency range of one to ten megacycles. To speed up variable-frequency tests, which at times had to be performed under reduced atmospheric pressure to simulate high-altitude flight conditions, a fixed network was designed which matched the actual antenna both for resistance and reactance at all frequencies.

Basis for Design

While theoretical considerations in this paper are general, this discussion is limited to a band from approximately one to twenty mc. The antenna for which an equivalent circuit is desired is the single-conductor type operating against a ground. The configuration of the wire may be horizontal, vertical, straight, or folded V. The quarter-wave resonant frequency of such a radiator usually lies between 5 and 10 mc. The characteristics of the antenna which must be known are given in Table I. A typical impedance characteristic is shown in Fig. 1.

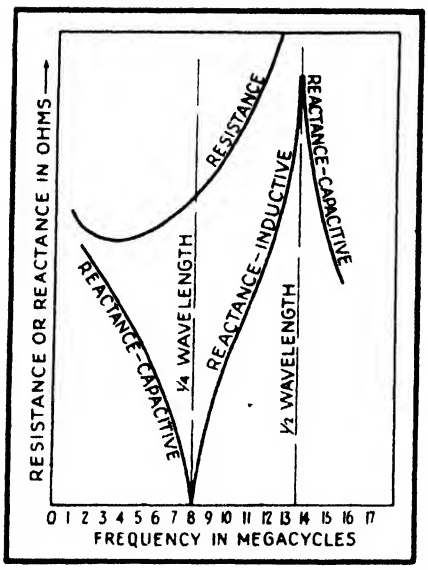

FIG. 1—Typical impedance variation of an antenna of fixed length when the frequency is varied showing reactance variation as a tangent function of frequency

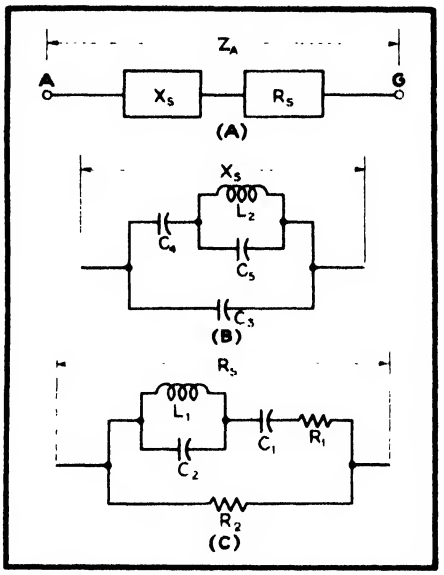

FIG. 2—(A) Antenna impedance can be represented by variable series reactance and resistance. (B) The reactance component and (C) the resistance component can be simulated by lumped constants

To properly evaluate various requirements of a good dummy antenna, it is necessary to understand the way in which the impedance of an actual antenna varies with frequency. The equivalent circuit of an antenna is that of a series reactance X_s and series resistance R_s as shown in Fig. 2A. These two components of impedance change with frequency. The variations of X_s and R_s with frequency given in Fig. 1 apply to all types of antennas where size and geometry remain fixed, while the frequency is changed. To simulate such an antenna at a given frequency it is only necessary to connect the proper values of resistance and either inductive or capacitive reactance in series.

If I_A is the current flowing in the artificial antenna circuit, the power output of the transmitter would be $P = I_A^2 R_s$. If the values of X_s and R_s are correctly chosen, P will be true power output of the transmitter into the actual antenna at the same frequency.

Using fixed *R-C* and *L-C* combinations to simulate the antenna is accurate and simple, but lacks flexibility where a continuous frequency band must be covered. The circuit consists of either a fixed capacitor or coil in series with a non-reactive resistor. The constants of the inductor or capacitor and resistor are calculated from the given antenna reactance, radiation resistance, and frequency.

The fixed resistance is made equal to the antenna resistance. The series capacitance is $C_s = 1/2\pi f X_A$ where X_A is negative. For positive values of X_A the antenna is inductive and $L_s = X_A/2\pi f$.

To provide an arrangement that is easier to work with when the frequency is frequently changed, the reactive and resistive components are made adjustable as, for example, a variable capacitor in series with a carbon compression resistor. When the antenna is inductive, a variable inductor is substituted for the capacitor. To further increase the versatility of the artifical antenna, both an inductor and a capacitor can be included in the series circuit, and a switch provided to short the unwanted element.

Although these adjustable circuits are theoretically sound, they seldom are satisfactory over a wide frequency range. In addition to their stray capacitance to ground,

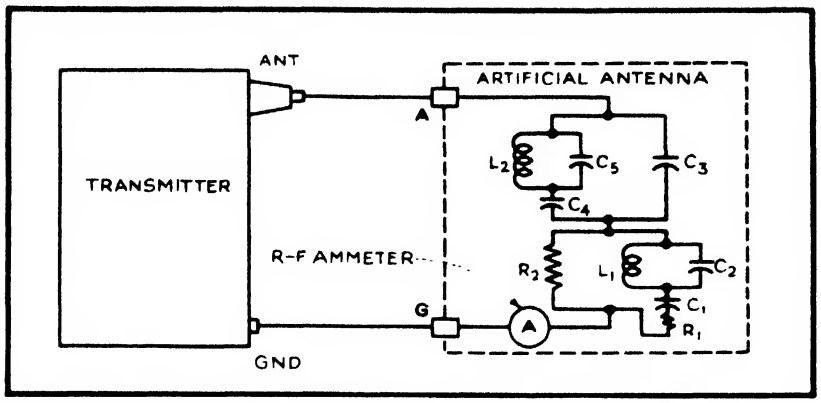

An r-f ammeter can be included in the artificial antenna for power measurements. Stray capacitances must be held to a minimum

adjustable inductors have a high distributed capacitance. This may give rise to spurious resonances. Variable capacitors of high maximum capacitance must be extremely large to withstand the high r-f potentials.

Not only are there practical electrical difficulties, but there are the operational disadvantages which require the manipulation of two controls for each change in output frequency. An error in setting of either the reactor or resistor results in unreliable measurements and a loss of time in rechecking results.

Composite Series Circuits

In contrast to the foregoing circuits that utilize variable components, the proposed artificial antenna is composed of fixed elements. When these elements are properly chosen, the reactance and resistance seen at the terminals of the network (Fig. 2A) will match those of the actual antenna at every frequency within the assumed limits.

It is the plan of this paper to treat each portion separately and finally to show how they are connected in series to form the desired circuit. The portion marked X_s will automatically duplicate the series reactance of the given antenna, while R_s will produce the resistance variation with frequency. Although in practice it is not possible to isolate resistance and reactance completely, it is assumed that the equivalent series resistance of the reactance section is low enough to be negligible and the equivalent series reactance of the resistance section can be disregarded in comparison with that contributed by the reactive circuit.

Network Equations

A combination of reactances which can have an equivalent series reactance variation with frequency similar to that shown in Fig. 1 is represented in Fig. 2B. The corresponding frequency characteristic is shown in Fig. 3A.

The problem is to select values of C_3, C_4, C_5, and L_2 to yield a reactance variation which duplicates that of any given antenna. While C_3 is theoretically unnecessary to obtain the simulated curve, in practice it was found that the stray capacitance from the antenna terminal to ground introduced a large error in reactance at the low-frequency end of the band. Using a controlled value of C_3 eliminates the effect of this unavoidable capacitance. Thus some value is selected for C_3 greater than the supposed stray capacitance to ground and if the final capacitance to ground is smaller than the assumed value, a trimmer capacitor can be inserted to make up the difference. A practical value for C_3 is about 10 $\mu\mu$f.

Design equations for this reactance network are derived in Appendix I and summarized in Table II.

In a similar manner, the network of Fig. 2C provides the required resistance variation. Design equations for this network are derived in Appendix II and summarized in Table III. The quantities referred

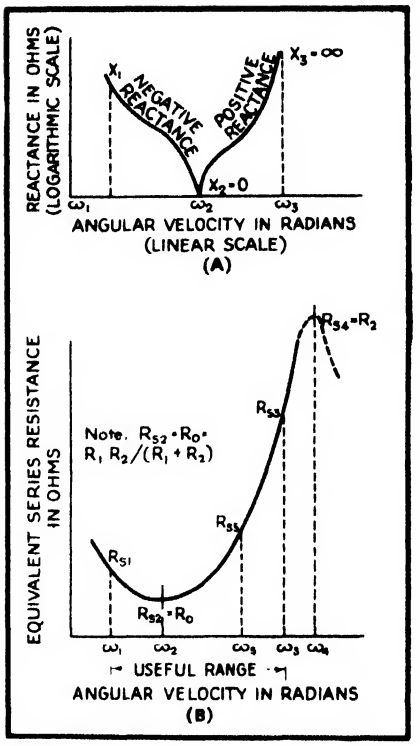

FIG. 3—Critical frequencies and their associated reactances (A) and resistances (B) of the antenna to be simulated are used to obtain values for the artificial antenna elements

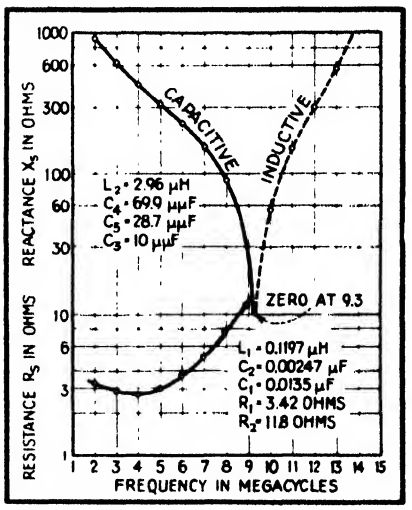

FIG. 4—An artificial antenna built from the design equations was tested and had these reactive and resistive characteristics; compare with Fig. 1

TABLE II—REACTANCE NETWORK DESIGN EQUATIONS

Units are in farads, henrys, cycles, and ohms.

1) Assume a value for C_3

)

(2) $$C_3 = \frac{(\omega_2^2 - \omega_1^2)(-X_1\omega_1 C_3 - 1) - X_1 C_3 \omega_1 (\omega_3^2 - \omega_2^2)}{X_1(\omega_1\omega_3^2 - \omega_1^3)}$$

where $C_3 = C_4C_5/(C_4 + C_5)$
ω_1 — angular velocity at lower limit
ω_2 — quarter-wavelength angular velocity
ω_3 — half-wavelength angular velocity
X_1 — antenna reactance at ω_1 (proper sign must be used for X_1 when substituting into equation)

(3) $C_4 = C_3(\omega_3/\omega_2)^2 - C_3(\omega_2 L\omega_3)^2/\omega_2^2$

(4) $C_5 = C_3C_4/(C_4 - C_3)$

5) $L_2 = 1/\omega_2^2(C_4 + C_5)$

Note: (A) If ω_3 is unspecified it can be assumed to be 1.67 ω_2, as stated in Table 1 (5); (B) The Q of L_2 should be as high as possible, at least 300; (C) Distributed capacitance of L_2 should be subtracted from the calculated value of C_5 to determine the physical value for C_5.

(6) To check accuracy of computed components, plot X_3 vs angular velocity from the following equation, and compare this curve with the given antenna reactance curve

$$X_3 = \frac{\omega^2 L_2(C_4 + C_5) - 1}{\omega C_3[1 - \omega^2 L_2(C_4 + C_5)[- \omega C_4(\omega^2 L_2 C_5 - 1)}$$

to in this table are made clear by Table I and Fig. 3B.

Example of Network Design

Pertinent data concerning the reactive characteristics of an antenna is: Lower limit frequency = 2 mc, reactance at lower limit frequency = $-j$ 930, quarter-wave frequency = 9.3 mc, and half-wave frequency = 15.5 mc.

From this data, values for substitution into Table II are: $\omega_1 = 2\pi(2 \times 10^6)$, $\omega_2 = 2\pi(9.3 \times 10^6)$, $\omega_3 = 2\pi(15.5 \times 10^6)$, $X_1 = -930$, and let $C_3 = 10^4 \times 10^{-12}$. Solving for the reactive network components, we obtain $C_3 = 20.3\ \mu\mu f$, $C_4 = 69.9\ \mu\mu f$, $C_5 = 28.7\ \mu\mu f$, and $L_2 = 2.96\ \mu h$.

If these values are substituted into the equation for X_3 and reactance plotted against frequency, the upper curve of Fig. 4 is obtained. Checking the value of X_3 against actual antenna reactance at any frequency shows that the error at any point is well within the limits of engineering accuracy. In this particular example, the reactance error at any frequency is less than two percent.

To complete the sample calculations, the significant resistance values of the given antenna with reference to Fig. 3B are: $R_{s1} = 3.2$ ohms, $f_1 = 2$ mc or $\omega_1 = 2\pi(2 \times 10^6)$, $R_o = 2.7$ ohms, $f_2 = 4$ mc or $\omega_2 = 2\pi(4 \times 10^6)$, $R_{s2} = 6$ ohms, $f_3 = 7.5$ mc or $\omega_3 = 2\pi(7.5 \times 10^6)$, $R_{s3} = 11.5$ ohms, and $f_4 = 9$ mc or $\omega_4 = 2\pi(9 \times 10^6)$.

Substitution of the preceding constants into the equations of Table III gives $R_2 = 11.8$ ohms, $f_4 = 9.275$ mc, $C_1 = 0.0135\ \mu f$, $L_1 = 0.1197\ \mu h$, $C_2 = .00247\ \mu f$, and $R_1 = 3.42$ ohms.

If these values are substituted in the equation for R_3 and the resultant values plotted against frequency, the lower curve of Fig. 4 is obtained.

The actual artificial antenna is the series combination of the resistive and reactive networks.

Lumping the reactive elements of the resistance network of Fig. 2C into a single reactance X_1, we find that the reactance of the resistance network is

$$X_3 = X_1R_2^2/|(R_1 + R_2)^2 + X_1^2| \qquad (1)$$

To find the greatest value that X_3 can ever reach, differentiate Eq. (1) with respect to X_1

$$\frac{d(X_3)}{dX_1} = \frac{|(R_1 + R_2)^2 + X_1^2|R_2^2 - (X_1R_2^2)2X_1}{|(R_1 + R_2)^2 + X_1^2|^2}$$

Setting the numerator equal to zero, and solving for X_1

$$X_1 = R_1 + R_2 \qquad (2)$$

Substituting Eq. (2) into Eq. (1)

$$X_{3max} = R_2^2/2(R_1 + R_2) \qquad (3)$$

In a typical case where $R_2 = 11.8$ ohms and $R_1 = 3.42$ ohms, the maximum value of X_3 is 4.56 ohms inductive. Substituting Eq. (2) in Eq. (10) from Appendix II gives

$$R_3 = \frac{R_2(R_2 + 2R_1)}{2(R_1 + R_2)} \qquad (4)$$

Using the same numerical values for R_1 and R_2, $R_3 = 7.2$ ohms.

Referring to the antenna resistance curve of Fig. 4B, we see that $R_3 = 7.2$ ohms at a frequency of 7.9 mc. At this frequency the antenna reactance is $-j100$ ohms. Thus, in the given example, the maximum error introduced by the reactance of the resistance variation circuit occurs at 7.9 mc and has a value of $X_{3max}/X_A = 4.56/100 = 4.56$ percent.

Antenna Operation

The simulative network discussed in this paper is, strictly speaking, only an approximation of the antenna which it is intended to replace. At any frequency the simulated reactance and resistance will differ from the actual values by a finite amount. The magnitude of these discrepancies will vary depending on the antenna, but in general it will be found that the reactance curve can be made to match within two percent, while the resistance may deviate as much as ten percent from the true value.

Effect of mismatch on the tuning of the transmitter output circuits may for all practical purposes

be neglected. However, the setting of the coupling control, being sensitive to the resistive component of the antenna impedance, will differ slightly at some points from its position when working into an actual antenna.

The network may be used for measuring power output if a radio-frequency ammeter is connected in series with the circuit. The power output is $P = I_A^2 R_s$ where P is power output in watts, I_A is amperes rms, and R_s is equivalent series resistance of entire network. The value of R_s at each frequency should be determined by measurement on either a Q meter or a suitable r-f bridge, between terminals A and G.

To get reliable indications of antenna current, the stray capacitance of the input terminal and of C_1 to ground must be reduced to as low a value as possible. Careful arrangement of the elements of the network, together with a short input lead, will increase the accuracy of power output measurements.

There are several precautions to be taken in connection with the design, construction, and use of the artificial antenna described here. The various components of the network must be carefully chosen to give satisfactory service. This caution is particularly applicable to capacitor C_1 which may be subjected to extremely high r-f potential, even with low-power transmitters. For example, at two megacycles, a transmitter which produces 20 watts in an antenna resistance of three ohms causes a current of 2.57 amperes rms to flow. Using the value of C_1 in our typical case, 69.9 $\mu\mu$f, the current in C_1 would be 2.25 amperes. The peak voltage across C_1 with 100-percent modulation is $2 \times 1.4 \times 1140 \times 2.25 = 7{,}160$ volts.

In conclusion, while the antenna network presented here falls considerably short of perfection, it does have a substantial field of usefulness from an engineering point of view. The effort consumed by its design and construction is small indeed when one considers the amount of time which can be saved in the development and testing of multi-frequency transmitters.

TABLE III—RESISTANCE NETWORK DESIGN EQUATIONS

Units in farads, henrys, cycles, and ohms.

(1) Solve for R_2 from the following equation, using given values from the antenna to be duplicated

$$\pm N[A(R_2 - R_{S5})]^{1/2} \mp M[F(R_2 - R_{S1})]^{1/2} = (N - M)[R_2 - R_{S3}]^{1/2}$$

where $A = \dfrac{(R_{S3} - R_O)/(R_{S5} - R_O)}{\left[\dfrac{\omega_5}{\omega_3}\left(\dfrac{\omega_2^2 - \omega_3^2}{\omega_2^2 - \omega_5^2}\right)\right]^2}$

$$F = \frac{(R_{S3} - R_O)/(R_{S1} - R_O)}{\left[\dfrac{\omega_1}{\omega_3}\left(\dfrac{\omega_2^2 - \omega_3^2}{\omega_2^2 - \omega_1^2}\right)\right]^2}$$

$$M = \omega_5^2 - \omega_3^2$$

$$N = \omega_1^2 - \omega_3^2$$

(2) Having found R_2, solve for ω_4 from

$$\omega_4 = [(\pm \omega_5^2 B - \omega_3^2)/(B - 1)]^{1/2}$$

where $B = \left[\dfrac{R_2 - R_{S3}}{A(R_2 - R_{S5})}\right]^{1/2}$

(3) $C_1 = \left(\dfrac{\omega_2^2 - \omega_5^2}{\omega_5^2 - \omega_4^2}\right)\left(\dfrac{\omega_4^2}{\omega_2^2\,\omega_5 R}\right)$

where $R = \dfrac{R_2^2}{R_2 - R_O}\left[\dfrac{R_{S5} - R_O}{R_2 - R_{S5}}\right]^{1/2}$

(4) $L_1 = (\omega_4^2 - \omega_2^2)/\omega_4^2\omega_2^2 C_1$

(5) $C_2 = 1/\omega_4^2 L_1$

(6) $R_1 = R_O R_2/(R_2 - R_O)$

(7) To check accuracy of the calculated components, plot R_s vs angular velocity from the following equation and compare this curve with the given antenna resistance curve

$$R_s = \frac{(R_1 R_2)(R_1 + R_2) + R_2 X_s^2}{(R_1 + R_2)^2 + X_s^2}$$

where $X_s = (-1/2\pi f C_1) + \dfrac{2\pi f L_1}{1 + (4\pi^2 f^2 L_1 C_2)}$

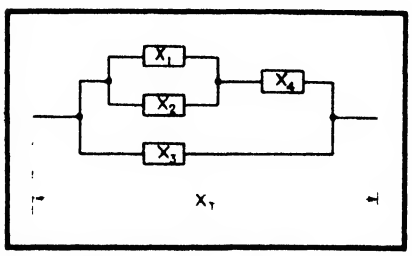

FIG. 5—Assumed circuit from which reactive network is developed

Appendix I Simulation of Reactance Curve

Neglect the resistance in the circuit. The reactive portion of the simulated antenna can be represented by Fig. 5. The total circuit reactance is

$$X_T = \frac{X_1 X_2 X_3 + X_3 X_4 (X_1 + X_2)}{X_1 X_2 + X_4 (X_1 + X_2) + X_3 (X_1 + X_2)} \quad (5)$$

let $X_1 = +\omega L_2$
$X_2 = -1/\omega C_5$
$X_3 = -1/\omega C_3$
$X_4 = -1/\omega C_4$

Substituting these values into Eq. (5) gives

$$X_T = \frac{\omega^2 L_2 (C_4 + C_5) - 1}{\omega C_3 [1 - \omega^2 L_2 (C_4 + C_5)] - \omega C_4 (\omega^2 L_2 C_5 - 1)} \quad (6)$$

when $\omega = \omega_3$, $X_T = 0$

$$\omega_3^2 L_2 (C_4 + C_5) - 1 = 0 \quad (7)$$

when $\omega = \omega_3$, X_T = infinity

$$C_3 [1 - \omega_3^2 L_2 (C_4 + C_5)] - C_4 (\omega_3^2 L_2 C_5 - 1) = 0 \quad (8)$$

when $\omega = \omega_1$, $X_T = X_1$

$$X_1 = \frac{\omega_1^2 L_2 (C_4 + C_5) - 1}{\omega_1 C_3 [1 - \omega_1^2 L_2 (C_4 + C_5)] - \omega_1 C_4 (\omega_1^2 L_2 C_5 - 1)} \quad (9)$$

Equations (7), (8), and (9) are now solved simultaneously for unknowns C_4,C_5, and L_2, giving the equations of Table II.

Appendix II
Simulation of Resistance Curve

In the network of Fig. 6A the equivalent series resistance, R_s, as shown at Fig. 6B is a function of the branch reactance X_1 which in turn is some function of frequency; thus

$$R_s = \frac{(R_1 R_2)(R_1 + R_2) + R_2 X_1^2}{(R_1 + R_2)^2 + X_1^2} \quad (10)$$

This circuit is satisfactory for our purpose because the equivalent series reactance X_s can at all times be made small compared to either the total series resistance or the total series reactance. This total series reactance includes the reactance developed in Appendix I. We are primarily concerned with the duplication of a resistance variation. The magnitude and importance of X_s is considered elsewhere.

The minimum value of R_s in Eq. (10) occurs when $X_1 = 0$ and $R_s = R_0 = R_1R_2/(R_1 + R_2)$. If Eq. (10) is solved for X_1 we obtain

$$X_1 = \pm \left[\frac{(R_1 R_2)(R_1 + R_2) - R_s (R_1 + R_2)^2}{R_s - R_2}\right]^{1/2} \quad (11)$$

From the condition for a minimum value of R_s, $R_1 = R_0R_2/(R_2 - R_0)$, which, substituted into Eq. (11), gives

$$X_1 = \left(\frac{R_2^2}{R_2 - R_0}\right)\left[\frac{R_0 - R_s}{R_s - R_2}\right]^{1/2} \quad (12)$$

Now if in Fig. 6A, X_1 assumes the configuration of Fig. 6C.

$$X_1 = \frac{1 - \omega^2 L_1 (C_1 + C_2)}{\omega C_1 (\omega^2 L_1 C_2 - 1)}$$

Substituting this value of X_1 into Eq. (12) yields

$$\frac{1 - \omega^2 L_1 (C_1 + C_2)}{\omega C_1 (\omega^2 L_1 C_2 - 1)} = \frac{R_2^2}{R_1 - R_0}\left[\frac{R_0 - R_s}{R_s - R_2}\right]^{1/2} \quad (13)$$

If ω_1 is the angular frequency at which the L_1C_2 loop is in parallel resonance, that is: $L_1C_2 = 1/\omega_1^2$, and similarily, if ω_2 is the angular frequency at which the circuit of Fig. 6C is in series resonance so that $L_1 (C_1 + C_2) = 1/\omega_2^2$, Eq. (13) can be written in terms of resonant and antiresonant angular velocities.

There are three unknowns in this resultant equation, namely, R_s, ω_1, and C_1. If three conditions are known, a corresponding number of simultaneous equations can be set up. The most convenient boundary conditions are the two limit frequencies and one intermediate frequency, and the corresponding antenna resistances. Using these values to solve this equation gives the design equations of Table III.

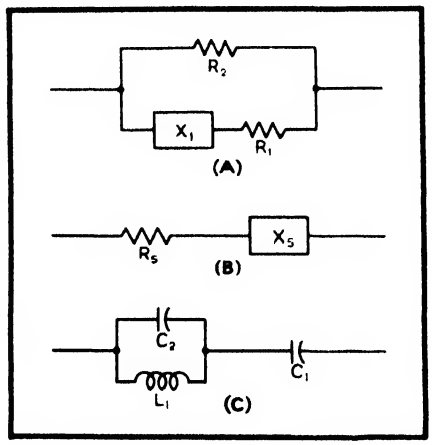

FIG. 6—Circuit from which resistive network is developed: (A) the assumed circuit, (B) the equivalent series circuit, and (C) the final design

Microwave Antenna Beam Evaluator

Development, adjustment, and routine maintenance of microwave antenna systems require a means for plotting the radiation pattern quickly. This system uses simple potentiometers but requires no nonlinear circuit elements. The recorded pattern is independent of transmitter power fluctuations and high sensitivity is realized without tuned amplifiers

By H. LeCAINE and M. KATCHKY

IN THE DEVELOPMENT of high-gain microwave antennas, numerous radiation patterns are required when checking critical adjustments to feeds, radiators and reflectors before optimum conditions for beamwidth and side lobes are found. Manual pattern-taking is a slow, laborious process, as it is generally necessary to measure received or transmitted power at each of many angles, and to calculate and plot each pattern. To speed up this type of work, an automatic recorder was developed at the National Research Council of Canada, with some unique features.

Although the recorder plots the square root of the detected signal, only simple wire-wound potentiometers in which resistance varies linearly with angle are required. Furthermore, since no circuit elements with nonlinear amplitude characteristics are used, an accuracy of 1 percent in the trace is realized in daily operation. The pattern is made independent of fluctuations in transmitted power by an unusually simple method. The received signal is merely balanced against a monitor voltage. The recorder does not respond to, nor is it jammed by interference encountered around a radar establishment, and a high receiver sensitivity is

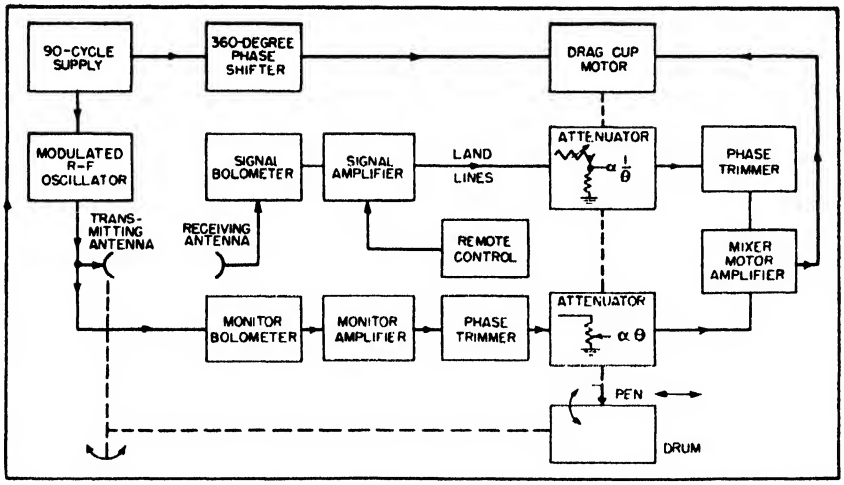

FIG. 1—Block diagram of the automatic recorder. Mechanical linkages between transmitting antenna and recording drum and between the attenuators and the recording pen are indicated by dashed lines

realized without the necessity of using tuned amplifiers. These characteristics are achieved by using the pen motor in a synchronous detector circuit.

Arrangement of Equipment

All the equipment illustrated with the exception of the receiving antenna and its associated detector and amplifier, is located in a room under the antenna turntable. The block diagram of interconnections is shown in Fig. 1. Several receiving antennas for different bands and at various distances are available to increase the flexibility of the system, and all are remotely controlled from the recorder room. The receiving antennas have directional characteristics to reduce the influence of undesirable reflections.

In operation, modulated radio-frequency energy is transmitted from the test antenna, which is located on the turntable. As this antenna is rotated, the varying field strength at the receiver is used to control the movement of a pen which traces the pattern on a rotating drum geared to the turntable drive shaft.

A power pattern of a high-gain antenna is not satisfactory because the side lobes are not given sufficient prominence. Field strength patterns overcome this objection and can be used directly to represent a contour of constant power or constant field strength. As the only suitable detectors give an output proportional to the power in the received signal, a direct-recording system with a linear potentiometer would give power patterns. To obtain the desired field strength patterns, a special attenuator could be used, but this would result in a recording sensitivity which varies with pen position. Since speed and accuracy place severe restrictions on the sensitivity, such a system would be satisfactory over a small range of signals only. In the circuit to be described, field strength patterns are obtained with constant recording sensitivity.

The transmitter most commonly used with the recorder is a klystron oscillator which is modulated by 90-cycle square waves from the multivibrator circuit shown in Fig. 2. The choice of 90 cycles was made to avoid power line frequency interference, and because there were no other users of 90-cycle frequency in the vicinity.

Part of the output from the multivibrator is amplified and applied to one field of the motor. A phase adjuster is provided to obtain the correct phase between the voltages on the two fields of the motor.

The signal bolometer and am-

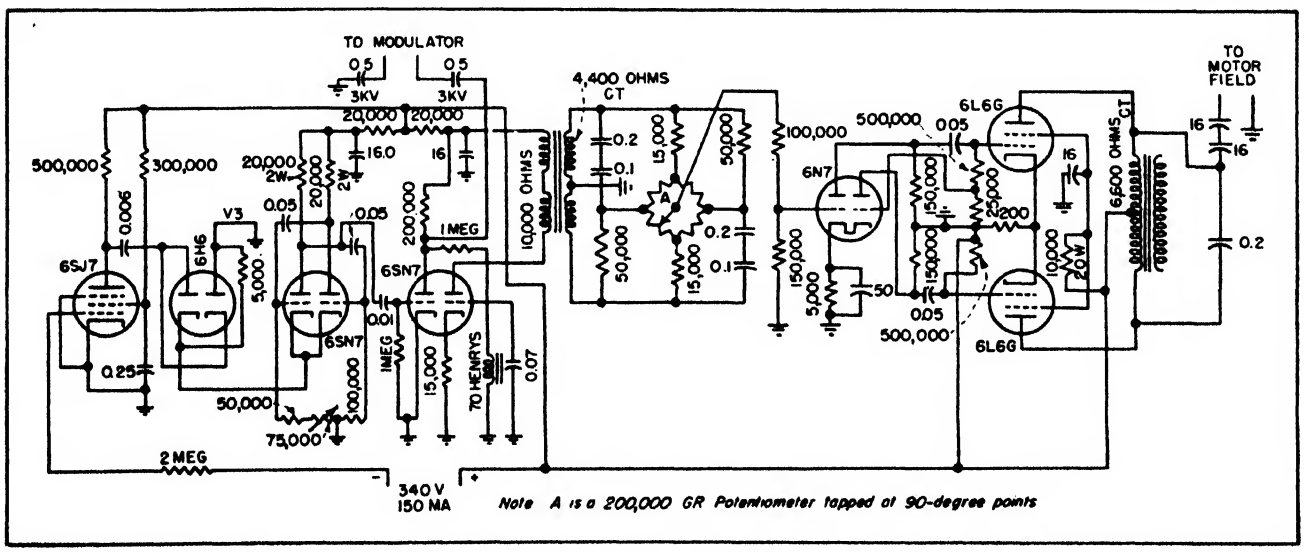

FIG. 2—The 90-cycle supply comprises a multivibrator circuit locked to the powerline frequency. Output from the unit modulates the r-f oscillator. A second output reaches the motor by way of a phase shifter and amplifier.

plifier are located near the receiving antenna. The bolometer is a Littelfuse element acting as a square-law detector. These elements have been in use for a number of years, and repeated tests by various methods and observers have proven them to be very accurately square-law up to several milliwatts. Thus the detected voltage is proportional to the radio-frequency power in the received signal.

The associated amplifier is well shielded to avoid blocking by any heavy radar interference picked up in the early stages. The synchronous detector circuit to be described makes unnecessary the use of tuned amplifiers. The overall gain can be varied from 40 decibels to 110 decibels in order to accommodate various antennas. Coarse adjustments in gain, covering a 50-decibel range in nine steps, are made at the receiving sites, while fine adjustments over a 20-decibel range are made remotely at the recording room. The gain of the amplifier is made stable by the use of inverse feedback, which also ensures a linear response. By careful design and shielding, a low noise level in the amplifier is achieved, allowing a high signal-to-noise ratio even for many low-gain antennas. Ratios of 100-to-1 in field strength, therefore, can be measured easily, and at maximum gain a receiver sensitivity of about 0.003 microvolt across 500 ohms is realized.

The output from the field amplifier is carried into the recording room by a 500-ohm line which is balanced to ground. The next stage is a cathode follower which presents the required low impedance to the attenuator.

A monitor device consisting of either a probe in the feed line. or a fixed antenna, picks up a portion of the transmitted signal. This fraction is then detected by a bolometer, giving an audio-frequency voltage proportional to the transmitted power. Any fluctuation in the transmitter output will affect both the signal and monitor voltages to the same extent, leaving the ratio of the two unchanged. As will be seen later, the pen position at balance is dependent on this ratio; therefore fluctuations in output do not alter the recorded pattern.

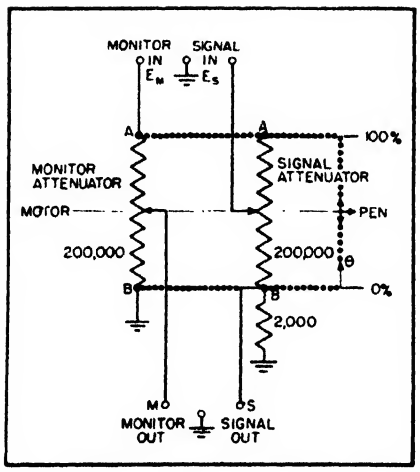

FIG. 3—One-tenth of the monitor attenuator output is compared with ten times the signal attenuator output and the resultant difference voltage drives the pen motor until the two quantities are equalized

The Attenuator System

The attenuators consist of two linear potentiometers with moving contacts ganged on the same shaft that drives the recording pen. The monitor and signal voltages are applied to these attenuators in the manner shown in Fig. 3. The two outputs from the attenuators are then added out of phase, and the resultant difference voltage is amplified and applied to one field of the motor, causing it to rotate. This moves the recording pen, and at the same time, moves the contacts in such a direction that the difference voltage is reduced to zero, at which point the motor ceases to rotate. This is the balance position. The proper direction of rotation is obtained by means of the 360 degree phase adjuster in the 90-cycle supply.

It can be shown that the pen traces out a field strength pattern which is not affected by power fluctuations in the transmitter. Let θ represent the pen position expressed as a fraction of the maximum pen displacement. It will also represent the position of the two potentiometers expressed as a fraction of their maximum displacement. Then for a monitor voltage of E_m and a signal voltage E_s at the attenuator inputs (Fig. 3)

$$\text{Output of signal attenuator} = \frac{2{,}000}{\theta \times 200{,}000 + 2{,}000} E_s$$

$$\text{Output of monitor attenuator} = E_m\theta$$

The circuits that follow compare one-tenth of the output of the monitor with ten times the output of the signal attenuator. When these quantities are equal

$$\frac{E_m\theta}{10} = 10 \times \frac{2{,}000E_s}{\theta \times 200{,}000 + 2{,}000}$$

$$\theta(\theta + 0.01) = E_s/E_m$$

$$\theta \simeq (E_s/E_m)^{1/2}$$

When the pen position is adjusted to be correct at full scale, the error introduced by the above approximation is negligible (within 0.1 percent full scale) down to a pen position of 1 percent of full scale. Further, since E_s and E_m are both proportional to the oscillator output power, their ratio, and therefore the pen position, is independent of the oscillator power.

At a given instant, the voltage applied to the motor is proportional to

$$V = E_m\theta - E_s/\theta$$

Taking the recording sensitivity S as being equal to the change in voltage per unit change in pen position, it is seen that

$$S = -\frac{\partial V}{\partial \theta} = E_m + \frac{E_s}{\theta^2}$$

but

$$E_s/\theta^2 = E_m$$

therefore

$$S = 2E_m$$

Thus the sensitivity is independent of the pen position. It is however, proportional to the monitor voltage, but the fluctuations in output normally encountered do not produce significant changes in sensitivity.

Recording Circuits

The circuit diagram for the mixer and recording motor is shown in Fig. 4. Where it is necessary to have a transformer before the point where the two voltages are added, great care must be taken, as it is essential that there should be no change of phase with amplitude. The first stage is a signal amplifier

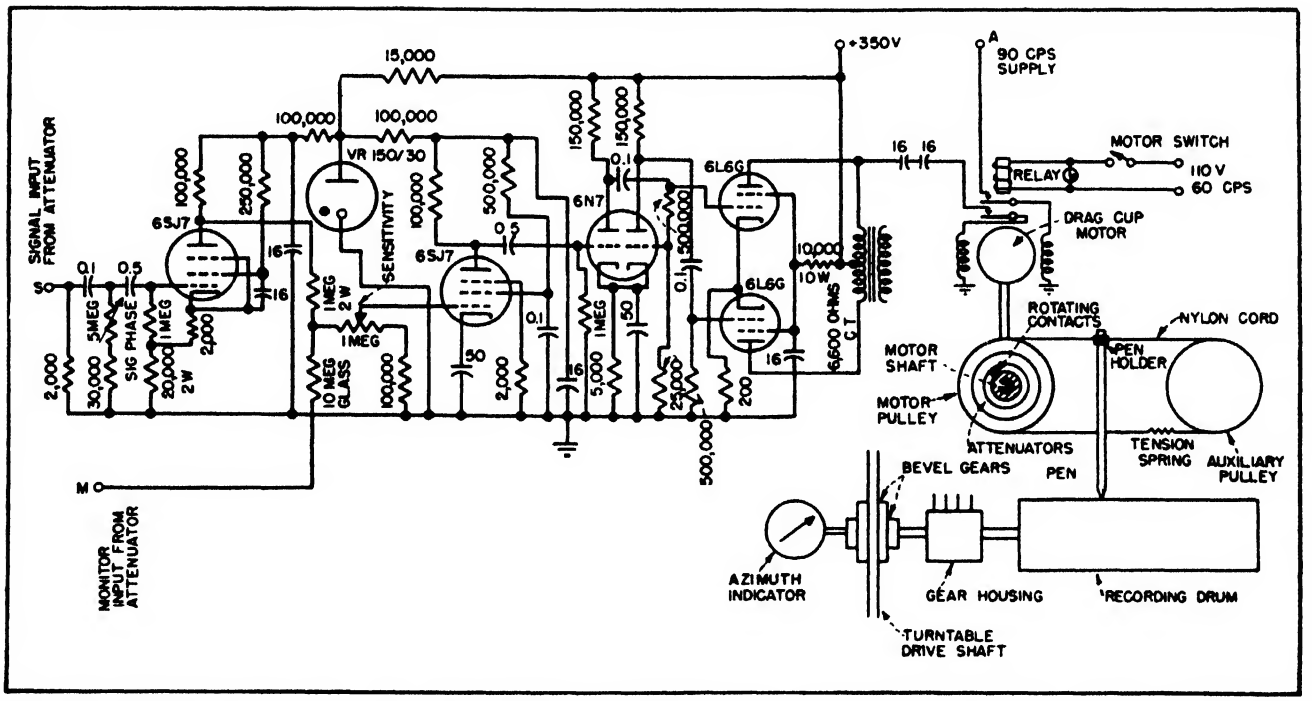

FIG. 4—The signal mixer, motor amplifier and recording apparatus are shown schematically and their interconnections to the other units are indicated

with cathode feedback. Following this, the two voltages are added in a circuit containing only simple resistance. Phase trimmers are provided in both monitor and signal lines to obtain the correct phase relationship. The remaining stages amplify the difference voltage before it is applied to the motor. The gain is adjusted for optimum recording sensitivity after the monitor voltage has been set at the required value.

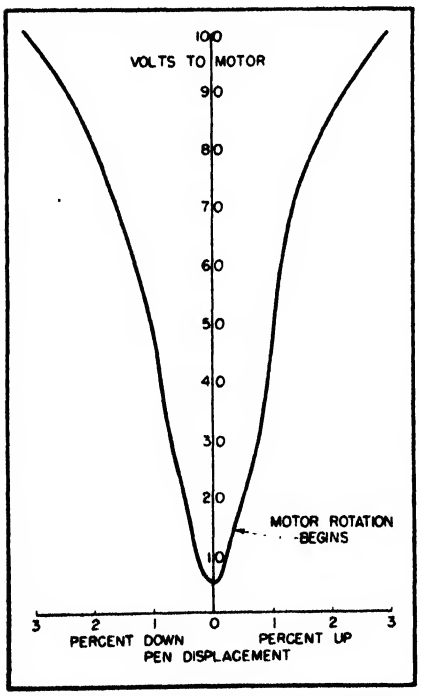

FIG. 5—The voltage at the motor terminals is shown as a function of pen position in percent of full-scale displacement from balance

The recording motor is a small alternating-current drag cup motor which has two field windings on the stator surrounding a cup-shaped rotor. The rotating shaft drives the ganged attenuator contacts and also a pulley which moves the recording pen in a straight line parallel to the axis of the cylindrical drum. Great care is taken to avoid mechanical backlash between the motor and the attenuator.

One field of the recording motor is fed by a constant voltage from the 90-cycle supply; the other by a control voltage derived by adding the attenuated monitor and signal voltages out of phase. With this arrangement, the motor responds only to frequencies within ± 2 cycles per second of the modulation frequency. Even for interfering signals within this bandwidth, the motor simply oscillates about the true value, producing a slight broadening of the pen trace. This behavior has proven to be of immense value, allowing reliable operation at times when an oscilloscope on the signal lines showed a confused mass of heavy radar interference. It is, of course, necessary to be able to obtain the correct phasing of the monitor, signal, and supply voltages, but once this has been accomplished, readjustments need only be made following replacement or interchange of a major system component. Small phase errors cause sluggish movement of the recording motor, which is easily spotted and corrected.

Plotting Antenna Pattern

In order to take a pattern, a sheet of graph paper with rectangular coordinates (which is most suitable for high-gain antennas) is placed on the drum so that the abscissa is along the circumference and the ordinate is parallel to the axis of the cylinder. The abscissa is, therefore, proportional to the angular rotation of the antenna. The drum turns through an arc length of ten inches (to fit the scale of the graph paper) and by shifting gears on

the gear housing, it is possible to take patterns for 20, 40, 200, or 400 degrees on this length of arc. In this manner, the operator is able to select the azimuthal expansion most suitable to the width of the radiated beam.

Before taking the pattern, the antenna under test is turned to the position of maximum gain, which is indicated by a vacuum-tube voltmeter on the signal line at the input

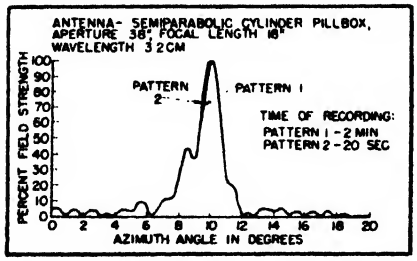

FIG. 6—The effect of increasing recording speed is shown in pattern 2, wherein a 5 percent error has been introduced by changing the field strength by 60 percent of full scale in one second

to the attenuators. The monitor and signal voltages are adjusted until the pen is on the 100 percent ordinate position, and the gain of the motor amplifier is set to give optimum recording sensitivity (this setting is determined experimentally and is rarely changed). When the preliminary adjustments are completed, the desired selection of azimuthal gearing is made, and the pattern is taken by rotating the antenna.

It has been stated that the bolometer and amplifier make a negligible contribution to the error in the pattern. Linear wire-wound potentiometers from stock give an attenuator unit in which the systematic error never exceeds 0.5 percent. The remaining factor in the accuracy of the recorder is the response of the recording motor to changes in field strength. The motor starts rotating at 15 volts, which corresponds to approximately 0.3 percent pen displacement, as shown in Fig. 5.

If a higher recording sensitivity is used in an attempt to reduce this figure, the motor will tend to hunt at the recording speed most commonly used. This effect will necessitate a lower speed to avoid sudden changes in field strength. If a lower sensitivity is used, the percent displacement over which the recording motor will not respond is increased, thus giving less accuracy in the pattern. The sensitivity used is a compromise between these factors, and allows accuracy within 1 percent, along with a high recording speed, without hunting.

It would also be possible to feed back in phase opposition the voltage from a second motor driven by the first and acting as a generator. This would have the effect of reducing the effective inertia of the mechanical system, and increasing the permissible pen speed. The drag-cup motor has such a good ratio of torque-to-inertia, however, that the feedback was considered unnecessary.

It has been found that for accurate patterns, the rotation speed of the antenna under test should be such that the field strength does not change by more than 40 percent of full scale per second. In general, adequate recording speed has always been found available. A 20-degree pattern with a 2-degree beamwidth at 6 decibels down can be taken easily in about one minute, and a 400-degree pattern of the same antenna in five minutes. Two 20-degree patterns recorded at different speeds (one in 2 minutes, the other in 20 seconds) are shown in Fig. 6. The two patterns are practically identical, except for a 5 percent error where the field strength changed 60 percent of full scale in one second at the faster recording speed.

In actual pattern taking, the accuracy has always been within one percent at all times and under varying conditions.

AUDIO

Crystal Pickup Compensation Circuits

From consideration of recording practice, record properties, pickup frequency characteristics, and listener acceptance, the appropriate corrective network for connecting crystal pickup to amplifier input to give desired overall frequency response is determined

By B. B. BAUER

IN THE DESIGN of phonograph equipment, quality performance is not automatically assured by choosing better-grade components for the playback mechanism. The circuit connecting the pickup to the amplifier plays an important part in the satisfaction which the user obtains from the instrument. A clear understanding of the latest trends in recording characteristics is essential to the selection of this circuit. In this article general consideration is given to the frequency response of phonograph playback equipment, with particular attention to the design of circuits for connecting piezoelectric pickups to playback amplifiers.

Recording Characteristics

To reproduce a record in the manner intended by the recording director, the characteristic of the playback system should match the characteristic of the recording system. Recording characteristics are specified in terms of the lateral or hill-and-dale amplitude and velocity of the modulated record groove.

Peak velocity of groove modulation, which is a function of signal frequency is commonly known as the modulation velocity. If modulation velocity is to remain constant, amplitude must decrease with the frequency.

Recording characteristic of a system is defined by the velocity-frequency or amplitude-frequency curve obtained by cutting a disk with a sinusoidal voltage of constant amplitude and varying frequency applied to the input terminals of the recording amplifier. In this manner a test record is obtained which can be used for calibrating playback systems.

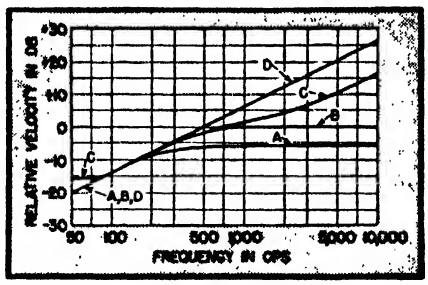

FIG. 1—Theoretical recording characteristics for (A) 250-cps turnover, (B) 500-cps turnover, (C) N.A.B. lateral recording, and (D) constant-amplitude recording

Shortly after the introduction of electrical recording, cutting heads and recording circuits were adjusted in such a manner that a constant velocity characteristic was obtained at frequencies above 250 cps, and a constant amplitude characteristic was obtained below this frequency (known as the turnover point). This recording characteristic is shown by curve A in Fig. 1. Maximum modulation velocity above the turnover point was limited—by the ability of the relatively heavy pickup needle chucks to turn the corners of the modulated groove at high frequency—to approximately 2.5 inches per second. The modulation amplitude below the turnover point was limited by the pitch of the grooves to approximately 0.002 inches. Disks recorded with this characteristic gave satisfactory tonal balance with equipment available at the time.

Extension of the frequency range by lightening the moving system of phonograph pickups, together with the development of wide-range loudspeakers for home use, led to the increase of the high-frequency modulation velocity to peaks of 5 to 7 inches per second. This resulted in a substantial improvement of the signal-to-noise ratio. Because of groove spacing limitations, maximum low-frequency modulation remained unchanged and the turnover point was shifted upward to 500 cps in home records. Such a recording characteristic is shown by curve B in Fig. 1. Because the surface-noise energy is contained principally above 1000 cps, this recording characteristic provides an improvement of signal to surface-noise ratio over the 250-cps turnover point characteristic of approximately 6 db.

High-Frequency Pre-Emphasis

To diminish the audibility of surface noise in transcriptions, it became common practice to accentuate the high-frequency characteristic in the cutting-head amplifier, and conversely, to attenuate the high-frequency response of the pickup. An example of such a recording characteristic is the orthoacoustic characteristic employed by the National Broadcasting Company, which provided for a 16-db rise at 10,000 cps. In 1942 the National Association of Broadcasters' recommended as standard the characteristic shown by curve C in Fig. 1, which corresponds closely to this

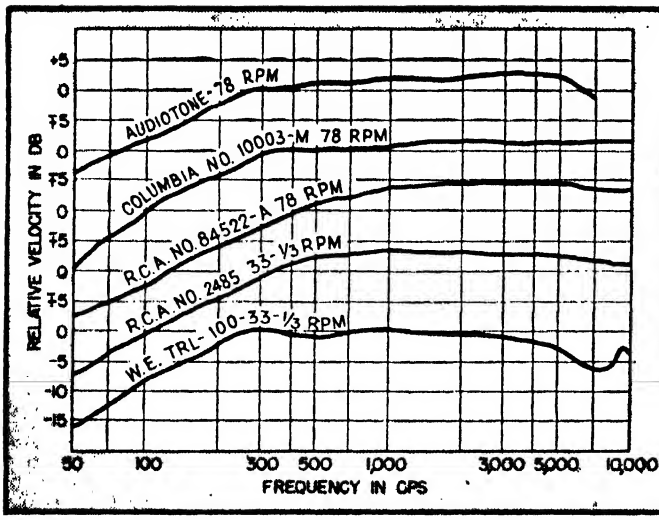

FIG. 2—Measured velocity-frequency characteristic of several test records

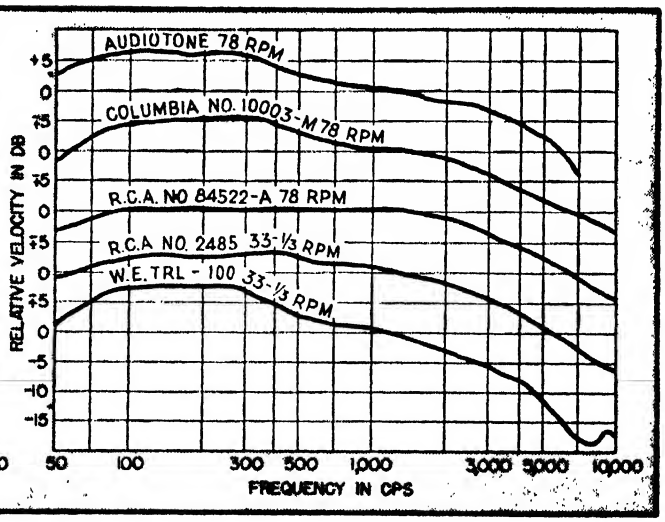

FIG. 3—Playback characteristics of test records in terms of N.A.B. response

orthoacoustic characteristic.

In addition to high-frequency pre-emphasis, the recommended standard indicates a low-frequency pre-emphasis. When compensated in the appropriate manner, low-frequency pre-emphasis, tends to diminish effects of turntable rumble and line frequency hum.

If the recorded amplitude is kept at a low value, it is possible to employ a constant-amplitude recording characteristic shown by curve D in Fig. 1. Such a characteristic has a number of advantages, among them that of efficiently utilizing the available record surface and of providing a high signal-to-noise ratio. This characteristic has not been extensively applied.[8]

The manufacturer of home records is confronted with a number of factors which have a bearing upon response-frequency characteristics. Home records are employed in an extremely wide variety of record players with different characteristics, in coin-operated machines, and in broadcast work. Such factors as needle tracking, recorded level, and surface noise, all of which are interdependent with response characteristics, are given different weight by various manufacturers and users. One finds, as a result, a difference between response-frequency characteristics of records manufactured under various brand names. Because of these differences in recording characteristics, a single playback response cannot meet all requirements and a compromise must be sought. It is to be expected that standardization work may be done in the future to remedy this situation.

Many recent recordings exhibit a good tonal balance when played back with a pickup adjusted to conform to the N.A.B. Standard. Other records provide a better balance when reproduced with a pickup which is flat on a velocity basis beyond the 500-cycle turnover point. However, surface-noise considerations in shellac-type home records dictate a reduction of high-frequency response of the playback roughly in accordance with the N.A.B. Standards. For reasons which are stated later, attenuation greater than prescribed by N.A.B. Standards is often desirable beyond 4,000 to 5,000 cps. There is little doubt that useful frequency content in commercial records beyond

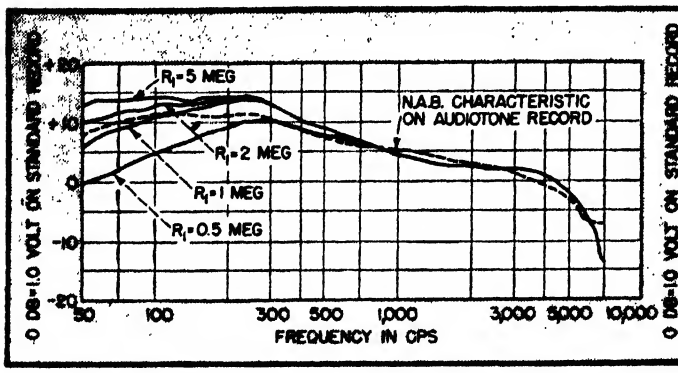

FIG. 4—Terminating resistance affects the low-frequency response of crystal pickups and therefore can be used to adjust overall response

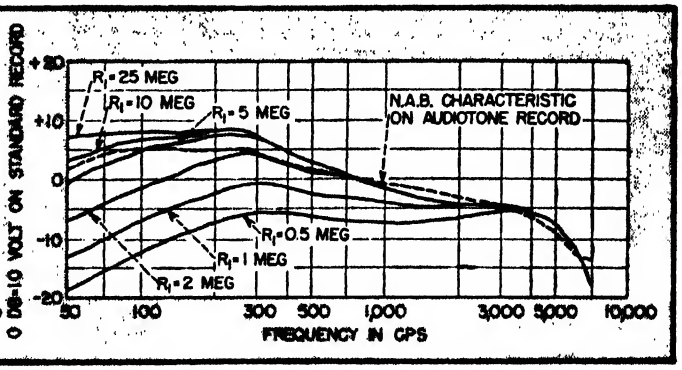

FIG. 5—By choosing terminating resistance used with PN type cartridge, N.A.B. characteristic can be approached. Five megohms gives best match

8,000 cps is negligible.

Test records provide convenient and precise means for testing and adjusting the response of playback systems. The test record need not be recorded with the exact characteristic which is desired for the playback system, as long as its characteristic is known. Most test records are recorded with a constant amplitude characteristic up to the turnover point, and a constant velocity characteristic above the turnover point.

Among American-made lateral test records are Audiotone No. 78-1 (250 cps turnover), Columbia Frequency Record No. 10003-M (300 cps turnover), and R.C.A. Frequency Record No. 84522 (500 cps turnover). These are 78-rpm records intended for use with home record players. For broadcast test work R.C.A. Orthoacoustic No. 2485 (500 cps turnover) and Western Electric Test Record TRL-100 (250 cps turnover) 33⅓ rpm records are available.

Frequency characteristics of test records are sometimes supplied by the manufacturers, but they can also be obtained by measurement of the width of reflected light pattern[3], or by measurement with a phonograph pickup which is known to be substantially flat and to have low needle-point impedance.

Velocity-frequency characteristics of the above test records, as measured in the Shure Laboratory, are shown in Fig. 2.

Procedure for obtaining the playback characteristic of a test record in terms of a given recording curve is to subtract the desired recording characteristic from the frequency characteristic of the given test record. The resultant curve is the overall characteristic which will be exhibited by the playback mechanism when reproducing the test record with the playback adjusted to match the desired recording characteristic. This subtraction has been performed for the first five test records mentioned above in terms of the N.A.B. Standard. The resulting curves are shown in Fig. 3.

Precise adjustment of the playback characteristic requires measurement of the acoustical output of the loudspeaker when the pickup is playing the test record. In practice, when suitable acoustical measurement facilities are not available the pickup output voltage is measured across the amplifier volume control; the characteristic of the amplifier and the loudspeaker is then added to these readings to obtain the overall characteristic.

Crystal Pickup Characteristics

Two types of piezoelectric crystals are employed in phonograph pickups, the x-cut rochelle salt type and a new crystal developed by the Brush Development Company known as the PN type. Rochelle salt crystal pickups are characterized by high output voltage and high internal capacitance. PN crystal pickups have acoustical characteristics similar to the crystal pickups, with the added advantage of withstanding extremely high ambient temperatures without deterioration. On the other hand, PN crystal pickups have a low internal capacitance which requires careful design of the input circuit for optimum operation.

From the electrical standpoint, a piezoelectric pickup can be represented as a zero-impedance generator connected in series with a capacitance which is numerically equal to the capacitance of the crystal. This capacitance is approximately 1000$\mu\mu$f in the case of rochelle salt pickups, and is approximately 100 $\mu\mu$f in the case of PN pickups. The addition of a capacitive cable to the pickup terminals results, therefore, in a loss of output voltage without change in frequency characteristic. The loss in output can be calculated by considering pickup capacitance C_o and cable capacitance C_1 as forming a capacitive voltage divider. The loss due to cable, in decibels, is 20 log $(1 + (C_1/C_o))$, indicating the desirability of connecting the pickup to the amplifier with a cable having the lowest possible capacitance.

Phonograph pickups are generally connected to potentiometer-type volume controls. Because the internal impedance of the pickup is capacitive (and therefore increases at low frequencies), the addition of the volume control across the pickup causes a drop in output at low frequency. The added loss due to the shunting effect of the volume control resistance, in decibels,

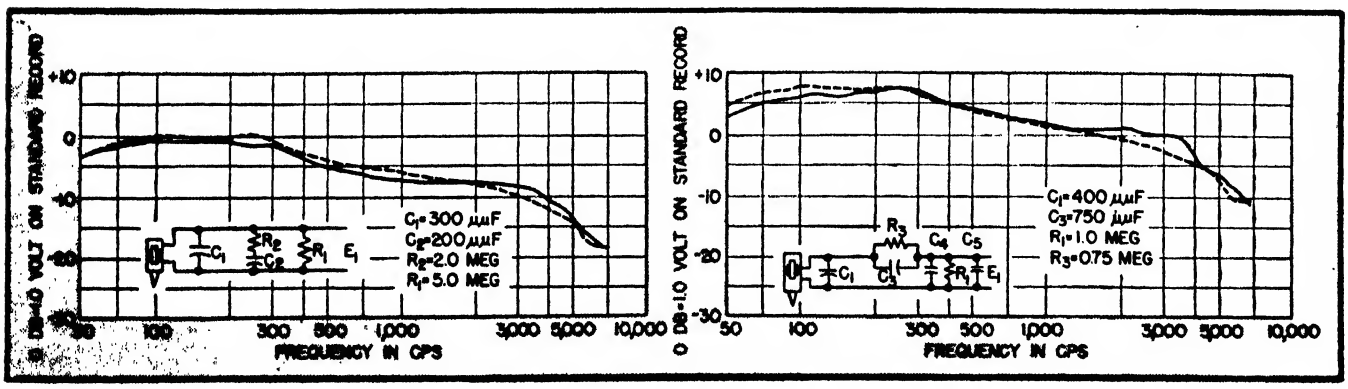

FIG. 6—Solid line is response of PN pickup cartridge with compensating network; dash line is Audiotone record response adjusted to N.A.B. Standard

FIG. 7—Similar curves to those of Fig. 6 but for crystal pickup. Both the curves of Fig. 6 and this figure are for response with bent-shank aluminum needle

equals 20 log $[1 + (1/\omega CR_1)^2]^{\frac{1}{2}}$ where C is the sum of the capacitance of pickup and cable $(C_0 + C_1)$ in microfarads, and R_1 is the volume control resistance in megohms.

Input-Circuit Loading

To illustrate the point, Fig. 4 shows the characteristic on an Audiotone record of a Shure P-87 rochelle salt pickup cartridge connected across resistances of 0.25 megohms to 5.0 megohms. In dotted line is shown the playback characteristic which should be attained on an Audiotone record in order to match the N.A.B. Standard Characteristic. (This is obtained from Fig. 3.) It is seen that with this particular rochelle salt pickup, a 1.0 megohm volume control provides the best fit to the N.A.B. characteristic.

Figure 5 shows the characteristic of a PN-87 type pickup cartridge connected across resistances of 1.0 megohms to 10 megohms. In this instance, a 5-megohm termination resistance provides the most satisfactory performance. (It should be noted that the 100-$\mu\mu$f capacitance of the vtvm leads has doubled the effective generator capacitance.) Where such high termination resistance is not desirable, it is permissible to connect a 0.0008-microfarad capacitor across the PN pickup. This expedient results in a 15-db drop in the output voltage, but good performance can then be obtained with a 1.0 megohm termination resistance or potentiometer volume control.

Pickup input circuits of the simple potentiometer type do not, in general, provide completely satisfactory performanee, but they can be employed in low-cost sets.

Low-Frequency Compensation

One of the earliest circuits employed for low-frequency compensation in piezoelectric pickups is shown in Fig. 6. The pickup is shunted by a series combination of capacitor C_2 and resistor R_2. At low frequency, R_2 is less than the capacitance of C_2, and therefore R_2 can be neglected. C_0, C_1, and C_2 form a capacitive voltage divider which reduces the low-frequency response evenly without frequency discrimination. At higher frequency, $X_{C_2} < R_2$ and the effects of the capacitor become gradually less important. In the design of this circuit, C_2 can be calculated from loss = 20 log $[1 + (C_2/C)]$ db, where C is the sum of the capacitances of pickup and cable, $(C_0 + C_1)$, based upon the desired low-frequency loss R_2 is adjusted to equal X_{C_2} at the frequency above which compensation is no longer desired.

Because of changes of capacitance of x-cut rochelle salt crystals with temperature, low-frequency compensation can vary several decibles over the temperature range of 76° to 90° F; however, if PN crystals are used this is not encountered. On the other hand, this circuit has the advantage of not being adversely affected by cable capacitance between the parallel branch and the volume control.

Figure 6 shows the Audiotone record response of a Shure PN-87 pickup cartridge connected to a network having the indicated circuit components. Response of this circuit matches well the playback characteristic of the Audiotone record adjusted to the N.A.B. Standard Characteristic.

Another low-frequency compensating circuit, introduced by the writer several years ago for use with rochelle salt crystal pickups, is shown in Fig. 7. It consists of a parallel combination of a capacitor C_3 and a resistor R_3 connected in series between pickup and volume control. This circuit presents a high impedance to the crystal at low frequency and therefore diminishes the effects of capacitance-temperature variations. In computing this circuit, R_3 and R_1 are treated as a voltage divider at low frequency. X_{C_3} is then made equal to R_3 at the frequency above which compensation is no longer desired. Stray capacitance C_4 and C_5 should be kept to a minimum to avoid a shunting effect upon R_1 at high frequency.

By the way of example, Fig. 7 shows the response-frequency characteristic of a Shure P-87 pickup employing a version of this circuit in which the network elements have the indicated values. By comparison with the N.A.B. Standard shown in broken line, it is seen that the two are in substantial agreement.

High-Frequency Compensation

Because the recording characteristic varies from one record to another, it is not feasible to specify with precision what response is apt to produce the most faithful reproduction. As has been pointed out, records appear to produce best fidelity when the response above 1,000 cps is flat on a constant velocity basis. Some of the newer recordings provide excellent results when played with a pickup adjusted in accordance with the N.A.B. Standards. For maximum flexibility, it appears best to have a pickup with an inherent high-frequency response somewhat higher than that required by the N.A.B. Standards. This response can be lowered, if necessary, by means of a conventional tone control circuit incorporated in later stages of the amplifier.

The high-frequency range most acceptable to the listener is determined, to a large extent, by surface noise. The surface noise energy content for various recording materials is shown in Fig. 8. Surface noise energy is distributed over practically all of the audible range on the basis of approximately equal energy content per cycle. Therefore, the effects of surface noise can be eliminated most easily by removing the higher end of the frequency spectrum, which contains the most surface noise energy per octave in the range where the ear is most sensitive to low level sounds.

Listener Tests

Distortion is another factor which has an important bearing upon the optimum high-frequency cut-off of the pickup. The origin of this distortion is (a) the relatively large radius of needle tip required

to track properly in conventional record groove[5], (b) distortion inherent in the process of duplicating commercial records, and (c) distortion which takes place in playback equipment. Distortion due to these causes can attain values as high as 15 to 20 percent on a direct measurement basis (not including intermodulation effects). Removal of response at high frequency is instrumental in reducing the annoyance caused by this type of distortion.

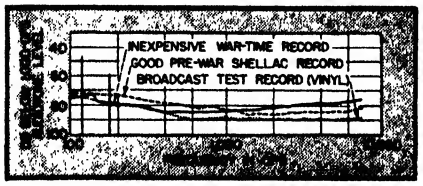

FIG. 8—Energy level per cycle of noise for various types of record material

The author has conducted a number of tests to determine the preference of listeners to high-frequency cut-off in the reproduction of home records. The tests were given to 100 non-technical listeners, and to over 100 radio engineers.[6] While a description of these tests is outside the scope of this article, the results given in Table I, although not conclusive, indicate that in the reproduction of home records, response above 5 kc exaggerates the effects of surface noise and distortion out of proportion to the improvement in fidelity. High-frequency cut-off can be obtained through the use of specially designed needles, or it can be obtained electrically with conventional low-pass filters.

The situation is, of course, totally different in the reproduction of broadcast-type transcriptions produced on low surface noise material and carefully processed to keep the sources of distortion to a minimum.

The author is grateful to the following persons for helpful discussion and for information regarding response characteristics: J. Dickert of Decca Records, Inc.; W. R. Dresser of the Audio-Tone Oscillator Company; H. S. Knowles of the Jensen Radio Corp.; V. J. Liebler of Columbia Recording Corporation; R. A. Miller of Bell Telephone Laboratories; A. A. Pulley and H. I. Reiskind of the Radio Corporation of America.

TABLE I—PREFERRED HIGH-FREQUENCY CUT-OFF

	Cut-off Frequency	Non-tech. Listeners	Technical Listeners
	3,000 cps	71%	13%
	5,000 cps	21%	58%
above	5,000 cps	8%	29%

REFERENCES

(1) Technical Standards and Good Engineering Practices for Electrical Transcription and Recordings for Radio Broadcasting, National Association of Broadcasters, Washington, D. C., Mar. 1942.
(2) Williams, A. L., Further Improvements in Light-Weight Record Reproducers and Theoretical Considerations Entering into Their Design, *Journal of the Society of Motion Picture Engineering*, Aug. 1939, p 203–222.
(3) Buchmann, G., and Meyer, E., A New Optical Method of Measurement for Phonograph Recordings, *E. W. T.*, 7, p 147, 1930.
(4) The method of obtaining this information and other factors affecting fidelity of phonograph reproduction were described by the author in a paper presented before the Chicago Section of the I.R.E. on Dec. 15, 1944.
(5) Pierce, J. A., and Hunt, F. V., On Distortion in Sound Reproduction from Phonograph Records, *Journal of the Acoustical Society of America*, 10, p 14, 1938.
(6) Method of administering preference tests and the results obtained were described in a paper presented by the author before the Acoustical Society of America on May 12, 1945.

Automatic Gain Control and Limiting Amplifier

An agc amplifier regulates the audio signal applied to a peak limiter so that the output is held constant to provide a high percentage of modulation in a transmitter or high level for recording or public address. A memory circuit holds the gain constant for a predetermined time to preserve dynamic range of program

By WILLIAM M. JUREK and JOHN H. GUENTHER

The automatic gain control and limiting amplifier (Progar) to be described was designed to bridge the gap between the physical limitations of broadcasting, recording, and public address equipment and the ability of operating personnel to maintain an efficient program level within these limits.

In broadcasting, dynamic limits are sometimes exceeded because of an operator's desire to maintain a high percentage of modulation at all times. Early attempts to alleviate this situation made use of peak limiting or compressor amplifiers at the transmitter. Unfortunately, this led to relaxing of critical monitoring. Operators relied upon the peak limiter to maintain a high average percentage of modulation, disregarding the fact that this statement holds true only when the proper signal level is fed into the peak limiter.

The Langevin 119-A unit was designed to be inserted between studio audio facilities and the transmitter. (Several have also been built by Royal S. Howard of the

Associated Broadcasting Company in San Francisco.) Figure 1 shows the sections into which it is divided, consisting essentially of an automatic gain control or guardian amplifier that provides a regulated audio flow and an improved type of peak limiter amplifier.

The input signal is first fed into the guardian amplifier and from there branches into two circuits, part going to the peak limiter and part going into the rectifying and memory circuit. The output of the rectifying and memory circuit controls the gain of the guardian amplifier. The output of the limiter also branches into two circuits, part going to the output load and part to the rectifier and bias control circuit which provides fast gain reduction action of the peak limiter amplifier.

Figure 2 shows the combined action of the guardian and limiter circuit. The lower graph represents the guardian action. The vertical axis represents the peak value of the input signal, and the horizontal axis represents the peak value of the signal at the output of the guardian circuit, which is also the input to the peak limiter. The vertical axis of the upper graph represents the peak value of the output signal.

Gain Control Action

The input controls are adjusted so that the average peak input signal is −31 db. The average peak into the limiter occurs at point *A*, which is at the knee of the curve, and the average peak output is +22 db, which is made equivalent to 80 percent modulation. As the body of the program material falls below the average peak, the full dynamic range of the material is reproduced due to the linear action of both amplifiers. Any transient peaks above the average peaks are compressed in the limiter section.

If the average peak value of the input should increase and remain there for any reason, as from −31 db to −21 db, the input to the limiter will increase to *B* and the average peak output will be +23 db, or 90 percent modulation. Under this condition, part of the body of the program below the average peaks will be compressed in the limiter. The gain of the guardian amplifier is then reduced to the −10 db control line so that the increased input produces an output from the guardian back at *A*, and the output from the limiter is again back at +22. The time for the guardian section to decrease its gain is much slower than the limiter attack time but is still too fast to be detected by the ear.

If, while the limiter is in this condition, the operator changes the input level back to normal (to −31 db), the input to the limiter will drop to *C* and the output signal to +12 db. The guardian section does not act immediately, but the memory circuit holds the gain constant for a predetermined time and then allows the gain to increase gradually to normal as represented by the zero control line. This wait time is relatively long and in present models is adjustable from 2 to 8 seconds. This long delay is provided to allow for station breaks and fadeouts as used in dramatic shows. If the action were extremely fast, the amplifier would try to maintain constant output continually and destroy the dynamic range of the program.

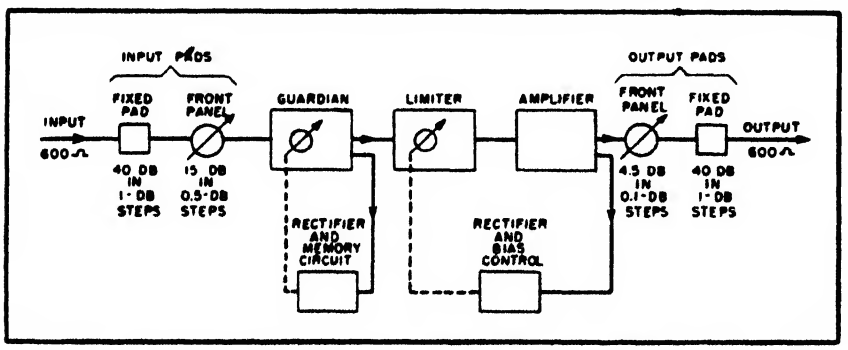

FIG. 1—Functions of the various stages in the amplifier

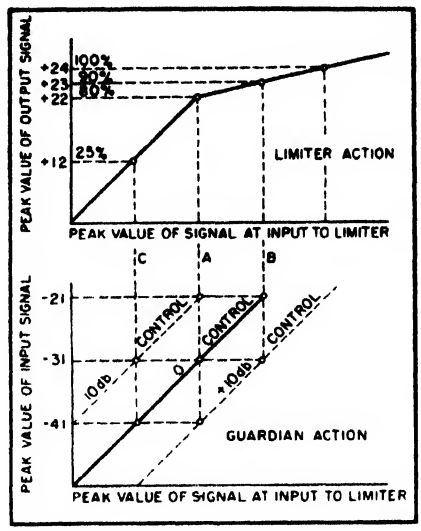

FIG. 2—Circuit action of the combined amplifiers at various levels

Should the average peak input signal level drop below its normal value, as from −31 to −41 db, with the corresponding output of +12 db, the guardian amplifier gain will again be held constant by the memory circuit for the predetermined time and will then slowly increase to the +10 db control line, bringing the output of the guardian amplifier back to normal. Upon restoring the input signal to normal again, the input to the limiter will be at *B*, and the limiter will instantly reduce this increased input signal to a safe output value until the guardian gain changes again.

The combination of the two amplifiers maintains a steady audio flow into the transmitter at all times. As is seen from the lower graph in Fig. 2, the gain-changing action of the guardian amplifier is not strictly of the compressor type, due to the action of the memory circuit. Therefore, even though the average dynamic range is changed, as it will be in any gain-changing amplifier, the dynamic expression is not affected.

Circuit

Figure 3 shows a schematic of the complete unit. The audio section of the amplifier consists of four push-

pull cascade stages with transformer input and output. The first two tubes are the guardian control section; the second stage is the limiter amplifier control section; the third stage is the linear amplifier section; the fourth stage is the power output section.

The control circuit for the guardian section consists of a two-stage resistance-coupled pushpull linear amplifier operating into a full-wave rectifier. The output of the rectifier feeds an RC circuit which builds up the d-c potential in proportion to the incoming program level. A portion of this potential is fed through the conducting diode, V_{12B}, into capacitor C_{22}. The voltage across C_{22} is then fed into the guardian amplifier control tubes. With the correct input signal applied to the tubes (−31 db), the bias of the tubes is established by the control circuit, mentioned above, to set the gain of the tubes in the center of the operating range. The purpose of this condition is to allow the tubes to increase or decrease amplification by approximately 15 db, thereby effecting the agc action.

If the incoming signal should be increased, additional potential is developed in the first RC circuit of the control section. Portions of this voltage are almost instantly transferred through conducting diode V_{12B} into C_{22}, increasing the control voltage on the tubes and thereby reducing the gain of the first stage and reducing the signal to the proper level going into the second stage. This circuit may be referred to as a reverse-acting control circuit whereby the operation of the circuit depends upon permissible error, which in this case is 1-db change in the output for a 10-db change in the input. Therefore, the action taken by the control circuit must be such that it produces enough control signal to reduce the incoming signal 9 db with only a 1-db increase in the output.

If the average peak of the input signal should drop from its normal value, the charging voltage will be reduced across C_{20}. If the signal is slightly reduced, no effective change will be produced on C_{22} because this capacitor may only be charged by V_{12B}, or discharged by V_{12A} and then only if the voltage of C_{22} equals the voltage of C_{20}.

This circuit is the heart of the guardian circuit, and is referred to as the memory circuit. This explains the reason why during a symphony concert the pianissimo passages are not affected, as some portions of it keep the first RC (C_{20}) charged sufficiently so as to prevent C_{22} from being discharged, thereby keeping the gain constant in the guardian circuit. Should the program drop completely, capacitor C_{20} would start discharging because no signal is being fed into the control circuit. As soon as the voltage across C_{20} equals the voltage across C_{22}, the conducting diode (V_{12A})

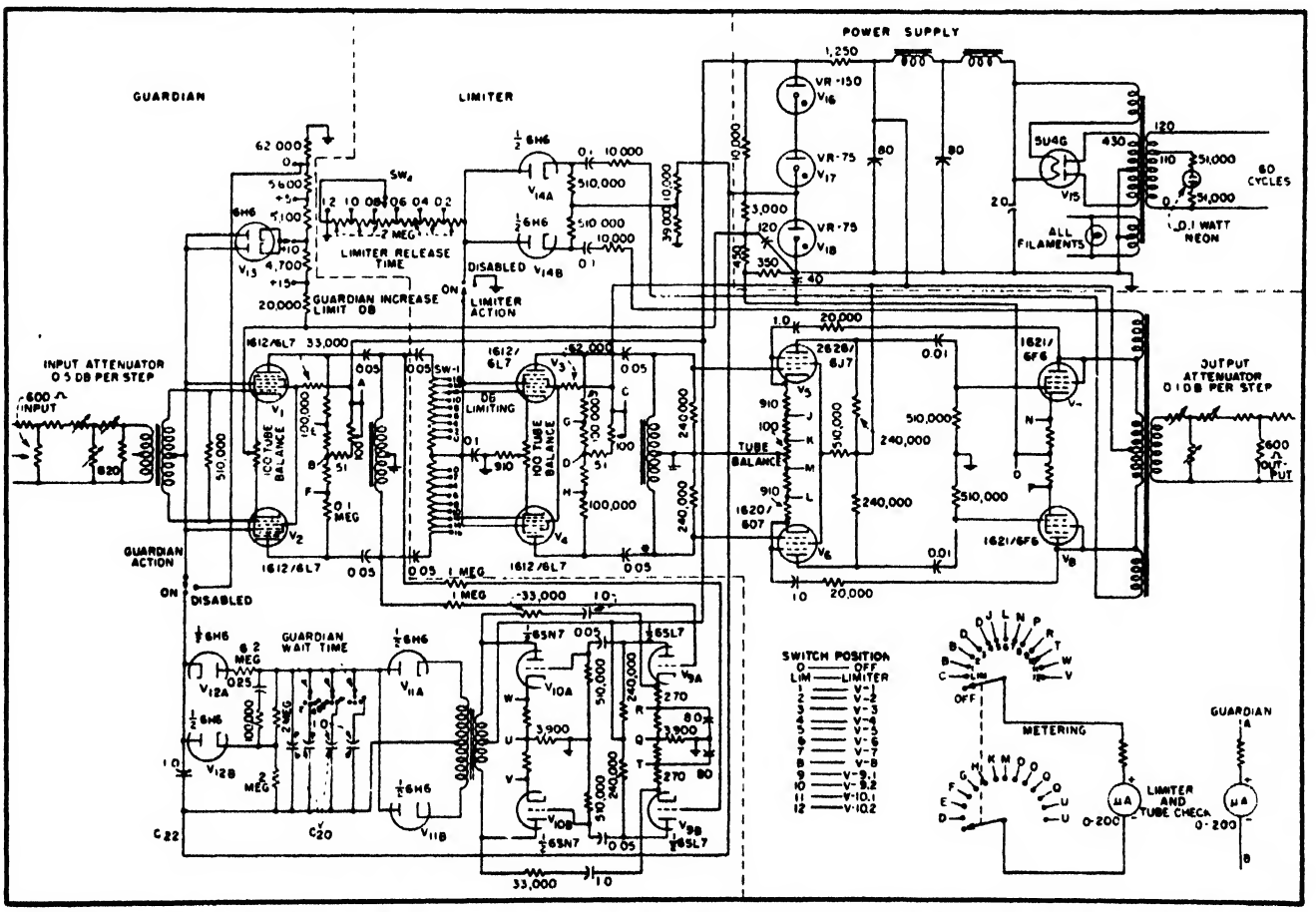

FIG. 3—The complete circuit is basically a four-stage audio amplifier, with added control circuits for the special functions

would start discharging C_{2a} at the same rate along with C_{2b}. This would reduce the control voltage, allowing the gain to increase in the guardian stage. This gain will increase to the limit determined by the setting of the guardian increase limit control. The purpose of the guardian increase limit control is to limit the maximum gain of the control amplifier when no signal is present. In average studio conditions, a 5-db limit is recommended. Ten and 15-db limits are provided for unattended service if the noise level of the preceding equipment will allow this additional gain.

A Guardian Action Disabling switch is provided for testing this circuit for normal gain conditions and for tube balance checks. This switch substitutes a fixed bias in place of the control circuit bias.

Guardian action is observed by measuring the combined plate currents of the guardian control tubes. This measurement is only relative as it measures the plate current of the tubes and is calibrated in terms of audio signal. A calibration control is provided to set the meter at zero position when the guardian action switch is in the disabled position.

The peak limiter section is composed of the last three pushpull stages, with a biased diode rectifier connected across the output. This rectifier rectifies a portion of the output voltage whenever that voltage exceeds the predetermined amount and applies that rectified voltage as a bias to the limiter input stage.

The limiting action is also a reverse-acting control circuit, and is designed to operate at a 10:1 control ratio, whereas a 10-db increase in input signal produces only a 1-db increase in output signal above the predetermined peak value.

The output of the guardian section is so adjusted that when the limiting control is in the zero position no limiting action takes place on normal program material. Due to the slow attack time of the guardian circuit normal transients appearing in the signal have no effect on the guardian control circuit and are passed on to the limiting section where they are reduced by the control action of the limiter. This also explains why steep wave front tones such as certain piano tones and cymbal crashes have little or no effect on the guardian action, and if dangerous to the transmitter are reduced to a safe value by the limiting action.

Circuit Tracking

Reverse-action control circuits were selected for both of the control circuits in place of forward-acting control circuits because of the extended range of control without cutting off the amplifier. Forward-acting circuits give difficulty in maintaining the control action over a range greater than 13 db. After that point, they have a tendency to cut off the controlled amplifier completely, thereby producing noticeable holes in the program material if the peaks should exceed the normal operating range encountered in practice.

The forward-acting control circuits receive their control voltage from the input of the amplifier and must develop the control voltage that will track along with the control action of the variable-gain tubes. The control circuit rectifiers produce a voltage that is linear to the input voltage, while the controlled tubes require a logarithmic voltage. Therefore, the tracking of a forward-acting circuit is difficult to control over an extended range.

In the reverse-acting control circuit, tracking is no problem as the circuit is selfbalancing, working on permissible error, and control action is automatically extended beyond the required 30 db.

Semifixed and variable attenuators are provided at the input and output to adjust the input signal and provide the unit with the proper input signal of −31 dbm (db referred to a zero level of 1 milliwatt), and to adjust the output of + 22 dbm to correspond to 80 percent modulation at the transmitter. These input and output levels must be established before putting the unit into operation.

Semifixed pads with a 40-db range are provided at the input and output to allow the unit to be substituted in place of the conventional line or program amplifier or inserted as a zero-gain device at the transmitter audio input.

Common Power Source

The power supply is conventional with VR regulator tubes stabilizing the critical voltages such as the guardian circuit and the limiter diode bias. It is recommended that the power supply be operated from the same a-c power source as the modulating stage of the transmitter. This is to allow for the variations in the line voltage that will change the modulation capabilities of the transmitter and will also change the output capabilities of the Progar, and will therefore maintain a uniform maximum operating point of both units simultaneously. If a well-regulated power supply is used, a constant fixed output will be maintained, and as the line variations affect the modulation capabilities of the transmitter the full benefits of the control action could not be utilized.

For network operation, it is advisable to use one unit at the studio with the limiter action disabled, and a second unit at the transmitter with the guardian action disabled. The reason for this recommendation is that if the two limiters are used in cascade with different release times, a pumping action will be noticeable on some program material.

Dynamic Suppression of Phonograph Record Noise

By controlling the bandwidth of an audio amplifier automatically in accordance with the characteristics of the recorded music, suppression of high and low-frequency noise may be achieved without noticeable injury to the realism of reproduction

By H. H. SCOTT

THE MOST OBVIOUS shortcoming of ordinary reproduction of music from phonograph records is the presence of the high-frequency background noise level caused by minute irregularities on the surface of the record. Although this noise is more or less random in character, the most annoying part of it is concentrated in the same frequency range as the upper musical harmonics. Any attempt to reduce it has heretofore been accompanied by a serious attenuation of these harmonics and often of some of the higher musical fundamentals also.

For years, it has been recognized that the most satisfactory simple means of controlling noise is by controlling bandwidth, using as sharp a cutoff as possible beyond the desired band and a minimum of attenuation within the band. The reproduction of phonograph records represents about the only phase in the field of electrical reproducing where this precept has been generally disregarded. There are several reasons for this. One is that the commonly used crystal pickup, when operated into a high-resistance load, provides conveniently a drooping frequency characteristic or high-frequency rolloff without the use of any additional parts. Another is that phonograph records have been made with various degrees of high-frequency preemphasis, and a single tone control adjusting the rate of rolloff can be used either to compensate for the recording characteristics or to reduce noise, the latter of course always at the expense of fidelity. The third and perhaps most important reason is that a sharp cutoff frequency sufficiently low to reduce the noise level appreciably makes such a deep excursion into the range of lower overtones and higher fundamentals of the music as to produce an extremely unnatural and mechanical quality at high volume levels.

To a secondary degree there are also present low-frequency noises or rumbles, which may be in either the record or the turntable, and which are noticeable during soft passages which do not contain many low frequencies. The present tendency to use large amounts of bass boost or automatic low-frequency compensation greatly exaggerates any rumble that may be present.

High-frequency and low-frequency noises are present at substantially constant level during the playing of a record. Hence they are most noticeable during soft passages and least noticed (often masked completely) during loud passages. The noise suppressor described in this paper is a device which controls the bandwidth of reproduction automatically and continuously as a function of the volume and frequency characteristics of the music, extending the band during the loud passages and contracting it during the low-level portions, the variation in bandwidth being independently controlled at both ends of the spectrum. Thus the noise is reduced when it would be most noticeable, and full bandwidth is used when it is most necessary, at high levels. This automatic contraction and extension of the bandwidth has but a negligible effect on the apparent realism of reproduction, because of the threshold characteristic of the ear and the distribution of energy in musical sounds as described below.

Music and Hearing

Curve *a* in Fig. 1 shows the threshold of hearing[1] for an average person, in terms of frequency. Sounds below this curve are inaudible. The distribution of the most probable amplitudes of the various frequency components involved in typical orchestral music[2] is shown by curve *b*. This may be moved up and down by varying the volume level of the reproduction as shown in curve *c*, but it will be noted that it always intersects curve *a* at definite points in both the low and high-frequency ranges. For any particular position of curve *c* and for the type of signal represented by curve *c*, all frequencies above and below these high and low-frequency limits, respectively, may be neglected so far as being of any importance to the listener is concerned, since he will not be able to hear them.

As a practical matter, if the reduction of volume is obtained by the musicians playing more softly, the shape of curve *c* will actually be altered to something more like curve *d*, showing still greater reduction in amplitude at the higher frequencies. This is the result of the well known fact that most musical instruments produce purer tones (less harmonics) when played softly than when played loudly. It

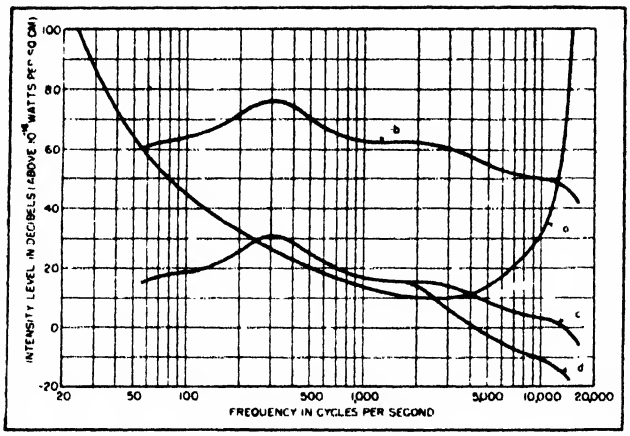

FIG. 1—Typical threshold of hearing (a) and most probable distribution of frequency components in music at high levels (b), with volume control turned down (c) and with orchestra playing softly (d)

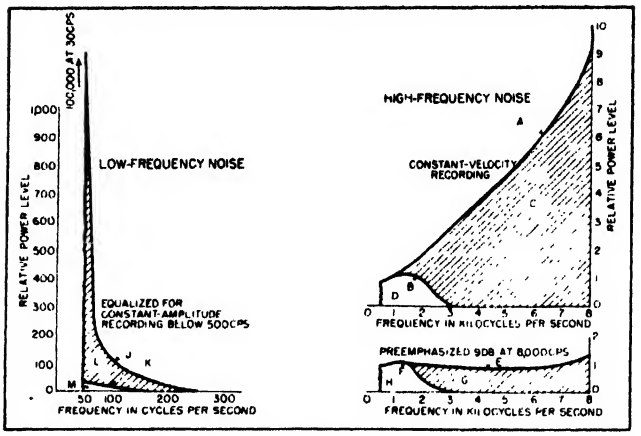

FIG. 2—Relative noise level per cycle bandwidth at high and low frequencies, when reproducing shellac records with and without dynamic noise suppressor. Shaded areas represent degree of noise reduction

will be noted that at low levels curve *d* may cross the threshold curve at a high-frequency limit as low as 2500 cycles.

Theoretically, then, when listening to low-level orchestral music of the type indicated, insertion of a 2500-cycle low-pass filter will produce little or no change which is obvious to the listener. This is actually borne out by listening tests. But the introduction of the filter results in a tremendous decrease in needle scratch. This is true because most of the scratch noise is high-frequency noise and its level is well above the threshold of hearing.

A similar situation exists at the low-frequency end of the range. Here again, reproduction of those components which fall below the threshold of hearing results in no worthwhile improvement in the quality of the signal but may cause rumble noise which is considerably louder than the desired signal components.

If, therefore, some system is devised which automatically cuts off sharply in response characteristics for the ranges including those components of a signal which are at too low a level to be heard, the apparent quality of reproduction will not suffer, and the signal-to-noise ratio will be improved to a worthwhile degree. The present state of the electronic art allows practical accomplishment of this objective in several different ways, with varying elaborateness of equipment.

Degree of Noise Reduction

The amount of audible noise reduction obtained with the system under discussion is difficult to express in simple terms, since it depends so much upon the high-frequency hearing of the individual, the effect of auditory masking of the small remaining noise by the music signal, and various psychological factors dealing with annoyance and personal preference.

A relatively simple system can be made to give more than 20-db attenuation to high-frequency and low-frequency noise, with substantially no attenuation within the pass band. A narrow band of noise is all that is left, and it is so situated (in shellac records) that it coincides with the point of minimum noise energy. It also lies within the musical spectrum, so that it is easily masked by even low-level music. In general terms, it may be said that the suppressor reduces the noise level from a point where it is distinctly annoying to a point where it is practically eliminated on the best records and practically unnoticeable on the worst records.

The only fair proof of the effectiveness and true value of the dynamic noise suppressor is in actual listening tests. Figure 2 has been prepared in an attempt to give a graphical portrayal of the amount of noise reduction. Curve *A* represents typical noise level per cycle bandwidth on a standard-grade shellac record.[3] The variation among records is very great, and while some high-quality records, particularly of the Vinylite type, may be noticeably quieter, many records, particularly if at all worn, produce far higher noise levels in the high-frequency range.

Curve *A* represents the relative noise level at various frequencies in terms of power level, as reproduced with a flat overall characteristic from a constant-velocity recording. The total area *C* plus *D* under curve *A* represents the total noise, since a linear frequency scale is used. Similarly, curve *B* represents the remaining noise spectrum when using the dynamic noise suppressor and the area *D* under this curve represents the remaining noise energy. Visual comparison of the area *D* with the total area *C* plus *D* gives some idea of the amount of noise reduction obtained on the physical basis of overall noise energy. It will be noted that the area *C*, representing the amount of noise eliminated by the dynamic noise suppressor, comprises all but a very small portion of the total noise energy, and that the most annoying noise, which

occurs in the higher frequency ranges, is eliminated entirely.

Preemphasized recordings have been used increasingly in recent years as a means of obtaining an improved signal-to-noise ratio. While record companies have not published data as to the exact amount of preemphasis used, indications are that 9 db at 8000 cycles is typical of records which have been widely sold. If the reproducing system is provided with an equivalent amount of deemphasis, the curve *A* becomes the curve *E*, and curve *B* becomes curve *F*. The total area *H* plus *G* represents the total noise, while *G* represents the relatively large proportion eliminated by the suppressor and *H* is the relatively small amount of remaining noise, which is even smaller than the equivalent area *D* without preemphasis.

Figure 2 shows also the low-frequency noise taken from Bauer's data (which were on a constant-velocity basis), adjusted for the normal reproducing characteristic used with a 500-cycle turn-over point between constant-amplitude and constant-velocity recording. It should be noted that the scales for the low-frequency chart are different from the high-frequency charts in order to provide satisfactory illustration of the noise-reduction effect. The break between the low and high-frequency charts was positioned at 500 cycles, which is a conventional crossover point in recording characteristics. It will be noted from curve *J* that low-frequency noise increases rapidly below 200 cycles, reaching a power level 1000 times as high at 50 cycles as at 1000 cycles, and still 100 times higher at 30 cycles. This illustrates why many record-reproducing systems have incorporated low-frequency cutoff circuits to reduce rumble trouble and acoustic feedback.

The action of the noise suppressor is the opposite of the low-frequency noise characteristic in that the noise attenuation increases as the frequency is decreased. Consequently, the remaining noise is approximately as shown by curve *K*, and is negligible at even very low frequencies. The total area *L* plus *M* represents the total low-frequency noise, the area *L* being that eliminated by the suppressor, and the area *M* representing the remaining noise. It will be noted that *M* represents a negligible part of the total noise area. Use of the suppressor is consequently of tremendous benefit in systems having extended or boosted bass response, and the suppressor becomes more important as the bass response is improved.

Aural Balance

There is a further important advantage in the simultaneous control of the low and high frequencies which is totally independent of the noise-suppression effect but is of prime importance in presenting what to the ear appears to be constant reproduction of a wide frequency range.

It is well known that restriction of one end of the frequency range is less noticeable if the other end of the range is also restricted, thus maintaining substantially constant the product between the high-frequency and the low-frequency cutoffs of the system. Of course, if the noise-suppression system were perfect, and the frequency ranges attenuated always fell beyond the range of audibility, the question of maintenance of aural balance would be of no importance, since, so far as the ear could determine, there would be no restriction of the frequency range. As a practical matter, however, this theoretically ideal condition is not always obtained.

Many people like to operate their radios or phonographs at a fairly high level, and, particularly where a high degree of compression is used in the transmission or the recording, the low-level portions of the program may be heard at a higher level than normal. This is also true for people sitting unusually close to the loudspeaker when the volume is adjusted for satisfactory level in a fairly large room. Under either of these conditions, the range during the low-level portions of the program may be restricted somewhat within the audible limits. Also, all program material will not follow exactly the actual frequency distribution of the curve *d* of Fig. 1. In fact, the actual frequency distribution of the music is constantly varying not only from orchestra to orchestra or from instrument to instrument, but also from instant to instant. Any curve such as those of *c* or *d*, therefore, represents merely an average condition.

Since these particular curves are based upon most probable levels, variations will normally fall below the curves, but occasionally variations will fall above the curves, and under these conditions also, if the variations occur at very high or very low frequencies, the aural balance might be upset. Independent control of low-level high-frequency cutoffs provides best fidelity for a wide range of signal types and best aural balance for variations in listening conditions.

A third condition goes back to the generally accepted reaction of the average listener in regard to noise versus high fidelity. Under conditions where a choice between fidelity and noise must be made, the listener will generally choose that condition which keeps the noise level practically inaudible during the actual program. With extremely noisy records, this may make desirable the setting of the control and gate circuits so as to provide somewhat greater frequency-range restriction, particularly at low levels, than that implied from theoretical considerations of curves *a* and *d*.

These conditions indicate the desirability of a system controlling both low and high frequencies, a desirability sufficiently great, in fact, to warrant control of both ends of the frequency spectrum even under conditions where noise is encountered at only one end.

Gate and Control Circuits

The heart of the noise-suppression system is a controlled bandpass filter known as the gate circuit. It has extremely sharp cutoff charac-

teristics, particularly for the elimination of high-frequency noise. For varying applications, depending upon the type of signal and the type of noise, lowpass, bandpass or band-elimination characteristics may be desired. For the disc record application a bandpass characteristic is preferred, with a sharp cutoff at the high-frequency end. The sharpness of the low-frequency cutoff is of somewhat less importance, but a slope steeper than that obtained with the ordinary single-stage R-C tone control is desirable. The gate circuit is capable of rapid control without introducing audible thumps into the output.

The control circuit which actuates the gate circuit adjusts independently and continuously both high and low cutoffs of the system, so that they always coincide with the respective points of intersection of the curves for the threshold of audibility and the frequency distribution of the particular signal. The control must be sufficiently fast to permit satisfactory reproduction of transient sounds and to follow each individual note in the music, so that noise shall not be heard in the background between adjacent notes in music of a staccato or percussion character, such as from the piano. When properly operated, the system shows no noticeable evidence of a rising and falling background noise varying in accordance with the musical signal.

The noise levels encountered in the upper and lower frequency ranges over which the cutoffs may be varied are considerably higher than the musical components existing in those ranges, except during a small portion of the playing time. Consequently the sensitivity of the control circuit must be reduced in the ranges over which the cutoffs are controlled in order that control shall reside in the signal, rather than in the noise or rumble. This is very satisfactorily arranged when the reproduced signal is music, since the extremely high harmonics exist only with fundamentals of somewhat lower frequency, and control of the high-frequency cutoff can be exercised in accordance with musical components below the controlled range. Similarly, the deep bass fundamentals are accompanied by harmonics of appreciable amplitude which may be used to control the low-frequency cutoff.

Practical Equipment

The noise suppressor for home phonograph use involves only three vacuum tubes, two in the gate circuit and one in the control circuit, and this third and latter tube may often be combined with one of the tubes already in the set. Furthermore, the gate circuit may be made with an adjustable maximum bandwidth or rolloff and thus may be used to replace some of the usual tone-control circuits in the receiver and the 10-kc whistle filter for a-m reception, so that the additional parts required to include the suppressor in a radio-phonograph are few in number.

Further elaboration of the gate and control circuits will produce many advantages such as wider frequency range, lower distortion, lower hum level, greater flexibility of control, and the ability to cope satisfactorily with a wider range of signal and noise types. The first three of these characteristics are of relatively little importance in home radio-phonograph, since even the simpler circuits exceed the normal requirements of home radio-phonograph design in these respects. The other improvements involve too many extra parts and tubes for inclusion in the average home receiver. On the other hand, for broadcast applications, the best possible performance is more important than the actual cost of the equipment, and for these applications, a considerably more elaborate form of the noise suppressor has been designed and is pictured here.

References

(1) Smoothed version of data presented by Steinber, Montgomery and Gardner. Results of the World's Fair Hearing Tests, *Bell Sys. Tech. Jour.*, 19, p 533, October 1940.

(2) Prepared by Ralph P. Glover, based upon data published by the Bell Telephone Laboratories. See also "Frequency Range and Power Considerations in Music Reproduction", published by the Jensen Radio Mfg. Co., and Harvey Fletcher, Hearing, the Determining Factor for High-Fidelity Transmission, *Proc. IRE*, 30, p 266, June 1942.

(3) Smoothed version of data used by B. B. Bauer, Crystal Pickup Compensation Circuits, ELECTRONICS, p 128, Nov. 1945.

Dynamic Noise Suppressor

Complete technical details of a system that provides essentially noise-free reproduction from phonograph records and transcriptions. Circuits are given for a 2-tube phonograph version and a 10-tube broadcast model

By H. H. SCOTT

A DYNAMIC band-pass system for separating signals from noise, as exemplified in the dynamic noise suppressor described here, provides what many consider the most satisfactory method of utilizing the maximum frequency range of a modern phonograph record or transcription while minimizing rumble, needle scratch, and other extraneous noises usually associated with recorded music.

The dynamic noise suppressor is now in regular use in a number of broadcast stations, both a-m and

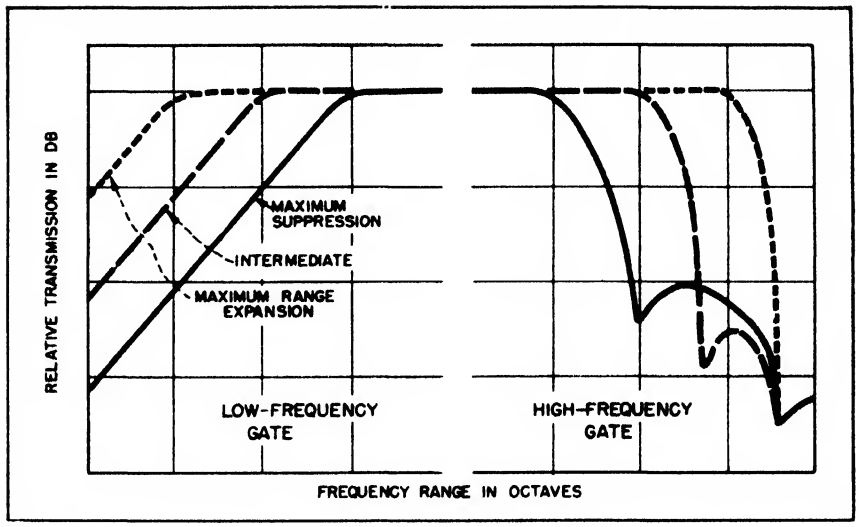

FIG. 1—Transmission characteristics of dynamic noise suppressor for conditions of maximum range expansion, intermediate suppression, and maximum suppression

f-m. The suppressor has also been adopted by several manufacturers of high-fidelity radio-phonographs, and the circuits are now being engineered into less expensive sets.

It should not be inferred that the system to be described is the only one which has ever been proposed. Although little has appeared in technical literature, a number of investigators have worked on the problem. Included among these investigators are Carlisle, Devine, Hammond, Heising, Llewelyn, Olson, and Purington.

The systems proposed have included volume expanders, circuits nonlinear with respect to amplitude, and automatic tone controls. Some of these have been used in commercial equipment. For instance, the volume expander or dynamic amplifier was used in certain models of RCA phonographs and is still used in some public address amplifiers. The automatic-tone-control type of noise-reduction system was used for several years in prewar receivers manufactured by the Scott Radio Laboratories.

Basically, noise-reduction systems fall between two extreme types—the dynamic band-pass system, in which the frequency range or pass band is varied in accordance with some characteristics of the signal, and volume-expander types in which the overall amplification or gain of the system, either effective or actual, is increased and decreased in accordance with some characteristics of the signal. In terms of the overall transmission-versus-frequency characteristics of a system as plotted in a conventional manner with a horizontal frequency scale and a vertical transmission scale, the dynamic band-pass system represents a horizontal change, while the volume-expander system represents a vertical change.

Noise reduction systems may also be designated as class A or class C, the terminology being borrowed from the similar applications in amplifiers. A class-A system is one in which, except for any filtering action, the output wave-form is a replica of the input wave-form. Such a system is linear with respect to amplitude so far as any cycle of the signal wave-form is concerned. A class-C system is one in which the output current flows only during a portion of the cycle of the input voltage. For very small input voltages, practically no output current will flow, and hence noise or signals below a certain level will be attenuated. This type of system depends upon amplitude nonlinearity for its noise-reducing action, which naturally results in distortion.

When only a single sine wave is being transmitted, the output wave-form of a class-C system can be restored by means of filters, and octave band-pass filters are conventionally used. However, even the best octave filter will not eliminate many higher-order intermodulation products such as $2f_1 - f_2$ or $2f_2 - f_1$ which may be of considerable magnitude in such a system when reproducing low-level signals.

Vertical noise-reduction systems include both class-A and class-C systems, the former being the volume expander in various modifications and the latter utilizing biased rectifiers or other barriers to obtain a class-C transmission characteristic.

The first requisite of a noise-reduction system is ability to reduce noise. To this end it is often desirable to control the transmission characteristics in accordance with some features of the signals not present in the noise. In the dynamic noise suppressor and other class-A systems this is possible because the control function may be divorced entirely from the controlled circuits.

Fuzz and Swish

Any noise-reduction system has certain limitations. The maximum bandwidth should be restricted somewhat when the noise level is excessive, so that in the loudest portions of the signal the noise is not heard superimposed on the music as a fuzz. A system with definite time constants is desirable, but if the time constants are made too long, loud notes may also be followed by an annoying swish.

Both fuzz and swish may be kept at a minimum only when the bandwidth transmitted at any instant is limited to that required by the signal. This is possible in the dynamic band-pass or horizontal type of system. In a vertical system, transmission in an entire frequency band increases and decreases as a unit

This paper was presented at the 1947 National Electronics Conference in Chicago.

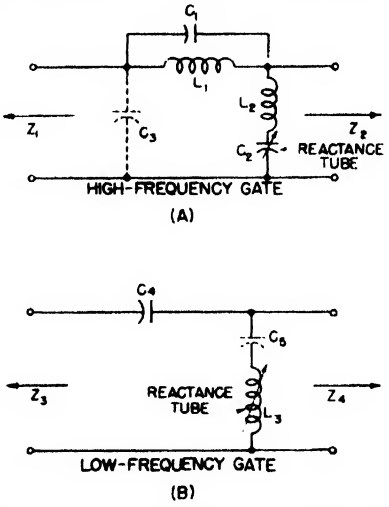

How It Works

Signal-controlled reactance tubes in these basic filter circuits act as gates that move the ends of the audio response curve inward and outward continuously and independently to let only the desired audio modulation through.

All noise signals in portions of the spectrum not having audible music components at a particular instant are suppressed.

Fundamentals of desired high-frequency notes are filtered out and rectified by a control circuit to change bias and hence capacitance of C_2 in high-frequency gate, and harmonics of desired low-frequency notes similarly vary inductance of L_3

FIG. 2—Basic gate circuits used to provide the continuously shifting response curves of Fig. 1

whether or not the entire band is required. This causes considerably more fuzz than in a horizontal type of noise suppressor.

The amount of objectionable fuzz is also a function of the smoothness with which the transmission characteristic is altered. In this respect, class-A systems are preferable to class-C systems, since with the latter the noise tends to pop in and out instantaneously at a given volume level.

The class-A horizontal system can be designed with an opening time-constant sufficiently long to provide suppression of loud clicks and similar transient disturbances, but not long enough noticeably to alter the reproduction of musical transients such as the crashing of cymbals. In similar cases where a high degree of suppression is used, the closing time-constant can be made long enough to prevent any effect of deadness resulting from removal of reverberation.

In actual practice, the closing time-constant is adjusted for the best compromise between reverberation and freedom from swish. Such factors are not controllable in the usual class-C noise-reducing system which operates instantaneously, tending to transmit all loud transient noises such as clicks and, when set for a high degree of suppression, to remove considerable reverberation.

In the vertical type of class-A system (the volume expander), such time constants sometimes provide serious problems in regard to the correct reproduction of musical transients, but with the class-A horizontal system (the dynamic noise suppressor), reproduction of musical transients is easily accomplished since the transmission is not altered in the frequency range which contributes most to the loudness of the signal.

Performance of Dynamic Noise Suppressor

In general, the dynamic noise suppressor causes less difficulty with fuzz than other types. It allows complete freedom of choice in any compromise which may have to be made between loss of reverberation and swish, while simultaneously allowing significant reduction in the amplitude of clicks and transient noises as well as the hissing type of surface noise. If volume expansion is desired for its own sake, the expander performance will be noticeably better when used with a dynamic noise suppressor, since the resulting reduction in noise level will tend to eliminate swishes resulting from the volume expander.

There are other noise-reducing systems intermediate between the true vertical and horizontal types and operating in much the same manner as automatic tone controls; in other words, the high-frequency end of the transmission characteristic is rolled off at a slight angle which decreases as the signal amplitude increases. Such systems are of the class-A type, but more closely resemble the vertical than the horizontal in general performance characteristics. If the noise reduction here is sufficient to be worthwhile, the change in tonal balance generally becomes noticeable because of the varying attenuation of signal components in the middle portion of the frequency spectrum.

While the dynamic noise suppressor makes previously useless records usable again, music lovers will generally find it an even greater advantage on modern high-quality records, where the noise level is not excessive but is still noticeable and annoying. Such records have a sufficiently wide frequency range to render undesirable any noticeable range restriction as a means of reducing noise. Playing such records with a wide-range dynamic noise suppressor eliminates the background noise without impairing tonal quality.

Response Curves

The number of circuits which can be used to obtain a dynamic band-pass system is almost limitless, but in any practical application it is desirable to secure the maximum of performance with a minimum of cost. It is therefore necessary to determine the minimum operating characteristics that will provide satisfactory performance, and use the minimum number of components to obtain these characteristics.

The first operating requirement is a sharp cutoff, particularly for the high-frequency gate circuit, since the most annoying scratch noise is concentrated in the high-frequency portion of the spectrum. Typical gate circuit curves which can be obtained with simple circuits and which have proved satisfactory

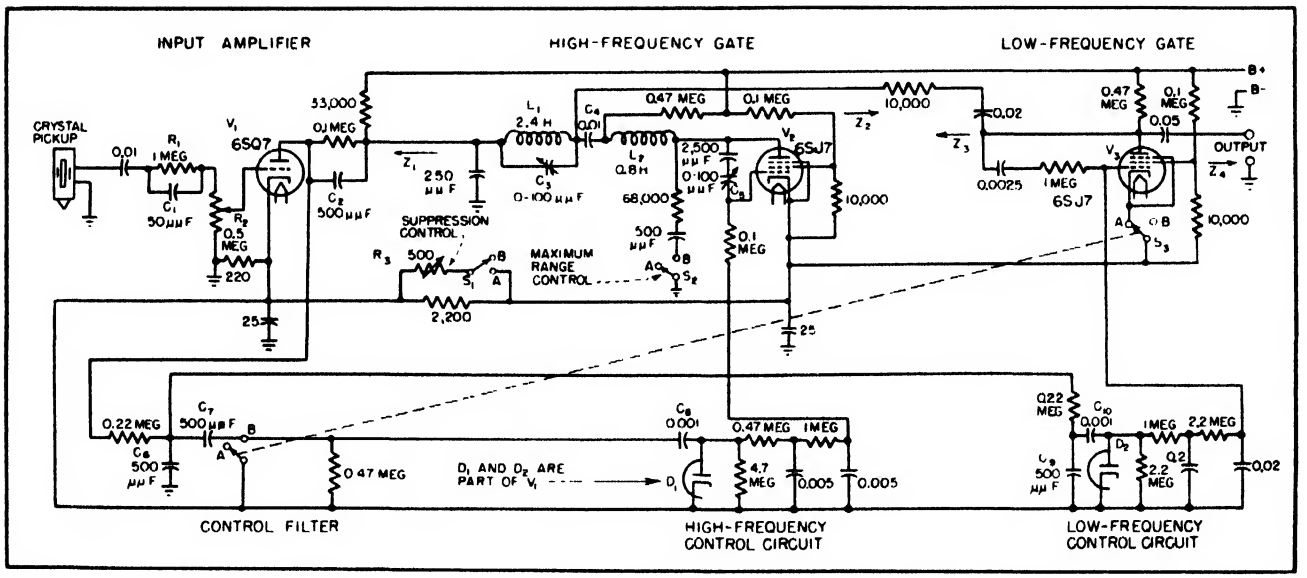

FIG. 3—Circuit of two-tube dynamic noise suppressor as incorporated in a home phonograph, with additional amplifier stage for coupling crystal pickup to suppressor circuit

in actual commercial applications are shown in Fig. 1. In normal suppressor operation, these are not static transmission characteristics, but vary rapidly from one extreme to the other in accordance with the requirements of the music or other signal. The vertical scale may typically represent 10-db intervals, while the horizontal scale may typically represent octaves.

The shape of these curves can be controlled considerably by proper choice of circuit constants and terminating impedances. If the shape of the curve in the neighborhood of the high-frequency cutoff is changed too abruptly, a disagreeable ringing may result, although with a dynamic system much more of this can be tolerated than with a static system.

Beyond cutoff, a maximum suppression of approximately 20 db below the normal flat response curve provides adequate noise reduction. Any further attenuation is definitely beyond the point of diminishing returns unless the system is capable of being adjusted to provide considerable high-frequency or low-frequency boost.

The function of the low-frequency gate circuit is to suppress hum, rumble, and other low-frequency noises and to maintain tonal balance, even under conditions of extreme noise suppression. A cutoff sharper than a simple RC or LR circuit affords is desirable. While exactly the same types of curves may be obtained at the low end as at the high end if economically justified, in practical applications the general shapes shown for the low-frequency gate are adequate. This is partly a result of the general nature of low-frequency noises —hum, rumble, etc—which tend to be harmonic in character rather than random.

High-Frequency Gate

A simple gate circuit that can be varied to provide the high-frequency cutoff and attenuation curves of Fig. 1 is given in Fig. 2A. Such a circuit may be considered roughly as a combination of a series m-derived and a shunt m-derived filter. The points of high attenuation caused by resonance in the series and shunt arms do not coincide except momentarily and in a random fashion while the cutoff frequency is varied by the signal. Normally, when the greatest suppression is taking place the points of high attenuation are separated by an octave or more.

Varying C_2 in Fig. 2A changes not only the cutoff frequency, but also the point of high attenuation determined by series resonance between L_2 and C_2 in the shunt arm. This provides a sharp cutoff with a high degree of attenuation just above the cutoff frequency.

In a practical gate circuit, C_2 is a reactance tube. The series-arm parallel resonance between L_1 and C_1 provides a fixed point of high attenuation which maintains attenuation at higher frequencies and provides high attenuation above the normal operating range or, when used on a-m, serves as a whistle filter.

Addition of C_3 maintains attenuation at still higher frequencies above the upper (fixed) null point when necessary. In more elaborate gate circuits, C_3 may be replaced by another reactance tube to provide still greater control range.

Impedance-Matching Problems

According to classical filter theory, filters should be terminated in certain definite impedances in order to provide satisfactory operating characteristics and freedom from undesired resonances. Where one of the important filter elements such as C_2 is variable, this poses a serious problem.

Impedance Z_1 across the input is most critical when C_2 is at a maximum and the cutoff point is, accordingly, at a minimum. Under these conditions Z_1 may be selected

to control the shape of the cutoff curve so that a wide range of possible contours can be obtained, ranging from a gradual roll-off to a resonant type of cutoff having a definite peak. The effect of varying Z_2 will then be relatively unimportant so long as Z_2 is maintained reasonably high.

On the other hand, when C_2 is reduced in capacitance and the cutoff frequency consequently increased, the circuit impedance increases, and the shunting effect of Z_2 becomes important. Under these conditions, the shape of the cutoff curve is controlled mainly by Z_2 and only secondarily by Z_1. By proper selection of operating impedances, therefore, the curves for minimum and maximum high-frequency response can be adjusted more or less independently, with a gradual transition at intermediate bandwidths.

For wider-range suppressor action, a second reactance tube may be added in place of C_2. For greater suppression, as in systems with unusual amounts of high-frequency noise or high-frequency boost, other sections may be added to the gate circuits.

A typical low-frequency gate circuit is shown in Fig. 2B. The variable inductance is obtained at low cost by means of a reactance tube. Such a circuit will provide low-frequency cutoffs approximating those shown in Fig. 1. Again, through proper selection of terminating impedances Z_3 and Z_4, it is possible to control the cutoff shapes to a high degree over a wide range of cutoff frequencies. If desired, the circuit can be expanded to m-derived and more complex forms.

Home Phonograph Model

The circuit of Fig. 3 shows a complete dynamic noise suppressor unit such as might be used on a phonograph, including an amplifier stage for coupling the crystal pickup to the gate circuit and for providing the necessary driving signal voltage for the control circuit.

Amplifier stage V_1 is not required

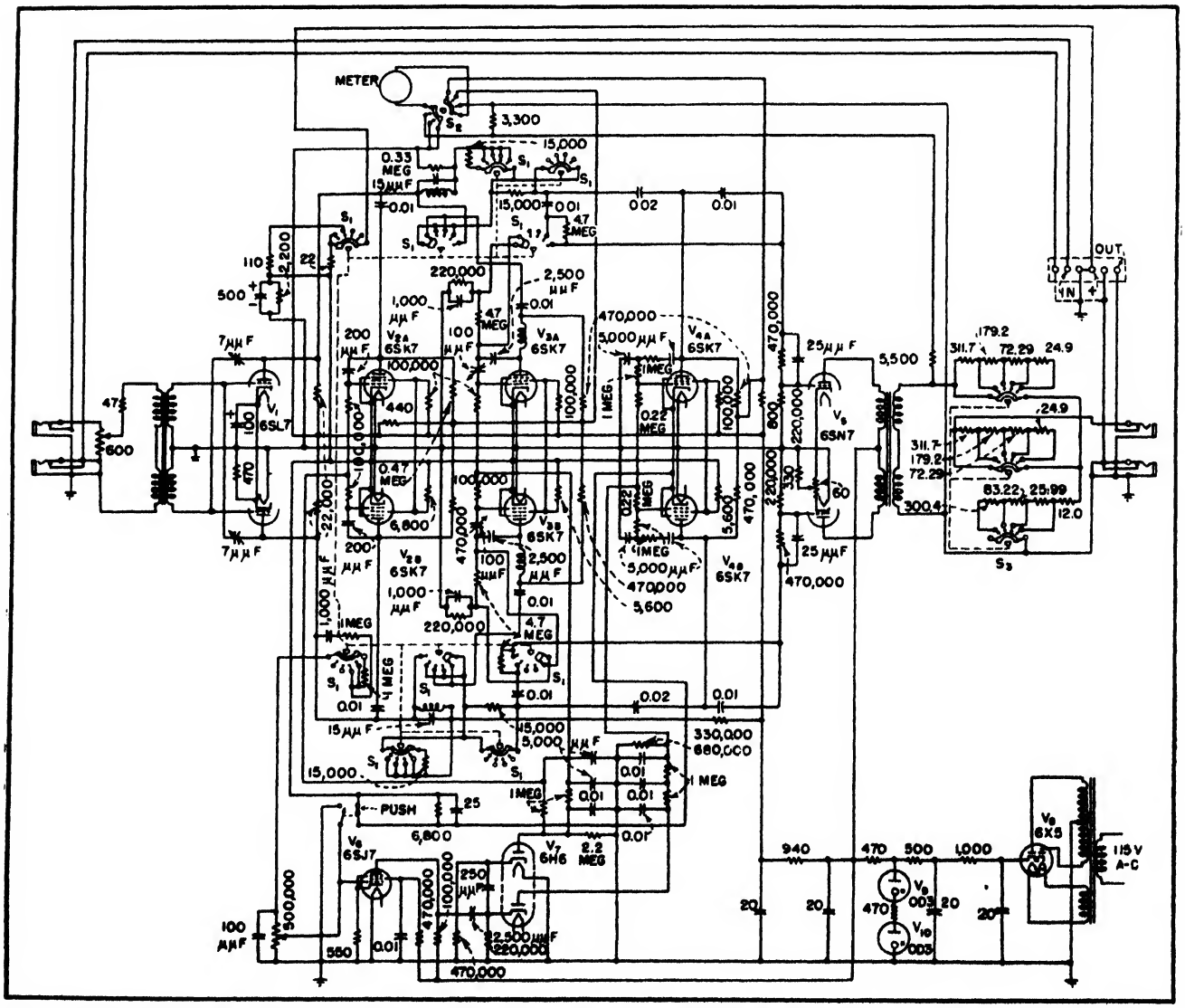

FIG. 4—Circuit of Scott model 310-A dynamic noise suppressor as designed for broadcast station use. Balanced 600-ohm input and output circuits are optional in place of the unbalanced terminations shown

when the suppressor is designed as an integral part of a complete amplifier system. The gate circuit then becomes merely an interstage coupling circuit. Suitable voltage for feeding the control filter can be obtained from some other amplifier stage, either preceding or following the gate circuit. The relative amplitudes of the voltages applied to the control circuit and to the gate circuit depend upon the types of tubes used in the gate circuits and their control characteristics.

Diodes D_1 and D_2 are sections of V_1. In a radio receiver or amplifier design, these diodes can be in any other amplifying tube or in tubes V_2 and V_3. Under this latter condition, the degree of suppression can be controlled by varying the screen voltages rather than the cathode resistors of V_2 and V_3.

Switch S_1 allows the suppressor to be opened, providing maximum range when no suppression is desired. When S_1 is closed, R_8 controls the amount of suppression by adjusting the degree to which the gate circuits close. For bad records, switch S_2 allows restriction of the maximum frequency range.

Switch S_3, included mainly for demonstration purposes, closes the high-frequency gate and leaves the low-frequency gate open, thus giving the effect of a low-pass filter providing the same scratch reduction as the dynamic noise suppressor but no rumble suppression. Comparison of tone quality for the normal (A) and filter (B) positions shows the superiority of the dynamic noise suppressor over a fixed filter of equivalent scratch reduction. For best results, both maximum and minimum bandwidths should be adjustable.

Control of Gate Circuits

Speed of control is particularly important on the high-frequency gate, which must open rapidly enough to provide satisfactory reproduction of high-frequency transients such as cymbals and triangles.

Ordinarily it would be considered impossible to provide such fast operation through grid-bias control in an unbalanced circuit, but certain features of the circuit shown in Fig. 3 make this possible. Any control voltage applied to the grid of reactance tube V_2 will produce a change in the plate current of that tube, causing a low-frequency transient voltage to appear in the plate circuit. Capacitor C_4, however, may be sufficiently small to prevent transfer of that voltage to the output terminals, and the low value of shunting impedance Z_1 further improves this action.

In other words, C_4, in conjunction with the low impedance Z_1 to which it is connected through the low inductance L_1, provides in effect a high-pass filter. Components of the control voltage, which because of previous filtering will be entirely low frequencies, will not actually appear in any appreciable amplitude across the output terminals of the gate circuit. This allows extreme rapidty of control of the high-pass filter used in the high-frequency gate, without introducing thumps or other objectionable transients into the reproduction and without the necessity of resorting to a push-pull stage.

The control circuits shown in Fig. 3 are simple but allow considerable discrimination between the desired signal and noise. Capacitor C_6 in the control filter restricts the high-frequency response of the two grid bias control circuits to prevent opening on loud high-frequency noise, while C_7 and C_8 restrict the low-frequency response of this control circuit.

The high-frequency sensitivity of the low-frequency control circuit is further restricted by C_9, and C_{10} prevents this control circuit from opening the low-frequency gate on loud low-frequency rumbles.

The over-all curve for the high-frequency control circuit approximates the response of the human ear. The control therefore resides in the desired signal rather than in the noise. This is possible because musical tones contain a fundamental and a series of harmonics. Opening the extreme high-frequency range of the gate to transmit high harmonics is controlled mainly by the corresponding fundamental tones. Opening the extreme low-frequency range to transmit low fundamentals is controlled mainly by the corresponding harmonics. This provides a high degree of discrimination against usual record noise, which tends to be greatest at extreme high and low frequencies. Of course, more elaborate filters may be used to restrict the operating ranges of the control circuits under extreme operating conditions.

For a typical home-type phonograph pickup having a replaceable needle or a bent stylus, a suppressor like that in Fig. 3 is designed to have a maximum range of 6,000 cycles. Components R_1 and C_1 in the pickup coupling circuit, as well as C_2, may be adjusted to provide the best over-all response characteristics.

Experience has shown that equalization which plays the low-frequency end of Columbia test record 10,004 reasonably flat provides a good average bass response for American recordings.

The overall response of the system at the high-frequency end of this record should theoretically roll down to approximate the NAB characteristic, since pre-emphasis of this general magnitude is used on most present U. S. recordings. Such a roll-off would droop above 1,000 cycles, being down approximately 10 db at 5,000 cycles. Unless a high-grade loudspeaker is used with the system, however, it may be found that this roll-off is too much and that a flatter high-frequency response is desirable to obtain sufficient brilliance. For best suppressor operation, however, the overall response of the system should be as smooth as possible and free from sharp peaks.

Resistor R_2 is normally adjusted so that the gate circuits are open during the louder passages of the music and closed during the quiet passages in order to suppress noise. Some experimentation with the setting of this control will be necessary on any new system.

Trimmer C_3 should be adjusted for a minimum of response at 9 kc

or, if the unit is to be used also for a-m reception, at 10 kc. With switch S_3 thrown to position B and R_3 set at 0, trimmer C_5 should be adjusted for a minimum response at 4 kc. An a-f oscillator and an oscilloscope or vacuum-tube voltmeter are desirable for these adjustments. For maximum effectiveness the noise suppressor should be engineered as part of a complete reproducing system.

Broadcast Station Model

Since the dynamic noise suppressor does not introduce any volume expansion, it is ideally suited for broadcast station use. The complete circuit of the type 910-A unit made particularly for this purpose is given in Fig. 4. Additional high-frequency reactance tubes extend the range up to 8 kc, which accommodates most present-day shellac records, and improve high-frequency noise suppression. The high-frequency cutoff in the expanded position is not as sharp as in the simpler model of Fig. 3, allowing appreciable transmission at 10 to 12 kc. However, in this wider-range unit provision is made for restricting the frequency range when playing badly distorted records. A somewhat more elaborate control circuit is also used.

The suppressor shown in Fig. 4 is built push-pull in order to minimize such factors as hum and residual vacuum tube distortion, and to provide the very highest degree of performance for broadcast station use. The reasons for using the push-pull circuit in this instrument are exactly the same as for using push-pull circuits in other broadcast station equipment.

Extended-range transcription models, based upon the broadcast unit, have been developed providing substantially flat response to 14 kc and utilizing somewhat different suppression characteristics and time constants in order to provide the best performance on high-quality recordings and transcriptions. Such units are usable not only on music but on speech and practically any other type of program material.

Other Applications

It is probable that in practically any instance where the desired signal varies in its bandwidth characteristics, the dynamic band-pass principle can be used to maintain an optimum signal-to-noise ratio. The flexibility of the control arrangements possible with a system of this type permits a high degree of discrimination between the desired signal and the noise, particularly in those cases where the signal and the noise have different distinguishing characteristics.

In the field of recorded music, the combination of new recording techniques, improved pressing materials, and the dynamic noise suppressor provides a realism of reproduction which is almost indistinguishable from a live program.

Audio Noise Reduction Circuits

Simple circuit employing germanium diodes as nonlinear elements reduces phonograph record-noise without substantially affecting desired signal. Single-channel unit up to 6,000 cycles and a three-channel 0-to-12 kilocycle version for broadcast stations are described

By HARRY F. OLSON

NOISE is one of the most disagreeable forms of distortion that occurs in sound reproducing systems. Therefore, any means which reduces or mitigates noise is extremely useful and important.

There are many ways of increasing the signal-to-noise ratio thereby reducing the deleterious effects of noise. A few of the systems that have been used may be listed; (1) a system in which the high-frequency response is attenuated; (2) a system with suitable pre-compensation and post-compensation so that the high-frequency response is accentuated in recording or transmitting and attenuated in reproducing or receiving; (3) a system using two channels—one channel is used to carry the signal and the other channel to control the amplitude of the signal in reproduction; (4) a system in which the high-frequency cutoff of the reproducing system is automatically made a function of the general level of the signal.

The use of two channels, in which one is used as a volume control, has been applied in some special cases but, in general, is impractical because two channels are not available in conventional reproducing systems.

Systems in which the high-frequency response is accentuated in recording or transmitting and attenuated in reproducing or receiving are used in phonograph and sound motion-picture reproduction as well as frequency-modulation radio broadcasting. This procedure is quite effective, but in some systems it is also necessary to reduce the frequency transmission band in order to obtain a substantial reduction in noise.

A system in which the high-frequency range is limited introduces frequency discrimination against high-frequency sounds, regardless of whether the high-frequency cutoff is fixed or is automatically con-

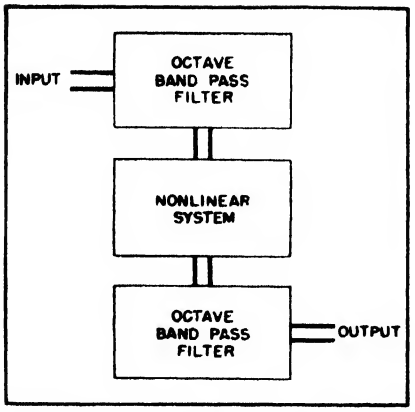

FIG. 1—Noise reduction system elements

trolled by the signal. Of course, in the case of the automatic system frequency discrimination occurs only when the amplitude of the signal is small. Nevertheless, this discrimination may be serious for certain sounds.

The noise reduction system to be discussed here employs a nonlinear element. The nonlinear element allows the useful signal to pass and discriminates against noise. This system lowers the ground noise level and thereby increases the signal-to-noise ratio without discrimination against the useful part of the signal.

Principle of System

A block diagram of the system is shown in Fig. 1. Band-pass filters which pass frequencies over a range of an octave are used at the input and output of the nonlinear element. The amplitude characteristic of the nonlinear element is illustrated in Fig. 2. As will be described later, this amplitude characteristic can be obtained with a properly biased diode vacuum tube or crystal rectifier. By using this method the system will exhibit high attenuation to signals of small amplitudes.

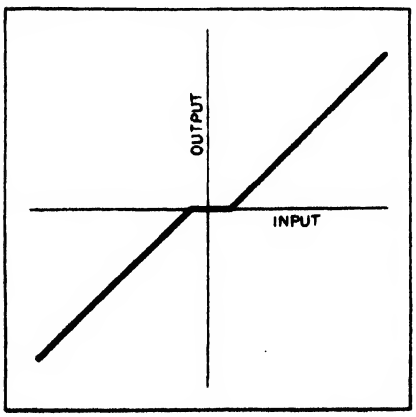

FIG. 2—Amplitude characteristics of a simple nonlinear element

The response of the noise reduction system to noise and a sine wave is depicted in Fig. 3. If the amplitude of the noise is kept below the response range of the noise reduction system, the noise will not be reproduced. The response of the noise reducing system to a sine wave signal is also shown. The output of the nonlinear element contains the fundamental, harmonics, and subharmonics of the fundamental. However, since the pass band of the input and output band-pass filters is an octave, the harmonics and subharmonics will not be transmitted by the system. The output wave, then, is a sine wave of the same frequency as the input sine wave. If two sine waves of different frequencies are impressed upon the system, the two frequencies must lie within the pass band octave in order to be admitted by the input band-pass filter. The output of the nonlinear element contains harmonics and subharmonics of the two fundamental frequencies, but these are rejected by the output band-pass filter. The output of the nonlinear element also contains the sum of the two frequencies and the difference of the two frequencies. Since the input is confined to an octave, the band-pass output filter will reject the sum and difference frequencies.

To summarize; if the input and output band-pass filters are confined to one octave or less, there will be no distortion produced by the system in the form of spurious harmonics, overtones, subtones and sum or difference tones. There will be some amplitude discrimination against signals of small amplitude. This discrimination may be reduced to a negligible quantity by employing the amplitude characteristic of Fig. 4. In this case, the transition from no response to a constant input-output relationship occurs very suddenly.

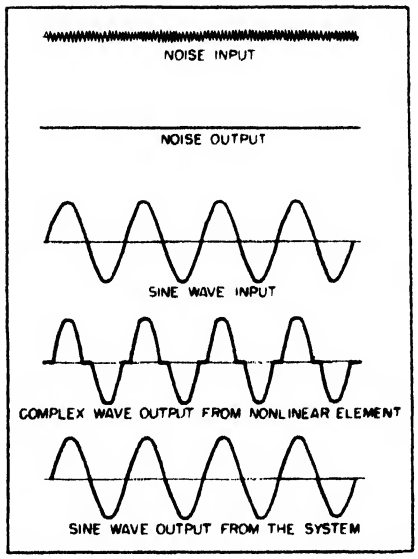

FIG. 3—Response of noise reduction system to noise and sine wave input

The gain in signal-to-noise by the use of a noise discriminating system employing a nonlinear element is depicted in Fig. 5. The amplitude ranges of the signal, the noise and the useful part of the signal are shown in Fig. 5A. The portion of the signal amplitude which is equal or less than the amplitude of the noise may be considered to be lost and of no value. By means of the nonlinear element, it is possible to eliminate the reproduction of all amplitudes below a certain level. If this amplitude corresponds to the maximum amplitude of the noise, the noise will not be reproduced. This condition is depicted in Fig. 5B. It will be seen that the noise

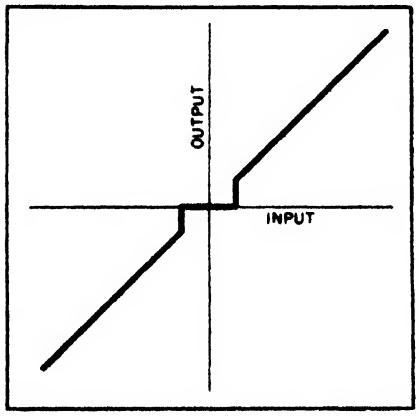

FIG. 4—Amplitude characteristics of a complex nonlinear element

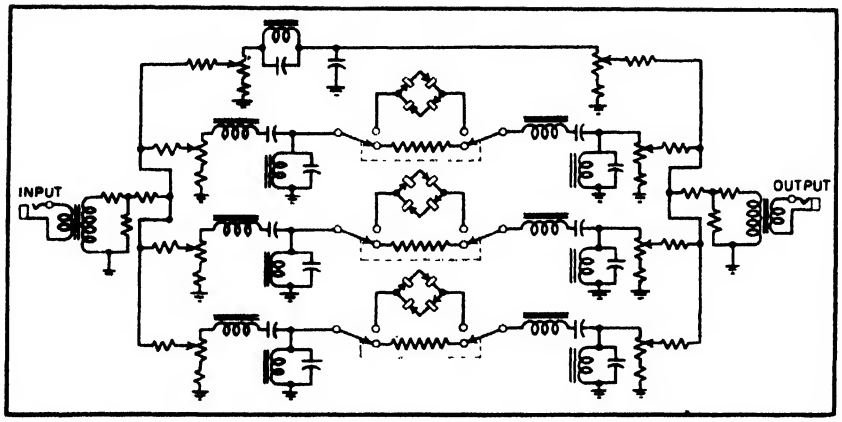

Schematic wiring diagram of ABC three-channel noise suppressor. Any of the channels can be switched to suppression or straight-through operation and the two top bands can be switched off entirely

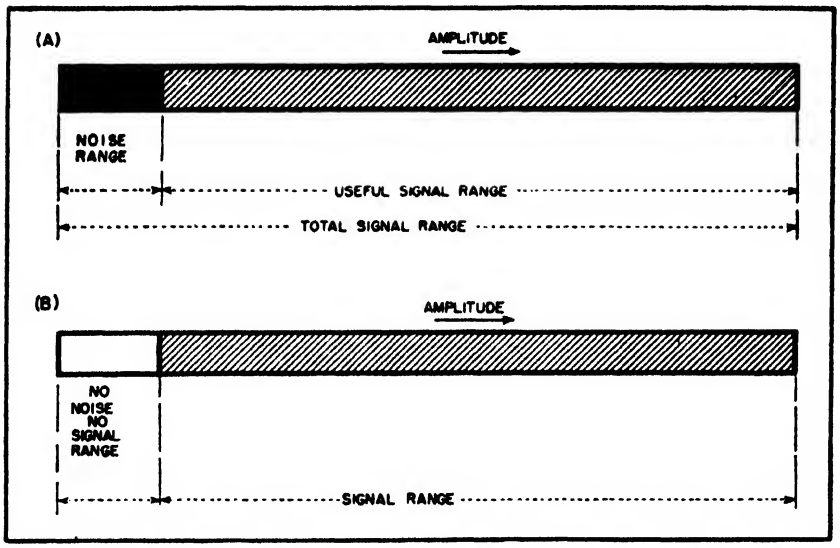

FIG. 5—(A) Amplitude ranges of total signal, noise, and useful signal in a conventional reproducing system; (B) amplitude ranges in a system with noise reduction

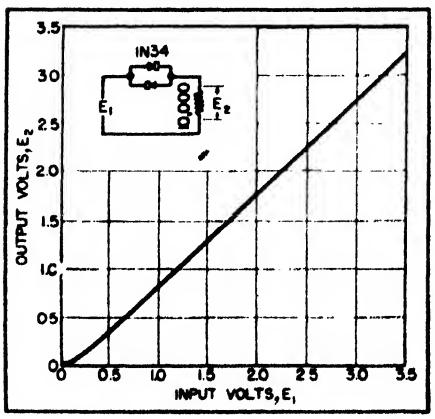

FIG. 6—Input-output voltage characteristics of two opposed germanium diodes

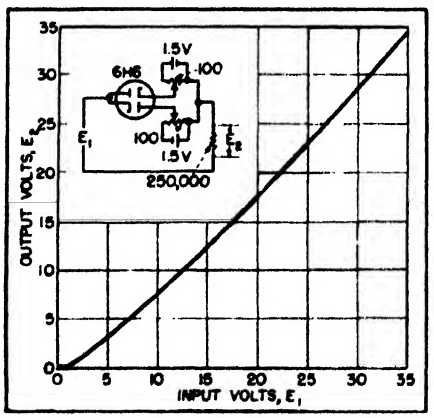

FIG. 7—Input-output voltage characteristics of two opposed biased tubes

reducing system reduces or eliminates the noise but does not increase the dynamic range of the signal. In effect, the nonlinear system separates the signal and noise in amplitude.

Nonlinear Elements

One way of obtaining the amplitude characteristics of Figs. 2 and 4 is by the use of unilateral conducting devices. These may be vacuum tube, crystal, copper-oxide or selenium rectifiers. Use of the vacuum tube diode and the germanium crystal rectifier as the nonlinear element is described below.

The input versus output voltage characteristics of two opposed germanium crystal rectifiers with a resistance load is shown in Fig. 6. It will be seen that the ratio of the output to the input voltage decreases rapidly below an input of 0.1 volt. This is due to the contact potential in these rectifiers. Supplying a bias voltage of about 0.1 volt.

The input-to-output voltage characteristic of two opposed biased vacuum-tube diode rectifiers is shown in Fig. 7. Below the bias voltage, the impedance of the rectifier is practically infinite because the reverse current in a vacuum-tube rectifier at audio frequencies is negligible.

The nonlinear elements of Figs. 6 and 7 approximate the amplitude characteristics of Fig. 3. The characteristics of Fig. 4 can be approximated using two sets of opposed biased diodes, one in series with the line and the other in shunt with the line. By a suitable choice of diodes, resistances and bias voltages, the characteristics shown in Fig. 8 can be obtained.

Thermal noise energy per cycle is independent of the frequency. However, in a phonograph record, the noise per cycle increases with increase of frequency, as indicated in Fig. 9. A consideration of the noise spectrum of a conventional shellac phonograph record, together with typical living-room noise spectrum and the response-frequency characteristics of the ear, indicates that a relatively sharp

cutoff is required at about 4,500 cycles in order to obtain tolerable reduction of the noise level in a conventional phonograph reproducing system. In view of the characteristics of phonograph reproduction, it was felt that the threshold type of noise reduction system would be particularly effective in reducing noise produced by records.

A block diagram of a phonograph reproducing system employing a simple audio antinoise system is shown in Fig. 10. The noise reduction takes place in the octave between 3,000 cycles and 6,000 cycles. This allows reproduction to 6,000 cycles with the low noise characteristics of a 3,000-cycle cutoff. The circuit diagram including the preamplifier, the filters and the nonlinear elements is shown in Fig. 11. The system consists of two crystal rectifiers, one vacuum tube, four inductors, eight capacitors, two potentiometers and five resistors. The response-frequency characteristics of the low-pass channel, the band-pass channel and the combination are shown in Fig. 12. Referring to the block diagram of Fig. 10, it will be noted that the input and output potentiometers are complementary and ganged together so that the overall gain is not changed by varying the potentiometer setting. In this way, the low response range of the nonlinear system can be adjusted to correspond to quiet, medium and noisy records by varying the ganged potentiometers. Noise reduction in the unit described is about 15 db for shellac home-type records.

The threshold noise reduction system described possesses advantages as contrasted to any system in which the high-frequency cutoff is a function of the general level of the sound. In such systems rectifiers are employed to supply the control bias of the tubes in the filter system. The retreat time of these rectifiers is relatively large, which means that with high-level sounds of short duration the high frequency cutoff may not follow the sound. If the cutoff remains at a high frequency after the level of

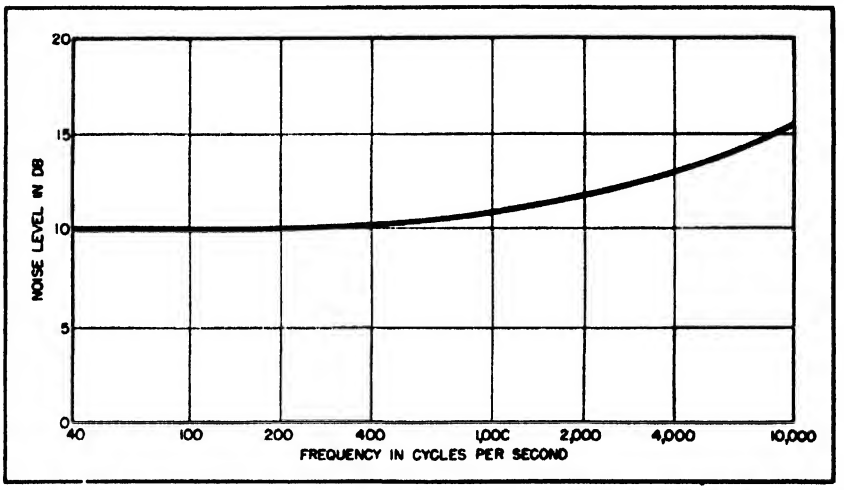

FIG. 9—Noise per cycle response-frequency characteristics of a phonograph record

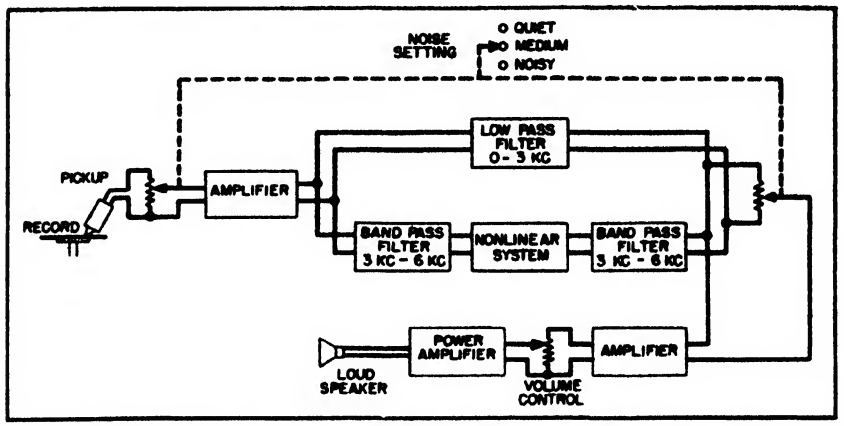

FIG. 10—Phonograph reproducer with simple audio noise reduction

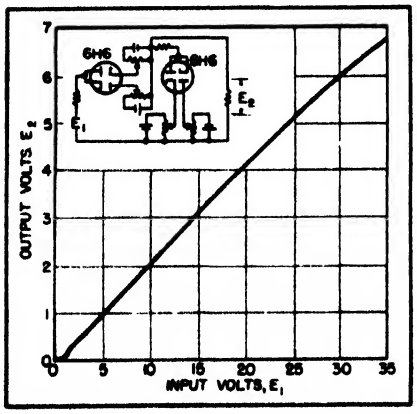

FIG. 8—Characteristics of two sets of opposed biased diodes specially connected

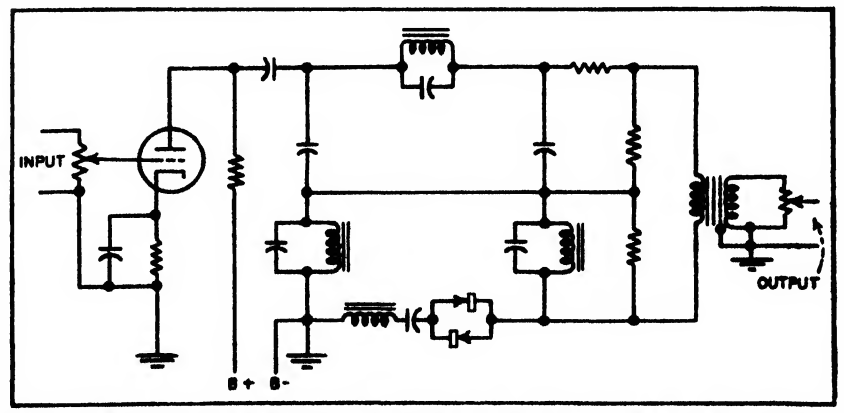

FIG. 11—Circuit diagram of block system in Fig. 10, showing amplifier, 3-6 kc low pass filter, band-pass filters, and nonlinear system

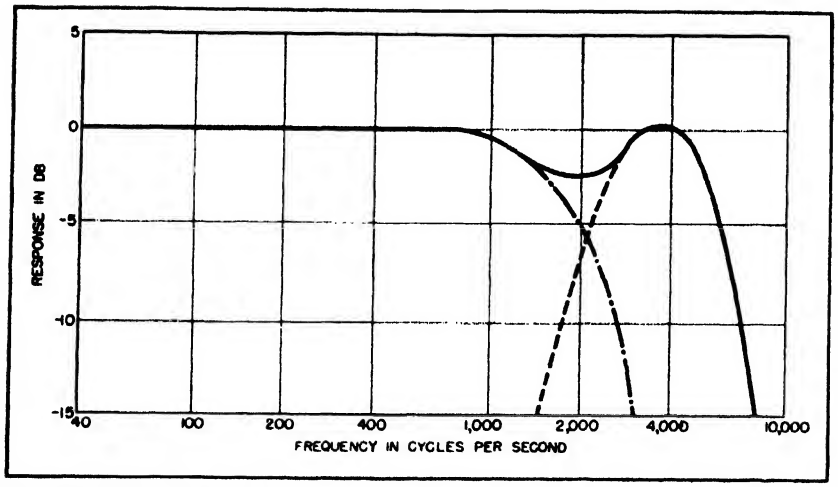

FIG. 12—Voltage response frequency characteristic of low-pass, band-pass (broken lines) and combined channels for the circuit of Fig. 11

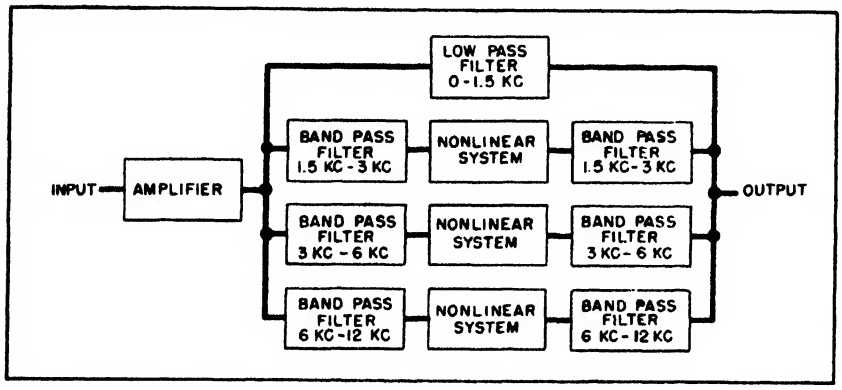

FIG. 13—Wide-range noise reduction system for 0-to-12 kc use

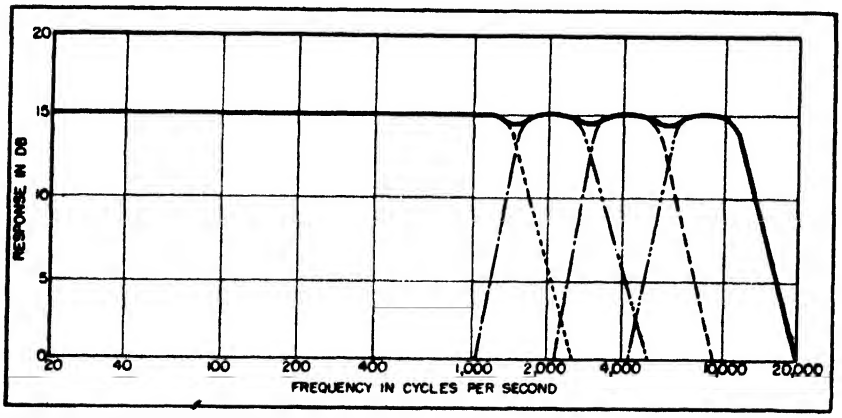

FIG. 14—Overall characteristics of three-channel system in Fig. 13. Band-pass channels are indicated by broken lines

the sound has returned to a low level, the result is an audible swishing of the noise. With sounds having a low general level, the high-frequency cutoff will be relatively low regardless of the overtone structure, with a resulting loss of overtones. In the system here described the output of the nonlinear element in the transmitting region corresponds to the input because the operation of the nonlinear element is instantaneous as far as audio frequencies are concerned. Therefore, there will be no swishing on high amplitude sounds of short duration. Furthermore, it transmits any sound which lies above the noise level. Therefore, there is no discrimination against any frequency band in this domain regardless of the general level of the sound.

Multiple Channel System

The system described, with an upper cutoff frequency of 6,000 cycles, has a much wider frequency range than the conventional home phonograph reproducing system, and the noise level is also lower. Extending the range beyond this frequency requires increased power output and improved loudspeaker systems. However, for wider range transcription phonographs an even wider frequency range is desirable.

A system with an upper cutoff of 12,000 cycles and three channels of noise reduction is outlined in the block diagram of Fig. 13. This system uses the nonlinear elements of Fig. 8. Each nonlinear system is equipped with a separate bias control so that the noise can be reduced in each band without discrimination against the useful signal. The response-frequency characteristic of the separate channels and the overall response is shown in Fig. 14. Conventional band-pass filters are used to confine the response to octave bands. A two-stage input amplifier overcomes the loss in the filters and nonlinear elements. Noise reduction of up to 20 db can be obtained in each of the channels.

The audio noise reduction system described is particularly effective in phonograph reproduction because the noise per cycle increases with the frequency. However, it may be applied with good results in other sound reproducing systems, as for example, sound on film, magnetic wire or tape, and radio broadcasting.

Background Noise Suppressor

HIGH-FREQUENCY NOISE is bypassed in the absence of high-frequency signals by a reactance-tube circuit, but when desired high-frequency audio signals are present, a disabling network renders the bypassing circuit inoperative. The suppressor can be used to remove record surface noise and noise introduced by the phonograph pickup. Under such conditions, h-f audible noise is constant and readily determined. During reproduction of quiet passages, noise is objectionable and therefore is suppressed. However, during passages when h-f signals of appreciable amplitude are present, noise is sufficiently below the reproduction level to be unobjectionable. A two-tube circuit

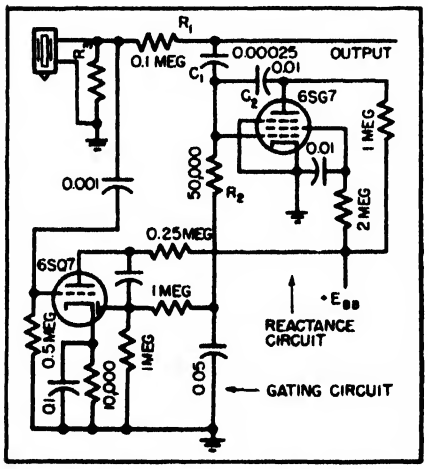

Reactance tube 6SG7 bypasses high-frequency noise. Gating tube 6SQ7 disables the shunting action of the reactance tube when h-f signals are present

acts to suppress background noise during such quiet passages, but to pass desired high frequencies if they are present at amplitudes above the noise level. The circuit is similarly applicable in any audio channel in which the noise level is constant.

Disabling Circuit

In the accompanying circuit diagram, a crystal phonograph pickup delivers a signal to the output. A circuit associated with the 6SG7 provides capacitive reactance between output and ground, which, in conjunction with series resistor R_1, acts as a low-pass filter. The circuit associated with the 6SQ7 acts to gate the reactance tube, decreasing its capacitance to ground in the presence of high frequencies to the left of R_1.

A resistance-capacitance divider so proportioned that it passes only high frequencies feeds the grid of the 6SQ7. Likewise the bypassing capacitor for the self-biasing cathode resistor of the 6SQ7 is proportioned to shunt only high frequencies so that the triode is degenerated for low frequencies but amplifies high frequencies. Also the diode-section anode of the 6SQ7 is driven from the triode-section anode through a high-pass resistance-capacitance network. These three high-pass R-C networks pass only frequencies above approximately 600 cps to the rectifier.

The diode section of the 6SQ7 develops a direct-current bias that disables the reactance tube in the presence of high frequencies. To delay the disabling action until the h-f amplitude exceeds the noise level (that is, until wanted signals are present), the cathode resistor of the 6SQ7 is made quite large, the exact magnitude depending on the noise level into the channel. The diode charges a capacitor in the grid circuit of the 6SQ7 to provide a negative biasing potential that reduces the tube's gain in the presence of frequencies above about 600 cps and at intensities higher than the noise level below which quieting is required and in proportion to the amplitude of these signals.

Resistance R_1 and vacuum tube 6SG7 constitute a low-pass filter of variable cut-off frequency. Capacitor C_1 is a coupling capacitor, and C_2 is a feedback coupling from anode to grid to enhance the reactive effect of the 6SG7 at higher frequencies. Furthermore, the capacitor between screen and cathode is small so that at low frequencies the gain of the pentode is degenerated by its screen, but at high frequencies the screen is held at ground potential, permitting normal tube gain. The capacitance (as distinguished from capacitive reactance) of the tube is thus a function of frequency.

In addition, the gain of the 6SG7 is controlled by the gating action of the disabling circuit so as to adjust the h-f shunting effect of the tube. The time constant of the grid biasing circuit is relatively short so that disabling bias can be rapidly applied and as quickly removed.

Although the switching action is so fast as to be substantially imperceptible to the human ear, the control action is relatively slow compared to the period of the frequencies being gated so that there is negligible distortion.

Coupling resistance R_2 between the disabling circuit and the reactance circuit serves two purposes. It is made sufficiently small so that the apparent level of the output from the complete suppressor circuit is not appreciably changed as the reactance tube becomes more or less capacitive. In addition, R_2 with C_1 acts as the usual tone compensating network used with crystal phonograph pickups to reduce the midfrequencies in proportion to the reduction of low frequencies provided by resistor R_2.

Should cathode bias be necessary in the reactance tube, the screen bypass capacitor is grounded instead of being connected to the cathode. Furthermore, the cathode bypass capacitor is made small as that at low frequencies there is cathode degeneration. The result is that the impedance of the reactance tube to low frequencies is very high and to high frequencies is quite low in the absence of a disabling bias from the gating circuit. Usual precautions of h-f circuits should be observed in the layout and wiring of the suppressor. (U. S. Patent 2,369,952 granted Feb. 20, 1945 to George F. Devine, assignor to General Electric Co.)

Audio Mixer Design

High and low-impedance circuits for mixing multiple inputs to an audio system. Features of the various arrangements are included, as well as possibility of cross-talk, hum problems, calculation of insertion loss and impedance matching

By RICHARD W. CRANE

IN the design of studio equipment and public-address systems, it is usually necessary to incorporate circuits capable of mixing anywhere from two to eight or more input elements, and these circuits must operate in such a manner that (1) the input and output impedances will be constant for any setting of the controls, (2) there will be no crosstalk, and (3) a variation in the setting of one control will not affect the attenuation of the other positions.

Mixer circuits in use today fall pretty well into two classes, the high-impedance type used in public address amplifiers and the low-impedance type used in broadcast and recording equipment. Two of the most common networks of the high-impedance type are shown in Fig. 1 and 2. The first circuit utilizes a double triode, such as a 6C8G or a 6F8G, and is excellent for a two-position mixer. It can also be used for three or four positions by using two tubes and, since all inputs are completely isolated from one another, there can be no crosstalk or other interaction.

As the plate resistances of the two sections are in parallel, one section sees a load consisting of the other section's plate resistance in parallel with the load resistance, giving an insertion loss whose exact value will depend on the circuit constants, but which will be not more than 6 db in the two position circuit shown. There is no real insertion loss, of course, since the tube amplifies, but it is obvious that the gain of the two sections connected as in Fig. 1 will be less than that of a single section alone and can never be greater than $\mu/2$, for the load resistance one section sees is always less than R_p. Similarly, for a three-position mixer $\alpha<\mu/3$, and for a four position mixer $\alpha<\mu/4$.

Figure 2 represents a circuit that works quite well for any number of positions. The series resistors should have the same value as that of the potentiometers, and the maximum insertion loss = $20\log n$ where n is the number of positions in the mixer.

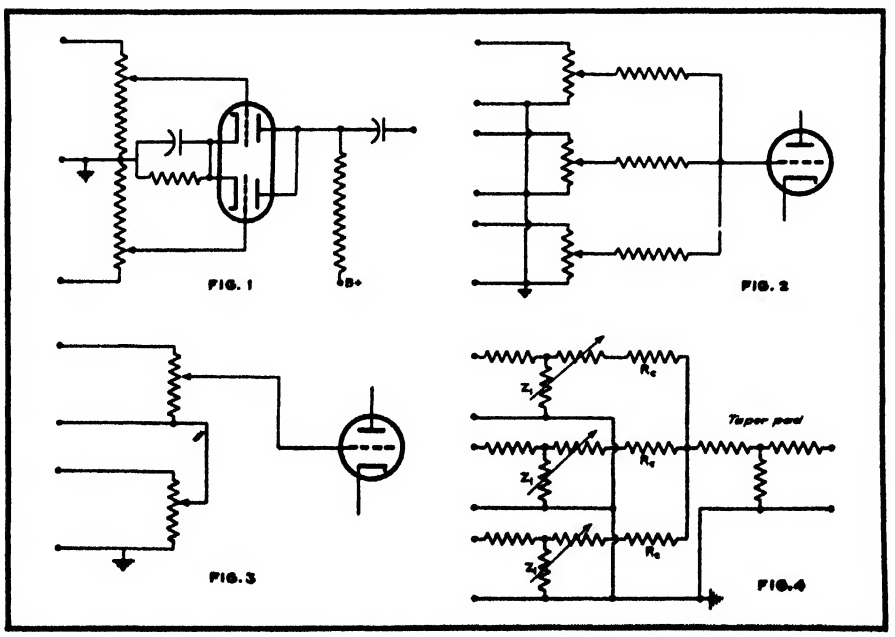

FIG. 1—Two-position high-impedance mixer feeding a double triode

FIG. 2—Three-position high-impedance mixer, parallel type

FIG. 3—Two-position high-impedance mixer, series-type

FIG. 4—Three-position low-impedance mixer, parallel type

Insertion Loss

The main disadvantage of this circuit is that the insertion loss will vary, depending on the setting of the potentiometers; for a four-position mixer, for example, the insertion loss of one channel may be only 8 db if the other three controls are wide open, while it will be 12 db if they are all in the off position. However, the maximum variation in insertion loss any one potentiometer can cause will range from 2.5 db for a two position circuit to 1.7 db for an eight-position mixer. (These figures are obtained by assuming that position 1 is the generator, calculating the insertion loss with all the controls wide open, then calculating the insertion loss with one potentiometer closed, and subtracting one from the other.) This variation will be quite a bit smaller if the source impedances are low compared to the values of resistance used in the mixer, and, in general, this circuit is useful in sound systems where too exact control is not needed.

Another type of high-impedance mixer is one in which the controls

are connected in series as in Fig. 3. Such a circuit requires that all inputs except one be ungrounded, but since this tends to develop hum and crosstalk, such networks should be avoided.

In these high-impedance circuits, there is no attempt made to match impedances; instead they are designed using potentiometers whose resistance is high (usually ½ to 1 megohm) compared to the source impedance of the preamplifier, phono pickup, or microphone. A source whose impedance is very low in relation to the mixer input impedance, such as an 8-ohm magnetic pickup, or a 250-ohm line, will require an input transformer.

Low-Impedance Types

There are many types of low-impedance mixers used and four of these are shown in Fig. 4, 5, 6, and 8. All four of these networks will give an exact input-to-output impedance match for any position of the controls.

Figure 4 is a parallel-type mixer where Z_1 is a variable, symmetrical T-pad whose input impedance = output impedance, as it is in all four low-impedance mixers.

Unit R_c is a fixed resistor, and a taper pad is used to convert the mixer's output impedance to the desired output impedance (this pad may be replaced by a transformer if one with the correct impedance ratio is available). For this network the following relations hold[1]:

$$R_c = Z_1\left(\frac{n-1}{n}\right)$$

$$Z_2 = Z_1\left(\frac{2n-1}{n^2}\right)$$

Insertion loss = $10 \log(2n-1)$ where Z_2 is the impedance looking back into the mixer (without the taper pad connected), n is the number of positions, and insertion loss is the mixer loss in db, not including the taper pad.

Example

Thus if we want a three-position, 500-ohm input, 500-ohm output mixer, R_c = 333 ohms, Z_2 = 278 ohms, insertion loss = 7 db; and we would use three 333 ohm resistors and a 278 to 500 ohm taper pad (which would give an additional loss of about 7 db). The procedure for the design of taper pads is given in ELECTRONICS for November, 1941[2].

Figure 5 shows a series-type mixer and for this circuit

$$R_c = Z_1\left(\frac{n}{n-1}\right)$$

$$Z_2 = Z_1\left(\frac{n^2}{2n-1}\right)$$

As in Fig. 4, the insertion loss = $10 \log(2n\text{-}1)$. This circuit differs from Fig. 4 in that it must be grounded at only one point, and thus only one input can be grounded.

Figure 6 shows a bridge-type mixer and is the best circuit for a four-position system, provided that the inputs can be ungrounded (although the system can be grounded at some one point). Figure 7 represents the equivalent circuit when position 1, for instance, is the generator. From this it can be seen that $Z_1 = R_c = Z_2$. Thus a master gain control identical with the individual attenuators can be used as an integral part of the mixer. If a master gain control is not used, the circuit should be arranged so that the mixer sees a resistive load equal to Z_1 otherwise the bridge will not balance. This circuit has an insertion loss of 6 db, which is less than that of any other four-position mixer.

The circuit of Fig. 8 can be used for any even number of positions from four up, and in this circuit[1]:

$$Z_2 = \frac{4Z_1(2n-3)}{n^2}$$

$$R_c = \frac{Z_1(n-3)}{n}$$

Insertion loss = $10 \log (2n-3)$ The taper pad in this network is an ungrounded H pad. This is an especially good design to use for a six-position circuit for in that case $Z_2 = Z_1$.

Crosstalk

As to crosstalk in mixers, it may be said that circuits with grounded inputs, such as Fig. 1, 2, 4, and 8, will not develop any, but Fig. 3, 5, and 6 may develop some, depending on the physical design of the equipment (shielding, placement of parts, etc.).

References

(1) Microphone Mixer Circuits, *Jour. Soc. of Motion Picture Engineers*, June, 1937, p. 604-613.
(2) Attenuator Design, ELECTRONICS, Nov. 1941, p. 51-54.

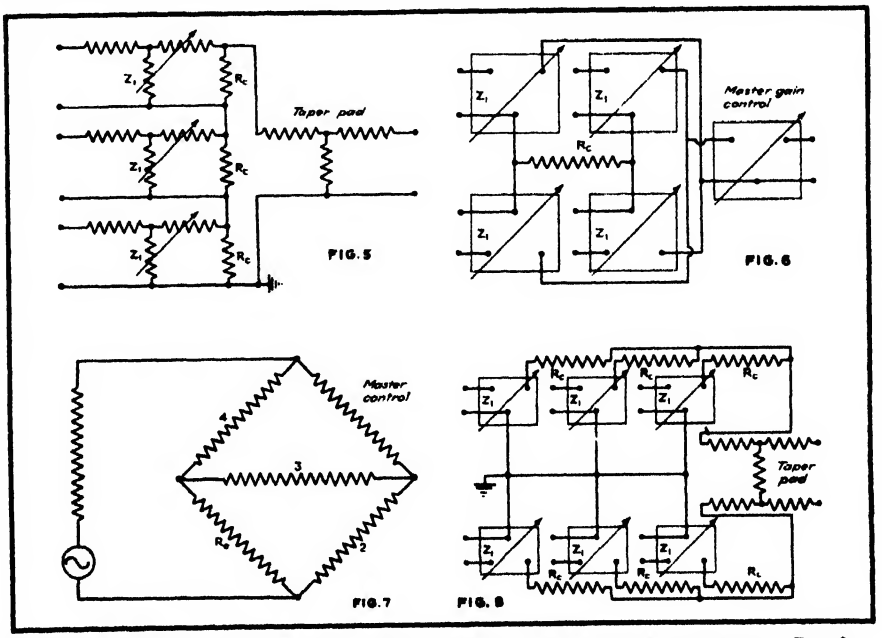

FIG. 5

FIG. 6

FIG. 7

FIG. 8

FIG. 5—Series-type low-impedance mixer for three inputs

FIG. 6—Bridge-circuit mixer with T-pads for four positions

FIG. 7—Equivalent circuit of bridge-type mixer

FIG. 8—Series-parallel mixer network of T-pads

Automatic Fader

By DAN HUNTER

THE device to be described automatically fades a program either completely or partially in or out, at predetermined rates, without the use of motors. The only moving parts consist of three relays, and individual fade-in and fade-out timing is easily adjusted.

The automatic fader is used to fade the nemo, a remote or network program for a local broadcast, or to join a remote or network program already under way. In the studio, it is also convenient for announcing a remote program. These operations involve strict cooperation between the master-control operator and the announcer unless the program is routed through a studio having a studio operator. This close cooperation demands the type of attention very difficult to achieve in any master control.

Circuit

The automatic fader was designed to operate from the nemo and announce tally lights plus an installed fade key and tally. As shown in Fig. 1, the fader is essentially an amplifier adjusted for zero gain, with time-delayed bias for control. The amplifier tube is biased to cut-off for complete fade-out, at an intermediate point for partial fade-out or in, and normal for complete fade-in. The bias is obtained from the two potentiometers in the bleeder circuit.

Two variable timing controls are included (slotted shaft for screwdriver adjustment), one for complete fadeout and one for complete fade-in. Timing of a complete fade is adjustable from 1 to fifteen seconds. The timing for the background level or partial fade is fixed at approximately two seconds.

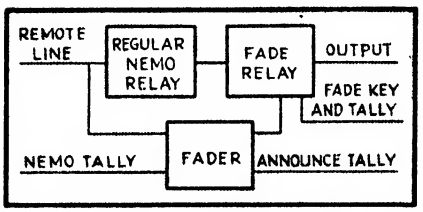

FIG. 2—Essential elements of the automatic fader system

The 6C5 is operated at a plate current of 0.5 to 0.6 ma to obtain a smooth fade. This quiescent point places the operation of the tube slightly above the point where the amplification begins to vary. This imposes a definite limitation on the maximum permissible input level at which the fader may be operated without distortion. The input is 10,000 ohms bridging, while the output is 500 ohms. The fader and its power supply were mounted on 3.5-in. rack-mounting panels.

At WMAL, the fader is in the nemo circuit, as shown in the block diagram of Fig. 2. The input of the fader is bridged across the nemo line and the fade relay switches either the nemo or the fader to feed the equipment. This switching can be done any time during a program provided a relay with grounding resistors is used. At WMAL an Automatic Electric relay is used, with 50,000-ohm resistors from all contacts to ground.

The relay L-2 which gives complete fades obtains its battery from the nemo tally light. This was done so that the fader would always be ready to perform. If the nemo is down, the fader is ready to fade in and vice versa.

The partial fade or background-level relay L_1 connects to the battery supplying the announce tally through a contact on relay L_2. This allows a background level only when both announce and nemo are set up. Since the tally lights and set-up buttons are on the announcers switching, console, (delite), the fade key and tally were also placed on the delite. This enables the announcer to completely fade in or out a program or announce over a background level without an operator.

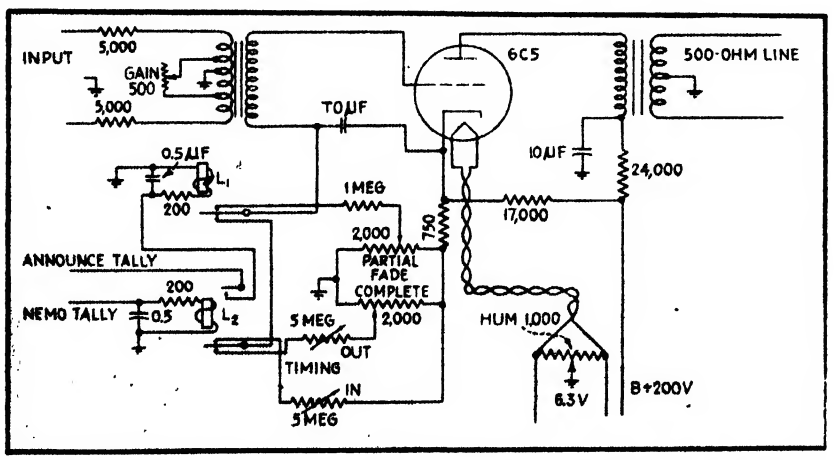

FIG. 1—Vacuum-tube circuit for complete or partial automatic fading of programs

Operation

If a fade is desired, the fade key is turned on; the fade tally gives indication. When nemo is released, the program is faded out, or if nemo is set up, the program is faded in. If announce is set up at the same time, then the program is either faded in or out but to a background level.

It was found that a partial fade of 10 db of tone (500 cycles) gave a good background level. The level is adjustable to −58 db when using the circuit shown in Fig. 1.

Volume Expander Design

An electronic volume expander provides full expansion of a wide range of program material in about ten milliseconds and return to normal gain in one second. The problems encountered, methods of solution, and results of experimental work are included

By ROBERT W. EHRLICH

MANY people, having listened to volume-expansion amplifiers, have found them to introduce undesirable wows, gasps, pops, or just plain distortion in the reproduced output. There is, however, ample justification for volume expansion in the fact that a certain amount of volume compression is used in making a majority of recordings and sometimes in broadcast work. In addition, the reduction of amplification at low levels helps to reduce record scratch and background noise during such passages.

This paper represents the results of a series of experiments to find the answers to expander design. The expander to be discussed is the electronic type, wherein the signal is rectified and the resulting d-c voltage is used to control the gain of a variable-gain stage as shown in Fig. 1. There are many other ingenious ways of introducing volume expansion, but it is felt that this type provides the necessary flexibility for application to varied types of program material.

The expander illustrated in Fig. 2 was developed in connection with these experiments. It has been found to give satisfactory results with a wide range of program material, and, even when improperly adjusted, it does not have many of the undesirable characteristics experienced with other circuits. The complete circuit of the expander is shown in Fig. 3.

Requirements

The design of an electronic volume expander involves a number of interesting problems beyond those ordinarily encountered in amplifier work. The variable-gain stage must

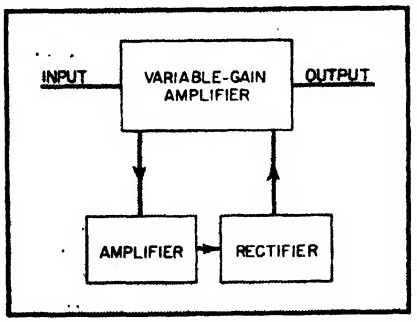

FIG. 1—Block diagram of an electronic volume-expander circuit in which the rectified signal is used to control gain

operate at not just one point on its characteristic, but rather over the complete range of its characteristics without introducing distortion. The amplifier which feeds the rectifier circuit must have means for adjusting its gain without any audible indication, and this gain must be variable to suit the various input signal levels.

Finally, the rectifier must be capable of rectifying a complex a-c signal without introducing objectionable ripple into the signal circuit. Moreover, the time constants throughout the expander circuit must be so adjusted that full expansion can be obtained in something like 5 to 15 milliseconds, while the time taken to return to normal gain is about one second. By careful attention to all of these requirements, satisfactory operation can be obtained.

Choice of Circuits

The variable-gain stage is the heart of the expander, and its selection is the first consideration in design. Perhaps the most widely used tube for this purpose is the 6L7, in which the d-c bias voltage on grid number 3 controls the gain of the tube with respect to grid number 1. Another popular method

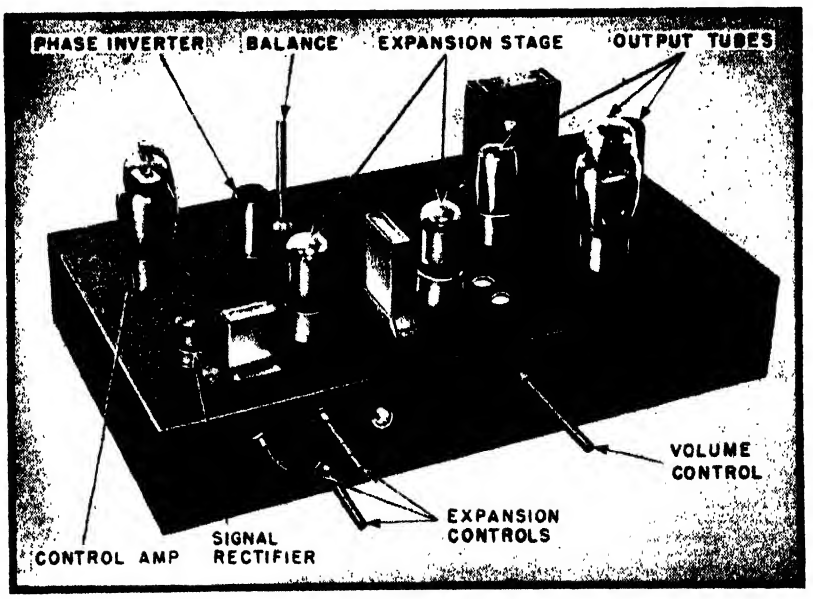

FIG. 2—Chassis of the experimental expansion amplifier

is to use a variable-mu tube such as the 6SK7 and let the d-c bias on the signal grid control the gain.

A less common but very ingenious circuit uses a triode tube as one leg of a voltage divider for the signal. The other leg is a fixed resistor. By varying the bias on the triode, the tube assumes different values of plate resistance, and thus there is a variation of the relative signal voltage which is taken off across the triode.

Because of the complex biasing problems on multi-element tubes, and because of the wide range of tube characteristics involved in the expansion stage, many of the circuit constants for that stage will have to be determined by trial and error.

During experimentation with the expansion stage, circuits were considered where the input to the control circuit is taken from the output of the expanding stage rather than the input. This type of circuit would have the advantage of reducing the amplification necessary to drive the control circuit. It was found to be unsatisfactory, however, because of dynamic instability caused by the regenerative action. Any delay in expansion was greatly accentuated. Moreover, since the control voltage was proportional to the square of the signal input, the curve of gain vs signal was very steep at higher levels. With one circuit tried, the action of the expander was delayed by one or two seconds, after which the expansion would take place very suddenly. The result was that the gain had no relation to signal strength with a typically variable input signal.

The push-pull circuit for the expander of Fig. 3 was selected after several disappointing experiments with single-ended circuits. Not only do the latter have a tendency to distort due to curvature of the tube characteristic, but they also are affected by any residual ripple that may come through from the rectifier. These effects are largely cancelled out in a push-pull stage.

Advantages of Push-pull

Another advantage, though not apparent at first, is the possibility of avoiding the use of bypass capacitors. Changes of screen and cathode voltages in an expanding stage are in such a direction as to oppose the change in gain caused by a change in grid bias. If the cathode or screen voltage variation is retarded by a large bypass capacitor, it is possible for the gain of the stage to increase before this capacitor can change its charge. When it does charge, it pulls the gain down. The result is that the amplifier gain overshoots its final mark and there is a tendency for thumps to be heard in the output. Figure 4 is an oscillogram which illustrates this type of transient response.

Effect of Transients

Another difficulty inherent in single-ended circuits is the possibility of introducing low-frequency transients or thumps in the output, due to rapid expander action. Such transients are cancelled out in a push-pull stage, since the control bias is applied to both grids simultaneously. Even with push-pull operation, however, it is still necessary to keep the transients in the output of the individual expander tubes from becoming so large as to cut off the following stage. This can be accomplished by transformer coupling, a

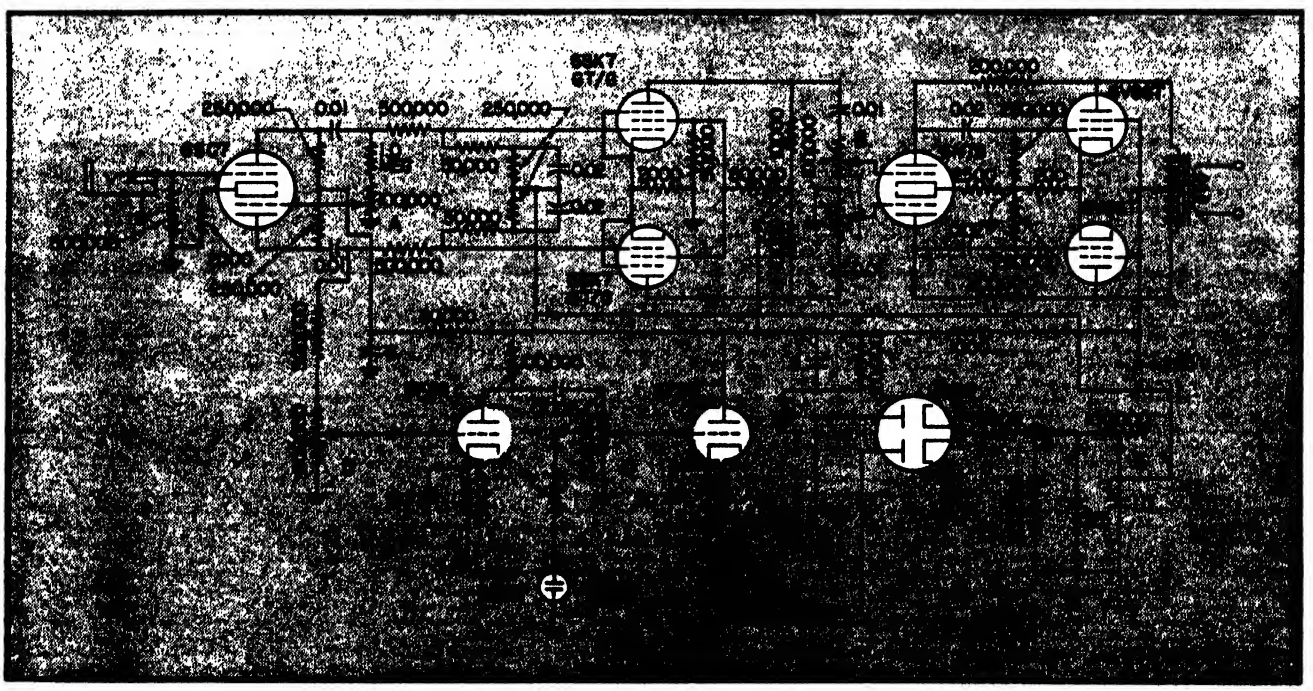

FIG. 3—Final circuit of the expansion amplifier. The lettered controls are identified as follows: *A*-balance; *B*-volume; *C*-input level; *D*-expansion; *E*-time constant

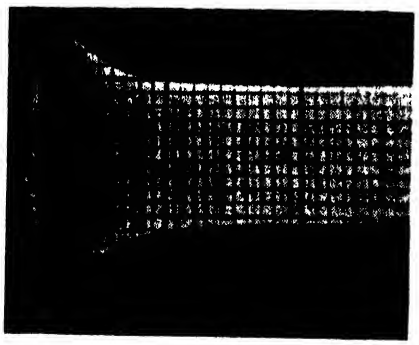

FIG. 4—This oscillogram shows the overshooting of gain caused by a 10-μf cathode bypass capacitor connected across a 10,000-ohm cathode resistor

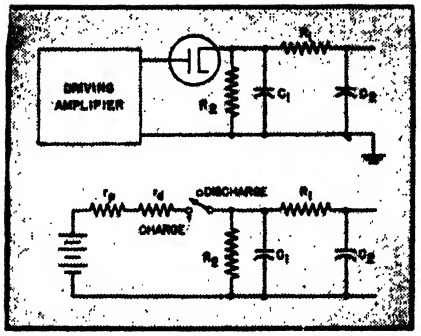

FIG. 5—A simple rectifier and filter circuit is shown at the top. Its equivalent circuit shows the factors that determine the charging and discharging time

special phase-inverter tube[1], or, as in Fig. 3, through the use of low values of plate load resistance and low values of coupling capacitors. The loss in low-frequency response is compensated for by the *RC* networks in the grid circuits.

In the control amplifier circuit of Fig. 3, there are two gain controls. One is used to vary the amount of expansion, and the other compensates for major differences in input signal level. A more common means of controlling expansion is the use of a potentiometer in the rectifier circuit, but this was found unsatisfactory because of its effects on the time constants in the rectifier.

Rectifier Problems

The rectifier with is associated filter is perhaps the most important section of the amplifier, for it is here that the dynamic nature of the entire unit is determined. Improper consideration of these factors can lead to serious volume distortion. The problem is to get an *RC* filter circuit which will react very rapidly to impulses of signal, and still eliminate all traces of rectifier ripple from the signal circuit. The solution is to make all resistors through which the capacitors charge very small, and those through which they discharge very large.

Figure 5 shows the type of rectifier circuit to be considered, along with its equivalent circuit. The charging time is determined principally by the internal impedance of the driving amplifier, r, the plate resistance of the diode, r_d and R_1; along with capacitors C_1 and C_2. The discharge time is determined by resistors R_1 and R_2 and capacitors C_1 and C_2. It is important also to remember that any other capacitors associated with the expander circuit can affect the time constants.

Calculation of the exact time constants of a circuit such as that of Fig. 5 is rather complex, but the following simple formulas developed by E. W. Kellogg and W. D. Phelps[2] will give the necessary values closely enough.

Charging time constant =
$(r + r_d)\ C_1 + (r + r_d + R_1)\ C_2$

Discharge time constant =
$R_2\ C_1 + (R_1 + R_2)\ C_2$

Adjustment of values should be made so that the minimum charging-time constant will not be over 15 or 20 milliseconds and the discharge-time constant not less than 0.5 second. In addition, the total resistance between the controlled grid and ground should, if possible, be kept below the maximum value specified for the tube used. The use of a cathode-follower circuit in the driving amplifier circuit of Fig. 3 makes the driver impedance very low and makes it easy to obtain a low charging time. Control of the time constant is obtained by making resistor R_1 in Fig. 5 variable.

Figure 6 shows an oscillographic determination of the minimum charging time for the expander of Fig. 3. A 500-cycle signal was keyed into the circuit with expansion full on, the 3000-ohm series resistor shorted, and the time-constant control set at its minimum value.

The number of cycles required for 64-percent expansion indicates the charging-time constant, eight milliseconds in this case. In practice, the insertion of the 3000-ohm buffer resistor was found valuable in materially reducing rectifier ripple. This resistor brought the

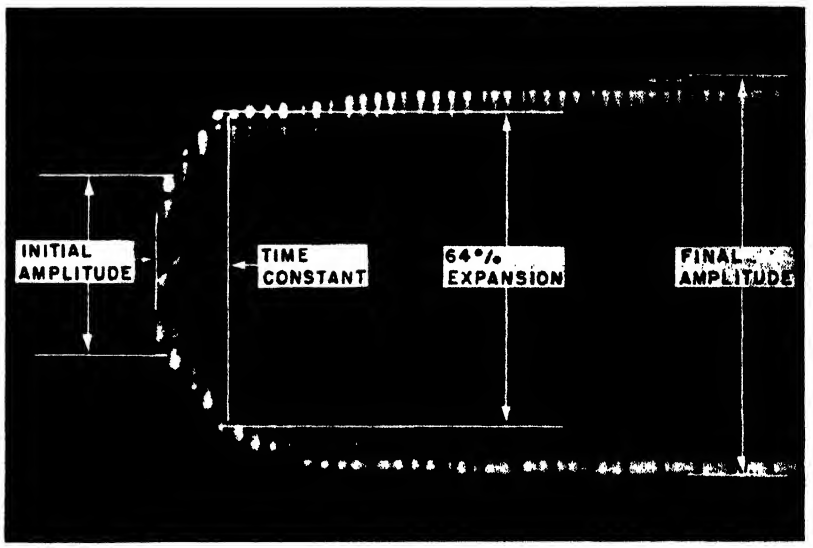

FIG. 6—Oscillogram showing the shortest possible transient response for the circuit of Fig. 3. The notch at the left was caused by masking tape over the stationary spot on the screen

time constant up to 12 milliseconds.

Performance is determined by testing for change in gain, or expansion, with respect to control voltage. For this test, control voltage is most easily obtained from a battery and potentiometer. A gain curve for the expander is shown in Fig. 7. The points to be noted are first, that the maximum change in gain without distortion must be at least about three times (10 db), and second, that the curve of gain versus voltage should be fairly straight over the range selected.

To compensate theoretically for a typical compression characteristic, all of the expansion would have to take place in the upper two db (20 percent) of the control voltage swing. This characteristic is neither necessary nor desirable. For one thing, the input level to such a circuit would be very critical, necessitating many readjustments of input level. Furthermore, this type of curve can lead to undesirable dynamic characteristics, especially in connection with overlong time constants. This combination will make the expansion come on suddenly, many milliseconds after the initial input impulse. The effect is difficult to describe, but it is unquestionably unpleasant.

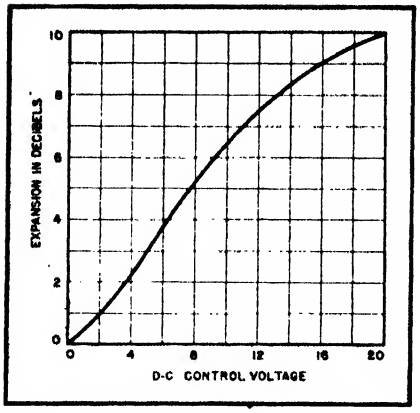

FIG. 7—Static gain versus control-voltage characteristic of the push-pull expansion stage shown in Fig. 3

Operation

Setting of the amount of expansion and the time constant is complicated by the fact that it is practically impossible to detect the action of a properly adjusted expander. There is a natural tendency to advance the expansion control to the point where the effects of the expander can be heard, for if time and effort have been put into the construction of such a circuit, one likes to hear it work. As a matter of fact, the only way to tell accurately how well an expander is operating is to play the same passage twice, once with expansion on and once with it off. This is only possible with phonograph records, for which reason records are probably the best source of program material for one who is learning to use an expander.

Once some experience has been gained with the expander, the two gain controls *C* and *D*, and the neon indicator in Fig. 3 can be used to advantage in setting up the expander for operation with any type of signal. The resistors associated with the neon lamp are so adjusted that the lamp begins to glow when the signal voltage is large enough to drive the expander to full expansion. The level at this point is adjusted by control *C* in such a way that the lamp will blink at peaks of modulation. For any radio station or record, this adjustment can usually be made in a few seconds, and it will hold as long as the same input source is maintained. With the signal level in the expansion control circuit so adjusted, it is then possible to set the second gain control, *D*, in terms of its own panel calibrations to give the number of decibels expansion desired for the particular program material.

Typical Control Settings

Actual settings of the expansion and time-constant controls will naturally vary for different types of program material. Symphonic selections are perhaps easiest to expand. This type of music will take all the expansion the amplifier can give, at the shortest time constant, without any unpleasant reaction. The only limit here is the point where soft passages are too soft to hear and loud ones uncomfortably loud. Martial band music also falls into this category.

TABLE I. RECOMMENDED EXPANDER SETTINGS

Program Material	Expansion	Time Constant
Symphonic Music, Band Music	Full	Short
Dance Music (slow)	Medium	Short
Organ Music	Low	Short
Speech, Dance Vocals	Low	Short
Swing Music (fast)	Medium	Long
Operatic Vocal Solos, Instrumental Solos	Not Recommended	

Dance music is a little more difficult to handle, and expansion should be used cautiously. The time constant should be short when the music is slow; but if the music is fast and hot, a long time constant is required to swamp out the rapid volume impulses and prevent jerkiness.

Speech is also difficult to handle but expansion can still be used to advantage if it is used sparingly. Time constants on speech should be kept short to preserve the natural expression. An over-long time constant and excessive expansion can lead to a very undesirable gasping or breathless effect.

One type of material for which expansion is not recommended is a vocal or instrumental solo. The performer puts in his own volume expression, and expansion will seriously distort it. The effect is at its worst when the expansion control circuit has peaks in its frequency response so that certain notes are expanded out of proportion to the rest.

Table I indicates in convenient form the expander settings recommended for various types of material.

References

(1) Weidemann, Lt. Henry K., USNR, A Volume Expander for Audio Amplifiers, *QST*, p 19, Aug. 1945.

(2) Kellogg, E. W., and Phelps, W. D., Time Delay in Resistance-Capacity Circuits, ELECTRONICS, p 22, Feb. 1937.

Surgeless Volume Expander

By A. NELSON BUTZ, JR.

WITH FEW EXCEPTIONS, volume expander systems have utilized the change in transconductance of a vacuum tube, as a function of one of grid voltages, to vary the amplification in such fashion as to enhance the dynamic range of the program being reproduced.

For the expansion action to be as unobtrusive as possible, the attack time must be made sufficiently rapid to permit complete expansion almost immediately upon the beginning of a loud passage. Decay of the expanded level, however, must occur considerably slower lest rapid increases and decreases of level, in staccato passages in particular, should modulate lower-level intervals. Another reason for requiring a fairly slow decay time is to permit a realistic decay of reverberation in reproducing music produced in live concert halls or studios. It is obvious that a rapid decay of expansion would accentuate the decay of reverberation and deaden quite effectively the normal studio characteristics.

Need for Pushpull

In securing expansion through variation of transconductance, a change of plate current in the expander stage necessarily occurs. If an expander circuit is constructed in as simple a form as possible, with a single controlled tube, this dynamic change of plate current appears as a component of the program being reproduced. As a result, the time constant of expansion attack must be made sufficiently long to place the components of the plate current surge in the subaudible region. In an amplifying system with good low-frequency response, this factor necessitates a minimum attack time of about 0.5 second, which is so slow as to produce a noticeable gradual increase in the louder passages.

The problem is aggravated by the fact that the absolute plate voltage change caused by expansion is usually considerably larger in magnitude than the desired signals. The obvious method of avoiding the effect of plate current surges has been incorporated in certain systems which use a pushpull expander stage. In this case, the d-c surge in each expander tube is cancelled out in the pushpull transformer of the expander system. However, the expense of a high-quality output transformer for such a system would place it beyond the economic reach of many users. In addition, a pushpull input transformer would be required to secure rapid expansion action because an RC input circuit would necessarily introduce an undesirable system time constant.

Single-Ended System

The expander circuit shown in Fig. 1 represents a method of balancing out changes in plate current while maintaining the entire system single-ended with respect to ground and eliminating the necessity of using expensive transformers. In addition, the inherent system distortion is extremely low over a controlled range of approximately 15 db. The attack time may be made extremely short without causing undesirable surges, while the release time may be made as long as desired.

The audio signal is applied to grid 1 in a conventional fashion while the variable expander bias is applied to the suppressor. As the suppressor is made more positive, from a given negative value, the screen current decreases while the plate current increases. In the 6SJ7, the negative transconductance to the screen and the positive transconductance to the plate match closely when the plate transconductance is changed over a wide range without altering the total cathode current. Unfortunately, as the suppressor bias is varied, the sum of control grid to screen and control grid to plate transconductances

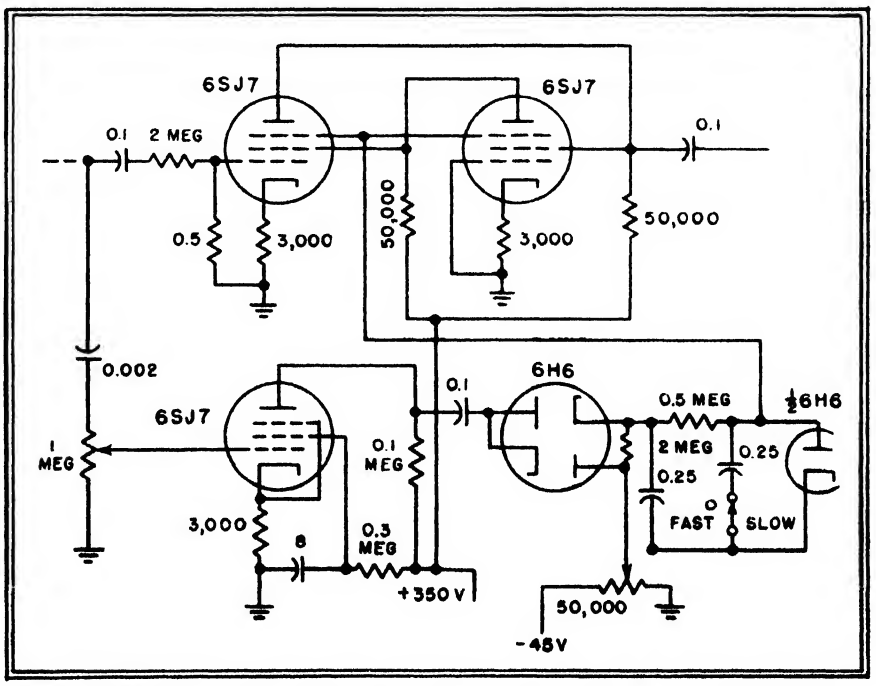

Fig. 1—Circuit of single-ended volume expander that requires no pushpull transformer for canceling out the d-c surge in each expander tube

remains constant, and if screen and plate of a single tube were tied together, no appreciable variation of overall gain will occur.

Use of Dummy Tube

The plate of the signal amplifier is connected to the screen of a dummy 6SJ7, and since expansion voltage is applied to the suppressor of both tubes, the dynamic change in plate current in the signal amplifier is balanced by the opposite change of screen current in the dummy. In a similar fashion, screen current change in the signal amplifier is cancelled by plate current change in the dummy. Consequently, variation of the effective transconductance of the signal amplifier is secured without introducing current surges in the signal circuit.

The maximum signal input to the expander stage is approximately 0.25 volt, and the maximum signal output of the system is of the order of several volts. The diode rectifier incorporated in the suppressor circuit prevents the expander rectifier from driving the suppressor positive, which would produce blocking and loss of expansion control. The time constants of the expansion rectifier systems are such that 75 percent of final gain is achieved in the *Fast* position in approximately 0.02 second. This time constant is tripled in *Slow* position. The two decay times are about 0.5 and 1.2 second respectively.

Three-Band Variable Equalizer

Versatile pre-equalizer provides gain or attenuation adjustment in one-db steps independently in the low-, high-, or mid-frequency bands of the audio spectrum. Applications include recording, rerecording, sound system compensation, and broadcast station equipment

By L. D. GRIGNON

THE variety of corrective networks used in audio equipment is due to the great number and extent of required corrections and to the difficulty of adequately and rapidly analyzing undesirable features in the signal being transmitted, recorded, or reproduced. In designing a single equalizer of sufficient flexibility to meet the diverse requirements usually encountered, one must decide what frequency characteristics are to be used, particularly if the total number of units is to be minimized.

The material which follows describes a suitable equalizer system which has been found easier to use and more effective for the purpose intended than any of the many types previously employed by the writer. In addition to this description, brief design information is given so that others may modify the circuits shown to suit particular conditions.

Characteristics

Experience with sound systems and in recording indicates that the majority of desired corrections exist in either or both the low or high ends of the frequency range. Intelligibility must be maintained at all times and, since this is most easily accomplished by emphasizing the mid-spectrum frequencies, a means must be provided to perform this function. Conversely, suppression of the mid-band can frequently be used to make harshness more tolerable, provided intelligibility is not degraded.

An important operating feature, too frequently excluded from corrective network design, provides that the 1000-cycle insertion loss shall not change appreciably as changes in the response characteristic are introduced. A few moments of operation with a network having this feature are sufficient to prove the point. Further, if the network is arranged so as to be inserted in various circuits, it must introduce no insertion gain or loss.

Accepting the above fundamentals, the unit was designed so that low- and high-end emphasis or suppression are in discrete steps achieved by a shelf effect arranged to shift the frequency of one-half loss or gain further toward the extremes of the signal band or nearer the mid-frequencies, thereby affecting the normal circuit characteristics only to the extent required by the necessary correction. (This differs from the usual manner in which only the slopes of the characteristic are changed, the hinge frequency remaining fixed.) Maximum suppression is 4 to 6 db, maximum emphasis is 8 to 10 db, and the change between steps is approximately 1 db, measured at 100 cps and 7,000 cps.

Mid-frequency correction is a maximum at 2,750 cps and is variable in steps of ½ db up to a total of 5 db suppression or emphasis. Frequency characteristics obtainable by the networks are shown in Fig. 1. Any combination of low-, mid-, and high-frequency responses can be obtained. Insertion loss of the system of networks can be made zero by a suitable choice of fixed attenuators.

Suppression at any of the three bands is introduced by rotating a control in a counter-clockwise direction from a normal setting and emphasis is applied by rotating the same control from the normal setting in a clockwise direction. In either case, suppression or emphasis is made progressively greater as the control is manipulated further from normal. As suppression or emphasis is introduced into any of the three frequency

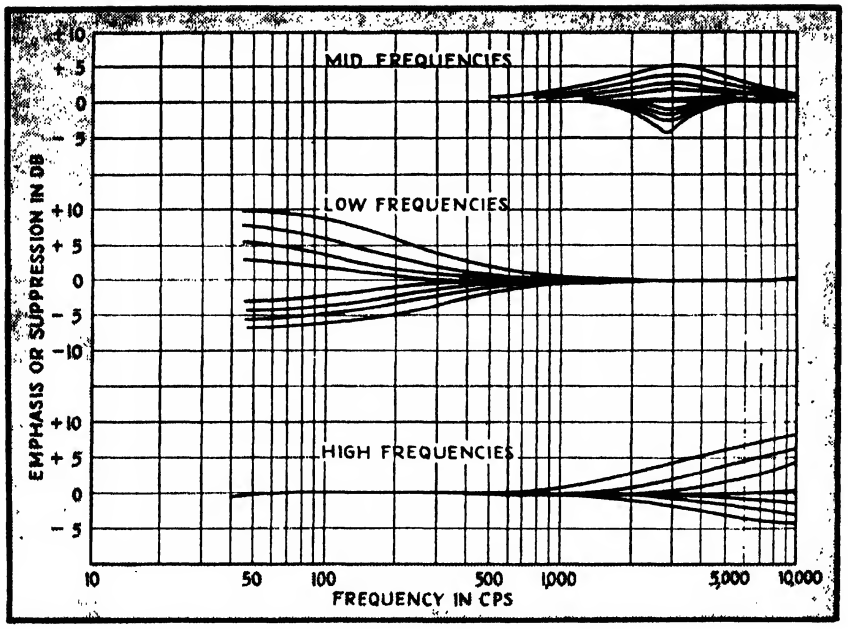

FIG. 1—Representative frequency characteristics obtainable with the three-band variable equalizer. Combining three curves, one from each group, gives the over-all response

bands, the insertion loss at 1,000 cps does not vary more than 1 db.

Dial stops, which are readily adjustable, are provided on each control to permit pre-setting or to provide limits.

The system may be inserted into a circuit without affecting normal transmission, manipulations or usage and, as previously specified, volume corrections need not be made simultaneously with equalization, although under some circumstances, particularly when low-end corrections are applied, there will be an apparent level change.

Mid-Frequency Section

Two constant-impedance networks are used for mid-frequency control. One is a suppression network of the required shape and fixed in amount at the desired maximum; the second is an emphasis network connected in series and variable in equalization by an amount equal to the sum of the maximum amounts of desired suppression and emphasis. At an intermediate point in the setting of the variable attenuator the frequency characteristics of the two networks are inverse and the net applied frequency correction is zero.[1]

To maintain constant insertion loss at all correction settings, a second variable attenuator having a 10-db maximum is mounted on the same shaft with the correction network attenuator, connected in series with the other two networks, and mechanically arranged to maintain the total attenuator loss at 10 db. The circuit as described above is shown in Fig. 2.

Feedback

Having introduced a loss of 10 db by the introduction of the mid-frequency networks, it is necessary to use at least 10 db of gain to maintain zero insertion loss. By providing amplification of greater than 10 db, low- and high-frequency correction can be realized by negative feedback.[2, 3]

The fundamental equation pertaining to negative feedback is

$$\text{Net gain} = A/(1 - KA) \qquad (1)$$

where A is voltage amplification without feedback and K is the ratio of input feedback voltage to the output voltage. Examination of this equation discloses that a two-fold change in K will nearly provide 6 db change in gain, provided that the product KA is sufficiently large. Further, by selecting the proper value for KA, the slope of the gain change can be adjusted to a maximum of approximately 6 db per octave when simple reactive combinations are used. However, when K varies with frequency because of reactive elements in the circuit, the phase angle around the feedback loop must be considered when computing resulting frequency characteristic changes.

Figure 3 depicts a two-stage amplifier with parallel feedback from the second plate circuit to the input cathode resistor. Feedback factor is determined by the ratio of Z_1 to $Z_1 + Z_2$. If either Z_1 or Z_2, or both, are made a function of frequency, as they are in Fig. 3, the frequency characteristic of the amplifier will vary accordingly.

Low- and high-end suppression or emphasis can be controlled by capacitor-resistor combinations such as are shown in Fig. 3. With a suitable choice of resistors, capacitors, over-

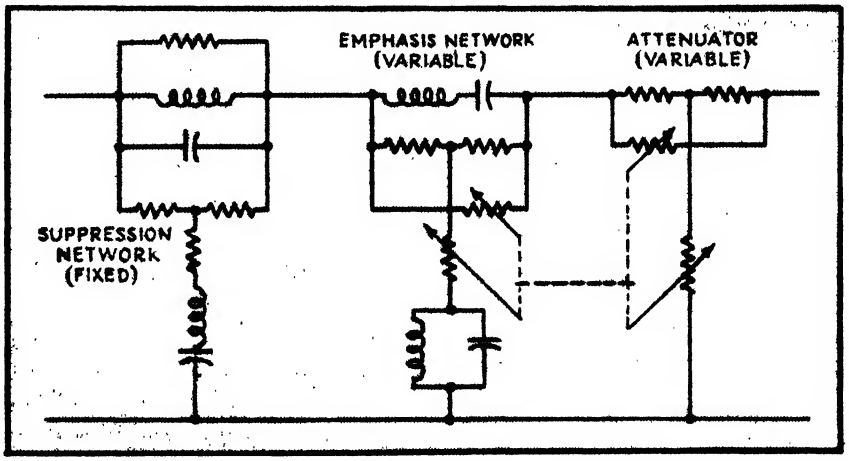

FIG. 2—Mid-frequency equalizer network

all gain without feedback, and feedback factor the specified frequency characteristics can be obtained by increasing or decreasing C_1, C_2, C_3, or C_4 in discrete steps, as follows:

Low-end suppression: Decrease C_1
Low-end emphasis: Decrease C_2
High-end suppression: Increase C_4
High-end emphasis: Increase C_3

Capacitors C_1 and C_2 are connected into the circuit with a single switch which is arranged to maintain C_1 constant while C_2 is being decreased to produce low-end emphasis and, conversely, C_2 is held constant as C_1 is decreased to give low-end suppression. Capacitors C_3 and C_4 are switched in the same manner except that either is held at the minimum value while the other is increased, in steps, to obtain high-end emphasis or suppression.

So that the feedback path does not adversely shunt the plate-cathode branch of the output tube, it is desirable to keep the minimum impedance of the path about twice the nominal plate impedance of the output tube. At first thought, such a relatively low-impedance path may seem unduly small, but in use the effective plate impedance is considerably lowered by the feedback factor and by the fact that as the path impedance is lowered to achieve equalization, plate impedance is likewise lowered. Obviously, there must be a limit and R_7 serves the purpose.

Because of the foregoing facts, large values of A (Eq. 1) are used, amounting to a voltage gain of 350 (measured without bypass on R_3) exclusive of input and output transformers. With the particular coils used, the over-all gain is 50 db, which is then reduced by the no-equalization feedback to 30 db. The greatest change in net gain is then from 24 db to 40 db, leaving 10 db minimum feedback to insure stability and maintenance of characteristics.

Circuit Details

Theoretically, a two-stage amplifier with only resistive feedback cannot oscillate even though very large values of KA are used. In practice, this is modified by phase shifts within the amplifier due to coupling, bypass, and stray impedances so that care must be exercised in design to minimize such effects. A satisfactory solution, when reactive elements are included in the feedback path as in this application, results when the amplifier is flat in frequency characteristic within two db from 20 to 20,000 cps and has no abrupt changes in gain.

The approach to the design of a corrective amplifier such as shown in Fig. 3 naturally depends upon how many types of correction are to be supplied and the order of magnitude.

The design approach for the unit being described will be used as an example.

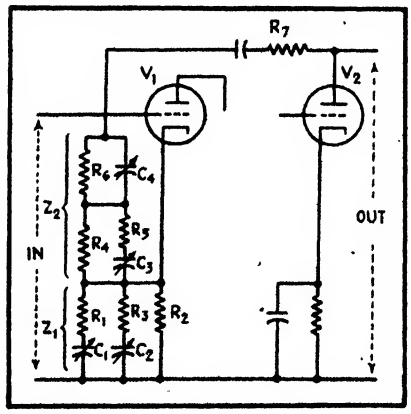

FIG. 3—Method of connecting resistors and capacitors in feedback path of two-stage amplifier providing low-frequency and high-frequency suppression or emphasis

First, determine the slopes of the gain changes to be obtained, keeping in mind that simple resistor-capacitor networks have a maximum reactance change of 2 to 1 for a corresponding frequency change and may be limited to less than this ratio by choice of configuration. Assuming a given tube complement, the cathode resistor of V_1 is determined within certain limits and the minimum feedback impedance can be determined, since the difference in gain establishes the maximum sum of desired suppression and emphasis.

From all of these facts the product of KA and of each factor can be established. Obviously, there is more than one combination which will satisfy the conditions. Determination of the values of the capacitor-resistor networks can most easily be made by recourse to the charts of Di Toro.[4] Some trial values and computations are indicated. Note that the zero-equalization conditions are determined principally by R_7, R_6, R_4, R_5, R_1, and R_2 in Fig. 3 since both C_1 and C_2 are made large for this condition and C_3 and C_4 are made very small.

Once the approximate components are determined, the remainder of the work is best done experimentally.

Nominally, the blocking capacitor in the feedback path is made relatively large in order that appreciable changes in feedback phase angle, or reduction of the feedback factor, occur at very low frequencies where the amplifier gain is low and the stability requirements established by Black[3] and Bode[5] are met. The use of networks as described permits an appreciable reduction in the capacitances of the coupling capacitor and C_2 due to the reverse effects of C_1 which is made smaller than might be expected to accomplish the desired result. Proper proportioning of the capacitors maintains the feedback factor nearly constant over the useful frequency range when set for zero correction.

As previously mentioned, the amplifier at zero equalization gives a gain of 30 db which must be reduced to zero by attenuators. The system of networks is assembled as in Fig. 4 with these attenuators, three fixed and one variable (in the mid-frequency section), located so as to make the input and output essentially resistive.

Because the feedback network is not of abnormally high impedance the network controls can be placed in a separate unit which contains the two capacitor accumulator switches, the mid-frequency network attenuator with the compensating ganged attenuator, and the feedback network capacitors.

Due to the potential differences which gather on the switch contacts, there will be some noise unless these potentials are reduced by connecting resistors between adjacent switch contacts. These bleeder resistors can be made sufficiently low to reduce noise without seriously affecting the frequency characteristic. A further aid in maintaining low noise from

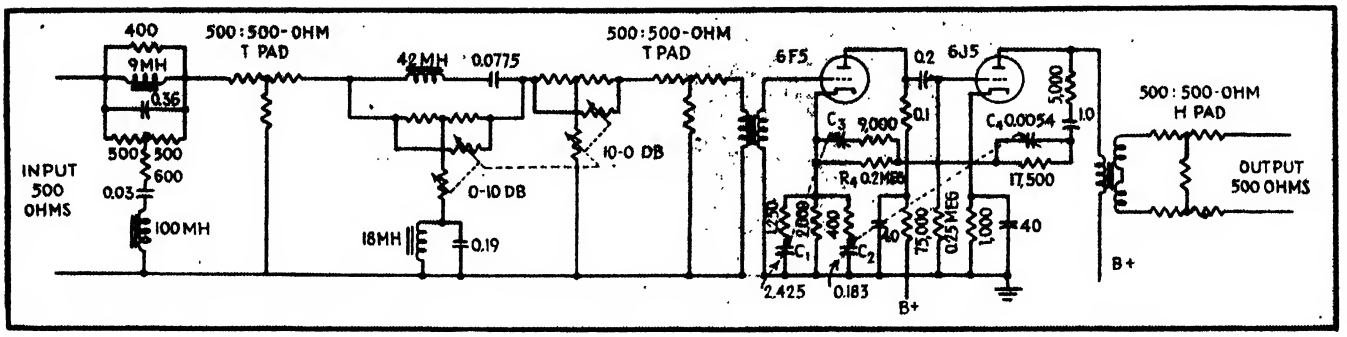

FIG. 4—Complete circuit of three-band variable equalizer. To raise lows, reduce C_3; to raise highs, increase C_2; to lower lows, reduce C_1; to lower highs, increase C_4. Fixed resistors shunting rheostats are 500 ohms each

the switches is the small difference in attenuation between steps.

The mid-frequency variable network has the usual characteristic of varying the frequency at which one-half attenuator loss occurs. As a result, the emphasis characteristic does not have the same shape as that obtained for suppression. The characteristic shown has been found satisfactory, but if this network were of the so-called constant B type as described by Miller and Kimball[6] there would not be the difference indicated.

Frequency characteristics do not change with tube replacement nor with a 10-percent change in plate supply voltage. Total noise, measured at the output of the system, is 87 db below 0.001 watt, which is sufficiently low to work into high-gain circuits for recording or rerecording. The minimum output capacity, including the output attenuator, is 8 db above 0.001 watt.

There has been some apprehension that feedback amplifiers with reactive networks in the feedback path are apt to be less stable and more susceptible to trouble than other conventional designs, but experience has shown that this is not the case. There has also been some aversion to the use of other than constant-impedance equalizers or additional amplifiers for frequency correction purposes, which has probably been due to ill effects caused by changing impedance conditions or poor transient response in such circuits. Both these faults are minimized in this system, as indicated by square-wave and intermodulation tests.

References

(1) Design information on networks as described may be found in "Motion Picture Sound Engineering," D. Van Nostrand Co. Inc., New York, Chapter XVI.
(2) Black, H. S., U. S. Patent 2,102,670.
(3) Terman, F. E., "Radio Engineers' Handbook," McGraw-Hill Book Co., New York.
(4) Di Toro, M. J., Equalizer Design, ELECTRONICS, p 118, April 1944.
(5) Bode, "Network Analysis and Feedback Amplifiers," D. Van Nostrand Co. Inc., New York.
(6) Miller and Kimball, *Journal of the Society of Motion Picture Engineers*, 43, No. 3, p 187, Sept. 1944.

Automatic Audio Phase Reverser

By ALVIN H. SMITH

IT IS a well known fact that the waveform of most speech and some music is not symmetrical. When such a nonsymmetrical signal modulates an a-m transmitter, it is possible for the modulation envelope to undergo excursions below the unmodulated level that are greater than the envelope excursions above this level. Such a condition is referred to as negative modulation. Most broadcast transmitters can accommodate positive modulation peaks in excess of 100 percent, but in no case can the negative modulation peaks exceed 100 percent, or serious distortion and interference to other radio services will result. Moreover, most detector distortion in modern broadcast receivers occurs on the negative portion of the detection curve. Thus, if a nonsymmetrical modulating signal can be made to produce more positive than negative modulation peaks, the coverage of a radio station may be increased, and, at the same time, overall distortion can be reduced.

The purpose of this a-f phase reverser is to adjust automatically the polarity of the audio input signal to the transmitter to produce the desired modulation polarity. This device is particularly useful when the modulating signal is of local studio origin; after an audio signal has passed through a number of repeater amplifiers, as in the case of a network program, phase and amplitude distortion cause the lack of waveform symmetry to be less pronounced

Circuit Operation

The circuit of the automatic phase reverser is shown schematically in the accompanying illustration. Basically, the device consists of a two-stage bridging audio amplifier using 6C5 tubes, a balanced rectifier, consisting of a 6H6 with one cathode grounded, and an R-C delay network, the output of which is connected to the control grid of

a 2050 thyratron. The firing of this thyratron actuates a polarity-switching relay.

A dpdt sense switch is connected in the input of the phase reverser unit. This switch is used to preset the phase reverser so that on modulation peaks, the transmitter will be modulated more positively than negatively. Once the proper switch position is selected, no further adjustment is required and the operation of the device is entirely automatic.

Conventional audio amplifiers are used and are designed to produce minimum distortion, since the waveform of the incoming audio signal must be preserved as nearly as possible. The 6H6 balanced rectifier operates in such a manner that for low audio input voltages, the potentials across the two halves of the output load are approximately equal. Under this condition, the net voltage across the R-C delay network is nearly zero.

On input voltage peaks, the rectification efficiency increases, and the diode having the higher input voltage peak develops the larger voltage across its load. As a result, a voltage is impressed across the input of the delay network having a polarity that is determined by the predominance of negative or positive peaks at the rectifier input.

Plate voltage for the 2050 thyratron is supplied by one-half of the high-voltage winding of the power-supply transformer through the winding of the polarity-switching relay. The thyratron normally conducts on every positive half-cycle of its plate voltage. Whenever the net voltage from the balanced rectifier is such that the grid voltage of the thyratron is approximately 3 volts negative, the thyratron ceases to fire and the relay switches to its unenergized position, reversing the polarity of the audio signal delivered to the transmitter.

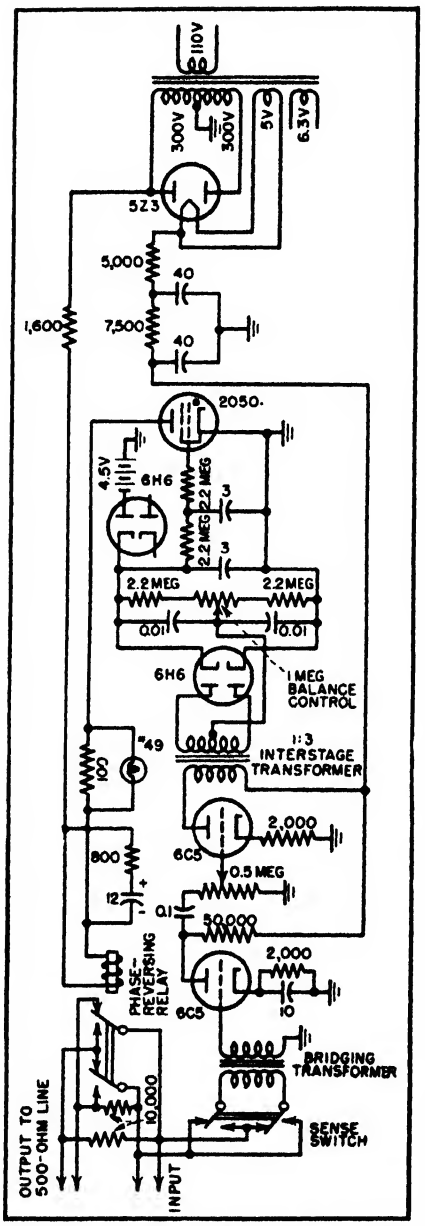

Automatic phase reversal of an audio signal is done by this circuit

A two-section R-C delay network is connected to the grid of the thyratron. This delay network aids in preventing chattering of the relay and delays switching until several peaks of the same polarity have occurred. Two 10,000-ohm resistors across the relay contacts act to reduce key clicks in switching; relay contacts should be set as close as possible for the same reason. The combination of the 12-μf capacitor in series with the 800-ohm resistor also acts to prevent relay chattering.

Control of Switching Time

A 6H6 clipper tube prevents the delay-network capacitors from charging negatively to such a degree that the switching action of the thyratron can not follow rapidly the peak polarity changes of the audio signal. The grid circuit of the thyratron performs this function for positive capacitor charges. Adjustment of the audio input to the balanced rectifier also affects the time required for switching.

The value of the resistor in series with the plate of the 2050 depends upon the characteristics of the particular relay used. This resistor should have as high a value as will give good switching action. A desired switching delay can be obtained by changing the values of the circuit constants in the R-C delay network. The only limitation is that the resistance in series with the 2050 grid must be at least 300,000 ohms.

The automatic phase reverser neither adds to the distortion nor increases the noise level of the audio circuit with which it is connected. This condition results from the fact that the audio circuit has only a dpdt relay added to it.

Low-Distortion Crossover Network

If placed between the output stage and the low-frequency output transformer, an audio crossover network for woofer-tweeter loudspeakers reduces distortion due to nonlinearity of transformer inductance and makes special transformer designs unnecessary

By PAUL W. KLIPSCH

TRANSFORMERS are recognizable as sources of distortion due to the nonlinearity of the inductance, which gives rise to an exciting current that contains components other than the fundamental. The same nonlinearity also produces intermodulation distortion.

The crossover network can be used to reduce transformer distortion by placing at least part of the low-pass filter between the power source and the low-frequency output transformer, instead of between the output transformer and the load.

Consider an output transformer operating between a high-impedance tube source and a 5,000-ohm load (referred to the primary side). Assume the primary inductance to be 26 henrys. At 30 cycles $\omega = 190$ and $\omega L = 5{,}000$. The shunt reactive load, equal to the resistive load, would produce a response which is 3 db down at 30 cycles. This is considered good response.

Next consider that the exciting current contains a considerable harmonic content. At ordinary power levels the third harmonic would typically be about one-third the amount of the fundamental current. This harmonic current, flowing in the generator impedance, produces a distortion voltage which is then fed to some other load, such as a high-frequency channel.

Evidently, a much higher primary inductance is required for reasonable distortion than would be required merely to give a flat response.

The circuit of Fig. 1A is an approximate equivalent of a tube source G_1 having a tube impedance R_P, feeding a transformer having a winding resistance R_T and primary inductance L. The distortion components are considered as being produced by generator G_2. This added generator produces harmonic voltages and intermodulation products.

The crossover network arrangement of Fig. 1B accomplishes two major purposes. First, the low-pass filter $L_1 - C_1$ attenuates high frequencies propagating in either direction. Voltages produced by G_2 are attenuated before reaching tube impedance R_P, so that relatively less distortion voltage is available at R_P for transmission to the high-pass channel.

Second, $L_1 - C_1$ attenuates high frequencies from G_1 propagating to the transformer, so that a narrow range of frequencies is received by T_1. The modulation products generated in T_1 (represented by G_2) are therefore of lower order than would be the case if the transformer were required to handle the entire spectrum. Furthermore, such modulation products from G_2 are again attenuated in their transmission back to the impedance of the tubes.

Obviously, both these effects reduce the distortion which can be fed to the high-frequency channel. The most annoying distortion generally appears as a form of high-frequency noise, and reduction of transmission of low-channel distortion to the high channel reduces this form of distortion.

This network system, by limiting the distortion produced by the nonlinear exciting current of the low-frequency output transformer and by limiting the transmission of such distortion back into the rest of the system, offers a double-dose cure for over-all distortion.

The network of Fig. 2 has already been described in some detail.[1] This circuit was originally developed primarily for purposes of economy. Since the original publication, some of the reasons for the superior performance have been studied, with the result that the advantage of lower distortion is now recognized as of greater importance than the reduced cost.

For the conventional tube output

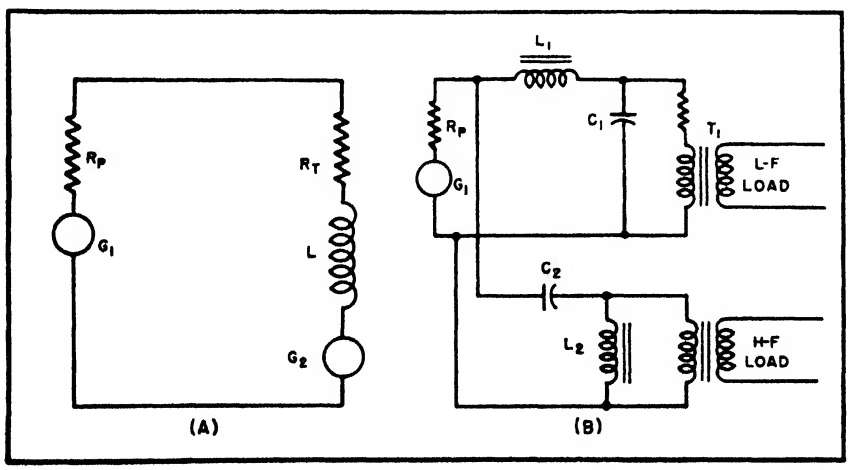

FIG. 1—Equivalent circuit of output tube, and recommended crossover network arrangement for reducing distortion due to inductance of output transformer

circuit one may set up transformer requirements. Taking the exciting current as composed of a fundamental component $I_1 = E/\omega L$ and a third harmonic content $I_3 = (1/3)\ I_1$, consider a tube source with R_p of 2,000 ohms working into a load of 5,000 ohms, and consider a low-end cutoff of 31 cycles. Assume we want to limit third harmonic distortion to 0.5 percent or 0.005 per-unit of the fundamental.

The inductance can be determined from

$$L = R_p/3\omega_1 D \qquad (1)$$

where L is the primary inductance of the transformer, R_p is the plate impedance, ω_1 is the angular velocity of the lowest frequency, and D is the per-unit distortion. (Distortion D is the product of the harmonic component of exciting current times the tube impedance, divided by the fundamental voltage. The exciting current (fundamental) was $I_1 = E/\omega_1 L$. I_3 is taken as $I_1/3$, so $I_3 = E/3\omega_1 L$. $I_3 R_p = DE$ so $D = 1/3\omega_1 L$ or $L = 1/3\omega_1 D$.)

Putting in numerical values, $L = 2{,}000/3 \times 200 \times 0.005 = 667$ henrys. This is a difficult value to achieve, doubly so if the leakage inductance is to be held to a minimum dictated by a top limit of transmission of say 15,000 cycles.

If the transformer is required to transmit only the lower part of the total spectrum the leakage inductance limitation is removed and a transformer with realizable ratio of primary-to-leakage inductance can be designed. Therefore, placing the low-pass filter ahead of the transformer relaxes its design requirements relative to maximum primary-to-leakage inductance ratio.

Placing the filter ahead of the transformer also reduces the required primary inductance for a stipulated distortion. First, the filter attenuates in each direction, so that harmonics and other distortion products arising in the transformer are attenuated before getting back to the generator where they can be transmitted to the high channel. Second, the higher frequencies are attenuated in a forward direction so that the distortion products arising in the transformer are of low order.

Thus, conventional transformers with primary inductance values of the order of 100 to 200 henrys can be used, instead of special designs with values like 667 henrys. Further, since the transformer is required to transmit only up to the crossover frequency, say 500 cycles, the leakage inductance is not a severe design requirement and the transformer may be a relatively low-priced unit.

Appendix

An examination of Eq. 1 and its derivation indicates the desirability of keeping the plate impedance low. Triodes, with or without feedback, and the more efficient beam tubes with voltage feedback, both offer the desirable low impedance. Either can be designed for any desired characteristics. It should be noted, however, that reducing the driver stage impedance to zero would still leave the transformer winding resistance, so a loudspeaker would never look back into zero impedance.

In the numerical example, the figures chosen would apply either to a pair of 2A3 (6B4G) tubes in push-pull without feedback, or to a pair of 6L6 tubes with about 15 db of voltage feedback.

To reduce the plate impedance to zero or near zero values might appear to be highly desirable. However, the characteristics of the driven loudspeakers are such that some source impedance is desirable. Even in highly developed horn loudspeakers, the efficiency and impedance vary, and the source impedance tends to smooth out the resulting response. In the case of direct radiators with the 20 to 1 variations in impedance a constant-voltage source is not the best.

Thus, feedback to reduce output impedance would appear capable of being carried too far. Feedback for distortion reduction can be applied simultaneously as voltage feedback which tends to reduce the tube impedance (make it constant voltage) and current feedback which tends to increase the impedance (make the source constant current). A happy combination of the two might prove to be the best overall.

Here one is faced with the desirability of an optimum impedance for operation of the loudspeakers, and a minimum impedance from the standpoint of distortion in the transformers. The crossover arrangement discussed here offers the possibility of minimizing transformer distortion while maintaining the tube impedance at optimum levels from the standpoint of loudspeaker operation and distortion.

Either voltage or current feedback reduces distortion in the tube system (and both together reduce distortion to the same extent as would the same amount of total feedback of either type by itself). A combination of both affords any desired impedance, so it appears that the designer is free to design the amplifier for optimum loudspeaker performance, relying on the described crossover to hold the distortion from reasonably good transformers within tolerable levels.

In the numerical example, a low cutoff of 31 cycles was chosen. There are very few loudspeakers that will reproduce a 30-cycle fundamental. If one is dealing with direct radiators of moderate size cutting off around 70 to 90 cycles, the improvements afforded by the present crossover will be but slightly noticeable. But if one starts working with organ reproduction or generation where low-C performance is demanded, some very annoying distortions crop up. It is particularly for the users of reproducers capable of 30-cycle performance[2] that this article is written.

References

(1) P. W. Klipsch, Crossover Network, Electronics, Nov. 1945.
(2) P. W. Klipsch, Design of Compact Two-Horn Loudspeaker, Electronics, Feb. 1946.

Technique for Distortion Analysis

Modification of clipped sine waves by circuits under observation is displayed on a cathode-ray oscilloscope for quick analysis of audio response. Typical patterns are given, and a simple equipment comprising biased crystal rectifiers is described

By SAMUEL SABAROFF

DISTORTION in a linear circuit can be separated into two general categories: nonlinear distortion; and frequency distortion. Nonlinear distortion is caused by impedances that are functions of current or voltage. A sine wave introduced in such an impedance will be distorted in waveform because of the harmonics generated. These nonlinear impedances are generally resistive, like those encountered in a tube or crystal.

A sine wave introduced in a circuit containing only reactance will not be distorted in waveform, but may be changed in phase and amplitude. This phase shift and amplitude change may also vary with frequency. Harmonics are not generated in this kind of a circuit, though they may be selectively diminished or accentuated.

Circuits in general have both nonlinear distortion and frequency distortion. The amount and kind of distortion that can be tolerated in a circuit depends on its use. Communication circuits, in which intelligibility is paramount, can have considerable distortion, whereas broadcast circuits should have negligible distortion.

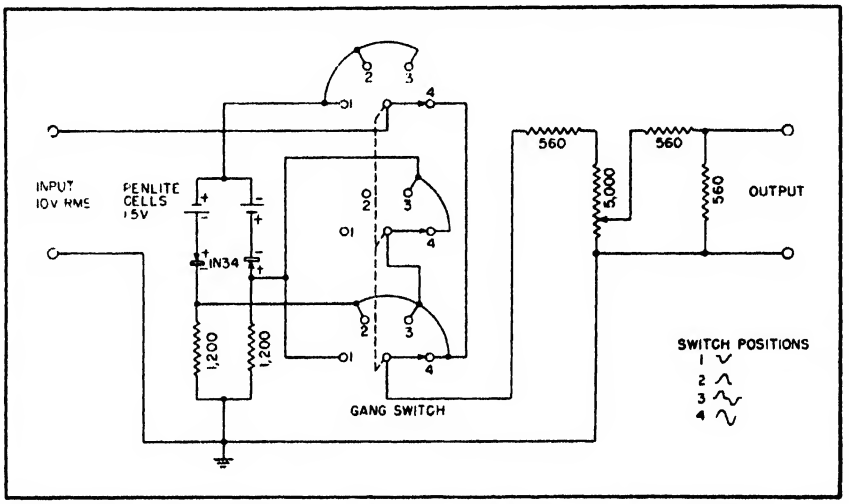

FIG. 2—Circuit diagram of a sine wave clipper with output waveforms for various switch positions indicated

There are various ways of determining distortion in a circuit in order to indicate its suitability for a particular application. One well-known method utilizes the circuit response to a sine wave. Nonlinear distortion is measured by noting the percentage of harmonics generated in the circuit for various frequencies and amplitudes. The effect of reactance is measured by the variation in gain as the frequency is varied.

The interdependence of the two kinds of distortion is not always clearly stated. The harmonics generated by nonlinear distortion will be influenced by the frequency characteristic, so that the sine wave analysis is correct only if either the nonlinear, or the frequency distortion is found to be negligible.

The sine wave analysis is of great utility however, in that definite and reproducible quantities

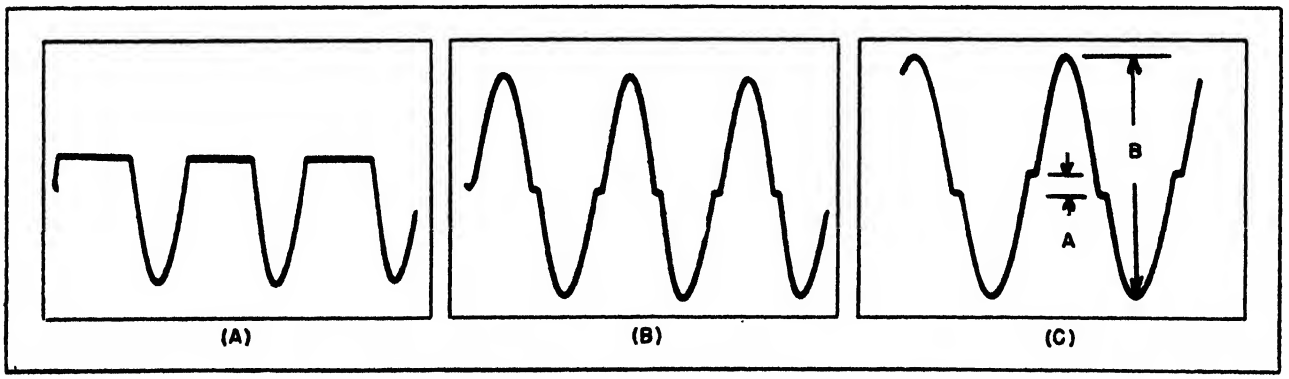

FIG. 1—Clipped sine wave (A); double clipped sine wave (B); double clipped sine wave showing phase shift (C)

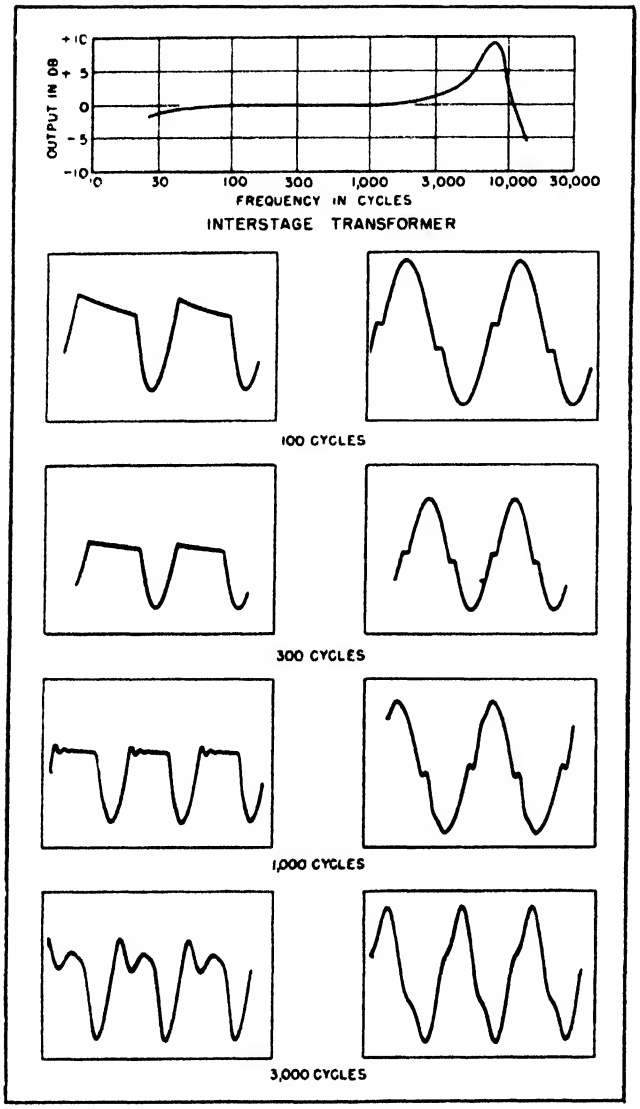

ABOVE

FIG. 3—Response of an interstage transformer in conventional graphic form and by means of clipped, and double clipped, sine waves

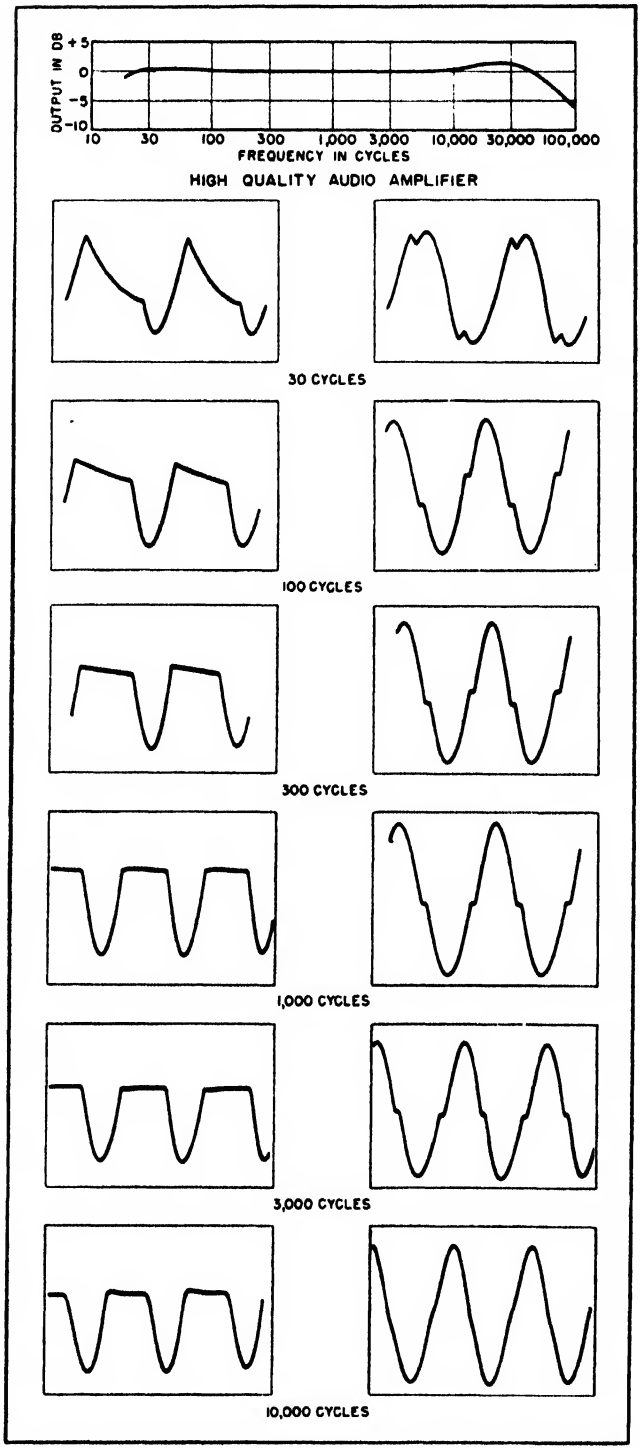

RIGHT

FIG. 4—Graph of high quality audio amplifier characteristics with clipped (left) and double clipped (right) oscillograms of response at spot frequencies

are obtained. In experimental, and developmental work it is sometimes tedious and time consuming.

Standard Waveform Method

A quick and simple qualitative anlysis of a circuit can be made by noting the change in shape of certain standard waveforms. Waveforms with a high harmonic content are particularly suitable for investigating the effect of frequency distortion in wide-band circuits. One example is the square wave, which is of great utility in the investigation of video circuits. The square wave can be considered to simulate an extreme case of the kind of signal the circuits are required to handle.

Most signals encountered in audio circuits are complex in that they are composed of a fundamental and its harmonics. A test waveform that simulates such a signal, and that has been particularly useful in audio circuit analy-

sis is shown in Fig. 1A. It is a portion of sine wave and is therefore called a clipped sine wave. Two such clipped sine waves can be placed back to back, as shown in Fig. 1B. This waveform has been termed a double clipped sine wave.

One great advantage of the clipped sine wave is in the economy and simplicity of its generator for which the circuit diagram is given in Fig. 2. A sine wave of the proper amplitude, is fed into the unit and clipping is done by means of biased crystal rectifiers.

The frequency range of the driving voltage is determined by the kind of equipment being tested. For high quality circuits, the frequency range may be approximately 100 to 10,000 cycles. For communications circuits, it can be 300 to 3,000 cycles. The frequency range need not be continuously variable. For most purposes, the discrete frequencies of 100, 300, 1,000, 3,000, and 10,000 cycles will suffice.

From Fig. 1A it is seen that the clipped sine wave is composed of successive flat portions with sharp corners, interconnected by portions of a sine wave. Analysis of this wave shows it to be the fundamental plus an infinite series of harmonics with the even harmonics predominating.

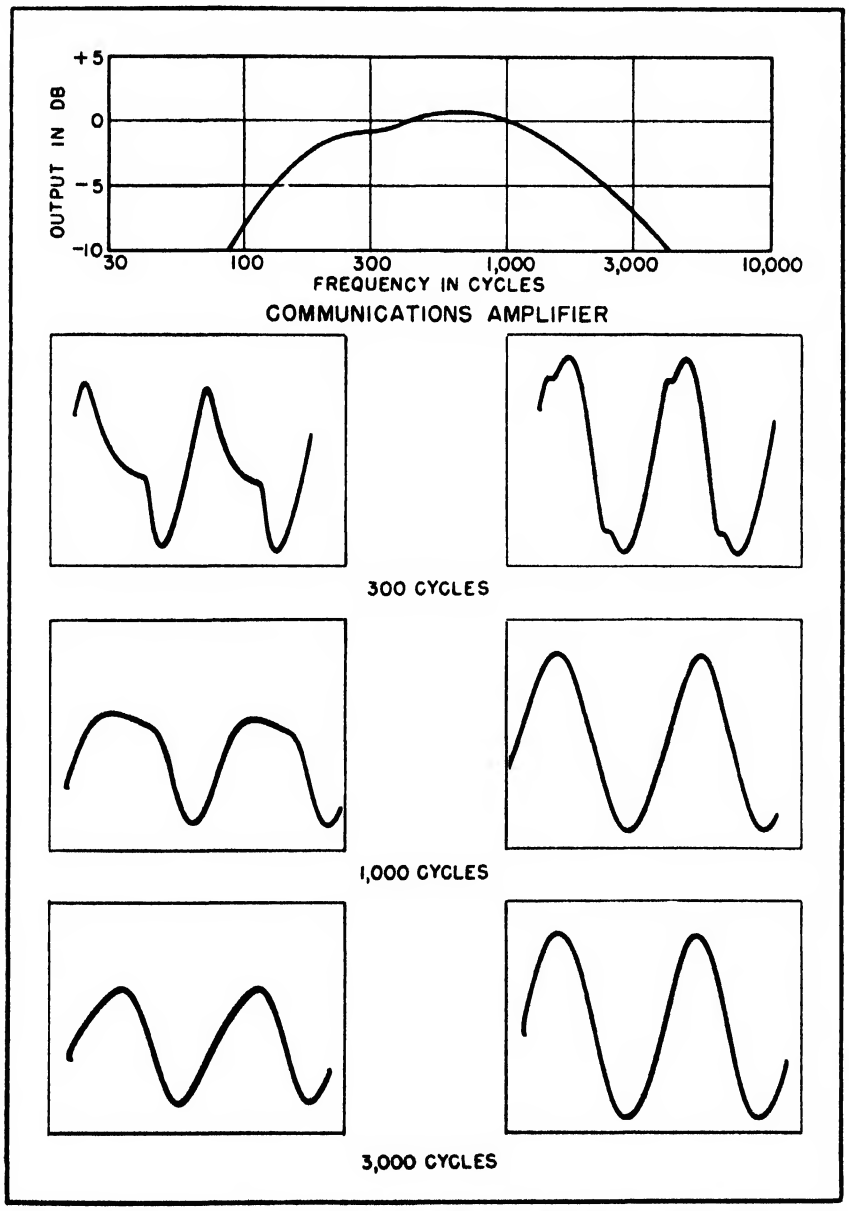

FIG. 5—Response of a communications amplifier. Oscillograms at left show effect on clipped sine waves and, at right, on double clipped waves

The flat portion and the sharp corners of the clipped sine wave are similar in shape to a half square wave, and the effect of a circuit on this portion of a clipped sine wave is similar to the effect on the square wave. Square wave experience can therefore be transferred almost intact to analysis with the clipped sine wave.

The asymmetry of the clipped sine wave is of great help in avoiding mistaken analysis due to amplitude saturation. Amplitude saturation is easily noted by a flattening of the peaks of the sine wave portion. Asymmetrical amplitude saturation can be investigated by reversing the polarity of the clipped sine wave. This feature has been useful in the investigation of class-B amplifiers. For the analysis, it is sometimes advantageous to reduce the duration of the sine wave portion by decreasing the ratio of driving voltage to back bias.

Double Clipped Sine Wave

The double clipped sine wave is useful in determining phase shift at low frequencies. It is composed of the fundamental and an infinite number of harmonics, with the odd harmonics predominating. This waveform, (Fig. 1B), is seen to be a sine wave with a small step at the points of zero voltage. Phase shift in a circuit is indicated by a vertical displacement of these steps, as shown in Fig. 1C. The approximate phase shift can be calculated from the following formula

$$\phi = \sin^{-1} (a/b)$$

where ϕ is phase shift; a is the vertical displacement of step portions; and b is the peak to peak amplitude.

It is possible of course, to formulate and plot the effect of various circuits on the clipped sine wave and the double clipped sine wave. For qualitative analysis, however, it is practical to illustrate the effect

of several typical circuits on these test waveforms by means of oscilloscope displays.

Interstage Transformer

The frequency characteristic of an inexpensive interstage transformer is shown at the top of Fig. 3. This transformer is essentially flat from 30 to 3,000 cycles, but with a large peak in the response at 8,000 cycles. The effect of this transformer on the clipped sine wave is shown at the left. At 100 cycles, there is sufficient high-frequency response to keep the corners sharp. At 300 cycles, a transient has become evident, becoming larger at 1,000 cycles.

The flat portion of the clipped sine wave is slightly less than a half period. Estimating the number of half waves of the transient on the flat portion and multiplying by two gives the approximate ratio of the transient frequency to the driving frequency. In this case it is estimated to be seven half waves for a 1,000-cycle half period, giving an approximate frequency of 7,000 cycles for the transient. It is interesting to note the correspondence of the transient frequency to the point of high gain on the frequency characteristic. The 3,000 cycle clipped sine wave indicates that the transient frequency has been more closely approached.

In Fig. 3 at the right are shown the effects of the transformer on the double clipped sine wave. The transient is beginning to be evident on the flat portions at 300 cycles. The 1,000-cycle wave is appreciably distorted by the transient, and the steps are practically obliterated at 3,000 cycles owing to dropping high-frequency response.

High Quality Amplifier

The graph in Fig. 4 shows the frequency characteristic of a high quality, multistage, resistance-coupled amplifier. This amplifier is essentially flat between 20 and 50,000 cycles. The series of oscillograms at the left shows the effects of this amplifier on the clipped sine wave. At 30 cycles, the slope of the flat portion illustrates the effect

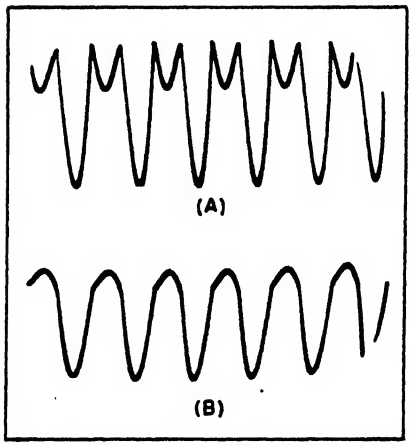

FIG. 6—Clipped sine wave with fundamental partially suppressed (A); and with fundamental partially accentuated (B)

of phase shift. The sharpness of the corners indicates the presence of higher order harmonics. At 100 cycles, the phase shift has decreased and the high-frequency response is still good. The oscillogram for 300 cycles is a good replica of the clipped sine wave, as it is at 1,000 cycles. At 3,000 cycles the effect of high-frequency attenuation is beginning to make itself felt, while at 10,000 cycles high-frequency cutoff has rounded the corners appreciably. The important feature in this analysis is the gradual change in shape of the clipped sine wave over the frequency range. There are no distinct resonant circuits or sharp discontinuities indicated, nor would they be expected in high-quality circuits.

The effect of this amplifier on the double clipped sine wave is shown in the oscillograms at the right. Phase shift, as indicated by the displaced flat portions, is evident at 30 cycles. This characteristic decreases with increasing frequency until it is negligible at 1,000 cycles. At 3,000 cycles the phase shift has reversed direction. Above 3,000 the lack of sufficient high-frequency response tends to obliterate the steps, as shown in the oscillogram for 10,000 cycles..

Figure 5 shows the frequency characteristics of an amplifier used for communication purposes. The response of this amplifier is maximum at approximately 700 cycles. It is down 1 db at 300 cycles, up 1 db at 700 cycles and down more than 7 db at 3,000 cycles. Zero level is taken at 1,000 cycles.

The oscillograms of the effect of this amplifier on the clipped sine wave are shown at the left in Fig. 5. At 300 cycles, phase shift is indicated by the slope of the flat portion, and the lack of high-frequency response by the blunted corners. The oscillogram for 1,000 cycles shows a rise in gain at somewhat less than 1,000 cycles, and the corners are further obliterated. At 3,000 cycles, the effect of a poor high-frequency response is evident. It is interesting to note in this amplifier also, the lack of any tendency toward transients. The clipped sine wave analysis indicates a broadly resonant circuit, with maximum gain at less than 1,000 cycles, and no significant frequency discontinuities outside the pass band.

To the right are the oscillograms showing the effect of this amplifier on the double clipped sine wave. The large phase shift at 300 cycles is shown by the vertical displacement of the flat portions. These steps are increasingly obliterated by the lack of high-frequency response at 1,000 cycles and 3,000 cycles.

Tuned Circuit at Driving Frequency

The examples just given illustrate the ordinary use to which one may put the clipped and double clipped sine wave. The effect of a circuit tuned to the fundamental frequency of the clipped sine wave was not clearly exemplified, and is therefore illustrated. Fig. 6A shows the shape of the clipped sine wave with the fundamental partially suppressed, and (B) with the fundamental partially accentuated. The flat portions have now become concave in A and convex as in B.

When the driving frequency is shifted slightly from that of the tuned circuit these convex and concave portions will be displaced to one side. An example of this effect is shown in Fig. 5 (1,000 cycles, at the left) illustrating the effect of a communications circuit on the clipped sine wave.

Beat-Frequency Tone Generator with R-C Tuning

By J. W. WHITEHEAD

THE PRINCIPLES of resistance-capacitance tuning of oscillators may easily be adapted to the design of tone generators using the heterodyne technique. Such a circuit has several advantages over tuned-circuit generators. For example, no difficulty is experienced in covering wide frequency bands with good frequency stability and low distortion and with simple frequency control. Furthermore, there is an extremely low degree of coupling with neighboring components. Remote control of frequency can also be arranged.

Circuit Details

The circuit shows two R-C tuned oscillators feeding the appropriate grids of a hexode mixer. The output from each oscillator is obtained by a suitable tap on the final resistance of each of the phase-shifting networks. A refinement (not shown) would be to leave a portion of the automatic bias resistance to each oscillator tube unshunted in order to introduce a degree of feedback for the purpose of limiting the amplitude of oscillation.

Control of the frequency generated by the tube V_1 in the variable frequency section is achieved by altering the effective resistance of one element in the phase-shifting network. This could be done by inserting a normal variable resistance in series with one of the fixed resistances, but here the same effect is secured by varying the grid bias of tube V_2. This tube is a cathode follower, the output impedance of which shunts the center resistance of the phase-shift network. The output impedance is a function of the grid bias on the tube that is controlled by potentiometer R. In short, the frequency of the oscillations generated by the variable oscillator, and hence the resulting tone frequency, is determined by the setting of R.

Potentiometer R may be mounted at any desired distance from the apparatus. The lead from its slider carries no current and can therefore cause no instability, however long it is. The potentiometer dial can be calibrated in frequency.

In practice, both oscillators are set to the same frequency (about 100 kc) with V_2 biased almost to cutoff, but if V_2 has a variable-mu characteristic it need not be biased so far back as might otherwise be necessary.

Instead of a cathode follower for frequency control, a negative-resistance transitron could be used and in this case the magnitude of the negative resistance is a function of the grid bias.

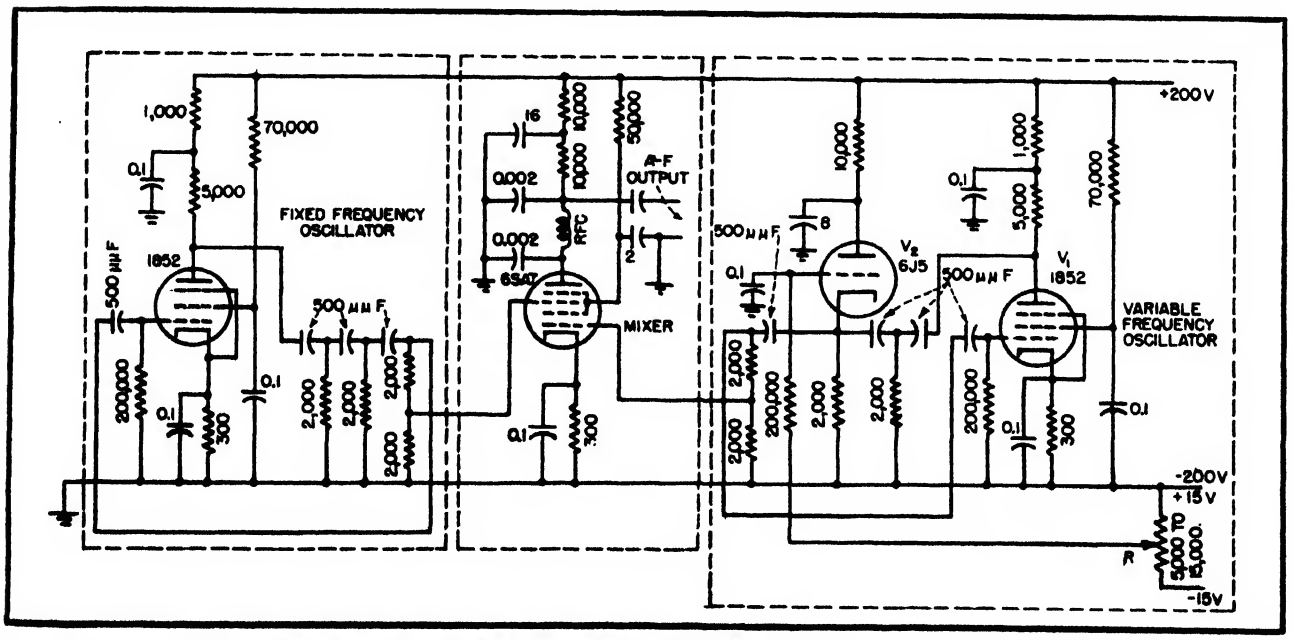

The values shown in the diagram provide oscillator frequencies of about 92 kc and the resulting beat-frequency variation is from a few cycles to over 20 kc. A voltage-regulated plate supply is preferable

Design of Loudspeaker Dividing Networks

Four-parameter chart gives directly the required values of L and C for a parallel-connected constant-resistance dividing network, at any desired crossover frequency and line impedance, when separate low and high-frequency loudspeakers are employed

By EARL R. SCHULER

With divided-range loudspeaker systems, an electrical dividing network must be used to separate the low and high frequencies into two bands so that each may be reproduced by the proper loudspeaker unit. To approximate the ideal network transmission characteristics of Fig. 1, the parallel-type constant-resistance dividing network of Fig. 2 is favored for its simplicity since both inductors (and both capacitors) have the same values.[1,2] The chart in Fig. 3 gives these values of L and C directly for various values of crossover frequency f and line impedance R_o.

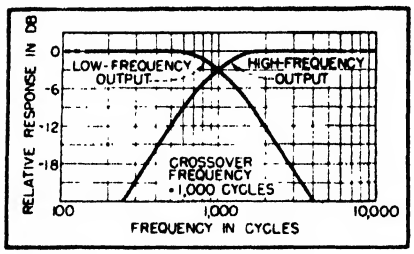

FIG. 1—Ideal transmission characteristics of a 1,000-cycle dividing network

Although the values of L and C may be computed easily from the simple formulas given in Fig. 2, the chart will be found very useful for preliminary design problems. The chart may be used beyond the ranges shown by employing one of the following sets of multiplying factors for the scales:

R_o	f	L	C
1	10	0.1	0.1
10	1	10	0.1
10	10	1	0.01

To prevent the generation of harmonics and intermodulation products by the network, the inductance of the coils must be independent of the signal level. Since air-core inductors are inherently free of this difficulty they are usually preferred over iron-core types. They must be rather large, however, and must be wound with heavy wire in order to obtain a reasonably high Q. A value of 20 at the crossover frequency is satisfactory. Information on the design of air-core inductors may be found in the literature[3,4].

EXAMPLE 1: A dividing network is required for use in a 15-ohm line, the crossover frequency to be 1,000 cycles. From the point of intersection of the diagonal 15-ohm and 1,000-cycle lines on the chart, read out to the left and upper edges of the chart to the values 3.37 mh and 7.50 μf for L and C. Coils may be wound especially for this value, and standard-size capacitors may be connected in parallel to make up the required capacitance within 5 to 10 percent.

It is permissible to redesign the network for a slightly different crossover frequency to permit use of standard capacitors. New values taken off the chart, starting from the intersection of the 15-ohm and 8-μf lines, are 938 cycles and 3.60 mh.

EXAMPLE 2: A dividing network is required for use in a 600-ohm line, the crossover frequency to be 500 cycles. This installation will require the use of separate auto-transformers to match the low- and high-frequency units to the 600-ohm outputs of the network. Since 600 ohms does not appear on the chart, preliminary values must be determined from the intersection of the 60-ohm and 500-cycle lines; these are found to be 27 mh and 3.75 μf. Since the value for R_o must be

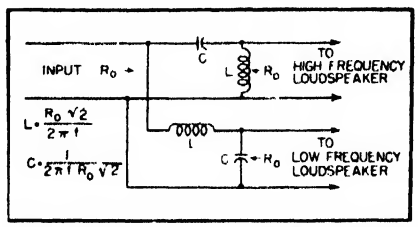

FIG. 2—Circuit of parallel-type constant-resistance dividing network, with design equations (L is in henrys, C is in farads, f is crossover frequency in cycles, and R_0 is impedance in ohms of input and each output branch of the network)

multiplied by 10 and there is no change to be made in the frequency (f multiplied by 1), the conditions for determining the final values are met by applying the multiplying factors on line 2 of the table. This gives final values of 600 ohms, 500 cycles, 270 mh, and 0.375 μf for the network.

REFERENCES

(1) John K. Hilliard, Loudspeaker Dividing Networks, ELECTRONICS, p 26, Jan. 1941.
(2) "Motion Picture Sound Engineering", chapter XX, D. Van Nostrand Co., New York, 1938.
(3) H. A. Wheeler, Simple Inductance Formulas for Radio Coils, *Proc. IRE*, p 1938, Oct. 1928.
(4) E. S. Purington, Simplified Inductance Chart, ELECTRONICS, p 61, Sept. 1942.

FIG. 3—Chart giving values of L and C for desired crossover frequency and line impedance in a parallel constant-resistance network

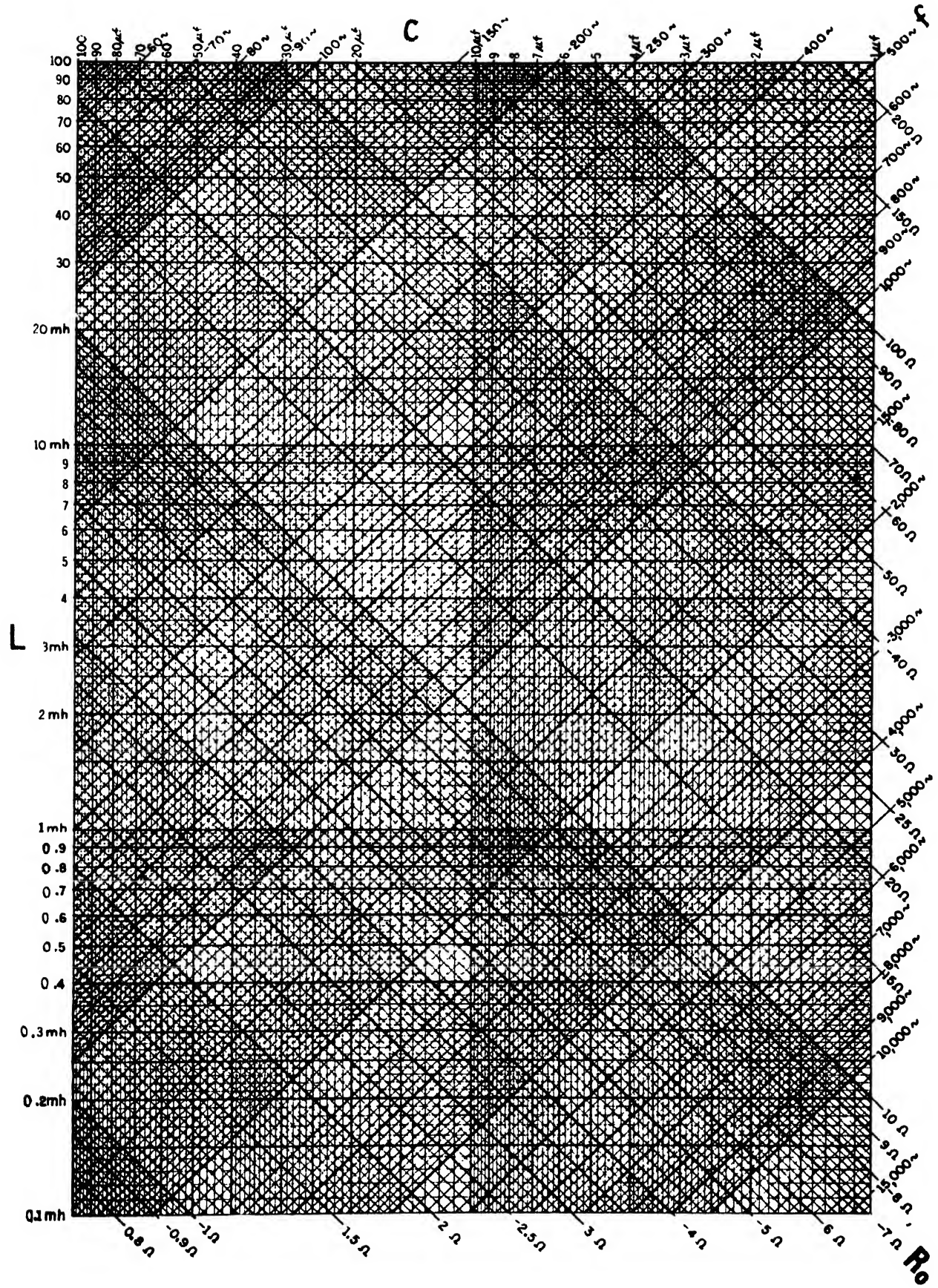
C
f
L
Ro
100
90
80
70
60
50
40
30
20 mh
10 mh
9
8
7
6
5
4
3mh
2 mh
1 mh
0.9
0.8
0.7
0.6
0.5
0.4
0.3 mh
0.2mh
0.1 mh
500~
600~
700~
800~
900~
1000~
1500~
2000~
3000~
4000~
5000~
6000~
7000~
8000~
9000~
10,000~
15,000~
100 Ω
90 Ω
80 Ω
70 Ω
60 Ω
50 Ω
40 Ω
30 Ω
25 Ω
20 Ω
15 Ω
10 Ω
9 Ω
0.8 Ω
0.9 Ω
1 Ω
1.5 Ω
2 Ω
2.5 Ω
3 Ω
4 Ω
5 Ω
6 Ω
7 Ω

Simple Harmonic Wave Analyzer

Speed of testing and inspection of audio frequency devices is facilitated through use of a simple amplifier-filter-rectifier instrument, designed to read directly the amount of second and third harmonic distortion

By R. F. THOMSON

THE primary requisites of any audio amplifier are uniform frequency response and freedom from distortion. The frequency response can readily be found by point to point measurements with relatively inexpensive equipment. The harmonic distortion is a difficult problem to solve, since it is done by analysis of the wave shape, which is a tedious job, or by means of a wave analyzer which involves an expensive piece of apparatus.

A simple and relatively inexpensive harmonic wave analyzer has been designed and constructed which provides a means for determining the second and third harmonic content of an amplifier or similar piece of apparatus operating in the audio frequency range. Fundamentally the method is based on the assumption that the harmonic content of the equipment under discussion is reasonably independent of frequency. This assumption is fulfilled quite well in audio amplifiers so long as the output load is a pure resistance. The instrument for making these harmonic measurements operates on the same principle as that of a wave analyzer. An adjustable sinusoidal voltage of fixed frequency is applied to the equipment under test and a variable gain amplifier incorporated as part of the wave analyzer is adjusted until the output meter, fed through a filter of fundamental frequency, reads 100 percent. The reading is also obtained for the magnitudes of the second and third harmonics, respectively, by noting the meter reading when the appropriate filter is switched into the circuit.

As shown in the block diagram of Fig. 1, the fundamental parts of this instrument are an isolating amplifier, band-pass filters, a voltage amplifier, a rectifier and meter. The first amplifier is used to isolate the instrument from the circuit under test. The band-pass filters are tuned to pass only the desired fundamental, second or third harmonic frequencies. Following the filters is a two-stage audio amplifier feeding a diode rectifier which in turn actuates a milliammeter having a range of 0-1 ma.

A schematic wiring diagram of the wave analyzer, complete with power supply is shown in Fig. 2. A type 6J7 connected as a triode, and transformer-coupled to the filter, is used in the first stage. This stage must be free from harmonics and must be capable of feeding sufficient voltage into the filter. Several methods of feeding the filter without a transformer were tried but none were satisfactory due to the low impedance of the filter. The matching transformer T, has a turns ratio of 3.6 to 1 and is a universal plate-to-line transformer of good quality. This reflects a load of approximately 7,500 ohms back to the plate. The filters provide a reactive load at frequencies removed from the pass frequency so this stage has to be matched near the point of maximum power transfer.

Filter Considerations

The band-pass filters used in this instrument were of the conventional constant K prototype T section type. The input or characteristic impedance of this filter was 600 ohms and the bandwidth 500 cps. As the input and output inductances, $\frac{1}{2}L_1$, are independent of the frequency and a

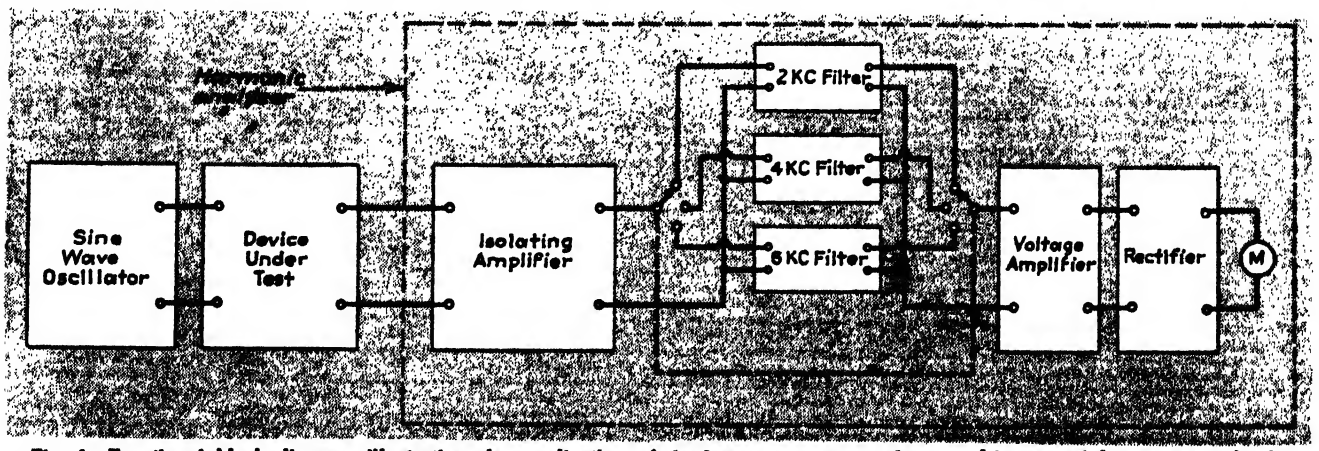

Fig. 1—Functional block diagram illustrating the application of the harmonic wave analyzer and its essential component circuits

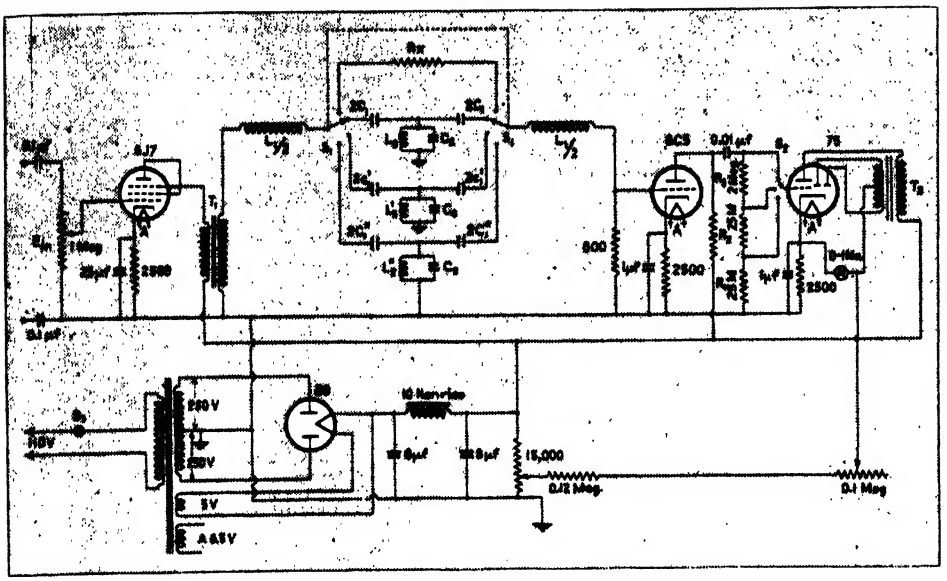

Fig. 2—Schematic wiring diagram of the harmonic analyzer

function of only the characteristic impedance and bandwith, they were connected directly into the circuit ahead of the band switch. The inductance used in this part was a telephone retardation coil with the iron core removed. These coils have an inductance of 0.191 henry and a comparatively high Q. The coils L_2 were receiving type radio frequency choke coils with sufficient turns removed to give the desired inductance. These inductances were measured by resonating them at the desired frequency with laboratory standard condensers. The filter condensers were chosen by again resonating them, with the corresponding inductance, at the desired frequency. This procedure was followed with each of the three arms of each filter. It is essential that the coils of the filters be of a relatively high Q to lessen the losses throughout the pass band. For this reason available iron-core coils were not feasible. The Q of these coils is about 10 which provides an attenuation of about 16 db over the pass band. Values for the various parameters of the filters are given in Fig. 3. These filters gave approximately 71 db attenuation at the unwanted frequencies.

Because the voltage output of the filters is very small (a maximum of 0.07 volts), two additional stages of amplification are necessary to raise this voltage to a reasonable amount. This is accomplished by means of a 605 connected as a conventional voltage amplifier, and resistance coupled to the succeeding stage. Distortion in this stage is of no consequence as the change of wave shape would only tend to cause a slight change of the meter reading which would automatically be compensated for in the calibration.

The signal is then amplified by the triode portion of a type 75 and is then fed into the diode section of the tube which acts as a full wave rectifier. The rectified current is read from the 0-1 milliammeter. This type of metering circuit was used as it gave very nearly a straight line scale. It was thought that this system would also require no zero adjustment. This did not prove true as a steady current of about 0.05 milliampere had to be bucked out by feeding a small voltage back from the power supply. The tap on the voltage divider is determined by trial as the current to be bucked out varies for different tubes.

Since the calibration of the voltmeter was very nearly linear, it was found convenient to provide three ranges having full scale distortion readings of 100 percent, 50 percent and 10 percent. These scales will give readily ascertainable readings of harmonics to a low as 0.2 of 1 percent. The scale change was accomplished by means of a series of resistors and a three point tap switch connected as the grid resistor of the 75 triode. With R_1 and R_2 equal, and R_3 equal to 8 R_1, the full scale readings of the meter will be 100, 50, and 10 percent.

Instrument Calibration

Calibration of this instrument is a rather simple procedure and can be done in either of two ways. The first method used was to feed a 2000 cps signal of adjustable amplitude into the instrument and to determine the output meter reading in terms of the input voltage. This procedure was then repeated with adjustable voltages of 4,000 and 6,000 cps. The harmonic distortion was then calculated and calibration curves were then plotted showing the percent of harmonic distortion against the output current. With this method there will be little error introduced by aging of the tubes.

The second method of calibration uses two oscillators, the first of which must be free of harmonics. Such a sinusoidal oscillator may be obtained by inserting a 2000 cps band-pass filter in the output of the laboratory oscillator or generator. The output of the second oscillator is fed into the instrument in series

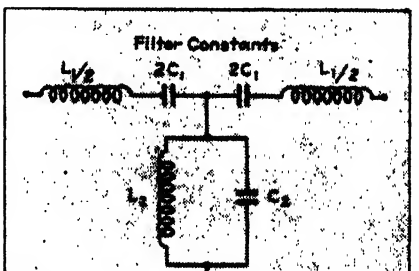

	Resonant Frequency of Filters		
Arm	2,000 cps	4,000 cps	6,000 cps
$\frac{1}{2}L_1$	0.191 h	0.191 h	0.191 h
L_2	5.96 mh	1.49 mh	0.662 mh
C_2	1.06 μf	1.06 μf	1.06 μf
$2C_1$	0.0332 μf	0.0083 μf	0.00379 μf
Z_0	600 ohms	600 Ohms	600 Ohms
Band Width	500 cps	500 cps	500 cps

Fig. 3—Diagram of band pass filters, with circuit constants for filters for fundamental, second harmonic and third harmonic frequencies

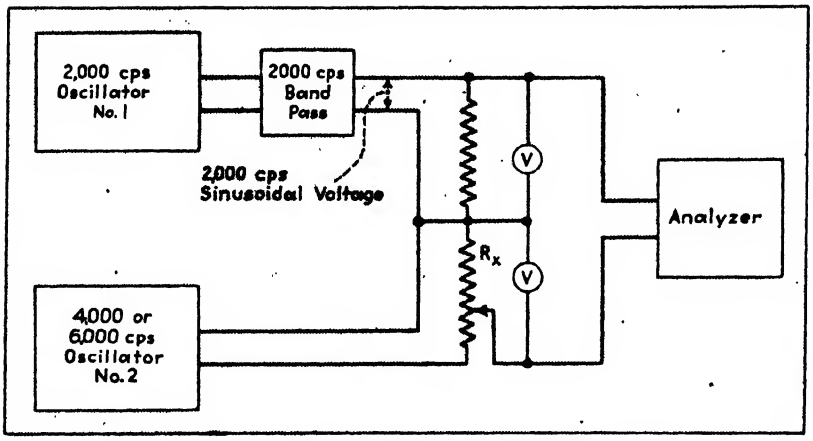

Fig. 4—Circuit connections used in calibrating the harmonic analyzer

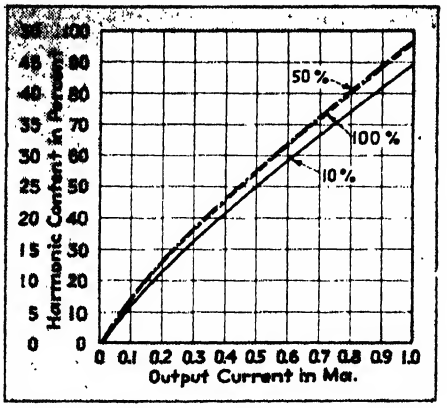

Fig. 5—Typical calibration curve for analyzer. The harmonic content in percent is directly readable from meter indication

with that of the 2,000 cps oscillator as shown in Fig. 4. Meters are placed across the output of both oscillators and the harmonic voltage, which is thus artifically generated, can be read directly. It is important that the mixing resistances be linear (i.e., independent of voltage or current) to prevent modulation of one oscillator by the other.

The voltage of the No. 1 or distortionless oscillator is adjusted for full scale reading of the meter with the 2000 cps filter connected in the wave analyzer. The 4000 cps filter of the analyzer is then cut in. The voltage of the 4000 cps oscillator is gradually increased and a curve of harmonic voltage against output current is plotted for second harmonic distortion. This procedure is repeated for the third harmonic and the percentage distortion is determined as in the previous method. These two methods of calibration checked with a maximum difference of 2 percent, which occurred near full scale readings. Calibration curve for the second harmonic is shown in Fig. 5. The third harmonic calibration was practically identical.

By properly apportioning the scale changing resistances R_1, R_2 and R_3, as previously described, a single calibration curve may be used for the instrument if all filters have the same mid-frequency attenuation. The mid-frequency attenuation of the filters may be adjusted by connecting an appropriate resistor across the shunt arm inductance, L_2. In this instrument, it was necessary to shunt the 4000 cps filter with a 220 ohm resistance to make the attenuation equal to that of the 6000 cps filter.

Operation of this analyzer is relatively simple and rapid. The device to be measured is supplied with a 2000 cps distortionless or sinusoidal voltage and the output from the device connected directly to the analyzer. With the 2000 cps filter in the circuit and the meter switched to the 100 percent position, the gain control of the analyzer is adjusted to give full scale reading of the meter. The 4000 and 6000 cps filters are then switched in and the magnitudes of the second and third harmonic voltages are read respectively. The minimum voltage necessary to operate this instrument is approximately 4 volts.

This instrument has been found very useful in measuring the harmonic content of various amplifiers constructed in the laboratory and in other experiments.

Wow Meter for Turntable Testing

A toothed wheel rotating between two pickup coils connected for maximum output generates a tone. Output is fed through a peak clipper to a discriminator and rectifier. Instantaneous speed variation is shown directly on a calibrated meter

By G. L. SANSBURY and E. W. PAPPENFUS

IN DISC RECORDING a common but annoying fault in reproduction is instantaneous speed variation of the turntable commonly called wow. Everyone is familiar with the discordant quavering of sustained piano or bell tones that are encountered in the reproduction of phonograph music. This is the direct result of turntable speed variation.

Wow can be detected by the listener when it occurs at a relatively low cyclic rate. One to three cycles per second in variation of frequency at 1,000 cycles seems to give the most noticeable wow at that frequency. The amount of wow that is detectable varies with frequency. A small amount is noticeable at high frequencies but only larger amounts at low; that is, a larger percentage of variation in frequency is tolerable when a low frequency is being reproduced.[1] In general, three-tenths of one percent instantaneous speed variation is the maximum that can be tolerated at any frequency without introducing noticeable frequency change in the reproduced tone.

Causes of Variation

There are a number of reasons for wow in turntables and these may be classified by the type of drive used.

In the rim-driven turntable eccentricity of the spindle, oval shape of the turntable, line frequency or between the spindle and the surface of the turntable, line frequency or voltage fluctuation, as well as variations in friction of any part of the driving mechanism during a portion of a revolution result in wow. In the spindle-driven turntable, out-of-round shaping of the turntable does not cause wow, but eccentricities in the driving gears or an eccentric spindle drive contribute to wow. Again, nonuniform bearing friction, variations in line frequency and voltage, and any inaccuracies in the drive mechanism tend to produce speed variation. Another factor that is somewhat difficult to control on the spindle-driven turntable is mechanical damping of the mechanism as the turntable is started. Frequently the turntable comes up to speed and overshoots slightly, then oscillates about the desired speed for a short time before it settles down to its constant-speed operation. In both types of turntable, variation in groove amplitude of the record causes a variation in torque that results in instantaneous speed variation if the drive motor does not have sufficient power or if the inertia of the turntable and its associated mechanism is not sufficient to carry through the momentary periods of greater torque requirements. This effect is similar to the problems involved in the design of a flywheel to maintain a required stability.

Since the requirements for constancy of speed in the phonograph turntable are so rigorous, it is important that a convenient means be devised for measuring instantaneous speed variation.

There are a number of methods by which the wow of a turntable might be measured.

Testing Methods

A method that comes to mind immediately is the familiar stroboscopic disc which is viewed in a 60-cycle light source. By observing the position of the dots or lines on the disc as the turntable is rotated, it is possible to check the average speed of the turntable. This method, however, is not practical for checking the instantaneous speed variation with an accuracy which is necessary in order to have a quantitative measure of turntable performance. It is true that the stroboscope disc does show up variations in turntable speed in the advancing rotation or reverse rotation of the virtual marks of the stroboscopic disc; but the motion is not easily measured because it ordinarily varies at a rate equal to that of turntable rotation. Since this method necessarily involves visual inspection, the observer errors are large.

Another method is to play a constant-tone record on the turntable using a conventional pickup, amplifier, and a frequency measuring system. There are a number of reasons why this is not entirely practical except as a rough approximation. This system must necessarily include any wow which is present in the original recording. It also includes wow contributed by any eccentricity of the record owing to off-center stamping of the blank or clearance in the center hole. These contributions to instantaneous frequency variation may add to or subtract from that present in the turntable being tested.

Another suggested means is to use a purely mechanical differentiating speedometer to measure instantaneous speed variation. This would be a rather difficult mechanical problem because the mechanism of the wow meter itself must be better at all times than the mechanism of the turntable. Building any measuring device to measure to within one-tenth of one percent is a major design problem. The differentiating speedometer must contribute no

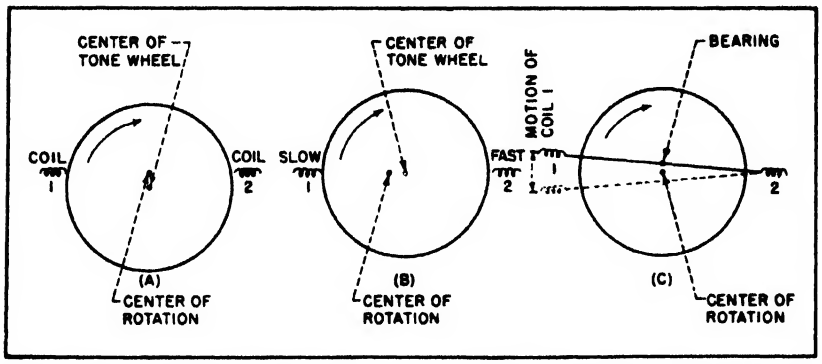

FIG. 2—Effect of wow on a single pickup coil (A and B) and upon a pair bearing on the center of the tone wheel (C)

friction to the turntable itself and it must have low inertia so that it does not reflect into the turntable a speed variation which is not present normally.

The most practical means by which the instantaneous speed variation of a turntable can be measured seems to be the method suggested by H. E. Roys[8] in which a gear blank is cut with a suitable number of teeth so that by using magnetic pickup from the teeth a convenient tone is generated. This tone is fed into an amplifier and a frequency measuring circuit that operates a meter indicating the instantaneous speed variation. A gear is admirably suited for the generation of a constant tone because it is possible to machine the teeth accurately so that the errors in tooth spacing contribute very little to the error of measurement. The centering of the gear can be accurately maintained because the inside framework is constructed of metal as shown in Fig. 1.

Gear Dimensions

The gear wheel is cut from a plate of cold-rolled steel and mounted on an aluminum wheel having its center at the center of the turntable. The gear has a pitch diameter of 13.750 inches, and a diametral pitch of 56, giving an output of 1,004 cps at 78 rpm and 427 cps at 33⅓ rpm. A center-drilled shaft brings about alignment of the centers of the tone wheel and the turntable record-centering pin. Three screws are used for leveling the wheel on the turntable so that the pole piece of the pickup coil is in horizontal alignment with the teeth of the tone wheel.

At first thought it might seem that a single magnetic pickup from the tone wheel would be satisfactory. This, however, is not true. A single pickup coil would introduce a variation in tone generated by the gear itself owing to eccentricities that might be present. This effect is shown in Figs. 2A and 2B, in which the center of the tone wheel and the center of the turntable do not coincide. With the turntable and the tone wheel in the position 2A, the peripheral velocity at coil 1 is equal to the average speed of the turntable, while at 2B it is seen that because of the decreased radius the peripheral velocity adjacent to coil 1 is lower than the average. At coil 2 the velocity and hence the tone is higher than the average.

This effect suggests the spacing of two pickup coils at diametrically opposite points in the circumference of the tone wheel, so phased that a double voltage is obtained. Assuming a sinusoidal voltage from the coil (the output is actually very close to a sine wave), then the voltage from coil 1 is $E_{max} \sin(\omega t + \theta)$ and the voltage from coil 2 is $E_{max} \sin(\omega t - \theta)$ where θ is a variable which varies throughout the revolution. The two expressions for the voltage output from the pickup coil are seen to be phase modulated and the voltage from either of the coils would therefore result in an erroneous answer from any simple form of indicating circuit. If the two voltages are added together the sum is $2E_{max} \sin \omega t \cos \theta$. This operation demonstrates that the phase modulation drops out, leaving an amplitude term $\cos \theta$. Thus by using two coils an output voltage is obtained, the frequency of which is directly proportional to the speed of rotation of the turntable.

Originally, for the sake of convenience, the pickup coils were suspended on a bearing at the center of the tone wheel with one end of the pickup coil assembly prevented from rotating with the turntable by abutment with a fixed stop. In Fig. 2C is shown the result of having the pickup coil assembly eccentric with regard to the center of rotation of the turntable. If coil 2 is fixed in space, coil 1 oscillates between the solid and the dotted positions indicated in Fig. 2C, resulting in a variational output that is not balanced out even through the addition of the two coil output voltages.

The coils are made from number 30 wire, scramble wound, approximately 1,500 turns. A pole piece of cold-rolled steel projects through the pickup coil and is magnetically coupled to a permanent magnet of the type used in a moving coil meter and to the teeth of the gear. The exact magnetic structure of the pickup coil assembly is not important, since a satisfactory output is obtained with no difficulty.

Centering the Assembly

At the center of the assembly is a tapered centering shaft that is pressed down to engage with the center hole of the tone wheel so that the pickup coil assembly is properly positioned. Upon release of the centering shaft, the pickup coil assembly is supported at its extremities from the surface of the turntable cabinet. Adjusting screws are provided so that the pole pieces and pickup coils can be shifted slightly to obtain maximum voltage from the system. A maximum voltage is secured when the two coils are in corresponding positions with regard to gear teeth, giving an output voltage from each coil so phased that they combine additively.

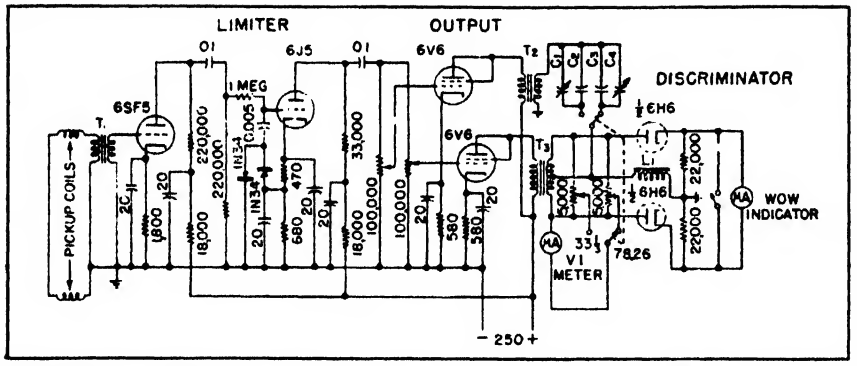

FIG. 3—Schematic circuit diagram of the wow meter. Shorting switch across the indicating meter prevents damage when turntable is started

A wow meter developed by the writers for production testing of transcription turntables is built for mounting in a standard speech rack and is selfcontained except for the power supply. Provision for checking the turntables at both 33⅓ and 78 rpm is included. At the left of the practical instrument is a meter directly calibrated in percent wow. On the right is a volume indicator for establishing the proper level for satisfactory operation. Below the volume indicator are two locking potentiometers for zeroing the volume indicator at both frequencies of operation. Below the wow indicating meter on the left is a meter shorting switch and the master gain control, as well as the 33⅓ and 78 rpm changeover switch.

In the schematic diagram of Fig. 3 may be seen a conventional voltage amplifier upon which no particular effort was expended to secure extended frequency response beyond 1,000 cycles and below 400 cycles. The input transformer matches the output of the pickup coils to the input grid with an impedance ratio of approximately 250 to 30,000 ohms. The first stage of the voltage amplifier uses a high-mu 6SF5 tube. The audio is then fed into a limiter circuit of the biased-diode type using germanium 1N34 diodes. This is in reality a peak clipper in which the diodes are biased with a voltage obtained from the cathode circuit of the second amplifier stage. A series grid resistor of 1 megohm provides a high impedance source so that effective peak clipping occurs whenever the peak a-c voltage exceeds the bias provided by the cathode circuit. The second amplifier stage consists of a 6J5 feeding the two output tubes. Since high frequency response is not required, it is satisfactory to feed the two 6V6 grid circuits in parallel. One 6V6 feeds the push-pull and the other the series portion of the discriminator circuit. A single 6H6 serves as a discriminator rectifier feeding a zero-center microammeter with an undamped movement. Two sets of capacitors, C_1 and C_2 for 33⅓ and C_3 and C_4 for 78 rpm, makes possible a more flexible wow meter for use with both turntable speeds. The variable portions of this tuned circuit C_1 and C_4 are high-capacitance variable ceramic capacitors that are convenient in this application. A volume indicator is connected across the output of one of the 6V6 tubes so that the proper voltage may be fed into the discriminator for satisfactory operation. This meter is switched with the variable capacitors used to tune the discriminator. Two 5,000-ohm potentiometers are used to adjust the volume indicator to zero at the level at which calibration was made. A shorting switch must be provided to protect the meter as the turntable comes up to speed. With a sensitive circuit such as must be used to detect wow of 0.1 percent, excessive deflection occurs with large frequency differences that are present before the turntable reaches its correct operating speed. Without the shorting switch severe pinning of the meter occurs during the starting of the turntable. The resonant circuit of the discriminator must use a high-Q audio coil at L_1 to secure adequate sensitivity. Since the inductance of L_1 varies with the a-c voltage present across it, it is necessary to hold the level into the discriminator at a value corresponding to that which was used during calibration.

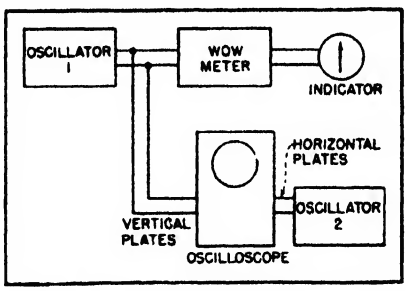

FIG. 4—Method of calibrating the meter by Lissajous figures

Standards of Calibration

The block diagram in Fig. 4 shows a method by which the wow meter can be calibrated. Oscillator 1 is fed into the wow meter and the vertical plates of an oscilloscope, while oscillator 2 feeds the horizontal plates of the scope only. With the two oscillators at the same frequency, the usual circular pattern is observed on the screen.

Before indicating how to measure minute frequency variations accurately, the fundamental relationship of Lissajous figure should be reviewed. The figure seen when there is a slight variation in frequency between the two input voltages applied to an oscilloscope progresses from a circle to a straight line, to a circle to a straight line, and so on. The figure passes through two straight line portions a second for a frequency difference of one cycle a second. By using a stop watch and counting for a period of a half minute or so, it is possible to measure the frequency of the oscillator accurately even to a portion of a cycle a second as is required in practical wow measurements. In a like manner, for each frequency difference at which the meter is to be calibrated the reading of the discriminator is recorded. This plot of

readings gives an accurate calibration of the wow meter. By repeating the process it is possible to calibrate the meter to read both at 78 and 33⅓ rpm. Since the microammeter used is undamped, the meter swings up and down scale in synchronism with the wow frequency during the operation of the instrument. The peak wow is half the total deflection plus and minus from the average position of the meter.

REFERENCES

(1) E. G. Shower and B. Biddulph, Differential Pitch Sensitivity of the Ear, *Jour. Acous. Soc. Amer.*, Vol. 3, p 275, Oct. 1931.
(2) H. E. Roys, The Measurement of Transcription Turntable Speed Variation, *Proc IRE*, p 52, Feb. 1943.

Microphone Calibrator

Simple, rapid and reasonably accurate method of measuring sensitivity, frequency response and polar response without a costly free-field anechoic chamber. Below 1,000 cycles a long wood tube absorbs unwanted sound. Higher frequencies are pulsed and recording is done before reflected sound returns to microphone

By D. H. BASTIN

THE FIELD CALIBRATION of a microphone requires that the microphone be placed in a plane sound field of known intensity. This type of calibration differs from a pressure calibration in that the effect of diffraction around the microphone is charged up as part of the response of the microphone. It is therefore the most useful type of calibration for microphones used in broadcasting.

Inexpensive Dead Room

Obtaining the required sound field indoors is a matter of some difficulty because reflections build up standing waves to give a nonuniform sound field. The usual method of obtaining the sound field by the use of free-field or anechoic chambers was felt to be too expensive for the present project, so two less expensive devices are used to obtain the required field, one operating from 30 to 1,000 cycles and the other unit operating from 1,000 to 15,000 cycles.

The two measuring techniques involved, outlined below, were developed for use on all microphones used in CBC studios across Canada. In both, the microphone being tested is compared against a standard microphone by a two-channel logarithmic voltmeter that automatically plots the response in decibels against frequency. The system can also be used for recording loudspeaker response and polar diagrams.

Low-Frequency Chamber

The frequency response from 30 to 1,000 cycles is measured by placing the microphone three feet from the end of a wooden tube 30 feet long and 11 by 11 inches in cross section. A drawing of the tube is shown in Fig. 1. At the end of the tube near the microphone is a loudspeaker. That part of the tube on the far side of the microphone contains curtains of cotton quilting hung across the tube in increasing amounts to form an acoustic resistance to absorb the energy of the sound passing from the loudspeaker. The treatment is adjusted

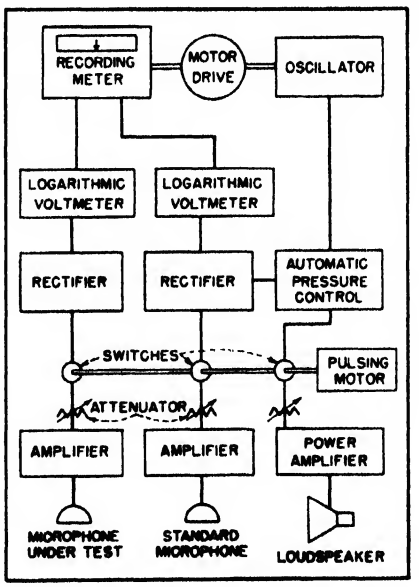

FIG. 2—Block diagram of microphone calibration rack used in CBC laboratories

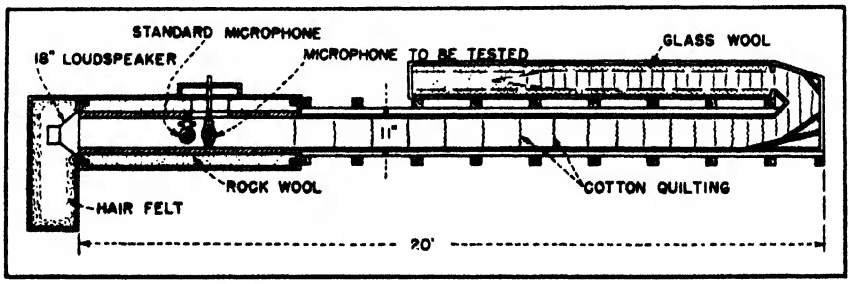

FIG. 1—Cross-section of 11-inch-square hollow wood tube used to absorb sound energy below 1,000 cycles from loudspeaker and thereby prevent reflection back to microphone being tested

until the acoustic impedance looking into the tube is approximately that of open air.

Mounted beside the microphone being tested is a small standard microphone, having flat response over the 30 to 1,000-cycle range, and of known sensitivity. The outputs of the two microphones are fed to the measuring rack and as the frequency of the loudspeaker signal is slowly changed the response curve is automatically plotted.

High-Frequency Pulse System

Over the range above 1,000 cycles a pulsing system is used to obtain effective free-field conditions. The microphone to be tested and a small loudspeaker are set up about three feet apart in a studio or small room. Midway between the microphone and loudspeaker is placed a small standard microphone.

A short pulse of sound at the desired frequency is transmitted from the loudspeaker, and the resulting output from the microphone is measured before enough time has elapsed for reflected sound from the nearest wall to arrive back at the microphone. The pulse is repeated at intervals long enough to allow reflections to die out between pulses. During the pulsing the frequency of the oscillator driving the loudspeaker is slowly changed and the response curve is automatically plotted by a logarithmic recording voltmeter. By rotating the microphone undergoing test a polar diagram of the response at any frequency can be plotted.

Pulse Length

The length of the pulse that is used is 10 milliseconds and the pulse is repeated 10 times every second. With a pulse of 10 milliseconds length and a sound velocity of 1,100 feet per second the sound path before the first reflection can reach the microphone is 11 feet. This means that the microphone can be half this distance or within 5½ feet of the nearest wall, hence a comparatively small room is suitable for the measurement.

At 1,000 cycles a pulse of 10 milliseconds consists of only 10 cycles, of which the first and last few cycles are obscured by transients, so that 1,000 cycles is about the low-frequency limit of this pulsing system. In a larger room a longer pulse could be used, and consequently a lower frequency could be reached. On the microphone channels the beginning and end of the pulses are clipped to remove transients from the pulses before comparing the two signals.

No special treatment is required on the walls of the room used for this part of the test, for the repetition rate of 10 per second allows sufficient time between pulses for reflected sound to drop to a negligible value before the next pulse is transmitted.

The sound source used for the high-frequency test is a small dynamic loudspeaker that was found to have adequate output up to 15 kc. As will be noted later, the response of the source is not critical in this method.

Standard Microphone

The standard microphone is a small type M101 crystal unit § by 15/16 inch in size, manufactured by Massa Laboratories.[1] The preamplifier housing supports the standard microphone in the position for minimum diffraction effect, with the end of the crystal unit parallel to the sound axis. In this position the diffraction effect is negligible below 10 kc, and the response can be considered flat. A reciprocity calibration on this unit gave a value of sensitivity in good agreement with the value stated by the manufacturer.

The preamplifier housing contains a 9002 tube connected as a cathode follower, acting as an impedance changer between the high impedance of the crystal and the low-impedance output. Terminals are provided on the preamplifier for injecting a signal in series with the crystal for making overall electrical calibration of the associated equipment.

Tests have shown that at the testing distances used, 15 inches to the standard microphone and 30 inches to the other microphone, neither microphone has appreciable influence on the sound intensity at the other, and for the period of the pulse each microphone is in a progressive sound wave, the pressure at the nearer microphone being twice that at the other. In the low-frequency tube an inexpensive crystal microphone is used as the standard, and is checked at intervals against the Massa standard.

The absolute accuracy of the measurements depends upon the

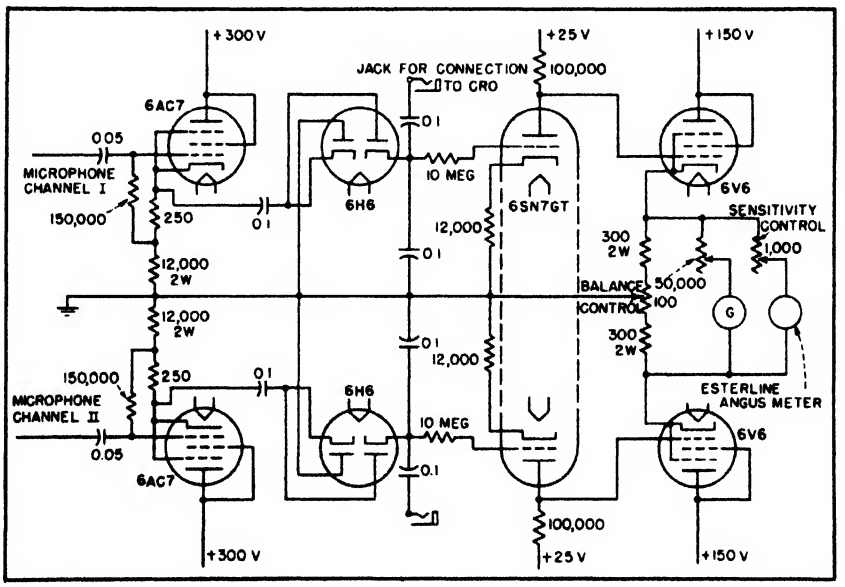

FIG. 3—Circuit of voltmeter providing logarithmic amplification over range of 46 db as required for plotting response curves in db

standard microphone, but the type of crystal microphone used appears to be stable, and a reciprocity calibration can be made upon it at any time if required.

Rack Equipment

Both parts of the calibration method require the comparison of the outputs of the two microphones. This comparison is carried out in the rack of equipment shown in the block diagram in Fig. 2.

The rack contains amplifiers for the two microphone channels, a logarithmic voltmeter which compares the outputs of the two microphones, a recording meter, an audio oscillator with a motor drive on the frequency dial, a power amplifier to drive a loudspeaker, an automatic pressure control, pulsing switches and a cathode-ray oscilloscope for waveform examination.

The two microphone channels are similar, each consisting of an amplifier, attenuator, rectifier and logarithmic stage. The attenuator controls are marked directly in decibels on the front panel. Each amplifier is followed by a cathode follower, using a 6AC7 as shown in Fig. 3 to provide a low-impedance source and so avoid peak clipping by the rectifier action. The 6H6 rectifiers are connected as voltage doublers. The maximum undistorted signal available from the cathode follower is about 100 volts, hence the peak d-c output from the rectifier is about 200 volts, or 46 db above the minimum usable output of 1 volt. Below 1 volt the initial current from the diodes becomes important, introducing nonlinearity.

Since only the amplitudes of the pulses are compared, the rectifier circuit has a short charge time constant, in order that the amplitude of the signal can rise to full value during the first millisecond of pulse. The discharge time constant is long, however, in order that the rectified level does not fall appreciably during the tenth second between pulses.

Logarithmic action is obtained by applying the positive voltage from the rectifier through a 10-megohm resistor to the grid of a 6SN7GT triode section operating with 25 volts plate supply. Because the emission velocities of the electrons given off by a hot cathode follow a Maxwellian distribution, the grid current which flows bears a logarithmic relation to the applied voltage. This logarithmic change in grid current produces a corresponding change in grid-to-cathode voltage, which is amplified and appears as a change in plate potential. The circuit as developed by Walter Ives[2] is accurately logarithmic over about 46 db, the limitations lying not in the log tube but in the rectifier and amplifier ahead of the log tube.

The direct-current output of the two logarithmic stages is further amplified by direct-coupled 6V6 tubes connected as cathode followers and fed to the recording milliammeter, which is a standard 5-ma Esterline-Angus meter. A potentiometer at the midpoint of the cathode resistors of the 6V6 tubes enables the two channels to be balanced so that equal signals on the two channels give center-scale deflection of the meter. This meter responds to the difference between the output of the two channels, and so is equivalent to the difference of the logarithms of the two microphone signals, and hence to the ratio of the two microphone responses. Since the response of the standard microphone is known to be flat, the result is the response curve of the unknown microphone plotted in db against frequency on the recording meter chart.

Recording Method

A sensitivity control in series with the meter can be set so that one division of the chart paper represents one db. The absolute sensitivity represented by the center line on the chart is found by subtracting the difference in gain of the two microphone channels, easily read off the two panel attenuators, from the sensitivity of the standard microphone. The two-channel construction tends to balance out effects of line voltage variation. In addition, electronic regulation is used on the plate supply for the logarithmic stage and direct-coupled amplifier. The stability of the gear is sufficient so that measurements remain accurate to within one db over long periods.

A small motor synchronized with the paper drive on the recording meter slowly changes the frequency of the oscillator driving the loudspeaker. The speed at which the oscillator frequency can be varied is dependent on the time constant of the rectifiers, which is relatively long. Even with this restriction, however, it only takes three minutes to traverse the frequency range from 30 to 15,000 cycles.

The curved coordinates produced by the meter are not as convenient to use as rectangular coordinates, but when a transparent scale marked in frequency is laid over the chart the sensitivity at any frequency can readily be read off.

For the low-frequency test in the tube no pulsing is used. The oscillator frequency is simply varied slowly as the response is plotted. For the high-frequency test the loudspeaker signal must be pulsed. This is done by a motor-driven commutator-type switch which shorts the oscillator signal except for the period of the pulse. Other commutators mounted on the same shaft short the microphone channels for a slightly longer period, clipping the transients from the beginning and end of the loudspeaker pulse. These commutators have to be phased on the shaft to allow for the time interval taken by the sound in travelling from the loudspeaker to each microphone.

It is difficult to find a loudspeaker or any sound source that has an output independent of frequency, but since this method compares the outputs of two microphones it does not greatly matter what variations occur in the sound output of the loudspeaker. However, to maintain approximately constant sound level at the microphone and to insure that the 46-db range of the voltmeter is not exceeded, a portion of the output of the standard flat-response microphone is fed to the automatic pressure control, a variable-gain amplifier in the loud-

speaker circuit. Here it controls the signal fed to the loudspeaker, increasing the output when the loudspeaker response drops, and decreasing the output when it tends to increase.

The cathode-ray oscilloscope mounted in the rack is useful for visual checks on wave form. It quickly shows up, for example, the characteristic distortion produced in a velocity microphone when the ribbon strikes a pole piece during part of a cycle. The picture of the pulse received by a microphone will show up excessive distortion if present, but unfortunately the pulsing system is not easily adapted for distortion checks, although very satisfactory for response measurements. When checking loudspeakers the shape of the pulse is very useful for giving a qualitative measure of the transient response.

Polar Response Curves

For normal tests the microphone is terminated at the input of the rack in a resistive load of 500 ohms, corresponding to the input impedance of standard speech equipment. The response curve then includes the loading effect of the termination on the internal impedance of the microphone, an effect which in most microphones reduces the sensitivity at the higher frequencies. If desired, other terminations may be selected by a panel switch. The stand carrying the microphone under test can be rotated by a small motor for the automatic plotting of polar response curves.

Besides measuring the response of microphones, the equipment using the pulsing system can be used to measure the response and polar distribution of loudspeakers above 1,000 cycles. For this test the standard microphone is placed in front of the loudspeaker to be tested, and a portion of the voltage applied to the voice coil is fed to one of the microphone channels in the rack. The curve plotted is the acoustic output of the loudspeaker for constant voltage on the voice coil, corresponding to the response that would be obtained if the loudspeaker were fed from a source having zero internal impedance. The response curve for other source impedances can be calculated from impedance measurements, or quickly plotted by placing the desired impedance in series with the voice coil after the point at which the comparison voltage is picked off.

The equipment described has been in routine use for almost a year. Since the calibration procedure is rapid and almost automatic the effects of adjustments on the microphones can be quickly seen and the best adjustment readily made.

The equipment has also been used to check new models of microphones, to measure the response and directional pattern of monitor loudspeakers, and for miscellaneous measurements, such as finding the transmission loss of loudspeaker grille cloth. If in the future a free-field room should become available the equipment can be used as it stands, simply by not using the pulsing switches. The equipment can also be readily adapted for more general laboratory purposes, such as measuring and plotting the response of filters or pickups.

References

(1) Frank Massa, Working Standard for Sound Pressure Measurements, *Journal of the Acoustical Society of America*, vol 17, p 29, 1945.

(2) Walter Ives, A Logarithmic Indicating Instrument for the Measurement of Radio Noise Voltages, Master's Thesis at McGill University, Sept. 1946.

Thermistor-Regulated Low-Frequency Oscillator

Phase-shift oscillator with four cathode follower stages and a thermistor maintains output level within 10 percent over entire range of 0.9 to 10,000 cycles. Practical circuit with values of components is supplemented by design considerations and cathode follower theory

By LAWRENCE FLEMING

THE DEVELOPMENT of instruments for vibration measurements, magnetic testing, geophysical exploration, and many other purposes requires a good low-frequency oscillator. The compact and reliable oscillator described covers the frequency range of 0.9 cycle to 10,000 cycles in four decade ranges, with a tuning dial that varies the frequency continuously over a ratio of 0.9 to 10. The same dial engraving serves for all four ranges, and accuracy of frequency setting is within 5 percent.

Automatic amplitude control by means of a thermistor maintains the output level constant within approximately 10 percent throughout the frequency range and keeps the distortion close to 1½ percent at all frequencies where it can be measured.

The regulating action of the thermistor amplitude control is well damped, so that the output level of the oscillator has no tendency to hunt or overshoot in response to power line surges or to manipulation of the frequency dial on the range switch. The output is also completely free from any tendency to jump about.

The principle of the oscillator circuit is shown in Fig. 1. The *R-C* phase-shifting network is connected

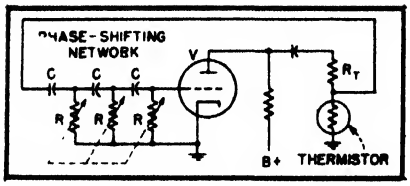

FIG. 1—Basic circuit of phase-shift oscillator

in the usual way between the plate and grid circuits of the triode. Roughly speaking, if the gain of the tube is greater than the loss through the network at that frequency where phase shift through the network is 180 degrees, oscillation will occur.[1, 2, 3] For this circuit the gain required for oscillation is 29 and the frequency is $f = 1/2\pi RC\sqrt{6}$ if the three sections of the network are alike.

For given values of R and C, the oscillating frequency is six times lower for the type of network shown than for the configuration having series resistors and shunt capacitors.

A thermistor, connected as the lower half of a voltage divider which includes resistor R_T in the feedback circuit, is employed to regulate the amplitude of oscillation. If the amplitude of oscillation increases, the current through the thermistor rises. As its temperature rises its a-c resistance goes down, reducing the percentage of signal fed back. The static characteristics of the Western Electric 1A thermistor are approximately as in Table I.

The complete circuit of a practical oscillator is given in Fig. 2. The frequency control dial rotates a three-gang potentiometer P_1 which with capacitors C_1 to C_6 forms the controlling network of the phase-shift oscillator. Sets of capacitors are selected by a three-circuit four-position range switch to provide the four frequency ranges. To compensate for the effect of stray capacitance on the highest frequency range, part of one of the capacitive legs of the network (C_6) is made adjustable.

The dial scale tends to be crowded at the high-frequency end because the frequency is inversely proportional to the resistance in the network. The scale shape was improved by using special inverse square law tapered three-gang potentiometers. A logarithmic taper would have produced a logarithmic dial scale, having the same percentage accuracy of setting at all points.

Cathode Followers

The oscillator circuit employs a single amplifier stage V_1, operating at high level, and four cathode followers. Each of the latter has a definite use.

The amplifier tube operates with no bypass, coupling, or decoupling capacitors whatever. Stray phase shifts outside the controlling network made up of ganged potentiometers P_1 and capacitors $C_1 - C_6$ affect the operations of the oscillator profoundly and must be avoided. The screen and bias voltages for the 6J7 tube are semi-fixed. The voltage divider current was selected after some experimentation to give the best compromise between high gain and stability. The gain is 80.

Cathode follower V_2, direct-coupled to the plate of V_1, is employed to drive the thermistor without loading down tube V_1.

The thermistor amplitude control circuit is like that of Fig. 1 except for a special method of returning the low-potential end of the thermistor to ground. The thermistor is returned to the cathode of one section of the double triode V_3. The series combination of R_T and the thermistor thus extends between the cathode of V_2 and the cathode of one section of V_3. These two cathodes are maintained at the same d-c potential by a path through 3-megohm resistor R_3, through which the grids of the two triodes are kept at the same potential. Signal voltage is kept from the grid of the ground-return section of triode V_3 by filter combination $R_2 - C_7$.

The a-c impedance to ground of the cathode of the section of V_3 being discussed is about 1,000 ohms since the tube is essentially a cathode follower. This special ground return arrangement is necessary because of practical considerations of leakage in large capacitors. The thermistor could have been returned to ground through a large capacitor, about 100 μf, but an electrolytic capacitor in this application gives trouble due to its variations in d-c leakage. The leakage causes the operating point of the thermistor, and hence the signal level, to drift about. The combination of one section of triode V_3 with R_2 and C_7 is really a scheme for making a small capacitor plus a tube act as a substitute for a very large capacitor.

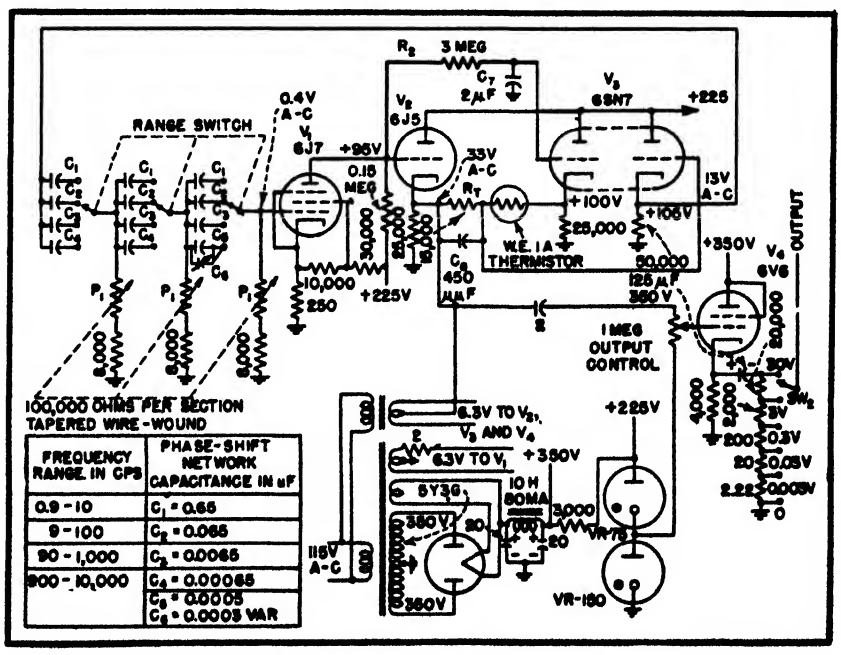

FIG. 2—Complete circuit of practical phase-shift oscillator

Table I—Static Characteristics of W.E. 1A Thermistor

Current in ma	Voltage in volts	A-C resistance in ohms
below 0.2	....	50,000
0.5	15	30,000
0.8	16	20,000
1.0	16	16,000
2.0	14	7,000
3.0	12	4,000
5.0	10	2,000
10.0	7	700

The junction of R_T and the thermistor is connected to the grid of the second triode section of V_3, whose cathode acts as a low-impedance source for feeding the phase-shifting network. Thus, tube characteristics are made to have very little effect on the frequency of oscillation.

All the above tubes receive their plate voltage from a pair of voltage-regulator tubes. The reduction of coupling due to the common impedance of the power supply is very necessary to avoid degeneration at low frequencies, but decoupling capacitors produce phase shifts that cause distortion and mistracking at the lowest frequencies. The rest of the power supply is conventional.

The output stage uses a 6V6 tube, V_4, operated as a cathode follower. There is no need for amplification here, but considerable need for isolation and low output impedance. A step attenuator is provided in the output of V_4 for convenience in obtaining small output voltages.

Tubes V_2, V_3, and V_4, whose cathodes operate at high d-c potentials above ground, are heated from a separate filament winding whose center tap is connected to the cathode of V_3.

Capacitor C_6 is connected across R_T to compensate for phase shifts at high frequencies due to the plate-ground capacitance of pentode V_3. Such phase shifts make the oscillation amplitude drop and make the frequency too low at dial settings of P_1 above 3 kc on the highest frequency range. Capacitor C_8 has the opposite effect. It can be chosen to give proper amplitude and dial scale tracking up to 10 kc. If C_8 is too large, the frequency and amplitude will be too high for the dial setting.

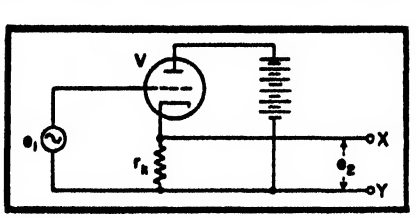

FIG. 3—Basic cathode follower circuit

General Design Considerations

The effect of stay phase shifts on the performance of a phase-shift oscillator is important. In resistance-capacitance coupled amplifiers the output voltage tends to lead in phase the input voltage at low frequencies and to lag at high frequencies. The phase lead is introduced by interstage coupling capacitors, plate and screen *RC* decoupling networks, cathode bypass capacitors, and the common capacitive impedance of the power supply. The phase lag at high frequencies is due to the shunt capacitances to ground across the plate and grid circuits of the tubes.

In a phase-shift oscillator employing a main network of the phase-leading type, such as the circuit of Fig. 1 and 2, additional leading phase shifts, such as those due to decoupling networks and the like, will increase the frequency of oscillation and decrease the gain required for oscillation (increase the amplitude and distortion). Stray lagging phase shifts, as those due to shunt circuit capacitance, will decrease the frequency below that which the main network would dictate, and increase the gain required to maintain oscillation (tend to make the device go out of oscillation). In an oscillator employing a network of the phase lag type these stray phase shifts have the converse effect.

The undesirable effects of stray phase shifts become noticeable in oscillator circuits of this type perhaps two octaves nearer the midband frequency of the system than any amplitude effects of frequency response. Thus, in the oscillator described the amplifier portion is flat to well over 12,000 cycles, yet compensation is required for proper oscillation amplitude and tracking above 3,000 cycles.

For fixed-frequency or narrow-range phase-shift oscillators, the leading type of phase-shifting network is best for low frequencies, because the stray phase shifts usually present tend to aid oscillation. Conversely, for high frequencies the lagging or low-pass type of network is the easiest to get working.

It is not recommended that the type 1A thermistor be employed as an amplitude control for frequencies lower than 1 cycle. This thermistor requires about 1.5 seconds to follow a change in current 90 percent of the way to equilibrium. Accordingly, the thermistor would introduce distortion at 1 cycle were it not for the degenerative properties of the oscillator at harmonics of the oscillating frequency. Slower thermistors are made, but are less sensitive and less readily available than the type 1A. The design problem is one of compromising lowest distortion at the lowest frequency with the convenience of a fast-acting amplitude control.

Measuring distortion at frequencies below 20 cycles is difficult. The waveform of the oscillator at 1 cycle looks like a pure sine wave when recorded on a Brush recorder, indicating an actual distortion of less than 5 or 10 percent at this frequency.

Cathode Follower Theory

In Fig. 3, if μ is the amplification factor of tube V, r_p is the plate resistance of the tube, and r_k is the cathode load resistor, the a-c resistance R_o looking at terminals X-Y is

$$R_o = \frac{r_p}{1 + \mu + r_p/r_k}$$

The gain VG of the stage then is

$$VG = \frac{e_2}{e_1} = \frac{\mu}{1 + \mu + r_p/r_k}$$

Values of bias, load resistor r_k, and maximum power and/or voltage output of a cathode follower are governed by exactly the same considerations as if the tube were operated as a conventional resistance-coupled amplifier. The values of μ and more particularly of r_p used should be the true values at the plate current at

which the tube is operating, not the published nominal values.

The input capacitance of a cathode follower is

$$C_i = C_{gp} + C_{gk}\ (1 - VG)$$

where C_i is the input capacitance, C_{gp} is the grid-plate capacitance, and C_{gk} is the grid to shell and heater capacitance.

REFERENCES

(1) Gintzon and Hollingsworth, Phase-Shift Oscillators, *Proc. IRE*, 29, 43–49, Feb. 1941.

(2) Note on above paper, *Proc. IRE*, 32, p 641, Oct. 1944.

(3) Nichols, U. S. Patent 1442781, Jan. 16, 1923.

(4) Shepard and Wise, Frequency Stabilized Oscillators, *Proc. IRE*, 31, p 256–258, June 1943.

Volume Compressor for Radio Stations

A unique audio compressor circuit that permits boosting the average percentage modulation of a short-wave transmitter up to 90 percent. Response is flat to 14,000 cycles

By GEORGE Q. HERRICK

THE preponderance of sudden volume peaks in foreign-language programs and the desirability of operating U. S. short-wave transmitters with the highest possible average percentage modulation for effective competition in international broadcasting made it highly desirable to use volume compressors on all programs.

The special compressor circuit developed for this purpose is shown in Fig. 1. The input and output transformers are standard models, connected as shown at (a) in Fig. 2 so that the windings have the indicated polarity. Between the crosswires at P are resistors R_1 and R_2, each shunted by one section of the 6N7 double-triode control tube.

Under normal conditions, when there are no peaks, the combined resistance of R_1, R_2 and the tube is low because the triode sections have a small negative bias (only developed across the 2000-ohm cathode resistor) and hence have fairly low plate resistance values. The two crossed wires can then be considered as connected together at P, placing the windings in series aiding as in Fig. 2b and giving signal transfer from input to output as required. The insertion loss under this normal condition is only 7 vu, easily made up in other amplifiers.

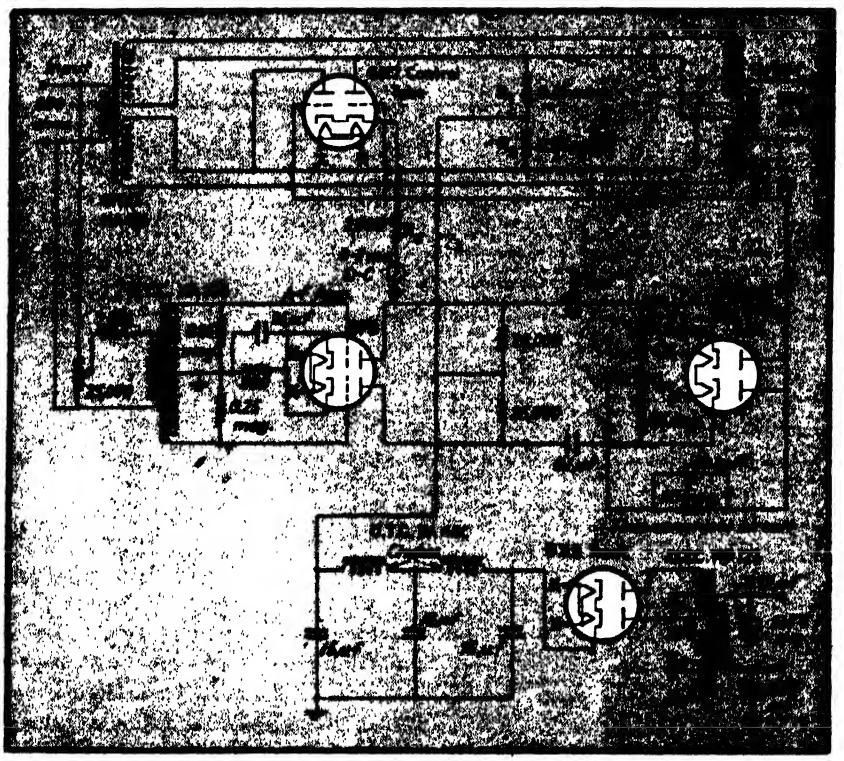

FIG. 1—Circuit diagram of volume compressor

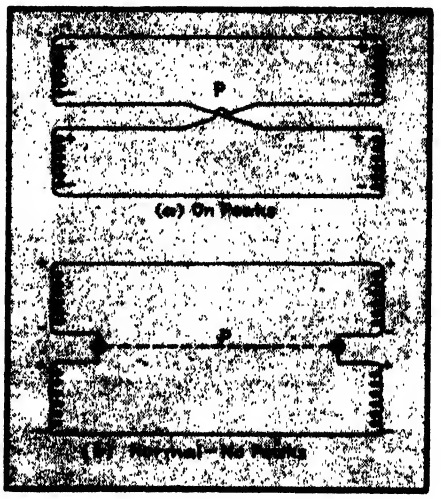

FIG. 2—Simplified diagrams of transformer connections

The input signal is also applied through the 25,000-ohm potentiometer to the 6F8 push-pull voltage amplifier stage, providing input voltage for the 6H6 signal rectifier tube. Diode plate current develops across the time constant circuit a voltage drop that acts in series with the

automatic C bias voltage across R_3 and aids that voltage, thereby driving the control tube grids more negative. Under normal-signal conditions, this merely drives the operating point slightly farther down on the characteristic curve without bringing it to cutoff.

Signal peaks increase the plate current through the time constant circuit of the signal rectifier in proportion to signal peak intensity, thereby increasing the negative bias on the control tube. As this bias approaches the cutoff value, the plate resistances increase rapidly and the feed-through circuit approaches that shown in Fig. 2a, where there is no connection between the crossed wires at P. (Actually there is still 0.5 meg between the wires due to R_1 and R_2, but this can be considered infinitely high for purposes of explanation.) Now the polarity of the two secondaries of the transformer is such that they oppose each other and provide the desired suppression on signal peaks.

Initial adjustment involves setting the input potentiometer to zero, feeding in an audio signal tone of a strength such as to give a compressor output of 9½ vu, then advancing the potentiometer until the output drops to 8 vu. This sets the threshold at which effective compression begins. A compression ratio of 10 to 1 will then be provided on strong peaks, meaning that a 10 db increase in input level will be limited to a 1 db increase in output level.

The circuit requires no critical voltages, hence the simple and conventional 6 X 5 rectifier circuit is entirely adequate as a power supply. It has extremely low inherent distortion, with phase-shift distortions not even noticeable on an oscilloscope and with a frequency response that is flat within 1.5 db over the entire range from 40 to 14,000 cycles. Tube failures or other defects in the compressor cannot interrupt the program; in fact, when a compressor tube is pulled out, the level automatically drops about 5 db to protect the transmitter against peaks.

Frequency Response of Magnetic Recording

Magnetic properties, physical dimensions and velocity of a magnetic recording medium are discussed and evaluated. Features and performance of electroplated wire and powder-coated tape are described

By OTTO KORNEI

Research Department
The Brush Development Company
Cleveland, Ohio

THE MOST REVEALING information about the mechanism of the phenomena which control any recording method may be obtained from an investigation of the reproducing process. Previous investigators have analyzed the response by empirical curve fitting[1] or theoretical considerations.[2,3]

Assume that a sinusoidal signal has been linearly recorded with a ring head (Fig. 1) on a uniformly moving medium and that the recording was done with constant current through the recording head, independent of frequency; that is, essentially, with constant peak induction in the recording medium.

The resulting record may be looked upon as a longitudinal arrangement of bar magnets of an individual length equal to one-half of the recorded wave, sinusoidally magnetized and with like poles joining.

The flux lines representing the internal magnetization B_i of these magnets must all close through the space surrounding them, thereby passing through their surface, creating there a certain surface flux density B_s. The latter determines the induction B_h in the magnetic circuit of the ring head contacting the recording medium. The reproducing voltage, e, generated in the head winding is proportional to the rate of change of the flux passing through the head.

The trend of this voltage, as a function of frequency, is derived, under simplifying assumptions, in Fig. 2 (at bottom). The reproducing voltage for very long wavelengths has theoretically a tendency to rise at a slope of 18 db per octave and this slope, with decreasing wavelength, gradually changes into 6 db per octave. A very long wave is one whose length is great compared with the longitudinal extension of the zone of magnetic interlinkage between recording medium and heads; that is, roughly, the length of the contact area between the two or about the longitudinal head dimensions (see Fig. 1). This wavelength range almost always lies below the range of practical interest.

Demagnetization

The observed shape of the frequency response curve follows this simplified prediction only to a limited extent. There is good agreement in the very low and part of the medium frequency range, but with increasing frequency the slope of the observed curve falls more and more short of the predicted 6 db-per-octave line. The curve even reverses its trend eventually and starts to fall gradually as the frequency increases further. Conse-

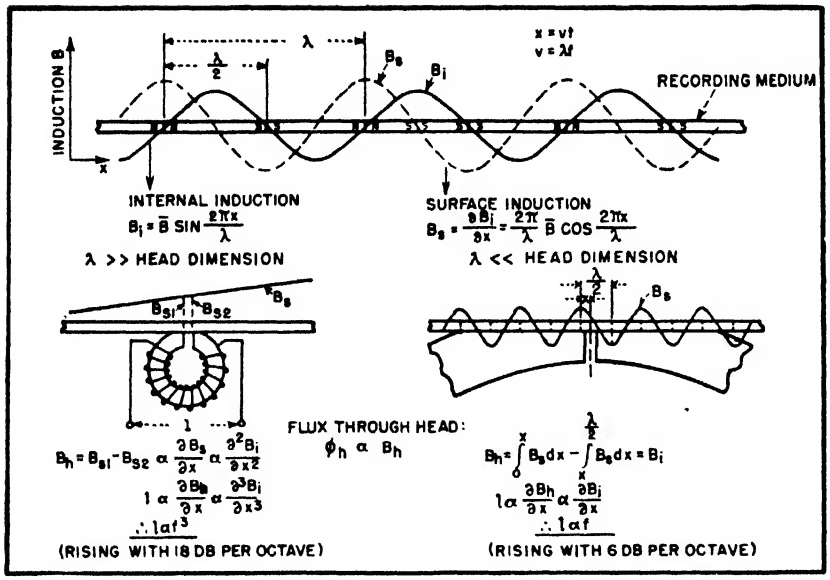

FIG. 1—Interaction between the recording magnetic medium and the reproducing ring head with a sinusoidal signal

quently, there must be certain effects, responsible for this deviation.

The most important of these effects is the self-demagnetization of the described elementary bar magnets. It is well known that the magnetomotive force available across the ends of an open bar magnet, or the useful induction which it can generate, decreases due to its own magnetization. The figure which relates this decrease to the magnetization is called the demagnetizing factor; it depends almost entirely on the physical shape of the magnet and becomes smaller as its ratio of length to diameter increases.

Figure 2 shows the familiar graphic method of finding the decreased induction of a magnetic structure when its intrinsic hysteresis loop and its demagnetizing factor N are known. A straight line, called the shearing line, is drawn through the origin at an angle whose tangent is proportional to the demagnetizing factor. The intersection P of this line with the hysteresis loop then gives the induction B'_r effective in the magnet, as compared with the highest induction B_r which would exist if the magnet were either closed or infinitely long.

The reduced induction values of all other points of the intrinsic hysteresis loop may be found in a similar manner. The locus of the new points describes the behavior of the open magnetic circuit and is called the sheared hysteresis loop. It is of importance in the investigation of all magnetic circuits containing portions of increased reluctance, including powder-coated recording media.

The demagnetizing effect is one reason for the response of a magnetic frequency record to decrease below the predicted 6 db-per-octave line. As the frequency increases, the length of the elementary bar magnets decreases which, in turn, causes an increase of the demagnetization. The demagnetizing factors in the case of magnetic recording are not exactly predictable because the adjacent elementary magnets interact with each other and are shunted during the playback process by the reproducing head. An approach to the solution of this problem has been made by Camras.[3]

It was pointed out that the slope of the shearing line depended only upon the demagnetizing factor; that is, in this case, upon the recorded wavelength. The ordinate B'_r at the intersection of the shearing line with the demagnetization curve is approximately proportional to the reproduced voltage and will decrease more slowly with increasing demagnetizing factor, the flatter the demagnetizing curve of the recording medium. The average flatness may be roughly defined by the ratio of coercive force to remanence. Accordingly, an improvement in the high-frequency response can be observed, with an

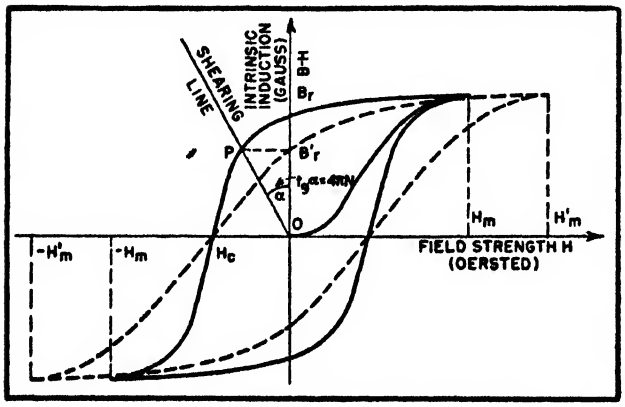

FIG. 2—Magnetization of a ferromagnetic material. The solid curves apply to a closed magnetic circuit and the dashed curves to an open magnetic circuit

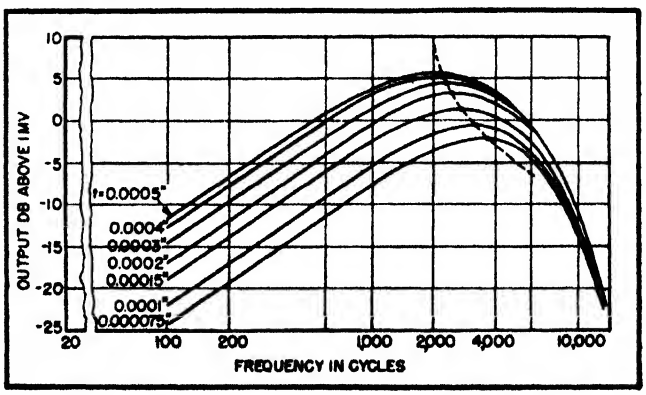

FIG. 3—Frequency response of electroplated brass tape operating at a velocity of two feet per second. Thickness is represented by t

increasing ratio of coercive force to remanence, irrespective of their absolute magnitudes.

From several materials with the same ratio of coercive force to remanence, the one with the highest absolute values (within practical limits) of the two quantities will still be the more desirable. The reason is that this material will yield the highest absolute reproducing level, because of its high remanence, and that it will offer the greatest resistance to accidental demagnetization by external fields because of its high coercive force.

Penetration

Based on the concept of the demagnetizing effect, the response of a thin recording medium might be expected to be superior to the response of a thicker one. However, experiment does not always verify this expectation since the response curves of all media within usual dimensions (thicknesses of a few thousandths of an inch) are found to be substantially alike, other conditions being equal. In an attempt to clarify this apparent contradiction, certain measurements were made whose results are represented in Fig. 3. Here are shown the response curves of several recording media, which differ only in their thickness. The absolute values of the thicknesses are very small.

Disregarding the absolute reproducing level, the frequency response of these very thin media actually does improve with decreasing thickness. Since all the curves have substantially the same shape, the position of the maxima of these curves forms a simple criterion for their frequency characteristic. The dotted line connecting these maxima shows that the improvement of high-frequency response is more rapid in the range of the thinnest media than in the range of the relatively thicker ones, tending toward no change at all for still thicker media.

This peculiar behavior can be explained by the assumption that the physical depth of magnetization of the recording media is dependent upon the recorded wavelength. The phenomenon may be termed penetration effect.

All wavelengths penetrate magnetically into the recording medium only to a limited depth; the longer ones penetrate more than the shorter ones and the absolute magnitude of this penetration is normally in the order of under one thousandth of an inch. Accordingly, the frequency response of the relatively thick commercial recording media is hardly affected by limited thickness variations since most of their cross section is inactive, that is, not penetrated by useful magnetic flux. When the thickness of the medium is substantially reduced to the order of the depth of penetration, the low frequency range will be impaired first, which means that the upper frequency range will be relatively favored.

In extremely thin carriers where complete penetration can be assumed over a wide frequency range, there is no selective influence of the penetration effect any longer. The frequency response is then controlled by the demagnetizing effect alone. Because of the increasing dimensional ratio of the elementary magnets, a thickness reduction by a certain ratio should have the same effect upon the response as an increase of the medium velocity by the reciprocal ratio. The absolute reproducing level, however, will drop by the same ratio because of the decreased cross section. This statement seems to be verified by the trend of the dashed line in Fig. 4, which approaches a slope of minus 6 db per octave for progressively decreasing thicknesses.

The penetration effect is another important factor which causes deterioration of the high-frequency response of commercial recording media since it results, with decreasing wavelength, in a gradual decrease of the effective cross section of the recording medium. (Shunting of the magnetized layer due to the presence of the inactive material does not seem to be serious.)

The penetration effect must not be confused with the magnetic skin effect since it has been found that the penetration is a function of the wavelength only, and not of the frequency. Its mechanism may be explained by the geometry of the flux lines entering the medium in the recording process. The course of these flux lines, which determines the depth of penetration, appears to depend primarily, for a given wavelength, upon the gap width and the permeability of the recording medium—greater gap width and lower permeability favoring deeper penetration.

One particular question that arises is that if the penetration decreases with rising frequency how is it possible to erase and to bias[4,6] with very high frequencies? The answer is probably that in the erasing process the recording medium has to be carried into saturation; in this range, however, its permeability approaches unity so that sufficiently deep penetration becomes possible for evident reasons of flux distribution. A somewhat similar condition prevails in the case of high-frequency bias. In this situation the recording medium works essentially within the toe of its normal magnetization curve where the permeability is also very low.

Gap Effect

Another effect which contributes to the loss of the reproduced level as the frequency increases is the almost purely geometric influence of the finite gap width of the reproducing head. The effect exists basically in any method of scanning a recorded signal. Figure 4 shows a representation of the function relating this loss to the ratio of gap width to recorded wavelength. It can be seen that no reproduction takes place when this ratio equals unity (or any integer).

The loss as shown describes the conditions for the reproducing process only.

It should be emphasized that the effective gap width of the reproducing head is not identical with the physical dimension of the gap. Magnetic leakage causes a certain spread of the zone of mutual influence between recording medium and gap, resulting in an effective

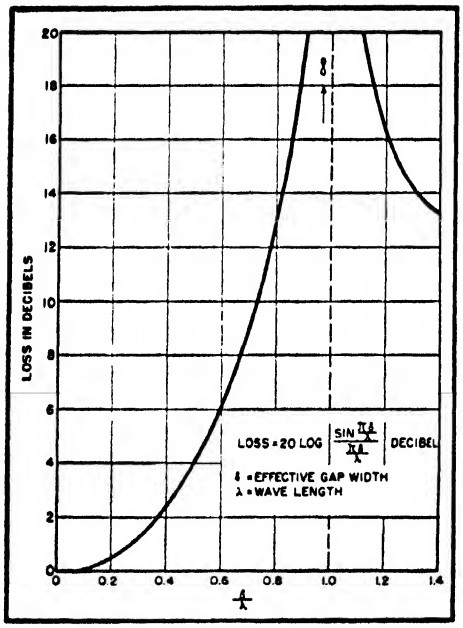

FIG. 4—Playback loss due to gap effect

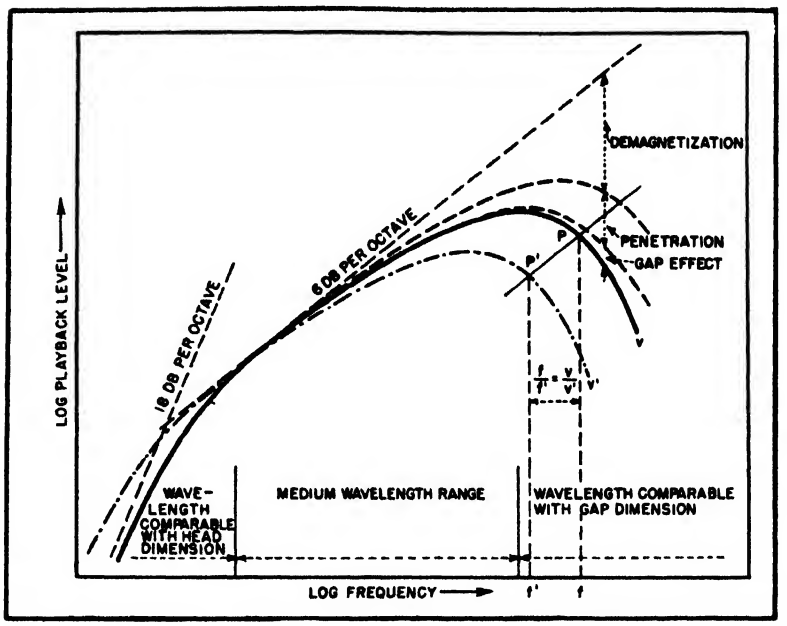

FIG. 5—Synthesis of the response curve of a magnetic recording medium

gap width which may be determined to be up to about 40 percent larger than the physical gap width.

Figure 5 shows, in a qualitative manner, the three discussed effects which control the shape of the frequency-response curve of magnetic recording as obtained with ring heads. The solid curve gives the general appearance of an observed response. The vertical distances between this curve, the two dotted curves, and the theoretical 6 db-per-octave line indicate the respective loss contributions of demagnetization, penetration, and gap effect.

Velocity

Figure 5 also indicates a convenient graphic method of converting a response curve established at a velocity v of the recording medium into the curve at some other velocity v': A 6 db-per-octave line is drawn through any point P of the given curve, plotted in the conventional double logarithmic system. On this line, point P' is found by spacing it from P at a horizontal distance which equals, as a frequency ratio, the ratio of the two velocities. The new curve (dash-dotted) is then found by shifting the original curve bodily along the 6 db-per-octave line to its intersection at P'. (The points P and P' on the two curves correspond to frequencies with equal wavelengths.)

The noise originating from a magnetic recording medium is evidently generated by random flux variations picked up by the reproducing head. These variations may have two different causes. The first one is the random fluctuation of the reluctance across the gap of any or all of the heads, brought about by either mechanical vibration or surface roughness of the recording medium. The second cause is the inherent grain structure of the recording material. Here, the magnetic discontinuities at the boundaries of the individual grains or domains will also cause minute flux variations.

Vibration and surface roughness of the medium can be minimized by appropriate design of the drive mechanism and by careful preparation of the medium.

The noise reproduced from a given recording medium will depend upon the magnetic state of the medium. A completely demagnetized medium will result in the least noise as evidenced by the low noise level obtained from an a-c erased in contrast to a d-c erased recording medium.

An important consequence arises from this recognition. A recording medium—after a-c erasing and subsequent recording—is demagnetized only in the portions where no signal is recorded. Wherever there is a signal, there will be magnetization corresponding to the instantaneous value of this signal. The signal itself, consequently, causes noise which follows the instantaneous signal level in its magnitude. This type of noise, closely related to but less objectionable than the continuous noise after d-c erasing, has been termed modulation noise or noise behind the signal. Its magnitude depends on the factors discussed before and noise values up to about 15 db above the no-signal-noise have been measured at the crest of a maximum signal.

For the generation of noise it is immaterial whether the recording medium or the associated reproducing head is magnetized since the two form one magnetic circuit during the reproducing process. An accidentally magnetized reproducing head will therefore also cause noise and great care has to be taken to reduce or eliminate the remanent magnetization of the reproducing head. This can be done by proper selection of the core material, by the introduction of an additional air gap into the magnetic circuit or by purposely demagnetiz-

ing the head whenever required.

Most magnetic recording media until now have had the form of fine wires or of thin tapes. Originally, plain carbon steel was used but has been replaced by various alloy steels, particularly the ternary alloys of iron and nickel-chromium, nickel-copper or cobalt-copper. The coercivity of these materials has thus been increased from about 25 oersteds for carbon steel to about 150 to 250 for various commercial recording media and up to over 400 for some experimental media.

All these recording media are produced by rather closely controlled drawing or rolling operations combined with a suitable heat treatment to effect and maintain the desired physical and magnetic properties. These procedures are difficult and expensive, particularly since the required magnetic hardness of the materials is usually accompanied by physical hardness.

One quite successful solution to this problem has been found to be the electroplating of a ductile, nonmagnetic base material with a ferromagnetic layer.[6] The base material for plated recording media is, ordinarily, brass in the form of fine wires or tapes. However, other shapes, for instance, disks or cylinders, may be processed just as readily which is of importance for special applications.

The plated layer usually consists of a cobalt-nickel alloy, applied to a thickness of about 0.0003 inch. This dimension provides a practical compromise between frequency response, reproducing level and production cost. The material has a coercivity of over 200 oersteds and a retentivity of about 10,000 gausses. The plating is very uniform and ductile, has a mirrorlike surface and fine grain structure, as evidenced by a low noise level. No heat treatment is required since the internal stresses, necessary in any permanent magnet material, are automatically created in the plating process.

The frequency response curves shown in Fig. 4 may be considered representative of the performance of the present plated media. Plated recording wires can now be produced at a rate of about 150 feet per minute, and up to 500 feet per minute have been experimentally obtained.

Magnetic Tape

The ability of a recording medium to exhibit a good high-frequency response depended primarily on its ratio of coercive force to remanence. This ratio determines the specific magnetic reluctance of the recording material and has definite limitations in most homogeneous materials. However, it can be artificially increased by using the ferromagnetic material as a fine powder, uniformly dispersing this powder in a suitable binder, and coating the resulting mixture on an inert base material to form the recording medium.[7] The magnetic reluctance of such material, when measured in bulk, will be very greatly increased by the presence of the minute interstices separating the individual particles. The effective induction will, consequently, be reduced from the intrinsic value of the powder while the coercive force remains unchanged (sheared hysteresis loop), thus giving the desired result of a greatly decreased slope of the demagnetization curve. If both particle size and their separating distances are made small in comparison with the shortest wavelength to be recorded, such a disperse material will behave like a homogeneous material.

The ferromagnetic powders for recording media may be produced from any suitable permanent-magnet material but experience has shown that various magnetic iron oxides are most readily and economically applicable. These powders, with a particle size of about 1 micron and an intrinsic coercive force[8] between 100 and 250 oersteds, are now predominantly used for the commercial production of powder-coated recording media in the form of tapes or sheets. The remanence of the iron oxide coating is usually between 400 and 800 gausses, about one order of magnitude below that of the more common homogeneous recording media.

The coating, containing between 25 and 40 volume percent of magnetic powder, is applied with a thickness of about one-half thousandth of an inch to a base of paper or thin plastic. The resulting recording medium exhibits extremely low background noise and a frequency response far superior to any homogeneous medium now in use. For a given frequency response powder-coated media can be run with roughly about one-half of the speed required for homogeneous media.

The reproducing level from powder-coated media is inherently low because of their low effective induction; but this deficiency can be compensated for by using a correspondingly wider recording track.

This paper is based, in part, on work done for the Office of Scientific Research and Development under Contract OEMsr-254 with The Brush Development Company. A number of facts presented in this paper were first published, in essence, in OSRD Report No. 5325, of June 30, 1945.

References

(1) H. von Lubeck, *Akust. Zeitschr.*, 2, p 273-295, Nov. 1937.
(2) D. E. Wooldridge, *AIEE Trans.*, 65, p 843-852, June 1946.
(3) M. Camras, *Proc. I.R.E.*, 34, p 320-326, Aug. 1946.
(4) Toomim, Hershel & Wildfeuer, *Proc. I.R.E.*, 32, p 664-668, Nov., 1944.
(5) L. C. Holmes and D. L. Clark, ELECTRONICS, 18, p 126-136, July, 1946.
(6) P. O. Pedersen, U. S. Patent 836,839, granted, Nov. 1906.
(7) J. A. O'Neill, U. S. Patent 1,653,467, granted, Dec. 1927.
(8) G. W. O. Howe, *Wireless Eng.*, 20, p 469-472, Oct. 1943.

Reverberation Time Nomographs

Areas of materials in room are measured and number of absorption units of each material is found with first nomograph. Total absorption units are then combined with room volume on second nomograph to obtain directly the reverberation time in seconds

By R. C. COILE

REVERBERATION TIME is the length of time required for the intensity of a sound to drop to one-millionth of its original intensity, which corresponds to a change of 60 decibels. The reverberation time of a room may be computed, knowing the dimensions of the room and the acoustical absorption coefficients of the different surfaces, from

$$T = \frac{0.049V}{A \log_e \left(\frac{1}{1-\bar{\alpha}}\right)} \qquad (1)$$

where T is the reverberation time in seconds, V is the volume of the room in cubic feet, A is the total surface area in square feet, $\bar{\alpha}$ is the average absorption coefficient of the room and is equal to $(A_1\alpha_1+A_2\alpha_2+\ldots)/(A_1+A_2)$, and α_1 is the absorption coefficient of area A_1.

This expression may be simplified[1] into an approximate expression accurate enough for the calculation of reverberation time of most rooms

$$T \cong 0.049\frac{V}{a} \qquad (2)$$

where V is the volume of the room in cubic feet, and a is the number of absorption units in the room computed by adding the absorption of each surface: $a=A_1\alpha_1+A_2\alpha_2\ldots$

Two nomographs have been designed to facilitate rapid calculations of reverberation time. The number of absorption units in a room may be found by using the acoustical absorption nomograph in Fig. 1. Then, knowing the absorption units and the volume, the reverberation time is given by the reverberation time nomograph in Fig. 2.

Find the reverberation time of a room 9 feet wide and 12 feet long, with a ceiling height of 8 feet. The walls and ceiling are of plaster on wood lath. One wall has a window 4 feet by 5 feet. Another wall has a glass door 3 feet by 7 feet. The floor is covered with a pile carpet on ½-inch felt. One adult person is in the room.

(a) Compute areas in square feet, as follows:

Carpet	9×12	= 108	floor
Glass	4×5	= 20	window
	3×7	= 21	door
		41	
Plaster	9×12	= 108	ceiling
	(8×12)	$-$ 21 = 75	wall minus door
	9×8	= 72	wall
	9×8	= 72	wall
	(8×12)	$-$ 20 = 76	wall minus window
		403	

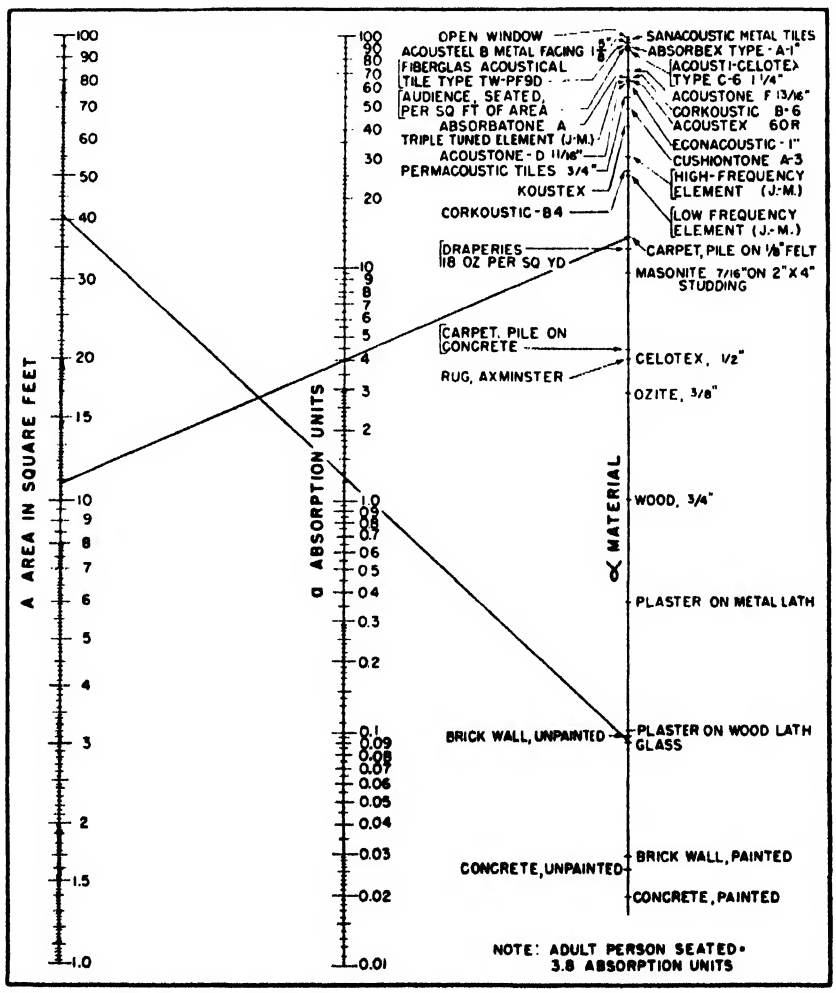

FIG. 1—Acoustical absorption nomograph, based up $a = A\alpha$, where α is the acoustical coefficient of the material

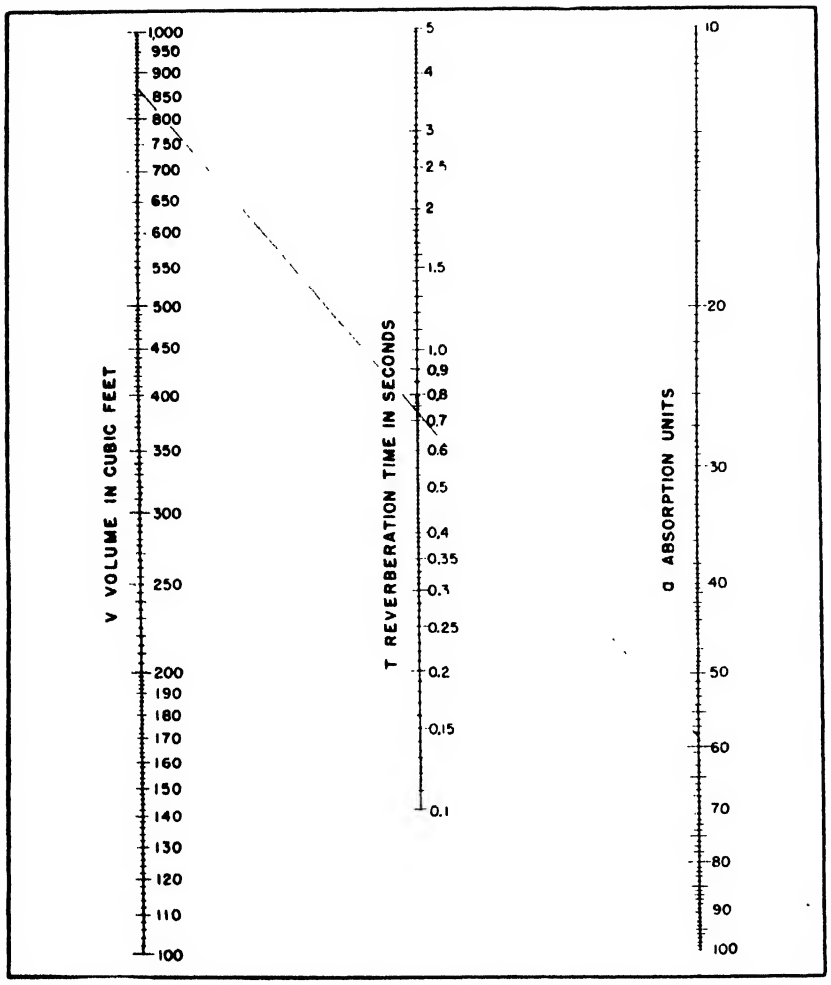

FIG. 2—Reverberation time nomograph, based upon $T = 0.049\ V/a$

(b) Compute absorption units, by first laying a straightedge between 41 on the area scale and glass on the material scale of the acoustical absorption nomograph in Fig. 1. Read the answer of 1.2 absorption units at the intersection of the straightedge with the absorption units scale.

The range of this nomograph can be extended by multiplying the area scale and the absorption unit scale by the same factor, such as 10. For example, to find the absorption units of the carpet area of 108 square feet, connecting a line between 10.8 on the area scale and carpet pile on ½ inch felt on the material scale gives 4.0 absorption units. Multiplying 4.0 by a factor of 10 gives the answer of 40.0 absorption units.

Similarly, 13.3 absorption units are obtained for 403 square feet of plaster on wood lath, and 3.8 absorption units constitute the allowance for one person. Adding then gives a total of 58.3 absorption units.

(c) Compute volume of room: $9 \times 12 \times 8 = 864$ cubic feet.

(d) Compute reverberation time by laying a straightedge between 864 on the volume scale and 58.3 on the absorption units scale of the reverberation time nomograph in Fig. 2. Read the answer of 0.72 second at the intersection of the straightedge with the reverberation time scale.

The range of the reverberation time nomograph may be extended by multiplying the volume and time scales by the same factor, such as 10, or by multiplying the absorption scale by a factor such as 10 and the time scale by the factor's reciprocal, 1/10.

The acoustical absorption nomograph was designed by using acoustical coefficients for 512 cycles. For more accurate computations of reverberation time at other frequencies, acoustical coefficients for those frequencies should be employed. The effect of humidity should also be taken into consideration.

REFERENCE

(1) Morse, Philip M., "Vibration And Sound", McGraw-Hill Book Co., page 301.

Voice-Operated Electronic Relay

By LT. CARL J. QUIRK

RADIO ENGINEERS often have need for a relay system that permits automatic turning on of recorders and transmitters for break-in operation. The voice-operated relay to be described was designed for the purpose of turning on or off any 115-volt a-c operated device whose requirements are within the current-carrying capacity of the relay contacts and connecting wires. By using a different pair of contact than those used here, any d-c operated device may be controlled in the same manner.

An ordinary magnetic-type earphone was used for the microphone. This necessitated a high-gain am-

plifier to provide positive control of the relay. A type 6SL7 tube, with both triodes in cascade, provides the necessary gain.

The purpose of the 884 thyratron is to energize or deenergize as desired, the main relay which is designated in the circuit diagram as relay *A*. Once relay *A* is energized, the 884 become deionized and a pair of holding contacts connects one side of the relay coil to the a-c line; since the other side of the coil is tied directly to the other side of the a-c line, relay *A* will remain energized.

The current that energizes relay *A* flows through the normally closed contacts of relay *B*. Thus, if these contacts become open, relay *A* will be deenergized and likewise the con-

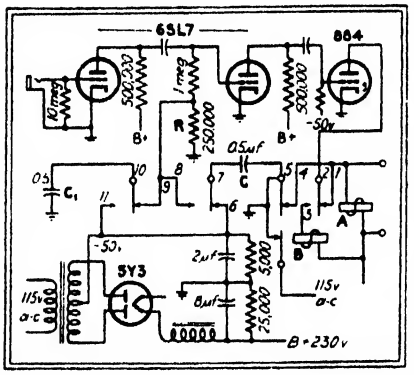

Circuit of electronic relay for actuating equipment by voice signals

trolled equipment will be turned off. To turn off the controlled device, it is necessary to energize relay *B*, thus opening its contacts. For this reason, when relay *A* becomes energized, the plate of the 884 is disconnected from the coil of relay *A* and connected to the coil of relay *B*, so that when the 884 is fired again, it energizes relay *B* instantaneously, opening its contacts and deenergizing relay *A*.

To turn on the controlled equipment, the following sequence takes place: a single word is spoken into the mike and the resultant voltage is amplified by the 6SL7 and applied to the grid circuit of the normally cut-off 884, overcoming the bias and causing it to fire. Since the plate-cathode circuit of the 884 is in series with the coil of relay *A* through contacts 1 and 2 of relay *A*, it completes the a-c circuit, thus energizing the relay. When this happens, the holding contacts 4 and 5 replace the circuit of the 884 and thus keep relay *A* energized. At the same instant, the plate of the 884 is connected to the coil of relay *B* through contacts 2 and 3 of relay *A*, but now the tube is no longer ionized since its plate circuit was opened by means of relay contacts 1 and 2. This is the sequence of events that turns on the controlled device and it remains on until another sound is made.

To turn off the controlled equipment, the above sequence of events is repeated, except that this time the 884 plate-cathode circuit is in series with the coil of relay *B*, so when the 884 is fired, it energizes relay *B* and opens its normally closed contacts, thus deenergizing the main relay and returning the controlled device to the off position.

In order to stabilize the operation of this circuit, some means must be provided to prevent the 884 from becoming ionized when it is switched from one relay coil to the other. It is very difficult to speak even one syllable before the main relay switches the 884 to relay *B* or back again, for if sound is still entering the microphone after the 884 is switched, then the 884 would become deionized again and switch the circuit back to the position it maintained before the sound was applied to the mike.

Stabilization Circuit

A "decaying bias" circuit is used to prevent the possibility of the above-mentioned instability from occurring. This circuit consists of two 0.5-μf capacitors designated *C* and C_1 and resistor *R*. One capacitor is used when the controlled equipment is turned on, to prevent the 884 from ionizing twice from one sound impulse and turning the controlled device off again. The other capacitor is used in the same manner, except it is used when the equipment is turned off, to prevent it from being turned back on from the same sound impulse with which it was desired to turn it off.

The circuit works in the following manner: during the period when relay *A* is deenergized, capacitor *C* is connected to the minus 50-volt bias supply through relay contacts 6 and 7 on relay *A*. When relay *A* is energized, the movable contact, 7, disconnects *C* from the bias supply and connects it through contact 8 to the grid circuit of the second half of the 6SL7 across resistor *R*.

Since the capacitor was charged up to bias voltage, it will cause the second half of the 6SL7 to be cut off, preventing any signal from getting through and thus preventing the possibility of the 884 becoming ionized and thus deenergizing the main relay. However, since this bias is due solely to the charge on the capacitor, it decays exponentially due to the discharge of the capacitor through *R*, the time constant of which will be determined by the size of *C* and *R*. This time constant may be varied to suit any type of operation.

Capacitor C_1 is charged in the same manner by the bias voltage through the relay contacts of relay *A* and applied to *R* when relay *A* is deenergized, so it will not be turned on again by the same sound impulse. Although a negative 25 volts is sufficient to cut off the 884 when using 115 volts of a.c. on the plate, approximately minus 50 volts was used in this circuit to prevent the possibility of any oscillation that may occur in the 6SL7 from firing the 884.

Instrument for Intermodulation Measurements

By GEORGE DANIEL

INTERMODULATION measurement makes possible important findings on the subject of distortion not available by other methods. In intermodulation, the interaction of two frequencies is studied, the purpose being to discover the degree to which one frequency is modulated by the other.

More versatile than its predecessor, a new Western Electric equipment for making these measurements consists of a signal generator in which two independent frequencies are produced and combined and an analyzer in which the degree of modulation of the higher frequency by the lower is determined.

A novel feature of this measuring system is the inclusion of a phase meter which indicates whether compression is occurring on the positive or negative half of the input signal by comparing the phase relationship between the output of the low-pass filter and the low-frequency signal at the input to the analyzer.

Oscillators

In the signal generator two oscillators, each made of a 2C51 miniature dual triode in a resistance—capacitance tuned oscillator circuit, generate the low and high frequencies. Combinations of capacitors provide frequencies of 40, 60, 100, and 150 cycles from the low-frequency oscillator, while similar provision is made for the selection of high frequencies of 1,000, 2,000, 7,000, and 12,000 cycles. Each oscillator circuit includes a 1A type thermistor, or thermally sensitive resistor, which operates on one of the cathodes of each of the 2C51's and, together with a voltage divider, provides negative feed back. The thermistors increase the stability of the oscillator outputs by minimizing variations occurring with changes in gain.

Each oscillator feeds a three-stage amplifier consisting of both halves of a 2C51 and a final push-pull stage. The amplified high frequency is attenuated to 0, 6, 12, or 30 db in relation to the low-frequency output and the two outputs combined in a hybrid coil. The use of a hybrid coil makes possible the combining of the two frequencies with a minimum of intermodulation because each of the amplifiers is separated from the other. At low outputs and for most frequency combinations, this intermodulation is less than 0.2 percent.

In the third stage of the initial amplifier, the plate load is a filter which may be selected by a switch as a band-pass filter of 1,500–2,500

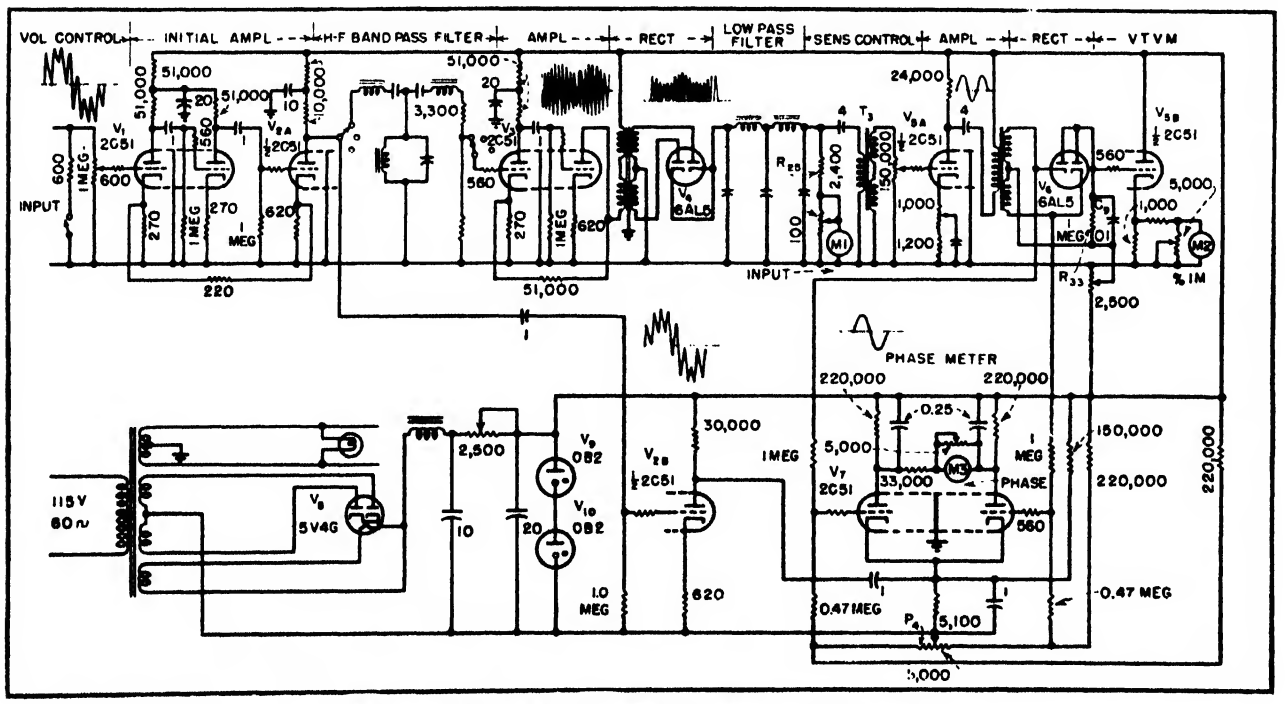

Schematic of the analyzer section of the intermodulation meter

cycles or a high-pass filter of 6,500 cycles. This signal is amplified by both halves of a 2C51 to produce an output of the high-frequency signal modulated by the low-frequency signal to a degree dependent upon the amount of intermodulation in the input signal.

The output of the high-frequency amplifier is rectified and filtered through a low-pass filter with a terminating resistor of 2,400 ohms, R_{25}. The amplitude of the low-frequency voltage impressed on this resistor is relative to the degree of intermodulation in the input signal, while the average current passing through R_{25} indicates the amplitude of the high-frequency input signal.

The low-frequency component from the low-pass filter is impressed upon the primary of transformer T_3, the secondary of which is connected to a variable attenuator which has provision for settings of 5, 15, 50, and 100-percent intermodulation, allowing full-scale intermodulation readings. The output of the attenuator is amplified by one-half of a 2C51 and this output rectified by the 6AL5 full-wave rectifier.

The voltage developed across R_{33} is applied to the grid of the other half of the 2C51 used in the low-frequency amplifier—a space-saving feature made possible by the shielding of the individual sections within the tube—and the triode used as a vtvm in connection with M_2, on which the percentage intermodulation is read directly. In the preceding rectification, the voltage polarity developed is always such as to make the grid negative with respect to ground. The cathode voltage is adjusted by a control on the front panel so that M_2 will read zero percent intermodulation by applying positive d-c voltage to the grid, increasing plate and cathode voltage.

Since the output of the rectifier V_4 is such as to make the grid of the vtvm more negative as the amount of intermodulation increases, the plate current and cathode voltage decrease with intermodulation increase, causing the pointer of M_2 to move.

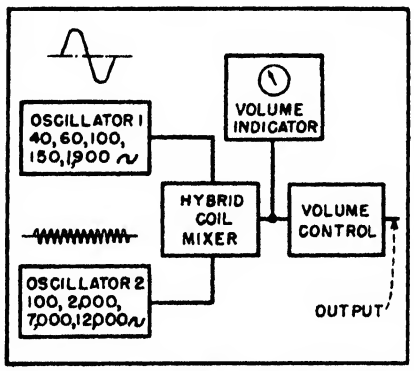

Essential stages of the system for measuring intermodulation distortion

Although the new system will be of value in many fields where audio frequencies are used, it will be of particular importance in the measurement of intermodulation on variable density sound track where intermodulation occurs not only during recording, but within the film itself.

Application

To determine optimum processing and recording techniques, the output of the signal generator is adjusted so as to modulate the light valve about 1.5 db below the clash point, or the point at which the two ribbons of the light valve overlap in the path of the light beam, thereby providing the maximum safe modulation. Recordings are then made at several recorder lamp intensities and the negatives processed for various values of gamma. Positive prints are next made for each negative at several printer light values in a region which past experience has shown to be acceptable.

Each of the several positives is then run on a suitable reproducer and the output fed into the intermodulation analyzer. The print which gives the optimum reading in terms of intermodulation percentage is then used as a guide in making further, more specific tests by the same method, with printer light values and values of gamma of the negatives only a small amount greater or smaller than those previously found most satisfactory.

Intermodulation Testing

Fidelity of audio amplifiers, especially those used in f-m transmitters and receivers, is best determined by intermodulation tests. Correlation with actual listener tests is higher for intermodulation tests than for harmonic distortion tests

By JOHN K. HILLIARD

STANDARDS of good engineering practices concerning f-m broadcasting, published by the Federal Communications Commission, specify an audio frequency bandwidth of from 50 to 15,000 cycles. These standards indicate that it is the intention for f-m broadcasters not merely to transmit the designated wide audio band but also to transmit this band with minimum distortion. To obtain this objective it will be necessary for most engineers to alter radically their audio frequency design and measuring techniques, and to revise their concepts of high fidelity.

In transmitting signals covering a wide frequency range, it is necessary that all the elements of distortion be reduced to a very low degree.

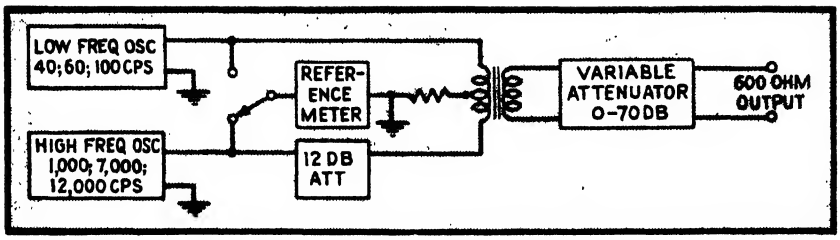

FIG. 1—Signal generator for intermodulation testing consists of two independent oscillators and a linear circuit for mixing their outputs

This requirement is particularly true when the frequency range approaches the full capabilities of the human ear. If distortion is not satisfactorily controlled, the results of extending the frequency range will be to produce a quality which is less pleasing than that obtained with a limited bandwidth.

The error of transmitting a wide band without sufficient reduction of distortion has been repeated many times and in each case the public has reacted unfavorably to what was expected to be an improvement. Experience in the sound motion picture field has indicated that widening of the frequency range should be the last step in design improvement. Reduction of distortion comes first and then, with proper experience, if the distortion and noise level are sufficiently low, the frequency band can be extended. If the new standards of the FCC are to be properly met, a new set of standards for measuring permissible distortion is essential. I refer not only to distortions of frequency and amplitude, but also to distortions caused by hum, noise, and distortion caused by interaction of complex frequencies, which has come to be known as intermodulation.

Tests for Fidelity

For an amplifier system to provide excellent quality without distortion while transmitting the band from 50 to 15,000 cycles, the complete amplifier system should be capable of passing the following tests:

(1) Total hum and other noises measured throughout the entire band should be at least 66 db below the full modulation or overload point.

(2) As determined by means of an oscillator and oscilloscope, the maximum sine wave carrying capacity for the system should be determined for all frequencies in the transmitted band. It is desirable for the amplifier system to have reserve sine wave carrying capacity of at least six decibels beyond full modulation over the entire pass band.

(3) Frequency response runs should be made at maximum operating level as determined by the preceding test. Additional frequency response measurements should be made at 30 db below that point and 60 db down from the maximum operating level. There should be no significant difference in the frequency response of the amplifier system at these three levels of output power.

(4) Determine intermodulation products of the amplifier system by methods outlined herein. For direct transmission, six percent intermodulation should not be exceeded anywhere in the frequency band. If the signal is to be recorded and re-recorded, or if it is to be transmitted through a network of amplifier systems, it is desirable for the intermodulation products to be held below four percent. Amplifier systems which will meet all of these requirements can be built, but they require much greater attention to design than they have been previously accorded.

Amplifier systems which will not meet these tests will fail to meet the objective of truly high-quality reproduction. Measurements of hum and other noises, measurement of maximum sine wave carrying capacity for the entire band, and measurement of frequency response at the designated levels all utilize techniques with which the audio-frequency engineer is familiar.

Intermodulation tests consist of transmitting simultaneously two known frequencies through the equipment under test and then measuring the degree of interaction and distortion of these two frequencies by determining the magnitude of new frequencies which have been generated.

Two known frequencies are applied to the input of the amplifier under test from a signal generator. The output attenuator of the signal generator is adjusted to produce the required power from the amplifier under test. The output of the amplifier or system being tested is connected to the input circuit of the intermodulation analyzer. The input attenuator on the analyzer is then adjusted until a carrier level meter reads 100 percent. An intermodulation percentage meter then reads directly the amount of distortion present.

Signal Generator

Figure 1 shows a block diagram of a conventional signal generator used for intermodulation testing. It contains two independent resistance-capacitance sine-wave oscillators. We have a choice of 40, 60, or 100 cycles from the low frequency oscillator and 1,000, 7,000, or 12,000 cycles from the high-frequency oscillator. The output level of each oscillator is independently controlled. A reference meter can be switched to either oscillator for metering its level. The output of each oscillator is transmitted by a cathode follower to a hybrid coil which combines the two oscillator outputs.

A 12 db fixed attenuator is provided in the high frequency oscillator output so that the low frequency is transmitted 12 db higher than the high frequency. This differential ratio of low to high frequency amplitudes is arbitrary and is used to obtain the maximum low-frequency sensitivity of the test.

For other test conditions, in particular where distortion is predominantly at high frequencies, it may be advisable to use other amplitude ratios for the two test frequencies.

An output meter, a variable attenuator of 30 db range, and fixed attenuation of either 20 or 40 db are available by means of a selector

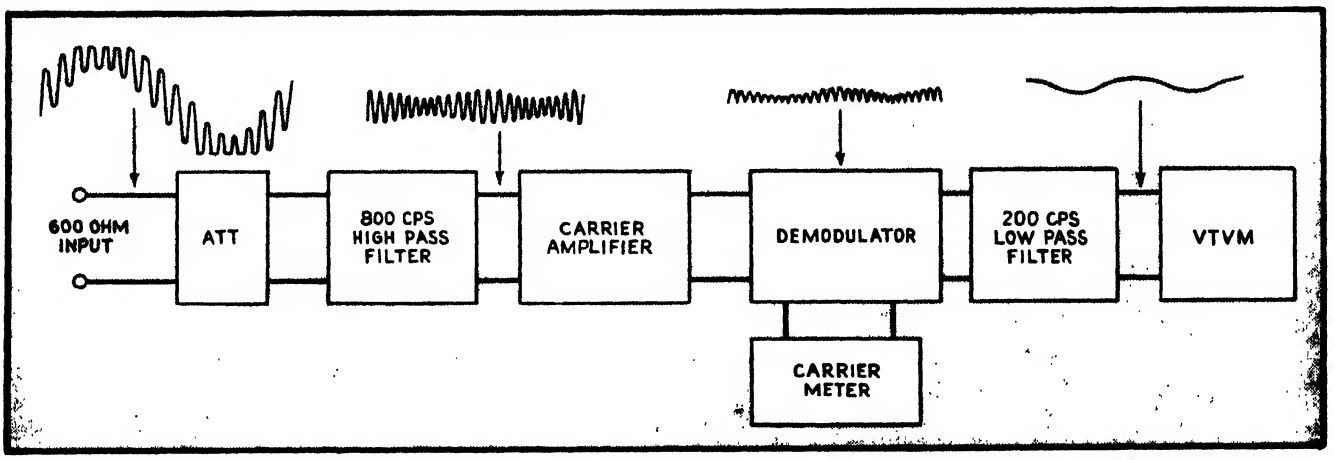

FIG. 2—Intermodulation analyzer detects high frequency modulation developed by nonlinearity of amplifier under test. (Word received from author explains that 1,000 cps in test oscillator has been replaced by 2,000 cps so analyzer accepts more sidebands—bandwidth is now 500 instead of 200 cps—eliminating tendencies for cancellation of sidebands of 100 cps)

switch to control the output. A ganged dual potentiometer at the input of cathode followers gives a vernier adjustment of output power.

A block diagram of an intermodulation analyzer is shown in Fig. 2. The input attenuator system is adjustable over a 90 db range in one decibel steps, and is capable of dissipating 50 watts. The input impedance is 600 ohms.

Intermodulation Analyzer

Equipment under test receives its input from the signal generator and delivers its output to the analyzer. The output of the equipment under test consists of a low frequency with a high frequency superimposed upon it, plus harmonics of the original tones, plus intermodulation distortion. In order to measure this intermodulation, it is necessary to remove the original low frequency component. This removal is accomplished by an 800 cycle high pass filter which follows the attenuator. The output of the filter consists of what may be termed a carrier and its resultant sidebands. This carrier is then amplified to a predetermined level and demodulated. The reference level is obtained by adjusting the input attenuator to provide a 100 percent reading on the carrier meter. The output of the demodulator is transmitted through a 200-cycle low-pass filter which removes the carrier frequency and transmits only sideband components up to 200 cycles.

Discussion in the literature has indicated that both first and second-order intermodulation components generally are present in the distortion of audio frequency transmission equipment. For this reason it is considered essential that measuring equipment should record many such components rather than limit itself to only first order components.

The 200 cycle cutoff frequency has been set so that at least the second order terms will be accepted for all the original low frequencies, more being accepted for the 60 and 40 cycle tones.

The choice of the 800 cycle cut off for the high-pass filter has been dictated by the requirement that at least 60 db of discrimination be inserted against all low frequencies in order that values of intermodulation can be measured down to 0.1 percent.

The ripple components or intermodulation products are amplified and measured by a vacuum-tube voltmeter. The meter is calibrated directly in percentage total intermodulation and has six ranges with full scale sensitivities of 0.3, 1.0, 3.0, 10, 30 and 100 percent. The analyzer can also be used as a voltmeter by bridging the filters. The frequency range as a millivoltmeter is flat within 1 db from 20 to 20,000 cycles per second and on the voltmeter scale its range is flat from 20 to 50,000 cycles.

The inclusion of the vacuum-tube voltmeter provides a method of accurately measuring signals or noise levels. The meter scales read in volts, with maximum sensitivity cor-

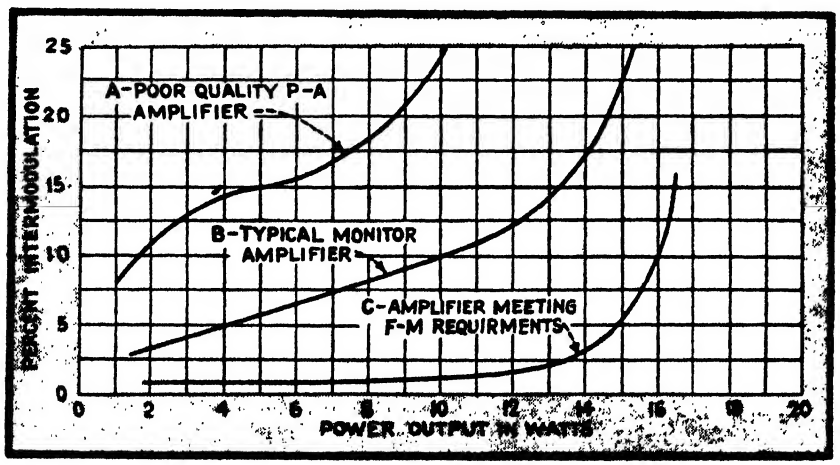

FIG. 3—Intermodulation tests indicate the increasing nonlinearity of amplifiers as they are called upon to handle larger signals

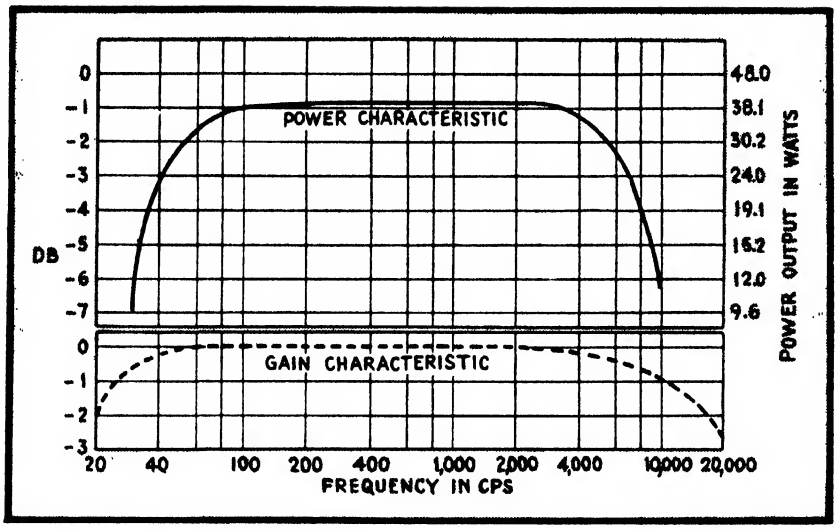

FIG. 4—Maximum undistorted power obtainable for a particular amplifier falls rapidly at low frequencies

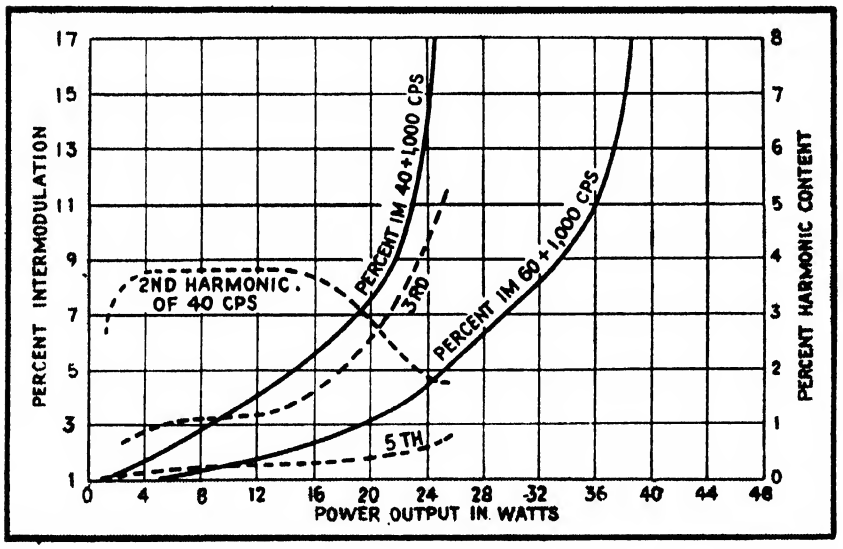

FIG. 5—Intermodulation and harmonic distortion of the amplifier whose characteristics are given in Fig. 4

responding to a full scale reading of 0.3 mv, and in db relative to one milliwatt across 600 ohms. In shifting from the measurement of percentage intermodulation to voltage, the termination of the amplifier under test is not altered.

Sensitivity for zero on the db scale has a range from minus 70 to plus 40 dbm in 12 steps of 10 db each. Because the scale is calibrated so that a −20 db point is readable, a range down to −90 dbm is possible.

Frequency response curves and noise levels can be obtained by using the voltmeter and millivoltmeter. Two scales enable data to be taken in either decibels or volts. A bridging jack is provided so that the vacuum tube voltmeter can be bridged across any portion of a circuit where a shunt of 1.4 megohms will not influence circuit conditions.

Apparent cancellation of intermodulation effects (usually near amplifier overload point) is a phenomenon which has been observed in some cases. In these cases it has been found that the pass band of the intermodulation analyzer was not sufficiently wide to accept the higher order distortion terms.

Calibration of the intermodulation analyzer is made using two frequencies, namely 1,000 and 1,060 cycles. A 20 db attenuator is switched into the 1,060 cycle oscillator output so that when these two frequencies are combined, the 1,060 cycle output will be 20 db below the 1,000 cycle output. By definition this is a condition of ten percent intermodulation. This complex signal is then transmitted directly to the analyzer with the range switch set for ten percent intermodulation. The input level is then adjusted for a ten percent reading on the intermodulation meter, and the carrier meter is set to 100 percent.

Calibration of the voltmeter is accomplished by checking against a standard a-c voltmeter. By inserting a 60 db attenuator ahead of the analyzer, the same voltage can be used to check the millivolt range.

Low Frequency Overloading

The writer wishes to stress the importance of linear transmission of amplitudes and wave forms of the low frequencies which occur simultaneously with the higher frequencies of speech and music. These low frequency components originate in drums and other percussion instruments, in the reproduction of gun shots, explosions, thunder and earthquakes.

Unless a transmission system has the carrying capacity at low frequencies to handle these sound effects, distortion results. Therefore, it is considered essential to test a transmission system in such a manner as to stress these low frequencies. Transformers and other devices which change their impedance at low frequencies are a major cause of distortion, because this impedance change limits the carrying capacity of the tubes. For this reason, limited power capacity will appear at low frequencies more readily than in the midrange.

Analysis indicates that all types of systems show least distortion near the middle portion of their transmission band. Therefore, test equipment is designed so that test frequencies lie near the outer portions of the frequency band.

Apparatus which shows low intermodulation distortion at 40 cycles

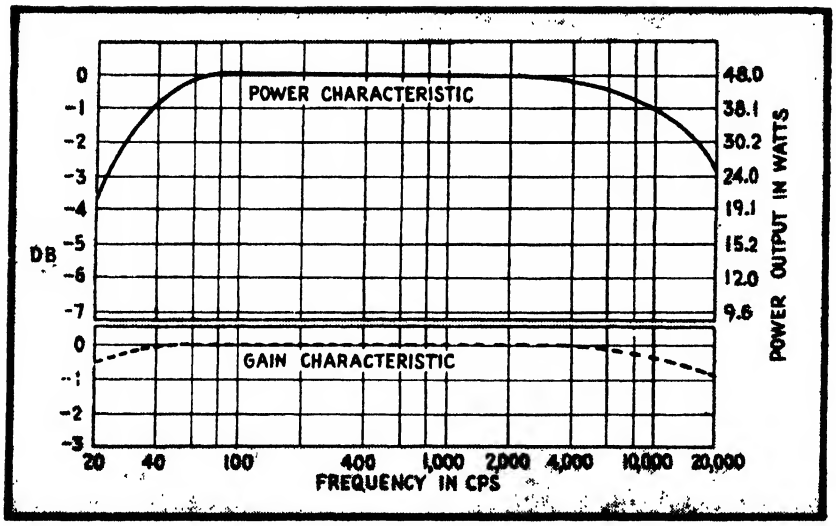

FIG. 6—Although not rated for as high power as the amplifier of Fig. 4 and 5, this amplifier has better high and low frequency response

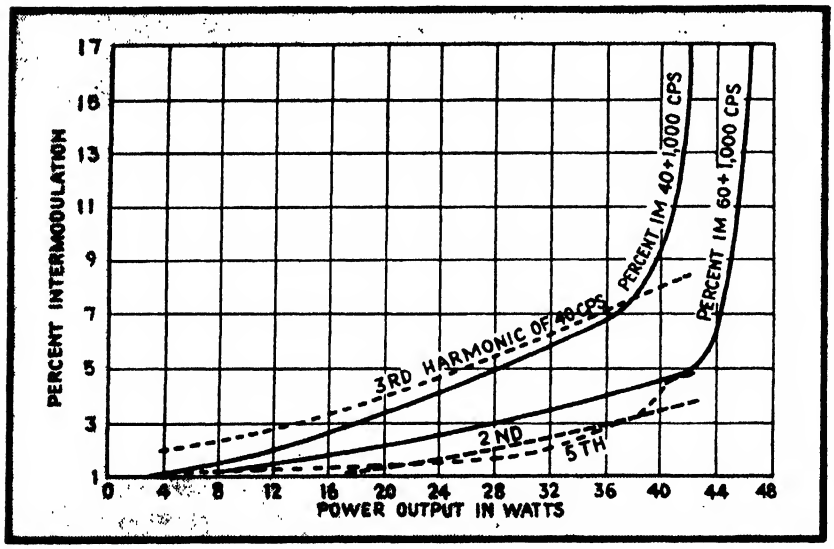

FIG. 7—Intermodulation distortion of the amplifier whose characteristics are shown in Fig. 6 remains low up to its rated output power

will meet the most rigid low frequency demands, while systems which pass the intermodulation test only at 60 or 100 cycles should be used only where a corresponding sacrifice in quality is permissible. This information, together with a corresponding study of high frequency properties, will determine the bandwidth for which a particular system is suitable.

Figure 3 shows intermodulation curves on three classes of amplifier. Curve A represents a poor public address amplifier which is not suitable for any application even though the amplifier is rated at 14 watts, because distortion is excessive at one or two watts. Curve B is representative of the average, high grade amplifier now used for radio station and recording purposes. Curve C is an amplifier which will meet the rigid specifications called for by f-m standards of good engineering.

Correlation of Harmonic and Intermodulation Distortions

Figure 4 shows the power and gain characteristic of a pushpull parallel 6L6 amplifier rated by its manufacturer at 50 watts. The power curve is obtained by observation of the maximum power that can be generated before departure of the output from a sine wave is observable on an oscilloscope. The gain characteristic had to be measured at a low level so as to be within the limitation of the power curve.

Figure 5 shows the distortion analysis for this amplifier, giving the 40 cycle harmonic analysis for 2nd, 3rd, and 5th harmonics as well as the percentage intermodulation for 40 and 1,000 cycles and for 60 and 1,000 cycles. It will be observed that the 40 cycle intermodulation products rise very rapidly in the vicinity of 25 watts. For this particular amplifier the 3rd harmonic shows a rapid increase at the same power. The fact that the 60 cycle intermodulation curve is lower for the same power indicates a deficiency in the output transformer as was indicated in Fig. 4 by the reduction in power handling capacity at low frequencies.

Figure 6 shows power and gain characteristics for an amplifier having a manufacturer's rating of 40 watts. In this case the power and frequency response are more uniform over a wider frequency range. Figure 7 shows the harmonic content at 40 cycles for 2nd, 3rd and 5th harmonics together with the intermodulation curves for 40 and 1,000 cycles and for 60 and 1,000 cycles. It will be noted in this case that the harmonic distortion for all orders of terms increases gradually with power. Because both total harmonic and intermodulation distortion are low, except near its rated maximum power, the amplifier can be considered to be comparatively free of distortion.

In our design and development work on amplifiers, we have found that proper design and adjustment are attained only when the curve shows low values of intermodulation at low levels and rises gradually as maximum power is reached.

A good example of how the intermodulation method can be helpful in design work is shown in Fig. 8. Here are shown three intermodulation curves showing the effect on intermodulation of improper bias of the

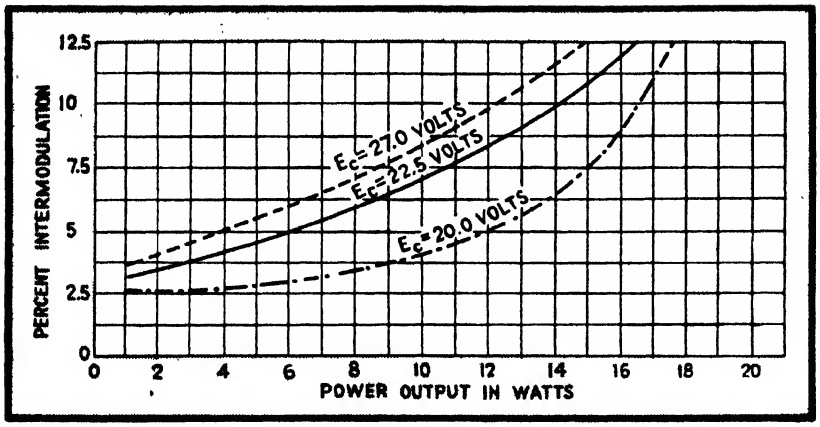

FIG. 8—Effect of cathode bias on linear operation of output tubes is shown by intermodulation tests

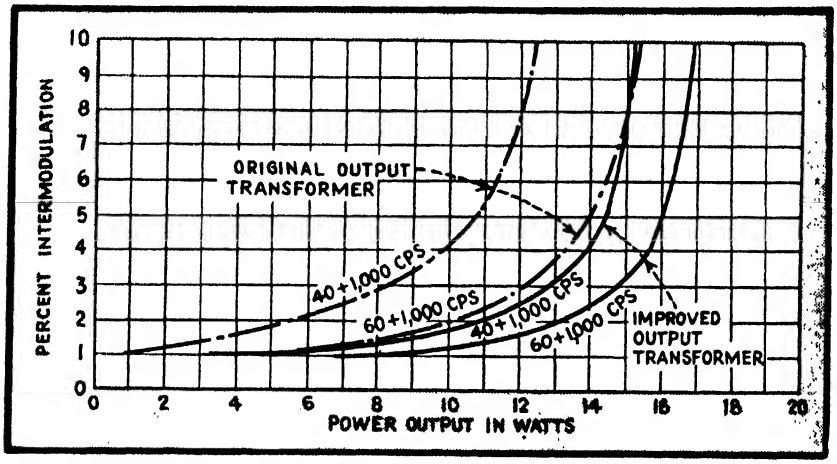

FIG. 9—Intermodulation testing shows the importance of the output transformer at low frequencies

amplifier's power stage. The requirement of low intermodulation products at low operating levels forces the bias nearer the condition of strictly Class A operation in amplifiers. In other words, excessive bias must be avoided for highest quality performance in the operating range.

Intermodulation testing has facilitated advancements in transformer design. Figure 9 shows the improvement which can be made in an amplifier by substituting an improved output transformer. It will be observed that the low frequency carrying capacity has been increased and the distortion has been reduced for all levels of operation.

Most of these curves have shown conditions where overload occurs first at low frequencies. In some amplifiers high frequency distortion predominates. To test these amplifiers the two frequencies from the signal generator are adjusted to be of equal amplitude. The intermodulation measurements will indicate the presence of high frequency distortion when it is not masked by low frequency distortion.

Without exception it has been the writer's experience that listening tests will confirm the relative intermodulation test figures. All other things being equal, critical listeners will select the system having the lowest percentage of intermodulation in a performance test.

The intermodulation test does not of itself provide all information required by engineers. It needs to be supplemented by frequency response, noise, and power tests mentioned earlier in this paper. When used in conjunction with these other tests, it is the writer's belief that this intermodulation method of testing represents a major tool, essential in design, production, and maintenance of amplifier systems which meet FCC standards of good engineering practice.

The writer wishes to acknowledge the important work done by W. C. B. Evans, who has shared the responsibilities of designing the equipment and who has supplied much of the laboratory data used in this paper.

Phase-Shift Oscillator Design Charts

For test equipment requiring either a fixed or variable audio-frequency voltage source, the simple one-tube phase-shift oscillator offers frequency stability and good wave form at low cost. With the nomograms given here, its design reduces to simple arithmetic

By WALTER W. KUNDE

IN designing various types of test equipment a voltage source operating at a fixed frequency other than 60 cycles is often desired. The single-tube phase-shift oscillator has found wide application in this field due to its simplicity, excellent stability and good wave form. When followed by an amplifier designed to furnish the required output voltage, it can be used to supply power for a-c bridge measurements, insulation

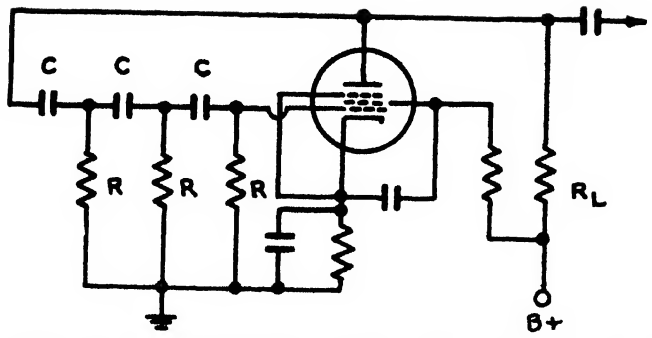

FIG. 1—Basic circuit of the phase-shift oscillator. The output frequency is determined by the values of R and C, and these are given in the accompanying nomograms. Other circuit values follow conventional practice and hence are not given. In a variable-frequency audio oscillator, a three-gang variable capacitor can be used for C or ganged rheostats can be used for R

tests, testing aircraft transformers and their associated equipment, and many other purposes.

The basic circuit for an oscillator of this type is shown in Fig. 1. When using ordinary resistors and capacitors the actual frequency obtained may differ slightly from the computed value, due to manufacturing tolerances of the components used. Any one of the resistors or capacitors in the phase-shift network may be varied slightly to compensate this effect. This is accomplished very nicely by making one of the resistors semi-variable.

The constants used in the phase-

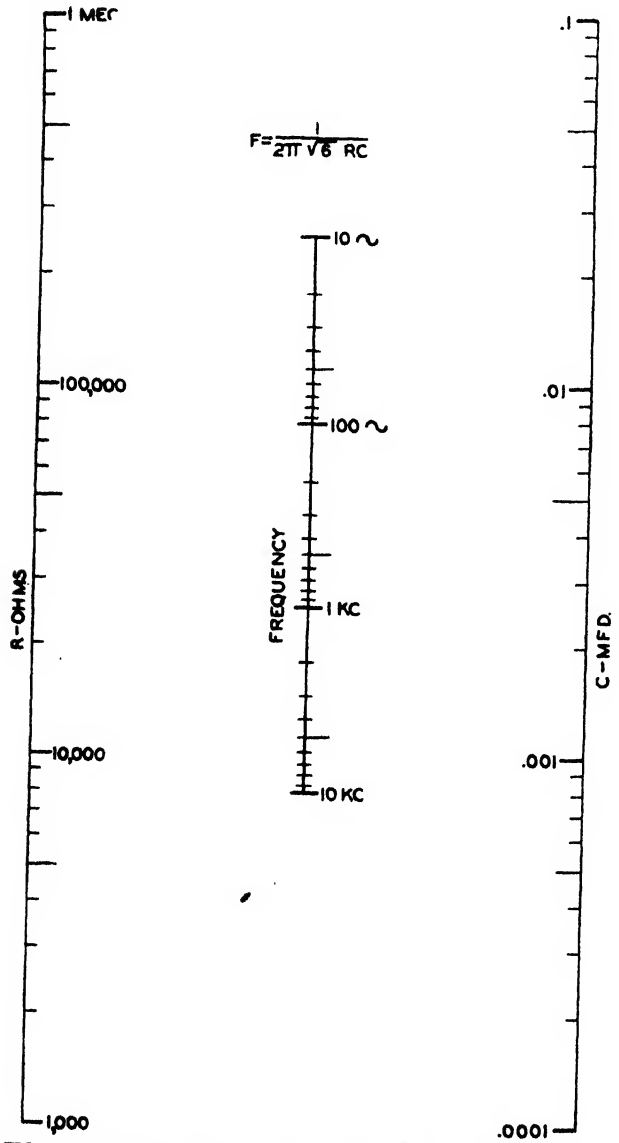

FIG. 2—Nomogram for determining values of R and C in the phase-shift oscillator circuit of Fig. 1. The ranges of values are appropriate for a fixed-frequency oscillator, permitting a choice of convenient values for the fixed resistors and capacitors

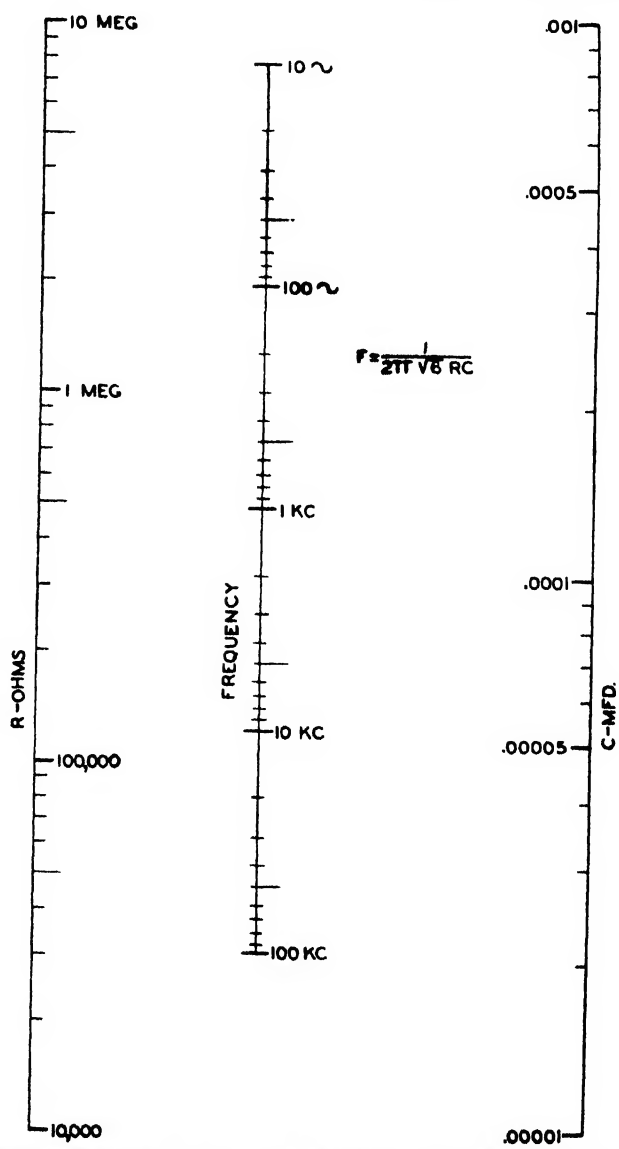

FIG. 3—Nomogram for the same conditions as Fig. 2, but with a range of capacitance values more appropriate for a variable-frequency oscillator in that it covers variable capacitor ranges that are readily obtainable. The frequency can go up to 100 kc

shift network to obtain a desired frequency are determined by the formula

$$f = \frac{1}{2\pi\sqrt{6}RC} \quad (1)$$

The alignment charts shown in Fig. 2 and Fig. 3 were developed to minimize errors and give a rapid, visual indication of possible RC combinations which would give the desired frequency.

It was shown by Ginzton and Hollingsworth* that the circuit gain must equal a minimum of 29 for oscillation to take place. This condition is readily met provided that $R >> R_L$, where R_L is the equivalent parallel value of the plate resistor and the grid resistor of the following amplifier tube. This is apparent when we consider the equation

$$A = 29 + 23\frac{R_L}{R} + 4\left(\frac{R_L}{R}\right)^2 \quad (2)$$

where A is the gain required for oscillation to start. A is independent of frequency when $R >> R_L$. For example, let $R = R_L$ for some given frequency. One can readily see that the required gain for oscillation to start is aproximately double that required when R is much greater than R_L.

The chart shown in Fig. 2 is used primarily for fixed low-frequency oscillators when a high-gain tube such as the 1851 is used. Lower values of R_L are used for a tube of this type, consequently R can be made smaller for a given frequency and C is in the range of the more commonly available values.

Figure 3 is a more universal chart and is used for both fixed and variable-frequency oscillators. Note that the values of C correspond closely to the values of variable capacitors considered to be common. For variable-frequency oscillators, either the resistors R or the capacitors C may be variable and ganged together. In a laboratory oscillator requiring more than one frequency range, variable capacitors with a 10-to-1 range may be used with a switch that changes the entire set of resistors in decade steps.

Example 1: The desired frequency is 1 kc. Assume R_L = 50,000 ohms. Using either Fig. 2 or Fig. 3, determine suitable values for R and C as follows: Remembering that R must be very much greater than R_L, assume a value of 650,000 ohms for R. Place a straight edge on 1 kc and on R = 650,000 ohms, and read 0.0001 μf as the required capacitance.

Example 2: To design a variable-frequency oscillator using variable capacitors whose range is 20 to 500 $\mu\mu$f, assume R = 1,000,000 ohms for the middle range of frequencies, and use Fig. 3 as follows to determine suitable values of R & C: Using the assumed value of R as a pivot point, allow the straight edge to slide between the maximum and minimum values of C. The frequency range is determined immediately without any lengthy calculations, being approximately 130 to 3200 cps.

* Ginzton, E. L. and Hollingsworth, L. M., Phase-Shift Oscillators, *Proc. I. R. E.*, p. 43, Feb. 1941.

Telephone Recording

Electronic dictating machines can be used to record important telephone conversations. Either direct or induction connection to the line is suitable. Design considerations are given

By K. L. MacILVAIN

TELEPHONE lines carry not only speech signals, but also interfering noise, ringing and other operating voltages. Any connection to a recording circuit should eliminate interference between the telephone pair and ground, provide isolation for direct current, and should not affect or be affected by the operating voltages nor should appreciably load the telephone line.

A typical direct connection is shown in Fig. 1A. The capacitor provides d-c isolation; the transformer blocks longitudinal current

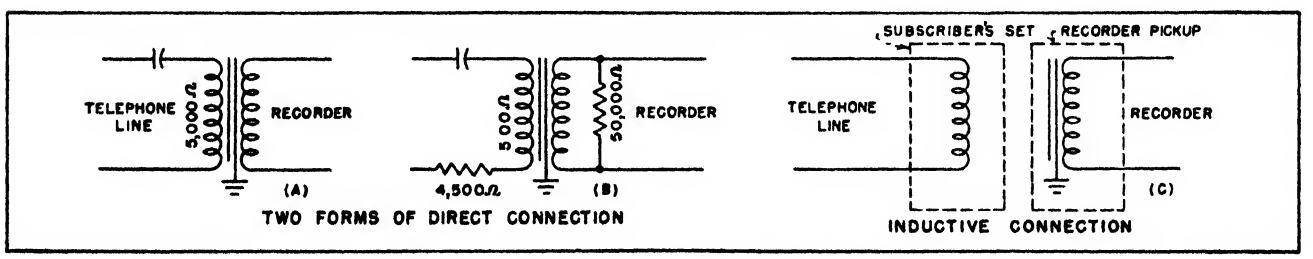

FIG. 1—Recorder can be either connected directly or by induction to telephone

(produced by voltage between the telephone pair and ground). Transformer input impedance should be sufficiently high not to appreciably load the line. If the transformer input impedance is low, for example 500 ohms, a series resistor added in the primary circuit, 4,500 ohms in Fig. 1B, prevents loading.

Although speech levels to be expected from a telephone line vary widely, signals available with the direct connection range from +10 db (where 0 db equals 6 milliwatts) for peak levels to −40 db, with good local voice levels averaging around 0 db but with many between −10 and −15 db. Regardless of the high standards at which telephone lines are maintained, wide ranges in speech levels are to be expected because of conditions beyond control of telephone engineers. The recording equipment must, therefore, be designed to record satisfactorily a 40-db range, although the extreme range might be as great as 60 db. To keep the recording level within the range of the recording medium, automatic control circuits should be incorporated in the recorder.

Inductive Pickup

With the inductive connection, shown in Fig. 1C, the telephone terminal equipment forms one winding of a transformer and the recorder pickup is the other. The pickup is formed into a flat unit that can be placed under the subscriber's set. The transformer so formed has low coupling between primary and secondary because of the relatively large spacing. The inductive pickup should be electrostatically shielded to eliminate effects of undesirable fields in the vicinity. From 40 to 60 db are lost in this form of coupling, so the recorder amplifier must have greater gain than for the direct connection. Hum-bucking arrangements can be added to neutralize fields from local motors and transformers, but because such fields are neither constant in magnitude nor direction, complete cancellation is difficult.

Either method of connection is satisfactory, and now that recording telephone conversations has been made legal many applications for this technique will be realized.

CIRCUIT THEORY

Cathode Follower Circuits

A comprehensive analysis of recently-developed cathode follower circuits, which serve as highly efficient transformers for coupling high-impedance sources to low-impedance loads. The circuits discussed are strictly power amplifiers. Voltage amplification is always less than unity

By WALTHER RICHTER

THE placement of a resistor in the cathode circuit of a single tube, or of a pair of tubes having their cathodes connected together, produces certain effects which have been put to good use in many applications. This discussion attempts a summary and analysis of these circuits, so that their behavior may be visualized and predicted.

Suppose a signal Δe_s is applied to a tube as shown in Fig. 1. Evidently the actual grid voltage change, that is the voltage change between grid and cathode, will not be as large as Δe_s. If the signal voltage makes the grid more positive, for instance, more plate current will flow; this will cause an increase of voltage across r_c, making the cathode also more positive. The cathode "follows" the grid, so to speak.

The mathematics of this case have been presented in this magazine once before[2], but will be repeated here for the sake of completeness.

If Δi_p is the plate current change due to the signal voltage change Δe_s, the actual grid voltage change will be given by

$$\Delta e_g = \Delta e_s - \Delta i_p r_c \qquad (1)$$

The fundamental relation between plate current change, grid voltage change and plate voltage change is given by the well known equation

$$\Delta i_p = \frac{\mu \Delta e_g + \Delta e_p}{r_p} \qquad (2)$$

An increase Δi_p in plate current causes a decrease—or negative increase—of plate voltage given by

$$\Delta e_p = -\Delta i_p (R + r_c) \qquad (3)$$

Substituting Eqs. (1) and (3) into Eq. (2) gives

$$\Delta i_p = \frac{\mu (\Delta e_s - \Delta i_p r_c) - \Delta i_p (R + r_c)}{r_p} \qquad (4)$$

When this equation is solved for Δi_p, we obtain

$$\Delta i_p = \frac{\mu \Delta e_s}{R + r_p + (\mu + 1) r_c} \qquad (5)$$

It is worthwhile to study Eq. (5) in detail. With $r_c = 0$, the equation assumes the familiar form

$$\Delta i_p = \frac{\mu \Delta e_s}{R + r_p} \qquad (5a)$$

In this case, representing fixed bias, signal and grid voltage change are of course identical. Comparing Eqs. (5) and (5a) we note that the introduction of r_c in the cathode lead has the same influence on the plate current change due to a signal voltage change, as if the tube were operating with fixed bias, but a resistor of the value $(\mu + 1)\, r_c$ had been added in the plate circuit. Another, sometimes more convenient, way to visualize the influence of the cathode resistor, can be deduced as follows: if we substitute Δi_p from Eq. (5) into Eq. (1), we obtain

$$\Delta e_g = \Delta e_s \frac{R + r_p + r_c}{R + r_p + r_c + \mu r_c} \qquad (6)$$

Now $R + r_p + r_c = R_t$ is the total resistance in the plate circuit, since obviously r_c is just as much a part of the plate circuit as R. However, r_c is also part of the grid circuit, and

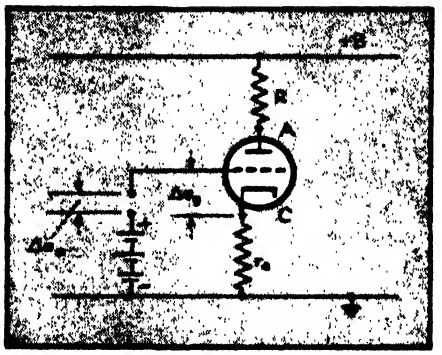

FIG. 1—Fundamental schematic wiring diagram of tube used as degenerative amplifier for phase inverter or cathode follower

its presence there causes the actual grid voltage change to be less than the signal voltage change in the ratio

$$\Delta e_g = \Delta e_s \frac{R_t}{R_t + \mu r_c} \qquad (6a)$$

We can therefore also state the influence of a cathode resistor by saying that its presence reduces the value of the signal voltage in the ratio given by Eq. (6) or Eq. (6a) before it reaches the grid.

While Eqs. (1) to (6) were set up for resistive values in the plate and cathode circuit, they are just as valid if the resistances are replaced by impedances (provided, of course, that there is a path for the direct-current component of the plate current). Thus the influence of a resistor by-passed with a condenser can be calculated by means of Eqs. (5) or (6) by simply replacing the value

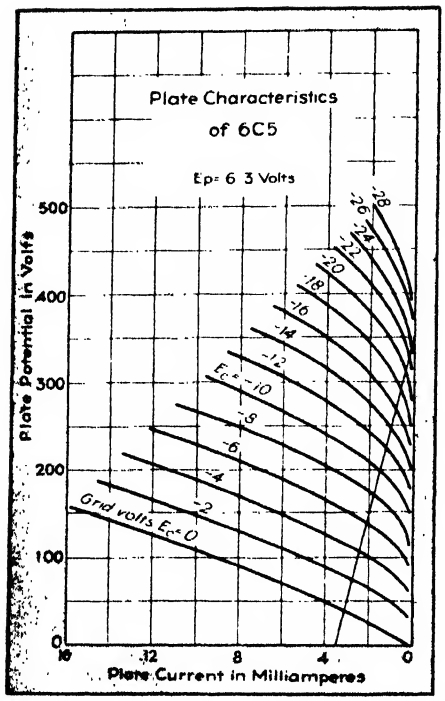

FIG. 2—Family of plate characteristics for triode, illustrating the operation of cathode follower

r_c with the complex value of the impedance representing the parallel combination of resistor and condenser.

Cathode Follower Arrangement

The case of a true "cathode follower," or impedance changing tube is obtained for $R = 0$. The question arises how much signal we shall obtain across r_c in this case.

The voltage change Δe_c across r_c due to the signal voltage change Δe_g is of course simply equal to the current change Δi_p, obtained from Eq. (5), multiplied by r_c; we have therefore

$$\Delta e_c = \Delta i_p r_c = \frac{\mu \Delta e_g r_c}{r_p + (\mu + 1) r_c} = \frac{\mu \Delta e_g r_c}{r_p + \mu r_c + r_c}$$

$$= \Delta e_g \frac{\mu r_c}{\mu r_c + r_p + r_c} \qquad (7)$$

Since the denominator is always larger than the numerator, the fraction will always have a value less than unity. This means that we cannot obtain voltage amplification with this circuit.

If R is made equal to r_c, the voltages across R and r_c will be equal, since the same current flows through them. But an increasing current will swing point A of Fig. 1 more negative, while point C will swing more positive. These two points may be capacity-coupled to a push-pull stage furnishing the 180 deg. phase displaced signals required for such a stage.[1]

The procedure of designing such a stage may best be shown on an example. Suppose 350 volts is available for the stage and that a 6C5 is to be used. If we were to design a conventional resistance-capacity coupled stage, we would draw a load line with the chosen value of the load resistance and decide on a proper operating point. This is exactly what we do now, except that the load resistance will be split into two equal parts, one to be placed into the plate lead, the other into the cathode lead. However, it might be desirable to hold the load to lower values than usual, to minimize the effect of cathode leakage and capacity. (For an excellent discussion of the effect of cathode capacity on the performance of cathode follower circuits, see C. E. Lockhart, "The Cathode Follower".[1]) Suppose we take a load of 100,000 ohms. Figure 2 shows the plate characteristic of the 6C5 with the load-line representing 100,000 ohms and inspection shows that a good operating point is 2 ma, with 150 volts across the tube and 200 volts across the 100,000-ohm load. The actual grid voltage for this condition would have to be about −7 volts, as seen from Fig. 2. Splitting the 100,000 ohm load into two resistors of 50,000 ohms results in the circuit shown in Fig. 3a. The operating—or quiescent—current of 2 ma causes a drop of 100 volts across r_c, and in order to have an actual grid voltage of −7 volts, a bias of +93 volts will be required.

The output voltage obtainable from such a stage for a given signal voltage can be determined in two ways, just as for a conventional circuit. For small signal voltages the equivalent plate circuit theorem will give us the answer, that is, Eqs. (5) or (6) can be used, which have been derived on the basis of this theorem. For larger signals the use of the load line will be indicated. Assuming at first a small signal, say 1 volt, the application of Eq. (5) or (6) requires the plate resistance to be known. At the operating point chosen in the example, this value would be about 16,000 ohms (determined from the cotangent at the operating point).

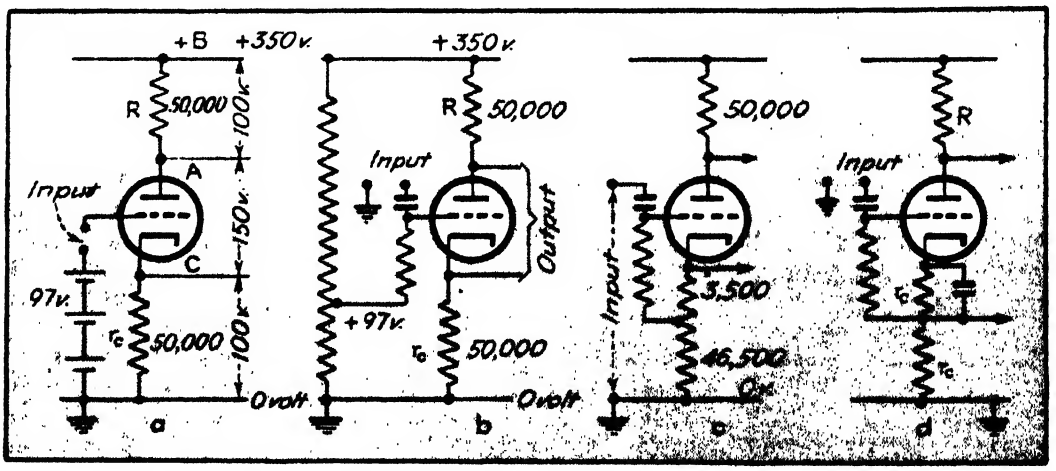

FIG. 3—Various circuit connections for phase inverter circuits

The plate current due to a signal of 1 volt would be given by Eq. (5):

$$i_p = \frac{20 \times 1}{50{,}000 + 16{,}000 + 21 \times 50{,}000} = \frac{20}{1{,}116{,}000} = 17.92 \times 10^{-6} \quad (5)$$

The signal appearing across the cathode (or plate) resistor will be given by

$$e_c = 50{,}000 \times 17.92 \times 10^{-6} = 0.896 \text{ volt}$$

We could have used Eq. (6a), to give us first the actual grid voltage change:

$$e_g = 1 \times \frac{116{,}000}{116{,}000 + 1{,}000{,}000} = 0.1039 \text{ volt} \quad (6a)$$

If 0.1039 volt were applied to a 6C5 tube with 100,000 ohm load, the voltage across the load would be

$$e_L = \frac{\mu \Delta e_g R_L}{R_L + r_p} = \frac{20 \times 0.1039 \times 100{,}000}{116{,}000} = 1.795$$

Half of this voltage, or 0.896 volt, will appear across r_c and R. Note that there is not only no amplification, but that the phase inverted output voltages are actually smaller than the input voltage.

Use of Curves for Large Voltage Variations

For larger voltages, the use of the characteristic curves is advisable. Here the actual grid voltages are best used as a starting point. Suppose that on the basis of Fig. 2 we decided to cause an actual grid voltage swing from −2 to −12 volts. What signal voltage will be needed and what will the output voltage be? The load line tells us that the tube voltage will swing between 75 and 225 volts, while the voltage across the load will swing between 350 − 75 = 275 and 350 − 225 = 125 volts. Half of these values, that is 137.5 and 62.5 volts, will represent the limits of the voltage swing across the cathode (and plate) resistor. The limits of the signal voltage swing can now be found. At the instant when the drop across r_c is 137.5 volts, the grid must be 2 volts negative with respect to the cathode, or 137.5 − 2 = 135.5 positive with respect to the negative end of the power supply; the other limit is correspondingly 62.5 − 12 = 50.5 volts. The total swing of the grid with respect to the negative end of the power supply is therefore 135.5 − 50.5 = 85 volts. Therefore, to obtain a swing of 75 volts of the two output voltages across r_c and R, an input voltage swing of 85 volts is needed. The ratio is 75/85 = 0.8823 and is the same as found for small signals, within the limits of accuracy of reading the characteristics. This indicates the extremely low distortion produced by such a stage, as would be expected from the highly degenerative effect of the cathode resistor. Another indication of the low distortion is found in the comparison of the midpoint of the signal swing, which is (135.5 + 50.5)/2 = 93 volts with the zero signal bias, which had been determined also to be 93 volts.

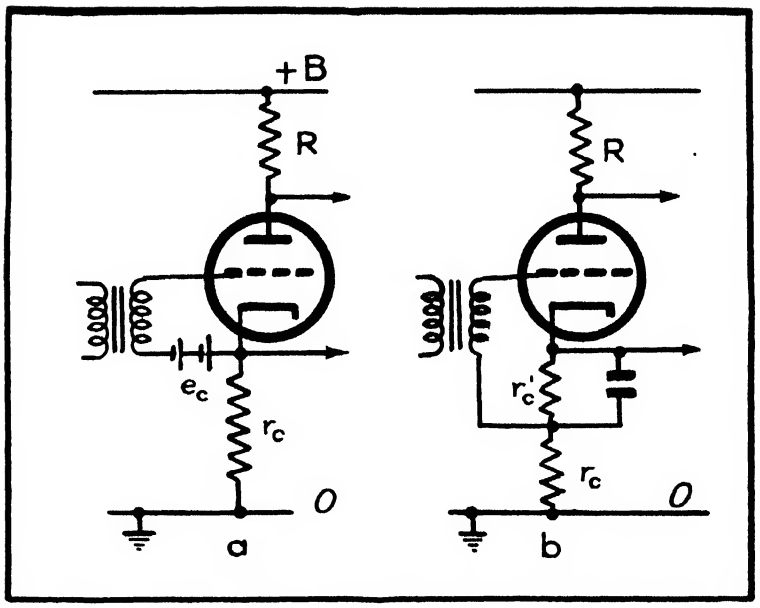

FIG. 4—Transformer input connections to phase inverter tube

To come back to this bias, Fig. 3a showed this bias as obtained from a battery. If a bleeder circuit across the power supply is available it may be conveniently tapped at the desired point, as shown in Fig. 3b, or the bias may be obtained by tapping r_c at a point furnishing the desired voltage. In the above example, with an operating current of 2 ma r_c would have to be tapped at 46,500 ohms (Fig. 3c) to furnish proper bias. The remaining 3,500 ohms are not by-passed by a condenser; such by-passing would destroy the balance of the signals while not serving any useful purpose. The inconvenience of tapping r_c, or splitting it into two odd-size resistors, however, usually makes the biasing arrangement shown in Fig. 3d preferable; R and r_c are again equal for push-pull output, but an additional resistor r_c' has been added, solely for the purpose of furnishing bias. A condenser is usually shown by-passing this resistor, but its effect is so slight on the performance of the stage (since it is usually small compared to r_c) that it may as well be omitted.

It was shown that such a stage cannot furnish amplification, i.e., that the two output voltages—or even a single one—appearing across r_c and R (with $R = r_c$) can never exceed the signal voltage. It should be pointed out that this is true only if the signal is introduced with respect to a point of fixed potential in the d-c system, such as is always the case in capacity coupled stages. If transformer coupling is used, as shown in Fig. 4a, the signal is seen to be introduced with respect to the cathode; under this condition the signal current flowing through r_c does not degenerate the signal and the stage will furnish the same amplification as a conventional stage with a load $R + r_c$ would, except of course, that the output is evenly divided between R and r_c. In this case, if self bias is used as shown in Fig. 4b, a by-pass

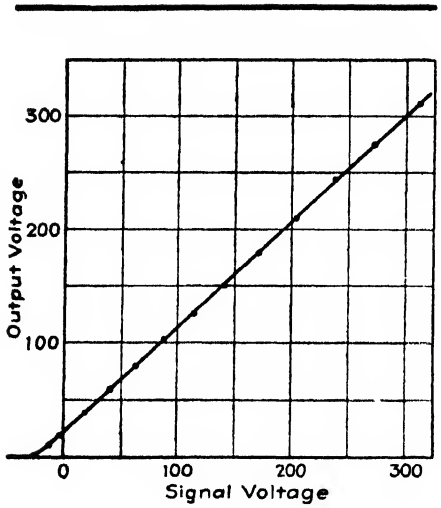

FIG. 5—Signal voltage, output voltage characteristics of cathode follower, showing wide range of linear operation

condenser must be used, if degeneration is to be avoided.

Applications of Cathode Follower

As already mentioned, the true "cathode follower" or "infinite impedance" circuit is represented by the condition $R = 0$. Such circuits are of interest, for instance, when it is required to place a voltage divider for the purpose of voltage adjustment across a source not permitting any current drain. A well known case of this kind is the saw-tooth voltage obtained across the condenser in the usual sweep circuit for cathode-ray oscilloscopes. To adjust the sweep amplitude a voltage divider is needed across the condenser, which upsets the linearity of this voltage with time for low sweep frequencies. Such a stage can also be used as an infinite impedance detector, with a very linear characteristic. In both cases a graph showing the output voltage as a function of the input voltage is desirable. Such a graph is easy to construct if we use again the actual grid voltage as an intermediate link and as the independent variable. This procedure has at the same time the advantage of giving that value of the signal voltage at which we might expect grid current.

Example of Calculation of Cathode Follower

Suppose we use a 6C5 with a 350 volt supply, placing a 100,000 ohm resistor in the cathode lead. These values have been chosen so that we may use Fig. 2, which was representing the same case. We then prepare a table as shown below, using e_g as independent variable.

e_g	e_t	e_{rc}	e_s
0	41	309	309
−2	76	274	272
−4	108	242	238
−6	141	209	203
−8	172	178	170
−10	200	150	140
−12	225	125	113
−14	248	102	88
−16	271	79	63
−18	292	58	40
−20	312	38	18
−22	330	20	−2
−24	340	10	−14
−26	350	0	−26

In this table e_g = actual grid voltage, e_t = voltage across tube, e_{rc} = voltage across resistor in series with tube, and e_s = signal voltage. The signal voltage e_s, given in the last row, is obtained by adding the actual grid-to-cathode voltage e_g, given in the first row (negative values) to the voltage across r_c, given in the third row. The linearity, as shown in Fig. 5, from zero up to about 290 volts, where the table shows the actual grid voltage to be about −1 volt and where we might approach the point of grid current, thus losing the infinite impedance characteristic, is almost unbelievable. The use of a high quality resistor for r_c will convert a precision d-c milliammeter into a vacuum tube d-c voltmeter capable of high precision. To obtain a very linear detector or a-c vacuum-tube voltmeter capable of handling large signals, all we have to do is to apply the signal with a bias of 26 volts, as shown by the graph.

Of the greatest interest is the use of a cathode resistor common to two tubes, as shown in Fig. 6. The very valuable properties of this circuit were first recognized by Goldberg[5] and Schmitt,[6] apparently independently of one another.

Two Tubes as Cathode Phase Inverter

In the circuit shown in Fig. 6 the grid of tube II is held at a fixed potential with respect to ground by the bias voltage e_c (shown as obtained from a battery) while to the grid of tube I the same bias plus the signal is applied. Consider the time when the signal makes the grid of tube I more positive. The current in tube I then tends to increase; but this increase of current, passing through r_c, would like to make the cathode "follow," as explained before, and, with the two cathodes connected, the cathode of tube II will therefore become more positive with respect to its grid, or, what amounts to the same thing, the grid will become more negative with respect to its cathode. This causes a decrease of current in tube II; this decrease must be less, however, than the increase of current in tube I, otherwise the total current flowing in the cathode resistor would decrease, and the cathode could not change its potential in the direction just reasoned. The plate potentials of the two tubes, that is, the potential of the points A and B of Fig. 6 therefore change in the opposite direction: A becomes more negative, B more positive. The question arises immediately what these potential changes will be in relation to the signal applied to the first grid, and in relation to each other.

Before going into the exact treatment of this case, a quick insight may be had by a simple assumption. Let r_c be infinite, or at least very large. This would of course call for a very high voltage supply, since the drop across r_c must be covered by the supply. Under this condition the current i_c must remain substantially constant, since even a very small

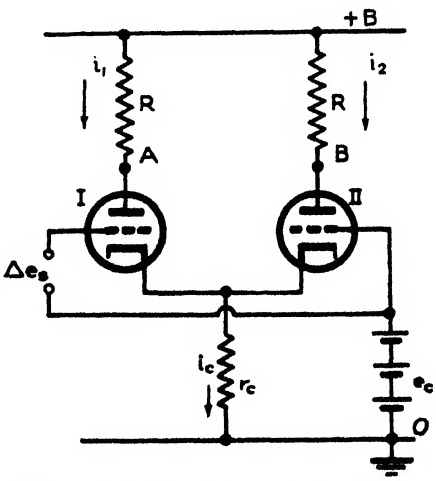

FIG. 6—Cathode resistor common to two tubes in parallel, with signal fed to grid of one tube

change would cause a large change of cathode potential. But since i_c is equal to the sum of i_1 and i_2, this means that any increase in i_1 must be accompanied by an equal decrease in i_2, and the cathodes have no other choice in responding to the application of the signal to the first grid, than to adjust their common potential to such a point that this condition will be fulfilled. For infinite r_c and linear operation of the tubes, this would obviously be the case, if the cathodes will "follow" just one half of the signal voltage change applied to the first grid. Thus, if the instantaneous value of the signal applied to the grid of tube I makes this grid let us say 4 volts positive, but if the cathodes follow 2 volts, then the actual grid voltage change on tube I will be 2 volts positive, on tube II 2 volts negative. Linear operation of the tubes assumed, the two plate currents will change equal amounts in opposite direction, thus keeping the current flowing in the common cathode resistor constant. The potential changes of point A and B are then also equal, but opposite in direction.

The exact treatment of this case can be made rather involved, but it can also be made very simple by the proper method of attack.

Suppose we investigate what happens if we introduce signal voltages to both grids. Let us confine ourselves, however, to a condition where the same amount of signal voltage change is impressed on both grids, but once the two voltage changes are in phase, the other time out of phase.

If we change both grid potentials the same amount and in the same direction (by tying the two grids together, for instance) the two tubes will act just like one, with an r_p equal to one half of the r_p of each tube, and a load resistance also equal to one half of the load resistance of each tube. The total current change, due to a signal change $\Delta e_c'$ applied to both grids will be given by Eq. (5), with the proper values substituted. We obtain

$$\Delta i_c' = \Delta (i_1 + i_2) = \frac{\mu \Delta e_c'}{\frac{1}{2} R + \frac{1}{2} r_p + (\mu + 1) r_c} \quad (8)$$

The plate current change of each tube will be one half of the value given by Eq. (8), that is

$$\Delta i_1' = \Delta i_2' = \frac{\frac{1}{2} (\mu \Delta e_c')}{\frac{1}{2} R + \frac{1}{2} r_p + (\mu + 1) r_c} = \frac{\mu \Delta e_c'}{R + r_p + 2 (\mu + 1) r_c} \quad (9)$$

If we excite the grids in push-pull, that is, make grid II negative exactly the same amount that we make grid I positive, then, linear operation assumed, the current in tube I will increase as much as the current in tube II decreases. For i_c remaining constant, the cathode will not change its potential at all, and the current changes taking place can be calculated by means of the equivalent plate circuit theorem, as if the tubes were operating with fixed bias. Therefore, if we make grid I more positive by $\Delta e_c''$ while making grid II the same amount $\Delta e_c''$ more negative, the plate current changes will be

$$\Delta i_1'' = \frac{\mu \Delta e_c''}{R + r_p}; \quad \Delta i_2'' = -\frac{\mu \Delta e_c''}{R + r_p} \quad (10)$$

These two cases are therefore easily enough managed mathematically, but they are not what we are interested in. We want to know what happens if Δe_c is applied to one grid, while the other remains at a constant potential. But this desired change in grid potentials could be considered as the result of two steps: at first, we make both grids an amount $\Delta e_c/2$ more positive, while in the second step we make grid I an additional $\Delta e_c/2$ more positive, while making grid II more negative by the same amount. The total result of these two steps is obviously a change of Δe_c volts on the first grid, and zero change on the second grid. The current changes taking place during the first step are found by Eq. (9), substituting $\Delta e_c/2$ for $\Delta e_c'$, while the current changes due to the second step are found in a similar way by means of Eq. (10), with the substitution of $\Delta e_c/2$ for $\Delta e_c''$. Adding the results of these substitutions into Eq. (9) and Eq. (10) we obtain the total current changes Δi_1 and Δi_2:

$$\Delta i_1 = \frac{\mu \Delta e_c}{2} \left(\frac{1}{r_p + R} + \frac{1}{r_p + R + 2 (\mu + 1) r_c} \right) = \frac{1}{2} \times \frac{\mu \Delta e_c}{r_p + R} \times \left(1 + \frac{r_p + R}{r_p + R + 2 (\mu + 1) r_c} \right) \quad (11)$$

$$\Delta i_2 = -\frac{\mu \Delta e_c}{2} \left(\frac{1}{r_p + R} - \frac{1}{r_p + R + 2 (\mu + 1) r_c} \right) = -\frac{1}{2} \frac{\mu \Delta e_c}{r_p + R} \times \left(1 - \frac{r_p + R}{r_p + R + 2 (\mu + 1) r_c} \right) \quad (12)$$

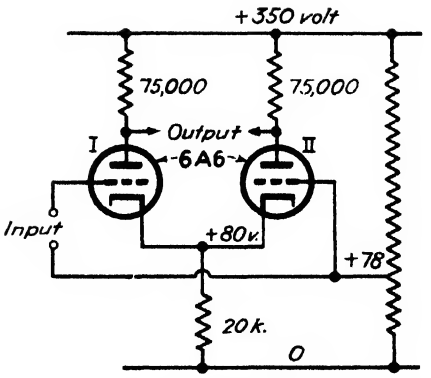

FIG. 7—Schematic circuits used to illustrate practical design of cathode follower arrangements

Designating

$$F = \frac{r_p + R}{r_p + R + 2 (\mu + 1) r_c}$$

we could call this factor the "deviation factor from true push-pull output." For $r_c = \infty$ the value of this factor becomes zero, and the two current changes are equal in size and opposite in sign, as we had already reasoned out for this case. The amount of change is seen to be the same as if one half of the signal, i.e. $\Delta e_c/2$ had been applied to each tube under fixed bias condition.

Often the voltage between points A and B alone is of interest, without regard of the distribution. This voltage is given by:

$$\Delta e_{AB} = \Delta i_1 R - \Delta i_2 R = \frac{1}{2} \frac{\mu \Delta e_c R}{(r_p + R)} (1 + F + 1 - F) = \frac{\mu \Delta e_c R}{R + r_p}$$

This is an important result: it shows the total output voltage to be independent of the cathode resistor and just as large as if the signal had been applied to one tube only, this tube working with conventional fixed bias condition.

Example of Design Procedure

Again an example may show most

quickly the relations and procedure. For each triode section of a 6A6 the following values were read from the curves:

$e_p = 120$ volts
$e_c = -2$ volts
$i_p = 2$ ma
$\mu = 35$
$r_p \leqq 25{,}000$ ohms

Suppose a 350 volt d-c supply is available for the operation of the stage, and that we were willing to let the load consume 150 volts. Load and tube would therefore take 270 volts, leaving 80 volts for the cathode resistor. A current of 2 ma in each tube and 4 ma in the cathode resistor gives then the resistor values shown in Fig. 7. The grid bias will have to be −78 volts. If a one-volt signal is placed on the grid of the first tube, according to Eq. (12) the *total* output voltage (that is the voltage e_{AB}) will be,

$$e_{AB} = \frac{35 \times 1 \times 75{,}000}{75{,}000 + 25{,}000} = 26.25 \text{ volts}$$

If the output were true push-pull, the voltage change of point A and of point B would each be exactly one half of the total output, or 13.125 volts. Actually the voltage swing of points A and B (Fig. 6) will be:

$$e_A = 13.125 \times (1 + F)$$
$$e_B = 13.125 \times (1 - F)$$

The two output voltages are of opposite polarity, or, in the case of a-c, of opposite phase. In our case F is

$$F = \frac{r_p + R}{r_p + R + 2(\mu + 1) r_c}$$
$$= \frac{25{,}000 + 75{,}000}{25{,}000 \times 75{,}000 + 72 \times 20{,}000}$$
$$= \frac{100{,}000}{100{,}000 + 1{,}440{,}000}$$
$$= \frac{100}{1{,}540} = \frac{1}{15.4} = 0.065$$

Therefore

$$e_A = 13.125 + \frac{13.125}{15.4}$$
$$= 13.125 + 0.852 = 13.977$$
$$e_B = -13.125 + \frac{13.125}{15.4}$$
$$= -13.125 + 0.852 = -12.273$$

Improving Balance

For many applications this unbalance of approximately 14 percent would not be of any consequence. If a closer balance is required, it is of course possible to tap the load resistor of the first tube at the appropriate place, and take the output from this tap instead of point A. Another method of improving the balance, used by Goldberg in later modifications of his high gain d-c amplifier, is based on replacing r_c by a pentode. Since in all our derivations we are interested only in variational resistances, that is in the ratio of voltage change to current change, use can be made of the very high plate resistance of a pentode, approaching values near one megohm, without the need of the high voltage supply which a regular one megohm resistor would require. If values of several hundred thousand ohms are introduced in the expression for the deviation factor, F, it is seen to approach zero for all practical purposes. Since the plate characteristics of pentodes remain flat to relatively low plate voltages, the advantage of a high r_c can be had without sacrificing a large amount of voltage over it.

Cascaded Cathode Phase Inverters

If two or more stages with cathode resistors are cascaded, as shown in Fig. 8, a considerable improvement of balance results, due to the fact that the signal applied to the grid of the second stage is already essentially a push-pull signal. The small unbalanced part of this signal—in the above discussed example about 14 percent—will again be mostly converted into a push-pull signal, so that the unbalance of output in the second stage could be called of second order. In this particular case calculations show that with an over-all amplification of $26.25^2 = 689$ for two identical stages, the two 180 deg. out-of-phase output voltages will differ less than one percent from each

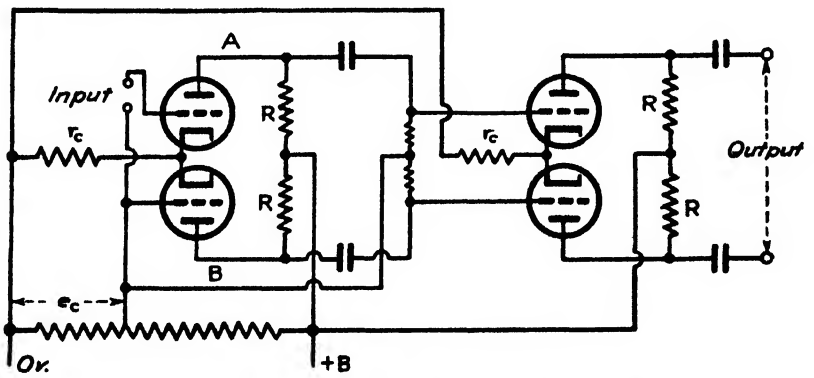

FIG. 8—Two stages of cascaded cathode followers

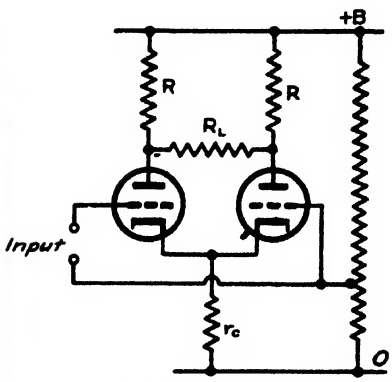

FIG. 9—Wiring diagram of two tubes in cathode follower circuit, with load taken between the two plates in a bridge arrangement

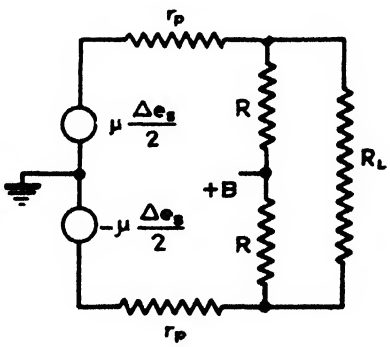

FIG. 10—Equivalent circuit for bridge type cathode follower circuit of Fig. 9

other. With the tolerances of commercial resistors and with the tubes hardly matching that closely, this is obviously an entirely theoretical value; the actual unbalance might be more or less than this calculated value.

Another interesting arrangement results if a load is connected between points *A* and *B*. This load may be a milliammeter such as found in vacuum-tube voltmeters of the type of the RCA Voltohmyst. The fundamental circuit is shown in Fig. 9. The current in the load, and the current changes in the resistors *R* due to the application of an input voltage can again easily be predicted by means of the same reasoning as in the open circuit case. The application of Δe_s on the grid of the first tube can be considered as the result of two steps, as before: (1) Voltage of both grids changed by $\Delta e_s/2$ in the same direction; (2) Voltage of first grid increased an additional $\Delta e_s/2$ in the same direction, second grid $\Delta e_s/2$ in the opposite direction. During the first step the current in both plate resistors will increase the same amount, but no load current will result; the second step represents pure push-pull operation, on which the value of r_p has no influence. The equivalent circuit for this case is shown in Fig. 10. The current in the load is given by

$$i_L = \frac{\mu \Delta e_s}{2r_p + \frac{2RR_L}{2R + R_L}} \times \frac{2R}{2R + R_L} \qquad (13)$$

$$= \frac{\mu \Delta e_s R}{r_p(2R + R_L) + RR_L}$$

$$= \frac{\mu \Delta e_s}{R_L\left(1 + \frac{r_p}{R}\right) + 2r_p}$$

If the load is a relay, instead of a meter, it will be desirable to make its resistance of such value that the maximum power will be obtained in the coil, or stating it in a different manner, that operation will result with the smallest possible input. The value of R_L giving the best match can be found by forming the expression for the power in the coil, $P = i_L^2 \times R_L$, with the value for i_L from Eq. (13) substituted into this expression, then differentiating P with respect to R_L and equating to zero, in the well known procedure to determine maxima and minima. The value will be found to be

$$R_{L_{opt}} = \frac{2r_p R}{r_p + R} \qquad (14)$$

If R_L is given, that is, cannot be chosen, no attempt must be made to satisfy Eq. (14) by giving R a value such that Eq. (14) will be satisfied. A little thought will show that R should always be as large as possible; for R approaching infinity, $R_{L_{opt}}$ will approach the value $2r_p$. Since the plate current flows through R, however, large values would make a high voltage d-c supply necessary.

Due to the balanced condition as far as plate supply is concerned these circuits seem to show the way to the solution of the d-c amplifier problem, as shown in Goldberg's paper. It is hoped that this discussion will help workers in this field to become a little more familiar with the characteristics of them.

Bibliography

(1) Lockhart, C. E., The Cathode Follower, *Electronic Engineering*, (London), 15, pg. 287, Dec. 1942, 16, pg. 375, Feb. 1943 and 16, pg. 21, June 1943.
(2) Richter, W., Mathematical Treatment of the Grid Bias Resistor, ELECTRONICS, 10 pg. 62, Nov. 1937.
(3) Goldberg, H. A., High Gain D-C Amplifier for Bio-Electric Recording, *Transactions of the A.I.E.E.*, 59, pg. 60, Jan. 1940.
(4) Richter, W., Resistance Coupling for Push-Pull Amplification, ELECTRONICS, 8, pg 40, Oct. 1935.
(5) Schmitt, O. H., Cathode Phase Inversion, *Jour. of Sci. Instr.*, 15, pg. 100, March 1938.

Reference

Schmitt, O. H., Electrical Control of Galvanometer Characteristics, *Jour. of Sci Instr.* 15, pg. 234, 1938.
Schmitt, O. H., Cathode Phase Inversion, *Rev. of Sci. Instr.* 12, pg. 548, Nov 1941.
Rahm, W. E., Electroencephalography, ELECTRONICS, 12, pg. 11, Oct. 1939.
Geohagen, W. A., An Improved C-R Oscilloscope Design, ELECTRONICS, 13, pg. 26 Nov. 1940.
Gilson, W. E., A Versatile Oscilloscope, ELECTRONICS, 14, pg. 22, Dec. 1941

Graphical Solutions for Cathode Followers

Survey of cathode follower input circuits and a method of computing design data for the desired circuit from the conventional load line. Plate-loaded and cathode-follower amplifiers are compared. Several examples are given

By HERBERT L. KRAUSS

THE LITERATURE contains a number of articles on cathode followers,[1-7] covering various aspects of their operation. Two methods of graphical solution have been presented.[4,7] The method which follows is thought to be somewhat simpler than the others, in that only the conventional family of plate characteristics for the tube and a load line are required. Special scales for cathode voltage and signal voltage must be determined for each value of load resistance, but this is not difficult after the quiescent operating point has been located. Once the signal-voltage scale has been provided, an analysis for voltage or power output and harmonic distortion may be made by conventional methods.

Assumptions

The load on the tube is assumed to be a pure resistance in all cases. Coupling and by-pass capacitors are assumed to have zero reactance; shunt capacitances due to tube elements, are assumed to have infinite reactance. Where transformers are

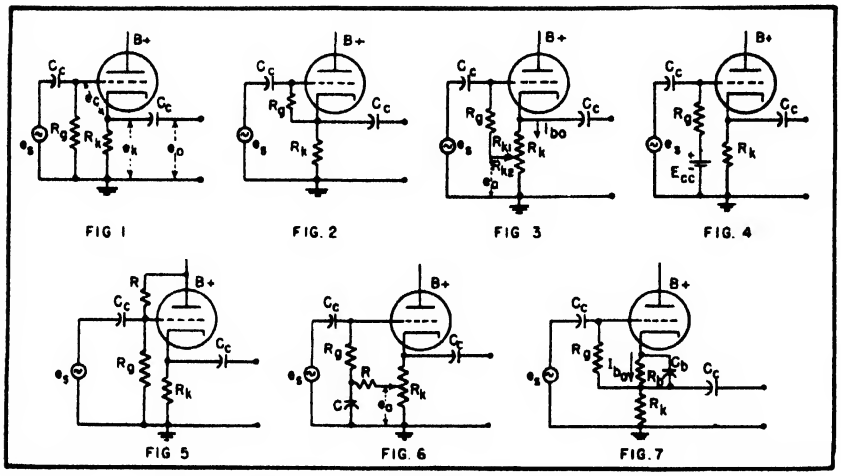

FIG. 1-7—Types of input circuits for cathode followers

used for coupling, they are assumed to be perfect, that is, to have zero winding resistance and leakage reactance, unity coupling, and infinite primary and secondary inductance with a finite ratio of transformation. For the sake of generality the source of signal voltage is assumed to be an amplifier stage which must be capacitance-coupled to the grid of the cathode follower. In some of the examples the circuit may be simplified if capacitance coupling is unnecessary.

Quiescent Operating Conditions

Figures 1 to 7 show common forms of the cathode-follower circuit, differing only in the method of obtaining grid bias. If high input resistance is required the circuits of Fig. 2 and 7 are best, because in these circuits the alternating voltage across R_g is $E_s - E_o = E_g$, the lowest possible value, and thus very little current will flow in R_g. On the other hand, in Fig. 1 the voltage across R_g is E_s. Since $E_g \cong 0.1\ E_s$ in many cathode followers, a given value of R_g will look approximately ten times as large to the signal source in the circuit of Fig. 7 as it would in that of Fig. 1. The circuits of Fig. 3 and 6 would give intermediate values.

To illustrate the graphical solutions for the quiescent operating points, the characteristics of a 6J5 tube will be used, with $R_k = 10{,}000$ ohms, and a plate supply voltage, $E_{bb} = 300$ volts. The steps in the solution are illustrated in Fig. 8. (1) Draw a load line with slope equal to $-1/R_k$ through the point E_{bb} on the plate characteristics of the tube. (2) For convenience in computation, add a scale for e_k below that for e_b, using the relation

$$e_k = E_{bb} - e_b. \qquad (1)$$

(3) Locate the quiescent operating point ($e_s = 0$) for the particular circuit used. The method of doing this is indicated below for each of the circuits.

In Fig. 1 the grid is at ground potential under quiescent conditions. Thus

$$E_{c_0} = -E_{k_0} \qquad (2)$$

defines the quiescent operating point. From an inspection of the operating characteristics in Fig. 8 this is seen to occur approximately at the point where $E_{c_0} = -14$ volts, $E_{k_0} = +14$ volts. It is labeled point A in Fig. 8.

In the circuit of Fig. 2, $E_{c_0} = 0$ because the grid leak connects the grid directly to the cathode. This gives the operating point indicated by B in Fig. 8. At this point $E_{k_0} = 163$ volts.

The circuit of Fig. 3 gives an operating point that lies between those of the previous examples. The grid is at the potential E_{c_0} above ground where E_{c_0} is the quiescent value of e_c. The condition to be satisfied is that

$$E_{c_0} = -I_{b_0} \times R_{k_1} = -(E_{k_0} - E_{c_0}) = -E_{k_0} \times R_{k_1}/R_k$$

where $R_k = R_{k_1} + R_{k_2}$ (3)

As an example, suppose that the quiescent operating point is to be located where $E_{c_0} = -6$ volts, and $E_{k_0} = 89$ volts. Then from Eq. 3, $R_{k_1} = R_k\ (E_{c_0}/-E_{k_0}) = 10{,}000 \times 6/89 = 674$ ohms, and

$R_{k_2} = 10{,}000 - 674 = 9{,}326$ ohms.

This gives the operating point labeled C in Fig. 8.

In the circuit of Fig. 4 the operating point may be chosen at will by adjustment of the bias voltage, E_{cc}. From inspection of the circuit it is seen that the condition

$$E_{cc} = E_{k_0} + E_{c_0} \qquad (4)$$

must be satisfied. If the operating

Symbols

- e_b = total instantaneous plate-cathode voltage
- i_b = total instantaneous plate current
- e_c = total instantaneous grid-cathode voltage
- e_k = total instantaneous cathode-ground voltage
- e_o = total instantaneous voltage developed across a portion of R_k, as shown in Fig. 3 and 6
- e_s = total instantaneous signal voltage, applied between grid and ground
- E_{c_0} = quiescent grid-cathode voltage
- E_{k_0} = quiescent cathode-ground voltage
- E_{b_0} = quiescent plate-cathode voltage
- E_{cc} = bias supply voltage
- E_{bb} = plate supply voltage
- $e_g = e_c - E_{c_0}$ = instantaneous varying component of grid-cathode voltage
- $e_o = e_k - E_{k_0}$ = instantaneous varying component of cathode-ground voltage
- I_{b_0} = quiescent plate current
- E_s = effective value of a-c signal voltage
- E_g = effective value of a-c grid-cathode voltage
- E_o = effective value of a-c cathode-ground (output) voltage
- μ = amplification factor of the tube
- r_p = dynamic plate resistance of the tube
- R_g = grid leak resistance
- R_k = cathode load resistance
- R_{pp} = plate-to-plate load resistance of a push-pull amplifier
- R_L' = plate load resistance of a transformer-coupled, single-tube amplifier, or $= R_{pp}/4$ for a push-pull amplifier

point used in Fig. 3 ($E_{c_0} = -6$ volts, $E_{b_0} = 89$ volts) is chosen, $E_{c_0} = 83$ volts.

The operating bias for the circuit of Fig. 5 is obtained by means of the voltage divider R and R_1 connected from B+ to ground. By proper choice of these resistors a quiescent grid-to-ground voltage of any desired value (equivalent to the E_{c_0} of Fig. 4) may be obtained. Locate operating point as before.

The operating point for the circuit of Fig. 6 is determined in the same manner as that in Fig. 3.

For Fig. 7, $E_{c_0} = -I_{b_0} \times R_k$ (5)
If $R_k + R_b = 10{,}000$ ohms and operating point C is assumed, $I_{b_0} = 8.9$ milliamperes and $R_b = 6/(8.9 \times 10^{-3}) = 674$ ohms. Thus $R_k = 9{,}326$ ohms. These results are the same as those obtained in Fig. 3. Since R_b is bypassed by C_b in Fig. 7, the a-c load resistance (R_L) is less than the d-c resistance ($R_k + R_b$). If R_k were to be kept at its previous value of 10,000 ohms, a new d-c load line corresponding to $R_k + R_b$ would have to be drawn. If the a-c load line passes through operating point C the value of R_b may be found as before. The d-c load line would now pass through the operating point and the point $E_{bb} = 306$ volts. Thus the operating point may be selected on the a-c load line and the plate-supply voltage increased above the previously chosen value of 300 volts by the amount of the bias voltage. This correction, which would also apply to a plate-loaded amplifier with a cathode bias resistor, will generally be so small as to be negligible for all practical applications.

The choice of the operating point is governed by the same considerations as in plate-loaded amplifiers. If the point is too near $E_{c_0} = 0$ (point B of Fig. 8) the quiescent plate dissipation may be excessive or the grid may be driven positive and grid current caused to flow. If the operating point is too near the other end of the load line (such as point A of Fig. 8) nonlinear distortion is increased and the tube may be driven to plate-current cutoff with a relatively small signal voltage. Operating point C represents a good compromise since it allows large voltage swings in both directions with low distortion.

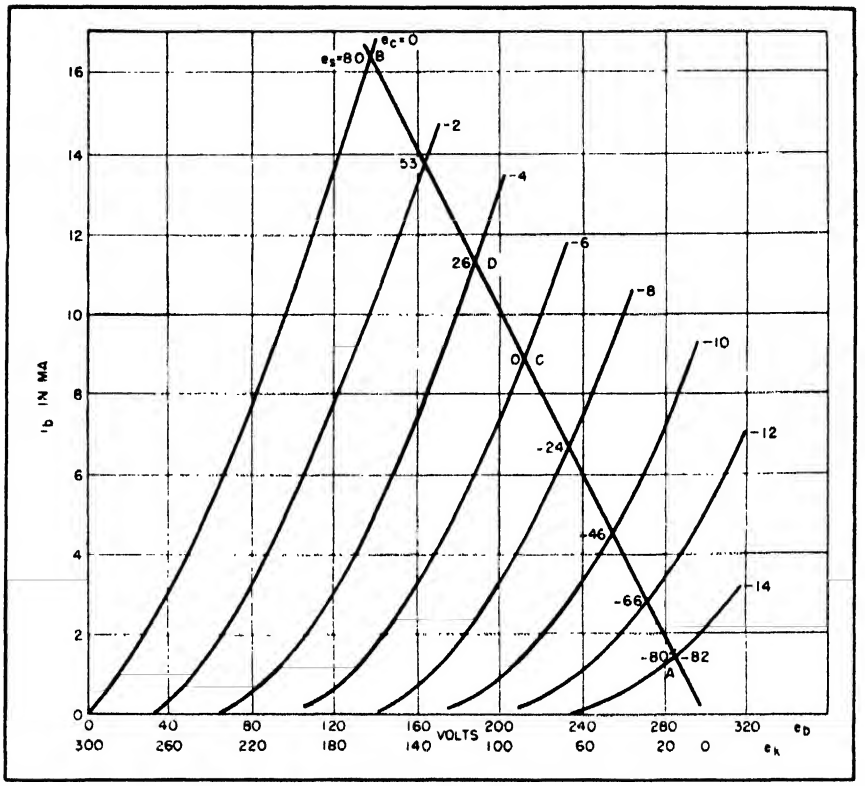

FIG. 8—A type 6J5 tube as cathode follower with R_k equal to 10,000 ohms and E_{bb} equal to 300 volts

Dynamic Operating Conditions

Once the static load line has been found and the quiescent operating point located, the dynamic load line may be drawn through the operating point. The a-c load resistance will be smaller than the d-c load resistance whenever a load is connected between the output terminals of Fig. 1 to 7, or when a by-passed bias resistor is used, as in Fig. 7. In many applications the difference between these two load lines is negligible, and it is so assumed in the example which follows.

Using the load line in Fig. 8 and operating point C, the required signal voltage (e_s) is to be determined for various instantaneous operating points along the line. A convenient method consists of determining the amplitude of the signal voltage at each intersection of the load line and the tube characteristic lines. The instantaneous values of e_s may be found from the relation

$$e_s = e_c - E_{c_0} + e_k - E_{k_0} \quad (6)$$

where E_{c_0} and E_{k_0} are the values at the quiescent operating point. The above equation is equivalent to the expression

$$E_s = E_g + E_k \quad (7)$$

involving only the a-c components. Thus in Fig. 8 at point D, $e_g = -4$ volts, $e_k = 113$ volts, and $e_s = -4 - (-6) + 113 - 89 = 26$ volts. Other values for e_s are found similarly and are indicated in a scale along the load line. Once the scale has been determined for e_s, additional points on the scale may be found by interpolation where necessary. Because of the low distortion obtained in cathode followers, a linear interpolation of values of e_s between the points previously found is sufficiently accurate for most purposes.

Distortion Analysis

A sinusoidal signal voltage may now be assumed, and the output voltage or current may be analyzed

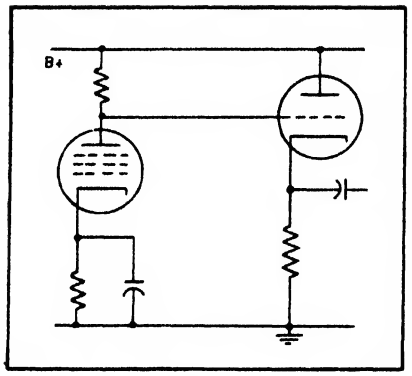

FIG. 9—A direct-coupled circuit

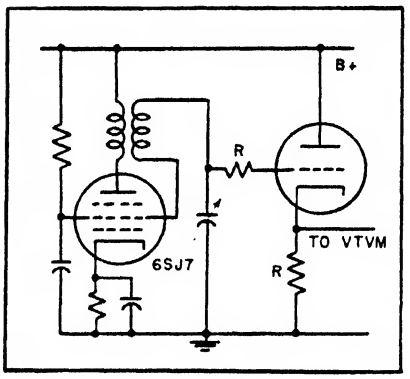

FIG. 10—Vacuum-tube voltmeter

for fundamental-frequency and harmonic components by the methods usually employed for power amplifiers.[8] It is important to note that the signal voltage (e_s) scale must be used for this analysis rather than the e_g-scale which is used for conventional amplifiers.

Using operating point C in Fig. 8 a signal amplitude of 80 volts is necessary to drive the grid to zero bias, at which point $e_b = 163$ volts and $e_o = e_b - E_{bb} = 74$ volts. When the instantaneous signal voltage is 80 volts negative (this point is indicated on the load line), $e_b = 17$ volts and $e_o = -72$ volts. Thus the amplitude of output voltage is nearly the same on the positive and negative half-cycles, indicating very little distortion. The voltage amplification of the circuit is: $A = \sqrt{2}E_o/\sqrt{2}E_s = 73/80 = 0.91$.

By contrast, if the circuit were operated as a plate-loaded amplifier with the same operating point and $\sqrt{2}E_s = 6$ volts, the corresponding values of amplitude of output voltage would be 74 for the positive half-cycle and -60 for the negative half-cycle, giving a fairly large percentage of second-harmonic distortion.[9]

The conclusions to be derived so far are that the cathode follower has inherently low distortion because of its negative feedback; high input impedance which is advantageous if the previous stage is sensitive to loading; low output impedance desirable for driver-stage applications; but the disadvantage of requiring a signal input slightly larger than the output voltage.

Many useful applications of the cathode follower as a coupling stage between a high-impedance source and a low-impedance load or as a video amplifier stage have been cited in the literature.[1-7] The possibility of direct coupling to the grid of the cathode follower from the previous stage as indicated in Fig. 9 should be considered because it permits the elimination of the coupling capacitor and grid leak usually required. If the direct grid-to-ground potential of the cathode follower can be the same as the quiescent plate voltage of the previous stage, direct coupling should be feasible. Figure 10 shows another direct-coupled circuit which has been used successfully in our laboratory, where it was desired to make selectivity measurements on a tuned r-f amplifier stage. Since a diode-type vacuum tube voltmeter would cause appreciable loading of the tuned circuit, and a consequent reduction in gain and selectivity, a cathode-follower stage was inserted as shown. The screen grid of the 6SJ7 may be operated at 75 to 100 volts, which is a convenient range for the quiescent grid-to-ground voltage of the cathode follower. The resistor R was necessary in the grid lead to prevent oscillation of the cathode follower stage.[7] A value of R between 100 and 1,000 ohms is generally sufficient to prevent oscillation.

A-M Detector

The circuit of Fig. 11, with a high value of R_k and an r-f bypass capacitor C, will act as a detector for amplitude-modulated waves. The large value of R_k will cause the tube to be biased near cutoff under quiescent conditions. Thus the action is similar to that of a diode detector with the added advantage of high impedance presented to the signal source. The disadvantage of this circuit as a detector is that, no matter how high R_k is made, the bias voltage for the grid must be developed across R_k, and a negative signal equal to this bias voltage must be applied before the tube will cut off. Thus for small applied signals no rectification will occur. This difficulty can be avoided by applying enough direct voltage in the grid circuit to bias the tube to cutoff, but this is not always a convenient solution. The output voltage of this detector is positive with respect to ground, and there-

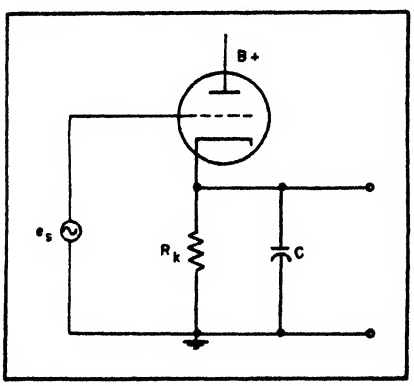

FIG. 11—A high-impedance detector circuit

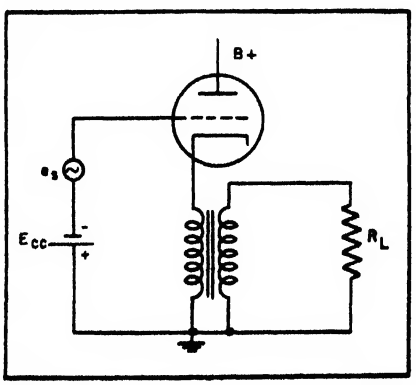

FIG. 12—A transformer-coupled amplifier

Table I

Fundamental-frequency power output and second harmonic distortion of a triode amplifier, plate-loaded and cathode-loaded. Triode-connected 6L6 tube with E_{bb} = 255 volts, E_{cc} = − 22.5 volts, $\sqrt{2}\,E_g$ = 22.5 volts

	Plate-loaded		Cathode-loaded		
R_L' ohms	P_o watts	Percent 2nd harmonic	P_o watts	Percent 2nd harmonic	$\sqrt{2}\,E_s$ volts
1,700	1.78	14.2	2.06	13.2	122.5
3,400	1.71	7.5	2.06	2.4	148.5
5,000	1.53	5.5	1.80	0.6	160.0

Table II

Triode-connected 6L6 tubes in push-pull, with E_{bb} = 255 volts, E_{cc} = − 22.5 volts, $\sqrt{2}\,E_g$ = 22.5 volts

	Plate-loaded		Cathode-loaded		
R_L' ohms	P_o watts	Percent 3rd harmonic	P_o watts	Percent 3rd harmonic	$\sqrt{2}\,E_s$ volts
500	3.72	0.41	3.75	0+	83
1,000	4.20	0.36	4.20	0+	114
1,500	4.02	0.23	4.02	0+	131

(In the push-pull amplifier R_L' is the equivalent load resistance presented to the composite tube, and is equal to one-fourth the plate-to-plate load resistance)

fore is not useful for avc purposes.

Because of the low output impedance of the cathode follower, it is sometimes useful as a power amplifier if the load impedance is subject to variation. The circuit diagram of a power amplifier with the load transformer-coupled into the cathode circuit is shown in Fig. 12. Although fixed bias is indicated, cathode resistor bias such as that used in Fig. 7 may be more convenient as long as the operation is restricted to class A. A graphical solution for the circuit of Fig. 12 is similar to that for a plate-loaded amplifier, except that scales must be provided for e_s and e_k as they were in Fig. 8. The quiescent operating point is determined from the plate-supply voltage and bias voltage exactly as it would be for a plate-loaded amplifier. Similarly, the slope of the load line is determined by the reflected load resistance (R_L') seen in the primary circuit of the transformer.

Figure 13 shows the graphical construction for a type 6L6 tube operated as a triode with E_{bb} = 255 volts, E_{cc} = −22.5 volts, and with load resistances of 1,700 and 5,000 ohms on the primary side of the transformer. A scale for e_k appears below the e_b-scale, and values of e_s are indicated along the two load lines. Note that e_k = 0 at the operating point; thus e_s is easily determined at any point along the load line from the relation

$$e_s = e_k + e_g \qquad (8)$$

Table I summarizes the results of calculations with three values of load resistance for both plate loading and cathode loading. The same grid-cathode voltage ($\sqrt{2}\,E_g$ = 22.5 volts) was used in all cases, the corresponding values of $\sqrt{2}E_s$ being given in the table for the cathode-loaded amplifier. The fundamental-frequency power output and percent second harmonic distortion were calculated by the method given in reference number 8, with the assumption that harmonics higher than the third were negligible. Note that $r_p \simeq$ 1,700 ohms at the operating point—thus the values of load resistance used correspond approximately to $R_L' = r_p$, 2 r_p and 3 r_p.

For the 1,700-ohm load the cathode loading does not reduce the distortion appreciably below the value obtained with plate loading, because the signal amplitude is such as to cause the tube to be cut off during part of the cycle (i.e., $i_b = 0$ at $e_s = -90$ volts). If the signal amplitude is reduced to 90 volts ($=\sqrt{2}E_s$) with the 1,700-ohm load, P_o = 1.31 watts and the second harmonic distortion = 5.1 percent.

With the other values of load resistance the harmonic distortion is reduced considerably by cathode

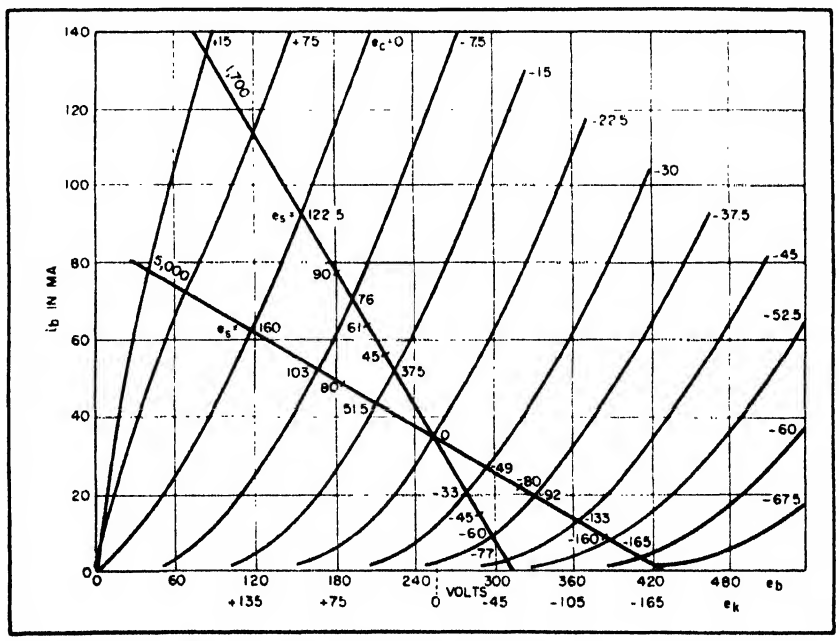

FIG. 13—A type 6L6 tube used as a transformer-coupled cathode-loaded power amplifier with R'_L equal to 1,700 ohms (upper curve) and 5,000 ohms. E_{bb} is 255 volts and E_{cc} is −22.5 volts

Table III

Triode-connected 6L6 tubes in push-pull, with E_{bb} = 255 volts, E_{cc} = − 30 volts, $\sqrt{2}\,E_g$ = 30 volts

	Plate-loaded		Cathode-loaded		
R_L' ohms	P_o watts	Percent 3rd harmonic	P_o watts	Percent 3rd harmonic	$\sqrt{2}\,E_g$ volts
500	3.66	4.75	3.83	1.07	93
1,000	4.30	3.59	4.57	0.35	126
1,500	4.37	2.84	4.60	0.22	147
1,700	4.28	2.82	4.53	0.0+	154

Table IV

Triode-connected 6L6 tubes in push-pull, with E_{bb} = 255 volts, E_{cc} = − 37.5 volts, $\sqrt{2}\,E_g$ = 37.5 volts

	Plate-loaded		Cathode-loaded		
R_L' ohms	P_o watts	Percent 3rd harmonic	P_o watts	Percent 3rd harmonic	$\sqrt{2}\,E_g$ volts
1,000	3.72	11.0	4.35	2.9	133
1,250	3.80	10.9	4.52	1.8	145
1,500	3.81	10.0	4.48	1.7	155
2,000	3.72	9.0	4.26	1.8	170

loading and the power output is increased about ten percent. In all cases the large values of signal voltage required for cathode-follower operation are a definite disadvange.

Push-Pull Power Amplifier

The circuit for the cathode-loaded push-pull power amplifier is shown in Fig. 14. An examination of the conditions to be satisfied for both quiescent and dynamic operation shows that they are identical with the conditions for a plate-loaded push-pull amplifier. The conditions are:

quiescent—$i_{b1} = i_{b2}$, $e_{c1} = e_{c2} = E_{cc}$, $e_{k1} = e_{k2} = 0$, and $e_{b1} = e_{b2} = E_{bb}$ (9)

dynamic—$\Delta e_{c1} = -\Delta e_{c2}$, $\Delta e_{k1} = -\Delta e_{k2}$, $i_{b1} - i_{b2} = i_d$; therefore $\Delta e_{c1} = -\Delta e_{c2}$, $\Delta e_{b1} = -\Delta e_{b2}$ (10)

In these relations the subscripts 1 and 2 refer to the two tubes of the push-pull circuit, and i_d is the net flux-producing component of current in the transformer primary. This current is defined in the conventional manner[9] so that

$$i_d \times N_p = i_2 \times N_s \qquad (11)$$

where N_p is the number of turns on one-half the primary, and N_s is total secondary turns.

Since the conditions to be satisfied are the same for both cathode loading and plate loading, the graphical solution for plate-loaded push-pull amplifiers is applicable. A signal-voltage scale must be provided along the load line on the composite characteristics. Two 6L6 tubes, triode-connected, were used for this analysis. A comparison of fundamental-frequency power output and third harmonic distortion for plate-loaded and cathode-loaded amplifiers under various operating conditions is given in Tables II to V.

Conclusions

From the results of these calculations the following conclusions are drawn concerning cathode loading versus plate loading for power amplifiers:

The advantages in all cases of cathode follower operation are the high input impedance (with negative grid operation) and low output impedance. The latter is particularly desirable when the load impedance may vary with frequency and a constant load voltage is desired. The disadvantages in all cases of cathode-follower operations are the large signal voltages required and the possibility that the maximum allowable cathode-to-filament potential of the tubes will be exceeded under maximum output conditions. For the single-tube amplifier, cathode loading will increase the power output and reduce the distortion compared to plate loading, provided the signal voltage used for cathode-follower operation does not drive the tube to plate-current cutoff (see Table I).

If the distortion is low for the plate-loaded case (either single or push-pull tubes) cathode loading will not increase the power output appreciably (see Table II). This is logical since if the distortion were negligible, the instantaneous excursions along the load line would be exactly the same for either type of loading. If the distortion is high in push-pull plate-loaded operation, cathode loading will reduce the distortion considerably and may increase the power output by more than ten percent. (See Tables III to V.) The increase in power output occurs because the negative feedback with cathode loading acts to increase the amplitude of the fundamental-frequency current while reducing the harmonic currents. The value of equivalent load resistance (R_L') which gives maximum power output is approximately the same for both cathode loading and plate loading in each case considered. With a fixed operating point and fixed grid voltage amplitude this result would be expected, since the excursions along a given load line are approximately the same for both types of loading.

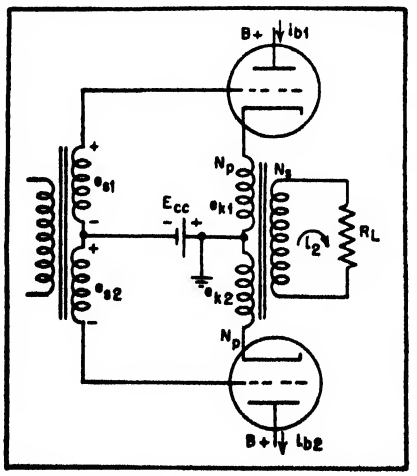

FIG. 14 — A cathode-loaded push-pull power amplifier circuit

Table V

Triode-connected 6L6 tubes in push-pull, with E_{bb} = 255 volts, E_{cc} = − 37.5 volts, $\sqrt{1}\ E_g$ = 45 volts (grid driven 7.5 volts positive)

	Plate-loaded		Cathode-loaded		
R_L' ohms	P_o watts	Percent 3rd harmonic	P_o watts	Percent 3rd harmonic	$\sqrt{2}\ E_s$ volts
1,000	6.27	10.7	7.37	2.2	169
1,250	6.34	10.2	7.43	1.8	181
1,500	6.35	9.2	7.39	1.5	196
2,000	6.08	9.0	7.00	1.6	215

The internal impedance of a tube acting as a cathode follower is $r_p/(1 + \mu)$.[10] If the Maximum Power Transfer Theorem is applicable, a load resistance equal to the internal resistance of the tube would give maximum power output. However, this theorem holds only for strictly linear operation of the tube with a constant voltage generated in the equivalent plate circuit, and thus restricts the grid swing to small values for the plate-loaded amplifier. This restriction is not so severe for cathode loading because of the reduced distortion. The equivalent generator for a cathode follower produces a voltage $\mu E_s/(1 + \mu)$[10]; thus it is the signal voltage E_s that must be kept constant in this case rather than E_g, while the load resistance is varied to obtain maximum power output. This follows also from Shapiro's graphical solution[4] involving equivalent plate characteristics for the cathode follower, wherein the input signal is represented by the grid-to-plate alternating voltage which is identical with the E_s used here.

Although the above arguments are theoretically sound, certain practical considerations prevent operation of the cathode follower with load resistances comparable to $r_p/(1 + \mu)$ in order to obtain more power output than is possible with plate loading. The plate power dissipation of the tube under both quiescent and dynamic conditions must not exceed its rated value. This will locate the operating point relatively low on the family of plate characteristics (see the operating point of Fig. 13, which is near the maximum-plate-dissipation point). Then for small values of R_L' the maximum allowable value of E_s (which will not produce grid-current flow or plat-current cutoff) will be quite small. With E_s limited to such a small value the power output will be less than the maximum value obtained with the load values and signal amplitudes noted earlier.

In conclusion it should be pointed out that this method of graphical analysis may also be applied to any amplifier that has combined plate and cathode loading, or for negative-feedback amplifiers. The scales for e_s and e_k would be determined in such a case by the amount of feedback voltage developed in the grid or cathode circuit. Once these scales are determined the analysis proceeds in the manner previously given.

Acknowledgment

The author wishes to thank Professor H. J. Reich and P. F. Ordung of the Department of Electrical Engineering, Yale University, for their helpful comments during the preparation of this paper.

REFERENCES

(1) Reich, H. J., "Theory and Applications of Electron Tubes", McGraw-Hill Book Co., 2d Edition, p 164, New York 1944.
(2) Reich, H. J., Features of Cathode Follower Amplifiers, *Electronic Industries*, p 74, July 1945.
(3) Richter, W., Cathode Follower Circuits, ELECTRONICS, p 112, November 1943.
(4) Shapiro, D. L., The Graphical Design of Cathode-Output Amplifiers, *Proc IRE*, p 263, May 1944.
(5) Greenwood, H. M., Cathode Follower Circuits, *QST*, p 11, June 1945.
(6) Goldberg, H., Some Considerations Concerning the Internal Impedance of the Cathode Follower, *Proc* IRE, p 778, November 1945.
(7) Schlesinger, K., Cathode Follower Circuits, *Proc IRE*, p 843, December 1945.
(8) MIT Staff, "Applied Electronics", John Wiley and Sons, p 412, New York 1943.
(9) MIT Staff, "Applied Electronics", John Wiley and Sons, p 438, New York 1943.
(10) MIT Staff, "Applied Electronics", John Wiley and Sons, p 537, New York 1943

Analysis of Cathode Follower

EQUIVALENT CIRCUITS for input and output impedance and equations for the gain of a cathode follower are derived by C. N. Jeffery in the *A.W.A. Technical Review*, March 1945. It is assumed that the input signal is small enough to ensure linear operation and that grid-cathode conductance due to transit-time and dielectric loss is negligible.

Input Impedance

Symbols are identified in Fig. 1 and Table I. From conventional circuit analysis the input impedance is found to be

$$Z_{in}' = [r_p Z_1/(r_p + Z_1)] + Z_{gk} + \frac{}{g_m Z_{gk}[r_p Z_1/(r_p + Z_1)]} \quad (1)$$

The equivalent circuit for input impedance is that of Fig. 2.

At low frequencies where interelectrode and distributed reactances are considerably greater than resistances in parallel with them the equivalent circuit is that of Fig. 3A. The conditions represented in this circuit are that the grid-cathode bias is obtained through R_{gk} to a tap on R_k, this tapped portion being small enough compared to R_k to be neglected; and that x is the ratio of the effective output load to the normal output impedance, $1/g_m$ (a fact to be deduced later). This circuit indicates that input resistance is increased, particularly if x is large. In practice the load is generally a resistance of

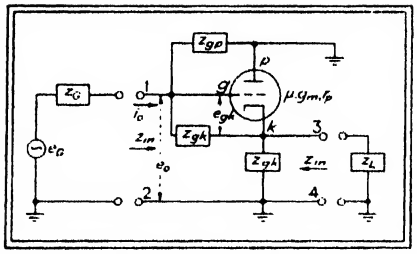

Fig. 1—Terms and symbols used in text. Inter-electrode capacitances are understood to be a part of the various impedances

the order $1/g_m$, thus the input resistance is $2R_{gk} + 1/g_m$.

At high frequencies where interelectrode reactances are much less than their associated resistances, if the load is capacitive the equivalent circuit is that of Fig. 3B. The negative resistance term may produce oscillation if the generator and input impedances combine to form a resonant circuit. The negative resistance can be neutralized by a series resistance whose value is

$$R_s = \frac{(1\ g_m)\ (C_3C_{gk}/C_{gp}^2)}{1 + (\omega^2/g_m^2)\ (C_3 + C_{gk} + C_3C_{gk}/C_{gp})^2} \qquad (2)$$

Because there will be some damping by the tuned circuit, the required grid stopper resistance is less than this value. From Eq. 2 it can be seen that R_s decreases with increasing frequency therefore parasitic oscillations at high frequencies require only a small grid stopper.

Some control may be exercised over C_3 which should be kept low. An example arose in practice: Output of a cathode follower was connected to a long cable. On disconnecting the cable load oscillation in the cathode follower commenced due to the large capacitance of the unterminated cable.

Table I—Cathode Follower Circuit Symbols

- Z_{gp} — Grid-plate impedance (assumed to be $-j/\omega C_{gp}$)
- Z_{gk} — Grid-cathode impedance, a capacitance $-j/\omega C_{gk}$ which may be shunted by resistance R_{gk}
- Z_{ck} — Cathode-earth impedance, normally resistor R_k, considerably greater than $1/g_m$, shunted as discussed
- Z_G — Internal impedance of generator of emf e_G connected to terminals 1, 2
- Z_L — Impedance of load connected to terminals 3, 4
- Z_1 — Z_L, Z_{ck} in parallel
- Z_2 — Z_G, Z_{gp} in parallel
- Z_3 — Z_L, Z_{ck}, r_p in parallel
- Z_{in}' — Input impedance without Z_{gp} in parallel
- Z_{in} — Input impedance with Z_{gp} in parallel

If the cathode-earth impedance is effectively a resistance R_k of value x/g_m, the equivalent circuit is that of Fig. 3C, which is also the equivalent circuit for low frequencies where grid bias is obtained by returning the grid resistor to a bias battery. If the grid-earth network is reduced to a parallel R-C, the resistance is

$$R_p = R_3 + (1 + x)^2\ R_3C_{gk}^2\omega^2 \qquad (3)$$

The damping effect of this on a tuned circuit is less in the case of a triode than for a pentode.

If the cathode follower load is inductive, the equivalent circuit is that of Fig. 3D.

Output Impedence

From analysis of the equivalent circuit, the general output circuit of a cathode follower is reduced to that of Fig. 4. At low frequencies where in normal practice $R_{ck} > 1/g_m$, $\mu > 1$ or $r_p > 1/g_m$, and provided $R_G > R_{gk}$ the output is a resistance $1/g_m$ and the circuit reduces to that of Fig. 5A.

In Fig. 5B where the generator impedance is a capacitance C_G the input capacitance is increased. If the generator impedance is an inductance L_G and the frequency is such that the equivalent input impedance is also inductive (L_{in} is L_G and C_{gp} in parallel as in Fig. 5C), the shunting term can be either zero, negative, or positive depending on the ratio f/f_s where f_s is the resonant frequency of the series circuit L_{in}, C_{gk}. If L_{in} is very large, oscillations can occur due to the negative resistance term.

If the input is a tuned circuit of dynamic resistance R_d the equivalent circuit is that of Fig. 5D. If Z_{ck} is capacitive, resonance can occur in the cathode circuit, but can be prevented by making the cathode impedance more resistive or inductive or by damping the input circuit. If it is essential that the output impedance be as nearly as possible a resistance $1/g_m$, then R_d at the highest operating frequency is restricted to very low values.

Gains

Two types of gain will be considered; the stage gain—defined as the ratio of output voltage to grid-earth voltage; and the overall gain—defined as the ration of output to

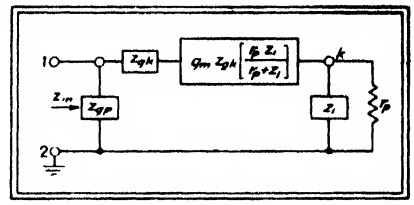

Fig. 2—Generalized equivalent input circuit of cathode follower

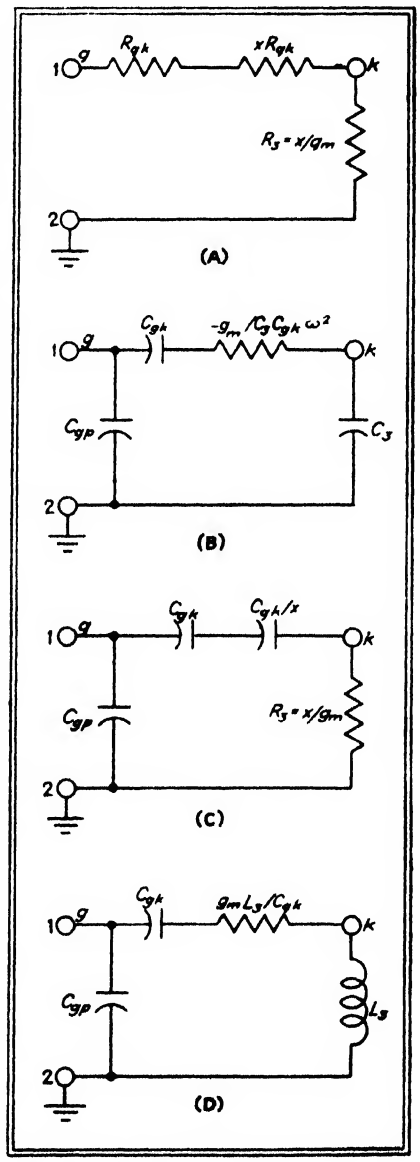

Fig. 3—Cathode follower input circuits for (A) low frequency, (B) capacitive load, (C) resistive load, and (D) inductive load

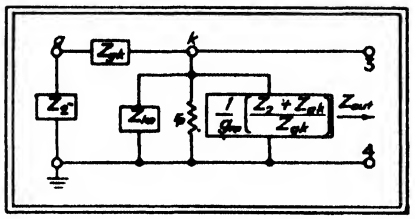

Fig. 4—Generalized equivalent output circuit of cathode follower

generator input voltages.

The stage gain is

$$\left|\frac{v}{e_0}\right| = \left|\frac{1 + 1/g_m Z_{gk}}{1 + (1/\mu) + (1/g_m Z_{gk}) + 1\ g_m Z_1}\right| \quad (4)$$

The overall gain is

$$\left|\frac{v}{e_0}\right| = \left|\frac{[Z_{gp}/(Z_{gp} + Z_0)]\,[1 + 1/g_m Z_{gk}]}{1 + \frac{1}{\mu} + \frac{1}{g_m Z_{gk}} + \frac{1}{g_m Z_1} + \frac{Z_{gp}\,(r_p + Z_1)Z_0}{(Z_0 + Z_{gp})r_p Z_1 g_m Z_{gk}}}\right| \quad (5)$$

For low frequency operation Z_{in} is very large thus the stage gain is used. Normally Z_{gk} and Z_1 are considerably greater than $1/g_m$ and if $\mu \gg 1$, the stage gain tends toward unity. If in addition $Z_1 = 1/g_m$, the stage gain is ½.

At high frequencies the input impedance must be considered. Normally the cathode follower is designed to feed a resistive load of value $1/g_m$, Z_{gk} and Z_{gp} are usually capacitive, and if $\mu \gg 1$, the stage gain becomes $|(1 + j\omega_{gk}/g_m)/(2 + j\omega C_{gk}/g_m)|$. The overall gain can similarly be reduced to a simpler expression.

Conclusions

It is difficult to define a figure of merit for comparing valves to be used in cathode follower circuits. However the following requirements are required at the higher frequencies: low output impedance for connection to concentric cable or low-impedance network (g_m high).

Output impedance independent of generator (input) impedance (C_{gk} low).

Freedom from oscillation if cathode impedance becomes capacitive, as from removing the load at the end of a transmission line connected to the cathode follower ($g_m/C_{ke}C_{gk}$ high).

High input resistance when output is correctly terminated (g_m/C_{gk}^2 high).

From these requirements a tentative figure of merit of $g_m/C_{ke}C_{gk}^2$ is suggested. Applying this figure of merit to typical valves indicates that the triode is approximately 50 percent better that the pentode.

Where input capacitance is important C_{gk} should be considered. If this parameter is included in the figure of merit, the triode is 25 percent better than the pentode. For additional material on cathode followers the reader is referred to Lockhart, C. E. writing in *Electronic Engineering* 15, 287; 15, 375, and 16, 21 (1942-1943).

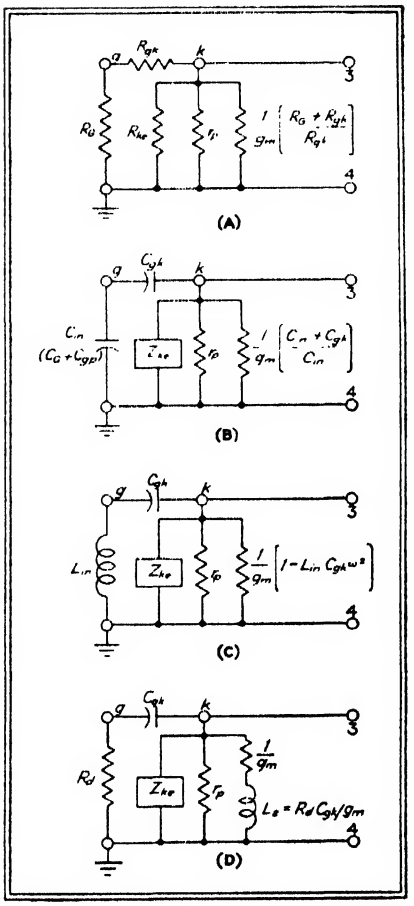

Fig. 5—Cathode follower output circuits for (A) low frequency, (B) capacitive input, (C) inductive input, and (D) resistive input

Cathode Follower of Very Low Output Resistance

A POSITIVE SQUARE WAVE applied to the input of a conventional cathode follower has its leading edge well reproduced, but its trailing edge is badly distorted. A two-tube circuit that overcomes this fault has an output impedance of 30 ohms at frequencies up to 30 mc and an output voltage that is higher than with a single-tube circuit.

Circuit Operation

To develop the two-tube circuit, consider a two-stage, resistance-coupled amplifier with 100-percent feedback from the second tube to the first as shown in Fig. 1A. The cathode resistor R_k must be large not to unduly decrease the gain of the second stage. The cathode degeneration in the first stage is therefore large. If R_k is of the order of the plate resistance of the tubes employed in the circuit, one of the tubes could be substituted for R_k as at Fig. 1B, which is the new circuit under discussion.

The equivalent circuit for that of Fig. 1B is shown in Fig. 2. Analysis of this circuit indicates that the ratio of output to input voltages is

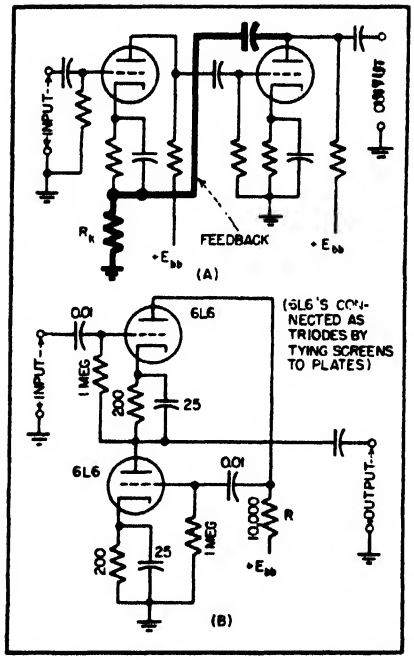

FIG. 1—By rearranging a two stage feedback amplifier (A) the plate resistance of the second tube can serve as the cathode resistor in the stage of the first tube (B)

$$\frac{E_{out}}{E_{in}} = \frac{\mu^2 + \mu\,(r_p/R)}{(\mu^2 + \mu + 1) + (\mu + 2)\,(r_p/R)}$$

and the output conductance is

$$G_{out} = \frac{1}{R_{out}} = \frac{\mu + 1}{r_p + R} + \frac{1 + \dfrac{\mu\,(\mu + 1)}{(r_p/R) + 1}}{r_p}$$

When R is large compared to r_p the first term of the conductance equation becomes negligible and the second term becomes approximately equal to the product of the amplification factor of the tube and the transconductance

$$G_{out} = (\mu^2 + \mu + 1)/r_p \approx \mu g_m$$

The value of output conductance represents an improvement over the conventional cathode follower by the factor μ. However, in driving low load impedances from this circuit, the signal must be small enough not to overdrive the lower tube.

Circuit Characteristics

The circuit with the values shown in Fig. 1B was examined at various frequencies from 10 kc to 30 mc. The output approached unity as the output load approached 1,000 ohms. The output was essentially uniform to about 10 mc, but fell above that frequency, falling faster with lower load resistances. A pronounced rise in output (an actual voltage gain) was obtained with a capacitive load of 0.0001 μf at approximately 10 mc. The rise occurred at lower frequencies as the capacitive load was increased. With 0.01 μf there was a slight rise at about 800 kc and practically no response at 1,000 kc. The fidelity of response to a pulse was definitely superior to that of a single-tube circuit and the effect on sine waves was also good. (Cathode Follower, by Calvin M. Hammack, Report 469, Radiation Lab., MIT, Cambridge, Mass.)

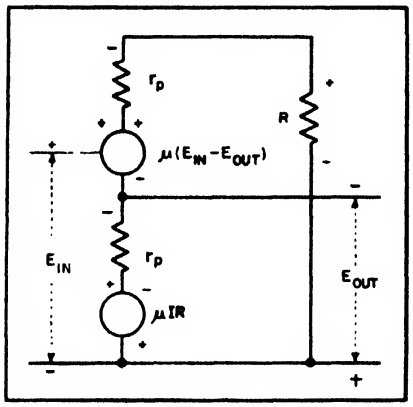

FIG. 2—Equivalent circuit of the low output impedance cathode follower

Bandwidth vs Noise in Communication Systems

Reporting an IRE symposium on the reformulation of the Hartley Law. New theory places limit on the extent to which bandwidth can be traded for signal-to-noise ratio, shows extent to which a-m, f-m, ptm and pcm make use of communication channel

THE BASIC QUESTION in communications is the relative value of various schemes of modulation, amplitude modulation, frequency modulation, pulse-time modulation and pulse-code modulation, to name but a few. New light on this question was shed at a symposium by the New York Section of the IRE. At this meeting, C. E. Shannon of the Bell Telephone Laboratories presented an extension of the theory of communication in the form of a general relation between the bandwidth used by a system, its capacity to transmit information, and the signal-noise ratio present. Using this relationship, three other speakers (B. D. Loughlin of Hazeltine, A. G. Clavier of Federal, and J. R. Pierce of BTL) drew conclusions concerning the relative efficiency of a-m, f-m, ptm and pcm systems as carriers of information.

Influence of Noise

The first statement of the new law to appear in print was published in an editorial[1] in ELECTRONICS quoting W. G. Tuller. In essence, the new law is a reformulation of the Hartley law,[2] which says that

the amount of information which can be transmitted in a given time is proportional to the bandwidth occupied by the communication channel. The revised law says that the amount of information which can be transmitted in a given time is also determined by the logarithm of the signal-noise ratio plus one.

The original Hartley law, as applied to television, for example, states that a 525-line, 30-frame image, having equal vertical and horizontal resolution, must occupy a channel at least 4.5 mc wide. The new law states that, if we are willing to increase the signal relative to the noise, at whatever cost, the bandwidth can be reduced below 4.5 mc, without reducing the total amount of pictorial information conveyed in a given time.

This relation between bandwidth and noise is not a new subject. Prior to 1935, it was believed that the information-carrying capacity of a circuit was dependent upon its bandwidth, and there the theory stopped. But in that year, before a technical world hardly ready to accept the concept, E. H. Armstrong proved that the signal-noise ratio of a broadcasting station could be improved materially by assigning a wide band to it.[6] His method was frequency modulation, whereby a spectrum 150 kc wide was occupied by a broadcast station operating with a 15-kc modulating signal, or about 5 times as wide as would be required by a double-sideband amplitude-modulation station.

The effect can be expressed, in somewhat idealized form, as follows: if the bandwidth utilized by an f-m station is doubled, other factors remaining unchanged, an improvement of 6 db in signal-noise ratio can be ideally achieved. Thus for each doubling of the bandwidth, 6 db is *added* to the signal-noise ratio.

The new law shows that this improved performance of an f-m system over an a-m one is still far from the ideal case. The ideal system, the best permissible under the new concept, is one in which the number of db improvement in signal-noise (for high signal-noise ratios) is *directly proportional* to the bandwidth employed. In other words, the number of db improvement is *multiplied* (rather than added, as in the f-m case) when the bandwidth is increased. Thus in the ideal system, doubling a given bandwidth may add a 10 db improvement in signal-noise ratio. If the band is then doubled again, the improvement is 10 times 10, or 100 db, a vast improvement, relative to the additive system typified by f-m. It turns out that the pulse-code modulation system,[4] alone of the schemes now known, is a multiplicative system. From a strictly theoretical point of view, pcm is thus the preferable system to use, when economy in the use of the ether spectrum is the primary consideration. If other economic factors (such as cost of equipment) are present, as they are in broadcasting, pcm may lose its advantage.

The new law (which has not yet received a name, but in which Tuller, Shannon, Sullivan and Wiener, of MIT, BTL, CalTech and MIT respectively, have had a hand) takes the following simple form

$$C = W \log_2 (1 + P/N) \qquad (1$$

Here C is the capacity of the channel to carry information per unit time (strictly speaking, the number of binary digits which can be transmitted in unit time), W is the bandwidth of the communication channel, and P/N is the signal-noise ratio in power units. The law states that if the capacity of the channel is to be increased, this may be done by increasing the bandwidth W, or equally well (cost not considered) by increasing the signal power relative to the noise. Alternatively, if we are satisfied with a given capacity, we may trade off bandwidth for signal-noise ratio. We may reduce the bandwidth W, if we are willing and able to increase the signal-noise ratio (by adding transmitter power or reducing noise). Or we may increase the bandwidth, and thereby permit a reduction in transmitter power, or an increase in noise, without harm to the capacity (e.g. quality of reproduction) of the circuit.

All this trading is possible in an ideal system, of which Eq. 1 is descriptive. Nonideal systems exist, in which increasing the bandwidth may *increase* the noise, as in the nonlimited a-m system. But if the system is clever enough to take full advantage of the ideal law, then bandwidth and signal-noise may be traded as indicated in Eq. 1. Pcm is one such clever system.

Underlying Logic

The proof of the law is not a simple matter, since it involves multidimensional spaces not familiar to the communication engineer. But the thread of the argument may nevertheless be followed from the reasoning presented by Shannon, which is herewith reported as given at the IRE meeting.

Figure 1 shows a typical communication system in which the initial information, in the form of a message, is transformed, by a transmitter using some form of modulation, into a signal. While the signal is

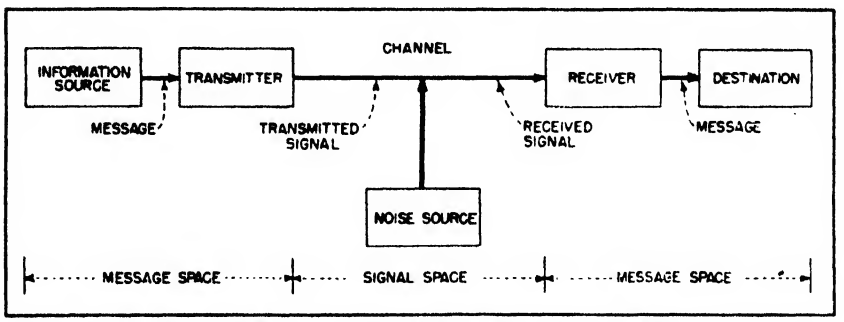

FIG. 1—Essential elements of a communication system, used by Shannon as a basis for treatment of bandwidth-noise problem. The transformation from message to signal is accomplished by some form of modulation

in the communication channel, noise is imposed upon it. Noise is defined as a statistical variation imposed on, but not correlated in any way with, the signal. The receiver transforms the signal-plus-noise back into a message which is perceived at the destination.

We now assign a bandwidth W cps to the communication channel, and put the channel to use for a period of T seconds. We inquire into what sorts of signals may be handled within this bandwidth and within this time. While it is impossible to construct exactly any signal function (except zero) which has no spectrum components outside the bandwidth W and no temporal existence outside the time T, some fair approximations may be so constructed.

A generalized example is shown in Fig. 2. Here we have a signal waveform plotted against time. Such a signal (of duration T seconds) may be passed through the system having W bandwidth, if its narrowest hump (half-wave component) is no narrower than $1/(2W)$ seconds. Moreover, if we sample the amplitude at intervals of time equal to $1/(2W)$, the sample amplitudes, taken throughout the duration of the signal, serve to specify the signal uniquely. Since we have taken T as the duration of the signal, it follows that there are $T/(1/(2W)) = 2WT$ sample amplitudes in the whole length of the signal function.

To take a concrete example, if a video waveform depicts a television program for an hour (3,600 seconds) over a bandwith of 4,000,000 cps, there are $2 \times 3{,}600 \times 4{,}000{,}000 = 28.8$ billion sample amplitudes in the signal. If we knew all these sample amplitudes, we could reconstruct the program exactly, even though we did not have the actual video waveform for reference. It thus takes $2WT$ different quantities to specify uniquely all the different types of signals which might be sent over a channel of bandwidth W cps during T seconds.

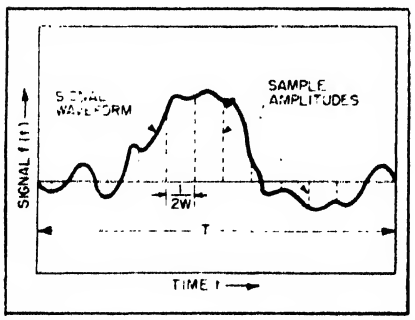

FIG. 2—Signal waveform can be specified by sampling the amplitude at regularly spaced intervals

Coordinates of Communication

Whenever such a large and general description of a quantity is encountered, it has proved most informative to adopt geometric methods of thinking. So, (and here is a big step so far as engineers are concerned) each possible signal capable of transmission through the system is imagined as a *point* in multidimensional space. Since a point is specified in space by its coordinates, and since the signal point (for the complete program) has $2WT$ different numbers required to specify it, it follows that the appropriate space has $2WT$ dimensions. In the television case previously cited, the space has 28.8 billion dimensions.

While such a space cannot be visualized (any more than four-dimensional space can be visualized), its properties may be deduced by the symbolized logic of mathematics, and examples may be visualized by reducing the problem to one, two, or three dimensions. For example, if we have a signal point in multidimensional space, it has the following coordinates: $x_1, x_2, x_3 \ldots \ldots x_{2WT}$ and its average energy is proportional to the sum of the squares of its coordinates. This energy is proportional to the square of the distance of the signal point from the origin of the space, regardless of the number of dimensions we consider. So we have a convenient relation between the ordinates which describe the signal and the average energy of the signal.

To take a three-dimensional case (a 3-cps channel in use for one second, for example), consider Fig. 3. All the possible signals which may be transmitted are represented as points in three dimensional space. Surrounding each such possible signal is a region of uncertainty (the boundary of which becomes sharper as the number of dimensions increases), which represents the effects of noise.

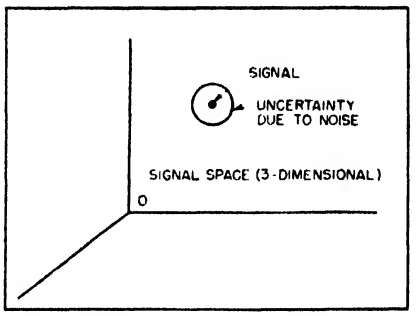

FIG. 3—Representation of a signal by a point in a three-dimensional signal space. The noise surrounds the signal point

In other words, the noise adds to or subtracts from the ordinates specifying the signal point in a random way which makes it impossible to know exactly where the signal point is after the noise has been added in the transmission system. But, if we know the average value of the noise energy, which we recall is proportional to the square of a distance connecting points in the space, we know the radius of the roughly spherical region within which the signal point is located. The same concept applies in a space of any number of dimensions, even though the shapes may not be visualized. So we have a *signal-space* inhabited by points representing possible signals, each point surrounded by a region of uncertainty which represents the random effects of noise.

We now consider the *message* before its translation into a signal. The message, for example, may be the audio waveform before application to a frequency-modulated transmitter, the f-m wave radiated being the corresponding signal. Each message has a spectrum of frequencies contained within a band W, cps (usually equal to or smaller than the channel bandwidth

W). Moreover the message lasts a time T_1 seconds, which may be shorter or longer than the signal duration T. Acting on the same logic as in the signal space, we imagine a *message space* of $2W_1T_1$ dimensions. Each point in this space represents a possible message having the given message spectrum W_1 and message duration T_1. In Fig. 4 we depict a two-dimensional space (a message having a 2-cps spectrum which lasts one second, for example).

Moreover, we may imagine groups of messages which are indistinguishable from one another when perceived at the destination of the system. For example, we may shift the phase of the harmonic components of a speech waveform without changing the sound of the speech as perceived by the ear. If we represent all such indistinguishable messages as points on an arc of a circle centered on the origin, we may specify all such messages by a single quantity, the radial distance from the origin to the arc, as shown in Fig. 4. In this case the message space is reduced to one effective dimension.

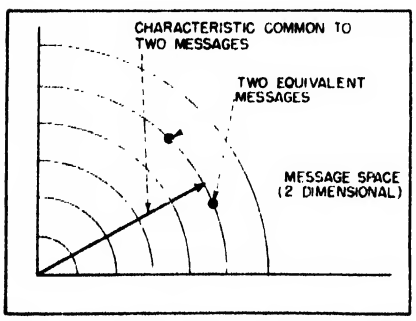

FIG. 4—Representation of equivalent messages as a point in a two-dimensional message space

Function of Modulation

Having, by dint of some exercise of the imagination, dreamed up two spaces, one containing the message, the other the corresponding signal, we now inquire concerning the translation process from message to signal at the transmitter and vice versa at the receiver. This translation, in geometric terms, is known as *mapping* the one space into the other. An example is given in Fig. 5A. If the transmitter employs single-sideband a-m, the mapping procedure is a one-to-one translation, changing only the position on a frequency scale. If double-sideband a-m is used, two sidebands are produced for each modulating harmonic component, so a message space of N dimensions is thereby translated into a signal space of $2N$ dimensions.

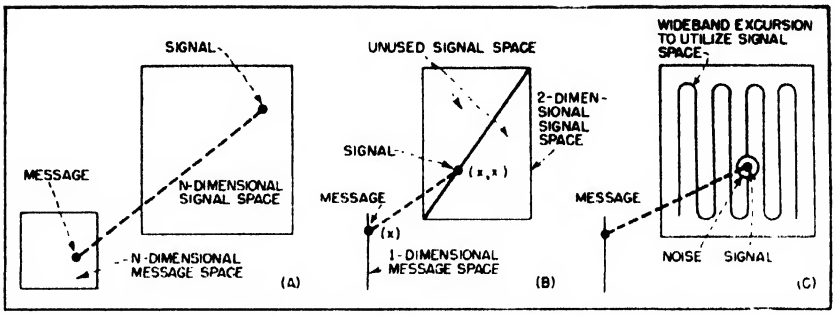

FIG. 5—Mapping is the process of transformation from message space to signal space. (A) Single-sideband a-m in two dimensions. (B) Double-sideband a-m from one to two dimensions. (C) Filling in unused space in double-sideband case, by utilizing a wideband modulation system

The simplest possible case is show in Fig. 5B. Here a message space of one dimension, the line shown, contains a message represented by the point whose coordinate is x. When translated by a double sideband a-m system into a signal, the signal space becomes two dimensional, as shown, but, since the sidebands are symmetrically disposed about the carrier, the same number describes each, and the corresponding signal point has coordinates x,x. Hence all signals lie on the diagonal line shown. So all possible messages in double sideband a-m are translated from a line to a line. All the signal space outside the line is unused in the double-sideband a-m system. This is the reason why this system of modulation cannot make the fullest possible use of the channel bandwidth.

In Fig. 5C, the wavy line represents a translation (corresponding to that introduced by pulse-code modulation, for example), which makes fuller use of the signal space available, and hence is more efficient than a-m as a modulation system. Efficient modulation systems all operate in this manner, although the shapes cannot be visualized in the multidimensional case.

In Fig. 5C, surrounding the message point is a circle representing the uncertainty introduced by noise. If the wavy lines are placed too close, so that the noise circle overlaps two lines, then the effect of the noise is multiplied. This overlapping means that the wideband system, typified by the wavy line, has a threshold value of signal, below which the effect of noise becomes rapidly worse, more rapidly than in the simple a-m case. This effect has been observed in wideband f-m, pcm and ptm systems. The theory shows that this is a general property of all wideband systems.

System Capacity

Finally, we come to the derivation of the modified Hartley law, Eq. 1. Dr. Shannon illustrated the three-dimensional case shown in Fig. 6. The transmitter power is P watts, and the random noise

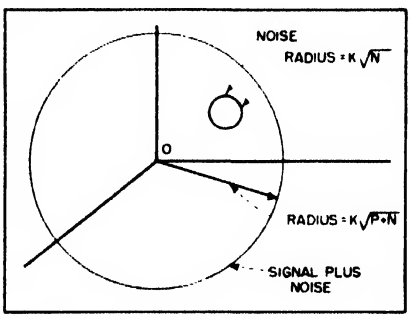

FIG. 6—Derivation of revised Hartley law is based on a spherical signal space, with radius squared proportional to sum of signal power plus noise power

(white noise) is N watts. The channel has a bandwidth W cps; the signal duration is T seconds. At the receiver, after the signal and noise have become mixed, the signal space is represented as a sphere whose radius squared is proportional to $(P + N)$. To find out how many signal points may be distinguished within this space, we fill it with small spheres representing the noise, each of radius squared proportional to (N). The maximum number of noise spheres which will fit into the multidimensional signal space is then the generalized volume of the message space $K\sqrt{P + N}^{2TW}$ divided by the generalized volume of the noise spheres $K\sqrt{N}^{2TW}$. We thus obtain the number of messages M which may be distinguished at the receiver

$$M = \frac{K\sqrt{P+N}^{2WT}}{K\sqrt{N}^{2WT}} = \left[\frac{P+N}{N}\right]^{TW} = (1 + P/N)^{TW} \quad (2)$$

We can rewrite Eq. 2 in logarithm form, using for convenience the log to the base 2

$$\log_2 M = TW \log_2 (1 + P/N) \quad (3)$$

Taking a cue from the pcm system, Dr. Shannon then introduced the binary digit system.[4] If S binary digits are available, the number of messages that can be carried by these digits is $M = 2^S$, from which $S = \log_2 M$. Then, Eq. 3 becomes

$$S = TW \log_2 (1 + P/N) \quad (4)$$

But S/T, the number of binary digits transmitted per second, is the capacity C of the channel to carry binary digits, so

$$C = W \log_2 (1 + P/N) \quad (5)$$

which is the law to be proved. Whew! While the law was proved for a system transmitting messages by the binary digit code, it can be shown to apply generally to all classes of systems.

Dr. Shannon pointed out that, while bandwidth can be saved (in the ideal system which makes full use of the signal space) at the expense of signal-noise ratio, the saving is very expensive, because of the fact that the logarithm changes very slowly with changes in the power P. Thus it might be necessary, in a particular case, to increase the transmitter power two times to secure a 10 percent reduction in bandwidth without harm to the signal. But, if one can afford it, one can do it.

A final form of the equation which shows the multiplicative nature of the decibel improvement, previously mentioned, is

$$C = KW\ 10 \log_{10} (1 + P/N) = K\ W\ n \quad (6)$$

where $n = 10 \log_{10} (1 + P/N)$ is the number of db expressing the signal-noise ratio plus 1, and K is a proportionality constant.

A lively discussion followed the meeting, participated in by Harold Wheeler, who stated his opinion that the number one should be eliminated from the argument of the logarithm. W. G. Tuller, and Herbert Sullivan also participated in the discussion. A summary of the analysis presented by A. G. Clavier, comparing the transmission efficiencies of various modulation schemes,[5] showed that, for operation well above (60 db) the noise, the utilization efficiency of pcm is independent of bandwidth, and that the only known system in which utilization efficiency increases with bandwidth is pulsed frequency modulation.—D.G.F.

References

(1) Cross Talk, ELECTRONICS, p 79, Aug 1947.
(2) R. V. L. Hartley, Relations of Carrier and Side-Bands in Radio Transmission, *Proc. IRE*, p 34, Feb 1923.
(3) E. H. Armstrong, A Method of Reducing Disturbances in Radio Signalling by a System of Frequency Modulation, *Proc. IRE*, p 689, May 1936.
(4) Coded Pulse Modulation Minimizes Noise, ELECTRONICS, p 126, Dec 1947.
(5) Effect of Modulation on Transmission Efficiency, ELECTRONICS, p 136, Jan 1948.

Wideband Phase Shift Networks

Design criteria are presented for L-C and R-C phase shifting networks that develop a constant phase difference over a wide frequency band. The technique is to introduce two phase shifts such that, although they vary with frequency, their difference does not

By R. B. DOME

IT IS frequently desirable to derive from a given voltage two new voltages of the same frequency but with the phase angle between the new voltages held substantially constant over a wide frequency range, each derived voltage having an amplitude characteristic linearly variable with the amplitude of the input voltage independently of frequency.

To produce the phase difference between the two voltages, two networks whose phase angles increase substantially linearly with the logarithm of the frequency are used. Thus, if the two networks are properly matched, the phase difference between them remains nearly constant over a wide range of frequency.

Network Development

One way of producing the two voltages is to derive both of them from a single source and arrange that the output of either channel is

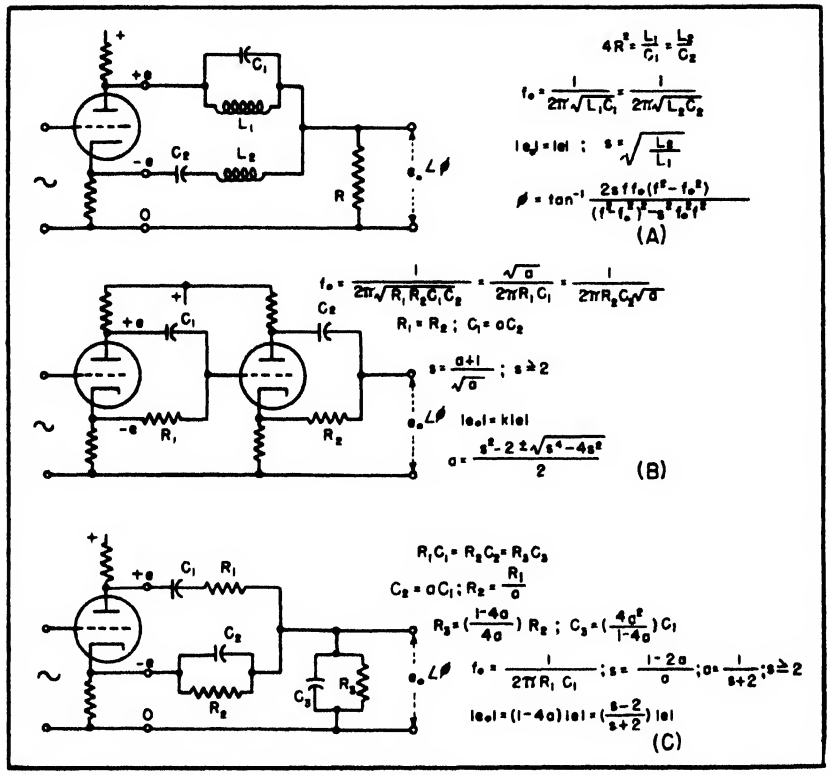

FIG. 1—Three networks for producing phase shift. Networks are used in pairs to obtain two outputs which have a constant phase difference over a wide range of frequency. Phase shift equation given for network of Fig. 1A holds for other two networks

independent of frequency, but that both have phase angles with respect to the input voltages varying in such a way that over a wide band of frequencies

$$\phi_1 - \phi_2 = K \qquad (1)$$

where ϕ_1 : phase angle of output No. 1
ϕ_2 : phase angle of output No. 2
K : a constant
ϕ_1 and ϕ_2 are each their own function of f, the frequency

One possible configuration for these functions is

$$\phi_1 = C + \log f \qquad (2)$$

$$\phi_2 = C + \log kf \qquad (3)$$

where C and k are constants

Substituting Eq. 2 and 3 in Eq. 1

$$\begin{aligned}\phi_1 - \phi_2 &= C + \log f - C - \log kf \\ &= \log f - \log f - \log k \\ &= -\log k \equiv K \end{aligned} \qquad (4)$$

Thus it is only necessary to find a network configuration which will yield a phase angle which varies as the logarithm of the frequency over a wide range of frequency. The network must also have no change in output amplitude with frequency. The latter limitation usually restricts the final network configuration to lattice types because finite ladder types with any phase shift must be accompanied by amplitude variations. In order to avoid the use of transformers in the lattice structure, a half-lattice will be chosen with the input terminals excited by two equal voltages 180 degrees out of phase. Such voltages are readily available from vacuum tube phase inverters consisting of a tube with equal cathode and anode loads.

L-C Lattice

A circuit having enough independent parameters to permit the designer to shape the phase angle curve to the required logarithmic form and the basic design equations of the circuit are shown in Fig. 1A. It will be noted from the equation for the phase angle (Fig. 1A) that an arbitrary factor s is included. The choice of s is up to the designer.

If s lies between 3 and 5, a fairly straight line for ϕ is obtained when plotted against a logarithmic frequency scale. As will be shown later, if a second curve for a second similar network, but with a resonant frequency f_0 which is 4.53 times the resonant frequency of the first curve, is plotted, the phase angle difference between these two curves is maintained within 90 ±4 degrees over a fairly wide range of frequency if $s = 4$, and is quite satisfactory for voice frequencies because the upper to lower frequency ratio is approximately 28 to 1, as for example would occur in a band from 130 to 3,600 cps.

The band can be widened indefinitely by adding more elements to the bridge arms with the result that the frequency range is expanded more until remarkably good performance is obtained over the full audio range from 30 to 15,000 cps.

The use of inductances in filters is to be avoided if possible because of the inability to obtain a pure inductance; there are always the inevitable series resistance and shunt capacitance. Other objections to the use of inductors are that they may pick up unwanted signals from stray magnetic fields and that they are not constant in inductance with applied voltage. As a consequence, a resistance-capacitance type of half-lattice network would be preferable providing the required type of phase curve were obtainable from them.

R-C Lattice

In order to provide a wide range of operation, two simple resistance-capacitance networks can be used in cascade with isolating tubes between them as shown in Fig. 1B. A single network has restricted bandwidth. No terminating resistor can be used in this type of network.

The phase angle of the final output voltage can be adjusted exactly as in the L-C circuit of Fig. 1A because the phase angle equation is identical. The only limitation with this network is that s must be greater than 2, however as previously found, for best results s

Table I—Determination of Network Parameters

First Network	Second Network
$f_{01} = 1488$ cps	$f_{02} = 329$ cps
$s = 4.00$	$s = 4.00$
$a = 0.1666$	$a = 0.1666$
$R_1 = 20{,}000$ ohms	$R_1 = 20{,}000$ ohms
$C_1 = \frac{1}{2\pi f_{01} R_1} = \frac{1}{2\pi 1488 \times 20000}$ $= 0.00535\ \mu f$	$C_1 = \frac{1}{2\pi f_{02} R_1} = \frac{1}{2\pi 329 \times 20000}$ $= 0.0242\ \mu f$
$C_2 = a C_1 = 0.166 \times 0.00535$ $= 0.000892\ \mu f$	$C_2 = a C_1 = 0.166 \times 0.0242$ $= 0.00403\ \mu f$
$C_3 = \left(\frac{1a^2}{1 - 1a}\right) C_1 = 0.333\ C_1$ $= 0.333 \times 0.00535$ $= 0.001785\ \mu f$	$C_3 = \left(\frac{1a^2}{1 - 1a}\right) C_1 = 0.333\ C_1$ $= 0.333 \times 0.0242$ $= 0.00806\ \mu f$
$R_2 = \frac{R_1}{a} = \frac{20000}{0.166}$ $= 120{,}000$ ohms	$R_2 = \frac{R_1}{a} = \frac{20000}{0.166}$ $= 120{,}000$ ohms
$R_3 = \left(\frac{1 - 1a}{1a}\right) R_2$ $= \left(\frac{1 - 0.666}{0.666}\right) 120{,}000$ $= 60{,}000$ ohms	$R_3 = \left(\frac{1 - 1a}{1a}\right) R_2$ $= \left(\frac{1 - 0.666}{0.666}\right) 120{,}000$ $= 60{,}000$ ohms

should be approximately 4, and hence lies well above 2.

The number of stages included in cascade may, of course, be increased to any desired number. When six such stages are used, the frequency ratio for which a phase angle difference between two sets of networks can be maintained within 90 degrees ±3 degrees becomes approximately 200 to 1, or what would cover an audio frequency band of 50 to 10,000 cps, which is adequate for high quality broadcast service.

Another R-C network, which does not require an isolation tube, is shown in Fig. 1C. This network somewhat resembles the L-C network of Fig. 1A but differs in output voltage. The output voltage is a proper fraction of the input voltage. The factor a must be less than 0.25, or s must be greater than 2, when using this network. As previously pointed out, for best results s should be approximately 4, or $a = 0.167$, which will yield an output voltage of about 0.83 times the input voltage.

The phase angle equation (Fig. 1A) is seen to be identical to those for the previously described networks. In order to find the proper values for f_0 in the two networks which are to yield a phase angle difference of 90 degrees, assume a geometric mean frequency between the upper and lower frequency limits of usable phase angle difference. This mean frequency is not critical, but a value of 700 cps has been suggested as a practical frequency (O. B. Hansen, Down to Earth on 'High Fidelity', Radio Technical Planning Board, Report on Standards and Frequency Allocations for Post-War FM Broadcasting, Panel 5, June 1, 1944, Section VIII). Having decided on the mean frequency of the system, it is merely necessary to design the two phase shift networks so that one has a phase angle of 180 − 45 degrees at 700 cps, and the other a phase angle of 180 + 45 degrees at 700 cps.

Basis for Design

Suppose the value for f_0 of the first network is to be determined, then, designating f_0 of the first network as f_{01} and letting f equal the mean frequency, designated as F, the phase angle equation (Fig. 1) becomes

$$\tan \phi = \frac{2sFf_{01}(F^2 - f_{01}^2)}{(F^2 - f_{01}^2)^2 - (sf_{01}F)^2}$$

Setting $\phi = 135$ degrees and $s = 4$, clearing fractions and solving for f_{01} gives $f_{01} = 2.126F$, which, for $F = 700$ cps, gives $f_{01} = 1{,}488$ cps.

By reciprocal relationships, the value of f_{02}, the f_0 of the second network, is $f_{02} = F/2.126$; at $F = 700$ cps, $f_{02} = 329$ cps.

The parameters of the two networks can now be calculated. For convenience and to establish values of impedance into which vacuum tubes can work satisfactorily, assume that $R_1 = 20{,}000$ ohms in each network. The calculations are summarized in Table I.

The phase shift curves for these two networks are shown in Fig. 2. Note the long frequency range over which these curves are substantially parallel. The difference angle is plotted to facilitate comparison. Note that this difference angle holds fairly close to 90 degrees over a range of frequencies from 130 to 3,600 cps. This range is quite adequate for a voice frequency channel.

Such a network can be used to build a simple single sideband transmitter without the necessity of using sharp cut-off filters and double or triple modulation. This simplification may be done by combining the outputs of two balanced modulators: one balanced modulator is fed with radio frequency cos ωt and audio frequency $m\cos(\mu t - \theta)$, and the other balanced modulator is fed with radio frequency cos $(\omega t \pm \pi/2)$ and audio frequency $m\cos(\mu t - \theta \pm \pi/2)$. If the plus signs are used and the balanced modulator outputs are added, the resultant output would be $m\cos[(\omega - \mu)t + \theta]$, which is the lower sideband.

Single Sideband Telephony

An experimental system of this type has been constructed and operated using carrier frequencies in the broadcast band. No untoward difficulty was encountered and re-

sults were fully up to expectations. The transmitter was modulated with audio signals taken from the output of a broadcast receiver. The single sideband transmission was received by a second broadcast receiver into whose input terminals was also fed an unmodulated continuous wave radio frequency from a signal generator to furnish the missing carrier. The signal generator frequency was adjusted until the reproduced program sounded most natural. No auxiliary filters were used in the radio section of the transmitter to aid in reducing the unwanted sideband.

The question may arise as to how much of the unwanted sideband is permitted to get through the system if not exactly 90 degrees phase difference is obtained between the two audio channels. The ratio of the weaker sideband to the stronger sideband is given by the equation

$$\text{RATIO} = \sqrt{\frac{1-\cos\delta}{1+\cos\delta}} \fallingdotseq \frac{\delta}{2}$$

where δ is the deviation of the difference phase angle from $\pi/2$, with δ expressed in radians for the approximate formula. A deviation from 90 degrees of 6 degrees is required before the weaker sideband becomes 5 percent as strong as the stronger sideband, so that the phase angle curve of Fig. 2 is probably commercially useful over a range in frequencies included between 84 degrees on the low side of the center to 84 degrees on the high side of the center.

A second application for the system is that of providing a closer-to-zero frequency single sideband telephone or broadcast transmission when filters are used. For example, a single sideband transmitter may be constructed along conventional lines with a quartz crystal type of band-pass filter to operate on 100 kc. Suppose the pass band extends from 100,600 to 108,000 cps. It is seen that frequencies below 600 cps are attenuated in such a system. Now if the single sideband system described in the present paper were to be used in conjunction with a filter, the filter could transmit from 100,000 to 108,000 cps, and the region between 27 and 600 cps could be taken care of by the audio phase shift system, letting the filter remove the undesired sideband from 99,400 down to 92,000 cps. Thus the resultant radiation could contain single sideband components corresponding to an audio frequency range of 27 to 8,000 cps instead of being limited to a range of 600 to 8,000 cps. The addition of the 27 to 600-cps range will add considerably to the naturalness of male speech and organ music. Frequencies between 0 and 27 cps should be removed from the original audio being fed into the system.

High Efficiency Transmitter

A high efficiency broadcast transmitter can be constructed by employing three power amplifiers and three antennas arranged so that an unmodulated carrier is radiated on a central antenna and the upper and lower sidebands are radiated respectively on two side antennas, which are on a straight line through the central antenna but on opposite sides equidistant from it. The sidebands are generated in much the same manner as described in the preceding section. Only one set of audio phase-shift filters are required, for the upper and lower sidebands can be obtained by simply adjusting the phases of the radio frequencies fed into the two sets of balance modulators.

This system of transmission could be accomplished with the following installed relative power capacity

Carrier	1.00
Upper Sideband	0.25
Lower Sideband	0.25
Total	1.50

When modulating 100 percent, this system will have an overall efficiency of about 66 percent, resulting in a d-c power consumption of 2.25 maximum. This consumption graduates down to 1.5 for zero modulation. For an average modulation of 50 percent the power consumption would thus be about 1.875.

The conventional double sideband plus carrier class-B amplifier must have an installed power capacity of 4.0 for handling the peaks of 100 percent positive modulation and the transmitter runs at 33 percent efficiency, requiring a continuous input power of 3.0 from the d-c supply. Thus the saving in d-c power consumption would be about 1.125 based on the carrier rating, or for a 50-kw transmitter, the saving would amount to 56.25 kw. Besides the savings in power costs, the system would have lower first costs in the water cooling system, power rectifiers and transformers,

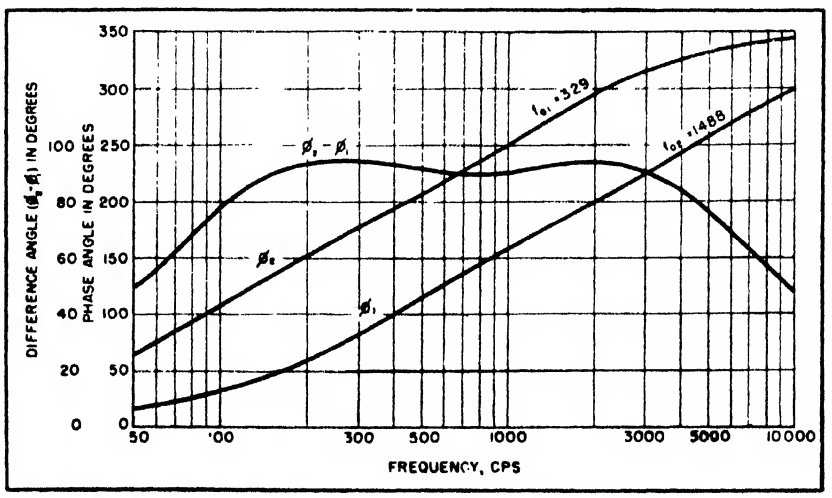

FIG. 2—Phase shift characteristics of networks whose values are given in Table I

and in high power vacuum tubes. The replacement tube cost also would be less.

In the operation of emergency communications transmitters it is often desirable to change the radiated carrier frequency a few hundred or a few thousand cycles to avoid either intentional or accidental jamming, yet it is also desirable to retain the benefits of precise frequency control such as is provided by a quartz crystal. One solution is to have available a large number of crystals lying on closely adjacent frequencies selectable by a rotary switch. Another scheme might be to adjust the air gap or shunt capacitance across the crystal. All of these methods have their objectionable features.

Adjustable Carrier Frequency

An alternative arrangement is to make use of the single sideband generator already described. By way of example, suppose the assigned frequency of a transmitter were 4,500 kc. One could then use a crystal oscillator on 4,498 kc in conjunction with the balanced modulator and a 2-kc variable frequency oscillator to produce the required 4,500-kc carrier. The oscillator could then be adjusted to other nearby frequencies to avoid jamming, by having it cover a range of roughly 0 to 4 kc and thus be able to change the radiated frequency plus or minus 2 kc about the assigned frequency.

The frequency stability of the system would be quite similar to the master quartz frequency stability and hence could be classified as precise. Wider ranges of control could of course be obtained by utilizing submultiple crystal frequencies or wider oscillator range, within the limits of stability of the final frequency.

Frequency Shift Keying

A transmitter equipped as above could be easily converted into a telegraph transmitter with precise frequency shift keying. By way of example, suppose the 4,500-kc transmitter were required to radiate 4,499.9 kc with the key down and 4,500 kc with the key up. All that would be necessary would be to shift the low frequency oscillator from 2.0 kc to 1.9 kc. This shift could be accomplished by keying in a shunt capacitance, and the resulting frequencies would be both precise and stable, maintaining the 0.1-kc difference quite accurately over long periods of operation.

Other Applications

The two 90 degree phase angle displaced voltages can be fed into the X and Y deflection plates of an electrostatic deflection type of cathode-ray tube to obtain a circular trace. The pattern will remain circular for wide changes in frequency if one of these phase-shift networks is used. The circular pattern is a useful indication of the closeness to 90 degrees of the phase shift obtained from these circuits and can be used to determine their performance.

By employing the 90 degree phase angle displaced voltages and a reversed Scott connected transformer, three phase power can be developed from a single phase source. Such a circuit could be used to control the speed of a three phase synchronous motor. Varying the frequency of the original source would vary the motor speed.

Stabilized Negative Impedances

Negative impedance is produced from a positive impedance of the desired type by positive feedback through an amplifier stabilized with negative feedback. Basic circuits and fundamental equations indicate the regions and limits of stability for ideal conditions

By E. L. GINZTON

INVERSE FEEDBACK is one of the most important developments in communication-network technique since the invention of the vacuum tube. Evolution of this principle can be traced along several independent courses two of which form the basis for this three-part article.

One of these courses culminated in Black's[1] disclosure in 1934 of negative feedback by means of which amplifiers can be stabilized and improved in many ways. A somewhat earlier contribution was made by Aiken[2], and Crisson[3] who discovered that by an appropriate application of positive feedback a two-terminal negative impedance could be obtained.

By combining the stabilizing feature described by Black and the negative-impedance concept introduced by Crisson and Aiken, it is possible to obtain a negative impedance that can be used as a stable circuit element. Thus by adding negative resistance, negative capacitance, and negative inductance to the list of positive impedances, the engineer now has at his disposal six elements for design instead of the usual three, making possible not only an improvement in some of the present circuit applications, but also opening an en-

tirely unknown field of design.

The first two parts of this article show how stabilized circuit elements can be obtained and investigate their stability and reliability. A few practical applications are described in the final part —not to give an air of completeness, but merely to illustrate some of the ways in which the negative circuit elements can be used.

A positive resistance R is defined by Ohm's law as the constant of proportionality between the voltage across and the current flowing through that resistance. That is, $R = E/I$ where E and I are voltage and current, respectively. According to Joule's law, power will be dissipated in resistance R at rate P where $P = I^2R$.

Nature of Negative Resistance

From these two laws a definition of negative resistance may be formed. If R is replaced by $-R_n$, it will be seen that Ohm's law will still hold, for voltage and current will still be proportional to each other. Joule's law will state, however, that instead of dissipating power, the negative resistance will generate power, introducing it into the circuit at the rate I^2R_n.

Obviously, if any device is to show a negative-resistance characteristic, it must contain a source of power, such as a battery, and a means of controlling that power source so that Ohm's law will be followed. Since, in any practical case a source of power is limited, the negative-resistance characteristic will be shown by the device only over a limited range of voltage or current.

Negative Reactances

The definition of negative inductance and negative capacitance may be formed analogously. The reactance of inductance X_L is defined by an extension of Ohm's law to alternating currents. Thus $X_L = E_L/I = j\omega L$ where E_L is the voltage across the inductance, I is the current through the inductance, and L is the inductance in henrys. As is shown by this relation, a positive inductance is one whose reactance increases with frequency.

If L is replaced by $-L_n$, the impedance is $\omega L_n/j$. This equation may be used as a definition of a negative inductance. Thus, it is seen that a negative inductance is equivalent to a capacitive reactance whose magnitude increases with frequency.

A negative capacitance may be defined in the same way. It will be found that a negative capacitance is equivalent to an inductance whose reactance decreases with frequency.

In passing, it should be noted that positive and negative inductances and positive and negative capacitances can store energy equally well. But in the case of the negative impedances, the amount of energy that can be stored is limited by the amount of voltage or current that the negative-impedance-producing element can supply.

Because amplifiers will be used to produce the negative impedances it will be necessary to consider their limits of linearity and power handling capacity. This consideration will be taken up in Part II; for the present we will assume that an amplifier which is linear within the range of operation required for the production of the required negative impedances can be built.

Negative Resistance Sources

There are many sources of negative resistances known at present. Some of them occur in natural phenomena such as in gaseous discharges, others are produced by artificial means such as a source of energy and a control device arranged to maintain current and voltage in their required ratio.

An example of the latter is a direct-current series generator which shows a negative-resistance characteristic because current flowing through the generator excites its field and the generator produces a voltage which tends to increase the current.

Sources of negative resistance which are useful in communication circuits were described by Herold[4] and others. Some of these are: Arc discharge, the dynatron, retarding-field type of negative resistance[5], a space-charge grid tube which operates with a temperature-limited cathode, the split anode magnetron, and a low gas-pressure triode.

None of these methods of obtaining negative resistances are capable of producing pure negative reactances. Moreover, examination of the various methods reveals that in most cases the resistance is not linear, but depends greatly upon the magnitude of the applied voltage or current.

A different method of obtaining negative circuit elements has been suggested by Crisson, Dudley, and Mathes by means of which it is possible to obtain linear negative resistances of any value whatever and also pure negative reactances. The following section will discuss the methods suggested by Crisson.[6]

There are two ways in which it is possible to obtain negative impedance provided a positive of this impedance can be constructed in the form of a two-terminal network. The two methods can be used to produce the same impedance, but it will be found that only one of them can be used in any particular application. This consideration will be discussed in greater detail later.

First, equations will be determined for the input impedances of the two circuits which have been found to give negative impedances. This analysis will indicate the range and limiting factors of the negative impedances so produced.

Shunt Negative Impedance

Consider the amplifier shown in Fig. 1. The square labelled A represents an ideal amplifier with a voltage amplification A and an output resistance R_1. (Output impedance R_1 in this paper will mean the impedance looking into the output terminals of the amplifier. It is not necessarily equal to the physical output impedance of the amplifier because it may be affected by the

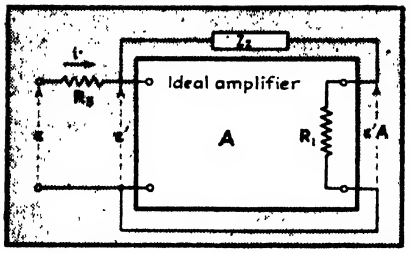

FIG. 1—Circuit for producing shunt negative impedance across its input terminals

presence of negative feedback in the amplifier.)

By an ideal amplifier is meant an amplifier which has a uniform frequency response from zero to infinity cycles per second, infinite power handling ability, zero phase shift for all frequencies, and an output resistance R_1 which is independent of frequency.

Let

e = voltage applied to the amplifier
e' = voltage at the input terminals of the amplifier (see Fig. 1)
Z_2 = any positive impedance, the negative of which it is desired to obtain
R_s = a resistance placed as shown in Fig. 1
i = current taken from the source of voltage e

The circuit shown in Fig. 1 may be rearranged by means of Thevénin's theorem. If this is done, the output of the amplifier as shown in Fig. 1 may be replaced by the equivalent voltage $e'A$ in series with the output resistance R_1. With this transposition in mind, the following relations can be written. The net voltage acting across the output impedance R_1 and impedance Z_2 is $(e' - e'A)$, according to the convention of polarities of voltages indicated in Fig. 1 by means of arrows. Hence, the current that flows through R_1 and Z_2 in series is

$$i = \frac{e' - e'A}{Z_2 + R_1} = \frac{e'(1 - A)}{Z_2 + R_1} \tag{1}$$

Solving for e'/i

$$\frac{e'}{i} = \frac{Z_2}{1 - A} + \frac{R_1}{1 - A} \tag{2}$$

This ratio represents an impedance at the amplifier terminals where e' is measured. The impedance offered to the source of voltage e must be the sum of R_s and this apparent amplifier input impedance. Defining the impedance offered to the source e by the entire circuit as Z_n

$$Z_n = e/i = R_s + e'/i$$

$$Z_n = R_s + \frac{Z_2}{1 - A} + \frac{R_1}{1 - A} \tag{3}$$

If R_s is adjusted so that $R_s = R_1/(A - 1)$, then $R_s + R_1/(1 - A) = 0$, and therefore Eq. (3) becomes

$$Z_n = Z_2/(1 - A) \tag{4}$$

If the amplification A is positive and greater than unity, then the input impedance of the circuit of Fig. 1 is negative and determined in character only by the nature of Z_2. Crisson attributes this type of a negative impedance to Dudley and for reasons which will be explained later calls this type of negative impedance the *shunt negative impedance.*

Series Negative Impedance

The second method of obtaining negative impedance is illustrated in Fig. 2. In this case Z_2 is the positive impedance the negative of which is the desired result. R_s is a resistance whose function is similar to that of R_s in the previous case.

If e is the voltage applied at the terminals of the circuit as is shown in Fig. 2, then a current i will flow through the circuit. The following equation can be written.

$$e = i(R_s + Z_2 + R_1) - i(R_s + Z_2)A \tag{5}$$

From which

$$Z_n = (e/i) = Z_2(1 - A) + R_s(1 - A) + R_1 \tag{6}$$

If R_s is adjusted so that $R_1 = R_s(A - 1)$, then $R_1 + R_s(1 - A) = 0$, and therefore

$$Z_n = Z_2(1 - A) \tag{7}$$

If A is positive and greater than unity, the input impedance of the circuit is negative and determined in character only by the nature of Z_2. This type of a negative impedance is called a *series negative impedance.* Crisson attributes its discovery to Mathes.

From the preceding discussion it is evident that by means of application of positive feedback in an ideal amplifier it is possible to obtain negative impedances without depending upon natural phenomenon such as gas discharge or secondary emission, or upon a device which may be inherently nonlinear.

Reliability

The elementary picture given above is not sufficient for a practical application of negative impedances. One can readily observe that both of these circuits are essentially members of the same family and involve positive feedback, and one would be rightly justified in raising the question of stability and how the deviations from the assumed ideal amplifier will affect its performance. These questions will be discussed later where it will be shown that negative circuit elements can be made to possess extraordinary stability, and that the deviations of an actual ampilfier from the ideal modify the results only in special regions.

In addition to the positive feedback that is obviously necessary to obtain the negative impedances, the amplifiers themselves can be stabilized with negative feedback. It will be shown that simultaneous application of positive and negative feedback in an amplifier may be made use of to produce negative impedances which are just as stable and reliable as ordinary commercially available circuit elements. Nor in this simultaneous application of positive and negative feedback does the effect of one cancel the effect of the other. Amplifier

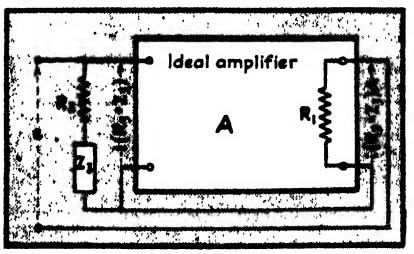

FIG. 2—Circuit for producing series negative impedance across its input terminals

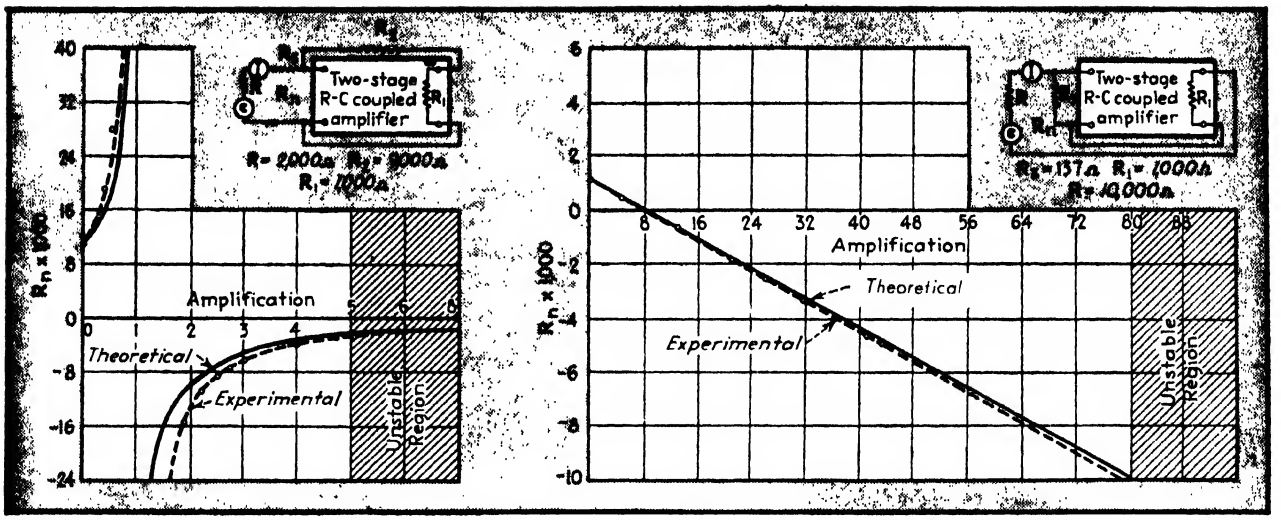

FIG. 3—Gain of amplifier determines magnitude and sign of negative resistance produced across its input although a single positive resistance is used

FIG. 4—A wide range of negative resistances can be produced by choice of amplification and of either shunt or series circuits

gain does, however, play a major part in determining the magnitude and stability of negative impedance. The effect is different for negative impedances produced by the two methods, as the following considerations will show.

Amplifier Gain in Shunt Circuits

If the amplification in Fig. 1 is zero, the input impedance offered to the source of a voltage e is the sum $(R_s + Z_s + R_1)$, and the current flows from the source of voltage, being entirely determined by this sum. If A is increased positively from zero towards infinity, the current will decrease and when A is of such a magnitude that the output voltage of the amplifier just equals e, the current must be zero and therefore the input impedance Z_n must be infinite. This is also observed from Eq. (3) and (4), because when $A = 1$, Z_n becomes infinite.

If A becomes greater than unity, the current reverses and flows into the source of voltage e and the circuit exhibits negative impedance characteristics. When A reaches a value so that the resultant current flowing into the voltage source e supplies all the losses in its path, oscillations will result.

An example of this kind of a negative impedance is illustrated in Fig. 3, where Z_s was chosen to be a pure resistance so that the input impedance of the amplifier is a pure negative resistance. The shaded region indicates the values of A for which the amplifier is unstable and in which case current is limited only by the power handling ability of the amplifier. It is seen from Fig. 3 that the negative resistance supplied by the amplifier in the stable region is greater in magnitude than the resistance R in parallel with which it is connected, and approaches an open circuit.

It should be observed at this point that a combination of a positive resistance in parallel with a larger negative resistance results in a positive resistance, although the series combination of the same two resistances will result in a negative resistance.

From interpretation of the performance of the circuit it was found that the arrangement of Fig. 3 is stable as long as the negative resistance supplied by the amplifier is greater than the positive resistance across which it is connected, i.e., in the region where the parallel combination of the two is positive. Because of this phenomenon, the type of the negative impedance supplied by the arrangements shown in Figs. 1 and 3 is called a shunt negative impedance.

Amplifier Gain in Series Circuits

The situation in the case of Fig. 2 will be found to be different. If the amplification is zero, then the input impedance of the amplifier consists of the sum $(R_s + Z_s + R_1)$. As A is increased from zero to unity, the voltage developed across the output terminals of the amplifier will be of such a direction that it will aid the applied voltage and the current will increase. When $A = 1$, the input voltage just equals the output voltage, and the voltage drop across the entire arrangement will be zero, which corresponds to zero input impedance. The current at this point will be limited entirely by the internal impedance of the source of voltage e.

If A is larger than 1, there will be a negative drop across the amplifier and its input impedance will be negative as defined by Eq. (6) and (7). If A is increased to the point where the current is so large that it supplies all the losses in its path, instability will be reached. As is shown in the special case illustrated in Fig. 4, the current for a constant voltage will continuously increase, from a value determined by $(R_s +$

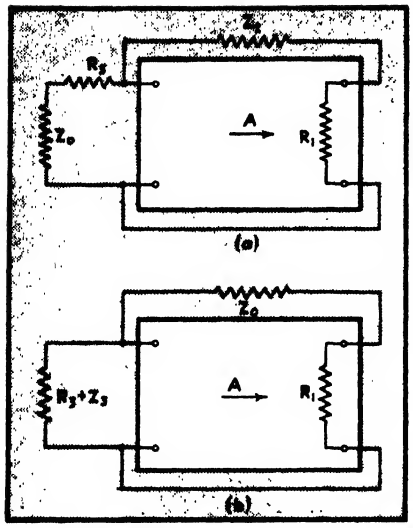

FIG. 5—Rearrangement of Fig. 1 and 2 shows that both shunt and series negative impedance are obtained from the same basic circuit. (a) corresponds to Fig. 1. (b) to Fig. 2

$R_1 + Z_2$) when $A = 0$ to infinity when all the losses are supplied by the amplifier.

As is clearly evident from these considerations and Fig. 4, the negative impedance will be stable and finite as long as its value is smaller in magnitude than the impedance in series with which it is connected. Thus, in the stable region of operation, the series combination of positive and negative impedance is positive, and for this reason, this type of a negative impedance is called a series negative impedance.

Negative-Impedance Limits

From this discussion it is evident that across a given positive resistance any value of negative resistance may be placed, from zero to infinity, and providing the negative resistance is of the right kind (shunt or series), a stable result will be obtained. It is plain that the ordinary concept of resistance is incomplete; a prediction regarding the behavior of the combination of positive and negative impedances cannot be made without complete information regarding the method used to supply the negative element. A more complete, but not any more rigorous, discussion will be found in the literature.[3, 4, 6]

In Fig. 1 and 2 resistances R_1 and R_2 are not essential parts of the negative impedances and Eq. (3) and (6) show that negative impedances will result whether these two resistances are present or not. However, due to the finite magnitude of the output impedance of the amplifier the negative impedance obtained by means of the amplifier alone will contain a term which is due to the output impedance of the amplifier. By placing proper positive resistances in series with the negative impedance the resistive component of this term will be cancelled and a pure negative impedance can be obtained. In the case of an ideal amplifier this cancellation can always be done; in the discussion which follows, it will be invariably assumed to have been done. Errors due to this assumption in the case of an actual amplifier will be discussed and analysed in Part II.

Stability

Before launching into the discussion itself, the particular sense in which the terms are used will be defined.

Conventional technical terminology is often confusing, the word stability having more than one meaning. In this paper there are discussed two kinds of stability and, although somewhat related, their meanings are different.

Operation of an amplifier is generally termed stable if introduction of an infinitesimal voltage anywhere in the amplifier will result in a transient which will decrease with time. If, on the other hand, the introduction of such voltage will produce currents which will increase indefinitely with time (or until limited by saturation of some element), operation of the amplifier is said to be unstable but in this paper such a result will be termed oscillation.

The second type of stability will be defined by the word stability itself, and will refer to the amount that the negative impedance can change due to a small variation in amplification of the amplifier, as for example by power supply voltage variation.

Conditions for Oscillation

Because positive feedback around an amplifier is used to produce negative impedance, it is to be expected that oscillation will occur for some conditions; in fact the previous qualitative examination of the effect of amplifier gain indicated, that for large amplification, oscillation does take place; therefore a more rigorous analysis of the conditions for oscillation will be made.

Figures 5(a) and 5(b) are rearranged forms of schematic circuits shown in Fig. 1 and 2 in which Z_0 is the internal impedance of the source e. From these it is seen that the actual circuits which develop negative impedances are identical in character, the difference being merely in the two points across which the desired negative impedance is developed.

On the basis of the criterion given by Nyquist' the possibility of oscillation may be determined by considering the circuits as positive-feedback circuits in which the impedance Z_0 is the impedance which is actually used across the terminals of the negative impedance. In general, it is impossible to predict whether oscillation will or will not occur except by applying Nyquist's criterion. In simple cases, however, it is possible to examine the circuits in the following manner.

The oscillations cannot occur unless there is a value of the positive feedback factor αA equal to or greater than unity, where A is the amplification parameter of the amplifier and α is the fraction of the output voltage of the amplifier that appears across its input. In the case of shunt negative impedance, α is defined as follows

$$\alpha = \frac{R_2 + Z_0}{Z_0 + R_2 + Z_2} \tag{8}$$

And in the case of series negative impedance

$$\alpha = \frac{R_2 + Z_2}{Z_0 + R_2 + Z_2} \tag{9}$$

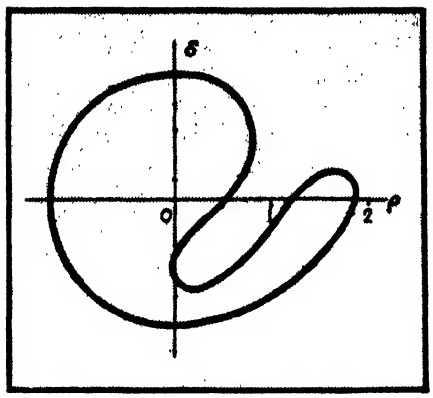

FIG. 6—Oscillations can not occur unless point (1, 0) of the Nyquist diagram is enclosed by the feedback-factor curve

The positive-feedback factor αA is a complex number and is a function of frequency in a way which is determined by the type of amplifier used and the character of the feedback network. It can be divided into a real and an imaginary part $\alpha A = \rho + j\delta$.

A not sufficient but a necessary condition for oscillation is that $\delta = 0$. There may be several frequencies at which this condition is satisfied, say, at $f_1, f_2, f_3, \ldots f_n$. If the real part of αA at any one of these frequencies exceeds unity, then oscillations will exist. Hence, the condition for oscillation may be stated as

$$\rho(f_1, f_2, f_3 \ldots f_n) \gtrless 1 \qquad \delta = 0$$

The one possible but unusual and seldom met exception to this rule may occur as is shown in Fig. 6 where, according to Nyquist's criterion, oscillations cannot occur. On the other hand, if the smallest value of $\rho(f_1, f_2, f_3 \ldots f_n)$ is greater than unity, then re-entrant curves around the point ($\rho = 1, \delta = 0$) are impossible and oscillations will necessarily exist. This is by far the most usual case.

If, for instance, the source impedance Z_0 is zero in the case of the series negative impedance, then according to Eq (9) $\alpha = 1$ and $\alpha A = 1$. In the ideal amplifier (or in a practical one at the point where the phase shift is zero) A is a real constant so that $\delta = 0$. If A is greater than unity, then oscillations must occur. In the case of a shunt negative impedance, if the source impedance Z_0 is made infinite, then $\alpha A = 1$ and oscillations must occur. This is seen to be in agreement with the physical interpretation of the negative impedance previously described.

Stabilization of Negative Impedances

Behavior of the negative impedance obtained in the manner illustrated in Fig. 1 and 2 depends only upon two factors, namely, the amplifier and the positive impedance. The positive impedances Z_a and Z_b are ordinary impedances constructed from resistors, inductors, and capacitors. The resultant negative impedance will obviously possess all the characteristics of these elements such as impedance change with temperature or with the amount of current or voltage applied to them. But in addition to these, the negative impedance is also dependent upon the gain of the amplifier used to supply that negative impedance.

In ordinary amplifiers the amplification often changes because of voltage fluctuations of the power supplies. Slow changes in tube characteristics and aging of the components of the amplifier also produce slow variations in the gain of the amplifier, and these, of course, will change the magnitude of the negative impedances. However, all of these factors may be greatly reduced by sufficient negative feedback within the amplifier itself. As will be shown later, the characteristics of the negative impedance can be easily made dependent, not upon the properties of the amplifier that supplies it, but upon the variations of the positive impedances Z_a and Z_b in the way mentioned previously.

The stabilization of the amplifier that supplies the negative impedances is well known and does not need to be fully described here.[1, 8, 9, 10] Important properties of stabilized amplifiers of particular interest in connection with the negative impedances will be taken up in Part II. Simplified diagrams of possible ways in which feedback can be applied to amplifiers supplying negative impedances are shown in Fig. 7(a) and 7(b).

Effect of Negative Feedback

The amplifier shown in both cases is a two-stage amplifier with all sources of power and filter network omitted for the sake of simplicity. A two-stage amplifier is necessary because the output and the input must be of the same relative polarity. A fraction β where $\beta = R_6/(R_6 + R_7)$ of the output voltage of the amplifier is returned to its input in such a manner that negative feedback is developed in the amplifier and its gain is stabilized by the factor $A\beta$, where A is the amplification of the amplifier with all feedback networks omitted. Except for the introduction of negative feedback, these circuits will be found to be the same as the schematic representations shown in Fig. 1 and 2.

The negative impedance developed by the amplifiers shown in Fig. 7 may be found in the same manner as in Eq. (4) and (7) if

A = amplification of the amplifier without negative feedback
β = fraction of the output voltage returned to the input of the amplifier as negative feedback
G = gain with negative feedback

$$G = A/(1 - A\beta) \tag{10}$$

and R_3 and R_4 so adjusted that

$$R_3 = R_1/(G - 1) \tag{11}$$
$$R_4 = R_1/(G - 1) \tag{12}$$

then, the shunt negative impedance will be given by

$$Z_n = Z_2/(1 - G) \tag{13}$$

and the series negative impedance by

$$Z_n = Z_3(1 - G) \tag{14}$$

In the material that is to follow, it will be assumed that R_3 and R_4 are so adjusted that Eq. (11) and (12) hold and Eq. (13) and (14) will be used with this implication in mind. For the sake of simplicity, all diagrams shown from this point on will not show resistances R_5 and R_6, although their presence is im-

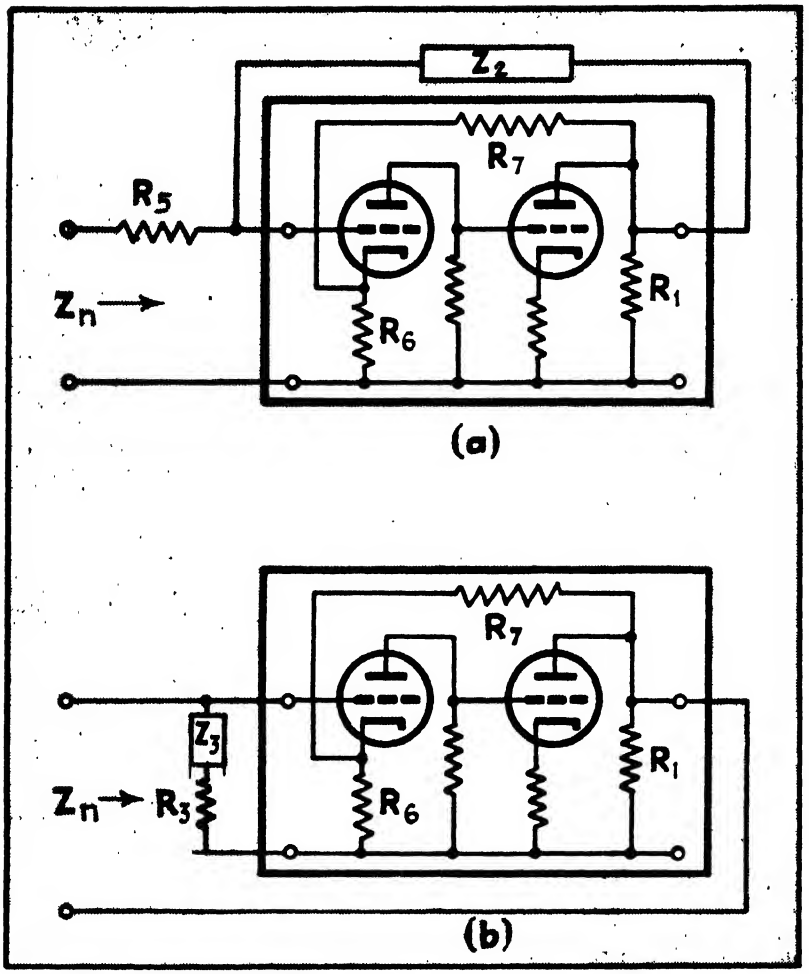

FIG. 7—Feedback to stabilize amplifiers used to produce negative impedance is produced by R_6 and R_7 at (a) for shunt and at (b) for series negative impedance

plied in all cases where a pure negative impedance is desired.

Stability of Negative Impedances

At first sight it may be thought that simultaneous application of positive and negative feedback in the same amplifier will simply produce cancellation, and if equal feedback factors are used the result would be the same as if no feedback were used at all. However, this is not so, as will become apparent as the discussion progresses.

As was seen in the above derivations and discussions, circuits shown in Fig. 1 and 2 produce negative impedances. By application of negative feedback internally to the amplifier its gain may be stabilized in the conventional manner. The extent to which the negative feedback stabilizes the negative impedances will now be determined quantitatively.

Stability of a negative impedance may be defined as the fractional change in negative impedance produced by a small change in gain of the amplifier which supplies that negative impedance. Stated algebraically $\partial Z_n/Z_n = k\partial A/A$ where A is the gain of the amplifier, ∂A is a small change in the gain, ∂Z_n is the change in the negative impedance, and k is a coefficient of stability, obviously dependent upon the amount of negative feedback utilized in the amplifier.

The coefficient of stability k describes to what extent negative impedance is affected by small changes in the propagation parameter of the amplifier. The ideal case would be obtained if k were zero, i.e., when a small change in the propagation parameter of the amplifier would produce no change in negative impedance.

As will be seen presently, stability of the shunt and series negative impendance is different, and the analyses will be divided into separate parts.

Stability of Shunt Negative Impedance

The shunt negative impedance is dependent upon the gain of the amplifier in the way expressed by Eq. (13). Substituting the value of G given by Eq. (10) in Eq. (13) one obtains for negative impedance the expression

$$Z_n = Z_2 \frac{1 - A\beta}{1 - A\beta - A} \tag{15}$$

The stability coefficient may be obtained from this expression by differentiating with respect to A giving change in Z_n to change in A

$$\frac{\partial Z_n}{\partial A} = Z_2 \frac{\beta(A\beta + A - 1) + (1 - A\beta)(\beta + 1)}{(1 - A\beta - A)^2} = Z_2 \frac{1}{(1 - A\beta - A)^2} \tag{16}$$

and therefore

$$\frac{\partial Z_n}{Z_n} = \frac{\partial A}{(1 - A\beta - A)(1 - A\beta)} \tag{17}$$

From which, the stability coefficient may be recognized as

$$k = \frac{A}{(1 - A\beta - A)(1 - A\beta)} \tag{18}$$

This important relation states that shunt negative impedance is stabilized by a factor which does not contain Z_2 and hence, the stability of shunt negative impedance is independent of its magnitude.

Investigation of the properties of the stability coefficient shows that there is an optimum value of β for any given value of A. The best value of β may be obtained by maximizing Eq. (18) with respect to β, as follows

$$\frac{\partial k}{\partial \beta} = \frac{A[(1 - A\beta - A)A + (1 - A\beta)A]}{(1 - A\beta - A)^2 (1 - A\beta)^2} = 0 \quad (19)$$

Solving this for β

$$\beta_{opt} = \tfrac{1}{2}\left(\frac{2}{A} - 1\right) \quad (20)$$

from which the optimum value of β for any given value of A may be obtained. The stability coefficient at β_{opt} is

$$k_{opt} = -4/A \quad (21)$$

Another critical point occurs when the denominator of Eq. (18) becomes zero, i.e., when $(1 - A\beta - A) = 0$. This is the case when

$$\beta = (1 - A)/A \quad (22)$$

At this value of β the stability coefficient is infinite and a small change in gain would produce an infinite change in the negative impedance. However, at this value of β the gain of the amplifier is unity and the negative impedance is infinite and obviously this critical point is of no importance.

Stability Calculations

Figures 8 and 9 show Eq. (18) in graphical form as a function of A and β. From Fig. 8 it is seen that the larger the propagation constant of the amplifier, the better the stability of the shunt negative impedance. If A is very large, then $\beta = -0.5$ gives the best k, but there is little improvement beyond $\beta > 0.1$ and in all practical cases this is the most satisfactory value due to the difficulty of obtaining a high value of A and a higher value of β than 0.1 due to the shunting effects of the β network.

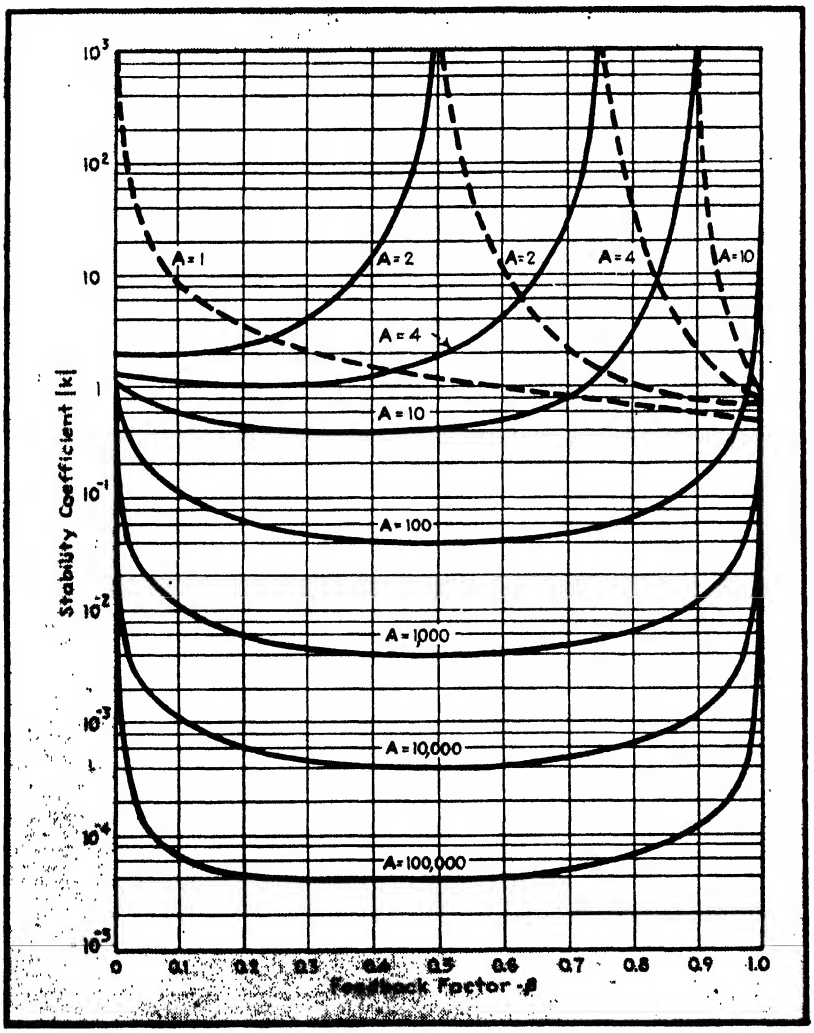

FIG. 8—Stability coefficient as a function of amplification and negative feedback shows regions in which best stability of negative impedance can be obtained

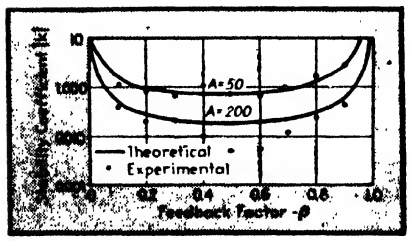

FIG. 9—Experimental determination of stability verifies the theoretical predictions

With present day tubes it is easy to obtain an amplification of 10,000. If enough negative feedback in the amplifier is used to make $\beta = -0.1$, then, according to Eq. (18) or Fig. 8, the stability coefficient is nearly 10^{-3}.

A test of a simple amplifier has shown that a 20 percent change in the supply voltage of a typical amplifier produced an 8 percent change in amplification. Hence, the change in the negative impedance supplied by this amplifier would be in the neighborhood of eight parts in 100,000. This stability is better than that encountered with ordinary circuit elements in cases where no temperature compensation is provided.

Effects of small changes in amplification of the amplifier which supplies the series negative impedance may be obtained in a similar manner. Series negative impedance is dependent upon the gain of the amplifier as given by Eq. (12) and (14). Combining this with the Eq. (10) which takes into account the negative feedback in the amplifier

$$Z_n = Z_3'\left(\frac{1 - A\beta - A}{1 - A\beta}\right) + R_1 \quad (23)$$

where $Z_3' = Z_3 + R_3$

From this, the stability coefficient may be obtained by differentiation

$$\frac{\partial Z_n}{Z_n} = \frac{-\partial A}{(1 - A\beta)\{(1 - A\beta[(R_1/Z_3') + 1] - A\}} \quad (24)$$

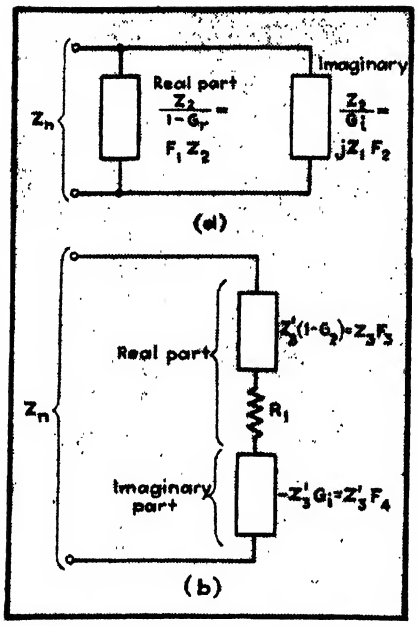

FIG. 10—Effect of phase shift in the amplifier is to produce a change in magnitude of the real component of the negative impedance, and to introduce an imaginary component (a) in parallel with shunt negative impedance, or (b) in series with series negative impedance

The stability coefficient is

$$k = \frac{-A}{(1-A\beta)\{(1-A\beta)[(R_1/Z_3')+1]-A\}} \quad (25)$$

This relation is different from the corresponding one for the shunt negative impedance because it involves the terms Z_3', which means that the stability of a series negative impedance depends upon the magnitude of the negative impedance developed by the amplifier. A physical interpretation of this dependence may be seen by examining two boundary cases.

If the output impedance of the amplifier $R_1 << Z_3'$, then the stability coefficient becomes very much the same as the one in the shunt negative impedance. If $Z_3' = R_1 = R_1/(G-1)$, the second bracket in the denominator of Eq. (25) reduces to zero. In this case, the stability coefficient becomes infinite. This latter case is of not much practical importance, for it corresponds to zero series negative impedance offered by the amplifier. In a practical amplifier, the output impedance of the amplifier can be made small, and for any given value of the negative impedance, the stability coefficient may be made as small as is desired by increasing A sufficiently. Rewriting Eq. (25) shows this more clearly

$$k = \frac{-1}{(1-A\beta)[1-(1-A\beta)/A][(R_3/Z_3')-1]} \quad (26)$$

If A is made very large, then

$$k \approx \frac{1}{A\beta[1+\beta][(R_3/Z_3')-1]} \quad (27)$$

and the stability can be made as good as desired by making A large enough.

For any given value of R_1/R_1' and A there is a best value of β. This critical value may be obtained by maximizing k as given by Eq. (25) with respect to β. This leads to the result.

$$\beta_{opt} = -\tfrac{1}{2}(1 - 4R_3/AZ_3') \quad (28)$$

This again differs from the best value of β in the shunt negative impedance as given by Eq. (22) because Eq. (28) involves the factor R_3/Z_3', i.e., it depends upon the value of the negative impedance developed by the amplifier. The stability coefficient for the series negative impedance at the best value of β is obtained by combining Eq. (28) with Eq. (25) or (26). This gives

$$k_{opt} = -\frac{4}{A}\frac{1}{[(2R_3/Z_3')^2 - 1][(R_3/Z_3')-1]} \quad (29)$$

which differs from the optimum value of the stability coefficient in the case of shunt negative impedance in the same general manner discussed above in connection with Eqs. (25) to (28).

Most Stable Condition

It is interesting to notice that if $R_3/Z_3' << 1$, then the optimum value of β in the case of the series negative impendance is $-\frac{1}{2}$. This is also true (exactly so, however) in the case of the shunt negative impendance. Remembering the fact that the gain of the negative-feedback amplifier approximates $-1/\beta$ it is seen that if the optimum value of feedback is used for best stability, the gain of the amplifier supplying negative impedance is just equal to 2. Hence, from Eq. (13) and (14) it is seen that the negative impedances developed by the amplifier in the two possible manners are

shunt type $Z_n = -Z_2$
series type $Z_n = -Z_3$

In other words, if the most stable operation of the negative impedance is desired, the value of the negative impedances obtained are merely the negative values of the positive impedances Z_2 and Z_3.

Amplifier Phase Shift

The simplest type of amplifier suitable for producing negative impedances is a two-stage, direct-coupled amplifier the power for which is supplied by an essentially zero-impedance source. Even in this simple case there are shunting capacitances in the tubes and wiring so that although at low frequencies the amplification is real, at higher frequencies, there is phase shift and obviously the character of the negative impedances that can be obtained by means of such an amplifier will not be the simple negative of the positive impedance which is used in conjunction with that amplifier.

If one considers a high gain amplifier with pentode tubes which utilize filter networks in the screen grid and cathode circuits and rectifier-type power supplies, the phase shift may take a complicated form and the resultant negative impedance will differ greatly from the simple form which would be expected if the phase shift were neglected.

In general, a properly designed amplifier will have a region where the amplification parameter is nearly constant and where the simple equations developed in the Part I hold. Outside of this region phase shift will occur, and the gain of the amplifier will contain an imaginary component. If G is the actual gain of the amplifier, G_0 is the absolute value of the amplifier

gain in the region where the phase-shift is zero or negligible, and θ is the phase shift in degrees referred to the zero phase-shift region, then the gain may be expressed as $G = G_o(\cos\theta + j\sin\theta)$. This can be written as

$$G = G_r + jR_i \quad (30)$$
where $G_r = G_o\cos\theta$
$G_i = G_o\sin\theta$

Both G_o and θ must be known for all frequencies before the nature of the negative impedance can be completely specified.

Substituting the vector relation for amplifier gain given by Eq. (30) in Eq. (13) (Part I), one obtains for negative impedance the equation

$$Z_n = \frac{Z_2}{1 - (G_r + jG_i)} \quad (31)$$

Which can be rewritten in the form

$$\frac{1}{Z_n} = \frac{1}{Z_2/(1 - G_r)} + \frac{1}{jZ_2/G_i} \quad (32)$$

Equation (32) is a familiar expression for two impedances in parallel, and the corresponding circuit is shown in Fig. 10(a). The real part is recognized as the shunt negative impedance proper, and the imaginary part represents an imaginary term which disappears when the imaginary part of the amplifier gain is zero. For the sake of convenience, the functions which determine the real and imaginary parts of the shunt negative impedance will be defined as follows

$$Z_n = \frac{1}{(1/Z_2F_1) + (1/jZ_2F_2)} \quad (33)$$

where $F_1 = \frac{1}{1 - G_r}$

$$F_2 = \frac{1}{G_i}$$

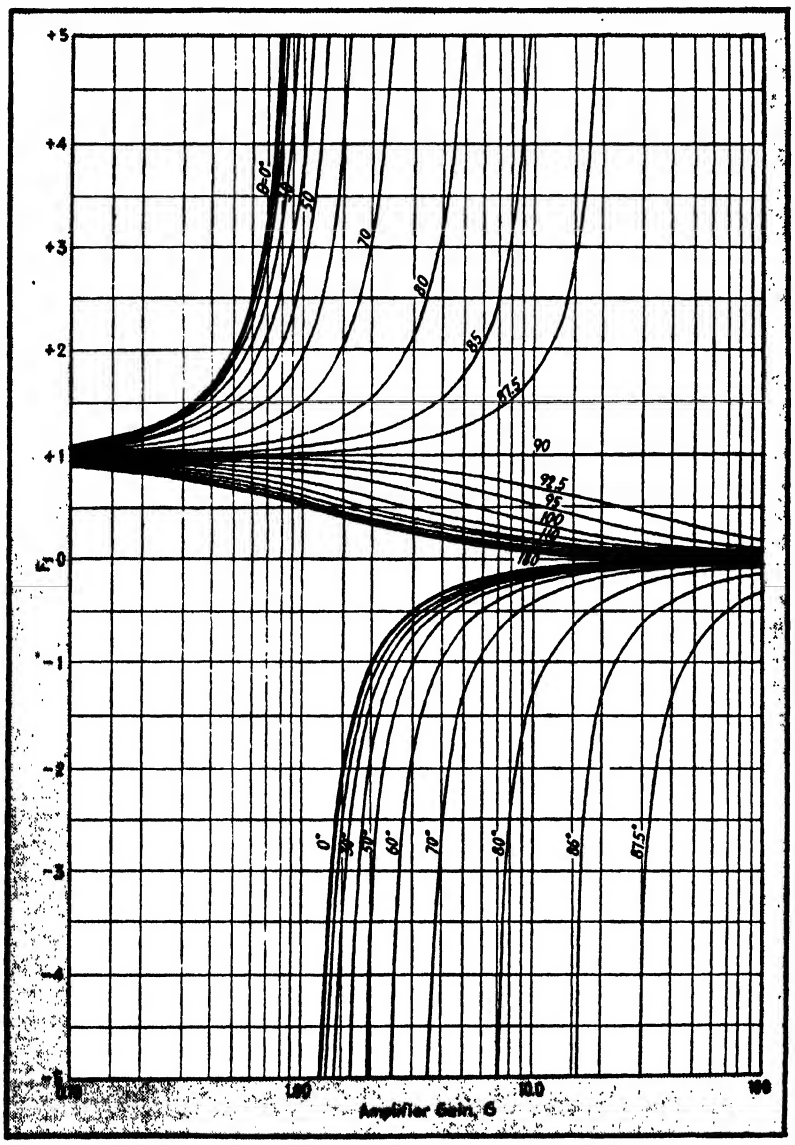

FIG. 11—Variation of F_1 with amplification for use in predicting effect of phase shift on negative impedance

Phase Shift Effect on Series Negative Impedance

The effect of phase shift upon the character of the series negative impedance can be obtained by substituting Eq. (30) in Eq. (14) and letting $Z_3' = Z_3 + R_3$ as was done in Eq. (23).

$$Z_n = Z_3'(1 - G_r) + R_1 - jZ_3'G_i \quad (34)$$

where R_1, the output impedance of the amplifier as before, must now be considered a function of frequency. This equation can be rewritten as

$$Z_n = Z_3'F_3 + R_1 + jZ_3'F_4 \quad (35)$$

where $F_3 = 1 - G_r$
$F_4 = -G_i$

The series circuit expressed by Eq. (35) is shown in Fig. 10(b). When $G_i = 0$, the complex form of the series negative impedance reduces to the simple conception of the negative impedance discussed earlier. The resistance R_3 must be so adjusted that in the region where $G_i = 0$ the negative resistance due to R_1 just cancels the output impedance of the amplifier. This cancellation obviously cannot hold outside this region because both the magnitude of the series negative resistance due to R_3, and the output impedance of the amplifier are changing and in general these changes will not counteract one another. The variation of output impedance of the amplifier with frequency due to phase shift and negative feedback is discussed later.

If the phase shift and the abso-

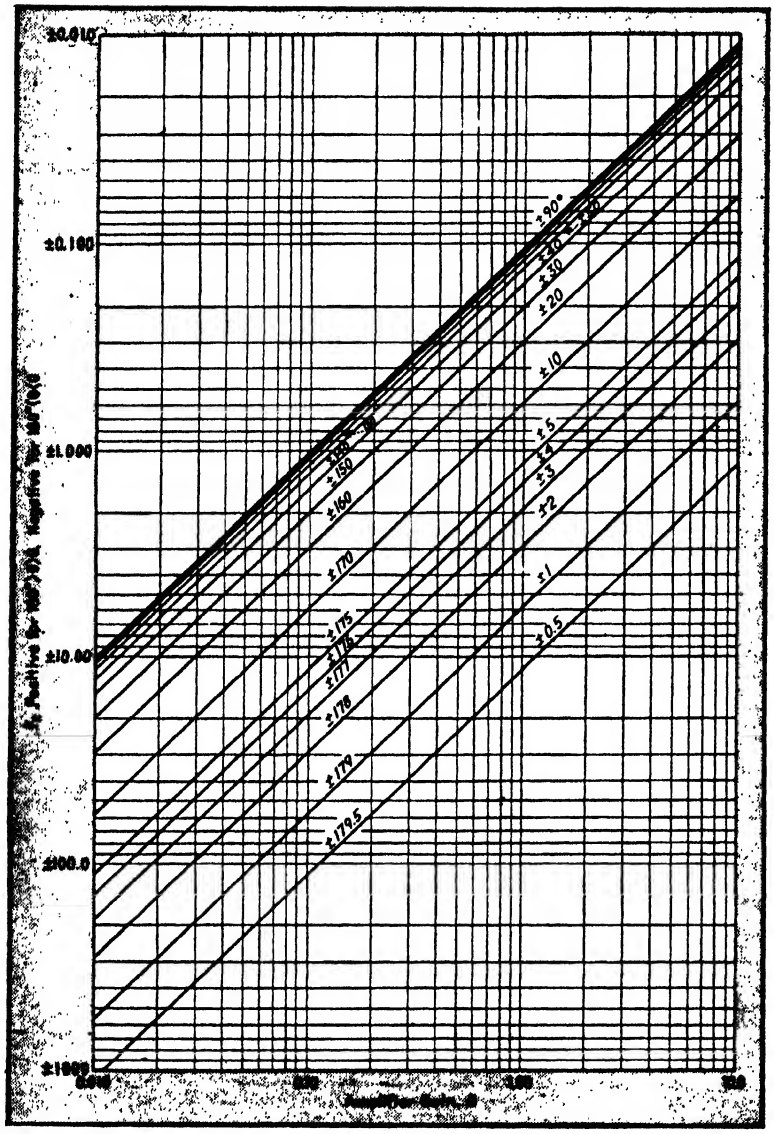

FIG. 12—Variation of F_2 with amplifier gain. Figures 11 and 12 are for shunt negative impedance

lute magnitude of the gain G of an amplifier are known, then functions F_1, F_2, F_3, and F_4 can be computed and the nature of the negative impedance outside the domain of constant G can be determined. This means that the exact nature of the amplifier and the types of coupling must be known, as well as the amount of negative feedback used within the amplifier.

To facilitate computation of the above functions, Fig. 11, 12, 13 and 14 give the functions in terms of the amount of phase shift and gain G.. These are merely graphical forms of the Eq. (33) and (35) from which the effect of phase shift and the gain for any amplifier on the character of either the shunt or series negative impedance may be obtained.

As an example, Fig. 15 shows a two-stage amplifier with resistance-capacitance coupling and utilizing a moderate amount of negative feedback. The phase shift and the absolute magnitude of the gain for this amplifier are also shown. From these curves and Fig. 11 and 12, F_1 and F_2 were obtained as functions of frequency, and are shown in Fig. 16.

Fig. 16 shows that the function F_1, which determines the character of the real part of the shunt negative impedance, changes sign abruptly at both low and high frequencies and thus changes the negative impedance into a positive one. In the mid-frequency region, F_1 remains remarkably constant, which means that the negative impedance also is very nearly constant. On the other hand, the imaginary component of the negative impedance introduces an appreciable effect long before the real part changes sign. Once Fig. 16 has been obtained for an amplifier the exact nature of the negative impedance that will be developed by means of that amplifier can be obtained by Eq. (33) or (35).

Illustration of Effect of Phase Shift

An example of a shunt negative resistance, obtained by means of the amplifier shown in Fig. 15 whose characteristics are described by Fig. 15 and 16, is shown in Fig. 17. These curves were obtained by the method outlined above and checked experimentally by measuring the input impedance of the amplifier as a function of frequency by means of a Wheatstone bridge.

These curves show that the real part of the negative resistance, in the region between 600 and 30,000 cps, is negative. Between approximately 1,000 and 15,000 cycles its value could have been obtained directly by Eq. (13), neglecting phase shift in the amplifier. At frequencies lower than 60 and higher than 30,000 cps the negative resistance changes sign and actually becomes positive. At the extreme frequencies, i.e., at zero and infinity, the amplification of the amplifier is zero, and the input impedance of the amplifier is simply R_s in series with the output impedance of the amplifier.

These curves also show that even at mid-frequencies the input impedance of the amplifier contains a reactive component. In accordance with the sign of function F_2 shown in Fig. 16 the reactance is capacitive at the high frequencies

and inductive at the low frequencies. As will be observed from Fig. 16 and 17, the reactive component of the negative resistance is minimum at approximately the same points where the real component becomes infinite.

Limitations Imposed by Phase Shift

In the region between 400 and 5,000 cps the reactive component is ten or more times the real component, therefore the former may be neglected in this region. In the case of negative resistance, the useful range of the negative resistance on the frequency scale must be inside these types of limits, and what happens outside may or may not be of importance. However, if it were a negative reactance that were obtained by means of this amplifier, it is obvious that the imaginary component will contribute a resistance component to the desired negative reactance. In this case it is imperative to know the behavior of the imaginary component for all values of frequency and not merely be satisfied with the knowledge that the resistive component is negligible in the useful range.

The reason for this is that either at the low or high frequencies, depending upon what kind of reactance is being developed by the amplifier, the imaginary component will produce a negative resistance which may cause oscillations in the amplifier. It is plain, therefore, that in no case may the quadrature component of a negative reactance be disregarded, but, on the contrary, its behavior as a function of frequency must be studied carefully, especially in the neighborhood of the point where the real part of the negative reactance becomes infinite in the case of the shunt negative reactance or zero in the case of the series negative reactance.

Advantages of Direct-Coupled Amplifier

A two-stage resistance-capacitance amplifier shown in Fig. 15 has 180-degree phase shift at the low-frequency end, which, according to Fig. 16, means that a nega-

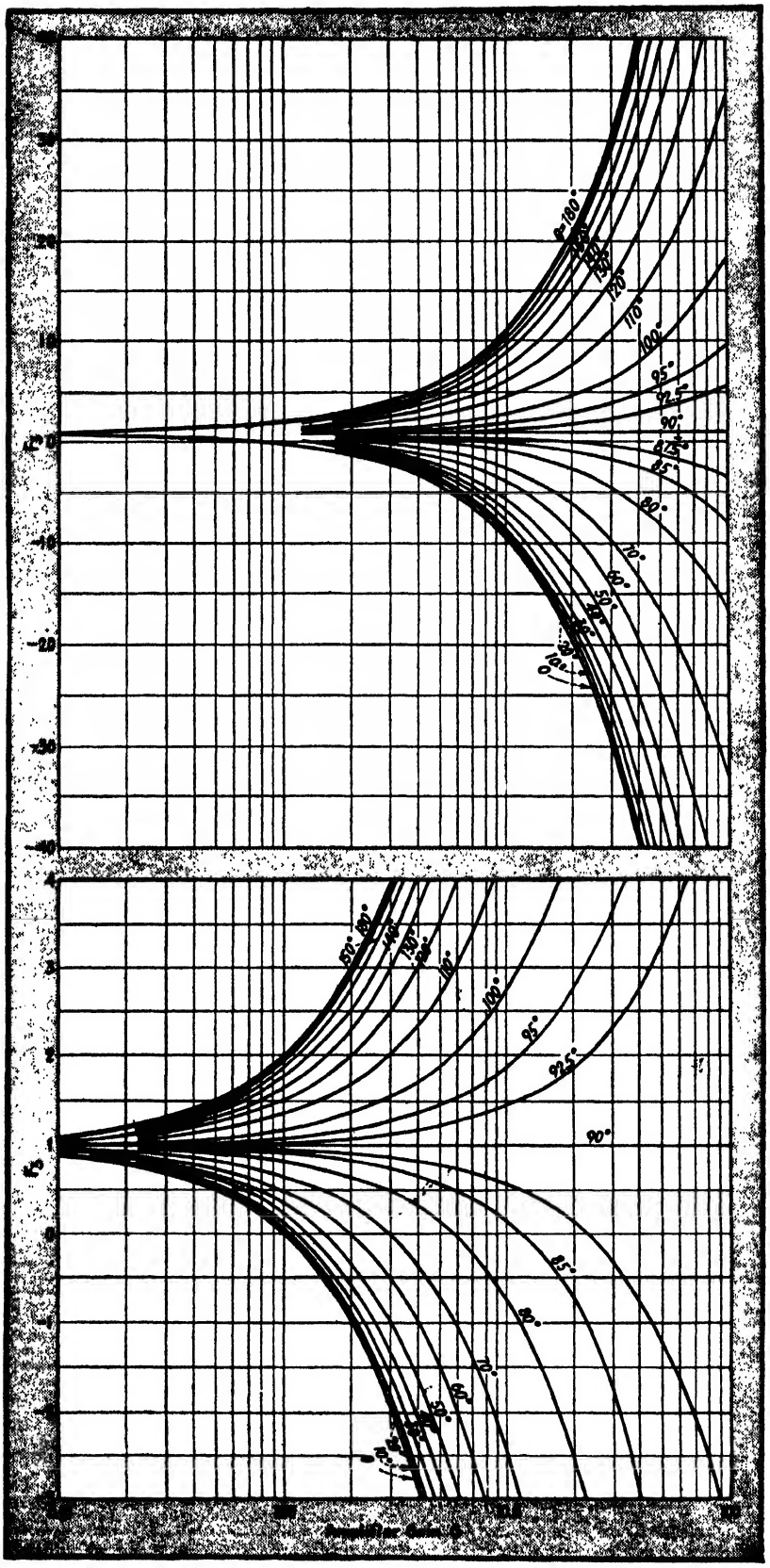

FIG. 13—Variation of F_s with magnitude and phase of amplification, below is a detail of the middle portion

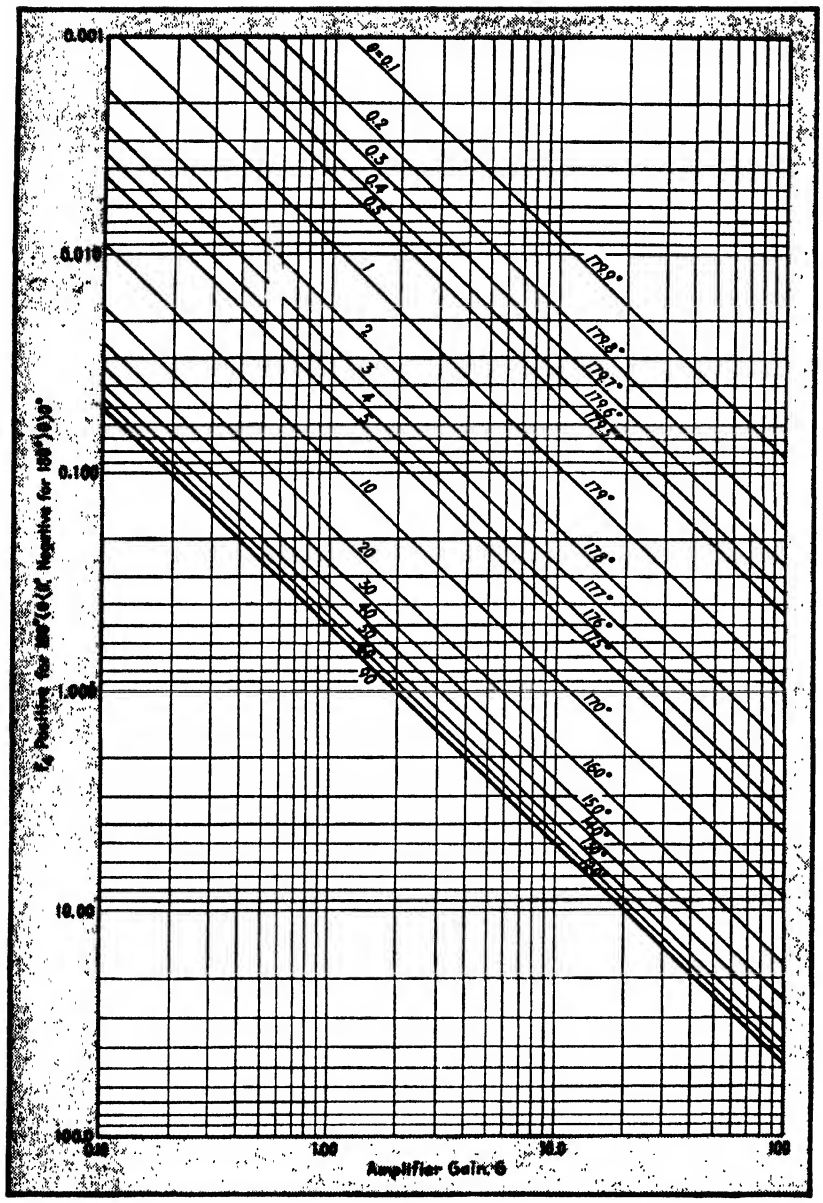

FIG. 14—Variation of F_4 with amplification. Figures 13 and 14 apply to series negative impedance

tive resistance will be developed by a shunt negative inductance circuit of magnitude L_2F_3, where L is the inductive reactance. The complete results are too complicated to present in a general form. In a special case of a two-stage amplifier with resistance-capacitance coupling, Table I summarizes what is to be expected.

Table I shows that the resistive component developed by a negative reactance in the case of an amplifier capable of 180-degree phase shift at either end of the frequency range is always negative at one end or the other. Therefore, extreme caution must be used in combining negative reactance with other elements.

By means of a direct-coupled amplifier it is possible to obtain negative reactances which do not have a negative resistance component. Referring to Table I, it is seen that a shunt negative inductance has a negative resistance component at the low frequencies. If a direct-coupled amplifier is used, the negative inductance will not have a resistive component at the low-frequency end; only a positive resistive component at high frequencies will be present. Similarly, a negative capacitance may be obtained which does not have a negative resistive component if a direct-coupled amplifier is used to produce series negative capacitance.

Negative resistance, according to its definition, must be able to supply power to the circuit to which it is connected. This involves a source of power in the network and because all actual devices have a finite source of power, the range of the negative characteristic must be necessarily limited. The magnitude of negative reactance exhibited by the device is also limited by the same factors as the negative resistance because negative reactances must supply power to the circuit on one half of the cycle and absorb power on the other half cycle.

Energy Storage of Negative Reactances

If a sinusoidal voltage whose crest value is e forces a current of crest value i through an impedance Z, then the following relations may be written

$$P = e^2\,2Z \qquad (36)$$

$$P = i^2Z\,2 \qquad (37)$$

where P is average power dissipated during the cycle in the case of resistance, and average energy stored in inductance or capacitance during the cycle in the case of reactance.

Power Limit of Series Negative Impedance

In the case of series negative impedance it is easiest to think in terms of the current that the amplifier can handle. This current is determined by the properties of the amplifier in the following manner.

If E_o is the maximum output voltage of the amplifier, then the maximum input voltage that can be developed at the input of the amplifier is E_o/G, where G is the voltage

gain of the amplifier. Let I be the maximum current that it is desired to obtain from the negative resistance. It is obvious that impedance Z_s' must not exceed the value which will make the voltage developed across it equal to the maximum allowable voltage. Thus Z_s' must not be greater than

$$Z_s'_{max} = E_0/GI \qquad (38)$$

Substituting this value of Z_s' into Eq. (12) and (14), it is seen that the magnitude of the negative impedance is determined by the factory E_0/I

$$Z_{nmax} = R_1 + (E_0/GI)(1 - G) \qquad (39)$$

This equation states that the magnitude of the negative impedance a given amplifier is capable of developing depends upon the current that it is desired to draw from the amplifier.

From Eq. (37) it is plain that the power-handling capability is proportional to the magnitude of the impedance of the circuit and the square of the current through the circuit. Combining Eq. (37) and (39), the power-handling capacity of the series negative impedance is

$$P = \tfrac{1}{2}I^2R_1 + (E_0I/2G)(1 - G) \qquad (40)$$

For any given amplifier there is a value of current at which the maximum possible P (measured in volt-amperes) can be developed by the negative impedance. This critical current may be obtained by differentiating Eq. (40) with respect to I and equating the result to zero. This gives

$$(\partial P/\partial I) = IR_1 + (E_0/2G)(1 - G) = 0$$

$$I_{max} = \frac{E_0}{2R_1} \cdot \frac{G - 1}{G} \qquad (41)$$

TABLE I
Resistive Component of Negative Reactance

Frequency Region	Resistive Component	
Shunt Produced Negative Reactance		
	$Z_2 = j\omega L_2$	$Z_2 = 1/j\omega C_2$
low	−	+
high	+	−
Series Produced Negative Reactance		
	$Z_3 = j\omega L_3$	$Z_3 = 1/j\omega C_3$
low	+	−
high	−	+

From which the maximum volt-amperes that can be developed by a series negative impedance is

$$P_{max} = -\frac{E_0^2}{4R_1} \cdot \frac{1 - G}{G} \qquad (42)$$

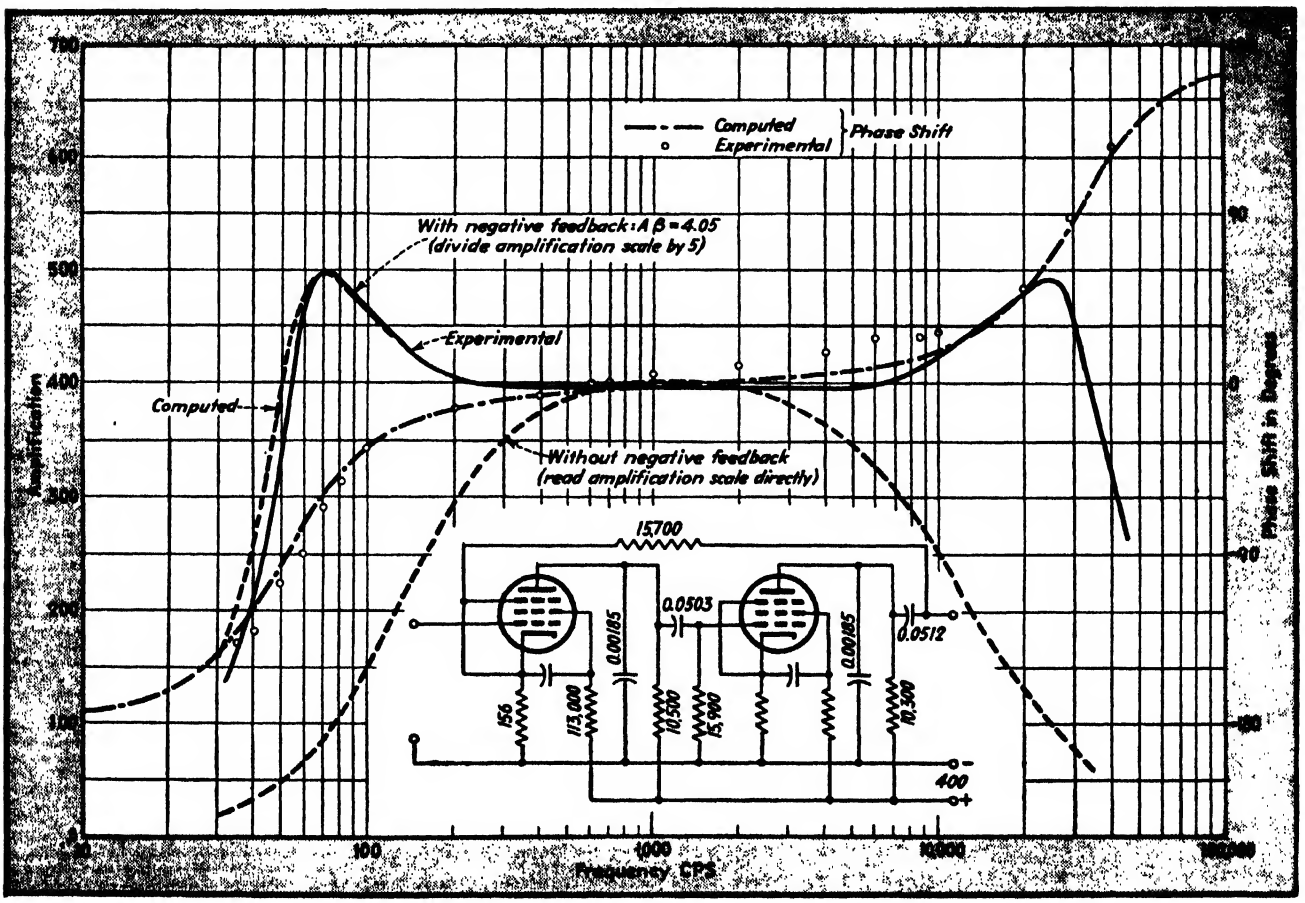

FIG. 15—Magnitude and phase shift of an amplifier from which shunt negative impedance is produced must be known as a function of frequency. The dot-dash curve is phase shift with negative feedback, other curves are gain

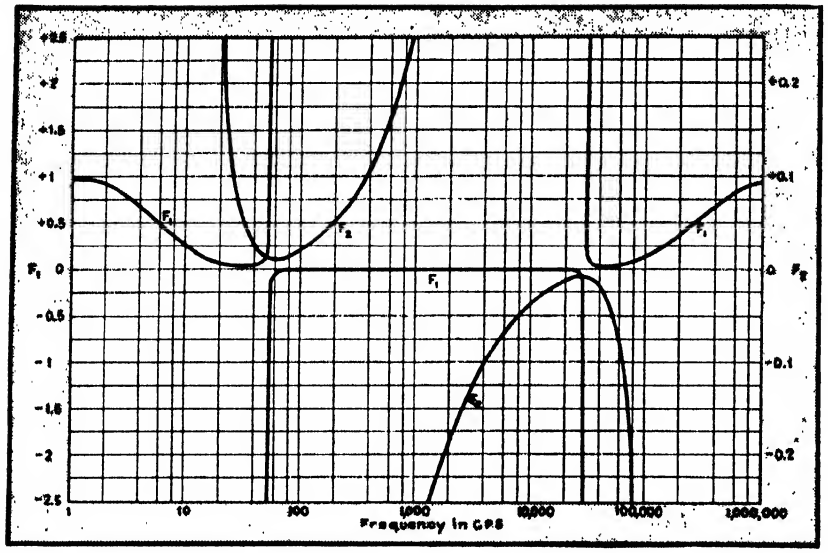

FIG. 16—Variation with frequency of gain functions of the amplifier of Fig. 15

If the maximum current I approaches the value for which Eq. (40) becomes zero, the power capability also approaches zero.

An example of a negative resistance that can be developed by an amplifier, together with its power capability is plotted in Fig. 18. It shows, for instance, that the actual amplifier cannot handle unlimited values of current; and that for any given amplifier and for any given maximum current, it is possible to obtain any magnitude of series negative resistance smaller in magnitude than the maximum given by Eq. (39).

Power Limit of Shunt Negative Impedances

It was assumed in the derivations of all equations that in this type of negative impedance the grid of the tube does not draw any grid current. Therefore, the peak value of the voltage that appears across the terminals of the negative impedance must not exceed the maximum allowable amplifier input voltage. This voltage is determined by two factors, namely, the direct current bias of the first tube, and secondly, the amount of negative feedback used in the amplifier. If e is the maximum voltage that can be applied to the input of the amplifier without producing distortion in the output of the amplifier in the absence of feedback, and $A\beta$ is the feedback factor, then the maximum voltage that can appear across the input terminals of the amplifier is

$$e_{max} = e\,(1 - A\,\beta) \qquad (43)$$

This equation determines the maximum allowable voltage, and the power capability of the negative impedances will then be given by Eq. (36).

The most convenient type of an amplifier suitable for supplying a negative impedance is a two-stage resistance-capacitance coupled amplifier, shown in Fig. 19. It is usually desirable to stabilize such an amplifier with negative feedback to improve its stability and frequency response. The effect of negative feedback on the frequency characteristic must be precisely known because the frequency characteristic determines the phase shift introduced by the amplifier and this, in turn, determines the type of impedance that results in the frequency region outside the desirable one.

In the following analysis, this notation will be used

S = Effective mutual conductance of the tube
G_m = mutual conductance of the tube
R_p = Plate resistance of the tube

$$R_{eq} = \frac{R_c}{1 + (R_c/R_{g1}) + (R_c/R_p)}$$

$R = R_{g1} + R_c/(1 + R_c/R_p)$
$X_c = 1/2\pi fC_c$ = the reactance of the coupling capacitor
$X_s = 1/2\pi fC_s$ = the reactance of the shunting capacitor from plate to ground of each stage, including stray, wiring and tube capacitances
A = voltage amplification of a stage without feedback
A_o = voltage amplification in the mid-frequency region
$L = X_c/R$ = frequency variable for low frequencies

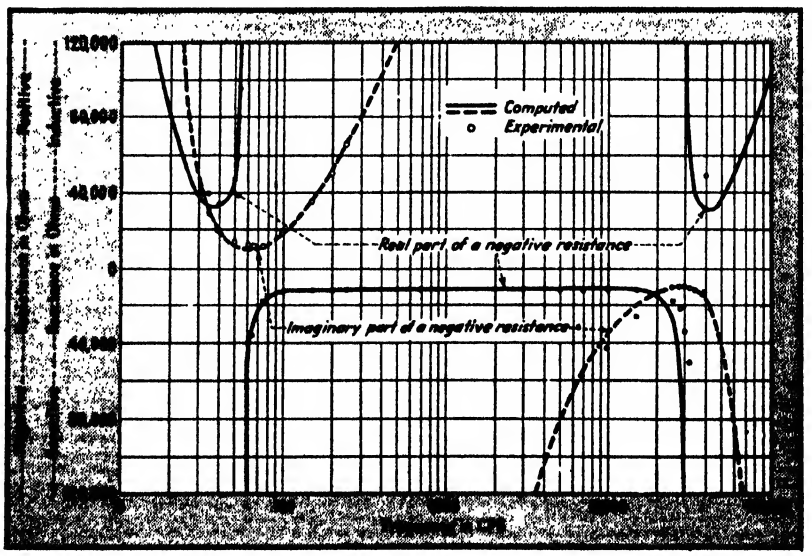

FIG. 17—Real and imaginary components of shunt negative resistance produced by the amplifier of Fig. 15

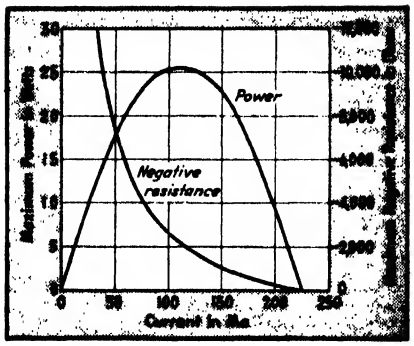

FIG. 18—For a given amplifier there is a limit to the power that can be developed by each value of negative resistance so produced

$H = R_{eq}/X_c$ = frequency variable for the high frequencies

The above notation will refer to the first stage, and if the symbols are primed, they will refer to the second stage. Thus, A is the amplification of the first stage and A' is the amplification of the second stage.

Effect of Bias Circuits

If the cathode resistors in Fig. 19 are unbypassed, then there will be a loss of gain in the stage due to current negative feedback. In the pentode amplifier, this does not modify the frequency characteristic appreciably, so that the only result will be a reduction of the mutual conductance of the tube. It can be easily shown that the effective mutual conductance of a tube is

$$S = \frac{G_m}{1 + G_m R_c} \tag{44}$$

It will be assumed in this derivation that either the cathode is not by-passed in which case Eq. (44) holds, or that it is adequately bypassed in which case $S = G_m$. The intermediate case is of no importance because it produces additional phase shift in the amplifier and should be avoided. The additional phase shift due to the improper bypassing of cathode resistor and also of the screen grid dropping resistor is discussed in the literature.[11]

The voltage gain of an amplifier in the mid-frequency region where zero phase shift occurs is given by Terman as[12]

$$A_o = SR_{eq} \tag{45}$$

The voltage amplification at the low frequency end of the frequency range is

$$A = \frac{A_o}{1 - jL} \tag{46}$$

and for the high frequency end.

$$A = \frac{A_o}{1 + jH} \tag{47}$$

These equations refer to the amplification of the first stage of the amplifier shown in Fig. 19. A similar set of equations may be written for the second stage, using the notation given above. It must be remembered that the amplification of the second stage must take into account the shunting effect of the resistances R_6 and R_7.

Calculation of Amplifier Response

The total voltage amplification of the amplifier will be

at low frequencies

$$AA' = \frac{A_o A_o'}{(1 - jL)(1 - jL')} \tag{48}$$

at high frequencies

$$AA' = \frac{A_o A_o'}{(1 - jH)(1 + jH')} \tag{49}$$

The voltage gain of the amplifier including negative feedback will be

$$G = \frac{AA'}{1 - \beta AA'} \tag{50}$$

Combining Eq. (48), (49), and (50), the following results, at low frequencies

at low frequencies

$$G = \frac{-A_o A_o'}{\beta A_o A_o' - (1 - jL)(1 - jL')} \tag{51}$$

at high frequencies

$$G = \frac{-A_o A_o'}{\beta A_o A_o' - (1 + jH)(1 + jH')} \tag{52}$$

Also, assume that the second stage is a times better than the first, at the low frequencies, and b times better at the high frequencies. Or symbolically,

$$a = L'/L$$
$$b = H'/H$$

Interpretation of Response Equations

Hence, Eq. (51) and (52) can be written

at low frequencies

$$G = \frac{-A_o A_o'}{\beta A_o A_o' - (1 - jL)(1 - jaL)} \tag{53}$$

at high frequencies

$$G = \frac{-A_o A_o'}{\beta A_o A_o' - (1 + jH)(1 + jbH)} \tag{54}$$

These are vector expressions for the gain in terms of the frequency variables L and H. The absolute value of the amplification and phase shift will be found in Table II. If the absolute value of the amplification is differentiated with respect to the frequency variable, it will be found that the frequency response curve of the amplifier has peaks at the low and the high end. Table II summarizes all the pertinent information regarding the response characteristics of the negative-feedback amplifier of the type

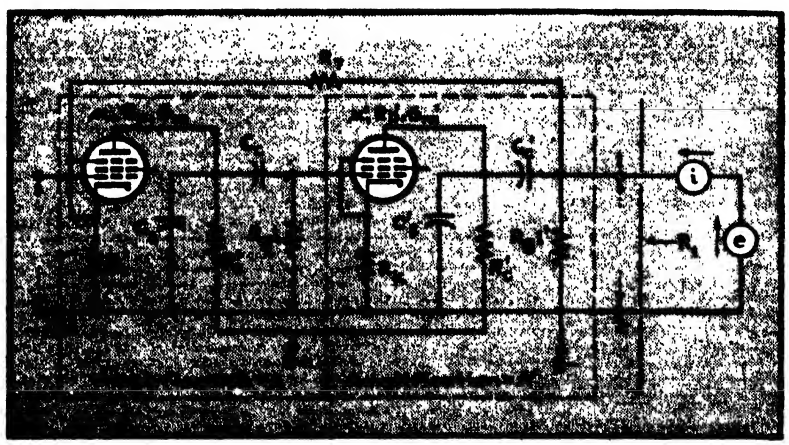

FIG. 19—Typical negative-feedback amplifier the frequency response of which must be known in order to predict the negative impedance that it will produce as a function of frequency

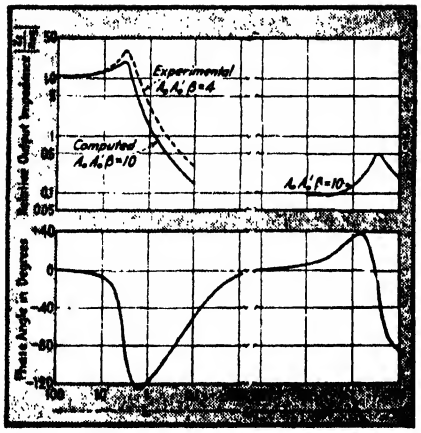

FIG. 20—Variation of amplifier output impedance with frequency affects the magnitude and angle of negative impedance

shown in Fig. 19. Figure 15 shows a typical response curve of the feedback amplifier.

Output Impedance of Amplifier

Negative impedances obtained by feedback amplifiers invariably contain a term due to the output impedance of the amplifier. If the amplifier is not stabilized by negative feedback, the output impedance R_o consists only of the parallel combination of R_{g1} and R_r in the mid-frequency range, and is affected by the coupling capacitance C_c at the low frequencies and by C_s at the high frequencies. Thus, even in the simplest possible case the output impedance is a function of frequency and is not at all constant.

When negative feedback is utilized in the amplifier, the picture becomes more complicated. As is well known, the effect of voltage feedback is to reduce the output impedance of the amplifier in the frequency range where the phase shift in the amplifier is negligible. But if phase shift in the amplifier is not neglected, there will be frequency regions where the output impedance is increased

Effect of Feedback

Roughly speaking, output impedance of the amplifier is affected by three factors. First, if no feedback is used R_o, the physical output impedance, is a function of frequency as explained above. Secondly, in the presence of negative feedback in the amplifier, the output impedance is reduced in the mid-frequency range, but when the amplification begins to fall, the output impedance will be increased because (due to phase shift) the negative feedback will actually become positive. Thirdly, due to the coupling between the two stages, the amplification will be zero at the extreme frequency regions, the feedback effects will disappear and the output impedance will be governed by the physical output impedances.

From this it is evident that the problem of determining the output impedance of an amplifier is not simple and the exact expression must depend not only upon the characteristics of output elements but also upon the coupling between the two stages. It is possible to analyze the output impedance of an amplifier completely in the general case where the two stages of the ampilfier are different. However, the results obtained from such an analysis are so complicated that they become of little actual value and it is simpler to handle each amplifier separately. But to show the type of results that can be expected due to the various effects, a special case will be considered where the two stages of the amplifier are alike in their frequency re-

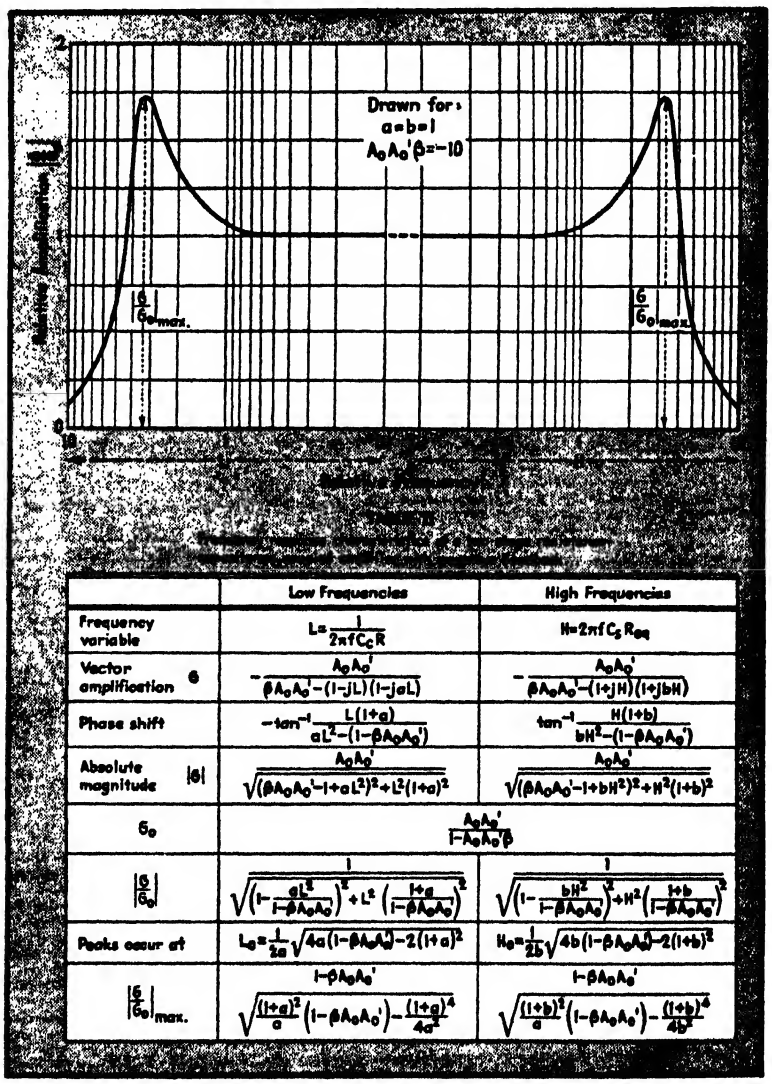

	Low Frequencies	High Frequencies
Frequency variable	$L=\frac{1}{2\pi f C_c R}$	$H=2\pi f C_s R_{eq}$
Vector amplification ϵ	$-\frac{A_0A_0'}{\beta A_0A_0'-(1-jL)(1-j\alpha L)}$	$-\frac{A_0A_0'}{\beta A_0A_0'-(1+jH)(1+jbH)}$
Phase shift	$-\tan^{-1}\frac{L(1+\alpha)}{\alpha L^2-(1-\beta A_0A_0')}$	$\tan^{-1}\frac{H(1+b)}{bH^2-(1-\beta A_0A_0')}$
Absolute magnitude $\lvert\epsilon\rvert$	$\frac{A_0A_0'}{\sqrt{(\beta A_0A_0'-1+\alpha L^2)^2+L^2(1+\alpha)^2}}$	$\frac{A_0A_0'}{\sqrt{(\beta A_0A_0'-1+bH^2)^2+H^2(1+b)^2}}$
ϵ_0	$\frac{A_0A_0'}{1-A_0A_0'\beta}$	
$\left\lvert\frac{\epsilon}{\epsilon_0}\right\rvert$	$\frac{1}{\sqrt{\left(1-\frac{\alpha L^2}{1-\beta A_0A_0'}\right)^2+L^2\left(\frac{1+\alpha}{1-\beta A_0A_0'}\right)^2}}$	$\frac{1}{\sqrt{\left(1-\frac{bH^2}{1-\beta A_0A_0'}\right)^2+H^2\left(\frac{1+b}{1-\beta A_0A_0'}\right)^2}}$
Peaks occur at	$L_0=\frac{1}{2\alpha}\sqrt{4\alpha(1-\beta A_0A_0')-2(1+\alpha)^2}$	$H_0=\frac{1}{2b}\sqrt{4b(1-\beta A_0A_0')-2(1+b)^2}$
$\left\lvert\frac{\epsilon}{\epsilon_0}\right\rvert_{max.}$	$\frac{1-\beta A_0A_0'}{\sqrt{\frac{(1+\alpha)^2}{\alpha}\left(1-\beta A_0A_0'\right)-\frac{(1+\alpha)^4}{4\alpha^2}}}$	$\frac{1-\beta A_0A_0'}{\sqrt{\frac{(1+b)^2}{b}\left(1-\beta A_0A_0'\right)-\frac{(1+b)^4}{4b^2}}}$

sponse. While the relative magnitudes of the various effects will be different for an amplifier with dissimilar stages, the general picture will be the same. Effects due to common power-supply impedance, additional phase shift due to cathode and screen by-passing will be entirely neglected because, by proper design, they can be eliminated.

Calculation of Output Impedance

The output impedance of an amplifier without negative feedback may be defined as the impedance looking into the terminals 1 - 2 in Fig. 19 with the first tube of the amplifier disconnected. It will be noticed that the resistances $R_k + R_7$ are in parallel with resistance G_{g1}'. Resistance R_7 will ordinarily be so high that it will not shunt R_{g1}' appreciably, but if it does then R_{g1}' must be corrected.

at low frequencies

$$R_o = \frac{R_{g1}'(R_o' - jX_o')}{R_{g1}' + R_o' - jX_o'} \qquad (55)$$

at high frequencies

$$R_o = \frac{-jX_s'R_o'R_{g1}'}{R_o'R_{g1}' - jX_s'R_o' - jX_s'R_{g1}'} \qquad (56)$$

If the impedance R_1 is measured by means of the voltmeter-ammeter method with current supplied from an infinite impedance source, then the following relations are true. The current i flowing through the impedance R_o produces a voltage drop iR_o. A fraction β of this voltage, determined by the ratio $R_k/(R_k + R_7)$, appears between the grid and cathode of the first tube and is amplified by the amplifier and forces a current to flow in the impedance R_o in the opposite direction to the current flowing due to the source of voltage e. Thus, the conventional feedback equation may be written $e = iR_o - iR_o \beta AA'$.

If this equation is solved for e/i, which is R_1, and values of R_o, A and A' are substituted into it, the output impedance of the amplifier is obtained as a function of frequency. For comparison with measurements it is convenient to express the results in polar form, giving the magnitude and phase of the amplifier output impedance.

The nature of the impedance variations given by such equations is shown in Fig. 20 which gives computed and experimental curves for the output impedance of a typical amplifier.

Improvement of Diode Detector

A practical diode-detector circuit is shown in Fig. 21. The diode is used as a rectifier, being substantially a short circuit on one-half cycle, and an open circuit on the other half. The load circuit consists of a network which has several functions. The load resistance is shunted by capacitor C_1 which is large enough to act as an effective short circuit for the radio-frequency voltages and yet in an ideal case must not shunt the load resistance for the highest modulation frequency that the detector is to handle. R_1 and C_2 form a filter which isolates the radio-frequency voltage that may exist across C_1 and allows only the modulation-frequency voltage to appear across the output R_2 of the circuit. Capacitor C_4 in conjunction with the resistance R_4 separates the modulation-frequency voltage from the direct-current voltage which is present across the load circuit, a filter arrangement which is often necessary to keep d-c voltage from the following amplifier grid and to utilize the d-c voltage for automatic volume control in a radio receiver. R_3 and C_3 form a filter which isolates the modulation-frequency voltage that exists across R_2 and allows only direct voltage to appear at the a-v-c terminal.

Diode Characteristics

Operation of the diode detector has been described in literature and does not need to be repeated here.[14] It has been shown that if the radio-frequency voltage is large enough, in the neighborhood of 20 volts, then the distortion due to detection is negligible, provided that the diode-detector circuit has a pure resistance in its load for the modulation frequencies and an effective short circuit to the radio frequencies. A diode detector under these ideal conditions may be considered as distortionless.

An actual detector circuit shown in Fig. 21 is far from being ideal and will produce serious distortion. The manner in which the actual circuit shown here deviates from the ideal detector can be seen from a study of Fig. 21. The load circuit of the detector, due to various capacitors in the circuit, presents a lower impedance to the modulation frequency than it does to the direct current.

Let Z_m be the impedance offered by the diode load circuit to the modulation frequencies, and R_o the resistance offered by the same circuit to the direct current. While it is not readily obvious, Terman has shown that the maximum per-

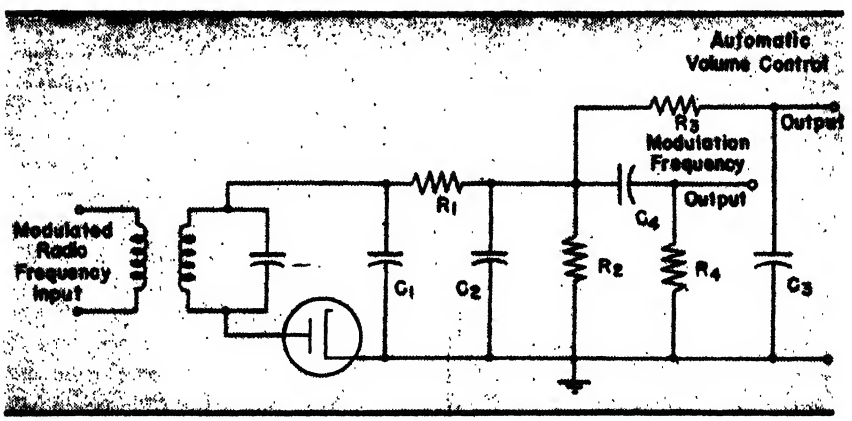

FIG. 21—
Typical diode-detector circuit which can be improved by addition of negative impedance

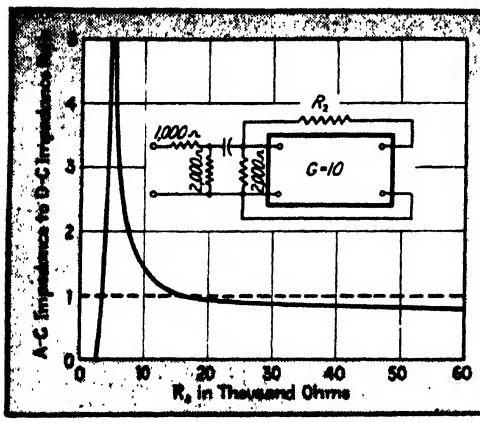

FIG. 22—Addition of negative resistance to diode detector improves the a-c to d-c impedance ratio

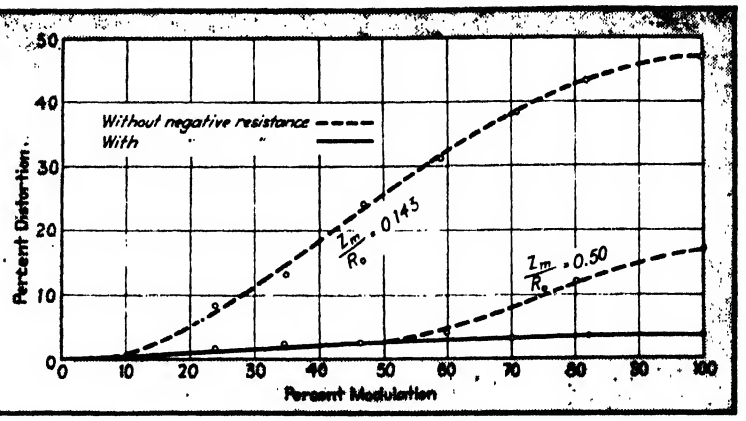

FIG. 23—Negative resistance added to a diode detector decreases distortion near 100 percent modulation

centage of modulation m that the diode detector with a given load can rectify without distortion is

$$m = Z_m/R_o \qquad (57)$$

If the actual percentage of modulation of the applied radio frequency signal exceeds this value, the rectified output will be distorted. The nature of the distortion depends upon the nature of the ratio Z_m/R_o. If this is a reel constant, then the distortion will be in the nature of clipping of the negative peaks of the modulation frequency wave. If the load is such that the above ratio (commonly called the a-c to d-c ratio) has a phase angle, then the distortion will be clipping of the negative peaks at an angle with respect to the axis of the rectified wave. The wave-shape of the distortion is not important in this discussion.

The important fact is that the diode detector deviates from the ideal distortionless detector in two ways: (1) Modulation-frequency impedance does not equal the d-c resistance of the diode load. This produces clipping of the negative peaks if the actual degree of modulation exceeds Z_m/R. (2) Modulation-frequency impedance has a phase angle due to the fact that the shunting capacitor C acts as a partial short circuit at the higher modulation frequencies. This causes diagonal clipping of the negative peaks.

Improvement by Using Negative Resistance

The two effects which cause deviation of an actual diode-detector circuit from the ideal detector can be eliminated by the application of stabilized negative impedances.

The first of the two effects can be eliminated entirely by means of a negative resistance of the shunt type placed across the diode load at the output terminals.[25] The negative resistance may be so adjusted that its value is just equal to the shunting resistance which causes the difference between Z_m and R_o. This will make the ratio given by Eq. (57) just equal to unity which, in turn, means that 100 percent modulated signals can be rectified without distortion.

The second of these deviations from the ideal may be eliminated by using a negative capacitance supplied by an amplifier which has a uniform response up to the highest modulation frequency that it is intended to use, and yet which cuts off considerably below the carrier frequency. By means of this arrangement it is possible to make the net capacitance across the load, as far as modulation frequencies are concerned, just zero and there will be no diagonal clipping even for 100 percent modulated signals. And yet, because the amplifier cuts off at some intermediate frequency, the negative capacitance will be absent above cut-off and the net capacitance offered to radio frequencies across the load will be equal to something greater than C_1.

Measurements of Improved Detector

It is seen that by means of two kinds of negative impedances an ordinary diode detector can be made to approach the ideal one very closely. The principle is illustrated experimentally by means of a diode detector which was purposely made to have a very poor a-c to d-c ratio. Figure 22 shows the a-c to d-c ratio of the diode load (measured by an ohmmeter to determine R_o, and by the voltage-current method to measure Z_m) as a function of the negative resistance placed across the diode load. It is seen from this graph that the proper amount of negative resistance across the diode load causes the a-c to d-c ratio to become unity.

Figure 23 shows the distortion produced by a diode detector as a function of degree of modulation for a detector which again had a purposely poor Z_m/R_o ratio in one case, and a typical one in another. In both cases the distortion of 100 percent modulated signals is very high. By means of a proper amount of negative resistance placed across the diode load, the Z_m/R_o ratio was made unity in each case and the distortion measurements repeated. The results are

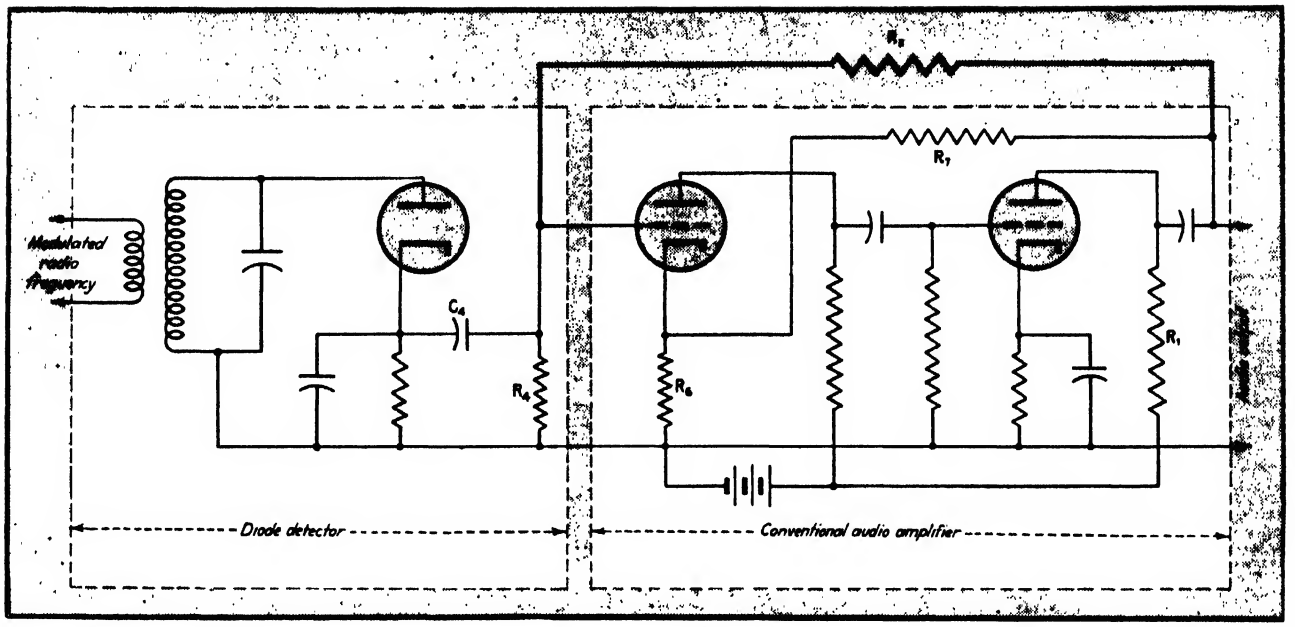

FIG. 24—Application of negative resistance to improve diode detector in conventional radio receiver requires addition of only one resistor

indicated by the solid curve.

It should be mentioned that the distortion was measured by a wave-analyzer at the output of the amplifier that supplied the negative resistance. The measured distortion in each of the three curves is the sum of all distortions due to the modulation-frequency oscillator, the modulator, the radio-frequency amplifier, the diode, and the audio-frequency amplifier used to supply the negative resistance.

The amplifier that supplies the negative resistance does not need to be a separate amplifier. The conventional radio receiver usually has two stages of audio frequency amplification after the diode detector. An addition of one resistor of proper value may be sufficient to make the Z_m/R_o ratio equal to unity and eliminate a large part of the distortion that results when high percentages of modulation are present.

Typical circuit of a diode detector and two-stage amplifier that might be found in a commercial radio receiver is shown in Fig. 24. The amplifier may be stabilized by negative feedback for better performance, but that is not essential, although highly recommended. A proper value of R_s will develop a negative resistance of the shunt type and in combination with R_4 will form an open circuit so that the Z_m/R_o ratio will be unity.

Capacitance Multiplication

It was shown that if an impedance Z_s was connected between the input and the output terminals of an amplifier, the input impedance of the amplifier was given by Eq. (13). If Z_s is a pure capacitance, the input impedance of the amplifier will be a capacitive reactance whose magnitude is given by

$$Z_n = \frac{1}{j\omega C_2(1 - G)} \tag{58}$$

If the amplifier is so arranged that the output of the amplifier will be of opposite relative phase to its input, then the gain of the amplifier will be a negative number, and so this equation becomes

$$Z_n = \frac{1}{j\omega C_2(1 + G')} \tag{59}$$

where G' indicates that it is a negative of the previously used symbol G. The input impedance is thus a capacitive reactance, with the equivalent value of

$$C_{eq} = C_2(1 + G') \tag{60}$$

which means that the capacitance C_2 is multiplied by the factor $(1 + G')$. It must be remembered, however, that in series with this capacitance there is a resistive component due to the inevitable output resistance of the amplifier.

Use of Negative Impedance Techniques

A pure capacitance multiplication can be obtained by a scheme similar to the method used in obtaining a pure negative reactance, If a capacitance is found to possess a certain series resistance, this can be eliminated by placing a negative resistance of the series type in series with the amplifier in the manner previously described. By making the negative and positive resistances just equal, a pure capacitance can be obtained. Another possible way of obtaining a pure negative capacitance is by utilizing a zero-output impedance amplifier.[16]

In some cases it is desirable to have a two-terminal impedance which will be small for all audio-frequencies and yet act as an open circuit for direct currents. Such an impedance may be obtained in the manner described above. In

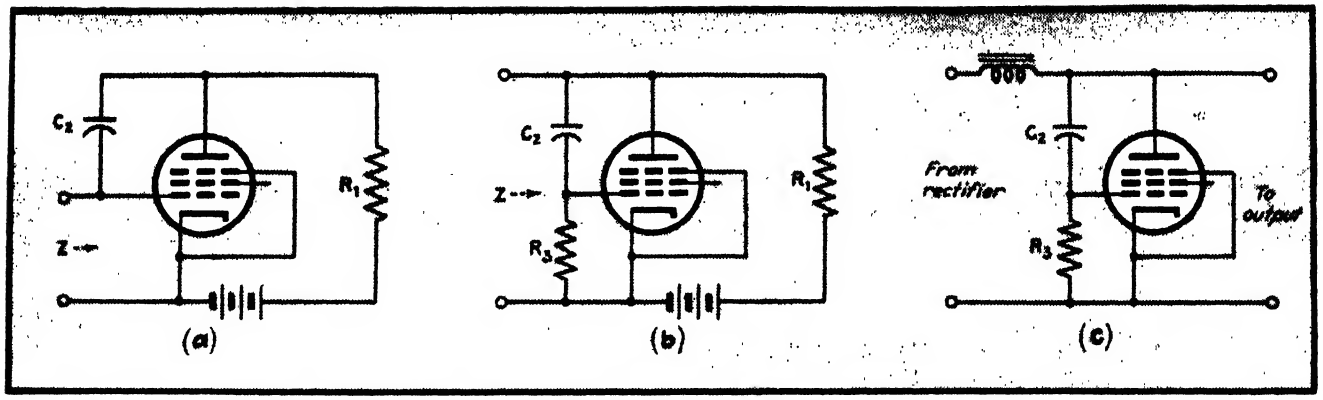

FIG. 25—Using principles on which negative impedance has been discussed, a single tube can be used to multiply capacitance as at (a) for a-c circuits, or as at (b) for combined a-c and d-c circuits for such applications as filters (c)

the frequency region where the amplifier supplying the multiplied capacitance has a uniform frequency response, the resistive component will be constant and its magnitude is given by Eq. (11) with G replaced by G'.

$$R = R_1/(1 + G') \qquad (61)$$

If C_2 is so large that the resultant circuit is merely a resistance to all frequencies for which the amplification G' is constant, the amplifier will act as a low a-c resistance, but will not pass direct current. Such an element is useful in power supply filters where it may be desired to use it as a voltage regulator or where it is desired to produce better filtering than can be done without resorting to very large capacitors. This use is illustrated in Fig. 25.

In Fig. 25(a) is shown a single-stage amplifier which has the proper phase relations to act as a capacitance multiplier. The amplification is best obtained by means of a pentode which has a high mutual conductance. The voltage gain of this amplifier is $G' = G_m R_1$, so that the input impedance of the amplifier is

$$Z = \frac{1}{j\omega C_2(1 + G')} + \frac{R_1}{1 + G'} = \frac{1}{j\omega C_2(1 + G_m R_1)} + \frac{R_1}{1 + G_m R_1} \qquad (62)$$

where G_m is the mutual conductance of the tube. If the reactance of capacitor C_2 is large enough, the input impedance of the amplifier will simply be $Z = 1/G_m$ providing the voltage amplification is much larger than unity.

Tubes such as 6AC7 or 6SG7 have a mutual conductance in the neighborhood of 10,000 micromhos so that it is possible to obtain an input resistance of 100 ohms for all frequencies for which the assumption made above regarding the magnitude of C_2 is true. This means that a tube of this sort is equivalent to a capacitance of 26.5μf at 60 cycles, or to a capacitance of nearly 1600 μf at a frequency of 1 cps. The capacitance of C_2 merely needs to be large in comparison to R_1 at these frequencies, which is simple because R_1 can be made as large as one desires.

A slightly different arrangement shown in Fig. 25(b) differs from the amplifier just discussed in two respects. If in the amplifier shown in Fig. 25(a) a very large resistance R_3 is placed across the input terminals, it will not affect the validity of the equations derived above. Also, if C_2 is very large, then it does not make any difference on what side of C_2 the input impedance is measured, and therefore, the equations derived for Fig. 25(a) are true for Fig. 25(b). Figure 25(b) has the advantage that a direct-current voltage may be impressed upon the device without disrupting the normal operation of the tube. Thus, this arrangement can be utilized in a power-supply filter in the same manner as an ordinary capacitor.

Further modification of the circuit is shown in Fig. 25(c) where the device is shown in a conventional power-supply filter circuit. The power supply itself supplies the necessary current for the tube and the parallel combination of load and power supply resistances constitute the equivalent of resistance R_1 of the former two circuits. In Fig. 25(b) and 25(c) the capacitor C_2 needs to be large enough only in comparison with R_3 which makes it particularly simple to obtain a device which will filter at the very low frequencies.

Negative Resistance Increases Tuned-Circuit Q

Consider a parallel combination of an inductor L and a capacitor C. If L is a pure inductance, and C is a pure capacitance, then the impedance at resonance becomes infinite. If the circuit L contains resistance R, then the impedance at resonance will be determined by the figure of merit of the circuit, commonly known as Q, which is defined as $\omega L/R_o$, and the impedance at resonance will be $R_o = \omega LQ$.

Often it is desirable to have a higher shunt impedance than can be obtained by the best coil that is available. This difficulty can be overcome by introducing either a series negative resistance in series with the coil, or a shunt negative resistance in parallel with the coil. By properly adjusting the magni-

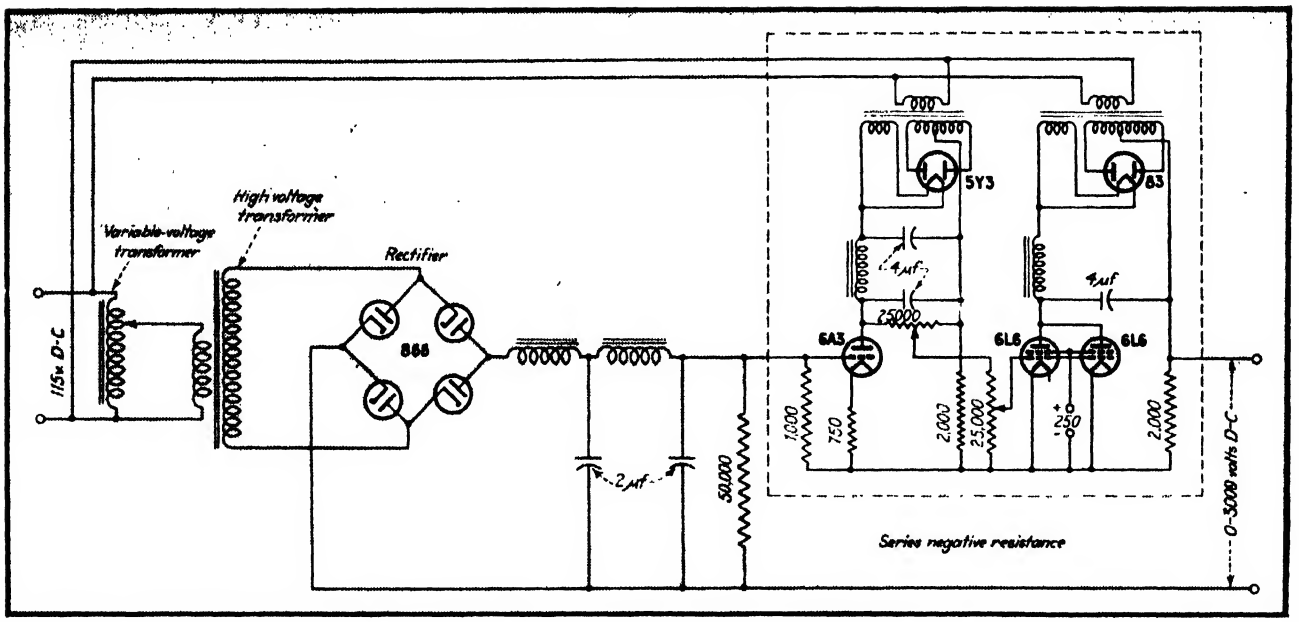

FIG. 26—Continuously-variable regulated-output power supplies can be built using negative resistance to give zero internal impedance

tude of the negative resistance, any value of Q can be obtained from the original one up to infinity. If, for example, we let R_0' be the shunt impedance of the tuned circuit at resonance, and assume that a shunt type negative resistance of magnitude R_n is placed across the tuned circuit, then

$$R_0' = \frac{R_0 R_n}{R_0 + R_n} \tag{63}$$

$$\frac{R_0'}{R_0} = \frac{R_n}{R_0 + R_n} \tag{64}$$

and the effective Q of the combination will be

$$Q_{eff} = Q \frac{R_n}{R_0 + R_n} \tag{65}$$

The stability of this increased Q must depend upon the actual increase in Q. This may be found as follows:

$$\frac{\partial Q_{eff}}{\partial R_n} = Q \frac{R_0}{(R_0 + R_n)^2} \tag{66}$$

$$\frac{\partial Q_{eff}}{Q_{eff}} = \frac{\partial R_n}{R_n} \left[\frac{R_0}{R_0 + R_n} \right] \tag{67}$$

From Eq. (67) it is plain that as R_n approaches R_0 the stability becomes very poor and at the point where Q_{eff} becomes infinite, the stability becomes infinite (See Eq. (18) and (27) and oscillations must take place. But due to the fact that the negative resistance may be stabilized very well by means of negative feedback, a considerable increase in Q is possible with reasonable stability. For instance, some stability figures were previously given for a typical amplifier. It was found that a 20 percent change in supply voltage produced a change in A of 8 percent. With $\beta = -0.1$, and $A = 10{,}000$, the stability coefficient was found to be nearly 10^{-3}, or $\partial R_n/R_n$ from Eq. (17) is $(1/1000)(8/100) = 8 \times 10^{-5}$ If it is further assumed that L is wound with copper wire and that a 10°C variation in temperature may take place, the original Q of the coil may vary by 4 percent. If Q_{eff} is regenerated to the point where the 20 percent variation in supply voltage will produce a 4 percent change in the Q, then $R_0/(R_n + R_n) = 500$.

This means that by this method it is possible to increase the selective properties of a tuned circuit by a factor of 500 and still have a resultant stability which is not worse than the stability of the original coil due to temperature variations. Actually, such an increase in Q_{eff} cannot be used without providing temperature compensation.

Tuned circuits regenerated in this way have many applications. They can be used in filters, wave analyzers, or in any other application where it is desirable to have a higher degree of selectivity than is made possible by ordinary coils.

Improvement of Power-Supply Regulation

In certain applications it is sometimes necessary to have a power supply which has negligible voltage variation with changing current, or in other words, a power supply with zero internal resistance. This can be accomplished by various types of well known voltage regulators. For use with Klystrons for instance, another feature is sometimes essential: a

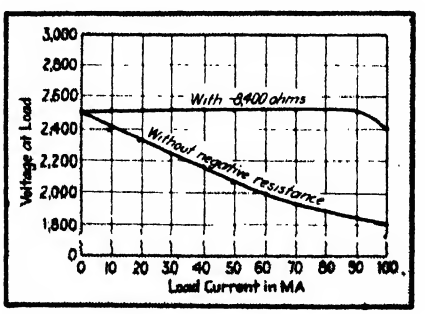

FIG. 27—Improved regulation obtained with negative resistance in Klystron power supply

method of controlling the voltage of the power supply continuously from zero to maximum with voltage regulation over the entire range. This requirement eliminates most of well known regulators and makes others impractical.

If a negative resistance is placed in series with a power supply and its magnitude adjusted so that it just cancels the internal resistance of the power supply, then the power supply in conjunction with the negative resistance will have a zero internal impedance and a varying load will not affect output voltage.

Figure 26 shows a schematic diagram of a power supply and a series negative resistance. Such an arrangement will make the output voltage of the power supply independent of current taken from the power supply over a wide range of voltages, because the internal impedance of power supply approximates quite well a constant. Figure 27 shows the improvement of voltage regulation of the power supply shown in Fig. 26.

References

(1) Black, H. S., Stabilized Feedback Amplifiers, *A.I.E.E. Trans.*, 53, No. 1, p. 114-120, Jan. 1934.

(2) Aiken, C. B., The Alteration of Residence, Inductance, and Capacity by Means of Resistance Coupled Amplifiers, *Jour. Optical Soc. of America*, 15, p. 85-95.

(3) Crisson, G., Negative Impedances and the Twin 21-Type Repeater, *B. S. T. Jour.*, 10, p. 485-513, July 1931.

(4) Herold, E. W., Negative Resistance and Devices for Obtaining It, *Proc. I. R. E.*, 23, No. 10, p. 1201-1223, Oct. 1935.

(5) Brunetti, C., The Transitron Oscillator, *Proc. I. R. E.*, 27, No. 2, p. 88-94, Feb. 1939.

(6) Steimel, K., Stability and Self Oscillation of Electric Circuits, *Zeit. fur Hochfrequenz*, 36, p. 161, 1930.

(7) Nyquist, H., Regeneration Theory, *B. S. T. Jour.*, 11, p. 126-147, July 1932 (This is a theoretical paper experimental verification of which is contained in a paper by Peterson, Kreer, and Ware, Regeneration Theory and Practice, *Proc. I. R. E.*, Oct. 1934).

(8) Terman, F. E., Negative-Feedback Amplifiers, ELECTRONICS, Jan. 1937.

(9) Cocking, W. T., Negative Feedback Amplifiers, *Wireless World*, Nov. 6, Nov. 13, and Dec. 25, 1936.

(10) Terman, F. E., and Wen-Yuan Pan, Frequency Response Characteristics of Amplifiers Employing Negative Feedback, *Communications*, March 1939.

(11) Terman, F. E., Hewlett, W. R., Palmer, C. W., and Wen-Yuan Pan, Calculations and Design of Resistance-Coupled Amplifiers Using Pentode Tubes, A. I. E. E. Technical Paper 40-52, Dec. 1939.

(12) Terman, F. E., "Radio Engineering," 2nd ed., McGraw-Hill Book Co., Inc., New York, 1937.

(13) Sturm, T., Verfahren zur Klirrverminderung (linearisierung), *Funktechnische Monatshefte*, Mar. 1937, pp. 77-82.

(14) Terman, F. E., "Radio Engineering," 2nd ed, McGraw-Hill Book Co., Inc., New York, 1937, p. 425-533.

(15) Terman, F. E., Buss, R. R., Hewlett, W. R., and Cahill, F. C., Some Applications of Negative Feedback with Particular Reference to Laboratory Equipment, *Proc. I. R. E.*, 27, No. 10, p. 649-655, Oct. 1939.

(16) Sturm, T., Verfahren zur Klirrverminderung (linearisierung), *Funktechnische Monatshefte*, Mar. 1937, p. 77-82; and Mayer, H. F., Control of the Effective Internal Impedance of Amplifiers by Means of Feedback, *Proc. I. R. E.*, 27, No. 3, p. 213-217, Mar. 1939 (Other authors have also described methods of making the output impedance of the amplifier equal to zero.).

Constant-Current Circuits

Exponential circuits can be made to carry more nearly constant current for longer times if corrective networks are used. Design equations and actions of these circuits are derived, and their advantages in magnetron pulse circuits are illustrated by a numerical example

By O. T. FUNDINGSLAND and G. J. WHEELER

EXPONENTIAL charging and discharging currents in resistance-capacitance or resistance-inductance circuits can be made approximately constant for short durations by inserting low-loss networks. Such networks permit reducing the capacitance by a factor of four or more for a given pulse duration, or increasing the pulse duration four times for a given capacitance and percent drop in current during the pulse. Similar results can be achieved in inductive circuits.

Reduced size of the reactive element made possible by these networks results in reduction of cost, bulk, and weight of the constant-current circuit. In applications where frequency stability of a self-excited magnetron oscillator is dependent upon tube current, the improved uniformity of current from these networks gives more stable operation.

The Problem

When a capacitor is charged or discharged through a resistor, the resultant current is an exponential function of time. However, in sawtooth sweep circuits, discriminating counter circuits, and other circuits involving pulses of constant amplitude, it is sometimes necessary or desirable to maintain constant current through a resistor, or resistive load for an arbitrarily short period of time. This requirement is especially necessary in one type of radar transmitter in which part of the energy stored in a capacitor is periodically discharged into a magnetron oscillator in the form of rectangular pulses. Approximately constant current can be obtained by inserting a parallel resistor-inductor network in series with the resistor-capacitor circuit.

To determine optimum values of these circuit parameters, consider the case of a capacitor C charged to potential E and then discharged through resistor R_0 when the switch of Fig. 1A is closed. It is desired to have the current through R_0 remain constant for a short interval ΔT. An inductor and resistor are inserted as in Fig. 1B. The relationship of the various parameters is determined by the following analysis.

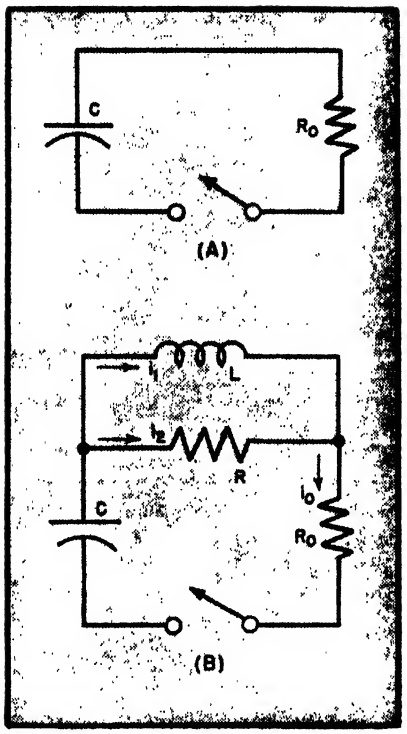

FIG. 1—(A) Exponential circuit, and (B) compensated circuit from which constant current can be obtained

By Kirchhoff's Laws

$$L\frac{di_1}{dt} = Ri_2 \tag{1}$$

$$i_0 = i_1 + i_2 \tag{2}$$

$$\frac{q}{C} + L\frac{di_1}{dt} + i_0R_0 = 0 \tag{3}$$

Because it is assumed that i_0 is constant, that being the desired condition, let i_0 equal I_0, a constant. Then from Eq. 1 and 2

$$L\frac{di_1}{dt} = R(I_0 - i_1)$$

or

$$\frac{di_1}{dt} + (R/L)i_1 = (R/L)I_0 \tag{4}$$

The complementary solution of Eq. 4 is $i_1 = Ae^{-(R/L)t}$ where A is an arbitrary constant. The particular solution is $i_1 = I_0$. The complete solution is therefore

$$i_1 = Ae^{-(R/L)t} + I_0 \tag{5}$$

Conventionally, this equation indicates that I_0 is a steady-state condition, which is obviously impossible. However, because the time interval under consideration is very short, no steady-state condition is reached, and thus Eq. 5 is legitimate.

When $t = 0$, $i_1 = 0$. Therefore, in Eq. 5, $A = -I_0$, and

$$i_1 = I_0(1 - \epsilon^{-(R/L)t}) \tag{6}$$

Differentiating Eq. 6 with respect to time and multiplying by L, we obtain

$$L\frac{di_1}{dt} = I_0R\epsilon^{-(R/L)t} \tag{7}$$

Substituting this equivalent into Eq. 3 gives

$$\frac{q}{C} + I_0R\epsilon^{-(R/L)t} + I_0R_0 = 0 \tag{8}$$

Differentiating Eq. 8 and substituting I_0 for dq/dt gives

$$\frac{I_0}{C} - \frac{I_0R^2}{L}\epsilon^{-(R/L)t} = 0 \tag{9}$$

If L/R is much greater than ΔT, then $\epsilon^{-(R/L)t}$ is approximately unity during the pulse interval. Thus Eq. 9 reduces to the familiar relationship: $R = \sqrt{L/C}$ or $L = R^2C$.

Circuit Modification

It is evident in the foregoing analysis that the value of R_0 does not affect the result. Consequently, if R_0 is replaced by a biased diode as in Fig. 2, it would be expected that for constant current the same relationships of the parameters must hold. In this case capacitor C is given, charged to a potential E, which is to be discharged through a load with constant current for a time interval ΔT after the switch is closed. The load in this case is a diode in series with a battery. Resistance R_0 represents the sum of the diode resistance, the switch resistance, and any other resistance in the circuit. The R-L network is inserted as before and the analysis is similar.

A new term, E_0, will appear in Eq. 3 and 8. However, this term disappears when Eq. 8 is differentiated, resulting in the same Eq. 9 and consequently the same two relationships: $R = \sqrt{L/C}$, and $\Delta T \ll L/R$.

If it is desired to close the switch and maintain a constant current through R_0 for a short period of time ΔT in the series circuit of Fig. 3A, a choke and resistor are again inserted as in Fig. 3B. Equations are again identical with those for a discharging circuit, except that the right-hand side of Eq. 3 and 8 is E_0 instead of zero. This term disappears when Eq. 8 is differentiated. Thus the analysis is the same as before, and the same relationships hold.

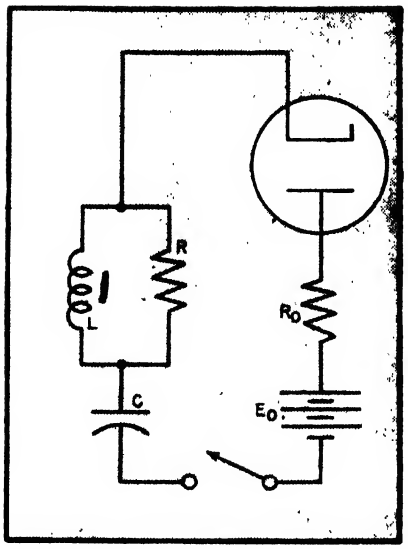

FIG. 2—A biased diode can be a part of the load through which constant current is passed

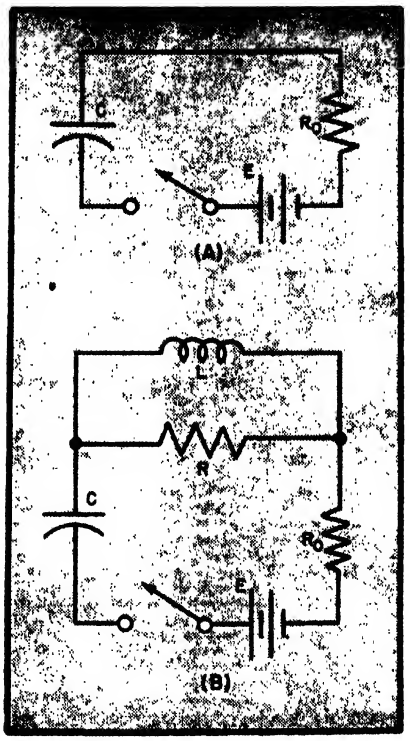

FIG. 3—Instead of discharging a capacitor, as in Fig. 1, the capacitor can be charged in the manner shown here

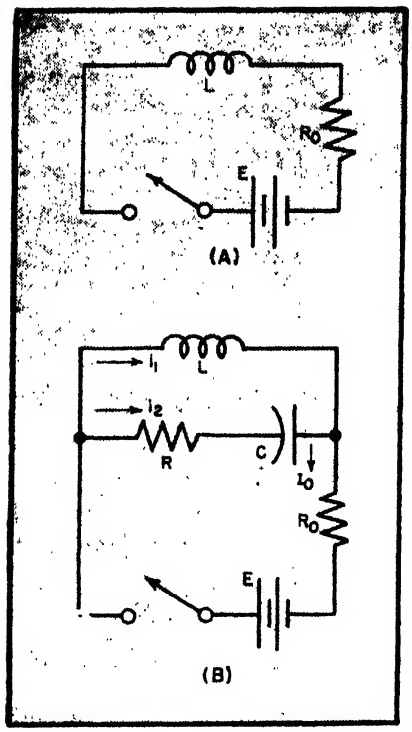

FIG. 4—(A) An inductor can replace the capacitor of Fig. 3. Corrective network (B) contains inductance

Although it is not a resistor-capacitor circuit, the following analysis is included here because it is also a case of maintaining a constant current in an exponential circuit.

In a circuit including resistor, inductor, and battery as shown in Fig. 4A it is again desired to close the switch and maintain a constant current through R_0 for a short time ΔT. This result is accomplished by inserting a resistor and capacitor as shown in Fig. 4B. Just as before, and for similar reasons, ΔT must be short compared to the time constant of the inserted network. That is, $\Delta T \ll RC$.

Although the characteristics of this circuit are comparable to those of the resistor-capacitor circuit previously analysed, the mathematical analysis for this resistor-inductor circuit is included here. As before, by Kirchhoff's Laws

$$L\frac{di_1}{dt} + I_0R_0 = E \tag{10}$$

$$R\frac{dq}{dt} + \frac{q}{C} + I_0R_0 = E \tag{11}$$

$$i_1 + i_2 = I_0 \tag{12}$$

From Eq. 10

$$\frac{di_1}{dt} = \frac{E - I_0R_0}{L}$$

From which by integration

$$i_1 = \frac{E - I_0R_0}{L}t + A$$

When $t = 0$, $i_1 = 0$, thus $A = 0$, and

$$i_1 = \frac{E - I_0R_0}{L}t \tag{13}$$

Likewise, from Eq. 11

$$q = B\epsilon^{-(1/RC)t} + (E - I_0R_0)C$$

As in the original circuit analysed, this simplification is permissible because $\Delta T \ll RC$. When $t = 0$, $q = 0$, thus $B = -(E - I_0R_0)C$, and

$$q = C(E - I_0R_0)\,(1 - \epsilon^{-(1/RC)t})$$

But $i_2 = dq/dt$, and therefore

$$i_2 = \frac{E - I_0R_0}{R}\epsilon^{-(1/RC)t} \tag{14}$$

Substituting the values of i_1 and i_2 given by Eq. 13 and 14 into Eq. 12 gives

$$\frac{E - I_0R_0}{L}t + \frac{E - I_0R_0}{R}\epsilon^{-(1/RC)t} = I_0 \tag{15}$$

Diqerentiating Eq. 15 gives

$$\frac{E - I_0R_0}{L} - \frac{E - I_0R_0}{R^2C}\epsilon^{-(1/RC)t} = 0 \tag{16}$$

During the short interval ΔT, $E - I_0R_0$ does not equal zero. Also, if ΔT is very small compared to RC, $\epsilon^{-(1/RC)t}$ is approximately unity. Therefore Eq. 16 reduces to the same relationship as previously obtained: $R = \sqrt{L/C}$. It should be noted that in this case, as before, the result is independent of the value R_0.

Magnetron Application

The circuit in Fig. 2 is similar to a discharge circuit used in some radar transmitters, and the load represented is essentially the equivalent circuit of a magnetron. The magnetron impedance is nonlinear, having a volt-ampere characteristic similar to that shown in Fig. 5. In general, the dynamic impedance is not constant over a wide range of voltage and current. However, over a small operating range the magnetron can be represented to a good approximation by the circuit shown in Fig. 6, consisting of a linear resistance equal to $\Delta E_M/\Delta I$, a perfect

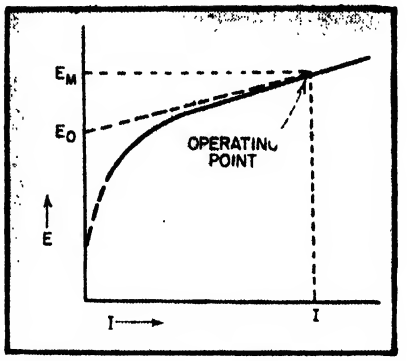

FIG. 5—Load characteristics of d-c anode circuit of magnetron can be simulated by battery and resistor

rectifier, and a battery E_0, where E_0 is the voltage intercept of a line drawn tangent to the curve at the operating point.

In one application the capacitor is charged between pulses through a resistance from a d-c source. The switch is a vacuum tube which is normally nonconducting but is turned on at regular intervals to discharge part of the stored energy into the magnetron in the form of rectangular pulses. With a constant magnetic field applied to the magnetron, the output frequency of the magnetron is a function of its peak current. Consequently, to prevent frequency shift during the pulse, it is important that the discharge current be maintained very nearly constant.

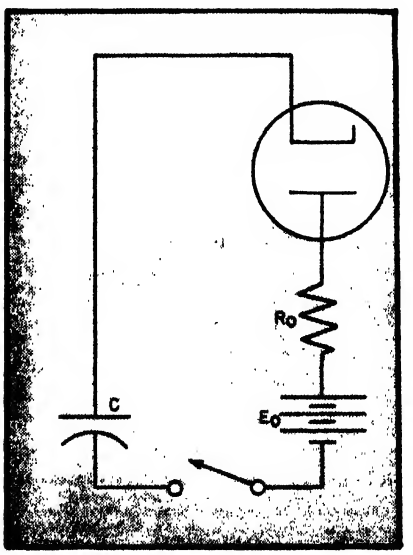

FIG. 6—An equivalent magnetron pulsing circuit containing a storage capacitor

Of course, the current can be held nearly constant by making the capacitor C very large. However, high-voltage capacitors are physically large and heavy, and therefore present serious difficulty in aircraft sets where space and weight are at a premium. Addition of the resistance-inductance network permits the use of smaller capacitors for a given pulse duration, or with a given size capacitance the pulse generator can produce longer pulses. These advantages are best illustrated by numerical example.

First consider the case without the addition of the resistance-inductance network. The current is found by simple circuit analysis

$$i = \frac{E - E_0}{R_0} \epsilon^{-(1/R_0C)t} \qquad (17)$$

Typical values are
E = 14,000 volts
E_0 = 11,500 volts
R_0 = 200 ohms
C = 0.1 microfarad

Thus

$$i = \frac{14{,}000 - 11{,}500}{200} \epsilon^{-(10^6/20)t}$$

At the moment of closing the switch the current is 12.5 amp. After one microsecond the current is 11.9 amp. This change represents a current drop of about five percent, which is barely tolerable with some magnetrons.

Now an R-L network is inserted, giving the circuit of Fig. 2 with $L = R^2C$. The resistance might be 50 ohms. The inductance must be 250 μh, and $(L/R) = 5 \times 10^{-6}$. By conventional circuit analysis the current as a function of time is found to be

$$i = \frac{E - E_0}{R + R_0} (1/2\beta) \times [(\beta - \alpha)\epsilon^{-(\beta+\alpha)t} + (\alpha + \beta)\epsilon^{-(\alpha-\beta)t}] \qquad (18)$$

where $\alpha = 1/2RC$

$$\beta = \alpha \left[\frac{R_0 - 3R}{R_0 + R}\right]^{1/2}$$

At the moment of closing the switch the current is now ten amperes. After one microsecond it has fallen to 9.96 amp. In this case the current drop is less than 0.5 percent.

If it were desirable to maintain the same magnetron operating point as before with an average pulse current of approximately 12.2 amp, it is only necessary to raise the voltage on C to 14,550 instead of 14,000 volts. The initial current is then 12.20 amp, and at the end of one microsecond i = 12.15 amp, still less than a 0.5-percent droop.

With the voltage raised to 14,625 volts, the initial current is again 12.5 amp, but it takes four microseconds for it to drop to 11.9 amp, the value reached in one microsecond without the addition of the resistance-inductance network. Thus the R-L network permits increasing the pulse length by a factor of four, provided the same percentage droop in current can be tolerated as for the shorter pulse.

If C =0.025 μf and R remains 50 ohms, L must be 62.5μh. Then with E = 14,625 volts, the initial current is 12.5 amp, and at the end of one microsecond, i = 11.9 amp. Thus, for one microsecond pulse duration the capacitance can be decreased by a factor of four without causing a greater droop than was obtained without the R-L network.

It may be noticed that the values of L/R in all these examples do not perfectly satisfy the requirement that $L/R \gg \Delta T$, and that the assumption that $\epsilon^{-(R/L)t}$ equals unity for the duration of the pulse is not quite true. As a result, the current pulses are not constant but droop slightly. To fulfill this condition rigorously and also have $L = R^2C$, it would be necessary to choose higher values for R and L. Then this droop would be practically eliminated, but as R is increased, the power supply potential E must be increased, and the power loss in R becomes greater. In practice, the selection of values of R and L is a compromise between minimum current droop and minimum power loss.

The requirement that $L = R^2C$ is also not critical. When the condition $L/R \gg \Delta T$ is rigorously fulfilled, a value of L less than R^2C would cause the current to rise linearly during the pulse, whereas if L were greater than R^2C, the R-L network would not be entirely effective in minimizing the current droop. In some cases it may be better to choose L less than R^2C, and L/R of the same order as, or even less than, ΔT so that the current, although remaining within an allowable percentage deviation from a specified mean value, first rises and then falls as shown in Fig. 7.

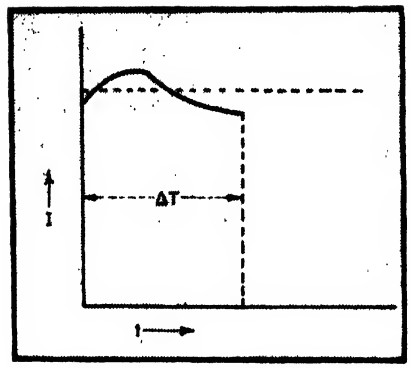

FIG. 7—Percent deviation from a constant level over a given time can be reduced by adjusting the corrective network

Practical Design

By more comprehensive circuit analysis or by experimentation, values of R and L can be determined for any given set of conditions which will permit increase in pulse duration ΔT or decrease in the required value of storage capacitance up to a factor of eight or ten, with very small loss of power. To obtain best results, the choice of R and L can also be influenced to some extent by other practical considerations not mentioned here. For example, it is conceivable that under certain conditions stray capacitance across the pulse generator switch and across the magnetron may form a resonant circuit with L and give rise to undesirable postpulse oscillations. A compromise in the choice of R and L may be necessary to produce the necessary damping.

Work was done by B. Chance, R. M. Walker, and others at Radiation Laboratory and elsewhere on improvement in linearity of voltage rise across capacitors used in timing circuits, beginning in 1942. One method employed inductance in series with resistance and capacitance, with appropriate tube switching to select only a small, linearly rising portion of the exponential

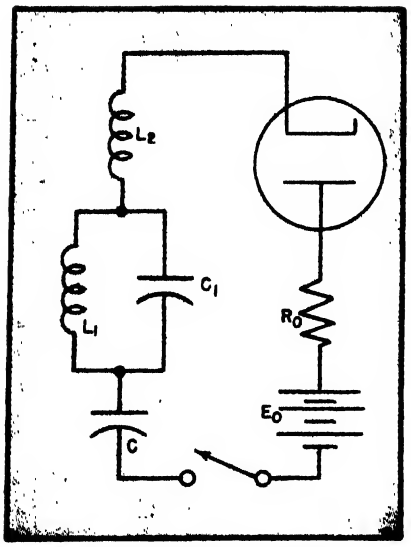

FIG. 8—A corrective network can be made entirely of reactive elements

voltage. However, in these low-level circuits power loss is usually an unimportant consideration and magnitudes of resistance, inductance, and capacitance differ appreciably from those recommended by the preceding analysis.

Dissipationless Circuit

Another method for minimizing magnetron pulse current drop has been suggested both at Radiation Laboratory and elsewhere. A. A. Varela, Naval Research Laboratory, Washington, D. C., described the use of an *L-C* network composed only of passive elements L_1, L_2, and C_1, as shown in Fig. 8. The network is used in place of the parallel *R-L* unit. Such a network will accomplish the desired result but has the disadvantage of requiring one more circuit element including a second capacitor of medium voltage rating. Although this type of pulse-forming network is composed of lossless elements, the voltage drop during the pulse due to the network surge impedance causes an effective loss in pulse power which is comparable to losses in equivalent *R-L* networks. The energy remaining in L_1, C_1, and L_2 at the end of the pulse may be dissipated in post pulse oscillations. Therefore, in view of these considerations, it seems advisable for most applications to use the simpler *R-L* network.

This paper is based on work done for the Office of Scientific Research and Development under contract OEMsr-262 with the Radiation Laboratory, Massachusetts Institute of Technology.

Design of Phantastron Time Delay Circuits

Detailed step-by-step explanation of how the phantastron circuit provides precision microsecond time delays that vary linearly with control voltage. Factors affecting performance are analyzed, along with use of control circuits, cascading for longer delays, and calibration techniques

By RICHARD N. CLOSE
and MATTHEW T. LEBENBAUM

THE phantastron is a simple electronic circuit which produces a variable time delay free from short-time jitter and stable over relatively long periods. In addition, the delay is a linear function of control voltage, so that an accurate calibration is relatively simple. In a particular circuit, the ratio of maximum to minimum delay attainable without sacrificing linearity is of the order of 50 to 1.

The need for time-delay circuits has become of importance in the past few years with the increasing applications of radar and of pulse-type navigational aids. In these systems, measurement of time intervals to a high order of accuracy is required, and a circuit such as the phantastron is extremely useful for such purposes.

A simple example will serve to illustrate the use of a time-delay device. Assume two pulses are received which are separated by a time interval Δt. These are presented on an oscilloscope as X and Y in Fig. 1A. The first received pulse, X, triggers a time-delay circuit which produces a marker pulse Z at a controllable time after triggering. The marker pulse may be adjusted until it coincides with Y. The time interval between X and Y may then be read as a function of the control voltage on the delay circuit. Control voltage can be obtained from a potentiometer, calibrated to read Δt directly.

A single-shot multivibrator with an adjustable width of pulse may be used as a time delay with the first signal initiating the action, and the trailing edge of the multivibrator output being used to develop a marker. The width of the pulse may be controlled readily and so a delay time may be introduced. This delay multivibrator[1,2] is simple and the delay is roughly linear with the setting of a linear potentiometer over a wide range. However its deviations from linearity (several percent) and short-time instability (of the order of 0.5 percent) are definite limitations in applications where high accuracies are involved. The phantastron, on the other hand, can be made linear to about 0.1 percent

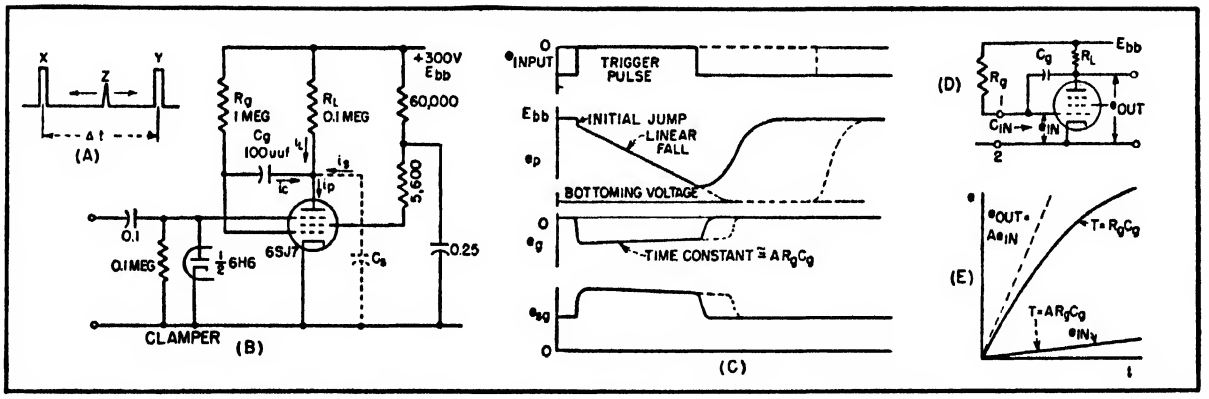

FIG. 1—In waveform A, a phantastron triggered by pulse X produces a controlled-position marker pulse Z. To measure time delay, phantastron control voltage is set so pulse Z coincides with Y. Other diagrams here apply to the Miller circuit

of maximum delay and has a short-time jitter of less than 0.05 percent.[5,6] Other circuits, such as the bootstrap sweep circuit with a comparator diode, produce results of equal precision, but are considerably less economical in the number of tubes employed.

Miller Sweep Circuit

The heart of the operation of a phantastron lies in the production of a voltage at the plate which decreases linearly with time for almost the entire period after the initiating trigger. To understand the mechanism of this linear variation, it is useful to analyze in some detail another circuit, the so-called Miller fed-back time base. This circuit, shown in Fig. 1B, can produce an extremely linear time base.

In the quiescent condition, the suppressor is sufficiently negative to cut off plate current. The grid is at zero because of the positive grid return. Except for a very small grid current, all of the space current goes to the screen.

If the suppressor is suddenly brought up to zero by the trigger, the time base is initiated. The circuit wave forms are shown in Fig. 1C. The solid lines are for the case of plate current cutoff before the plate has bottomed (see the following discussion); the dotted lines are for termination of the time base after bottoming.

The plate current is the sum of the three currents shown in Fig. 1B: the discharging current i_s from the stray capacitances, the discharging current i_c from C_g, and the current i_L through the load resistance. When the suppressor is brought up to zero, a large fraction of the space current must flow to the plate as in a normal pentode. Since the grid side of C_g is tied to B+ through the large grid resistor R_g, the discharging current from C_g will be limited to approximately E_{bb}/R_g.

At the first instant, the strays supply most of the plate current, which is fairly large since the tube was operating at zero grid bias before the trigger.

As the strays discharge, the plate voltage drops and current flows through R_L. This drop is transmitted to the grid, since the voltage across C_g cannot change rapidly. As a result, space current is reduced. Since the plate can only fall a few volts before the tube is cut off, and because R_L is quite large, i_L will be small.

An equilibrium point is soon reached where the plate current is the normal fraction of the existing space current, and the fall of plate voltage is arrested.

Actually, the plate voltage continues to fall, as is shown below, but the rate of change of grid voltage goes through zero and becomes positive as C_g discharges through R_g. This occurs when the rate of fall of plate voltage is exactly equal to the rate of change of voltage across C_g. As the grid rises and space current increases, the plate current also increases and the plate voltage continues to drop, but at a slower rate. This drop, reflected to the grid through C_{gp} retards the rise of grid voltage. It is this feedback path which is responsible for the almost linear fall of plate voltage after the initial jump.

Miller Effect

One simple way of looking at this is to redraw the circuit as in Fig. 1D and consider what the impedance looking in at the terminals 1-2 must be. The input capacitance of a tube, as expressed by the well-known Miller effect equation, is

$$C_{in} = C_{gk} + C_{gp}(1 + A\cos\theta) \quad (1)$$

where C_{gk} is the grid-cathode capacitance, C_{gp} is the grid-plate capacitance, A is the gain of the tube and $\cos\theta$ is the phase angle of the load (unity for a resistance load).

Normally, C_{gp} is extremely small in a pentode, but in this circuit we have deliberately added a capacitance between plate and grid. Since $A >> 1$, the capacitance appearing across terminals 1-2 will be very closely $A \times C_g$. We have, therefore, an RC sweep generator with an extremely long time-constant, and we use only a very small portion of the exponential rise in voltage across C_{in} as the input voltage. This portion is so small that it has a practically linear variation with time.

Figure 1E shows the relative shapes of the voltages. The exponential curve with time-constant of R_gC_g would be the input voltage

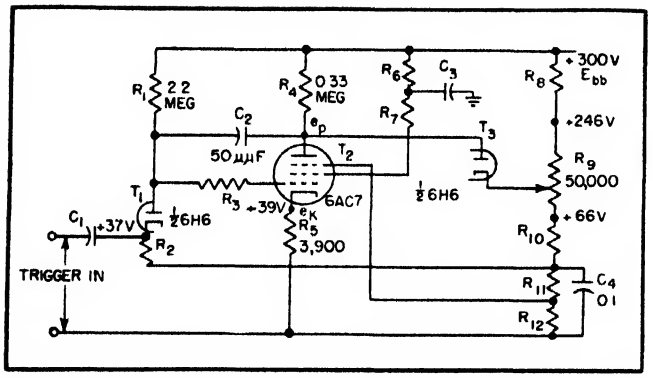

FIG. 2—Simple pentode phantastron circuit as developed in England

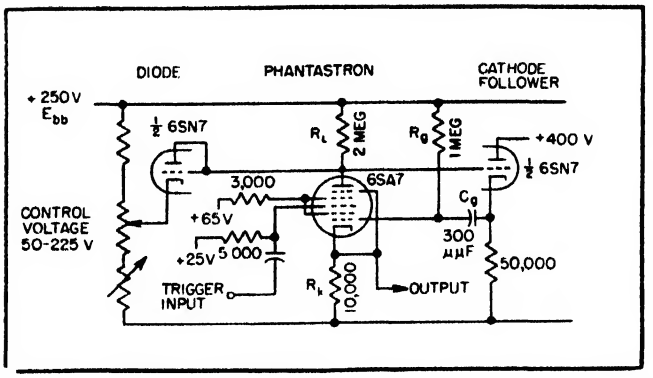

FIG. 3—Pentagrid converter adaptation of phantastron, with cathode follower

if C_g were connected from grid to ground. With the grid-to-plate connection, the input voltage rise has a time constant of $A \times R_gC_g$. The output voltage is simply e_{in} times the gain.

More formally, one may express the rate of change of plate voltage mathematically. This is useful, for it shows immediately the necessary conditions for linearity, and indicates the region in which we must operate the tube in order to obtain the best results.

The variation in plate current of a pentode for small grid variations may be expressed as

$$i_p = g_m\left(e_g + \frac{e_{sg}}{\mu_{sg}} + \frac{e_p}{\mu_p}\right) \qquad (2)$$

where e_g, e_{sg}, and e_p are the instantaneous control grid, screen grid, and plate potentials, μ_{sg} and μ_p are the screen grid and plate amplification factors respectively, and g_m is the plate-control grid transconductance. If we let v_c be the voltage across C_g at any instant, then from Eq. 2

$$i_p = g_m\left[(E_{bb} - R_Li_L - v_c) + \frac{e_{sg}}{\mu_{sg}} + \frac{E_{bb} - R_Li_L}{\mu_p}\right] \qquad (3)$$

Solving for i_L and noting that $i_p = i_L + i_s + i_c$, we obtain

$$i_L = \frac{g_m\left(E_{bb} - v_c + \frac{e_{sg}}{\mu_{sg}} + \frac{E_{bb}}{\mu_p}\right) - i_c - i_s}{1 + g_mR_L + g_mR_L/\mu_p} \qquad (4)$$

In order that di_L/dt (and therefore de_p/dt) be constant, each term of the denominator of Eq. 4 must be constant and the terms of the numerator must be constant or vary linearly with time. Since R_L is large and only a small grid change is required to produce a large output voltage, if operation is above the knee of the e_pi_p characteristic of the tube, g_m, μ_p, e_{sg} and μ_{sg} are relatively constant. The current i_c flowing into C_g is $(E_{bb} - e_g)/R_g$, and since the change of e_g is small compared to E_{bb}, to a high degree of accuracy i_c is a constant, as follows

$$i_c = \frac{E_{bb} - e_{gav}}{R_g} = \frac{E_{bb}'}{R_g} \qquad (5)$$

Now, $dv_c/dt = i_c/C_g$, so from Eq. 5 we have

$$dv_c/dt = E_{bb}'/R_gC_g \qquad (6)$$

During this stage, e_p is falling relatively slowly, and i_s is small compared to i_c if $C_g >> C_s$, as it is chosen to be. In any event, if e_p is falling linearly, i_s is constant.

Differentiating Eq. 4 with respect to time and multiplying both sides by R_L, we obtain

$$R_L\frac{di_L}{dt} = \frac{de_p}{dt} = -\frac{g_mR_L}{1 + g_mR_L(1 + 1/\mu_p)}\frac{E_{bb}'}{R_gC_g} \qquad (7)$$

Making the further assumption that $\mu_p >> 1$ and $g_mR_L >> 1$, Eq. 7 reduces to

$$de_p/dt = -E_{bb}'/R_gC_g \qquad (8)$$

This indicates that if our assumptions are valid, the fall of plate voltage is linear. The rate of fall is easily calculated from the circuit parameters. In the circuit shown, for example, the fall is approximately $300 \div 10^6 \times 100 \times 10^{-12}$, or 3 volts per microsecond.

Bottoming of Plate

When the plate voltage in the Miller circuit falls to a very low value, our initial assumptions are no longer justified. At low plate voltages, g_m drops rapidly and μ_p approaches 1, and the plate drop departs from linearity. At some point, the rate of change of e_p becomes zero, and the plate is said to have bottomed. This is equivalent to operating below the knee of the pentode characteristic. In this region a drop in plate voltage reduces the fraction of space current flowing to the plate, so that although the total space current is increasing (grid voltage rising), the net plate current change is zero. At this point in the cycle there is no feedback through the plate-grid capacitor, and the grid now rises towards B+ at a rate determined only by the simple time constant, R_gC_g. This increases the total space current and screen current until the grid is caught at zero by the flow of grid current. The initial conditions then exist except that the plate voltage remains almost constant at its bottomed value. In this circuit, the plate can only rise to its initial value if the suppressor grid cuts off the plate current.

If this plate current cutoff could be made to occur when the plate first bottomed, the rise of the grid and screen to their initial values would be greatly accelerated. The increase in plate voltage as plate current is cut off would be reflected back to the grid, greatly increasing the rate of rise of grid voltage. As will be shown later, this can be accomplished simply by use of the phantastron circuit. This sharp rise

can then be differentiated and used as an output pulse.

We would then have almost all the elements of a time-delay circuit: (1) A voltage falling linearly with time; (2) A relatively fixed voltage at which the fall is arrested; (3) A method of obtaining a sharply rising voltage at this terminating point for developing into a marker.

If we could control the plate voltage at which the cycle starts, we would have the last element required, for then the total plate voltage drop (and therefore the time) is controllable. There remains only to investigate the linearity of the time delay as a function of the control variable, and the stability of the various stages of the cycle.

Simple Pentode Phantastron

Before this is done, the workings of a simple pentode phantastron circuit will be analyzed in order to draw together the principles discussed above and to indicate wherein it differs from the Miller circuit. The circuit is shown in Fig. 2. Control grid initiation is used instead of suppressor grid triggering. The initial voltages are shown on the schematic, the plate voltage being determined by the setting of R_6. The plate attempts to rise to B+, but when its voltage equals that on the cathode of T_2 (which is variable from 66 to 246 volts), T_2 conducts, catching the plate at that voltage. This is the usual method of controlling the starting voltage of the cycle, and for the values given in this circuit, controls the delay from about 20 to 75 microseconds. Since T_1 is conducting, it holds the phantastron grid at 37 volts. The suppressor is at 20 volts, determined by a bleeder chain; it is almost 20 volts negative with respect to the cathode, cutting off plate current.

Following the British custom, the sequence of phantastron operation will be divided into six stages. The conditions set forth above characterize the quiescent period, stage VI. When a negative trigger of approximately 30 volts peak with a steep leading edge is applied to the grid of T_2 through T_1, stage I is initiated. Since bias resistor R_6 is not bypassed, the voltage on the cathode follows the grid voltage as in a cathode follower. Drop in cathode voltage is equivalent to a suppressor voltage rise, and at some point plate current begins to flow. The resulting drop in plate voltage is reflected through C_2 to the grid. This stage will then be recognized as the initial-jump period of the Miller time base. Only one point of difference is important: the grid (and therefore the plate) must fall considerably farther than in the Miller circuit to establish the first equilibrium point because the cathode voltage follows closely the grid voltage, the actual bias developed being equal to $\Delta e_g(1-A)$ where Δe_g is the change in grid voltage, and A is the gain of the tube as a cathode follower. This initial jump is of the order of 30 to 40 volts, dependent upon the setting of the control voltage.

With plate current equilibrium established, stage II begins. During this stage, the plate voltage drops linearly in exactly the same fashion as in the Miller circuit. It should be noted that T_1 and T_3 are both cut off after the initial trigger by the drop in grid and plate voltage respectively, and are cut off during stages I, II, III, and IV. The tube bottoms at the end of stage II.

Stage III is the period during which the grid voltage rises towards the supply voltage with time constant R_1C_2, as discussed previously. During this stage, the plate current change is practically zero, and plate voltage remains almost constant. As the grid voltage (and therefore, cathode voltage) rises, the suppressor falls with respect to the cathode. The end of stage III is defined as the point where the suppressor voltage has fallen sufficiently to commence cutting off plate current.

During stage IV, the grid rises rapidly, as the plate rise is reflected onto the grid. It is during this stage that the useful output is developed, since the cathode voltage is rising steeply enough to trigger a marker circuit, such as a conventional blocking oscillator. Stage IV ends when the grid rises to the voltage on the cathode of T_1; this diode conducts, catching the grid.

In stage V, the plate voltage rises till it is caught by T_3, and the circuit is ready for triggering again. The speed with which the plate can return to its initial value so that the circuit can be triggered again is determined by the rate at which grid-plate coupling capacitor C_2 and the strays from plate to ground can be charged through the load resistance.

In this phantastron, then, it is possible to obtain an output delayed in time from the initiating trigger by 20 to 75 microseconds, depending on the setting of the 50,000-ohm linear potentiometer. This delay is closely a linear function of the potentiometer setting.

Pentagrid Phantastron

Chance and his associates at the MIT Radiation Laboratory adapted the original pentode phantastron (developed by the Telecommunications Research Establishment, Gt. Malvern, Worcs., England) to the American type 6SA7 pentagrid converter.[8] In this pentagrid circuit, shown in Fig. 3, grids 2 and 4 (tied internally) are used as the screen grid, grid 3 is used as the grid controlling plate current (the suppressor grid of Fig. 2), and grid 5 is used as a normal suppressor grid (tied to cathode).

One of the advantages of the 6SA7 is that the $e_{p3}i_p$ characteristic exhibits a very sharp cutoff. During stage IV, then, when the suppressor voltage drop begins to cut off the plate current, the rate of cutoff (and therefore the rate of rise of plate voltage) is more rapid than in the normal pentode. This plate voltage rise, reflected to the grid, causes the cathode voltage to rise steeply, producing a sharply defined output pulse.

The addition of the cathode follower allows the plate to return to its initial value much more rapidly than in the simple phantastron. In the latter circuit, the grid-plate coupling capacitor and strays must

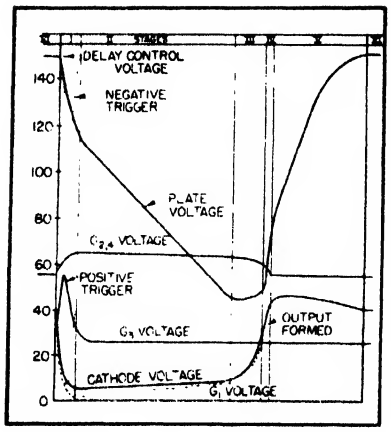

FIG. 4—Phantastron waveforms, divided into six stages according to British custom. Stage VI is quiescent condition

charge through the high load resistance. With the cathode follower circuit of Fig. 3, the cathode follower charges C_g and only the strays charge through R_L, so the rate of rise of plate voltage is extremely rapid. The wave forms in this phantastron are shown in Fig. 4.

Maximum Duty Cycle

The duty cycle is defined as the ratio of delay time to the time between successive triggers. Since the recovery is an exponential charging toward B+, the maximum control voltage is normally limited to less than 90 percent of the supply voltage; otherwise, the recovery time would be undesirably long. When this limitation exists in the simple circuit of Fig. 2, the recovery time at maximum delay approximately equals the delay time (50 percent duty cycle).

If a cathode follower is used to charge C_g during recovery (stage V), the duty cycle is limited only by the time required to charge the stray capacitance between the phantastron plate and ground through the large plate resistor as mentioned above.

Maximum Delay

If the phantastron is pressed beyond the maximum permissible duty cycle (stage V incomplete), the delay is no longer a linear function of the control voltage; if pressed far enough, erratic triggering will result. In cases where 100 percent duty cycle is required, two phantastron delays may be employed in series, or a fixed video delay line may be inserted in series with the phantastron trigger.

The maximum delay may be calculated from the approximate formula $T_{max} = R_g C_g (V_{max} - V_o)/E_{bb}$, where V_{max} is the maximum value of control voltage and V_o is the minimum control voltage which results in delay (40 to 60 volts).

Minimum Delay

When the phantastron is triggered by a positive trigger applied to grid 3, the delay may be reduced smoothly to zero by continuously lowering the control voltage. When a negative trigger is used, the minimum delay is a function of the trigger width and amplitude. In either case, however, linearity of the delay with control voltage begins to suffer when the value of delay becomes less than 2 percent of the maximum delay.

Linearity

A linearity error of ± 0.1 percent of T_{max}, when T_{max} is greater than 200 microseconds, is obtainable under laboratory conditions, while a linearity error of 0.25 percent has been achieved in mass production. Linearity error is defined as the maximum difference between the actual delay and the delay value determined by straight-line interpolation between two calibration points located near the maximum and minimum delays respectively. The linearity obtainable becomes poorer as the value of T_{max} decreases. Thus, for a phantastron operating between 3 and 50 microseconds, 0.5 percent linearity error is the smallest easily attainable.

Table I—Nonlinearity Errors in 300-Microsecond Phantastron

Cause of Error	Approximate Nonlinearity Introduced
Variation of duration of stage I with control voltage	+0.1%
Variation of magnitude of stage I	−0.4%
Nonlinearity of slope and variation in bottoming voltage in stage II	+0.1%
Variation of duration of stage III	−0.8%
Control voltage potentiometer loading	+1.0%

In order to obtain the above linearities, careful selection of circuit values is necessary. This is particularly true since there are unavoidable nonlinearities in the various phases of operation whose effects can be eliminated only by carefully balancing as closely as possible one against the other, and deriving the necessary additional compensation from the loading of the control voltage potentiometer

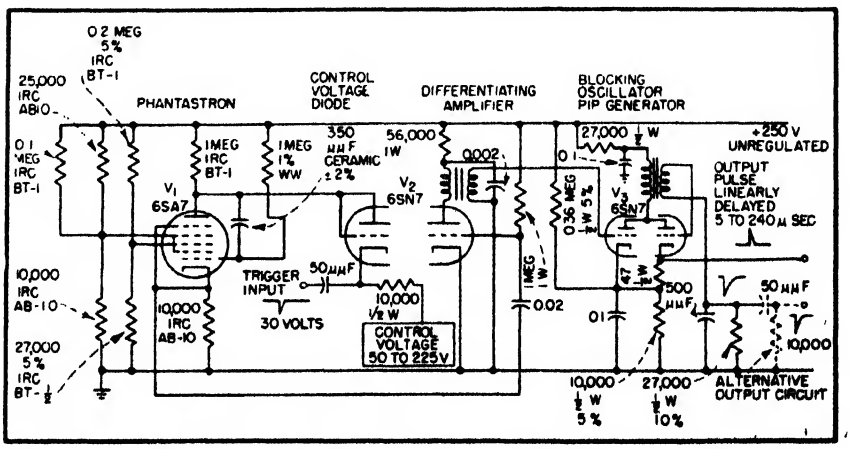

FIG. 5—Phantastron time delay circuit providing 240 microseconds maximum delay. Resistor types specified give the required temperature compensation. Both pulse transformers are Utah X124-T2 or equivalent

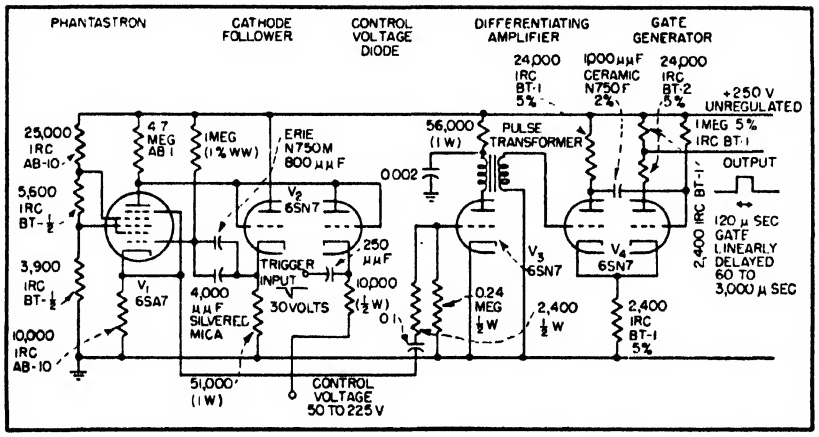

FIG. 6—Phantastron delay circuit with cathode follower and gate output, providing 60 to 3,000 microseconds delay. Pulse transformers are the same type as in the circuit of Fig. 5

by the phantastron plate resistor. Table I summarizes these sources of nonlinearity and roughly indicates their magnitude and direction for the case of a 300-microsecond phantastron.

Particularly important in obtaining good linearity are the values of quiescent screen voltage (on grids 2 and 4), the second control grid voltage (on grid 3), and the values of the plate and cathode resistors. Table II gives recommended component values for four different values of maximum delay.[8] Obviously, if the linearity of the phantastron is to be utilized, a calibrated potentiometer or other type of control circuit of very high accuracy must be employed to convert voltage into a dial reading or a mechanical computer input.

Temperature Compensation

To retain linearity and calibration at widely different ambient temperatures, special care must be exercised in the choice of resistor and capacitor types used. Types indicated in Table II and in the circuit diagrams of Fig. 5 and 6 were chosen so that the effects produced by their variation with temperature would balance as nearly as possible. Both positive and negative coefficient resistors and capacitors are specified.

Unfortunately, it has been found difficult to reproduce results of temperature cycling tests when temperatures are carried to the extremes required by Service specifications. Apparently, a hysteresis type of effect or permanent change in temperature coefficient of some of the standard carbon resistors occurs which upsets the compensation after several temperature excursions. Also, variation in the temperature coefficients of the carbon resistors from lot to lot is common. The best results achieved in practice showed a variation of roughly 0.5 percent in the phantastron calibration over the temperature range of −50C to +70C, with most of the variation at the extremes of temperature.

If it is desired to reduce the temperature effect over moderate ranges of ambient temperature, the types indicated in the table should be satisfactory. If a more rigid compensation is desired, it is recommended that an investigation be made for that purpose. This is particularly true since the local temperature surrounding each component is the significant factor in determining its behavior, and this depends greatly on chassis layout.

Supply Voltage and Tube Variations

Variation of the plate supply voltage over a ±10 percent range produces a change in the delay value of roughly ±0.1 percent of maximum delay. Variation of heater voltage over a ±10 percent range produces roughly a ±0.1 percent change, but in the opposite direction. For this reason an unregulated supply is normally used with the phantastron, since heater and plate-voltage changes very nearly compensate for one another when the line voltage is altered. The control voltage must

Table II—Recommended Values of Phantastron Circuit Components

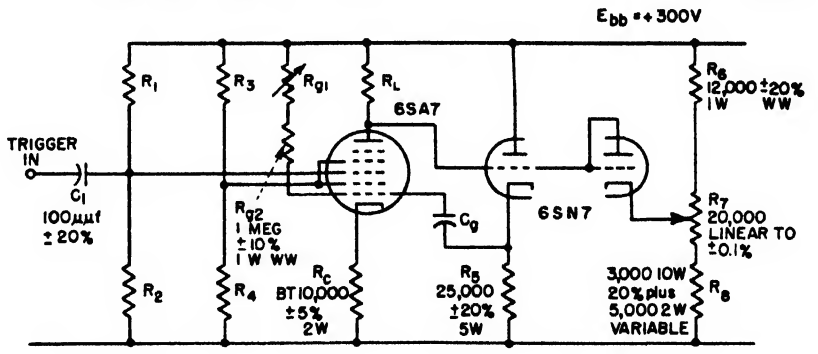

Parameter	Resistor Type for Temp Comp	500-μsec Phantastron	2,500-μsec Phantastron	10,000-μsec Phantastron	50,000-μsec Phantastron	Tolerance
R_1	BT	68,000 (2w)	68,000 (2w)	50,000 (2w)	50,000 (2w)	5%
R_2	WW	5,600 (1w)	6,200 (1w)	5,000 (1w)	5,000 (1w)	5%
R_3	WW	20,000 (10w)	20,000 (10w)	15,000 (10w)	15,000 (10w)	5%
R_4	BT 50% / Erie 50%	8,200 (1w)	6,200 (1w)	5,600 (1w)	5,600 (1w)	5%
R_L	BT	1 meg (1w)	2 meg (1w)	5 meg (¼w)	5 meg (¼w)	20%
R_{g1}	WW	0.1 meg (2w)	0.1 meg (2w)	0.1 meg (2w)	0.1 meg (2w)	20%
C_g	Temp coeff	90 μμf N150	475 μμf N150	2,000 μμf N270	5,000 μμf N270	10%

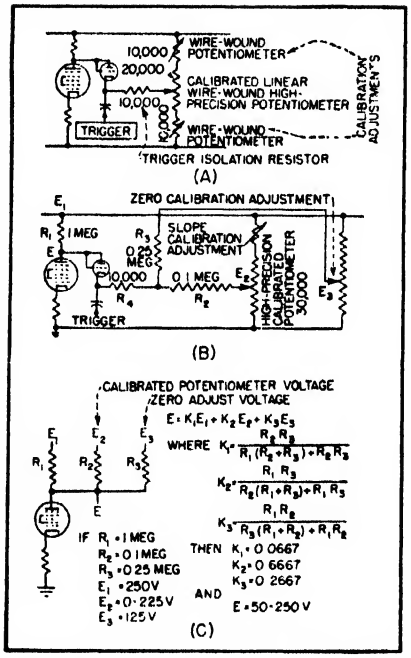

FIG. 7—A simple control circuit for the phantastron is shown at A, with a voltage-addition network for the same purpose at B and, at C, a simplified version of the network that neglects the diode and R_4

be derived from voltage-divider type networks operating from the same supply as is used for the phantastron circuit itself, so that it drifts exactly in proportion to the plate and screen voltages.

Linearity is not adversely affected by change of tubes, but calibration may change several percent. Calibration adjustments are provided in the control circuit for this reason.

Trigger Requirements

A trigger of at least 30 volts amplitude is recommended. A positive trigger may be supplied to grid 3 or a negative trigger supplied to grid, plate, or cathode. Injecting the trigger through the control voltage diode has the advantage of removing the effect of the triggering circuit once the operation has begun. The 10,000-ohm resistor shown in series with the diode (Fig. 5) is provided in order to isolate the trigger from the stray capacitance which exists if the control voltage lead travels any appreciable distance to the control circuit, which may often be in a remote location. A duration of at least 2 microseconds is recommended for the positive trigger to ensure reliable operation. The negative trigger may be somewhat shorter.

Control Circuits

As has been mentioned previously, the control circuit is a network designed to produce a voltage varying from roughly 50 volts, where plate bottoming and hence zero delay occur, to a value somewhat less than the supply voltage. This voltage may be derived from a calibrated potentiometer used in a voltage divider circuit, as in Fig. 7A. The rheostats in series with each end of the potentiometer are varied until the voltages at the ends, or at two calibration points near the ends of the potentiometer, are correct. Since the rheostats interact on each other, several successive settings of each rheostat must be made before a solution is converged upon.

In certain applications it is desired to produce the control voltage from an electronic computer whose output may be the sum or product of several variable quantities. Here it is often inconvenient or impossible to supply the 50 volts of zero-delay voltage in the simple way described above.

Figure 7B shows a resistance mixing or linear voltage addition network which allows the addition of any number of variable or fixed voltages to produce the desired control voltage. The plate resistor of the phantastron is considered as part of the network and is actually used to contribute most of the zero voltage by the current it draws from the network.

Figure 7C is an equivalent circuit of the adding network. The diode resistance and the 10,000-ohm trigger isolation resistor are ignored since they have no effect on linearity and have only a second-order effect on the calibration, which may be ignored initially.

As seen from the equations in Fig. 7C, the resultant voltage on the phantastron plate is composed of definite fractions of the calibrated potentiometer voltage E_2, the supply voltage E_1, and the zero calibration potentiometer voltage E_3. When the calibrated potentiometer arm is grounded, the zero-calibration potentiometer contribution plus the supply voltage contribution should produce the voltage required for zero delay. A slope calibration adjustment is also provided in series with the top end of the calibrated potentiometer. These two adjustments are virtually independent of one another.

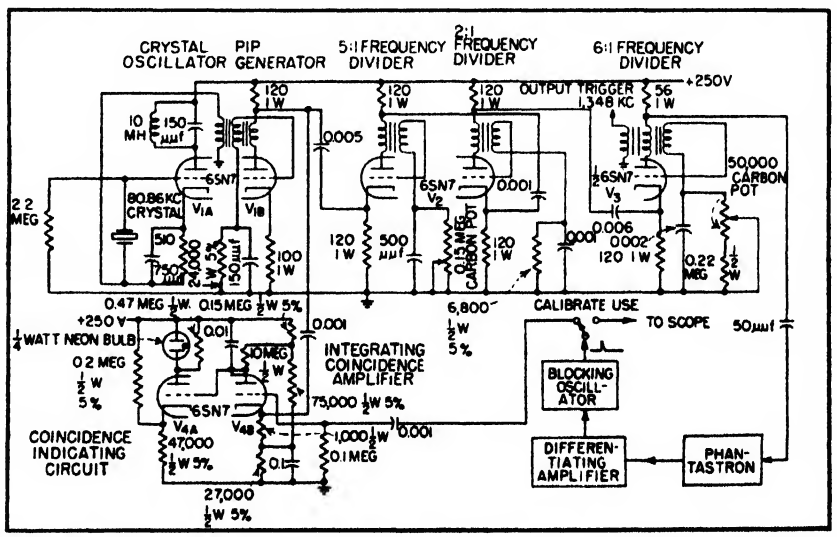

FIG. 8—Crystal-controlled trigger source and neon lamp coincidence calibrating circuit for use in conjunction with a phantastron delay. All pulse transformers are the same type as in the circuit of Fig. 5

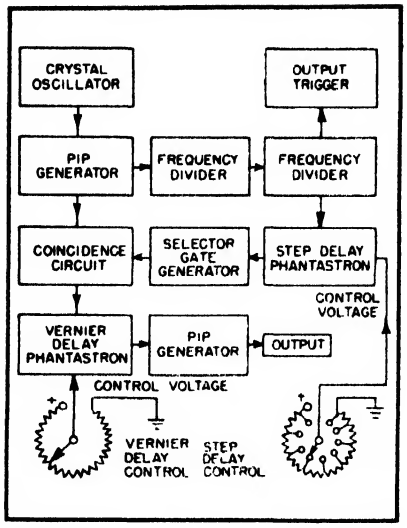

FIG. 9—In two-scale delay circuit, step-delay phantastron produces uniformly spaced pips to trip vernier phantastron

If desired, additional branches may be supplied to add additional voltages, and the slope calibration rheostat may be used as a multiplier control to multiply the calibrated potentiometer reading by any desired factor. If the latter is done, the slope calibration rheostat should be replaced by a low-impedance potentiometer connected across the supply voltage, in order not to change the impedance at the slider of the calibrated potentiometer.

The phantastron exhibits sizable calibration drifts with ageing of tubes and should be calibrated against a frequency standard or other timing standard at intervals of 20 to 50 hours of operation. Figure 8 shows a crystal-controlled timing circuit and a calibration indicator which may be built into the phantastron chassis for this purpose. It consists essentially of a crystal-controlled oscillator synchronizing a frequency-divider chain which produces a trigger at a submultiple of the oscillator frequency. This trigger is used to trigger the phantastron and any external equipment it is desired to synchronize with it.

The oscillator has a frequency of 80.86 kc, so that negative synchronized pips 12.37 microseconds apart (exactly one nautical mile of radar range) are produced at the output of V_{1B}. These pips are fed into the cathode of V_{1B}, which is normally biased well beyond cutoff, and are of sufficient amplitude so as to bring the grid almost up to cutoff. In this condition, a positive pulse applied on the grid will cause conduction of plate current and will appear amplified at the plate. A positive pulse appearing at any other time will not appear at the plate unless it is of very large amplitude.

A large time constant composed of an 0.01-μf capacitor and a 10-megohm plate resistor is used in the plate circuit so as to integrate the amplified pulses into a steady d-c voltage. The voltage is directly coupled to the grid of V_{1A}, which is essentially a cathode follower normally biased so as to draw sufficient current to light the 0.25-watt neon bulb in its plate circuit.

The delayed pulse controlled by the phantastron circuit is fed into the grid of V_{1B}. As the delay is adjusted so as to coincide with the first one-mile interval of the pip generator, the phantastron delayed pulse comes into coincidence with the first one-mile pip and a voltage is built up across the plate load. This lowers the bias on V_{1A} and causes the neon lamp to dim. The bias on V_{1A} is set so that the lamp does not completely extinguish, since the voltage required to restart the glow discharge is appreciably higher than its extinction voltage, and dead space or electronic backlash would be introduced.

By selecting two crystal-controlled pips—one near each end of the delay range to be covered—the zero and slope may be set by setting the calibrated potentiometer to read the proper value and adjusting the calibration adjustments until the neon lamp dims. The one-mile pip is used rather than the zero pip since the phantastron is nonlinear in the region of zero delay. The proper pip may be chosen by counting the number of times the light blinks as the calibrated potentiometer is turned through its range.

Cascade Delay

Where a long delay of very high precision is required, the 0.1-percent accuracy of the phantastron may be improved by using two or more of them in a cascade delay (Fig. 9). The first phantastron is controlled by a step-type potentiometer calibrated so as to produce equal increments of delay as it is advanced from one position to the next. The output of this phantastron fires a narrow selector gate which is injected into the cathode of a coincidence amplifier. Crystal-controlled pips are fed into the grid, and the desired pip appears amplified at the plate. The position of this pip is independent of the calibration errors of the phantastron (so long as these are not larger than half the width of the selector gate), and is accurate within the precision of the crystal oscillator. This accurately delayed pip is then used as a trigger for the second or vernier phantastron, which covers the time interval between pips. In this way a long time interval can be measured with the precision normally achieved in measuring a much shorter time interval. One of the drawbacks encountered in this method is the nonlinearity of the vernier phantastron at the lower end of its range. This can be overcome by overlapping the vernier phantastron into the second pip interval.

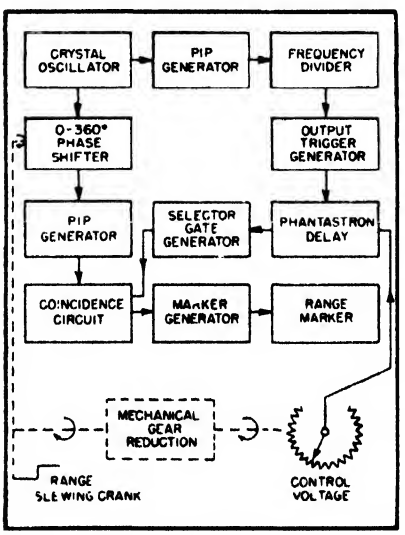

FIG. 10—Block diagram of precision phase-shift delay circuit using a phantastron as an ambiguity resolver

A more convenient type of two-scale delay employs a precision RC phase-shift network to shift the phase of the crystal oscillator continuously through 360-degree cycles (Fig. 10). This produces a set of synchronized pips which appear to travel continuously in time as the capacitor is rotated continuously through many cycles of phase shift. By using a phantastron and selector gate to follow a particular pip and exclude all others, a continuously variable delay of high precision is obtained. In practice, the phase-shift capacitor is geared mechanically through a speed reduction box to the phantastron control voltage potentiometer so as to provide tracking.

Automatic Tracking

Where it is desired to measure a changing time interval continuously, such as in an antiaircraft radar, the delayed pip may be made to follow the target pulse automatically. A simple version of such a system is shown in Fig. 11. Two gates adjacent in time, called the early and late gates respectively, are positioned by the phantastron. Through an electronic or electromechanical servo loop the phantastron voltage is continuously adjusted so as to keep the target pulse exactly split between the early and late gate.

The area of the pulse falling in the early gate is measured by a coincidence amplifier gated by the early gate, while the area falling in the late gate is measured by a coincidence amplifier gated by the late gate. The two coincidence amplifier d-c voltages may then be used to operate a small d-c motor which through suitable gearing turns the range voltage potentiometer (and phase-shift capacitor in the case of a two-scale delay) so as to correct the position of the gates.

Adequate damping must be employed to prevent oscillation or hunting of the servo system. Rate-measuring circuits may be included in conjunction with memory circuits to maintain a continuous rate of change of delay in absence of signal or when the scanning radar beam is off the target.

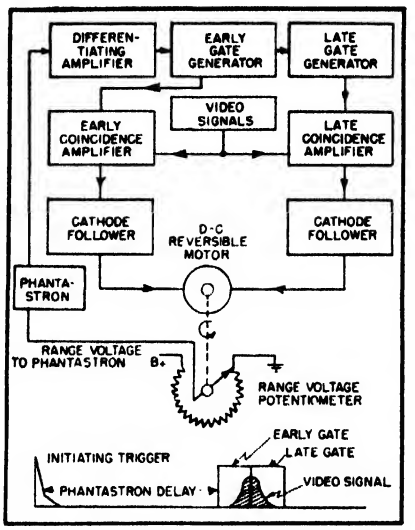

FIG. 11—Block diagram and timing diagram of a phantastron delay for automatic tracking of moving radar signals

REFERENCES

(1) MIT Radar School Staff, "Principles of Radar", p 2-53, McGraw-Hill Book Co., New York, N. Y.
(2) B. Chance, Some Precision Circuit Techniques used in Wave Form Generation and Time Measurement, *Rev. Sci. Inst.*, p 396, Oct. 1946.
(3) Kelner, Hughes, Berg, Hinkle, and Chance, An Adaptation of the Phantastron Delay Multivibrator Circuit to the 6SA7 Tube, *MIT Radiation Laboratory Report No. 63-21.*

Self-Switching R-F Amplifier

Multivibrator circuit using two pentodes amplifies and automatically switches two circuits into common indicator for direction finding and similar uses. Design considerations, switching ratios, and input resistance variations are discussed

By H. M. WAGNER and J. F. HERRICK

CERTAIN TYPES of electronic equipment require the switching of radio-frequency energy between two circuit elements. Examples of such equipment are radio direction finders and beacons, for which various mechanical and electronic means have been employed to accomplish the desired switching.

This paper presents a few of the observed and measured characteristics of a particular multivibrator type of switch, including the measurement of the instantaneous input resistance. While the measurements reported were made at frequencies between 20 and 60 megacycles per second, the same general type of circuit can be used at lower or higher frequencies.

A schematic diagram of the electronic switch on which tests and observations were made is shown in Fig. 1. The tubes function both as an amplifier for radio frequencies in the range from 20 to 60 megacycles per second and as an audio-frequency generator at approximately 200 cycles per second. The circuit appears similar to that of a conventional r-f amplifier. However, in contrast to regular

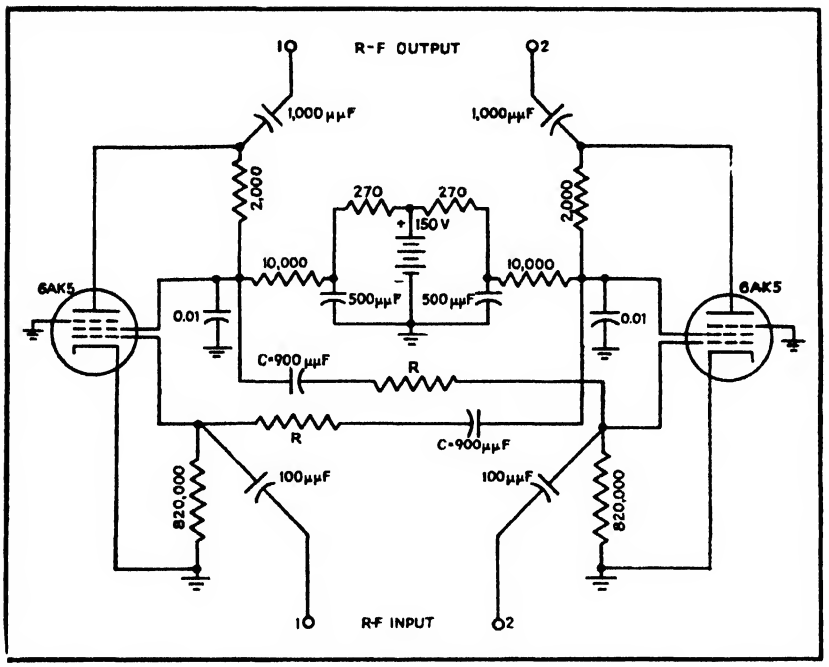

FIG. 1—Schematic circuit diagram of multivibrator switch

r-f amplifiers having fixed operating potentials, the amplification here is accompanied by cyclical changes in bias and operating potentials imposed by the voltages of multivibration.

A resistor R in series with capacitor C form the audio-feedback path between the plate-screen of each tube and the grid of the other tube. This resistor serves the dual purpose of preventing r-f coupling between tubes and of limiting the d-c grid current. Its value has an important effect both on the multivibrator wave shape and on the input impedance of the switch. If r-f decoupling were the only consideration, a choke might be used in place of this resistor. A bypass capacitor from the screen-grid to ground is needed for r-f amplification but tends to reduce the sharpness of the square wave multivibrator voltages. The capacitor used should be large enough to provide r-f bypassing but small enough to maintain square-wave sharpness.

Multivibrator Voltage and Wave Forms

Before studying the performance of the multivibrator switch at radio frequencies, it is advisable to examine the performance of the switch simply as an audio-frequency oscillator. In order to do this, oscillograms of the voltage pattern at each electrode (anode, screen and control grid) of one tube, and at the junction of the feed-back capacitor C and resistor R were recorded. Separate tests were made using values of 100,000 ohms, 820,000 ohms and 2 megohms for R. The results for the first two cases are shown in Fig. 2 and 3. Horizontal lines in each oscillogram represent fixed voltages applied for calibration purposes. All voltage outputs were applied directly to the plates of an oscilloscope having 20 megohms internal resistance.

The high plate potentials of approximately 150 volts correspond to the cutoff condition of the tube. The low plate potentials correspond to the operating interval. The potentials on the tube during the conducting period determine at any instant its operating characteristics as an amplifier.

The contour of the grid voltage variation demonstrates the grid-voltage limiting action which tends to maintain nearly zero bias on the grid during the conducting period. During the conducting period the input resistance of the control grid is low in comparison to the current-limiting resistance R; and the grid voltage goes positive only a very small fraction of the voltage applied at the other end of R (compare Fig. 2 C and D or Fig. 3 C and D). It is desirable to keep this positive swing as small as possible, both for the sake of the a-f waveform and to minimize r-f input circuit loading that increases with the grid current. The grid current may be determined from the oscillograms which give the voltages at either end of resistor R. The peak grid currents are 300 microamperes, 75 microamperes and 33 microamperes when R is 100,000 ohms, 820,000 ohms, and 2 megohms respectively. (The variations in grid current

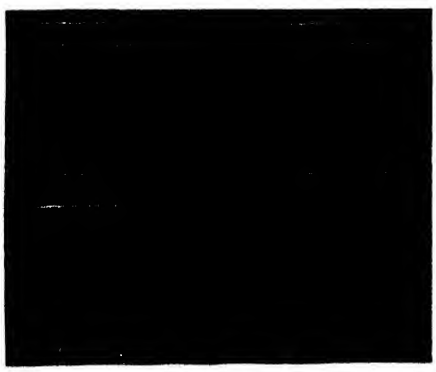

FIG. 2—When R is 100,000 ohms the multivibrator voltages are as shown: (A) at anode, (B) at screen, (C) at grid, (D) at junction of R and C

FIG. 3—When R is 820,000 ohms the multivibrator voltages are as follows: (A) at anode, (B) at screen, (C) at grid, (D) at junction of R and C

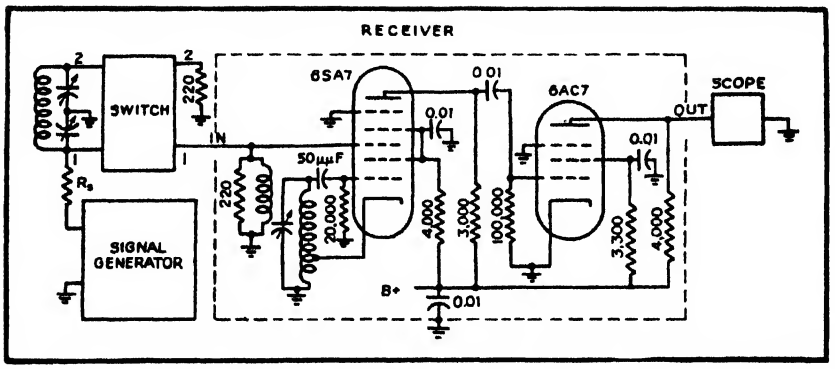

FIG. 4—Schematic circuit diagram of the receiver used for measuring characteristics of the switch, and block diagram of test connections

throughout the conducting portion of the cycle are shown in Fig. 7C. The magnitude of the peak grid current and the rate at which the grid current drops throughout the cycle increase as the value of R is decreased.)

Amplification Characteristics

Since the state of multivibration imposes varying potentials of appreciable magnitude on the electrodes of the tube, the r-f amplification may be expected to vary also. The amplification has been investigated using the arrangement shown in Fig. 4. Because the r-f voltages used are at too high a frequency to apply directly to the usual oscilloscope, the output of the switch is first fed to a superheterodyne receiver that converts the r-f to a lower frequency.

Figure 5 is a typical oscillogram obtained when the input signal is from a low impedance source (R_s approximately 20 ohms). Under these conditions the input signal remains practically constant and independent of the connected load. Hence, any variation in signal output results from the amplification characteristics of the switching tube. The variations in height of the r-f envelope presented on the scope indicate the variations in r-f amplification of the switch. As can be seen, the amplification remains relatively constant throughout the conducting portion of the multivibrator cycle, in spite of the appreciable variations in plate and screen voltages (shown in Fig. 2 and 3). The waveform of the r-f envelope is essentially rectangular and has steeper sides than those of the corresponding multivibrator plate and screen voltages.

Switching Ratio Characteristics

Switching ratio is defined as the on-off ratio of r-f voltage appearing at the output circuit, and is measured from an oscillogram such as Fig. 5. Dimension A corresponds to the r-f voltage available when the switch is closed; when the tube is functioning as an r-f amplifier. The distance B corresponds to the r-f voltage leaking through the switch when it is open; that is, when the tube is cut off.

One technique used in measuring switching ratios involves the measurement of four factors as shown in the following

$$\text{switching ratio} = (A\ B)(E_B/E_A) \quad (1)$$

in which A and B are the measured oscilloscope deflections indicated as A and B in Fig. 5, and E_A and E_B are the output readings of the signal generator in microvolts when measuring the heights of A and B respectively.

If desired, the measurements can be reduced to two quantities as follows: The deflections A and B may be measured for a constant signal-generator voltage ($E_A=E_B$), or the signal-generator voltages, E_A and E_B, may be recorded for equal oscilloscope deflections ($A = B$). The former procedure presented a practical difficulty because the deflection B was smaller than the thickness of the normal oscilloscope trace. In the latter procedure the deflection should be chosen so that its magnitude insures reliable readings without overloading the receiver. Under the conditions of this particular experiment it was found advisable to measure all four quantities.

As a check on the method used, the switching ratio was measured under simulated conditions with multivibration stopped by biasing one tube to cutoff. The factor by which the signal had to be increased in order to equal the height of the oscillogram when the tube was operating as an r-f amplifier was taken as the switching ratio. The results were approximately the same as those measured under conditions of multivibration.

Representative values for switching ratios obtained with the circuit arrangement used (Fig. 4) were 170 at 28 megacycles and 65 at 60 megacycles per second.

Input Resistance

When the output impedance of the source of constant signal is made comparable to the input impedance of the switch, for example, by inserting a series resistor, the r-f envelope departs considerably from that obtained when the source impedance is negligible. Figure 6 shows pairs of oscillograms which demonstrate such departures. The left-hand oscillograms designated

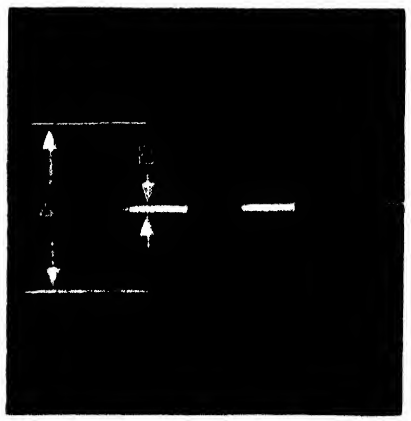

FIG. 5—Amplification characteristics and off-on ratio of the switch at 60 mc when R is 820,000 ohms

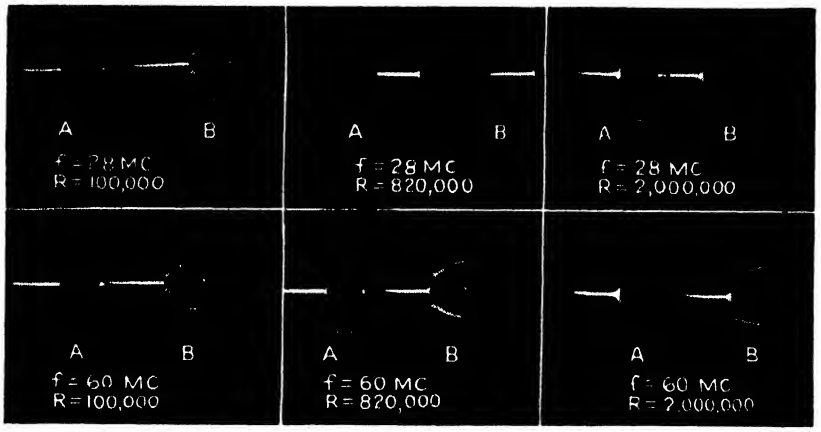

FIG. 6—Radio-frequency envelopes produced by switch under varying circuit conditions. Each left-hand picture (A), was obtained with the switch input connected to a low-impedance source, while at the right (B) it was connected to a 3,000-ohm source

by the letter *A* show the characteristic amplification pattern with R_s approximately 20 ohms, which is negligible; the right-hand oscillograms designated by the letter *B* show the corresponding results when R_s equals 3,000 ohms. In the latter case, R_s and the input resistance of the switch form a voltage divider that reduces the r-f voltage available for amplification. The input resistance of the switch varies continuously throughout the conducting portion of the multivibrator cycle as demonstrated by the fishtail shape of the right-hand oscillograms.

The particular application contemplated when this investigation was undertaken was such that the switch input would come from a push-pull circuit tuned to the r-f signal. For this reason a tuned input circuit (Fig. 4) was chosen to simulate the expected condition of operation. Since the circuit is tuned to the signal frequency, the reactive component is tuned out, except for a slight variation in input capacitance during the switching cycle, and the resistive component of the input impedance is measured.

The input resistance actually measured is that between one end of the tuned circuit and ground rather than that across the tuned circuit. It is the combined load of operative tube, inoperative tube, and circuit. Care was taken to balance the input circuit and the switch. The input resistance is measured in the following manner: first a signal voltage is applied directly to input 1 or input 2 (Fig. 4) from a generator of negligible internal impedance. The microvolt reading of the signal generator is the actual voltage applied. The height of the resulting square wave envelope is observed on the oscilloscope. Then a known resistance is placed in series with the signal generator and input 1 or input 2, thus producing an oscillogram having a fishtail contour. If the generator microvolt-reading is kept the same as before, then the difference between the height of the square wave and the height of the fishtail at any instant serves as a measure of the voltage drop across the known resistance in series with the signal generator. These data may be used to calculate the input resistance of the switch at any instant of the cycle, as given by the following equation

Input resistance=

$$R_s/[(H_0/H_R) - 1] \qquad (2)$$

in which H_0 is the height of the grid voltage-current curve for the particular tube was established. The slope of this curve was measured to determine the d-c incremental input resistance. The values of grid current, at which the slope was determined, were 300, 75, and 33 microamperes, which are the peak grid currents as determined above. It was found that the d-c incremental input resistances thus determined were of the same order of magnitude as the minimum r-f values.

Straight Amplifier Comparison

A comparison was made of the input resistance of the tubes during multivibration and of the same pair of tubes operating as an r-f amplifier (nonswitching). This was done in order to ascertain how the instantaneous impedance of a multivibrator deviated from the familiar

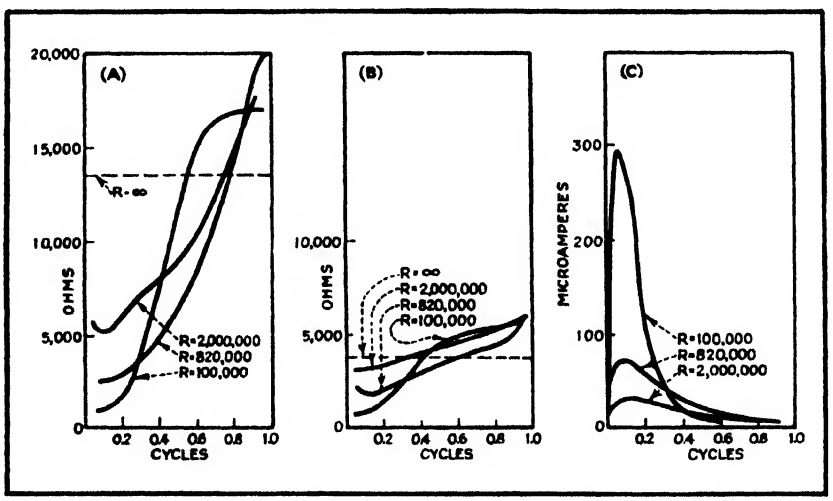

FIG. 7—(A) shows input resistance of the switch at 28 mc; (B) that at 60 mc. Grid current is shown in (C). Time interval is the cycle of conduction of either tube, which is about 2.5 milliseconds when R is 820,000 ohms

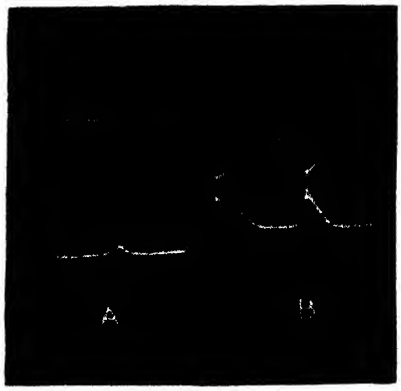

FIG. 8—Successive radio-frequency envelopes produced by the switch for parallel output connection at 60 mc when R is 100,000 ohms. At (A) the switch is connected to a low-impedance source; at (B) to a 3,000-ohm source

constant input impedance of an r-f amplifier. Measurements of input-resistance were made when $R = \infty$, that is, when the grid current was negligible. Fig. 7A and 7B indicate the results of these measurements by the horizontal lines marked $R = \infty$. These lines show that at 28 megacycles per second the input resistance of the switch is lower, throughout most of the switching cycle, than while functioning as an r-f amplifier. At 60 megacycles per second the input resistance is lower or higher depending upon the value of the feedback resistor R.

The prime cause for low input resistance of the switch is the fact oscillogram at a particular instant of the cycle for negligible impedance of the signal source, and H_R is the height at the same instant of the cycle when a known impedance R, is placed in series with the signal generator. The heights used in the formula should include correction for the thickness of the oscillograph line.

Variation During Switching

The variation of input resistance of the switch throughout a switching cycle is shown in Fig. 7. The data for these curves were obtained by applying Eq. 2 to oscillograms (Fig. 6). Care was taken to maintain constant output of the signal generator throughout the recording of each pair of oscillograms. The particular value of R (the resistor in the feedback path of the multivibrator circuit) for each oscillogram is indicated in the figures as is also the frequency of the signal. It will be noted that there is considerable variation of input resistance during a switching cycle. The range of this variation decreases as the signal frequency and the value of R are increased. It is interesting to know how the grid current varies during the same switching cycle, so the curve showing this variation is given in Fig. 7C.

A comparison was made of the minimum value of the r-f input resistances shown in Fig. 7A and 7B with the value of d-c input resistance of one tube at the peak grid currents shown in Fig. 7C. The that when either tube conducts its grid is driven slightly positive by the voltages of multivibration, resulting in grid-current loss. The loading of the switch is thus mostly that of one conductive tube, as compared with an amplifier with two tubes giving equal loading. The absence of electron flow in one tube of the switch permits the input resistance to exceed that of the amplifier under certain conditions already shown. When the loading produced by electron transit time becomes high at high frequencies, its absence in one of the switching tubes has a greater effect on the input resistance than at lower frequency where the grid current loading predominates.

It should be noted that when the tubes are used in the reference amplifier they are operated with small grid bias and at a plate current slightly above rated value. These conditions of operation are comparable to those in the switch but result in lower values of input resistance than those realized in normally biased amplifiers.

Since the measurements of input impedance have been made on a balanced circuit, the condition of balance was investigated. This was done by observing the oscillograms produced when the outputs 1 and 2 of the switch were connected in parallel. Fig. 8 demonstrates circuit performance.

References

(1) R. Keen, "Wireless Direction Finding," 3rd edition, Iliffe and Sons, Ltd., p 540, Fig. 428.
(2) E. Cole, and R. E. McCoy, Radio Adaptor Unit, U. S. Pat. 2,397,128, March 26, 1946.

Frequency Control for Low-Impedance Oscillator Tanks

By V. M. ALBERS

THE CONVENTIONAL arrangement for a variable-resistance frequency control tube used to control the frequency of an oscillator is shown in Fig. 1. Tube V is in series with capacitor C, and varies the effective value of its capacitance as a part of the oscillator tank circuit as the control grid voltage of V is varied.

Figure 2 is a variation of the circuit in which a diode is used in place of the resistor in the plate circuit of the frequency control tube. The diode conducts during a part of the negative half-cycles of the oscillator, and causes a positive voltage to be developed at point A in Fig. 2. The voltage developed can

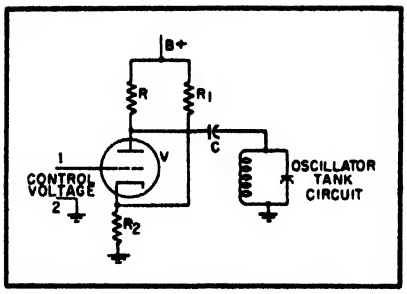

FIG. 1—Conventional circuit using a variable-resistance type frequency control tube

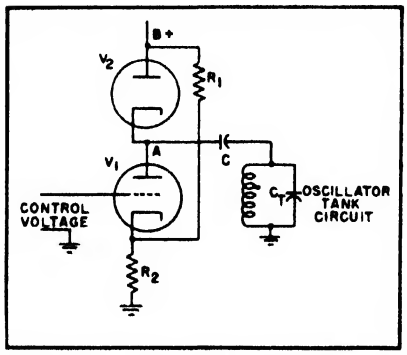

FIG. 2—Improved circuit using a diode in the plate circuit

leak to ground by way of the frequency control tube V_1 during the remainder of the cycle. The average potential which is retained at A is determined by the control voltage applied between points 1 and 2.

The effective value of C is then determined by the fraction of the negative half-cycle during which the diode conducts rather than by the effective resistance in series with C. The value of C used is about 20 percent of the value of C_T which is the fixed tank circuit capacitance.

For low-impedance tank circuits, this frequency control circuit offers considerable improvement over that shown in Fig. 1. It does, however, cause some variation in the oscillator frequency for a given control voltage applied between terminals 1 and 2 when the heater voltage for tubes V_1 and V_2 varies.

Stabilizer

To eliminate the effect of variations of heater voltage, the device has been further modified by replacing tube V_2 by a copper-oxide rectifier. The rectifier used by the author is the Varistor D-157873, containing four rectifiers which can be connected in series. The use of four rectifiers in series decreases the voltage applied across each rectifier. Figure 3 shows a schematic of the circuit using this rectifier. The values of the resistors were chosen to set the frequency control tube at the center of its range when zero voltage is applied between terminals 1 and 2.

The curves in Fig. 4 indicate the relative frequency change plotted as a function of the voltage applied to the frequency control tube grid for both the 6SN7 tube and the 7F8 tube. The sensitivity of the 7F8 tube is somewhat higher to small voltages applied to the control tube grid. However, the range of frequency control is about the same with either tube.

When the plate supply voltage was varied from 200 to 300 volts with the voltage applied to the frequency control tube grid maintained constant, the variation in oscillator frequency using the 7F8 tube was 0.07 percent, and using the 6SN7 tube the oscillator frequency variation was 0.02 percent. When the heater voltage was varied from 6.3 to 5.7 volts, the frequency change using the 7F8 tube was 0.2 percent, and using the 6SN7 tube it was 0.07 percent.

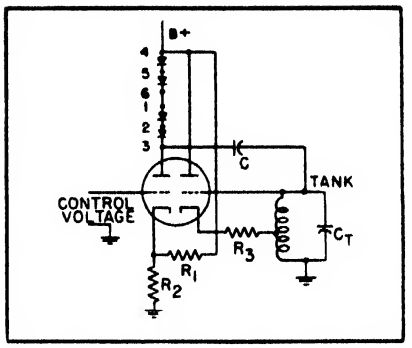

FIG. 3—Final circuit with the Varistor in the plate circuit. Values of R_1 and R_2 are 33,000 and 1,500 ohms respectively for a 6SN7 and 35,000 and 1,000 ohms for a 7F8. Numerals indicate Varistor terminals

The 7F8 tube is a more sensitive frequency control tube than the 6SN7 but it has a correspondingly higher sensitivity to the effects of plate and heater voltage variation. These effects of heater and B-supply voltage variation are the combined effects on both the oscillator and frequency control sections.

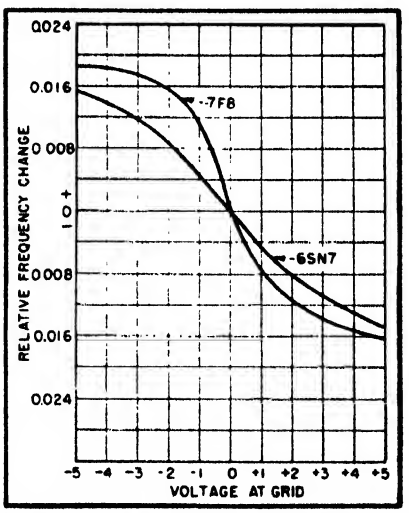

FIG. 4—Curves showing the variation of oscillator frequency as a function of control voltage

Conversion from Series to Parallel Impedance

By GERSHON J. WHEELER

IMPEDANCE MEASUREMENTS made on r-f bridges are usually determined in series form $R \pm jX$, but in many applications, it is desirable to know the equivalent parallel impedance; that is, that value of resistance and reactance in parallel which will have an impedance equivalent to that measured on the bridge. The

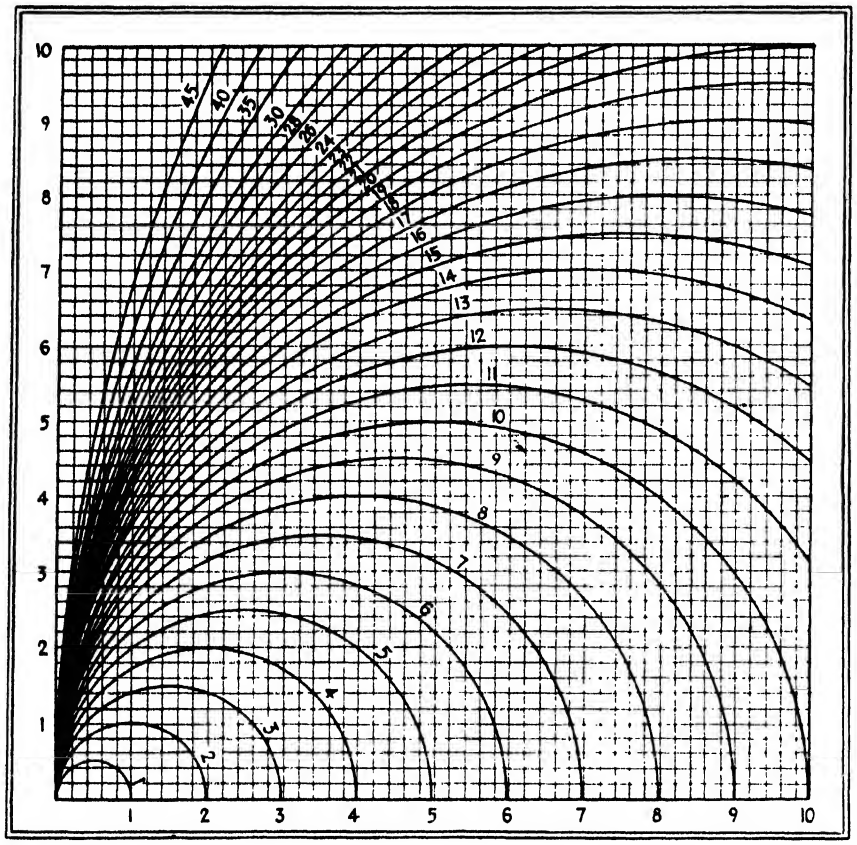

Graph for converting resistive and reactive series-impedance components into equivalent parallel-impedance elements is constructed from circles the locus of whose centers are on the horizontal axis of a rectangular coordinate system

accompanying graph presents a quick method for determining the equivalent parallel resistance R_p and reactance X_p when the series resistance R_s and reactance X_s are known.

To determine the value of *parallel resistance*, enter the value of series resistance on the horizontal axis and the value of series reactance on the vertical axis. The number at the right-hand end of the arc at which these coordinates intersect is the value of the parallel resistance.

To determine the value of *parallel reactance*, enter the value of series reactance on the horizontal axis and the value of series resistance on the vertical axis. The arc now indicates parallel reactance.

The arc indicates the parallel value of whichever series component was entered on the horizontal axis. The units may be ohms, tens of ohms, megohms, or anything else, but must remain the same throughout.

If the value of the series resistance is more than ten times or less than one-tenth the series reactance, the graph should not be used. Instead, the following relationships which hold within one percent produce the required result more quickly. With small R_s, $R_p = X_s^2/R_s$ and $X_p = X_s$. With large R_s, $R_p = R_s$ and $X_p = R_s^2/X_s$.

Illustrations

EXAMPLE I: R_s is 42 ohms, X_s is 58 ohms. Find R_p and X_p. The numbers on the graph will be used to indicate tens of ohms. Enter with 4.2 on the horizontal axis and 5.8 on the vertical. These coordinates intersect just above the arc numbered 12. The value of R_p is about 122 ohms. Next enter with 5.8 on the horizontal axis and 4.2 on the vertical. The intersection is just below the arc numbered 9. The value of X_p is about 89 ohms.

EXAMPLE II: R_s is 400 ohms, X_s is 70 ohms. Find R_p and X_p. Here, the numbers on the graph must indicate hundreds of ohms. Enter with 4 on the horizontal axis and 0.7 on the vertical. The intersection indicates that R_p is about 410 ohms. Enter with 0.7 on the horizontal axis and 4 on the vertical. The intersection is on arc 23, thus, X_p is 2300 ohms.

The graph may be used for either capacitive or inductive reactance. The parallel reactance, of course, has the same sign as the series reactance.

Graphical Determination of Percent Harmonic Distortion

By ROBERT W. BUCHHEIM

IN DESIGNING resistance loaded amplifiers or analyzing vacuum tubes the relation between load resistance and harmonic distortion is frequently needed. Usually numerical calculations based on values read from characteristic curves are made to find this relation; however a graphical method can be

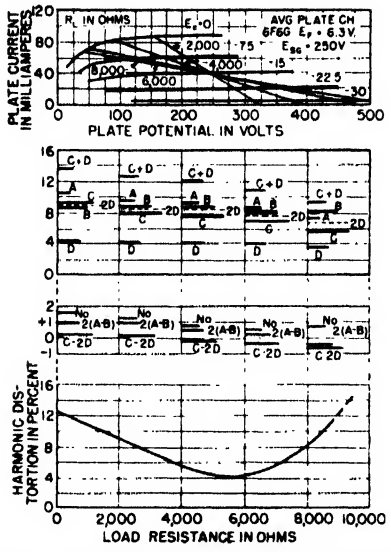

FIG. 1—Using currents from tube characteristic, combinations are plotted and differences and quadratic sumes obtained giving quantities from which percent harmonic distortion is obtained

used that is simpler. Furthermore, this graphical method has the advantage that it uses the distances from the characteristic curve directly without the necessity of converting them to numbers, and it has an accuracy that is more compatible with the original data than is the arithmetical computation.

Basis for the Method

The commonly used expressions for harmonic distortion are

$$D_2 = \frac{(I_H + I_L) - (I_X + I_Y)}{(I_H - I_L) + (I_X - I_Y)} \qquad (1)$$

$$D_3 = \frac{(I_H - I_L - 2(I_X - I_Y)}{2(I_H - I_L) + (I_X - I_Y)} \qquad (2)$$

where D_2 is the ratio of the second harmonic to the fundamental and D_3 is the ratio of the third harmonic to the fundamental currents; I_H is the plate current at the positive peak of the grid swing, I_L is the plate current at the negative peak, I_X is the plate current when the grid signal voltage is at half its positive peak, and I_Y is the plate current at half the negative grid swing. Total harmonic distortion D_0 as a fraction of the fundamental is given by

$$D_0 = (D_2^2 + D_3^2)^{1/2} \qquad (3)$$

A plot of D_0 vs R_L is required.

For ease of notation let: $A = (I_H + I_L)$, $B = (I_X + I_Y)$, $C = (I_H - I_L)$ and $D = (I_X - I_Y)$, then Eq. 3 can be written

$$D_0 = \frac{\{[2(A-B)]^2 + [C-2D]^2\}^{1/2}}{2(C+D)} = N_0/2(C+D) \qquad (4)$$

where $N_0^2 = [2(A-B)]^2 + [C-2D]^2$

The quantities N_0 and $(C + D)$ can be obtained graphically.

Consider a family of plate characteristics for a 6F6G power pentode as shown in Fig. 1. The operating point is chosen at the intersection of the $E_B = 250$-volt coordinate and the $E_G = -15$-volt curve. Load lines corresponding to several likely load resistances are drawn through this operating point.

A sheet of coordinate paper is arranged as in the rest of Fig. 1 with vertical lines labeled with the various values of load resistance to be considered. The ordinate of the top coordinate section is in milliamperes; its scale can be arbitrary or it can be transferred directly from above with dividers. Distances representing I_H, I_L, I_X, and I_Y are transfered in this way so that a plot of these quantities vs R_L is obtained. There is no need to draw a careful curve through these values, but a free-hand curve helps in identifying them.

From these intermediate curves, curves of A, B, C and D can be obtained by graphical addition and subtraction in accordance with their definitions. Next, in a similar manner, curves of $2D$, $(C - 2D)$, $(C + D)$, $(A - B)$ and $2(A - B)$ are constructed.

To obtain N_0 a quadrature addition of $2(A - B)$ and $(C - 2D)$ is made by measuring these quantities at right angles to each other; the diagonal joining their ends is N_0. As shown in the diagram, the graph becomes crowded when the currents have been added to give their sums and differences. Hence the constructions are transferred, as made, to a clear section of the graph below. The distance of N_0 is also plotted in this section.

When N_0 and $2(C + D)$ have been obtained D_0 is determined from slide rule manipulation using Eq. 4. Because D_0 is the ratio of quantities of the same dimensions, the scales of the ordinates can be whatever is convenient. The factor 2 can be eliminated from the final expression for D_0 if the scale of lower work graph is half that of the top section; $(C + D)$ must then be plotted in the lower part.

This construction is carried through for each R_L and a plot of D_0 vs R_L made as in Fig. 1; plots of D_2 and D_3 can also be made conviently. This graphical method is fast and direct. A regular routine should be followed in carrying it out; many of the combinations can be made without changing the setting of the dividers. Errors are easily detected as the construction progresses by any radical singularities in the intermediate curves.

Optimum Conditions for an R-C Oscillator

By H. A. WHALE

RESISTANCE-CAPACITANCE NETWORKS of the type shown in Fig. 1 occur in many electronic circuits. The network is used in feedback oscillators of the Wein bridge type, in which case the components can be proportioned in accordance with relations presented in this discussion to provide optimum frequency stability. Although these relations are derived for the particular bridge oscillator under examina-

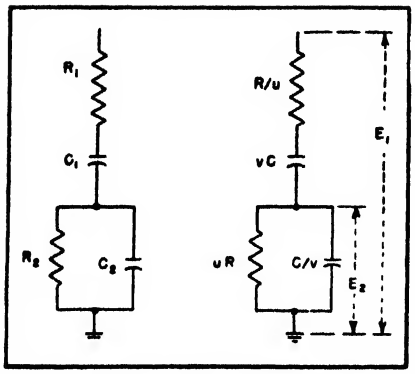

FIG. 1—Circuit under consideration is common to many applications

tion, they are also valid for a resistance-capacitance amplifier made frequency selective by choice of coupling or where feedback is used to give an amplifier having rejection for a narrow band of frequencies.

Wein Bridge Oscillator

In the common R-C cathode-coupled oscillator of the Wein bridge type[1], the components of the feedback network are proportioned so that R_1C_1 equals R_2C_2, under which condition the ratio of output voltage E_2 to input voltage E_1 varies with frequency in the manner shown in Fig. 2 by curve for $U^2 = 1$[2,3]. The frequency selectivity of this particular type of oscillator is due to the comparatively rapid change with frequency of the phase between the input and output voltages in the vicinity of the oscillating frequency, $1/[2\pi(R_1R_2C_1C_2)^{1/2}]$ cycles per second.

In designing such oscillators for the greatest frequency stability, the conditions for the most rapid change of phase with frequency and for the most sharply peaked $|E_2/E_1|$ curve are required. These conditions can be found by replacing R_1 C_1, R_2, C_2 respectively by R/u, vC, uR, and C/v, in which case the oscillating frequency is $f_0 = 1/2\pi RC$. For any frequency f

$$\frac{E_2}{E_1} = \frac{y(f/f_0)^2 + j(f/f_0)[1 - (f/f_0)^2]}{[1 - (f/f_0)^2]^2 + y^2(f/f_0)^2} \quad uv \quad (1)$$

where $y = (u^2 + v^2 + u^2v^2)/uv$. Let $(f/f_0) = x$, then

$$\left|\frac{E_2}{E_1}\right| = \frac{uvx}{[(1 - x^2)^2 + (xy)^2]^{1/2}} \quad (2)$$

$$\phi = \tan^{-1}(1 - x^2)^2/xy \quad (3)$$

For maximum rate of change of phase with frequency, differentiate ϕ with respect to x. Inasmuch as interest is in values near $\phi = 0$ at which $x = 1$

$$\phi = (1 - x^2)^2/xy \quad (4)$$

therefore

$$\frac{d\phi}{dx} = -(x^{-2} + 1)/y \quad (5)$$
$$\approx -2/y \quad (\text{near } x = 1)$$

Because x is nearly unity near the oscillating frequency

$$\left|\frac{E_2}{E_1}\right| = \frac{uv[1 - (1 - x^2)^2/2(xy)^2]}{y} \quad (6)$$

The magnitude of the term $(1 - x^2)^2/2(xy)^2$ determines the sharpness of the resonance peaks, for the smaller is y the more rapid the change with x. Thus, as would be expected, the rate of change of phase and the sharpness of the resonance peak both depend on the same parameter y.

The problem is to determine the values of u and v for which y is a minimum. To do so, let $v^2 = 1$, in which case $C_1 = C_2$, and then $y = (2u^2 + 1)/u$. This relation is a minimum when $u^2 = 0.5$. Various calculated amplitude, and phase curves for $v^2 = 1$ and different value of u^2 are shown in Fig. 2 with the value of u^2 indicated for each curve.

For any general value of v^2 there is an optimum value of u^2 and vice-versa. The general expressions are obtained.

$$\frac{dy}{du} = \left(\frac{d}{du}\right)\frac{u^2 + v^2 + u^2v^2}{uv} \quad (7)$$

$$= -(v/u^2) + (1/v) + v \quad (8)$$

which equals zero when

$$u^2 = v^2/(1 + v^2) \quad (9)$$

Similarly, for a given value of u^2 the optimum value of v^2 is

$$v^2_A = u^2/(1 + u^2) \quad (10)$$

Carrying the logic further, put Eq. 9 into the expression for y, then

$$y^2 = 4(1 + v^2) \quad (11)$$

which has its minimum when $v^2 = 0$, and then $u^2 = 0$. Thus the criteria for the sharpest resonance curves and the most rapid change of phase near the resonant frequency are that u and v are as small as possible consistent with maintaining either Eq. 9 or 10. When u and v are both small, they are nearly equal.

Figure 3 presents curves for various values of (u^2, v^2). These curves include the cases for u^2 and v^2 both vanishingly small; that is, the theoretically best conditions that can be obtained. Also included in Fig. 3 are some experimental points obtained with the indicated values.

For the conventional case at $x = 1$

$$u^2 = v^2 = 1; \quad d\phi/dx = -2/3$$

while for the optimum case at $x = 1$

$$u^2 = v^2 \to 0; \quad d\phi/dx = -1$$

Practical Considerations

The foregoing analysis indicates that for maximum stability the ratios C_2/C_1 and R_1/R_2 should be as large as possible consistent with a given (frequency) relationship between them. In oscillators employ-

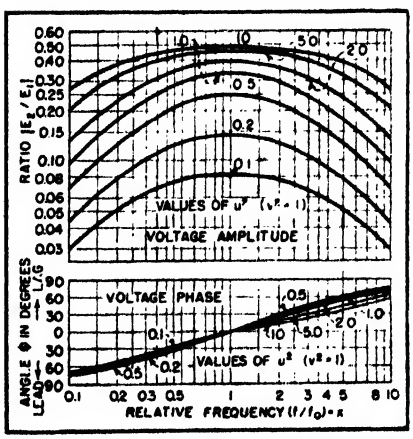

FIG. 2—Normalized amplitude and phase characteristics of circuit

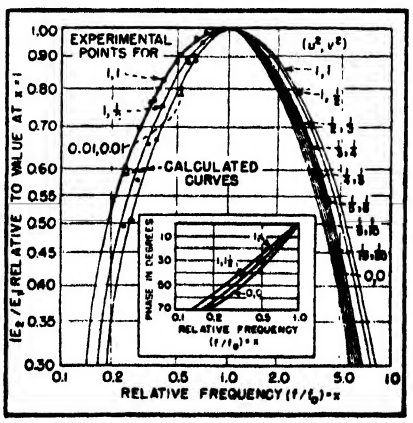

FIG. 3—Experimental points fall close to the calculated resonance curves

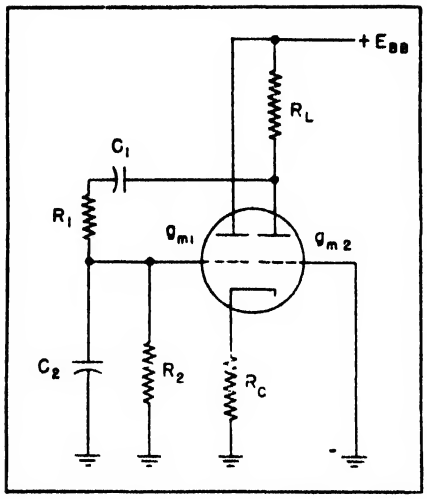

FIG. 4—Typical oscillator circuit to which design can be applied

ing this type of feedback circuit; condition for oscillation is

$$1 + R_1/R_2 + C_2/C_1 < A \qquad (12)$$

where A is the gain in the auxiliary amplifying circuit. Using the foregoing notation, this condition can be expressed as

$$1 + 1/u + 1/v < A \qquad (13)$$

Thus the minimum values of u and v that can be employed are determined by the gain that is available from the amplifier.

For example, in the cathode-coupled oscillator[4] shown in Fig. 4, the condition for oscillation is

$$E_2 > AE_1 \qquad (14)$$

or

$$\frac{uv}{y} > A = g_{m1}g_{m2}R_c R_L \qquad (15)$$

which means that

$$1 + 1/u + 1/v < g_{m1}g_{m2}R_c R_L \qquad (16)$$

where g_{m1} and g_{m2} are the mutual conductances of the two triode sections under the operating conditions.

If the oscillator is to cover a range of frequencies, the ratio C_2/C_1 must remain constant over the band. This consistancy can be accomplished by using a ganged tuning capacitor with, for example, C_2 consisting of three sets of plates in parallel and C_1 the other set. Then $v^2 = 0.33$. Thus for optimum stability with this value of v^2, $u^2 = 0.25$. The condition for oscillation becomes

$$g_{m1}g_{m2}R_c R_L > 8 \qquad (17)$$

For usual triodes, R_o is approximately 500 ohms, and g_m is approximately 2,000 microhms, therefore R_L should be greater than 4,000 ohms.

(1) H. H. Scott, A New Type of Selective Circuit and Some Applications, *Proc. I. R. E.*, p 226 Feb. 1938.
(2) F. E. Terman, R. P. Buss., W. R. Hewlett, and F. C. Cahill, Some Applications of Negative Feedback with Particular Reference to Laboratory Equipment, *Proc. I. R. E.*, p 649 Oct. 1939.
(3) F. E. Terman, "Radio Engineers' Handbook", McGraw-Hill Book Co., New York, p 505 1943.
(4) Keats A. Pullen, The Cathode Coupled Amplifier, *Proc. I. R. E.*, p 402 June 1946.

Pulse-Modulated Oscillator

Method and circuits are presented for pulsing a high frequency oscillator so that all waves are of the same amplitude. Pulse rate is variable over wide limits independently of oscillator frequency. Calibration and marking of sweeps with the equipment are described

By ALLAN EASTON

AN IMPROVED METHOD for generating a train of sine waves, in which the first cycle is identical to the following cycles, is described. The train may be initiated from an outside trigger and may therefore operate over a wide range of pulse repetition frequency. Large peak-to-peak amplitudes are available requiring but small power input.

Rapid development of equipments utilizing pulse techniques has made necessary precise methods of time measurement. The cathode-ray oscilloscope using slave sweeps has become a common tool for accurate pulse work[1, 2, 3, 4].

Various means have been suggested for calibration of time bases[5, 6, 7]. The method described in this paper provides a readily adjustable means of generating a sinusoidal wave train of uniform amplitude under control initiated by externally applied triggers.

Pulsed Resonant Circuit

The most elementary type of sine wave sweep calibrator is shown in Fig. 1A. Operation depends on the transient oscillation which results from sudden interruption of a steady current flowing through an inductance shunted by a capacitance. Should the current I_p be suddenly cut off by application of a negative gate to the triode grid, an oscillatory voltage appears across the capacitance such that

$$e_c = -I_p(L/C)^{1/2}\epsilon^{-\omega t/2Q}\sin \omega t \qquad (1)$$

where the symbols are defined and derived in the appendix.

The exponential term of Eq. 1 determines the rate of decay of the oscillation. If Q were very high, oscillations would persist, dying out gradually. However, with ordinary commercial inductors having practical values of Q, oscillations decay in a relatively short time, as shown in Fig. 1B.

The magnitude of Q required to give an amplitude Ke_0 to the nth cycle of oscillation (derived in appendix) is

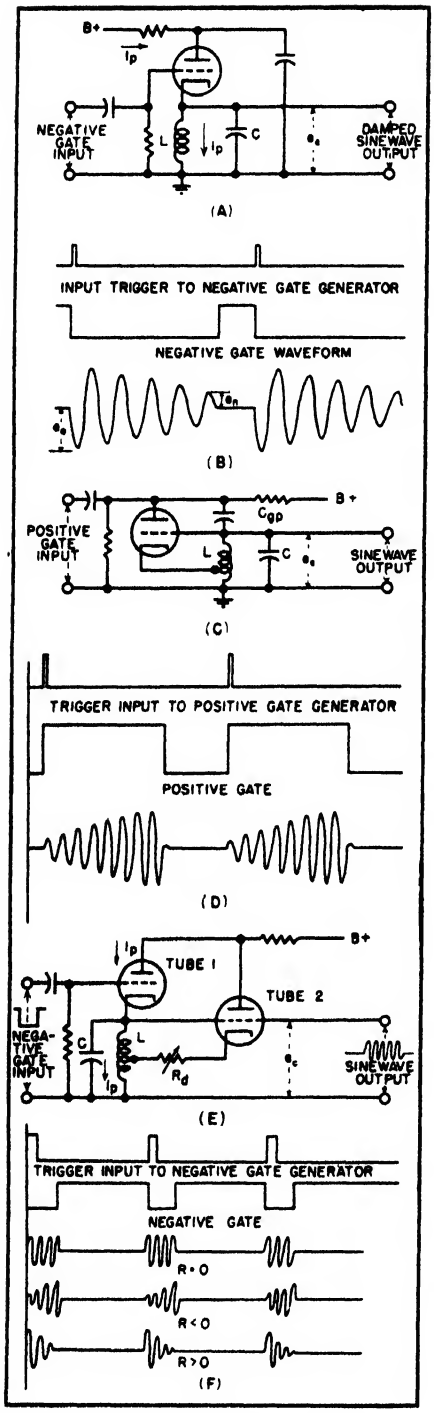

FIG. 1—By combining a pulsed resonant circuit (A) giving a damped wave train (B) with a keyed oscillator (C) giving a wave train that builds up (D), a pulsed oscillator (E) that can generate a wave train of constant amplitude (F) is obtained

$$Q = \frac{(n-1)\pi}{\ln(1/K)} \qquad (2)$$

Thus to obtain e_n equal to $0.9e_s$, that is K equals 0.9, where n is 21 cycles, Q must nearly equal 600 (This relation incidentally provides a method of measuring Q of an inductor[4].)

Limitations of the damped train as an accurate source of sweep calibration markers are numerous and some superior means have been developed.

Keyed Oscillator

It is possible to develop a sine wave train by the method shown in Fig. 1C. A Hartley type oscillator is connected so that application of a positive gate to the triode plate will result in the growth of oscillations such that

$$i = (e_s/\omega L)(\sin \omega t) \exp R_n t/2L \qquad (3)$$

Oscillations grow at a rate determined by the magnitude of negative resistance R_n introduced by the oscillator tube. This circuit may be difficult to synchronize well. The degree of synchronization depends upon factor e_s of Eq. 3. If sufficiently high frequency components are present in the rising edge of the positive gating pulse, synchronizing pulses can be obtained in the tuned circuit through the triode grid-to-plate capacitance. At best, locking with the trigger is precarious and, in addition, time delay involved in waiting for oscillations to reach final amplitude, as illustrated in Fig. 1D, may be prohibitive for many applications.

Combination Circuits

An ingenious combination of both circuits described above was developed by Radiation Laboratory, Massachusetts Institute of Technology.

The circuit, shown in Fig. 1E, may be analyzed qualitatively by considering the oscillator tube (tube 2) as a source of negative resistance. If the oscillator were not present, the circuit would be similar to that of Fig. 1A, the damping resistance in this case is greater than zero and therefore the wave train will decay exponentially as mentioned. As the magnitude of the negative resistance (controllable by degeneration potentiometer R_d) causes the equivalent circuit resistance to approach zero (Q approaches infinity), the envelope of the oscillations more nearly approaches a pair of parallel horizontal straight lines. Should the effective circuit resistance become negative, oscillations will build up from their initial value to some final value determined by circuit parameters. These conditions are illustrated in Fig. 1F.

The magnitude of the peak voltage of the first cycle is

$$e_{max} = I_p(L/C)^{1/2} \qquad (4)$$

Equation 4 predicts an oscillator voltage proportional to the d-c plate current and to the square root of the L to C ratio. Substituting typical values into the equation where $C=100\mu\mu f$, $L=250\mu h$, $I_p=0.010$ amp, and $f=1.006$ mc gives e_s equal to 15.8 volts peak or 31.6 volts peak-to-peak.

If this voltage is inadequate for a particular application, it is then necessary to increase I_p. The upper limit to the L to C ratio is determined by stability requirements and therefore cannot be increased indefinitely.

At about 10 mc this circuit becomes expensive and unwieldy. Suppose $C = 25\mu\mu f$, $L = 10\mu h$, $I_p = 0.010$ amp, and $f=10.06$ mc, then e_s is equal to 6.32 volts peak. To obtain the same value of e_s at 10 mc as was realized at one megacycle, plate current should be more than doubled and yet circuit stability would be poorer because of the higher L to C ratio. Should really large marker voltages be desired, excessive plate currents would be required.

Pulsed Oscillator

For reasons of economy and simplicity another approach to the problem, which extends the operating range to well over twenty megacycles, was tried. The principal difference circuitwise is the inclusion of a gas thyratron such as a type 2D21, 2050, 6D4, or 884 and associated circuits shown in Fig. 2.

Theory of operation is as follows. Three tubes are employed, a shock tube V1, a clamp tube V2, and an

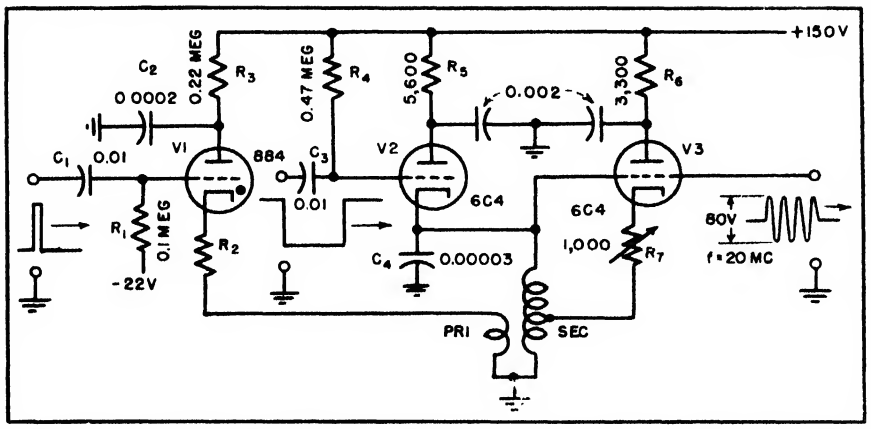

FIG. 2—Circuit of a pulsed oscillator that delivers pulses of high, uniform amplitude

oscillator tube V3. The shock tube V1 has the characteristic of being able to pass large surges of current (in excess of five amperes) for a short interval and then remain in the ready state with the passage of a small current (in the order of microamperes). Clamp tube V2 has the characteristic that its resistive impedance from cathode to ground (the plate is held at a-c ground by a capacitor), which is in parallel with the tuning coil of the oscillator, is very high when the tube is nonconducting (control grid biased negative), and very low (about 300 ohms or less depending on tube type) when the tube is conducting. Oscillator tube V3, with its circuit, is permitted to oscillate or prevented from oscillating by the clamp tube by virtue of the tube resistance which shunts the tuned circuit.

In operation the circuit is in the ready state when C_2 is fully charged through R_3 to the supply potential. Tube V2 is conducting and tube V3 is therefore in the nonoscillating condition.

Sequence of Circuit Functions

When it is desired to set off a train of oscillations each of the same amplitude, a sharp positive pulse is applied to the thyratron grid through R_1C_1, causing the gas to ionize and C_2 to discharge through the interelectrode space and the primary of the high frequency transformer. Simultaneously with the positive pulse on the thyratron grid, a negative gate is applied to the grid of the clamp tube through C_3R_4 causing the clamp tube to become nonconducting and permitting oscillations to build up.

Oscillations will, therefore, not have to build from low amplitude gradually, but can be equal or even larger than succeeding oscillations.

When the positive pulse which was impressed on the thyratron grid decays, the gas tube deionizes by virtue of R_3C_2 in the plate circuit, and the tube disconnects itself from the circuit except for the cathode to ground capacitance across the tuned circuit. Oscillations will continue until the negative gate on the clamp tube grid is removed, permitting the clamp tube to become conducting thereby quickly damping the oscillations.

Rate of decay is determined by the magnitude of the resistance the clamp tube shunts across the tuned circuit. Type 6J4 which has a very high value of transconductance will damp the oscillations faster than will type 6C4. (In all cases decay time may be longer than rise time.) Meanwhile C_2 will be recharging through R_3 preparatory for the next cycle of operation.

Circuit Characteristics

This circuit has been constructed and tested using component values indicated in Fig. 2. With a positive plate voltage supply of 150 volts, it was possible to obtain as much as 80 volts peak to peak at 20 mc. This large voltage was possible chiefly by virtue of the tremendous surge of current delivered by C_2 through the thyratron tube into the tuned circuit as explained above. The circuit as shown is capable of operation at pulse repetition frequencies ranging from less than one cycle per second to slightly over 5,000 cps. Total average plate current consumption of the three tubes does not exceed ten milliamperes at the highest frequency of operation.

Some necessary precautions for obtaining optimum performance are:

The positive trigger which actuates the thyratron grid should have a steep rise, preferably in the order of 1,000 volts per microsecond.

The negative gate which actuates the clamp tube must rise quickly enough so that the clamp tube current is cut off at the same time that the gas tube fires.

The transformer primary must be connected to the cathode of the shock tube by short leads. The primary must be closely coupled to the secondary; the primary turns numbering one half of the secondary turns, approximately.

R_7 is adjusted for flattest topped wave trains.

R_3 should be selected of sufficient resistance to limit peak current in the thyratron to a safe value as specified by the manufacturer. R_3 may be used to determine the initial amplitude of the generated sine wave train.

Applications

The most obvious application of the pulse modulated oscillator is for time base calibration. In the commonest case a saw-tooth sweep of somewhat indeterminate length is used to measure characteristics of a pulse display. The sine wave train is fed into vertical deflecting plates of a cathode-ray tube and horizontal deflection sensitivity is adjusted to give a full deflection. Thus with the period of the calibrating waves known, the time scale in microseconds per inch is

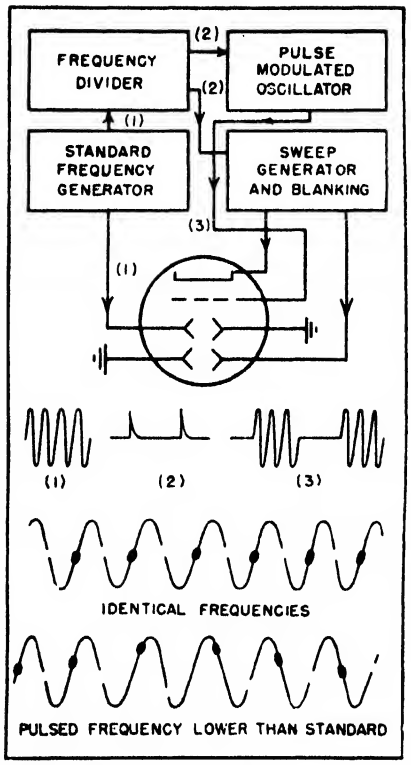

FIG. 3—Using the method shown at the top, the patterns shown below are obtained to indicate the frequency of the pulsed oscillator

determined. Calibrating markers are virtually indispensable where the sweep velocity is not constant.

The pulse to be measured may be observed simultaneously with the calibrating markers. Controllable delay and negative gate duration may be adjusted to cause the markers to coincide with the pulse.

Intensity grid modulation of the cathode-ray beam is a popular means of utilizing sweep markers. The sine wave train may be mixed with blanking pulses or may be connected to the cathode or grid of the cathode-ray tube while the blanking pulses are connected to the unused element. Alternate bright and dark spots facilitate measurement of pulses without distorting the shape of the display.

A convenient possibility is to use one pulsed oscillator for making one microsecond dots and another for making 0.1 or 0.05 microsecond dots and then mixing the two to give marker dots.

A particularly interesting extension of testing amplifiers by square wave analysis[9] is made possible with the pulse modulated oscillator. In present television receiver practice an intermediate frequency of about 21 mc has been accepted as standard. Overall bandwidths of 3 to 5 mc are used and some means for testing transient response of intermediate frequency amplifiers is needed. It is customary to use a sweep oscillator and cathode-ray oscilloscope[10] for this purpose. This method gives little information concerning transient response whereas the pulse modulated oscillator when injected into the grid circuit of the i-f amplifier enables direct observation of pulse response of all circuits after the mixer. Vertical or horizontal synchronization pulses can be used to trigger the pulsed oscillator.

Methods of Calibration

In order to utilize fully the pulse modulated oscillator, some means of accurately setting or measuring the sine wave frequency is needed.

Common is the zero beat method in which a crystal oscillator or standard signal generator is made to zero beat with the unknown frequency. Caution must be maintained to avoid synchronization of the pulsed oscillator by the standard frequency source or the reverse. It is possible for the pulsed oscillator to begin oscillating at a frequency determined by its own circuit constants and then be forced into another frequency of oscillation by the calibrating voltage. At 20 mc, small stray capacitances may cause considerable coupling. Synchronization of either pulsed oscillator or calibrating oscillator by one another or by an external stray signal must be avoided if useful results are to be obtained[11]. The zero beat method gives no information about the spacing of individual sine waves of the pulsed train but measures average frequency. If the first few oscillations had a different period from the succeeding cycles, a situation which is quite possible, the zero beat method would not reveal this fact.

The fact that the sine wave train is pulsed, that is, interrupted periodically, gives rise to a spectrum of frequencies, any one of which may give zero beat with a calibrating frequency. Only one of these beats represents the center frequency of the wave train[12].

Another method of calibration utilizes the cathode-ray tube oscilloscope to obtain a Lissajou figure[13]. When two voltages of slightly different frequencies are compared, one connected to each pair of deflecting plates of the cathode-ray tube, a stationary pattern will appear either if the two frequencies bear a harmonic relationship, or if they have a harmonic in common.

When the two frequencies are equal, a stationary geometric figure such as a circle, ellipse, or straight line can be obtained. The same precautions against unwanted synchronization must be observed in this case. The characteristic circle denoting equal frequencies can be obtained by comparing the calibrating frequency with any one of the spectral sideband components of the pulsed wave. Frequency difference between successive spectral components depends upon pulse repetition frequency. Advantage may be taken of this fact in calibrating by Lissajou figures. If the characteristic circle is obtained, change the pulse rate slightly; only the center component, that is the nominal sine wave frequency, will remain unchanged and will continue to give the circle. Any spectral sideband components will change frequency when the pulse rate is altered.

An excellent method of calibration, first demonstrated to the author by R. D. Scheldorf of Radio Corporation of America, is illustrated in Fig. 3. A crystal oscillator or other type of standard frequency generator is connected to a frequency divider which generates a synchronizing pulse to trigger the pulse modulated oscillator and slave sweep of the cathode-ray oscilloscope. The standard frequency voltage is connected to the vertical plates through the vertical

amplifier, and the pulse modulated oscillator to the intensity control grid (Z axis). If the two frequencies differ but slightly, a very easily recognized result appears. The difference frequency shows up as a wave of bright spots whose period is equal to the reciprocal of the difference. Precautions must be taken as usual to prevent oscillator pulling. No trouble is experienced with sidebands. It is also possible to determine whether any shift in frequency of the pulse modulated sine waves occurs when the pulse rate or duration of the train is altered. In the case where only a few cycles of the train are desired, the above methods do not give sufficient accuracy for the most precise requirements.

The most accurate calibrating procedure developed to date to the author's knowledge is the method described in a previous paper[14]. This paper describes a rapid, accurate determination of spacing between pulses or sine waves having production line simplicity and laboratory precision. It is possible to ascertain whether the first cycle has the same period as the succeeding cycles. This information is important where maximum precision is desired.

Mathematical Appendix

A simplified equivalent circuit of the keyed oscillators discussed in the text is shown in Fig. 4. Switches S1 and S2 are provided to indicate various stages in the operation of the circuits.

CASE A considers the buildup characteristic of the elementary pulsed sine wave generator of Fig. 1A for which S1 and S2 are normally closed, but at $t = 0$ S2 is opened. The differential equation describing the subsequent action is

$$L\frac{di_2}{dt} + R_L i_2 + q/c = 0 \qquad (1A)$$

or

$$(DL + R_L + 1/PC)i_2 = 0 \qquad (1B)$$

Where $1/P = \int_0^t dt$

The general solution[15] of Eq. 1 is

$$i_2 = (\exp - \alpha_1 t)\,[A_1 \sin \beta t + A_2 \cos \beta t] \qquad (2)$$

In order to evaluate the arbitrary constants of integration the following boundary conditions are substituted, neglecting $I_p R_L$ drop

$t = 0, q = 0, i_2 = -I_p$, and $\left(\frac{di_2}{dt}\right) = \left(\frac{\alpha_1}{\beta_1}\right) I_p$.

The complete solution is therefore

$$i_2 = -I_p (\exp - \alpha_1 t)\,[\cos \beta_1 t - \alpha_1/\beta_1 \sin \beta t] \qquad (3)$$

We are primarily concerned with the potential across the capacitance

$$e_c = \frac{1}{c}\int i_2\, dt \qquad (4)$$

$$e_c = \frac{I_p}{C}\cdot\frac{\alpha_1}{\beta_1}\int (\exp - \alpha_1 t) \sin \beta_1 t\, dt - \frac{I_p}{C}\int (\exp - \alpha_1 t) \cos \beta_1 t\, dt \qquad (5)$$

Performing the indicated integration and evaluating the constant of integration gives

$$e_c = \frac{-I_p}{\beta_1 C} (\exp - \alpha_1 t) \sin \beta_1 t \qquad (6)$$

If Q is very much greater than unity,

$$\beta_1 = \omega, \text{ and } \alpha_1 = \frac{\omega}{2Q}, \text{ and}$$

$$e_c = -\frac{I_p}{\omega C} (\epsilon^{-\omega t/2Q}) \sin \omega t \qquad (7A)$$

or also

$$e_c = I_p (L/C)^{1/2} (\epsilon^{-\omega t/2Q}) \sin (\omega t + \pi) \qquad (7B)$$

Equation 7 describes an oscillation whose decay properties depend upon the magnitude of Q. If Q is very high but R_L is still larger than zero e_c decays slowly (see Fig. 1B and 1F). If Q is infinite, that is, if $R_L = 0$

$$e_c = -I_p (L/C)^{1/2} \sin \omega t \qquad (8)$$

This equation expresses the case shown in Fig. 1E and 2 where the oscillator tube is adjusted to cause the effective circuit resistance to vanish. If Q is negative, that is, if R is less than zero, then oscillations build up indefinitely. Actually losses in the circuit due to nonlinearity of the oscillator tube will limit the amplitude of oscillations.

In using the circuit in Fig. 1A, assume one wishes to ascertain the Q required to sustain oscillations for n cycles so that

$$e_n = Ke_0 \qquad (9)$$

then

$$e_0 = I_p (L/C)^{1/2} (\exp - \omega t_n/2Q) \sin \omega t_0 \qquad (10A)$$

and

$$e_n = I_p (L/C)^{1/2} (\exp - \omega t/_n 2Q) \sin \omega t_n \qquad (10B)$$

but

$$\omega t_0 = \frac{\pi}{2} \text{ and } \omega t_n = 2(n-1)\pi + \frac{\pi}{2}$$

then

$$K = \frac{e_n}{e_0} = \exp - \frac{(n-1)\pi}{Q} \qquad (11)$$

from which

$$Q = \frac{(n-1)\pi}{l_n (1/K)} \qquad (12)$$

Figure 5 is a plot of K versus Q for several typical values of n.

The amplitude of the first cycle of oscillation may be readily obtained from the Eq. 7A. Let $\omega t = \pi/2$ and $Q >> 1$ then $e_{cmax} = I_p (L/C)^{\frac{1}{2}}$. As a check this can be deduced from energy considerations where

$$\frac{1}{2} L I_p^2 = \frac{1}{2} C e_c^2 \qquad (14)$$

and

$$e_{cmax} = I_p (L/C)^{1/2} \qquad (13)$$

CASE B refers to Fig. 1C for which S2 in Fig. 4 is open throughout. Before $t = 0$ S1 is closed. At $t = 0$ S1 is opened causing circuit resistance to become negative. Synchronizing pulse e_s causes transient oscillation to begin such that

$$i\,(DL + R_n + 1/PC) = e_s \qquad (15)$$

from which

$$i = \epsilon^{-\alpha t}\,[A_1 \sin \beta t + A_2 \cos \beta t] \qquad (16)$$

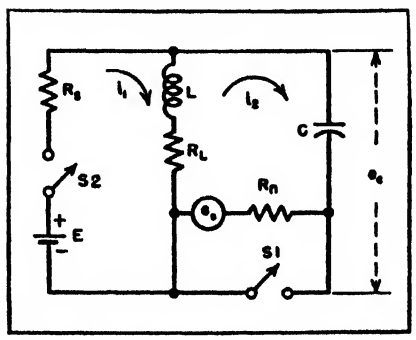

FIG. 4—Equivalent circuit of pulsed oscillator

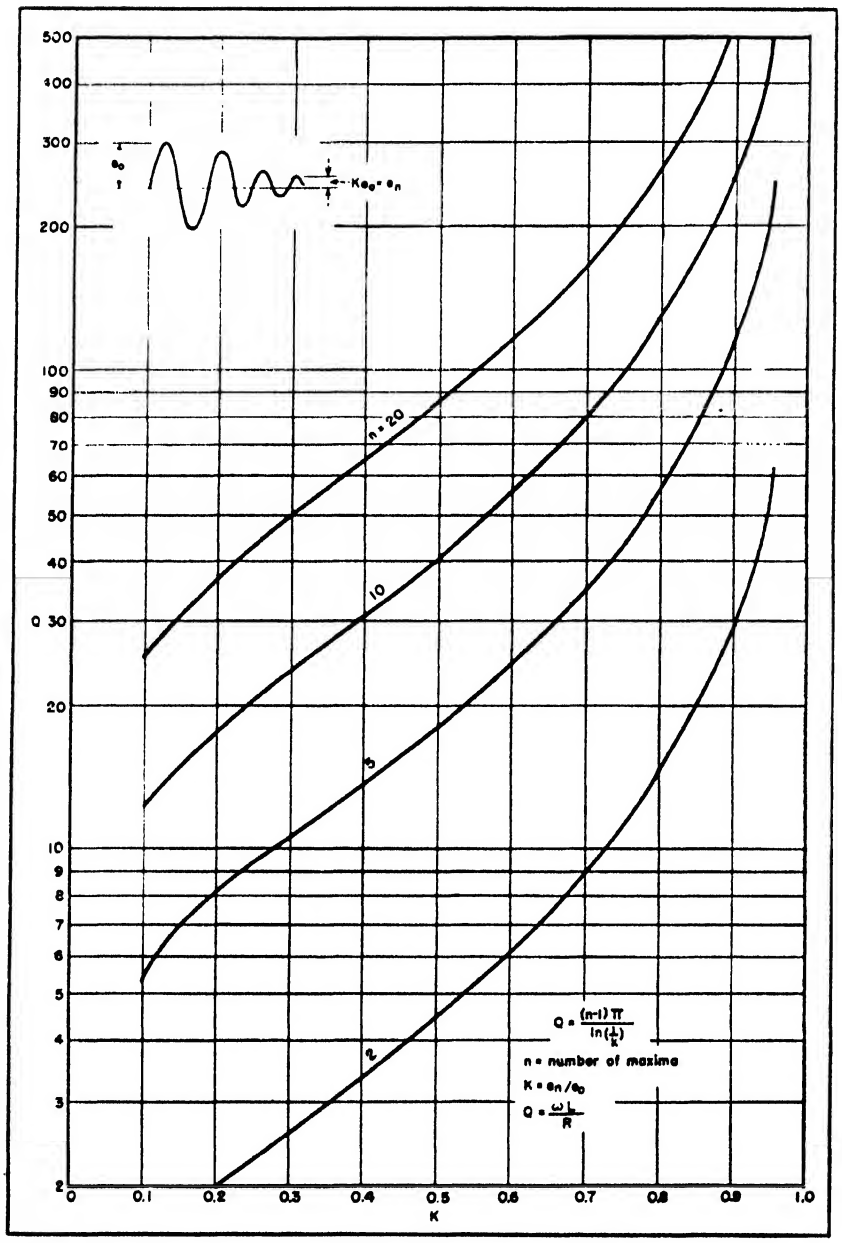

FIG. 5—Graph shows the quality (Q) of a resonant circuit if the oscillations initiated by shock are to decay to a particular fraction (K) of their initial value in a given number (n) of cycles

We are not concerned with steady state condition because e_s is negligible compared with the amplitude of the resulting oscillation. Boundary conditions are $t = 0$, $q = 0$, $di/dt = e_s/L$ giving

$$i = \frac{e_0}{\beta L} e^{-\alpha t} \sin \beta t \qquad (17)$$

and if $Q>>1$, and $R<0$ then

$$i = \frac{e_0}{\omega L} (\exp R_n t/2L) \sin \omega t \qquad (18)$$

This expression is the equation of an oscillatory current which builds up from zero to some final value determined by tube nonlinearity.

CASE C considers oscillations after application of the negative gate to the grid of the clamp tube. Oscillations will continue in a manner determined by the magnitude and sign of the effective circuit Q. When the negative gate is removed and the cathode follower is permitted to become conducting, oscillations will be damped at a rate determined by the magnitude of R_s. When S2 is closed (corresponding to removal of the negative gate), equations describing the currents in the two meshes are

$$E = i_1 (R_s + DL) - i_2 (DL) \qquad (19)$$

$$0 = - i_1 (DL) + i_2 (DL + 1/PC) \qquad (20)$$

(R_L is neglected as its effect is negligible compared with R_s). Equations 19 and 20 may be solved simultaneously for i_2 giving

$$i_2 \left(D^2 + \frac{D}{R_s C} + \frac{1}{LC} \right) = 0 \qquad (21)$$

Roots of the auxiliary equation are

$$\left.\begin{matrix} r_1 \\ r_2 \end{matrix}\right| = \alpha_2 \pm \beta_2$$

It is not necessary for the purpose of this analysis to complete the particular solution for i_2. It is sufficient to observe that when $\beta = 0$ the circuit is critically damped and current in the capacitor can decay to zero without oscillatory overshoot; this is the borderline condition. The value of R_s required to give critical damping is deduced from

$$\beta = \left(\frac{1}{4R_s^2 C} - \frac{1}{LC} \right)^{1/2} = 0 \qquad (22)$$

For the overdamped condition

$$R_s < \frac{1}{2} (L/C)^{1/2} \qquad (23)$$

It should be noted that in circuits shown in Fig. 1E and 2 there are two transients. There is the transient resulting from current I_s which flows when S2 is closed, and the residual alternating current which remains when S1 is closed. By the principle of superposition each condition may be considered separately. Both conditions give similar differential equations but have different boundary conditions, which do not affect the analysis because we are not concerned with currents but rather with rates of decay of currents. It is evident that for rapid damping at high oscillator frequencies a cathode follower having low cathode to ground resistance is essential. Otherwise decay time may be considerably longer than rise time of the pulse

modulated oscillator waveform envelope.

If R_1 can be made very small so that $(1/4R_1^2C^2) >> (1/LC)$ then $i_2 = A_1 (\exp -t/R_1C)$ and i_2 will decay exponentially to a value of $1/e$ in R_1C seconds.

Substitution of typical values into the last equation gives the following data: either $f = 1$ mc, $C = 100\mu\mu f$, $L = 250$ μh, $R = 790$ ohms, and $t = R_1C$ 7.9×10^{-8} sec, or $f = 10$ mc, $C = 25$ $\mu\mu f$, $L = 10$ μh, $R = 316$ ohms, in which case $t = 7.9 \times 10^{-9}$ sec.

REFERENCES

(1) "Time Bases", O. S. Puckle, John Wiley.
(2) "The Cathode Ray Oscilloscope in Radio Research", Watson Watt, H. M. Stationery Office London, 1938.
(3) "Cathode Ray Tubes and Their Applications", Cristaldi, P. S. *Proc I.R.E.*, p 373, June 1945.
(4) "Ultra High Frequency Techniques", Brainerd, D. Van Nostrand, p 208.
(5) Time Base Calibration, Ludman, W. W., ELECTRONICS, p 117, Sept. 1945.
(6) "Time Bases", O. S. Puckle, John Wiley, p 100.
(7) Measurement of Television Synchronizing Pulses, Monfort, R. A. and Somers, F. J., *RCA Review*, Jan. 1942.
(8) Impedance Measurement With Square Waves, Rockett, F., ELECTRONICS, p 138, Sept. 1944.
(9) Amplifier Testing by Means of Square Waves, Swift, *Communications*, Feb. 1939.
(10) Factory Alignment Equipment for Frequency Modulated Receivers, Rice. *Proc I.R.E.*, Oct. 1941.
(11) Synchronized Oscillators as FM Receiver Limiters, Carnahan, C. W. and Kalmus, H. P., ELECTRONICS, p 108, Aug. 1944.
(12) Note on the Fourier Series of Several Pulse Forms, Lattin, W. J., *Proc I.R.E.*, Nov. 1945.
(13) "Electrical Engineer's Handbook", Pender, John Wiley, p 10.
(14) Measuring Pulse Characteristics, Easton, A., ELECTRONICS, p 150, Feb. 1946.
(15) "Introduction to Electric Transients", Kurtz and Corcoran, John Wiley.

Equivalent Series and Parallel Impedances

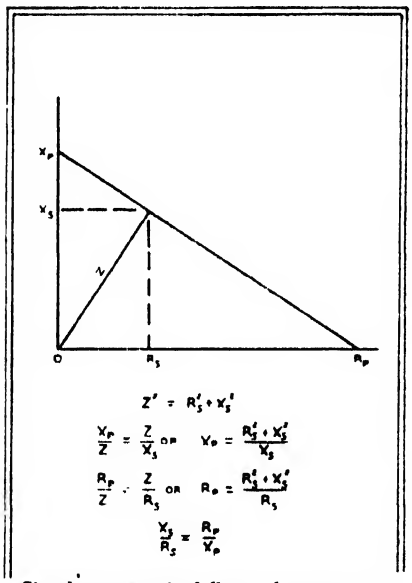

Simple geometrical figure for representing impedance relations

By R. L. PEEK, JR.

IN IMPEDANCE computations, it is frequently necessary or convenient to express an impedance $R_s + jX_s$ in terms of a resistance R_p and reactance X_p which have, when connected in parallel, the impedance $R_s + jX_s$. The reverse operation is similarly frequently required. It is the purpose of this note to describe a simple geometrical construction that represents the relation between these impedances. This relation is:

$$X_p = R_s^2 + X_s^2/X_s$$
$$\text{and } R_p = R_s^2 + X_s^2/R_s$$

The corresponding geometrical construction is shown in the illustration. Here R_s and X_s are the sides of a rectangle, of which Z is the diagonal. The perpendicular to Z cuts X_s and R_s prolonged at X_p and R_p respectively. The proof that the relation between X_s and X_p and R_s and R_p is that given by the above equations follows from the equal ratios of corresponding sides of similar triangles, as noted in the figure.

By laying off lengths on ordinary cross-section paper, this construction may be used to determine X_p and R_p when X_s and R_s are given or vice versa. Aside from its utility in computation, the construction permits visualization of the relative magnitude of the four quantities involved, including the useful corollary that $X_s/R_s = R_p/X_p$.

Design Curves for Parallel-T Network

Chart presents generalized design curves from which transmissions at various deviations from resonant frequency can be read directly. Design equations are also presented, and conclusions as to properties of parallel-T networks under usual conditions are drawn

By DAWKINS ESPY

PARALLEL-T NETWORKS are coming into common use because of their simplicity, economy and effectiveness. To simplify their design, generalized transmission curves for conditions ordinarily encountered are presented.

Resonance equations for the general parallel-T network are given in Table I, which contains other pertinent equations and the circuits which they describe. The analysis

Table I—Design Equations for Parallel-T Network

General Parallel-T Network

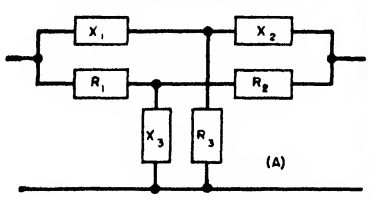

Capacitive Parallel-T Network

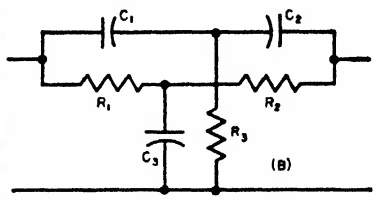

General Resonance equations

$$X_1X_2 = (R_1 + R_2)R_3 \quad (1A)$$

$$R_1R_2 = (X_1 + X_2)X_3 \quad (1B)$$

Relationships between parameters

$$X_1 = mR_1;\ R_2 = kR_1 \quad (2)$$

$$X_2 = kR_1 = kX_1/m \quad (3)$$

$$R_3 = [mk/(1+k)]R_1 \quad (4)$$

$$X_3 = [k/(m+k)]R_1 \quad (5)$$

Resonance frequency of network

$$f_0 = \frac{1}{2\pi[R_1R_2\{C_1C_2/(C_1+C_2)\}C_3]^{1/2}} \quad (8)$$

Design of capacitive network, all components related to R_1 or C_1

$$C_1 = 1/2\pi f_0 mR_1 \quad (9A)$$

$$C_2 = mC_1/k;\ R_2 = kR_1 \quad (9B)$$

$$C_3 = (m+k)/2\pi f_0 kR_1 = m(m+k)C_1/k \quad (9C)$$

$$R_3 = mkR_1/(1+k) \quad (9D)$$

General expression for transmission through a parallel-T network

$$T = \frac{1}{1 + j\dfrac{(f/f_0)}{1-(f/f_0)^2}\dfrac{\alpha+\beta\gamma^2}{\alpha\beta\gamma}} \quad (6)$$

$$\alpha = \frac{R_2}{R_1+R_2} = \frac{k}{1+k} \quad (7A)$$

$$\beta = \frac{X_2}{X_1+X_2} = \frac{k}{m+k} \quad (7B)$$

$$\gamma = \frac{X_1+X_2}{R_1+R_2} = \frac{m+k}{1+k} \quad (7C)$$

need not be restricted to symmetrical networks in which $R_1 = R_2$ and $X_1 = X_2$ or even to the condition that $R_1 = X_1$ at resonance. For the general case the parameters m and k can be defined at resonance by the two relations of Eq. 2, and with the aid of Eq. 1 the relations of Eq. 3, 4, 5 can be derived.

The general expression for transmission through a parallel-T network is given by Eq. 6 where f is the operating frequency and f_0 is the resonant frequency of the network; the other terms are defined by the relations of Eq. 7. Usually the parallel-T network is made using capacitors for the reactive arms. The resonant frequency of such a network is given by Eq. 8; R_3 does not appear in this relation because it is uniquely determined by the other parameters. The arms of the capacitive network can be designed from the relations of Eq. 9.

Considerable information about the network can be obtained from an examination of part of Eq. 6

$$\frac{\alpha+\beta\gamma^2}{\alpha\beta\gamma} = \frac{1+m+2k}{k} \quad (10)$$

which, for $m = 1$, reduces to $2(1+k)/k$ and for $k = 1$ reduces further to $3 + m$.

These relations show that the larger the magnitude of Eq. 10, the less the selectivity of the network. Increasing m for a fixed value of k increases the value of Eq. 10, decreasing the selectivity, while increasing k causes Eq. 10 to decrease, approaching 2 as a limit, and consequently increasing the selectivity. The effect can be seen in the design chart in which Eq. 6 is plotted for various values of k and m; only the low side of resonance is shown because the curves are symmetrical.

An approximate transmission formula when $k = m = 1$ for the frequency range from $f = 0.9f_0$ to $f = 1.1f_0$ is

$$T = j\,[(f/f_0) - 1]/2 \quad (11)$$

This equation also illustrates the fact that there are approximately 90 degrees of phase shift near resonance, lagging at frequencies below, leading at frequencies above.

The parallel-T network loads the driving circuit at all frequencies, and at resonance presents an input impedance of $R_1/2$ for any value of k when $m = 1$. Below resonance this impedance increases and above resonance it decreases. Loading the output of the network with an external load reduces the transmission on both sides of resonance, although the effect is greater on the low-frequency side. However, loading with a value as low as $3(1+k)R_1$ reduces the transmis-

Table II—Comparison of Computed and Measured Transmissions

Frequency in cycles per second	Transmission in Decibels: k = 1 and m = 1 Computed	k = 1 and m = 1 Measured	k = 1 and m = 1 Measured*	k = 1 and m = 5 Computed	k = 1 and m = 5 Measured
1,000	——	−65	(1,000 −65.7)	——	——
950	−31.6	−32	(1,053 −32.7)	−37.6	——
900	−25.6	−26.5	(1,110 −26.4)	−31.6	−33
850	−22.0	−22.1	(1,170 −22.3)	−27.5	——
800	−19.1	−19.4	(1,250 −19.2)	−25.0	−26.5
700	−14.9	−15.3	(1,430 −15.2)	−20.8	−22.0
600	−11.9	−12.0	(1,670 −11.8)	−17.5	−19.0
500	− 9.15	− 9.5	(2,000 − 9.4)	−14.8	−16.0
300	− 4.35	− 5.0	(3,300 − 4.8)	− 9.0	−10.0
100	− 0.7	− 1.9	(10,000 − 0.9)	− 2.5	− 3.0

* These two columns give the symmetrical frequency on the high side of resonance as compared to the frequency of the extreme left-hand column and the corresponding transmission. The transmissions indicate the degree of symmetry of the response.

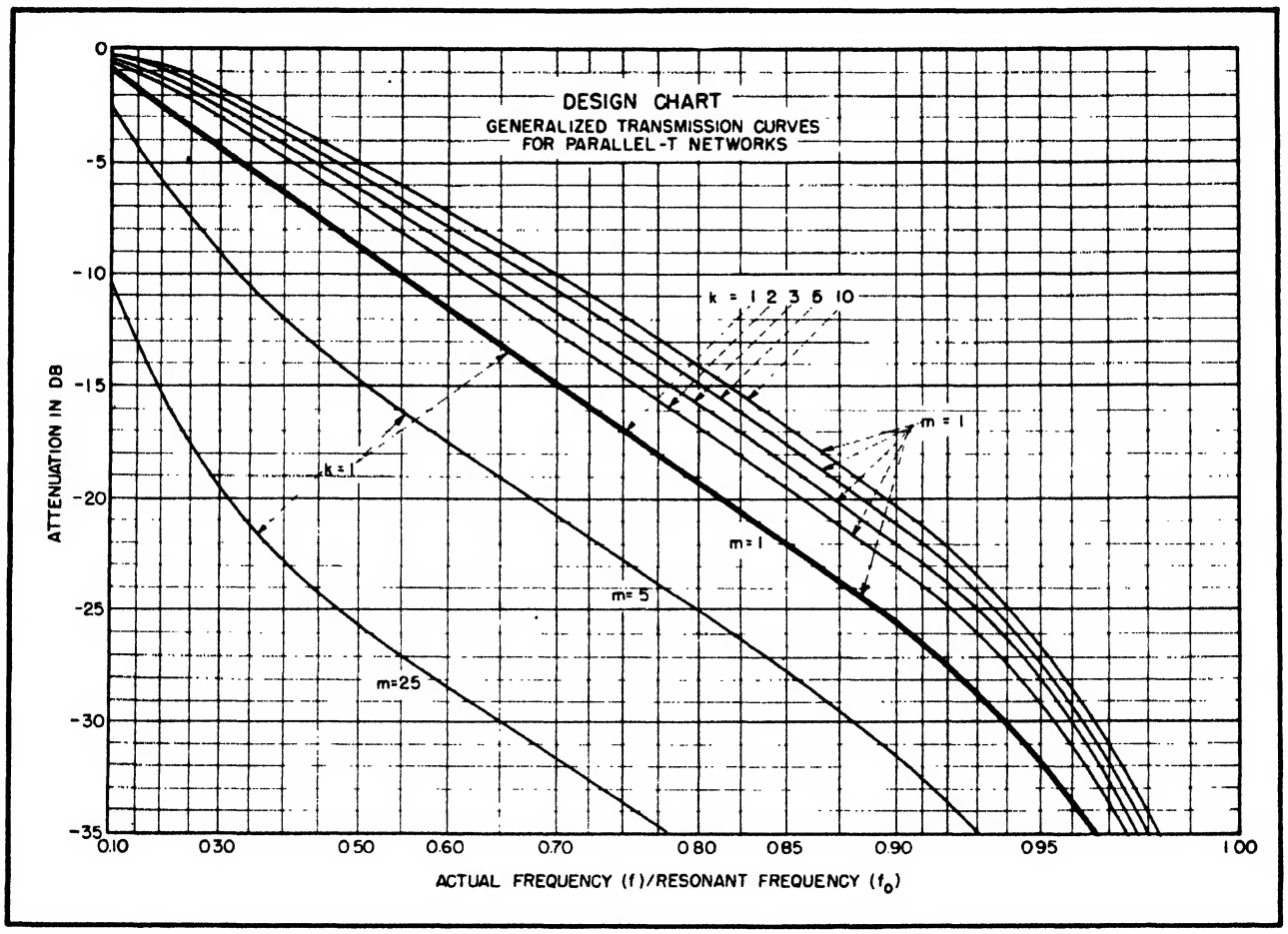

sion less than a decibel in the region from $f = 0.5f_0$ to $f = 2f_0$.

Varying R_3 and either R_1 or R_2 allows sufficient adjustment to tune the network to resonance. Each component contributes approximately 0.5-percent change in f_0 for each 1-percent variation from the specified value. An adjustable element should have a range of ± 4 times the individual element tolerance to assure the ability of resonating the network.

A parallel-T network resonant at 1,000 cps and with $k = m = 1$ was built from the foregoing equations. From Eq. 9 $R_1 = R_2 = 16{,}000$ ohms, $R_3 = 8{,}000$ ohms, $C_1 = C_2 = 0.01$ μf, and $C_3 = 0.02$ μf. With ±1-percent tolerance capacitors, actual values of the resistances required for resonance were $R_1 = 15{,}800$ ohms, $R_2 = 16{,}000$ ohms, $R_3 = 8{,}000$ ohms. The computed transmissions (from the design chart) and the measured values are presented in Table II. Results for a similar network, but for which $m = 5$, are also given in this table.

The measurements at resonance were remade by filtering out the second and third harmonics with parallel-T networks and rejecting hum frequencies with a high-pass filter. Under these conditions an attenuation of 115 db was measured.

Cathode-Coupled Half-Shot Multivibrator

By ROBERT K. F. SCAL

IN CONNECTION with the construction of synchronization equipment for the Stanford University multifrequency ionosphere recorder, the author developed a frequency divider which is simple in construction, dependable in operation with either continuous, intermittent series or individual actuating pulses, and which has already proved valuable in several other applications. Due to its original application as a pulse-frequency halver it was referred to as a pulse-halver. However, it is more broadly

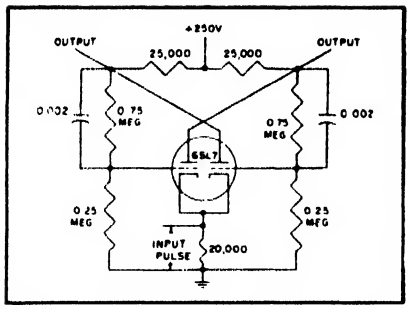

FIG. 1—Circuit of the half-shot multivibrator

referred to as a half-shot multivibrator, from the fact that it is developed from the basic Eccles-Jordan multivibrator circuit and that one-half an output cycle is obtained for each complete input cycle.

The circuit developed by the author is simple in construction and does not require a large negative voltage from a separate power supply. It operates with any plate supply voltage from 125 to 325 volts and the cathode potential will not exceed eighty volts with respect to ground or heater.

Uses

One application of this circuit is for frequency division, where any frequency (from practically zero on up into the lower r-f range) may be divided by any power of two simply by using the required number of stages in series, the output of each stage being applied to the input of the next through a simple R-C differentiating circuit. By means of a single-pole selector switch a versatile circuit may be constructed to give either rectangular waves or pulses, by connecting the taps either ahead of or following the differentiators, or both, at a number of different frequencies.

The half-shot multivibrator may also be employed as an electronic switch, which operates each of two external circuits by means of the output voltage of either or both of the plates. For this purpose the circuit supplies two rectangular waves 180 degrees out of phase.

Circuit Operation

The basic circuit is shown in Fig. 1. This circuit is symmetrical and is stable with either triode conducting, and the other one cut off. This means that it is possible for a single input pulse to actuate it for one-half cycle.

As this circuit is activated only by a negative pulse whose magnitude is limited to a reasonable value, it may be triggered by a differentiated rectangular wave, each cycle of which gives a single operating pulse and thus one-half of an output rectangular wave cycle. In this way, two input rectangular wave cycles (pulses) give a single output rectangular wave cycle. If alternate negative input pulses are equally spaced, the output will be a square wave, but by controlling the spacing of the input pulses, rectangular waves of various proportions may be obtained from the output.

Action With Positive Pulse

In either stable condition, one triode is conducting and the other is cut-off. If a positive pulse is applied to the cathodes the conducting tube will tend to conduct less current. However, this tendency is counteracted by the fact that any decrease in this grid-cathode potential causes less grid current to flow, and the drop in the cathode, the grid-to-plate, and the plate-to-plate supply resistors causes the grid voltage to return to nearly zero with respect to the cathode.

As the cathode and grid go positive as a unit, the plate does likewise, and due to the coupling capacitor the grid of the cut-off tube is forced to go more positive. However, the grid-cathode potential of the cut-off tube remains about the same and this tube is held beyond cut-off even with a positive pulse on the cathode. Therefore the circuit is not actuated by positive pulses as long as the coupling capacitor's discharge time constant is large compared to the pulse width, and the pulse is of reasonable magnitude.

With a positive input pulse, a very small positive pip is visible on the plate waveform during both the cutoff and conducting portions, since the drop in grid current of the conducting tube also causes the latter's plate voltage to rise. These pips are visible only with large vertical amplification of the plate voltage waveforms.

Effect of Negative Pulse

If a negative pulse is applied to the cathodes, the tube that is conducting will continue to do so, but the other tube will start to conduct, causing its plate voltage to be decreased. Due to the coupling capacitor, the grid potential of the conducting tube will be slightly decreased also, so that it starts to cut off, causing its plate voltage to rise, which in turn raises the grid-cathode potential of the formerly conducting tube still more through the other coupling capacitor.

This action is cumulative and instantaneous, amounting to a complete switching of tubes. Another negative pulse applied to the cathodes will switch the tubes back to their original condition, in a similar manner, and repeated pulses result in rectangular waveforms on each plate of one-half the frequency of the negative triggering pulse. The output of either or both plates may be used, as desired.

The resistance values are calculated with the aid of the tube characteristic curves to give a steady-state condition which can be easily switched by the available cathode pulse so that when one tube has zero grid-cathode potential the other will be held just beyond cut-off.

The limitations on the operating frequency range are due to the charging and discharging of the coupling capacitors. Above the upper frequency limit the circuit acts like a conventional frequency divider whose operation depends on the charging rate of a capacitor, and thus its factor of frequency division is a function of the input pulse width and R-C time constants.

For normal operation, the size of the coupling capacitors is not critical. The capacitance must be great enough so that little charging and discharging can take place while the pulse is applied to the

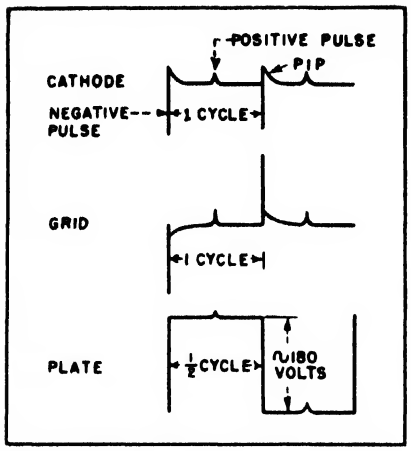

FIG. 2—Waveforms at elements of one triode. The pip at the cathode is due to charging effects of an isolating capacitor in the input pulse circuit

cathodes. Otherwise the circuit becomes unstable and does not know which way to go because each triode will be conducting an equal amount of current and it will be a matter of chance which tube gains control and causes the other tube to be cut off. The capacitors must be small enough so that they can charge and discharge sufficiently between pulses to be prepared for the next pulse. Fig. 2 shows the waveforms of the circuit when actuated by a 60-cycle input pulse.

Tubes Critical

Either a high-mu (6SL7) or a medium-mu (6SN7) twin triode may be used. The wider the frequency range over which a particular circuit is to operate, the more constant the plate supply voltage must be, and for best results in such applications a regulated power supply is indicated.

Particular tubes of the same type will not always operate in this circuit, and sometimes it is not possible to obtain operation by adjustment of the resistor network alone. However, the circuit can always be made to work by connecting small external capacitances across the tube elements by trial and error. Adjustment of circuit resistance or external capacitance to make a particular tube operate is not recommended. It has been found that when a circuit has once been made to work properly, and no external capacitance other than stray capacitance is present, approximately 60 percent of the dual triodes selected at random will operate. The use of individual triodes may be preferred to facilitate obtaining properly matched pairs of triodes.

The very large rectangular wave output is capable of producing so-called r-f burns, even with a repetition frequency as low as 15 cps.

Voltmeter Loading

Simple nomograph gives true voltage in high-impedance circuit when measurements are made with two different voltage ranges of an ordinary low-sensitivity voltmeter. Underlying equations for voltmeter error are given, with examples of use

By R. E. LAFFERTY

MEASURING voltages across high - impedance circuits with voltmeters of sensitivities in the order of 1,000 ohms per volt will give readings that are appreciably less than the true voltages.

The higher the input resistance of a voltmeter, the lower will be the required deflection current and hence the smaller the error. With voltmeters of 20,000 ohms per volt sensitivity or greater, the error is usually negligible.

There are many voltmeters in use of the 1,000 and 5,000 ohms per volt class, and frequently these are the only instruments available when it is desired to know the actual voltage across a circuit.

The purpose of this paper is to provide an equation (suitable for slide rule calculations) and a nomograph (which only requires a straightedge) that will quickly yield the true voltage in a circuit after two measurements are taken with a voltmeter of low sensitivity. The only requirement of the voltmeter employed is that the internal resistance of the meter be directly proportional to the voltage range selected. All of the common type of current-operated voltmeters come under this classification.

The circuit shown in Fig. 1 represents a voltmeter with two ranges connected to a simple network. In practice, circuits are usually more complex than this, but they can be reduced to an equivalent circuit similar to that in Fig. 1.

Let E = true voltage across R_n with voltmeter disconnected
E_H = voltage measured across R_n on highest meter range that will give an accurate reading
E_L = voltage measured across R_n on next lower range
E_G = source of constant voltage

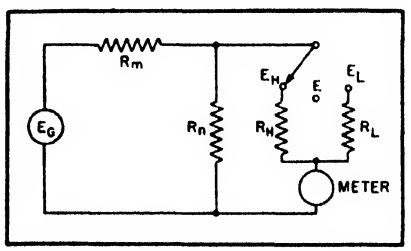

FIG. 1—Circuit of two-range voltmeter used as example

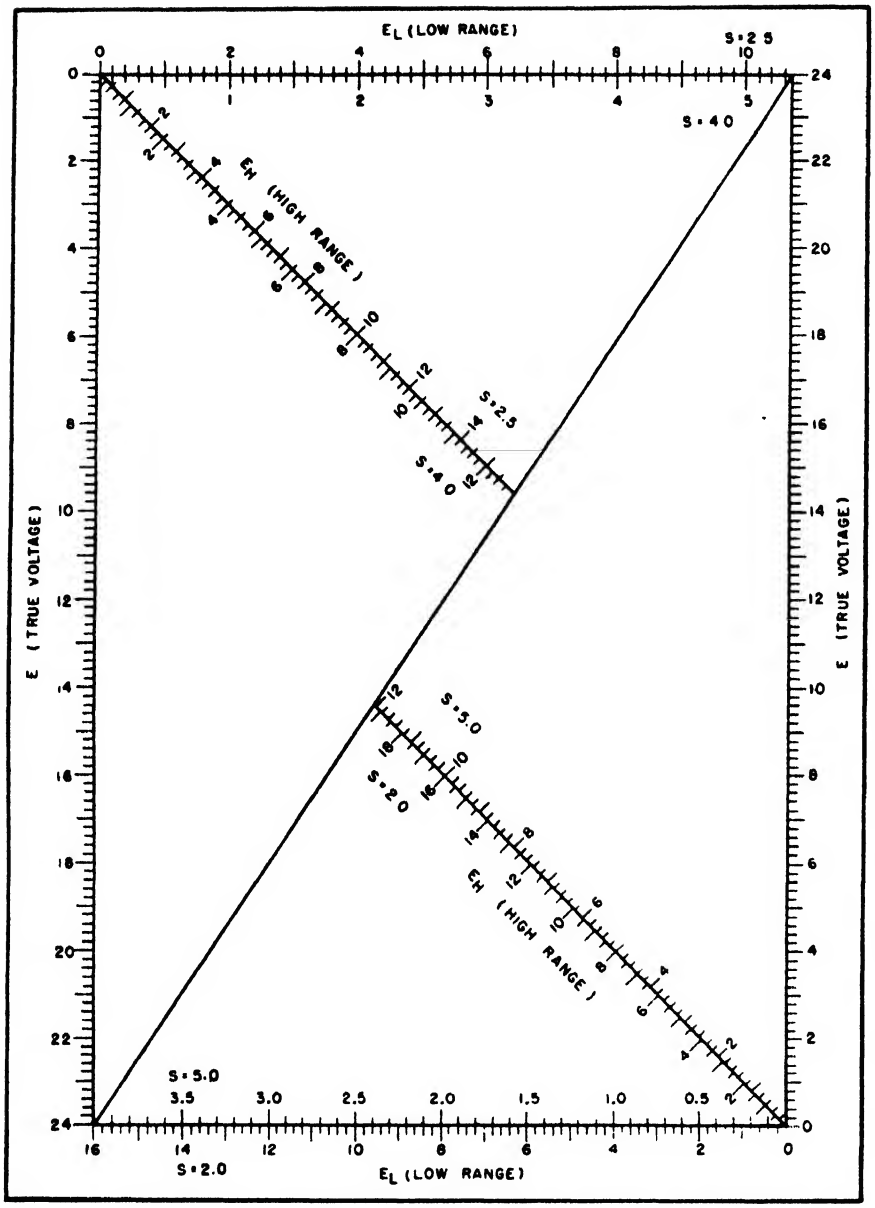

FIG. 2—Voltmeter loading nomograph. Take voltage readings on two ranges, divide higher range scale by lower to get S (either 2, 2.5, 4, or 5 on standard volt-ohm-milliammeters), then place straightedge on measured values (E_L and E_H) for S scale in question and read true voltage on adjoining E scale. If range of any scale is inadequate, multiply all scale values by 10, 100, or any other convenient factor

R_H = internal resistance of voltmeter when measuring E_H
R_L = internal resistance of voltmeter when measuring E_L
S = ratio of two scales used; $S = R_H/R_L$
R_n = resistance across which output voltage is developed
R_m = series dropping resistance that accounts for difference in E_L, E_H, and E.

Derivation of Equation

Simple circuit theory allows us to write

$$E = E_0 \frac{R_n}{R_n + R_m}$$

$$E_H = E_0 \frac{R_H R_n}{R_H R_m + R_H R_n + R_m R_n}$$

$$E_H = E \frac{R_m + R_n}{R_m + R_n + (R_m R_n / R_H)} \quad (1)$$

$$E_L = E \frac{R_m + R_n}{R_m + R_n + (R_m R_n / R_L)} \quad (2)$$

Substituting SR_L for R_H in Eq. 1 and solving for E in both equations, we have

$$E = E_H \frac{R_m + R_n + (R_m R_n / SR_L)}{R_m + R_n} \quad (3)$$

$$E = E_L \frac{R_m + R_n + (R_m R_n / R_L)}{R_m + R_n} \quad (4)$$

Rearranging Eq. 3 and 4

$$(R_m + R_n)(E - E_H) = E_H \frac{R_m R_n}{SR_L} \quad (5)$$

$$(R_m + R_n)(E - E_L) = E_L \frac{R_m R_n}{R_L} \quad (6)$$

Dividing Eq. 5 by Eq. 6

$$SE_L (E - E_H) = E_H (E - E_L)$$

$$E = \frac{(S - 1) E_H}{S - (E_H / E_L)}$$

This equation is particularly suited to slide rule calculations.

Example 1: A voltmeter, when placed across two terminals, reads 105 volts on its 200-volt range. The meter is switched to the 100-volt range and reads 70 volts. Divide 105 by 70 and subtract the quotient from the scale ratio of 2.0. This gives us 0.5 for the denominator. It should be noted at this time that when the scale ratio is 2.0, the term $(S - 1)$ in the numerator equals 1.0. Now divide 105 volts by 0.5 and the result is the true voltage of 210 volts.

Example 2: A voltmeter reads 50 volts on its 150-volt range. On the 60-volt scale it reads 40 volts. $E_H/E_L = 50/40 = 1.25$. Subtract this from the scale ratio of 2.5 and the denominator equals 1.25. Divide this into E_H (50 volts) and multiply the quotient by (2.5 − 1) or 1.5. The true voltage is 60 volts.

Use of Nomograph

Although this equation is not difficult to use when one has become familiar with it, still it is less trouble and quicker to lay a straightedge on a nomograph and read the unknown value directly.

The nomograph presented in this paper is divided diagonally into two parts. Each half is used in the same way. The graph was divided to facilitate reading the four scales for $S = 5$, 2, 4, and 2.5. These values of S were chosen after 26 volt-ohm-milliammeters of 10 manufacturers were examined for their most popular switching ratios of both d-c and a-c ranges. The favorites are 5 and 2, with 4 and 2.5 used least. The ratio of 10 was used so seldom that it was not included in this nomograph.

As in the case of the equation, the best way to explain the use of the nomograph is with example problems. To compare the results of the equation with that of the nomograph, use the same problems as before.

Example 1: $E_H = 105$ volts and $E_L = 70$ volts. Place a straightedge between these values on the E_H and E_L scales for $S = 2.0$ and let it extend to the E scale. The straightedge will pass through 210 volts on the E scale, which is the true voltage. Note: This lower right half of the nomograph is also used when $S = 5$. Since values here are beyond range of nomograph, values on all three scales were multiplied by 10.

Example 2: $E_H = 50$ volts and $E_L = 40$ volts. This solution requires the use of the upper left half of the nomograph since $S = 2.5$. Using the scales for $S = 2.5$, with all scale values multiplied by 10, the true voltage is found to be 60 volts on the E scale.

The equation and nomograph will yield the true voltage only when the measurements are taken across linear circuits. Should lowering the voltage, due to voltmeter loading, change the network resistance, the nomograph can not be used.

The question arises as to how well the nomograph will apply to vacuum-tube circuits. Placing a current-operated voltmeter between a tube element and ground will lower the voltage on that element. Experiment shows that when the tube is operated with fixed bias the element resistance changes considerably with changes in element potential and the nomograph should not be used.

When cathode bias is employed, the reduction in voltage is accompanied by a proportional reduction in current. Thus the resistance of the tube remains substantially constant within the normal limits of operating voltage for the tube. In this instance the nomograph may be used, but with reserve. The resulting error is usually less than 5 percent but higher errors have been encountered. However, the error before using the nomograph was in some cases as high as 60 percent.

Reactance Networks with Resistance Terminations

A general treatment of bisectable reactance networks with equal resistance terminations, especially with the reactors ideal; illustrated by working out the detailed performance of four-element networks commonly used for simple low-pass purposes. Illustrative curves and numerical examples are given for determining the reactor elements required to produce a specified curve, and for determining the curve corresponding to a given set of elements

By E. S. PURINGTON

MANY electrical circuits consist of a bisectable symmetrical network of reactor elements inserted between two equal resistance terminations. These are exemplified by the simple but important arrangement of Fig. 1A, where the network comprises the reactor elements L_1, C_1 and C_2, and the driving voltage E in the sending arm R produces an output current I_r in the receiving arm which is also a resistor R. Also indicated is the first half portion of the system resulting from bisection, and the electrical connectors by which power can be transferred to the second half portion. With the reactor elements dissipative, the insertion properties of the network are most readily derivable from the termination impedance R, and the impedances Z_s and Z_r looking from the termination R into the first half portion, first with the connectors opened, then closed by shorting them together, using

$$\text{Insertion ratio} = \frac{E/2R}{I} = \frac{(1 + Z_s/R)\ (1 + Z_r/R)}{(Z_s/R - Z_r/R)} = M + jN \quad (1)$$

This equation becomes greatly simplified if ideal conditions are stipulated, with the terminations R of pure ohmic resistance independent of frequency, with each reactor element free from dissipative loss, and with the numerical impedance of each inductor proportional to frequency and of each capacitor inversely proportional to frequency. By reference to Fig. 1B, Z_s and Z_r become pure reactance impedances jX_s and jX_r, and simple right angle triangle type vector diagrams result showing the circuit relation for the open and closed conditions. The ratio X_s/R is the tangent of the phase angle by which voltage E leads the current I_s, and X_r/R is the tangent of the angle by which voltage E leads the current I_r. These angles θ_s and θ_r cannot differ from zero by more than 90 electrical deg., but can be positive or negative. For the

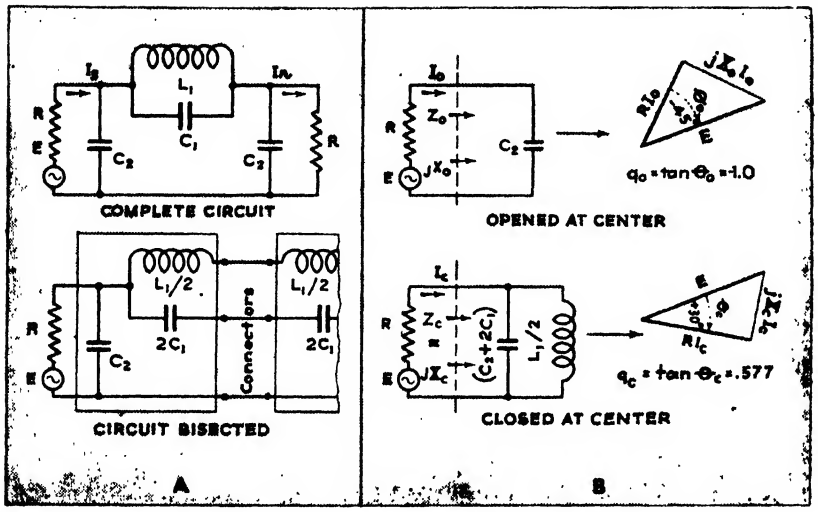

Fig. 1—Bisectable reactance networks with equal resistance terminations

case illustrated, θ_o is negative for all frequencies, but θ_c is positive for low frequencies and negative for high frequencies. The ratios X_o/R and X_c/R will be here termed q_o and q_c from analogy to the quality factor Q expressing the reactance-resistance ratio for coils or condensers. These q's in general are complex functions of frequency, with values ranging from negative infinity to positive infinity. The vector diagrams of Fig. 1B depict conditions for a combination of elements which for some frequency makes $\theta_o = -45$ deg., $\theta_c = 30$ deg., for which the tangents are $q_o = -1.0$ and $q_c = 0.577$.

With this stipulated simplification, Eq. 1 becomes

$$\text{Insertion ratio} = \frac{E/2R}{I_r} = \frac{(1 + jq_o)(1 + jq_c)}{j(q_o - q_c)} = M + jN \qquad (2)$$

and because the q's do not involve $j = \sqrt{-1}$, this simplifies to

$$\text{Insertion ratio} = \left|\frac{q_o + q_c}{q_o - q_c}\right| \angle + j\left[\frac{q_o q_c - 1}{q_o - q_c}\right] = M + jN \qquad (3)$$

so that M and N are directly computable from the q's. For the sample values given above, $M = 0.268$, $N = 1.0$, and since M and N are both positive the insertion ratio vector is in the first quadrant, with the termination current I_r lagging behind the reference current $E/2R$ and therefore behind E itself by less than 90 electrical deg. The insertion loss in decibels, $10 \log_{10} (M^2 + N^2)$ is 0.3 db, and the insertion lag, $\tan^{-1} (N/M)$ is +75°. In terms of the q's, in general

$$\text{Loss} = 10 \log_{10} \left\{1 + \left[\frac{1 + q_o q_c}{q_o - q_c}\right]^2\right\} \qquad (4)$$

$$\text{Lag} = \tan^{-1}\left[\frac{q_o q_c - 1}{q_o + q_c}\right] \qquad (5)$$

These equations are especially useful if the loss and lag are to be computed after expressing the q's for any specific circuit as algebraic functions of frequency. For single point computations, especially simple equations result by substituting $q_o = \tan \theta_o$ and $q_c = \tan \theta_c$ in Eq. 4 and 5, and simplifying to yield

$$\text{Loss} = 10 \log_{10} \operatorname{cosec}^2 (\theta_o - \theta_c) \qquad (6)$$

$$\text{Lag} = (\theta_o + \theta_c) \pm 90 \text{ deg.} \qquad (7)$$

In Fig. 2 is given a chart and explanatory matter for quickly evaluating the insertion loss by Eq. 6, applying to any bisectable symmetrical network with equal resistance terminations. By its use the insertion loss for any specific choices of elements such as L_1, C_1 and C_2 of Fig. 1A inserted between specified resistance terminations R can be most rapidly evaluated. Substantially all that is required is computation of the angles θ_o and θ_c by which the driving voltage E leads the current produced by that voltage for the two conditions with the circuit as a whole opened and closed at the center of symmetry.

The more important problem usually is to predetermine what values must be assigned to the elements to be inserted between specified terminations R so that the loss and possibly the lag will be a suitable function of frequency. For this purpose it is desirable to use equations in terms of the q's, survey the entire possibilities of curve shapes afforded by a given network arrange-

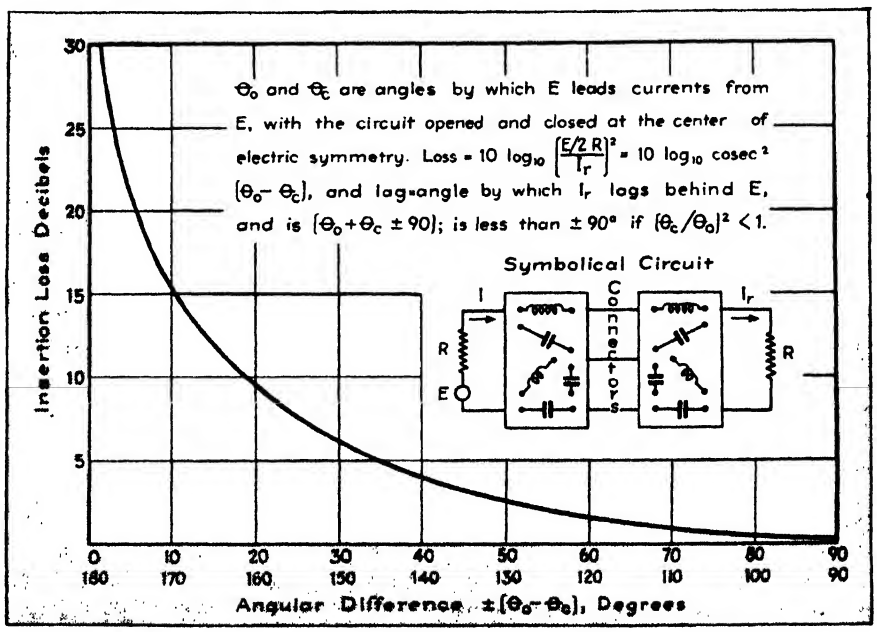

Fig. 2—Loss and lag characteristics for bisectable R-X circuits

ment, choose the shape that is most satisfactory, and evaluate the reactor elements which for the specified R will yield that shape. Before carrying through the necessary routine using Fig. 1, it will be helpful to study Eq. 4 and 5 in greater detail.

Quick inspection of Eq. 4 shows the loss is zero for any frequency making the product of the q's negative unity, and the loss is infinite for any frequency making the q's equal. Less obviously, zero loss is approached for any condition making one of the q's a very large value and the other a very small value. Such is the case in the cited example of Fig. 1B for frequencies near zero, making q_o highly negative and q_c only slightly positive. Less obviously also the loss is very great for any condition making both of the q's very small, as is the case in Fig. 1B for very high frequencies with the q's only slightly negative. Inspection of the circuit configuration often reveals conditions of zero and infinite loss. In Fig. 1A, the loss is of necessity infinite for the frequency of antiresonance of elements L_1 and C_1, corresponding in fact to the q's of Fig. 1B being algebraically equal. Inspection of a circuit configuration will always fail to disclose the condition of zero loss due to the product of the q's being negative unity, since not all combinations of elements will result in such a condition existing.

It is noteworthy that the loss equation involves the product and the difference of the q's, while the lag equation involves the product and the sum. The quotient of the q's is not as yet specifically involved, but for the present has the hidden value of clearing up the equational ambiguity as to the quadrant location of the phase angle. In Eq. 5, if the tangent of the phase lag angle is positive, the angle may be in the first or third quadrant, but if negative, in the second or fourth. Referring back to Eq. 2, $M = (q_o + q_c)/(q_o - q_c)$ is positive provided the quotient (q_c/q_o) is within the limits -1 to 1. Therefore if $(q_c/q_o)^2$ is less than unity, or correspondingly $(\theta_l/\theta_o)^2$ is less than unity, the lag angle must be located in the first or fourth quadrant for which M is positive, otherwise it must be located in the second or third quadrant for which M is negative.

Absolute determination of the lag angle must be based upon agreement as to lag for some specified frequency. Since in Fig. 1A all the network currents for very low frequencies are in the inductor L_1 directly connecting the two terminations, so that the network produces no effect at zero frequency, it will be agreed that the lag is zero at zero frequency, and not, for example 360 deg. But at infinite frequency the loss approaches infinity and the lag angle approaches the boundary between the first and second quadrants. Absolute lag, as for example 90, 450, or—270 deg., can be found only by applying the physical doctrine of continuity and integrating the phase changes as the frequency progresses from zero to infinity. Unfortunately Eq. 3 points out that as frequency changes in such a way as to make $(q_o - q_c)$ change sign, the vector $(M + jN)$ changes by 180 deg. No physical discontinuity is involved because at the same time the insertion loss is infinite. What happens is a reversal of the load current I_r as it passes through a condition of zero magnitude, analogous to the change of direction of current in the galvanometer arm of a bridge in passing through a condition of balance. Nevertheless there is no short method of checking whether 180 deg. must be added or subtracted when the frequency passes through the critical value. Apparently the only satisfactory procedure to clear up this point, if important, is to compute the performance at least once with an element such as L_1 of Fig. 1A slightly dissipative, using the more general Eq. 1, useful when Z_c/R is a complex imaginary. The lag performance under this condition will serve as a guide to what should be done in the limiting case with the element L_1 mathematically free from loss.

Solution of Specific Problem

The procedure necessary to develop loss and lag equations for any network to which the preceding theory applies will be illustrated by working out the complete solution for Fig. 1A. Here is a circuit with four differently choosable electrical elements, the terminations R, and the network reactors L_1, C_1 and C_2. It is required to develop the insertion performance equations covering all possible combinations, survey the possible curve shapes and tabulate information as to how any selected curve shape may be realized.

If a set of values is randomly assigned to the circuit elements, the performance as here defined will not be modified by multiplying the impedance of each element by a given factor, as for example by doubling R, doubling L_1 and halving the capacitances of C_1 and C_2. But the performance will be altered if the terminations R are held constant while the impedances of the network elements are doubled, since the q's will be doubled. To provide for various impedance levels of the network elements with respect to the terminations, an impedance level parameter h is introduced to which in the equations the q's will be proportional.

With a fixed specified value for R, the only way that the elements of the network may be modified without curve shape changes is by multiplying the network reactor values L_1, C_1 and C_2 all by the same factor, as by doubling. What previously happened at frequency f will subsequently happen at a frequency $f/2$, thereby shrinking the curve if plotted on a frequency basis. If however some significant reference frequency F_o is set up, as for example the cutoff frequency of the curve shape if used for filtering purposes, and the curve is plotted in terms of the ratio of any frequency to the reference frequency, change of the reference frequency will not change the curve shape. In the present example the significance of F_o as the cutoff frequency is chosen to give the simplest possible loss equation, but its cutoff significance appears only after specific curve shapes are plotted. The ratio f/F_o will be here given

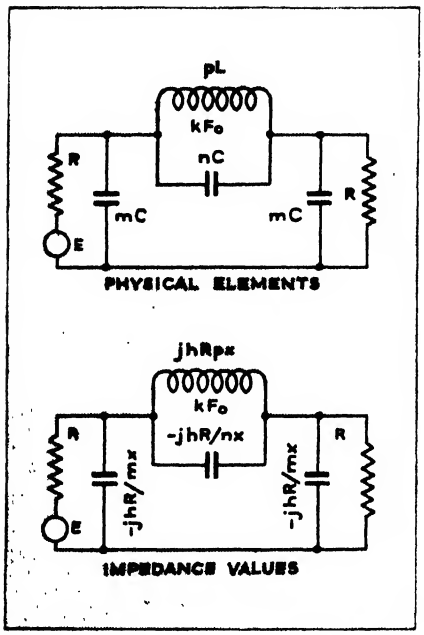

Fig. 3—Circuit designations showing relation between physical elements and impedance values

the designation x customarily applied to the abscissa in curve plotting.

With a fixed R, and choices of h and F_o which must be held constant, variations in elements L_1, C_1 and C_2 are still possible. L_1 and C_1 determine a finite frequency for infinite insertion loss. The ratio of this frequency to F_o will be termed k, the infinite loss parameter. Changing k requires modification of L_1, C_1 or of both, and with the requirement that h and F_o will not be changed, it develops that all three reactor impedances must be altered, but not in a proportionate manner.

In place of the three physical elements L_1, C_1 and C_2 it becomes necessary, therefore, to deal with three abstract elements F_o, h and k, to yield performance equations in terms of x, h and k. It must be possible to evaluate the reactors for the specified R, the value desired to represent F_o corresponding to $x=1$, and the values chosen for the parameters h and k determining and identifying the curve shape to be duplicated.

It works out most advantageously to designate reactor values as functions of R, F_o, h and k in two steps. Basic values of inductance and capacitance designated L and C are defined as those having numerical impedances hR at F_o, thereby involving everything except k. The various inductor and capacitor elements in the network are then these basic values multiplied by factors m, n and p, for example, which involve only k. In terms of inductance, element L_1 of Fig. 1A is replaced in Fig. 3 by element pL, for example, but because of the definition of L on an impedance basis, the element is also capable of being assigned an impedance designation $pL=jhRpx$. Similarly for example C_2 can be designated $mC=-jhR/mx$, and $C_1=-jhR/nx$. Designations here used for basic values of L and C differ from other practices in standard texts, but this seems justifiable because of the greater simplification of results and because of the direct physical significances in terms of impedances. The general equations universally useful for computing basic L and C values, together with the various combinations of units with which they may be used, are

$$L = 0.1592\,hR/F_o \qquad C = 159{,}200/hRF_o$$

F	R	L	C
cps	ohms	henry	μf
kcs	ohms	mh	$m\mu f$
Mcs	ohms	μh	$\mu\mu f$

For example, to be at an impedance level of $h=4$ with respect to a 500-ohm termination at 200 cycles, the basic value of L must be 1.592 henry. Or a 100-$\mu\mu f$ condenser operating at $F_o=10$ mc may be considered to be at an impedance level of $h=2.2$ with respect to a 72-ohm resistance impedance.

For determining what functions of k the multiplying factors m, n and p of Fig. 3 must be, one requirement is that pL and nC must be of equal numerical impedance for the special frequency value kF_o for which $x=k$. This requires the relation $pn=1/k^2$. Two other relations must be found. Inspection of Eq. 4 indicates the desirability of making q_o q_o as simple an algebraic function as possible. Using the impedance designations of Fig. 3, routine algebraic procedure yields for the q's and their product

$$q_o = \frac{-h}{mx}\,;\quad q_o = \frac{-hpx}{[(m+2n)\,px^2-2]}\,;$$

$$q_o\,q_o = \frac{h^2}{[m\,(m+2n)\,x^2 - 2m/p]}$$

The product function q_o q_o will take on the simplest possible form $h^2/(x^2-1)$ provided the relations $m(m+2n)=1$ and $p=2m$ are met as well as the previously established relation $pn=1/k^2$. These three relations are met if m, n and p are the following function of k

$$m = \sqrt{1-k^{-2}}\cdot$$
$$n = 1/2k\sqrt{k^2-1} = 1/2mk^2$$
$$p = 2\sqrt{1-k^{-2}} = 2m \qquad (8)$$

With these functions of k now replacing m, n and p, the q's become

$$q_o = \frac{-h}{\sqrt{1-k^{-2}}\,(x)}\,;$$
$$q_o = \frac{-h\sqrt{1-k^{-2}}\,(x)}{(x^2-1)} \qquad (9)$$

The four combinations of the q's which determine the circuit performance are

$$q_o\,q_o = \frac{h^2}{(x^2-1)}\,;$$
$$(q_o - q_o) = \frac{h\,(k^2-x^2)}{k\sqrt{(k^2-1)}\,(x)\,(x^2-1)} \qquad (10)$$

$$q_o/q_o = \frac{(1-k^{-2})\,x^2}{(x^2-1)}\,;$$
$$(q_o + q_o) = \frac{h\,[k^2-(2k^2-1)\,x^2]}{k\sqrt{k^2-1}\,(x)\,(x^2-1)}$$

Substitution of the product, difference and sum functions of the q's in Eq. 4 and 5 yield the loss and lag equations which when reduced to simplest form are recorded as part of the Chart. These permit loss and lag curve shapes to be computed and plotted as functions of $x=f/F_o$ for all possible combinations of h and k within the allowable ranges of these parameters. The loss is zero db for any condition making $F_{1,2}$ zero, including the two conditions $x=0$ and $x=a=\sqrt{1-h^2}$, the latter of which occurs only if h is less than unity for this type of circuit. This condition is a function of the net-

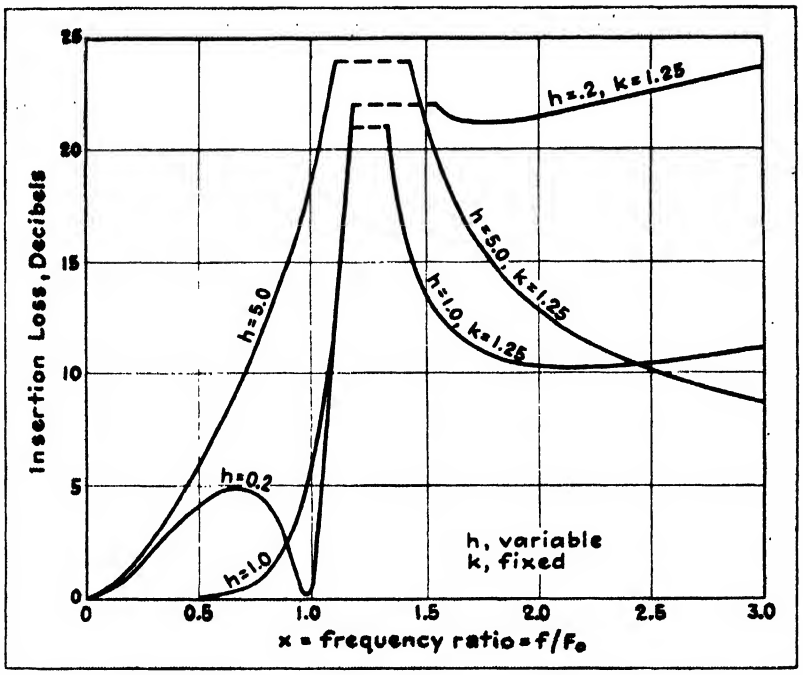

Fig. 4—Low-pass filter characteristics; effect of changing impedance level

work and of the termination. Infinite loss requires the loss function to be infinite, including the two conditions $x = k$ and $x =$ infinity, which are determined by the network only. Information is included also to enable the network elements to be computed corresponding to any specified value of R, any frequency F_o desired to correspond to $x = 1$, and any curve shape specified by numerical values of h and k.

Included with the Chart are loss curves for $h = 0.6$ and $k = 1.1$, 1.5 and infinity, illustrating choices of parameters which give circuit element values suitable for low-pass filter purposes. With the sharpest cutoff curve ($k = 1.1$) there is only 6 db difference between maximum loss in the pass range and the minimum loss in the attenuation range. For higher values of k, greater filtering effect in the two ranges is accompanied by lesser sharpness of cutoff. At $k =$ infinity, factor n becomes zero, and the element nC is therefore not required. The other limiting condition with k = unity results in the network being entirely absent with the two terminations direct connected to give zero loss and lag at all frequencies.

Fig. 4 shows the effect of changing the impedance level using a fixed value of $k = 1.25$, and three choices of h. Values of h less than unity, say in the vicinity of $h = 0.6$ are most desirable if low loss is desired over the greatest possible frequency range.

Figure 5 gives more detailed information for parameter values $h = 0.6$, $k = 1.25$, and includes information for a dissipative case computed by the more complex equations required, based on Eq. 1. Various loss and lag points cover an assumed case with inductor element pL including in series a resistor sufficient to make the Q of the inductor arm the reasonable value of 20. The effect of dissipation is of most importance just below cutoff. Comparison of the loss curve for the dissipative case with the curve of Fig. 4 for $h = 1$ will serve to emphasize that choice of impedance level of the network with respect to the terminations may be of more practical importance than choice of kind and amount of material necessary to give extreme values of quality factors of reactor elements. In Fig. 5, the lag points for the dissi-

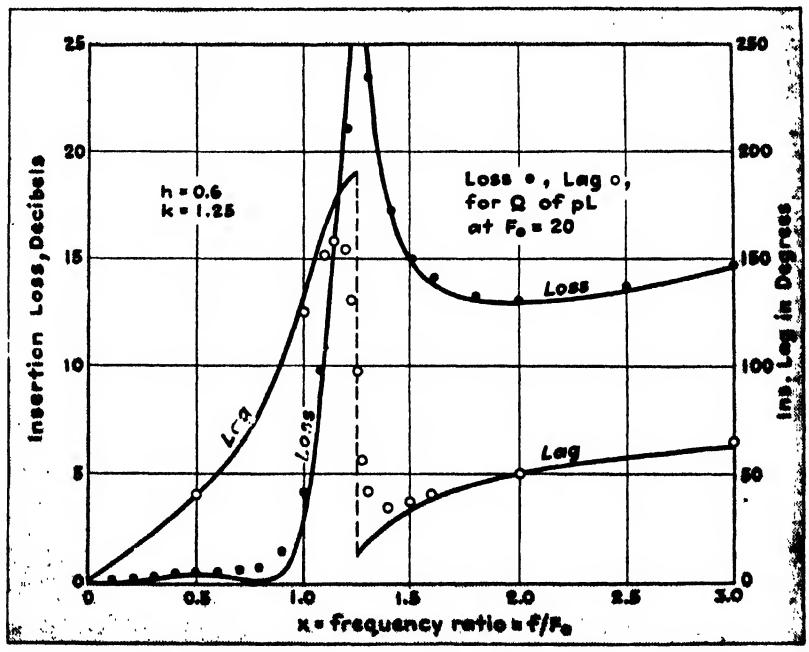

Fig. 5—More detailed data for parameter values h=0.6, k=1.25

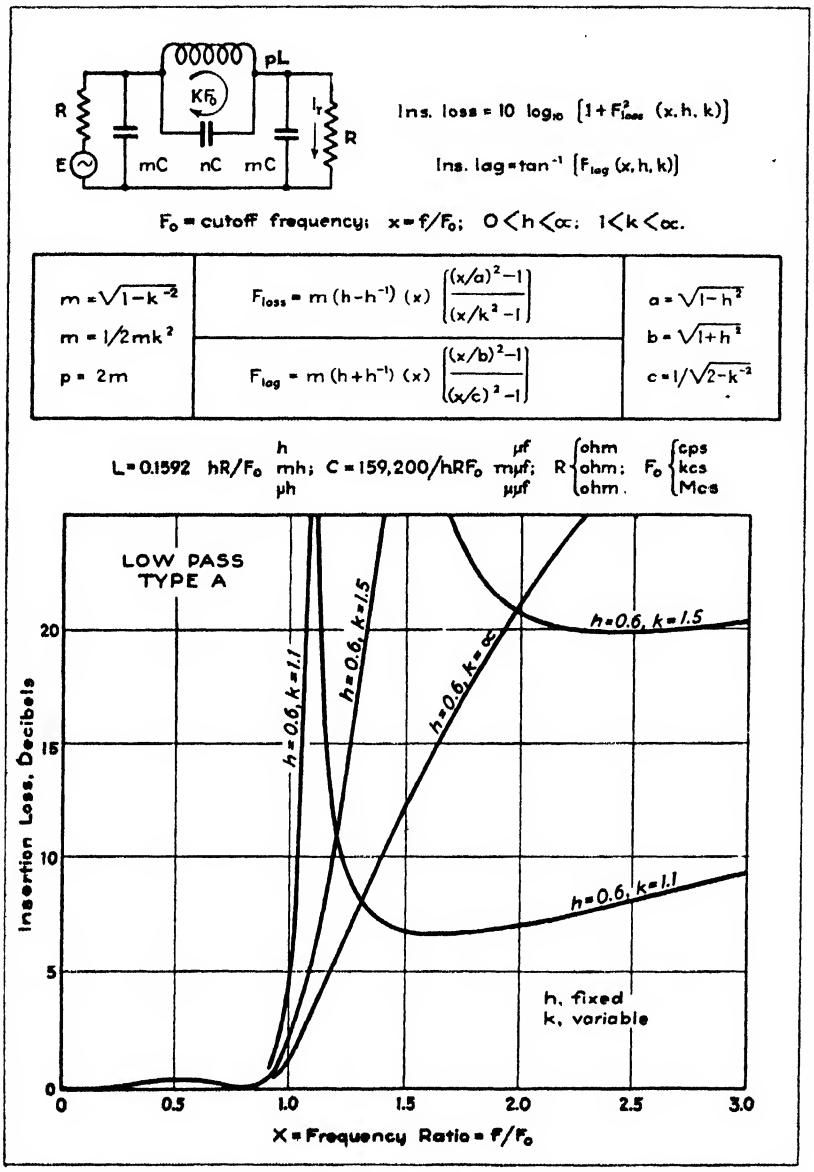

Fig. 8—Characteristics of low-pass filter unit with several values of h

pative case justify the phase reversal for the limiting non-dissipative case at $x = k$ being interpreted as a decrease of lag with increasing frequency, thereby making the lag for infinite frequency 90° instead of 450°. This should not be considered to rule out the possibility of other and more complex networks yielding integrated lag changes of more than 360° over the entire frequency range.

The information of the Chart is arranged for ready evaluation of reactor elements corresponding to any curve shape and specified values of terminations and cutoff frequency. For example, for terminations 5000 ohms, impedance level $h = 0.6$, and $F_c = 10$ kc, the basic values of L and C are 47.7 mh and 5.31 mμf. Values of the multiplicative factors for values of k greater than unity herein mentioned are given below.

k	m	n	p
1.1	0.416	0.99	0 832
1.25	0.600	0.533	1.200
1.50	0.745	0.298	1.490
Infinite	1.000	0.000	2.000

Noting that the sum of all three capacitors $(n + 2m)$ C is practically independent of k, and that over a limited range of inductance the amount of material is practically independent of pL provided the coil quality Q is kept constant, it follows that economics does not enter into the choice of k. For the choices of R, F_c and h given above and the additional choice $k = 1.25$, the network is found to require an inductor $pL = 55.3$ mh, two condensers, $mC = 3.19$ mμf, and one condenser $nC = 2.84$ mμf.

The inverse problem of determining the curve shape and cutoff frequency for a specified set of circuit values is somewhat more complex, but will be carried through to indicate that all combinations are cared for in the general solution here given. Given for example $R = 500$ ohms, $mC = 0.1$ μf, $nC = 0.2\mu$f, $pL = 2$ h, it is required to determine R, F_c, h and k. Knowing that pL and nC resonate at kF_c, it follows that $kF_c = 159.2/\sqrt{(pL)\ (nC)} = 252$ cps. Study of Eq. 8 shows k can be determined from the two condenser values mC and nC, since $k = \sqrt{1 + mC/2nC}$, that is $k = 1.12$. Therefore $F_c = 225$. Also from Eq. 8, values of m, n and p for $k = 1.12$ are 0.447, 0.894 and 0.894 respectively. Therefore from the known values of the circuit elements, $L = 2.24$ h and $C = 0.224$ μf. Using the formulas for L or for C in terms of h, R and F_c, h in either case is 6.31. Therefore, $R = 500$, $F_c = 225$, $h = 6.31$ and $k = 1.12$. For this combination the curves could be plotted if desired, but the loss curve would not be radically different in nature from Fig. 4, $h = 5$, $k = 1.25$.

Cathode Follower Nomograph

Gain, amplification factor, and the ratio of cathode load resistance to tube plate resistance are related

By MELVIN B. KLINE

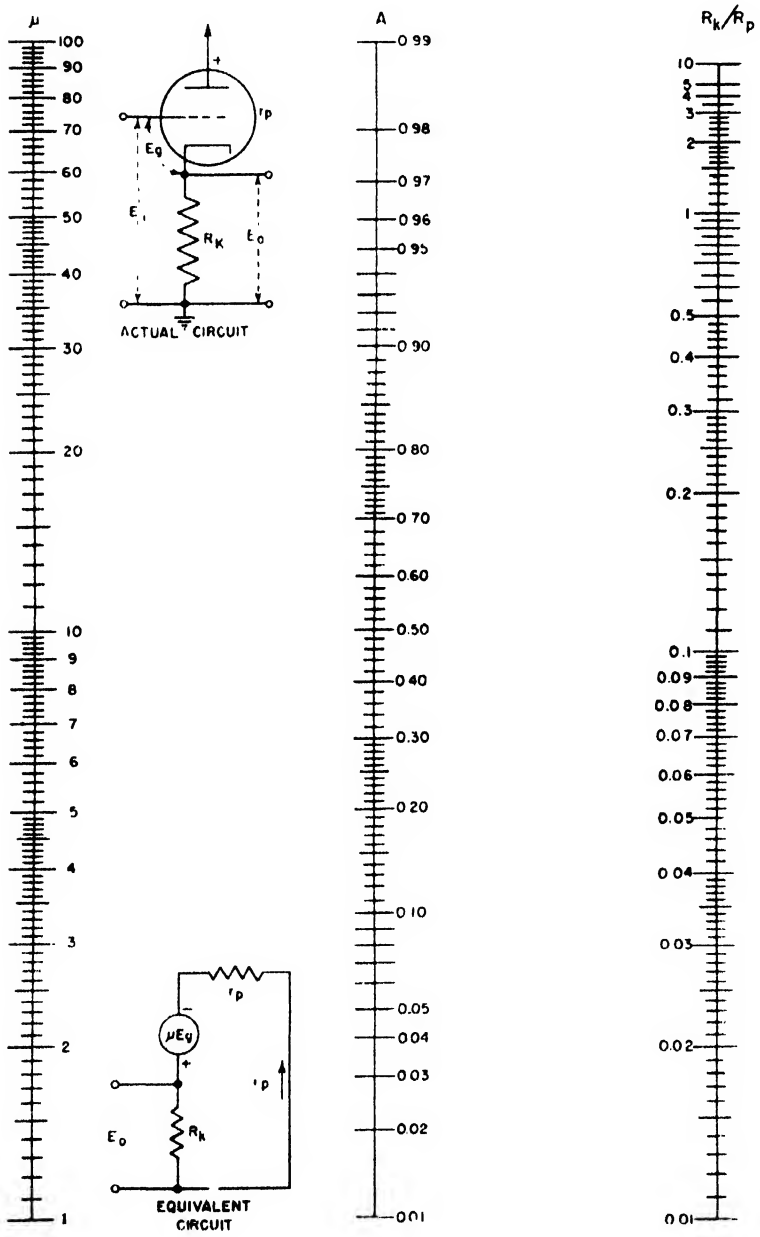

THE CATHODE-FOLLOWER has become one of the most useful tools of the electronic engineer because of its desirable characteristics as an impedance transformer.

Neglecting the effect of interelectrode and other shunting capacitances, the actual and equivalent circuits of the cathode-follower are as shown on the nomograph. Circuit equations are

$$\mu E_g = (R_k + r_p)\, i_p \qquad (1)$$

$$E_o = R_k i_p \qquad (2)$$

$$E_i = E_g + E_o \qquad (3)$$

Since the gain A is the ratio of output voltage to input voltage, solution of these equations results in the following expression for the gain of a cathode-follower

$$A = \frac{E_o}{E_i} = \frac{\mu R_k}{r_p + R_k(\mu + 1)} \qquad (4)$$

Dividing by R_k and letting $R_k/r_p = n$

$$A = \frac{\mu}{\mu + 1 + (1/n)} \qquad (5)$$

When n is very large ($R_k >> r_p$), the gain approaches a maximum value of 1.

Very often, the engineer wants to know how much gain (actually loss) he will get from a cathode-follower using a specific tube and cathode resistor. The nomograph relates tube amplification factor μ, gain A, and the ratio n of cathode load resistance R_k to tube plate resistance R_p.

Cathode Follower Nomograph for Pentodes

Gain, transconductance, and cathode load resistance are related in this nomograph

By MELVIN B. KLINE

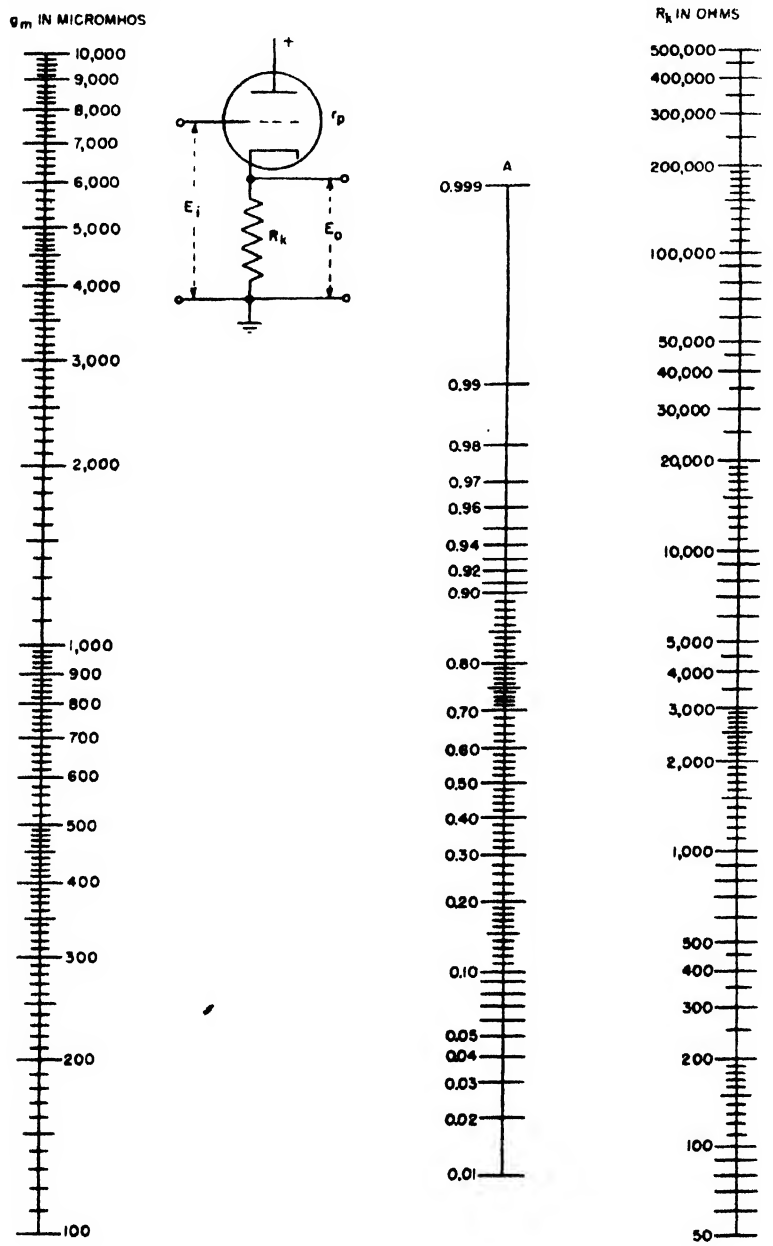

WHEN USING PENTODES as cathode followers, it is generally easier to work with transconductance than with amplification factor in computing gain and output impedance. The gain A of a cathode follower is

$$A = \frac{E_o}{E_i} = \frac{\mu R_k}{r_p + R_k(\mu + 1)} \qquad (1)$$

where μ is the amplification factor of the tube, r_p is the tube plate resistance, and R_k is the cathode resistor value. Dividing both numerator and denominator of this equation by r_p and substituting $g_m = \mu/r_p$, the equation for gain becomes

$$A = \frac{g_m R_k}{1 + g_m R_k + (R_k/r_p)} \qquad (2)$$

Since most pentodes are characterized by a relatively large plate resistance, and since within the normal range of cathode resistance $R_k << r_p$, this equation may be simplied to

$$A = \frac{g_m R_k}{1 + g_m R_k} \qquad (3)$$

A nomograph for this equation is given. While it assumes R_k to be much smaller than r_p, actually little error is made in using Eq. 3 instead of Eq. 2 even when R_k is as large as r_p. Also, little error is made even up to several mc despite neglect of effects of shunt capacitances across R_k.

Cathode Follower Impedance Nomograph

Output impedance, transconductance, and cathode load resistance are related

By MELVIN B. KLINE

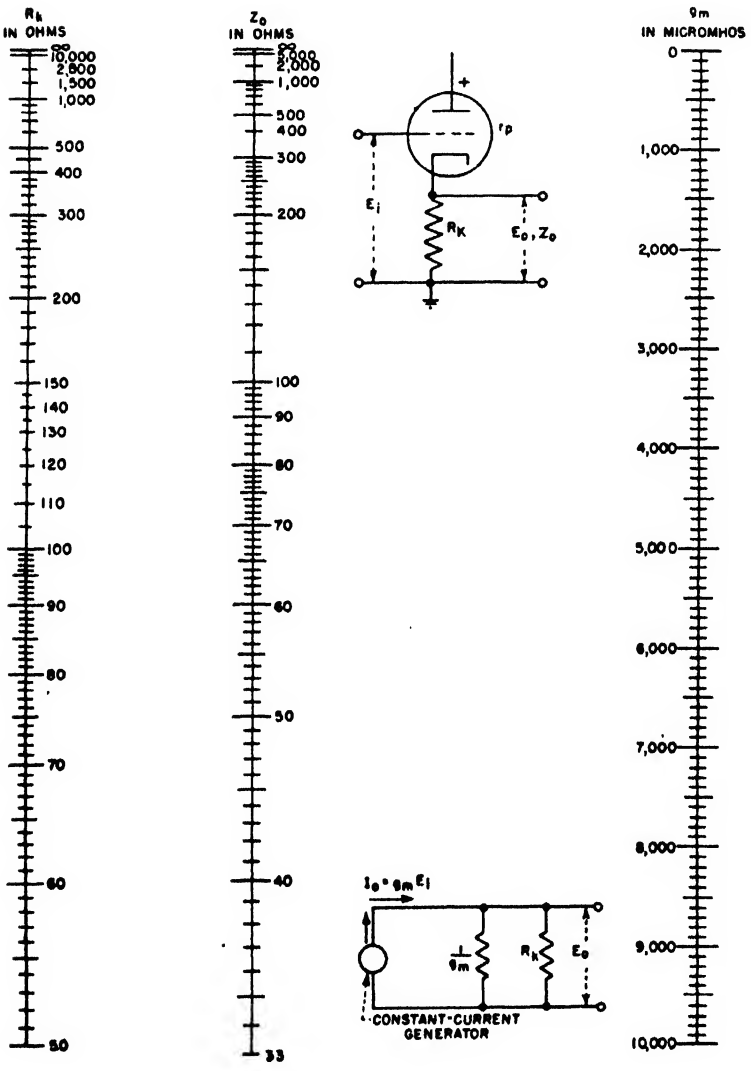

THE OUTPUT IMPEDANCE of a cathode-follower is readily found with the aid of the accompanying nomograph if transconductance and cathode load resistance are known. The pertinent design equation is obtained by starting with the relation for gain in terms of transconductance. When $R_k << r_p$

$$A = \frac{E_o}{E_i} = \frac{g_m R_k}{1 + g_m R_k} \qquad (1)$$

Rewriting gives

$$E_o = \frac{(1/g_m)\, R_k}{(1/g_m) + R_k}\, g_m E_i \qquad (2)$$

This represents a parallel resistance combination consisting of two resistances, $1/g_m$ and R_k, through which flows a current $g_m E_i$, as indicated in the constant-current form of the equivalent circuit on the nomograph.

Equation 2 states that the output voltage E_o is a result of an output current ($I_o = g_m E_i$) flowing through an output impedance

$$Z_o = R_k/(1 + g_m R_k) \qquad (3)$$

This Z_o is the output impedance of the cathode-follower as given by the nomograph.

This chart should be of particular value in providing the proper termination for transmission lines and coaxial cables.

DB Gain-Loss Calculator

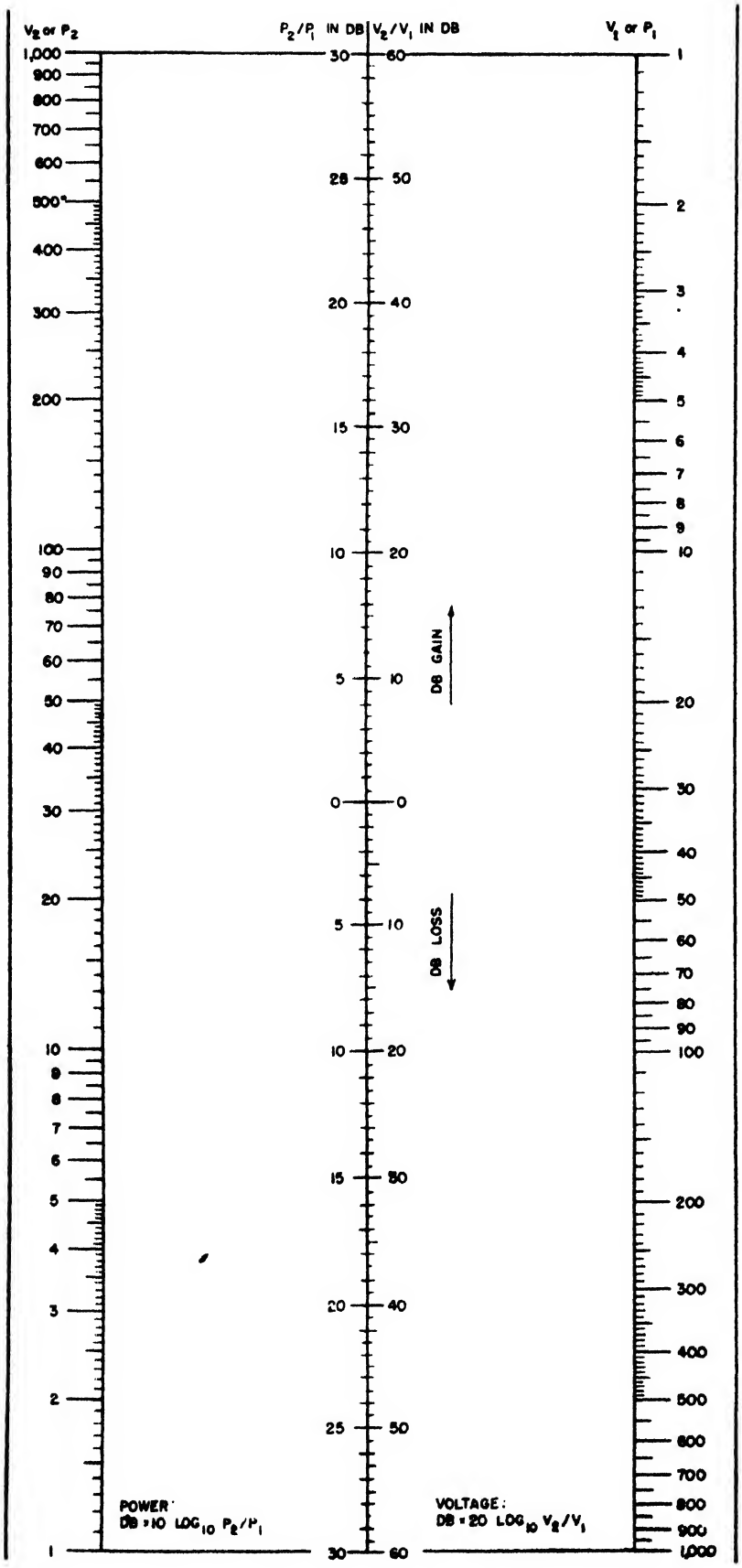

By LLOYD A. LOHR

IN WORKING with communications equipment, it is often desirable to know the db gain or loss ratio of two voltages, currents, or powers with a minimum amount of calculation. This nomograph will give the db value directly for any voltage, current, or power ratio up to 1,000 to 1 with only one setting of a straightedge, and the range can readily be extended by using multiplying factors. The converse problem, of finding a ratio that will give a desired db gain or loss, can just as readily be solved.

If V_1 and V_2 are known, place the straightedge to connect their values on the outer scales and read voltage gain or loss in db on the right side of the center scale.

If P_1 and P_2 are known, place the straightedge to connect their values on the outer scales and read voltage gain or loss in db on the left side of the center scale.

If the db value and one voltage or power value are known, connect these values with a straightedge and read the other voltage or power value on the third scale.

The range of the nomograph can be extended by applying a multiplier to one of the log scales and adding to the db scale values as follows:

Multiplier for one log scale	Add to values on P_2/P_1 scale	Add to values on V_2/V_1 scale
10	10	20
100	20	40
1,000	30	60
10,000	40	80
100,000	50	100

Example: What is the db gain for a voltage ratio of 100 to 5? From the nomograph, the db gain is approximately 26.1 db. Checking, db = 20 log V_2/V_1 = 20 log 20 = 26.06 db.

Impedance Nomograph

By GERSHON J. WHEELER

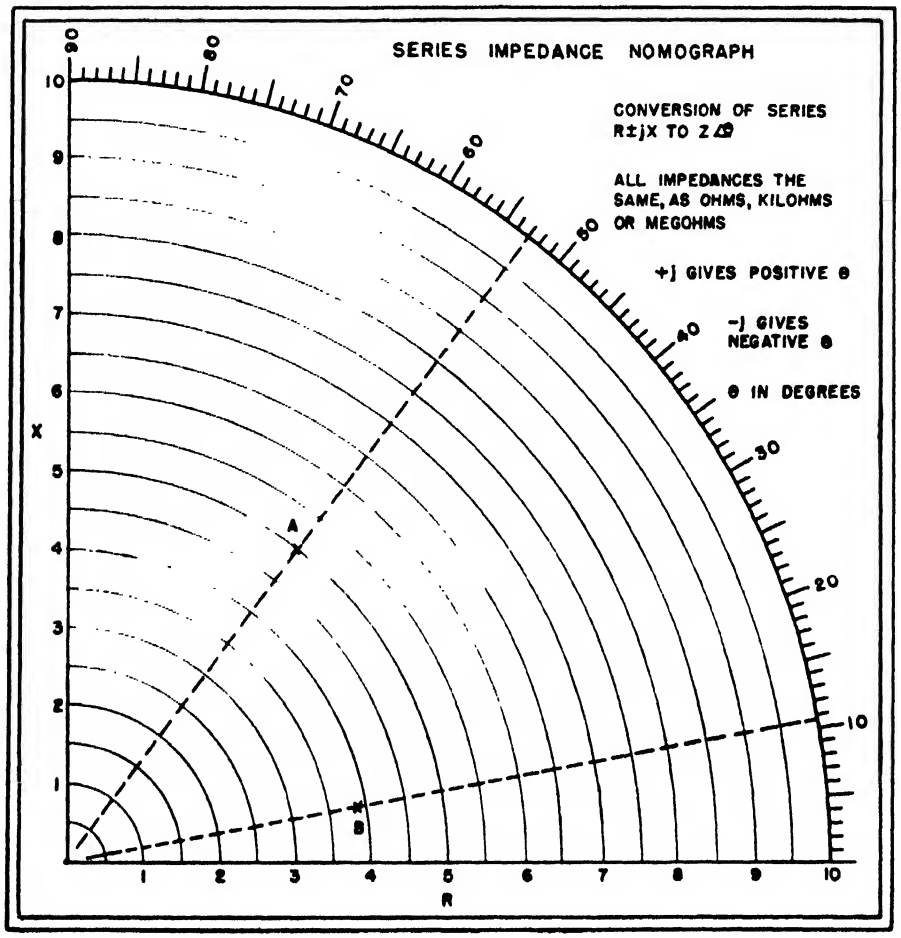

THIS NOMOGRAPH presents a simple means for converting $R \pm jX$ to Z/θ or vice versa. Enter the graph with the value of R as the abscissa and the value of X as the ordinate. The point so located lies on or near an arc which represents a value of Z to be read at either end of the arc. The angle θ is found by laying a straight edge through the origin and the point found above. The value is read on the outside quadrant.

For example: R is 3 ohms, X is 4 ohms. The point located as above is point A on the graph. It lies on an arc which has a 5 at either end. A straight edge through A and the origin intersects the quadrant at about 53 degrees. Thus Z is 5 ohms and θ is 53 degrees. If R is 30 and X is 40, then Z would be 50. That is, the units may be ohms, tens of ohms, fractions of ohms, etc, as long as R, X, and Z are in the same units.

If R is 38 ohms and X is 7 ohms, the intersection is now at point B. Here the units are tens of ohms. Z is approximately 39 ohms and θ is about 10.7 degrees.

If Z/θ is given, the process is reversed.

If R is ten times X or greater, or if X is ten times R or greater, then Z is approximately equal to the larger value, and θ cannot be determined accurately but is larger than 84 degrees or smaller than 6 degrees as the case may be.

If X is negative, θ is negative.

Impedance-Admittance Conversion Chart

Simple chart for quickly converting $Z = R \pm jX$ to $Y = G \mp jB$ and vice versa when combining impedances in parallel. One-decade range requires use of multipliers for most problems, but accuracy is adequate for quick, rough estimating work

By ROBERT C. PAINE

WHEN impedances are to be combined in parallel it is necessary to convert them to admittances so they can be readily added together. Such conversions can be conveniently performed with reasonable accuracy by the aid of the chart shown. Resistance R is plotted in a horizontal direction and re-

actance X in a vertical direction, being considered positive or negative depending on whether it is inductive or capacitive. Passing through each impedance point $R \pm jX$ is an arc centered on the horizontal axis for conductance G, and another arc centered on the vertical axis for susceptance B of the corresponding admittance $Y = G \mp jB$. The susceptance is read as negative for inductances and positive for capacitances.

Examples of Use

(1) Impedance $Z_1 = R + jX = 8 + j5$. On the chart this corresponds to an admittance $Y_1 = G - jB = 0.09 - j0.057$.

(2) Impedance $Z_2 = 2 - j1.5$. The corresponding admittance is $Y_2 = G + jB = 0.32 + j0.24$. Because Z_2 lies near the origin, greater accuracy can be attained by using a multiplier such as 4. Then $4Z_2 = 8 - j6$, the corresponding value of Y is $0.08 + j0.06$, and this value multiplied by 4 gives the correct value, $Y_2 = 0.32 + j0.24$.

(3) The impedances of examples 1 and 2 are combined in parallel. The sum of their admittances is $Y_3 = Y_1 + Y_2 = 0.41 + j0.183$. Changing the scale by a factor of $\frac{1}{4}$ we obtain $\frac{1}{4} Y_3 = 0.102 + j0.046$, and $Z_3 = \frac{1}{4}(8.2 - j3.6) = 2.05 - j0.9$.

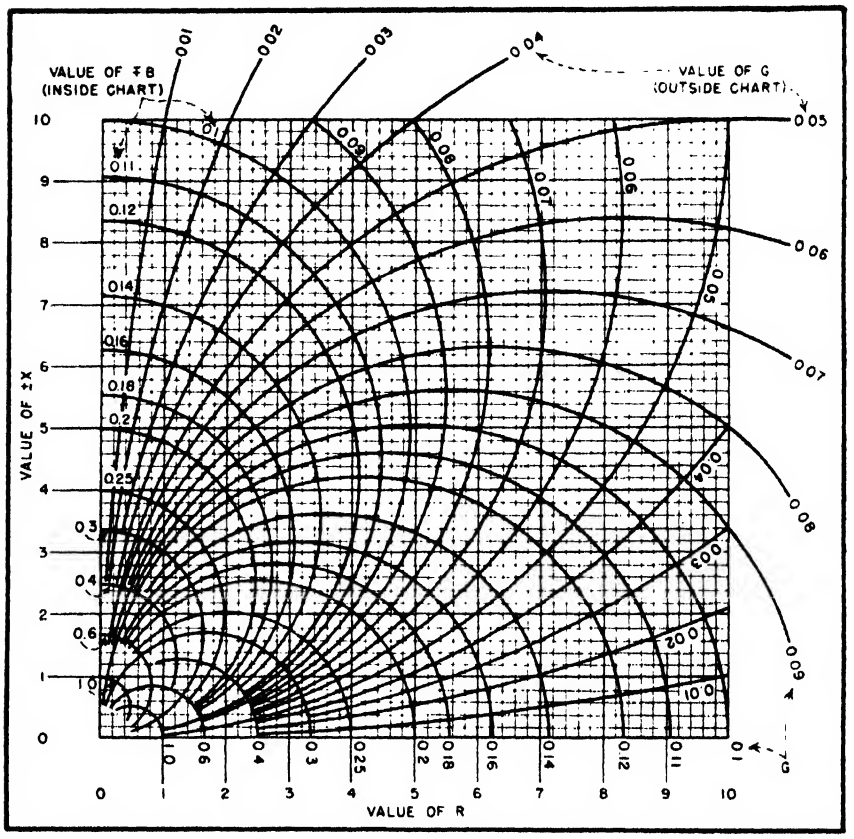

When known values are outside range of chart, multiply by any convenient value that brings them within range, find equivalent values from chart, and multiply them by that same multiplier to get final answer. Values of R and centers of circles for corresponding G values are on horizontal reference axis. Values of X and centers of circles for corresponding B values are on vertical reference axis

(4) Impedance $Z_4 = 20 - j15$. Multiply Z_4 by 1/10 to get values within range of chart, find admittance values as in example 1, and multiply them by 1/10 to get $Y_4 = 0.032 + j0.024$.

Theoretical Signal-to-Noise Ratios

Signal-to-noise ratios are derived in terms of the frequency bands of the signal and of the transmitted radio carriers. Resulting equations indicate merits of various combinations of modulation and multiplex with respect to noise. Frequency and amplitude modulation systems are compared

By J. ERNEST SMITH

COMPARATIVE ANALYSIS shows the signal-to-noise ratios obtainable in multichannel amplitude modulation and frequency modulation transmission systems. This discussion applies particularly to ultra and super high-frequency radio relay circuits for point-to-point communication. Equations are derived which indicate, among other things, that, for equal transmitted powers and radio frequency bandwidths, double f-m systems offer advantages over double a-m systems.

Ultra and super high-frequency

radio relays are being planned for transmission of television, high quality programs, multiplex telephony and telegraphy, facsimile, radiophoto, and business machine data. Design of such facilities requires knowledge of the modulation methods that provide optimum signal-to-noise ratios in the individual channels of a multichannel system. Knowing the signal-to-noise ratio of a channel, the designer of a system that is to transmit different types of intelligence can allocate to each channel only as much of the total transmitted energy as is required for satisfactory reception of each type of intelligence. By thus weighting each channel, an optimum number of channels can be obtained for a fixed transmitted power and bandwidth.

Types of Modulation and Noise

Several types of transmission can be employed, all using either a-m or f-m. In a single modulation system the intelligence modulates the transmitted carrier. In a double modulation system the intelligence signal modulates a subcarrier which, in turn, modulates the transmitted carrier. For single channel transmission, only one intelligence signal is used.

Two types of noise can affect radio transmission. Impulse noise, accurately represented by a unit impulse, can be considered, at the higher frequencies, as a finite bandwidth of components having equal amplitudes and the same phases. This interference produces transients in the receiver, but being of local-origin its effects can be reduced by shielding the noise source or relocating the receiver's antenna.

On the other hand fluctuation noise, due largely to shot effect, thermal agitation, and antenna pickup (site) noise, cannot be removed. Above 300 mc shot noise predominates to the extent that thermal and site noise can be neglected. Within the acceptance band of the receiver, fluctuation noise can be considered as a finite bandwidth of components having equal amplitudes but random phases.

Define noise power density as the noise power per unit of bandwidth (watts per cycle). Noise power generated by the receiver is directly proportional to bandwidth. The equivalent fluctuation noise voltage N is proportional to the square root of bandwidth. This noise voltage, wherever it is generated, will be referred to the antenna input terminals. To include the bandwidth in which this noise exists, use the nomenclature N_f, where N is the peak value of the fluctuation noise in the frequency band f.

Noise Determination

The signal to noise ratio $(C/N)_{2f_r}$, where the notation is explained in Table I, can be obtained by measurement: Connect an r-f generator directly to an a-m superheterodyne receiver and amplitude modulate the r-f generator 100 percent with an audio tone. Because the tone fully modulates the carrier, the detected signal S is a precise audio measurement of the magnitude of the r-f carrier. We have assumed the existence of a noise magnitude N_{2f_r} at the receiver input terminals. This magnitude will be different at the mixer due to the antenna coupling circuits. However, the modulated carrier will be modified also so that $(C/N)_{2f_r}$ remains unchanged. We assume that the mixer has a linear conversion characteristic. The intermediate frequency carrier-to-noise ratio will then equal the r-f carrier-to-noise ratio if $f_i = f_r$. This latter equality is not obtained in practice. In fact, receiver selectivity is almost entirely determined by f_i and, in general, f_i will be much less than f_r. A portion of the noise is thus rejected by the i-f band, consequently

$$\left(\frac{N2f_i}{N_{2f_r}}\right) = \left(\frac{f_i}{f_r}\right)^{1/2}$$

The intermediate frequency carrier-to-noise ratio as modified by the i-f pass-band is expressed as

$$\left(\frac{C}{N}\right)_{2f_i} = \left(\frac{f_r}{f_i}\right)^{1/2}\left(\frac{C}{N}\right)_{2f_r} \qquad (1)$$

Equation 1 gives the carrier-to-noise ratio that is applied to the receiver detector. The function of the detector is to reproduce the original modulating tone by folding the lower sidebands upon the upper sidebands so that they add in phase to produce a resultant S equal in magnitude to C. The sidebands of noise are filled with components of equal amplitude and random phase. When the lower sideband is folded on the upper, the noise power in the band zero to f_i from the detector is twice that of the upper sideband alone. Normally, the detector output contains a low-pass filter of cutoff frequency f_a where f_a is much less than f_i. Accordingly, this filter will reject all noise components greater than f_a and the output noise power is reduced by the factor f_a/f_i, therefore

$$\begin{aligned}(S/N)_{f_a} &= (C/N)_{2f_a} \\ &= (f_i/f_a)^{1/2}(C/N)_{2f_i} \\ &= (f_r/f_a)^{1/2}(C/N)_{2f_r}\end{aligned}$$

or

$$(C/N)_{2f_r} = (f_a/f_r)^{1/2}(S/N)_{f_a}$$

Noise Measurement

The ratio $(S/N)_{f_a}$ is obtained directly by measurement. With the

C	: peak amplitude of radio frequency carrier
C_a	: peak amplitude of subcarrier in double modulation system
f_a	: transmission bandwidth of intelligence portion of system
f_d	: peak frequency deviation of carrier or subcarrier from unmodulated frequency
f_a	: transmission bandwidth of multiplex system
f_s	: frequency of subcarrier
$2f_i$	: transmission bandwidth of intermediate frequency portion of system
$2f_r$	: transmission bandwidth of radio frequency portion of system
f_1	: lower limit of a given channel within a multiplex system
f_2	: higher limit of a given channel within a multiplex system
m	: percent modulation in an amplitude modulation system
N	: equivalent fluctuation noise voltage; subscript refers to bandwidth over which particular noise voltage is developed
n	: number of channels in a multiplex system
S	: voltage of detected intelligence signal

deviation ratios of frequency modulation systems are indicated by $(\ )_{r\text{-}f}$ to indicate deviation of radio carrier frequency, and by $(\ )_{s\text{-}f}$ to indicate deviation of the subcarrier frequency

Table I—Nomenclature used in equations

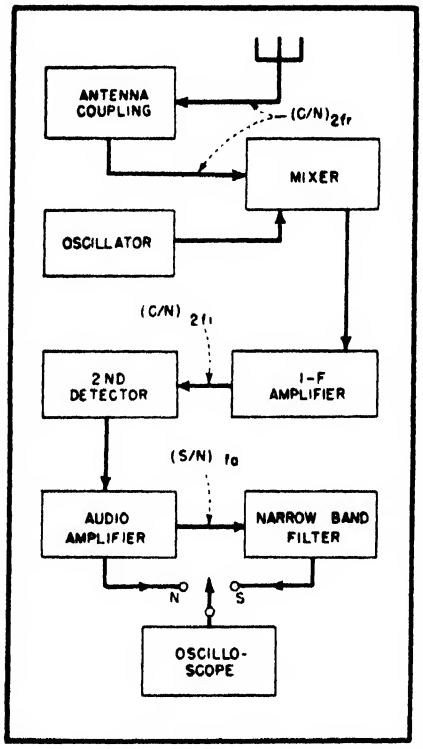

FIG. 1—How noise at the receiver input is measured in the field

switch of survey receiver shown in Fig. 1 in position N and no modulation of the r-f generator, the oscilloscope will trace the fluctuation noise output of the receiver. With the switch in position S and 100 percent modulation of the r-f generator, the signal S will be shown on the oscilloscope. The audio band-pass filter minimizes noise during the signal measurement so that the ratio of the vertical deflections obtained gives the desired signal-to-noise ratio in the band f_a. The a-m receiver described can be used as a survey receiver. Reliable C/N measurements are made at the receiving sites with transmitting and receiving antenna gains calibrated with respect to the actual radio circuit equipment. Noise factor of the survey receiver should be known relative to that of the proposed relay receiver.

Threshold Relations

In the previous section we assumed that S/N (detected carrier-to-noise ratio) at the output of the a-m detector was linearly proportional to C/N at the input to the detector. It has been demonstrated experimentally that this relation holds as long as

$$(C/N)_{2f_i} > 1 \tag{2}$$

We may define Eq. 2 as the threshold condition for an amplitude modulated signal. Crosby has shown that the corresponding threshold condition in frequency modulation requires that

$$(C/N)_{2f_i} \leq 2 \tag{3}$$

In a particular radio relay link the radiated power, distance of transmission, and receiver i-f bandwidth must be correlated to satisfy the threshold relations and the desired S/N in a particular intelligence channel. The information needed to meet these requirements with a simple survey measurement is derived in succeeding sections.

Single Modulation A-m

In a single modulation a-m system the i-f band need be only $2f_a$ wide to pass the modulated carrier. Actually, due to Q limitations of the circuits, it usually exceeds this value.

Assume that, in the mixer or first detector stage of the receiver, the local heterodyne oscillations are of high amplitude compared with the incoming signal, i.e., the mixer does not affect C/N.

At the input to the second detector one might say that three waves exist; namely, the carrier C, the noise N and the signal S. For 100 percent modulation, S equals C in magnitude. Thus, the output of the a-m detector has an S/N equal to C/N in the i-f band when $f_i = f_a$. When f_i is greater than f_a, we consider only C/N within the portion of the i-f band $2f_a$ wide because all other noise components are rejected by the detector output circuit.

We may then write for 100 percent modulation $(S/N) = (C/N)_{2f_a}$. For less than 100 percent modulation, S/N is directly proportional to the modulation index. Thus

$$(S/N)_{f_a} = m\,(C/N)_{2f_a} \tag{4}$$

Double Modulation A-m

In a double modulation a-m system the intelligence signals amplitude modulate their respective subcarriers. These subcarriers amplitude modulate the transmitted r-f carrier. The r-f and i-f bandwidths of the receiver must be at least $2f_s$ wide, where $f_s = f_a + f_b + \ldots f_n$, to pass the modulated carrier without distortion. Then C/N in the r-f band is

$$(C/N)_{2f_r} = (f_a/f_r)^{1/2}(C/N)_{2f_a} \tag{5}$$

Similarly C/N in the i-f band becomes

$$(C/N)_{2f_i} = (f_a/f_i)^{1/2}(C/N)_{2f_a} \tag{6}$$

To determine the subcarrier-to-noise ratio after the group detector, we again consider the noise within the i-f band extending f_s on either side of the central frequency, because all other noise components are rejected by the low-pass filter following the detector. Thus

$$\begin{aligned}(C/N)_{2f_a} &= (f_i/f_a)^{1/2}(C/N)_{2f_i} \\ &= (f_a/f_a)^{1/2}(C/N)_{2f_a}\end{aligned} \tag{7}$$

Writing C_c for the peak amplitude of any subcarrier and temporarily assuming that the subcarrier modulates the radiated r-f carrier to 100 percent, we obtain from Eq. 4

$$(C_c/N)_{f_a} = (C/N)_{2f_a} \tag{8}$$

for the subcarrier-to-noise ratio in the bandwidth of the total group of intelligence signals f_s.

The arrangement assumed in Eq. 8 would not permit transmission of intelligence because an increase in the amplitude of the subcarrier due to modulation by the intelligence signal would cause the subcarrier to overmodulate the r-f carrier. Therefore, to allow an intelligence signal to modulate its subcarrier 100 percent we must reduce C_c. For n channels, C_c equals $C/2n$ to avoid over modulation during the intervals when all subcarriers add in phase. Rewriting Eq. 8 for n intelligence channels gives

$$(C_c/N)_{f_a} = (1/2n)\,(C/N)_{2f_a} \tag{9}$$

In the group band each channel occupies a band $2f_c$ wide. Because the noise is equally distributed over this band, the effect of filtering any channel will be to reduce the noise in that band to

$$N_{2f_a} = (2f_a/f_s)^{1/2}N_{f_s} \tag{10}$$

Substituting Eq. 7 and 10 into Eq. 9 gives

$$\left(\frac{C_s}{N}\right)_{2f_s} = \frac{1}{2n}\left[\left(\frac{f_s}{2f_s}\right)\left(\frac{f_s}{f_s}\right)\right]^{1/2}\left(\frac{C}{N}\right)_{2f_s} = \frac{1}{2n\sqrt{2}}\left(\frac{C}{N}\right)_{2f_s} \quad (11)$$

It should be noted in this case that the noise in any filtered channel does not depend upon its position in the frequency spectrum but only upon the channel bandwidth and this bandwidth need never exceed $2f_s$. After final detection of this channel signal, the signal-to-noise ratio becomes, for 100 percent modulation of the subcarrier

$$(S/N)_{f_s} = (C_s/N)_{2f_s} = (1/2n\sqrt{2})\,(C/N)_{2f_s} \quad (12)$$

and for m percent modulation of the subcarrier

$$(S/N)_{f_s} = (m/2n\sqrt{2})\,(C/N)_{2f_s} \quad (13)$$

For a double modulation system in which only one intelligence is transmitted $n = 1$. Inserting this value in Eq. 13 and comparing the result with Eq. 4, we note that the double a-m system has a worse S/N than the single a-m system by a factor of $2\sqrt{2}$ or nine decibels. Six decibels of this loss is due to the energy required to transmit the subcarrier. The remaining three decibels are accounted for by the fact that the single a-m system has a noise acceptance band of $2f_s$, whereas the double a-m system has two noise acceptance bands, each of bandwidth $2f_s$ in the r-f spectrum and, consequently, the latter accepts $\sqrt{2}$ times more noise. If the subcarrier and one sideband are suppressed as in some single sideband systems, the double a-m system is, in effect, converted to a single a-m system and the nine decibels are regained.

Single Modulation F-m

Mathematical analysis of a frequency modulated carrier shows that an infinite number of sidebands are produced. Therefore, a finite receiver i-f bandwidth must introduce some distortion due to sideband clipping. This type of distortion appears as concomitant amplitude and phase modulation of the i-f carrier. The limiter erases the amplitude modulation. In a wideband system ($f_d/f_s > 1$), the writer believes that the phase distortion will be negligible as long as the r-f and i-f bandwidths are not less than $2f_d + 4f_s$. In narrow band f-m systems ($f_d/f_s < 1$), these bandwidths can be reduced to $2f_d + 2f_s$.

In the i-f band we have as before

$$(C/N)_{2f_i} = (f_r/f_i)^{1/2}(C/N)_{2f_r} \quad (14)$$

which must satisfy the f-m threshold condition of Eq. 3.

The signal is now impressed upon an f-m detector having a frequency fidelity band from zero to f_s. Assuming fulfillment of the threshold requirement, we are concerned only with C/N in a portion of the i-f band $2f_s$ wide. This ratio is

$$(C/N)_{2f_s} = (f_r/f_s)^{1/2}(C/N)_{2f_r}$$

To determine the signal-to-noise after detection, we use the relation

$$\left(\frac{S}{N}\right)_{f_s} = \sqrt{3}\left(\frac{f_d}{f_s}\right)_{r\text{-}f}\left(\frac{C}{N}\right)_{2f_s} \quad (15)$$

where $(f_d/f_s)_{r\text{-}f}$ is the deviation ratio of the r-f carrier at the highest modulating frequency.

Double Modulation F-m

In a double frequency modulation system the channel is identical with the single f-m system insofar as the first f-m detector action at the receiver is concerned. However the frequency band from zero to f_g is wide enough to contain several subcarriers which are themselves frequency modulated by independent intelligence signals.

To determine the ratio of any one subcarrier to the noise in the total band from zero to f_g, we rewrite Eq. 15 substituting f_g for f_s.

$$\left(\frac{C_s}{N}\right)_{f_g} = \frac{\sqrt{3}}{n}\left(\frac{f_d}{f_g}\right)_{r\text{-}f}\left(\frac{C}{N}\right)_{2f_g} = \frac{\sqrt{3}}{n}\left(\frac{f_d}{f_g}\right)_{r\text{-}f}\left(\frac{f_s}{f_g}\right)^{1/2}\left(\frac{C}{N}\right)_{2f_s}$$

Any one subcarrier is frequency modulated within the channel band $f_2 - f_1$. The noise in this band is less than that in the total band zero to f_g so that the ratio C_s/N in this band is improved by a bandwidth factor.

To determine this factor, we recall that the noise out of the detector varies linearly with frequency as shown in Fig. 2A. Consequently, the noise power density is a parabolic function of frequency and the ratio of noise energy in the total band to that in the band $f_2 - f_1$ is equal to the ratio of the area under the parabola to the shaded area of Fig. 2B. This ratio is obtained by integration

$$\frac{\int_0^{f_g} f^2 df}{\int_{f_1}^{f_2} f^2 df} = \frac{f_g^3}{f_2^3 - f_1^3}$$

The rms and, consequently, the peak voltage ratio is equal to the square root of the energy ratio. Therefore, the improvement factor due to filtering the frequency band $f_2 - f_1$ is $[f_g^3/(f_2^3 - f_1^3)]^{\frac{1}{2}}$. The subcarrier-to-noise ratio in this band then becomes

$$\left(\frac{C_s}{N}\right)_{f_2 - f_1} = \frac{\sqrt{3}}{n}\left(\frac{f_d}{f_g}\right)_{r\text{-}f}\left(\frac{C}{N}\right)_{2f_s} \times \left[\left(\frac{f_s}{f_g}\right)\left(\frac{f_g^3}{f_2^3 - f_1^3}\right)\right]^{1/2} \quad (16)$$

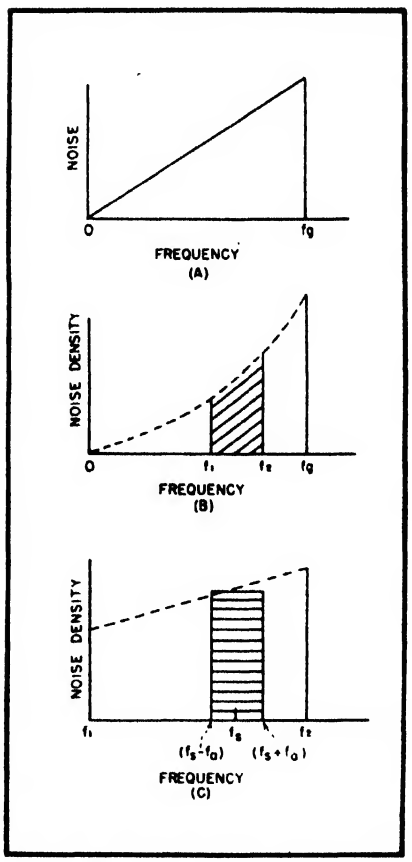

FIG. 2—Noise-frequency relations used in computations

Basic signal-to-noise equations derived in text for a bandwidth f_a

Amplitude Modulation

Single: $\left(\frac{S}{N}\right)_{f_a} = m\left(\frac{C}{N}\right)_{2f_a}$

Double: $\left(\frac{S}{N}\right)_{f_a} = \frac{m}{2n\sqrt{2}}\left(\frac{C}{N}\right)_{2f_a}$

Frequency Modulation

Single: $\left(\frac{S}{N}\right)_{f_a} = \sqrt{3}\left(\frac{f_d}{f_a}\right)_{r\text{-}f}\left(\frac{C}{N}\right)_{2f_a}$

Double: $\left(\frac{S}{N}\right)_{f_a} = \frac{1}{n}\sqrt{\frac{3}{2}}\left(\frac{C}{N}\right)_{2f_a} \times \left(\frac{f_d}{f_s}\right)_{r\text{-}f}\left(\frac{f_d}{f_a}\right)_{s\text{-}f}$

Comparing one system with another gives

$$\frac{\text{Double a-m}}{\text{Single a-m}} = \frac{1}{2n\sqrt{2}}$$

$$\frac{\text{Single f-m}}{\text{Single a-m}} = \frac{\sqrt{3}}{m}\left(\frac{f_d}{f_a}\right)_{r\text{-}f}$$

$$\frac{\text{Double f-m}}{\text{Single a-m}} = \frac{1}{mn}\sqrt{\frac{3}{2}}\left(\frac{f_d}{f_s}\right)_{r\text{-}f}\left(\frac{f_d}{f_a}\right)_{s\text{-}f}$$

$$\frac{\text{Double f-m}}{\text{Double a-m}} = \frac{2\sqrt{3}}{m}\left(\frac{f_d}{f_s}\right)_{r\text{-}f}\left(\frac{f_d}{f_a}\right)_{s\text{-}f}$$

$$\frac{\text{Double f-m}}{\text{Single f-m}} = \frac{1}{\sqrt{2n}}\left(\frac{f_d}{f_s}\right)_{s\text{-}f}$$

The last ratio is for identical intermediate frequency bandwidths

Table II—Comparison of Modulation Systems

Equation 16 may be described as the threshold equation for the second f-m detector, i.e., the value of C_s/N must be equal to or greater than two in order that the S/N out of the second detector be a linear function of the subcarrier-to-noise ratio into the detector.

In general, the bandwidth $f_2 - f_1$ is determined by the frequency deviation of the subcarrier and it may be considerably greater than $2f_a$ where f_a is the fidelity band of the second f-m detector. As in the single f-m modulation case, we need to know the ratio of subcarrier-to-noise in the band $2f_a$.

Define the subcarrier frequency, f_s, as the arithmetic mean frequency in the band $f_2 - f_1$, or $f_s = \frac{1}{2}(f_1 + f_2)$. As before, the noise in the band $2f_a$ wide with f_s as its center frequency will be less than the noise in the total band $f_2 - f_1$. Observing Fig. 2C, it will be evident that the noise accepted in the band $2f_a$ wide will vary with the location of f_s.

Starting with Eq. 15 and writing the improvement factor in the same manner as in the derivation of Eq. 16, the subcarrier-to-noise ratio in the band f_a either side of f_s referred to the total first detector band

$$\left(\frac{C_s}{N}\right)_{(f_s+f_a)-(f_s-f_a)} = \frac{\sqrt{3}}{n}\left(\frac{f_d}{f_0}\right)_{r\text{-}f}\left(\frac{C}{N}\right)_{2f_a} \times \left[\left(\frac{f_a}{f_0}\right)\left(\frac{f_0^3}{(f_s+f_a)^3-(f_s-f_a)^3}\right)\right]^{1/2} \quad (17)$$

the fraction within the square root bracket of this equation can be simplified to

$$\left(\frac{f_a}{f_0}\right)\left(\frac{f_0^3}{6f_s^2f_a\left(1+f_a^2/3f_s^2\right)}\right)$$

Because f_s must be at least $3f_a$ to reproduce the signal wave shape, we can neglect the term $f_a^2/3f_s^2$ compared with unity, and Eq. 17 further simplifies to

$$\left(\frac{C_s}{N}\right)_{(f_s+f_a)-(f_s-f_a)} = \frac{1}{\sqrt{2n}}\left(\frac{f_d}{f_s}\right)_{r\text{-}f}\left(\frac{C}{N}\right)_{2f_a} \quad (18)$$

Again using the standard Eq. 15

$$\left(\frac{S}{N}\right)_{f_a} = \sqrt{3}\left(\frac{f_d}{f_a}\right)_{s\text{-}f} \times \left(\frac{C_s}{N}\right)_{(f_s+f_a)-(f_s-f_a)}$$

Substituting Eq. 18 into this result

$$\left(\frac{S}{N}\right)_{f_a} = \frac{1}{n}\left(\frac{3}{2}\right)^{1/2}\left(\frac{f_d}{f_s}\right)_{r\text{-}f} \times \left(\frac{f_d}{f_a}\right)_{s\text{-}f}\left(\frac{C}{N}\right)_{2f_a} \quad (19)$$

Results of these derivations are summarized in Table II which shows signal-to-noise ratios that can be obtained in each of the systems analysed and the manner in which channel frequencies affect these ratios.

Two-Terminal Oscillator

Negative transconductance provided by a two-stage amplifier gives the phase reversal necessary for circuit oscillation. Only two points in the circuit are needed for connection of a simple tuned circuit to provide several oscillator arrangements

By MURRAY G. CROSBY

THE PHASE REVERSAL which exists between the input and output of a vacuum-tube amplifier operates as somewhat of an inconvenience in design of an oscillator circuit. The requirement of phase inversion which is required to produce the proper feedback for oscillation has been met in various ways. The most common is the use of a coupled circuit between the plate and grid which furnishes the phase reversal as well as the tuning elements.

Another means of setting up oscillations is by means of a negative transconductance tube, or circuit, which does not give the usual phase reversal between the input and output. The dynatron, transitron, and multistage amplifier are examples[1] of this type. These circuits have the advantage that they may be connected as oscillators by merely connecting a simple two-element tuned

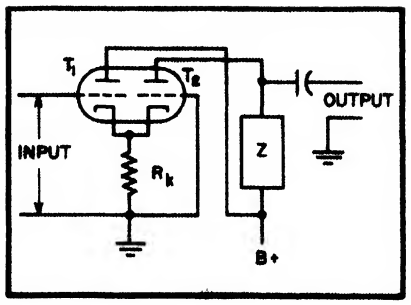

FIG. 1—Basic circuit of the oscillator. Tube T_1 operates as a cathode follower to drive T_2

circuit between two points in the circuit.

The circuit to be described[2] is the multistage amplifier type in which two stages are connected in cascade amplification to eliminate the phase reversal effected by a single stage. The method of coupling between stages has many advantages over the prior types.

Basic Circuit

Figure 1 shows the fundamental circuit. A twin triode is connected with one triode acting as a cathode follower driving the cathode of the second triode through coupling effected by the common cathode resistor R_k.

A positive voltage applied to the grid of T_1 causes more current to flow in the plate circuit of T_1 and consequently more current through the common cathode resistor. The increased current through the cathode resistor raises the potential of the cathodes in the positive direction.

An increased positive potential on the cathode of T_2 is equivalent to an increased negative potential on the grid of T_2. Thus a positive voltage applied to the grid of T_1 is converted, by the coupling system, to an equivalent negative potential on the grid of T_2. This phase reversal, together with the phase reversal effected between the grid and plate of T_2, forms a complete 360-degree phase rotation, so that the input is in phase with the output.

The transconductance between input and output is therefore negative, so that all that is required for oscillation is to place a tuned circuit in the output plate circuit and couple it back to the input grid circuit.

Characteristics

Figure 2 shows the plate-current-grid-voltage characteristics obtained between the grid of T_1 and the plate of T_2. It will be noted that the slope of the transconductance is negative, and that both positive and negative saturation are obtained in the negative-grid region. In other words, the circuit operates as a class A limiter which does not draw grid current. For this type of operation, the grid of input triode T_1 is biased to point a on the characteristic.

The operation of a class A limiter[3] is as follows: The negative half cycles of the input wave are limited by negative cutoff at the grid of T_1. Positive half cycles on the grid of T_1 are converted to negative half cycles on the grid of T_2 by the phase inversion existing due to the cathode coupling. Hence, the positive half cycles are limited by negative cutoff on the grid of T_2. The result is negative cutoff limiting of both half cycles of the input wave. This is accomplished without grid current as long as the input is made less than a peak voltage which draws current on the positive half cycles at the grid of T_1. In the usual limiter arrangement, grid current is not drawn until the input is of the order of 50 volts rms.

FIG. 2—Characteristics of the plate current of T_2 and the grid voltage of T_1

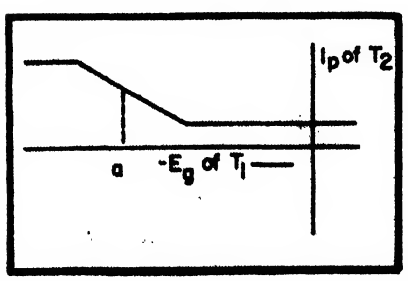

Values of Components

Figure 3 shows how the feedback connection is made to form the oscillator circuit. Capacitor C_1 couples the output to the input and acts as a blocking capacitor to keep the plate voltage off the input grid. The value of C_1 is chosen to provide a reactance which is small in comparison to either R_g or the reactance of the input capacitance of T_1. Resistor R_g is a grid-return resistor (0.5 megohm or less) and, for low frequencies, may consist of the output potentiometer. Cathode resistor R_k may be varied to control the amplitude of oscillation. Maximum output is usually obtained with an R_k of about 500 ohms with dual-triode receiving tubes.

The 6J6 miniature dual triode is perhaps the most ideally suited, especially for the higher frequencies, but tubes of the 6SN7GT, 6SL7GT, 6N7 and similar types may also be used. Frequencies as high as 130 megacycles have been obtained with the 6J6, but it is felt that frequencies much higher are possible.

Factors controlling the maximum oscillation frequency are the magnitude of impedance inserted in the output plate circuit, and the degree of shunting effect of the cathode-to-ground capacitance on the cathode resistor. The cathode-to-ground capacitance of the 6J6 is approximately seven micromicrofarads. When a 500-ohm cathode resistor is used with the 6J6, the cathode-to-ground capacitance does not become appreciable until frequencies above 50 megacycles are obtained.

As an audio oscillator, this circuit generates a waveform which has substantially less harmonic content than that obtained with conventional oscillator circuits. This is especially true for the higher values of common cathode resistor, R_k. Values of the order of 10,000 ohms may be used.

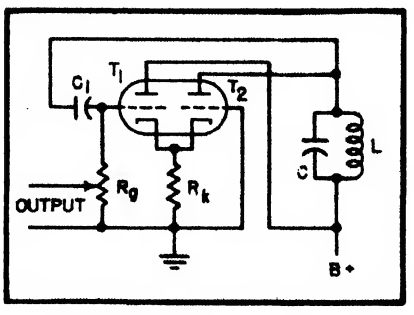

FIG. 3—Capacitor C_1 provides feedback to the grid of T_1 and also blocks the plate voltage

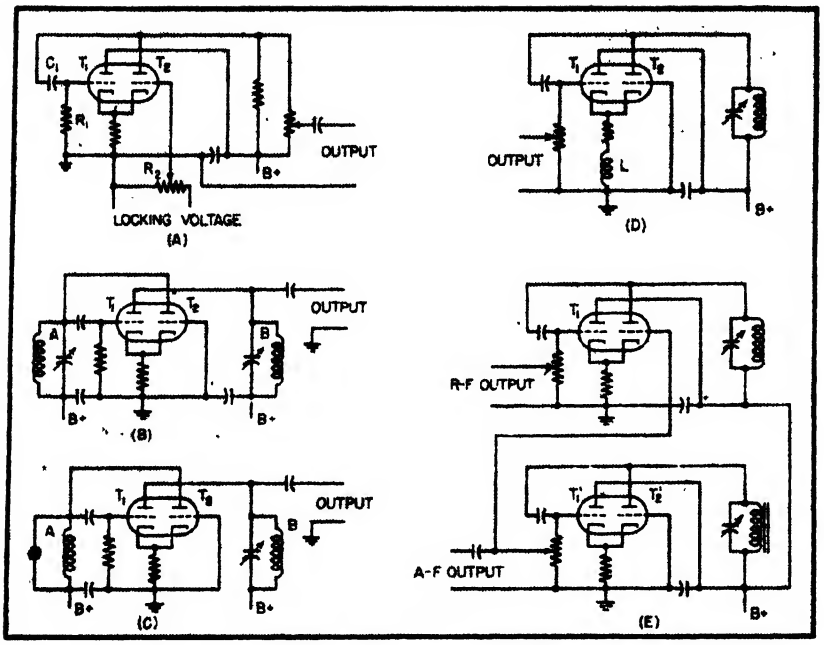

FIG. 4—Five useful circuit arrangements for the two-tube oscillator

These higher values also result in reduced output voltage.

Applications

The circuits of Fig. 4 are various arrangements taken from the author's U. S. Patent 2,269,417. Figure 4A is a multivibrator circuit in which resistance and capacitance take the place of the tuned circuit. This multivibrator circuit has the advantage that its output waveform is a true square wave, and does not have the exponential decay at the top of the square wave as is characteristic of the usual multivibrator circuit. Hence, it may be used for a square waveform generator. Frequency control may be obtained by varying resistor R_1 and capacitor C_1. Locking voltage may be applied to potentiometer R_2 to hold the oscillations in step with an external oscillator. The percent mark or duty cycle, of the square-wave pulse may be controlled by feeding positive or negative voltage to potentiometer R_2.

Figure 4B shows how fundamental frequency oscillation may take place in tuned circuit A, while harmonic output is obtained from tuned circuit B. The cathode-follower action of triode T_1 is not affected by tuned circuit B, because B is tuned to a harmonic.

Figure 4C shows how a crystal may be inserted as the fundamental oscillating element of the circuit of Fig. 4B. Such an arrangement has obvious advantages in crystal oscillator operation where harmonics are usually desired.

Figure 4D shows the original oscillator circuit with an inductance L inserted in the common cathode circuit to form a peaking coil to extend the frequency range limited by the cathode-to-ground capacitance of the common cathode circuits.

Figure 4E shows r-f and a-f twin-triode oscillators arranged to provide either r-f output, a-f output, or modulated r-f output. Modulation applied as shown in the circuit diagram is quite linear up to the point where the overall gain is modulated below an amount sufficient for oscillation.

This circuit was developed while the author was in the employ of RCA Laboratories.

References

(1) Herold, E. W., Negative Resistance and Devices for Obtaining It, *Proc. IRE*, 23, p 1201, Oct. 1935.
(2) Crosby, Murray G., Cathode-driven Oscillator, U. S. Patent 2,269,417, filed May 13, 1939, issued Jan. 6, 1942.
(3) Crosby, Murray G., Limiting Amplifier, U. S. Patent 2,276,565, filed May 23, 1939, issued Mar. 17, 1942.

COMPONENTS

Frequency Stability of Tuned Circuits

Data on the performance of coils tuned by air-dielectric capacitors, during variations in air density and humidity such as are encountered when equipment is operated over a wide range of altitudes. The effect of varying carbon-dioxide content, encountered in dry-ice test chambers, is also discussed

By G. V. ELTGROTH

IN ORDER to retain standards of accuracy initially imposed upon radio and other electronic equipment employing circuits tuned by air-dielectric capacitance, the effects of natural variations in the dielectric must be understood and taken into account. This is particularly true where equipment is to be used at high altitudes and under adverse weather conditions.

There are three characteristics of air as a dielectric which may affect the resonant frequency of a tuned circuit situated in this dielectric. (In this discussion, the effects of mechanical variation of components with varying conditions will not be considered.) They are:

1. *Density.* The dielectric constant of air varies with pressure and, therefore, with altitude. The dielectric constant also varies with temperature, since this too affects the density of a gas.

2. *Composition.* The relative humidity of air is constantly changing and has a decided effect on the dielectric constant at higher temperatures (above 10 deg C). In tests where dry ice is used, the carbon-dioxide content of the surrounding medium also may rise to 60 percent or 70 percent as compared with its normal value of 0.03 percent. This will increase the dielectric constant.

3. *Saturation.* Air almost saturated with water vapor will deposit thin films on objects situated in it. This should not be confused with condensation, which occurs when the air becomes supersaturated at the temperature of the body with which it is in contact.

Each of these effects will be thoroughly discussed in the following sections.

We shall first develop a few simple required relations:

$C = He$ — C = Capacitance of capacitor

$dC = Hde$ — H = Constant determined by mechanical construction

$\frac{dC}{C} = \frac{de}{e}$ — e = Dielectric constant of dielectric medium

Thus the percent change in C = percent change in e.

$f = \frac{A}{\sqrt{C}}$ — f = resonant frequency of circuit being investigated

$df = -\frac{1}{2}\frac{A}{\sqrt{C}}\frac{dC}{C}$

$\frac{df}{f} = -\frac{1}{2}\frac{dC}{C}$ $\qquad A = \frac{1}{2\pi\sqrt{L}}$

Thus the percent change in $f = \frac{1}{2}$ the percent change in C, and is negative, signifying that an increase in C decreases f.

The dielectric constant of dry air for pressures below 1000 lb per sq in. is given by $e = 1 - 18.25\ P \times$

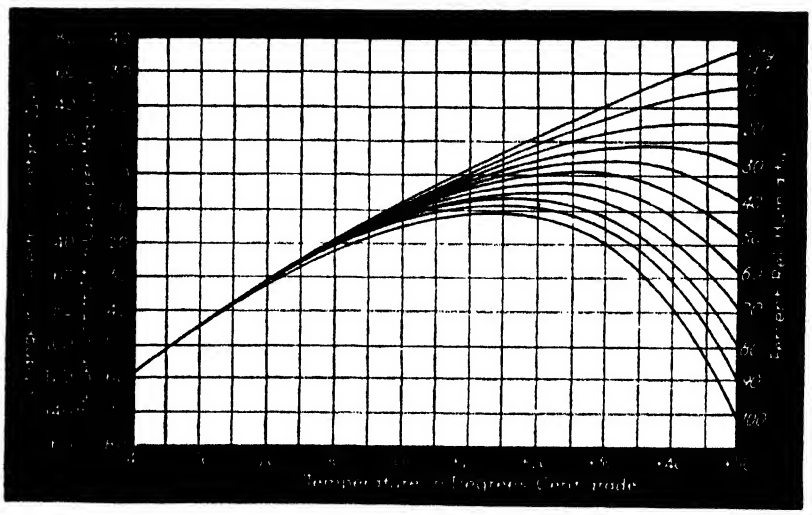

FIG. 1—Change in frequency and dielectric constant with temperature, using various values of relative humidity as a parameter. The air reference is air at 20 deg C and 50 percent relative humidity ($e = 1.00058565$)

$10^{-6} \times \frac{292}{t}$, where P is expressed in in. Hg and t in deg. K.

$$\frac{\delta e}{\delta P} = 18.25 \times 10^{-6} \times \frac{292}{t}$$

Assuming $t = 292°K$ (19°C) we have

$$\frac{\delta f}{\delta P} = -9.125 \times 10^{-6}$$

for constant relative humidity and temperature.

The frequency will drop 9.125 cps per Mc per in. Hg pressure increase. Reducing the pressure from 30 in. to 10 in. Hg (equivalent to an altitude of 27,500 ft) will increase the frequency 20 × 9.125 or 182.5 cps per Mc, which is 0.01825 percent.

Let $P = 20$ in. Hg, and let the temperature vary over a narrow range about 292 deg K.

$$e = 1 - 547.5 \times 10^{-6} \times 292/t$$

$$\frac{\delta e}{\delta t} = -\frac{547.5 \times 10^{-6} \times 292}{t^2}$$

$$\frac{\delta e}{\delta t} = -1.875 \times 10^{-4}$$, for constant relative humidity and pressure.

From this it is evident that the frequency will increase 0.9375 cps per Mc per deg C rise in air temperature for dry air. This is negligible in comparison with other changes normally encountered.

(a) *Humidity.* If the relative humidity is held constant at various values, and the temperature of air varied, it will be found that the curve e vs. *temperature* will vary in form.

$$e_{air} = 1 + 209.66 \frac{P}{t} \times 10^{-6}$$

$$e_{vapor} = 1 + 966.83 \frac{P}{t} \times 10^{-6}$$

P is here expressed in mm Hg, t in deg K

From these equations was derived the equation $e = 1 + [209.66 \times 760/t + 757.174\ V.P./t] \times 10^{-6}$. Setting the portion in brackets equivalent to V gives $e = 1 + V \times 10^{-6}$. This relation was used in calculating the values of V in Table I for different values of temperature and relative humidity. The right-hand column labelled ΔV contains values of the total change in V in going from 0 to 100 percent relative humidity. Values of vapor pressure $V.P.$ in mm of Hg corresponding to the indicated values of temperature and relative humidity are found in meteorological tables.

Allowance for water-film deposit on electrodes is not included. Such deposits will add to the shift in capacitance.

A curve interpreting the data in Table I in terms of change in dielectric constant in parts per million, and resonant frequency shift in cycles per megacycle, is shown in Fig. 1.

(b.) *Carbon dioxide content.* When cold tests are run with dry ice as the cooling agent, the air in the cooling chamber will have its carbon-dioxide content materially increased. The dielectric constant for carbon dioxide differs materially from that of air, the values at 19 deg C and 762 mm mercury pressure being 1.0005475 for air and 1.000921 for carbon dioxide.

Table II gives the variations in e and f with varying carbon dioxide content, for a constant temperature of 19 deg C and a pressure P of 30 in. (762 mm) of Hg.

From this table it is seen that the presence of CO_2 in the air dielectric of capacitors may produce frequency shifts up to 0.0186 percent, a very appreciable amount in a transmitter being designed for an accuracy of 0.03 to 0.05 percent. The figures apply to dry air, at 19 deg (292 deg K) C and 762 mm Hg. Values of Δe and Δf may be readily obtained for any other temperature or pressure by multiplying by the factor $292P/762t$, where P is in mm Hg and t is in deg K.

A graph of the data in Table II is shown in Fig. 2. It is important to note that with 60 percent carbon dioxide content, the frequency shift is over 0.01 percent. At −40 deg C, when the carbon dioxide content is only 50 percent. the frequency will be 0.0117 percent lower than with air.

Saturation

Recent experimental work has shown that moisture films form on objects situated in moist air even though conditions may be such that no condensation takes place. We shall derive the effect of water-film formation on a capacitor formed by two or more parallel plane surfaces.

The capacitance of such a capacitor may be expressed as $C = He/S$, where H is a constant de-

TABLE I—VALUES OF *V* FOR AIR AT VARIOUS HUMIDITY AND TEMPERATURE VALUES

(Dielectric constant $e = 1 + V \times 10^{-6}$)

Temp. °C	Relative Humidity 0%	10%	20%	30%	40%	50%	60%	70%	80%	90%	100%	Δv
−40	682	682	682	682	682	682	682	682	682	682	682	0
−30	655	655.08	655.16	655.24	655.32	655.4	655.48	655.56	655.64	655.72	655.8	0.8
−20	629	629.232	629.464	629.696	629.928	630.16	630.392	630.624	630.856	631.088	631.32	2.32
−10	605	605.56	606.12	606.68	607.24	607.81	608.37	608.93	609.49	610.05	610.61	5.61
0	583	584.27	585.54	586.81	588.08	589.35	590.62	591.89	593.16	594.43	595.7	12.7
+10	562	564.46	566.92	569.38	571.84	574.3	576.76	579.22	581.68	584.14	586.6	24.6
+20	543	547.53	552.06	556.59	561.12	565.65	570.18	574.71	579.24	583.77	588.3	45.3
+30	525	532.95	540.9	548.85	556.8	564.75	572.7	580.65	588.6	596.55	604.5	79.5
+40	508	521.4	534.8	548.2	561.6	575	588.4	601.8	615.2	628.6	642	134
+50	493	514.7	536.4	558.1	579.8	601.5	623.2	644.9	666.6	688.3	710	217
+60	478	512	546	580	614	648	682	716	750	784	818	340
+70	464	515.5	567.0	618.5	670	721.5	773	824.5	876	927.5	979	515

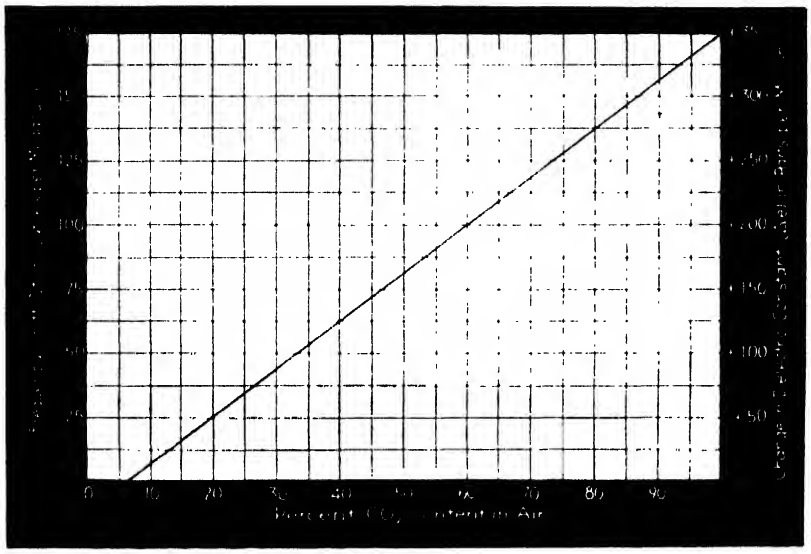

FIG. 2—Variation of dielectric constant and frequency with volume percentage of CO_2 in air. Here P is 762 mm Hg and t is 292 deg K (19 deg C)

pending on size of plates and system of units employed, e is the dielectric constant of the medium, and S is plate spacing.

Let the dielectric constant for the normal dielectric be e_1, and let that for the material in the film formed on the plates be e_2. Also, call C_0 the normal capacitance, C' the capacitance with film on plates, and y the film thickness. Now, with plane plates and a uniform film thickness, the film-air interface will correspond to an equipotential surface, and

$$C_1 = \frac{He_1}{S - 2y} \qquad C_2 = \frac{He_2}{2y}$$

These relations are set up by assuming a metal surface of infinitesimal thickness, at the equipotential surface of the water-air interface, and then calculating the effective capacitance on each side thereof.

The two capacitances are effectively connected in series, so we may obtain C' from the series capacitance relationship:

$$C' = \frac{C_1 C_2}{C_1 + C_2}$$

$$\text{i. e. } C' = \frac{He_1 e_2}{2y(e_1 - e_2) + e_2 S}$$

The fractional change in capacitance will then be

$$\frac{C' - C_0}{C_0} = \frac{e_2 S}{2y(e_1 - e_2) + e_1 S} - 1$$

and

$$\frac{\delta}{\delta y}\frac{C' - C_0}{C_0} = -\frac{2e_2 S(e_1 - e_2)}{[2y(e_1 - e_2) + e_2 S]^2}$$

We are interested in the action of thin films of foreign dielectric and will therefore confine our calculations to the region where y is less than or equal to 0.01 S. This permits the use of the following simplified equation

$$\frac{\delta}{\delta y}\frac{C' - C_0}{C_0} = \frac{2}{S}\left[1 - \frac{E_1}{E_2}\right]$$

On the basis of this assumption, the fractional change in capacitance is

$$\frac{C' - C_0}{C_0} = \frac{2y}{S}\left[1 - \frac{e_1}{e_2}\right]$$

Now, for a practical application of this expression, assume a spacing between plates of $S = 0.05$ cm (0.020 in.) and a downward frequency shift Δf of -100 cps per Mc, which corresponds to 200×10^{-6} for $\Delta C'$. The normal dielectric is air ($e_1 = 1$) and the foreign dielectric is water ($e_2 = 81$). Let us find the required film thickness for the given frequency shift.

Solving the foregoing equation for y, substituting in it the known values, and simplifying gives a value of 5.06×10^{-6} cm for the film thickness y.

Thus, a film thickness of 5.06×10^{-6} cm or 0.00001285 in. produces a frequency shift downward of 0.01 percent. This is a film approximately 120 molecules in depth, and is quite undetectable by ordinary methods since its thickness is only about one-tenth the wavelength of green light. It is obvious at once that the formation of *actual visible condensation* on the plates of a tuning capacitor will result in shifts very many times this in magnitude, and should be strenuously avoided.

For a given film thickness, the frequency shift is inversely proportional to the spacing of the plates.

Experiments have shown that on a clean polished metal surface, films up to 30 or 40 molecules thick may be formed at 98 percent relative humidity with a temperature around 30 deg C. On a good dielec-

TABLE II—VARIATIONS IN e and f WITH VARYING CARBON-DIOXIDE CONTENT

% CO_2 by Vol.	e	Δe (mult. by 10^{-6})	Δf in cps per Mc
0	1.0005475	0	0
10	1.00058485	37.35	−18.68
20	1.0006222	74.7	−37.35
30	1.00065955	112.05	−56.03
40	1.0006969	149.4	−74.7
50	1.00073425	186.75	−93.38
60	1.0007716	224.1	−112.05
70	1.00080895	261.45	−130.73
80	1.0008463	298.8	−149.4
90	1.00088365	336.15	−168.08
100	1.000921	373.5	−186.25

tric material, the films formed under the same conditions were up to 180 molecules in depth. Since oils and greases are dielectrics, capacitor plates should be kept scrupulously free of them.

Coils and Wiring

Impregnation of insulated wires with wax prevents moisture absorption by the insulation covering (thereby decreasing the effective moisture film thickness) and moves the wax-air interface out from the conductor, thus situating the inevitable moisture film in a region of lesser electric intensity where it has less effect on the capacitance of the circuit.

Frequency shift with humidity would seem to be due to surface changes, in view of the relatively short time required for recovery of normal characteristics. This indicates the necessity for keeping the wax-air interfaces out of any region of strong electric field intensity. The foregoing statement applies particularly to coils, which should be covered with a sufficient thickness of wax to keep the interface out of any region of strong electric intensity caused by potentials existing between adjacent turns. It is evident that the greater the spacing of turns, the smaller will be the ratio between coil distributed capacitance and total tuning capacitance, and therefore the less important will be the removal of the wax-air interface. In addition, increased spacing will diminish the electric field between adjacent conductors thereby decreasing the effect of moisture film deposits.

The films build up to depths of 25 molecules on dielectrics at 40 deg C and a relative humidity of 85 percent. A coil wound with flat wire spaced 0.005 in. and with no protective covering other than enamel on the wire would have its distributed capacitance increased 0.01 percent under these conditions.

In view of the fact that moisture films have such large effects when compared with their dimensions, it is interesting to note here that if by some means the interior of a device being tested were maintained 5 deg C above the external temperature, then the interior relative humidity could not exceed 80 percent even though the external temperature might range up to 60 deg C at 100 percent relative humidity.

Conclusions

Listed below are the effects on resonant frequency of each of the variables which are due to dielectric changes only.

1. *Pressure.* For air at 19 deg C the coefficient is −9.125 cps per Mc per in. Hg, or 0.01825 percent change in frequency for altitude change from sea level to 27,500 feet.

2. *Temperature.* For air at 19 deg C, 30 in. Hg., the coefficient is +0.9375 cps per Mc per deg C. (This is negligible and need not be considered in design.)

3. *Relative Humidity.* We give below the total frequency shift in cps per Mc, as air at the specified temperature and 760 mm Hg pressure is varied from 0 to 100 percent relative humidity.

deg C.	cps/Mc
−40	−0
−30	−0.4
−20	−1.16
−10	−2.8
0	−6.35
+10	−12.3
+20	−22.65
+30	−39.75
+40	−67.00
+50	−108.5
+60	−170.00
+70	−257.5

4. *Carbon Dioxide.* Mixed with air at 19 deg C and 30 in. Hg pressure, the coefficient is −1.868 cps per Mc per percent of carbon dioxide. Also 53.5 percent of carbon dioxide is required to shift the frequency downward 0.01 percent. This effect becomes greater at lower temperatures.

5. *Moisture Film Deposits.* Deposits at 98 percent relative humidity and 30 deg C on perfectly clean capacitor plates (0.020 in. spacing) are sufficient to lower the frequency 0.0025 percent. The presence of oil or grease films may increase this to 0.015 percent.

6. Wherever wax is used for sealing against moisture, wax-air interfaces must be kept out of strong electric fields.

R-F Inductance Meter

Two r-f oscillators, one with unknown L in series and the other with standard C in parallel, are tuned to zero beat. Value of unknown inductance at selected test frequency is then read directly on scale of capacitor with accuracy within 1 percent for 1 μh to 100 mh

By HAROLD A. WHEELER

THIS direct-reading r-f inductance meter is designed for quickly and accurately measuring inductance of a radio coil. Errors in readings are within about one percent of the observed value for the rated range of inductance, which is unusually close when applied to one-tenth of full scale. This tolerance of error is based on the usual types of radio coils with fairly small inherent capacitance and at least a mod-

erately high ratio of reactance to resistance.

The measurement of small capacitance is a valuable byproduct use of the instrument. It is direct-reading in terms of the difference of two scale readings, and its errors are only those of the precision capacitor included in the inductance meter. This measurement is made at radio frequencies whose values are chosen for convenience and reliability.

The block diagram in Fig. 1 shows the arrangement of the inductance meter. Two similar oscillators are tuned to the same frequency by observing a zero-beat indicator. Each oscillator contains a resonant circuit with fixed inductance L_o and fixed capacitance C_o. One oscillator also has a calibrated variable capacitor C connected in parallel. The other has provisions for connecting unknown inductance L in series.

With the standard capacitor C at its reference value (taken as zero) and the unknown inductor L on short-circuit, the two oscillators are tuned to resonance by a fine adjustment. Then the unknown L is inserted and the standard C is increased to restore zero-beat. The latter condition satisfies the equation of resonance of the two oscillators: $(L + L_o)C_o = (C + C_o)L_o$. From this the calibration formula is derived, giving $L = CL_o/C_o$. The factor L_o/C_o is adjusted to be a decimal multiplier, and the scale of C is direct-reading in micromicrofarads, so the value of the unknown L is obtained merely by shifting the decimal point.

The circuit of the r-f oscillator and buffer amplifier is given in Fig. 2. The two oscillators and amplifiers are alike except for the differences in the tuned circuit, one including the standard capacitance C and the other the unknown inductance L. The standard inductors L_o are the pair of plug-in coils, one for each oscillator, whose values are equal to the maximum inductance of each range. Each oscillator has a regulator circuit which limits the amplitude of oscillation to a suitable value for the buffer amplifier.

The beat-note circuit is given in Fig. 3. Direct-current coupling of the amplifier to the rectifier-meter combination provides response down to very low frequencies. The full-wave rectifier causes the meter pointer to vibrate at double the beat frequency.

The response curves of the meter are shown in Fig. 4. The curve of Fig. 4A shows the wide peak obtained while tuning one oscillator past the frequency of the other, and the curve of Fig. 4B is an enlargement of the valley near zero beat.

The zero-beat indicator gives essentially a wide peak having a narrow valley in the center. The width of the peak is ±5,000 cycles from the center, so it cannot be passed in

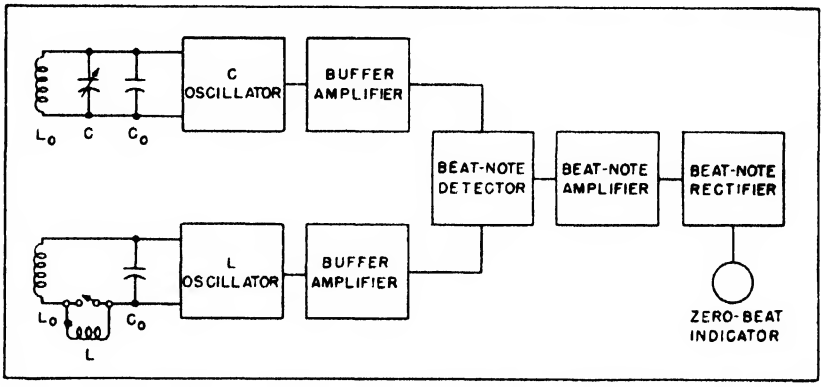

FIG. 1—Block diagram of direct-reading radio-frequency inductance meter

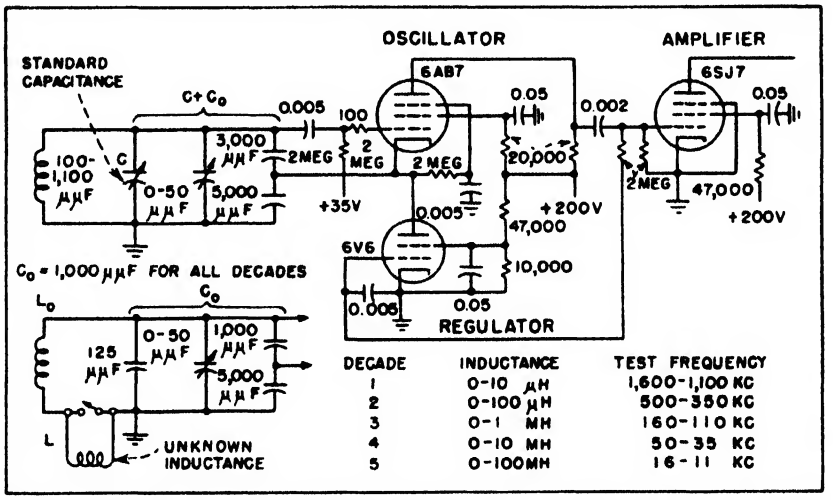

FIG. 2—Circuit for one of the oscillators with its buffer amplifier. Both are identical except for the tank circuits; one has the standard capacitance in parallel, and the other has the unknown inductance in series as shown at left

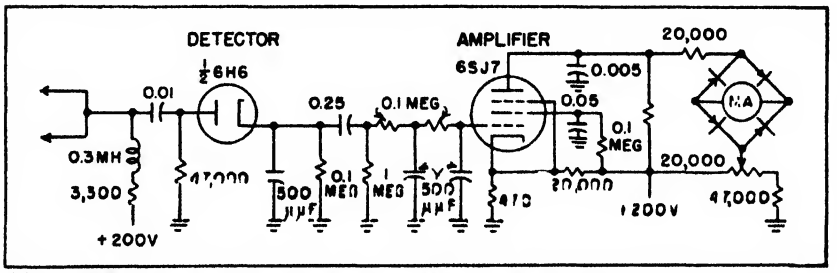

FIG. 3—Circuit of beat-note detector, amplifier, rectifier, and 0-1 ma d-c indicator serving the pair of r-f oscillators

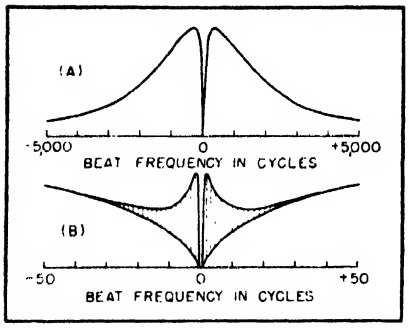

FIG. 4—Response of zero-beat indicator is shown at A, and enlarged view of valley near zero beat appears at B

quick tuning. The width of the valley is ±100 cycles, the pointer vibrations are within ±10 cycles, and the dead spot in the center is within ±1 cycle. The wide peak is used to find the narrow valley, after which the dead spot gives a reliable indication of zero beat.

This indicator has been found well adapted for use by nontechnical personnel. It cannot be overloaded in normal use. Being visual, it neither causes nor suffers from noise in the laboratory or factory.

Test Frequencies

The choice of test frequencies which are best adapted for the usual radio coils in the respective decades of the inductance range is a compromise which fortunately is not too critical. The final selection is influenced also by the stability of C_0 and L_0 and by convenience in the use of the decimal values.

The basic value of the inductance of a simple coil in open space is determined by the magnetic energy in the vicinity of the coil but outside the cross-section of the conductor itself. If a shield can is used, this space is confined to the inside of the shield. The inductance would have this basic value if the coil and shield were made of perfect conductors, and its actual value is not much different at the higher radio frequencies.

The resistance of the wire and the shield causes an increase in the actual or apparent inductance of the coil, in proportion to the magnetic energy which is allowed to penetrate inside of either conductor and outside of the shield to the surrounding space. The internal capacitance increases only the apparent inductance, by virtue of the approach to self-resonance.

The magnetic energy in the wire increases the inductance by a constant amount at low frequencies, and by a decreasing amount at higher frequencies. The transition occurs at the frequency where the skin depth is one-fourth the wire diameter if the wires are well separated, and at a slightly lower frequency if they are close together. In the case of fine wire, such as in stranded (Litz) conductors or in multilayer coils, this effect is constant at all frequencies up to the operating frequencies, so it causes no error in inductance measurements at lower frequencies. In a coarse wire, such as the conductors of a transmission line, this effect varies slowly with frequency as governed by the skin effect, so a measurement at a lower frequency is subject to a slight error relative to the operating frequency.

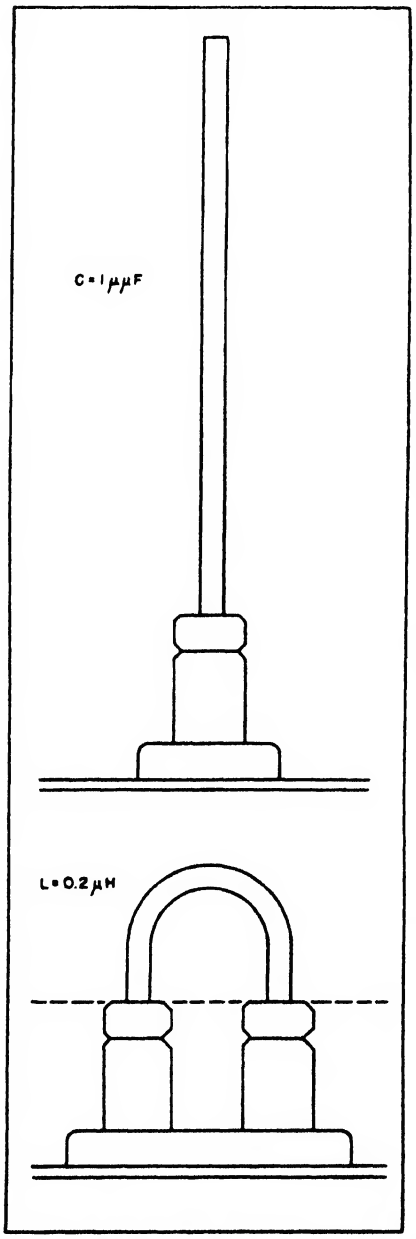

FIG. 5—Examples of small values of capacitance and inductance, shown actual size here, that can be measured with the r-f inductance meter

A perfect shield decreases the inductance by a substantial amount, while the imperfection of the shield conductor causes a relative increase. As the frequency is lowered, the inductance increases gradually as governed by the skin effect in the shield, then rapidly as the conductive shielding fails, and finally approaches the value of the inductance without the shield.

The internal capacitance causes the apparent inductance to increase rapidly as the frequency approaches self-resonance in the coil. This is the factor which makes impossible the direct measurement of inductance by a single observation at the operating frequency.

The best frequency for a direct measurement of inductance, with least error from all causes combined, should be much lower than the frequency of self-resonance but much higher than the frequency of shield failure. Fortunately these two frequencies are usually far apart. Three decades is a typical separation in the case of small coils in shield cans, operating around 1 mc.

The internal capacitance is the most typical characteristic for small radio coils, since it is determined mainly by the size, the leads, and the terminals. The typical range of internal capacitance is within 10 $\mu\mu f$, so the inductance meter is standardized for about 5 $\mu\mu f$ with a tolerance of ±5 $\mu\mu f$ to maintain the rated limits of error.

Since there are many causes of error and it is desired to hold the total error within one percent, the

test frequencies are chosen low enough so that ±5 $\mu\mu$f causes less than ±0.25 percent error. In other words, the unknown inductance would resonate at the test frequency with more than 2,000 $\mu\mu$f capacitance, so the test frequency is about 1/20 the frequency of self-resonance, or lower.

The 5,000-division continuous linear scale is available only in the precision capacitor, as distinguished from the inductor and the resistor. Therefore the capacitor is the ideal variable standard in any system of measurement, and especially in a direct-reading system. The inductance meter is a simple way of utilizing the capacitor to read directly in proportion to the unknown inductance.

By making the test at the highest frequency permissible for each decade of the inductance range, it is possible to take full advantage of the long scale of 5,000 divisions for 1,000 $\mu\mu$f, by reading to about ½ division or 0.1 $\mu\mu$f.

In the first three decades (up to 1 mh), the test frequency is above 100 kc so it is possible to take advantage of the low range of the precision capacitor, having 50 divisions per $\mu\mu$f, or the equivalent of 50,000 divisions for full scale. This refinement is available only for a range of 4,000 divisions. Therefore it is useful for absolute measurements only to 8 percent of full scale.

By the addition of fixed capacitors in parallel, this expanded scale becomes available for differential tests of coils nearly alike. By this method, any inductors within the range of 1 μh to 1 mh can be compared to within 1/5,000 of their values, or 0.02 percent. Any larger inductors up to 100 mh can be compared on the standard scale within 1/500 of their values, or 0.2 percent.

Examples of the absolute sensitivity of this instrument, which is attained by the long scale and the beatnote comparison at radio frequencies, are given in Fig. 5. These diagrams are shown actual size.

The capacitance C is a small antenna inserted in the capacitance terminal. Its value is 1 $\mu\mu$f, which is 5 divisions on the regular scale or 50 divisions on the expanded scale.

The inductance L is a small loop of heavy wire connected to the inductance terminals. As compared with a short-circuit (a large flat disc at the dotted line) the inductance is 0.02 μh, corresponding to 10 divisions on the regular scale or 100 divisions on the expanded scale.

By indicating inductance values on the expanded scale of a precision capacitor and using r-f oscillators with a zero-beat indicator, an inductance meter is obtained which has an unusual degree of absolute and differential stability as well as high accuracy.

Temperature Coefficients in Electronic Circuits

Factors influencing frequency-temperature stability of tuned circuits are analyzed to determine design criteria for circuit elements. Application of these criteria permitted development of an airborne transmitter having negligible frequency drift

By CHESTER I. SOUCY

Of the few studies of the effects of temperature coefficients on electronic circuits which have been published during recent years, some have presented views which conflict with respect to theoretical principles, or which are in disagreement with experimental results. These disagreements are due chiefly to the disregard of theoretical factors whose importance has been recognized only recently.

Of major interest in governing the resonant frequency of an R-L-C circuit are (1) inductive temperature coefficients of coils, leads and wiring; (2) capacitive temperature coefficients of fixed and variable capacitors, inter-electrode capacitances in tubes, and capacitances between terminals, switch contacts and wiring; and (3) resistive temperature coefficients of resistors. Resistive coefficients are of importance because changes in circuit resistances affect tube operating voltages and can thus produce frequency changes.

Parameter and Frequency Coefficients

If f represents the frequency, and L and C the inductance and capacitance, respectively, of an L-C circuit, then it can be shown that

$$\frac{df}{f} = -\frac{dL}{2L} \text{ or } -\frac{dC}{2C} \qquad (1)$$

Equation 1 is valid for frequency, inductance and capacitance changes, all occurring over the same range of temperatures.

From Eq. 1, it follows that

$$a \text{ or } b = 2\left|\frac{df}{f}\right|, \qquad (2)$$

where a is the capacitive temperature coefficient, equal to $-|dC/C|$ and b is the inductive temperature coefficient, equal to $|dL/L|$.

Where inductance and capacitance in the tuned circuit both change as a result of thermal variations, the frequency temperature coefficient is

$$\left|\frac{df}{f}\right| = \left|\frac{dC}{2C}\right| + \left|\frac{dL}{2L}\right| \quad (3)$$

Frequency Drift Compensation

Design of coils and capacitors with low temperature coefficients for use in fixed-frequency circuits, or the compensation of these elements is relatively simple. But for variable-frequency circuits the design problem is complicated by the fact that inductive temperature coefficients of coils vary with frequency and corresponding coefficients of variable tuning capacitors change with rotor position. Few discussions of drift compensation have pointed out the fact that in a variable-frequency circuit using a fixed inductor, the inductive temperature coefficient must be compensated by an inductive component over the frequency range of tuning.[1] If a capacitor should be used for compensation, its capacitance change Ca would have to vary according to the inverse square of the frequency, an impossible requirement for a single compensator. Thus, despite the fact that the use of a single compensating capacitor would permit simpler and more economical design, the most satisfactory solution to the problem of reducing frequency drift in variable-frequency L-C circuits is to design fixed inductors with an inductive temperature coefficient as near as possible to zero. On the other hand, with variable inductance tuning and variable permeability tuning,[2] the use of capacitors for compensation proves more satisfactory.

Inductive Coefficent Components

It is important to realize the error in the common conception that the inductive temperature coefficient depends solely or even principally upon the thermal coefficients of linear expansion of the conductor and coil form. In addition to the factor of linear expansion, Groszkowski showed in 1937[3], that the inductive temperature coefficient is influenced by eddy current or "internal inductance" effects, as well as by skin effect in the conductor and self capacitance as noted by previous investigators.

Bloch[4] investigated the relative magnitude of the different components. Measurements on a small coil of 68 turns of No. 28 copper wire indicated an inductive temperature coefficient of $(20 \pm 1) \times 10^{-6}$ per degree C. Conductor skin effects and Groszkowski's eddy-current effects were grouped together as the internal inductance component, since both effects depend upon penetration of the turns of the conductor by the magnetic field and upon the coefficient of resistivity of the conductor which affects such penetration. The calculated values of the components of inductive temperature coefficient were: component due to linear expansion of coil, 8×10^{-6} per degree C; internal-inductance component, 13×10^{-6} per degree C; and self-capacitance component, 1×10^{-6} or 2×10^{-6} per degree C.

Figure 1 shows the variation in inductive temperature coefficient with number of turns for two coils having small self capacitance, each wound on a skeleton glass-bonded mica form with small axial expansion coefficient (8.8×10^{-6} per degree C).[5] The discrepancy between calculated and measured values is accounted for by the internal inductance component. Note that the temperature coefficient varies almost linearly with the number of turns. This fact is significant for the case of variable-inductance tuning, and for tapped and variometer coils.

Self Capacitance of Coils

In some coils, the conductors are embedded in grooves or in slots in the supporting insulation, or the conductors may be fired or deposited electrolytically on ceramic or

Table I—Temperature Coefficients of Dielectrics

Material	Temperature Coefficient (Parts per Million per Degree C)		Permittivity (Dielectric Constant)
	Permittivity	Expansion	
Polyvinyl Chloride (Geon No. 2016)	7,140[a]	30	3.5
Phenolic, molded[12] (BM-120 Bakelite)	3,940	30 to 40	4.2
Glass, white flint[5]	2,000		7.5
Phenolic, laminated	1,055 to 1,290[b]	17 to 30	5.5
Glass, Pyrex[5]	600	3.2	4.5
Ebonite[5] (hard rubber)	500	70 to 80	3.0
Cordierite[17], ceramic (Alsimag No. 202)	500	1.6	5.0
Porcelain[5]	500	3.5	5.4
Phenolic, mica-filled aniline formaldehyde (Resinox No. 7013)	400[c]		4.3
Steatite[5]	150	8.0	6.5
Mica[5]	20 to 100	3.0	7.0
Fused silica[16]	50	0.5	3.85
Mycalex[d]		10 to 11	7.5 to 9.2
Polystyrene[18] (Victron white)	−35	70	2.4 to 2.9
Titanium Dioxide[11,12]	−1,800 (max)	6 to 10	90 to 170
Paraffin wax[12]	−1,930[c]	130	2.5
Water[11,12]	−3,600[e]	195	80

Notes: [a]Data from mfgr. Varies widely with temperature and frequency. This figure valid for 15–70 C, 60 cps.
[b]Figure obtained from tests on bandswitches.
[c]Approximate only.
[d]Data from mfgr.
[e]Approximate data. Varies with temperature and becomes positive above 10^{10} cps. This figure valid at 25 C, up to 100 mc.
Numerical superscripts refer to references cited in text.

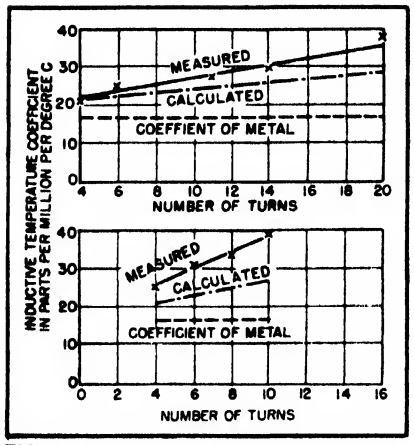

FIG. 1—Inductive temperature coefficient as a function of number of turns for two coils having small self inductance, wound on low-expansion forms. Difference between measured and calculated values is the internal inductance component

glass forms. Such coils will have greater distributed capacitance than those consisting of a single self-supporting layer or of round conductor wound on a smooth form. Multilayer coils and closely wound solenoids have higher values of distributed capacitance because of the decreased spacing and replacement of air between turns by solid insulation of higher permittivity.

Distributed capacitance of a coil increases its effective inductance to a value L', as indicated by the formula

$$L' = \frac{L}{1 - \omega^2 C_o L} \qquad (4)$$

in which C_o is the distributed capacitance, ω is the angular frequency, and L is the inductance when C_o is not taken into account. The distributed capacitance of a single-layer solenoid can be calculated readily, and rather surprisingly, does not depend upon the number of turns but upon the turn spacing and the coil and conductor diameters. Distributed capacitance does not include that of the mass of the coil to ground or the capacitance between leads or terminals.

The inductive temperature coefficient γ due to self capacitance[4] is

$$\gamma = \frac{k + \omega^2 L C_o \sigma}{1 - \omega^2 L C_o} \qquad (5)$$

where k is the composite temperature coefficient of expansion determined by the coil form and the conductor, and σ is the temperature coefficient of permittivity of the coil form or other dielectric between turns. Equation 5 indicates that the inductive temperature coefficient will increase with frequency, with the temperature coefficient of permittivity of the dielectric, including that of any impregnant or finish, and with the magnitude of the distributed capacitance.

The magnitude of self-capacitance effects at frequencies above one-tenth of the natural resonance frequency may be noted from Fig. 2. This curve shows the variation in inductive temperature coefficient with frequency, calculated and measured by Thomas[5] for a small coil having the conductor deposited electrolytically in grooves in a ceramic form. As the natural frequency of this coil, 10.9 mc, is approached, the temperature coefficient rises from a low value of 8×10^{-6} per degree C, approximately equal to the expansion coefficient of the ceramic, to nearly $1{,}000 \times 10^{-6}$ per degree C. Components other than expansion and self capacitance were small in this particular coil.

Not only is it important that a coil have small distributed capacitance, but also that the insulation have a small temperature coefficient of permittivity. The scarcity of data on this coefficient prompted the writer to collect the information presented in Table I.

Practical Coil Construction

The writer's test on receiver and small transmitter coils, using finishes having a neutral effect, covered a range of temperature coefficients from 4.1×10^{-6} per degree C, for a special coil with silvered-invar conductor and low-expansion ceramic, up to 60×10^{-6} per degree C for a low-frequency antenna coil. Temperature coefficients as low as 1×10^{-6} per degree C have been obtained by others by the use of more complicated designs.[5, 6, 7]

One of the basic problems in coil

Table II—Temperature Coefficients of Commercial Capacitors

Type of Capacitor	Temperature Coefficient (Parts per Million) per Degree C)	Notes
Fixed ceramic compensating	−1,600 to +150	Linear and stable; coefficient varies at low frequencies[2,12]
Molded mica	+50 to −500	Writer's measurements. Aging has somewhat variable effect on capacitance shifts[9,13].
Molded silvered mica	−250 to +250	Writer's measurements. Aging effect about 1/5 that of mica type.
Mica compression trimmer	+400 to +800	Writer's measurements.
Molded paper (JAN spec)	−20,000 to +20,000	Variable. Large aging effect.
Paper (impregnated and sealed)		Vary widely with temperature, frequency, and type impregnant[14,15,19]
Variable air dielectric:		
Ganged receiver type (ceramic insulation, no trimmer)	+98 to +28	Writer's measurements. See Fig.4.
Trimmer (ceramic insulation; at midposition)	+136	Writer's measurements.
Vacuum type (GE Type GL-1L38, 50 μμf, 7,500 v)	+27	Manufacturer's rating. Probably linear and stable.

Note: Numerical superscripts refer to references cited in text.

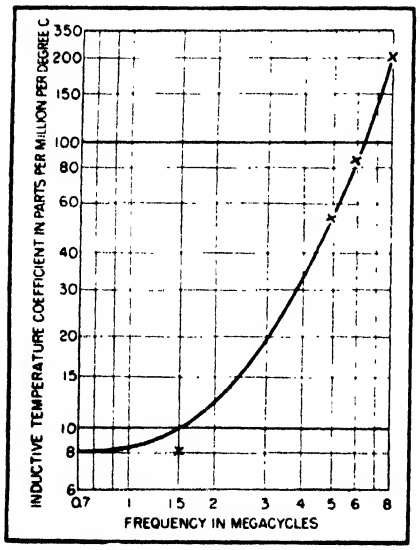

FIG. 2—Self-capacitance effects cause this variation with frequency of inductive temperature coefficient of a small coil

design is that of obtaining inductance that is stable cyclically with temperature variations and also has secular, or long term, stability. For example, self-supported single-layer coils are found to have poor cyclical stability. Figure 3 shows results of a complete temperature cycling test at 1.5 mc on an oscillator coil wound with silvered nickel-alloy conductor on a ceramic form having a small expansion coefficient.

Temperature Coefficients in Capacitors

Fixed and variable air-dielectric capacitors have been constructed, after careful design, to have temperature coefficients as low as 1×10^{-6} per degree C, and to have excellent retrace characteristics as well as secular stability.[7, 8, 9, 10] However, such special and expensive constructions, some of which require low-expansion plates and spacing elements and bimetallic compensators, are seldom used commercially.

Considerable use has been made of ceramic compensating capacitors in tuned circuits of receivers and transmitters,[1, 2] despite the difficulties and compromises in compensation usually involved. Although they are stable, ceramic types have higher r-f losses than air-dielectric types,[10] and their temperature coefficients cannot be predicted as accurately as desired before firing. Ceramic compounds of higher permittivity are now being made of various mixtures of titanium dioxide and barium titanate, which has a permittivity of 1,200, or other combinations with strontium and calcium titanates.[11] Many of these compounds have linear characteristics with temperature and frequency at above 10 to 50 cps.[5, 10]

The capacitance - temperature shift of a low-priced, ganged receiver tuning capacitor, employing phenolic insulation for the stator and attached trimmers, was found to be much greater than that of a similar unit using ceramic insulation. Capacitance shift and temperature coefficient as functions of rotor position for the ceramic-insulated capacitor are shown in Fig. 4.

Humidity Effects

Changes in capacitance of air-dielectric capacitors due to the temperature coefficient of permittivity of air are negligible in most cases, being only 1.87×10^{-6} per degree C for dry air at 20 C. The effect of humidity becomes appreciable at higher temperatures, amounting to 217 parts per million for a change in relative humidity from 0 to 100 percent at 50 C.

Moisture Films

Of more importance, is the effect of films of moisture on capacitor plates or over the outer surfaces of coils, that is, lying within the electric field between turns. Such films are of particular importance when they are formed over thin films of oil or grease on metals, thereby increasing the effective film thickness. Table I shows that water has a very high temperature coefficient of permittivity as well as a high dielectric constant. Consequently, frequency shifts due to such invisible moisture films may exceed 100 cycles per mc even before absorption of moisture occurs in insulating materials. Obviously, the much thicker films formed by visible condensation will have even more substantial effects.

It is generally known that the absorption of moisture by solid insulating materials increases their permittivities, but the fact that water has a large negative temperature coefficient is not so well known, nor has its wide variation with temperature and with certain temperature-frequency combinations been widely recognized.[11, 12]

Table II presents data on the temperature coefficients of capacitors of various types. Tests made by the writer showed the variation of temperature coefficient for commercial mica and silvered-mica types over the extreme working range, differences between units of the same type and make, and their erratic changes with time.[13] Unfortunately, the bulk of commercial grades of mica and silvered-mica capacitors, such as are used commonly in radio receivers, differ greatly from the high grade components referred to by some writers,[7, 10, 11] and enjoy a better reputation for low temperature coefficient, cyclical reliability, and permanence than their performance under adequate temperature tests warrants.

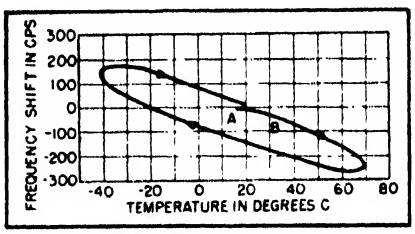

FIG. 3—Temperature cycling measurements yielded data for this frequency shift-temperature characteristic of a small low-expansion coil. Thermal lag of coil parts causes segment AB to deviate from main part of curve and results in displacement of retrace curve

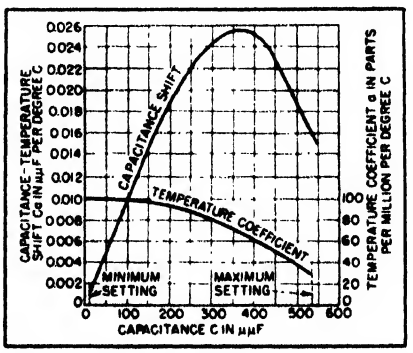

FIG. 4—Capacitance-temperature shift and temperature coefficient for a ceramic-insulated ganged tuning capacitor as functions of capacitance setting

The input capacitance of a 7A4 tube changes about 0.17 $\mu\mu$f during the first fifteen minutes of operation. For a 6J5, the change is about twice as great. In receiver r-f tubes, the change in interelectrode capacitance is about one-fifth to one-eighth of these values.[15]

For an assumed circuit capacitance of 25 $\mu\mu$f, such tube-capacitance shifts cause frequency shifts of 3.4 kc to 6.8 kc at a nominal frequency of 10 mc for 7A4 and 6J5 oscillators, respectively. When circuit capacitance is large, the effect of tube-warmup shift is minimized, and a similar order of capacitance change in bakelite wafer-type switches, sockets, and the like, is also minimized.

Wiring and Switching Devices

From the data in Table I, it can be seen that stray circuit capacitances, particularly those involving dielectric materials such as phenols and other plastics, can cause very large circuit temperature coefficients when stray capacitance is a large fraction of total circuit capacitance. Ceramic tube sockets and ceramic and glass-bonded mica insulation for contacts and terminals are probably the best materials where frequency stability is critical.

Tuned-Circuit Resistance

Wiring and leads to coils and capacitors also undergo changes in inductance with temperature due to expansion and skin effect. The latter varies with frequency and size of conductor, and as a result, inductive temperature coefficients in the order of 20×10^{-6} to 60×10^{-6} per degree C can occur.[16]

The resonant frequency of an R-L-C circuit, when the resistance is taken into account is given by

$$f = \frac{\sqrt{4LC - R^2C^2}}{4\pi LC} \qquad (6)$$

The more familiar formula, $f = 1/2\pi\sqrt{LC}$, takes no account of the small effect of circuit resistance upon the frequency.

An example will illustrate the contribution of resistance in a practical case of an R-L-C circuit in which $L = 100$ μh, $C = 100$ $\mu\mu$f and $R = 10$ ohms. The resonant frequency is approximately 1,592 kc. The resistance factor in the numerator of Eq. 6 reduces this frequency 12.5 parts per million, or 19.9 cycles in this example. For a resistive temperature coefficient for annealed copper wire of $3{,}930 \times 10^{-6}$ per degree C at 20 C, the resulting frequency temperature coefficient would amount to less than one part per million.

This low calculated value checks with the maximum value found by Thomas[7] in checking the effect of coil resistance in a test oscillator. Under the poorest operating condition, he found the maximum frequency temperature coefficient to be 1.2 parts per million.

Therefore, it is apparent that the only serious effect due to changes in coil resistance with temperature are the resulting changes in eddy currents in the conductor which affect the internal inductance coefficient, as described above.

Resistor Variations

Resistors that control tube operating voltages often have appreciable resistive temperature coefficients. In a reasonably well designed commercial radio receiver, the oscillator frequency drift is not likely to exceed 300 parts per million for a change of 10 percent in line voltage, and shifts as low as 25 parts per million are reported for permeability-tuned oscillators.[2] Therefore, it is unlikely that shifts greater than a few parts per million per degree C can be ascribed either to carbon resistors having temperature coefficients, usually negative, between 600×10^{-6} and $8{,}900 \times 10^{-6}$ per degree C, or to wire-wound resistors having coefficients of 200×10^{-6} to 500×10^{-6} per degree C.

The mechanical design of sets and components must be such that stressing of materials beyond elastic limits at extreme temperatures does not occur. For example, wire on a coil form may be stressed when the coil form has a much higher coefficient of expansion than the wire. Buckling of chassis or structural members must also be avoided. The nonlinearity of curve 1 in Fig. 5 is probably due to such unequal expansion effects. In drift tests on a military radio receiver, the writer found that a radical change or reversal of the temperature coefficient occurred at a temperature below freezing. This effect was traced to leads on an air-dielectric trimmer capacitor which were too taut, distorting the stator assembly.

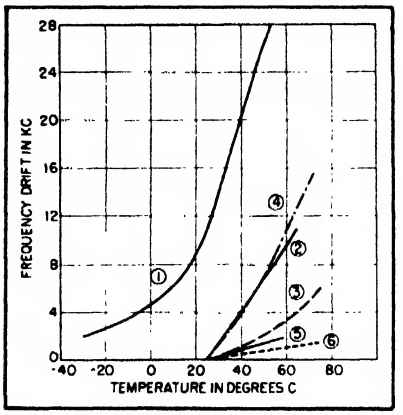

FIG. 5—Frequency drift-temperature curves illustrate analysis of drift in development of an airborne transmitter. Curve 1: total circuit drift due to original coil with bakelite endpieces; curve 2: component produced by coil frame; curve 3: drift from relay contact plate; curve 4: drift from toggle switch; curve 5: component from rotor coil; curve 6: drift obtained with revised coil construction

Test on Developmental Transmitter

A number of the factors involved in causing frequency drift are illustrated in Fig. 5 which depicts the history of the laboratory development of a radio transmitter for military aircraft use. This experience and the analysis of drift factors resulted in replacement of standard commercial parts with components having lower temperature coefficients. Many laboratories probably reached similar conclusions in solving such design problems during the war.

Each component under investigation was mounted in the temperature-controlled test chamber and was used to control the frequency of an oscillator beating with a crystal-controlled oscillator. Curve 1 of Fig. 5 shows the frequency

drift with temperature at a frequency of 3 mc for the original oscillator coil assembly. Despite the fact that this variable inductor was wound on a grooved ceramic form, a frequency drift of 630 cycles per degree C, or 210 parts per million, was observed above room temperature. This measurement confirmed the original suspicion that the coil contributed largely to the bad drift characteristics observed in the initial model of the complete transmitter. The reduced rate of drift at low temperatures was probably due to nonlinear expansion effects in the coil assembly.

The coil frame endpieces, on which the terminals were also mounted and which were constructed of high-grade laminated phenolic, were tested separately. Curve 2 indicates that these endpieces contributed to the circuit a component of frequency temperature coefficient equal to 90×10^{-6} per degree C. This component is nearly half that due to the whole coil assembly, and results from the high temperature coefficient of permittivity of the phenolic, shown in other tests to be of the order of $1,000 \times 10^{-6}$ to $1,300 \times 10^{-6}$ per degree C. Other components employing phenolic insulation were a toggle switch, used to select quartz crystals for fixed-frequency operation, and the contact mounting plate of a band-change relay. Curves 3 and 4 show that these parts added drift components of 110×10^{-6} and 41×10^{-6} per degree C to the overall result. Although each of these circuit elements contributed only a few $\mu\mu f$ of capacitance to the circuit, their capacitance changes with temperature were large enough to affect seriously even the stability of circuits employing large tank capacitors.

The large frequency drift was remedied by a new coil design. The new coil, of slightly reduced size and inductance, employed a silver-jacketed nickel-alloy conductor with a temperature coefficient of linear expansion of 1×10^{-6} per degree C. This coil was wound on an Alsimag No. 202 grooved ceramic form having a very small expansion coefficient of 1.88×10^{-6} per degree C as compared to a coefficient of 6.34×10^{-6} per degree C of the coil form previously used. The bakelite endpieces were replaced by aluminum plates into which ceramic bushings were inserted for insulated parts. The new coil had a frequency temperature coefficient of only 19.5×10^{-6} per degree C, including 4.1×10^{-6} per degree C due to a rotor coil as shown in curve 5, indicating an improvement of more than ten to one. The drift curve obtained with this new coil is shown in curve 6.

The toggle switch was replaced with a rotary type employing ceramic insulation and the relay contacts were mounted on a piece of glass-bonded mica. A large ceramic capacitor with a very small negative temperature coefficient was used to compensate the remaining positive drift components due to the coil, wiring and oscillator tubes.

References

(1) H. Sherman, Temperature Compensation, ELECTRONICS, p 125, April 1944.
(2) T. A. Hunter, Precision Master Oscillators, *Tele-Tech*, p 71, 125, 126, Feb., 1947.
(3) J. Groszkowski, the Temperature Coefficient of Inductance, *Proc IRE*, p 448, April 1937.
(4) A. Bloch, On the Temperature Coefficient of Air-Cored Self Inductances, (correspondence) *Wireless Engr and Eng Wireless*, p 359, Aug. 1944.
(5) H. A. Thomas, The Stability of Inductance Coils at Radio Frequencies, *Jour IEE*, p 702, Nov. 1935.
(6) W. H. F. Griffiths, Recent Improvements in Air Cored Inductances, *Wireless Engr*, p 8-18, Jan. 1942; p 56, Feb. 1942.
(7) T. Slonozewski, High Accuracy Heterodyne Oscillators, *BSTJ*, p 407, July 1940.
(8) H. A. Thomas, The Electrical Stability of Condensers, *Jour IEE*, p 297, Sept. 1936.
(9) H. A. Thomas, Variable Air Condenser with Adjustable Compensation for Temperature, *Jour IEE*, p 277, August 1937.
(10) W. G. F. Griffiths, Temperature Compensation of Condensers, *Wireless Engr*, p 107, March 1942; p 148, April 1942.
(11) A. von Hippel, R. G. Breckenridge, F. G. Chesley and L. Tisza, High Dielectric Constant Ceramics, *Ind and Eng Chem*, p 1,097, Nov. 1946.
(12) A. von Hippel, Tables of Dielectric Materials, NDRC Div 14, *Report No 237, Contract OEMsr-191; Report V*, MIT, Feb. 1944.
(13) C. I. Soucy, Trends in Development of Parts and Components, *Tele-Tech*, p 52, 105, 107, June 1947.
(14) M. Brotherton, "Capacitors: Their Use in Electronic Circuits," D. Van Nostrand Co.
(15) S. W. Seeley and E. I. Anderson, UHF Oscillator Frequency Stability Considerations, *RCA Rev*, p 77, July 1940.
(16) H. A. Thomas, The Dependence on Frequency of the Temperature Coefficient of Inductance of Coils, *Jour IEE*, 81, p 101.
(17) F. E. Terman, "Radio Engineers' Handbook." First Edition. McGraw-Hill Book Co., Inc., p 111, 1943.
(18) J. M. Miller, Thermal Drift in Superheterodyne Receivers, ELECTRONICS, p 24, Nov. 1937.
(19) L. J. Berberich, C. V. Fields and R. E. Marbury, Characteristics of Chlorinated Impregnants in Direct-Current Capacitors, *Proc IRE*, p 389, June 1945.

Mutual Inductance of Concentric Coils

For air-core transformers with greater length than diameter, such as are generally used in r-f service, this nomograph provides pertinent design data in three settings of a straightedge and clearly shows the effects of changes in parameters

By THOMAS C. BLOW

MUTUAL INDUCTANCE between two concentric single-layer air-core solenoids is a circuit value that defies simple analysis. Mutual inductance is dependent on coil dimensions in such an involved manner that design of a radio-frequency transformer is difficult. This nomogram facilitates the design of these transformers.

Examination of the relationship for coaxial solenoids (Circular C74, National Bureau of Standards, Jan. 1937, p 281-282) reveals that for values of D/l less than unity the

formula reduces approximately to

$$M = 0.0251 \frac{d^2 Nn}{(D^2 \times l^2)^{1/2}}$$

The accuracy of this approximation is within three percent for most conditions. From this formula a simple nomograph, which allows an investigation of the effects of the parameters, can be plotted. For given coil dimensions, M is directly proportional to the product of primary and secondary turns. For a given value of d, the outer diameter D does not greatly influence the mutual inductance, and the length of the shorter coil has no effect on the mutual inductance.

To show the use of the chart, consider a design where the outer coil is to be the shorter. Choosing l as 8 in., d as 3 in., and D as 4 in., draw a line (1) through $l = 8$ and $D/l = 0.5$ extending to the M scale. Connect this intersection on M to $d = 3$ with a straight line (2). Use the resulting intersection with the l scale as a turning point for selecting compatible values of Nn and M, draw a straight line (3). If, as shown, the mutual inductance is to be 2 mh, the turns product should be 80. With 16 turns on the longer coil, 5 turns would be required on the shorter one. It should be noted that the 5 turns can be wound with any spacing without materially changing the value of M. The chart can be used to determine any one of the variables l, d, D, Nn, or M when the others are known as long, as the sequence of operations is preserved, namely 1,2,3 or 3,2,1.

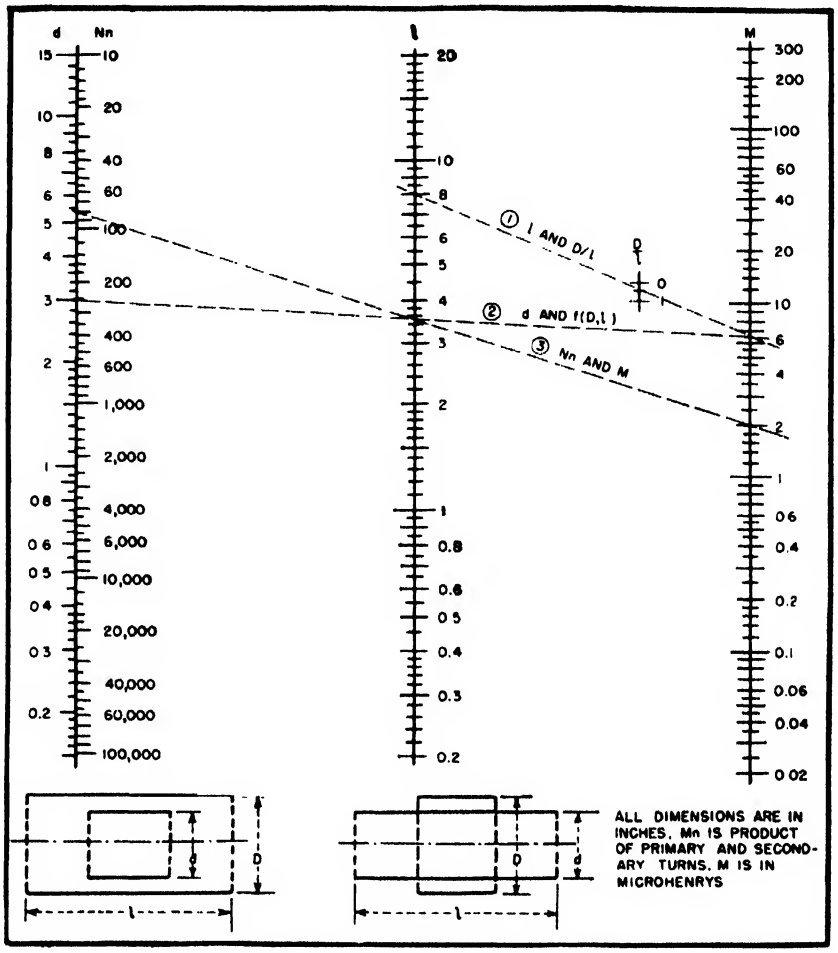

Resonance in Mica Capacitors

By A. P. GREEN
and
C. T. McCOMB

In numerous high-frequency electronic applications the requirement exists that several physically separated points in a circuit be established at a common potential. To satisfy this condition most efficiently it is necessary to operate by-pass capacitors in a series resonant condition.

The simple capacitor element is composed of an effective capacitance in series with an inductance; this inductance is composed not only of the inductance of the associated leads but also the inherent inductance of the foil or plates of the capacitor itself. From this it is seen that for any particular capacitor size or shape there will be associated with the capacitance an absolute minimum of effective series inductance. At low frequencies the magnitude of the inductive component of reactance is so small that it is negligible in comparison to the capacitive component. As the frequency is increased the capacitor element behaves as an ordinary series resonant circuit.

For the most efficient application of a by-pass capacitor to function at a given frequency or band of frequencies, the best unit will be

the largest practical capacitance that will meet both the physical and resonance requirements. The physical requirement will be fixed by the space available and the necessary lead length. With the lead length factor being determined by circuit requirements, the size of capacitor for resonance is then fixed by the frequency.

The above consideration has been applied to the case of the common postage-stamp mica capacitor. An experimental determination of the resonant frequency variation as a function of lead length has been carried out using mica capacitors with leads of No. 20 tinned copper wire. The accompanying chart gives the results of measurements conducted over the practical range of lead lengths for numerous sizes of mica capacitors. The characteristic shape of the curves demonstrates the existence of the above-discussed inherent inductance of the capacitor element. Since the functional variation of resonant frequency is plotted with respect to actual lead length, the residual inductance of the unit manifests itself as an asymptotic maximum resonant frequency for any particular capacitor.

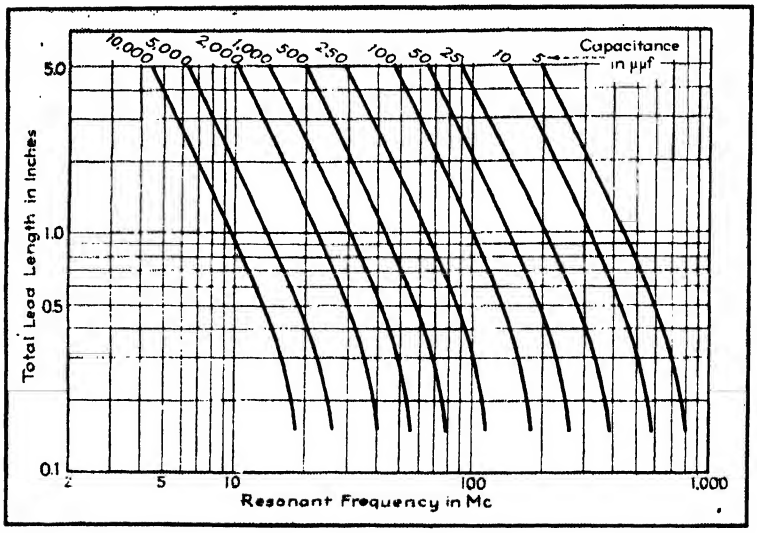

The chart gives lead lengths and capacitance values for series resonance at any frequency from 5 to 800 Mc, for postage-stamp mica by-pass capacitors with No. 20 tinned copper leads

Example of Use of Chart

A by-pass capacitor is desired for 100 Mc. Reference to the chart shows that there are four capacitor sizes that exhibit a usable resonance at this point, these being represented by the four curves that intersect the vertical 100-Mc line. The largest capacitance is most desirable as discussed above, but the choice of unit will be determined partially by the lead length requirement. It is seen from the chart that the range of available capacitances varies from 250 $\mu\mu$f with a total lead length of 0.31 inches to 25 $\mu\mu$f with a lead length of 4.0 inches. Assuming that a lead length of 1.0 inch would be most desirable for the circuit, a 100-$\mu\mu$f capacitor would be chosen.

An examination of the chart reveals an interesting yet expected relationship. It is seen that for a constant lead length the resonant frequency varies inversely as the square root of the capacitance. Thus for a 1.0-inch lead length, 500 $\mu\mu$f is resonant at 43.5 Mc, and 5 $\mu\mu$f is resonant at 435 Mc.

High-Q Iron-Cored Inductor Calculations

From analytic development, equations for the conditions at which inductor Q will be at its highest are derived. Using these equations, core and coil dimensions for an iron-cored inductor are calculated and the effects of varying its parameters are studied

By STEPHEN L. JAVNA

IRON-CORED audio-frequency inductors of good Q can be designed with reasonable accuracy, and their performances over a range of frequency and voltage can be predicted by the method to be described herein. Intuition regarding these matters develops with experience, and model theory may be applied, nevertheless it is desirable to approach the subject from an analytical point of view.

Literature is replete with general information on the subject but there does not seem to be a completely organized method of solution. It is the object of this paper, therefore, to present a "cook-book"

method for inductor design aimed at obtaining a design that will give an optimum value of Q.

The approach is to write down all pertinent equations, making a few simplifying assumptions so that all the variables that enter into them will be analytic. These equations are substituted, one into another, and the result then differentiated and equated to zero in such a manner as to obtain the optimum design conditions. Thus, although the final design equations are suitable for blind substitution of the given coil parameters and direct solution for the remaining parameters, they will be based on mathematical development.

Design equations for direct substitution simplify such design problems as determining the manner in which each coil dimension affects the coil Q, and thus aid in determining the changes in design that will lead to the required inductor improvements.

The utility of the equations has been tested in design by comparing the calculated with the measured characteristics.

The development will be directed toward finding an answer to the following problem.

Given: Required inductance
Maximum allowable coil dimensions
Operating voltage
Operating frequency
No d-c in the coil

To find, for a condition of optimum Q:

Number of turns
Wire size
Lamination size and stack
Lamination material
Q
Effect of parameters on Q and inductance

Table I.—Symbols for coil and core parameters used in the text

A	— Effective cross-sectional area of magnetic-flux path, in square inches
A_c	— Gross cross-sectional area of magnetic path, in square inches
a	— Empirical constant, see Eq. (1)
B	— Maximum flux density within the core, in maxwells per square inch
c	— Area of coil conductor, in square inches
F	— Fraction of core-window area occupied by copper wire of coil
f	— Frequency, in cycles per second
g	— Actual gap length, in inches
I	— Current through coil, in amperes
k	— Empirical constant, see Eq. (1)
L	— Inductance of iron-cored coil, in henrys
l	— Mean length of magnetic path, in inches
L'	— Length of coil conductor, in inches
m	— Mean length of a turn of the coil, in inches
$\mu\Delta$	— Incremental permeability of core with respect to air at operating frequency, in gilberts per inch
N	— Number of turns in coil
n	— B&S wire size number of conductor
$R_{a\text{-}c}$	— Apparent alternating-current coil resistance caused by core loss, in ohms
$R_{d\text{-}c}$	— Copper-loss resistance, in ohms
R'	— Reluctance of air gap assuming no fringing, in gilberts per maxwell
ρ	— Resistivity of conductor, in ohm-inches (0.6788×10^{-6} for copper)
s	— Total lamination window area, in square inches
t	— Tongue width, in inches, see Fig. 1(a)
V	— Voltage across coil, in volts
w	— Weight of core, in pounds

Inductor Construction

Generally speaking, inductors used in communication equipment such as wave filters include a coil of wire that is wound over a suitable form in a manner described elsewhere.[1] The coil is mounted over an iron core which among other forms may comprise a toroidal dust core, Hipersil loop, conventional E-I laminations, or any one of the innumerable other lamination forms and shapes, none of which affects the design procedure.

A popular and easily available shape is the scrapless E-I lamination. These are so called because two Es and two Is are stamped simultaneously from a single blank as shown in Fig. 1(a), with no scrap. Fig. 1(b) gives the dimensions of a choke coil utilizing scrapless laminations of such a quantity as to provide a square cross-sectional area of magnetic path. These laminations are described in greater detail in manufacturers' handbooks.[2]

A magnetic path of square cross-section is desirable because it can be shown that for a given cross-sectional area of magnetic path, the rectangular configuration which gives the shortest mean length per turn of wire is a square. Due to burrs and scale on the laminations, the effective or net cross-sectional area of the stack and tongue width is about 0.9 of this product.

Laminations may be stacked by interleaving, or by stacking all the E pieces in the same direction, and butting the I pieces against them as shown in Fig. 1(b). If an air gap is required, a nonmetallic gap

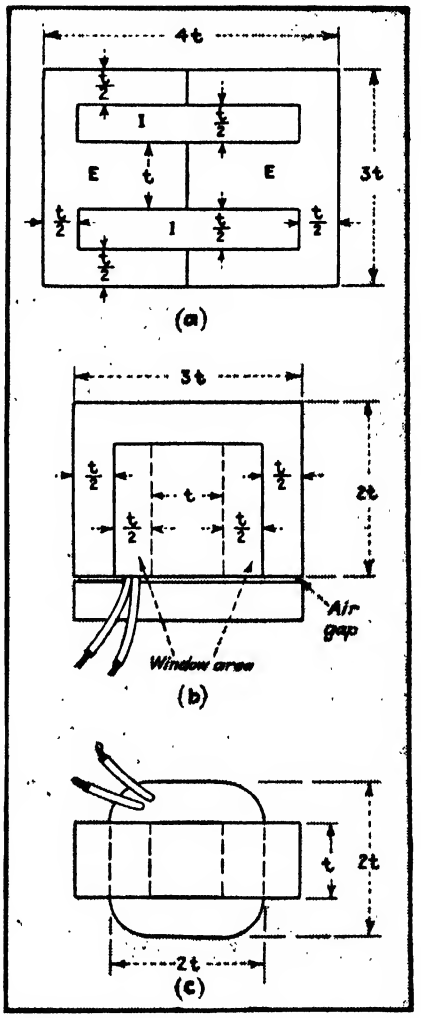

FIG. 1—(a) Layout for stamping scrapless E-I laminations. (b) Plan shows assembly of core from laminations. (c) Elevation of completed transformer, showing coil wound on core

FIG. 2—Equivalent circuit of iron-cored inductor at a fixed frequency and voltage

spacer of proper thickness is inserted in the joint between each E and I, and the assembly mechanically clamped together. The coil is always designed to fill the window of the closed lamination, as Fig. 1(c) indicates.

Development of Design Equations

At a given set of conditions of frequency and voltage the equivalent circuit of an iron-cored inductor may be represented by Fig. (2). R_{a-c} is a fictitious value of resistance which, if multiplied by the square of the coil current, will give the core loss of the inductor. Thus, the losses in the inductor may be represented by $I^2R_{d-c} + I^2R_{a-c}$, where I^2R_{d-c} includes copper losses, and I^2R_{a-c} includes core losses.

In developing design equations, we will first derive expressions for the alternating-current and direct-current resistances of the inductor. By combining these two resistance equations with the equation for the Q of the inductor, we will obtain the design equations.

To determine the alternating-current resistance let us assume that core loss of an inductor can be expressed in the form

$$P_{cl} = kB^a \text{ watts per pound} \quad (1)$$

Quantities represented by symbols used in this and subsequent equations are given in Table I. Total core loss in the inductor is then

$$P = kB^a w \text{ watts} \quad (2)$$

But by Ohm's law, core loss is also given by

$$P = I^2R_{a-c} \text{ watts} \quad (3)$$

Equating Eq. (2) and (3) and solving for R_{a-c}, we obtain

$$R_{a-c} = kB^a w/I^2 \text{ ohms} \quad (4)$$

Since the Q of the coil will usually be greater than 10, practically no error is introduced by setting

$$I = V/2\pi fL \text{ amperes} \quad (5)$$

Substituting Eq. (5) in Eq. (4) and solving, we obtain

$$R_{a-c} = 39.5kB^a w(fL/V)^2 \text{ ohms} \quad (6)$$

Direct-current resistance of any conductor can be represented by the equation

$$R_{d-c} = \rho L'/c \text{ ohms} \quad (7)$$

Where L' can be found from

$$L' = mN \text{ inches} \quad (8)$$

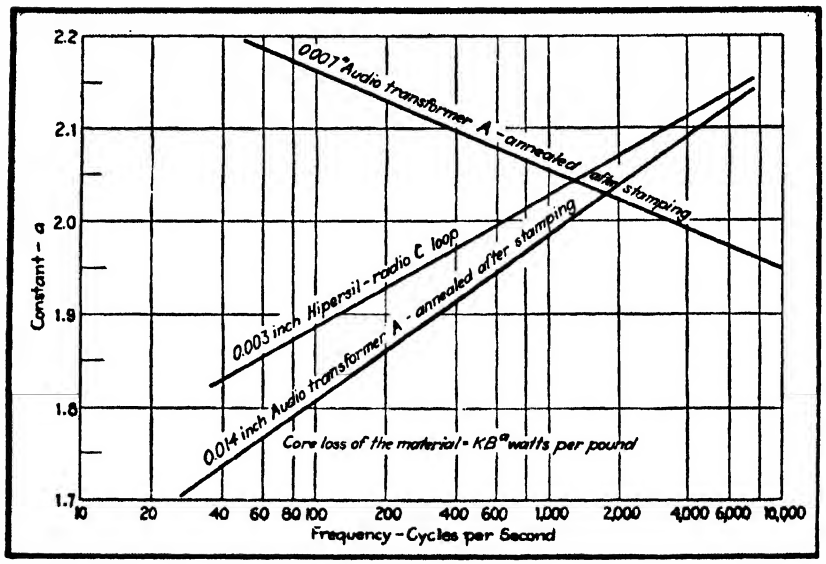

FIG. 3—Experimentally determined curves show values of a in Eq. (1) for three types of core material as a function of frequency

For any coil the conductor cross-sectional area can be computed from the winding window area by

$$c = sF/N \text{ square inches} \quad (9)$$

Substituting Eq. (8) and (9) into Eq. (7) and solving for the direct-current coil resistance we find that

$$R_{d-c} = (mN^2/sF)0.6788 \times 10^{-6} \text{ ohms} \quad (10)$$

The basic equation for induced emf in a coil is $V = 4.44fNBA \times 10^{-8}$ volts, or

$$N = (V/4.44fBA)10^8 \text{ turns} \quad (11)$$

Substituting Eq. (11) into Eq. (10) we obtain

$$R_{d-c} = (m/sF)(V/fBA)^2 \times 3.44 \times 10^8 \text{ ohms} \quad (12)$$

Equations (6) and (12) give us the alternating-current and direct-current resistances of the inductor in terms of primary design parameters.

Inductor design is to be such that the Q will be as high as possible. Q is given by the definition

$$Q = 2\pi fL/(R_{a-c} + R_{d-c}) \quad (13)$$

It is apparent that Q will be a maximum when $(R_{a-c} + R_{a-c})$ is a minimum. Differentiating $(R_{a-c} + R_{d-c})$ with respect to B, setting the derivative equal to zero, and solving for B will give the value of B at optimum operation. Thus

$$\frac{d(R_{a-c} + R_{d-c})}{dB} = 0 =$$

$$39.5akB^{a-1}w(fL/V)^2 - (m/sF)(V/fBA)^2B \times 6.88 \times 10^8$$

Solving this expression for B we obtain

$$B = \left[\frac{17.4mV^4 \times 10^8}{akwf^4(LA)^2sF}\right]^{1/a+2} \text{ maxwells per square inch} \quad (14)$$

Air Gap Calculations

Resistance per foot of copper wire at 20°C may be written

$$R = 2^{n/3} \times 10^{-4} \text{ ohms per foot} \quad (15)$$

Solving for wire size we find that $n = 50.79 + 10\log R$, but $R = R_{d-c}/mN$, and therefore

$$n = 50.79 + 10\log(R_{d-c}/mN) \quad (16)$$

A well-known expression for inductance is

$$L = 3.19N^2 \times 10^{-8}(R' + l/\mu\Delta A) \quad (17)$$

In the subject case R' may be approximately expressed as $2g/A$, where g is the width in inches of the actual air gap between E and I pieces at the butt joint. This neglects fringing. Roters[3] has developed a method for computing air gap reluctance which takes fringing into account. By this means g may be corrected analytically. For ordinary manufacturing purposes all that is required is a general idea of gap size, and the approximate method will usually be found quite sufficient. As a matter of fact, after the coil is manufactured and assembled the gap is adjusted so that the coil inductance will be exactly the value desired.

Substituting the foregoing ap-

proximate value of R' in Eq. (17) we obtain for gap width

$$g = (N^2A_g/2L)\,3.19 \times 10^{-8} - (lA_g/2\mu\Delta A) \text{ inches} \quad (18)$$

Measured Quantities

Experimentally obtained curves for k and a for a number of magnetic materials are given in Fig. (3) and (4) respectively. These curves are obtained as follows. A sample stack of the material to be tested is obtained and a coil of any convenient size and number of turns is mounted over the core. The core is butt stacked with a gap. Inductance and Q of the test unit are measured at a number of representative voltages—enough to cover a sufficiently wide range of flux densities—for several values of frequency as parameters. (The author has used a General Radio impedance bridge with good results.)

The effective resistance as obtained from Eq. (13) is

$$R_{a-c} + R_{d-c} = 2\pi fL/Q \quad (19)$$

R_{d-c}, the direct-current resistance of the coil is easily measured. R_{a-c}, the effective alternating current of the coil can then be computed from Eq. (19) using the measured value of Q.

To determine core loss, coil current is obtained from $I = V/2\pi\ fL$ where V is the sinusoidal voltage measured directly across the coil after the bridge has been balanced. Obviously the input impedance of the voltmeter used for this measurement should be much greater than $2\pi fL$. Knowing the coil current, the core loss can be calculated from Eq. (3). The core should be weighed or its weight computed by counting laminations. Core loss is then

$$P_{cl} = I^2R_{a-c}/w \text{ watts per pound} \quad (20)$$

From Eq. (10) $B = (V/4.44fNA) \times 10^8$.

With this information, core loss curves can be plotted as in Fig. 5, with frequency as parameter, on log-log paper. These curves will all be nearly straight lines. The slope of these curves is the exponent a, and k can be computed for the corresponding frequency by taking the core loss at any flux density on the curve and substituting in Eq. (1). From the data of Fig. 5 and similar curves, Fig. 3 and 4 are obtained. These curves justify the original assumption that core loss may be represented by $P = kB^a$. To complete the data necessary for designing an inductance, a typical curve of incremental permeability vs flux density is reproduced in Fig. 6, but it will be seen later that these values are not critical.

Design Procedure

A typical problem will be solved to illustrate design procedure.

Given:

- Required inductance of 5 henrys
- An available space of 2¼ × 2 × 1¾ inches
- Operating voltage of 10 volts
- An operating frequency of 1,000 cycles per second
- Core material available is Allegheny audio transformer A steel, annealed after stamping, laminations in 0.014-inch thickness (29 gage)

To find:

- Number of turns in coil
- Wire size for winding
- Lamination size and stack
- Gap width
- Q of coil

Designing for a square core cross-section, we see that a scrap-

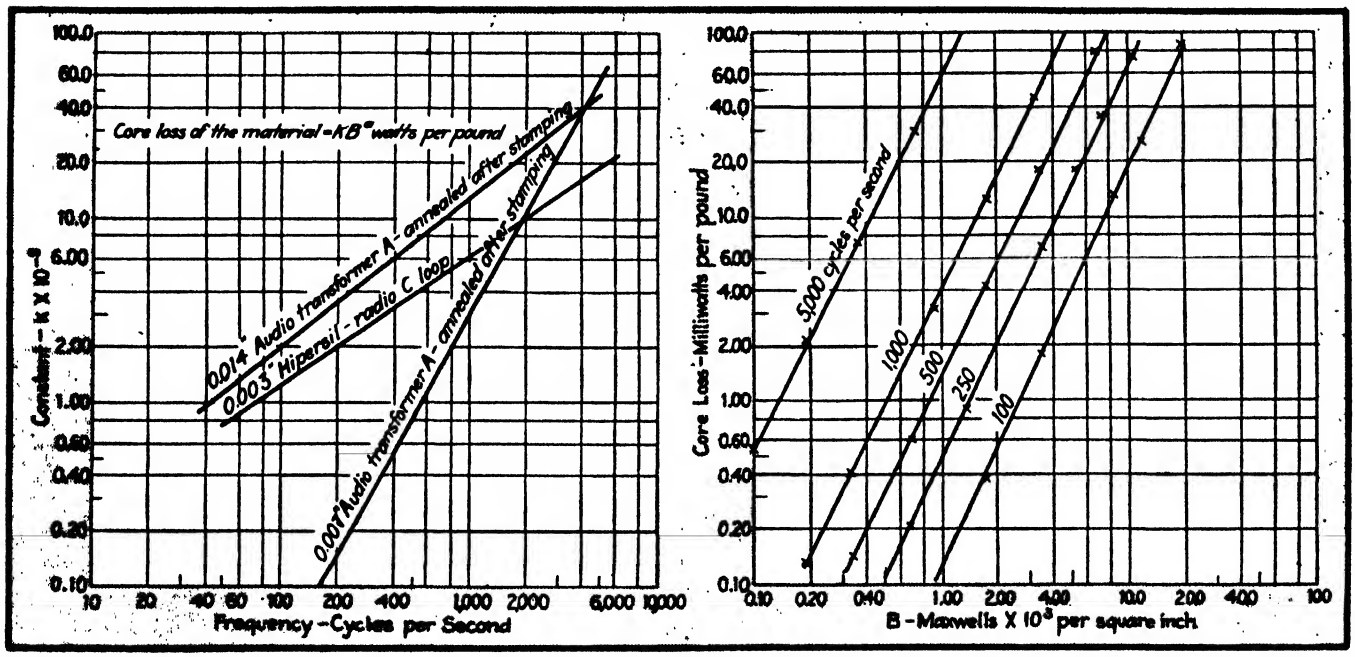

FIG. 4—For use in determining core loss in inductor calculations, k as determined experimentally for three different materials is given here as a function of frequency

FIG. 5—Core loss measured at several frequencies for a small sample of 0.007-inch high-silicon steel, Allegheny audio transformer A, annealed after stamping

less lamination with $t = \frac{3}{4}$ inch will fit the space allowed. Finished dimensions will require a space $2\frac{1}{4} \times 1\frac{7}{8} \times 1\frac{1}{2}$ inches as illustrated in Fig. 7.

First the physical design parameters will be calculated from the required conditions and the previously developed equations, and then the coil and core will be designed. Utilizing the same notation as previously, from the dimensions of Fig. 7 we obtain

$$m = 2\left(1\frac{1}{2}\right) + 2\left(\frac{3}{4}\right) = 4.5 \text{ inches}$$

$$l = 4\left(1\frac{1}{8}\right) = 4.5 \text{ inches}$$

$$w = 0.615 \text{ pounds}$$

$$A = \left(\frac{3}{4}\right)\left(\frac{3}{4}\right)(0.9)$$

$$= 0.505 \text{ square inches}$$

$$A_g = \left(\frac{3}{4}\right)\left(\frac{3}{4}\right) = 0.563 \text{ square inches}$$

$$s = \left(1\frac{1}{8}\right)\left(\frac{3}{8}\right) = 0.422 \text{ square inches}$$

It will be assumed that the ratio of copper area in the window to window space area is 0.3. This is usual, somewhat less with smaller laminations, and somewhat greater with larger laminations. From Fig. (4) for 0.014-inch audio transformer A steel, annealed after stamping, k at 1000 cycles is 1.3×10^{-4}. From Fig. 3, $a = 1.987$.

From Eq. (14) B is calculated to be 89.2 maxwells per square inch. From Eq. (6) and (12), R_{a-c} and R_{d-c} are calculated, giving $R_{a-c} = 592$ ohms and $R_{d-c} = 600$ ohms respectively. Q is calculated from Eq. (13) using the previously determined values of resistance. This gives $Q = 26.3$.

The total number of turns is found to be 5,000 from Eq. (11), and the coil is to be wound of number 35 wire as determined from Eq. (16). Using the value of B determined previously, $\mu\Delta$ is found from Fig. 6 to be 1050. Equation (18) gives a gap length of 0.038 inches.

It should be noted that the value of $\mu\Delta$ need not be accurate for even if it varies by 100 percent, the gap is barely affected.

The coil is designed to fit a window length of $1\frac{1}{8}$ inches with $\frac{1}{8}$ inch on each side for a margin. Usable winding length is then $\frac{7}{8}$ inch. The nominal diameter of number 35 wire is 0.0061 inch, and thus turns per layer $= (\frac{7}{8})/0.0061 = 143.5$ turns. Allowing 5 percent for irregularities, we can expect the turns per layer to be (0.95) (143.5) = 136 turns. From previous calculation we found that 5,000 turns were required, therefore the number of layers will be 5000/136 = 37 layers.

It should be noted that R_{a-c} and R_{d-c} come out nearly equal. This will verify the rule followed by most designers that for optimum Q the fixed losses represented by R_{d-c} should be equal to the variable losses represented by R_{a-c}. If in Eq. (14) a is set equal to 2, the same result is obtained as when Eq. (6) and (12) are equated and solved for B. In other words, the rule is accurate if $a = 2$. Actually, a is usually nearly 2.

The coil as designed above was constructed and with the gap adjusted to give $L = 5$ henrys at 1,000 cycles and 10 volts, Q was found to be 25.9, which represents an error of 1.5 percent. The gap was actually found to have been adjusted to be about 0.060 inch as against about 0.04 inch computed. This discrepancy is due to fringing.

Suppose that it is desired to reduce the size of the inductor by using a $\frac{1}{2}$-inch scrapless E-I lamination with a $\frac{1}{2}$-inch stack. What is the effect of this change in physical constants on the characteristics of the coil if the inductance is to remain 5 henrys at 10 volts and 1,000 cycles? Taking $F = 0.25$ we find that

B = 209 maxwells per square inch
R_{d-c} = 994 ohms
R_{a-c} = 935 ohms
Q = 16.3
N = 4,790 turns
n = No. 39

This is obviously not as good as the first coil because the Q is lower and number 39 wire is harder to handle.

Suppose the same $\frac{1}{2}$-inch lamination is used but with a one-inch stack, what then? The results are

B = 135 maxwells per square inch
R_{d-c} = 796 ohms
R_{a-c} = 800 ohms
Q = 19.7
N = 3,710 turns
n = No. 38

This coil is better than that obtained with a $\frac{1}{2}$-inch stack but not so good as that obtained with the $\frac{3}{4}$-inch lamination.

Following this lead, suppose the coil is redesigned to use a 1-inch scrapless lamination, with a one-inch stack. Taking $F = 0.35$,

B = 48.5 maxwells per square inch
R_{d-c} = 413 ohms
R_{a-c} = 415 ohms
Q = 38
N = 5,180 turns
n = No. 32

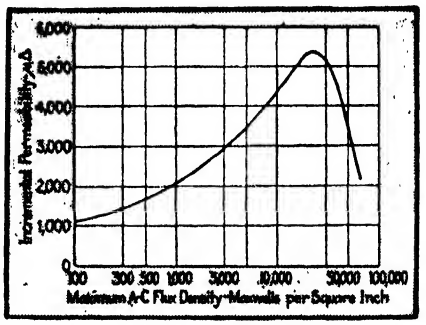

FIG. 6—Incremental permeability characteristic of 0.014-inch Allegheny audio transformer A core steel

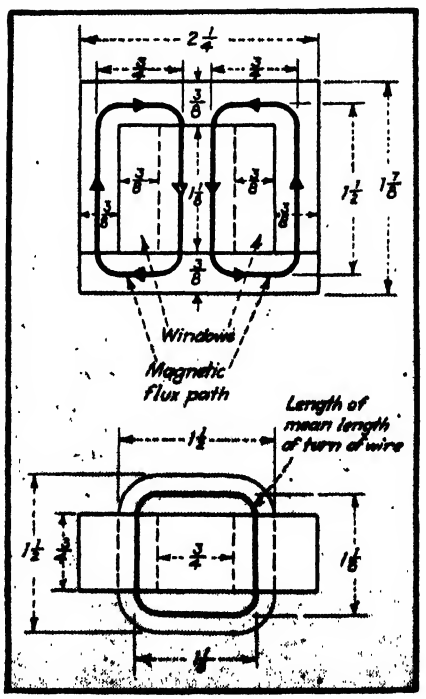

FIG. 7—Dimensions of inductor calculated by method developed in text

If a Q of 26 is not high enough for the first case that was computed and more space is not available, will using an 0.007-inch lamination thickness in the same size lamination, i.e., ¾-inch scrapless, improve the coil? New values of a and k are found from the graphs. The results are

B = 117.5 maxwells per square inch
R_{d-c} = 362 ohms
R_{a-c} = 312 ohms
Q = 46.6
N = 3,880 turns
n = No. 34

As might have been expected, a thinner lamination will improve the Q.

Taking the original coil, 5,000 turns of number 35 wire on a ¾-inch E-I ¾-inch stack, Allegheny audio transformer A steel, annealed after stamping, 0.014 inch thick, operated at 10 volts, what happens if the frequency is changed to 500 cycles? Results are

B = 226 maxwells per square inch
R_{d-c} = 600 ohms
R_{a-c} = 385 ohms
Q = 15.95
L = 5.02 henrys

If the frequency is maintained at 1,000 cycles, but voltage is increased to 20 volts, what is the effect?

B = 178 maxwells per square inch
R_{d-c} = 600 ohms
R_{a-c} = 586 ohms
Q = 26.5
L = 5.01 henrys

It should be noted that due to the large air gap, the inductance remained practically independent of voltage and frequency.

Thus the basic design equations may be used and applied to almost any magnetic material, regardless of shape or size, and the effects of various parameters may be easily computed.

References

(1) Roters, H. C., "Electromagnetic Devices", John Wiley and Sons, Ins., New York City, 1941, Chapter VI.
(2) Allegheny Ludlum Steel Corp., Technical Bulletins EM-1 EM-2 and EM-3, Brackenridge, Pa., 1939.
(3) Roters, H. C. "Electromagnetic Devices", John Wiley and Sons, Inc., New York City, 1941, Chapter V.

Bibliography

(1) Roters, H. C., "Electromagnetic Devices", John Wiley & Sons, New York, 1941.
(2) Allegheny Ludlum Steel Corporation Technical Bulletins EM1, EM2, EM3.
(3) Arguimbau, L. B., Losses in Audio Frequency Coils, *General Radio Experimenter*, 11, 6, Nov., 1936.
(4) McElroy, P. K., and Field, R. F., How Good is an Iron Cored Coil?, *General Radio Experimenter*, 16, 10, Mar., 1942.
(5) E. E. Staff, M.I.T. "Magnetic Circuits and Transformers", John Wiley and Sons, New York, 1943.
(6) Spooner, Thomas, "Properties and Testing of Magnetic Materials", McGraw-Hill Book Co., Inc., 1929.
(7) Everitt, W. L., "Communications Engineering", McGraw-Hill Book Co., Inc., 1937.
(8) Terman, F. E., "Radio Engineering Handbook", McGraw-Hill Co., Inc., 1943.
(9) Hanna, C. R., Design of Reactances and Transformers Which Carry D. C., *Electrical Engineering*, Feb., 1927.
(10) Dagally, W., Alternating Current Inductance Coils and Transformers, *Wireless Engineering*, Jan., 1936.
(11) U. S. Steel, Electrical Steel Sheets, Technical Bulletin No. 2.

Measuring Coil Characteristics Without an Impedance Bridge

Use of the cathode-ray oscilloscope to measure inductance, Q, impedance, power factor, effective resistance of coils—especially useful when changes are being made in the coils under measurement. Method would also make useful demonstration set-up for technical schools

By H. D. BRAILSFORD

MANY occasions arise where it is desired to measure inductance, impedance, or other characteristics of coils but a conventional impedance bridge is not immediately available. A cathode-ray oscilloscope may be employed as the indicating device in conjunction with simple, readily obtainable circuit components to accurately perform all the functions of conventional bridges. The basic idea involves connection of the oscilloscope so that the pattern on the screen graphically compares the voltage across the unknown impedance in phase and amplitude to that across a non-inductive resistance. When two sine voltages are simultaneously applied, one to the horizontal and one to the vertical deflection plates of an oscilloscope, the spot motion developed is a mechanical resultant of the two driving forces and is termed a Lissajous figure. (See any text on sound or physics). Two measuring techniques employing these figures will be discussed.

Calibrating the Horizontal and Vertical Amplifiers

The methods to be described require an equal deflection sensitivity for the vertical and horizontal amplifiers in the oscilloscope. To make this calibration, the horizontal and vertical deflection input terminals

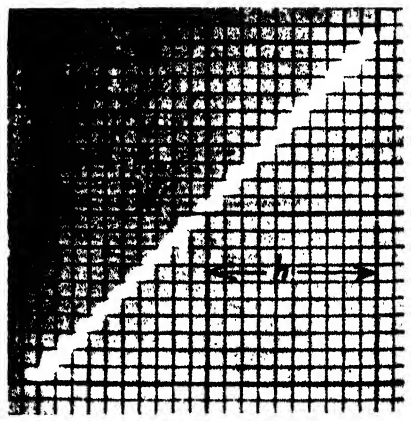

FIG. 1—Proper adjustment of horizontal and vertical gain controls on the oscilloscope will produce equal deflections, with the resultant straight line inclined at an angle of 45 degrees

should temporarily be connected together and a deflecting voltage of any convenient value applied between these terminals and ground. The horizontal and vertical amplifier gain controls are then adjusted so that the pattern appears as Fig. 1, that is, a straight line inclined at an angle of 45 deg. ($v = h$). If a large number of measurements are to be made it is a good idea to seal the gain control knobs in this position with a piece of tape to prevent their inadvertent shift.

Resistance Comparison Method

Impedance. The circuit for direct impedance measurement is given in Fig. 2; R is a variable resistor, L is the coil under test, and R_L represents the total effective resistance of the coil. The alternating voltage supply may be from any convenient source. If an oscillator with output voltage control is available, the potentiometer shown will not be necessary. The pattern on the screen will take the form of an ellipse. The driving voltage should be varied until the horizontal deflection (h) has any convenient value. Resistor R is now adjusted until the vertical deflection is equal to the horizontal ($v = h$ as of Fig. 3). At this position the voltage drop across resistor R is exactly equal to that across the unknown impedance Z, therefore Z is equal to R. If an uncalibrated resistor is used, its resistance at this adjustment may be measured on an ohmmeter. A calibrated resistance will of course give the value directly in ohms of impedance Z. The voltage across R, (E_R) lags E_s by an angle, θ, dependent upon the power factor of Z.

Power Factor. The Lissajous figure may be solved to yield the power factor and other characteristics of Z. At unity power factor θ is zero and the pattern becomes the straight line of Fig. 1. At zero power factor θ is 90 deg. and the pattern becomes a circle. In Fig. 4 is shown the change in appearance of the pattern due to increased power factor by the addition of a series resistance in the coil circuit. The general equation[1] for this ellipse is

$$v^2x^2 - 2vhxy\cos\theta + h^2y^2 = v^2h^2\sin^2\theta \quad (1)$$

Where x and y are the coordinates of any point, θ is the phase difference in degrees between the two voltages, v and h are the maximum vertical and horizontal spot displacements respectively.

If we choose a point where the ellipse crosses one of the axes, then the other ordinate becomes zero and the equation reduces to

$$\sin\theta = \pm\frac{y}{v} \text{ for a point on the } y \text{ axis.} \quad (2)$$

$$\sin\theta = \pm\frac{x}{h} \text{ for a point on the } x \text{ axis.} \quad (3)$$

Referring to Fig. 4; if $v = 10$, $y = 7$.

Therefore:

$$\sin\theta = 0.7$$
$$\theta = 44° 26'$$

Power Factor of $Z = \cos\theta = 0.714$

A vector diagram constructed to scale as in Fig. 4-A will graphically give the value of inductance and total effective resistance. A more direct method of measuring inductance and effective resistance will be described.

In cases where Z has a very low power factor, that is, θ approaching 90 deg., as in Fig. 3, a considerable error may result due to the inability accurately to locate y. The use of a finer trace will help. A better method, however, is to use a low power factor condenser in place of R in the circuit of Fig. 2. A paper capacitor in the audio range may, for practical engineering purposes, be considered to have zero power factor. The pattern will then be the graphical reciprocal, so to speak, of that attained with the resistance, that is, for zero power factor, $\theta = 180$ deg. and the trace shows a straight line; for unity power factor $\theta = 90$ deg. and a circle appears on the target. Thus;

Power Factor $= y/v$

For the coil shown in Fig. 3 the power factor determined by this method was found to be 0.2 ($\theta = 78° 45'$).

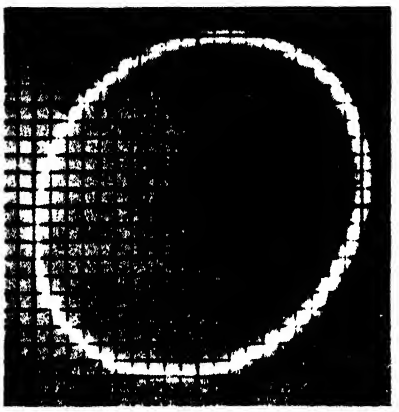

FIG. 3—Oscillogram when the coil has a low power factor. Fine trace will aid in making the measurement; a better plan is to use a condenser of low power factor in place of R in Fig. 2

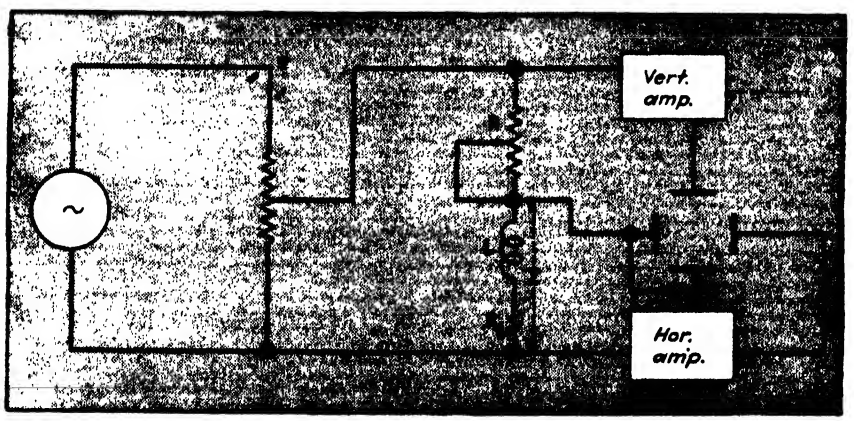

FIG. 2—Circuit in which impedance of the coil L is determined. At proper value of R, the 45-deg deflection will be secured. Then $R=Z$

Resonance Method

Inductance. The circuit employed to determine inductance is given in Fig. 5. A variable oscillator will be required of appropriate frequency range. The coil to be measured is connected in series with a paper or mica capacitor of known value. Resistor R is adjusted to give a con-

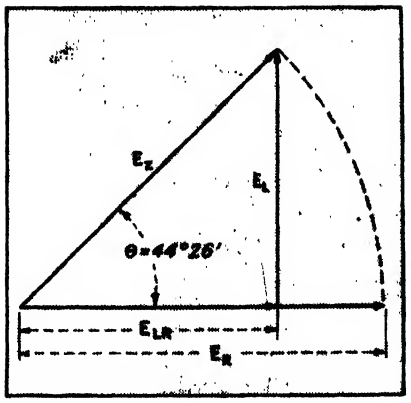

FIG. 4-A—Vector diagram of the situation occurring in Fig. 4

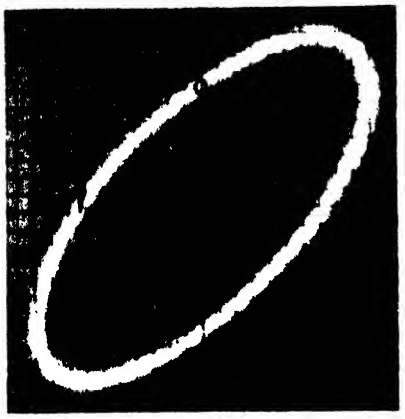

FIG. 4—Appearance of trace when the coil has appreciable resistance

venient vertical deflection. The oscillator is started at its lowest frequency and gradually advanced until the Lissajous ellipse closes into a straight line as in Fig. 6 denoting zero phase shift between E_R and E_Z. This will be the fundamental resonant frequency of the LC circuit. The apparent inductance L may readily be determined by reference to any standard impedance chart and is that value of inductance having a reactance equal to C at the resonant frequency. A more accurate determination is given by the simple equation

$$L = \frac{\left(\frac{5033}{f}\right)^2}{C} \qquad (4)$$

Where f is the resonant frequency, L is in millihenries and C is in microfarads.

It should be noted that at the balance position shown in Fig. 6, the horizontal deflection is at a minimum. This is so because at resonant frequency the reactance of a series resonant circuit is zero and the voltage drop (E_R) is solely due to effective resistance. Figure 6-A is a vector diagram for the condition of Fig. 6; E_C and E_L are equal and 180 deg. out of phase; θ is the phase or power factor angle of the coil; E_{LR} is the drop due to effective resistance of the coil and is seen to be identical to E_R.

It should be noted that the magnitude of E_L and E_C may vary through wide extremes with respect to the driving voltage, depending upon the effective resistance in the LC circuit.

Effective Resistance. Referring to Fig. 6, the amount of horizontal deflection h, as stated, is due to the voltage drop across the effective resistance of the coil at resonant frequency. (Condenser losses may be neglected throughout the audio and lower radio frequency range.) To measure this directly it is only necessary to readjust R until the vertical deflection again equals the horizontal deflection, at which position R is equal to the effective resistance of L at the frequency at which the measurement is made. For coils having a fairly high Q, the effective resistance may be quite small and to get a reasonably accurate measurement the output voltage of the oscillator should be increased to expand the pattern.

Inductance Measurement by Parallel Resonance. Where the inductances under investigation have a very high Q, the exact resonant frequency may more easily be determined by connecting capacitor C in parallel with the inductance. The operating technique is the same, the difference being that at resonance the voltage across the LC circuit is at a maximum and the cathode trace is substantially more sensitive to frequency shift, thus making it easier to set the oscillator at the exact resonant frequency.

When using the shunt resonance method it should be borne in mind that the distributed capacitance of the coil will be, in effect, added to that of the tuning condenser and the indicated inductance will be higher than the true value. For this reason coils having a high distributed capacitance should preferably be measured by series resonance. The coil of Fig. 3, for example, which was a 4000-turn layer wound solenoid, measured 150 millihenries by series resonance and 155 millihenries by shunt resonance. The tuning capacitance was 1.0 microfarad and the resonant frequencies 410 and 404 cycles respectively.

Determination of Q. Having established inductance and effective resistance of a coil by the foregoing methods, the figure of merit or Q is readily determined by the familiar equation:

$$Q = \frac{2\pi fL}{R} \qquad (5)$$

It should be mentioned that the output impedance of the driving os-

FIG. 5—Resonance methods of measuring inductance of a coil

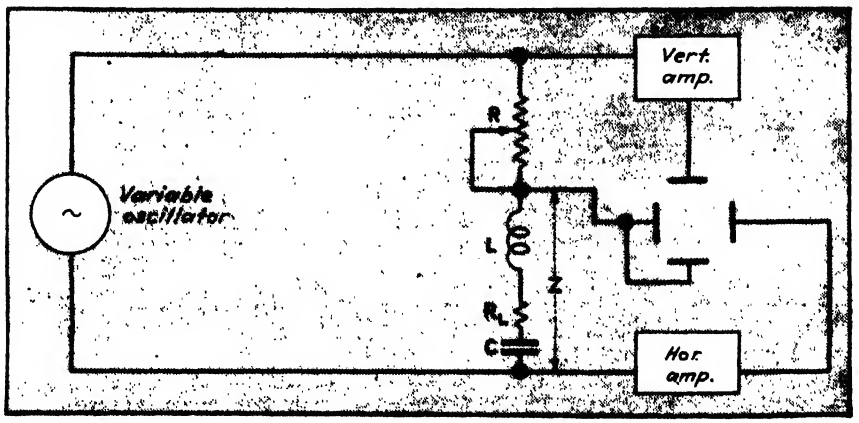

cillator should be high with respect to that of the coil under test at the resonant frequency, otherwise the *LC* circuit will tend to generate harmonics. It will not then be possible to close the pattern which will assume an irregular configuration, the exact shape being a function of the order and amplitudes of the harmonics. For example, Fig. 8 illustrates the pattern obtained with an oscillator output impedance of 250 ohms as compared to the pattern of Fig. 6 obtained with an output impedance of 5000 ohms. The coil under test in this case had an output impedance of 240 ohms at the resonant frequency. Harmonics may also be excited by the application of too high a voltage.

Distributed Capacitance. The distributed capacitance of a coil may be measured by locating its resonant frequency from the circuit of Fig. 2 although, as Terman,[2] points out, the value obtained in this way will be somewhat smaller than the true value. The results are however usually accurate enough for most engineering applications.

$$\text{Distributed Capacitance } C_D = \frac{\left(\frac{5033}{f}\right)^2}{L} \quad (6)$$

where C_D is in microfarads, and L is in millihenries as measured by the series-resonant method.

It has been the writer's experience at this Laboratory that once the fundamental theory of the foregoing technique has been thoroughly grasped, the setup time and operating procedure compare favorably with conventional impedance bridge measurements. We frequently use these methods in preference to a bridge, particularly where it is desired to study the progressive effect on the characteristics of a coil of changing frequency and/or influences in its magnetic field. One investigation in particular involved a study of the behavior of layer-wound solenoid coils with plunger cores of different materials and configuration and in one case where the magnetic plunger was shielded by a nonmagnetic sleeve of conducting material. Wave filter elements and other resonant circuits are likewise readily tuned to the desired frequency by this method.

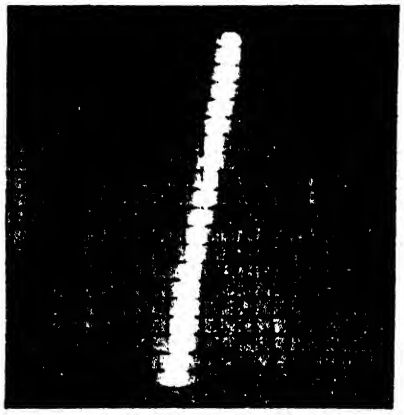

FIG. 6—Using the circuit of Fig. 5, applied frequency is increased until this pattern appears. This will indicate the fundamental resonant frequency of the coil

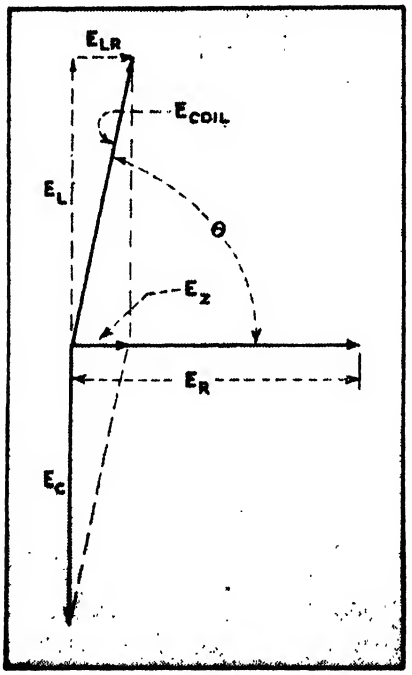

FIG. 6-A—Vector diagram for the condition of Fig. 6

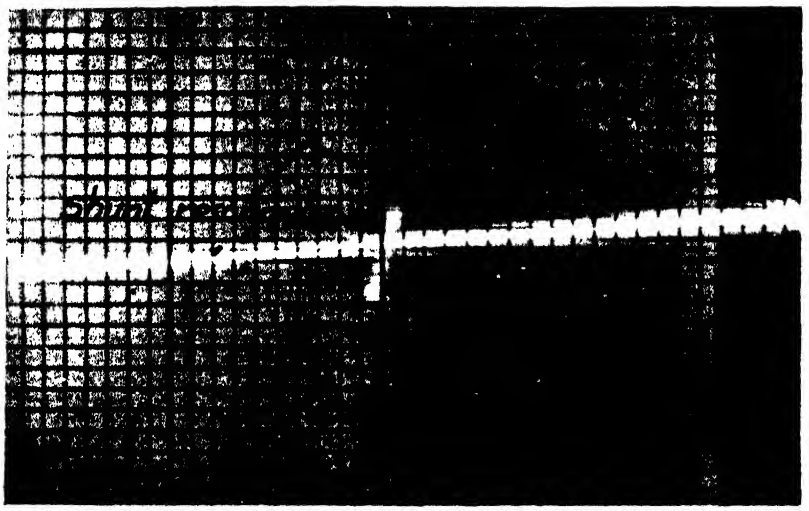

FIG. 7—Composite diagram showing comparison of series and parallel resonant methods of measuring coil characteristics

REFERENCES

(1) Watson, F. R., "Sound", p. 58, John Wiley and Sons, New York, N. Y.
(2) Terman, F. E., "Measurement in Radio Engineering", McGraw-Hill Book Co., New York, N. Y.

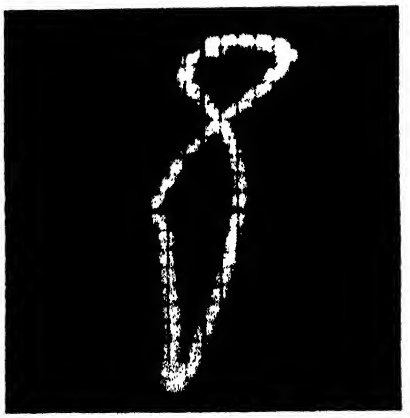

FIG. 8—Effect of using oscillator output impedance low in value, showing generation of harmonics

Crystal Rectifiers

Recent developments in the manufacture of germanium and silicon crystals have provided a new, efficient rectifying device, necessary for radar and of increasing usefulness in commercial microwave applications

By W. E. STEPHENS

THE demands of microwave radar necessitated the development of more than thirteen different types of crystal rectifiers which were produced by the million. Basic improvements in stability and performance may enable the crystal to displace the diode tube in many applications, particularly because of its effectiveness at high frequencies. Even at low frequencies, certain kinds of crystals may prove more stable, have less weight and take up less space than a diode and filament transformer.

What a Crystal Rectifier Is

A modern crystal rectifier consists of a small-area contact between a metal like tungsten and a suitable semiconductor such as galena, germanium, or silicon. Many names have been used to describe these rectifiers, such as silicon-crystal rectifier, dry-point contact rectifier, barrier-layer rectifier, point-contact semiconductor rectifier, converter crystal, mixer crystal, video crystal, and detector crystal. These differ from copper-oxide and selenium rectifiers in having a small contact area and usually a smaller power-handling capacity. On the other hand, their reduced capacitance makes them very useful at high frequencies.

A typical crystal rectifier is shown diagrammatically in Fig. 1. The ceramic cartridge with brass ends holds the whisker and semiconductor in stable contact. The pointed whisker is soldered into the pin end and the semiconductor, soldered on the end of a stub, is pushed in from the other end till the contact is made. The whisker spring is compressed slightly and the stub locked by a set screw. The cavity is then filled with wax to make the contact moisture-proof.

Semiconductor Properties

Although the contact area is critical, probably the most important part of the rectifier is the semiconductor. Semiconductors are materials having a high electrical resistance, between that of metals and insulators, usually with a temperature coefficient of resistance different from that of metals. Semiconductors are much more sensitive to small amounts of impurities or imperfections in the crystal lattice than metals.

The addition of a fraction of a percent of certain other elements will lower the resistance of some semiconductors to that of poor metals. In this condition, good rectification can often be obtained by making small-area contact to the surface of the semiconductor with a suitable metal. It is thought that the difference in work function between the metal and semiconductor produces a potential barrier to the flow of electrons. This barrier drops slowly on the semiconductor side owing to the space charge effect of the unneutralized impurity ions present in the semiconductor, and practically stops the flow of electrons from the metal to the semiconductor under any conditions. However, the electrons can flow from the semiconductor if the electronic potential of the semiconductor is raised enough to allow the electrons to pass over the barrier. This also requires

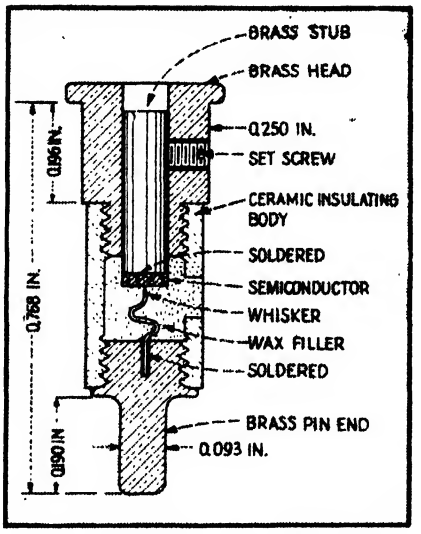

Fig. 1—Cross-section of a typical crystal rectifier. The dimensions are approximate

that appreciable voltage drop occur at the semiconductor contact, which is achieved by making the contact area small and producing a spreading resistance in the semiconductor. Consequently, the barrier will allow current to pass in one direction and not in the other, as shown in Fig. 2. Similar effects occur at the back surface of the silicon. For good rectification, the contact area at the back surface must be large in order to eliminate any spreading resistance over which a potential drop can occur. This approximate description of the rectifying action indicates that a major part of the art of crystal rectifier production lies in the preparation of the semiconductor and its surface. Two typical curves of the current-voltage characteristic at low frequency for a properly prepared crystal are shown in Fig. 3.

This work was done in part under contract OEMsr-888 between the Trustees of the University of Pennsylvania and the Office of Scientific Research and Development, which assumes no responsibility for the accuracy of the statements contained herein.

The primary attribute of the crystal rectifier which makes its use for microwave radar imperative is the small area of the region where rectification occurs. Very probably this region is smaller than 10^{-4} cm in thickness. Consequently, the time for electrons to cross this film will be small enough to eliminate transit-time effects, even at microwave frequencies. Furthermore, since these crystals have small capacitance in the contact, their rectifying properties are little affected by frequencies up to several megacycles.

So far there have been three main uses for crystal rectifiers—as detectors of microwaves, as mixers or converters of microwaves, and as higher-voltage low-frequency diodes. This classification is not profound, but serves to illustrate the different electrical characteristics required of the crystal types developed for these purposes.

As a detector, the crystal is connected between the receiving antenna and ground across the input to the video amplifier. Used in this fashion, microwave powers of the order of 10^{-7} watt picked up by the antenna can be detected. When smaller amounts of power are to be received, a local oscillator, usually producing 0.7 volt at 30 or 60 mc from the signal, is connected to the crystal. Then the two signals are mixed by the crystal and the converted intermediate frequency fed into the i-f amplifier. Used in this fashion, microwave signals as small as 10^{-15} watt can often be detected.

Crystals are also used at frequencies lower than those corresponding to microwaves. As a second detector, the crystal converts the intermediate frequency of 30 mc into d-c. This service requires crystals which will stand higher voltages than the normal limit of 1 or 2 volts. Other low-frequency uses include d-c restorers and voltmeter rectifiers.

Table I—Composition of Crystal Rectifiers

Bulk material	Impurities added: High-frequency mixer crystals	High-back voltage crystals	Low-frequency rectifiers
Silicon	Aluminum Boron	Germanium also Ni Sn Bi Ca	Aluminum Boron Germanium also Mo Ta Zr Co W Re Be Fe
Germanium	Antimony also P Fe	Tin also Ca Ni Sr Bi N	Antimony Tin
Galena	Unknown	None known	Unknown
Iron pyrites	Unknown	None known	Unknown

Preparation of Crystals

Most present-day crystals are made from silicon which is initially prepared in a very pure form by crystallization at a high temperature from silicon tetrachloride. The resulting needles are melted in a quartz crucible in a good vacuum (10^{-5} mm Hg) at about 1,500 C with a small amount of the desired impurity added to the melt, as indicated in Table I. After slowly cooling from the bottom the melt is cracked loose from the crucible and sawed into slabs about 1 mm thick. Both sides of the slab are rough-ground flat. One side is finished with fine carborundum and then polished with No. 000 emery paper to a mirror-like surface. The slab is then heated to about 1,050 C in air for several hours until a blue color appears, indicating the formation of a thin oxide layer. The unpolished side of the slab is next electroplated with nickel. The slab is broken or sawed into small pieces about 2 mm square. These small pieces are then soldered onto the brass stub (see Fig. 1), trimmed, and the oxide washed off the polished surface with hydrofluoric acid. The semiconductor is then ready for assembly.

Tungsten Catwhisker

The whisker is usually made from pure annealed tungsten wire of diameters up to 10 mils. The desired lengths are plated at one end with gold or other material suitable for soldering. The wire is next soldered into the pin and formed in the correct shape by a crimper. The point is sharpened by electrolytic polishing or by grinding on an Arkansas stone to a smooth cone of about 60 deg included angle. The whisker and silicon are then assembled in the cartridge. The set screw is tightened somewhat and the stub pushed in till the whisker makes contact with the semiconductor surface. This position is detected by continuously measuring the resistance between the ends of the crystal or watching the current-voltage curve on an oscilloscope. The stub is pushed in about a mil farther to compress the crimped

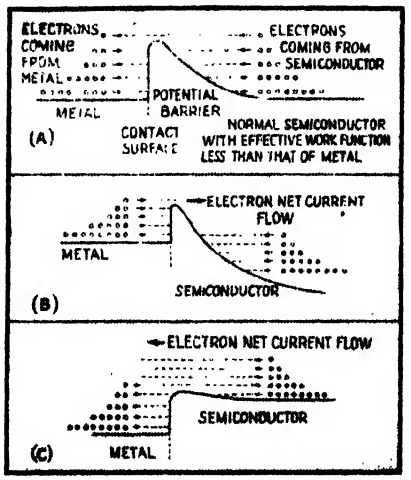

Fig. 2—Schematic diagram showing contact between metal and germanium semiconductor. In A, no voltage is applied, and hence the two electron flows are just equal. At B, the semiconductor has been made positive, lowering its electronic potential and decreasing electron current from the semiconductor, so that a slight net current flows. The semiconductor has been made negative at C, raising its electronic potential and increasing current from the semiconductor

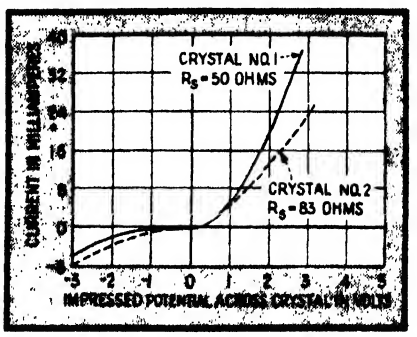

Fig. 3—Current-voltage curves for two different crystals

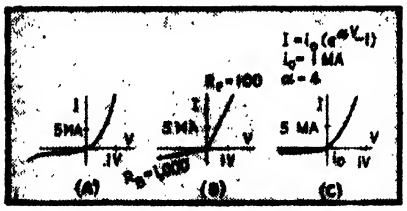

Fig. 4—The experimentally observed current-voltage curve at A agrees reasonably well with the curve deduced from front and back resistance constant at B and that from diode theory at C

wire and make firm contact. The cartridge is usually tapped to stabilize the contact. Then the cavity in the ceramic body is vacuum impregnated at elevated temperature with a mixture such as opal wax and paratac. Sometimes the hole is plugged up with alundum cement. The crystal cartridge is tested, labeled, and then packed in a metallic shield to protect it from picking up electric charges which might injure it. Care must always be taken in handling a crystal to avoid any appreciable discharge through it.

In describing the electrical characteristics of crystals we shall refer mainly to rectifiers made from silicon doped with aluminum and/or boron and prepared as described above. Other techniques and materials can be used, but most crystals are at present made in this fashion.

The d-c rectification curve in Fig. 3 shows that the difference between the resistance in the front and back direction is a measure of ability to rectify, and the back-to-front ratio was an early criterion of a good rectifier. The ratio of back resistance at 1 v to the front resistance at 0.3 v is greater than ten to one for a good crystal. The rectification curve can be well approximated by a simple formula with two constants:

$$i = i_0(\epsilon^{\alpha V} - 1)$$

where i is the instantaneous current and V the instantaneous voltage across the contact, i_0 and α being constants. The value of α varies from 2 to 20 volts^{-1} in ordinary crystals although it has been observed larger; i_0 is of the order of milliamperes, but varies from crystal to crystal.

Figure 4 shows typical approximations compared to a typical observed current-voltage curve. At low frequencies the rectification depends primarily on α. Actually, for appreciable current carried in the forward direction the applied voltage does not all appear across the contact. A voltage drop occurs across the spreading resistance owing to the small size of the contact to the semiconductor (this is evident from Fig. 3), and the fact that the semiconductors do not have as high a conductivity as metals. This spreading resistance R_s varies from 5 to 100 ohms depending on the diameter of the whisker and, consequently, necessitates a correction $(V_{\text{applied}} - iR_s)$ to the voltage across the contact. The slope of the current-voltage curve at zero bias is the low-level or video resistance and varies from several thousand to fifty thousand ohms.

Temperature Variations

These resistances vary appreciably with temperature. In fact, the low-level or zero-bias resistance varies exponentially with the reciprocal of the temperature. This variation is essentially the same as that of a thermistor. This is because of the change with temperature of i_0 which can be expressed as $i_0\epsilon^{-\phi/kT}$ where ϕ is an effective barrier height in electron volts and kT is the thermal energy in electron volts. (At room temperature kT is 1/40 e-v). The value of ϕ is usually between 0.1 and 0.4 e-v and $k = 8.6 \times 10^{-5}$ e-v per degree Kelvin.

The curve in Fig. 5A shows the calculated variation of the low-level or zero-bias resistance with temperature of a typical crystal. The only practical way found so far to reduce this variation is to control the crystal temperature. A reduction in ϕ which will reduce the temperature coefficient of resistance also decreases the sensitivity of the crystal as a detector.

The front and back resistances and spreading resistance do not vary as rapidly with temperature as the low-level resistance. Typical variations of front and back resistance are +20 percent at −20 C and −40 percent at +70 C from the room temperature value 22 C.

Square-law rectification is to be expected of any rectifier as long as the voltage swing is limited to the region where departure from linearity of the characteristic curve is small. Most crystals show square-law rectification up to powers of the order of several microwatts or voltages of the order of 0.1 v. Below this level, the short-circuit rectified current i_{d-c} is directly proportional to the input a-c power, in the relation:

$$i_{d-c} = SP_{a-c}$$

where S (Fig. 5B) is the sensitivity. This low-frequency sensitivity is greater than 2 for good crystals. Actually, at low frequencies, S should be one-half of α.

As the power level is increased above microwatts, the rectified current becomes more nearly proportional to the square root of the input power. If the load resistance is not small, the crystal will bias itself and reduce the rectification. As rectified currents of milliamperes are reached, the voltages increase to the order of whole volts and the resistance in the back direction may start decreasing. This puts a limit on the amount of input power which can be used without saturation of rectification. Fur-

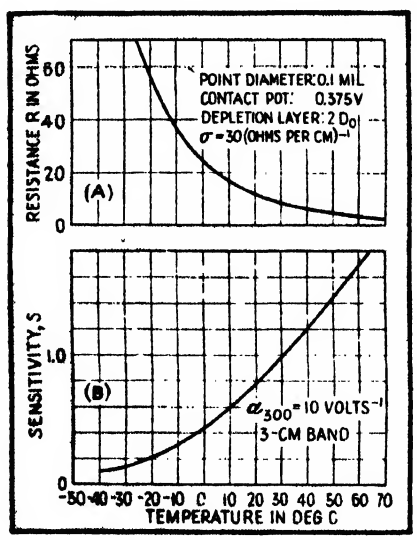

Fig. 5—Variation of resistance (A) and sensitivity (B) of a representative crystal with temperature

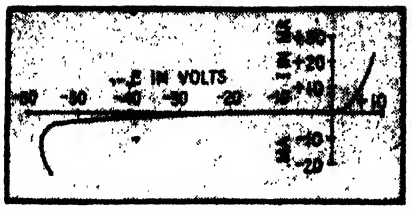

Fig. 6—The typical d-c characteristic curve of a high-back-voltage silicon crystal

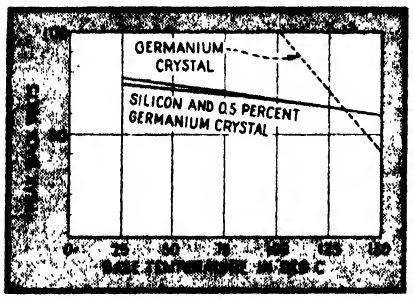

Fig. 7—A comparison of peak back voltage as a function of base temperature for two crystals of different composition

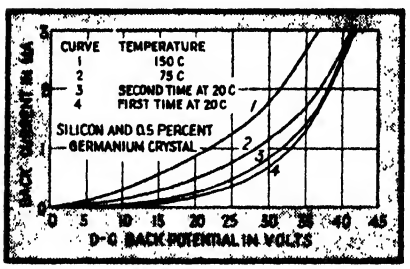

Fig. 8—D-c back voltage characteristic curves at different temperatures for the silicon crystal shown in Fig. 7

ther increase of voltage may damage the crystal. In fact, voltages of the order of 4 v or rectified currents of greater than 30 ma will damage the more sensitive types of crystals.

High-Back-Voltage Crystals

When certain impurities are added, both germanium and silicon have been found to withstand large voltages in the back direction. A typical curve is shown in Fig. 6. In general, hbv germanium gives much better back-to-front ratios than have been found so far with hbv silicon. Consequently, most high back voltage crystals are at present made from germanium. Silicon, on the other hand, shows promise for temperature-insensitive and frequency-insensitive high-back-voltage crystals. Silicon has much better rectifying properties at microwaves and less variation of back resistance and peak back voltage with temperature than most hbv germanium. A typical variation of peak back voltage with temperature is shown in Fig. 7. The variation of back current with temperature is shown in Fig. 8.

These hbv crystals are in many cases better for rectifiers than diodes such as the type 6H6. For several volts of 60-cps input, hbv crystals give more rectified current than a 6H6 with both plates in parallel. The change in rectified current as the frequency is increased to 30 mc is shown in Fig. 9A. The variation of rectified current with temperature is shown in Fig. 9B. Germanium hbv crystals still in development have better low-level rectification and give larger currents in the forward direction.

Noise

By careful control of manufacture, the noise generated by crystals has

Table II. Crystal Characteristics

	Mixer Crystals				
	Least sensitive	Medium sensitivity	More sensitive	Most sensitive	High burnout
30				*L*	*1N25** Less than 8.0 db
				t	Less than 2.5 *x*
				NF_r	Less than 13.4 db
				B_p	7 w d-c
				B_d	26 w d-c
10	1N21 (obsolete)	1N21A	1N21B*	1N21C	1N28*
	L Less than 8.5 db	Less than 7.5 db	Less than 6.5 db	Less than 5.5 db	Less than 7 db
	t Less than 4 *x*	Less than 3 *x*	Less than 2 *x*	Less than 1.5 *x*	Less than 2 *x*
	NF_r Less than 15.5 db	Less than 13.5 db	Less than 11.3 db	Less than 9.5 db	Less than 11.8 db
	B_p	0.3 erg	2 ergs	2 ergs	5 ergs
3	1N23	1N23A	1N23B*		
	L Less than 10 db	Less than 8 db	Less than 6.5 db		
	t Less than 3 *x*	Less than 2.7 *x*	Less than 2.7 *x*		
	NF_r Less than 16.0 db	Less than 13.7 db	Less than 12.2 db		
	B_p 0.3 erg	1.0 erg	0.3 erg		
1	1N24 (obsolete)	1N26* coax-shielded cartridge			
	L Less than 14 db	Less than 8.5 db			
	t	Less than 2.5 *x*			
	NF_r	Less than 13.9 db			
	B_p	0.1 erg			

L: loss
t: noise temperature
B_p: burnout proof test
B_d: burnout design test
NF_r: noise figure of receiver (3 db receiver)
* Army-Navy preferred list
A and B crystals are physically interchangeable

High-Back-Voltage Crystals		
Second detector crystal pigtail cartridge	d-c restorer (r-f) crystal pigtail cartridge	d-c restorer crystal pigtail cartridge
W. E. D171561	W. E. D171612	W. E. D172925

been greatly reduced. In many cases, the i-f noise observed from a crystal used as a mixer is no more than that experienced from a resistance of equivalent magnitude. However, crystals often give more noise than would be expected from thermal agitation and shot effect. This has been designated extra noise, and is observed when either d-c or r-f voltage is imposed on the crystal.

The spectrum of this extra noise is not uniform in the manner of thermal agitation. Much more low-frequency noise is observed than that at high frequencies, varying inversely with frequency from 50 cps to 1 mc, when it tapers off and approaches thermal agitation noise. Consequently, at an i-f of 30 mc the noise is not bothersome, whereas for i-f values in the audio range the extra noise from the crystal is very large.

High-Frequency Operation

At high frequencies, the capacitance across the blocking layer (barrier) becomes important because it can bypass the barrier if its impedance becomes less than the resistance of the barrier, as indicated in Fig. 10. This happens first in the back direction and reduces the back-to-front ratio. The high-level rectification efficiency is then measured by the ratio of the back resistance (shunted by the capacitance) to the front resistance. This begins to decrease when $1/\omega C$ becomes less than R_b. The value of C has been measured at about 0.2 $\mu\mu$f so that $1/\omega C$ becomes less than 1,000 ohms at a frequency of 1,000 mc.

Figure 11 shows the decrease in rectification efficiency with decrease of wavelength (increase in frequency) for two early crystals. The

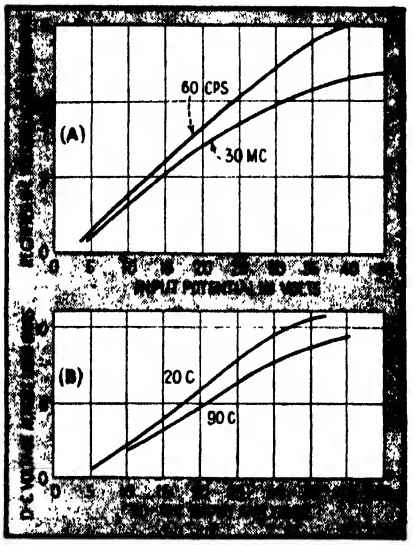

Fig. 9—Rectified d-c from a high-back-voltage silicon crystal as a function of input voltage as affected by frequency (A) and temperature (B)

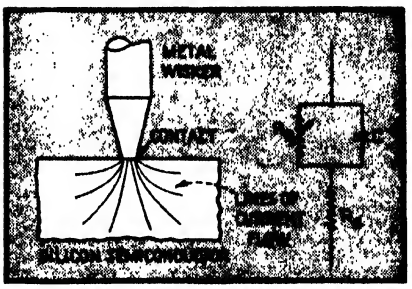

Fig. 10—Lumped parameter circuit to approximate crystal contact. R_s and C are resistance and capacitance of the contact and R_s is the spreading resistance in the semiconductor caused by small area of contact

According to Wavelength Used

High-Back-Voltage Crystals

E_1 more than 5 v E_2 more than 0.10 v E_3 more than 15 mv V_b more than 50 v	E_1 more than 15 mv R_b more than 0.1 meg (− 1 v) V_b more than 50 v R_{30} more than 2,000 ohms	E_1 more than 15 mv R_b more than 0.06 meg (− 50 v) More than 0.25 meg (− 5 v) I_F more than 5 ma (+ 1 v) R_{30} more than 2,000 ohms

Video Crystals

cm				Medium high burnout
30		1N29 L_{10} less than 8.0 db R_{d-c} greater than 6,500 ohms at 40 mv		
10	M R_{d-c} B_d	1N27 Greater than 60 0 to 4,000 ohms	1N32* Greater than 100 5,000 to 20,000 ohms 0.3 w d-c	1N33 Greater than 30 but less than 140 2,000 to 10,000 ohms 2.5 w d-c
3	M R_{d-c}	1N30 Greater than 55 7,000 to 21,000 ohms	1N31* Coax-shielded cartridge Greater than 55 6,000 to 23,000 ohms 0.02 w d-c	M: figure of merit R_{d-c}: d-c resistance at + 5 mv

Crystal diode pigtail cartridge

1N34
V_r less than 10 v
I_F less than 5 ma (+ 1 v)
R_b less than 0.025 meg (− 50 v)
R_b less than 0.2 meg (− 10 v)
V_b less than 50 v

Instrument Rectifier

1N22

Sylvania	W. E.
R_b more than 2,000 ohms	L less than 10 db
R_F less than 60 ohms	l less than 6 x
I_{10} more than 0.45 ma	I_{10} more than 0.4 ma
I_1 more than 0.4 ma	
B_p 0.3 erg	B_p 0.3 erg

E_1 : d-c output voltage with 24.7 v peak 30-mc input
E_2 : a-c output voltage with 24.7 v peak 30-mc modulated 0.92 v peak as input
E_3 : d-c output voltage with 0.5 v peak 30-mc input
V_r : d-c voltage at the output with 30 v rms 60-cps input; (the capacitor is omitted and the load resistance is 500 instead of 1,000 ohms)
V_b : peak back voltage the crystal is required to stand
R_b : static d-c resistance at the back voltage indicated
R_{30} : impedance at 30 mc
I_F : d-c in the forward direction at the voltage indicated

crystal with the larger capacitance shows a faster drop in rectification efficiency. Newer crystals have better rectification efficiencies than are shown in these examples.

A corresponding decrease in efficiency occurs in mixer performance and low-level detection. In general, the lower the contact capacitance, the better the high-frequency performance. Consequently, except for problems of r-f and i-f match, a crystal good at high frequency is also good at lower frequencies.

Low-level sensitivity drops even faster with increasing frequency than mixer performance or rectification efficiency. Whereas rectification efficiency might be expected to vary roughly as $1/(1 + R_s\omega C)$, low-level sensitivity should drop as

$$1/(1 + \omega^2 C^2 R_s R_s).$$

Actually, in many cases, crystal performance does not decrease as fast as expected with frequency.

The stability of present-day crystals is well displayed by the mechanical, electrical, and exposure tests which production samples are required to stand.

The mechanical design test involves dropping the crystal three times from a height of 30 in. onto a wood block, twisting the crystal ends with a torque of 1.5 in.-lb so as to unscrew the parts, and applying a force of one pound to the tip of the crystal at right angles to the axis of the crystal while the head is clamped. A crystal must withstand immersion in warm water for fifteen minutes, in room-temperature water for fifteen minutes, and several cycles of heating and cooling between 70C and −40 C. The electrical burnout tests are described below. After being subjected to all of these tests the performance of 80 percent of the samples is required to be within specified limits, but 90 percent of the samples must be within the limits after any single design test.

There are two types of burnout tests intended only to indicate rough differences in ability to withstand overloading and to ensure production quality. The first consists in discharging a charged concentric line through the crystal. By this means, a pulse of approximately three microseconds width is sent through the crystal. This time is determined by the length of the line and is chosen to be shorter than the time constant for heat dissipation of the crystal contact. The energy contained in this pulse is determined by the capaci-

Table III. Results of

VIDEO OR LOW LEVEL CRYSTALS

RMA No.	Description and band in mc	Test freq in mc	Test holder	Maximum test power in milliwatts	Minimum figure of merit	Range of video resistance in ohms	Burnout test
1N27	For pulse discrimination 10	3,295	Rad. Lab. drawing B3424 tunable	5	60	0 to 4,000	
1N29	Special use 30	10 cm	1N21 type	Same as 10 cm mixers	Conversion loss at 10 cm 8 db max	6,500 min at + 40 mv	
1N30	Original 3	9,375	TPX—56GM tunable	5	55	7,000 to 21,000	Proof test 0.3 erg
1N31	Improved stability 3	9,375	Rad. Lab. drawing B7389 fixed tune	5	55	6,000 to 23,000	Design test 0.02 w d-c 1-μsec pulse
1N32	Improved sensitivity 10	3,295	Rad. Lab. drawing B7389 fixed tune	5	100	5,000 to 20,000	Design test 0.03 w d-c 1-μsec pulse
1N33	Improved burnout 10	2,880	Hazeltine fixed tune	5	40 min 130 max	2,000 to 10,000	Design test 2.3 w d-c 1-μsec pulse

HIGH-BACK-VOLTAGE CRYSTALS

Western Electric No.	Description	Freq	Rectification in test circuit				60 cps conversion at high level		Peak back voltage min d-c	30 mc impedance in ohms	d-c resistance
			Low level		High level						
			In	Out min	In	Out min	In	Out min			
D171561	2nd detector	30 mc	0.5 v peak 30 mc	15 mv d-c	24.7v peak 30 mc	5 v d-c	0.92 v peak 60 cps modulation	0.10v 60 cps	50 v		
D171612	D-C restorer (r-f)	30 mc							50 v	2,000	0.1 meg at − 1 v
D172925	D-C restorer	30 mc								2,000	0.06 meg at − 50 v 0.25 meg at − 5 v

tance of the line and the voltage to which it is charged. If the voltage is very high, some dissipation of the pulse energy seems to be experienced when the contact is made for the discharge which simulates the spike which gets through the transmit-receive gas tube before it breaks down to protect the crystal from the transmitted radar pulse.

Another method of testing crystals for burnout consists in exposing the crystal to a d-c pulse of about one-microsecond width, obtained by discharging an artificial line through a thyratron into the crystal. A circuit for accomplishing this is shown in Fig. 12. Only a rough correlation exists between these methods of testing crystals for burnout because multiple pulses have more effect than single pulses and the method is less erratic. The match of the crystal to the pulsing circuit is important for reliable testing and in actual radar practice additional protection can often be afforded by r-f mismatch in the holder to overload pulses. Design tests which are given to samples of production crystals are also usually more stringent than the proof tests which are applied to every crystal produced.

Design Tests on Crystals

HIGH-BACK-VOLTAGE CRYSTALS

RMA No.									
1N34	Crystal diode	60 cps	30 v (rms) | 10 v d-c (500 ohms load resistance; no capacitor)					50 v	0.025 meg at − 50 v 0.2 meg at − 10 v

MIXER OR LOCAL OSCILLATOR DRIVEN CRYSTALS

RMA No.	Description and band in cm	Test freq in mc	Test holder	Test power level in milliwatts	Max Conversion loss in db	Min noise ratio	i-f impedance in ohms	Min rectified current ma	Burnout proof test in ergs
1N21	Obsolete 10	3,060	Bell Labs ES4	0.5	8.5	4 x	Approx 400		
1N21A	Standard 10	3,060		0.5	7.5	3 x			0.3
1N21B	Improved sensitivity and burnout 10	3,060		0.5	6.5	2 x		0.4	2.0
1N21C	Most sensitive 10	3,060		0.5	5.5	1.5 x			2.0
1N23	Standard 3	9,375	TPX-36GM	1 0	10	3 x	Approx 400		0.3
1N23A	Improved sensitivity	9,375		1.0		1.7 x	400		1.0
1N23B	Most sensitive 3	9,375		1.0	6.5	2.7 x	400		0.3
1N24	Obsolete	1-cm band	Mounted in wave guide		14				
1N25	High burnout 30	1,000		1.25 0.9	8	2 5 x	100 to 400		7 watts 1-μsec pulses
1N26	Coax-shielded cartridge 1	24,000	TPK-15 HU	1.0	8.5	2.5 x	300–600 measured at 3 cm	0.5	0 1
1N28	High burnout 10	3,060		0.4	7	2 x	Approx 250	0.4	5
1N22	Instrument rectifier at 10 or 3	Western Electric		10 cm	10	6 x		0.4	0.3
		Sylvania		3 cm			10 cm 3 cm	0.45 0.4	0.3

Crystal Types

Table II shows the present crystal types grouped in horizontal rows according to the wavelength band for which they are recommended. The grouping in vertical columns is according to use, sensitivity, and burnout. Mixer crystals are for use with local oscillators, whereas video crystals are for detector use. Table III gives test specifications.

The characteristics listed in the tables are further defined below. L is the loss in db of the crystal used as mixer.

$L = 10 \log_{10} l$ where l is the ratio of r-f signal power input to i-f power output. A perfect diode might be expected to have an efficiency of 50 percent ($l = 2$) or $L = 3$ db.

The noise temperature t of the crystal is the ratio of the average of the square of the noise voltage produced by the crystal to the thermal agitation or Johnson noise voltage squared of a resistance equal to the i-f impedance of the crystal.

$$t = \frac{V_c^2}{V_r^2} = \frac{V_c^2}{RW(1.6 \times 10^{-20})}$$

where R is the i-f impedance and W is the integrated bandwidth of the mixer and amplifier, V_c is the crystal noise, and V_r the noise voltage from

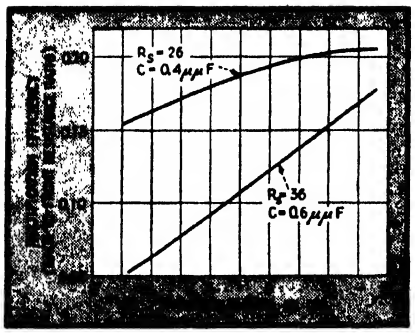

Fig. 11—Rectification efficiency (back-to-front resistance ratio) of two different crystals as a function of wavelength. The lower curve shows the effect of larger contact capacitance

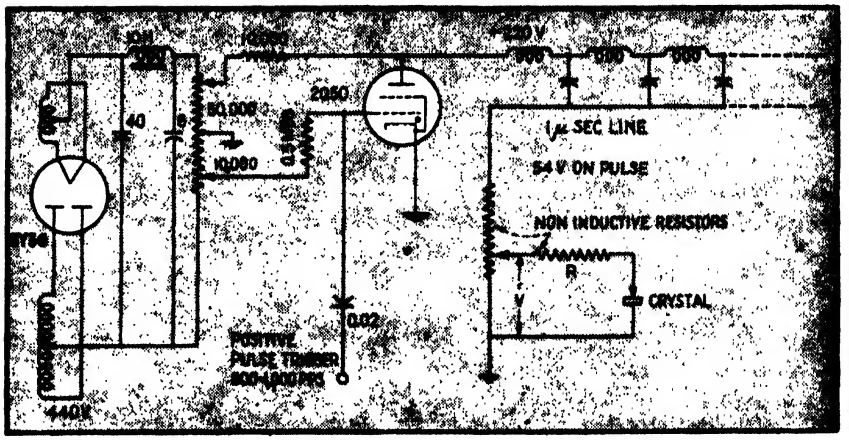

Fig. 12—The d-c pulser circuit used in the burnout tester

an equivalent resistance. The value of t is usually given as a ratio, and appears in the tables as $t = 2x$ where x indicates it is a ratio; a crystal would be considered perfect if t were equal to unity.

An overall criterion of performance is NF_r, the noise figure of the receiver, which gives the ratio of the average of the output noise voltage squared to the output signal voltage squared when the input signal power is just equal to the thermal agitation noise power

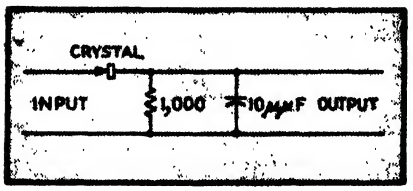

Fig. 13—Circuit used for measuring second detector characteristics

$$NF_r = l(NF_{1\text{-}t} + t - 1)$$

where all the terms are ratios. Assuming the noise figure of the average amplifier $NF_{1\text{-}t} = 2x$ (or 3 db), then in db, $NF_r = 10 \log_{10}[l(t+1)]$ where l and t are ratios. The best NF_r of a perfect diode would be 6 db for a 3-db receiver, with image matched. The noise figure in db of the crystal by itself (NF_c) can be expressed as

$$NF_c = 10 \log_{10}(tl)$$

where t and l are ratios.

The video impedance $R_{d\text{-}c}$ is measured at 5 mv in the forward direction. M is the figure of merit of a crystal as used for the input to a video amplifier. It is a measure of the output signal voltage V_0 to the output thermal agitation noise voltage V_N (background).

$$\frac{V_0}{V_N} = \frac{P_i R_{d-c}}{\sqrt{W}\ 1.26 \times 10^{-10} b \sqrt{R_{d-c} + r}} = \frac{P_i M}{1.26 \times 10^{-10} \sqrt{W}}$$

where $M = R_{d\text{-}c}/b(R_{d\text{-}c} + r)^{\frac{1}{2}}$, $i = SP$ (input r-f), P_i is r-f input power, and r is a fictitious series resistance of the grid of a first tube which would give a noise equivalent to the amplifier noise. An s equal to one is desirable and r is of the order of 1,200 ohms.

B_r and B_d are the proof and design burnout test required for the crystal. The number of ergs given is the energy in a spike or pulse of roughly 3 microseconds duration from a Torrey concentric line pulser used to proof test each crystal. The power in watts is the peak available (or matched) power in r-f or d-c microsecond pulses.

D-C AMPLIFIERS

Survey of D-C Amplifiers

Analysis of causes of drift in direct-current amplifiers, descriptions of methods used to neutralize or prevent drift, and typical industrial applications

By MAURICE ARTZT

THE quest for a stable d-c amplifier is an old one, and will probably continue as long as tube characteristics wander with changes in voltage and temperature. A rapidly expanding literature on the subject gives evidence that considerable progress has been made in overcoming drifts and instabilities usually associated with d-c amplifiers. As their advantages in certain applications become more apparent, still further progress is to be expected.

Causes of Drift

There are three primary causes of zero or steady-state drift in the usual d-c amplifier circuit. The first of these, and the one easiest to eliminate, is drift due to changes in the plate supply voltage. This can be balanced out by either of two methods: by complete regulation of the B supply, or by devising a tube circuit in which the plate current is exactly proportional to the B voltage. Where regulation of the B supply is the method chosen it can usually be carried to as high an accuracy as needed, though this results in a rather bulky unit.

The second method is to be preferred wherever possible, for it permits the use of an unregulated voltage supply. It can be readily seen that when the plate current of a tube is exactly proportional to the B voltage, then the voltage developed between the plate of this tube and a proper tap on a B supply bleeder will remain zero as the B voltage varies. A bridge balance is thus substituted for an accurately regulated source of plate power.

The other two causes of drift are directly related and result from changes in cathode temperature. The first of these—contact potential—is the most troublesome, and has an effect similar to a change in grid bias as cathode temperature changes. This same change in cathode temperature will also cause the equivalent plate impedance of the tube to vary. But these two characteristics do not change by a definitely fixed amount with cathode temperature. They both have rather large components interrelated with plate current and plate voltage.

Where the tube is used only in the center of its linear range, and excursions in plate current due to signals are small, then the R_p of the tube can be considered constant and the effect of these two variables lumped and treated as a shift in grid bias with cathode temperature. Where the operating conditions are not so limited, both must be considered. This is readily seen in the voltage-current equations of a tube.

It is usual to express the voltage-current equation of a tube as follows

$$i_p = \left[\frac{E_p + \mu E_g}{R_p}\right]^n \qquad (1)$$

For a limited operating range in the linear portion of the tube curves, the exponent n can be considered to be unity, and R_p can be considered as the slope of the E_p/i_p curve at this point. This is usually written then as

$$E_p = i_p R_p - \mu E_g \qquad (2)$$

The contact potential drift can then be added as a voltage V_f, varying with filament voltage, to give the expression

$$E_p = i_p R_p - \mu E_g + \mu V_f \qquad (3)$$

This equation can be used over a limited range in deriving the expression for overall performance of an amplifier, and will give a reasonably accurate indication of the drift to be expected as V_f changes. It is so used in deriving the balance conditions and gain equations for a number of the d-c amplifier systems described later.

That Eq. (3) cannot possibly hold over any large range of voltage variations is shown by the tube curves in Fig. 1. This set of curves was taken on one of the triodes in a 6SN7GT/G tube of average g_m. The curves are definitely moved to the left in the linear range by an increase in filament voltage, and this gives some weight to the use of the contact potential drift voltage

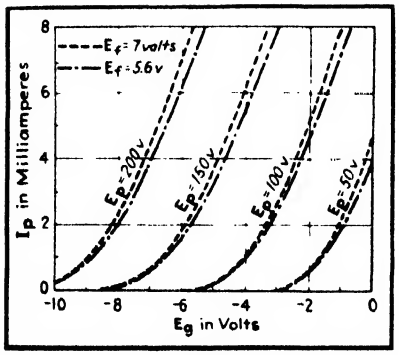

FIG. 1—Effect of filament voltage on characteristics of a 6SN7GT/G tube

V_f assumed in Eq. (3). But account is not taken of the fact that the slope of the curves also changes, for apparently R_p has decreased as E_f was increased. What has actually happened in Eq. (1) for this change in filament voltage is that the exponent n has changed, for the tangent point of intersection of the curves in Fig. 1 has not shifted appreciably. The two sets of curves become more nearly parallel at the higher values of I_p, so Eq. (3) becomes increasingly more accurate as I_p increases.

From these tube curves and equations it may be seen that while drifts due to B supply are a first-order effect, those due to cathode temperature are considerably more complicated, and greater care in design is necessary for their elimination.

The four general classifications of d-c amplifiers are (a) simple cascaded amplifiers, (b) modulation systems, (c) compensated d-c amplifiers, and (d) bridge-balanced d-c amplifiers. Each type will be briefly described in turn here.

Simple Cascaded Amplifier

In the simple cascaded amplifier, succeeding stages are usually stepped up a B supply bleeder, or coupled with a potentiometer divider with consequent loss in gain. These are illustrated in Fig. 2(a) and 2(b) and, supplied with unregulated voltages, are notorious for drift. They are seldom used without some form of correcting or compensating system.

One form of drift control can be obtained by adding 100-percent degenerative feedback to obtain a current amplifier with unity voltage gain. This circuit is so applied in a commercial sensitive microammeter.[1]

The circuit in Fig. 2(b) has been used in various ways with feedback[2] and with correction for the loss in voltage gain,[3, 4] but in either case careful regulation of plate and filament supplies is required to eliminate drift.

Modulation Systems

While modulation systems are not strictly d-c amplifiers, they are so used in many applications and have considerable merit. In this type the d-c signal to be amplified modulates a carrier wave, and after sufficient amplification the wave is detected to obtain the amplified signal. Such systems are well known and the literature is fairly complete.[5, 6, 7]

Where the required frequency response is very high, these systems become awkward because the high carrier frequency requires elaborate shielding. It is therefore more limited in its applications than the two types that follow.

In a modified form, the input signal itself is chopped. This can be done by a light shutter for phototube amplifiers, or by vibrators or tubes for other types of signals.[8]

In compensated d-c amplifiers some variable characteristic of the amplifying tube is balanced against the same variations in another tube,

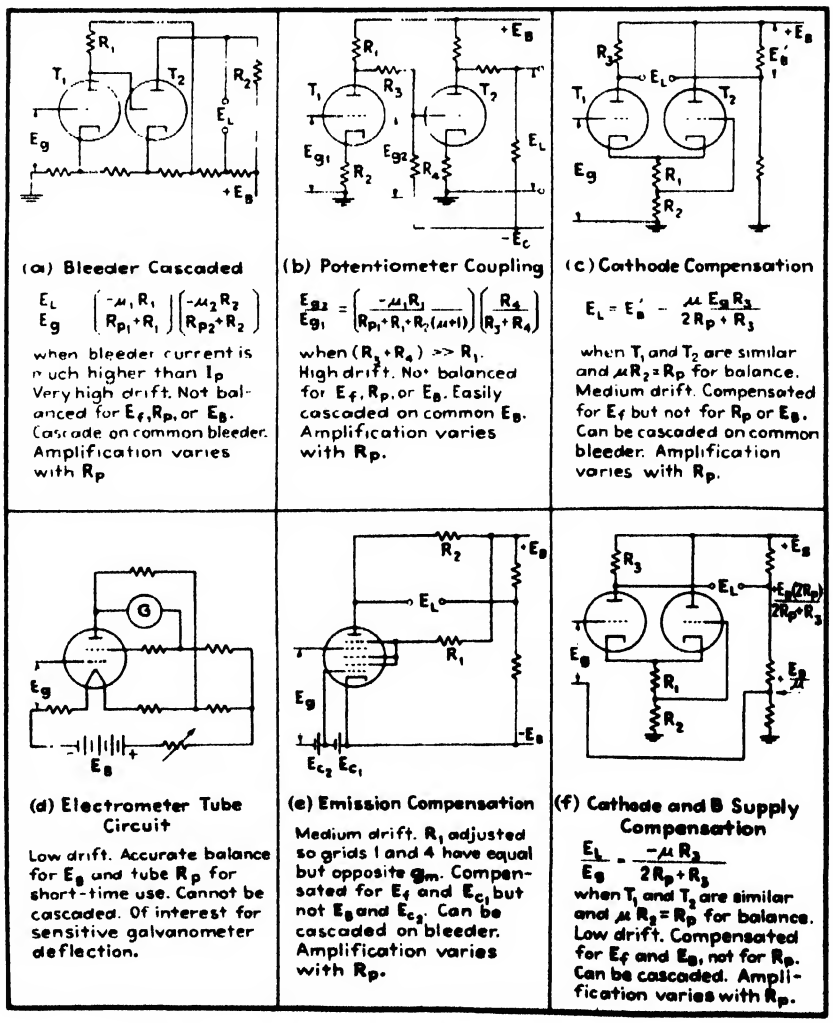

FIG. 2—Fundamental and compensated d-c amplifier circuits

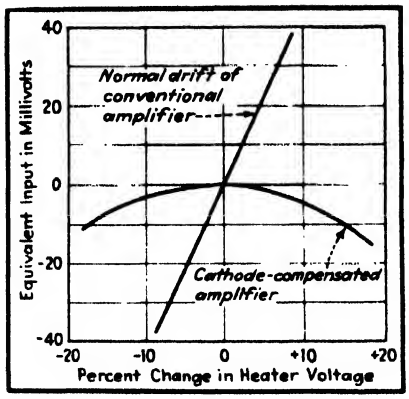

FIG. 3—Characteristic of cathode-compensated d-c amplifier circuit shown in Fig. 2 (c)

or against a different characteristic of the same tube. This system compensates for contact potential drift in the cathode-coupled amplifier system, as illustrated in Fig. 2(c).[9, 10, 11, 12, 13] When used with an accurately regulated power source a stable system results.

Compensated D-C Amplifiers

This cathode-compensated amplifier can be considerably improved and still greater freedom from drift obtained if the input voltage includes a tap on the B supply bleeder at the value of E_B/μ, as shown in Fig. 2(f). This addition makes the zero-signal output current directly proportional to plate voltage. When the output is then returned to the proper point on the bleeder, the effect of changing E_B is eliminated, and the plate supply need not be regulated.

The drift characteristic of amplifiers of this type as compared to a conventional amplifier is shown in Fig. 3. The balance obtained is a tangential one, and holds over only a limited range of filament supply variation. For this reason, even with E_B compensation as in Fig. 2(f), only a limited supply voltage change can be allowed if resetting of the zero point is to be avoided.

By a fortunate choice of constants this compensation for filament and plate voltage can be obtained in the amplifying tube itself, as in the electrometer tube circuits.[14, 15] One form of this circuit is shown in Fig. 2(d). As this circuit cannot be readily cascaded, it is chiefly of interest for use with a sensitive galvanometer.

Compensation for changes in emission, whether due to heater voltage change or to a random effect, can be obtained in a pentagrid type of tube as shown in Fig. 2(e)[16]. Here the value of R_1 is adjusted to make grids 1 and 4 have equal but opposite transconductance to the plate, and the compensation therefore includes all circuit elements common to both grids, but does not include the plate supply. In this circuit, as in the cathode-compensated circuits, with the two control grids having equal but opposite effects on the plate current, signals can be applied to either grid, or to both at the same time to obtain a differential amplifier. If grid 4 in Fig. 2(e) is returned to a tap on a bleeder across the plate supply, correction for changes in E_B will be obtained in a manner similar to that applied to the circuit in Fig. 2(f).

While this brief resume of compensating systems is not complete, it includes the better known methods and will serve to illustrate how compensation for filament supply can be obtained, and show that compensation for plate supply can usually be added for increased stability.

A distinction is made between compensated and bridge-balanced d-c amplifiers, for in bridge-balanced circuits all variables in the

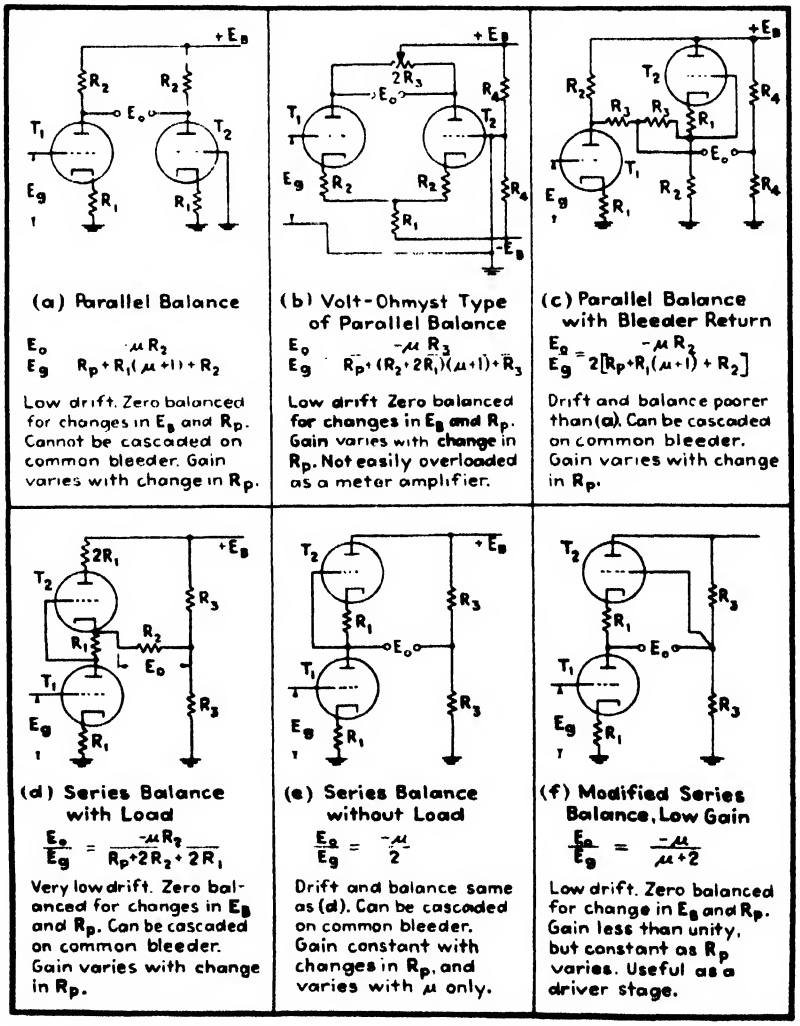

FIG. 4—Fundamental circuits of balanced d-c amplifiers

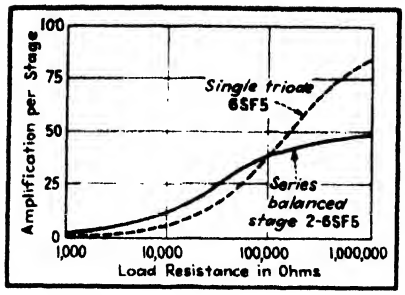

FIG. 5—Variation of amplification with load resistance for a single triode stage and a two-tube series-balanced stage. In both instances no bypass capacitor was used on the cathode bias resistor

changes, it has been found experimentally that such a balance is no more difficult to obtain than the balance for contact potential alone as used in the compensated circuits.

Bridge-Balanced D-C Amplifiers

The advantages of this type of balance are that regulation of plate and filament supplies becomes unnecessary except where extreme precision is required, and the balance holds for any part of the tube curves. Operation becomes less critical and more consistent.

The conventional type of balanced d-c amplifier is shown in Fig. 4(a). It is the equivalent of returning the output voltage to a bleeder in which the bleeder proportioning changes in the same manner as the amplifying tube. This type of amplifier will balance perfectly if the two tubes remain identical in characteristics as supply voltages change. It is often used in tube voltmeter circuits.[17]

A modification of this circuit, in Fig. 4(b), is found in the well-known Volt-Ohmyst circuit for voltage and resistance measurements.[18] While having some of the features of the cathode-coupled circuits, the main balance is still between the two tubes in parallel, with the common coupling resistor R_1 assisting in maintaining a constant zero position.

Neither of these two circuits can be cascaded as shown, and both are most useful as meter amplifiers, etc. Where higher gain is required than one stage will give, the circuit in Fig. 4(a) can be modified to that in Fig. 4(c) to allow cascading. The output then is returned to the B supply bleeder and additional stages can be stepped up the bleeder in the usual manner. In this case the gain per stage has been cut in half from that of the circuit in Fig. 4(a), and the high-frequency response has been impaired by the high value of series resistors R_s that feed the output. For proper balance the circuit requires that four pairs of resistors as well as the tubes remain constant and it will therefore have slightly more drift than the circuit of Fig. 4(c) under similar conditions.

These disadvantages in Fig. 4(c) can be eliminated and several important advantages gained by shifting T_s and its cathode resistor over to replace the plate resistor for T_1 as shown in Fig. 4(d) and 4(e).[19] Here the balance is no longer for tubes in parallel, but rather in series, and both pass the same plate current at the zero-signal position. The balance for changes in E_s and R_p is more nearly perfect than in Fig. 4(a), 4(b), and 4(c). A differential change in contact potential between the two tubes will shift the zero position as in any other balanced arrangement, but with the same plate current in each tube this effect is much less pronounced than in the parallel systems.

If the value of load resistor R_s

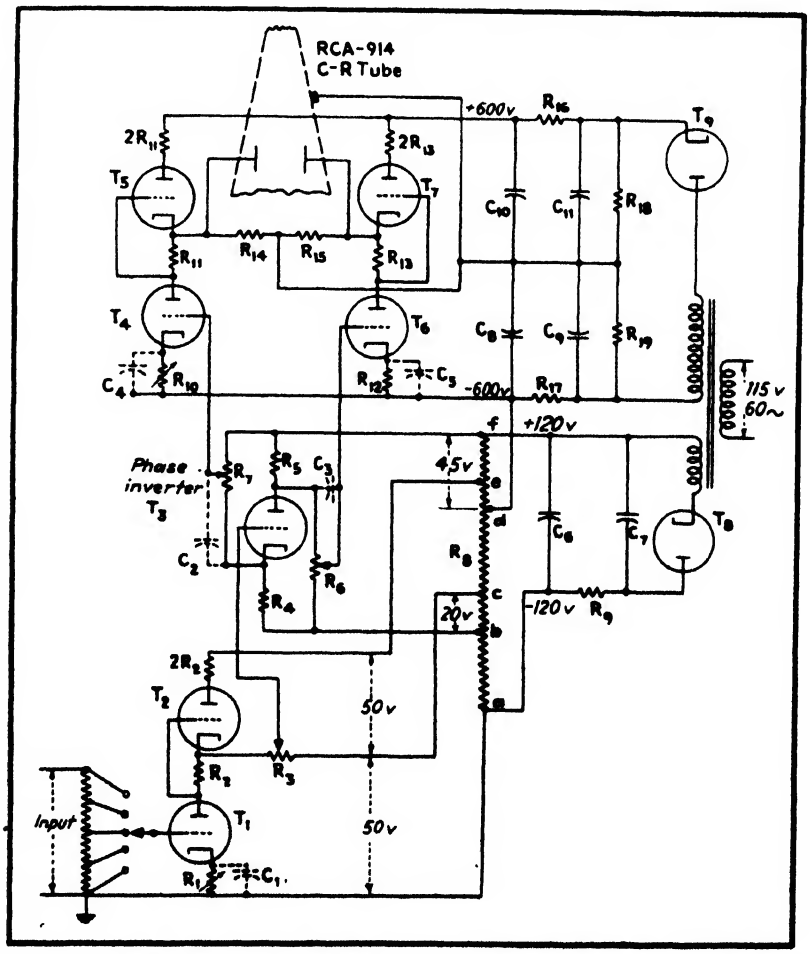

FIG. 6—Series-balanced d-c amplifier circuit arranged for feeding a pair of deflecting electrodes in a cathode-ray tube of an oscilloscope

is low, somewhat higher amplification will be obtained with the circuit in Fig. 4(d) than with the simplified version in Fig. 4(e). In Fig. 4(d) the load current flows through the cathode resistor of T_2 in a regenerative direction. However, for all practical purposes, if a load resistor equal to or greater than the R_p of the tubes is used, there is little difference and the simpler arrangement of Fig. 4(e) with its fewer parts is preferred.

In both Fig. 4(d) and 4(e) the cathode resistor of T_1 is usually made variable as a balance adjustment. The range of adjustment is purposely made small, ±15 percent from the value of the cathode resistor of the upper tube. Under these conditions it has been found that if R_1 can be set within this range so that $E_o = 0$ with no input to the grid of T_1, the two tubes are sufficiently well matched for all practical purposes, and hold this balance over very wide changes of filament and plate voltages. When properly balanced in this manner a sensitive voltmeter can be connected across E_o and will show no deflection even when the line voltage supplying filament and plate power is switched off and on.

A third arrangement of the series-balanced system is shown in Fig. 4(f). Here the upper grid is returned to the bleeder instead of to the plate of T_1, and the voltage gain is reduced to slightly less than unity. This is useful as a current amplifier for meters, or as a driver phase inverter. The inverter stage obtains its plate power from the bleeder on a second d-c source of 120 volts, again unregulated and half-wave rectified. The input stage, employing 6SF5 tubes for T_1 and T_2, draws plate power from the same low-voltage bleeder that feeds the phase inverter. This bleeder is 10,000 ohms and has fixed taps providing the voltages shown. No bypassing is used between any taps on the bleeder. This prevents any one section from having a different time delay on build-up or decay with a changing line voltage. Half-wave rectifying for the two power supplies is possible because all hum is balanced out for the zero-signal condition, and rises to only a few percent when sweeping a nine-inch screen.

The process of balancing the amplifier is simple, and the cathode-ray tube itself is used as the indicator. The two load resistors, R_{14} and R_{15}, are shorted, and the zero position of the cathode-ray spot is marked. The grid of T_4 is then shorted to minus 600 volts and the short on R_{14} removed. R_{10} is adjusted to bring the spot back to its zero position. Then the grid of T_5 is shorted to minus 600 volts, the short on R_{15} removed, and R_{12} adjusted to recenter the spot.

The output stage is now balanced and the phase inverter can be adjusted. Short R_2 so the inverter has zero input, remove the short between the grid of T_4 and minus 600 volts, and adjust R_7 to center the spot, then remove the short on the grid of T_5 and adjust R_6 to again center the spot. Now with the input control at zero, the short across R_2 can be removed and R_1 finally adjusted to center the spot again. The entire amplifier is now balanced and ready for use.

The amplifier as described will have a flat response from pure direct current to over 20,000 cycles. By the addition of the five capacitors shown in dotted lines, the upper limit is raised to over 100,000 cycles. The values of these are determined by the circuit constants and the various capacitances to ground.

In use this amplifier shows remarkable stability of image, there being no breathing with widely changing line voltages, and no capacitance couplings to cause transients that jump the image off the screen on change of input. Turning off the power and later turning it on causes the image to fade out and then fade in without appreciably changing location on the screen.

It has been found that with the oscilloscope in daily use for many hours at a time any readjustment of balance was unnecessary for

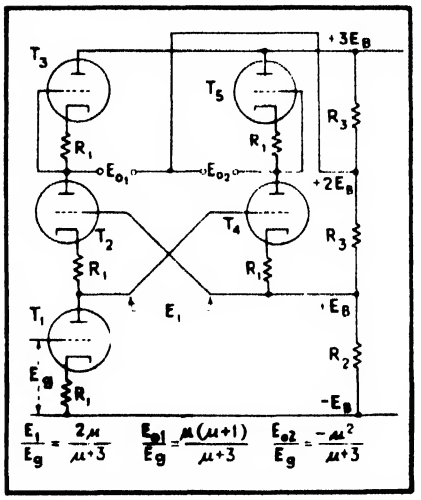

FIG. 7—Circuit illustrating use of the modified series-balanced low-gain driver stage of Fig. 4 (f) to obtain push-pull output from single-ended input

periods of six months or more, and the spot position over this time and from cold to hot never varied over 0.1 inch. As the deflection sensitivity is approximately 0.1 volt per inch, this shows an overall long-time drift of not over 10 millivolts as referred to the input. When it is considered that ordinary tubes and resistors are used and that neither plate nor filament supplies are regulated, this performance becomes remarkable.

Push-Pull Driver for Oscilloscope

A second type of deflection amplifier was built with the stage shown in Fig. 4(f) as a push-pull driver. The method of obtaining push-pull from this driver is shown in detail in Fig. 7 Here the driver tube T_1 passes the full plate current of that side of the output having tubes T_3 and T_4 in series. As the grid of T_3 is connected to the B supply bleeder, it forms a cathode drive for T_3. At the same time the second half of the output stage has the lower cathode returned to the bleeder and the lower grid is driven by T_1. Thus T_3 and T_4 are driven in opposite phase to obtain push-pull output. While the balance of zero position is correct with this type of drive, the two output voltages E_{o1} and E_{o2} are not quite the same, but differ by the ratio of $(\mu + 1)/\mu$. However, this

is not serious, as it amounts to only three percent with 6SH7 tubes as triodes in the output stage. This is as close to a true balanced push-pull as is ordinarily obtained in any circuit unless the tubes are especially picked.

The complete deflection amplifier with this drive system is shown in Fig. 8. This second system has the advantage over the first that the two plate power sources are connected plus to minus rather than at an intermediate point as in Fig. 6. Thus both upper and lower supplies can be obtained from a single power transformer winding. In addition the driver stage has nearly unity gain, rather than a 2 to 1 loss as in the phase inverter, so additional sensitivity can be obtained.

This amplifier was built with 6SJ7 tubes for T_1 and T_2 and 6SH7 tubes for T_3, T_4, T_5, T_6, and T_7. All were connected as triodes with suppressor and shell connected to cathode, and screen to plate. The four bleeder voltages *ab*, *bc*, *cd*, and *de* are equal, and in this case 300 volts each. The three capacitors shown dotted bring the flat response up to 250,000 cycles, with a slow drop-off above this. The amplifier is usable at 500,000 cycles with about fifty percent of the deflection at zero frequency or direct current.

Comparison of Oscilloscope Circuits

The balance conditions obtained with the circuit of Fig. 8 are not quite as good as in the first method because tube T_3 must balance through T_6 and T_7 in series, but the spot is still within 0.2 inch of its cold position after an eight-hour run. The deflection sensitivity is less than for Fig. 6, as tubes with a lower μ are used to get better high-frequency response.

One precaution is necessary here that was unnecessary with the first amplifier; namely, adjustment of the time constants of the two power supplies to be equal and thus prevent breathing with line voltage changes. As upper bleeder *cde* has the heavier tube load across it, the overall value of R_{11} and R_{12} must be somewhat less than the sum of R_{13}, R_{14}, and R_{15}. The value is easily determined by using a Variac in the supply line, and adding additional load from *a* to *c* until breathing is eliminated with sudden line changes. Once determined, a fixed load can be put across *a* to *c*, as amplifying arm, including tube characteristics and supply voltages, are balanced against similar variables in a second arm of the bridge. Thus if the parameters of the non-amplifying arm vary in the same manner as those in the amplifying arm, a complete balance for E_f, E_b, R_p and contact potential is obtained. While it may be argued that no two tubes will balance for all of these this is not critical and need not be made variable for future adjustments.

The drift performance of this amplifier with changes in line voltage is shown in Fig. 9 where the equivalent input in millivolts is plotted against the power line voltage. Between the line voltage limits of 105 to 140 volts this drift is only ± 2.5 millivolts, and represents a spot movement of ± 0.008 inch on the nine-inch screen. This is considerably better than is obtained with most a-c deflection amplifiers even with carefully regulated plate supplies.

Both of these deflection amplifiers are shown without the usual centering control. The resistor R_1 is used for centering in either case by throwing the amplifier off balance the required amount to move the zero position of the spot anywhere on the screen. This is an instantaneous movement and does not have the high time delay of motion obtained with the centering control on an a-c deflection amplifier.

In both amplifiers the second anode of the cathode-ray tube is above ground, by 375 volts in Fig. 6 and by 900 volts in Fig. 9. This voltage, therefore, adds to the usual high negative voltage supplying the cathode of the cathode-ray tube to give the total cathode-to-anode accelerating voltage. The reason for not grounding the second anode is, of course, to allow one side of the signal input to be grounded.

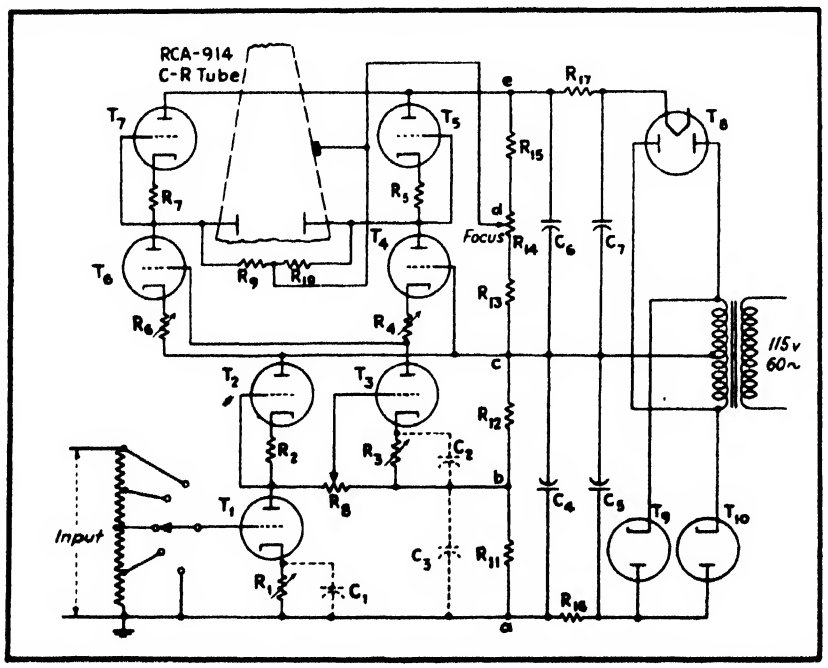

FIG. 8—Alternative method of using a series-balanced d-c amplifier for oscilloscope deflection

Photoelectric Light Meter

One interesting application of the series-balanced circuit should be noted. This is a light meter

that can be calibrated as an exposure meter or the like. The circuit in Fig. 10 is almost self-explanatory, for the two tubes are operated as in the other circuits described, but with a-c plate supply. The phototube is connected grid to grid to obtain additional amplification. The two grid resistors are equal and one megohm each, and the meter is one milliampere full scale. R_4 is 500 ohms and R_3 is 400 ohms fixed and 200 ohms variable.

With this arrangement and with an RCA 918 phototube, a full-scale deflection can be obtained with 0.1 lumen through a $\frac{1}{8}$-inch diameter aperture. Other scales can be provided by switching meter shunts, grid resistors, or apertures. As no transformers or rectifiers are used, a compact instrument results.

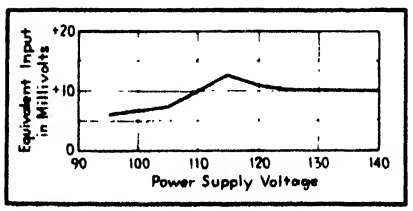

FIG. 9—Effect of variations in power supply voltage on drift in the oscilloscope deflection amplifier of Fig. 9

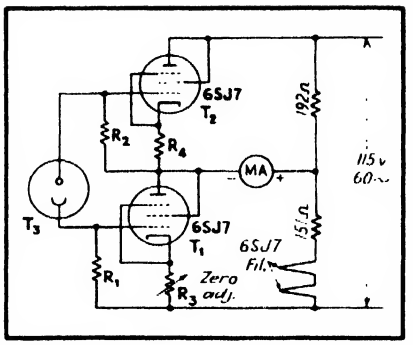

FIG. 10—Series-balanced amplifier used as a light meter

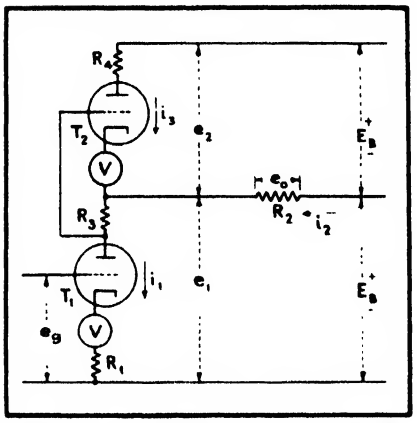

FIG. 11—Derivation of series-balanced conditions in an amplifier

REFERENCES

(1) RCA ultra-sensitive d-c meter No. 9819.
(2) Brubaker, W. M., D-C Amplifier, *Bulletin of the American Physical Society*, Vol. 14, No. 6, Dec. 7, 1939.
(3) Mezger, G. Robert, Feedback Amplifier for C-R Oscilloscopes, ELECTRONICS, p. 126–131 and 254, Apr. 1944.
(4) Mezger, G. Robert, A Stable Direct-Coupled Amplifier, ELECTRONICS, p. 106–110 and 352–358, July 1944.
(5) Balanced Modulator, U. S. patent 1,988,472, Jan. 1935.
(6) Whitaker and Artzt, Development of Facsimile Scanning Heads, "Radio Facsimile," RCA Institutes Technical Press, published Oct. 1938.
(7) Black and Scott, A D-C Amplifier, *Proc. I.R.E.*, June 1940.
(8) Vacuum-Tube Chopper, U. S. patent 2,323,966, July 1943.
(9) Miller, S. E., Sensitive D-C Amplifier with A-C Operation, ELECTRONICS, p. 27–31 and 105–109, Nov. 1941.
(10) Williams, Emerys, The Cathode-Coupled Double-Triode Stage, *Electronic Engineering*, London, Vol. XVI, No. 195, p. 509–511, May 1944.
(11) Ginzton, E. L., D-C Amplifier Design Technique, ELECTRONICS, Mar. 1944.
(12) Goldberg, A High-Gain D-C Amplifier for Bioelectric Recording, *Electrical Engineering*, Vol. 59, p. 60–64, Jan. 1940. This circuit has some of the features of the cathode-balanced circuits in combination with a push-pull balance. A high cathode resistor is used to obtain push-pull from a single-ended input. This resistor was later replaced by a pentode to get the effect of an infinite cathode resistance without excessive voltage drop.
(13) Richter, Walter, Cathode Follower Circuits, ELECTRONICS, p. 112–117 and 312, Nov. 1943.
(14) Penick, D. B., Direct-Current Amplifier Circuits for Use with the Electrometer Tube, *Review of Scientific Instruments*, p. 115–120, Apr. 1935.
(15) Huntoon, R. D., An Inexpensive Direct-Current Amplifier, *Review of Scientific Instruments*, p. 322–326, Oct. 1935.
(16) Bousquet, A. G., Random Emission Compensation, *General Radio Experimenter*, May 1944.
(17) Thurston, J. N., An A-C Operated Vacuum-Tube Voltmeter, ELECTRONICS, p. 102–104 and 224–232, Oct. 1943.
(18) RCA Volt-Ohmyst, No. 165A.
(19) Series-Balanced Amplifier, U. S. patent 2,310,342. Feb. 1943.

D-C Amplifier Design Techniques

Design equations with practical examples, stabilization of negative feedback amplifiers. cathode follower and phase inverter considerations. tube drift problems in high-gain d-c amplifiers, and operation of multistage amplifiers from common power supplies

By EDWARD L. GINZTON

A METHOD of directly coupling successive stages of a vacuum-tube amplifier without using a common B-supply has been described by W. M. Brubaker.[1] Except for the verbal description in this note, the circuit does not seem to have appeared in print in spite of its usefulness and simplicity. In the simplified version of this circuit given in Fig. 1a, a battery is shown tapped near the middle, with a resistor connected across the entire battery. It is obvious that regardless of the position of the tap on the battery, there is always a point on the resistance which is exactly at the same potential as the tap on the battery. Thus, it is possible to tap a source of voltage $(E_1 + E_2)$ and, regardless of the load placed upon the source of voltage, find a point on the load which will be at the same potential as the tap.

In Fig. 1b, this tap has been applied to the amplifier coupling. A source of voltage $(E_1 + E_2)$ is tapped, and this point is connected to the cathodes of the two tubes.

Then resistances R_1, R_2, R_3, and the (d-c) plate resistance R_p of the tube are so chosen that the junction between resistors R_2 and R_3 is at the same potential as the tap on the source of voltage $(E_1 + E_2)$. Any number of tubes may be cascaded in this manner, all using the same power supply.

This method makes it possible to eliminate the zero-signal d-c component from any similar circuit. Several other modifications are illustrated in later sections of this article, with circuit data.

Design Equations

The equivalent diagram of Fig. 1b, together with the symbols which are used below, is shown in Fig. 2. It should be noted that R_p is the d-c plate resistance of the tube, equal to the d-c voltage E_c at the plate of tube divided by d-c plate current I_p. The analysis of this circuit should show how the voltage E_2 depends upon the various constants shown in Fig. 2, and how this voltage can be adjusted to any desired value. Applying Kirchhoff's Law to Fig. 2, one has:

$$\left.\begin{aligned} i_p (R_p + R_1) + i_2 (R_1) &= E_1 \\ i_p (R_1) + i_2 (R_1 + R_2 + R_3) &= E_1 + E_2 \end{aligned}\right\} \quad (1)$$

$$\text{But } i_p = \frac{E_c}{R_p} \text{ and } i_2 = \frac{E_2 - E_3}{R_3}$$

By combining these equations and rearranging their terms,

$$R_2 = R_1 \frac{E_c + E_2}{E_1 - E_c (1 + R_1/R_p)} \quad (2)$$

$$\text{and } R_3 = R_1 \frac{E_2 - E_3}{E_1 - E_c (1 + R_1/R_p)} \quad (3)$$

Equations 2 and 3 are the design equations. If one designs an amplifier for given supply voltages E_1 and E_2, and a given plate voltage E_c, and if one knows R_1, then R_2 and R_3 may be computed to produce the required E_2. Sometimes, however, one knows all voltages; i.e., E_1, E_2, E_c, and E_3, but R_3 must not exceed a certain value. Then Eq. 3 can be inverted:

$$R_1 = R_3 \frac{E_1 - E_c}{E_2 - E_3 + E_c (R_3/R_p)} \quad (4)$$

Now, from Eq. (2) and (3),

$$R_2 = R_3 \frac{E_c + E_2}{E_2 - E_3} \quad (5)$$

in comparison to the supply voltage. As an example, a 6SJ7 may be operated under the following conditions:

$E_2 = 400$ v, $E_1 = E_2 = 200$ v,
$E_c = 100$ v, $E_3 = 0$ v, $R_1/R_p = 0.5$.

Using Eq. 8, the comparative amplification is found to be 71.4 percent. By means of more careful design, efficiencies in the neighborhood of 80 percent can be realized.

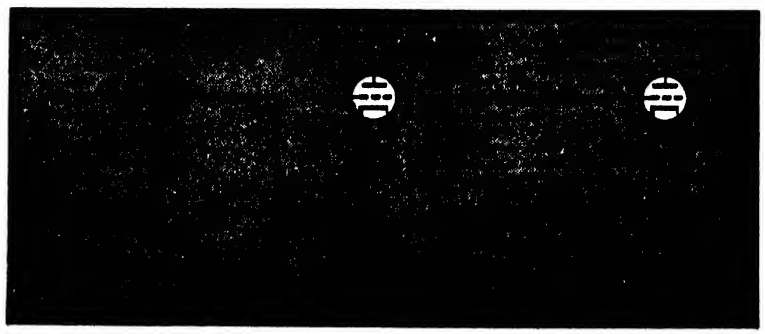

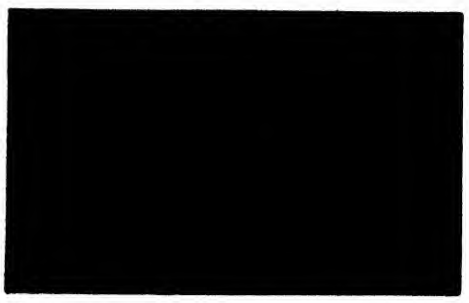

Fig. 1—Basic bridge circuit, and bridge version used for interstage coupling

Fig. 2—Equivalent circuit of the coupling network in Fig. 1b

As an example, Fig. 3 shows a two-stage amplifier using two 6J7 tubes. Suppose a 400-v power supply is available. From a tube manual, one finds the recommended operating conditions for such a tube forming an alternate set of design equations.

If a resistance-capacitance coupled amplifier is designed to produce a certain amplification A_c, and is converted into a d-c amplifier by means of the circuit described above, the amplification A of the d-c amplifier will be less than A_c due to the voltage drop across R_2. "Efficiency" of amplification may then be defined as $\eta = A/A_c$. While an exact expression for the efficiency can be derived, it is more significant to use an expression based upon a few assumptions. If the resistance-capacitance coupled amplifier is a pentode tube with an infinite dynamic plate resistance, load resistance R_1, and grid leak resistance R_3, and a trans-conductance g_m, its amplification is:

$$A_c = g_m \frac{R_1 R_3}{R_1 + R_3} \quad (6)$$

If a d-c amplifier is now designed using the same load resistance R_1 and the same grid leak resistance R_3, then the amplification of the d-c amplifier will be:

$$A = g_m \frac{R_1 (R_2 + R_3)}{R_1 + R_2 + R_3} \frac{R_3}{R_2 + R_3} = g_m \frac{R_1 R_3}{R_1 + R_2 + R_3} \quad (7)$$

The efficiency of amplification η can be computed by combining Equations (3), (5), (6), and (7), giving

$$\eta = \frac{1}{1 + \dfrac{E_c + E_2}{E_2 - E_3 + E_1 - E_c (1 + R_1/R_p)}} \quad (8)$$

The significance of this relation can be seen more clearly when $E_3 = 0$ and the supply voltage $E_2 = (E_1 + E_2) \gg E_c (1 + R_1/R_p)$, all of which is accurate enough for qualitative discussion, remembering that R_p can be considered infinite. Then

$$\eta \approx \frac{1}{1 + E_c/E_2}$$

This means that for best efficiency,

E_0 should be as small as possible (older manuals, such as RCA-RC-12 give more complete information than the later ones). For 6J7:

Plate supply voltage.....180 v
Screen voltage .....30 v
Grid voltage .....1.55 v
Plate voltage (E_0).....60 v
Plate current (i_p).....0.24 ma
Screen current .....0.08 ma
Plate load (R_1) .....0.5 meg
Grid leak (R_g) .....0.5 meg
Cathode resistor .....4850 ohms
Voltage amplification 93
Transconductance g_m .....375 μ mhos

The d-c amplifier operating under similar conditions will have the following modifications in its design formulas, obtained from the above data and the notation previously given:

$$R_p = \frac{E_0}{i_p} = \frac{60}{0.24 \times 10^{-3}} = 0.25 \text{ meg}$$

$E_0 = 60$ v $\quad E_2 = 150$ v
$R_1 = 0.5$ meg $\quad E_1 = 250$ v $\quad E_3 = 0$ v

E_3 may be any practical value, zero being the most convenient. From Eq. (2) and (3), $R_2 = 1.07$ meg and $R_3 = 0.428$ meg. The amplification per stage can be computed from Eq. (7), and is found to be 100. This is higher than the corresponding resistance-capacitance coupled stage because of the higher grid leak resistance. If the resistance-capacitance coupled amplifier were to use the same grid-leak resistance, its amplification would be about 125 for the same value of plate current.

It should be noticed that in single-ended amplifiers with cathode resistors, there is a loss in amplification due to negative feedback introduced by the cathode resistors, so that the effective amplification per stage is $A_{eff.} = A_0/(1 + R_c g_m)$, where R_c is the cathode resistance. In the example shown in Fig. 3, this reduction in amplification is from 100 to 87. If the screen voltage is obtained by means of a series dropping resistor, even a further reduction of gain could be expected.[3]

The decrease in amplification due to negative feedback introduced by the cathode and screen resistors can be eliminated either by using push-pull amplifiers, in which case there is no degeneration, or by using fixed grid bias and screen supplies.

The amplifier shown in Fig. 3 should have an overall amplification of about 1400, a uniform frequency response from zero to 20,000 cps, and should be able to deliver about 50 v peak without appreciable distortion.

Stabilization of Negative Feedback Amplifiers

Since the output of the Brubaker amplifier can be adjusted to have a zero d-c component, conventional negative feedback circuits can be used to stabilize the amplifier. The principles involved in applying negative feedback are now so well known that it is not necessary to say very much about either the method or the final results. A few remarks, however, might be helpful in realizing the best performance.

In applying negative feedback in a multi-stage amplifier of the Brubaker type, the same oscillation criterion applies as in the case of the ordinary resistance-capacitance coupled amplifiers: unlimited feedback can be applied in one or two stages without any oscillation troubles, and over a larger number of stages if proper care is taken.[3] In general, application of feedback to one stage does not produce great benefits, and more than two stages require a compromise design between frequency response and the degree of stabilization. It is the two-stage amplifier that is easiest to handle *if audio frequencies as well as d-c have to be amplified.*

If negative feedback is applied to a two-stage amplifier, (or any even number of stages), such as shown in Fig. 4 the feedback resistor R_f has to be connected from the plate circuit of the last stage to the cathode resistor of the first stage. As a result of this, there is an undesirable loss of amplification due to two effects: (1) the un-bypassed cathode resistor R_c in the first stage, and (2) the loss in gain of the second stage due to the shunting of the plate load by $(R_f + R_c)$.

As was shown in the preceding section, the first of these could be appreciable, while the effect of the second depends upon the magnitude of the feedback desired. These two effects are inter-related in such a way that the greater one attempts to make β (the fraction of output that is introduced into the input), the lower is the amplification of the two stages. This just means that in order to obtain a high degree of the stability, and at the same time the highest possible amplification, these two effects must be minimized.

In practice, this can be done by (1) designing the output stage to operate with the lowest possible impedance so that the shunting effect of a given $(R_f + R_c)$ is as small as possible, (2) designing the input stage with the highest possible impedances so that for a given β, R_f becomes as high as possible, (3) adjusting the operation of the first stage so that its gain is obtained for the lowest possible value of g_m, to reduce the degenerative effects

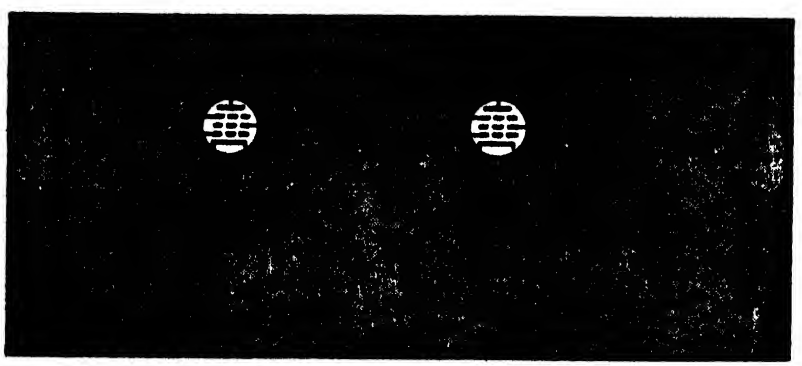

Fig. 3—A two-stage d-c amplifier using pentode tubes

of R_r, the un-bypassed cathode resistance of the first stage; (4) obtaining the bias for the second stage either with a bias cell, or merely by choosing the proper value of E_s.

If properly designed, it is possible to obtain both a stabilization factor of 100 and an amplification of approximately 100 with a two-tube pentode amplifier. Figure 4 shows the circuit and frequency response of an amplifier similar to one of Fig. 3, but stabilized by means of negative feedback. It will be observed that in order to connect resistance R_4 without disturbing the potentials of the circuit, a tap on resistance R_2 had to be used which had the same potential with respect to ground as the upper terminal of R_4 of the first stage.

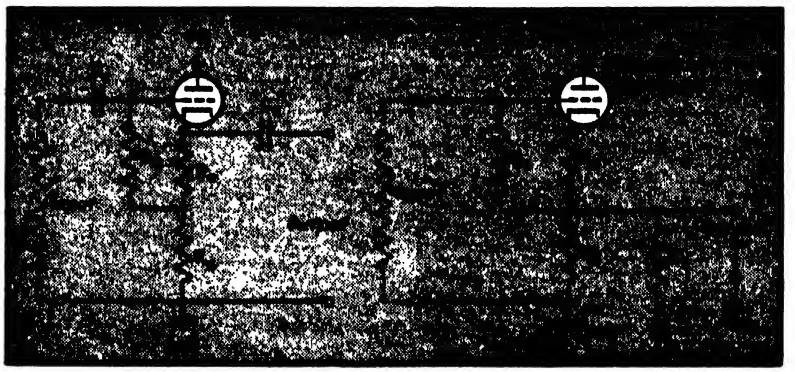

Fig. 5—The conventional R-C coupled cathode follower (a) and the Brubaker equivalent of the conventional cathode follower (b)

Cathode Follower Considerations

Cathode followers of the type shown in Fig. 5a find application in circuits where a high impedance has to be converted into a low one without the use of transformers. In most such cases, in addition to the bias resistor R_c, a resistance R_a is added which allows greater output voltages and at the same time develops degenerative feedback which tends to stabilize the action of the tube against voltage and tube characteristic changes.

In conventional cathode followers, the proper bias voltage developed across R_c is introduced to the grid through the resistance R_g. The voltage across R_a is kept from altering the situation by a blocking capacitor C_1 on the input side. Capacitor C_2 prevents the direct voltage across $(R_c + R_a)$ from appearing at the output terminals.

Figure 5b shows the d-c equivalent of Fig. 5a. Here the capacitors are omitted and the undesired direct voltage across R_a is eliminated by connecting R_7 to E_s, which may be the same voltage as is used in the amplifier proper. The proper value of resistance R_7 is chosen so that the current supplied from E_s through R_a and R_7 just equals the total cathode current of the tube; that is,

$$i_b = \frac{E_s}{R_a + R_7} \text{ or } R_7 = \frac{E_s}{i} - R_a \quad (9)$$

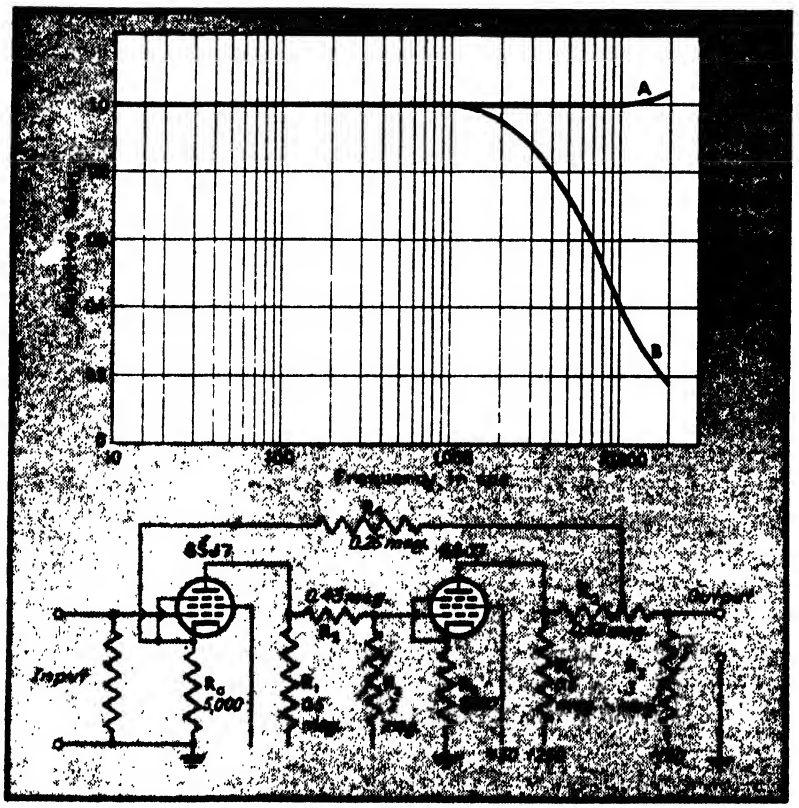

Fig. 4—A two-stage direct-coupled amplifier employing negative feedback. Curve A shows the frequency response with feedback; B, without feedback

Phase Inverter Considerations

Push-pull arrangements have even greater advantages in d-c amplifiers than in resistance-capacitance coupled ones. Single-ended input voltages can be converted to push-pull ones by means of phase inverters, which are shown in Fig. 6. It will be seen that these are again merely modifications of the well known a-c circuits.

Figure 6a shows a push-pull amplifier in which one grid is driven by the unbalanced input and the second grid from the output circuit of the first one. The circuit to the left of the line *a-a* is designed in the obvious manner, using formulas previously given. If this is done, then the d-c potential from point *b* to ground will be zero, and point *c* can be chosen so that the ratio $(R_{10} + R_{11})/R_{10}$ equals the voltage amplification of the driven stage. If properly designed and

adjusted, the input to both tubes will be balanced, there will be no degeneration due to cathode resistance R_c, and the gain will be the highest possible with the tubes used.

The phase inverter shown in Fig. 6b is perhaps the more useful of the two. If one were to bisect the circuit by a horizontal line into two symmetrical parts, then each one would again be designed along the general principles outlined before. Each half of the circuit could possess a high degree of stability due to degenerative feedback developed by the resistor R_c. In the form shown in Fig. 6b the lower tube is driven by the signal voltage developed across R_c due to the driver tube. If

$$\frac{R_t R_s}{R_c + R_s} g_m > 1,$$

then the output of the device will be balanced to the same degree as the above inequality. The balance, of course, can be made perfect by adjusting the tap b to the proper point.

It should be pointed out that resistors R_{11} and R_{12} provide the proper bias voltages for the two tubes, whereas R_c and R_s are so adjusted as to give the highest possible value of $R_c R_s/(R_c + R_s)$ and still maintain the potential from point a to ground zero, to provide for the condition that $R_c R_s/(R_c + R_s) >> R_{11}$ or R_{12}. Other types of phase inverters often used in a-c circuits can be easily converted for d-c applications.

Tube Drift Problems in High-Gain Amplifiers

The most difficult problem in a high-gain d-c amplifier is the change in the plate current of the first tube due to random changes in the work function of the cathode surface. These current changes are usually small, but are always present. Negative feedback cannot eliminate these changes because they act as if they were input signal variations and as such cannot be distinguished from the signal itself.

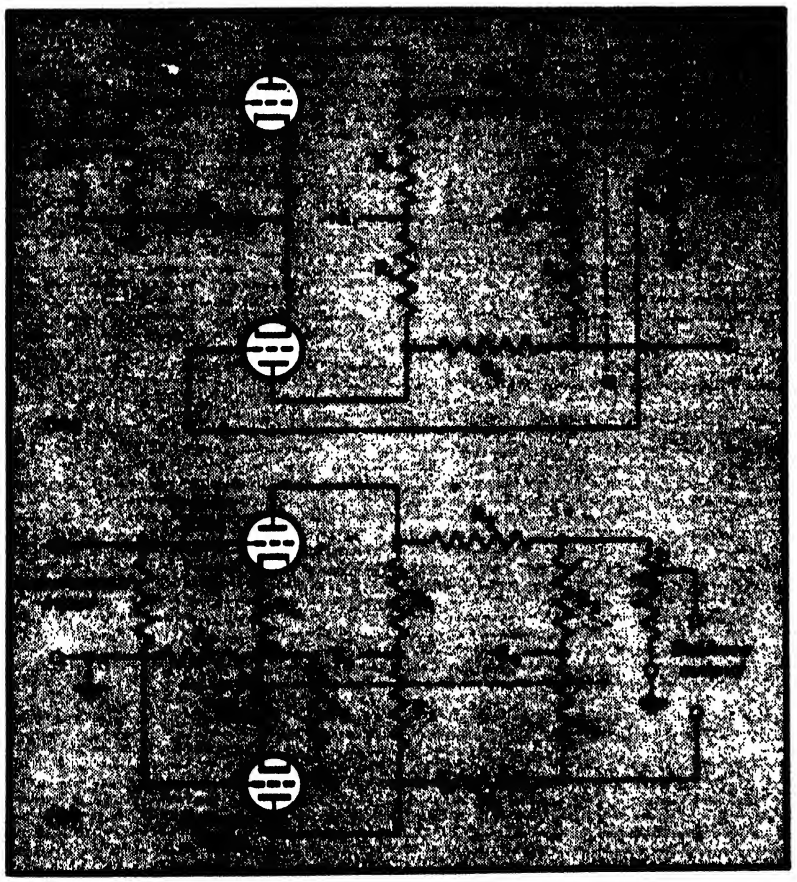

Fig. 6—Two types of d-c phase inverters. The tubes can be either triodes or pentodes in the circuit at (a)

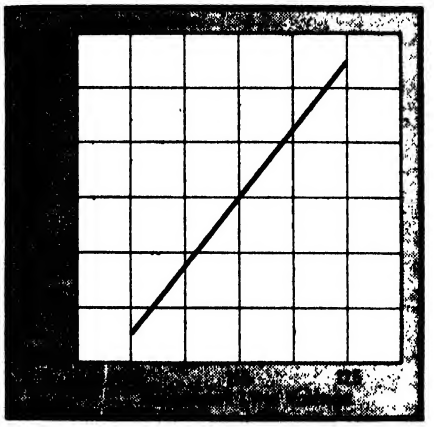

FIG. 7—Output voltage variation of the amplifier shown in Fig. 4 due to filament voltage changes

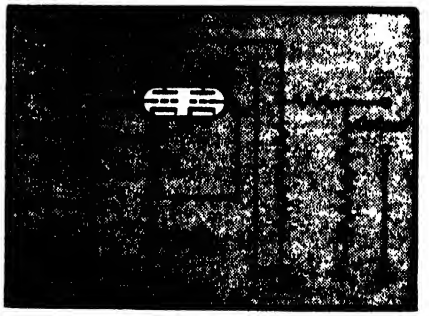

FIG. 8—The basic Miller circuit which improves the drift problem of the input stage of the d-c amplifier. If g_2 is the transconductance of T_2, then R_2 is nearly equal to $1/g_2$

The most serious immediate cause of these current changes is the filament voltage, although ambient temperature affects the current also. (In addition, there seem to be other causes which are not yet understood.) To illustrate the magnitude of these changes, Fig. 7 shows the variation of the output voltage due to changes in filament voltage. The ordinate is an equivalent input voltage; i.e., change in output voltage amplification.

A great improvement can be realized by means of a circuit described by Miller.[4] Miller uses a double triode with a common cathode, and the circuit is so arranged that if one triode behaves in the same manner as the other, cancellation of the variation takes place. The

basic circuit is shown in Fig. 8. If $R_2 = 1/g_2$, then $\Delta e = \Delta i_1 R_1 - (g_2 \Delta i_1 R_1) R_2 = O$; and changes in emitter characteristics that are common to both sections will produce no net change in the plate current of the active amplifier T_1. An amplifier built with the first stage modified in this manner is shown in Fig. 9. Figure 10 shows the variation of the output voltage (again referred to input) as a function of the filament voltage of the first tube. It is seen that for a proper value of the resistance R_2, a marked improvement is produced.

Operation of Multi-Stage Amplifiers from Common Power Supplies

If many stages are used in an amplifier, currents flowing through the source of voltage (E_2 and E_1) from the last stages can introduce voltages into the earlier stages. This causes regeneration which can express itself either in oscillation or other undesirable effects. There are two ways to avoid the trouble: (1) use of low-impedance power supplies, (2) separately filtered lines to groups of stages. The former can be accomplished by means of either batteries or properly designed electronic voltage regulators, and the second by voltage regulator tubes such as VR-105.

The general method described is useful in extending practically all known techniques now used in a-c amplifiers to zero frequency. These methods are not restricted to amplification alone.

One of the objectionable features of this method is the necessity of two voltages, positive and negative with respect to ground. Miller[4] attempts to get around this difficulty by using cold-cathode regulating tubes as circuit elements. The use of these tubes in this manner brings up other problems, however. The VR-tubes need a fairly high voltage to start them and draw heavy currents. This causes troubles in design, adjustment and operation. The VR-tubes also tend to be noisy, so that their use is usually restricted in amplifiers, at least as circuit elements. The two required voltages can be obtained from one power supply and do not require additional parts.

References

(1) Brubaker, W. M., D-C Amplifier, *Bulletin of the American Physical Society*, Vol. 14, No. 6, Dec. 7, 1939. (Program for the University of California meeting.)

(2) Terman, F. E., Hewlett, W. R., Palmer, C. W., and Wen-Yuan Pan, Calculation and Design of Resistance-Coupled Amplifiers using Pentode Tubes, *Transactions of the A. I. E. E.*, Vol. 59 (1940).

(3) Terman, F. E., ELECTRONICS, Jan. 1937.

(4) Miller, Stewart E., Sensitive D-C Amplifier with A-C Operation, ELECTRONICS, Nov. 1941.

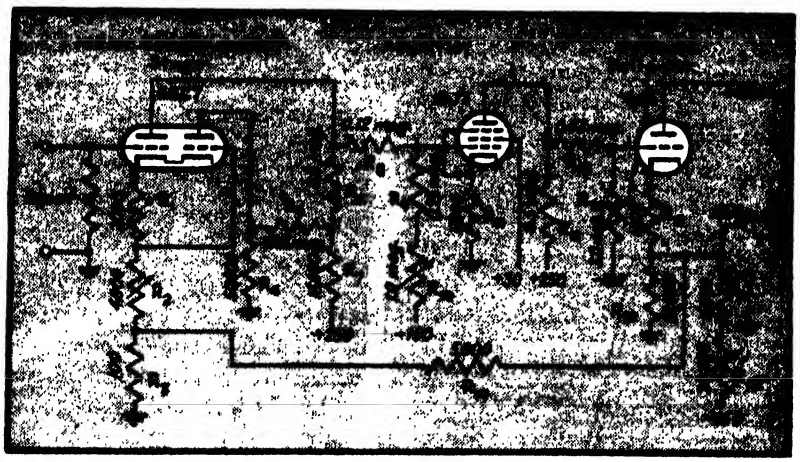

FIG. 9—A two-stage d-c amplifier using a Miller compensated stage, a cathode follower, and stabilized negative feedback

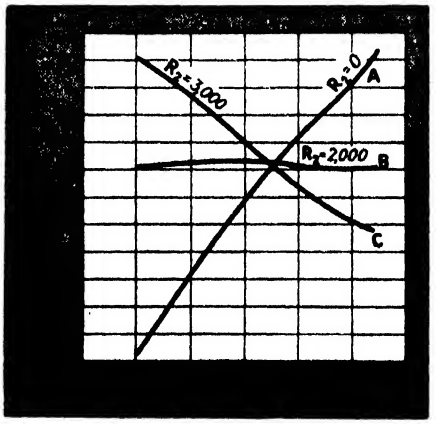

FIG. 10—The effect of Miller on the stability of the amplifier shown in Fig. 9, in respect to filament voltage changes

Bridge-Balanced Amplifiers

Inherently stable with respect to tube and supply-voltage variations, the d-c voltage and current amplifier circuits described lend themselves ideally to the design of vacuum-tube voltmeters and photoelectric light meters

By Y. P. YU

THE MAXIMUM sensitivity obtainable with a vacuum-tube voltmeter is limited by the stability that can be achieved. The difficulty in maintaining an accurate zero base line is due to these major causes: (1) variations in values of the circuit parameters, such as resistances; (2) variations of supply

voltages; (3) variations of tube factors, such as plate resistance and amplification factor.

Variations in circuit parameters result chiefly from changes in temperature of resistors. They can be minimized by the use of thermally compensated resistors and the proper placement of component parts. Fluctuations of line voltages affect both the heater and the plate supply voltages. Tube factors are dependent upon operating voltages, upon cathode emission, and upon the aging of the tube. The effect of variations in supply voltages and tube factors on zero deflection of the output meter can be minimized by the use of balancing circuits.

Voltage Amplifier

Figure 1 shows the basic circuit of a d-c bridge-balanced voltage amplifier. Tube T_N serves as an inverse-feedback amplifier in which the degeneration is provided by the I-R drop across the bias resistor R. Other tubes, T_1 to T_{N-1}, serve to balance out variations of tube factors and supply voltages.

The cathodes of all tubes are heated from the same source. The balance will be perfect if all tubes remain identical in characteristics as supply voltages and other conditions change. Physically, R_1, R_2, T_N, and other tubes of the amplifier circuit perform as the four arms of a balanced bridge, in which R_1 and R_2 correspond to the ratio arms, T_N to the unknown arm, and $T_1 - T_{N-1}$ to the standard arm. Any change in voltage drop across the arm T_N due to variations in tube factors or in supply voltages will be accompanied by an identical change in voltage drop across each tube of the arm $T_1 - T_{N-1}$; therefore, the ratio of E_1 to E_2 remains constant, and the balance of the bridge holds for any part of the tube curves.

Current Amplifier

The output terminals of the bridge-balanced voltage amplifier are at high quiescent d-c potential above ground. In order to couple this output directly to the input of the next stage, it is necessary to establish the correct bias voltage between the grid of the next tube and its cathode. Furthermore, the gain of the bridge-balanced voltage amplifier decreases rapidly as the load resistance decreases, becoming extremely small when the load resistance is lower than the cathode resistance R because excessive degeneration is developed by the cathode resistors. In order to couple the output to an indicating meter of low internal resistance, it is necessary to reduce the amount of degeneration.

The d-c bridge-balanced current amplifier circuit of Fig. 2 was developed to satisfy these requirements. In this circuit the correct grid-bias voltage of T_3 is established by the voltage drop across resistor R_1, and the amount of degeneration is reduced by eliminating cathode resistors. The grid-excitation voltages of T_3 and T_4 are opposite in phase. Therefore, the signal components of plate currents of T_3 and T_4 cancel in the biasing resistance R_1; there is no loss in amplification even when R_1 is very large.

Millivoltmeter Circuit

The schematic diagram of a vacuum-tube millivoltmeter is shown in Fig. 3. Two 6SL7 tubes are used as a d-c bridge-balanced voltage-amplifier stage and two 6SN7 tubes are used as a d-c bridge-balanced current amplifier. Balance adjustment of the output stage is accomplished by adjusting the grid biases of T_3 and T_4. The potentiometer R_7 is used as a panel zero control. The potentiometers R_5 and R_6 are used to take care of large zero shifts such as may be encountered when the tubes are changed. An L-attenuator consisting of two resistors, R_1 and R_2, is used as a voltage multiplier to give a constant input resistance of 10 megohms at all voltage ranges.

Care in construction is essential in a sensitive vacuum-tube voltmeter of this type. It was found necessary to provide good ventilation, to choose tubes of similar characteristics, and to use low-temperature-coefficient precision resistors. Furthermore, the temperature coefficient of all resistors except R_1, R_2, R_3, and R_4 should be identical. Stabilization of the plate-supply voltage is obtained by the use of an electronic voltage-stabilizing circuit.

This instrument gives a full-scale meter reading of one millivolt d-c on its most sensitive voltage range. In conjunction with a special probe (diode detector), the instrument may be used to make exact measurements from d-c up to radar frequencies. By connecting the instru-

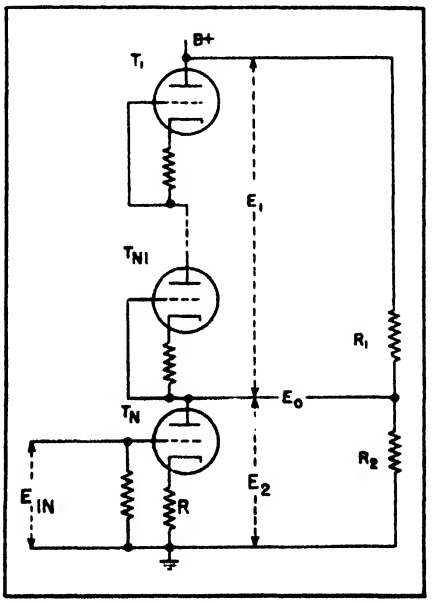

FIG. 1—Basic circuit of d-c bridge-balanced voltage amplifier

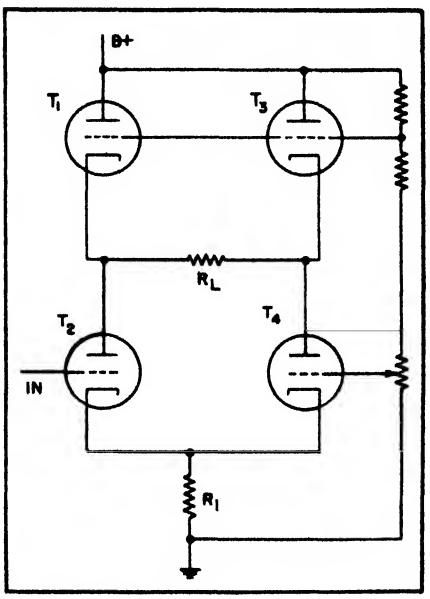

FIG. 2—Basic circuit of d-c bridge-balanced current amplifier

ment across proper resistors a very sensitive microammeter is obtained. For example, it is possible to obtain a full-scale deflection for 0.001 microampere by connecting the instrument across a 1.111 megohm resistor, making the resultant input resistance one megohm. When used with an external battery and proper resistors, the instrument will measure resistances from 0.001 ohm up to 1,000,000 megohms. Line-voltage variations from 105 volts to 120 volts will affect the meter reading by less than 4 percent.

Coupling Between Stages

When a single plate supply is employed, coupling between stages is one of the major difficulties in the design of multistage d-c amplifiers. Three methods which are particularly adaptable in bridge-balanced arrangements will be described here.

One method utilizes a cold-cathode voltage regulator tube as shown in Fig. 4. When all the tubes in the circuit are similar, the overall voltage gain of this amplifier is $\mu^2/3$, where μ is the amplification factor of the tubes. A voltage gain of 64 db with good stability was obtained from this amplifier circuit by using two and one-half 6SL7's. But noise is generated by glow discharge in the voltage regulator tube, and a highly regulated plate-supply is needed to give good stability to this amplifier.

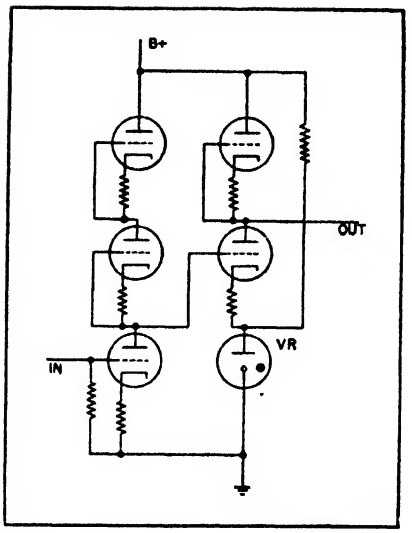

FIG. 4—Coupling two stages of a bridge-balanced amplifier by using a voltage-regulator tube

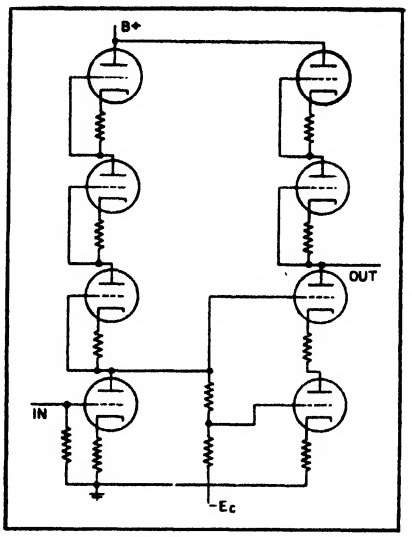

FIG. 5—Another method of coupling between stages in a d-c bridge-balanced amplifier

The second method employs a separate bias-supply, as shown in Fig. 5. When all tubes are similar, the design equation of this amplifier is

$$R_1/R_2 = E_{BO}/E_C = N-2$$

where N is the number of tubes in series, and E_{BO} is the quiescent plate voltage. The overall voltage amplification of this circuit is $\mu^2/2$, where μ is the amplification factor of the tubes. The disadvantage is that two highly regulated power supplies are needed.

The third method employs a push-pull phase-inverter arrangement wherein a large cathode bias may be employed without the usual attendant disadvantage of excessive negative feedback. The basic circuit of this type of arrangement is shown in Fig. 6. The overall voltage gain of this amplifier is $2\mu_1\mu_2/3$, where μ_1 and μ_2 are the amplification factors of the tubes employed in the first and the second stages respectively. A voltage gain of 56 db with very low noise level was obtained from this circuit by using one and one-half 6SL7's as the first

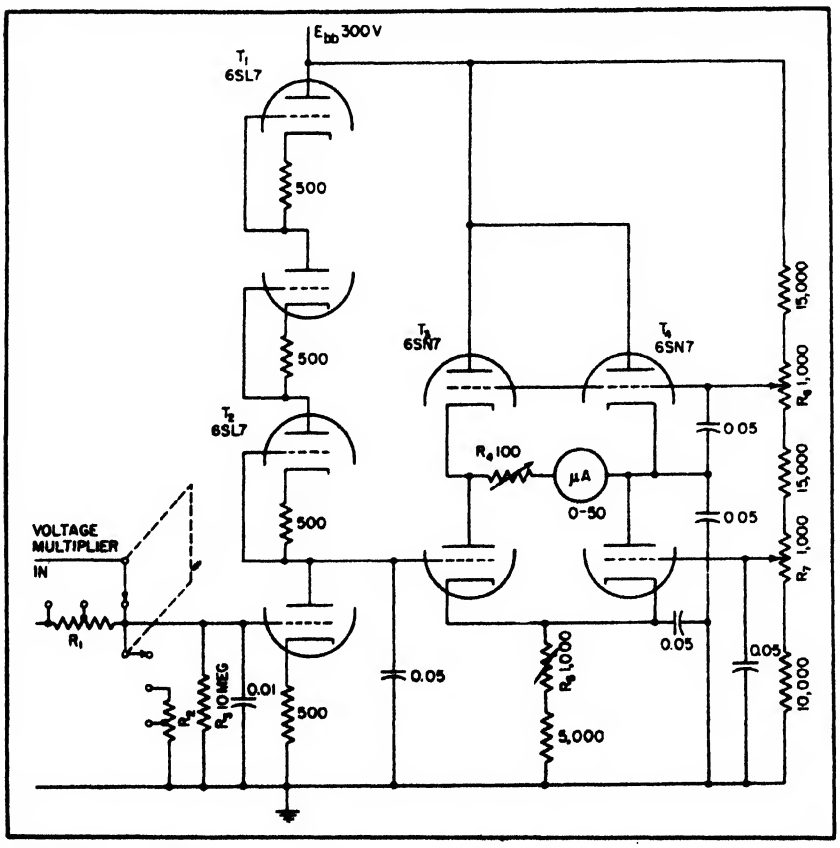

FIG. 3—Circuit of practical vacuum-tube millivoltmeter employing a balanced amplifier to obtain extreme stability

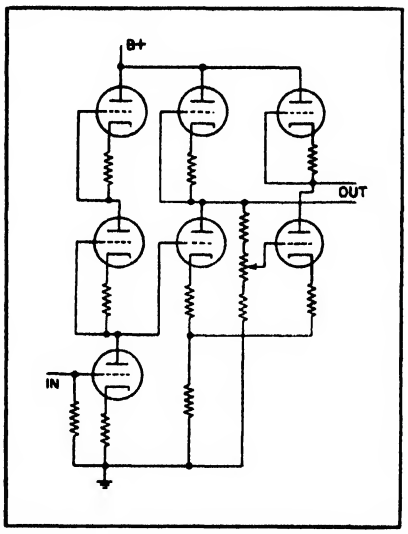

FIG. 6—Using a phase inverter to couple two stages improves amplifier performance.

stage and two 6SN7's as the inverter stage.

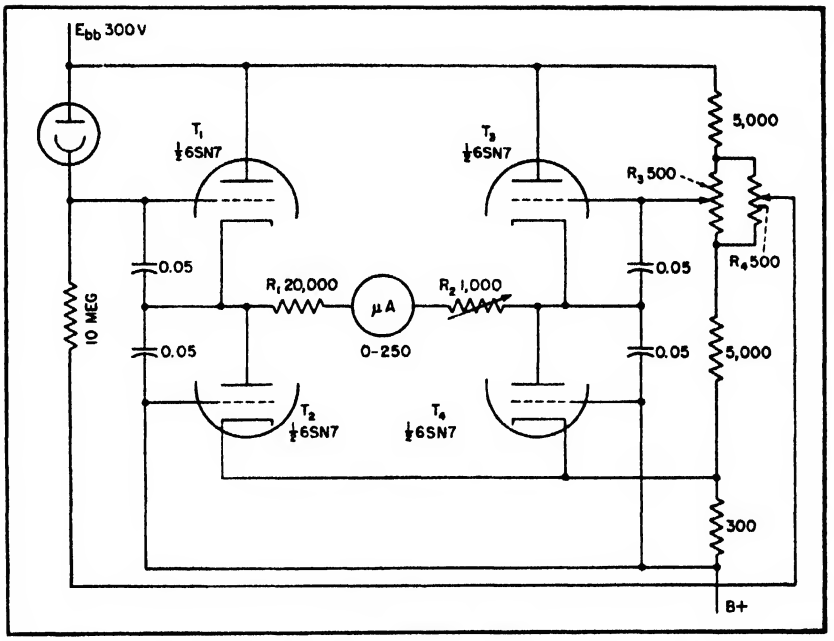

FIG. 7—Degenerative-balance light meter circuit employing a balanced amplifier to obtain high stability

Light-Meter Circuit

A bridge-balanced circuit with negative feedback, for measurement of very small illumination, is shown in Fig. 7. The bridge arrangement of the circuit makes zero setting practically independent of supply-voltage variations. The amount of degeneration developed by resistor R_1 is sufficient to prevent tube changes from affecting the calibration of the instrument. This circuit can measure illumination with full-scale sensitivity corresponding to a phototube current of 0.5 microampere.

The process of balancing the circuit is simple. Connect the grid of T_1 to the center tap of potentiometer R_2, and adjust R_3 to bring the meter reading to its zero position. Then reconnect the grid of T_1 to its original position, and again bring the meter reading to zero by adjustment of R_4. The circuit is then ready for operation. Variable resistor R_3 is used for adjusting the calibration of the output meter in case it is necessary to change the phototube. Potentiometer R_4 is used as a panel zero control. This circuit has proved itself simple to build, reliable in indication, and stable in operation.

D-C Amplifier for Low-Level Signals

Bandwidths of only a few cycles, input impedances not over 20 ohms, and averaging rectifiers are used to minimize noise when amplifying signals below a microvolt. Speed of amplifier response is analyzed. Construction of two laboratory amplifiers is described

By CHARLES B. AIKEN and W. C. WELZ

AMPLIFIERS for extremely low input levels are often required in the measurement of physical quantities in both research and materials testing laboratories. One important field of instrumentation where such amplifiers are required is the measurement of various forms of radiation.

Design Considerations

The conventional method of using an a-c amplifier instead of a d-c type is to modulate a local high-frequency carrier with the input signal, amplify the modulated a-c, and finally obtain the signal by detection. Recently the thermal time constants of bolometers and thermocouples have been substantially reduced, so it is possible to inter-

rupt the radiation falling on them, by means of a mechanical shutter for example, and thus directly obtain an a-c output that is proportional to the incident radiation.

To measure minute amounts of radiation, such as those involved in astronomical investigations, it is necessary to deal with signals of the order of millimicrovolts. To distinguish such signals in the presence of noise, it is necessary to employ an exceedingly narrow bandwidth in the amplifier. The frequencies of operation of the newer bolometers and thermocouples range from 5 to as high as 150 cycles. During the course of work on a National Defense Research Committee contract, amplifiers for use with these bolometers and for general testing at low frequencies were developed; the amplifiers operate at frequencies below 50 cps with bandwidths less than 5 cps wide. Although these units are of specialized nature, they do have many uses in instrumentation beyond the purposes for which they were originally designed.

In electrical design, it is desirable to operate at as low a frequency as possible, because the minimum achievable bandwidth becomes narrower as the operating frequency is lowered, thus reducing the noise against which the signal must compete. But too low a frequency presents apparatus problems, particularly in the design of the input transformer and in the size of the by-pass capacitors. Frequencies in the vicinity of 60 cycles are to be avoided because of the universal presence of hum fields from power circuits.

One of the most important design aspects affecting the level of circuit noise is the rectifier used at the amplifier output to convert the a-c into d-c for actuating an indicator or recorder. Peak-type diode voltmeters accentuate the noise component more than averaging rectifiers, so the averaging type is preferred. Perhaps the best rectifier from the standpoint of minimizing noise is the mechanical rectifier; it is a motor-driven switch operated from the same shaft that drives the mechanical shutter. The switch thus reverses the polarity of the amplifier output in synchronism with the a-c signal generated by the shutter so that the output is rectified on a purely average basis, independently of the absolute value of the signal. The mechanical rectifier is strictly linear, and when used with a filter, provides selectivity dependent only on the characteristic of the filter.

Input Circuits

Balanced input circuits and a suitable input transformer are essential if maximum sensitivity is to be realized when the amplifier is connected to thermal receivers or other devices of low impedance. The stepup of this transformer should be high, so that the irreducible thermal noise across its input terminals is made large enough to override by a substantial margin the noise generated in the first vacuum tube. For operating frequencies of 10 cycles or above, this condition is easily fulfilled, and it is then unnecessary to take extreme precautions to reduce tube noise to the lowest possible level.

The transformer used is the Thermador Type TG-3, originally intended for geophysical use. It has a six-element shield and a rated secondary inductance of 2,400 henries ±10 percent, at low voltages. The stepup obtainable from a balanced 10-10 ohm input circuit is 150 at 50 cycles, 107 at 12 cycles, and 84 at 7 cycles, the secondary being tuned for maximum output in each case. However, unless the secondary Q is greater than two, tuning the secondary provides little improvement.

The layout of the amplifier should take account of the obvious precautions required in any high-gain device, such as in-line sequence of stages, adequate separation of high-level and low-level regions, and shielding of critical elements. Moreover, at the gains involved here, certain additional precautions are necessary, especially in the first stage, although it has been found that elaborate constructions are not always necessary. In some cases, protection provided by the sextuple shielding on the transformer, the metal case of the first tube, and a standard metal chassis enclosing the transformer tuning capacitor and the wiring has proved

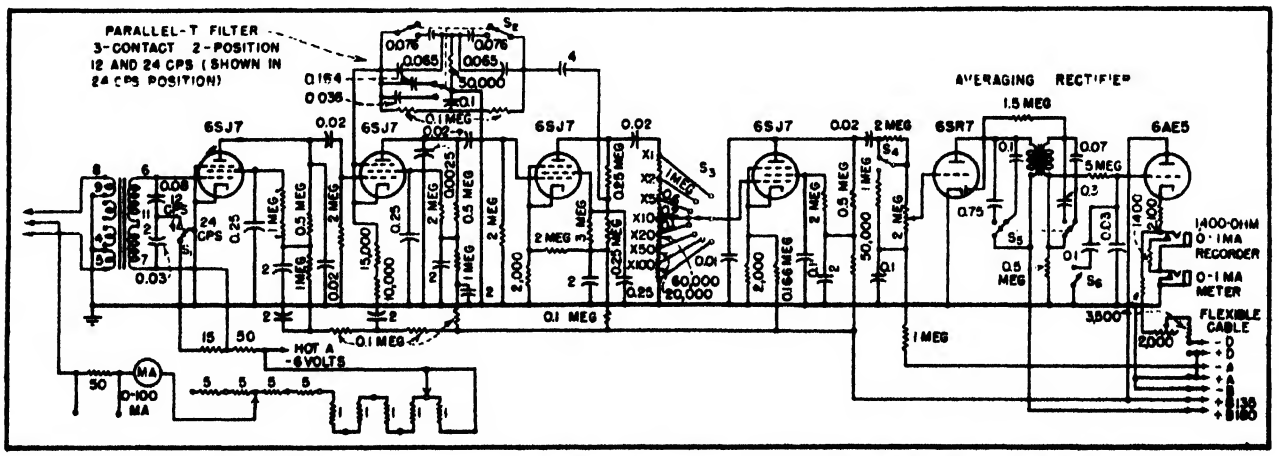

FIG. 1—Parallel-T filter and averaging rectifier minimize noise in this amplifier for use with bolometers

satisfactory, provided the device is not subjected to severe electrical interference. In other cases, moderate additions to this shielding have been necessary.

Tubes recommended for the first stage are the 6SJ7 and the 1620. It is desirable to test tubes for electrical and microphonic noise, and to select the quietest units, because individual tubes differ greatly.

A very substantial plate decoupling filter is required in the first stage; the second stage is also apt to call for special attention in this regard. The necessary filtering can be realized either by using two or three sections of R-C filter (multiple sections require less total R and less total C than a single section of the same effectiveness), or by using gas voltage-regulator tubes, which act as excellent low-frequency by-pass elements.

It is well to use precision wire-wound resistors in all parts of the first stage, except the sections of decoupling filter which precede the last section. Oil-filled by-pass capacitors should be used, and very high resistance mica coupling capacitors; capacitors having even a small leak can cause severe noise. The use of one-point grounds, as is common in high-gain radio-frequency amplifiers, is especially desirable.

Selective Circuits

In the first amplifiers constructed in our laboratories, inductance-capacitance selective circuits were used. Besides tuning the input-transformer secondary, the grid circuit of the third stage, which utilized the primary of a Thermador Type TG-26 transformer, was tuned. This type of tuning is simple and results in a fairly high gain. However, the inductance of the coil changes slightly with voltage level, thereby causing detuning and moderate nonlinearity.

In the later amplifiers, a twin-T selective feedback circuit has been employed for tuning purposes, usually from the plate of the third stage to the cathode of the second. Feedback from the third plate to the suppressor-grid of the first stage has also been successfully used. In most cases, a well balanced twin-T network gives sufficient selectivity. However, in some cases a narrower band was required; it was achieved by increasing the shunt capacitance in the twin-T circuit above the normally used value, which makes the feedback voltage regenerative near what would normally be the zero transmission frequency of the twin-T.

Signal Rectifier

Considerable use has been made of a simple peak-type diode rectifier, which is satisfactory unless it is necessary to measure signals just above circuit-noise level. Circuit noise contains peaks that are several times the average noise level. These peaks register on a peak-type voltmeter, and keep the rectified noise voltage unnecessarily high.

This difficulty can be remedied by arranging the diode to respond to the true average of the impressed alternating voltage by using a circuit in which no by-pass capacitors are used across the resistors in series with the diode. With amplification adjusted so as to obtain the same sinewave output in both cases, the average noise level with a peak rectifier was 74 percent greater than with the average-type rectifier, and in addition, the latter gave a more uniform noise level, relatively free of surges, than the peak type.

As has been mentioned, synchronous mechanical rectifiers have also been employed. This rectifier has been used successfully in the amplification of direct potentials that are interrupted, fed into an alternating-current amplifier, and then synchronously rectified. The rectifier and the filter to which its output is delivered give an effective selectivity to the amplifier which is determined entirely by the characteristics of the filter.

In order to get full output from a

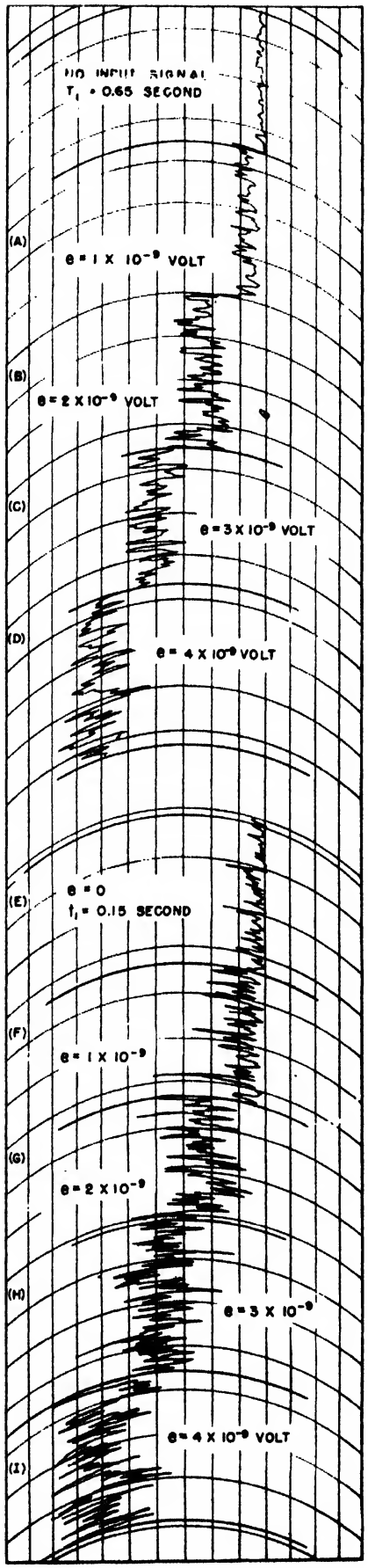

FIG. 2—Output from amplifier of Fig. 1

synchronous rectifier, the phase of the impressed voltage must be correct. For this reason the amplifier should be provided with a continuously variable phase adjusting network so that the correct relationship between signal and rectifier phase can be easily reached, and so that effects of small drifts in the tuning of the amplifier, or slight changes in the operating frequency, can be compensated.

If full advantage is to be taken of the useful characteristics of the rectifier-filter system, it is essential that there be no interference, either microphonic or electrical, from the rectifier itself. Such interference, being synchronous, is very detrimental and great care must be taken to avoid it.

Speed of Response

There is no simple relation between the effective overall time constant of the amplifier and the bandwidth at some specified amplitude, such as 3 decibels down, or 6 decibels down. However, certain simple formulas make it possible to decide on the approximate value of bandwidth to be employed when a given response speed is required.

When a sinusoidal electromotive force is suddenly impressed upon a series-tuned circuit, the resulting current consists of a steady-state term plus a transient term, which gradually dies away. The transient is of the form of a damped sine-wave, and the time constant t_1 of the circuit is the time required for the amplitude of the transient to decrease to 37 percent of its initial value. Let f_2 and f_1 be frequencies at which the resonant curve of the tuned circuit falls to a fraction F of its maximum. If X is the total reactance around the circuit at either one of these frequencies

$$F = 1/(1 + X^2/R_1^2)^{1/2} \qquad (1)$$

from which two relations follow

$$(2\pi f_2 L/R_1) - (1/2\pi f_2 CR_1) = (-1 + 1/F^2)^{1/2} \qquad (2)$$

and

$$(1/2\pi f_1 CR_1) - (2\pi f_1 L/R_1) = (-1 + 1/F^2)^{1/2} \qquad (3)$$

adding these two expressions

$$[2\pi f_2 L + 1/2\pi f_1 C] - [2\pi f_1 L + 1/2\pi f_2 C] = 2R_1(-1 + 1/F^2)^{1/2}$$

furthermore $2\pi f_2 L$ is very nearly equal to $1/2\pi f_1 C$, and $2\pi f_1 L$ is equally close to $1/2\pi f_2 C$, hence

$$f_2 - f_1 = (R_1/2\pi L)(-1 + 1/F^2)^{1/2} \qquad (4)$$

in addition, the rise of current in the circuit is determined by the time constant t_1 which is $2L/R_1$; this term can be used to eliminate L/R_1 from Eq. 4 giving, on rearrangement

$$t_1 = (-1 + 1/F^2)^{1/2}/\pi(f_2 - f_1) \qquad (5)$$

which equation relates time constant to bandwidth. For half-amplitude bandwidth $F=0.5$ and Eq. 5 gives

$$t_1 = 0.552/(f_2 - f_1)$$

showing that a frequency response one cycle wide at half amplitude gives an effective time constant of slightly over half a second. If bandwidth is considered to be between the 3-db points, then $F=0.707$

$$t_1 = 0.318/(f_2 - f_1)$$

which results indicate that, for a given definition of bandwidth, the time constant depends, as does the noise, on the absolute bandwidth.

The synchronous rectifier used with this amplifier and its associated filter also has an effect on the response time of the system. When the voltage impressed on the mechanical rectifier is synchronous with the rectifier switching, as will always be the case with the desired signal, the output will contain a direct-current term. If a signal is suddenly impressed on the rectifier, the voltage appearing across the output of the filter will require some time to reach its maximum value. The time constant t_1 is the interval required for the output to reach 63 percent of its final value.

If the filter consists of two identical resistance-capacitance networks, the ratio of the instantaneous output voltage to the impressed direct voltage is

$$e_2/E_0 = 1 - e^{-1.81t/RC} \times [1.342 \sinh(1.118t/RC) + \cosh(1.118t/RC)] \qquad (6)$$

from which it can be found that the output reaches 0.63 of its final value when $t/RC=3.03$, hence t_1 is $3.03RC$ for this filter.

To relate this time constant to the effective selectivity, let f_0 be the synchronous frequency, and f_1 and f_2 be the higher and lower frequencies of the incoming signal at which the filter output is reduced to

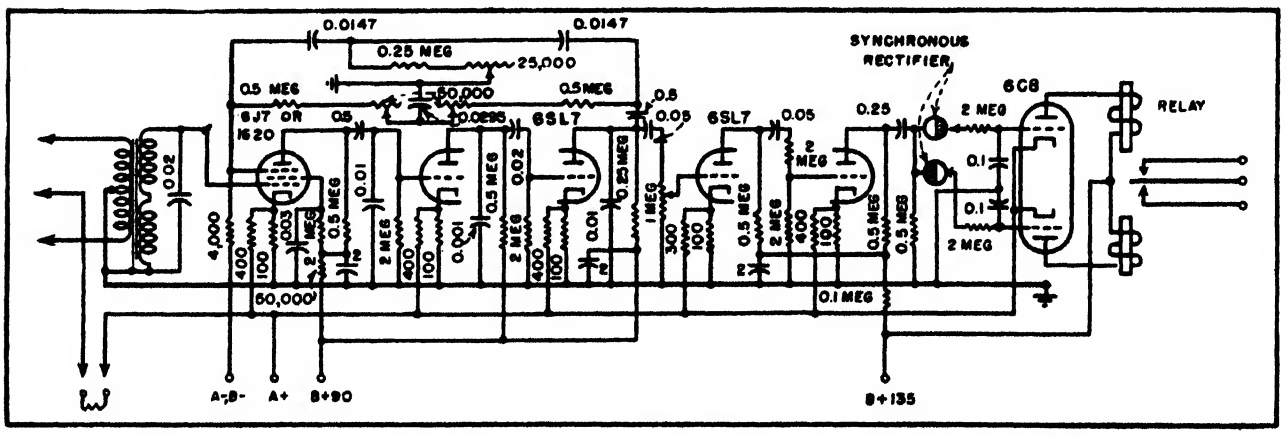

FIG. 3—Synchronous rectifier, consisting of two rotating commutators, averages noise in amplifier output

a fraction F of its maximum steady state value. Then

$$F^2 = 1/\{1 + 28[\pi RC(f_2 - f_0)]^2 + 16[\pi RC(f_2 - f_0)]^4\} \quad (7$$

and also an identical expression in which $(f_0 - f_1)$ appears in place of $(f_2 - f_0)$. Eliminating f_0 between these two similar expressions and eliminating RC by means of the previously obtained time constant

$$t_1 = [3.03/\pi(f_2 - f_1)] \times [-3.5 + (11.25 + 1/F^2)^{1/2}]^{1/2} \quad (8)$$

which, for $F = 0.5$, gives

$$t_1 = 0.614/(f_2 - f_1)$$

corresponding roughly to the time constant of the tuned circuit at its half-amplitude bandwidth. The time constant of the two-mesh filter is slightly greater than that of a single-mesh one, however this disadvantage is offset by the greater attenuation of the synchronous frequency provided by the two-mesh filter.

Description of Amplifier

The circuit of a two-frequency laboratory amplifier is shown in Fig. 1. A spring suspension used to support it has sufficient stiffness to provide a period of 0.8 second for oscillations in the vertical direction. This gives adequate protection against ordinary mechanical disturbances. Construction and layout are not greatly different from those of any ordinary low-gain amplifier, the chief difference being that the output transformer (which feeds the rectifier) is mounted in an entirely separate box to prevent objectionable magnetic coupling with the input.

It is to be noted that both the bolometer current and the grid bias for the first stage and for the fifth stage are obtained from the A-battery, without developing trouble from feedback. The bias connection to the fifth stage is rather heavily filtered, however.

No by-pass capacitor is provided in the rectifier circuit, so that the direct voltage developed is proportional to the average value of the signal. A part of this voltage is impressed, through a low-pass filter, upon the grid of the output tube. Switch S_6 allows the time constant of this filter to be set at either 0.15 seconds or 0.65 seconds.

The frequency of maximum amplification can be changed from 12 to 24 cycles by switching capacitances in the twin-T network, across the secondary of the input transformer, and across each winding of the output transformer. Because maximum amplification is often not required, the switch S_4 has been provided to lower the gain by a fixed amount. Further adjustment to a desired sensitivity is made by the volume control in the grid circuit of the fourth stage which is composed of precision wirewound resistors, and provides attenuations up to 100 times, as indicated in the circuit diagram.

Performance Data

Full-scale deflection of the output meter is obtained with 0.05 microvolts developed in a 10-ohm resistor in one side of the balanced input circuit, with the attenuator at 0.1. When there is no attenuation, and the impressed signal is reduced to 0.005 microvolt, the total deflection obtained is greater than full-scale (because of the addition of the circuit noise to the signal), but we can rate the maximum full-scale sensitivity as 0.005 microvolt. When 24-cycle tuning is used, the sensitivity is 0.0042 microvolt.

Figure 2 shows a record of the 12-cycle circuit noise made with a recording milliammeter when the input cable is terminated in a pair of 10-ohm wire-wound resistors. The average noise voltage is 1.1×10^{-9} volt. Figures 2B to 2D, inclusive, show the result of adding successively greater amounts of signal. It will be noticed that a signal of 0.001 microvolt can be very definitely detected, although it is not greatly above noise level. In these runs the time constant switch was in the 0.65-second position. Figure 2E to 2I, inclusive, show similar data except that the switch

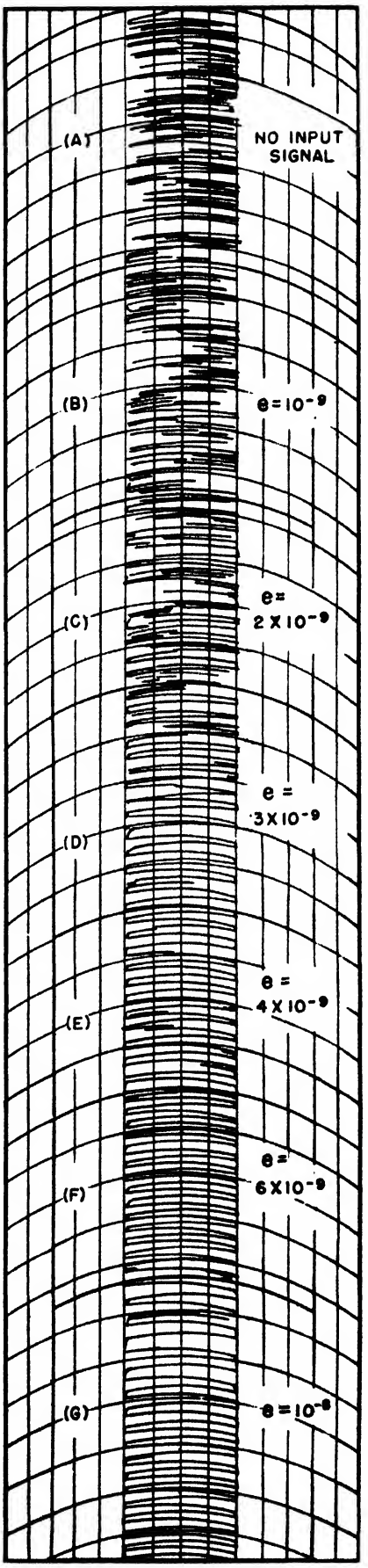

FIG. 4—Output from amplifier of Fig. 3

S_e is in the 0.15-second position, and hence the oscillations of the recorder needle are more rapid.

Records of the noise level made with the secondary of the input transformer short-circuited, show it to be 3×10^{-10} volt, in terms of the equivalent primary circuit voltage or approximately a quarter the circuit noise developed with 10-10 ohm resistors at the input cable.

The average noise level indicated by the recordings is 1.1×10^{-9} volt on the 12-cycle channel, and 1.3×10^{-9} on the 24-cycle channel. The half-amplitude bandwidth of the former is 2.0 cycles, while the latter is 5.4. The root-mean-square thermal noise voltage in an idealized frequency band 2-cycles wide, generated by a 20-ohm resistor, is 0.8×10^{-10} volt, while that corresponding to a 5.4-cycle bandwidth is 1.3×10^{-9} volt. It is necessary to consider the full 20 ohms of the two 10-ohm resistors in the input circuit, because the voltages they generate are in series with the primary, in the same way that the signal voltage developed in a 10-ohm thermal receiver is in series with the primary. The above figures show that the total noise of the amplifier approaches thermal limit.

The root-mean-square voltage across the secondary of the rectifier transformer corresponding to full-scale deflection of the recording milliammeter in the output of the direct-current amplifier stage is 46 volts. This means that the total voltage amplification from 10-ohm input circuit to transformer secondary is 9.2×10^{9}. Of course, not all of this gain is effectively used, because there is a four-to-one voltage division in the rectifier circuit proper, and because the direct voltage developed is proportional to the average value of the impressed alternating voltage, or to $2^{\frac{1}{2}}/\pi$ times the root-mean-square impressed alternating current. Hence the rectified voltage applied to the filter is only 5.2 volts, and the useful voltage gain may be taken as 1.04×10^{9}. However, the larger figure, relating to the transformer secondary voltage, is effective in determining the possibility of there being stray feedback of alternating voltages within the amplifier itself.

A Compact Amplifier

Figure 3 shows a small amplifier, having only four tubes, intended to be used with an external synchronous rectifier (shown as part of the diagram). The unit is designed for nominal 24-cycle operation, and the half-amplitude bandwidth is 4.0 cycles. Tuning over a 10 percent range is provided by the ganged variable resistors in the twin-T network.

The first three stages take a total B-battery current of less than 0.6 milliampere at 90 volts, and hence a small separate B-battery is used for them. Using a battery greatly reduces the amount of plate-circuit filtering that is required and avoids the necessity for numerous bulky capacitors.

Because (1) no proportionality of output versus input was required with this device and (2) a rather wide range of input voltages had to be handled, the last stage was provided with a series grid resistor, and thus acted as a limiter. The next to last stage also limits somewhat on strong signals. The resulting phase shift with amplitude, while appreciable, is not enough to interfere with the action of the synchronous rectifiers. Ranges of input voltage in excess of one-thousand to one can be handled without difficulty.

There are two half-wave sections in the rectifier, each of which feeds a separate filter and a triode direct-current amplifier, so that one triode will respond to a signal of a certain phase, and the other to one of opposite phase. A differential relay with one winding in series with each output-tube plate is provided.

The amplifier was designed to give reliable operation on input signals down to 10^{-9} volt acting in one side of a 10-10-ohm balanced circuit. Actually, it does rather better than this, as is indicated by Fig. 4. Figure 4A shows the operation of a recorder connected to the differential relay. The pen moves in one direction when the relay closes due to current through the upper triode section and in the opposite direction when the relay closes on the other side. Because of the very high gain, circuit noise keeps the relay in operation always.

The frequency of the signal recorded in Fig. 4B was adjusted to differ by 0.2 cycle per second from that of the mechanical rectifiers, so that with a strong signal the relay and recorder move regularly back and forth. In Fig. 4B the change in the character of the record clearly shows the presence of a signal of 10^{-9} volt, although the operation can hardly be described as satisfactory. With twice as much input voltage, the regular pattern becomes more evident (Fig. 4C) although noise is still quite troublesome. With 3×10^{-9} volt (Fig. 4D), the operation is fairly good, and at 6×10^{-9} or more, it is substantially perfect.

A Stable D-C Amplifier

An aperiodic coupling element permits response to zero frequency and to high frequencies limited only by conventional limitations in RC coupling. Useful in CR-tube deflection; has a voltage gain of 5,000

By G. ROBT. MEZGER

THE DESIGN of high-gain, wide-frequency-range direct-coupled amplifiers always has been hindered by a number of factors which are difficult to control. The term "direct-coupled" as used in this paper embodies any type of interstage coupling system for vacuum-tube amplifiers which permits response of the system to signal potentials of zero frequency. It is not restricted to the case of zero-resistance connection between the output terminal of one vacuum-tube stage and the input terminal of a following stage.

The problem of maintenance of proper electrode potentials in direct-coupled amplifiers usually has occasioned the necessity for having either the output or the input terminals average the signal component of their output about some potential other than that of ground. The use of transformers or capacitors as interstage coupling elements destroys the feature of response to signals of zero frequency.

Direct-coupled amplifiers of high gain often are troubled with uncontrollable drifts in output potential. The term drift is used here to indicate any change, usually uncontrollable, which will cause an undesired variation of either the a-c or the d-c component of the output of an amplifier. It is used in contradistinction to the term "noise" which is reserved for reference to short-time disturbances.

Drifts in direct-coupled amplifiers have been known to achieve such magnitude that attempts to correct them have carried the tubes in the latter stages of the amplifier beyond their operating range. Circuit arrangements which have been used to maintain proper electrode potentials usually involve the placement of power supplies or batteries in such a manner that they are required to carry signal potentials. As a result, these large masses, with their high stray capacitance to ground, shunt the high-frequency components of the signal and destroy the high-frequency performance of the amplifier.

Solutions for the Problem

A circuit which has been widely used of late for direct interstage coupling is shown in Fig. 1. In this circuit, a voltage divider is placed between the plate of the first stage and a potential source which is highly negative with respect to the grid of the second stage. The two resistors in the divider, R_1 and R_2, are so chosen that the potential of point a is exactly the operating potential desired for the grid of T_2. Attenuation of the signal originating at the plate of T_1 will appear at the grid of T_2 because of the IR drop across R_1.

As the negative-potential source at which R_2 is terminated is made more negative, R_2 must be increased to maintain the same average potential at point a. The attenuation therefore becomes less. If the plate of T_1 were operating at an average potential of +100 volts, and if R_2 were terminated at a source which was negative by 1000 volts with respect to ground, only ten percent attenuation of the signal would occur.

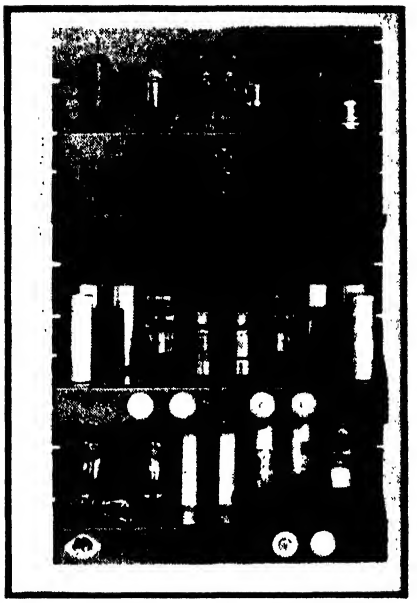

Back elevation of the amplifier as constructed at the David W. Taylor Model Basin

By inspection of Fig. 1, it can be seen that if it were possible to control the flow of current through R_1 and R_2 so that it is absolutely constant, i.e., so that there would be no *change* in potential drop through R_1 regardless of signal-potential variations, the signal originating at the plate of T_1 would then appear unattenuated at point a. This would be accomplished, for instance, if R_2 were increased to infinity, as is implied in the foregoing, so that the current flowing through the network would be constant at all times. It is also equivalent to saying that if a signal were

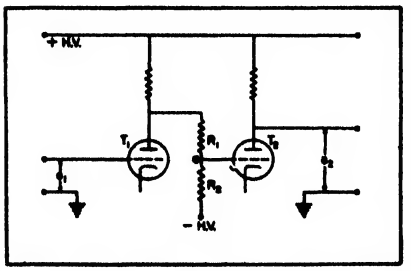

FIG. 1—Hypothetical circuit for direct coupling between two tubes

applied at point a which was equal in both magnitude and phase to the signal at the plate of T_1, then regardless of the current flowing through R_1 the signal potential at point a would be the desired potential.

A Direct-Coupling Circuit

The application of just such a signal at point a is accomplished by the circuit of Fig. 2. In this circuit, T_2 operates as the infinite resistor previously described; the IR drop through R_1, which is produced by the flow of the plate current of T_2, provides the proper average potential at point a while introducing no signal attenuation.

In Fig. 2, the main elements of the coupling device between T_1 and T_2 are resistor R_1, which has the same function as does R_1 in Fig. 1, and triode T_2 which, with its cathode-load resistor, replaces R_2. T_3 operates to maintain the potential of point a exactly equal in magnitude and phase to the potential which originates at the plate of T_1.

Consider the coupling element first as a voltage divider made up of the series combination of R_1, r_p of T_3, and R_4. Then, neglecting any effects caused in T_2 by R_2, the signal at point a would be the plate signal of T_1 reduced by the factor $(r_p + R_4)/(R_1 + r_p + R_4)$. If, however, the plate current of T_2 is decreased just sufficiently, with any increase in e_3, to permit T_2 to develop across R_1 a signal potential of the proper magnitude to compensate exactly for the attenuation produced by this voltage divider, the desired condition for potential at point a will have been obtained. In this manner, R_1 will simulate a resistor which provides a potential drop but which carries no current. This is accomplished by maintaining constant the plate current of T_2 regardless of changes in e_3.

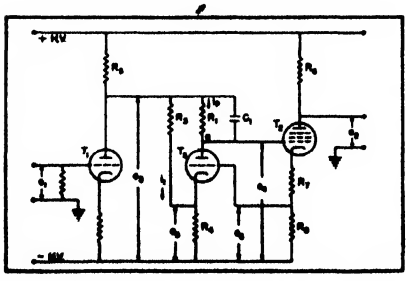

FIG. 2—Basic circuit in which a tube, T_3, stabilizes the amplifier

Control of plate current of T_2 to maintain it absolutely constant is effected by varying the cathode potential of the tube by an amount which will vary r_p just sufficiently to compensate any change in plate current which would be caused by variations in e_3. Resistor R_3 is added, therefore, as shown in Fig. 2, to develop the control potential necessary across the cathode of T_3. The value of R_3 is so chosen that, when operating in series with R_4 as a voltage divider across the input potential e_3, the voltage drop across R_3, with constant plate current simultaneously flowing through R_4, is just sufficient to alter the parameters of T_2 to compensate any change in plate current. When this condition prevails, the signal potential originating at T_1 will cause the signal component of the potential at point a to equal exactly, in both magnitude and phase, the output signal from T_1; and i_p of T_2 will be absolutely constant. The average potential of point a, furthermore, can be controlled by design to be exactly the desired operating potential for the grid of T_2.

Analysis of the Circuit

This circuit may be analyzed rigorously as follows: From the definition of μ, constant plate current requires that $\Delta e_g = -\Delta e_p/\mu$, where $e_g = e_a - e_3$ and $e_p = e_4 - e_3$. Both e_g and e_p depend upon e_3. Therefore, introducing e_3 as independent variable and passing to infinitesimals in place of the finite variations, the condition for constant i_p becomes

$$\frac{\partial e_g}{\partial e_3} = -\frac{1}{\mu}\frac{\partial e_p}{\partial e_3} \qquad (1)$$

The two partial derivatives occurring in Eq. (1) can be readily evaluated by applying Kirchhoff's laws to the circuit of Fig. 2:

$$e_3 = i_p R_1 + e_p + i_p R_4 + i_1 R_4$$

$$i_1 = \frac{e_3 - i_p R_4}{R_3 + R_4}$$

$$e_p = e_3\left[1 - \frac{R_4}{R_3 + R_4}\right] + i_p\left[\frac{R_4^2}{R_3 + R_4} - R_1 - R_4\right]$$

$$\frac{\partial e_p}{\partial e_3} = 1 - \frac{R_4}{R_3 + R_4} = \frac{R_3}{R_3 + R_4} \qquad (2)$$

Similarly,

$$e_g = e_a - (i_1 + i_p)R_4 = e_a - i_p R_4 - \left(\frac{e_3 - i_p R_4}{R_3 + R_4}\right)R_4$$

For the purpose of this discussion, e_a can be assumed constant. In the circuit actually used, this is assured by the adoption of a push-pull circuit. Then

$$\frac{\partial e_g}{\partial e_3} = -\frac{R_4}{R_3 + R_4} \qquad (3)$$

Substituting Eq. (2) and (3) into Eq. (1), the condition for constant i_p becomes

$$-\frac{R_4}{R_3 + R_4} = -\frac{1}{\mu}\frac{R_3}{R_3 + R_4}, \text{ or } R_4 = \frac{R_3}{\mu}$$

The value of R_3, then, is equal to μR_4, where $\mu = g_m r_p$ at the conditions under which the tube is operated. The value of R_3 is not found to be critical in practice. It may vary as much as 15 percent with little change in operation of the circuit. R_3 may be determined empirically by measuring the plate current of T_2 while varying simultaneously the plate-supply for T_3 at the common junction of R_3 and R_1.

The proper grid-bias potential for T_2 is taken from the cathode-load resistor of T_3 by adjustment of R_7 and R_8. The circuit between the grid of T_2 and the cathode of T_3 is degenerative and operates only to maintain a constant bias potential on the grid of T_3, so that a rise in grid potential (rise and fall of potential are given here with respect to *signal* ground potential, which is at a level of —400 volts with respect to absolute ground in the amplifier described) of T_3 increases the plate current of T_3.

The potential of point a with respect to ground (signal) is thus reduced, and the grid potential of T_2 is reduced an equal amount, thereby reducing the cathode potential of T_2 and the grid potential of T_3 by an amount just sufficient

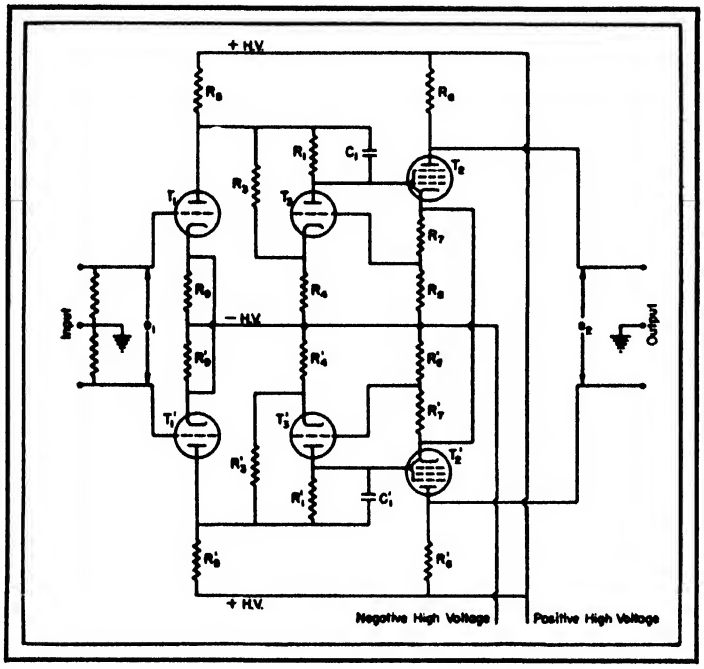

FIG. 3—Complete basic circuit for the stabilized amplifier. Resistors R_7, R'_7, R_8 and R'_8 are combined into a single resistor: the same is true of R_9 and R'_9.

to compensate for the original rise. It is this self-stabilization of the coupling element, operating to compensate stage by stage for undesired variations of circuit conditions, which permits these stages to be cascaded without danger from long-time drifts rendering the amplifier unusable.

An inspection of Fig. 2 will show that the compensating action described will occur not only for variations in the parameters of T_2 and T_3, but that it will occur also for any signal which appears at the plate of T_1. This circuit, then, while it is extremely stable, will pass no signal and will not function as an amplifier.

Elimination of Degeneration

A means for permitting the circuit to be self-compensating but nevertheless allowing it to function as an amplifier is shown in Fig. 3. In this circuit, an amplifier, identical in every respect to the amplifier of Fig. 2, has been added to the original circuit to provide a push-pull circuit. It will be noted, however, that, by use of the parallel connection of the cathodes of each amplifier tube in each stage, a variation in cathode potential of one tube in a stage will cause a change in i_p of the other tube, and a signal caused by such a change will appear in balanced form in the output circuit. If an unbalanced input signal, then, is applied to the input of the amplifier of Fig. 3, the common connections of the cathodes of T_1 and T'_1 and T_2 and T'_2 will cause a balanced signal potential to appear at the output terminals.

The circuit in this form is suitable only for push-pull output potentials, which adapts it ideally to deflection of a cathode-ray tube. This may restrict its usefulness for some other applications. The input signal may be either balanced or unbalanced with respect to ground in this circuit.

By the self-compensating action described in the foregoing, any variation of cathode temperature, which changes r_p and g_m and which has been a main cause of drift and variation of amplification in direct-coupled amplifiers, has been virtually eliminated. The part of the circuit of Fig. 3, therefore, which consists of all elements following the plate terminals of T_1 and T'_1, may be viewed as a single unit for a direct-coupled amplifier consisting of a self-compensating coupling element and an amplifying stage. The coupling element has the advantage of introducing no signal attenuation, and it operates to correct continuously for any of the usual circuit variations which cause drift in the output signal.

Stages may be cascaded to provide increased gain. It is significant that the self-compensating feature of the coupling element permits stages to be cascaded without the effects of individual stage drifts becoming cumulative due to succeeding amplification. The number of stages which can be cascaded is limited only by the de-

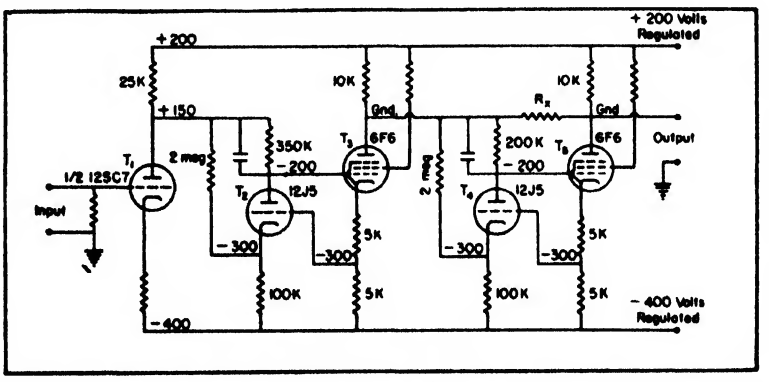

FIG. 4—Cascaded direct-coupled amplifier, showing voltages with respect to ground. For reasons stated in text, this circuit proved impractical

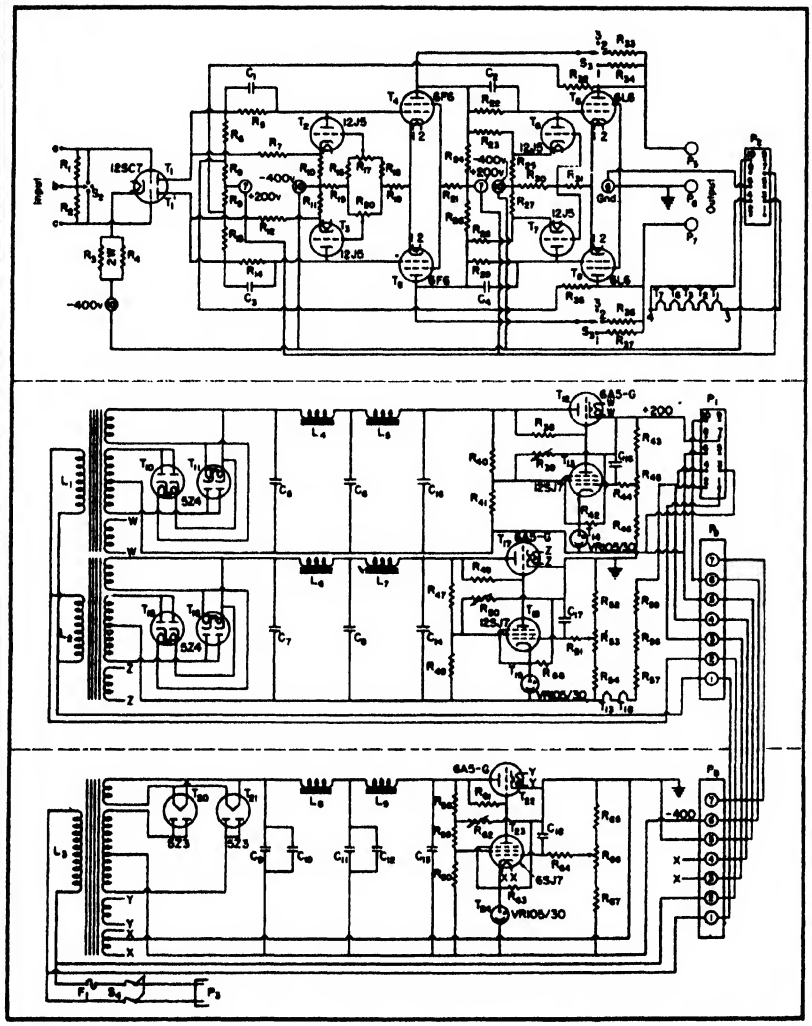

FIG. 5—Schematic of complete stabilized direct-coupled amplifier. Parts list is given in the accompanying text

PARTS LIST FOR FIG. 5

R_1, R_{13} — 1 meg, 1 w
R_2, R_4 — 200,000, 1 w
R_3 — 300,000*
R_6 — 20,000, 1 w
R_7 — 2 meg, 1 w
R_8, R_9 — 25, 1 w
R_{10}, R_{11} — 100,000*
R_{12} — 2 meg, 1 w
R_{14} — 20,000, 1 w
R_{14} — 300,000*
R_{15} — 2,000, 10 w
R_{16} — 1,000, 1 w
R_{17} — 50, pot.
R_{18} — 1,000, 1 w
R_{19} — 2,000, 10 w
R_{20} — 250, pot.†
R_{21} — 25,000, 1 w
R_{22} — 200,000, 1 w*
R_{23} — 2 meg, 1 w
R_{24} — 10,000, 10 w
R_{25} — 100,000, 1 w
R_{26} — 10,000, 10 w
R_{27} — 100,000, 1 w
R_{28} — 2 meg, 1 w
R_{29} — 200,000*
R_{30}, R_{31} — 2,500, 10 w
R_{32} — 10,000, 10 w
R_{33} — 100,000, 1 w
R_{34} — 35,000, 1 w
R_{35} — 10,000, 10 w
R_{36} — 100,000, 1 w
R_{37} — 35,000, 1 w
R_{38} — 1 meg, 1 w
R_{39} — 20,000, pot.
R_{40}, R_{41} — 100,000, 1 w
R_{42} — 5,000, 10 w
R_{43} — 75,000, 1 w
R_{44} — 1 meg, 1 w
R_{45} — 15,000, pot
R_{46} — 75,000, 1 w
R_{47}, R_{48} — 100,000, 1 w
R_{49} — 1 meg, 1 w
R_{50} — 20,000, pot.
R_{51} — 1 meg, 1 w
R_{52} — 75,000, 1 w
R_{53} — 15,000, pot.
R_{54} — 75,000, 1 w
R_{55} — 150, 10 w
R_{56}, R_{57} — 300, 10 w
R_{58}, R_{59}, R_{60} — 100,000, 1 w
R_{61} — 1 meg, 1 w
R_{62} — 100,000, pot.
R_{63} — 15,000, 10 w
R_{64} — 1 meg, 1 w
R_{65} — 250,000, 1 w
R_{66} — 75,000, pot.
R_{67} — 75,000, 1 w

C_1, C_2, C_3, C_4 — 0.1 μf, 600 v
C_5, C_6, C_7, C_8 — 8 μf, 600 v, elec.
C_9, C_{10} — 2 μf, 1000 v, oil
C_{11}, C_{12}, C_{13} — 4 μf, 600 v, oil
C_{14}, C_{15} — 8 μf, 600 v, elec.
C_{16}, C_{17}, C_{18} — 1.0 μf, 600 v, oil
S_1 — Two-gang rotary, each gang SP, eleven-position
S_2 — SPST rotary
S_3 — Two-gang rotary, each gang SP, three-position
S_4 — DPST toggle
L_1, L_2 — Power Transformer, 180 va, 400-0-400 v, 200 ma d. c., 5 v-amp, 6.3 v — 5.14 amp, Thordarson T-13R16.
L_3 — Power transformer, 590-0-590 v, 200 ma d.c., 6.3 v-3 amp, Kenyon T-247.
L_4, L_5, L_6, L_7, L_8, L_9 — Filter choke, 12 h at 0 ma, 5 h at 200 ma, d.c., 80 ohms, 1600 v insulation test, Thordarson T-67C49.
F_1 — 5 amp, Type 3AG
P_1, P_2 — Ten-terminal flush female chassis connector, Jones S-310-FP.
P_3 — Flush female chassis connector
P_4 — Three-terminal female chassis connector, Amphenol PC3F.
P_5, P_6, P_7 — Banana jack
P_8, P_9 — Seven-terminal terminal strip

* Precision-type, (IRC Type WW-4), wire-wound resistors.

† R_{20} consists of ten 25-ohm, ½ w resistors, connected in series across the terminals of an 11-position rotary switch, and isolated from the remainder of the circuit with a 1000 ohm, 10 watt resistor at either end of the switch.

mands for economical power-supply design and by the noise which is introduced by the first stage, which noise is not eliminated by the circuit. By suitable design of the circuit, the proper value of R_s generally may be provided to obtain the requisite frequency response, gain, and average output level which may be desired.

In practice it has been found that R_1 is relatively high. Accordingly, the stray circuit-capacitance and the interelectrode capacitances of T_s and T_3 operate as a shunt to ground for the high-frequency components of the signal at point *a*. By the addition of C_1, the effect of these stray capacitances is neutralized. Limitations on high-frequency response of the stage, then, become the same as those governing the operation of conventional resistance-capacitance-coupled amplifiers. The value of C_1 must be large with respect to the sum of stray circuit-capacitances and the interelectrode capacitances of T_2 and T_3. In practice, a capacitance of 0.01 μf or more has been found satisfactory for circuits of the type shown here.

Distribution of Potential

The circuit of Fig. 4 illustrates the type of potential-distribution problem encountered in the application of the direct-coupled amplifying unit to a three-stage cascaded direct-coupled amplifier.

The first stage, which consists of T_1 alone, is a conventional direct-coupled amplifier. Its output signal is superimposed upon its average plate potential of +150 volts. T_2 operates as a coupling element to the grid of T_3, which is an amplifier. T_4 and T_5 operate in like manner to T_2 and T_3. The average potential, with no signal applied to the input circuit, is given for all significant points in the circuit. It will be noted that the output level of each stage, exclusive of the input stage, is at ground potential.

The feedback resistor R_{22}, which is shown in Fig. 4, has no function in the distribution of average potential. It is employed, rather, in the final design of the amplifier

TABLE I. Overall Amplifier Gain as a Function of Attenuator Setting and Actual Amplifier Gain

Attenuator Setting	Amplifier Gain Setting		
	1000	2000	5000
0	0	0	0
1	1	2	5
2	2	4	10
3	5	10	25
4	10	20	50
5	20	40	100
6	50	100	250
7	100	200	500
8	200	400	1000
9	500	1000	2500
10	1000	2000	5000

as a gain-control element.

Design for a Typical Amplifier

Figure 5 illustrates schematically a complete design for a direct-coupled amplifier. The maximum voltage-gain of the amplifier is 5000 times. Its input impedance is 100,000 ohms. The high-frequency response of the unit is given in Fig. 6. The low-frequency response of the amplifier is uniform, at the maximum value shown in Fig. 6, to zero cps.

The amplifier has been designed for direct deflection of a Du Mont Type 5LP5 cathode-ray tube, which is operated with a second-anode potential of 1000 volts and an intensifier-electrode potential of 2000 volts. Instability of gain and drift cannot be observed on the screen of the cathode-ray tube. The amplifier is operated entirely from alternating-current power.

Input Circuit

A balanced input attenuator (Fig. 7) is provided in the amplifier for reduction of the input signal to an amplitude which is proper for the grid of the first stage and for control of the magnitude of the output potential. The attenuator gives steps in gain in the ratio of 2 to 1 as closely as could be obtained with available values of standard commercial resistors. Eleven fixed positions of the input attenuators are available which, with three fixed values of amplifier gain, give a total of 33 gain positions. The maximum attenuation, exclusive of the "OFF" position, is 10^{-4}. The gain settings available are given in Table I.

Immediately following the input attenuator in the circuit is a three-position switch which will ground either side of the amplifier input for use with signals which are unbalanced with respect to ground. An ungrounded position is provided for use of the amplifier in the conventional balanced manner.

Balance of the Amplifier

The term "balance" is used to refer to the overall adjustment of any or all of the characteristics of an amplifier to readjust the output-circuit performance to compensate variations such as drift, change in gain, change in output level, and other factors. Practically all direct-coupled amplifiers require a balance control of some type for final adjustment of the operation of the amplifier. The balance of the amplifier shown in Fig. 5 is controlled by adjustment of potentiometers R_{17} and R_{20}. The balance control for this amplifier is merely an adjustment for the potential of the grid of T_2, Fig. 2, which adjustment is obtained by varying its position along the cathode resistor of T_2, Fig. 2. Potentiometer R_{20}, Fig. 5, has a wide range of control, and it is mounted on the chassis of the instrument for adjustment only during servicing and maintenance,

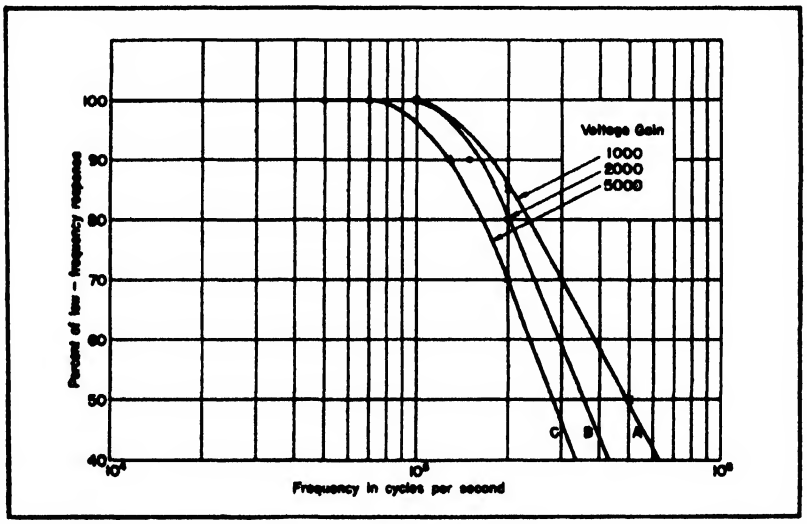

Fig. 6—High-frequency response characteristic of the amplifier

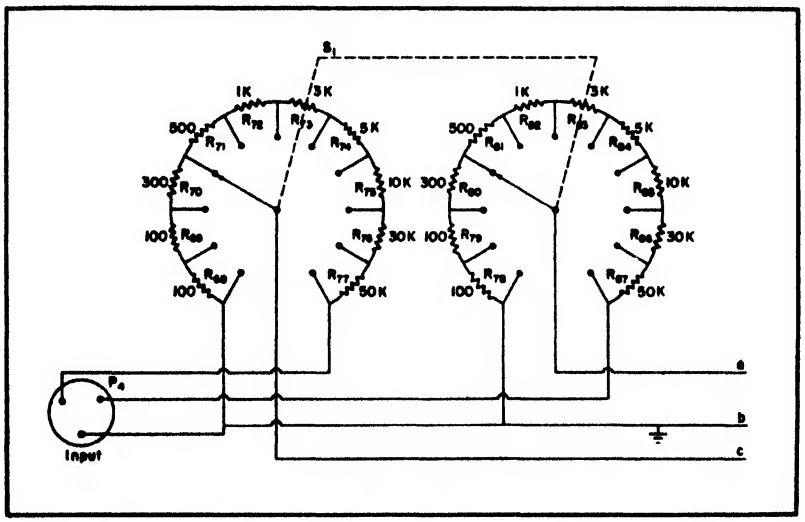

FIG. 7—Input attenuator detail. Each resistor is a ½-watt unit

or when tubes are changed. Potentiometer R_{17} functions as a vernier on R_{20}, and it is mounted on the front panel of the amplifier for use as a spot-position or pattern-centering control.

Feedback Circuits

Negative voltage-feedback is employed in this amplifier to vary the voltage gain, to stabilize the voltage gain, to reduce drift, to broaden the frequency response, and to reduce the effective output impedance of the unit.

One feedback circuit extends from the plates of the output tubes to the plates of the input tubes. To obtain the proper polarity for negative feedback, the two balanced sides of the amplifier must be cross-connected. This type of feedback minimizes differential variations between the two sides of the push-pull amplifier. The feedback elements between T_8 and T_1', for example, consist of R_{32} and R_9.

Negative voltage-feedback also is employed to control voltage gain of the amplifier. This is accomplished through feedback used independently on each phase of the balanced unit. T_8 feeds signal voltage back to T_4, and T_9 feeds back signal to T_5. S_2 is a two-section gang switch which controls the feedback simultaneously on each channel. Positions are provided for voltage gains of 1000, 2,000, and 5000 times.

Direct-Current Heater Operation

Since the interstage coupling elements T_2, T_3, T_6 and T_7 are the most likely single sources of instability in the amplifier, their internal characteristics are kept as nearly constant as possible by operation of their heaters from a regulated d-c source. This precaution has been found to contribute greatly to the freedom from drift found in this amplifier. Much of the drift problem in this design depends upon the constancy of the operating parameters of these coupling elements. In this connection, also, it was found highly desirable to employ commercial "precision" resistors, such as IRC Type WW-4, for the plate-load resistors of the coupling tubes because of their low temperature-coefficient of resistance.

Inasmuch as the input stage receives no compensation of any type, and to reduce a-c ripple in the amplifier output, the heater of this tube also is operated from a d-c source.

Amplifier tubes T_4, T_5, T_8 and T_9 all are operated from a conventional alternating-current source.

Power Supplies

Power for the complete amplifier is supplied by three separate rectifier-filter systems. The output of each system is controlled by an electronic regulator. The first system, reading from the top of Fig. 5, has an output of +200 volts. The second system furnishes regulated power for operation of all heater circuits which require direct-current operation. The third system has an output potential of −400 volts for operation of the amplifier.

Acknowledgments

The concept and design of the basic coupling circuit and the development of the final amplifier unit are the work of Mr. George W. Cook of the Electronics Section of the David Taylor Model Basin. The mathematical analysis of the circuit was performed by Mr. Westley F. Curtis of the Structural Mechanics Section.

A D-C Amplifier of High-Current, Low-Impedance Output

By LAWRENCE FLEMING

THE PROBLEM of making a d-c amplifier which will deliver a large current to a low-impedance load is difficult to solve by conventional means. Ordinarily the load of a d-c amplifier must be connected directly in the space-current path of the last tube, because a matching transformer cannot be employed. Power tubes require at least 100 volts between plate and cathode in order to conduct sizeable currents; when the drop across the load is but a few volts the efficiency of the system becomes very low. If output currents of more than about 200 milliamperes are needed, an inconvenient number of large tubes in parallel must be used.

Direct-current driving amplifiers are often required for oscillographic work. The amplifier here described delivers up to one ampere to an oscillograph element of three ohms impedance, with a frequency range of zero to several thousand cycles. Since it was clearly impractical to parallel enough power tubes to conduct one ampere (several channels were required), the expedient was employed of using a carrier-current system terminating in an output transformer and a dry-disc rectifier.

Performance

Specifications of general interest are: Maximum output, 1.2 amperes into 3 ohms. Input signal for maximum output, 10 volts d-c. Input impedance, 10 megohms. Frequency range, 0 to 4000 cycles.

The linearity of the input-output relation is shown in Fig. 3. The stability is high and the system operates for months at a time without adjustment.

Figure 1 shows the system in block-diagram form. An oscillator supplies carrier excitation to the grid of modulator tube V_1. This tube is operated as a class C amplifier, so that its carrier-frequency output is proportional to its plate voltage. The plate voltage of tube V_1 is supplied by the d-c input signal through a cathode follower V_2. The carrier output of modulator tube V_1 passes through a bandpass filter which passes the carrier frequency and the sidebands, thence through a power amplifier, an output transformer, and a dry-disc rectifier. The d-c output of the system is taken from the rectifier.

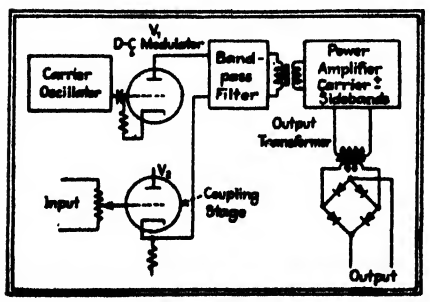

Fig. 1—Functions of the several stages of the oscillator-amplifier arrangement for supplying up to one ampere of direct current to a three-ohm load

Modulator Circuit

The class C type of modulator used has a higher order of stability than the more conventional diode, varistor, or square-law type of balanced modulator. To minimize the residual carrier voltage appearing at the output of the modulator when its plate voltage is zero, the modulator stage may be neutralized, or it may be operated as a frequency multiplier without neutralization. In practice, the latter is simpler and just as effective.

The best tube for use as a modulator is a high-mu triode. The excitation voltage is not critical. Operating constants for the modulator in the system shown are: Grid excitation, 20 volts. Plate voltage operating range, 0 to 10 volts. Load (filter) impedance, 7500 ohms.

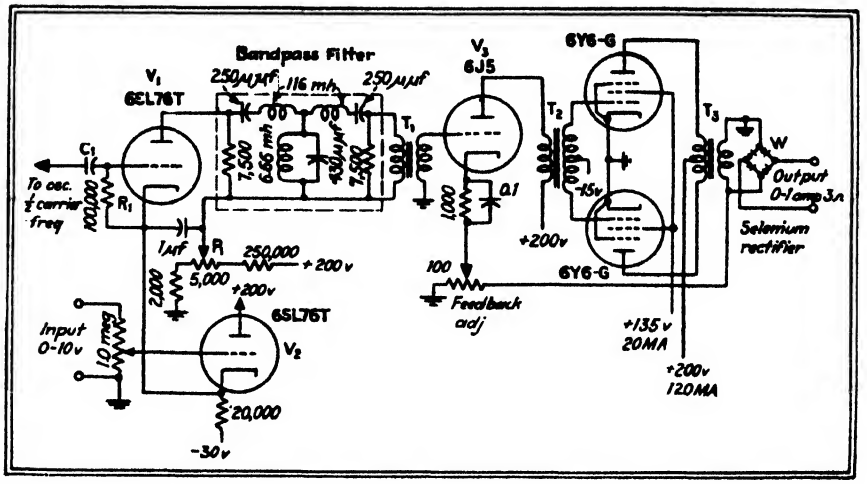

Fig. 2—Complete circuit of the direct-current amplifier. Use of a carrier-current system provides one ampere d-c output without using several tubes in parallel to conduct such a large current

Details of Circuit

Figure 2 is a schematic diagram of a complete amplifier channel. The modulator tube V_1 is biased conventionally by means of grid leak R_1 and capacitor C_1. The no-signal plate voltage of V_1 is adjusted by potentiometer P_1, which permits utilizing input signals of either polarity. The cathode follower V_2 is here arranged to drive the cathode of V_1 instead of the plate. A negative signal at the grid of V_2 thus increases the voltage between the plate and cathode of V_1.

The bandpass filter should pass the carrier frequency and the upper and lower sidebands. If the percentage bandwidth is small, a tuned circuit can be substituted for the filter.

In this particular case, an overall response of 0 to 4000 cycles was required. The carrier frequency chosen was 30 kilocycles. The filter was designed for a nominal bandwidth of 25 to 35 kilocycles.

Because of the high carrier frequency, special transformers had to be built for use at T_1, T_2, and T_3. At 10 kilocycles and below, ordinary audio transformers should be satisfactory.

The rectifier W at the output of the system is a Federal selenium unit, type 5B1AV1. At 30 kilocycles, the efficiency of dry-disc rectifiers is about half that obtained at lower frequencies. Hence if a lower maximum frequency of overall response is usable, a lower carrier frequency can be employed with a consequent reduction in the size of the power amplifier.

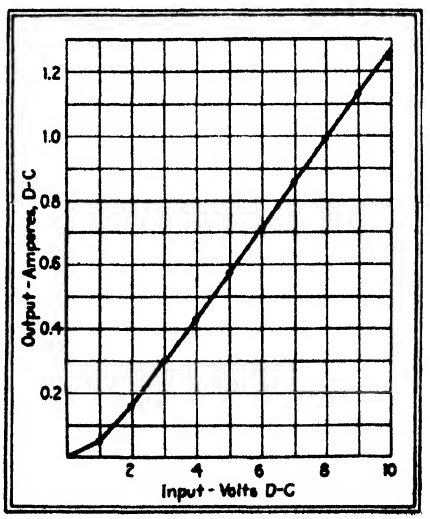

Fig. 3—Input-output characteristics of the direct-current amplifier

Gas-Tube Coupling for D-C Amplifiers

Combining a cathode follower with a gas diode gives a stable and efficient coupling network. Evolution and operation of the circuit are explained

By FULVIO IANNONE and HOWARD BALLER

PROBLEMS of supplying operating potentials to direct-current amplifier stages connected in cascade are bothersome. Each additional stage of amplification requires extra potential from the power supply and frequently causes trouble with insulation and voltage drift. Negative feedback is helpful in reducing drift but the difficulties of cascading direct-current amplifiers usually require the designer to minimize the total number of stages.

Figure 1 illustrates several methods of coupling. The circuit at Fig. 1A introduces no loss in transferring the signal from the plate of the first stage to the grid of the following stage, although it is very susceptible to drift introduced through supply voltages. The circuit at Fig. 1B uses a glow tube or neon lamp as a coupling element. Choice of the value of R_g in this circuit is a compromise; ordinarily R_g should be smaller than the d-c resistance (R_n) of the gas tube and larger than its a-c resistance (r_n) so that a smaller percent of the d-c voltage present on the plate of the first tube will be coupled to the grid of the second tube than the percent of a-c voltage that is so coupled. In addition, direct current flowing through the gas tube is limited by its rating and by the voltage drop caused in the plate load resistor of the first stage. As a result of these limitations on the design. R_g must sometimes be chosen in such a way that substantial coupling loss occurs. The VR type of tube with rated average current is ordinarily not considered for this application because its d-c resistance is of the same order of magnitude as the plate load resistors which may be desired.

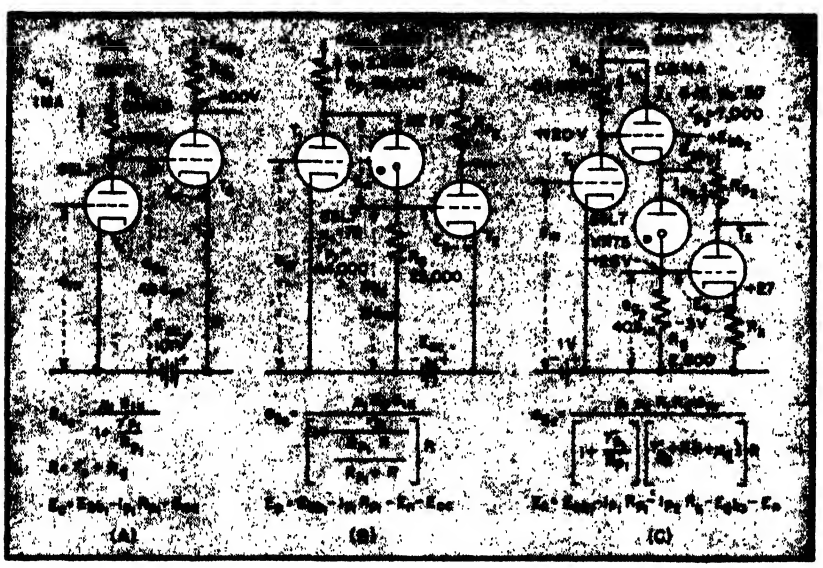

FIG. 1—Conventional d-c amplifier circuit and two methods of using gas tubes for coupling between stages. Typical values for the networks are given

Improved Coupling Circuit

The circuit illustrated in Fig. 1C suffers from none of these disadvantages. An additional tube is used as cathode follower with its cathode impedance composed of the VR tube and resistor R_p. With this arrangement there is no d-c load on the first amplifier and the input impedance of the cathode follower is so high that it does not affect the gain of the first stage. Most of the d-c voltage drop in the cathode circuit of the follower stage occurs across the VR tube while almost all of the signal drop appears across R_p. Because the current through the VR tube flows in a path separate from the d-c plate current of the first stage, the design of the first stage is independent of the d-c resistance of the VR tube. The only requirement is that R_g must be much larger than the dynamic impedance of the VR tube. Coupling loss of signal voltage from the first amplifier plate to the second amplifier grid is only slightly greater than the ordinary cathode-follower loss. Figure 1C also shows how a negative feed-back resistor (R_k) can be inserted in the cathode of the second amplifier to increase stability.

The gas tube coupling should only be applied in circuits where the signal level is high enough so that noise from the gas discharge will be negligible. A conservative figure is to keep the total signal change more than 50 mv. Maximum signal change allowable across the VR tube is a function of current

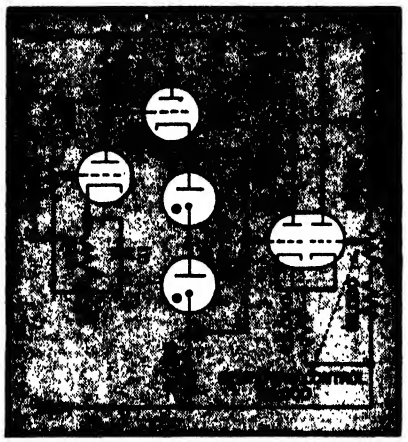

FIG. 3—Circuit of direct-coupled amplifier for an oscilloscope. The novel coupling system provides a response flat within one db to ten kilocycles

and, to a slight degree, frequency. For design purposes the change of voltage across the VR tube should be held to less than 0.5 volt. When neon tubes are used, the maximum allowable signal voltage drop across them is approximately one or two volts, depending on the type of tube and the d-c operating current. This limit must be observed because the signal current variations through the glow tube may be sufficient to drive it to the point of extinction on negative signal current peaks or to overload it on positive signal currents. Distortion of the waveform occurs as a result of either of these conditions.

Impedances of Gas Tubes

Magnitude and phase angle of impedance were measured for the four VR types, VR75, VR90, VR105, and VR150, and for two common neon tubes, rated at 1/25 watt and ½ watt. The frequency range was from 20 cycles to 20 kc. The data show that impedance does not vary much at the lowest frequencies, and tests confirm the fact that the magnitude of the impedance given on the curves for a frequency of 20 cycles is very close to the value at frequencies from zero up to 20 cycles.

The results in all cases indicate (1) that there is a steady increase of the ohmic impedance with increased frequency; (2) the phase angles are always inductive, that is, the current lags the voltage by an angle between zero and 180 degrees (angles greater than 90 degrees indicate negative resistance); (3) for a given tube operated within ratings, the impedance is reduced by increasing the average current.

Figure 2 illustrates the approximate values of impedances and phase angles to be expected from typical gas tubes. All the tubes tested were made by leading manufacturers and were in good condition. However, impedances differed by as much as 20 or 30 percent when other tubes of the same type and manufacturer were substituted. Consequently, the curves should only be construed as approximate, and exact values from them cannot be relied on. This is no serious disadvantage, because the circuits in which they are applied do not require exact ohmic values, a 20 percent change in gas tube impedance producing about one percent change in grid voltage.

Bypass capacitors should be connected across the gas tubes if the rise of impedance at high frequency causes difficulty. The graph of phase angle, which is also approximate, was drawn by averaging the data on each tube for the three operating currents 10, 20, and 30 ma. There is no significant change in phase as a function of average current except for subnormal average currents, which produce negative resistances at low audio frequencies.

An application of gas tubes is illustrated in the circuit of Fig. 3, which is a direct-coupled amplifier for use in feeding a pair of deflection plates in an oscilloscope. It has a gain of about 400 and is flat within 1 db to 10 kilocycles.

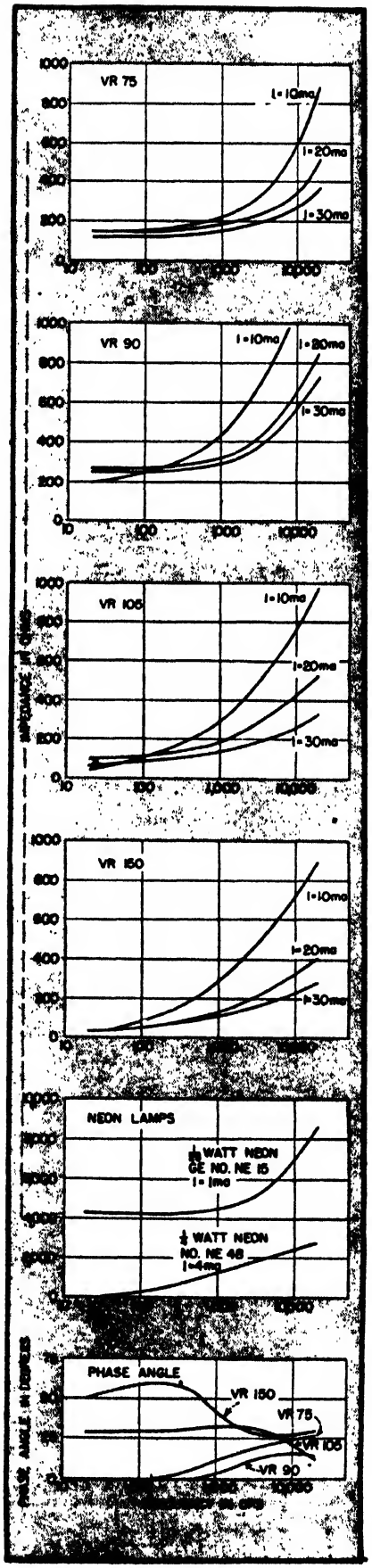

FIG. 2—Characteristics of voltage-regulator gas tubes and neon lamps

High-Gain D-C Amplifier

By W. G. SHEPARD

UNBALANCE resulting from shifting grid bias is eliminated by a parallel balanced directly coupled amplifier that has high gain, low drift, flat response from 0 to 50,000 cps, and negligible phase shift to 20,000 cps.

Counteracting Unbalance

Figure 1 shows several directly coupled amplifiers. The amplifier in Fig. 1A is of the push-pull type in which the signal is of equal amplitude but opposite phase in the two channels. Because drift voltage is in phase in each channel it does not add to the signal. Common cathode resistors in each stage tend to equalize the signal in each channel. When several stages are cascaded to give very high amplification, adjustments on any one stage seriously disturb other stages by affecting the bleeder current common to all stages. To obtain amplifier stability, these interrelating biases need to be eliminated.

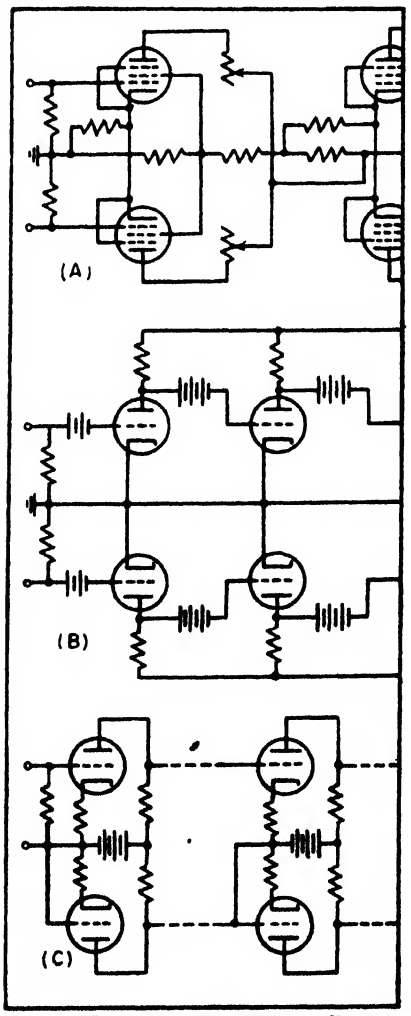

FIG. 1—The top two circuits illustrate common types of direct coupling; the lower one shows an improved method

In a circuit such as that of Fig. 1B where individual batteries are used to furnish the voltage drop between the plate of one tube and the grid of the next, any drift voltage in a stage appears equally on the grids of the next stage and therefore does not interfere with the signal. However, the drift does change grid biases of subsequent stages. As this change in grid bias is amplified by subsequent stages, it may reach proportions that shift the bias of final stages beyond satisfactory operating limits. Were common cathode resistors used, the effect would be decreased, but would not be eliminated.

Difficulty of adjustment and the passing on of drift voltages can be eliminated by the circuit of Fig. 1C. The amplifier consists of a series of independent stages linked with only two connections (shown dotted). One connection carries the signal; the other, the reference voltage. To keep each stage separate, individual power supplies are used. Only one side of each stage carries the signal, the other being to cancel drift voltages. Any drift affecting both tubes of a stage equally will not produce a change in voltage at the coupling out of that stage.

Because only one channel of the balanced amplifier carries signal, no special shielding or placement of parts is necessary in the nonsignal channel. Furthermore there can be no interaction between a nonsignal half of a stage and any other stage, or, because no common cathode resistor is used, between nonsignal and signal halves of a

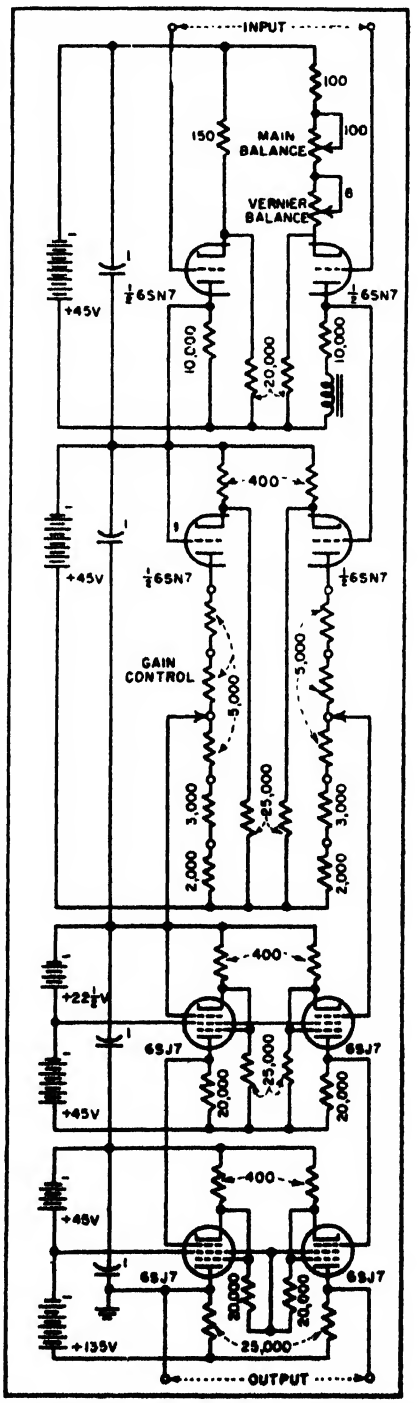

FIG. 2—Four stage directly coupled amplifier is stabilized against drifts

single stage. As a result the nonsignal halves of the stages can be adjusted without affecting the rest of the amplifier, and once it is adjusted, that half of the amplifier can be forgotten. (It is assumed that there is no grid current in the signal channel. If there is grid current, low plate loads can minimize its effect.)

Because it is impractical for components of both channels to exactly correspond, some adjustment is necessary. Fortunately adjustment of grid bias in the first stage will satisfactorily correct all succeeding stages. If corresponding components of both channels are closed matched, changes in grid bias from such a single adjustment will not move the tubes out of operating limit.

Figure 2 shows a four-stage version of this type amplifier; filament wiring and battery disconnects are omitted. The voltage gain is about 10,000. A final amplifier stage (not shown) has been used to bring the over-all amplification to either 250,000 or 1,000,000.

Two variable resistors in the cathode circuit of the first stage provide balancing adjustment. Cathode degeneration is reduced by using bleeder resistors. A stepped gain control is introduced between the second and third stages that does not destroy amplifier balance or drift cancelation. The capacitors, by lowering a-c impedance between power supplies, prevents oscillation. A dual type tube was chosen for the first stage as the two sections, being in the same envelope, are more apt to be subjected to the same changes. Because of the high gain, battery power is used to avoid hum. Medium size B-batteries (Burgess No. 5308) have shown a surprisingly long life. A 6-volt storage battery supplies the heater current. The final stage can be operated from an a-c powered supply.

Construction and Performance

Two amplifiers were constructed using standard parts. Resistors were of the ordinary metallized variety, each one in the signal channel being matched to within two percent of the corresponding one in the nonsignal side. To obtain the necessary fineness of adjustment, the 8-ohm vernier was a specially made spiral slide wire. Signal-carrying wiring was kept isolated from other parts where possible; a shield was put between stages. Input and output leads were kept well separated. The 6SN7 tubes were tested to obtain those having the least drift and being the least microphonic; so the 6SJ7 tubes were selected in matched pairs. Both amplifiers have performed very well for over two years.

Amount of drift depends largely on how closely the input tubes are matched and how long a warm-up is allowed. Because most of the drift is caused by change of cathode temperature, the heater current is turned on first. Tests with carefully selected tubes indicate that, after 10 minutes of warm-up, a drift equivalent to about 0.5 millivolt input signal can be expected over two hours. After the first hour, if no overloading has occurred, the equivalent drift has decreased to about 50 microvolts over a two-hour period.

The frequency response is essentially flat from zero to at least 50,000 cps, and could be further extended if compensation in addition to the 85-mh inductance in the first stage were added. This inductance, wound on a high permeability iron core, reduces phase shift, which comparison of input and output signals on an oscilloscope shows to be less than 10 degrees at 20,000 cps. The use of screen-grid tubes accounts for the high-frequency response with high gain because low plate resistances can be used without sacrificing amplification, as would be the case with triodes. This circuit lends itself to the use of screen-grid tubes, whereas in many d-c amplifiers their use is difficult.

The amplifier output is necessarily at a relatively high positive potential (150 to 200 volts) with respect to the input. Thus, only the input or the output, not both, can be grounded; the other must be well insulated from ground and handled accordingly. If the amplifier drives an oscilloscope, it is ordinarily more satisfactory to ground the output of the four stages shown in Fig. 2, allowing the final amplifier plates, which should be connected directly to the deflection plates of the cathode-ray tube, to assume a positive potential with respect to ground, and the input to the four-stage amplifier to assume a negative potential.

Stabilized D-C Amplifier with High Sensitivity

By H. S. ANKER

THIS amplifier is designed to measure very small currents or voltages from a high-impedance source. Special features incorporated are a new input tube, increased linearity, good stability, and a regulated power source.

The input tube of the amplifier was carefully selected, as low grid current is necessary and high amplification desirable. Of many tube types tested, the miniature tube 12BE6 was found to be the most suitable. It has a grid current only slightly higher than that of special

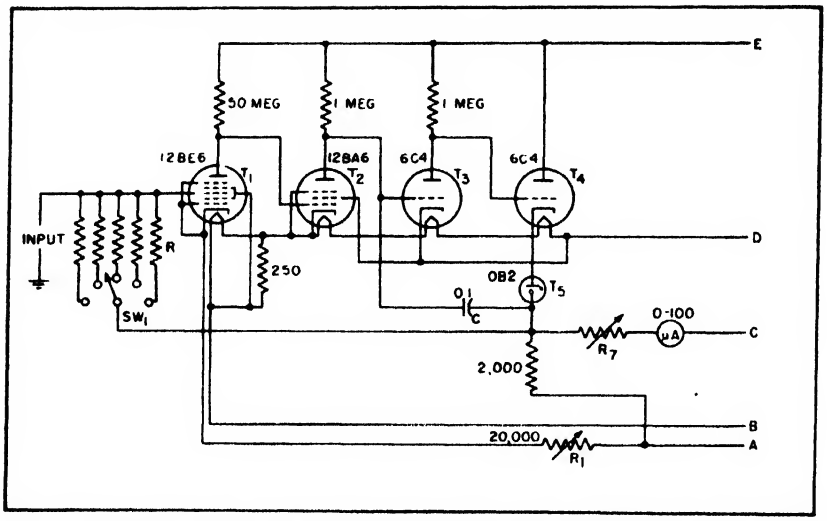

FIG. 1—Input ranges are determined by choosing values of R from 10 to 100,000 megohms. Lettered leads correspond to those shown in Fig. 2

electrometer tubes and at the same time has the advantage of a high amplification factor in addition to being generally available and much less expensive. Only small variations were found in the operating characteristics of the several tubes tested.

At the most satisfactory operating point, the plate voltage is 12 volts, the screen voltage (grids 2 and 4) is approximately 7.5 volts, and the control grid (grid 3) is negatively biased to 2.5 volts. Grids 1 and 5 are connected to the cathode. The heater current is reduced to 105 ma. Under these conditions, the grid current is about 10^{-13} to 10^{-11} amperes and the amplification factor is between 200 and 300. The tube must be well shielded from light and coated to prevent surface leakage.

Amplifier

The amplifier circuit shown in Fig. 1 is based on an amplifier described by Roberts[1]. Three stages of voltage amplification are used, following by a cathode follower as the last stage. For stability, the tubes are heated from the regulated power source.

The sensitivity is changed by a Shallcross No. 4765 switch in which the bakelite baseplate has been replaced by one of polystyrene. Zero adjustment is made by means of R_1. The meter together with the series resistor R_7 forms a 1.0-volt meter. A 100-μa d'Arsonval type meter is satisfactory but the author prefers to use a galvanometer such as Leeds and Northrup No. 2420, especially when using the decade to be described, because the galvanometer can withstand a substantial overload without being damaged.

For more accurate readings, a decade may be inserted into the power source bleeder, and R_7 changed to make a 0.1-volt meter. The decade replaces part of R_8 for a positive or part of R_{10} for a negative input such that its total resistance is adjusted to give a voltage drop of one volt, permitting partial backing out of the signal. Each step of the decade corresponds to a voltage change of 0.1 volt. Under these conditions, the galvanometer will be on scale for only one setting of the decade for any input current. This setting of the decade is the first digit of the reading, the second and third digits being read on the galvanometer.

The input tube is washed carefully with absolute alcohol and dipped into polystyrene lacquer. It must be well shielded against stray pick-up, light, and protected from sudden temperature changes. It is preferable to mount the input tube inside an evacuated vessel. A polystyrene tube socket is used for it, and all input leads are insulated by means of polystyrene.

Capacitor C is used to quench oscillations. Depending on the layout, it may be necessary to change the connections and/or size of this capacitor to suppress oscillations.

Power Source

All supply voltages are obtained from the regulated source shown in Fig. 2 which is powered from the 115-volt a-c line. The filaments of the regulator tubes in the source as well as the filaments of the tubes in the amplifier form part of the bleeder.

The limiting factors of the stabi-

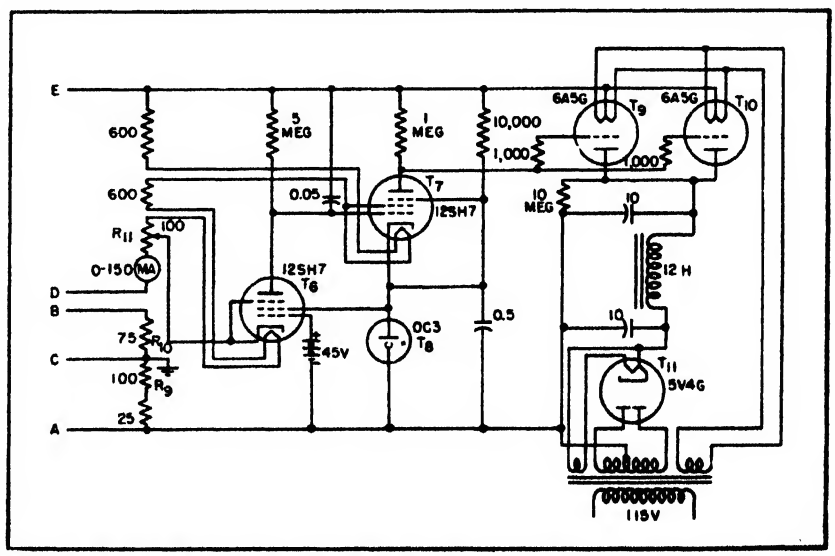

FIG. 2—Stabilization ratio greater than 25,000 is provided by this power supply

lization obtainable are the temperature variations of the resistors and of the characteristics of T_{1a}. To minimize these effects, the resistors, particularly those in the bleeder, were Advance wire wound. If it is desirable to increase the stabilization still further the power supply and the amplifier would have to be placed in a constant temperature chamber.

The stabilization ratio is greater than 25,000. If slightly reduced performance can be tolerated, the battery may be eliminated and the grid of T_a returned to the midpoint of a 100,000-ohm resistor connected across T_a. The stabilizer current through the milliammeter is adjusted by varying R_{1a}, and should be set to operate at 135 ma.

After preliminary adjustment of the power source, it and the amplifier should be allowed to run for 24 hours. During this baking period the tube characteristics will largely stabilize. Final adjustment can then be made. If the instrument is to be used continually, it is best to operate it 24 hours a day as there tends to be a small drift during the first two hours of operation. Variation in line voltage of 10 percent has a negligible effect.

(1) S. Roberts: *Rev. Sci. Inst.* 10, p. 181 (1939).

Cathode Follower Coupling in D-C Amplifiers

New screen-coupled cathode follower and phase inverter circuits permit design of three-tube d-c amplifier operating from a single 250-volt power supply, providing a gain of 60 db with flat response from 0 to 20,000 kc and almost unmeasurably low circuit noise level

By Y. P. YU

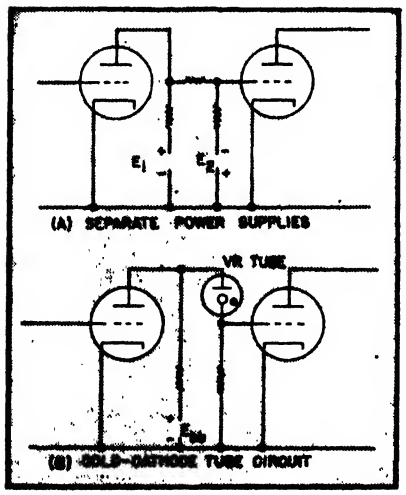

FIG. 1—Two conventional methods of coupling between stages in a d-c amplifier

THE method of coupling between stages is one of the difficulties in the design of d-c amplifiers with a single power supply, because the output of a given stage is usually at a high quiescent d-c potential above ground. In order to couple this output to the next stage, the high d-c potential must be cancelled in some manner.

One method employs a separate power source, as shown in Fig. 1A[1]. Here feedback through the power supply introduces oscillation or other undesirable effects, and highly regulated power supplies are needed.

Another method utilizes a type VR cold-cathode gas tube, as shown in Fig. 1B[2]. The defects of this arrangement are noise due to discharge in the gas, and heavy current drawn by the VR tube.

In order to overcome these difficulties, two methods are introduced in this paper. One is a pushpull phase inverter arrangement wherein a large cathode bias may be employed without the usual attendant disadvantage of negative feedback, and the other involves coupling the plate of one stage to the screen of a cathode follower stage.

Phase Inverter Circuit

The quiescent d-c cathode potential of a vacuum tube can be raised to a high value by means of a large resistance connected from the cathode to ground. In Fig. 2, the cathode quiescent d-c potential of T_2 or T_3 is equal to the voltage drop across resistor R_k. Also, E_k is equal to E_{b1} (the quiescent plate potential of T_1) plus E_{cc} (the bias voltage of T_2 or T_3).

In an ideal phase inverter, the input of T_2 should be equal to and 180 degrees out of phase with the input of T_3. Likewise, the output of T_2 should be equal and 180 degrees out of phase with the output of T_3. Therefore, the negative feedback produced in R_k by the plate current of T_3 is canceled completely by the

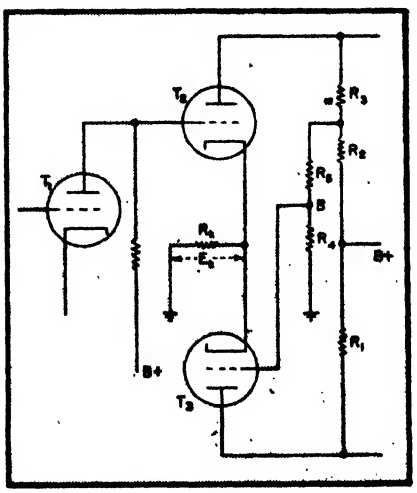

FIG. 2—Pushpull phase inverter circuit for d-c amplifier

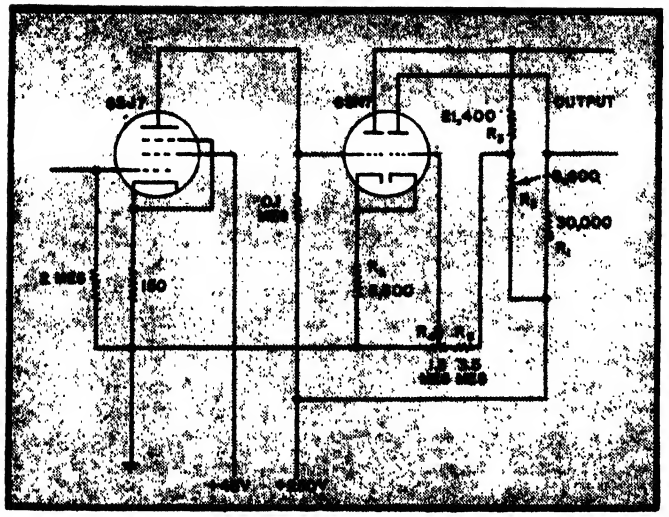

FIG. 3—Practical d-c amplifier circuit employing phase inverter stage and requiring only 250-volt plate supply

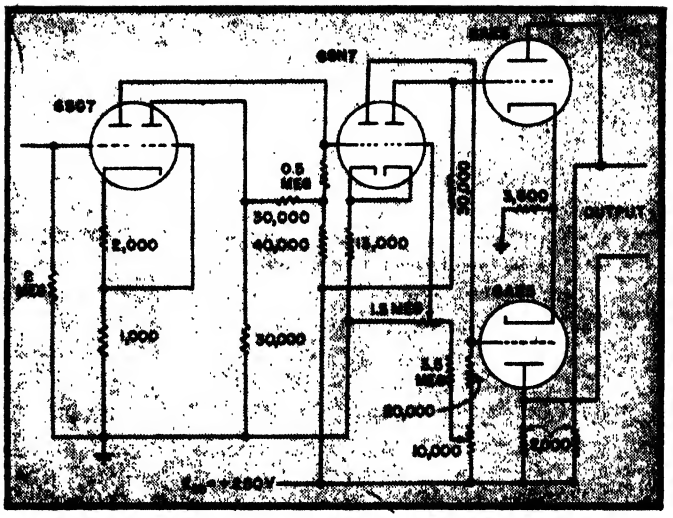

FIG. 4—Direct-current amplifier using double triode ahead of phase inverter to cancel plate current changes in first stage due to changes in cathode surface

negative feedback produced in R_5 by the plate current of T_2, since they are equal and 180 degrees out of phase.

The values of R_1, R_2, R_3, R_4, R_5, and R_6 in the circuit of Fig. 2 can be calculated as follows:

$$R_2 + R_4 = R_1 \tag{1}$$

$$R_k = \frac{E_{b01} + E_{cc}}{2I_{b02}} \tag{2}$$

where E_{b01} is the quiescent plate voltage of T_1, E_{cc} is the bias voltage of T_2 or T_3, and I_{b02} is the quiescent plate current of T_2 or T_3. For ideal phase inversion, the input of T_3 has its quiescent d-c potential equal to E_{b01} and its instantaneous signal component equal to minus e_{g2}, which is the signal component of the grid potential of T_2. Since the input of T_3 is taken at point B, we have

$$\frac{E_{bb} - I_{b02}R_2}{-g_2 e_{g2} R_2} = \frac{E_{b01}}{-e_{g2}} \tag{3}$$

$$g_2 = \left.\frac{\delta i_{p2}}{\delta e_{g2}}\right]_0 \tag{3a}$$

$$R_2 = E_{bb}/(g_2 E_{b01} + I_{b02}) \tag{4}$$

where $(E_{bb} - I_{b02}R_2)$ is the quiescent d-c potential at point B, E_{bb} is the B power supply voltage, g_2 is the transconductance of T_2 at the operating point, i_{p2} is the instantaneous signal component of the plate current of T_2, e_{g2} is the instantaneous signal component of the grid potential of T_2, and $-e_{g2}R_2g_2$ is the instantaneous signal component of the potential at point B.

The magnitude of the input voltage at the control grid of T_2 is set by adjusting the ratio of R_4/R_5, where R_4 and R_5 are simply arranged as a potentiometer. In other words, the ratio E_{b01}/e_{g2} determines the values of R_2, and the magnitude of E_{b01} or e_{g2} determines the value of the ratio R_4/R_5.

The value of $R_4 + R_5$ should be very large in comparison to R_2, because the potential at point B should not change appreciably after connection of resistors $R_4 + R_5$ from point B to ground. Also, the value of R_4 should not exceed the allowable grid leak value of T_2. About 8 to 7 megohms for $R_4 + R_5$ is satisfactory in most cases.

The ratio $R_4/(R_4 + R_5)$ may be expressed in two ways:

the characteristics of these two tubes, we have:

6SJ7		6SN7	
E_{b01}	= 50 volts	E_{b02}	= 85 volts
E_{g01}	= 40 volts	E_{cc2}	= − 2 volts
E_{cc1}	= − 0.5 volt	I_{b02}	= 4 ma
I_{b01}	= 2 ma	g_2	= 500 × 10^{-6}

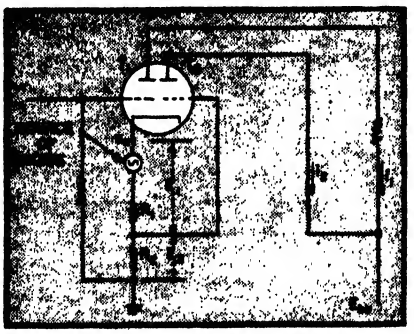

FIG. 5 (above)—Basic double-triode circuit used to cancel effects of cathode noise

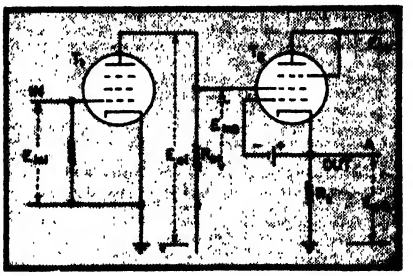

FIG. 6 (upper right)—Basic screen-coupled cathode follower circuit

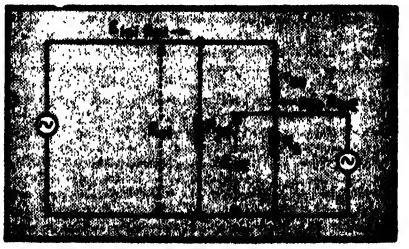

FIG. 7 (lower right)—Equivalent circuit of screen-coupled cathode follower

Calculation gives the following values for the resistors:

$$E_k = E_{bo1} + E_{co2} = 50 + 2$$

$$R_k = \frac{E_{bo1} + E_{co2}}{2\,I_{bo2}} = \frac{50 + 2}{2 \times 4 \times 10^{-3}} = 6{,}500 \text{ ohms}$$

$$\frac{R_4}{R_4 + R_5} = \frac{E_k}{E_{bb} - I_{bo2}\,R_2} \qquad (5)$$

$$\frac{R_4}{R_4 + R_5} = \frac{1}{R_2\,g_2} \qquad (6)$$

Design Considerations

Suppose a d-c amplifier is to be designed by using a 6SJ7 as T_1 and a double triode 6SN7 as T_2 and T_3, with a plate supply voltage E_{bb} of 250 volts, as shown in Fig. 3. From manufacturer's specifications giving

$$R_2 = \frac{E_{bb}}{g_2\,E_{bo1} + I_{bo2}} = \frac{250}{500 \times 10^{-6} \times 50 + 4 \times 10^{-3}} = 8{,}620 \text{ ohms}$$

If $R_4 + R_5 = 5$ megohms is used, from Eq. 6 $R_4/5$ megohms $= 1/(8{,}620 \times 500 \times 10^{-6})$, $R_4 = 1.14$ ohms, and $R_5 = 5 - 1.14 = 3.86$ ohms.

If the exact values of resistance are not obtainable, a potentiometer may be used for R_4 and adjusted to the right value. The total voltage gain of this amplifier is about 67 db, with uniform gain up to 12 kilocycles. A high-gain stage should not be used for this type of phase inverter circuit because when the ratio R_1/R_2 is very high, stability may be poor unless temperature-compensated resistors are used.

Low Noise Level Circuit

In Fig. 4, a double-triode 6SC7 is used instead of a 6SJ7, in order to cancel the change in plate current of the first stage due to the changes in work function of the cathode surface of the tube.[2] The basic circuit is shown in Fig. 5, and the function of this circuit is explained as follows:

$$E_1 = e_n - (i_1 + i_2)\,R_1$$
$$E_2 = (i_1 + i_2)\,R_2$$

where i_1 and i_2 are plate currents of T_1 and T_2 respectively. When the signal input to the grid of T_1 is zero, $i_1 = g_1\ (E_1 - E_2)$ and $i_2 = g_2 E_2$, where g_1 and g_2 are the transconductances of T_1 and T_2 respectively. Therefore

$$E_1 - E_2 = E_1 - [g_2\,E_1 + g_1\,(E_1 - E_2)]\,R_2$$

By rearranging and simplifying the above expression, we obtain an equation from which the performance of the circuit can more readily be deduced:

$$E_1 - E_2 = \frac{E_1 - g_2\,E_1\,R_2}{1 + g_1\,R_2}$$

When R_2 is equal to $1/g_2$, $E_1 - g_2 E_1 R_2 = 0$ and $E_1 - E_2 = 0$. The net change in plate current i_1 due to random changes in work function of the cathode surface or changes in heater voltage is therefore zero. A gain of 30 to 32 db can be expected from a 6SC7 in this type of operation.

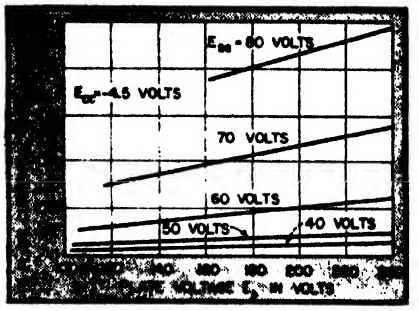

FIG. 11—Static characteristics of 6J7 for 4.5-volt bias

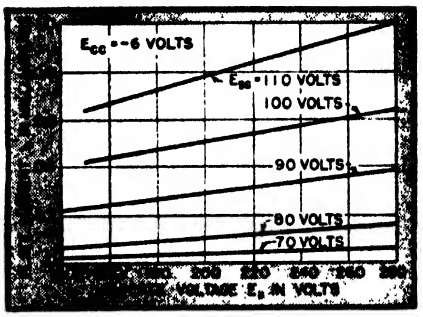

FIG. 12—Static characteristics of 6J7 for 6-volt bias

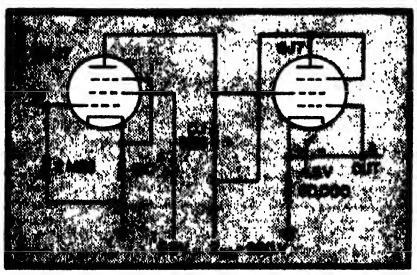

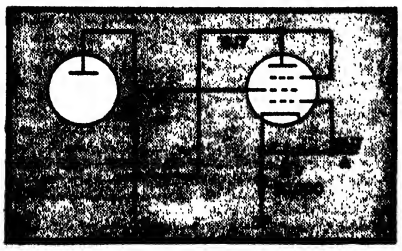

FIG. 8 (upper left)—Practical version of screen-coupled cathode follower

FIG. 9 (lower left)—Screen-coupled cathode follower with higher negative bias

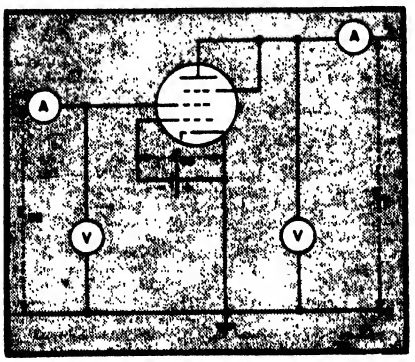

FIG. 10 (above)—Laboratory circuit used to obtain screen characteristics of 6J7

The noise level in the amplifier circuit of Fig. 4 is down to practically zero (about 0.01 microvolt referred to the input) with the input terminals shorted. The voltage gain is 70 db with a flat frequency response up to 12 kilocycles and less than 1 percent distortion for 5 millivolts sensitivity. Only one regulated 250-volt power supply is required. Good stability (practically constant output) has been had for a five-hour run after the initial warmup period. Feedback can be provided from the output of 6AE5 to the bias resistor of 6SC7 when wider frequency response is desired.

The remarkable feature of this method of coupling is that the noise level and the distortion percentage can be reduced to an extremely low value. The operation also can be stabilized to a very high degree if

Table I — Mathematical Analysis of Screen-Coupled Cathode Follower Circuit

E_{in1} = input voltage to T_1
E_{in2} = input voltage to T_2
E_{o1} = output signal voltage from T_1
E_{o2} = output signal voltage from T_2
r_{sg} = screen grid resistance of T_2
g_{m1} = control grid-to-plate transconductance of T_1
g_{m2} = control grid-to-plate transconductance of T_2
i_{sg} = screen current of T_2
R_{b1} = load resistor in plate circuit of T_1
R_k = bias resistor for T_2
g_{2p} = screen grid-to-plate transconductance of T_2

$$E_{o2} = (g_{2p} E_{in2} + i_{sg}) R_k \qquad E_{in2} = E_{o1} - E_{o2}$$

$$i_{sg} = \frac{E_{in2}}{r_{sg}} = \frac{E_{o1} - E_{o2}}{r_{sg}} \text{ so } E_{o2} = (E_{o1} - E_{o2})(g_{2p} + 1/r_{sg}) R_k$$

$$E_{o1} = (g_{m1} E_{in1} - i_{sg}) R_{b1} = g_{m1} E_{in1} R_{b1} - \frac{E_{o1} - E_{o2}}{r_{sg}} R_{b1}$$

$$E_{o1} = \frac{g_{m1} E_{in1} R_{b1} + E_{o2} R_{b1}/r_{sg}}{1 + (R_{b1}/r_{sg})}$$

$$E_{o2} = \left(g_{2p} R_k + \frac{R_k}{r_{sg}}\right)\left(E_{o1} - E_{o2}\right)$$

$$E_{o2} = \left(g_{2p} R_k + \frac{R_k}{r_{sg}}\right) E_{o1} \Big/ \left(1 + g_{2p} R_k + \frac{R_k}{r_{sg}}\right)$$

$$E_{o2}\left[\left(1 + g_{2p} R_k + \frac{R_k}{r_{sg}}\right) - \frac{\left(g_{2p} R_k + \frac{R_k}{r_{sg}}\right)\frac{R_{b1}}{r_{sg}}}{1 + (R_{b1}/r_{sg})}\right] =$$

$$\left(g_{2p} R_k + \frac{R_k}{r_{sg}}\right)\left(\frac{g_{m1} E_{in1} R_{b1}}{1 + (R_{b1}/r_{sg})}\right)$$

$$E_{o2} = \frac{g_{m1} E_{in1} R_{b1} (g_{2p} + 1/r_{sg})}{\left(\frac{1}{R_k} + g_{2p} + \frac{1}{r_{sg}}\right)\left(1 + \frac{R_{b1}}{r_{sg}}\right) - \frac{R_{b1}}{r_{sg}}\left(g_{2p} + \frac{1}{r_{sg}}\right)}$$

when $r_{sg} >> R_b$, $r_{sg} >> R_k$ $\qquad E_{o2} = \dfrac{g_{m1} R_{b1}\left(g_{2p} + \frac{1}{r_{sg}}\right)}{\frac{1}{R_k} + g_{2p}} E_{in1}$

all resistors are temperature compensated and all heater voltages are carefully regulated.

The objectionable feature of this method of coupling is that the plate supply voltage available for the last stage is low (only 95 volts in the circuit of Fig. 4). This defect can be avoided by the method of coupling next to be discussed.

Screen-Coupled Cathode Follower Circuit

If the input of a cathode follower circuit is coupled to the screen grid instead of the control grid as in the usual arrangement, a circuit is obtained which steps down the quiescent d-c potential to as low as a few volts at the output of the stage.

In Fig. 6, the input from the plate of the preceding stage feeds directly to the screen grid of T_2. The output of T_2 is taken from R_k and directly feeds to the control grid of the next stage. The quiescent d-c potential at point A, equal to R_k $(I_{b2} + I_{sg})$, can be made less than a few volts.

The equivalent circuit of Fig. 6 is shown in Fig. 7. The equation for the voltage gain can be obtained by a mathematical analysis of this circuit, as given in Table I.

When the value of $1/r_{sg}$ is very small in comparison with the other terms, the voltage gain equation may be simplified to

$$E_{o2} = g_{m1} E_{in1} R_{b1} g_{2p} \Big/ \left(\frac{1}{R_k} + g_{2p}\right)$$

Then the gain for the screen-coupled cathode follower stage alone is

$$\text{gain} = g_{2p} \Big/ \left(\frac{1}{R_k} + g_{2p}\right)$$

Therefore the maximum gain for the screen-coupled cathode follower stage (being equal to one) can be obtained when $g_{2p} >> 1/R_k$. When the plate current and the screen current both are small, R_k can be made large because even with a large R_k the cathode-to-ground potential, equal to R_k $(I_{b2} + I_{sg})$, is still not too large to make difficult the coupling into the next stage.

The plate current and the screen current of a tube can both be lowered by increasing the negative bias voltage on the tube. Unfortunately, when the negative bias voltage increases, the screen grid-to-plate transconductance g_{2p} decreases.

In Fig. 8, where a 6SJ7 is used as the first stage and a 6J7 is used as the screen-coupled cathode follower stage, the total voltage gain E_{o2}/E_{in1} is 30 db with 0.85 volt peak output. The quiescent d-c potential at point A, the output terminal, is minus 1.5 volts. This negative 1.5 volts can be utilized as the bias volt-

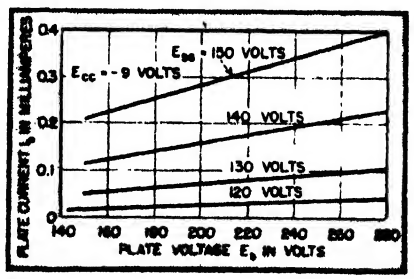

FIG. 13—Static characteristics of 6J7 for 9-volt bias

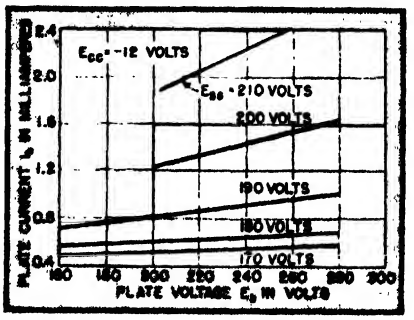

FIG. 14—Static characteristics of 6J7 for 12-volt bias

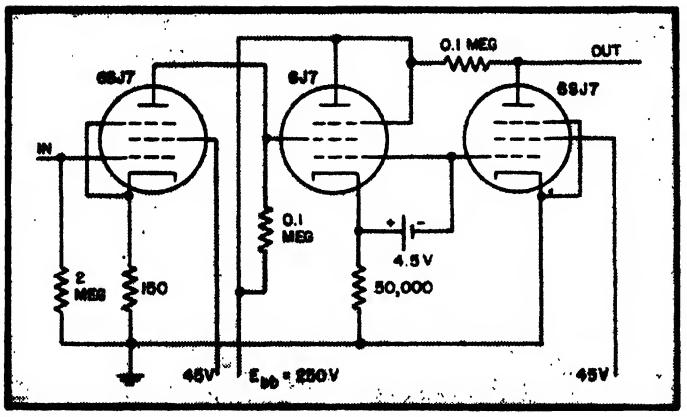

FIG. 15—Screen-coupled cathode-follower in d-c amplifier having 76 db voltage gain and flat response up to 12 kc

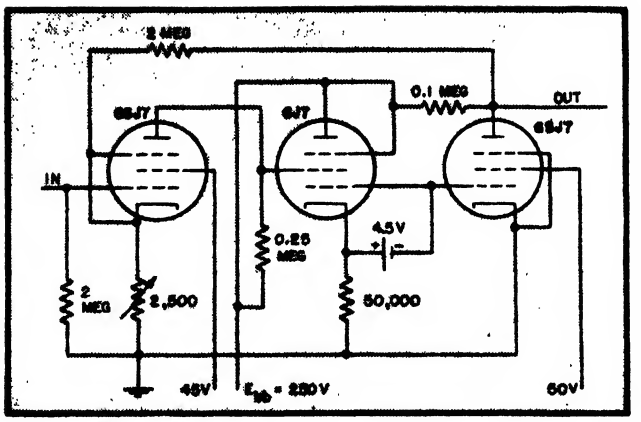

FIG. 16—Circuit of Fig. 15 with feedback resistor, giving 60 db gain but extending flat response up to 20 kc

age for the succeeding stage, and therefore point A can be connected directly to the control grid of the next stage.

In Fig. 9, with the negative bias increased to 12 volts, the quiescent d-c potential at point P, the input terminal, is 210 volts; after the screen-coupled cathode follower stage, the quiescent d-c potential at point A, the output terminal, is minus 1.5 volts. Point A can be connected directly to the control grid of the succeeding stage, utilizing this minus 1.5 volts as the bias voltage. About 8 db loss in voltage gain resulted from the screen-coupled cathode follower stage.

The screen characteristics of a type 6J7 tube were obtained by use of the laboratory setup shown in Fig. 10, with results as given in Fig. 11, 12, 13, and 14. The portions of the curves from zero plate potential to near the values of the screen grid potentials have been neglected, because the screen currents are so high in these ranges that the preceding stage might be overloaded; also, the curvatures of the plate characteristics are so high that large percentages of distortion may be expected. Many other types of pentodes no doubt are able to serve in this kind of arrangement. The choice lies mainly in the specification required.

Results and Discussion

The amplifier circuit in Fig. 15, with a 6SJ7 as the first stage, a 6J7 as a screen-coupled cathode follower stage, and another 6SJ7 as the final stage, has a total voltage gain of 76 db with 2.5 percent total distortion at 15 volts peak output. The frequency response is flat up to 12 kilocycles. The amplifier circuit in Fig. 16 is essentially identical except that a feedback resistor is provided from the output of the last stage (the plate of the 6SJ7) to the cathode of the first stage. The frequency response is raised to 20 kilocycles with a voltage gain of 60 db, and the distortion is reduced to less than one percent at 15 volts peak output.

The operation of screen-coupled cathode followers is stable with wide-band frequency response, because the circuit is highly degenerative. There is no appreciable change in output for a six-hour run after the initial warmup period.

A small percentage of distortion is to be expected in screen-coupled cathode follower circuits due to the nonproportional change of screen

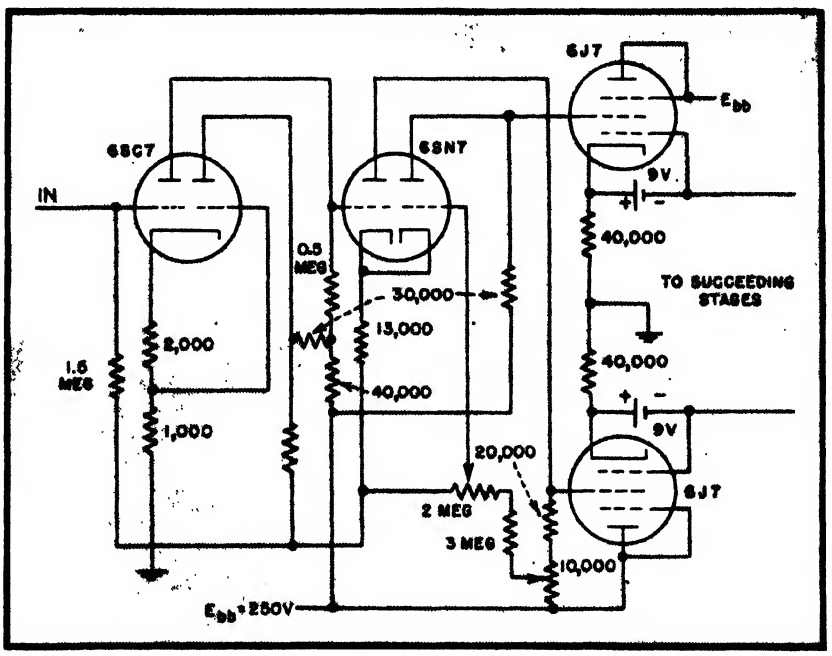

FIG. 17—Practical circuit combining screen-coupled cathode follower with pushpull phase inverter to give high-gain, wide-band operation with only a single conventional 250-volt power supply

current with respect to change of screen potential; in other words, the screen grid resistance is not exactly constant when the screen potential is varying; also, the screen grid-to-plate transconductance g_{sp} is not exactly constant when the screen potential is varying. About 0.5 percent distortion is produced by the screen-coupled cathode follower circuit in Fig. 8 when the output is 0.85 volt peak value.

Conclusions

Fortunately, most of the total distortion in a screen-coupled cathode follower circuit (about 85 percent of the total distortion in the amplifier circuit of Fig. 8) can be cancelled by a pushpull phase inverter arrangement such as the amplifier circuit shown in Fig. 17. Therefore, the pushpull arrangement which has been discussed in the early part of this paper may be incorporated with the screen-coupled cathode follower circuit to solve the problem of coupling between stages in a high-gain d-c amplifier using one common power supply of limited d-c voltage output.

The author wishes to acknowledge that this paper was prepared in the Electrical Engineering Department of Lehigh University with valuable advice from Professor E. M. Mode.

References

(1) Ginston, Edward L., D. C. Amplifier Design Techniques, ELECTRONICS, Mar. 1944
(2) Miller, Stewart E., Sensitive D. C. Amplifier for A. C. Operation, ELECTRONICS, Nov. 1941.

FILTERS

Resistance-Capacitance Filter Chart

Values of R and C for both low-pass and high-pass filters are given in terms of the amount of rejection desired at any given frequency from 1 millicycle to 1,000 megacycles. Chart also gives the reactance of a capacitor at any frequency

By ERNEST FRANK

RESISTANCE-CAPACITANCE filters are frequently used when a sharp cutoff characteristic is not required and, in the low-pass case, when the voltage drop across the series resistor can be tolerated. Applications of the low-pass R-C filter include decoupling from a common power supply for a multistage vacuum-tube amplifier, smoothing filters for power supplies when a large voltage drop across the filter is not objectionable, and inexpensive hash filters to attenuate high-frequency disturbances on electrical leads. High-pass R-C filters are often used as interstage coupling networks.

The circuits of Fig. 1 show the R-C low-pass and high-pass filter connected to an a-c generator. The generator resistance is assumed to be negligible compared with R, and d-c voltages are omitted for the purposes of an a-c analysis. R and C form a voltage divider, and the complex output voltage is given by

$$\text{Low-pass: } E_o = \frac{-jX_cE_i}{R - jX_c} \qquad (1a)$$

$$\text{High-pass: } E_o = \frac{RE_i}{R - jX_c} \qquad (1b)$$

The magnitude of the ratio of E_i to E_o is

$$\text{Low-pass: } \left|\frac{E_i}{E_o}\right| = \sqrt{1 + \left(\frac{R}{X_c}\right)^2} \qquad (2a)$$

$$\text{High-pass: } \left|\frac{E_i}{E_o}\right| = \sqrt{1 + \left(\frac{X_c}{R}\right)^2} \qquad (2b)$$

Solving the above equations for the generator frequency f gives

$$\text{Low-pass: } f = \frac{1}{2\pi RC}\sqrt{\left|\frac{E_i}{E_o}\right|^2 - 1} \qquad (3a)$$

$$\text{High-pass: } f = \frac{1}{2\pi RC}\frac{1}{\sqrt{\left|\frac{E_i}{E_o}\right|^2 - 1}} \qquad (3b)$$

When the reactance of C is equal to R, the ratio $|E_i/E_o|$ is equal to $\sqrt{2}$. This condition occurs at a frequency f_s that is equal to $1/2\pi RC$ and corresponds to the frequency at which the output voltage is 3 db down from the input voltage, ignoring impedance levels (db = 20 $\log_{10}|E_o/E_i|$). Therefore

$$\text{Low-pass: } f = f_s\sqrt{\left|\frac{E_i}{E_o}\right|^2 - 1} \qquad (4a)$$

$$\text{High-pass: } f = f_s\frac{1}{\sqrt{\left|\frac{E_i}{E_o}\right|^2 - 1}} \qquad (4b)$$

In low-pass applications the ratio $|E_i/E_o|$ is often selected to be 10 or greater. Therefore, Eq. (4a) becomes

$$f \simeq f_s\left|\frac{E_i}{E_o}\right| \quad ; \quad \left|\frac{E_i}{E_o}\right| \geq 10 \qquad (5)$$

because $|E_i/E_o|^2 \gg 1$. The value of f is given to an accuracy of about 1 percent by Eq. (5) when $|E_i/E_o| = 10$. When $|E_i/E_o| = 100$, f is given to an accuracy of about 0.1 percent. The error resulting from the use of Eq. (5) is in the pessimistic direction since the true value of f, obtained from Eq. (4a), is always smaller than the value of f given by Eq. (5).

Use of Chart

In high-pass applications, the value of f_s is usually of primary interest, and is given by $f_s = 1/2\pi RC$. The chart in Fig. 2 enables f_s to be read directly in one operation for a given value of R and C in either the low-pass or high-pass case. When a value of $|E_i/E_o|$ equal to or greater than 10 is desired in the low-pass case, the value of f_s determined from the chart can be multiplied by $|E_i/E_o|$. The chart can also be used to determine the reactance of a capacitor at any frequency. The fol-

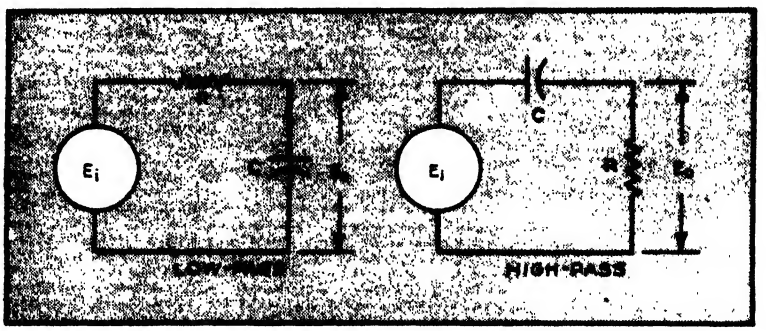

FIG. 1—Low- and high-pass R-C filters shown connected to a-c generator

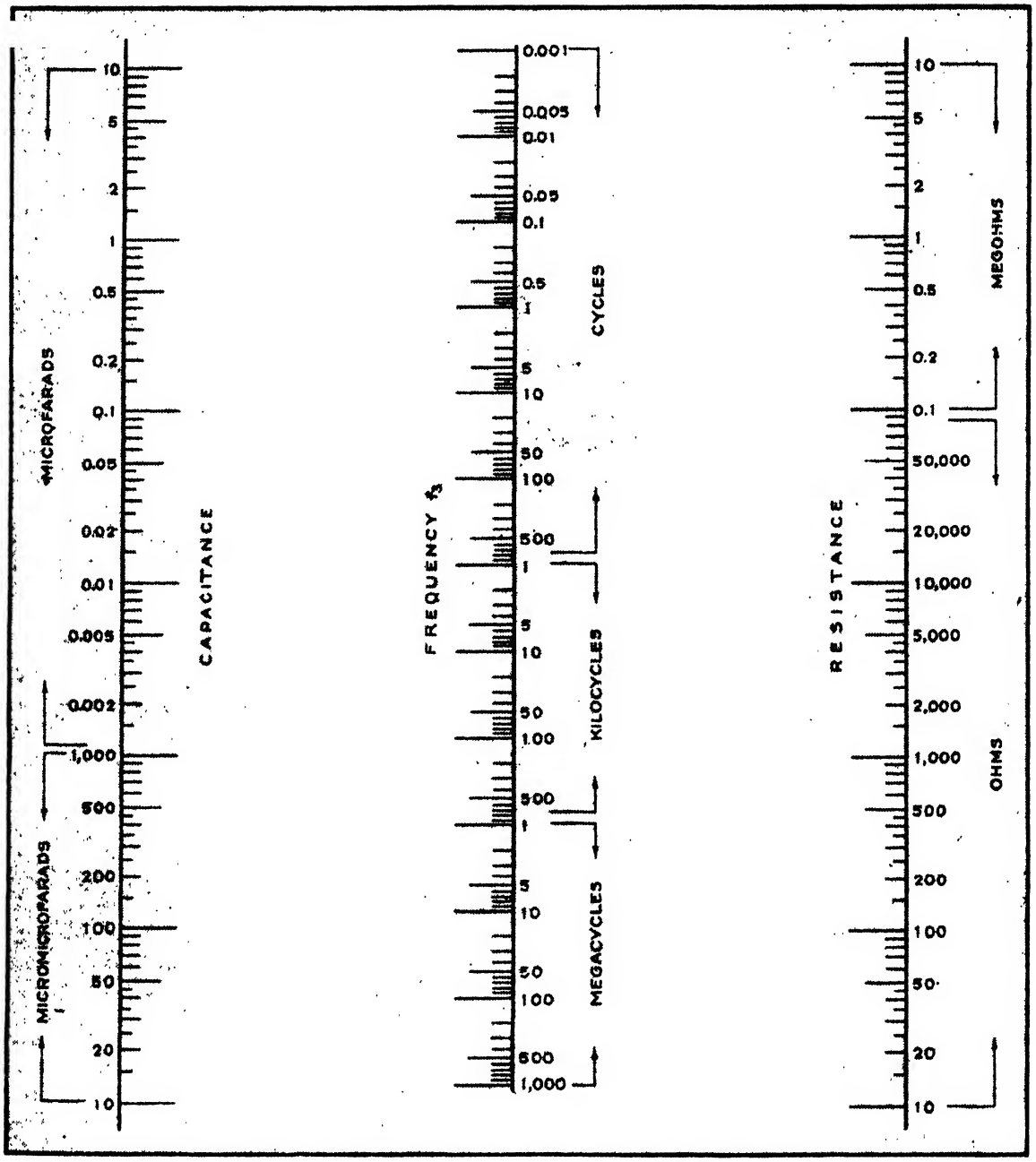

FIG. 2—Resistance-capacitance filter chart based on the relation $f_s = 1/2\pi RC$, where f_s is the frequency at which the filter provides an attenuation of 3 db. To find the reactance of a capacitor, place ruler on known capacitance and frequency values and read the reactance value on the resistance scale

lowing examples illustrate the use of the chart.

Example 1

A plate decoupling *R-C* filter must attenuate frequencies above 50 cps by a voltage ratio of 10:1. The value of R cannot exceed 4,000 ohms to avoid an excessive loss in d-c voltage. What value of C is required? From Eq. (5), $f_s = 50/10 = 5$ cps. From the chart, draw a line through $f_s = 5$ cps and $R = 4{,}000$ ohms. Read $C = 8\mu f$.

Example 2

The low-frequency end of the 3-db pass-band of a resistance-capacitance coupled amplifier must be 100 cps. A 0.01-μf coupling capacitor is available. What value of output resistance must be used? Draw a line through $C = 0.01$ μf and $f_s = 100$ cps. Read $R = 0.16$ meg.

Example 3

What is the reactance of a 0.002-μf capacitor at 1 megacycle? Draw a line through $C = 0.002$ and $f_s = 1$ mc, and determine $R = 80$ ohms.

Construction of Chart

The chart covers a wide range at the sacrifice of accuracy in readability. If greater accuracy is desired, it is simple to construct a chart which covers a limited range.

1. Use two sheets of log paper, one of which has twice as many cycles as the other; for instance, two-cycle and four-cycle paper. Each complete scale must be the same total length.

2. On opposite edges of the two-cycle paper, write down the resistance and capacitance values including the desired range.

3. Cut a strip of the four-cycle paper and prepare to paste it equidistant from, and parallel to, the R and C scales, in an inverted sense.

4. Compute f_s for one value of R and C included on the scales.

5. Match the four-cycle frequency scale to the line joining these values of R and C and paste the scale in place.

6. Label the frequency scale, using the computed value of f_s as a guide to the major scale values.

High and Low-Pass Filter Design

By C. J. MERCHANT

MUCH of the arithmetical drudgery of high- and low-pass audio-filter design can be eliminated by the use of a reactance slide-rule. For example, the formulas for L and C in a single constant-K high-pass T-section are $L = R/4\pi f_o$, $C = 1/\pi f_o R$, where f_o is the cut-off frequency and R is the terminating resistance. A simple rearrangement of these expressions gives $2\pi(f_o/R)L = 1/2$ and $1/2\pi(f_o R)C = 1$ or, in other words, L is the inductance whose reactance at the frequency f_o/R equals 1/2 ohm, and C is the capacitance whose reactance at the frequency $f_o R$ equals one ohm.

The method can be extended to other types of sections, and a multi-section filter can be designed with only two settings of the reactance slide-rule, once at f_o/R for the inductances and once at $f_o R$ for the capacitances. In multi-section filters the sharpest cut-off consistent with high attenuation outside the pass-band is realized by using terminating m-derived half-sections with m = 0.6, a full m-derived section with m = 0.8, and one or more constant-K sections.

Figure 1 gives the values of the reactances in ohms in such sections, the coils being evaluated at f_o/R and the capacitors at $f_o R$.

For example, to design a three-section low-pass filter of T-sections with R = 500 ohms and f_o = 1000 cps, first set the rule at 1000/500, or 2 cps, and find the inductances whose reactances at 2 cps are those given on the chart. To find the ca-

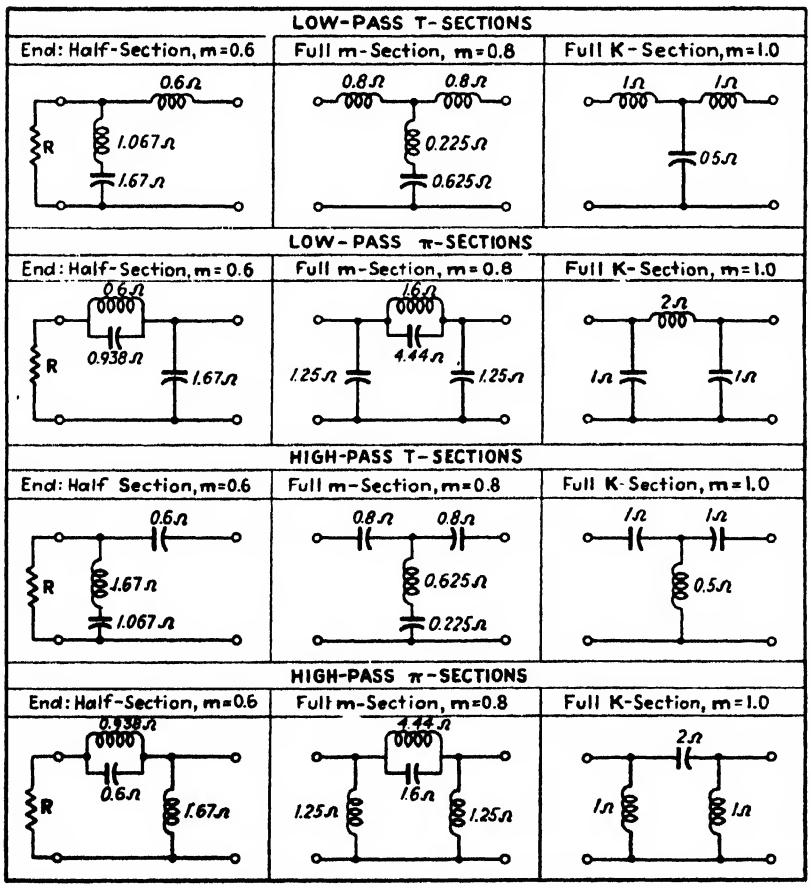

FIG. 1—Generalised impedance chart from which impedances are calculated by reactance slide-rule if terminating impedance and cut-off frequency are given

pacitances, reset the rule at 1000 × 500, or 500 kc, and find the capacitances whose reactances at 500 kc are those given on the chart. The complete filter and its attenuation characteristic are given in Fig. 2.

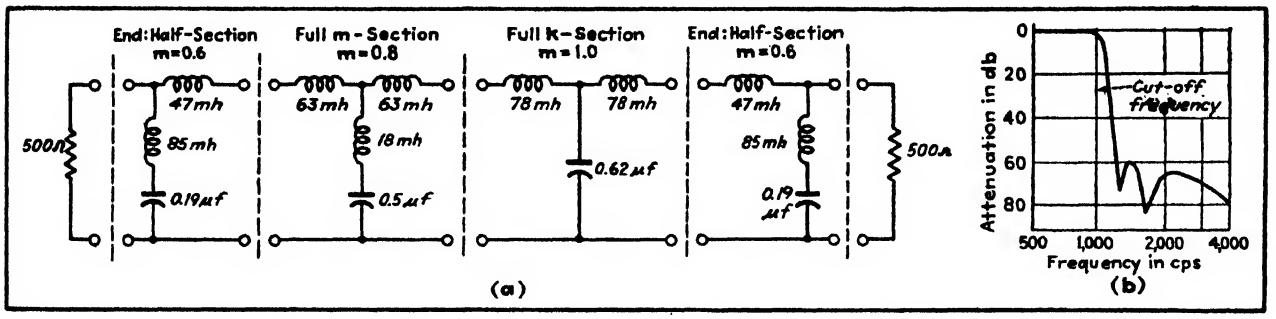

FIG. 2—Illustrative filter design values and attenuation characteristics of low-pass filter designed by use of Fig. 1

R-C Bandpass Filter Design

Relationships between circuit parameters of a parallel-T R-C network, used as the feedback loop in an amplifier that gives the narrow bandpass characteristics of an L-C circuit, are determined. Design curves and applications to low-frequency filters are presented

By JACK L. BOWERS

AN ELECTRONIC FILTER with narrow bandpass characteristics can be made using the R-C parallel-T network in a feedback amplifier. By choice of component values different from those that produce the usual null characteristics, the bandpass characteristics obtained with this circuit are more desirable for many applications than those produced by the usual L-C filter.

Selective Negative Feedback

Considerable interest has been shown in the application of resistance-capacitance parallel-T networks for feedback in vacuum tube amplifiers. The arrangement was first presented by H. H. Scott[1] for use as a selective circuit, and more recently A. E. Hastings[2] has offered an excellent theoretical analysis. However, most of the effort in this field has been toward the use of the parallel-T network with parameters chosen to produce an absolute null at the operating frequency. The purpose of this paper is to describe the excellent practical results achieved using the circuit in a selective frequency filter under different operating conditions.

As commonly used, with the circuit designed to produce a complete null, the output of the network can be used as a source of degenerative feedback voltage for all frequencies except that at which null occurs. Transfer characteristics so produced are sharply selective forming a cusp shaped curve at the desired frequency. Though this shape is excellent for selected applications such as wave analyzers, engineers find that most needs demand the ordinary L-C type of resonance curve of broader top and steeper sides. Less stability is then required of all frequency determining circuits and yet adequate attenuation is realized at short distances from the selected frequency. As will be shown, this type of operation can be obtained from parallel-T networks when the circuit parameters are chosen properly.

Circuit Analysis

It will first be advisable to review the equations which describe the operation of the parallel-T network and establish design constants. For simplification, in the circuit shown as Fig. 1, the series resistances will be considered equal, as will the series capacitances. The shunt impedances will bear relations to be

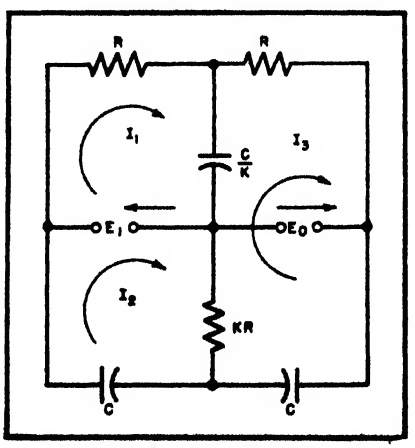

FIG. 1—Basic parallel-T R-C filter

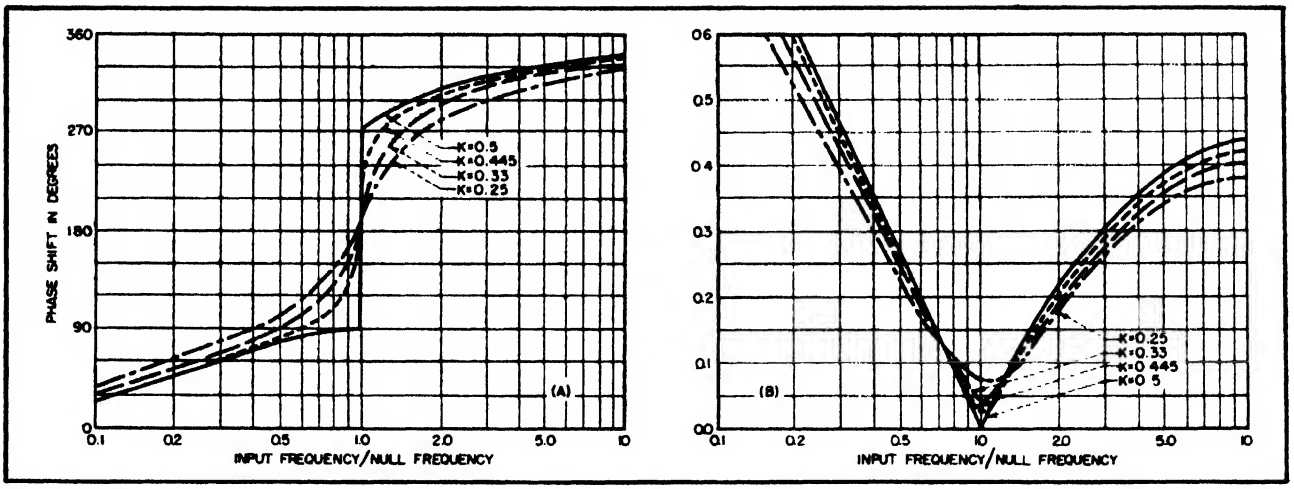

FIG. 2—By choice of the K the phase and amplitude characteristics of an R-C filter can be made similar to those of an L-C filter

proven, that produce the frequency characteristics described in this paper.

The following four circuital equations can now be written substituting βE_1 for E_0

$$E_1 - I_1(R - jK/\omega C) + I_2(-jK/\omega C) = 0$$
$$E_1 + I_2(KR - j/\omega C) - I_3 KR = 0$$
$$\beta E_1 + I_2(R - jK/\omega C) - I_1(-jK/\omega C) = 0$$
$$\beta E_1 + I_2 KR - I_3(KR - j/\omega C) = 0$$

If the determinant of the coefficients of the variables E_1, I_1, I_2, and I_3 in the above four equations is set equal to zero and the resulting equation solved for β, the following relation obtained is the necessary condition to be met if the variables are to have values other than zero

$$\beta = \{KR^2 - (2K^2R/\omega^2C^2) + j[(K/\omega^2C^2) - (2K^2R^2/\omega C)]\} / \{KR^2 - (2KR/\omega^2C^2) - (2K^2R/\omega^2C^2) - (R/\omega^2C^2) + j[(K/\omega^2C^2) - (2K^2R^2/\omega C) - (2KR/\omega C) - (R^2/\omega C)]\}$$

If R is set equal to $1/\omega C$, then

$$\beta = \{(K - 2K^2) + j(K - 2K^2)\} / \{(K - 2K - 2K^2 - 1) + j(K - 2K - 2K^2 - 1)\}$$

which reduces to

$$\beta = \frac{2K^2 - K}{2K^2 + K + 1}$$

This equation shows that at a frequency where $R = 1/\omega C$, β is real and has a magnitude dependent only on K. If $K = 0.5$, $\beta = 0$, and the circuit exhibits a complete null. It has been shown elsewhere that under these conditions the network produces an abrupt phase reversal, changing from 90 degrees to a value of 270 degrees at the null point. If K is less than 0.5 there is only a partial null, and network phase shift attains a value of 180 degrees as is shown by the real, negative value of β. Reversal from 90 degrees to 270 degrees occurs more gradually as the slope of the curve decreases with K.

Figure 2A shows the resulting effect of K on the network phase characteristic, and Fig. 2B indicates its effect on the attenuation vs frequency characteristic. Data for both sets of curves were obtained experimentally. Discrepancies which are evident in measurement of attenuation in Fig. 2B compared to the derived relation of β are attributed to experimental error and the finite resistance of capacitors used.

Filter Circuit

If the parallel-T network is used for a source of feedback in a vacuum tube amplifier, a small amount of regeneration will be obtained at the selected frequency when $K <$ 0.5. At frequencies on either side, the magnitude of the feedback signal increases, but its phase is then approaching 90 or 270 degrees, and so the regenerative effect decreases. As the frequency moves farther from the center value, the phase becomes such that degeneration occurs and the amplifier produces a large degree of attenuation.

When gain of the amplifier is kept below the value which will produce oscillation due to regeneration at the center frequency, an excellent filter is obtained whose characteristic is similar to that of L-C circuits. Opposing effects of attenuation and phase characteristics at the center frequency produce a relatively broad topped curve, while its sides are steep. A filter circuit may be designed with values of effective Q up to 100 and at frequencies well removed from the center the attenuation is greater than that of an L-C circuit. Typical filter characteristics are shown in Fig. 3.

Filter Amplifier Design

A filter amplifier can be designed

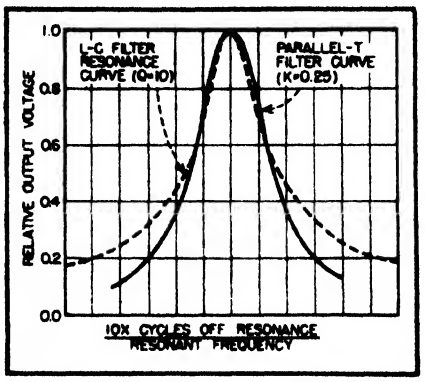

FIG. 3—Comparison of R-C and L-C filter characteristics

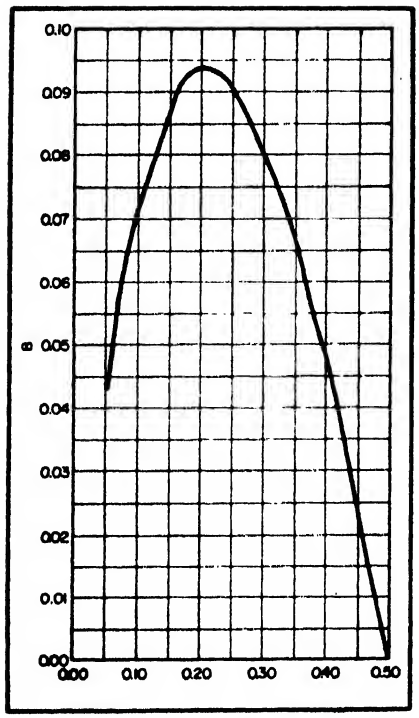

FIG. 4—Feedback as a function of filter selectivity (abscissa is K)

from the formulas derived above. Sharpness of the selectivity will be proportional to the effective gain of the amplifier, so this is the first consideration. Depending upon whether a moderate or a very large Q is desired, a triode or a pentode amplifier will be chosen. For a high degree of stability, the amplifier may have three stages and employ a large amount of additional degenerative feedbacks which is not a function of frequency.

After design of the amplifier and calculation of its gain A a value of K will be chosen that gives a network transmission β substantially less than $1/A$, so that oscillation or instability is avoided. This value of K can be determined from the graph of Fig. 4. Upon examination of the curve, it may be seen that β increases in value until a maximum is reached at $K = 0.207$. At this point β has a value of 0.0934, which is the largest practical value for filter amplifier design. The circuit resistances and capacitances are then chosen according to the desired frequency $f_o = 1/2\pi RC$. Further adjustment of the selectivity can then be made by varying the amplifier gain, or by changing the value of K, which involves the simultaneous change of the two shunt arms KR and C/K. If only one of the shunt arms is changed, there will be an accompanying change in frequency as well as selectivity.

A typical pentode amplifier circuit with parallel-T feedback appears in Fig. 5. For f_o of 60 cps with R of 265,000 ohms, C of 0.01 μf, and a K of 1/3, Q was between 2 and 20 depending on the amplifier gain controlled by the screen potential. Such a filter would present very difficult design problems with L and C components and would be very large and heavy. A particular design problem of this type of filter is that of maintaining zero phase shift in the amplifier at its low operating frequency. This condition is obviously necessary, because it is the phase characteristic of the network that controls filter operation. A d-c amplifier would most efficiently solve this problem by eliminating all low-frequency phase shift and removing the need for bulky coupling capacitors.

Advantages of Filter

A filter designed in this manner has advantages of small circuit components at all frequencies and a very desirable selectivity characteristic. Because only resistive and capacitive components are required, the problem of temperature compensation is relatively simple and moisture has little effect. Due to these features, this circuit is vastly superior to an L-C filter at audio and low ultrasonic frequencies. At higher frequencies, it will operate equally well, but the L-C networks begin to show their advantages. Compared to other types of R-C filters, the circuit described in this paper has definite advantages in circuits demanding a selectivity of relatively broad peak and steep sides. Also, consideration of attenuation and phase characteristics shows that with an amplifier of fixed gain, a higher amplitude ratio of passed to rejected frequencies is obtained, because degeneration is about the same in either case, while the parallel-T filter supplies additional gain due to regeneration at the passed frequency.

The author acknowledges research done by Kenneth Jenkins of Oakland, California, who upon the author's suggestion carried out work which culminated in the development of the subject circuit.

References

(1) Scott, H. H., A New Type of Selective Circuit and Some Applications, *Proc IRE*, p 226 Feb. 1938.
(2) Hastings, A. E., Analysis of Resistance-Capacitance Parallel T Network and Applications, *Proc IRE*, p 126P March 1946.

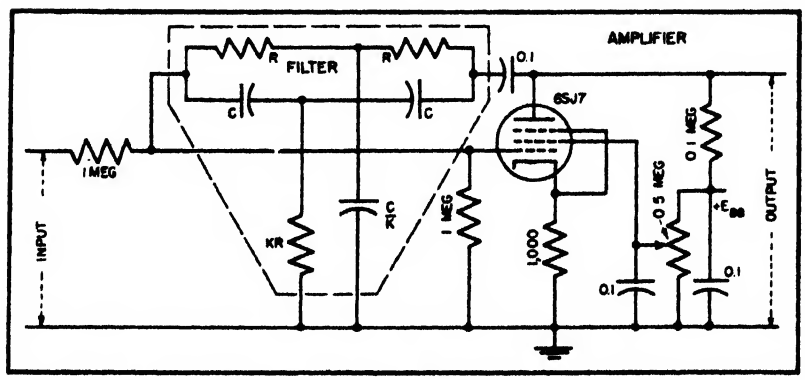

FIG. 5—Typical low-frequency electronic filter in amplifier with R-C network for feedback

The Effect of Incidental Dissipation in Filters

Where exact predictions of filter performance are necessary, account must be taken of the losses in the network components. The paper presents a method of ascertaining the effect of these losses on propagation factor, reflection factor and interaction factor

By E. A. GUILLEMIN

IN the design of filters it is customary to assume that the network itself (apart from the terminating resistances) is lossless. In constructing the filter it is, therefore, essential to use coils and capacitors having losses which are as small as practicable in order that the behavior predicted by the theory be at least approximately realized. Since the size, weight, and cost of a circuit element increase as its incidental losses are reduced, it is significant to know quantitatively the effect of incidental loss upon the filter behavior in order that a satisfactory compromise may be achieved.

It is not necessary that one be able to calculate exactly the effect of incidental dissipation inasmuch as the design procedure used for the lossless structure is quite commonly rather approximate. Thus, if one designs a filter on the basis of its attenuation function alone, the so-called reflection and interaction losses are for the moment regarded as being of secondary importance. If the reflection losses are considered at all, their effect upon the net insertion loss is usually regarded as being significant only over the attenuation band where the terminal conditions depart significantly from the hoped-for matched condition. The interaction losses are rarely regarded to be of sufficient importance to warrant their consideration in the design calculation. In cases where such procedures are inadequate it is better to abandon the conventional methods entirely and design for insertion loss directly. The conventional methods, then, are primarily suited to situations where the prediction of exact performance is unessential. In such cases the conventional methods are greatly to be preferred because of their comparative simplicity.

Effect of Incidental Losses

1. The theoretically infinite peaks in the attenuation loss and the reflection loss remain finite. The finite value of the attenuation (in nepers) at such a peak is given by Eq. 25 which shows the effect of the nearness of the peak to the cutoff and the dependence upon Q. Equation 50 gives the finite reflection loss (in nepers) at its peak for a filter with a single *m*-derived image impedance. For filters with more complicated image impedance, the peak reflection loss is given (in nepers) by the natural logarithm of Eq. 46 or Eq. 47 according to whether the lossless image impedance is respectively zero or infinite at this point.
2. Incidental losses cause the attenuation to be nonzero in the pass band. Here the phase is also somewhat different from its lossless value. Equations 14 and 15 may be used to compute the modified values of attenuation and phase not only within the pass band but also within the stop band where, however, the effects are less significant and of less importance (except at the peaks as already mentioned). Equations 14 and 15 apply everywhere except near attenuation peaks or near the cutoff where the special formulas given by Eq. 31 and 32 must be used.

In applying these results to a composite filter the effect upon the net attenuation loss is most expeditiously computed by considering each filter section separately and adding the losses thus found. The Q's of the various sections need not be alike. The effect upon the reflection loss depends only upon the terminal image impedance and hence involves only a single calculation regardless of the number of sections forming the composite filter.

The present discussion relative to the effect of incidental dissipation applies specifically to the interpretation of filter behavior according to the conventional methods, whence it is consistent to adopt the point of view that these effects need be determined only to a first order of approximation. The simplicity of the resulting formulas reveals the appropriateness of this attitude.

Insertion Loss

Before proceeding with the theoretical discussion it is essential to recall the expression for insertion loss. With reference to Fig. 1, the insertion ratio is defined as E_2'/E_1; that is, as the ratio of the load voltage that would be obtained without the filter (Fig. 1B) to the load voltage that results when the filter is inserted between the source and load resistances R (Fig. 1A). It is implied here as usual that the filter is electrically symmetrical with regard to its input and output terminals.

Denoting the image impedance of the filter by Z_0, and its normalized value by $z_0 = Z_0/R$, the reflection coefficient common to both terminal-pairs becomes

$$r = \frac{1 - z_0}{1 + z_0} \tag{1}$$

Writing for the propagation function $\gamma = \alpha + j\beta$, where α and β are respectively the attenuation and phase functions, the insertion ratio reads

$$E_2'/E_1 = e^{\gamma}(1 - r^2)^{-1}(1 - r^2 e^{-2\gamma}). \tag{2}$$

It is customary to refer to the

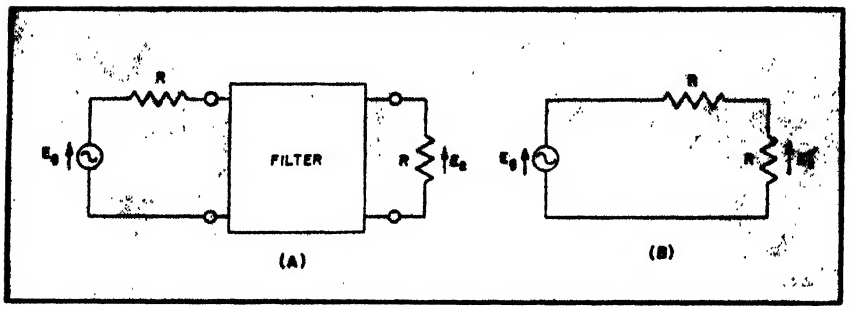

FIG. 1—Significance of insertion ratio, which is ratio of load voltages without filter to load voltage obtained with filter between source and load

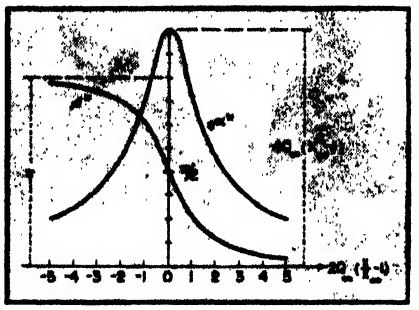

FIG. 2—Plots of attenuation factor and phase for Eq. 23 and 24

separate factors in this expression as follows:

e^{γ} = propagation factor
$(1 - r^2)^{-1}$ = reflection factor (both ends)
$(1 - r^2e^{-2\gamma})$ = interaction factor.

With reference to the factor $(1 - r^2)^{-1}$ it may be well to recognize that

$$(1 - r^2)^{-1} = \left[\frac{1}{2}\left(\sqrt{z_0} + \frac{1}{\sqrt{z_0}}\right)\right]^2 \quad (3)$$

the quantity in the square bracket being the more familiar expression for the reflection factor at one end of the network.

Ordinarily the propagation factor e^{γ} is of first order importance in the insertion ratio expression, while the reflection and interaction factors are regarded as being of second order. One might, therefore, consider it worth while to determine the effect of incidental dissipation only upon the factor e^{γ}. After some reflection, however, one recognizes that this conclusion is not quite correct since there are some critical frequencies (such as the cutoff frequency or the zeros or poles of Z_0) at which the values of $(1 - r^2)^{-1}$ and $(1 - r^2e^{-2\gamma})$ are important. The latter factor is not important in the attenuation range where α is large or in the transmission range where $z_0 \cong 1$ and hence $r \cong 0$; but neither of these conditions obtain in the immediate vicinity of the cutoff frequency. Here the combined factor $(1 - r^2)^{-1}(1 - r^2e^{-2\gamma})$ must be considered and the question as to whether the effect of incidental dissipation upon its values may be significant, must be more carefully investigated.

The factor $(1 - r^2)^{-1}$ is not important over the transmission range where $z_0 \cong 1$ and $r \cong 0$, but in the attenuation range where z_0 is imaginary the conventional analysis shows that this factor introduces a maximum negative loss of about 6 db wherever $|z_0| = 1$, and an infinite positive loss wherever z_0 is critical (has a zero or a pole). One may conclude that it is not essential to consider the effect of incidental dissipation in this factor except at the critical frequencies of z_0. Here this effect is definitely of importance because it limits the reflection loss to a finite value which must be determined.

To summarize the discussion so far, one may say that the effect of incidental dissipation upon the insertion ratio, Eq. 2, should be investigated for

e^{γ} over the entire frequency range
$(1 - r^2)^{-1}$ at the critical frequencies of z_0 only
$(1 - r^2)^{-1}(1 - r^2e^{-2\gamma})$ at the cutoff frequency only

In the following paragraphs these items are considered in the order given.

The Propagation Function

Filters to which the present discussion is pertinent are designed without regard for the resulting phase characteristic; that is, the attenuation requirement is of primary importance. In such cases any desired result may be obtained by cascading a suitable number of simple m-derived structures with appropriately chosen m-values. It is significant to observe in this connection that the effect of incidental dissipation upon the resultant attenuation and phase shift depends only upon the form of the propagation function and not at all upon the structure of the network or upon the form of the image impedance. If, for the purpose of calculating the effect of incidental dissipation, one assumes a specific network configuration, the results are not restricted in their application to that structure but apply equally well to any other configuration having the same propagation function. Since the overall attenuation loss is addi-

Table I—Symbols used in this Article

Z_0 = image impedance
R = source or load resistance
$z_0 = Z_0/R$ = normalized value of the image impedance, or the image impedance referred to a one-ohm level
r = reflection coefficient (common to both ends since a symmetrical network and equal source and load resistances are implied)
E'_2/E_2 = insertion ratio (voltage)
$\gamma = \alpha + j\beta$ = propagation function (or constant)
α = attenuation function (or constant)
β = phase function (or constant)
e = base of natural logarithms
e^{γ} = propagation factor
e^{α} = attenuation factor
ln = natural logarithm
$*$ = distinguishes any quantity when the effect of loss is included
$x = f/f_c = \omega/\omega_c$ = ratio of any frequency to the cutoff frequency of the filter (assumed low pass)
$\omega_\infty = 2\pi f_\infty$ = frequency of (theoretically) infinite attenuation
$x_\infty = f_\infty/f_c$
$Q = \left(\frac{R}{L\omega} + \frac{G}{C\omega}\right)^{-1}$ = uniform combined Q of coils and capacitors
$Q_c = Q$ for $\omega = \omega_c$; $Q_0 = Q$ for $\omega = \omega_0$; etc.
m = constant appearing in Zobel's theory of m-derived filters

tive, the consideration here may be restricted to a single m-derived filter constituent, for which the propagation function is given by the expression

$$\gamma = ln \frac{y_0 + 1}{y_0 - 1} \tag{4}$$

in which

$$y_0 = \frac{(x^2 - 1)^{1/2}}{mx} = \frac{(1 - x^2)^{1/2}}{jmx} \tag{5}$$

For the low-pass filter

$$x = \omega/\omega_c = f/f_c \tag{6}$$

where f_c is the cutoff frequency. The analysis pertinent to the band-pass and other filter classes may be obtained by making appropriate frequency transformations.[1]

The basis for the approximate consideration of incidental losses is given by the statement[2] that if the function $z\ (j\omega)$ is the driving point impedance of a lossless network then $z(j\omega + \delta) = z^*(j\omega)$ is approximately the impedance of the corresponding uniformly dissipative network,[3] where

$$\delta = \frac{1}{2}\left(\frac{R}{L} + \frac{G}{C}\right) \tag{7}$$

is the average uniform dissipation ratio. The asterisk is here used to designate the dissipative function, not the conjugate value. The process applies in unaltered form also to admittances and propagation functions.

The propagation function, according to Eq. 4 and 5, is a function of the frequency variable jx. If the propagation function of the corresponding uniformly dissipative network is denoted by $\gamma^*(jx)$, one has

$$\gamma^*(jx) = \gamma\ (jx + \delta/\omega_c) \tag{8}$$

and a Taylor expansion about the point $\delta = 0$ yields

$$\gamma^*(jx) = \gamma(jx) - j\left(\frac{d\gamma}{dx}\right)\frac{\delta}{\omega_c} - \frac{1}{2}\left(\frac{d^2\gamma}{dx^2}\right)\left(\frac{\delta}{\omega_c}\right)^2 + \ldots. \tag{9}$$

According to Eq. 4 and 5 the derivatives appearing here are found to be

$$\frac{d\gamma}{dx} = \frac{2m}{[1 - (1 - m^2)x^2][x^2 - 1]^{1/2}} \tag{10}$$

and

$$\frac{d^2\gamma}{dx^2} = -\frac{2mx\,[1 + 2(1 - m^2) - 3(1 - m^2)x^2]}{[1 - (1 - m^2)x^2]^2\,(x^2 - 1)^{3/2}} \tag{11}$$

Substitution of these expressions into Eq. 9 yields the desired results.

Before carrying out this step it is useful to observe according to Eq. 7 that

$$\frac{2\delta}{\omega_c} = \frac{R}{L\omega_c} + \frac{G}{C\omega_c} = \frac{1}{Q_c} \tag{12}$$

where Q_c is a quantity which measures the quality of the coils and capacitors. The tacit assumption in the approximate analysis used here is that the Q-values are the same throughout the network. However, if the filter is realized as a cascade of component networks then it is clear that the contribution (to the total attenuation) of a given component depends only upon the Q-values of that component. If the capacitors are essentially lossless (as may usually be assumed), Q_c is the familiar expression for the Q of the coils evaluated at the cutoff frequency.

In Eq. 10 and 11 it is expedient to introduce the frequency of infinite attenuation by means of the relation (applying to m-derived filters)

$$\frac{\omega_\infty}{\omega_c} = \frac{f_\infty}{f_c} = x_\infty = \frac{1}{(1 - m^2)^{1/2}} \tag{13}$$

With the use of these relations, substitutions of Eq. 10 and 11 into Eq. 9, and subsequent separation into real and imaginary parts yields the following results for the attenuation and phase functions of the dissipative filter

$$\left.\begin{aligned} &\alpha^* = A(x); \quad \beta^* = \beta - B(x); \\ &\quad \text{for } x < 1 \text{ (pass band)} \\ &\alpha^* = \alpha + B(x); \quad \beta^* = \beta - A(x); \\ &\quad \text{for } x > 1 \text{ (stop band)} \end{aligned}\right\} \tag{14}$$

where

$$\left.\begin{aligned} A(x) &= \frac{m}{Q_c|1 - x^2|^{1/2}\,(1 - x^2/x_\infty^2)} \\ B(x) &= \frac{mx[3(1 - x^2/x_\infty^2) - 2m^2]}{4Q_c^2|1 - x^2|^{3/2}(1 - x^2/x_\infty^2)^2} \end{aligned}\right\} \tag{15}$$

x_∞ in Eq. 13. In the relations of Eq. 14, α and β are the attenuation and phase functions of the lossless structure.

These results are, of course, not applicable to points in the immediate vicinity of the cutoff ($x = 1$) or to points in the vicinity of the infinite attenuation peak. For these regions it is necessary to derive special relationships. It is observed that the effect of dissipation is to add correction terms to the attenuation in the pass band and to the phase in the stop band which are inversely proportional to the first power of Q_c, while the corrections to α in the stop band and to β in the pass band are of second order since they are inversely proportional to Q_c^2. It should also be observed that the correction terms are increased as the frequency of infinite attenuation is moved closer to the cutoff ($x_\infty \to 1$). The results apply also to the constant-k filter since the latter is obtained for $m = 1$ or $x_\infty = \infty$.

The Attenuation Peak

The effect of dissipation in the vicinity of the infinite attenuation peak is considered next. Since this is the frequency at which the quantity y_0 of (Eq. 5) passes through unity, one may write for this vicinity

$$y_0 \cong 1 + \left(\frac{dy_0}{dx}\right)_{x=x_\infty}(x - x_\infty) \tag{16}$$

Denoting the corresponding function for the dissipative network by $y_0^*\ (jx)$, and following the pattern of Eq. 8 and 9 pertaining to the propagation function, yields the analogous relations

$$y_0^*\ (jx) = y_0\left(jx + \frac{\delta}{\omega_c}\right) \tag{17}$$

$$y_0^*\ (jx) = y_0(jx) - j\left(\frac{dy_0}{dx}\right)\frac{\delta}{\omega_c} - \frac{1}{2}\left(\frac{d^2y_0}{dx^2}\right)\left(\frac{\delta}{\omega_c}\right)^2 + \ldots. \tag{18}$$

Here only the first two terms of the Taylor expansion are needed. Use of Eq. 16 thus gives for the vicinity of the point $x = x_\infty$

$$y_0^* = 1 + \left[(x - x_\infty) - j\frac{\delta}{\omega_c}\right]\left(\frac{dy_0}{dx}\right)_{x=x_\infty} \tag{19}$$

According to Eq. 5, 6, and 13, the derivative of y_0 appearing here is found to have the value

$$\left(\frac{dy_0}{dx}\right)_{x=x_\infty} = \frac{1}{x_\infty(x_\infty^2 - 1)} \tag{20}$$

so that Eq. 19 becomes

$$y_0^* = 1 + \frac{(x - x_\infty) - j\frac{\delta}{\omega_c}}{x_\infty\,(x_\infty^2 - 1)} \tag{21}$$

The desired behavior of the propagation function for the vicinity of the point $x = x_\infty$ is obtained through substitution of this value of y_0^* into Eq. 4 in place of y_0 (and

denoting the result by γ^*). In connection with this step it should be observed that the fractional term in Eq. 21 has a value small compared to unity throughout the frequency range of interest here and that this term, therefore, while significant in the evaluation of $y_0^* - 1$, may be ignored in considering the value of $y_0^* + 1$. Making use of the relation expressed by Eq. 12 (with ω_c replaced by ω_∞), one thus obtains the result

$$\gamma^* = ln\left\{\frac{4Q_\infty(x^2_\infty - 1)}{2Q_\infty\left(\frac{x}{x_\infty} - 1\right) - j}\right\} \quad (22)$$

Separation into real and imaginary parts gives

$$\alpha^* = ln\left\{\frac{4Q_\infty(x^2_\infty - 1)}{\left[1 + 4Q^2_\infty\left(\frac{x}{x_\infty} - 1\right)^2\right]^{1/2}}\right\} \quad (23)$$

and

$$\beta^* = \frac{\pi}{2} - \tan^{-1}\left[2Q_\infty\left(\frac{x}{x_\infty} - 1\right)\right] \quad (24)$$

Plots of the functions e^{α^*} and β^* are shown in Fig. 2 for assumed values of $Q_\infty = 50$ and $x_\infty = 5/4$, $(m = 0.6)$. In contrast to the behavior of the lossless network it is observed that the attenuation (α^*) remains finite at the point $x = x_\infty$, and the phase (β^*) varies continuously from the value π to zero instead of having a discontinuity at this point. Equations 23 and 24 are, of course, applicable only to frequencies in the immediate vicinity of the attenuation peak. Of primary interest is the value of this peak, that is

$$\alpha^*_{max} = ln\,[4Q_\infty(x^2_\infty - 1)] \quad (25)$$

As might have been expected, this value increases with Q_∞ and decreases as the theoretically infinite attenuation peak is moved closer to the cutoff; that is, as the value of x_∞ approaches unity (the value of m approaches zero). The purpose of using an m-derived section with a value of x_∞ near unity is to obtain a rapid increase in attenuation beyond the cutoff. One observes that unless the value of Q_∞ is sufficiently large, however, the desired effect cannot be realized. Equation 25 presents a simple means for controlling the significant factors in a contemplated design.

Behavior at the Cutoff

At the cutoff $x = 1$ and the value of y_0, according to Eq. 5, is zero. One may expect that the effect of incidental dissipation is to yield a function y_0^* having a nonzero value at the cutoff. It is reasonable to assume, however, that this value is small compared to unity so that one may use the approximation

$$\frac{y_0^* + 1}{y_0^* - 1} \cong -(1 + 2y_0^*) \quad (26)$$

and hence, according to Eq. 4, obtain for the value of the propagation function at the cutoff

$$\gamma_c^* = ln\,(1 + 2y_0^*) + j\pi \cong 2y_0^* + j\pi \quad (27)$$

To obtain the desired value of y_0^*, it is convenient first to write Eq. 5 in the form

$$y_0 = \frac{[1 + (jx)^2]^{1/2}}{jmx} \quad (28)$$

whence y_0^* is had through replacing jx by $jx + \delta/\omega_c$. Since the denominator in Eq. 28 does not behave critically in the vicinity of the point $x = 1$, it is moreover essential only to replace jx by $jx + \delta/\omega_c$ in the numerator, and since $(jx + \delta/\omega_c)^2 \cong -x^2 + 2jx(\delta/\omega_c)$, one has for $x = 1$

$$y_0^* = \frac{(j\,2\delta/\omega_c)^{1/2}}{jm} = \frac{1}{m(jQ_c)^{1/2}} \quad (29)$$

in which Eq. 12 is also used. Substitution of this result into Eq. 27 yields the desired value of the propagation function at the cutoff, thus

$$\gamma_c^* = \frac{2}{m(jQ_c)^{1/2}} + j\pi. \quad (30)$$

Separation into real and imaginary parts gives the formulas

$$\alpha_c^* = \frac{1}{m}\left(\frac{2}{Q_c}\right)^{1/2} = x_\infty\left(\frac{2}{Q_c(x^2_\infty - 1)}\right)^{1/2} \text{ (nepers)} \quad (31)$$

and

$$\beta_c^* = \pi - \frac{1}{m}\left(\frac{2}{Q_c}\right)^{1/2} \text{ (radians)} \quad (32)$$

For $m = 0.6$ $(x_\infty = 5/4)$, and $Q_c = 50$, one finds $\alpha_c^* = 1/3$ neper or 2.9 db and $\beta^* = \pi - 1/3$ radians or 161 degrees. It is significant to observe that the choice of a small m-value (attenuation peak near the cutoff) yields a larger attenuation at the cutoff and thus partially defeats the purpose for which such an m-derived section is normally used unless the factor Q_c can be made large enough.

Reflection Loss at the Critical Frequencies of z_0

Since the complete filter structure to which the present discussion is relevant may be a composite one having a fairly elaborate image impedance at its input and output terminals, it is necessary to assume for z_0 an expression of the form

$$z_0 = \frac{(1 - x^2)^{1/2}(1 - x^2/x_2^2)\ldots}{(1 - x^2/x_3^2)(1 - x^2/x_4^2)\ldots} \quad (33)$$

Inasmuch as the reflection factor reads $(1 - r^2)^{-1}$ and according to Eq. 1

$$r^2 = \left(\frac{1 - z_0}{1 + z_0}\right)^2 = \left(\frac{1 - 1/z_0}{1 + 1/z_0}\right)^2 \quad (34)$$

it is clear that the end results are the same whether Eq. 33 or its reciprocal is used for z_0; that is, it is immaterial whether z_0 is assumed to be midseries (as in Eq. 33) or midshunt.

The critical frequencies of z_0 are those corresponding to $x = x_2$, x_3, . . . etc. At these points either z_0 or $1/z_0$ becomes zero. In the vicinity of these points the value of r^2 according to Eq. 34, may be evaluated considering z_0 or $1/z_0$ to be small compared to unity, thus obtaining either

$$r^2 = 1 - 4z_0, \text{ (for } x = x_3, x_5, \ldots) \quad (35)$$

or

$$r^2 = 1 - 4/z_0, \text{ (for } x = x_2, x_4, \ldots) \quad (36)$$

The reflection factor may, for these vicinities, be represented by

$$(1 - r^2)^{-1} = 1/4z_0, \text{ (for } x = x_3, x_5, \ldots) \quad (37)$$

or

$$(1 - r^2)^{-1} = z_0/4, \text{ (for } x = x_2, x_4, \ldots) \quad (38)$$

The next step is to replace z_0 in these expressions by the corresponding dissipative function z_0^*, which is accomplished in the usual manner through use of the approximate relation

$$z_0^*(jx) = z_0\left(jx + \frac{\delta}{\omega}\right) = z_0(jx) - j\left(\frac{dz_0}{dx}\right)\frac{\delta}{\omega} + \ldots \quad (39)$$

or

$$\frac{1}{z_0^*(jx)} = \frac{1}{z_0\left(jx + \frac{\delta}{\omega}\right)} = \frac{1}{z_0(jx)} - j\left(\frac{d}{dx}\frac{1}{z_0}\right)\frac{\delta}{\omega} + \ldots \quad (40)$$

according to whether z_0 or $1/z_0$ is

zero at the point in question. Use of Eq. 33 yields

$$\left(\frac{dz_0}{dx}\right)_{x=x_k} = -\frac{2}{x_k}\left[\frac{z_0}{1-x^2/x_k^2}\right]_{x=x_k}$$
for $k = 3, 5, \ldots$ (41)

and

$$\left(\frac{d}{dx}\frac{1}{z_0}\right)_{x=x_k} = -\frac{2}{x_k}\left[\frac{1/z_0}{1-x^2/x_k^2}\right]_{x=x_k}$$
for $k = 2, 4, \ldots$ (42)

Writing (by analogy to Eq. 12)

$$\frac{2\delta}{\omega_k} = \frac{1}{Q_k} \quad (43)$$

one thus finds

$$z_0^* = \frac{j}{Q_k}\left[\frac{z_0}{1-x^2/x_k^2}\right]_{x=x_k}$$
for $k = 3, 5, \ldots$ (44)

and

$$\frac{1}{z_0^*} = \frac{j}{Q_k}\left[\frac{1/z_0}{1-x^2/x_k^2}\right]_{x=x_k}$$
for $k = 2, 4, \ldots$ (45)

Substitution of these expressions into Eq. 37 and 38 respectively yields the desired results for the reflection factor of the dissipative network at the critical frequencies of z_{in}, thus

$$(1-r^2)^{-1} = \frac{Q_k}{4j}\left[\frac{1-x^2/x_k^2}{z_0}\right]_{x=x_k}$$
for $k = 3, 5, \ldots$ (46)

and

$$(1-r^2)^{-1} = \frac{Q_k}{4j}\left[\frac{1-x^2/x_k^2}{1/z_0}\right]_{x=x_k}$$
for $k = 2, 4, \ldots$ (47)

As an illustration one may consider z_0 to be the midseries image impedance of the single shunt-derived filter; that is

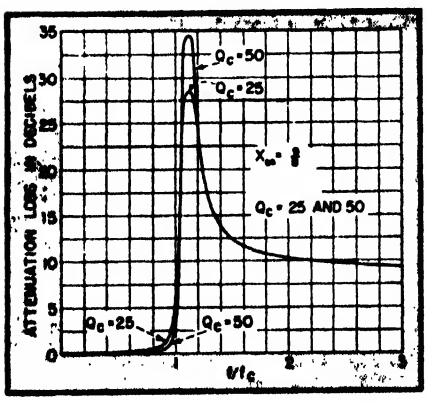

FIG. 3—Attenuation curve of network for two values of Q; m = 0.458

$$z_0 = \frac{(1-x^2)^{1/2}}{(1-x^2/x_2^2)} \quad (48)$$

Then Eq. 47 gives

$$(1-r^2)^{-1} = \frac{Q_2}{4}(x_2^2-1)^{1/2} \quad (49)$$

The reflection loss at this point is

$$ln\left[\frac{Q_2}{4}(x_2^2-1)^{1/2}\right] \text{ nepers} \quad (50)$$

In this simple filter section the critical frequency x_2 is controlled by the value of m chosen for the determination of x_∞, so that one has in this case $x_2 = x_\infty$; that is, the peak in the attenuation loss coincides with the peak in the reflection loss. The net loss at this point is given by adding the results expressed by Eq. 25 and 50, thus

$$\text{net loss} = ln\,[4Q_\infty(x_\infty^2-1)] + ln\left[\frac{Q_\infty}{4}(x_\infty^2-1)^{1/2}\right]$$
$$= ln\,[Q_\infty^2(x_\infty^2-1)^{3/2}] \text{ nepers} \quad (51)$$

For the numerical values: $Q_\infty = 50$, $x_\infty = 5/4 (m = 0.6)$ one has

$$\text{net loss} = ln\,112.5 + ln\,9.37 = ln\,1{,}054 \quad (52)$$

or in decibels

$$\text{net loss} = 41 + 19.4 = 60.4 \text{ db} \quad (53)$$

While the contribution due to the reflection loss is moderate, it nevertheless is a significant help toward providing a satisfactory peak loss particularly when x_∞ is chosen near unity. This fact is clearly appreciated from a comparison of the resultant loss as expressed by Eq. 51 with that provided by the attenuation function alone, Eq. 25.

Combined Reflection and Interaction Factor at Cutoff

This factor reads

$$F = \frac{1-r^2e^{-2\gamma}}{1-r^2} \quad (54)$$

with r^2 given by Eq. 34, and

$$e^{-2\gamma} = \left(\frac{1-y_0}{1+y_0}\right)^2 \quad (55)$$

as is evident from inspection of Eq. 4. According to Eq. 33, z_0 in the vicinity of the cutoff ($x = 1$) is very small, and hence r^2 may be approximated by Eq. 35. The function y_0, according to Eq. 5, is also very small in this vicinity and hence one may use the approximation

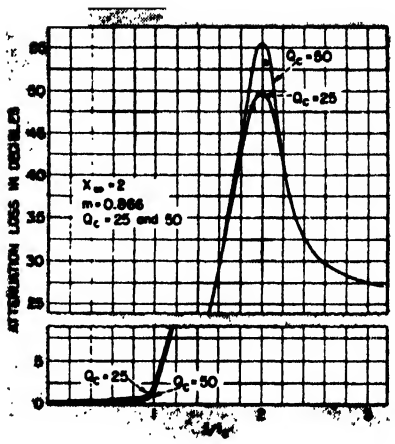

FIG. 4—Attenuation curve of network for two values of Q; m = 0.866

$$e^{-2\gamma} = 1 - 4y_0 \quad (56)$$

so that

$$r^2e^{-2\gamma} = 1 - 4(y_0 + z_0) \quad (57)$$

Thus an approximate expression for F, useful for the vicinity of the cutoff, becomes

$$F = \frac{y_0 + z_0}{z_0} = 1 + \frac{y_0}{z_0} \quad (58)$$

Although both y_0 and z_0 become zero at the cutoff, their ratio is finite. For example, using Eq. 5 for y_0 and Eq. 48 for z_0 gives

$$F = 1 + \frac{(1-x^2/x_2^2)}{jmx} \quad (59)$$

If $x_\infty = x_2$, this expression becomes for $x = 1$

$$F = 1 - jm = 1 - j(1-x_\infty^{-2})^{1/2} \quad (60)$$

Since this result for the nondissipative network is finite while the attenuation at the cutoff is zero unless the effect of dissipation is considered, one may conclude that the incidental dissipation has a second order effect upon the factor F and should, therefore, be neglected inasmuch as the effect of dissipation upon γ at the cutoff has been evaluated to a first order only.

Illustrations

Figures 3 and 4 illustrate the resulting formulas given by Eq. 14,

15, 23, and 25 for several different values of Q and x_∞ or m. Each figure shows a pair of low-pass attenuation-versus-frequency curves for the same value of x_∞ or m but for Q's of 25 and 50. Specifically these figures indicate the appearance of attenuation curves for $x_\infty = 9/8$ ($m = 0.458$), and $x_\infty = 2$ ($m = 0.866$) respectively.

These attenuation curves are those obtained from physical component networks whose theoretical propagation functions are given by Eq. 4 and 5 regardless of the corresponding image impedance. For example, a component network may be any one of the familiar forms of single m-derived sections shown in Fig. 5. Alternately the component network may be the shunt derivation of the network of Fig. 5C as shown in Fig. 6A; or it may be the corresponding midseries section shown in Fig. 6B. Again one might consider the series derivation of the network of Fig. 5B as shown in Fig. 6C, or the corresponding midshunt form shown in Fig. 6D. All of these networks have fundamentally the same attenuation function, namely one having a single attenuation peak as given analytically by Eq. 4 and 5. It is important to recognize that the effect of incidental dissipation upon the resulting attenuation function depends only on the uniform dissipation ratios R/L and G/C and not at all upon the network configuration or the number of inductances or capacitors involved in the particular filter.

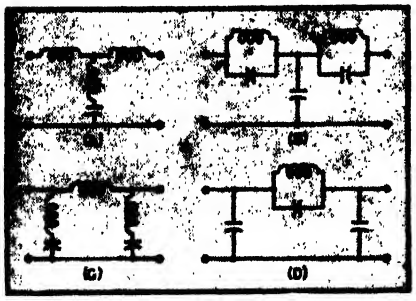

FIG. 5—Forms of single m-derived sections

Figure 7 illustrates the resulting insertion loss obtained from cascading two sections like the one shown in Fig. 5A or two sections like the one shown in Fig. 5D, with $x_\infty = 9/8$ and $x_\infty = 2$ respectively. The component network for $x_\infty = 9/8$ is assumed to have a Q of 50 while that for $x_\infty = 2$ is assumed to have a Q of 25, the point being that a higher Q is needed for that component network having its attenuation peak nearer the cutoff. The insertion loss shown in Fig. 7 is calculated by adding to the sum of appropriate curves of Fig. 3 and 4 the reflection and interaction losses of the lossless constant-k filter calculated according to established methods, the effect of dissipation upon the latter being negligible (the only peak in the reflection loss in this case occurring at infinite frequency).

Band-pass Filters

In dealing with band-pass filters it is customary to make all calculations in terms of the so-called equivalent low-pass filter which is obtained by simply regarding the midband frequency of the band pass as the origin of the frequency scale for the low pass. This procedure is, of course, valid only when the band width is small compared to the midband frequency, but a large number of practical cases are thus accommodated.

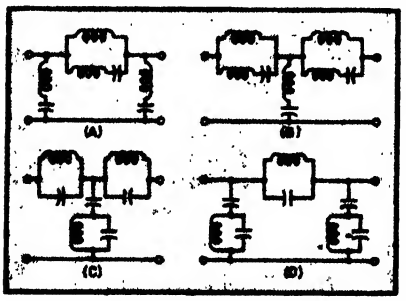

FIG. 6—Double m-derived sections obtained through performing a second m-derivation upon networks of Fig. 5B or C

It is clear that the cutoff frequency ω_c of the low pass is the equivalent of half the bandwidth of the band pass. If the bandwidth of the band pass is denoted by w and the midband frequency by ω_0, one observes that Eq. 12 for the band pass becomes

$$\frac{2\delta}{w/2} = \frac{2\delta}{\omega_0}\left(\frac{2\omega_0}{w}\right) = \frac{2\omega_0}{w} Q_0^{-1} \qquad (61)$$

Hence in applying the preceding formulas to a band-pass filter one must recognize that the pertinent Q is Q_0 multiplied by the factor $w/2\omega_0$, Q_0 being the value appropriate to the band-pass structure at its midband frequency. Since $w/2\omega_0$ is small, it is clear that the band-pass structure must have a much larger Q (at its mean frequency) for the net results to be comparable to those of an equivalent low-pass filter.

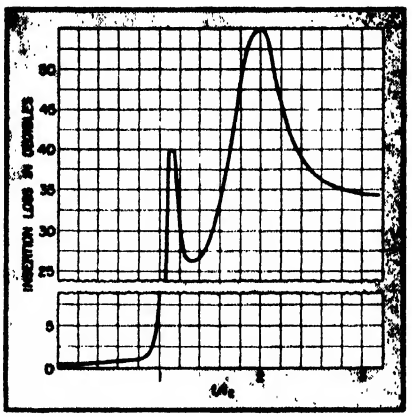

FIG. 7—Insertion loss of a composite filter consisting of two single m-derived sections in cascade having the values m = 0.458 and 0.866 and Q's of 50 and 25 respectively

References

(1) Guillemin, E. A., "Communication Networks", John Wiley and Sons, Inc., Vol II, p. 420.
(2) loc. cit. p 445.

Filters for Electronic Equipment

By GERSHON J. WHEELER

MANY MODERN INDUSTRIAL electronic devices and auxiliary units are sources of r-f noise covering a wide range of frequencies. As such they interfere with radio communications in all bands. This interference is picked up by the antenna of the receiver or is fed back into the power lines. If the noise generator is in a well-shielded box, then power-line filters should eliminate the interference.

There are a few practical precautions which are not mentioned in the textbooks. Most filters for this application are broadband pi-type configurations consisting of two capacitors and a choke (Fig. 1). Although the larger the choke, the higher will be the attenuation, care must be taken not to make this too large. If the reactance of the choke at the line frequency is too high, the resultant voltage drop would prevent the equipment from operating properly. For example, a 250-microhenry choke in a 110-volt, 800-cycle line (this is not an uncommon line frequency today) would have a reactance of 1¼ ohms. If the equipment draws 20 amperes, the drop across the choke would be 25 volts.

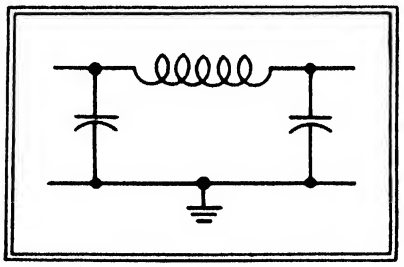

Fig. 1—Popular pi-type of filter under discussion

In a-c circuits, and especially at line frequencies greater than 60 cycles, care must be taken not to use large capacitors. If the capacitive reactance of the capacitor is too small, the power source may be called upon to deliver more current than it is capable of handling.

Care must also be taken to prevent resonance at a frequency within the rejection band of the filter. The coil and second capacitor form a series-resonant circuit (Fig. 2) and, at the resonant frequency, a high r-f voltage may be developed across the capacitor.

These problems in design vanish if readily available commercial filters are used, but there still arise problems in installation. The filter must be well grounded. If there is an impedance of any type between the filter ground connection and the actual ground, r-f energy will be fed through the filter back into the line. (Fig. 3).

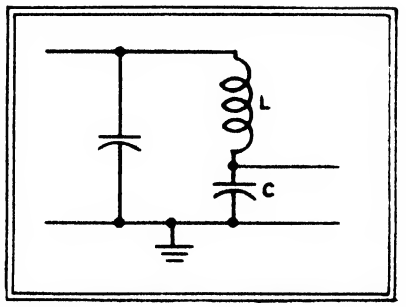

Fig. 2—Redrawing a pi-network shows the resonant circuit formed by *L* and *C*

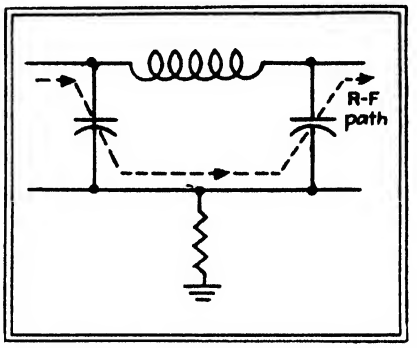

Fig. 3—Passage of r-f current through a filter when the unit is connected to a poor ground

Lastly, it is important to shield the input of the filter from the output. If this is not done, the unfiltered portion of the line will radiate and this radiation will be coupled into the filtered side.

Pi Networks as Coupled Tank Circuits

A development of the theory of pi networks as they apply to r-f output circuits of transmitters. A design procedure is outlined and curves are given to simplify matching the output stage directly to the transmission line or antenna, without an output transformer

By FREDERIC D. SCHOTTLAND

THE use of a π configuration of reactances to couple a class C power amplifier to its load is not new. However, the proper handling of such a network in this application is far from being common knowledge to engineers who design or operate transmitting equipment. This lack of knowledge generally

results in a circuit containing few of the obtainable advantages, and one whose harmonic attenuation leaves much to be desired.

New Approach Needed

Unfortunately for the transmitter engineer, design information on π networks is to be found principally in texts concerning themselves with filter and transmission-line theory. As a consequence, the subject is not approached in such a manner as to apply directly to the problem at hand. When following the customary design procedure, an infinite number of solutions are indicated. Cut-and-try methods of adjustment are extremely laborious, and modifications appear to give totally uncorrelated results. The underlying theory as presented in texts is in such form as to give little help, since the means for imposing the further conditions necessary to obtain the single desired solution are by no means apparent.

If the π network is to replace the coupled tank circuit, obviously it must perform the same functions. In general, the basic requirements of the circuit are:

1. It must transform the load to some predetermined impedance.
2. It must deliver a prescribed amount of energy at some maximum or required efficiency.
3. It must provide a preselected degree of harmonic attenuation.

Review of Matching Problem

Figure 1(a) is a simplified schematic of a vacuum tube coupled through a plate-tuned transformer to a load which may be an antenna at resonance or a properly terminated transmission line. Figure 1 (b) accomplishes the same coupling through the use of a π network. Both will perform the functions listed above.

In the coupled tank circuit of Fig. 1(a), the first function is controlled by correctly choosing the turns ratio of L_1 and L_2 and the amount of mutual inductance. The second function is accomplished by having the proper ratio of L_1 to C. Finally, we obtain sufficient harmonic attenuation by keeping the circuit above some minimum value of Q. In other words, we couple in a resistance with a definite relationship to either reactance. All of these points are well covered in existing literature, and this knowledge is basic to the transmitter engineer.

Inspection of the π network of Fig. 1(b) does not immediately reveal how all this is accomplished. We know that a π network will transform impedances and act as a coupling device, but how to control the efficiency and the Q of the circuit is not indicated, nor is this design information available in convenient form.

Reduction of π to L

In any actual circuit we are not concerned with the internal impedance of our tube as such, but rather with the impedance into which it must work. As a limiting case it becomes that impedance which will give the maximum transfer of radio-frequency power under the specific operating conditions of grid bias, excitation and plate voltage employed, without exceeding the rated plate dissipation of the tube. In the circuit of Fig. 2, therefore, R_o will be taken to mean the impedance with which we wish to terminate our generator, and not the internal impedance of the generator itself.

The values of X_T and X_o to match R_A to R_o are obtained from the relations*

$$X_T = \frac{-R_o X_L}{R_o \pm \sqrt{R_o R_A - X_L^2}} \quad (1)$$

$$X_o = \frac{-R_A X_L}{R_A \pm \sqrt{R_o R_A - X_L^2}} \quad (2)$$

To avoid an imaginary value for X_T or X_o,

$$X_L^2 \leq R_o R_A \quad (3)$$

To make X_o infinite in value so the output capacitor will drop out, we must choose the negative sign for the radical and use a value of R_o such that

$$R_A = \sqrt{R_o R_A - X_L^2} \quad (4)$$

This in no way changes the performance of the network, but the circuit simplifies to the L network of Fig. 3, which may be more easily analyzed.

The L network shown in Fig. 3 is of extreme interest. It is not only the equivalent circuit of a π network, but if R_A is taken as the reflected resistance of the load, it is the equivalent circuit of a coupled tank network as well. Here, then, is common ground and a means of correlating the two circuits. At resonance, X_T is equal to X_L. R_o was defined as the impedance into which we are to work. That is, it is the image impedance of the network, so

$$X_L = X_T = R_o/Q \quad (5)$$

$$R_A = X_L/Q \quad (6)$$

From Eq. (5), at any desired Q the value of X_L is fixed, and consequently the value of X_T is also fixed. The value of R_A is given by Eq. (6). From Eq. (5) and (6) we see that

$$R_o = X_L^2/R_A \quad (7)$$

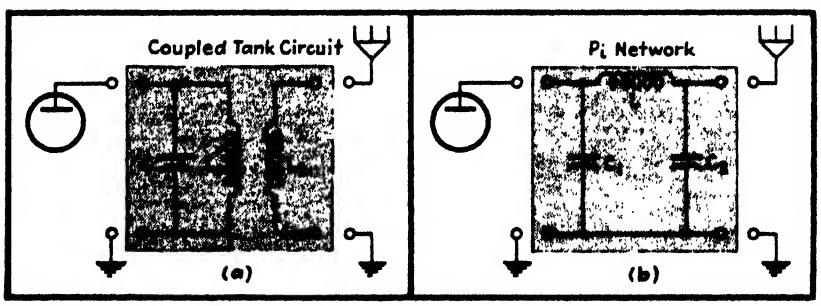

FIG. 1—Simplified representation of a class C r-f output stage feeding a transmission line or antenna at resonance through a coupled tank circuit (a) and through an equivalent pi network (b)

*Everitt, W. L., Output Networks for Radio Frequency Power Amplifiers. *Proc. I.R.E.*, 19, No. 5, p. 725–737, May 1931.

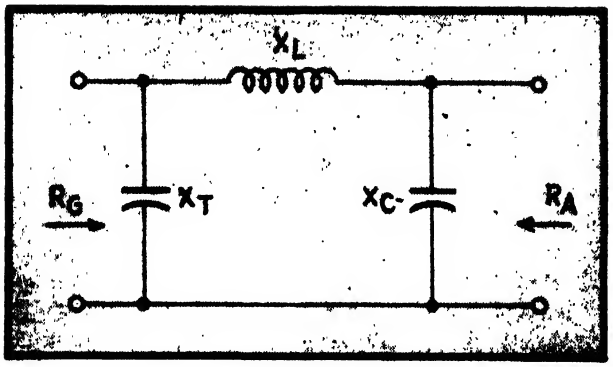

FIG. 2—Pi section used as a low-pass coupling network

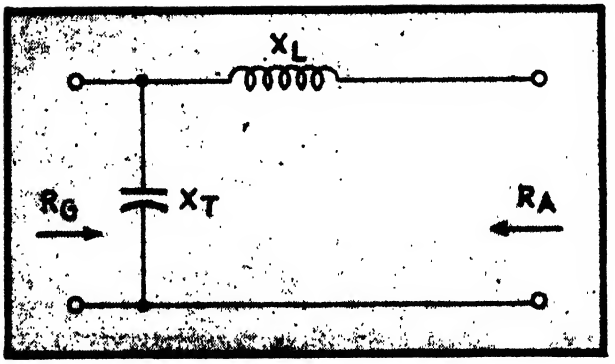

FIG. 3—Equivalent circuit of pi coupling network

Limitations of L Network

We formerly intended to find a network which would match R_G to whatever antenna we had. Because of the restriction of Eq. (4), however, we must now match our antenna to our network. This by no means destroys the usefulness of the network, for the value of R_A which has been obtained is the minimum impedance into which we may work under the given operating conditions. This minimum is entirely independent of the restrictions of Eq. (4).

If the actual load has an impedance greater than R_A it can be made to look like R_A so far as its resistance is concerned, by shunting it with the proper value of reactance. Naturally we shall choose a capacitance for this purpose, since it will act to increase the harmonic attenuation. If the actual antenna has an impedance smaller than R_A, there is nothing we can do about it. Obviously, to increase the impedance we must insert a reactance in series with R_A. If this is a capacitance, it will subtract from X_L, and if an inductance it will add. We may, therefore, view the addition of a series reactance as a change in the value of X_L. If we reduce X_L to obtain the required Q, the QX_L is reduced and R_G is not matched. Similarly, if X_L is increased, we again obtain a mismatch.

Fortunately, it is seldom necessary to couple into an antenna whose impedance is much below that usually found to be the proper terminating impedance of the network. At low radio frequencies, of course, this difficulty may very well be encountered. Although the normal antenna in this case may be so short electrically as to have low resistance, its capacitance in general will also be quite low. To resonate such an antenna, considerable inductance will be required in the loading coil. The resistance of such a coil will be comparable to the antenna itself, and added to it, will bring the resistance into which the network is coupled to a higher value. Of course, this added resistance represents a loss, but that loss was inherent in the circuit and not added by the coupling network. The whole matter may be resolved as follows:

At low frequencies (such as radio beacon frequencies below the broadcast band), it is desirable to use a class C amplifier whose generator impedance is as low as possible, such as a low-voltage, high-current tube or tubes in parallel. This will make R_G and consequently R_A lower. If R_A is still greater than the effective antenna resistance, the resulting circuit would have a higher Q than required, and would, in effect, be undercoupled.

When the actual load, which we shall call R_L, is greater than R_A, the problem has a complete solution. A reactance in parallel with R_L will give a circuit whose impedance is lower than R_L. By properly choosing this reactance, the resistive component may be made equal to R_A, something which was impossible to do with additions of series reactances. This reactance should be capacitive, to increase harmonic suppression.

Development of π Circuit

It is interesting to note that we are throwing off the yoke of Eq. (4), since we are now resynthesizing the original π network of Fig. 2. However, for simplicity, and to maintain the analogy to coupled tank circuits, we shall continue to use the L network of Fig. 3. We shall treat this newly formed parallel circuit as an entity in terms of its series equivalent.

Figure 4(a) shows this parallel circuit, where R_L is a load greater than R_A, and X_C is the compensating capacitive reactance necessary to make the total circuit resistance look like R_A. Figure 4(b) is the series equivalent, where X_E becomes the effective series reactance of Fig. 4(a). It will be as though X_L had been reduced. To compensate, either X_L or the tuning capacitance must be increased. To maintain the original conditions, we will naturally increase X_L.

From Fig. 4(b),

$$R_A - jX_E = \frac{-jR_L X_C}{R_L - jX_C} \qquad (8)$$

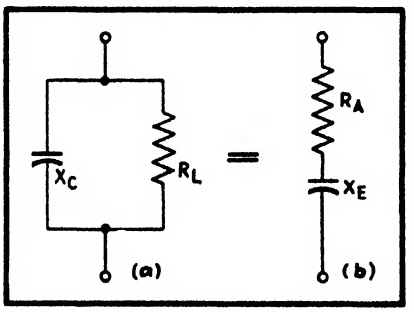

FIG. 4—Load with reactance in parallel (a), and its equivalent series circuit (b)

Clearing j from the denominator,

$$R_A - jX_s = \frac{R_L X_C^2 - jR_L^2 X_C}{R_L^2 + X_C^2}$$

$$R_A = \frac{R_L X_C^2}{R_L^2 + X_C^2} \quad (9)$$

$$X_s = -\frac{R_L^2 X_C}{R_L^2 + X_C^2} \quad (10)$$

Solving Eq. (9) for X_C now gives

$$X_C = -R_L\sqrt{\frac{R_A}{R_L - R_A}} \quad (11)$$

Equation (11) gives the value of compensating capacitive reactance X_C which will transform R_L into R_A. Figure 5 is a family of curves for this relationship, where R_L is plotted versus X_C for selected values of R_A.

In using Fig. 5, the range may be extended by multiplying all of the quantities by the same factor. For example, assume that it is required to find the reactance which will transform an actual resistive load R_L of 60 ohms into one of 20 ohms. Since there is no curve in the range of $R_A = 20$, we will use the $R_A = 2$ curve and assume that R_L and X_C are also ten times their given values. We enter the graph from the left at the point $R_L = 6$. Traveling to the right we find that the intersection with $R_A = 2$ occurs at $X_C = 4.2$. Multiplying by ten, our answer is 42 ohms.

Equation (10) gives the series equivalent reactance introduced by X_C, this being the value by which X_L will have to be increased to compensate. Figure 6 is a family of curves for this relationship. This curve is also used in extended ranges by multiplying all of the quantities by the same factor. Proceeding with the above example, we enter the curve at $X_C = 42$, and find the intersection with $R_L = 60$ at $X_s = 28$ ohms. No factor was involved and the answer is read directly.

Since the design procedure for a coupled tank circuit holds for the equivalent circuit of Fig. 3, any calculations which the engineer is accustomed to make to determine the proper reactances to use for a coupled tank circuit hold equally well for the π network. Of course, in most cases only X_C would remain the same, while X_L would have to be increased by an amount equal to the value of X_s. Knowing X_C and Q, R_A could be readily obtained.

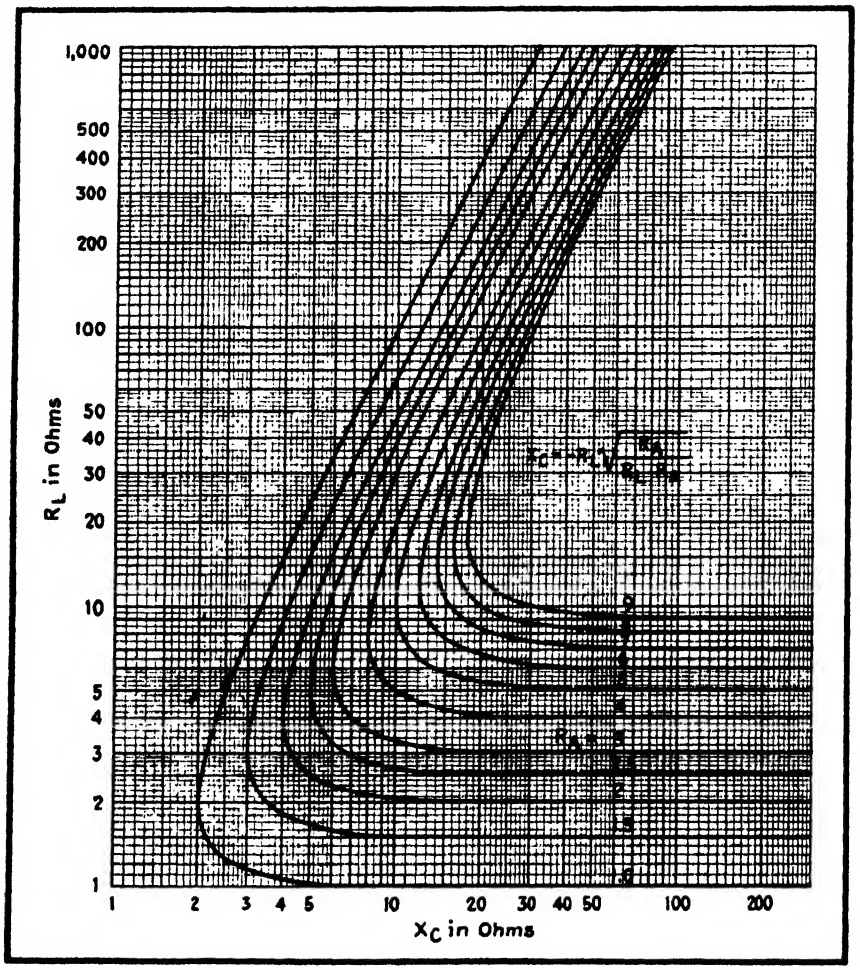

FIG. 5—Chart giving value of compensating capacitive reactance X_C required to make load circuit have correct resistance for matching purposes

Terminating Impedance

At best, the calculation of the generator impedance of a class C power amplifier is only an approximation. An actual measurement under operating conditions is much to be preferred. While we cannot do precisely that, we are able to do what is even more to the point. The circuit lends itself admirably to a measurement of R_G, the resistance with which we actually wish to terminate the vacuum tube.

The circuit of Fig. 3 is set up with sufficient metering to obtain plate current, plate voltage and load current. In place of R_A we may use any convenient value which we shall call R_X. The circuit is then tuned by means of X_T and the output and input powers calculated. If we have not exceeded or equaled the rated power dissipation capabilities of the tube, X_L is reduced and the circuit retuned. This procedure is continued until, at resonance, either maximum or required power output is obtained within the limitations of tube power dissipation. In the case of pentodes, the screen as well as plate dissipation must be watched, particularly if the ratio of X_L to R_X is large. Having adjusted the circuit we have terminated it with the proper R_G. Since we know R_X or can measure it, by measuring X_L or X_T we are able to calculate R_G. From this data R_A is fixed according to the circuit Q which is to be used.

If R_X is much different from R_A it is necessary to repeat the adjust-

ments and measurements using some value of R_x nearer to the calculated R_A. Just when it is necessary to repeat the measurements may easily be determined. If R_x is quite large, upon adjusting the circuit for proper impedance the resulting Q will be a low value. If it becomes much below 10, the conditions of maximum impedance and unity power factor will not occur simultaneously, and the harmonic generation will be appreciable. Consequently, erroneous measurements will result. If, on the other hand, R_x is too low, X_L will be large in order to bring R_0 to its proper value. This will result in a condition of undercoupling. The tube will be delivering full output possible under the conditions, but that output will be low as will be the input power. Since the internal impedance of a vacuum tube is a function of the operating conditions, R_0 will be different from that under the required load conditions.

Antenna Measurement

In many cases, the actual antenna resistance R_L is not known. This too may be found experimentally. Since we already know R_0, by replacing R_x with the actual antenna, adjusting for the required power, and measuring X_L or X_T we have sufficient data to calculate the unknown load resistance. Here again we should have comparable values of load, and the first measurement will generally have to be repeated using a value of R_x more nearly the same as R_L. Of course, if equipment is available, the measurement may be made by the substitution method. This means, in most cases, having available power resistors, continuously variable, and with neglible or tunable reactance. The first method is quite accurate and more adaptable to the equipment of the normal laboratory or transmitting plant.

Note that for the antenna measurement, we are not concerned with R_0 as it will finally exist, but simply wish to keep it constant for the two measurements, the one with R_x and the other with R_L. To be most accurate, therefore, all meter readings should be the same for both measurements. Low power may, of course, be used in this antenna resistance measurement.

The following outline summarizes the procedure to be followed in the design of a π coupling network.

1. Set up the circuit of Fig. 3 with any value of R_A, such as R_x. Adjust X_L until when tuned by X_T the required power output within dissipation limits is obtained. Measure R_x and X_L or X_T. The required load impedance R_0 is given by Eq. (7).

2. Select a value of Q for the required harmonic attenuation and calculate X_L and X_T from Eq. (5).

3. Find the value of R_A from Eq. (6).

4. Replace R_x by R_L, the actual load, and adjust the circuit for the required power output. Measure X_L or X_T, and using the value of R_0 found in step 1, calculate R_L from Eq. (7) solved for R_A, which in this case is R_L.

5. Replace this value of R_L by an R_x of approximately the same value and repeat steps 1 and 4.

6. If neither the value of R_x used in step 1 nor the value in step 5 is approximately equal to R_A, repeat steps 1, 2 and 3 using an R_x more nearly the same as that of R_A as found in step 3.

7. Find X_C from Fig. 5 or from Eq. (11).

8. Find X_E from Fig. 6 or from Eq. (10).

9. Increase X_L by X_E.

If reasonable care has been exercised, the circuit will be found to tune within a small percentage of the calculated X_T, and the final adjustments will be easy to make.

If X_T was varied very much in achieving tuning, this will alter the

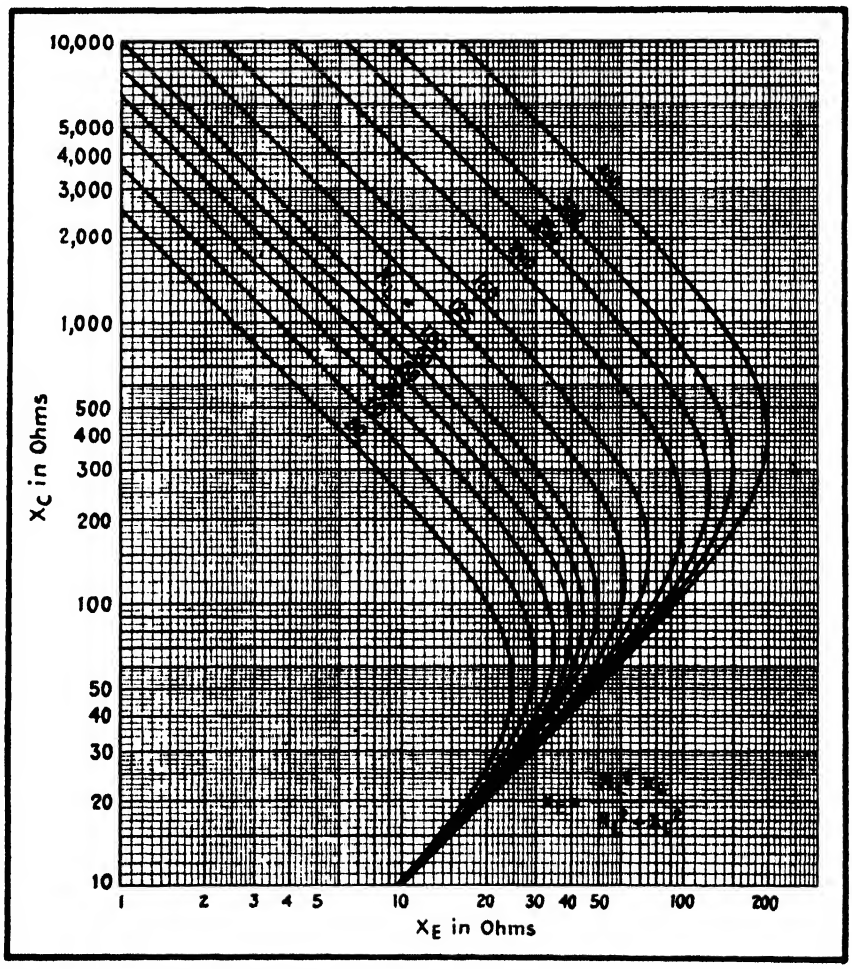

FIG. 8—Chart giving reactance value X_E by which the inductive reactance X_L in the network must be increased to give correct tuning

Q and should be corrected. Let us examine the case where X_T was increased for tuning, knowing that if it were decreased the reverse procedure would hold. In order to decrease X_T (increase the capacitance), either X_A must be increased or X_L decreased. The effect on the power output will clearly indicate which is required. An examination of Fig. 6 will show whether X_C is to be increased or decreased to cause the proper change in X_A. It will be seen that up to the point where X_C is equal to R_L an increase in X_C will cause an increase in X_A. When the value of X_C is greater than R_L a decrease in X_C is needed to cause an increase in X_A. Incidentally, it is just this effect that makes the adjustment of a π network by cut-and-try methods so confusing to the uninitiated. Not only can tuning be accomplished by any of the three reactances, but the change in the direction of the effect of changes in X_C produces apparently uncorrellated results.

Example

Probably the best method of explaining the design procedure is to work out a typical design. The following example is actual observed data.

1. The circuit of Fig. 3 is set up, choosing initially for R_A the value $R_A = 60$ ohms. X_L is adjusted for maximum power output, then measured and found to be 308 ohms. From this, $R_G = X_L^2/R_T = 94{,}900/60 = 1580$ ohms.

2. Using a Q of 12, $X_L = X_T = R_G/Q = 1580/12 = 132$ ohms.

3. $R_A = X_L/Q = 132/12 = 11$ ohms.

4. Inserting the actual antenna and readjusting for maximum power output, X_L is found to be 413 ohms. From this, $R_L = X_L^2/R_G = 171{,}000/1580 = 108$ ohms.

5. Steps 1 and 4 are repeated using $R_T = 108$ ohms. Upon readjustment, X_L is found to be 425 ohms, and $R_G = X_L^2/R_T = 181{,}000/108 = 1660$ ohms. Replacing R_T by R_L and again readjusting, X_L is measured as 417 ohms, and $R_L = X_L^2/R_G = 174{,}000/1660 = 105$ ohms.

6. Since R_L and both values of R_T are quite different, we will repeat steps 1, 2 and 3 using $R_T = 15$. When adjusted now, $X_L = 149$ ohms, and $R_G = X_L^2/R_T = 22{,}200/15 = 1480$ ohms. At a Q of 12, $X_L = X_T = 1480/12 = 123$ ohms, and $R_A = X_L/Q = 123/12 = 10$ ohms.

7. Using Fig. 5, we enter at $R_L = 10.5$ ohms, and the intersection with $R_A = 1$ occurs at $X_C = 3.4$. Since a factor of 10 has been used, $X_C = 34$ ohms.

8. Using Fig. 6 we enter the curve at $X_C = 340$ and, assuming a curve $R_L = 105$ to exist slightly above $R_L = 100$, we can estimate the intersection to occur at $X_A = 30$. Since a factor of 0.1 was used, $X_R = 3$ ohms.

9. X_L is, therefore, increased to 126 ohms.

Our final circuit has $X_T = 123$ ohms, $X_L = 126$ ohms, and $X_C = 34$ ohms. It properly terminates our tube when loaded by a resonant antenna of 105 ohms, yielding a circuit Q of 12. In actual practice, this tuned almost perfectly as calculated, and the change in X_T to produce exact tuning was too slight to warrant any further changes.

Conclusion

The foregoing assumes that means for making reactance and resistance measurements are at hand. In the field, particularly using emergency equipment, this will not be so. However, it is hoped that sufficient light has been thrown on the subject to enable "blind" tuning to be accomplished logically and rapidly.

As a suggestion, start with an L network, resonate the antenna, and then add output capacitance as required. Up to a point, increases in capacitance and inductance will bring up the antenna current. Thereafter, the current will start to drop off. In other words, at first R_L is too large to achieve a low enough R_G. As X_C reduces the effective R_L the current will increase to the point of overcoupling and excessive power output, as evidenced by excessive plate current. Further reduction of R_L or increase in X_L will be in the direction of low coupling and high Q, which is, of course, more desirable. For safety, then, adjustment is continued in this direction until the plate meter indicates that not too great a plate input is being delivered to the tube.

Single-Sideband Crystal Filters

X-cut crystals are used in multiple-section filters for the upper and lower sidebands and the carrier frequency. The carrier filter has a passband 16 cycles wide between 3-db points and the sideband filters are flat within 0.6 db for nearly 6 kilocycles

By PAUL K. TAYLOR

ONE PROBLEM involved in the development of an improved type of radio receiver for twin-channel, single-sideband reception was the design and construction of three crystal filters. These were used to separate the carrier from the sidebands of an amplitude-modulated wave train at

an intermediate frequency of 100 kc and to isolate each of the two sidebands.

Specifications called for a carrier filter less than 25 cycles wide at points whose response was 3 db down from maximum, and 175 cycles wide at points 50 db down, with a maximum attenuation of over 70 db available.

Since both speech and musical programs were to be received with high fidelity, each sideband (channel) filter was specified to have a passband 6 kc wide, flat within ±0.5 db except at the edges where a 2-db drop from maximum response could be tolerated. These edges were taken to be 100 cycles and 6 kc respectively from the intermediate carrier frequency of 100 kc.

A maximum relative attenuation of at least 85 db was desired at all frequencies separated by more than 4 kc from the passband midfrequency. This would provide for a 40-db attenuation of adjacent-channel signals of equal strength in addition to a possible unfavorable selective fading differential of 45 db between the two channels.

A piezoelectric crystal such as quartz acts electrically[1] like the LC circuit shown in Fig. 1. For a range near the resonant and antiresonant frequencies of this electrically equivalent circuit, the crystal presents a reactance whose variation is shown by the full-line graph of Fig. 4. Suppose that two crystals are so cut that the resonant frequency of one coincides with the antiresonant frequency of the other. The reactances of both crystals are then as depicted by the full-line and dashed-line graphs of Fig. 4.

Theory

If these crystals be connected in a bridge circuit similar to Fig. 6, or its equivalent lattice, Fig. 2, we have the structure of a simple narrow bandpass filter. The dashed-lines in Fig. 2 indicate lattice arms of the same type as those actually shown. In Fig. 6, the dashed-lines indicate that *XX* are the two halves of a single crystal having divided plating. Likewise for *YY*.

The bridge circuit of Fig. 6 is that of a pure reactance bridge. This will be perfectly balanced when the reactance between points 1 and 2 of the circuit is equal to that between 1 and 4 and of the same sign. The same is true for the reactance between 2 and 3 and that between 3 and 4. There are two frequencies at which this will occur. On Fig. 4, these are designated $f\infty_1$, and $f\infty_2$, for the attenuation (theoretically) reaches an infinite value at these frequencies. Actually, the attenuation will merely rise to a maximum value, called an attenuation peak, at each of the two frequencies of balance as shown in Fig. 5. As the frequency of an input signal is increased from $f\infty_1$, toward f_A, the attenuation will continuously decrease until it (theoretically) reaches zero at f_A, the series-resonant frequency of one of the pairs of crystals.

For frequencies between f_A and f_B the reactances of the two pairs of bridge arms are at each point of opposite sign. Hence, signals whose frequencies lie within this range will pass through the filter (theoretically) with no attenuation. Actually some attenuation is experienced in this range, the amount depending on the Q factor of the crystals and associated circuit elements. For this reason, characteristics of the filters developed in this work are shown as relative attenuation versus frequency rather than actual attenuation. The region between f_A and f_B, as shown in Fig. 5, is the passband of the filter.

In practice, capacitors C_A are placed in parallel with input and output terminals of the filter. Others, C_B, of much smaller capacitance, are connected from input to output as bridging capacitors.

The parallel capacitors adjust the separation between resonant and antiresonant frequencies of the bridge arms and hence control the width of the passband. The bridging capacitors change the shapes of the reactance graphs of the bridge arms somewhat, thereby changing the frequencies at which the two reactance curves cross where of like sign. Adjustment of the bridging capacitors, therefore, controls the frequencies of the attenuation peaks of Fig. 5.

The resonant and antiresonant frequencies of a quartz crystal are separated by only about 0.4 percent of resonant frequency (for X-cut crystal). Since, as seen in Fig. 4, the passband is only double this amount, some other circuit element must be introduced if wide passbands are desired. Such an element may be an inductance placed in series or in parallel with each crystal of the circuit. These two types of connection result in filters having low image impedance and high image impedance, respectively.

To avoid stray couplings in the channel filters herein described, a reasonably low image impedance was chosen. This choice called for a coil to be connected in series with each crystal of the filter circuit. The widening of the filter passband by the use of coils is due to the fact that their addition produces a large increase in the separation of resonant and antiresonant frequencies of the bridge arms and furthermore extends the upper edge of the passband considerably beyond the higher of the two antiresonant frequencies of the bridge circuit, Fig. 9 and 10.

For the passband region, the image impedance of the filter is a pure resistance whose value changes from near zero at the passband edges to a maximum midway between them. Terminating resistances considerably lower than the midband impedance are used in the filters actually built to secure[2] a better average impedance match over the whole passband.

If all the coils used in the wideband filter are wound to have equal resistances, or if supplementary resistors are inserted to make all arms of the equivalent bridge circuit have equal resistances, it is possible[1] to consider these resistances as being brought outside the bridge circuit proper and incorporated in the terminating resistors. This leaves the bridge as a pure

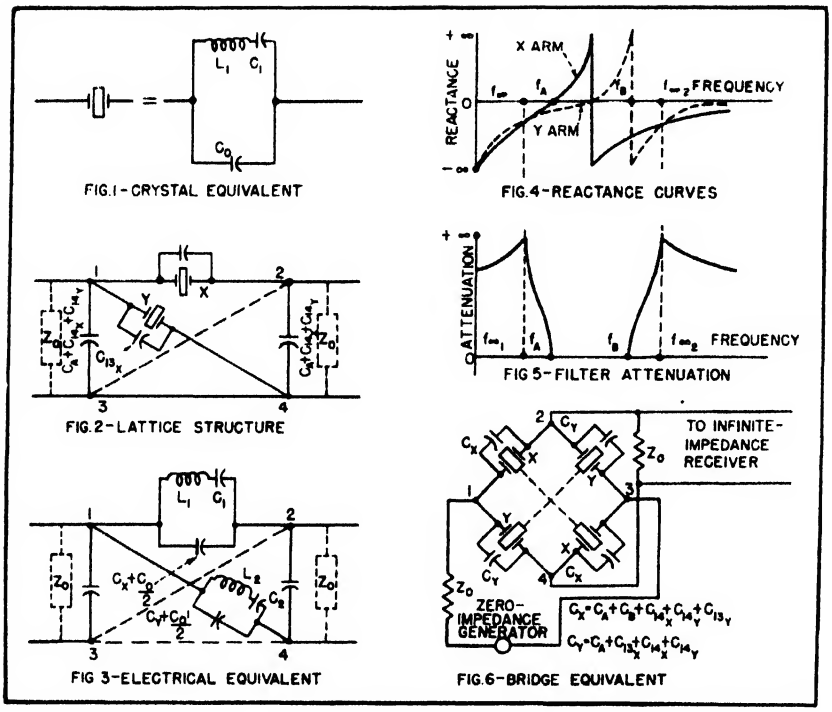

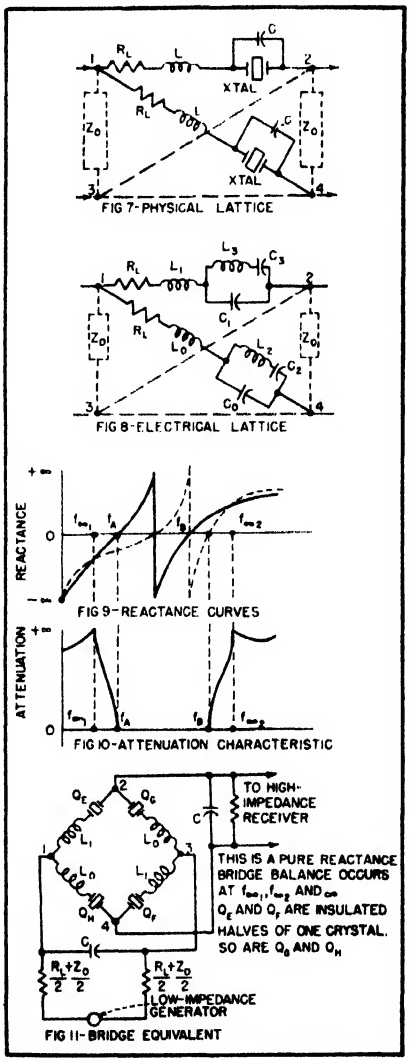

Table I—Effect of Temperature on Attenuation Characteristic

db Down	Frequency (kc) of Lower Side		Difference cps	Frequency (kc) of Upper Side		Difference cps
2	93.92	93.93	+10	99.890	99.868	−22
6				100.060	100.035	−25
10	93.58	93.62	+10	100.152	100.127	−25
20	93.41	93.44	+30	100.300	100.278	−22
30	93.29	93.35	+60	100.405	100.360	−45
40	93.16	93.21	+50	100.505	100.480	−25
	Average		+38	Average		−27

reactance bridge. Under this condition neither the sharpness of the cutoff at the passband edges, nor the steepness of the attenuation characteristic of the filter is impaired by the resistances of the coils inserted in the filter lattice.

Mason[1] has given mathematical formulas from which the values of the circuit components of a filter section can be computed after certain constants have been chosen. These are (1) the frequencies of the edges of the passband, (2) the frequencies of the peaks of infinite attenuation, and (3) the midband image impedance of the desired filter. The formulas refer to the electrical equivalents of the crystal filter lattice as shown in Fig. 3 and 8.

A sample 6-kc filter calculation using the wideband filter formulas, resulted in the following values. Chosen

$Z_0 = 2{,}000$ ohms
$f_A = 99.50$ kc; $f_B = 106.70$ kc
$f_{\infty_1} = 98.70$ kc; $f_{\infty_2} = 107.50$ kc; $f_{\infty_3} = \infty$

Having obtained the values of the equivalent electrical components of a crystal filter section, the next step is to transfer the computed series resonant frequencies f_s and f_s of the crystals to actual dimensions of the quartz crystals themselves. Equations for accomplishing this depend upon the type of crystal cut decided upon.[2, 3] Calculated

$L_0 = L_1 = 44.22$ mh
$C_0 = 52.84\ \mu\mu f$; $C_1 = 54.88\ \mu\mu f$
$L_2 = 20.73$ h; $C_2 = 0.1206\ \mu\mu f$; $f_s = 100.70$ kc
$L_3 = 18.58$ h; $C_3 = 0.1284\ \mu\mu f$; $f_s = 105.28$ kc

The −18.5-deg X-cut crystal had previously been generally used as a filter crystal due both to its high Q and freedom from the troublesome face shear mode of oscillation. However, this cut has quite a large temperature coefficient of over 20 parts per million per degree centigrade.

The +5-deg X-cut crystal with a width-to-length ratio of 0.35 has a temperature coefficient of only about 4 parts per million per degree centigrade.[4] Moreover, it is easily cut from the mother quartz (involving rotation only about the X or electrical axis). It has the disadvantage of having a relatively large coupling to the face shear mode when wide crystals are used.

Because of the two advantages mentioned, the +5-deg X-cut crys-

tal was chosen for the present filter construction. A single-section channel filter was found to have a spurious resonance due to the coupling to the shear mode. The response occurred at a frequency approximately 116 percent of the passband midfrequency and reduced the attenuation to within 11 db of that of the passband itself.

When a filter of four sections was tested, however, no observable indication of any secondary response at all was present. This is evident in the graphs of Fig. 14 and Fig. 15 where the attenuation is 87 db or greater for all frequencies more than 1.2 kc (1.1 percent) higher than the upper edge of the passband. This desirable result was due to the slight differences in crystal frequencies for the four filter sections resulting from the choice of different peaks of maximum attenuation for each section.

By the use of equations given by Atwood [3] we find for the +5-deg X-cut crystal that $f = 110.5/y'$ kc.

This equation is strictly accurate for only very narrow crystals, of which y' is the length. The crystals were designed to have a width/length ratio of about 0.35 in order to secure the +5-deg X-cut crystal minimum temperature coefficient of 4 parts per million per degree centigrade previously mentioned. As X-cut crystals of larger and larger widths are used, the crystal frequency constant decreases somewhat from that of a very narrow crystal.[5] For a width/length ratio of 0.35 the decrease is 1.8 percent. Hence the equation is modified for the crystals used in the present project to

$$f = 108.5/y' \text{ kc}$$

A preliminary study of the effect of interelectrode and stray capacitances together with midband frequency and bandwidth requirements for the 6-kc bandpass filters dictated the use of very thin crystals. Having chosen a minimum feasible thickness and a width/length ratio of around 0.35 the equivalent motional capacitance of a sample crystal was found by measurement of its static capacitance together with its resonant and antiresonant frequencies. Substitution of this value for C_2 or C_3 in Mason's equations determined the image impedance Z_0 of the filter. This value of Z_0 was, therefore, used in calculating all the electrical components of the 6-kc bandpass filters.

To obtain the sharp cutoff and large attenuation required by the specifications, a filter of four sections was built for each of the 6-kc channel filters. Two shielding cans were used as containers for each complete filter, each can containing two filter sections. After the filter was mounted, dry air was passed through the can which was then hermetically sealed.

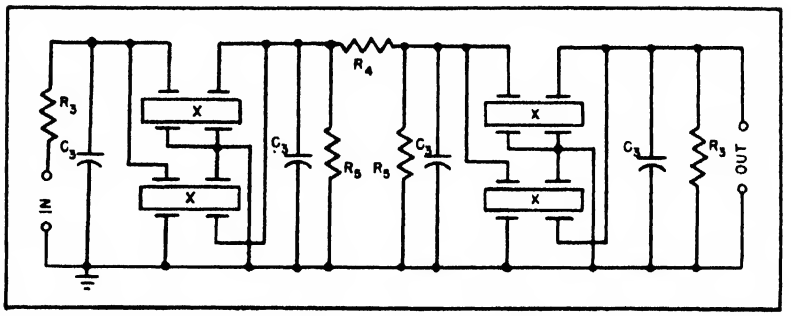

FIG. 13—A double-section 20-cycle crystal filter. Capacitors C_3 control passband width, R_3 are terminating resistors, R_4 and R_5 are interstage impedance-matching resistors and X are +5-deg X-cut crystals. These components are shown in the illustrations on this page

Each single-filter section consists of two crystals with divided plating, two coils in shielding cans, each equipped with adjustable powdered-iron cores, two small, fixed, molded mica capacitors and a tiny bridging capacitor. The latter is formed by two short lengths of bus bar mounted about ¼-inch apart on the bottom of the Bakelite crystal mounting base.

The circuit of each double-section filter is shown in Fig. 12. Resistor R_2, shunted between the interconnection of each two sections and the chassis, together with the resistances of the input and output coils, provides a T pad to serve for interstage impedance matching. External terminations were used with each double section filter.

Each series coil is a universal-wound coil on a ½-inch-diameter Isolantite form. The coil is equipped with an adjustable powdered-iron core, and in use is mounted in the shielding can.

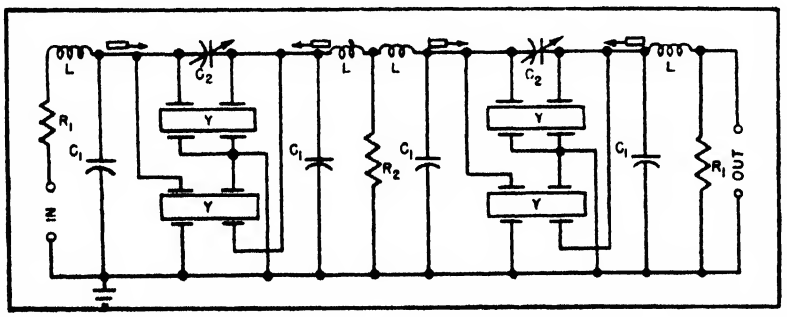

FIG. 12—A double-section 6-kc-channel crystal filter. Capacitors C_1 permit fine adjustment of passband width, C_2 fine adjustment of attenuation peaks, L are passband widening coils, R_1 are terminating resistors, R_2 are interstage impedance-matching resistors and Y are +5-deg X-cut crystals

Construction of Carrier Filter

The narrow-band filter for the 100-kc intermediate-frequency carrier was much simpler in design and construction than the channel filters described above.

Calculated values of the motional capacitance together with the chosen theoretical passband width of 40 cycles, and the chosen fre-

quencies of the attenuation peaks, determined the value of image impedance.

Here, again, as for the 6-kc channel filters, terminating resistors of smaller size than the image impedance were used to give a better impedance match throughout the passband. Figure 13 is a schematic diagram of the wiring of this double-section narrow-band filter.

Each single section consists merely of two divided-plating crystals, two small mica capacitors and the terminating resistors. The three resistors (at the center of the under-chassis view) constitute a pi-type attenuation pad of about 7 db between the two sections. Input and output terminating resistors are mounted externally to the shield can.

Results and Conclusions

Each of the two complete four-section 6-kc channel filters had an insertion loss within the passband itself of about 24 db. To compensate for this loss, the filter was fed from and into vacuum-tube circuits. The tube supplying the signal to the input of the filter was a 6J5 used in a cathode-follower circuit for easy impedance matching. The output of the filter was fed to a 6SK7 pentode amplifer. The result was a gain within the passband of 1.5 db measured from input to cathode follower to output of the pentode amplifier. The same type of tube-circuit arrangement was used with the carrier filter.

The attenuation characteristics of the lower and upper channel four-section crystal filters are shown in Fig. 14 and 15. The average characteristics are as follows:

Width of passband between points 2 db down, 5.94 kc; 2-db point adjacent to carrier, 134 cycles from carrier, passband flat within ±0.6 db over a bandwidth of 5.73 kc; bandwidth at 85 db down, 8.10 kc; attenuation greater than 87 db for all frequencies separated more than 4.17 kc from the passband midfrequency. Tests of the 6-kc channel filters at 25C and 50C respectively show a slight narrowing of the passband with rise in temperature averaging about two-and-one-half cycles per centigrade degree of temperature change. This is shown in Table I.

In Fig. 16 are shown two passband and attenuation characteristics of the double-section carrier filter. These were measured respectively at 25C and 50C. A rise of temperature is observed to cause the characteristic as a whole to shift to slightly lower frequencies. The shift averages only 0.44 cycles per deg. The bandwidth of the filter characteristic measured at room temperature is 16 cycles at a relative attenuation of 3 db, 22 cycles at 6 db, 86 cycles at 50 db and 180 cycles at 78 db. The latter attenuation is maintained for all frequencies outside the 180-cycle band mentioned.

The author desires to express his appreciation for helpful guidance, valuable suggestions, and continued interest to E. D. Blodgett, Thomas Jacobi and L. L. Lakatos of the Engineering Products Department of the RCA Victor Division. He is also thankful to the staff of the RCA Crystal Engineering Department for preparation and mounting of the crystals, and to the RCA-Victor Division of the Radio Corporation of America at Camden, New Jersey, whose facilities made possible the development herein described.

References

(1) W. P. Mason, "Electromechanical Transducers and Wave Filters," Chap. VIII, D. Van Nostrand Co., Inc., 1942.
(2) E. A. Guillemin, "Communication Networks," Vol. II, Chap. VIII, Art. 6; Chap. X, Art 2, John Wiley and Sons, 1935.
(3) J. B. Atwood, The Equivalent Electrical Circuit of Quartz Crystals, RCAC Eng. Report F-72-7, 1/19/39, Sheets 6, 12, and 15.
(4) R. A. Heising, "Quartz Crystal Applications," p 538, D. Van Nostrand Co., Inc., 1946.
(5) W. P. Mason, Electrical Wave Filters Employing Quartz Crystals as Elements, *B.S.T.J.* 133, p 410, July 1934.

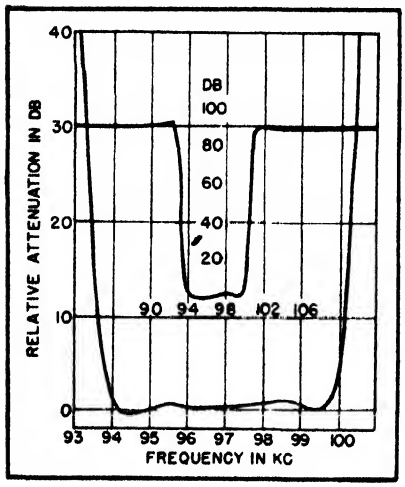

FIG. 14—Attenuation characteristic of a four-section crystal channel filter for 94-99.9 kc

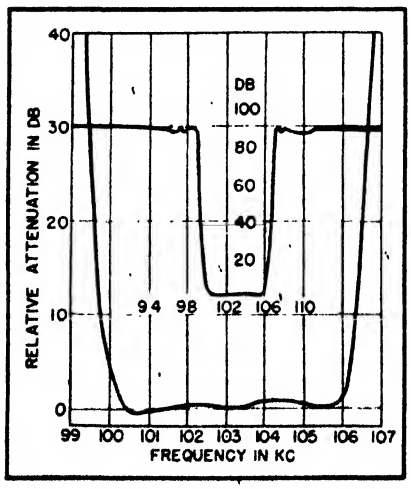

FIG. 15—Attenuation characteristic of a four-section crystal channel filter for 100.1-106 kc

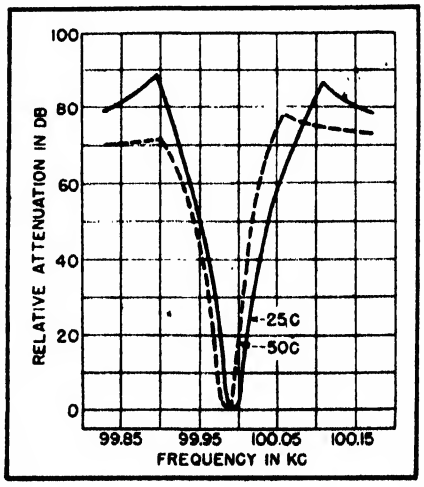

FIG. 16—Attenuation-frequency characteristic and effect of temperature change on the 100-kc 2-section carrier filter

Phase-Shifter Nomograph

Bridge-type phase-shifting network covering the full range from zero to 180 degrees has many applications even though it requires ground isolation. The nomograph reduces design calculations to one reading with a straight-edge and a simple arithmetic calculation

By RAYMOND E. LAFFERTY

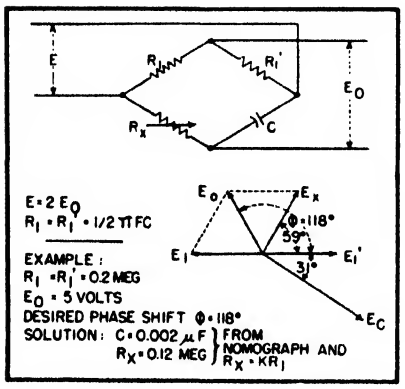

FIG. 1—Bridge-type phase-shifting network, and vector diagram for the example set forth

THE bridge-type network shown in Fig. 1 is useful for shifting the phase of the output voltage to any desired value between 0 and 180 degrees with respect to the input voltage. The amplitude of the output voltage remains constant at one-half the input voltage value for all degrees of phase shift.

In practice, a fixed value of C is employed and the value of R_x is varied between infinity and zero ohms. When R_x is infinity, the phase-shift angle ϕ is 0 degrees; when R_x is equal to R_1, ϕ becomes 90 degrees; when R_x is zero, ϕ is 180 degrees.

The accompanying nomograph facilitates determining the value of R_x required to provide a desired phase shift angle with a particular set of values for R_1, C, and frequency. A straight-edge is placed on the known values of f and R_1, and the required value of capacitance for C is read on the C scale. This nomograph is based on the fact that the reactance of C must equal the resistance of R_1, making C equal to $1/2\pi fR_1$. Next, on the ϕ-K column read the value of K corresponding to the desired value of phase shift ϕ. Since $K = R_x/R_1$, the required value of R_x is readily computed as $R_x = KR_1$.

For the example set forth in Fig. 1, the nomograph gives the value of C directly as 0.002 μf and, for ϕ = 118 degrees, gives K = 0.6. Multiplying this value of K by the 0.2-meg given value of R_1 gives 0.12 meg as the required value of R_x. The vector diagram in Fig. 1 illustrates the phase relations of the various voltages in the network for this particular example.

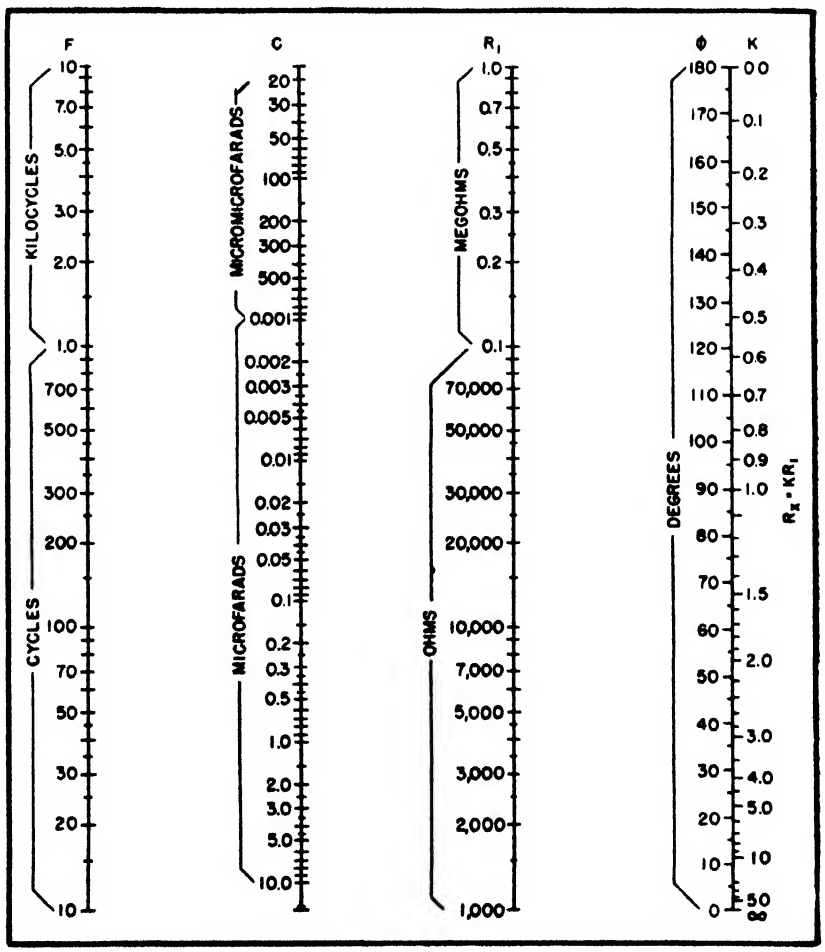

The Swinging Filter

Engineering comments on the purpose, proper design and correct use of variable inductance chokes for filtering the output of rectifier systems. Optimum performance of swinging choke depends upon its use in circuits meeting specifications for which it was designed.

By ROBERT M. HANSON

THE SO-CALLED swinging choke is often used by designers of rectifier-filters as the first element of a choke input filter. This type of reactor was so named because of the characteristic wide variation of inductance as the direct current component is varied. This discussion will cover the design principles and the application of this type of choke from both the theoretical and practical standpoint. A large part of the material will apply to the ordinary smoothing reactor as well.

Inductance may be defined as follows: A coil has an inductance of one henry when an electromotive force of one volt is induced by a uniform current-change of one ampere per second.

Any change of current through the winding will result in the generation of a voltage across the coil having a polarity opposing the voltage causing the current change. The definition of inductance gives the magnitude of this voltage as a measure of the inductance. This voltage will be zero when the current in the coil is constant. Consequently the application of inductance will be to circuits where the current is subject to change. The electromotive force induced in the coil is commonly referred to as its excitation voltage. Alternating current equipment is usually specified in terms of root-mean-square sine wave terminology, and a choke specification is not complete unless the excitation voltage and frequency are specified as well as the inductance and the average value of the direct current flowing through it.

TABLE OF RECTIFIER CIRCUIT CHARACTERISTICS

	Type of Circuit			
	Single phase full wave		Three phase half-wave	
	Using 2 tubes	Bridge using 4 tubes	Using 3 tubes	Bridge using 6 tubes
Ratio of ac voltage to dc output voltage				
1. Transformer secondary rms volts per leg	1.11	1.11	0.86	0.43
2. AC components of rectifier output, rms				
At ripple frequency	0.47	0.47	0.18	0.04
At ripple 2nd harmonic	0.10	0.10	0.04	0.01
At ripple 3rd harmonic	0.04	0.04	0.02	....
Ripple frequency, where f is supply frequency	$2f$	$2f$	$3f$	$6f$
Ratio of tube currents to direct current				
Peak anode current	1 00	1.00	1.00	1.00
Average anode current	0.50	0.50	0.33	0.33

A manufacturer's catalog will seldom list the rating of excitation voltage for an iron core filter reactor. In the normal application the maximum choke excitation voltage will be determined by the direct voltage of the power supply and the type of rectifier circuit chosen. The insulation test voltage of the choke is usually given and the unit recommended for operation in rectifier circuits where the direct voltage is from thirty to fifty percent of this rms test voltage. The unit will have been designed to withstand the excitation voltages encountered in this service. It would be bad practice to insulate the core of a low test voltage choke by mounting it on standoff insulators and to connect the coil in a high voltage rectifier filter, unless it had been determined that the permissible excitation voltage would not be exceeded. Such a condition would be characterized by the noisy operation, poor filtering, erratic rectifier tube operation (possibly with the load shifting from tube to tube). and early failure of internal coil insulation.

The manufacturers of filter chokes usually catalog the swinging and smoothing reactors in sets rated according to the direct current capacity. As the requirements of different applications will vary, the ratings have been standardized by listing the inductance of the smoothing choke at maximum rated direct current, and giving the inductance of the swinging choke at both maximum and at 10 percent of the maximum rated direct current. Typical design values would be 10 henries for the smoothing choke and a swinging choke with 6 henries at rated current and 15 henries at 10

percent of rated current. An alternate set of values might be 12 henries for the smoothing choke and 5 to 20 henries for the swinging choke. The companion set of swinging and smoothing chokes will usually be found to be exactly the same overall size, and to have identical coil construction. Curve 1 of Fig. 1 shows a typical curve for a 1 ampere swinging choke.

Ratings of Filter Chokes

Curve 2 of Fig. 1 shows the inductance-current characteristic of the regular smoothing reactor where the unit is designed for optimum inductance at rated current. The inductance at maximum rated current is approximately twice that of the swinging choke but the increase of inductance is only about 20 percent at 10 percent rated current.

Curve 3 of Fig. 1 shows the inductance-current curve of a filter reactor designed for constant inductance. These three curves were plotted from measurements made on reactors having identical coil and core sizes. The only difference was in the design of the magnetic circuit of the three units. The swinging choke has a relatively small air-gap in series with the magnetic circuit compared to the gap in the unit set for optimum inductance.

The inductance of an iron core filter choke may be determined by the following expressions:

$$L = KN^2\mu'b \qquad (1)$$

where, L is inductance in henries,
K is factor expressing core area, units, etc.,
N is number of turns in winding,
μ is permeability of core steel, and
b is equivalent length of magnetic circuit flux path including effect of air gap

All of these factors except the core permeability are essentially independent of the magnitude of the direct current in the winding. However the permeability factor is variable depending upon the direct current magnetization of the core, and also upon the a-c flux density in the core. An increase of the d-c magnetization tends to decrease the permeability, while an increase of the a-c flux density increases the permeability up to a certain value after which further increases of flux density results in rapid decrease of permeability. The silicon steel commercially used in filter chokes can give a permeability change of as much as 30 to 1 over the extremes of d-c magnetization, and a change of 10 to 1 with variations in a-c flux density.

The flux density in the core resulting from the direct current in the winding is expressed by the following formula:

$$B_{dc} = 0.4\pi NI\mu, b \qquad (2)$$

where, B_{dc} is flux density in gauss,
π is 3.14,
N is number of turns in winding,
I is direct current in amperes,
μ is permeability of core under operating conditions,
b is equivalent length of magnetic path including effect of air-gap.

This flux represents energy stored in the magnetic field and once established, no additional energy is required to maintain it.

This filter reactor will have an alternating voltage applied to the winding that is dependent upon the amount of ripple voltage requiring filtering. The frequency of this voltage will depend upon the power line frequency and upon the type of rectifier circuit selected. With a 60 cps single phase, full wave, two tube rectifier, the principle component will be 120 cps with smaller 240 and 480 cps components.

The fundamental relation between magnetic flux ϕ and induced voltage E is:

$$E = 10^{-8}KNf\phi = KNfAB_{ac} \qquad (3)$$

where, E is effective voltage, in volts,
K is constant,
N is number of turns in winding,
f is frequency in cps,
ϕ is total flux in core,
A is area of core cross section, and
B_{ac} is flux density (maximum)

Rearranging Eq. (3) we find

$$B_{ac} = 10^{-8}E/KNfA \qquad (4)$$

The maximum instantaneous flux density in the core will be the sum of B_{ac} and B_{dc}. The design must be such that this total does not exceed the saturation value for the core material used. It is evident from Eq. (2) and (4) that the designer may set the values of a-c and d-c flux densities at any desired value within

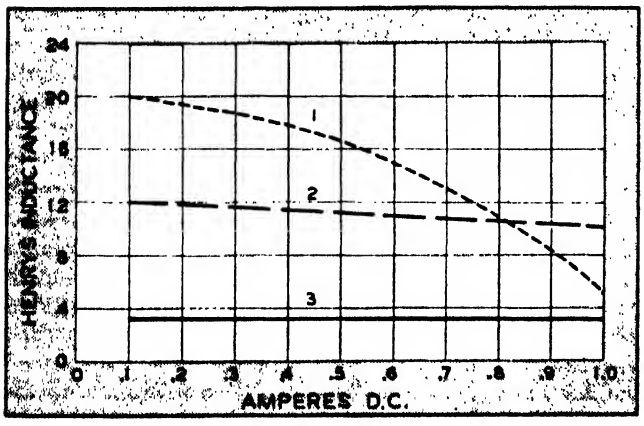

Fig. 1—Inductance of typical iron core coils intended for use in power supply filter circuits. Curve 1 represents desirable characteristics for one type of swinging choke. Curve 3 represents characteristics of coil whose inductance is independent of current through it. Curve 2 represents compromise between 1 and 3

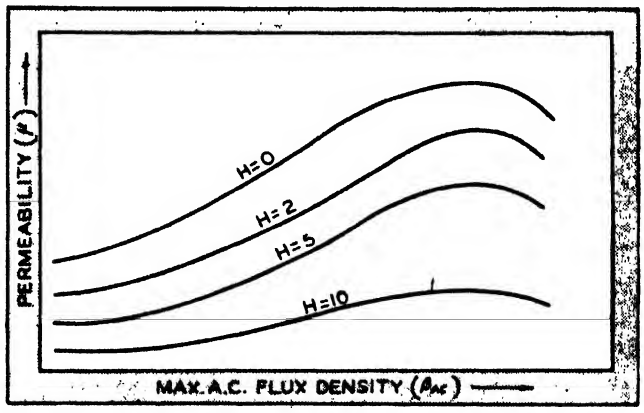

Fig. 2—Curves representing the variation of permeability plotted against maximum a-c flux density for iron core coils with varying degrees of magnetic intensity, H, resulting from direct current flowing through the coil. The relative values of H for each case is indicated on the individual curves of the family

limits by proper selection of the design elements of number of turns, core area, length of magnetic path in iron, length of magnetic path in air, grade of core material, and operating point of magnetic material.

The d-c magnetomotive force in gilberts per centimeter will be

$$H_0 = 0.4\pi N I/b \qquad (5)$$

where H_0 is the force establishing the flux in the magnetic material having a mean length of path b.

The relative effects of d-c magnetization, and of a-c flux density upon the permeability of a core material are shown in Fig. 2. The abscissa represents the range of a-c flux density from low values to the saturation point, the ordinate is proportional to permeability, and the family of curves shows the effect of various degrees of d-c magnetization. It can be seen that for any constant value of a-c flux density the permeability is a maximum for zero direct current, and decreases as the direct current is increased.

Design of Swinging Chokes

The problem in designing a swinging choke is to cause the inductance to increase when the direct current in the winding is decreased, and assuming the a-c excitation voltage to be kept constant. Reference to Eq. (1) shows that the change must be accomplished by a change in the permeability μ. From Eq. (4) we see that the a-c flux density will not change when the direct current is changed and the a-c voltage, E, is kept constant. However, Eq. (5) shows that the d-c magnetomotive force is directly proportional to the direct current in the winding. Therefore, when the direct current is decreased, the value of H from Eq. (5) will decrease, the resultant permeability shown on Fig. 2 will be increased, and consequently the inductance will increase as shown by Eq. (1).

If the magnetic path of the reactor consisted entirely of iron the change of inductance would be directly proportional to the change in permeability. This sets the absolute limit for the inductance ratios of a swinging choke at the permeability ratios resulting from the maximum and minimum values of magnetomotive force.

A reactor with no air gap in the magnetic circuit, and carrying direct current, would have a relatively large value of H and therefore a low permeability. Placing an air gap in the circuit would increase the effective length of path shown as b is Eq. (5) and result in greatly decreased H. This increased effective length of magnetic circuit, and the value of increased permeability due to decreased H, may be substituted in the inductance formula Eq. (1). It may be found that the increased permeability more than compensates for the increased magnetic path and the result is that the choke with the air gap will have a higher inductance when carrying direct current than the choke with a closed magnetic circuit. It will also be found that there is an optimum value of air gap giving a maximum inductance and this value will be different for each value of direct current. As the amount of direct current is increased the optimum air gap will also become larger.

Swing Choke Adjustments

The swinging choke is adjusted with an air gap that is at the optimum value giving high inductance at the lowest current and consequently the gap will be smaller than optimum at the high current and the inductance at high current will be low. Reference to Fig. 1 shows this effect clearly. Curve 1 shows a reactor with a small air gap giving 20 henries at 0.1 ampere d-c and only 5 henries at 1 ampere. Curve 2 shows the gap adjusted for the maximum inductance of 10 henries at 1 ampere. This large air gap minimizes the effect of permeability variations and the inductance only increases to 12 henries at 0.1 ampere dc. Curve 3 shows the effect of a very large air gap resulting in an inductance below the maximum at 1 ampere, but it is practically constant regardless of variations of direct current.

The engineer designing the swinging reactor will calculate the inductance at both the low and high currents. The design is modified until these two inductances are the values specified. Further investigation must then be made to be sure that the core material is not saturated at the high value of current. After the reactor is assembled the air gap may be adjusted until the inductance at the high current is the exact value specified. The inductance at the low current is then measured. If this value of inductance did not meet the specifications it would be necessary to correct the entire design as both inductances cannot be independently adjusted by means of the air gap.

Ripple Voltage Considerations

The value of the a-c excitation voltage is necessary in designing these reactors. Figure 2 shows the permeability change with flux density, and indicates how it drops to a very small value after the density exceeds a certain value. This means that a reactor might be designed and tested to give a specified inductance at an excitation of 10 volts r.m.s. 60 cps, and yet when the choke is installed in the filter where the excitation is 1500 volts 120 cps it could be unsatisfactory. However the practice of measuring the choke at such low excitation is perfectly satisfactory providing it has been designed for the operating conditions, and this measured inductance is considered as a figure of merit for the reactor rather than the actual operating inductance to be used in circuit design.

The references on the subject of filter design, given in the bibliography, explain in detail how to determine the size of reactor and condenser required for a specific ripple percentage, and for proper limitation of peak rectifier tube current. A portion of the standard table of rectifier design data will be given here for discussion purposes. The data of this chart was determined assuming choke-input filter with infinite inductance, zero voltage drop in tubes and choke, and perfect regulation in power transformer and supply line.

The chart shows that the rectifier

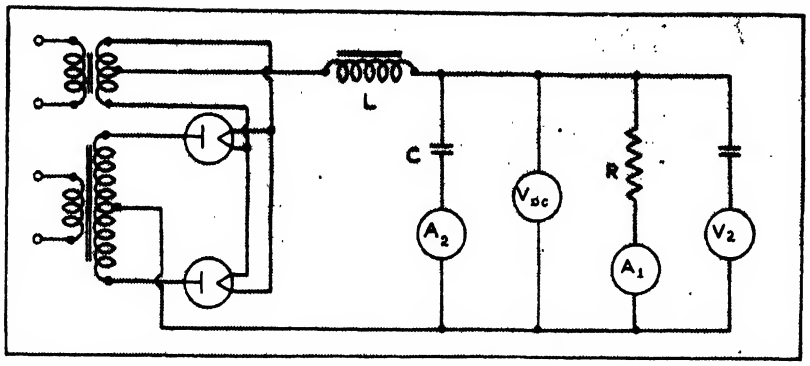

Fig. 3—Schematic wiring diagram of single-phase, full-wave rectifier, filter and load

output will have a fundamental ripple frequency that is dependent upon the supply frequency and the type of rectifier circuit used. With a 60 cps supply the regular full-wave circuit will have a principle ripple voltage at 120 cps and the magnitude of this ripple voltage is shown to be 47 percent of the direct voltage. The three-phase half-wave circuit would have a fundamental ripple voltage at 180 cps and have a root-mean-square value equal to approximately 18 percent of the direct voltage. The three-phase full-wave bridge rectifier would have a fundamental ripple voltage at 360 cps and an r-m-s value equal to 4 percent of the direct voltage.

The exact magnitude of the various ripple components will differ from the values given in the chart in actual practice because of non-sinusoidal waveform of supply voltage, reactance in the power transformer, resistance in filter reactor, voltage drop in rectifier tube, and an input reactor with an inductance that is not relatively infinite.

A single-phase full-wave rectifier circuit is shown in Fig. 3. The output of the rectifier is delivered to the load R through a single section choke input filter consisting of the reactor L and the condenser C. This 6-μf condenser will have a reactance of approximately 220 ohms at 120 cps. The load resistance R was adjusted from 1000 to 10,000 ohms to give a direct current range of 1 ampere to 0.1 ampere when V_{ac}=1000 volts. There will be a flow of direct current through the reactor and the load resistor R. There will also be a flow of alternating current through the reactor L and the parallel impedance of the condenser C and the resistance R. However the reactance of the condenser is so much smaller than the resistance of the load that the actual load resistance has little effect upon the magnitude of this alternating current.

The peak value of the excitation voltage of the filter reactor L will be equal to the product of its reactance and the alternating current flowing in the winding *i.e.*, $\sqrt{2}E_{ac} = 2\pi fLI_{ac}$ volts.

Avoiding Resonance Effects

If this current is to be calculated the circuit must be solved by the use of complex algebra as the reactor consists of an inductive reactance in series with a resistance depending upon the Q of the choke, and the condenser is in series with these two elements and consists of a capacitive reactance. As the inductive reactance of the choke becomes smaller with decreased inductance it will approach equality with the reactance of the condenser and the voltage across the reactor will increase. If the reactance of the choke and condenser become equal we have a condition of series resonance and the voltage across the reactor may become much greater than the actual ripple voltage from the rectifier. This condition of series resonance must be avoided as it will result in high peak current through the rectifier tubes, excessive voltage across the filter choke, and high ripple voltage at the load.

The vector relationships between the filter input voltage E_{ac}, the choke excitation voltage E_{ch}, and the output ripple voltage across the condenser E_c are shown in Fig. 4. If the choke is a pure reactance the voltage induced will lead the current by 90 deg. The voltage drop of the condenser will lag the current by 90 deg. The input voltage E_{ac} will be the vector sum of these two voltages. Examination of the vector diagram shows that the choke excitation voltage will tend to be greater than the filter input ripple voltage. It is also evident that a decrease of inductance will result in increased voltage drop across the choke as well as increased ripple voltage across the condenser.

Under operating conditions with the usual rectifier-filter combination, the excitation voltage for the input

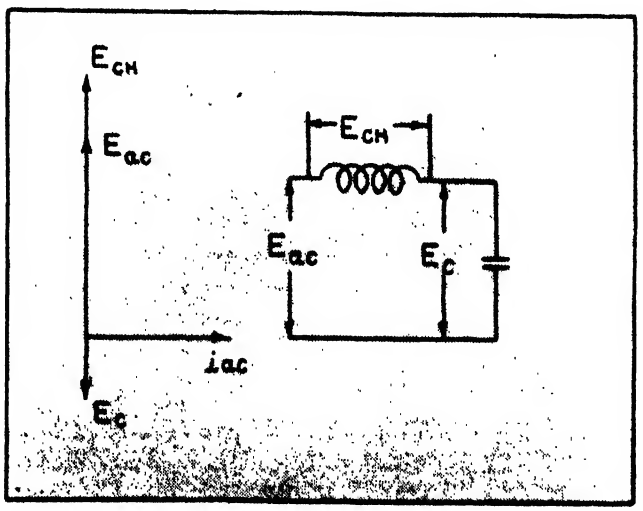

Fig. 4 — Vector diagram of voltages across elements of simple L-type filter, illustrating the possibility of attaining resonance

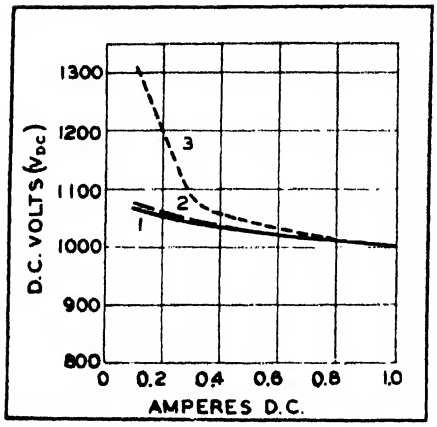

Fig. 5—D-C voltage regulation for the full wave rectifier circuit of Fig. 3, for the three chokes whose variation of inductance with saturation current is shown graphically in Fig 1

filter reactor will have an approximate root-mean-square value equal to 50 or 60 percent of the d-c output voltage. This means that the choke excitation voltage for a filter in a single-phase full-wave supply delivering 3000 volts d-c would be about 1500-1800 volts r.m.s., at 120 cps if the supply is 60 cps. The reactor for this service must be designed with sufficient turns and adequate core area to avoid excessive flux density and saturation of the core. A 5-henry, 1-ampere reactor designed for service in a 400 volt d-c supply would not operate in place of a 5-henry, 1-ampere reactor designed for use in a 3000 volt d-c power supply. However the high voltage unit would be satisfactory in the low voltage supply providing the low excitation did not result in low inductance. It is also perfectly possible that both units might measure 5 henries at 1 ampere dc and an excitation of 10 volts 60 cps.

The actual current in the winding of the input filter reactor has been shown to consist of a steady current to the load with a superimposed alternating current flowing through the filter condenser. If the reactance of the condenser be considered negligible compared with the reactance of the reactor, this alternating current will be $E_{ac}/2\pi fL$, where E_{ac} is the ripple voltage at the filter input. The peak value of this current will be equal to $\sqrt{2}E_{ac}/2\pi fL$ amperes. Now as long as this peak value of current is less than the direct current flowing in the reactor there will never be a period of zero current in the choke. But if the direct current be reduced in value to less than this peak alternating current there will be a period of zero current for a part of each cycle. The rectifier tubes pass current in one direction only and prevent passage of the negative part of the alternating current. The action is somewhat similar to overmodulation of a high level class C radio frequency amplifier. During these periods of zero current through the reactor, the load current must be supplied by the filter condenser charge. At the beginning of the next conducting cycle the rectifier current will rise to a high value and restore the condenser charge. The limiting condition is obtained when the load has been removed entirely and then the filter condenser will become charged up to the peak value of the transformer secondary voltage.

This analysis indicates that as the load current is decreased the rectifier will operate properly with good regulation until the point where the direct current has a magnitude equal to the peak alternating current flowing in the filter reactor, and then as the current is further removed the direct voltage will rise until it equals the crest value of the transformer voltage as a limit. As the direct current is reduced below this critical point part of the alternating current cycle will be cut off, consequently its r-m-s value will be decreased. This will result in decreased IX drop in the filter condenser and a lower value of measured ripple voltage.

Curves 3 of Figs. 5, 6 and 7 show measured values of these effects using the circuit of Fig. 3, and a 3-henry reactor shown on curve 3 of Fig. 1. The approximate formula for determining the critical direct current in amperes was given as follows:

$$I = \sqrt{2}\,E_{ac}/2\pi fL \qquad (6)$$

As this was a 1000-volt rectifier we take, from the table, 0.47 times 1000 to get the value of the 120 cps ripple voltage E_{ac}. Substituting in Eq. (6) gives us

$$I = \frac{\sqrt{2} \times 470}{6.28 \times 120 \times 3} = 0.3 \text{ ampere}$$

The measurements show this to be the critical current. Curve 3 of Fig. 5 shows a sudden rise in direct voltage as the direct current is reduced below 0.3 ampere. Curve 3 of Fig. 6 shows a sudden decrease in the condenser displacement current as the direct current is reduced below 0.3 ampere, while Fig. 7 also shows the corresponding sudden decrease in ripple voltage. It must be remembered that the current of Fig. 6 is an average value over the complete cycle and actually the peak value through the rectifier may be increasing seriously.

Equation (6) may be rewritten to give the minimum value of inductance in henries that is required for

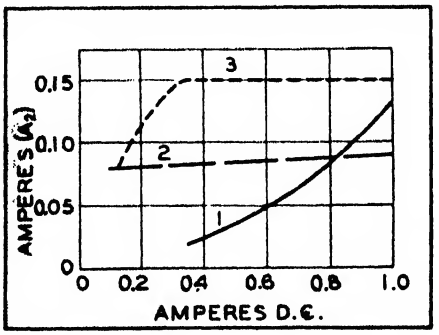

Fig. 6—Current through the filter condenser, C of Fig. 3, for choke coils whose characteristics are given in Fig. 1. The numbered curves have the corresponding significance in Figs. 1, 5, 6, and 7

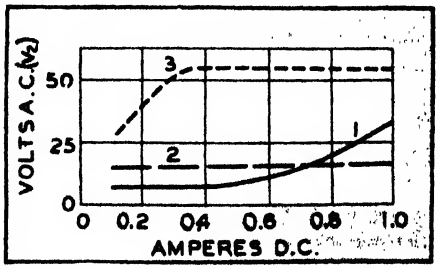

Fig. 7—Ripple voltage, measured by voltmeter V_2, across the load, R, for the three types of choke coils given in Fig. 1

a given set of voltage and current operating conditions:

$$L = \frac{\sqrt{2}\, E_{ac}}{2\pi f I} \qquad (7)$$

The minimum inductance for our filter operating from 0.1 to 1 ampere d-c is determined from Eq. (7). At 1 ampere L must be more than 0.9 henry and, at 0.1 ampere L must be more than 9.0 henries.

Curve 2 of Figs. 5, 6 and 7 show the operation with choke 2 of Fig. 1. The inductance varies from 10 to 12 henries. The regulation is satisfactory, the condenser current decreases very slightly due to the 20 percent increase of inductance, and there is a corresponding slight decrease in ripple voltage as the direct current is decreased. The ripple voltage is approximately one fourth that obtained with the 3-henry reactor. This reactor would have adequate inductance at every current to permit proper operation of the filter.

Solution of Eq. (7) above showed that the inductance must be at least 0.9 henry at 1 ampere d-c and increase to 9.0 henries at 0.1 ampere. If filter reactors were to have a constant inductance that was independent of the magnitude of the direct current, it would be necessary to install a 9-henry reactor. But if a unit could be constructed to have 0.9 henry at 1 ampere, 9 henries at 0.1 ampere dc and be above the critical inductance for all intermediate current values, it would serve the purpose and quite possibly would be smaller and cheaper than the 9-henry constant inductance unit. The swinging choke is the answer to this problem.

The selection of the proper input filter reactor requires consideration of several factors. If the direct current requirement of the load circuit is constant there would be no purpose in installing a swinging input choke. The smoothing type would provide higher inductance, better filtering and lower choke excitation voltage. If the direct current is subject to variation over wide limits, a swinging choke will undoubtedly be the proper choice. If the future current requirements cannot be predicted it would be wise to install the swinging choke as a precaution. The approximate formula, Eq. (7) should always be used to determine the minimum permissible inductance at the maximum and minimum current conditions.

BIBLIOGRAPHY

Magnusson, C. E., "Alternating Currents," McGraw-Hill Book Co., N. Y.
McIlwain & Pender, "Electrical Engineers Handbook," Vol. V., John Wiley & Sons, N. Y.
Eastman, "Fundamentals of Vacuum Tubes," McGraw-Hill Book Co., N. Y.
Smith, F. Langford, "Radiotron Designers Handbook," RCA Mfg. Co., Camden, N. J.
Fowle, Frank F., "Standard Handbook for Electrical Engineer," McGraw-Hill Book Co., N. Y.
Reich, H. J., "Theory and Application of Electron Tubes," McGraw-Hill Book Co., N. Y.

Transient Delay Line

Design criteria for a pulse-delay network useful in radar, television, or test oscilloscope work. With highest frequency component of the transient known, a simple, graphical solution is possible for required values of inductance and capacitance

By JOHN M. LESTER

WHEN designing special electronic equipment, it is often necessary to provide some method of delaying or storing electrical information for a given length of time. If this memory time is in the order of microseconds, an electrical network with special characteristics can be designed and constructed quite easily. Except for a small amount of attenuation, the signals applied to the network input will be faithfully reproduced at the output after the required time has elapsed.

By choosing the correct value of m in an m-derived low-pass filter, it is possible to obtain a phase-shift characteristic that is fairly linear with frequency for almost the entire pass band. If a transient signal is passed through this filter, it will be delayed in time by an amount equal to $\beta/2\pi f$ where β is the phase shift in radians at a frequency f. No phase distortion will occur if the phase characteristic of the filter is linear up to the highest frequency included in the transient signal. By placing sections of these filters in cascade any desired delay can be obtained.

The effect of m on the phase-shift characteristic of one section is shown by the solid-line curves in Fig. 1. β is plotted against ω/ω_c for various values of m. The broken-line curves in Fig. 1 show how the slopes of the solid-line curves vary with ω/ω_c. The ordinate is expressed in terms of $T\omega_c$. Because $\beta = \omega T$, this also equals $\beta/(\omega/\omega_c)$. We see that when m equals 1.4, the phase shift is fairly linear up to 95 percent of the cutoff frequency, and the average value for $T\omega_c$ can be taken from the curve as 2.73. $T\omega_c$ will never vary more than $\pm$ 2.93 percent from this value for frequencies below 95 percent of cutoff.

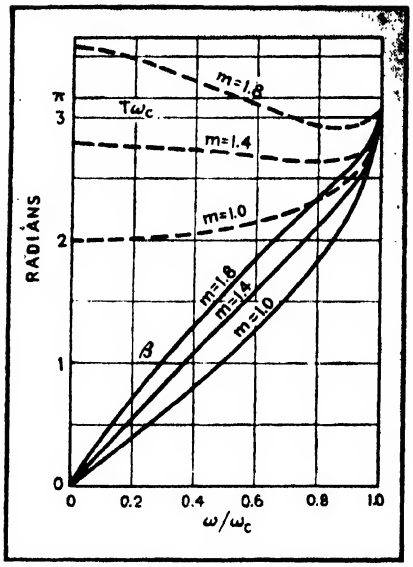

FIG. 1—Phase-shift characteristics for one section are shown by the solid lines. The dashed lines show how the slopes vary as the cutoff frequency is approached, expressed in terms of $T\omega_c$.

Figure 2A shows a T section of an m-derived low-pass filter. Substituting a value of 1.4 for m, we get

$$L'_1 = mL_k/2 = 0.7L_k \quad (1)$$

$$L'_2 = \frac{(1-m^2)}{4m} L_k = -L_k/5.6 \quad (2)$$

$$C' = mC_k = 1.4C_k \quad (3)$$

We can see that L'_2 is negative. This negative value of L'_2 can be obtained by using the network shown in Fig. 2B. The network with mutual inductances is equivalent to the network of 2C. Therefore

$$\left(\frac{1-m^2}{4m}\right) L_k = -M \quad (4)$$

$$mL_k/2 = L/2 + M \quad (5)$$

$$mC_k = C \quad (6)$$

Substituting Eq. 4 in Eq. 5 we get

$$L = mL_k + \left(\frac{1-m^2}{2m}\right) L_k = \left(\frac{m^2+1}{2m}\right) L_k \quad (7)$$

Letting $T\omega_c = 2.73$ which is the value we previously determined from Fig. 1, then

$$T = \frac{2.73}{\omega_c} \quad (8)$$

or

$$f_c = \frac{2.73}{2\pi T} = \frac{0.435}{T} \quad (8a)$$

Cutoff Frequency

This derivation shows that T is inversely proportional to the cutoff frequency. Referring to Fig. 2C, the cutoff frequency of an m-derived filter is

$$f_c = \frac{1}{\pi\sqrt{(L+2M)C + 4C(-M)}}$$

Since k (coefficent of coupling) $= M/L$

then

$$f_c = \frac{1}{\pi\sqrt{(LC+2kL)C + 4C(-kL)}}$$

$$= \frac{1}{\pi\sqrt{(LC+2kL)C - 4kLC}}$$

$$= \frac{1}{\pi\sqrt{CL(1-2K)}} \quad (9)$$

or

$$\omega_c = \frac{2}{\sqrt{CL(1-2k)}} \quad (9a)$$

Substituting Eq. 9a in Eq. 8, we get

$$T = 1.36\sqrt{CL(1-2k)} \text{ when } m = 1.4 \quad (10)$$

With the use of Eq. 10 the time delay of an m-derived filter, when $m = 1.4$, can be calculated.

Terminating the Filter

So that no reflections will occur, it is necessary to terminate the filter correctly. Assuming the filter consists of pure reactances, then the terminating resistance,

$$R_0 = \sqrt{L_k/C_k} \quad (11)$$

Substituting Eq. 6 and 7 in Eq. 11

$$R_0 = \sqrt{\frac{L\frac{(2m)}{(m^2+1)}}{C/m}} = \sqrt{\frac{L(2m^2)}{C(m^2+1)}} \quad (12)$$

Since $k = M/L$, then from Eq. 4 and 7

$$k = \frac{\frac{(m^2+1)}{(4m)}L_k}{\frac{(m_2+1)}{(2m)}L_k} = \frac{m^2-1}{2(m^2+1)} \quad (13)$$

or

$$2k(m^2+1) = m^2 - 1$$

$$2km^2 + 2k = m^2 - 1 \quad (14)$$

and

$$m^2 = \frac{1+2k}{1-2k} \quad (14a)$$

Substituting in Eq. 12, we get

$$R_0 = \sqrt{\frac{L(1+2k)}{C}} \quad (15)$$

Substituting the value of 1.4 for m in Eq. 14a, we see that $k = 1/6$.

The chart shown in Fig. 3 is based on Eq. 10 and 15 which, when reduced to their simplest form, are

$$T = 1.11\sqrt{LC} \quad (16)$$

$$R_0 = 1.15\sqrt{L/C} \quad (17)$$

when $m = 1.4$

Use of Chart

Knowing the delay time for one T section and the terminating resistance, the correct inductance and capacitance for the filter can be determined from the chart. As many sections as desired may be added in cascade to give any time delay desired. The total delay will be T times the number of sections.

It must be remembered that the chart is fairly accurate only if it is used for frequencies below 95 percent of cutoff.

Using Eq. 8, we see that

$$f_{max} = \frac{0.435 \times 0.95}{T} = \frac{0.41}{T} \quad (18)$$

Suppose we have a transient signal which we want to delay one microsecond. We want the impedance of the network to be 1,000 ohms. Also, the highest frequency contained in the transient signal is one mc. What will be the constants of the network?

Example

Knowing f_{max}, we first determine

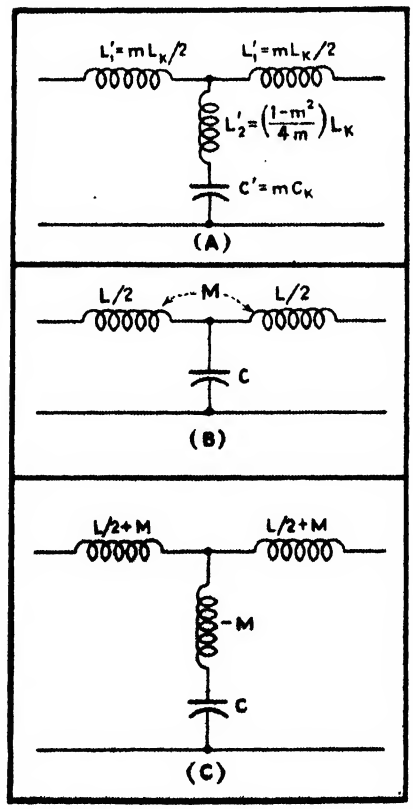

FIG. 2—Development of a T section of an m-derived low-pass filter. (A) The value of L'_2 is shown to be negative and is obtained in practice by the circuit of (B). (C) demonstrates the derivation of the cutoff frequency

the maximum delay T per section realizable.

$$f_{max} = \frac{0.41}{T} \text{ or } T = \frac{0.41}{1 \times 10^6} = 0.41 \times 10^{-6} \text{ sec}$$

The number of sections will be the total time divided by T, or $10^{-6}/(0.41 \times 10^{-6}) = 2.44$.

Therefore, three sections are the minimum to be used. With three sections we will have $(10^{-6}/3) = 0.33 \times 10^{-6}$ seconds delay per section. From the chart we can determine L and C. We see that $L = 260\mu h$ and $C = 340$ $\mu\mu f$. Therefore, the networks will have the constants shown in Fig. 4, when $k = 1/6$.

The following are practical problems that must be taken into consideration when constructing a delay filter:

(1) Providing small attenuation.

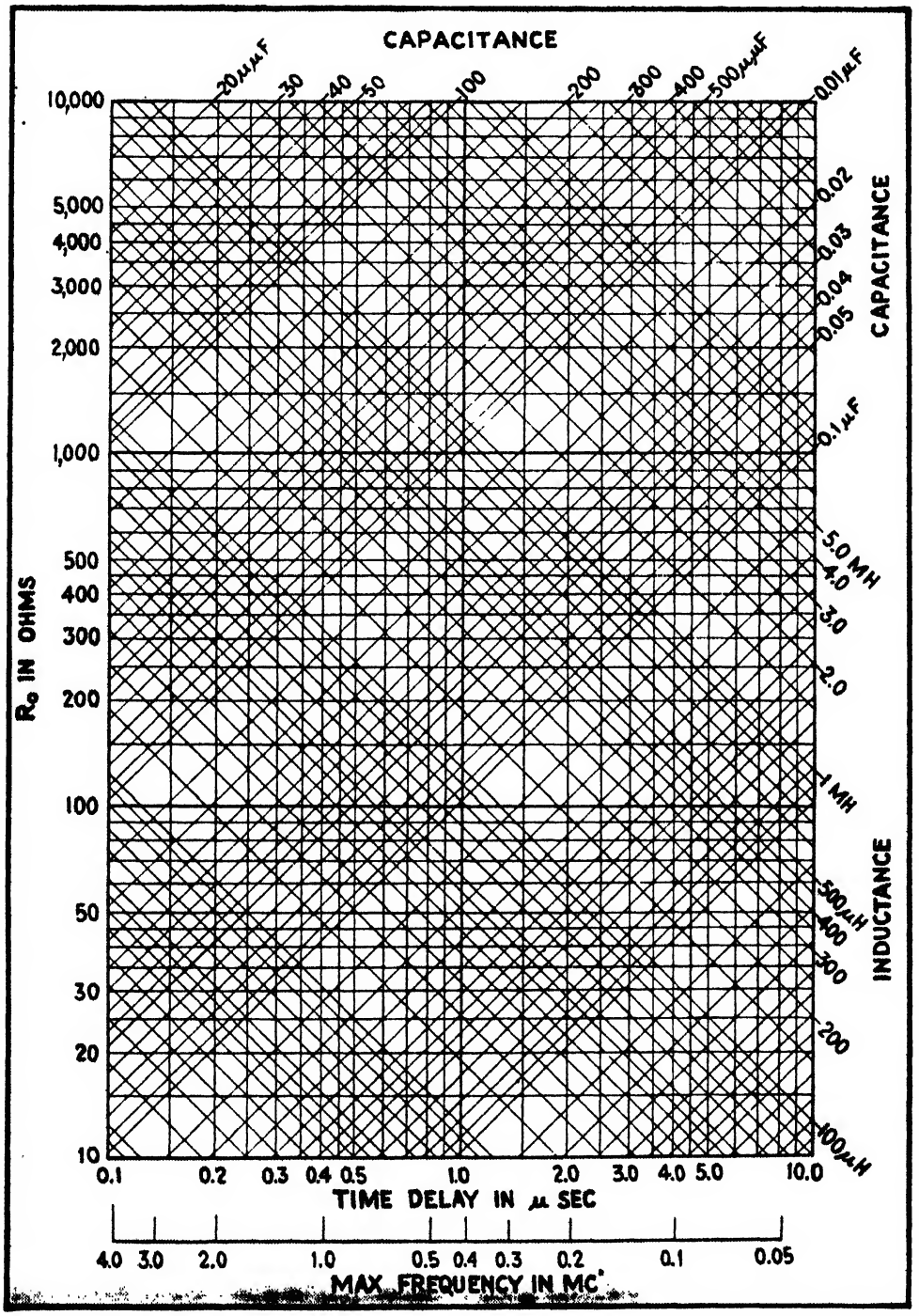

FIG. 3—Chart used in determining the value of inductance and capacitance of the filter when time delay T and terminating resistance R_0 are known, accurate only when used for frequency below 90 percent of cutoff

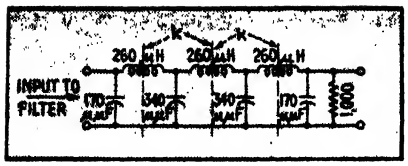

FIG. 4—Three T sections form a filter network to delay a transient signal 10 microseconds. Impedance of the network is 1,000 ohms and the highest frequency contained in the transient is 1 mc

(2) Obtaining the correct coefficient of coupling.

(3) Preventing reflections.

The attenuation of the network depends upon the Q of the capacitors and inductors. Usually the loss due to the capacitors is negligible and can be neglected. The attenuation for frequencies lower than 95 percent of cutoff is approximately equal to $\omega T/2Q_L$ nepers, where T is the delay time in seconds. Q_L can be increased in several different ways. The size of the wire used for winding inductors can be large. However, this will increase the physical size of the filter and hence increase stray capacitance between coils. If the frequencies involved are in the order of 100 kc to 4 mc, the use of litz wire will help to increase Q_L. Also, Q_L can be increased by using powdered-iron cores.

The coefficient of coupling can be controlled by varying the spacing between adjacent coils. The spacing should be adjusted so that the coffficient of coupling is equal to 0.16.

Unless the network is terminated in its characteristic impedance or a close approximation to it, echoes or reflections will occur when transient signals are inserted. Usually when several sections are used in cascade, a sufficiently good termination will be obtained when both ends of the network are terminated with capacitors equal to $C/2$. However, if a more perfect termination is desired, a half-π section where $m = 0.6$ can be used.

It is good design practice to try to use a network as low in impedance as possible. This reduces the size of the inductors and hence reduces the stray capacitance between coils and permits an increase in the Q of the coil, in turn producing less phase distortion and less attenuation.

Bibliography

(1) Guillemin, E. A., "Communication Networks," John Wiley & Sons, Inc., p 824.

(2) Starr, A. T., "Electric Circuits and Wave Filters," Pitman Publishing Corp., p 242.

(3) Pierce, G. W., "Electric Oscillations and Electric Waves," McGraw-Hill Book Co., p 321.

IONOSPHERE

Propagation of Very Short Waves

A definitive statement, based in part on the experience of the MIT Radiation Laboratory, of some of the factors governing propagation at frequencies from 100 to 30,000 mc

By DONALD E. KERR

THE accelerated wartime development of radar and associated equipment has brought to light new and interesting information concerning the mechanism of propagation of radio waves at frequencies above 100 mc. In many respects these very short waves behave like visible light, but in other respects they behave quite differently. Accurate description of the mechanisms involved necessitates borrowing techniques from such widely separated fields as physical optics, quantum theory, and meteorology. This article is intended to outline briefly some of the problems involved, and to present a few of the principles employed in their solution. The experimental data quoted here were obtained by the Propagation Group of the MIT Radiation Laboratory operating under Contract No. OEMsr-262, but the general information summarizes the activities of many investigators in various parts of the world.

One-Way Propagation in Free Space

The most useful way of expressing the radiation of energy from an antenna is in terms of the antenna pattern function or radiation pattern, $f(\theta,\phi)$. It expresses the ratio of field strength radiated in the direction θ, ϕ to the field radiated in the direction of maximum transmission (where $\theta = \phi = 0$). In general f is a complex quantity, but in the interest of simplicity this fact will be ignored in the following treatment. The generalization to complex f is obvious. For the special case of a uniform or isotropic radiator, f is unity for all angles, but for the usual directive antennas f is unity along the axis of symmetry ($\theta = \phi = 0$), and decreases with increasing values of either angle. The power gain G of a particular antenna relative to a reference antenna is easily shown to be*

$$G = \frac{\int f_r^2(\theta,\phi)\, d\Omega_r}{\int f^2(\theta,\phi)\, d\Omega} \qquad (1)$$

where Ω is the solid angle occupied by each antenna pattern and f_r is the pattern of the reference antenna. If the reference antenna is isotropic the numerator of Eq. 1 is 4π. All antenna gains used here are referred to the isotropic radiator.

The power gain in Eq. 1 is evidently related to the power flow from the antennas, given by the Poynting vector S. The magnitude of this vector giving the power flow across a unit area normal to the direction of transmission from a directive antenna in free space is given in terms of the radiated power P_t, distance R, gain G_t and pattern function f_t by

$$S = \frac{P_t G_t}{4\pi R^2} f_t^2(\theta,\phi) \qquad (2)$$

where the subscript t serves to distinguish the transmitting antenna from a receiving antenna of different characteristics.

It is frequently desired to find the three-dimensional coverage diagram of a given antenna. This is the locus in space of all points at which either the electric field or Poynting vector assume some particular assigned value. These values may be stated in absolute measure (in volts per meter or watts per square meter), or they may be specified relative to the value of either of these quantities at some reference distance from the antenna. In mks units, the rms electric field E and time average of the Poynting vector are related by $S = E^2/120\pi$. Then Eq. 2 yields

$$\left|E\right| = \frac{\sqrt{30 P_t G_t}}{R}\left|f_t(\theta,\phi)\right| \text{ volts per meter} \qquad (3)$$

A familiar special form of Eq. 3 is that for the field strength in the equatorial plane of a half-wave doublet, for which $G = 1.64$;

$$E = 7\sqrt{P_t}/R \text{ volts per meter} \qquad (3a)$$

In particular, if we denote by E_r and S_r the field strength and Poynting vector at a reference distance R_r in the direction of maximum

* For further discussion of antenna directivity and gain see Schelkunoff, "Electromagnetic Waves," Chapter 9, D. Van Nostrand and Co., New York.

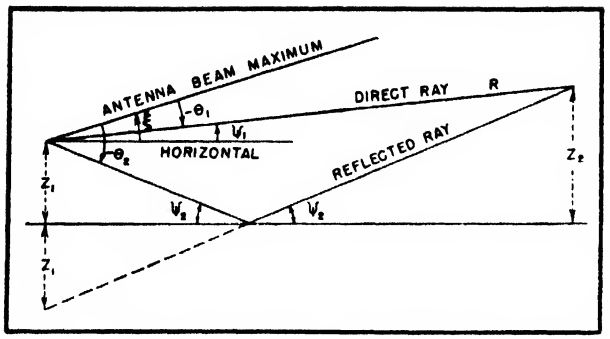

FIG. 1—Geometry of reflection from a plane earth. The simple properties of this figure can be applied to the real earth as shown in Fig. 3

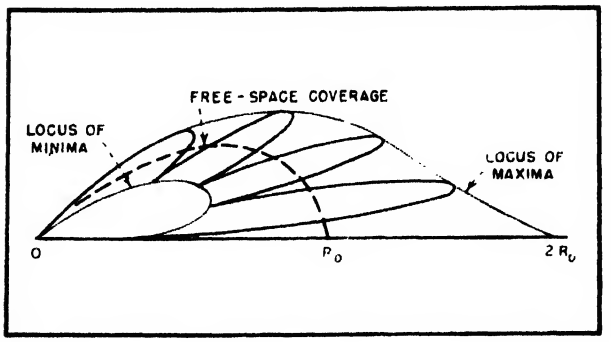

FIG. 2—Coverage diagram, over a plane earth, for vertical polarization. In the case shown, the reflection coefficient decreases with increasing angle of incidence

transmission Eq. 2 and 3 lead to

$$\sqrt{\frac{S}{S_s}} = \left|\frac{E}{E_s}\right| = \frac{R_s}{R}\left|f_t(\theta,\phi)\right| \qquad (4)$$

These three relations may be summarized by one simple equation

$$R = R_f\,|f_t(\theta,\phi)| \qquad (5)$$

where

$$R_f = R_s\left|\frac{E_s}{E}\right| \qquad (6)$$

Equation 5 specifies the distances defining the locus of points at which the field strength has a specified value E. This locus is a surface with the shape of the antenna pattern, enclosing a volume depending upon the particular value of E.

In order to abstract energy from the radiated field, a receiving antenna is oriented in the general direction of the transmitter. It may be characterized by its effective area A_r or by its gain G_r, which depends upon A_r and upon the wavelength λ by $G_r = 4\pi A_r/\lambda^2$. The effective area is commonly ½ to ⅔ of the geometrical area, and refers to orientation for maximum reception; see Schelkunoff, first footnote. The power intercepted by the antenna, P_r, is the product of the incident Poynting vector, the effective area, and the square of the receiving antenna pattern function:

$$Pr = \frac{P_t G_t G_r \lambda^2}{(4\pi R)^2} f_t^2(\theta,\phi)\, f_r^2(\theta',\phi') \qquad (7)$$

where the angles describe the orientations of the two antennas relative to the line joining them.

Assuming that both antennas are aligned for maximum reception ($f_t = f_r = 1$), we may determine the maximum range to which satisfactory reception can be obtained. This maximum range will be called the free-space detection range R_0. At this range the received power P_r will be reduced to the minimum useful (barely perceptible) value, denoted by P_{min}. The determination of P_{min} is often a difficult process, and is outside the scope of this paper. For the present purpose we assume P_{min} to be known. Then Eq. 7 becomes

$$R_0 = \frac{\sqrt{G_t G_r}\,\lambda}{4\pi}\sqrt{\frac{P_t}{P_{min}}} \qquad (8)$$

This important equation states the relations between the system parameters and the best possible free-space performance. The free-space range R_0 has become a generally accepted yardstick of performance. It is instructive to consider a numerical example to obtain orders of magnitude likely to be encountered. Assume that a microwave communications system has the following characteristics: $P_t = 10$ watts; $P_{min} = 10^{-12}$ watts; $\lambda = 10$ cm; antenna diameters = 1 meter and effective areas $2/\pi = 0.637$ times the geometrical value, giving a gain of 200π. These values, inserted into Eq. 8, give a free-space range of 50,000 km, or 31,000 miles! Such fantastic ranges are never observed in practice, of course, because of the effects of the presence of the earth, which will be described presently.

It should be noted that if $R_0 = R_f$ in Eq. 5 and 6, these equations define the volume in free space inside which satisfactory reception can be obtained, and the maximum permissible space attenuation of electric field. In particular, if we confine ourselves to the vertical plane ($\phi = 0$), a polar plot of $R = R_0 f(\theta)$ is called the free-space coverage diagram. As will be seen later, the earth and atmosphere usually distort it to a marked degree.

In this section we shall assume that the earth is plane, and that its effects can be expressed by a plane-wave reflection coefficient, $\Gamma = \rho e^{-j\phi}$, the ratio of field strength in a plane wave reflected from the surface to the field incident upon it. The reflected wave is attenuated by the factor ρ and is retarded in phase by an angle ϕ. Both ρ and ϕ depend upon the earth constants, wavelength, polarization, and angle of incidence as discussed in the second installment of this paper.

The modification of the free-space distribution of field strength may be expressed conveniently in terms of a quantity termed the pattern-propagation factor, represented by F. It is chosen to express as nearly as possible all of the factors external to the system, i.e., those involving the antenna pattern and propagation effects alone. Its definition is: F is the absolute value of the ratio of electric field at a point under stated physical conditions to the maximum possible free-space field at that point. In symbols,

$$F = \left|\frac{E}{E_0}\right| \qquad (9)$$

where E_0, the maximum free-space

field, is given by Eq. 3 with $f_t(\theta, \phi) = 1$. Because of its usefulness we shall focus our attention primarily on F, or on $20 \log_{10} F$, the actual field strength relative to free-space field strength expressed in decibels. The significance of F will become clear from the following illustrations. (Note that under free-space conditions F is just $|f|$).

As shown in Fig. 1, energy travels from one terminal to the other by two routes, one the direct-ray path and the other the reflected-ray path. Along the latter path, the energy appears to come from the image of the source below the surface, and it traverses a path length R_2 that is greater than R_1. The resultant field strength is the vector sum of the fields traversing the two paths, and an interference pattern is formed in space because of the spatial phase relationships.

The field from the energy traveling along R_1 is

$$E_1 = E_s \frac{R_s}{R_1} e^{-jkr_1}$$

where $k = 2\pi/\lambda$. If the antenna is isotropic the field incident on the surface is as strong as that radiated along the direct-ray path, and after reflection it appears at the field point as

$$E_2 = E_s \frac{R_s}{R_2} \rho e^{-j(kR_2 + \phi)}$$

The derivation is limited to small angles and ratios of heights to range (the usual approximations). Then in the denominator we may set $R_1 = R_2 = R$, but of course cannot do so in the numerator, as the difference $R_2 - R_1 = \Delta R$ is the quantity required. Then the total field is

$$E = E_1 + E_2 \simeq E_s \frac{R_s}{R} e^{-jkR_1} [1 + \rho e^{-j(k\Delta R + \phi)}]$$

But the coefficient of the quantity in brackets is just the free-space field; consequently the magnitude of the quantity in brackets is F for this case. Elementary geometry shows that $\Delta R \simeq 2z_1z_2/R$, so F becomes

$$F = |1 + \rho e^{-j\alpha}| = \sqrt{1 + \rho^2 + 2\rho \cos \alpha} \quad (10)$$

where

$$\alpha = \frac{4\pi z_1 z_2}{\lambda R} + \phi \quad (11)$$

This shows that the field strength is periodic with height, oscillating between $1 + \rho$ and $1 - \rho$ times the free-space field.

In this installment ρ will be assured constant in order to simplify the discussion.

An important special case occurs when $\rho = 1$ and $\phi = \pi$, which occurs at grazing incidence. Then Eq. 10 becomes

$$F = 2 \left| \sin \left(\frac{2\pi z_1 z_2}{\lambda R} \right) \right| \quad (12)$$

which shows that the field strength is twice the free-space value when $2z_1z_2/\lambda R = n/2$, where n is an odd integer, and is zero when $2z_1z_2/\lambda R = n$, where n is an integer. The complete variation of field strength with range for this case is given by

$$\left| E \right| = \left| E_0 \right| F = 2 \frac{R_s}{R} \left| E_s \sin \left(\frac{2\pi z_1 z_2}{\lambda R} \right) \right| \quad (13)$$

which shows that as R increases the field oscillates out to where $z_1z_2/\lambda R = 1/4$, after which it decreases without oscillation. In this latter region, as $2\pi z_1z_2/\lambda R$ becomes very small, the sine may be approximated by its argument, and Eq. 13 becomes

$$E = E_s R_s \frac{4\pi z_1 z_2}{\lambda R_2} \quad (14)$$

the familiar result for the so-called "inverse square law" region. This is a useful approximation for wavelengths that are not too short and for ranges small enough that the earth's curvature is not important. (The temptation to use this simple formula may easily lead one astray, however.)

Equations 10 to 13 may be easily modified to give the complete expression for F including the antenna pattern. As may be seen from Fig. 1, the fractions of field strength radiated along the direct and reflected ray paths are $f(\theta_1)$ and $f(\theta_2)$, respectively. Then a derivation similar to that for Eq. 10 shows that

$$F = |f(\theta_1) + \rho f(\theta_2) e^{-j\alpha}| = \sqrt{f^2(\theta_1) + \rho^2 f^2(\theta_2) + 2\rho f(\theta_1) f(\theta_2) \cos \alpha} \quad (15)$$

Both antenna pattern and reflection coefficient now limit the range of variation of F, the limits of which are $f(\theta_1) \pm \rho f(\theta_2)$. To calculate F in a specific case the behavior of ρ and ϕ must be known (see second installment) and θ_1 and θ_2 must be determined. From Fig. 1 we see that

$$\left.\begin{aligned} \theta_1 &= \psi_1 - \xi \\ \theta_2 &= -\psi_2 - \xi \\ \tan \psi_2 &= (z_1 + z_2)/R \end{aligned}\right\} \quad (16)$$

The arrows indicate the positive directions for the angles, except for ψ_2, which is always positive. The calculation of field strength above a plane earth is simple and straightforward, and is expressed (except for reflection coefficient) in Eqs. 3, 9, 15 and 16.

The relation of a coverage diagram to F may be derived by recalling the definition from Eq. 9, $|E/E_0| = F$. But $|E_0| = |E_s|R_s/R$; therefore $R = R_s|E_s/E|F$. From Eq. 6 $R_s|E_s/E| = R_f$. If we set $R_f = R_0$ the free-space detection range, then the coverage diagram is a polar plot of the equation

$$R = R_0 F \quad (17)$$

This is an implicit relation, as F is a function of R. For many practical purposes this is unimportant, because for small elevation angles and ranges greater than a few miles F can be expressed approximately as a function of γ, the angle of elevation, by noting that $\psi_1 \approx \psi_2 \approx \gamma$. Consequently, a polar plot of F may be converted into a coverage diagram by introducing R_0 as a scale factor. As $0 \leqq F \leqq 2$, the operating range of a system over a plane earth may at most be twice the free-space range, or may be reduced to zero, although the range of variation is in practice always less than this, as shown by Eq. 15. Figure 2 shows a sketch indicating qualitatively how a coverage diagram may appear when the antenna pattern and decrease of ρ with the angle ψ_2 are important in influencing F.

Equation 7 for received power in free space may now be modified to include F. The Poynting vector incident on the antenna is $S = E^2/120\pi = E_0^2F^2/120\pi$, from which

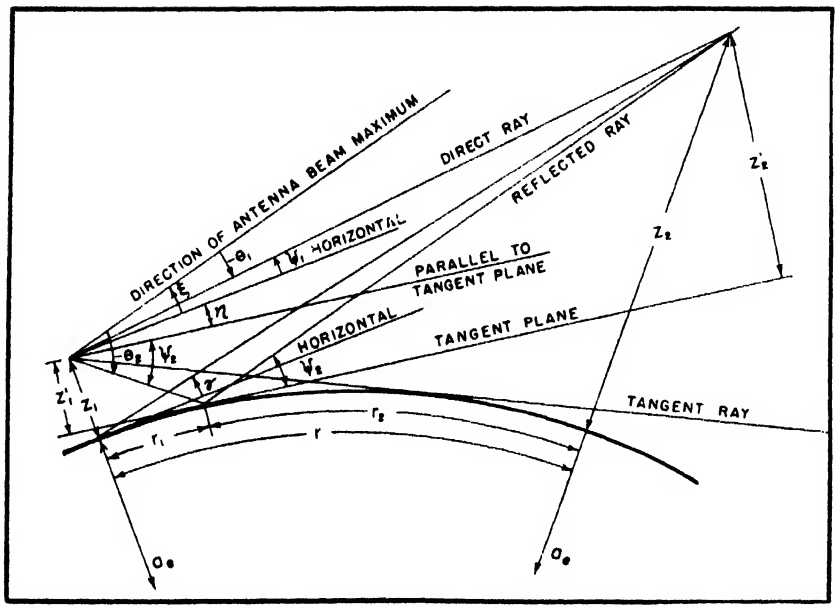

FIG. 3—Geometry of standard propagation over a sperical earth, in the interference region

it may be shown that the new expression is

$$P_r = \frac{P_t G_t G_r \lambda^2}{(4\pi R)^2} F^2 f^2_r(\theta', \phi') \qquad (18)$$

One-Way Propagation Over Spherical Earth

The spherical shape of the earth introduces complications into the problem of field strength computation which will only be outlined briefly here.** The region in Fig. 3 above the tangent ray is called the interference region because, as in the case of the plane earth, interference between direct and reflected waves produces interference patterns. The region below the tangent ray is called the diffraction region, because energy penetrates it by diffraction around the bulge of the earth. The radius a_e is the effective radius of the earth, different from the true radius as a result of atmospheric refraction, and is discussed in the second installment of this paper.

In the interference region the formula for F is similar in form to that for the plane earth, but differs in some details. Because the reflected wave strikes a convex rather than a plane surface, upon reflection it is spread out, resulting in a weaker field than that reflected from a plane surface. This weakening of the reflected field is expressed by the divergence factor D, which now appears in combination with ρ where ρ appeared in the plane-earth formulas. At high elevation angles D is essentially unity, but it falls to zero rather abruptly in the vicinity of the tangent ray. A second difference appears in the formula for ΔR, which as can be seen from Fig. 3, is $\Delta R \simeq 2z'_1 z'_2/R$, where z'_1 and z'_2 are the heights of the terminals above the plane tangent to the earth at the point of reflection, and are less than the true heights above the earth's surface. It is easily shown that for $z/a_e \ll 1$ and $r/a_e \ll 1$,

$$z'_{1,2} \simeq z_{1,2} - \frac{r^2_{1,2}}{2a_e} \qquad (19)$$

Before ΔR, D, or the other required quantities can be calculated r_1 must be obtained; unfortunately this requires solution of the cubic equation

$$r_1^3 - \frac{3}{2} r r_1^2 + \left[\frac{1}{2} r^2 - a_e(z_1 + z_2)\right] r_1 + a_e z_1 r = 0 \qquad (20)$$

Although simple in theory, the procedure is laborious and is awkward numerically. (Graphical methods have been devised to give r_1 and all quantities depending on r_1, and are described in detail in the book mentioned in the second footnote.)

The relations necessary to obtain θ_1, θ_2, and D are given by

$$\left.\begin{aligned} \theta_1 &= \psi_1 - \xi \\ \theta_2 &= -\psi_2 - \xi - \eta \\ \eta &= r_1/a_e \\ \tan\psi_2 &= (z'_1 + z'_2)/r \\ D &= \frac{1}{\sqrt{1 + \dfrac{2z'_1 z'_2}{a_e r \tan^2\psi_2}}} \end{aligned}\right\} \qquad (21)$$

Once r_1 is known, Eq. 21 can be used to calculate field strength for the spherical earth from the appropriate expression for F, which is,

$$F = |f(\theta_1) + D\rho f(\theta_2) e^{-j\alpha}| = \sqrt{f^2(\theta_1) + D^2\rho^2 f^2(\theta_2) + 2D\rho f(\theta_1) f(\theta_2) \cos\alpha} \qquad (22)$$

where

$$\alpha = \frac{4\pi z_1' z_2'}{\lambda R} + \phi \qquad (23)$$

Thus the field strength distribution in the interference region above a spherical earth is qualitatively similar to that above a plane earth. The lobes occupy somewhat different positions from those over a plane earth because of the modified form for α given by Eq. 23 and 19, and the range of variation of F is further limited by D, which predominates near the tangent ray.

A coverage diagram illustrating

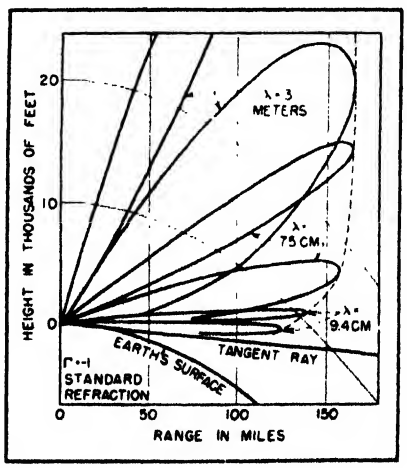

FIG. 4—Contours of field strength 103 db below that at a distance of one meter, from an isotropic antenna 110 feet above the surface (two lowest lobes are shown for each wave length; R = 88 miles)

** Details of new methods for rapid computation of field strength are given in Vol. 13 of the forthcoming Radiation Laboratory Series, "Propagation of Short Radio Waves," to be published by McGraw-Hill Book Co., Inc., New York.

the general features described above is given in Fig. 4, which has been drawn for an isotropic radiator and $\rho = 1$, $\phi = \pi$. Only the two lowest lobes are shown for each of the three wavelengths. The effect of D is shown by the dotted line, which approaches zero near the tangent ray. Since we have assumed $\rho = 1$, F approaches 2 in the lobe maxima, i.e., the maximum range is twice the free-space range at high angles, while it approaches zero at the minima. (As pointed out above, the combination of D, ρ, and f always reduces the range of variation in a practical case, although for wavelengths of roughly 1 meter or more the conditions shown in the diagram are often closely approached over water.)

Perhaps the most striking and important feature of Fig. 4 is the comparison of wavelengths that it affords. Note that transmitter height is fixed and wavelength is varied. The angular elevation of a given lobe increases with (but not in direct proportion to) the wavelength and decreases with increasing height. The superiority of short wavelengths for operation at low elevation angles is clearly indicated. The accompanying penalty consists of having the high coverage for the shorter wavelengths broken up into many fine lobes. This important fact must be considered in choices of wavelength for applications in which the detailed structure of the coverage diagram is important.

Description of the field in the diffraction region requires an entirely different approach from the simple methods of geometrical optics employed up to this point; physical optics must be applied. It is now necessary to sum infinite series, which in the region of the tangent ray usually requires an inordinately large amount of labor. Fortunately, in the diffraction region sufficiently far below the tangent ray only the first term of the series is important, and we shall limit our discussion to this special case, for which

$$20 \log_{10} F = 20 \log_{10} [V(X)] + 20 \log_{10} | U(Z_1) | + 20 \log_{10} | U(Z_2) | \quad (24)$$

where V and U are called the range-attenuation and height-gain functions respectively, and the dimensionless variables X and Z are obtained by introducing scale factors as follows:

$$X = R \Big/ \left(\frac{a_e^2 \lambda}{\pi}\right)^{1/3} \quad (25)$$

$$Z = 2z \Big/ \left(\frac{a_e \lambda^2}{\pi^2}\right)^{1/3} \quad (26)$$

The components of Eq. 24 are shown in Fig. 5 and 6, the solid lines referring to the situation considered here. Thus we see that in the region well below the tangent ray the field strength may be calculated rather more easily than in the interference region. It should be noted in passing that no distinction is made here between horizontal and vertical polarization, because in the microwave region the diffraction field depends only slightly on polarization, and negligible error results from treating both polarizations alike. This is far from true at low frequencies, of course.

We shall now consider all the characteristics of the reflection coefficient, $\Gamma = \rho\, e^{-j\phi}$, as expressed by Fresnel's equations for specular reflection of a plane wave from a plane surface. If ϵ is the dielectric constant of the earth σ is its conductivity in mhos per meter and λ is in meters, and if $|\epsilon - j60\lambda\sigma| \ll 1$, then Γ is given approximately by

$$\Gamma_v = \rho_v e^{-j\phi_v} \simeq \frac{\sqrt{\epsilon - j60\lambda\sigma}^{-1} \sin \psi_2 - 1}{\sqrt{\epsilon - j60\lambda\sigma}^{-1} \sin \psi_2 + 1} \quad (27)$$

$$\Gamma_h = \rho_h e^{-j\phi_h} \simeq \frac{\sin \psi_2 - \sqrt{\epsilon - j60\lambda\sigma}^{-1}}{\sin \psi_2 + \sqrt{\epsilon - j60\lambda\sigma}^{-1}} \quad (28)$$

where v and h denote vertical and horizontal polarization, respectively. It is well known that for soil ϵ and σ vary widely in a rather unpredictable manner, and we shall not attempt to discuss these variations here; but for sea water the variations are smaller and the values are more definitely known. Fig. 7 shows ρ and ϕ as given by Eq. 27 and 28, for sea water, using the best data available. The striking feature of these figures is the slight dependence of ρ and ϕ on wavelength and grazing angle for horizontal polarization, as contrasted with the marked dependence for vertical polarization. For the latter, ρ_v experiences a minimum at the complement of Brewster's polarizing angle familiar in optics, and ϕ_v undergoes its most rapid change. The phase lag ϕ_h is not shown, as it increases over 180° by less than 1°. It is important to notice that at grazing inci-

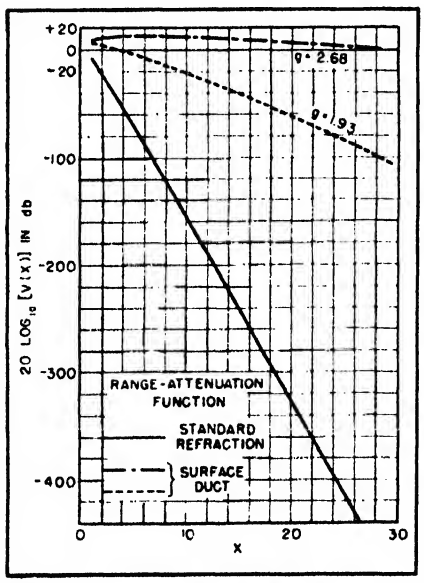

FIG. 5 — Range-attenuation function for standard refraction, and for two surface ducts (see text for significance of duct parameter g)

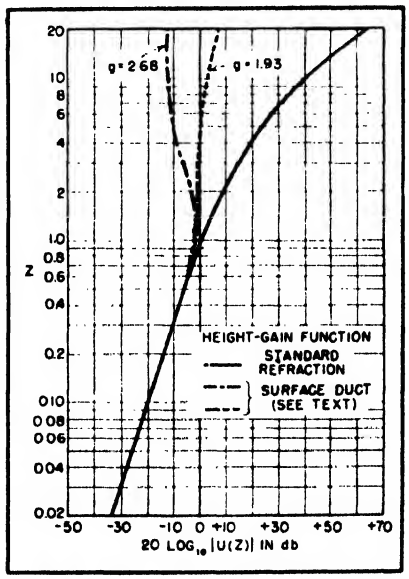

FIG. 6—Height-gain function for standard refraction and for two surface ducts, corresponding to range-attenuation function of Fig. 5

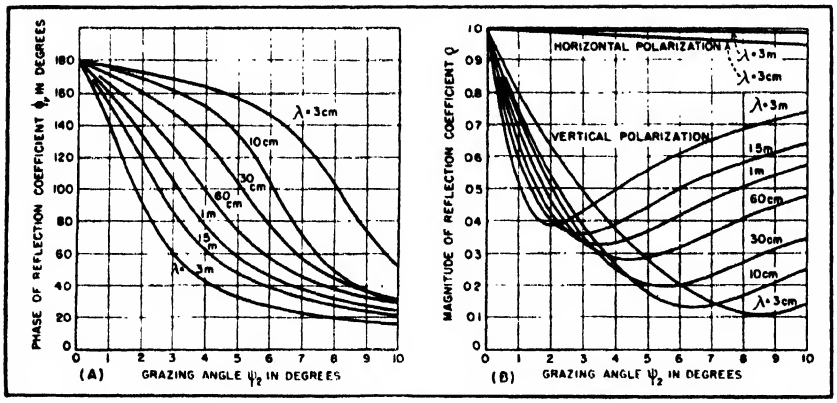

FIG. 7—Phase (A) and magnitude (B) of reflection coefficient as a function of grazing angle for a smooth sea. The phase curves are for vertical polarization

dence ($\psi_s = 0$) the two polarizations behave alike; all the incident radiation is reflected and is retarded in phase by π; thus $\Gamma = -1$ and the field is zero at the surface. This is true as long as ϵ and σ remain finite, but if σ is assumed to be infinite $\Gamma = +1$ for all ψ_s. Thus the assumption that $\Gamma = +1$ is not justified for the microwave region.

For relatively long wavelengths —say 1 meter or longer—the assumption of a smooth earth surface is reasonably valid, as attested by the large amount of practical data from meter-wave radar. As the wavelength becomes shorter, however, roughness of the surface becomes more important than ϵ and σ in determining the amount of specular reflection obtained; the tendency is, of course, toward diffuse scattering, which does not produce a well-defined interference pattern. No accurate method for determining the effects of roughness is known, but an estimate can be obtained from a criterion suggested by Lord Rayleigh. If h is the height of a surface irregularity, the surface tends to give specular reflection if $h \sin \psi_s < \lambda/8$, and tends to give diffuse reflection if the inequality sign is reversed. Although not pretending to numerical accuracy, this criterion predicts the correct trend, showing that surface irregularities increase in importance as wavelength is decreased or grazing angle is increased.

The maximum and minimum values of field strength in the interference pattern are a measure of ρ. If the antenna pattern is so broad that it can be neglected, and if the lobe spacing is so small that ρ does not change appreciably between adjacent maxima and minima, Eq. 22 (Part I) gives

$$\rho = \frac{1}{D}\frac{F_{max} - F_{min}}{F_{max} + F_{min}} \qquad (29)$$

Measurements of relative field strength in the maxima and minima thus afford an experimental means of determing ρ. Such measurements have been made by several methods. Figure 8 shows data obtained by flying a receiver at constant altitude through the interference pattern from a transmitter at the sea shore. Lack of accurate means of measuring the state of sea roughness precludes any but qualitative statements, but the scatter of points is believed to be attributable to reflections from time-varying rough wave patches, which tend to "fill up" the minima, increasing F_{min} and causing the indicated value of ρ to decrease. This is particularly true for horizontal polarization, because in the minima the direct and reflected waves are 180° out of phase and are very nearly equal in magnitude, and even a small "stray" reflection takes control and determines F_{min}. Similar results were obtained concurrently on 3 cm.

Corresponding measurements over land show that *most* terrain produces diffuse scattering of 10- and 3-cm waves, and no well-defined interference pattern exists. Important exceptions are airport surfaces, flat desert country, and the like, which are often sufficiently smooth to give efficient specular re-

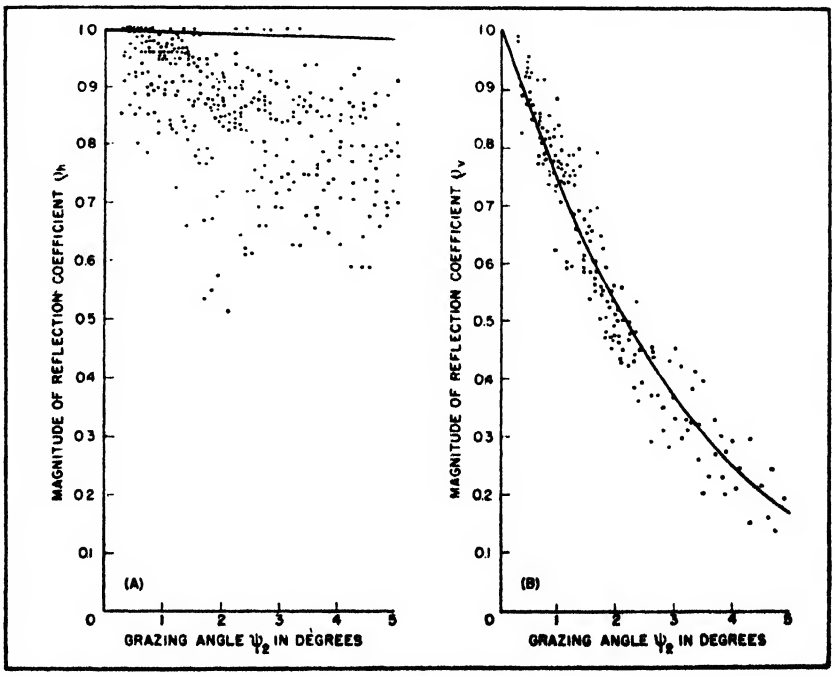

FIG. 8—Measured values of reflection coefficient over sea water at 10 cm, with horizontal (A) and vertical (B) polarization. Lines show theoretical values for smooth sea

flection. Radar experience on meter waves indicates that a dependable interference pattern can be obtained if sufficient care is exercised in the choice of the site.

Propagation in Radar Problems

Extension of the above results to radar requires introduction of the effective scattering cross-section of the target, σ. It is defined *for free-space conditions* as the area intercepting that amount of incident energy which, if scattered isotropically, would give an echo equal to that from the target. That is,

$$\sigma = 4\pi R^2 \left| S_r/S_i \right| \tag{30}$$

where S_i and S_r are the incident and reflected values of the Poynting vector. The value of S_i is given by Eq. 2 (Part I), $S_r = \sigma S_i/(4\pi R^2)$, and the received power $P_r = S_r A f_r^2 (\theta, \phi) = S_r G \lambda^2 f_r^2 (\theta, \phi)/4\pi$. Combining, we have the radar transmission equation *for free space*

$$P_r = P_t \frac{G^2\lambda^2}{(4\pi)^2} \frac{f^4(\theta,\phi)}{R^4} \sigma \tag{31}$$

where identical transmitting and receiving antennas are assumed. Comparison of this expression with the parallel expression for one-way transmission, Eq. 7, (Part I) shows that P_r depends in the same way on all corresponding variables except for range and antenna pattern function.

The free-space *radar* detection range may be found directly from Eq. 31, setting $f(\theta, \phi) = 1$, and $P_r = P_{min}$

$$R_0 = \sqrt[4]{\frac{P_t}{P_{min}} \frac{\sigma}{4\pi}} \sqrt{\frac{G\lambda}{4\pi}} \tag{32}$$

Another numerical example is of interest. Assume that a 10-cm radar system transmits a peak power of 100 kw, the minimum useful received power is 10^{-12} watts, the antenna is identical with that given in the example (Part I), and the target cross-section is 20π sq. meters. Equation 32 indicates a free-space range of about 60 km, or 37 miles. (Had this radar system been used as a one-way communications system its free-space range would have been almost one million miles.)

The modification of the free-space radar equation to include the effects of the earth and atmosphere may be made easily for a *point* target in a manner analogous to that employed for one-way transmission. The antenna pattern function is replaced by F, giving

$$P_r = P_t \frac{G^2\lambda^2}{(4\pi)^3} \frac{F^4\sigma}{R^4} \tag{33}$$

Unfortunately this treatment is in reality not as simple as it appears at first glance, because σ is only a convenient mathematical fiction for any but the simplest of targets. The simplest target is a perfectly conducting sphere, for which σ is essentially the geometrical cross section, πr^2, for r/λ greater than about 4. Most targets consist of a large number of scattering surfaces, the reflections from which interfere and cause the echo to fluctuate in amplitude over wide limits with small changes in target aspect. This effect becomes more pronounced as the ratio of object size to wavelength increases. The microwave scattering pattern from an aircraft, for instance, contains a very large number of fine lobes in the solid angle 4π; consequently the echo fluctuates very rapidly and the radar is likely not to "see" the target every time it scans the region of the target if the scan rate is rapid. (This echo fluctuation is *in addition to* that arising from the passage of the aircraft into and out of the lobes of the interference pattern.) As a result it is necessary to establish arbitrary definitions of σ appropriate to the type of target, radar, method of display of data, the minimum allowable percentage of "hits," and many other parameters. Once these conventions are established numerical values for σ can be obtained which allow estimation of performance by Eq. 32. Subject to these limitations, radar coverage diagrams may be prepared from the equation $R = R_0 F$ just as for one-way transmission, and the region enclosed by the diagram is that inside which the target is detectable with the degree of certainty agreed upon. Useful values of σ for wavelengths of 10 or 3-cm range from under 100 sq ft for small aircraft to roughly 700 sq ft for heavy bombers.

An additional complication enters if a target with appreciable height such as a ship is very near the earth's surface, because of the variation of the incident field with position on the target. Assuming a plane earth with $\Gamma = -1$, this variation is given by Eq. 12 (Part I). If the target were "lumped" at a height z_2, then Eq. 33 would give

$$P_r = P_t \frac{G^2\lambda^2\sigma}{4\pi^3 R^4} \sin^4\left(\frac{2\pi z_1 z_2}{\lambda R}\right)$$

and for sufficiently small values of the argument of the sine function

$$P_r = P_t \frac{4\pi G^2\sigma}{\lambda^2 R^8} (z_1 z_2)^4$$

It is found experimentally with microwave radar at low altitudes that if appropriate care is exercised in treating the rapid fluctuations of echo strength, a ship echo varies on the average as $1/R^4$ out to some reasonably well defined range, beyond which it varies roughly as $1/R^n$, and in many practical cases falls below the detection limit while varying according to this law. Such behavior would be expected from a point target at a fixed height above a plane earth, from a vertical flat sheet, and from certain other simple models. The actual values of σ are not constant, but vary with radar height, target size and aspect, wavelength, range, and other factors; but by judicious division of the range of the variables approximate values of σ for ships have been determined, and may be used to obtain estimates of radar performance on ship targets.

Atmospheric Refraction

Thus far the effects of the atmosphere have been neglected. It is well known that the gradual decrease of the atmospheric index of refraction with increasing altitude and the accompanying increase of phase velocity cause a slight distortion of the wave front and a tendency for the waves to follow the earth's curvature. If the index decreases essentially linearly with

height the effect is as if the propagation occurred over an earth with no atmosphere but with an effective earth's radius greater than the true radius.* If the effective radius a_e is known the methods described above can be applied by substituting a_e for the true radius a. The generally accepted value of a_e/a is 4/3, giving $a_e = 5{,}280$ statute miles. The refraction in this case is called *standard* refraction and gives rise to *standard* propagation.

Considerable work has been done in an attempt to discover geographical and seasonal variations of the effective earth's radius. It is now clear that such investigations are not particularly significant, however, because when marked variations of the refractive index gradient occur the concept of an effective earth's radius loses its validity, and other methods are necessary to give a meaningful description of refraction phenomena.

Large variations in refractive index gradient are best expressed in terms of a parameter called the *modified* index of refraction, N, defined by

$$N = h\,(1 + z/a) \simeq n + z/a \qquad (34)$$

where n is the atmospheric index of refraction at the height z (n departs from unity by only about 3×10^{-4}). The modification consists of adding the term z/a, thereby introducing the curvature of the earth into the refraction problem. The modified index is useful because it permits treatment of the complicated problem of a spherical earth with atmospheric index of refraction n as the simpler problem of a plane earth and equivalent index of refraction N. It is also important because it is a clearly defined boundary between the meteorological side of the problem, which takes the meteorologist as far as determining n as a function of height, and the electromagnetic side, which begins with n (or N) and concerns the effect of a given variation of N with height upon field strength. Neither phase of the problem can be given in detail here, but a few of the most important features and some interesting practical results may be outlined.

The absolute value of n is not important, but the vertical gradient of n or N

$$\frac{dN}{dz} = \frac{dn}{dz} + \frac{1}{a}$$

determines the characteristics of the propagation. In the absence of atmospheric stratification dn/dz is essentially independent of z, and

$$\frac{a_e}{a} = \frac{1}{a\dfrac{dN}{dz}} = \frac{1}{1 + a\dfrac{dn}{dz}}$$

When dn/dz varies with z, marked transmission abnormalities are likely to occur and give rise to *nonstandard propagation*. (The term *anomalous* propagation is also frequently employed, but it has been so abused that it is avoided here.) Some basic forms of N as a function of z, called *modified index profiles*, are shown in Fig. 9. In each case the region in the vicinity of the atmospheric "layer" in which the slope departs from the constant value for the remainder of the profile is responsible for transmission vagaries.

The regions marked a—b show marked affinity for very short radio waves; if the wavelength is sufficiently short, energy may be guided for great distances with very low spatial attenuation, and is often said to be "trapped."

The "trapping" layers, a—b in Fig. 9, are also called "ducts" because of their wave-guiding properties; in fact they may be likened to a parallel-plane wave guide with a leaky top. The analogy to such a wave guide is useful because: (1) it renders plausible the *increase* of trapping effects as wavelength *decreases;* (2) it suggests that complicated field strength distributions may be formed by superposition of a number of transmission "modes"; and (3) it illustrates the importance of the position of the energy source in determining the degree of excitation of the modes. The analogy is unsatisfactory in a quantitative investigation, and a correct analysis requires extension of the theory for the diffraction region to include the effects of irregularities of the modified index profile. It yields expressions for the field strength similar in form to Eq. 24, (Part I) but differing in detail to express the trapping effect and distortion of field strength by the duct. For example, the broken lines in Fig. 5 and 6 (Part I) apply to a modified index profile of type D in Fig. 9 that has been approximated by two straight lines, the top sec-

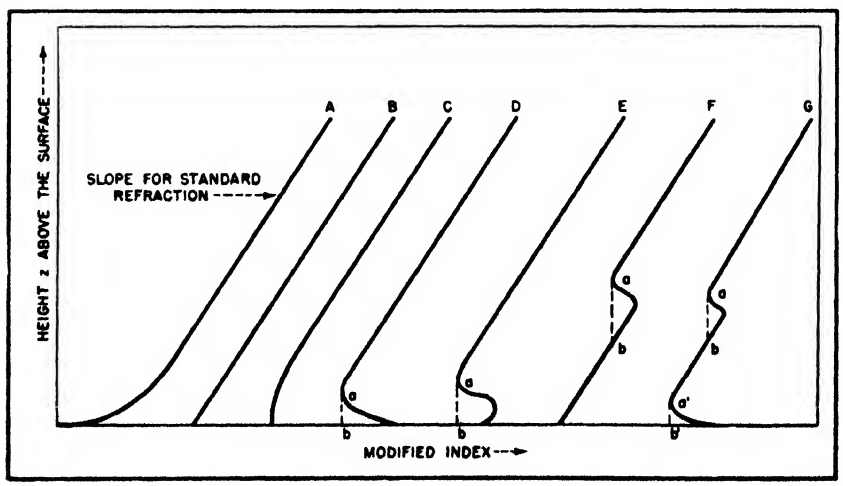

FIG. 9—Idealized modified index profiles: *A*, substandard surface layer; *B*, standard refraction; *C*, superstandard surface layer; *D*, same as *C* with surface duct; *E*, elevated superstandard surface layer with surface duct; *F*, same as *E* with elevated duct; *G*, surface and elevated superstandard layers with ducts. In each case, the duct extends from a to b, and a' to b'

* Schelleng, Burrows and Ferrell, "Ultra Short Wave Propagation," *Proc IRE* vol 21, p 427, 1933.

tion having the slope corresponding to standard refraction and the bottom section having the negative of this slope. The height h of the joint between the two lines (called the height or the depth of the duct) is $h = \frac{g}{2}\left(\frac{a_e\lambda^2}{\pi^2}\right)^{1/3}$ where g is 1.93 and 2.68 in the curves shown. (These values apply only to the lowest order transmission mode, which predominates sufficiently far below the tangent ray.)

Figure 5 (Part I) shows that the duct causes the field strength to decrease very much less rapidly with range in the diffraction region than it does with standard refraction, and Fig. 6 (Part I) shows that within and near the duct the height-gain function is distorted. It suggests a reduction of field strength above the duct. When the height-gain and range-attenuation functions are combined, however, the field is seen to be enormously stronger, both above and in the duct, than with standard refraction.

A numerical example will illustrate the gain in signal strength at low heights. Suppose a duct 64 ft deep occurs over a 10-cm transmission circuit 41.5 miles long with terminal heights of 100 and 15 ft. From Eq. 25 and 26 (Part I), $X = 5$, $Z_1 = 3$ and $Z_2 = 0.45$. The 64-ft duct corresponds to the middle curve in Fig. 5 and 6 (Part I). Then

$$20\log_{10}F = 20\log_{10}|V(5)| + 20\log_{10}|U(3)| + 20\log_{10}|U(0.45)| = -3 - 1 - 6 = -10 \text{ db}$$

For standard refraction, however, the first two terms would have been −69 and +15, and the total would have been −60 db; that is, the duct has increased the signal level by 50 db.

By contrast with the situation in a simple wave guide, each transmission mode, although guided by the duct, "leaks" out of the top of the duct; the greater the degree of trapping the smaller is the rate of leakage. Increasing the duct height (more correctly, the quantity g) increases the degree of trapping, causing the "bulge" in Fig. 6 (Part I) to become more pronounced and the rate of attenuation with range to decrease. (It also encourages the presence of higher-order transmission modes, not considered here.) If the transmitter is in the duct or not far from it, the general effect is to produce a long "finger" in the coverage diagram coinciding roughly in position with the duct, often extending for great distances. Two common cases in which the duct rests on the surface are shown by D and E in Fig. 9.

The terms employed above are only crudely descriptive of the complete mathematical formulation of the problem, which is too involved to give here. (The same mathematical problem occurs in connection with potential barriers in quantum theory.) Most writers base elementary explanations of trapping phenomena upon the methods of geometrical optics, using Fermat's principle and tracing ray paths through the inhomogeneous layers. Such ray methods have the advantage of pictorial simplicity, but they represent an oversimplification of the true problem and they may easily lead to erroneous conclusions if they are interpreted without full knowledge of their limitations. These methods have been avoided and the more difficult but correct wave theory is used in this brief discussion. A complete discussion of the problem requires application of both ray and wave solutions in the regions for which each is valid.

It should be emphasized that only energy leaving the transmitter at *very small* angles of elevation is affected by ducts. The field at angles above roughly 1° is not affected appreciably.

When the duct is considerably above the transmitter, as in F of Fig. 9, energy may also be propagated beyond the horizon. The rigorous theory for this case has not yet been carried to a numerically useful state, however, and approximate methods are necessary. One of the best known of these methods describes the propagation in terms of a *plane* wave reflected from a *plane* layer in which n varies with height. If the layer is not too thick (in terms of wavelength), strong reflections may occur at *very small* grazing angles. In this case the longer wavelengths experience the greatest effect, by contrast with the trapping discussed previously.

Early investigators sought explanations of refraction effects in terms of "reflections from air-mass boundaries," which in current terminology would be called refraction by (or reflections from) the elevated irregularities in the modified index profile. (These irregularities are by no means limited to boundaries between different air masses in the meteorological sense, however.) It seems clear now that the early results included the combined effects of profiles of types D, E, and F of Fig. 9.

The effect of the layer represented by the bottom of profile A of Fig. 9, in which dN/dz is greater than the standard slope, is to decrease the field strength below the standard level near the surface, hence it is called a *substandard* layer; this is the opposite of the effect of superstandard layers in which dN/dz is less than the standard slope and fields in and near the duct are above the standard level.

The meteorological phase of the refraction problem is vastly complicated; it requires the answers to many questions that are new in meteorology and defy analysis in terms of existing knowledge. Consequently it was necessary during the war to start from scratch in the new field of radio-meteorology, developing experiment and theory simultaneously with the application to the radio problem. Study of the dynamics of the lower atmosphere was begun experimentally by meteorological soundings employing methods capable of revealing great detail in atmospheric structure. Meteorological analysis based upon the soundings and upon other weather information has brought to light the fundamental principles of the processes involved, but working out their application is a problem for the future.

Figure 10 shows atmospheric soundings, made in an aircraft over the ocean with specially developed

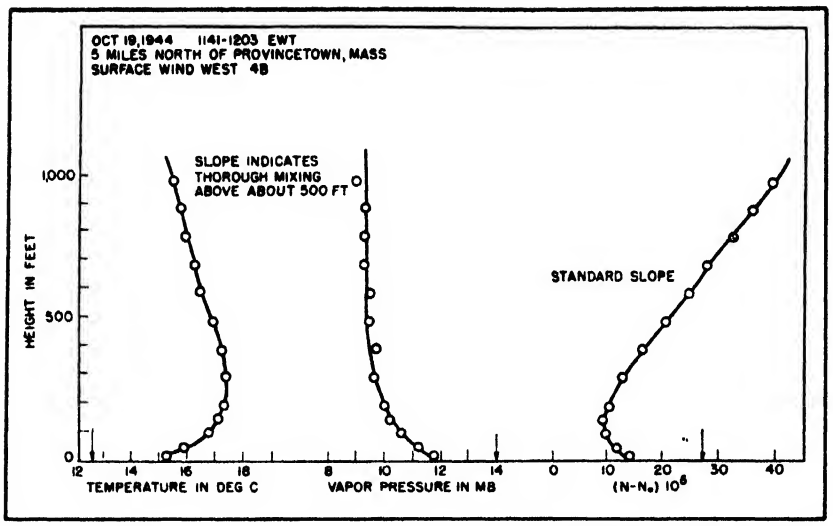

FIG. 10—Atmospheric sounding, showing variations in temperature vapor pressure and index of refraction with height, taken in an aircraft. Arrows on baseline indicate water surface values, determined by water temperature

instruments when warm, dry air was blowing over the water from the land on a hot summer afternoon, forming a surface duct capable of producing strong trapping on wavelengths of roughly 10 cm or less. Several thousand soundings of this general nature have been made in various localities by several groups of investigators.

The atmospheric index of refraction n depends upon pressure, temperature and humidity but is *independent of wavelength* down to about 1 cm (where atmospheric absorption becomes important.) The index gradient, dn/dz, involves both the gradients of the atmospheric quantities and their absolute values, with the result that a very wide range of effects on the modified index profile is possible. We may summarize the most important of these effects very briefly as follows:

(a) In an atmosphere that is completely mixed vertically dN/dz is nearly constant, and is approximately 0.04 per ft; but complete mixing is rare and 0.036 is the value commonly defined as that giving standard refraction. (Type *B* of Fig. 9.)

(b) An increase of temperature with height (temperature inversion) tends to make $dN/dz < 0.086$ per ft, and tends to give profiles of Types *C* through *G* of Fig. 9.

(c) A decrease of water vapor pressure or concentration (specific humidity or mixing ratio) with height tends to make $dN/dz < 0.036$ per ft, and tends to give profiles of Types *C* through *G* in Fig. 9. Relative humidity is an essentially useless quantity in this work because it is not a conservative property of the atmosphere.

(d) An increase of humidity with height tends to make $dN/dz > 0.036$ per ft, and tends to give profiles of Type *A* of Fig. 9.

When (b) and (c) combine dN/dz may easily become negative and strong ducts may be formed; this is particularly prevalent along a coast, where warm dry air from the land may flow out over cold sea water. If, on the other hand, the air is warmer than the water but is extremely moist, the reverse situation (d) is likely to occur, giving substandard surface layers.

Any of the profiles of Fig. 9 may also occur over land as a result of numerous meteorological processes. The most pronounced effects over land occur as part of the diurnal cycle of daytime solar heating of the earth's surface and nocturnal cooling by radiation. During the middle of the day the air is mixed by convection from solar heating, but at night radiational cooling of the surface chills the air from below, and if the sky is clear and winds are light a temperature inversion is likely to form. Humidity gradients may also occur, and depending upon their sign and magnitude, either ducts or substandard layers may result. The result is that overland transmission as a rule becomes variable at night, often producing a wide range of signal strengths as a result of the continually varying nature of the atmospheric stratification.

A general feature of both overwater and overland transmission between terminals near or below the horizon is that when ducts occur at or near the surface the *average* signal level tends to rise, often to the vicinity of the free-space level, but it tends to decrease under the influence of substandard layers. Superposed on this shift in average level is scintillation or fading which may be small or may encompass a range of as much as 40 or 50 db. The maximum levels reached in most cases reported so far are from 10 to 15 db above the free-space level. The mechanism of the fading is not clearly understood, but in the light of existing information it is reasonable to believe that it results from superposition of a number of

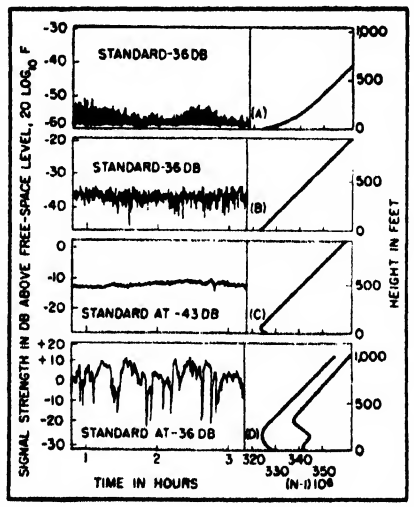

FIG. 11—Variations in signal strength associated with modified index profiles identified in FIG. 3. The standard signal strength is indicated in each diagram

transmission modes, the relative amplitudes and phases of which are continually varying as a result of time variations in the microstructure of the atmosphere.

Figure 11 shows typical behavior of 10 and 3 cm one-way transmission on a nonoptical overwater transmission path. Each signal type was found to occur when the indicated modified index profile predominated on the path, which in this case was 41 miles long, between Provincetown and Gloucester, Massachusetts. High average signal with deep "roller" type fading was unfailingly characteristic of ducts roughly 100 feet or more in depth, but when the ducts were shallow, about 50 feet or less, the average signal was lower, and fading was slight. In the second case only the lowest order transmission mode is important (on 10 cm), and freedom from interference by higher order modes is presumably responsible for the increased steadiness of the signal. These shallow ducts are believed to prevail over most of the open oceans, and may be of considerable importance in microwave radar and communications at low altitudes.

Measurements by low-power radar from a height of 50 feet at Provincetown made simultaneously with the one-way measurements and on the same wavelengths showed wide variations in maximum detection range on ships and coastal surface targets. With standard modified index profiles detection was limited to targets within horizon range (15 miles or so), while substandard surface layers reduced this coverage somewhat. Shallow ducts increased the detection range by roughly 20 or 30 percent, but deep ducts permitted ranges very far beyond the horizon. Echoes were received at one time from Nova Scotia, 280 miles distant, and ranges between 100 and 200 miles were common.

A most interesting and significant feature of this particular path was that during the *summer* standard profiles and signal levels occurred only about 2 or 3 percent of the total time. During the rest of the time either deep ducts and high fading signal or substandard conditions prevailed in this particular location, often for two or three days at a time; but trapping conditions accounted for the major fraction of the period. Diurnal effects, predominant in overland transmission, were barely noticeable. As cold weather approached standard refraction occurred an increasing fraction of the time, and the departures from standard signal level and radar ranges decreased. Other measurements during the winter indicate that fairly small variations are to be expected then (in this region). This seasonal trend is to be expected because of the corresponding seasonal variation in the air-water temperature and humidity contrasts which determine the modified index profile.

This is only a small sample of a large amount of information accumulated from all parts of the world from which reports on radar operations are available. Ranges up to 400 miles on coastal targets have been reported in the Mediterranean Sea, and comparable ranges have been obtained off the northwest coast of Africa, in the vicinity of Australasia, in the South Atlantic, and in numerous other places. Perhaps the most startling report comes from a 1.5-meter radar at Bombay, which obtained echoes intermittently over a period of several weeks from the coasts of Arabia, about 1,700 miles away.

This brief outline of some of the problems of propagation can do no more than to suggest the kind of information needed for successful design and operation of equipment in the microwave range. Other equally important problems not discussed here are those of radar echoes from meteorological phenomena and attenuation by the atmospheric gases and by such hydrometeors as rain, hail, snow, and fog. These subjects form a new field that has hardly begun to be explored, and offer fascinating opportunities for further research.

2-Mc Sky-Wave Transmission

A simplified review of present ionospheric knowledge and a critical survey of the information resulting from an empirical use of the night-time *E* layer. Its relative stability, as disclosed by loran operations, is little affected by ordinary disturbing phenomena

By J. A. PIERCE

THE ionosphere is usually defined as "that region of the earth's atmosphere which is ionized sufficiently to affect the propagation of radio waves." For practical purposes it may be thought of as all the atmosphere above the stratosphere, or, more specifically, the atmosphere between 30 and 300 miles above the surface of the earth.

The atmosphere at such heights consists primarily of the same constituents as at sea level, nitrogen and oxygen. Above 60 miles the oxygen presumably exists in atomic rather

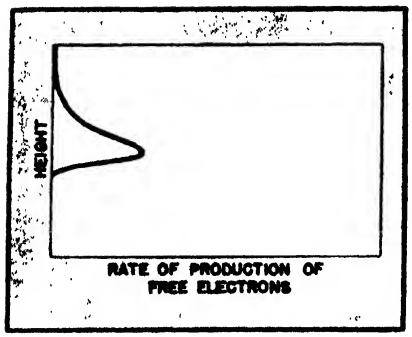

FIG. 1—Chapman curve showing vertical distribution of free electrons

than molecular form because the ultraviolet light from the sun disassociates the atoms much faster than they recombine. Nitrogen may be disassociated at, say, 200 miles but the evidence for that is less clear.

There is little to indicate that the heavier elements settle out at the lower altitudes. Probably all the components of the atmosphere are quite well mixed, except for the change from molecular to atomic oxygen at 60 miles. It may be that hydrogen and helium escape into space; there is no strong evidence that they form much of the upper air.

The pressure at which these gases exist decreases exponentially with increasing height to very small values. At 60 miles it is about one millionth of the sea level pressure, while at 200 miles it is probably thousands of times again as small. The mean free path, at 60 miles height, may be taken as one centimeter while at 200 miles it may be as much as a mile or more. This mean free path is the distance a particle—molecule, atom, heavy ion or electron—will travel, on the average, before it collides with another particle. It is a very important quantity.

The temperatures in the ionosphere are high. This does not mean that there is much heat in the upper air, because there are very few particles to contain heat, but it does mean that the particles travel rapidly. At sea-level temperatures the air molecules travel at about 0.5 kilometer per second, while at 200 miles altitude they move several times as fast. The temperature, after falling to about −70 F in the stratosphere, increases to nearly the sea-level value at about 30 miles. Then there is a sharp drop to about −140 F at 50 miles. Above that the temperature (velocity of particles) rises rapidly to somewhat more than 80 F at 60 miles and to perhaps 1,400 F at 200 miles.

Production of Ionization

If a certain wavelength of solar ultraviolet light excites one of the electrons in an atom so that it breaks away from the atom and exists alone, the atom is ionized. The electron may be called a negative ion and the positively-charged remnant of the atom is called a heavy or positive ion. The electron is small and light. It will travel, independent of the heavy ion, at great speed until it finds another heavy ion with which it can unite or until it finds an atom or molecule to which it can stick temporarily.

Let us assume that ultraviolet light of some ionizing wavelength is falling upon the atmosphere. There will be, in general, enough energy at this wavelength to penetrate some distance into the air but not enough to reach the surface of the earth before it has all been expended in ionization. At several hundred miles above the surface very little ionization will be produced because there are very few atoms there to absorb the energy. The ionization will therefore increase as the height decreases because there is more and more material which can be ionized. As the height decreases further, however, a substantial fraction of the original ultraviolet energy has been used up so that, although the number of atoms continues to increase very rapidly, the number of electrons set free does not increase so rapidly. At still lower heights the number of free electrons actually begins to diminish and, lower yet, decreases to zero when all of the suitable incoming energy has been used up.

This behavior can be calculated, under certain simplifying assumptions, and gives a curve of the shape of Fig. 1 which is known as the Chapman distribution. The height at which the free electrons are produced and the thickness of the layer of electrons depend upon the kind of ionizing energy, the kind of atoms which are ionized and the temperature of the air. The number of free electrons produced depends upon the same things but especially upon the total energy available in the ionizing ultraviolet light.

The true picture of the vertical distribution of free electrons is much more complicated. A separate distribution, of the form of Fig. 1, is produced for every combination of ionizing ultraviolet wavelength and atomic constituent in the atmosphere. Many of these distributions overlap each other but some are quite well separated. Furthermore, these Chapman curves define the rate at which free electrons are produced. There is some diffusion from the heights at which they are produced and the electrons at lower levels recombine faster than those above. Both of these factors operate to cause the heights at which the density of ionization is maximum to be greater than the heights at which the electrons are set free most rapidly.

Formation of Layers

Figure 2 shows the approximate distribution of free electrons as they exist by day and by night. The maximum at about 250 km is called the *F* layer, or Appleton layer. The small bump on the lower side appears only in the day time in the summer, because it recombines quickly at night and is swamped in the body of the *F* layer in the winter. When it appears it is called the F_1 layer and the remainder of the *F* region is known as the F_2 layer. The *F* layer varies

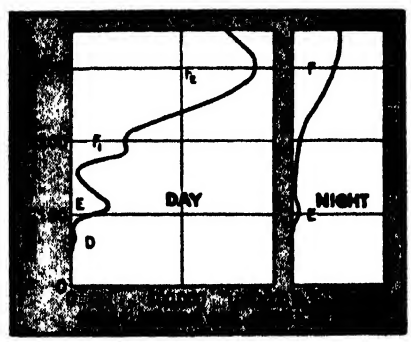

FIG. 2—Night and day distribution of free electrons showing disappearance of the *D* layer and combination of the F_1 and F_2 layers at night

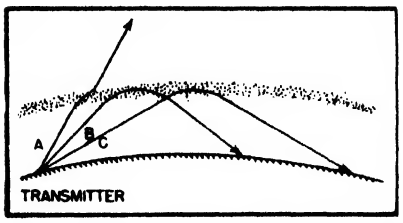

FIG. 3—A simplified representation of an ionospheric layer showing the effects of rays entering at different angles. Ray A has left the earth at too steep an angle to be turned back

greatly in height, thickness, and density of ionization.

The *E*, or Kennelly-Heaviside layer at about 100 km, is much more stable. Its density of ionization follows the altitude of the sun quite closely, except that some ionization remains throughout the night when the sunlight does not fall on the layer. We shall be primarily concerned with the *E* layer.

The tail of the E layer, perhaps at about 70 km above the earth, sometimes shows a small maximum which is called the *D* layer. The density is low, so that only low frequency waves can be reflected from it. The *D* layer is primarily of importance because it absorbs energy from radio waves.

Reflection

If a radio wave penetrates obliquely into the ionosphere the phase velocity, which determines the direction of the wave front, increases as the index of refraction decreases. At the same time the group velocity, which is the velocity with which the energy travels, decreases in the same ratio. Thus the upper part of the wave front travels faster as the wave penetrates into an ionized layer because the density of ionization is increasing. The wave is therefore refracted so that it curves back toward the earth, but it travels more slowly while being refracted.

In Fig. 3 we have postulated an ionospheric layer whose density (number of free electrons per cubic centimeter) is roughly indicated by the density of dots. Three rays of radio frequency energy are shown entering the layer. If the frequency is such that reflection can occur at oblique incidence but not at vertical incidence on the layer the behavior will be as shown. A ray C departing at a small angle to the horizontal will only require a modest amount of refraction before it is turned parallel to the surface of the earth. It will therefore not need to penetrate far into the layer and will span a long range in a single hop. Another ray, B, departing more steeply from the earth will penetrate the layer more deeply because it must be turned through a greater angle. If the required bending cannot be achieved, because the frequency or departure angle is too high or the density of the layer is too low, the ray A will penetrate the layer, traveling on a path which is concave downward until the height of maximum ionization is reached and concave upward beyond that height. This ray, of course, leaves the earth completely unless it is turned back later by a higher layer. The effect of the penetration is to establish the well known skip distance within which sky-wave signals are not received. Outside a layer, rays travel straight lines.

Single-Hop Limit

There is a definite maximum range which can be spanned by single hop transmission. This is the distance covered by a ray departing horizontally (or as nearly horizontally as antenna radiation can be effective) and is about 1,500 miles in the case of *E*-layer transmission. At greater distances the signal is cut off by the earth itself. This shadow effect can be seen clearly in the sharp drop in the 1-hop sky-wave field-intensity curve of Fig. 4.

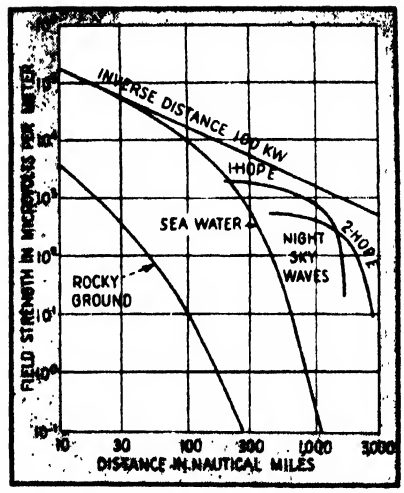

FIG. 4—Field strength as a function of distance from a 100-kw transmitter, over sea water and rocky ground. The 1-hop *E* sky waves can not be safely used beyond 1,400 miles because their strength falls rapidly below those of the 2-hop *E*

A rough diagram indicating the typical action of both *E* and *F* layers is given in Fig. 5. Here we have assumed a number of rays at different radio frequencies, all departing from a transmitter along the same path. The medium frequencies shown, 500 kc and 2 mc, are both reflected by the *E* layer, but the 2-mc ray pen-

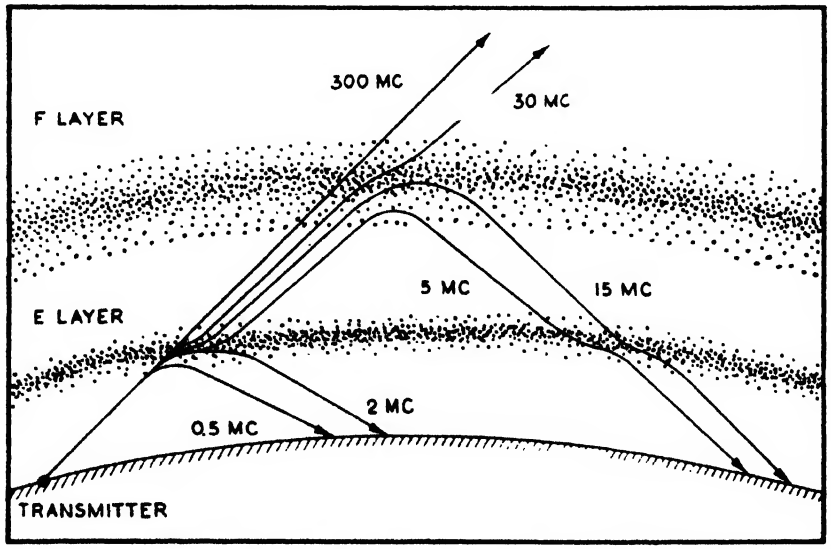

FIG. 5—Typical behavior of rays at various frequencies in the *E* and *F* layers. At the higher frequencies the rays are less affected by the ionosphere

etrates much more deeply and travels somewhat farther. At 5 mc, the ray is refracted strongly in the *E* layer but does penetrate it, and is easily reflected by the *F* layer. The 15-mc ray is less affected by the *E* layer and penetrates more deeply into the *F* layer, but the general behavior is much the same as at 5 mc. Thirty mc, however, is too high a frequency to be returned, under the conditions we have postulated. The ray passes the *E* layer with very little refraction, and is refracted strongly by the *F* layer but without being turned back toward the earth. The energy at this and all higher frequencies, such as 300 mc, escapes into space. As the frequency increases the deviation of the ray in the layers decreases until at microwave or optical frequencies the effect of the ionization is not at all perceptible.

The whole structure of Fig. 5 depends upon the density of ionization in the layers and upon the angle of departure of the original rays. At a lower angle the 5-mc ray might often be reflected from the *E* layer while the 30-mc ray would be returned from the *F* region.

The reflection of radio waves in the ionospheric layers is only half of the process of radio transmission by sky waves. The absorption of energy from the waves is of at least the same importance.

Some mention was made above of the mean free path of an electron (or other particle) in the upper atmosphere. This quantity, or more properly the inversely-varying collisional frequency, controls the energy lost by a radio wave. While there may be a million free electrons per cc in a highly ionized layer there are typically a million times as many neutral atoms or molecules with one of which an electron may collide at any instant. Suppose, for example, that on the average an electron can move freely only for a millionth of a second before bumping into a heavy atom. If the electron is being vibrated by a radio frequency field at 1 mc there is only about one chance in two that the electron can complete a cycle of oscillation before its motion is interfered with.

The collision is important for this reason. Some energy is abstracted from the radio wave to provide the kinetic energy contained in the moving electrons. This energy is, in effect, lost to the radio wave only for a half cycle because the moving electron, since it constitutes a moving charge, reradiates an electro-magnetic field whose energy is equal to the energy absorbed by the electron. As the radio wave passes through the ionosphere the energy reradiated by all the electrons adds in phase to constitute a wave traveling in the same direction as the original wave. If the electrons can move freely, tiny elements of the energy in the wave flow back and forth between electrostatic and kinetic states, but the total energy in the wave remains the same.

Energy Lost by Collision

If, however, an electron rebounds from an atom while temporarily carrying some of the energy two things happen. One is that the direction of motion of the electron is changed. The energy is then reradiated in a different orientation, so that the phase relation with the radiation from other electrons is damaged. Even more serious is a real loss of radio frequency energy because the atom is accelerated slightly and carries off part of the kinetic energy which had been loaned to the electron. This energy is completely lost to the radio wave and remains in the atmosphere in the form of increased kinetic energy, or heat.

If the probability of collision and loss of energy is high enough the radio wave will be completely attenuated in the ionized layer. The degree of absorption is less as the frequency is increased because the electrons are more likely to be able to complete their half cycles of oscillation before a collision occurs. In the *F* layer there is little collisional friction because the mean free paths are long and the collisional frequency is low. In the *E* layer collisions are frequent enough so that waves of frequency below 2 or 3 mc are completely absorbed in the daytime. At night the density of ionization in the *E* layer decreases to perhaps a tenth of the daytime value. The absorption goes down to low values because the chance of a collision between an electron and some other particle is similarly reduced.

We may summarize the situation thus: Ionization is needed to reflect radio waves but ionization at low heights in the atmosphere absorbs energy from the waves. The higher the frequency the stronger the ionization required for reflection and the less the absorption.

Little Ionization at Night

Since most ionization in the atmosphere is produced by the action of ultraviolet light from the sun there is little new ionization created at night. The free electrons recombine, but slowly enough so that a substantial number of them remains throughout the night. Thus the maximum ionization occurs at or soon after noon and the minimum at sunrise. Similarly the ionization is more intense in summer than in winter because the sun shines more perpendicularly upon the atmosphere and the ionization increases as does the temperature.

Whether radio transmission is better by day or by night, in winter or in summer, is a question of frequency. At high frequencies, say 20 mc, the weak ionization may prevent sky-wave transmission completely in the winter or at night, while in summer or daytime the stronger ionization will support transmission when absorption is so small as to be unimportant. At broadcast frequencies, absorption is complete in the daytime so that only ground wave ranges are useful. At night, long distance transmission is possible, and the decreased absorption in the winter makes communication better than in the summer.

2-mc Sky-wave Loran Transmissions

During the war, much practical information was obtained from the use of *E*-layer transmissions which extended the night-time range of the loran navigational system. The balance of this paper describes some of the phenomena encountered.

Figure 6 shows typical variations of the critical frequencies (which are proportional to the square roots of the maximum densities of ionization)

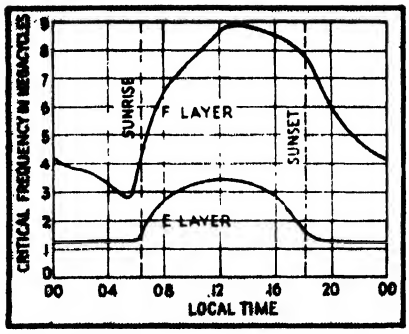

FIG. 6—Critical frequencies for the *E* and *F* layers at various times of the day. These plots are particularly important in showing that ionization in the *E* layer is not entirely dependent upon solar radiation

in the *E* and *F* regions throughout the day. Recombination is slow in the *F* region that the maximum occurs well after noon although all of the ionizing energy appears to come directly from the sun. The smooth decrease throughout the night is another manifestation of the fact that some free electrons have lifetimes of many hours in the *F* layer.

The behavior of the *E* layer at night is not understood. At the height of the *E* layer complete recombination takes only a few minutes, so that the density of ionization adapts itself very quickly, in the daytime, to the amount of energy being received from the sun. The *E* layer curve of Fig. 6, between sunrise and sunset is nearly proportional to the fourth root of the cosine of the sun's distance from the zenith. This is so exactly true that without question the ionization would go almost to zero at night if ultraviolet light from the sun were its only source.

The energy brought into the earth's atmosphere by meteoric bombardment may possibly be enough to sustain this night-time ionization.[1] In any case, meteoric effects are definitely perceptible and certainly cause many of the variations in the density and distribution of free electrons in the *E* layer even though they are probably not the major cause of the ionization. The random variations in the density of the *E* layer are of the first importance in the propagation of loran signals by sky waves, because they control the errors of the system.

Sky-wave Delay

The transmission time of a sky wave is greater than the transmission time of the ground wave, primarily because of the greater distance traveled but also because the wave travels more slowly during the process of refraction. The difference between the two times is called the sky-wave delay. The delay observed at a point very near the transmitter (if penetration does not occur) is essentially equal to the transmission time of the sky wave. As the distance increases the transmission time of the the sky wave increases but the transmission time of the ground wave increases more rapidly. The delay therefore decreases as the distance of transmission increases and, in fact, becomes very nearly constant at distances of a thousand miles or more. Figure 7 shows the standard delay curve for loran, which is drawn for reflection from the *E* layer. The curve is a mean for night conditions at a frequency just below 2 mc. It is never drawn back to zero distance because a 2-mc wave nearly always penetrates the night-time *E* layer at short distances and because the delay becomes more variable as the distance decreases. At distances less than 1,200 μ sec (about 200 nautical miles) the delay is completely unreliable. Fortunately for loran the ground-wave service of the system is ordinarily available at distances up to those at which the *E*-layer transmission becomes satisfactory.

The stability of the reflection becomes greater at longer distances partly because grazing reflection is better than reflection at a steep angle, but primarily because a change in the height of reflection does not greatly change the total distance traveled by the ray. At a distance of a thousand miles the length of the sky-wave path increases only 1.78 miles for a change in the height of reflection of 5 miles. This is a change in the time of transmission of less than 10 μsec or about one-fifth of the corresponding change at a short distance.

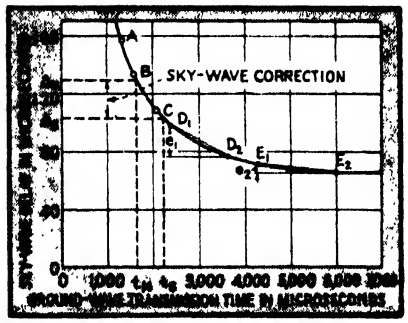

FIG. 7—Delay in reception of a sky wave after reception of a ground wave from the same transmitter is shown as a function of distance of the receiving point from the transmitter. The curve has been calculated to distances beyond ground-wave reception in terms of the travel time of radio waves

Variations of five miles in the height of reflection are rare, but do occur at times. Their effect upon standard loran is not too large because such an extreme variation is likely to exist over a large area. It will therefore operate to increase (or decrease) the transmission times from both stations of a pair so that the time difference measured by the navigator does not vary as much as the individual delays.

The discussion in the last few paragraphs has been specifically applicable to the *E* layer. Only this layer is used in loran because the *F* layer is too variable to permit prediction of the times of transmission with the necessary accuracy. A comparison between the layers is given in Fig. 8 which shows the apparent variation of the line of position through a point in Bermuda. These observations were made as part of first experiments on loran. For ob-

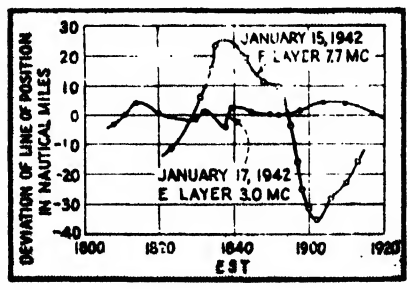

FIG. 8—Apparent deviation of a line of position with time using signals reflected from the *E* and *F* layers. As a result of this study, the *E* layer was chosen for loran work

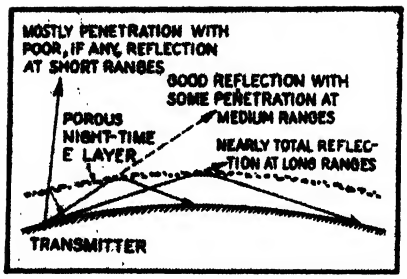

FIG. 9—The porous character of the night-time *E* layer is illustrated by the reflection at long ranges, the penetration at short distances

vious reasons work involving the *F* layer was discontinued after that time. The example shown is typical of the behavior of both layers although the time of day was not favorable to maximum stability of either. The average deviations of the line of position are 18 miles for the *F* layer and 2 miles for the *E*. The distance was 625 miles from the stations, so that the equivalent average errors in the bearing of Bermuda, as seen from near New York, were 1.7 deg for the *F*-layer experiment and 0.2 deg for the *E*-layer.

As will be seen from the notation on Fig. 8, the layer can be selected by proper choice of frequency. At the time of these experiments 7.7 mc penetrated the *E* layer while 3.0 mc did not. The loran frequency is chosen as one which will be reflected by the *E* layer at all times at all distances which will not be adequately served by ground waves. It is possible that frequencies as high as 2.5 mc might satisfy this criterion, but both ground-wave range and sky-wave stability are improved by using lower frequencies. (The lower limit of frequency, incidentally, is that at which it becomes too difficult to generate and radiate a sufficiently short pulse for loran purposes. With the criteria adopted for standard loran, this frequency is probably about 1 mc).

Choice of Loran Frequency

It should be noted that the last paragraph did not state that signals at the loran frequency would not penetrate the *E* layer. They almost always do penetrate at short distances and part of the energy usually penetrates the layer at long distances. This seems to be because, in contradiction of what has been suggested above, the *E* layer is not really a smooth homogeneous layer at night, although it is in the daytime. At night the layer is porous, even gauzy. It seems to consist of many nuclei or clouds of ionization chiefly at about the same height—a little below the height of the daytime or normal *E* layer—with either spaces or patches of sparse ionization between them. The density of the ionization in the clouds is not very great so that 2-mc rays pass vertically through the layer partly because of penetration of the clouds and partly by passing between them. At more grazing angles the probability of passing through the spaces becomes smaller and usually goes nearly to zero for transmission over the longer distances. A diagram showing this effect is given in Fig. 9.

In general some energy will be reflected by the porous night-time *E* layer and some will pass through it and be reflected from the *F* layer. Multiple-hop transmission is possible in both cases so that the pattern of received pulses may be very complex. The structure of some of these components of the received pattern is shown in Fig. 10A. The way the corresponding signals look on a linear time base is indicated at B. This diagram is idealized.

The spotty character of the night-time *E* layer gives rise to pulses whose shape is not the same as that of the pulses when they leave the transmitter. Several of the small clouds of ionization in the neighborhood of the midpoint of the transmission path may reflect the pulse. While each reflection may be a complete and perfect reproduction of the transmitted pulse, the overlapping components arriving at the receiver may combine to give a very complex form indeed. This is particularly true at very short distances, say up to 100 miles, where often a family of ten or a dozen contiguous or overlapping pulses may be seen. As the range increases the weak multiple pulses move toward each other and coalesce into a single strong pulse which occasionally has a more or less serious distortion of its shape. Figure 11 shows some of the typical reflection patterns received between, say, 100 and 400 miles from a loran transmitter. The reason for not using sky waves at very short distances is clear.

The Delay Curve

The standard technique in loran is to measure to the first visible component of a pulse even though the

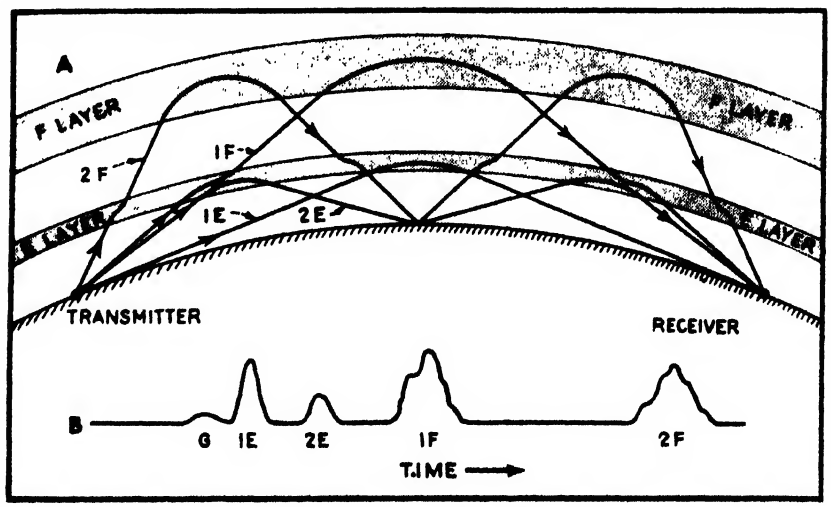

FIG. 10—Multiple-path transmissions occur in many combinations, only a few of which are shown. Their appearance on the loran indicator scope is suggested at B. Only the ground wave, G, and the 1-hop *E* will have any semblance of stability over a period of time

pulse be complex. As seen in Fig. 11B this may be quite different from measuring to the dominant component. This decision was first made on theoretical grounds and was based on the belief that if a pulse should be simultaneously reflected from a number of clouds of ionization the part arriving first must travel by the simplest and most direct path and should therefore be the most reliable. This thesis has been amply confirmed by experiment, as measurements made on the first component exhibit smaller mean deviations than those made in any other way.

At the start of the loran program the night-time E layer was scarcely known to exist and its properties could not be predicted. It was necessary, therefore, in the interest of speed, to determine the necessary factors empirically. More than this has not yet been done. Fortunately the layer was found to be remarkably stable. That is, its characteristics change very little from one hour of the night to another. More surprisingly, the properties of the layer seem to be essentially the same at all latitudes, and to vary only simply and moderately between winter and summer. These auspicious discoveries greatly facilitated the use of sky waves for loran.

The delay curve already cited was determined by making loran observations on sky waves at accurately known points and comparing the observed readings with time differences calculated (for the locations where they could not be directly measured) in terms of ground-wave transmission.

Charts and tables for Standard loran are computed in ground-wave time differences even though the distances are so great that ground waves cannot be received.

Sky-wave Corrections

A correction must be applied when sky waves are used. The correction can be read from the sky-wave delay curve if the distances to the two stations are known. Suppose that t_M in Fig. 7 represents the distance of the navigator from the master station while t_S is the distance from the slave. The first-hop E layer sky wave from the master will arrive Δ_M μsec after the ground wave and the corresponding slave pulse will be Δ_S μsec later than its ground wave. Since the navigator measures the time difference between the M and S pulses his sky-wave reading will differ from his ground-wave reading (if he has made one) by $(\Delta_M - \Delta_S)$ μsec. This amount is the sky-wave correction. In this case (closer to the master station) the sky-wave reading is smaller than the ground-wave reading. The correction is therefore called positive, so that when it is added to the sky-wave reading the ground-wave time difference, which is shown on the charts, will be obtained.

The sky-wave corrections can, of course, be calculated easily at the time the charts are prepared. They are ordinarily exhibited on the charts as small numbers printed at the intersections of the whole degrees of latitude and longitude. The magnitude of the corrections is small so that interpolation by inspection is adequate. On the centerline of the pair and at long distances from both stations the corrections are zero because the master and slave delays cancel each other.

The delay curve was constructed through study of many thousands of loran sky-wave readings made at various distances from the stations. At short ranges both sky and ground waves could be received. Measurements of both against the ground wave of the other station of the pair gave two average readings whose difference was the delay at the distance of the station whose sky wave was used. Points derived in this way are shown at A, B, and C of Fig. 7. For longer ranges, where ground waves could not be used, an inverse process had to be employed. The sky-wave readings of a pair were averaged and compared with the calculated ground-wave reading at the monitor station. The discrepancy (e_1 or e_2 in the figure) was, of course, the sky-wave correction. Since the two distances were known, the correction gave the slope of a chord of the delay curve, as shown at $D_1 - D_2$ or $E_1 - E_2$. Many lines of this slope could be drawn in

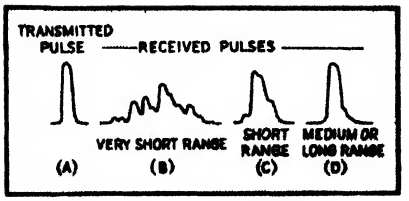

FIG. 11—Within 100 miles of a transmitter the pulses reflected from the E layer are complex and useless for accurate timing techniques. At 300-400 miles, the pulses have achieved sufficient stability

an effort to find the vertical position of the line which would fit its end points into a smooth curve with the end points of other similar lines at other distances. If enough observations are available, at enough distances, the curve can easily be constructed.

Empirical Formula for Delay

The curve which, after three years experience in various latitudes, seems to be the best average approximation to the true values has been shown in Fig. 7. This curve is described by the equation: delay in μsec

$$= D + 0.3\left(\frac{7{,}000 - t}{1{,}000}\right)^2 + 0.18 \times 10^{-6}\left(\frac{7{,}000 - t}{1{,}000}\right)^{11}$$

D is the minimum sky-wave delay which varies between 65 μsec in the winter and 75 μsec in the summer

t is the transmission time of the ground wave in μsec

This formula applies for distances less than about 1,130 nautical miles (where $t = 7{,}000$). For greater distances the delay equals D. This equation has no mathematical justification.

As shown by the variation of the quantity D, the layer height is somewhat greater in the summer. However, the delay curve, for all practical purposes, simply moves upward so that the correction, which is always the difference between two delays, is not affected. There is an error introduced by this change in two cases; when the navigator may occasionally wish to measure the time difference between a sky wave and a ground wave, and in the case of the synchro-

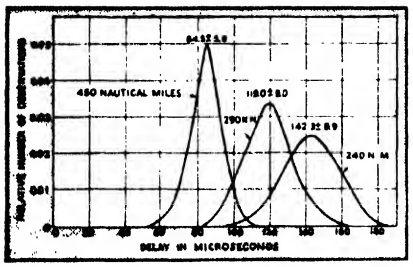

FIG. 12—As shown by the three sets of observations, the average sky-wave delay diminishes as distance from the transmitter increases and the spread of readings decreases proportionately

nization path in SS Loran[2, 8] which will be discussed below.

The only significant latitude effect which has been isolated is that the delay curve may be used at shorter distances at low latitudes. That is, near the equator fairly reliable operation may be had at as little as 150 nautical miles, while at 45 deg latitude about 250 miles is the minimum safe distance. The curve itself does not seem to vary appreciably over the range from 25 N to 63 N within which it has been carefully checked.

Variation in the Sky-Wave Delay

Since we propose to examine closely the averages and the mean deviations of the sky-wave delay and sky-wave corrections, it is necessary to test the accuracy with which transmitter synchronism can be maintained. An example, somewhat better than normal, is given by readings from a pair of stations in the Northwest Atlantic Chain observed at a monitor station where the computed reading was 3510.6 μsec. The mean, as is usual, agrees with the computation within 0.2 or 0.3 μsec, and the average deviation is of the order of 0.6 μsec. A series of sky-wave readings usually shows an average deviation at least four or five times as great. It is, therefore, nearly always satisfactory to assume that the synchronism of the transmitting stations is rigid and that any deviations observed are the result of variations in sky-wave propagation. Exceptions to this assumption are usually obvious.

Three distribution curves of observations of the sky-wave delay are given in Fig. 12. The curves are drawn to have the same area and exhibit clearly the two important facts of sky-wave transmission for loran. The average delay diminishes as the distance increases, as shown by the delay curve, and the spread of the readings also decreases in about the same proportion. The probable errors in this set of observations are: 9.9 μsec at 240 nautical miles, 9.0 μsec at 290 nautical miles, 5.8 μsec at 450 nautical miles. The first two are somewhat below the normal scatter at these distances.

Layer Height Correlations

At long distances it is impossible to measure delay directly. Distribution curves of the sky-wave reading (not delay) compared with the computed reading at distances of 870 and 1,350 nautical miles show that the corresponding probable errors are 2.1 and 2.4 μsec, although a smaller error would be expected at the greater distance. These are errors in the sky-wave *correction*. As remarked above, major changes in the height of reflection of a sky wave may be expected to affect both transmission paths in the same way and therefore to cancel to some extent. In other words, there should be a correlation between the two delay patterns, and the errors of a sky-wave measurement would be smaller than if the two reflection points behaved independently. For instance, the probable error of delay at a thousand miles averages about 3.9 μsec. If every point in the reflecting layer varied independently, the probable error of a sky-wave reading would be about $\sqrt{2} \times 3.9$ μsec, or 5.5 μsec. Actually, for base-line lengths of about 250 or 300 miles, the probable error of a reading is usually between 1.5 and 2.0 μsec for a thousand-mile range. This indicates a fair degree of correlation in the behavior of the layer at points separated by a hundred miles or more.

The probable error of *delay* is shown in Fig. 13 as determined from monitor station readings on many different pairs of stations. The points for ranges greater than could be served by ground waves were determined during the American trials of the SS Loran system.[2, 8] The equa-

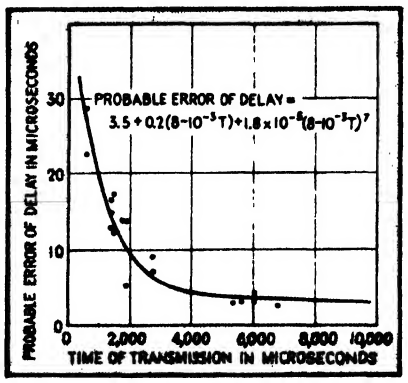

FIG. 13—Probable error of delay has been determined by actual observations at monitor stations of various pairs of transmitters

tion given on the diagram defines the smooth curve but has no other significance.

If no correlation existed between the layer heights at the two points of reflection, the probable error of a sky-wave reading would be found by taking the square root of the sum of the squares of the two values of probable error of delay for the two distances involved. Since there is a correlation, an estimate of the probable error of a reading can be made by multiplying the no-correlation value by a factor smaller than unity which can be obtained by experiment. This factor is given in Fig. 14 where it is plotted against the electrical length of the base line. The positive slope means simply that the greater the separation of the stations the less the variations in delay tend to cancel each other. The factor, "Probable error of synchronization", is given in the equation on the figure because

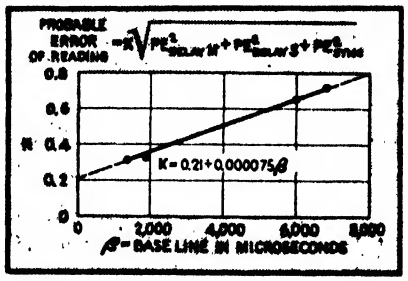

FIG. 14—The increasing value of the correlation factor, K, indicates that as the separation of transmitters increases, variations in delay tend to cancel less. This also shows that over great distances the ionosphere does not move uniformly

sometimes, as in SS Loran, the absolute accuracy of synchronism cannot be assumed. In SS Loran, of course, the probable error of synchronization is equal to the probable error of delay at the distance separating the stations.

Sky-wave Accuracy Patterns

The accuracy (or average error) with which a sky-wave loran reading can be made can be estimated by the method of the preceding section. This average timing error may or may not correspond to a significant number of miles depending upon the distance from the stations and their orientation with respect to the navigator.

Ordinary geometrical methods permit the calculation of the number of miles corresponding to a change in reading of one microsecond. These formulas may be combined with the methods of this article to yield the average error of a sky-wave reading in miles.

The probable error of a sky-wave line of position (in nautical miles) varies over the service area of a loran pair, whether standard or SS. It is of special interest to note that the errors increase very slowly with distance along the center line of the pair. This is because the timing errors are nearly inversely proportional to distance and almost cancel the increasing geometrical error. Beyond the 1,400 mile limit or within 250 miles of the stations it is not safe to use sky waves because of ambiguity in the first case and erratic behavior in the second.

The accuracy of SS Loran is greater than the sky wave accuracy of standard loran, because the long base lines greatly improve the geometrical accuracy, or miles per μsec of timing error. The timing error itself is not so good as in a standard loran, primarily because of sky-wave variations on the synchronizing path, but the timing error is not increased as much as the geometrical factors are improved. The total area served by an SS pair is not so great but the errors are smaller and more constant except along the base line extensions.

One of the outstanding anomalies in the *E* region is the existence of sporadic ionization. This takes the form of clouds of free electrons, at a very constant height, which are sporadic in both time and space. They may appear at any time, day or night, and last for a few minutes or for hours. Their size may be anything up to hundreds of miles across. They sometimes appear to move with very great velocities and at other times they seem nearly stationary. The density of ionization is often low but occasionally is very great indeed —even greater than is ever observed in the *F* layer. On at least one occasion the density has been observed to be enough to reflect signals up to 110 mc over a thousand-mile path.

These clouds are probably caused by corpuscular bombardment of the atmosphere by particles shot off by the sun, in much the same way that northern lights are formed. While sporadic *E*-region ionization may appear at any time, it is most likely in the summer and at times of sunspot maximum. It is most probable at high latitudes and is very seldom if ever observed at the magnetic equator—again like the aurora.

In the early days of loran it was feared that signals from one station of a pair might be reflected from a cloud of sporadic *E* ionization while the other signals would be transmitted by the normal night-time *E* layer, thus leading to large and unpredictable errors. Fortunately this is not the case, apparently because the normal reflections occur at a height somewhat below that of the sporadic *E*, so that the signals never are propagated by the sporadic clouds.

At very short distances sporadic *E*-region ionization frequently does cause strong steady reflections. Since the height of reflection differs from the normal, this contributes to the unreliability of sky-wave transmission at short distances at 2 mc.

The best evidence to this effect is given in the table which exhibits the average value and probable error of sky-wave readings when sporadic *E* ionization is and is not present. These data were taken in Ottawa, Canada, by the Canadian Navy, in May, June, and July, 1948, the season of maximum sporadic ionization. During this period the sporadic *E* layer appeared about one-third of the time at Ottawa. Of course there is no proof that sporadic ionization existed at the points of reflection at the same time they were observed at Ottawa, but it is more likely to have existed there then than when it was not observed at Ottawa. As the table shows, there was no significant change in the loran reading at times when sporadic *E*-region ionization was observed. The probable errors (or average errors) of the readings were actually smaller at those times, but the difference is not large enough to be significant except in the sense that it may be taken as proof that the errors were not larger in the presence of sporadic ionization.

Effect of Sporadic *E* on Loran Readings

	Normal		
Pair	No. of Observations	Mean Reading	Probable Error
MF	561	2932.1	3.2
MB	422	3816.3	4.4
DB	368	1342 5	3.7
	1351		

	During Sporadic E			Computed Reading
Pair	No. of Observations	Mean Reading	Probable Error	
MF	305	2932.6	2.9	2932.4
MB	256	3816.8	3.6	3814.7
DB	206	1341.8	3.1	1342.4
	767			

Magnetic Activity

The effect of sudden or large variations in the earth's magnetic field upon loran transmissions is known, but will not be discussed in this paper. It seems, however, that none of the ordinary phenomena which disturb radio transmissions have any appreciable effect upon the accuracy of loran sky-wave readings, although the reliability of the service may suffer in operating too near the magnetic pole.

References

(1) Pierce, J. A., Abnormal Ionization in the *E* Region of the Ionosphere. *Proc. IRE*, p 892, July, 1948.

(2) Fink, D. G., The Loran System, ELECTRONICS, p 94, Nov. 1945.

(3) McKenzie, A. A., Loran, *QST*, p. 12, Dec. 1945.

Ionosphere Measuring Equipment

The pulse-reflection technique of ionosphere investigation requires a transmitting and receiving system which sweeps the region from 1 to 20 megacycles rapidly. Equipment described utilizes a common oscillator to facilitate tracking, and broad-band response to obviate tuning

By P. G. SULZER

THE pulse method of ionosphere investigation[1] employs a series of radio signals of short duration which are transmitted, reflected, and received, as in radar. The pulses are longer, however, and the distances (and elapsed times) are greater. Much lower frequencies are used, as the purpose is the investigation of the ionospheric characteristics on all frequencies between 1 and 20 megacycles.

It is necessary to make measurements over the entire frequency range in as short a time as possible, so that the ionosphere will not change noticeably during the recording. This paper describes a system which eliminates nearly all mechanical problems and provides perfect tracking of the transmitter and receiver.

Systems Now in Use

One system which is used in equipment developed by The Bureau of Standards[2] has a pulsed transmitter linked to a receiver by a beat-frequency system. The output of a variable-frequency oscillator is mixed with the output of an oscillator operating at the intermediate frequency of the receiver. The difference of these two frequencies is selected and amplified in the transmitter. Signals to be received are mixed with the output of the variable oscillator, the frequency difference then being the receiver intermediate frequency which is amplified and detected in the usual manner.

In this instrument the variable oscillator, converter and power amplifier are tracked by means of cams. This system appears to have the usual disadvantages that are connected with mechanical tuning arrangements. One very good characteristic of the system, however, is the heterodyne scheme which insures that the receiver and transmitter are always operating on the same frequency.

Another system currently employed is that in the Type 249 equipment of National Physical Laboratory (British) design, which uses the frequency-modulation method of developing pulses.[3] The transmitter is tuned rapidly by a motor-driven rotating capacitor through the frequency on which the receiver is operating; the receiver is therefore subjected to a pulse whose shape and duration depend on the bandwidth of the receiver and the rate of change of transmitter frequency. The portion of the energy in the pass band of the receiver which is radiated and returned to the installation by the ionosphere will be recorded as a pulse. The frequency modulation method as employed in this equipment is inefficient as compared to pulse methods since the transmitter is operating continuously and only a portion of the total received energy is utilized by the receiver. Another disadvantage of the system is the fact that the effective pulse width will in general not be constant, unless the rate of change of the transmitter frequency is maintained at a uniform level over the frequency range, which is usually not the case. As a result the height resolution of the equipment varies over the frequency band employed. To produce narrow pulses, the transmitter frequency must be varied rapidly across the receiver frequency range by a high speed motor-driven inductor or capacitor.

Experimental System

The system to be described employs a heterodyne method similar to that used in the Bureau of Standards equipment in that the receiver and transmitter are linked by a beat-frequency arrangement. In the new system, however, complicated tuning arrangements are avoided by the use of untuned receiver input and transmitter circuits. Figure 1 shows a block diagram of the system. It will be noted that the common oscillator (common to both the transmitter and the receiver) is tuned from 31 to 50 megacycles. In the transmitter these frequencies are mixed with the output of a 30 megacycle pulsed oscillator. The difference frequency, which

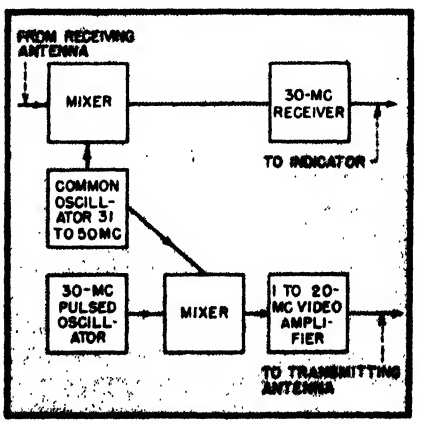

FIG. 1—Block diagram of the ionosphere sounding equipment, showing the common oscillator

varies from 1 to 20 megacycles, excites an untuned wide-band amplifier, which feeds the antenna. In the receiver, incoming signals whose frequencies vary from 1 to 20 megacycles are mixed with the 31 to 50 megacycles from the common oscillator. The difference frequency, which is constant at 30 megacycles, is amplified and detected with a superheterodyne receiver. Since the transmitter and receiver are controlled by the same oscillator they are always operating on the same frequency.

The system under discussion has no serious mechanical limitations; there are no variable capacitors rotating at high speed and there are no cams. The frequency range may be covered as rapidly as desired, since it is necessary to rotate only one small variable capacitor to tune the transmitter and receiver from 1 to 20 megacycles. It is comparatively easy to obtain high output power.

There are, however, two undesirable features of the system. In the first place the untuned receiver input circuits permit cross-modulation from local stations, generating a series of interfering voltages at frequencies throughout the entire frequency range. This has not been sufficiently serious to prevent good records from being obtained. Second, because the transmitter is untuned a large number of stages of amplification is necessary to obtain high power. This does not seriously decrease the overall efficiency.

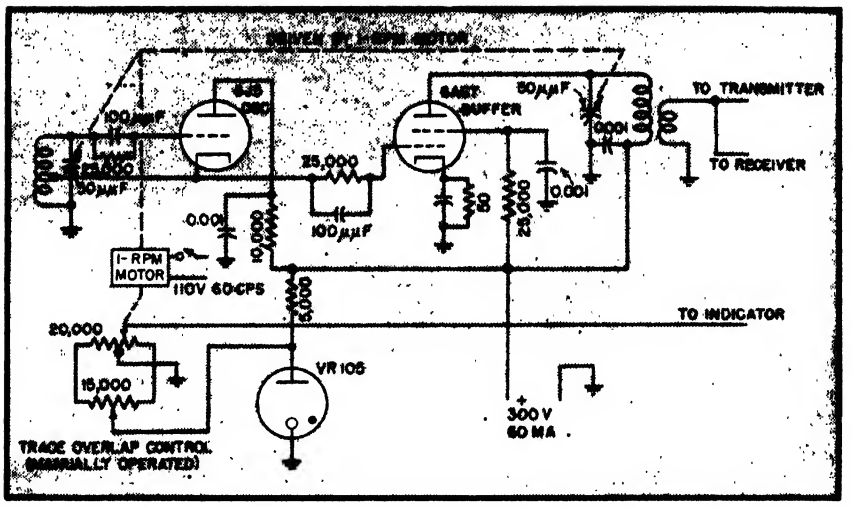

FIG. 2—Simplified schematic wiring diagram of the common oscillator

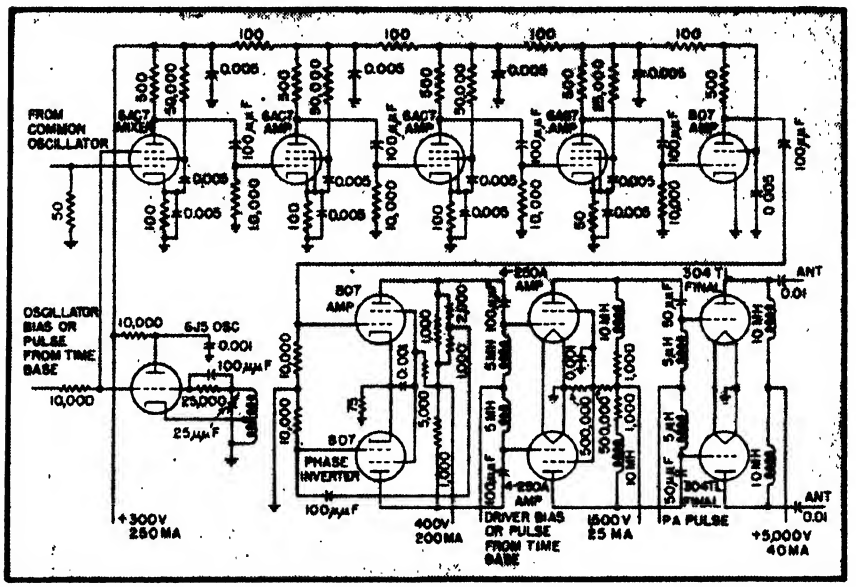

FIG. 3—Schematic circuit diagram of the wide-band pulsed transmitter

Basic Units of New System

The experimental model of the system, which will be described below, consists of five basic units; the common oscillator, transmitter, receiver, time base, and indicator. As illustrated in Fig. 2, the common oscillator uses a 6J5 tube connected in the cathode-tap Hartley circuit. Voltage from the cathode drives the buffer 6AG7 isolating the oscillator from the transmitter and receiver circuits. The oscillator and buffer capacitors are ganged and driven by a 1-rpm motor. Since these capacitors have semi-circular plates, the complete frequency range is covered in 180 degrees rotation of the capacitor shafts, which takes 30 seconds. Link coupling is used between the buffer tank circuit and the coaxial lines to the transmitter and receiver. The motor also drives a center-tapped potentiometer that is connected to develop a positive voltage. This voltage is zero when the oscillator is operating on 31 megacycles, and increases to +50 volts at 50 megacycles. It is used to drive the horizontal deflection circuits in the indicator, deflection depending on the operating frequency of the equipment. Since the tuning capacitors are always rotating in the same direction, the oscillator will pass through a given frequency once when the capacitor plates are meshing and once when they are unmeshing. It is necessary that the horizontal deflection voltage supplied to the indicator be the same for these two positions. A trace overlap control is provided to correct for errors in the location of the potentiometer center-tap.

Limitations to Rate of Frequency Sweep

With this arrangement there is a limitation to the speed in covering the frequency range—the speed with which the capacitors can be rotated. However, if the operating frequency

is changed too rapidly, it is found that by the time the echoes return to the receiver the common beating oscillator is tuned to another frequency, and the echo signals are received on the slope of the selectivity curve of the i-f amplifier, resulting in a loss of sensitivity and distortion of the received pulse. If the frequency range from 1 to 20 megacycles is covered in 30 seconds, echoes from a height of 1,000 kilometers will be detuned 4.2 kilocycles. This amount of detuning is not considered to be serious and the use of the 1 rpm appears to be satisfactory.

The transmitter, Fig. 3, begins with a pulsed Hartley oscillator, using a type 6J5 operating at 30 megacycles. The time base supplies a bias of −150 volts to the oscillator grid; this fixed bias is removed during the pulse, when the tube operates. This oscillator drives the suppressor grid of a 6AC7 mixer, the control grid of which is driven by the common oscillator. The mixer is of the plate-detector type, and operates with a 500-ohm load resistance. This low value was chosen to provide uniform gain over the band of frequencies covered by the equipment. The most important frequency appearing across this load is the difference-frequency, which varies from 1 to 20 megacycles. Since the output of the mixer is down 3 db at 15 megacycles, any sum or higher-order frequencies are of little importance. Following the mixer are two stages of amplification using 6AC7's which also have 500-ohm load resistors. Next is a 6AG7 amplifier with a 500-ohm plate resistor. This stage is slightly overdriven, the result of which is a limiting action that helps to maintain constant output. The 6AG7 drives a single 807 amplifier, with zero bias and high plate current (150 milliamperes). This tube develops 30 volts rms across 500 ohms, which is sufficient to excite the push-pull 807 stage. This stage is in effect, a phase inverter, the grid of the lower tube on the diagram being driven by the plate of the upper tube. These tubes develop 120 volts plate-to-plate, which is enough to excite the 4-250A stage, which is a pulsed class-A amplifier. Normally the time base supplies sufficient bias for plate current cutoff; when the transmitter is pulsed the bias is −10 volts and each tube draws 500 milliamperes of plate current on peaks. Continuous operation under these conditions would, of course, be out of the question because of plate dissipation and power supply limitations. The 4-250-A's drive the final amplifier, push-pull 304TL's, which have a plate supply of 5,000 volts and a normal grid bias of −1,000 volts. This is decreased to −50 volts when the transmitter pulses, and each plate draws 2.5 amperes peak current during the pulse. The load on this stage is a vertically directed rhombic antenna, which presents an average impedance of 800 ohms over the frequency range used. The power output at 1 megacycle is 7 kw peak in a 1,000-ohm load, decreasing to 1 kw at 20 megacycles.

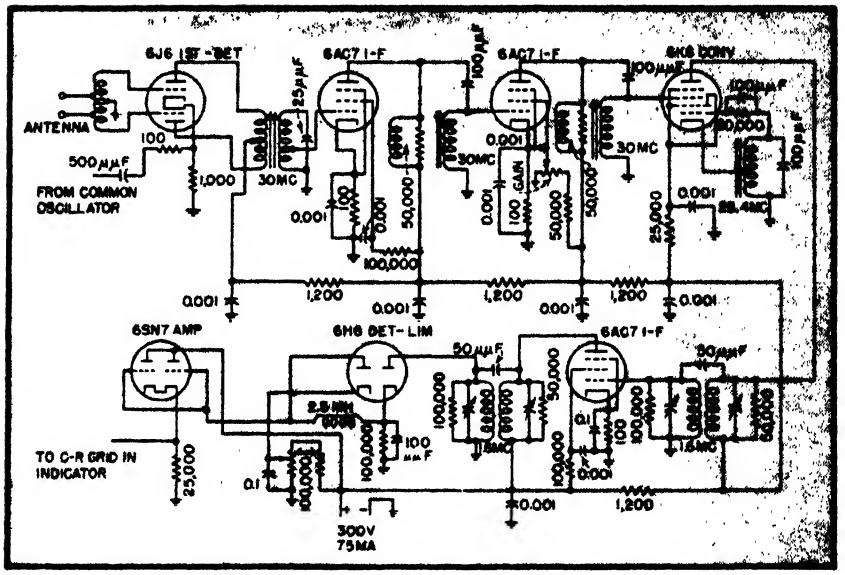

FIG. 4—Circuit diagram of the wide-band receiver used to measure the delay between the transmitted signal and that reflected from the ionosphere

Receiver Design

The receiver, Fig. 4, is a double intermediate frequency superheterodyne. The first detector uses a 6J6 operated as a balanced mixer. Voltage from the common oscillator is applied to the cathodes of this tube in parallel, while the incoming signals are applied to the grids in push-pull. The plates are also connected in push-pull, with the plate coil inductively coupled to the first i-f grid circuit. It was found that cross modulation from stations operating in the broadcast band was serious in this stage, and it was necessary to use a high-pass filter to decrease the strength of these signals. In its present form this is merely the shunt coil shown in the diagram, which also acts as a transformer to connect the receiving antenna to the mixer grids. Like the transmitter, the receiver also uses a vertically directed rhombic antenna. It was found that the sensitivity of the first receiver model was very poor below 2 megacycles. This was caused by the blocking of the first i-f stage by the common oscillator, which is near the 30-megacycle i-f when the equipment is working in this frequency range. The sensitivity was improved by increasing the selectivity of the tuned circuit in the grid of the first 30-megacycle i-f stage by tapping the grid down on the coil, as shown in the diagram. The 30-megacycle i-f amplifier consists of two stages employing 6AC7 tubes. The gain of the receiver is controlled by varying the screen voltage of the second stage. Following these is the 6K8 second converter, which changes the i-f to 1.6 megacycles. Then there is one 6AC7 i-f stage at the 1.6 megacycle frequency. Following it is a detector using one section of a 6H6, the other half of which is used as a limi-

ter. The bandwidth of the receiver is 20 kilocycles for 3 db down, while the sensitivity is better than 1 microvolt for 1-volt output over the entire frequency range.

The present experimental model receiver is not entirely satisfactory for the following reasons: low sensitivity between 1 and 2 megacycles; cross modulation between the common oscillator and harmonics of the receiver local oscillator used to convert to 1.6 megacycles (Result is many dead spots across the band. This effect could probably be eliminated by better shielding).

Time Base Generator

The functions of the time base, Fig. 5, are synchronized to the power-line frequency. Tube V_1 is a distorting amplifier, whose output is a square wave. This is differentiated and used to drive V_2, a conventional trigger circuit. The plate voltage of V_{2a} is a positive pulse whose duration can be easily controlled. In this equipment it is 3,300 or 6,600 microseconds long, depending on whether the range switch is set at 500 or 1,000 kilometers. This pulse drives an inverting amplifier, V_{3a}, which operates the sweep generator and height-marker generator. The output of the sweep generator is a sawtooth wave, which gives a linear sweep in the indicator. The height-marker generator contains a switch tube, a negative-resistance oscillator, a squarer, and an amplifier. The oscillator, V_5, is of the negative-resistance type, with cathode coupling. This is switched on by means of a cathode follower, V_{6a}. The sine wave from the oscillator is squared by V_{6b} and V_{7A}. The square wave is differentiated and applied to the grid of V_{7B}, an amplifier whose output is a series of positive pulses, one for each cycle from the oscillator. These are applied to the grid of the cathode-ray tube in the indicator, producing lines at the proper intervals. Since 100-kilometer markers were desired, the total distance the waves will travel between markers will be 200 kilometers, corresponding to a time of 200/300,000 or 1/1,500 second. The oscillator frequency was therefore set at 1,500 cycles.

The trigger tube, V_{2A}, also drives the gate amplifier, V_{8A}, whose output is a negative pulse. This is applied to the cathode of the cathode-ray tube, increasing its intensity during the sweep.

The transmitter pulsing circuit uses the so-called bootstrap amplifier, used in the modulators of some of the early loran and radar transmitters. The 60-cycle square wave from the plate of V_{1B} is differentiated and used to drive the grid of V_8, an amplifier, with an output of positive pulses. These are passed through V_9, a diode, to the grid of V_{10}, a thyratron. This tube effectively connects a charged artificial transmission line across a load resistance. The discharge of the line is in the form of a positive rectangular pulse, whose duration depends on the constants of the line. The pulse is applied between the control grid and cathode of V_{11},

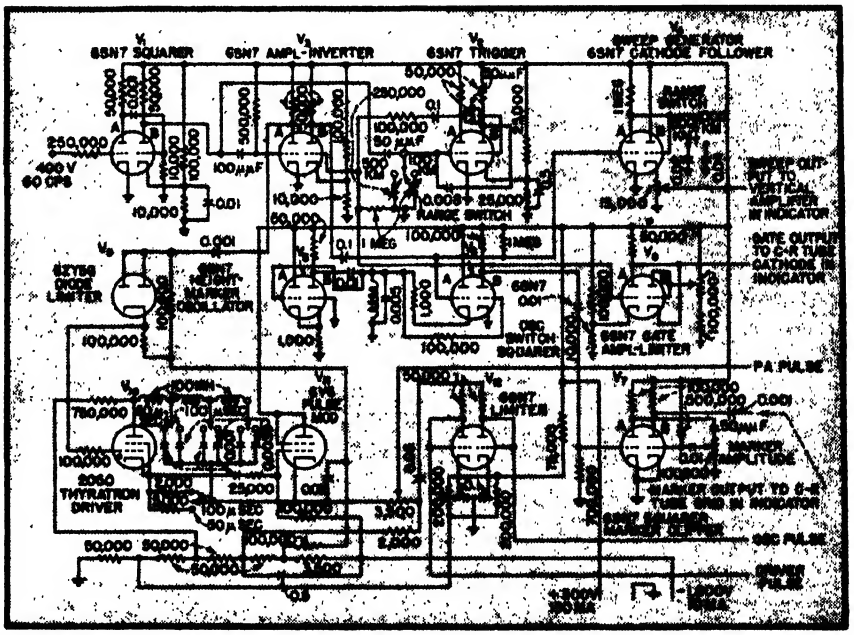

FIG. 5—Timing circuits used to trigger the transmitter and provide time marks

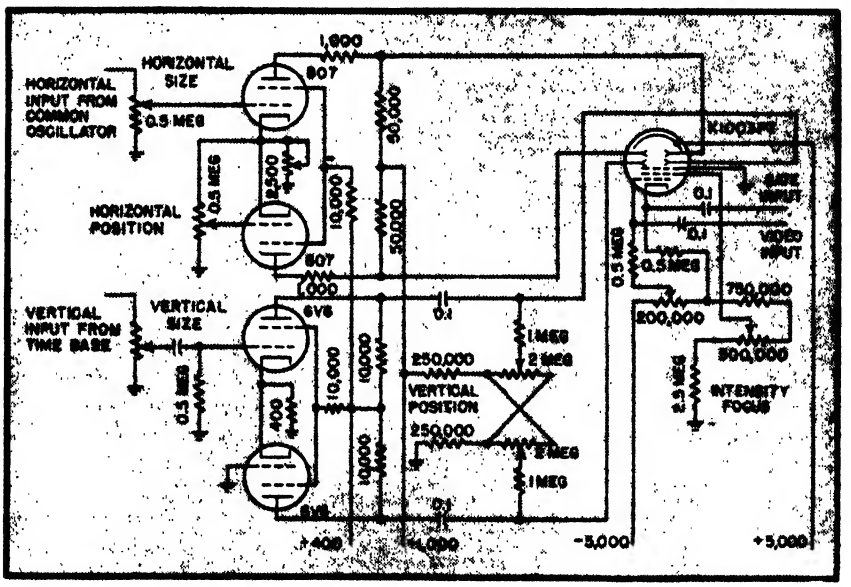

FIG. 6—Simplified schematic diagram showing the signal inputs to the plates of the cathode-ray tube indicator used to display the ionosphere characteristic information

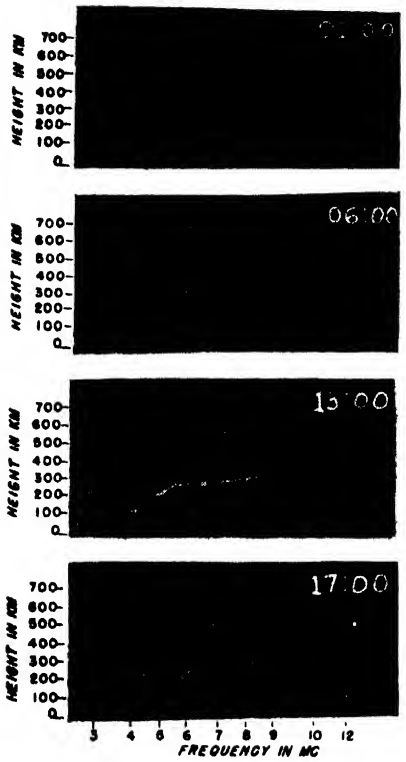

FIG. 7—Photographs of cathode-ray tube patterns obtained with the ionosphere measuring equipment. Layer heights are plotted vertically and frequency horizontally

the modulation tube, which has its load resistance in its cathode circuit. The output is a positive pulse of 1,000 volts amplitude, which is used to pulse the power amplifier. The modulator might at first appear to be a cathode follower; there is, however, no degenerative action, since cathode voltage is not subtracted from the driving voltage. The thyratron, with its associated circuits, follows the cathode potential of the modulator hence the name bootstrap. There are two other pulse outputs, obtained from a tap on the modulator load. The amplitudes of these pulses are controlled by the two halves of V_{12}, which are connected as diode limiters. One of these pulses operates the 30 megacycle oscillator in the transmitter, while the other controls the 4-250-A stage.

When the cathode of the modulator goes positive, the cathode and plate of the thyratron also go positive. If the grid of the thyratron were connected directly to the pulse circuits of V_{11}, it would remain negative for a time, and would be bombarded by positive ions. The combination of the diode V_8, and various decoupling resistors allows the grid to go positive also, preventing this bombardment.

The indicator, Fig. 6, uses a K1003P7 12-inch cathode-ray tube, with a total accelerating voltage of 10,000. Video signals from the receiver and height markers from the time base are applied to its grid with positive polarity. The cathode-ray tube is gated by means of negative pulses applied to its cathode. The vertical deflection amplifier, which is driven by voltage from the potentiometer in the common oscillator unit, uses a pair of 807's in push-pull. It was necessary to use direct coupling between these tubes and the horizontal deflection plates because of the low sweep frequency used (1/30-second). Positioning is obtained by varying a positive bias on the control grid of one of the 807's; this system is similar to that used in some DuMont oscilloscopes. The vertical deflection amplifier, which uses 6V6's, is driven by the sweep output of the time base. Positioning is obtained in this case by the usual dual potentiometer.

Recording Ionosphere Characteristics

The record now obtained in ionosphere sounding usually takes the form of an *h'-f* curve, in which the vertical heights *h'* are plotted as a function of frequency *f*. These data are normally recorded on film or paper. In the new equipment permanent records have not been made automatically, although there is under development a system for doing this. The *h'-f* curve appears on the screen of a long-persistence cathode-ray tube. The vertical sweeps take place every 1/60-second, and have durations of 3,300 or 6,600 microseconds, to give full-scale virtual heights of 500 or 1,000 kilometers. The vertical sweep line is moved across the face of the tube as the frequency changes, giving a two-dimensional record. Although automatic photographic recording has not yet been provided, it is possible to take time-exposure photographs of the runs, a few of which are included in Fig. 7. The height markers appear as horizontal lines, while the frequency markers are dots along the bottom of the record.

The record marked 13:00 shows the layers that usually appear during the day. Proceeding from left to right, the E-layer starts at 3 megacycles and extends slightly past 4. The increase in height from 100 kilometer to 140 indicates an E critical frequency. Immediately above this the F_1 layer starts at a height of 220 kilometers. The height decreases slightly as the frequency is raised, and then increases to 260 kilometers at 5 megacycles; this is the F_1 critical frequency. From here on the record shows F_2 layer which splits at 7.5 megacycles because of the earth's magnetic field. There are two critical frequencies associated with this, the ordinary at 8.5 megacycles and the extraordinary at 9.2 megacycles. The F_1 layer is frequently split, but that does not appear on this record. A multiple reflection may be seen above the F_1 and F_2 regions. In this case the down-coming echo has been reflected by the earth and makes one more trip up and down. The vertical lines are interference from stations in the operating range of the equipment.

The writer wishes to acknowledge the cooperation of the Department of Terrestrial Magnetism, Carnegie Institution of Washington, whose facilities were used in the construction and testing of the equipment.

References

(1) Breit, G., and Tuve, M., A Test for the Existence of the Conducting Layer, *Physical Review*, Sept. 1926.
(2) Gilliland, T. R., Field Equipment for Ionospheric Measurements, *Journal of Research, National Bureau of Standards*, May 1941.
(3) "Technical Description and Operating Instructions for Radio Equipment Type 249 (To NPL Design)", Baddow Research Laboratories, West Hanningfield Road, Great Baddow, Chelmsford, Essex, England.
(4) Szikiai, G. C., and Schroeder, A. C., Cathode-Coupled Wide-Band Amplifiers, *Proc. IRE*, p 701, Oct. 1945.

Ionosphere Equipment for Field Use

A simplified technique for pulsed ionosphere measurements uses unattended recording equipment. The receiver is remotely located from the variable-frequency transmitter but automatically follows frequency excursions throughout the signal spectrum

By GLENN H. MUSSELMAN

IN INVESTIGATIONS of the ionosphere the relationship between the E-layer critical frequency and time, during a solar eclipse, is of fundamental importance. The radiation received from the sun decreases and then returns to normal in a cycle that consumes a few hours, at the most, compared with the period of the normal day-and-night cycle. Comparison of eclipse observations with data taken on normal days yields information that aids materially in understanding the behavior of the ionized regions above the earth's surface.

The partial solar eclipse of November 23, 1946, was observed in the Boston area about noontime. On a normal day there is a flat maximum of the E-layer critical frequency at about local noon; this eclipse, therefore, promised to show a dip in an otherwise relatively flat curve as illustrated. The dip results from reception of decreased solar radiation,[1] and the magnitude and shape of the curve are related to the variation of the exposed area of the sun during the eclipse period. The critical frequency in this case dropped from about 3.4 mc to 2.8 mc, which is commensurate with a 50-percent eclipse taking place at noon.

Ionosphere Measurement Systems

As there is no known method of postponing an eclipse, limited time was available for the design and construction of a complete working system, and some of the more elaborate and involved equipment arrangements were avoided in favor of simpler gear capable of obtaining the necessary data with reasonable accuracy.

One possible arrangement is to place the transmitter beside the receiver with the controls located so that both units are hand-turned by an experienced operator. This probably represents the simplest design, but requires a skillful and patient manipulator, if not a crew of them, for any extended operation. A second system is one in

Circuit diagram of the receiver used in ionosphere measurement work and described in detail in the text

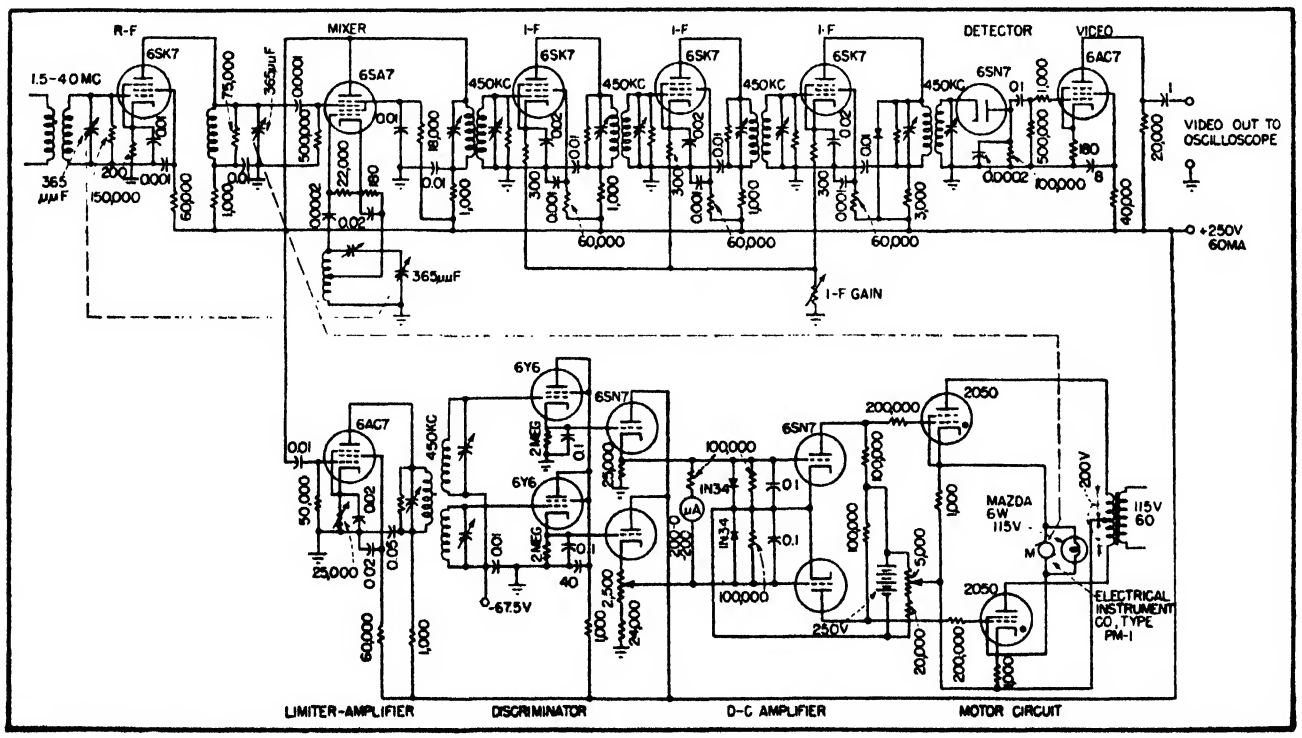

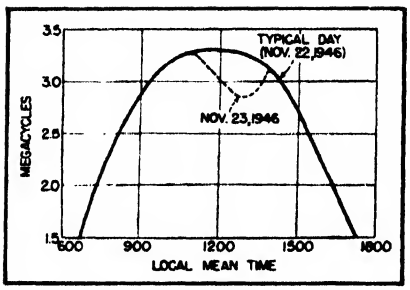

FIG. 1—Variation of E-layer critical frequency with time

which both the transmitter and receiver are individually driven by synchronous motors operating from a common power main. This is used widely in present day sweep-frequency gear and is exceedingly reliable. The disadvantage is that the tuning characteristics of the two units must be carefully tailored to match throughout the entire frequency range.

Probably the most modern, integrated design is one in which a common motor-driven tuned oscillator, in conjunction with heterodyning, serves to control both transmitter and receiver frequencies.[2] Good results are obtained by this method but the complexity is justified only where a wide frequency range is mandatory, and if the equipment is intended for continuous operation over a long period.

Field Requirements

The equipment requirements for eclipse observations are as follows:

(1) Since all of the activity centers around the receiver and recording equipment, it is desirable to locate the transmitter with its high-voltage circuits apart from these. Some separation between the transmitting and receiving antennas is also desirable to reduce the amplitude of the ground wave, or main bang, in the receiver. Unless specially gated attenuator circuits are contained in the receiver, operation of the two units in the same room results in terrific receiver overloading.

(2) The receiver should be substantially automatic in its tuning, leaving the operating personnel free to develop the records and plot the data as secured.

(3) The entire equipment should be simple so as to reduce construction time, and so that it may be easily set up at any distant point.

Transmitting Equipment

The transmitter consists of a pulsed variable-frequency power oscillator of about 10-kw peak power, coupled into a long-wire resistance-terminated horizontal antenna. The primary features of this antenna are that it will radiate some power over the frequency range used, and that the input impedance characteristics are such that the antenna does not materially influence the oscillator frequency. The frequency range is 1.5 to 4.0 mc. The transmitter sweeps continuously between these two limits, requiring four minutes for the complete cycle. The emitted pulses rise in 30 microseconds, are about one hundred microseconds long, and are spaced one-tenth of a second apart.

Recording the Signals

The recording equipment was installed in another building about a half-mile away, and comprised servosweep circuits, an oscilloscope fitted with a continuously recording camera, and the sweep-frequency receiver described below. The trace of the scope is horizontal and is intensity-modulated by the video output of the receiver, combined with height markers.

The sweep-frequency receiver uses a folded doublet half-wave horizontal antenna cut for 2.9 mc and fed with a 300-ohm twin lead transmission line. The tube lineup consists of a 6SK7 r-f amplifier, a 6SA7 mixer, three 6SK7 broadband i-f amplifier stages, a 6SN7 diode detector and a 6AC7 video amplifier. The r-f, mixer, and oscillator circuits are tuned by a three-gang 365 $\mu\mu$f-per-section tuning capacitor. The shaft of this capacitor carries an 8-inch diameter aluminum disk dial. The edge of the disk is grooved for a dial drive cord, and the face is covered with cardboard, suitably marked with a frequency calibration. Slots are cut in the cardboard so that an electrical contact can complete a relay circuit, thus providing frequency marks on the record as the receiver tunes.

Circuit Analysis

The r-f and mixer stage gain is fixed as indicated in Fig. 2. The i-f stage gain is adjusted by a resistor common to the cathodes. The total bandwidth of the i-f section is about 40 kc at the half-power points. The overall bandwidth is less than this due to the selectivity of the r-f and mixer circuits, and consequently varies with frequency. If the r-f and mixer circuits are damped heavily, the overall bandwidth approaches that of the i-f alone, but this is accompanied by a degradation of the desired signal-to-image response ratio. Corresponding to the selectivity curves shown, the image response is down 54 db when the receiver is tuned for a desired signal of 2.0 mc, and 32 db when tuned for 4.0 mc. The overall gain against frequency is essentially constant as shown in Fig. 3.

The output of the mixer stage, besides feeding the i-f channel, also feeds a 6AC7 limiter-amplifier tube which in turn excites a three-coil frequency discriminator. The peaks of the discriminator are spaced about 15 kc above and below the center i-f. The usual diode detectors are replaced by 6Y6 tubes connected as so-called infinite impedance detectors. In order to realize a satisfactory average rectified volt-

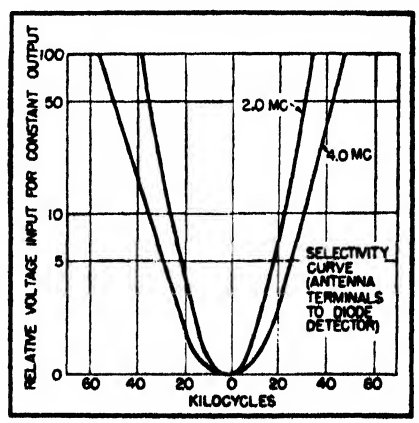

FIG. 2—Overall bandwidth of receiver

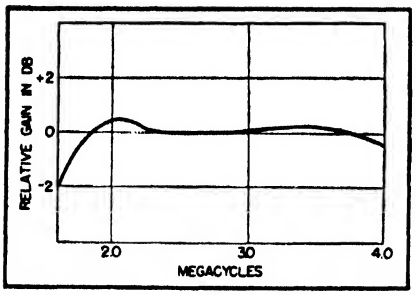

FIG. 3—Receiver gain as a function of desired frequency

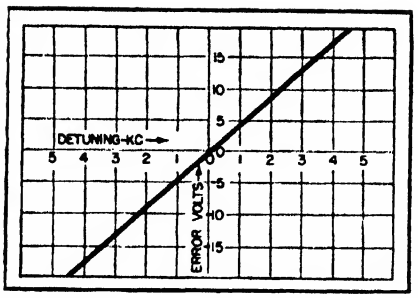

FIG. 4—Discriminator output characteristics with 100-microvolt signal at antenna

age across the detector loads, it is necessary to employ a time constant in excess of the recurrence interval of the r-f pulses. A conflicting requirement is that if the load voltage is to be able to follow the variations in amplitude of successive pulses, a small time constant is indicated. The design was compromised at 0.2 seconds with a 2.0-megohm resistor and 0.1μf capacitor. If the leakage resistance were no problem a higher impedance circuit with the same time constant—say, 20 megohms and 0.01 μf—would require less charging current from the tube for the same voltage output. A 6SN7 tube connected as a pair of cathode followers is used as an isolation stage. Across these latter cathodes is connected a zero-center voltmeter that serves as a tuning indicator. The voltmeter reads zero when the receiver is properly tuned so that the pulses fall in the center of the i-f pass band. The magnitude and polarity of the voltage are proportional to detuning over a range of about 10 kc either side of the center frequency as shown in (Fig. 4).

In order to suppress the effects of varying signal strength (resulting from changes in radiated power from the transmitter and varying antenna efficiencies at both receiver and transmitter as a function of the frequency) it is desirable to provide limiting in the 6AC7 tube. This same limiting, of course, tends to remove the selectivity effects of the front-end circuits to a certain extent. A rather subtle disadvantage of limiting is that since the desired r-f pulses are short compared to the recurrence interval (100 μsec compared to 100,000 μsec) continuous carrier signals of much smaller amplitude can produce equivalent discriminator action during the long interval between pulses. In other words, with a given desired pulse voltage at the antenna terminals, the more limiting, the more sensitive the discriminator is to weak, undesired, continuous-wave signals. The relationship between antenna terminal voltage and the voltage at the plate of the limiter amplifier is shown in Fig. 5. The received ground-wave pulses average about 100 millivolts, so that there is sufficient limiting to take care of changes in signal strength of 2 to 1 or 3 to 1. There is another factor that tends to favor the c-w signals. The detector load capacitors charge up to produce an average d-c voltage which more nearly approaches the peak value of the signal voltage when that signal voltage is continuous rather than pulsed.

Automatic Tuner

The difference voltage caused by detuning, hereafter called error voltage, is amplified by a 6SN7 d-c amplifier. The plates of this tube are connected to the normally biased-off grids of two type 2050 thyratron tubes. The thyratrons are connected with a power transformer and a small motor in a bridge circuit. The motor has a permanent-magnet field so that the direction of rotation of the armature depends on the polarity of the voltage applied to it. If either grid of the 6SN7 is made negative with respect to the cathode, the appropriate thyratron grid goes positive and plate current flows through the motor armature. The motor will, of course, rotate in the opposite direction when a negative voltage is applied instead to the opposite 6SN7 grid. Having one 6SN7 grid go positive is undesirable, so two 1N34 diodes are arranged to convert the entire error voltage into a negative component appearing at one 6SN7 grid only. It will be seen that the diodes force the 6SN7 cathode reference potential to follow whichever grid is more positive with respect to ground. This feature doubles the sensitivity of the servo amplifier.

Figure 6 shows the motor speed as a function of error voltage. The flat spot in the center of the characteristic is deliberate, and can be varied by adjustment of the thy-

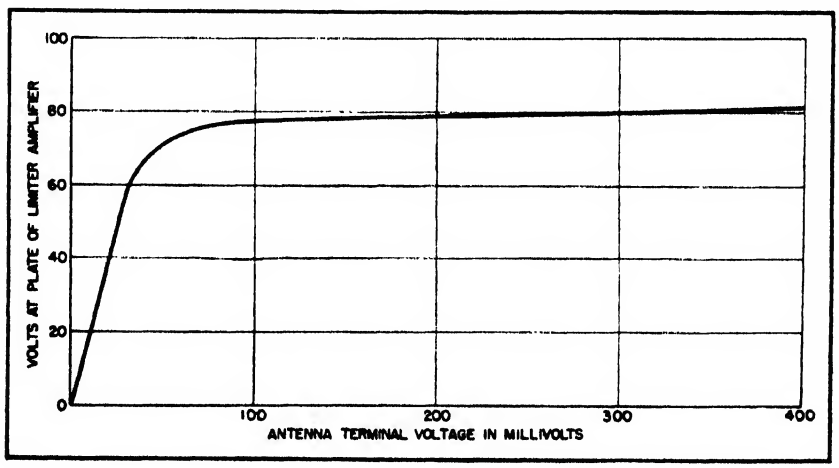

FIG. 5—Linearity characteristics from antenna terminals to discriminator input

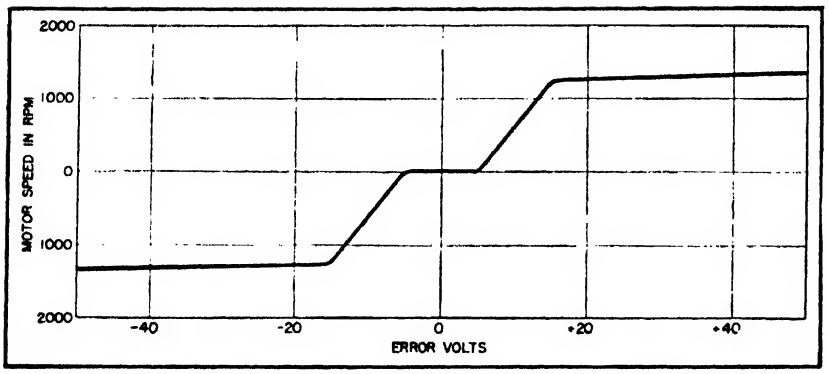

FIG. 8—Motor speed as a function of error voltage applied to d-c amplifier

ratron grid bias. A nonlinear resistance in the form of a 6-watt 125-volt lamp is connected across the motor armature and this, in conjunction with the flat spot, practically eliminates hunting. When the error voltage decreases to about 5 volts, the voltage applied to the armature approaches zero, the lamp filament cools, and its resistance decreases. The low resistance dissipates the power generated by the coasting armature, thereby acting as a brake and preventing overshoot.

The motor drives an 80-to-1 worm gear reduction box terminating in a ¾-inch diameter pulley. This pulley cord drives the main tuning dial.

When the pulse signals are properly tuned in with appropriate adjustments, the motor-driven tuning follows the transmitter frequency faithfully. Since the ground wave from the pulse transmitter is at least 100 times greater than the strongest reflection (this statement concerns the arrangement described and would not hold true for a greater separation between transmitter and receiver), discriminator action, and consequently receiver tuning, tracks on the ground wave only.

Observation of the tuning meter indicated that the receiver tuning was generally within 2 kc of the transmitter frequency. The shape of the reflections as observed on a monitor scope indicated that this amount of detuning was in no way detrimental.

It must be remembered that the receiver as described needs to be located so close to the transmitting antenna that the ground-wave signals greatly override all noise bursts and signals from other sources.

In order to make the receiver less sensitive to general channel interference, the limiter-amplifier circuit might be gated so as to be operative only for a period of a few hundred microseconds at the time of each ground-wave pulse. Synchronization with the transmitter timing would then be required, but this could be obtained readily from the oscilloscope sweep circuit. An improvement along this line would allow greater separation between transmitter and receiver. The attendant advantage is that the ground wave would be greatly reduced in amplitude, possibly to the extent that it would be comparable to the E-layer reflection. Loran pulse-matching technique demonstrates the improved measuring accuracy obtainable when pulse amplitudes are equalized. It is reasonable to expect that in the future some adaptation of this technique will find its way into ionosphere sounding equipment.

References

(1) Harang, L., Radio-Echo Observations at Tromsö during the Solar Eclipse on July 9, 1945, *Terr. Mag. and Atmos. Elec.*, **50**, No. 4, 1945.

(2) Sulzer, P. G., Ionosphere Measuring Equipment, ELECTRONICS, p 137, July 1946.

Recording Sky-Wave Signals

Description of monitoring station set up by Canadian government to investigate sky-wave interference occurring when two or more broadcast stations share the same channel. Signal strength of a station is recorded on strip chart for several hours, and photoelectric scanner then determines percent of time signal exceeds any selected value

By WILBERT B. SMITH

A GOOD DEAL of the energy radiated from standard-band broadcasting stations is reflected from the ionosphere and returns to earth at a distance from the station. This phenomenon is an advantage in the case of clear-channel stations since it augments the coverage, but where channels are shared by two or more stations in the same region it may produce interference which seriously limits the coverage otherwise obtainable.

In the broadcast allocation structure, due cognizance must be taken of the effects of sky-wave signals. Ground-wave propagation is calculated from verified theoretical

curves, but because of the many indeterminable factors involved in sky-wave propagation, no corresponding curves exist, and calculations must be made from entirely empirical curves. These curves are plotted from measured data on the sky-wave signal intensities of distant stations over an extended period, and are based on the signal exceeded for certain percentages of time.

Early curves took no separate account of variations due to latitude, or between north-south and east-west propagation, or of ionospheric focusing, but assumed an average propagation characteristic for all sky-wave signals. The early curves are the ones which have been in use up to the present time, under the North American Regional Broadcasting Agreement, Havana, 1937.

The Modus Vivendi, Washington, 1946, which extends the above-mentioned agreement, recognized the need for more up-to-date information on which to base new technical standards to be drafted in 1948, and charged the signatory countries with making the necessary studies towards this end. A program of sky-wave recording was therefore drafted by the Canadian authorities to determine the propagation characteristics of sky-wave signals in Canadian latitudes.

Sky-Wave Recording Technique

Equipment for the recording of sky-wave signals must be accurate and stable, yet simple enough to be used in outlying stations. It must produce records which are readily analysed in terms of the absolute field intensity of the radio wave, in microvolts per meter.

The essential components of field-intensity recording equipment are the radio receiver and antenna, comparison standard signal generator or other calibration means, and the graphical recorder.

In the system as finally developed by the author for the Canadian recording program, the incoming signal is received on a National HRO receiver which has been peaked for maximum i-f response, and from which the avc voltage is fed to a vacuum-tube amplifier which drives a 5-ma graphical recorder. In series with the graphical recorder is a device which periodically returns the recorder pen to zero so as to blank in the area between the curve and zero to facilitate analysis of the graphs. The incoming signal as delivered by the antenna is compared with the output of a standard signal generator for calibration of receiver output. The antenna itself is calibrated by comparison with a field-strength meter of known accuracy.

Analysis of the charts is accomplished by means of an electronic scanner, in which a spot of light rapidly traverses the chart along the time scale. The reflected light operates, through a phototube and amplifier, an electronic gate which permits current to flow through a meter calibrated directly in percentage only during the periods when the spot is on the blanked-in portion of the chart. In this manner the scanner integrates the time during which a particular value of signal was exceeded. Suitable scales used in conjunction with calibration marks placed on the charts permit direct determination of the field intensity exceeded for any specified percentage of time.

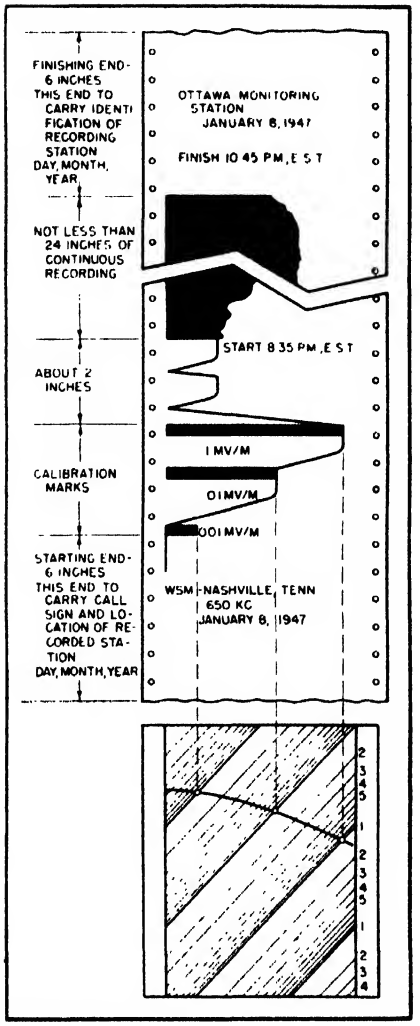

Format followed in recording signal strength of broadcast station on strip chart, and (below chart) method of obtaining calibration curve used in connection with electronic scanner

Signal Generator

The circuit diagram of the standard signal generator is shown in Fig. 1. It is a straightforward design, the only unique features being the shielding, the use of a coupling tube between the r-f sources and the receiver, and the vacuum-tube voltmeter circuit.

Effective shielding is achieved by locating the oscillator and the circuits associated with it in individual cast aluminum boxes which are insulated from ground, connected together in sequence at one point only, and grounded to the main chassis at one point only. Circuits entering the boxes are individually filtered by means of chokes and capacitors, and control shafts entering the boxes are broken with insulated couplings. Circuits within the box are grounded at one point only, near where the r-f voltages are finally delivered.

Under the provisions of present international agreements the lowest sky-wave field which has any significance is 25 microvolts per meter, so there is little advantage in making studies on field intensities much less than this. Therefore the signal generator was designed to deliver calibrated r-f voltages only down to 10 microvolts, which with the usual broadcast type of antenna permits accurate recording of fields as low as 5 microvolts per meter.

In order to simplify operation and minimize effects of antenna va-

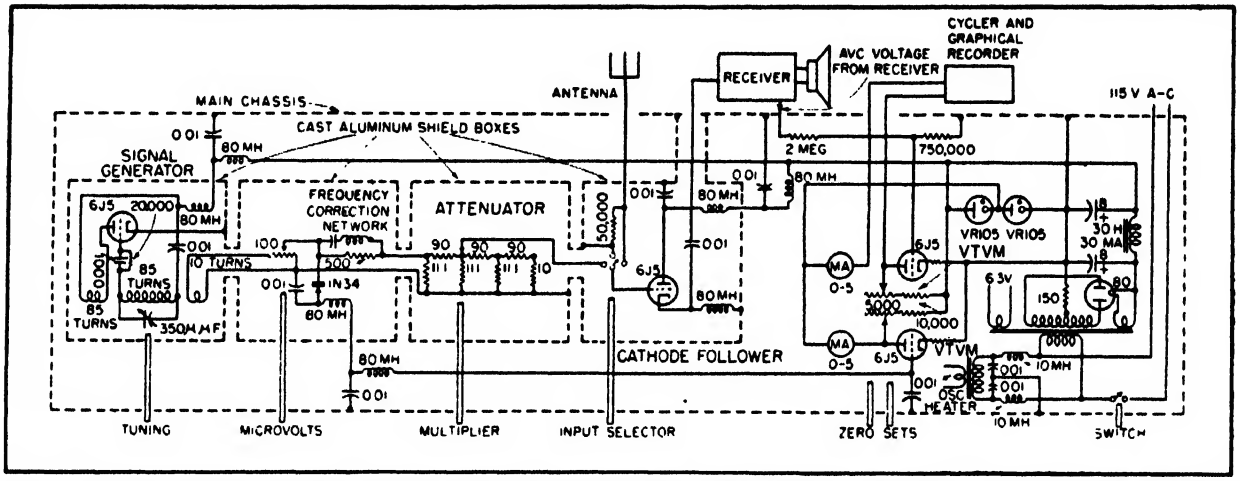

FIG. 1—Circuit of signal generator used for calibration in connection with recording of sky-wave signals, showing elaborate shielding technique employed and relationship to other units of recording system

riations, a cathode-follower coupling tube is included in the circuit between the r-f sources and the receiver input, with a switch to change the input from antenna to signal generator for calibrations. Since this tube is in the circuit for both calibration and recorded signals, it is in effect part of the receiver and is calibrated with it. It does not introduce spurious effects unless subjected to r-f signal intensities of the order of 2 volts, which may drive the tube beyond its range of linearity. Localities where high signal strength exists are avoided in selecting a site for the recording equipment.

Two similar vacuum-tube voltmeters are provided, one for measuring the r-f voltage applied to the attenuator, and the other for operating the graphic recorder from the received avc voltage. They consist of triodes with the indicating meters bridged between their plates and the midpoint of two voltage regulators in series. The tubes are operated under conditions of no input voltage with about 0.8 volt bias, obtained from a cathode resistor. The plate resistances are varied for zero reading on the respective meters, as zero-sets. For any negative voltage applied to the triode grid, the plate current will decrease a proportionate amount over the corresponding portion of the tube characteristic, which in the case of the 6J5 triodes is quite linear. The change in plate current will result in the difference current flowing through the meter, giving after calibration the measure of the applied voltage.

Provides Protection

This circuit was selected to utilize the negative avc voltage from the receiver, and to provide protection against accidental overload of the meters or recorder from excessive input voltage. Excessive input voltage can only drive the triode to cutoff, when the meter will be called upon to carry not more than the normal plate current of the triode, which is approximately 8 ma and not dangerous for a 5-ma meter.

The vacuum-tube voltmeter which reads the r-f voltage applied to the attenuator obtains its grid voltage from a germanium crystal rectifier. No return resistance path is provided for this rectified voltage as the germanium rectifier itself has a sufficiently low resistance in the reverse direction to permit the grid charge to leak off. Since the voltage applied to the tube grid is very nearly equal to the peak value of the r-f voltage applied to the attenuator, the original calibration of the signal generator can be against a standard cell, although comparison against a laboratory standard signal generator may be more convenient.

The second vacuum-tube voltmeter obtains its grid voltage from potential-dividing resistances across the avc circuit of the receiver. The values of these resistances are such as to bring the range of the meter onto the portion of the receiver gain characteristic which

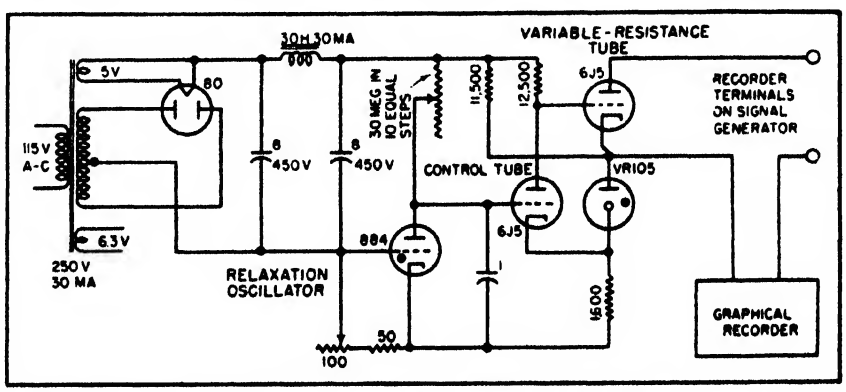

FIG. 2—Cycler circuit for sweeping pen of recorder periodically back to zero, to black in entire area between signal strength curve and zero. Rate of sweep may be varied from once per second to once every 5 seconds by adjusting 30-megohm resistor

is most nearly logarithmic. It is therefore possible to get better than two complete ranges, or a ratio of 100:1 within the scale of 0-5 ma, using a National HRO receiver.

The circuit for blanking in the area on the chart between the curve and the zero for analysis by means of an electronic scanner is shown in Fig. 2. Electrically it consists of a small resistance in series with the graphical recorder, which resistance remains constant for about four-fifths of the cycle, and then increases to infinity over the remaining fifth, after which it suddenly returns to its previous value and the cycle starts over again.

The resistance which performs in this unusual manner is the plate resistance of a 6J5 triode, the grid of which is held about 4 volts positive for the first four-fifths of the cycle. Under these conditions the tube shows a linear plate resistance characteristic of about 300 ohms for currents as high as 8 ma.

The grid of the output or variable-resistance tube is connected to the plate of another 6J5 triode which acts as a control tube to translate the voltage developed by the relaxation oscillator into an increasing bias. Since the control tube is biased well beyond cutoff for four-fifths of the cycle developed by the relaxation oscillator, it does not come into action until the last fifth of the cycle. It then diverts the current previously flowing through the grid circuit of the output tube, permitting the bias of that element to increase to cutoff.

The relaxation oscillator is conventional, being a capacitor charged through a high resistance and discharged through a type 884 thyratron. By using a tapped 30-megohm resistance and a 1-μf oil-filled paper capacitor, good stability was obtained with periods from 1 to 5 seconds long.

For chart speeds of 1 foot per hour the 5-second period is required, but for faster speeds a correspondingly faster rate applies.

An Evershed-Vignoles graphical recorder with 5-ma range and clockwork drive is used. This instrument is fitted with an oil dashpot so that control can be had over damping, which is important for the cyclic operation to which the instrument must respond. Wrinkling of paper was overcome by using No-Rinkle ink and Albanene paper produced by Keuffel & Esser. The combination of a red ink and a blue-sensitive phototube in the electronic scanner was found to give best results.

A substantial part of the information to be gleaned from the chart is statistical and involves the determination of the signal exceeded for certain percentages of time, during certain periods relative to sunset. Heretofore, the method of analysis has been to step off with dividers and scales the time increments corresponding to certain signal intensities, replot the values so obtained and from the resultant curve read off the required information of the signal exceeded for certain percentages of time. Needless to say, this manual method is tedious and inefficient, and opens wide the door to personal error which it is almost impossible to check. Fortunately, however, when a great deal of data is so analyzed most of the errors balance out in the subsequent statistical mathematical treatment, but there still remains the tedious labor of the manual analysis.

The electronic scanner was developed for the dual purpose of speeding up analysis and eliminating largely the personal error. Due to the shortness of time during which the Canadian program could operate before the data would be required for the production of propagation curves, speed and accuracy of analysis were essential.

The circuit of the scanner is shown in Fig. 3. The chart to be scanned is wound around the scanning drum, which will accommodate 24 inches of chart for each operation. The lamp-house contains a carriage which slides along ways under the control of a crank on the front of the lamp-house. Mounted on this carriage is a light source consisting of a 32-candlepower automobile lamp, condenser lens, diaphragm with a 1-mil aperture, and

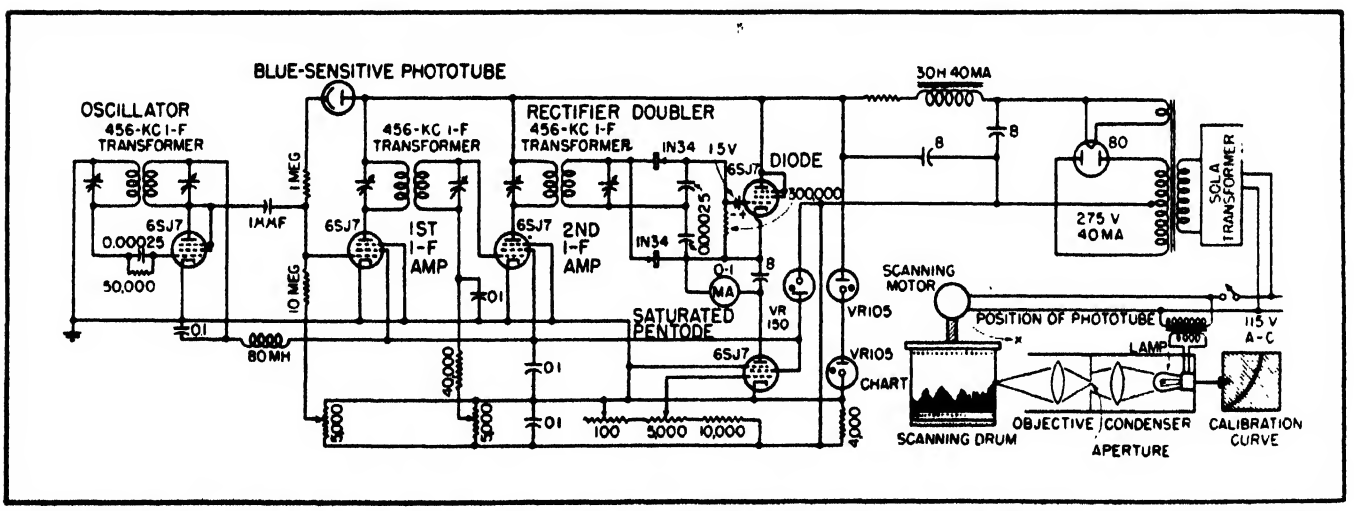

FIG. 3—Circuit of electronic scanner used for analysis of charts. Arrangement of optical system is shown at lower right; phototube is mounted on carriage along with lenses and lamp, and picks up light reflected from spot on chart

an objective lens which focuses the image of the aperture as a small spot of light on the chart undergoing analysis. Also mounted on the carriage is a phototube so arranged as to pick up diffused reflected light from the spot on the chart. The top of the lamp-house carries a special logarithmic graph under roughened plastic to take pencil lines. Crossing the chart is a pointer which is connected to the carriage and arranged to track with the position of the spot of light. The near side of the pointer acts as a straight edge to place the calibration lines on the graph, and to read off the values of signal exceeded.

The electronic section consists of an amplifier responsive to the standard i-f value of 456 kc but normally biased slightly beyond cutoff. This amplifier is supplied with 456-kc excitation from an oscillator through a small capacitor, but does not come into action until the bias on its first stage is reduced by illumination of the phototube. The output of the amplifier is rectified by two germanium rectifiers in a doubler circuit, and applied to the grid of a triode-connected 6SJ7, which is in series with a 6SJ7 saturation pentode and the percentage-of-time meter.

When the phototube is not illuminated there is no appreciable output from the amplifier and the grid of the triode is maintained at zero potential by a flashlight battery, permitting the full saturation current of 1 ma to flow through the saturation pentode and give a full-scale reading on the percentage-of-time meter. This condition corresponds to the scanning of a completely inked-in portion of a chart undergoing analysis.

When the phototube is illuminated the amplifier comes into action and produces at the output of the germanium rectifier 50 volts or more, which produces immediate cutoff of the triode. For the period when this condition prevails no current flows through the percentage-of-time meter. This corresponds to the scanning of a blank portion of the chart.

Since the percentage-of-time meter is of the uniform scale type, it will read the average current flowing through it, provided the cycle is fast enough to prevent the meter movement from following the individual fluctuations. Hence it follows that in the scanning operation the meter will read directly the percentage of time during which the phototube has not been illuminated, which is the percentage of time a certain signal strength has been exceeded.

The instrument can be made unresponsive to residual room illumination by judicious adjustment of the amplifier bias controls, so that no special precautions are necessary in regard to room lighting. A Sola constant-voltage transformer supplies the electronic circuits. This transformer combined with the voltage regulators used to obtain the various internal voltages gives maximum stability and the instrument can be easily read to an accuracy within 1 percent.

The image of the aperture in the diaphragm on the chart being scanned is about 0.03 inch in diameter, which is about the width of the line traced by the pen on the graphical recorder. Consequently, the scanner can resolve and analyse any record normally taken by the recorder. The accuracy with which the percentage-of-time meter and the calibration on the graph can be read is about 2 percent.

In using the scanner, the chart to be analysed is first placed on the drum with the zero side to the front and with the calibration marks showing on the outside. The pointer is then wound successively to the top of each calibration mark and a short pencil line drawn along the straight-edge intersecting an appropriate unit line on the graph. These points are then joined up by a smooth curve which provides the scale from which signal intensities pertaining to that particular chart are read. The curve so plotted is in reality the received signal versus avc voltage curve, and consequently provides the means for reading directly in microvolts per meter the field intensity from the recorded values of the resultant avc voltage. A new curve is drawn for each chart analysed.

After the calibration curve is established, the chart is moved around the drum until the portion of which the analysis is desired is on the outside and visible to the scanning spot. The drum is then started rotating and the percentage-of-time meter checked for zero and full scale. The scanning spot with its attendant pointer is then wound across the chart until the meter reads the desired percentage of time, when the corresponding field intensity can be read off directly from the intersection of the straight edge of the pointer.

Measurement of VHF Bursts

Sudden increases in strength of signals received beyond line-of-sight range are believed due to meteors passing through upper atmosphere. Pulse techniques gave path lengths

CONTINUOUS recordings of signal strength of selected f-m and television stations, made at distance ranging from 100 to 1400 miles, have at times revealed unexpectedly strong signals that could not be attributed to reflections from aircraft or to undulating tropospheric discontinuities. These sig-

Typical signal strength recording, showing two distinct examples of bursts. This record was obtained at Laurel, Md. for f-m station WGTR 337 miles away at Paxton, Mass., operating on 44.3 Mc with power of 83 kw, during the early morning hours of Nov. 11, 1943 while Leonid meteor showers were near a peak. Signal strength at this distance is normally insufficient to give good aural reception. The accompanying account is abstracted from Exhibit 4 of the Frequency Allocation Hearings in Washington and is published with the approval of the FCC Engineering Department

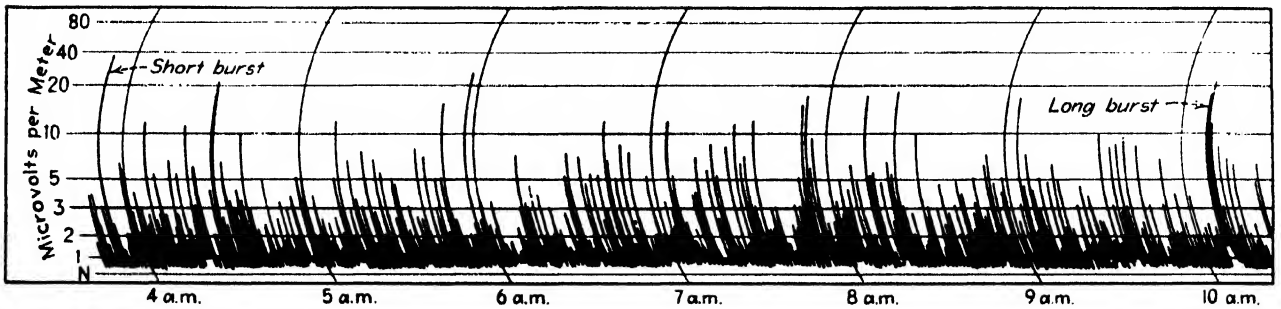

nals, which have been designated as bursts, usually involve a sharp rise in signal strength over a period of a few tenths of a second, but occasionally the burst may be sustained for several seconds or more.

Measuring Path-Length of Bursts

In order to determine the propagation path-lengths of the burst pulses, a series of tests was made by transmitting a steady signal having evenly spaced reference pulses. When the path length for the momentarily strengthened signals or bursts is longer than for ground wave signals, these burst pulses appear between the reference pulses, and the measured path differences are a clue to the origin of the bursts.

The method of pulsing involved frequency-modulating the transmitter ±75 kc by a continuous 170-cycle tone. The f-m signal was received on a Hallicrafters S-27 receiver, the i-f output of which was fed to a Hammarlund Super-Pro receiver tuned to a narrow pass band at the lower end of the swing. The resulting sharp pulses were fed to the vertical plates of a cathode-ray oscilloscope. The horizontal sweep was set at one-half the tone frequency so that two reference pulses appeared simultaneously on the screen, as shown on the accompanying diagram. Any difference in path length D causes the burst signal to be delayed by a time interval D/c where c is the velocity of propagation, so that the pulse of the delayed burst occurs between the ground wave pulses.

During the tests the path differences ranged from about 150 to 900 miles, corresponding to total path lengths of from 350 to 1100 miles.

Cause of Bursts

The greater distances can be interpreted as reflections from media of height comparable to the E layer but lying to each side of the great-circle plane. This correlates quite well with the assumption that bursts are produced by ionization caused by passage of meteors through the upper atmosphere.

Visual correlation of bursts and meteors was obtained by engineers on several nights. In one instance a brilliant meteor with a persistent visible train was observed along the plane of the signal path, with sufficient inclination of the track to reflect the signal back at an acute angle, and the increase in signal strength was sustained for about ten seconds.

Bursts have also been recorded at Laurel, Md. on 71.75 Mc from television station WRGB. They are less frequent than at 44.3 Mc, and have a shorter average duration. Engineers have concluded, however that bursts are not sufficiently prevalent to impair the usefulness of that portion of the v-h-f spectrum in which they occur.

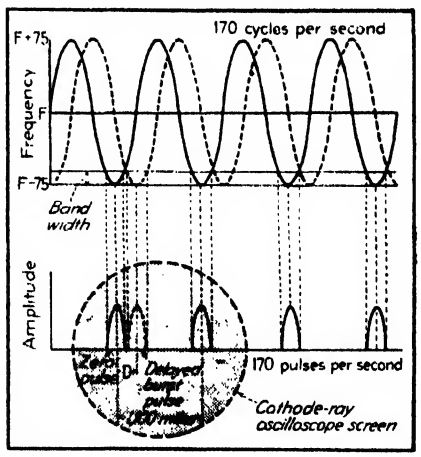

Method used for measuring path lengths of v-h-f bursts

MEASUREMENTS

R-F Bridge for Broadcast Stations

Versatile unit incorporates variable-frequency signal generator, calibrating oscillator, bridge circuit, detector and batteries in a single lightweight unit. Principles of operation are outlined and constructional data are given

By FRED SCHUMANN and CHARLES DUKE

ONE OF THE most useful pieces of equipment in a broadcast station is a reliable, easily portable radio-frequency bridge. This is particularly true for the station with a multi-element antenna array where checks on self and mutual antenna impedances, driving-point impedances, and common-point impedance are frequently desirable.

The bridge to be described contains an oscillator crystal-controlled at the station frequency, in this case 980 kc, and an electron-coupled oscillator which can be calibrated at the station frequency by means of the crystal oscillator and then varied about 60 kc each side of this frequency. The oscillator is modulated at 1,000 cps. Following the oscillator is the bridge proper and then a sensitive receiver with an audio amplifier sharply peaked at 1,000 cps. The latter arrangement is particularly to be desired when making antenna measurements during times of heavy static.

The power supply consists of batteries which are contained within the apparatus. The compactness of this arrangement will be appreciated by anyone who has had to make the usual setup of a signal generator, bridge and receiver upon a small antenna base on a cold night.

Theory of Operation

The basic bridge circuit, shown in simplified form in Fig. 1, is similar to the a-f hybrid coil type 4-A used for some years by the Bell System.

Assume that L_A equals L_B and that equal voltages are induced in both arms. Then i_A will equal i_B in magnitude and phase provided the self impedance of mesh A equals the self impedance of mesh B. For this condition the bridge is balanced and no voltage appears across the detector terminals.

In practice, before making a measurement an initial balance is made with the unknown terminals shorted and the self-contained standard resistance R_s set at zero. This balance is made with C_A and C_B set as close to maximum capacitance as possible. If great care is used in balancing capacitances to ground in construction, the values of C_A and C_B in the initial balance will be practically equal. Assume now that the initial balance has been made and the two capacitance values are C_{A_1} and C_{B_1}. Suppose an unknown impedance consisting of R_s and C_s in series is connected to the unknown terminals. To again balance the bridge it will be necessary to add a resistance (R_s) in the A arm equal to R_s. Also, since capacitive reactance has been added in the B arm, it will be necessary to add an equal capacitive reactance in the A arm. This is done by changing C_A from C_{A_1} to a lower value C_{A_2}. The unknown capacitive reactance is then

$$X_{C_s} = X_{A_2} - X_{A_1} \tag{1}$$

$$\frac{1}{\omega C_s} = \frac{1}{\omega C_{A_2}} - \frac{1}{\omega C_{A_1}} \tag{2}$$

$$C_s = \frac{C_{A_1} C_{A_2}}{C_{A_1} - C_{A_2}} = \frac{D_1 D_2}{D_1 - D_2} K_A \tag{3}$$

where D_1 and D_2 are the dial divisions corresponding to C_{A_1} and C_{A_2} and K_A = calibrating constant of C_A where $C_A = D_A K_A$. If the unknown capacitive reactance is required this is:

$$X_{C_s} = \frac{1}{\omega C_s} = \frac{D_1 - D_2}{\omega K_A D_1 D_2} \tag{4}$$

Suppose the unknown impedance consisted of R_s and L_s in series. In this case, in addition to the resistance balance it will be necessary to add capacitive reactance in the B arm to balance the positive reactance of the unknown. The unknown positive reactance therefore equals the change in negative reactance, or

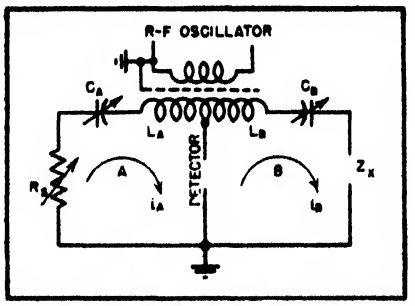

FIG. 1—Basic circuit used in r-f bridge

$$X_{L_s} = X_{B_2} - X_{B_1} = \frac{1}{\omega C_{B_2}} - \frac{1}{\omega C_{B_1}}$$

$$= \frac{C_{B_1} - C_{B_2}}{\omega C_{B_1} C_{B_2}} = \frac{D_1 - D_2}{\omega K_B D_1 D_2} \quad (5)$$

and $$L_s = \frac{D_1 - D_2}{\omega^2 K_B D_1 D_2} \quad (6)$$

where K_B is the calibrating constant of C_B.

In the bridge built by the authors, K_A and K_B were equal within less than 1 percent error and had a value of 1.87 $\mu\mu$f per division. The dials used had 200 divisions and the capacitors were of the straight-line capacitance type. The calibrating constants were determined by first making an initial balance and then adding specific values of known capacitances in shunt with C_A and C_B and noting the change in C_A and C_B to again balance the bridge. A curve was plotted which turned out to be an exceedingly straight line, and its slope was used in determining the values of K.

The r-f bridge, signal generator, and receiver are constructed in a single aluminum cabinet with dimensions of 22 inches by 14 inches

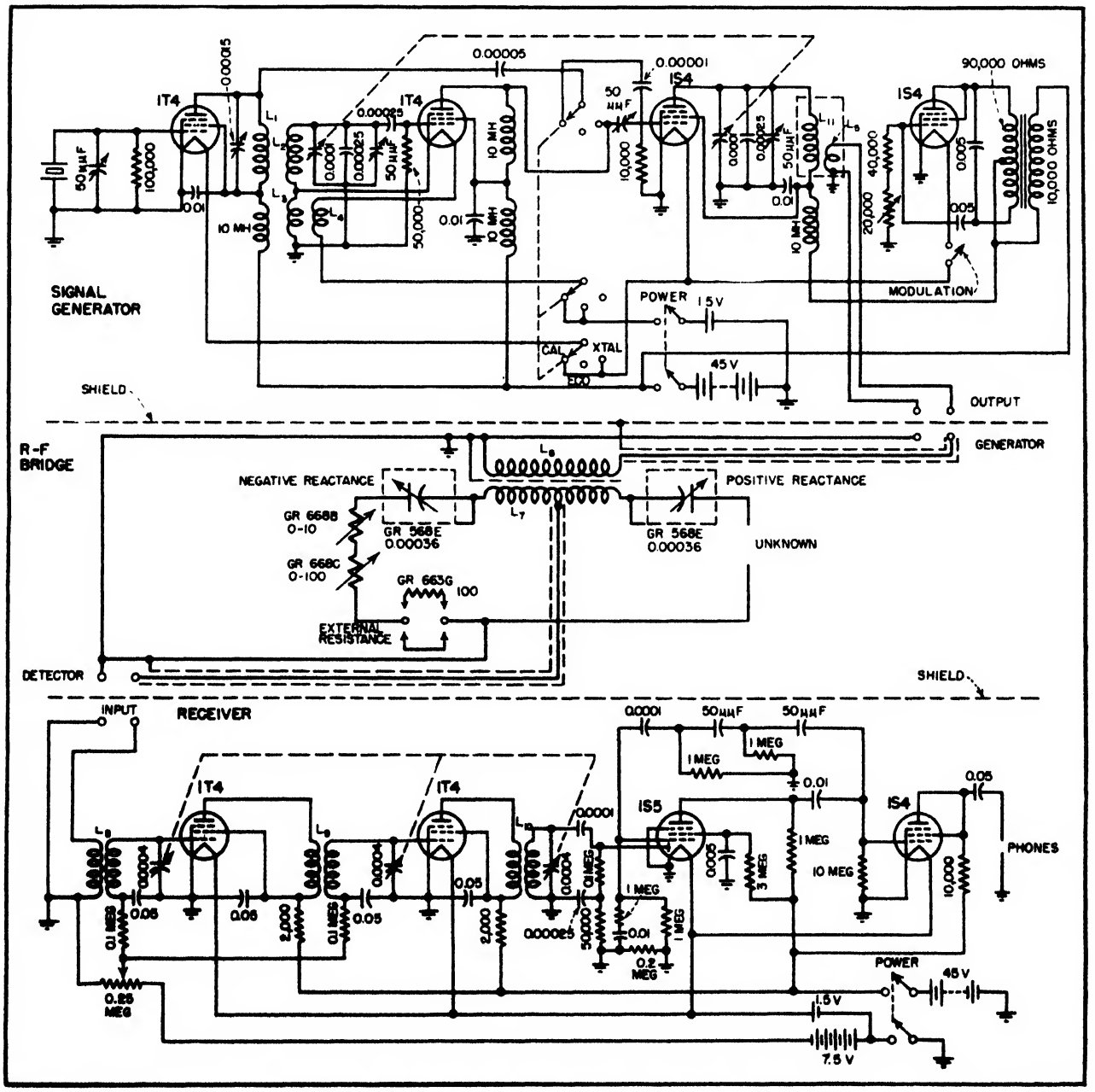

FIG. 2—Complete schematic diagram of bridge unit

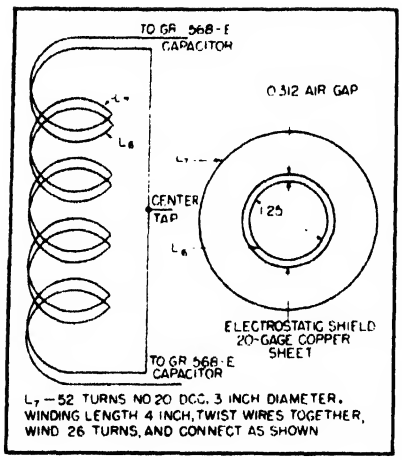

FIG. 3—Construction of bridge-circuit inductor is shown at left; assembly of inductors and electrostatic shield is shown at right

by 8 inches. This cabinet is divided into three sections by aluminum shields and the signal generator and receiver are also individually shielded. It is necessary that no coupling exist between signal generator and bridge and between bridge and receiver except through the external connections. Stray coupling will result in a false resistance balance when measuring 100 ohms or greater.

The construction is such as to minimize the capacitances to ground of all components and to keep these capacitances equal in each of the arms. For the purpose of eliminating changes in stray capacitances as the rotors are turned, the reactance balance capacitors are fitted with shields connected to their rotors.

Shielding

The circuit is shown in Fig. 2. Analysis indicates that all induced voltages across the two parts of L_7 are kept equal and the electrostatic shielding between L_6 and L_7 is made adequate by the construction shown in Fig. 3. Since the maximum value of resistance that can be measured with the internal components is 110 ohms, binding posts are provided for connection of external standards to facilitate the measurement of large resistances or to obtain steps of less than one ohm. All grounds are made to the cabinet at a single point to prevent introduction of undesired voltages from the signal generator through common ground-return impedances.

Plug-in type coils are used throughout the signal generator built into this apparatus and new bands of frequencies can be added if desired. An r-f isolation amplifier is used to minimize oscillator frequency change with varying load conditions and its tuning control is ganged with the electron-coupled oscillator control for single-dial tuning. The electron-coupled oscillator is capable of maintaining its frequency calibration with good accuracy over considerable periods of time and can be adjusted to zero beat with the crystal oscillator at 980 kc by operating the oscillator control switch to the CAL position and adjusting the 50 $\mu\mu$f trimmer in the grid circuit.

The modulator uses a Hartley oscillator circuit and is tuned to 1,000 cps. Small variations in frequency are corrected by adjustment of the grid resistor. The r-f output voltage, which can be modulated approximately 50 percent, is one volt across 50 ohms impedance. The B-battery drain is 10 ma and the A drain is 250 ma under normal operating conditions.

The receiver, employing a trf circuit, can be tuned over the broadcast band. A feedback network between plate and grid of the first audio stage sharply peaks the audio response at 1,000 cps, greatly facilitating measurements on antennas in the presence of atmospheric static and interference from other stations. The B-battery drain is approximately 6 ma and the A drain is 250 ma.

Accuracy

While it is not claimed that this bridge is more accurate than others, it is believed that the obvious advantages offered by its compact arrangement will make its use worthwhile. The bridge, when checked against one of known high accuracy, proved to be within 2 percent for reactance and resistance values in the ranges commonly used in broadcast work.

The authors wish to acknowledge the valuable suggestions received from several members of the technical staff of WSM during the construction of this device.

Table I—Coil Winding Data

Circuit Symbol	Number of Turns	Size dcc Wire	Winding Diam. (inches)	Notes
L_1	90	32	1.5	Closewound. For 980-kc crystal
L_2	44	32	1.5	Closewound. For eco range of 920–1,050 kc
L_3	12	32	1.5	Interwound with L_4 at end of L_2
L_4	12	32	1.5	Interwound with L_3 at end of L_2
L_5	12	22	1.5	Closewound at end of L_{11}
L_6	45	20	1.25	Closewound. See Fig. 3
L_7	52	22	3	Length 4 inches. See Fig. 3
L_8	Commercial antenna coil to cover broadcast band with tuning capacitance used			
L_9, L_{10}	Commercial r-f coils to cover broadcast band with tuning capacitance used			
L_{11}	54	26	1.5	Closewound. For tuning range of 920–1,050 kc

FCC Frequency Measurement Techniques

Received signals up to 500 mc are quickly referred to markers emanating from a standard that is accurate to better than one part in ten million. Frequency subdivision to 50 cycles allows comparison between the standard and time signals. Sense of the final interpolation between 10-kc markers is by means of a lower frequency standard

By ALFRED K. ROBINSON

ONE DUTY of the Federal Communications Commission is measuring frequencies of radio transmitters at central monitoring stations. It is important, therefore, that the accuracy of the reference standard surpass the frequency tolerance required of the transmitting stations and that the means of comparing the received signal with the standard be simple, quick, and accurate.

Basically, the system used depends upon a primary standard that will maintain an accuracy of better than one part in ten million over long periods of time, and is capable of being compared frequently with time signals from the Naval Observatory. In practice, 10-kilocycle markers are derived from the primary standard by frequency division and the incoming signal is caused to beat with the nearest marker. The beat note, always less than 5,000 cycles, is measured by an audio interpolation oscillator.

Accurate Comparison

Audio comparison can be made at any frequency by use of an audio-frequency oscillator, similar to the General Radio type 617, variable from 0 to 5,000 cycles. This instrument has a maximum error of plus or minus 2 cycles throughout the range and the error remains constant regardless of the frequency of measurement. However, even this slight error can be reduced if outputs from the standard at 1,000 cycles and 50 cycles are made available for interpolation. The only remaining source of error is the ability of the engineer to match the audio tone (resulting from the nearest standard 10-kc point beating with the signal) to the audio interpolation oscillator. This error can be serious and depends largely upon the experience of the engineer in matching tones and the care he takes. Even experienced engineers have frequently matched the second harmonic of one tone with the fundamental of another.

Complete elimination of the human error in matching these tones therefore represents a definite forward step in measurement work The system devised to eliminate this error entails energizing the vertical plates of an oscilloscope with the i-f signal from the last i-f amplifier stage of the receiver and sweeping horizontally with the audio-frequency voltage from the audio interpolation oscillator. Proper adjustment of the scope amplifiers (it is only necessary to preset this adjustment once for all signals) will result in a trapezoid pattern when the difference between the incoming signal and the closest standard 10-kc point is matched by the audio frequency of the interpolation oscillator. This trapezoid will result only when the two frequencies are identical, thereby eliminating the error possible from use of a meter indicator by comparing the audio frequency with a harmonic or subharmonic of the fundamental frequency.

When the trapezoid is stationary on the screen the two signals are matched. Any difference between them will cause the pattern to revolve one way or another. Accordingly, the engineer has merely to stop this pattern to obtain exact zero beat. Actual frequency comparisons using this method are practical when the difference between the standard and signal are as low as 5 cycles using a 5-inch Dumont oscilloscope. This is true even on comparatively weak signals. As it is easy to count accurately well beyond this figure it is obvious that the so-called blind spot (10 to 50 cycles), where receiver audio systems and human hearing are undependable, is completely eliminated together with all the auxiliary apparatus necessary to overcome it by other means.

Overmodulation Check

The usefulness of such a system in the accurate measurement of broadcast station frequencies or any station with close tolerance requirements is readily apparent. Proper adjustment of the standard signal level will result in blanketing a large portion of the modulation of A3 signals, thus permitting a sharply defined trapezoid even under heavy modulation. Any type of A0, A1, or A3 signal can be measured in this fashion.

Further advantage results from the fact that the signal being measured can be continuously monitored at the audio output of the receiver, and that overmodulation present in an A3 signal is immediately apparent. The scope pictures the radio-frequency envelope of the signal in much the same manner as if the equipment were coupled directly to the transmitter.

Local Substitution Oscillator

When the signal is on for an extremely short interval as is the case with aircraft transmissions, the

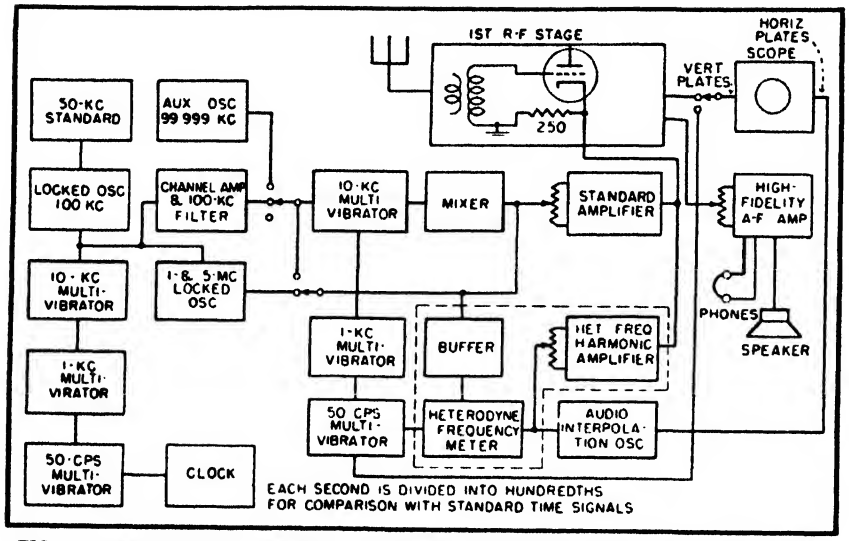

FIG. 1—Block diagram showing the primary standard and divider chain that permits comparison with Naval Observatory time signals. The auxiliary oscillator is used to determine sense of the final audio interpolation

above procedure cannot be employed. The length of time required to turn the audio oscillator from one end of the dial to the other is greater than the time the station remains on the air. In such cases a heterodyne frequency meter is used. This equipment comprises a stable calibrated oscillator whose fundamental or a harmonic is tuned to the frequency being measured. The output from this oscillator must be evenly controlled and injected into the receiver in the same manner as the standard. Once the signal from this oscillator is at zero beat with the station signal the oscillator frequency is measured in exactly the same manner as an A0 signal at the received signal frequency. The calibration of the oscillator is therefore unimportant except to indicate the order of harmonic and for identification of 10-kc points in the very high frequency range as explained later. The errors in setting this oscillator to zero together with that introduced by possible interim drift are much greater than by a direct comparison of the standard with the signal. However, in the event of off-frequency operation the frequency may be checked exactly by setting up according to the heterodyne frequency meter measurement technique and remeasuring on the next transmission using the direct beat method. The audio interpolation oscillator dial would only have to be shifted slightly to obtain the trapezoid. This same method can be used in the case of A2 or carrier shift signals. Exact measurements follow the preliminary heterodyne frequency measurement technique whenever greater accuracy is desired.

Identifying Markers

It is noteworthy that the only computation necessary in this method of measurement is that of identifying the nearest 10-kc point. The point is checked by counting the number of 10-kc points above or below the nearest 100-kc point, which in turn is readily identified from the receiver calibration or from the nearest 1,000-kc marker. This method can be used up to approximately 50 mc. Above this frequency it is best to use the heterodyne frequency meter technique by zero-beating at a harmonic of the heterodyne meter, measuring the fundamental of the heterodyne frequency, and then multiplying by the harmonic order. The actual frequency can be measured with the same degree of accuracy by beating directly against the standard once the 10-kc point used is identified. To simplify computation the tenth harmonic of the heterodyne frequency oscillator is normally used.

The useful output from the conventional multivibrator is limited to approximately 15 mc. This range was formerly extended to perhaps 25 mc by the use of tuned r-f amplifiers. There are several disadvantages to such tuning. The principal ones are the time element, the variable level due to tuning, and the inconvenience of adjustment.

Harmonic Amplifier

To provide strong, clean standard 10-kc points up into the ultrahigh-frequency range without tuning, a harmonic or distortion high-gain amplifier was designed. The principal design characteristics are in accordance with published[1] high-frequency resistance-coupled amplifier requirements with the exception that here high distortion is desirable as a harmonic producer. The unit comprises three stages of amplification with a single bias control that gives smooth 100 percent control. Output levels of individual harmonics of the standard are largely constant irrespective of frequency.

Bias control is the principal one for all measurements. Once a signal is tuned in, the standard injection level is set by means of this control to the same as that of the signal, thereby modulating the incoming signal at the audio-frequency difference. This difference is then matched by means of the audio interpolation oscillator as explained previously. The audio difference as matched is plus or minus from the nearest 10-kc point.

Determination of the sense is quickly found by throwing a switch marked standard-auxiliary to the auxiliary position. In this position the standard has been disconnected and an auxiliary crystal oscillator slightly lower in frequency is connected. All multivibrator outputs are shifted a like percentage. Therefore the beat between the nearer 10-kc marker and the station signal will increase or decrease in frequency depending upon whether the

station is high or low in frequency.

When the audio beat is as high as 4,000 cycles, this slight change in tone may be hard to detect by ear. Readjustment of the audio interpolation oscillator to obtain the stationary trapezoid in the auxiliary position will give the same sense indication by an increase or decrease in dial setting. Determination of the 10-kc point used can be checked by counting to the nearest 100-kc marker.

Zero beating the heterodyne frequency meter with the signal requires that strong clean harmonics be available. Since a sine-wave output is available, whereas the standard multivibrators have a distorted wave to start with, a four-stage untuned harmonic generating amplifier was found necessary to extend the useful range of this instrument from 10 mc to well above 500 mc. Bias for level adjustment is controlled in exactly the same manner as on the standard.

Many refinements have been added to fit the particular needs of the monitoring station. For example, both the standard and heterodyne frequency meter outputs are injected into the receivers at the cathode of the first r-f tube. Several gains important to monitoring station operation are thus realized. Interunit connections are made at low impedance and the cathode connection isolates the standard and heterodyne meter outputs from the antenna circuit. Undesirable radiation that might interfere with reception at other monitoring positions is eliminated. The cathode connection also allows the antenna or grid circuit of the receiver to be shorted, eliminating the incoming signal while still permitting the heterodyne frequency meter and standard outputs to be mixed in the receiver.

Another useful refinement allows switching the 50-cycle multivibrator output (that drives the primary standard clock) to the vertical plates of the scope, and switching the output from the 50-cycle multivibrator (used for audio interpolation) to the horizontal plates. As each of these units is controlled in turn by successive multivibrators a quick check is possible of the correct operation of all control equipment. The figure on the scope is almost a perfect square which remains absolutely fixed providing all apparatus is functioning normally.

The inputs and outputs of all apparatus are brought to a central switching panel in front of the engineer, permitting instantaneous operation of various receivers, disc and tape recorders, filters, and other special equipment. An antenna switching arrangement in use at one of the monitoring stations permits pushbutton selection of any antenna on the reservation.[2]

REFERENCES

(1) F. E. Terman, "Radio Engineers' Handbook", McGraw-Hill Book Co., New York, 1943.
(2) Alfred K. Robinson, Automatic Antenna Switching, *QST*, p 38, April 1945.

Components of UHF Field Meters

Tuning limitations of resonant circuits, tunable doublet antenna, uhf voltmeters, cavity attenuators, power-supply stabilizer of early model of field-strength meter, and standard-signal generator are described

By EDUARD KARPLUS

FREQUENCY LIMITS of electronic equipment were rapidly pushed into the hundreds of megacycles during war development. To learn about propagation and equipment capabilities a field strength meter was developed for the range from 300 to 1,000 mc. This meter was intended for measurements in the laboratory or field. It had to be quickly tunable to any frequency within its range. A sensitive receiver, which could be calibrated by a standard signal generator, was required to measure the voltage induced by an unknown field in an antenna of known characteristics.

In using the field strength measuring equipment the antenna and receiver are tuned to the incoming signal; the antenna is disconnected from the receiver and replaced by a dummy antenna and a standard signal generator which is adjusted to give the same receiver response. The field strength ϵ in microvolts per meter is related to the standard signal generator voltage E in microvolts by

$$\epsilon = E\frac{1}{h_e}$$

where h_e is the height of the antenna in meters. If the antenna is adjusted to half-wave resonance

$$h_e = 0.636l = 0.636\,\frac{\lambda}{2} = \frac{95}{f}$$

to a first approximation, where f is the operating frequency in megacycles. Therefore the unknown field strength is

$$\epsilon = 0.0105\,f\,E$$

The receiver and the standard signal generator have since found wide application in other fields, and, although the original models are obsolete today, many of their components will be found useful in similar applications.

Tuned Circuits

The butterfly circuit, as well as its

application in negative-grid triode oscillators, has been described in detail,[1] but the wide interest shown in this development justifies a few further remarks.

The butterly circuit used in the signal generator has 2½-inch outside diameter and 5 and 6 plates on the rotor and stator respectively, has a tuning range of 220 to 1,100 mc and is equipped with terminals for grid and plate of the oscillator tube. The butterfly circuit can be considered a parallel combination of inductances and capacitances. This combination is seen in the schematic diagram of Fig. 1 where the capacitive branch is represented by two series capacitors and the inductive branch by two parallel inductors between terminals one and two. Variation of both capacitance and inductance is brought about by rotation of the inner, butterfly shaped, member. The capacitive branch is the familiar series-gap tuning capacitor. Variation of the two identical inductive branches is achieved as the rotor progressively blocks out the area through which a magnetic field can pass.

At 220 mc, with the plates fully meshed, the effective inductance of the circuit is 0.011 μh, the effective capacitance is 48 $\mu\mu$f, and the effective Q is 650. The corresponding values at 1,100 mc are 0.004 μh, 5 $\mu\mu$f, and a Q of 300.

Common to all butterfly circuits is a series-gap capacitor for capacitance variation across two fixed terminals, which eliminates the necessity of sliding contacts, and the direct incorporation of a parallel inductive path into the structure of this capacitor. This integral design is important in reducing metallic losses at points where capacitive and the inductive paths of the tuned circuit join and makes it possible to use lumped parameter elements at these high frequencies. The eddy-current shielding effect of the rotor plates, which reduces the effective inductance in the high frequency position, helps to obtain very wide tuning ranges, but increases the losses to some extent.

If low losses are important, and wide tuning ranges are not required, butterfly circuits should not be used. Better results can be obtained with a cylinder circuit.[2] This circuit can be represented by a diagram similar to Fig. 1 with a single and fixed inductive branch. The tuning ranges of cylinder circuits are considerably smaller than the ranges obtained with butterfly circuits, but their losses are lower and their Q's are practically constant. A cylinder circuit with cylinders one inch in diameter and two inches in length has a tuning range of approximately 500 to 1,000 mc with a Q of 1,200.

In a broadcast receiver a three-to-one frequency variation is ordinarily produced by a 180 degree rotation of the capacitor shaft, but a typical butterfly circuit varies from 220 to 1,100 mc between two rotor positions which are only 90 degrees apart. To compensate for this difference, and for an uneven frequency distribution, the angular precision of the drive has to be about seven times better in the butterfly circuit than in a comparable variable capacitor circuit. The precision required to prevent axial movement of the plates is the same in both cases provided the air gap and the care used in centering the plates are equal. This relation is based on percentage accuracy and has to be multiplied by the ratio of frequencies if frequency increments are considered. In our example this ratio would be 1,000.

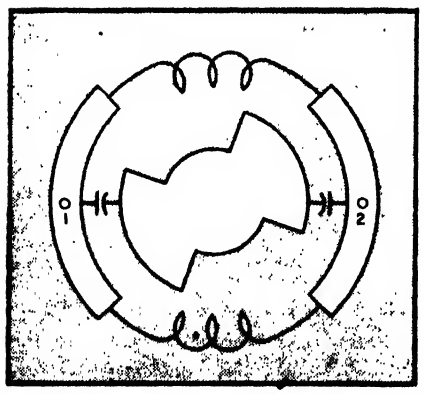

FIG. 1 —Left—Schematic diagram of butterfly circuit indicates that high resonant impedance appears across points 1 and 2

FIG. 2 —Below—(A) Tunable antenna and (B) attenuator coupling are principal uhf features of equipment

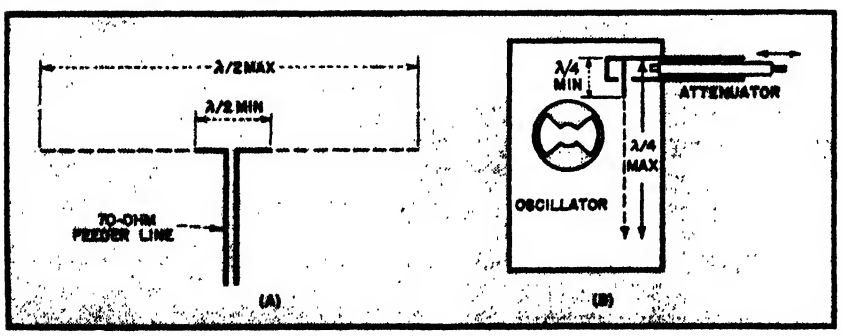

Frequency Limits

The 220 to 1,100 mc butterfly circuit has an air gap of 0.04 centimeter, which is not adequate for high-power applications. If this air gap were changed to 0.2 centimeter, the maximum capacitance across the terminals would be reduced to one fifth its previous value and the frequency range would be 500 to 1,000 mc, to a first approximation. This large reduction in tuning range cannot be offset by an over-all increase in the size of the unit. A 50 percent increase in diameter would increase both capacitance and inductance by a factor of about 2.3 and would approximately restore the bottom frequency of 220 mc, but the top frequency would have dropped to under 700 mc. An increase in the number of plates would seem to be a possible solution, but unfortunately butterfly circuits with more than a certain number of plates have spurious modes which interfere with their proper operation. It appears, therefore, that the maximum size and the maximum number of plates that can be used in a butterfly circuit are limited by the top frequency, and that the bottom frequency is then determined by the air gap.

In practice it is very hard to com-

FIG. 3 —Experimental drive systems for flexible conductors used (A) to couple from oscillator into attenuator cavity and (B) to tune doublet antenna

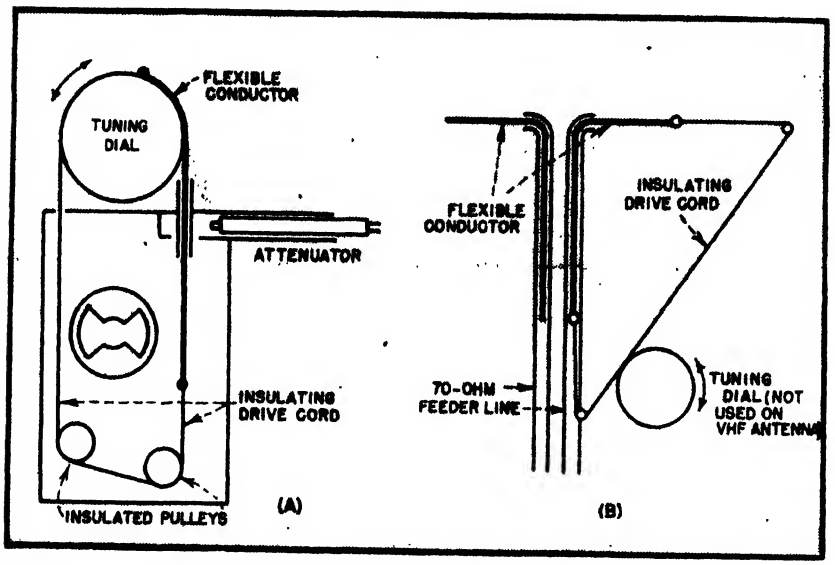

pute the top frequency of a butterfly circuit without a good deal of experimental data taken from similar designs because the mechanical shapes determining both capacitance and inductance are too complicated for simple approximations. The bottom frequency can be obtained with reasonable accuracy if the capacitance of the series gap capacitor is computed as in any low-frequency application and the inductance as

$$L = 4.9\, r \log_{10} (r/t + w)\, 10^{-9} \text{ Henry's}$$

where r is the inside radius of the butterfly stator plates and t and w are thickness and width of the stator stack, all in centimeters. To arrive at an estimate of the top frequency of a butterfly circuit, a range factor is used which varies between two and 12 for the circuits that have been built so far. The range factor increases as frequency and air gap are reduced.

Tunable Resonator

Another component of general usefulness is a tunable resonator which is incorporated in the signal generator and in the receiver of the field strength measuring equipment. In both cases resonators with a five-to-one frequency range were required and adjustment by turning a dial seemed desirable. Figure 2 shows schematically these two applications.

In Fig. 2 A a 70-ohm feeder line is connected to a doublet antenna, the length of which has to be $\lambda/2$ at the operating frequency. In Fig. 2 B a mutual inductance type attenuator is coupled to a 220 to 1,100 mc butterfly oscillator. A quarter-wave resonator with the current loop in the attenuator produces a strong field of the desired mode and reduces in proportion undesirable modes which might otherwise cause errors in attenuation.

This same system was used in a 1,000 to 3,000 mc signal generator to select, in addition, the second and the third harmonics of a 500 to 1,000 mc oscillator. In this particular case the oscillator used a quarter-wave open line and could be driven much harder for harmonic generation than would be possible with a butterfly oscillator.

In both cases conventional telescoping tubes could have been used, but for a five-to-one frequency range at least five joints would have been required. The solution adopted consists, instead, of a short fixed guide and a long flexible conductor which is pushed through the guide by the amount required to produce resonance. In the attenuator, which is illustrated in Fig. 3 A, the remaining part of the conductor, which is not required at a particular frequency setting, does not constitute a problem because it passes through the oscillator shield into the outer space and cannot interfere with the components inside the shield. Good contact between conductor and guide is important. As shown, the flexible conductor can be tied to an insulating drive cord and be guided and driven by pulleys operated by a conveniently located dial. By proper choice of the location and size of the insulated pulleys inside the oscillator housing, coupling between the resonator and the oscillator can be adjusted over the frequency range.

Conditions in the tunable antenna are somewhat different because no ground plane is available for separating the used and the unused parts of the resonator. In that case, the flexible resonator is fed through a hollow feeder line as shown schematically in Fig. 3B. The feeder line is composed of two tubes spaced to provide the desired characteristic impedance of 70 ohms and bent at the upper end to give the flexible resonator a right angle deflection. The unused parts of the resonators are within the feeder lines and do not disturb the field of the antenna.

To avoid complications, a driving mechanism has been omitted in the 220 to 1,100 mc doublet antenna. The feeder lines of this antenna are aluminum channels spaced for 70-ohm characteristic impedance by a polystyrene bar. The flexible conductors are self-supporting flat strips of slightly curved spring material, similar to the strips used in the familiar steel rules. Adjustment of antenna length is easily made by hand using pins which are fastened to the conductors and project through the aluminum channels.

Crystal Detectors

After a careful study of uhf voltmeters, it was decided to use a crystal detector as the rectifying element because, in spite of all their shortcomings, voltmeters of this type can be built with lower corrections for frequency than any of the others. A suitable crystal detector had to be developed for this application in 1941, but today completely sealed detector cartridges with standardized dimensions and reliable performance are available.

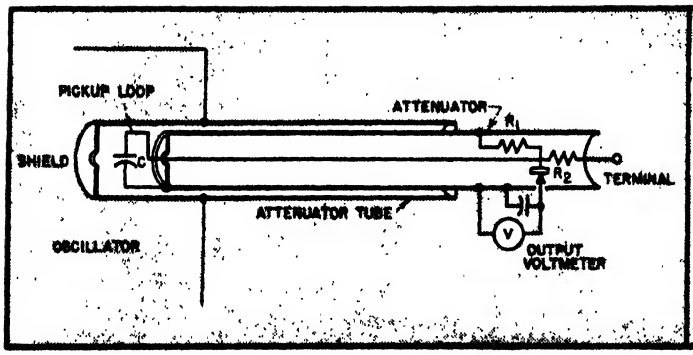

FIG. 4—Output meter of standard-signal generator can be located at output of attenuator

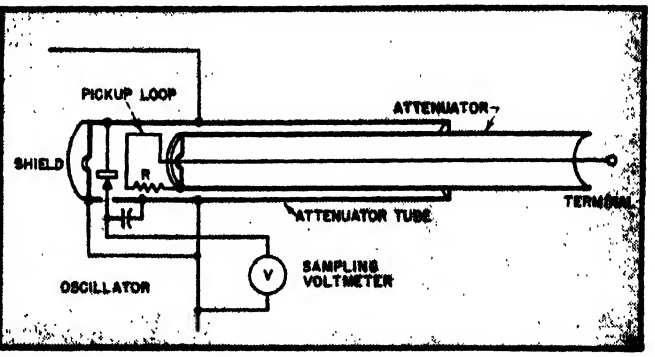

FIG. 5—Output meter of standard-signal generator can be located at input to attenuator

Up to a few thousand megacycles the action of the detector junction is independent of frequency if precautions are taken in its manufacture and the frequency characteristic of a crystal detector type voltmeter is determined by its resonant frequency. Series resonance of the shunt capacitance of the detector junction and the lead inductance between voltmeter terminals increases the voltage E appearing across the detector junction with respect to the terminal voltage e and causes a corresponding frequency error F such that

$$F = \frac{E}{e} = \frac{1}{1 - (f/f_0)^2}$$

where f and f_0 are operating frequency and resonance frequency of the voltmeter respectively. In any particular voltmeter design the resonant frequency f_0 varies only slightly with individual detector cartridges. In a typical application, using the type 1N21-B detector, which is the most suitable for this purpose, the resonant frequency varies from 3,500 to 3,900 mc, corresponding to a frequency error of 9 to 7 percent at 1,000 mc.

Erratic variation or drift of crystal detectors have been largely reduced by modern design and it has been found that in most cases the drift is independent of frequency. Because this assumption is certainly correct for small drift, detectors can be checked periodically and corrected at any convenient frequency, for instance at 60 cps.

Another peculiarity of crystal detectors which sets them apart from vacuum-tube voltmeters and thermocouples, ordinarily used at lower frequencies, has to be mentioned as it bears on their application. Vacuum-tube voltmeters can be built for a wide range of voltages, and their circuits can be so designed that no permanent damage is done by overloads. Thermocouples can be built for a wide range of currents. They are readily burned out, but this damage is immediately obvious. Most crystal detectors will not stand more than a few volts, and great care has to be taken to prevent overloads which might change the characteristic of their junction before it is made ineffective or burned out.

Attenuator

A voltmeter placed at the input to the attenuator of a signal generator will read independently of attenuator setting, but a voltmeter placed at the output terminal will read only over a limited range of low attenuation. It would seem, therefore, that the first location, which is always used at low frequencies is more desirable, but at ultrahigh frequencies the second method will give more accurate results.

In both cases the accuracy at low output voltages depends on the attenuator calibration, which can be computed precisely for the mutual inductance type attenuator commonly used at ultrahigh frequencies. The quarter-wave resonator described in connection with Fig. 3B is not required, and better results are obtained if the end of the attenuator tube is fitted with a shield to exclude undesirable modes and is pointed toward a part of the oscillator circuit which carries current in the plane of the pickup loop. The field of this current passes the shield and enters the attenuator tube where it is attenuated logarithmically, decreasing by 32 db for each diameter traveled.

If a voltmeter is placed at the output side of a line connected to the pickup loop, a reference point of attenuator output voltage can be established for any position of the pickup loop that provides sufficient voltage to make the meter read, and accurate lower output voltages can be obtained by moving the pickup loop by accurately determined amounts. A complete output system of this type includes resistors, R_1 and R_2 and capacitor C, as shown schematically in Fig. 4. Resistor R_1 is required to terminate approximately the short line between pickup loop and voltmeter in order to prevent excessive voltage rise which might overload the crystal detector, if the proper load is not connected. Resistor R_2 is a matching resistor to provide desirable values of output impedance. It will ordinarily be determined by the characteristic impedances of the cable connecting the load and was 70 ohms in the field strength measuring equipment tc simulate the radiation resistance of the doublet antenna. Capacitor C is sufficiently large to be ineffective at radio frequencies and has been inserted only to facilitate low frequency calibration of the crystal detector.

In this output system, the accuracy of output voltage at the reference point is determined by the voltmeter alone and does not depend on any other circuit elements. The accuracy of the output impedance is determined by R_2 alone because this resistor is immediately preceded by

the output voltmeter, which can be considered a zero-impedance source. Obviously no signal generator could have sufficient power to meet this requirement, but as long as its output voltmeter is reset to the same value whenever the load is changed, the terminals of the voltmeter have all the characteristics of a zero-impedance source. In operation, therefore, the reference level of the logarithmically calibrated attenuator has to be established with the load connected, and as we have seen, this has to be done at a high output level to provide a reliable reading of the output meter. If, for some reason, the load changes with the signal amplitude, the attenuator calibration will be in error.

Alternative Output Circuit

To follow the more conventional output system the voltmeter is placed at the attenuator input as shown in Fig. 5 where it samples the field in the attenuator tube. This field decreases within the attenuator according to the same logarithmic law as before. Output voltage depends on the size and position of the pickup loop, the output impedance on the characteristic impedance, and length of the short line connecting the pickup loop with the output terminals. To eliminate a frequency dependent effect, this line has to be terminated at the pickup loop. Resistor R is inserted for this purpose, but because the reactance of the pickup loop itself is included in the termination, an accurate solution of this problem is difficult at uhf.

If an adequate solution is possible at lower frequencies, however, or over a limited range at some high frequency, two advantages are obtained, compared to the output system shown in Fig. 4. That the output meter reads at all attenuator settings is convenient as mentioned before. In addition the generator voltage is now independent of the load because it is determined by field strength in the attenuator tube.

Both these disadvantages of the simpler and more accurate system, which uses the meter at the output terminal, can be overcome. The crystal-detector type output meter has to work at a low level to prevent damage to the crystal junction and will not be able to indicate modulation peaks. By coupling a high-level peak-reading diode voltmeter to the oscillator, modulation can be determined accurately. In addition, a permanent indication of oscillator amplitude is obtained which is useful for monitoring purposes even if it cannot be made proportional to the output voltage. To eliminate errors caused by a load that changes its impedance at high levels, an attenuation pad can be inserted between the terminal of the signal generator and the load, or resistance R_1 and R_2 of Fig. 4 can be rearranged to give a fixed initial attenuation.

No matter which attenuator output system has been used, terminals for connecting the load have to be provided. At uhf this connection is always a matched concentric cable, and no particular advantage is obtained by locating the signal generator output terminal at the end of another cable as is customary at lower radio frequencies. The output terminal, in form of a concentric cable fitting, can be located on the front panel of the instrument.

Regulated Power Supply

Another problem encountered in the design of the field strength measuring equipment concerns the power supply. The equipment was built for 60-cps operation, but for at least part of the time the power required had to be produced by a motor-generator set driven from a storage battery. Under these conditions both voltage and frequency vary widely. Some means had to be provided to regulate filament and plate supplies.

The regulated power supply adopted for the field strength measuring equipment presents a solution of this problem by magnetic and electronic means. The fundamental schematic diagram is shown in Fig. 6.

The two outer a-c windings of the regulator are connected in series with the power transformer. A d-c winding is energized from a twin triode tube T_1 which acts as a grid-controlled rectifier. The reactance of the regulator is determined by the d-c current in the middle winding and automatically varies to maintain the primary voltage of the transformer constant.

Control voltage for the rectifier tube T_1 is derived from the main B-supply. At normal line voltage the grids of tube T_1 are slightly negative with respect to its cathode and allow some current to flow through the d-c winding of the regulator. At higher line voltages the grids become more negative because the voltage across the glow tube T_3 does not change. The rectified current through T_1 then decreases and the impedance of the regulator increases to bring the

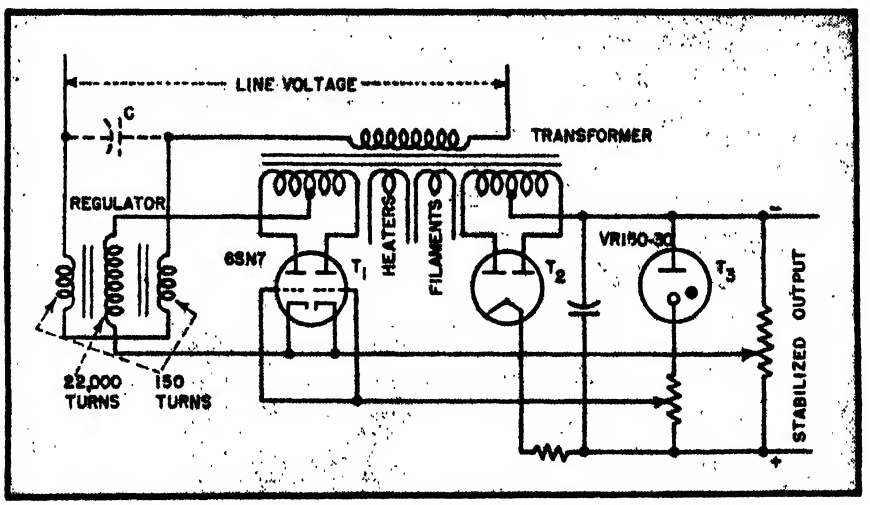

FIG. 6—Power-supply stabilizer, to regulate both filament and heater as well as high-voltage supply, uses controlled saturable reactor in power input circuit

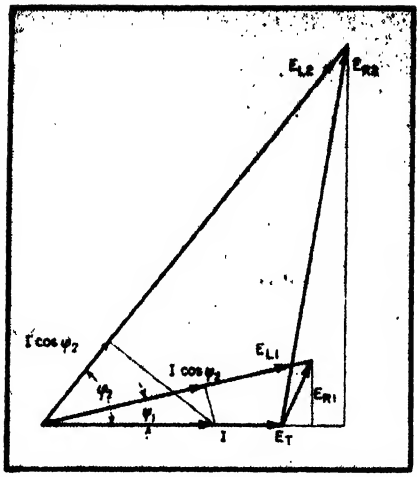

FIG. 7—Vector diagram shows that reactor absorbs the change in input voltage

primary voltage of the transformer back to its previous value.

Regulator Design

Figure 7 shows voltage and current relations of the system for minimum and maximum line voltage E_{L1} and E_{L2}. Line current I and transformer voltage E_T are independent of line voltage. E_{R1} and E_{R2} are the voltages across the regulator which are out of phase with the line current except for a small component which covers the a-c losses in the regulator and increases slightly with line voltage. Input power, therefore, is essentially constant including a regulator loss of about ten percent. The phase angle of the input power varies between ϕ_1 and ϕ_2 and can be corrected for average line voltage by a fixed capacitor across the line terminals.

To compute the regulator characteristics, the power required by the instrument and the expected line voltage variations have to be known. By assuming a minimum voltage drop E_{R1} in the regulator, the operating voltage of the transformer E_T, the line current I, and the maximum volt-amperes IE_{R2} that the regulator has to handle can be established. For good regulation, the flux density in the regulator should be kept low. At high flux densities, considerable distortion of current waveform results, which causes poor regulation in the filament and heater supplies. It should be remembered that the regulation control voltage is derived from the main B-supply, which is proportional to the rms value of heater current only as long as the waveform of the power source remains constant. Depending on filter circuit and load, output voltage of the B-supply will be determined by average or peak values of the power source rather than by its rms value. The flux density of the regulator is determined by its ampere-turns IN_1 and the length of its magnetic path l_1 where N_1 is the total turns of the two outer a-c windings and l_1 is the outer circular path of the core. The maximum regulator voltage E_{R2} is determined by the cross-section of the core, the flux density, and the total turns of the a-c windings.

To reduce the regulator voltage to its minimum E_{R1}, the core material is saturated by d-c current in the middle winding. The ampere-turns required are now determined by the shorter path l_2 through the center leg and the two outer legs in parallel. Because the magnetizing current is furnished by a vacuum tube, the d-c resistance of the middle winding can be high and its number of turns N_2 can be many times larger than N_1. The two halves of the outer winding have to be well balanced because no a-c voltage should appear across the middle winding.

Magnetizing current is produced in the grid-controlled full-wave rectifier T_1. The plate voltage of this tube is derived from the main power transformer and should be high enough to allow the maximum current required for regulator saturation to flow without grid current. Control voltage for this tube is obtained from the glow tube and potentiometer combination across the B-supply of the instrument. Ordinarily the gain in the grid-controlled rectifier T_1 will be sufficient to change the magnetizing current of the regulator over its full range with a very slight variation of the B-supply output voltage, but there is no reason why additional gain could not be inserted between T_2 and T_1.

The characteristic curves of the power supply used in the signal generator are given in Fig. 8. The power requirement of the main instrument transformer is 70 watts, and it operates at 75 volts. It will

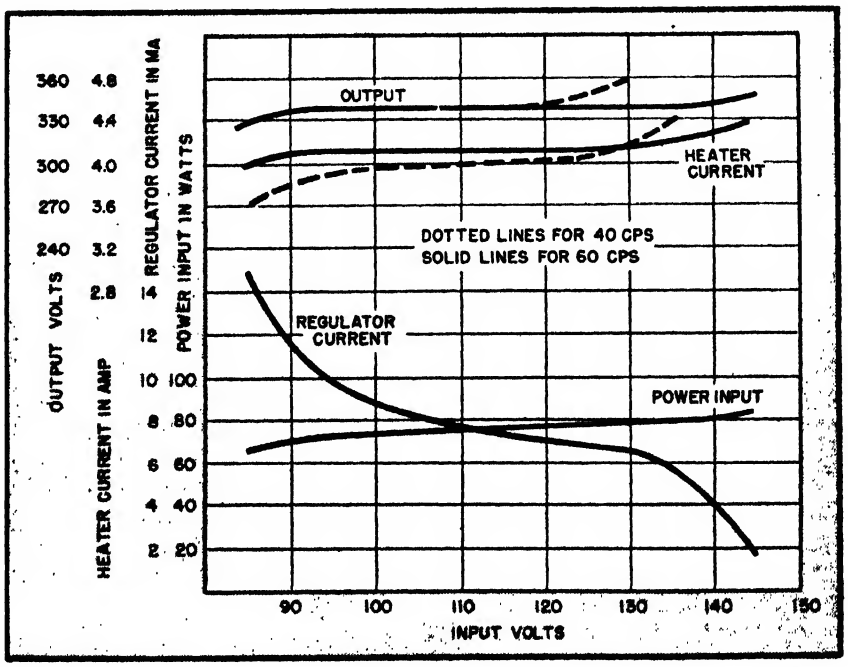

FIG. 8—Measured characteristics of power supply show the wide range over which the stabilizer operates

be seen that the operating range of the regulator is extremely wide at 60 cps and is still adequate at 40 cps. Regulation of the heater supply is not as good as that of the B-supply, particularly at 40 cps. This inadequacy is due to distorted waveform of line current and has been partly corrected by capacitor C of 6 μf across the regulator.

REFERENCES

(1) Karplus, E., Wide Range Tuned Circuits and Oscillators for High Frequencies, *Proc. of I.R.E.*, p 426, July 1945.
(2) Gross, Ervin E., Jr., Coaxial Butterfly Circuits, ELECTRONICS, p 156, April 1946.

Design of F-M Signal Generator

Requirements of a reactance modulator for producing constant deviation of a variable oscillator are developed. Design data is given for an f-m signal generator covering 54 to 216 megacycles. Operation from 100 kilocycles to 25 megacycles is provided

By DONALD M. HILL and MURRAY G. CROSBY

IN the design of a frequency-modulation signal generator, the choice of the general type of circuit is considerably affected by the problem of modulation calibration. The usual reactance-modulator circuits produce deviations of the oscillator frequency which vary with the oscillator frequency. Since it is necessary to permanently calibrate the deviation obtained from the instrument, some means must be employed to maintain a constant modulator sensitivity over the frequency range. Two systems are available for accomplishing this purpose: the heterodyne system and the constant-deviation variable-oscillator system.

Heterodyne System

The basic operating principle of the heterodyne system is indicated in the block diagram of Fig. 1, which is reproduced from a paper[1] by A. W. Barber, C. J. Franks, and O. W. Richardson. In this system, frequency modulation of the fixed oscillator is controlled by variation of the modulating voltage applied to the reactance tube by means of a deviation control potentiometer. When the desired deviation has been chosen, this is necessarily held constant regardless of the output frequency, since it is the fixed oscillator that is modulated, and its frequency deviations are transferred unaltered to both the sum and difference frequencies which are generated in the mixer stage. The desired sum or difference frequency is amplified to obtain the required output voltage.

It is possible to gang the deviation control potentiometer to the variable tuning element of the variable oscillator to produce a constant deviation of the variable oscillator and to heterodyne this with an unmodulated fixed oscillator; however, modulation of the fixed oscillator is obviously preferable.

Although the many desirable features of the heterodyne system made it convenient for the original f-m broadcast band (42-50 mc), it is not well suited for a generator covering a large part of the vhf region. In addition to the desired sum or difference frequencies, the mixer output contains the harmonics of the two oscillators and the sum and difference frequencies of the various harmonics. These spurious frequencies are not harmonically related to the desired output frequency and, in fact, sometimes coincide with it[2]. To keep the output signal reasonably free from spurious signals over a wide frequency range, it is necessary to use the difference frequency and operate the oscillators at frequencies so high that frequency stability would be a major problem.

If sufficient oscillator stability could be attained, there would remain the problem of amplifying the desired signal in the mixer output. In the vhf region, this would require a tuned r-f amplifier. The problem of ganging the variable oscillator with an amplifier operating at the difference frequency is not very inviting since the rate of change of the output frequency is considerably different from the rate of change of the variable-oscillator frequency.

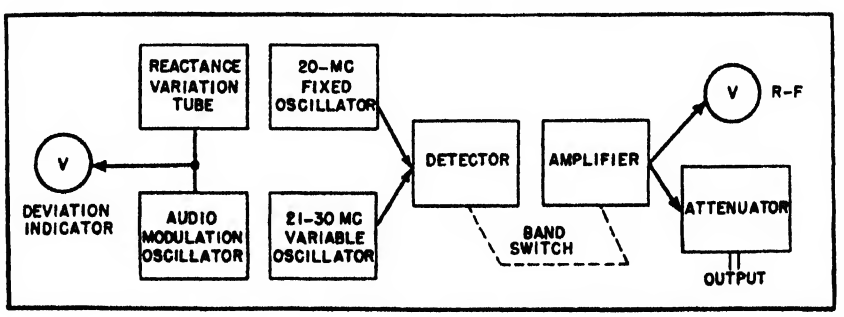

FIG. 1. Essential stages of f-m signal generator employing the heterodyne system

Constant-Deviation Variable-Oscillator System

If a constant-deviation modulation system is utilized, the signal generator does not require the step of heterodyning with its attendant spurious responses. Either an oscillator operating directly at the output frequency or a master-oscillator-multiplier arrangement may be used. Such arrangements confine the spurious responses to harmonics or subharmonics which are inherently low in output and are simply related to the output frequency so that they may be readily identified.

The constant-deviation system gives a greater output per tube used in the signal generator. With the elimination of the heterodyne step, only a single oscillator is required. Also, the efficiency of amplifiers or multipliers is considerably greater than that of a frequency converter.

In reactance-tube frequency modulation, there are two general types of reactance tubes employed. One type appears as a controllable inductance and the other as a controllable capacitance. The equivalent inductance or capacitance produced by the usual reactance tube with a two-element phase shifter results in an equivalent inductance or capacitance which is independent of frequency[8]. The reactance tube is placed in parallel with the tuned circuit to be modulated so that the inductive type may be considered as adding a controllable inductance in parallel with that of the tuned circuit while the capacitive type adds a controllable capacitance in parallel with the tuned-circuit capacitance.

For the inductive type of reactance tube, the resulting total tuned-circuit inductance is that of the tuned circuit and the reactance tube in parallel or

$$L_t = L_e L/(L_e + L) = L/(1 + L/L_e) \quad (1)$$

where L is the fixed inductance of the tuned circuit and L_e is the effective inductance of the reactance tube.

When Eq. 1 is inserted in the expression for the resonant frequency of the tuned circuit, the frequency is given by

$$f = 1/[2\pi\sqrt{LC/(1 + L/L_e)}] = f_r(1 + L/L_e)^{1/2} \quad (2)$$

in which C is the fixed capacitance of the tuned circuit and $f_r = 1/(2\pi\sqrt{LC})$. The quantity L/L_e is normally small in comparison to unity, so that Eq. 2 simplifies to

$$f = f_r(1 + L/2L_e) = f_r + f_r L/2L_e \quad (3)$$

The second term in Eq. 3 is the frequency deviation which results from the reactance-tube modulation. It is seen to be proportional to the resonant frequency f_r and the ratio L/L_e between the tuned-circuit inductance and the effective inductance of the reactance tube.

For the capacitive type of reactance tube, the resulting total tuned-circuit capacitance is that of the tuned circuit and the reactance tube in parallel. The frequency is then given by

$$f = 1/[2\pi\sqrt{L(C + C_e)}] = f_r(1 + C_e/C)^{-1/2} \quad (4)$$

For the practical case, C_e/C is small compared to unity, so that

$$f = f_r(1 - C_e/2C) = f_r - f_r C_e/2C \quad (5)$$

It is thus seen that the frequency deviation produced by the capacitive type of reactance tube is proportional to the resonant frequency f_r and to the ratio C_e/C of equivalent reactance-tube capacitance to tuned-circuit capacitance.

The manner in which the frequency deviation varies with resonant frequency is also dependent upon which element of the tuned circuit is varied. If the tuned circuit is of the variable-capacitance, fixed-inductance type, and the reactance tube is of the inductive type, the frequency deviation may be taken from Eq. 3 which is $f_r L/2L_e$. In this type of circuit, L is fixed and L_e is independent of frequency. The result is a fixed percentage variation of inductance which produces a fixed percentage frequency variation. The frequency deviation in cycles is therefore proportional to the resonant frequency.

If the tuned circuit is of the variable-capacitance fixed-inductance type, and a capacitive reactance tube is used, the percentage capacitance variation varies with frequency as the tuning capacitor is varied. That is, the ratio C_e/C varies with frequency since C is varied. The value of C is varied in accordance with the formula $f_r = 1/(2\pi\sqrt{LC})$, which may be rewritten

$$C = 1/[L(2\pi f_r)^2] \quad (6)$$

Substituting Eq. 6 in Eq. 5 gives

$$f = f_r - 2\pi^2 C_e L f_r^3 \quad (7)$$

In the frequency deviation given by the second term in Eq. 7, the quantities C_e and L are independent of frequency for the fixed-inductance type of tuned circuit. The percentage frequency deviation is thus proportional to the square of the resonant frequency. The deviation in cycles is proportional to the third power of the resonant frequency.

If the tuned circuit is of the variable-inductance fixed-capacitance type and the reactance tube is inductive, the ratio L/L_e varies with frequency. The tuned circuit inductance L is tuned in accordance with $f_r = 1/(2\pi\sqrt{LC})$, which may be rearranged to

$$L = 1/[C(2\pi f_r)^2] \quad (8)$$

Substituting Eq. 8 in Eq. 3 gives

$$f = f_r + 1/[(2\pi)^2 L_e C f_r] \quad (9)$$

The values of L_e and C are independent of frequency for this combination so that the frequency deviation is inversely proportional to the resonant frequency. The percentage frequency deviation is therefore inversely proportional to the square of the frequency.

When the fixed element of the tuned circuit and the reactance tube type are the same (both capacitive or both inductive), the deviation sensitivity is proportional to the operational frequency. With fixed C in the tuned circuit and an inductive type reactance tube, deviation is inversely proportional to frequency. With fixed L in the tuned circuit and a capacitive type reactance tube, the deviation is directly

proportional to the third power of the frequency.

The nearest approach to constant-deviation operation that may be obtained with the conventional reactance-tube circuits is a deviation which is either directly or inversely proportional to the operational frequency. Two combinations of reactance tube and tuning element produce deviations proportional to frequency. One of these is obtained by the familiar variable-capacitance tuned circuit in combination with an inductive reactance tube, and the other is obtained by a variable-inductance (such as a permeability-tuned) circuit in combination with a capacitive reactance tube. When either one of these combinations is employed, the deviation increases with frequency so that some means must be provided to reduce the deviation sensitivity as the frequency is increased.

Correction Methods

Various means may be applied for correcting the inherent deviation variation with frequency. One method is to gang a modulation input potentiometer with the tuning dial as shown in Fig. 2. Potentiometer P is designed to have a resistance taper such that, when ganged to the shaft of tuning capacitor C, the modulation sensitivity is maintained constant as the frequency is varied. For the circuit shown, the potentiometer reduces the modulation input as the frequency is increased.

Figure 3 shows how the modulation sensitivity may be maintained constant by ganging an element of the reactance-tube phase shifter to the shaft of the tuning dial. For the inductive-reactance tube and variable-capacitance tuned circuit shown, phase-shifter capacitor C_1 is ganged to tuning-capacitor C in such a manner that C_1 is increased as C is decreased. This increases the phase-shifter attenuation as the frequency is increased so that the degree of modulation produced by the reactance tube falls off with frequency sufficiently to produce constant deviation. A particular shaping of the plates of C_1 with relation to those of capacitor C is required.

In the circuit of Fig. 3, the attenuation of the phase-shifter is mechanically varied to produce constant-deviation operation. It is also possible to arrange constant-deviation sensitivity over a given frequency range by means of a particular phase-shifting network which inherently produces the required phase shift and has the proper attenuation characteristic. The requirements of such a network may be seen from the following analysis.

Equivalent Circuits

In the reactance-tube circuit of Fig. 4, the plate circuit of tube T appears as a reactance by virtue of, the reactive current it draws due to the phase-shifted voltage fed from the plate to the grid. The impedance looking into the plate circuit is given by

$$Z_e = E\,e^{j\omega t}/i_p \tag{10}$$

If the input impedance of the phase-shifter is assumed to be negligibly high, the current i_p is

$$i_p = e_g G_m \tag{11}$$

in which G_m is the transconductance of tube T. The grid voltage e_g is

$$e_g = BE\,e^{j(\omega t + \phi)} \tag{12}$$

in which B is the attenuation of the phase-shifter, expressed as a fraction less than unity, and ϕ is the phase shift produced by the phase-shifter. Substituting Eq. 12 in Eq. 11, then substituting the resulting plate current in Eq. 10 gives

$$Z_e = E\,e^{j\omega t}/G_m BE\,e^{j(\omega t + \phi)} = e^{-j\phi}/BG_m \tag{13}$$

$$Z_e = (\cos\phi - j\sin\phi)/BG_m = R_e + jX_e \tag{14}$$

in which

$$R_e = \cos\phi/BG_m \tag{15}$$

and

$$X_e = -\sin\phi/BG_m \tag{16}$$

Thus the impedance looking into the plate circuit of the reactance tube is composed of a series combination of a resistance R_e and a reactance X_e. If ϕ is between zero and +180 degrees (leading) the equivalent reactance is negative and therefore represents a capacitance. Likewise, if ϕ is between zero and −180 degrees (lagging), the equivalent reactance is positive and represents an inductance. For the practical case in which ϕ is close to ±90 degrees, the resistive component may be neglected and the reactance becomes

$$|X_e| = 1/BG_m \tag{17}$$

In the case of the inductive type of reactance tube, the equivalent inductance is

$$L_e = X_e/\omega = 1/\omega BG_m \tag{18}$$

When the equivalent inductance of

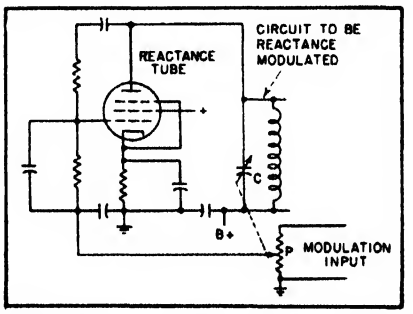

FIG. 2. Constant deviation is obtained by ganging a modulation input potentiometer with the tuning capacitor

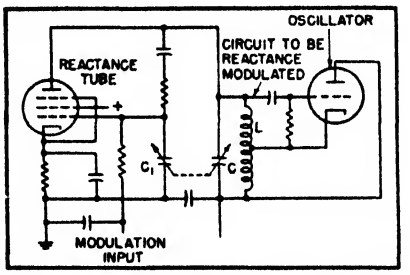

FIG. 3. Method of obtaining constant deviation by ganging an element of the phase shifter with the tuning capacitor

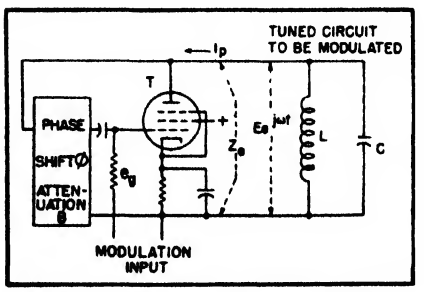

FIG. 4. Fundamental reactance-tube circuit

Eq. 18 is inserted in 3, the frequency is

$$f = f_r + f_r\omega LBG_m/2 = f_r + \pi LBG_m f_r^2 \quad (19)$$

Thus, with a fixed phase-shifter attenuation B and tuning inductance L, frequency deviation is proportional to the square of the resonant frequency f_r. Hence, by using an inductive reactance tube with a phase-shifter attenuation inversely proportional to the square of the frequency, constant-deviation operation may be obtained with a fixed-inductance, variable-capacitance tuned circuit.

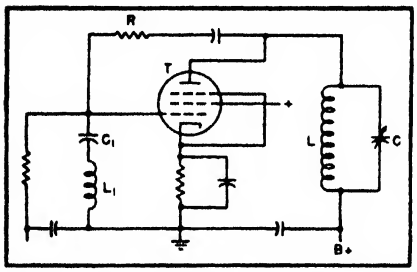

FIG. 5. Constant-deviation reactance-tube circuit. Phase shifter R, C_1, and L_1 produces an attenuation inversely proportional to the square of the frequency over the tuning range

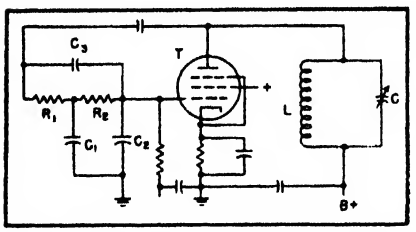

FIG. 6. In this constant-deviation network, the required inverse-square attenuation is obtained by the bridged-T phase-shifting network R_1, R_2, C_1, C_2, and C_3

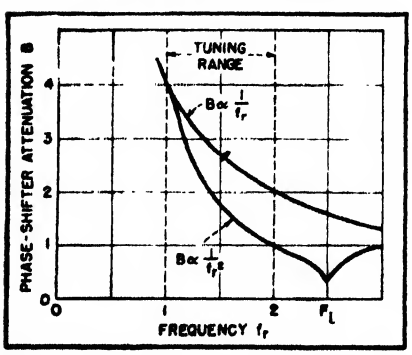

FIG. 7. Attenuation $B \propto 1/f_r$ produced by conventional two-element inductive reactance-tube phase shifter and attenuation $B \propto 1/f_r^2$ required by an inductive reactance tube for constant deviation of a capacitance-tuned circuit

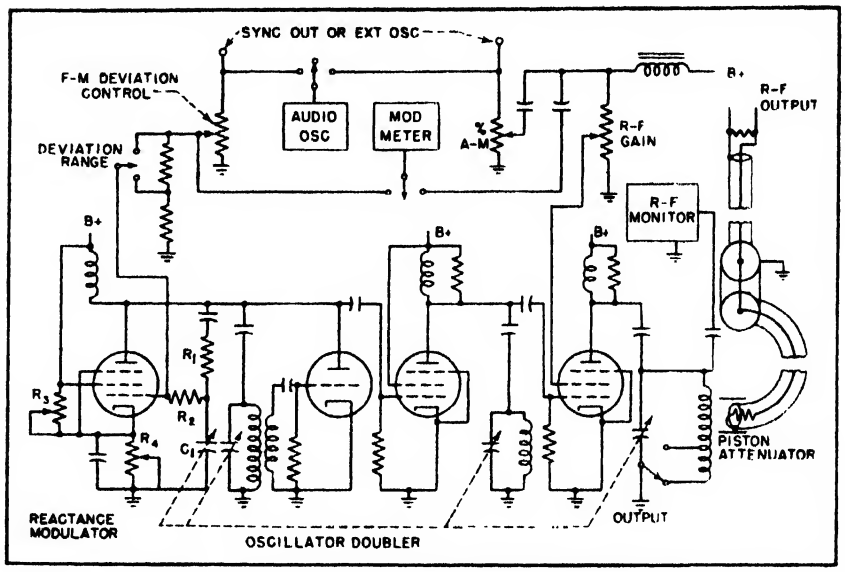

FIG. 8. Simplified diagram of the f-m signal generator

In the case of the capacitive reactance tube, the equivalent capacitance is

$$C_e = 1/\omega X_e = BG_m/\omega \quad (20)$$

Inserting C_e from Eq. 20 in Eq. 5 gives

$$f = f_r - f_r BG_m/2\omega C = f_r - BG_m/4\pi C \quad (21)$$

The deviation term $-BG_m/4\pi C$ in Eq. 21 shows that the deviation is independent of frequency if the phase-shifter attenuation B and the tuned circuit capacitance C are also independent of frequency. Hence, constant-deviation operation may be obtained by the use of a fixed-capacitance, variable-inductance tuned circuit and a capacitive-type reactance tube employing a phase-shifter having an attenuation independent of frequency.

Figures 5 and 6 show capacitance-tuned circuits and inductive-reactance tube arrangements which produce constant frequency deviation over a range of frequencies. The resulting phase-shifter attenuations have the general shape shown in Fig. 7. The attenuation is such that the phase-shifter output amplitude is inversely proportional to the square of the frequency over the tuning range ($B \propto 1/f_r^2$, assuming constant phase-shifter input). The normal attenuation produced by conventional two-element phase-shifters is an output amplitude inversely proportional to the first power of the frequency, $B \propto 1/f_r$. In Fig. 5, this inverse square-law characteristic is obtained by tuning L_1C_1 to frequency F_t in Fig. 7. Tuned circuit L_1C_1 operates on the capacitive side of resonance and therefore appears as a capacitance to produce an inductive-reactance tube.

In Fig. 6, the bridged-T network R_1R_2 and $C_1C_2C_3$ is tuned to locate its rejection frequency at the frequency F_t. This network is capable of constant-deviation operation over a frequency range of about two-to-one, while the network of Fig. 5 covers a range of about 1.5 to one. The exact magnitude depends upon the constancy of deviation required.

Over-All Design

A frequency coverage of two-to-one can be obtained by coupling an attenuator to the modulated oscillator. This system is not suitable for a wider frequency coverage since the phase-shifting network and the oscillator tank coil have to be switched. The network is rather critical and switching of this circuit at very high frequencies would

probably lead to trouble.

A design which permits a four-to-one frequency coverage without switching oscillator and modulator circuits is obtained by following the oscillator with a class-C stage whose tank coil is switched to operate either as an amplifier or as a doubler. This design permits the oscillator and modulator to operate at half the frequency of the high output-frequency range. At lower frequencies, the effects of stray and residual reactances are not as troublesome as they would be at the higher frequencies. It also permits amplitude modulation of the output stage.

This design is not entirely satisfactory because some undesired amplitude modulation is produced during frequency modulation of the oscillator and the oscillator voltage is not sufficient to permit the class-C stage to remove this spurious amplitude modulation by limiting. A second objection is that amplitude modulation of the class C stage produces a considerable amount of spurious frequency modulation of the oscillator. Both of these objections can be removed by adding a second class-C stage.

The design which proved to be most satisfactory is shown in Fig. 8. The reactance-modulated oscillator operates from 27 to 54 megacycles. This is followed by a doubler stage and an output stage. The output stage operates either as an amplifier or as a second doubler (quadrupler), thus providing frequency coverage from 54 to 216 megacycles. This design provides the maximum of stability and simplicity since the oscillator and modulator operate at a relatively low frequency and the only r-f switching required is to switch a ground contact on the output coil.

The reactance tube uses a bridged-T type network similar to that of Fig. 6, in which C_2 and C_3 are replaced by the input capacitance and the grid-to-plate capacitance of the reactance tube. Capacitor C_1 is made variable and ganged with the tuning capacitor to provide the precision of deviation calibration required in a signal generator.

The slotted stator of C_1 is visible in the foreground of Fig. 9. By bending the sections of the stator, the deviation can be made as constant as desired over the entire frequency range. Resistor R_4 is bypassed for r-f only so that it causes degeneration at modulation frequencies and is used as a modulation sensitivity control. Resistor R_5 controls the cathode bias by bleeding current through the cathode resistor and is used to adjust the modulator tube to its most linear operating point. Total rms distortion of less than one percent at 75-kc deviation can be obtained with a modulating signal containing less than one-half percent distortion.

Doubler Tracks

A conventional self-biased class-C doubler is used. This stage tracks with the oscillator if the inductance of the tank coil is made one-fourth that of the oscillator tank and an identical capacitor section is employed. However, a higher tank circuit impedance can be obtained by decreasing the capacitance and correspondingly increasing the inductance. The requirements for tracking are that the shape of the capacitor plates be identical and that the ratio of maximum capacitor-and-circuit capacitance to total minimum-capacitance in the doubler circuit be the same as for the oscillator circuit.

Amplitude modulation is produced by modulating the screen circuit of the output stage. Since the power required is small and comparable with that required for frequency modulation, a simple resistance-tuned modulating oscillator serves for either amplitude or frequency modulation. Distortion is less than 3.5 percent for amplitude-modulation depths up to 50 percent. Due to the effective buffer action of the doubler stage, the spurious frequency modulation produced during amplitude modulation is small.

Frequency range switching is accomplished by providing the output tank coil with two contact points, one or the other of which is grounded by spring-contact fingers actuated by the frequency range switch. This method avoids most of the mechanical and electrical difficulties of coil switching.

In the output tank circuit, a high Q was desired to reduce the harmonically-related spurious output signals, while a low Q was desired to reduce the amplitude modulation introduced on frequency-modulated signals by the selectivity of the circuit. In the final design, the damping was adjusted to reduce spurious signals to more than 35 decibels below the desired signal. The resulting amplitude modulation at 75-kc deviation is about two percent.

A mutual-inductance (piston) attenuator's is coupled to the tank-circuit inductor of the output stage. This is a simple and accurate attenuator for the vhf range since the rate of attenuation is dependent only on the inner diameter of the attenuator tube after sufficient attenuation has been introduced to suppress undesired modes of propogation of the electromagnetic field in the tube. The attenuator dial is calibrated from 0.1 microvolt to 0.2 volt; correction being made for a slight nonlinearity at the high-voltage end of the range.

Figure 10 shows the design of the output system. The voltage induced in the attenuator coupling loop L_3 in Fig. 10A is

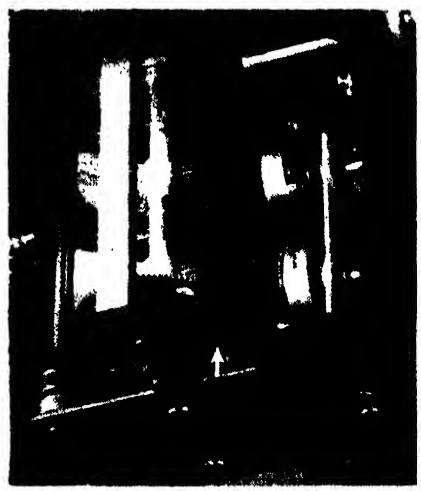

FIG. 9. Mechanical details of the r-f assembly. The arrow indicates the slotted stator of C_1

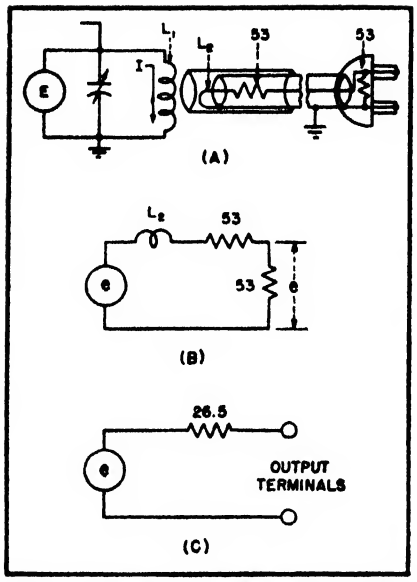

FIG. 10. Circuit (A) is the output system in which the D-shaped coil L_1 is used. The equivalent circuit of the attenuator is shown at (B) and the equivalent circuit of the signal generator at (C)

$$e' = I\omega M = \frac{E}{\omega L_1}\omega k\sqrt{L_1 L_2} = EK\sqrt{L_2} \tag{22}$$

where $\omega = 2\pi$ times the frequency and k is the coefficient of coupling between L_1 and L_2.

This equation shows that e' is a function of the tank voltage E and the coefficient of coupling k only. The attenuation law of the piston attenuator controls k. Voltage E is monitored by a voltmeter of the set-to-line type, the level being adjusted by a control in the screen circuit of the output tube. The output tank coil is physically flattened on the side facing the attenuator to present a more uniform field to the attenuator and permit larger values of k than are obtainable with a coil of circular cross-section. Although tank voltage E is smaller when doubling, the transformer ratio ($\sqrt{L_2/L_1}$ of Eq. 22) is larger and the allowable Q is greater. By placing the attenuator in proper relation to the tank coil, equal output is obtained on the two frequency ranges with very little change in the gain control setting.

A switch, ganged with the frequency range switch, actuates a precision voltage divider to halve the frequency-modulating voltage when the high-frequency range is being used since otherwise the deviation would be double that on the low-frequency range. A section of this unit switches calibrating resistors in the r-f monitoring voltmeter circuit.

Standard 53-ohm RG58/U cable is used for the output cable. To keep the output impedance of the generator constant, a 53-ohm resistor is placed in series with the coupling loop and another is used to terminate the output cable. From Fig. 10B, the voltage e across the terminating resistor is then:

$$|e| = \left|\frac{53\,e'}{106 + j(\omega L_2)}\right| = \frac{53\,e'}{\sqrt{(106)^2 + (\omega L_2)^2}} \tag{23}$$

Since L_2 is less than 0.01 microhenry, $(\omega L_2)^2$ can be neglected in comparison with $(106)^2$ and $e = e'/2$.

Neglecting L_2 in Fig. 10B, an application of Thevenin's theorem yields the equivalent circuit of the signal generator, shown in Fig. 10C. Thus the generator can be represented as a source e in series with a resistance of 26.5 ohms. The attenuator is calibrated in terms of the open-circuit output voltage e.

If the load impedance is not large compared with 26.5 ohms, the voltage applied to a load attached to the output terminals can be calculated by using the equivalent circuit of Fig. 10C.

To provide frequencies below the range of the signal generator, a converter consisting of a fixed oscillator operating at 70 mc, a linear mixer, and an amplifier which has flat response from 100 kc to 25 mc has been constructed. When the signal generator is tuned from 70.1 to 95 mc, the difference frequency of 100 kc to 25 mc is obtained from the converter. With frequency modulation the useful low-frequency limit is obviously dependent on the deviation employed.

By adjusting the over-all conversion-amplification of the converter for unity gain, the output voltage can be read directly from the attenuator dial of the signal generator without requiring an additional monitoring system or attenuator. Provision is also made for an uncalibrated voltage with about ten times the amplitude of the input signal. The fixed oscillator is provided with a calibrated incremental trimmer capacitor for selectivity measurements.

References

(1) Barber, A. W., Franks, C. J. and Richardson, A. G., A Frequency-Modulation Signal Generator, ELECTRONICS, April 1941, p 36.
(2) Badessa, R. S., Mixer Frequency Charts, ELECTRONICS, August 1946, p 188.
(3) Hund, August, "Frequency Modulation", p 166, McGraw-Hill Book Co.
(4) Harnett, D. E. and Case, N. P., The Design and Testing of Multirange Receivers, *Proc. IRE*, 23, June 1935, p 578.

Wide-Range Sweeping Oscillator

Single test oscillator covers all frequencies from upper video range through standard a-m broadcast, police, aeronautical, f-m broadcast, and television bands to the citizen's band. Basically the circuit is a beat-frequency oscillator using two 3-cm klystrons

EXPANSION of the commercially useful electromagnetic frequency spectrum, accelerated by wartime developments, has made an extremely wideband sweeping oscillator a laboratory necessity. For example, the maintenance man alternately faced with servicing a standard a-m broadcast receiver

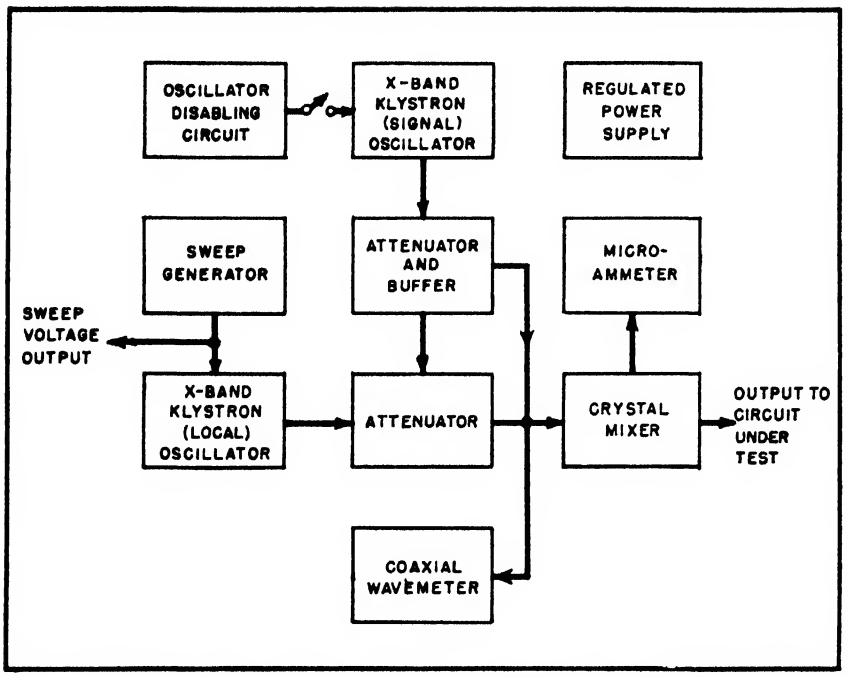

FIG. 1—Block diagram shows principle of operation

and next a television receiver needs an oscillator covering a wider frequency range than provided from previously available signal generators. The research worker needs a laboratory instrument covering an even greater frequency spread.

To meet a need for such test equipment a wide-range sweeping oscillator has been developed. It has output frequencies between 50 kc and 500 mc immediately available at approximately a 50-ohm impedance level and with an amplitude of about 0.1 volt maximum.

Receiver Alignment

Frequency excursion per sweep is adjustable to a maximum of approximately 40 mc. A sawtooth sweep voltage adjustable between 50 and 100 cps is available at front panel terminals to be used either as such or as a synchronizing source for another sweep generator. A precision coaxial wavemeter is included with the front panel controls. Thus the sweeping oscillator in combination with any cathode-ray oscilloscope provides a receiver alignment tool that is at once precise and extremely flexible. For example, a television or f-m broadcast receiver can be aligned with equal ease.

In aligning a receiver, the sweeping oscillator produces a signal of nearly constant amplitude but with a cyclic time variation in frequency. A sweep voltage whose amplitude variation is synchronized with the signal frequency variation is also furnished by the sweeping oscillator. With the frequency excursion approximately centered in the passband of the receiver, the vertical amplifier of the oscilloscope is connected to some convenient monitoring point in the audio or video section of the receiver. The sawtooth sweep voltage output available at the oscillator is connected to the horizontal amplifier of the oscilloscope, or the internal sweep of the oscilloscope, properly synchronized, is used. The pattern on the screen is a graph whose abscissa is frequency and whose ordinate is receiver response.

This method of alignment is more rapid than the point-by-point technique. What is usually more important, the effect of the adjustment or variation of any of the receiver parameters on the response at all frequencies is immediately apparent. The possibility of missing a hump or some other asymmetry in the response is eliminated, as the output of the sweeping oscillator has no discontinuities within its particular spectrum.

Calibration of the frequency coordinate of the receiver response frequency plot on the oscilloscope screen is most conveniently accomplished by means of the precision absorption type wavemeter. When the sweeping oscillator passes through the frequency to which the wavemeter is set, there will be a dip in the response pattern, thus effecting the calibration.

Oscillator Components

Figure 1 gives the block diagram of the sweeping oscillator, which is a heterodyne-type generator combining the outputs of two X-band (3-cm) reflex klystrons (the Sheppard-Pierce type) in a mixing network. One klystron, called the signal generator, is at a fixed frequency during operation of the instrument. The other, designated the local oscillator, is swept in frequency by the application of a sawtooth wave to its repeller. The two outputs are heterodyned in a microwave crystal mixer and the resulting difference frequency made available at the output terminals.

The sawtooth is generated by a gas tube relaxation oscillator and serves not only to modulate the local oscillator but also to develop sweep voltage for use in synchronization of an oscilloscope sweep. An efficient electronically regulated power supply furnishes plus 300 volts, minus 300 volts (both regulated), and filament power. Ripple is kept very low so as to obtain stable klystron operation.

Sweeping Oscillator

Figure 2 shows the simplified schematic diagram of the sweeping oscillator. All adjustments are available at the front panel. The sawtooth sweep voltage generator is a conventional gas tube relaxation oscillator utilizing the miniature 2D21 gas tetrode. The sweep rate control varies the capacitor charging time-constant to make available sweep rates from approximately 50 to 100 cps. The sweep amplitude

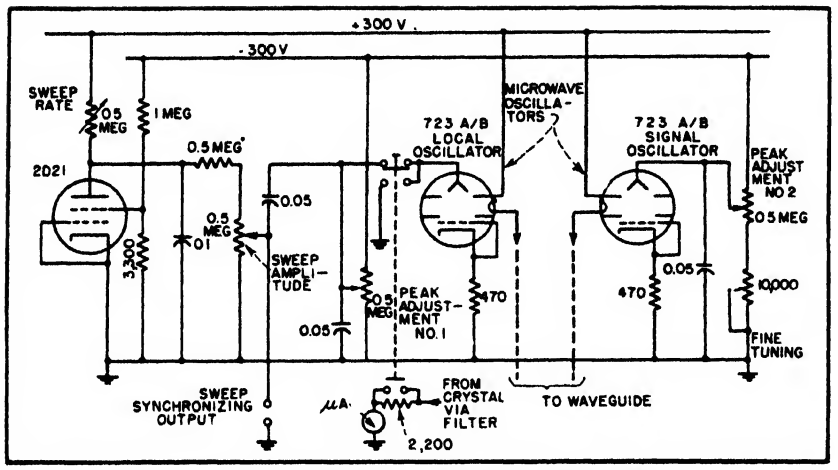

FIG. 2—Schematic of sweeping and tuning circuits

control adjusts the output frequency excursion up to a maximum of 40 mc by controlling the magnitude of the sawtooth voltage applied to the local klystron oscillator repeller electrode. The use of this adjustable relaxation oscillator for the production of both frequency and oscilloscope sweep has not only added to the flexibility of the system, but has also eliminated the inconvenient phasing adjustments necessary when the line supply voltage is used for the same purpose.

It is also possible to frequency modulate the klystron from an external source by removing the 2D21 and feeding the external modulating signal into the instrument through the sweep output jacks.

Reflex Klystron Characteristics

The literature is sufficiently rich in klystron references to make any detailed review of klystron theory inappropriate. However, maximum efficiency in the utilization of this sweeping oscillator requires that certain klystron characteristics be kept clearly in mind. Figure 3 gives two plots, both against the magnitude of negative repeller voltage, as the abscissa (repeller voltage increasing in negative value to the right); one graph is with output as the ordinate, the other with frequency as the ordinate.

The plot of output against repeller voltage indicates that oscillations can be sustained over certain ranges of repeller voltages. Note that the average magnitude of the output over the two ranges shown is greater for the higher repeller voltage. The mode with the greater output, as would be expected, is associated with the lesser time of the electron bunches in the space between the bunching grids and the repeller. The two voltage modes are only representative; there may be more or fewer depending on the electrode voltages obtainable.

The plot of repeller voltage against frequency illustrates the frequency sweeping principle of this instrument. If the repeller voltage is varied over a range within the limits imposed by a voltage mode, then the frequency of the local oscillator will vary in magnitude as well as frequency, as between points A and B of Fig. 3. This variation in magnitude might seem to introduce an unwanted amplitude modulation characteristic in the output. Actually such is not the case, for reasons to be mentioned in the next section.

The natural resonant frequency of the cavity of either klystron is not affected by the variation of the repeller voltage; such variation merely drives the cavity off resonance up to a limit imposed by the effective Q of the cavity. The actual resonant frequency is adjusted by changing the grid spacing and thus the physical conformation of the cavity. The grid spacing of either klystron can be changed, but only a control for the local oscillator is brought out to the front panel as the coarse tuner.

Mixing Oscillator Outputs

The principal design problem associated with mixing the outputs of the two oscillators in the waveguide system involved the efficient isolation of the oscillators from each other to minimize pulling. Furthermore, sufficient decoupling between the oscillators and their load was required. Figure 4 illustrates the waveguide system that was used. The chief feature of this system is the broadband directional coupler, which consists physically of three holes in the wall between the two waveguides.

Directional couplers are designed to provide transmission between two waveguides (or transmission lines) in one direction only. For this particular system, the directional coupler allows energy from the signal oscillator to reach the crystal mixer, but ideally no energy from this source reaches the local oscillator. Similarly a minimum amount of energy from the local oscillator reaches the signal oscillator. Transmission from one waveguide to the other is directed to the termination and is almost completely absorbed. Thus local and signal oscillators are isolated and the possibility of locking or pulling is minimized though not entirely eliminated, as later explained.

Signal from the signal oscillator undergoes about 10 db attenuation in passing through the directional

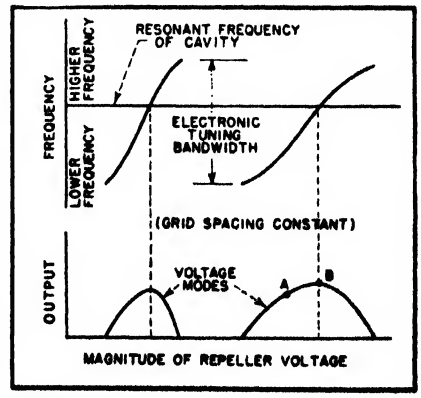

FIG. 3—Frequency and amplitude of klystron output are affected by varying its repeller voltage

coupler and, constrained by the one-way properties of the coupler, reaches only the crystal mixer assembly. There is little reflection of this particular signal in either of the waveguides because the crystal assembly is in the shorter waveguide, and a carbon coated termination card is in the other. Both provide loads of approximately the characteristic impedance of their waveguides. The signal from the local oscillator travels directly to the mixer. The portion of the signal from this source entering the longer waveguide by way of the three-hole coupler is directed only toward the termination, where it is completely absorbed.

The attenuator between the local oscillator and mixer decouples this oscillator from its load. As a matter of fact, the attenuator action is incidental, the isolating action being the primary consideration. The attenuator in the signal oscillator path is actually the output attenuator; that is, its adjustment controls the amplitude of the output from the sweeping oscillator. This action is possible because the output of the sweeping oscillator results from the heterodyning of two signals, one much larger than the other; the heterodyned output amplitude is substantially independent of the larger. The smaller of the two signals at the mixer is that of the signal oscillator, as this one is attenuated more in passing through the directional coupler. Hence, adjustment of the transmitted amplitude of the signal oscillator controls the output of the sweeping oscillator. This arrangement also prevents the previously mentioned amplitude modulation of the local oscillator signal, associated with the frequency modulating process, from appearing in the output. With the signal oscillator producing an output of constant amplitude, the output of this instrument is therefore substantially independent of variations in the amplitude of the local oscillator.

Frequency Calibrating Circuit

The frequency calibrating circuit of this instrument is built around a precision coaxial absorption wavemeter. The outer conductor of the coaxial line is silver plated on its inner surface, and the moveable center conductor is an invar rod successively copper, nickel, and silver plated. This type of construction, together with close mechanical tolerances, insures high Q, negligible temperature coefficient, and high overall precision.

The crystal current indicated on the microammeter is a function of the rectified output of both the local and signal oscillators. Normally, however, the highly attenuated signal of the signal oscillator contributes a negligible amount to the total crystal current. Hence in order to monitor the output or measure the frequency of the signal oscillator it is necessary to deactivate the local oscillator and increase the meter sensitivity by a pushbutton switch on the front panel.

In the operation of this instrument, a reading proportional to the local oscillator frequency is taken and recorded, with the sweep amplitude at zero. The pushbutton is then depressed, and a reading is taken of the frequency of the signal oscillator. The output frequency is then the difference multiplied by a proportionality factor.

After the oscilloscope pattern is properly located and centered appropriately to the equipment under test, the calibration of the frequency axis of this pattern is accomplished by first recording the wavemeter reading proportional to the wavelength of the signal oscillator. This measurement involves tuning the wavemeter until the entire visible pattern decreases. The wavemeter is then varied until a moveable dip is seen on the pattern. The movable dip is an indication of the frequency of the local oscillator and is used to measure the width of the passband and, in conjunction with the signal oscillator reading, the absolute frequency. This procedure eliminates the use of any switching.

The midpoint of the frequency excursion can be readily adjusted to a maximum of 500 mc. This limit is not imposed by the frequency range of the two klystrons. Indeed, if only the range of the two oscillators were considered, a maximum midpoint frequency of nearly 1,000 mc could be reached. This last figure arises from the fact that each oscillator has a frequency range of about 1,000 mc, covering the band 8,700 to 9,700 mc. The upper frequency limitation of the instrument is determined by the properties of the output circuit. Much above 500 mc, the unavoidable capacitances in the crystal mixer output circuit take their toll and the output amplitudes fall off. If, however, a coaxial output circuit is used, it is possible to push the frequency limit up another octave to 1,000 mc.

The sweep amplitude adjustment gives continuous control of the frequency excursion per sweep from zero up to a maximum of 40 mc. This large frequency excursion, together with the frequency coverage, gives ample and flexible coverage for most if not all commercial vhf applications, including color television.

With the local oscillator sweeping a frequency range that just or nearly includes the constant frequency of the signal oscillator, it is possible to obtain output frequencies close to the audio range. Ideally, of course, the complete audio band could be covered. This is not practically feasible, however, because even with a carefully designed waveguide system there is some pulling or interaction between the two oscillators when their frequencies are close. This interaction can be ascribed to the small departure of the waveguide terminations and crystal mixer assembly from the ideal flat waveband loading. It is this pulling which limits the low end of the frequency range.

In addition to the use of the sweeping oscillator as an aligning instrument, it is also possible to utilize the oscillator without the sweeping feature by the simple expedient of turning off the sweep amplitude. This instrument so operated becomes a c-w signal source with the above-mentioned ranges.

This instrument is well suited for instructional purposes as it pro-

duces visual indications of the frequency characteristics of receivers and transducers when used in conjunction with a suitable oscilloscope having a conventional circuit.

No complete attempt to enumerate the capabilities of this instrument has been made. It is the opinion of the designers that this instrument is intrinsically so flexible that numerous additional uses will suggest themselves to the user.

VHF Impedance Measurements

Equipment for making impedance measurements in the range from 50 to 150 mc is described and its probable errors are analyzed. Construction and operation of the equipment and method of making measurements are explained

By D. STANLEY HENRY

AN INSTRUMENT with which to measure impedance in terms of resistance and reactance through the range of frequencies which have been assigned to the commercial f-m and television services is needed. Below this range r-f bridges are satisfactory and above this range slotted-line measurements are convenient.[1]

The instrument to be described is small and compact so that it can be used in many places inaccessible with conventional equipment. The grounding problem, which is always important and often critical at these frequencies, offers little difficulty principally because the device is complete in itself.

The range can be quickly varied to suit the particular problem so that in most cases it is unnecessary to supplement the unknown impedance with a known reactance in order to bring the unknown impedance within range of the instrument. However, greatest accuracy is obtainable through the resistance and reactance ranges commonly encountered in antenna and transmission line measurements. The resistance range is approximately 30 to 1000 ohms, and at 100 mc the reactance range is approximately ±15 to 500 ohms. The reactance range depends on the capacitance range of the capacitor used for C_2 in Fig. 1 and 2.

Resistance measurements are made in terms of a ratio of the voltage developed across a resonant circuit to the voltage resulting when the unknown resistance is introduced into the circuit. The unknown reactance is measured in terms of the variation of reactance of an accurately calibrated capacitor that is required to return the measuring circuit to resonance.[2]

The most logical means of measuring voltage and indicating resonance is a vacuum tube voltmeter connected to a resonant circuit L_1C_1 as shown in Fig. 1. Because a voltage ratio is used, the voltmeter need not be calibrated if its law of deflection is known. One of the adjustments requires tuning to produce 70.7 percent of the voltage at resonance. This voltage would be one-half of the voltmeter reading at resonance if the voltmeter were square-law. The added sensitivity of this type of voltmeter is convenient for increased tuning accuracy.

A balanced-modulator circuit will insure square-law operation because only second-order terms appear in the plate circuit. A 100-μa meter with at least 50 dial divisions is satisfactory for the meter. The required balanced voltage for the voltmeter is obtained from the balanced circuit L_1C_1.

Assume Q_2 of resonant circuit L_2, C_2, C_3 is reasonably high so that R_2 can be neglected. Let Z_2 be the impedance seen by a series generator in circuit 2 of Fig. 1 when it is isolated from circuit 1, then

$$Z_2 = \frac{Z_R Z_X}{Z_R + Z_X}$$

When circuit 2 is coupled to circuit 1, the impedance appearing in circuit 1 due to circuit 2 is[3]

$$\frac{(\omega M)^2}{Z_2} = \frac{(\omega M)^2}{Z_R} + \frac{(\omega M)^2}{Z_X}$$

This equation shows that the various shunt impedances affect circuit 1 independently and any one may be added or removed without

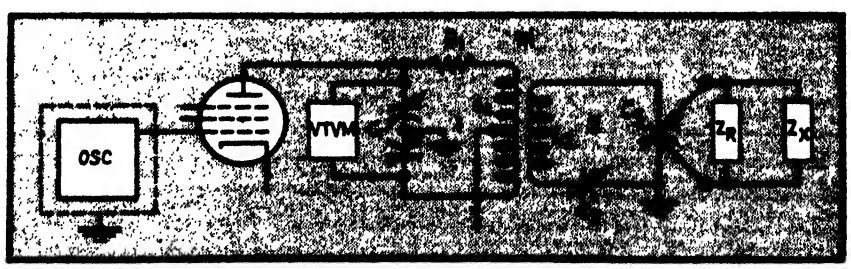

FIG. 1—The principle of measurement is that of a Q meter. The pentode prevents reaction of the measuring circuit on the oscillator and gives the generator a nearly infinite internal impedance

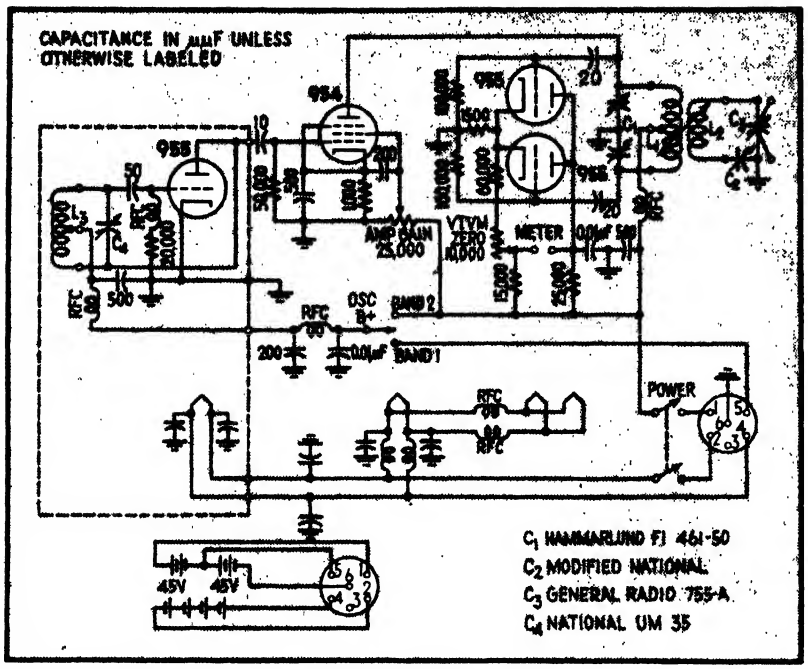

FIG. 2—A balanced, square-law vacuum-tube voltmeter is built into the instrument to measure the voltage across the resonant circuit

changing the effect of the others. Regardless of the physical arrangement of the unknown impedance, circuit 2 sees the equivalent resistance in parallel with the equivalent reactance. In cases where the series components are more desirable and useful, the parallel combination can be changed to the series equivalent.

It should be noted that the minimum capacitance of C_2 will appear across C_3 as an unknown reactance but the effect of this reactance is constant and will not modify the value of the unknown because it has been shown that unknown components across C_2 affect circuit 1 independently.

It is important to connect the unknown directly to the terminals of C_2 rather than to electrically equivalent points, to eliminate error which would be introduced by the inductance of the leads connecting circuit 2 to C_2. The method of tuning circuit 2 described below will show that the circuit inductive reactance is tuned out.

Care must be taken to maintain the Q of circuit 2 as high as possible because the principal assumption in this method of measurement is that the resistance of circuit 2 is negligible. Consideration of this resistance would make the measurements unnecessarily tedious. Experience has shown that very practical and useful results can be obtained with such an assumption.

The resistance R_1 of circuit 1 is used as a starting point for making measurements but it is not necessary to know the ohmic value. At one point in the tuning procedure, circuit 1 will be detuned from resonance until the square-law voltmeter indicates one-half the reading at resonance. This indicates a voltage 70.7 percent of maximum and shows that a reactance equal to R_1 has been added to circuit 1. This reactance will then be replaced by an equal reactance of opposite sign which can be accurately determined from C_2. The constant driving voltage is effectively in series with L_1 and C_1 because this circuit is driven by a pentode which is practically a constant-current generator. The inductive coupling between L_1 and L_2, which presents resistance and reactance components to circuit 1, need not be known.

In using the vhf impedance measuring circuit of Fig. 2, the following procedure is used:

1. Detune C_1 until it has no effect on the voltmeter and set the voltmeter to zero.

2. Set C_2 to minimum so that $\Delta C_2 = 0$.

3. Tune C_1 for maximum voltmeter reading and adjust the amplifier gain for a convenient reading, probably full scale. Circuit 2 is so far from resonance that it will have negligible effect on circuit 1 at this point.

4. Short C_2 by inserting a strip of crimped copper between the plates. This must be done at the plates rather than across the terminals to avoid the error caused by the inductance of a relatively long shorting bar across the terminals.

5. Tune C_2 for minimum voltage indication.

6. Remove the shorting strip and check C_1 for resonance.

7. Note the maximum voltmeter reading in dial units as V_1.

8. Detune circuit 1 by decreasing C_1 until the meter indicates one-half the maximum reading. At this point $X_{C_1} = R_1$.

9. Retune circuit 1 to resonance by increasing C_2. This indicates that an impedance equal to R_1 has been presented to circuit 1 from circuit 2. Note (ΔC_2).

10. Add the unknown directly to the terminals of C_2.

11. Retune C_2 to cancel the added reactive component. Call the new setting of C_2 $(\Delta C_2')$. Note $(\Delta C_2')$ and the new voltmeter reading V_2.

12. $1/\omega(\Delta' C_3) - (\Delta C_2) = (\Delta' C_3)$ is the unknown reactance, where $(\Delta' C_3) = (\Delta C_2') - (\Delta C_2)$. From step 9 above

$$\frac{(\omega M)^2}{1/\omega(\Delta C_2)} = R_1 \qquad (\omega M)^2 = \frac{R_1}{\omega(\Delta C_2)}$$

The voltages developed across C_1 are inversely proportional to the effective circuit resistances so that

$$\frac{E_1}{E_2} = \frac{R_1 + \omega^2 M^2/R}{R_1} = 1 + \frac{1}{R\omega\,(\Delta C_2)}$$

$$R = \frac{1}{\left(\frac{E_1}{E_2} - 1\right)\omega\,(\Delta C_2)}$$

Let $P = (E_1/E_2) - 1$, and $V =$

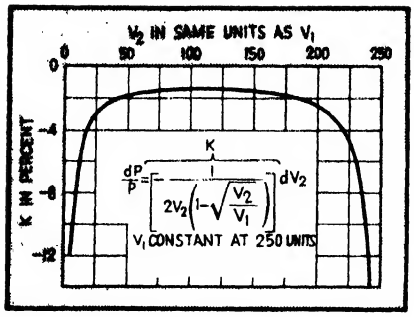

FIG. 3—Adjust coupling between circuits 1 and 2 of Fig. 1 to keep V_2 within the range of least relative error K which can be introduced by inaccuracies in reading voltages when measuring resistances

voltmeter deflection in a square-law device, then $P = \sqrt{V_1/V_2} - 1$: $R = 1/P\omega(\Delta C_s)$: $X = 1/\omega(\Delta' C_s)$.

Analysis of Errors

From the above equations for R and X, we see that the accuracy of the measurements depends on a knowledge of frequency, (ΔC_s), and the voltage ratio used to find P. For greatest convenience in using an instrument of this type, it is necessary that the source of frequency be an integral part of the unit. The oscillator shown was calibrated with a heterodyne frequency meter, the fundamentals of which were referred to a frequency standard. Tuning circuit 1 through resonance may cause a frequency change of about 0.002 percent. It is safe to assume that errors in frequency will be negligible as compared with other probable errors.

By means of differentials, the relative effect of errors in the calibration or use of C_s can be shown from $X = 1/\omega(\Delta' C_s)$. Assuming that $\Delta\omega = 0$, and taking logs we obtain $\log X = \log 1 - \log\omega - \log(\Delta' C_s)$; and differentiating obtain $dX/X = -d(\Delta' C_s)/(\Delta' C_s)$.

This result shows that the relative error in measuring reactance is inversely proportional to $(\Delta' C_s)$ and directly proportional to the error in finding $(\Delta' C_s)$. This is particularly serious for large inductances and small capacities because $(\Delta' C_s)$ is equal to the difference in the two settings of C_s. The resistive component of the unknown lowers the Q of the circuit so that the exact setting of this capacitor for resonance is more difficult. Sometimes it is better to tune through resonance until the voltmeter reading indicates the same point but on the other side of the resonance curve. Then one-half of the change in C_s will be required $(\Delta' C_s)$.

The measurement of the resistive component involves the square root of the voltage ratio and also (ΔC_s) as the principal causes of error because again these errors will probably be large compared to the error in frequency. It is doubtful that C_s can be set within about 2 or 3 percent because of the broadness of resonance.

The relative error in finding R which results from error in the voltage ratio is more easily predicted by considering the error in finding P. Let V_1 and V_2 be the meter deflections in any units and assume V_1 constant as the starting point, then $P = \sqrt{V_1/V_2} - 1$, taking logs; $\log P = \log(\sqrt{V_1/V_2} - 1)$, and differentiating

$$\frac{dP}{P} = -\frac{\left(\frac{1}{2V_2}\right)\sqrt{\frac{V_1}{V_2}}}{\sqrt{\frac{V_1}{V_2}} - 1} dV_2 =$$

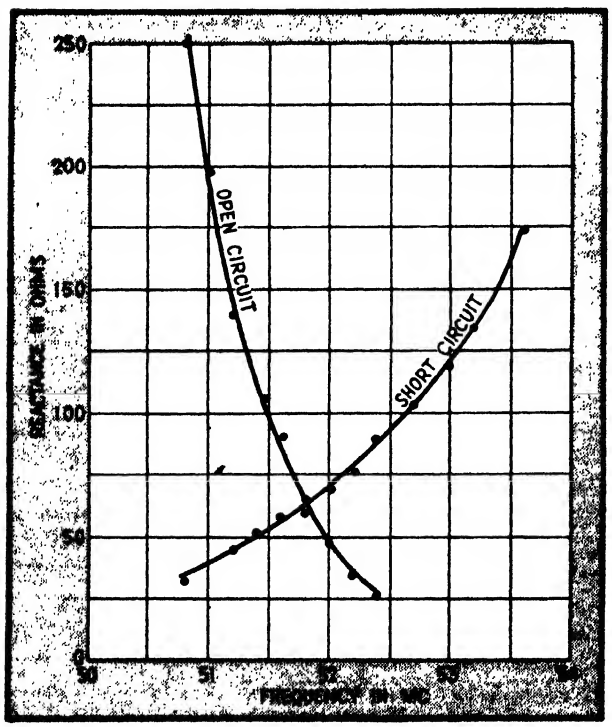

FIG. 4—Measurement of coaxial-line reactance made with the instrument

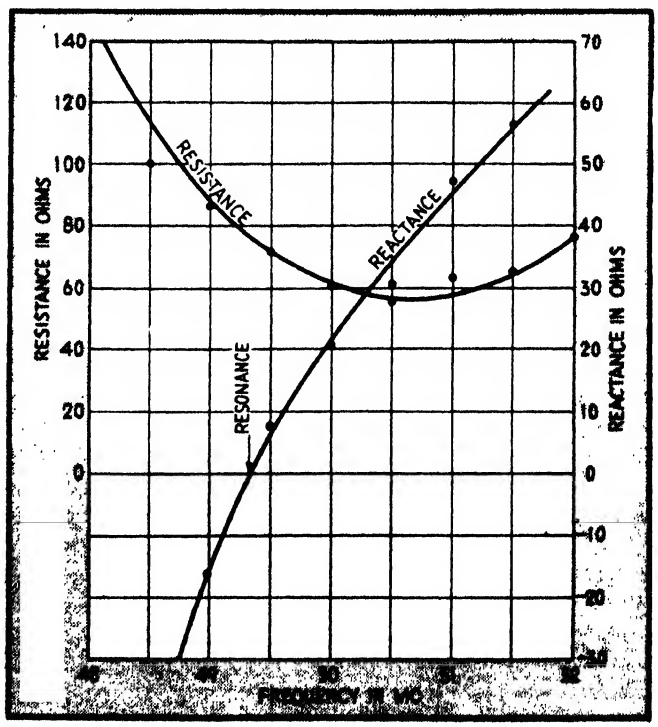

FIG. 5—Impedance of a dipole antenna as measured with the test instrument

$$-\left[\frac{1}{2V_2\left(1-\sqrt{\frac{V_2}{V_1}}\right)}\right]dV_2$$

The factor inclosed in brackets is plotted as a function of V_2 in Fig. 3. This curve indicates the range through which V_2 may be read for minimum error. The values of V_2 and (ΔC_3) are interdependent and can be adjusted toward optimum by varying the coupling between L_1 and L_2. This adjustment also is convenient in the measurement of reactance. If a large capacitance is to be measured, the coupling is made small so that (ΔC_3) will be large. Conversely, for a large inductance, the coupling is made close. This adjustment effectively doubles the useful range of C_3. Errors in determining P or (ΔC_3) affect R in just the same manner as an error in $(\Delta' C_3)$ affects the measured value of X. Of course, the errors can tend to cancel or to accumulate, depending on the relative sign of the differential value.

If the power leads are filtered, no r-f will get to L_1 except through the pentode amplifier which approximates a constant-current generator. A butterfly circuit[4] oscillator is an ideal source of power for such a device because of its range, small size and simplicity.

The upper frequency limit of this particular unit is 150 mc. This limit is determined by the necessary inductance of the leads to C_3 because the terminals of C_3 must be available for connecting the unknown. L_2 must be large enough to couple sufficiently with L_1.

The square-law vtvm is best checked by plotting the square root of the meter deflection as a function of the applied voltage. If the meter response is square-law, this plot gives a straight line.

In use, the balance of the L_1C_1 circuit can be conveniently checked by tuning C_1 to resonance and then touching each stator section of C_1 in succession. The voltmeter reading should drop to nearly zero in each case. Small amounts of unbalance can sometimes be compensated by adjusting the center-tap by-pass capacitor. Choice of tubes or of bias operating point is relatively unimportant.

In making any measurement, it is comforting to be able to make it by at least two radically different methods. Because the range of this instrument overlaps the upper limit of the General Radio 916-A r-f bridge, a complete comparison of the two methods at 50 mc was possible. The average difference for random measurements was within five percent and in many cases less than two percent.

Figure 4 shows the results of a group of measurements to determine the characteristic impedance[5] of a 50-foot length of concentric line. The open-circuit and short-circuit reactances of the line are plotted as a function of frequency without regard to sign.

Figure 5 gives the characteristics of a dipole fed with a length of EO1 cable. As this is a balanced impedance and the instrument is an unbalanced device, the measurement is tedious but the curves indicate the results that can be expected and demonstrate the consistency of the measurements. The value of about 76 ohms resistance at resonance is reasonable.

References

(1) Marchand, N., and Chapman, R., UHF Impedance Measurements, Electronics, p 97, June, 1945.
(2) Seeley, S. W., and Barden, W. S., A New Method for Measurement of Ultra-High Frequency Impedance; "Radio at Ultra-High Frequencies," *RCA Institutes Technical Press*, 1940, p 272-293.
(3) Terman, F. E., "Radio Engineer's Handbook," McGraw-Hill Book Co., 1943, p. 149.
(4) Karplus, Eduard, The Butterfly Circuit, *General Radio Experimenter*, 19, No. 5, Oct. 1944.
(5) Sinclair, D. B., Measuring Balanced Impedances with the R F Bridge, *General Radio Experimenter*, 17, No. 4, Sept., 1942.

Wide-Range Signal Generator with Automatic Amplitude Control

By HOWARD T. STERLING

After experimenting with various types of amplitude control for L-C oscillators involving shunting of the tuned circuit, with results not wholly satisfactory, the following scheme was worked out with much better success. It was inspired by the use, in General Radio's model 605 signal generator, of plate voltage control to set oscillator output to the desired amplitude.

Referring to the circuit illustrated, the output of the oscillator, V-1, is rectified by the diode, and the positive voltage resulting is fed to the grid of V-4. This tube is operated at low current, the variable cathode resistor R providing sufficient bias despite the positive voltage at the grid due to oscillator output. Variations in oscillator output are amplified by V-4 to control the bias on V-5 and hence the oscillator plate voltage.

The signal voltage at V-4 grid can be applied to a vtum to read oscillator (and signal generator) output. Since the control depends upon change of amplitude, regardless of the level, it will be seen advisable to operate the oscillator at a relatively high level. In practice, twelve to fifteen volts peak was found most satisfactory. With a fairly high-Q variable capacitor (such that amplitude does not fall below this value at the low-frequency end of a band) the output of the generator

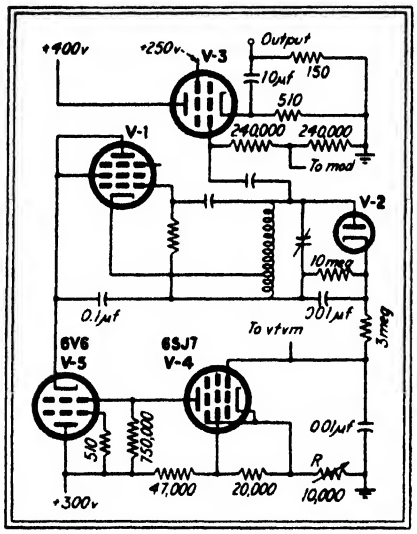

Circuit of a system of automatic amplitude control of an oscillator in a signal generator

can be kept constant plus or minus 2 percent from 50 kc to 50 Mc.

The tube finally chosen for *V*-1 was a 6AC7. Everything from a 6J5 through a 6L6 was tried, but the 6AC7 behaved most consistently and provided highest output. Any convenient diode can be used for *V*-2. A 6L6 was used at *V*-3 for high output.

Power Supply

The oscillator plate and *V*-4 screen supply should be regulated, although it is not entirely necessary. The control circuit is essentially degenerative so that the output will not vary much with change in the line voltage. The screen potential on *V*-4 will affect the gain of that stage, though the plate voltage need not be regulated. Tube *V*-4 and its associated bleeder draw about 5 ma and this is the only additional plate current drain introduced by this control circuit.

Any doubts as to the advisability of changing the plate voltage of the oscillator may be set at rest; the resulting slight shift in frequency is far less than the one-percent tolerance that must be expected in the best of wide-range signal generators.

The output can be adjusted by *R*; in practice this should be set and locked, although a vernier control of comparatively low resistance may be placed in series with it and brought to a knob on the panel to correct for residual amplitude changes of one and two percent if desired. With distortion, 100 percent modulation of *V*-3 is possible, but 50 percent modulation is very clean and requires about 15 volts peak of audio.

The line termination at the generator consists of the cathode impedance of the tube and the 500 and 150-ohm resistors in parallel. Twelve volts r-f to the grid of *V*-3 will result in 2.5 volts output with a termination of 73 ohms at the far end of the line.

High-Accuracy Signal Generator

By J. J. BANN

UNUSUAL accuracy in a signal generator can be accomplished using quartz crystal frequency control. In the instrument illustrated, output at any fundamental frequency from 100 kilocycles up to about 12 megacycles is determined only by the crystals available.

In addition, the small degree of correction necessary for a crystal which is either slightly low or slightly high in frequency can be done by the switching circuit shown. A variable capacitor permits final adjustment of the crystal circuit to zero beat against WWV or a secondary frequency standard.

This adjustment enables the operator to use the crystal harmonics as standard frequency markers throughout the radio spectrum up to 30 megacycles. If the same results are desired at higher frequencies, up into television channels, they can be achieved with crystals of higher fundamental frequencies ground to the same accuracy as the 100-kc standard supplied with the instrument.

With a crystal at 10.7 mc, f-m discriminators and ratio detectors can be aligned to their respective center frequencies. A 10.8 and a 10.6-mc crystal can then be used successively to check the balance in the negative and positive directions, and also the band limit amplitudes. The 10th harmonic of either of these i-f crystals provides the frequency for alignment of the 108-mc end of the r-f section in the receiver. The 10.7-mc signal is unsuitable since it will ride through the i-f stages.

For television receiver alignment, five crystals can be employed at the five frequencies equal to one-half the frequencies required for stagger tuned i-f peaking. For example, RCA receivers are aligned at 21.8, 22.3, 23.4, 25.2 and 25.3 mc. Ordinary peaking methods are employed with an amplitude-modulated signal at the above points. Five crystals, at 10.9, 11.15, 11.7, 12.6, and 12.65 mc, will double to the desired frequencies. In addition, a crystal for tuning each of

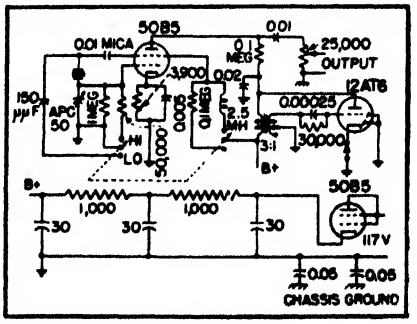

In the circuit of the generator, the ganged switch permits correction of the crystal frequency by a variable capacitor when it is either above or below a standard frequency

the trap frequencies to minimum is useful. These frequencies are 19.75 and 21.25 mc, for which the crystal frequencies for doubling would be 9.875 and 10.626 mc.

Where peaking adjustments are being made the set is trimmed for maximum detector output (or avc voltage) at each of the peak frequencies, and when trap adjustments are made the traps are tuned for minimum output at the trapped frequencies.

Aligned by zero beating against WWV at 2.5 or at 5.0 mc, the 100-kc frequency can be used as a direct source of harmonics at 100 kc or as a sine wave generator for a multivibrator. A similar application for higher frequency use would employ a 1,000-kc crystal or one at 5.0 or 10 mc. In each instance after alignment by the zero-beat method against WWV standard frequency transmissions, harmonics of the fundamental crystal frequencies can be used up into the vhf region.

Television receiver local oscillators can be adjusted to their proper fixed frequencies for each channel by use of crystals at a lower frequency with a harmonic at the desired frequency. For example, a channel 4 local oscillator in recent receivers is set at 93 mc by zero beating it against the 10th harmonic of a 9.3 mc crystal. A prewar television receiver would have a channel 4 local oscillator setting of 80 mc. This can be adjusted against the 10th harmonic of 8.0 mc or 8th harmonic of 10 mc.

Direct-Coupled R-F Amplifier

By EARLE TRAVIS

ANYONE who has ever used a bridge for measuring antenna resistance knows that a strong signal generator is essential. Otherwise the null is buried under noise and the signal of any transmitter on that frequency. As the average signal generator has a rather low output, an amplifier for it is a decided advantage.

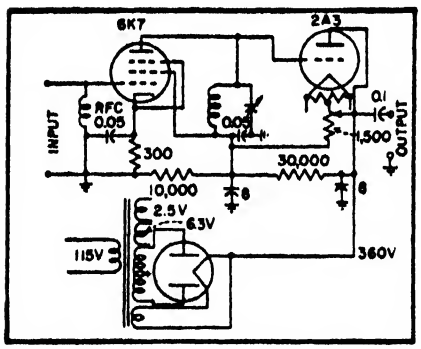

Circuit of high-gain direct-coupled amplifier for use with a signal generator

An amplifier for this purpose should be completely shielded and nonoscillating. It is an advantage to have a low-impedance output to match the low-impedance cables furnished with the bridge. The circuit shown in the diagram meets all these specifications. The reason for making it direct coupled is that this does away with all untuned circuits between the 6K7 and the 2A3, allowing the 6K7 to produce a relatively high gain.

If it is desirable to have a constant output impedance, the output voltage of the amplifier may be varied by detuning the tuned circuit. No values are shown in the diagram for the tuned circuit as its values depend on the frequencies over which the amplifier will be used.

Power Measurements at Very High Frequencies

By WILLIAM MARON

THIS PAPER DESCRIBES a means for measuring r-f power between 20 and 40 watts at 100 megacycles.

Figure 1 shows a single-ended class C amplifier stage, using long lines. The antenna coupling circuit, consisting of L_1 and C, is designed to match a 70-ohm coaxial line to feed the antenna. The load should, therefore, be in the vicinity of about 70 ohms. A 60-watt, 110-volt lamp operated below full wattage has a resistance of about 70 ohms; any slight discrepancy is compensated by the point of attachment to the coupling circuit.

If a photoelectric cell *PE* is placed in the path of light from the lamp, a direct current will be generated by the photocell which can be measured by a microammeter. The amount of current given by *PE* is dependent on the quantity of light produced by the lamp, which in turn is a function of the magnitude of r-f flowing through it. By calibrating the microammeter it is

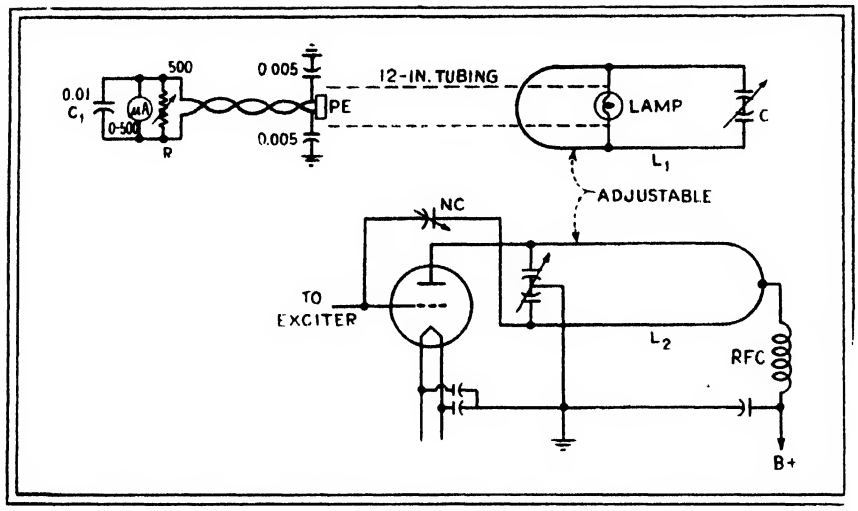

Fig. 1—Photoelectric method of measuring r-f power at 100 megacycles

possible to find the amount of r-f power produced by the amplifier.

Construction Details

As some photoelectric cells are damaged if subject to temperatures above 120 F, it is advisable to separate the cell from the lamp by at least twelve inches. This is particularly important if measurements are to be made over an extended length of time.

A piece of Bakelite tubing with an inside diameter sufficient to accommodate the lamp is cut to proper length. A series of small holes is drilled in the tubing to provide ventilation. A hood over the holes prevents entrance of extraneous light. The photocell is mounted at the other end of the tubing and bypassed for r-f as shown in Fig. 1. The length of leads going to the microammeter is of no relative importance; the leads, preferably, should be shielded. Bypassing the meter is also desirable to prevent burn-out due to stray r-f current. The meter shunt R may or may not be necessary, although it is a precaution to include it.

The bulb is debased to cut down capacitance and the cement and insulation removed between the center contact and outside contact. turbing the position of it in regard to the photocell, connect the low-frequency a-c. Adjust the voltage with the autotransformer and read the microammeter. Plot the wattage

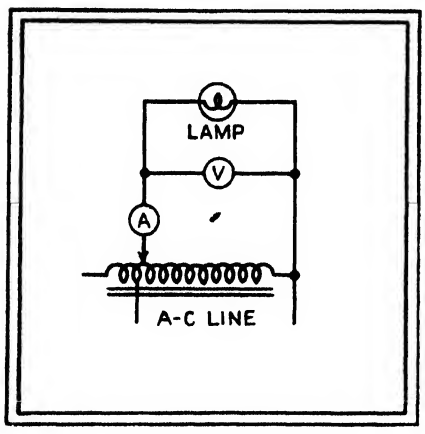

Fig. 2—Circuit for calibrating the lamp from an a-c line. If the lamp is replaced, recalibration is necessary

Calibration

Figure 2 illustrates a calibration circuit for lighting the lamp from the a-c line. The meters are used for computing the power input to the bulb; a wattmeter may be used if available.

To calibrate, remove one leg of the bulb from L_1 and, without disturbing the position of it in regard to the photocell, connect the low-frequency a-c. Adjust the voltage with the autotransformer and read the microammeter. Plot the wattage input to the lamp versus meter reading. Should the pointer go off scale before the maximum wattage range is reached, then R is adjusted to keep the meter on scale.

The calibration obtained holds only for each individual lamp and distance between the lamp and the photocell. Any change makes recalibration necessary. Figure 3 is a typical calibration chart

After calibration has been completed, reconnect the lamp to L_1. The transmitter is turned on and L_1 coupled to L_2 so as to make the tube draw normal plate current. The plate tank is repeatedly retuned for minimum plate current while C is being adjusted for maximum plate current. The connections from the lamp to L_1 should be tried in several places for correct impedance match. The proper place is where the meter indicates maximum for the required input to the tube.

Once the proper connections of the lamp to L_1 and the correct relationship between L_1 and L_2 has been established, L_1 should be fixed in position. To determine the r-f power, observe the meter reading and refer to the calibration chart.

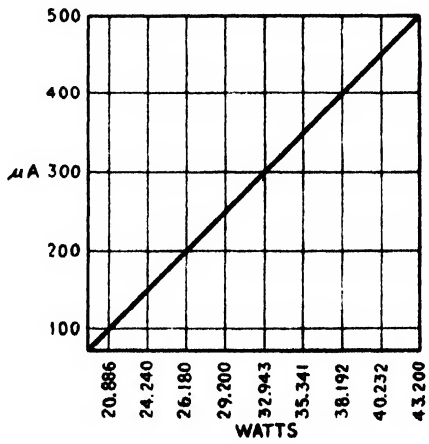

Fig. 3—Typical calibration chart obtained by use of the circuit shown in Fig. 2

Frequency-Scanning VHF Impedance Meter

Instrument using principle similar to that employed in aircraft f-m terrain-clearance indicators scans bandwidths up to 30 mc in the range between 10 and 250 mc. Details of design are given and the method of operation is described, using termination of an r-f transmission line as an example

By LESTER L. LIBBY

IMPEDANCE MEASUREMENTS can be made at radio frequencies by several methods and techniques, using such instruments as the radio frequency bridge, the slotted line, the Q meter and the combination of a calibrated signal-generator with standardized r-f ammeter, voltmeter or reference impedance. Each of these methods has its own particular type of utility. However, in determining the impedance-versus-frequency curve of a particular device, all require tedious point-by-point measurements.

A new instrument has been developed which provides an instantaneous and visually-presented determination of impedance versus frequency. The design of the instrument is such as to enable it to handle almost all of the devices encountered by the radio engineer in the design and development of present-day vhf and h-f equipment. The instrument is a frequency-scanning reflection meter designed for operation anywhere in the range from 10 to 250 megacycles. At any frequency within this range it will rapidly scan a bandwidth of up to 30 megacycles. Its output signal, suitable for use with any oscilloscope, is proportional to the amount of energy reflected from the end of a transmission delay line to which the device or system under test has been connected.

Principle of Operation

The meter principle was originally used in the terrain clearance meter.[1] It consists essentially of a wide-range sweeping oscillator[2] which is arranged to propagate a frequency-modulated signal through a transmission system of finite propagation time. This propagation time is such that at any instant the reflected energy received back from the far end of the system will be of a measurably different frequency from that being fed into its input.

The pitch of the beat note produced by combining the incident and reflected waves in an internally-contained detector circuit is proportional to the rate at which the frequency is being varied and to the propagation time of the transmission system. The amplitude of the beat note is proportional to the amplitude of the reflected wave.

With reference to Fig. 1 and 2, the conditions which prevail are as follows:

(1) An r-f voltage of amplitude A is linearly frequency-modulated between the limits f_1 and f_2 by a sawtooth waveform of period T.

(2) This voltage is applied to a transmission line whose terminating impedance Z_L does not equal its characteristic impedance Z_o.

(3) The reflected energy due to this inequality is received back at the input after a delay time τ equal to twice the propagation time along the transmission line.

When attenuation in the transmission line is assumed to be negligible and ρ is taken as the transmission-line reflection factor equal to $(Z_L - Z_o)/(Z_L + Z_o)$ the voltage amplitude of the reflected wave will be ρ times the amplitude of the applied wave. The total frequency excursion Δf of the reflected wave will be the same as that of the applied wave. The frequency of the beat note is given by

$$F = \frac{\tau}{T}(f_2 - f_1) = \frac{\tau}{T}\Delta f \qquad (1)$$

The beat note exists for a length of time equal to $T - T'$, where T' is the time of the return sweep. At the end of this time, for the brief interval T', a transient frequency is set up as the applied wave snaps back from f_2 to f_1 to repeat the sweeping sequence.

To a first order of magnitude, it is necessary that the beat-note

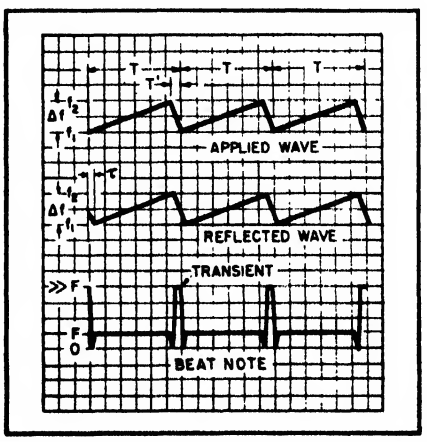

FIG. 1—Frequency vs time relationships existing at the beat-note detector

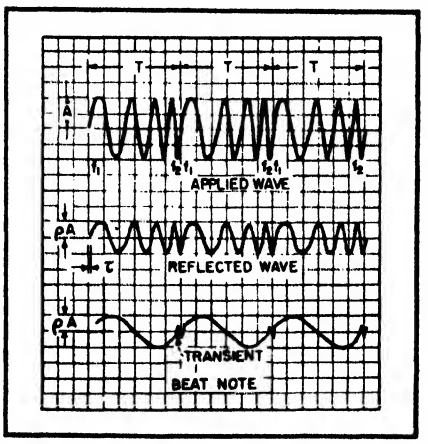

FIG. 2—Amplitude vs time relationships existing at the beat-note-detector

frequency be such that at least one full cycle of the beat note is completed during the time interval T. As is apparent from Fig. 3, this condition must be fulfilled if a closely sinusoidal beat-note waveform is to be obtained. Therefore

$$T \geq 1/F \quad (2)$$

For the case where $T = 1/F$, substituting for T in Eq. 1 gives

$$\Delta f = 1/\tau \quad (3)$$

In order, therefore, to secure at least one full cycle of beat note, the total frequency deviation must equal the inverse of the total propagation time outward and back through the transmission line. The amount of frequency excursion during one cycle of beat note will determine the frequency resolution of a particular reflection measurement.

Description of Instrument

In the instrument, a band-pass audio amplifier with variable gain is used in conjunction with the beat-note detector. This combination results in high sensitivity of measurement of reflected energy. In order to reach the best compromise between high gain, good stability and low susceptibility to disturbance from unwanted signals, the amplifier is designed with a pass band of from 300 to 6,000 cycles per second. The beat-note detector is a silicon-crystal diode and the frequency-sweeping signal generator is an oscillator[2] plus an auxiliary 2,000-cps sawtooth modulator of the phantastron type. Three fixed lengths of RG-58/U coaxial transmission line are included internally to provide a suitable transmission delay for most of the applications generally encountered. The propagation velocity along this type of line is about 660 feet per microsecond.

The diagram of Fig. 3 shows the essential elements of the frequency-scanning reflection meter. The portion within the dotted line is the oscillator with its normal 60-cps sawtooth frequency modulation applied to the high-level (local) oscillator. The frequency excursion can be adjusted to as high as 30 megacycles or more. The adjustable output of the 2,000-cps sawtooth modulator is applied to the low-level (signal) oscillator, permitting sweep excursions of up to 5 megacycles. The 60-cps sweep rate is intended for very-high-frequency (30 to 250 megacycles) broadband work, whereas the 2,000 cps sweep rate is designed for high-frequency (10 to 50 megacycles) medium and narrow-band work.

With the various combinations of transmission line lengths included in the instrument, total delay times of 0.2, 0.4, 0.6, 0.8 and 1.0 microseconds are available. From Eq. 3 the respective sweep widths for obtaining one complete cycle of beat note output are 5.0, 2.5, 1.67, 1.25 and 1.0 megacycles. For the condition of two full cycles of beat-note output per sweep, the above sweep widths are doubled; for three full cycles of beat note, the sweep widths are tripled; and so on. This permits operation of the instrument under a wide variety of conditions, using either the high-frequency sweep rate or the low-frequency sweep rate as the individual case may dictate, and patching in suitable lengths of internal or external transmission line as required.

Applications

One typical use of the instrument is described in the following paragraphs.

Suppose it is necessary to evaluate the impedance of a coaxial-sleeve broad-band vertical dipole antenna designed for operation in the 50 to 60 megacycle region from 53.5-ohm coaxial transmission line. The antenna is mounted on an elevated support about 80 feet from the point at which the test instrument is most conveniently located, and an attached 100-foot length of 53.5-ohm coaxial cable is brought down to the test location. It is desired to observe visually the reflected energy from this antenna over the frequency range of 40 to 70 megacycles, and this information is desired with a frequency resolution of about 2 megacycles.

The ratio of total sweep width to desired frequency resolution is $30/2 = 15$, so that 15 full cycles of beat-note output per sweep are required. Hence, modifying Eq. 3 for this case.

$$\Delta f = 15\,(1/\tau) \quad (4)$$

so that

$$\tau = 15/30 = 0.5 \text{ microsecond} \quad (5)$$

The same figure may be arrived at by noting that the 2-megacycle resolution requirement is equivalent to saying that the applied frequency must shift at the rate of 2 megacycles per beat-note cycle. It then follows directly from Eq. 3 that $\tau = \frac{1}{2}$ microsecond.

A two-way delay of 0.5 microsecond requires a one-way length of solid-dielectric coaxial cable of 166 feet. Since the 100-foot feeder

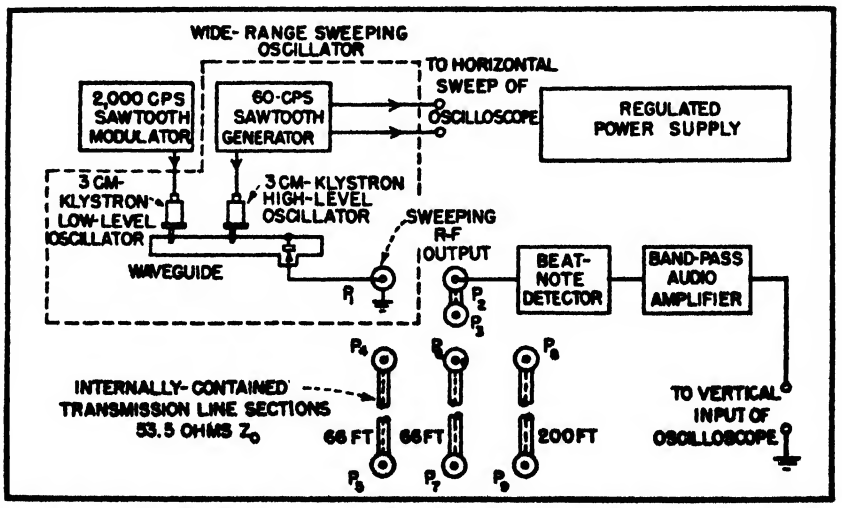

FIG. 3—Block diagram of the frequency-scanning vhf impedance meter showing lengths of transmission line available within the instrument

cable is already available externally, it is only necessary to add a single 66-foot length of internal cable from that available in the instrument to make up the necessary transmission system. The setup is as follows:

A patching cable is connected between connectors P_1 and P_2. Another patching cable is connected between P_3 and P_4. The feed cable from the antenna is connected to P_5. The sweeping output is set up for a center frequency of 55 megacycles, with the 60-cps sawtooth generator set for 30 megacycles of total sweep width (the 2,000-cps sweep is set to zero for this particular application). The 60-cps sawtooth-sweep output terminals are connected to the horizontal sweep input of any commercial oscilloscope, and the output of the band-pass audio amplifier is connected to the vertical input of the oscilloscope.

The visual pattern of the desired data will resemble the sketch of Fig. 4. The 15 complete beat-note cycles, swept every 1/60 of a second ($F = 900$ cps), are modulated by an envelope whose amplitude represents the amount of reflected energy as a function of instantaneous frequency. As can be seen, the reflected energy approaches zero in the region of 55 megacycles, at which point the antenna impedance closely matches the characteristic impedance of the transmission line. At either extreme of the frequency excursion the reflected energy approaches that which would be obtained if the transmission line were terminated in an open circuit. It is thus possible to tell at a glance just how effectively a given antenna matches its transmission line, and over how wide a frequency band it does so.

Transmission-Line Attenuation

Since attenuation is present to some extent in all practical transmission systems, the amplitude of the reflected voltage wave as received back at the beat-note detector is not strictly equal to ρ times the voltage amplitude of the applied wave, but is $\eta^2\rho$ times this amplitude, where η is the voltage attenuation ratio suffered by the wave in traversing the length of the line one way. However, it remains true that the amplitude of the reflected wave received back at the beat note detector is proportional to the magnitude of the reflection factor. For an open-circuited or short-circuited termination of the transmission line the magnitude of ρ is always unity. For an arbitrary terminating impedance it is possible to evaluate the magnitude of the reflection factor, and hence the magnitude of the terminating impedance, by the following procedure:

First, the transmission line to be used is terminated in a short-circuit, corresponding to a reflection factor of amplitude unity, and the amplitude of the resultant beat note is adjusted to any convenient reference value, such as two inches peak-to-peak. Then the arbitrary terminating impedance is connected across the transmission line in place of the short-circuit and the peak-to-peak height of the resultant beat-note wave displayed on the oscilloscope screen is measured. The ratio of the height at any particular frequency to the two-inch reference height is then the magnitude of the reflection factor at that frequency. The phase angle of the reflection factor may be obtained by comparing the phase of the beat-note wave at any particular frequency to the phase of the two-inch reference wave. With this information, the terminating impedance may then be calculated with the aid of the Smith Chart.

From the above description it is apparent that a knowledge of the transmission-line attenuation is not essential to the operation of the instrument. However, excessive transmission line attenuation is to be avoided since there is a practical limit even in the most carefully manufactured delay cable or transmission line to the uniformity of characteristic impedance with length. The minute irregularities in Z_0 which exist cause small reflections to occur early in the line which may completely mask the reflection due to the terminating impedance when the cable attenuation per unit length is high and the line length large. It is fortunate that for vhf applications, where the transmission line attenuation is rather high, it is generally satisfactory to work with frequency resolutions of the order of about three megacycles.

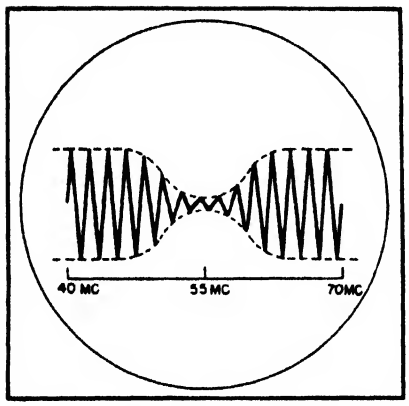

FIG. 4 —Typical visual presentation of reflected energy on an oscilloscope screen

Transmission-line lengths of the order of 100 feet may then be employed without excessive total attenuation. For frequencies below the vhf range the transmission-line attenuation is conveniently low, so that longer lengths may be used to achieve the finer absolute frequency resolution which is usually desired here. A relative frequency resolution of from 2 percent to 5 percent of the center frequency is satisfactory in most cases. The sum of the lengths of cable contained within the instrument provides a minimum absolute frequency resolution of about one megacycle. For narrower resolutions than this, the addition of a suitable length of external transmission line is required. Similarly, if resolutions of less than about 2 megacycles are desired in the upper portion of the vhf band it will probably be necessary to use a suitable length of lower-loss transmission line than that contained within the instrument.

Operation With Balanced Circuits

For measurement of balanced impedances two methods have

proved satisfactory. The first method involves the use of coaxial transmission line in conjunction with a suitable balanced-to-unbalanced transformer to connect the impedance to be measured to the line. The second method makes use of an external length of balanced transmission line of the twin-lead type developed for use with present-day television and f-m receivers. This transmission line may be set up in the laboratory by stringing a suitable length back and forth between pegs located on the walls in such positions that the sections of line thus formed are spaced two or three feet from each other. The balanced impedance to be measured may then be connected to one end of this line, while the other end of the line is connected to the coaxial output connector of the instrument.

Tests have shown that this type of balanced transmission line arrangement then acts as its own balanced-to-unbalanced conversion system to a satisfactory degree. Futhermore, tests have also shown that transmission-line impedances of from 50 to 300 ohms may be used without encountering trouble from second-time reflected waves.

REFERENCES

(1) Lloyd Espenschied and R. C. Newhouse, A Terrain Clearance Indicator, *Bell Syst. Tech. Jour.*, Jan. 1939.
(2) Wide Range Sweeping Oscillator, Kay Electric Co. Eng. Staff, ELECTRONICS, p 112, August 1947.

Calibrating Laboratory Standards Against WWV

By GARDNER P. WILSON

FREQUENCY STANDARDS in laboratories can be simply and rapidly calibrated against radio station WWV's short-wave broadcasts by using an oscilloscope as a watch with a second hand revolving 100 times a second. The technique reduces observational errors.

Propagation Effects

At great distances from WWV, signals are received by sky-wave reflections from the ionized layers. Variations in apparent elevation of these layers change the path length of the radio waves. Often these variations in path length are rapid so that the standard carrier or tone arrives at the receiver at a different frequency from the original. This Doppler effect introduces considerable error on short observations made several thousand miles from the transmitter. For long duration observations, average received frequency is identical to that transmitted.

Because the standard frequency arrives at the receiver by several different paths, fading occurs, which at times causes the signal to disappear and reappear with large phase shifts. The phase shift is very apparent when using an oscilloscope to view the received wave. These fades and shifts make it extremely difficult to observe sinusoidal waves for enough time to determine average frequency and keep a particular reference crest or hollow of the received signal on oscilloscope screen.

Attempts to use either carrier or modulation of WWV as reference for calibration of laboratory standards in Pasadena, California, approximately 2,500 miles from the source, gave unreliable results because of the above difficulties. Doppler frequency shifts of about one part in 10,000 were observed on all short waves and on the tone modulation frequencies.

Observational Method

One possibility of minimizing effects of fading and momentary frequency shift is to divide the ticks transmitted for 0.005 sec every second by WWV to run a synchronous electric clock. This procedure requires extra equipment and necessitates taking observations over a period of many days to obtain suitably high accuracy; it gives no information about short time errors in the laboratory standard, such as crystal oven temperature cycling or line voltage variations.

A more satisfactory method is to feed the 100 cps signal from the laboratory standard, which usually has outputs of 10,000, 1,000 and 100 cps in addition to the generated 100,000 cps, to the vertical plates on an oscilloscope, and to the horizontal plates by way of a 90 deg phase shifting circuit (an 0.05 μf capacitor in series with a 4,000 ohm resistor) so as to produce a 100 cps circle on the oscilloscope, comparable to a hand of a watch that makes 100 rps. In addition, audio output of a communications receiver tuned to WWV is applied to one set of deflection plates of the oscilloscope. One second tick from WWV then appears as a wave extending half way around the circle and repeating itself every 100 revolutions. If the laboratory standard is precisely on frequency, the wave will appear stationary, however any drift will appear multiplied 100 times, simplifying observation of errors. If the beginning of the tick is used as the reference point, and if the reference point drifts 36 deg. in 100 sec., the laboratory

standard is in error one part in 100,000. Shorter intervals can be used for observations and good accuracy obtained for checking oven cycling and line voltage variation effects on the laboratory standard.

Accuracy of the one second tick from WWV for any one second is within 0.00001 sec. (one part in 100,000). An observation 100 sec. long will reduce this error to one part in 10,000,000. The longer the observation, the smaller the error becomes in comparison with other fixed errors. Changes in radio path length affect arrival time of ticks in the same manner as they do the carrier. The variation introduces random movement of the tick wave around the 100 cps circle, usually within five degrees of arc. However, the average point can readily be seen. Fading will often cause the tick wave to disappear in part or altogether, but it will reappear and the reference cycle can easily be identified.

It is wise precaution when making these measurements to make a rough check that one second ticks are not appearing every 99 or every 101 revolutions of the oscilloscope trace. A Lissajou pattern using the tone modulation and the local 100 cps will give a quick check. Best receiver tuning for viewing the tick is with the receiver exactly centered on the carrier frequency, half way between tone modulation sidebands. This tuning can easily be verified by oscilloscopic observation as the receiver is tuned.

Checking UHF Oscillator Stability

Design of a simple mixer that permits heterodyning an uhf oscillator against a crystal-controlled multiplier. The difference frequency is fed to a conventional receiver to observe frequency shift

By L. E. PINNEY

FOR COMPARING oscillator frequencies by the heterodyne method, the simple circuit shown in Fig. 1 has been used with excellent results. The device is used with an ordinary all-wave radio, or better, with a communications receiver which responds to the difference frequency of the two oscillators. Audible response is obtained by heterodyning the intermediate frequency of the receiver to a suitable audio frequency, as in c-w telegraph reception, or by modulating one of the oscillators.

The antenna post of the receiver is connected through a capacitor to the plate circuit of the mixer shown in the diagram. The mixer antenna is a suitable length of heavy wire, ordinarily about three feet.

Optimum values of external grid bias for the mixer range from 2 or 3 volts with 100 volts on the plate to zero at 45 volts on the plate. Since operation at the lower voltage is often quite satisfactory, it has been found convenient in such cases to connect terminals 1 and 2 together and to use a 45-volt B battery. The plate current at this voltage is about one milliampere. Grid-leak bias might also be used at higher plate voltages by omitting the grid-return capacitor and adjusting the grid resistor.

The oscillator whose frequency stability is to be observed is operated in the same room with the mixer (which is connected to the receiver) and a crystal-controlled frequency multiplier that gives a very stable signal at about 112 mc.

The oscillator under test is adjusted to a frequency such that the difference between it and the frequency of the crystal-controlled multiplier may be tuned in on the receiver. Thus, if the oscillator under test operates at a frequency of 100 mc, and the receiver is capable of detecting frequency variations of 1 kc, frequency instability amounting to 1 part in 100,000 may be observed. For maximum sensitivity, the difference frequency should fall in the range of highest resolution of the receiver. For most receivers, this optimum value is in the lowest frequency band.

Since the mixer is essentially untuned, it will respond to all the lower frequencies used in communications. Nearby broadcasting stations may be heard at almost any setting on the receiver dial by operating an ordinary test oscillator, adjusted to a suitable frequency, in the vicinity of the mixer.

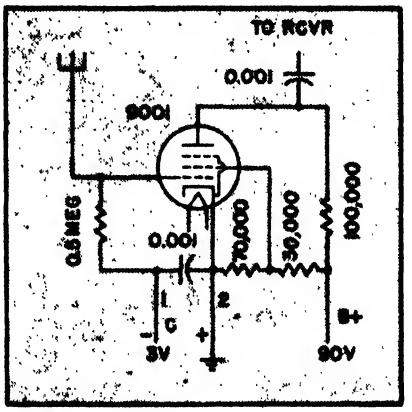

FIG. 1—Untuned mixer for comparing the frequency of an uhf oscillator with that of a crystal-controlled multiplier. Terminals 1 and 2 may be connected together if a plate potential of 45 volts is used

VHF Transmitter Power Measurements

By LEONARD R. MALLING

INCREASING USE of the vhf spectrum has resulted in the need for an accurate and convenient method of measuring r-f power at frequencies ranging from 100 to 500 mc and powers ranging up to 100 watts.

Line of sight limitations, low weight requirements, the use of directive antennas and the need of portability has lead to a figure of the order of 50 watts maximum continuous power output for transmitters designed for vhf use. Pulse power of the order of kilowatts may be conveniently measured if the pulse rate is made low for output power tests.

Except when extreme portability is required, vhf transmitters are designed to work into coaxial cables feeding dipole arrays, so that for maximum efficiency the antenna system should be purely resistive. If we terminate the transmission line in a purely resistive load the power output of the transmitter can be determined by a knowledge of the power dissipation in this resistor. Maximum convenience is obtained by having a power measuring device that does not require tuning.

Resistive Termination

Two difficulties arise in the termination of a transmission line with a resistor; power dissipation in the resistor, and correct matching of the resistor to the transmission line. The power dissipated in the resistor may be found from a measurement of temperature rise, voltage or current. Of the three, voltage measurement is the most convenient but the capacitive input of the voltmeter must then be compensated to obtain effective resistive termination of the transmission line.

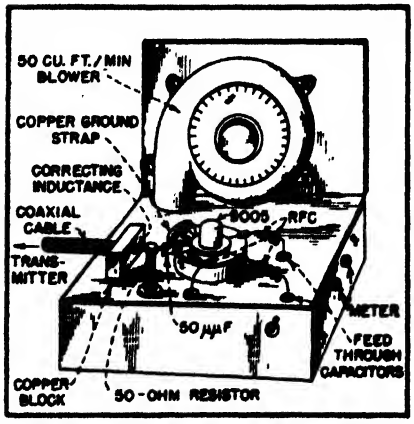

Mounting of components in wattmeter

For the termination, one type of resistor is of particular interest, a ½-watt carbon resistor having brass endcaps and contained in a ceramic case. The length of the carbon mix between brass caps is 0.5 cm, the diameter 0.3 cm.

Assuming a resistor of 50 ohms with these dimensions, the resistance per cm cube is seven ohms and the skin depth is 0.6 cm. The skin effect may thus be neglected as we can expect substantially uniform current distribution.

Knowing the current distribution enables us to determine the inductive effect of the resistive rod, a value of 0.001 microhenry or an inductive reactance of 2.5 ohms at 500 mc. Thus the terminating impedance gives a standing wave ratio of 1.05 on the transmission line. Sufficiently accurate power measurements may be made when the standing wave ratio is less than 1.1, a value rarely achieved even with the best antenna designs.

The 9005 diode having a resonant frequency of 1,500 mc and a voltage rating of 117 volts maximum makes a peak diode voltmeter for the measurement of voltage across the resistor. For the moment we are concerned with the input capacitance of this diode and, allowing for socket and stray capacitance, a value of one $\mu\mu$f may be assumed. The mismatch due to this capacitive reactance may be neutralized by a corresponding inductive reactance.

The shunt capacitive reactance may be converted to an equivalent series reactance of three ohms at 200 mc for which the equivalent inductance is 0.002 microhenry. Difficulties in making a completely noninductive connection to the transmission line are now avoided as we may leave a short length of the inner conductor equivalent to this value for making the connection to the resistor. With RG-8/U 50-ohm concentric cable, having a 7/21 copper conductor, the length of conductor is approximately 0.5 cm from the end of the cable to the resistor.

With the relatively small values of correction used the slope of the inductive and capacitive reactance curves may be assumed to be constant so that the compensation will hold over a wide band of frequencies, certainly from 100 to 500 mc. The correction is made in approximately the middle of this band.

Accuracy

With a high resistance load, one megohm, and a small r-f bypass capacitor of 100 $\mu\mu$f, the meter reading will indicate peak voltage across the terminating resistor. Because of electron transit time and internal diode resonance, the meter indication at 500 mc will be a few percent low with correspondingly less error at lower frequencies. This error has been described as the premature cutoff error and is dependent on the characteristics and geometry of the tube.

Diode resonance is caused by the series inductance of the tube leads resonating with the plate-to-cathode capacitance. Resonance checks are best made by a variable-frequency signal generator as unavoidable external lead inductance will lower the resonant frequency of the diode. Resonance with the 9005 may thus occur at 1,000 mc. At 500 mc, the meter indication may be 30 percent high, at 100 mc the error will be one percent. A

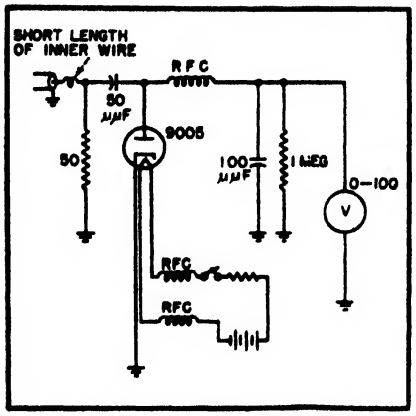

FIG. 1—Circuit of vhf wattmeter

calibration chart may be made covering the band.

Construction Detail

To aid heat dissipation in the resistor, the diode assembly may be placed on a copper plate to which the resistor is soldered using an ample supply of metal. This ensures good thermal and radio conductivity. With an air blower supplying 50 cu ft/min to the copper plate, the resistor may be operated at ten or twenty times its normal rating in free air or much higher for short periods.

Figure 1 shows the wiring arrangement of the diode power head. Use of a battery for heater power avoids long a-c supply leads. The meter may be any high-resistance d-c voltmeter, preferably with a multiplier switch. For peak pulse power measurements the voltmeter may be replaced by a calibrated oscilloscope.

If large resistors introduce error because of excessive inductive reactance, the resistor may be sunk in a hole in the copper as shown in Fig. 2 to provide reversal of current in the restricted area.

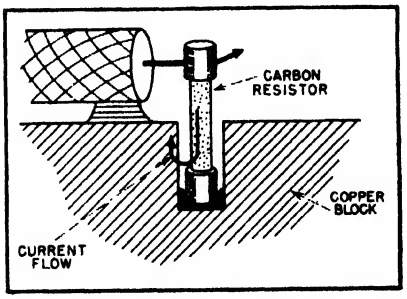

FIG. 2—Method of reducing the effective inductance of a carbon resistor

Static for Radio Receiver Tests

A fluctuating audio signal from a gas tube is peaked, amplified, and applied to a spark coil that discharges at irregular intervals. The resulting r-f signal may be used to simulate click, thunderstorm, hiss or grinder static

By J. C. R. LICKLIDER and E. B. NEWMAN

GOOD PERFORMANCE is based on good testing. In no field is this statement truer than it is in the design of radio receivers. Receiver performance has improved at a pace set by the development of testing methods and equipment.

One big gap in radio testing procedures became evident during the war. There were no established methods of imitating atmospheric static in the laboratory. This paper describes methods which were developed to fill in the gap. It presents a simple quantitative method of specifying the characteristics of static which are important for receiver design, and it describes apparatus which simulates the various types of static.*

The intense static from local thunderstorms, and probably most other types of atmospheric static, arises from very brief electrical or electro - magnetic disturbances. These disturbances are transients of extremely short duration. They often occur in bursts, trains, or crashes. Their times of occurrence are highly irregular, if not completely random. They are irregular also in amplitude. Each pulse scatters energy continuously through a wide band of the radio-frequency spectrum.

The atmospherics encountered at any given station depend not only on local conditions but also upon conditions in remote regions, especially upon propagation between these regions and the receiving station. For this reason the characteristics of atmospheric static are by no means simple. They vary from one geographical location to another and from one frequency band to another. They vary with the time of day, from day to day, and from season to season.

Measurements of intensity alone fail to indicate just what static is. Equivalent microvolts do not tell what a burst of static will do to a sensitive radio receiver.

Static Density

It is most useful for the present purpose to think of atmospheric static as a series of transient impulses which set resonant circuits into oscillation. The important characteristics of the impulses are, first, their intensity, and, second, their spacing or distribution in time. If the impulses follow one another closely, we speak of *dense* static; if they occur so infrequently that the after-effects of one impulse are gone

* This work was begun under Contract OEMsr-858 between OSRD and Harvard. Contract NSori-76 with the U. S. Navy Office of Naval Research.

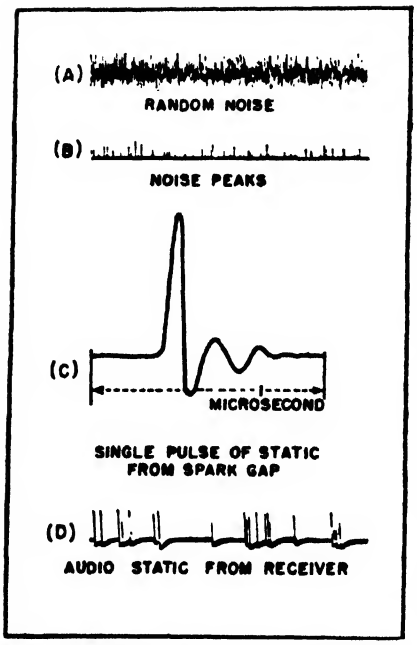

FIG. 1—Random noise (A) is put through a circuit which passes only noise peaks (B). The peaks are amplified and activate a spark gap. One pulse of the resultant r-f static has, when observed on a video oscilloscope, the waveform shown at (C). The audio static output of a receiver under test (D) results from a series of pulses

before the next impulse comes along, we speak of *sparse* static. The significance of static density in determining its interference value has not always been well understood, and contradictions have resulted from failure to specify the density of the static under discussion.

Static density may be designated conveniently in terms of a notation borrowed from radar: pulse repetition frequency. Although the number of pulses per second may vary within quite wide limits, it is possible to think of a particular sample of static as having an average prf. For various samples, the average prf may range from near zero to exceedingly high values. When the prf is low and the pulses are widely spaced, the intermittent character of static is emphasized. On the other hand, when the prf is high and the pulses are closely spaced, static takes on the character of fluctuation noise (recently called white noise).

The static density determines the way in which we must look at receiver performance. When it is dense and is observed through a narrow-band receiver, the individual pulses are broadened by passage through the narrow-band circuit and pile up on each other's heels. Dense static gives rise, therefore, to an irregularly fluctuating wave instead of an irregular sequence of spikes. With dense static, consequently, receiver performance can be predicted fairly accurately by assuming that we have an r-f carrier modulated by a continuous spectrum of noise. Sparse static, on the other hand, brings into play the time constant of each of the circuits in the receiver. The ring time of resonant circuits, the time constants of squelch circuits, avc circuits, and noise limiters, the regulation of the power supply, are all interrelated in the transient response of the receiver.

For most tests of radio receivers, the shape of the static spectrum is quite unimportant. The passband is always narrow relative to the overall frequency range covered by the static, and within the passband the average distribution of static energy is essentially uniform. It is ordinarily not necessary, therefore, in simulating static for receiver tests, to match the spectrum of natural atmospherics.

Standards for Measuring Static

The following procedure has been adopted as a standard method of specifying atmospheric static. If the static is relatively homogeneous, it is expressed in terms of two measures: (1) the intensity in a band 10 kilocycles wide, centered at the frequency to which the receiver is tuned, and (2) the average prf. The first quantity is usually calculated from measurements made with a receiver of known selectivity. The second quantity is determined with

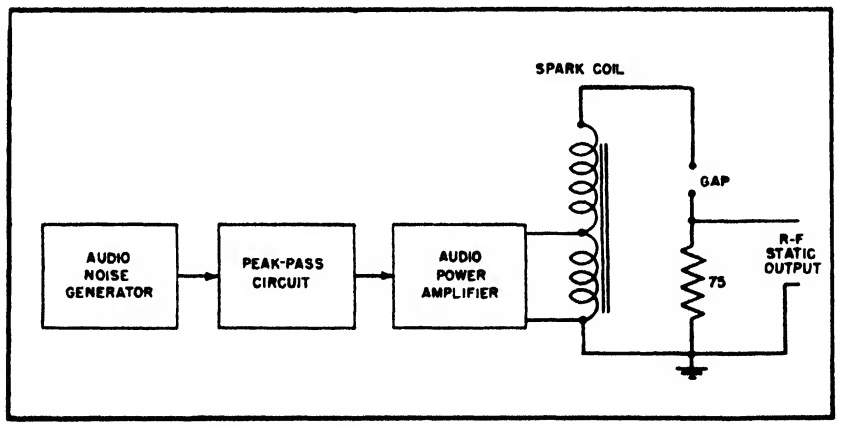

FIG. 2—Block diagram of the static generator

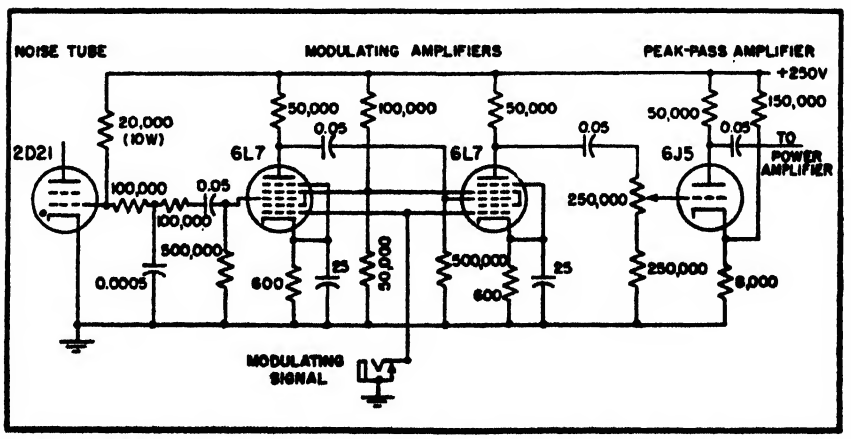

FIG. 3—Schematic diagram of the audio noise generator and peak-pass circuit

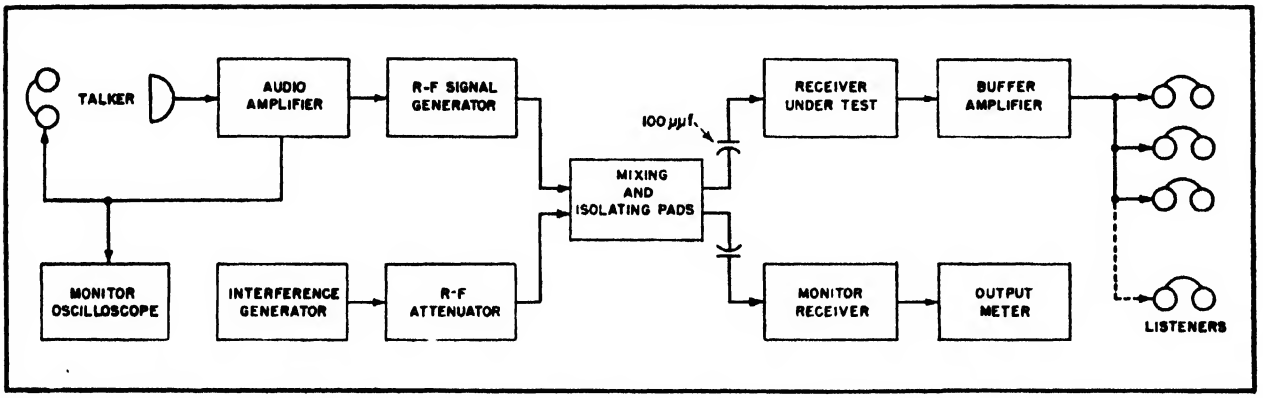

FIG. 4—Setup used in articulation tests of radio receivers. One such test is shown in progress in the two photographs which appear elsewhere in these pages

the aid of a pulse-counting meter and a wide-band receiver.

The relation between designations based on this method of specification and the nomenclature which has been used widely in previous discussions of atmospheric interference is fairly direct. The correspondence is approximately as follows: *click static*—weak, very low prf; *lightning* and *local thunderstorm static*—intense, low or medium prf; *hiss static*—weak, very high prf.

To describe the static frequently referred to as *grinders*, a third characteristic of natural static must be taken into account. Grinders are essentially bursts of pulses. In specifying the characteristics of grinders, the measures of intensity and density can be either short-time averages within bursts or long-time averages including a number of bursts. In either instance, it is necessary to describe the static in terms, for example, of the percentage of the time occupied by bursts and their average frequency of recurrence.

Simulation of Local Static

The method used in simulating local thunderstorm static and click static is illustrated schematically in Fig. 1. A block diagram of the apparatus is shown in Fig. 2, and the circuits of the audio noise generator and the peak-pass amplifier are shown in Fig. 3.

As indicated (Fig. 1) the first step involves the production of a fluctuating audio-frequency wave (A) provided by a gas-tube noise generator. This wave is fed into a peak-pass amplifier, which gives it the form shown at (B), and then is applied to the primary of a spark coil. The secondary of the spark coil is connected through a small series resistance to a spark gap. When the voltage developed across the gap by the secondary reaches the breakdown value, there is a very brief surge of current through the gap and through the resistor. The voltage thus developed across the resistor is a series of very short pulses (C) which occur at irregular intervals and which vary irregularly in amplitude.

The irregularity in time and in amplitude is derived from a random noise wave containing only audio - frequency components, whereas the sharpness of the output pulses (which accounts for the fact that the spectrum extends high into the radio-frequency range) is due primarily to the suddenness with which the resistance of the spark gap breaks down when the critical voltage is exceeded.

The intensity of the simulated static is adjusted by means of a video attenuator of conventional design, and the intensity level per cycle (or per 10-kilocycle band) is determined with the aid of a receiver of known selectivity, by measuring the equivalent noise sideband input and correcting for bandwidth. The density of the simulated static is controlled by adjusting the gain of the peak-pass amplifier. When the gain is increased, more of the peaks of the voltage wave from the gas-tube generator are passed, and more output pulses are produced.

The average prf is indicated by a pulse-counting circuit connected to the output of a wide-band monitor receiver. With very low prf, the interference consists of a succession of randomly spaced clicks. With prf's between 20 and 2,000 pulses per second, the interference sounds like typical thunderstorm static.

Simulation of Other Types

To provide simulated static of the grinders type, it is necessary only to introduce slow, random, amplitude modulation of the audio noise delivered to the peak-pass amplifier. This is done by applying an irregularly fluctuating wave to the No. 1 grids of the 6L7 amplifiers (Fig. 3). With this arrangement, the equipment under test may be subjected to irregular bursts of static pulses very similar to natural grinders. These irregular bursts are useful in showing up irregularities of performance due to unstable avc circuits.

Hiss static can be simulated with the spark-gap generator by applying high-prf excitation and thus forcing almost continuous discharge, but under these conditions the output is not stable. For hiss static, therefore, it is better to take advantage of the fact that when viewed through circuits of limited bandwidth irregularly spaced pulses at very high prf resemble fluctuation noise. Methods of generating

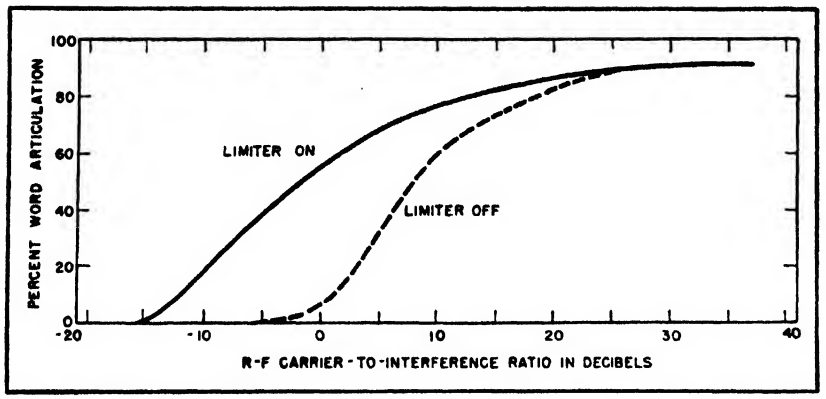

FIG. 5—Results of a series of tests on a receiver employing a series-diode noise limiter

wide-band fluctuation noise with the aid of gas-filled tubes were developed during the war in connection with radar jamming.[1]

Use In Receiver Tests

The simulated static has been used extensively in laboratory tests designed to evaluate the performance of radio receivers and of noise-reducing circuits. In most of the work, articulation tests have been used to measure the intelligibility of speech transmitted over a radio link of which the receiver or the noise-reducing circuit comprised a part.

By way of illustration, a typical test setup is shown in Fig. 4, and the results of a typical test are presented in Fig. 5. The receiver under test was equipped with a Wasmansdorff series-diode audio noise limiter which could be switched on or off.[2] The aim of the test was to measure the effectiveness of the limiter in overcoming the effects of impulsive static with an average prf of 1,000 pulses per second. Two talkers alternately read standardized lists of words (the Psycho-Acoustic Laboratory PB Lists) over the test circuit to a group of experienced listeners who recorded the words as they heard them. Tests were conducted with various r-f carrier-to-interference ratios, half of the tests with the limiter operating and half with the limiter disconnected.

As shown, the listeners were able to understand many more of the words when the limiter was used; the advantage provided by the limiter was approximately equal to that which would have resulted from a 10-db increase in carrier power.

References

(1) J. D. Cobine, Noise Output of the Sylvania 6D4 Gas Triode at Audio and Supersonic Frequencies, Harvard University Radio Research Lab. Report 411-92, 1944. (Available through the Office of Technical Services, U. S. Dept. of Commerce, Washington, D. C., PB 14163)

(2) Emerick Toth, Noise and Output Limiters, ELECTRONICS, p 114, Nov. 1946.

Noise Generator for Receiver Measurements

Diode noise generator permits simplified procedure in the measurement of noise figures and receiver input resistance. The receiver bandwidth need not be known and measurement is independent of the response curve of the receiver

By PETER G. SULZER

TWO significant sources of noise are associated with a radio receiver. One is made up of all of those within the receiver itself, such as shot effect and partition noise. The other source is the thermal agitation (Johnson) noise supplied by the resistive component of the antenna impedance. The noise figure[1, 2] of a receiver is defined as the ratio of the sum of these two to the second, or,

$$F = \frac{P_r + P_a}{P_a} \qquad (1)$$

where P_r is the equivalent noise power output of the receiver referred back to its input terminals (that part in excess of thermal noise), and P_a is the thermal noise supplied to the receiver by the antenna. A perfect receiver would have P_r equal to zero, and the noise figure would be unity. This definition is not very explanatory; the reader should see the first two references for a full discussion of the subject.

It is easy to calculate P_a, but P_r is difficult to determine directly. However, the sum $P_r + P_a$ may be determined by a simple expedient. The noise power output of the receiver is measured when a resistance R_a, which is substituted for the antenna, is connected across the antenna terminals. Next, a temperature-limited diode is connected as shown in Fig. 1 and the direct diode current I is adjusted by varying the filament temperature to such a value that the noise power from the diode doubles the

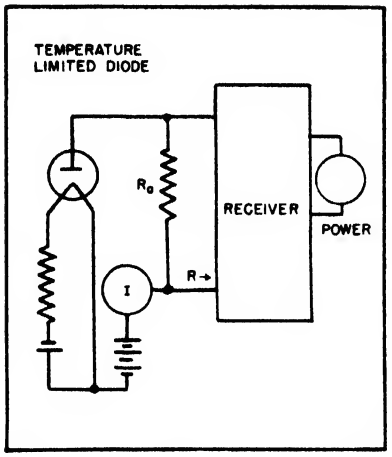

FIG. 1—Basic circuit for measurement of noise figure with a noise diode

power output of the receiver.

Under these conditions, $P_{diode} = P_r + P_a$, and

$$F = (P_r + P_a)/P_a = P_{diode}/P_a \quad (2)$$

It is now necessary to evaluate P_{diode} and P_a. The rms fluctuation current from a temperature-limited diode is[3]

$$i^2 = 3.18 \times 10^{-19} IB \quad (3)$$

where i is the rms fluctuation current in amperes, I is the direct diode current in amperes, and B is the bandwidth in cycles per second. If the input resistance of the receiver is R, the diode sees a load resistance R_aR/R_a+R, and the diode delivers to the receiver a power

$$P_{diode} = 3.18 \times 10^{-19} IB (R_aR/R_a + R)^2 1/R \quad (4)$$

A resistance will develop a thermal-agitation voltage across its open-circuited terminals $e^2 = 4KTR_aB$, where K is Boltzmann's constant, 1.374×10^{-23} joules per degree Kelvin, T is the absolute temperature of the resistor in degrees Kelvin, and B is bandwidth in cycles per second. It is assumed that R_a is constant over this frequency band.

The resistor will deliver a power to the receiver

$$P_a = \frac{4KTR_aB}{R_a + R}\left(\frac{R}{R_a + R}\right) \quad (5)$$

Substituting Eq. 4 and 5 in Eq. 2,

$$F = \frac{5,790}{T} IR_a \quad (6)$$

For a temperature $T = 289$ degrees Kelvin, 19 C,

$$F = 20 IR_a$$

Since the bandwidths cancel, noise figure measurements made in this manner are independent of the response curve of the receiver. Since quantity R, the input resistance of the receiver, does not appear, the measurements are not in error because of the mismatch between R_a and R, and the effects of such mismatch on noise figure can be studied.

The factor R_a in the expression requires some attention. A temperature-limited diode should, at first glance, appear to have an infinite a-c plate resistance. However, the work-function of the filament surface depends on the anode voltage[5]. The result is that emission increases with increased anode voltage, and the a-c plate resistance becomes finite. When high values of R_a are used, the plate resistance must be considered in parallel with it.

Resistance R must have the desired value, and must remain constant over the frequency range used. At the higher frequencies, the use of film-type resistors is desirable.[6] It has been found by slotted-line measurements that Allen-Bradley fixed resistors and Type J potentiometers of 1,000 ohms or less resistance are suitable at least as high as 400 megacycles.

Use of Diode Generator

It was stated that measurements are made by noting the diode current necessary to double the output of the receiver. Thus, the use of an output meter is indicated. However, calibration is usually necessary because of the nonlinearity of the detector. If a signal generator is available, it can be used. If not, the diode generator itself will serve the purpose.

The noise diode and R_a are connected to the receiver, and the diode itself is turned off. The r-f gain control of the receiver is turned down until the output meter nearly indicates zero. Under this condition the gain is so low that the noise obtain sufficient input to the receiver for this calibration.

The input resistance R of a receiver can be measured by a method given by A. van der Ziel.[7] A somewhat simplified version of his method follows.

The noise diode is connected to the receiver input terminals, with the diode inoperative, and with $R_a = \infty$. The receiver gain is decreased until the output indicator drops nearly to zero. The diode filament temperature is increased until a current I is obtained, and the output reading is noted. With reference to Eq. 3, the input power to the receiver is given by

$$P = 3.18 \times 10^{-19} I_1 BR$$

Next, a finite value of R_a is used, and the diode current I is adjusted for the same output reading as before. It will be necessary to use a higher value of I, I_2, because part of the diode power output is absorbed by R_a. The power input to the receiver is given by Eq. 3, and is the same as that obtained with I_1 when $R_a = \infty$. Equating the powers,

$$3.18 \times 10^{-19} I_1 BR = 3.18 \times 10^{-19} I_2 B \left(\frac{R_aR}{R_a + R}\right)^2 1/R$$

Solving for R,

$$R = R_a\left(\sqrt{\frac{I^2}{I^2 - I_1^2}} - 1\right) \quad (8)$$

The procedure can be simplified if $I_2 = 4I_1$. Then $R = R_a$. In making the measurement in this manner, an output reading is obtained for a diode current I. The diode current is then increased to $4I$, and R_a is decreased to give the same output reading. Detector calibration is unnecessary for this test.

Noise Generator Design

In the noise generator circuit of Fig. 2 a type 708A triode is used as a diode, the control grid being used as the anode. The plate is not connected. The 708A was chosen because it has high grid-dissipation capabilities, low grid-filament capacity, and a thoriated tungsten filament whose temperature responds rapidly to changes in applied voltage.

Filament voltage is controlled by

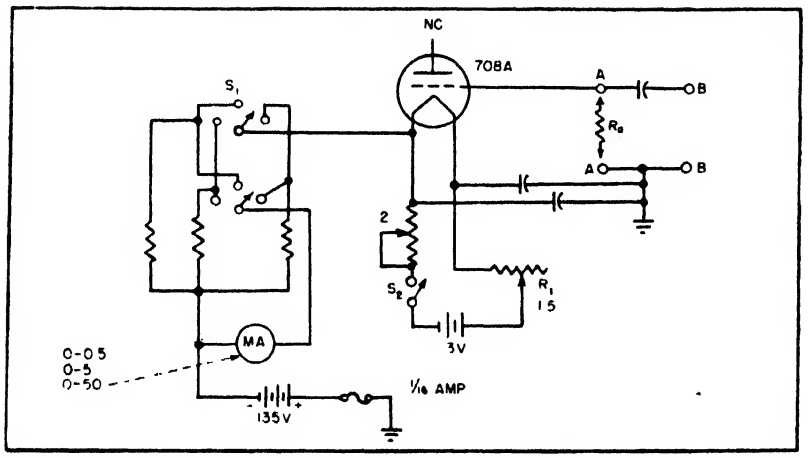

FIG. 2—Schematic diagram of the diode noise generator. The receiver connects to points *A-A* normally, to *B-B* if d-c isolation is required

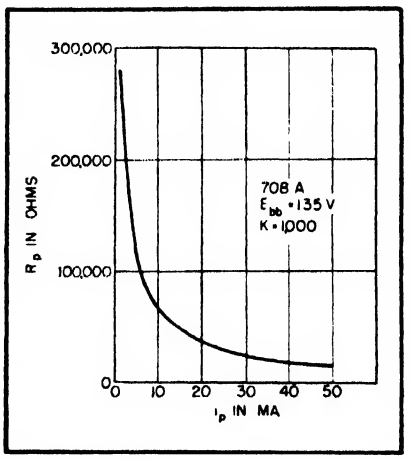

FIG. 3—Plate resistance versus plate current for the 708A tube

a rheostat R_1 which is used to set the diode current I to the desired value. In practice it may be necessary to measure noise figures as high as 50 with values of R_a as low as 50 ohms. This requires direct diode currents as high as 50 milliamperes. The meter was provided with shunts for full-scale currents of 50, 5, and 0.5 milliamperes.

The tube is mounted on an insulated panel with terminals for R and for connection to the receiver. Every effort has been made to keep the output capacitance as low as possible $-10\mu\mu f$ in this case. At

The input resistance was measured by two independent means to provide a check on theory. The noise diode gave a value of 200 ohms; 220 ohms was obtained by substitution with a signal generator.

The 6J4 preamplifier shown in Fig. 4B gave a minimum noise figure of about 2. This is not quite as good as the 6J6, but the circuit has the important advantages that the tuning of the input circuit is not critical and neutralization is not required.

Input resistances of 140 ohms and 130 ohms were obtained with the diode and signal generator refrequencies where the reactance of this capacitance becomes comparable to R, it is necessary to tune it out by means of a coil or, at very high frequencies, a Lecher wire system.

Figure 3 is a plot of R_p versus i_p for the 708A. It can be seen that R_p will be much higher than R_a under almost all circumstances.

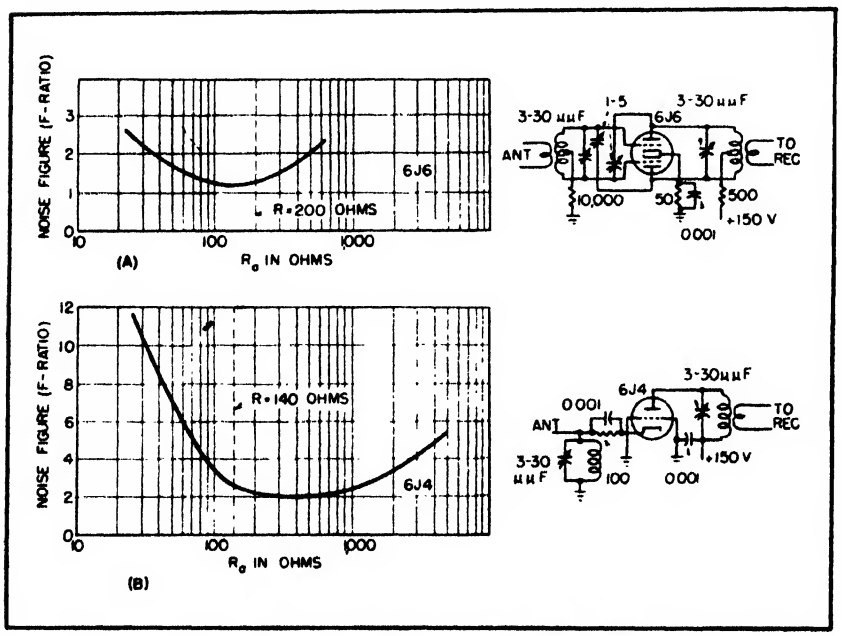

FIG. 4—Preamplifier circuits and measurements

Results

The choice of a diode for this use is a difficult one because almost all small diodes made in this country have oxide cathodes and are not suitable. It is to be hoped that a tube designed specifically for this application will be manufactured. A small diode constructed from the plate and filament of a 316A doorknob tube and mounted in a tubular envelope for probe use should be ideal for measurements, at least up to the vhf range.

The results of some measurements made with the diode noise generator are shown in Fig. 4A and 4B. The two amplifier circuits shown were used as preamplifiers for a Super-Pro receiver. The push-pull neutralized 6J6 gave the lowest noise figure; a ratio of about 1.2. This value is doubtful to about ±0.2 because of the external noise pickup. The minimum noise figure was obtained with a value of R_a less than the input resistance R; 150 ohms as compared with 200 ohms.

spectively. The measurements were made at 20 megacycles.

The assistance of Arthur H. Benner in the construction and measurements is gratefully acknowledged.

REFERENCES

(1) H. T. Friis, Noise Figures of Radio Receivers, *Proc IRE*, 32, p 419; July 1944.
(2) Shepard Roberts, Some Considerations Governing Noise Measurements on Crystal Mixers, *Proc IRE*, 35, p 257; Mar. 1947.
(3) W. Schottky, Spontaneous Current Fluctuations in Various Conductors, *Ann. Physik*., 57, p 541; 1918.
(4) J. B. Johnson and F. B. Llewellyn, Limits to Amplification, *Elect. Eng.*, 53, p 1,449; Nov. 1934.
(5) L. R. Koller, "Physics of Electron Tubes," 2nd Ed., McGraw-Hill Book Co., New York; 1937.
(6) J. M. Miller and B. Salzberg, Measurement of Admittances at Ultra-High Frequencies, *RCA Rev*, 3, p 486; Apr. 1939.
(7) A. van der Ziel, Measurement of Noise Ratios and Noise Factors, *Phillips Res. Rep.* 2, p 321; 1947.

Noise Meter

AN AUDIO NOISE METER designed for use in quantitative test of noise components in aircraft radio equipment is shown in the diagram. The

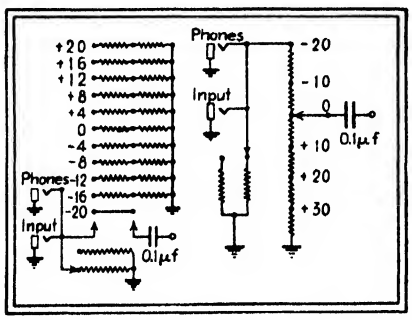

Two attenuator circuits that may be used at the input circuit of the audio noise meter. Phones permit monitoring of the signal

instrument consists of a vacuum-tube voltmeter that is connected to the regular receiver in the plane. This eliminates switching problems and permits the measurements to be made from points where interference is being generated, remote from the receiver. The meter is described in a paper by Fred Foulon on the subject of radio noise elimination in all-metal aircraft, and was presented at the AIEE national technical meeting at Salt Lake City in September, 1943.

The instrument indicates the quasipeak value of the noise signal rather than the rms value since only the nuisance value of the noise signal present in the audio output of the receiver is of interest. The proper response is accomplished by the use of a resistance-capacitance network that requires a 10-millisecond charge time and a 600-millisecond discharge time in accordance with the standard time constant for noise-measuring instruments.

To prevent a false reading by a signal from a radio station that may be inadvertently tuned in, the audio signal is monitored at the input of the noise meter by headphones inserted in the jack provided. This is also of value in identifying the source of radio noise since certain units of noise-producing equipment in aircraft cause a characteristic audio signal in the receiver.

A starting point in the measurement of radio noise is the evaluation of the background level of the receiver with all noise sources inoperative, the receiver antenna lead disconnected, and the antenna terminal grounded to the receiver chassis through a capacitor whose value equals that of the antenna. The background level is then determined throughout the frequency range of the receiver. The relative noise output of the various electrical devices in the plane may be measured and steps taken to reduce the coupling paths to the receiver.

For measurement of ignition noise reaching the receiver via the antenna, the background level is measured with the antenna and lead-in connected normally. In this case it must be remembered that the atmospheric noise level is the limiting background level. If noise from equipment inside the plane is reduced to the atmospheric noise level in one location, it may be above the atmospheric noise level in another location.

The circuit includes a filter to limit the frequency response of the instrument to the audio range necessary for intelligible transmission of speech. The meter is calibrated in db using a 0-db reference

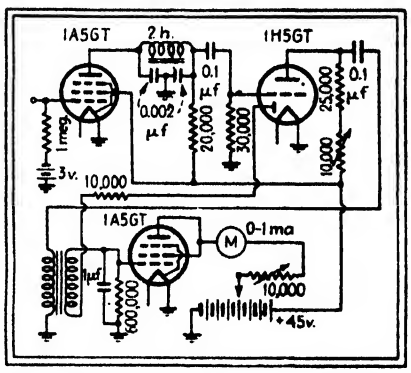

Circuit of vacuum-tube voltmeter that connects to the plane's receiver and allows noise measurements at remote points

level of one milliwatt in 600 ohms. An input attenuator circuit is shown that extends the fullscale range of the meter in steps of 4 db. An alternative attenuator circuit is also given that provides steps of 10 db. High sensitivity is used to indicate the background level of the receiver used in conjunction with the meter, since this is one factor of the basis on which quantitative audio noise measurements are made.

Oscilloscope for Pulse Studies

The wideband instrument described incorporates a triggered sweep, time delay of the signal to permit the triggered sweep to get under way, beam blanking during stand-by, and time-interval marking of the trace by beam-intensity modulation

By HORACE ATWOOD, JR. and ROBERT P. OWEN

THERE IS AN increasing interest in electronic circuits which generate, shape or otherwise make use of sharp voltage and current pulses. The exact form of these pulses is of great interest to the investigator, but observation of them is often difficult or impossible with previously developed commercial cathode-ray oscilloscopes. Such instruments are generally not capable of reproducing, distinctly and without distortion, pulses having extremely steep fronts and of low and irregular repetition rate.

It was therefore decided to develop a portable cathode-ray oscilloscope which would not only be suitable for conventional applications, but would also be particularly effective for the observation and measurement of pulse waveforms.

As is always the case with a new instrument, many problems arose and were solved in the process of design and development. Too often ideal performance of one circuit can be obtained only by limiting the operation of another equally important circuit. For example, the requirements of high gain and wide bandwidth in amplifiers are always incompatible. Perhaps the most difficult problem facing the design engineer is the reconciliation of such conflicting circuit requirements. Satisfactory compromises can be reached only through careful consideration of the entire field of application of the instrument.

Figure 1 shows the functional layout of the oscilloscope in block diagram form. The horizontal deflection, vertical deflection, and beam modulation circuits are designated here, as they are on the front panel of the instrument, by the coordinate symbols X, Y, and Z. This nomenclature emphasizes the function of the cathode-ray oscilloscope as an extremely versatile curve-tracer, working in effect in three dimensions.

Except for the input cathode-followers, all vertical and horizontal amplifier stages are mounted on a heavy vertical phenolic panel. This construction minimizes stray capacitance to ground and saves space, since bulky insulated terminals and lugs are unnecessary. Conventional mounting strips are used underneath the metal horizontal chassis to support less critical components.

The cathode-ray tube selected

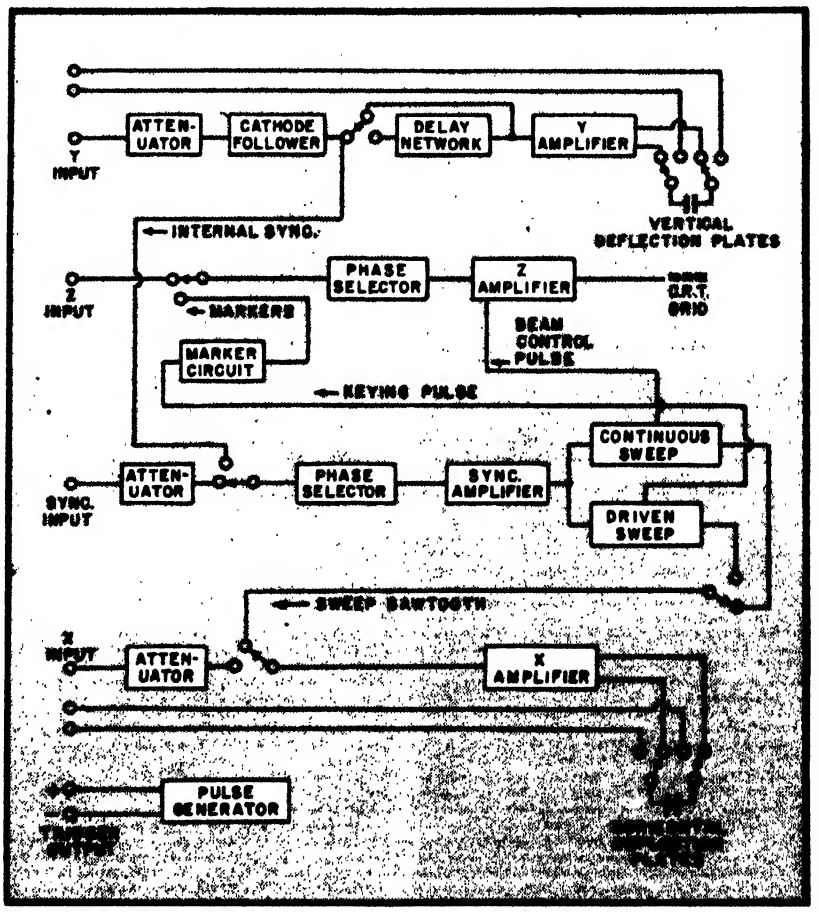

FIG. 1—Block diagram of the oscilloscope, showing the several ways in which the signals and sweeps can be handled

was the Type 5JP- which has a five-inch diameter screen and is available with either short, long, or medium persistence characteristics. To improve the utility for high-frequency applications, the deflection plate connections are brought out directly to terminals on the neck of the tube, minimizing capacitance and cross-coupling effects. An intensifier electrode allows high overall accelerating potentials without excessive beam deflection factors.

A double-primary transformer and high-voltage rectifiers normally supply a negative 2000 volts for the cathode and a positive 2000 volts for the intensifier, the second anode and deflection plates being near ground potential. When high deflection sensitivity is of greater importance than image brilliance, the second half of the power transformer primary can be switched in series with the first half. This change in connections reduces voltages by one-half, thus approximately doubling the deflection sensitivity.

If the waveform to be investigated has a peak to peak amplitude of from 20 to 300 volts, it can be satisfactorily observed by feeding it directly to the deflection plates of the cathode-ray tube. There are terminals on the front panel for this purpose, and coupling capacitors in the deflection-plate leads allow the beam positioning controls to function without interference from applied d-c potentials. These coupling circuits introduce no distortion above ten cycles per second, and the upper limit of usefulness for the tube when used in this way is several hundred megacycles.

Ordinarily, the signal must be amplified before reaching the cathode-ray tube. Amplification is advisable if the input is single-ended, even though the original signal is of considerable amplitude, so that balanced signals may be applied to the deflection plates. Of course, amplifiers are of value only within their frequency response range. The Y-axis amplifier of this instrument is useful for sinusoidal signals between five cps and 10 Mc.

Input can be effected through a test probe and five feet of coaxial cable, or to a terminal on the front panel. There is a twenty-to-one attenuation ratio in the probe as a result of a necessary compromise between probe input capacitance and cable length. Input impedance of the probe is five megohms in parallel with 10 $\mu\mu f$. A 0.01 μf, 1000 volt capacitor prevents d-c loading of the circuit under observation. Insulated clips permit safe use on peak voltages up to the rating of the input capacitor.

Immediately following the input terminal and probe socket is an isolating capacitor and a three-position *RC* attenuator having ratios of 1:1, 10:1, and 100:1. This attenuator, as well as the one in the test probe, is compensated for high frequencies and introduces negligible distortion within the frequency range of the amplifier.

A continuously variable attenuator is necessary in an instrument of this type, but here compensation is impossible because the resistances are not fixed. Sources of distortion and methods of compensation are discussed later. Stray capacitances must be rendered ineffective by a relatively low-resistance potentiometer (1000 ohms).

The problem of matching this power from the receiver and from R_s can be neglected, and the output power of the receiver will then be directly proportional to I.

The diode current I is then increased until some convenient output reading—say one volt—is obtained. The diode current I is then doubled, and the output reading is noted. If the detector is linear, the reading will be 1.41 volts. If not, it will probably be higher—perhaps 1.5 or 1.6 volts. The increase from 1 volt to the higher value does indicate a true doubling of the input power.

If the receiver has an a-f or video gain control, its setting must not be changed after this calibration is made, since it is necessary that the detector operate over the same part of its characteristic. It may be necessary to use a high value of R_s to low-impedance control to the high-impedance stepped attenuator is

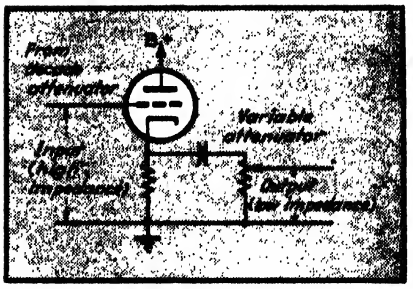

FIG. 2—Cathode-follower circuit acts as an impedance transformer between the high-impedance decade attenuator and the low-impedance continuously variable attenuator

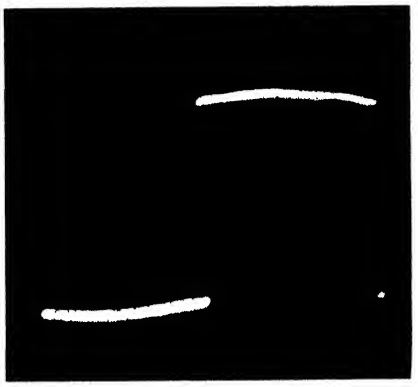

FIG. 3—A 30-cps square wave, as reproduced by the vertical axis amplifier

solved very conveniently by the insertion of a cathode follower, shown in Fig. 2, as an impedance transformer, with the additional advantages of extremely low input capacitance and the ability to handle large signals. To take full advantage of the three-position decade-attenuator, the gain control is limited to a maximum attenuation of ten to one. This feature also prevents overloading of the input stage by strong signals, as long as the resulting deflection on the cathode-ray tube screen is less than three inches peak to peak.

Vertical Amplifier

Immediately following the variable attenuator are two amplifying stages, the first employing a 6AC7 pentode, the second, a 6AG7. Both plate circuits include compensating filters for low frequencies which, with slight individual adjustment to take care of component variations, make it possible for the

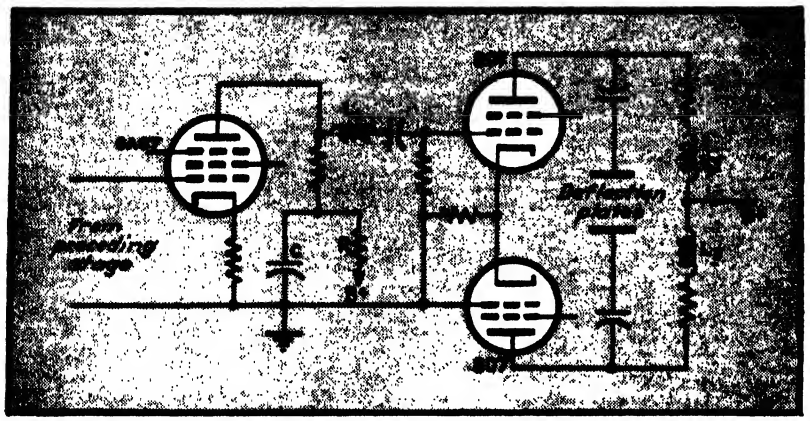

FIG. 4—Y-Axis amplifier is low-frequency compensated by the *RC* network, and high-frequency compensated by the series inductor L_1 and the shunt inductors L_2 and L_3. The X-axis amplifier is similar

amplifier as a whole to pass a 30-cycle square wave with only the slight distortion shown in Fig. 3. High frequency compensation is also provided, shunt peaking being used with the 1000-ohm plate load of the Type 6AC7 stage and series peaking with the 1300-ohm load resistor of the Type 6AG7. A type of compensation allowing a larger plate load for the desired frequency range is used in the latter stage in order that the maximum possible output can be obtained from the deflection amplifier which it drives. Transient response is equal to that of the shunt peaked stage.

The deflection amplifier consists of two 807's, cathode-coupled to give a balanced output. Because of low output capacitance it was found possible to use 1500-ohm plate loads and shunt peaking without reducing frequency response below that of previous stages. The last two stages of the vertical amplifier are shown in Fig. 4. Over three inches of undistorted deflection is available with 4000 volts accelerating potential on the cathode-ray tube.

Response of the Y-axis amplifier is down less than ten percent at five Mc, and is ten percent of the mid-frequency gain at ten Mc. Compensation is adjusted to give faithful reproduction of high frequency pulses without overshoot or oscillation. The oscilloscope input deflection factor is approximately 0.07 volts rms per inch of peak to peak deflection, with the higher accelerating potential.

High gain is not required in the X-axis or horizontal amplifier, so a cathode follower and gain control driving a balanced deflection amplifier similar to that of the Y-axis is all that is necessary. Response is down about 25 percent at two Mc, and the deflection factor is 2.5 volts rms per inch.

Signal Time-Delay

When using a driven or start-stop type of sweep, it is often necessary to trigger the time-base by means of the signal which is to be observed. Although sweep circuits such as the one used in this oscilloscope get under way in a small fraction of a microsecond, part of the wavefront is obliterated as shown in Fig. 5(a) unless there is a short time-interval before the signal appears at the vertical deflection plates.

A delay of about one-half microsecond can be obtained by switching in a delay network ahead of the variable attenuator. This network of the low-pass filter type has a characteristic impedance of 200 ohms to match the output of the cathode-follower, and a cutoff frequency of twelve megacycles in order that it will be essentially distortionless up to approximately six megacycles. With the signal delayed by this network, the trace is as shown in Fig. 5(b).

Time Bases

Two linear time-bases are provided. One, providing the usual continuous sweep, is shown in Fig. 6, and is a modified form of the high-vacuum circuit first described by Puckle. It has a range of 15 cps to 150 kc when running free and is exceptional in its ability to synchronize steadily at high signal-to-sweep frequency-ratios. Stable operation with more than 100 cycles of the signal on the screen can be obtained at medium frequencies. Operating frequencies as high as 300 kc or more are attained by moderate synchronizing with high frequency signals.

The second time-base incorporated in this oscilloscope is of the driven or start-stop type. Each stroke must be initiated by an external signal. Its great usefulness is in detailed inspection of waves occurring at relatively long and inconstant intervals, and having short durations. Any one of four sweep durations (5, 25, 100, or 1000 microseconds) may be selected by means of a switch on the front panel. This sweep can be triggered repeatedly at rates up to approximately the frequency corresponding to the sweep period. The previously mentioned delay network greatly increases the utility of this time-base (Fig. 5).

A stage of amplification following a phase-selector stage, (Fig. 1), in the synchronizing circuit insures that the foregoing time-bases

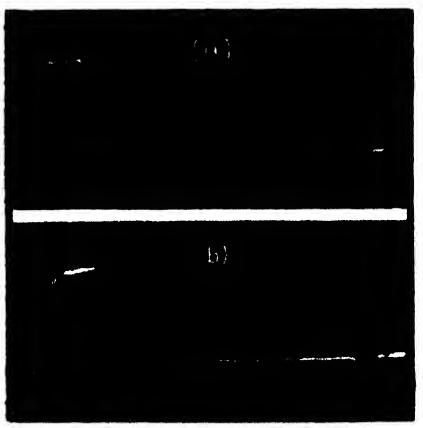

FIG. 5—Pulse reproduced with (a) and without (b) time delay for the signal. Marking spaces are 1 μ sec apart

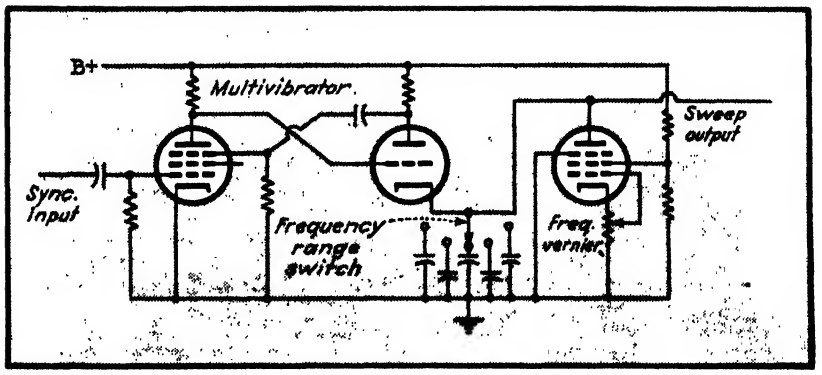

FIG. 6—Simplified wiring diagram of the vacuum-tube sweep circuit indicates the principle of operation. The triode of the multivibrator periodically charges one of the frequency-range capacitors. The constant-current pentode, which includes the frequency-vernier control, linearly discharges the frequency-range capacitor

can be synchronized or initiated by small signals of either polarity. One volt peak will trigger the driven sweep.

Generally, driven sweeps of short duration and low repetition rate are limited to one-half of the horizontal deflection distance that is available to the continuous sawtooth sweeps or other symmetrical signals. However, when this instrument employs driven sweeps, the operating points of the X deflection amplifiers are shifted along their dynamic characteristics to allow full deflection.

The Z-axis or beam modulation amplifier, illustrated in Fig. 7, makes use of a phase-selector as its input stage, thus making possible blanking or intensifying of the beam by either a positive or negative signal. This amplifier, together with the time-bases, acts as a beam control circuit serving to blank the return trace of continuous sweeps, and to drive the beam from cut-off during stand-by to full intensity during sweep when the driven time base is in use.

It is very necessary that adequate beam brightening be provided on short-duration strokes if the image is to be photographed, otherwise the beam intensity must be increased to a high level to make an infrequently repeated trace visible. As a result, the beam rest position will be so bright as to obscure the remainder of the trace. The cut-off of the beam during stand-by avoids this difficulty.

To allow for the use of the Z-axis with video frequency signals, the response of the amplifier was made uniform to four megacycles.

For use in conjunction with the Z-axis there is provided an oscillator and pulse-forming circuit which together furnish sharp pulses at intervals of one, ten, or 100 microseconds. Figure 8 is a block diagram of this marker circuit. The oscillator is synchronized with driven sweeps, and is used to indicate elapsed time along the X-axis by introducing brightening or blanking markers (Fig. 5) into the trace. Direct application of the signal to be investigated to the vertical deflection plates in no way affects the use of this timing circuit. The transitron oscillator is designed to be keyed on by the initiation of the driven sweep, but it is also useful over most of the continuous-sweep frequency range.

An unusual feature of this instrument is the inclusion of a pulse generator for use in triggering and testing other equipment. There are available at terminals on the front panel positive and negative pulses of about 100 volts peak amplitude and less than a microsecond duration, at a rate continuously variable between 200 and 3000 pulses per second.

Attenuator Distortion

Initial deformation of the signal takes place when it is reduced from its original value by the test probe or the stepped attenuator. Both of these voltage dividers are compensated at the high frequencies by means of adjustable capacitors shunting the fixed resistors. These capacitors are adjusted for minimum distortion of a 10 kc square wave, this frequency usually being the most sensitive to attenuator misadjustment. Even at the best possible setting, however, there will be a slight but

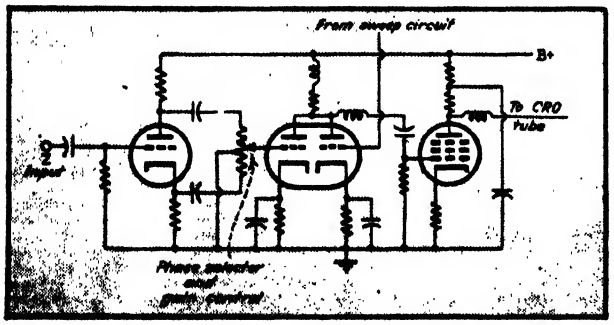

FIG. 7—The Z-axis or beam modulation amplifier blanks the return trace by means of a pulse from the sweep circuit (see Fig. 1). This blanking pulse is superimposed upon any external modulation signal by the dual-triode mixing stage. Phase selection of the external signal is accomplished by the balanced phase-inverter and potentiometer preceding the mixer stage. Both shunt and series high-frequency compensation are used in the final stage

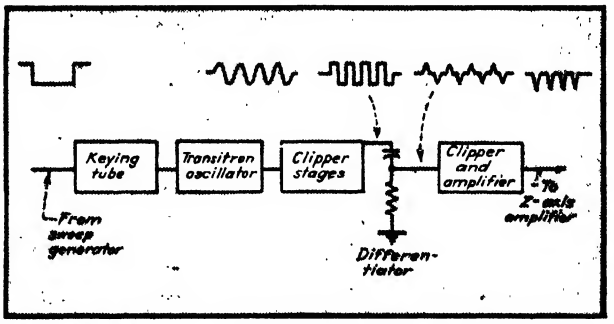

FIG. 8—The oscillator of the time-interval marker circuit is keyed on for the duration of each driven sweep. Wave shapes show the manner by which the oscillations are converted to marker pulses

noticeable rounding of the leading corners of square waves at 100 kc and higher. This distortion is probably caused by phase shift at frequencies above one megacycle. While generally negligible, this effect cannot be entirely eliminated. Equal attenuation at all frequencies is an engineering ideal that can be approached only at the expense of input impedance.

Additional distortion takes place in the delay network, mainly because of the more rapid transmission of the frequency components above approximately two megacycles, and because of resistive and dielectric losses. Fortunately, this deformation in a well designed and correctly matched lumped-constant delay network is of the same order as that occurring in the attenuators, and can usually be neglected at frequencies below one-half the theoretical cut-off of the delay network.

The amplifiers themselves cause little or no frequency and phase distortion within their range of uncompensated, flat response. By proper compensation this range can be greatly extended at each end, but over-compensation must be avoided. The low-frequency and high-frequency equalizing circuits correct both gain and phase characteristics, but the most extended region of uniform gain and the most linear phase-shift characteristic cannot be attained with the same circuit constants. If a wide-band amplifier is adjusted for minimum distortion of square waves at both ends of its frequency range, it will generally be found that the correction made is a compromise between that necessary for optimum gain and for optimum phase characteristic, but much closer to the latter than to the former. This will be the case at both low and high frequencies. Linear phase-shift at low frequencies requires more compensation than is needed for flat gain. The reverse is true at high frequencies.

Phase and frequency distortion in under-compensated amplifiers will appear respectively as sawtooth and concave bowing of the top and bottom portions of low-frequency square waves, and as rounding of the corners of high-frequency square waves. An over-compensated amplifier shows the even less desirable symptoms of upward slope and convex bowing of low-frequency square waves, and over-shoot, or even a train of oscillations, following the wave front of a high-frequency wave or pulse.

The Y-axis of this instrument will pass a thirty cps square wave with only slight convex bowing (Fig. 3) and compensation is so adjusted that there is no over-shoot on even the most abrupt wave fronts.

Amplitude distortion is always present in oscilloscopes, but seldom to an objectionable extent, as such distortion does not change the wave form in a manner that is very obvious to the eye. Interaction, or cross-coupling, between amplifiers is a serious problem. However, it can be solved by careful component and wiring layout, the provision of metallic shields where necessary, and the use of low output-impedance power supplies.

Oscilloscope amplifier performance is too often specified only in terms of sinusoidal frequency response, but this tells only part of the story of the actual fidelity of reproduction. The phase characteristics of the amplifier are of at least equal importance and should be given full consideration. For example by specifying the square wave response.

The authors wish to acknowledge the valuable contributions of Mr. Bernard Amos and Mr. Charles Puckette to the development of this instrument.

Direct-Coupled Oscilloscope

Examination of low-frequency phenomena encountered in servo techniques and electromedical work requires a high-sensitivity oscilloscope employing d-c amplifiers. Design considerations are given for a portable device useful in observation of waveforms up to 3 megacycles

By J. H. REYNER

THE requirements of modern servo technique and electromedical work call for the examination of very low frequencies. The use of conventional a-c amplifiers involves circuits having long time constants, but such circuits are seriously disturbed by transient impulses, which cause displacement of the image, often off the screen altogether, for periods lasting several seconds. The only real solution is to use a direct-coupled system. A further important requirement in a modern oscilloscope is that it shall be able to record potential differences between two points in a network, but

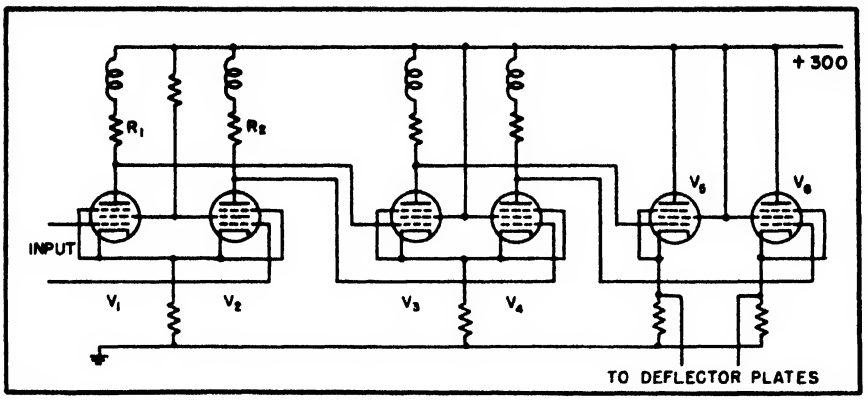

FIG. 1—Simplified schematic diagram of direct-coupled amplifier stages

should disregard fluctuations in the general level of network potential.

The instrument to be described achieves both these features in a practical fashion. The system is indeed so stable that it is not necessary to use stabilized power supplies. Although attention was primarily concentrated on the lower-frequency requirements, the circuits were found to be effective up to comparatively high frequencies. In the design of the finished instrument, therefore, attention was paid to constructional details and layout in such a manner as to maintain the frequency response substantially uniform up to 1 mc or, at some sacrifice of sensitivity, up to 3 mc. The amplifiers are provided with a simple link by means of which the user can choose whichever condition he wishes.

Special CRT

The instrument uses a cathode-ray tube of a type developed for radar. The particular tube has the merit of giving a brilliant trace and a sharply focussed spot with an anode voltage of only 1 kv. Because of this relatively low anode voltage the sensitivity of the tube itself is high. Electrostatic deflection is used, vertical deflectors having a sensitivity of 2.2 mm per v while horizontal deflectors are approximately half this sensitivity. The screen diameter is 3.5 in. with a nearly flat face. Four standard types of screen are available; blue trace with afterglow approximately 1 microsecond; green trace with afterglow approximately 1 millisecond; yellow trace with afterglow approximately 6 seconds; and blue trace with yellow afterglow lasting approximately 20 seconds.

Although the screen diameter is smaller than on many oscilloscopes the extremely small spot diameter (approximately 0.25 mm) at full brilliance results in such sharp traces that the effectiveness of the display is better than on many larger diameter screens.

The c-r tube sensitivity permits a high amplifier sensitivity to be obtained with a maximum gain of only 700. This condition results in a screen deflection of 1.5 mm per mv rms input to the amplifier. The sensitivity on the horizontal amplifier is only about half this figure.

The focus and intensity controls are independent and the focus is sharp over the whole screen. This effect is accomplished by the manner of connecting the deflector plates to the amplifying network, which ensures that the mean deflector potential is the same as the final anode voltage of the cathode-ray tube. This requirement is critical and provision for adjustment is explained later.

The two amplifiers, which are identical in all but minor particulars, each consist of three pairs of symmetrically arranged push-pull tubes. The basic circuit is shown in Fig. 1. The tubes V_1 and V_2 constitute a symmetrical cathode follower or "long-tailed pair". The anodes of the tubes are directly coupled to the grids of tubes V_3 and V_4 which are a similar long-tailed pair arrangement, and these anodes are again coupled directly through the grids of the final pair, which are simple separate cathode-follower stages, the voltage across the cathode resistors being fed direct to the deflector plates of the cathode-ray tube.

All three pairs of tubes are fed from the same supply line but the circuit is so arranged that the cathodes of the first pair are at a low potential, those of the second pair are at an intermediate potential, while in the third pair the whole of the signal voltage is developed in the cathode circuit, there being no anode resistor in either tube.

This symmetrical arrangement provides not only the discrimination previously mentioned but also contributes to the stability because there is no signal current in the B+ line. A symmetrically-applied signal to the input causes circulating currents around the network $V_1R_1R_2V_2$ and there is no signal current either in the high-voltage line or in the cathode resistor. The cathode resistor thus has no effect on the amplification for symmetrical signals, but to any asymmetrical signal it becomes operative and introduces heavy negative feedback; the resulting discrimination in the actual amplifiers is of the order of 1,000 to 1 at the maximum gain setting.

A similar action takes place in the second and third pair of tubes, though advantage of the symmetry here is more in the avoidance of signal currents in the B+ line, since these are now of greater magnitude. Because of this circuiting there is no interaction between one stage and the next or between one amplifier and the other and since, as will be seen later, the time base is operated on a similar principle, the whole instrument can be fed from a common power supply without any appreciable interaction among the circuits.

Since the whole network is directly coupled it operates from zero frequency upwards. Small corrector chokes are included in the anode circuit, so proportioned as to maintain the response level until

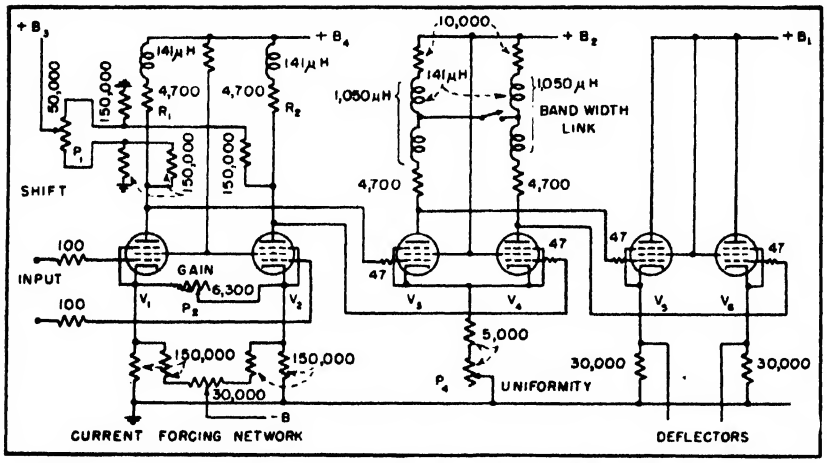

FIG. 2—Detailed circuit schematic of direct-coupled amplifier showing controls

the cutoff point is reached after which rapid attenuation sets in.

Functional Controls

Figure 2 shows the amplifier network in greater detail. Variation in the sensitivity of the amplifier is accomplished by providing separate cathode resistors for the first two tubes and bridging the cathodes with a variable resistance. When this resistance is zero, so that the cathodes are connected together, the two cathode resistors operate in parallel and the circuit is effectively the same as that of Fig. 1 and develops its maximum gain. Increasing the value of the gain control inserts resistance into the circulating anode current ring, the voltage drop acting to oppose the push-pull component of the input signal and thus reducing the push-pull sensitivity of the stage. The push-push sensitivity is not affected and therefore the discrimination tends to fall off as the gain is reduced, but since maximum discrimination is required at maximum sensitivity this constitutes no serious disadvantage in actual practice.

The actual voltage on the anode of the tubes V_1 and V_2 is determined mainly by the voltage drop in the anode resisters R_1 and R_2. An additional source of voltage, however, is applied to these two anodes through a symmetrical network from another source, actually taken from the power supply unit a little earlier in the smoothing chain. This voltage is fed through buffer resistors having a high value compared with the anode resistors, so that the amplification of the network is not appreciably affected. It will be noted, however, that the potential is actually introduced via the slider of potentiometer P_1. At the midpoint of this potentiometer, the potential applied to each tube is the same, but as the slider is moved a condition of unbalance is introduced, which has the effect of making one anode slightly more positive and the other slightly more negative. This unbalance is transferred through the next two pairs of tubes and produces a shift of the spot on the cathode-ray tube screen irrespective of any movement which is being produced by the signal. A smooth and wide range of control is obtained by this means, the important feature being that the change of position is instantaneous so that the location of the image is both positive and rapid.

Bandwidth Adjustment

It has already been mentioned that at the option of the user the frequency response can be varied from 1 to 3 mc. The adjustment is accomplished in the second pair of tubes, the anode resistors for which are in two portions. When both portions are in operation the amplifier maintains its response level up to practically 1 mc, being actually only 3 db down at this frequency. If the link shown in the diagram is closed, however, the upper portions of the two anode resistors are short-circuited and only the lower portions are effective. Under these conditions the frequency response is maintained up to 3 mc but the gain of the stage is reduced by approximately three times. From the symmetry of the arrangement it will be seen that the link short-circuits two points at the same d-c potential so that no circulating currents result.

Figure 3 shows the performance of the amplifier with the link in the 3 mc position. It will be observed that the response is completely uniform from zero up to a frequency very close to the cutoff frequency, after which rapid attenuation occurs. There is no phase shift in the lower frequency portions but some phase shift becomes noticeable a little above 500 kc and the phase angle is approximately 75 deg at 3 mc. Because of this phase shift at the limiting frequency the locus of the operating point on the tube characteristics at this point is no longer a straight line but is an ellipse of fairly large eccentricity. Consequently the volt-ampere requirements are considerably greater than at the lower frequencies where there is no phase shift.

Because of this fact it is not possible to develop the full screen deflection at the highest frequencies and at 3 mc the maximum deflection obtainable is a little over 2 cm. The position rapidly improves as the frequency is reduced. About double this deflection is available at

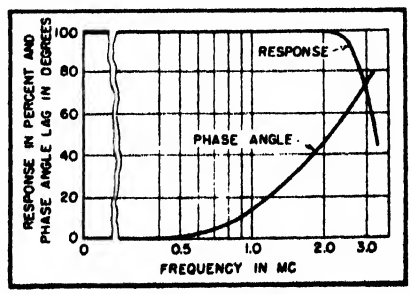

FIG. 3—Frequency response and phase angle of amplifier with link adjusted for 3-mc band

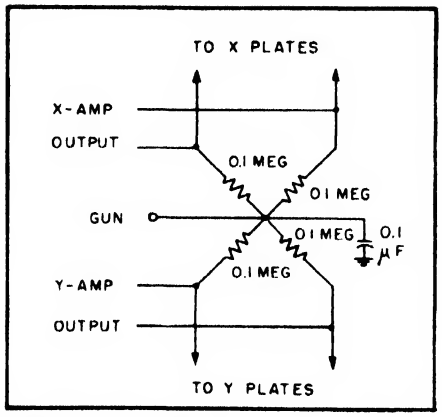

FIG. 4—Gun and deflector plate hookup

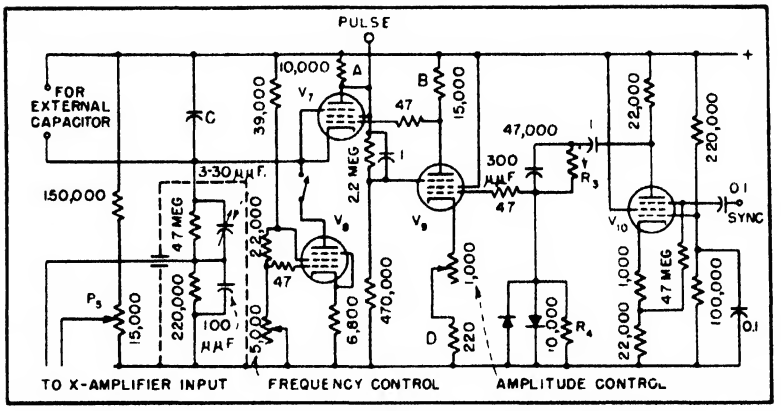

FIG. 5—Simplified schematic diagram of time base generator

1.5 mc and at a little under 1 mc the full screen can be filled. While this limitation might appear serious, in practice the need for a good high-frequency response is determined mainly by the need to handle the harmonics of a fundamental operating on a much lower frequency. The relative strength of these harmonics will, in any case, be small so that not more than about 10 percent of the screen will be required. Actually, approximately 25 percent of the screen can be filled even at the highest frequency and this amount is considered satisfactory.

Current-Forcing Circuit

In order to obtain the discrimination required in the input stage it is necessary that the cathode resistors of V_1 and V_2 shall be of high value. This would normally result in the cathode potential being appreciably positive to ground, so that if the grids on the first stage are operating near ground potential they would be so negative with respect to the cathode as to reduce seriously the effective conductance of the tubes V_1 and V_2. It is, therefore, necessary to maintain the anode current through V_1 and V_2 at a suitable value, and in order to accomplish this current is forced through the cathode resistors from a negative source of current. This supply is effectively a constant-current supply and forces into the network a current which divides equally through the two cathode resistors. The current is actually fed through the slider of a potentiometer. When the instrument is set up the slider is adjusted until the potential of the two cathodes, with the gain control at the maximum resistance, is equal. Without this adjustment operation of the gain control would produce a disturbance in the datum anode current that would be indistinguishable from a genuine signal.

To maintain sharp focus and freedom from astigmatism the final anode of the the cathode-ray tube must be at the same potential as the mean potential of both pairs of deflector plates. To achieve this condition the final anode of the cathode-ray tube is not solidly grounded but is connected to each of the four deflector plates through four equal resistors of 0.1 megohm as shown in Fig. 4. The mean outputs of the two amplifiers are then equated by appropriate adjustment of the anode current of the second stage in the amplifier at P_4. (Fig. 2). This adjustment is necessary on but one amplifier and is therefore incorporated in the horizontal amplifier only.

Time Base

A symmetrical construction is adopted in the time base which is shown in simplified form in Fig. 5. The capacitor C is charged through the pentode tube V_8. Across the capacitor is the discharge tube V_7, the grid of which is held at a potential determined by the network B, V_9 and D. When the capacitor C is discharged, the cathode of V_7 is near the B+ potential so that the grid of the tube is considerably negative with respect to the cathode and the tube is non-conducting. As the capacitor charges up, the cathode potential falls until it becomes only slightly positive with respect to the grid and the tube commences to conduct. As soon as current flows in this circuit a potential is developed across A which reduces the screen potential of V_8, causing a rise in anode potential which makes the grid of V_7 more positive. This change increases the conductance of V_7 so that the discharge is accelerated and a rapid flyback is obtained.

The action of V_7 and V_8 results in an effective transfer of the cathode current of V_8 from the anode to the screen so that the total drain from the supply line remains constant. This is an important feature since it not only avoids interaction between the time base and the amplifiers but it also renders the operation of the time-base circuit independent of the time-constant of the high voltage supply line. Because of this condition the circuit continues to function satisfactorily down to indefinitely low frequencies. Capacitor C is actually a series of eight of gradually increasing value in order to give discrete ranges of frequency, and for the sake of reasonable portability the largest capacitor is such as to provide a minimum sweep frequency of 2 cps. A two-pin socket is provided, however, to make the time-base voltage available externally, or for single-sweep operation as ex-

plained below. Additional capacitors can be added across the socket to extend the time base frequency downwards to at least to 0.2 cps.

Fine control of the frequency is obtained by varying the current through the pentode tube V_8 via the grid potential. The voltage across the time-base capacitor is transferred through a high-resistance potentiometer to the input of the horizontal amplifier. This arrangement permits the width of the scan on the cathode-ray tube screen to be varied from about one half to five screen diameters. The highest time-base frequency is 150 kc and since the horizontal amplifier frequency response extends to at least ten times this value the saw-tooth waveform is satisfactorily maintained throughout the full frequency range. The potentiometer is compensated for stray capacitances so that the correct ratio is maintained throughout the full frequency range. To offset the d-c component of the time base signal the other X-amplifier input terminal is supplied with a steady voltage adjusted by the potentiometer P_5 to equal the mean d-c value of the signal.

Synchronism

The synchronism is automatic. Synchronizing signals are applied through the tube V_{10} to the grid of tube V_8. These signals control the current of V_8 and hence the grid potential of V_7. A positive synchronizing impulse will thus drive the grid of V_7 positive and initiate the discharge.

The pulse of current through V_{10} does produce some slight modulation of the high voltage line but this is limited by the rectifier network in the bottom half of the potentiometer which transfers the voltage from V_{10} to V_8, and also by the inclusion of a high value of resistance in the cathode. As a result, the current of V_{10} is, in practice, substantially constant.

The main function of the two rectifiers just mentioned, however, is to limit the synchronizing pulse to a suitable value. The resistors R_3 and R_4 are so chosen that for small signals the rectifiers are of relatively high resistance. As the voltage on R_4 rises, however, the rectifiers begin to conduct and thus to shunt the bottom half of the potentiometer and limit the voltage applied to V_8. It is thus not possible to produce over-synchronism with consequent shortening of the time-base sweep. This feature is valuable in practice because with conventional methods a change in amplitude of the signal under examination causes a change in the point at which the time base triggers, with consequent unsteadiness of the image. With the present arrangement the image remains quite steady, irrespective of the changes of amplitude and the arrangement is so successful in practice that no synchronizing control is provided. It is merely necessary to apply to the sync terminal a signal either from the output of the vertical amplifier or direct from some part of the circuit under examination.

The negative pulse developed across A is brought to a terminal at the rear of the instrument and may be connected to the modulator grid on the cathode-ray tube, if desired. In this condition the spot is blacked out during the flyback.

Constructional Features

The power supplies and time-base components are mounted on the main chassis while the two amplifiers, which are assembled as separate units, are mounted in antivibration mountings on either side of the cathode-ray tube. All main controls are available on the front panel. The four deflector plates are connected to terminals along the bottom of the front panel and four switches immediately above permit each plate individually to be connected to ground, to the terminal either directly or through a capacitor, or to the output of the appropriate amplifier. The leads to the deflector plates are spaced from each other and from the chassis in order to reduce the stray capacitance. Where minimum plate capacitance is essential, however, connections can be made to four terminals at the back of the instrument. These terminals are normally strapped to adjacent terminals connected to the front terminals but by opening the links the additional capacitance of the wiring is removed. The gun and modulator electrodes are also accessible at the rear, together with the pulse output for flyback suppression.

Symmetrical input is provided on each amplifier with a ground terminal in between and each input is provided with a multiposition switch. This switch allows direct connection; direct connection through a resistance attenuator that reduces the sensitivity approximately fourteen times; and direct or attenuator connections including an isolating capacitor of 0.1 microfarad with 1.2 megohms to ground.

The horizontal amplifier switching has two additional positions. The first of these connects the amplifier input to the time base while the second is for single-sweep operation, the time base still being connected but the discharge tube rendered inoperative.

The single sweep referred to is not electronic in character. The time-base controls are set to operate at the required sweep speed and the time-base terminals are then short-circuited externally. On removal of the short-circuit the spot will sweep across the screen and will stay in its final position until restored by re-imposing the short-circuit across the capacitor. The d-c positioning of the spot and the gain control of the horizontal amplifier can be manipulated to include the whole of the sweep on the screen or any portions thereof. The internal time base is rendered inoperative when the amplifier is connected for external signals.

A graticule with millimeter rulings is located in front of the tube face, being held in position by a cover plate which incorporates a telescopic light shield. This cover plate can be removed completely and replaced by a camera, either for single shots or for continuous recording.

Cathode-Ray Q Meter

By RUDOLF FELDT

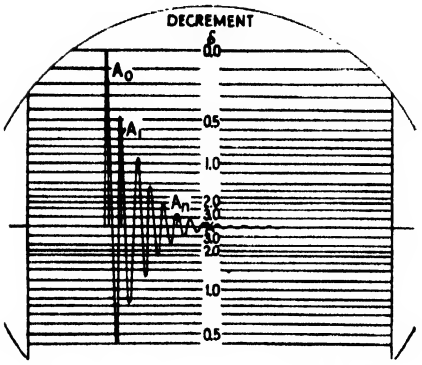

Fig. 1—Decrement is determined from the amplitudes of successive peaks of a free running, oscillating circuit

LOGARITHMIC DECREMENT and Q can be measured by the cathode-ray oscilloscope. This method of plotting damped oscillations as fixed images on the cathode-ray tube has both electrical and mechanical significance.

Theory

Any system which is able to oscillate will generate damped oscillations if excited by shock. The frequency of these oscillations is determined by the inductance and capacitance of the system, and the damping of the oscillations by losses in the system. A damped oscillation is expressed by

$$A_t = Ae^{-\alpha t}\cos \omega t \qquad (1)$$

where A_t is the voltage across the circuit at any time t

A is the voltage at the moment of excitation, time T

ω is the natural angular velocity of the circuit

α is the decrement factio given by $\alpha = R/2L$

R is the equivalent total series resistance of the circuit

L is the equivalent series inductance of the circuit

Logarithmic decrement δ is defined as the natural logarithm of the ratio of maximum voltage during any given cycle of oscillation to the maximum voltage of the next cycle. Logarithmic decrement is equal to decrement factor α divided by natural frequency f. Referring to Fig. 1

$$\delta = \alpha/f = R/2fL = (1/n)\ln (A/A_n) \qquad (2)$$

From Eq. 2

$$Q = \pi/\delta = n\pi/\ln (A/A_n) \qquad (3)$$

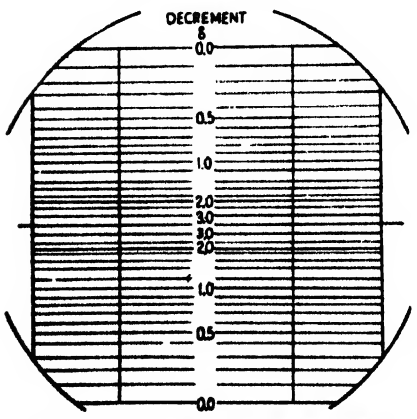

Fig. 2—Scale for measuring decrement directly

Measurement

Shock excitation of tuned circuits can be obtained either by applying square waves or by differentiating the saw-tooth wave of the sweep generator, which is a part of almost every cathode-ray oscilloscope, thereby obtaining repetitive pulses. These square waves or pulses are then fed to the oscillatory circuit. The damped oscillations that are generated are applied to the vertical amplifier of the oscilloscope. Sweep is applied to the horizontal amplifier in the usual manner. If pulses from the saw-tooth generator are used, synchronism is necessarily maintained.

Values of decrement and quality can be obtained from the pattern of the damped oscillation or by means of transparent scales placed in front of the cro screen. These

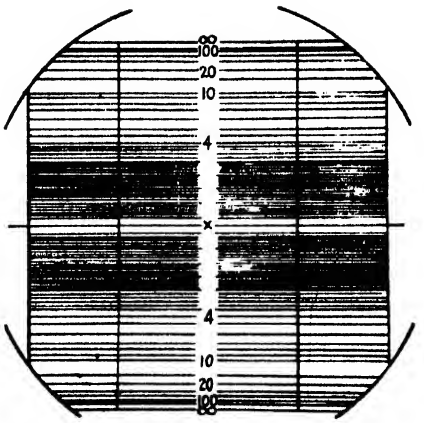

Fig. 3—Scale for measuring quality directly

scales are drawn from Eq. 2 for δ, and from Eq. 3 for Q. Figure 2 shows such a scale calibrated for logarithmic decrement and Fig. 3 shows a scale for quality.

To measure decrement, the pattern of the damped oscillation is centered on the line marked X on the scale. Amplitude of the oscillations are adjusted (conveniently by the gain of the oscilloscope amplifier) so that one peak touches the zero reference line. The amplitude of the next peak indicates on the scale the value of δ. If the value at the nth successive peak is read, divide by n to obtain δ.

Quality can be determined in a similar manner using the scale of Fig. 3. In this case the reference line is marked X. The pattern is adjusted so that one of the amplitudes of the damped oscillation touches the reference line. The next amplitude indicates on the scale the value of Q or if the scale is read at the nth amplitude it is multiplied by n to obtain Q.

For accurate measurements precautions must be taken to avoid loading of the resonant circuit by the pulse generator and the oscilloscope.

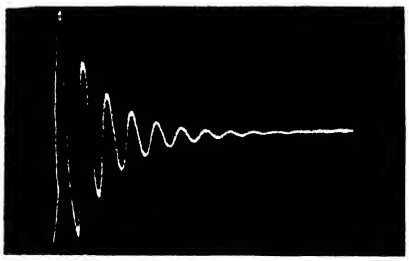

Fig. 4—Typical trace from which decrement and quality can be measured

In Fig. 4 the trace obtained from a vedeo peaking coil having a decrement of about 0.6 is shown. If the voice coil of a loudspeaker is excited by a square wave without introducing electrical damping, the trace indicates damping of the loudspeaker membrane and its resonant frequency.

Any mechanical device which can be excited by shock to produce vibrations can be measured by this method. If the shock is synchronized with the sweep circuit of the cro and the mechanical vibrations converted into electrical signals by piezoelectric pickups, or electromechanical or photoelectric devices, a steady trace can be produced as in measuring electrical circuits; otherwise an adaption of single trace technique can be made.

Time-Base Calibration

Time-displacement linearity of oscilloscope sweeps can be measured at tenth-microsecond intervals by using a crystal-controlled, driven multivibrator chain. Circuit provides sweep-triggering pulse and constant-amplitude, continuous calibrating signal

By WALTER W. LUDMAN

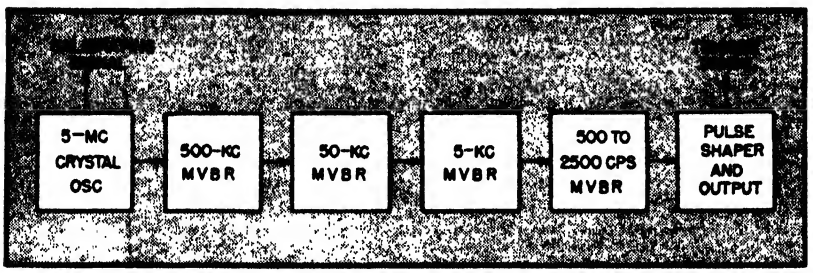

Time-base calibration requires a constant-frequency calibrating signal and a synchronized pulse to trigger the sweep. A crystal-controlled oscillator provides the calibrating signal; multivibrator frequency-dividers provide the relatively long-period, short-duration synchronized triggering pulses

TESTING of certain electronic equipment requires the measurement of the width or duration of extremely narrow, rectangular, recurrent pulses. Some of these pulses may have durations as short as one-half microsecond. It may be necessary to measure the duration of such pulses to an accuracy of 2 per cent.

Synchroscope

Measurement of such short-duration pulses is usually accomplished with the aid of a device generally known as a synchroscope. This is primarily an oscilloscope with a triggered sweep circuit supplying, for the horizontal deflecting plates of a c-r tube, a deflection voltage which varies at an unusually high speed and has a very linear rate of change. Provision is made for applying the pulse to be measured directly to the vertical deflecting plates of the c-r tube.

The horizontal sweep voltage or time base varies at a rate such that its total voltage swing may occur in a time interval of only 3 or 4 microseconds; the time between successive sweeps may however be very long in comparison, 1000 microseconds in the example shown in Fig. 1.

The time interval between successive sweeps is controlled by the recurrence rate of the trigger signal which starts the sweep circuit functioning. This trigger signal can be supplied by circuits within the synchroscope or from some external source, but it must be in synchronism with the recurrence rate of the signal to be viewed.

When a pulse having a duration of only one microsecond is viewed on an oscilloscope provided with a sweep having a duration of 3 microseconds, a pattern is obtained as shown in Fig. 2. Very accurate measurements of the actual duration of the pulse at any amplitude can be made if the exact time rate of change per unit of deflection of the horizontal sweep is known. Various methods can be used for calibrating such a time base in terms of microseconds per inch of deflection.

Calibration Techniques

Most calibrating schemes are based on the application of a sine-wave signal of known frequency to the vertical channel of the oscilloscope. If the frequency is known, the time interval between successive cycles of the sine wave is sim-

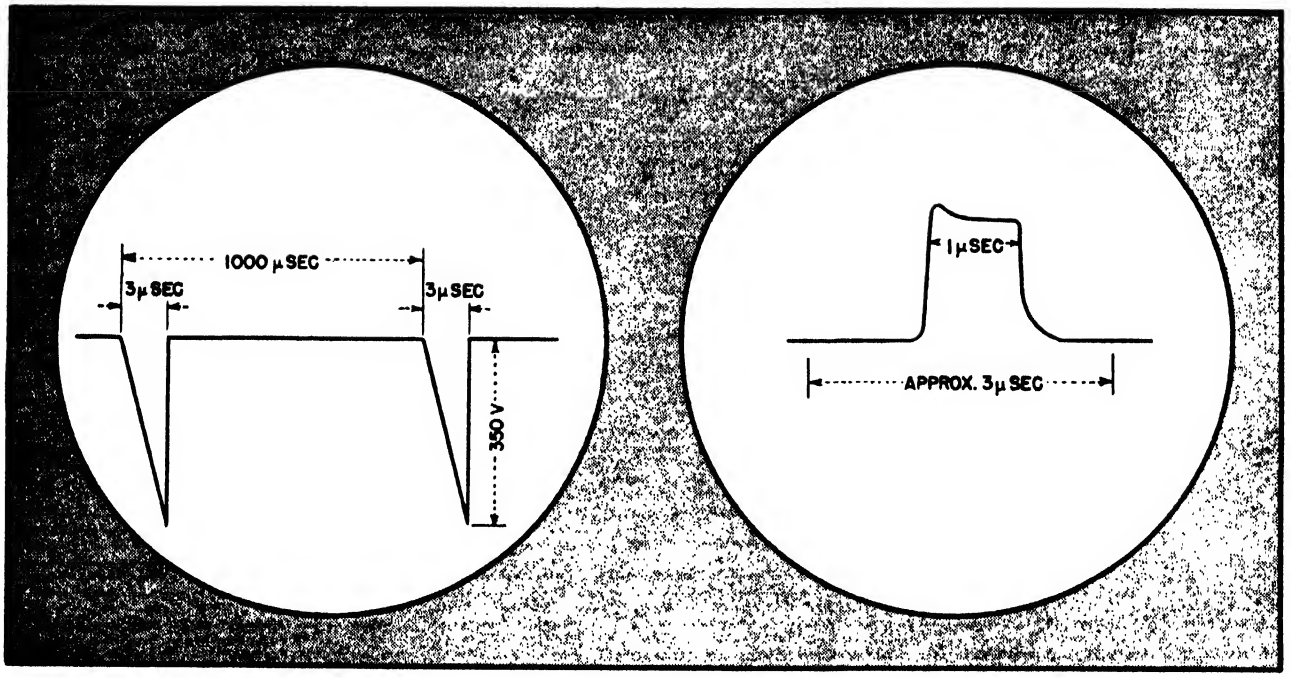

FIG. 1—Typical pulse sequence, showing the long and short periods that must be accommodated by a time-base calibrator

FIG. 2—One-microsecond pulse can appear distorted when viewed on a high-speed time base if the sweep is non-linear

ply $T = 1/F$ seconds or $10^6/F$ microseconds. Thus a frequency of one megacycle would have a time interval of one microsecond between successive cycles.

In order to make use of such a sine-wave calibrating signal it is necessary that the signal be synchronized with the trigger signal which starts the time base. This requirement has led to the general adoption of various forms of shock-excited oscillators. Circuits of this type are arranged to deliver a damped wave train of oscillations when excited by the same trigger voltage which initiates the sweep oscillator. The time interval between successive cycles of the damped wave is governed by a tuned circuit which is resonant at the desired frequency.

The disadvantages of this method are: (1) Since the frequency is determined by a simple tuned circuit, its alignment must be checked frequently. (2) The frequency of the tuned circuit can only be checked while it is operated in a continuous-wave oscillator circuit. Whether the resonant frequency remains the same under conditions of shock excitation is questionable. (3) A damped wave train may introduce errors because the time interval of each cycle is not the same.

To overcome these drawbacks the system shown in the block diagram is used. The unit contains a 5-mc crystal-controlled oscillator which supplies the calibrating signal. Because the time interval between cycles is 0.2 microsecond, calibrating intervals of 0.1 microsecond are readily available.

Following the crystal oscillator is a series of multivibrators used as frequency dividers. The first, operating at 500 kc, is synchronized directly from the crystal oscillator. It, in turn, synchronizes a 50-kc stage which in turn locks in a 5-kc multivibrator. The output of this multivibrator synchronizes a fourth, whose frequency is variable in synchronized steps from 500 to 2500 cps.

The output of the last multivibrator is fed through a pulse-shaping amplifier, a variable delay network and finally a cathode-loaded output stage. The function of the frequency dividers and pulse-shaping stage is to produce a pulse which is synchronized with the calibration signal and suitable for use as a trigger pulse to trigger the sweep circuit in the oscilloscope.

When the oscilloscope sweep is triggered by this pulse and the calibrating signal from the crystal oscillator applied to the vertical plates of the c-r tube, the stationary sine wave pattern of Fig. 3 is obtained. The variable delay control in the input to the cathode-loaded

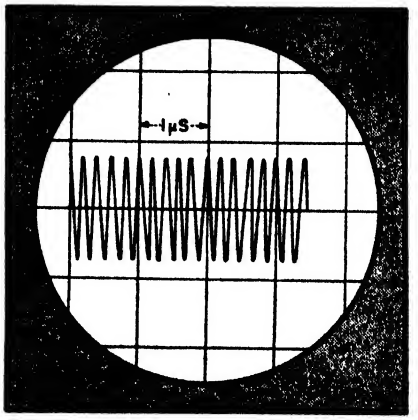

FIG. 3—Constant-amplitude, fixed-frequency sine wave serves to mark microsecond intervals on sweep for linearity calibration

output stage permits positioning the calibration signal anywhere along the time base.

As previously pointed out, the time interval between successive peaks of the same polarity is 0.2 microsecond. If the sweep speed is adjusted until exactly five peaks coincide with one inch of deflection, the time base can be considered to have an accurate calibration of one microsecond per inch of deflection. If the sweep speed is adjusted for 10 peaks per inch, the calibration is equivalent to 2 microseconds per inch.

Calibrator Circuit

The circuit shown in Fig. 4 is, with few exceptions, straightforward and requires little explanation. The final multivibrator is made variable in frequency so that the oscilloscope sweep circuit can be triggered at the same repetition rate while being calibrated as when being used for measurements. This multivibrator is also of the unbalanced variety, i.e., the circuit constants of the two sections of the dual tube comprising the multivibrator are considerably different. As a result, one half-cycle of the signal is much shorter in duration than the other half. This permits obtaining a pulse of comparatively short duration. Because the shorter part of the cycle appears as a negative pulse on the plate of the left-hand triode, the output of this section is applied to a zero-bias amplifier which permits the negative half-cycle to be amplified while tending to clip the positive half-cycle. The amplitude of the negative peak is sufficient to drive the amplifier grid to cutoff thus squaring the peak.

The combination of the 25,000-ohm rheostat and 15-$\mu\mu$f capacitor produces a phase shift which is capable of making the signal applied to the grid of the cathode-loaded stage lag the signal at the plate of the preceding tube by almost one microsecond.

The output signal is a positive pulse having an amplitude of approximately 20 volts peak and a duration at 80 percent of peak of about 12 microseconds. The output of the crystal oscillator is approximately 70 volts peak to peak.

Use of Calibrator

To insure utmost accuracy of calibration and measurement certain precautions have to be observed. First, before the time base is calibrated, the sweep should be positioned by means of the position control so that the start of the sweep is at some definite reference point. Once this adjustment is made and the calibration performed for this setting, all measurements should be made with the sweep starting at the same reference point.

Second, when calibrating the time base, the calibration should be made for a certain definite portion of the sweep (usually the one inch nearest the center of the oscilloscope). All future measurements should then be made on the same portion of the sweep. These two precautions eliminate possible error due to non-linearity of the sweep or non-linearity of the c-r tube deflection.

Also, it is advantageous to use the peaks of the calibration signal which are nearest the vertical portion of the c-r tube face used in making measurements. Thus if negative pulses are to be measured on the scope, the negative peaks of the calibrating signal would be nearest to the portion of the tube face on which the measurement is to be made. If measurements are made at the vertical center of the screen, it may be an advantage to use the zero crossover portion of the sine wave.

Advantages of Calibrator

The equipment described has certain desirable features not found in calibrators using such methods as

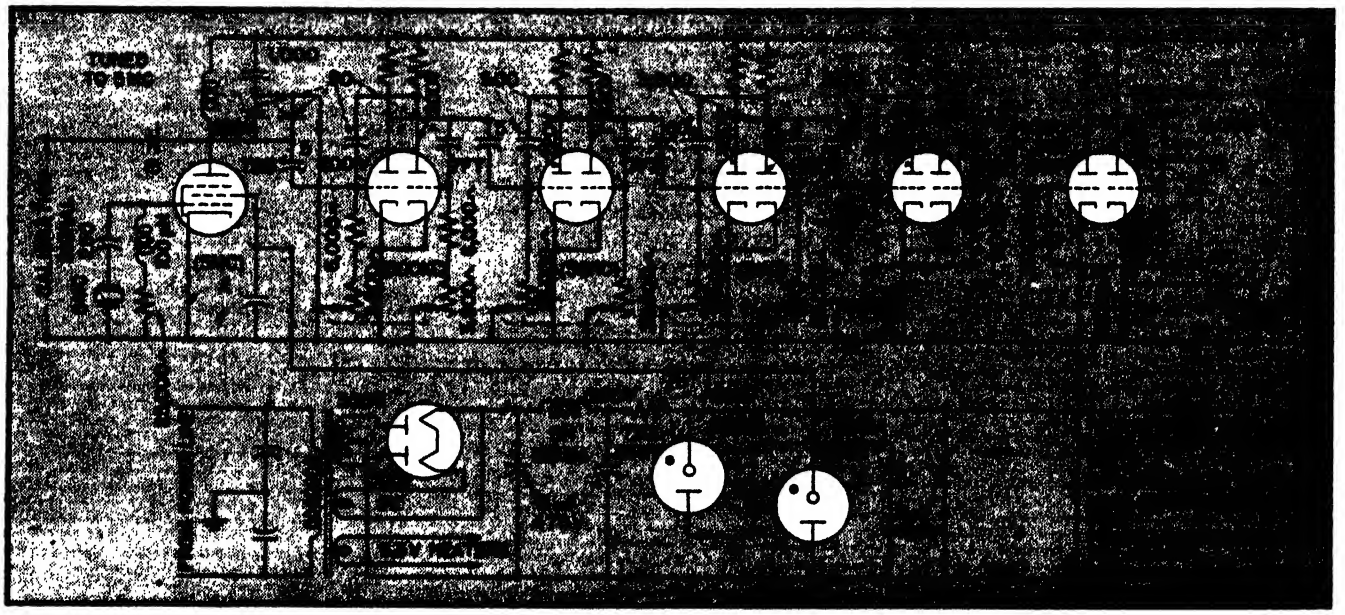

FIG. 4—Circuit of self-contained time-base calibrator which can be built for rack mounting or test-bench use

triggered shock-excited oscillators. First of all, because the calibration signal is crystal-controlled and operates continuously, the calibration signal covers the entire duration of the sweep and has a constant amplitude over the whole sweep.

The use of a 5-mc calibrating signal enables the calibration of the sweep to be done at points of one microsecond and one-half microsecond per inch of sweep with high accuracy. The unit can also be easily adapted to the calibration of slower speed sweeps by utilizing the output of the intermediate multivibrators for a calibrating signal. For example, the 500-kc multivibrator could be used for obtaining 2-microsecond time intervals, 20-microsecond points can be obtained from the 50-kc multivibrator and 200-microsecond intervals from the 5-kc multivibrator.

To make use of the intermediate frequencies for calibrating purposes it would be desirable to pass the output of the multivibrator through an amplifier which has a differentiating network in its grid circuit. This practice would provide sharp, spike-like pulses that would permit sharper calibration.

In setting up the unit and adjusting the multivibrators to synchronize on the proper frequencies a single or multiple loop Lissajou pattern can be produced on an oscilloscope by using the multivibrator output and a standard signal generator. The dual potentiometer in the grid circuit of the multivibrator is varied until the Lissajou pattern is synchronized; that is, appears stationary. An alternate method is to use the output of the crystal oscillator or the preceding multivibrator in place of the signal generator. The final multivibrator can best be checked for frequency range by comparing its output to an audio-frequency signal on the oscilloscope.

Units of this type have been in use by the writer for several years for calibrating oscilloscopes. The results have been consistently reliable. Few readjustments of the multivibrators have been necessary.

Pulse Transmission in Amplifiers

An economic evaluation of single and double-tuned coupling circuits in pulse amplifiers is possible by setting standards for comparison of steady-state and transient response. The experimental results obtained at medium frequencies are valid much higher in the spectrum

By ARTHUR E. NEWLON

THE SUBJECT of pulse transmission has been rather thoroughly treated in the literature from an analytical standpoint, but the observational and experimental aspects have not received as wide attention. This paper gives the findings of an experimental investigation made to determine bandwidth requirements for the transmission of rectangular pulses through a communication channel.

The work was motivated by a need to determine the relative advantages of single-tuned versus double-tuned coupling circuits in amplifiers used for pulse transmission.

With new uncrowded regions of the spectrum available for wideband transmissions it becomes desirable to investigate the use of amplifiers employing relatively unselective, but simple, single-tuned coupling circuits. If they can be used in place of the double-tuned type without too much loss in gain for equal pulse transmission, a considerable advantage in simplicity of manufacture, alignment and servicing of wideband amplifiers will accrue.

Experimental Procedure

Analytical demonstration can be made of the validity of frequency scaling in the study of pulse transmission. This fact was utilized, making possible the experimental use of a narrow-band, low-frequency amplifier whose band-pass characteristics were easily controlled. This test procedure permitted the use of long pulses whose shape and length could be determined accurately.

A block diagram of the test setup is shown in Fig. 1. The circuits to be tested are incorporated in an amplifier with their pass bands centering about 460 kc. A 460-kc signal, pulse modulated, is applied to the amplifier, the output of which is demodulated and observed on a wide-band oscilloscope. The pulse modulating voltage is mixed with the output of the amplifier to provide accurate timing marks on the oscilloscope pattern. The patterns for each test condition have been standardized in size and photographed for subsequent analysis.

The apparatus is capable of passing a pulse less than one-half the length of the shortest used in taking the test data, without a measurable deviation from squareness in the oscilloscope pattern.

Before outlining the measuring technique, two terms used in specifying pulse shapes will be defined. Figure 2 shows a typical output pulse shape. The terms defined in the figure are percent rounding and percent width. Percent rounding is the percentage of the time duration of the input pulse required for the output pulse to reach 90 percent of its

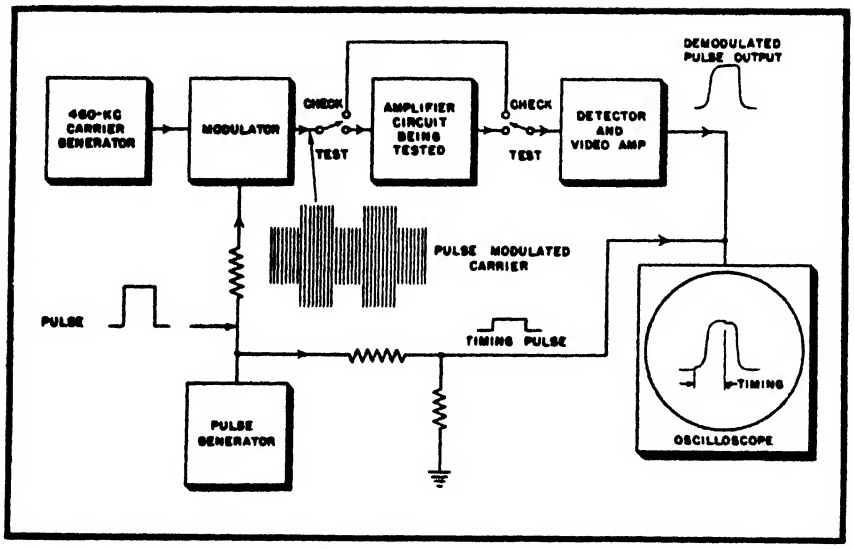

FIG. 1—Block diagram of the test equipment used in determining the response of amplifiers to pulsed signals. The pulse generator also supplies timing markers to the oscilloscope

final amplitude. Percent width is the percentage of time duration of the input pulse required for the output pulse to go from 10 percent of its final amplitude, through 100 percent and back down to 10 percent.

The pulse-modulated signal is applied to the amplifier under test. Pulse length is then adjusted to give an output pulse having a specified amount of rounding. After adjusting the oscilloscope pattern size to a standard value, the figure is photographed. A series of such data has been taken for each circuit tested, with several values of pulse length to give various degrees of rounding of the output pulse.

Experimental Results

Pulse transmission was measured on four amplifiers having band-pass characteristics as shown in Fig. 3. The term response as used here is the steady state response of the circuit to an impressed sine wave of voltage. It should not be confused with the circuit's response to pulses.

Data was taken for pulse lengths varying increasingly from that length which just produced a perceptible decrease in the output pulse amplitude. That is, the pulse lengths were always sufficiently long to permit the output pulse to build up to its flat top portion.

Figure 4 summarizes pulse rounding data taken on the four amplifier circuits whose band-pass characteristics are shown in Fig. 3. Quadratic equations were fitted to the observed data to a precision of better than 5 percent. These equations are tabulated below.

Transmission characteristic A
$$L = 1{,}807 - 45.7R + 0.36R^2 \quad (1)$$

Transmission characteristic B
$$L = 1{,}521 - 41.0R + 0.32R^2 \quad (2)$$

Transmission characteristic C
$$L = 909 - 23.7R + 0.18R^2 \quad (3)$$

Transmission characteristic D
$$L = 897 - 23.6R + 0.19R^2 \quad (4)$$

The above equations are identical in form, differing only by a multiplying factor. The group can be specified by the following characteristic equation

$$L = K(1{,}000 - 26.2R + 0.20R^2) \quad (5)$$

where, L is length of pulse in microseconds; R is percent rounding; and K is a factor representing a function of the steady state response characteristic of the circuit. Equation 5 is plotted in Fig. 5. Equations 1 to 5 are valid for values of R in the range 10 to 60 percent.

Rounded Pulse Transmission

In some applications the widening of a pulse in transmission through a channel is of more interest than the time of rise; particularly is this true if clipping removes the rounded top of the pulse. It was expected that pulse width would bear a more or less

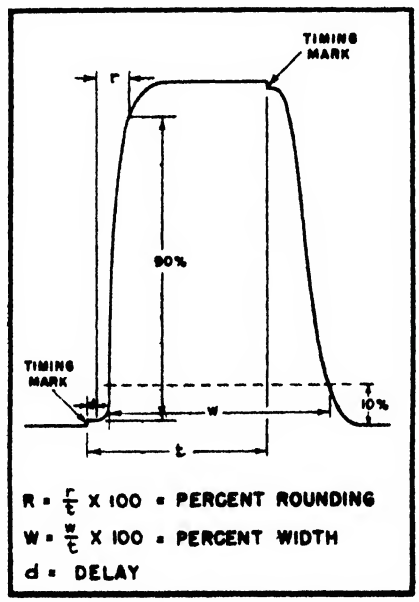

FIG. 2—Typical output pulse with the percent rounding and percent width defined. The delay between the timing mark and the initiation of the output pulse occurs in the amplifier and other circuits

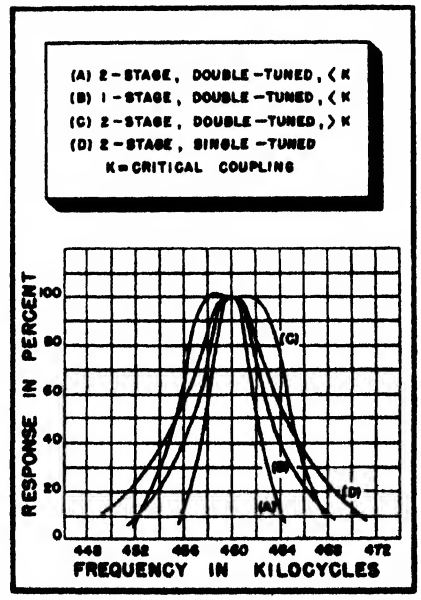

FIG. 3—Response characteristics of several amplifiers for steady-state or sine-wave amplification. The response to pulses is described in the text

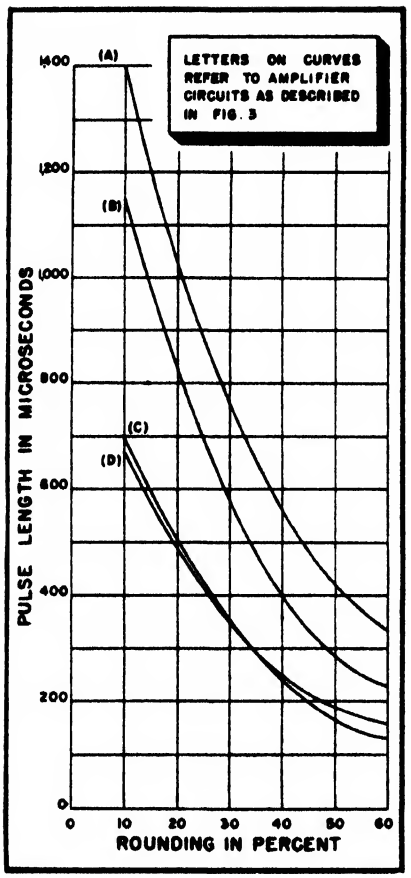

FIG. 4—As a circuit rounds the output shape of a square-wave input pulse, the length of the pulse must be increased or else the output amplitude will decrease

simple relation to pulse rounding and the curves plotted in Fig. 6 show this to be true. Adjusting all the data to a common linear trend line, the following equation is arrived at

$$W = 109 + 0.75R \qquad (6)$$

where W is percent width, and R is percent rounding. Or, the pulse width is increased by approximately the percent rounding.

Frequently in practice we have to deal with only nominally square pulses. It is therefore of interest to know how much bandwidth requirements may be relaxed if the system is not to be required to handle perfectly square pulses. A series of measurements was made with a half-wave, rectified sine wave input pulse as representing a typical rounded pulse. Table I summarizes the results of these measurements.

Off-tune operation is frequently encountered in practice due to time and temperature drift or to faulty tuning adjustment. Pulse transmission through amplifiers having characteristics A and C was investigated for several degrees of detuning and a comparison made with corresponding on-tune operation. Table II summarizes the results of these measurements.

Discussion of Experimental Findings

The derivation of Eq. 5 shows the length of pulse which can be transmitted with a specified amount of rounding through a circuit follows the same law of variation for both single- and double-tuned stages when the bandwidth is varied. This permits prediction of the effect of changes in the bandwidth of a circuit upon output pulse shape, after drawing a family of such curves for various values of K. If circuits of the same configuration and the same pass-band shape are being compared, direct scaling may be employed after

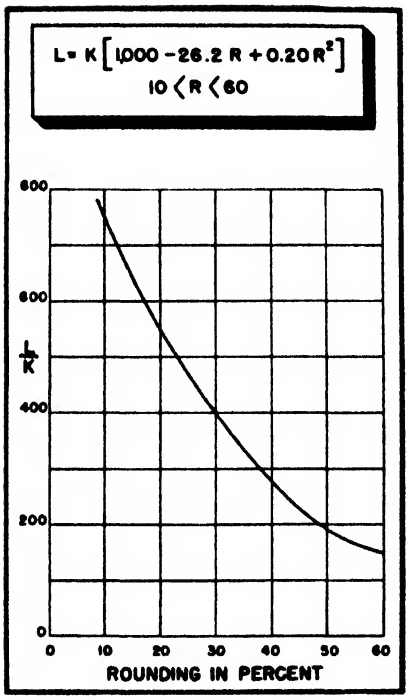

FIG. 5—Graphical representation of Eq. 5 showing percent rounding in relation to the quotient of pulse length divided by circuit response to sine waves

Table I—Comparison of Transmission of Square and Half-Sine Wave Pulses

Pulse Length μsec	Pulse Width (percent) Square Pulse	Sine-wave Pulse	Respons Characteristic (see text)
1,300	122	108	A
600	140	121	A
680	116	96	C
260	134	117	C
220	147	132	D

Table II—Comparison of On-Tune and Off-Tune Transmission

Pulse Length (μsec)	On-Tune Rounding (percent)	On-Tune Width (percent)	Off-Tune Rounding (percent)	Off-Tune Width (percent)	Off-Tune Amplitude (percent)	Deviation (kc)	Response (percent)
			Transmission Characteristic A, Fig. 3				
1,300	13	122	11	120	92	+0.81	89
1,300	13	122	7	119	60	+1.71	60
1,300	13	122	4	118	24	+2.80	33
			Transmission Characteristic C, Fig. 3				
260	39	134	35	133	87	+1.94	99
260	39	134	20	134	62	+3.74	78
680	10	116	11	117	100	−1.72	101
680	10	116	5	120	55	−4.79	48

Note: Amplitude is the amplitude of output pulse compared to amplitude when on tune
Deviation is the displacement of carrier from center of pass band
Response is the steady state sine-wave response of amplifier at stated deviation

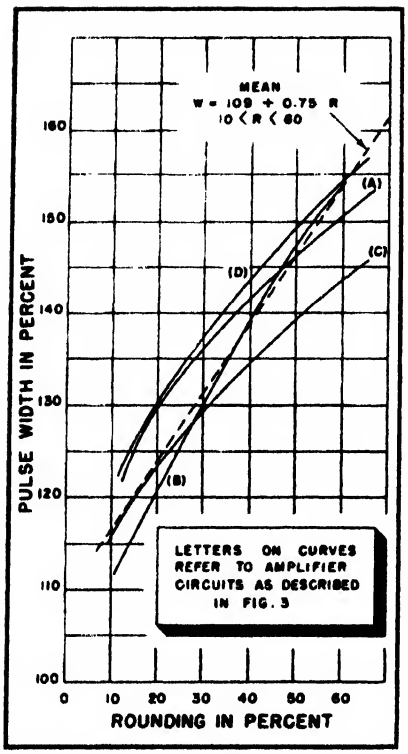

FIG. 6—Output pulse percent width as a function of percent rounding

K has been determined for a single bandwidth.

As an illustration of the use of Eq. 5, a computation was made to show the cost of improving the output pulse shape by progressive increases in bandwidth of a single-tuned amplifier, all the time maintaining a constant gain by increasing the number of stages. The gain, G, of a multistage, single-tuned amplifier, all stages of which are alike, is given by

$$G = \left[\frac{G_m}{\Delta\omega C}\right]^n \left[\frac{1}{P^{2/n}} - 1\right]^{n/2} \qquad (7)$$

where

G_m = transconductance of amplifier tubes
P = percent response at which overall band width is measured, expressed as a decimal
C = total circuit capacitance per stage
n = number of identical stages
$\Delta\omega$ = 2π times band width at point P

For the purposes of computation the following assumptions were made:

G = 56,400
G_m = 10,000 μmhos
C = 20 $\mu\mu$f
P = 0.5
$\Delta\omega$ = 10^7 when rounding is 60 percent

The first computation made for $\Delta\omega = 10^7$, with an output pulse rounding of 60 percent, shows 3 stages to be required in the amplifier. Reference to Fig. 5 shows L/K is equal to 145 for 60 percent rounding. To compute the bandwidth required for, say, 30 percent rounding we note that L/K equals 396, giving the new bandwidth requirement of $\Delta\omega_{30} = 396/145\ \Delta\omega_{60} = 2.73 \times 10^7$. The value of n for 30 percent rounding may now be determined from Eq. 7. Figure 7, curve I, shows the complete data for the range of 10 to 60 percent rounding for the conditions assumed.

Curve II in Fig. 7 shows how the overall gain of a 5-stage amplifier of the above characteristics varies as its bandwidth is adjusted to yield output pulses with varying degrees of rounding. The data is plotted as loss of gain compared to the gain at a bandwidth giving 60 percent pulse rounding.

The data presented in Fig. 7 show that relatively perfect transmission of square pulses comes at a high price, and indicates that very good economic reasons must be advanced to justify pulse transmission of a better quality than that which will give 30 to 40 percent rounding.

The data given in Table I show that a square-wave pulse is increased in width more than a sine-wave pulse of the same length, when passed through the same amplifier, the average difference being 17 percent in these data. For the case of the amplifier whose gain was computed in the example above, this would mean a saving of one stage if 50 percent rounding were permissible, see Fig. 7, curve I; or, referring to Fig. 5, a pulse 47 percent shorter in duration could be transmitted if the input pulse were one-half sine wave instead of square wave in form.

An examination of Table II reveals that off-tune operation has several effects: the time of rise is decreased, pulse amplitude is decreased, and pulse width changes very little if at all.

Comparison of Single-Tuned and Double-tuned Coupling Circuits

To examine the relative merits of single-tuned and double-tuned coupling circuits from the standpoint of pulse transmission, it is first necessary to determine at what common response point the bandwidths of the respective circuits should be measured. That the comparison is markedly influenced by the choice of this point will be evident from data to be given later. In setting up the circuit having response characteristic D, Fig. 3, the bandwidth was so chosen that the pulse transmission through this circuit was identical to that through the circuit having response characteristic C. Figure 4, curves D and C, will show the similarity in performance of these two circuits.

First, considering the problem qualitatively, transmission through a circuit would be expected to vary in some manner related to the area under its frequency response characteristic. It would also be expected that of two response characteristics of equal area, if one had very wide flaring skirts, and the other steep skirts, better pulse transmission would be obtained with the latter. This is because an appreciable portion of the characteristic having flaring skirts is at frequency locations remote from the center of the band. The areas under the four response characteristics in Fig. 3 were deter-

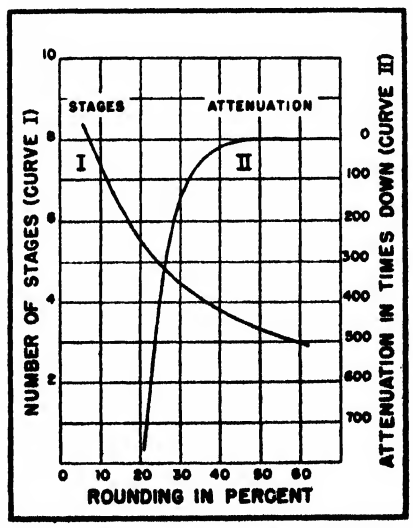

FIG. 7—Curves showing the number of stages needed and attenuation as a function of percent rounding for single-tuned amplifiers

Table III—Areas Under Response Characteristics

Response Characteristic (see text)	Area (square units)
A	460
B	800
C	1,020
D	1,090

Table IV—Comparative Center-Frequency Gains of Single and Doubled-Tuned Circuits

Coupling, Double-Tuned Circuits	Gain Per Stage 1-Stage Single	1-Stage Double	5-Stage Single	5-Stage Double	10-Stage Single	10-Stage Double
Critical	66	61	20	34	14	28
Overcoupled, 2 percent dip	66	70	20	42	14	36
Overcoupled, 8 percent dip	66	82	20	54	14	48

mined as listed in Table III.

The manner in which the pulse length that may be transmitted varies with the area under the response curve of the circuit is then shown in Fig. 8, with percent rounding as a parameter. These curves show the area under the response characteristic of a circuit is important in determining its pulse transmission capabilities. However, the discontinuities present in the curves indicate the shape of the transmission characteristic is also of importance. Comparing the data for transmission characteristics A and B in Fig. 8, a certain rate of improvement in going from A to B is noticed. Now, comparing the performance with characteristics B and C, a much greater rate of improvement is found. Last, comparing data on characteristics C and D, a lower rate of improvement or actual deterioration is obtained. Thus, going from a circuit having a response shape with narrow skirts to one with flaring skirts, but greater area, much less improvement in pulse transmission is effected than in making a proportional change of area from flaring skirts to narrow skirts. It is evident the transmission shape exerts an appreciable influence upon the ability of a circuit to transmit square pulses.

Table III shows transmission characteristics C and D to have substantially equal areas, and curves C and D in Fig. 4 show these two circuits to have practically identical pulse transmission characteristics. Therefore, we may obtain from these two transmission characteristics a common crossover point for which a bandwidth specification may be stated. In this case, crossovers occur at 42 percent and 50 percent on either side of center in Fig. 3. That is, both amplifiers have identical response at 455.3 kc (50 percent) and at 465.5 kc (42 percent). Then, on the average, the comparison point may be said to be at approximately 46 percent response.

More of the experimental data may be used in the determination of

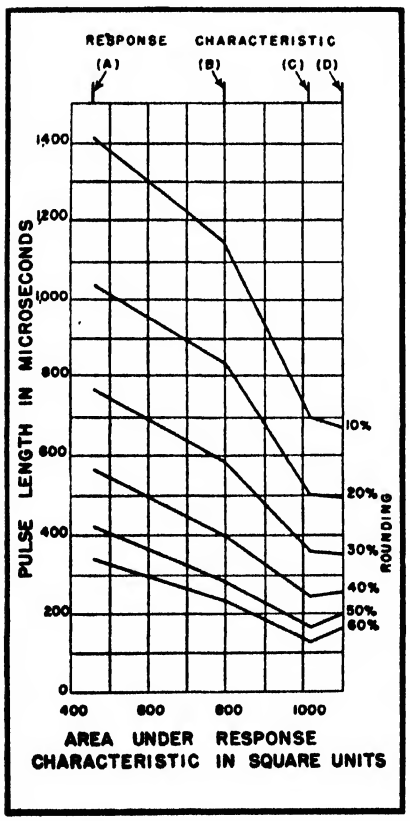

FIG. 8—Minimum pulse length expressed in terms of the area under response characteristic for several amplifiers at different percent rounding

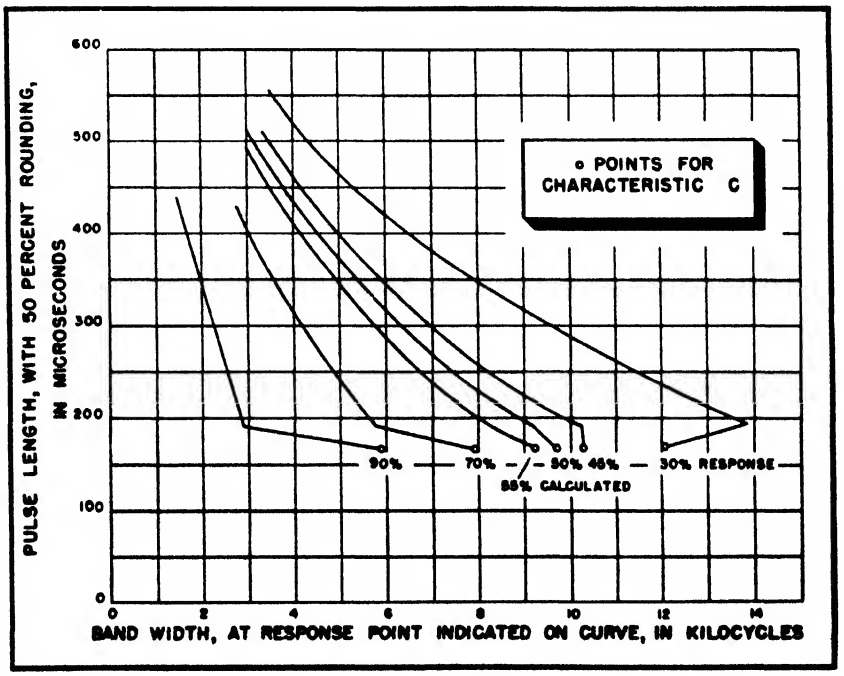

FIG. 9—Permissible pulse length as a function of bandwidth

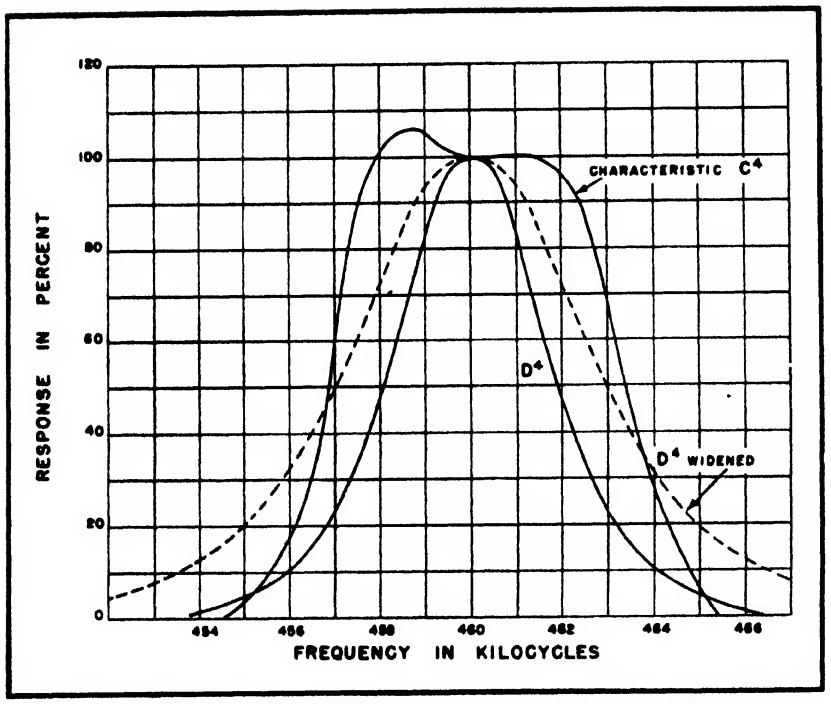

FIG. 10—Transmission characteristics of an 8-stage amplifier

the comparison point between single-tuned and double-tuned circuits if another method is employed. Progressing through characteristics A, B, and D, in the order listed, the pass band becomes progressively wider and the skirts flare in increasing degree, as shown in Fig. 8. These three characteristics are, broadly speaking, similar, differing mostly as to bandwidth. Bandwidth, as measured from these characteristics, is plotted against pulse length, with the percent response at which the bandwidth is measured as a parameter, in Fig. 9. The smooth curves connecting these points for a given percent response are extrapolated to the region where data from response characteristic C would fall. Now, the extrapolated curve most nearly passing through an observed point for characteristic C would indicate at what percent response the single- and double-tuned circuits should be compared. This response point turns out to be 55 percent, as compared with the 46 percent determined by the method above.

The above determination of the response point at which comparisons of single-tuned and double-tuned circuits should be made was derived on the basis of a 1- or 2-stage amplifier. In practice, an amplifier will frequently have a greater number of stages. Consequently the overall response characteristics will have steeper skirts as the number of stages is increased, and it would be expected that the basis of comparison for the two types of circuits would vary somewhat with the number of stages in the amplifier. Accordingly, transmission characteristics C and D were raised to the fourth power to give the equivalent frequency response of an 8-stage amplifier, with the results shown by the solid curves in Fig. 10. The area under the D^4 curve was then increased to be equal to that under the C^4 characteristic, see dotted curve, making the two characteristics approximately equally efficient for transmitting square pulses. For this moderate shift the previous data permits a comparison on the basis of equal areas. This assumption will not be rigorously justified, but it is believed in the present case the small amount of extrapolation necessary does not unduly reduce the accuracy of the results. After this adjustment, the average crossover point is at 40 percent response. Comparing this with the 55 percent crossover point for two stages it is seen that increasing the number of stages in an amplifier decreases the value of the response point on the frequency characteristic at which a comparison of single-tuned and double-tuned circuits should be made. The above calculations may be generalized by saying that in the average multistage amplifier the pulse transmission capabilities of an over-coupled and double-tuned amplifier and of a single-tuned amplifier will be identical if their steady state frequency response characteristics have the same bandwidth at approximately the 45 percent response point.

An analytical expression comparing single-tuned and double-tuned, over-coupled circuits would be too cumbersome for practical use. Therefore, a comparison will be made on a computed experimental basis. Computations have been made for single-tuned and double-tuned circuits typical of those likely to be encountered in wide band i-f amplifiers. The following characteristics were assumed:

f_o = 30 mc

Capacitance = 22 $\mu\mu$f total for single-tuned amplifier

= 12 $\mu\mu$f per circuit for double-tuned amplifier

G_m = 9,000 μmhos

Stages = 1, 5, 10

Response at which bandwidth is measured = 45 percent

Primary and secondary circuits identical in double-tuned amplifier

Couplings = critical, over-coupled 2 percent dip at center, over-coupled 8 percent dip at center

Pulse rounding = 50 percent

Pulse length = 1 μsec

Bandwidth Requirements

Referring to Fig. 3 and 4, curves D, it is seen the bandwidth required to transmit a 1-μsec pulse is 0.0103 x 190 = 1.96 mc. That is, a single-tuned circuit, or an equivalent double-tuned circuit, 10.3 kc wide at 45 percent response will transmit a pulse 190 μsec long with 50 percent rounding. Therefore, 190 times this bandwidth is required to transmit a 1-μsec pulse. This is the overall bandwidth required regardless of the

number of stages. Thus, each stage of a 10-stage amplifier would be 1.96 mc wide not at 45 percent response, but at $0.45^{0.1}$ which equals 92.3 percent response. Table IV summarizes the results of these computations.

These data show that for a single-stage amplifier there is very little choice between the single- and double-tuned type of coupling circuits. However, as the number of stages is increased the double-tuned circuit shows an increasing advantage in gain over the single-tuned circuit. Whether the increased complexity of double-tuned circuit elements is offset by the increased gain available can only be decided by a knowledge of the circumstances surrounding a given application.

As a matter of interest, Fig. 11 shows a series of curves giving bandwidth requirements for transmitting pulses varying in length between 0.1 and 7 μsec with three different degrees of rounding. Bandwidth is specified at the 45 percent response point.

Pulse transmission through several types of single- and double-tuned amplifiers is investigated experimentally. The length of pulse that can be transmitted through a circuit with a given percent rounding, R, is found to be given by: $L = K(1{,}000 - 26.2R + 0.20R^2)$, where K is a function of the transmission characteristic of the circuit. Increase in width of a pulse is found to be approximately equal to the amount of rounding. Amplifier design requirements are found to be appreciably eased if pulse input is of the form of a half sine wave. Off-tune operation is found to result in a decreased rise time and a decreased output pulse amplitude. It is shown that bandwidths of single and double-tuned circuits should be compared at approximately the 45 percent response points in determining their pulse transmission capabilities. In a multistage amplifier, double-tuned coupling circuits are shown to offer appreciable advantages from the standpoint of gain.

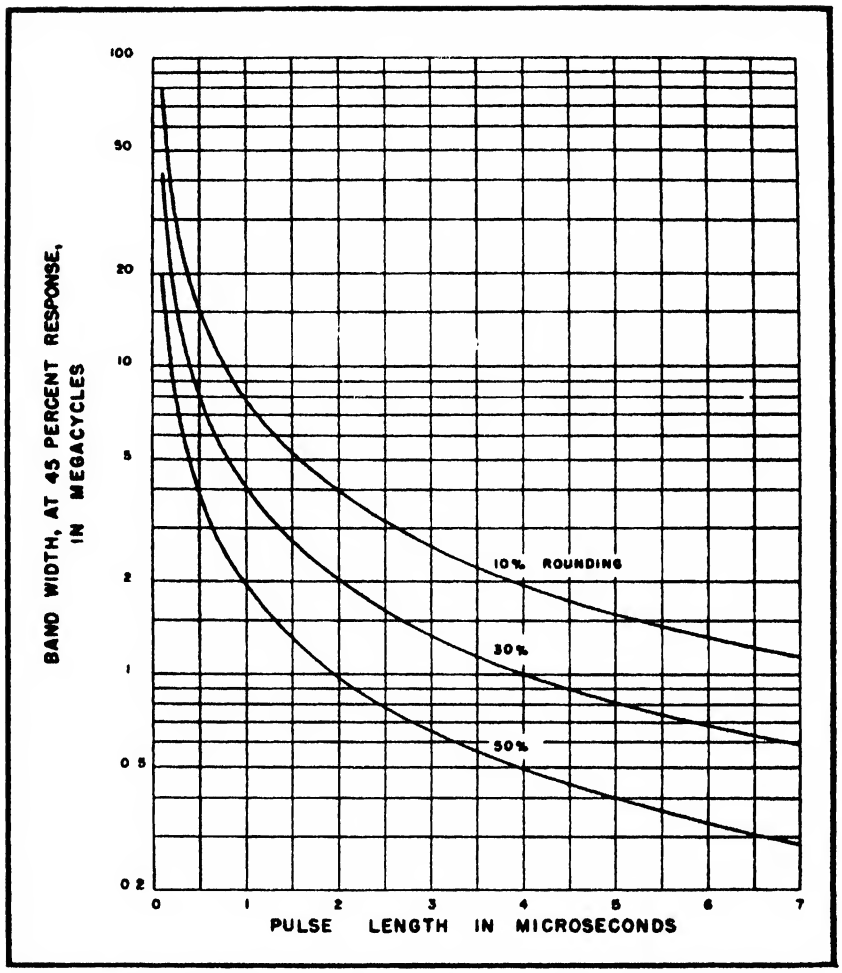

FIG. 11—Bandwidth required as a function of pulse length for three different percent rounding

Electronic Switch for the Production of Pulses

Circuit provides variable pulse length, variable pulse rate, variable delay of synchronizing pip, and a means for introducing a steady-state signal upon which pulses may be superimposed, in a generator designed for laboratory use

By C. R. SMITLEY and R. E. GRABER

IN RECENT YEARS, laboratory work in the audio and ultrasonic frequency ranges has required the use of pulse techniques in many acoustical and electrical experiments. Various types of pulsers have been described in the literature[1]. Five desirable characteristics, however, are not all included

in the devices described to date. These desirable factors are:

(1) Pulse length variable, by means of a calibrated adjustment, over a suitably wide range.

(2) Pulse rate similarly adjustable over a suitably wide calibrated range.

(3) Pulse length and rate adjustments entirely independent of one another.

(4) Synchronizing pip for oscilloscope trace synchronization, the pip occurring a suitable and adjustable length of time before the beginning of the pulse. Control independent of pulse rate and length.

(5) A means for introducing a steady-state signal upon which pulses may be superimposed, often required in studying high-gain systems utilizing automatic volume control.

The device described below was built to meet the above requirements and for general laboratory use. In addition, the following specifications were set up and are fulfilled:

(a) Pulse length, or closure time, adjustable in steps between 5 milliseconds and 250 milliseconds.

(b) Pulse rate, or interval between closures, adjustable in steps between 0.6 second and 2.9 seconds, with an auxiliary control providing intermediate repetition rates throughout this rane.

(c) Delay between the initiating pip, which is also used for oscilloscope sweep synchronization, and the start of the pulse adjustable in steps between 5 milliseconds and 250 milliseconds.

(All of the above adjustments are independent of one another).

(d) Frequency range of the signal to be switched, 1 kc to 100 kc.

(e) Maximum peak output voltage, approximately 5.

(f) Dynamic range of pulse output, 30 db.

(g) Steady state non-pulsed signal, automatically pulsed signal or a hand-keyed output pulse available by the operation of suitable switches.

(h) A visual signal indicating when a pulse is initiated.

Operating Principle

A block diagram of the circuit components employed in the pulser appears in Fig. 1. Voltage waveforms, and times of occurrence, observed in various portions of the system are indicated above the components.

A gas-tube R-C sawtooth oscillator is used as the rate control. The oscillator output is differentiated and the resulting negative voltage pulses are used to trigger a delay multivibrator and to provide synchronizing pulses for oscilloscope sweep synchronization.

The delay multivibrator remains fired for the interval of time t_1 to t_2. The differentiated output consists of a positive pip at time t_1 and a negative pip at time t_2 as shown. The negative pip triggers the length multivibrator at time t_2 and this remains fired for the time interval t_2 to t_3.

The rectangular, positive output pulse from the length multivibrator is impressed through a d-c restorer to the suppressor grids of the switch tubes. The restorer provides a suitable cutoff bias for the switch tubes except during the interval t_2 to t_3, when the switch tubes are rendered conducting by the positive length-multivibrator pulse.

The switch circuit has been described elsewhere[2]. This circuit has a useful dynamic range of about 30 db and has negligible switching transient output over the range of signal levels employed.

The signal input may be connected for steady, automatic, or hand-key operation by means of a selector switch. With this switch in position *1* the input signal is applied directly through the level potentiometer and the mixer amplifier to the grid of the output cathode follower. This position is incorporated for convenience in observing the non-switched input signal and, in effect, shorts out the electronic switch.

With the selector switch in position *2*, a non-switched output of any level from zero to maximum may be obtained as in position *1*. The output of the switch tubes is added to this in the mixer amplifier. An auxiliary control regulates the maximum amplitude of the switch-tube output. By means of the two controls, any desired relative level of pulsed and non-pulsed signals may be obtained.

In position *3*, a hand key may be used to turn the output on and off.

The schematic diagram of the pulser appears in Fig. 2. The gas-

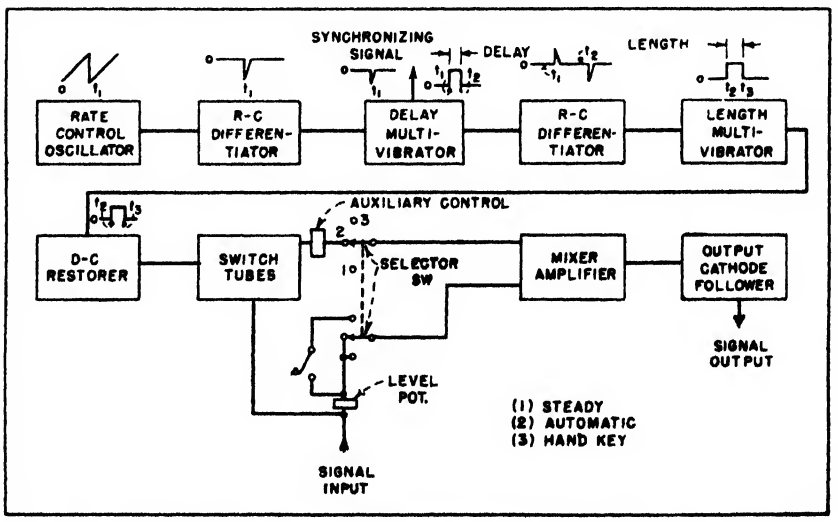

FIG. 1—Block diagram of pulser

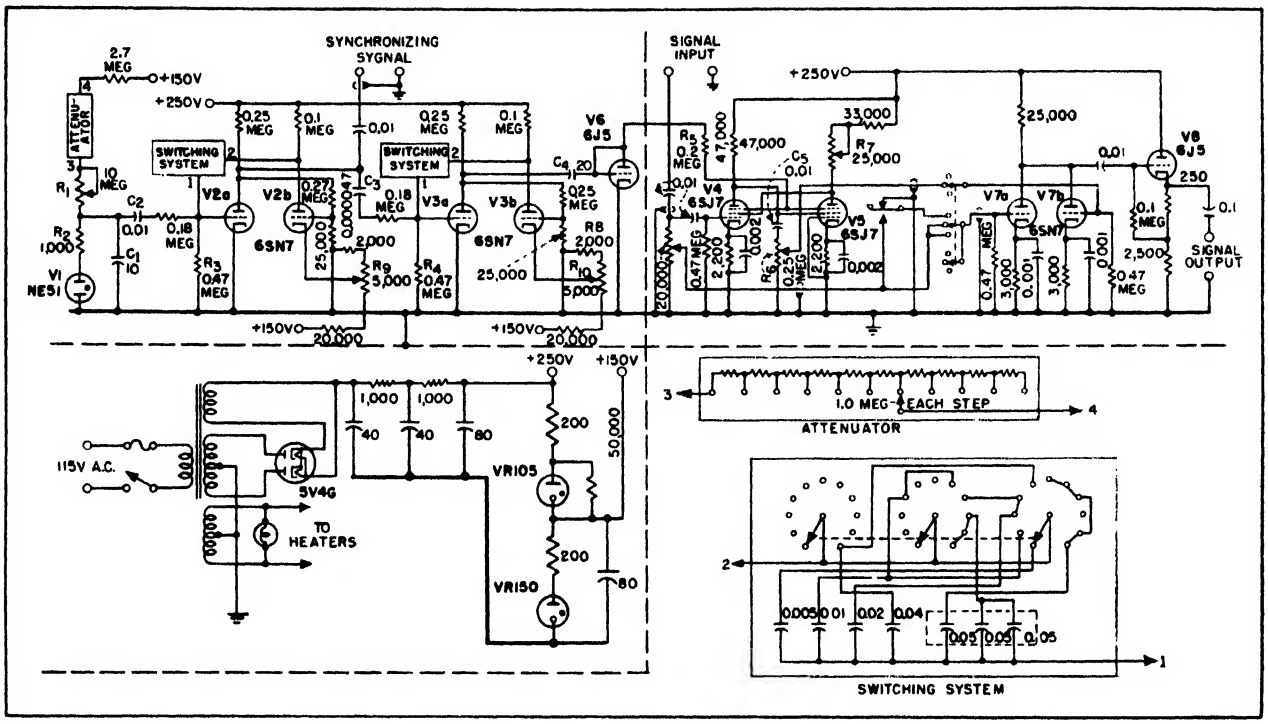

FIG. 2—Schematic diagram of pulser

tube R-C sawtooth oscillator comprised of V_1, C_1, and R_1 plus the attenuator will be noted in the upper left of the figure. In operation, C_1 charges through R_1 and the attenuator until the drop across C_1 reaches the ignition voltage of V_1. Tube V_1 then fires and discharges C_1 through protective resistor R_2 until the extinction voltage of V_1 is attained, after which the above cycle is repeated. The repetition rate is determined by the calibrated attenuator and the intermediate control R_1.

The discharge time constant of R_2C_1, is very much smaller than the charge time constant so that a sawtooth oscillator output voltage is obtained. This is differentiated by C_2 and R_3 and the resulting negative voltage pip is used to trigger the delay multivibrator V_{2a} and V_{2b}. The length of the positive delay multivibrator output pulse appearing at the plate of V_{2a} is controlled by the associated capacitor switching system. The front edge of this pulse occurs at the instant V_1 fires and is used for synchronizing.

The delay multivibrator output is differentiated by C_3 and R_4 and the negative voltage pip resulting at the end of the pulse is used to trigger the length multivibrator V_{3a} and V_{3b}. The length of the positive length multivibrator output pulse appearing at the plate of V_{3a} is controlled by the associated capacitor switching system.

It is evident from the above that the repetition rate, delay, and length of pulses are all independently adjustable.

The switching pulses from the length multivibrator are impressed on the suppressor grids of the switch tubes V_5 and V_6 through C_4 and R_5. The output side of C_4 is connected to ground through V_8, which acts as a d-c restorer or charging rectifier. By this means, the suppressors are maintained at a sufficient average negative potential with respect to ground as to cut off the switch tubes except during the pulse intervals.

The operation of the switch tubes is described in detail elsewhere[5]. The signal to be pulsed is impressed on the grid of V_4. The output pulses appear at the plate of this tube and are impressed across R_6 through C_6. Resistor R_7 is an adjustable type which is used in initially adjusting the switch for minimum, no-signal, switching transient output.

The operation of the selector switch was described under the discussion of the block diagram. Tubes V_{7a} and V_{7b} are the mixer tubes previously mentioned, and V_8 is the output cathode follower. A VR-stabilized power supply, details of the attenuator, and the capacitor switching system complete the diagram.

In the alignment process the device is first turned on and allowed to warm up. The vertical plates of an oscilloscope are connected to the sync output terminals and the delay multivibrator control, R_{9}, is adjusted until rectangular output pulses are observed on the oscilloscope for all positions of the rate and delay control settings. In addition, it should be noted that the flashing of V_1 occurs simultaneously with the synchronizing pulses. The oscilloscope is then connected to the output terminals and the length multivibrator control R_{10} is adjusted

so that symmetrical output pips are obtained for all combinations of rate, delay, and length settings.

After the multivibrators have been adjusted, the switching transient control R_7 in the plate of V_4 is adjusted for minimum no signal output with an oscilloscope connected to the output terminals.

Waveforms that should be obtained for each of these adjustments are indicated on the block diagram of this instrument.

REFERENCES

(1) Scheuch, D. R., and Cowan, F. P., Laboratory Pulse Generator With Variable Time Delay, *Rev. Sci. Inst.*, p 223, June 1946.

(2) Butz, Jr., A. N., Surgeless Volume Expander, ELECTRONICS, p 140, Sept. 1946.

Stable Voltmeter

By means of a compound feedback circuit extreme stability is obtained in a conductively coupled electronic instrument. Positive feedback produces an effectively infinite gain that is highly degenerated by negative feedback

By R. W. GILBERT

VACUUM TUBE amplification to extend the sensitivity of direct indicating electrical instruments has attracted the attention of numerous investigators, resulting in many effective methods for obtaining stability beyond that normally required for sound amplification. The impedance coupled alternating-current instrument amplifier has been particularly highly developed, largely by properly applied degeneration effective over the frequency range desired. The conductively coupled amplifier, responsive to both alternating and direct current, has however proved more difficult because of circuit limitations imposed by the necessity for both amplifying and degenerating through the conductively coupled circuit loop.

Condition for Stability

Broadly the attainment of stability in the face of variable tube coefficients is a problem of sacrificing a maximum of inherent amplification by degeneration, resulting in less gain but a proportionately greater stability. From this viewpoint it is apparent that the optimum combination is an infinite inherent gain which is completely degenerated, resulting in an amplifier having a nominal overall gain and first order independence of variations in tube coefficients.

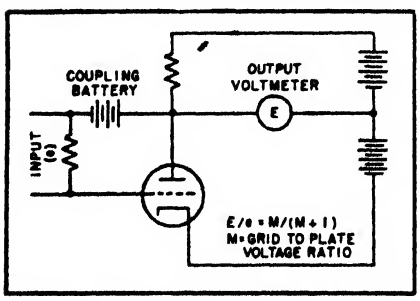

FIG. 1—Degenerative coupling from plate to grid, through a battery to preserve the required operating potentials on grid and plate, stabilizes the tube circuit

At first it would appear possible only to approach but not obtain this condition because infinite gain considered as a separate function would be on the threshold of self-sustained oscillation. However, the superposition of degeneration exerts a stabilizing influence, and, unless inhibited by the time constants of the circuit, a stable overall system is possible. The present circuit is capable of adjustment to and beyond this ideal condition, and in practice reduces the influence of tube variables entirely to a second order effect.

Consider the circuit of Fig. 1 wherein the plate of the triode is conductively coupled to the grid through a battery equal to the voltage normally existing between these elements in a conventional amplifier circuit. Coupling of this nature is essentially degenerative in direction inasmuch as any plate voltage variation is transmitted to the grid as a corrective control to partially restore the original plate voltage. If an input voltage e is injected in series with the grid the voltage change E appearing at the plate is in a direction to reestablish the original grid voltage through the coupling battery. Thus the plate voltage shift is a measure of the input voltage, but less by an amount that is a function of the amplification factor.

For this condition the feedback relationship (Regeneration Theory by H. Nyquist, *B.S.T.J.*, 11, 1932, Jan., p 126) applies

$$\text{Overall voltage ratio} = \frac{E}{e} = \frac{M}{Mb + 1} \qquad (1)$$

where M is the amplification factor (voltage ratio) of the tube proper in its circuit without feedback, and b is the transfer characteristic of the feedback loop, in this case the plate-grid degenerative connection. But here plate voltage changes are transmitted entirely to the grid so b is unity, and Eq. 1 becomes

$$\frac{E}{e} = \frac{M}{M + 1} \qquad (2)$$

From this equation it is apparent that as M becomes larger the overall amplification factor approaches unity and, which is more important, becomes more independent of changes in M.

This circuit is similar in function to the conventional cathode follower circuit except that the

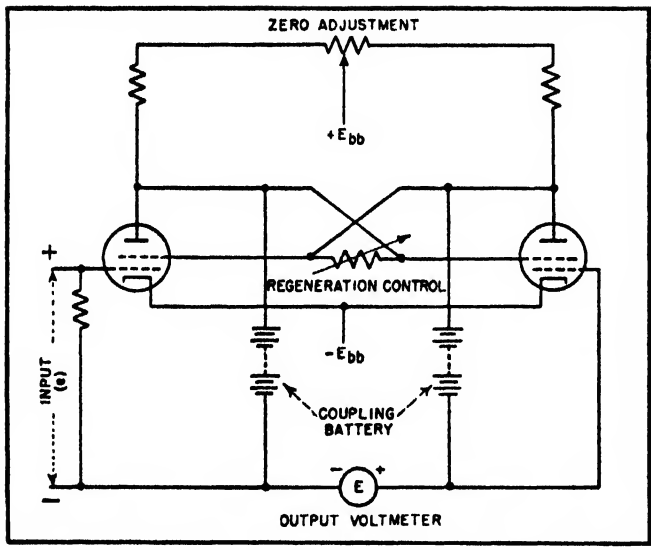

FIG. 2—Regenerative feedback to auxiliary grids increases amplification. Balanced circuit is used to obtain necessary phase reversals

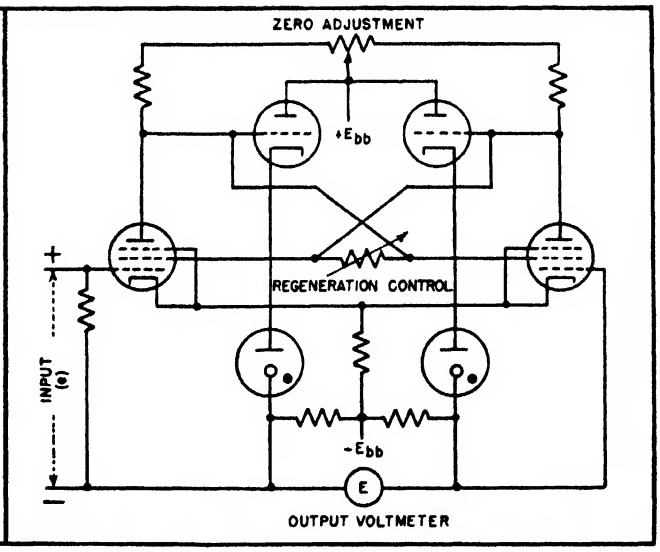

FIG. 3—Practical circuit incorporates cathode-coupled isolation tubes and gas tubes in place of batteries for maintaining proper biases

resistance mutual to the input and output circuits is in the form of a plate resistor rather than a cathode resistor. The circuit may thus be considered as a "plate follower" in distinction to the cathode follower type of circuit.

Realizing the Conditions

The absence of cathode resistance permits the introduction of additional tube elements without involving their operation with the degenerative function of the control grid. In the two-tube circuit of Fig. 2 this feature of independence allows the introduction of a second grid to obtain regeneration, resulting in an effective increase in *M*. The second grid of each tube is crossed to the plate of the opposite tube to obtain regeneration in a manner similar to the action of a multivibrator. An adjustable plate-to-plate shunting resistor allows adjustment of the degree of regeneration. In practice the second grid is most conveniently the screen grid of a standard pentode, which is designed to operate at voltages comparable to the plate voltage without secondary emission complications.

If the control grids are temporarily made ineffective, for example by disconnecting and biasing from a separate source, and the regeneration control increased, a point of instability will be reached where the circuit will fall over, one tube blocking and the other conducting in the manner of a half cycle of multivibrator operation. At this point the circuit is critically regenerated and is essentially an amplifier of infinite gain. If the control grids are then reconnected to the degenerative coupling batteries all tendency toward instability will be restrained by superimposed degeneration and the circuit will function as the circuit of Fig. 1 containing a tube of infinite *M*. In fact the regeneration control may be further advanced and the circuit operated in the seemingly impossible region of greater than infinite (negative) internal gain.

With the circuit adjusted to this point of critical regeneration, the control grids exert only a transient type of control upon the tube space paths, while the regenerated screen grids and plates do the actual work of establishing the output voltage. If the control grid-cathode voltages are observed while an input voltage is applied, no change is noticeable, and this condition of zero grid excursion may be used in practice as the criteria for adjustment of the regeneration control. If the regeneration control be adjusted above or below the critical point while the circuit is subjected to an input variation, a control grid excursion will appear but of a polarity with respect to the input dependent upon the direction of misadjustment.

In a practical instrument amplifier the feature of zero grid excursion for a tangible plate voltage output means a materially more linear relationship between input and output because the plate and screen grid variational factors are more constant over wider voltage excursions than the control grid. Also the tubes can be operated at the quiescent grid current point throughout the range of input, minimizing grid current demand in sensitive direct-current applications.

Significance of Circuit Characteristics

When critically regenerated, the circuit also has the interesting property of behaving as an output voltage source of zero variational resistance within functional limits. In operation with an input voltage applied, the output voltmeter may be shunted to demand more output current without affecting its reading. Conversely series resistance may be added to the coupling battery circuits without affecting the

output reading. In either case the plate to screen-grid regenerative action supplies the additional output energy without requiring any static change in the control grid potentials, so the overall voltage ratio remains constant. Insufficient regeneration causes a positive variational resistance to appear, and excessive regeneration causes a negative variational resistance. In the latter case shunting the output voltmeter will increase its reading. Naturally if regeneration is increased beyond the critical point to where the negative resistance looking into the output end of the amplifier is greater than the positive resistance within the output voltmeter, the circuit will become unstable and fall over. Also as regeneration is increased from the optimum critical point to the point of instability the overall voltage ratio varies to infinity. These effects have no probable practical significance but serve to demonstrate the fact that considerable latitude exists between the point of optimum adjustment and the region of instability. In fact unless the resistance of the output voltmeter is quite low, complete removal of the regeneration control resistor will not produce instability in standard pentode type tubes.

When used as a d-c amplifier the question of zero stability becomes of interest. No material advantage over conventional d-c amplifier circuits is apparent in respect to stability, but in general the usual precautions apply. Use of two tubes in opposition reduces the effect of contact potential variations to a differential rather than a direct effect, so that regulation of the heater supply voltage, if necessary, is really effective. The major cause of zero drift then becomes the differentials between the two tubes that change with time, which fundamentally cannot be compensated and can only be reduced by the use of matched tubes.

Practical Circuit

The circuit of Fig. 3 is essentially the circuit of Fig. 2 reduced to a practical arrangement. The coupling batteries are replaced by cold-cathode gas voltage regulator tubes which have sufficiently low internal variational resistance not to load the output circuit unduly. The input tubes are followed by a stage of cathode followers primarily to remove the output load and the regulator tube current from the regenerative portion of the circuit. Without the buffer action of the cathode followers it might prove impossible to supply the desired output without loading the input tubes to the point where critical regeneration is not attainable. While a battery plate supply is shown for simplicity, the circuit is particularly adaptable to service power supply with a minimum of filtering because the regulator tubes effectively regulate the element voltages. This regulation together with the zero resistance output characteristic removes virtually all supply voltage ripple from the output.

The gas regulator tubes unfortunately have a small equivalent internal inductance due to the total ion mass in the space path. In an alternating-current amplifier this inductance causes an additional output loading factor that manifests itself increasingly with increasing frequency. This inductance is in the order of six millihenrys in small tubes (Type 991, etc.) and 80 mh in larger tubes such as the VR series, at normal operating current. Capacitive bypassing has limitations because, if sufficiently heavy, the tubes may be damaged when starting. Also resonance against the internal equivalent inductance can actually increase the loading at

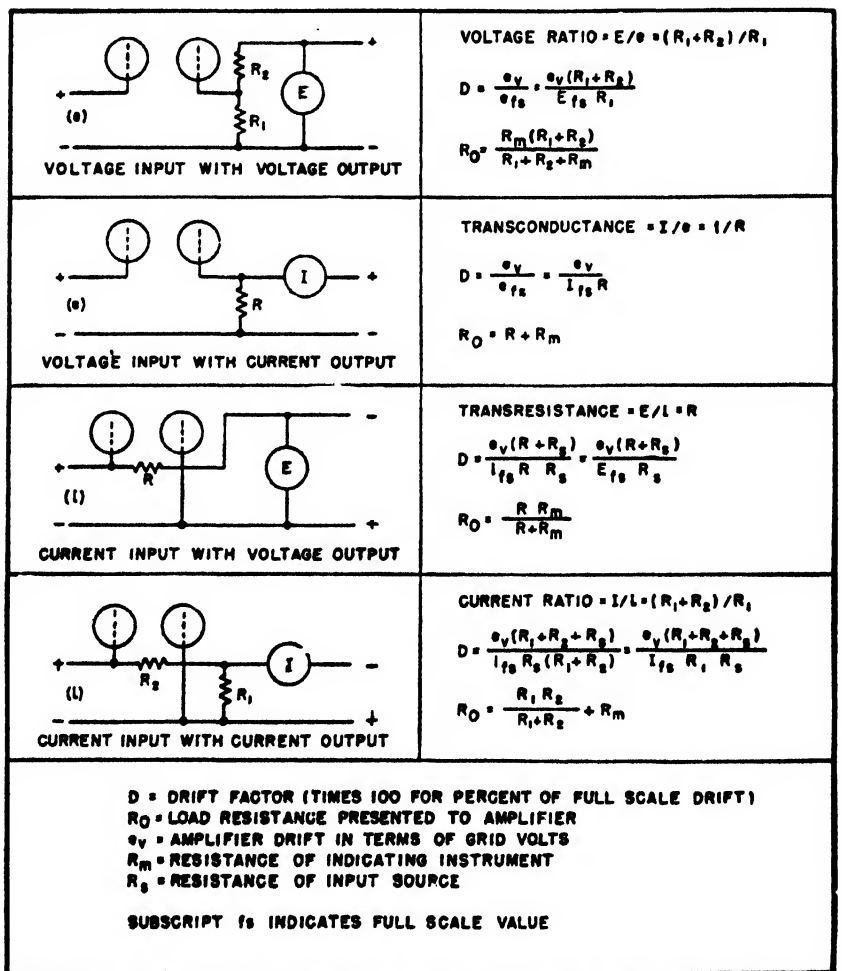

FIG. 4—Variations in the degeneration network of Fig. 3 adapt the instrument to various combinations of input and output. Equations indicate drift and loading.

the resonant frequency. However, as an instrument amplifier application is limited largely to d-c and a-c not exceeding audio frequency, where this inductive loading effect is not serious.

For simplicity of explanation it is assumed that the circuit of Fig. 3 is arranged to provide a voltage ratio of unity, whereas any voltage ratio is possible by incorporating a degenerating network rather than a simple mutual resistance. Also four basic operating combinations are possible; voltage input with voltage output, voltage input with current output, current input with voltage output, and current input with current output. These combinations are shown in Fig. 4 as changes to the circuit of Fig. 3, together with the expressions for the gain in each case. Note that for current input a current balance network is employed rather than adapting the voltage input circuit to current by passing the input current through an input shunt. This current balance arrangement balances the input terminals to zero potential, maintaining effectively zero resistance looking into the input end of the amplifier. Thus in the case of current as well as voltage inputs the circuit demands no energy from the input source.

Drift

In common with all conductively coupled amplifiers the circuit is inherently a high input impedance device and is at a disadvantage from the standpoint of zero stability when operated from low impedance, low voltage sources such as a thermocouple. The tendency to zero drift is caused principally by contact potential variations within the input tubes, but all circuit components contribute more or less to the total drift. However, for simplicity the amount of drift that can be expected from the tube circuit proper is best expressed as the equivalent grid potential variation, or the amount of grid potential change required to rebalance the circuit after drift has taken place. The effect of this potential change in terms of output can then be calculated from the constants of the degenerating network, and expressed as a drift factor D for any set of conditions. The expression for the drift factor is given in Fig. 4 for the four basic degenerating networks in terms of the equivalent grid potential drift variations e_v. Note that in the case of current input the resistance of the input current source is effectively in parallel with the grid circuit and enters the expression. The drift factor expresses the ratio of expected drift to full scale output or input, and can be multiplied by 100 to obtain the expected drift in percent. Note also that the load presented to the amplifier output R_0 does not enter the drift expression because an optimum adjustment of regeneration is assumed; in case of misadjustment the load resistance will have a small second order effect upon drift.

In practice e_v can be determined experimentally by setting up the unity gain circuit of Fig. 3 with the input terminals short circuited. As the circuit drifts, e_v is read directly on the output voltmeter.

An experimental design of electronic d-c voltmeter using the compound feedback circuit was built. This particular instrument includes features of convenience such as input polarity reversal and center zero switch positions, and means for calibration and zero adjustment without disconnecting the input. It contains an input network for four voltage ranges from 100 millivolts to three volts. An experimental companion instrument for current measurements down to 0.1 microampere full scale, similar in appearance to the electronic voltmeter, was also designed.

Pulse Response of Diode Voltmeters

Corrections necessary in the calibration of a typical peak-reading, vacuum-tube voltmeter used to measure pulse amplitudes are determined from theoretical analysis and checked against measurements. Means are suggested for calibrating, and improving performance

BY ALLAN EASTON

PEAK VALUES of pulse voltages must frequently be measured in such circuits as radar and pulse-modulation systems. There are several methods, the most popular being the cathode-ray oscilloscope and the diode, vacuum-tube, peak voltmeter. Each instrument has its own particular advantages, and is selected partly for its technical factors, partly for its convenience.

The familiar vacuum-tube, peak voltmeter, based upon the rectifying properties of a diode, has been used for many years for measurements of sinusoidal voltages. References in the literature are frequent and the nature of its shortcomings has been discussed.[1, 2, 3] It is only possible to use this type of vacuum-tube voltmeter for pulse voltage measurements if sufficient information concerning the characteristics of the instrument, as well as the na-

TABLE J – DEFINITIONS OF SYMBOLS

C	—capacitance
e	—base of natural logarithm
e_1	—maximum value to which capacitor charges
e_2	—minimum value to which capacitor discharges
e_0	—peak amplitude of measured pulse
E_{DC}	—direct voltage resulting from rectification and integration of pulse waveform
α_1	—time constant during t_1
α_2	—time constant during t_2
f	—pulse repetition frequency
k	—correction factor for vtvm
R_1	—total resistance during charging
R_2	—total resistance during discharging
R_D	—diode conducting resistance
R_s	—source resistance
t_1	—duration of charging interval
t_2	—duration of discharging interval
T	—period of pulse

ture of the source to be measured, is available.

A circuit diagram of a typical vacuum-tube voltmeter is shown in Fig. 1A. Many variations of the circuit exist but the basic analysis is similar for each type. The magnitude of the direct voltage output (a measure of the source potential) is indicated by a d-c microammeter either directly, or through an amplifier. This part of the circuit is not shown as it has little bearing on the analysis to be presented.

Fig. 1B is the equivalent circuit. In order to derive an expression for the relationship between E_{DC} and e_0, defined in Table I, several assumptions are required. It is assumed that the source resistance R_s can be combined with the diode resistance R_D to form R_1. The diode is regarded as perfect, that is, the resistance in the conducting direction is constant and equal to R_D, and the resistance in the nonconducting direction is infinite. Leakages in capacitor C and in the rest of the circuit shunting C are combined in R_2. The duration of the pulse is assumed to be short compared with the period.

The positive pulse voltage, shown in Fig. 2A is impressed across the terminals marked 1 and 2 in Fig. 1B. During the charging interval t_1, C is charged through R_1 and then for a time t_2 partially discharged through R_2. The phenomenon is repeated periodically and eventually reaches the steady state condition depicted by Fig. 2B.

The maximum value to which C can be charged is

$$e_1 = e_2 + (e_0 - e_2)\,(1 - \epsilon^{-\alpha_1 t_1}) \qquad (1)$$

$$= e_0 + (e_2 - e_0)\,\epsilon^{-\alpha_1 t_1}$$

The minimum potential to which C can fall is

$$e_2 = e_1 e^{-\alpha_2 t_2} \qquad (2)$$

Equations 1 and 2 can be manipulated to obtain

$$e_1 = \frac{e_0\,(1 - e^{-\alpha_2 t_2})}{1 - e^{-\alpha_1 t_1} e^{-\alpha_2 t_2}} \qquad (3)$$

and

$$e_2 = \frac{e_0\, e^{-\alpha_2 t_2}\,(1 - e^{-\alpha_1 t_1})}{1 - e^{-\alpha_1 t_1} e^{-\alpha_2 t_2}} \qquad (4)$$

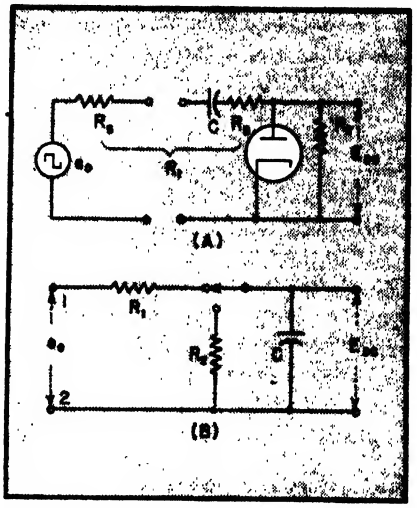

FIG. 1—(A) At the left is the rectifier portion of a typical diode voltmeter. At the right is the equivalent of a circuit under measurement. (B) The simplified, equivalent circuit of a diode voltmeter uses a switch to represent the diode

Practical Simplifications

It is desired to obtain an expression relating E_{DC} and the several factors appearing in the equations. The d-c potential across C is

$$E_{DC} = \frac{1}{T}\int_{t_0-\epsilon}^{t_1} e_1 dt + \frac{1}{T}\int_{t_1}^{(t_1+t_2=T)} e_2 dt \qquad (5)$$

Integrating, evaluating, and simplifying, we obtain

$$E_{DC} = \frac{e_0 t_1}{T} + \frac{e_1}{\alpha_1 T}\,(e^{\alpha_1 t_1} - 1) - \frac{e_0}{\alpha_1 T}\,(e^{\alpha_1 t_1} - 1) + \frac{e_1}{\alpha_2 T}\,(e^{-\alpha_2 t_1} - e^{-\alpha_2 T}) \qquad (6)$$

Equation 6 is an exact expression for E_{DC} limited only by the simplify-

FIG. 2—(A) Pulse applied to diode voltmeter, and (B) pulsating d-c developed across meter capacitor

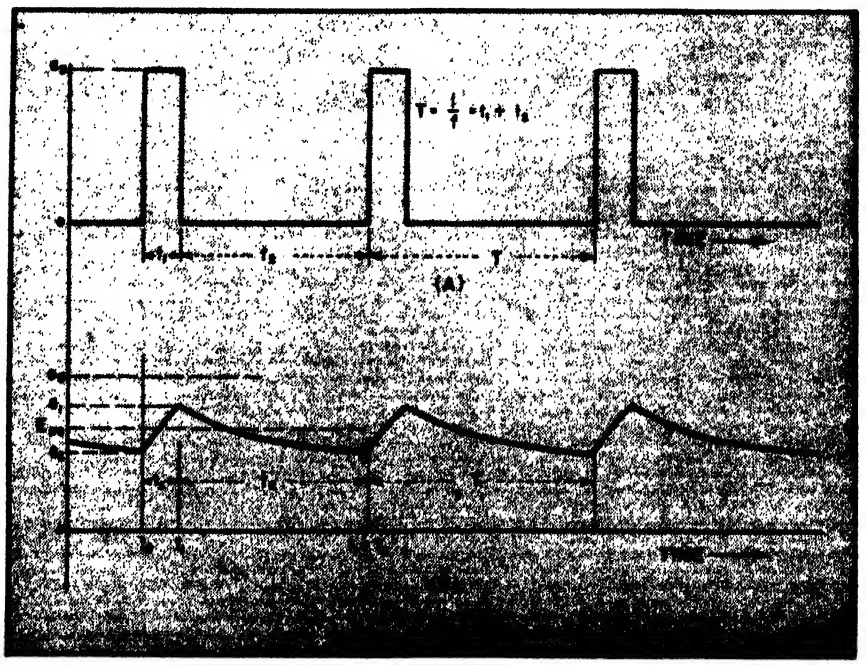

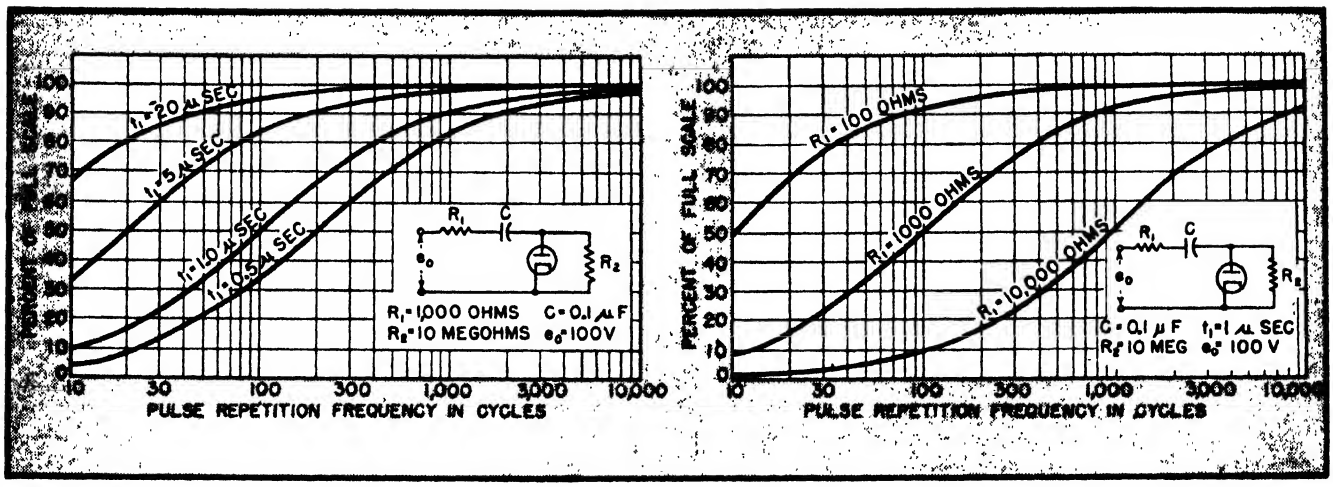

FIG. 3—Effect of pulse width on meter indication

FIG. 4—Source impedance affects meter indication

ing assumptions stated above. The equation in this form is unwieldy but may be simplified considerably if

$$\begin{aligned} \alpha_1 t_1 &< 1 \\ \alpha_2 t_1 &< 1 \\ \alpha_2 T &< 1 \end{aligned} \tag{7}$$

This simplification is justified because the pulses under discussion are relatively short in duration. However the voltmeters will perform accurately with long pulses, as will be demonstrated later. Also α_1 and α_2 may be made as small as desired by increasing the size of capacitor C. This practice will be justified later in the discussion.

If Eq. 7 is correct, the approximation $e^x = 1 + x$ may be employed. Equation 6 then reduces to

$$E_{DC} \simeq e_1 \tag{8}$$

Equation 3 may be simplified, using the same assumptions, to

into Eq. 7 will show that over the larger part of the range of narrow pulse width and pulse repetition frequencies the approximation is not in great error.

Figures 3, 4 and 5 are plots of Eq. 11. Note the effect of the various parameters on the meter calibration. It can be seen from these curves that, unless the four factors can be evaluated, the diode vacuum-tube voltmeter may indeed be quite misleading. The curves of Fig. 4 and 5 are identical in shape indicating that it is possible to improve meter accuracy for any given values of t_1 and t_2 by either making R_1 small or R_2 very large. In practice, R_2 is not usually made more than 10 megohms because of leakage difficulties. In certain military equipment destined for operation in

$$e_1 \simeq \frac{e_0 \alpha_1 t_1}{\alpha_1 t_1 + \alpha_2 t_2} \tag{9}$$

From which

$$E_{DC} \simeq \frac{e_0 \alpha_1 t_1}{\alpha_1 t_1 + \alpha_2 t_2} \tag{10}$$

Equation 10 may be restated, in terms of the original quantities, as

$$E_{DC} = e_1 = \frac{e_0 t_1 R_2}{t_1 R_2 + t_2 R_1} \tag{11}$$

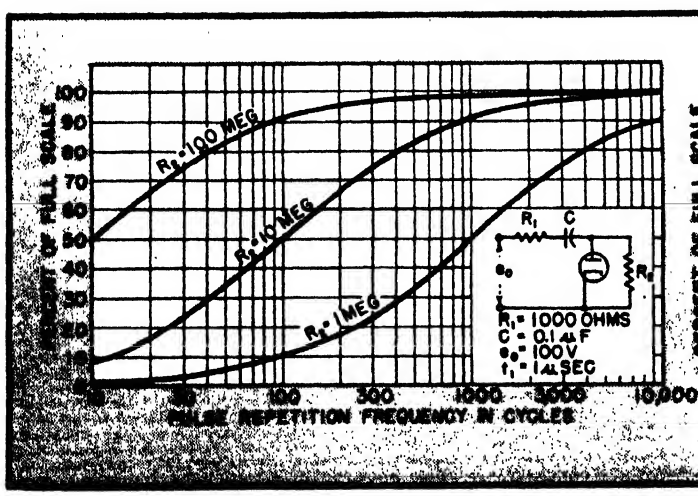

FIG. 5—Magnitude of capacitor discharging resistor affects meter calibration

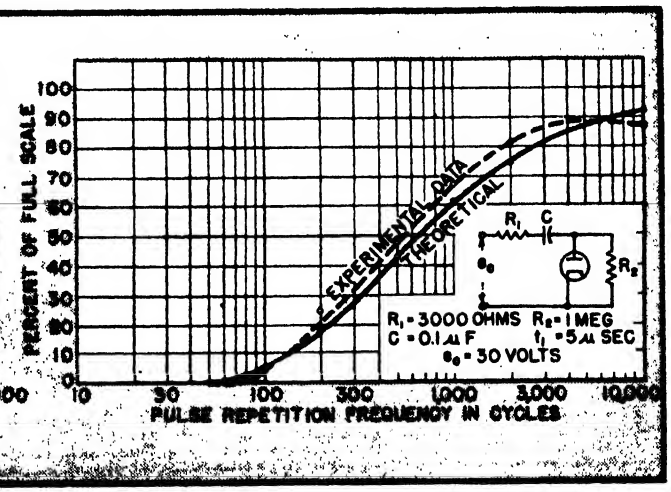

FIG. 6—Experimental data verifies the results of the theoretical circuit analysis

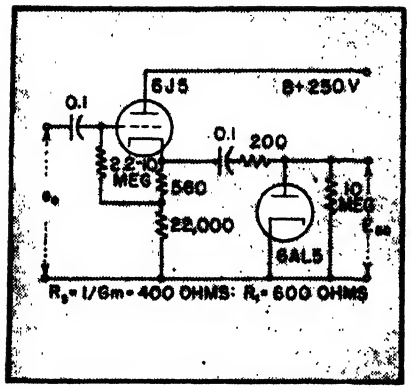

FIG. 7—A cathode-follower reduces circuit loading by the meter and prevents circuit impedance from affecting the meter indication

It should be noted at this point that E_{DC} is independent of C as long as C is sufficiently large to make Eq. 7 valid. Intuitively, one might suspect from examination of the circuit that one could replenish the loss in amplitude of the charging voltage due to the long charging time constant by making C larger. Equation 2 shows this is not the case. Substitution of typical values humid climates, use of resistors larger than one megohm is undesirable. The limiting value of R_1 is the diode resistance plus the source impedance.

Corrections

A typical commercial diode-type vacuum-tube voltmeter uses approximately the following constants

R_1 = 1000 ohms
R_2 = 10 megohms
C = 0.01 μf

Reference to Fig. 4 indicates that this instrument will read approximately half the peak pulse value when a one microsecond pulse of 100 cps repetition frequency is impressed on its terminals, therefore a correction factor should be determined.

Equation 11 may be restated in a slightly different form

$$e_0 = kE_{DC} \tag{12}$$

$$e_0 \simeq E_{DC}\left[1+\left(\frac{t_2}{t_1}\right)\left(\frac{R_1}{R_2}\right)\right] \tag{13}$$

and if $t_2 \simeq T$

$$e_0 \simeq E_{DC}\left[1+\left(\frac{T}{t_1}\right)\left(\frac{R_1}{R_2}\right)\right] \tag{14}$$

Because the usual commercial, diode, vacuum-tube voltmeter is calibrated in rms values, that is 0.707 of peak, Eq. 14 should be modified to

$$e_0 \simeq \sqrt{2}\, E_{DC}\left[1+\left(\frac{T}{t_1}\right)\left(\frac{R_1}{R_2}\right)\right] \tag{15}$$

and

$$k = \sqrt{2}\left[1+\left(\frac{T}{t_1}\right)\left(\frac{R_1}{R_2}\right)\right] \tag{16}$$

Equation 16 gives an expression for a multiplying factor by which the meter reading must be corrected to indicate the pulse amplitude.

A circuit was set up similar to that shown on Fig. 1A. A 6AL5 diode with an R_p equal to 300 ohms, was used. Figure 6 shows the experimental results compared with the theoretical values computed from Eq. 16. The agreement is fairly close, within plus or minus ten percent.

It can be seen from the above discussion and from study of the curves that this type of voltmeter has anything but high input impedance under pulse conditions. The impedance of the diode voltmeter may be arbitrarily specified as being equal to the source impedance when

$$E_{DC} = \frac{1}{2}\, e_0 \tag{17}$$

It is difficult to define this impedance precisely because it is dependent on the pulse duration, repetition frequency, and amplitude, as well as circuit constants. Reference to Fig. 3, 4 and 5 shows that the input impedance may be well below 1000 ohms even though R_2 is equal to 10 megohms.

Improving Voltmeter Performance

Utility of Eq. 16 is limited by the difficulty in evaluating the magnitude of R_1. In most cases it is possible to estimate the source resistance with fair precision; but the diode resistance is difficult to deter-

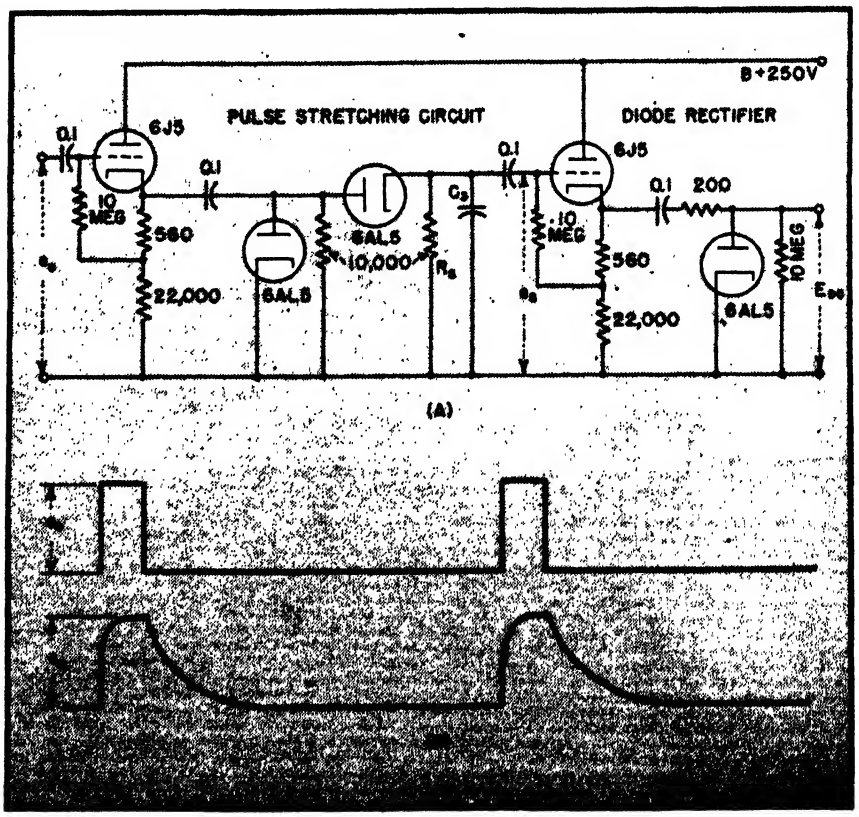

FIG. 8—(A) When measuring exceedingly short pulses, the reliability of the meter can be improved by introducing a pulse-stretching circuit ahead of the diode rectifier. The circuits are connected through cathode followers to prevent interaction. (B) The applied pulse shown at the top is stretched into a longer pulse by the circuit

mine. The diode resistance differs from tube to tube and, what is worse, is dependent on current. Thus R_1 depends on the magnitude of e_0 as well as values of α_1 and α_2.

A simple cathode follower similar to that shown in Fig. 7 will help improve the diode performance in some measure. Variations in R_s will have no effect on meter calibrations, providing R_s is small compared with the input resistance. Under this condition R_1 will be quite small, possibly 600 ohms or less. This low resistance will enable calibration of an instrument and computation of a correction curve based only on pulse width and repetition frequency.

Pulse stretching can sometimes be utilized as a means of making the instrument usable on narrower pulses. Figure 8 illustrates a possible arrangement. It is necessary to proportion R_s and C_s so that complete recovery, 99 percent, can occur between successive pulses. At the highest repetition frequency, C_s should be small enough to permit e_c to reach at least 99 percent of final value during the narrowest pulse to be measured. These precautions are necessary to minimize loss of peak amplitude and consequent loss of accuracy.

BIBLIOGRAPHY

(1) Aiken, C. B., Theory of Diode Voltmeters, *Proc. I. R. E.*, **26**, p 859, July 1938.
(2) Terman, F. E., "Radio Engineers' Handbook", McGraw-Hill Book Co., Inc., New York, 1943, p 929–937.
(3) Rider, J., "Vacuum Tube Voltmeters", John F. Rider Publisher, Inc., New York.

High-Frequency Crystal Voltmeter

By B. F. TYSON

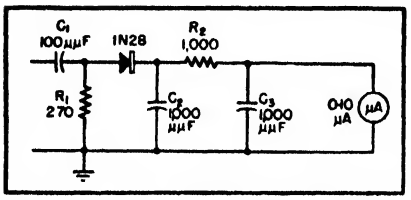

FIG. 1—Circuit diagram of crystal voltmeter

A CRYSTAL voltmeter is useful in measuring the gain and response characteristics of the r-f and i-f circuits in f-m and television receivers. Such an instrument is physically small, and when built in probe form can be easily connected to the point of measurement. Inherently, it has high sensitivity and when used with a 10-microampere meter will indicate r-f voltages as low as 0.05 volt.

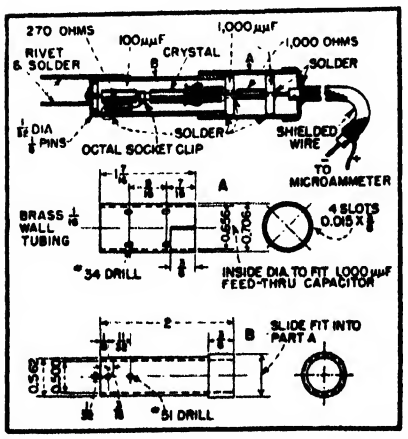

FIG. 2—Crystal probe assembly consists of two cylinders machined so the end of one slides inside the other for rapid replacement of crystal cartridge

The voltmeter described here uses a type 1N28 crystal rectifier connected as shown in the circuit diagram of Fig. 1. Other crystals such as types 1N21 or 1N25 can also be used. On the input side, load resistor R_1 and a ceramic d-c blocking capacitor C_1 are built into the probe. On the output side, the r-f components of the rectified current are bypassed to ground through a button mica capacitor C_2 and the direct current to the microammeter is filtered by resistor R_2 and a button mica capacitor C_3.

The physical arrangement of the various parts is shown in the cross-section assembly view of Fig. 2. The smaller diameter half of the probe has the ground and high potential input tabs and contains the blocking capacitor and load resistor. The shielded microammeter lead is brought out of the other half which houses the button-type bypass and filter capacitors and the filter resistor. Note that the large end of cylinder *B* is made to slide fit into cylinder *A* and a clip from an octal socket is soldered to the end of the 100-$\mu\mu$f Ceramicon capacitor to receive the contact of the crystal. The larger, probe end of the crystal is held firmly by a finger contactor. Thus, the entire probe is separable near its center for easy insertion of the crystal cartridge.

Fig. 3 is a typical calibration curve of the crystal voltmeter using a 1N28 crystal. Measured characteristics of several 1N28 crystals

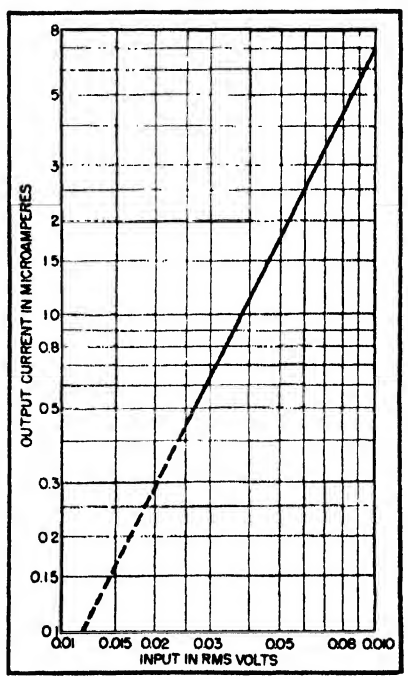

FIG. 3—Typical calibration curve of the crystal voltmeter using a 1N28 crystal

indicate that their sensitivities are in the order of 700 to 1,200 microamperes per volt squared and that they have square-low input-output characteristics only for inputs up to approximately 0.1 volt. The compact construction of the probe, minimizes lead inductances and stray capacitances, and the low value of load resistance, 270 ohms, serve to maintain an input-output characteristic substantially independent of frequency from 50 mc to at least 250 mc. At frequencies below 50 mc, the response falls off gradually.

The crystal voltmeter has been checked for susceptibility to burnout. Peak surges of 500 volts d-c or 130 volts, 60-cycle a-c have shown no effect on the calibration. Likewise, it has been determined that the crystal can withstand r-f voltages to produce approximately 1 ma of direct current, without effect on calibration. Higher r-f voltages, or mechanical shocks may, of course, cause a change in calibration or permanent damage.

The crystal voltmeter is intended for observation of r-f voltage across low impedances such as the output terminals of a signal generator or a low-resistance plate load of an amplifier tube. Care should be exercised in connecting the probe for high radio-frequency measurements to avoid excessive lead length and the addition of stray capacitance. When making measurements at low frequencies, say below 50 mc, it should be remembered that the 100-$\mu\mu$f d-c blocking capacitor has appreciable series reactance. It will be observed that the action of the microameter needle is somewhat sluggish due to damping by the crystal resistance. A short time should therefore be allowed for the needle to come to rest before reading the meter.

Measuring Complex Components

Real and imaginary components of unknown voltage are directly indicated in sign and magnitude relative to reference voltage by audio-frequency vacuum-tube voltmeter. Instrument simplifies measurements on amplifiers and filters. Operation is described

By GEORGE E. PIHL

THE INSTRUMENT discussed in this paper is a vacuum-tube voltmeter that indicates directly the real and imaginary components of an unknown voltage, in terms of a reference voltage. The voltmeter has full-scale ranges of 1, 5, 10, and 50 volts and the frequency range extends throughout the audio spectrum, 20 to 20,000 cycles per second.

There has long been a need, particularly in the field of communications, for an instrument that would measure unknown alternating voltage in terms of its real and imaginary components, with respect to a second voltage used as reference. This need is especially true in measurements on filters, attenuators, and amplifiers where a knowledge of phase shift may be important. The instrument will perform such measurement at any frequency within the audio range. Its operation is based upon the well known fact that the magnitude of the vector sum of a large voltage and a small voltage is very nearly equal to the sum of the large voltage and the in-phase component of the small voltage.

Let e_t be a voltage of large magnitude used as reference. Let e_r and e_j be the magnitudes of the real and imaginary components of the unknown voltage e_x. If we put e_t on the real axis, then the vector sum e_t of the two voltages will be

$$e_t = e_t + e_x$$
$$e_t = e_t + e_r + je_j$$

The magnitude of e_t is

$$|e_t| = [(e_t + e_r)^2 + (e_j)^2]^{1/2}$$

If e_t is sufficiently large in comparison to e_j, then $(e_j)^2$ becomes negli-

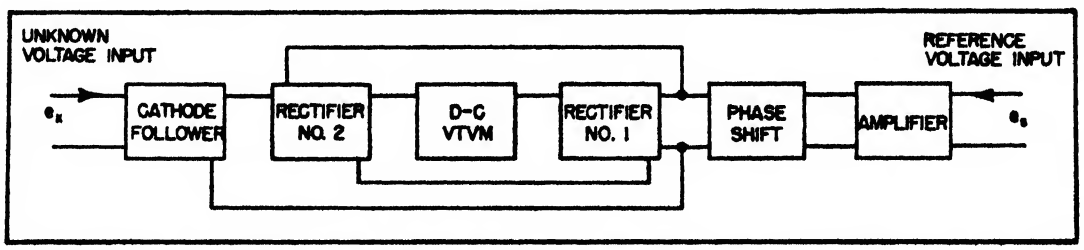

FIG. 1—Block diagram of meter for indicating real and imaginary components of a complex voltage

Table I—Comparison of true and measured values of voltage

Value of either the real or the imaginary components			
True	Measured	True	Measured
0.00	0.01	0.60	0.61
0.10	0.11	0.70	0.70
0.20	0.21	0.80	0.80
0.30	0.31	0.90	0.90
0.40	0.41	1.00	1.00
0.50	0.51		

Measured values are tabulated to two decimal places to correspond with the precision of indicating instrument used in actual circuit.

gible with respect to $(e_s + e_r)^2$ and the magnitude of e_i is approximately

$$|e_i| = [(e_s + e_r)^2]^{1/2} = e_s + e_r$$

Therefore, e_r is approximately

$$e_r = |e_i| - e_s$$

It is therefore possible to measure the real component of the unknown with respect to a large voltage used as reference by providing an instrument that reads the difference between the magnitude of the vector sum of the unknown and reference and the magnitude of the reference alone.

In a similar manner, if the reference voltage is advanced in phase by exactly 90 degrees, then the indication of the instrument will be the imaginary component of the unknown with respect to the original reference axis.

The block diagram of a system which will perform as indicated by the preceding is shown in Fig. 1. The reference voltage e_s is fed into an amplifier to make the resultant amplitude large in comparison to e_x. The amplified reference is applied to a phase-shift circuit which allows the output voltage to be either in phase, or in leading quadrature with respect to e_s, thus providing for measurement of both e_r and e_j. Output of the phase-shift network is applied to rectifier No. 1, producing at its output terminals a d-c voltage proportional to the magnitude of the amplified reference.

The unknown voltage is applied (through a cathode follower) in series with the output of the phase-shift network to the input of rectifier No. 2. At the output of this rectifier there appears, therefore, a d-c voltage proportional to the vector sum of the unknown and the amplified reference. The outputs of the two rectifiers are connected in series opposition to a d-c vacuum-tube voltmeter which therefore measures the voltage component desired. Multiple range can be obtained through a voltage divider in the e_x input circuit.

Inherent Error

If the reference voltage has an amplitude of 50 volts and the amplitude of the unknown is limited to a maximum of one volt, then the inherent error of this method for various assumed phase angles can be determined as follows

$$e_s = 50 + j0$$
$$e_x = e_r + je_j \text{ where } (e_r^2 + e_j^2)^{1/2} = 1.0$$

If we let e_r have the values given in the Table I, the true value of e_j can be computed from

$$e_j = [(1.0)^2 - e_r^2]^{1/2}$$

The magnitude of the vector sum will be

$$|e_i| = [(e_r + 50)^2 + e_j^2]^{1/2}$$

Therefore the measured values of e_r and e_j will be

$$e_r = [(e_r + 50)^2 + e_j^2]^{1/2} - 50$$
$$e_j = [e_r^2 + (50 + e_j)^2]^{1/2} - 50$$

Obviously the error in the measurement of either component will be the same for the same component value. As Table I shows, inherent error due to the method of measurement is not serious because the maximum error of 0.01 volts is only one percent of full scale. Furthermore, it is possible to reduce this error in the actual operation of the instrument as will be explained later.

Rectifier Circuits

Because the method of operation of this instrument is based upon the measurement of a small voltage difference between two large voltages, it is apparent that the two rectifier circuits must have characteristics as nearly identical as possible. This condition is not difficult to satisfy as each rectifier is operating linearly because the applied a-c voltages are large. In addition, although the voltage applied to rectifier No. 2 is a variable, depending upon e_x, the variation is never greater than two percent under all conditions. Because both rectifiers operate linearly, a simple zero set control can be provided in the d-c vacuum-tube voltmeter circuit to take care of slight unbalance of the rectifier circuits which may develop as the frequency is varied.

It is evident from the foregoing that the heart of the instrument is the rectifier system. The circuit diagram of Fig. 2 satisfies all of the requirements. In this circuit the amplified reference is rectified by T_1 acting as a linear peak diode, the resulting d-c voltage appearing across R_1 with the polarity indicated. The vector sum of the unknown and amplified reference is applied to T_2 also acting as a linear peak diode, the resulting d-c voltage appearing across R_2. The difference of these two d-c voltages then appears across C_3 as is evident from the above connections. Diodes T_1 and T_2 may conveniently be a dual diode, both diodes included in the same envelope. This circuit has the advantage over other possible solutions in that both signal sources and the vtvm have a common low potential or ground side.

Phase Shift Networks

From the description of the method given, it is apparent that

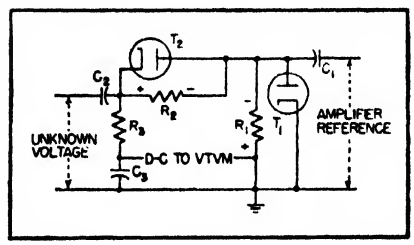

FIG. 2—Reference and unknown voltages are rectified and combined. Combination is effectively the algebraic sum of reference and the in-phase component of the unknown voltage

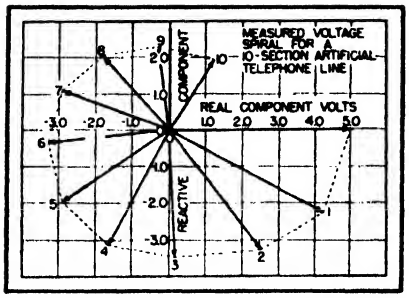

Angle and amplitude of voltages across sections of an artificial transmission line can be quickly determined using the complex voltmeter

if the reference is a source of low voltage, it must be amplified before being applied to the rectifier system. Furthermore, for the measurement of e_r, the amplified reference must be exactly in phase with e_i and for the measurement of e_j the amplified reference must be exactly 90 degrees leading with respect to e_i. Because some phase shift within the amplifier is inevitable over an extended frequency range, two phase-shift controls are necessary. One is provided to secure the in-phase reference, the other for the 90-degree reference.

The reference is first shifted approximately 45 degrees in a leading direction by a resistance-capacitance circuit. The phase control for the measurement of e_r consists of a resistance-capacitance network to shift the phase in a lagging direction so that the net phase shift is zero. The phase control for the measurement of e_j consists of another resistance-capacitance network to shift the phase an additional amount over the original 45 degrees so that the net phase shift is 90 degrees.

Complete Circuit

The diagram of the instrument is shown in Fig. 3. Tube T_1 is a double triode, each section being used as a cathode follower. The first section provides a means of changing the voltage range by the voltage divider in the cathode circuit. Range is selected by S_1. The second section provides a divided output voltage at constant impedance for introduction into the rectifier system.

Tube T_2 is the double rectifier which works into the d-c vacuum tube voltmeter, T_3. The latter has a range of plus or minus one volt, center zero. The switch S_2 provides a means of opening one rectifier circuit in order to set the magnitude of the amplified reference voltage at 50 volts, allowing it to be read by the same vtvm because S_2 also changes vtvm range from one volt to 100 volts. The magnitude of the reference is controlled by R_1.

The reference is applied to the first section of T_5, another double triode. The first section provides low output impedance for working into the phase-shift network controlled by S_6 and R_2. This network, when properly set, provides a leading phase shift of approximately 45 degrees.

The second section of T_5 works into two phase-shift networks, one controlled by R_3 and S_5 providing a lagging phase shift of approximately 45 degrees and its output providing the reference for measuring e_r. The other network out of T_5 controlled by S_4 and R_4 provides an additional shift of approximately 45 degrees leading for the measurement of e_j. The proper reference for the component to be measured is selected by S_3 and applied to T_4, the voltage amplifier which then works into the rectifier system.

In all three of the phase-shift networks, the proper capacitance depends upon the frequency only. Therefore S_4, S_5, and S_6 are ganged together and labelled as a frequency control, to be set for the frequency range desired. Potentiometers R_2 and R_3 are ganged together and used as the phase control for the real component. The setting which gives in-phase reference results in the lead and lag 45-degree shifts mentioned above. After this control is set, the control for measuring the imaginary component, R_4, is set for an additional 45 degrees.

Potentiometer R_5 is simply the zero set for the d-c vacuum-tube voltmeter. Voltage regulator tubes insure stable operation.

Controls and Method of Setting

The following is a summary of all controls:

RANGE: Ranges of 1, 5, 10, and 50 volts full scale plus or minus are provided.

ZERO SET: With USE-CAL switch on USE, reference voltage applied, and unknown terminals shorted, this control is set for zero voltmeter indication. With the switch in the USE position, R_7 having a resistance of 9,500 ohms is used as the voltmeter multiplier. This multiplier gives the input to T_3 a sensitivity of two volts. However, the micrommeter scale has been altered to give a center zero, and the needle is adjusted to this point by R_8, the ZERO SET control. The ZERO SET

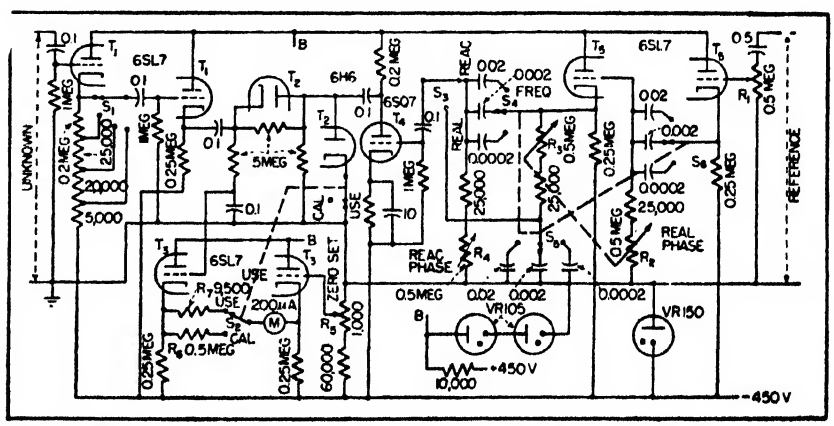

FIG. 3—Complete circuit diagram of the complex voltmeter indicates use of cathode followers to feed vacuum tube voltmeter

Table II—Calculated and measured phase shift of an R-C circuit

Calculated Values		Measured Values		Operating Frequency
e_r	e_j	e_r	e_j	In cps
0.07	0.61	0.10	0.60	200
0.44	1.42	0.50	1.45	500
1.39	2.24	1.50	2.20	1,000
3.03	2.44	3.05	2.40	2,000
4.53	1.46	4.60	1.50	5,000
4.87	0.78	4.90	0.80	10,000

See Fig. 4 for circuit and equation

applies about one volt to the grid of the second section of T_3 by this adjustment. Thus the actual range of the input to T_3 is ±1 volt.

REFERENCE AMPLITUDE: With USE-CAL switch on CAL, this control is adjusted for a voltmeter reading of 50 volts. Resistor R_6 of 0.5 meg gives the meter a full scale range of 100 volts, therefore the adjustment is made for center scale. Because R_7 has been previously set to give about one volt deflection, this voltage produces negligible deflection with the new multiplier in the circuit. The microammeter is therefore at its extreme left or zero-current position with no input voltage. The 50-volt point is therefore center scale which is marked zero on the microammeter face.

FREQUENCY: This control must be set to the appropriate range. The ranges provided are 20 to 200, 200 to 2,000, and 2,000 to 20,000 cps.

REAL PHASE: With S_3 on REAL, and an external lead used to connect the reference voltage to both the reference and the unknown terminals, this control is set for a maximum value as indicated by the vtvm.

REACTIVE PHASE: With S_3 on REAC, and an external connection as above, this control is set for zero value as indicated by the vtvm. This adjustment assures a reading of zero for the imaginary component of a pure real unknown and minimizes the inherent error of the method discussed previously.

Although there may seem to be a large number of controls to be set, these do not have to be disturbed after they are once set providing the frequency is not changed. Therefore in the analysis of a complicated circuit at a single frequency, the operation is very simple, only the REAL-REAC switch and the RANGE switch being used.

For example, the complete voltage spiral of a twenty-section artificial telephone line may be obtained in about 15 minutes. On the other hand, if the frequency response characteristic of a network is desired, in general all of the above controls need to be reset at each new frequency. While this resetting slows down the procedure, the method is faster than others.

The agreement between measured and calculated results for the voltage across the resistance in a simple R-C circuit, as a function of frequency, is given by tabulated

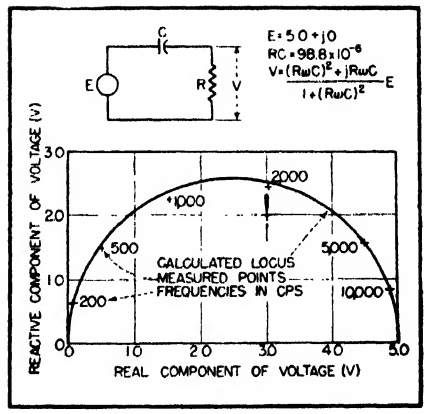

FIG. 4—Comparison of calculated and measured voltages shows utility of meter

values in Table II and the curve in Fig. 4. Input voltage was maintained at five volts and was used as the reference.

The instrument described has been in service for a considerable period and has proved itself to be stable in operation and reliable in indication. It represents what is believed to be the first instrument that reads directly the complex value of a voltage in the rectangular coordinate system and establishing polarities of the real and imaginary components as well as their magnitudes. Its limitations are similar to those for any electronic measuring instrument, namely that controls must be set with care and voltages under measurement must be of good sinusoidal waveform and reasonably good frequency stability.

Impedance Measurements

ELECTRICAL IMPEDANCES, whether they are resistances, inductances, or capacitances, can be quickly measured by varying a known impedance to produce a squarewave trace on a cathode-ray oscilloscope. The circuit for making such measurements is shown in the accompanying drawing, where the two capacitors could be replaced by two inductors if desired. It should be noted that if inductors are used, their inherent resistances can be used for R_1 and R_2, obviating the need for connecting separate resistors.

The circuit operates as a balanced attenuator. A squarewave of any convenient frequency is applied to the input. The output is connected to the vertical deflection channel of an oscilloscope the sawtooth sweep of which is synchronized to the squarewave. Impedances

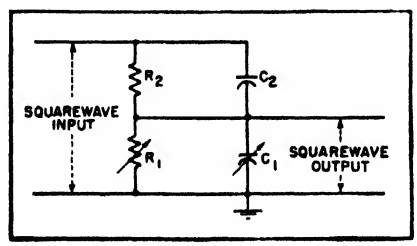

Impedances can be measured in a balanced attenuator by adjusting for the condition at which a complex input waveshape is reproduced in the output

of the measuring network are adjusted until a squarewave is displayed on the oscilloscope, under which condition $R_1C_1 = R_2C_2$ or $R_1L_2 = R_2L_1$, where these values are effective, including stray impedances. Any of the impedances can be varied, preferably one that is grounded. If the reactance across the lower portion of the network is too large, the output squarewave will be peaked at its rising edge; if that reactance is too small, the output will be rounded at the rising edge. (U. S. Patent 2,409,419 granted 15 October 1946 to Peter S. Christaldi, assignor to Allen B. DuMont Lab., Inc.)

Grid-Dip Oscillator

ONE of the most useful instruments in an electronic laboratory is the grid-dip oscillator with a vhf frequency range. Strangely enough, however, these have not been generally available as a commercial product until recently. Since the early days of radio, however, they have been constructed by the individual engineer to fit particular applications when needed.

The grid-dip oscillator consists of a variable-frequency oscillator with an indicating milliammeter in its grid circuit. When the oscillator tank circuit is coupled to a second resonant circuit, usually by holding the tank inductance near the second tuned circuit, a dip in the grid current indicates the frequency at which power is drawn from the oscillator. A frequency-calibrated dial on the oscillator then indicates the frequency at which resonance occurs.

The resonant frequency of any coil and capacitor combination, alone or connected into circuits, resonant lines, wave traps, r-f chokes, and antennas, can thus be determined quickly and changes made to tune them to the desired frequency. Additional capacitance of tubes and wiring needs to be taken into account however if the unit being measured is not connected to its final operating circuit. The frequency change due to tube heating, which is particularly large at the i-f and front-end frequencies used in f-m and television receivers, can be readily determined with the grid-dip oscillator. The frequency at which wiring between components resonates may also be determined.

The circuit of one of the grid-dip oscillators recently announced by De Vine Laboratories is shown in the accompanying diagram. In addition to operation as a grid-dip oscillator it permits the addition of earphones in the grid circuit so that the instrument becomes an oscillating detector for beating against an unknown signal for determining its fundamental and harmonic frequencies.

Use of the headphones also permits operating the tube without plate voltage to form a diode detector for modulated signals from a transmitter or signal generator. Removing the headphones in this instance switches the meter back in the grid-cathode diode circuit and permits use as an absorption frequency meter or a field strength meter.

The instrument shown employs seven plug-in coils to cover a frequency range from 1.9 mc to slightly over 200 mc. Each coil is mounted inside a polystyrene cylinder so that it can be inserted in and near tank coils having high voltage without contact to the turns of the coil. The coils are tuned by a split-stator capacitor having specially designed plates to allow a nearly linear dial calibration in terms of frequency.

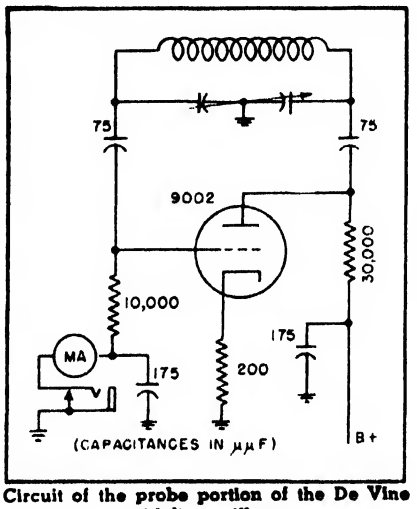

Circuit of the probe portion of the De Vine grid-dip oscillator

Elements of the circuit shown are mounted in a narrow metal case so that the coil, tuning capacitor, grid meter, and a drum dial are arranged in line. Thus the unit is practically a probe with its coil at one end, and dial at the other end. Having the meter mounted on this unit permits readings to be made while watching the dial when tuning through the range.

Phase Meter

By E. O. VANDEVEN

THE PHASE METER is a device that measures the phase angles of a low or high frequency polyphase voltage supply. Essentially this is accomplished by developing on the screen of a cathode-ray oscilloscope a circular sweep at the polyphase supply frequency. Each phase voltage of the polyphase supply is then separ-

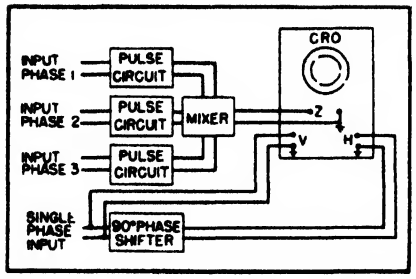

FIG. 1—Block diagram of phase detector

ately amplified, clipped, differentiated and again amplified.

In the output of each phase amplifier are pulses which are established in time by their respective phase voltage. These pulses are mixed and applied to the Z-axis amplifier of the oscilloscope to intensity modulate the circular trace, causing a dark or bright spot to appear for each phase voltage. The angular displacement between the spots is then a measure of the angular displacement between corresponding phase voltages. The phase angles can be read by calibrating the oscilloscope screen radially in degrees.

A block diagram of the phase meter is shown in Fig. 1. One phase of the three-phase supply is applied to a device which shifts the phase by 90 degrees. This is done, since to obtain a circular sweep it is necessary to apply to the horizontal and vertical amplifiers voltages of the same frequency but separated in phase by 90 degrees. The pulse forming and mixing circuits are also indicated.

The phase meter was developed for work with the 2H21 phasitron tube, used to generate crystal-controlled f-m. The phasitron has three-phase r-f applied to the deflector electrodes. A crystal oscillator at approximately 230 kilocycles is the signal source. This single-phase voltage is transformed to three-phase by employing a modified Scott transformer connection.

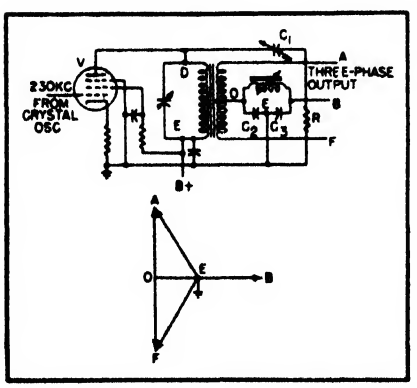

FIG. 2—Single-phase to three-phase transformation circuit and phase diagram

The single- to three-phase transformation circuit, with the associated phase relationships, is shown in Fig. 2. Amplifier tube V supplies a transformer load, the secondary of which is center tapped. Secondary voltage, AF, is shown vectorially on the phase diagram. The OB vector, displaced 90 degrees from AF, is obtained by shifting the phase of the primary voltage DE by 90 degrees. Since DE and AF are in phase, vector OB is then 90 degrees from AF.

Resistor R is essentially connected from B to E which is part of a tuned circuit. Therefore by detuning the tuned circuit slightly from the resonant point the reactance from B to E can be made to appear inductive. This inductive reactance is in series with C_1, and by proper adjustment of these two parameters the voltage BE will be displaced from the supply voltage DE by 90 degrees. By properly establishing the ratio of C_2 to C_3, the point E is selected along the OB vector. Point E is grounded providing a neutral point for the balanced three-phase system.

For the phasitron to operate with minimum distortion it is necessary that the exciter supply phase voltages of equal magnitude and angular displacement. The phase meter was developed to facilitate the adjustment of the exciter supply for perfect three-phase output.

Circular Sweep

Figure 3 shows the circuit used to obtain circular sweep. The single-phase, 230-kc signal feeds a pentode amplifier. The amplifier plate circuit has a tuned transformer which, when resonated, gives a 90-degree phase shift between primary and secondary. Proper adjustment of the secondary tuning

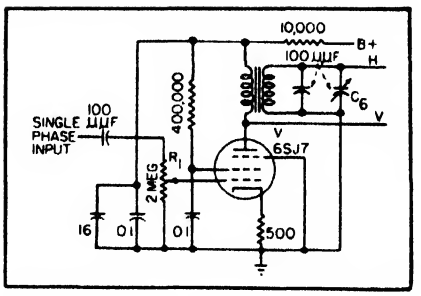

FIG. 3—Circuit of circular sweep generator

capacitor is accomplished by observing the pattern on the c-r tube. When this capacitor, and the horizontal and vertical gains, are correctly set, the result will be a circular trace on the cro screen.

The pentode amplifier is run class A and with an unbypassed cathode resistor. This is to minimize distortion of the voltages applied to the vertical and horizontal amplifiers. The cro amplifiers must also have low distortion, or it will be impossible to obtain perfect circu-

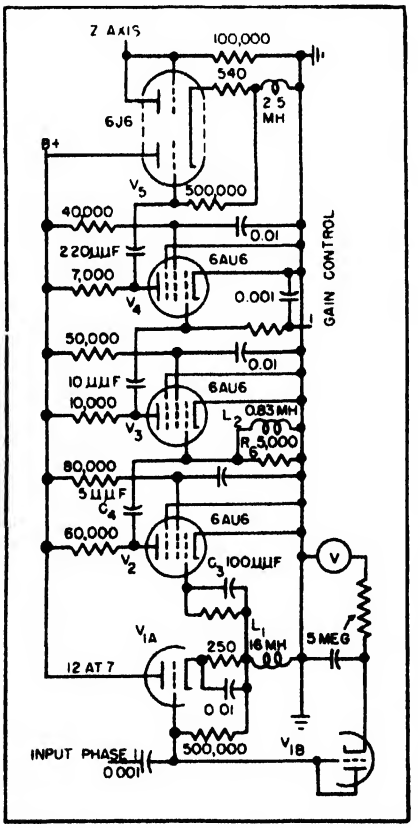

FIG. 4—Pulse generator for one phase

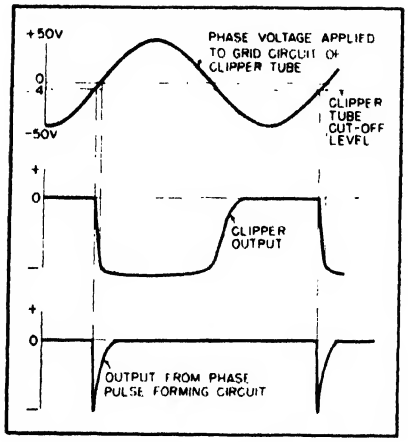

FIG. 5—Phase relations in pulse-forming circuit

lar sweep. Circle size is controlled by R_1.

One of the pulse-forming circuits is shown in Fig. 4. Phase voltage is applied to V_{1A}, a cathode follower. This tube transforms from high-impedance input to low-impedance output across L_1.

Operation

Accuracy of the meter depends more than anything else on the coupling circuit between V_{1A} and V_2, and the operation of V_2. The voltage developed across L_1 is at least 30 volts rms. Therefore the grid of V_2 swings from minus 50 volts to 50 volts plus, less the drop across R_2C_2. The tube begins to conduct when the input voltage rises to approximately −4.5 volts. When it reaches zero volts, grid current begins to flow, resulting in a voltage drop across the grid resistor.

The output of V_2 therefore is a pulse whose leading edge is very steep. It is important that this leading edge be definitely established in time with respect to the phase input voltage.

Tube V_2 is directly coupled to L_1, since a blocking capacitor would have a discharge time constant which would develop grid-bias on V_2 and change its operating point with respect to the phase input voltage. Filter R_2C_2 has a time constant which is short compared to the period of one cycle. Thus, as the voltage across L_1 rises from its peak negative value, V_2 should begin to conduct at a point determined entirely by its cutoff potential.

If the magnitude of the phase voltage is varied, this point will shift slightly, which is part of the inherent error of the device. If all phase voltages are varied by the same amount however, no net error should result. All operating points will have shifted by the same amount and in the same direction.

C_1 and R_1L_2 constitute a differentiating circuit, the voltage on V_3 grid consisting of narrow positive and negative pulses. Since V_3 is zero biased, its grid presents low impedance to the positive pulses and high impedance to the negative ones. In the output, positive pulses predominate.

Tube V_4 is an amplifier-inverter, biased beyond cutoff. The pulses are also narrowed in this stage. Output of V_4 is applied to V_5, a cathode follower. The negative pulses developed across the cathode-follower load impedance cannot be fed to the Z axis input directly. If this were done the cathode-follower loads of all phase circuits would essentially be in parallel. When one cathode follower were pulsing the remaining two would present excessive loading. The result would be insufficient pulse output voltage.

Circuit Isolation

Therefore the second section of V_5, is diode connected. Under these circuit conditions, the cathode load impedances of the inoperative cathode followers are isolated from the load impedance of the one that is operating.

Tube V_{1B} is diode-connected to form part of a peak-reading voltmeter circuit. The meter is calibrated to read rms phase voltage.

Figure 5 shows the phase relationship between the sine wave input to the phase circuit and the output pulses appearing at the Z-axis input to the cro. The leading edge of each pulse is determined by the cutoff point of the first clipper tube in the corresponding phase circuit.

Other possible uses of the phase meter principle include the measurement of phase shift through amplifier circuits.

Construction of Shielded Room in VHF Field

By CECIL C. PINE

PRESENT-DAY development of vhf and uhf equipment necessitates the modernizing of the conventional screened room. In fact, an ordinary double or triple shielded room utilizing copper or galvanized iron mesh is ineffectual when subject to interference such as that caused by uhf radiations of extremely high peak power.

The shielded room to be described was the outgrowth of an effort to provide a means for testing radio direction-finding equipment under conditions of very severe local disturbances, and to date it has proved adequate in all respects.

The first requirement in aligning and testing automatic d-f equipment is to provide a means of coupling a signal of known field strength into the loop and vertical antenna input circuits. This must be done in a manner simulating ideal field conditions and should be free from all uncontrollable factors such as variation of field strength or interference from unwanted signals.

The elimination of interfering signals is usually accomplished by

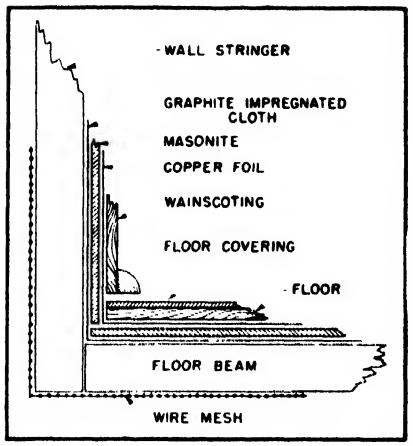

FIG. 1—An expanded view of a portion of the shielded room showing constructional details

employing a combined system of shielding and filtering. The test room is generally constructed with either two or three shields consisting of wire mesh or copper foil spaced from two to four inches apart and connected together at but one point. This technique normally attenuates any radiation exterior to the room from 60 to 100 db. However, any r-f voltage superimposed on the power lines leading into the room will be radiated inside the room and cause trouble. An r-f filter consisting of chokes and capacitors interposed between the power line and the load is generally considered an adequate means of eliminating interference from this source.

An ordinary pi network consisting of two 0.5 μf and two r-f line chokes placed in the power lines leading into the screened room was of little value when the lines exterior to the room were subject to bombardment from a pulsed uhf source. A test receiver connected to the bench conduit, and even to points along the internal shield, registered interference over most of the frequency band for which the room was to be used.

Another interesting fact was revealed when tests were made in a room triply shielded with ½-inch galvanized mesh. Here a small loop connected to the test receiver could be used to take a bearing on the source of external interference although the generating equipment was enclosed in another triple shielded room some distance away.

Construction

Some of the more particular aspects considered in the construction of the new room are the methods of obtaining sufficient shielding and filtering. To obtain a high degree of attenuation, three shields are used. The outer shield consists of ½-inch galvanized mesh, the second or center shield is a graphite-impregnated cloth, and the inside of the room is lined with copper foil which forms the third or inner shield. The outer and inner shields are connected together at one point, the neutral leg of the power line.

The center shield, consisting of the graphite-impregnated cloth, is used to attenuate the uhf leakage. This material is extensively used for its ability to absorb any high frequency energy that terminates upon it, and is here used as a floating shield which merely acts to dissipate the currents flowing in it rather than conducting them to a common ground point as is the case with the other two shields. Fig. 1 gives a general illustration of the construction carried on throughout the room.

The framework of the room is constructed of well-seasoned 2 by 3-inch members, the exterior of which is covered with the galvanized mesh. The impregnated cloth is glued to the back of tempered masonite sheets which in turn are nailed to the inside of the framework to form the walls, floor and ceiling. The joints in the cloth backing are overlapped to form a continuous shield, and all nails used in securing the masonite are countersunk.

Copper foil is cemented to the masonite with a heavy Bostick cement. All panelling, light fixtures, and other supported items are held in place by small angle strips which are soldered directly to the copper foil.

Inasmuch as the shielding must be continuous throughout the entire surface of the room, the door is constructed in a similar manner and is provided with special metal stripping which assures a good bond to the respective shields. Ventilating holes cut through the copper and cloth shields are covered with fine copper mesh.

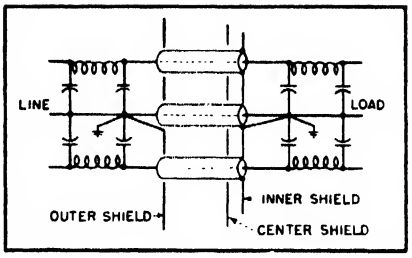

FIG. 2—Schematic diagram of all-wave filter system. The cylindrical forms in the center represent the microwave filters

Filtering

A special microwave line filter is used, in conjunction with the more conventional types, to obtain a high degree of attenuation over the entire r-f spectrum. Figure 2 shows the circuit arrangement.

The first filter section consists of a pi network utilizing 0.5-μf oil-filled capacitors and low-frequency chokes and is installed in a copper-clad box mounted on the outside of the room. The second section makes use of the microwave filters, which are placed in each leg of the power line (including the neutral leg). These filters form the connecting means from the outer box to the interior of the room. Inside the room is another copper-clad box, in which is located a third filter section consisting of 0.5-μf oil-filled capacitors and high-frequency chokes.

As shown in Fig. 2, the outer and inner shields are connected together by means of the neutral wire through one of the microwave

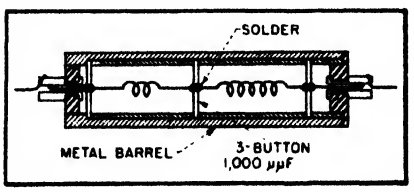

FIG. 3—Details of the microwave filter

chokes. A more detailed illustration of the microwave choke is given in Fig. 3.

A test receiver placed in a room of the type described was unable to detect any type of interference over the entire band from 200 to 1,600 kilocycles; although, by opening the door by as much as one-eighth of an inch several broadcast stations could be received with considerable volume. Moreover, the uhf type of interference was reduced to a negligible amount when the door of the room was securely closed.

Radiation from R-F Heating Generators

By ARTHUR G. SWAN

INDUSTRIAL USERS of electronic heating equipment that have encountered problems in minimizing the amount of radiation from the units can benefit by the work done in Hawaii for solving a similar problem.

During the war, the military governor of the Territory found it advisable to control the use of diathermy equipment by licensing for use only diathermy equipment whose radiated signals were sufficiently attenuated. Details of the control were passed to a board of Army officers, who, with the cooperation of the FCC, set up standards for maximum allowable radiation, and recommended a type of shielded room to limit this radiation.

Tests showed that a room consisting of two concentric shields, both floating above ground, and having an a-c service entrance filtered as in Fig. 1, gave satisfactory results. The filter box is grounded to the inside room-shield. Access to the room was by means of a door constructed with shielding on both sides. When closed, there was no interruption in the continuity of the shields throughout the room.

Many such installations were constructed throughout the Islands, and with proper attention to details and some experimental modifications to suit local conditions, all but a few proved very satisfactory.

Attenuation was estimated by listening to the diathermy signal on a Hallicrafters S-29 receiver carried out along radials from the diathermy equipment. In most cases, the signal was undetectable at distances greater than fifty yards from the offending unit.

Construction

The type of shielding material used was not critical. Copper fly screening was best, but was hard to obtain at that time. Ordinary steel fly screening, or hardware cloth up to half-inch mesh, worked satisfactorily. Wood spacers separated the inside from the outside shields by one or two inches and separated the outside shield from any possible external ground. In a few cases a ground on either the inside or outside shield helped, but in a large majority of cases attenuation was greatest with both shields ungrounded. No objection was found to running as much a-c wiring as was desired from the filter around the inside of the room, but there could be no exposed wire between the filter and the a-c entrance to the room. Radiation along the power line outside the room was sometimes troublesome, and in some cases could be followed nearly a mile along pole lines before proper shielding was accomplished.

A minimum number of doors should be built into the shielding. Best results were obtained where only one door opened into the room, and this, when closed, had to make good electrical contact on all four sides. The hinged side was provided with several flexible straps to connect the respective door shields to room shields.

Wood used as insulation between shields and between outside shield and ground had to be thoroughly dry. It was necessary to insulate between the outside ground and any plaster, concrete, linoleum, etc.

The filter was mounted flat against the inside shield directly over the spot at which the a-c line entered the room. The box was constructed of heavy gauge metal with all seams soldered. Commercially built filters were not satisfactory.

Close proximity of the room to open house wiring had to be avoided and installations on ground floors or in basements worked best. Those in frame buildings were hardest to attenuate. The smaller the room, the easier it was to attain good attenuation. Care had to be exercised in construction to see that no nails or strands of wire shorted between shields. All seams in shielding had to make continuous electrical contact.

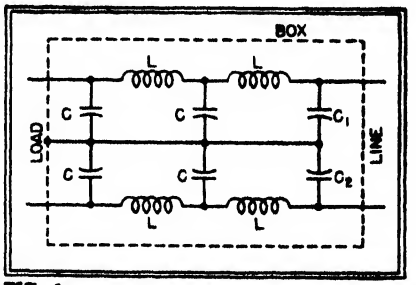

FIG. 1
Capacitors C_1 and C_2 were not always necessary in the filter. All capacitor values were 0.1 μf but lower values were sometimes satisfactory. The inductors marked L consisted of 20 turns wound on a one-inch diameter form

Measuring and Monitoring Broadcast Frequencies

The beat note between the harmonic of a multivibrator synchronized with the station frequency and a signal from WWV is measured by means of a counter or frequency meter

By LARRY S. COLE

THIS PAPER describes a method for measuring or monitoring radio frequencies against the Bureau of Standards primary frequency emissions from WWV without the use of an intervening standard. The method is particularly applicable to frequencies which are integral multiples of ten kilocycles, such as standard broadcast station frequencies, and it offers an unusually high degree of accuracy.

Principle of Operation

The process is illustrated in the block diagram of Fig. 1. The signal to be checked is taken from the oscillator or buffer stage in the transmitter and is used to synchronize the multivibrator. One of the multivibrator harmonics is compared with one of the emissions of WWV by means of an ordinary radio receiver. The resulting beat frequency can be measured by any of several commonly used methods, such as an electronic frequency meter or a counting mechanism.[1, 2]

To determine the frequency deviation from the assigned frequency the following analysis is used: Let

F = frequency under measurement

F_m = fundamental frequency of multivibrator

$N = F/F_m$ = synchronization ratio

F_s = standard frequency emission used

$n = F_s/F_m$ = order of the multivibrator harmonic used

$f = F_s - nF_m$ = beat frequency in receiver

Then $F_m = F/N$, and the signal compared with F_s is $nF_m = (n/N)F$

Let ΔF be the deviation between correct (assigned) and actual value of F; then the signal compared with F_s is $(n/N)(F - \Delta F)$, and the measured beat will be

$$f = (n/N)F - (n/N)(F - \Delta F)$$
$$= (n/N)\Delta F \text{ or}$$
$$\Delta F = (N/n)f \qquad (1)$$

For example, consider a broadcast station with an assigned frequency F of 1230 kc and a multivibrator having a frequency F_m of 10 kc and synchronized at a ratio N of 123/1. The 1500th harmonic of the multivibrator is then beat in the receiver against the standard frequency emission from WWV at 15 megacycles (F_s). Suppose the beat between the two latter signals ($F_s - nF_m$) to be 18 cps. Substituting these values in Eq. 1, we get $\Delta F = (123/1500)18 = 1.476$ cps.

The method offers no way of determining the sign of ΔF, or whether the measured frequency is above or below the assigned frequency. However, raising or lowering the transmitter frequency a cycle or so and noting whether the beat frequency increases or decreases will yield this information.

Equipment

The multivibrator frequency F_m was chosen at 10 kc as this value contains harmonic components which fall on all standard emissions from WWV as well as those of broadcast stations. While, for the majority of frequencies involved in the band, synchronization of the multivibrator could be accomplished in two or more steps with reasonably low synchronization ratios, there are 19 frequency channels which are prime multiples of 10 kc. In these latter cases, synchronizing the 10-kc multivibrator must be done in one step—involving

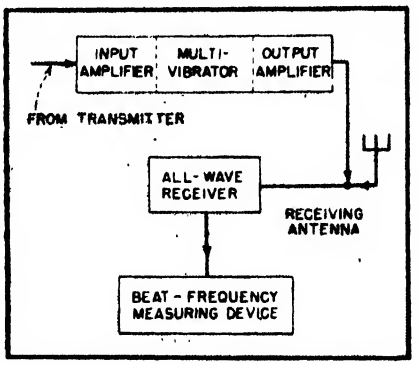

FIG. 1—Functional block diagram of the monitoring system

synchronization ratios of from 59/1 to as high as 149/1.

All the available information at hand indicated a practical synchronization ratio limit at about 50/1. Therefore the first problem was to investigate the possibility of practical synchronization at ratios of at least as high as 150/1. To accomplish this, the natural unsynchronized frequency of the multivibrator had to possess a high degree of inherent frequency stability and it also had to be isolated from any reactions due to adjustments or variations in the input synchronizing circuit and the output circuit.

The first problem was solved by using high-quality resistors of ample rating and an extremely stable voltage regulator. The regulator used was adapted from that developed by Bousquet[3], and produced an unusually high degree of regulation of the d-c output voltage.

Pentode tubes in the input and output circuits provided ample isolation when their operating voltages were also regulated. Gain of these stages could not be controlled by any

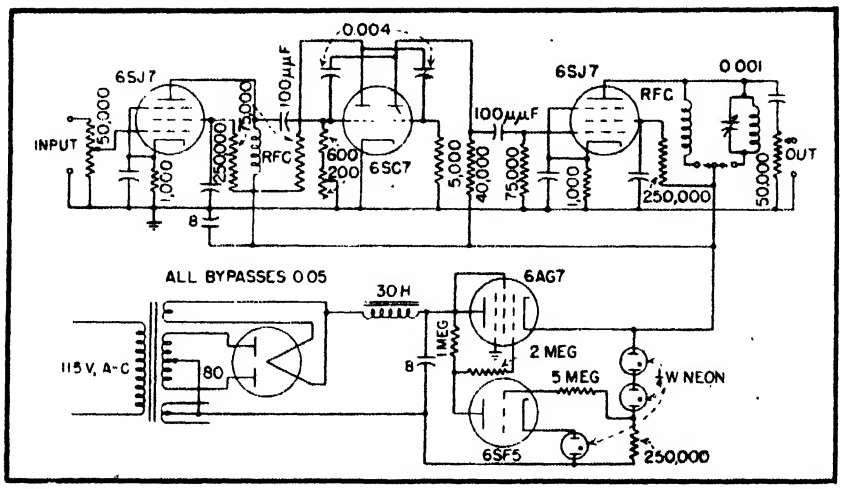

FIG. 2—Complete circuit of the multivibrator unit

variation of the operating voltages such as would result from a conventional cathode-bias control.

To obtain sufficient output on high harmonics, it was necessary to tune the plate circuit of the output amplifier over the range from 5 to 15 mc. Below 5 mc, the circuit is untuned as shown in the circuit of Fig. 2.

Synchronization of the unit at a particular ratio is achieved with various combinations of natural uncontrolled multivibrator frequency and synchronizing voltage amplitude. The combination resulting in the greatest stability is found by noting when the adjustment on the multivibrator frequency can be shifted the greatest amount without the loss of synchronism. As a typical example, this resulted with a natural multivibrator frequency of approximately 9.5 kc when synchronized to 10 kc using a 100/1 ratio.

No attempt was made to find a limit of synchronization ratio, but the unit constructed has been synchronized with complete stability at ratios as high as 200/1.

The unit was installed experimentally at a local broadcast station (KVNU, 1230 kc) for a thorough test under operating conditions. The input synchronizing voltage was obtained by bridging the low-impedance transmission line to the station frequency monitor from the crystal oscillator stage of the transmitter. The output of the multivibrator was connected to the antenna terminal of an all-wave receiver. A short horizontal antenna outside the transmitter building was used to pick up WWV and other signals.

After the multivibrator unit had become reasonably stabilized as to temperature, no further adjustments were necessary over a period of several days. During daylight hours, the 10 and 15-mc signals from WWV were used to check the operation of the unit. At night, the 5 and 2.5-mc signals were used. Other broadcast stations were also used as check frequencies both day and night. For a strong beat frequency in the receiver, a reasonable relationship between the strength of the received radio signal and the harmonic of the multivibrator is maintained by adjustment of the output control of the multivibrator unit.

In the modern broadcast station, the frequency control of the transmitter and the usual frequency monitor are of the same order of stability and should a large frequency deviation be indicated by the monitor, there may exist a reasonable doubt as to which is in error. In such cases, the immediate determination of the true transmitter frequency is of considerable value. For this particular application, an audible check of the beat frequency in the receiver would suffice for checking and for resetting the transmitter to assigned frequency.

References

(1) Case, N. P., A Precise and Rapid Method of Measuring Frequencies From Five To Five Hundred Cycles Per Second, *Proc. I.R.E.*, 18, p 1586, Sept. 1930.

(2) Hunt, F. V., A Direct-Reading Frequency Meter Suitable for High Speed Recording, *Rev. Sci. Inst.*, 6, p 43, Feb. 1935.

(3) Bousquet, A. G., Improving Regulator Performance, ELECTRONICS, 11, p. 26, July, 1938.

Measuring Pulse Characteristics

Method and equipment for rapid, accurate determination of pulse characteristics have laboratory precision and production-line simplicity. Basically, circuits and techniques measure time by obtaining coincidence with a standard time interval

By ALLAN EASTON

MEASUREMENT of pulse characteristics has been developed to a high degree of precision in the past few years. The relatively crude method of measurement using a linear saw-tooth sweep has been supplanted by more sophisticated means such as circular, spiral, or expanded sweeps.

By using the principle of coincidence the method described herein is capable of high accuracy without requiring great skill on the part of the operator, and therefore lends itself to production testing. In the

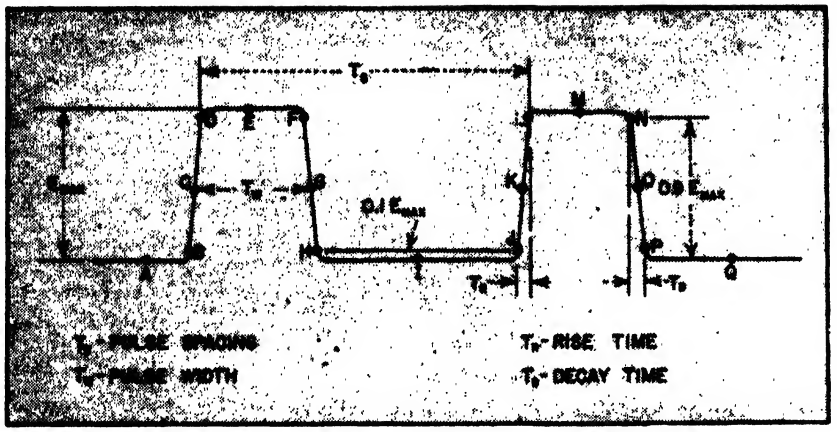

FIG. 1—Critical points from which pulse characteristics are measured

laboratory it is valuable because of its adaptability to measurements in the 0.1- to 100-microsecond range.

Particular applications of this method of measuring pulses are in metering velocity of light, delays at discontinuities in filters and transmission lines, in television, in radar ranging, and for calibrating linear sweeps.

Measuring Pulse Spacing

This method of pulse measurement is intended to increase the realizable accuracy and ease of measuring (1) time intervals between two or more pulses, (2) pulse duration, and (3) pulse growth and decay times.

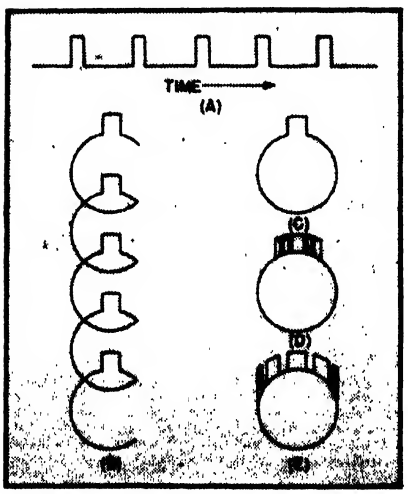

FIG. 2—To observe the pulse sequence shown at (A), a circular sweep, shown expanded at (B), can be used. At synchronism the trace appears as at (C); off synchronism it appears as at (D) or (E)

Pulse spacing T_S in Fig. 1 is the time interval between any two corresponding parts of two successive pulses in one trigger cycle. The duration of the pulse, T_W, is arbitrarily defined as the time difference between the 50-percent amplitude points. The rise time T_R is the time required for the pulse to increase from 10 percent to 90 percent of its full amplitude. Decay time T_D is the time required for the pulse to decrease from 90 percent to 10 percent of full amplitude. It is assumed throughout this discussion that the entire phenomenon to be measured occurs in one repetition period and is periodic in nature.

Figure 2A shows a train of pulses as they would appear on a suitable linear saw-tooth sweep. The distance between successive pulses is proportional to their time spacing. Imagine this same sweep wound like a rope so that it appears as a pile of coils as in Fig. 2B. If these traces are superimposed upon each other and if the circumference of each sweep is the same as the distance between pulses, the picture will appear as in Fig. 2C. If the length of each sweep is too short or too long the result will appear as in Fig. 2D or 2E. In other words, when the length of one circumference is just equal to the pulse spacing only one pulse will appear. When the length of the sweep is held constant corresponding to some predetermined amount of time, the pulse spacing can be varied until coincidence occurs. On the other hand, if the pulse spacing is held fixed, the frequency which determines the length of the circular sweep can be altered until coincidence results.

Thus this technique provides a system for either measuring or adjusting pulse spacing. The method requires a setting of frequency until coincidence is obtained. The accuracy, therefore, is dependent on frequency primarily and on the setting or resolution error in obtaining coincidence. No complicated judgments or measurements are required on the part of the operator—a desirable fact for production measuring equipment.

The pulse spacing is given by the equation

$$T_S = 1/f_C \qquad (1)$$

where T_S is the pulse spacing, and f_C is the coincidence frequency.

Measuring Pulse Width

Pulse width can be measured in two ways, both of which are based on the spacing measurement just described. Referring to Fig. 3A one sees a pulse with fairly steep sides shown along with its derivative. This derivative can be obtained in

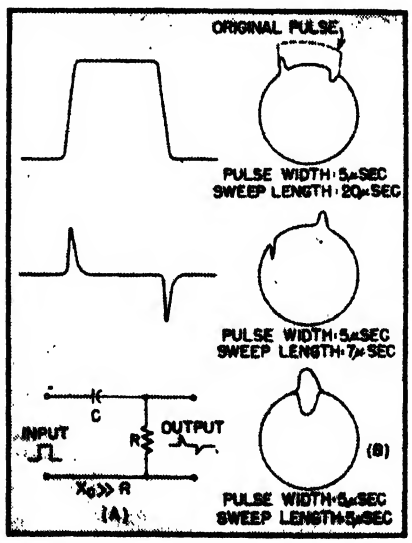

FIG. 3—(A) Left—If the pulse to be measured, as shown at the top, is differentiated by such a circuit as this, the derivative pulses, shown in the middle, are obtained. (B) Right—To measure pulse width, the derivative pulses are placed on a circular sweep and either the sweep or pulse generator adjusted until coincidence is obtained

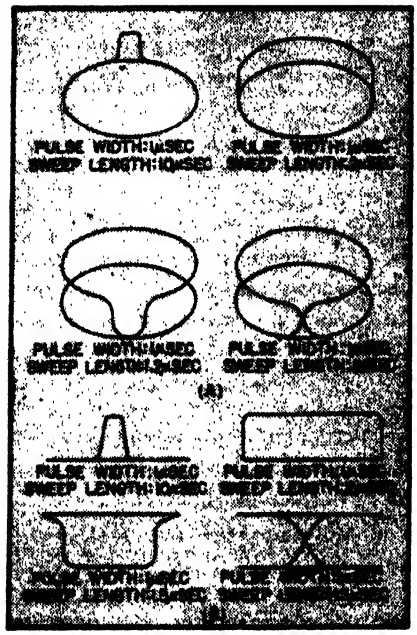

FIG. 4—Using either an elliptical (A) or a horizontal sinusoidal (B) sweep, one can determine pulse length by adjusting the sweep period relative to the pulse duration, giving the simple patterns shown at the right. Crossover is at the 50 percent point

several ways, one of which is shown. When the differentiated pulse is impressed on the variable-frequency sweep, patterns similar to those on Fig. 3B result. Essentially the pulse width measurement consists of measuring the spacing between the two pulses obtained by differentiating the leading and lagging edges of the original pulse.

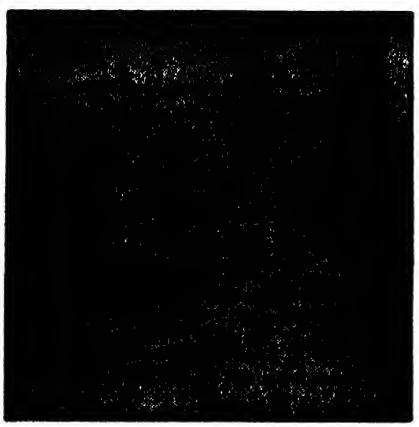

FIG. 5—When growth and decay times are approximately equal, they can be determined from measurements of pulse duration at the 10- and 90-percent amplitude points as shown here

An alternative method of determining pulse width is perhaps more suitable for many purposes. This is illustrated by Fig. 4. The figures are self-explanatory and show the effect on the pattern of increasing the sweep frequency. The method can be applied successfully with either elliptical, circular, or flat sinusoidal sweeps. This method enables determination of pulse width between points of any required percent of maximum pulse amplitude.

Measuring Growth and Decay Times

One method of measuring growth time depends upon the procedure previously described for pulse width measurements. If the pulse width is measured as described, at the 10- and 90-percent points, the rise time is determined as follows

$$T_R = T_D = \frac{(1/f_{0.1}) - (1/f_{0.9})}{2} \qquad (2)$$

where T_R is the rise time from 0.1 to $0.9E_{MAX}$, T_D is the decay time from 0.9 to $0.1E_{MAX}$, $f_{0.1}$ is the frequency corresponding to the width at $0.1E_{MAX}$, $f_{0.9}$ is the frequency corresponding to the width at $0.9E_{MAX}$, and E_{MAX} is the peak value of the pulse as indicated in Fig. 1.

The accuracy of Eq. 2 depends upon the equality of T_R and T_D. Figure 5 illustrates this method used with linear sweeps.

In cases where T_R does not equal T_D, an alternative method may be superior. Refer again to Fig. 3A. The shapes of the pulses shown are proportional to the rate of change of the measured pulse (if X_C is very much greater than R). Thus the width of the pulse at the base is proportional to rise or decay time. Measuring the width of the positive and negative derivative pulses by the methods previously described will give the values of T_R and T_D.

Accuracy of Measurement

The precision of the spacing measurement depends primarily on frequency. Errors which are due to sweep irregularity and resolution are quite small. However, at the present state of the art, frequency can be measured or set to better than one part in one million. In practice,

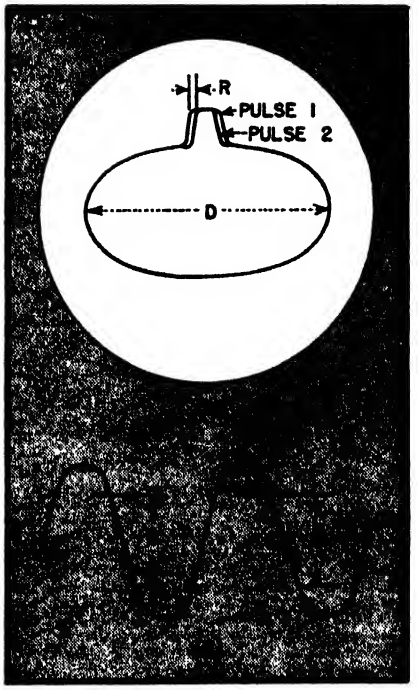

FIG. 6—For minimum error of measurement, the pulse (A) should be located on the most linear portion of the sinusoidal sweep (B)

therefore, the resolution of the coincidence setting determines the maximum accuracy.

Figure 6A shows the face of a cathode-ray tube with an eliptical pattern. An elliptical trace is used with conventional cathode-ray tubes because it insures best utilization of the screen area. Width of the trace limits the precision with which coincidence can be set. With a good cathode-ray tube, the thickness of the trace can be made less than 0.0312 inch. The length of one cycle of the elliptical trace depends upon tube diameter. A 5-inch cathode-ray tube will accommodate a trace length of approximately 12 inches.

Figure 6B shows two sine-wave cycles. The sections A and A' represent the maximum-velocity portions at the top side of the elliptical trace. It is on this part of the elliptical trace that the pulses should be set. The sections A and A' include about plus and minus 45 degrees. On the elliptical sweep 90 degrees at the maximum-velocity portion corresponds to approximately two-thirds of the horizontal deflection. If the coincident pulses are located on this maximum-velocity section,

the resolution error can be computed from

$$\epsilon = (R/\pi D)T \text{ seconds} \quad (3)$$

where ϵ is the resolution error, R is the resolution in inches, D is the width of the sweep pattern in the horizontal direction, and T is the period of one sweep cycle.

Equation 8 can be used with equal accuracy whether the sweep is elliptical, circular, or flat simple harmonic in character. The only requirement is that the displayed pulses be set to the maximum-velocity portion of the sweep.

Substituting the following typical values into Eq. 3

$R = 0.312$ inch
$D = 4$ inches
$T = 1$ microsecond

one obtains $\epsilon = 0.0024$ microsecond error, or an error of 0.24 percent.

In many applications the spacing between trains of pulses is required. In this case the error would be divided by N-1 where N is the number of pulses in the train. It can be seen that the error in measuring the spacing of a train of eleven pulses spaced one microsecond apart would be in the order of 2.4 ten thousandths of one microsecond or 2.4×10^{-10} second.

The accuracy of the measurement can be improved if necessary by using larger cathode-ray tubes and higher accelerating potentials to obtain larger and finer traces. The limits to the size and complexity of the equipment are an economic factor which must be evaluated in each application. The accuracy figures shown above do not require skillful manipulation of the test equipment or careful judgment in reading anything but frequency.

The method described in the preceding sections has been used by the author with excellent success. Equipments of several types have been constructed and are now in use.

Practical Systems

Fundamentally, there are two ways of using the outlined method. The first is to measure any of the quantities indicated, requiring variable frequency. The second is to set other equipments by means of the method, usually requiring fixed frequencies. However in either case the fundamental principles are identical.

Figure 7 shows a simplified block diagram of a typical system and a typical circuit for each of the less standard units. The requirements and characteristics of each unit follow.

STANDARD-FREQUENCY GENERATOR may supply either fixed or variable frequencies in whatever ranges are required. This unit should be capable of high precision.

FREQUENCY DIVIDERS are a necessary component in any system in which the elliptical sweep must be synchronized with the display. The sweep frequency is usually much higher than the pulse recurrence frequency, and therefore frequency dividers are utilized.

TRIGGER GENERATOR is used to sharpen the output of the frequency dividers and to privide a sharp, precise initiating pulse.

MANUAL PHASE SHIFTER is useful in rotating the display with respect to any fixed point. This enables locating the pulses on the maximum-velocity portion of the trace. In an oscilloscope which utilizes radial deflection, this circuit might be deleted.

SWEEP AMPLIFIERS are required because most standard-frequency generators do not develop sufficient voltage to deflect the beam of a cathode-ray tube directly.

PHASE SPLITTERS are used in obtaining an elliptical sweep. It is necessary to phase-shift the horizontal deflecting potential 90 degrees with respect to the vertical deflecting potential. The horizontal deflecting potential is usually fed push-pull while the vertical phase is connected single-ended to one vertical deflecting plate.

CATHODE-RAY TUBE is the heart of the equipment. The size of the tube depends on the accuracy required as well as upon economic factors.

VIDEO AMPLIFIER may or may not be required, depending upon the application. It usually is connected single-ended, into one vertical plate of the cathode-ray tube.

VARIABLE WIDTH INTENSIFIER is an essential part of the system. The display to be observed may occur in only a few sweep cycles of each trigger recurrence cycle. If all the sweeps were permitted to appear, very low contrast would result. The intensifier, analogous to the blanker used in television practice, is introduced into the grid or cathode circuit of the cathode-ray tube. It is made variable in duration so that any number of sweep cycles can be viewed at will. The possible ambiguity, which can occur if the sweep length is half of the pulse spacing, is removed by use of the intensifier. Only when the correct sweep length is used can the pulse appear as in Fig. 2C, that is, with an open base line under the pulse.

MANUAL DELAY MULTIVIBRATOR is used in many applications where the phenomenon to be viewed is delayed with respect to the trigger pulse. If this is the case, it may be desirable to delay the intensifier pulse a corresponding amount so that no more sweep cycles are illuminated than are necessary.

PULSE COUNTER is incorporated if it is desirable to know the pulse recurrence frequency.

Variations of Method

It is not necessary to confine oneself to deflection methods to measure pulse characteristics. It is possible to obtain coincidence using intensity modulation as well. In this case a circular sweep is used, but the video pulses are connected to the grid circuit of the cathode ray-tube, while the intensifier pulses are impressed on the cathode. A bright spot will appear on the dimmed trace corresponding to each pulse instead of a deflection of the trace. When the bright spots merge, coincidence is obtained.

There is a limitation to the foregoing method. In those instances where the triggering pulse, which

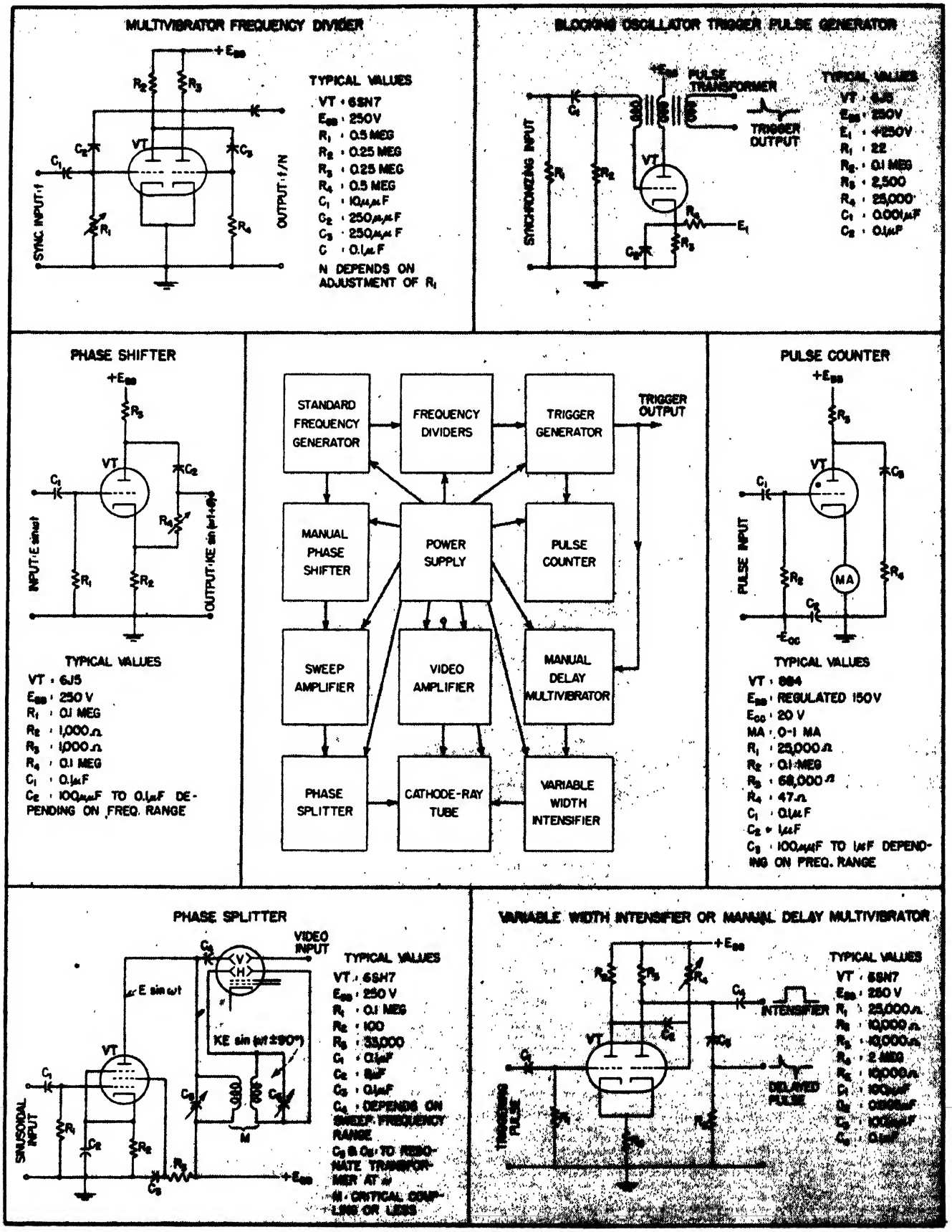

FIG. 7—The block diagram indicates the functioning of the equipment used in measuring pulses. The individual circuits are illustrative of the types of units comprising the system. Blocks for which no circuits are shown are conventional. See the bibliography for additional circuits suitable for each unit in the system

initiates the phenomenon to be measured, is derived from the sweep frequency, the pulse rate will change as the sweep length is altered to obtain coincidence. The pulse rate must be an integral submultiple of the sweep frequency, therefore at high pulse rates it may not be possible to obtain a desired value of pulse repetition frequency. For example, if the sweep frequency is 100 kc, it is not possible to obtain a pulse rate of 10.5 kc. The closest that one could approach the desired rate is 10.0 kc or 11.1 kc.

BIBLIOGRAPHY

Frequency Dividers

(1) Appleton, E. V., Automatic Synchronisation of Triode Oscillators, *Proc. Cambridge Phil. Soc.*, p 231, 1922.
(2) Carnahan, C. W., & Kalmus, K. P., Synchronized Oscillators as Frequency Modulation Receiver Limiters, ELECTRONICS, p 108, Aug. 1944.
(3) Beers, G. L., A Frequency-Dividing Locked-In Oscillator Frequency-Modulation Receiver, *Proc. IRE*, p 730, Dec. 1944.
(4) Koga, I., A New Frequency Transformer or Frequency Changer, *Proc. IRE*, p 669, Aug. 1927.
(5) Groszkowski, J., Frequency Division, *Proc. IRE*, p 1960, Nov. 1930.
(6) Andrew, V. J., Adjustment of the Multivibrator for Frequency Division, *Proc. IRE*, p 1911, Nov. 1931.
(7) Andrew, V. J., A Simplified Frequency Divider, *Proc. IRE*, p 982, July 1933.
(8) Sterky, H., Frequency Multiplication and Division, *Proc. IRE*, p 1153, Sept. 1937.
(9) Miller, R. L., Fractional Frequency Generators Utilizing Regenerative Modulation, *Proc. IRE*, p 446, July 1939.
(10) Builder, G., A Stabilized Frequency Divider, *Proc. IRE*, p 177, Apr. 1941.
(11) Stansel, F. R., A Secondary Frequency Standard Using Regenerative Frequency Dividing Circuits, *Proc. IRE*, p 157, Apr. 1942.
(12) Puckle, O. S., "Time Bases," John Wiley & Sons, Inc., New York, p 129-138, p 184-189, 1943.
(13) Ludman, W. W., Time-Base Calibration, ELECTRONICS, p 117, Sept. 1945.
(14) Shenk, E. R., Multivibrator Applied Theory and Design, ELECTRONICS, p 137, Jan. 1944; p 140, Feb. 1944; p 138, Mar. 1944.

Cathode-Ray Tubes and Circuits

(15) Brainerd, J. G., UHF Techniques, D. Van Nostrand & Co., Inc., New York, p 208-228, 1942.
(16) Puckle, O. S., "Time Bases," John Wiley & Sons, Inc., New York, p 139-160, p 70-80.
(17) Muller, Garman, Droz, "Experimental Electronics," Prentice Hall, p 293-322.
(18) Watson Watt, "Cathode Ray Tubes in Radio Research," H. M. Stationery Office, London.
(19) Richter, W., Beam Blanking Circuit for Oscilloscopes, ELECTRONICS, p 128, 1944.
(20) Atwood, Horace J., & Owen, R. P., Oscilloscope for Pulse Studies, ELECTRONICS, p 110, Dec. 1944.

Pulse Counters

(21) Case, N. P., Precise Method of Measuring Frequencies from Five to Five Hundred Cycles, *Proc. IRE*, p 1566, Sept. 1930.
(22) Hunt, F. V., Direct Reading Frequency Meter, *Review of Scientific Instruments*, p 43, Feb. 1935.
(23) Guarnaschelli, F. & Vecchiacchi, F., Direct-Reading Frequency Meter, *Proc. IRE*, p 659, Apr. 1931.

Video Amplifiers

(24) Wheeler, H. A., Wide Band Amplifiers for Television, *Proc. IRE*, p 429, July 1939.
(25) Terman, F. E., "Radio Engineers' Handbook," McGraw-Hill Book Co., New York, p 413-434.
(26) Zworykin, V. K., & Morton, G. A., "Television: The Electronics of Image Transmission," John Wiley & Sons, Inc., New York, p 394-440.
(27) Seely and Kimball, Analysis and Design of Video Amplifiers, *R.C.A. Review*, p 171-183, Oct. 1937; p 290-308, Jan. 1939.
(28) Everest, F. A., Wide-Band Television Amplifiers, ELECTRONICS, p 16-19, Jan. 1938.

Phase Splitters

(29) Mesny, R., Generator of Polyphase Oscillations, *Proc. IRE*, p 471, Sept. 1925.
(30) Barrett, R. M., N Phase RC Oscillators, *Proc. IRE*, p 541-545.
(31) Terman, F. E., "Radio Engineers' Handbook," McGraw-Hill Book Co., New York, p 154-164.
(32) Hershenberger, W. D., Generating Circular Traces, *Proc. IRE*, p 205, Apr. 1944.

Phase Shifters

(33) Puckle, O. S., "Time Bases," John Wiley & Sons, Inc., New York, p 190-191, 1943.
(34) Muller, Garman, Droz, "Experimental Electronics," Prentice Hall, p 299-305.
(35) Everest, F. A., Phase Shifting up to 350 Degrees, ELECTRONICS, p 46, Nov. 1941.
(36) Terman, F. E., "Radio Engineers' Handbook," McGraw-Hill Book Co., New York, p 949-950.

Trigger Generators

(37) Zworykin, V. K. & Morton, G. A., "Television: The Electronics of Image Transmission," John Wiley & Sons, Inc., New York, p 949-950.
(38) Brainerd, J. G., "UHF Techniques," D. Van Nostrand & Co., New York, p 168-207, 1942.
(39) Puckle, O. S. "Time Bases," John Wiley & Sons, Inc., New York, p 36-62, p 63-69, p 184-189, 1943.
(40) Muller, Garman, Droz, "Experimental Electronics," Prentice Hall, p 287-290.
(51) Phelps, B. E., Dual-Triode Trigger Circuits, ELECTRONICS, p 110, July 1945.
(52) Kiernan, E. F., Microsecond Pulse Generator, ELECTRONICS, p 141, Sept. 1944.

Standard Frequency Generators

(53) Terman, F. E., "Radio Engineers' Handbook," McGraw-Hill Book Co., New York, p 480-516, p 951-957.
(54) Terman, F. E., "Measurements in Radio Engineering," McGraw-Hill Book Co., New York.

Measurement of Velocity of Propagation in Cable

In determining electrical length of vhf lines, it is necessary to know the velocity of propagation in the particular cable that is used. A simple, resonant, substitution measurement made with the instrument described gives that information

By B. KRAMER and FRED STOLTE

ONE OF THE important characteristics of an ultrahigh-frequency transmission line is the velocity at which an electromagnetic wave propagates through it. Not only is knowledge of this velocity essential in determining the lengths of solid dielectric tuning stubs used for impedance matching, but it is also vital

TABLE I—DEFINITION OF SYMBOLS

c	— wave velocity in air, 3×10^{10} cm per sec
f	— frequency, see text preceding each equation
k	— dielectric constant
l	— length of line, in cm
v	— wave velocity in line, in cm per sec
Z_o	— characteristic impedance of line, in ohms
Z_l	— input impedance of line, in ohms
λ	— wavelength in line, in cm

when the line is used as a harness where exact physical lengths must represent exact electrical lengths.

For these reasons and as a method of quality control it is necessary to measure the velocity of propagation of each reel of transmission line. This becomes a large scale operation where, for example, over two million feet of polyethylene insulated transmission line is manufactured in a month.

Velocity of propagation varies inversely as the square root of the dielectric constant of the material separating the inner and outer conductors of a coaxial, transmission line. The relative velocity of propagation is found by the relation $v/c = 1/\sqrt{k}$ where the significance of the letters is given in Table I. Thus it can be seen that any change in the dielectric constant will result in a variation in the velocity of propagation.

The two following expressions from transmission line theory are the basis for the method of measuring the velocity of propagation, which is described in a Naval Research Laboratory report, "Methods of Measuring the Electrical Characteristics of Transmission Lines at Ultra High Frequencies".

The velocity of propagation is equal to the wavelength times the frequency in cycles per second or $v = \lambda f$, and the input impedance of an open-circuited, low-loss line is given by the expression $Z_l = jZ_o \cot (2\pi l/\lambda)$. It can be seen that when l is equal to an odd number of quarter wavelengths the quantity $\cot 2\pi l/\lambda$ is equal to zero and therefore the line will act as if its input end were short circuited.

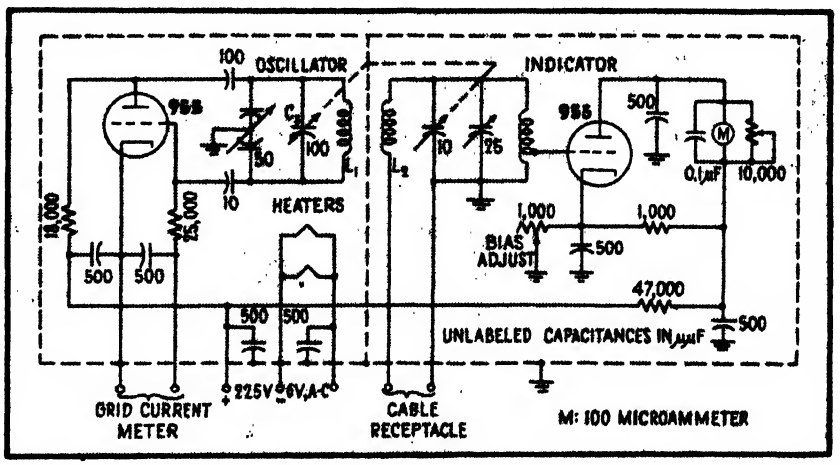

FIG. 2—Complete circuit of the velocity of propagation measuring instrument

Method of Measurement

Referring to Fig. 1, which is a simplified schematic of the velocity-of-propagation meter circuit, one sees that two circuits L_1C_1 and L_2C_2 will resonate at the same frequency if the transmission line acts as a short circuit. This will occur only when the frequency of the generator is such that the electrical length of the transmission line is exactly an odd number of quarter wavelengths.

This condition of zero impedance is approached by first tuning capacitor C_1 so that the whole circuit is in resonance and then short circuiting the input end of the transmission line. If resonance is disturbed the circuit is returned with capacitor C_2. The procedure is repeated until open and short circuiting the transmission line does not disturb the resonant condition of the measuring circuit. By measuring the frequency at which no resonant disturbance occurs and, knowing the physical length of the transmission line, the velocity of propagation can be determined.

The method just outlined is obviously not adaptable to mass production methods which require accurate results, rapidly obtainable by unskilled personnel. The Naval Research Laboratory, recognizing this, developed an instrument for precise measurement which they have called

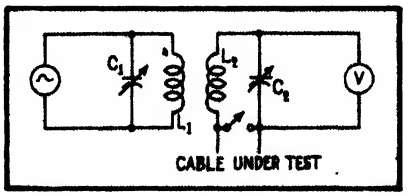

FIG. 1—Frequency is adjusted until cable under test presents a short circuit to the instrument

the VP Meter. In this instrument, which employs the principles outlined, it is only necessary to insert the prepared end of a transmission line of predetermined length and adjust a single dial until a maximum indication is shown on the meter. The relative velocity of propagation is then read directly from the frequency dial or from a calibration table.

The instrument developed and built by Federal's engineers is based on this design but is modified to enable it to be used for a wide variety of sizes of coaxial and dual transmission lines, and to have a finer tuning control.

The sample of solid polyethylene transmission line is cut exactly 150 cm long which represents $\frac{3}{4}$ of a wavelength at approximately 100 megacycles for the velocity of propagation of this particular cable.

The velocity of propagation in percent is calculated as follows when frequency is in mc $v/c = \lambda f \times 10^6/c$. From the above values, $l = \frac{3}{4}\lambda = 150$ cm, thus $\lambda = 200$ cm. Substituting this value of wavelength into the foregoing equation gives $v/c = 200f \times 10^6/3 \times 10^{10} = \frac{2}{3}f$. Thus the

relative velocity is a direct function of the resonant frequency.

The speed of measurement on the VP Meter is due to the fact that the oscillator and indicator circuits are ganged together and always tuned to the same frequency when the transmission line receptacle is short circuited. As before, this condition will occur when the frequency is such that the cable is exactly $\frac{3}{4}\lambda$ and is indicated by a maximum reading on the vacuum-tube voltmeter which is a sensitive, resonance indicator.

Figure 2 is a schematic circuit of the VP Meter. On the lefthand side is the oscillator circuit which can be tuned from 95 to 105 megacycles by means of capacitor C_3. The inductor L_1 is very loosely coupled through an electrostatic shield to inductor L_2 in the indicator circuit. Padding capacitors are provided in each circuit to obtain close tracking throughout the frequency range.

To insure the accuracy of results, it is only necessary to check the frequency calibration of the dial and the tracking between the two circuits. Frequency calibration is easily checked against a calibrated frequency standard. Tracking is checked by merely inserting a copper shorting rod in the line receptacle and noting the change in meter deflection over the frequency range. A two-percent change in meter deflection would still represent negligible error in measurement. No change in meter deflection indicates perfect tracking.

Three calibrated, test samples are used for frequently checking the calibration of the instrument. The samples consist of solid dielectric lines that have been pulled into a tight fitting copper tube and sealed, the tube serving as the outer conductor. The velocities of propagation in these samples have been adjusted so as to bracket the range of the instrument.

The time required to measure the relative velocity of a prepared cable sample with this instrument is only about ten seconds. The total error due to working limitations is estimated to be less than two percent. The standard deviation in the measurement of a large number of samples of a single type of transmission line does not exceed 0.08 percent, the major part of which is due to variations in the samples themselves.

High-Resistance D-C Voltmeter

Design of a reflex vtvm for measuring voltages of sources having an internal resistance as high as 1,000 megohms. The maximum error on any scale is less than eight percent and, for the upper sixty percent of scale, less than five percent. At 100 megohms internal resistance, the errors are five and two percent respectively

By D. L. WAIDELICH

A d-c vacuum-tube voltmeter with a very high input resistance was developed and found to be quite useful in general electronics laboratory work. The resulting instrument has a linear scale substantially independent of tube characteristics; it possesses over-voltage protection; it has a very high input impedance; and it is particularly unique in that an electrical zero adjustment is not used.

The circuit is that of a reflex voltmeter[1,2] and has found application lately in a commercial vacuum-tube voltmeter[3]. The voltmeter to be described differs from this one mainly in that over-voltage protection is furnished and no electrical zero adjustment is used.

The abbreviated circuit of the voltmeter is shown in Fig. 1A. The voltage to be measured is E, and the negative feedback introduced by the resistance R makes the voltmeter linear over a large range of voltages. The simplified equivalent circuit of the voltmeter is given in Fig. 1B if the assumption of linear tube characteristics is made. By solving the circuit equations, the current through the meter is

$$i_p = \frac{E + (1/\mu)\, E_b}{R\,(1 + 1/\mu) + 1/g_m} \qquad (1)$$

where $g_m = \mu/r_p$.

If the tube used has both a high amplification factor μ and a high mutual conductance g_m, the current i_p becomes

$$i_p = E/R \qquad (2)$$

This indicates that for large values of applied voltage E, the meter current i_p is substantially independent of the characteristics of the tube and of the plate voltage supply and depends only on cathode resistance R. This property of the circuit will largely eliminate the problem of tube replacements, because no recalibration will be necessary when the tube is replaced.

Residual Current

When applied voltage E is zero,

TABLE I—EXPERIMENTAL RANGE DESIGN

Voltage Range	Resistor R, Megohms	Plate Voltage	Residual Current, μa	Saturation Current, μa	Open-Circuit Current, μa
0–50	0.5	162	5.7	285	135
0–100	1.0	278	4.3	275	195
0–250	2.5	370	2.3	155	125

the meter current i_p becomes

$$i_{pr} = \frac{(1/\mu)\, E_b}{R\,(1 + 1/\mu) + 1/g_m} \qquad (3)$$

which might be called the residual current. In most cases $R \gg 1/g_m$ and $\mu \gg 1$, and hence

$$i_{pr} = \frac{(1/\mu)\, E_b}{R} \qquad (4)$$

This residual courrent can be balanced out by means of a circuit involving a zero adjustment, or the current can be kept as low as possible by making the plate voltage E_b small and making the amplification factor large. This latter method is the one adopted for this voltmeter in that it completely eliminates any zero adjustment, but it does mean that a small residual current is always present with the input terminals of the voltmeter shorted. The current through the meter given by Eq. 1 will be proportional to applied voltage E except for the residual current of Eq. 3.

If the residual current is made small, the maximum error should occur at the lower end of the meter scale, and the error should be smallest at the top end. To make R large means that the current meter used must have a full scale current that is as low as possible. A compromise in the interests of ruggedness was a panel-type microammeter.

Saturation for Safety

The voltmeter circuit will start to saturate when the grid voltage e_g is zero. When the circuit equations are solved under these conditions, it is found that the applied voltage E is

$$E = \frac{R}{R + r_p} E_b \qquad (5)$$

and, because $r_p \ll R$,

$$E = E_b \qquad (6)$$

The voltmeter thus starts to saturate when the applied voltage becomes equal to the plate voltage of the tube.

Grid current actually flows before the point $e_g = 0$ is reached, and hence to prevent the grid current from making the voltmeter non-linear and from reducing the input impedance, the plate voltage E_b is made somewhat larger than the full applied voltage E. When E is made larger than E_b, the voltmeter starts to draw grid current, saturation sets in, and the meter current stops increasing. Hence, this property of saturation can be used to prevent meter overloads.

In all cases, E_b was adjusted so that the meter current with overloads did not become more than three times the full-scale current. The meters withstand this amount of overload current without injury. The full scale deflection of the meter used should occur when

$$E = E_b \qquad (7)$$

If the grid current of the tube is neglected, the input resistance R_i of the circuit can be calculated from Fig. 2A in which R_c is the paralleled resistance of the measuring cable of the tube and tube socket to ground, and of any resistance that may be added for reasons to be given later. The resistance between the grid and the cathode terminals of the tube and the tube socket is shown as R_{gk}, while that between grid and plate is R_{gp}. Both the resistances of the cable and of the tube are usually several thousand megohms.

Varying Input Resistance

The solution of the circuit equations along with the use of the approximation $V_g \ll R$ shows that the input impedance of the voltmeter appears to be composed of three resistances in parallel as given in Fig. 2B. Two of the resistances are negative, while the third is positive. Because the positive resistance R_c is usually smaller than the two negative resistances in parallel, the input resistance R_i is positive and slightly greater than R_c. It should be noticed that R_i varies with the voltage E to be measured, and increases in magnitude as E decreases. Grid current flow which becomes large as E approaches E_b will reduce the input resistance R_i. Positive ion flow to the grid also becomes important as E approaches E_b.

If the input terminals of the voltmeter are open-circuited, no current can flow into the meter, and an equilibrium point must be reached such

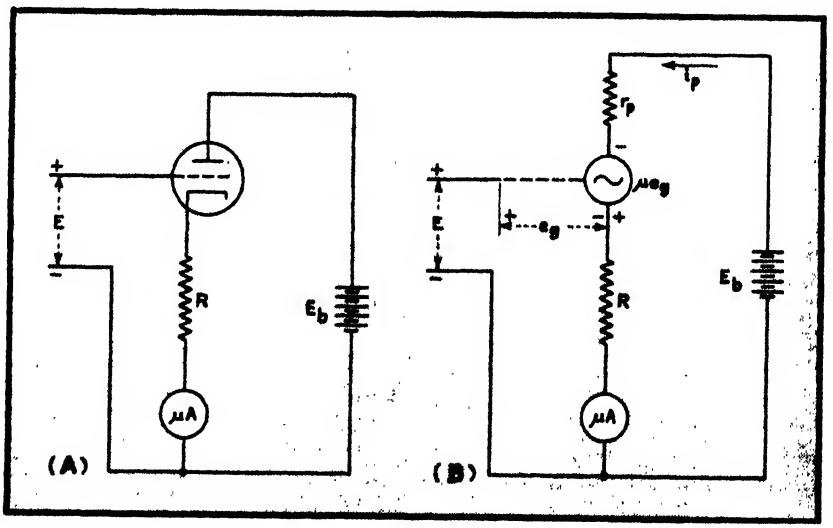

FIG. 1—(A) Basic circuit diagram of the d-c voltmeter. (B) Basic equivalent circuit arranged for analysis

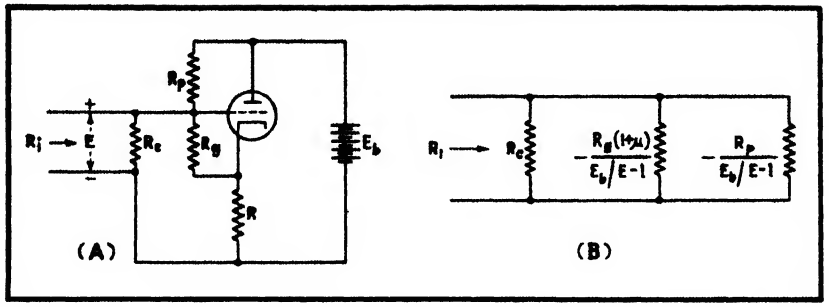

FIG. 2—(A) Circuit for calculation of the input resistance of the d-c voltmeter. (B) Equivalent input circuit composed of two negative resistances and one positive resistance

that the negative resistances must be equal to the positive resistance. Neglecting grid current, this equilibrium point occurs when

$$\frac{E}{E_b} = \frac{\dfrac{1}{\dfrac{1}{R_g(1+\mu)} + \dfrac{1}{R_p}}}{\dfrac{1}{R_c} + \dfrac{1}{\dfrac{1}{R_g(1+\mu)} + \dfrac{1}{R_p}}} \qquad (8)$$

Equilibrium will occur when E approaches E_b if R_c is very large, and as E approaches zero if R_c is very small. This indicates that on open-circuit the meter may indicate full scale or even more, but the pointer will not go past the saturation point in any case. The open-circuit reading can be reduced by decreasing R_c, but this will also reduce the input resistance of the voltmeter. Equation 8 also indicates that as the internal resistance of the voltage to be measured approaches the parallel resistance of R_c, $R_g(1+\mu)$, and R_p, the accuracy of measurement will become poor.

An experimental circuit was constructed using a 6F5G tube because this had a high amplification factor and a fairly high mutual conductance. A 0-100 microampere, d-c instrument was chosen to indicate the applied voltage, and three scales of 50, 100, and 250 volts were decided upon. Table I indicates the design and experimental results for each of these ranges.

The cathode resistor R is determined by dividing the range in volts by the full-scale current in amperes of the meter used. The plate voltage used must be large enough so that no appreciable grid current flows over the useful range of the meter but small enough so that neither the residual current, nor the saturation current, is too large.

The open-circuit current was found always to be somewhat smaller than the saturation current except for the 50-volt range, where it is much smaller than the saturation current. The reason for this is that grid current flows in larger quantities just above full scale, and this has the effect of reducing R_c.

A twenty-volt full-scale was found successful, but was not used. Any range below this could not be used, because the conditions for linearity, residual current, and saturation current could not be met adequately. Ranges above 250 volts are very successful and are limited only by what plate voltages the tube must withstand.

It was found that for voltage sources whose internal resistance was 100 megohms or below, the maximum error on any scale was less than 5 percent, while for the upper sixty percent of the scale the error was less than two percent. When the voltage sources had a resistance of 1000 megohms, the errors became eight and five percent respectively.

To keep the open-circuit reading of the voltmeter below full-scale, a 10,000-megohm resistor from the grid of the 6F5G tube to ground was successful.

Any alternating voltage superimposed on the direct voltage to be measured is kept out of the meter by the use of a simple low-pass filter consisting of a high resistance in the probe and the shunt capacitance of the cable to the voltmeter. An additional mica capacitor may be necessary in some cases.

The circuit diagram of the voltmeter constructed is shown in Fig. 3. No voltage regulator is needed in the power supply because the reading of the voltmeter is not affected by small changes in the plate voltage. Precision resistors are used in the cathode circuit in series with the microammeter, because on these resistors to a large extent depends the accuracy of the instrument. The heater of the 6F5G tube was left floating. Changing tubes had no effect on the calibration.

In addition to the advantage of high input resistance, the vacuum-tube voltmeter described can have its tubes changed without affecting calibration and poor regulation of supply voltages does not affect operation. It was found to be simple to build and to operate and also features a linear scale and over-voltage protection.

Its disadvantages are that it measures positive direct voltages only; is

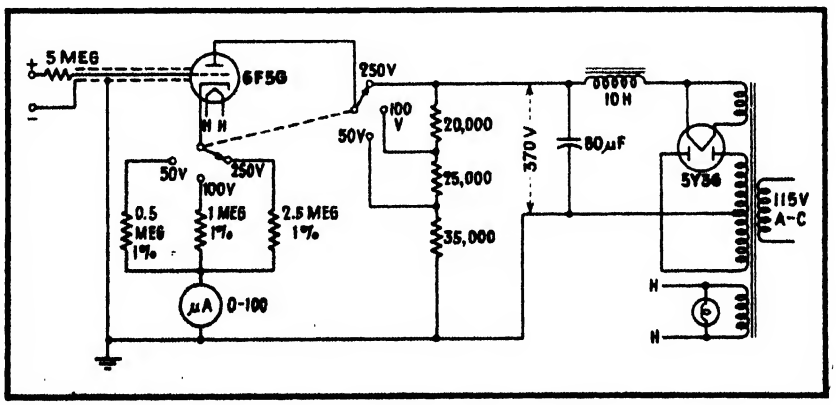

FIG. 3—Complete circuit of the high input resistance d-c voltmeter

not suitable for use on low voltages; has a residual current indication; and indicates a reading with the input open-circuited.

REFERENCES

(1) Medlam, W. B., and Oschwald, U. A., The Thermionic Voltmeter, *Wireless Engineer*, p 664–673, 3, Nov. 1926.

(2) Medlam, W. B., and Oschwald, U. A., Further Notes on the Reflex Voltmeter, *Wireless Engineer*, p 56–60, 5, Feb. 1928.

(3) Bousquet, A. G., A D-C Vacuum-Tube Voltmeter, *General Radio Experimenter*, p 1–4, 19, Dec. 1944.

Measuring Mutual Inductance and Capacitance

By A. W. SIMON

MOST STANDARD METHODS OF measuring mutual inductance become inaccurate when applied to the measurement of mutual inductances corresponding to small coefficients of coupling, such as those commonly encountered in radio circuits. This is true in particular of the widely used method of determining mutual inductance in terms of self-inductance, by connecting the two windings series-aiding and series-opposing.

For example, to determine mutual inductance accurately to 1 percent by this method, for a case where the coefficient of coupling is 5 percent, the self-inductance has to be measured with an accuracy of 0.5 percent, which is beyond the accuracy of ordinary inductometers and bridges. It is readily seen that an error of 0.5 percent in the latter, under the same conditions, could lead to an error of 10 percent in the mutual inductance.

The method of simple opposition devised by Felici is not subject to this difficulty and enables the mutual inductance to be determined with an accuracy equal to that of the inductometer used. Furthermore, if an inductometer of the Brooks type is employed, the range of the Felici method can be extended in the direction of lower inductances by incorporating a switch, by means of which one winding of the inductometer can be reversed; the unknown inductance is then equal to one-fourth of the difference of the inductometer readings for the two positions of the switch.

Unfortunately, if the two coils to be measured are enclosed in a shield can, the simple Felici arrangement fails to give a perfect null. This is due to the fact that the shield introduces an out-of-phase component, which cannot be balanced out by mutual inductance alone. In this case, it is necessary to resort to Campbell's modification of the Felici circuit, in which this component is balanced out by a portion of the primary voltage introduced into the secondary by means of a slide wire potentiometer. With an inductometer of the Brooks type, this arrangement also can be extended in the direction of lower mutual inductances by incorporating a reversing switch and taking one-fourth of the difference of the corresponding readings.

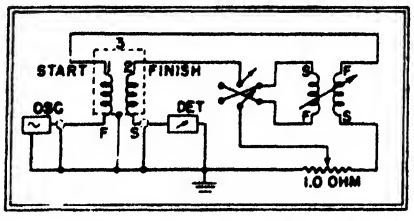

Fig. 1—Useful circuit for measuring mutual inductance between coils having small coefficient of coupling

Improved Circuit

A practical circuit is given in Fig. 1 for the measurement of mutual inductance between coils, both unenclosed and enclosed in shield cans. This circuit is based on the Campbell modification of the Felici circuit and employs an inductometer of the Brooks (or other ±2M) type and reversing switch. It is particularly suitable for the accurate measurement of mutual inductance between coils with small coefficients of coupling such as are frequently encountered in radio work, and enables such a measurement to be carried out with an accuracy equal to that of the inductometer used. It can also be used to set coils very quickly and accurately to a predetermined mutual inductance or coefficient of coupling—a feat which is only difficultly accomplished by means of a bridge. The circuit is particularly recommended to the radio industry for use in connection with the determination of the coefficient of coupling of i-f transformers, instead of the now widely used but inaccurate method employing a self-inductance bridge.

Operation

To make a measurement of mutual inductance, the inductometer is read for the two positions of the reversing switch. The unknown inductance is then equal to one-fourth of the difference between the corresponding self-inductance readings. To get a perfect null in both positions, the manner of connection of the unknown must be carefully preserved. If a perfect null is obtained for only one throw of the switch, the connections of one coil of the unknown should be reversed. For the measurement of coils unenclosed in shield cans, the slider is set to the zero position.

Analysis of the circuit of Fig. 1, as well as that employing a self-inductance bridge, reveals that for coils enclosed in shield cans, the "mutual

inductance" actually measured is the quantity

$$M_{12} - \frac{M_{13}M_{23}}{L_3}\frac{Q_3^2}{(Q_3^2+1)}$$

where M_{12} is the mutual inductance between the coils 1 and 2, M_{13} and M_{23} are the mutual inductances between the respective coils and the shields, and L_3 and Q_3 are the self inductance and Q respectively of the shield itself.

For setting the coupling between two coils to a definite value k, the self-inductance L_1 and L_2 of the coils is first measured on a bridge and the required mutual inductance M calculated from the equation

$$M = k\sqrt{L_1L_2}$$

The reading L of the inductometer for the neutral position of the inductometer coils is then determined, and the inductometer set to a self-inductance reading given by

$$L_a = L + 2M$$

One of the coils is then moved until the null point is reached. The setting can be checked by throwing the reversing switch and observing whether a null point occurs at the reading L_b given by

$$L_b = L - 2M$$

The given procedure is very useful in making up standards for i-f transformers and other units.

Mutual Capacitance

For control of the capacitive coupling of coils enclosed in shield cans, particularly i-f transformers, a measurement of the "mutual capacitance" or intercoil capacitance (more correctly, the coefficient of electrostatic induction between the coils) becomes desirable. This measurement can be carried out as follows (Fig. 2):

(A) Capacitance $C_{12,13}$ of coils 1 and 2 connected together with respect to the shield (grounded) is measured.

(B) Capacitance C_{11} of coil 1 with respect to the shield and coil 2 (both grounded) is measured.

(C) Capacitance C_{22} of coil 2 with respect to the shield and coil 1 (both grounded) is measured.

The "mutual capacitance" or coefficient of electrostatic induction C_{12} of coil 1 with respect to coil 2 is then given by

$$C_{12} = 0.5\,(C_{12,13} - C_{11} - C_{22})$$

In accordance with electrostatic theory, the quantity C_{12} is negative.

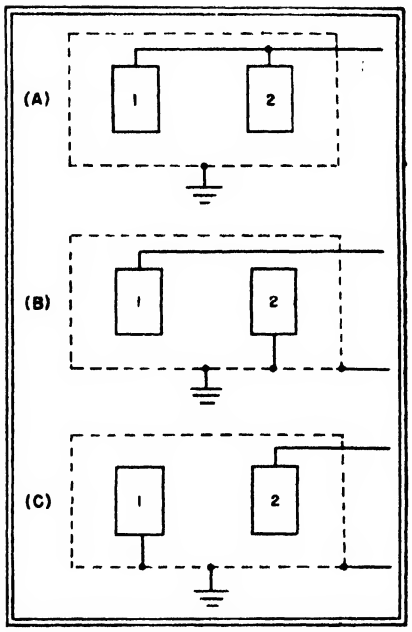

Fig. 2—Three steps for determining mutual capacitance between two coils

Carrier-Frequency Voltmeter

Strength of signals received over power lines, telephone lines and cables in the range between 20 and 500 kc is directly indicated in db, using a fixed-gain double-superheterodyne receiver. A built-in calibration oscillator is provided

By PAUL BYRNE

THE carrier-frequency voltmeter to be described was developed primarily for making measurements on power lines, telephone lines and cables in the region between 20 and 500 kc. The specifications to which the instrument performs are based on the requirements of the Pacific Gas and Electric Company. Special features were suggested by engineers of the Bell Telephone System.

The instrument is essentially a fixed-gain double-superheterodyne radio receiver covering the required frequency range. The d-c output of the final detector operates a microammeter calibrated in db. A variable attenuator, connected between the input terminals and the first grid, provides a wide range of measurable voltages. An injection oscillator, in effect a signal generator, is included to facilitate calibration.

Circuit Details

Referring to the block diagram of Fig. 1 and the complete schematic of Fig. 2, the input filter is of the bandpass variety. The attenuator consists of a wire-wound section and a carbon-resistor section, and operates in 10-db steps.

The variable-frequency oscillator beats with incoming signals in the carrier-frequency range and produces a 1,500-kc signal at the input of an adjustable-gain i-f amplifier. Temperature stabilization of the vfo is accomplished by means of a variable capacitor consisting of two fixed plates about ¼ inch by 1½

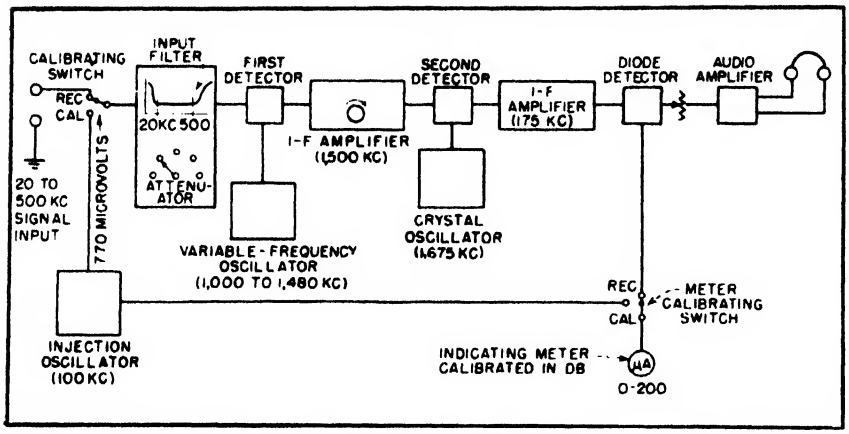

FIG. 1—Functional block diagram

inches in size and an intermediate movable plate operated by a 2½-turn spiral of thermostatic bimetal. The output of the 1,500-kc amplifier combines in a second detector with that of a 1,675-kc crystal oscillator to produce a 175-kc signal which is fed to a fixed-gain i-f amplifier. Output of the 175-kc amplifier goes to a third detector. The audio output of this detector drives an a-f amplifier operating a headset used for monitoring. The d-c output of the third detector operates the indicating meter, which is a 0-200 microammeter.

The injection oscillator delivers 0.77 volt (0 db) to the input circuit of the instrument, operating at 100 kc. A switch permits the output of the injection-oscillator monitoring diode to be read on the indicating meter for calibration purposes. Adequate signal input is provided so frequency calibration of harmonic points above 100 kc on the dial can be checked from the injection oscillator.

The carrier-frequency voltmeter will handle from 77 microvolts to 77 volts at the input, or 80 db below to 40 db above zero level (1 milliwatt into 600 ohms). Selectivity characteristics are approximately 6 db down at 1 kc off resonance, 18 db down at 3 kc off resonance and 40 db down at 7 kc off resonance.

Input impedance is 10,000 ohms in the rejection band, and approximately 20,000 ohms in the pass band.

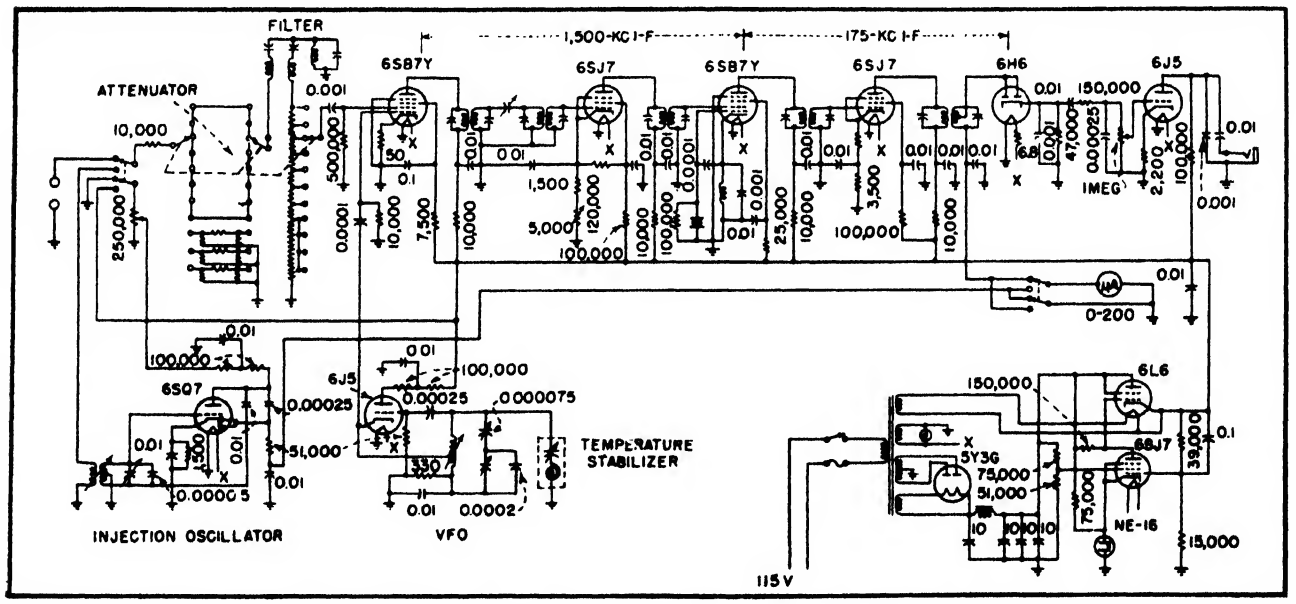

FIG. 2—Complete circuit diagram of the instrument

MICROWAVES

Engineering Approach to Waveguides

Practical considerations in the choice and fabrication of wave guides are considered from the engineering viewpoint. The advantages of hollow, rectangular guides are described by comparison with coaxial cable characteristics at super high frequencies

By THEODORE MORENO

UNTIL A FEW YEARS AGO, wave guides were a type of transmission line having considerable theoretical interest but little practical utility. The basic physical principles governing their operation were developed and published before the war,[1, 2, 3, 4] but widespread use during the last few years has reduced their seemingly complex behavior to a set of engineering principles, sufficient for most microwave transmissions.

Choice of Conductor

When a transmission line is to be chosen for microwave frequencies, the choice must usually be made between rectangular wave guide and coaxial line. The coaxial line may be either rigid line or flexible cable, but both are operated with the principal mode (*TEM*) carrying energy, along with the first of the higher order modes ($TE_{1,1}$) that will be able to carry energy as the wavelength is reduced. The cutoff wavelength of this higher mode is given to a good approximation by $\lambda_c = 2\pi\sqrt{\epsilon}(b + a)/2$, where a is the outside diameter of the inner conductor and b the inside diameter of the outer conductor. A coaxial line is normally operated below cutoff for this higher mode. For a given operating frequency, a maximum limit is therefore set on the transverse dimensions of the line.

A practical wave guide is usually rectangular in cross section and is operated with the first of the higher order modes carrying energy. This is the $TE_{1,0}$ mode, also known as the dominant mode in rectangular wave guide. It is illustrated in Fig. 1, along with some of the possible higher modes. To carry energy in the dominant mode, a rectangular wave guide must exceed certain minimum dimensions, but to avoid the higher modes, must not exceed certain maximum dimensions.

Circular wave guides are usually avoided because there is a very narrow frequency range over which any given size of guide is above cutoff for the dominant ($TE_{1,1}$) mode but will not carry energy in any of the other higher modes. Furthermore, any ellipticity or obstacle in the wave guide is likely to elliptically polarize the traveling wave, making it difficult to handle at the output.

Sometimes the $TM_{0,1}$ mode in circular wave guides is used because it combines circular symmetry with high power-carrying capacity, but care must be taken to avoid the lower modes, especially when the guide is long and resonances are likely to be encountered. Other odd shapes of wave guide offer possibilities of

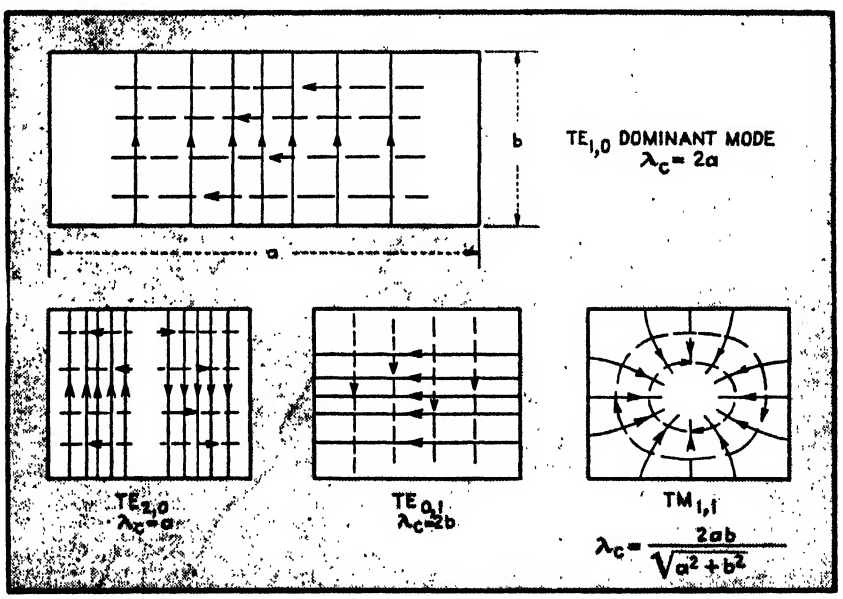

FIG. 1—The distribution of the transverse electric (solid) and transverse magnetic (dashed) waves in wave guides of various rectangular cross sections. The geometry of the guide is usually such that only the dominant mode ($TE_{1,0}$) is above cutoff. A few of the higher modes are shown

smaller size or greater bandwidth, but to the present time rectangular guides have been most widely used, and the subsequent discussion will be confined to guides of this type.

Low Attenuation in Guides

One of the principal advantages offered by rectangular wave guides is their low attenuation. The losses in a rigid, air-dielectric coaxial line will usually be at least half again as great as the losses in a wave guide, and the losses in standard coaxial lines are usually about three times as great as in standard wave guides operating at the same frequency. A flexible cable with polyethylene dielectric has even greater losses, usually about twenty times the loss in a wave guide.

TABLE I—Comparison of Transmission Lines for 5,000 mc

Type of line	Rectangular wave guide	Rigid Coaxial line	Flexible cable
Army-Navy type no.	RG-49/U	RG-76/U	RG-9/U
outside dimensions	2 × 1 in.	5/8 in. diam	0.420 in. diam
conductor material	brass	brass	inner conductor 7/21 AWG silvered copper outer conductor double braid, inner silvered copper, outer copper
surface finish	silver	silver	silver
dielectric	air	air	polyethylene
weight lb per ft	1.40	0.292	0.150
attenuation db per ft	0.011	0.035	0.23
recommended power rating	1.2 megawatts	0.3 megawatts	4,000 volts rms max 66 watts continuous

High-Power Capacity

An additional advantage offered by wave guides is their high power-carrying capacity. The power-carrying capacity of a wave guide will be from three to ten times as great as in a standard coaxial line, if the limit is set by the dielectric strength of the insulator. A large flexible cable will be able to handle peak powers that are comparable to those handled by an air-dielectric coaxial line, but the average power is greatly limited by the heating of the inner conductor, and will be several thousand times less than the capacity of a wave guide.

A still further advantage of wave guides is their mechanical simplicity. This arises chiefly from the fact that with a coaxial line it is necessary to support the center conductor. This can be a severe mechanical problem if the support must at the same time have good mechanical strength and not interfere with the electrical properties of the line.

The advantages that are offered by a wave guide may be offset by its size. For a given operating frequency, there is a minimum limit set on the dimensions of a wave guide, while no such restriction applies to coaxial lines. At frequencies much lower than 3,000 mc, the size and weight of wave guides become prohibitively large for all but certain limited applications. At higher frequencies wave guides lose their awkwardness, and above 10,000 mc, their size becomes an advantage. Methods of fabrication approaching jewelers' techniques are needed for coaxial line structures operating under similar conditions.

Disadvantage of Limited Bandwidth

Another great disadvantage of wave guides is their restricted bandwidth. A given wave guide is limited by theoretical considerations to a 2:1 frequency range, if both cutoff and higher modes are to be avoided. The practical necessity of avoiding the high attenuation region near cutoff still further lowers this figure, and in practice it is necessary to limit a wave guide of fixed dimensions to about a 1.5:1 frequency range. A coaxial line, on the other hand, can be operated, in theory at least, at any frequency for which the higher modes are below cutoff. But this range is usually restricted because supports must be provided for the center conductor. A flexible cable, in which the center conductor is continuously supported by the flexible dielectric, does not encounter the same limitation, but when air dielectric is used, dielectric beads or stub lines must be used for support. A broad-band stub support is usually not operable over much greater than a 1.5:1 frequency band, and paired or multiple bead supports are even less satisfactory at microwave frequencies. Undercut dielectric beads have been designed which are satisfactory at all frequencies below several thousand megacycles, but they offer mechanical difficulties in long lines.

Cables, by their flexibility, have advantages over wave guides, but to offset this, a variety of designs of wave guide have been developed which are usually flexible enough for most practical applications, and have attenuation that is not greatly in excess of the rigid guides.

For purposes of comparison, the properties of a typical rectangular wave guide, rigid coaxial line, and flexible coaxial line at a frequency of 5,000 mc (6 cm wavelength) are summarized in Table I.

When a rectangular wave guide is chosen for a particular frequency or band of frequencies, the larger inside dimension of the guide must be greater than a half free-space wavelength for the lowest frequency signal to be passed, if the dominant mode of transmission ($TE_{1,0}$) is to be above cutoff. But that dimension must not exceed a full wavelength or one of the higher modes ($TE_{2,0}$) will also be above cutoff.

Dimensions vs Application

The smaller of the inside dimensions of the guide should be kept below a half wavelength or another

mode of transmission ($TE_{0,1}$) will be above cutoff. There is no minimum limit on this dimension of the guide, for the cutoff wavelength of the $TE_{1,1}$ mode is independent of the smaller dimension of the guide. It is desirable, however, to make this dimension very nearly a half wavelength, as the attenuation will then be kept at a minimum and the power-carrying capacity maximized. Attenuation will be an inverse function of the height of the guide, and power-carrying capacity a direct function.

The wall thickness of the guide is determined solely by considerations of strength, weight, and ease of fabrication. Wall thicknesses in common use vary from 0.040 in. for the smallest guides to 0.081 in. for the largest.

Standard Sizes In Use

A number of sizes of wave guide have been picked as standard guides by the Army-Navy R-f Cable Coordinating Committee. The frequency ranges over which these guides can be used are shown in Fig. 2, along with the more recent allocations of the microwave spectrum by the Federal Communications Commission. Although the standard guide sizes overlap and cover the spectrum continuously, bands which have been allocated are not completely covered by any one size of guide. This is unfortunate in that more sizes of wave guide will have to be brought into widespread use.

Wave Guide Materials

The material most commonly used for wave guides is cold-drawn rectangular brass tubing. Different alloys have been used, but a red brass alloy of about 90 percent copper and 10 percent zinc is usually preferred for reasons of strength and corrosion resistance. Brass has been found suitable, for its mechanical strength is combined with good machineability and ease of fabrication, and its electrical properties, though generally satisfactory, can be readily improved by electroplating. The tubing is not free of stresses, and unless annealed may warp seriously when slotted.

Rectangular brass tubing is available in a wide variety of sizes and dimensions from a number of manufacturers. But most of this tubing has heretofore been used primarily for decorative purposes, and is held to no tolerances. The dimensions are likely to vary widely from sample to sample, and the tubing will be unsatisfactory for any applications that are at all critical. Most of the standard wave guides listed in Fig. 2 are generally available at manufacturing tolerances that are sufficiently close for most microwave applications. These close-tolerance guides are generally called radar tubing because they were first developed for radar applications. They are available for only slightly greater cost, and should be used for microwave work whenever possible. The tolerances vary with the particular dimensions and with the guide sizes, but the dimensions are generally held to within 0.005 in. or less.

Aluminum tubing has been rather widely used because its weight is less than a third that of the corresponding brass tubing. But this lightness is gained at a sacrifice in ease of fabrication. Methods of assembly such as dip brazing which assure a strong mechanical bond are carried out at such high temperatures that the wave guides will usually warp. Various methods of joining pieces at lower temperatures are also used. For example, an anodized aluminum guide may be copper

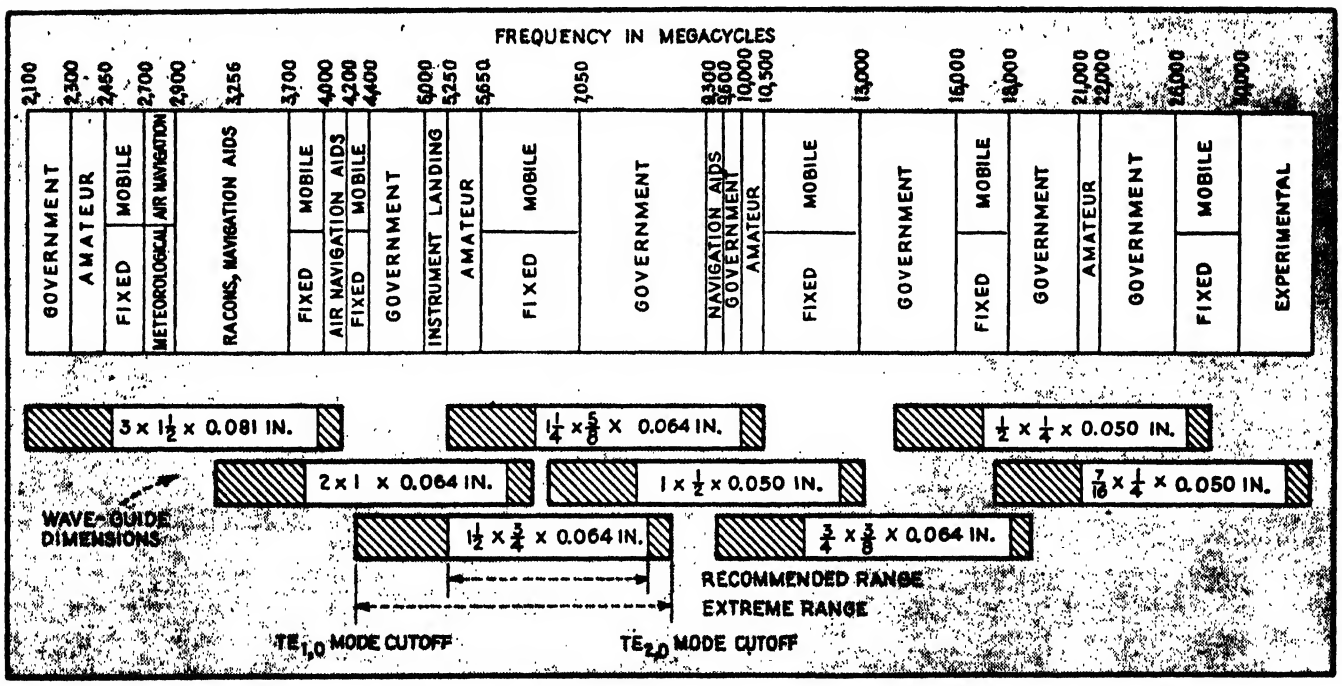

FIG. 2—Federal Communications Commission allocations in the microwave region and standard wave guides suitable for use at various frequencies. Dimensions on the wave guides indicate outside cross section and wall thickness

plated and soft soldered. But these low-temperature techniques are in general more difficult and less satisfactory than the corresponding techniques for brass guide.

Solid silver guide has been used at very high frequencies for applications where low attenuation is important, but its cost is generally prohibitive. Other types of construction have been proposed, such as plated plastic tubing, but these have not been extensively used or tested.

Metal Finishes

The electrical properties of a brass or aluminum wave guide may be considerably improved by the type of finish applied which may also greatly improve the corrosion resistance of the guide. The skin depth in most metals is so small at microwave frequencies that if one metal is plated on another to a depth of less than a thousandth of an inch, essentially all of the conduction current in the metal will flow in the plated surface. The guide losses will then depend upon the plated surface metal rather than the base metal. For this reason a silver plate is often used, because silver's exceptionally high conductivity is coupled with good resistance to corrosion. But both the electrical and mechanical properties depend to a considerable extent upon the type and quality of the silver plate, and the type of plate that gives the best electrical characteristics is not necessarily the most satisfactory from the standpoint of appearance and resistance to corrosion.

Plating Techniques

It has been found that the resistance to corrosion of a silver-plated surface is greatly improved and the electrical properties essentially unchanged if the silver is in turn coated with a flash plate of palladium or rhodium. These rare metals have poorer conductivity than silver, but when they are applied in an exceedingly thin plate, much less than the skin depth, essentially all of the conduction current flows in the silver underneath, and the losses are correspondingly low. The thin flash plate greatly improves the ability of the wave guide to withstand salt spray without corroding.

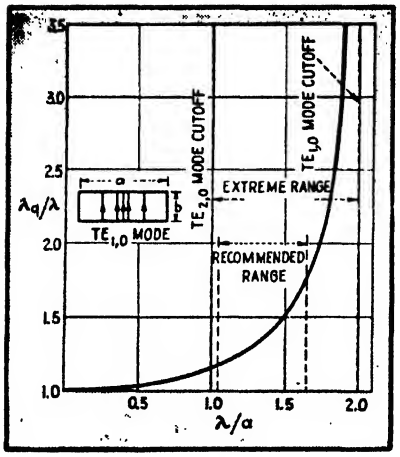

FIG. 3—Wavelength characteristics of a rectangular wave guide operating in the dominant mode. The ratio of wavelength in the guide to wavelength in space (ordinate) is plotted against the ratio of wavelength to the wider dimension (abscissa)

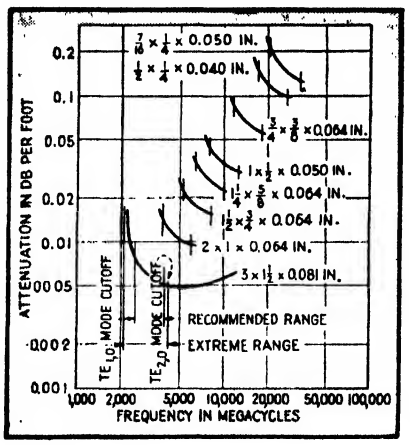

FIG. 4—Theoretical attenuation of copper wave guides over their operating frequency range for the dominant mode. Dimensions are outside measurements and wall thickness. Curves show the extreme ranges possible with each type of guide

A gold plate has also been extensively used. Although gold has somewhat poorer conductivity than silver, the losses in gold surfaces are very little different from the losses in silver-plated surfaces, and the corrosion resistance of gold is very good, but its cost is relatively high.

In general, the effective resistivity of a plated surface is somewhat higher than the low-frequency resistivity of the metal, and the losses will therefore be somewhat greater than predicted by theory. This effective resistivity will vary greatly with the plating solution and rate of deposition, as well as with the type of base metal and its surface finish. The losses are also affected by ageing, tarnishing, and corrosion, and for these reasons, exceptions may be drawn to almost any general statement about losses in plated surfaces. But the following remarks are usually applicable.

Losses in Plated Surfaces

The difference between theoretical and measured losses will usually increase with increasing frequency. But at even the highest frequencies, the losses in a plated surface of high quality will usually be less than half again as great as predicted by theory, and will seldom exceed twice the theoretical value. If the plating is of poor quality or has corroded, the losses may be much greater. To get minimum losses in a plated surface, the thickness of plating should be many times the skin depth. For example, at 9,000 mc, 0.5 mils minimum thickness of silver plate is recommended—this is more than one hundred times the theoretical skin depth.

If the surface of a wave guide is coated with a thin, protective layer of insulating material, the conduction current in the surface will flow in the metal under this protective layer, and the attenuation will not be greatly affected. For example, if aluminum wave guide is anodized, the losses will not be greatly changed, and may even be less than in the unanodized guide which has a very thin layer of nonconducting aluminum oxide on the surface. And the inner surface of any wave guide, brass or aluminum, can be coated with a protecting lacquer which will not affect the attenuation but will greatly improve the corrosion resistance.

The weights of the various standard wave guides of Fig. 2 are listed in Table II. The weights given are for brass guide, aluminum will weigh about 31 percent as much as brass.

Because a wave guide does not operate in the principal (*TEM*)

mode of transmission, the wavelength in the guide λ_g will in general be greater than the wavelength in free space λ. The wavelength for any mode in any air-dielectric wave guide is given by $\lambda_g = \lambda/\sqrt{1-(\lambda/\lambda_c)^2}$. For rectangular guide the cutoff wavelength of the dominant mode is $\lambda_c = 2a$, when a is the larger inside dimension. For this mode, the ratio λ_g/λ is plotted as a function of the ratio λ/a in Fig. 3.

The fact that the wavelength in the wave guide is greater than the wavelength in air may lead to the erroneous conclusion that the electromagnetic energy travels through the wave guide at a rate exceeding the speed of light. Actually, the phase velocity v_p is greater than the speed of light c by the factor λ_g/λ, but the energy travels through the guide at the group velocity, v_g, given by $v_g = c^2/v_p$.

The attenuation of the various standard wave guides of Fig. 2 is plotted as a function of frequency in Fig. 4. It is interesting to note that although the losses are greater in the higher frequency wave guides, the losses in any particular wave guide will actually decrease with increasing frequency over the normal frequency range. The values given in Fig. 4 are all theoretical values for copper wave guide, and represent minimum limits that are approached to a greater or lesser extent by actual guides. If the wave guide is constructed of, or plated with some metal other than copper, the losses in the guide will increase as the square root of the ratio of the resistivity of the metal to that of copper. The relative attenuation of the various metals compared to that of copper is given in Table III.

TABLE II—Weights of Standard Brass Wave Guides

Outside dimensions × wall thickness in inches	Weight in pounds per foot
3 × 1 1/2 × 0.081	2.63
2 × 1 × 0.064	1.40
1 1/2 × 3/4 × 0.064	1.03
1 1/4 × 5/8 × 0.064	0.848
1 × 1/2 × 0.050	0.531
3/4 × 3/8 × 0.064	0.468
1/2 × 1/4 × 0.040	0.198
7/16 × 1/4 × 0.050	0.217

TABLE III — Relative Attenuation in Metals at High Frequencies

Metal	Attenuation relative to copper
Aluminum	1.28
Brass	2
Cadmium	2.09
Chromium	1.23
Gold	1.19
Lead	3.57
Magnesium	1.63
Manganin	5.05
Palladium	2.52
Phosphor-bronze	2.47
Platinum	2.41
Rhodium	1.71
Silver	0.97
Tin	2.58
Zinc	1.89

Power Limitations

The theoretical power-carrying capacity of a rectangular wave guide is $P = 3.85\ ab(\lambda/\lambda_g)10^6$ watts when the dimensions of the guide, a and b, are in inches. This equation assumes a breakdown potential of 30,000 volts per cm for the air dielectric, a value that has been experimentally checked, and also assumes that there are no standing waves in the wave guide. If there are standing waves present, the power-carrying capacity of the guide will be reduced by a factor representing the voltage standing wave ratio in the wave guide. The recommended maximum power to be carried in a wave guide is about one-fourth the theoretical maximum.

Breakdown at High Altitude

The breakdown potential in air will be lowered if the air pressure is decreased, and if a wave guide is operated at high altitude without pressurization, its power-carrying capacity will be greatly reduced. The reduction factor is given as a function of altitude in Fig. 5.

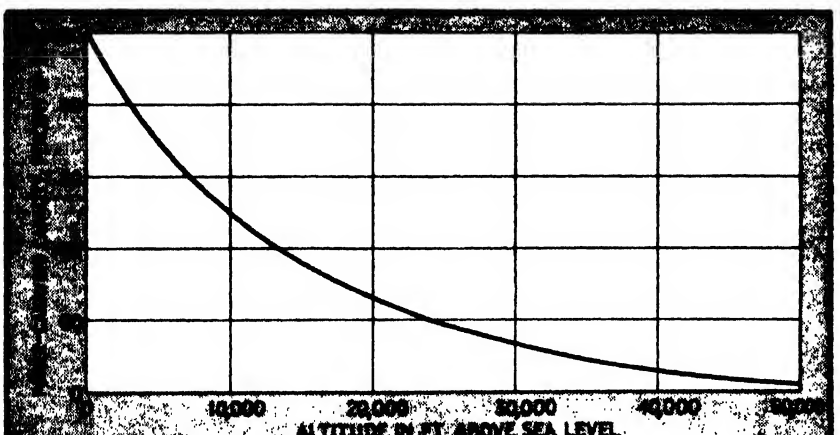

FIG. 5—Percentage decrease in the power-carrying capacity of a wave guide with increasing altitude (decreasing pressure)

References

(1) Barrow, W. L., Transmission of Electromagnetic Waves in Hollow Tubes of Metal, *Proc. I.R.E.*, Oct. 1936, p 1298.

(2) Southworth, G. C., Hyper-frequency Wave Guides—General Considerations and Experimental Results, *B.S.T.J.*, April 1936, p 284.

(3) Carson, J. R., Mead, S. P., and Schelkunoff, S. A., Hyper-Frequency Wave Guides—Mathematical Theory, *B.S.T.J.*, April 1936, p 310.

(4) Chu, L. J., and Barrow, W. L., Electromagnetic Waves in Hollow Metal Tubes of Rectangular Cross-Section, *Proc. I.R.E.*, Dec. 1938, p 1520.

Waveguide Data

Dimensions of rectangular copper waveguides covering the entire microwave spectrum in accordance with FCC frequency allocations, with cutoff frequencies, curves of attenuation and power-handling capacity for each size, and performance equations

By LEONARD E. SHERBIN

THE MICROWAVE FIELD has reached that stage of development where it is now desirable to standardize on various waveguide sizes. Since the physical dimensions of a waveguide determine the frequency range over which it can most satisfactorily operate, it is desirable that waveguide dimensions be standardized according to frequency allocations. This would avoid need for two waveguide sizes to cover a band of frequencies allocated to one service, as well as to obtain the maximum efficiency from a transmission line.

A number of systems for determining standards for waveguide sizes have been put forth, all of which are based upon the following factors: (1) To use as few waveguide sizes as possible; (2) To have the waveguides operate over as wide a band as is practical; (3) To choose the dimensions so that the inherent losses are as low as possible; (4) To standardize on waveguides having the highest possible power-carrying capacity; (5) To choose the waveguides with characteristics compatible with FCC frequency allocations; (6) To use waveguide sizes for which tubing is available; (7) To choose dimensions so that the waveguide has the necessary mechanical strength.

Cutoff Frequency

The cutoff frequency is that frequency below which a waveguide will not transmit any energy. That is to say, the wave will not propagate if it is below the cutoff frequency of the waveguide. This is borne out by the fact that the characteristic wave impedance is a pure imaginary quantity for frequencies below the cutoff frequency of a waveguide.

The attenuation in a waveguide below cutoff is a reactive attenuation. The waveguide looks like a pure reactance to the source and therefore the energy is reflected back from the waveguide. The action of a waveguide below cutoff is analogous to that of a high-pass filter below the pass band of the filter. The characteristic wave impedance for a transverse electric wave is

$$Z_{TE} = \nu_1 / \sqrt{1 - (f_c/f)^2} \qquad (1)$$

where Z_{TE} = characteristic wave impedance for a transverse electric wave, $\nu_1 = \sqrt{\mu_1/\epsilon_1}$ = intrinsic impedance of the dielectric, ϵ_1 = dielectric constant, μ_1 = permeability, f_c = cutoff frequency, and f = frequency.

For values where $f_c > f$ the characteristic wave impedance is a pure imaginary and hence no energy can be propagated along the waveguide. When $f = f_c$ the characteristic wave impedance is infinite and for an ideal waveguide would represent a sharp transition from an imaginary characteristic wave impedance to a real one. However, for practical waveguides with imperfect conductors there is a small amount of phase shift below cutoff and some attenuation above cutoff. Above cutoff, practical wave guides have a real attenuation factor and a phase shift along the axis of the guide.

The above discussion shows the impracticability of using waveguides at frequencies below cutoff for the transmission of energy. At frequencies close to and just above the cutoff frequency for a given waveguide the attenuation-vs-frequency curve has a steep slope with a relatively high attenuation factor. This makes it undesirable to use waveguides in this region. The expression for the cutoff frequency for a transverse electric $TE_{m,n}$ or transverse magnetic $TM_{m,n}$ wave is

$$\lambda_c = \frac{2}{\sqrt{\left(\frac{m}{a}\right)^2 + \left(\frac{n}{b}\right)^2}} \qquad (2)$$

where λ_c = wavelength at cutoff, m and n are the subscripts for a given mode, and a and b are the inside dimensions for the wide and

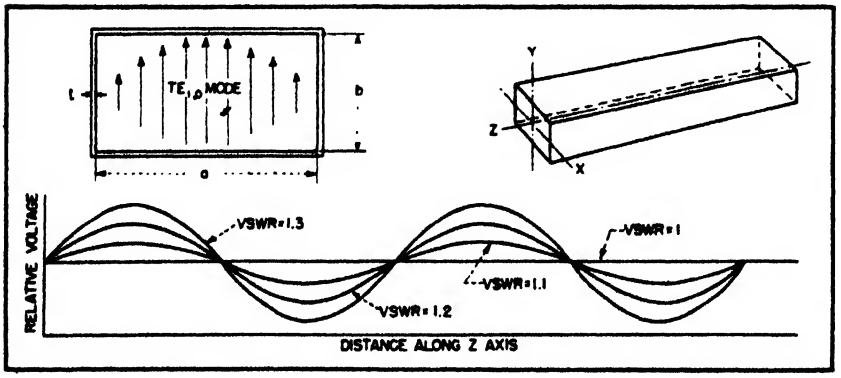

FIG. 1—End view of electric field distribution in rectangular waveguide, and curves showing voltage along longitudinal axis Z of a rectangular waveguide for various voltage standing wave ratios

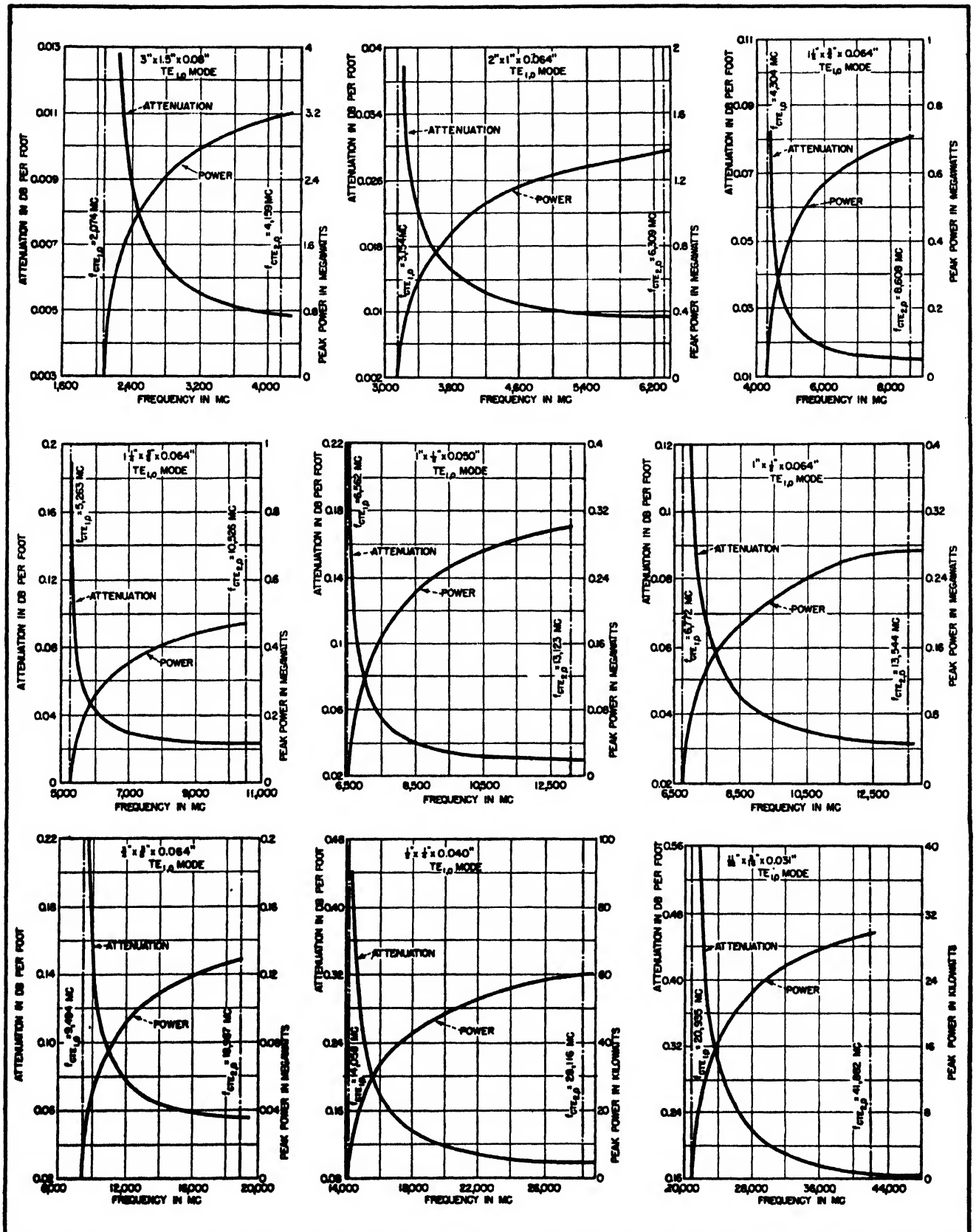

FIG. 2—Attenuation and power curves plotted against frequency for rectangular copper waveguides having the length, width, and thickness dimensions indicated. All operate in $TE_{1,0}$ mode. Two sets of curves for 1 x 1½-in. size show effect of wall thickness

narrow sides respectively as indicated in Fig. 1.

For the $TE_{1,0}$ wave, which is the one used in practically all cases, Eq. 2 reduces to

$$\lambda_c = 2a \quad (3)$$

This equation shows that for the $TE_{1,0}$ mode the a dimension of a rectangular waveguide is the only physical factor determining the cutoff frequency. The cutoff frequencies of the waveguides included in the various recommendations for standardization are given in Fig. 2.

Operation at Higher Modes

In order to operate a waveguide at its optimum efficiency the dominant mode is usually used. The dominant mode is the lowest-frequency mode that will propagate down the waveguide. The propagation of more than one mode in a waveguide is undesirable as it results in impedance mismatches for the various modes, along with reflections and the generation of spurious frequencies other than the desired one at discontinuities. If these spurious frequencies can propagate down the waveguide they will have many detrimental effects. This results in the loss of energy propagated down the waveguide, high standing wave ratios in the waveguide, and very inefficient transmission of the microwave energy.

Therefore, it is essential that the physical dimensions of a waveguide be so chosen that all modes, other than the desired one, cannot propagate. This places the limitation on the highest frequency at which a waveguide can be most efficiently used.

The $TE_{2,0}$ mode is the next higher mode that could be propagated. By simplifying Eq. 2 the cutoff wavelength for the $TE_{2,0}$ mode becomes equal to a. This places a limit on the highest frequency of the band for which a given waveguide is suitable.

In practice, the upper frequency limit is usually lower than the theoretical limit, so that moding difficulties are avoided. The lowest transverse magnetic wave which can exist is the $TM_{1,1}$ mode and since it occurs at a higher frequency than the $TE_{2,0}$ mode in the recommended waveguide sizes, there is no need to investigate further.

The b dimension is subject to compromise on many points. The larger the b dimension the lower the attenuation and the greater the power-handling capacity of the waveguide. However, there is a limit as to how large b can be made before difficulties are encountered with modes other than the dominant mode. The b dimension has to be such that it will not support any mode other than the $TE_{1,0}$. In practice the ratio of the b dimension to the a dimension is usually less than 0.5 to avoid any possibility of the waveguide supporting a mode other than the $TE_{1,0}$.

Power-Carrying Capacity

The maximum power that a waveguide can carry for the $TE_{m,0}$ mode is

$$P = E_{max}^2\, 6.63 \times 10^{-4}\, ab \left(\frac{\lambda}{\lambda_g}\right) \quad (4)$$

where P = maximum power for the $TE_{m,0}$ mode in watts, E_{max} = maximum permissible voltage gradient, λ_g = guide wavelength, λ = free space wavelength, and a and b are waveguide inside dimensions in cm. This gives the theoretical power that a waveguide can handle if the voltage standing wave ratio is 1, and is valid for given humidity and air pressure conditions only.

The maximum field intensity occurs where the electric field is greatest. The greatest electric field is parallel to the narrow side (b dimension). in the center of the broad side (a dimension). Therefore, the b dimension limits E_{max} since it determines the field intensity at which a voltage breakdown will occur. The maximum power is proportional to the cross-sectional area ab of the waveguide and the ratio λ / λ_g.

A value of 15,000 volts per cm will be used in the calculations for E_{max}. This value has been arrived at empirically and is used by the Army and Navy in applying power ratings to waveguides. Any increase in voltage standing wave ratio will decrease the power-handling capacity of waveguides since the field intensity will then have varying values along the waveguide axis, with the maximum value of field intensity being greater than if the voltage standing wave ratio were unity. Any sharp corners, bends, twists, etc, would tend to lower the maximum power rating. Figure 1 shows (at upper left) the electric field distribution across a waveguide for the $TE_{1,0}$ mode, along with curves portraying the increase in peak voltage due to increasing standing wave ratios.

The graphs in Fig. 2 give the maximum power-carrying capacities under ideal conditions and assuming an E_{max} of 15,000 volts per cm for the $TE_{1,0}$ mode.

In a rectangular copper waveguide with air dielectric and for the $TE_{1,0}$ mode the attenuation is

$$\alpha_{copper} = \frac{0.01107}{a^{3/2}} \left[\frac{\frac{1}{2}\frac{a}{b}\left(\frac{f}{f_c}\right)^{3/2} + \left(\frac{f}{f_c}\right)^{-1/2}}{\sqrt{\left(\frac{f}{f_c}\right)^2 - 1}} \right] \quad (5)$$

where α_{copper} = attenuation in db per ft for a copper waveguide for the $TE_{1,0}$ mode.

For metals other than copper, Eq. 5 must be multiplied by K, where K is equal to the square root of the ratio of the resistivity of the metal used to the resistivity of copper.

The values for attenuation in waveguides as obtained by measurements run somewhat higher than the values obtained by solving Eq. 5. This is caused by such conditions as variations in plating, impurities in the metal, dust, varying atmospheric conditions, and corrosion.

Curves of attenuation vs frequency are also given in Fig. 2 for various waveguide sizes, based on Eq. 5. These curves indicate that it is not desirable to operate a waveguide at frequencies close to cutoff. The attenuation is high in this region and decreases rapidly to the point where it is fairly constant. Also, wide-band operation

in this region is undesirable as it would cause considerable distortion.

For narrow-band operation near cutoff the attenuation is so much greater that considerably larger transmitters would have to be used to obtain a comparable input to the antenna for most practical waveguide installations. In receiving applications the increased attenuation results in lower effective signal input to the receiver, thereby decreasing the signal-to-noise ratio and sensitivity of the installation.

Minimum Attenuation in Waveguides

Tabulation of design equations covering attenuation, development of simplified versions applying to specific practical air-core guides most often encountered, and graphical construction for determining conditions for minimum attenuation at exciting frequency

By EDWIN N. PHILLIPS

IN recent literature dealing with the phenomena of signal transmission through air-cored waveguides, the conditions for propagation have been adequately dealt with, but the conditioning of the cross-sectional dimensions to obtain minimum attenuation at the exciting frequency has generally been dismissed with but a brief treatment. Since this aspect is of direct concern to the designer using waveguides, this paper presents the necessary formulas for predicting cross-sections giving minimum attenuation.

Practical formulas concerning attenuation in air-cored guides are listed by Sarbacher and Edson in their book, "Hyper- and Ultra-High-Frequency Engineering." These formulas, as converted into English units, appear in Table I. For material other than copper, multiply the value of attenuation by $\sqrt{\rho/\rho_c\mu}$, where ρ is the specific resistivity of the guide material, ρ_c is the specific resistivity of copper, and μ is the permeability of the guide material. It will be noted that the formulas for the $H_{0,m}$ and the $H_{n,m}$ excitation modes in rectangular cross-section guides and the H_1 mode in

TABLE I. DESIGN FACTORS FOR COPPER-WALLED AIR-CORED WAVEGUIDES

	TYPE	MODE	CONFIGURATION	CUTOFF FREQUENCY f_c IN MC PER SEC	ATTENUATION α IN DB PER FOOT OF AXIAL LENGTH	$\frac{f_{MIN}}{f_c}$	α_{MIN} IN DB PER FT OF AXIAL LENGTH
RECTANGULAR	H WAVES	$H_{n,m}$ n≠0	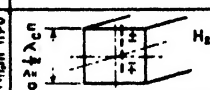	$5905.5\sqrt{\left(\frac{n}{a}\right)^2+\left(\frac{m}{b}\right)^2}$	$0.01119\frac{\sqrt{m}}{\sqrt{(b^3)}}\cdot\frac{\left\{\frac{b}{a}+\left(\frac{n}{m}\right)^2\left(\frac{b}{a}\right)^3\right\}\left(\frac{f}{f_c}\right)^{\frac{3}{2}}+\left\{1+\left(\frac{n}{m}\right)^2\left(\frac{b}{a}\right)^2\right\}\left(\frac{f}{f_c}\right)^{-\frac{1}{2}}}{\left\{1+\left(\frac{n}{m}\right)^2\left(\frac{b}{a}\right)^2\right\}^{\frac{3}{2}}\sqrt{\left(\frac{f}{f_c}\right)^2-1}}$	$\sqrt{\frac{6}{2}\sqrt{1+\left(\frac{k_2}{k_1}\right)^2+\sqrt{\left(\frac{k_2}{k_1}\right)^4+\frac{14}{9}\left(\frac{k_2}{k_1}\right)^2+1}}}$ $\frac{k_2}{k_1}=\frac{\frac{a}{b}+\frac{\left(\frac{n}{m}\right)^2}{\left(\frac{a}{b}\right)^2}}{1+\frac{\left(\frac{n}{m}\right)^2}{\left(\frac{a}{b}\right)^3}}$ $\frac{k_2}{k_1}=2\frac{a}{b}$	α_{MIN} IS TO BE DETERMINED SEPARATELY FOR EACH CASE
		$H_{0,m}$ n=0	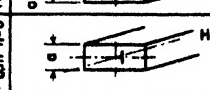	$\frac{5905.5}{b^2}$ LOWEST CUTOFF FREQ	$0.01119\frac{\sqrt{m}}{\sqrt{(b^3)}}\cdot\frac{\frac{b}{2a}\left(\frac{f}{f_c}\right)^{\frac{3}{2}}+\left(\frac{f}{f_c}\right)^{-\frac{1}{2}}}{\sqrt{\left(\frac{f}{f_c}\right)^2-1}}$ LOWEST ATTENUATION		
	E WAVES	$E_{n,m}$	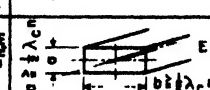	$5905.5\sqrt{\left(\frac{n}{a}\right)^2+\left(\frac{m}{b}\right)^2}$	$0.01119\frac{\sqrt{m}}{\sqrt{(b^3)}}\cdot\frac{1+\left(\frac{n}{m}\right)^2\left(\frac{b}{a}\right)^3\left(\frac{f}{f_c}\right)^{\frac{3}{2}}}{\left\{1+\left(\frac{n}{m}\right)^2\left(\frac{b}{a}\right)^2\right\}^{\frac{3}{2}}\sqrt{\left(\frac{f}{f_c}\right)^2-1}}$	$\sqrt{3}=1.732$	$0.01804\frac{\sqrt{m}}{\sqrt{(b^3)}}\cdot\frac{1+\left(\frac{n}{m}\right)^2\left(\frac{b}{a}\right)^3}{\left\{1+\left(\frac{n}{m}\right)^2\left(\frac{b}{a}\right)^2\right\}^{\frac{3}{2}}}$
CIRCULAR	H WAVES	H_0	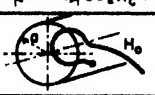	$\frac{7167.7}{a^2}$	$\frac{0.0061769}{\sqrt{(a^3)}}\cdot\frac{\left(\frac{f}{f_c}\right)^{-\frac{1}{2}}}{\sqrt{\left(\frac{f}{f_c}\right)^2-1}}$	∞	THIS WAVE IS UNSTABLE O AND CAN BE USED ONLY IN STRAIGHT TUBING
		H_1	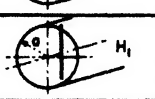	$\frac{3458.8}{a^2}$ LOWEST CUTOFF FREQ	$\frac{0.0042746}{\sqrt{(a^3)}}\cdot\frac{0.42\left(\frac{f}{f_c}\right)^{\frac{3}{2}}+\left(\frac{f}{f_c}\right)^{-\frac{1}{2}}}{\sqrt{\left(\frac{f}{f_c}\right)^2-1}}$	$\sqrt{\frac{6}{2}\sqrt{1+\left(\frac{k_2}{k_1}\right)^2+\sqrt{\left(\frac{k_2}{k_1}\right)^4+\frac{14}{9}\left(\frac{k_2}{k_1}\right)^2+1}}}$	$\frac{0.0041848}{\sqrt{(a^3)}}$ LOWEST MINIMUM ATTENUATION
	E WAVES	$E_{0,1}$	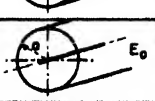	$\frac{4520.85}{a^2}\rightarrow\frac{4521}{a^2}$	$\frac{0.0049}{\sqrt{(a^3)}}\cdot\frac{\left(\frac{f}{f_c}\right)^{\frac{3}{2}}}{\sqrt{\left(\frac{f}{f_c}\right)^2-1}}$	$\sqrt{3}=1.732$	$\frac{0.0078953}{\sqrt{(a^3)}}$
		E_1	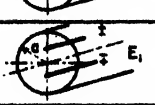	$\frac{7167.7}{a^2}$	$\frac{0.0061769}{\sqrt{(a^3)}}\cdot\frac{\left(\frac{f}{f_c}\right)^{\frac{3}{2}}}{\sqrt{\left(\frac{f}{f_c}\right)^2-1}}$	$\sqrt{3}=1.732$	$\frac{0.00995476}{\sqrt{(a^3)}}\cdot\frac{0.01}{\sqrt{(a^3)}}$

circular cross-section guides can be expressed in the form

$$\alpha = k_1 \frac{\left(\frac{f}{f_c}\right)^{1.5}}{\left[\left(\frac{f}{f_c}\right)^2 - 1\right]^{0.5}} + k_2 \frac{\left(\frac{f}{f_c}\right)^{-0.5}}{\left[\left(\frac{f}{f_c}\right)^2 - 1\right]^{0.5}} \quad (1)$$

where α is in db per foot and k_1 and k_2 are constants dependent on the material and the dimensions of the guide.

For copper guides, the ratio k_2/k_1 for various excitation modes is

$H_{0,m}$ . . . rectangular cross-section	$2a, b$
$H_{1,1}$ . . circular cross-section .	2.38
$H_{n,m}$ . . rectangular cross-section	$\dfrac{\left(\frac{a}{b}\right) + \frac{\left(\frac{n}{m}\right)^2}{\left(\frac{a}{b}\right)^2}}{1 + \frac{\left(\frac{n}{m}\right)^2}{\left(\frac{a}{b}\right)}}$

where a is the thickness of the rectangular cross-sectioned guide in inches or the radius of the circular guide, b is the width of the rectangular cross-sectioned guide, and n and m are subscripts defining the order of the wave propagated within the guide.

By differentiating Eq. 1 with respect to the frequency ratio f/f_c, where f represents the exciting frequency and f_c the cutoff frequency below which the guide will not transmit electromagnetic waves, and setting the resulting expression equal to zero, the following expression for f_{min}, the frequency of minimum attenuation, is obtained

$$\frac{f_{min}}{f_c} = \frac{\sqrt{6}}{2}\sqrt{1 + \frac{K_2}{K_1} + \sqrt{\left(\frac{K_2}{K_1}\right) + \frac{14}{9}\left(\frac{K_2}{K_1}\right)} + 1} \quad (2)$$

Because an approximate solution to this equation may be sufficiently accurate in certain cases, and to provide a rough check on computations, the equation has been plotted as Fig. 1.

Because of the relative ease of excitation and the low overall attenuation, the $H_{0,m}$ excitation mode is often used. For this case, Eq. 2 simplifies to

$$\frac{f_{min}}{f_c} = \frac{\sqrt{6}}{2}\sqrt{1 + 2\frac{a}{b} + \sqrt{4\left(\frac{a}{b}\right)^2 + \frac{28}{9}\left(\frac{a}{b}\right) + 1}} \quad (3)$$

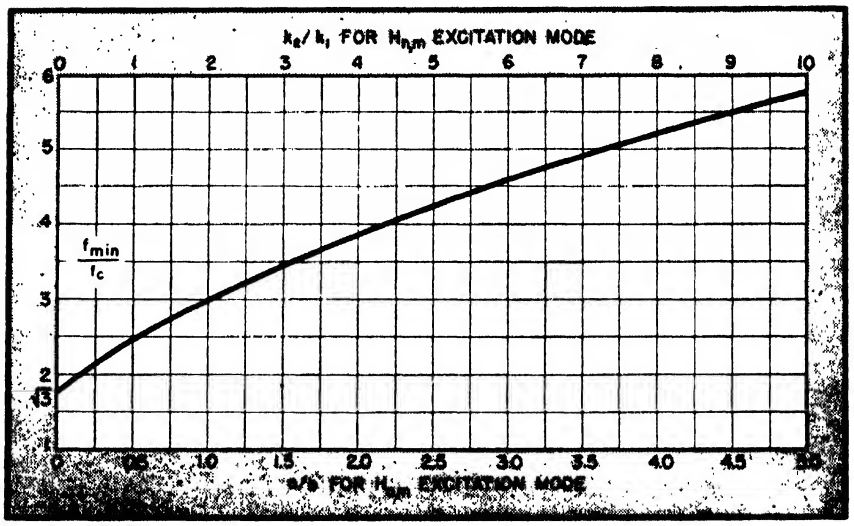

FIG. 1—Minimum attenuation in air-cored waveguide in terms of dimensional parameters

While Eq. 2 and 3 are useful for fixed guide dimensions and variable input frequency, often the input frequency is fixed and the guide dimensions must be varied to secure minimum attenuation. Manipulation of Eq. 2 and 3 to isolate the dimensional factor gives for the general case

$$\frac{k_2}{k_1} = \frac{\left(\frac{f}{f_c}\right)^4 - 3\left(\frac{f}{f_c}\right)^2}{3\left(\frac{f}{f_c}\right)^2 - 1} \quad (4)$$

and for the $H_{0,m}$ mode

$$\frac{a}{b} = \frac{\left(\frac{f}{f_c}\right)^4 - 3\left(\frac{f}{f_c}\right)^2}{6\left(\frac{f}{f_c}\right)^2 - 2} \quad (5)$$

In all these formulas, the condition for minimum attenuation is independent of the guide material, and dependent only on the cross-sectional dimensions of the guide and the order of the transmitted wave.

Formulas for E Modes

Treating the formulas for the $E_{n,m}$ excitation mode in rectangular cross-sectioned guides and $\underline{E}$ excitation modes in circular cross-sectioned guides in a similar manner, the general formula is

$$\alpha = k \cdot \frac{\left(\frac{f}{f_c}\right)^{1.5}}{\left(\left(\frac{f}{f_c}\right) - 1\right)^{0.5}} \text{ db per ft} \quad (6)$$

Setting the first derivative equal to zero gives

$$f_{min}/f_c = \sqrt{3} \quad (7)$$

Note that here the condition for minimum attenuation is independent of both the guide material and the guide dimensions. It will further be noted that Eq. 7 is the limit of Eq. 2 obtained when k_2/k_1 equals zero, indicating in the $H_{0,m}$ mode a zero guide thickness.

Thus, when the thickness a equals the width b of the guide and it is excited in the $H_{0,m}$ mode, Eq. 3 gives f/f_c equal to 2.96; for a cutoff frequency of 1.5 x 10^9 cps, the frequency of minimum attenuation is 4.44 x 10^9 cps. For a guide of the same cross-section excited in the $H_{1,1}$ mode, k_2/k_1 will be unity, and Eq. 2 gives 2.416 for f/f_c; for a cutoff frequency of 2.12 x 10^9 cps, the frequency of minimum attenuation will be 5.12 x 10^9 cps. For the same cutoff frequency, Eq. 7 gives 3.67 x 10^9 cps as the frequency of minimum attenuation in a rectangular guide which is excited in transverse magnetic mode.

Approximate Plots

By means of Eq. 2, 3, and 7, approximate plots of the attenuation-vs-frequency relationship for air-cored waveguides can easily be

made. The cutoff frequency f_c forms a vertical asymptote on a log-log grid, the point of minimum attenuation forms a horizontal asymptote, and since at a frequency much higher than that giving minimum attenuation the guide behaves as any metallic conductor whose attenuation varies as the square root of the frequency, a third boundary to the curve is formed. To illustrate this, Fig. 2 gives the attenuation curve of a brass guide (square root of the resistivity-ratio of brass to copper is 2.015) with inside dimensions of 1.34 x 2.84 inches. This data combines with the formulas in Table I to give, for $H_{0,1}$ excitation, f_c = 2,084 mc, f_{min} = 4,960 mc, α_{min} = 9.42 db per thousand feet, and α = 110 db per thousand feet at $f = 10^{13}$ cps. The resultant curve closely approximates a point-by-point plot, and saves much time.

Once the attenuation per unit length and the guide length are known, the transmission-line efficiency in percent is obtained from

$$\eta = 100/\left(\log^{-1}\frac{\alpha l}{10}\right) \qquad (8)$$

where l is line length in feet. A plot of this is shown in Fig. 3.

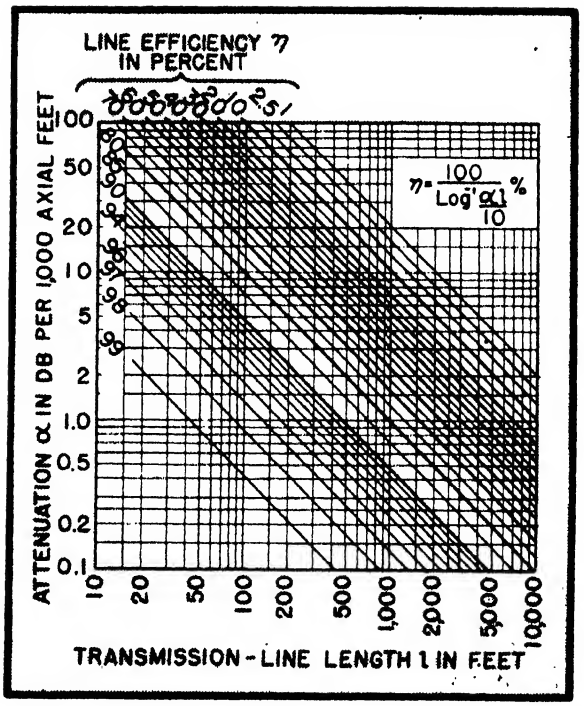

FIG. 3—Transmission-line efficiency in terms of cable length and attenuation per unit length

Also plotted in Fig. 2, as a matter of pertinent interest, are the attenuation curves of a zero-conductance brass concentric line for which D/d = 3.59, with the same inner periphery as the guide (α = 200

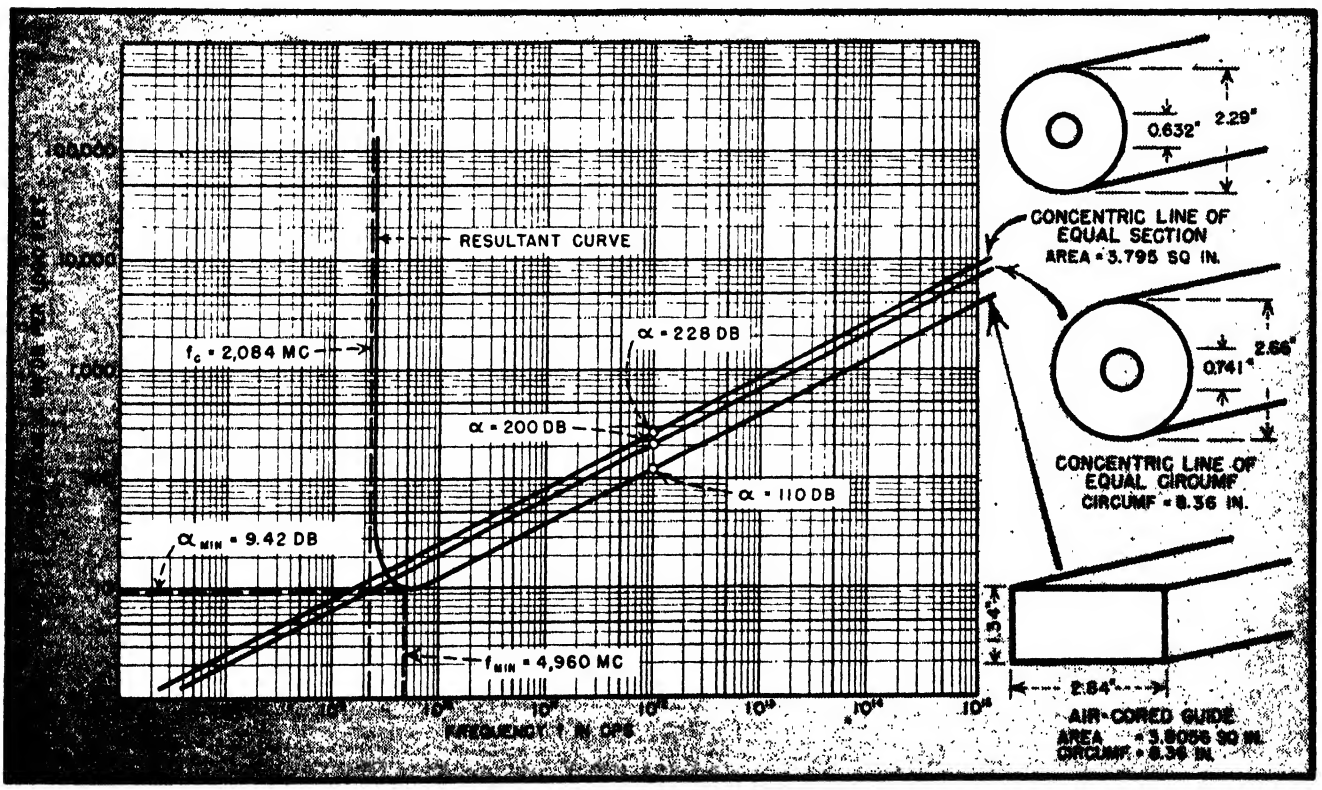

FIG. 2—Graphical construction of attenuation curve for 1.34 by 2.84-inch rectangular waveguide, and corresponding curves for two types of concentric lines

db per thousand feet at 10^{10} cps), and a zero-conductance brass concentric line for which $D/d = 3.59$, with the same dielectric area as the guide cross-section ($\alpha = 228$ db per thousand feet at 10^{10} cps).

Pertinent points to be mentioned as general guides in the use of waveguides of this type are (1) an infinite number of cross-sections will give minimum attenuation at any prescribed frequency, but the cross-sectional dimensions are not independent of each other and both depend on the cutoff frequency chosen; (2) the lower the cutoff frequency chosen, the lower will be the attenuation, the larger the guide dimensions will be, and the broader will be the bell of the curve at the minimum point in the H propagational modes, giving less distortion in the output of a complex wave or a modulated carrier.

Concerning this last point, most of the present-day applications use pulsed modulation, and it can be shown that when the ratio of the carrier (or pulsed) frequency to the pulsing frequency is great, the sidebands are negligible, and attenuation can be computed for the carrier alone.

Circular Waveguide Fields

To facilitate the design of exciting elements and grids for filtering particular modes, field patterns for five modes having the lowest cut-off frequencies are plotted. Diagrams show direction and relative magnitude of fields in the transverse plane

By GEORGE R. COOPER

THE diagrams presented in this paper describe the electric and magnetic fields inside circular wave guides for certain modes of transmission.

For each mode considered there are curves showing the direction and relative intensity of the transverse fields and the relative intensity of the longitudinal field. The direction of the longitudinal field is, of course, always along the axis of the guide.

The five modes of transmission presented here are those which have the lowest cut-off frequencies.

These curves find practical application in designing many types of wave guide equipment. For example, the design of devices for initiating and receiving the various modes, either independently or simultaneously in a single guide, is aided by a knowledge of the locations of regions of maximum field strengths and their associated directions.

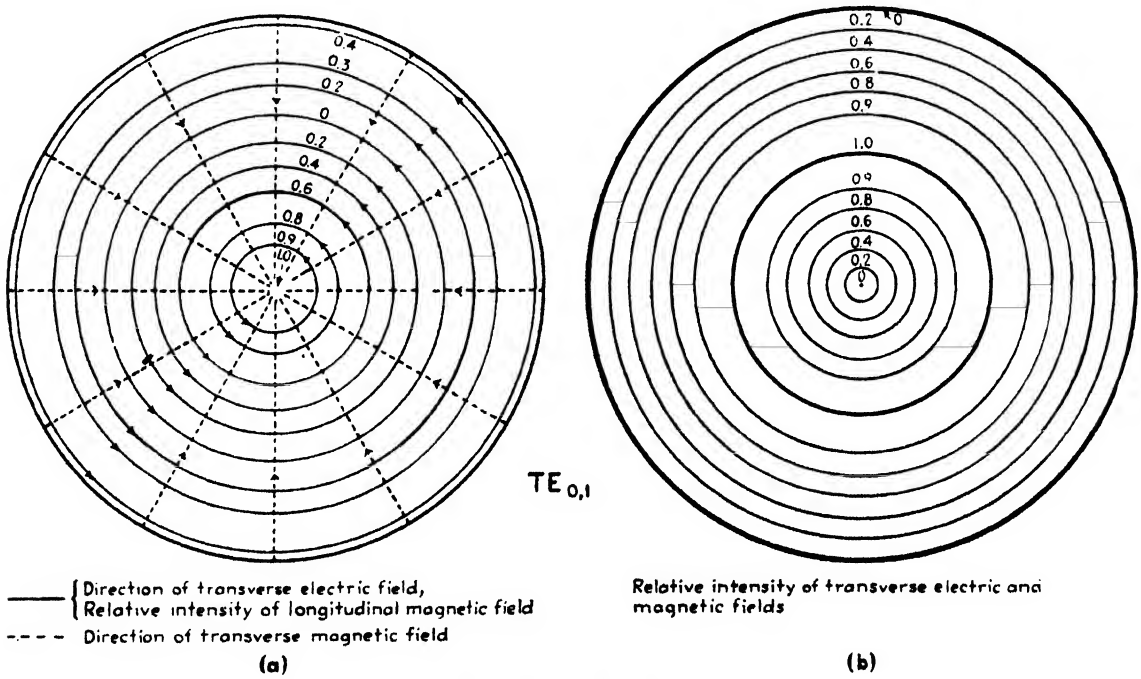

FIG. 1—The wave guide field pattern of the simplest transverse electric wave

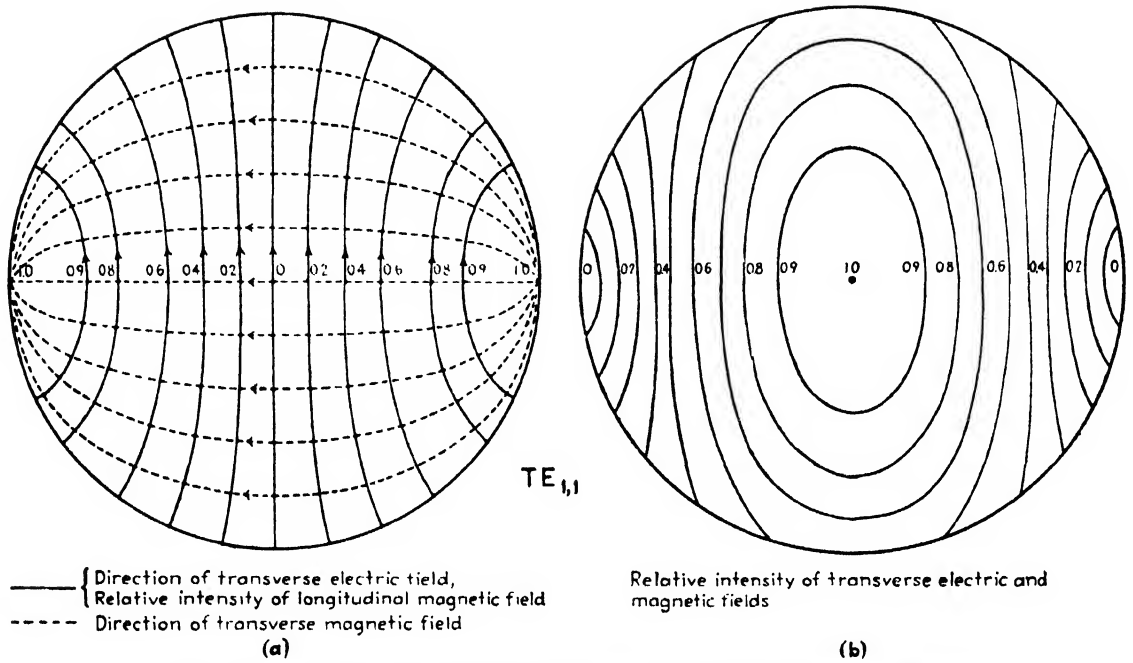

FIG. 2—For a given wave guide radius, this mode will transmit the lowest frequency

Likewise, the design of filters for passing a desired mode or modes and attenuating undesired modes is materially aided by this information. A further use might be the design of coupling units of all sorts. One application in which these curves have been of considerable benefit is the design of a transducer for changing from one mode of transmission to another.

The curves are of considerable theoretical interest and it is hoped that they will add to the existing knowledge of wave guide transmission.

In a circular, air-filled guide of perfect wall-conductivity at a frequency well above the cut-off frequency, the transverse electric waves ($TE_{n,m}$) are defined by the following equations:

$$E_z = 0 \tag{1}$$

$$H_z = AJ_n(K_m' r/a)\cos(n\theta)\cos(\omega t - \beta x) \tag{2}$$

$$E_\theta = (377A)(f/f_0)[J_n'(K_m' r/a)\cos(n\theta)\sin(\omega t - \beta x)] \tag{3}$$

$$H_r = -A\sqrt{(f/f_0)^2 - 1}\,[J_n'(K_m' r/a)\cos(n\theta)\sin(\omega t - \beta x)] \tag{4}$$

$$E_r = (377A)(n/K_m')(a/r)(f/f_0)[J_n(K_m' r/a)\sin(n\theta)\sin(\omega t - \beta x)] \tag{5}$$

$$H_\theta = A(n/K_m')(a/r)\sqrt{(f/f_0)^2 - 1}\,[J_n(K_m' r/a)\sin(n\theta)\sin(\omega t - \beta x)] \tag{6}$$

where

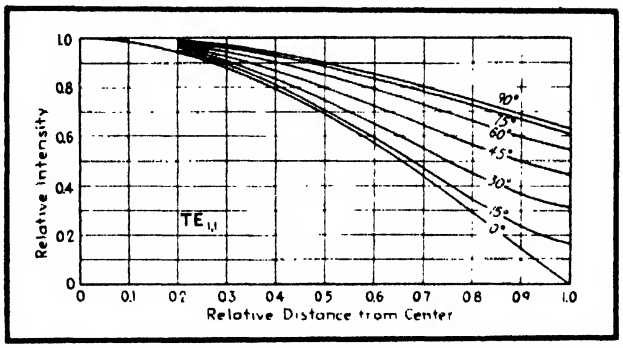

FIG. 3—As an aid to plotting relative transverse field intensity, this intermediate graph is used

E = the electric field intensity in volts per meter along the axis indicated by the subscript

H = the magnetic field intensity in ampere-turns per meter along the axis indicated by the subscript

A = a constant determining the maximum amplitude of the field

a = the diameter of the guide

r/a = the relative radial distance from the center of the guide

x = the distance along the axis of the guide

θ = the angle in the transverse plane

$J_n(\ )$ = the Bessel function of the first kind of order n

$J_n'(\ )$ = the first derivative of $J_n(\ )$ with respect to its argument

K_m' = the mth root of $J_n'(K) = 0$

f_0 = the cut-off frequency

f = the frequency of transmission

$\omega = 2\pi f$

β = the phase shift in the guide in radians per meter

In these equations the factors which determine the phase of the components are of no importance in calculating the field direction and relative intensity beyond indicating that all transverse components are in phase. For that reason these factors are omitted throughout the following discussion.

The direction of the transverse electric field is given at every point inside the guide by the differential equation

$$r\,d\theta/dr = E_\theta/E_r \tag{7}$$

If the expressions for E_θ and E_r from Eq. (3) and (5) are substituted in Eq. (7) and the integra-

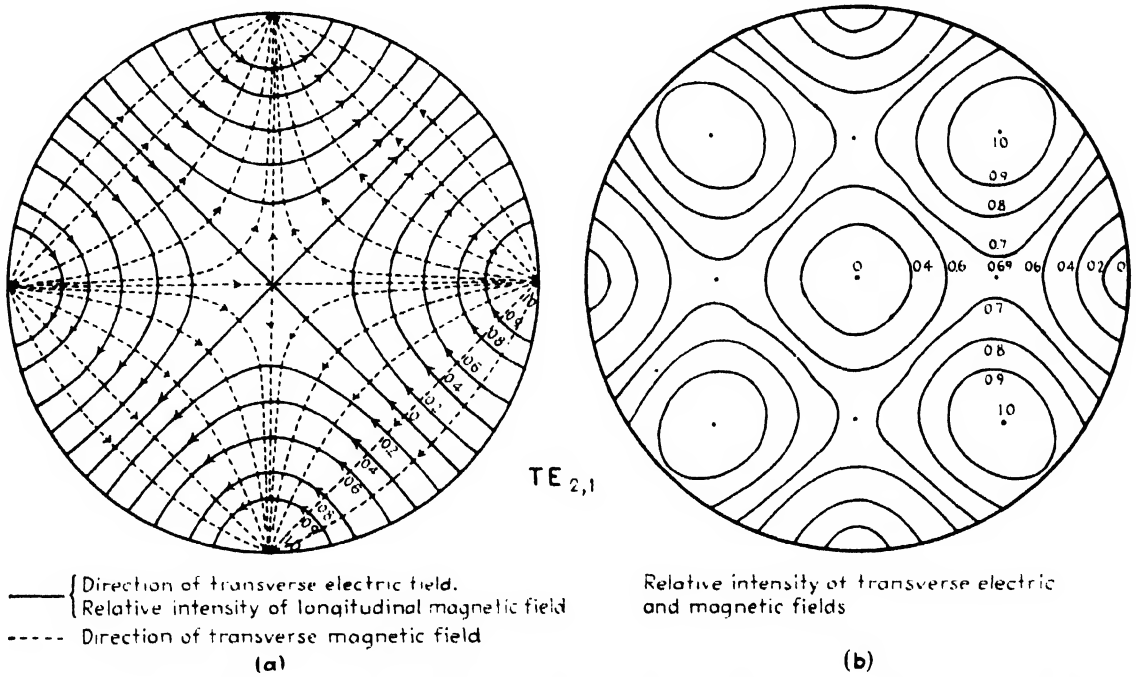

FIG. 4—To excite guides, probes can be aligned with the electric field at points of maximum intensity

tion carried out the resulting equation is

$$J_n(K_m' r/a)\cos(n\theta) = C \qquad (8)$$

where C is an arbitrary constant. Except for a constant multiplier, the left side of this equation is also the expression for H_r. Therefore, Eq. (8) defines a family of curves which at every point determines the direction of the transverse electric field and also, with appropriate choices of C, give the contours of relative intensity for the longitudinal magnetic field, H_r.

The results of evaluating Eq. (8) for the $TE_{0,1}$, $TE_{1,1}$, and $TE_{2,1}$ modes are shown by the solid lines in Fig. 1(a), Fig. 2 (a), and Fig. 4(a) respectively. The number near each line is the relative intensity of H_r for that particular contour. The tangent to the line at any point is the direction of the transverse electric field at that point.

The same figures also show with dotted lines the direction of the transverse magnetic field. These curves are not calculated but are simply sketched in as the orthogonal trajectories of the first set. In fact, calculated curves for the $TE_{1,1}$ and $TE_{2,1}$ modes would be difficult to obtain as the family is represented mathematically by a slowly convergent infinite series.

The next items of interest are the contours of relative intensity for the transverse electric and magnetic fields. In the case of the $TE_{0,1}$ mode where E_r is zero, these curves are easily obtained by setting the expression for E_θ equal to an appropriate set of constants. The results are shown in Fig. 1(b).

For the $TE_{1,1}$ and $TE_{2,1}$ modes the problem is more difficult as there are two components to consider and the total transverse field is the re-

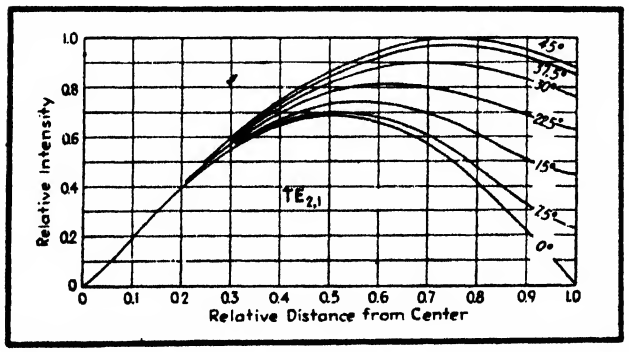

FIG. 5—This intermediate graph gives relative intensity, but not direction, of the transverse field

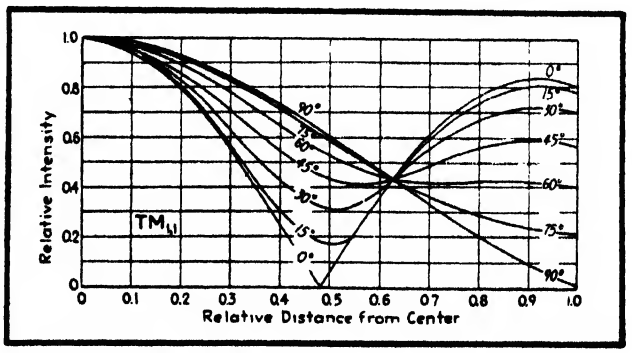

FIG. 6—Replotting these curves on polar coordinates as in Fig. 3(b) gives intensity contours

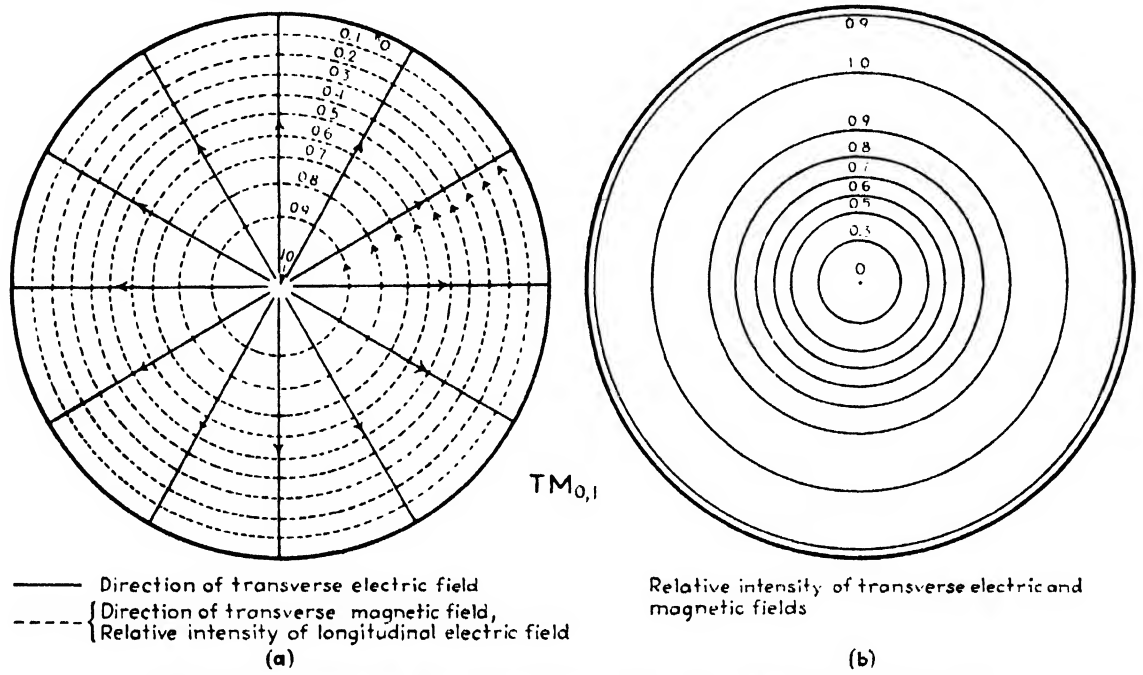

FIG. 7—Of the *TM* modes, this one transmits the longest wavelength in a given guide

sultant of these two. The first step is to evaluate E_θ and E_r for a number of values of r/a and θ and to find the resultant field by taking the square root of the sums of the squares of these two components. The resultant values, expressed as relative intensity, are then plotted as a function of r/a with θ as a

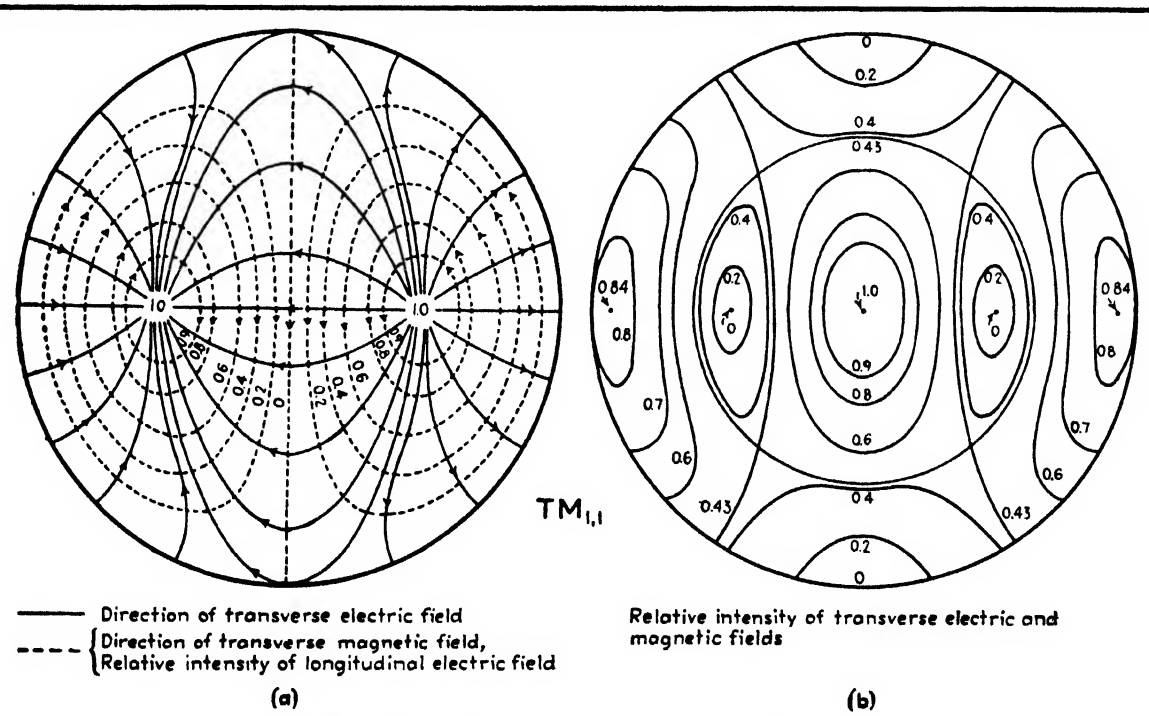

FIG. 8—This $TM_{1,1}$ mode has the same cut-off frequency as the $TE_{0,1}$ mode shown in Fig. 1

parameter. These intermediate curves are shown in Fig. 3 and Fig. 5. From these curves it is possible to read the values of r/a and θ needed to plot the contours of relative intensity. These contours are shown in Fig. 2(b) and Fig. 4(b).

Although the contour intensity curves were calculated from the electric field equations, they apply equally well to the transverse magnetic field because of the constant ratio between orthogonal field components. It is obviously impossible to represent the intensity or direction of the total magnetic field with a single set of curves as the longitudinal and transverse components are ninety degrees out of time phase.

The transverse magnetic waves ($TM_{n,m}$) may be represented by the following equations:

$$H_z = 0 \tag{9}$$

$$E_z = A\, J_n (K_m r/a) \cos (n\theta) \cos (\omega t - \beta x) \tag{10}$$

$$H_\theta = -(A/377)(f/f_c)[J_n' (K_m r/a) \cos (n\theta) \sin (\omega t - \beta x)] \tag{11}$$

$$E_r = -A \sqrt{(f/f_0)^2 - 1}\,[J_n' (K_m r/a) \cos (n\theta) \sin (\omega t - \beta x)] \tag{12}$$

$$H_r = -(A/377)(n/K_m)(a/r)(f/f_0)[J_n (K_m r/a) \sin (n\theta) \sin (\omega t - \beta x)] \tag{13}$$

$$E_\theta = A\,(n/K_m)(a/r) \sqrt{(f/f_0)^2 - 1}\,[J_n (K_m r/a) \sin (n\theta) \sin (\omega t - \beta x)] \tag{14}$$

where

K_m is the mth root of $J_n (K) = 0$

By a method similar to that used previously it is possible to show that the equation

$$J_n (K_m r/a) \cos (n\theta) = C \tag{15}$$

defines a family of curves which gives the direction of the transverse magnetic field and, also, contours of relative intensity for the longitudinal electric field. These curves for the $TM_{0,1}$ and $TM_{1,1}$ modes are shown by the dotted lines in Fig. 7(a) and Fig. 8(a) respectively. The directions of the transverse electric field are shown by the solid lines drawn in the same figures.

The contours of relative intensity for the transverse electric field are determined by the same general method as was used for the TE waves. Since no intermediate curves are needed for the $TM_{0,1}$ mode, the final result is plotted immediately in Fig. 7(b). For the $TM_{1,1}$ mode intermediate curves are necessary and these are shown in Fig. 6. The contours of relative intensity for this mode are then plotted in Fig. 8(b). As in the case of the TE waves, these curves apply equally well to the magnetic field.

The author gratefully acknowledges the encouragement and assistance given by Professor R. P. Siskind of the School of Electrical Engineering, Purdue University.

Apertures in Cavities

Size and placement of apertures and slots in walls of resonators affect loading, internal field distortion, and efficiency of energy transfer from cavity to load. Experimental results indicate effects of opening size for wanted and unwanted radiation

By J. H. OWEN HARRIES

ELECTROMAGNETIC energy, when generated in a cavity by a beam of electrons, has to be guided out of the cavity and into a load. To extract energy a loop can be coupled to the internal magnetic field. Another method is to project the end of either a tuned or terminated transmission line into the internal electric field. But probably the neatest way, and the one which is perhaps the most likely to be used for most engineering purposes, is that of cutting an aperture in the wall of the resonant cavity at an appropriate place. Energy will travel out through such an aperture to a greater or lesser degree, and with differing radiation patterns according to position, size, and shape of the aperture in relation to the mode of oscillation within the cavity.

Slots and Apertures

Typical experimental results indicate the operation of this latter method. A rectangular resonator shown in Fig. 1A and having the dimensions $x = z = 59.8$ cm, and $y = 15.0$ cm was set into oscillation at its lowest frequency (H_{011} mode; subscripts here indicate the number of standing waves in each of the three cavity dimensions). Under this condition the electric field was wholly in the y direction. The current antinode was around the vertical sides of the box; the voltage antinode was in the center of the x-z sides. The measured resonant wavelength was 81.8 cm.

A slot a-b was cut as shown so that dimension b was normal to the lines of current flow. Dimension a was 1.5 cm. The slot dimension b was varied from zero (no slot) to 20 cm. The Q of the cavity varied with b in the manner shown in Fig. 2A. Wavelength remained almost constant, increasing only to 82.3 cm as b was increased to 20 cm. The electric field shape within the resonator is very little affected over this range of dimension b.

A slot at the current antinode

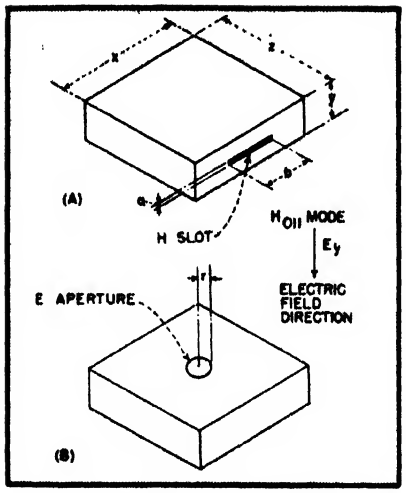

FIG. 1—Openings in cavity serve to extract electromagnetic energy

operates by virtue of disturbing the magnetic field at the wall of the resonator, and is therefore referred to an H slot.

Instead of using an H slot at the current antinode, electromagnetic energy can be withdrawn through an aperture positioned at the electric antinode. This hole in the cavity wall is called an E aperture. Such an arrangement is illustrated in Fig. 1B.

An experimental curve of the Q of the same resonator as used with the H slot, but with an E aperture used instead, is also plotted in Fig. 2A. It was found that if the diameter of this aperture was increased much beyond three or four centimeters the electric field was severely distorted.

In most resonators used in conjunction with electron beams, the electrons are injected at the electric antinode and it is necessary, as far as possible, to preserve a fairly even distribution of electric field in that neighborhood. Moreover, it is generally convenient to separate the point at which the electron beam enters the resonator and the place where the electromagnetic energy is withdrawn. Therefore the H slot is generally the more useful of the two methods of loading the cavity. For this reason the plot of E aperture in Fig. 2A has not been carried to larger diameters.

Loading Factors

In any resonator the maximum instantaneous value of the energy stored in the field is given in mks units by

$$W_P = \frac{\epsilon_0}{2} \int E^2 dv \qquad (1)$$

where ϵ_0 is the specific inductance-capacitance of free space, E is the maximum instantaneous value of electric field in the cavity, and v is the volume of the resonator. The selectivity factor of the resonator is:

$$Q = \frac{\omega W_P}{P_R} \qquad (2)$$

where $\omega = 2\pi C/\lambda$, C being the velocity of the electromagnetic wave and λ the electromagnetic wavelength, and P_R is the power lost in the internal surface of the resonator.

If a load is added in which power P_L is dissipated, the selectivity factor becomes

$$Q_L = \frac{\omega W_P}{P_R + P_L} \qquad (3)$$

which can be rewritten as

$$\frac{1}{Q_L} = \frac{P_R}{\omega W_P} + \frac{P_L}{\omega W_P} \qquad (4)$$

or

$$\frac{1}{Q_L} = \frac{1}{Q} + K_1 \qquad (5)$$

where K_1 may be referred to as the aperture loading factor.

From the measurements presented in Fig. 2A we see that the Q of the unloaded cavity is 13,700. The load Q when loaded can be obtained from these curves. Using Eq. 5 the respective loading factors can be plotted for the H slot or the E aperture used in this resonator at the H_{011} mode. Aperture loading is plotted in Fig. 2B for both cases. Further studies show that dimension a of the slot has comparatively little effect upon the loading.

Coupling to a Resonant Load

The loading factor K_1 applies only when the aperture is radiating into free space. If instead the slot is arranged to couple the resonator to another tuned element, the phenom-

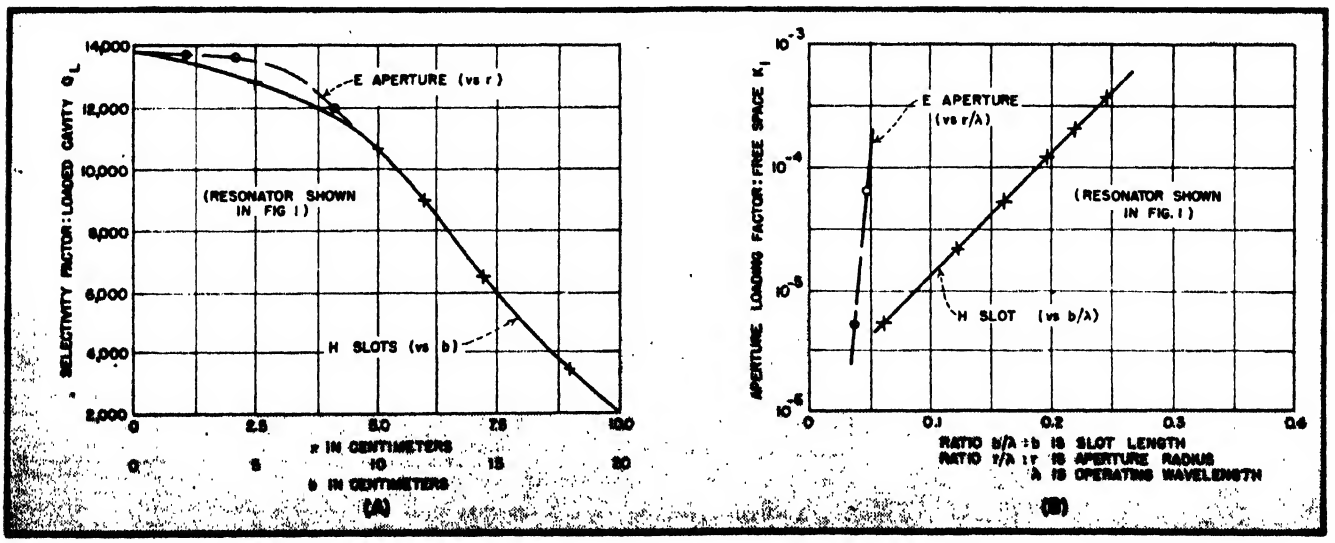

FIG. 2—Loading is affected by size of opening in resonator

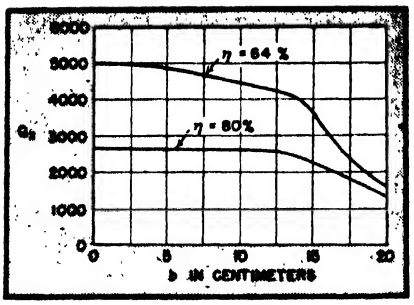

FIG. 3—Size of opening affects unwanted leakage lost through it

enon will be modified in a more or less complicated way depending upon the relative damping of the two resonators and the coefficient of coupling. If, as will be described later, a dipole aerial, which is tuned to the resonant wavelength, is arranged with its current point near the H slot or one of its voltage points in the E aperture, the loading factor will increase very much more rapidly with either b or r than is indicated in Fig. 2B. This phenomenon enables much smaller values of b or r to be used for a given loading, and correspondingly less disturbance of the internal field within the resonator is produced.

It can be shown that the efficiency of a resonator and load in combination is given by

$$\eta = \frac{P_L}{P_L + P_s} = 1 - \frac{Q_L}{Q} \qquad (6)$$

from which it follows that Q_L/Q should be roughly not more than one-tenth.

Unintentional energy leakage through apertures must also be considered. It is often necessary not only so to arrange an aperture that considerable energy is guided from the cavity, but in addition to arrange other apertures through which electrons may be injected into or removed from the cavity, so that they do not allow appreciable energy to leak out.

If we indicate by K_s the loading factor of a slot through which energy must not be appreciably radiated from the cavity, we can write for the reciprocal of the selectivity factor

$$\frac{1}{Q_x} = \frac{1}{Q_L} + K_s \qquad (7)$$

where, as before, Q_L is the selectivity factor of the loaded cavity, and Q_x is the selectivity factor of the cavity losing energy both to a load and by leakage.

To avoid leakage of energy, the value of either b or r must be such that Q_x tends to equal Q_L, so that K_s is small compared to $1/Q_L$. It will be observed in Fig. 2B that this condition can be met quite readily in practice. However the accidental presence of an external resonant structure might easily upset these conditions.

Figure 3 shows the variation of Q_x with the slot dimension b in the resonator of Fig. 1A. Two cases are shown, one when the resonator is so loaded that $\eta = 64\%$, the other when $\eta = 80\%$. In the latter case an H slot length of 10 cm can be used, for example, to inject electrons without permitting appreciable radiation loss.

Tuned Loads

Consider again the design of an aperture for withdrawing wave energy from a resonator. One of the factors that has to be taken into account is whether the distortion of the internal electric field caused by the aperture in the cavity wall is

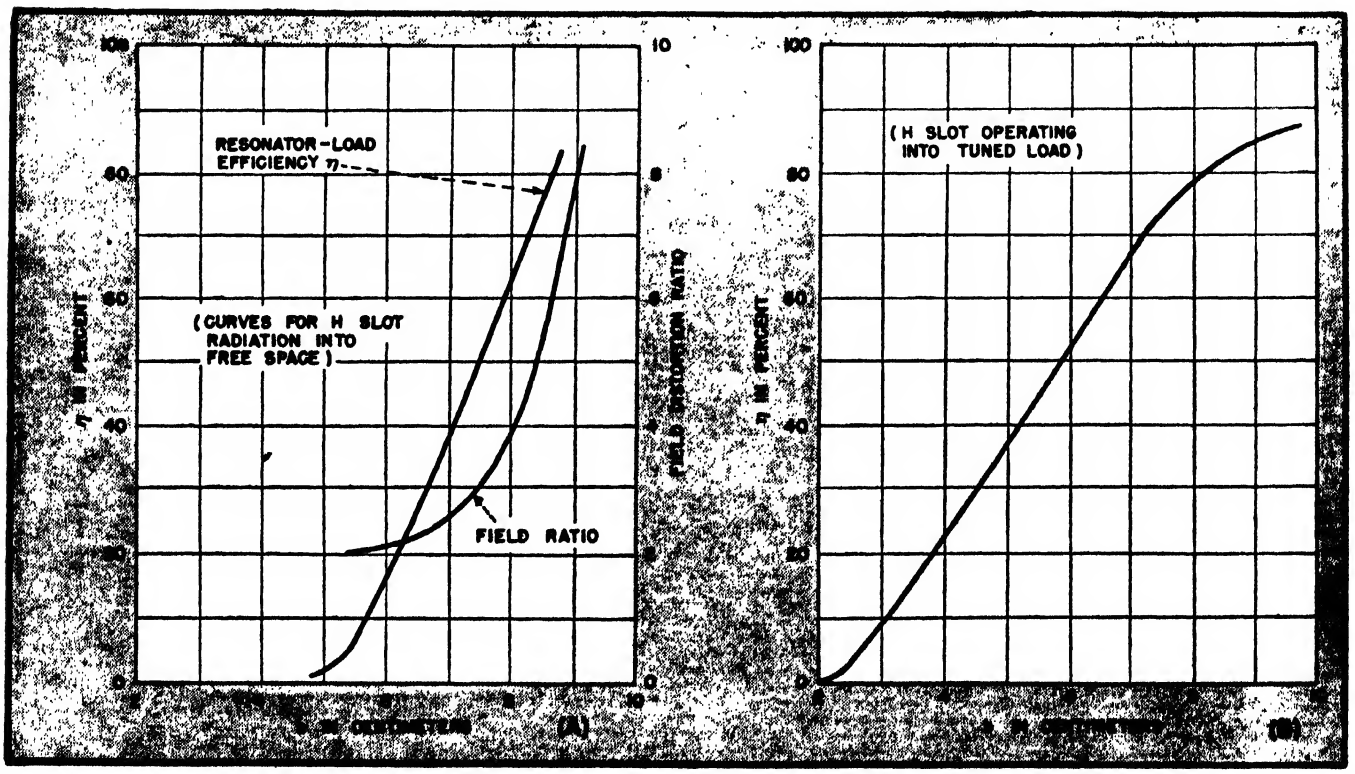

FIG. 4—Energy transfer to the load varies with size of opening

sufficiently small to be tolerable. The following experimental results illustrate this point.

A roughly cylindrical resonator was arranged to operate in the H_{111} mode on about a 78 cm wavelength. An H slot was cut in one of the flat ends, and Q and Q_L as functions of b were measured. The ratio between electric field magnitudes at two points, each near one of the two flat ends of the resonator, was also measured as a function of b as an indication of the disturbance of the field by the slot.

Utilizing Eq. 5, the resonator load efficiency was plotted together with a curve of the internal field ratio as shown in Fig. 4A. It will be observed that the field became severely distorted when the slot was made sufficiently large to give reasonable efficiency. This trend is largely because the unloaded Q was only 2,000. Had it been higher, a lesser value of b would have sufficed to give a good efficiency.

In this experiment the walls of the resonator consisted of copper foil about 0.01 inch thick. The wall near the slot was next thickened to about six inches, whereupon no appreciable radiation from the resonator to free space was observed even with b at its maximum of ten inches.

The current antinode of a dipole that was tuned to the operating wavelength was next placed near the slot. Adequate energy could then be withdrawn to give good values of resonator-load efficiency, and negligible distortion of the internal field of the resonator was observed. The graph of resonator-load efficiency against b under these circumstances is given in Fig. 4B.

The tip of a tuned dipole was exposed to the field immediately outside an E aperture of such a resonator as that illustrated in Fig. 1B operating in the H_{011} mode. Very small loading was produced unless the aperture was made so large as to distort the field of the cavity. It is in general necessary to insert the dipole or tuned rod a considerable distance into the resonator, or even to connect it to the internal wall opposite the aperture to obtain reasonable resonator-load efficiency.

Hybrid Slots

Some slots are intermediate between the E aperture and the H slot. An example of the use of such a hybrid slot is of interest. It is placed between points of magnetic and electric antinodes of the resonator.

A cylindrical resonator that is depicted elsewhere in this article and whose dimensions are given in Fig. 5 was operated in the E_{010} mode—that is, with the electric field in the axial direction. A circumferential slot was arranged as shown, and bridges were provided to join the center of the flat upper side to the vertical sides of the cylinder.

With 20 bridges, Q_L closely approached Q, the unloaded Q value, which equaled 1,000. With only ten bridges, as illustrated, Q_L dropped to 630. With only two bridges, which were positioned at opposite ends of a diameter, Q_L was reduced to 200. With ten bridges, the thickness of the top was increased from 2.5 to 5.0 cm, and the height of the sides and the thickness of the bridges increased the same amount. However Q_L was unchanged, within the accuracy of measurement, from the previous 630. These results are applicable to the problem of coupling a circular wave guide to a cylindrical resonator.

Because a resonator designed for practical engineering applications seldom leads to analytically tractable shapes, the design of apertures seems to be performed best by experiment, and usually on model resonators the results of which can be scaled down to apply to the operative wavelength. Once the general phenomenon is understood, it is easy to produce desired degrees of loading by trial, with little error.

There does not seem to be an adequate published mathematical analysis of the properties of apertures, although an interesting paper by Neyman has been published in Russian (*Izvestiya Elektroprom. Slab. Toka,* 1940, No. 6, pp 1-16) which provides an admittedly approximate theory and quotes some experimental results.

It is not within the scope of this paper to deal with mathematical theory of apertures, but the following comments on Neyman's paper may be of interest.

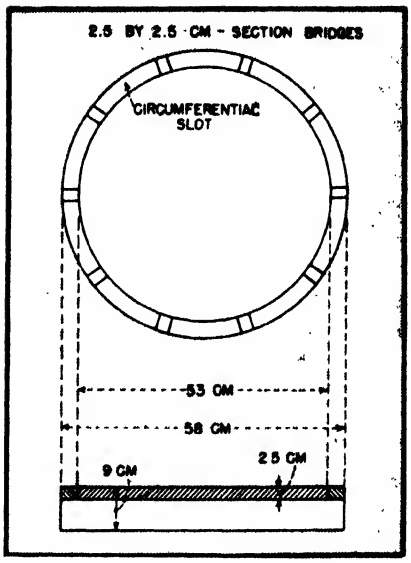

FIG. 5—Cavity used to study coupling to cylindrical resonators

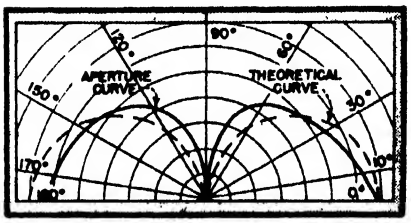

FIG. 6—Neyman compared the patterns of an aperture and a theoretical dipole

Neyman points out that a rigorous solution of the problem presents mathematical difficulties. He therefore presents an approximate solution for the E aperture, for which he gives experimental confirmation.

He concludes that the radiation resistance into free space of an E aperture situated at the electric antinode and having a radius r, small compared to the wavelength, is approximately $10^4(r/\lambda)^4$. This radiation resistance is referred to the maximum current in a cylindrical resonator operating in the E_{010} mode.

He also states that performance of an H aperture can be represented by a system of equivalent dipoles for which he derives formulas, but there does not seem to be experimental confirmation of these results nor of the statement that, for b equal r, the radiation from an E aperture is thousands of times greater than that

from an H slot. He also presents an expression for power radiated by an H slot which varies as b^6 and a^2. This result does not seem to be confirmed by this reviewer's experiments.

Neyman points out that loading can be increased by external tuned elements such as the dipole, or by resonance of the external surroundings of the resonator or of its own external contours. He also points out that radiation patterns can be produced that are the resultant of the fields from several slots.

The radiation pattern from an E aperture at the electric antinode is similar to that of a dipole. Neyman has shown this to be the case experimentally by the plot shown in Fig. 6.

The present author expresses his thanks to Rediffusion Ltd., at whose Electronics Department the experiments were performed, for permission to publish this paper.

Cavity Oscillator Circuits

Design of re-entrant type cavity oscillators using disk-seal tubes for uhf c-w or pulse operation takes into consideration methods of tuning and of extracting power. Dimensions and tuning characteristics of 10-cm oscillators are given

BY A. M. GUREWITSCH

DISK-SEAL TUBES are particularly adapted to the grid-separation circuit (also designated in the literature as grounded-grid or grid-return circuit), as contrasted to the conventional circuit usually used at lower frequencies. The differences between the two circuits are illustrated in Fig. 1A and 1B. The circuit usually used at lower frequencies is shown in Fig. 1A. Here the signal is introduced between the cathode and grid and the load is placed between the plate and the cathode. At frequencies where lumped circuit elements are generally used, this circuit performs satisfactorily. However, at higher frequencies where one is forced to use cavity resonators, the conventional circuit becomes impractical. The problems of shielding between input and output and of controlling exchange of energy between input and output become of prime importance.

Grid Separation Circuit

The grid-separation circuit shown in Figure 1B represents a practical solution. This circuit can also be used at lower frequencies; that is, its usefulness is not limited to cases where cavity resonators must be used. It is readily seen that, if the resonant elements are formed by resonant cavities as in Fig. 2, the grid plane forms a separation between the two resonant spaces; namely, the cathode-grid space and the grid-plate space. The only means by which energy can be exchanged between the two resonators is through the electron stream and by means of the coupling through the grid.

Computations on a circuit like this are similar to those on conventional circuits. For example, the power gain G is given by the expression

$$G = \frac{\mu + 1}{R_l + R_p} R_l$$

and for $R_p \gg R_l$, $\mu \gg 1$

$$G = G_m R_l$$

where G_m and μ are the transconductance and amplification factor respectively, R_p is the plate impedance of the tube at the frequency used, and R_l is the impedance of the load.

In oscillators an external coupling (feedback) of some kind between the two resonators is usually necessary, as indicated in Fig. 2. For amplifiers a regenerative control must be used in some cases. This coupling, called the feedback or regeneration circuit, has the job of taking a definite amount of energy from the grid-plate resonator and delivering it at a proper phase to the grid-cathode resonator. Generally a circuit like this is frequency-sensitive and represents a design problem for tunable oscillators, particularly if a single control

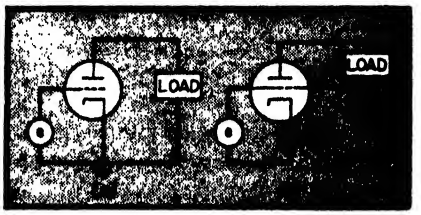

FIG. 1—(A) Grounded-cathode circuit conventionally used at low frequencies, and (B) grounded-grid circuit used at high frequencies

tuning is desired over an appreciable frequency range. Various designs of this coupling are possible.

Re-entrant Oscillator

This article deals with an oscillator of a design named the re-entrant type oscillator. This oscillator is simple mechanically. It can be tuned by a single control over a considerable range with fairly constant power output. The efficiency and reliability of this circuit, especially in the higher frequency range (around 3000 mc), became evident early in its development. It has been used successfully in a number of practical applications both as c-w and pulsed power sources. Different modifications of this circuit as applied to tubes of types 2C40 and 2C43 (see McArthur, E. D., Disk-Seal Tubes, ELECTRONICS, Feb. 1945, p. 98) are shown in Fig. 3 to 9.

TABLE I—C-W OPERATION OF CAVITY OSCILLATOR

f in mc	l_g	l_p	l_d
	all in inches		
3300	1.37	2.0	1.17
3000	1.75	2.4	1.55
1500	3.8	6.2	2.35
1000	5 6	9.4	1.78

See Fig. 3 for dimensions, d_p: 9/16 in., d_g: 13/16 in., d_a: 1-1/2 in.

As shown in Fig. 3, the oscillator consists of an outer cylinder which makes contact over the base of a disk-seal tube. An inner rod makes contact with its plate cap. A finger or capacitive type plunger closes the resonant space. The grid connection consists of a cylinder which clamps around the grid ring of the disk-seal tube. A d-c connection for the grid bias is made at the proper points on the grid cylinder. The frequency of oscillation depends primarily upon the length of the grid cylinder as shown by Table I. The plunger has to be placed at a proper position to obtain optimum performance. There are, however, other modes of operation in which plunger position is more important than grid cylinder length in setting the frequency.

For the circuit of Fig. 3, a d-c plate potential of 250 to 500 volts is recommended. A power output of 100 to 150 milliwatts can be obtained from a 2C40 tube at 3000 mc with a plate voltage of 250 volts.

Tuning can be accomplished in various ways. One method is to make the grid cylinder telescopic and to move it together with the plunger as shown in Fig. 4. Tuning can also be accomplished by moving the plate contact assembly including the plunger along the anode cap as shown in Fig. 5.

Figure 6 shows an oscillator which has a movable tuner on the plate rod and a separate plunger. The tuner

TABLE II—PULSED OPERATION OF CAVITY OSCILLATOR

f in mc	l_g	l_a	l_d	l_p
	all in centimeters			
3300	2.7	2.28	2.2	5.4
3000	3.5	2.5	3.0	6.2

See Fig. 7 for dimensions, d_a: 1-15/32 in., d_p: 9/16 in., d_g: 1-1/4 in., d_p: 13/16 in.

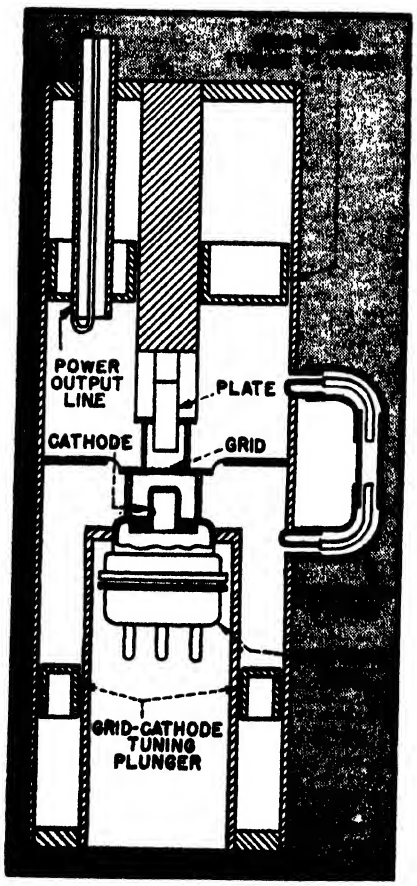

FIG. 2—In this grounded-grid cavity circuit, the grid and grid mounting ring form a separating plane between cathode and anode cavities

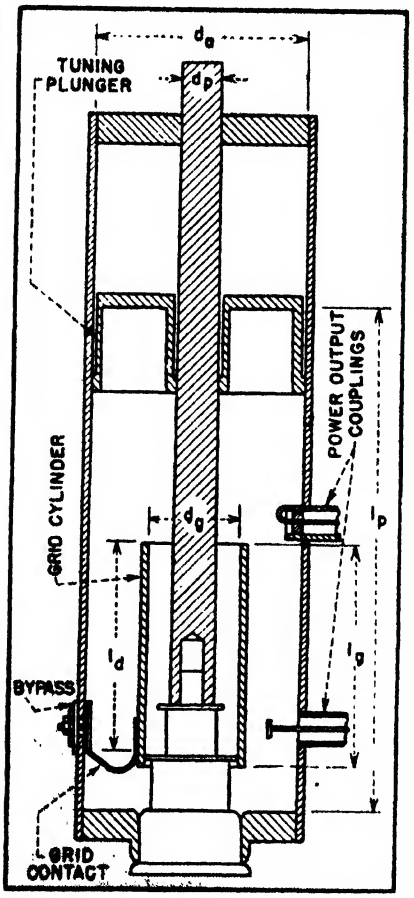

FIG. 3—Length of the grid cylinder determines the frequency of this cavity oscillator. The tuning plunger is set for optimum performance

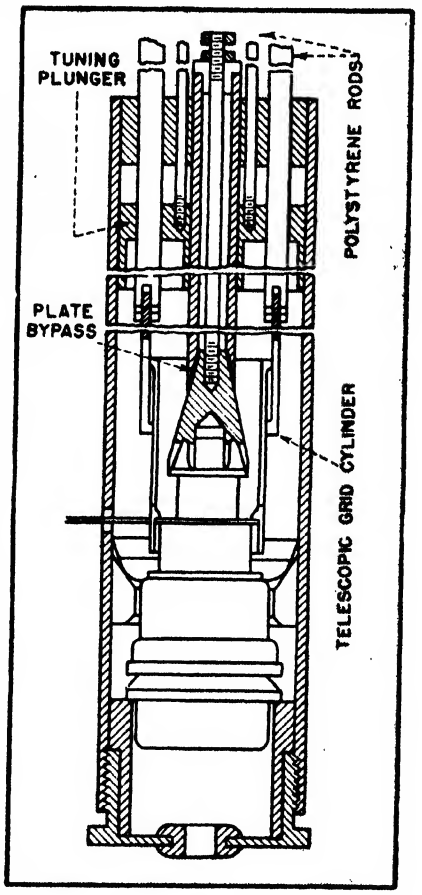

FIG. 4—As the telescoping grid cylinder tunes the cavity oscillator, the tuning plunger also moves to maintain optimum conditions

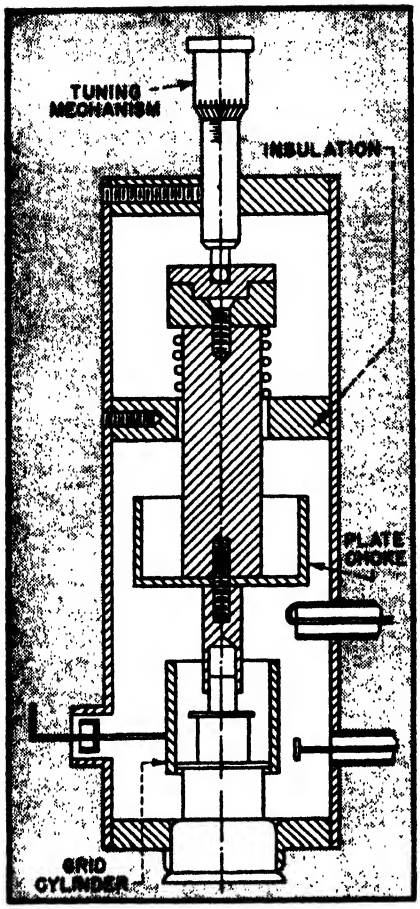

FIG. 5—This tuning method requires a sliding contact at the anode cap that must pass d-c and withstand the high anode temperature

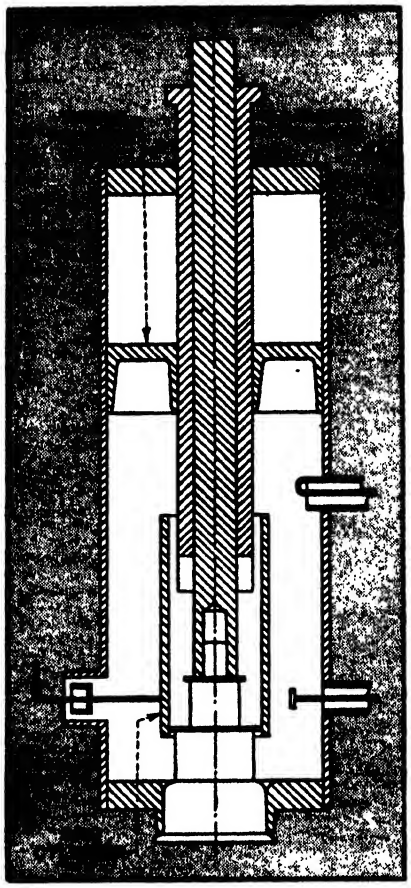

FIG. 6—To obtain a more reliable sliding contact than that of Fig. 5, the tuning plunger is mounted on a sleeve that slides on the plate rod

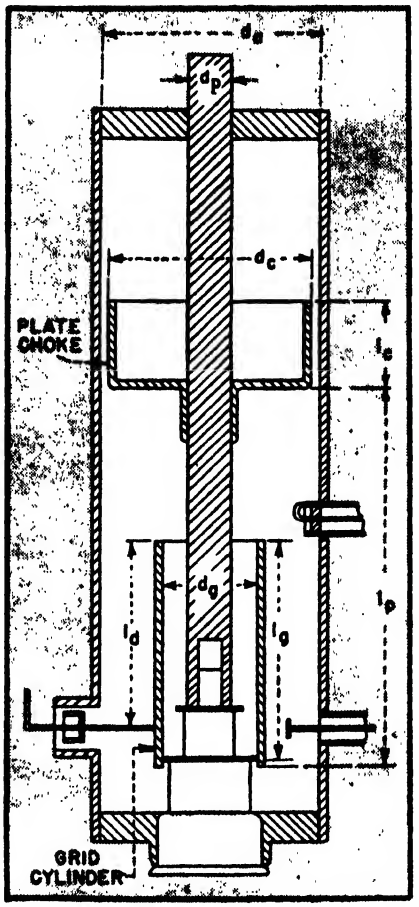

FIG. 7—Whereas tuning plungers have both inside and outside sliding contacts, plate chokes must slide only on their inside faces

on the plate rod is first put as near the plate of the tube as possible and the plunger adjusted for optimum operation. Then the plate tuner and the plunger are locked rigidly together and moved simultaneously for tuning.

The problem of power extraction from such an oscillator is, of course, one of matching the desired load impedance to the impedance that the oscillator requires for optimum operation. This can be accomplished in any of the well-known ways of impedance matching over the necessary range. Preferably, points for power extraction should be chosen which are physically convenient. The adjustments of the impedance matching system will then be best accomplished experimentally. For example, the loop near the end of the grid cylinder nearest the plate side or a probe near the grid ring have been used successfully. The adjustment was accomplished by moving these probes or loops radially and axially. These different methods are illustrated in the drawings of the several types of oscillators.

For pulsed operation with the 2C43, the data for the oscillator shown in Fig. 7 is presented in Table II. A plate voltage peak of 2.5 to 3 kv was used with these circuits. A power output in the order of 1 kw

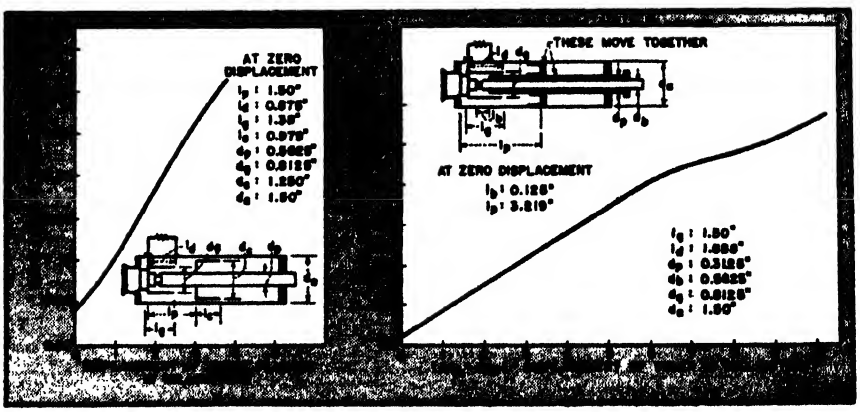

Left. Frequency characteristics of re-entrant oscillator of the type shown in Fig. 5. Right. Frequency characteristic of re-entrant oscillator tuned by the method illustrated in Fig. 8

can be obtained with 3 kv at the plate, 1,000 pulses per second, and 1-microsecond pulse duration.

The frequencies given in this article are, of course, only approximate for the indicated dimensions. The actual frequencies will depend on which type of tube is used and will vary somewhat among tubes.

Waveguide Transmission Systems

The useful transmission of power from a microwave oscillator to an antenna invariably requires a multiplicity of joints and bends. These components must be carefully engineered and fabricated to avoid undue losses or standing waves arising from discontinuities

By THEODORE MORENO

A RECTANGULAR WAVE GUIDE system that connects a microwave transmitter or receiver to an antenna may contain a considerable number of cascaded wave guide sections and components. Some of the components that might be found in a typical system are shown in Fig. 1, and include straight sections, bends, twists, right angle corners, rotating joints, and coaxial line to wave guide adaptors. In addition, the components must be assembled with the use of connectors which join together the various wave guide sections.

To operate at maximum efficiency, the transmission system should have minimum attenuation. Furthermore it should be electrically smooth and free from impedance discontinuities, otherwise standing waves will be set up in the line with a consequent increase in the attenuation. A more serious effect of these discontinuities in the line may be the resulting impedance mismatch between the transmitter or receiver and antenna. These mismatches may lead to very serious decreases in transmitter power output or receiver sensitivity. Furthermore, if there is a guide very many wavelengths long between the discontinuity and transmitter, the load impedance presented to the transmitter may be a very rapidly varying function of frequency, with resulting instability in the transmitter output.

The maximum allowable attenuation for the transmission system, and the maximum allowable input voltage standing wave ratio ($\eta_s = E_{max}/E_{min}$) to the system with a matched load on the far end are determined by the required overall performance of the receiver or transmitter. Once the performance requirements of the transmission system have been established, and the number of components in the system are known, the required attenuation and standing wave ratio of each component may be estimated.

If there are no resonances in the system, the overall system attenuation, expressed in db, will be the sum of the attenuations of the individual components and connectors. The reflection introduced by each component will add to or subtract from the reflected wave already present in the system, depending upon their phase relationships. The input standing wave ratio to the entire system cannot be predicted unless the phase relationships of the reflections introduced by each component are known. Usually this information is not available; only the standing wave ratios introduced by the components are known. But if there are n components and connectors, each introducing a standing wave ratio (η_1) into a matched line, the maximum standing wave ratio (η_{max}) for the entire system, which will be encountered if all reflections add in phase, will be given by

$$\eta_{max} = (\eta_1)^n$$

The most probable standing wave ratio for the entire system (η_{pr}), assuming random phase addition of all reflections, is given to a good approximation by

$$\eta_{pr} = (\eta_1)^{\sqrt{n}}$$

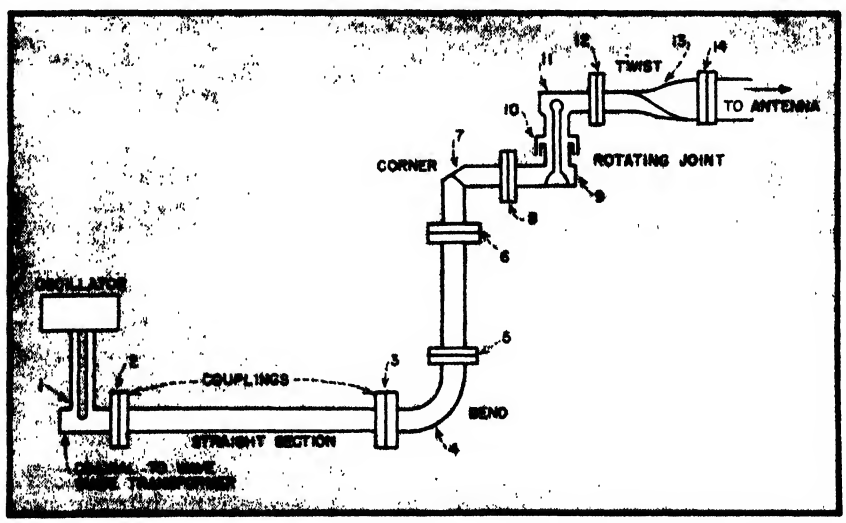

FIG. 1—Typical wave guide transmission system. The numbers indicate the possible discontinuities encountered in such a structure

if the number of components or the reflection from each component is not excessively large.

It is apparent that if the overall system requirements are strict, and there are a considerable number of components and connectors in the system, the requirements imposed on the performance of each component may be quite severe. For example, if there are 10 elements in a microwave system, each with a loss of 0.1 db and capable of introducing a swr of 1.05 into a matched line, the total loss in the system will be $10 \times 0.1 = 1.0$ db or 21 percent of the input power. The most probable input swr will be 1.17 and the maximum possible swr will be 1.63. But if each component has a loss of 0.3 db and introduces a swr of 1.2, the total loss will be 3.0 db or 50 percent of the input power, the most probable swr will have risen to 1.78, and the maximum possible swr will have reached 6.2, in general a prohibitively large value for satisfactory system operation.

Each connection between the various components of a wave guide transmission system is a possible discontinuity in the transmission line, and the connectors must therefore be carefully designed if the system is to operate at maximum efficiency.

Wave Guide Connectors

If the ends of two sections of wave guide are machined off square and then clamped tightly together, the resulting butt joint will generally be electrically smooth and free from loss. The only discontinuity offered by such a butt joint will result from misalignment and differences in the guide dimensions on either side of the joint. These are usually negligible if the wave guides are held to close tolerances during manufacture, and both the loss and reflection will be so small as to be very difficult to measure.

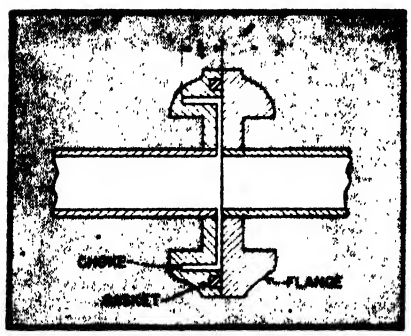

FIG. 2—A choke-flange coupling used for connecting sections of rectangular wave guide

The efficiency of such a connection depends critically upon the tightness of the joint between the wave guides. If the ends of the guide are not finished square and smooth, if the guides are misaligned or not clamped tightly together, the loss and reflection may be relatively large. And if the joint is not mechanically satisfactory, it is impossible to predict accurately what its electrical performance will be without careful measurement, although losses in the order of 1.0 db have been measured. So while the simple butt joints may be very satisfactory, and are even preferred when accurate measurements are being performed, they must be assembled with considerable care and mechanical accuracy.

The assembly of wave guide components is greatly facilitated with the use of choke couplings, as illustrated in Fig. 2. These may be designed to offer a minimum reflection and loss, and offer great advantages in flexibility and reliability. The L-shaped cavity between the choke and flange may be considered a half-wave shorted line in series with the wave guide, which presents a short circuit at the input and offers therefore a minimum electrical discontinuity. The circular slot in the choke is a quarter wavelength deep. This places the contact between choke and flange at a point of zero current; therefore the contact does not have to be good. The distance from the slot to the wave guide must be determined experimentally, but it is electrically equivalent to a quarter wavelength. For maximum bandwidth, the width of the slot should be appreciably greater than the separation between choke and flange faces.

A choke-flange connection of this type when properly designed will introduce a swr less than 1.05 over most of the usable range of the wave guide. The loss will be in the order of 0.001 to 0.01 db, increasing with decreasing guide size, and independent of the tightness with which the choke and flange are clamped together.

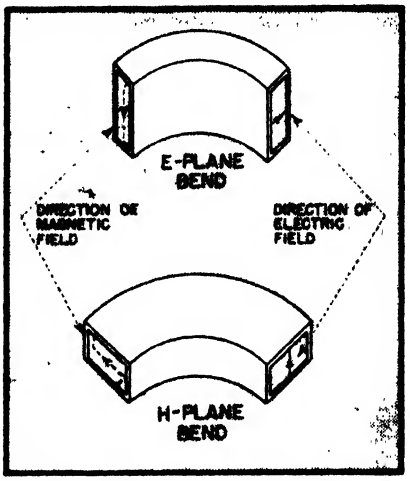

FIG. 3—Bends used to change the direction of rectangular wave guide

Transmission through a choke-flange joint will be satisfactory even if the choke and flange faces are separated and misaligned to a certain extent, or if these joints are used for nonrigid couplings such as are required when a shock-mounted chassis is connected to a rigidly mounted line. If a clearance of $\frac{1}{4}$ wavelength is allowed between choke and flange, a sidewise displacement of up to $\frac{1}{4}$ wavelength will not raise the loss above 0.3 db, or the swr above 1.3.

Two chokes paired together will generally form a satisfactory connection, and may allow a greater separation for a nonrigid joint. But with paired chokes there is usually a resonance encountered near the design wavelength, which is marked by a sharp rise in the loss and swr. Also the swr over a band of frequencies is generally higher than for the choke-flange combination.

Wave Guide Bends

The direction of transmission in a wave guide system may be changed by bending the wave guide. The bend may be in the plane of either the electric or magnetic fields, and is correspondingly called an E or H plane bend (Fig. 3). The radius of the bend is not critical and may be quite small.

If the inner radius of the bend is

greater than a guide wavelength, λ_g, the swr will be under 1.05 over the normal operating range of the wave guide. A much smaller radius, down to $\lambda_g/4$ or less, will produce a swr in general under 1.1, but considerable care must be applied to the fabrication of the bend to achieve these results. A simple theory predicts that best results will be found with bends whose mean length is an integral number of half wave guide wavelengths, but the effects of irregularities in fabrication are usually much more important.

Several techniques of fabricating bends are widely used. The tubing may be filled with a low melting-point alloy and bent around the desired inner radius. For small radii, the cross-section will be distorted from a rectangular into a trapezoidal shape, which will increase the reflection, but the desired cross-section may be maintained by forcing rollers through the guide after the bend has been made.

Small radius bends are also fabricated from sheet brass by silver soldering, but this must be done with care, or irregularities will mar the inside surface. Electroforming[1] is satisfactory, giving bends with a uniform, rectangular cross-section and smooth inside surface.

Wave Guide Twists

A rectangular wave guide may be twisted about its axis to rotate the direction of the electric field. No great standing ratio will be set up if the guide is not deformed in the process (Fig. 4). Filling the guide with low melting-point alloy before twisting is a common method of fabrication, and electroforming is also satisfactory. If the twist is $2\lambda_g$ or more in length for a 90 degree rotation, the swr will generally be under 1.1, and shorter twists are satisfactory if carefully made.

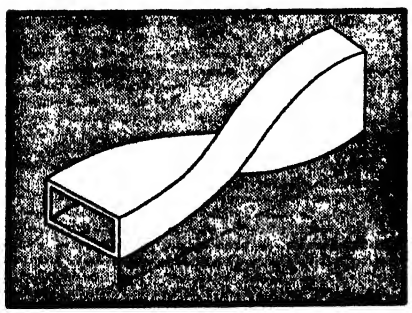

FIG. 4—A twist in rectangular wave guide

Wave Guide Corners

Changing the direction of transmission in a wave guide system by an abrupt corner is generally not satisfactory, as an appreciable reflection will be set up. But if the desired angular change is accomplished by using two simple corners (Fig. 5), spaced apart approximately a quarter wave guide wavelength ($L/\lambda_g = \frac{1}{4}$), the reflections from the two corners will cancel each other. For E plane corners, the optimum spacing is given very closely by $L/\lambda_g = 0.25$ for angles up to 90 degrees, but for H plane corners, this optimum spacing is slightly different, and is plotted as a function of λ/a in Fig. 5 for a 90-degree total change in direction.

The bandwidth over which these corners will introduce a standing wave ratio less than 1.05 is generally plus or minus three decreased by 10 percent of the center frequency for a 90 degree bend, increasing as λ/a decreases, and is greater for smaller angles. Circular bends are preferred for larger angles and greater bandwidths.

It is also possible to eliminate the reflection at an abrupt corner by modifying the corner as illustrated in Fig. 6, and the bandwidth will be very nearly the same as for the double corner. The required dimensions for the corner are plotted as a function of the angle for both E plane corners and H plane corners in Fig. 6. This type of corner must be held to rather close manufacturing tolerances to attain the optimum performance.

Tee Joints in Wave Guides

Tee joints in rectangular wave guides are similar to stubs in conventional transmission lines. A stub that branches from the broad side of a rectangular guide in the E plane is in series with the main guide, and a stub that branches from the narrow side in the H plane is in shunt with the main guide (Fig. 7).

The presence of the fringing fields

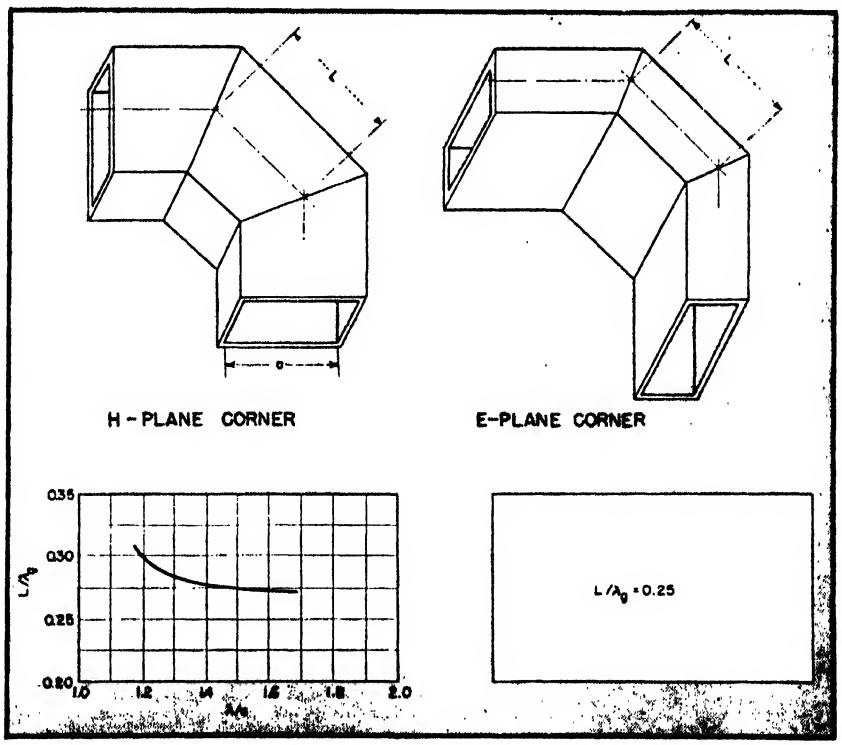

FIG. 5—Ninety-degree corners in wave guide designed for minimum reflection. Optimum spacing for E-plane corners is determined from the expression in the box; that for the H-plane corner from the graph

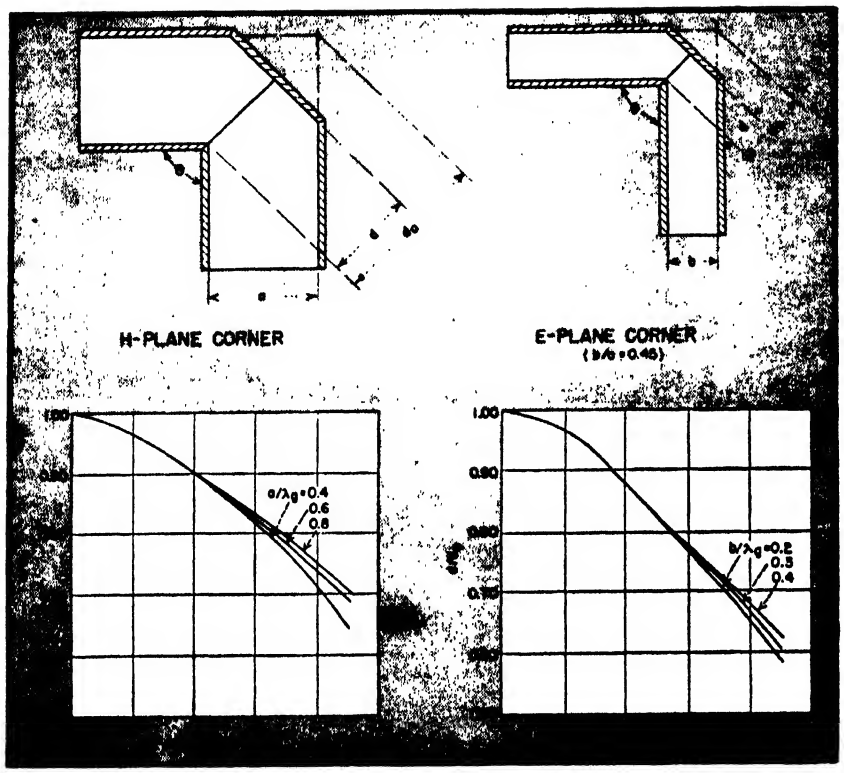

FIG. 6—Single-corner with minimum reflection. Required dimensions for both types of corner are plotted as a function of the angle

at the corners somewhat modifies the action of the tees. With the series or E plane tee, a short circuit placed $\lambda_g/2$ away from the junction should allow perfect transmission past the stub, and a short $\lambda_g/4$ away should cause complete reflection at the stub. For the shunt or H plane tee, a short $\lambda_g/4$ away should give perfect transmission, and a short $\lambda_g/2$ away should cause complete reflection. It is actually possible to find positions of the short in both branch arms which give perfect transmission and complete reflection, but the locations are slightly different from the above values, and depend upon the ratio of wave guide dimensions to wavelength.

With the idealized tees, it should be possible to locate a short in branch one to allow perfect transmission from branch two to stub arm branch three, or to cause a complete reflection at the junction. With the actual tees, it is possible to locate the short to give a complete reflection for an input signal from branch two or three, but there is no short location which will give perfect transmission between these arms. The minimum swr which can be attained will depend upon the ratio of wavelength to guide dimensions, and upon the type of tee, but will usually be of the order of 1.5. For perfect transmission, it is necessary to modify the tee by the addition of some sort of matching structure, such as the metallic diaphragm indicated in Fig. 7.

In the design of wave guide components, it is often necessary to employ some sort of matching device to remove the reflected wave that results from a discontinuity. This may be accomplished by introducing an additional discontinuity, the reflection from which is of the proper magnitude and phase to cancel the undesired reflected wave. Thin metal diaphragms or metal posts are widely used for this purpose; these are equivalent to susceptances that shunt the transmission line.

The required normalized susceptance may be determined by measuring the swr in the line that is to be reduced, and is given by

$$|B/Y_0| = \eta_v - 1/\sqrt{\eta_v} \qquad (2)$$

The susceptance should then be placed at a distance d_1 from a voltage minimum, given by

$$\frac{d_1}{\lambda_g} = \frac{90 - \tan^{-1} \frac{1}{2}|B/Y_0|}{720} \qquad (3)$$

where the arctangent is expressed in degrees. The matching susceptance if inductive should be placed at this distance on the load side of a voltage minimum, if capacitive it should be located an equal distance toward the signal input from minimum. For minimum frequency sensitivity, it should be located as near as possible to the source of the undesired reflection, and it should be kept in mind that voltage minimums are spaced apart $\lambda_g/2$ along the input guide to the source of reflection.

One of the most commonly used

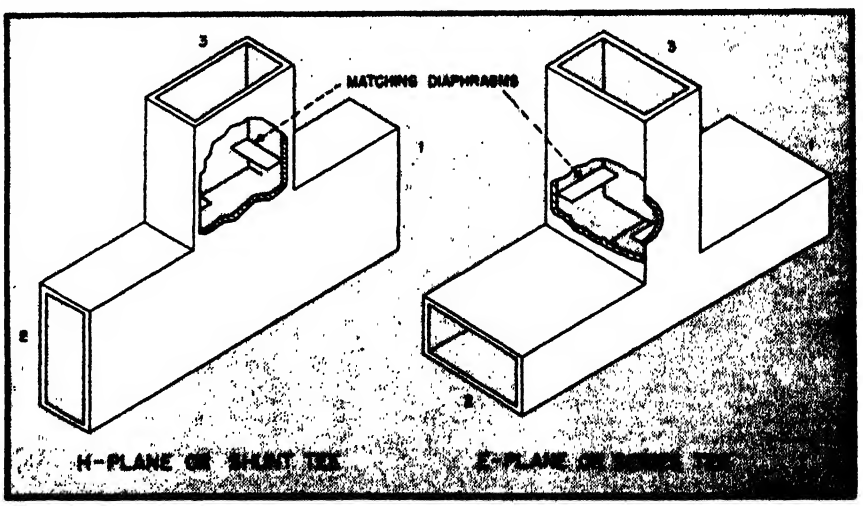

FIG. 7—Tee joints in rectangular wave guides, showing matching diaphragms

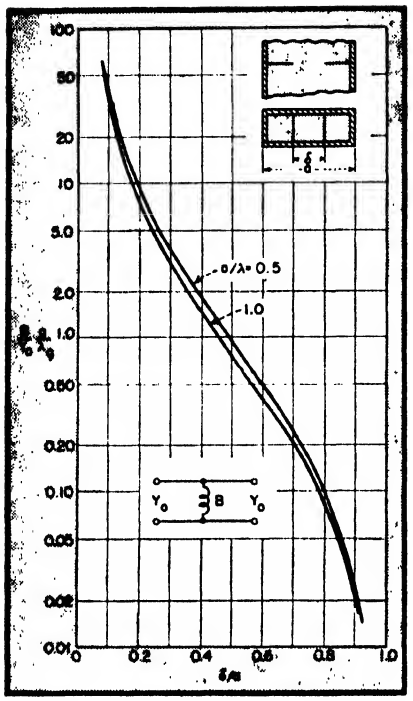

FIG. 8—Susceptance of the inductive diaphragm used for impedance matching in rectangular wave guides as a function of dimensions

matching susceptances is a thin metal diaphragm placed transversely across the wave guide, with an opening symmetrically located and extending across the wave guide parallel to the narrow dimension (Fig. 8). This type of diaphragm is equivalent to an inductive susceptance shunting the guide. The magnitude of this susceptance depends upon the size of the opening in the diaphragm, and may be obtained from the figure.

Another matching susceptance that is widely used is a metallic post or tuning screw centrally located in the broad side of the guide and extending part way across parallel to the electric field. This screw is equivalent to a shunting capacitive susceptance whose magnitude increases with probe depth. A resonance is reached when the probe depth is approximately a quarter wavelength, and for greater lengths the probe is inductive, but practically it is never used in the inductive region.

The output of many microwave oscillators is delivered into a coaxial line, and some sort of coaxial line to wave guide transformer must be used to send the signal through a wave guide transmission system. The most suitable transformer section is one that introduces no reflected wave when a signal is fed between the coaxial line and wave guide in either direction. If losses are low, reflectionless transmission in one direction is a guarantee of reflectionless transmission in the other.

The simplest coaxial line to wave guide transformer is constructed by extending the center conductor of the coaxial line into the wave guide to form a probe antenna in the wave guide, parallel to the electric lines of force (Fig. 9A). This transition will introduce no reflection at a single frequency if the probe antenna is of the proper length and the proper distance from the wave guide short. Both of these dimensions are roughly a quarter wavelength, but must be determined experimentally for satisfactory results.

The bandwidth over which the transformer is satisfactory is made greater by increasing the size of the coaxial line and the diameter of the antenna, and also by rounding the end of the antenna. It is still further increased by modifying the probe as shown in Fig. 9B, to end in a metal sphere, and by flaring the outer conductor of the coaxial line into the inner wall of the wave guide. A transformer of this type can be designed to introduce a swr below 1.2 over most of the useable range of a wave guide.

Two additional designs of fixed-tuned broadband transformers are shown in Fig. 9C and D. Type C is called a doorknob transformer, and has been designed to handle high powers. Both C and D provide a support for the center conductor of the coaxial line, and also a direct current return, which are advantages for some applications. Both of these designs have good bandwidth, but the optimum dimensions must be found experimentally for different sizes of coaxial line and wave guide.

Reference

(1) Hassell, F., and Jenks, F., Electroforming Microwave Components, ELECTRONICS, p 134, March, 1946.

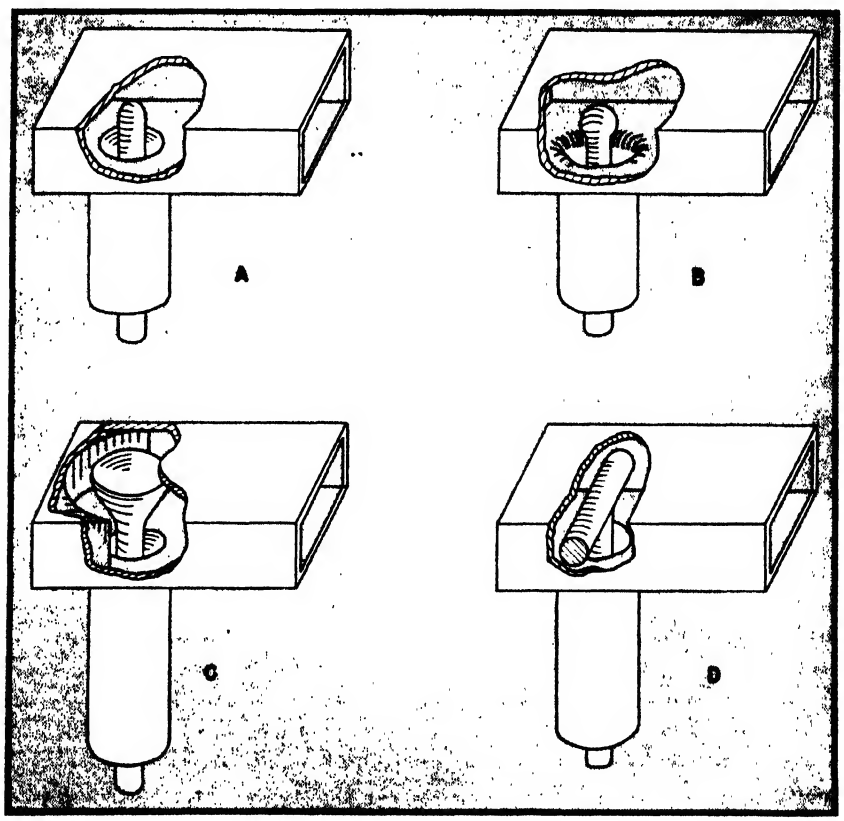

FIG. 9—Broad-band, fixed-tuned coaxial line to wave guide transformers. These methods of construction are necessary to provide reflectionless transmission

Coaxial Butterfly Circuits

Coaxial versions designed to fit over the type 2C43 lighthouse tube serve as wide-range uhf signal generators suitable for general laboratory use in the range from 500 to 1,600 megacycles. A single control varies feedback and frequency for either c-w or pulsed operation

By ERVIN E. GROSS, Jr.

IN SPITE of the large increase in production and use of high-frequency equipment during the war, simple and convenient laboratory apparatus such as variable oscillators and standard-signal generators, for frequencies above 500 megacycles, have not progressed commensurably. Much equipment has been built and used at frequencies well above 500 megacycles, but most of it has been for special purposes and is not suitable for general laboratory use.

During the emergency period, when speed was essential, it proved much quicker and easier to build a series of fixed-frequency test oscillators for specified frequencies and uses than to build multiple-purpose wide-range variable oscillators.

While fixed-frequency or limited-range oscillators were being used as an expedient, development work was continued on wide-range variable oscillators. This paper is a report on one such development, using the type 2C43 lighthouse tube. The oscillators developed have a single tuning control, wide tuning ranges, good output, and no sliding contacts.

Original Butterfly Circuit

Simple negative-grid triode oscillators using a single tuned circuit between grid and plate can be made to operate at frequencies approaching the resonant frequency of the tube if the tube has properly proportioned grid-cathode and plate-cathode capacitances. A compact tuning unit such as the butterfly circuit[1] is connected with a minimum of lead inductance between grid and plate, while feedback to sustain oscillation is determined by the effective grid-cathode and plate-cathode capacitances.

Because of the low ratio of plate-cathode to grid-cathode capacitance of the disc-seal or lighthouse tubes, efforts to use these in simple oscillator circuits were not successful above 700 megacycles. However, of the available high-frequency triodes, the lighthouse tube seems to have power ratings best suited for use in laboratory oscillators, when maximum frequency and good output are required. Although this tube does not work well in the simple oscillators using a single tuned circuit, it will oscillate to higher frequencies than other available tubes, with good efficiency, when used in oscillators employing multiple tuned circuits.

Coaxial Version

To build a tuning unit to fit the lighthouse tube in a convenient manner, a much different mechanical structure from the original butterfly circuit was required. Since the tube was designed for use in coaxial-line resonators, it seemed desirable to try to build variable oscillators using elements of coaxial lines as resonant circuits. The resulting tuning unit is known as the coaxial butterfly.

Figure 1 illustrates the basic form of the coaxial butterfly tuning unit, showing the high-frequency position of the rotor at the left and the low-frequency position at the right. This unit consists of a coaxial line shorted at one end and open at the other. The outer conductor is not a full cylinder, but has two 105-degree sections cut away. Rotating between inner and outer conductors are two 75-degree sectors which vary the frequency.

In operation the tube is connected across the open end of the line and acts as a capacitive load foreshortening the line. The length of the line at resonance is much less than a quarter-wavelength because of this loading. As the two rotor sectors are rotated, the characteristic impedance of the line is varied. This means that the amount of foreshortening caused by the tube grid-plate capacitance changes, and hence the resonant frequency is varied.

Figure 2 shows a basic unit equipped with terminals for connection to the plate and grid of the lighthouse tube. In addition to the loading

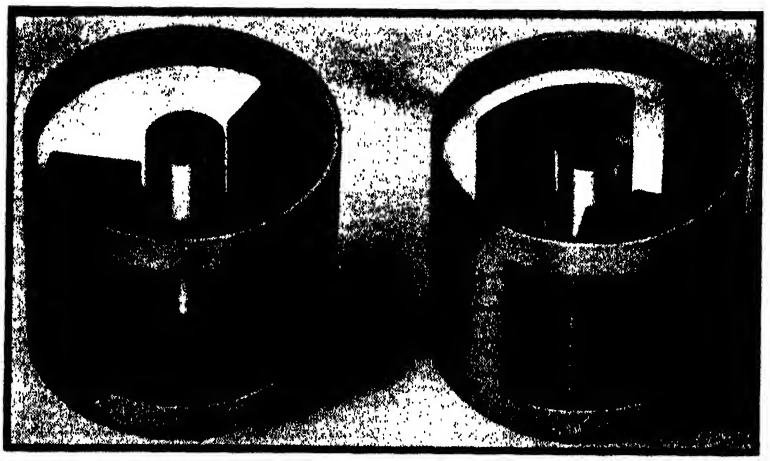

FIG. 1—Basic form of coaxial butterfly circuit. High-frequency setting is shown at left, low-frequency setting at right

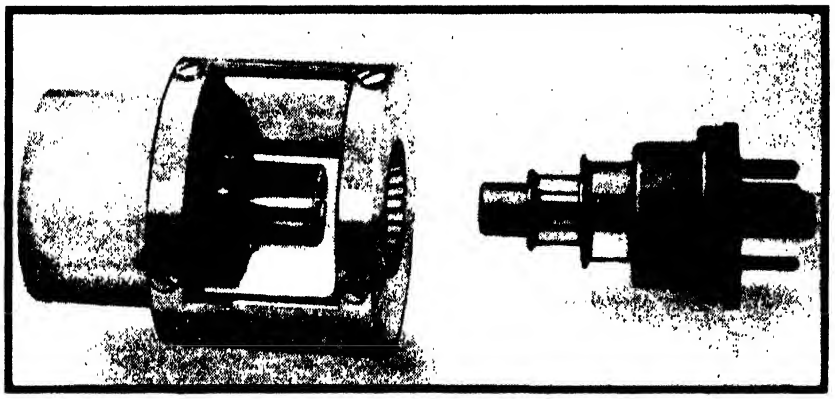

FIG. 2—Coaxial butterfly unit, designed to make plate and grid connections automatically when pushed over the lighthouse tube

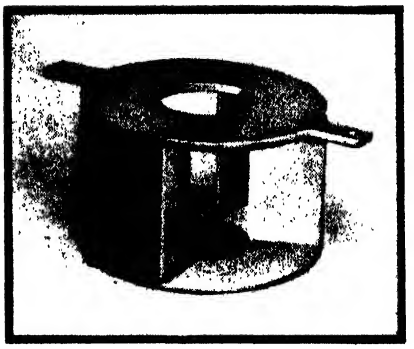

FIG. 4—Coaxial butterfly rotor construction which has given widest frequency ranges in uhf oscillators

caused by the tube grid-plate capacitance, there is some capacitance added across the open end of the line by the rotor segments.

Frequency-Capacitance Chart

To get a better understanding of these tuning units, the plot shown in Fig. 3 was made. Values of loading capacitance required for a line of unit cm length are plotted versus frequency for a range of Z_0 from 10 to 500 ohms.

Besides showing that there is not much to be gained in frequency range by making the loading capacitance larger than the tube grid-plate capacitance, the chart can be used as a means of finding the resonant frequency for a line of known impedance Z_0, known length, and a given loading capacitance, or to obtain the proper loading capacitance for a desired frequency with a line of given Z_0 and length.

The chart has proved very useful in designing some of the coaxial tuning units. For example, with the dimensions and spacings that are considered practical in these tuned circuits, Z_0 can be varied from about 30 ohms to 150 ohms. If we make the tuned circuit 2 cm long, what frequency range should we get if the total effective loading capacitance is 4 $\mu\mu$f. This makes $n = 2$; the chart is adapted for this line length by multiplying capacitance scale values by 2. The original 2-$\mu\mu$f line on the chart now represents 4 $\mu\mu$f, the value at hand, and the frequency values obtained will be divided by 2. For $Z_0 =$ 150 ohms the frequency then is 1,600/2, and is 3,200/2 at $Z_0 =$ 30 ohms, giving a frequency range of 800 to 1,600 megacycles for the unit.

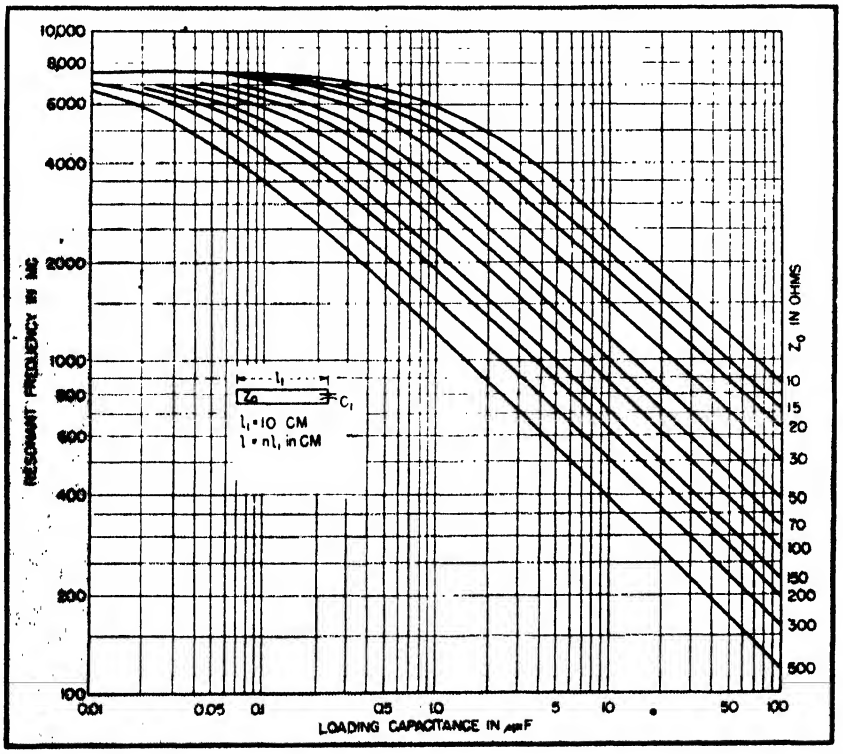

FIG. 3—Calculated curves of resonant frequency as a function of loading capacitance and Z_0 for a line of unit cm length. For a line n cm long, multiply capacitance scale values by n and divide frequency scale values by n before using chart

Figure 4 shows the rotor construction which has given the widest frequency ranges. The two full metal rings at the ends not only make a stronger and more easily supported rotor than is shown in the basic units, but serve to keep the lumped inductance at the ends of the line at a minimum so that it is possible to take advantage of most of the change in Z_0 caused by the rotor segments.

Wide Frequency Ranges

The most effective means for getting wide frequency ranges has been to reduce all spacings between the rotor and the fixed portions of the tuned circuit. This decreases the effective Z_0 when the rotor is meshed with the outer conductor. In addition, the effective loading capacitance is increased. At low frequencies, Z_0

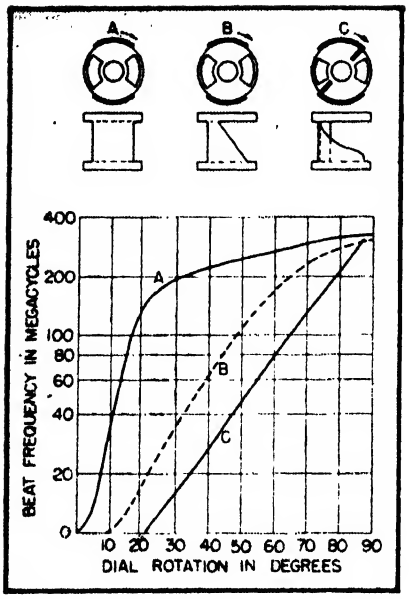

FIG. 5—Example of frequency variation versus dial rotation that is possible with coaxial butterfly units. Curves A, B, and C apply when stator or outer conductor of unit is shaped as in sketches A, B, and C respectively

is unchanged, and the resonant frequency is reduced. At high-frequency settings the resonant frequency is increased because the decrease in Z_0 has greater effect than the increase in loading capacitance.

Stator Design

The stator or outer conductor of the line can be altered or shaped to provide a desirable law of frequency variation. While this lowers the top frequency for a given unit, the consequent reduction in the low-frequency limit produces an increased frequency range. Figure 5 illustrates one possibility. Here a 1,000-1,300 megacycle oscillator was designed for beat operation with a fixed 1,000-mc oscillator. A logarithmic variation of beat frequency was desired between 10 and 300 megacycles. Curve A shows the variation obtained before shaping, with most of the frequency change occurring in the relatively small region where the rotor segments are just beginning to pass under the outer conductor. Curve B shows the results of shaping the stator as indicated in sketch B, and curve C shows the final curve obtained with the outer conductor shaped in the manner shown in sketch C. It will be noted that rotation has been reduced from 90 degrees to slightly less than 70 degrees.

The Q obtained with a coaxial butterfly circuit is low when compared with that obtained in coaxial tuners of optimum dimensions. Measurements on a tuning unit with a range of 620-1,350 megacycles indicate that the Q is about 350 at the low frequency and about 200 at 1,000 megacycles.

Feedback Circuits

The basic feedback circuit used with coaxial butterfly oscillators is shown in Fig. 6. The coaxial butterfly unit supplies a high resonant impedance between grid and plate of the tube. The outer cylinder, with tube and tuned circuit forming part of the inner conductor, makes up a coaxial resonator between grid and cathode of the tube. The fields of the two circuits are linked through the openings of the coaxial butterfly. Proper feedback for oscillation is obtained by adjusting the two disc-shaped plungers within the outer cylinder.

In addition to the frequency-determining rotor, this system requires two adjustable elements which have multiple sliding contacts. This circuit can be simplified if the plungers are properly located for the highest oscillator frequency and feedback for lower frequencies is maintained by adding capacitance C_r between a point on the tuning unit and a point on the outer chamber.

Sliding contacts can be eliminated if this capacitance is added, as shown in Fig. 7, by a series of adjustable metal fingers (a) which mesh successively with a tab on a ring (d) which is carried by the rotor. While multiple tuning elements are required, a variable oscillator with a single tuning control is the result. Oscillators with capacitive feedback adjustments such as this work satisfactorily over frequency ranges of about 1.6 to 1. Coaxial butterfly tuning units can be conveniently built to cover ranges of 2 to 1.

To make use of ranges available for grid-plate tuning units, an additional element to the feedback circuit was found necessary. This addition, shown in Fig. 8, consists of added grid-cathode capacitance produced by a series of adjustable fingers (b) mounted on the cathode stub which mesh successively with the shoe (c) mounted on the feedback ring (d).

As will be demonstrated, the feedback circuits outlined affect the coupling between the grid-plate tuning unit and the grid-cathode resonant circuit as well as keep the grid-cath-

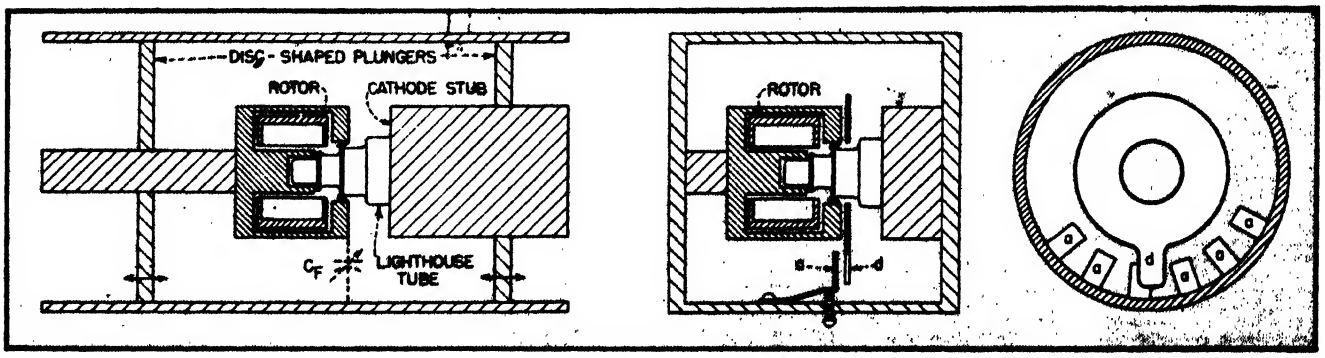

FIG. 6—Basic feedback circuit used with coaxial butterfly oscillators described in this article

FIG. 7—Cross-section and end views of oscillator, showing C_r of Fig. 6 added to eliminate sliding contacts

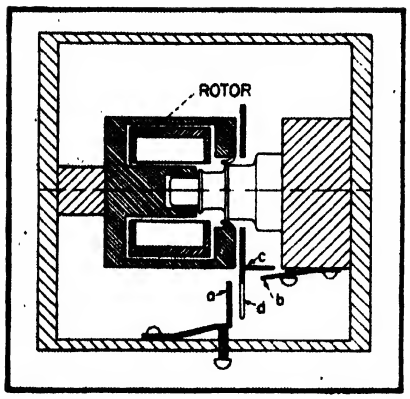

FIG. 8—Feedback circuit for wide-range coaxial butterfly oscillator, with no sliding contacts

ode circuit properly tuned. Variations in coupling are caused by the relation of the feedback fingers (a) to the openings in the coaxial butterfly unit. For this reason, and because the coupling varies with the rotor position, some amount of experimenting and compromising is required before a continuously variable oscillator with a frequency range of 2 to 1 can be obtained. The final result, however, is an oscillator that has a wide tuning range, good efficiency, a single tuning control, and no sliding contacts.

Steps in the development of oscillators using the coaxial butterfly circuit have been outlined. Operating characteristics and descriptions of some of these oscillators follow.

The first oscillators developed using the coaxial butterfly unit were for use in a beat-frequency oscillator having a fixed 1,000-mc oscillator beating with a variable 1,000 to 3,000-mc oscillator to produce an output frequency of 10 to 300 mc.

Beat-Frequency Oscillator

The beat-frequency oscillator was suggested as a means for obtaining pulses with extremely short rise time at low frequencies where conventional oscillators do not have sufficiently rapid starting or buildup time. The fixed oscillator was to operate as either a c-w oscillator or a pulsed oscillator.

Pulsing requires more than the usual feedback to obtain the short rise time, and early experiments using the sliding end discs for feedback adjustment showed that a change in feedback was required if the oscillator was to be shifted from c-w operation to pulsed operation. It was noted that the change was accomplished by keeping the length of the outer cylinder constant and moving the tuning unit with respect to the end discs.

It was also found that the results could be duplicated by using the capacitive-type feedback. To reduce drift, the two oscillators were kept as much alike as possible. Outer chamber dimensions were kept the same. Adjustable capacitive-type feedback was retained for the fixed oscillator to obtain the required change in feedback, and the fixed oscillator grid-plate tuning unit was built as a coaxial butterfly with the rotor omitted.

Oscillator Buildup Time

Figure 9 demonstrates rather clearly that the capacitive adjustment does more than keep the grid-cathode chamber properly tuned. By shifting the point at which the capacitance is produced, frequency stability and oscillator starting or buildup time are markedly modified. As indicated by the upper right-hand sketch, the oscillator buildup time has been broken up, for convenience, into two components, which have been called T_D and T_R (delay time and rise time). Good stability required for c-w operation results when the capacitance is produced in line with the solid portion of the tuning unit, while rapid rise time and short delay time required for pulsed operation result when the capacitance is produced in line with the opening of the tuning unit.

As a pulsed oscillator, delay time was reduced to about 0.05 microsecond and the rise time was reduced to less than 0.05 microsecond. Many things was tried in an effort to improve the rise time of the oscillator under pulsed conditions. Loading the oscillator in an effort to reduce the Q of the tuned circuit was one device that was effective. The effect was not noticeable, however, until feedback had been adjusted for optimum pulse shape.

As a means to pulse the oscillator, a relatively low-power negative pulse was produced across the cathode resistor. This method was simple, worked very well, and did not require the high power that would be needed for plate pulsing.

As a c-w oscillator, the stability factor or frequency change in parts per million caused by a 30-percent change in plate voltage was reduced to 1,000. Power output of 1.7 watts with an efficiency of 30 percent was obtained with 250 volts on the plate. While operation is possible for all positions of the feedback capacitance, stability is poor when feedback is optimum for pulsing, and oscillator rise time is bad when feedback is optimum for c-w operation.

Variable Oscillator

Power output of an experimental model of the 1,000-1,300 megacycle variable oscillator for use in the beat-frequency oscillator varied from 0.3 watt to 0.7 watt with a plate voltage of 250 volts, while efficiency varied from 6 percent to 15 percent. A sizeable loss of power output and efficiency is the price paid for variable-frequency operation.

Wide-Range Oscillator

After completing work on the beat-frequency oscillator, it was decided to try to make an oscillator having a

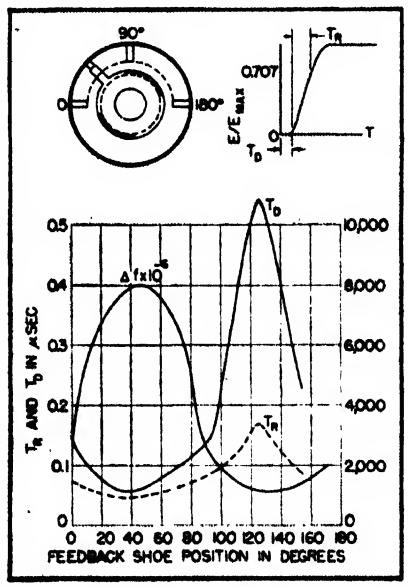

FIG. 9—Variations in oscillator stability and buildup time as a function of feedback capacitance location with respect to openings in the coaxial butterfly unit

wide range that would be suitable for laboratory use. As has already been pointed out, ranges could be made much wider than were required for the beat-frequency oscillator. Experiments showed that because of the space required by the outboard drive for the rotor, the maximum frequency for which the outer resonant circuit could be adjusted was about 1,350 mc. To get as wide a range as possible for experiments, the lower frequency was reduced. The final frequency range obtained with this oscillator was 620 to 1,340 mc. This range was again obtained with a single tuning control, with no sliding contacts.

Position of Coupling Loop

Location of an output coupling loop for this oscillator was determined experimentally. It was first roughly determined that maximum output could be obtained if the loop were located in the end disc of the outer chamber, opposite the adjustable feedback fingers.

Figure 10 illustrates the method used to locate the optimum position for the loop. At several frequencies throughout the range the oscillator end disc was rotated so that loop X was moved through the arc subtended by the feedback fingers (area ABCD). By this means it was discovered that maximum output for any frequency was obtained when the output loop was opposite the acting feedback finger. The fixed loop position which will give best output over the frequency range is then at 36 degrees, or opposite the 1,000-mc active feedback finger.

Power output obtained over the frequency range varies between 0.15 and 0.30 watt. Here again increased frequency range is gained with a reduction in power output.

Getting Higher Frequencies

To extend the useful range of these oscillators to higher frequencies, a coaxial butterfly tuning unit for a range of 800 to 1,600 mc has been built. The unit has a more compact and simple rotor support and drive than was used on previous models. Portions of the plate end or short-circuited end of the line have been cut away to allow the rotor supports to turn. Also, portions of the grid-end disc have been sliced off to make way for the supports which hold the feedback ring to the rotor. Other mechanical changes have simplified the assembly of the unit appreciably. Oscillations have been obtained over the frequency range of this unit with about the same vigor as are obtained from the lower-frequency unit. Tests have not been completed on this oscillator, but it is hoped that a mechanically simplified feedback circuit can be devised.

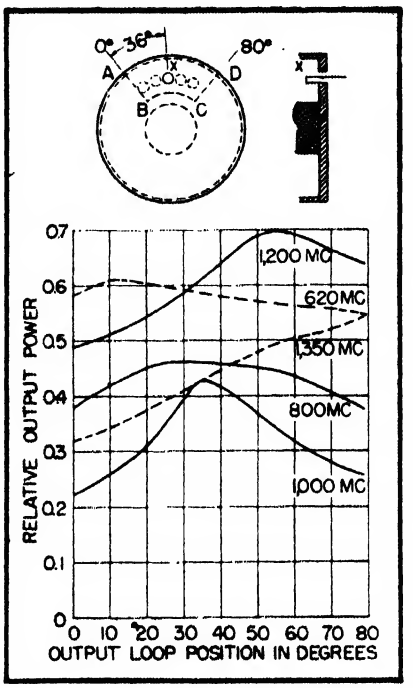

FIG. 10—Oscillator output as a function of output loop location with respect to active feedback fingers

Conclusions

The oscillators described in this paper, while not of the more desirable single tuned circuit type depending upon the tube electrode capacitances for feedback, do operate with a single tuning control and are somewhat more efficient. Sliding contacts have been eliminated and wide ranges have been maintained. The oscillators have high enough output to be used as laboratory oscillators or in standard-signal generators.

New tubes may soon make these circuits obsolete, but for the present they are useful and their performance is comparable to that of oscillators operating at much lower frequencies.

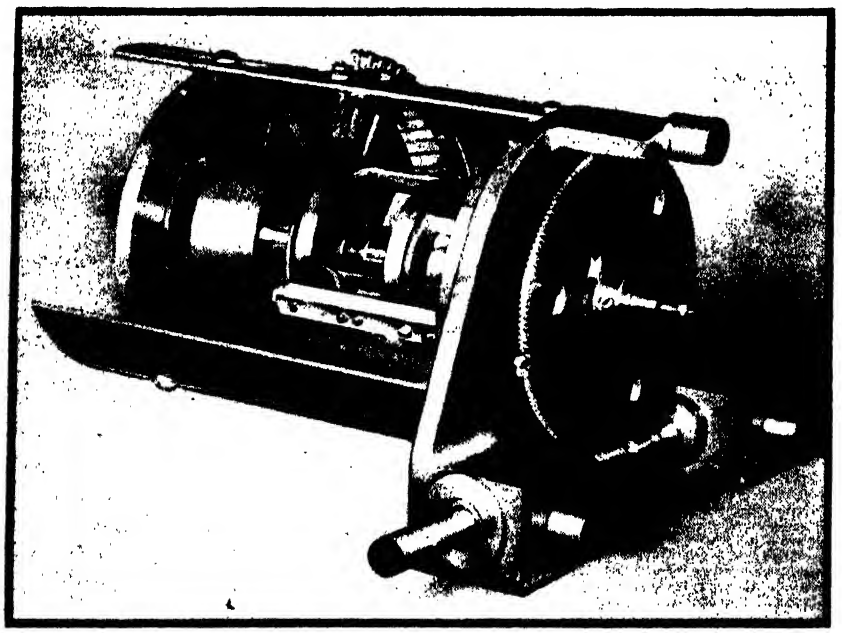

Coaxial butterfly oscillator for 1,000 to 1,300 megacycles

References

(1) Karplus, Eduard, Wide-Range Tuned Circuits and Oscillators for High Frequencies, *Proc. IRE*, p 426–441, July, 1945.

Simplified Microwave AFC

Combinations of motor and electronic afc action for microwave oscillators are discussed. Methods of automatic and manual correction scanning complete the design considerations for a 3,000-mc radio-relay system that remains within 200 kc of assigned frequency

By F. A. JENKS

The afc system to be described is relatively simple, compact, easy to adjust, and can operate with either tunable klystrons or tunable magnetrons.

Most of the relay systems on microwave channels are rather wide band, in the order of 2 mc or more. Consequently, if the transmitter carrier is held to within about ± 200 kc of the assigned frequency, it will remain well within the channel limits. A simplified motor-operated afc system will serve.

In all automatic frequency control systems, the frequency of the controlled oscillator is compared with a known reference frequency, and any discrepancy between the two, as indicated by the detection circuit, is used to apply a correction to the afc oscillator. One method uses a cavity resonator as the reference frequency standard. The resonator is used in such a way as to obtain a sensing or directioning of the oscillator drifts for applying the proper corrections. This correction may be accomplished by coupling the resonator to a waveguide bridge circuit.[1]

The type of sensing used in the system to be described is somewhat novel because it applies a sensing modulation to the reference resonator itself. This sensing modulation provides a means of detecting the magnitude and direction of frequency shift of the oscillator. The signal carrying this information is used to shift the oscillator back to the correct frequency setting. Either mechanical or electronic means can be used to tune the tube, or both can be used in combination.

Several useful afc systems are discussed: motor afc system alone; motor and reflector afc system combination; pushbutton scanning means for such systems; automatic scanning means. Their discussion is preceded by an analysis of certain basic operating principles.

Method of Sensing

If the resonant frequency of an excited resonator is moved back and forth at a given rate, the resulting signal from a crystal detector coupled to the cavity is in phase with the signal producing the resonant frequency shift when the carrier is effectively detuned to one side of resonance, and 180 degrees out of phase when it is detuned to the other side of resonance. As far as the crystal detector is concerned, variation of the cavity resonant frequency is equivalent to frequency modulation of the carrier generator. When the carrier is exactly in tune with the resonator, the detector output is entirely the second harmonic of the sweep rate, with no fundamental component present.

Figures 1 and 2 illustrate these basic sensing functions graphically. Figure 2 shows that increasing the carrier detuning will enhance the voltage of the fundamental frequency-modulating frequency obtained from the crystal detector until the detuning has gone about one-quarter of the resonator bandwidth, at which point the voltage of the fundamental begins to drop off, although remaining in the same phase. The output signal from the detector crystal is a reversing-phase variable-magnitude voltage of the same frequency as that used to modulate the resonator.

Figure 2 is correct for small frequency deviations of the resonator frequency, a condition which is employed in the present afc system. Wider deviations move the fundamental peaks out to about the half-power points on the resonance curve. The slope of the fundamental curve at or near resonance is called the conversion factor or sensitivity of the resonator-detector unit, dE_c/df, and is stated in volts per cycle for a given radio-fre-

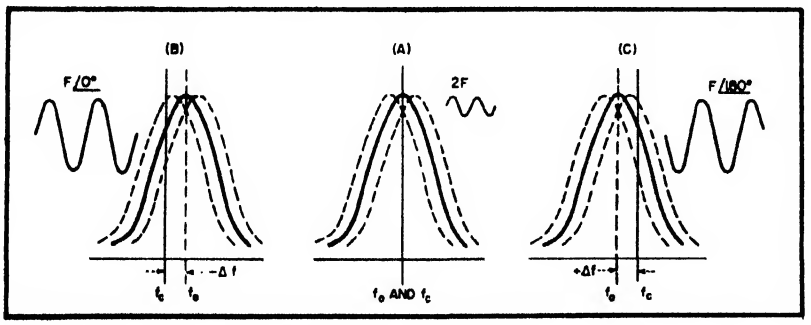

FIG. 1—Phase method of obtaining frequency drift sense

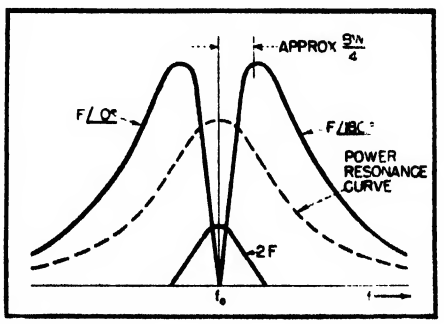

FIG. 2—Resonator-detector output

quency power into the resonator and a given frequency deviation.

To prevent modulation of the cavity from reacting on the oscillator, careful adjustment of the coupling between the two is necessary. It is desirable to use only a small amount of power in the resonator, as this aids in meeting the decoupling requirement by allowing loose coupling and avoids absorbing too much energy from the oscillator.

Basic Motor AFC

To illustrate each functional section of the complete afc system, the two methods of control will be discussed separately. Figure 3 shows a block diagram of the essential elements of the motor afc without antihunt. Since the resonator-detector output is a reversing-phase variable-magnitude voltage of the fundamental sweep frequency, it is suitable for operating a two-phase motor. If one winding is excited with a constant voltage of fixed phase, and the other, called the control winding, is excited by a variable-magnitude voltage of either 0 or 180-deg phase relationship with respect to the first winding, the direction of rotation of the motor will depend upon whether 0-deg or 180-deg phase voltage is in the control winding. The speed at which the motor runs is dependent upon the amplitude of the voltage in the control winding, with zero voltage producing no rotation, even though full voltage is maintained on the first or reference phase winding. The motor, in essence, becomes a phase detector in this type of afc system.

From the diagram of Fig. 3, it is seen that the resonator-detector signal is amplified and applied directly to the control winding of the motor. The fixed phase winding derives its excitation from the same source that is used to produce the resonator frequency deviations for the sensing operations.

Since the two-phase motor is a mechanical device, it is subject to certain evils, namely bearing friction, inertia, and unbalance. In a good motor the rotor will be balanced rather carefully, and static inertia troubles will not begin to appear until the static friction in the bearings has been virtually eliminated. Owing to this friction, a finite signal voltage E_m at the motor winding is needed to overcome these forces and produce rotation. Usually the rotational friction is lower than the static friction, and consequently it is not the important factor in the problem.

Assuming then that the system is exactly in tune, no fundamental voltage will appear at the motor winding. As the oscillator begins to drift, the error signal on the motor winding has to reach a value of E_m volts before motor-operated afc action takes place. Therefore, the unavoidable frequency error owing to friction is the frequency drift required to produce E_m volts at the motor.

Referring again to Fig. 3, the terms used to describe the action around the feedback loop may be summarized and defined. E_m is the motor voltage required to overcome static friction; dE_c/df is the resonator-detector voltage frequency sensitivity, near resonance; A_m is the gain of the motor amplifier section; Δf is the frequency deviation error without afc.

To cause afc action to take place the error signal must equal E_m, and that quantity may be evaluated by

$$E_m = A_m (dE_c/df) \Delta f \quad (1)$$

Solving for the frequency error produced by the motor afc because of frictional forces gives

$$\Delta f_m = \pm(E_m/A_m) (df/dE_c) \quad (2)$$

The error shown in Eq. 2 is the long-time error encountered in the motor-operated type of afc system (assuming negligible resonator and modulator drift), since the motor will drive until the error voltage on its winding has reached some value less than E_m. Driving toward the correct frequency, the inertia of the mechanical system will carry the tuning well into the region where the error signal is less than E_m. The fact that rotational frictional at slow speeds is less than static friction emphasizes this condition.

It may happen that the mechanical inertia of the gear train actually carries the tuning through the correct value and to a reverse voltage greater than E_m. This new error signal drives the system in the other direction and the overrun may then be encountered a second time. This can result in hunting, where the motor oscillates the tuning back and forth around the correct frequency setting.

The problem of eliminating hunting will be taken up in a later section. The correction response time of the motor afc is usually slow due to the mass and drag of the mechanical linkages.

Basic Electronic AFC

Using electronic afc, for example by varying the reflector voltage of a reflex klystron, a residual error signal is required to produce a correction voltage with which the afc must operate. This is unlike the motor-operated afc in which the error signal would go to zero if no static frictional forces existed. Figure 4 shows a block diagram of an electronic afc section. The essential difference between this and the previous case is the replacement

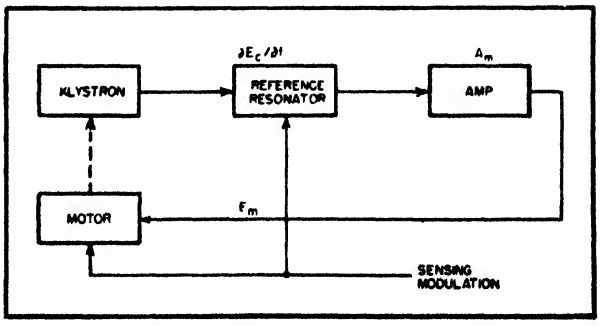

FIG. 3—A basic motor-operated automatic frequency control

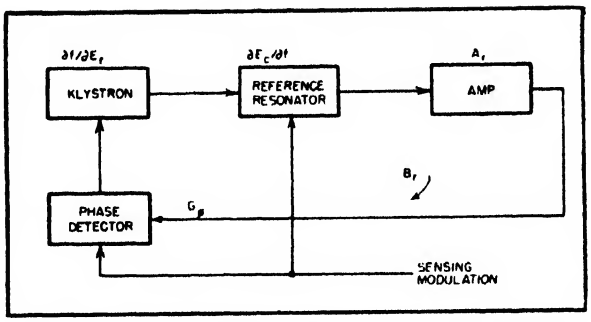

FIG. 4—A basic electronic automatic frequency control

of the motor by a phase-detector whose output is coupled directly into the reflector circuit of a klystron. Since the reflector is frequency-voltage sensitive, the control loop is complete to provide afc action.

As such an electronic afc system does not have any mechanical circuits, it can be treated in the usual feedback manner. The terms used around the feedback loop in Fig. 4 are defined as follows:

G_ϕ = conversion gain of phase detector
df/dE_r = klystron reflector frequency—voltage sensitivity
dE_c/df = resonator-detector voltage-frequency sensitivity near resonance (as before)
A_r = gain of reflector amplifier section
Δf = frequency deviation error without afc
B_r = feedback gain around loop, excluding amplifier A_r

The residual error in the electronic afc is the frequency error drift divided by the total loop gain

$$\Delta f_r = \frac{\Delta f}{\text{loop gain}} = \frac{\Delta f}{A_r B_r} \quad (3)$$

$$A_r B_r = A_r \left(G_\phi \frac{df}{dE_r} \frac{dE_c}{df} \right) \quad (4)$$

Substituting Eq. 4 in Eq. 3

$$\Delta f_r = \frac{\Delta f}{A_r G_\phi \dfrac{df}{dE_r} \dfrac{dE_c}{df}} \quad (5)$$

The residual error signal can be made smaller by increasing the gain around the feedback loop ($A_r B_r$).

Combination Motor and Electronic AFC

The motor and electronic afc systems have one interesting thing in common; neither afc system can produce complete error correction. The motor system is afflicted with frictional troubles, and the electronic system requires some error signal to produce afc action. Operating in combination, however, the electronic afc has to handle all transient errors greater than the maximum frequency error allowed by the motor friction given by Eq. 2. Its long-time error signal will be less than this amount. Consequently, the resulting long-time error of the combined systems is given by substituting Eq. 2 into Eq. 5

$$\Delta f_{mr} = \frac{\Delta f_m}{A_r B_r} = \frac{(df/dE_c)\,(E_m/A_m)}{(df/dE_r)\,(dE_c/df)} \quad (6)$$

$$\Delta f_{mr} = \left(\frac{df}{dE_c}\right)^{-1} \left(\frac{dE_r}{df}\right) \left(\frac{E_m}{A_m A_r G_\phi}\right) \quad (7)$$

Several things are gained when the electronic afc system is combined with the motor-operated afc. First, the response of the electronic system is faster than its mechanical counterpart. This feature relieves the motor of trying to respond to transients which it can not handle. Second, the quicker action of the electronic system acts as an anti-hunt circuit for the motor afc. If the motor inertia carries the corrective tuning past the center frequency, the electronic afc corrects this situation by electronic tuning, thus wiping out or materially reducing (by an amount equal to $-\Delta f/A_r B_r$) the reverse error signal which the motor winding would have otherwise seen. Action such as this removes any tendency to hunt or oscillate about the center frequency, and gives a smoothly damped motor operation. Third, when the combined system is in tune, the output from the phase detector is zero.

This last condition is most important in transmitters whose modulation characteristics are critical as to distortion, and the oscillator must be operated at the center of a mode as dictated by the reflector characteristics. Consider a step-function frequency disturbance. The action of the electronic afc causes it to make its best possible correction as given by Eq. 5. During this time the motor has also begun to operate, to wipe out the error voltage on its winding. As the system approaches the correct mechanical tuning of the klystron, the error voltage is reduced. When the correction is complete, the output of the phase detector goes essentially to zero, thereby putting no additional voltage from electronic afc action onto the already existing reflector potential. In this way, the best modulation characteristics are maintained, even under rather severe afc hold-in conditions.

Motor Circuit Antihunt Control

When the motor-operated afc is considered alone, some means of reducing the tendency to oscillate about the center-frequency must be introduced. One of the most satisfactory methods is to couple an eddy current generator to the motor shaft, and excite one of its fields at the motor frequency. The amplitude of the resulting voltage in its output winding will be proportional to the speed of the motor, and its phase will be either 0 or 180 deg with respect to the exciting voltage, depending upon the direction of rotation. No slip rings are needed so no additional friction forces are incurred.

The eddy-current generator signal is introduced into the motor control circuit in such a way that its phase is in opposition to that of the error signal. When a frequency disturbance occurs, the motor operates to reduce the error as usual, but some signal of opposite phase proportional to the motor speed is supplied by the generator to reduce the apparent error signal. Such a reduction in error voltage slows down the motor, which pro-

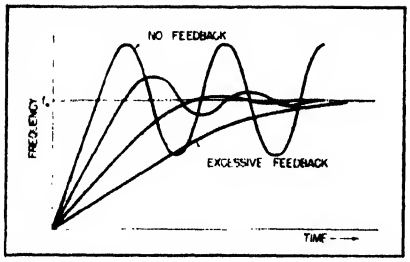

FIG. 5—Motor tuning time plotted against corrective feedback

cedure in turn reduces the injected antihunt voltage.

Should the inertia of the mechanical system carry the correction too far, and cross the center frequency, the error signal will change phase. This condition puts both error and antihunt signals in phase, and the sum of the two act to brake and reverse the direction of rotation. Once this reversal is accomplished they are again out of phase, because the phase of the generator voltage depends upon the direction of shaft rotation only, and the antihunt signal is again tending to slow down the motor. One important point should be noted; the antihunt signal becomes less and less as the motor slows down when approaching the correct tuning, and it is zero when the motor arrives at a dead stop. In this latter condition the system has its greatest sensitivity.

The amplitude of the antihunt signal plays a large part in determining the characteristics of the motor afc system. In Fig. 5 is shown a series of curves for different amounts of speed feedback voltage. It is possible to go from the case of oscillation with no antihunt voltage through a gradual approach to the condition with no overshoot, and beyond to a point using excessive antihunt signal. The proper adjustment is somewhere between the two extremes, depending upon the operating requirements of the individual equipment.

Hold-in Tightness

From Eq. 2 it is apparent that the motor error caused by static friction varies inversely as the gain of the motor amplifier, A_m. Figure 6 illustrates a family of curves which show increasing tightness of afc control (that is, less frequency error) with increasing amplifier gain. The section near the center, before overloading occurs, is most interesting. As the gain increases, the motor-error width decreases accordingly.

The ability of the system to respond to transient disturbances is dependent upon the electronic afc. Assuming that a 400-cps motor is used, and the same sensing frequency is used for both motor and electronic afc, it is apparent that the error information is arriving into the system at only a 400-cps rate. This relatively slow rate of gathering information puts a definite limit upon the transient response of the electronic afc. If at least 20 complete information cycles are needed for reproducing error data of a transient pulse, then the transient response that can be handled by such a system is in the order of 0.1 second, or longer.

The difficulty in filtering out 400 cps from the output of the phase detector to prevent 400-cps frequency modulation of the klystron necessitated a brute-force filter, which would preclude attempting to raise the transient response when using such a low sensing frequency. It is entirely possible to use two sensing frequencies to overcome this trouble, such as 400 cps for motor control and 50 kc to 100 kc for electronic control, with good transient response.

Motor AFC with Antihunt Generator

The simplest form of afc system that has been discussed is one using just motor control, with antihunt signals supplied by an eddy-current generator. A block diagram of this arrangement is shown in Fig. 7. The performance to be expected from this circuit is given by Eq. 2, and the response to transients is relatively poor. However, such an afc is characterized by extreme simplicity, low power drain, compact size, and a wide tuning range.

The mechanical details are most important, such as good linkages between the motor shaft and the tuning member, stable frequency-temperature characteristics of the reference resonator, and stable resonator-modulator characteristics. Some means of reducing the second harmonic voltage of the sensing frequency is necessary to prevent overheating the motor winding with a signal that contributes no rotational torque.

A slightly different type of motor-operated afc is possible by coupling the motor to a potentiometer which in turn varies the reflector voltage of the reflex klystron. No mechanical work is done on the klystron, consequently less torque is needed

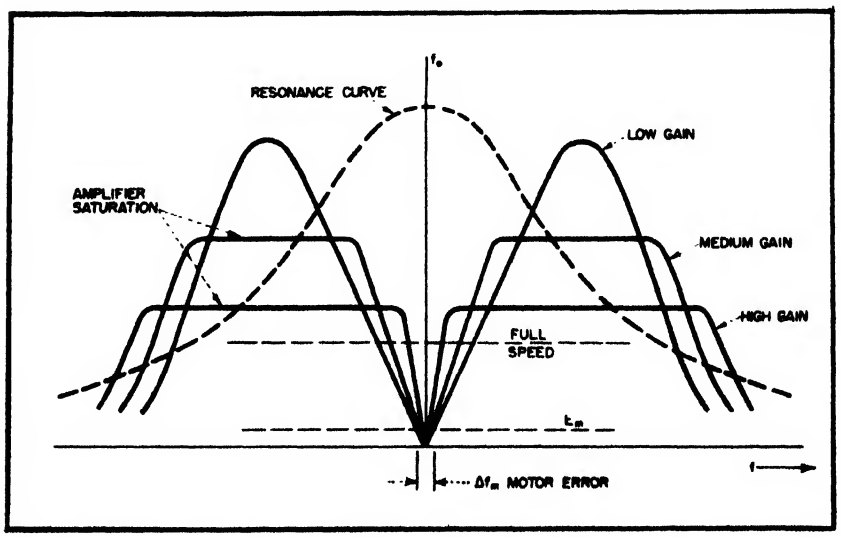

FIG. 6—The hold-in characteristic versus motor-amplifier gain indicates how well motor error can be compensated

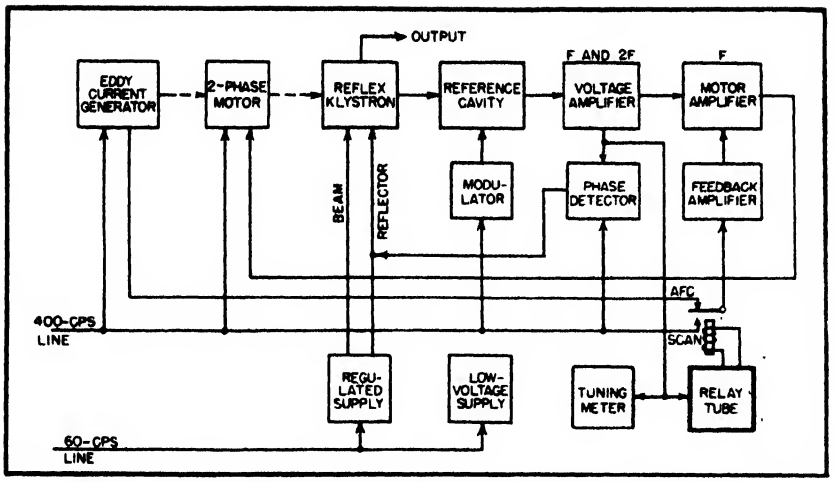

FIG. 7—Block diagram of a motor afc system connected for antihunting

from the motor. The frequency control range of this system is limited, however, to the electrical tuning of the reflector circuit. Unlike the electronic afc, no sensing voltage has to be filtered from the reflector circuit.

Motor-Electronic System

The combination of motor and electronic afc systems gives more flexibility of operation. Figure 8 shows a block diagram of this combination system. Note that the antihunt signals for the motor are now amplified in a separate stage and fed into the signal amplifier at a point beyond where the phase detector signals are picked off. The change in antihunt injection is necessary to prevent the generator voltage from getting into the phase detector circuit.

Several points of caution are necessary to observe if this combination afc is to function properly. Referring again to Fig. 8, the phase of the signal at the motor winding should be either 0 or 180 deg with respect to the voltage on its fixed phase winding. The phase of the amplified antihunt signal should be 180 deg with respect to the signal voltage at the point of injection into the motor amplifier chain. Last, the phase of the signal voltage at the secondary winding of the pushpull transformer of the phase detector should be either 0 or 180 deg with respect to the reference voltage in the center leg of the phase detector. Also, the frequency response around the electronic afc loop should drop to unity before the phase shift has reached 180 deg, otherwise the reflector afc will oscillate at the frequency where the 180-deg shift occurs.

Pushbutton Scanning

The two systems described above will pull into frequency if the drifting oscillator signal is within the skirts of the reference resonator response. However, the oscillator may not be within this frequency range, especially with a tunable reference resonator as used in signal generator applications. To make the motor tune the oscillator without error signal from the resonator, a switch or pushbutton arrangement can be used to inject scanning voltage into the motor amplifier and to disconnect the motor antihunt signals during the scanning operation.

The simplest method is to allow the motor to drive always in the same direction during scanning. If the resonator is tunable or channelled, a better method is to connect a set of contacts to the frequency-shifting mechanism which selects the proper phase of the scanning voltage for driving in the correct direction. Such a scheme will be described in more detail in a later section.

Certain applications require that the afc system automatically search and lock onto the signal if it should

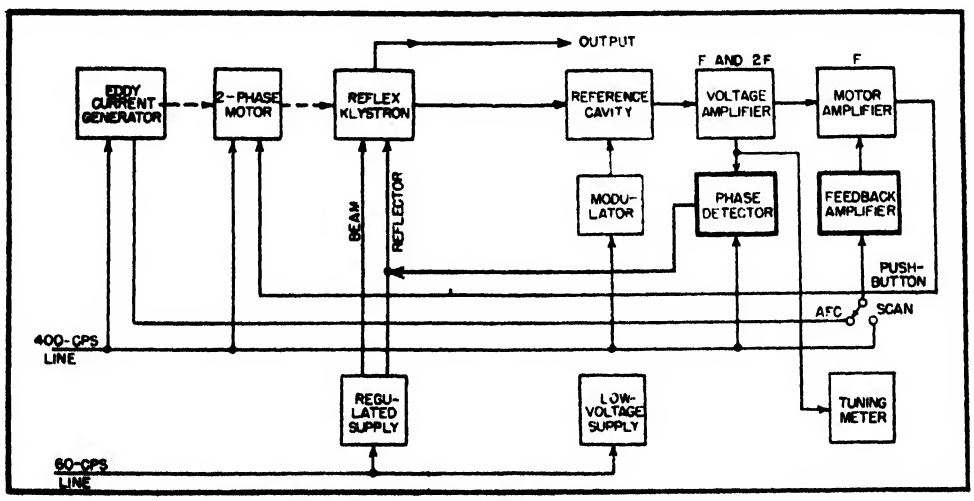

FIG. 8—Block diagram of motor and electronic afc system

not be within the pass-band limits of the reference resonator. This type of operation is relatively easy to accomplish with the afc equipment under discussion.

Figure 2 shows the output voltages from the resonator-detector within the resonant characteristics of the cavity. Notice that the second harmonic of the sensing modulation frequency peaks at resonance, while the fundamental goes to zero. It is obvious then that if both the fundamental and second harmonic frequencies are amplified and rectified, a control bias can be developed whenever the carrier lies within the resonator limits. Should the carrier drop out of the pass band of the resonator, no bias will be produced and scanning can be made to commence. An automatic scanning system is shown in block diagram form in Fig. 9.

First, it is important that the d-c bias developed by this rectified sensing signal be sufficiently great at resonance to cut off the control or relay tube with a reasonable margin of safety. Second, if this bias is used to cut off a scanning tube (instead of operate a relay tube) it must be great enough to eliminate completely all trace of scanning voltage in its output circuit; otherwise the afc system will remain slightly off to one side or the other of resonance. During scanning, some means to reduce or eliminate the speed feedback voltage is required. If this reduction is not effected the scanning will be slow and jerky.

A more desirable method than cutting off a vacuum tube is to use the bias voltage to operate a relay tube. The relay, when relaxed, allows the generator feedback voltage to be applied in the normal manner, and when energized it injects scanning voltage into the system instead of antihunt voltage from the generator.

As mentioned earlier, the phase of the scanning voltage can be selected automatically so that the motor will drive in the shortest direction to pick up the signal. A pair of contacts operated by the

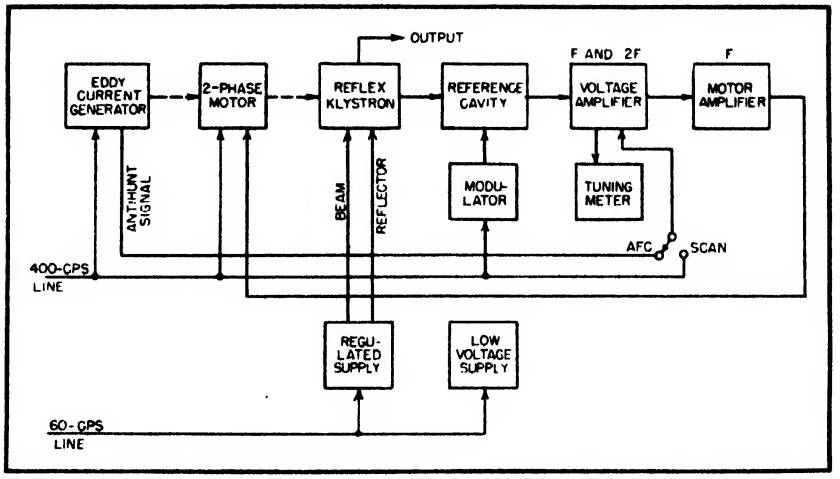

FIG. 9—Block diagram of an afc system with automatic scan

resonator tuning or channeling mechanism though a clutch will work satisfactorily for this phasing operation.

The Reference Resonator

One of the most critical components in the entire afc equipment is the reference resonator. The important characteristics of this component are: frequency-temperature coefficient; stability of sensing modulation method; means of coupling to the microwave tube; tuning range or channelling and the mechanism required. Each of these factors has to be carefully considered so that the completed resonator unit will have sufficient frequency stability within itself to act as the reference for the afc system. All of the above-mentioned resonator characteristics are treated in some detail in another paper[8].

Since the type of afc system being discussed is not a precision system, the required stability of the reference resonator is not as great as if it were used in a system attempting to compete with crystal control performance. Nevertheless, it is desirable to make the frequency-temperature coefficient of the cavity as low as conveniently possible. The use of Invar or Nilvar steels will produce a resonator whose frequency-temperature coefficient will be only several parts per million per degree Centigrade.

This accuracy can be achieved, however, only after the certified material is double checked for proper coefficient of thermal expansion, and then making certain that the resonator is machined from the measured stock. A chemical or spectrographic analysis is not enough. A piece of the actual material to be used must be measured for coefficient of thermal expansion. All soldering operations must be done in an oven and with soft solder. After machining and soldering, the piece should be artificially aged to remove the greater part of the material creep which would otherwise occur.

Materials such as plated fused quartz, Multiform, or Vycor can be used if satisfactory fabrication methods are available. Another approach is to make a temperature-compensated resonator from two different pure metals, such as copper and molybdenum. Each of these metals has a relatively stable coefficient of thermal expansion over a wide temperature range. By proper choice of the geometry of the compensated resonator, it can be made more stable than an Invar resonator. If operation over a wide ambient temperature is required, some means of temperature control for any of the resonators may be needed to keep it within frequency tolerance.

The stability of the sensing modulation method means the ability of the modulating device to be dimensionally stable. If a diaphragm or

plunger is moved in the resonator it will produce tuning, and when moved sinusoidally at the modulation rate it provides the sensing signal.

Figure 10 illustrates two modulating methods. It is important that the vibrating member always oscillate at the same place within the cavity, else the center-frequency tuning will shift as a result of such movement. Usually, if the drifting of the mean position of the modulating member is limited to approximately one-hundredth of the amplitude of vibration, it will be accurate enough for the type of afc systems being discussed.

If the sensing modulation is produced by an electrical means, such as a silicon rectifier in a transmission line, it is again necessary to use a unit whose stability is good over long periods of time. Any change in the crystal characteristic will reflect a reactive component into the cavity, thereby causing a shift in its resonant frequency. The advantage of the crystal rectifier type of modulation is that the sensing frequency can be anywhere between the low audio range and the low radio frequency range; the upper limit being dependent upon the sideband attenuation due to the resonator Q.

Coupling the resonator to the microwave source is sometimes a problem, since it is necessary that the modulated resonator shall not pull or react on the oscillator to produce a similar modulation on the outgoing carrier. Loose coupling consistent with suitable energy into the resonator is about the average condition. It might be desirable to add a series impedance between the two, to locate the resonator characteristic at a more suitable spot on the oscillator's load-power output diagram.

The tuning range or channelling required is entirely dependent upon the intended application of the equipment. Fixed-station point-to-point operation may demand a single frequency, or possibly two or three, while portable-mobile equipment may need ten to a hundred channels. Laboratory apparatus usually requires continuous tuning over the available frequency band. Whichever type of tuning is required, it is important that the tuning mechanism (the mechanical device which positions the tuning member inside the resonator) be given considerable engineering thought.

Schemes are now available whereby a resonator can be tuned smoothly over a large frequency range, or it can be channelled at equal frequency intervals. With relatively close spacing between channels, it is necessary that the tuning member have a rather low mechanical tuning rate in megacycles per inch to achieve good frequency repeatability.

Figure 11 shows two methods of tuning reentrant type resonators. If remote channel selection is desired, the indexing device which operates the tuning member should not require high angular tolerances on the shaft rotation. The design should be such that ordinary detent tolerances can be used.

The method of obtaining mechanical and electrical tuning will depend largely upon the type of microwave oscillator used, such as magnetron, klystron, or special triode. This discussion is based on klystron oscillators, since all the experimental work was done with such tubes.

Klystrons like the 2K28, using cavities which are external to the vacuum section, can employ a simple paddle or plunger system to provide mechanical tuning. Designs where the tuning member is inside the vacuum or is part of the vacuum enclosure, as for example the 2K57 for the former and the 2K41 for the latter, require a somewhat more complicated tuning mechanism. Some means of maintaining a vacuum is needed, and bellows or diaphragms are ordinarily used. These devices add a considerable amount of extra work for the motor tuning mechanism, since producing a tuning motion requires that the devices be deformed. However, such tuning systems have been used successfully without experiencing detrimental effects due to work hardening, provided the tuning correction motion of the motor afc is a small fraction of the total available tuning travel.

An important requirement of the tuning characteristic of the microwave tube is that the tuning curve does not reverse in slope over the range of travel to be covered by the afc system. A change in slope of this curve is not too serious, since

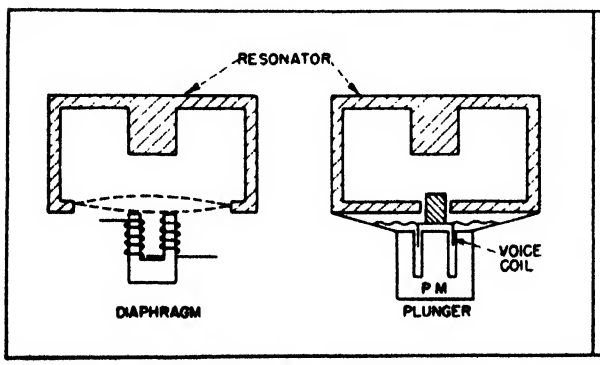

FIG. 10—Methods of frequency-modulating a resonator cavity with loudspeaker units

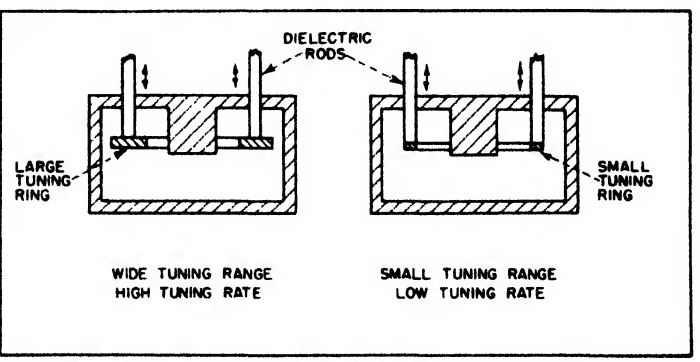

FIG. 11—Methods of resonator tuning that give different rate and range characteristics

this merely changes the system gain, but a reversal of slope would mean that the afc would drive away from that frequency region.

Some mechanical tuners use a screw thread which actuates the tuning member. Upon reaching the end of travel, the direction of rotation has to be reversed to repeat the tuning cycle. When using motor afc with this tuning method, provision must be made to reverse the motor at the end of travel during scanning, otherwise the system will drive to the end and jam. A more suitable method is to use a cam to actuate the tuning member. The tuning cycle can be repeated by just rotating the cam in the same direction, and no intricate limit-stop reversing switches are necessary.

The angular tuning rate (megacycles per degree of shaft angle, using a cam drive) is quite often determined by the total tuning range required and the allowable physical size of the mechanism. Of course, the greater the angular tuning rate the more accurately positioned the shaft must be for setting to a given frequency. Too low a rate may make the correction response time too long. A compromise between several factors is usually required in each individual application.

Motor-Generator Unit

The choice of the motor-generator unit depends upon several factors: sensing frequency; output torque required for tuning operations; physical size; constructional details. The sensing frequency is determined by the choice of motor for other reasons than frequency, as motors are available at 60 cps or 400 cps. There is little difference in system performance between 60 cps and 400 cps, and other factors are usually more demanding, such as weight, size, and availability.

The output torque is determined by the type of tuner mechanism employed on the klystron. However, most small motors have a reasonable amount of torque after going through a gear reduction of 1,000 to 1 or better. The speed of the output shaft is directly related to the correction response time. There should be minimum backlash between the klystron tuning member and the motor shaft. Any backlash in the gear train should occur as near to the motor shaft as possible, and not near the klystron tuning member.

The physical size of the motor-generator unit is dictated primarily by the required output torque, duty cycle, and the sensing frequency. For special applications where light weight and compact size are paramount, small 400-cps units are available. If the generator has to be coupled to the motor shaft as a separate unit, the overall size may be greater than desired.

The constructional details of the motor-generator unit are important, since good bearings, good alignment and balance, and small rotor diameter, all tend to reduce the frictional forces which the signal voltage has to overcome. From Eq. 2 (Part I), Δf_m will be smaller if the value of E_m is smaller. Good dynamic balance is necessary to prevent damage both to the bearings and the alignment by vibration during high-speed scanning. To avoid warp and twist between the motor and the klystron tuner, both should bolt solidly to each other. If it is necessary to fasten them to a third member, the design of this third member should be such as to provide maximum stiffness and rigidity.

A Practical Design

During the experimental work on afc systems of the type under consideration, several laboratory models were constructed. One of these illustrated is a 3,000-mc signal source of 200 to 300 milliwatts output, using pushbutton scanning.

The reentrant type reference resonator is made of Invar steel, and is tuned by an annular ring that moves coaxially inside the resonator adjacent to the center post section, similar to that shown in Fig. 11. Three polystyrene rods support this tuning ring, and they in turn are fastened to a spider on top of the resonator. A smooth cam moves this spring-loaded spider through the tuning range.

In the sample model the tuning range was 100 mc, with a total travel of about 0.375 inch. A vernier dial with gear reduction was used to operate the cam. Connected to the dial shaft, between the dial and the gearing unit, is a clutch plate that operates either of two pairs of switch contacts for small angular motions of the dial. One pair closes with motion in one direction, the other closes with motion in the other direction. These contacts are connected to the scanning circuit, and put the correct phase of 400-cps voltage into the scanning switch so that the motor will scan in the direction of frequency shift caused when the dial is turned. The correct adjustment of the clutch spring is such that only one pair of contacts is kept closed at all times.

The resonator is modulated by a simple miniature dynamic speaker unit, mounted so that its metal diaphragm is concentric with and just under the bottom section of the resonator. A small plunger about $\frac{1}{4}$ inch in diameter and $\frac{1}{2}$ inch in length is connected to the center of the diaphragm and protrudes through a hole in the bottom of the cavity, as shown in Fig. 10. When this plunger is vibrated by the diaphragm, it cyclically changes the distribution of the electric field in the resonator gap space, thus producing frequency modulation.

The tuning dial and gear reduction are mounted above the Invar resonator, and beneath the panel is the dynamic modulator unit. The 2K41 reflex klystron is mounted horizontally with its tuning cam just below the base end. The motor-generator unit and its gear train are under the klystron mount.

In designing this sample unit, a small 400-cps motor-generator from the Sperry A-12 pilot turn-control was chosen because it was compact, had a suitable gear train, and delivered sufficient torque. A 400-cps motor was used because it is easier to make an amplifier free from hum

pickup at that frequency than at 60 cps. Any 60-cps pickup in the 400-cps amplifier is greatly reduced by the tuned circuit used to attenuate the second harmonic before it is applied to the motor. It is still necessary to keep the amplifier relatively free from hum to prevent overloading of the input stages.

The gear train supplied with the motor was modified slightly to allow the tuning cam to come out at right angles to the motor shaft, as shown. The klystron tuner was redesigned to permit the tuning lever to be operated by a cam. A small roller is located at the end of this lever to provide free motion over the cam surface, especially on the steep backside. This tiny roller is just visible in the illustration. The torque required to move the tuning lever over the cam surface is about 2 ounce-inches.

The complete block diagram of Fig. 8 shows the afc system for the entire equipment as given in Fig. 12. Triode tubes are used throughout. From the input of the amplifier (the crystal detector) to the motor winding there is a gain for small signals of 90 db, and from the same input to the phase detector there is a gain of 93 db. A tuned circuit is used at the input of the push-pull motor-amplifier to introduce a 20-db attenuation at 800 cps, the second harmonic of the sensing frequency. Since the second harmonic is a maximum when the system is exactly in tune with the reference resonator, it is necessary to avoid putting second harmonic power into the motor. No rotational torque is produced by this frequency, but but it would heat the motor and reduce the allowable fundamental frequency dissipation. A small amount of second harmonic energy is desirable at the motor, however, since it keeps the rotor jittering slightly and helps to reduce the static friction in the bearings. In this way the value of E_m is made smaller, consequently improving the motor error.

A transformer-coupled stage with 40-db gain is provided for the antihunt voltage from the eddy-current generator. This tube envelope also contains a diode which is used to rectify some of the signal to operate a tuning meter. In automatic scanning systems this diode provides the scanning bias, as will be explained later. Meter indication is obtained when the tuning of the klystron is within the skirts of the resonator. It takes a slight dip when the system is correctly in tune.

The pushbutton scanning switch disconnects the antihunt generator, and puts scanning voltage into its amplifier instead. The phase of this scanning voltage is determined by the two pairs of contacts operated through the clutch on the reference resonator tuning shaft. Scanning is

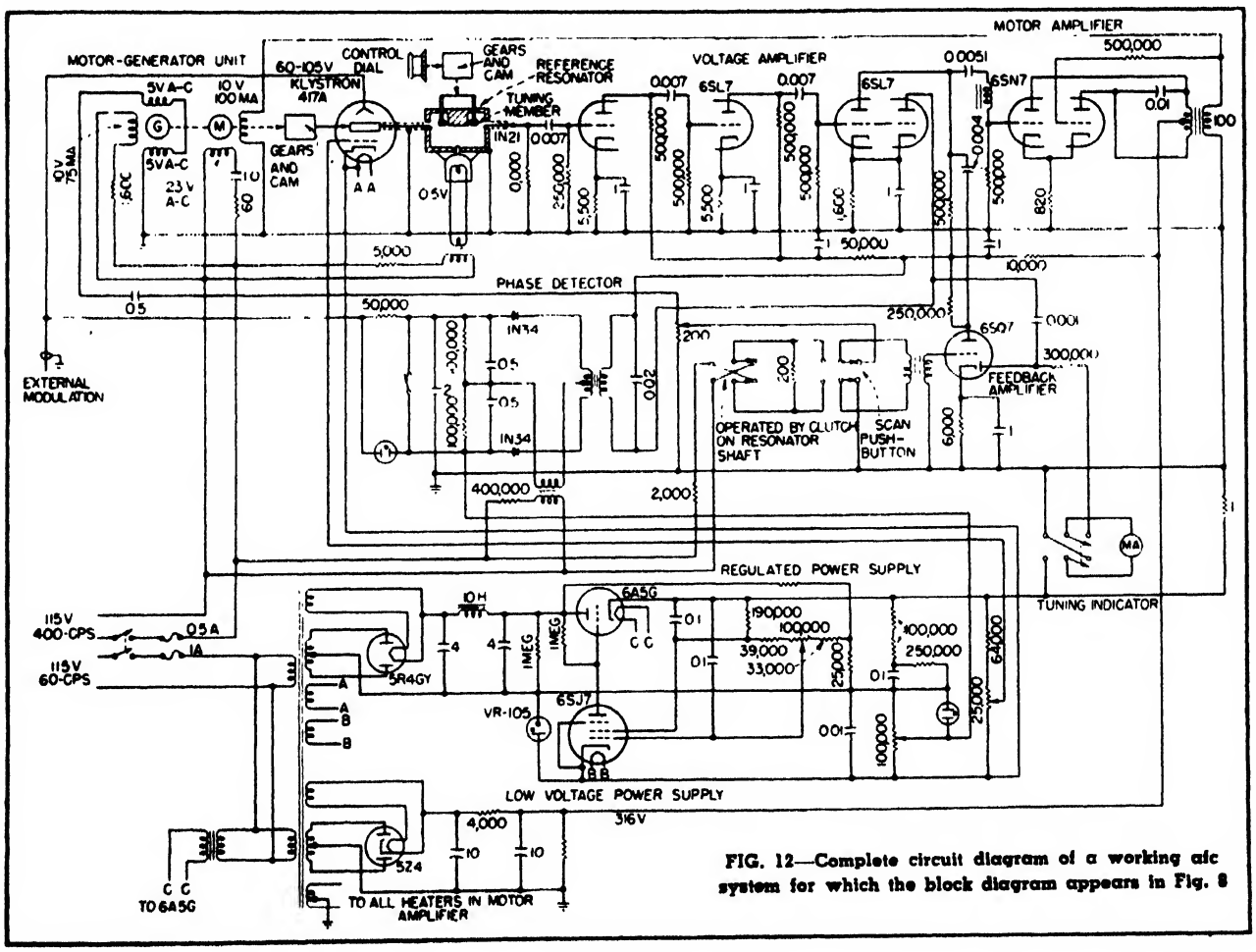

FIG. 12—Complete circuit diagram of a working afc system for which the block diagram appears in Fig. 8

produced by injecting the voltage into the last stage of the motor-amplifier by way of the feedback amplifier circuit. This allows the remainder of the circuits to respond to the resonator-detector signal as soon as the system drives within frequency range. When the tuning meter shows a reading, the scanning button can be released and the system will pull in of its own accord.

The motor-amplifier output stage is push-pull connected to avoid d-c saturation of the transformer core. Signal voltage for the second grid is obtained from the output winding of the transformer. The 6SN7 tube supplies a maximum of one watt to the motor control winding.

Transformers in the phase detector circuit are insulated at the secondary to withstand 1,500 volts d-c working voltage. This is necessary since the reflector potential of klystrons is negative with respect to ground by a rather high value. An electrostatic shield between the core and the pushpull output winding is desirable to distribute the capacitances equally to ground. The center-leg transformer supplies the reference voltage directly from the 400-cps line.

Small crystal diodes (a 1N35 balanced pair) are used as rectifiers in the phase detector. Vacuum tubes could be used equally well, except that isolating heaters at high negative voltages is not always convenient. A brute-force capacitance filter is used to reduce any 400-cps voltage which might get onto the reflector. In this unit an impedance was provided in the reflector circuit across which external modulation could be applied to the reflector. A switch is connected across the output of the phase detector for turning off the electronic afc system, but it does not affect the external modulation circuit.

Since rather high value resistors are used in the reflector circuit, it is advisable to have some means of preventing the reflector from drawing excessive current should the reflector voltage momentarily go positive. The simplest method is to connect a 0.25-watt neon bulb across the output of the phase detector. A more desirable way is to use a diode between the reflector and the cathode of the klystron. Any tendency of the reflector to go positive with respect to the cathode is prevented immediately by conduction of the diode.

Six Channels with Automatic Scan

Another experimental model had six channels spaced 30 mc apart at 3,000 mc and incorporated the automatic scanning feature. It used a cutoff tube to control the scanning, but a more satisfactory method is to use a relay tube to perform the scanning function similar to the pushbutton system just described.

The reference cavity, method of modulation, klystron tuning mechanism, and control amplifier were essentially the same as the previous unit. The only major changes are in the resonator tuning cam and the scanning control means. The special cam is made in six steps, each step at a constant radius for the particular channel. This type of construction does not require close angular tolerances when changing channels, and ordinary switch-type detent mechanisms can be used. It may be necessary to couple a wafer switch to the cam shaft, so that a correction in the d-c reflector voltage can be made at each channel to peak the power output.

The diode previously used to provide signal for the tuning meter is now also used to bias the relay tube to cutoff. During scanning no signal is in the control amplifier, and hence no bias is developed by the diode. As the klystron frequency gets within the resonant skirts of the cavity, bias is developed and the relay shifts to the afc position and the system takes hold. With this type of control it is most important that the second harmonic signal alone provide enough bias voltage to keep the relay in the afc position.

For unattended operation, it is desirable to select a relay which is hermetically sealed. An unsealed relay can accumulate dirt and dust on the contacts, and fail to operate in low-voltage, low-current circuits. It is also desirable to have the relay relaxed, not energized, during normal afc operation. This latter condition automatically occurs in this circuit since the bias voltage cuts off the relay tube except when scanning.

Reference

(1) R. V. Pound, Electronic Frequency Stabilization of Microwave Oscillators, Rev. Sci. Instr., p 490, Nov. 1946.

(2) F. A. Jenks, Sperry Report 5225-1053, Design Considerations of Reentrant Type Precision Resonators for AFC (Unpublished).

Impedance Measurements at VHF

A slotted line, used in conjunction with a variable-reactance line that balances out reactive impedances, is readily adapted to measurements of impedance, antenna phasing, and directivity comparisons. Equipment for unbalanced and balanced loads are described

By E. G. HILLS

RADIO-FREQUENCY MEASUREMENT in the two lower television and frequency-modulation bands cannot be conveniently made using the equipment and techniques of either the lower-frequency bands or the microwave region. However, in this region from 44 to 216 megacycles the slotted transmission line is a simple device for measuring impedances, especially if it is used somewhat differently than it is normally used in the microwave region.

Accuracy of Standing Wave Measurements

A slotted line is most accurate when used in measuring impedances that are of the same order of magnitude as the characteristic impedance of the line itself. For impedances greatly different from that of the line, the attenuation of the transmission line, if any, connecting the slotted line to the impedance being measured comes into the picture. This necessitates cumbersome corrections. Fortunately, at these frequencies coaxial cable is available that has sufficiently low attenuation so that several feet of it can be connected between the slotted line and the unknown impedance without necessitating correction for impedances that cause standing-wave ratios (swr) up to 15 to one, and still give reasonable accuracy.

Attenuation in the slotted line itself also causes errors in measurement. These errors normally appear as errors in the measured swr and in the position of a voltage or current minimum as measured with respect to some reference point, such as the point at which the unknown impedance is connected. A small percentage error in determining the position of the minimum can cause an extremely high percentage error in the measured impedance for impedances causing high swr on the measuring line.

As an example, if an impedance of 100 + j300 ohms is to be measured on a 50-ohm slotted line, a 2-percent error in swr can give a 10-percent error in resistance and a 3-percent error in reactance. An error of 2 percent of a half wavelength in determining the position of a voltage or current minimum, however, can cause a 150-percent error in resistance and a 43-percent error in reactance.

Impedance Measuring Equipment

Figure 1 shows an equipment arrangement for measuring impedance by means of two swr measurements and no position measurement. A sleeve is placed around the coaxial cable connecting the unknown impedance to the slotted line. The distance from the load end of this sleeve to the point where it is shorted to the outside of the coaxial cable is movable by means of a sliding plunger. This sleeve forms the outside conductor of a second coaxial line, which has as its inner conductor the outside conductor of the coaxial line leading from the load to the slotted line. This second larger coaxial line is shorted by the plunger at one end and has its other end connected in series with the outer conductor of the coaxial line leading to the slotted line and the unknown impedance. By varying the position of the sliding plunger the reactance introduced by the shorted line can be varied through all values both positive and negative, limited only by the Q of the line.

By sliding the plunger until the minimum swr is obtained, the reactance of the unknown impedance will be tuned out. The swr with this tuning then indicates the resistive component of the unknown impedance by itself. The value of this resistance is the characteris-

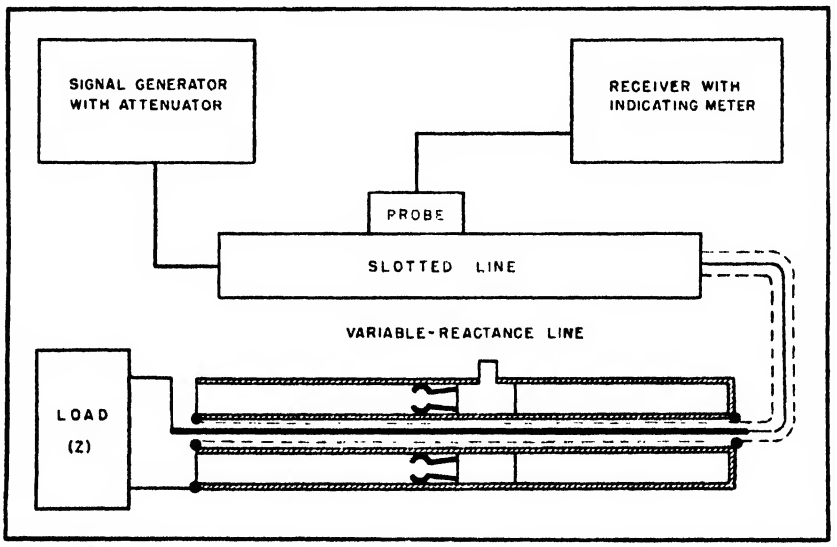

FIG. 1—Basic measuring connection includes slotted line connected to load through specially-constructed variable-reactance line

tic impedance of the slotted line either multiplied or divided by the swr, depending upon whether the resistive component of the unknown impedance is larger or smaller than the characteristic impedance of the slotted line.

Checking Conditions

To check which of these two conditions exists, it is only necessary to short-circuit the inner coaxial cable at the load and note the position of the minimum on the slotted line. If the position is the same as it was before the short was made but after the plunger had been adjusted for minimum standing wave ratio, the resistance of the load is on the same side of the characteristic impedance of the slotted line that a short circuit is, namely lower, so that a division must be performed to get the value of the resistance. If the minimum with the short-circuit in place is 90 degrees away, the resistance is higher than the characteristic impedance of the line and a multiplication must be performed to obtain the value of the resistance.

Reduction of Data

In order to get the reactance, it is necessary to refer to one of the various transmission line charts, such as the Smith chart, which are plotted in a variety of handbooks and periodicals. Although these charts appear in several different forms and look quite different they are just different conformal transformations of the same relationships between voltages and currents at different points of a transmission line, and contain the same information.

Figure 2 shows a form of transmission line chart in which the horizontal axis represents resistance and the vertical axis represents reactance. The two circles shown represent points of constant swr which degenerate into a point at Z_0 when the swr ratio is unity.

In the measurement just described, the smaller circle corresponds to the swr measured with the reactance of the unknown

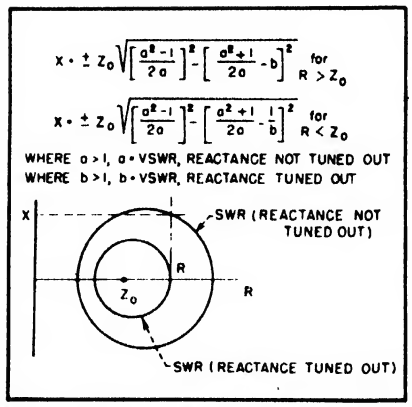

FIG. 2—Circle diagram is used to obtain reactance from two standing-wave ratio measurements, or equations can be used

tuned out. One of the two points at which this circle crosses the real axis represents the resistive component of the unknown impedance. By projecting vertically upward or downward from this point until the larger circle, which corresponds to the swr of the unknown impedance with its reactance not tuned out, is reached, the point on the complex plane representing the unknown impedance is obtained. The vertical distance from the real axis gives the reactance of the unknown.

As there is a question as to whether to go upward or downward, or what is the same thing, whether the sign of the unknown reactance is positive or negative, the rough position of the plunger must be noted. If this plunger is less than a quarter wavelength from the load end of its line an inductive reactance is being used to tune out the reactance of the unknown, so the unknown reactance must be negative. If the plunger is more than a quarter wave but less than a half wave from the open end, the unknown reactance is positive. For making this check on sign as well as for other uses of this variable-length coaxial line, it is convenient to place callibration marks along the line, labeling the frequencies at which different plunger positions are a quarter wavelength from the end of the line.

Sequence of Measurement

Summarizing the above, the procedure to follow in a measurement is to:

(1) Short-circuit the variable-length transmission line and measure the swr of the unknown.

(2) Also short-circuit the unknown and find the position of a minimum on the slotted line.

(3) Remove both of the above short circuits and adjust the plunger until the minimum of the slotted line is either at the same point as it was in step 2, or if this is impossible, until it is 90 degrees away on the slotted line. In the latter case there will be two positions of the plunger that will give a minimum. One of these two minimums is much lower than the other and occurs with the plunger at a quarter wave point, at which position it is throwing a parallel resonant circuit in series with the unknown, essentially open-circuiting it. The other plunger position giving a minimum should be used.

(4) Take the standing wave ratio.

(5) Determine the resistive component of the unknown, which is the characteristic impedance of the slotted line either multiplied or divided by the standing wave ratio of step 4 depending upon the position of the minimum of step 3.

(6) Determine the reactance of the unknown from a transmission line chart, using the knowledge of the resistive component and swr of the unknown impedance, or determine it from the formula of Fig. 2 which is derived from the geometry of the circle diagram.

(7) Note the sign of the reactance from the position of the plunger in step 3.

Measuring Balanced Impedances

The equipment arrangement as shown in Fig. 1 can be used only for measuring the impedance of unbalanced circuits, that is, circuits in which one side is grounded or can be grounded without disturbing the impedance of the unknown. If a balanced antenna, the impedance of which is to be measured, can be cut in two and half of it mounted above a ground plane as in Fig. 3A, the impedance as measured with the equipment arrangement shown will be half the impedance of the

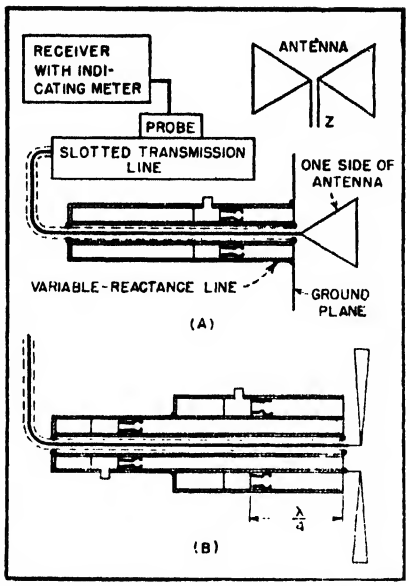

FIG. 3—The method of Fig. 1 can be used to measure unbalanced antennas by feeding energy to the system by radiation to the antenna (A). Balanced impedances can be measured using a double-section variable reactance line (B)

balanced antenna in both its resistive and reactive components.

An arrangement as shown in Fig. 3B could, of course, be used directly to measure balanced impedances.

Figure 4 shows a variable reactance that has been used very successfully for impedance measurements. It is constructed of two concentric brass tubes with a variable-position plunger short-circuiting the two together. A piece of coaxial cable is run through the center tube and its braid is soldered to this tube at the open end of the large coaxial line so formed. The length of the variable reactance must be at least a half wavelength at the lowest frequency at which it is to be used.

Another method of measuring balanced impedances, which requires no expensive special equipment and which gives quite accurate results, consists of stretching tautly a piece of 300-ohm parallel line between the impedance to be measured and a line balancer which may be one of the variable reactances of Fig. 4 with the plunger set at a point 90 degrees from the open end, and moving a pickup probe along the parallel line in order to measure swr.

Figure 5 shows a pickup probe fastened to the end of a second line balancer. If the signal generator used is not balanced and is not connected to the parallel line through a balancer, or if the pickup probe is not balanced, the results obtained will be so erratic as to be useless. Available polyethylene extruded parallel line seems to be sufficiently uniform along short lengths and to have sufficiently low losses and radiation up to 216 megacycles to give good results when impedance is computed from a measured swr and a measured minimum position.

Impedance measurements using either the two swr measurement with an unbalanced unknown or the 300-ohm parallel line with a balanced unknown can be made to an accuracy of 15 percent in both resistance and reactance for swr up to ten to one, and more accurately for lower swr.

The design and adjustment of antenna arrays can be facilitated immeasurably if suitable phase measuring equipment is available. A system for measuring phase in the 44-216 mc region, an adaptation of a method used at lower frequencies for a long time[1], is illustrated by the equipment arrangement of Fig. 6. This method uses the principle that the only variation between signals taken from various points of a slotted line perfectly matched to a load is one of phase, and that phase change is linear with distance as measured along the line.

In this system the output of a signal generator is connected to both a slotted line and the device under test, such as the antenna array. The slotted line is terminated in a matched resistance so that the amplitude of current along the line is constant. A sampling probe at the end of a balancer, similar to that described for measuring swr on the open parallel line, is connected through an attenuator to the sliding pickup of the slotted line.

A receiver is also connected through a flexible coaxial line to this same slotted line pickup probe in such a way that the receiver input is the sum of the signals extracted from the slotted line and brought into the sliding probe from the sampling probe. Because of this connection, the attenuator can be adjusted so that the signal sampled from, say, a dipole in the array under test is of the same amplitude as that removed from the slotted line. The position of the slide on the slotted line can be adjusted so that the phase of the signal from the slotted line is such that cancel-

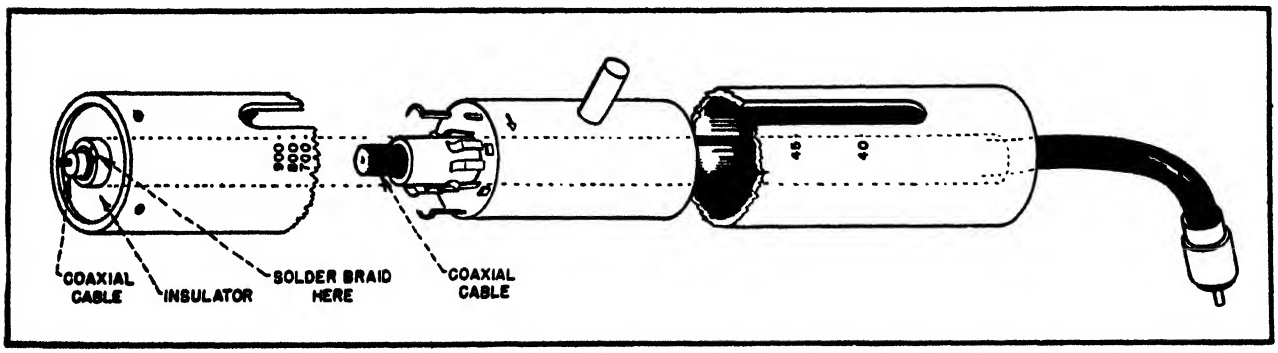

FIG. 4—Variable reactance shown in diagrams is constructed from coaxial cable over which brass tubing is fitted

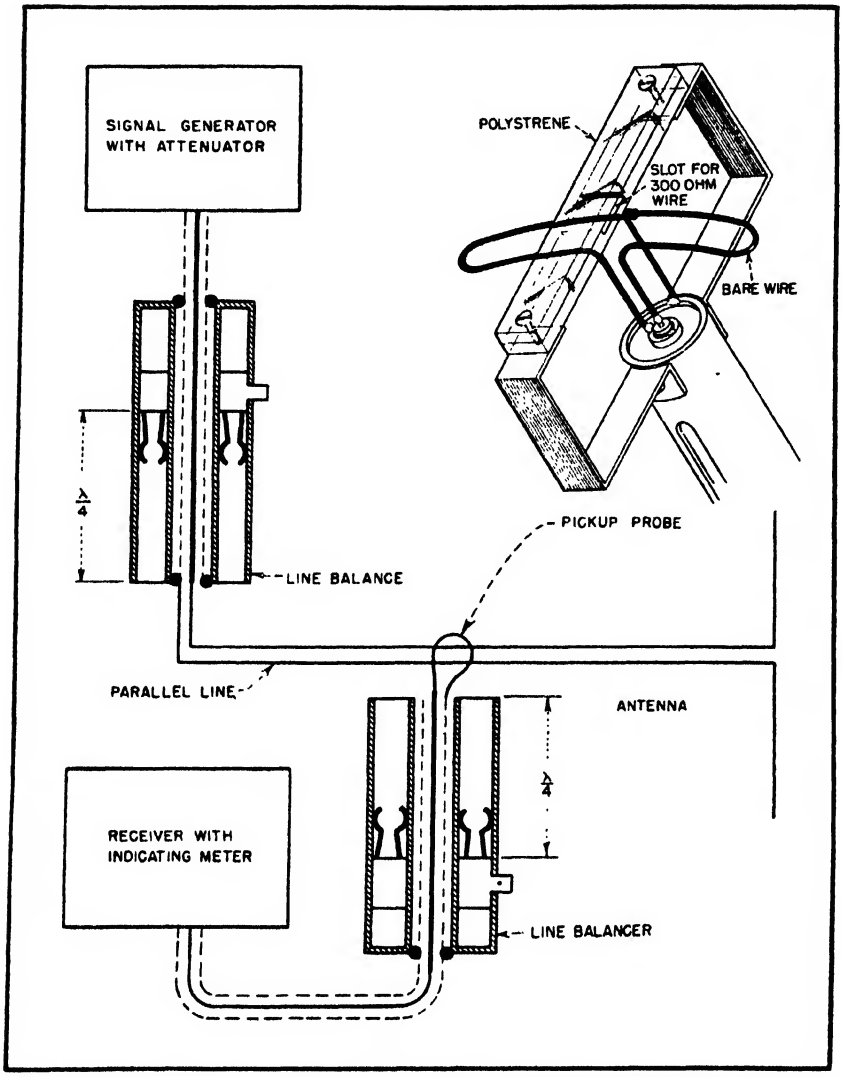

FIG. 5—Standard 300-ohm parallel line can be used with pickup probe to measure balanced impedance in this connection

lation of the signal from the antenna dipole under test occurs.

If the balanced probe is then moved so as to sample energy from a different dipole and the position of the sliding probe is moved to that now required for cancellation, the amount it is moved along the slotted line gives the phase difference between the two dipoles. From a knowledge of the wavelength in the slotted line this difference can be expressed in degrees.

With this equipment arrangement, a minimum point is found along the slotted line every wavelength rather than every half wavelength, as in the case in swr measurements. This difference does not mean, however, that the slotted line has to be twice as long because the sampling probe can be rotated 180 degrees if the minimum tends to fall out of range of the slotted line.

The accuracy with which phase can be measured by this method depends largely upon how good the slotted line is and how well it is terminated. A slight rotation of the sampling probe is of no importance as it does not normally change the phase, but only the amplitude of the picked up signal. An accuracy of measurement of between $\pm$ 3 and $\pm$ 5 degrees has been consistently obtained over the 44 to 216 megacycle range.

There are many different manners in which antenna gain (directivity) has been measured[1,2]. Results of such measurements can be expressed in terms of the directivity of a half-wave dipole or an isotropic (completely nondirectional) radiator. The latter is used in expressing absolute gain of antenna arrays. The gain of a half-wave dipole over an isotropic radiator is 2.15 db along the centers of its major lobes.

Figure 7 illustrates an arrangement of equipment for measuring the gain of an antenna over that of a half-wave dipole quite accurately and simply. In this arrangement a signal generator is connected through a slotted line and a line balancer to the antenna under test. A signal is radiated from this antenna to a receiving antenna which is connected through a balancer to a receiver.

It is necessary that both antennas be balanced carefully in order to be sure that no currents flow on the outsides of the coaxial lines leading to the signal generator and receiver. If currents do flow on these lines, they will radiate from line to line or from line to antenna and make the readings meaningless.

It is also necessary that the signal generator have an output impedance equal to the characteristic impedance of the slotted line, as will become apparent later. Because most signal generators have low output impedances, it may be necessary to connect a resistance in series with the generator output or otherwise modify the generator to obtain the required output.

With the equipment arranged as described, the signal generator attenuator should be set to such a value that a convenient output from the receiver is obtained. The antenna under test is then replaced with a half-wave dipole, not necessarily of the same impedance as the antenna under test or even a known impedance. The signal generator attenuator must then be reset until the receiver output becomes the same as it was when the antenna being tested was in use. The db difference between the two attenuator settings gives the antenna gain over a half-wave dipole, if the two antennas had exactly the same mis-

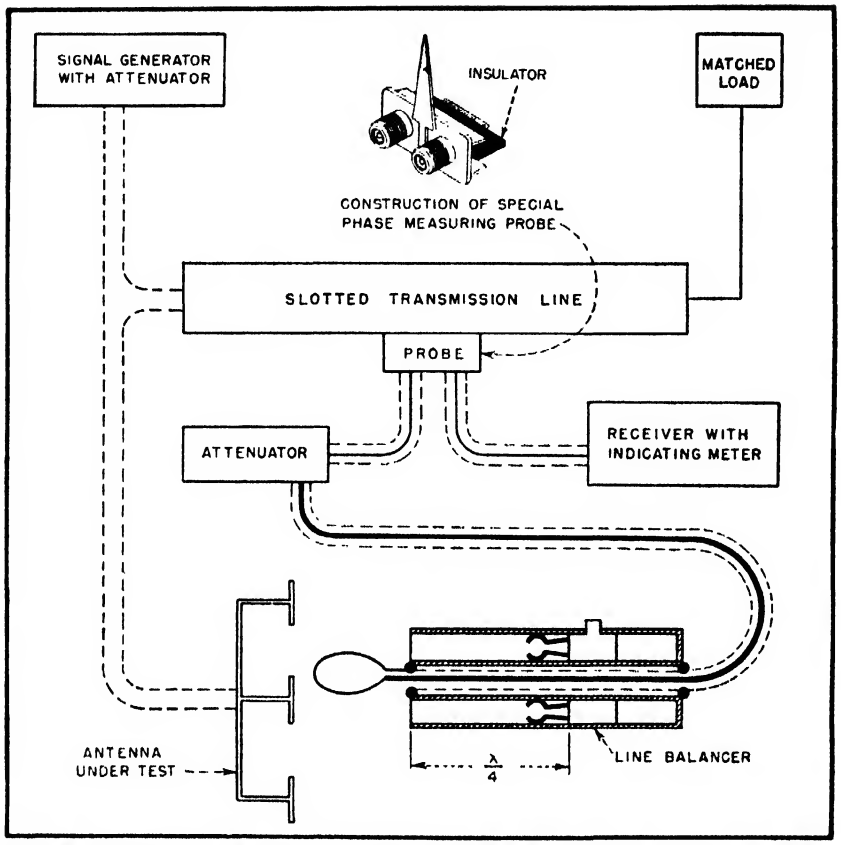

FIG. 6—Phasing of antennas in an array can be measured by utilizing the linear phase shift with distance along a flat slotted transmission line by this connection built about a special probe

matches to the slotted line. The swr of the two antennas can then be measured and the ratio of the power transmission coefficients computed from the two swr values. The absolute gain of the antenna under test can then be computed as the sum of 2.15 db, the difference of signal generator attenuator settings in db and the ratio of power transmission coefficients of the two antennas expressed in db. Figure 7 gives the formula for this last quantity in terms of the two measured swr.

The measuring methods herein described lend themselves quite well to quick changes of frequency, even over several octaves, as is desirable for broad-band antenna work. The accuracy seems sufficiently good for most engineering purposes. There is still an ever increasing need for a piece of high-frequency impedance measuring apparatus that approximates the ohmmeter in its simplicity of operation. At present when a change is made in, say, a television antenna, it may be necessary to measure its impedance over the entire frequency range 44 to 216 megacycles to determine if the change is desirable. This measurement is obviously a time-consuming procedure.

In the setting up of a new development program there is always the problem of what fraction of the available time should be spent in constructing test equipment and what fraction of the time spent using it. The best solution to this problem as applied to antenna development may eventually result in much more convenient methods of impedance measurement. Increased accuracy is, of course, always to be desired.

References

(1) J. F. Morrison, A Simple Method of Observing Current Amplitude and Phase Relations in Antenna Arrays, *Proc IRE*, p 1310, Oct 1937.

(2) J. C. Schelleng, C. R. Burrows, and E. B. Ferrell, Ultra-Short Wave Propagation, *Proc IRE*, p 427, March 1933.

(3) F. M. Colebrook and A. C. Gordon-Smith, The Design and Construction of a Short-Wave Field-Strength Measuring Set, *Jour IEE*, p 388, 84, 1939.

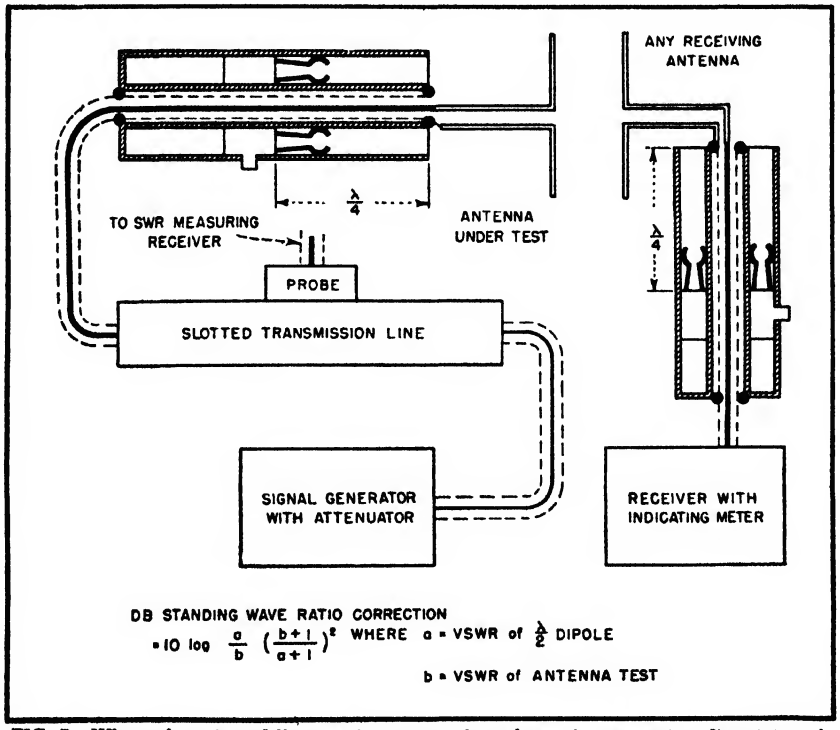

FIG. 7—Where there is a difference in antenna impedance in comparing directivity of two antennas, correction can be made based on standing-wave ratio measurements

UHF Impedance Measurements

By measuring standing waves on transmission lines, the terminating impedance can be determined. Low-power equipment can be used if the measuring probes have high impedance. Resonance and loose coupling are used to obtain high-impedance probes

By N. MARCHAND and R. CHAPMAN

MEASUREMENT of impedances at ultrahigh frequencies by the standing-wave method is well known. The majority of these measurements are made on power equipment where the energy consumed by the measuring device does not disturb the system.

When the power available begins to approach the power consumed by the measuring device, conventional equipment begins to decrease in accuracy until a point is reached where the measurements are meaningless. All types of receiving apparatus and receiving antennas fall in this latter group. Measuring the impedance of these devices calls for a new type of equipment.

Improved Equipment

The equipment described in this article is primarily a high-impedance voltage-reading device usable at frequencies from 150 to 1000 megacycles. The average accuracy of these measurements is in the order of 10 percent, although accuracies of five percent are possible under optimum conditions.

An oscillator is used to excite a transmission line of known impedance. The unknown impedance is used to terminate the standard line. The standing-wave ratio and the positions of several nulls on the line are noted with the aid of a high-impedance probe coupled to the input of a receiver. A reference point for calculating the phase angle of the load is established by shorting the standard line at the termination.

Although designed primarily for the impedance measuring equipment, the high impedance probes were found useable for several other interesting applications. Voltage distribution and balance were accurately checked on dipoles, folded dipoles, loops and various other assemblies.

The standard lines in use are a 50-ohm coaxial line, and a 95-ohm balanced line. The coaxial line is slotted along its length to permit insertion of the probe. The balanced system is equipped with a mechanical means of marking nulls. The same system of indicating nulls could be applied to the coaxial system, but in the coaxial case it was found relatively easy to measure the nulls directly with a meter stick. The standard lines are shown in Fig. 1 and in several photographs.

Generator and Receiver

The signal source may be any stable, well-shielded oscillator which covers the necessary range. The frequency calibration is not important as the frequency may be measured experimentally on the standard line, but an accurate, easily-read attenuator is essential. A single-ended output on the generator is desirable; for making coaxial measurements it is necessary.

In making measurements with the balanced system it is best to rely on an unbalance-to-balance converter to properly excite the lines, even though a generator with a so-called balanced output is available.

If a balance box (balance-to-unbalance converter, essentially a device for transferring from a coaxial system to a balanced system) is used when exciting any type of balanced system, the balance to ground will be preserved. This is generally safer than relying on the balance of the output of the generator, especially where accurate measurements are being made. Design data and general characteris-

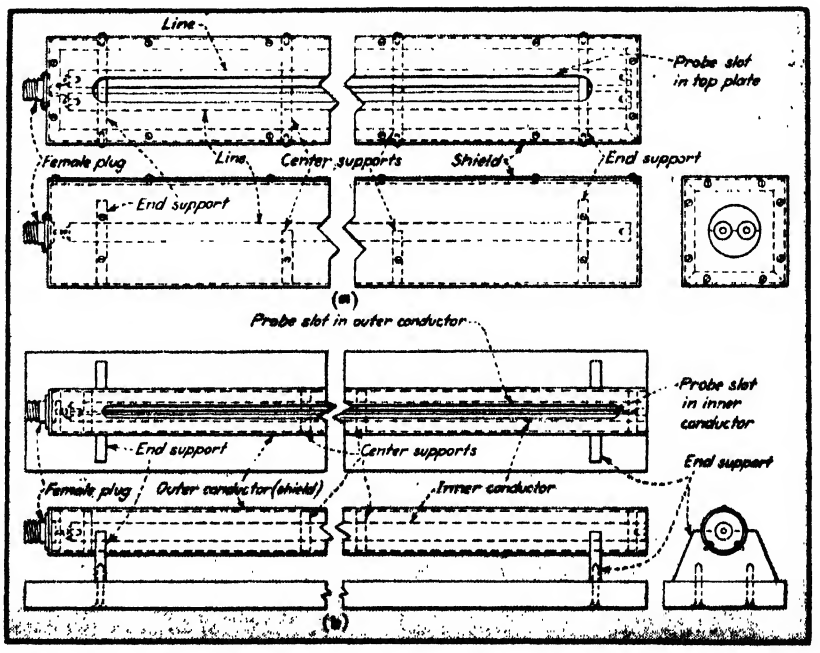

FIG. 1—(a) Balanced line used in impedance measurements, constructed in a trough for shielding. (b) Coaxial line construction

tics of this type of converter have already been discussed and analyzed.

The receiver, like the oscillator, may be any model which will cover the desired range. Similarly, it must be well shielded. It should contain a diode-type output meter. This meter need have no special calibration as it is used only for indicating nulls.

High Impedance Probes

The probe which is connected to the receiver input is the critical part of the system. It must be an easily tuned, high-impedance device which will consume negligible power from the standard line. Two types are used. For the low-frequency range (150 to 350 megacycles) standard *LC* tuning is employed. In the high-frequency ranges (350 to 1000 megacycles) coaxial and balanced lines are tuned by means of sliding shorts.

The greater the characteristic impedance of the shorted quarter-wavelength line section of the probe, the less critical the tuning becomes. When the line is tuned to exactly one-quarter of a wavelength, the impedance is real and very high. As long as the input impedance of the probe remains in the order of twenty-five times the impedance of the standard line it will produce no detrimental effects (for standing wave ratios of five or less). This means that the characteristic impedance of the probe will determine the ease with which it may be tuned, as indicated by the relation $Z = jZ_0 \tan (2\pi l/\lambda)$. This, and the obvious mechanical limitations, set the value of the characteristic impedance of a practical probe at 100 ohms.

Output from the probe is obtained by loosely coupling to the high-current end of the quarter-wavelength section with a loop connected to a coaxial line.

Loose coupling is necessary for several reasons:

The probe can consume only a small amount of power from the standard line. The amount of power being consumed can be adjusted by varying the coupling to the receiver. The coupling can be adjusted by varying the pickup-coil ductor, or its orientation with respect to the center conductor. The lowest value of coupling which will give a suitable reading on the receiver output meter is used.

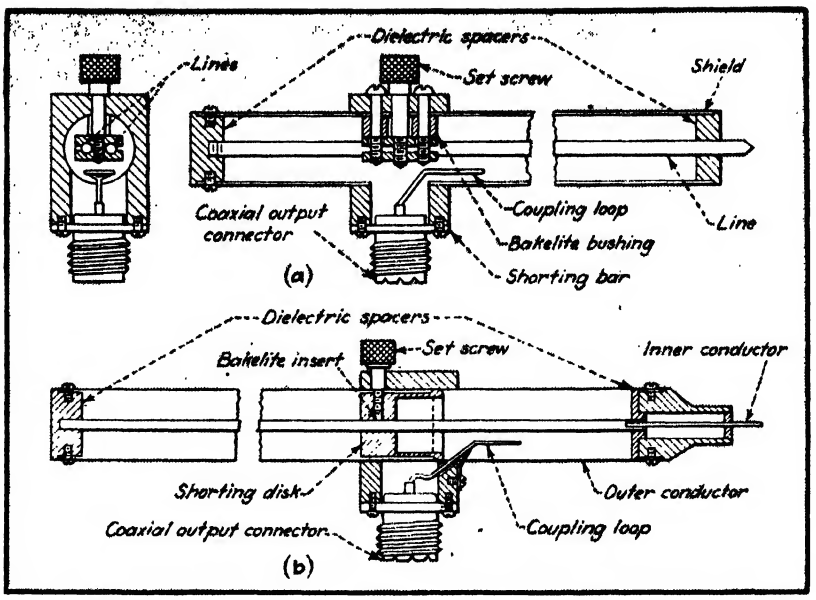

FIG. 2—(a) Balanced u-h-f probe construction provides a movable shorting bar and a pickup loop assembled inside a shield. (b) Coaxial probe is similarly constructed, with shorting disk and pickup loop inside the outer conductor of the probe

Of secondary importance is the unbalance which the pickup loop introduces into the system. Each side of this loop presents a different impedance to ground. This lack of symmetry, if the coupling becomes excessive, will unbalance the tuned section. Consequently the balanced line begins to look like a coaxial line. The two lines look like the inner conductor, in conjunction with the shield, of a coaxial line. This produces several effects. As shield currents begin to flow, a solid connection to the standard-line shield from the probe shield becomes essential to prevent detuning. When this connection does not exist, the circuit is completed by capacitance between the probe shield and the standard line. As the unbalpacitance is being constantly changed by the position of the operator, it is impossible to take an accurate reading.

Another effect of coupling is upon the standard line. As the unbalance increases, the two central conductors look increasingly like a single line, and introduce unbalance errors in the measurements.

In the event that extremely close coupling is necessary, the unbalancing effect of the loop may be removed by installing a balanced-to-unbalanced converter loop as a pickup. This type of pickup presents the same impedance to ground from either side of the line.

When the probe is used in conjunction with a sensitive receiver, the coupling may be maintained at a value small enough to avoid any of the previously mentioned effects.

Construction

The size of the coupling loop is such that it will resonate at approximately 2000 megacycles. This eliminates sharp changes in sensitivity over the range of the probe.

The tuning short of the probe is controlled by a knurled setscrew, which is used to lock and adjust it. This setscrew is an integral part of the block upon which the output plug and pickup loop are mounted. The pickup loop moves with the

short, and is always at the low-current end of the dual line.

The balanced probe illustrated in Fig. 2(a) is basically a dual line with a shield. A short, controlled from outside the shield, may be used to tune this line to one-quarter of a wavelength between 350 and 1000 megacycles.

The probe used on the 150 to 350 megacycles portion of the range consists of a length of balanced line tuned with a variable capacitor as shown in Fig. 3(a). An adjustable short is shunted across the line to permit the probe to be used on several ranges with a low tuning capacitance.

The coaxial probe is similar to the balanced probe in most respects. It consists of a single conductor, a shield, and a short controlled from outside the shield for tuning as shown in Fig. 2(b). Energy is removed by means of a pickup loop mounted directly under the short. The major axis of the pickup is on the shield diameter. The 150-to-350 megacycle coaxial probe is capacitor tuned as illustrated in Fig. 3(b).

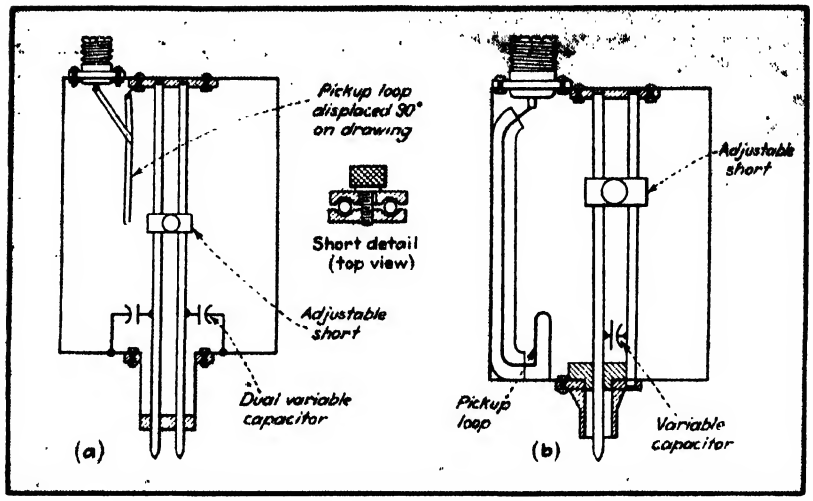

FIG. 3—For operation at v-h-f, capacitor-tuning supplements the shorting-bar tuning used at u-h-f as in (a) the balanced probe and (b) the coaxial probe

Measuring Procedure

When making measurements, the standard line is shorted at the point where the unknown impedance is to be placed. The oscillator is fed into the standard line. The receiver-input cable is connected to an auxiliary pickup. This may be any device which can be used to couple loosely to the standard line. The best position is approximately halfway between points of maximum and minimum pickup.

With the auxiliary pickup in this position, any disturbance on the line will produce a deflection on the receiver-output meter. The probe may now be tuned by sliding it along the standard line and adjusting the short until no visible deflection is produced on the receiver-output meter. When this condition is reached the probe is tuned to one-quarter wavelength and presents a high impedance to the standard line. The auxiliary pickup is now replaced with the probe.

With the short in place, the probe is used to determine the positions of several nulls.

If the receiver and oscillator are well shielded, the ratio of maximums to minimums should be extremely high. At the minimum, the voltage should be zero. If this is not the case, there is direct pickup between oscillator and receiver.

One of the ways of minimizing direct pickup is to run the oscillator at the lowest level consistent with accurate readings. Direct pickup has no effect on the positions of the nulls, except to make them less pronounced, but causes a serious discrepancy in the measurement of the ratio of voltage maximum to voltage minimum.

After several nulls have been located the frequency may be calculated. These same nulls are used as reference points for measuring the unknown impedance. The short is removed and the unknown impedance is placed at the end of the line. The positions of the new nulls are noted. The relation of the null obtained when the line was shorted to the latter null is noted. It is also necessary to note whether the first null, obtained when the line was shorted, is toward the generator or toward the load in relation to the null obtained with the line terminated in the unknown impedance. It may be measured in either direction as long as the direction is noted.

The last piece of information necessary is the standing-wave ratio. With the short removed, the probe is placed at a minimum. The signal-generator attenuator setting and the receiver output meter reading are noted. The probe is moved to a maximum. The signal-generator attenuator is adjusted until the receiver output meter returns to its former reading. The signal-generator attenuator reading is again noted. The standing-wave ratio is equal to the maximum signal-generator attenuator reading over the minimum attenuator reading. From the information obtained about the frequency, the null shift and the standing wave ratio, the characteristics of the load may be calculated.[2, 3]

When making measurements with the coaxial system the balance box is not used in feeding the transmission line. This is the only physical difference between the two systems.

References

(1) Marchand, N., Transmission-Line Conversion Transformers, ELECTRONICS, p. 142, Dec. 1944.
(2) Stewart, Measurement of Antenna Impedance, *QST*, p. 80, Dec. 1943, also Notes on Transmission Lines, *QST*, p. 25, Aug. 1943.
(3) Terman, F. E., "Radio Engineers' Handbook," McGraw-Hill Book Co., 1943, p. 172–192.

Comparator for Coaxial Line Adjustments

High-frequency line impedance measurements in laboratory or field can be simplified by this compact comparison instrument that essentially replaces the slotted coaxial line and sliding-probe voltmeter technique for checking match or determining standing-wave ratio and reactive component

By O. M. WOODWARD, Jr.

IN matching a load with several adjustable elements, such as an antenna array, to coaxial transmission lines the process may prove to be tedious using the conventional slotted line and probe indicator. At low frequencies such lines become long and inconvenient to construct.

The simple instrument illustrated in Fig. 1 is a comparator consisting of a coaxial T-junction with a current pickup loop symmetrically placed to couple magnetically to the center of the junction. The T-junction joins the generator, the load whose characteristics are to be obtained, and a line terminated with a resistance or reactance equal to its characteristic impedance.

Electrostatic shielding between the coaxial lines and the loop is provided by a number of slots cut in each of the three lines near the center of the junction. The loop may be rotated in the plane of the junction to assume the various positions shown in Fig. 2. The output of the loop is fed to an indicator.

Referring to Fig. 3 the three lines have a common voltage $\bar{E}$ at the center of the T-junction. Hence the impedance of the load line at the junction L is

$$\bar{Z}_L = \bar{E}/\bar{I}_L \qquad (1)$$

Since the opposite line is matched,

$$Z_c = \bar{E}/\bar{I}_c \qquad (2)$$

and

$$\bar{I}_L = \bar{I}_c\,(Z_c/\bar{Z}_L) \qquad (3)$$

The impedance at a voltage minimum is a pure resistance equal to the product of the standing-wave ratio P and the characteristic impedance Z_c of the line, where P is taken to be the ratio of the minimum voltage to the maximum voltage.

By means of the usual impedance transfer equation the impedance may be determined in terms of the resistance at a voltage minimum X located a distance of ρ electrical degrees on the load line.

$$\bar{Z}_L = \frac{P Z_c + j Z_c \tan \rho}{Z_c + j P Z_c \tan \rho} Z_c \qquad (4)$$

Combining Eq. 3 and 4

$$\bar{I}_L = \bar{I}_c \left(\frac{1 + j P \tan \rho}{P + j \tan \rho} \right) \qquad (5)$$

With the loop in position D (Fig. 2) parallel to the load and matched lines, a voltage will be induced in the loop producing a current $\bar{I}_p$ proportional to the vector difference of the load and matched line currents.

$$\bar{I}_p = T\,(\bar{I}_L - \bar{I}_c) = (T\bar{I}_c)\left(\frac{1 + j P \tan \rho}{P + j \tan \rho} - 1 \right) = (T\bar{I}_c)\,\frac{(1 - P)\,(1 - j \tan \rho)}{(P + j \tan \rho)} \qquad (6)$$

where T is a proportionality constant depending upon the frequency, physical dimensions of the comparator components, and the input impedance of the receiver.

After rectification in the receiver the output current I'_p will be proportional to the absolute magnitude of Eq. 6, or

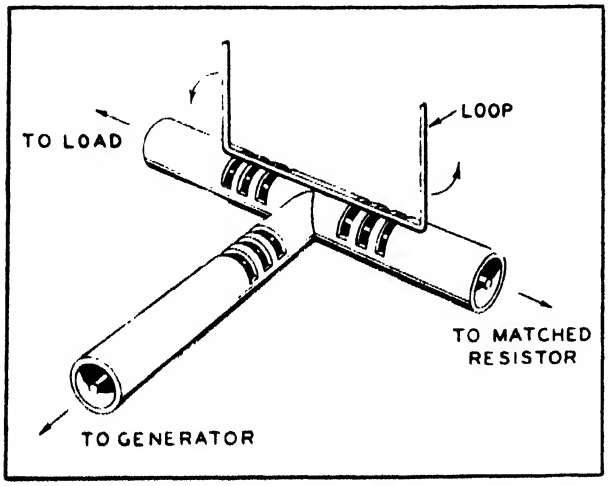

FIG. 1—Simplified drawing of T-junction, showing connections and the pickup loop that can be rotated to couple to them

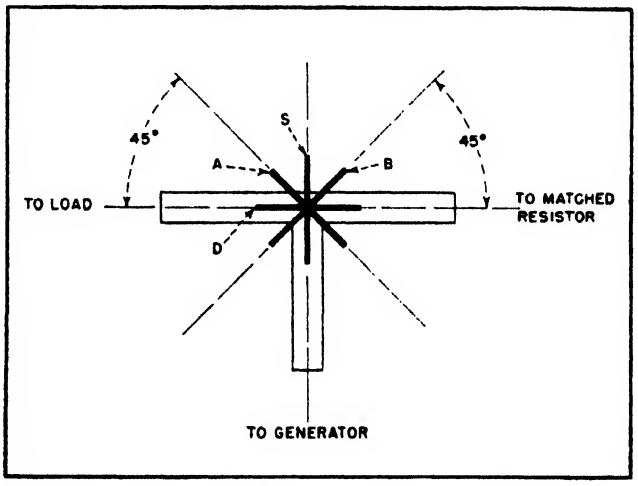

FIG. 2—Detail of the pickup loop positions with relation to the junction, and the notation used in designating position

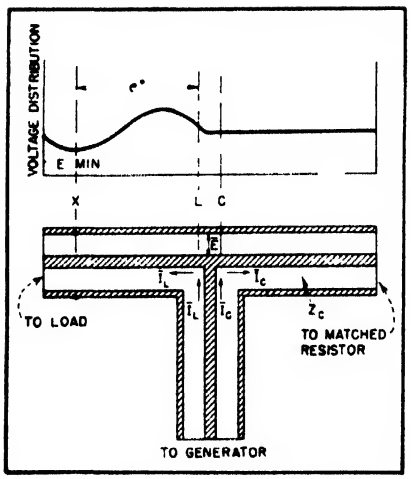

FIG. 3—Graphical representation of the standing wave formed on one arm of the T-junction when the load is not matched

$$I'_D = T'|I_e|\left(\frac{1+\tan^2\rho}{P^2+\tan^2\rho}\right)^{1/2}(1-P) \quad (7)$$

where the proportionality constant T' also includes the receiver gain factor. Similarly, with the loop in position S parallel to the generator line a voltage will be induced in the loop producing a current $\bar{I}_s$ proportional to the vector sum of the load and matched line currents.

$$\bar{I}_s = T(\bar{I}_L + \bar{I}_C) = (T\bar{I}_e)\frac{(1+P)(1+j\tan\rho)}{(P+j\tan\rho)} \quad (8)$$

The receiver output current will then be

$$I'_s = T'|I_e|\left(\frac{1+\tan^2\rho}{P^2+\tan^2\rho}\right)^{1/2}(1+P) \quad (9)$$

$$\frac{I'_D}{I'_s} = \frac{1-P}{1+P} = K \quad (10)$$

The ratio of the receiver output currents for the two coil positions is equal to the magnitude of the reflection coefficient K on the load line.

In practice, the loop is placed in position S and the receiver gain or generator power adjusted to produce full-scale reading on the receiver output meter. The loop is then rotated to position D and the reflection coefficient is directly indicated on the meter as the percentage of full-scale reading. Equation 10 shows that the reflection coefficient reading obtained is independent of the relative position of the standing wave with respect to the comparator. If the receiver is not linear, suitable correction of the meter calibration must be made.

This relationship also may be shown in another manner. The loop currents for the two positions D and S are

$$\bar{I}_D = T(\bar{I}_L - \bar{I}_e) = \frac{T\bar{E}}{Z_L}\left(1-\frac{\bar{Z}_L}{Z_e}\right) \quad (11)$$

and

$$\bar{I}_S = T(\bar{I}_L + \bar{I}_e) = \frac{T\bar{E}}{Z_L}\left(1+\frac{\bar{Z}_L}{Z_e}\right) \quad (12)$$

The well-known transmission line equation expressing the current at a point down the line in terms of the load characteristics and line constants is

$$I_p = \underbrace{\frac{I_L}{2}\left[1-\frac{\bar{Z}_L}{Z_e}\right]\epsilon^{\gamma P}}_{\text{Reflected wave}} + \underbrace{\frac{I_L}{2}\left[1+\frac{\bar{Z}_L}{Z_e}\right]\epsilon^{-P\gamma}}_{\text{main wave}} \quad (13)$$

Hence the ratio of the receiver output currents for the two loop positions D and S is seen to be the ratio of the reflected wave to the main wave, or the coefficient of reflection.

$$\frac{I'_D}{I'_S} = \left|\frac{\left(1-\frac{\bar{Z}_L}{Z_e}\right)}{\left(1+\frac{\bar{Z}_L}{Z_e}\right)}\right| \quad (14)$$

Assuming that a matched line may be provided, correct operation is independent of frequency up to the range where the loop couples to an appreciable fraction of a wavelength on the lines. In this region the loop current will not be a function of the currents flowing in the lines at the immediate T-junction only.

To obtain an experimental check on the accuracy of operation, a slotted measuring line was inserted between an adjustable load and the comparator. Standing-wave ratio readings obtained from the two instruments for various loads and frequencies are comparable as shown in Fig. 4 and 5.

Fixed Loop for Matching

For certain applications, such as final matching adjustments of antennas in the field, the comparator may be simplified by fixing the loop in position D. In use, the load matching elements are adjusted in rotation for a null on the receiver output meter. Referring to Eq. 7 it is seen that a null is obtained only when P is unity.

In comparators of this type covering the frequency range of 400 mc to about 1,700 mc, the receiver is replaced by a fixed crystal and microammeter. The loop consists of an adjustable quarter-wave tuning stub to which is coupled the fixed crystal. The matched load is a selected resistor equal to the characteristic impedance of the lines.

For a given standing wave on the load line the load current and hence the loop current will be a function of the relative position of the standing wave with respect

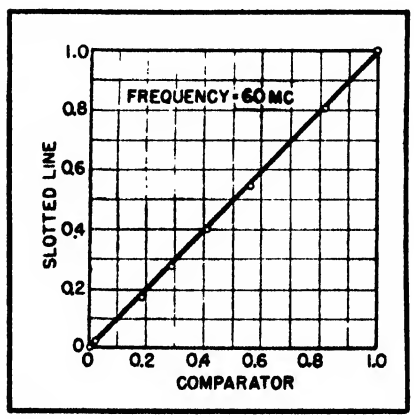

FIG. 4—Standing-wave ratios obtained with a slotted line inserted between adjustable load and comparator at 60 mc

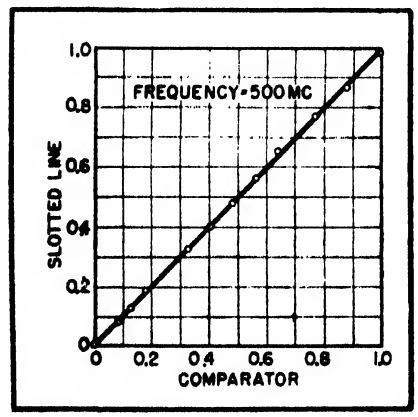

FIG. 5—Good agreement is found at 500 mc between slotted-line and comparator measurements of standing-wave ratios

to the T-junction. If the line between the load and the comparator is of such a length as to give a voltage minimum at the T-junction ($\rho = 0$) the loop current from Eq. 7 is seen to be proportional to (1-P)/P. For the same load a change in line length of one-quarter wavelength will result in a voltage maximum appearing at the T-junction ($\rho = 90$), and the loop current will be proportional to (1-P).

The ratio of the minimum loop current to the maximum loop current for a given load and a variable shift of the standing-wave along the load line is seen to be equal to the standing-wave ratio.

$$\frac{I_D \text{ min.}}{I_D \text{ max.}} = \frac{(1 - P)}{(1 - P)/P} = P \qquad (15)$$

Thus, as a match is approached on the load line by adjustment of the matching elements, the possible meter deflection diminishes rapidly.

Using a square-law crystal detector the relative meter deflection as a function of the standing-wave ratio and its position on the load line is plotted in Fig. 6. The shaded area indicates the possible deflection change for any shift of the standing wave along the line. A constant T-junction voltage E is assumed for these calculations.

Absolute Magnitude of Load Impedance

Other load characteristics may be obtained from the comparator with the rotating loop. The absolute magnitude of the load impedance $|Z_L|$ at the T-junction is found by taking the ratio of the linear receiver output readings for two additional loop positions. From Fig. 2 it is seen that with the loop in position B the loop current is

$$\bar{I}_B = T\left(\frac{\bar{I}_c}{\sqrt{2}} + \frac{\bar{I}_c}{\sqrt{2}}\right) = \sqrt{2}\, T \bar{I}_c \qquad (16)$$

since the loop is at an angle of 45 degrees and couples equally with both of the T lines. Components of the load current in the loop are equal and opposite in this case. Similarly, with the loop rotated 90 degrees to position A, the current is

$$\bar{I}_A = T\left(\frac{\bar{I}_L}{\sqrt{2}} + \frac{\bar{I}_L}{\sqrt{2}}\right) = \sqrt{2}\, T \bar{I}_L \qquad (17)$$

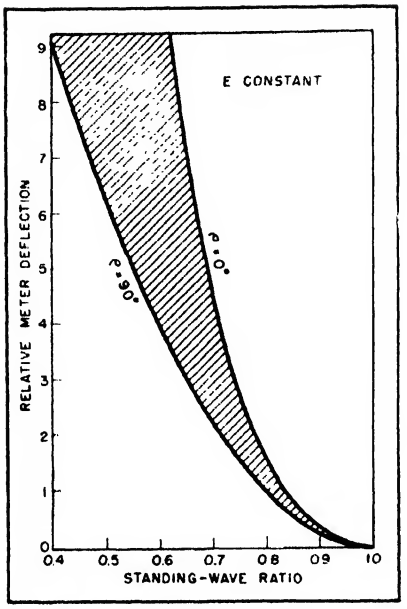

FIG. 6—Relative meter deflection shown as a function of standing-wave ratio and its position on the load arm of the T-junction

Forming the ratio and combining with Eq. 3,

$$\frac{I'_B}{I'_A} = \frac{|Z_L|}{Z_c} \qquad (18)$$

where $|Z_L|$ is expressed in terms of the characteristic impedance of the lines. In practice the receiver output meter is set to full scale at the loop position giving the larger reading. The loop is then rotated 90 degrees to the other position and the ratio of $|Z_L|/Z_c$, or $Z_c/|Z_L|$ as the case may be, is read directly on the meter as the percentage of full scale deflection.

Resistive Component of Load Impedance

Having obtained the reflection coefficient K and the absolute magnitude of the load impedance $|Z_L|$ from the four loop positions, the resistive component R_L of the load impedance may be found. From Eq. 4

$$\frac{\bar{Z}_L}{Z_c} = \frac{P + j \tan \rho}{1 + j P \tan \rho} = \frac{R_L + j X_L}{Z_c} \qquad (19)$$

Equating the real terms and imaginary terms respectively

$$R_L - X_L P \tan \rho = Z_c P \qquad (20)$$

and

$$R_L P \tan \rho + X_L = Z_c \tan \rho \qquad (21)$$

Eliminating tan ρ and solving for R_L/Z_c

$$\frac{R_L}{Z_c} = \left(\frac{P}{P^2 + 1}\right)\left[\left(\frac{|Z_L|}{Z_c}\right)^2 + 1\right] \qquad (22)$$

since $P = (1 - K) / (1 + K)$

$$\frac{R_L}{Z_c} = \frac{(1 - K^2)}{2(1 + K^2)}\left[\left(\frac{|Z_L|}{Z_c}\right)^2 + 1\right] \qquad (23)$$

Although the arithmetic value of the reactive component X_L may be derived knowing R_L and $|Z_L|$, the algebraic sign of X_L is not found since the same loop reading of ρ and $|Z_L|$ will be obtained whether the reactive component is positive or negative. Also for some values of the load impedance having a small phase angle, low accuracy is obtained in determining the arithmetic value of X_L.

To obtain the algebraic value of the reactance, the matched resistor (Fig. 3) is replaced with a shorted coaxial line one-eighth wavelength long having the same characteristic impedance Z_c as the T-junction lines. Since the reactance of the eighth-wave shorted stub is $+ jZ_c$,

$$\bar{I}_c = \bar{E} / + j Z_c \qquad (24)$$

$$\text{Hence } \bar{I}_c = \bar{I}_L\left(\frac{X_L}{Z_c} - j\frac{R_L}{Z_c}\right) \qquad (25)$$

With the loop in position D,

$$\bar{I}_D = T(\bar{I}_L - \bar{I}_c) = T\bar{I}_L\left(1 - \frac{X_L}{Z_c} + j\frac{R_L}{Z_c}\right) \qquad (26)$$

Likewise, with the loop in position S,

$$\bar{I}_S = T(\bar{I}_L + \bar{I}_c) = T I_L\left(1 + \frac{X_L}{Z_c} - j\frac{R_L}{Z_c}\right) \qquad (27)$$

Designating the ratio of the receiver output currents in this case by K'

$$K' = \frac{I'_D}{I'_S} = \left[\left(1 - \frac{2X_L}{Z_c} + \frac{|Z_L|^2}{Z_c^2}\right) \Big/ \left(1 + \frac{2X_L}{Z_c} + \frac{|Z_L|^2}{Z_c^2}\right)\right]^{1/2} \qquad (28)$$

Solving for X_L/Z_c,

$$\frac{X_L}{Z_c} = \frac{(1 - K'^2)}{2(1 + K'^2)}\left[\left(\frac{|Z_L|}{Z_c}\right)^2 + 1\right] \qquad (29)$$

The ratio of the receiver currents for the loop positions B and A will be the same whether the stub or the matched resistor is used. It is seen that the equations

for the resistive component and the reactive component are identical in form. The adjustable stub may be calibrated in terms of frequency for convenience in use.

Since the reactance of a shorted line θ electrical degrees in length is given by

$$X = +jZ_s \tan\theta \qquad (30)$$

it is seen that the stub may be somewhat shorter than an eighth-wave in length if its characteristic impedance is raised, the only requirement being that its reactance be equal to the characteristic impedance of the load line.

For a particular frequency of operation the stub length to give the required reactance may be found quite easily without the use of the slotted measuring line equipment. The load line is replaced by the stub, and the matched resistor connected to the opposite side of the comparator. Since it was shown in Eq. 18 that the absolute magnitude of the load impedance in terms of the characteristic impedance was equal to the ratio of the loop currents for loop positions B and A, the stub is simply adjusted until this ratio is unity.

A chart is given in Fig. 7 from which the resistive and reactive components of the load impedance may be obtained from the various loop positions of the comparator.

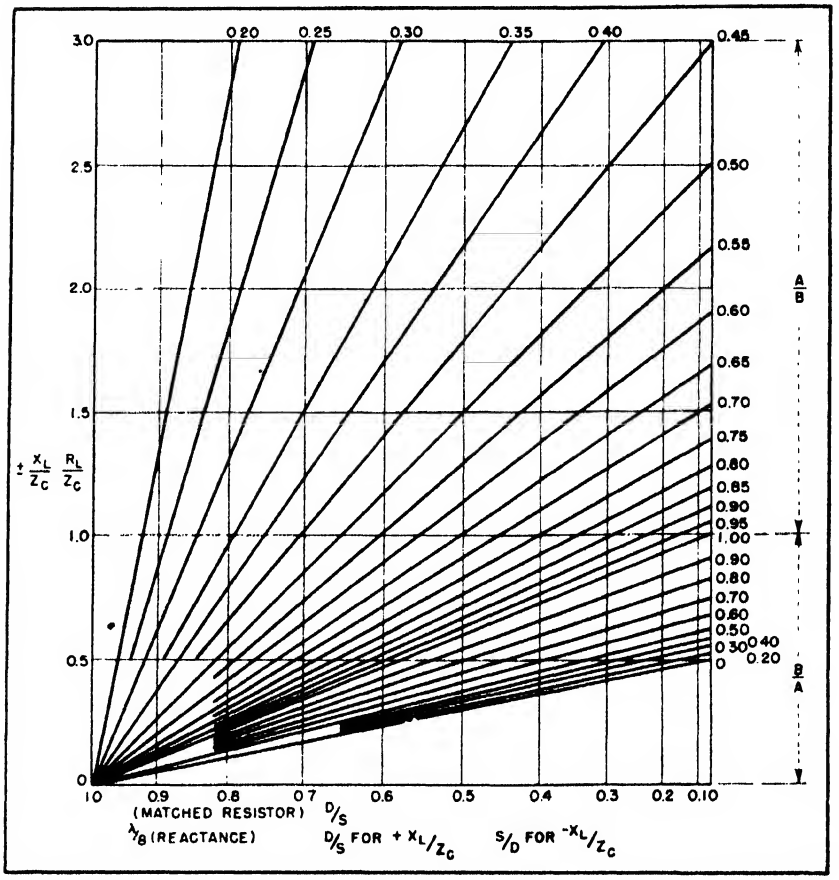

FIG. 7—Chart showing resistive and reactive components of the load impedance as obtained from various loop positions and detector voltage readings

Example

As an example of its use, an unknown load and the matched resistor are connected as shown in Fig. 2. The loop is rotated in the four positions to give the current ratios of D/S and A/B (or B/A). For a D/S ratio of 0.46 and a A/B ratio of 0.65 the resistive component of the load impedance in terms of the characteristic impedance is found to be 1.10. The matched resistor is then replaced by the eighth-wave stub and the current ratio D/S (or S/D) determined. Using the same A/B value of 0.65 previously found, it is seen that the reactive component of the load impedance in terms of the characteristic impedance is equal to -0.75 for a S/D ratio of 0.62. For a characteristic impedance equal to 52 ohms the load impedance is then equal to

$$(1.10 - j0.75)(52) = 57.2 \text{ ohms} - j\,39 \text{ ohms} \qquad (31)$$

An adjustable impedance was measured with the comparator and the slotted line apparatus at a frequency of 200 mc to provide an experimental check of the accuracy of the comparator. The results are tabulated below.

Comparator	Slotted Line
$18.3 + j\,6.5$	$18.2 + j\,6.5$
$44.7 - j\,70.4$	$44.8 - j\,67.2$
$36.2 - j\,20.3$	$38.4 - j\,19.3$
$58.3 - j\,100.0$	$56.8 - j\,101.0$

Acknowledgment

The author wishes to acknowledge the useful suggestions and valuable contribution by Dr. G. H. Brown in the development of the comparator.

SHF Heterodyne Frequency Meter

Description of a portable instrument that can be used in the range 450 to 10,000 mc with a maximum error not exceeding 0.05 percent. The butterfly oscillator is checked at 5-mc points with a crystal that allows use of the equipment as a frequency standard accurate to 0.001 percent

By CARSON D. JEFFRIES

THE heterodyne frequency meter to be described was developed primarily for use in the range 2,000 to 10,000 mc. It has, however, a useful range of 450 to 10,000 mc, the fundamental range of the heterodyne oscillator being 450 to 900 mc.

The incorporation of a crystal calibrating circuit makes possible frequency measurements with a maximum overall error of ±0.05 percent; the heterodyne oscillator may be finely tuned by a gear reduction system, allowing measurements of frequency modulation and frequency increments of 0.01 percent.

Measurement Methods

Frequency in the range 2,000 to 10,000 mc is commonly measured with tunable resonators, or wavemeters, of several types: coaxial-line, cylindrical-cavity, or transition. These devices may be used as transmission or absorption elements. They are relatively small, light-weight, and simple.

The instrument described in this paper is considerably more complex than the devices named above, but it has greater utility, greater sensitivity, is self-calibrating, and operates over a wide frequency range. It can also be used as a low-power-level frequency standard of ±0.001 percent accuracy.

The block diagram of the heterodyne frequency meter shown in Fig. 1 illustrates the components of the instrument and their function.

The unknown frequency F_1 in the range 450 to 10,000 mc is coupled into mixer no. 1, which is also coupled to the heterodyne oscillator. This oscillator has a calibrated dial and its frequency F_2 can be continuously varied between 450 and 900 mc. Thus F_1 may be measured by the usual heterodyne method; a series of values of F_2 is observed for which an audio beat note with F_1 is heard in the phones connected to amplifier no. 1.

In general, audio beats are heard if $nF_2 = mF_1$, where $n = 1, 2, 3 \ldots$, and $m = 1, 2, 3 \ldots$. In this case the audio beat notes are loudest when $m = 1$. If F_2' and F_2'' are values of F_2 for two adjacent values of n, and if $m = 1$, then

$$nF_2' = F_1 \qquad (1)$$

$$(n+1)F_2'' = F_1 \qquad (1a)$$

and

$$F_1 = \frac{F_2' F_2''}{F_2' - F_2''} \qquad (2)$$

If F_1 is known approximately, then n is known for a particular value of F_2 and it is only necessary to determine the value of F_2 in order to determine F_1. It can be done in a single operation, thus making the measurement a simple one. The accuracy of measurement of F_1 is equal to the accuracy of determination of F_2, which in this case is ±0.5 percent—the normal dial calibration accuracy of the heterodyne oscillator.

Crystal Calibrator

In order to determine F_2 more accurately it is necessary that a special calibration circuit be employed. A crystal oscillator whose frequency F_4 is 5 mc ±0.001 percent is used as a standard and coupled to mixer no. 2. Also coupled to this mixer is a 20-mc oscillator whose frequency F_3 may be slightly varied. The coupling between these two oscillators is sufficient to allow F_3 to be locked-in with $4F_4$ when they are adjusted to zero beat by means of the mixer, audio amplifier no. 2, and earphones. The heterodyne oscillator is also coupled to mixer No.

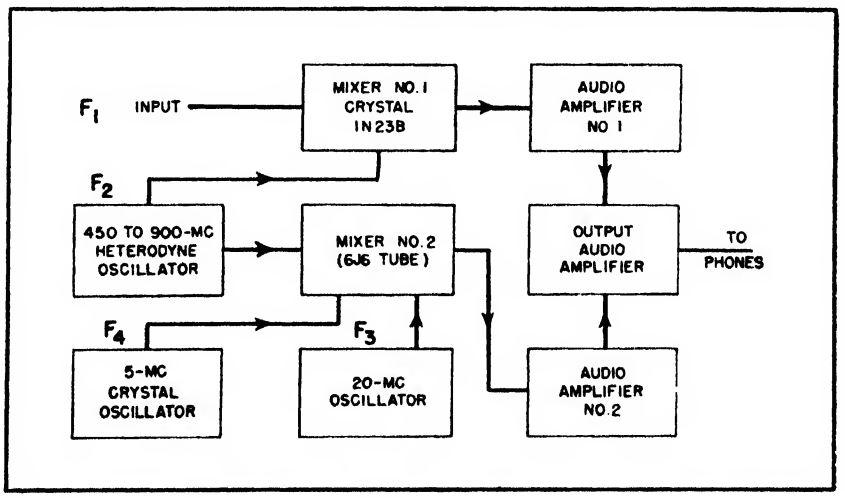

FIG. 1—Block diagram of the frequency meter. Gain controls allow the user to select the desired beats to be fed into the output audio amplifier

2, and as F_2 is varied, there will be heard in the phones audio beat notes every 5 mc in the range of the heterodyne oscillator. These check points are beats between F_2 and nF_4 and accurate to within ± 0.001 percent. By linear interpolation between them F_2 may be determined at any point on the dial to within ± 0.05 percent.

Because the heterodyne oscillator dial calibration accuracy is only ± 0.5 percent, it is possible for 5-mc check point frequencies to be ambiguous over most of the range; such an impasse is avoided by turning off the crystal oscillator and first finding a reference point with only the 20-mc oscillator.

Separate audio channels and gain controls for the two mixers are used so that the instrument can be used without the calibration circuit for rapid measurements without high accuracy, and the dial calibration of F_2 may be quickly checked without hearing interfering beats with unknown frequencies. Adjacent check points and a beat with an unknown frequency can be identified separately and then heard together with minimum interpolation errors.

The instrument may be used as a frequency standard by setting F_2 to any of the 5-mc check points in its range. This will determine F_2 to an accuracy of ± 0.001 percent. Mixer No. 1 will generate harmonics of these standard frequencies up to 10,000 mc and these signals can be taken from the F_1 input connector.

The complete schematic diagram of the instrument aside from the conventional power supply, is shown in Fig. 2 and described below.

The heterodyne oscillator is a type 6F4 triode tube operating in a butterfly circuit[1] that combines mechanical simplicity with compactness and avoids sliding r-f contacts. The butterfly rings are 2 inches in diameter and there are three in the stator stack. The rotor is also a stack of three plates and has an insulated shaft and ball bearing support. The rotor requires 90 degrees rotation to vary the frequency from

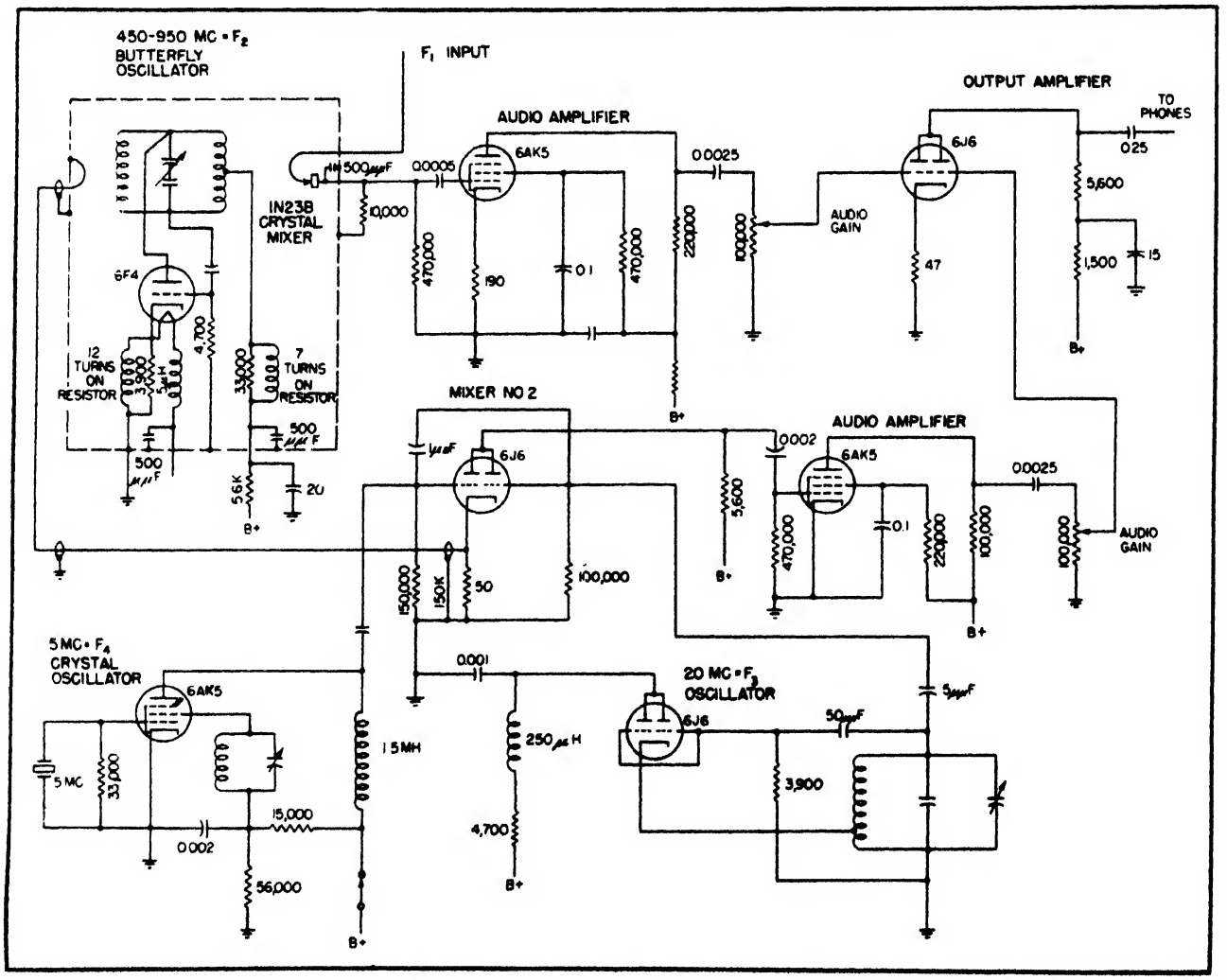

FIG. 2—Complete schematic diagram of the heterodyne frequency meter. The power supply, not shown, has two outputs suitably isolated to prevent coupling between units of the equipment

450 to 900 mc and is coupled to the panel tuning control by a 30-to-1 reduction worm gear; it is also connected through a 450-to-1 reduction to the panel fine tuning and interpolation dial control.

The frequency dial is 6½ inches in diameter and is directly calibrated in terms of F_2; the interpolation dial is 4½ inches in diameter and has 100 equal divisions and a hair line index. The whole mechanical system is spring loaded in order to eliminate backlash.

Frequency Stability

The oscillator has good mechanical and plate voltage stability. The plate, heater, and cathode chokes have been experimentally chosen to give smooth oscillator operation over its entire range. Incidental frequency and amplitude modulation is very small, the check points being very pure beat notes over the entire range. Since there are no sliding contacts, no noise is evident as the oscillator is tuned.

Adequate r-f shielding of the oscillator is obtained by use of the cast housing and tight cover, L-C filters in all power leads entering the oscillator cavity, and additional shielding of the worm gear system. It is necessary to prevent leakage of r-f power in order to avoid a serious noise problem; many parts of the oscillator drive mechanism could be paths of random r-f current flow, giving rise to broad bands of noise to be picked up by the mixers and amplifiers.

Mixer no. 1 as illustrated consists of a type IN23B crystal coupled inductively to the heterodyne oscillator and in series with the coaxial line input of F_1, the unknown frequency. A d-c load resistance across which are developed audio beat frequencies is mounted outside of the casting.

The 5-mc crystal oscillator is of conventional electron-coupled design. It uses a 6AK5 miniature pentode and a 5-mc temperature-compensated quartz plate with a variable pressure plate that allows the frequency F_4 to be set against a primary or secondary frequency standard. This oscillator will maintain its accuracy to within ±0.001 percent for normal (±20 C) temperature variations. A panel switch cuts the plate supply on or off.

Secondary Calibrator

The 20 mc oscillator is a conventional Hartley circuit using a type 6J6 miniature dual triode with the elements connected in parallel. It is slightly tunable by means of a panel trimmer control.

Mixer no. 2 is a type 6J6 miniature dual triode using each grid and the cathode as three separate inputs. The crystal oscillator and the 20 mc oscillator are each capacitively coupled to a grid and to each other. The heterodyne oscillator is coupled in by means of a loop in the cavity feeding a 50-ohm coaxial line terminated in a 50-ohm disc resistor that is also the cathode resistor of the 6J6 tube. This connection gives low impedance coupling and prevents reaction on the heterodyne oscillator.

Audio amplifiers no. 1 and no. 2 are each conventional resistance-capacitance coupled 6AK5 pentode amplifiers with separate gain controls on the panel. They each feed into separate grids of the 6J6 output audio amplifier to which high impedance earphones are capacitively coupled.

The power supply is quite conventional, with resistance-capacitance filters used to decouple various components. The method of decoupling has not been indicated in the diagram, all leads to the plate power supply being marked B+.

Limitations to Accuracy

It has been stated that the maximum overall measurement error of this heterodyne frequency meter is ±0.05 percent, and this can be simply proved. The accuracy of measurement is the accuracy of determination of F_2. Points of ±0.001 percent accuracy are placed on the F_2 dial every 5 mc by the calibration circuit. Linear interpolation must be used to determine F_2 between these points. The tuning curve of F_2 is not truly linear, the deviation from linearity in the vicinity of 450 mc being −0.03 percent of frequency at the midpoint between two adjacent check points; at 750 mc the deviation is 0.0 percent; at 900 mc it is +0.02 percent. Any backlash errors can be eliminated by proper technique. The interpolation dial can be accurately read only to about ¼ of a division, thus causing an error of about ±0.01 percent of frequency. Thus the total error arrived at by adding ±0.03 percent for dial nonlinearity, plus ±0.01 percent for interpolation dial errors, plus ±0.01 percent for other errors gives ±0.05 percent. Because of the improved F_2 dial linearity this total error is only ±0.02 percent in the F_2 range of 650 to 800 mc.

By improving the dial linearity of the heterodyne oscillator and by using more closely spaced check points, it is possible to construct a frequency meter similar to this one with an error of measurement of 1 part in 10^5.[2]

No adequate measurements of the sensitivity of this instrument have been made; it varies widely over the range and is of the order of 0.01 microwatts at 200 mc and 10 microwatts at 10,000 mc.

Acknowledgment

The author wishes to acknowledge the helpful suggestions of H. E. Overacker, A. P. G. Petersen, and W. B. Wholey.

References

(1) Karplus, Eduard, Wide Range Tuned Circuits and Oscillators for High Frequencies, *Proc. IRE*, p 426, July 1945.

(2) Essen, L., and Gordon-Smith, A.C., The Measurement of Frequency in the Range 100 mc to 10,000 mc, *Jour. IEE*, 92, p 201, 1945.

Direct-Reading Wavemeter Design

Construction details of direct-reading wavemeters for the range from 2 to 75 cm (15,000 to 400 mc). Theory behind maintaining linearity of wavelength-change-to-conductor-displacement is given for cavity devices of finger-contact and re-entrant line short-circuit type

By G. E. FEIKER and H. R. MEAHL

THE development of wavemeters for use in the centimeter-wavelength range was accelerated after 1939, before which Lecher wires were probably in greatest use. Development of resonant coaxial transmission line and resonant wave guide cavity types followed.

All forms of the Lecher wire wavemeter require that two or more observations of resonance be made and that the distance of motion of a short-circuiting bar or plunger between points of resonance be measured to get data from which the signal wavelength can be calculated. A 5- to 30-centimeter searching wavemeter was developed to replace the various forms of Lecher wire device in order to conserve space and man-hours.

The back-panel appearance of the direct-reading 5- to 30-cm searching wavemeter is shown in Fig. 1. The device will agree with a primary standard of wavelength of frequency within 0.1 cm and will repeat a reading made using a crystal-controlled signal source within 0.05 cm.

A cross-section of the resonant cavity of this wavemeter is shown in Fig. 2. A coaxial transmission line resonator operates in its quarter-wave mode. Finger contacts are used on the inner conductor, the length of which is adjustable by means of a rack and pinion. The visual indication of resonance is obtained by converting a small amount of microwave energy to direct current with either a thermocouple or a crystal rectifier and applying it to a d-c microammeter. An input of approximately 20 milliwatts is required for full-scale deflection with a thermocouple and approximately one milliwatt when a crystal rectifier is used.

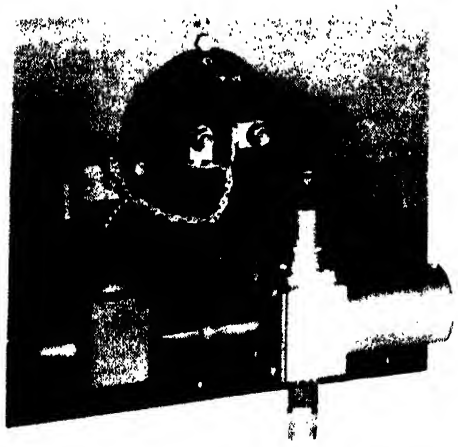

FIG. 1—A 5 to 30-cm searching wavemeter with finger contact to inner conductor

In order to obtain better accuracy and precision in another equipment, the size and shape of the contacting fingers were chosen to cause a minimum departure from a linear characteristic over a range from 30 to 75 cm. In addition, the coupling loops were adjusted to give uniformly good sensitivity over the whole range together with a characteristic sufficiently linear to allow the direct reading scale to be guaranteed accurate to within 0.5 percent.

In order to increase the effective scale length, the wavelength dial is rotated nearly two revolutions. The slope of wavelength versus conductor displacement was adjusted so that one set of graduations could be used with two sets of color-coded numerals. The correct scale is indicated by a colored target near the upper left edge of the dial.

Shielding for Accuracy

Experience with the 5- to 30-cm wavemeter showed a need for shielding against extraneous fields. Any r-f voltage induced in the nominally d-c path between crystal and microammeter is rectified to give a deflection. A combination bypass capacitor and instrument connection, together with grounding the input coupling and tuning shaft to the case, provided adequate shielding in the vicinity of high r-f fields.

A design similar to that of the 5- to 30-cm wavemeter has been made for the 2- to 8-cm range with the scale direct reading to within 0.05 cm between 3 and 8 cm.

Precision Wavemeters

An early form of laboratory wavemeter built for the dual purpose of investigating the characteristics of quarter-wave resonators as wavemeters of high precision in the 8- to 12-cm wavelength band and of measuring the output spectra of magnetron oscillators is shown in Fig. 3. Since the existence of discrete narrow spectra was suspected, a vernier tuning control shown at

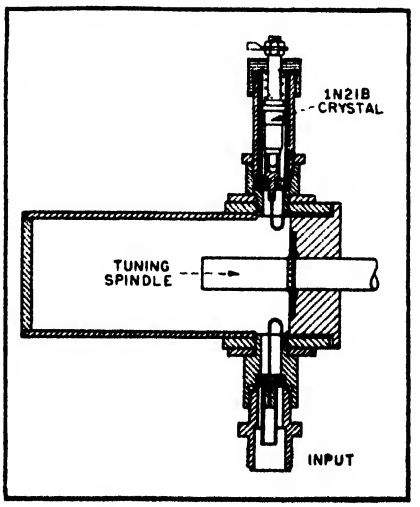

FIG. 2—Cross-section of 5 to 30-cm searching wavemeter

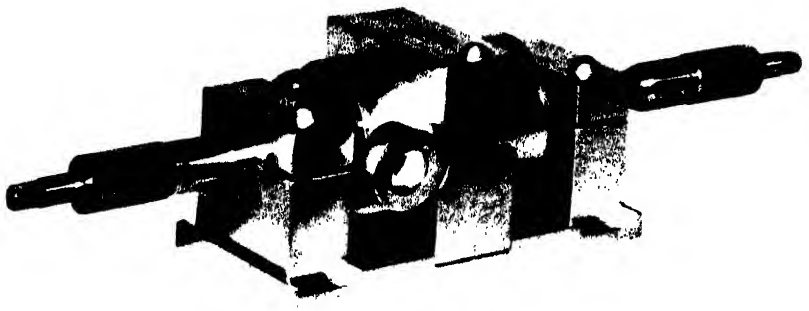

FIG. 3—A developmental 8 to 12-cm precision wavemeter with conductors for coarse and fine tuning

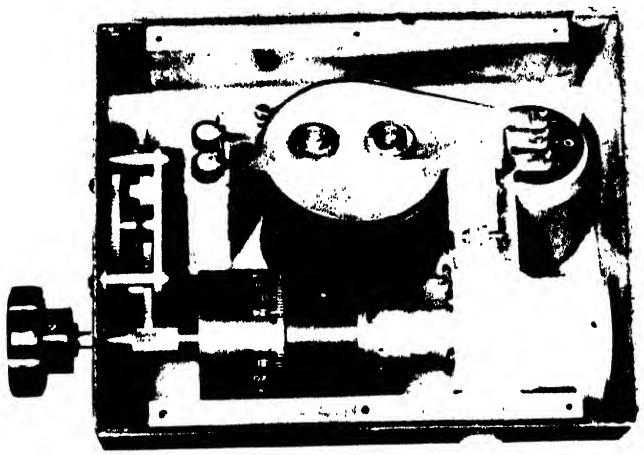

FIG 4—Field type precision wavemeter. Indicating meter is at upper center

the right was included. However, the main tuning control proved adequate and tests showed that the resolution obtainable with a coaxial resonator employing a silver-plated micrometer spindle as adjustable center conductor was sufficient for all but the most specialized measurements in the 8- to 12-cm range.

Quantitative analysis and test of the performance of this laboratory wavemeter provided guidance in the design of wavemeters for field use. Improvements were made in the coupling loops, the contact between the micrometer-head mounting plate and the body of the wavemeter, the contact between the mounting plate and the micrometer spindle and in the body of the wavemeter itself. The measuring equipment had good sensitivity, full scale deflection for approximately 1 milliwatt input, and a wavelength versus displacement characteristic linear within 0.05 percent over the wavelength range of 8 to 12 cm. Positive low resistance contact is necessary both between the micrometer-head mounting plate and the body of the wavemeter as well as between the mounting plate and the micrometer spindle. It was found that the stiffness of a wavemeter body made of standard brass tubing was inadequate. Changes as great as 0.03 percent in tuning were caused by pressure on the clamp that held the body to the base.

In field wavemeters satisfactory contact between the micrometer-head mounting plate and the body of the wavemeter resulted from the combination of silver plating both parts and turning a lip approximately 0.005 inch high on the body of the wavemeter at its inner edge.

A satisfactory contact between the mounting plate and the micrometer spindle was obtained by making the micrometer spindle of sterling silver and the finger contacts of silver-plated phosphor bronze or beryllium copper. Motor driven accelerated wear tests indicated that a year of trouble free performance could be expected from this combination. However, the re-entrant transmission line type of short-circuit which is described below is superior to the finger-type contact in having low manufacturing cost and more uniform and stable electrical characteristics.

Adequate stiffness in the wavemeter body has been obtained by means of a sturdy bronze casting, silver plated for high conductivity, shown in Fig. 4. This casting is securely bolted to the sloping panel to provide a sturdy mount for the input jack, output coupling loop, crystal rectifier unit, and tuning control.

Re-entrant Short Circuit

One of the most valuable features of the field type precision wavemeter is the re-entrant transmission line short circuit between inner and outer conductors of the resonator, shown in cross-section in Fig. 5. This accomplishes the same purpose as the finger contacts of earlier designs but without a mechanical contact between conductors of the main resonant cavity. The re-entrant portions of the cavity are proportioned so that the reactance at the input to the re-entrant line is zero at some intermediate wavelength in the band. At other wavelengths, the reactance is small in proportion to that of the main cavity. The rotating joint between micrometer spindle and head is at a low current point, so that the effect of this variable resistance contact on the wavemeter performance is negligible.

This design has resulted in an ideal working condition for the micrometer screw, since there is no load on the spindle. The construction provides a close approximation to the ultimate in uniformity and stability of both electrical and mechanical characteristics.

Further features of the field-type precision wavemeter are the direct-reading wavelength scale, accurate within 0.1 percent and resettable within 0.002 centimeter, and the combined shielding and bypassing that protect the wavemeter from

strong radio-frequency fields and prevent responses to other than the impressed signal.

The appearance and construction of a postwar 8- to 12-cm precision wavemeter for general laboratory use is illustrated on the first page of this paper. Comparison with Fig. 4 will show that the gear-stop and sensitivity control of the field type have been omitted and that a less expensive bypass capacitor has been used across the microammeter, but that the primary structural and shielding features have been retained. The electrical characteristics of the two wavemeters are identical. Many of the benefits that accrue in designing for field use are not visible, but require a comparative study of the designs developed here and in England.[1] It is believed that the use of friction to hold the positions of the drum, the thimble, and the extension piece fixed relative to the spindle is indication that field use was considered secondary during the British development. The use of a 0.002-inch clearance for a distance of from $\frac{1}{2}$ to $\frac{3}{4}$ inch in the noncontacting plunger type also points in the same direction.

It is interesting to note the differences in electrical design, also. In the designs described herein the cavity beyond the end of the adjustable inner conductor has been chosen to be below cutoff for all operating wavelengths; whereas in the British design, the cavity is in the pass band for operating wavelengths. This difference apparently resulted from considering the direct-reading feature more important than width of tuning range while developing these designs.

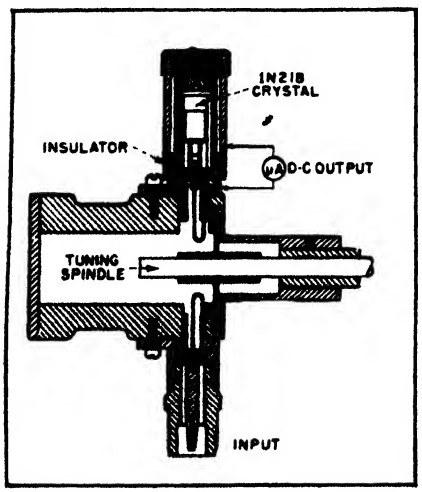

FIG. 5—Cross-section of re-entrant transmission line short circuit type

A 12- to 17-cm precision wavemeter operating on the same principles as those for the wavelength range 8- to 12-cm has the same quality of performance as detailed in Table I.

The precision type wavemeters are unusually well adapted for field service where extreme conditions of temperature, humidity, high-power radio-frequency fields in and out of the wavemeter range, vibration and shock are encountered. For example, the micrometer heads have been lubricated with a special oil which allows free movement at −60 C and yet does not evaporate at 50 C. Extensive use of these wavemeters for several years has shown that the wavelength calibration is maintained well within the 0.1 percent specification.

The devices have also been used as power indicators without modification, as receivers after connecting an audio amplifier across the crystal rectifier, and even as tunable band-pass filters after removing the crystal rectifier and connecting directly to the output loop.

Theory

The most important property of direct-reading wavemeters is the linearity of wavelength change to conductor displacement. The underlying theory of this property is presented below for those wavemeters employing finger contacts and those with a re-entrant transmission line short circuit.

It is an experimental fact that properly designed wavemeters having a resonator of the type shown in Fig. 6A have the property that a one centimeter increase in the length of the center conductor changes the fundamental resonant wavelength by four centimeters. It may at first seem obvious that this is the case, since the wavemeter is resonant in its quarterwave mode. Actually, however, the line is considerably shorter than a quarter wavelength because of the end-loading capacitance of the inner to outer conductor. This foreshortening may

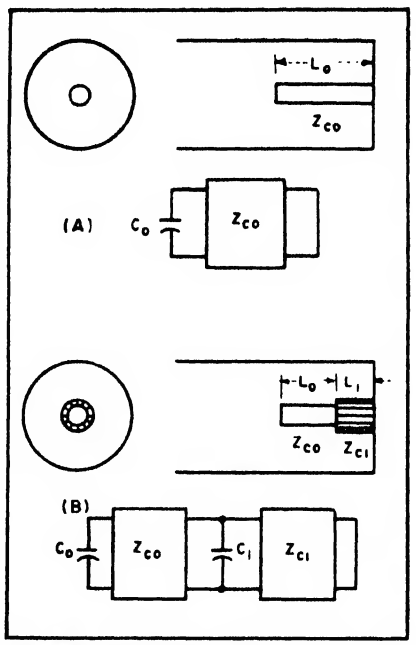

FIG. 6—Cross-section and equivalent circuit (A) of finger-contact type and (B) re-entrant type wavemeter

be as great as 18 percent of the quarter wavelength, and yet the rate of change of wavelength to conductor displacement is within 1 percent of the four-to-one relation.

It is difficult to make a good disc-type electrical contact of the kind needed in the resonator although such a contact was used in the early designs. The cylindrical type shown in Fig. 6B has been used in more recent designs requiring finger contacts because of its simpler construction. Resonators having a contact of this kind depart from the four-to-one relation and are not linear over the complete range of extension of the center conductor, but can be made direct reading within a fraction of one percent over a two-to-one wavelength range.

The resonator of Fig. 6A is a special case of that shown in Fig. 6B, the analysis of which is given below. The equivalent circuit for the latter consists of two cascaded sections of transmission line of characteristic impedances Z_{c1} and Z_{co}. The former is short-circuited at its input end, and the latter is terminated in an equivalent end-loading capacitance C_0, representing the effect of the fringing field between the end of the center conductor and outer conductor. A

capacitance C_1 is added to account for the step in the center conductor.[8]

The electrical length $\theta_0 = \beta L_0$ of the extensible portion of the center conductor can be related to the frequency and constants of the circuit. Referring to Fig. 6B, resonance will occur when the reactance of the parallel combination of line L_1 and fringing capacitance C_1 is the conjugate of the reactance of line L_0 terminated in the equivalent discontinuity capacitance C_0.

The input reactance of line L_1 is

$$X_{L1} = Z_{c1} \tan \theta_1$$

where Z_{c1} *and* θ_1 are the characteristic impedance and electrical length, respectively of line L_1.

Combining with the capacitive reactance $X_{c1} = 1/\omega C_1$,

$$X_1 = \frac{X_{L1} X_{c1}}{X_{c1} - X_{L1}} = \frac{(Z_{c1} \tan \theta_1)(1/\omega C_1)}{(1/\omega C_1) - Z_{c1} \tan \theta_1}$$

The input reactance of line L_0 terminated in the capacitance C_0 is

$$X_2 = -\frac{1/\omega C_0 - Z_{c0} \tan \theta_0}{1 + (1/\omega C_0 Z_{c0}) \tan \theta_0}$$

where Z_{c0} and θ_0 are the characteristic impedance and electrical length, respectively, of line L_0.

The condition for resonance, $X_1 = -X_2$, gives for θ_0 the relation

$$\tan\theta_0 = \frac{\frac{X_{c0}}{Z_{c0}} - \frac{Z_{c1}}{Z_{c0}} \tan \theta_1 \left(\frac{C_1}{C_0} + 1\right)}{1 - \frac{Z_{c1}}{Z_{c0}} \tan \theta_1 \left(\frac{Z_{c0}}{X_{c1}} - \frac{X_{c0}}{Z_{c0}}\right)} \quad (1)$$

The relation for the special case of Fig. 6A is obtained from Eq. 1 by setting $\theta_1 = 0$, in which case

$$\tan \theta_0 = \frac{X_0}{Z_{c0}} = \frac{1}{\omega C_0 Z_{c0}} = \frac{\lambda}{2\pi C_0 Z_{c0}} \quad (2)$$

where v is the velocity of propagation and λ the wavelength in cm.

If it were possible to eliminate end-loading so that $C_0 = 0$, the electrical length θ_0 would be 90 degrees. The magnitude of the effect of end-loading capacitance can be seen from Fig. 7, in which values of θ_0 are plotted for a wavemeter operating in the 8- to 12-cm range.

Of more importance is the expression for the rate of change of conductor displacement with wavelength, which can be found by differentiating the expression for the length L_0 of the extensible line.

$$L_0 = \theta_0/\beta = (1/2\pi)(\theta_0 \lambda)$$

$$\frac{dL_0}{d\lambda} = \frac{\theta_0}{2\pi} + \frac{\lambda}{2\pi}\frac{d\theta_0}{d\lambda} \quad (3)$$

The second term is obtained from the expression for tan θ_0,

$$\frac{d\theta_0}{d\lambda} = \frac{1}{D}\left[\frac{dN}{d\lambda} - \frac{N}{D}\frac{dD}{d\lambda}\right] \cos^2\theta_0 \quad (4)$$

where N is the numerator and D the denominator of Eq. 1.

For the case in Fig. 6A, the expression for the rate of change of wavelength to conductor displacement reduces to

$$\frac{dL_0}{d\lambda} = \frac{\theta_0 - 1/2 \sin 2\theta}{2\pi} \quad (5)$$

Let

$$\theta_0 = \frac{\pi}{2} - \epsilon$$

Then

$$\sin 2\theta_0 = \sin(\pi - 2\epsilon) \leqq 2\left(\epsilon - \frac{2}{3}\epsilon^3\right) \quad (6)$$

for $\epsilon < 0.5$ radian.

Therefore,

$$\frac{dL_0}{d\lambda} \leqq \frac{1}{4} - \frac{\epsilon^3}{3\pi} \quad (7)$$

The percent deviation from a 4-to-1 slope has been calculated from Eq. 7 and plotted in Fig. 7 for the 8- to 12-cm range.

When the projecting type of contact is used, the rate of change is no longer four to one. The slope versus wavelength for a 30- to 75-cm wavemeter, and conductor length versus wavelength, have been plotted in Fig. 8. This wavemeter employed a contact line 5.25-cm long. The ratio of characteristic impedances Z_{c0}/Z_{c1} was 1.15. A reduction in the length of the contact line to 3.2 cm made the characteristic linear to within ±0.5 percent over the range of 30 to 75 cm.

A cross section of a cavity type used in the 8- to 12-cm and 12- to 17-cm wavemeters is shown in Fig. 9. The main part of the cavity consists of two transmission lines, one having the variable length *AB* as inner and *MN* as outer conductor, the other having *JK* as inner and *LM* as outer conductor. The former line is terminated in a fringing capacitance from *A* to the outer conductor; the latter line is shorted by the plate *KL*.

The re-entrant portion of the cavity consists of the short-circuited line *HI*, *GF*, and the line *CD*, *FE*. The two parts of the cavity are connected by the choke line *BC*, *JI*. The center conductor rotates in its bearing at point *D*, this being the only point of mechanical contact between the outer shell and center conductor. The electrical quality of this contact is not important, since it is at a low current point relative to the current in plate *KL*.

An equivalent circuit for the cavity can be drawn, showing the interconnection of the five different transmission lines having characteristic impedances Z_{c1}, Z_{c2}, Z_{c3}, Z_{c4}, Z_{c5} and the discontinuity capacitances. The capacitance C_{03} represents the fringing capacitance from the end of the center conductor to the shell. Capacitances C_1, C_{12}, C_{23}, C_{34}, C_4, C_5 are those associated with the discontinuities at the junctions of the various transmission lines. These capacitances can be calculated from the dimensions.[8]

The following procedure is followed in calculating the wavemeter characteristic. The reactance ap-

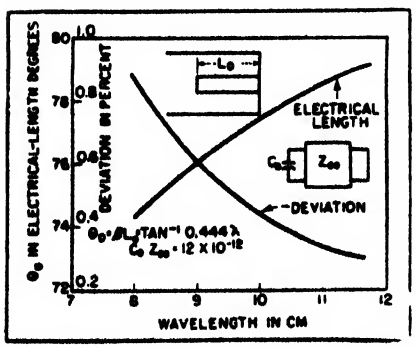

FIG. 7—Electrical length and deviation from the 4-to-1 slope in a finger-contact wavemeter

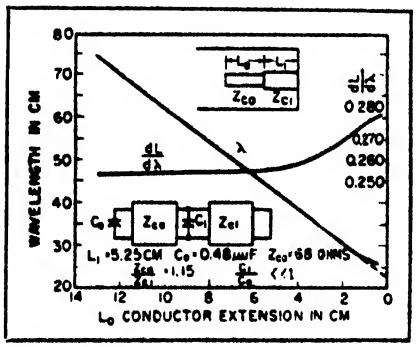

FIG. 8—Resonant wavelength versus conductor extension and slope for a re-entrant type wavemeter

Table I—Characteristics of 12- to 17-cm Wavemeter Calculated From Equivalent Circuit

λ	$\Delta\lambda/\Delta L_2$	I_{05}/I_{01}	P_1	P_2	P_3	P_4	Q
12		0.046	8.8	1.8	11.0	0.19	2250
13.25	3.540						
14.50	3.566	0.073	8.6	3.5	10.3	0.15	2260
15.75	3.550						
17.00	3.555	0.104	8.3	5.3	9.7	0.22	2280

$\Delta\lambda\ \Delta L_2$ = slope of wavelength versus conductor displacement
I_{05}/I_{01} = ratio of current through rotating joint to maximum current
$P_{1,2,3,4}$ = power loss in various portions of cavity shown in Fig. 9
Q = Q-factor of overall resonator

pearing between terminals S and T due to the combination of networks 1, 3, 4, and 5, where each network consists of a transmission line and associated discontinuity capacitances, is calculated, ignoring losses. The electrical length of line of characteristic impedance Z_{c2} necessary to give the conjugate reactance across these two points is then determined. This calculation is carried out for several wavelengths over the band of operation to obtain the characteristic of extension AB versus wavelength. Matrix formulation simplifies the procedure of calculation.

The equivalent circuit can also be used to calculate other properties of the resonator. The ratio of current I_{05} in the rotating joint at D to current I_{01} in the short-circuiting plate KL is of importance in the design. Distribution of loss in various parts of the cavity and the Q value of the resonator can also be calculated.

Table I gives values of slope of wavelength versus conductor displacement, $\Delta\lambda/\Delta L$, current ratio I_{05}/I_{01}, Q, and loss distribution for a 12- to 17-cm cavity.

In order to make the wavemeter direct reading, utilizing a standard micrometer screw thread, a slope of $\Delta\lambda/\Delta L = 3.543$ was required. The dimensions of the cavity were varied in initial trial calculations until the following series was obtained in which all dimensions are the same except the diameter of the center conductor of line L_1.

diameter (inches)	$\Delta\lambda/\Delta L$ (average)
0.320	3.58
0.330	3.55
0.340	3.53

The experimental value of average slope for the final design with a diameter of 0.330 inch was 3.536. The calculated value is in error by less than 1 percent. The experimental value is somewhat affected

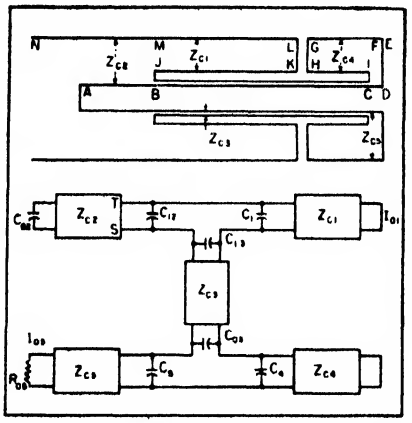

FIG. 9—Equivalent circuit for re-entrant type wavemeter

by the coupling loops, so that better agreement could hardly be expected.

It should be pointed out that the analysis is valid only for loose coupling, since over coupling can greatly change the calculated characteristics.

Acknowledgement

The authors take this opportunity to acknowledge P. E. Hosegood's contribution of the expanded scale feature to the precision wavemeters, F. J. Moles' development of the 5- to 30-cm and 2- to 8-cm searching wavemeters, and E. D. Cook's encouragement during the course of these developments.

References

(1) L. Essen, Cavity Resonator Wavemeters, *Wireless Engineer*, p 126, May 1946.
(2) J. R. Whinnery and H. W. Jamieson, Equivalent Circuits for Discontinuities in Transmission Lines, *Proc IRE*, Vol. 32, p 98, Feb. 1944.

Buzzer Signal Generator for 3,000 Mc

DAMPED OSCILLATIONS in a tunable concentric line resonator are produced by a battery-operated buzzer in a microwave signal generator developed under auspices of Panel 15 of OSRD.

When the buzzer is operating, the interruptions at the armature contacts produce pulses of r-f energy of complex wave form. The actual r-f energy produced is very small; it may be considered to be in the form of recurring damped oscillations with the recurrence frequency determined by the frequency of vibration of the armature of the buzzer. This frequency is adjustable between 1000 and 2,000 cps, subject to mechanical limitations of the buzzer.

The recurring pulses of r-f energy produced by the buzzer are fed to the tuning unit through a short length of concentric line connected to a coupling loop within the resonator. This coupling loop is shunted by a 50-ohm disc resistor to reduce spurious resonance in the coupling loop.

The tuning unit is a concentric line type resonator, the center conductor of which can be varied in length by means of a rack and pinion drive. This drive is controlled by the main frequency control on the front panel. Variations in the length of the portion of the center conductor that is within the fixed-length outer conductor change

the resonant frequency of the resonator from 1,000 to 3,500 mc.

The pulses of r-f energy from the buzzer apparently have steep wave fronts which are capable of shock-exciting the resonator. In the complex wave form, components of many frequencies are present but the introduction of the high-Q resonant circuit causes the r-f energy at the resonant frequency to predominate. This sets up an r-f field in the resonant line of the tuning unit at the moment of each pulse. Some of this pulsed r-f energy is fed to the output circuit through an attenuator.

Some of the magnetic flux developed in the resonator extends into the end of the attenuator cylinder. This flux within the cylinder decreases exponentially with increasing distance from the resonator. Therefore, as the coupling loop is moved up and down the tube, a varying amount of magnetic flux is linked by the loop; this results in a variable pickup of energy. Maximum pickup occurs when the coupling loop projects out of the tube just into the resonant cavity. An output of several hundred microvolts into a 50-ohm load is provided.

A piston-type attenuator is used, consisting of a cylinder and a piston which carries the output coupling loop. A coaxial cable connects the loop to the output connector. This assembly is attached to a port on the resonator cavity. The position of the piston coupling loop in the cylinder is adjusted by means of a rack and pinion connected to the attenuator control on the panel.

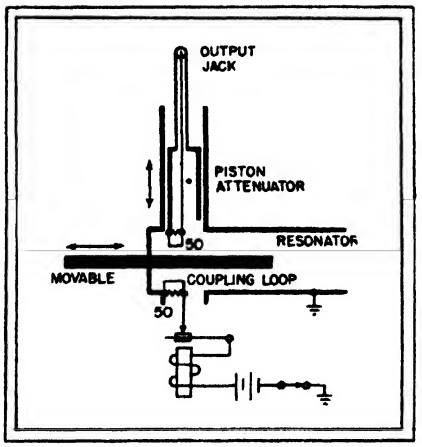

Circuit of simple microwave signal generator

Improving Stability of UHF Oscillators

Mathematical analysis of the factors governing frequency stability of uhf oscillators during load impedance changes, and method of reducing frequency variations in a 1,000-mc oscillator by means of a series capacitor in anode circuit

By CARL A. HELBER

CERTAIN APPLICATIONS for microwave oscillators require that they maintain frequency within specified limits under various conditions. Such conditions involve, among others, changes in the oscillator tube interelectrode capacitance and changes in the load impedance.

The latter condition is of particular interest in applications where it is necessary to tune a microwave oscillator by using a dummy load, such as before installing the oscillator in an airplane. Besides the initial difference in impedance which may occur between the dummy load and the antenna system to which the oscillator is finally connected, a further change in load impedance may occur as a result of antenna icing under extreme conditions.

For these reasons it is desirable to determine the measurable factors which are responsible for the frequency stability of uhf oscillators. An even more desirable goal is the determination of the frequency stability of a particular oscillator in terms of its physical dimensions and the electrical characteristics of the oscillator tube. An analysis of these factors has led to the development of simple triode oscillators having stability characteristics which can be calculated accurately enough for most engineering purposes.

Frequency Pulling

Oscillator frequency variations due to variations in load admittance are due to the fact that the admittance as seen by the oscillator tank circuit is not a pure conductance, but may have a susceptive component. If the susceptive component is capacitive, it decreases the oscillator frequency; if inductive, it increases the oscillator frequency.

Usually the oscillator is connected to a transmission line of characteristic admittance G_0 through some kind of a coupling system. Specifications usually indicate the maximum load mismatch which can be expected in terms of the maximum standing wave ratio S on the transmission line. Since the line may be of any arbitrary length, it is conceivable that conditions may obtain whereby the maximum susceptive component of the line input admittance may be presented to the oscillator.

The maximum susceptive component is a function of the standing wave ratio S; from the admittance

plot in Fig. 1A, this can be seen to be

$$\Delta B = \pm 0.5\,(S - 1/S)\,G_0 \qquad (1)$$

The equivalent lumped circuit of the oscillator tank circuit is given in Fig. 1B, where C is the equivalent lumped circuit capacitance of the oscillator tank circuit.

Usually the oscillator does not work directly into the transmission line, but rather into a coupling network which is connected to the line. The admittance actually connected across a tank circuit is generally only a small fraction of the admittance seen looking directly into the line. If we call the transformed characteristic admittance G_0', then it can be shown that the maximum susceptive component presented to the oscillator tank circuit will be

$$\Delta B' = \pm 0.5\,(S - 1/S)\,G_0' \qquad (2)$$

The oscillator frequency for a purely conductive load will be the familiar

$$f = 1/2\pi\sqrt{LC} \qquad (3)$$

Squaring this expression, differentiating with respect to C, and simplifying gives

$$\frac{df}{dC} = -\frac{f}{2C} \qquad (4)$$

or differentiating in terms of a change in susceptance dB, the result is

$$\frac{df}{f} = -\frac{dB}{4\pi fC}$$

Substituting for dB the value in Eq. 2 and changing df to Δf, we obtain a formula which relates the maximum frequency shift obtainable by load phase variation to the standing wave ratio S, the load conductance G_0' presented to the tank circuit for $S = 0$, and the equivalent capacitance C of the oscillator tank. Thus

$$\frac{\Delta f}{f} = \pm\frac{(S - 1/S)\,G_0'}{8\pi fC} \qquad (5)$$

Now S is usually fixed by the antenna designer and G_0' is a function (for maximum power output) of the oscillator tube characteristics. Hence C is the only one of these factors which depends upon the physical dimensions of the oscillator.

In a simple lumped-element circuit, C consists entirely of the tube plate-grid capacitance in parallel with any capacitance provided by the feedback circuit and any capacitance which might have been added for tuning purposes.

For practical purposes G_0' in high-voltage pulsed oscillators may be replaced by $2P/E_{bb}^2$, where P is the power delivered to the load and E_{bb} is the peak pulse voltage applied to the anode of the tube. This substitution is justified if the peak plate-grid voltage swing is nearly equal to E_{bb}. In practically all cases encountered, this assumption appeared to be very nearly correct when the oscillator was delivering maximum power to the load. To a good approximation then

$$\frac{\Delta f}{f} = \pm\frac{(S - 1/S)\,P}{4\pi fC\,E_{bb}^2} \qquad (5a)$$

When the tank circuit is made up from a section of transmission line, the equivalent capacitance will be greater than for the simple lumped circuit case because of the distributed capacitance of the line.

Coaxial-Line Tank Circuit

In the 1,000-megacycle region, coaxial line tank circuits for triode oscillators are generally used because the radiation loss is lower than is obtained from open-wire lines; consequently, we shall devote our attention entirely to the discussion of coaxial line circuits.

For simplicity let C in Fig. 1C represent the entire lumped capacitance placed across the end of the coaxial line of characteristic impedance Z_0. For a condition of resonance,[1] we find that

$$\frac{\lambda}{2\pi c}C = Z_0 \tan\frac{2\pi l}{\lambda} \qquad (6)$$

where λ = wavelength in centimeters, l = length of tank in centimeters, and $c = 3 \times 10^{10}$ centimeters per second.

If we find the value of $d\lambda/dC$ for this case, we can then equate this value to $d\lambda/dC$, for the equivalent lumped circuit case. We will then have a means of working with the rather complicated equations for the coaxial line in terms of constants applied to a simple lumped circuit. This gives a value for C which can be used in Eq. 5 to predict the behavior of a particular

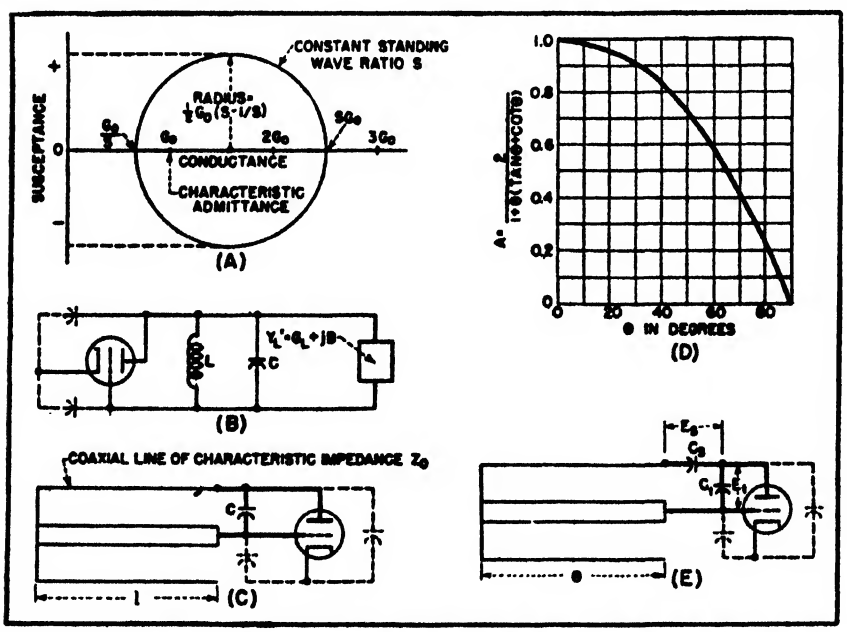

FIG. 1—(A) Locus of all possible admittances looking into transmission line; (B) simplified equivalent lumped circuit of Colpitts oscillator; (C) equivalent tank circuit of coaxial line oscillator, in which resonance occurs when reactance of C is equal to the inductive reactance of the section of closed coaxial transmission line; (D) variation of factor A with electrical length θ of coaxial line; (E) circuit of series-capacitance method of stabilization

oscillator toward load impedance variations.

Differentiating Eq. 6 gives

$$\frac{d\lambda}{dc} = \frac{\lambda}{C\,[1 + \theta\,(\tan\theta + \cot\theta)]} \qquad (7)$$

where $\theta = 2\pi l/\lambda$ = electrical length of the line in radians. The value of $d\lambda/dC_s$ for the lumped-element case is simply

$$\frac{d\lambda}{dC_s} = \frac{\lambda}{2C_s} \qquad (8)$$

Equating Eq. 7 and 8 and solving for C_s gives

$$C_s = \frac{C}{2}[1 + \theta\,(\tan\theta + \cot\theta)] \qquad (9)$$

Since it is easier to plot a function which goes to zero rather than one which goes to infinity, let us plot the function

$$A = \frac{2}{1 + \theta\,(\tan\theta + \cot\theta)}$$

as a function of θ as in Fig. 1D. Thus

$$C_s = C/A \qquad (10)$$

As an example of the application of Eq. 10, if we have an oscillator for which C = 3$\mu\mu$f and θ = 66 degrees at λ = 30 centimeters (Z_o = 24 ohms), we find that C_s = 6.1$\mu\mu$f. In many applications this is too small a value to give the required stability as determined by Eq. 5 and thus we might try to raise C_s by increasing θ. Doing this is not always feasible, however, because of the increased difficulty of providing tuning in the closer-spaced lines required in order to satisfy Eq. 6. Increasing C_s on the other hand, may cause l to become too small to allow efficient tuning. In order to circumvent these difficulties and still achieve a sufficiently large C_s, an additional capacitance in series with the tank circuit has been used.

Use of Series Capacitance

We can best analyze this method by using the concept of energy storage in the circuit capacitances. The total energy stored in all the capacitances in the circuit will be found and equated to the energy stored in a single lumped capacitance having the same applied voltage as the tube load impedance.

The series capacitance circuit is shown schematically in Fig. 1E.

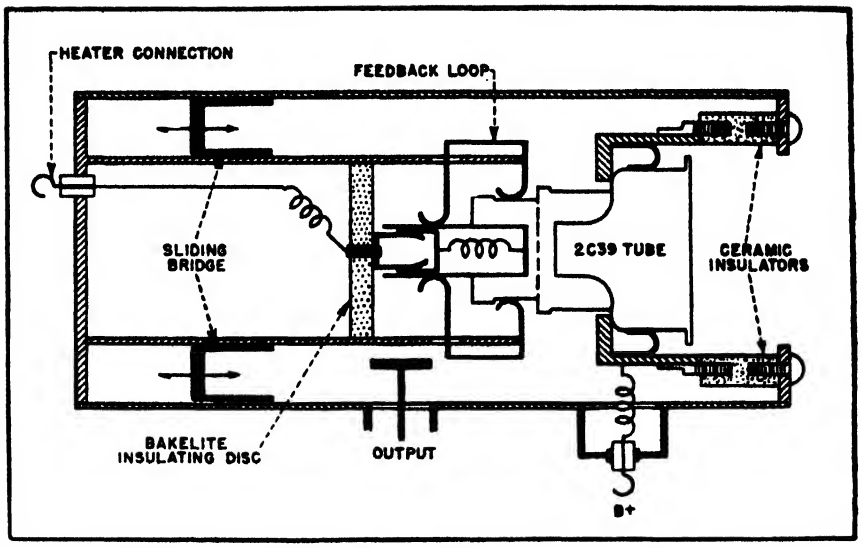

FIG. 2—Cross-section of 1,000-mc oscillator assembly using series capacitance method of stabilization

Since the current through C_s in a high-Q circuit is the same as that through C_t, the voltage developed across C_s is

$$E_s = E_t C_t/C_s \qquad (11)$$

The total voltage across the line will be $E_s + E_t$ or $E_t\,(1 + C_t/C_s)$. We have shown previously that the equivalent lumped capacitance of a resonant coaxial line circuit is given by Eq. 10. In this case C is made up of C_s and C_t in series or

$$C = \frac{C_s C_t}{C_s + C_t} \qquad (12)$$

The energy stored in the entire tank is then

$$W = \frac{E_t^2\,(1 + C_t/C_s)^2\,C_s C_t}{A\,(C_s + C_t)} = \frac{E_t^2\,C_t\,(C_s + C_t)}{AC_s} \qquad (13)$$

Equating this expression to the energy stored in a simple lumped capacitance C_s with voltage E_t across it, we arrive at an expression for the equivalent capacitance seen by the tube and the load

$$C_s = \frac{C_t\,(C_s + C_t)}{AC_s} \qquad (14)$$

If we use the same impedance line and make C_t equal to 3$\mu\mu$f as in the previous example (Z_o = 24 ohms), with C_s = 2.2$\mu\mu$f, θ will increase to 79 degrees because of the fact that C_t and C_s in series are tuning the line. For θ = 79 degrees, A is found to be 0.24 and thus C_s will be 29.5$\mu\mu$f as compared to 6.1$\mu\mu$f obtained without the use of the series capacitance.

It should be remembered, however, that increasing the equivalent capacitance of the tank circuit is not without undesirable effects. As the capacitance increases the tank circuit losses also increase, and thus a compromise between stability and efficiency must be made. For a particular application 25 to 35$\mu\mu$f was considered sufficient. An oscillator was built using the values for C_t and C_s given above. The measured equivalent capacitance was about 25$\mu\mu$f which is in good agreement with the theory. This same general theory, when applied to several other types of oscillators, yielded equally good results.

Practical Oscillator

The oscillator shown in Fig. 2 is an example of one that was built on the basis of the foregoing theory. A 2C39 triode was used with 2,000-volt, one-microsecond pulses applied to the anode through the coil and capacitor shunt feed illustrated. Under these conditions about 1,600 watts peak power was obtained at 1,000 megacycles.

Feedback was obtained in this particular design by means of loops tied to the cathode and extending into the plate-grid cavity. The capacitance equivalent to C_s consists of the short section of open-ended

coaxial line surrounding the anode of the tube. The anode radiator on the 2C39 was removed in order that the series capacitance could be reduced to about 2$\mu\mu$f. Tuning was accomplished by means of a sliding metallic bridge which was used to vary the length of the coaxial line tank circuit.

The overall efficiency of the oscillator was about 35 percent at 2,000 volts. Operation at 300 volts and 120 milliamperes gave an output of about 4 watts or 11 percent efficiency as an unpulsed oscillator. For pulsed operation, peak power output in watts increases with peak pulse voltage in an essentially linear manner, with power going from about 350 watts to about 2,400 watts as voltage is increased from 1,000 volts to 2,500 volts.

The author wishes to express his indebtedness for the assistance and encouragement given by Dr. A. J. Ruhlig of Naval Research Laboratory during the preparation of this paper.

Reference

(1) Brown, Hugh A., Frequency of Capacitance Tuned Lines and Resonant Line Oscillators, *Communications*, May 1945.

Variable-Frequency Oscillator for 25 Centimeters

To increase frequency in the average uhf oscillator, the inductance and capacitance of the tuned circuits are decreased. This method of frequency control is adequate to frequencies of 10 to 60 megacycles, but above this range, the inductance of the tube leads and the inter-electrode capacities become appreciable and eventually, with increasing frequency, the oscillator reduces to the tube and its inherent capacity and inductance. Above 60 megacycles, the loss in efficiency and power output is due to these three main factors:

(a) Transit time of electrons between cathode and plate, which increases the effective grid-conductance of the tube and shifts the phase of the plate current with respect to the grid voltage.

(b) Limitation, by the physical structure of the tube, of the extent to which the parameters of the oscillator circuit can be reduced.

(c) Increase of power loss in the oscillating circuit as a result of skin effect; large capacitance charging current, which results in large I²R loss; electromagnetic radiation from the circuit; dielectric losses in the tube base and envelope.

In an oscillator constructed by George Pihl at Northeastern University and described by H. G. Ryan in a paper delivered before the Boston AIEE, it was found that most of these factors could be controlled by the choice of a proper tube. The Western Electric 368A was the only commercial tube available which met the requirements of the oscillator as to frequency and stable output. This was used in the tuned-grid tuned-plate oscillator circuit shown in Fig. 1.

The tuning elements are coaxial stubs and a sliding capacitor. The use of the stubs results in a negligible radiation loss since the field is confined to the inside of the elements, and the high frequency current is confined to the inside of the lines. This arrangement also simplifies the problem of applying direct voltages to the elements without allowing the high frequency currents to flow in the supply lines. Using these stubs also eliminates body capacity effect. The filament circuit also has tuned stubs to isolate the high frequency currents and to keep the center of the filament at zero r-f potential.

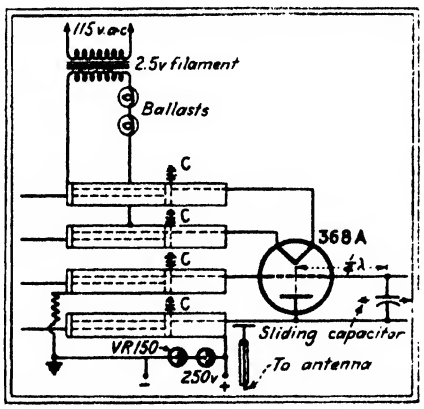

FIG. 1—Circuit of 25-cm oscillator for demonstration of wave guides and resonant cavities

The sliding capacitor, used between the grid and plate for frequency variation, varies the length of a ¼ wave section, since at high frequencies, the reactance is very small and the capacitor acts effectively as a shorting bar.

Two WE ballast tubes are used in the filament circuit to stabilize the current through the filament. Two VR150 regulator tubes are used to limit the voltage variations in the oscillator, since voltage variations in a self-excited oscillator are one of the main reasons for instability.

Mountings

The oscillator tube is mounted on an aluminum bracket composed of two sections with a semi-circle cut in each section of the bracket; the completed circle has the same diameter as the tube. The tube fits in the hole in a vertical position and is rigidly mounted. This method allows convenient mounting of the tuning stubs and sliding capacitor.

The tuning stubs are mounted on another aluminum bracket by means of a clamping sheet of polystyrene.

Bypass capacitors must be used between the grid and ground and plate and ground. Flanges of sufficient area were soldered to the ends of the stubs, and the stubs were clamped to a sheet of aluminum with a suitable dielectric to provide the required bypassing.

The stubs are 3 inches long to tune the oscillator to resonance at the desired frequency. The stubs consist of sections of coin-silver tubing with an outside diameter of $\frac{3}{8}$ in. The center conductor is another section of coin-silver tubing, O.D. of 0.05 in.

To provide a low-resistance path for the high-frequency current, a section of coin-silver tubing was arranged to telescope into the main tube. This contact tube was slotted to compensate for any irregularities in the main tube's diameter and to provide a tight, wide-area contact. To connect the outer tube to the inner tube, this section of tubing was soldered to a brass plug, a hole was drilled in the brass plug, and the plug slotted to permit a sliding fit over the center conductor.

To provide bypassing, $\frac{3}{4}$-in. flanges were soldered to the end of the outer tube to provide the necessary capacitance to ground.

The handles for tuning consisted of two brass rods soldered to the sliding contacts and brought out to a piece of polystyrene rod. These rods were fused into the polystyrene piece to complete the stub, and a brass end plate soldered on the outer tube.

The sliding capacitor was built to slide on an extension of the grid and plate leads, essentially a short Lecher wire system. Alternate sheets of copper and mica were soldered to two brass sleeves which form the sliding contact. The whole assembly is mounted on a piece of sheet polystyrene.

To vary the frequency of the oscillator over its whole range, the capacitor has to be moved only a very short distance. At (a) in Fig. 2 is shown the method of mounting it so that rotation of the polystyrene shaft moves the capacitor along the Lecher wires.

For stops, a free collar and a fixed collar were put on the $\frac{3}{4}$-in. shaft. To the collars, were affixed arms that permitted two complete revolutions of the shaft, the free collar being stopped by a projecting screw on the mounting bracket in one revolution and the fixed collar being stopped by a projecting screw on the free collar, permitting the second revolution of the shaft. These two revolutions of the shaft give the oscillator a frequency range of 10 megacycles at 1500 megacycles. With this frequency range and control, it was found that the oscillator fulfilled all the requirements for fine frequency control and frequency limits.

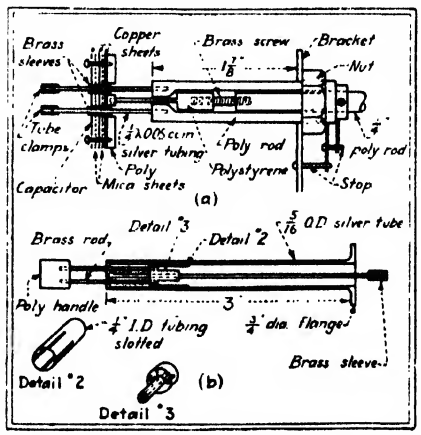

FIG. 2—At (a) is shown the sliding capacitor and its mounting details. Construction of the tuning stubs is shown at (b). The section of Detail #3 was turned down on a lathe and soldered inside Detail #2 at the unslotted end

Adjustment and Tuning

In an oscillator of this type, the grid current is the best indication of oscillation (the plate current not being changed appreciably since the losses are rather high).

To tune the oscillator for oscillation, a low value of plate voltage is used and all the tuning stubs set at approximately the same position. The setting of the plate and grid stubs is varied until the grid current starts to flow. In an oscillating condition, this current will be approximately 1.4 ma. In a non-oscillating condition, the grid current will be negligible.

Once the oscillator is in an operating condition, the grid current meter is removed from the circuit and the filament stubs tuned for resonance. This is done by means of a crystal rectifier and microammeter lightly coupled to the Lecher wires. A maximum indication on the microammeter shows that the oscillator is tuned to resonance.

In the initial adjustment of the oscillator, the capacitor is not touched other than to have it at approximately a $\frac{1}{4}$ wavelength from the center of the plate. However, the oscillator should be slightly detuned so that the output of the oscillator is fairly constant. In this condition, the capacitor does not tune through resonance which would increase the output sharply.

Uses

This oscillator was built to provide a means of measuring the Q of resonant cavities. In the past, the Q of cavities has been measured by using a fixed frequency and tuning the cavities through resonance, varying the cavity dimensions to do so, but the Q is changed somewhat by this method since the dimensions and input of the cavity must be constant and so a true curve of the cavity is not obtained. With this oscillator, a closer and truer picture of cavities can be obtained.

Another important use of the oscillator is to use it in conjunction with demonstration wave guides. At the frequency of operation (25 em), large sections of wave guides may be excited and the field pattern and distribution may be probed, since at 25 cm the guide may be 10 inches in diameter. In our case, ordinary tinned iron stove pipe was used.

Stabilizing Frequency of Reflex Oscillators

By GEORGE G. BRUCK

MICROWAVE GENERATORS can be stabilized in frequency in several ways. The method to be described is advantageous in that it is all electronic, uses fewer circuit components than some methods, and incorporates several simplifications of the plumbing. Used with a 10-kmc oscillator, this circuit maintains the frequency within one part in 10^6.

Duplex Heterodyne

The operating principle can be followed through the block diagram. Microwave energy from the oscillator enters the main waveguide G by way of the probe P and flows in the indicated direction. The energy is tapped through the first iris I_1, which admits a small amount of energy to the upper cavity C_1. This cavity has low Q (of the order of 1,000) and serves chiefly to isolate the subsequent portions of the circuit from the main guide.

A fraction of this energy is admitted to the first crystal X_1 (such as a 1N/23B) where it mixes with energy from the intermediate-frequency amplifier output (approximately 30 mc). The resulting sum (or difference) frequency is transferred into the second cavity C_2 through the third iris I_3. This cavity has a high Q and is used as the frequency reference. The energy in the second cavity is coupled through the forth iris I_4 to the second crystal X_2 where it is mixed with energy from the first cavity coming through the fifth iris I_5. The result is the intermediate frequency, which is returned to the i-f amplifier input to produce oscillation through the system at or near the intermediate frequency.

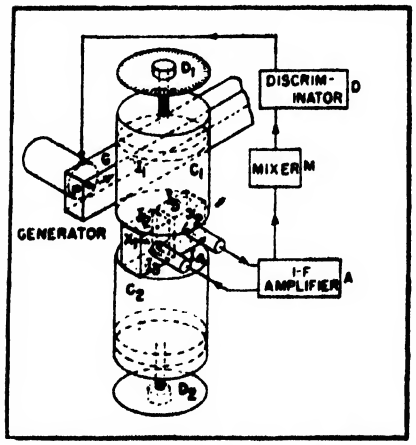

Microwave plumbing is shown pictorially in block diagram of stabilizer

Oscillation occurs only if the microwave generator delivers sufficient power to the mixer crystals, which condition is dependent upon the coupling of the irises. Because the crystals require voltages of a given magnitude for best operation as mixers, the irises have optimum size, but are not critical. The choice of cavity and coupling in the upper section should be such as to sufficiently attenuate the uhf generated in the first crystal, so that feedback through any channel but the high Q cavity is avoided. Using the highest possible i-f will make attenuation of this uhf easier.

Criteria for Oscillation

The system will oscillate at the nominal frequency of the amplifier if the phaseshift through the two crystals and the second cavity is zero. A change in phaseshift will change the intermediate frequency. If f_1 is the original microwave frequency, f_2 is the heterodyne frequency produced in the first crystal and to which the second cavity is resonated, f_3 is the nominal frequency of the amplifier, δ_2 is the phaseshift in the second cavity and its associated couplings, and δ_3 is the phaseshift in the amplifier and its associated elements, then $f_2 = f_1 \pm f_3$ and, for oscillation, $\delta_2 + \delta_3 = 0$, with the second cavity tuned to f_2. Furthermore, where Q_2 is the loaded Q of the second cavity, δ_2 near resonance is

$$\delta_2 \approx 2(\Delta\omega_2/\omega_2)Q_2$$

where $\Delta\omega_2$ is the deviation from resonance. By introducing Q_3, defined as the equivalent over-all Q of the amplifier, δ_3 can be expressed as

$$\delta_3 \approx 2(\Delta\omega_3/\omega_3)Q_3$$

Using these expressions for phase shift in the criteria for oscillation, selecting the positive sign, and simplifying, one obtains an expression for the frequency deviation of the amplifier

$$\frac{\Delta f_1}{\Delta f_3} = 1 - \frac{Q_3}{Q_2} + \frac{f_1 Q_3}{f_3 Q_2}$$

If the negative sign is taken, all terms of the righthand side of the equation are negative. There are two other possible combinations of signs, but they represent unstable conditions.

For the relationship between frequency deviation of the amplifier and the microwave oscillator to be independent of the circuit elements, Q_3 must be small; that is, the phase changes very little with frequency near resonance; Q_3 can be made zero over an appreciable bandwidth, which, although not indespensable, is desirable. Almost any 30-mc radar i-f strip can be adapted for the purpose, giving an i-f deviation approximately half the microwave deviation, which is favorable for proper stabilization. Because grid current in the amplifier will cause noticable detuning, such nonlinear elements as Thermistors or Thyrites should be introduced to limit the amplitude of oscillations so that detuning is unnoticeable.

Recovery of information from the i-f strip is straightforward. Any discriminator, separated by a buffer stage, supplies sufficient output to control a reflex oscillator. The oscillator control completes a negative feedback loop from generator through guide to first cavity through the mixers and second cavity to the oscillating i-f amplifier, hence through the discriminator back to the generator. Phaseshifts throughout this loop must not introduce f-m oscillations in the overall system.

Frequency modulation can be introduced by injecting the audio-frequency signal through an additional mixer between the i-f amplifier and the discriminator. The i-f output (30 mc) is mixed with a frequency-modulated auxiliary oscillator (10 mc); the resulting difference frequency (20 mc) drives the discriminator. Drift in the auxiliary oscillator will, of course, affect the microwave oscillator, the microwave deviation being about twice that of the auxiliary oscillator.

The complete circuit is easy to adjust and operate. The microwave components are not critical, can be assembled in advance, and need no adjustments. The two cavities can be coupled mechanically for tuning. The second or reference cavity must have an effective Q higher than 10,000 and high thermal stability; it is preferably constructed from such low expansion alloys as Invar. The coupling irises should be small. The amplitude control of the i-f amplifier must keep the d-c in the two mixer crystals constant. In testing the circuit, two oscillators were easily kept within 100 cps of each other. The circuit was developed while the author was with Raytheon Mfg. Co., Waltham, Mass, and the inventions are assigned to that organization.

3-Cm Continuous-Range Oscillator

By IRVING M. GOTTLIEB

DESIGN AND TESTING of r-f plumbing components in the 3-cm band can be greatly facilitated by means of a signal generator capable of providing continuous calibrated tuning over the desired frequency range. With the laboratory oscillators available, it is a very tedious and laborious process to plot frequency characteristics of a mixer unit or to obtain the Q of a resonant cavity. The desirable requirement that power output remain constant over the frequency band involved in the measurement procedure is difficult to satisfy, inasmuch as the reflector potential adjustment for the reflex klystron affects both power and frequency.

The system described delivers constant power at any frequency within the range of 8,800 to 9,500 mc by tuning a calibrated dial to the desired frequency. A precision-calibrated tunable cavity is employed as a wavemeter to check the tuning dial calibration from time to time. Once the tuning dial has been calibrated, one merely selects the desired frequency increments and records the corresponding microwave power output from the component under test. The plumbing setup used is shown in the photograph.

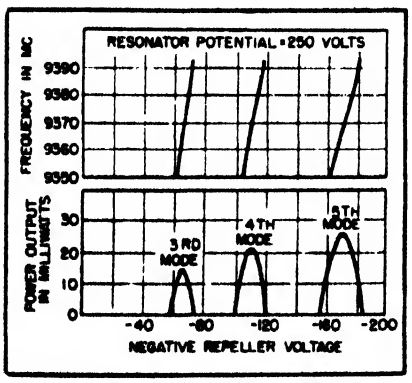

FIG. 1—Power output and oscillation frequency of a 723A/B klystron vary with repeller voltage in the three voltage modes shown

Klystron Operation

Both the power output and frequency of oscillation of a klystron can be adjusted by varying the negative voltage on the repeller electrode. The tube will oscillate only within certain ranges of repeller voltage, known as voltage modes. Figure 1 shows power output and frequency as functions of repeller voltage for a type 723A/B klystron oscillator. Of the three voltage modes shown, the one for the range of repeller voltages between −150 and −180 volts gives the greatest power output. Consequently, this circuit is designed to deliver voltages within that range to the repeller of a 723A/B.

The klystron can be tuned over a relatively narrow frequency range by changing its repeller voltage alone; wide changes in frequency are obtained by mechanically tuning the resonant cavity of the klystron and simultaneously adjusting the repeller voltage. This simultaneous adjustment is not easy to accomplish by the most obvious expedient of gearing a potentiometer to the cavity tuning screw. The exact value of repeller potential required at any given frequency does not coincide exactly to that indicated by the curve, but is rather erratic, and at the same time, critical. The electronic system described, automatically provides the correct repeller potential for constant output over the entire tuning range.

Circuit Design

The circuit of the automatically controlled repeller voltage supply is shown in Fig. 2. Tube V_1 is one section of a 6J6 connected as a grid-controlled rectifier. When no signal voltage is applied to the grid of this tube its quiescent output causes

The next tube V_2 is a 2D21 thyratron. Its grid bias is adjusted by means of R_1 so that the tube is just on the threshold of ionization. Thus, a slight positive voltage appearing across the crystal can cause

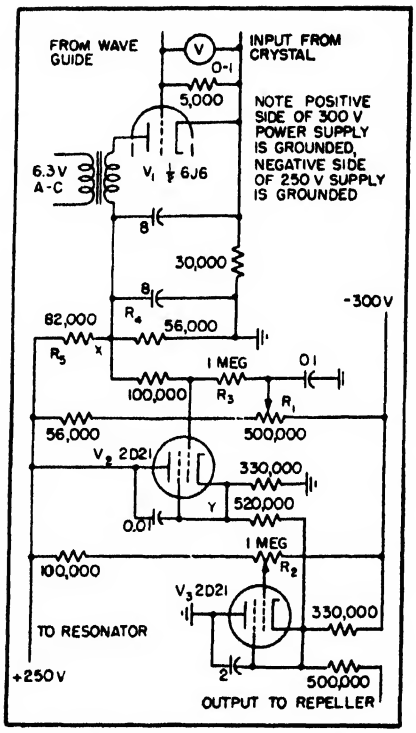

FIG. 2—Circuit of the automatically controlled repeller voltage system includes grid-controlled rectifier, control thyratron, and relaxation oscillator thyratron

this thyratron to fire with the result that point Y becomes about 200 volts positive with respect to ground.

The last tube V_3 is also a 2D21 thyratron. It serves as a relaxation oscillator to generate negative-going sawtooth waves of about 1 cps frequency and with a peak negative amplitude adjustable by means of R_2 to the vicinity of 200 volts. For most 723A/B tubes, the repeller voltage range for the fifth mode will be approximately from 150 to 190 volts. The exact value of repeller voltage is obtained by halting the generation of sawtooth waves. Suppose that the relaxation oscillator attempts to develop a negative sawtooth having a negative amplitude of about 200 volts. Also, assume that the klystron will operate only in the fifth mode and that for a particular adjustment of the cavity screw, maximum r-f output will occur at –165 volts.

Now, as the negative sawtooth approaches 165 volts, the klystron begins to deliver microwave power and a positive emf appears across the monitoring crystal. This occurrence upsets the balance of point X with respect to ground so that a positive voltage is impressed upon the control grid of V_2. If R_1 is so adjusted that this tube is near its threshold of firing, the emf delivered by the crystal will continue to increase, as will the positive voltage impressed on the thyratron grid. At some value of microwave power close to the optimum for fifth mode operation, V_2 will fire and cause point Y to suddenly become positive with respect to ground. The sawtooth is thus caused to reverse and to go in the positive direction, resulting in a decrease in the output of the klystron. Consequently, the control thyratron deionizes and allows the relaxation oscillator to again begin generating a negative sawtooth. As before, the klystron output increases, causing V_2 to fire, and the cycle of operation is repeated.

Once the system has searched for and found the region of optimum repeller potential, the subsequent small oscillations about this potential are of very minute amplitude, less than 0.1 volt. Variation in the klystron oscillator frequency with respect to repeller voltage is about 2 mc per volt. Therefore, the hunting action of V_3 produces deviations in klystron frequency of only 0.2 mc, of negligible importance in the vicinity of 9,300 mc.

Preliminary Adjustment

The 0–1 d-c voltmeter connected across the monitoring crystal indicates oscillation and is handy for the initial tuning up of the system. A 300–0–300 volt midget type power transformer is used with the 6.3-volt filament winding connected to the filament supply. The conventional 120-volt primary winding is unused.

As previously mentioned, point X should be at zero potential with respect to ground with no signal input to the 6J6 grid. This voltage should be measured with R_3 disconnected. If this condition is not obtainable, either R_4 or R_5 should be changed from the values designated in the schematic diagram. A vacuum-tube voltmeter should be connected from the repeller voltage output to ground and with V_2 removed from its socket, R_2 should be adjusted to yield a sawtooth voltage having a negative peak of approximately 200 volts. This voltage can be easily observed on the vtvm, inasmuch as the sawtooth frequency is about 1 cps. Next, with all tubes in place, adjust R_3 until the needle of the vtvm ceases to fluctuate, then back off just sufficiently to permit oscillation of the relaxation oscillator. It will now be found that a slight positive potential impressed upon the 6J6 grid will prevent oscillation of the 2D21 relaxation oscillator. The sawtooth will "freeze" somewhere in the vicinity of 100 volts. If the repeller voltage output is now connected to the klystron repeller and the monitoring crystal is connected to the input, the system should be immediately operative. Figure 3 shows how the repeller voltage is automatically controlled to produce nearly constant microwave power output while the klystron is mechanically tuned.

The dial should be calibrated by means of the cavity wavemeter which is always available for checking the frequency. The attenuating section should be adjusted so that a 0–100 microammeter can be used in conjunction with the output crystal. It will then be found that negligible reaction exists between the component under test and the amount of

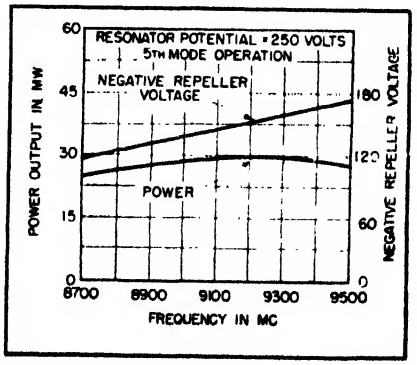

FIG. 3—As the klystron cavity is mechanically tuned, the automatic control varies potential on repeller as shown by upper curve to provide fairly constant power indicated by curve below

energy flowing through the waveguide. An added refinement would involve a combination of resistors and tuning stubs such that the standing wave ratio throughout the guide would be at a minimum. However, it was observed that this condition is approached sufficiently for the purpose by employment of the single attenuating section.

Mode Selection

The searching range covered by the relaxation oscillator is such that with 250 volts applied to the klystron resonator, there will be little opportunity for operation in a mode other than the fifth. If the 723A/B shows a tendency to jump to the fourth or sixth mode, as evidenced by an abrupt change in the tuning calibration, this effect can be corrected. Operation in the fourth mode can be rendered impossible by backing R_1 away from the threshold of firing of V_2, thus making necessary the stronger input from fifth mode operation to actuate this tube. Operation in the sixth mode can be halted by adjusting R_2 so that the peak amplitude of the negative sawtooth will not be high enough to support sixth mode operation. However, with most 723A/B tubes, this trouble will not be encountered, and it is a simple matter to record the frequency characteristics of a plumbing unit.

Two power supplies are required: one to deliver 300 volts at 10 ma, and the other, stablized with respect to line voltage fluctuations, to furnish 250 volts at 30 ma. The 300-volt supply is employed as a source of negative potential for the klystron repeller and the relaxation oscillator and for bias voltages for the two thyratrons. The 250-volt supply furnishes positive voltage for the various electrodes in a conventional manner and also powers the klystron resonator electrode.

Bolometer Amplifier

Compact tuned amplifier designed for use with bolometer or crystal microwave detectors uses high-Q toroid coils to obtain narrow pass band and high gain. Sensitivity approaches thermal noise and gain is adequate for use with a suitable voltmeter

By D. D. KING, JOHN TAYLOR and W. H. FAULKNER Jr.

A STANDARD arrangement for detecting microwave signals makes use of a bolometer or crystal detector whose output is fed through an amplifier and thence to a voltmeter. Crystals permit the use of an unmodulated source of microwave energy; then modulation usually is inserted at the amplifier input before amplification. In case a modulated source is used, the crystal or bolometer output can be coupled to an audio amplifier. The amplifier described was specifically designed for use with modulated signals.

The principal requirements for such an amplifier are: linear response over the full range of amplitudes to be handled; adequate gain; minimum noise level.

The first of these requirements is easily fulfilled over a voltage range of 80 db with standard design practice and adequate plate voltage. Likewise, the proper number of stages of amplification will furnish sufficient gain to drive any voltmeter. The fundamental limitation rests in the noise level.

In designing the present amplifier several precautions were taken to minimize the noise level. Bandpass amplifiers have long been used for this purpose; usually an RC network serves to peak the amplifier response. As may be seen on the circuit diagram in Fig. 1, the response of the amplifier described is determined by a tuned load in each plate circuit. Toroids with Polyiron cores are used as inductors. Several advantages accrue from this design.

In the first place, the toroids have a high Q of 60 which yields a very narrow pass band with the simplest circuit. The frequency response of the amplifier is shown in Fig. 2. The large effective plate

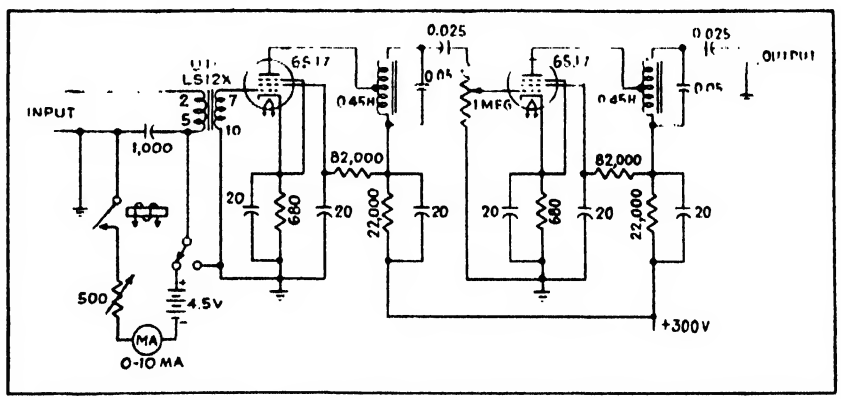

FIG. 1—Tuned plate load circuits use toroid inductors having Polyiron cores. The relay at the left disconnects the bolometer battery circuit when the tube filaments are turned off

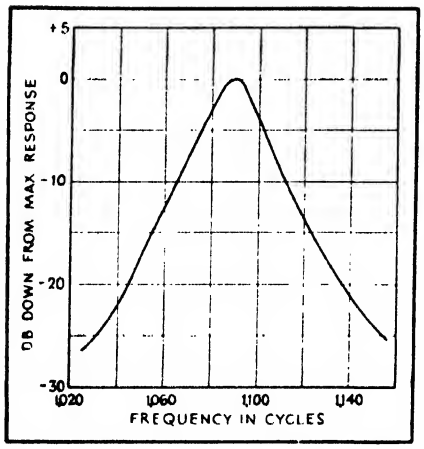

FIG. 2 — Amplifier frequency-response curve shows a bandwidth of less than twenty cycles at a point 3 db down from maximum response. This high selectivity results from the use of the high-Q toroids

load also permits full utilization of the tube gain. Toroids are insensitive to outside fields; hence no particular precautions need be taken in mounting them. The circuit with constants as shown in the diagram yields a voltage gain of 107 db with a pass band as shown of less than 20 cycles at 1.09 kc.

The circuit given uses a center-tap connection to the tube plate. An increase in gain of some 5 db per stage is obtained by connecting the plate to the top of the toroid. The pass band then appears to be very slightly increased. Since the amplification is adequate, the center tap was used in this instance.

A further reduction of bandwidth may be obtained by inserting more tuned circuits. However, this approach imposes severe frequency stability requirements on the modulator of the source without a commensurate improvement in the noise level. The rms noise voltage from a resistance R at an absolute temperature T is given by $V=7.41\times10^{-13}(TR\Delta f)^{\frac{1}{2}}$ where Δf is the frequency band. The square-root term in the formula shows that a reduction in band from, say, two percent to one percent is relatively unprofitable. On the other hand it is essential that the band exclude 60 cycles and its principal harmonics.

Having eliminated noise sources outside the chosen frequency band, it remains to reduce contributions at the modulation frequency. Since bolometers require a d-c source, the input circuit is complicated by the presence of a battery and milliammeter. As shown in Fig. 1, a relay is also provided to open the battery circuit when the tube filaments are switched off. It was found that a 1,000-μf capacitor in parallel with these components reduces the noise level. Leads in the input circuit are kept short, shielded, and close to the chassis. This last precaution minimizes ground loops in the low-impedance input circuit.

The only resistor in the input circuit is in the cathode of the first stage. Its value is not critical but it must be wire-wound. Carbon resistors carrying current become noisy after a period of service.

Another difficulty inherent in a high-gain tuned system is that of microphonic resonances. A particularly effective tube shield against microphonic resonances is used in this amplifier. Instead of screwing a shield can over the shock-mounted tube, the shield forms an integral part of the metal tube. This construction is accomplished by filling in the space between the tube envelope and shield can with Wood's metal. The resulting heavy unit is extremely insensitive to microphonics. The low melting point of the metal filler makes tube changes relatively easy.

The particular unit described is designed for use with a Ballantine voltmeter. In this service the performance data are given in Table I.

The resistance of the bolometer is roughly 200 ohms. Taking the operating temperature as 400 K and substituting in the equation, one obtains a value of noise approximately equal to 10^{-6} volt. Evidently the theoretical limit of performance has been approached. Comparison with a thermistor bridge and calibrated attenuator indicates that the minimum detectable microwave power at 3000 mc is of the order of 10^{-9} watt for the bolometer. The crystal is substantially more sensitive, of course.

Table I—Amplifier Performance Data

Type of Input	Noise Level in db (0 db 1 volt)
Short Circuit	−160 db
Bolometer (10 ma Littelfuse) carrying 10 ma	−155 db
Crystal (1N21B)	−145 db
Gain	107 db
Maximum Output	100 v

Measurements were made of the amplifier output as a function of microwave input to a bolometer. For this purpose, an attenuator was used which consisted of a waveguide operated beyond its cutoff frequency and calibrated in terms of a Ballantine voltmeter. From the measurements obtained, amplifier output was found to vary linearly with bolometer input.

Various noise levels were measured with a 0 to 1-ma recording milliammeter. This measurement was made by coupling the a-c output of a Ballantine meter to the recorder through a copper-oxide bridge rectifier. With the amplifier input short-circuited and carrying no current, the noise level at the input was found to be about 0.6×10^{-6} volt. This voltage remained practically unchanged when a direct current of 10 ma flowed through the short-circuited input. When a bolometer carrying no current was connected to the amplifier input, the noise increased to about 1.0×10^{-6} volt. Noise of about 1.4×10^{-6} volt was measured when the bolometer carried 10 ma.

Considerable improvement in the signal-to-noise ratio is obtainable with adequate rapidity of response for most applications through the use of several microfarads of shunt capacitance.

The presence of a signal increases the apparent noise, hence the voltage levels given above were measured with the aid of an attenuator in the output circuit. A signal of 10^{-7} volt is, however, well above the noise on the meter, or on the recorder using no shunt capacitor.

Piston Attenuator

Deviation from ideal attenuation at any frequency in vhf, uhf, and shf bands is given directly on nomograph for piston diameters from 0.25 to 4 inches

By RAYMOND E. LAFFERTY

PISTON ATTENUATORS are used as variable attenuators in the very high, ultrahigh, and superhigh frequency bands. The attenuation per unit length is linear when calibrated in db and may be computed from theory[1,2,3] when the physical dimensions and mode of operation are known.

Although there is some variation of attenuation with frequency in all piston attenuators, this error can be minimized by proper selection of frequency range and pipe diameter. The accompanying nomograph gives directly the extent of this attenuation error, as a convenient guide for the design of new attenuators. The $TE_{1,1}$ scale is for the mutual inductance type of attenuator with coplanar coils, and the $TM_{0,1}$ scale is for the mutual capacitance type.

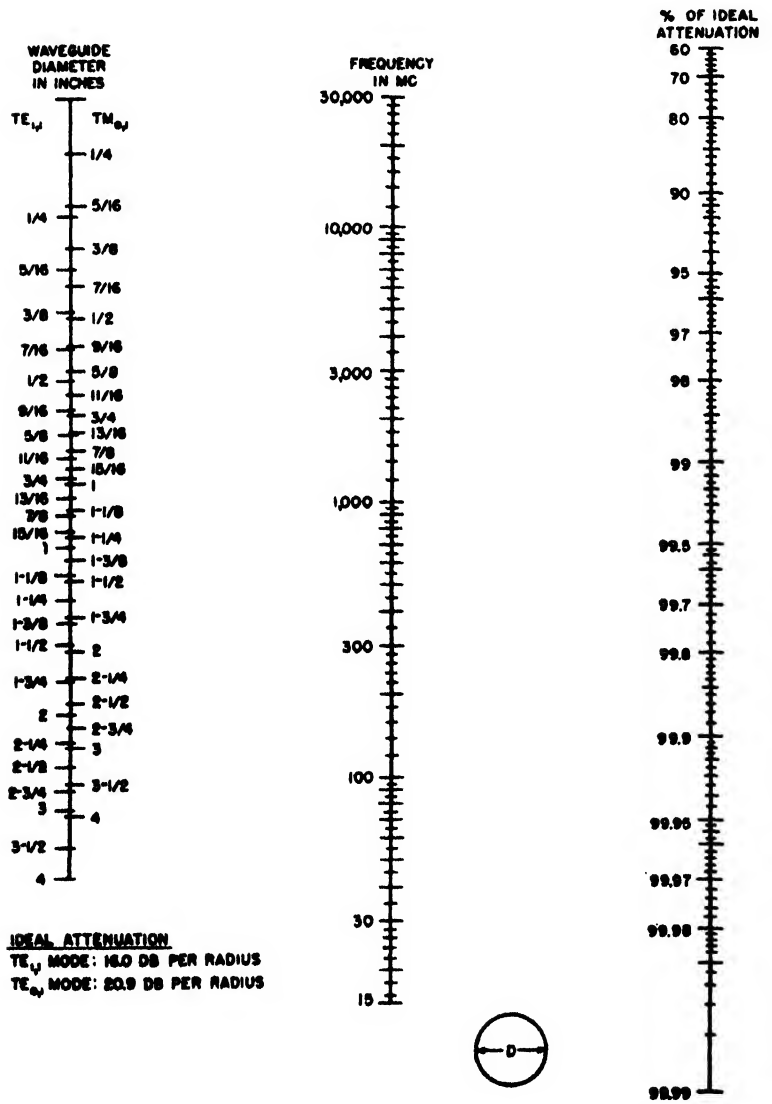

To use this chart, locate the pipe diameter on the scale for the proper mode, place a straightedge on this value and on the frequency value (center scale), and read the percent of ideal attenuation where the straightedge intersects the righthand scale. Multiplying the ideal attenuation (see bottom of chart) by this percentage factor gives the true attenuation in db per radius for the given frequency.

Example: A signal generator uses a $TE_{1,1}$ half-inch diameter piston attenuator. The frequency range is from 1,000 to 8,000 mc. What is the attenuation over this range? At 1,000 mc the attenuation is 16 times 0.9974, or 15.96 db per radius. At 3,000 mc it is 16 times 0.976, or 15.62 db per radius. This is a variation of approximately 0.33 db for each radius of travel (0.25 inch) of the piston. If the piston travels 1.5 inches from the 0-db starting point the difference in attenuation between the frequency limits will be approximately 2 db.

References

(1) D. E. Harnett and N. P. Case, The Design and Testing of Multi-range Receivers, *Proc. IRE*, p 578, June 1935.
(2) E. G. Linder, Attenuation of Electromagnetic Fields in Pipes Smaller Than Critical Size, *Proc. IRE*, p 554, Dec. 1942.
(3) F. E. Terman, "Radio Engineers' Handbook," p 881, McGraw-Hill Book Co., New York, N. Y., 1943.

Standing Wave Meter

The power reflections caused by mismatch at the junction of waveguide components are measured automatically by a device which gives a direct meter indication of the standing wave ratio

By HEINZ E. KALLMANN

THE meter to be described is an automatic standing wave detector of moderate accuracy designed for quick and simple operation in situations such as production tests and adjustments of microwave equipment. It has proved helpful in a survey of the effects of various parameters on the matching of a waveguide transition. The study was typical of the many cases where only the standing wave ratio is wanted, not the position of the maxima and minima. In this device the problem is simplified by providing a constant and matched source of microwave power. It is then only necessary to know the difference between the maximum and minimum amplitude, which is proportional to the amplitude of the reflected power. If a mechanism periodically moves the position of the standing wave detector probe past the position of the maxima and minima or vice versa, then a peak-to-peak voltmeter fed by the detector will yield readings directly proportional to reflected voltage E_r. With a given input E_o, the meter may be calibrated in voltage standing wave ratio, η_v, from $\eta_v = (E_o + E_r)/(E_o - E_r)$.

Standing wave minima are spaced at intervals of half a guide wavelength λ_g; relative movement of the probe and minima by at least $\lambda_g/2$ will thus insure that at least one maximum and one minimum are passed by the probe wherever they happen to be in relation to the position of the probe. To assist the performance of the peak voltmeter circuit, however, it is preferable to increase the relative movement of the probe and standing waves from one-half guide wavelength to two or more guide wavelengths.

To simplify the design of the microwave components, the probe is mounted in a fixed position and its electrical distance from the load varied by means of a periodical line stretcher, in this case a strip of low-loss dielectric periodically dipped into the guide through a slit in its top wall. Insertion of a dielectric is equivalent to an increase of the guide width, thus reducing the guide wavelength λ_g. The arrangement used for a guide of 0.5 x 0.25-inch outside dimensions is sketched in Fig. 1; it offers a long taper of the dielectric in a small space. The guide is bent, in the E plane, to U shape with an outside diameter of 2½ inches. A central slit 0.092 inch wide is cut along the curved inside part of the U. Into this slit dips the edge of a circular polystyrene disk, 0.075 inch thick, which is mounted 0.10 inch off-center on the spindle of a small 30-rps motor (not shown). The configuration of a U-shaped guide and circular disk makes a very slim taper, minimizing the discontinuities and thus the reflection; bevelling of the dielectric disk further minimizes the discontinuities. When the motor rotates, the eccentric rim of the polystyrene disk periodically penetrates the center of the U guide nearly to the opposite wall and is withdrawn to the edges of the slit.

The sketch of Fig. 1 shows strips of lossy material, such as conducting rubber, cemented along the edges of the slit to absorb radiation through it and also small pieces of lossy material, such as molded polyiron powder, wedged into the ends of the slit. The latter are needed to absorb slot waves, spurious standing waves set up between the two edges of the slit as on a balanced line.

The main limitation to the accuracy of the meter is imposed by re-

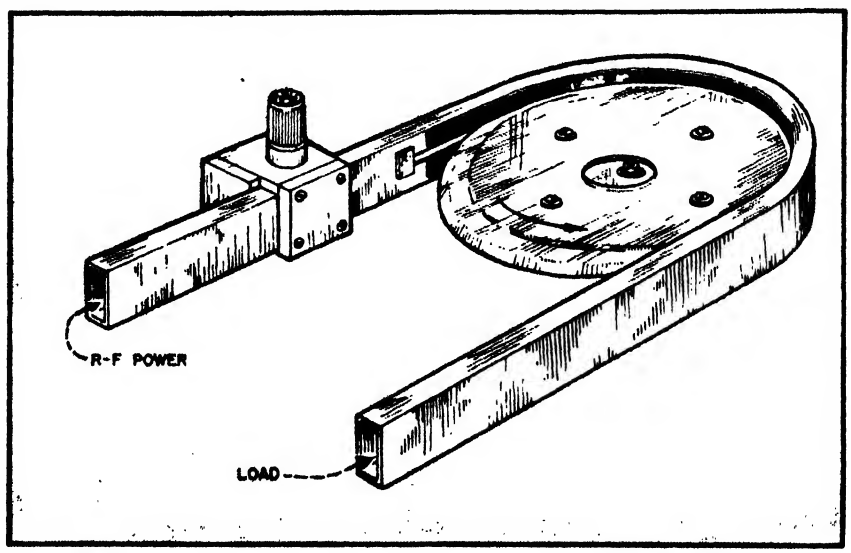

FIG. 1—Measurement probe (left of center) and eccentric dielectric rotor which dips through a slot in the U-shaped wave guide when driven by a small motor. This insertion of a dielectric gives the effect of alternately stretching the guide to a greater length and returning it to its original dimension

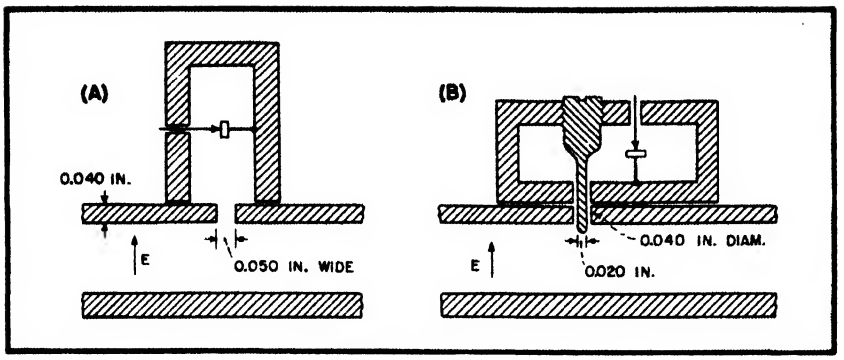

FIG. 2—Probe and crystal detector for measuring magnitude of power reflections. At (A) the crystal is coupled by means of an E-plane tee, whereas at (B) a coaxial coupling and wire probe are employed

flections from the point where the dielectric dips into the waveguide. Direct reflection of oscillator power at this point is observed as residual standing wave ratio even if the load is perfectly matched. Furthermore, waves reflected from an unmatched load are reflected forward again at this point. Second reflections at the load interfere constructively or destructively with the first ones, dependent upon the distance between line stretcher and load. The larger the mismatch at the line stretcher, the more does the observed standing wave ratio vary around the proper value. Oscillator mismatch that might affect the accuracy of the measurement is usually kept low by padding.

Crystal Detector

The probe is placed immediately before the line stretcher. It couples a crystal detector to the waveguide with about 15 db attenuation, assuming a power level of about 1 milliwatt at this point of the guide. The crystal may either be coupled in by an E-plane tee with a slot 0.050 inch wide across the whole width of the 0.040-inch guide wall, as shown in Fig. 2A, or by means of a coaxial coupling between the main and a short auxiliary guide consisting of a 0.020-inch wire probe in a hole 0.060 inch in diameter, as in Fig. 2B. The coupling should be nondirectional, but imperfection in this respect will not affect the result.

The crystal detector is operated substantially without load. It can be shown that under this condition and for the relatively high power level in this device, it acts as a linear detector.

The amplifier and voltmeter circuit are shown in Fig. 3A. All plates are fed with about 250 volts, with very low ripple, from a regulated power supply (Fig. 3B) employing a Thyrite bridge; total current drawn is 3 milliamperes, exclusive of that for the microwave oscillator. The first amplifier stage, a pentode, and the second stage, a triode, provide about 70 db gain in a conventional audio-frequency design; the response extends low enough to minimize phase distortion at 30 cps. The amplifier feeds into a voltage-doubler rectifier employing a double diode.

The reading of the meter is unaffected by the distance of the load only to the extent that its rectifier circuit approximates a perfect peak rectifier, that is, one whose output is independent of the shape and spacing of the peaks. In particular, loading of the rectifier is undesirable since it affects mainly the shape of the peaks. To minimize this effect,

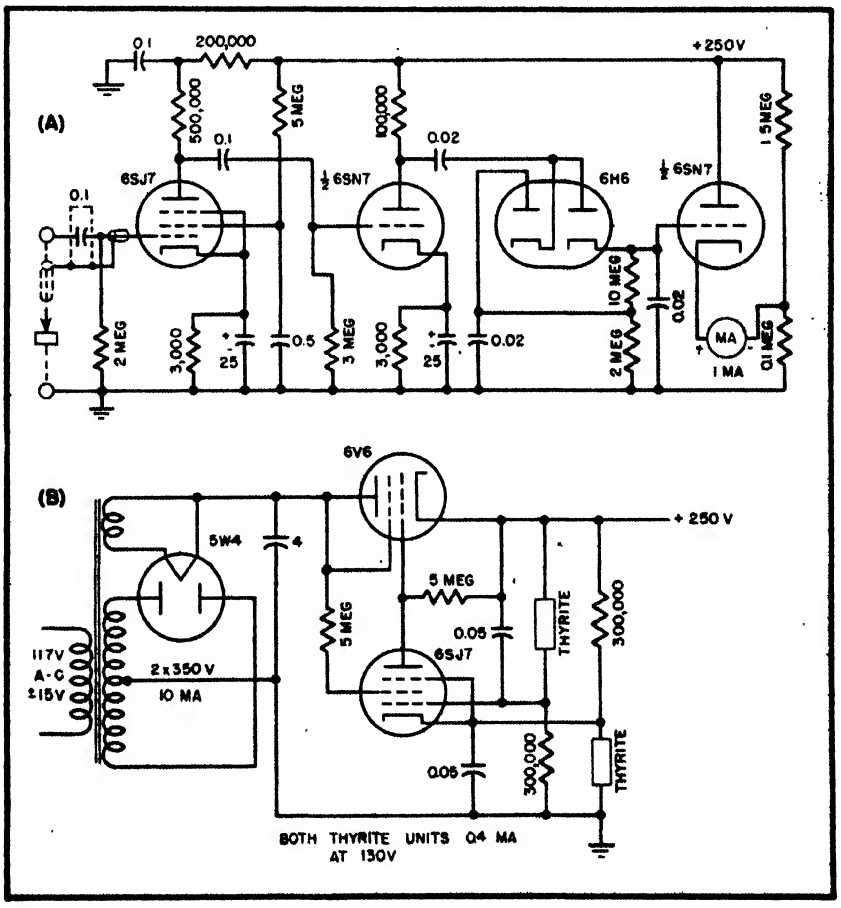

FIG. 3—Fundamental standing wave meter circuit diagram (A) and Thyrite bridge regulated power supply (B) used to operate the unit

very high load resistances are necessary which entail long time constants and slow meter response and whose insulation is difficult. To ease these requirements without sacrifice in accuracy, the following steps were taken.

Instead of the required minimum of a half guide wavelength, the line was stretched periodically by two or more guide wavelengths. The effect is illustrated in Fig. 4 where the

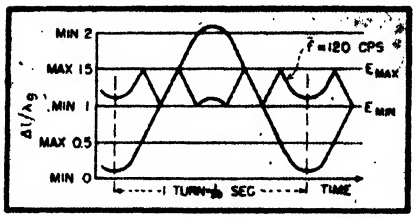

FIG. 4—The effect of changing line length as indicated by the signal at the probe. Rounded peaks occur when the line stretcher reverses its action

sine-shaped curve represents the change of line length Δ_l/λ_g as a function of time t for one turn of the motor in 1/30 second. Since the change extends over two whole guide wavelengths, the signal at the probe will then be the same as if the amplitude had changed about four times as often back and forth between one minimum and the next maximum with the average frequency f approximately equal to 120 cps, as shown in the zigzag curve of Fig. 4.

Round peaks occur in the zigzag curve whenever the line stretcher reverses its action; their height depends on whether this happens near a maximum or minimum, or in between—that is, on the position of the load. The sharp peaks of the zigzag curve, on the other hand, are unaffected in height and shape by the position of the load. The larger Δ_l/λ_g, the more sharp peaks are interposed between each two round peaks and the less will the response of an imperfect peak voltmeter be affected by the varying height of the latter. It can be seen that deformation of the U-shaped guide or of the circumference of the polystyrene disk merely affects the spacing of the sharp peaks but does not affect their number or their height.

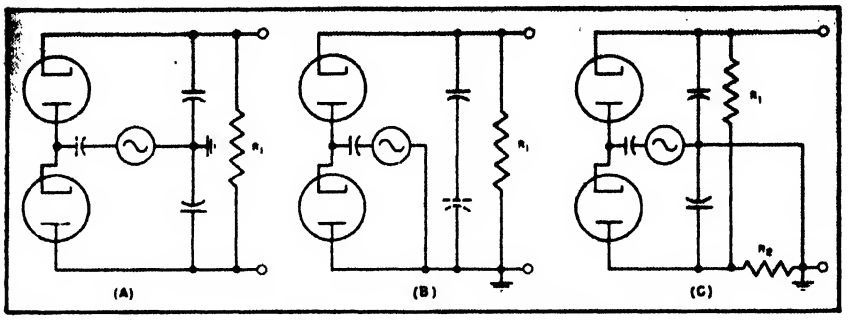

FIG. 5—Voltage-doubler rectifier circuits. At (A) is shown a full-wave doubler, with a half-wave circuit at (B). The circuit at (C) combines advantages of both types

Rectifier Circuit

There are two main forms of the voltage-doubler rectifier, the full-wave doubler of Fig. 5A and the half-wave doubler of Fig. 5B. Both yield the same output—twice the peak-to-peak voltage. They differ in that the former draws energy evenly from both the positive and negative peaks of the supplied oscillations, but does not permit of both single-ended input and output without the help of a transformer; the opposite is true for the half-wave doubler.

The circuit of Fig. 5C was developed by combining most of the relevant advantages of both Fig. 5A and Fig. 5B. It differs from that of Fig. 5A only in that one output terminal is grounded through resistor R_3 which is too large to affect the operation of the rectifier circuit. The new circuit has single-ended input and output; it still yields fully twice the peak-to-peak voltage for any load resistance which is large compared with $R_1 + R_2$. It provides approximately even loading of both the positive and negative peaks as long as R_3 is large, and offers a dis-

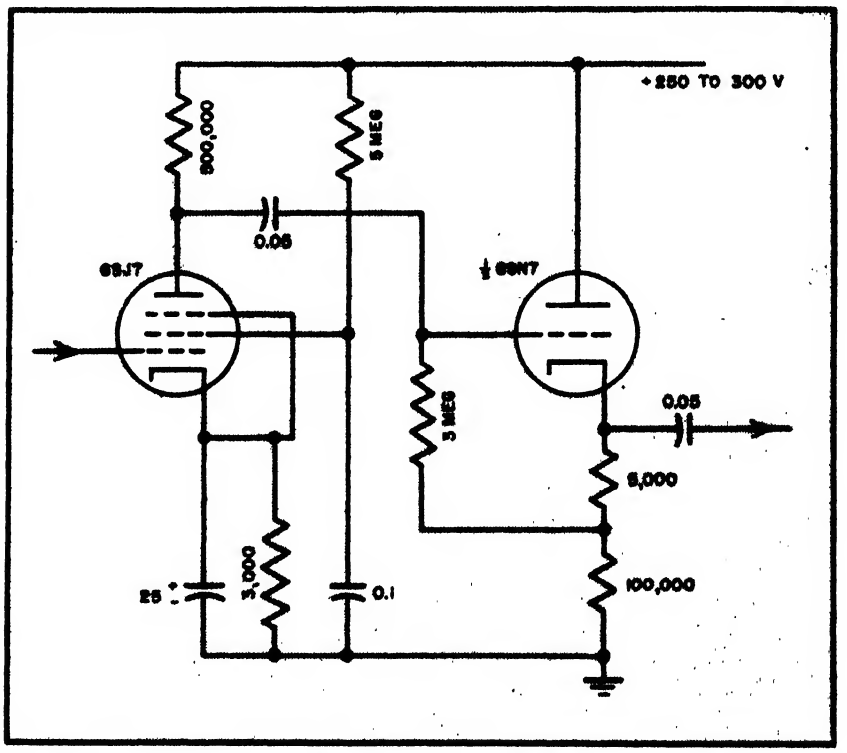

FIG. 6—Improved amplifier to replace the single stage shown in Fig. 3. Low impedance output is obtained with the cathode follower

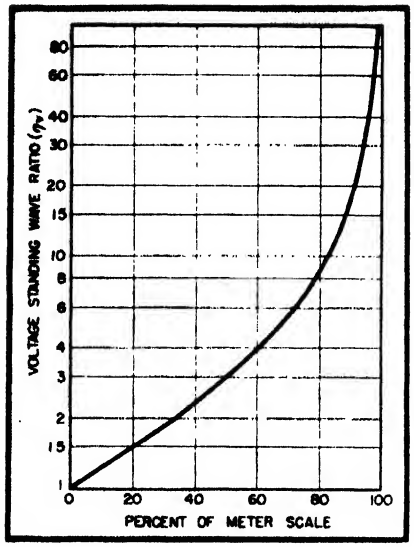

FIG. 7—Calibration of the meter dial in terms of voltage standing wave ratio

tinct improvement in the accuracy of the standing wave meter. In the circuit of Fig. 3, this voltage-doubling rectifier employs a value of 2 megohms for R_1.

Two further refinements tested and used in more elaborate equipment were not needed in the simple unit here described. The second amplifier stage in Fig. 3 was replaced by the two stages shown in Fig. 6. Replacing the amplifier triode by a pentode increases the sensitivity by about 20 db without reaching the limits of instability or circuit noise.

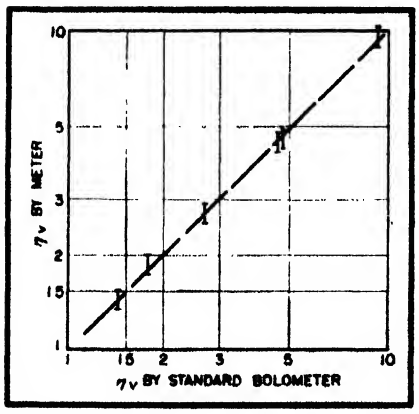

FIG. 8—Voltage standing wave ratio observed on the meter in comparison with measurements by means of a standard bolometer. Vertical lines indicate the spread of the readings

In addition, this amplifier stage was coupled to the voltage-doubler rectifier via a cathode-follower stage with the low output impedance of $1/g_m$ approximately equal to 500 ohms so that the deformation of the voltage peaks due to rectifier loading was further reduced.

The output of the voltage-doubler rectifier is of the order of 100 volts for full scale, but is of such high impedance that direct measurement with a d-c voltmeter is undesirable. It is, therefore, transformed down to a more convenient impedance level by means of a cathode-follower tube. Due to the degenerative resistance of 0.1 megohm in its cathode circuit, the plate current of this triode is strictly proportional to its grid potential, with an effective mutual conductance of 10 micromhos. A bleeder resistance from B + to its cathode holds the standing plate current to cutoff.

Any meter system with a sensitivity of 1 milliampere for full scale deflection may be used. Its scale is calibrated according to the curve of Fig. 7; voltage standing wave ratio $= (1 + E_r)/(1 - E_r)$, if full scale (100 percent) is to indicate an infinite ratio. The detector characteristic, amplifier, and rectifier may all be assumed as linear.

Comparison With Bolometer

The calibration thus computed was checked for various loads against a standing wave detector employing a standard bolometer, with results as in Fig. 8. A load with a standing wave ratio adjustable from 1.02 to greater than 70 was built, as shown in Fig. 9, consisting of a choke-type metal plunger movable in a high-loss waveguide, molded of polyiron powder. A slotted-section line stretcher inserted between this calibrated load and the matchmeter was varied and the variations in the meter readings noted. Short lines straddling the expected straight line are marked in Fig. 8, indicating the range of these variations. The deviations never exceed plus or minus 10 percent of the correct standing wave ratio and, in most cases, are much less. The error is typical for reflections between line stretcher and load; it seems low considering that there were two choke-flange joints and that the polystyrene disk of the tested instrument did not even have a bevelled edge.

Circuit Elements not Critical

The assumption of a linear overall characteristic was thus confirmed. Changes in gain with aging have thus no influence on the calibration provided it is set to full scale for $\eta_v = \infty$. Adjustment may equally well be made by control of the input power or by a voltage divider (not shown) in place of the grid resistor of the first amplifier stage.

No tuned or frequency-sensitive parts are used. All circuit components are of standard type and tolerance. The instrument as described can easily be built into an 8-inch cube using standard components. No more space is needed even if the microwave oscillator is included, fed from the same power supply.

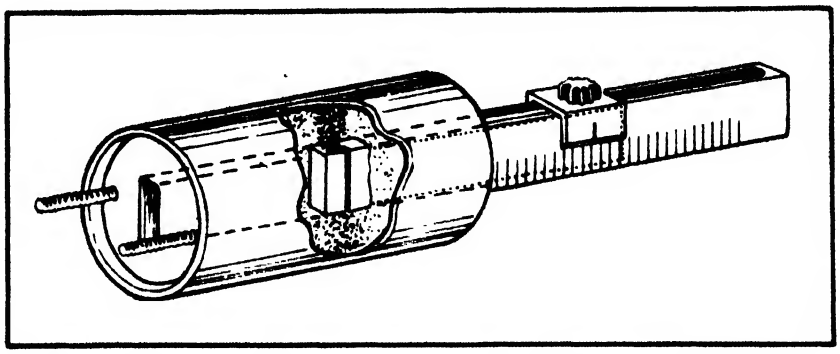

FIG. 9—Artist's drawing of an adjustable standing wave ratio load used in calibrating the meter as shown in Fig. 8

POWER SUPPLIES

Analysis of Full-Wave Rectifier and Capacitive-Input Filter

Some simplifying assumptions make it possible to express results in terms of two general parameters. Data are presented for tube angles, output voltage, ripple, and peak tube currents. Filter resonance, pulsed current, and continuous current operation are included

By D. L. WAIDELICH

THE FULL-WAVE rectifier circuit with a capacitive-input filter is probably the most common of all rectifier circuits.

Freeman and Terman[1] have made an analysis of this circuit using as their chief assumption the idea that the filter inductance was infinitely large. They have presented curves which could be used in the design of the rectifier and filter circuit, but unfortunately the curves are valid only at lighter loads and at one frequency, that of sixty cycles per second. Stout[2] made an analysis which presented the waveforms in the circuit but gave no characteristic curves suitable for use in design, while Mitchell[3] assumed an infinitely large inductance in his analysis.

This paper presents the results of an investigation made to determine the effects of a finite filter inductance on the operation of the rectifier and filter circuit. The results may be used in the design of the rectifier and filter circuit for any frequency and with any load from open circuit to short circuit.

The analysis of the circuit was made using the newly developed steady-state operational calculus[4]. It was found that approximate values of the portion of a cycle that each tube was conducting would be helpful in the analysis, and these were obtained by setting up the circuit and observing the tube currents by means of a cathode-ray oscilloscope. With these approximate values as a starting point, the exact portion of each cycle that the tube was conducting could be determined from the analysis.

The schematic diagram of the rectifier and filter circuit is shown in Fig. 1. Tube T_1 conducts during the first half cycle of the applied alternating voltage and charges capacitor C_1 almost to the peak value of the alternating voltage.

Current flows from capacitor C_1 through the filter inductor L to charge capacitor C_2. The load resistor R has the same voltage as the second capacitor C_2. During the second half cycle of the alternating voltage, the second tube T_2 conducts, and capacitor C_1 is charged again to repeat the process. The filter may be thought of as a low-pass filter which passes direct current but greatly attenuates the alternating currents.

To make a mathematical analysis feasible, certain simplifying assumptions are necessary:

(1) The transformer and filter-inductor resistance is zero. The tube resistance is zero when it is conducting.

(2) The leakage reactance of the transformer is zero.

(3) Both filter capacitors have the same capacitance.

The errors caused by the first of these assumptions will be corrected for in a manner to be described.

Two equivalent circuits were used as shown in Fig. 2. When the tube is conducting Fig. 2A applies, while Fig. 2B should be used when the tube is not conducting. The equations for the currents and voltages in the circuits were set up and then solved by the use of the steady-state operational calculus. The solution showed that the tube conduction angle γ of one tube depends only on the two independent variables $\omega^2 LC$ and ωCR where ω is

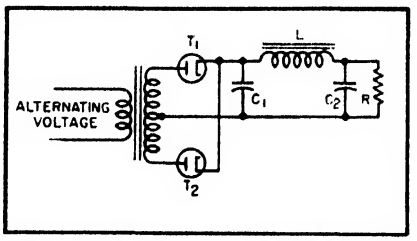

FIG. 1—Schematic circuit of the rectifier and filter

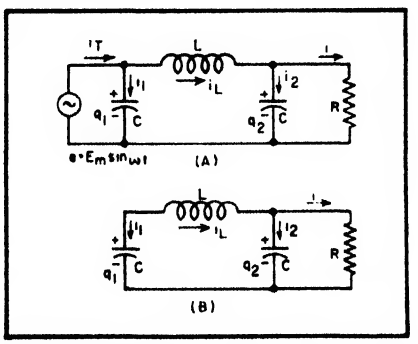

FIG. 2—Equivalent circuits of the rectifier and filter. (A) tube conducting; (B) tube not conducting

2π times the supply frequency. L is the inductance in henries of the filter inductor, C is the capacitance in farads of one filter capacitor, and R is the resistance in ohms of the load resistor. The variable ω^2LC may also be regarded as the ratio of the reactance of the filter inductor to the reactance of one filter capacitor, while ωCR is the ratio of the load resistance to the reactance of one filter capacitor. The solution showed furthermore that all characteristics of this rectifier circuit depend on these two variables alone.

Filter resonance seems to occur at $\omega^2LC = 0.5$, for then the sum of the reactances of the two filter capacitors and of the inductor is zero. This assumes that the reactances are calculated at the fundamental ripple frequency which is twice the supply frequency. The problems of practical importance at present always have ω^2LC greater than 0.5 and for this reason it was decided to use 0.6 as the lowest value of ω^2LC.

Two special cases of the general solution were considered separately because of the significance of the results. The first of these is that for ω^2LC infinitely large which implies that the filter inductance is infinitely large and that the current through the inductor has zero ripple.

The other special case might be called the non-cutoff or the continuous-current case in that each tube is conducting 180 degrees and the current entering the filter never cuts off or drops to zero. The current in each tube is stopped by conduction starting in the other tube, and a form of commutation between the tubes is set up in which the current switches from one tube to the other and back again.

The main problem for this second special case is not that of finding γ which is known to be 180 degrees, but that of finding the boundary or dividing line between the cut-off or pulse-current and non-cut-off or continuous-current cases. In the analysis it was found that the boundary occurred at approximately $\omega CR = 0.6$ with the continuous-current case occurring for smaller values of ωCR and the pulsed-current case for larger values of ωCR.

The characteristics of the circuit that are of the most use in the design of the circuit and predetermining its properties are the tube angles, the average output voltage, the ripple, the peak and average tube currents, and the peak inverse voltage on the tubes.

The angle γ during which the tube conducts is presented in Fig. 3 as a function of ω^2LC for various values of ωCR. For a fixed value of ω^2LC this angle varies from zero degrees at open circuit (ωCR infinitely large) to 180 degrees for the continuous-current case which includes values of ωCR from approximately 0.6 to zero (short circuit). With ωCR fixed, the angle γ varies little for values of ω^2LC above ten, but for ω^2LC less than ten the variation is considerable, especially as filter resonance is approached ($\omega^2LC = 0.5$).

The angle β at which the tube stops conducting is presented in Fig. 4 and the manner of variation is similar to that for angle γ. For a fixed value of ω^2LC, angle β varies from ninety degrees at open-circuit to 180 degrees for values of ωCR from approximately 0.6 to zero (short circuit). The angle α at which the tube starts conducting may be found by the use of the relation, $\alpha = \beta - \gamma$. Increasing the load of the rectifier circuit has the effect of increasing both angles β and γ, while α is decreased. The effect of approaching resonance in the filter is similar in that angles β and γ are increased, while α is decreased.

One of the most important characteristics of a rectifier circuit is the average output voltage. This voltage may be obtained from the ratio of the average output voltage to the maximum value of the sinusoidal voltage across one-half of the transformer secondary, E_{dc}/E_m. The ratio E_{dc}/E_m is given in Fig. 5 as a function of ω^2LC for various values of ωCR. For a fixed value of ω^2LC, the ratio decreased from a maximum of unity for ωCR infinitely large (open circuit) to 0.637 for ωCR equal approximately to 0.6. For values of ωCR from 0.6 to zero (short circuit) the continuous-current case applies, and $E_{dc}/E_m = 0.637$. The voltage ratio E_{dc}/E_m varies little for large values of ω^2LC, but changes considerably as ω^2LC approaches the resonance value of 0.5. Both increasing the load and approaching filter resonance have a similar effect, that of making the voltage ratio approach 0.637.

The ripple voltage across the load resistor of the rectifier circuit is another important characteristic. It may be obtained from the percent ripple r which is defined as 100 times the ratio of the effective value of the fundamental ripple voltage appearing across the load resistor to the average voltage E_{dc} across the same resistor. In practice only the fundamental ripple voltage is sufficiently large to warrant consideration, and for a full-wave circuit, the fundamental ripple frequency is twice the supply frequency.

For large values of ω^2LC and ωCR it was found possible to give a partly empirical and partly theoretical expression for the percent ripple across the load resistor. This is

$$r = \frac{31.5 + 67.25\,\omega^2LC}{(\omega^2LC)\sqrt{4\,(\omega^2LC)^2 + (\omega CR)^2\,(4\,\omega^2LC - 1)^2}} \qquad (1)$$

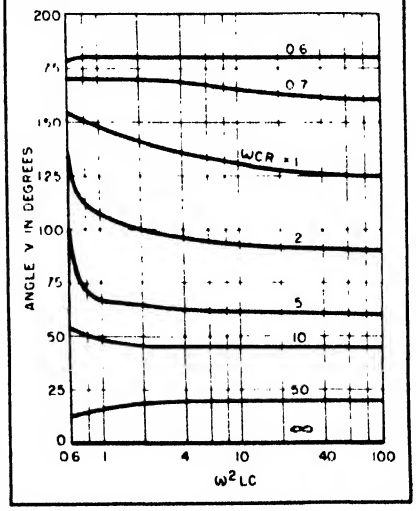

FIG. 3—Angle during which the tube conducts

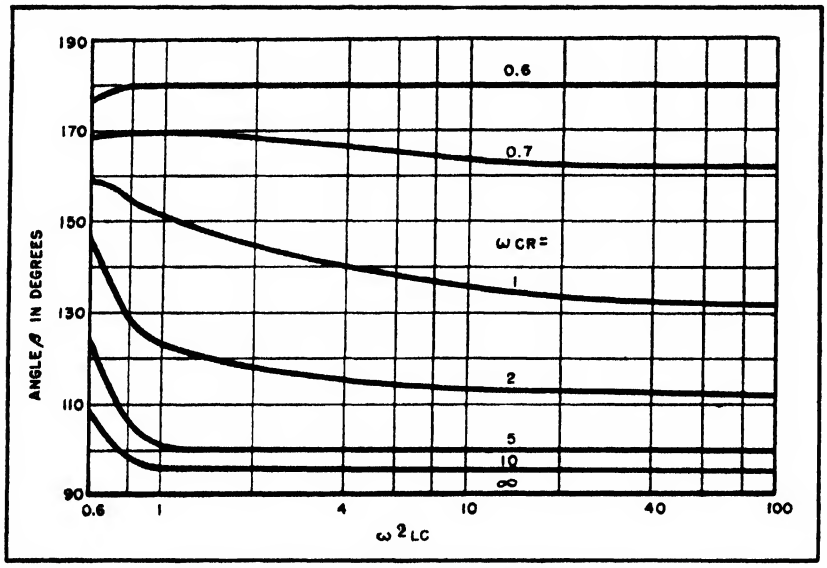

FIG. 4—Angle at which the tube stops conducting

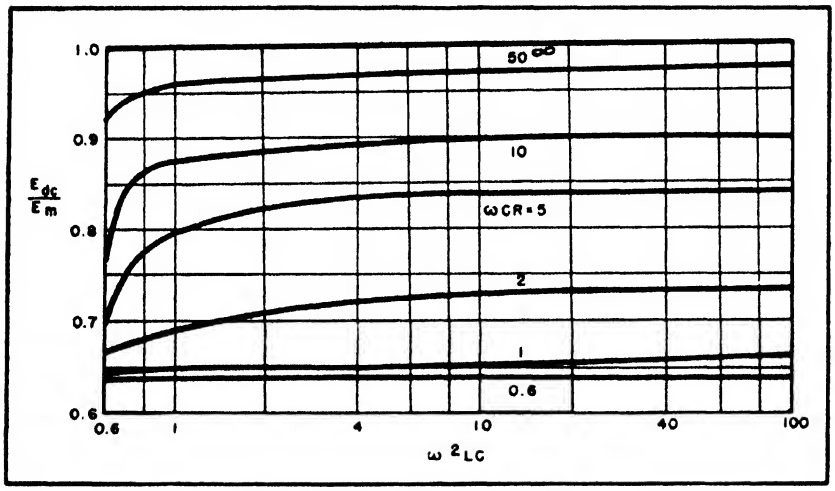

FIG. 5—Average output voltage

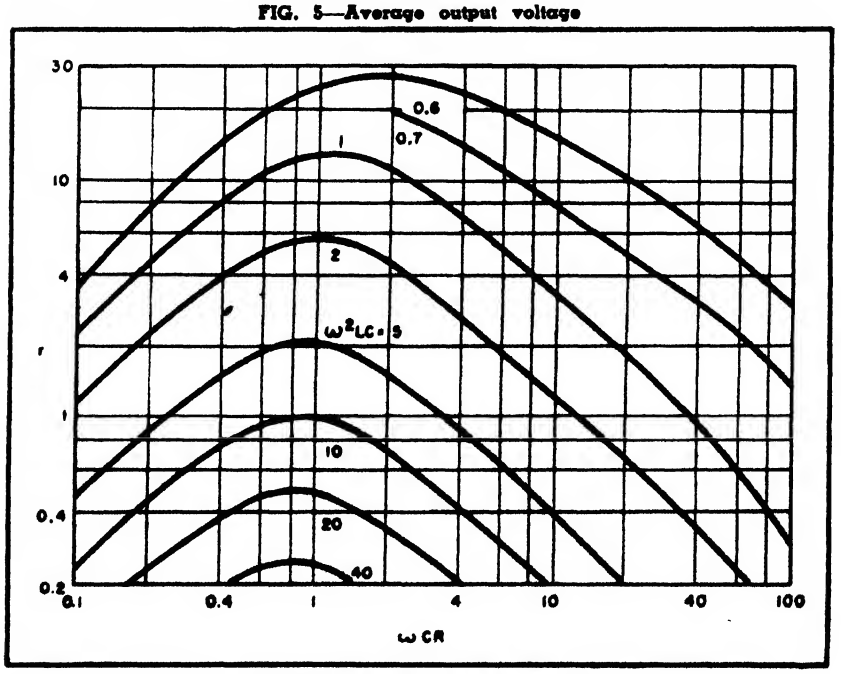

FIG. 6—Percent of ripple voltage

and the error in the percent ripple will be less than five percent if $\omega^2LC \geqq 2.0$ and $\omega CR \geqq 5.0$.

Equation 1 will be applicable in many of the problems encountered in practice, particularly those in which the circuit is lightly loaded. It expresses the percent ripple for the region where each tube is firing only a short time, the output voltage is high, and the charges on the filter capacitors do not vary much during one cycle.

For heavier loads, the percent ripple is shown as curves in Fig. 6. For ω^2LC constant, the ripple increases from zero for ωCR approaching infinity (open circuit) to a maximum in the vicinity of ωCR equal to unity and then approaches zero again as ωCR approaches zero (short circuit). For a fixed value of ωCR, the percent ripple increases from zero for ω^2LC approaching infinity (infinitely large inductance) toward a maximum as ω^2LC approaches 0.5 (filter resonance). For very heavy loads ($\omega CR < 0.6$) the continuous-current case applies and the percent ripple r is given by

$$r = \frac{47.14\ (\omega CR)}{\sqrt{4\ (\omega^2LC)^2 + (\omega CR)^2\ (4\ \omega^2LC - 1)^2}} \qquad (2)$$

The percent ripple approaches zero as ωCR approaches zero (short circuit) because most of the ripple voltage appears across the inductor and very little of it appears across the output load resistor, while all of the average voltage appears across the load resistor.

The peak tube current may be obtained from the ratio P_T of the peak tube current to the average current for one tube. An empirical equation was fitted to the calculated values of P_T and this equation is

$$P_T = 5.016\ (\omega CR)^{0.4655} \qquad (3)$$

where $\omega CR \geqq 0.6$. For values of ωCR from 0.6 to zero, P_T varies from four to a minimum of two.

The inverse peak voltage applied to each tube is always the maximum value of the transformer secondary voltage.

The circuit was set up to obtain experimental verification of the foregoing calculated results. Measurements were made with a sixty-cycle source of alternating voltage

and with a filter having $\omega^2LC = 2.0$. This value of ω^2LC was chosen so that a large range of ωCR could be obtained. Filters with other values of ω^2LC were also used with good agreement.

Various quantities such as average output voltage, ripple voltage, and the tube angle γ were measured. Figure 7 shows the calculated and experimental results for the average output voltage ratio with the calculated results shown as a solid curve and the experimental points as circles. Agreement is good except for low values of ωCR which correspond to heavy loads.

For heavy loads the resistance of the rectifier tube, transformer, and filter choke become appreciable in comparison to the load resistance. These resistances were measured and were added to the load resistance to give an equivalent load resistance. The tube resistance was taken as the voltage across the tube at rated current divided by the rated load current of the tube. The average output voltage is then the product of the average output current and the equivalent load resistance.

The new value of ωCR is increased since the equivalent load resistance is larger than the load resistance alone. The resulting compensated experimental values are shown as crosses in Fig. 7, and the agreement between the experimental points and calculated curve is quite good even for heavy loads (small values of ωCR).

Similar results for the percent ripple are shown in Fig. 8. Since the percent ripple is inversely proportional to the average output voltage, the compensated values of percent ripple are smaller than the uncompensated ones. Again agreement between the calculated curve and the compensated experimental points is good.

The peak tube currents will be somewhat in error for high values of ωCR even though compensation is used. Equation 8 will give somewhat high values of peak currents in this case.

One very common design problem is that in which the maximum ripple, the load current and voltage,

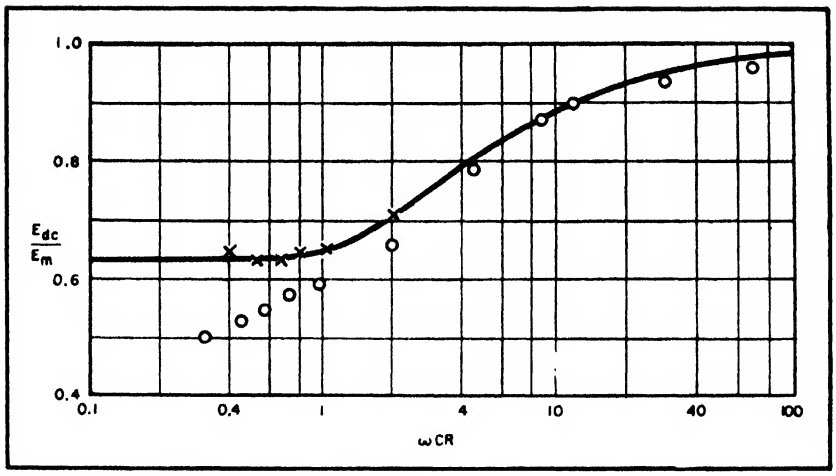

FIG. 7—Average output voltage for $\omega^2LC = 2.0$. The solid curve is calculated, the circles are uncompensated experimental points, and the crosses are compensated experimental points

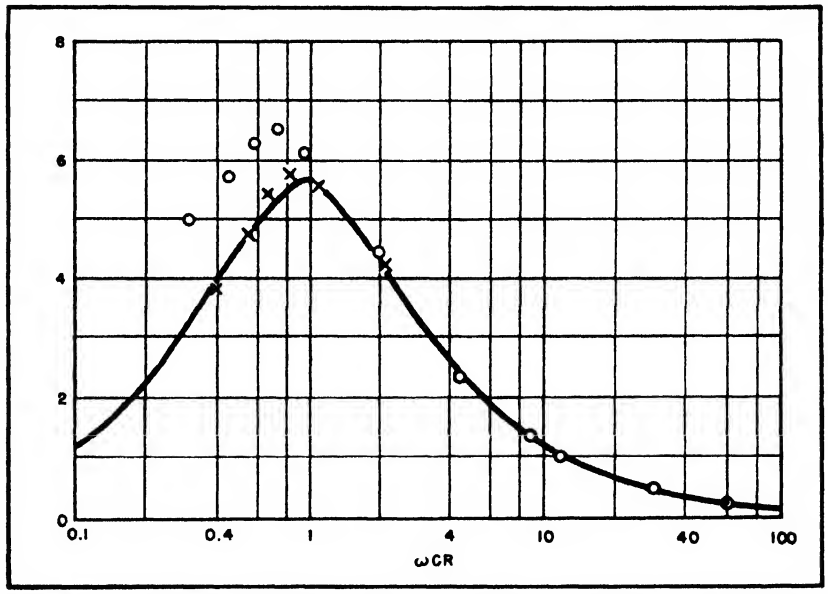

FIG. 8—Percent ripple voltage for $\omega^2LC = 2.0$. The other conditions are the same as illustrated in the graph of Fig. 7

and input alternating voltage and frequency are known and the filter components, tube and transformer are to be selected. If a size of filter capacitor is selected, ωCR may be calculated. From the ripple characteristics of Fig. 6 the value of ω^2LC may then be selected to give the maximum permissible ripple. The inductance necessary may then be obtained from ω^2LC. If an inductance of this size is not available, a different value of capacitance C should be selected and the whole procedure repeated.

Once the values of ωCR and ω^2LC have been obtained the secondary voltage of the transformer may be found from the average voltage characteristics of Fig. 5. The tube or tubes may be selected by the use of Eq. 3. If the tube, transformer, and choke resistances are appreciable, they should be taken into account.

References

(1) F. E. Terman, "Radio Engineer's Handbook", First Edition, McGraw-Hill Book Co., Inc., 1943, p 602-605.
(2) M. B. Stout, Analysis of Rectifier Filter Circuits, *Trans. A.I.E.E.*, 54, p 977, Sept. 1935.
(3) R. G. Mitchell, Vacuum Rectifiers Working with Condenser Input, *Wireless Engineer*, 20, p 414, Sept. 1943.
(4) D. L. Waidelich, The Steady-State Operational Calculus, *Proc. I. R. E.*, 34, p 78, Feb. 1946.

Thermionic Rectifier Circuits

Circuit and performance data for five d-c power supplies operating from a 115-v 60-cps line: a gas-tube bridge circuit delivering 9 amp at 90 v; three transformerless B supplies having high current ratings; a simple high-voltage bridge rectifier for cathode-ray tubes

By RICHARD C. HITCHCOCK

THE PURPOSE of this article is to give details and performance characteristics of five rectifier tube circuits which have proven satisfactory in use over a period of several years.

The electronic circuits proposed are mainly adaptations of well-known theory[1,2,3] but emphasis is placed on four points; (1) the use of inexpensive tubes and components; (2) the attainment of relatively high current output; (3) light-weight construction, making for portability; (4) operation from 115-v, 60-cps source of power.

One power supply employs four argon charger-type tubes in a bridge circuit whose input connects directly to the a-c line, and will supply 9 amp at 90 v d-c It can supply d-c equipment having 110 v nominal rating, and is particularly suited for operation of arc-lamps, electrolysis, etc. Three transformerless B supplies include a half-wave rectifier connecting directly to the a-c line and delivering 400 ma at 90 v; a half-wave doubler providing one common connection between a-c line and d-c load and delivering 130 ma at 150 v; a full-wave doubler giving 200 ma at 180 v. Finally, an eight-tube bridge circuit is represented that has proved satisfactory for obtaining 2000 v d.c. at 250 ma. It uses receiver-type tubes in an unorthodox design—a simple and economical means of supplying a cathode-ray tube.

Gas-Type High-Current Rectifier

Since a d-c arc gives about four times the light output when operated on d-c as on the same current from an a-c source it is advisable to provide d-c operation.[4] A bridge circuit originally designed to supply d.c. for a carbon arc is shown in Fig. 1. Six-ampere bulbs having high crest inverse voltage and high d-c output voltage suitable for this circuit are: Westinghouse Style No. 289416 and General Electric Cat. No. 189049. (Not all 6-ampere charger bulbs have the proper operating characteristics for this circuit).

A multiple-winding filament transformer is needed; two of the secondaries supply a single filament each (2.2 v at 18 amp), and the third feeds two filaments in parallel (2.2 v at 36 amp). The a-c line goes directly to the tubes without a transformer. Note that the d-c output cannot be grounded.

To start this circuit, the main switch is closed first. The load switch is closed after the filaments are up to operating temperature. This procedure is necessary because gas-filled tubes with oxide-coated filaments must not have plate voltage applied when cold. In the completed unit shown in the photograph, a "mark time" switch is employed; one SPST switch closes immediately, and a second SPST switch closes after a 45-sec interval.

Two fuses are shown in Fig. 1. The load fuse should be chosen to permit the desired load current to flow (not more than 12 amp) and the main fuse should be somewhat higher in rating since it must also supply current for the filaments. The purpose of using two fuses is to be sure that an overload will blow only the load fuse, while the filaments still remain heated by the transformer. An inexpensive bimetal circuit breaker was used in place of the load fuse.

The smoothing choke must have low resistance and fairly high inductance, considering that the current passing through it saturates the core. The unit used has an inductance of 0.04 h at 60 cps with its

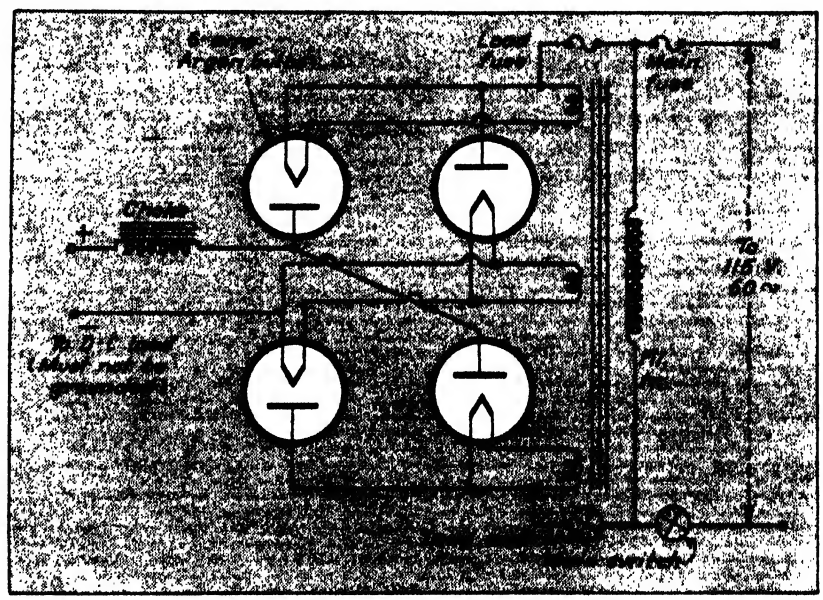

FIG. 1—Schematic diagram of high-current rectifier circuit, using four gas-type tubes to provide d-c outputs up to 9 amp at 90 v

core (0.0036 h without core) and a d-c resistance of 0.5 ohm, obtained with a coil having 490 turns of No. 12 B & S dcc wire. Coil dimensions are 1.63 in. inside diam, 3 in. outside diam and a length of 6 in. Core dimensions are 1.063 in. diam and a length of 18 in., obtained with 350 pieces of 0.05-in. diam soft iron wire.

A convenient advantage of rectification with this circuit is that an impedance may be placed in series with the load fuse to reduce the d-c output. This impedance effectively reduces the d-c output without wasting power, as would be the case with a series resistor. A range of inductance values ove ra 11:1 ratio may be obtained by inserting or removing the core from the choke.

Still greater flexibility of operation may be obtained through the use of two identical coils and cores. In the first coil the core is fixed for use as the d-c filter choke of Fig. 1. The second coil, arranged with a movable core, is connected in series with the load fuse as an a-c impedance. When the circuit is used to supply an arc lamp it has been found possible to put most of the reactance in the a-c side, and to use only a low resistance in the d-c part of the arc circuit.

Porcelain mogul sockets are needed for the 6-ampere bulbs. Due to the high operating temperatures of these bulbs, the use of flameproof or asbestos-covered wire is recommended for connections.

The characteristics of this gas-type high-current rectifier are shown in Fig. 2. The dashed load lines are for 8, 10, 20, and 40 ohms, about one-fifth the weight of a motor-generator of equal capacity.

Circuits using single 25Z5 and 25Z6 tubes are well known[5]. Often such circuits use a resistance in series with the heater for operation while the three solid lines are for a-c input voltages of 100, 110, and 120 v. From these curves we see that with 110 v. a-c input and a load of 8 ohms, the d-c output is 10 amp and 80 v.

The total weight of the unit, including the steel cabinet, is 39 lb—

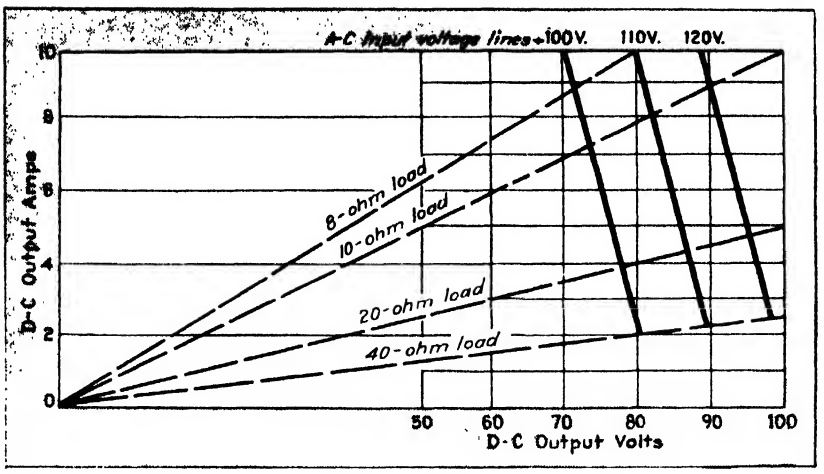

FIG. 2—Operating characteristics of high-current rectifier circuit of Fig. 1

directly from the 115-v line. However, the circuits of Fig. 3, 4 and 5 each use five heaters in series and therefore require no additional series resistor. Only four 25Z5 or 25Z6 tubes are used as actual rectifiers, although five heaters must be used in series across a 115-volt a-c line. Of course, one heater may be replaced by an 83-ohm resistor.

A single tube—the 117Z6GT—may also be used with these circuits. This is a two-cathode, two-plate tube with a 117-v heater element[6], requiring no series resistor on a 117-v line.

A half-wave rectifier which needs no transformers for operation from a 115-volt a-c line is shown in Fig. 3 along with its output characteristics. The d-c side of the circuit is automatically grounded with the a-c supply. For example, if the lower side of the a-c

SUMMARY OF RECTIFIER CHARACTERISTICS

Description	Tubes Used	Transformer Sec. Windings	Circuit in Fig.	Typical D-C Output	Notes
High-current gas-type full-wave bridge	Four 6-amp Rectigon or Tungar	3 Fil.	1	90 v, 9 amp	Neither side of d-c output can be grounded
Half-wave	Four 25Z5 or 25Z6	None	3	90 v, 0.4 amp	One side of d-c output is grounded by grounding a-c line
Full-wave doubler	Four 25Z5 or 25Z6	None	4	180 v, 0.2 amp	Neither side of d-c output can be grounded
Half-wave doubler	Four 25Z5 or 25Z6	None	5	150 v, 0.13 amp	One side of d-c output is grounded by grounding a-c line
High-voltage bridge rectifier	Eight 80	8 Fil. 1 Plate	7	2500 v, 0.25 amp.	Either side of d-c output can be grounded. For 5Z3 tubes, output current is 0.45 amp

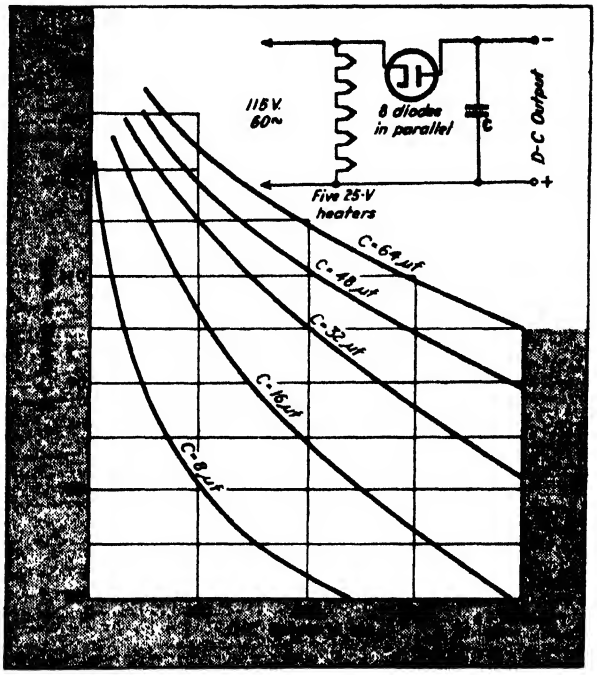

FIG. 3—Half-wave transformerless rectifier circuit using four 25Z5 or 25Z6 tubes, with operating characteristics

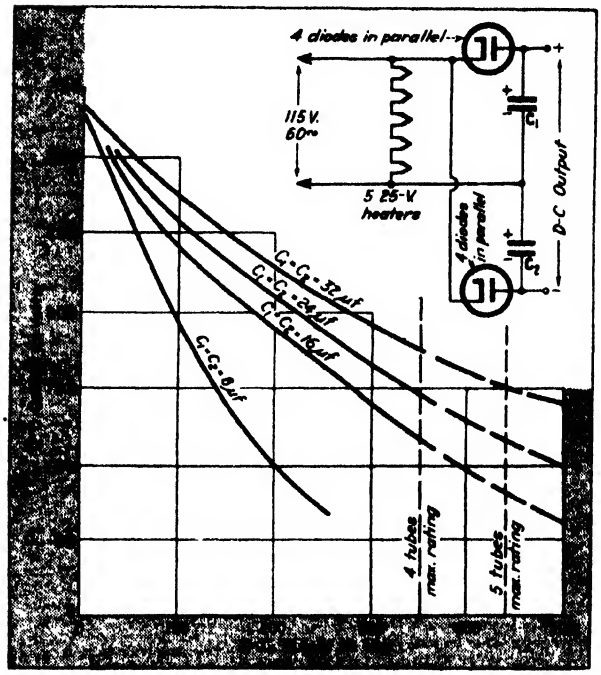

Fig. 4—Full-wave voltage-doubler rectifier circuit and performance characteristics. Output terminals cannot be grounded

supply in Fig. 3 is grounded, the negative d-c terminal is also grounded. Note that all eight of the plates and all eight of the cathodes (2 each per tube) in Fig. 3 are connected in parallel.

Comparing the half-wave circuit of Fig. 3 with the full-wave voltage doubler circuit of Fig. 4, it will be seen that the output of the half-wave circuit is less than that of the voltage-doubler circuit, even when using the same total capacitance. The major advantage of a half-wave circuit is that its output becomes grounded whenever the a-c input is grounded. This is important for high-gain amplifiers which do not have interstage transformers, since pick-up voltages must be minimized.

Four tubes are used in the full-wave voltage-doubler circuit[1] of Fig. 4, four cathodes and four anodes (2 tubes) being connected in parallel in each half of the circuit. As in the circuit of Fig. 3, there are five heaters rated at 25 v each in series across the 115-v a-c line, although only four tubes are connected in the rectifier-doubler.

The capacitance marked on each curve in Fig. 4 is half the total capacitance required. For example, the 24-μf value at 100 and 500 ma means that two 24-μf capacitors are needed. Also note that the maximum output rating for 4 tubes is 350 ma.

If electrolytic capacitors are used in the circuit of Fig. 4, they must be polarized as shown. It is impossible to use a dual electrolytic of the 16-16-μf type if the negative leads are common. Such a dual capacitor can of course be used as a single 32-μf unit, in series with a similar one correctly connected.

Half-Wave Doubler Circuit

A half-wave doubler circuit[2, 7] in which one side of the a-c input is connected to one side of the d-c output is shown in Fig. 5. Capacitor C_1 is rated 150 v d.c., and preferably has a paper dielectric, but C_2 may be either a paper or electrolytic 800-v unit. For light d-c loads C_1 may be a polarized electrolytic capacitor with the negative lead connected to the a-c line. For heavy d-c loads (above about 190 ma at 110 v), the voltage on C_2 reverses, and an electrolytic is not suitable.

The three curves in Fig. 6 permit direct comparison of the three circuits, each of which uses a total capacitance of 48 μf, and four 25Z5 or 25Z6 tubes as rectifiers. In all cases the full-wave rectifier-doubler gives the highest output voltage and current. Of the three circuits, the half-wave doubler has the poorest regulation and the half-wave rectifier has the best regulation.

The choice between the half-wave doubler and the half-wave rectifier may be based either on the required d-c output or the regulation, considering that both have one d-c terminal at the same potential as one a-c terminal. The d-c outputs of these two circuits are equal at 190 ma, 110 v. For lower current values, the half-wave doubler permits higher voltages; for higher output currents, the better regulation of the half-wave rectifier appears advantageous in giving higher output voltage.

In general the vacuum-tube rectifiers are self-protecting to a great extent and require no preliminary heating of their cathodes, so that the circuits of Figs. 3, 4 and 5 may be connected simultaneously to the d-c loads and the a-c lines.

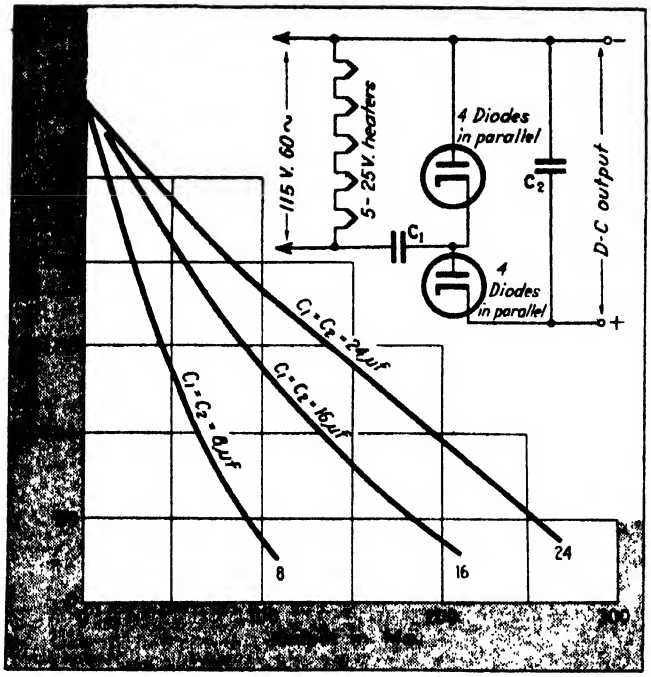

Fig. 5—Half-wave voltage-doubler rectifier circuit and performance characteristics. One side of output can be grounded

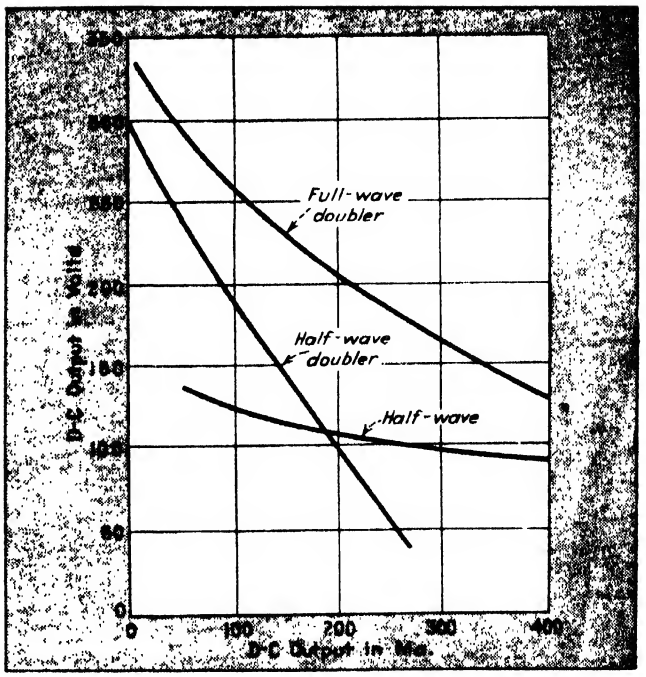

Fig. 6—Comparison of output characteristics of rectifier circuits in Fig. 3, 4, and 5

An eight-tube bridge rectifier using receiving-type tubes is shown in Fig. 7. The output data for this circuit, when type 80 tubes are employed, are given in Fig. 8. A maximum output of 0.450 amp instead of 0.250 amp is possible if 5Z3 tubes are used instead of type 80 tubes. Both filament and plate transformers are needed for this circuit, and for experimental use at different voltages, a Variac supplies the plate transformer.

The filament transformer must be insulated for 5,000 volts both to ground and between the various filaments. If type 80 tubes are used, the rating of each of the eight windings is 2 amp at 5 v. Usually such windings can be overloaded, however, for the 5-v, 3-amp filaments of 5Z3 tubes. Tubes 4 and 5 may be connected in parallel to a single secondary of a filament transformer having a double current rating.

While it is normally quite safe to apply plate and filament potentials simultaneously to vacuum tubes, it is perhaps better for this high-voltage device to light the filaments with the Variac set at 0 volts for the plate transformer primary. The primary voltage can then be increased until the desired output is reached. A radio-type transformer is used, the secondary being a 2,000-v winding with a center tap which is not needed for this circuit.

An essential part of the circuit of Fig. 7 is the use of eight resistors, *R*, which parallel each rectifier tube. These are 0.5-meg, 2-w carbon units. They serve the important function of dividing the back emf evenly among the tubes. In the forward direction those resistors are largely shunted out by the conductance of the tubes.

Output characteristics are shown in Fig. 8. The dashed lines indicate load resistances of 5,000 to 50,000 ohms. The curved lines are the a-c voltages which are impressed on the primary of the plate transformer as indicated. For instance, with 80 v a-c impressed on the primary, this curve shows that an output of 150 ma at 1,500 v is available with a 10,000-ohm load.

The weight of the eight-tube bridge rectifier is 98 lb. All capacitors are oil-impregnated paper units rated at 3,000 v.

The eight tube sockets may be

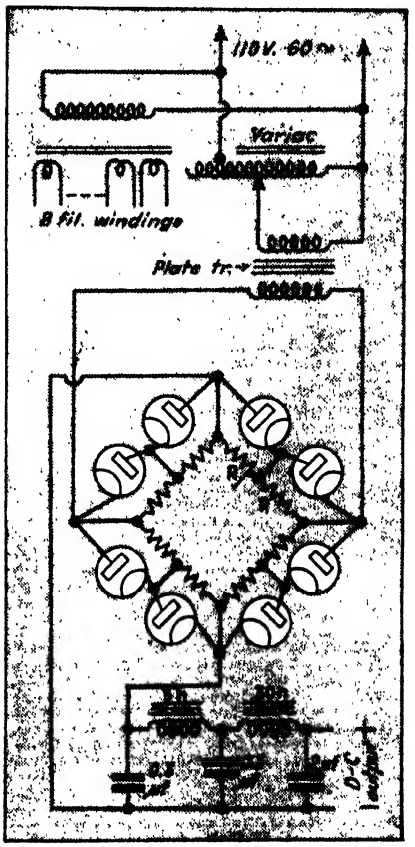

Fig. 7—High-voltage bridge rectifier circuit, using eight receiver-type tubes (type 80 or 5Z3) to provide maximum direct voltage of 2500 v with ample current for cathode-ray tube applications and experimental laboratory use

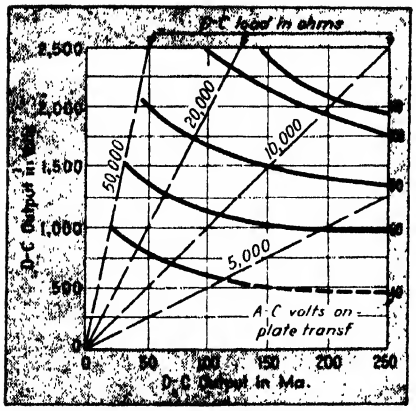

Fig. 8—Operating characteristics of high-voltage bridge rectifier circuit of Fig. 7

mounted on an insulating ring in the center of which is the filament transformer, allowing convenient, short leads. To be safe at the potentials used, auto ignition cable is suggested. Isolantite rods support the insulating ring from the metal panel on which all components are fastened.

A miniature switchboard-type voltmeter and ameter may be connected in the d-c output. A 5-ma (full scale) meter calibrated in volts is used in series with an external multiplier of eight 2-watt, 75,000-ohm units. This voltmeter and series resistor also serve to discharge the stored energy in the filter capacitor when the circuit is OFF.

REFERENCES

(1) Waidelich, D. L., The Full-Wave Doubling Rectifier Circuit, *Proc. I R E*, 554 558, Oct. 1941.
(2) Waidelich and Gleason, The Half-Wave Voltage-Doubling Rectifier Circuit, *Proc. I R E*, 535-541, Dec. 1942.
(3) Waidelich, D. L., Voltage Multiplier Circuits, ELECTRONICS, p. 28–29, May 1941.
(4) Gage, S. H., and Gage, H. P., Optic Projection, p. 68, Comstock, Ithaca, N. Y., 1914.
(5) *RC14 Receiving Tube Manual*, p. 26, p. 169, RCA Mfg. Co., Harrison, N. J. 1940.
(6) Ref. (5), p. 254.
(7) Ref. (5), p. 26, Fig. 38.
(8) K. Henney (Editor) "Radio Engineering Handbook," p. 501, McGraw-Hill Book Co., 3rd Ed. 1941.

Voltage-Regulated Power Supplies

A nonmathematical solution is traced from simplified theory. Actual values of circuit elements necessary to build a power pack and three-tube control are computed. Practical suggestions are given for physical layout and elimination of ripple

By PAUL KOONTZ and EARLE DILATUSH

SIMPLY stated, the action of a voltage regulated power supply is to cancel any attempted fluctuation of its output voltage whether caused by input (line) change, or output (load) change. One way to become familiar with the regulating action of this circuit upon input variations is to trace the path of the supply ripple. In the usual power supply, this disturbance consists mainly of 120-cycle sine-wave a-c, with amplitude from a fraction of a volt to several volts. In Fig. 1, this voltage appears across points A and B, and produces a flow of current through V_1 (whose initial action is that of a diode) and R_1. A portion of the voltage drop across R_1 caused by this current is applied as bias to the control grid of the amplifier tube V_2. Since V_3 holds the cathode of V_2 at a fixed point above ground, V_2 amplifies this variation, causing it to appear in inverted form across the load resistor R_2. Since R_2 also serves as the bias resistor for V_1, it produces through V_1 an inverted version of the original ripple current. Because this and the original ripple are approximately equal but opposite in phase, cancellation occurs, giving as the end result an almost ripple-free output across C and B. A similar cancellation is produced by any attempted fluctuation of input voltage to the regulator.

Attempted output voltage changes caused by load variations are similarly cancelled because they, too, are applied to the grid of the amplifier tube V_2.

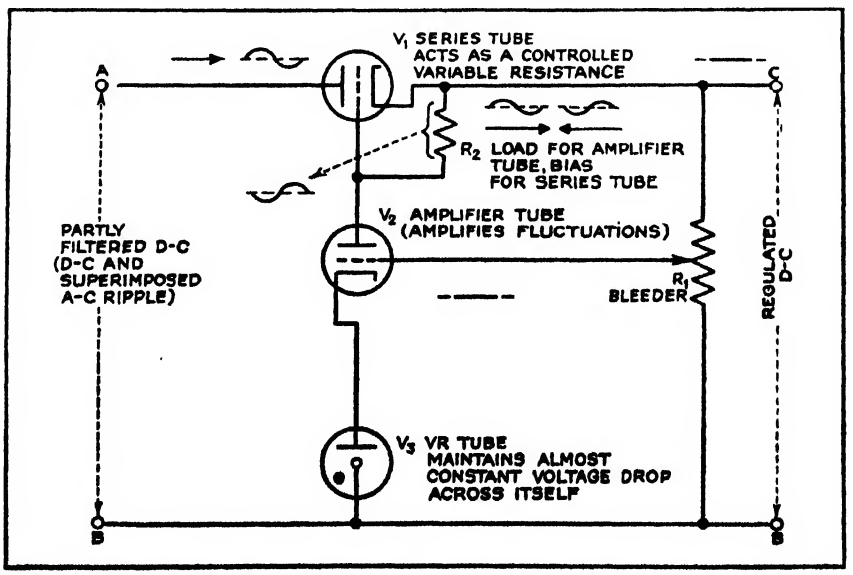

FIG. 1—Fundamental elements of a voltage-control designed to follow a conventional rectifier

It was assumed above that the grid of V_2 is the sole means of control. That is, that the change voltage applied to it by R_1 is the only acting control voltage, and that the grid of V_2 is the only point to which control voltage is applied. A complete analysis presents quite a different picture. Not only are other control voltages present, but they are introduced at several different points in the circuit.

Variations of the unregulated supply voltage can act as a control source when applied to any of the amplifier tube elements. When the screen of V_2 is fed by a bleeder from the unregulated supply as in Fig. 2, the variations of that supply voltage appear across the screen-to-cathode impedance of V_2 and are amplified by the screen which acts like a low-gain control grid. This control-effect produces across R_2 a voltage of the proper phase to effect cancellation of the input changes, but of an amplitude that is normally much greater than that needed for cancellation.

Similarly when V_1 is fed by a bleeder from the unregulated supply, a portion of the variation in that supply appears across V_3, which forms the cathode circuit of V_2. Hence V_2 has impressed on its cathode (in series with its grid return) a portion of the input change. The amplitude of these changes depends on the effective impedance of V_3, which is usually from about 200 to 1,000 ohms. The effect of these changes opposes that caused by the grid and screen controls.

The impedance of V_3 also causes the introduction of another voltage into the grid return of V_2. This additional control voltage, resulting from variations of the plate and screen current of V_3, acts degeneratively to reduce the gain of V_2.

Evaluation of Control Factors

The effectiveness of the control action of the grid may be expressed in its simplest form as

$$\text{Resultant fluctuation of the supply output} = \frac{\text{Attempted excursion}}{\text{Gain of the amplifier stage}} \quad (1)$$

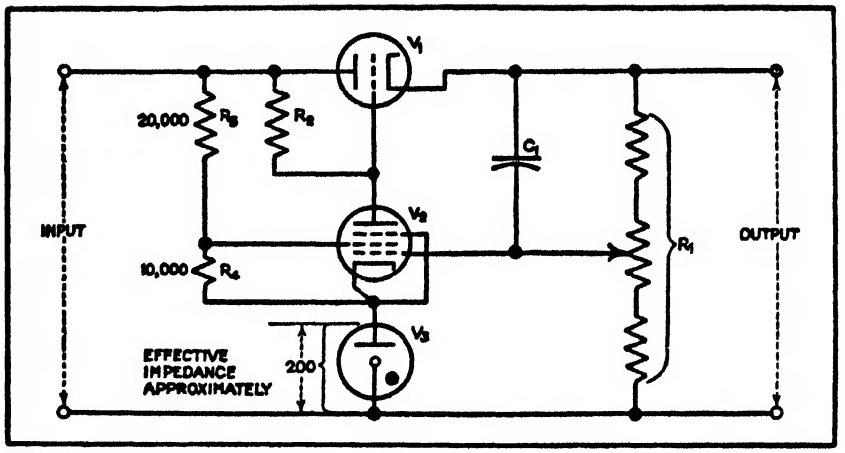

FIG. 2—A voltage-control circuit in which several elements of the control tube are fed from the unregulated input

The effect of the screen control, in the absence of grid control, may be stated as

$$\text{Resultant fluctuation of the supply output} = \text{Difference between (a) [attempted fluctuation] and (b) [portion applied to screen times screen gain]} \quad (2)$$

The composite output fluctuation, resulting from both grid and screen control may be found by considering the result obtained from Eq. 2 as the attempted excursion in Eq. 1.

$$\text{Resultant fluctuation of the supply output} = \frac{\text{(Original excursion) minus (portion applied to screen times screen gain)}}{\text{Gain of amplifier stage}} \quad (3)$$

For the moment, let us assume that the resultant fluctuation in Eq. 3 equals zero. In this event, the final fluctuation on the output is equal to that value which produces at the grid of V_2 an exact duplicate of the voltage present on the cathode.

$$\text{Resultant fluctuation of the supply output} = \text{Voltage on output which produces at the grid of } V_2 \text{ a change voltage duplicating that on the cathode.} \quad (4)$$

In the average power supply, the grid, in spite of the other controls, is able to reduce any ripple presented to it to a value comparable to that existing on the cathode. This is true even though the screen overcompensates in the usual case. The value existing on the cathode will vary widely when different V_2's of the same type are substituted in the same chassis. Conventional design for a supply furnishing an output of 250 to 300 volts d-c produces a ripple content of approximately 0.04 v rms. The d-c regulation is usually maintained within about ±2 volts.

Before designing any regulated supply, it is of prime importance to list the actual demands to be made on it. Instantaneous peak current demand (as distinguished from maximum average current demand) is probably first in importance. These supplies are not reservoirs, hence lose both control and effectiveness when subjected to any instantaneous load even slightly beyond their rated capacity. The frequency of demand is unimportant, however, if it lies below approximately 20,000 cycles per second. Above this frequency the effective impedance of the supply increases rapidly because of the inability of tube V_3 in the amplifier cathode circuit to regulate. A rise in supply impedance can be counteracted by shunting a paper capacitor of 1 or 2 microfarads across the regulated output. When this capacitor is in-

cluded, the supply can be used to feed equipment calling for microsecond pulses of high amplitude.

Selection of the output voltage to be provided is also important. To reduce the cost of components, an output range of 250 to 300 v is favored, when that is adequate for the equipment being fed. Higher output voltages are easily produced, but require more expensive components. A wide range of output voltage adjustment should also be avoided unless there is a specific need for it. The usual dependability of domestic supply lines makes it unnecessary to provide against large line voltage changes.

Design of Supply Section

For design purposes, supply and control circuits can be considered separately. The supply portion, as considered here, consists of the components shown in Fig. 3. This circuit differs from an ordinary unregulated power supply only in the addition of V_1, which may for the moment be considered as a variable series resistance introduced for control purposes.

To illustrate design procedure a set of requirement limits has been chosen based on commercial ratings for supply components.

The limits decided on are: output voltage, 250-300 v; output current range 75-200 ma; power line fluctuations of ±10 percent.

On the basis of these limits we may now choose the series tube, V_1; the rectifier tube, V_4; the filter choke, L_1; and the power transformer, T_1.

Tubes commonly chosen for series service include 2A3, 6A3, 6B4, 6L6, 6V6, 6Y6, and 807. For our supply the recently introduced 6AS7G, a twin triode expressly designed for this service is chosen. Their extremely low plate resistance allows the use of a lower voltage drop across them, hence a reduced high-voltage winding on the power transformer. The heater-cathode rating of ±300 v makes possible the paralleling of their filaments with that of the amplifier tube. Only two of these tubes are needed because of their current-carrying ability, with a resultant saving of space.

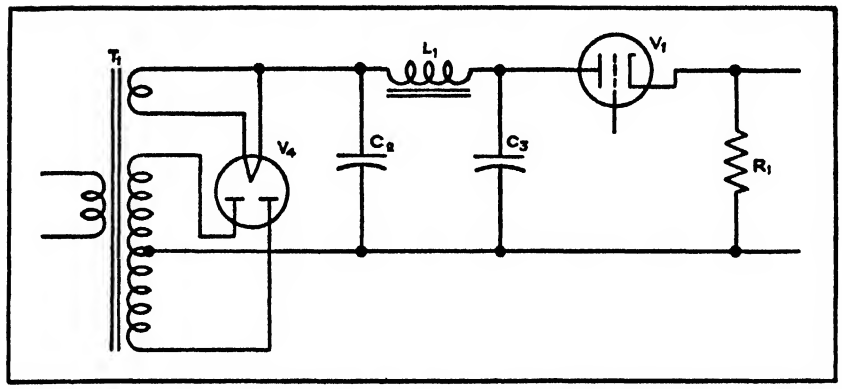

FIG. 3—Supply section of a voltage-regulated power unit with the series tube inserted to illustrate its action

A suitable filter choke will have low internal resistance and adequate current carrying capacity. Inductance rating is of secondary importance. A 5 to 10 henry choke with 50 to 200 ohms internal resistance, and rated to carry at least 225 ma will be satisfactory. The one selected for this example is rated at 5 henries at 225 ma with 100 ohms d-c resistance.

The rectifier selection is easy, for the 5U4G, 5Z3, 5T4, and the 5X4G can all handle the current and voltage requirements. The 5U4G is chosen because of its general availability.

Selecting a Power Transformer

In the selection of a power transformer, we must first determine the voltage needed out of the rectifier. This will consist of the sum of the voltage drops across the filter choke, series tubes, and output load. The use of the following procedure is necessary to determine that voltage:

1—Inspect the characteristic curves of the selected series tube. determine from them the lowest allowable plate voltage for the maximum current specified.

Example: Each side of a 6AS7G will deliver 56 ma at 20 v, so 2 6AS7G's in parallel will provide the required 225 ma total current, including approximately 25 ma current consumed internally by the power supply.

2—Increase the minimum working plate voltage by a sufficient margin to allow for possible component variations. This also is necessary to allow proper control of the series tube, since its bias must swing symmetrically about a center point and never drop to zero.

Example: 20 v plus 20 v margin equals 40 v minimum operating plate voltage.

3—Next determine the minimum voltage allowable at the plates of the series tubes. This is the highest power-pack d-c output voltage plus the voltage determined in step 2. Note that this must be delivered to the plates of the series tubes under the condition of lowest allowable line voltage and highest rated output current of the pack.

Example: 300 v pack output plus 40 v from step 2 = 340 v delivered at 225 ma total drain, and 105 v line input.

4—Add the voltage obtained in step 3 to the IR drop across the filter choke (at full 225 ma current) to find the voltage the rectifier must deliver at lowest line input.

Example: $E = IR = 0.225 \times 100 =$ 22.5 v choke drop. 340 v + 22.5 v = 362.5 v at 225 ma which the rectifier must supply at 105 v line input.

5—Refer to the characteristic curves of the rectifier selected. From them find the input voltage to the rectifier that will produce the output voltage determined in step 4. Be sure to take into consideration the type filter (choke or capacitor input) and the size of its components.

Example: 5U4G, capacitor input filter using 8μf input capacitor. 350 v a-c rms in, equals the required 362.5 v out at 225 ma.

6—Calculate the highest a-c input voltage to the rectifier that will result when the line input voltage is increased to its upper limit.

Example: Voltage ratio of the power transformer equals 362.5/105 or 3.33. 125 v × 3.33 = 416 v a-c out.

7—Again refer to the rectifier tube curves. Determine the d-c voltage out of the rectifier for the a-c voltage into it calculated in step 6.

Example: 416 v in = 435 v d-c out (at 225 ma drain).

8—See what the maximum wattage dissipation in the series tube will be, under the worst operating conditions; that is at maximum current drain, maximum line input voltage and lowest d-c output voltage.

Example: 435 v − 22.5 v choke drop = 412.5 v applied to the series tubes. This, minus 250 v (the lowest output voltage) = 162.5 v across the series tubes. Therefore, since $W = EI$, 162.5 v × 0.225 amp = 37 w total dissipation.

9—Using the maximum a-c input voltage to the rectifier (determined in step 6), and the minimum current drain (set by the limits), inspect the rectifier tube characteristics and find the d-c output voltage for these conditions.

Example: 5U4G, 416 v a-c, 100 ma total drain; the d-c out of the rectifier is 500 v.

This voltage, minus the lowest pack d-c output voltage set by the limits, is the maximum voltage that will appear across the series tubes.

Example: 500 v −10 −250 v equals 240 v maximum across the paralleled 6AS7Gs.

10—If the ratings of the series tubes (maximum wattage and plate voltage) are not exceeded under the conditions imposed by the limits, we may now easily determine the nominal voltage of the a-c high voltage winding on the power transformer, by multiplying its voltage ratio by the nominal line voltage.

Example: 3.33 × 115 = 383—so a rating of 380 v would be satisfactory.

Additional design considerations for the supply section stipulate rectifier tubes having good regulation (low internal voltage drop). If a capacitor input filter is used, the input capacitance should be at least 8μf. When a choke input filter is used a swinging choke is advisable following the rectifier tube.

Standard practice dictates the use of supressors in control grid and plate circuits (screens, too, if used) when series tubes are paralleled for greater current capacity. Their elimination would result in highly unstable or erratic operation. It is preferable that these supressors be mounted with one end directly supported by the tube socket lug to which it connects. Resistance values of 50 ohms for the plate, and 100 ohms for the grid and screen are satisfactory.

The control circuit shown in Fig. 4 is typical. A sharp-cutoff pentode is more suitable than a remote-cutoff pentode for use as the amplifier V_3. Its lower plate current allows the use of a high value of plate load resistance R_2, resulting in higher gain and less degeneration. The highest gain of the amplifier will be obtained when R_2 approaches the plate resistance of the amplifier tube. This suggests a value for R_2 of from 0.5 to 1 megohm.

The voltage reference source is usually a cold-cathode tube of the VR type, although batteries or a neon bulb could be used. Tubes are preferred because of their long life and low effective impedance. High impedances at V_3 will cause an increased ripple output, as well as poorer regulation because of increased degeneration in the amplifier stage. Impedances presented by tubes of the VR type approximate 200 to 1,000 ohms.

Selection of the specific tube for any given application depends on fulfilling the following requirements:

1—The amplifier tube V_3 must be provided with adequate plate voltage over the entire range of operation.

Example: (based on the limits used for computation in the supply section: 250 to 300 v at 75 to 200 ma external drain over 105 to 125 v line input.)

The amplifier plate voltage will be lowest with highest line and lowest output voltage and current—125 v line, 75 ma external drain at 250 v output. Reference to step 9 in the supply section shows 240 v across the 6AS7G's under this condition. Inspection of the characteristic curves for the 6AS7G shows that 130 v bias will be required to limit the current through each section to 25 ma (¼ of the 100 ma total). The voltage between the amplifier plate and ground is the output voltage of the supply 250 v, minus the bias voltage for V_1 130 v; or 120 v. A small voltage must be maintained between plate and cathode of the amplifier tube V_3.

2—The grid of the amplifier tube V_3 should receive as large a percentage as possible of the total fluctuation present on the output. Hence the highest voltage VR tube allowable by step 1 should be used.

Example: A type OC3/VR105 is indicated here.

The bleeder consisting of R_3 and R_4 must supply V_3 at least 8 ma of current, and must maintain the screen of V_3 at a suitable voltage above its cathode.

Example: Lowest unregulated d-c is approximately 340 v (at 105 v line input and 225 ma total drain), therefore the total resistance R_3 plus R_4 will be: (340-105) /0.008 = 235/0.008 = 30,000 ohms.

The section between the screen of V_2 and its cathode (plate of V_3) must have a drop of approximately 60 v for adequate screen supply. Thus R_4 will be: 60/0.008 = 7,500 ohms. This gives suitable values of R_3 and R_4 as 22,500 ohms and 7,500 ohms respectively. Wattage ratings of R_3 and R_4 must allow for the condition of highest unregulated supply voltage (500 v as determined in step 9 of supply). Therefore 500—105/30,000 = approximately 13 ma. Wattage dissipated in R_3 = 0.013 × 0.013 × 22,500 = 3.8 watts.

Therefore R_3 requires a 5 watt resistor. Similarly, R_4 calls for a 2 watt rating. Screen current has been neglected as negligible in these computations.

The amplifier grid bleeder consisting of R_5, R_6, and R_7 can be determined as follows: Its total resistance R_1 should be sufficient to allow the conservative use of small fixed carbon resistors at R_5 and R_7, and a standard potentiometer at R_6. However, if excessively high values are used, V_2 exhibits troublesome hum pickup from its grid wiring.

Example: If 300 v is the maximum pack output, a total suitable bleeder value will be approximately 0.25 megohm.

The necessary resistance values for R_5, R_6, and R_7 will vary with the regulated output voltage of the pack, and while they could be computed, a simpler method for determination is available. Substitute a 0.25 megohm potentiometer for R_1. With the pack operating, adjust the potentiometer to obtain a pack output voltage approximately 10 percent higher than the highest desired output voltage. Disconnect the potentiometer, and record the resistance from arm to positive end. Reconnect the potentiometer and set the pack in operation. Readjust it to give an output voltage 10 percent lower than the lowest desired output voltage. Again disconnect, and record the resistance from the arm to minus end. You now know the values of R_5, R_6, and R_7 that will produce the desired range. To make the resultant values of R_5, R_6, and R_7 fall on commercial resistance values, the total bleeder resistance R_1 may be adjusted upwards or downwards by a factor of plus or minus 25 percent.

Example: R_5, 120,000 ohms; R_6, 50,000 ohms; and R_7, 82,000 ohms for an approximate output range of 220 to 330 v for this particular supply.

The grid coupling capacitor, C_1, which presents a low impedance path to the grid for attempted high and medium frequency changes in the output, is usually about 0.25μf. Larger values, while transferring more of the low (ripple) frequency variations to the grid, may cause undesirable effects due to time lag in their transmission.

Design for Minimum Ripple

A ripple voltage of 0.02 to 0.05 v rms in the output of a standard voltage-regulated power supply is usually satisfactorily low. If troublesome, it may often be reduced by carefully selecting tube V_3 that is used as voltage reference, particularly when the screen and V_3 bleeder are connected to the unregulated supply voltage.

If unusually low ripple must be obtained, the circuit modification shown in Fig. 5 can be used. Analysis of the operation of this circuit will show that the degree of ripple reduction is not limited by the amplifier gain but may be made practically infinite. This effect is accomplished by feeding the screen of the amplifier tube V_2 a controlled amount of the input ripple. The screen, acting as a low-gain control grid, produces across the series tube a voltage equal to the original ripple but of opposite phase. Control of the amount of ripple fed to the screen grid is performed by the 0.5 megohm potentiometer.

The most satisfactory degree of ripple cancellation can be assured by placing the pack in operation with its actual load and an oscilloscope connected across the output. After all other adjustments have been made, the ripple can be cancelled by adjusting the potentiometer.

The degree of ripple cancellation does not depend on the amount of ripple present, and almost complete cancellation can usually be effected with ripple inputs of 50 v or less. One of the supply modifications this suggests is the reduction of the filter components to a single capacitor following the rectifier. Power-pack output ripple of 0.002 v or less can be obtained under these conditions. When a normal filter is used, the residual ripple may be too small to be observed on a sensitive oscilloscope.

Optimum Regulation

Variations in output voltage owing to changing load will be minimized by the use of a low impedance supply to the series tube. The use of a mercury-vapor type rectifier will often give the greatest improvement in that respect.

Any means of increasing the effective gain of the amplifier stage will also improve the regulation. Three schemes advanced for this purpose include: substitution of a constant voltage device (such as

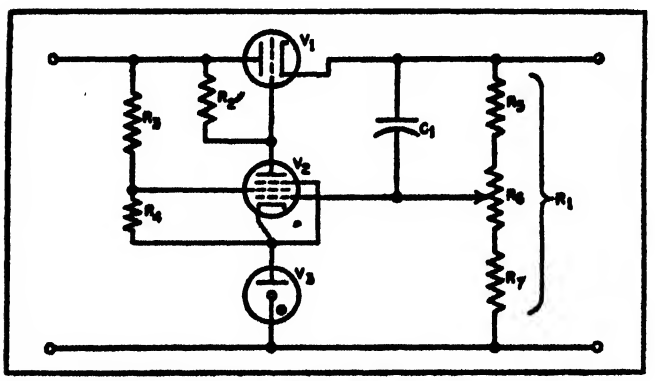

FIG. 4—Control section of a regulated supply. The text describes methods for selecting them

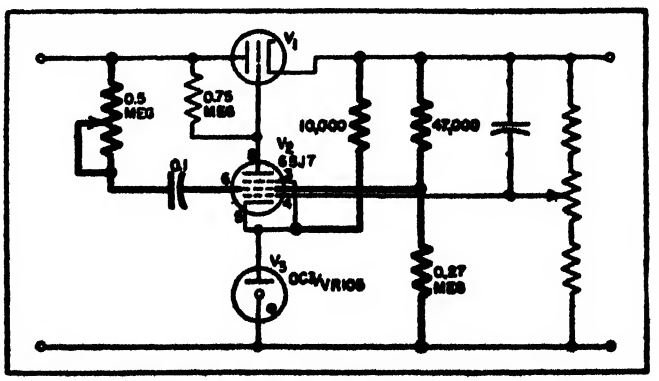

FIG. 5—Modification of the fundamental regulating circuit for extremely low ripple is shown by the heavy circuit lines

neon lamps, VR tubes, or batteries) for the portion of the amplifier grid bleeder between the grid and regulated B+; substitution of a constant current device (such as a pentode tube or inductance) for the portion of the amplifier grid bleeder between grid and B−; the use of a multiple stage amplifier.

Another method of improving regulation is to connect the screen of the amplifier tube to a bleeder from unregulated B+.

Physical Arrangement

Layout of the supply portion follows the established rules for power supplies. To avoid hum pickup by the control section it is desirable to place the entire supply section at one end of the chassis. Thus, no a-c wiring but that for the filaments need be close to the sensitive control circuits.

The series tube placement requires consideration of the problem of heat elimination. Nearly a fourth of the total power consumed by the entire supply is dissipated by the series tubes under some conditions of operation.

The control portion is more demanding in its placement and wiring needs. To realize full benefits from a supply of this type, hum pickup on the amplifier tube wiring must be eliminated. All wires to the grid of the amplifier should be short, and capacitance between them and other wires or chassis reduced to a minimum. The capacitor between the amplifier grid and regulated B+ should be mounted away from the chassis to avoid unwanted capacitance to ground. The voltage adjusting potentiometer should preferably be located on the chassis adjacent to the amplifier tube socket. If panel control is required a shaft extension is preferable to locating it on the panel. Hum pickup from 60 cycles on long leads to this control is often difficult to eliminate. A safe rule to follow is to consider the amplifier tube as an r-f amplifier, and to use appropriate wiring precautions.

An oscilloscope is the only satisfactory means of observing the minute fluctuations present on the output of a voltage-regulated power supply. It is also extremely useful for trouble shooting as well as for measuring the variations present.

Bibliography

(1) W. R. Hill, Jr., Analysis of Voltage Regulator Operation, *Proc. IRE*, Jan. 1945.
(2) F. V. Hunt, and R. W. Hickman, On Electronic Voltage Stabilizers, *Review of Sci. Inst.* 10, p 6.
(3) A. Abate, Basic Theory and Design of Electronically Regulated Power Supplies, *Proc.* IRE, *July* 1945.
(4) G. W. Davis, 0-300 Volt Regulated Power Supply *Radio News*, Sept. 1945.
(5) H. J. Reich, "Theory and Application of Electron Tubes," McGraw-Hill Book Co., p 590.

Multi-voltage Regulated Power Supplies

Two regulated output voltages at extreme values of current are provided by using glow discharge tubes in the proper combination

By J. R. MENTZER

SEVERAL VALUES of stable voltage are often required for the testing of equipment which is normally battery operated. These can be obtained from a conventional power supply by using four standard types of gas-filled voltage regulator tubes, the VR-75, VR-90, VR-105, and VR-150. They make it possible to secure any regulated voltage which is a multiple of 15 volts, up to the nearest multiple of 15 volts below the available output voltage from the power supply filter, which is necessary for ignition.

To obtain the various voltages it is necessary to use the tubes in combinations wherein the voltages across some are added and the voltages across others are subtracted. The problem of getting the desired voltage is one of finding two combinations of 75, 90, 105, and 150 volts whose difference is the desired voltage. Either combination may involve any or all of the four voltages. For example, assume that it is desired to have 165 volts regulated output. This may be obtained by subtracting 75 volts from the sum of 150 volts and 90 volts.

The method of getting the sum of any voltages is to put the tubes in series across the line with an appropriate dropping resistor in series with the tubes. The subtraction of any voltage from this sum is then accomplished by putting the combination of tubes whose voltage total is to be subtracted in series with the load. This is shown in Fig. 1, for an output of 165 volts.

In case more than one voltage output from a given power supply is desired, the method may be extended. Although the problem may be somewhat more complex, depending upon the output voltages de-

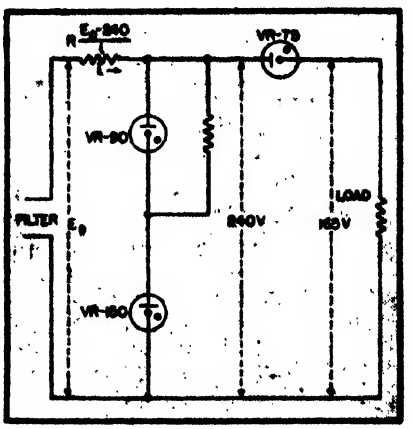

FIG. 1—Simple circuit for providing 165 volts of regulated output

sired, the same procedure can be applied. As an example, it might be desirable to have a power supply to be used for testing equipment which is designed to operate from battery voltages of 135 volts and 45 volts.

The higher voltage may be established by subtracting the voltage across a VR-105 from the sum of the voltages across a VR-150 and a VR-90 in series as shown in Fig. 2. The 45 volts may be obtained by subtracting the voltage across a VR-105 from the voltage across the VR-150 which is in series with the VR-90.

Current Variations

In Fig. 2, more current would normally flow through the VR-90 than would flow through the VR-150, so it is advisable to shunt the VR-90 with a resistor which will carry the excess current at the voltage established across it by the VR tube which it shunts. This equalizes the current operating ranges of the tubes in series.

The load current range for the circuit is determined by the fact that the current through the input series line resistor must be constant to produce the constant drop between the filter output and the two VR tubes in series across the line. As the load currents are caused to vary in any order, the current through the VR-150 must vary by an amount equal and opposite to the algebraic sum of the load current variations. Since the current through the VR-150 must not be less than 5 ma and not greater than 40 ma, the sum of the load current variations cannot be greater than 35 ma.

Although the current range of the single VR-150 sets a limit on the total variation of load current, the magnitude of the load currents available may be increased by shunting the series dropping tubes by suitable resistance. For example, if it is desired to have a load current of 100 ma available at 135 volts and 60 ma at 45 volts, the VR-105 in the 135-volt line should be shunted with a resistor which will carry the current in excess of the rated current through the VR-105.

If 100 ma is the maximum current required at 135 volts, a current well up in the operating range of the VR-105 may be selected. By allowing 30 ma through the tube, the resistor must carry the remaining 70 ma at 105 volts. This would require a resistor of 1500 ohms for shunting the VR-105.

If a current in the VR-105 in the 45-volt line is picked at 30 ma, this would then require a shunting resistor which would carry the remaining 30 ma of load current at 105 volts or a resistance of 3500 ohms across this VR-105. The series dropping resistor would then have to carry the total load current of 160 ma plus the current through the VR-150.

If the 160-ma load current is the maximum load current of a range of load currents, the current in the VR-150 should be of a minimum operating value. This would assure the maximum compensating value of the VR-150 current as it increases with decreasing total load current. Assuming a current in the VR-150 of 10 ma, the total filter current will be 160 ma plus 10 ma or 170 ma.

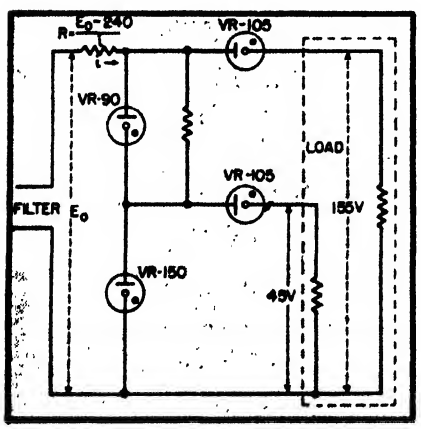

FIG. 2—Two widely different output voltages are provided by this arrangement

Table I—Procedure for Computing Values

Step	Method
1 Compute R_4	$R_4 = \frac{2E_4}{i_{L\max} + i_{L\min} - i_{t\max} - i_{t\min}}$
2 Compute R_3	$R_3 = \frac{2E_3}{i_{h\max} + i_{h\min} - i_{t\max} - i_{t\min}}$
3 Compute i_{R4}	$i_{R4} = \bar{i}_L - \bar{i}_t$
4 Compute i_{R3}	$i_{R3} = \bar{i}_h - \bar{i}_t$
5 Compute R_o	$R_o = \frac{\bar{E}_o - E_1 - E_2}{i_{R4} + i_{R3} + 3\bar{i}_t}$
6 Compute R_1	$R_1 = \frac{E_1}{\frac{\bar{E}_o - E_1 - E_2}{R_o} - i_{R3} - 2\bar{i}_t}$
7 Compute limit on $i_{h\max}$	$i_{h\max} \leqq \bar{i}_h + i_{t\max} - \bar{i}_t$
8 Compute limit on $i_{h\min}$	$i_{h\min} \geqq \bar{i}_h - (\bar{i}_t - i_{t\min})$
9 Compute limit on $i_{L\max}$	$i_{L\max} \leqq \bar{i}_L + i_{t\max} - \bar{i}_t$
10 Compute limit on $i_{L\min}$	$i_{L\min} \geqq \bar{i}_L - (\bar{i}_t - i_{t\min})$
11 Compute upper limit of $E_{o\max}$	$E_{o\max} \leqq (E_1 + E_2) + R_o (i_{h\min} + i_{L\min} + i_{t\max})$
12 Compute lower limit of $E_{o\min}$	$E_{o\min} \geqq (E_1 + E_2) + R_o (i_{h\max} + i_{L\max} + i_{t\min})$
13 Compute Z_{AC} back from high-voltage load	$Z_{hAC} \leqq R_{3AC} + R_{1AC} + R_{2AC}$
14 Compute Z_{AC} back from low-voltage load	$Z_{LAC} \leqq R_{4AC} + R_{2AC}$

$i_{h\max}$ and $i_{h\min}$, respectively, are the maximum and minimum values of the high voltage load current.
$i_{L\max}$ and $i_{L\min}$, respectively, are the maximum and minimum values of low voltage load current.
$i_{t\max}$ and $i_{t\min}$, respectively, are the maximum and minimum rated gas tube operating currents.
Denote the average values of all varying quantities by a bar above the quantity symbol, e.g., $E_{oav} = \bar{E}_o$.
Denote the a-c resistance of a given tube by R_{1C}, e.g., for V_1 use R_{1AC}.

The series dropping resistor at the filter output is computed by application of Ohm's Law:

$$R_s = \frac{E_o - 240}{0.170} \text{ ohms}$$

where E_o is the output voltage of the filter, and 240 volts is the voltage across the VR-90 and VR-150 in series.

The VR-90 should then be shunted by an equalizing resistor to make the currents in the VR-90 and the VR-150 equal. The resistor must carry all of the load current of the 45-volt output. This is 60 ma, and the resistor voltage will be 90 volts as determined by the tube. The resistor will be 1500 ohms. The schematic diagram will then be as shown in Fig. 3.

If the load current requirement from a regulator of this type is too low in one or more branches, a shunting bleeder of suitable resistance may be employed to increase the load drain to an operable value in the load branches involved.

Since the low voltage is obtained by taking the difference between two larger voltages, this may yield a larger tolerance on low output voltage on a percentage basis than the rated percentage tolerance of any of the individual tube voltages. The tolerance in volts, however, will not be greater than the sum of the voltage tolerances of the tubes which determine the low output voltage.

Table I gives a general method of solving for the circuit components when two output voltages and the extreme values of load currents are specified. Certain restrictions must necessarily be put on the output current variations. The solution yields the permissible input voltage variation for the range of load currents desired, and the internal a-c impedance looking back from the load.

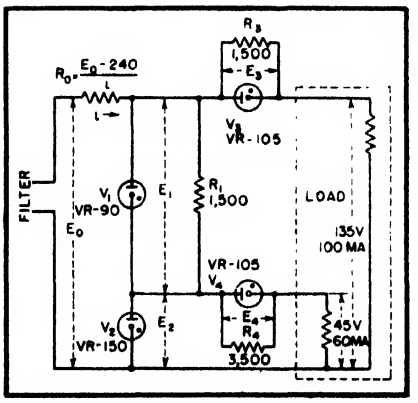

FIG. 3—For high-current requirements, resistors are shunted across the voltage-regulator tubes in series with the loads

The component symbols used in Table I apply to Fig. 3. Measured values of regulation were 2 volts variation of the 135-volt output and 1.3 volts variation of the 45-volt output for an a-c line voltage variation from 105 volts to 125 volts.

Versatile Power Supply

By WILLIAM B. MILLER

BOTH direct and alternating voltages for meter testing are provided by the circuit shown. The a-c output is continuously variable from 0 to 1,200 volts and the maximum d-c output is fixed and regulated at 500 volts. Lower d-c voltages are obtained by means of a variable voltage divider which allows smooth control down to zero volt.

Low ripple was not a factor in the design and only ordinary filtering was used. However, the action of the regulator section and a small amount of feedback resulted in a measured ripple of 0.4 millivolt. Regulation was important and is quite good. After the output was set at 500 volts, it held with no perceptible change, with a line variation from 90 to 125 volts and a load variation of from 0 to 200 milliamperes.

Four 6L6G's, triode connected, are used in parallel as the series regulators, and a 6SJ7 as the amplifier. Resistors in each plate lead of the 6L6's equalize the current distribution, and resistors in each grid lead help stabilize and limit the grid current. A total of 200 ma may be safely drawn from this combination.

The 6SJ7 control amplifier was considered as an r-f tube and care in wire placement was used to eliminate erratic operation and unwanted oscillations. Resistors R_2 and R_3 supply the screen voltage and also the keep-alive voltage for the VR150, the current through the latter being about 15 ma with no load on the supply. The divider network across the output supplies the control grid voltage for the 6SJ7 and also feeds the grid any fluctuations in the output voltage. The amplifying action of this tube provides the regulating effect. Any change on the grid of the 6SJ7 is amplified and transmitted as bias to the 6L6's, which changes their series resistance in the proper direction to counteract the fluctuation.

By varying P_1, the output voltage is brought to the exact value desired. The divider was calculated to put the grid 5 volts above the cathode, or 155 volts; P_1 has a range of about 50 volts. Potentiometer P_2 helps in reducing ripple, as it feeds the unregulated voltage to the regulated side and any ripple will be partially cancelled due to the 180-degree phase difference between the two.

Resistor R_1 and capacitor C_1 aid considerably in ripple reduction. A 500,000-ohm potentiometer was used for R_1 and adjusted for minimum ripple voltage. If the supply is used where the load changes rapidly, a 4-μf 600-volt oil-filled capacitor across the output helps in maintaining regulation.

The change from d-c to a-c is accomplished by means of a 4-pole double-throw relay. When the relay is energized, it disconnects the high-voltage windings from the rectifier tube and makes them available by means of a switch. The Variac, connected to the primaries of one filament transformer and the plate transformer, controls the a-c output. When the switch selects the filament transformer, a-c from 0 to 7.5 volts is available at the terminals. With half of the plate winding switched in, up to 600 volts may be had. With the full winding, 1,200 volts are available; each range being continuously variable. The Variac is turned down whenever a change is made to prevent arcing at the relay contacts.

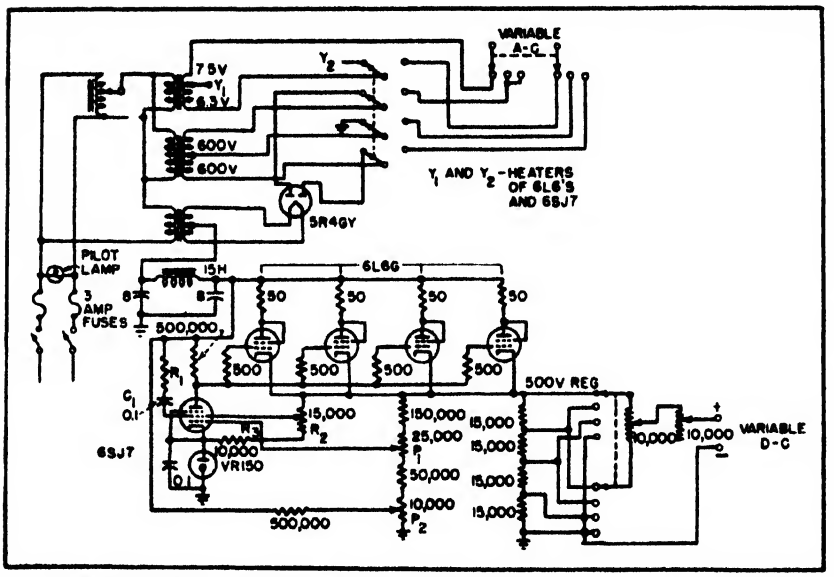

Up to 1,200 volts a-c and 500 volts d-c are available from the power supply

The resistance network across the output divides the 500 volts d-c into four ranges, each range being approximately a 125-volt step, depending on the current being drawn. Thus for the first range the voltage is 0 to 125, the second from 125 to 250, the third from 250 to 375 and the last from 375 to the full 500. The arrangement of the potentiometers gives a very smooth control between ranges and allows voltages as low as 0.05 to be easily obtained. The two 10,000-ohm potentiometers are General Radio type 314A, rated at 8 watts.

Power Supply for Microwave Equipment

Continuously variable from 300 to 5,000 volts, the voltage-regulated power supply described utilizes an electronically controlled servo motor to automatically adjust an autotransformer. The d-c output of the device has less than three millivolts ripple at all voltages

By OLIVER HOAG

DUE to recent trends toward high frequencies, power supply requirements have become more stringent. In microwave equipment, operating voltages must be extremely stable to maintain necessary frequency stability. This is particularly true in the case of laboratory equipment.

The requirements for an adequate voltage supply in the laboratory operation of the majority of microwave tubes are:

(1) It should have excellent regulation for line voltage fluctuation, less than five millivolts of ripple, and efficient control for load current fluctuation.

(2) The output voltage should be smoothly variable without steps through the entire voltage range.

(3) Operation should be convenient and simple, with a minimum number of controls.

(4) The supply should be fully protected for the safety of the operator and of the tube under test.

(5) To be useful for medium and high-power tubes, voltage and current range should be wide.

The common inverse-feedback regulator circuit can be designed to give the required regulation at low voltages. However, at higher voltages more glow-discharge, voltage-regulator tubes for the reference voltage are necessary. For an output of 5,000 volts, approximately 31 type OD3/VR150 tubes would be needed. Furthermore, most voltage-regulator tubes have small spasmodic variations in the order of 0.1 to 0.5 volt.[1] Because even the finest voltage-regulator tubes have some spasmodic variations, the chance of a voltage shift is multiplied by the number of voltage-regulator tubes in the string, and any changes that do occur will

appear in the output. Such disturbances can be observed in the output of all high-voltage regulators, and can usually be traced to the VR tubes.

Conventional low-voltage regulator circuits usually include some kind of compensation for input voltage variations but satisfactory compensation is not possible when the number of VR tubes in the circuit is changed frequently.

Another objection to a power supply using many VR tubes is the number of controls necessary for its operation. Three adjustments must be made for each voltage setting; a coarse tap-switch control, a transformer primary voltage adjustment to put the correct voltage across the regulator tube, and a fine control setting.

This paper describes a voltage regulator system of four main parts, meeting all five requirements of a high-voltage supply for laboratory use. The output is smoothly and continuously variable from 300 to 5,000 volts or higher, using one knob.

While designed for laboratory use on microwave oscillators and amplifiers, the characteristics of this regulated supply are such that it should prove useful for many other applications requiring high voltages with good flexibility and regulation, provided the positive output can be grounded.

The block diagram in Fig. 1 shows the four essential units. The servo-transformer unit consists of a three-phase autotransformer to vary the primary voltage of the high-voltage transformer (and thus the d-c input of the electronic regulator), a reversible servo motor geared to the autotransformer, and a control circuit.

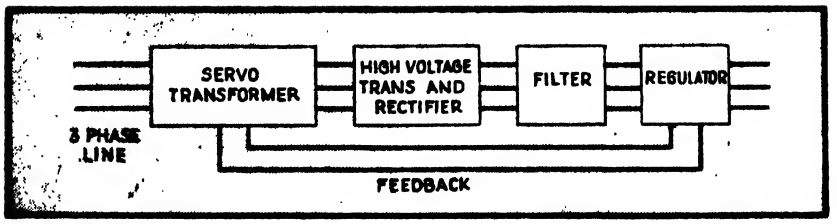

FIG. 1—Essential elements of the voltage regulator

The operation of the control circuit can be seen by reference to Fig. 2. The regulator-tube voltage appears across the divider R_1, R_2, R_3. The voltage appearing across R_1 is compared with the independent plate supply and the difference is the bias for V_1, the left-hand section of the double triode. Similarly, the difference between the voltage appearing across $R_1 + R_2$ and the plate supply is the bias for V_2, at the right. The value of this voltage is greater than that applied to V_1.

With normal regulator-tube voltage, V_1 conducts and V_2 does not. Then the contacts of both relays are open and the motor is not operating. As the regulator-tube voltage becomes lower, the V_2 bias becomes less negative, and this tube conducts, energizing the RAISE relay. The bias of V_1 is also decreased, but since V_1 was already conducting, the change has no affect on the LOWER relay. Thus, the motor operates to restore the regulator-tube voltage, until the restored voltage cuts off V_2.

When the regulator-tube voltage becomes too high, the increased V_1 bias cuts off tube V_1. This de-energizes the LOWER relay, thereby closing its contacts to operate the motor to lower the voltage to normal.

The normal voltage bandwidth can be adjusted by R_2. Its centerpoint is set by R_3. This servo control is necessarily a discontinuous type[2] because a primary voltage correction should be made only when the regulator tube is getting too near the limit of its ability. Narrower bandwidth is not desirable.

Before power is applied to the transformer, or before the 6SN7GT is warm, the relays are in a position to lower the autotransformer. The failure of either the 6SN7GT or the 5Y3GT tube would result in a lowering of the transformer primary to zero. Thus this control circuit is inherently safe. This servo-transformer arrangement can be made to work with existing regulator circuits as well as with the one described.

Rectifier and Filter

The rectifier of Fig. 1 is a conventional six-phase single-Y circuit with delta primary. The primary is rated at 208 volts, 60 cycles. The filter requires some special consideration because neither the positive nor the negative lead is grounded. Instead, the positive output after the regulator must be grounded in most

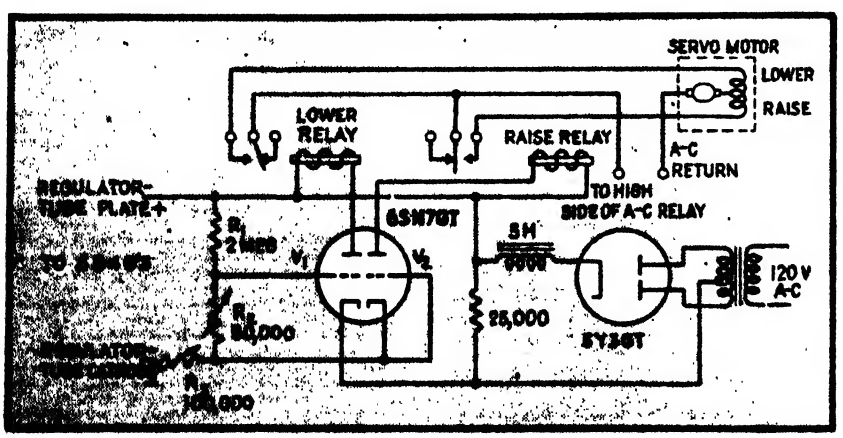

FIG. 2—Electronic circuit for control of the servo motor which is geared to the autotransformer

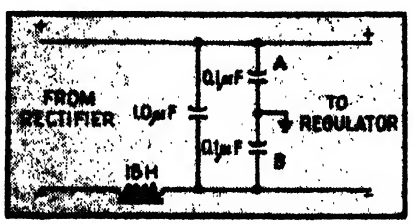

FIG. 3—Although the output of this filter cannot be grounded, capacitors *A* and *B* bypass to ground the high peaks caused by distributed capacitance of the transformer

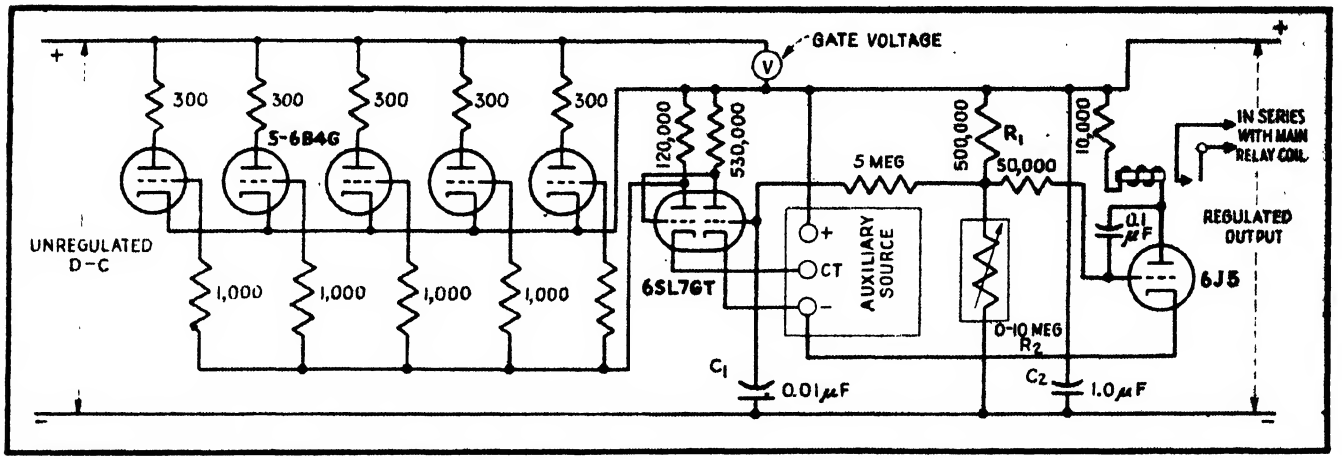

FIG. 4—Inverse-feedback type of regulator with auxiliary voltage source to supply the reference voltage

microwave work. Since the positive output is not common with any lead in the filter, the latter must float with respect to the ground. This would interfere with the filtering action and produce spikes too large to be corrected by ordinary regulator tubes. Figure 3 shows how the filter is bypassed in a way to eliminate the spikes caused by the distributed capacitances in the transformer. High alternating voltages are bypassed to ground through each 0.1 μf capacitor.

Regulator Circuit

The circuit of Fig. 4 shows an inverse-feedback regulator with some fundamental changes. To eliminate the long string of voltage-regulator tubes employed in older regulators, an independent regulated auxiliary voltage source is used. This serves two purposes; first, it supplies the reference voltage and it is extremely stable and constant; second, it is a constant plate supply for the regulator's direct-coupled amplifier.

The reference voltage is compared in the right-hand section of the 6SL7GT to that appearing across R_1. The difference is the signal which, when greatly amplified, drives the 6B4G regulator tubes. The auxiliary voltage source is constant for all output voltages.

When the regulator is operating at high voltages, $R_2 = 12 \times R_1$ and the magnitude of the d-c signal is reduced by the factor $R_1/R_1 + R_2$ or 1/13. At lower output voltages, this factor approaches unity. Actually, however, the gain of the amplifier (estimated to be greater than 15,000) is so large that this voltage division becomes negligible. Furthermore, the capacitor C_1 increases the factor to nearly unity for rapid changes in the divider by effectively shunting R_2.

Because of the high gain, the regulator has a strong tendency to oscillate, but the addition of capacitor C_2 across the output prevents the overcompensation caused by the high gain. The stabilization ratio is defined as dE_i/dE_o where E_i is the voltage applied to the regulator and E_o is the regulated output. Although difficult to measure accurately, this ratio of the changes in voltages is estimated to be over 10,000.

Assuming the reference voltage to be constant, the most likely cause of voltage drift is the divider R_1, R_2. Resistor R_1 is a commercial one-watt, ½-percent, wire-wound precision resistor. The other, R_2, is a special variable resistor. The divider carries only 0.5 ma of current and the resistors dissipate only about 13 percent of their rated values. Thus the temperature rise, and hence the resistance change, is held to a minimum.

Various attempts were made to measure the drift, and because of the necessity of maintaining a bucking or reference voltage more constant than the voltage being measured, the system shown in Fig. 5 was used.

The regulated reference supplies are extremely stable and were thoroughly warmed up before the measurements were made. The voltage to be measured is adjusted to a value close enough to the total reference voltage to make the difference within the range of the recording voltmeter. This method shows a drift of less than 0.1 percent during the first five minutes of warm-up of the regulator, and not more than 0.01 percent at any time thereafter.

Resistor R_2 in Fig. 4 is made up of ten two-watt composition volume controls connected as rheostats. There are 475 volts maximum across each one and 4,750 volts across the ten. They are rated at 500 volts each.

The ten volume controls are mounted on vacuum-impregnated linen Bakelite and driven by gears made of impregnated Bakelite. The normal backlash in these gears provides the basis for a combination coarse and fine control of the regulated voltage.

When the control knob, which has a 12 to 1 ratio to the volume control gears, is turned in one direction, the first volume control alone changes its resistance. Then the second takes, and later the third, until finally, when all the slack is taken up, all ten are turning. At first, the control is ten times as fine as when all the volume controls are moving. When the control knob is reversed, it is again a fine control. On the panel, the knob is labeled, MASTER CONTROL: (Coarse; turn continuously. Fine; rock back and forth).

The regulated auxiliary voltage source is indicated by a block in Fig. 4, and is shown in schematic form in

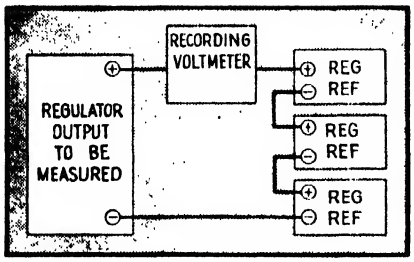

FIG. 5—Block diagram illustrating method of measuring drift

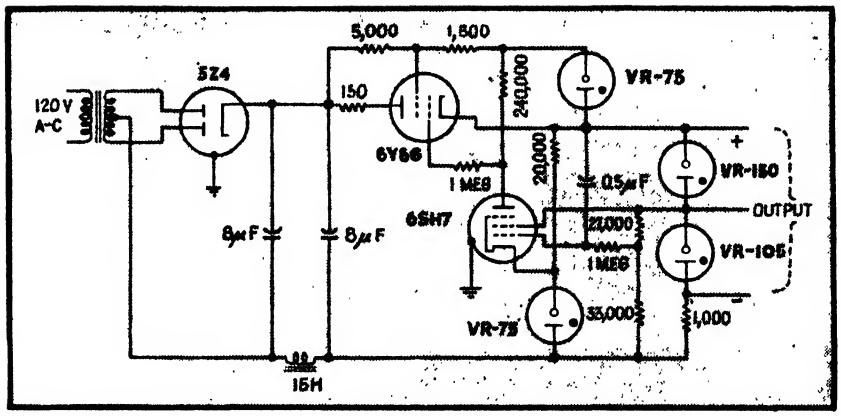

FIG. 6—Circuit of the auxiliary voltage source used for reference. This unit supplies plate voltage for the d-c amplifier of Fig. 4

Fig. 6. It is an independent constant voltage source, although it may be operated from the same a-c line. In this case, it is supplied by one of the 208-volt lines and neutral. Therefore, the primary on the transformer is wound for 120 volts, single phase.

The output of the auxiliary unit is first electronically regulated and then again regulated by the glow-discharge tubes. This inverse-feedback regulator does depend upon a glow discharge tube for its reference, but only one type VR75 is used and it is supplied from the regulated side of the 6Y6G tube. The VR75 was selected because of its freedom from spasmodic variation found in other glow-discharge tubes. The slope of the top VR75 provides excellent compensation for the slope of the bottom VR75[3].

For the safety of inexperienced or careless operators, and for safety in servicing, a closed cabinet is used with an interlock switch, which opens the main three-phase relay when the rear door is opened. The regulated auxiliary voltage source and all filaments, except those in the servo-transformer control circuit, operate with the interlock open. The opening of the interlock prevents the application of any voltage to the autotransformer and prevents the operation of its control circuit. The high-voltage output jacks are located inside the cabinet, and leads to them are brought in through separate grommets. When there is any output voltage, no work can be done on the supply, and high-voltage connections cannot be made.

If failure in the control circuit of the servo transformer allowed it to run to its highest position, many times the proper plate voltage would be applied to the regulator tubes. Since this would be beyond the ability of the electronic regulator to correct, the output voltage would also increase to an excessive value. Regulator tubes, and perhaps other valuable equipment, would be damaged. Two things were done to prevent such an occurrence.

First, the circuit shown in Fig. 2 is made inherently safe, in that failure of either tube to conduct will result in lowering the servo transformer to minimum, where it will remain. And second, included in the regulator circuit of Fig. 4 is a triode-operated relay which must be closed for the operation of the main high-voltage relay.

The grid of the 6J5 triode receives its bias from the difference between the voltage across R_1 and the auxiliary voltage source which is its plate supply. If this bias gets too high, (and it will if the servo transformer goes too high) the triode cuts off, opening its relay. The relay contacts are in series with the main high-voltage relay coil and thus all high voltage is removed. The main high-voltage relay (not shown) is so connected that it will not close except when the servo transformer is at minimum. When this main relay is open, the motor can lower the servo transformer, but cannot raise it. Thus, should the voltage across R_1 become excessive, the high voltage is shut off and cannot be applied except under safe conditions.

Ion bursts in some klystrons cause a sudden and severe surge in the beam current which may damage the power supply and its current meter. An over-current relay with contacts in series with the high-voltage relay coil, and a choke in series with the current meter, provide excellent protection from such overloading. The choke will delay meter deflection until the relay opens the main high-voltage relay. Tests indicate that with these safeguards, the power supply can be shorted or subjected to a sudden open-circuit without damage, that failure of any tube will not cause damage to any other part, and that interruption of the power line will safely shut the supply off. Magnetic breakers in the a-c lines provide additional protection against internal breakdowns and will operate within one-half cycle.

Tests show that the high-voltage regulator has a d-c output with less than three millivolts of ripple which is approximately the same at all output voltages. At 5,000 volts, this is 6×10^{-5} percent and at 300 volts it is 1×10^{-3} percent. When viewed on a high-gain oscilloscope, the output is practically free from transient jumps. It can handle a 3-ma or a 500-ma load with equal facility. The maximum output current of the regulator is limited only by the number of regulator tubes used.

REFERENCES

(1) Hogg, F. Livingston, Electronic Voltage Regulator, *Wireless World*, p 330, Nov. 1943.
(2) Middel, H. D., Electronics in Instrumentation, *Proc. of National Electronics Conference*, 1944, 1.
(3) Hogg, F. Livingston, Electronic Voltage Regulator, *Wireless World*, p 329, Nov. 1943

Filter Ripple Chart

Where choke input is used, output characteristics are readily predetermined. Curves are given for 50 and 60-cycle, half-wave and full-wave, and single and three-phase rectifiers. A rectifier attenuation table is included

By C. K. HOOPER

WHEN USING choke-input filters, the output ripple of rectifier-type power supplies can be predetermined from the accompanying chart.

It is necessary to know the inductance value, in henrys, and the capacitance, in microfarads, for each filter section. Knowing the product of these two terms, the amount of attenuation in db for each filter section can be read directly on the chart. Curves are given for 50-cycle (dashed lines) and 60-cycle (solid lines) power, for the four types of supplies most often used in industrial equipment.

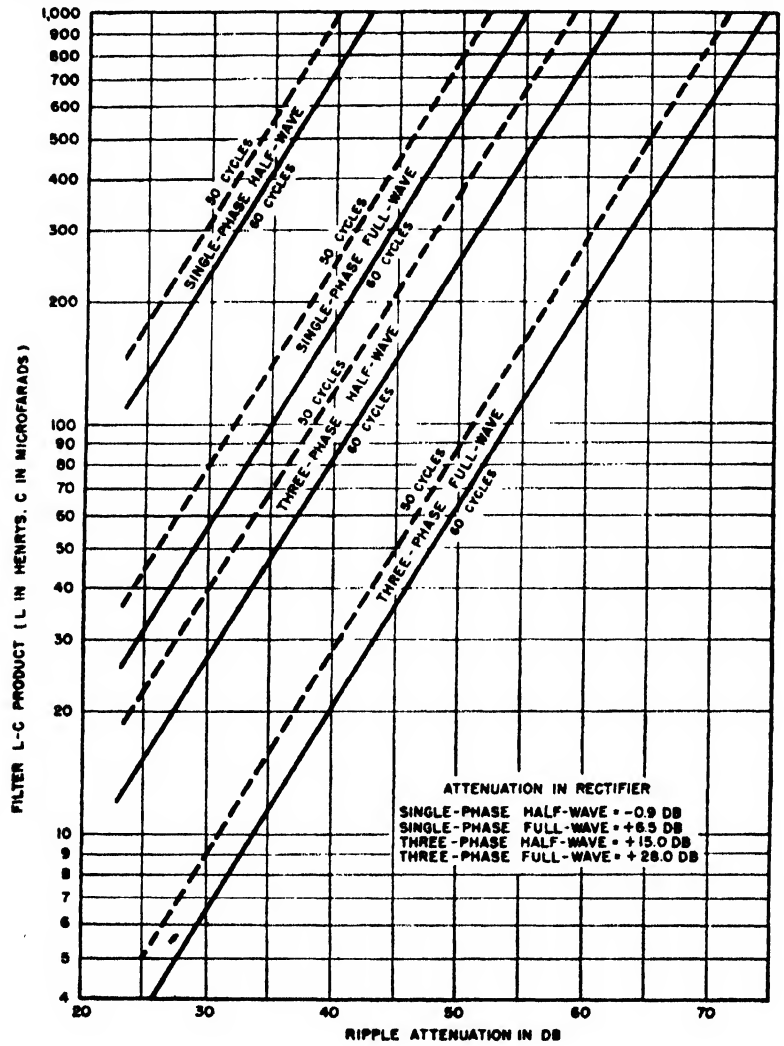

To obtain the total output ripple in db below the d-c level, the equivalent rectifier attenuation must be added to that of the filter sections.

Practical Example

The following example will illustrate the use of the chart. Assume that a single-phase full-wave rectifier operating from a 60-cycle supply has a two-stage choke-input filter. One of the filters consists of a 2-henry choke and 15-μf capacitor. The other filter consists of a 2-henry choke and 20-μf capacitor.

For the first filter, with an L-C product of $2 \times 15 = 30$, the attenuation is read as 24.5 db. The second filter has an L-C product of $2 \times 20 = 40$ and the attenuation is read as 27 db. From the table the equivalent rectifier attenuation of a single-phase full-wave rectifier is given as + 6.5 db.

The total resulting ripple attenuation is the sum of that of the individual filter sections plus that of the rectifier. In this case, the total is $24.5 + 27 + 6.5 = 58$ db rms below the d-c level.

Automatic Control of Battery Charging

By E. L. DEETER and A. C. PLAUTZ

TO OPERATE special electronic equipment designed for a-c line use it was necessary to convert the d-c available on a ship. Furthermore, it was imperative that storage batteries be utilized as an emergency source in case the ship's power supply failed. The automatic electronic control system herein described was

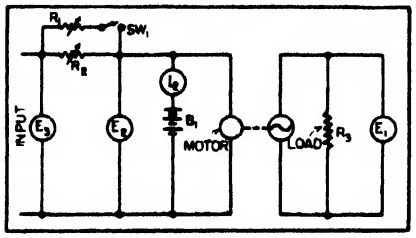

FIG. 1—Basic charging circuit in which a manually operated switch is used for illustration

developed to insure a constant d-c supply for the rotary converters.

In the basic circuit of Fig. 1, the rotary converter, supplying a-c to a fixed load, is connected on the d-c side to a power source having an emf considerably higher than that required to operate the converter properly. A series resistor, R_s, is varied to adjust the current and voltage. The emergency battery B_1 is connected across the converter input and will draw current when its voltage drops to a value below that of E_s. Connected in this manner, the battery affords an excellent filter for line voltage variations that are inherent in most d-c distribution systems.

Let us assume that the storage battery B_1 has been properly charged, and in this instance shows an emf of 36 volts. If the resistance of R_s is slowly decreased, the discharge current I_s of the battery will likewise decrease as the voltage across E_s increases. When E_s becomes 36 volts, no current will flow in or out of the battery, and it will float on the line.

However, this condition is not easily maintained and is not desirable with this control system. The resistor R_s is increased, or set to a value that allows a slight discharge of the battery. If, after the battery voltage has decreased to 35 volts, the switch SW_1 is closed, the battery will start its charging cycle, provided the resistor R_1 is of the proper value to raise the voltage across the battery. By proper choice of the resistors, and with a constant converter load, the times of the charge and discharge cycle may be made equal.

The function of the electronic control circuit is to operate SW_1, at the proper time intervals. The method by which this is accomplished may best be explained by reference to Fig. 2. In this schematic a battery B_2 is placed in series with, and its polarity opposing battery B_1.

The bias voltage on the 2050 gas tube will be the algebraic sum of the two battery potentials. Suppose the storage battery B_1 has been slightly discharged and has an emf of 35 volts. If the B_2 source is 33 volts, the gas tube will be biased to two volts negative and will not allow the tube to ionize on the positive peaks of the plate supply.

A further slight decrease in the emf of B_1 causes the bias to become less negative and the gas tube ignites to close the relay RL when the critical bias condition is reached.

Closing of relay RL places the resistance of R_1 in parallel with the R_2 resistance and initiates the charging cycle. It is also responsible for another change vital to the operation of the control circuit. The transfer switch SW_2 places a higher potential in series with the battery B_1, lowering the bias on the tube to a lower negative value than that causing the transfer. This incremental decrease determines the amount of charge (and emf increase) necessary to interrupt the charging cycle.

Using a battery as shown by B_2 in Fig. 2, the battery voltage of B_1 would vary 1½ volts between cycles, as the smallest increment usable would be 1½ volts. In the circuit of Fig. 3, this increment may be adjusted to any desirable value over a considerable range. Circuit resistances and associated voltage drops limit the minimum practical increment to about a half volt when the total battery is of the order of 36 volts.

In Fig. 3, a regulated d-c supply is substituted for battery B_2 of Fig. 2. Controls P_1 and P_2 of the regulated supply make it possible to adjust the starting and stopping point of the charge and discharge cycle.

The control unit operates from the a-c output of the converter, assuring constant filament voltage for the tubes.

A small time constant at the control grid of the 2050 tube is introduced by means of R_4 and C_4. The capacitor C_3 is essential in preventing chatter of the relay when the cycling increment is less than one volt.

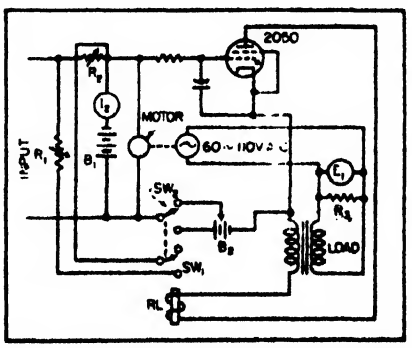

FIG. 2—Electronic charging control circuit with battery B_2 supplying a reference voltage

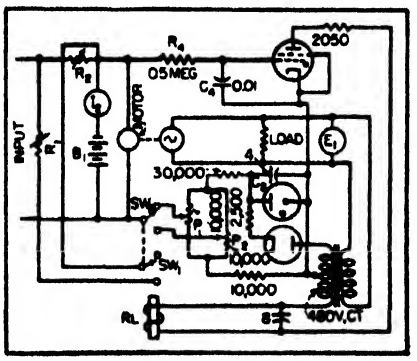

FIG. 3—Stabilized voltage source replaces the reference battery in the final circuit

Voltage-Stabilized Bias Supply for Power Tubes

WHEN VOLTAGE-STABILIZED power supplies are employed for bias on power tubes the flow of grid current of the power tube is in the reverse direction to current flow in the bleeder resistor of the bias supply and tends to remove the load from the supply. The diagram shows the circuit of a degenerative, shunt-type, voltage-stabilized bias supply that maintains a 65-volt output within very close limits on reverse current swings up to 200 milliamperes. This circuit was developed by George E. Pihl, and is described by him in Bulletin No. 10 published by the College of Engineering, Northeastern University, Boston.

In the conventional shunt type of voltage stabilizer circuit, two 2A3 tubes can produce an output of about 60 volts when handling a grid current swing of 100 milliamperes. With such a current swing an output voltage deviation of about 8 volts takes place. Using the same tubes in the amplified shunt stabilizer circuit shown in the diagram the change in output voltage becomes 0.2 volt with the same current swing.

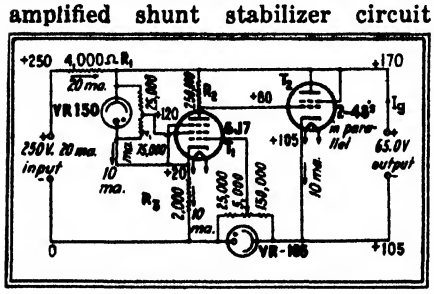

Changes in bias voltage caused by reverse grid current flow of the controlled tube are minimized by the voltage stabilizer shown here

Operation of the Circuit

When the circuit is used to supply bias to a modulator or other power tube the periodic increase of grid current causes a small change in the output voltage of the stabilized supply. This change in output voltage in turn is applied through the voltage regulator tubes, VR-150 and VR-105, in series with resistor P_3, to produce increased bias on the grid of T_1, a 6J7 tube. This action decreases the plate current of the tube, the plate becoming more positive. The positive voltage change is applied to the grid of T_2 and effectively lowers the plate-to-cathode resistance of the tube. The lowered resistance permits additional grid current of the power tube to flow through T_2 and stabilize the circuit.

To minimize the deviation of output voltage necessary for operation of the system the change of resistance of T_2 is made large for a small change of grid voltage of T_1. Tube T_2 must be capable of a total current variation of from 10 to 210 ma at a plate voltage of 65 volts without having its grid go positive. A pair of type 48 tubes operated in parallel as triodes can pass 210 milliamperes at 65 volts and zero bias, and were therefore used.

Operating potentials at various points in the circuit are indicated in the diagram and are referred to the negative side of the input voltage source. An initial current of 10 ma through the 48 tubes is permitted to stabilize the VR-105 tube. To maintain this current, a negative bias of 25 volts is necessary on the grids of the 48 tubes. Another 10 ma is allowed to flow through the VR-150 for stabilization.

The graph shows the change of output voltage plotted against grid current of the power tube. The rate of change of output voltage is approximately 0.002 volts per ma of current flow, according to the slope of this curve. This is the same result that a perfectly regulated source of voltage in series with two ohms would produce.

An unstabilized power supply would require a two-ohm bleeder resistor to obtain this result and the bleeder would be obliged to dissipate more than two kw of power.

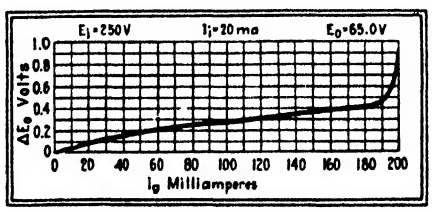

Curve of deviation in output voltage vs. grid current, plotted under operating conditions

A Variable-Frequency Electronic Generator

Device operated from 220 v a-c line turns out 1400 watts of power at any selected frequency between 300 and 3500 cps. Novel automatic control circuit keeps regulation within 1 per cent for output voltages between 85 and 125 v

By DANA A. GRIFFIN

THE ELECTRONIC GENERATOR to be described was developed to fill the growing need for a versatile source of a-c power. Several branches of the electronic industry require a device capable of delivering a reasonable amount of power to various loads, over a wide frequency range. Good waveform and good regulation under various load conditions are also essential requirements. The variable-frequency electronic generator was designed to take care of this problem.

The power output of the generator is 1400 watts over a frequency range of 300 to 3500 cps. The frequency stability is better than 2 percent after the initial warm-up period. Output voltage is adjustable between 85 and 125 v rms. The regulation is better than 1 percent from no load to full load. The waveform is substantially sinusoidal under operating conditions ordinarily encountered.

Typical Applications

Operating requirements of much airborne radio and radar equipment are such that the equipment must function properly even though the frequency of the power source varies through a wide frequency range. It follows, therefore, that a power supply that can quickly be shifted from one frequency to another is a practical necessity in a number of applications.

The design engineer requires such a power supply for development work. Transformer, capacitor and cable manufacturers also need a power source of this type in order to meet test requirements. Government specifications frequently call for complete systems tests on the production lines, over a wide range of power frequencies. The creation of high audio frequency vibrations for test purposes, employing magnetostriction devices actuated by the electronic generator, is another interesting application.

In addition to factory and laboratory applications there are others applying to maintenance and service. For example, radio installations in aircraft can be tested in the plane or serviced in the repair shop without resorting to the gasoline-driven aircraft power supplies ordinarily employed.

The basic approach to the problem of designing a variable-frequency electronic power source is well known to those familiar with the design of radio telephone transmitters. The generator employs a tunable audio oscillator and several stages of audio amplification in cascade, the final stage using a pair of power tubes operating as a Class B amplifier. Similar amplifier arrangements are used in many modulator systems in radio transmitters.

General Circuit Arrangement

The electronic generator differs from a transmitter modulator system in that a variable-frequency audio oscillator is connected to the input stage in place of a microphone. The frequency can then be adjusted by turning the frequency control knob of the oscillator. The only serious problem in design is the problem of regulation. Inasmuch as the impedance of the final amplifier stage is several thousand ohms, the regulation of such systems is ordinarily poor. Unless special provision is made to insure good regulation, output voltage may vary considerably from no load to full load.

An electronic control circuit employed in the electronic generator changes this picture completely. Through the operating range of the control circuit, the regulation is better than 1 percent, and the recovery time when the load condition is drastically altered is less than a second.

The block diagram across the top of the accompanying drawing shows the overall electronic generator circuit. Two of the three schematic diagrams appearing below within dotted lines constitute "blow-ups" of circuits within individual blocks to which they are appended. The other schematic, at the bottom, shows details of a regulated power supply unit to be discussed later. Blocks for which schematics are not shown are conventional and need no elaboration here.

The oscillator employs two tubes in a conventional *RC* circuit. Two frequency ranges are provided, 300 to 1000 cps and 1000 to 3500 cps. A switch is provided to select the range. The tuning dial is supplied with a double-ended pointer so that the calibration scale for each range may occupy approximately 180 deg.

The oscillator drives the 6L7 tube in the control circuit (shown schematically). Output of the 6L7 drives the phase-inverter 6SN7. The 6SN7 is followed by push-pull 6A3's in Class A, which drive 812's in Class B. The 812's drive the final stage, using 833-A's in Class B.

With a given amount of drive to the final amplifier, the output voltage at the secondary of T_1 will ordinarily vary through wide limits when control is not provided, being dependent upon the load. The solution is simple, if we approach the problem from the correct angle.

The maximum load to be used is connected to the output transformer. Then the drive to the final amplifier is adjusted to deliver the proper voltage to this load. This is accomplished by control of potentiometer P_3, in the grid of the 6L7 control tube. If the load is removed, the output voltage will rise quickly under ordinary circumstances. The function of the control circuit is to prevent this by reducing the drive to the final amplifier whenever the output voltage exceeds the predetermined level.

An isolation transformer T_2 feeds output voltage to the 6H6 diode in the control circuit. This transformer is used so that the output circuit may be kept independent of the ground system of the generator. The normal 120-v output at the secondary of T_1 is reduced to 40 volts at the diode by T_2. Potentiometer P_1, in the cathode circuit of the 6SJ7 d-c amplifier, is adjusted so that the positive bias normally generated by the diode is cancelled and the 6SJ7 is operating at a point close to plate current cutoff. A slight negative bias on the injector grid of the 6L7 results because of the small plate current of the 6SJ7. The control grid bias on the 6L7 control tube is adjusted by means of P_2. The latter is adjusted so that the output of the 6L7 is linear through the control range.

When adjusted as described, the control circuit operates as follows: The output of the diode increases when the load on the generator is reduced. The 6SJ7 grid bias becomes less negative and 6SJ7 plate current increases, which puts increased negative bias on the 6L7 injector grid. This reduces the drive to the final amplifier so that the output voltage is held to a value extremely close to that obtained under the full load condition.

Because the control circuit is connected from the input of the system to the output, the arrangement is one conducive to oscillation. For this reason the constants in the diode circuit must be such that the system will not "take off" in a low frequency oscillation. With the values given, tendency to oscillate is eliminated.

Naturally, the output voltage can be changed from zero to maximum (150 v) under load by the adjustment of P_4. Complete functioning of the control circuit, is, however, limited to the range between 85 and 140 volts at the secondary of T_1. This range of control is sufficient to cover most applications. Where additional voltage is needed with good regulation, the use of appropriate step-up or step-down transformers is indicated.

Bias Supply Details

One other design problem was the construction of a suitable grid bias power supply for the final amplifier.

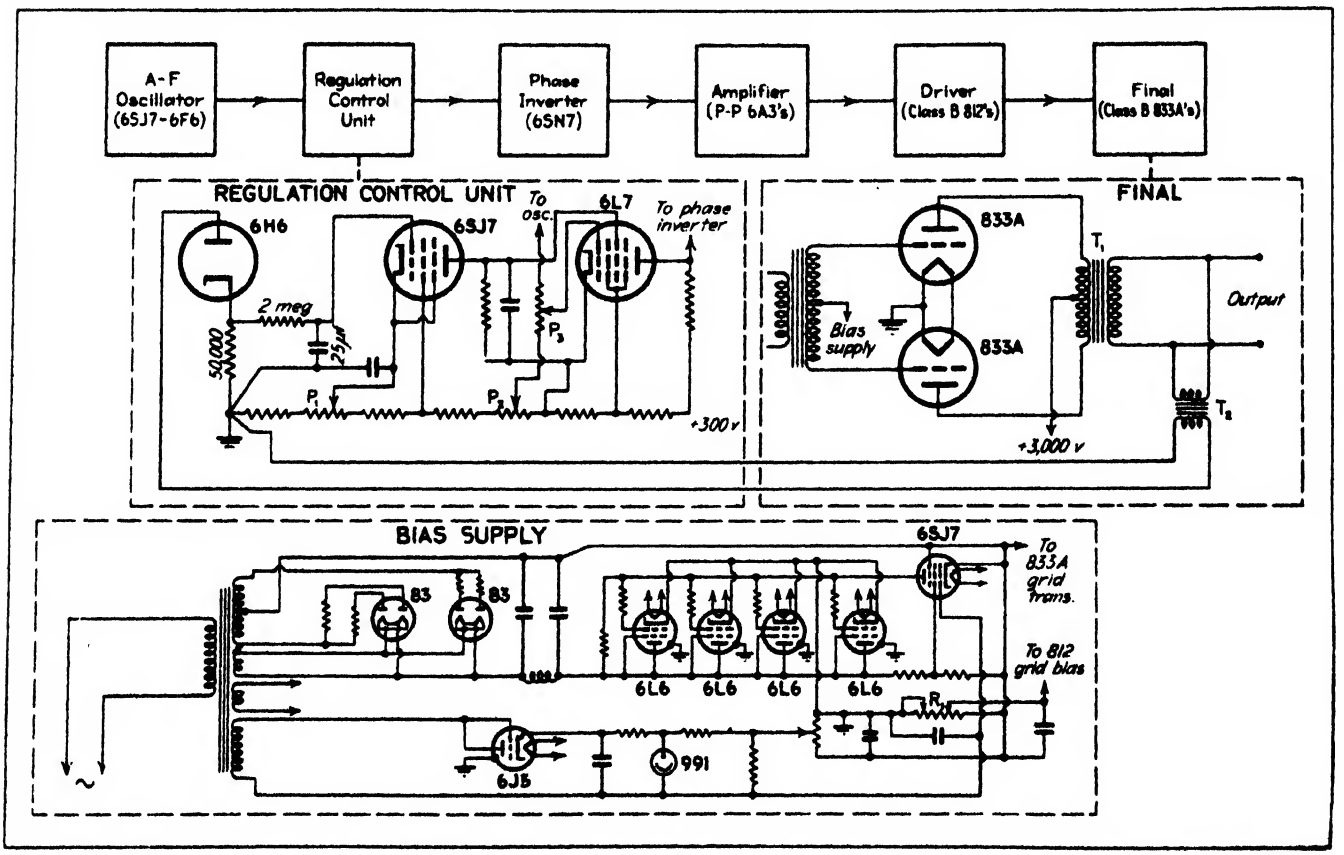

Combination block and schematic diagram of variable-frequency electronic generator. Blocks across top show overall circuit arrangement. The two schematics appearing immediately below, within dotted lines, show circuit details of the units to which they are appended, namely within the regulation control unit and within the final Class B amplifier unit. The schematic at the bottom shows details of a regulated power supply unit which provides bias for the driver and final amplifier

As the 833A tubes require a negative bias of 70 v and the peak grid current under full load is around 300 ma, it was necessary to consider the problem of securing a bias supply of good regulation. In ordinary times a small d-c generator might be considered for this application as such a generator satisfies the requirement of low impedance. The output voltage is not independent of line voltage, however, and the procurement situation at the moment is extremely difficult. For these reasons the electronic approach was again resorted to with excellent results.

Conventional regulator circuits did not appear to work well here as complete control was required at the low output voltage of 70 v. The 6J5 and the 991 tubes shown schematically at the bottom of the schematic provide a stabilized bias for the 6SJ7 bias supply unit control tube that operates above ground potential in a negative direction. The high voltage supply using a pair of 83 rectifiers, also shown schematically, delivers 250 v to the four 6L6 regulator tubes, so that a voltage of 70 volts at 350 ma is developed across R_1.

Of course, regulation is not a serious problem until the 833A tubes begin to draw grid current. Under such conditions increasing grid current tries to increase the voltage appearing across R_1. The control tube then increases the bias on the 6L6 regulator tubes so that the bias voltage is maintained at a constant value. As the system is independent of reasonable line voltage changes, and as the impedance is substantially zero insofar as variations in voltage caused by grid current are concerned, the supply affords an excellent answer to the bias problem.

Mechanical Design

The mechanical design of the generator was undertaken while keeping in mind the different requirements occasioned by different types of use. In a laboratory, complete control should be available for the engineer. In some shop applications where a fixed critical frequency is needed the controls should be made inaccessable to unskilled operators. For this reason the front door of the cabinet is provided with locks and the small door covering the control panel can also be locked if desired. The sides, back, and top of the cabinet are made of expanded metal to insure adequate ventilation. Openings are provided in the rear of the back panel so that a-c line input and power output cables can easily be brought in to fuse blocks on the lower deck.

The lower deck is given over to a 3000-v plate supply for the 833A tubes and a 1500-v plate supply for the 812 tubes. Control equipment includes a time-delay relay which delays the application of high voltages until the rectifier tubes have had an opportunity to warm up. An adjustable overload relay is also included. A safety interlock switch is operated when the front door is opened.

The chassis on the second deck includes a 300-v regulated supply for the low-level audio stages and the output voltage regulation control circuit. The audio oscillator and the C bias supply for the 833A and 812 tubes are also located on this chassis.

The top deck is devoted to the high level Class B output stage. As the heat dissipation from the tubes is quite large a polished baffle plate is located between the tubes and the output transformer to prevent the latter from overheating. Sufficient room is available on this deck to install corrective elements where the load is highly inductive.

The control panel includes all of the controls essential to operation once the switch from the power line has been closed. The plate switch on the left controls the high voltage to the two Class B stages. This enables the operator to cut off the power output, without shutting off the whole unit, to conserve the life of the 833A's. The power could, of course, be cut off by means of a line-switch in the output circuit but the method used is desirable from a tube conservation standpoint. If an overload occurs the overload relay operates, removing the high voltage. When the trouble is cleared, operation of the overload-relay push-button switch will again apply plate voltage to the power tubes. The third control from the left is the audio oscillator frequency range switch and the next, of course, is the frequency control dial. The audio gain control, at the right of the frequency control dial, is adjusted to give required output under full load. The last control, for diode threshold adjustment, permits the circuit to be externally adjusted for best regulation.

Electronic Generator Efficiency

The power requirements are 3.5 kw from a single-phase 60-cycle line. An auto-transformer is included in the unit so that voltages from 208 to 260 v can be used. Taps are provided on the transformer at 10-v intervals within this range. The overall efficiency of the system is better than 40 percent. This of course does not compare favorably with rotary machines but on the other hand the wide frequency range and excellent regulation cannot be secured by mechanical means.

In closing, it is well to point out that the design described was intended to cover as many industrial applications as possible consistent with reasonable cost. Different frequency ranges and power outputs are design variables that may be changed to meet special cases. The first is quite easy to shift within reasonable limits by changing the constants of the audio oscillator. Good performance can be expected through a frequency range limited in extent only by the performance of the Class B transformers.

Considering the second design variable, it is obvious that the number of watts per dollar will decrease at lower power outputs and increase with higher power outputs. This is true because the chief changes are related to the type of tubes used in the final amplifier and the size of the final amplifier voltage plate supply.

PRODUCTION

Sensitivity Limits in Radio Manufacturing

Statistical procedure for determining economical sensitivity limits of receivers coming off a production line, and use of a preselected average set of tubes to determine if rejection of a receiver is due to circuit trouble or to an unfortunate combination of tubes

By A. S. BLATTERMAN

EVEN with the most careful control in manufacture the performance of finished radio receivers of a given design will vary. The performance can be described in terms of various operating characteristics such as the selectivity, sensitivity, maximum power output, avc action, and distortion (using the terms in a very general sense). These characteristics are not independent of one another, nor are they all of the same importance.

The present discussion directs attention to the sensitivity alone, defining it in terms of microvolts input to give a stated output (in watts or in volts). The sensitivity will vary from one receiver to another, and the question arises as to how much variation should be expected or allowed. This question can be answered through straightforward statistical analysis.

Suppose we consider a more or less conventional six-tube receiver as indicated in Fig. 1. Here there are at least eleven variable factors in the circuit which will affect the overall sensitivity—the nine gain factors $\mu_1, \mu_2, \mu_3, \ldots \mu_9$ of the coupling circuits and tubes, the coupling resistor R, and the B supply voltage.

In the course of manufacture and assembly of receivers, suppose that each of the above eleven factors varies ± 10 percent. The total overall gain of the receiver (its sensitivity) might then, if we happen to get all low-value factors together first and all high-values factors next, vary in the ratio of $(1.1/0.9)^{11}$ and give a range of over 9 to 1 in sensitivity.

Standard Deviation Unit

It will now be shown that the principle just used, taking all the possible maximum and minimum limits for determining the limits of a complete assembly of parts, is not economically justified. It will also be shown how proper economic limits may be specified.

If the gain factor (the mutual conductance g_m) of a large number of supposedly identical vacuum tubes is measured, it will be found that there is a certain distribution of high, low, and intermediate values. Under commonly existing, controlled conditions of manufacture, the distribution will follow the normal or Gaussian law typified by the curve of Fig. 2. About 68 percent of all values of g_m will be within ± 1 standard deviation s from the average value, about 95 percent within ± 2 standard deviations $2s$, and 99.73 percent within ± 3 standard deviations $3s$ from the average.

The standard deviation s is a statistical measure of dispersion and by formula is the square root of the average of the squared differences from the arithmetic mean

$$s = \sqrt{\frac{(X_1-\overline{X})^2+(X_2-\overline{X})^2+\ldots.(X_n-\overline{X})^2}{n}} \qquad (1)$$

where n is the number of observations and $\overline{X}$ is the arithmetic mean of the n observations. The same sort of thing will happen for such other circuit elements as coils, resistors and capacitors if measurements are made of Q, R, or C.

Tube-Picking Probabilities

To go back to the vacuum tubes, suppose the average mutual conductance value of a certain kind of tube is specified as 1,000 micro-

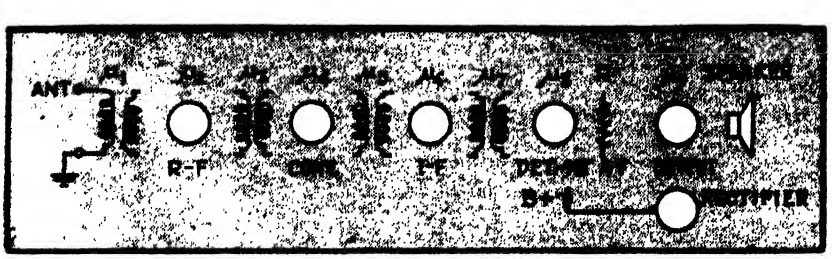

FIG. 1—Simplified diagram of six-tube receiver used as example in illustrating procedure for setting sensitivity control limits for production-line tests

mhos. If a lot of say 100 of these tubes is measured, it will be found that the average value is very closely 1,000 micromhos. The standard deviation s, when calculated, may be 10 micromhos. This means then that if we pick out tubes at random from a large lot we can be quite sure of not getting more than about 15 in 10,000 tubes having g_m greater than $1,000 + 3s = 1030$ micromhos, and no more than 15 in 10,000 with g_m less than 970 micromhos.

With this low probability of picking a tube having either extremely high or extremely low gain, the chances of ever getting a combination of say 5 such tubes into one receiver, all having highest gain or all having lowest gain in a given combination, is exceedingly remote indeed. The fallacy of setting performance limits of the assembled receiver on the basis of separately adding maximum and minimum limits of component parts is therefore obvious. One would expect almost all receivers to give performance very far within the extreme limits that such a calculation shows.

Suppose that coils, transformers, resistors, voltages, etc are held substantially constant so that receiver sensitivity is only affected by the tubes, and suppose there are n stages of these producing average stage gains of $\mu_1, \mu_2, \mu_3, \ldots \mu_n$ decibels with standard deviations of gain from each of the average values of $s_1, s_2, s_3, \ldots s_n$ decibels. Then for the combination of n tubes the value of average overall gain is

$$\bar{\mu} = \bar{\mu}_1 + \bar{\mu}_2 + \bar{\mu}_3 \ldots\ldots\ldots + \bar{\mu}_n \text{ db} \quad (2)$$

and the standard deviation of this overall gain is

$$s_\mu = \sqrt{s_1^2 + s_2^2 + s_3^2 + \ldots\ldots\ldots s_n^2} \text{ db} \quad (3)$$

The limits, then, of overall gain $\bar{\mu}$ between which we may expect to find all receivers except about 3 in 1000 are $\bar{\mu} + 3s_\mu$ and $\bar{\mu} - 3s_\mu$.

As a simple special case to illustrate the point of the discussion let us suppose that the individual stage gains (average) are all the same (μ_1) and that each has the same standard deviation s_1. Then Eq. (3) becomes $s_\mu = s_1\sqrt{n}$, and 99.73 percent of all receivers will show gains between the limit values $n\,\bar{\mu}_1 + 3s_1\sqrt{n}$, and $n\,\bar{u}_1 - 3s_1\sqrt{n}$.

Had we followed the plan described earlier of finding these limits from the $3s$ limits of each stage, the overall limit values would obviously have been $n\,\bar{\mu}_1 + 3s_1 n$ and $n\,\bar{\mu}_1 - 3s_1 n$, which is a variation from overall average gain $\sqrt{n}$ times as great. The extreme case where all tubes are on the low side or all on the high side may of course happen, but the point is that the probability of it happening is extremely small. The situation is shown in Fig. 3 for four stages ($n = 4$).

Practical Application

An important practical question that arises is, "In the quantity production of radio receivers of a given type, what high and low limits shall be established for sensitivity such that within these limits we can be sure that variations in sensitivity are due solely to normal variations in tubes?" The procedure is as follows:

(1) Select a receiver of the type to be dealt with which is known to be normal (although perhaps not exactly average) in regard to its component parts, wiring, etc., and

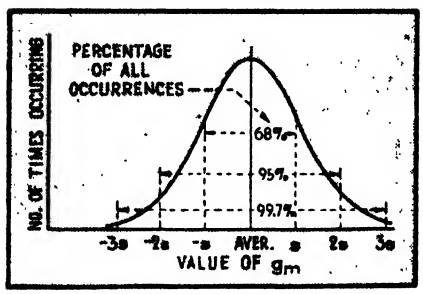

FIG. 2—Variations in mutual conductance values of supposedly identical tubes follow the normal or Gaussian distribution curve shown here

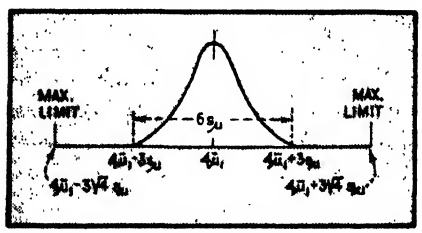

FIG. 3—Variation in overall sensitivity of four stages having equal gain. The maximum limit is twice the probable limit for four stages

allow it to come up to operating temperature with a random lot of proper type tubes in the sockets.

(2) Take successive readings of sensitivity (μv input for standard output) for say 100 different tubes inserted in socket No. 1. These, for example, could be 100 different type 6K7 r-f amplifier tubes taken at random from stock.

(3) Calculate the average sensitivity $\bar{X}_1$ (μv) of the 100 readings and the standard deviation s_1 in μv.

(4) Insert in socket No. 1 a tube which produces this average value of sensitivity, and leave it there.

(5) Take successive readings of overall sensitivity for 100 different tubes of the required type, inserted one after the other in socket No. 2. Again calculate average value of sensitivity $\bar{X}_2$ of these 100 readings and the new standard deviation s_2.

(6) Insert in socket No. 2 a tube which gives this average overall receiver sensitivity, and leave it there.

(7) Repeat for each successive socket until all sockets are equipped with average tubes.

(8) Measure sensitivity $\bar{X}_n$ (microvolts) of the receiver with the tubes in the sockets which have thus been selected as being average tubes.

(9) Calculate the expected standard deviation in sensitivity s_t of the receiver with randomly chosen tubes in production from

$$s_t = \bar{X}_n\sqrt{(s_1/\bar{X}_1)^2 + (s_2/\bar{X}_2)^2 + \ldots. (s_n/\bar{X}_n)^2}$$

(10) Set sensitivity limits for normal tube variations at $\bar{X}_n + 3s_t$ and $X_n - 3s_t$ μv.

Suppose that sensitivity limits are required for a six-tube set with the following tube complement: (1) r-f amplifier; (2) converter; (3) i-f amplifier; (4) detector—first audio; (5) output; (6) rectifier.

As the first step in the procedure, sensitivity is measured in microvolts at the antenna and ground input terminals, using 100 tubes in each socket in turn. The complete data and calculations (hypothetical) for the r-f amplifier stage are given at A in Table I. Similar measurements are then made and tabu-

TABLE I. DETERMINATION OF CONTROL LIMITS FOR SIX-TUBE SUPERHETERODYNE RECEIVER

(A) DATA FOR R-F STAGE (r-f tube changed 100 times—other tubes fixed)

X in μv	f freq. of occurrence	fX	$(X-\overline{X})$	$(X-\overline{X})^2$	$f(X-\overline{X})^2$
9.9	2	19.8	−0.4	0.16	0.32
10.0	4	40.0	−0.3	0.09	0.36
10.1	7	70.7	−0.2	0.04	0.28
10.2	20	200.4	−0.1	0.01	0.20
10.3	34	350.2	0	0	0
10.4	19	197.6	0.1	0.01	0.19
10.5	8	84.0	0.2	0.04	0.32
10.6	3	31.8	0.3	0.09	0.27
10.7	2	21.4	0.4	0.16	0.32
10.8	1	10.8	0.5	0.25	0.25
Total	100	1026.7			2.51

Av. $\overline{X}_1 = 1026.7/100 = 10.3$, and standard deviation $s_1 = \sqrt{2.51/100} = 0.159$

(B) AVERAGE VALUE OF MICROVOLTS INPUT $\overline{X}_1$ AND STANDARD DEVIATION s_n FOR STANDARD OUTPUT

Tube Disposition	No. 1 varied; 2, 3, 4, 5, 6 fixed	No. 2 varied; No. 1 at average	No. 3 varied; 1, 2 average	No. 4 varied; 1, 2, 3 average	No. 5 varied; 1, 2, 3, 4 average	No. 6 varied; others average
Averages $\overline{X}_{1,2,3,\ldots,n}$	10.3	18.5	14.6	16.0	12.1	14.3
Std. Dev. $s_{1,2,3\ldots n}$	0.159	0.304	0.180	0.215	0.120	0.106

(C) COMPUTATION OF CONTROL LIMITS FOR INPUT TERMINALS

Average overall sensitivity $\overline{X}_n = 14.3$ microvolts (measured with average tubes)

$$\text{Overall standard deviation } s_t = 14.3\sqrt{\left(\frac{0.159}{10.3}\right)^2+\left(\frac{0.304}{18.5}\right)^2+\left(\frac{0.180}{14.6}\right)^2+\left(\frac{0.215}{16.0}\right)^2+\left(\frac{0.120}{12.1}\right)^2+\left(\frac{0.106}{14.3}\right)^2} = 0.45\mu v$$

Control limits on this receiver: $\overline{X}_n \pm 3s_t = 14.3 + 1.35 = 15.7\ \mu v$ and $14.3 - 1.35 = 12.9\mu v$

lated for the other five stages, the results summarized as at B in Table I, and the control limits computed as at C.

The data in Table I also provides another check. It is common practice to measure the sensitivity at the control grid of the converter tube. We have, from the data, the standard deviations for the groups of 5 tubes (r-f tube eliminated): $s_2 = 0.304\ \mu v$; $s_3 = 0.180\ \mu v$; $s_4 = 0.215\ \mu v$; $s_5 = 0.120\ \mu v$; $s_6 = 0.106\ \mu v$. Suppose the sensitivity at the converter grid with average tubes is 170 microvolts. This gives for the combination

$$s_0 = 170\sqrt{\left(\frac{0.304}{18.5}\right)^2+\left(\frac{0.180}{14.6}\right)^2+\left(\frac{0.215}{16.0}\right)^2+\left(\frac{0.120}{12.1}\right)^2+\left(\frac{0.106}{14.3}\right)^2} = 4.67\mu v$$

Therefore the sensitivity limits at the converter grid to be taken as acceptable and due to normal tube variations in this particular receiver are $170 + 3s_0 = 184.0\ \mu v$ and $170 - 3s_0 = 156.0\ \mu v$.

We can go farther now and establish economic sensitivity limits where the variations are due to the combined effect of normal variations in coils, capacitors, resistors, wiring, etc. The procedure is as follows:

Using a set of average tubes determined as such by the measurements and calculations previously described, measure the sensitivity of say 100 different receivers each of which is known to have normally controlled components. Since the same tubes are used in each of the sets, variations in sensitivity between the sets will be due solely to variations in the sets themselves.

Calculate the average sensitivity $\overline{X}_s$ in microvolts for the lot of sets used and the standard deviation S_s of the sets in microvolts. If in production average tubes are used, the acceptable limits in sensitivity for set variations alone will be $\overline{X}_s + 3S_s$ and $\overline{X}_s - 3S_s$. If, on the other hand, tubes are taken at random, the limits in sensitivity covering normal expected variations of both tubes and sets will be

$$\overline{X}_s \pm 3\overline{X}_s\sqrt{(s_1/\overline{X}_1)^2+(s_2/\overline{X}_2)^2+\ldots\ldots(s_n/\overline{X}_n)^2+(S_s/\overline{X}_s)^2}$$

Having established sensitivity limits as described, a production receiver showing sensitivity beyond these limits must be immediately suspected as containing abnormal components or wiring or abnormal tubes. Insertion of a set of average tubes removes the possibility of abnormal tubes and if the sensitivity then exceeds $\overline{X}_s \pm 3S_s$ microvolts, the set must be suspected of abnormality in itself.

Sensitivity values as measured on 100 receivers coming from production, each using the set of average tubes measured in the first example, are $\overline{X}_s = 13.5\ \mu v$ and $S_s = 0.50\ \mu v$. Limits on sensitivity exclusive of tubes are $13.5 \pm 3 \times 0.5 = 12.0$ to $15.0\ \mu v$. Limits including both normal tube and set variations are

$$13.5 + 3 \times 13.5\sqrt{\left(\frac{0.159}{10.3}\right)^2+\left(\frac{0.304}{18.5}\right)^2+\left(\frac{0.180}{14.6}\right)^2+\left(\frac{0.215}{16.0}\right)^2+\left(\frac{0.120}{12.1}\right)^2+\left(\frac{0.106}{14.3}\right)^2+\left(\frac{0.50}{13.5}\right)^2} = 15.7 \text{ to } 11.3\ \mu v$$

Limits including tube variations only (see previous example) are

$$13.5 \pm 3 \times \frac{13.5}{14.3} \times 0.45 = 14.8 \text{ to } 12.2\ \mu v$$

Suppose now that a receiver comes through production with random tubes and shows a sensitivity of $16.0\ \mu v$. This is beyond the upper limit of $15.7\ \mu v$. Upon the insertion of a set of average tubes (selected as previously described), the sensitivity is $14.2\ \mu v$. This is within the 12.0–15.0 μv limit for receiver variations alone. We conclude that there was trouble with the original set of tubes.

Quality Engineering in Tube Manufacture

Testing of random samples can indicate when vacuum-tube production deviates from quality standards. Procedures given, applicable to other products as well, cover static and dynamic performance tests, life tests, mechanical tests, and checking of appearance

By EUGENE GODDESS

PRESENT-DAY mass production lends itself admirably to quality engineering practices. Although this article is centered on vacuum-tube manufacture, the approach and much of the technique are directly applicable to other phases of industry.

Quality Tests

In order to determine vacuum-tube *quality*, it is necessary to have a criterion of acceptability; in other words, the tube must pass some sort of a test. One method tests a random sample (typical of the day's production) for static characteristics and dynamic performance. All conditions of the test are recorded and readings are meticulously observed, with the exact nature of the test depending on the type of tube involved.

For the usual transmitting or receiving tube, test instructions should specify voltages for filament, plate, control-grid, screen-grid, and suppressor-grid as required to observe filament, plate, control-grid, and screen-grid currents. Emission, plate resistance, amplification factor, and mutual conductance should be determined; furthermore, it is desirable that interelement capacitances be measured also.

Cathode-ray tubes should be checked for light output, line width, deflection sensitivity, focusing voltage, leakage, gas ratio (or cross), interelement voltage breakdown, and anode currents.

Specifications for dynamic testing should include load resistance (or impedance), signal voltage, and power output at normal and reduced filament voltage. In addition, specifications should give operating voltage and current ranges for all other tube elements.[1]

Measurement of Interelectrode Capacitances

For the measurement of capacitances of 1 $\mu\mu$f or less, several methods are available. Perhaps the most accurate procedure uses a precise capacitance bridge. Another satisfactory method uses a vacuum-tube voltmeter to measure the voltage developed across a capacitance at a fixed frequency. Alternative methods are:

(1) Capacitance can be measured as part of a resistance-capacitance discharge circuit in which the tube capacitance discharges through a known resistance. Since $C = t/R$, the capacitance is easily determined. Both time (in the order of microseconds) and resistance (in the order of megohms) can be determined with reasonable accuracy.

(2) Capacitance can be measured as the terminating impedance of a coaxial transmission line. The reactance is measured by placing the tube in the transmission line as a terminating element. The line is then tuned to resonance by varying its length.[2]

Mechanical Performance Tests

Tubes must perform satisfactorily and must possess reasonable life; in addition, they must be rugged. This does not imply that it is permissible to play hockey with a two-inch u-h-f transmitting tube. On the other hand, it should not be necessary to transport the tube in a plush-lined case. The usual points of mechanical weakness can be divided into four main headings:

(1) Metallic bodies (filaments, grids, plates, etc.)
(2) Metallic joints (welds)
(3) Glass bodies (glass envelopes, beads)
(4) Glass joints (either glass-to-glass or glass-to-metal)

Among the methods used for checking the mechanical durability of the tube are: 1. Bump tests; 2. Vibration tests; 3. Thermal shock tests.

In a bump test, a pendulum of prescribed weight and length is allowed to strike the tube, which is so suspended that it swings freely on impact. The tube is then tested for mechanical failure, static characteristics and interelement capacitance (revealing changes in electrode spacings).

The vibration test is essentially the same as the bump test. Instead of causing acceleration through impact, the tube is placed on a shake table and is subjected to acceleration values that are several times that of gravity. Both of these tests can be made with voltages on the elements, so that results can be observed on a cathode-ray-tube oscilloscope. In this way, temporary interelement shorts and undue voltage excursions can be observed.

Thermal shock tests are concerned with the condition of the glass. In general, they reveal improper annealing or defective sealing.

The foregoing are the most common mechanical performance tests. It is possible to make as many tests as there are mechanical performance weaknesses.

Life Testing of Tubes

Tube life can be determined on the basis of either static or dynamic performance. In any event, the life will depend (among other factors) upon: 1. Filament voltage; 2. Tube operating temperature; 3. Amount and nature of the free resi-

dual gases in the tube and in the metallic parts.

Within a thoriated tungsten filament, thorium is diffused to and evaporated from the surface at a definite rate. The ideal filament voltage is one which causes a current flow of such magnitude that the heat produced establishes an equilibrium between these two rates.[8]

If the filament temperature is too low, insufficient emission will result. If filament temperature is too high, the rate of evaporation will exceed the rate of diffusion. Under this condition, the surface is stripped of its thorium and soon acquires the properties of a pure tungsten emitter, which is about 1/1000th the emission of a thoriated tungsten filament operated at equivalent temperature. As a result, the emission drops rather sharply and the tube ends its useful life abruptly and prematurely.

Such a tube can be brought to life again by means of the so-called "hot shot" treatment, which consists of operating the filament at a rather high temperature (2800 deg K) for a few minutes. This reduces some of the thoria (thorium oxide) within the filament to metallic thorium. Then, operation of the filament at a lower temperature (2200 deg K) diffuses the newly reduced thorium to the surface. However, life obtained by rejuvenation is not a true test of life, but rather is a test of the renewing process.

It has been pointed out that the voltage at which a filament is operated determines its temperature. Temperature determines the fraction of the surface which is covered with a monatomic layer of thorium. Emission may drop below acceptable limits as the fraction of the covered surface is reduced. Since good life depends upon good emission, any factors which disturb or deteriorate the emissive properties of the filament contribute to the early demise of the tube. Operation at excessive filament voltage is one such factor.

Another factor which can result

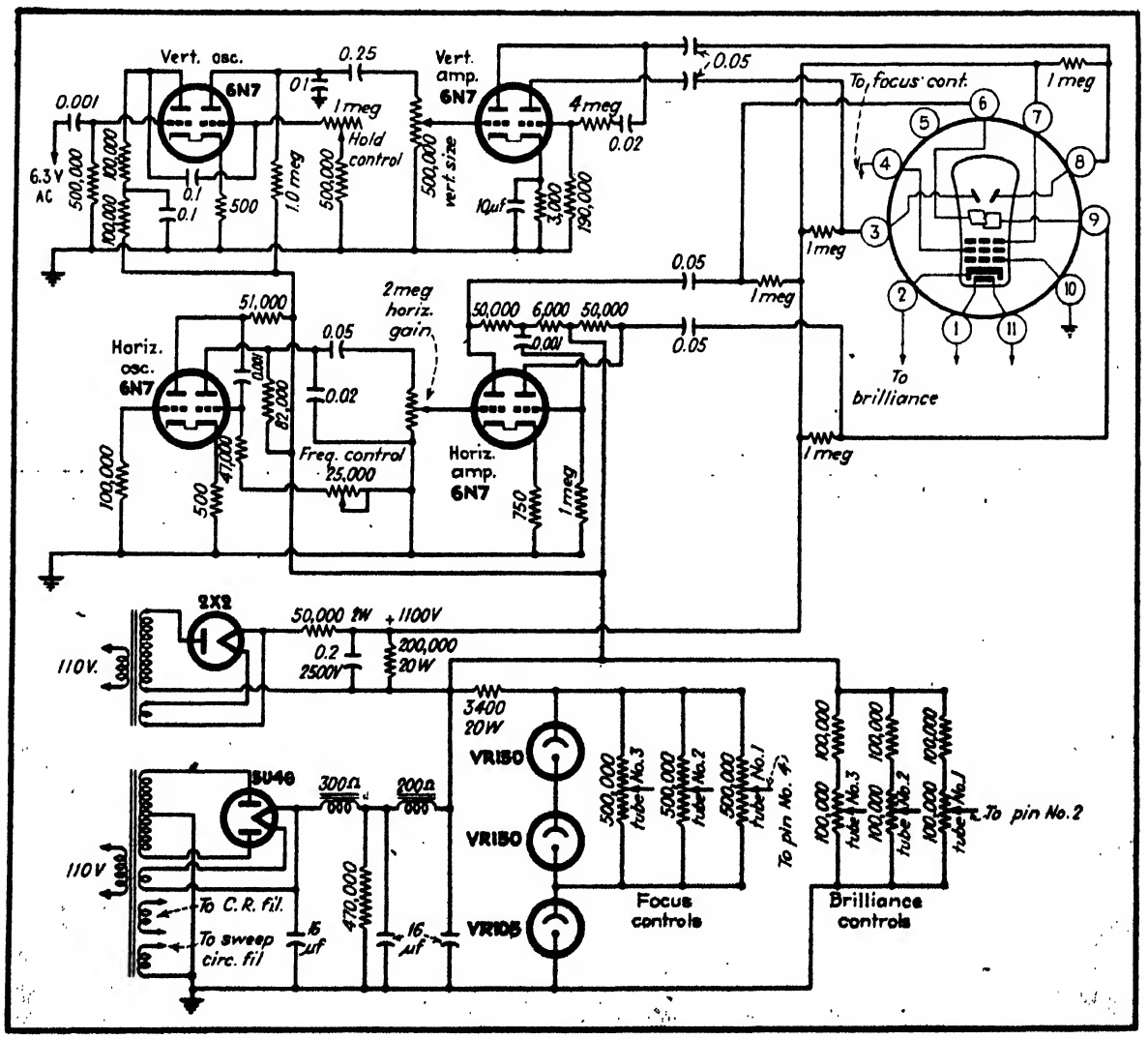

Schematic circuit of three-position life test set for use on type 2AP1 cathode-ray tubes

in reduced emission is the presence of excessive amounts of oxygen in the tube. Should this highly-active gas be available to form a chemical union, layers of thorium and tungsten oxides are formed. If this happens, emission quickly drops to the vanishing point.

If the power supply voltage varies over a considerable range, the life test will operate at various temperatures; in other words, anode and filament power dissipation will vary. It is therefore necessary that the power line voltage for life test equipment be regulated within close limits.

Complete and carefully prepared records should be kept of all test conditions and causes of failure. This latter point cannot be overemphasized since one of the primary objects of all life tests is to reveal the weaknesses which cause tube failure. For example, to state that a cathode-ray tube failed due to low light output is not enough; it is much more significant to point out that the low light-output was caused by a deteriorated cathode surface which resulted from the failure of a metal-to-glass seal.

The tube that performs properly is interesting and indeed welcome; nevertheless, it is the defective tube that uncovers weaknesses and helps us evolve new and better production techniques.

Other Tests

Samples should be selected and tested at periodic intervals, in order to ascertain the life of the shipped product. Factory engineers, design engineers, and persons responsible for maintaining production should be advised of all failures occuring in non-experimental tubes. All innovations in processing or structure should be successfully life-tested before becoming a regular part of the manufacturing procedure.

A sizeable quantity of tubes should be selected at random from the packing room and should be examined for appearance. This inspection should answer the following questions:

(1) Is the tube clean?
(2) Is the tube identification brand clean and legible?
(3) Is the company trademark clean and legible?
(4) Are the base pins neatly soldered? Has extra flux been wiped away?
(5) Is the tube base on straight?
(6) Are the critical dimensions within specification?
(7) On the basis of the perfect tube being rated as 100 percent, what is the rating of the average of these tubes?

The basic purpose in making this type of examination is to rate the tube's appearance from the standpoint of saleability.

It is inadequate to say that the vacuum-tube industry sells "tubes". We are offering measurements when we offer tubes. Some assurance must be given that the meters which check those measurements are correctly calibrated.

Tubes are saleable because they have certain characteristics—characteristics which are measureable by meter. Quality, as determined by electrical testing, implies the use of meters, and the testing is no bet-

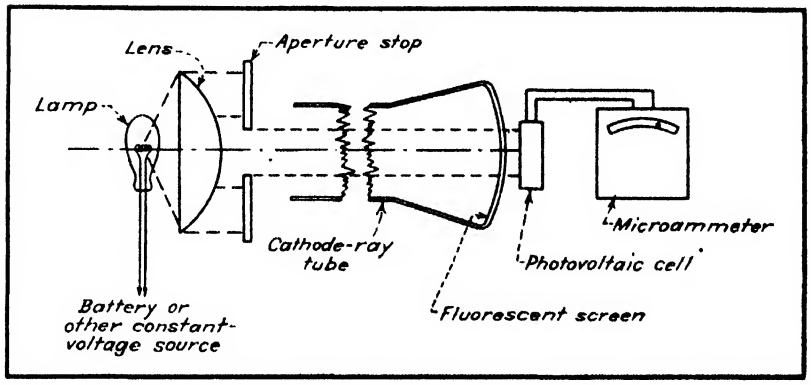

Arrangement used for measuring light transmission of a cathode-ray tube screen

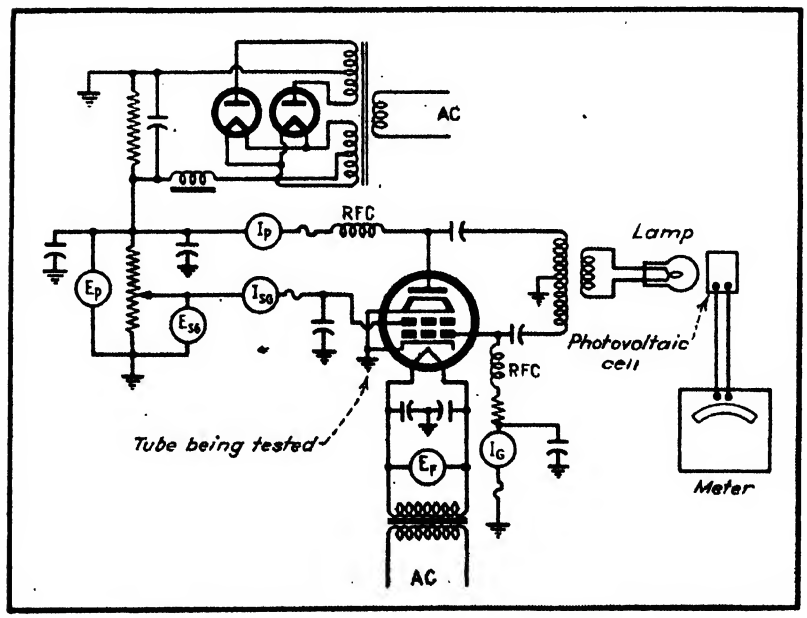

Simplified schematic of oscillator used to determine power output of a beam-power tube. The circuit is essentially a Hartley oscillator in which the inter-electrode capacitances of the tube under test serve as the capacitive elements of the tank circuit. The cathode is grounded to complete the plate circuit

ter than the meters that perform the work. Improperly calibrated meters give rise to three risks:

(1) The possibility that acceptable tubes may be rejected.
(2) The possibility that rejectable tubes may be accepted.
(3) The possibility (almost certainty) that the quality will be indeterminate.

Proper calibration of test meters is normally a function of a meter maintenance unit, acting under the jurisdiction of an equipment section. This meter-maintenance unit will generally have a set of secondary standards. However, the quality control activity is so definitely tied up with measurement problems that it is advantageous to have the primary standards retained by the quality engineering division.

Certified standard cells, high-precision potentiometers, volt boxes, current and voltage transformers, highly sensitive galvanometers and accurate wavemeters are a few of the primary standards which should be available to the quality control engineer. Then, when a question comes up involving the accuracy of factory readings, unquestionable evidence can be produced by the quality engineering laboratory. Unless a standards laboratory is set up to do the job, the quality engineering department should act as the "Bureau of Standards" for the factory.

With a test procedure set up, the next step in utilization of quality engineering is analysis of the test results to determine exactly where the trouble is when shrinkage (loss during production) exceeds permissible manufacturing limits. This subject will be taken up in the next issue, and will be followed by the final article covering process control charts and other statistical methods of controlling quality during manufacture.

REFERENCES

(1) Report published by Institute of Radio Engineers, New York. "Standards on Electronics, Methods of Testing Vacuum Tubes, 1938".
(2) Nergaard, L. S., A Survey of Ultra-High-Frequency Measurements, *RCA Review*, Oct., 1938.
(3) Koller, L. R., "Physics of Electron Tubes." McGraw-Hill Book Co., New York.

Shrinkage Analysis in Tube Manufacture

Procedure for isolating the factors responsible for rejected tubes, with examples of routine followed by Shrinkage Analysis Department and samples of typical reports

By EUGENE GODDESS

SUPPOSE 1000 stems for vacuum tubes are started in the mounting department and that only 800 actually became satisfactory tubes. Shrinkage analysis seeks to determine why 200 were lost en route. In contrast, quality control is concerned with variations in the performance of the 800 good tubes. Shrinkage analysis thus obtains information directly concerned with the reduction and removal of factors which cause industrial losses.

If the product is running close to a manufacturing limit, shrinkage analysis will never disclose that fact until the damage is done; quality control, however, observes the condition and reports to factory engineers who take steps to rectify the trouble. Should quality control warnings be ignored for one reason or another, shrinkage results. Shrinkage analysis, then, is the fact-finding procedure which informs factory engineering of the vital channels to be worked on to bring variables under control.

In cases where the shrinkage is localized, a positive indication is available which points to an inefficient or improper operation. Let us say that 5 percent is the normal shrinkage expectancy for open filaments over the entire operation. If this 5 percent loss occurs in only one operation, it is imperative that factory engineers correct the situation quickly. Regardless of this fact, the point being made is that localization of the disturbance to a single operational area is most easily recognized by a preliminary analysis.

Suppose a poor material is used. If twenty different operations each lose 0.5 percent of their tubes due to open filaments, an overall filament shrinkage of 10 percent results. Here the trouble-localizing or "where" analysis is small, but the "what" analysis discloses the hidden truth.

Once it has been ascertained factually that trouble exists, a secondary analysis must be performed in order to isolate it. Is it confined to a certain operator or machine or to a certain combination of operators and machines? Does it occur on any specific day of the week? Does it occur only during or following certain atmospheric conditions? Does it manifest itself only on certain work shifts?

The causes for shrinkage belong more properly in the domain of engineering, but often the shrinkage analysis department can disclose or confirm facts concerning such troubles. Good analysts are fundamentally curious.

Here, then, is a method of operation:

1. A primary or preliminary analysis is made for purposes of identification.

2. A secondary or detailed analysis is made for purposes of isolation. Summaries are made daily, weekly,

and monthly in order to detect shrinkage trends. An isolating analysis follows any time that the situation demands it.

It is desirable that shrinkage analysis work be performed by a single specially trained group rather than by individuals from different departments. The Shrinkage Analysis Department is not concerned so much with reduction of shrinkage as it is with presenting accurate facts concerning the condition. This information is then turned over to factory engineers whose main concern is to keep the factory running at high efficiency.

There is some question as to whether the completely tabular form of report is as digestible or as emphatic as the same report would be if results were integrated into conclusive thoughts. The analyst's opinions and conclusions are important for several reasons, namely:

1. The analyst has time to draw a summary. Most (not all) other persons give tabular reports a quick reading and generally do not stop to summarize.

2. The analyst's summary is objective—thus, results are viewed impartially.

3. The analyst often draws upon the experience of many engineers to make or confirm his conclusions.

Report value depends on two factors: 1. Factual content; 2. Thorough study of the findings. The first factor depends on the efficiency of the analyst; the second factor depends on the engineering personnel of the sections involved.

Failure of production and engineering personnel to utilize the potentialities of the Shrinkage Analysis Department may be ascribed to the natural reticence of anyone to bare his errors, and to misunderstanding concerning the function of the Shrinkage Analysis Department in the general scheme of factory operation. Since reticence can be overcome only when misunderstanding is clarified, it is imperative to discuss the main problem: "What relationship does the Shrinkage Analysis Department have to general factory activity?"

Development engineers set up specifications for making tubes, and factory engineers watch manufacturing procedure to be sure specifications are followed. Naturally, all specifications cannot be followed exactly — the slight changes that are necessary are termed variables. The Quality Engineering Department gives a dynamic picture of production by observing deviation of the variables; when deviation gets out of control, shrinkage will then occur.

The Shrinkage Analysis Department examines rejected material to reveal the cause of shrinkage. This information is conveyed to factory engineers and production personnel, who use the additional information to put the variables under control. That is the reason—the sole reason—for circulating reports. Departmental activities are completely objective and are aimed at pointing out failure only for the purpose of lighting the road so engineering and production personnel may achieve success.

As an example, let us assume that a transmitting tube fails because of low power output. The first step in performing a post mortem is to verify the failure in the following manner:

1. The test set must be checked with good tubes to show that it is operating properly.

2. The meters should be verified to remove any question about the effect of calibration on observed results.

3. If the tube is tested as a power amplifier, it is necessary to verify the power input before condemning the tube for poor power output.

These are some of the preliminary steps which, though they seem quite obvious, are easily overlooked.

Once the failure has been verified, it is desirable to determine whether low power output is due to low emission or to faulty construction in the tube. If emission is adequate, the tube should be checked to see if the grid is properly constructed. It is necessary also to verify whether power output is measured at a frequency at which inter-element spacing may be at fault. Similarly, filament construction must be examined.

If emission is low, gas content of the tube should be measured and it is worthwhile to investigate carburization of the filament. When the filament is over-carburized, emission is reduced and in some cases power output suffers. This condition can be checked by "flashing" the tube at a temperature slightly higher than normal; thus, some of the carbon is removed and power output can be redetermined. If power output comes up, the cause of failure is known. Should power output fail to come up, over-carburization is not at fault.

If the tube shows a slight gassy condition, the seals and beads should be carefully examined for wire leaks or faulty beads; metal-to-glass seals should be given special attention. Where tungsten is used as a lead, it should be examined for small fissures through use of a magnifying glass or microscope. In some cases it is desirable to use a fluorescent liquid penetrant which becomes visible under ultraviolet light.[1]

Where large volumes of gas cause the tube to be classed as an "air tube", the failure will generally be in the form of a large crack or fissure. Frequently, this can be discerned by eye with the aid of a bright light.

The above analysis does not pretend to be as complete or as detailed as might be desired. It does offer two advantages; it provides a simple pattern for new and untrained help, and it requires practically no expensive or elaborate test equipment.

As a second example, consider a cathode-ray tube which has been rejected for low light output. Here again, the rejection should be verified. One convenient method uses several test sets for checking the reject against a standard tube. A standardized test set is preferred on which heater current and anode voltages can be observed. The heater current can act as an index of cathode temperature. By reading second or third anode currents, as required, intensity of the beam

hitting the screen can be checked.

If anode currents are low, it is incorrect to assume that cathode emission is reduced. This value must be checked separately with a low positive voltage on the grid. Once it has been definitely established that cathode emission is inadequate, various beads and wires should be examined for cracks or failures that permit entrance of gas which destroys the emitting surface.

When the tube is opened, the cathode should be examined for ion spots. If none are present, it should be examined for other types of contamination such as chloride or oil, which also reduce emission.

Suppose, however, that emission is adequate but second anode current is low. In that case, the geometry of the electron gun should be examined for alignment and concentricity on the test set or by opening the tube if necessary; apertures should be checked for correct size. If emission and second anode current are adequate but light output is low, the tube should be opened to measure the light transmission of the screen. If the screen is too thick, then light intensity on the face of the tube will be materially less than on the inner surface of the screen. If light transmission is adequate, the screen may be inefficient for other chemical or physical reasons.

Basically, the luminescence of a phosphor is due to an unstable crystalline structure; this structure is disturbed by physical shock. When the phosphor comes from the oven during the manufacturing process, it is rather lumpy. Thus, it is necessary to reduce the diameter of particles to the order of 5 to 50 microns and this is generally done by ball milling. If ball milling continues over an extended period of time, the crystalline structure is disturbed by the physical shock. As a result, the phosphor becomes stable and loses its basic property of luminescence.

Impure chemicals used for synthesizing impair the efficiency and color of the phosphors. These characteristics may also be affected by improper crystallization temperatures. Now, all these things increase the amount of inert or non-luminescent material present in the phosphor and subsequently in the screen. Consequently, the efficiency of the entire screen is reduced because this inert material takes up space which normally would be occupied by luminescent material.

These are only a few of the factors which can cause low screen efficiency. Nothing has been said about reflectivity of the inner glass surface nor about glass thickness and bulb processing, which factors also affect the light output offered by the tube.

It is hoped that the material given so far in this series of articles will indicate the basic approach to these problems. It is more important to understand the approach than to understand the specific method, because the latter varies from problem to problem—the approach to shrinkage analysis problems generally remains the same.

REFERENCE

(1) Kulin, S. A., Fluorescent Inspection of Tungsten, ELECTRONICS, July 1943, p. 95.

Quality Control in Tube Manufacture

Discussion of problems involved in setting up a statistical method of controlling quality of tubes and component parts during manufacture, with instructions for using process control charts in connection with random sampling techniques to detect promptly when a process is out of control and causing excessive shrinkage

By EUGENE GODDESS

THE chief objective of a quality control system is to assure quality on an economic basis. Such a system should exercise its effect during manufacturing operations, through process control, and should insure the quality of the finished article by means of product control.

Effectiveness of the control can be determined in two ways: 1. By studying the presence or absence of critical attributes of the product; 2. By studying the variation of some mensurable characteristic of the product.

Sample Size

A statistical method of quality control requires consideration of the problem of sample size. Usually, this presents a difficult problem because the fundamental concept of the statistical approach is not clearly understood. When this difficulty is analyzed, the question of sample size resolves itself into a statement (on the part of management) concerning quality level to be maintained in the product. Once this level is established for interdepartmental or external shipments the percentage limits for defectives can be established and an intelligent solution to the sample-size question can be obtained.

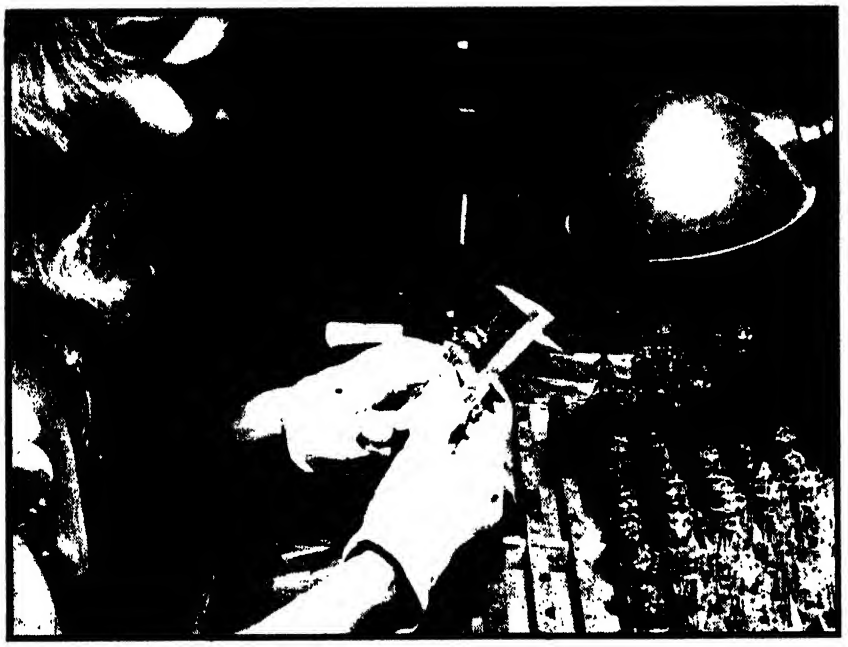

Go no-go inspection for dimensional accuracy of tube parts is performed on a sample quantity taken from the grand lot

As an example, management may decide to ship a finished product with a 9 to 10 probability that defectives will not exceed 30 per 10,000. Once management decides what risk it is willing to take to get a specific quality, the question of sample size can be rationally approached. If every unit shipped must be absolutely perfect, then 100 percent inspection and 100 percent efficiency are necessary. In mass production 100 percent inspection efficiency cannot be assured because of 1. Human judgment; 2. Prolonged work periods;[1] 3. Worker's skill; 4. Worker's concept of how the job should be done; and 5. Worker's attitude toward the work.

Because of these human factors controlling inspector efficiency, 100 percent inspection is not the practical solution for the problem.

Of course, most manufacturers desire to ship a product that is 100 percent perfect. How can it be done? In most cases (certainly in mass production), perfection in inspection is impractical and unattainable. Hence, the existence of merchandise returns from customers. It is a rare organization indeed which never has a product returned. However, though the manufacturer cannot achieve a 100 percent perfect product, he can certainly approach that condition. The essence of the technique is to obtain a random sample of good size and inspect it carefully. In this way, 100 percent inspection efficiency is obtained on the sample rather than partial inspection efficiency on 100 percent of the product.

Suppose management agrees it is permissible to have 100 defects in 10,000 parts; in other words, the fraction defective is 0.01 on the average. If this condition existed, a sample of 250 units would probably disclose two rejects.

If the lot had 200 defects per 10,000 on the average, then a sample of 250 could have four rejects and a sample of 500 could have nine rejects. This example shows that as the sample size increases, the fraction defective in the sample approaches the fraction defective in the lot. The answer to the question of sample size rests then with management, which must declare that the observed fraction defective in the sample must be accurate, $\pm X$ percent. The actual technique for selecting samples and interpreting the results can be found in suitable texts on statistics.[2] These methods should be diligently applied in order to protect the manufacturer.

Once the theoretical sample size has been computed, it becomes necessary to select the practical sample size, depending on the availability of the product. If the theoretical sample size is 189 and the product comes packed in groups of 25, it is convenient to take a sample which is a multiple of 25. In this case, either 175 or 200 would be suitable but it is good practice to use the larger sample.

Sample size does not depend on percentage. For example, if percentage were a criterion in selecting a sample, then 1 out of 5 would be as typical as 200 out of 1000, since both are 20 percent samples. Likewise, if sampling information were on a percentage basis, a sample of 1 from a lot of 10 would be more typical than a sample of 50 from a lot of 1000. Of course, these extreme cases reduce the percentage basis of sample selection to an absurdity but they were selected to make the argument more poignant.

The object in taking a sample from a grand lot is to obtain information about the quality of the grand lot, the assumption being that the sample has the same distribution of defects (or variables) as the grand lot. To be properly selected, a sample must be: 1. Taken at random so as to be typical; 2. Large enough that its distribution curve is not materially affected by sample size; 3. Composed of normal products and not containing engineering freaks.

In substance, sampling is safe if production on a product is running normally. When production becomes abnormal, units should be subjected to a manufacturing culling operation. The good product is then inspected on a sampling basis —actually, this amounts to inspecting a previous inspector's work.

Product Control

One of the problems which confronts quality control engineers is that of passing judgment on the

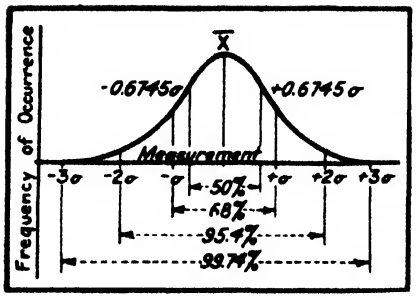

FIG. 1—Normal or Gaussian distribution curve relates frequency of occurrence with different values of deviation from the arithmetical mean $\bar{X}$ for a given measurement

grand lot. The lot can have one of three sources: (1) An outside supplier supplying a raw product; (2) A company department supplying a part to another company department; or (3) The company itself, offering its completed product for final inspection.

Regardless of where a grand lot comes from, judgment should be made in the same way. In evaluating the grand lot, the quality control department will feel pressure exerted upon it by: (1) The outside supplier, who feels his *good* product has been rejected; (2) The department head, who resents having a grand lot rejected because "a few bad ones showed up in the sample"; or (3) Over-anxious production men, who are trying to meet shipping schedules and contracts.

These pressures are only human and will always exist as long as humans play a part in the production picture. One of the best ways to overcome this situation is to sit with the persons involved and demonstrate the quality of the rejected product by detailed examination of the grand lot in question.

For example, although only 3 defects showed up in the sample of 250, there is a probability of 0.9 that the number of defectives per thousand will be between 21 and 7. If the detailed examination does not verify the prediction, something is wrong with the data. Usually, when the true condition of the product is once revealed and verified, the doubters accept future statistical results.

There is one other possibility of serious friction which cannot be ignored. Should the outside supplier insist that his product is *good* despite the rejection, it will probably be necessary to review the specification against which the examination was made.

The subject of product control is extensive indeed and will not be discussed further except for one additional warning. Be sure to select a *random* sample. If the grand-lot is thoroughly mixed, the random nature of the sampling is not critical. But if the grand lot is not thoroughly mixed, it is imperative that the sample be selected by a random operation. It is interesting to note that a random sample means a sample selected in a random manner; thus the reference is to the technique of sampling rather than to the sample per se. Obviously, the criterion of random selection is to give each unit of the grand lot an equal chance of being chosen.

Process control prevents the occurrence of industrial losses by showing the trend in quality as a

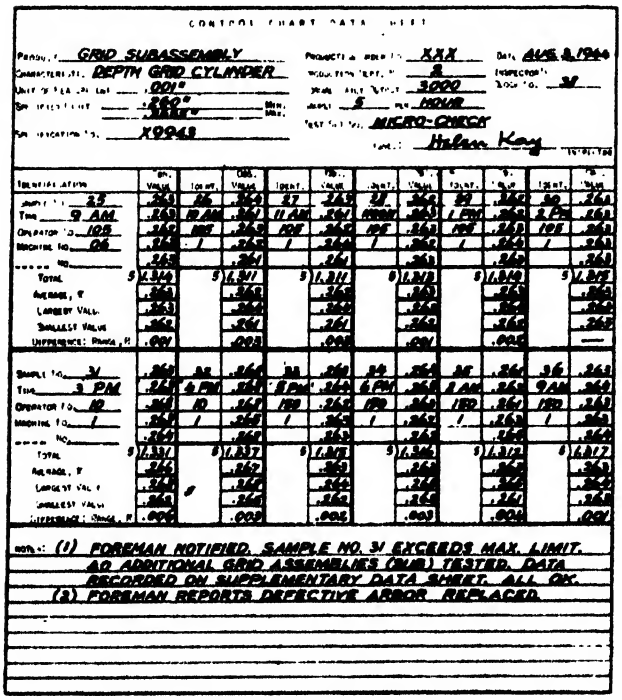
CONTROL CHART DATA SHEET

Product: GRID SUBASSEMBLY — Part: DEPTH GRID CYLINDER — Unit of Measurement: .001" — Specification: .260" ± .010" — Location: X9943 — Product No.: XXX — Date: AUG. 3, 1944 — Inspection Dept.: 8 — Inspector No.: 31 — Sample Size: 5 — Frequency: HOUR — Gage No.: MICRO-CHECK — Inspector: Helen Kay

Identification	Sample 1	Sample 2	Sample 3	Sample 4	Sample 5	Sample 6	Sample 7	Sample 8	Sample 9	Sample 10
Sample No.	25	26	27	28	29	30	31	32	33	34
Time	9 AM	10 AM	11 AM	Noon	1 PM	2 PM	3 PM	4 PM	5 PM	8 AM
Operator No.	105	105	105	105	105	105	105	105	105	105
Machine No.	06	06	06	06	06	06	06	06	06	06
Observations	.260	.260	.261	.260	.260	.260	.264	.260	.260	.260
	.260	.260	.260	.260	.260	.260	.260	.260	.260	.260
	.260	.260	.260	.260	.260	.260	.260	.260	.260	.260
	.260	.260	.260	.260	.260	.260	.260	.260	.260	.260
	.260	.260	.261	.260	.260	.260	.260	.260	.260	.260
Total	1.300	1.300	1.302	1.300	1.300	1.300	1.304	1.300	1.300	1.300
Average, $\bar{X}$	.260	.260	.260	.260	.260	.260	.261	.260	.260	.260
Largest Value	.260	.260	.261	.260	.260	.260	.264	.260	.260	.260
Smallest Value	.260	.260	.260	.260	.260	.260	.260	.260	.260	.260
Difference: Range, R	.000	.000	.001	.000	.000	.000	.004	.000	.000	.000
Sample No.	31	32	33	34	35	36	37	38	39	40
Time	3 PM	4 PM	5 PM	6 PM	7 PM	8 PM	8 AM	9 AM	10 AM	11 AM
Operator No.	02	02	02	02	02	02	02	02	02	02
Machine No.	1	1	1	1	1	1	1	1	1	1
Observations	.264	.260	.260	.260	.260	.260	.260	.260	.260	.260
	.260	.260	.260	.260	.260	.260	.260	.260	.260	.260
	.260	.260	.260	.260	.260	.260	.260	.260	.260	.260
	.260	.260	.260	.260	.260	.260	.260	.260	.260	.260
	.260	.260	.260	.260	.260	.260	.260	.260	.260	.260
Total	1.304	1.300	1.300	1.300	1.300	1.300	1.300	1.300	1.300	1.300
Average, $\bar{X}$	.261	.260	.260	.260	.260	.260	.260	.260	.260	.260
Largest Value	.264	.260	.260	.260	.260	.260	.260	.260	.260	.260
Smallest Value	.260	.260	.260	.260	.260	.260	.260	.260	.260	.260
Difference: Range, R	.004	.000	.000	.000	.000	.000	.000	.000	.000	.000

Notes: (1) FOREMAN NOTIFIED. SAMPLE NO. 31 EXCEEDS MAX. LIMIT. 40 ADDITIONAL GRID ASSEMBLIES (OUR) TESTED. DATA RECORDED ON SUPPLEMENTARY DATA SHEET. ALL OK.
(2) FOREMAN REPORTS DEFECTIVE ARBOR REPLACED.

FIG. 2—Depth measurements on grid cylinder are recorded in this manner on a typical control-chart data sheet. Computed average values $\bar{X}$ and range R provide points for plotting on control chart

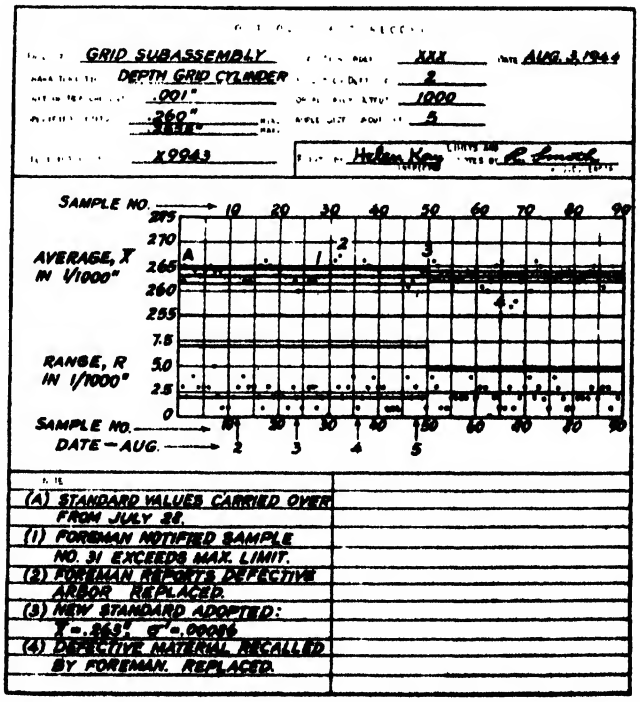

FIG. 3—Control chart record carries a plot of calculated values $\bar{X}$ and R from data sheet of Fig. 2. Points 25 to 36 are thus derived. Note point 31, which exceeds maximum limit established for this grid subassembly

function of either the attributes or the variables. This is best illustrated by an example. Several constants from the American Standards Association War Standard Z 1.3-1942 are used, and it is well to point out that if the sample size changes, the constants also change. The ASA has issued three excellent publications covering this entire problem,* which are valuable in setting up a quality control system.

Suppose it is desired to control the depth of a grid assembly for a cathode ray tube. In such a case, quality is to be measured by observing the trend in a variable, and one way to proceed is given here:

1. Each hour, determine and record the depth of a sample of five grid assemblies.

2. Compute average depth by adding the depths and dividing by 5. Call this value $\overline{X}$.

3. Determine the range, R, of the sample by subtracting the smallest value from the largest.

4. After n values of $\overline{X}$ have been computed, determine the average of the averages, $\overline{\overline{X}}$, which is found by the equation $\overline{\overline{X}} = \Sigma\overline{X}/n$ where $10 < n < 25$.

5. From the same data, compute $\overline{R}$, the average of the ranges using the equation $\overline{R} = \Sigma R/n$ where $10 < n < 25$.

6. Compute control limit values for $\overline{X}$ as

$$X_{L\ \text{upper}} = \overline{\overline{X}} + 0.577\overline{R}$$

$$X_{L\ \text{lower}} = \overline{\overline{X}} - 0.577\overline{R}$$

7. Compute control limit values for $\overline{R}$ as

$$R_{L\ \text{upper}} = 2.114\overline{R}$$

$$R_{L\ \text{lower}} = 0(\overline{R}) = 0$$

8. Prepare two charts, one for $\overline{X}$ and one for R. Show $\overline{\overline{X}}$, $X_{L\ \text{upper}}$, and $X_{L\ \text{lower}}$ on one chart. Show $\overline{R}$, $R_{L\ \text{upper}}$ and $R_{L\ \text{lower}}$ on the second chart.

9. Plot the values of $\overline{X}$ and R on the respective charts.

10. If 25 consecutive values of X and R fall between the upper and lower limits, we can say that control exists. If not more than 1 out of 35 successive values of $\overline{X}$ and R (or 2 out of 100) fall outside the limits, it may be safely concluded that excellent control exists.

11. If good control exists (as described in step 10 above), $\overline{\overline{X}}$ and $\overline{R}$ may be adopted as standard values, i.e. $\overline{\overline{X}} = \overline{X}'$ and $\overline{R} = R$.

12. If good control does not exist, use only that portion of the data which can be considered as representative to recompute $\overline{\overline{X}}$ and $\overline{R}$.

13. Compute sigma prime, the standard deviation, as $\sigma' = \overline{R}/2.326$. This is an index to the dispersion or spread of the individual measurements about their average.

14. Let the maximum specified limit be $X_{max.}$ Then, if

$$(X_{max.} - \overline{X}')/3\sigma' > 1$$

$\overline{X}'$ and σ' may be used for ensuing calculations.

15. On the basis of $\overline{X}'$ and σ' (from step 14) determine the central line for $\overline{X}$, which is the average of the (representative) averages $\overline{\overline{X}}$ (see step 12) and is equal to $\overline{X}'$.

16. Compute the limits for $\overline{X}$ as

$$X_{L\ \text{upper}} = \overline{\overline{X}} + 1.342\sigma$$

$$X_{L\ \text{lower}} = \overline{\overline{X}} - 1.342\sigma'$$

17. The central control line for R is

$$R_{\text{control line}} = 2.326\sigma$$

18. The control limits for R are

$$R_{L\ \text{upper}} = 4.918\sigma$$

$$R_{L\ \text{lower}} = 0(\sigma) = 0$$

19. Use the values of $\overline{X}$, $X_{L\ \text{upper}}$, $X_{L\ \text{lower}}$, $R_{\text{control line}}$, $R_{L\ \text{upper}}$, and $R_{L\ \text{lower}}$, as determined in steps 15 to 18, as control lines on their respective charts for the next 100 samples unless a major cause of failure is eliminated.

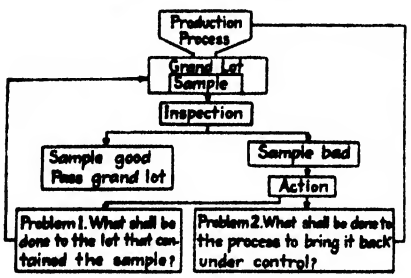

FIG. 4—Functional breakdown of situations resulting from a good sample lot and a bad sample lot under quality control

20. If a major cause of failure is eliminated, use the last 25 representative values to compute new control lines as indicated in steps 12 to 19.

21. If no major failure is eliminated in the next 100 values, then use the last 25 values to compute new control lines as indicated in steps 12 to 19.

22. Completed control charts should be filed.

An interesting observation can be made about step 14. The denominator of the fraction contains $3\sigma'$ because σ' is the standard deviation of the observed values from their average, and $3\sigma'$ includes 99.74 percent of the articles examined. Of course, this theory is based on a normal or Gaussian distribution curve, as shown in Fig 1. Thus,

$$\sigma = \frac{\sqrt{(X_1 - \overline{X})^2 + (X_2 - \overline{X})^2 + \cdots + (X_n - \overline{X})^2}}{n}$$

where X_1, X_2, $\cdots$ X_n are the observed averages and

$$\overline{X} = (X_1 + X_2 + X_3 + \cdots + X_n)/n.$$

Use of the Control Chart

A typical control chart data sheet is shown in Fig. 2. Values of the constants given in the example are correct so long as the sample size is 5. Should the sample size vary, the new constants should be determined as explained in ASA publication Z 1.3-1942.

A quality control chart as shown in Fig. 3 should not be kept secret. It should be posted where the factory engineers, quality control engineers, foremen, factory production heads and division managers can observe it at will. New data should be plotted as soon as it is obtained and verified. If newly-plotted points are inside the limits, the manufacturing process continues uninterrupted.

But suppose a point occurs outside the 3-sigma limits as determined in step 16. Since a normal distribution is assumed (based on the 25 consecutive satisfactory sam-

ples), the point outside the 3-sigma limits is due to an assignable cause —in other words, it was not a chance variation.

As shown in Fig. 4, an out-of-control condition presents two problems: 1. What should be done with the lot that contained the sample; 2. What should be done to the process to bring it back under control?

The lot can be judged as explained under sections covering sample size and product control. With respect to the process, the best procedure is to request foremen and factory engineers to investigate the cause for lack of control. Until control is re-established, sampling should be done at an accelerated rate, say once every 5 or 10 minutes. Once control is re-established (25 consecutive samples within limits), the sampling rate may be reduced to its original value.

REFERENCES

(1) Dutton, H. P., Quality Control, *Factory Management and Maintenance*, 93, No. 9, Sept. 1935.
(2) "Engineers' Manual of Statistical Methods," John Wiley & Sons, New York, N. Y., 1941, p. 84.
(3) Z1.3-1942, Z1.1-1941, and Z1.2-1941, American Standards Association, 70 W. 45th St., New York, N. Y.

Central Signal Generator for Production Testing

This central signal source supplies modulated frequencies to 25 test stations in a radio receiver manufacturing plant. Coupling, impedance matching, attenuator design, radiation, and leakage are discussed

By FRED MILLER

QUANTITY PRODUCTION of radio receivers requires a calibrated source of radio-frequency signals for aligning and testing. This can be supplied by equipment at individual testing stations or by placing the equipment in a central location and using transmission lines to the individual stations. The latter method provides a central location for all the tube equipment, where it can be maintained, adjusted and kept free of tampering by unauthorized personnel. Other factors are cost, uniformity of signals, delivery time, and economy.

The system to be described contains 24 test stations, about 7 feet apart, 12 to a floor (2 floors), with radio-frequency energy covering the intermediate frequency and several spots across the broadcast and short-wave bands. An additional station is provided in the engineering department. The r-f is controlled in amplitude and available in level from 1.0 μv to 0.1 volt.

A number of transmitters were built, one for each radio frequency and modulated with an identifying audio frequency. The frequencies chosen are:

Signal	Frequency	Modulation in cps
I-F	455 kc	1,500
Broadcast	1,740	300
	1,530	600
	960	800
	610	1,000
Short Wave	6 mc	2,000
	10	2,500
	18	3,000

These radio frequencies were chosen to supply the band limit, alignment points, and cross-over tracking points in each band, missing local broadcast stations. To prevent interruption of service, a spare transmitter unit is provided to replace temporarily any unit needing repair. It is equipped with plug-in coils to cover the radio frequency range and with a rotary switch to select the audio frequencies.

The transmitters employ the circuit shown in Fig. 1. A 6V6 crystal oscillator using an AT-cut crystal is followed by a 6V6 class-C amplifier modulated by a 6V6 Heising modulator. The radio-frequency output is link coupled to a 50-ohm line. Audio signal is supplied to the modulator by a 6SJ7 tube in a Colpitts audio oscillator. This circuit was chosen because only one tube is required, there is no need for a tapped inductance coil, and it permits ease of frequency change and uniformity of transmitters with different audio frequencies.

Panel jacks are provided for reading plate and grid currents and a rear jack for reading modulation voltage. The modulation control is screwdriver adjusted at the rear of the chassis. A meter panel, with a plate current meter and a grid current meter, is used for all units. Standard phone plugs and six-foot cords make connections. A separate power supply is used for each four transmitters, and supplies 200 volts at 0.5 ampere.

Thirty-percent modulation was used at first so that sensitivities measured on the assembly lines would correspond with the standard procedure used in engineering tests. However, the modulation percentage was later raised to about 50

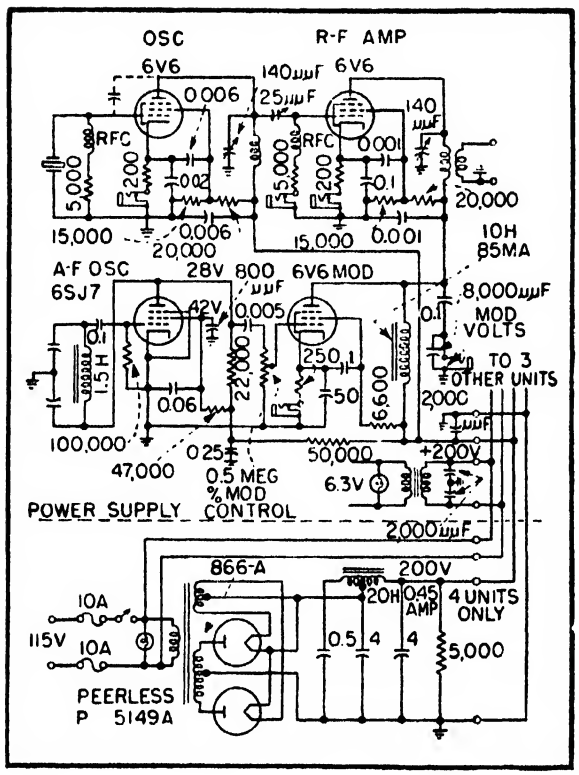

FIG. 1 — Complete circuit of one transmitter and a power supply for four transmitters

percent to approximate conditions of a broadcast station and resulted in a little clearer signal. The modulation voltage must be maintained constant or the apparent receiver sensitivity will also change.

A coupling unit was required to couple each transmitter of each frequency to the line, keep interaction of frequencies in the transmitters at a minimum, match the impedance of each transmitter to the line, and adjust the voltage level of each frequency on the line. Interaction of controls should be small and the voltage obtainable should be variable from one to several volts. A number of different methods, including cathode followers, were considered but the coupling was accomplished by means of the circuits shown in Fig. 2.

Basically, a series resonant circuit is used for each frequency, as it has the advantage of presenting a low impedance to the particular frequency while presenting a high impedance to the other frequencies. This makes it possible to connect such units in parallel to the line, a great advantage as it allows a common ground system and in addition makes impedance matching easy. A series connection would add the impedance of all elements in the circuit at the frequency being considered.

The final impedance match is obtained by adjusting values of a carbon resistor in the resonant circuit. The voltage level is adjusted by a variable capacitor used to vary the coupling to the transmitter. Link coupling is used and the links fed by a 52-ohm coaxial line. The impedance match is not critical at broadcast frequencies, because the line length represents such a small portion of a wavelength; so more attention was given to obtaining the desired voltages at the output of the coupling unit.

The short-wave links are more particular. The inductance of the tuning coil for each frequency is the same as the inductance of the transmitter tank coil for that frequency. The tuning capacitors are also the same value as used in the transmitters. The low impedance of the link circuit requires a large variable capacitance for coupling and a value of 450-μμf served.

One coupling unit is used for each floor (12 stations). Thus, two coupling units are fed from each transmitter. One chassis is used for both i-f units, one chassis per floor (two) for all broadcast frequencies and one chassis per floor (two) for all short waves.

Four coaxial cables are used for the transmission system. One handles the i-f to eliminate the possibility of beats with other frequencies. One is used for all broadcast frequencies, one for all the short waves, and one for use at a later date for an aligning signal. These cables feed an attenuator box at each test position. The transmission lines are required to carry r-f power from the coupling units to the individual test stations. As power delivery is required at the test stations and a number of frequencies per line are used, it is necessary to match the line impedance at the sending and receiving ends.

The effect of mismatch is reflection, which results in standing waves along the line, producing inconsistent voltages at points along the line, frequency discrimination at any one point along the line, and inability to obtain the correct amount of power from the line. As stations are required every seven

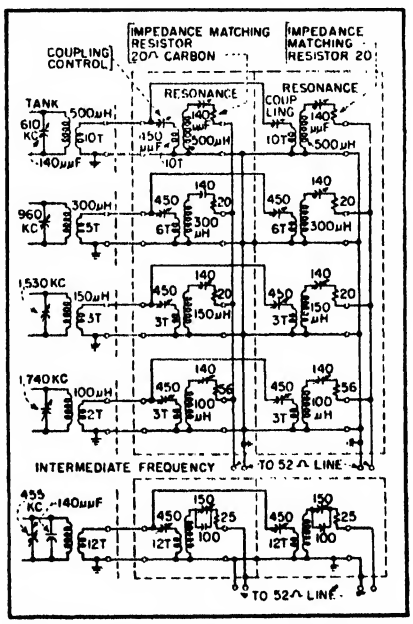

FIG. 2—Coupling circuits for feeding several transmitters to a common line

feet along the line, terminations become quite a problem. This can be seen from the following:

If a 50-ohm line is joined by another 50-ohm line, the impedance presented at the junction is that of two 50-ohm lines in parallel, or 25 ohms. This 25 ohms must match the previous single line of 50 ohms —an impedance ratio of 2 to 1.

As the line progresses another seven feet, another branch occurs with another impedance discontinuity. In addition, the two branches are also looking into 25 ohms, representing an impedance mismatch to the branches. The usual way such a condition is met is by use of transformers to match the different impedances. However, radio-frequency transformers are usually quite frequency selective, and as our lines carry a number of frequencies, transformers could not be used. If a resistive impedance-matching pad was used to match branch impedances, the loss in the number of pads required would be prohibitive.

The method used to accomplish the impedance matching is a combination of line loading and resistive impedance-matching pads. The formula for a distortionless line (one in which theoretically there is no frequency or delay distortion) is $\omega L/R = \omega C/G$, where L is inductance, C is capacitance, G is conductance and R is resistance. This can be written $LG = RC$. Physical lines do not usually approach this relationship, so it is possible to improve the line by loading, usually by increasing the inductance. The LG term may also be increased by increasing the conductance (lowering the leakage resistance across the line) and accepting the attendant greater attenuation.

Our lines use the principle of loading with conductance and then making that conductance the useful load on the line. The conductance used is 625 ohms every seven feet, resulting in an attenuation of six db per hundred feet of cable and changing the characteristic impedance of the cable from 52 to 50 ohms. Because this impedance change is small, it is possible to use unloaded line from the transmitters to the point where loading begins. The lines are terminated in 50 ohms. Figure 3 shows a block diagram of the system.

As the lines are run overhead and the test positions are some distance from the loading points, it is necessary to use another line, dropping from the main cable to the test positions. This line is matched at both sending and receiving ends, but on the longer wavelengths the characteristic impedance of the line itself is not matched. This was done to be able to use a more convenient and cheaper cable. The receiving end is terminated in the attenuator box, and the sending end is matched by an impedance-matching T pad.

The line loading is 625 ohms and power is taken off in this loading. The input impedance of the impedance-matching T pad is 625 ohms and used for the conductive loading, and the output impedance made to look like 100 ohms to feed the branch line. Minimum attenuation is required to reduce loss as much as possible. To meet this condition, one series arm of the pad is made zero. An unusual feature of this pad is that the input looks like 625 ohms to the line, but the line looks like only 50 ohms to the pad. The output looks like 100 ohms and also is terminated in 100 ohms. The pad was designed to have an attenuation of 20 db or a voltage ratio of 10 to 1.

These pads are contained in J boxes which in turn are placed in a larger box every seven feet along the line.

Attenuators are needed at each test station to reduce the signal level from the maximum available to a known and controlled value. Each test position is equipped with an attenuator box containing a switch for selecting one of the four lines (i-f, b-c, s-w, a-s), four variable T pads for adjusting the level of each line to 0.1 volt; a variable T pad to adjust voltage between steps of the attenuator; and a step, ladder-type attenuator producing output levels in steps of 10 from 10 μv to 0.1 volt. The four-position switch is

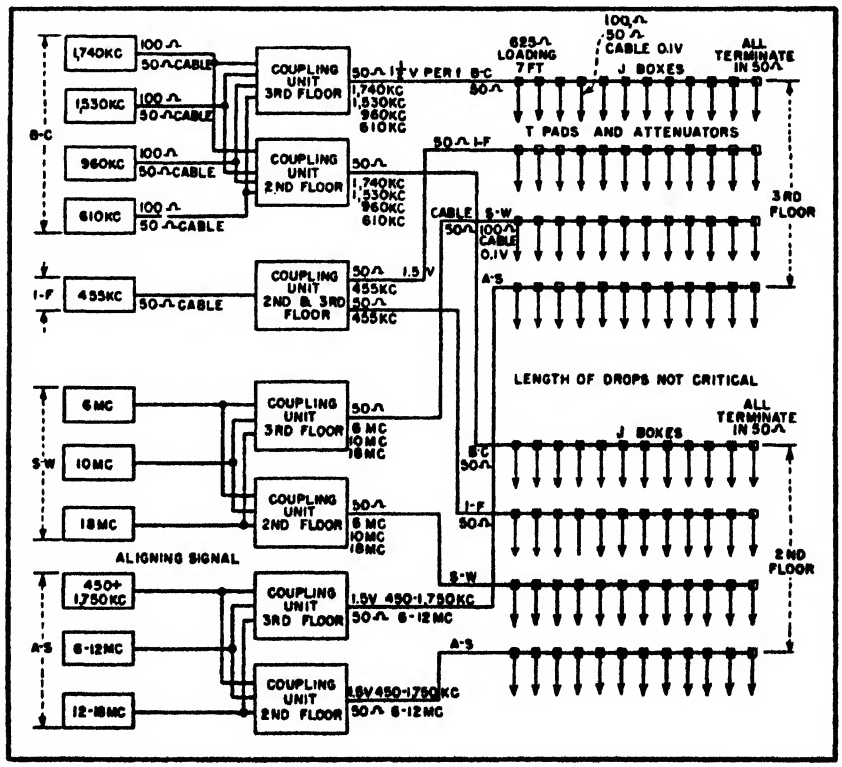

FIG. 3—Arrangement of transmitters, resonant-circuit coupling units, and J-box pads

arranged to terminate all unused lines in 100 ohms. A test connector is provided for using a vtvm in setting the input level.

It is desirable to purchase attenuators, but due to procurement problems, it was decided to build them. A simple design was required for ease of construction. The attenuator should have a flat attenuation ratio to 20 mc and steps of output voltage of 100,000 μv, 10,000 μv, 1,000 μv, 100 μv, and 10 μv. This represents a total voltage attenuation ratio of 10,000 or 80 db. If a very small amount of capacitive coupling exists across the attenuator, the attenuation ratio will change at the high-frequency end of the band to be covered. This would be undesirable as it would cause the attenuation to differ across the band. To reduce this effect the attenuation per stage is kept low (20 db) and each stage individually shielded. To reduce capacitance coupling, the switch was built into the attenuator. This allows the switch contacts to be shielded up to the actual surface of the contact itself and the spacing of contacts reduces the capacitance between them. Capacitance to ground should also be low.

The attenuator elements are formed by carbon resistors. The individual sections consist of a T pad with the series arm 82 ohms and the shunt arm 20 ohms. The circuit is shown in Fig. 4. The design follows that for any simple T pad.

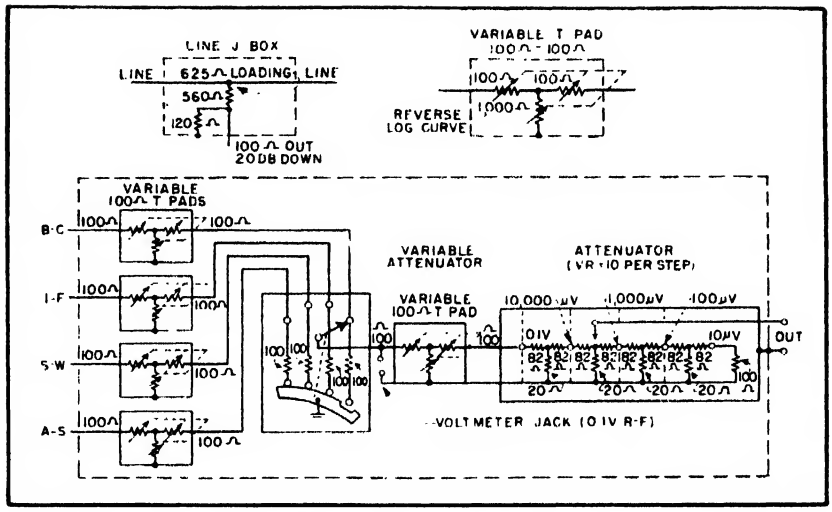

FIG. 4—Circuits of line J-box, variable T-pad, and step attenuator

Variable T Pad

Five variable T pads are used in each attenuator box. One is used on each of the four input lines to adjust the input voltage of the attenuator to exactly 0.1 volt. The voltage along the lines varies due to attenuation along the line and any slight reflections that may be present. The fifth variable T pad is used to control smoothly the voltage between steps of the ladder attenuator. It corresponds to the variable control on a signal generator and enables voltages other than steps of 10 to be obtained. All of these controls are screwdriver types so that the output voltage of the entire attenuator can be set to a value corresponding to the sensitivity of the receiver being tested, thus requiring no adjustment by the operator.

The requirements of this pad are 100-ohm input and output impedance $\pm$ 10 percent, a variable attenuation ratio of about 30 db and a reasonably flat frequency response to 20 mc. The variable T pad is made of three rheostats. Two are linear taper 100-ohm maximum value, clockwise rotation; one is log taper (curve A) 1000-ohm maximum value, counterclockwise rotation. Rheostats for radio frequency are difficult to obtain, so a number of tests were made and it was found that a wire-wound control possessed considerable inductance, and that a high-resistance control showed a capacitive effect. A low-resistance carbon-type control is as capacitive as a high-resistance one, but the capacitive reactance is shunted by a low resistance and becomes less important. Controls made of molded composition were quite satisfactory in the 100-ohm value tested.

The output of the attenuator may be wired directly to the receiver antenna terminal, using a dummy antenna, or it may be coupled to the receiver loop, using another loop as a radiator. The loop method is favored, as it allows a greater production speed because no connections are made to the receiver. A loop was designed, keeping the distributed capacitance low, to have an impedance of 100 ohms in the middle of the broadcast band. This loop worked very satisfactorily for the i-f and short waves as well. The receiver i-f response was naturally considerably less than the other frequencies due to no front-end gain in the receiver.

Radiation and Leakage

In a system comprising a number of watts of transmitter power and a large network of transmission lines, the problem is present of radiated radio-frequency energy getting to the receivers to be tested. This energy, arriving around or by-passing the regular system, causes trouble in a number of ways. Radiated signals are generally undesirable because of the possibility of causing local interference in nearby broadcast receivers, heterodyne whistles (in our case occuring only on very distant stations because of choice of signal frequencies), and in the case of the i-f frequency, heterodyne whistles on every signal tuned in.

More serious is the by-passing of the attenuator, thus causing the attenuation ratio to change, particularly on the 1 to 10 microvolt levels.

The problem can be divided into two main classifications: radiation, and leakage. The difference between these may not be apparent, so we will define leakage as local effects, such as leakage across an attenuator due to capacitive or inductive coupling, and radiation as energy arriving through the medium of space. Its field may be considerably distorted inside a building. Conduction along the main lines is included as leakage.

Radiation occurs mainly from the transmitter and associated equipment due to the large amount of power present there. It may also occur from long runs of unshielded coaxial lines. It was decided to attempt to control direct radiation by shielding each unit and, after the equipment was placed in operation, determine if it was necessary to add further controls, such as a shielded room. It was decided that with other controls used the equipment need not be placed in a shielded room and that even the shield cans may be left off to facilitate tube or other maintenance.

When unshielded loops are used to couple power to receivers under test, the large number of loops used contribute a field strength which may be higher than the residue radiation from the transmitters. It would be uneconomical to reduce radiation from the transmitters to a point greatly lower than that from the loops. No attempt has been made to shield loops used in the open on the assembly lines, although this might be done by placing the receiver in an open metal box. Shielded booths are used at test positions where sensitive receivers are aligned. These reduce radio noise disturbances from automatic screwdriver motors, fluorescent lights, and eliminate any residue signal leakage that may be present.

The booths are made of aluminum alloy sheets on an extruded angle frame. When all openings are closed, no broadcast stations can be received, but the booth is normally operated with no door and two openings for handling receivers. The receivers slide on a steel-topped bench equipped with a wooden insert under the coils of the receiver being tested. An 80-db line filter is installed. It is important that this filter and also the attenuator box be mounted directly on the booth metal wall to obtain a good ground. A wire or braid to ground is not sufficient. A Celotex lining improves the acoustical characteristics.

The greatest control of radiation by any single item was installing all coaxial cables in conduit. A completely closed conduit system (except for drop-off cables) was used, tying the whole system together with a common ground to the transmitter cabinets. It is unimportant whether this system is grounded to actual ground. The conduit also controlled coaxial cable radiation. This radiation occurred, not so much through the cable, but from the outside ground conductor of the cable acting as an antenna because of a slight potential difference between the outside coaxial conductor and the transmitter ground plane. As it is difficult to determine the actual point of equal potential (the ground plane), indeed if such a point exists, and because any connection to this point must be of extremely low r-f impedance at 20 mc, it is very difficult to control this type of radiation by a simple ground connection to the transmitter frame. A special filter was constructed by soldering a few feet of the outside coaxial conductor to a metal plate in an S shape and then grounding the plate. This filter is quite effective, but placing the cable in conduit is a much better answer.

If any appreciable signal is present on the main lines, it can radiate from them, as well as be conducted along them, and cause a very difficult control problem. This is prevented by the use of filters.

Simple r-f filters are used at the transmitter units. They consist of 0.002-μf mica capacitors from B+ to ground and from both sides of the main line to ground. These are installed where the wiring enters the chassis, and the lead lengths are kept to less than one-half inch. It was found unnecessary to use filters in the main power wiring to the power supplies. Filters in the shielded booths contribute to this control, as well as reduce noise from the countless number of fluorescent lights and machinery. These filters are installed, one in each main wire, and contained in a metal box which is grounded to the booth metal wall.

Low-Frequency Padding

In production aligning of radio receivers, part of the procedure may be accomplished more rapidly, and perhaps better, with inexperienced personnel, by the use of a wide-band signal. This allows trimmers to be tuned for maximum output without rocking the gang.

A number of disadvantages of the multivibrator for this use became apparent. One of the most glaring is the fall-off of radio-frequency voltage with frequency directly as the order of the harmonic. To maintain proper distribution of the harmonics, the fundamental frequency of the multivibrator should be in the audio range, say, 1,000 cps. If coverage is required to 20 mc, the output voltage falls to 1/20,000th of the fundamental and an amplifier to build this characteristic up to a flat curve and furnish an output level of about five volts to operate the system is a big order.

It was decided to use a radio-frequency oscillator sweeping across the band at an audio rate. A motor-driven capacitor was chosen for the sweep. During sweeping, the signal would appear on a receiver only a few microseconds every 1/100th of a second, and to increase the length of time the signal passed the receiver frequency, frequency modulation was added by means of a reactance tube. When the circuit was tested, f-m was found to be unnecessary, and it was also found that the motor speed could be reduced to 1,800 rpm, which results in an impulse every 1/30th of a second.

Coupling units represent a somewhat different problem from the other units, as they must handle a

band of frequencies. Cathode followers were chosen for this reason. They were designed to work into a 50-ohm load.

Additional Equipment

Since the equipment was first installed, some of the features added are padding signals, an audio system, additional test stations, changing location of test stations including one in the engineering department with an additional 50 feet of line, and split test stations. The latter consists in feeding part of the four cables of a station to another station, for example, taking the i-f signal to another test position to enable another test operator to prealign the i-f stages. Thus production can be increased on an assembly line by the use of two test operators.

Test operators report that they like the system, that it is much easier for them and results in faster testing.

Automatic Limit Bridge for Production Testing

Resistance of as many as 119 circuits are automatically compared with those of precision circuits in a standard chassis. Amplified output of a bridge is converted to square waves and applied to a thyratron whose bias is set for required acceptance tolerances

By R. D. CAMPBELL and E. J. TOTAH

NEED has long existed for a simple automatic bridge to serve as the master test position on production assembly lines of electronic equipment. Bridges previously available for this purpose* have required an inordinately long setup time and have therefore been useful only on runs of thousands of identical chassis.

The equipment to be described requires about 15 minutes setup time and is therefore advantageous even on short production runs. The instrument consists of a 3-gang, 120-position ratchet-driven switch, arranged to step once per second, plus the circuit shown in the block diagram of Fig. 1. The instrument is capable of making 119 independent measurements of resistance to ground. Connection to the chassis under test is made through tube sockets and by clips at test points.

Bridge Circuit Arrangement

The arrangement of the bridge circuit is dictated by the necessity for grounding both standard and chassis under test and so that a given percent unbalance produce a constant output voltage throughout the entire resistance measuring range. The latter requirement makes it impossible to insert the bridge voltage between the center point of the ratio arms and ground, since drastic loss of sensitivity in measurement of low resistance values would result. Accordingly, the bridge voltage supply must float above ground and be well insulated.

* ELECTRONICS, p 58, Feb. 1943.

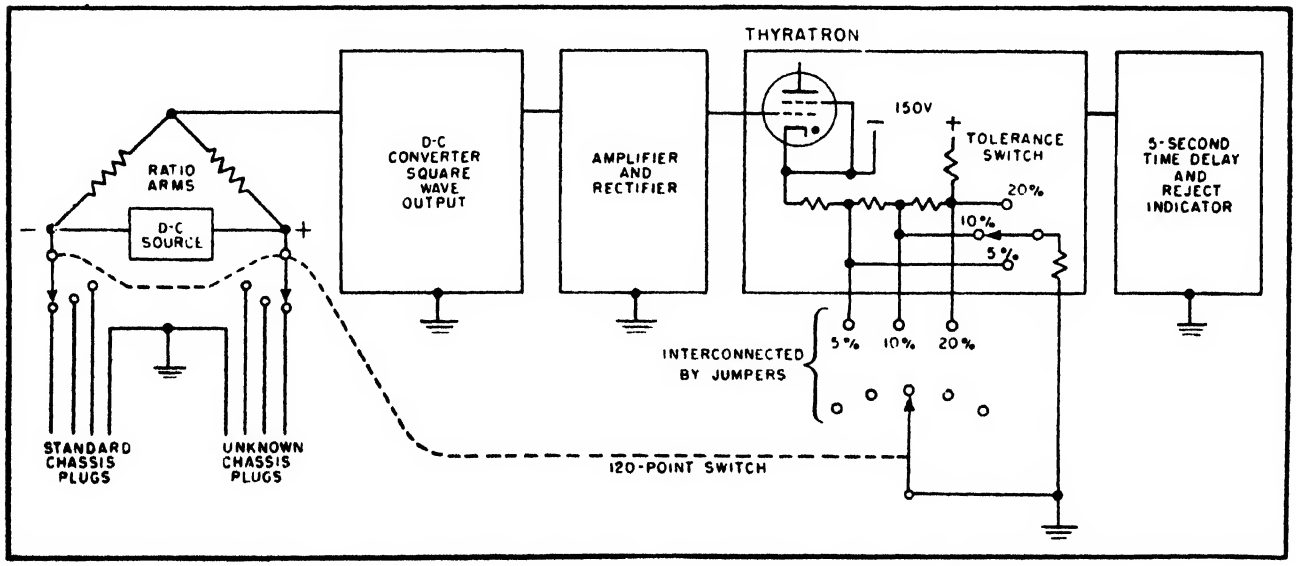

FIG. 1—Functions of the main stages of the automatic circuit tester

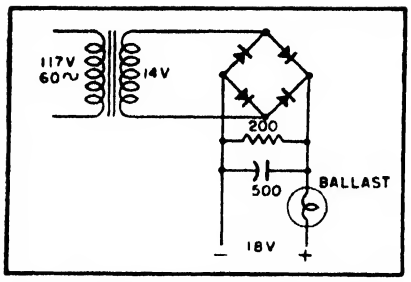

FIG. 2—Circuit of bridge voltage supply

The d-c unbalance voltage from the bridge is next amplified by a stage having high input resistance, and then converted into a-c for further amplification and rectification. Conversion to a-c is necessary, since the firing of the limit thyratron must be independent of the polarity of the original unbalance voltage.

The thyratron is provided with a tapped bias supply, to permit selection of several firing points corresponding to different amounts of bridge unbalance. The bias is controlled by a three-position tolerance switch and, in addition may be modified by the installation of jumpers on the main selector switch.

The final block includes a five-second time delay, which eliminates spurious rejects due to transients, and an indicator lamp which operates when a true reject occurs.

The circuit of the bridge voltage supply is shown in Fig. 2. The rectifier is made by reassembling commercial selenium 5-plate groups having a current rating of 200 ma and a peak inverse voltage of 70 volts per plate. The ballast lamp quickly limits short-circuit currents to approximately 0.7 ampere.

A curve of bridge voltage against load resistance is given in Fig. 3. No attempt is made to regulate the bridge voltage and it therefore varies in proportion to the line. The error due to this variation has been reduced to one of second order magnitude by methods to be discussed later in connection with thyratron performance.

The vital portion of the instrument is the detector. This device must have high input impedance, an efficient conversion of d-c to a-c, and excellent zero stability. The order of magnitude of unbalance voltages to be detected is as follows: 5 percent yields 0.25 volt d-c, 10 percent yields 0.5 volt and 20 percent yields 1 volt. Accordingly a d-c vacuum-tube voltmeter circuit is necessary having a zero drift small compared to 0.25 volt. In addition, the zero must be the same whether the input be grounded directly or connected to ground through several megohms. The detector circuit is shown in Fig. 4.

It has been found that many commercial 6C4 tubes have grid currents less than 2×10^{-10} ampere. In addition, careful measurement permits pairs of tubes to be selected whose unbalance due to changes in heater voltage is less than one-fifth the unbalance observed when a single tube is paired with a fixed resistance. A matched pair of tubes is used as the input circuit of the detector, one tube being used as the load of the other. A special plate supply is not required. An amplified d-c voltage is therefore available across points A and B of Fig. 4. The input tubes can henceforth be considered as a high resistance and battery in series as indicated in dotted lines in the circuit of Fig. 4.

Figure 5 indicates the method of diode operation. Since V_1 and V_2 conduct together, the voltages V_{1k} and V_{2k} are half sinewaves and occur at the same time. If E_0 is zero, and V_3 removed, the contact potential of V_4 appears across AB except when it is cut off by the voltage V_{1k}. At those times the voltage V_{1k} is zero. Similarly, if V_4 is replaced and V_3 removed, square waves of opposite polarity are generated across AB due to the contact potential of V_4.

If both V_3 and V_4 are replaced, E_0 may be adjusted for balance, since it discourages one diode and encourages the other. At balance, the voltage AB is zero except for insignificant spikes of brief duration at the end of each half cycle.

If E_0 is increased by 1.0 volt, one of the upper diodes will remain con-

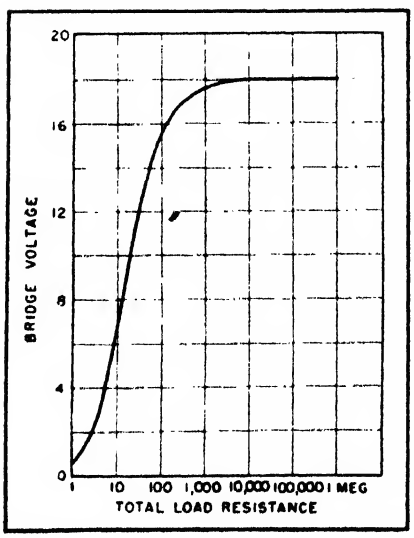

FIG. 3—Bridge voltage regulation curve

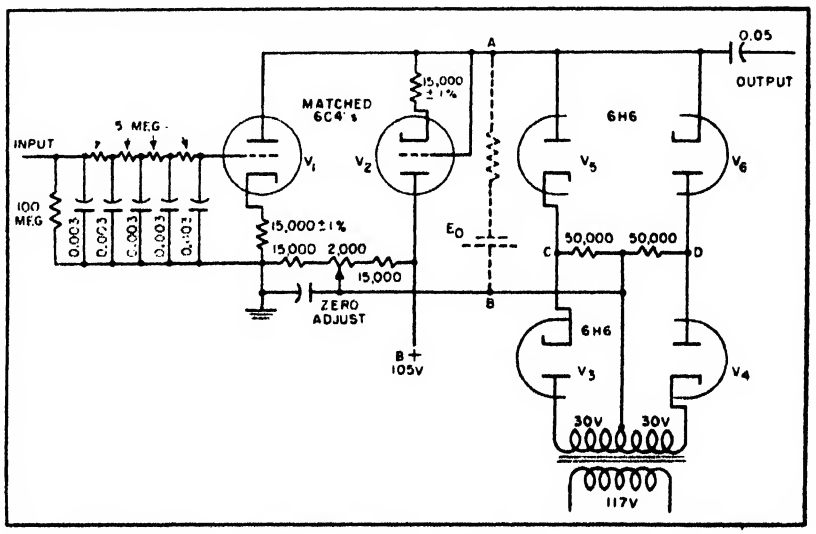

FIG. 4—This d-c amplifier circuit acts as the detector of bridge unbalance

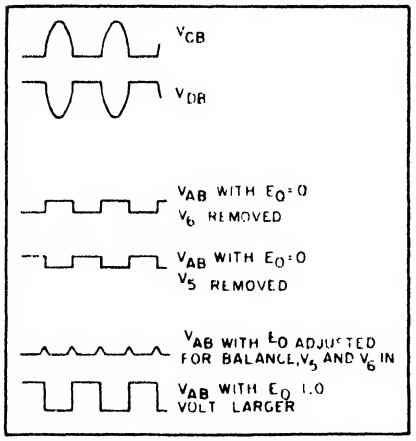

FIG. 5—Operation of the electronic shorting switch formed by the diodes of Fig. 4

ducting until the input voltage from the lower diodes has become one volt greater. The result is that diodes V_5 and V_6 act as switches which open and close across AB. Once E_0 has been set at balance, the output from the circuit will be square waves whose peak to trough amplitude equals any change in E_0. The battery and resistor across AB may now be forgotten and the circuit is seen to be a d-c amplifier plus an electronic shorting switch.

With suitable heater voltage control, the circuit of Fig. 4 will drift less than two millivolts after a warmup time of one-half hour. In this particular application no heater voltage regulation is necessary.

The amplifier, rectifier, and filter are indicated in Fig. 6. Half of a 6SN7 is used as the gain stage, the other half being used as a shunt rectifier. This yields an output of square waves standing on the axis, rather than being symmetrically disposed about it. Thus the final value of filtered d-c is twice as great as would have been obtained with a series rectifier.

The complete thyratron circuit is shown in Fig. 7. Essentially it is a normal a-c thyratron and relay circuit with a variable bias inserted between cathode and ground to permit selection of several firing points.

The tolerance switch on the instrument is grounded through 50,000 ohms, whereas the arm on the selector switch is grounded directly. Hence, when the selector hits a circuit where a jumper has been installed, the bias will be established by the jumper and not by the main tolerance switch.

The shunting effect of one circuit on the other creates negligible error. With the switch and jumpers as shown in Fig. 7, circuits 44, 47, 48, 49, and 50 will be measured to 10 percent tolerance. Circuit 46 will be measured at 5 percent, circuit 45 at 20 percent, and circuit 43 will not be measured at all since the bias available on the ∞ jumper point is greater than the maximum signal the amplifier can handle.

The VR75 and its associated resistors are inserted as a refinement to make the instrument nearly independent of line voltage. As pointed out, the bridge supply voltage is proportional to the line and one would therefore expect the signal at the thyratron grid to be proportional to the line. If this were true, and if the thyratron firing point did not vary with line voltage, the requirement would be satisfied by leaving the thyratron bias proportional to the line also.

The selector switch is stepped once per second by a tube-operated relay as long as circuits are encountered whose errors do not exceed the tolerances set up. However, when the thyratron fires, its relay prevents further stepping and the switch stops and waits upon that circuit. A reject is not immediately indicated. Instead voltage is applied to a 5-second delay circuit consisting of a resistor, capacitor, and another tube-operated relay. Upon operation of this relay a reject is indicated and the operator must manually step the switch to the next position by means of a key. If the unbalance had dwindled during the 5-second interval so that the thyratron went out, the switch would have continued on automatically. The delay is necessary to avoid spurious rejects of long time constant circuits where the resistors might be correct but the capacitors considerably different.

The bridge is arranged to be completely set up without accessory ap-

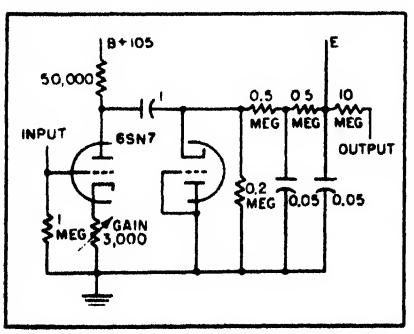

FIG. 6—Circuit of amplifier-rectifier stage

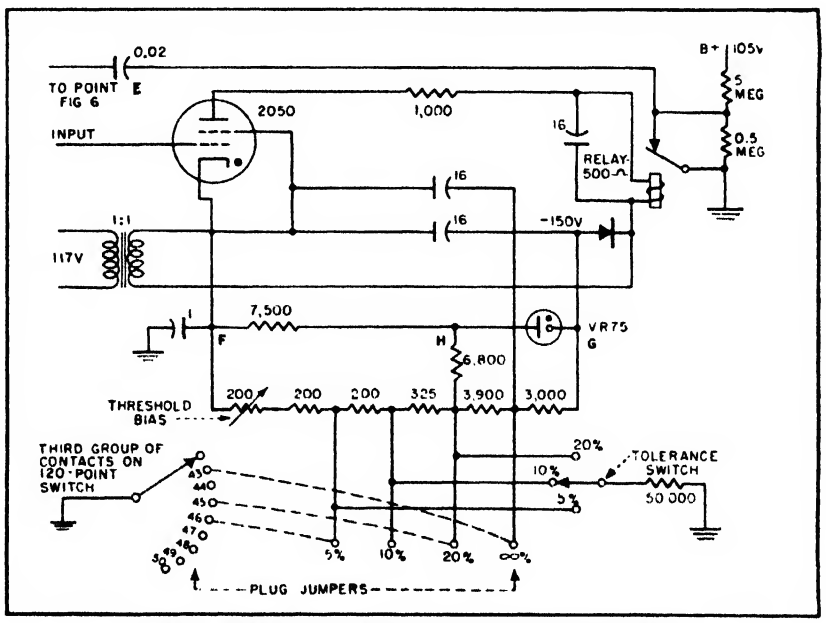

FIG. 7—Method of providing automatic tolerance selection

paratus. Accordingly, step 0 of the selector switch is occupied by standard resistors, normally set to represent a 10-percent unbalance. If the gain, bias, and balance adjustments are made using these standards, the available tolerances will be 5, 10, and 20 percent. One standard may be varied slightly by means of a calibrated rheostat. This makes possible a choice of tolerance groups at 4–8–16 or 6–12–24 percent. Similar groups between these limits may be chosen. It is assumed that the usual choice of a tolerance group will be 6–12–24, for chassis containing chiefly 10-percent resistors. The 24-percent tap will then be available for measuring volume controls, and the 6-percent tap for more precise circuits.

Standard Chassis

A standard chassis must be built to represent accurately the group of production samples to be measured. In general the standard need contain only precision resistors. However, considerable time will be saved by duplicating long time constant circuits so that the bridge will not need to hesitate so often. Accordingly large capacitors should also be included. Note from Fig. 1 that any polarized circuit elements should be electrically inverted in the standard chassis. Small air-core coils may well be used to represent themselves, but iron-core chokes and transformers may be replaced by resistors. Since the short-circuit current from the bridge supply is about 0.7 ampere, a check of low-resistance grounded circuits, such as r-f and i-f coils, will detect 0.4 ohm differences if the chosen tolerance is 5 percent. Thus, some shorted tuning and trimmer capacitors can be detected.

The resistor values used in a standard chassis are not the nominal values. A production run of chassis containing 1,000-ohm resistors cannot be properly checked if the standard chassis has precision 1,000-ohm resistors in the equivalent circuits.

A simple computation will indicate the reason for this. Consider the bridge of Fig. 1 with 20 volts as the bridge voltage and an unknown one percent different from the standard, such as 990 ohms and 1,000 ohms respectively. The computed unbalance voltage is 0.05 volt. Since the amplifier and detector are a linear system, the bridge will therefore recognize 5 percent as 0.25 volt, 10 percent as 0.5 volt, and 20 percent as 1.0 volt. Computing the unbalance for 1,200 ohms, or 20 percent high, the value becomes 0.91 volt. Computing the unbalance for an unknown of 800 ohms, or 20 percent low, the voltage calculated is 1.11 volt. Thus, a high value of resistance gives too little unbalance voltage and a low value gives too much.

The remedy is to choose the standard somewhat lower than 1,000 ohms. The proper size for the standard may be easily computed from the formula $P = 0.005\ Q^2$ where Q is the percent tolerance at which a resistor is to be checked and P is the percent low to select the standard. For example: if a 1,000-ohm resistor is checked to 10 percent tolerance, $P = 0.005\ (10)^2 = 0.5$. Therefore the standard should be 0.5 percent low or 995 ohms. For maximum accuracy the standards should be chosen in this manner. This consideration is particularly important when the tolerance setting is high. At 20 percent tolerance, if the nominal value were used as the standard, the bridge would accept resistors lying between 18.2 percent low and 22.2 percent high.

Direct-Indicating Comparison Bridge for Production Testing

DESIGNED FOR RAPID production testing where moderate accuracy is desired, the circuit shown in the illustration provides comparison of resistors, capacitors and inductors to a similar standard. It consists of an a-c slide-wire bridge and an electron-tube indicating circuit. The slidewire covers a range of approximately ±50 percent of the value of the standard.

Three working standards are used in calibration of the gear: one of nominal value and one each of upper and lower desired limits. Low and high values can be different. After adjustment, the separate indicating meter provides a within-limits reading up to a marked point on the scale or an outside-limits reading beyond. Thus the testing operator is not required to rotate dials or press buttons.

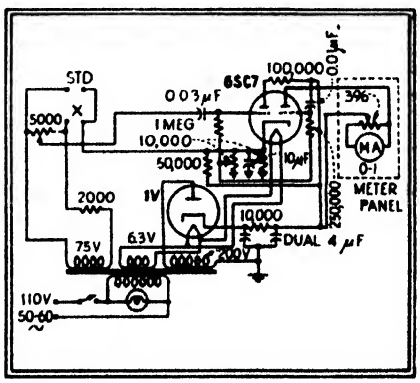

Schematic diagram showing use of type 1-V rectifier and 6SC7 null indicator in direct-indicating comparison bridge

Accuracy of the equipment is largely dependent on the care with which limits are set as well as variations in line voltage. However, sensitivity and stability are such as to permit successful operation with limits set as close as ±5 percent or as wide as ±50 percent of nominal. As made by Industrial Instruments, Inc., the range of measurement on capacitance is from 0.0001 to 1.0 μf; in resistance, from 2000 ohms to 20 meg; and in inductance, from 5 to 50,000 henrys.

Frequency Meter for Use by Factory Personnel

By W. R. STRAUSS

INDUSTRIES that use audio frequencies in measurement work have use for a frequency meter that measures from ten to 50,000 cycles and that can be operated by non-technical personnel, after a few minutes instruction. To fit these requirements, engineers at North American Philips designed the unit illustrated for use in their plant.

The frequency meter they developed has sufficient power to operate a strip-chart recorder without an auxiliary amplifier regardless of voltage variations between 2 and 200 volts.

The input circuit consists of a limiter as shown in the diagram. This stage employs resistor R_1 to bias the control grid of the input tube on the peaks of a cycle.

In clipping the peaks of a cycle, the output shows a square wave with steep fronts. The square wave results regardless of whether the input frequency is a pure sine wave or one with distortion and irregularities. In case of a badly distorted wave, the grid circuit will favor the predominant frequency over the lesser peaks by a ratio of about 3 to 1.

Floating Screen

Plate output voltage of tube V-1 is held constant by a floating screen grid. Since plate current changes are a function of screen voltage, increase of audio input voltage results in a decrease of screen voltage. This, in turn, is affected by the bias developed across R_1. Screen voltages reduce proportionately with increase of grid bias developed across R_1. Stabilization of screen resistor R_4 to ground, or B- with a bleeder resistor, would limit the range of constant output to a narrow band of frequencies. Capacitor C_2 is an audio bypass to prevent any part of the original wave shape from entering the plate circuit. The RC time constant of R_1 and C_2 is sufficient to delay any small part of the original wave from coinciding with the square wave, thus avoiding valleys and discharge peaks.

At V-1, a type 6AG7 was found to be best from the standpoint of high transconductance and high screen-grid wattage dissipation. The input sensitivity is slightly more than one volt, for almost all frequency ranges. Input impedance is greater than 100,000 ohms for most frequencies but not higher than the value of R_2.

Multivibrator as Amplifier

The multivibrator circuit formed by V-2 and V-3 is directly connected to the plate of V-1, and is at rest by virtue of bias-resistor R_6. The value of R_6 is selected to permit the multivibrator circuit to operate at the instant a square-wave voltage is present at the plate of V-1. The multivibrator circuit has no resonant characteristics; its function is to amplify the output of V-1 without alteration.

Amplified square waves are then fed into an RC integrating network (C_5,R_{12}, etc.) which determines the amplitude of the pulse that is to appear on the grid of V-4. Capacitors in the frequency-selector circuit are either air-type trimmers or silver-mica types having negative coefficients to minimize calibration drift caused by heat within the instrument.

Operation of the V-4 tube circuit is similar to class C audio amplification. The grid bias is adjusted to zero plate current with no signal input. This circuit functions as a linear amplifier in which plate current changes are directly proportional to grid voltages.

Safety Circuit

External and panel meters are protected from burnout by a relay in the plate circuit of V-4. The relay shorts the meter when current exceeds 10 ma and releases at about

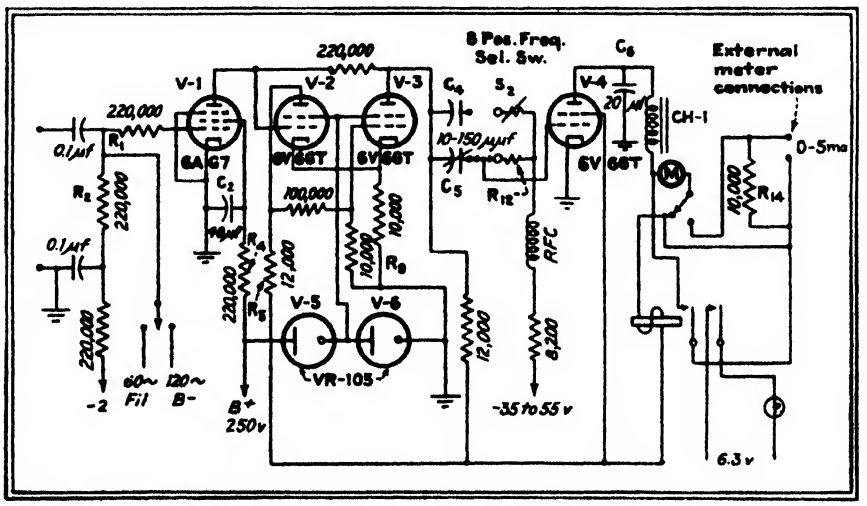

Circuit of electronic meter for production testing of frequencies between ten and 50,000 cycles. A linear direct-reading dial permits rapid reading by non-technical personnel

4 ma. The meter circuit is arranged to permit reading the panel and external meters simultaneously. Accurate frequency indication on the external meter is only limited by the meter itself. If a recorder is used, overshooting and undershooting of the pen (determined by chart paper travel) must be taken into consideration. If the frequency meter is accurately calibrated and stabilized, the inherent circuit error will be less than 2.0 percent of full scale over the entire range of 10 to 50,000 cycles.

An *RC* network having a long time constant (C_8, CH_1) is incorporated into the plate circuit of *V*-4. Without the *RC* network, some recorder pens resonate badly at 100 to 130 cycles with the selector switch (S_2) set on 100 or 500-cycle positions. External meters having a 5-ma movement and a coil resistance not exceeding 1000 ohms may be used without recalibration. An external meter-damping resistor, R_{14} of 10,000 ohms, was chosen as an optimum value.

For frequency calibration 60 cycles at 6.3 volts is obtained from the filament leg of the transformer and 120 cycles at 2.5 volts comes from the B-minus leg of the full-wave power rectifier through a 47-ohm resistor. The calibration switch is normally open (center position) as shown. Selector switch S_2 is placed on the 100 or 500-cycle range when making a calibration check.

The frequency meter has been used to measure audio-frequency differences in quartz crystal manufacturing, determine pulse frequencies, function for gamma, x-ray, and electron counting, determine a-c line frequencies for power and audio transformer design, and measure temperature-coefficient-drift on transmitters and receivers operating under test temperatures of from −40 to 200 deg F.

Pulse-Type Tester for High-Power Tubes

Motor-driven 5-rpm commutator in simple trigger circuit causes ignitron to fire and apply high-voltage pulse to grid of tube being tested. Resulting grid and plate voltage and current pulses are measured on high-persistence c-r tube by means of calibrating spot

By E. C. EASTON and E. L. CHAFFEE

THE purpose of the pulse-type high-power tube tester herein described is to obtain simultaneous measurements of plate voltage, plate current, grid voltage, and grid current at the crest of the grid-current curve of a triode when the grid current is made to vary as a pulse of very short duration.

An electrically operated commutator alternately applies to a cathode-ray oscilloscope a signal from the tube tester or a signal from a calibrating circuit. When the tube tester is connected to the oscilloscope, a voltage proportional to the grid current is applied to the horizontal plates while the vertical deflection is produced by either the plate voltage, plate current, or grid voltage as desired. The operator obtains readings of the peak values by matching a calibrating spot with the end of the characteristic curve as seen on the long-persistence screen of the oscilloscope.

The apparatus was designed to test tubes of the type used for loran. The tube can be supplied with plate-current pulses of 200 amperes at plate voltages up to 20,000 volts. The grid voltage may be varied from −5,000 to +10,000 volts.

Measuring Circuit

The measuring circuit is shown in Fig. 1. The grid current is measured in terms of the voltage across a noninductive shunt R_{10}. This voltage is applied directly to the horizontal plates of a cathode-ray oscilloscope. The plate current is measured in similar fashion by applying directly to the vertical plates of the oscilloscope the voltage across the noninductive shunt R_2. By means of switch SW_1, the vertical plates may be connected either across R_2 for plate current measurement, across R_4 for plate voltage indications, or across R_6 for determining the grid voltage. Complete shielding of all portions of the measuring circuits is most essential in this method because of the use of pulses having high rates of change of current.

The combination $C_3C_5R_3R_4$ forms a compensated voltage divider to supply a known fraction of the plate voltage to the oscilloscope. Similarly, $C_4C_6R_5R_6$ form another compensated voltage divider for the measurement of grid voltage. Each voltage divider is carefully adjusted with the aid of a square-wave generator so that when a square wave of voltage is applied across the divider, a good reproduction of the square wave appears across the low-voltage section.

The high-voltage section of each divider is enclosed in an aluminum shield. The low-voltage section plugs into sockets mounted on the shield. The shield and the bottom of the low-voltage section are grounded to a common point which

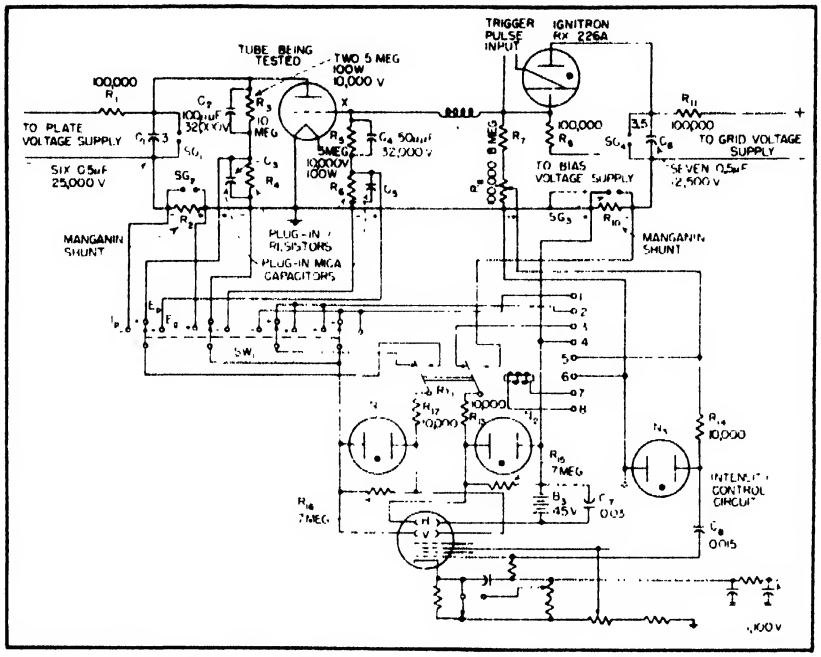

FIG. 1—Measuring circuit for pulse-type tube tester

also serves as the ground connection for the tube to be tested, the cage which holds the apparatus, and the shunts R_2 and R_{10}. By the use of a common ground point, ground currents are kept out of the cage and shields, and thus magnetic disturbances from ground currents are minimized.

Connections from the voltage dividers and shunts to the oscilloscope are made through coaxial cable. The grounded side of each shunt and voltage divider is connected to the outer conductor of the corresponding cable. All these cables run to a junction box which contains switch SW_1 and relay RY_1. The junction box is grounded to the common ground point, but all cable connections are insulated from the box. Thus, if, because of very heavy tube currents, the grounded side of a cable should be at a different potential from ground, no part of the tube current will flow through the outer conductor of the cable. With these precautions in grounding and shielding, no magnetic pickup or interaction between circuits is observed.

The impulse of grid current is controlled by the ignitron RX-226A. When the trigger circuit causes the ignitron to fire, the voltage on capacitor C_6 is applied between grid and cathode of tube X. The inductance L retards the rise and fall of grid current sufficiently to provide a grid-current pulse which rises rapidly and then holds a rounded peak for several microseconds before dropping.

Pulse-Forming Circuit

Before the ignitron is fired, the grid of the tube X is kept at a negative potential by a bias power supply acting through R_9. This negative bias is adjustable to a maximum of 5,000 volts and is set at a value sufficient to hold the plate current to a negligible value over the normal range of plate voltage.

By means of voltage divider R_7R_8 in Fig. 1, a portion of the grid voltage is fed to the intensity control of the oscilloscope. When the ignitron fires, the intensity of the electron beam is greatly increased, and the rapidly-formed trace is made visible on the long-persistence screen. (Battery B_3 serves to position the electron beam to the left of the center of the screen.)

The oscilloscope beam is deflected horizontally by the grid current, and vertically by either the plate voltage, plate current, or grid voltage, depending on the setting of SW_1. When the grid current is at its peak, the beam is deflected to a maximum horizontally. Hence, if observations are made on each vertical signal at the extreme of the horizontal deflection, all readings are obtained at the peak of the grid current.

Calibration Procedure

In order to calibrate the oscilloscope and thus obtain the true value of each measured quantity from the deflection on the screen, two variable d-c voltages are provided, as shown in Fig. 2. By means of battery B_1, potentiometer

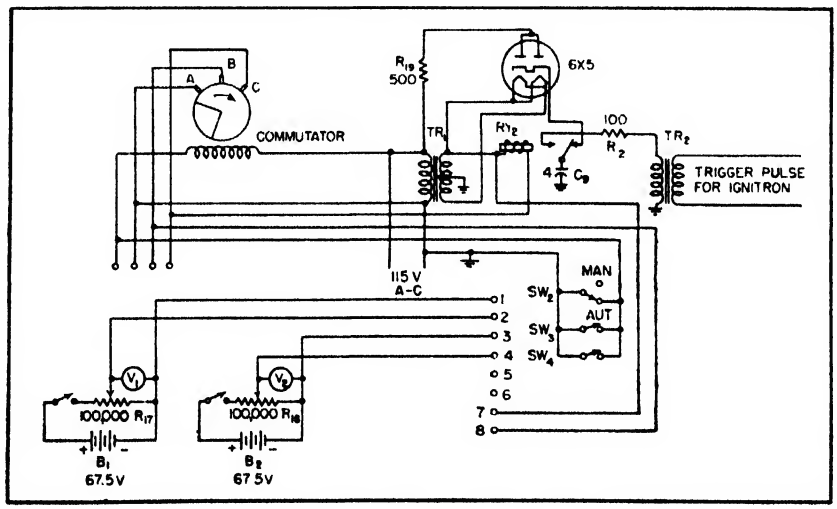

FIG. 2—Calibration and trigger circuit

R_{17}, and voltmeter V_1, a known voltage of any desired value can be applied to the vertical plates; B_2, R_{18} and V_2 supply a similar known adjustable voltage for the horizontal plates. When relay RY_1 is in the position shown in Fig. 1, these calibrating voltages are applied to the oscilloscope.

By adjusting R_{17} and R_{18}, the luminous spot may be moved to any point on the screen. Thus the spot may be moved to the end of the signal trace, and by reading V_1 and V_2, the vertical and horizontal deflection voltages can be determined at the peak of the grid current. Knowing these deflection voltages and the resistance of shunts R_2 and R_{10}, the plate and grid currents may be found. Similarly, knowing the voltage divider ratios, the plate and grid voltages may be determined.

In order to keep the outer conductors of all coaxial cables at ground potential, it is necessary to have the plate and grid voltages cause a deflection in the opposite direction from that caused by the plate current. Switch SW_1 reverses the polarity of the calibrating voltage whenever the polarity of the signal voltage changes.

Relay RY_1 switches the oscilloscope from signal to calibration. When the relay is energized, the signal is fed to the oscilloscope. When the relay coil current is removed, the oscilloscope is connected to the calibrating voltages.

The operation of relay RY_1 is controlled by the trigger circuit shown in Fig. 2. This circuit includes a mechanical commutator having three contacts. The commutator rotates at 5 rpm. The rotating Bakelite disc contains a brass insert which connects the contacts with each other as the disc turns. When contacts A and B are connected by the brass insert, relay RY_1 is energized by transformer TR_1, and the measuring circuit is connected to the oscilloscope.

When all three contacts are connected together, relay RY_2 is energized. This relay causes C_6 to discharge through the primary of

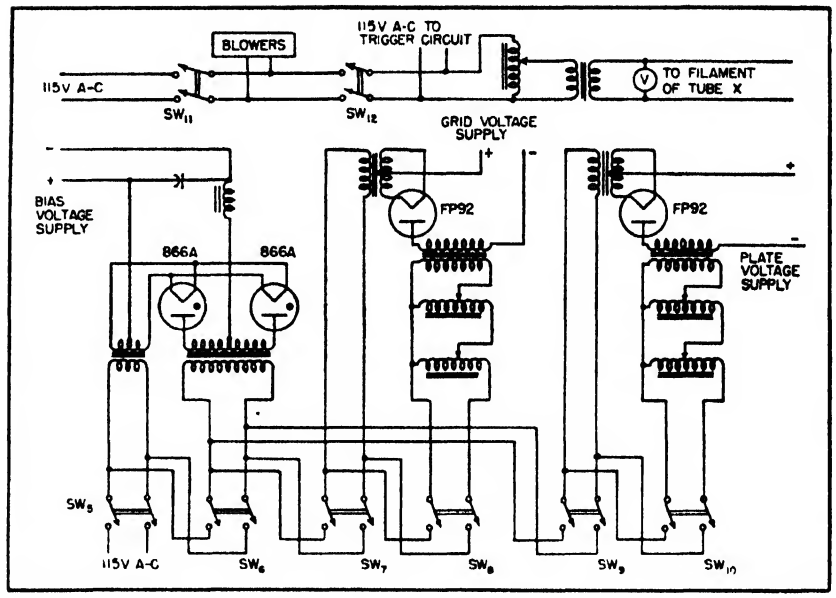

FIG. 3—Power system for pulse-type tube tester

transformer TR_2. The pulse of voltage from the secondary of TR_2 fires the ignitron and thus applies the grid voltage to tube X. As the commutator continues to rotate, both RY_1 and RY_2 are deenergized, and the calibration voltages are applied to the oscilloscope. Thus, five times a minute, the following cycle of operations takes place: RY_1 closes, RY_2 closes, the ignitron fires, RY_1 and RY_2 open. With RY_1 closed, the operator sees the tube characteristic on the oscilloscope screen. With RY_1 open, he sees the spot as positioned by the calibrating voltage.

The operation of the mechanical commutator is made automatic by setting switch SW_3 in Fig. 2 on AUT. When this switch is open (position indicated as MAN) the commutator does not rotate. With SW_3 open, the operation of the commutator may be controlled manually by pushbutton SW_3 on the main panel, or by SW_4 which is a remote trigger mounted at the end of a long cord. The 6X5 tube shown in Fig. 2 is a rectifier which charges C_6.

Protective Devices

To insure the safety of both operator and equipment, various protective devices are provided. In Fig. 1, N_1, N_2 and N_3 are ½-watt neon bulbs. Should a flashover occur in any of the high-voltage circuits these neon bulbs together with resistors R_{12}, R_{13}, and R_{14} will prevent the voltages applied to the oscilloscope from exceeding a value of approximately 70 volts.

Spark gap SG_1 is set to break down at 20,000 volts in order to protect C_1, which is rated at 25,000 volts. Gap SG_4 breaks down at 10,000 volts to protect the 12,500-volt capacitors at C_6.

Paper gaps SG_2 and SG_3 are designed to break down and form a mechanical short-circuit if excessive voltage should appear across either shunt R_2 or R_{10}. These gaps each consist of a spring whose pointed end presses against a brass plate. A piece of thin paper is placed between the point and the plate. If excessive current should be passed through the shunt, the paper is punctured, the spring makes contact with the plate, and the shunt is short-circuited.

In order to prevent the operator from applying plate voltage to tube X before the negative grid bias is connected, the power controls are interlocked as shown in Fig. 3. Closing switch SW_5 applies filament voltage to the 866A mercury-vapor tubes in the bias power supply. This switch also supplies voltage for SW_6. Closing SW_6 applies plate

voltage to the bias rectifier and thus provides the negative bias for tube X. After SW_8 is closed, voltage is available for the grid and plate power supplies.

The use of two autotransformers in the high-voltage parts of the grid and plate power supplies is an added safety feature. In each system, one autotransformer is placed out of the operator's reach and is set so that when the second autotransformer is adjusted by the operator, no dangerously high voltages may be applied to the tube X at any setting of the operator's control transformer.

Switch SW_{11}, mounted on the main panel, turns on the blowers which cool tube X and also provides voltage for SW_{12}. Closing SW_{12} applies voltage to the filament of tube X and also provides voltage for the trigger circuit.

When the tube tester is used for making measurements, it is advisable to keep the oscilloscope signal voltages between 25 and 50 volts. Voltages below 25 give deflections whose short length increases errors in measurement. Voltages much in excess of 50 volts may cause the neon protective bulbs to ignite and give a false indication.

To keep the oscilloscope voltages within the required range when measuring grid or plate voltages, each voltage divider is provided with several different low-voltage sections. Thus, the plate-circuit voltage divider has four low-voltage sections providing voltage ratios of approximately 50, 100, 200, and 400. These ratios cover the voltage ranges 0-2,500, 2,500-5,000, 5,000-10,000, and 10,000-20,000 respectively.

Similarly, shunts of different value are provided for R_2 and R_{10}. For R_2 the available resistances are approximately 2, 1, 0.5, and 0.25 ohms covering the current ranges 0-25, 25-50, 50-100, and 100-200 amperes respectively.

√ High-Speed Resistor Tester

Pigtail resistors are checked against a standard with a percentage limit bridge at a speed of 1,800 per hour. An electronic null detector and special fixtures reduce hand operations to a minimum

By A. W. DAUBENDICK

IN MANUFACTURE of electronic equipment, the percentage limit bridge with its usual accessories often fails to meet all resistor-testing requirements. In the design to be described, the instrument is arranged for maximum utility and speed of operation. The physical design of the equipment has been influenced primarily by job analysis and motion study.

The equipment consists of two assemblies so that maximum table space is made available to accommodate other testing operations. All major sources of heat are isolated from the operator, and from the calibrated components, by being mounted in the rear assembly. The front assembly shown in Fig. 1 contains the complete bridge circuit and the null-indicating instrument. This confines all points of operation to a small space and allows minimum motion of both hands and eyes. The sequence of motions by the operator are natural, rhythmical, and as nonfatiguing as possible.

An operator, when inspecting pigtail type resistors, takes them from stock a handful at a time. The individual resistor is delivered to the test clips while being held by its leads, one in each hand. After the resistor is inserted in the test clips, the operator's hands are removed from the test circuit while the limit measurements are being made by continuing the motion of the forearms downward. When the release motion is completed, the limit-switching operation follows automatically since the motion of the right arm is terminated by striking (with the bottom of the hand) a large Bakelite platform which is mechanically coupled to the limit switch.

The operator's cues to observe the indicator are the operations of releasing and switching. If the switching operation causes the indicator needle to cross zero (midscale) the resistor is known to be within the limits indicated by the settings of the limit controls. The resistor is then removed by a reversal of the insertion operations.

Although the limit-switching operation might be regarded as a motion that should be eliminated, it becomes useful in this arrangement as an inducement for the operator to remove his hands from R_x. At

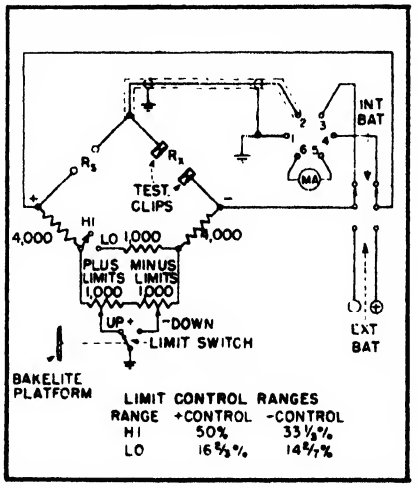

FIG. 1—Schematic of bridge assembly. The panel meter has a 0.5-ma zero-center range and the resistors are accurate to ±0.1 percent

the same time the switching operation has been reduced to a negligible loss.

Gross time study of the operation of this equipment, inspecting one-watt carbon resistors with axial leads, shows an operating speed of about 1,800 pieces per hour for a male operator.

Null Indicator

In the design of the electronic d-c null indicator shown schematically in Fig. 2, some sacrifice has been made in voltage sensitivity. But, since the input resistance to this instrument is 10 megohms, the current sensitivity is better than 0.001 microampere per least scale division. The voltage sensitivity is still great enough for 0.1 percent discrimination with as little as 5 volts applied to the bridge. The electronic null indicator allows the limit bridge to be applied proficiently to resistances ranging between 5 ohms and 50 megohms, a ten-million-to-one ratio.

The circuit of the null indicator consists of a series-balanced d-c voltage amplifier direct coupled to a parrallel-balanced current amplifier. The input of the voltage amplifier is actuated from the null terminals of the bridge through a light a-c filter.

The circuit quantities shown provide ample sensitivities, and zero drift is low enough not to require filament voltage regulation to stabilize contact potentials. At the same time the variable-mu grids obtain a semilogarithmic deflection pattern (see Fig. 3) which is considered most desirable in some applications.

Tube matching is the most critical provision for these circuits. If tube selections are favorable, the zero drift may be less than two degrees deflection (equivalent to about 10 mv) with line voltage variations of 10 percent. The first stage deserves the most favorable choice of tubes and it is also desirable that the input tube be a hard one to minimize the effects of input resistance variation. This latter requirement is not too critical, however, since the final zero adjustment may be corrected for any particular setup, after which the remaining errors will be entirely negligible.

Power Supply

The power supply is inadequate for operating the bridge through the very low end of the resistance range but it takes care of all battery requirements for values above 100 ohms, which include the wide majority of applications. It adjusts itself automatically to the ideal requirements throughout its applicable range.

There is no pretense of using the VR-75 for regulating purposes. Rather, this tube serves as an automatic voltage limiter which will not shunt the output circuit as maximum load current is approached. The maximum output voltage obtained was chosen as approximately the maximum which cannot be sensed by an operator's fingers. No greater voltage is ever required because of the high current sensitivity of the null indicator.

Maximum output power, obtained at the deionization potential of the VR-75, is about 1.75 watts. Since the multiplier consumes almost ¾ watt, there remains only one watt to be divided about evenly between the standard and the unknown. This feature provides ample protection against damaging overloads. The maximum current available to the test circuit is 25 ma. Whenever low resistance setups require more current than this, battery power will be more applicable.

The test clips are machined from ⅜-inch square stock. When made from hardened steel or finished in hard chrome plate they have been found to accommodate millions of insertions without noticeable wear. The two members of each contact assembly are bound together with a single screw against a compression spring. This arrangement provides for adequate adjustment of contact pressure, and convenience in dismantling for cleaning.

Reference

(1) Maurice Artzt, Survey of D-C Amplifiers, ELECTRONICS, p 112, Aug. 1945.

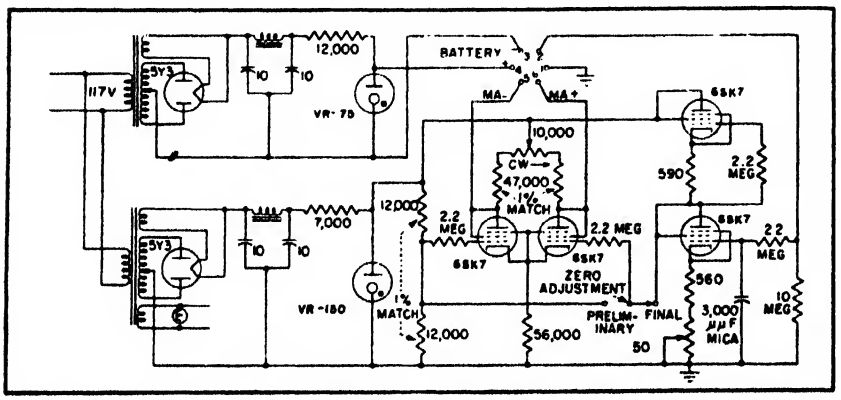

FIG. 2—Circuits of the voltage supply and null indicator amplifiers that form the accessory unit. This may be mounted away from the table area

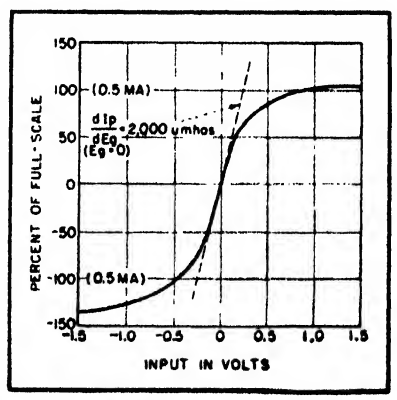

FIG. 3—Deflection curve of null indicator using remote cutoff tubes

Overvoltage Testing of Capacitors

Methods and equipment for testing paper-dielectric liquid-filled capacitors for direct-current service are described. In addition to precautions for personnel safety, testing techniques should limit charging and discharging currents and prevent oscillation

By R. J. HOPKINS

Because, in general, manufacturers of high-voltage capacitors electrically test 100 percent of their products, repetition of these tests by customers on 100 percent of their incoming capacitors should be unnecessary. Sampling procedures that insure a satisfactory average quality level (AQL) have been developed on a statistical basis and have been widely accepted by industry for quality control purposes.

A typical sampling schedule similar to that used by the U. S. Army for acceptance of d-c rated paper-dielectric capacitors is given in Table I. In the event that the number of defective capacitors in any sample quantity exceeds that allowed by the table, the lot from which the sample was taken can be tested 100 percent.

Overvoltage tests on capacitors include the following:

DIELECTRIC TEST: Voltage is applied from terminal to terminal, across the active dielectric.

GROUND TEST: Voltage is applied from each terminal to case where the case is not a terminal, and thus across the major insulation between dielectric assembly and case, including bushings.

MULTIPLE SECTIONS TEST: Voltage is applied between sections where there are more than one independent section in the same case.

When making terminal-to-terminal or dielectric tests, it is of greatest importance that charging and discharging currents be non-oscillatory. Direct-current capacitors are designed to operate with much higher voltage stresses across their dielectric than are a-c rated capacitors, and oscillation of either charging or discharging currents impresses oscillatory voltages across the capacitor which may exceed the a-c breakdown strength of the capacitor, thus causing failure.

Even though the charging and discharging currents are nonoscillatory, there is danger of damage due to high peak currents. Most capacitors designed for ordinary d-c operation are not intended to withstand high current surges, and such surges may cause arcing at the foil electrodes. This possibility of damage is recognized by various standards issued during the war to cover hermetically sealed paper capacitors. For example, AWS C-75.16 and JAN C-25 specify that charging and discharging currents be limited to one ampere. This limit has been widely adopted by the capacitor industry. The resistance required to hold the capacitor current within this limit is more than sufficient to suppress oscillations in the test circuits described later.

When testing, it is possible to allow the capacitor to remain charged but disconnected from the voltage source for the duration of the test. However, under these circumstances failure may occasionally occur at the instant of discharge after the test, even though the discharge current is nonoscillatory and limited to one ampere. It has been shown that these failures do not occur if the capacitor remains connected during the test.

Test Prod Type Equipment

Simplest and least expensive type of equipment for making tests at voltages below 5,000 volts d-c is the so-called test prod or test-sticker type of test set. This equipment includes a full-wave rectifier with plate voltage control to cover the voltage range desired, and a suitable voltmeter, with two test leads brought through flexible armor to a pair of insulated test handles. Rather than moving the work to the test leads, the prods can be used by the operator to apply voltage to a large number of capacitors without handling each individual capacitor.

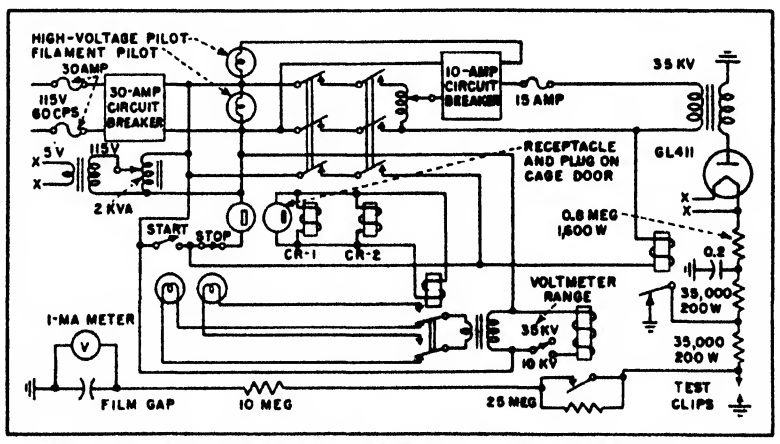

FIG. 1—Rectifier and controls of test prod equipment are straightforward

For the sake of safety, the cabinet access doors are usually interlocked, and the low-voltage supply circuit to the plate transformer is usually brought through a pair of push button contacts on each test handle, convenient to the operator's thumbs during normal use of the prod. It is thus difficult to obtain voltage at the test handles unless the operator has one in each hand.

A schematic diagram for such a test set is given in Fig. 1. This set uses 115-volt 60-cps power, brought through a cabinet door interlock and fuse block to a motor-driven time-delay relay that prevents application of power to the plate transformer until the tube filaments are heated. Provision is made so that filament power is on as long as the main line switch is closed independently of the plate power. Control of the plate voltage is obtained by a variable-voltage autotransformer in the low-voltage supply. Plate voltage is switched on and off by means of the two push-buttons in the low-voltage supply, which are physically located in the handles of the test prods.

The full-wave rectifier uses GL-866-A mercury-vapor tubes, and the d-c supply is filtered. A voltmeter and voltmeter multiplier, in this case a one-milliampere meter and five-megohm resistor, are connected across the test leads. Between the rectifier and the filter, and between the filter and the test prod, 5,000-ohm resistors have been installed to limit charging current to one ampere. The 60,000-ohm resistor connected across the test leads provides a discharge path for the test capacitor after the plate voltage is removed. This resistor is larger than is necessary to limit the discharge current to one ampere because, as it is permanently connected across the d-c output, it must be high enough to keep the current that is drawn to a fraction of the available rectifier output.

When testing with this type of equipment, the voltage must first be preset to the desired test level. This presetting is simplified by providing protective scabbards for the test prods, close enough together so that the operator can press both buttons in the handles with one hand, leaving the other free to adjust the voltage control. The prods are then applied de-energized to the terminals of the capacitors to be tested, and the buttons on the handles depressed, after which the voltage rises to the preset level. After the required time of application of test voltage, plate voltage is removed by releasing the buttons in the handles, and the capacitor discharges through the resistor connected across the test leads.

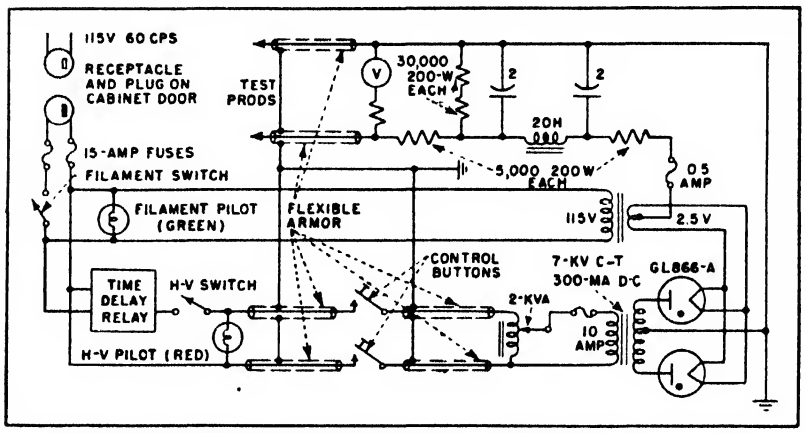

FIG. 2—Interlocks are major circuit features of this test cage equipment

Test Cage Type Equipment

For making tests above 5,000 volts, the interests of safety to the operator dictate using a test set with an interlocked test cage in which one capacitor at a time can be connected to the test leads. The wiring diagram of such a test set, rated 35 kv maximum, is Fig. 2.

This set includes a half-wave Kenotron rectifier, supplied through a variable-voltage transformer from a 115-volt 60-cps source. Failure protection is provided by both fuses and circuit breakers. Start and stop push buttons with suitable indicating lights are supplied to control the coil current to two contactors in series with the plate supply. Two contactors are provided to protect the operator in case one contactor sticks. Door and test cage interlocks open the coil circuit of these contactors.

Resistors are provided in series with the high-voltage lead between filter and discharge switch and between discharge switch and the test leads to limit charging and discharging currents to one ampere. An additional series resistance of 800,000 ohms is provided to limit the total plate current to the rating of the tube. In this set the discharge path is a solenoid-operated switch between the high-voltage lead and ground. The voltmeter has 10-kv and 35-kv scales with a solenoid-operated multiplier switch.

Testing with this type of set is quite simple. After the filament of the rectifier has been heated, one capacitor at a time is connected to the test leads. With the gate and the plate circuit closed, voltage is raised slowly to the desired level by means of the variable-voltage transformer and is held at that level for the desired time. At the end of the desired holding time, the voltage control is turned to the zero position and the plate power removed by pushing the off button. This button also closes the discharge switch, thus draining the charge on the capacitor quickly enough so that substantially no charge remains by the time the operator has opened the cage to change connections.

With this type of set, capacitors should not be connected in parallel for test. With two or more capacitors connected in parallel, failure of one capacitor allows the other parallel-connected capacitor to discharge through the resultant short circuit, with a discharge both oscillatory and of a high peak current.

Voltages to be used for over voltage testing of d-c capacitors have been standardized satisfactorily in the last few years. These voltages are now shown in proposed JAN C-25 Amendment 1, and it is anticipated that these same values will be recommended in industrial standards now being designed to cover capacitors for commercial use. Such test voltages include:

TERMINAL - TO - TERMINAL TEST VOLTAGE: 200 percent of rated d-c volts for 15 seconds, or 250 percent of rated d-c volts for one second.

TERMINAL-TO-CASE VOLTAGE: 400 percent of rated d-c volts for capacitors rated 600 volts d-c and below, and 200 percent of rated volts plus 1,000 volts for capacitors rated above 600 volts. The time of application of full test voltage is one second.

TEST VOLTAGE BETWEEN MULTIPLE SECTIONS: 200 percent of rated d-c voltage for a period of one second.

Table I—Capacitor Sampling Table for Overvoltage Tests

Lot Size	Number of Samples: First Sample	Number of Samples: Second Sample	Number of Samples: Combined Samples	Allowable Rejects: First Sample	Allowable Rejects: Combined Samples
Up to 299	25	50	75	0	1
300–499	35	70	105	0	2
500–799	50	100	150	1	3
800–1,299	75	150	225	2	4
1,300–3,199	100	200	300	2	6
3,200–7,999	150	300	450	3	9
8,000–21,999	200	400	600	4	11

If rejects from first sample exceed the allowable limit for a first sample, but do not exceed the allowable limit for combined samples, take second sample. If rejects from first sample or combined samples exceed the allowable limit for combined samples, reject lot for 100 percent tests.

If capacitors are not purchased in accordance with the specifications listed above, recommended test values should be obtained from the capacitor manufacturer. If test voltages that are used are in accordance with applicable specifications, if precautions are taken never to exceed a charging or discharging current of one ampere, and if the test voltage source remains connected to the capacitor under test throughout the test, there will be little trouble from damage or failure of properly designed and constructed capacitors.

Curve-Tracer for Acoustic Devices

Quality control over full-scale production output of handset receivers is obtained through the use of a powered-sweep bfo, a long persistence c-r tube, and suitable test fixtures

By R. K. HELLMANN

ACOUSTICAL DEVICES such as telephone handset receivers, loudspeakers, and microphones are now manufactured in accordance with performance specifications which call for a predetermined output-versus-frequency curve with comparatively narrow tolerance limits. In order to control production quality it is necessary to check the performance of each unit produced.

Among the various methods of recording a test curve the semi-permanent trace obtained with a cathode-ray tube of long screen persistence was found the most practical solution. A curve traced in this manner with a relatively slow sweep can be made visible between 3 and 15 seconds, which is long enough to produce the impression of the complete diagram, and short enough to cause no interference with a subsequent curve.

The curve tracer described here is based on this recording principle of operation. It has withstood the rough treatment on the assembly line over a period of five years while testing well over a million units justifies this report.

Operation of the curve tracer is shown in the block diagram in Fig. 1. The device under test is fed from a beat-frequency oscillator whose frequency is varied by a mechanical drive. The same drive also actuates a potentiometer which controls the horizontal deflection of the luminous spot in the cathode-ray tube. The device under test may be, for instance, a handset receiver.

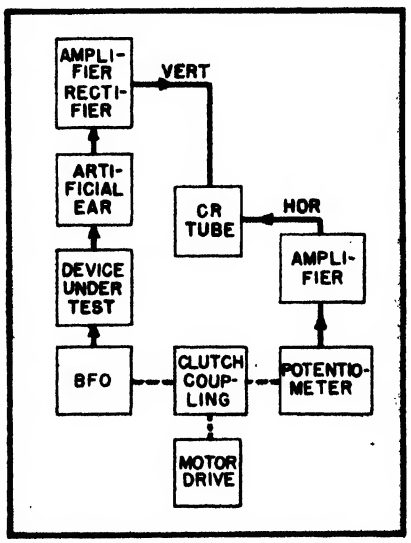

FIG. 1—Curve tracer includes these units. Artificial ear is a crystal or capacitor microphone

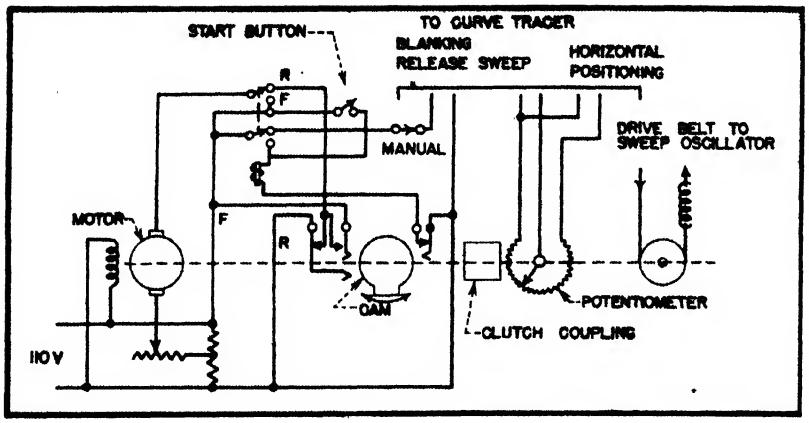

FIG. 2—Details of drive circuit. Cam and contact arrangement establishes start and stop positioning of mechanical train

It is coupled to an artificial ear. The output of the latter is amplified, rectified, and applied to the vertical deflection plates of the oscilloscope.

Frequency Sweep

The mechanical drive affords automatic scanning and consists of a reversible a-c motor with double gear reduction. On the slow shaft is a coupling device which, in the engaged position, connects the motor drive by means of a pretensioned metal belt with the pulley on the beat-frequency oscillator. Also on the slow shaft is a cam which operates two adjustable sets of contacts.

Figure 2 illustrates the operation of the drive circuit. When the starting button is pressed, the armature of the motor is energized through the contacts of the holding relay so the motor moves forward, starting the frequency sweep. When the cam opens the adjustable end contact, the holding relay releases and reverses the motor. This moves the beat-frequency oscillator toward its starting frequency.

Near the rest position, a cam-operated switch opens the armature circuit and stops the motor. If the inertia of the armature should carry the cam beyond the range of this rest position a second contact on the same adjustable arm closes and makes the motor rotate in a forward direction until it comes to rest between the two contacts.

When the end contact in the forward direction opens, a quick-acting relay lifts the bias of the cathode-ray tube. The bias is normally sufficiently negative to blank out the beam. In this manner a trace is produced on the screen only during the forward sweep. Since current density in the spot and accelerating voltage are high to make the afterglow of the trace last a long time, this precaution is necessary to prevent burning of the screen with a stationary spot.

Provisions are made to operate the drive and the frequency-determining potentiometer by hand so details of the diagram can be retraced. To this end the coupling device on the slow motor shaft can be pressed inward to disengage the metal belt from the shaft of the drive and the associated cam. However, engagement with the potentiometer which controls the horizontal beam displacement is retained. When released, an arrangement of spring pins relocates the oscillator control at the starting frequency as determined by the adjustable contact arm.

Since manual operation does not energize the holding relay the cut-off bias must be lifted in that case by pressing a button marked 'Manual'.

Potentials at both ends of the sweep potentiometer can be adjusted by two separate controls so the frequency range of the sweep, as set by the adjustable cam contacts, can be spread out to any desired length on the screen.

It will be realized that the curve tracer as a production testing device is only as practical as the auxiliary apparatus and fixtures.

Figure 3 shows the test fixture and circuit of a handset receiver. Since the cavities in the molded cap of the handset establish the shape of certain parts of the response curve, the test fixture consists of a handset with a special cap that is quickly detachable by means of a bayonet lock. A spring holds the unit against the coupler of the artificial ear with the prescribed pressure of 1 kilogram and also holds it safely in the loading position. The receiver under test is connected to the low-impedance output of the beat-frequency oscillator through a resistance equal to the nominal receiver impedance at 1000 cycles, and the voltage is adjusted at the same frequency so 1 mw is delivered to the receiver.

A crystal microphone made by Ballantine Laboratories and equipped with a coupler of approximately 12 cu cm has been found highly suitable for this application.

In order to stabilize the receivers magnetically a cam transfers the receiver leads momentarily to the source of stabilizing current during the closing of the handset arm in the fixture and restores them to the audio voltage just before the receiver seats itself on the coupler.

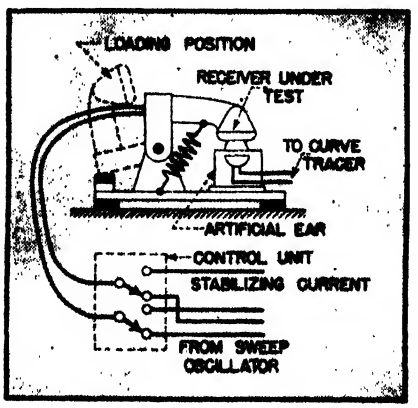

FIG. 3—Production test fixture duplicates physical arrangement of actual handset receiver

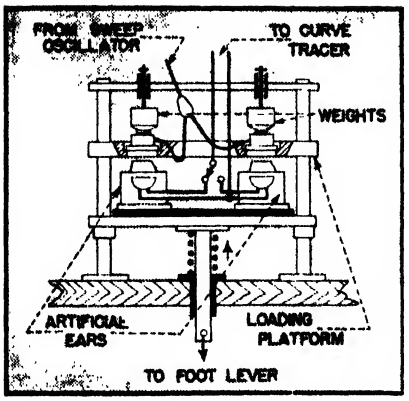

FIG. 4—Duplex fixture tests two receivers of a headset at once. Circuit is shown in Fig. 5

A somewhat more elaborate fixture is illustrated in Fig. 4. It accommodates the two receivers of a headset and is therefore equipped with two artificial ears. These are mounted on a support plate which can be lowered by a foot lever for loading. The receivers are placed in positioning recesses in the loading platform. When the pedal is released the ears are lifted by a spring which presses their couplers against the receiver units and the individual loading weights.

When used for testing high-impedance headsets of the resonant type, this fixture is associated with the circuit shown in Fig. 5. This was developed in accordance with the observation that sufficiently informative curve-tracer diagrams are obtained if both receivers, coupled to their respective ear cavities and connected in series, are run together. The output of each ear can be connected to the curve tracer input by means of switch T.

The data to be checked are the frequency and amplitude of the resonance peak, its width at 6 db down, and the impedance at peak output. Measuring the latter is at the same time an insurance that the output measurement in series connection does not introduce errors due to uneven voltage distribution. The test circuit can accordingly be arranged to provide four conditions which are selected by means of a 8-deck, 4-position switch, S.

After placing the headset in the fixture the operator proceeds as follows: position 1 of the main switch S is a calibrating position. Voltage E_1 is adjusted at 1000 cycles to a standardized value, and a fixed small fraction is fed directly into the curve tracer input whose gain is then adjusted against a calibrating mark on the screen.

In position 2, one-half of the standardized input is fed to the two receivers in series and the resonance peak is noted. Immediately, the curve is repeated with full input voltage in position 3. The location and magnitude of the main resonance can be noted as well as its width at a level 6 db below the peak, which will still be visible faintly from the trace taken in position 2.

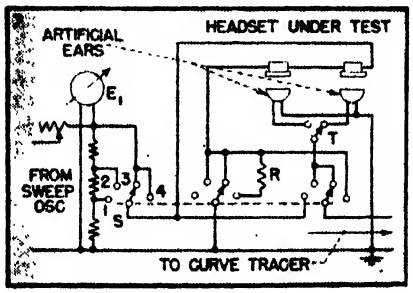

FIG. 5—Headset receivers are tested in series using the production fixture of Fig. 4. Individual outputs are connected to the curve tracer by switch T

By switching S to position 4 a comparatively small measuring resistance R is inserted into the circuit and the potential drop across it connected into the curve-tracer input. The resulting curve represents E_1R/Z and can, as R and E_1 are constant, be interpreted in terms of Z as a function of frequency. It is particularly convenient to read impedance at the output peak frequency, which has been set as a specification requirement.

When it comes to testing high-fidelity receiver units whose output level must be kept within narrow limits and is to be determined in terms of absolute sound pressure, the crystal microphone is no longer used.

Figure 6 shows a production line fixture using a Western Electric 640-A capacitor transmitter with a 6-cu-cm coupler, preamplifier and power supply.

The fixture is combined with a demagnetizer which reduces the initially fully-charged receiver magnet to a value indicated by the curve-tracer diagram.

The U-shaped laminated yoke of the demagnetizer is excited with 60-cycle a-c and can be lifted by means of a hand lever to expose the receiver magnet to a stronger or weaker alternating field. In the lowest position the exciting winding is disconnected.

For use with this fixture the standard curve tracer was modified slightly. The bias of the cathode-ray tube was adjusted so that a faint spot was normally visible instead of completely cut-off. The clutch mechanism was provided with a detent at the 1000-cycle point in the disengaged (manual) condition.

With this arrangement the first test operation is to set the sweep frequency by hand to 1000 cycles and adjust the input voltage E_1 so that the light pointer hits the zero-db level marked on the screen (see also Fig. 7B). The calibrated voltmeter will then indicate, in db above a reference level, the sound

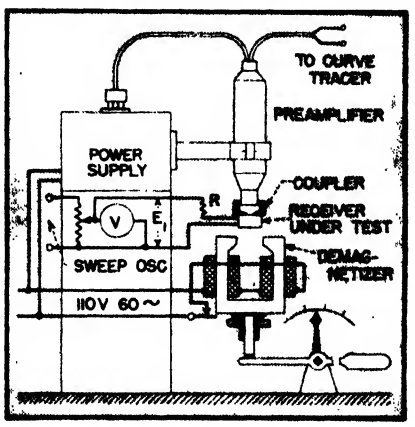

FIG. 6—High-fidelity receiver-units with narrow limits are tested in this fixture which combines a capacitor microphone and hand-actuated demagnetizer

pressure developed by the receiver under test. By gradual demagnetization, response can be brought between limits marked on the voltmeter dial.

The clutch is subsequently reengaged to the lower starting frequency and the sweep with a brilliant trace is initiated by pressing the starting button. The curve will, of course, go through zero at 1000 cycles and therefore represent deviation from that point.

To facilitate rapid interpretation of the diagrams produced by the curve tracer, the screen markings deserve special attention. Figure 7 illustrates three types of markings used.

Lines and symbols are usually drawn directly on the outside of the screen. The choice of a particular marking scheme depends, of course, largely on the test specifications. In Fig. 7A for example, which shows the pattern obtained with the fixture of Fig. 3, it was possible to describe the tolerances of the output curve simply by an upper and lower limit. The shaded areas were painted red so parts of the ordinarily bluish-green trace changed to that color as soon as they exceeded the permissible limits. It would be conceivable to utilize this for an automatic rejection feature by placing in front of the screen a phototube which has been made selectively responsive to red by suitable filters.

The two dashed frequency lines serve as calibration points for frequency adjustment, and the horizontal markings serve for gain adjustment by means of a standard unit.

In Fig. 7B, the curve will always go through the intersection of the 1000-cycle line and a zero-db horizontal. Again a number of calibration markers can be seen. Due to higher accuracy required with this test, the width of the trace had to be considered. Unless push-pull deflection amplifiers are used, the diameter of the luminous spot is likely to vary from one end of the curve to the other. If this is the case, the lines denoting the limits should be corrected so that the interference between any part of the spot and the limit line is not acceptable. To use for this purpose the imaginary center of the spot was generally found unsatisfactory in practice.

In Fig. 7C still another method of marking is indicated. A number of taut black wires are placed across the screen to denote such values as minimum amplitude and frequency limits. This method is particularly convenient for small production runs.

Referring to Fig. 7, a few typical clues to production faults as indicated by the curve tracer can be seen. In the high-fidelity receivers, Fig. 7A and 7B, the slight hump at about 2000 cycles is controlled by an acoustical coupling resistance which connects two cavities inside the receiver.

If this resistance is produced by a piece of silk, its porosity must be kept in a prescribed relation to the volume of these cavities to produce a flat response curve. Too little porosity will result in a pronounced peak in the curve, too much, in a dip. If the silk breather has come loose, this is usually revealed by a rake near the top of the hump.

The peak near the high frequency end is caused by acoustical cavities between the diaphragm and the earpiece of the receiver. In this space a moisture guard in the form of a thin diaphragm is usually placed. Slackness of this membrane may modify the shape of this peak considerably and it is therefore important to control its tension carefully. The shape of output curve in this region reveals to the skilled operator the nature of the required correction.

In the response curve shown in Fig. 7C the location and height of the resonance peak is influenced largely by the condition of the magnetic diaphragm. One of the common faults indicated by a shift in the resonance peak is distortion of the seating surface caused by insufficient lapping or faulty clamping. The degree of sag due to magnetic attraction determines the effective air gap of the receiver and is therefore revealed in both the output and impedance curves. Likewise the degree of magnetization can be determined.

Obviously there are many problems in quality control of acoustical devices where testing by the curve tracer can be applied advantageously. These include production testing of loudspeakers and radio receivers. For testing the latter, the sweep frequency generator can be used to modulate the signal generator, and the demodulated signal as picked off the voice coil of the receiver under test could be used for vertical deflection. Such a test would take only a few seconds but might present a better picture of the audio performance of a receiver than methods presently used.

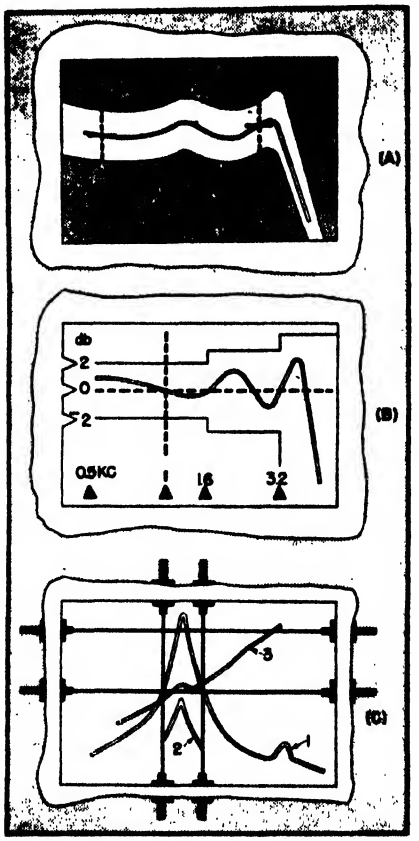

FIG. 7—Three alternative types of screen markings for production-line evaluation of curve-tracer readings. Pattern at A has shaded area painted red to show plainly any deviation of the trace from established limits. Marking B has limit lines established for contact with peaks in curve. Taut black limit wires are used at C for ease of changing on short runs

Tube-Seasoning Timer

Versatile unit for controlling the time schedule of cathode-ray tube seasoning racks up to 55 minutes. Various numbers of tubes can be seasoned on different runs

By M. SILVERMAN

MANY METHODS can be evolved for controlling the time schedule on cathode-ray tube seasoning racks, depending only on the ingenuity of the design engineer. Our company developed and has used for some time a satisfactory system.

Accuracy of time periods is not extremely critical and a spring-driven timer was found quite adequate for the job. The one we used was made by Walser Automatic Timer Co. Figure 1 shows the diagram of connections.

The switching arrangement throws resistors in and out of the heater circuit to change heater voltage. Minor variation in the number of tubes on the rack for different runs is no serious problem. A complete load of 20 tubes is standard practice. However, absence of one or two tubes from the rack does not affect current drawn through R_1 and R_2 materially. Voltage drop across the resistors is practically unchanged.

Switches can be adjusted either to open or close a circuit after a predetermined time interval. To start, proper settings are applied to all timers. This leaves the rack as shown in the diagram, with the a-c line connected and, in a typical cathode-ray tube test, with 11 volts impressed across the heaters. Operation then proceeds as follows:

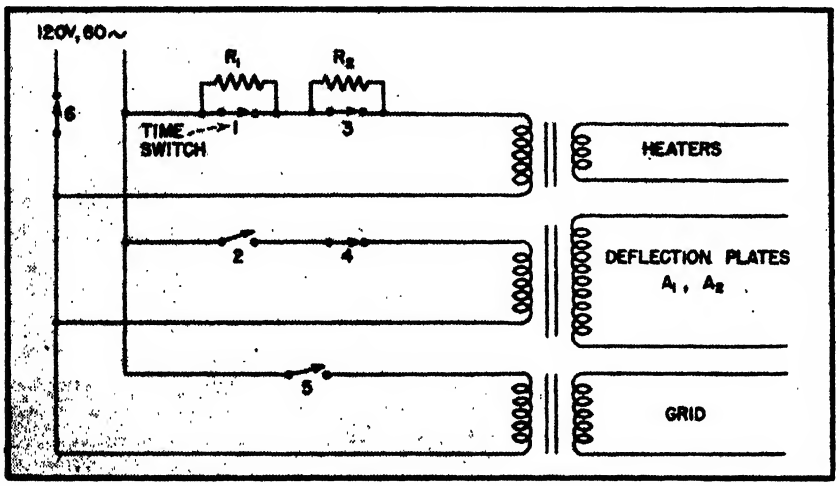

FIG. 1—Circuit showing the arrangement of switches, resistors and transformers

1 Opens after 10 minutes; Throws in R_1 and lowers heater voltage to 10 volts
2 Closes after 10 minutes; Turns on A_1, A_2, and deflection plates
3 Opens after 45 minutes; Lowers heater voltage to 9 volts
4 Opens after 45 minutes; Turns off A_1, A_2, and deflection plates
5 Closes after 45 minutes; Turns on grid
6 Opens after 55 minutes; Turns off a-c line

This type of timer is extremely versatile and permits considerable latitude in schedule changes.

Soldering Litz Ends

By EMERICK TOTH

THE WRITER had occasion to design a receiver for aircraft using coils of litzendraht wire. These coils ranged in diameter from 12 inches, wound with litz of about 180 strands of number 38 wire, to little fellows of ½ inch ID using 7/41 litz. Over 150 coils were involved, a total of more than 300 coil ends, thousands of individual strands that must be properly tinned and soldered.

Careful tests were made of the following three methods:

(1) Cautious removal of the silk and enamel from the coil end by abrasion against a relatively soft high-speed rotary wirebrush.

(2) Heating of the coil end in an alcohol or Bunsen-burner flame and subsequent plunging of the hot coil end into alcohol.

(3) Application of a small quantity of a paste of zinc chloride and water to the coil end and heating with a soldering iron, immediately followed by tinning with rosin-core

solder while the resulting zinc chloride and enamel mixture was still boiling. The silk insulation was burned and stripped off by a very short exposure to a flame, and subsequent wiping with a rag prior to application of the zinc chloride.

Method (1) was found to damage individual strands excessively, and did not clean all strands in sizes of litz with many strands, such as 70/38 and 180/38.

Method (2) was difficult to control. Insufficient exposure to the flame resulted in the enamel not cracking off when the hot coil end was plunged into cold alcohol. Overheating caused individual strands to burn off. Even when satisfactory cleaning was obtained, the copper was left so brittle that soldered coil ends would break easily.

Method (3) provides easy and effective tinning. The appearance of the tinned end was neat and clean after the residue of zinc chloride, enamel, rosin, and solder had been wiped off while still hot with a damp rag. The ease of tinning even 180/38 litz suggested that inside strands were not properly coated. Several samples were cut in cross-section but all strands appeared to be clean of enamel and tinned.

Samples were placed in a salt-spray chamber and subjected to the Navy's standard salt-spray test for two hours. It was found that except for a light accumulation of powdery salt the samples were in no way affected by the test and all 300 coil ends were processed as outlined in method (3) above.

Eighteen months after delivery, one equipment was examined which had been in service in Panama for a year. No trace of corrosion or any other damage was found.

Zinc chloride is very hygroscopic and should be kept in a suitable well-stoppered glass bottle, with only as much paste prepared at one time as is needed for a few hours use.

Concentricity Tester for Enamel Film on Wire

By ELMER F. HANSEN

AN ELECTRONIC CIRCUIT which makes it possible to measure the thickness or concentricity of enamel insulation on a sample of magnet wire in about one minute is described by Elmer F. Hansen in the Nov. 1942 issue of *General Electric Review*. The sample of wire is inserted in a turning chuck and placed over two brass plates mounted end to end in the same plane. An insulating block applies pressure to hold the wire flat against the plates. This gives two capacitances in series between the brass plates; the copper wire is the common conductor and each brass plate serves as a conductor, with the film of enamel acting as the principal dielectric for each capacitance. This series connection eliminates the necessity for scraping off insulation.

Changes in film thickness change the capacitance over a range of 5 $\mu\mu$f to 7 $\mu\mu$f for an average wire samples with varying degrees of concentricity. This change is measured by connecting the brass plates to the grid and plate circuits respectively of an oscillator, as shown in Fig. 1. An increase in film thickness causes a decrease in the connected grid-plate capacitance and an inversely proportionate increase in the d-c plate current of the oscillator. The deflection of the plate current milliammeter M_1 was found by test to be a linear function of film thickness.

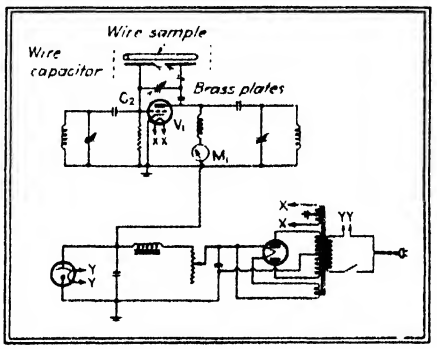

Fig. 1—Basic electronic circuit for measuring the thickness of enamel insulation on wire at production speeds

A calibration in terms of the ratio of maximum to minimum film thickness was found more suitable for production testing because it remains accurate regardless of normal changes in circuit parameters with age, and is also independent of slight changes in oscillator frequency. In making a test, the wire sample is rotated to get minimum meter deflection, and sensitivity control C_s is varied until a reading of 1.0 is obtained. The wire is then rotated for maximum deflection, and the ratio of maximum to minimum film thickness is read directly on the meter. The results are accurate to within about 5 percent.

B-H Curve Tracer for Lamination Samples

Magnetic characteristics of laminated material can be checked in a few minutes during production runs to detect wrong laminations in a-f transformer or choke assemblies, using a special four-tube amplifier and test jig with an ordinary cathode-ray oscilloscope

By ROBERT ADLER

THE characteristics of the magnetic material used in transformers and chokes are not easily measurable, and introduce a factor of uncertainty in the design and production of vacuum tube equipment.

Sometimes a deterioration in the characteristics of some complex circuit defies explanation until the change is traced to a change in characteristics of magnetic materials. By then, hundreds of assemblies may have been completed with the wrong laminations, and much valuable time may be lost.

Apparatus for rapid and easy testing of magnetic materials is extremely useful in such cases. But, to obtain such data as permeability, saturation, coercive force and hysteresis loss of magnetic alloys, special equipment which is not easily available has been necessary; and even with such equipment, comparatively large amounts of sample laminations are generally needed for test, and the measurements take considerable time and effort.

The oscillographic equipment described makes it possible to obtain this data with great rapidity. Comparison checks of a number of samples can be made within a few seconds. Initial and reversible permeability characteristics, or increase of loss with flux density can be directly observed on the screen when the current input to the sample is gradually varied—observations and measurements which take hours with older methods.

An additional advantage of the oscillographic method is that it permits the use of extremely small samples. A little washer punched from a single lamination is all that is needed. Less than one millivolt, produced in a few turns which are wound around this miniature ring, is sufficient to provide an indication of flux density in the sample. On the other hand, little power is needed to saturate so small a sample, and the whole equipment is compact and easy to handle.

The small size makes it possible to run tests at elevated temperatures by simply placing the sample with its holder on a heater a few inches in diameter. Such an arrangement is particularly valuable for tests on alloys with low permeability. Some of these alloys exhibit a large drop of permeability at high temperatures, and this characteristic is used for temperature compensation in watthour meters and other instruments. The equipment described here makes it easy to check the performance of such materials throughout the range of their operating temperatures.

The samples have about ⅛ inch minimum inside diameter. The ratio between inside and outside diameter should be small to maintain approximately uniform field intensity throughout the piece. A ratio of about 3:2 (for instance, ⅜ inch outside and ¼ inch inside) is good enough for most purposes.

Figure 1 shows a block diagram of the equipment. A 60-cycle current of low voltage and high intensity is

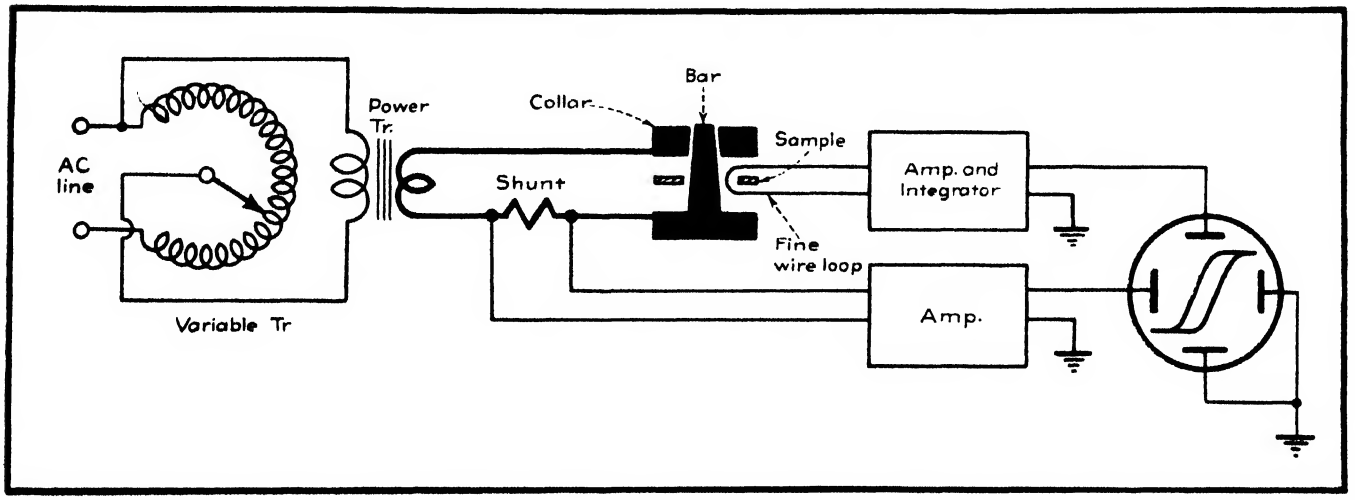

FIG. 1—Block diagram of complete B-H curve tracer. A washer-shaped sample of the lamination to be tested is slipped over the bar that forms a single-turn loop carrying a 60-cycle current of the order of 100 amperes, and the resulting magnetization is utilized by electronic circuits to produce the B-H curve of the magnetic material on the screen of the cathode ray oscilloscope

sent through a shunt resistance and a bar and collar arrangement by the secondary winding of the power transformer. The washer-shaped sample is slipped over the bar, and one or more turns of fine wire are threaded through the gap between sample and bar. The potential appearing across the little loop is fed into the input of an amplifier which also contains an integrator. The output of this integrator is connected to the vertical plates of an oscilloscope. The potential drop across the shunt is fed through a single-stage amplifier to the horizontal plates of the oscilloscope. A variable transformer serves to adjust the primary voltage supplied to the power transformer.

At any given moment, the current flowing through the bar develops a corresponding field intensity in the sample. At the same time, a proportional potential is produced across the shunt and appears amplified across the horizontal oscilloscope plates. As the flux in the sample changes, a voltage is induced in the little loop proportional to dB/dt, the rate of change of the flux. To obtain B from this voltage, it is necessary to carry out a process opposite to differentiation; in other words, pass the voltage through an integrating network. A simple network of this kind is shown in Fig. 2. The output from the loop is fed into a large capacitor through a large resistance. The time constant of these two elements is large compared to one period of a 60-cycle wave. If E designates the potential produced in the loop, the voltage appearing across the capacitor is proportional to $\int Edt$. Since E is proportional to dB/dt, the voltage across the capacitor is

$$\int Edt = \int \frac{dB}{dt}\,dt = \int dB = B$$

This derivation does not take into account various constant factors. It proves, however, that the output from the integrator stage is proportional to the flux density in the material. The proper voltage for the vertical oscilloscope plates must be obtained by selecting the right gain in the amplifier.

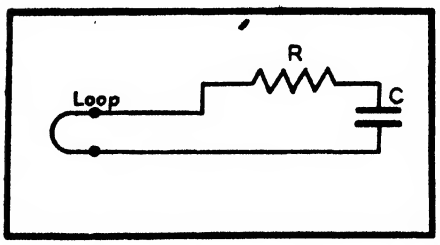

FIG. 2—Simple integrating network used to convert the induced voltage (proportional to dB/dt) to flux B

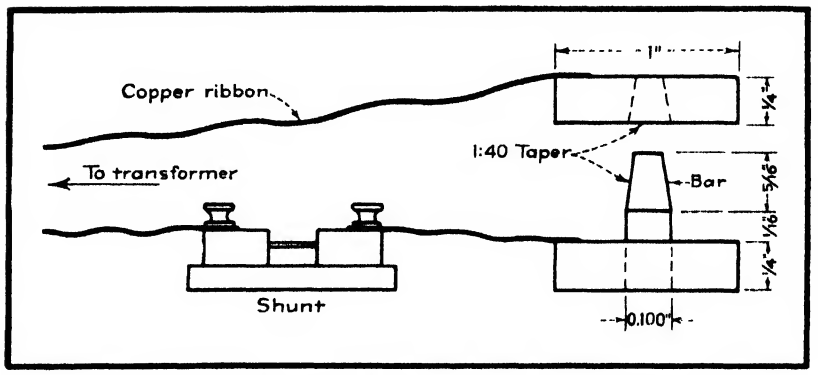

FIG. 3—Details of the bar and collar used for magnetizing the sample to be tested

Circuit Details

The power transformer is the type used in small radio sets, with a primary rating of approximately 40 watts. The secondary consists of a single turn formed by four strips of copper braid, ⅜ inch wide, all in parallel. The open-circuit voltage across this secondary turn is about 0.1 volt, and it can handle over 100 amperes without undue drop of voltage. At this high current intensity the power developed is only in the order of 10 watts.

Figure 3 shows the high-current circuit. The same four strips of copper braid are used throughout to avoid heating. The bar is made of copper, 0.100 inch in diameter, soldered into a ¼ inch copper plate, and the braided leads are soldered to this plate. The top portion of the copper bar is slightly tapered, and another ¼ inch copper plate with a correspondingly tapered hole is used for the return connection. Contact between bar and top plate is very good if the tapers are correct, and any heat developed in the copper rod is promptly dissipated into the two end plates. The total resistance of the high-current circuit is less than 0.001 ohm. Up to 150 amperes, it can be used for short periods without undue heating.

The shunt is selected according to the range of current required for the sample. In most cases it is the largest resistance in the high-current circuit. Most shunts produce a drop of 50 mv at full rated current, and a rating close to the required current intensity should be selected. Since the full voltage available is about 100 mv, such a combination permits easy adjustment within the desired range.

With an output voltage from the shunt of 30 mv, a gain of 30 is normally needed to get full deflection on the scope. A single 6SF5 high-gain triode supplies this gain.

The output voltage from the little loop depends on the saturation flux and on the cross-section of the sample, but in most cases it is a small fraction of one millivolt. The amplifier for the loop must therefore have high gain. It uses two 6SF5 triodes with the integrator section inserted between them. A detailed diagram of this amplifier and integrator is given in Fig. 4. The peculiar characteristics required in this amplifier make it somewhat unconventional, and therefore it is described in detail.

It would be very difficult, even with the largest available by-pass capacitors, to keep the time constant of the

cathode circuits large compared to one period of a 60-cycle wave; therefore, no cathode by-passes are used, even though the loss in gain is considerable. This disadvantage is somewhat compensated by greater stability of the overall gain.

The integrator stage consists of a 6SJ7 pentode with a plate load of 0.33 megohms shunted by a 1-μf capacitor. Under the operating conditions used, the internal plate resistance of the 6SJ7 is about 2 megohms, so that the effective resistance across the plate capacitor is about 0.25 megohms. The reactance of 1 μf at 60 cycles is about 2700 ohms, so that the plate load is predominantly capacitive, with a resistive component of only 1 percent. At the higher harmonics present in this channel the ratio is even better.

The total plate and screen current for all four tubes is about 3 ma. This small amount can safely be taken from the rectifier which supplies the amplifier and sweep circuits in the scope. The filaments are also fed from the power transformer in the scope, which, in most cases, will carry this slight overload without difficulty.

Large coupling capacitances of 0.1 μf and grid leak resistances of 1 megohm are used throughout to keep the low-frequency response high. It would be impractical to increase the size of these parts further, because small supply voltage variations with very low frequencies would then cause large vertical excursions on the scope.

The phase error caused by all these coupling elements adds up and distorts the trace very strongly, unless means are inserted to compensate it. Here is an approximate computation of the total phase error: At 60 cycles, the reactance of 0.1 μf is 27,000 ohms; combined with a resistance of one megohm, the tangent of the leading phase angle is:

$$\tan \phi = 2700/10^6 = 0.027$$

This corresponds to about 1.5 deg. There are altogether four such networks in the vertical channel, assuming that similar coupling elements are used in the amplifier stage contained in the scope. This gives a total phase shift of 6 deg. for 60 cycles. At the third harmonic the phase shift is only 2 deg. Since the voltage in the vertical channel contains very strong harmonics, a phase shift of 4 deg. and more between fundamental and harmonics is sufficient to confuse the result completely.

An equalizer is therefore inserted in the input to the first stage of the vertical amplifier. It is drawn in detail in Fig. 5a. The function of the equalizing network is to introduce a lag inversely proportional to frequency. At high frequencies the two capacitors simply act as a capacitive voltage divider without introducing phase shift, but at low frequencies part of the input current runs through the 4000-ohm resistor. Accurate phase compensation is best obtained by adjusting this resistor, since the phase shift caused by the scope itself is different with scopes of different manufacture. Directions for the adjustment of the phase equalizer are given later. It is interesting to note that the equalizer also compensates a small resid-

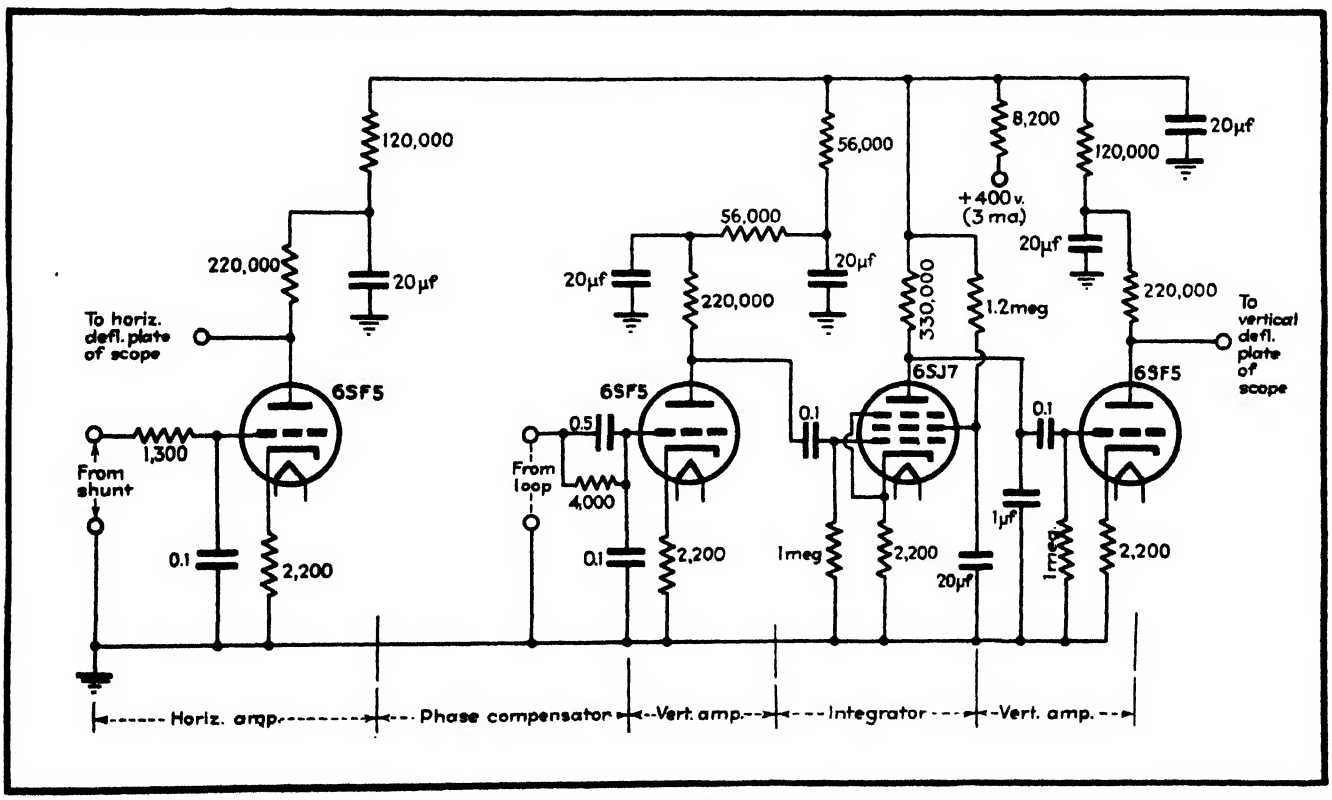

FIG. 4—Circuit used for the amplifiers and integrator

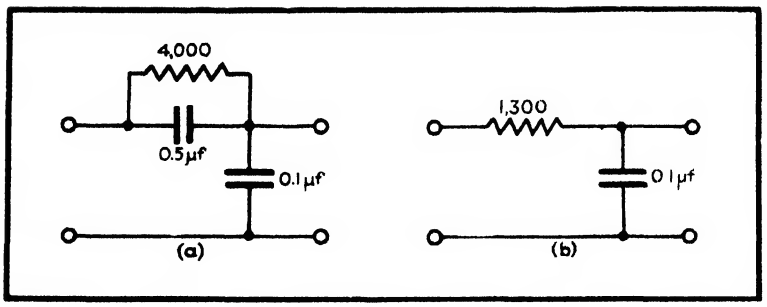

FIG. 5—Equalizing networks used to correct phase shift

ual phase error produced in the integrator stage of the equipment.

A smaller amount of phase shift is produced in the horizontal channel. The output voltage from the shunt is almost exactly a sine wave, and phase shift leads to a displacement of the horizontal time base on the screen, pulling the two steep portions of the hysteresis loop apart, so that the loss area appears larger. Equalization could be obtained by the same method as in the vertical amplifier, but the low harmonic content in this channel permits the use of a simpler network, as shown in Fig. 5b. Compensation with this network is possible only for one frequency. If the 60-cycle source contains strong harmonics, the type of equalizer shown in Fig. 5a should be used in both channels.

Adjustment of the equalizers is most easily accomplished by means of samples, using some characteristics inherent in B-H curves.

In Fig. 6, a normal hysteresis loop of ordinary transformer steel is shown (*a*), together with distorted forms resulting from incorrect vertical phase adjustment (*b* and *c*). When the equipment is first put into operation, curves resembling one of these distorted patterns are usually observed. By varying the input voltage to the power transformer, no change should appear in the correct curve (*a*), except that the saturated portions (*s*) stretch out when the current is increased. Incorrect vertical phasing spreads these portions and makes them appear like (*b*) or (*c*). By adjusting the vertical equalizer, a trace similar to Fig. 6a can be obtained. With a loop containing long saturated portions (*s*), vertical adjustment can thus easily be made of extreme accuracy.

If the current is now varied, the horizontal distance between the two steep portions, corresponding to the coercive force, should not vary after saturation has been reached. Variations, if they occur, are due to incorrect horizontal compensation.

To obtain accurate horizontal adjustment, a 2-inch diameter air-wound coil of about ten turns is substituted for the little loop, connected to the vertical amplifier, and coupled inductively with the high-current circuit. Care should be taken that no iron is present anywhere near this coil. Since the permeability of air is constant, independent of field intensity, a straight line appears on the screen (Fig. 6d); its slope depends on the voltage induced in the coil. Usually, a narrow ellipse (Fig. 6e) is obtained at first, rather than a single straight line. If the horizontal phase adjustment is now varied until the ellipse is reduced to a line, phasing is accurate and complete.

Practical Data

For a great number of applications, comparison of the characteristics of different materials is of primary interest. In these cases no absolute calibration of the equipment is necessary.

As long as washers made from different materials have identical dimensions, the curves on the screen permit numerical comparison. Differences in thickness can be compensated by using a correspondingly larger number of turns for the little coupling loop on thinner pieces. For many materials only one turn is needed, and in this case, if thicknesses are different, the vertical deflection is proportional to the thickness. The gain control on the scope can be used to equalize the calibration.

Eddy currents flowing in the sample tend to make the hysteresis loop appear wider, leaving the level of the saturated parts and the slope of the steep portions unchanged, but increasing the total area enclosed by the loop. With eddy current losses present, this area corresponds to the total core loss at 60 cycles, rather than to the hysteresis loss only. This is a valuable feature if total core loss is the object of interest, and in this case the sample should be of a thickness intended for actual use. If, however, the actual hysteresis loop and the real value of coercive force are required, samples of the smallest thickness available should be used to keep eddy current losses down to a minimum. This precaution is particularly important with high-permeability materials.

The average diameter of the sample washer determines the field intensity H produced by a given current. Washers of different average diameter, therefore, require proportionately different currents to obtain the same H. If the calibration is to be maintained for a larger washer, less horizontal gain is required. The equipment described provides enough current for saturating alloys even if the permeability is low, provided that small diameters are used.

For quick comparison, a number of samples can be slipped over the same fine wire loop and inserted one after the other around the copper bar.

Heat Runs

The holder assembly can be mounted on a heater unit for measurements at elevated temperatures. This unit consists of a heavy round iron casting with a heater winding on the inside. During the measurements the whole assembly is protected by a heat-insulating cover not visible in the picture.

The photographs of the four hysteresis loops in this article were taken during such a test, using a sample of low permeability, with the temperature rising in three steps from 80 deg. F (largest curve) to 200 deg. F (smallest curve).

To obtain permanent records, the curves can easily be photographed from the screen. With a curve of average size on a 3-in. tube with green fluorescence, an exposure of 1/50 second on high-speed panchromatic film with an f/4.5 lens gives satisfactory results. The screen should be illuminated from the outside just enough to make the mask with the calibration lines appear clearly on the print.

When the current is gradually increased from zero beyond saturation, the oscilloscope shows a hysteresis loop slowly growing out of a single point into the final curve. The changes of reversible permeability, represented by the average slope of the trace, from its low initial value to its larger "operating" value, and its final drop when saturation is approached, become clearly visible and measurable.

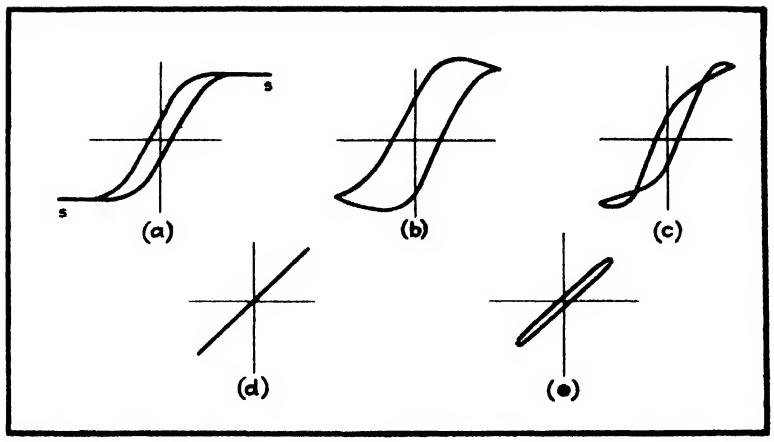

FIG. 6—Curves obtained during initial adjustments

Calibration

While the simplest way of calibrating the equipment consists of the use of samples with known characteristics, it is also possible to apply voltages of known magnitude to the vertical and horizontal inputs and thus obtain an absolute calibration. The following formulas are useful in this procedure; they are accurate only for narrow washers, with outside and inside diameters not too different, because of the error introduced by the assumption that the numerical average represents the true "magnetic average" diameter.

The following symbols are used in the formulas:

I = current through bar in amperes, rms.
E_h, E_v = voltages at horizontal and vertical amplifier inputs in millivolts, rms.
(A), (mv) = ratings of shunt in amperes and millivolts.
D_o, D_i = outside and inside diameter of sample in inches.
T = thickness of sample in inches.
n = number of turns in loop.
H = maximum field intensity in sample in oersteds.
B = maximum induction in sample in gausses (lines per cm²).

The current through the bar then becomes

$$I = E_H \frac{(A)}{(mv)}$$

The field intensity is

$$H = 0.45 \frac{I}{D_o + D_i}$$

The induced flux density is

$$B = 116 \frac{Ev}{(D_o - D_i)\, Tn} \text{ (for 60 cycles)}$$

To obtain an absolute calibration, the peak-to-peak deflection of the oscilloscope per millivolt is first established for both channels. The relation between millivolts and magnetic values is then used to convert the observed deflections into peak values of H and B.

RECEIVERS

Adjustable-Bandwidth F-M Discriminator

Use of a cathode follower in place of the pentode amplifier normally used to drive a Foster-Seeley discriminator provides easily adjustable bandwidth control, output-frequency characteristics complementary to the frequency-voltage characteristics of stabilized f-m microwave oscillators, and freedom from critical adjustments

By W. G. TULLER and T. P. CHEATHAM, Jr.

IN THE COURSE OF research on communication systems, the need arose for a discriminator to be used in frequency-modulation receivers having variable bandwidth. Almost simultaneously the mathematical analysis of a typical discriminator circuit showed a possibility of constructing a discriminator whose bandwidth would be readily adjustable by means of a tap switch, but whose output—frequency characteristics would have a shape independent (in normalized coordinates) of discriminator bandwidth.

This discriminator circuit has proved considerably more tolerant to misadjustment than conventional types, and has four other significant features: (1) the bandwidth is adjustable over more than a four-to-one range by means of a single tap switch; (2) the normalized output voltage-frequency characteristic is independent of bandwidth; (3) the normalized output voltage-frequency characteristic may be made the complement of the frequency-modulating voltage characteristic of a frequency-modulated stabilized microwave oscillator, thereby making possible very good overall system linearity; (4) the circuit is not as critical to slight mistuning as most other discriminators (particularly in mistuning the primary).

The discriminator has three compensating undesirable features: (1) one additional high-g_m tube may be required as compared to other discriminators; (2) sensitivity (output volts per megacycle of frequency deviation) is an inverse-squared function of bandwidth while peak output voltage is an inverse function of bandwidth; (3) larger bandwidths are required for a given amount of distortion than in the case of the Foster-Seeley discriminator.

Electrical Circuit

The circuit of a typical cathode-driven discriminator, given in Fig. 1, operates in the same fashion as the Foster-Seeley[1] discriminator except for one important fact—the stage preceding the rectifier acts as a constant-voltage source (cathode follower) instead of a constant-current source (pentode amplifier). This in general means that the tube driving the discriminator may not give good limiting action, so that the circuit may have to be preceded by a conventional limiter.

The coils forming the transformer in the cathode-driven discriminator may be coupled as tightly as possible, since the output of the discriminator is proportional to the coefficient of coupling between them and the bandwidth is independent of this coefficient. Circuit parameters given in Fig. 1 are for operation at a midfrequency of 60 mc, and all data given were taken about this midfrequency.

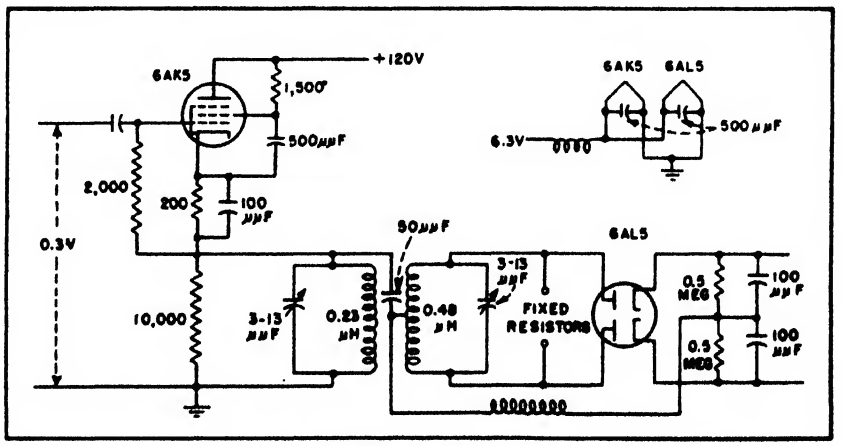

FIG. 1—Cathode-driven discriminator circuit, with values of components for center frequency of 60 mc

Theory of Operation

An analysis of the operation of a cathode-driven discriminator is partially given as an incidental part of a published analysis[1] of the Foster-Seeley discriminator, and the results of this analysis are of interest here. If the detectors are linear, the output voltage as a function of circuit parameters is

$$E_0 = \eta E_1 \left\{ \sqrt{\left[1 + \frac{\alpha Q_2 F}{2(1+Q_2^2F^2)}\right]^2 + \left[\frac{\alpha}{2(1+Q_2^2F^2)}\right]^2} - \sqrt{\left[1 - \frac{\alpha Q_2 F}{2(1+Q_2^2F^2)}\right]^2 + \left[\frac{\alpha}{2(1+Q_2^2F^2)}\right]^2} \right\} \quad (1)$$

where E_0 = d-c output voltage
η = rectification efficiency of rectifiers
E_1 = Peak r-f voltage across transformer primary
$\alpha = Q_2 K \sqrt{L_2/L_1}$
Q_2 = loaded Q of transformer secondary
K = coefficient of coupling
L_2 = inductance of transformer primary
L_1 = inductance of transformer secondary
$F = 2B/f_m$
B = deviation
f_m = midfrequency

Each radical in Eq. 1 represents the output of one of the two half-wave rectifiers. The expression may be simplified to

$$\frac{E_0}{\eta E_1} = \sqrt{1 + \alpha \frac{\frac{\alpha}{4} + Q_2F}{1+Q_2^2F^2}} - \sqrt{1 + \alpha \frac{\frac{\alpha}{4} - Q_2F}{1+Q_2^2F^2}} \quad (2)$$

Now if the detectors are square-law instead of linear, the effect on Eq. 2 is simply to remove each radical, leaving

$$\frac{E_0}{\eta E_1} = \frac{2\alpha Q_2 F}{1+Q_2^2F^2} \quad (3)$$

From this expression it is apparent that a plot of $E_0/\eta E_1\alpha$ as a function of Q_2F or, since $F = 2B/f_m$, as a function of Q_2B, should be independent of Q_2. The effect of a change in Q_2 will be to produce a proportional change in the peak amplitude reached by E_0 since α depends directly on Q_2, and to change $\Delta\nu_p$, the peak-to-peak bandwidth of the discriminator, inversely with Q_2 since the output will be a maximum for a given value of Q_2B independent of Q_2. The curve given by Eq. 3 is identical with the voltage-frequency characteristic of microwave discriminators, and hence complementary to the frequency—voltage characteristic of a frequency-modulated microwave oscillator stabilized by such a discriminator[2]. As can be seen from a comparison of Eq. 2 and 3, the use of linear detectors instead of square-law makes the shape of the output-frequency characteristic somewhat dependent on the value of α, and hence on the Q of the tuned circuit. For small deviations (normalized with respect to peak deviation), or for coefficients of coupling less than unity, the difference between linear and square-law rectifiers is negligible.

The results obtained from the circuit of Fig. 1 are shown graphically in Fig. 2 and 3. Figure 2 is a normalized plot of the output voltage—frequency characteristic of the cathode-driven discriminator for various loadings, in comparison with two curves taken at different loadings on a Foster-Seeley discriminator. The shape of the characteristic of the Foster-Seeley discriminator is a critical function of loading and coupling, optimum damping being somewhere between the no-load condition (circuit losses correspond to 3,200-ohm shunt resistor) and loaded condition (equivalent shunt resistance of 760 ohms) in the case studied. The normalized curves for the cathode-driven dis-

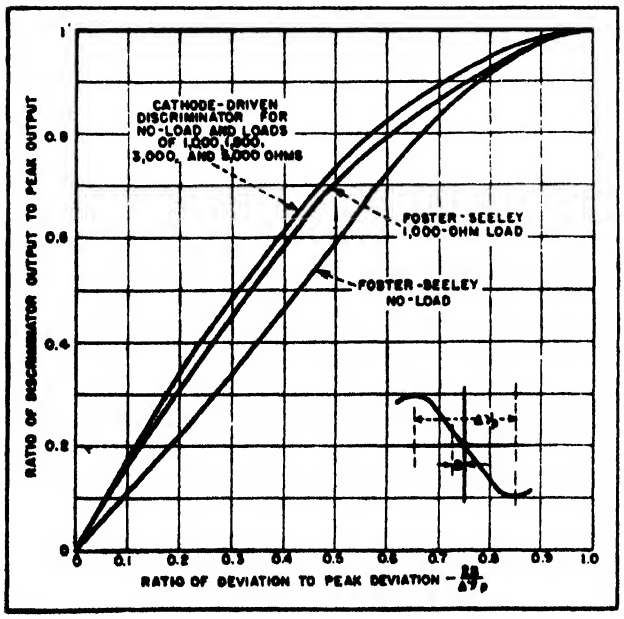

FIG. 2 (left)—Voltage-frequency characteristics of conventional and cathode-driven Foster-Seeley discriminators, showing that the cathode-driven discriminator is independent of loading

FIG. 3 (below)—Variation of bandwidth-load product with bandwidth for cathode-driven discriminator, showing how circuit losses provide lower limit to bandwidth obtained

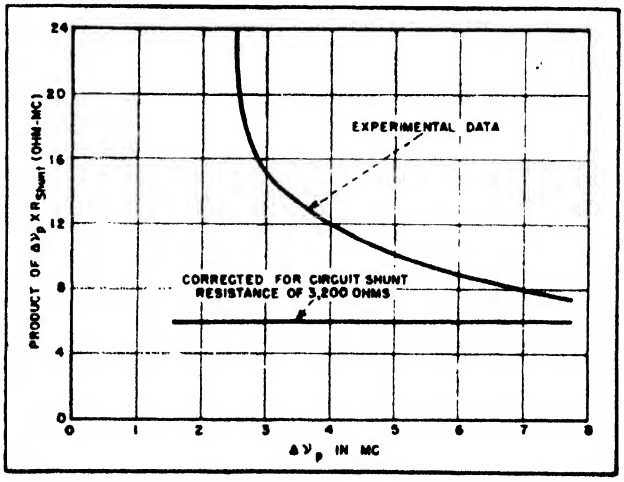

criminator, however, are independent of loading within experimental error, as shown in Fig. 2.

Figure 3 is a plot of the product of the bandwidth and load resistance as a function of the bandwidth. (Table I is included for supplementary data not included in Fig. 3.) If the circuit Q were infinite, so that all losses were supplied by the loading resistor, this curve should be a straight line parallel to the abscissa since in this case $Q_0 = \omega LR$. Therefore $R\Delta\upsilon_p$, where $\Delta\upsilon_p$ is peak-to-peak bandwidth, should be independent of R or $\Delta\upsilon_p$.

In practice, circuit losses provide a lower limit to the obtainable bandwidth. In the case investigated this came at 1.7 mc, equivalent to a shunting resistance of 3,200 ohms. This resistance was assumed to be included in parallel with the various load resistors.

The resistance of the parallel combination was computed for each case and a new curve plotted using the calculated resistance as the load. As is seen in Fig. 3, the resulting curve is within experimental error a straight line parallel to the abscissa. The load resistors used were measured at d-c rather than 60 mc, so that the a-c resistance of the highest-resistance units might be expected to be relatively lower than the a-c resistance of the lower units because of the Boella effect. This might explain the dropping off of the experimental points for small bandwidths.

Adjustment of the cathode-driven discriminator to give symmetrical curves was considerably easier than adjustment of the Foster-Seeley discriminator in all cases. This was especially true with respect to primary tuning in obtaining a sym-

Inasmuch as the cathode-driven discriminator is easy to adjust and not critical as to coupling coefficient, one might wish to use it in the detection of frequency-modulated signals from some linearly modulated source such as a broadcast station. In this application one is interested in the nonlinearity of the circuit, which will be somewhat greater than that of the Foster-Seeley discriminator.

Figure 4 shows the amplitude of the various important harmonic components in the output of the cathode-driven discriminator as a function of the ratio of deviation of incoming frequency to peak-to-peak bandwidth of the discriminator. These curves are an extension of the ones given previously in an analysis of microwave discriminators,[3] the extension having been carried out by twelve-point schedule analysis. As is shown by these curves, the peak-to-peak discriminator bandwidth must be five times the peak-to-peak deviation for 1 percent third harmonic distortion or 2.5 times the peak-to-peak deviation for 5 percent third harmonic distortion. These figures compare with the 1.7 ratio ordinarily used in commercial frequency-modulation receivers. The curves given apply for square-law detectors. If linear detectors are used, the ratio of 2.5 may be dropped to 2.1 for critical coupling. Distortion is always less with linear than with square-law rectifiers in this discriminator, but is somewhat dependent on coupling at high deviations.

TABLE I—Effect of Load Resistance on Bandwith

Physical Load Resistor (ohms)	Actual Shunt Resistance* (ohms)	$\Delta\nu_p$ (mc)
∞	3,200	1.7
87,000	3,090	2.0
12,000	2,530	2.5
5,000	1,950	3.0
3,000	1,550	4.0
1,500	1,020	6.0
1,000	760	7.6

* Corrected for 3,200 ohms circuit resistance.

This paper is based in whole or in part on the work done for the Office of Scientific Research and Development under Contract OEMsr-262 with the Massachusettts Institute of Technology.

REFERENCES

(1) D. E. Foster and S. W. Seeley, Automatic Tuning, Simplified Circuits, and Design Practice, *Proc. IRE*, p 289, March 1937.

(2) K. R. Sturley, The Phase Discriminator, *Wireless Engineer*, p 72-78, Feb. 1944.

(3) W. G. Tuller, Distortion in F-M Discriminators, Technical Report No. 1, March 8, 1946, NDRC Division 14, Research Laboratory of Electronics, Massachusetts Institute of Technology.

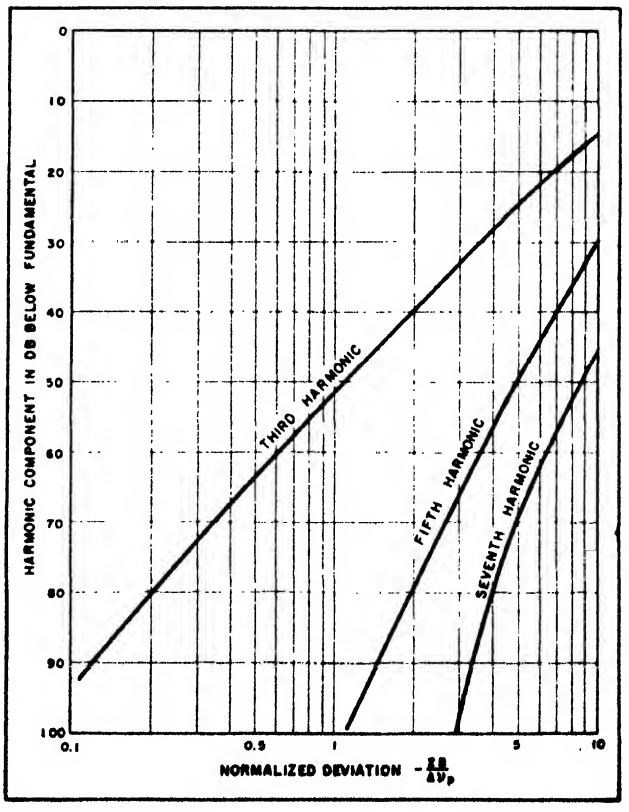

FIG. 4 — Distortion curves for cathode-driven discriminator, giving amplitudes of important harmonic components as function of ratio of frequency deviation to peak-to-peak bandwidth of discriminator

Single-Stage F-M Detector

Operating principles of a circuit that uses a special heptode tube arranged as an oscillator and phase detector. Output at full deviation is twenty volts, peak to peak, and response to amplitude variation is fifty db less than to frequency change

By WILLIAM E. BRADLEY

THE art has long had at its command a number of excellent single-stage circuits which very closely approximate the ideal amplitude-modulation detector, so constructed and arranged as to be highly responsive to variations in carrier-wave amplitude but not at all responsive to carrier-frequency deviation. It was concluded that further development of f-m methods and systems was being greatly impeded by the lack of a comparable tool in the frequency-modulation art. Accordingly, efforts were directed to the development of a single-stage frequency-modulation detector, so constructed and arranged as to be highly responsive to carrier-frequency deviation, but not at all responsive to carrier-amplitude variations.

The f-m detector to be described is responsive directly, and solely, to the frequency deviation of the received carrier signal. In practice, the full capabilities of the circuit are efficiently realized by the use of a special heptode tube having high transconductance and sharp cutoff characteristics together with shielding of the grid number 3 from other tube elements.

The minimum i-f input signal required to operate the detector is approximately one-half volt rms for full deviation, the voltage required varying linearly with deviation. The relation between the frequency deviation of the applied carrier wave and the audio output voltage is linear up to the limit of the detector characteristic, where a sharp break occurs. The output for full 75 kilocycle deviation is approximately 20 volts, peak to peak. The response of the circuit to amplitude variation is negligible and, with attention to shielding, is normally 50 to 60 db less than the f-m response.

A circuit diagram of the detector is shown in Fig. 1. The essential parts are the heptode tube and two tuned circuits reactively coupled. The output of the i-f amplifier is applied to one of the two control grids of the heptode, shown as grid 3, and audio is derived from the plate current of the tube.

Fundamental Circuit

One of the two tuned circuits is connected to the first grid of the heptode, while the other is connected to the heptode plate. Both tuned circuits are tuned approximately to the intermediate frequency, and the plate tuned circuit is damped so as to have a bandwidth approximately six times that of the useful deviation band.

The portion of the diagram shown dotted is a neutralizing circuit which may be used to remove the disturbing effects of capacitance coupling from grid 3 to the heptode plate. If the layout of wiring is reasonably good, no neutralizing is needed.

Because of feedback of energy from the electron stream to the input grid, it is desirable to drive the detector from a source of fairly low impedance. Thus a step-down transformer (having an effective turns ratio of about three to one) is ordinarily used at the input.

The first three elements of the tube, together with the tuned circuit *B*, comprise an oscillator. Since the screen is bypassed to ground, oscillator voltage appears on grid 1 and the cathode. The oscillator operates class C, so that the space current through the heptode consists of a series of pulses. It is highly desirable that the pulse duration be short compared to the time interval between pulses.

Phase Relation

The second control grid (3) of the heptode causes the tube to function as a phase detector. The proportion of a space current pulse reaching the plate of the heptode

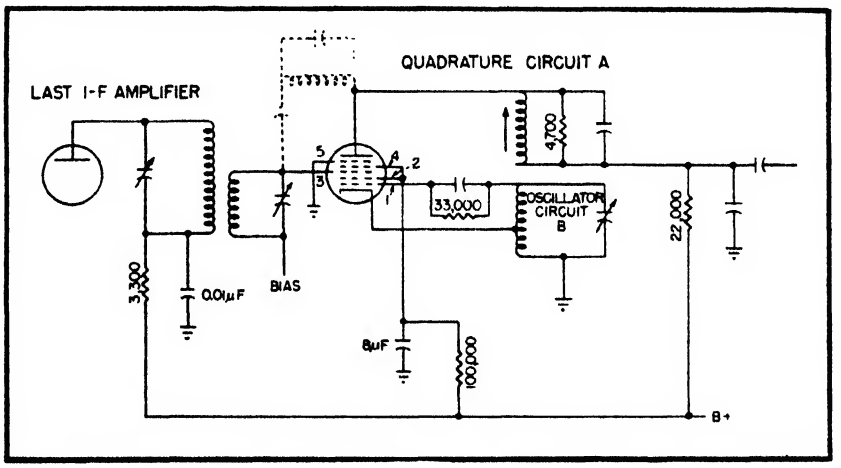

FIG. 1—Basic circuit of the f-m detector

depends on the potential of this control grid at the instant of arrival of the pulse. This instantaneous control voltage in turn depends on the sum of the bias and the incoming signal voltage, which may add to or subtract from the bias, depending on the phase relation between the oscillator and the incoming i-f signal.

The fundamental component of the resulting plate current is fed back to the oscillator through a tuned phasing circuit, which is reactively coupled to the oscillator tank. The adjustment of this phasing circuit is such that the effect of the feedback is reactive. When this is done, variations in plate current cause pure frequency modulation of the oscillator without any variations of loading to the first order, in other words, without changing the amplitude of the oscillator signal.

The phase of the feedback is unaffected by the incoming signal on the second control grid (grid 3). If the pulses of plate current through the tube are short, the incoming signal can only modify their magnitude, not their phase.

The oscillator circuit is shielded from the direct action of the incoming signal, so that the frequency of the oscillator is determined wholly by its fixed constants and the fundamental component of the heptode plate current. The circuit is so adjusted that, with no input, the oscillation is at center frequency. Provided that the phasing circuit is damped so as to be noncritical with regard to frequency, and so long as the oscillator has a constant amplitude, the variation of frequency as a function of plate current is linear.

Because the plate current consists of a train of pulses, it follows that the mean value of the current over any one cycle is substantially equal to one-half of the peak value of the fundamental component. This is true for any wave form of this type, and it does not depend on the exact shape of the pulse, provided only that the pulses be fairly short compared to the interval between pulses.

Oscillator Locks in Phase

The phase of the incoming signal with respect to the oscillator, by affecting the plate current magnitude, affects the oscillator frequency. This causes the phase relation to change, tending toward an equilibrium phase relation. It follows that the oscillator locks into a nearly fixed phase relation with the incoming signal. The oscillator frequency is consequently the same as that of the signal. But the oscillator frequency is directly proportional to the fundamental component of plate current, which alone governs it, so that this plate-current component must vary linearly with signal frequency deviation.

Finally, from the fact that the mean plate current is proportional to the fundamental component, it can be concluded that the mean plate current varies linearly with the signal frequency.

Put somewhat differently, if the fundamental component of plate current were not directly proportional to signal frequency, then the oscillator would not remain locked in phase with the signal. But it has been noted that there is a strong tendency for the oscillator to seek an equilibrium phase relation with the signal, so that as long as the incoming signal is strong enough to cause the oscillator to lock in, then the plate current must be proportional to signal frequency.

Effect of Signal

If the oscillation frequency of the detector, in the absence of signal, is at the center of the i-f band, and if a signal is applied at this frequency, then the oscillator must adjust itself to be in quadrature with the incoming signal. Only at the instant that the incoming sine wave passes through zero can a pulse of plate current pass through the tube without being either increased or decreased in size by the effect of the signal voltage, which would change the phase back toward quadrature. There are two such instants in each incoming signal cycle but only one corresponds to a stable lock-in condition, the other in effect repelling the pulse in phase until it moves to the stable condition. This situation is shown in Fig. 2A.

The manner in which the size of the plate current pulses vary with the relative phase difference between the oscillator and incoming signal is shown in Fig. 2B and 2C.

If the signal frequency changes to a new value within the i-f band, the phase slowly changes until a new plate current is established, which is consistent with the new frequency. With a large signal, only a very small phase variation between oscillator and signal is required to reach the new equilibrium; with weak signals, the variation of phase is greater. If the signal is too small and the frequency deviation too great, no phase may exist at which the instantaneous grid potential is sufficiently different from the bias potential to produce the required plate current, and the oscillator will fall out of synchronization. The signal strength required to maintain synchronization varies directly with deviation.

If, while the frequency is off center, the amplitude of the incoming signal is varied, the only effect is that the oscillator phase readjusts itself continuously to main-

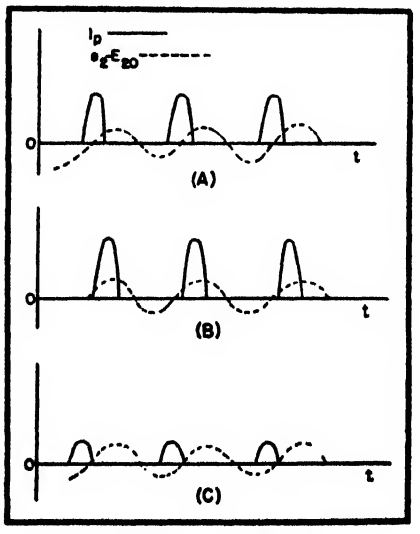

FIG. 2—Variation of plate-current pulse due to phase difference of oscillator and incoming signal

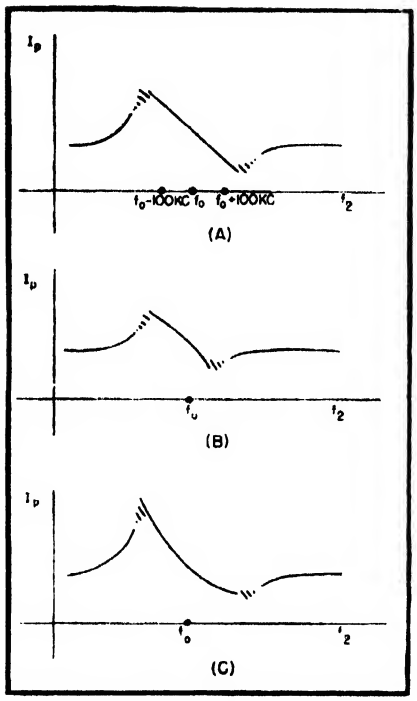

FIG. 3—Adjustment of the phasing circuit produces these curves of plate current plotted against frequency

tain the plate current demanded by the frequency.

Thus, the circuit functions as a detector with an extremely linear response to frequency modulation and with no response of the mean plate current to amplitude modulation, provided that the incoming signal is sufficiently large to synchronize the oscillator.

The shape of the plate current vs. frequency characteristic is shown in Fig. 3 for various adjustments of the phasing circuit; in Fig. 3A the circuit is adjusted for quadrature, while Fig. 3B and 3C show the effect of mistuning. It is worthy of note that the correct adjustment does not give the maximum lock-in range for a given input signal. The slightly detuned adjustment of Fig. 3C gives somewhat greater lock-in range.

A-M Response

An extremely small response to amplitude modulation may remain due to the presence of stray coupling between the input signal and the oscillator. This coupling is mainly capacitive and is composed of stray wiring capacity plus interelectrode capacitance from input grid to other tube elements. By special design precautions, the tube interelectrode capacitance has been made very small. In practice, it is essential to adjust the circuit primarily for linearity, relying on correct design and wiring layout to eliminate extraneous effects.

The neutralizing circuit (shown dotted in Fig. 1) consisting of a blocking capacitor in series with a nearly self-resonant choke, can effectively remove the residual response to amplitude modulation when it is uneconomical further to reduce stray capacitance. This has not been found to be noticeably better under field conditions, however, since the unneutralized circuit has negligible amplitude modulation response.

Mathematical Analysis

In exact mathematical analysis, the operation of the complete detector circuit even for steady state conditions is quite complex, involving the algebra of coupled circuits. Hence, the outstanding traits of the arrangement tend to be obscured by details of analysis.

The equivalent circuit shown in Fig. 4 is analytically much more clean cut and over a considerable range of frequency is equivalent to the actual circuit. This is true because, although the actual detector has two tuned circuits instead of one as in Fig. 4, the phasing circuit is very heavily damped, so that its bandwidth is approximately six times that corresponding to the maximum deviation expected. Hence, this circuit reflects a substantially unchanging loading and detuning into the oscillator in the relevant frequency range, while it shifts the plate current feedback phase through 90 degrees.

Using the circuit of Fig. 4, it is easy to show how the circuit ignores amplitude modulation and why its detection characteristic is inherently linear.

The negative conductance reflected by the tube in Fig. 4 across the tuned circuit is $-aI_k/E_1 = G$, where E_1 is the peak voltage across the tuned circuit, a is the effective stepdown turns ratio of the oscillator coil, and I_k is the fundamental component of cathode current, i_k.

It is a good approximation to represent the plate current as a function of i_k and e_2, the instantaneous voltage on the second control grid, by the expression $i_p = i_k F(e_2)$, where $F(e_2)$ is a function shaped somewhat like an integral sign.

The second control grid voltage is made up of the sum of a fixed bias and the sinusoidal incoming signal of magnitude E_2. Then $e_2 = E_{20} + E_{2(1)} \cos(\omega_0 t + \phi_{2(1)})$, where E_2 and ϕ_2 are functions of t varying slowly with respect to $\cos \omega_0 t$.

$F(e_2)$ may be expanded in a Taylor's series about $e_2 = E_{20}$, and terms beyond the second neglected. This approximation turns out to be rather good because of the fact that in normal operation i_k is zero except for a short time during which e_2 is within a half volt or so of E_{20}.

$$F(e_2) = F(E_{20}) + F'(E_{20})\, E_2 \cos(\omega_0 t + \phi_2)$$

The cathode current pulses occur at the time when the voltage on the first control grid is at a maximum. This voltage is of the form $e_1 = E_1 \cos(\omega_0 t + \phi_{1(1)})$. It maximizes when $\omega_0 t = -\phi_1$, so that the mean effective value of $F(e_2)$ during the occurrence of the current pulse is

$$F(e_2)\Big]_{\omega_0 t = -\phi_1} = F_0 + F' E_2 \cos(\phi_2 - \phi_1),$$

writing, for brevity, F_0 and F' for $F(E_{20})$ and $F'(E_{20})$ respectively.

Then the magnitude of the fundamental component of plate current can be expressed as a function of magnitudes and phases of signal

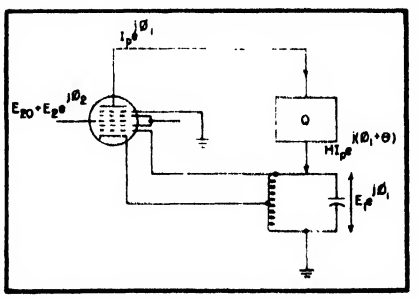

FIG. 4—Circuit of Fig. 1 arranged for mathematical analysis

and oscillator voltages as follows:

$$I_p = I_k[F_0 + F' E_2 \cos(\phi_2 - \phi_1)]$$

The above expression specifies the magnitude of I_p. The phase of I_p is substantially in exact opposition to that of the oscillator, due to the normal phase inverting action of the tube and the inability of the incoming signal appreciably to change the timing of the pulses of current.

The quadrature network, Q, represents the effect of the actual phasing circuit. It is here represented as merely applying to the oscillator from a high impedance source a current proportional to I_p but changed in magnitude by a factor H and shifted in phase with respect to the oscillator voltage by an amount θ.

The admittance which this current reflects across the tuned circuit is the ratio of the current to E_1

$$Y = \frac{H \epsilon^{j\theta} I_k[F_0 + F' E_2 \cos(\phi_2 - \phi_1)]}{E_1}$$

The conductance across the tube contributed by the oscillator elements, as noted above, is $G = -aI_k/E_1$. The admittance of the tuned circuit alone is $Y_1 = g_1 + j\omega C_1 + 1/j\omega L_1$. Near resonance this can be represented approximately by $Y_1 = g_1 + j2C(\omega - \omega_1)$, where ω_1 is the resonant frequency of the tuned circuit alone.

For steady oscillation, the total admittance across the tuned circuit must be zero.

$$G + Y + Y_1 = g_1 - \frac{aI_k}{E_1} + H\frac{I_k}{E_1}[F_0 + F' E_2 \cos(\phi_2 - \phi_1)]\cos\theta + j\left\{2C(\omega - \omega_1) + H\frac{I_k}{E_1}[F_0 + F' E_2 \cos(\phi_2 - \phi_1)]\sin\theta\right\} = 0$$

or substituting,

$$I_p = I_k[F_0 + F' E_2 \cos(\phi_2 - \phi_1)]$$

$$0 = E_1 g_1 - aI_k + H\cos\theta\, I_p + j\left\{E_1 2C(\omega - \omega_1) H \sin\theta\, I_p\right\}$$

Both real and imaginary parts of this expression must be separately equal to zero. Setting the imaginary part equal to zero gives

$$I_p = \frac{2C E_1}{H \sin\theta}(\omega - \omega_1).$$

The equation is important because it dictates that the plate current varies directly with frequency provided E_1 is constant. It also shows that the connection between plate current and frequency does not depend on E_2, again provided E_1 is constant.

Phasing Adjustment

Setting the real part equal to zero gives

$$E_1 g_1 - aI_k + H\cos\theta\, I_p = 0$$

In this equation g_1 and I_k are definite functions of E_1 alone, so that the equation represents a connecting relation between E_1 and I_p. For correct operation, it is desirable for E_1 to be constant and unaffected by I_p. It follows that the correct adjustment of the phasing circuit is that which causes cos 0 to be zero.

This adjustment can be performed readily by causing I_p to vary by means of an audio voltage applied to the signal input grid and adjusting the phasing circuit for a minimum of audio in the oscillator grid current. Since the phasing circuit has a low Q, the adjustment is not particularly critical.

Carrying on the above approximate mathematical treatment, the effect of stray couplings from the signal input to other parts of the circuit can be evaluated. The general result is that such couplings, if large enough, tend to cause the detector to respond slightly to amplitude modulation.

The effect of the finite duration of the pulses of cathode current can also be treated approximately by a slight extension of the above analysis. It has been found that, if the pulses have a duration of less than one quarter of a cycle, the detector operates for all practical purposes as if the pulses were ideally short. If the current pulses become longer than one third of a cycle, the operation of the circuit becomes more complex, with some residual distortion.

The width of the pulses is controlled by the loading reflected into the oscillator circuit by the phasing circuit. No more coupling to the phasing circuit should be used than enough to give the required deviation sensitivity, excessive coupling causing wide pulses.

Nonlinear Limiter

By EDMUND R. BRILL

A LIMITER CIRCUIT is usually included in the intensity modulation channel of cathode-ray tubes to prevent blooming from strong signals. However, the limiting action prohibits discriminating between signals of different intensities above the level of saturation. The problem arose in connection with radar intensity modulation presentation, such as the plan position indicator, to develop a limiter that would protect the phosphorescent screen, yet to permit resolution of signals over a wide dynamic range of input. A nonlinear limiter using germanium crystal rectifiers was developed whose current versus potential characteristic follows a cube root and thus gives, in combination with a cathode-ray screen whose transfer characteristic (spot brightness versus control voltage) follows a cube law (as most screens do), an overall transfer characteristic that is linear. This compensation greatly increases the dynamic range that can be usefully presented by intensity modulation methods. The technique is applicable to gamma (contrast) control of television video signals, for wide dynamic range meters, and wide range chart

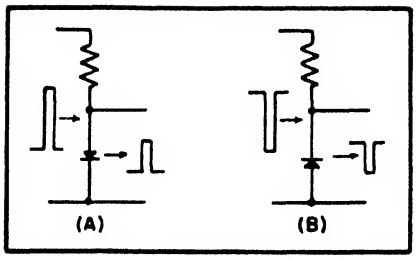

FIG. 1—Nonlinear compression circuits use crystal rectifiers

recording of such quantities as antenna patterns.

Circuits

The nonlinear limiter circuit is the voltage divider shown in Fig. 1 using a resistor and a crystal. The circuit at Fig. 1A is used for positive-going signals; that at Fig. 1B for negative-going signals. As the output is obtained across the crystal, it is desirable to make the ratio of crystal resistance to total divider resistance high. This characteristic can be obtained, without affecting the compression exponent, by using several crystals in series. The maximum input potential that can be applied to the divider is limited by the peak current that can be passed through the crystal without permanently altering its characteristic. At low input levels the circuits tend toward a linear transfer characteristic. Figure 2 shows the effect of the resistance of the resistor in a potentiometer using germanium crystals of the type manufactured by Western Electric.

Other compression exponents can be obtained by using vacuum diodes or silicon crystal rectifiers. Connecting the two sections of a 6H6 as shown in Fig. 3 and with both resistors 10,000 ohms, a square root response was measured between 1.00 and 100 volts input; the output was about 0.25 volt at an input of 10 volts. As the resistors are made smaller, the characteristic of the circuit changes from square root toward linear.

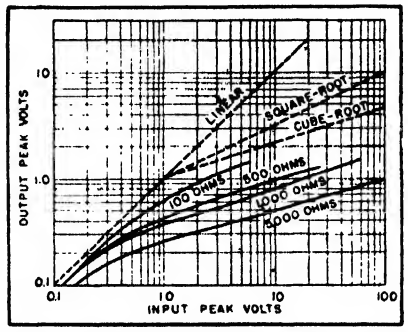

FIG. 2—Compression characteristic of germanium crystal divider varies with series resistance

A silicon crystal, of the type manufactured by Sylvania Electric Products, used in the circuits of Fig. 1 with a 1,000-ohms series resistor gave a compression exponent between a half and a third at higher voltages, but approached a linear characteristic at input potentials below one volt.

In general, the characteristic of the crystal circuit over a wide range of input levels is the reciprocal of the exponent of the current versus potential characteristic of the particular rectifier. Several nonlinear compression circuits can be cascaded to obtain a characteristic whose exponent is the reciprocal of the sum of the reciprocal exponents of each individual circuit. The circuits will have to be isolated from each other by amplifiers, which will also be necessary to maintain the signal level. (Ed. Note: By taking the output across the resistor element of the voltage divider instead of across the crystal, a nonlinear expander is obtained. The technique has possibilities in electrical computers.) Work reported herein was done at RRL under contract OEM sr-411 with OSRD.

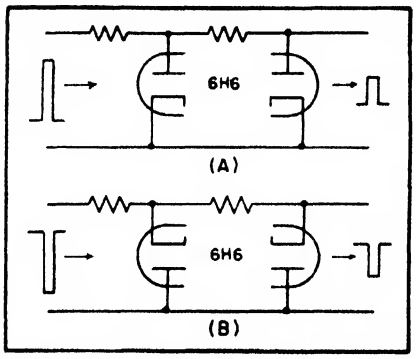

FIG. 3—Shunt diodes can be used in a nonlinear compression circuit

F-M and A-M Receiver for Comparison Tests

By WILLIAM F. FRANKART

THE RECEIVER TO BE described was designed to tune over the range of 15 to 170 megacycles and to have an overall sensitivity of two microvolts. It receives amplitude-modulated signals having high adjacent channel interference and also receives wideband frequency-modulation signals. It was used for making direct comparisons between frequency modulation and amplitude modulation reliability-of-communication tests.

The receiver had to be stable, of known sensitivity, known passband characteristics and rapid changeover from a-m to f-m. It is also suitable for the determination of maximum frequency and minimum phase deviation and of the mean carrier frequency tests as described by Crosby (pages 85-87, Hund, "Frequency Modulation"). For these tests, a receiver that has narrow passband characteristics on a-m is necessary and no commercial communication receiver in this frequency range was found suitable.

Crystal Diodes

Two separate i-f channels are used, tuned to ten megacycles. The a-m channel has a pass band of six kilocycles. Of special interest in this channel is the use of Sylvania 1N34 germanium crystal diodes. The crystals are used in a circuit that is, in

addition to being the second detector, a noise limiter that is very effective on pulses of steep wave front and short duration such as automobile ignition interference.

The second detector and noise-limiter circuit operation was greatly improved because the germanium crystal diode starts to work at much less signal level than the typical 6H6 diode. Also, the electrostatic capacitance of the crystal diode is much less than the 6H6. The blocking characteristic of the crystal is another factor that contributed to operation as a peak pulse noise limiter.

The f-m i-f channel has a passband of 300 kilocycles, this being wide enough for f-m reception. The circuit features the use of bifilar-wound single-tuned i-f transformers and germanium crystals in the Seely ratio detector. By using the bifilar-wound i-f transformer, certain advantages were had; more gain per stage, a high degree of stability, less components necessary, one circuit to align, and wider passband characteristics.

All bypass capacitors under 0.001 μf are silver mica and all capacitors below 0.011 μf are low-loss mica. The a-m i-f transformers are Aladdin No. 1201 with capacitors as called for in the schematic. These transformers are normally designed to operate on 12.6 megacycles and the capacitance increase was necessary to obtain the characteristics desired.

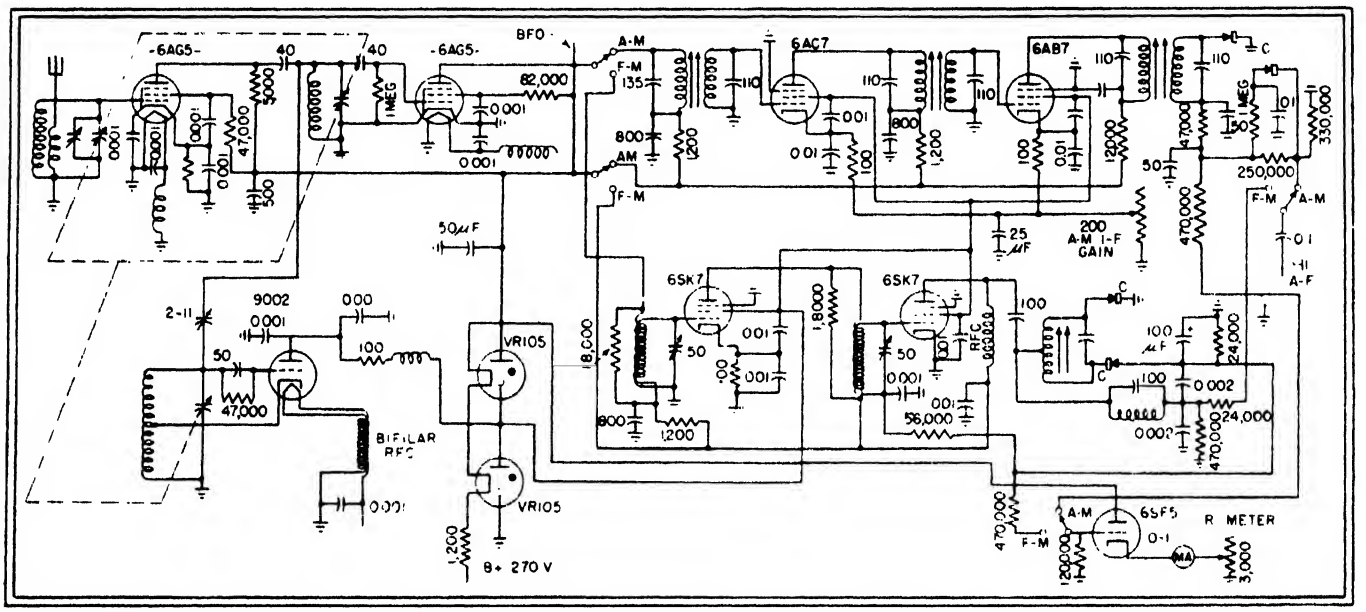

Circuit of the r-f and i-f stages of the combination receiver designed for convenient comparison of f-m and a-m signals

Synchronized Oscillators as F-M Receiver Limiters

An oscillator stage following the i-f amplifier and synchronized to a subharmonic of the i-f signal gives voltage gain, adjacent-channel selectivity, quieting sensitivity, and good amplitude-limiting action. Synchronizing voltage can be injected in several ways

By C. W. CARNAHAN and HENRY P. KALMUS

In prewar f-m receivers the only nonlinear element was the amplitude limiter. Distortionless amplification of an f-m signal is independent, within limits, of the amplitude characteristic of the r-f and i-f amplifiers. Accordingly, it was thought that some of the nonlinear but extremely sensitive amplifiers used in the early days and long abandoned for a-m reception might prove useful as limiters in f-m receivers.

Following this line, the Zenith Laboratories in 1941 started a

study of the possible advantages of synchronized oscillators in f-m reception. As used in an f-m receiver, the application comprises an oscillator stage following the i-f amplifier, with the oscillator frequency synchronized to the frequency of the i-f signal, or to a subharmonic of it. Thus, if frequency of the i-f signal deviates over 150 kc with a center frequency of 8.3 Mc, the synchronized oscillator may operate over the same range, or at a subharmonic such as 4.15 Mc, with a deviation of 75 kc. The practical application of subharmonic synchronization for frequency division is well known.[1]

Because of the priority of military work, research and development of this type f-m receiver have been on a limited scale. Unconventional ways have been found for using a synchronized oscillator to advantage, but these developments will have to wait for publication until practical application can be realized.

Interest in the phenomena exhibited by synchronized oscillators goes back to the early days of vacuum tubes and references are extensive. Several hundred papers, largely of a theoretical nature, have been written on the behavior of oscillators. Of these, a substantial fraction have dealt with synchronization and frequency division. A few of the best representatives of these references are listed in the bibliography at the end of this article. Papers on actual applications are scarce, for the reason that up to the present, the field has been relatively limited.

Some Actual Applications

There have been several suggested and actual applications to f-m receiver technique. Among these is British Patent No. 163,462, issued to Eccles and Vincent in 1920. It covers the use of an oscillator synchronized at the carrier frequency for the reception of narrow-band f-m, code and phone transmissions. The inherent selectivity of a synchronized oscillator seems to have been realized at this early date. Some work was also done about this time by H. G. Moller[7], who used a synchronized oscillator for f-m code reception.

The idea then seems to have languished until the middle thirties. In 1935, Armstrong[8] obtained a patent on the use of a synchronized oscillator at the intermediate frequency in an f-m receiver, with a limiter following the oscillator to remove amplitude variations. In 1938, the Japanese[9] described the use of a synchronized oscillator to separate the f-m component from a signal which contained both frequency and amplitude modulation. Their oscillator was adjusted so that it acted simultaneously as a fair amplitude limiter. Synchronization on a subharmonic of the received signal was tried, but unfavorable results were obtained.

In 1940 two Russian workers, Kisselgof and Knazev[10], suggested and built a synchronized amplifier for f-m receivers. The oscillator was synchronized at the intermediate frequency, and amplitude limitation was achieved by loading the oscillator with a pair of shunt-connected diode clippers. These investigators showed that normal amplifier gains could be obtained in an oscillator stage. The problem of injecting the synchronizing signal from the high-impedance circuit of a preceding amplifier was met by employing a pentagrid tube, the 6L7, with the i-f signal applied to the first grid and the oscillation circuit connected between the third grid and plate. By thus allowing only electron coupling between the source of injected voltage and the oscillator circuit they minimized interaction between the two circuits and thereby eliminated a major feedback problem.

Practically all the references on the synchronized oscillator are theoretical in nature, and highly mathematical, due to the non-linear differential equations involved. While a simplified explanation may lack rigor, at least it has the advantage of presenting a physical picture of the mechanism of synchronization for both fundamental and subharmonic operation.

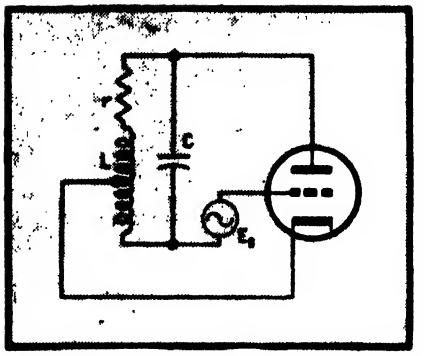

FIG. 1—Impedanceless generator in series with grid injects a synchronizing signal into a simplified Hartley oscillator

This analysis is based on a consideration of the actions occurring over one cycle of a synchronized oscillator. Such a treatment has been published recently for a free-running Hartley oscillator[11]. Referring to Fig. 1, consider a simplified Hartley oscillator with the tank circuit connected between plate and grid, and with the synchronizing signal injected by an impedanceless generator in series with the grid lead.

Theory of the Synchronized Oscillator

Figure 2(a) shows the plate current of the tube as a function of the instantaneous voltage across the tank circuit. The oscillator is assumed to operate class C without plate-current saturation. Figure 2(a) shows instantaneous oscillator voltage as the projection of a vector A of variable length, rotating in a counter-clockwise direction. For a free-running oscillator, i.e., $E_s = 0$, the angular velocity of this vector may be assumed constant over the cycle. From A_1 to A, the g_m of the tube is zero, the damping factor of the oscillation is positive, and the vector amplitude decreases exponentially.

From A to A_1, the amplitude must increase exponentially to its original value if oscillation amplitude is to remain stable. During this amplification period, when the tube is conducting, the damping factor is negative. The condition for stability in a free-running oscillator is that the loss in amplitude during the cut-off period, when the tube is

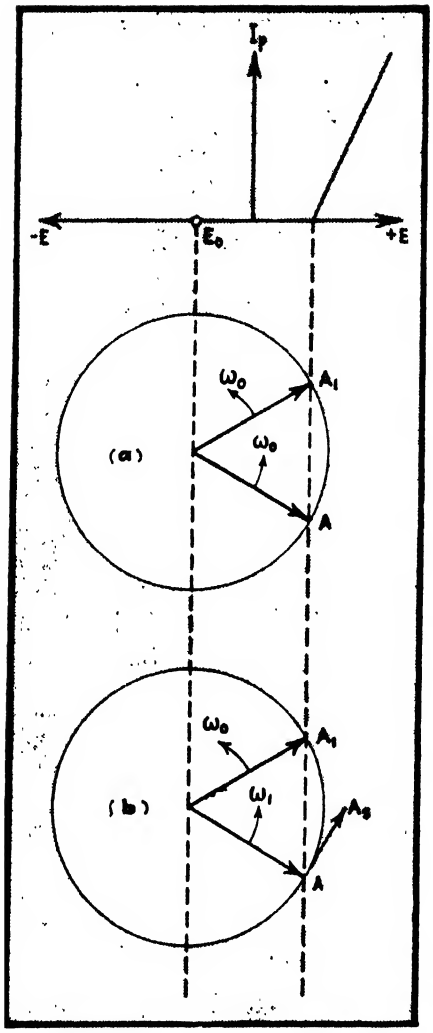

FIG. 2—Plate current of oscillator in Fig. 1 is a function of instantaneous voltage across tank circuit, which appears as the projection of vector *A*. For a free-running oscillator, (a) angular velocity is assumed constant. In (b), angular velocity of the synchronizing signal is greater and A_s is the tank-voltage component due to synchronizing voltage

not conducting, must be just equal to the gain in amplitude during the amplification period.

We have assumed that for a free-running oscillator the angular velocity of the amplitude vector is constant, and equal to the resonant angular velocity of the tuned circuit. Actually, angular velocity during the amplification period will differ from this, because of the changed circuit conditions during this period, with the result that the *average* angular velocity of the amplitude vector of a free-running oscillator over one cycle will, in general, not agree exactly with the resonant angular velocity of the tank circuit.

The possibility of a change in angular velocity during the amplification period gives the clue to what occurs during synchronization. For if E_s is not zero, and has an angular velocity not equal to that of the free-running oscillator, stable synchronization means that the average angular velocity of the oscillation amplitude vector must change until it is equal to that of the injected signal.

During the cut-off period, synchronizing voltage E_s can have no effect on the oscillation vector, the angular velocity of which during this period is, say, ω_o, the resonant angular velocity of the tuned circuit. During the amplification period, however, E_s causes a component of plate current which may change the phase angle of the oscillation vector. Thus the angular velocity of the oscillation vector during the amplification period may be decreased or increased, depending on whether the phase of the plate current produced by E_s is lagging or leading the phase of the free-running oscillation current at the start of the amplification period.

If the angular velocity of E_s is greater or less than ω_o, synchronization occurs only when the *A* vector rotates through 2π radians in exactly one cycle of E_s. The condition for stable synchronization is that the gain or loss in relative phase angle between *A* and E_s during the amplification period shall exactly balance the loss or gain in relative phase angle during the cut-off period.

Vector Relations

In Fig. 2(b), are shown the vector relations existing when the angular velocity of the synchronizing signal is greater than ω_o, the free-running angular velocity. Here A_s is the component of the tank voltage due to the synchronizing voltage E_s. This component is added in quadrature with the oscillation vector during the amplification period, so the angular velocity, ω_1, of the resultant is increased during this period. If ω_s is the angular velocity of the synchronizing signal, the average value of angular velocity of the resultant over a complete cycle must be equal to ω_s, for stable synchronization.

For a given difference between ω_o and ω_s, the angular velocity of E_s, the phase angle between E_s and *A* at the start of the amplification period will be 90 deg for the minimum amplitude of E_s required for synchronization. If the magnitude of E_s is less than this critical value, the gain in phase during the amplification period will not balance the loss in phase during the cut-off period, and the effect of E_s during the next conductive period will be reduced due to the discrepancy in correct phasing at the start. Thus the phase conditions never stabilize, and no synchronization exists.

If the magnitude of E_s is greater than that required at optimum phasing, the gain in phase during the amplification period will be greater than required, and the phase at the start of the next amplification period will be less than 90 deg, thus reducing gain in this period. This process will continue until the relative phase at the start of the amplification period is reduced to a value which remains stable with the given magnitude of E_s.

The phenomenon of stable synchronization is thus due to the fact that the oscillation vector can slip in relation to the synchronizing vector until stable phase and amplitude conditions are reached. If E_s is variable in frequency, but always of sufficient amplitude, the oscillator will adjust itself almost instantaneously to every change in frequency of E_s.

Synchronization with an injected signal whose frequency is a multiple of the free-running frequency can be explained in a similar manner. Figure 3 shows the phase relations which might exist during the amplification period and between the oscillation voltage and a synchronizing voltage of twice the

frequency. During the active period the double-frequency synchronizing wave is practically equivalent to a synchronizing wave with the frequency of the oscillator but twice the amplitude of the double-frequency wave. It is clear that if the amplification period extended beyond the boundaries marked in Fig. 3, the effect of the injected voltage at double frequency would be to decrease the desired change in oscillation vector phase, since the added portions would produce a reactance change in the opposite direction.

For subharmonic operation, the fraction of the oscillator cycle comprising the amplification period should be limited to a half cycle (or an odd multiple of a half cycle) of the synchronizing voltage.

Sensitivity of Synchronization

While the method of injecting synchronizing voltage shown in Fig. 1 cannot generally be realized in a practical f-m receiver, it can be used to illustrate the factors affecting synchronization sensitivity of the amplifier-limiter in practical circuits, since the same general principles hold for all.

Synchronization sensitivity may be defined roughly as the amplitude of the injected voltage required to synchronize the oscillator over a given frequency range of the synchronizing voltage, for a given oscillator frequency and amplitude.

Since the synchronization process is essentially that of adding a reactive component of current during a fraction of the oscillator cycle in order to slow down or speed up the angular velocity of the oscillation vector during this period, the action is similar to that of a frequency modulator of the reactance tube type. Factors affecting sensitivity are the same in both cases.

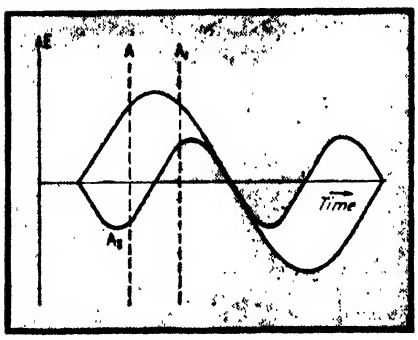

FIG. 3—Phase relations between oscillation and synchronizing voltage when the latter is of twice the former's frequency. Time lapse here represents the amplification period of the tube, during which the effect is that of a synchronizing wave of identical frequency but double amplitude

The L/C ratio of the tank circuit should be as high as possible, since then the reactive voltage developed across the tuned circuit is a maximum for a given amplitude of reactive plate current. The g_m of the tube during the amplification period should be as high as possible, to secure the required reactive plate current with the least injected voltage.

With the single-circuit oscillator shown in Fig. 1, sensitivity can usually be increased for low oscillator voltages by damping the tuned circuit. If damping is increased, the amplitude of the required reactive plate current remains the same for a given deviation from the resonant frequency, since the decrease in impedance of the tuned circuit is balanced by a decrease in the phase angle of the impedance. However, the g_m of the tube during the amplification period must be increased to maintain the same oscillator voltage, and hence the required synchronizing voltage on the grid of the tube is decreased. For optimum adjustment, damp the tuned circuit until, for a desired oscillator voltage, the plate current and the g_m of the tube are as high as possible.

In a single-circuit oscillator the required reactive current varies linearly with frequency deviation for a small range on either side of resonance, since it varies with the sine of the phase angle of the tuned circuit impedance. This phase-angle variation may be reduced by a large factor over a small range, and synchronization sensitivity correspondingly increased, by adding a tuned secondary to the tank circuit inductance, as shown in Fig. 4. If circuit Q factors and coupling are adjusted to give a band-pass char-

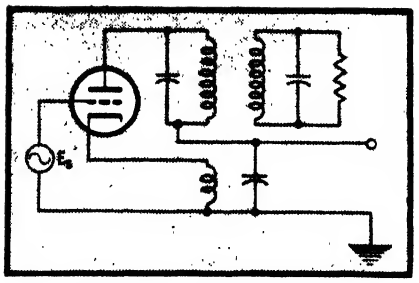

FIG. 4—Addition of a tuned secondary to the tank-circuit inductance increases synchronization sensitivity by reducing phase-angle variation of the primary impedance

acteristic over the desired frequency range, the phase angle variation of the primary impedance can be easily reduced by a factor of five or more, with a corresponding increase in the synchronization sensitivity.

Figure 5 shows the phase characteristics of the primary impedance for (1) a single circuit, (2) two circuits critically coupled, and (3) two circuits over-critically coupled. Even a moderate degree of coupling will provide considerable improvement of the sensitivity. This increase in sensitivity with a band-pass tank circuit was first noted by Sterky.[12] If the two circuits are over-critically coupled, giving the phase characteristic (3) of Fig. 5, the free-running frequency of the oscillator tends to rest on either side of the double bend in the characteristic, and synchronization sensitivity to a signal in the center is largely lost. This condition may also occur unintentionally through regenerative coupling to a preceding high-Q i-f circuit, and is to be avoided at all costs.

Difficulties with Subharmonics

All the factors discussed above, namely High L/C ratio, high g_m, and two-mesh tank circuits, which make for high synchronization sensitivity at the fundamental, also hold for synchronization at a subharmonic of the injected voltage. This is because, as discussed above, the action of the injected signal at a higher frequency than the oscillator, over a limited period of amplification, is exactly analogous to the action of a signal at the same

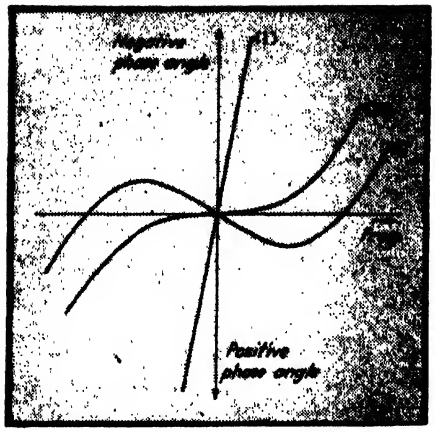

FIG. 5—Phase characteristics of primary impedance in Fig. 4 for a single circuit (1), two circuits critically coupled (2) and two circuits over-critically coupled (3). In curve (3), synchronization sensitivity in the center is largely lost

frequency as the oscillator. There is, however, some loss in sensitivity over operation at the fundamental, due to the restriction of the amplification period, and the only justification for subharmonic operation is that it avoids the practical difficulties of feeding an oscillator from a high-impedance source, and minimizes difficulties in oscillator alignment due to overall regeneration.

Some of the loss in sensitivity entailed in subharmonic operation can be recovered by a proper adjustment of bias on the oscillator, since this determines the length of the amplification period In general, however, fixed bias on the oscillator grid makes it difficult to start at the desired level of 5 to 10 volts, and not much latitude exists in bias voltage.

Suppression of Subharmonic Oscillations

An unpleasant feature which is associated with high sensitivity for subharmonic operation is the long-known fact that oscillations at the subharmonic frequency are suppressed if the injected signal rises to the same order of magnitude as the oscillator voltage. This is sometimes not recognized at first if a demodulated signal is viewed on an oscilloscope.

Distortion caused by suppression of the subharmonic at the center of the band then has a similar appearance to distortion caused by insufficient synchronizing signal and the consequent loss of synchronization over part of the modulation cycle. The effect appears to be due to upper bend saturation in the tube characteristic, so that too much injected voltage lowers the effective g_m of the tube to the point where the lower-frequency oscillations can no longer be sustained. While this effect is analogous to i-f overloading in an a-m receiver, the resulting audio distortion is much worse, and cannot be tolerated.

If minimum synchronizing voltage, delivered by the i-f amplifier, is of the order of a volt, suppression of the subharmonic oscillation by stronger signals can be satisfactorily overcome with a complete automatic gain-control circuit deriving voltage from rectification in the last i-f grid circuit before the limiter. If, however, full advantage is taken of the gain in a synchronized oscillator, the required minimum synchronizing voltage will be much less than one volt, and generally there will not be enough gain in the i-f amplifier to provide satisfactory gain control. Fortunately, special circuit means exist that will not suppress the oscillation until the voltage on the last i-f amplifier is high enough to cause this stage to act as a limiter and so prevent a further rise.

Advantages of the System

At this point, the advantages of using a synchronized oscillator in an f-m receiver can be summarized as follows:

1. Selectivity to adjacent channels —at least equal to the selectivity of two i-f stages.
2. If properly designed—a synchronization sensitivity sufficient to give a voltage gain (as an amplifier) considerably better than the conventional i-f amplifier.
3. An amplitude-limiting action better than that of a conventional limiter.
4. A quieting sensitivity inversely proportional to frequency deviation of the received signal.

The fact that overall regeneration is decreased as a result of subharmonic operation cannot be fairly counted as an advantage, since operation on the fundamental is practically impossible, and subharmonic operation may add to the receiver cost by requiring an automatic gain-control string.

Of the features listed, the first—selectivity—is an inherent property of any synchronized oscillator. It can be shown mathematically[18] that if two equal voltages, one lying within the synchronizing range of an oscillator, and one without, are injected into the oscillator so that it is synchronized by the first signal, the amplitude of the second signal will be greatly reduced. Physically, the explanation of this is that the effective g_m of the oscillator tube for the interfering signal is considerably reduced, since it can produce an effect only during the amplification period, which is not synchronous with the interfering signal.

With subharmonic operation, the only effect of an adjacent-channel signal is a very slight frequency modulation which may occur during the amplification periods. While the desirability of good adjacent-channel selectivity will be enhanced as the f-m band is filled up, it is doubtful whether this advantage alone is sufficient to justify the use of a synchronized oscillator, if it is used following an i-f amplifier which already has a good selectivity.

At present, no known oscillator-limiter circuit combines perfect amplitude limiting with high synchronization sensitivity and voltage gain. While it is possible to adjust an oscillator for a high amplitude, 20 volts or more, so that it limits very well for a signal at the center of the band, the amplitude still shows a variation over the band, and the sensitivity usually drops by a factor of ten or more.

On the other hand, an oscillator with a lower amplitude level, and designed for maximum sensitivity and voltage gain, can be followed with a very simple limiter stage of

the usual type, the combination giving excellent limiting action over the entire band. The use of a conventional limiter following the oscillator has the further advantage that the oscillator is separated from the frequency detector. If a conventional diode discriminator is connected directly to the oscillator through a secondary on the oscillator tank coil, the oscillator and discriminator alignments become interdependent, with consequent difficulties in production.

The last feature—a quieting sensitivity inversely proportional to frequency deviation—is of importance in the application of the synchronized oscillator-limiter to f-m services other than broadcast. These services generally employ a low deviation ratio, and a small quieting voltage on the limiter is very desirable because the r-f and i-f gains can be kept low and stable.

Injection of Synchronizing Voltage

In most of the previous applications of the synchronized oscillator, injection has been accomplished from low-impedance sources. Since the source of synchronizing voltage in a practical f-m receiver is the last i-f stage, problems arise because of the high impedance of this circuit. Coupling between the oscillator tank circuit and the synchronizing input circuit must be reduced to a minimum in order to obtain normal gain from the i-f stage.

Figure 6 shows a typical synchronized-oscillator circuit using a type 1852 tube with the synchronizing voltage developed in the grid circuit. Oscillation is maintained by a cathode tickler winding. Because of the grid-to-cathode capacitance, part of the oscillator voltage across the tickler is developed across the input tuned circuit which at the same time works as the plate load for the last i-f amplifier.

Normal gain of an i-f amplifier is $g_m Q\omega L$, which might be 50 for an f-m i-f amplifier. If the oscillator operates at the fundamental, the loading effect due to the reflected oscillator voltage is so great that the amplifier gain practically disappears. With subharmonic operation, a gain of 10 in the preceding i-f amplifier is obtainable. Thus most of the gain in the oscillator itself may be lost by the reduction of gain in the preceding stage.

As mentioned, the Russian solution to this problem was the use of a pentagrid mixer, in which the first section acted as a buffer between the input circuit and the oscillator. Unfortunately, with present tube structures this method has two disadvantages. First, it is impossible to obtain the desired g_m in the oscillator section if the electron stream is already limited by the first grid. Second, because of the low g_m, suppression of subharmonic oscillations occurs at a considerably lower level than is the case with high g_m pentodes. It is expected that by using different injection methods and tube structures, these difficulties will be overcome.

Even though the loading effect in the oscillator input circuit is reduced to a negligible amount, enough coupling may still exist between the oscillator and the i-f circuits to introduce hysteresis into the oscillator. The worst offender in this connection is stray coupling between the oscillator and the input to the i-f amplifier. An amount of coupling which ordinarily is acceptable in production will cause the oscillator to jump suddenly from one frequency to another during alignment, and make its correct adjustment impossible in production. Subharmonic operation overcomes this to a large extent, since the harmonic content of the oscillator is not large without an injected signal. Normal precautions must be taken to reduce overall feedback from the oscillator, however, even with subharmonic operation.

References

(1) Morrison, J. F., *Proc. IRE*, 28, No. 10, p. 444-450, Oct. 1940.
(2) Tucker, D. G., *Electronic Engineering*, Mar., Apr., June, Aug. 1943
(3) van der Pol, B., *Proc. IRE*, 22, p. 1051, Sept. 1934.
(4) Appleton, E. V., *Proc. Camb. Phil. Soc.*, 21, p. 231, 1922
(5) Groszkowski, J., *Proc. IRE*, 18, p. 1960 Nov., 1930.
(6) Tucker, D. G., *P. O. E. E. Jour.*, p. 75, July, 1940.
(7) Moller, H. G. *Jahrb. f. drahtl. Telegr.*, p. 256, 1921.
(8) Armstrong, E. H., U. S. Patent 2,116,501
(9) Hayasi, T., and Yamagiwa, S. *Nippon Elec. Comm. Eng.*, p. 436, Nov., 1938.
(10) Kisselgof and Knazev, *Izvest. Elektroprom. Slab. Toka*, No 10, p. 16, 1940.
(11) Record, F. A., and Stiles, J. L., *Proc. IRE*, p. 281, June, 1943.
(12) Sterky H., *Proc. IRE*, 25, p. 1153, Sept. 1937
(13) Tucker, D. G., *Electronic Engineering*, p. 114, Aug., 1943.

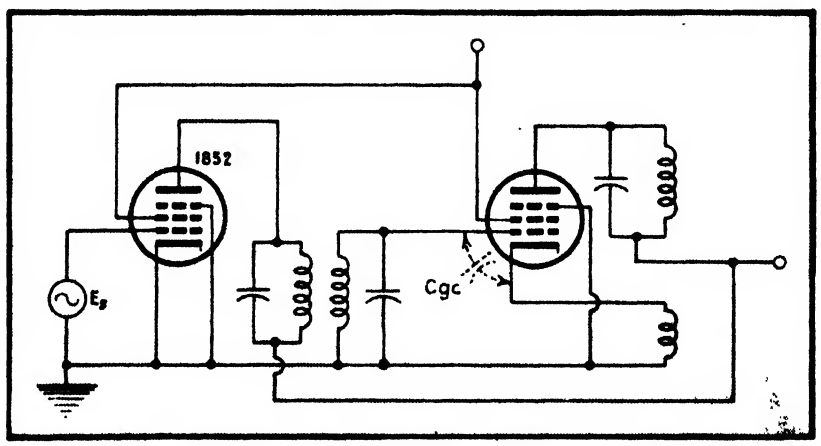

FIG. 6—Typical synchronized-oscillator circuit having synchronizing voltage developed in the grid circuit of the type 1852 tube while oscillation is maintained by a cathode tickler winding

Squelch Circuits for F-M Receivers

Simple circuits for disabling the audio amplifier of an f-m broadcast receiver between stations. In several arrangements described the second limiter is used as a d-c amplifier for supplying squelch voltage and no additional tubes are used

By C. W. CARNAHAN

SQUELCH CIRCUITS for disabling the audio amplifier in the absence of a received carrier have been used for some years in f-m communications receivers, where intermittent operation makes their use imperative. Noise output of an f-m receiver without an incoming carrier is relatively great owing to high i-f gain and the fact that the amplitude limiter becomes an efficient amplifier for receiver noise.

A common squelch method is to bias the first audio tube beyond plate current cutoff, using a control voltage derived from the i-f amplifier or detector. The additional amplifier required has generally been an economic impediment to the use of such circuits in f-m broadcast receivers.

No Extra Tubes

Several squelch circuits to be described provide adequate action without additional tubes if the receiver employs a genuine amplitude limiter.

Historically, the first form of such circuits[1] was used in prewar Zenith f-m receivers as shown in Fig. 1. Tubes V_1 and V_2 constitute a cascade limiter in which the signal from the i-f amplifier is clipped on one side by V_1 and on the other side by V_2. This circuit is like that of any other cascade limiter, except for the positive bias on the grid of V_2 arising from the connection to $B+$ through R_1. The positive bias, in combination with the poor regulation of the plate circuit, owing to R_2, greatly reduces audio noise in the absence of a signal resulting in a partial squelch action while tuning between stations.

The solid line (A) of Fig. 2 shows the plate voltage of V_2 as a function of signal input with R_1 connected to B+, while the dotted line (B) shows the plate voltage with R_1 grounded. The effect of the positive bias is to increase the plate current of V_2 for low signal levels, thus dropping the plate voltage to a point below the knee of the $e_p - i_p$ curves for a pentode. In this region the g_m of the tube is low, and the plate resistance is greatly reduced. These two effects combine to reduce the noise output of the discriminator. In addition, the grid-cathode impedance of V_2 is lowered due to the positive bias, decreasing the noise response of the tuned input circuit. As the desired signal increases, a negative bias is built up, the plate current decreases, and the d-c plate voltage rises. Thus in addition to its r-f limiting action the tube acts as a d-c amplifier with the rectified signal voltage as a d-c input.

Since the plate voltage change over the desired signal range is of the order of fifty volts, it is an easy matter to use this potential to disable the audio amplifier. Figure 3 shows the circuit used to disable a first audio stage consisting of a zero-bias high-mu triode.

The control voltage appearing across R_2 is divided by five through R_3 and R_4, and applied to the lower end of the audio grid resistor R_5. The cathode of the audio tube is biased positively by the divider R_6 and R_7. The cathode bias is adjustable and is set so that the audio grid is biased beyond plate current cutoff in the absence of a signal. When a signal is applied, the positive voltage across R_3 and R_4 is increased and the tube resumes normal operation.

Bypassing capacitors C_2, C_3, and C_4 are required to keep residual noise and hum off the audio grid. The time constant of R_5 and C_5 should be small enough so that the

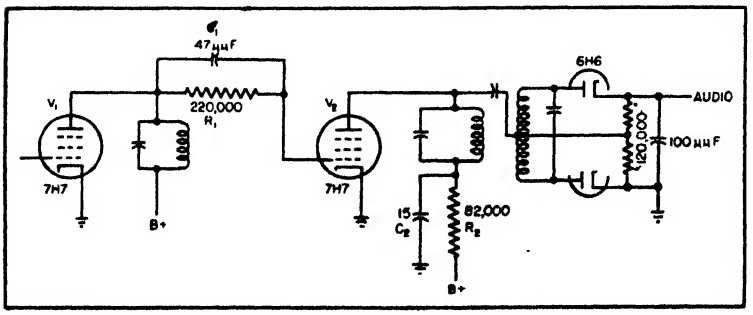

FIG. 1—A direct-coupled cascade limiter wired for partial squelch

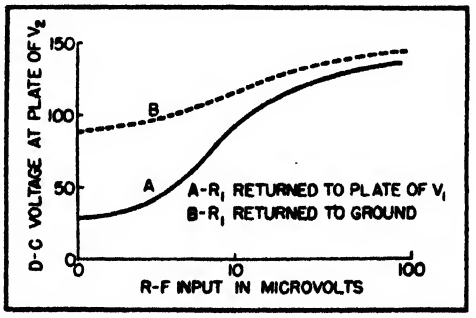

FIG. 2—Response for two limiter connections

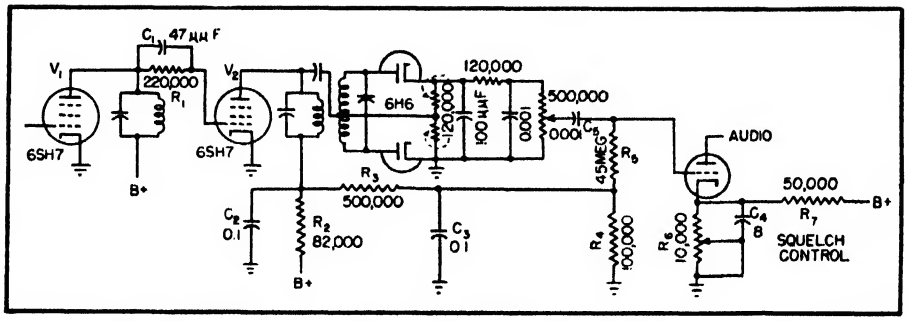

FIG. 3—Squelch circuit used to develop voltage for disabling audio amplifier

control voltage can respond to the average tuning rate. If this time constant is too large, it is possible to tune through a station before the squelch action ceases. To prevent the grid from going too far positive, R_5 is made large, at least 30 megohms. With the grid too positive and too small a coupling capacitance, some low frequency response is lost, owing to the decrease in grid-to-cathode impedance.

The squelch voltage can also be applied directly to the diode detectors, as shown in Fig. 4. Both diode cathodes are biased positively through the divider and squelch control R_5 and R_6, while the control voltage is applied without reduction to both diode plates through R_4. The diode plates are isolated from the cathodes for d-c by C_2. Adequate for communications service, this arrangement is not as satisfactory as the previous one for broadcast use because the audio level at the detectors is high. When tuning off a station some distortion results before suppression is complete.

Amplified Squelch

When the utmost in performance and ease of control is desired a single d-c amplifier can be added. In Fig 5 voltage across the second limiter plate resistor is taken from the divider R_5, R_6, and applied to the cathode of the d-c amplifier V_3. The grid of this tube is supplied with a variable positive bias from a potentiometer across the B supply. In the absence of signal, the grid is positive with respect to the cathode, and the tube draws full current. The resulting voltage drop across R_7 is applied to the grid of the first audio tube V_4, to cut off plate current. With a signal applied, the second limiter plate current is reduced, and the cathode of V_3 rises in potential respect to the grid, cutting off the plate current of this tube. This action in turn removes the bias from the first audio tube.

Reference

(1) U. S. Pat. 2,323,880, issued to C. W. Carnahan.

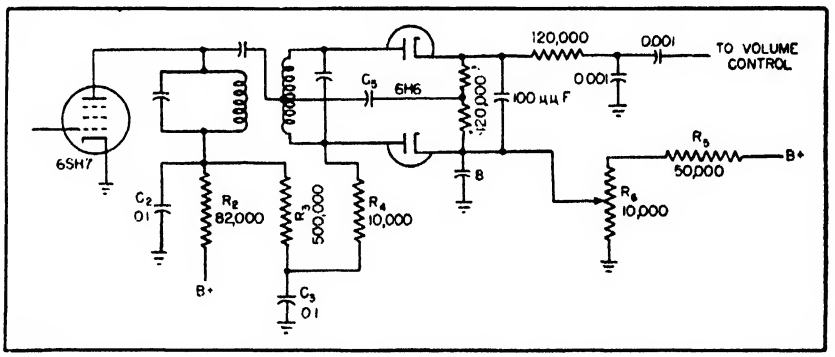

FIG. 4—Squelch developed by means of bias on the discriminator diodes

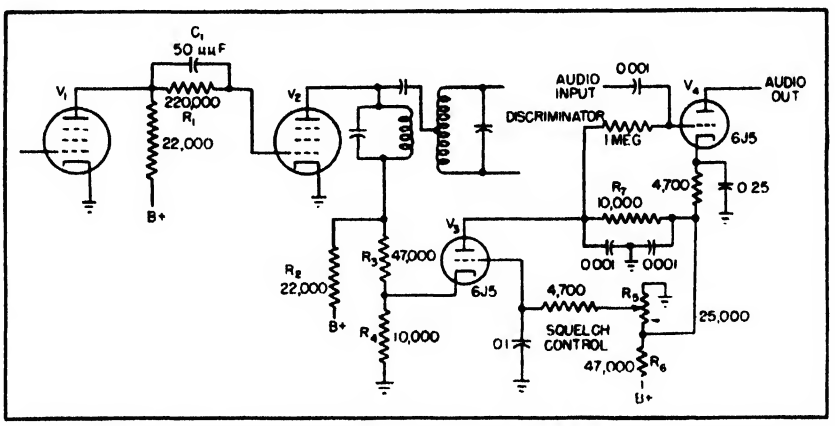

FIG. 5—Amplified squelch with extra tube, used in SCR-808 transmitter-receiver

Superregenerative Detection Theory

Operation of the superregenerative detector is developed, leading to the concept of a time aperture function. Bandwidth, signal-noise ratio, and other circuit properties are shown to depend on this function, whose values in turn depend on the quenching waveform

By WILLIAM E. BRADLEY

An investigation into the operating mechanism of the superregenerative detector, has used physical reasoning and results of measurements.

The specific object of the investigation was to develop a theory that would identify the factors controlling selectivity, optimum quenching, signal-noise ratio, and account for the difficulty of reproducing a given response from one design to another. Because most superregenerative detectors combine in one tube at least four distinct functions, it is not surprising that the behavior of the circuit is complex.

A superregenerative detector, the elements of which are shown in Fig. 1, ordinarily consists of an oscillator having a resonant circuit tuned to the frequency of the desired signal. This circuit is fed from an r-f stage, converter, or antenna, which can be considered a generator of current $i(t)$. The oscillator is caused to operate intermittently by means of a quenching signal supplied from an auxiliary oscillator or from low-frequency oscillation of the same tube. This quenching action can be represented by a varying conductance $g(t)$. The combination of resonant circuit and varying conductance constitute the active element. In addition there are the auxiliary elements, an oscillation detector and an audio or video amplifier. An automatic regeneration control feedback from beyond the oscillation detector to the active element may also be included.

The circuit performs four fundamental operations in sequence: (1) Quenching erases the effect of the previous cycle of operation, clearing the circuit for reception of new impressions; this is done by cutting off the oscillating tube or by damping the circuit. The varying conductance is positive during quenching. (2) Reception takes place when the incoming wave sets up a signal in the circuit as the quenching is withdrawn. (3) Amplification begins when the quenching is sufficiently withdrawn (conductance made negative) so that oscillations will grow in the circuit. This action continues until the overload level is reached or the circuit is again quenched. (4) Detection, usually in the form of a change in oscillator grid or plate current and sometimes using a separate crystal or vacuum diode or a change in quenching rate, produces an output that varies according to the rapidity with which full amplitude of oscillation is reached, and depends on the principle that the stronger the incoming signal the sooner the oscillation will reach full strength, usually several volts. At the end of this operation the varying conductance may fall to zero and the oscillations cease to grow, but nevertheless the requisite energy is delivered to the detector and amplifier.

Of the four operations, least is generally understood of the reception action. It is not obvious at what instant and in what manner the forced oscillation of the circuit produced by the incoming signal changes to free oscillation of the resonant circuit. To determine this and other circuit actions, an approximate solution of the differential equation of a tuned circuit with varying damping was made. Another rigorous approach, based on the superposition integral, has verified the results and indicated the trivial nature of the error in the approximate solution.

To obtain a detailed picture of the behavior of the active element during reception and amplification of an incoming signal consider that a current $i(t) = I \exp j\omega_s t$ is continuously applied. At negative time (during the quenching operation) the varying conductance $g(t)$ has a large positive value; it varies in some manner through zero at $t = 0$ to a generally negative value for positive values of t. The problem

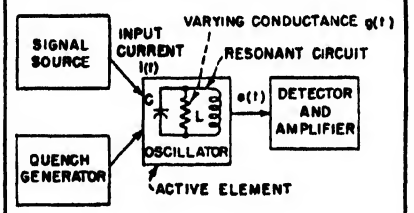

$$e'' + P(t)e' + [\omega_0^2 + P'(t)]\, e = i'(t)/C \quad (1)$$

where $P(t) = g(t)/C$ and $\omega_0^2 = 1/LC$

$$e'' + P(t)e' + \left[\omega_0^2 + \frac{P'(t)}{2} + \frac{P''(t)}{4}\right] e = 0 \quad (2)$$

satisfied by $e = \exp -0.5 \times \int P dt \pm j\omega_0 t$

$$E(t) = (1/j\omega_0 C) \times \int_{-\infty}^{\infty} F(t,\tau) i'(\tau) e^{-j\omega_0 \tau} d\tau \quad (3)$$

which for $i(t) = I\cos\omega_s t$, becomes

$$E(t) = (I/2C) \times \int_{-\infty}^{\infty} F(t,\tau) e^{j(\omega_s - \omega_0)\tau} d\tau \quad (4)$$

$$F(t,\tau) = \begin{cases} 0 \text{ for } \tau > t \\ \exp -0.5 \int_{\tau}^{t} P(t)dt \text{ for } \tau < t \end{cases} \quad (5)$$

FIG. 1—Chief element of superregenerative detector is resonant circuit with varying damping; the equations describe it

is to find the level of oscillation during the amplification operation.

The problem involves the solution of a linear second order differential equation with the coefficient of the first derivative varying with time. This is Eq. 1 (Fig. 1); the primes indicate differentiation with respect to time. The instantaneous voltage on the resonant circuit is $e(t)$; incoming signal is $i(t)$.

The rigorous solution of Eq. 1 is difficult to obtain and use because, to be mathematically complete, it must include the effect of the resistance on the resonant frequency and all of the phenomena that hold for large values of $P(t)$, the damping factor, including the transition between oscillating and nonoscillating states. For present purposes such a solution is unnecessary because, in the practical case $P(t) \ll \omega_0^2$ and, for quench frequencies low compared to the resonant frequency $P'(t) \ll \omega_0^2$.

Under these conditions a very similar second order equation (with its right hand member zero), Eq. 2, can be used for comparison. The first two coefficients of Eq. 2 are identical with those of Eq. 1 and the third is negligibly different; hence, over a limited time, the solutions of the two equations cannot be very different in nature. In fact in the practical case of a high-frequency superregenerative detector the third coefficients of the two equations differ by less than the error in measuring ω_0. For the purpose of this analysis the solution of the comparison equation Eq. 2 differs negligibly from the correct solution of the reduced or homogenous form of the circuit equation.

Knowing the two functions e_1 and e_2 that satisfy the reduced equation, the complete solution of the equation with right hand member can be found by the method of variation of parameters (Lester R. Ford, "Differential Equations", McGraw-Hill Book Co., New York, 1933, p 75.) The solutions are Eq. 3, 4 and 5.

Equations 3, 4 and 5 embody a complete solution to the problem. The function $F(t,\tau)$ is called the time aperture function and, as will be shown, is of basic importance in describing superregenerative detection. Equation 3 states that the voltage envelope amplitude across the resonant circuit at a particular instant of observation, t, depends on an integral of the product of the time aperture function and the input signal, the integration being performed over the preceding time, τ, so that each time element of input signal contributes to the output with a relative importance determined by the value of the time aperture function. Usually the time aperture function has one very large peak, at the moment when the damping passes through zero, and falls rapidly to small values on either side of this moment. Therefore the incoming signal at the moment of zero damping has the greatest effect on the output. This behavior gives rise to the sensitive period of the detector.

Equation 4 expresses the output due to a carrier that remains substantially constant in frequency and amplitude during one quench cycle. The integral is of the same form as the Fourier analysis integral that gives the frequency spectrum of a pulse. As a consequence the time aperture function is related to the selectivity curve of the superregenerative detector in the same way that the waveform of the envelope of a pulsed carrier is related to its spectrum. Thus, for example, a narrow time aperture function causes a broad band receiver and a broad function causes a narrow acceptance band.

The time aperture function is given by Eq. 5 provided the variation of damping with time is known; that is, when $P(t)$ is known. In geometrical terms, if a function of time is drawn having everywhere a slope of $0.5P(t)$ and intersecting the time axis at time t of observation of the resonant circuit voltage, the curve for time prior to t is the natural logarithm of the time aperture function. This process is illustrated in Fig. 2.

Suppose that a sine wave is used for quenching, and that it cuts off the oscillator tube for a large part of the cycle; this sort of operation is usual in some of the older separately quenched superregenerative detectors. Then $P(t)$, the exponent gand $F(t,\tau)$ are shown in Fig. 2B.

By sketching the form of $F(t,\tau)$ for various values of t it is discovered that the area under $F(t,\tau)$ increases rapidly with increasing t, showing that $E(t)$ is growing rapidly with time during the amplification phase. It is also found that the peak of $F(t,\tau)$ as a function of τ occurs at the instant that $P(t)$ passes through zero.

The theory developed in the foregoing analysis can be applied ex-

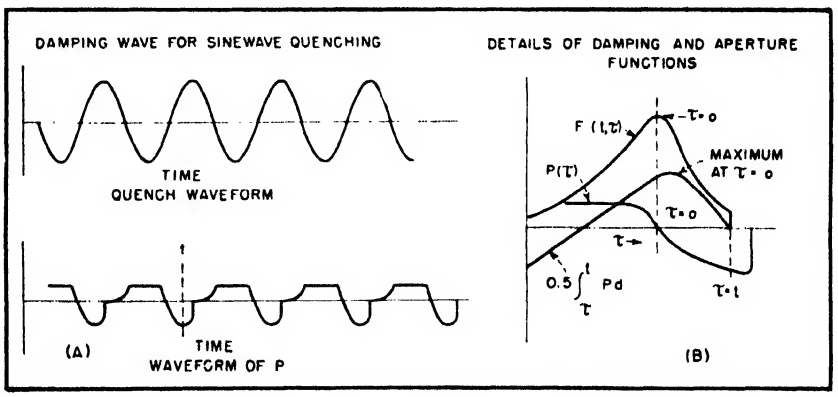

FIG. 2—Variation with time of the damping and aperture functions depends on the form of the quenching wave

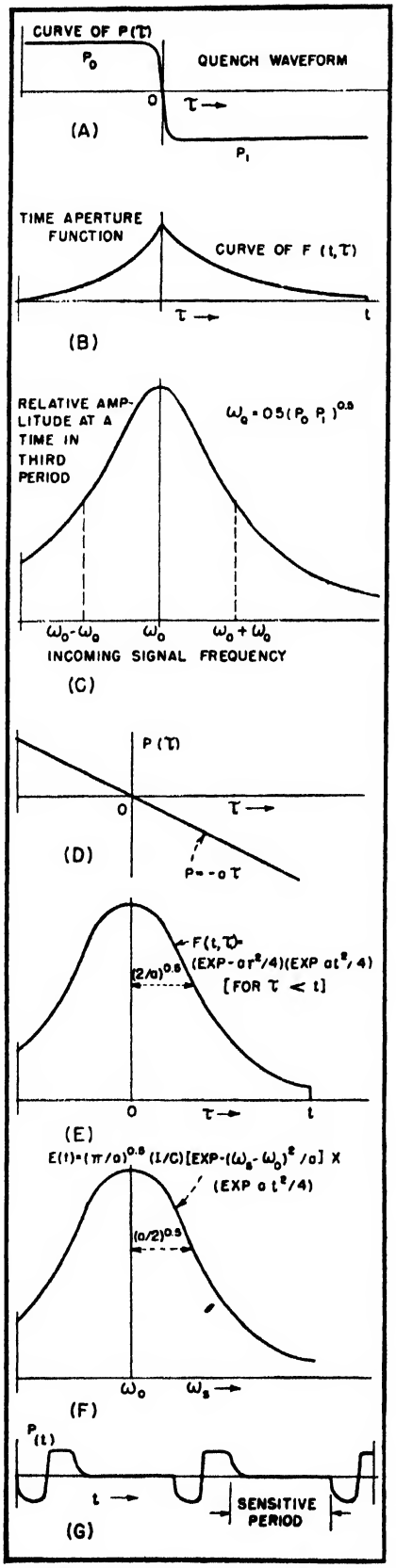

FIG. 3—Knowing the time variation of the damping, the aperture function and pass band can be determined. Optimum quenching waveform is given at (G)

actly in a few interesting cases. Suppose that a square quenching wave is used such that $P(t)$ is positive and equal to P_0 prior to $\tau = 0$ and that it is negative and equal to $-P_1$ thereafter. The quench waveform and time aperture function for this case are shown in Fig. 3A and B. The relative amplitudes of the signal in the amplification phase are also shown (Fig. 3C); this later curve is effectively the selectivity curve of the detector.

For a sensitive, narrow-band detector with a square quenching wave, $-P_1$ should be made as small as is consistent with the chosen quench frequency. For thorough quenching in a short interval P_0 must be large.

Another practical case is that of linearly changing $P(t)$. The commonly used sine wave quenching wave causes $P(t)$ to change from positive to negative nearly linearly. The bandwidth and time aperture function $F(t,\tau)$ depend on the rate of change of $P(t)$. If $P(t)$ has been changing linearly in a negative direction since $t = -\infty$ and at $t = 0$ passes through zero, the voltage $E(t)$ at time t due to an input $I \cos \omega_R t$ can be found as outlined at Fig. 3D through 3F. For this special case both the time aperture and the frequency response have the shape of a probability function.

The almost proverbial poor signal-noise ratio of superregenerative detectors is mostly due to the short effective duration of the time aperture function. In most cases the time aperture function has an effective duration, measured between points of half-peak sensitivity, much less than a tenth of the total quench period. Statistical theory indicates that the signal-noise ratio should vary directly as the square root of the ratio of the effective duration of the time aperture to the total quench cycle duration.

The narrowest band and greatest sensitivity as well as the best signal-noise ratio appear to be obtainable when $P(t)$ has a large positive value during the quenching period (first operation), which is made as short as is consistent with thorough quenching, followed by a value of zero during the entire reception period (second function), which is made as long as possible. The amplification (third function) and detection (fourth function) periods should be as short as is practical. To achieve this result, $P(t)$ should become quite negative so as to amplify quickly the voltage existing at the end of the reception period to a usable level. The required waveform is shown in Fig. 3G.

Certain additional precautions must also be observed in designing superregenerative detectors. The quenching must be complete, otherwise remnants of oscillation persist from the preceding cycle, spoiling the sensitivity of the receiver. Ringing or spurious modes of resonance associated with r-f chokes, quenching circuit coils, or other components can interfere with the quenching, retaining a remnent signal to compete with the new incoming one. Typical symptoms of this difficulty appear when a sharply resonant circuit such as a wavemeter is momentarily held close to the active element. Another effect, usually serious only in low-frequency superregenerative detectors, is shock excitation of the active element by the quenching wave. This action reduces the sensitivity; it is eliminated by restricting the frequency content of the quench.

A simple way of testing for the presence of any of these difficulties is to examine the shape of the selectivity curve with a weak incoming signal. The selectivity curve should be smooth and single peaked. Any of the above difficulties will cause peaks separated by an interval equal to the quench frequency.

Although superregenerative detectors may take a bewildering number of special forms depending upon application, the theory developed above has been found to explain the behavior of all forms investigated during the past five years in this laboratory. In each case the development centered around obtaining the prescribed aperture function. Once this had been accomplished the selectivity and signal-noise ratio measured on the detector agreed substantially with the calculations.

Superregenerator Design

Gain and selectivity of superregenerative receivers can be predicted by the principles that are developed. Circuit operation and the effects on operating characteristics of changing various components are explained. Effects of specific quenching waveshapes are discussed

By ALAN HAZELTINE, D. RICHMAN and B. D. LOUGHLIN

A SUPERREGENERATOR consists of a resonant circuit and an oscillator or regenerator tube, as shown in Fig. 1A. The resonator has a positive damping G_r consisting of the inherent and coupled losses of the tuned circuit. The resonator is also periodically supplied with an effective negative conductance ($G_r - G_r$) by regenerator tube, which is switched on and off by a quenching voltage to produce this effect.

Much prewar information on this circuit is vague, particularly that concerning gain and selectivity. Extensive war-time application of superregeneration in IFF equipment required a thorough investigation. Late in 1942, H. A. Wheeler developed the basic concepts that lead to a clarification of the characteristics of this device. A summary of this theory is given and it is shown how it can be used as a guide in designing superregenerative receivers.

The Superregenerator

In the circuit described above, transient oscillations, excited by a signal in the tank (Fig. 1B), build up exponentially during the period of negative conductance. When the quench voltage turns off the regenerator tube, a period of positive conductance results during which the oscillations are quenched. In most applications it is desirable for the transient oscillations of one quench cycle to almost completely die out so that the transient of the next quench cycle is started mainly by the applied signal.

In the linear mode of operation (Fig. 1C) the regenerator tube is turned off and oscillations are quenched before they reach saturation. The oscillations at the end of the negative conductance period, which are generally fed to a peak detector, are linearly related to the applied signal amplitude.

In the logarithmic mode of operation (Fig. 1D) the regenerator tube stays on until the oscillations reach saturation. The duration of saturation varies with the amplitude of the applied signal, giving, for separately quenched operation, a saturation pulse width that is approximately a logarithmic function of signal amplitude. For self-quenched operation a quench rate that is approximately a logarithmic function of signal amplitude results.[1] Detection of a-m in the logarithmic mode may be obtained by using a separate averaging detector or by using the variations in the regenerator tube electrode currents. The transient oscillation energy of a logarithmic-mode superregenerator has also been used to feed an f-m detector.[2] For studies of gain and selectivity it is convenient to ignore the detection action, and to consider the superregenerator as merely a carrier-frequency amplifier.

Calculating Gain

Action of the superregenerator as an amplifier can be described by considering the tank with its inherent and coupled positive conductance as being shunted by a periodically varying negative conductance, representing the regenerator tube. A general shape of conductance-time variation is shown for the two operating modes in Fig. 1C and D.

For calculating gain and selectivity, it is convenient to consider that a cycle of quench operation starts at T_A when the oscillations of the previous cycle are being damped out and the input current I begins to establish a normal signal in the tank, and that the cycle ends at T_B when the oscillations have again built up to maximum amplitude.

The superregenerative transient oscillation resulting from a short

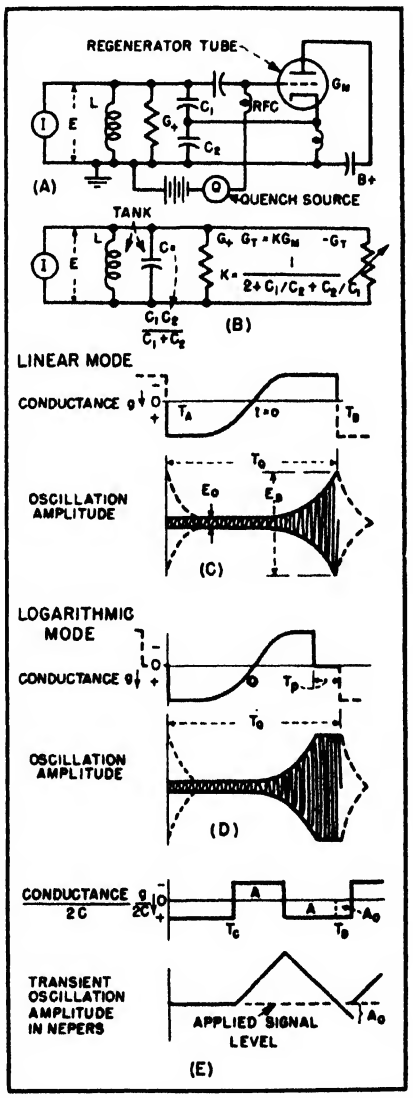

FIG. 1—Superregenerative circuit (A) and equivalent circuit (B) and relation of oscillation amplitude to waveshape of conductance (C), (D) and (E) under various conditions

r-f pulse at $t = 0$ (when $g = 0$) has an amplitude at time T_s of

$$E_s = E_0 \exp\left(-\frac{1}{2c}\int_0^{T_s} g\,dt\right) \qquad (1)$$

where E_0 is the amplitude at $t = 0$ and E_s is the amplitude at T_s. It is convenient to express the ratio of the superregenerative transient amplitude to the applied signal amplitude as a gain A in nepers (one neper equals approximately 8.7 db) so that

$$A = \ln\frac{E_s}{E_0} = -\frac{1}{2C}\int_0^{T_s} g\,dt \qquad (2)$$

Thus, $1/2C$ times the area under the negative conductance-time curve between $t = 0$ and $t = T_s$ represents the gain in nepers to a short r-f pulse applied at $t = 0$ and measured at $t = T_s$.

For the linear mode the total superregenerative gain is given by integrating the total negative conductance area. For the logarithmic mode the effective superregenerative gain is obtained by integrating the negative conductance area up to the time of saturation. This is illustrated in Fig. 1D where T_r is the period of the constant amplitude (saturation) oscillations of the logarithmic mode of operation.

The superregenerative gain just described is not the total gain for a continuous carrier at the frequency of the resonator. Some further gain results because the r-f signal is present during the entire quench cycle. This produces a regenerative gain R which is generally considerably less than the superregenerative gain.

Sensitivity Limitations

The manner of decay of the oscillations during positive conductance is similar to the transient build-up during negative conductance, and the same equations hold for the transient amplitude in the positive conductance area. With repetitive quench, as shown in Fig. 1E, the net transient amplitude at T_n due to the energy remaining in the tank from the previous transient of oscillation initiated in the tank at T_0 is given approximately by $1/2C$ times the net area under the conductance-time curve between T_c and T_D. *Thus, for the transient hangover to be less than the applied signal, the net area over a complete quench cycle must be positive.* This excess damping, shown as A_n in Fig. 1E, should be at least 3 to 5 nepers for most applications.

Sensitivity of a superregenerative receiver is determined by the minimum usable signal level. For the logarithmic mode, sufficient superregenerative gain is obtained to amplify thermal noise to saturate the regenerator tube. In this case the sensitivity is limited by the signal-noise ratio or by the signal level necessary to overcome hangover.

In a linear mode superregenerator, sensitivity may be limited by insufficient gain, as well as by signal-noise ratio or hangover. This is particularly true in applications using a very high quench rate, low-transconductance regenerator tubes, or high-capacitance resonators.

If a short r-f pulse is applied to a superregenerator, highest gain is realized if the pulse is applied when the conductance passes through zero going from positive to negative. If applied later, there is less remaining negative conductance area and thus less gain. If applied earlier, the oscillations decay again, giving less gain. Thus, the superregenerator can be considered to have a sensitivity which varies during the quench cycle, having a maximum at the time when $g = 0$ and is going from plus to minus.

Variation of sensitivity in nepers with time can be found directly from the conductance-time function, and from this a linear sensitivity-time pulse can be calculated, as in Fig. 2. The magnitude of the superregenerative selectivity curve has the same shape as the frequency spectrum of this sensitivity-time pulse. The corresponding frequency spectrum can be found by Fourier analysis or by Campbell and Foster's tables.[3] The four steps, ignoring effects of hangover and assuming high gain, in finding the bandwidth of a superregenerator with a known variation of conductance with time, are shown in Fig. 2; at the bottom of the figure the response in the presence of hangover is shown.

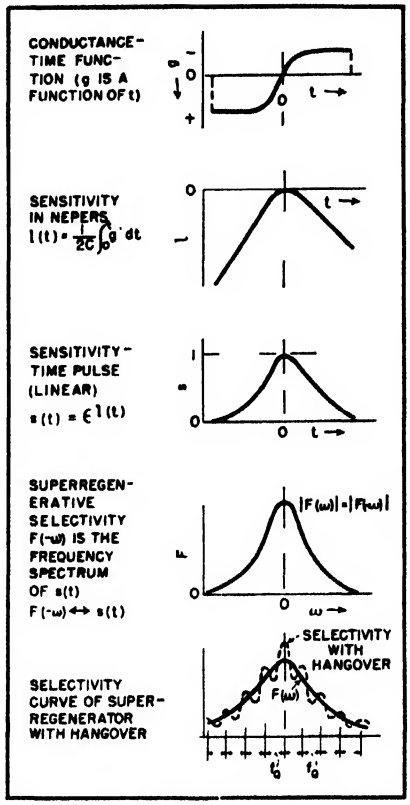

FIG. 2—Steps in the development of selectivity from waveform of conductance, as described in text, and, at bottom, effect of hangover on selectivity

To illustrate how these steps might be applied, consider the design of a superregenerator that is quenched as in Fig. 1A. From an assumed quench waveshape and a knowledge of the variation in transconductance with grid bias (as obtained from published tube data), the variation of transconductance with time can be found. By applying the equations of Fig. 1B, the variation of G_T can be found. This is subtracted from an assumed (or known) value of G_+ for the resonator, giving the net conductance-time function needed for applying the steps of Fig. 2. The sensitivity function $l(t)$ in nepers can be obtained by integrating (graphically, if necessary) the conductance-time function and multiplying by $1/2C$. The linear sensitivity-time pulse $s(t)$ is obtained by exp $l(t)$, where

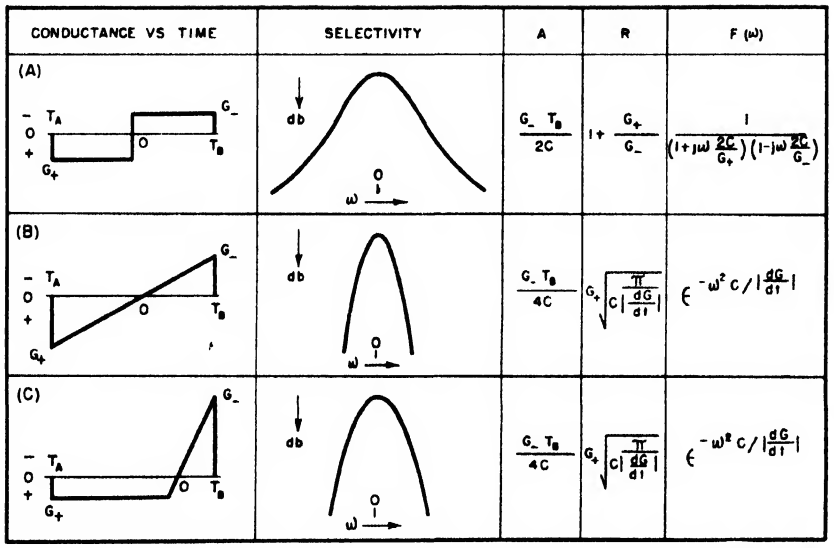

FIG. 3—Conductance waveform controls selectivity, as these specific examples show

$l(t)$ is conveniently taken to be zero at $t = 0$. The superregenerative selectivity shape is found from the frequency spectrum of $s(t)$. If $s(t)$ is not found in Fourier transform tables, an approximate answer may be obtained by graphical Fourier analysis.

If it is desired to calculate the selectivity of an existing superregenerator, it may be convenient to find the plate-current waveform of the regenerator tube (by inserting a small resistor in the plate circuit and observing the quench-frequency voltage waveform across it on an oscilloscope). Then the selectivity can be calculated as before.

Equations for Gain and Selectivity

The variation in superregenerative sensitivity with time means that the effect of the current supplied to the resonator varies with time. This is exactly equivalent to a variation in input current amplitude with time. It can be shown that the magnitude of the superregenerative selectivity response characteristic is equivalent to that of an unvaried and undamped resonator to which an a-m signal is applied. The spectrum of that a-m signal is continuous because each cycle of quench is independent of the others, if hangover is negligible. The selectivity characteristic of the superregenerator is exactly equivalent to the frequency spectrum of the amplitude modulated signal, or of the sensitivity pulse.

The sensitivity pulse is defined as

$$s(t) = \exp\left(\frac{1}{2C}\int_0^t g\,dt\right) \qquad (3)$$

where this relation holds for $T_A \leq t \leq T_B$, and $s\ (t) = 0$ outside of these limits.

The gain of the superregenerator, H, is defined as the ratio of the voltage existing at the peak of a superregenerative cycle to the voltage which would be developed across the tank at resonance if the conductance had remained at the value G_+. That is

$$H = E_B/(I/G_+) \qquad (4)$$

It can then be shown (for example, by conservation of energy or by superposition of the effects of a series of impulses) that

$$H = \exp(A)\,\frac{G_+}{2C} \times \int_{T_A}^{T_B} \exp\left(\frac{1}{2C}\int_0^t g\,dt + j\omega t\right) dt \qquad (5)$$

If hangover is ignored and the superregenerative gain is large, Eq. 5 reduces to

$$H = \exp(A)\,\frac{G_+}{2C}\int_{-\infty}^{+\infty} s(t)\exp(j\omega t)\,dt \qquad (6)$$

Equation 6, which ignores end effects, indicates that the selectivity of a superregenerator can be found from the inverse Fourier transform of the sensitivity-time pulse. The factor, $\exp A$, in Eq. 6 is the superregenerative transient gain where

$$A = -\frac{1}{2C}\int_0^{T_B} g\,dt \qquad (7)$$

The remaining factor, evaluated at resonance, defines the added gain that is obtained by regeneration. The regenerative gain ratio is

$$R = \frac{G_+}{2C}\int_{-\infty}^{+\infty} s(t)\,dt \qquad (8)$$

As before, these steps have ignored effects of hangover and assume that the superregenerative gain is large.

Effects of hangover can be computed from the net attenuation, A_0, and phase shift per cycle, $\exp(-A_0 - j\,\omega\,T_Q)$. The resulting selectivity is

$$S = F(\omega)/|1 - \exp(-A_0 - j\omega T_Q)| \qquad (9)$$

where $F\ (\omega)$ is the selectivity ignoring hangover. The curve at the bottom of Fig. 2, showing hangover, is plotted to a linear scale; the peaks are very nearly separated by $F_Q = 1/T_Q$ and the troughs are halfway between.

Figure 3 gives examples of three conductance-time curves with their corresponding selectivities as calculated by the foregoing method, as well as the equations for superregenerative gain A, regenerative gain R and selectivity $F(\omega)$, ignoring hangover and end effects.

In the case of symmetrical squarewave quench (Fig. 3A), a selectivity equal to that of two cascaded, isolated single-tuned circuits (one having conductance G_+, the other G_-) is obtained. When $|G_-| = G_+$ the equivalent phase characteristic of the selectivity has no phase distortion. This distortionless phase characteristic is produced by all conductance-time functions which have skew symmetry about $g = 0$ (Fig. 3A and 3B). When gain A is large, departure from exact skew symmetry in regions remote from $g = 0$ can be neglected.

The triangular conductance waveform of Fig. 3B produces a selectivity having the form of a probability curve. (A probability curve plotted to a db scale forms a parabola.)

The conductance waveshape of

Fig. 3C is similar to that found in the usual self-quenched superregenerator, particularly those using grid quench and having the grid leak returned to a positive bias. This waveform produces a selectivity following a probability curve, but considerably wider than that of Fig. 3B. The reason for this is that, for the same quench frequency and gain, the shape of Fig. 3C has a greater rate of change of conductance with time, giving a narrower sensitivity-time pulse and thus a wider frequency spectrum.

When a converting superregenerator is used, such as the Fre-Modyne circuit, an unusual result is obtained. The conversion efficiency varies during the quench cycle so that the r-f sensitivity-time pulse is the product of the i-f sensitivity-time pulse and the conversion efficiency pulse. This generally results in an r-f sensitivity-time pulse that is slightly narrower than the i-f pulse, and thus gives a slightly wider r-f bandwidth than i-f bandwidth.

In the foregoing discussion it has been assumed that the resonant frequency of the superregenerative tank circuit does not vary during the quench cycle. This gives symmetrical selectivity curves. If the superregenerative tank frequency varies appreciably during the period when the sensitivity-time pulse has significant amplitude, then a result much like a combination of simultaneous a-m and f-m is obtained, which can produce unsymmetrical selectivity curves.

It can be shown that the shape of the selectivity curve near the nose of the curve is determined mainly by the shape of the conductance-time curve near the time when $g = 0$. If the conductance waveshape is approximately a straight line in the vicinity of $g = 0$, then the selectivity curve is a probability curve to approximately as many db of attenuation as are represented by the superregenerative gain obtained during the linearly sloping part of the conductance wave form. This leads to the useful approximation that *the total bandwidth at one neper (8.7 db) from the peak is*[4]

$$f_w = (1/\pi)\ |(1/c)|dG/dt||^{1/2} \qquad (10)$$

where dG/dt is the slope of the conductance-time curve at g = 0.

In a separately quenched superregenerator, Eq. 10 shows that, in general, if the quench voltage amplitude is increased, the selectivity curve will become wider. Also, if the quench voltage frequency is reduced, keeping the same waveshape, that the selectivity curve will become narrower. However, if the quench amplitude is increased, or the frequency decreases, the available superregenerative gain will be increased, producing more total gain for a linear mode operation or producing an earlier saturation in logarithmic mode. *Thus for a given quench waveshape, and for a specified superregenerative gain, the narrowest selectivity is obtained by using the lowest possible quench frequency.* However the minimum quench frequency should be at least equal to twice the maximum modulation frequency of the received signal.

The question frequently arises of how to measure the selectivity of an existing superregenerator. Conventional methods may be applied in certain cases, but are generally inadequate. With certain types of superregenerators the problem is like measuring the selectivity of a conventional receiver having a very flat avc that cannot be disconnected. The following method is suggested as being applicable to substantially all forms of superregenerators normally used.

The audio output noise of the receiver, without an applied signal, is measured by an output meter (rms type preferred). A signal is applied at resonance and adjusted in level until the noise is suppressed by some convenient amount such as 10 or 20 db. Then the signal is detuned and readjusted in level until the noise is suppressed by the same amount. The difference between the two levels is the attenuation or selectivity at the detuned frequency. By this method of constant noise suppression, the complete selectivity curve may be measured (assuming an adequate signal generator) to as much as 80 to 100 db of attenuation.

References

(1) F. W. Frink, The Basic Principles of Superregenerative Reception, *Proc. IRE*, p 76, Jan. 1938. This paper gives a more complete description of the various modes of operation.

(2) H. P. Kalmus, Superregeneration—Its Possibilities and Limitations, *Proc. IRE*, Oct. 1944.

(3) Bell Telephone System Monogram B-584, Fourier Integrals for Practical Applications.

(4) MacFarlane and Whitehead, The Superregenerative Receiver in the Linear Mode, *Jour. IEE*, Part III A, No. 1, 1946.

Single-Sideband Converter

IN keeping with the current interest in single sideband reception, the circuit of the Millen adapter unit is shown in the accompanying diagram. It consists of a crystal-controlled low-frequency converter designed to adapt communication receivers for selectable single sideband reception. Eliminating one of the side bands by selection reduces interference, both from the standpoint of noise, and heterodyne signals, owning to the reduction of the normal receiver bandwidth to approximately 25 percent.

The unit consists of a crystal-controlled oscillator and a mixer which converts the normal 455-kc i-f to 50.5-kc; an i-f amplifier with four high-Q tuned circuits; a detector and audio amplifier, and a power supply. A lever-type switch mounted on the front panel switches the oscillator crystal to provide

either 49.5 or 50.5 kc to select the sideband which is to be passed.

The 455-kc output from the receiver is coupled to the sideband selector by a small loop on the input cable which is slipped around the diode plate pin on the receiver detector tube. The audio output of the selector can be used directly for headphone reception or the output may be fed into the audio amplifier in the receiver for loudspeaker reception.

The normal receiver audio gain control is turned off so that the output from the receiver detector does not get into the audio amplifier. In some receivers the leakage may be such that it will be necessary to disconnect the first audio amplifier tube.

The i-f transformers T_1 and T_2 are aligned to 50.5-kc and, with the switch in the upper sideband position, the response at 50-kc is about 5-db down.

When the switch is in the double sideband position, T_2 has been retuned by capacitor A to 49.5-kc and this (plus T_1, which is still tuned to 50.5-kc) results in a sharp-nosed curve ideally shaped for aural carrier tuning peaked at 50-kc. This double-sideband tuning position can be used for normal operation. Its selectivity is high enough to attenuate most high-frequency heterodynes lying above 2,000 cycles.

When the interference gets bad and the off-frequency carrier gets in closer so that the beat note drops to 1,000 or 500 cycles, one of the single sideband positions is switched in, and the tuning control rocked slightly. If the heterodyne persists, the other sideband is switched in and the tuning control rocked again. For maximum rejection it is necessary to climb up slightly on the low-frequency side of the curve to a point about 5-db below the peak.

The first section of the 6SN7GT operates as an infinite-impedance detector, and the second section of the tube is used as an audio amplifier. A high-pass filter having high attenuation to frequencies below 300 cycles is installed in the audio circuit. This filter not only removes undesired low-frequency beat notes, but makes speech sound natural by attenuating the lows in proportion to the highs. It also takes out some of the noise.

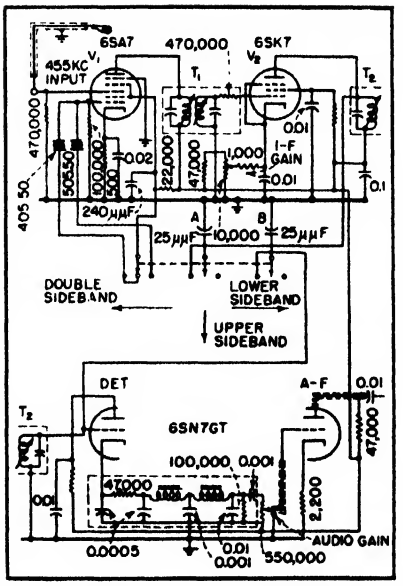

Circuit diagram of the single-sideband converter

Superregenerative Detector Selectivity

Experimental determination of characteristics of a superregenerative detector indicates that selectivity and sensitivity increase and noise decreases with decreasing quench frequency. Selectivity decreases with increasing quench amplitude

By ALLAN EASTON

THIS PAPER describes an experiment dealing with the effect of some circuit parameters on the selectivity characteristic of a superregenerative detector. Data is presented and some conclusions discussed, along with a brief qualitative explanation of the reasons underlying the observed phenomena.

The author was confronted with the problem that on a superregenerative receiver, designed and placed in production, it was found necessary to tighten the selectivity specification.

Receiver Circuit

The circuit diagram of the receiver is shown as Fig. 1. Components essential to the discussion are shown in detail. The receiver consisted of five basic parts: (1) selective antenna transformer; (2) buffer amplifier tube for reduction of reradiation; (3) superregenerative detector; (4) external sinusoidal quench oscillator; (5) audio amplifier.

The oscillator circuit which performs the superregenerative function is a conventional Hartley oscillator, with the tank connected between grid and plate of the tube. The frequency of operation is in the one hundred megacycle range. The sinusoidal quench voltage is impressed on the grid of the detector through a large resistance. The audio output voltage is taken from the grid circuit.

Selectivity Measurements

Several samples of the production receiver were carefully aligned and the selectivity measured. The curve of Fig. 2 labeled Typical Set repre-

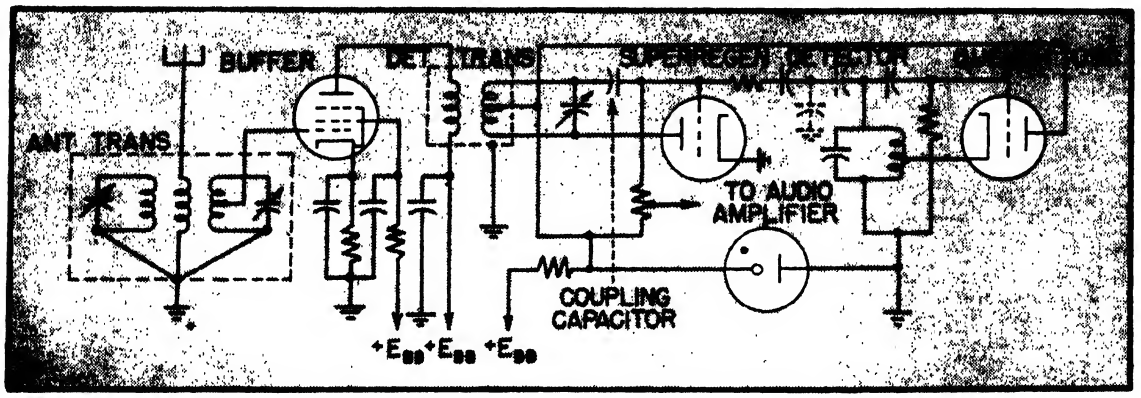

FIG. 1—Circuit of superregenerative receiver upon which tests were made. Dotted capacitors were added later to decrease bandwidth by reducing quench amplitude to the detector tube

sents this measured selectivity. The required selectivity dictated by the revised specification, and the selectivity obtained as a result of this investigation are also shown. Study of the obtained selectivity curve indicates plenty of leeway for production variations.

It was first necessary to ascertain the individual contribution of each stage to the total selectivity characteristic. The bandwidth of the detector alone was determined in the usual manner. A standard signal generator was connected to the grid of the r-f amplifier and the changes in frequency required to restore standard output for input voltage ratios of 2, 10, 100, and 1000 times the resonant value were observed. Figure 3 shows a plot of the overall selectivity of the typical set as shown on Fig. 2. The selectivity characteristic of the detector alone, and the bandwidth of the antenna transformer alone are also shown. The data for the antenna transformer curve was obtained by impressing a signal voltage, whose frequency was varied, across the antenna terminals and measuring the voltage appearing at the grid of the r-f buffer.

With this selectivity information, the following requirements were recognized as essential to improving the selectivity: (1) antenna coil selectivity might be sharpened; (2) leakage, if any, around the antenna coil could be reduced to obtain full benefit of the antenna coil selectivity; (3) the superregenerative detector selectivity might be increased to carry the entire selectivity specification by itself.

Several attempts were made to sharpen the antenna transformer selectivity. The grid tap of the antenna transformer was shifted to obtain the optimum position, higher-Q coils were tried, and the coupling was altered. Some improvements were realized in the transformer characteristic but the overall selectivity was not appreciably changed.

Experiment indicated definitely that while leakage broadened the selectivity curve slightly it was not a controlling factor.

Detector Selectivity

Next, factors affecting detector selectivity were studied. The design of the detector transformer was changed. The plate coupling coil was moved away from the grid winding. This change seemed to reduce loading on the grid winding, thereby increasing the Q. Selectivity improved somewhat, but the sensitivity declined. Oscillator excitation was decreased by changing the tap on the detector coil. This, in effect, reduced the negative resistance, resulting in increased Q. The selectivity at an input voltage ratio of 100 was 3.0 percent, compared with 3.5 percent previously observed. Again, however, sensitivity was decreased, this time by a factor of 10.

In order to study the effects of quench frequency and quench amplitude upon selectivity, apparatus was connected as indicated in the block diagram of Fig. 4. The quench frequency was varied over wide limits for several values of quench amplitude, and the bandwidth of the detector stage alone was measured. The results are shown in Fig. 5A. These curves are convincing evidence that selectivity is greatly influenced by both quench frequency and quench amplitude. The selectivity may be controlled over a five to one range by these parameters.

Figure 5B indicates a definite reduction in noise output as quench frequency is lowered. The usable sensitivity is much improved, and the signal to noise ratio, under these conditions, is higher. Figure 5C shows how detector sensitivity depends on quench frequency.

Figure 6 is a plot of detector bandwidth versus quench amplitude. The quench frequency was 60 kc. The data was taken at both ends of the carrier frequency band, that is at 50 and at 100 mc. The optimum value of quench frequency is roughly proportional to the carrier frequency. Bandwidth was measured where the required input signal was 100 times that at resonance for the same signal output in all bandwidth measurements.

Study of the various curves shows that best bandwidth is obtained with about a 50-kc quench frequency and two to three volts quench amplitude.

The production receiver was altered to accomplish the recommended changes. The original receivers used a quench frequency of 150 kc at 9.5 volts amplitude. These values had been chosen because the sensitivity

and selectivity were least affected by small changes in quench constants. The change consisted of increasing the size of the quench oscillator tank capacitor, inserting an iron core to increase the quench oscillator coil inductance, and reducing the quench amplitude by using a capacitance divider across the tank.

Effect of Strong Signals

Further tests on the production receiver indicated that detuning occurred when the input voltage was increased. This phenomenon is characteristic of oscillators with intermittent or pulsed modulation. When the duty cycle of the modulating pulse voltage is changed, there is a corresponding frequency shift in the oscillator. This shift, in effect, reduces the selectivity as measured by the interfering signal method. The percentage detuning was as much as 1.25 percent of carrier frequency as the input was increased from 50 to 20,000 microvolts, meaning that a receiver which passed a static selectivity test would probably fail when given a dynamic selectivity test.

A simplified equivalent circuit is shown in Fig. 7 along with some other tabulated data. Several sizes of coupling capacitor were installed in order to study the effect of decoupling the variable resistance presented by the oscillator tube from the tank circuit. For each size of coupling capacitor indicated, the following steps were taken.

The receiver was tuned to resonance with about 50 microvolts input and the carrier frequency for maximum audio output observed. The input was raised to 20,000 microvolts and the audio output measured without retuning. The first column shows the capacitance used. The second column shows the audio output variation versus coupling capacitor size to be as much as 4.5 to 1. The signal generator was retuned to obtain maximum audio output and again the audio measured. The third column shows this data. Observe that the audio output was nearly doubled by retuning.

The increment of frequency required to retune was recorded in column four. The detuning varied from 0.43 percent to 1.25 percent depending upon the size of the capacitor. The bandwidth was measured for each size of capacitor; results are tabulated in the last column. The bandwidth changed almost 2 to 1. Our conclusion is that the smaller the capacitor, the lighter the loading, and thus the higher the Q of the tuned circuit. Values of capacitance smaller than 10 $\mu\mu$f resulted in oscillator failure.

Theory of Operation

Precise, quantitative analysis of superregeneration is a risky procedure because of the difficulty in completely describing the phenomenon. The contradictory conclusions resulting from the several methods of analysis found in the literature (see bibliography) reflect this difficulty. The brief discussion which follows will, therefore, be qualitative in nature. The conclusions reached were deduced from the experimental work and were tested on the same equipment. Thus the conclusions are valid when applied to similar circuits, but should be examined carefully before being applied to other types of superregenerative detectors.

Refer to the detector circuit in Fig. 1. Assume the signal voltage and the quench voltage to be disconnected. When the plate potential is turned on, oscillations will build up exponentially. The equation describing the phenomenon is given by Frink[1] as

$$I_0 = \frac{e_R \omega_R}{\beta R} \epsilon^{-Kt^2/2} \qquad (1)$$

where

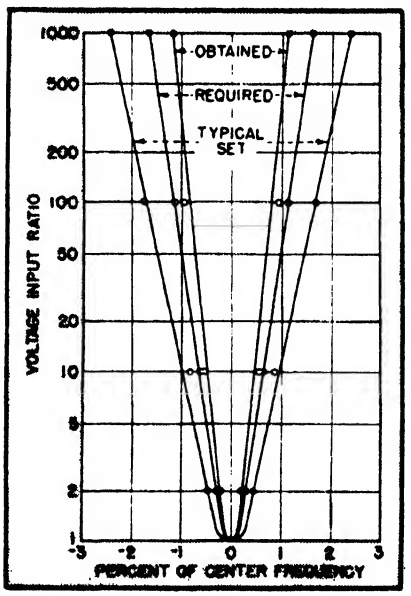

FIG. 2—Measured selectivities of superregenerative receiver

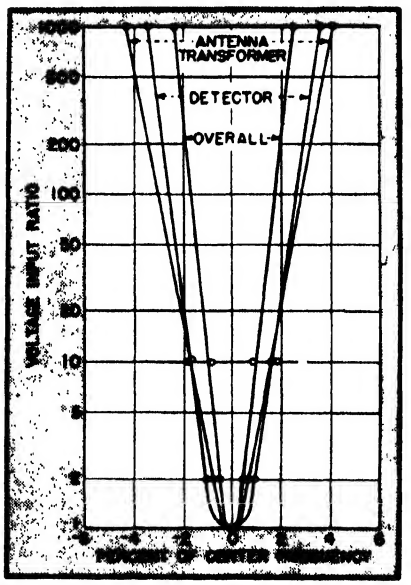

FIG. 3—Circuit contributions to receiver selectivity

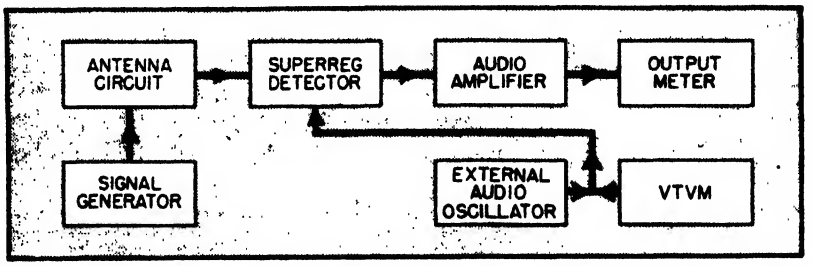

FIG. 4—Basic laboratory circuit used to study the effects on superregenerative detector of quench frequency and amplitude, and signal strength

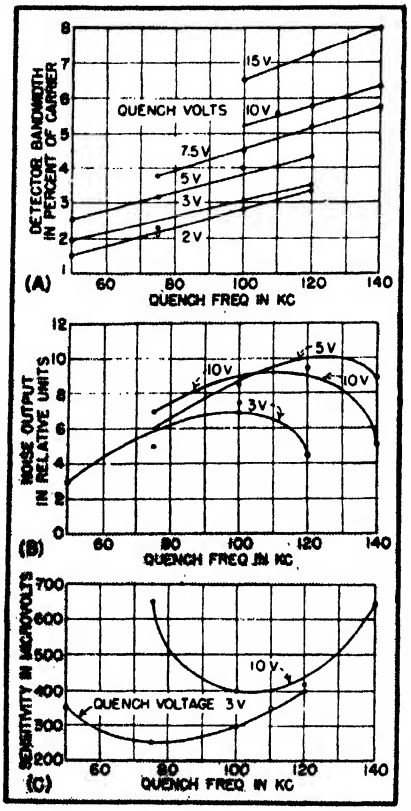

FIG. 5—Quench frequency affects detector bandwidth (A), detector noise output (B), and detector sensitivity (C)

I_0: amplitude of the oscillatory current
e_s: random noise amplitude (signal absent) or signal amplitude
ω_R: $2\pi \times$ resonant frequency
t: time
L: inductance in tuned circuits
C: capacitance in tuned circuits
R: total effective resistance in tuned circuits
$\beta = [(1/LC) - (R/2L)^2]^{1/2}$

The amplitude of the oscillatory current is proportional to the signal strength, e_s. In the initial conditions just postulated, e_s is random noise.

The rate at which oscillations grow, dI_0/dt, is also proportional to e_s; thus

$$\frac{dI_0}{dt} = \frac{e_s\,\omega_R}{2L\,\beta}\,\epsilon^{-Rt/2L} \qquad (2)$$

In the case of growth, R is negative. In the case of decay, R is positive.

These equations were derived assuming linear elements. The oscillations will actually reach saturation at a time somewhat different from that indicated by the equations, because of the nonlinearity of the detector grid circuit.

Instead of turning the plate voltage on and off, the grid bias can be varied periodically to produce a similar effect. In this case, the quench voltage will interrupt the oscillations. In Fig. 8 there is shown a plot of a square wave of quench voltage. Square-wave quench voltage is used on the figure for the sake of clarity. Immediately below this plot is the growth and the decay envelope of the oscillations for zero input signal. In this case, random noise triggers the oscillations. The detector output will consist of noise, the characteristic hiss usually associated with the superregenerative detector. Lower lines indicate the growth, with signal introduced. The rate of rise of the oscillations is greater the larger the incoming signal. The shaded areas indicate the contribution of the signal amplitude to the rise time.

The voltage appearing across the detector grid resistor, which constitutes the detector output to the audio amplifier, depends upon the average grid current, i_a, and is proportional to the area under the lower curves of Fig. 8. In addition

$$i_a = K\,(2L, R)\,\log_e\,(e_{s1}/e_{s2}) \qquad (3)$$

where i_a: change in detector current, K: constant for detector, e_{s1}/e_{s2}: applied signal voltage ratio.

The change in detector current varies as the logarithm of the applied signal ratio, which accounts for the desirable limiting action on strong signals and the comparative freedom from noise interference. If the superregenerative detector is to be operated on strong signals, the use of high transmitter modulation percentages is recommended. Equation 3 predicts that the output from the detector will drop as signal input is increased when low modulation levels are employed. Kalmus[2] has used the superregenerative detector in f-m receivers to obtain both amplification and limiting action.

The sensitivity of the superregenerative detector is a function of the i_a of Eq. 3. The sensitivity obtainable at high frequencies is considerably greater and could be obtained by other comparatively simple means. Noise muting sensitivities of 10 to 20 microvolts were realized with the receiver shown.

Choice of Quench Constants

The data presented indicates that it is possible to control the selectivity over wide limits by relatively simple changes in circuit constants. This possibility lends itself particularly well to production receivers. Quench frequency and quench amplitude are the parameters which have considerable effect on selectivity and are the easiest to control. Some changes in sensitivity occur simultaneously and are sometimes difficult to predict, as was illustrated in Fig. 5C. However, it is possible in most instances to arrive at a compromise which will result in good selectivity, sensitivity, and signal to noise ratio.

The most important factor in determining the quench magnitude and frequency is the decrement of the

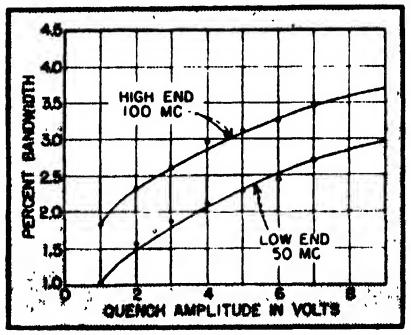

FIG. 6—Bandwidth is affected by quench amplitude

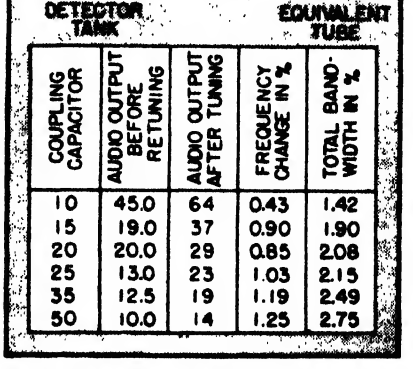

COUPLING CAPACITOR	AUDIO OUTPUT BEFORE RETUNING	AUDIO OUTPUT AFTER TUNING	FREQUENCY CHANGE IN %	TOTAL BANDWIDTH IN %
10	45.0	64	0.43	1.42
15	19.0	37	0.90	1.90
20	20.0	29	0.85	2.08
25	13.0	23	1.03	2.15
35	12.5	19	1.19	2.49
50	10.0	14	1.25	2.75

FIG. 7—Detuning of the superregenerative detector by strong signals can be minimized by using a small coupling capacitor between detector tank and superregenerative tube

tuned circuit. The oscillations should have time to decay to below the level of the weakest signal to be detected. If this is not done, a coherent state of oscillation results, in which the oscillations are continuous and do not decay completely. Consequently, the oscillator will beat with the incoming signal. Multiple responses, one for each sideband of the coherent oscillator, will result. This condition of multiple responses is brought about by excessive quench frequency or insufficient quench amplitude. The quench frequency should be low enough to permit the oscillations to reach maximum amplitude. The data taken in the performance of the experiments described above seems to indicate that a greater on period of oscillation, brought about by either lowered quench frequency and/or amplitude, will result in improved selectivity.

If the quench frequency is too high, the superregenerative detector will operate in the linear mode rather than the logarithmic mode. The linear mode of operation does not have the advantage of noise quieting and limiting on strong signals.

The quench frequency should be high enough so that no combination of quench frequencies and modulation frequencies can result in audible interference.

At high frequencies selectivities far greater than those possible with two and perhaps more tuned circuits alone can be obtained. The practical limit on selectivity comes from the problem of oscillator drift. An excessively sharp receiver is adversely affected by temperature, humidity, or voltage changes, which may result in complete loss of signal, whereas a less selective receiver will only lose sensitivity.

The superrengenerative detector is a very high gain device, consequently it does not seem advisable to rely on preselector stages for selectivity. Preselector stages are essential, however, for the reduction of oscillator reradiation.

When it is important to maintain constant percentage bandwidth over a large frequency range, it will be necessary to change the quench constants simultaneously with the frequency setting. If several bands are employed, switching of quench constants is desirable.

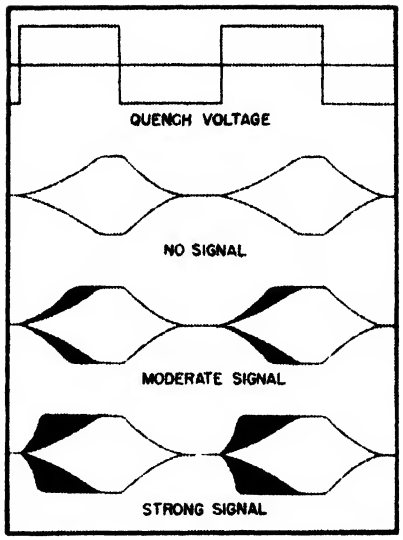

FIG. 8—Strength of the signal determines the rate at which detector oscillations grow

References

(1) Frink, Frederick W., The Basic Principles of Superregenerative Reception, *Proc. I.R.E.*, Jan. 1938, p 76.
(2) Kalmus, Henry P., Superregeneration—Its Possibilities and Limitations, *Proc. I.R.E.* Oct. 1944, p 591.

Bibliography

(1) Ataka, Hikosaburo, On Superregeneration of an Ultra-Short-Wave Receiver, *Proc. I.R.E.*, Aug. 1935, p 841.
(2) Meyerson, Art H., Super-Regenerative Detectors in U-H-F, *Communications*, Mar. 1943, p 16.
(3) Terman, Frederick E., "Radio Engineers' Handbook", McGraw-Hill Book Co., New York, p 662.
(4) Terman, Frederick E., "Radio Engineering", McGraw-Hill Book Co., New York, p 456.
(5) Russell, O. J., Super-Regeneration, *Wireless World*, Dec. 1944, p 361.
(6) Armstrong, Edwin H., Some Recent Developments of Regenerative Circuits, *Proc. I.R.E.*, Aug. 1922, p 244.
(7) Scroggie, Superregenerative Receiver, *Wireless Engineer*, Nov. 1936, p 581.
(8) Becker, Stewart, and Leeds, L. M., A Modern Two-Way Radio System, *Proc. I.R.E.*, Sept. 1936, p 1183.
(9) Maurice, Superregeneration for Broadcast Receivers, *Wireless Engineer*, Jan. 1938, p 4.
(10) Hulbert, E. O., On Super-Regeneration, *Proc. I.R.E.*, Aug. 1923, p 391.
(11) Hayasi, Problems of Superregeneration, *Nippon Elec. Comm. Eng.*, Aug. 1937, p 246.
(12) Uda, Noise Suppressing in Superregenerative Receivers, *Nippon Elec. Comm. Eng.*, Aug. 1937, p 237.

Superregenerative Circuit Applications

Survey of equipment utilizing superregenerative circuits includes iff gear, telemetering systems, radar beacons, remote-control devices and f-m receivers. Difficulties in analyzing basic circuit performance necessitate the empirical design considerations outlined here

By HARRY STOCKMAN

THE TECHNICAL TERM superregeneration was introduced in 1922 by E. H. Armstrong, who is also credited with the invention of the superregenerative receiver[1]. In simultaneous work, other engineers utilized the basic concept of superregeneration, intentionally or unintentionally, as illustrated by the contemporary patent literature. The collected patents and the few papers published outline the history of superregeneration up to the beginning of World War II. During the war, the most important applications were classified. Consequently, the war archives of the U. S. Government are now the repository of the complete and accurate story of the development.

Superregeneration can be defined

as the condition in a regenerative system that produces a growing transient of oscillation, prevented from becoming a sustained oscillation by means of a repeated quenching action. The envelope form and repetition rate of the transient or wave train depend upon the initial conditions, which may be controlled by a modulated wave in such a manner that later rectification of the transient yields the modulation signal. Simplified diagrams of self- and externally quenched superregenerative detectors are shown in Fig. 1.

An equivalent circuit can be drawn for the superregenerative detector, taking into account the inductance, capacitance, and resistance of the tank circuit, the varying impedance presented by the periodically quenched tube, and external impedance introduced into the circuit, as for example, reflected antenna impedance. Then, if a signal voltage is assumed to be impressed on the circuit, one can write a differential equation involving the instantaneous tank-circuit current and its derivatives. Finding solutions for this nonlinear differential equation is a difficult process, a fact that has hindered the superregenerative receiver designer.

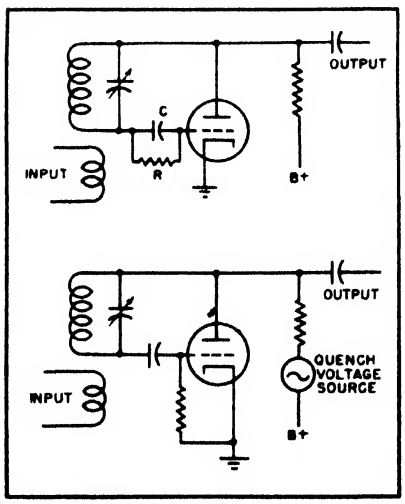

FIG. 1—Simplified circuit diagrams of basic superregenerative detectors. Relation between R and C permits periodic blocking in self-quenched detector (top); oscillation in externally quenched detector (bottom) is turned on and off by separate quench-voltage source

The complexities that arise in a rigorous mathematical treatment of this extremely nonlinear type of circuit may be bypassed by the use of graphical methods related to bench measurements. These methods are similar to those employed in the treatment of class-C amplifiers, large-signal detectors, and frequency converters. In many special phases of the general problem, however, advanced analytical methods are justified.

Many of the design requirements are contradictory to one another, so that the final design must often be a poor compromise among high sensitivity, high selectivity, high fidelity, efficient avc operation and fast recovery time. One reason for this vagueness in design is that not enough is known about the basic mechanism of superregeneration. The sometimes unpredictable behavior of these circuits is often due to incomplete information about circuit and tube fundamentals, such as the variation of effective dissipation during the quenching cycle, the influence of circuit Q, and the effect of variation of tube coefficients.

Inherent Noise

Although the superregenerative receiver is famous for high gain, its noise-muting sensitivity generally is not high enough. In addition, the characteristic noise produced in the superregenerative circuit in the absence of a signal or in the presence of a weak signal, is a serious defect. Such noise can be reduced by automatically or manually lowering the sensitivity of the circuit. Unfortunately, the use of a preamplifier does not generally improve the signal-to-noise ratio as shot effect and beating of an incoming signal with noise components reduce the noise-muting sensitivity to about the same value as is obtained without the preamplifier.

Radiation

Radiation is a typical defect, particularly noticeable when several superregenerative receivers operate close together. These effects can be minimized by reducing antenna coupling, quench-frequency voltage amplitude, and amplitude of oscillation. Such ameliorating changes generally result in poorer operation in other respects. A preamplifier ahead of the superregenerative circuit will reduce, and in some cases almost eliminate radiation.

A frequency converter can precede the superregenerative circuit to act as a buffer. Such an arrangement may not appreciably reduce radiation because of the recombination of sum and difference components inherent in a converter.

Bandwidth

Inherent avc in superregenerative circuits regulates the gain when the circuit is detuned from the mid-frequency of a given signal. This and other effects generally cause poor selectivity at medium and high frequencies. Multiple-resonance phenomena cause broad and nonuniform response, although this is not necessarily a disadvantage in some applications.

The quench frequency required increases with carrier frequency. Accordingly, the absolute bandwidth increases with carrier frequency. The important characteristic, however, is the bandwidth relative to the signal frequency. In general, a superregenerative receiver can be said to compare more favorably with other receivers at higher signal frequencies.

High distortion is a classical limitation of superregenerative circuits, particularly in logarithmic mode. Since the output of the superregenerative detector varies logarithmically with the degree of modulation of the signal, volume expansion occurs when the modulation rises above approximately 60 percent. This effect is undesirable in communications and broadcast receivers. In pulsed systems, distortion of the pulse shape occurs, limiting accuracy of triggering and coding and inhibiting fast operation.

Sources of Instability

Changes in antenna loading, which can occur when rotational antennas are used, as well as changes in the loading presented by

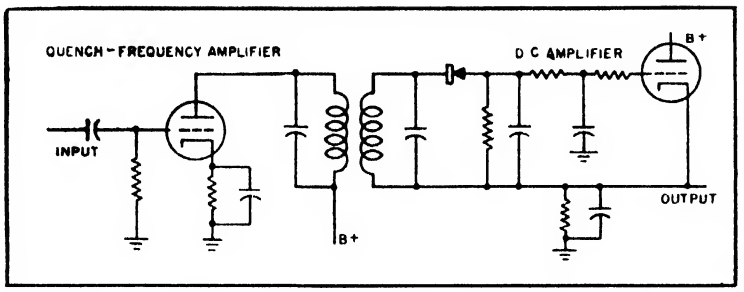

FIG. 2—Automatic gain stabilization (ags) circuit. When superregenerative-detector bias voltages drift, this feedback circuit acts to correct the deviation

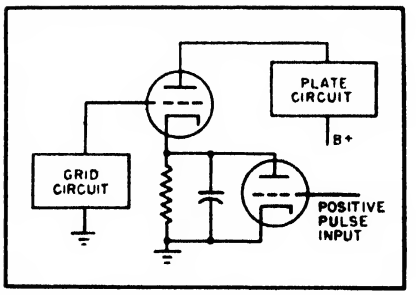

FIG. 3—Positive pulses fed to righthand triode speed transmitter-circuit recovery

the video or audio amplifier coupled through a rectifier to the oscillating circuit, can inhibit the superregenerative action.

In pulse reception, the sensitivity of the superregenerative circuit must be closely controlled so that uniform response to incoming pulses is secured and operation on weaker pulses and disturbances avoided. This control is accomplished by the automatic gain stabilization (ags) circuit, an example of which is shown in Fig. 2. The ags circuits regulate the amplitude of the noise-initiated oscillations by controlling either the bias of the superregenerative circuit or the quench-voltage amplitude.

The superregenerative circuit is subject to a number of forms of instability. One undesirable form is jitter, encountered in pulse reception and transmission circuits. Jitter is characterized by a nonuniform starting rate of the oscillation wave trains. Even slight mismatching between antenna and line, or line and receiver, can cause such disturbances because of reflection of wave-train oscillations at the point of mismatch. When the reflected oscillations arrive at the receiver, they start an additional wave train which interferes with proper operation of the receiver.

Centimeter-Wave Operation

In the centimeter-wave region, lighthouse tubes, reflex klystrons and magnetrons permit superregenerative operation and provide useful signal reception. At these frequencies, however, such receivers have serious limitations, such as high noise level and the need for extra tubes for control purposes.

The superregenerative receiver can be considered as an intermittently operating transmitter, and indeed the receiving-tube circuit is frequently used for transmission in transmitter-receiver equipment. Although such a design reduces size and weight, it has many shortcomings, particularly when the transmitter and receiver must be tunable within different frequency bands and when the transmitter must operate with high frequency stability. Automatic gain stabilization may not be applicable for pulse reception in a superregenerative transmitter-receiver because of troublesome time constants in common circuit elements.

Beacon and iff equipment, utilizing a common, transmitter-receiver, superregenerative circuit, may have a period of insensitivity, or dead time, amounting to several milliseconds following reply to a challenging signal. This large dead time is caused in part by the use of a single tube for receiving and transmitting. Fast-operating circuits have been designed to remedy this condition and can be arranged, for example, rapidly to discharge transmitter bypass capacitors, as shown in Fig. 3. The need for fast recovery enters into many applications of superregenerative circuits and is sometimes one of the hardest requirements to satisfy.

F-M Circuits

Superregenerative circuits can be utilized in many different ways for f-m reception, but not always with advantage. Slope detection can be utilized but may produce an undesirable form of the multiple-resonance curve and the response of the circuit to amplitude variations. For f-m receiver applications, a converter can be used to obtain an i-f that is higher than the frequency of the incoming signal, and a superregenerative amplifier can then be utilized in a lock-in type of circuit. A second converter provides the following discriminator with an input of sufficiently low frequency. Possibilities exist for developing good superregenerative f-m receivers, based on simplification of the designs suggested here, or on other approaches.

The use of superregenerative amplifier circuits as either r-f or i-f limiters in f-m receivers is of particular interest. An example of such a circuit is shown in Fig. 4. By the use of special quench wave forms, practically complete limiting can be obtained.[8] Cascade circuits with a second, time-delayed, superregenerative amplifier have proven useful. All these circuits operate on the basic principle that the percentage of a-m appearing in the r-f output of a superregenerative amplifier will be smaller than that existing in the incoming wave.

Gas-Tube Relay Circuits

Properly modified superregenerative circuits of conventional form are used to operate relays, particularly for the control of target aircraft. Superregenerative gas-tube circuits, using thyratrons, are also used for similar purposes, but have the following limitations: unreliable control due to lack of precision in gas-tube operation, dependence of tube on ambient temperature, critical bias voltages, and short tube life. Hard-tube superregenerative circuits can be de-

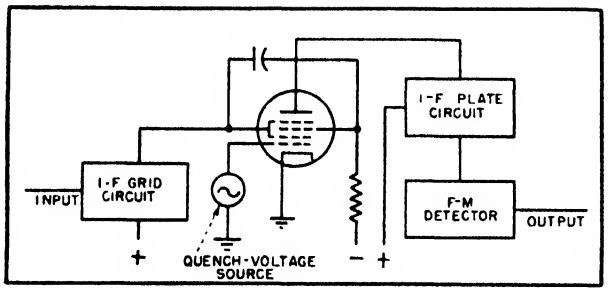

FIG. 4—Superregenerative i-f limiter circuit. Quench voltage of suitable waveshape permits nearly complete limiting

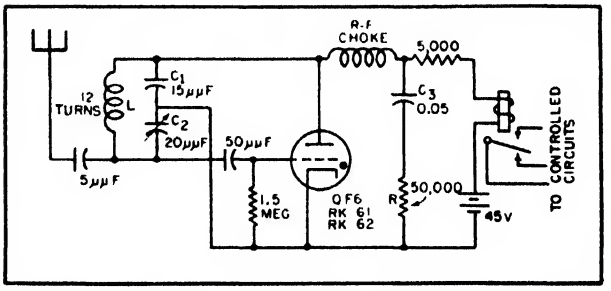

FIG. 5—Typical superregenerative gas-tube circuit affords compact, lightweight means of actuating relay by radio signal

signed to give sufficient plate-current variation with a small interrupted signal, or for a given amplitude or frequency change in a c-w signal.

Figure 5 shows a circuit diagram of one form of modern gas-tube superregenerative relay.[3] The tube in combination with the plate-voltage source, resistor R and capacitor C_3 constitutes an a-f sawtooth oscillator. Normally, a relatively large d-c flows through the relay winding and keeps the relay energized. In addition to its sawtooth oscillation, the tube also quenches at a superaudible rate, and therefore maintains an average negative potential on its grid. A third oscillation is present in the tank circuit L, C_1, C_2, consisting of wave trains of constant energy. When a sufficiently strong signal is impressed on the tank circuit through the antenna, the wave-train energy and repetition rate change so as to make the grid slightly more negative. This change in grid voltage prevents the tube from firing, so that the relay current drops to a very much smaller value, tripping the relay. The device can be operated with signal on or off for rest position of the relay.

Although small size and light weight are particular advantages of superregenerative circuits, their increasing use in balloon transceivers, guided missiles, and the like, now necessitates new inventions to reduce their weight still further.

The superregenerative circuit has important applications in remote control of missiles, telemetering of missile control data, target seeking, radar beacons, iff equipment, and a variety of circuits for remote control of switches and relays. Means for rapid coding, reception of secret messages, and insensitivity to certain types of interference and jamming are inherent advantages of the superregenerative circuit that are important for these applications. On the other hand, since such applications also give rise to more rigorous requirements on receiver stability and reliability under adverse weather conditions, the need for improvement in superregenerative receivers has become very great. A rich field for exploration is open here to the serious research worker and development engineer.

REFERENCES

(1) U.S. Patent 1,424,065, issued to E. H. Armstrong.
(2) U.S. Patent 2,273,090, issued to M. G. Crosby.
(3) U.S. Patent 2,383,119, issued to R. H. Packard.

Wideband I-F Amplifiers

Advantages of high gain with wide bandwidth can be obtained from stagger-tuned coupling networks provided compensation is made for extraneous frequency-selective feedback through the tubes. Design considerations and procedure are presented

By MATTHEW T. LEBENBAUM

IMAGE REJECTION ratio[1] is one of the important performance characteristics in the development of wide-range tunable superheterodyne receivers for the uhf and shf regions (300 to 30,000 megacycles). If a tunable receiver is to be a truly single-dial, single-signal receiver, all spurious responses, the most important of which is the image response, must be reduced to below the level where objectionable interference may be encountered.

Two major components of a system which introduces attenuation to the image response are (1) an r-f preselector and (2) an i-f amplifier which removes the image frequency sufficiently far from the desired signal frequency that advantage can be taken of the selectivity of the r-f preselector.

To determine the image rejection obtained with a given intermediate

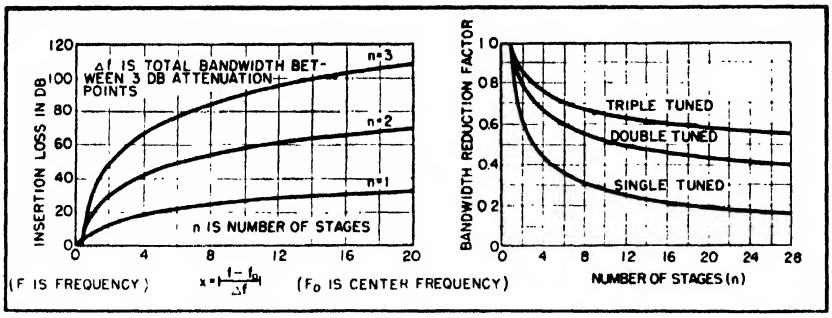

FIG. 1—Normalized curves for selecting number of preselector circuits for a specified skirt rejection

FIG. 2—Degree of narrowing of passband introduced by multiple couplings all tuned to the same center frequency

frequency, one simply determines the ratio of the response in the r-f passband to the response at two times the intermediate frequency from the passband. Increased rejection is obtained with higher i-f.

Design Parameters

Information required by a designer of an i-f amplifier is (1) frequency, (2) bandwidth, (3) gain, (4) off-band rejection. The frequency is obtained by joint agreement between preselector and amplifier designers. In receivers under consideration, a minimum image rejection ratio of at least 60 db is desired. A family of curves which aid in the selection of the required number of preselector circuits and intermediate frequency is shown in Fig. 1[9]. Curves are for maximum insertion loss in the r-f passband of three db (L_0) and give the insertion loss of the filter at any frequency f outside the center of passband f_0.

For example, if a 70-db image rejection ratio is required, and for design considerations of tracking and oscillator stability the r-f bandwidth is 50 mc, it can be seen from Fig. 1 for $n = 1$ that a single-tuned preselector will be unsatisfactory regardless of intermediate frequency. If two tuned circuits ($n = 2$) are used, the parameter $x = (f - f_0)/\Delta f$ is taken from the curve to be equal to 20 for 70-db rejection. Because $\Delta f = 50$ mc and $f - f_0 = 2f_{i\text{-}f}$, then $f_{i\text{-}f} = 20 \times 50/2 = 500$ mc. For three tuned circuits ($n = 3$) $f_{i\text{-}f} = 4.6 \times 50/2 =$ approximately 120 mc.

Agreement must be reached on the relative complexities involved in the two alternatives. In the particular case to which the above figures refer, a three-cavity preselector, and an i-f amplifier, centered at 160 mc were chosen. Bandwidth is generally dictated by the intelligence to be received. In this case, 20 mc was used.

The overall gain required is a function of the receiver application. For general monitoring of a portion of the radio-frequency spectrum, which was desired, reception of signals down to noise level is required. Sufficient gain must therefore be included to bring the receiver noise up to a level at which the second detector is operating linearly. Total gain is thus a function of the noise figure of the receiver. The 160-mc i-f amplifier used as an example in this article incorporated between 90 and 100-db voltage gain from input grid through the second detector.

Off-band rejection requirements are determined by the specific application, but in general, the requirement of high gain requires a large number of stages, and (as will be seen later) the circuits which must be used to obtain the combination of high gain and large bandwidth are such as to insure excellent skirt rejection.

Amplifiers Above 100 Mc

Design of amplifiers operating above 100 mc is one which is as much a mechanical problem as an electrical one, if lumped constant interstage networks are to be used. These networks must be kept compact with the fewest and shortest possible leads. If a design is used which deviates from these requirements, experience has shown that regeneration troubles invariably arise, and their elimination results in mechanical layouts which are cumbersome, difficult to build, and even harder to service. For the above reasons, a highly desirable type of coupling is the single-tuned network using tube and stray capacitances as shunt capacitance and a variable inductance for tuning. This network can be constructed in extremely small space with very short leads.

The disadvantage of this coupling is that the gain-bandwidth product[7] of a single-tuned network is low compared to more complex networks, off-band rejection is also low, and overall bandwidth of a series of single-tuned stages becomes rapidly smaller as the number of stages is increased. Figure 2 shows the degree of narrowing as a function of the number of cascaded stages for single-tuned coupling as well as for double and triple tuning. There is a definite advantage in the use of more complex coupling networks, completely aside from the fact that their gain-bandwidth products are higher to start with, because of less rapid narrowing with increasing number of stages, but unfortunately, these networks are difficult to realize at high frequencies.

If single-tuned circuits are used, it can be shown that if both high gain and large bandwidth are required, the resultant amplifier rapidly becomes uneconomical and under certain conditions impossible of construction. Figure 3 shows the number of stages required to realize given bandwidths and gains using cascaded single-tuned coupling. With gains of 100 db and bandwidths greater than 4 mc, the cascaded single-tuned amplifier is impractical.

Stagger-Tuned Circuits

To retain the simplicity of the single-tuned amplifier and to obtain the desirable gain-bandwidth product and slower narrowing of the overall bandwidth of multituned networks, stagger tuning is used.

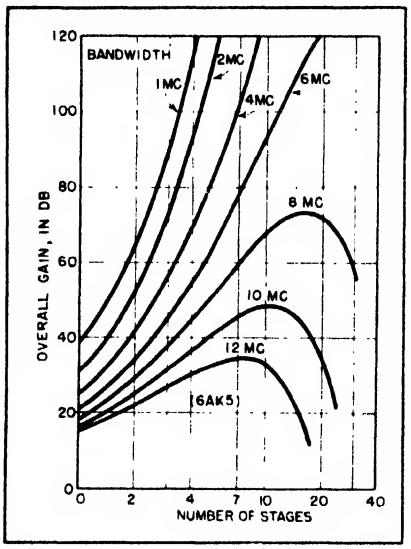

FIG. 3—Curves relate the three functions total gain, bandwidth, and number of stages for cascaded single-tuned couplings

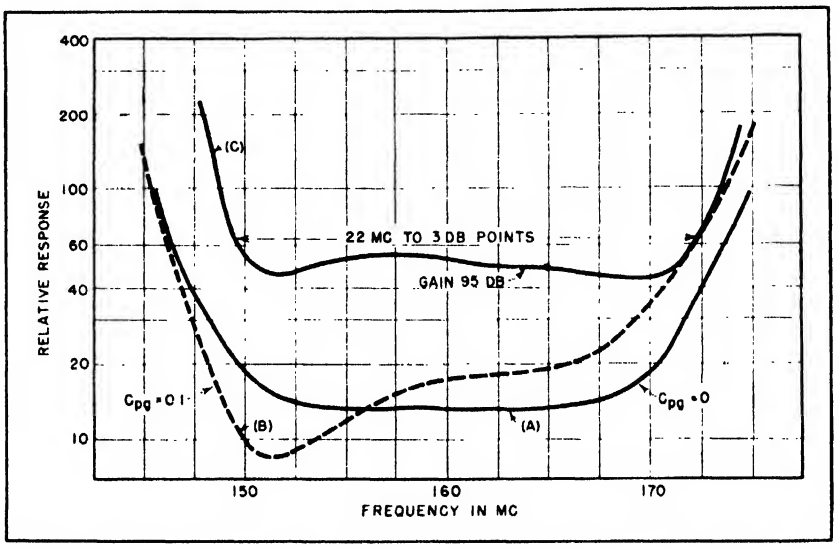

FIG. 4—Because of selective loading from feedback within the tube, the response (A) of a nine-stage amplifier of three triples was distorted (B) Response curve (C) of the amplifier after readjustment of staggered frequencies and damping

By properly adjusting tuning frequencies and damping of individual single-tuned stages, results approaching those obtainable with multituned coupling can be obtained with little sacrifice of simplicity.

The theory of stagger tuning has been adequately covered in the literature[4] so no derivations will be included in this paper. The method has proved to be exceedingly powerful in the simple solution of most present wideband, high-gain amplifier problems.

In discussing stagger tuning, it is convenient to express the gain-bandwith product in units of $g_m/2\pi C_T$ and call this the gain-bandwidth factor. The gain-bandwidth factor for a single-tuned stage is, therefore, unity[4].

A STAGGERED PAIR of overall bandwidth Δf and geometrically centered at f_0 consists of two single-tuned stages of dissipation factor $D = 1/Q$ and tuned at frequencies $f_0\alpha$ and f_0/α respectively. Where δ is less than 0.3

$$D = 0.707\delta$$
$$\alpha = 1 + 0.333\delta$$
$$\delta = \Delta f/f_0$$

The stage gain times overall bandwidth factor of this combination will be unity. Figure 2 shows that the corresponding factor for two cascaded stages is only 0.64. In addition, overall selectivity function of the staggered pair will be, in both absolute value and phase, that of a transitionally-coupled[5], double-tuned circuit. For this reason overall bandwidth decreases more slowly as staggered pairs are cascaded than for identically tuned stages. Figure 2 gives the narrowing factor for staggered pairs and triples by using the double-tuned and triple-tuned curves respectively where n is the number of pairs or triples.

A STAGGERED TRIPLE of overall bandwidth Δf and geometrically centered at f_0 consists of two single-tuned stages of dissipation factor D staggered at $f_0\alpha$ and f_0/α and one single-tuned stage of dissipation factor δ centered at f_0. Where δ is less than 0.3

$$D = 0.5\delta$$
$$\alpha = 1 + 0.433\delta$$
$$\delta = \Delta f/f_0$$

The stage gain times overall bandwidth factor of this combination will be unity, and the overall selectivity function will be, in both absolute value and phase, that of a transitionally-coupled triple-tuned circuit. Three cascaded single-tuned circuits would give a corresponding factor of only 0.54. It is also seen that the overall bandwidth decreases even more slowly as triples are cascaded.

It is possible to carry the staggering to n stages, but in the practical case the pair or triple is normally used and if more gain is required than can be obtained in this manner additional pairs or triples are used in cascade.

As an example of the design of an amplifier, the following requirements are set: $f_0 = 160$ mc, overall bandwidth $\Delta f_t = 20$ mc, overall gain $G_A = 100$ db. As a first approximation, assume four triples are required. From Fig. 2, each triple must be $\Delta f_T = \Delta f_t/0.76 = 20/0.76 = 26.3$ mc wide. For 6AK5's, $g_m = 5{,}200$ μmohs, $C_T = 11$ μμf, so that the stage gain (G_s) times the bandwidth per triple (Δf_T) is

$$G_s\Delta f_T = g_m/2\pi C_T = \frac{5{,}200 \times 10^{-6}}{2\pi 11 \times 10^{-12}} = 75 \times 10^6$$

and the stage gain is $75 \times 10^6/26.3 \times 10^6 = 2.86$ or 9.1 db, and overall gain (for four sets of triples giving 12 stages) is $9.1 \times 12 = 109$ db.

$\delta = \Delta f_T/f_0 = 26.3/160 = 0.158$
$f_1 = f_0\alpha = f_0(1 + 0.433\delta)$
$= 160(1 + 0.433 \times 0.158) = 170.9$ mc
$f_2 = f_0/\alpha = f_0/(1 + 0.433\delta)$
$= 160/(1 + 0.433 \times 0.158) = 150$ mc
$f_3 = f_0 = 160$ mc
$D = 1/Q = 0.5\delta = 0.5 \times 0.158 = 0.079$
$Q_1 = Q_2 = Q = 1/0.079 = 12.7$
$Q_3 = 1/\delta = 1/0.158 = 6.33$

$$R_1 = Q_1/2\pi f_1 C_T = \frac{12.7}{2\pi 170.9 \times 11 \times 10^{-6}} = 1{,}060 \text{ ohms}$$

$$R_2 = Q_2/2\pi f_2 C_T = \frac{12.7}{2\pi 150 \times 11 \times 10^{-6}} = 1{,}210 \text{ ohms}$$

$$R_3 = Q_3/2\pi f_3 C_T = \frac{6.33}{2\pi 160 \times 11 \times 10^{-6}} = 560 \text{ ohms}$$

The parameters of the amplifier are thus determined. (A staggered pair would be designed similarly by using the constants previously presented for it.) The selectivity of the tuned circuits must be realized, thus the calculated resistances must be changed to take into account the tube's input conductance and finite coil Q. In stagger-tuned amplifiers centered in the vicinity of 30 mc, it is customary to use damping resistors one five-percent RMA size higher than that calculated in order to compensate for losses external to the damping resistor.

Extraneous Damping

Unfortunately, at frequencies above 100 mc, the effect of the grid-plate capacitance becomes of increasing importance. The effect of this feedback path is to distort the selectivity curve, tilting it with greater gain at the low end of the band and less at the high. At frequencies below 100 mc, it is usually sufficient to compensate for conductive and susceptive components of fedback admittance by retuning the grid circuit to the proper frequency and readjusting the damping.

As the center frequency is raised, this type of correction becomes less effective. Figure 4 shows the calculated selectivity curves of an ideal amplifier using three triples to obtain a 20-mc bandwidth at 160 mc, and of the same amplifier with the feedback included and with the individual stages retuned to the calculated stagger frequency and with the damping adjusted to the theoretical values. This calculation must be carried out stage by stage as the effect is cumulative. Feedback capacitance was assumed to be 0.1 μμf, which is about twice the normal value in a 6AK5, and was chosen to magnify the effect. However, actual experimental results show this tilting to be of such magnitude as to require additional compensation.

If the values of tuning frequencies and loading are varied from the theoretical, the passband can no longer be maintained flat without great sacrifice in gain. However, if small dips and peaks are allowable, a good compromise can be obtained by designing the amplifier for a slightly wider band than required, about ten percent, and adjusting the damping empirically to obtain the optimum result. The new values of loading are difficult to calculate because of their dependence on the value of the grid-plate capacitance, which may vary from tube to tube and stage to stage by a considerable percentage. It can be shown that the fedback admittance has conductive and susceptive values of the form

$$G_f = B_{gp} \frac{g_m B_L}{G_L^2 + B_L^2}$$

$$B_f = B_{gp} \frac{1 + g_m G_L}{G_L^2 + B_L^2}$$

where G_f and B_f are the conductive and susceptive portions of the admittance of the grid circuit as the result of a grid-plate susceptance $B_{gf} = C_{gp}$. Also B_L and G_L are the conductive and susceptive portions of the plate load admittance. Because G_L must always be positive, it may be seen that the B_f is always positive (or capacitive). However, because B_L may take either sign, being negative below resonance of the plate circuit and positive above, the conductive component varies widely with frequency.

The effect is noted especially in the case of stagger tuning; if the grid circuit is tuned to a lower frequency than the plate circuit, grid-plate capacitive feedback produces a negative damping in the grid and when the grid is at a higher frequency, a positive damping. This loading changes with frequency and so the selectivity curve of the tuned circuit is distorted. This distortion, when magnified by successive stages, produces the results shown in Fig. 4.

Compensation

As mentioned above, it is difficult to calculate correction factors because of the uncertainty of the value of C_{gp}. Despite the importance of feedback with conventional tubes above 100 mc, a good compromise can be obtained by empirical adjustments. Figure 4 shows the selectivity curve of the 160-mc amplifier whose design was discussed. The following table shows the effect of feedback and tube loadings on the values of the parameters

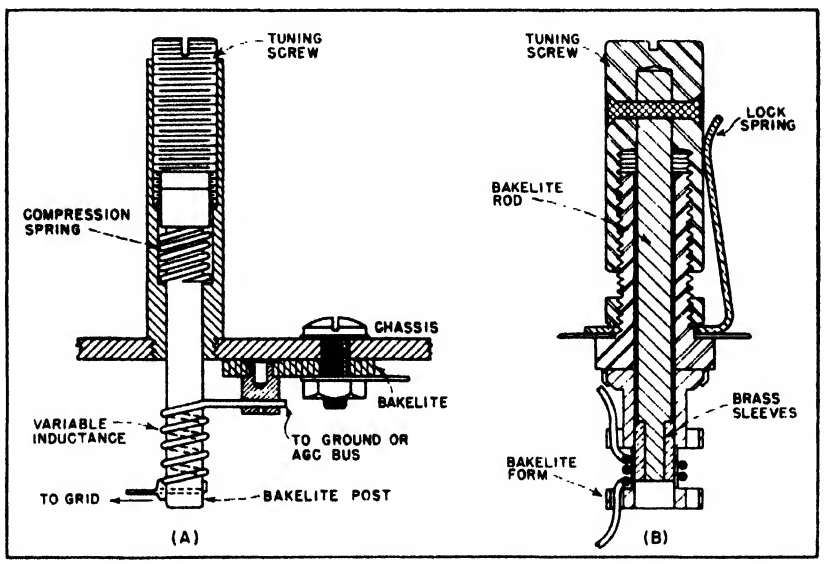

FIG. 5—Two methods of tuning inductors in the vicinity of 100 mc. (A) The coil length is varied. (B) The coupling to a loop is varied

	Frequency	
	Calculated	Adjusted
High	170 9	172.5
Low	150	149
Center	160	160

	Resistance	
	Calculated	Adjusted
High	1,060	2,700
Low	1,210	820
Center	560	820

This amplifier had a gain, including loss in the second detector, of about 95 db which is quite close to the predicted gain, showing that the compromise was made with but little sacrifice.

An important acheivement in the use of single-tuned circuits is in the mechanical construction. No interstage shielding is required, and the layout is relatively clean and simple. Several types of tuning mechanisms have been used as shown in Fig. 5. Fig. 5A shows a coil used at 200 mc, the inductance variation being accomplished by spreading the turns of the beryllium copper spring coil. The rod diameter was ⅛ in. Figure 5B shows a conventional brass slug-tuned coil used at 160 mc, which tuned over about 30 mc. The important features of the mechanical construction of the amplifier are the extremely short lead lengths, no wiring being used, the components themselves providing connecting wires, and the care in selection of grounding points.

References

(1) Image rejection, as used in this paper, is the ratio of input to the receiver required to produce standard output with that input signal different from the receiver midfrequency by twice the intermediate frequency to that input required to produce the same output with the input signal at the receiver midfrequency. The image frequency is higher than the desired signal when the receiver local oscillator is lower than the received signal, and vice versa.

(2) Richards, P. I., Universal Optimum-Response Curves for Arbitrarily Coupled Resonators. *Proc. I.R.E.*, p 624, 34.

(3) Gain-bandwidth product is the product of center-frequency voltage amplification times the bandwidth between 3-db points. For a pentode with a single tuned coupling network, it can be shown that this product is $g_m/2\pi C_T$, where g_m is the tube's transconductance and C_T is the total capacitance across the tuned circuit; this ratio is independent of center frequency.

(4) Wallman, H., Stagger Tuned I-F Amplifiers, Radiation Laboratory, Mass. Inst. Tech., Report 524, Feb. 1944. Also R. F. Baum, Design of Broad-Band I-F Amplifiers, Jour Appl Phys, Part I, p 519, Part II, p 721, 17. Wallman's analysis leads to the formulas given in this paper as well as those for any bandwidth regardless of center frequency, and are extremely simple to use to obtain flat-topped response. Baum's paper describes an interesting approach which leads to useful results for the general case of n-circuits with a response curve exhibiting peaks and dips within the passband.

(5) Transitional coupling is defined as that coupling at which the first three derivatives of the transfer impedance are zero.

AGC-Noise Considerations in Receiver Design

Automatic gain control is considered for communications receiver service from the standpoint of its effect on signal-to-noise ratio at various signal voltages. The desirability of employing high gain in controlled stages and the limitations of such use are pointed out

By JOHN B. MOORE

AUTOMATIC control of the output volume of radio receivers is so universally employed that there is apt to be a tendency to simply incorporate it in any design as a matter of course. It is the purpose of this present treatment to point out and discuss some of the factors that are not always obvious but that are important where the best possible performance must be obtained, as in commercial communications service; also, to deal with certain compromises that often must be made.

The simplified diagram given in Fig. 1 is a generalized schematic arranged to show the functional sub-divisions of a complete receiver. Control of the output volume is obtained in this generalized receiver by means of a manual volume control in the a-f amplifier (for phone service) or in the tone keyer (for telegraph service). The output volume thereby can be adjusted independently of the gain of the r-f and i-f amplifiers. For this reason, which is important in many types of equipment for commercial service, the commonly-used term *automatic volume control* (avc) is not applicable. The preferable term, which will be employed in this discussion, is *automatic gain control* (agc).

Figure 2 gives a generalized schematic circuit of a three-stage r-f amplifier, with agc, such as might be used in the complete receiver of Fig. 1. A particular fea-

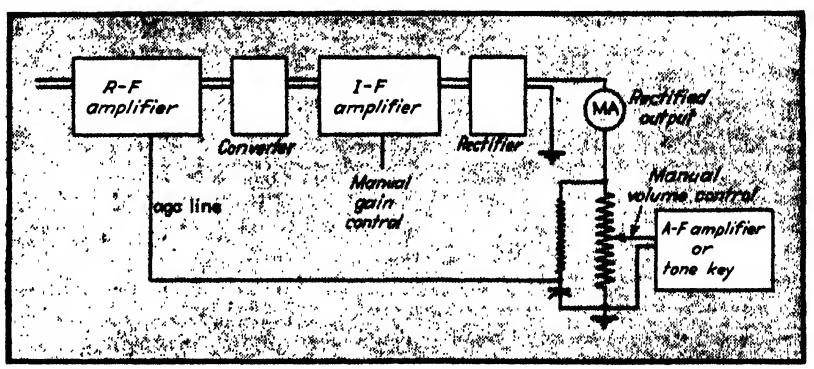

FIG. 1—Stages in a typical communications receiver having automatic gain control of the r-f amplifier

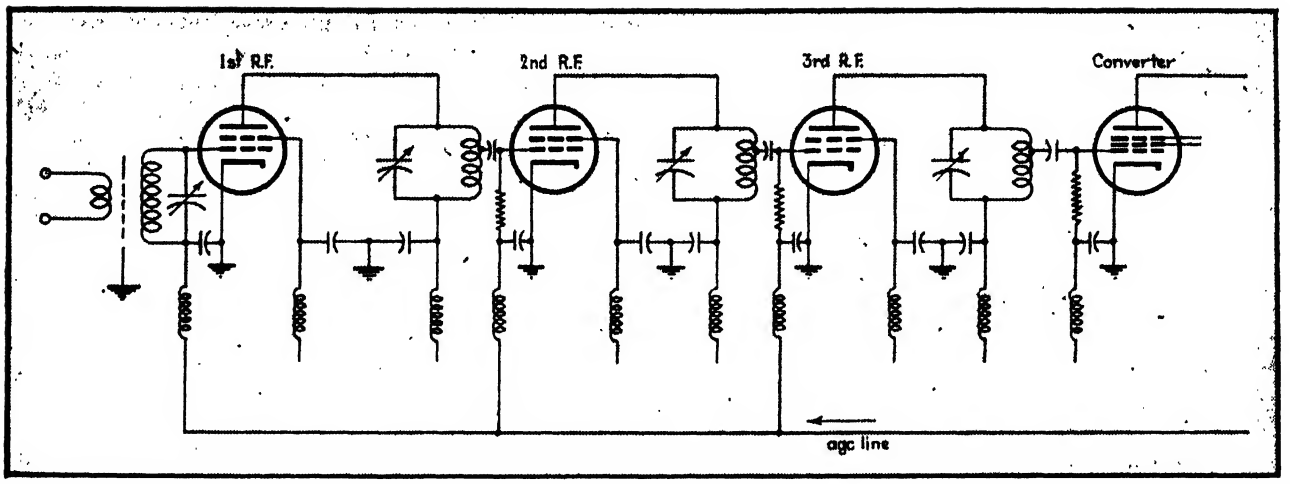

FIG. 2—Three-stage r-f amplifier and converter used for purposes of discussion by the author. Taps on the inductances permit adjustment for any desired value of gain without changing other operating conditions

ture to be noted in this circuit is the use of taps on the tuned-circuit inductances. The purpose of these is to make it possible to obtain any desired value of overall gain, up to the maximum, without the necessity for changing the tube voltages or operating points from their optimum values. Other features of the circuit are conventional, except perhaps for individual r-f filtering of the supply voltages to each tube. This latter is essential in any high-gain r-f amplifier operating at the higher frequencies.

Diode Output vs Carrier Amplitude

The usual criterion of agc action is the shape of the characteristic of rectified output vs r-f carrier input. Such a graph shows how nearly constant the output is maintained over the indicated range of r-f input voltage. For some purposes, this is sufficient. Such data do not, however, show what the signal-to-noise ratio in the output will be. For reasons which will be brought out in following paragraphs, this signal-to-noise performance may be quite different over a wide range of r-f input voltages than one would be led to expect from a statement of noise equivalent of the receiver.

In Fig. 3 are shown two typical graphs of output noise level, expressed in db below 100 percent modulation, plotted against r-f carrier input signal in microvolts. For the moment, let us consider only the general features of these two characteristic graphs.

Between the points indicated by *A-A'* and *B-B'*, the graphs are linear. A check of various points will show that the noise equivalent, in microvolts at the input of the receiver, is essentially constant over these linear portions of the graphs. For example, a noise level of 20 db below 100-percent modulation at a carrier input value of 2.6 microvolts (average) gives a noise equivalent of 0.26 microvolts at the receiver input. This method of expressing noise levels is convenient and useful because it provides a figure which can be compared directly with values of r-f signal input in microvolts.

The ideal condition is that one in which the noise equivalent, at the receiver input, is constant regardless of signal strength. Then, and then only, is the full benefit of increased signal strength realized. In the curves of Fig. 3, it will be observed that the characteristic does not continue linear at the higher

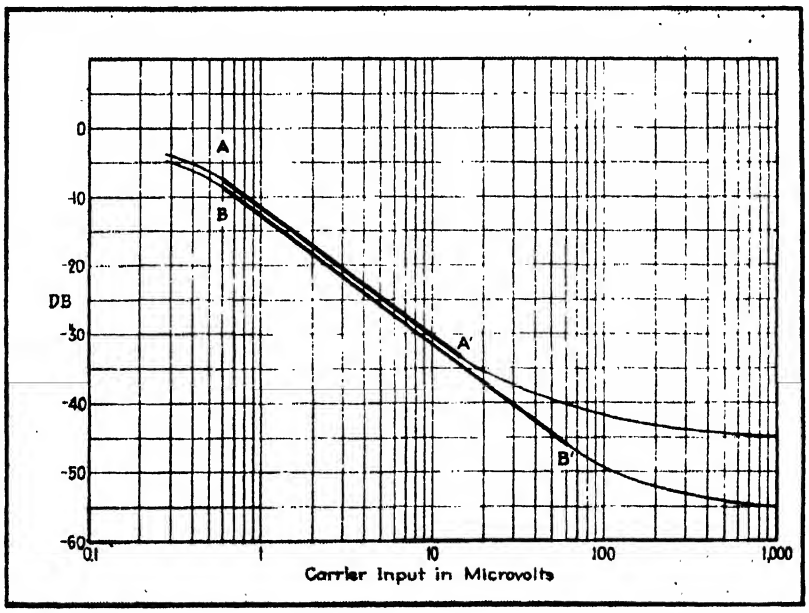

FIG. 3—Output noise level in db below 100-percent modulation, plotted against r-f carrier input signal in microvolts

values of input signal. Instead, each characteristic levels off. Increasing the signal input ten times, from 100 microvolts to 1,000 microvolts, does not produce a corresponding improvement in signal-to-noise output of the receiver. A further increase from 1,000 microvolts to 10,000 microvolts produces an even smaller improvement. As a practical matter, there is no object in having such characteristics continue linear down to extremely low levels in the design of radio receivers for general use. The level at which the characteristic will be permitted to flatten off is, therefore, determined by practical considerations of the performance required.

In order to compare different performance curves directly, some common base or starting point must be used when making the measurements. For the curves of Fig. 3, the starting point was a diode output of 0.1 ma for zero r-f input signal. The particular equipment used in the tests maintains a diode output of approximately 0.6 ma at normal operating values of signal strength. In other equipment, a similar ratio between normal output and starting-point output of the diode could be used. Adjustment to the desired value of rectified output for zero r-f signal input is obtained by means of the manual gain control associated with the i-f system as shown in Fig. 1.

The flattening-off level, for such curves as those of Fig. 3, is determined by the amount of r-f gain employed between a given input stage and a given converter (Fig. 1). Three stages are shown to give the required r-f selectivity and also the desired agc action as judged by constancy of output over a wide range of r-f signal input. The overall gain is fixed at a desirable value by proper choice of the positions of the taps on the coils of the tuned circuits. This permits obtaining the desired reduction of maximum gain without changing tube voltages and operating points and thereby sacrificing agc performance.

To explain the foregoing, let us assume some values of noise equivalent and of gain. The noise equivalent at the input of the receiver may be taken as 0.3 microvolt; and that at the grid of the converter as 3 microvolts. Assume a value of r-f gain, from receiver input to converter grid, of 1000/1 with agc acting and an input of 1 microvolt. This point is chosen from Fig. 3 as one which is near the start of the linear portion of both characteristic curves.

Converter Noise

The values of amplified signal and noise appearing at the converter grid for different values of r-f input are given in the accompanying table. These are based on the somewhat idealized assumption that the agc action holds an absolutely constant output and therefore a constant signal level at the grid of the r-f converter. The assumption also is made, for the purpose of this simplified illustration, that the second and third stages contribute no appreciable portion of the noise. For purposes of illustration, these assumptions are justifiable; the errors involved being too small to appreciably affect the validity of the illustration.

The tabulated figures show that at low levels of input signal the final signal-to-noise ratio in the output of the receiver is determined by the signal-to-noise ratio existing at the input of the receiver. As the signal input is increased, and the agc action comes into play, the amplified noise appearing at the converter grid becomes less in magnitude compared to the noise equivalent of the converter itself. The result is that, at the higher levels of signal, the signal-to-noise ratio of the output of the receiver is determined not by that existing at the input but rather by the noise equivalent of the converter. The agc-characteristic of signal-to-noise vs r-f input therefore flattens off as shown in Fig. 3.

In the lower portion of the table, the r-f gain is assumed to be 100 instead of 1000. This lower value of r-f gain results in poorer signal-to-noise ratios at the higher values of signal input. The curve for this case therefore would flatten off at a considerably higher level of noise. This is illustrated by the two curves of Fig. 3, which are plotted from actual data rather than from the assumed data tabulated in the table for purposes of simplified explanation.

Use of High Gain

The foregoing discussion indicates the desirability of employing high gain in the r-f amplifier to which agc is applied. There are certain limitations, though, to the amount of gain that can be safely used. One is stability, or freedom from self-oscillation, at all frequencies. A second is protection of the r-f converter tube from being overloaded by stronger signals on channels adjacent to the desired signal.

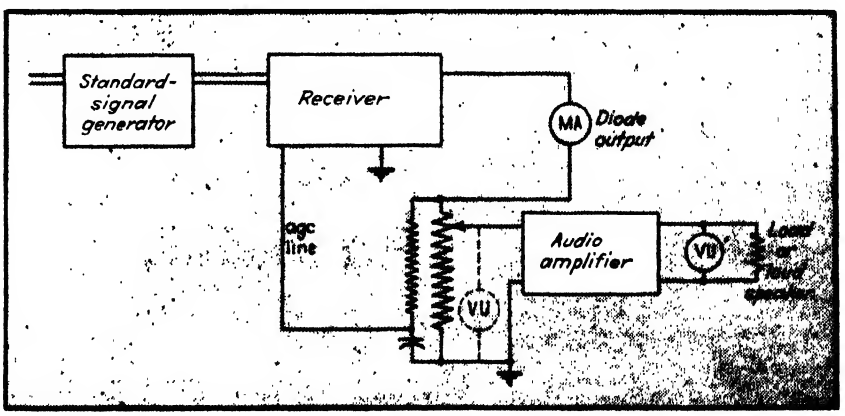

Arrangement of equipment used to determine the output current of a diode at various carrier signal levels

If the r-f gain and the agc hold the desired signal at 10,000 microvolts at the grid of the converter, and a signal 100 times as strong as the desired one is received on an adjacent channel, the interfering signal will have a voltage of about one volt at the grid of the converter. This is apt to produce serious overloading and interference.

In actual use of a receiver such as depicted in Fig. 1 and having agc-noise characteristics as shown in Fig. 3, it is customary to manually readjust the i-f gain in order to obtain optimum performance on very weak and also on very strong signals. In this way the agc-noise characteristic may be shifted from its positions shown on Fig. 3 to best handle existing conditions and ranges of signal strength, noise, and interference. Obviously, the design of the agc system should be such as to cover the greatest possible range of input signal without the need for manual re-adjustment of the i-f gain.

The final design generally must be a compromise between the various factors discussed; the exact compromise being determined by the performance required and the conditions under which the equipment will be used.

Table of Output Signal-to-Noise Ratios with Various Input Conditions

Input Signal, μv	R-F Gain	At Conv. Grid. Signal, μv	At Conv. Grid. Noise, μv	Converter Noise Equiv., μv	Converter Total Noise, μv	Signal Noise Ratio
1	1000	1000	300	3	300	3.3
10	100	1000	30	3	30	33.3
100	10	1000	3	3	4.2	238
1,000	1	1000	0.3	3	3	333
10,000	0.1	1000	0.03	3	3	333
1	100	100	30	3	30	3.3
10	10	100	3	3	4.2	23.8
100	1	100	0.3	3	3	33.3
1,000	0.1	100	0.03	3	3	33.3
10,000	0.01	100	0.003	5	3	33.3

Noise and Output Limiters

Comprehensive survey of instantaneous noise-peak and output limiters for a-m communications receivers, with representative values of components, analysis of operation, and conclusions as to usefulness.

By EMERICK TOTH

LIMITERS, as the name implies, are restrictive devices. The limiter circuits discussed in this report are curative means designed to mitigate the effects of undesired electrical disturbances of an impulse nature, such as static, ignition noise, and radar signals, on the output of radio receivers designed particularly for amplitude-modulated communications use.

Preventive means operating directly in the antenna circuit have not as yet been developed with any considerable degree of success. The circuits described below center at or near the final detector in a receiver, and the best of them, when properly designed and operated, can provide very considerable assistance in reception through many forms of noise.

Limiters are divided into three groups: (1) instantaneous noise-peak limiters, whose primary usefulness is in modulated-wave (mcw) reception such as speech and music; (2) output limiters, useful mainly for continuous-wave (c-w) reception, such as telegraph signals; (3) circuits not falling directly into the first two groups.

Limiters of this general group are actually operative only when the instantaneous value of the carrier exceeds some reference level, which may be a d-c bias voltage controlled from the front panel of the receiver or, better, the average value of the rectified carrier itself as it appears across the final detector load.

Essentially, an instantaneous noise-peak limiter usually involves two circuits, one having a time-constant corresponding to the usual detector load circuit, and the other having a much longer time-constant. The time-constant differential of these two circuits is responsible in large part for the successful operation of the limiter.

Most of the instantaneous limiters to be described are half-wave devices and operate on the modulation envelope resulting from recti-

fication of the positive half-cycles of r-f input to the detector. The usual form of half-wave diode detector does not respond substantially to the negative half-cycles of signal, and therefore suppresses also the negative half-cycle of r-f noise peak where it exceeds the equivalent of 100 percent modulation of the desired carrier. Full-wave limiters generally do not provide a substantial improvement when applied to such detector circuits on mcw operation, unless considerable clipping of the desired modulation is tolerable.

Series Noise-Peak Limiters

The most useful and successful of the instantaneous group are series noise-peak limiters. In contrast to others of this group, which have not been very effective on the longer wave-trains resulting from impulse excitation in receivers operating below about 10 mc, series-type limiters have been highly effective in receivers covering the signal range from 15 kc to over 400 mc. They also satisfy one general requirement for limiters intended for mcw use by not causing a degree of distortion which would affect the intelligibility of voice signals or seriously impair the quality of music, when the usual average values of carrier modulation are employed at the transmitters.

In addition, series limiters require very few components over those normally found in the usual half-wave diode detector, and are easily adaptable to automatic threshold biasing by the rectified voltage of such a detector. These limiters have also been found useful for c-w reception if care is taken to provide the proper value of beating or heterodyne voltage at the final detector.

Simple Series Limiter

Figure 1 shows the simplest form of series limiter, widely used in Navy shipboard receivers. It requires only one fixed capacitor, two fixed resistors, and an independent diode in addition to the normal components of a diode second detector. No front-panel control of threshold for varying carrier levels is required, threshold bias being automatic in the sense that it is directly derived from the rectified carrier. Its operation can be briefly described as follows:

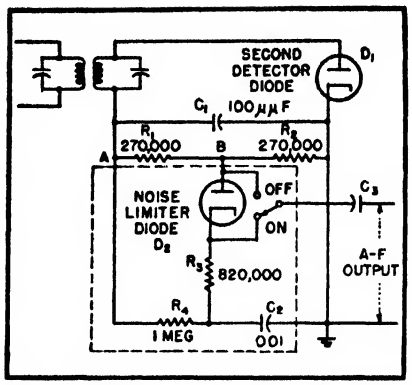

FIG. 1—Simple series limiter, requiring only the four additional components inside the dash-dash rectangle

Assume a rectified d-c potential of 10 volts developed across R_1 and R_2 in Fig. 1 by a constant carrier. The cathode of the limiter diode is then initially at about −10 volts with respect to ground because of its connection to point A through R_3 and R_4, while the limiter plate is at about −5 volts to ground. The plate is thus momentarily 5 volts positive with respect to the cathode and the limiter diode becomes conductive, its resistance being fairly low compared to the other resistance values in the circuit. Output capacitor C_3 is thereby connected through the conductive diode to junction B, so that a constant modulated r-f carrier input provides a-f output. This output is about 45 percent of what it could be without the limiter, but generally this reduction is of little significance since it usually affects only the reserve gain and not the sensitivity of the receiver.

Under the above conditions, capacitor C_3 is charged through 1-megohm resistor R_4 to a potential of about −7 volts. Any appreciable change in this potential would require about 0.01 second, due to the time-constant of R_4C_2. The time-constant of $(R_1 + R_2)C_1$ is, however, only about 50 microseconds, so that the potential at the limiter diode plate can change in about 1/200th of the time required for its cathode to assume a new potential. Therefore, if a noise potential of perhaps 100 volts suddenly appears across $R_1 + R_2$ and brings the plate of the limiter diode to −50 volts from ground potential, the diode plate becomes about 43 volts more negative than its cathode and the diode stops conducting. This in effect disconnects output capacitor C_3 from point B, and the a-f amplifier has no appreciable input for the duration of the noise modulation. By the time that the cathode of the limiter diode has assumed an effectively more negative potential, the noise pulse will usually have decayed and the limiter diode will have become conductive again, restoring the a-f input to the audio amplifier.

With this limiter, appreciable distortion can be seen on an oscilloscope only above approximately 40 percent modulation. In listening tests involving both speech and music, most personnel have found it extremely difficult to detect distortion by ear on transmission maintaining an average modulation level of between 30 and 40 percent, a condition commonly encountered. With the circuit constants shown in Fig. 1, the time-constant of recovery from surge input is very satisfactory, an

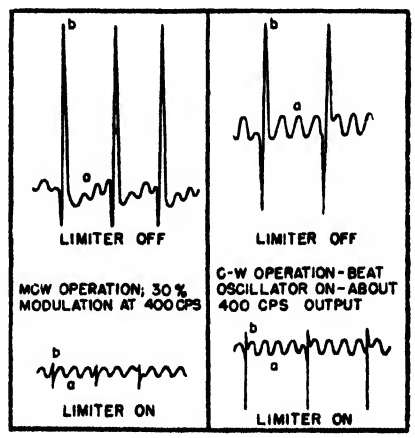

FIG. 2—Oscilloscope tracings of audio output of receiver, illustrating noise suppression of simple series limiter. Signal input to receiver is 80 microvolts, and avc is off

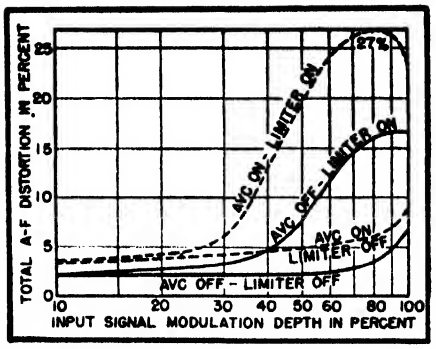

FIG. 3—Modulation distortion curves as measured at output of typical communications receiver using simple series limiter. The avc-off curves are substantially the same as for weak-signal avc-on operation. Signal input frequency is 4,000 kc, a-f output frequency is 1,000 cycles, and signal input level is 1,000 microvolts

item of importance, especially in shipboard receivers.

It should be noted that the modulation threshold value given above applies to distortion of only that half of the audio envelope appearing across the detector load which corresponds to increasing rectified current, the other half-cycle being unaffected with a half-wave limiter. This is likewise true of most of the limiters described below.

Oscilloscope tracings illustrating the operation of the simple series limiter on both mcw and c-w signals in a typical receiver appear in Fig. 2. On c-w, the beat oscillator acts to produce operation of the limiter similar to that with a very low percentage of desired signal modulation at the detector.

Modulation distortion under various conditions of mcw operation is indicated by the curves in Fig. 3. The change in threshold of limiter action between weak and strong signals is particularly evident.

Operation of the series limiter on c-w reception may be improved by the incorporation of some additional degree of r-f limiting in the i-f (or r-f) amplifier immediately preceding the final detector. This can take the form of an added grid leak and capacitor between the control grid and the i-f transformer of this amplifier stage. The resultant better i-f limiting will allow the use of a lower beat oscillator injection voltage to the detector without abrogating resonant overload performance, a condition favoring good operation of the limiter following the detector.

Series-Type Noise Limiter With Threshold Adjustment

With a potentiometer substituted for fixed resistor R_1 in the circuit of Fig. 1, the limiter threshold can be varied from about 65 percent modulation down to substantially zero percent (on half the modulation cycle). This control varies the d-c bias due to the rectified carrier at the cathode of the limiter diode, which bias determines the limiting threshold.

The modified circuit, shown in Fig. 4, may also include an additional diode. This is shunted

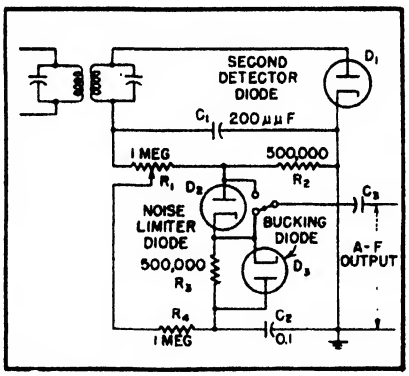

FIG. 4—Series-type noise limiter with threshold adjustment so that limiter operation can be set to start anywhere in range from 0 to 65 percent modulation

across resistor R_3 to buck the internal (thermionic) potential of the limiter diode, as this residual voltage reduces the effectiveness of the limiter at low carrier levels by raising the limiting threshold in terms of modulation percentage. The voltage built up across R_3 due to rectified direct current from the detector will, together with the time-constant of C_3 and the grid resistor in the first a-f stage, tend to maintain this additional diode biased to cutoff, except on weak signals. The price paid for this improvement in weak-signal limiting, however, is generally a considerable increase in audio distortion at all useful levels. Making the time-constant of C_3 and the audio amplifier grid leak equal to that of R_4C_2 will assist in keeping this increase in distortion to a minimum.

Low-Loss Series-Type Noise Limiter

The reversal of cathode and plate connections of the limiter diode in the variation of the series-type limiter shown in Fig. 5 necessitates the use of two more resistors and a capacitor (over those required by the simplest form) to provide the required biasing and *RC* delay circuits for the diode elements. It has, however, the advantage of providing the a-f amplifier with a higher percentage of the a-f voltage appearing across the detector diode load, as contrasted with the circuit of Fig. 1. For a comparable degree of modulation distortion, this improved transfer of a-f voltage will amount to about 2 or 3 db, which is usually not of great importance unless the receiver is deficient in reserve gain.

The cathode of limiter diode D_2 is biased negative relative to its plate by connection to the junction of detector-load resistors R_2 and R_3 through resistors R_4 and R_5. R_4C_2 provides a long time-constant circuit similar to R_4C_3 in Fig. 1 while R_5 serves as the cathode load resistor across which the limiter output voltage is developed in a manner similar to R_3 in Fig. 1. Capacitor C_3 provides a-f coupling to the plate of D_2 for the detector audio output voltage appearing between the junction of R_1 and R_5 and

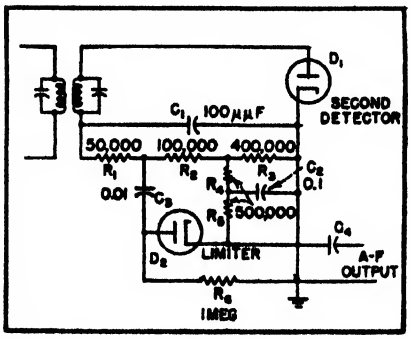

FIG. 5—Low-loss series limiter, requiring three more components than the simplest version in Fig. 1

ground. Resistor R_1 serves only as an r-f filter element. The action of this circuit in limiting peaks of noise or other modulation is identical to the circuit shown in Fig. 1, the plate of D_2 being free to follow variations in detector a-f output voltage, while the cathode circuit is held by the longer time constant of R_4C_2.

Hum is one of the serious difficulties in any system wherein audio signals are taken from a relatively high value of resistance load located in the cathode circuit of an a-c heated vacuum tube. The heater-cathode capacitance of the most widely used receiver tubes will be on the order of 5 to 10 $\mu\mu$f, which at 60 cps presents a capacitive reactance of 250 to 500 megohms. With a resistive load between cathode and ground of perhaps 0.5 megohm, about 0.1 percent of the heater-to-ground potential will appear across the cathode resistor. This would be about 6 millivolts with a 6.3-volt heater.

When using the simple series limiter circuit of Fig. 1 with a 6H6 duodiode, the hum voltage appearing across R_3 may be approximately halved by grounding that end of the heater which is closer to the cathode element used for the limiter diode, since in the 6H6 the individual diode heater windings are in series. With even fairly high-gain a-f amplifiers, however, the hum will usually be troublesome even though this precaution is taken.

The circuit arrangement in Fig. 6 has been found highly satisfactory for further reducing hum from the series limiter. The reduction obtained will generally be on the order of 20 db with normal commercial variations in tubes and other components. The cathode resistor of the a-f amplifier following the limiter will not be bypassed to ground, resulting in some decrease in the gain otherwise obtained from this audio stage, due to degeneration. Two additional capacitors and a resistor are required over those needed for a normal a-f amplifier input system with unbypassed cathode.

The equivalent circuit is that of

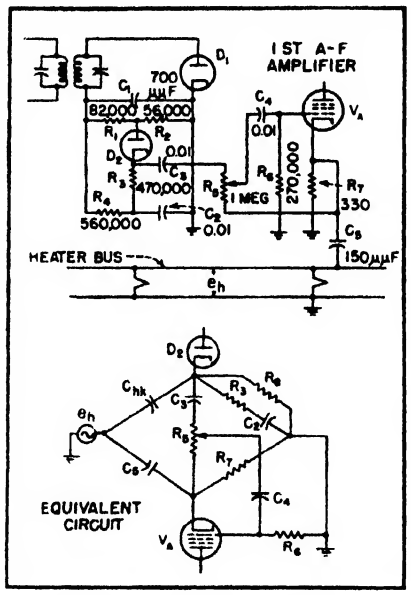

FIG. 6—Hum-reduction version of simple series limiter, with equivalent circuit arranged to show bridge configuration

a bridge, with e_h as the limiter diode heater voltage (normally grounded on one side in most receivers) and C_{hk} as the heater-cathode capacitance. R_3 and C_2 form another arm of the bridge and are shunted by the equivalent resistance R_e, which is a composite of R_1, R_2, R_4, the effective resistance of D_1, etc. R_7 is the cathode bias resistor for a-f amplifier tube V_A. The bridge configuration is completed by capacitor C_b, which is connected between the ungrounded side of the heater supply and the cathode of V_A. Fortunately, the value of C_b with the usual limiter circuit values is quite low; in the circuit shown it is only 150 $\mu\mu$f. It should be noted that this hum-bridge scheme allows normal location and operation of the a-f gain control R_6, even to the extent that despite unbypassed cathode resistor R_7, the gain control can reduce the input to V_A substantially to zero, since its low end returns to the cathode of V_A. It should also be noted that, if a LIMITER ON-OFF switch is used, two different values of C_b will be required, due to slight changes in bridge configuration when switching from the cathode to the plate of the limiter diode.

The circuit of Fig. 7 functions as a balanced bridge arrangement for detector voltages above the limiting threshold, with unbalance being maintained at all other times. It must be adjusted manually for each carrier level, but automatic operation can be achieved by adding another diode, as in Fig. 8.

When the contact arm of R_6 in Fig. 7 is at the grounded end of R_6 and R_1 is set equal to R_3 (47,000 ohms), R_1, R_2, R_3, and R_4 form a balanced resistance-bridge circuit which is fed from the i-f output through the second detector and noise limiter diodes. If both diodes rectify in phase and their loads are equal, the a-f output across R_6 is essentially zero. When the limiter diode is made inoperative by adjusting R_6 to bias its cathode with a positive d-c voltage, the bridge becomes unbalanced and a-f output is obtained when a constant modulated carrier input is present. If, now, a noise peak arrives that exceeds the limiter diode bias, the bridge will be rebalanced and substantially no a-f output will be obtained for that part of the noise peak during which it exceeds the diode bias voltage.

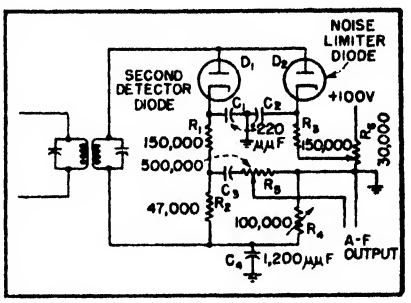

FIG. 7—Balanced-detector noise limiter

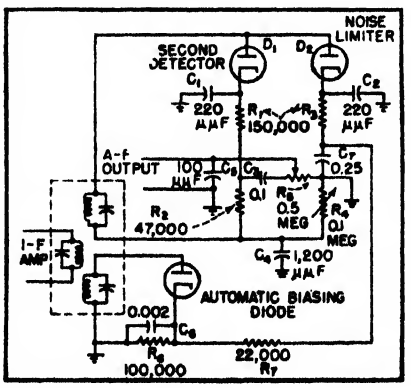

FIG. 8—Automatic balanced-detector noise limiter

The limiter normally is initially balanced by adjusting R_4, and is thereafter adjusted for each carrier level and desired modulation threshold only by means of front-panel control R_4. Adjustment of R_4, however, disturbs the balance of the bridge by varying the resistance of one arm, hence it may be desirable to gang a variable resistor with R_4 so as to hold its equivalent resistance constant. For most effective operation, the time-constant of $(R_1 + R_2)C_1$ should equal that of $(R_4 + R_1)C_2$ for all settings of R_4, and the capacitances of the two diodes should be equal.

During tests at U. S. broadcast frequencies, no improvement in receiver performance was discernible with this limiter, improvement becoming noticeable only above about 10 mc and only on ignition-pulse types of interference. The need for adjusting to changing carrier values makes this circuit practically useless on fading signals, unless limiter control settings such as would cause serious distortion are tolerable. No appreciable limiting was obtained on c-w reception employing a beat oscillator.

Automatic Balanced-Detector Noise Limiter

By adding another diode circuit to the arrangement of Fig. 7, automatic operation is obtained, eliminating adjustment of a balancing potentiometer with each change in carrier level. The additional diode is operated from a tertiary winding on the final i-f transformer, as shown in Fig. 8. This diode rectifies the i-f carrier to provide a d-c bias of about twice the mean rectified voltage furnished by the detector diode, so that limiting does not take place on modulation depths below about 100 percent. The bias voltage is applied to R_3 at the point where R_4 (Fig. 7) introduces the bias in the manually controlled circuit. The cathode delay bias on the noise limiter diode is thus maintained automatically at a substantially constant ratio with respect to the carrier input. The depth of modulation at which audio distortion begins is

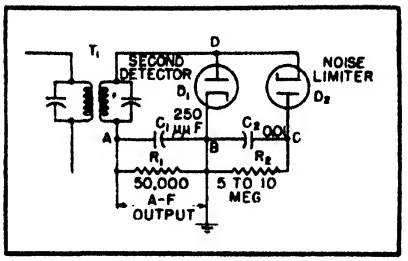

FIG. 9—Balancing-type noise limiter

mainly determined by the ratio of the rectified voltage supplied by the automatic biasing diode to that supplied by the detector diode. The limitations in performance of this circuit, however, are otherwise similar to those applying to Fig. 7.

Balancing-Type Noise Limiter

The balancing (or bucking) effect of a diode shunted across the second detector with reversed polarity is used in the circuit of Fig. 9. When the limiting threshold is passed, as on noise peaks, the variations in limiter diode current oppose the normal demodulation current in the second detector.

Assume that an unmodulated carrier produces a rectified potential of 10 volts across second detector diode load R_1, making point A 10 volts negative with respect to ground. Then, on positive peaks of carrier input, point D will be close to ground potential, because point A remains relatively constant over an r-f cycle and the 10-volt positive r-f peak across the i-f transformer secondary acts to cancel the negative 10 volts at A. On negative peaks, point D will therefore be about −20 volts with respect to ground.

The voltage impressed across the noise limiter diode in series with R_2 will then vary between substantially zero and −20 volts at an r-f rate. This builds up a potential of about −20 volts across capacitor C_3, thereby biasing the limiter diode plate 20 volts negative with respect to ground. The net effect is that the second detector diode is shunted by a high impedance, between about 2.5 to 5 megohms for the value of R_2 shown, until such a time as the i-f input voltage increases substantially above the 10-volt value, as on a noise peak or with modulation of the carrier. When this occurs, the limiter diode becomes conductive for all portions of the modulated wave having an instantaneous value in excess of 10 volts negative. It should be noted that the audio voltage appearing across R_1C_1 is added to the instantaneous negative voltage peaks appearing across the secondary of T_1, in addition to the mean value of rectified carrier voltage across R_1. Since the time-constant of R_2C_2 is long, about 0.05 to 0.1 second, C_2 will serve mainly as a coupling capacitance to R_1 as regards a-f variations. These variations, being of opposite polarity to those across R_1, will tend to cancel the latter on half the audio cycle. The magnitude of the cancellation effect will depend on the impedance of the limiter diode when conducting, which in turn will depend on the values of the impressed voltages and R_2, so that better cancellation will in general be obtained as R_2 approaches R_1 in value. This would necessitate increase of C_2 to a large value to maintain the time-constant of R_2C_2 at the desired magnitude, and would increase the a-c loading across R_1 as regards audio output, seriously affecting modulation distortion except with the limiter disabled.

The modulation distortion of this type of limiter is quite high, even on relatively low modulation depths, with effective limiting of noise peaks. Although the distortion can be reduced by various expedients, perhaps the most attractive feature of the circuit is its ability to provide about twice the normally obtainable avc voltage when the d-c potential across R_2 is utilized.

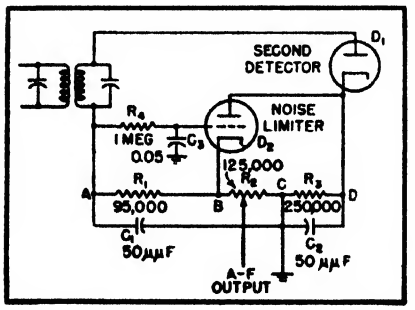

FIG. 10—Triode shunt-type noise limiter

The circuit of Fig. 10 employs the plate resistance of a triode shunted across a portion of the second detector diode load, the magnitude of the shunt resistance being controlled by the grid and plate voltages, which act in conjunction with differential time-constants.

Assuming a carrier input that produces a total rectified voltage of 10 volts across the diode load (between A and D), potentials relative to the second detector cathode will be -10 volts for A, about -8 volts for B, and about -5.8 volts for C. The triode plate is thus 8 volts positive with respect to its cathode, while its control grid (connected to A through R_4) is 2 volts negative. For a triode with a μ of 20, this produces plate current cutoff, so that the triode plate resistance is high and has little shunting effect on second detector load resistor R_1 and R_2. Now if a 100-volt noise pulse suddenly appears between points A and D, the triode plate-cathode voltage rises to 80 volts relatively long before the grid potential can change, since the plate circuit time-constant is about 12 microseconds while that of the grid circuit is about 50 milliseconds. The triode then becomes conductive and shunts section B-D of the detector load for the duration of the noise pulse, thereby reducing the audio output from the detector. The noise disturbance should subside before the control grid swings sufficiently negative to stop this limiting action.

The percentage of modulation at which audio distortion due to the limiter appears depends upon the type of triode used, the relative values of R_1, R_2, and R_3, the time-constants involved, and the absolute carrier level. The higher carrier levels produce no distortion (and no limiting). Serious distortion, however, has been observed for modulation as low as 10 percent with low signal levels. Effective limiting action is restricted to a narrow range of carrier input levels, generally being evident above 10 mc in carrier frequency.

In Fig. 11 is shown the simplest limiter of them all, requiring only

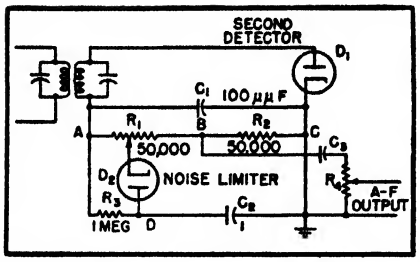

FIG. 11—Diode shunt-type noise limiter

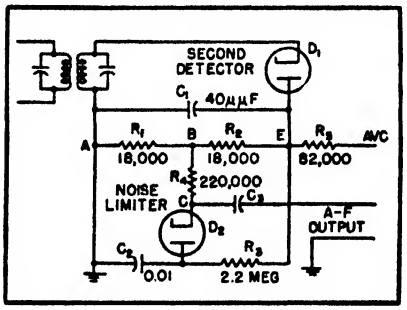

FIG. 12—Modified shunt noise limiter

an additional resistor and a capacitor, along with an independent diode.

Here R_1 and R_2, bypassed by C_1, provide a detector diode load with a time-constant of about 10 microseconds, to which is connected the cathode of the noise limiter diode. The limiter plate circuit time-constant is 1 second, so that the limiter diode conducts and shunts the detector diode load on noise (and modulation) peaks. During such peaks, the a-f output of the detector is reduced by an amount which depends on the value of R_2 plus the portion of R_1 between point A and the limiter cathode, the position of the variable contact on R_1, and the noise peak voltage. The depth of modulation above which distortion begins is determined by the relative values of R_1 and R_2 and by the setting of R_1. The performance of this limiter was not very good, some improvement being evident on pulse-type interference on signals above 10 mc. The shunting effect of the limiter diode is appreciable only when the variable contact on R_1 approaches point B.

Modified Shunt-Type Noise Limiter

The limiter circuit in Fig. 12 resembles the series-type limiter of Fig. 1 except that the plate of the limiter diode and the low end of its cathode resistor are interchanged. As a result, the limiter diode acts to shunt C, thereby reducing the a-f output voltage whenever a noise-peak makes the diode conductive. The arrangement shown permits grounding the low end of the i-f transformer secondary when desirable for stability reasons.

Assume a constant carrier making point E on the detector diode load 10 volts negative with respect to A (ground). Points B and C are then both -5 volts to ground because the limiter diode is nonconducting, its plate being effectively at the -10 volt potential of E. The plate circuit time-constant is much longer than that of the cathode circuit of the limiter, so that any noise surge in excess of 20 volts across

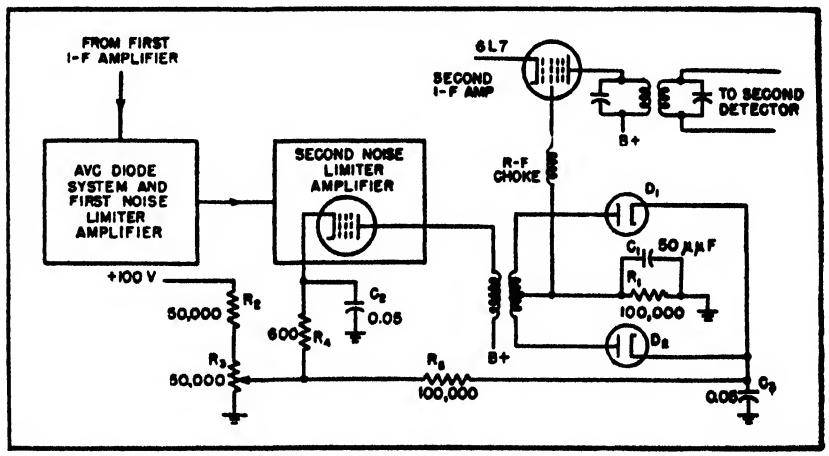

FIG. 13—Degenerative noise limiter, acting between first and second i-f stages

the entire detector load drives the cathode of the limiter diode more than 10 volts negative with respect to ground and the diode conducts, shunting the input to the following a-f stage. This shunting action is made more effective by series cathode resistor R_4, which with the limiter diode closed acts as part of a voltage divider to attenuate detector-load voltage peaks. Limiting action ceases when C becomes positive with respect to D due either to decay of the noise pulse or to charging up of C_2. The limiter will begin to cause audio distortion at about 100-percent modulation for the values shown. If R_2 equals 0.4 R_1, distortion will begin at about 40 percent modulation and a greater percentage of the a-f output developed across the detector load will be available to the following a-f amplifier. This limiter has been found to be much more effective than the simple shunt limiter, although not as good as the simple series-type limiter at the lower carrier frequencies.

Degenerative Noise Limiter

Degenerative feed to the i-f amplifier prior to final detection is used in the circuit of Fig. 13. A portion of the output from the first i-f amplifier is amplified in the first and second noise limiter amplifiers, and the resulting i-f output is coupled into a full-wave rectifier having R_1 as a load. The d-c voltage developed across R_1 provides the bias for the injector grid of a 6L7 pentode serving as the final i-f amplifier tube. Front-panel control R_4 provides a positive delay voltage for the diode cathodes, to prevent rectification until signal or noise peaks exceed this bias. Since the time-constant of the diode load is only 5 microseconds, the d-c potential across R_1 can fluctuate at a rate of up to about 200 kc.

If the normal carrier peak impressed across the diodes is 10 volts and the delay bias is 5 volts, the diodes do not rectify (since each gets only half the applied voltage) and the 6L7 injector grid then has substantially no bias relative to ground. Now if a 100-volt noise peak appears across the secondary of the diode transformer, the delay bias on each diode is exceeded by 45 volts and a negative potential of about 45 volts is therefore applied to the 6L7 injector grid. If this change in injector grid potential occurs simultaneously and in opposition to the change in the control grid potential of the 6L7 due to the same noise pulse and at the same rate, the effects of the noise pulse on the second detector can be reduced considerably by the resulting bucking action. Ideal phase and amplitude balance usually are, however, difficult to achieve, due in large part to the many circuits involved in the noise limiter amplifier and rectifier channel.

This limiter requires manual adjustment of the threshold of operation and is useless on fading signals. Circuits may be added to provide automatic biasing from an additional avc system, resulting, however, in almost prohibitive complexity. One version of this latter form has been found to be almost as effective as the simple series limiter at the higher signal frequencies. Modulation distortion is determined by the delay bias obtained from R_2 or by the accessory avc bias in the automatic form.

The a-f output limiters differ from the instantaneous noise-peak limiters primarily in that they simply present a continuous limit on the maximum power output from one or more amplifiers at some predetermined level. They are, in general, difficult to bias automatically to provide limiting at a desired depth of modulation of the carrier independent of the absolute carrier value, and are therefore mainly useful on c-w (telegraph) operation.

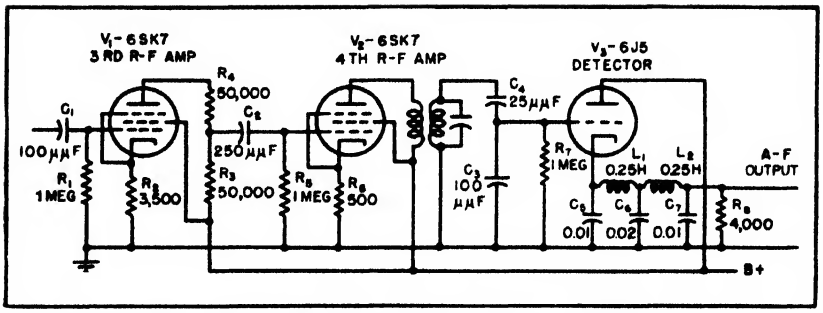

FIG. 14—R-f output limiter depending on plate current saturation in the last two r-f stages, with low-pass filter following the detector to further improve the signal-to-noise ratio of the receiver

R-F Output Limiter

R-f output limiting (with incidental r-f noise limiting) is quite satisfactorily achieved with the simple circuit arrangement of Fig. 14, which depends on vacuum-tube plate current saturation and control grid cutoff, with maintenance of a high input impedance in the control grid circuits of the saturated tubes. The third and fourth r-f amplifier stages are used as saturation limiters by operating with about 45 volts applied to both screen and plate circuits. The two stages combined provide the equivalent gain of one r-f amplifier stage at a much lower limiting level than is feasible with one stage alone, by virtue of r-f voltage dividers R_5-R_4 and C_5-C_6. The single tuned circuit following the fourth stage filters out r-f distortion caused by the preceding limiter circuits and provides further selectivity, while the low-pass filter following the detector further purifies the audio output and improves signal-to-noise ratio.

The initial a-c input resistance of the third r-f amplifier tube is about one megohm, until the applied signal voltage exceeds the negative bias supplied by the voltage drop across cathode resistor R_5 to the control grid, when it drops to about one-half megohm because the grid becomes, in effect, a diode rectifier conductive for that portion of the

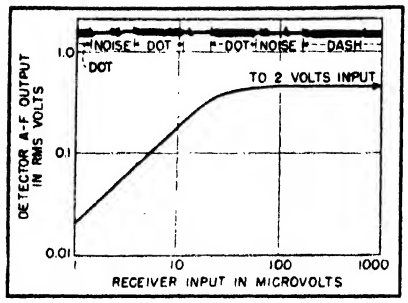

FIG. 15—Resonant overload characteristics of receiver using r-f output limiter for long-wave c-w reception, and oscillogram of letter V as received from an overseas transmitter in presence of 12-volt noise peaks. Input signal frequency is 16 kc, unmodulated; beat oscillator is on; a-f output frequency is 1,000 cycles. Distortion figures for detector output are 0.7 and 0.1 percent respectively for 2nd and 3rd harmonics with receiver input of 10 microvolts, and 2.9 and 0.9 percent for 500,000-microvolt input

positive half-cycle during which the signal exceeds the grid bias.

The negative bias thus developed across grid leak R_1 by grid rectification is applied to the control grid to limit the increase in space current. During a noise peak, then, the effective positive instantaneous voltage on the grid is the difference between the rectified voltage across R_1 (maintained by charging C_1) and the positive half-cycle voltage of the noise peak, with limiting effects in the plate circuit due to plate saturation.

On the negative half-cycle of r-f input, grid cutoff limits the change in plate current of the tube. The phase shift from grid to plate circuit results in the positive noise peaks applied to the grid of the third r-f amplifier tube appearing as modified negative peaks at the grid of the fourth r-f amplifier, where they are further limited by grid cutoff, the positive peaks at this point being also limited in the fourth amplifier plate circuit by saturation effects. The combined effect of the two limiter tubes thus is to limit both peaks of applied r-f voltage, whether due to signals or noise peaks.

Conventional bypass capacitors and screen filters are not shown in the circuit diagram but are actually used in the circuits themselves. The detector, an infinite-impedance or cathode-follower type, is used primarily for its low output impedance, and does not provide any desired limiting action. This saturation-type limiter is useful chiefly for c-w reception at very low carrier frequencies, though with a suitable saturation limit and an exceptionally good avc system controlling the preceding r-f gain to just below limiting level on the desired signal, distortion on mcw reception can be kept low over a considerable range of carrier input values.

Use is made in f-m receivers of similar limiting in the i-f system, except in those having limiting discriminators of the ratio type. Such i-f limiters usually do not, however,

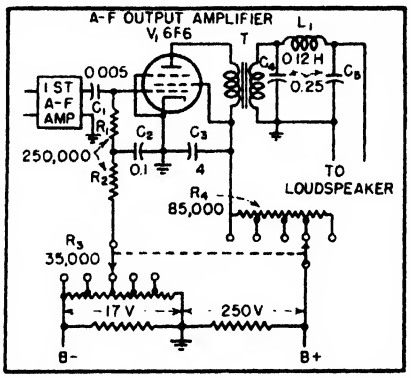

FIG. 16—A-f saturation-type output limiter

utilize voltage dividers. They are designed for higher limiting levels than the circuit of Fig. 14, and operate to reduce amplitude variations of the f-m carrier appearing at the discriminator to the greatest practicable extent. The avc voltage may be taken from the final limiter grid resistor, or the preceding one if there is more than one limiter stage.

Figure 15 shows the resonant overload and distortion characteristics of a receiver utilizing this type of limiter and oscillogram of the letter V as received at 16 kc from an overseas transmitter in the presence of 12-volt noise peaks.

A-F Saturation-Type Output Limiter

Control of the saturation level of the a-f output pentode tube at various screen, plate, and control grid voltages provides audio output limiting action without use of additional tube circuits (Fig. 16). A low-pass filter ($L_1 C_4 C_5$) filters out distortion produced in the output stage; its cutoff frequency is 1,200 cps, and hence for a 1,000-cps tone signal the harmonics will be filtered out to a considerable degree.

The control grid, screen, and plate voltages in this limiter are varied by a double-pole switch that contacts taps on resistors R_3 and R_4. The voltages thus obtained maintain the gain below saturation fairly constant for all switch settings, while at the same time permitting control of the limiting level. This circuit is useful for c-w reception only. Below limiting threshold, there is a change in gain of about 3 db for a 20-db range of limiting threshold. It is highly desirable with output limiters that the gain below limiting threshold remain as nearly constant as possible for all settings of the threshold control.

Modified A-F Saturation-Type Limiter

By using a partly fixed-bias and partly self-bias arrangement in the cathode circuit of the output tube, output saturation threshold control is obtained in the circuit of Fig. 17 by varying only the common d-c plate and screen grid voltage supply to the tube. This is done in steps giving changes of 5 db in output limiting level. Resistor R_7 in the control grid circuit of the output tube reduces a-c loading, and prevents excessively high direct current through the secondary

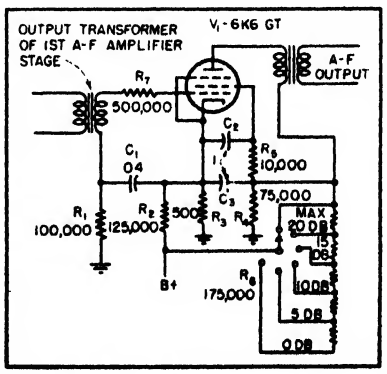

FIG. 17—Modified saturation-type limiter

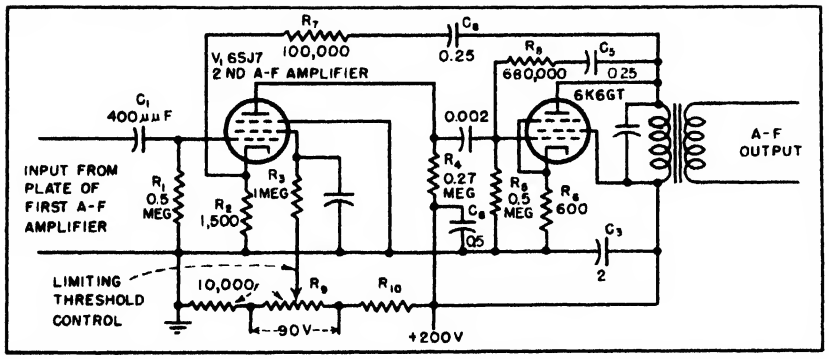

FIG. 18—Interstage a-f output limiter

winding of the interstage a-f transformer when rectification occurs in the grid circuit of the output tube. This limiter is useful for c-w reception only. There is some loss in gain below limiting threshold for the lower levels of limiting, amounting to about 5 db for about 21 db of threshold adjustment.

Interstage A-F Output Limiter

The circuit of Fig. 18 obtains its output limiting effect in the a-f stage preceding the output stage, and employs some degenerative feedback to the limiting amplifier from the output amplifier as an aid in maintaining the gain below the limiting threshold as nearly constant as possible.

Limiting is done interstage primarily because of the low limiting level of 60 microwatts required in this case for the minimum threshold value, this low level being difficult to obtain with the audio output tubes usually incorporated in Navy receivers. For a limiting level range of 20 db, this circuit gives a change in gain below threshold of about 10 db, and a change of 16 db for a limiting level range of 30 db. These comparatively large losses in gain for the lower limiting levels are due to the low minimum limiting level required.

Full-Wave Shunt A-F Output Limiter

Two diodes in a single 6H6 envelope, connected interstage as in Fig. 19, serve as a full-wave shunt type of audio output limiter. One diode shunts plate load R_4 of the interstage a-f amplifier tube for the positive and the other for the negative half-cycles of the audio signal. The diodes are biased in series with a d-c voltage obtained from R_7, which thus controls the threshold level above which they become conductive on audio peaks. The diode impedance when conducting at the usual operating audio voltage levels involved averages only a few thousand ohms (the actual value depending mainly on the resistance of that part of R_7 between the variable contact and ground, plus R_8, and also on the audio voltage values), so that the plate load of the preceding amplifier drops from a value of about 250,000 ohms below limiting threshold to perhaps 5,000 ohms during limiting action.

With a high plate-impedance tube, such a load change will produce about 30 db less amplification above the limiting level than below it. This loss of amplification, combined with normal saturation effects in the preceding amplifier tube, limits the output peak voltage to a value that cannot exceed the d-c limiting bias of R_7 by any considerable amount. This limiting system is considered to be among the best of the audio output limiters for c-w reception. For a limiting level range of about 20 db, the change in gain below limiting threshold is only 2 or 3 db.

Figure 20 shows the resonant overload characteristics of this type of limiter as used in a typical receiver. The change in gain from LIMITER OFF to ON condition is caused by switching out a pad in the a-f amplifier system.

The circuit shown in Fig. 21 was used to investigate the possibility of providing output limiting without serious audio distortion by virtue of exponential nonlinear response, the theory being that a logarithmic increment in output for a linear increment of input would not cause distortion sufficient to destroy intelligibility.

Logarithmic Limiter or Compressor

The arrangement consists of a two-stage a-f amplifier, with degenerative feedback from the plate circuit of the output tube to the cathode of the preceding stage. Two diodes are connected in series with the feedback path, in such a way as to provide a path for both positive and negative half-cycles of the feedback voltage. Potentiometer R_{10} across a battery provides d-c bias to the diodes for setting the limiting level. The diode d-c circuit resistance is kept low to take advantage of low diode internal impedance values varying at an exponential rate with applied voltage. Using the diodes in this

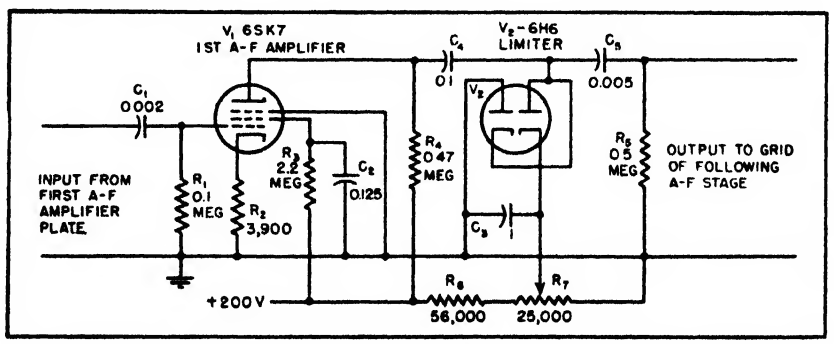

FIG. 19—Full-wave shunt a-f output limiter

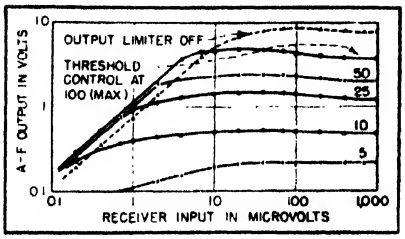

FIG. 20—Resonant overload characteristics of receiver using full-wave shunt a-f output limiter on c-w operation with unmodulated 500-kc input and 1,000-cycle output. Curves continue essentially flat out to 2 volts input

manner as feedback impedances is equivalent to varying the feedback percentage from a low value to a maximum as the instantaneous feedback voltage rises, with the reverse effect as the instantaneous feedback voltage falls.

When the instantaneous feedback voltage exceeds the region relative to diode impedance wherein that impedance is effective in determining feedback current, the circuit returns to linear operation. Within the nonlinear portions of the output characteristic, this circuit produces considerable distortion on speech or music but does not destroy intelligibility. Noise interference is reduced substantially, and almost as effectively in some cases as with a series noise-peak limiter, if the desired signal is kept within the first linear portion of the output characteristic while noise peaks extend into the compressed region beyond.

Figure 22 shows typical characteristic curves obtained with this limiter arrangement.

Other Limiter Arrangements

If a frequency-modulation receiver employing a discriminator of, perhaps, the Foster-Seeley type is tuned to amplitude-modulated signals, two peaks of maximum response will usually be evident, corresponding to the two points of maximum discriminator current. Since the two halves of the discriminator characteristic are the result of the differential voltage derived from two opposing detectors, the noise output of such a discriminator will be relatively low with no signal input as compared to an ordinary amplitude detector preceded by the same amplifiers. The discriminator provides a somewhat better signal-to-noise ratio on an amplitude-modulated signal tuned to one of the peaks of discriminator response, which is particularly apparent with relatively low modulation frequencies (narrow discriminator characteristic), and especially on keyed c-w signals. It should be noted that the discriminator used in this way reduces the useful bandwidth of the overall selectivity characteristic preceding it to about half of what it would otherwise be with the usual a-m detector.

The discriminator may be followed by a low-pass filter cutting off at about 200 or 300 cps and a d-c amplifier (capable of passing up to these frequencies) which operates a keyer tube controlling a local tone oscillator. Such an arrangement is capable of providing some really startling performance on keyed c-w signals in the presence of noise interference which would make reception with the usual receiving system, even with noise-peak limiters, absolutely hopeless. The use of the local keyer circuit eliminates one of the two peaks of reception, since the discriminator output polarities are opposite for its two maximum response points and the usual keyer tube circuit is arranged to respond to one polarity only. This scheme is subject to various disadvantages when adapted to a conventional a-m receiver, such as complexity and rather critical operating adjustments, but within its limitations has much merit. Figure 23 is typical of such circuits. The similarity of this arrangement to receiving systems for frequency-shift keyed signals is evident.

Using an f-m discriminator for a-m reception is, of course, a variation on the old proposal of providing two reception channels, one receiving signal plus noise and the other noise only, with the outputs of the two channels appropriately opposed or bucking. This proposal in its usual form does not work satisfactorily, due to the inherent difficulties of balance between such channels and the difference between them in decay time of the noise wave trains. The success (rather limited) of the discriminator version is mainly due to having a very small percentage difference in frequency between discriminator peaks of response as compared to the proposal mentioned, to inherently automatic balance when the discriminator characteristic is symmetrical, and to the single-channel amplifier preceding the discriminator.

Various other modifications of the general scheme of using a discriminator on a-m reception, some in conjunction with noise-peak and other limiters, have been evolved, and preliminary reports have indicated that considerable noise reduction effects have been obtained. The number of circuits and components involved, unfortunately, ap-

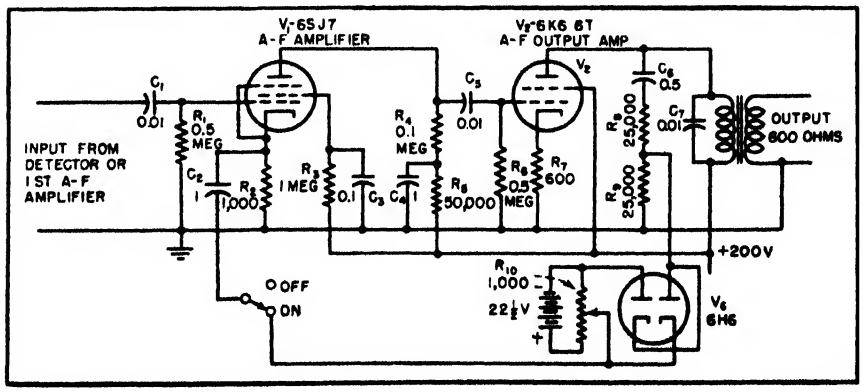

FIG. 21—Logarithmic limiter or compressor, employing two diodes in the degenerative feedback path

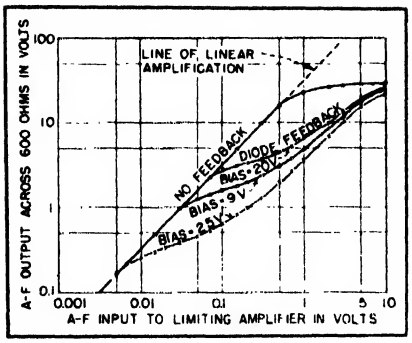

FIG. 22—Typical characteristic curves for receiver using logarithmic limiter, with 1,000-cycle a-f input

pears to have resulted in much additional bulk and complexity.

A diode of the thermionic type may be considered, for the purposes of this report, as a unidirectional variable resistor in series with an internally generated d-c potential due to cathode emission. For instance, in the 6H6 type of diode, this apparent internal potential appears to be about 1.2 volts and of such polarity as to result in electron flow from cathode to plate within the tube when the external plate-to-cathode path is completed. The effective value of the internal series resistance depends on both the d-c circuit resistance external to the diode and the external applied voltage.

If there is an external d-c circuit resistance of 1 megohm, for example, the internal resistance of each 6H6 diode is in the neighborhood of 600,000 ohms when 1 volt positive external potential is applied to the plate (as by a rising noise-peak), while at 10 volts it is about 35,000 ohms, as shown in Fig. 24. The curve is drawn as an average of quite widely scattered measured values.

Thus the measured shunting effect of the limiter diode is not very appreciable in a circuit like that of Fig. 11 until the noise peak voltage appearing across it approaches 10 volts. With a 1-volt desired signal also appearing across the detector diode load, it would seem to the operator as though the limiter were not functioning. In addition, during the period in which the limiter diode internal impedance is low, it provides a path effectively shunting out the resistance in the long time-constant circuit (R_3C_2 in Fig. 11), thereby accelerating the charging-up of C_2. As the voltage across C_2 approaches that appearing between the limiter cathode and ground, limiting ceases. From these considerations, it is apparent that the shunt-diode type of limiter will be peculiarly vulnerable to the modulation envelope set up by the longer wavetrains of interference occurring at the lower frequencies for a given pulse of excitation at the antenna.

Inserting a suitable value of resistor in series with the limiter cathode, as in Fig. 12, will extend the charging time of C_2 when the limiter diode impedance is low, in addition to providing voltage divider action relative to the succeeding a-f amplifier. It is for these reasons that the circuit of Fig. 12 out-performs the simple shunt limiter so greatly, although only approaching the performance of the simple series limiter.

The series type limiter operates to open the circuit to the a-f amplifier. Once the internal potential of the limiter diode itself plus the external no-signal potential applied to this diode by the associated detector diode has been overcome (as it may be by a relatively weak signal or even by inherent receiver noise), further negative biasing of the limiter diode by a noise peak will open it, so that it becomes, in effect, an extremely high resistance, resulting in practically no signal being transmitted to the succeeding a-f amplifier. Precautions should be taken to avoid shunting the limiter diode by the stray capacitance of wiring, switches, etc. Since the diode is open on noise peaks, it will not shunt the resistance of the long time-constant circuit (R_1C_2 in Fig. 1) and so will not abrogate the functioning of that part of the limiter. This characteristic makes it of great value even in receivers designed for as low as 15-kc carriers.

Where it is of importance, the diode internal potentials which may delay functioning of the series limiter in the presence of very weak signals may be bucked-out by, for instance, a suitable battery in series with the limiter cathode resistor. It should be noted that shunting this cathode resistance with any substantial value of capacitance in an attempt to obtain a capacitance voltage-divider for the open condition of the limiter diode should be avoided, as it generally results in increased distortion of the desired signal.

On weak signals, the insertion loss of the series limiter is perhaps 3 db, while on strong signals there is practically no such loss.

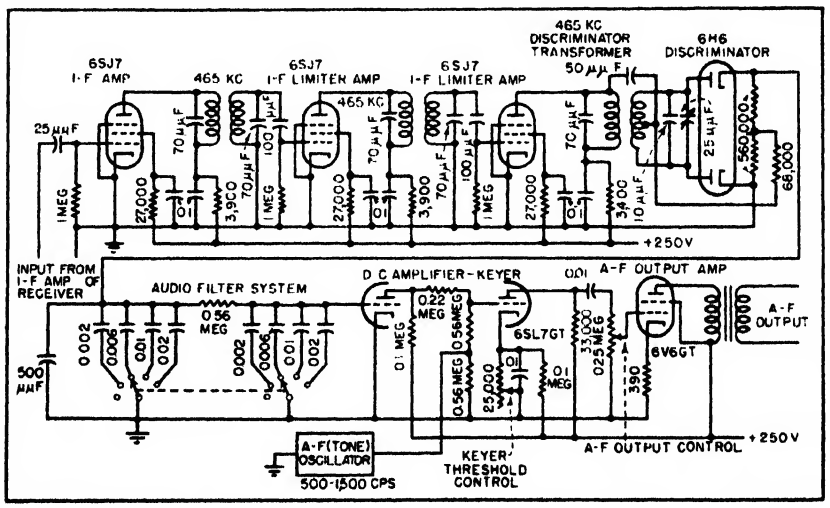

FIG. 23—Discriminator-keyer circuit arrangement for c-w operation

By insertion loss is meant the change in desired-signal gain of the receiver when switching from LIMITER OFF to ON condition, as measured with signal modulation percentage below the threshold of limiting. In the absence of noise peaks exceeding the preset threshold of limiter action, the limiter diode is biased to closed condition by a relatively low external voltage when a weak signal is present, resulting in a high value of internal resistance in this diode, with attenuation of input to the succeeding amplifier by voltage divider action. On a strong desired signal, however, the external diode biasing voltage is much higher, with much lower diode internal resistance, and the insertion loss is minimized.

Crystal Diodes

Diodes of the crystal type may be utilized in place of the thermionic type in the various limiter circuits designed for diode use. For such purposes, the crystal must be capable of operation without damage at relatively high impressed voltages and fairly large instantaneous currents. Crystals of the silicon and similar varieties are therefore unsuitable, due to their inadequate voltage and current handling capabilities, but germanium crystals may be considered for such service. It should be remembered, however, that the various crystal diodes have relatively low back resistance compared with thermionic diodes, and also that their inverse current characteristics have peculiarities of slope that cannot be neglected in some applications. Further, since the back-resistance is relatively unaffected by the d-c load resistance with which the crystal is used, while the forward resistance increases with increased load resistance, the actual values of resistance incorporated in limiter circuits using crystal diodes become of prime importance in determining limiter effectiveness. The temperature-sensitivity of crystal diodes will also have to be seriously considered for some applications.

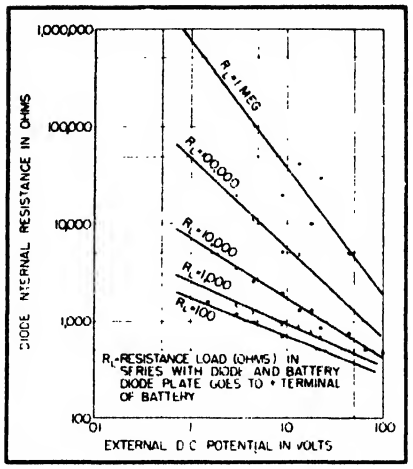

FIG. 24—Diode internal resistance at various external load resistances and applied d-c potentials, for a 6H6 diode element. Values are derived on basis of 1.2 volts diode apparent internal potential

In general, it is desirable to have control of the a-f gain following instantaneous limiters of any type. This, of course, is normal for AVC ON operation, but should also be true for AVC OFF or c-w operation. The shunt limiters operate better with low a-f gain following, and with a high r-f input level at the associated detector. The series diode limiters are usually inoperative, as regards limiting, until their internal diode potentials are exceeded, something also most readily accomplished with the highest possible signal input to the detector.

Progressive Limiting in Amplifiers

All amplifiers are, of course, limiters as their maximum output capabilities are approached. Advantage can be taken of this characteristic to prevent blocking, or a decrease of signal output from a receiver with increasing input during AVC OFF operation. The average r-f pentode of the semiremote or remote cutoff type will withstand an r-f input of about 10 times the value required to just initiate appreciable overload before its maximum output begins to drop. For example, by appropriate choice of plate load, it is possible even with normal d-c electrode potentials to have the i-f amplifier preceding a last i-f stage begin to overload before the last i-f stage begins to block, to have the amplifier preceding the next-to-last begin to overload in its turn, etc.

With five properly designed i-f or r-f stages preceding the final detector, for instance, it is possible to provide satisfactory protection against blocking in this way over a range of about five orders, or 100,000 times the input which initiates overloads of the last i-f stage. While of maximum utility on c-w operation, such a characteristic will also be of use on mcw operation with avc off, since even though distortion of voice signals is very high, their presence will nevertheless be evident. This means can also be very useful in protecting detectors and audio limiters against excessive overdrives which tend to abrogate their characteristics.

Linear Detection

Linear detection is to be preferred for the final detector stage, not only for the reasons of low distortion and discrimination against weak undesired signals in the presence of relatively stronger desired ones, but also because of behavior with regard to noise. In the linear region of detection, increase in the signal input level to the detector will not be accompanied by substantial increase in the noise output due to internal noise modulation of the carrier within the receiver, a highly desirable condition.

Desirable A-F Amplifier Characteristics

The frequency response of the a-f amplifier following the detector should be restricted to a range not exceeding the requirements for satisfactory voice reproduction, or the fidelity permitted by the selectivity preceding the final detector, whichever is the lesser. The high-frequency cut-off for good voice intelligibility is, however, about 3,500 cps, and the selectivity preceding the detector should not, in general, abrogate this requirement.

Audio systems which have poor transient reproduction characteristics may tend to magnify the effects of noise pulses. The tendency

toward damped oscillations or hangover on sharp peaks of input in such systems may be reduced by the use of low-impedance output tubes (triodes) or by a sufficient degree of degenerative feedback from the output, and also by the provision of properly designed output transformers, properly loaded.

Circuit Diagrams

The circuit diagrams in this report have been prepared with the intent of showing, as clearly as possible, the circuit configurations in their most readily comprehensible form. It has been the author's experience that this is absolutely essential for an understanding of limiter circuits particularly, and seemingly novel circuit arrangements have often revealed their similarity to or identity with one of those covered in this report upon redrawing.

Conclusions

From the overall viewpoint of simplicity, effectiveness, and low distortion, the series-type noise-peak limiter appears to be the best choice for mcw operation, while from the standpoint of effective limiting, minimum change of gain below limiting threshold over a wide threshold range, and relative simplicity, the full-wave a-f shunt output limiter appears best for c-w operation. The former may be combined with the latter for even more effective operation on c-w signals.

It should be remembered that no limiter is a cureall. When noise-peaks do not substantially exceed the desired carrier peak values and occur so frequently that they fill in the modulation, only some of the very elaborate limiter arrangements, such as, for instance, the discriminator-keyer combination types for c-w reception, will afford any considerable degree of relief. Within their inherent limitations, however, those limiters recommended above can be very useful additions to the communication receiver, and also to the broadcast receiver which must work under conditions of high ambient static or similar disturbances.

Simplified Single-Sideband Reception

Accessory designed for use with a conventional communications receiver exhibits advantages when receiving ordinary code signals, as well as single-sideband phone. Selectivity is approximately doubled by employing a demodulating oscillator, balanced detector, two 90-degree audio phase-shift networks and a low-pass filter

By OSWALD G. VILLARD, Jr.

ATTENTION has recently been drawn to 90-degree wideband audio phase-shift networks as a means of generating single-sideband radio signals.[1,2] Filters of the R-C type, such as those described by Dome[3], are simple and inexpensive to make. Moreover, radio transmitters incorporating them are flexible and easier to adjust than the conventional variety using sharp band-pass filters. It is reasonable to expect, in the light of these and other developments[4,5], a re-evaluation of the possibility of applying single-sideband transmission to a much wider group of radio services (aircraft, police, military and amateur) than those at present enjoying its advantages.

Practical 90-degree networks make possible an equally important simplification in single-sideband receiving technique. An arrangement is described in this article whereby the effective intermediate-frequency bandwidth of a radio receiver can be made exactly that of the passband of a low-pass audio filter, instead of approximately twice that passband as in conventional a-m practice. This technique, in effect, makes possible the design of single-sideband receivers in which audio selectivity is the equivalent of i-f selectivity. As a result, the cost of receivers having a square-sided band-pass response of sufficient sharpness to take full advantage of the saving in bandwidth afforded by single-sideband transmission need not be greater than that of present-day communication receivers. In addition, it is possible to convert existing equipment to take advantage of the new system.

Advantages

The circuit to be described offers some advantages in the reception of conventional code signals. All incoming noise or code signals higher, or lower, in frequency than the final beating oscillator can be virtually eliminated from the output. The effective bandwidth of the receiver is thereby halved, since signals are heard on one side of zero beat only. Moreover, it is possible to select the side of zero beat on which signals are heard simply by throwing a switch. Alternatively, it is possible to listen to signals on the two sides separately and simultaneously. Two

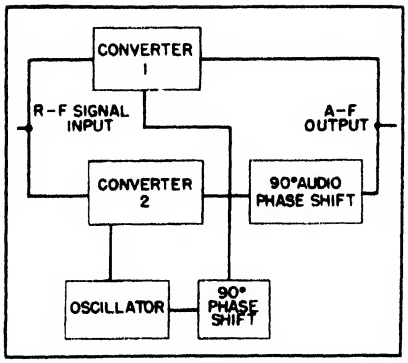

FIG. 1—Block diagram illustrating basic system

operators can listen without mutual interference to two different sets of transmissions coming from the output of a single receiver, one hearing all signals higher in frequency than that of the beating oscillator and the other hearing all signals lower in frequency. In the same way the system may be used to separate multiple single-sideband transmissions; conversations carried by the lower sidebands of a given suppressed carrier appear in one output channel, while those carried by the upper sidebands appear in the other.

Circuit Operation

Operation of the circuit is easily explained. First, it must be remembered that detection is essentially a process of frequency conversion. Signals become intelligible as soon as they are translated from the radio-frequency spectrum down to their correct place in the audio-frequency range.

Frequency conversion can be accomplished by either of two methods that are ordinarily equivalent but which have an important distinction from the standpoint of the present discussion. Basically, it is desired to generate difference frequencies falling in the audio range by combining an incoming radio-frequency signal with a local oscillation. The desired difference frequencies can be generated by superposition of signal and local oscillation and rectification of the resulting envelope, or by modulation of signal by local oscillation (or vice versa) whereby the lower sideband is the desired difference frequency. It is important, in single-sideband detection, to avoid the production of beats between the sidebands themselves or beats between the sidebands and adjacent interfering signals which might produce spurious audio-frequency output. Because this effect may readily take place with the first method as a consequence of the rectification process the second method is to be preferred for the present purpose because the incoming signal which is modulated by the local oscillation can be handled in a class-A amplifier possessing as nearly linear a grid voltage-plate current characteristic as possible.

Let the demodulating oscillator voltage be expressed by $E_1 \sin \omega_1 t$, and let an incoming sinusoidal single-sideband signal be $E_2 \sin \omega_2 t$. The incoming signal is fed simultaneously to two frequency converters. One of the converters is supplied with oscillator voltage and the other receives the same voltage shifted 90 degrees in phase, or $E_1 \cos \omega_1 t$. The output of the first converter is then

$$e = m E_1 \sin \omega_1 t \, E_2 \sin \omega_2 t = \frac{m E_1 E_2}{2} \cos (\omega_1 - \omega_2)t - \frac{m E_1 E_2}{2} \cos (\omega_1 + \omega_2)t$$

where m = modulation factor (a constant)

The right-hand portion of the second expression is the upper sideband, in which we have no interest. If $\omega_1 > \omega_2$, the left-hand portion is positive; if $\omega_1 < \omega_2$, it remains positive because $\cos(-\alpha) = \cos \alpha$. The output of the second converter is

$$e = m E_1 \cos \omega_1 t \, E_2 \sin \omega_2 t = -\frac{m E_1 E_2}{2} \sin (\omega_1 - \omega_2)t + \frac{m E_1 E_2}{2} \sin (\omega_1 + \omega_2)t$$

If $\omega_1 > \omega_2$, the left-hand portion of the second equation is negative; if $\omega_1 < \omega_2$, it becomes positive, because $\sin(-\alpha) = -\sin \alpha$.

Thus the first converter gives a difference-frequency output whose relative phase may be thought of as not changing as the incoming frequency passes from lower to higher than that of the oscillator. The second converter on the other hand gives an output whose relative phase does change by 180 degrees as zero beat is crossed. Now, by means of a 90-degree wideband phase shifter it is possible to delay the audio output of the second converter until it becomes

$$-\frac{m E_1 E_2}{2} \cos (\omega_1 - \omega_2)t.$$

This voltage, if added to the output of the first converter when $\omega_1 > \omega_2$, will produce cancellation,

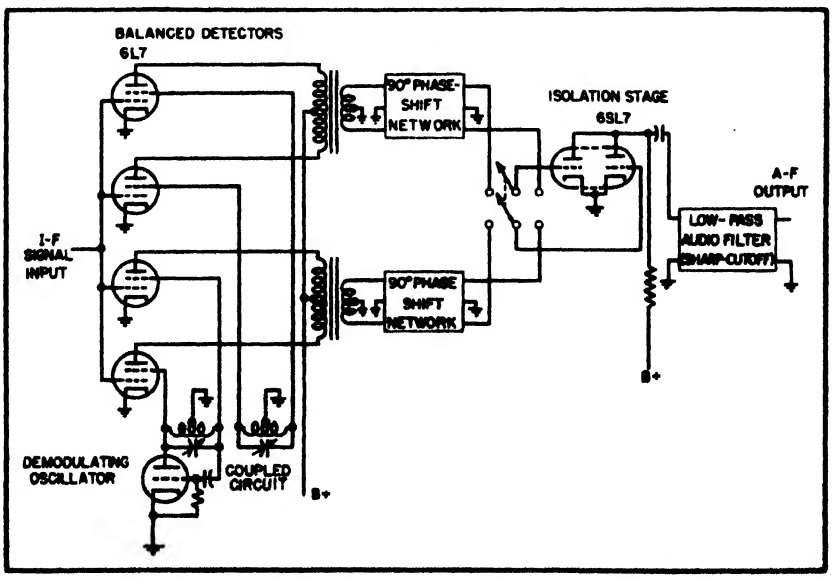

FIG. 2—Simplified schematic of single-sideband detector circuit

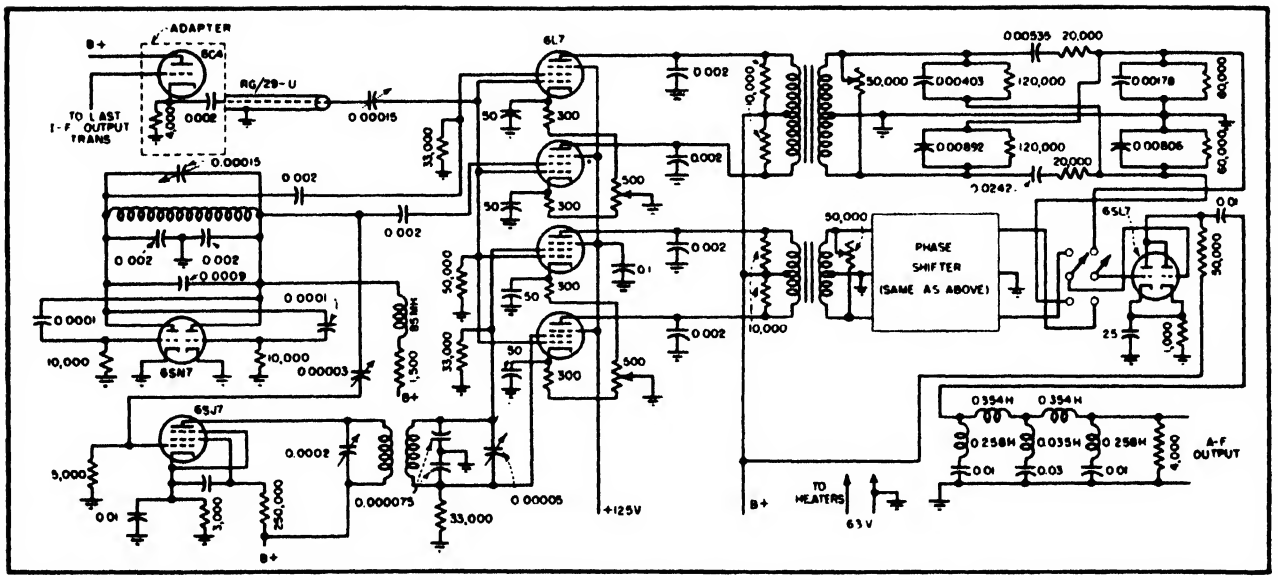

FIG. 3—Complete schematic of single-sideband reception accessory for communications receiver

whereas if $\omega_1 < \omega_2$ direct addition results. Thus, by means of a 90-degree wideband phase-shift network and two detectors fed by radio-frequency voltages in phase quadrature, it is possible to reject signals on one side of the beating oscillator and pass those on the other.

A block diagram of the basic method is shown in Fig. 1.

Practical Application

Balanced detectors are used in the practical circuit in order to reduce the likelihood of demodulating beats between components of the incoming signals, in addition to the beats between this incoming spectrum and the local oscillator. The balanced arrangement is particularly important where strong adjacent-channel interference may be encountered and where detection is done at relatively high signal levels (of the order of tenths of a volt.) Under these conditions curvature of the grid-voltage plate-current characteristic of most vacuum tubes will produce appreciable even-order distortion and even-order sum-and-difference frequencies. These effects result in spurious audio output since they may be produced by two radio frequencies anywhere in the input signal spectrum.

The balanced detector arrangement eliminates even-order distortion but does not affect odd-order distortion and odd-order sum-and-difference frequencies arising from the rate of change of curvature of the grid-voltage plate-current characteristic. However, odd-order distortion may be minimized by using tubes of the remote-cutoff type which are especially designed to have a low rate-of-change of curvature. The balanced detector using remote-cutoff tubes such as the 6L7 makes it possible virtually to dispense with i-f selectivity provided a highly selective audio filter is used, since only those beats between local oscillator and incoming signals which fall within the passband of the audio filter will be heard.

The 90-degree phase shift between the demodulating voltages fed to the injector grids of the pairs of detector tubes in Fig. 2 is conveniently obtained by taking advantage of the quadrature relationship between voltages across two coupled circuits tuned to resonance. For convenience in adjustment, a buffer tube is employed between the oscillator and the coupled circuits in the actual unit, since tuning the coupled circuit would otherwise affect the oscillator frequency.

The two 90-degree audio phase-shift networks shown are identical. While a network of this type produces two output voltages having a phase difference of nearly 90 degrees over a wide range of frequencies, the phase of these output voltages themselves bears no fixed relationship with that of the common input. It is therefore necessary to use two identical networks in order to obtain two voltages between which a 90-degree phase exists, assuming the two separate input channels to be in phase. In practice the phase of the two channels may be arbitrary, and a quadrature relationship is actually used.

Employment of two identical 300 to 3,000-cps networks connected to the outputs of the two balanced detectors also prevents any amplitude unbalance affecting the degree of undesired-signal cancellation arising from the variation in input impedance of each filter with frequency. Variation may affect the overall frequency response, since the 6L7 tubes may be considered as constant-current generators whose output voltage is proportional to the output impedance, but it does not affect the ratio of the outputs of the two detectors and therefore cancellation of the undesired signal. When the primaries of the audio trans-

formers are loaded with resistances low enough to damp out transformer resonances, it is found that the input impedance of the phase-shift networks has a negligible effect on the overall frequency response.

Figure 3 shows the complete schematic diagram of a single-sideband detector which may be added to a standard communications receiver. Connection is made by removing the receiver's second detector tube, plugging in an adapter, and then plugging the detector tube into the adapter. A 6C4 cathode follower couples i-f output into the single-sideband detector circuit without disturbing normal operation of the receiver except for a slight retuning of the secondary of the last i-f transformer.

Balancing controls for the two detectors are potentiometers in their cathode circuits. The secondary of the i-f transformer connected to the 6SJ7 buffer tube is resistance-loaded in order to broaden the tuning and make the phase setting less critical. Variable resistors shunted across the secondaries of the output transformers provide a convenient means of equalizing the magnitude of the detector outputs. The low-pass filter used in the common output is a home-made *m*-derived affair cutting off at 2,500 cycles per second and designed for a 4000-ohm characteristic impedance.

Circuit Adjustment

Tuning up the circuit is straightforward. The beat-oscillator voltage at the 6L7 grids can be set at 15 volts just as in conventional converter service. Detector balance is determined by turning off the oscillator and removing or disconnecting one pair of 6L7's. A strong steady signal, such as that from a broadcasting station, is tuned in and the balancing resistor of the remaining pair of tubes adjusted for minimum audio output. This process is then repeated with the first pair of tubes. With the correct adjustment the detector should produce a deafening output with the oscillator turned on, whereas there should be no audible output at all with it off.

Adjustment of the radio-frequency phase of the local-oscillator signal at the second balanced detector is easily made. With the secondary of the i-f transformer tuned for maximum voltage at the 6L7 injector grids the phase is approximately correct. This condition can be verified by connecting the horizontal and vertical plates of an oscilloscope to the secondaries of the audio-output transformers. If the amplitude balance is approximately correct a steady a-m signal such as a broadcast station will give a weaker beat note on one side of resonance than on the other. Tuning to the weaker side, the amplitude balance is set for greatest rejection and likewise the radio-frequency phase setting touched up. For any given pitch of beat note the balance may be made complete and the beat eliminated completely by adjustment of phase and amplitude. The procedure is exactly like that of balancing a bridge. However, since the 90-degree networks do not give a perfect 90-degree phase shift as well as a perfect amplitude balance at all frequencies it will be found that the rejection, while perfect at one frequency, is imperfect at others. As a compromise, it is best to adjust for complete cancellation at a frequency in the vicinity of 1,000 or 2,000 cycles, where the ear is most sensitive.

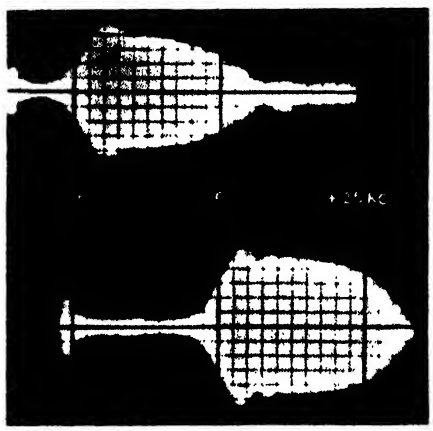

FIG. 4—Oscillograms showing rejection of upper sideband (top) and lower sideband (bottom)

The laboratory model for which the schematic is given could be considerably simplified. Dual triodes or even detector crystals could be substituted for the 6L7 mixers. If mixing is done at low enough levels the balanced connection could probably be dispensed with. The local oscillator could be simplified and the buffer tube eliminated by making the oscillator a pentode tube with electron coupling between the frequency-determining elements and the plate circuit to which the i-f transformer would be connected.

Figure 4 is an attempt to illustrate the properties of the circuit by means of the familiar frequency-modulated oscillator technique. Owing to the presence of the demodulating oscillator there is displayed on the oscilloscope screen a continuously-varying audio beat between the frequency-modulated test oscillator and the steady demodulating oscillator. The audio-frequency waveform has random phase because the two oscillator phases are unrelated, and hence does not remain stationary. The envelope of this waveform is an indication of the overall selectivity curve of the detector circuit. It is not entirely representative because at the oscillator sweep speeds available, transient response effects in the sharp-cutoff audio filter considerably distort the envelope. The patterns show spurious humps and are not as symmetrical as would be the case if the response curve had been plotted with a very slow rate-of-change of sweep-oscillator frequency. Rejection of the undesired signal is illustrated by the oscillograms.

References

(1) M. A. Honnell, Single Sideband Generator, ELECTRONICS, p 166, November 1946.
(2) B. E. Lenahan, A New Single Sideband Carrier System for Power Lines, *Elec. Eng.*, 66, p 549, June 1947.
(3) R. B. Dome, Wideband Phase Shift Networks, ELECTRONICS, p 112, December 1946
(4) *Tele-tech*, Vol. 7, No. 1, p. 62, January 1948.
(5) O. G. Villard, Jr., Single-Sideband Operating Tests, *QST*, p 16, January 1948.

Single-Signal Single-Sideband Adaptor

By E. W. ROSENTRETER

An ordinary superheterodyne receiver will demodulate a single sideband signal and its accompanying carrier so long as the ratio of carrier amplitude to sideband amplitude is kept sufficiently large, though not without distortion. If, however, the carrier is attenuated below a critical value, complete unintelligibility will result. Commercial single-sideband transmitters now in operation attenuate the carrier 20 db below the sideband level to conserve power and simplify equipment.

If a communications type of receiver is used to demodulate this type of signal some means of carrier reinforcement in the receiver is necessary. This can be done conveniently at the intermediate frequency by using the receiver's beat frequency oscillator to exalt the carrier. Exact tuning is required, as well as excellent stability of transmitter frequency, receiver local oscillator frequency and beat frequency oscillator. If the frequency of any of these varies, an audio beat will be produced.

If the carrier is completely suppressed, then the received single-sideband signal can be satisfactorily demodulated only if the beat frequency oscillator supplies the missing carrier. The critical value between the synthetic carrier and the signal must be maintained or exceeded for acceptable results. Since it is difficult to control accurately the frequencies of the oscillators in both transmitter and receiver, other arrangements usually are resorted to in conventional single-sideband receivers.

Figure 1 shows in block form a simple receiver system using low-frequency filters. With this arrangement, double conversion is necessary to change the higher radio frequencies used for communications down to the frequency of the filter.

The purpose of the two oscillators is to enable the pass-band filter to accept the desired sideband, whether it be upper or lower. This is done by switching one or the other oscillator into the second converter circuit.

Another single-sideband system, relatively simple in circuit elements, is shown in Fig. 2. This

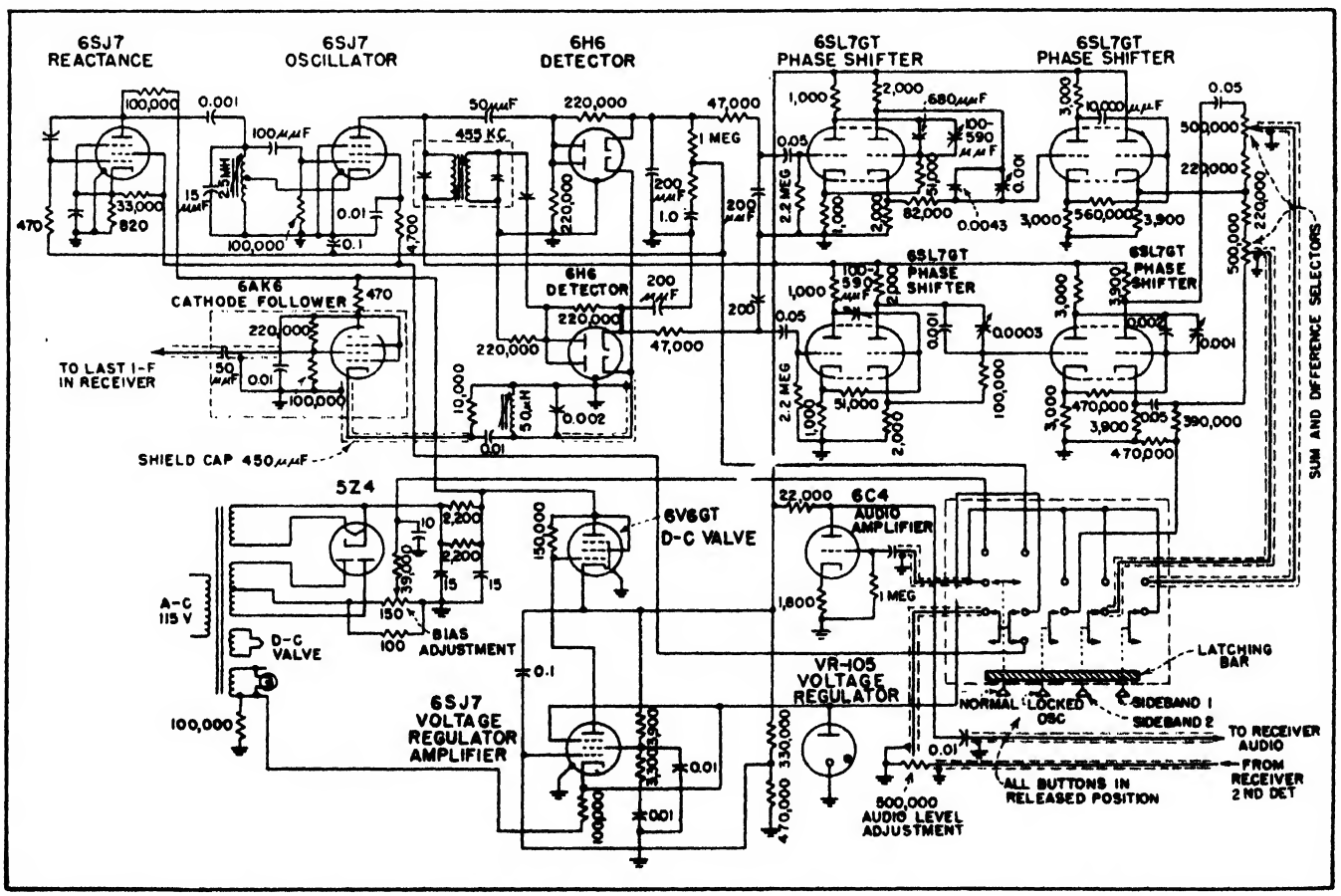

Complete circuit of the General Electric Selector for single sideband reception with a conventional communications receiver

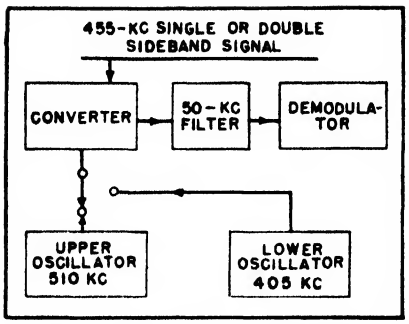

FIG. 1—Filter type of single-sideband receiver

arrangement is used in the General Electric Single Sideband Selector. Reception of a single-sideband signal with or without carrier, and selection of one or the other sideband in a conventional a-m signal, are among the types of transmission which the system handles.

Principle of Operation

Assume that a conventional a-m, double sideband signal is being received. Referring to Fig. 2, the signal from the receiver i-f channel, containing carrier and both sidebands, is fed into two special detectors; 1 and 2. Voltage from an oscillator operating at the same frequency as the i-f channel is also fed into the two detectors. A fixed phase shift of 90 degrees exists between the oscillator voltage applied to detector 1 and detector 2.

The oscillator voltage, or synthetic carrier, is many times greater in magnitude than the incoming signal voltage. Thus the two detectors demodulate the incoming signals at an effective low modulation factor and distortion products are small. Identical audio signals, corresponding to the sideband intelligence are obtained from the two detectors, except for a 90-degree phase difference between them. The amplitude of these signals is directly proportional to the amplitude of the sideband intelligence.

The audio voltages are fed into phase-shift networks A and B, where they undergo an additional 90-degree relative phase shift. The two outputs are fed into a sum and difference circuit, where they are added or substracted algebraically. It can be shown that the sum contains only upper sideband information, for example, and that the difference contains only lower sideband information. (See: Simplified Single-Sideband Reception O. G. Villard, Jr. ELECTRONICS, May 1948.) Selection of one or the other is easily done by a switch, which selects the additive or subtractive process. The same switch also selects an output containing both sidebands.

Lattice Networks

Since the oscillator operates at one frequency only, it is quite simple to create and maintain a 90-degree phase shift of its voltage for application to detector 2. To be of any practical value, the sidebands must be wide enough to carry the desired intelligence. Suppose for instance that an audio voice frequency range of 100 cycles to 4,000 cycles is desired. Then the two sidebands will each be up to 4,000 cycles wide, so that the A and B networks must maintain a 90-degree phase difference over the full 100 to 4,000-cycle audio band. The wideband phase-shift networks were devised by R. B. Dome, and were described in detail in ELECTRONICS, December 1946. Briefly, the manner in which they function is that phase shift increases nearly linearly with the logarithm of the frequency. Thus

$$\text{Phase A} = K + \log f$$
$$\text{Phase B} = K + \log tf$$

Substracting phase B from phase A

$$\phi A - \phi B = K + \log f - K - \log tf$$
$$= \log f - \log f - \log t$$
$$= -\log t$$

where K and t are constants and f is the frequency. Thus the difference in phase shifts between A Network and B Network is a constant, regardless of frequency.

With two networks composed of three RC lattices as shown in Fig. 3 and through proper choice of component values, a frequency coverage ratio of 100 to 1 may be accomplished. Figure 4 shows that although the applied voltages undergo total phase shifts up to several hundred degrees, depending on frequency, the difference in phase shift between the two outputs is approximately 90 degrees over a very wide range. This difference can be made to extend from 50 to 5,000 cycles per second, or it may be from 250 to 25,000 cycles per second, for example.

The choice of frequencies of say 50 to 5,000 cycles per second does not mean that the phase-shift networks will not pass frequencies beyond this range (higher or lower in frequency). It means simply that the 90-degree phase difference is not preserved outside this range. Frequencies above or below will have a phase difference other than 90 degrees and consequently, when applied to the sum and difference circuits, they will not combine algebraically to add or cancel completely. Incomplete suppression of the unwanted sideband corresponding to these extreme frequencies is the result.

Operating Unit

A single-sideband selector unit embodying the method shown in Fig. 2 and 3 is built for use in conjunction with existing a-m receivers having a nominal i-f frequency of approximately 455 kc.

The unit is attached to the re-

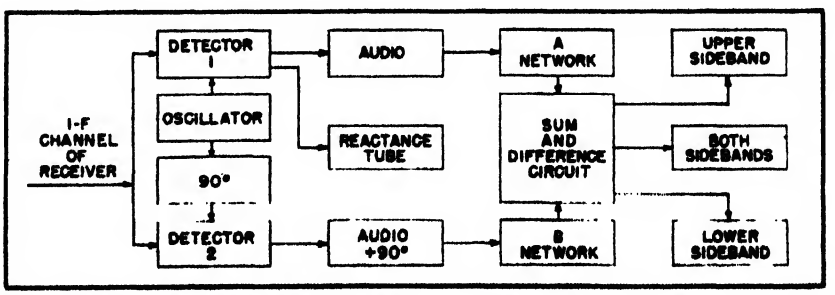

FIG. 2—Stage arrangement of the General Electric Selector unit for adding to a conventional communications receiver

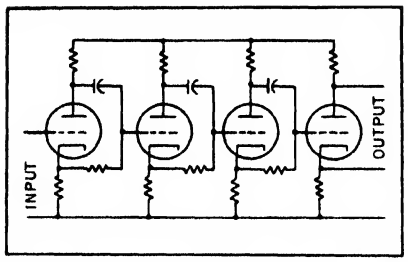

FIG. 3—Three-lattice A or B phase-shift audio network

ceiver by means of a small probe which is connected to the last i-f stage of the receiver through a short length of low-capacitance shielded cable. The high-impedance i-f signals are transformed to low-impedance level by means of the probe, and are then fed into the selector. The only other connections between the receiver and the unit are two shielded wires for audio.

The selector permits reception of single-sideband signals with carrier, single-sideband signals without carrier, conventional a-m signals (selecting the upper or lower sideband or both), dual single-sideband signals, that is, intelligence A on one sideband or intelligence B on the other sideband with carrier or attenuated carrier and conventional shortwave broadcasts employing exalted carrier.

Selection of any of these is done by four pushbuttons on the front panel. The phase-shift networks cover a frequency range of 70 to 7,000 cycles per second. Therefore, the quality of reproduction is usually only dependent upon the i-f pass-band characteristics of the receiver.

Locked Oscillator

Should the carrier frequency delivered by the receiver tend to deviate from that of the selector's oscillator, a d-c control voltage will be delivered by the combination of oscillator frequency, intermediate frequency, and detector.

This d-c control voltage, applied in a feedback loop back to the oscillator through a reactance tube, then serves to restore the i-f carrier and oscillator to frequency synchronism. Moreover, the time constant in the d-c circuit provides the equivalent of memory; should the i-f carrier temporarily disappear because of selective fading or transmitter troubles, the locked oscillator will not get away. This is especially useful in weak-signal, transoceanic communications, and a must when the receiver is unattended over long time intervals.

This feature minimizes the need for retuning against change in transmitter frequency, change in receiver local oscillator frequency, change in selector voltages or temperatures that normally would cause frequency drift.

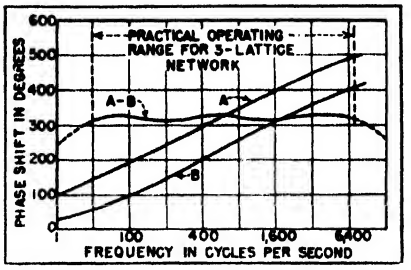

FIG. 4—Characteristics of three-lattice phase-shift network

Satisfactory locking action is produced when the carrier of the received signal, either because of suppression at the transmitter, or because of selective fading, is as much as 20 db below sideband level. When no carrier is transmitted, no locking or control voltage is generated, so that retuning of the receiver will be necessary from time to time. For this reason a small amount of carrier, say 1 or 2 percent of the sideband energy, should always be transmitted in single-sideband systems for use with this type of receiver.

The locking circuit permits listening to a weak signal, even though a strong signal is nearby (in frequency), without the selector oscillator being captured by the stronger signal. The degree of selectivity which this makes possible cannot be fully appreciated by anything short of an actual listening test in a band of crowded signals.

Tracking Permeability-Tuned Circuits

By A. W. SIMON

THE system of tuning shown in Fig. 1A employs ganged, identical variable capacitors with a series (padder) capacitor and a shunt (trimmer) capacitor to restrict the range of the oscillator section in superheterodyne receivers. It has its exact counterpart in permeability-tuned systems (ganged, identical, iron cores and coils) except that, on account of the inverse relationship between capacitance and inductance, the series capacitor is replaced by a shunt coil, and the shunt trimmer by a series coil, as indicated in Fig. 1B.

The theory of tracking, or maintainance of a constant frequency difference between the r-f and oscillator sections, has been discussed for the case of ganged capacitors by various authors. Two general methods of analysis have been presented, one of which is based on the solution of a cubic equation,[1] and the other on the properties of an equilateral hyperbola.[2] The latter method is much less laborious than the former, and is accordingly applied to the solution of the permeability-tuned system problem.

It should be noted, in connection with the circuit of Fig. 1B, that the series coil L_s could also be placed on the capacitor side of the shunt coil L_p, or coils could be placed in both

positions, without departure from three-point tracking.

If the problem is treated according to the method of Roder, we compute three pairs of values x_i, y_i (i = 1, 2, 3) according to the equations

$$x_i = 1/4\pi^2 f_i^2 C \quad (1)$$

$$y_i = 4\pi^2 F_i^2 C_1 \quad (2)$$

where f_i and F_i represent a pair of corresponding signal and oscillator frequencies, respectively, at which perfect tracking is desired (taken preferably in ascending order) and from these in turn compute three auxiliary parameters x_0, y_0 and K given by

$$x_0 = D_x/D \quad (3)$$

$$y_0 = D_y/D \quad (4)$$

$$K = (x_i - x_0)(y_i - y_0) \quad (5)$$

where

$$D_x = \begin{vmatrix} (x_1y_1 - x_2y_2) & (x_1 - x_2) \\ (x_2y_2 - x_3y_3) & (x_2 - x_3) \end{vmatrix} \quad (6)$$

$$D_y = \begin{vmatrix} (y_1 - y_2) & (x_1y_1 - x_2y_2) \\ (y_2 - y_3) & (x_2y_2 - x_3y_3) \end{vmatrix} \quad (7)$$

$$D = \begin{vmatrix} (y_1 - y_2) & (x_1 - x_2) \\ (y_2 - y_3) & (x_2 - x_3) \end{vmatrix} \quad (8)$$

The desired values of the circuit constants sought are then given by

$$L_p = K/y_0 \quad (9)$$

$$L_s = -x_0 \quad (10)$$

$$C_2 = C_1/K \quad (11)$$

A numerical example will make the foregoing clear. (In practice the $4\pi^2$ is best carried along as a factor since it cancels out in most of the operations.) The computations are carried out in practical units, — cycles, farads and henrys. Let it be required to calculate L_p, L_s and C_2 given that $C_1 = 80\mu\mu f$, $f_1 = 600$ kc, $f_2 = 1{,}000$ kc and $f_3 = 1{,}500$ kc, for an intermediate frequency of 455 kc, so that $F_1 = 1{,}055$ kc, $F_2 = 1{,}455$ kc. and $F_3 = 1{,}955$ kc.

Eq. 1 and 2 yield

$4\pi^2x_1 = 3.4723 \times 10^{-4}$
$y_1/4\pi^2 = 89.04$
$x_1y_1 = 3.0917$
$4\pi^2x_2 = 1.2500 \times 10^{-6}$
$y_2/4\pi^2 = 169.36$
$x_2y_2 = 2.1170$
$4\pi^2x_3 = 5.5556 \times 10^{-3}$
$y_3/4\pi^2 = 305.76$
$x_3y_3 = 1.6987$

so that we have

$D_x/4\pi^2 = +2.5275 \times 10^{-3}$
$4\pi^2D_y = -99.39$
$D = -2.4735$

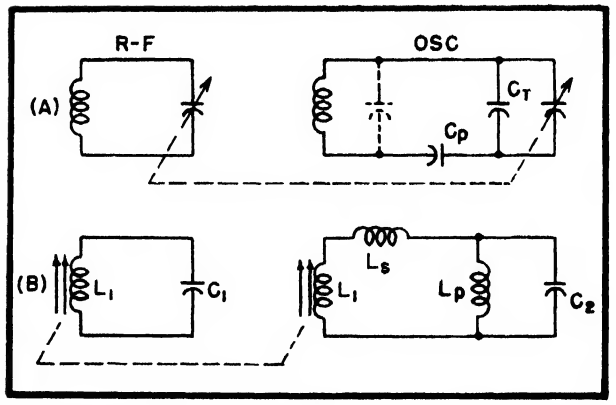

FIG. 1—Conventional variable-capacitance tuned r-f and local oscillator circuits (A) and equivalent permeability tuned circuits (B) as used in a superheterodyne receiver

the values of the auxiliary parameters are

$x_0 = 2.5884 \times 10^{-4}$
$y_0 = 1.5863 \times 10^{2}$
$K = 1.7476$

so that the required circuit parameters are

$L_p = 1127.3\mu h$
$L_s = 25.88\ \mu h$
$C_2 = 45.777\ \mu\mu f$

While the calculations are somewhat lengthy, they involve none but arithmetic operations. The use of logarithms greatly shortens the labor of computation.

REFERENCES

(1) Landon, V. D. and Sven, E. A., Solution of the Superheterodyne Tracking Problem, ELECTRONICS, p 250, August 1932.
(2) Roder, Hans, Oscillator Padding, *Radio Engineering*, p 7, March 1935.

Tracking the Permeability-Tuned Circuits

By A. W. SIMON

IN A previous article[1,2] the author has given simple formulas for the calculation of the padder and trimmer coils required to reduce to a minimum the mistracking between the oscillator and r-f sections of permeability-tuned superheterodyne receivers. By the application of these formulas, the maximum deviation due to mistracking between sections can be reduced usually to less than 1 db.

There is another cause of mistracking, namely, the reactance coupled into the r-f section by the antenna circuit. While the effect of this reactance is not serious in the case of a rod or wire antenna, it becomes quite marked for the now widely used loop antenna, due to the higher degree of coupling used. However, the reasoning which underlies the deduction of the above mentioned formulas also suggests how the effect of the antenna circuit can be neutralized.

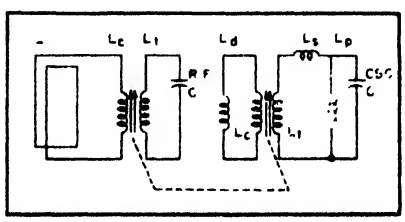

Method of neutralizing effect of loop antenna reactance on tracking of permeability-tuned receiver

The basic principle of the permeability-tuned circuit is that the inductance of the respective ganged coils be identical in every position, that is, at every frequency. The effect of the coupled reactance is to upset this condition. Hence a simple solution suggests itself, namely, to couple into the oscillator section a dummy coil of the same inductance as that of the loop antenna. The reactance coupled into both sections is then the same at every frequency and mistracking does not result. A typical circuit is shown. Here L_t, L_t represent identical coils and cores, L_c L_c identical primaries wound over them, and L_d the dummy coil simulating the effect of the loop L.

(1) ELECTRONICS, **19**, p 138, Sept. 1946.
(2) *Radio*, **30**, p 20, Nov. 1946.

Permeability Tuning of Broadcast Receivers

Analysis of permeability-tuned series loop and transformer-coupled loop circuits. Performance is compared with that of the familiar capacitance-tuned high-impedance type. Coil-winding data for obtaining proper pitch for oscillator tracking are also given

By L. O. VLADIMIR

PERMEABILITY tuning has been used widely in automobile receivers and has been found to be very satisfactory for such use. The advantages to be gained by this method of tuning rather than a gang capacitor are: smaller size, lower cost, and improved signal-to-noise ratio when tuning a small-capacitance antenna.

Of these advantages only lower cost would ordinarily be of great importance in the design of home receivers. Unquestionably, the greatest barrier to the wide acceptance of permeability tuning is the degradation of loop performance which is encountered, particularly in small table models.

At present there are two accepted methods of permeability tuning a loop antenna. In both cases the loop must be of the low impedance variety and is usually constructed of two to four turns of heavy copper wire or ribbon. The two methods which we will consider are:

1—The transformer-coupled circuit wherein the loop is connected to a small primary winding which is coupled to a secondary winding which in turn is tuned by an iron core. The schematic diagram appears in Fig. 1.

2—The series loop circuit wherein the loop is connected in series with the tuning coil. The schematic diagram of this connection appears in Fig. 2.

The analysis of the transformer-coupled circuit will follow very closely a previously derived method for the capacitance-tuned low-impedance loop[1]. The analysis of the series loop circuit will follow the method given by Polydoroff[2]. Gain and signal-to-noise ratio will then be compared for the two circuits and a further comparison made with the usual high-impedance capacitance-tuned loop antenna.

For the purposes of these comparisons, a table model receiver having an area of 82 square inches available for the loop will be considered. Knowing the loop area and the number of turns, the effective height of the loop is found from the formula

$$h_e = \frac{2\pi NA}{\lambda} \text{ in microvolts per meter} \quad (1)$$

The effective height of the loop mul-

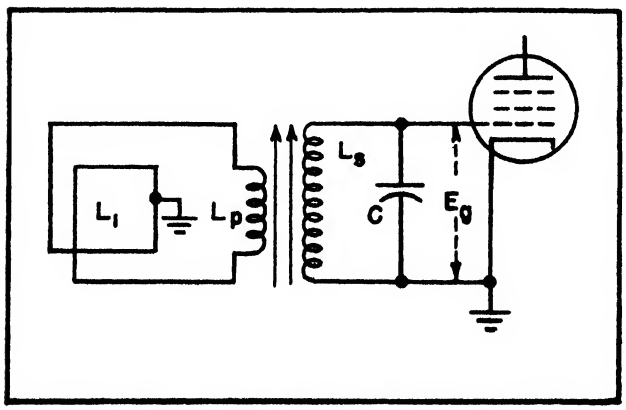

FIG. 1—Transformer-coupled loop circuit

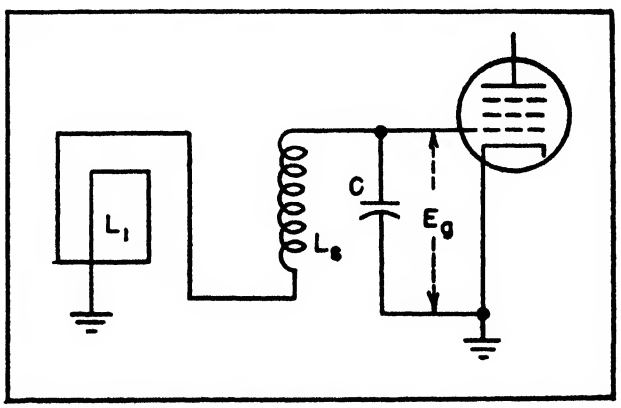

FIG. 2—Series loop circuit

Table I—Series Loop Circuit

Frequency in kc	Q	Loop Effective Height μv/m	Figure of Merit	Tuned Circuit Impedance, ωLQ
1,500	90	0.0093	0.836	145,000 ohms
1,000	95	0.0062	0.588	231,000 ohms
600	110	0.0037	0.408	418,000 ohms

tiplied by the gain of the input circuit is equal to the figure of merit of the loop.

To find the thermal-noise produced in the input circuit, the tuned circuit impedance must be known, and this will be calculated for each of the three type circuits compared here.

Analysis of Series Loop Circuit

The factor which determines the gain obtainable with the series loop is the tuning range available in the permeability-tuned coil. It was determined experimentally that a linear pitch, 130-microhenry, progressive-wound coil on Bakelite tubing having dimensions of 0.206 inch I.D. and 0.226 O.D., tuned with a commercially available iron core whose dimensions are 0.200 inch diameter and 1.5 inch long, could be made to have an inductance change of 11 to 1.

Inasmuch as the dial calibration which can be obtained with a linear pitch coil was found to be somewhat more crowded at the high-frequencies than is usual with a tuning gang and since this crowding was deemed to be unsatisfactory, a variable-pitch coil having three different pitches was designed and was found to be a great improvement over ganged capacitors insofar as dial crowding is concerned. Such a coil having an initial inductance of 180 microhenries was found to have an inductance change of 10.3 to 1.

Applying a formula[2] to find the size of the loop which may be tuned we have

$$L_1 = \frac{L_s\left[\mu_{eff} - \frac{(f_{max})^2}{(f_{min})^2}\right]}{\frac{(f_{max})^2}{(f_{min})^2} - 1} \qquad (2)$$

where L_1 = loop inductance
L_s = tuning coil air inductance

To tune the complete broadcast band with some allowance for drift and misalignment, f_{max} must be at least 1,610 kc and f_{min} at most 535 kc. This is a frequency range of 3.01 to 1 or the equivalent of a 9.06 to 1 inductance change. Substituting in Eq. 2 with a μ_{eff} of 10.3 for the variable pitch coil,

$$L_1 = \frac{130\,[10.3 - 9.06]}{9.06 - 1} = 20\ \mu h$$

For the 82 square-inch loop which is being used in this instance, it was found that 20 μh was obtainable with 5.6 turns. The effective height of this loop is calculated by the use of Eq. 1. The Q of the circuit is very nearly the Q of the tuning coil itself since it forms the greater part of the total inductance, and figure of merit equals $heXQ$.

Knowing that the total inductance at 1,610 kc is 130 + 20 or 150 μh, the inductance at other frequencies is found by multiplying 150 by the square of the frequency ratios. For example at 1,500 kc,

$$L = \frac{(1,610)^2}{(1,500)} \times 150 = 172\ \mu h$$

Some of the important characteristics of this input circuit are shown in Table I.

The factors which must be known for the calculation of the transformer-coupled loop[1]

- k = coefficient of coupling between primary and secondary. This value varies as the coil is tuned
- m = ratio of primary inductance to loop inductance
- L_{eqv} = total inductance as seen at the grid of the tube
- Q_{eqv} = total circuit Q as seen at the grid of the tube

While it is highly desirable to keep both m and k constant as L_s is tuned, this is not feasible. In order that k be as large as possible across the entire band, it was found desirable to wind part of the primary over the top of the secondary (top being considered the end of the secondary through which the iron core enters), the rest of the primary being concentrated at a point about half-way down on the secondary winding.

Theoretically, any number of turns of the low-impedance loop can be coupled into the secondary and the same signal obtained at the grid. Actually, however, larger loop inductances result in more primary turns which yield a somewhat higher coefficient of coupling than small primaries. For this reason when dealing with table model loops, a 4-turn loop gives better results than a 2-turn loop. Also, Q is improved with the increased turns. In the comparison made here, a 4-turn loop of 82-square-inch area having an inductance of 10 μh was used with the transformer-coupled input circuit.

Since the presence of the primary winding connected through the loop reduces the tuning range of the secondary, the size of the primary winding must be determined experimentally, although if the coefficient of coupling is known, the maximum size of the primary needed to maintain tuning range may be calculated. This primary inductance is usually of necessity smaller than the optimum value which should be used for the coefficient of coupling encountered. Actual values of k and m for a 130-μh variable pitch secondary coupled to a 10-μh loop are given below. These values were de-

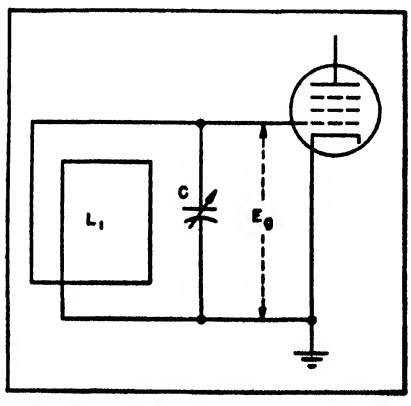

FIG. 3 — High-impedance capacitance-tuned loop circuit

TABLE II—Transformer-Coupled Loop

Frequency in kc	Transformer Gain	Loop Effective Height μv/m	Figure of Merit	Tuned Circuit Impedance $\omega L_{eqv} Q_{eqv}$
1,500	59.5	0.00664	0.395	108,500 ohms
1,000	116.5	0.00442	0.515	151,500 ohms
600	241	0.00265	0.640	247,000 ohms

TABLE III—Capacitance-Tuned Loop

Frequency	Q	Effective Height in μv/m	Figure of Merit in μv/m	Tuned Circuit Impedance ωLQ
1,500	70	0.0284	1.98	120,500 ohms
1,000	83	0.0189	1.57	95,500 ohms
600	70	0.0113	0.795	48,300 ohms

termined experimentally in order that the tuning range be covered.

Frequency	k	m
1,500 kc	47.%	0.28
1,000 kc	61.3%	0.34
600 kc	70.%	0.46

Purely theoretical considerations would have made $m = 0.75$ at 1,500 kc and $m = 0.47$ at 600 kc, thus[1]

$$Q_{eqv} = Q_s \frac{(1 + m - mk^2)}{(1 + m + 2mk^2)} \quad (3)$$

The assumption used in deriving this equation was that the total primary circuit Q made up of both loop and primary inductance is equal to $(\frac{1}{2})\ Q_w$. This is close to being the actual case and at

$$1{,}500 \text{ kc}, Q_{eqv} = 90 \frac{(1 + 0.28 - 0.062)}{(1 + 0.28 + 0.124)} = 78$$

$$1{,}000 \text{ kc}, Q_{eqv} = 95 \frac{(1 + 0.34 - 0.128)}{(1 + 0.34 + 0.256)} = 72.4$$

$$600 \text{ kc}, Q_{eqv} = 110 \frac{(1 + 0.46 - 0.225)}{(1 + 0.46 + 0.45)} = 71.2$$

$$L_{eqv} = L_s \frac{(1 + m - mk^2)}{(1 + m)} \quad (4)$$

Since at 1,610 kc, it was found that $k = 80.3$ percent and $m = 0.15$,

$$L_{eqv} = 130 \frac{(1 + 0.15 - 0.0138)}{(1 + 0.15)} = 128.2 \ \mu\text{h}.$$

Knowing the tuning inductance at 1,600 kc, the inductances at other frequencies can be calculated as before for the series circuit[1]

$$\text{Gain} = kQ_{eqv} (L_s/L_1)^{1/2} \left[\frac{m^{1/2}}{1 + m}\right] \quad (5)$$

From Eq. 5

$$L_s = \frac{L_{eqv} (1 + m)}{1 + m - mk^2} \quad (6)$$

Then

$$\text{Gain} = kQ_{eqv} \left[\frac{L_{eqv}}{L_1}\right]^{1/2} \left[\frac{m}{(1 + m)(1 + m - mk^2)}\right]^{1/2} \quad (7)$$

Knowing the gain of the input transformer, the figure of merit of the loop system is the effective height of the loop multiplied by the gain of the transformer. Pertinent characteristics for the transformer-coupled circuit are shown in Table II.

Capacitance-Tuned High-Impedance Loop

To satisfy tracking considerations, it was found that the capacitance-tuned high-impedance loop should have an inductance of 183 μh. Knowing that a 4-turn loop of this area had an inductance of 10 μh we may calculate the turns of the 183-μh loop as

$$\sqrt{\frac{183}{10}} \times 4 = 17.1 \text{ turns}$$

The figure of merit for this loop circuit is loop effective height multiplied by loop Q. Table III shows the characteristics for the capacitance-tuned high-impedance loop including the loop Q when mounted about two inches from its associated chassis. Figure 3 shows this type of loop circuit.

In most receivers sufficient intermediate-frequency gain is available so that actual gain of the antenna circuit is of minor importance compared with the signal-to-noise ratio of this circuit.

The input circuit noise[4,5] is

$$E_t = 1.28 \times 10^{-10} \sqrt{FR} \quad (8)$$

where E_t is the noise in volts

F = receiver bandwidth in cycles (7,000 cycles in the present analysis)

R = tuned circuit impedance in ohms connected to the input tube grid plus the equivalent input noise resistance of the input tube

The equivalent input noise resistance (shot noise referred to the grid circuit) is[6] 3,300 ohms for a 6SG7 tuned r-f amplifier. This noise resistance is negligible compared with the tuned circuit impedance. However, in the case of a 6SA7 converter tube used as the input tube, the equivalent noise resistance is 240,000 ohms and is of considerable importance in determining the signal-to-noise ratio.

If we divide the grid circuit noise as given by Eq. 8 by the figure of merit of the loop system, a measure of the signal-to-noise ratio for the receiver is obtained. In fact, by thus referring the noise to the input of the receiver, we have obtained the familiar ENSI (equivalent noise signal input) expressed in microvolts noise per meter which is usually used to express the signal-to-noise ratio of receivers. Using this method of analysis and the information previously derived for the three types of loop circuits, we can tabulate the performance of the loop circuits for two extreme types of input tubes as shown in Table IV.

Obviously, the permeability-tuned loop is inferior to the capacitance-tuned type with respect to both gain and signal-to-noise ratio.

When input tube noise is neglected, the actual value of tuned circuit inductance has no effect on signal-to-noise ratio, although gain is nearly proportional to the square root of inductance. When a 6SA7 is used as the input tube, it is desirable to build the tuned circuit im-

TABLE IV—Comparison of Circuits

Frequency in kc	Figure of Merit	Grid noise voltage 6SG7 Input Tube μv	ENSI μv/m 6SG7 Input Tube	Grid noise voltage 6SA7 Input Tube μv	ENSI μv m 6SA7 Input Tube
Series Loop Circuit					
1,500	0.836	4.06	4.86	6.62	7.9
1,000	0.588	5.14	8.73	7.35	12.5
600	0 108	7.15	17.5	8 86	21.7
Transformer-Coupled Circuit					
1,500	0.395	3.51	8.9	6.1	16.2
1,000	0.515	4.16	8.1	6.67	12.9
600	0.640	5.32	8.3	7.46	11.7
Capacitance-tuned High-impedance Loop					
1,500	1.98	3.71	1.87	6.4	3.23
1,500	1.98	3.3	2.1	6.17	3 9
600	0.795	2.35	3.0	5.75	7 25

pedance to as high a value as possible to overshadow tube noise..

For the foregoing analysis, the high inductance permeability-tuned coil was not considered, for it was found that a variable pitch winding could not be wound satisfactorily above 130 μh. It was found to be quite practical, however, to wind linear pitch progressive windings on a 0.226 diameter form with 250 μh inductance. Such a coil showed an inductance range of 10.6 to 1 (this compares with the 11 to 1 range for a 130-μh linear pitch coil).

An analysis of performance with this 250-μh coil is of interest, because it represents the best which we can do for a small permeability-tuned receiver with no r-f stage. Assuming use of the series loop circuit, the loop inductance can be calculated to be 47.7 μh consisting of 8.7 turns of the same area used for the previous loops. Table V is a summary of the performance characteristics using this tuning coil and loop.

Any improvement which can be made in either iron core or coil to improve tuning range will, of course, result in better performance for any of the loop-tuning circuits, insofar as signal-to-noise ratio is concerned.

One advantage which the transformer-coupled circuit enjoys over the series type, besides improved gain at the low frequencies, is the fact that the loop may be center-tapped to ground in order to provide balance to extraneous noise pickup. This is only a slight advantage, however, since the series loop is usually of low enough impedance so that noise pickup due to capacity effects is small.

With permeability tuning in a small table model receiver, the signal-to-noise ratio will be down from two to five times depending on the circuit used, the input tube and loop parameters. With some sacrifice of dial scale linearity, the gain need not be down more than two times, and this may often be regained in the i-f portion of the receiver.

A console receiver with a large area available for a low-impedance loop may have a signal-to-noise ratio equal to or better than a gang-capacitor tuned receiver, and may be done without any impairment of dial scale linearity.

While a mathematical approach[6] to the tracking of a permeability-tuned oscillator coil to the r-f coils is possible, the results are invariably inconclusive. The majority of development engineers will undoubtedly prefer an experimental approach just as they have done with gang capacitor tracking in the past. By using variable pitch oscillator coils, it is possible to obtain nearly perfect tracking, and, after a little practice, the design procedure is not lengthy.

The simplest case is one which involves a linear-pitch progressive-wound antenna coil with a series loop. If all iron cores are alike and a shunt inductance padder is used, this corresponds exactly with the gang capacitor case where all sections are alike and an oscillator series capacitance padder is used. An oscillator coil consisting of a solenoid of some convenient wire size and pitch should be wound on the same size tubing used for the antenna coil. The length of the oscillator coil should be equal to that of the antenna coil. It has been found that No. 34F, Formex or Formvar, wire with sufficient pitch to give an air inductance of about 18 μh works well. Such a coil covers too much range to track, and the range can be limited by inserting a fixed series inductance.

The alignment procedure should be as follows: With cores out of the coils by about $\frac{1}{8}$ inch, align the oscillator to the top frequency (usually about 1,610 kc). Peak antenna trimmer. Tune receiver to 1,000 kc and adjust iron core in antenna coil for maximum sensitivity. Tune receiver to about 580 kc and rock-in inductance padder for maximum sensitivity. Repeat entire procedure.

If it is found that mistracking occurs so that the antenna coil requires more capacitance (or inductance) at frequencies between 1,000 and 1,610 kc and further requires less capacitance or inductance at frequencies between 1,000 and 580 kc, the series inductance should be reduced to obtain tracking. Conversely, if it is found that the antenna coil requires less capacitance to align above the middle frequency and more capacitance to align below the middle, the series inductance should be increased.

After the correct value of series inductance has been determined, it may be measured along with the oscillator coil to find what total value of oscillator inductance is required. A new coil is then wound on a larger diameter tubing using the

Table V—250-μh Coil in Series Loop Circuit

Frequency in kc	Figure of merit	ωLQ	ENSI 6SG7 tube μv/m	ENSI 6SA7 tube μv/m
1,500	1.28	272,000 ohms	1.35	5.5
1,000	0.915	160,000 ohms	7.9	9.8
600	0.635	885,000 ohms	15.7	17.9

same wire size, pitch, and number of turns as before, but the diameter of the new coil is such that the correct total inductance is obtained.

As an example, it was found that a series inductance of 6.0 μh was required with an 18.0 μh-oscillator coil which had been wound on 0.226 O.D. tubing. A new coil having the same wire size and number of turns was wound on 0.260 O.D. tubing to have 24μh inductance. This coil tracked satisfactorily. It will be found that inductance increases as the square of the diameter, within narrow limits, for solenoids of the general configuration used for oscillator coils. If a tuned r-f coil is to be used in addition to the antenna coil, it should be wound on a suitable diameter tubing so that its inductance is equal to that of the antenna coil plus the loop.

When the antenna coil is a variable pitch winding, the oscillator coil must also have a variable pitch which corresponds. For the series loop it is only necessary that the pitch multiplying factors and proportion of turns in each section be the same for both antenna and oscillator coil. Beyond that the design procedure is the same as that previously used for the linear coils.

For example, the antenna coil consists of a progressive-universal winding of three separate pitches as follows: 83 turns at 177 turns per inch, 100 turns at 247 turns per inch, 157 turns at 363 turns per inch, for a total of 340 turns and a winding length of 1.375 inches.

Experience indicates that a convenient oscillator coil of around 20 μh should have about 130 turns. We then divide each of the above pitch figures by a factor of 2.5 to obtain the number of turns in each section of the oscillator coil. This comes out to be 33 turns, 40 turns and 63 turns. All that remains is to find the actual pitch of each section so that the total oscillator coil length is 1.375 inches. Since turns divided by TPI, turns per inch, equal winding length, we may set up an equation for TPI as follows

$$\frac{33}{\frac{177}{247}(\text{TPI})} + \frac{40}{\text{TPI}} + \frac{63}{\frac{363}{247}(\text{TPI})} = 1.375$$

solving, TPI = 94

The oscillator coil should then be wound

33 turns at $94 \times \frac{177}{247} = 67.3$ TPI

40 turns at 94 TPI

63 turns at $94 \times \frac{363}{247} = 138$ TPI

Such an oscillator coil is wound on thin-wall tubing and the required series inductance is determined in the same manner as was used for linear coils. A new coil of larger diameter may then be wound using the same number of turns and pitch to incorporate the necessary series inductance.

The transformer-coupled loop with variable pitch tuning coils is the most difficult type to track for the loop primary has a pronounced effect on the secondary tuning curve. Here it is best to start with an oscillator coil whose pitch variations correspond with those of the antenna coil as before, but mistracking will inevitably be found. The frequencies where this mistracking occurs as well as the direction of misalignment are noted.

As a general rule when more inductance is required in the antenna coil for alignment above the middle frequency (at around 1,200 or 1,300 kc), the oscillator coil winding pitch must be reduced (more turns per inch) at this end of the oscillator coil. When more inductance is required in the antenna coil below the middle frequency (around 700 or 800 kc) the middle pitch of the oscillator coil should be increased (less turns per inch).

To determine whether oscillator pitch must be reduced or increased at any particular frequency, 1,000 kc is used as the starting point since the iron cores are aligned there. Thus if more inductance is needed in the antenna coil at 1,200 kc for tracking, the oscillator core has moved too rapidly, up from 1,000 kc, and so the winding pitch must be reduced between 1,000 kc and 1,200 kc to correct.

Inasmuch as varying oscillator series inductance has somewhat the same effect as changing pitch, various combinations are possible which appear to give reasonably good tracking, but one particular combination will usually be best. Lag or lead of the oscillator core with respect to antenna core must be watched.

Very often the low-frequency pitch of the oscillator coil may be varied to correct for lead or lag, when a shunt inductance padder is used. Decreasing pitch at the low-frequency end of the oscillator coil will lower the shunt padder inductance, and this in turn will cause less oscillator core lag at 1,000 kc.

If a tuned r-f stage is used with the transformer-coupled loop, a primary winding similar to that used for the loop may also be wound on the r-f coil and a dummy inductance connected to this primary to simulate the loop.

References

(1) L. O. Vladimir, Low-impedance Loop Antenna for Broadcast Receivers, ELECTRONICS Sept. 1946.
(2) W. J. Polydoroff, Permeability Tuning, ELECTRONICS, Nov. 1945.
(3) W. J. Polydoroff and A. J. Klapperich, Effective Permeability of High Frequency Iron Cores, *Radio*, Nov. 1945.
(4) J. B. Johnson and F. B. Llewellyn, Limits to Amplification, *Bell Sys. Tech. Jour.*, Jan. 1935.
(5) W. A. Harris, Fluctuations in Vacuum Tube Amplifiers and Input Systems, *RCA Review*, Apr. 1941.
(6) A. W. Simon, Tracking Permeability-Tuned Circuits, ELECTRONICS, Sept. 1946.

Method of Plotting Tracking Error

By E. B. MENZIES

PLOTTING OF a tracking error curve is generally reckoned to be a more tedious procedure than the original calculations of correct oscillator inductance and padding capacitance.

A simple system for plotting tracking error has proved to have reasonable accuracy, and great flexibility. It is invaluable where it becomes necessary, in the design of superheterodyne coils, to make the small inductance changes necessary for perfect tracking.

It was proposed to wire the coils under test with their correct tuning and padding capacitors, and align them in the normal manner. A signal generator would be fed into the antenna coil (through the usual dummy antenna) and the frequency of the beat appearing in the mixer plate checked at various positions of the tuning capacitor, perfect tracking keeping the frequency of the beat more or less constant at the i-f frequency. The next step was to make the antenna coil produce its own signal at the frequency of the signal circuit by wiring it in an oscillator circuit, and do away with the signal generator input.

Thus, one section of the tuning gang tunes an oscillator at the signal frequency, and another section tunes the usual local oscillator. If these two are combined in the normal mixer circuit, we have a beat frequency in the plate circuit equal to the normal i-f. By beating this i-f signal with a signal of the same frequency from a signal generator, in a tube such as a 6L7, it is possible to listen with headphones in the 6L7 plate circuit to the tracking error.

The circuit is shown in Fig. 1. The antenna coil is wired in a Franklin oscillator circuit and the output of this signal-frequency oscillator is coupled to the signal grid of the 6K8. The 6K8 oscillator circuit is normal. The i-f signal appearing at the plate is coupled to the injection grid of a 6L7 detector. The output of a signal generator, tuned to the i-f frequency, is fed into the other input grid of the 6L7, and headphones are connected in its plate circuit.

Mixer Output

Although the signal in the 6K8 plate circuit contains beats equal to the sum and difference of the signal and oscillator frequencies, as well as traces of both their fundamentals and their harmonics, in practice the amplitude of the difference frequency (normally used as the i-f) is so large compared with the beats from other harmonics, that these latter may be almost disregarded. A bypass capacitor in the 6K8 plate circuit removes some of the higher order harmonics.

A gain control in the 6K8 cathode circuit enables the operator to compensate for high signal oscillator output driving the 6K8 signal grid positive.

Fig. 2A shows the constants required for loading the antenna winding. The free primary does, in most cases, show self-resonance at some point within the tuning range of the secondary. If there is self-resonance, and the coupling coefficient is of normal value, the coupled reactance of the primary may shift the resonant frequency of the secondary appreciably. Figure 2B shows a loading circuit for the primary of an r-f coil. The 10-$\mu\mu$f capacitor has been included as being a reasonably close approxima-

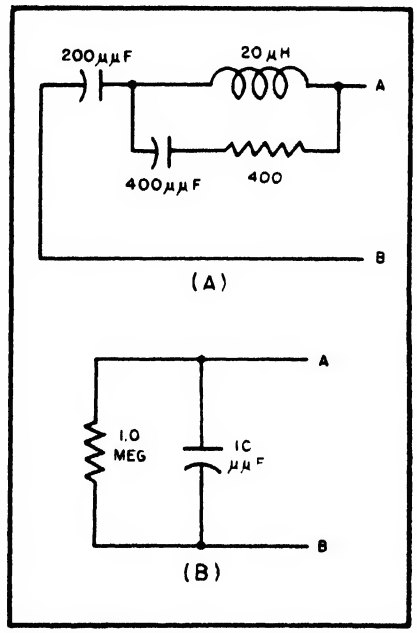

FIG. 2—Loading circuits for connection to the primaries of antenna and r-f coils

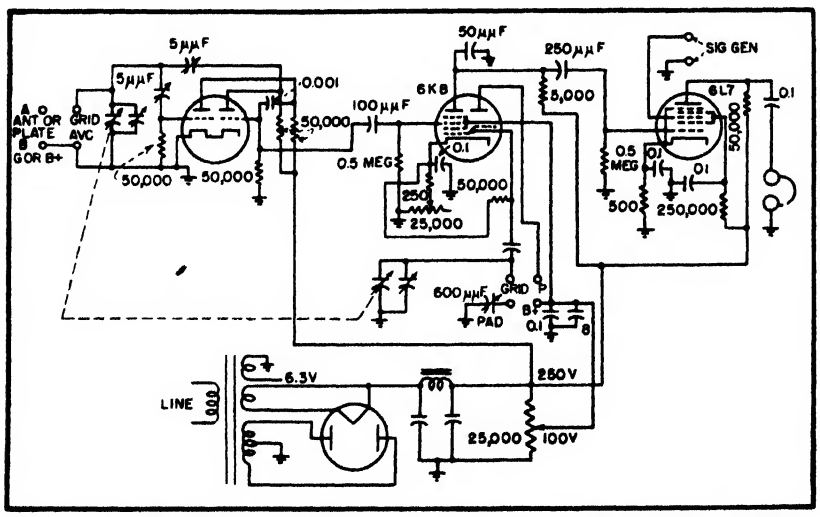

FIG. 1—Complete circuit for checking the tracking error in superheterodyne receivers. The coil terminals are lettered to indicate the corresponding connections in a typical receiver

tion to the output capacitance of most of the r-f pentode tubes in normal use.

A curve for normal oscillator tracking is shown in Fig. 3. In the case of a simple superheterodyne, we can assume that the original calculations called for the three points of perfect tracking as 600, 1,000, and 1,400 kc. These perfect tracking points show as crossovers on the curve.

While it may be possible to position the 1,400-kc crossover point correctly by adjustment of the parallel trimmers, and to position the 600-kc point by adjustment of the series padder, only correct oscillator coil inductance will position the 1,000-kc point correctly. The effect of too high an oscillator inductance is to make the two higher-frequency crossover points bunch together at the high-frequency end of the tuning range, and to make the tracking error large at the lower frequency end of the tuning range.

The procedure for taking a tracking error curve is quite simple. The antenna and oscillator coils are checked first. The signal generator is tuned to the correct i-f frequency and connected to feed the 6L7. As in normal alignment, the trimmer capacitors are adjusted at 1,400-kc, the padder at 600-kc, and the 1,400-kc point rechecked. The proper adjustment is indicated by zero beat in the headphones.

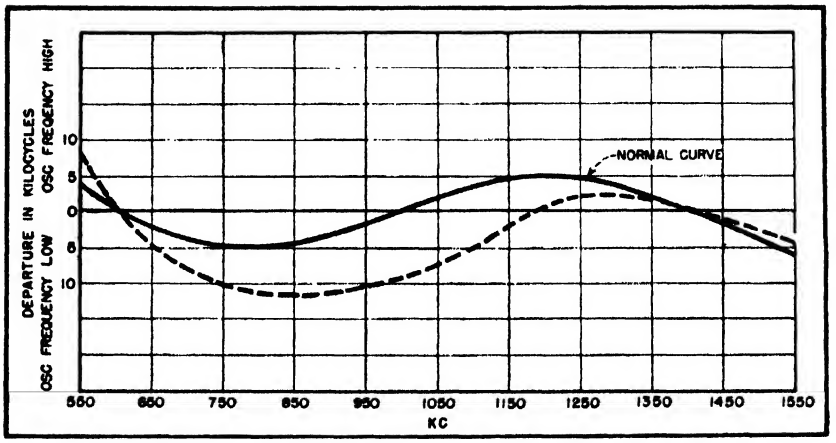

FIG. 3—Curves showing the departure of a receiver oscillator from perfect tracking. The dashed curve is that obtained when the oscillator inductance value is too great

When the gang is tuned from the full-in to full-out position, if the oscillator inductance is correct there should be three points of zero beat, 600, 1,000, and 1,400 kc. At other than these points the beat note in the phones will vary in pitch with the position of the tuning capacitor.

The deviation from perfect tracking at any point may be measured by leaving the gang set at that point and retuning the signal generator for zero beat. It is possible to determine exactly the deviation in kilocycles from perfect tracking, and to tell if the oscillator signal is high or low in frequency. It is then a matter of minutes to plot a curve. With an intermediate frequency of 465 kc, a deviation of about 5 kc appears in order, particularly with a standard gang which would be almost certain to show some inaccuracy in itself.

The procedure in the case of an r-f coil is to remove the antenna coil, substitute the r-f coil, and leave all trimmers set as they are. When the r-f coil primary is loaded correctly, rotation of the gang should produce a similar curve, with little or no alteration of the antenna trimmer.

If the equipment is made so that coil connections can be easily and quickly made, then a tracking error curve can be made in a few minutes. The system has proved itself here in a practical way, and the accuracy would appear to be well within the limits of mass-production manufacturing tolerance.

VHF Receiver Measurements

By HOWARD GORDON and LOUIS GEORGE

ADVANCE OF COMMUNICATIONS into the very high frequencies has made accurate measurements of receiver radio-frequency selectivity characteristics increasingly difficult. Standard signal generators available for use at these frequencies, up to the present, have no provision for accurately discerning the sufficiently small increments in frequency required for these tests. In many cases, the receiver under test has a relatively sharp selectivity characteristic—in the order of kilocycles, while the signal generator tuning dial divisions represent frequency differences in the order of megacycles.

The technique to be described was found to be superior to the usual method of reading the signal generator dial divisions for small frequency increments.

Referring to the block diagram shown in Fig. 1, the signal generator is resonated to the receiver frequency and the input level adjusted to produce some convenient rectified carrier voltage across the second detector load resistor. A calibrated communication receiver capable of tuning to the intermediate frequency is then coupled into the i-f amplifier of the receiver under test at some point where the signal level is of convenient amplitude. The calibrated receiver is then tuned to the inter-

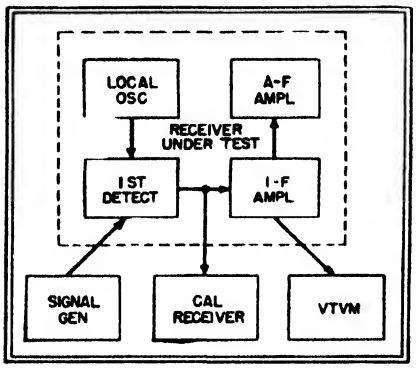

Fig. 1—Use of receiver calibrated at the intermediate frequency of the receiver under test

mediate frequency produced and the frequency and input level recorded.

Adopting the usual procedure, the signal generator is detuned in small frequency increments, at the same time increasing the input level to the value required to maintain the initial output voltage. At each point, the calibrated communication receiver is tuned to the intermediate frequency. The difference between any reading of the calibrated receiver and its initial tuning is equal to the difference between the corresponding and original signal generator frequency. This procedure is carried out above and below the receiver's resonant frequency as far as desired. The selectivity characteristic can then be plotted in terms of decibels below maximum response as shown in Fig. 2.

When the local oscillator in the receiver under test is crystal controlled, as found in spot-frequency receivers, then by knowing the intermediate frequency at any time, the signal generator frequency can be calculated. This method can also be used to advantage in checking signal generator frequency calibration and thermal drift.

It should be noted that the above procedure assumes that the receiver local oscillator will not change in frequency during the test. For practical purposes this is probably a reasonable assumption and certainly true if the local oscillator is crystal controlled. Any oscillator drift is easily measured, however, with the calibrated and comparatively low frequency receiver by beating a harmonic of its local oscillator with the high frequency oscillator fundamental and multiplying receiver tuning by the order of the harmonic used. It is not necessary to have any frequency calibration of the signal generator except insofar as this information may be needed for correcting attenuator settings. If the local oscillator frequency is known or can be accurately measured, that value and the intermediate frequency measured with the calibrated receiver will give the signal generator frequency.

An error in absolute value of frequency can be introduced when the auxiliary receiver is tuned to zero beat. The reason for this is that the

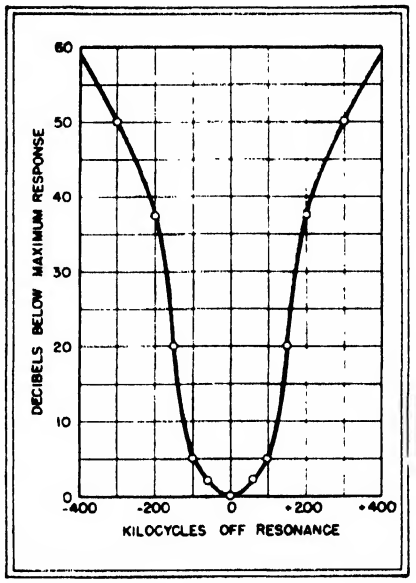

Fig. 2—Selectivity of vhf receiver measured between i-f stages by calibrated low-frequency receiver

beat frequency oscillator in the calibrated receiver may be tuned three or four kilocycles from the resonant frequency of the i-f amplifier. However, this difference is usually negligible at very high frequencies. When an available calibrated receiver will not tune to the intermediate frequency of the receiver under test, it may still be used by tuning so that a harmonic of its local oscillator beats with the i-f signal. All receiver frequency difference readings would then be multiplied by the order of the harmonic being used.

High-Level Detector

By J. C. RANKIN

METALLIC-OXIDE RECTIFIERS have been experimentally used for years in radio receivers, however, their use has been restricted to high-impedance circuits that are followed by audio frequency amplifiers. These amplifiers, unless carefully designed, introduce harmonic distortion. Coupling networks, especially the loudspeaker transformer, introduce frequency distortion.

To avoid these sources of distortion a low-impedance high-level detector system, the basic circuit of which is shown in Fig. 1, is suggested. It will be observed that all audio frequency amplification has been eliminated and that the only source of distortion is the detector.

This detector can be any single element metallic rectifier, such as used for battery chargers or toy trains. The output transformer operates at radio frequency and is constructed

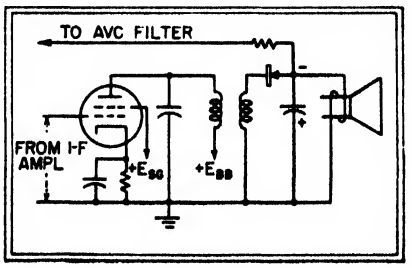

FIG. 1—Metallic-oxide rectifier simplifies audio output circuit

so that the tuned primary winding, in conjunction with the reflected impedance of the voice coil, substantially matches the plate resistance of the output tube. The radio-frequency impedance of the secondary winding is equal to the audio-frequency impedance of the loudspeaker voice coil.

The capacitance of the metallic oxide rectifier plates, which is detrimental in high impedance circuits, has little effect on this circuit. This capacitance may be in the order of 500 micromicrofarads but because it is in series with an impedance of approximately six ohms, it causes little loss.

The shunting capacitor C_1 can be 0.5 μf without affecting the audio frequencies; at 455 kc a 0.5μf capacitor has a capacitive reactance of approximately 0.6 ohms and will bypass any radio frequency voltage which may be fed through the capacitance of the rectifier plates.

The voltage applied to the loudspeaker voice coil can also be used as a source of voltage for automatic volume control. As the detector operates into a low impedance load, the avc can be applied to the cathodes of the i-f amplifier tubes instead of their grids.

The circuit, shown at Fig. 1, operates as a half-wave detector but greater output can be obtained by using a fullwave bridge rectifier, as shown in Fig. 2.

The metallic oxide rectifiers operate fairly efficiently at 455 kc but greater overall stability and gain can be obtained by using a second converter in the receiver to produce approximately 50 kc on the grid of the power tube.

A volume control of the wire wound type can be inserted between

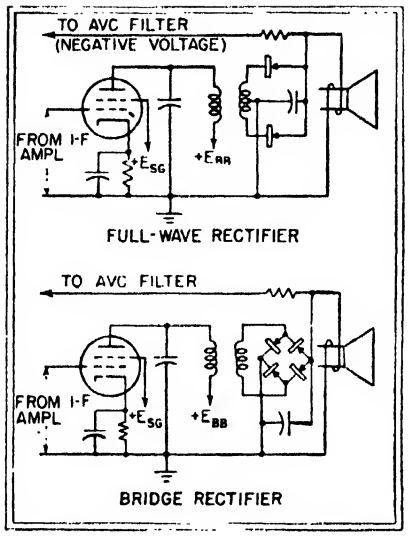

FIG. 2—Best results are obtained with a full-wave rectifier

loudspeaker voice coil and secondary winding of the output transformer. This control may be either a variable series resistance or a pad type attenuator. If a variable series resistance is used, when the volume is decreased the output transformer secondary no longer looks into a six-ohm load and the voltage across the secondary coil increases, consequently the avc voltage increases simultaneously with a decrease in volume at the loudspeaker. However, this feature cannot be utilized beyond a certain limit as it is necessary to maintain a load on the primary winding of the output transformer to prevent radiation and coupling between various stages of the receiver.

It will be noted that besides improving the fidelity, the use of a low-impedance high-level detector allows all tubes to contribute to the selectivity of the receiver.

Experimental Circuit

One experimental circuit used by the author was similar to that of Fig. 1; the output tube was a 6V6. This tube was fed from the final 455 kc i-f transformer of a small receiver. The primary winding feeding the 6V6 was a broadcast antenna coil approximately $\frac{3}{4}$ inch in diameter, with the antenna winding removed. A variable capacitor in series with a fixed one tuned this primary winding. The secondary winding consisted of 15 turns of 20-gauge enamel covered wire wound over the bottom end of the primary; the position of this winding was made adjustable as the coupling position is critical.

It was found that the loudspeaker winding presented an inductive load which was reflected across the transformer primary and because of this fact more tuning capacitance than is normally required was needed to retune the loaded circuit to 455 kc.

When the correct coupling position is obtained, only a small amount of shielding is required and it was found that radiation from the power stage did not affect another receiver placed three feet away.

The rectifier is a single copper plate that is oxidized over an area $1\frac{1}{4}$-inches square and pressed against a steel plate. Using the full-wave circuit, about two-watts output was developed from a 6V6. Listening tests indicated that fidelity was comparable to a console receiver.

The low-impedance high-level detector can be applied to phonograph amplifiers by modulating an oscillator with the pickup voltage, and amplifying and detecting as described above.

Directly Coupled Phase Inverter

By E. JOHNSON

DIRECT-CURRENT symmetry and stability of output are obtained from the phase inverter shown in the accompanying diagram. Because of these properties, the circuit is useful in handling flat-topped pulses, low frequencies and the like. The indicated values of the components, although considered optimum for the specific application for which this circuit was developed, should be taken as suggestions rather than absolutes.

The upper half of the inverter is recognizable as a cathode-cou-

pled amplifier[1,2]. The output of this half is in phase with the inverter input.

The lower half is the same as the upper half but with its grids interchanged. With respect to quiescent conditions, the lower half of the circuit behaves identically to the upper half. However, the output of the lower half is 180 degrees out of phase with the inverter input. The inherent gain of the lower half is about half that of the upper half so that an adjustment of the potentiometer R_3 is necessary to equalize the outputs of the two halves. Overall gain of the inverter is controlled by R_1.

Potentiometer R_4 is adjusted to make the d-c output voltage of each half of the circuit equal, the adjustment being made in the absence of signal and before R_2 is adjusted. The subsequent adjustment of R_2 does not necessitate any further adjustment of R_4, making the circuit very easy to balance. Essentially, each half of the circuit operates independently of the other half so that there is no tendency towards regenerative drifting and critical adjustment that characterize many comparable circuits.

With the typical values of components as shown, the circuit has a voltage gain of about 20 and handles inputs up to two volts without appreciable distortion. Use of 6SN7's would have reduced the gain to about seven. Graphical analysis offers a convenient means of investigating the performance of the circuit and provides a guide for selecting the components[3]

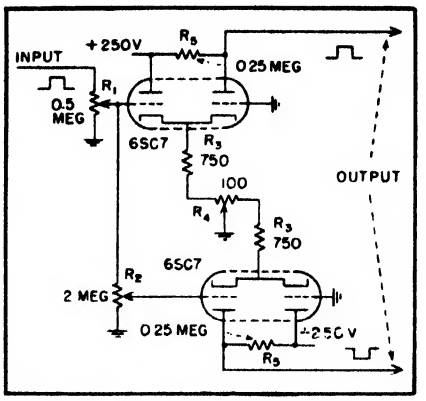

Phase inverter is directly coupled

REFERENCES

(1) G. C. Szikiai and A. C. Schroeder, Cathode-Coupled Wide-Band Amplifiers, *Proc IRE*, p 701, Oct. 1945.
(2) K. A. Pullen, The Cathode-Coupled Amplifier, *Proc IRE*, p 402, June 1946.
(3) M. S. Rifkin, A Graphical Analysis of the Cathode-Coupled Amplifier, *Communications*, p 16, Dec. 1946

Noise-Free Code Reception

Discrimination between the time constants of signal and noise allows continuous waves to trigger an audio tone generator feeding the loudspeaker. Amplitude and frequency variations have little influence on circuit operation

By D. L. HINGS

NEED for improved reception of continuous-wave signals at lower threshold levels, or in greater levels of impulse wave interference, has been felt by all communication men for many years. The various expedients to reduce shock from impulse waves, in the form of limiters, have proven this. Although limiters are very effective in some cases, it has been obvious that tone heterodyning from a beat-frequency oscillator was entirely unsatisfactory for noise-free or automatic communications under impulse interference of atmospheric or a man-made nature.

In the approach to this development, it was considered that the fundamental problem with present-day reception systems was involved in discrimination between the similar wave trains produced by noise and c-w signals. Therefore, if detection were possible when only one form of energy existed, this problem would be solved. This might be possible if receivers were made sufficiently sensitive and detection of amplitude changes during the signal interval were nonexistent.

It was further reasoned that electrical interference energy existed at all times in a communications receiver, either from antenna pickup or from front-stage noise in the receiver. A c-w signal is continuous, having on and off intervals and fading characteristics. Interfering impulse noise by contrast is discontinuous and the duration of the interfering impulses is much shorter than even high-speed c-w intervals.

Static impulses, ignition interference, and discharge interference have extremely short time constants at the antenna, but after amplification through r-f and i-f amplifiers these constants are increased several hundred times.

The effect of interference impulses on the receiver tuned circuits ahead of the detector is shown in Fig. 1. An impulse (*A*) will ring the tuned circuits of the first r-f amplifier to many times the duration of the initial impulse (*B*). This in turn excites the next stage which rings for a still longer duration, depending on the Q of the tuned circuits, and so on. (*C*).

The r-f and i-f amplifier circuit time constants will prevent the original impulse from being amplified, and instead of an impulse appearing at the second detector, there will be a wave train (*D*) that rises in amplitude in accordance with the circuit constants which remains for the duration of the

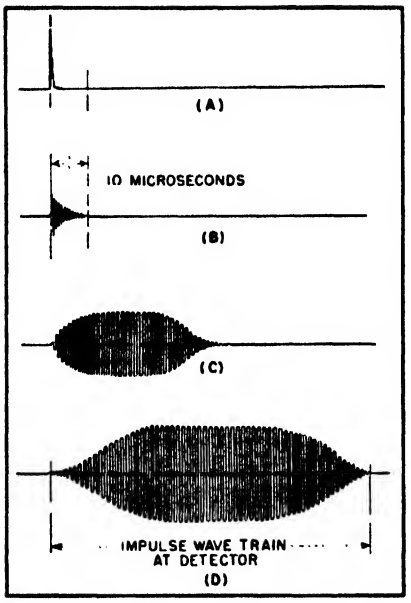

FIG. 1—Analysis of the action of an impulse through the tuned circuits of a receiver

ringing of the tuned circuits, falling to zero as dictated by the circuit characteristics. This may take from fifty to several hundred microseconds, depending on the amplitude of the original impulse, whereas this initial impulse duration (*A*) may be only a fraction of a microsecond.

In referring to impulse interference at the detector, it is necessary therefore to consider these interferences as discontinuous wave trains that vary in length in accordance with the amplitude of the original impulse. It is these receiver-generated wave trains that cause portions of the intelligence waves to be obliterated from the detector when the amplitude or audio beat is being detected.

In receiving locations having a high ambient impulse background noise, it would seem that these wave trains could be frequent enough to create a continuous wave if they followed each other very closely. Considering that each wave train, or circuit ring, is started by an impulse, and these impulses have no phase relation to each other, then it will follow that the random phase relation will cause conflicting phase angles between each wave train and, therefore, cannot make up a continuous wave. These phase differences between wave trains cause the amplitude to fall between each wave train. This condition marks the distinction between reception of a continuous wave and that of impulse wave trains at the detector circuit in receivers of conventional design.

If a c-w receiver is subjected to heavy ignition noise with repetition times of two or three hundred cycles per second, there will exist at least an equal number of wave trains, or even more if several arcs occur on one ignition discharge. This means that c-w intervals will be separated by a large number of wave trains of shorter duration.

The detector voltage from the discontinuous wave trains may be considerably greater than the voltage from the continuous waves, thereby preventing the use of an avc system. The amplitude of the discontinuous waves may be much greater than the continuous waves, thereby preventing a readable note from a bfo detector.

The fundamental difference between the discontinuous waves and the continuous waves is their relative duration. This phenomenon is illustrated in Fig. 2, showing the difference between continuous and discontinuous wave trains at (*A*).

When the rise and fall of the detector voltage produces audio energy, the greatest voltage change occurs when only the impulse wave trains exist. The detector audio voltage during the c-w intervals is produced by the impulse wave trains amplitude modulating the continuous waves.

To permit a clean demarkation between the marker and spacer intervals, it is necessary to erase this modulation during the marker, as it provides less audio energy than the spacer. Erasing c-w of the discontinuous wave trains necessitates very heavy limiting at the second detector, so that continuous waves will not permit a change in the detector audio voltage during the marker interval as illustrated in Fig. 2(B).

With satisfactory limiting of the detector, there will exist audio energy from the rise and fall of each end of a discontinuous wave train and a silent period during the relatively long c-w marker interval (*C*). This form of limiting permits clean demarkation between c-w and impulse noise. However, the audio energy obtained during the spacer interval does not have constant frequency characteristics, making it unsuitable for direct reproduction.

To reproduce the marker time interval, the spacer audio energy must be amplified, limited (*D*), rectified (*E*), then the d-c component used to trigger an audio tone generator to produce marker (*F*) or spacer tone intervals. The d-c may also be used to operate a teletype machine directly.

A simple method of producing a tone for the marker interval involves utilization of the d-c voltage that is derived from the spacer audio energy for biasing an audio tone amplifier to cutoff. Then the c-w interval interrupts the d-c voltage and the amplifier produces the desired tone.

In the practical application of this system, it is found desirable to have two or three filter time-constant adjustments in the d-c generating circuit. This provides for various speeds of reception so that

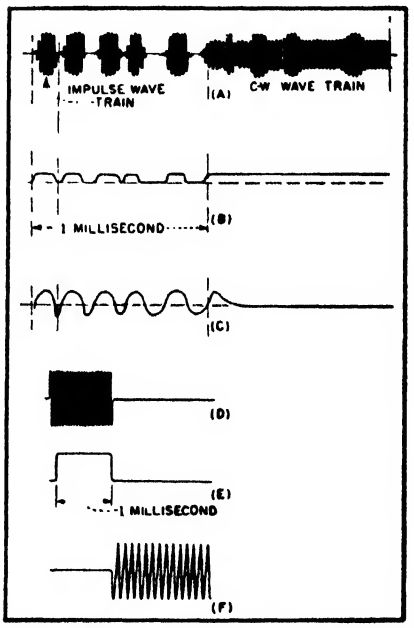

FIG. 2—Steps in the limiting and detection of a c-w signal

even when, for example, one hundred words per minute cannot be received due to very heavy impulse noise, a setting is available for lower speeds. Adjustable tone frequency is also provided to prevent operator fatigue. The receiving accuracy of the system is dependent on the shock and the ringing characteristics of the receiver circuits.

It is quite normal to get perfect reception through impulse noise from a c-w signal that is not discernible on orthodox reception systems. Conditions of reception have been noted under actual test, using standard communications receivers combined with this noise-eliminating device, where perfect reception was obtained even though S meter indications showed S9 interference levels against S1 signal intensity.

The schematic circuit diagram shown in Fig. 3 covers the arrangement for a unit primarily intended for aural reception and adaptable for connection to the i-f amplifier of a standard communications receiver. Tubes V_1 and V_2 are sharp-cutoff-type r-f amplifiers, V_2 functioning somewhat as a peak limiter. The diodes V_3 are represented in the detector circuit with one section acting as the demodulating diode, which prevents modulation on the carrier wave on any voltage exceeding the difference between the detector voltage and the 4½-volt bias system.

The circuit functions are illustrated in Fig. 3. Normal detection is provided by diode 1 until the amplitude is great enough to cause rectification to occur in diode 2 during the reverse cycle, at which time the energy in excess of the effective bias will be equal and opposite across the detector load circuit. The half-cycle difference will be absorbed by the filter network, thereby neutralizing any effective audio-frequency voltage change across the detector load resistance.

Tube V_4 is a high-frequency audio amplifier operating V_5 which is a square-wave amplifier. The output from V_5 is relatively constant in amplitude and rectified by diode V_6. The filter capacitor for the rectifier may be switched in value from 0.003 to 0.02 μf for various speeds of keying, and the d-c energy provides cutoff bias to V_6.

Tube V_8 is a phase-shift audio oscillator supplying energy to the grid of V_9, which in turn excites power amplifier V_9. The frequency and amplitude of the oscillator are controlled in the resistance network and the volume control is in the grid circuit of the power amplifier.

The system provides for reception of all detectable signals without interference. Controlled tone pitch and intensity reduce operator fatigue and greatly increase the accuracy of copying. All signals received are automatically reproduced in unvarying intensity, and absence of background noises permits the simultaneous operation of many receivers in the same room without disturbance to any of the operators.

During standby periods, the receiver is completely silent even though adjusted for maximum sensitivity.

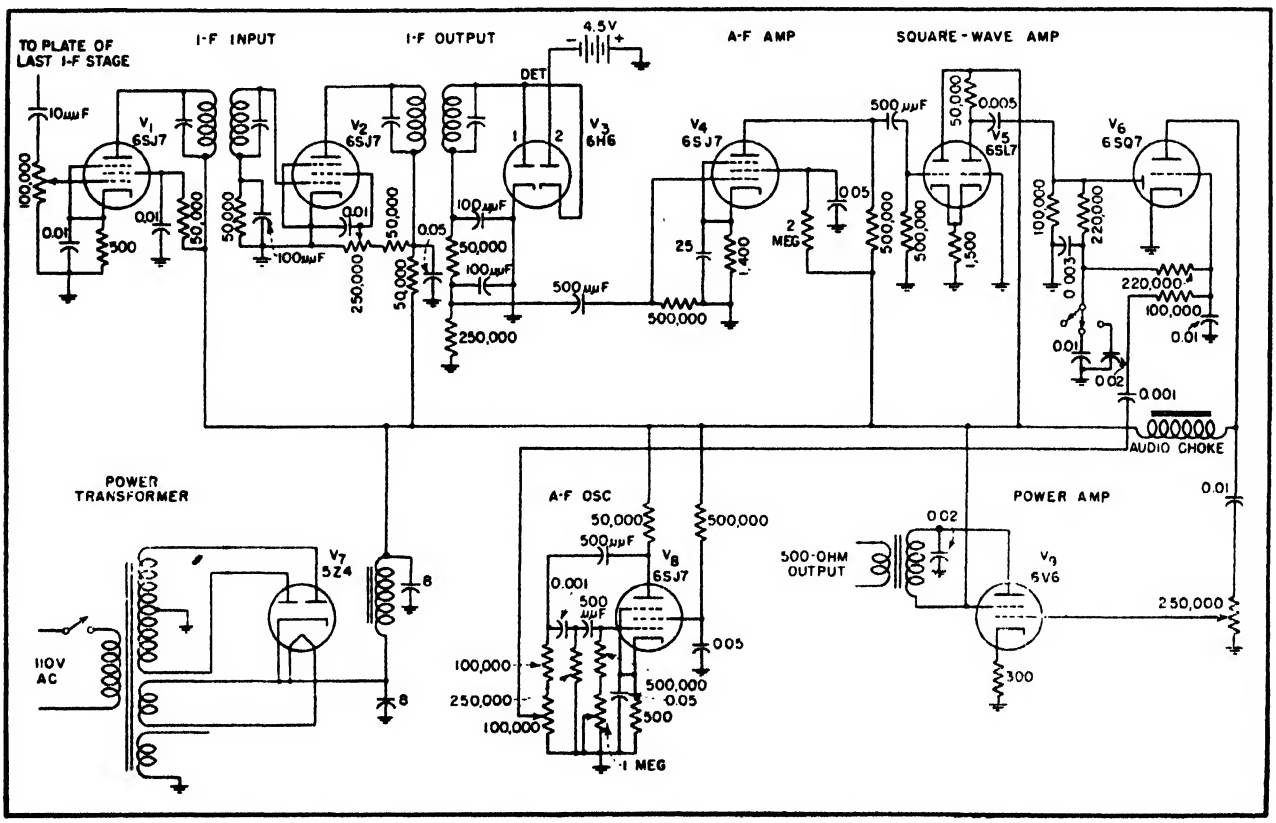

FIG. 3—Complete circuit of the system for eliminating noise from c-w signals by discriminating between the time constants of noise and the desired signal

Mixer Frequency Charts

By R. S. BADESSA

WHEN two frequencies, B and A, are mixed to produce the sum frequency $B + A$ or the difference frequency $B - A$, a possibility exists that some harmonic of B, or some harmonic of A, or some combination of the harmonics of B and A will produce unwanted components lying close to the desired frequency. In some cases the magnitude and frequency of these unwanted components are such as to present serious problems in selectivity, often to the extent of requiring a different choice of input frequencies.

The two charts shown provide a means of determining in advance the unwanted components capable of arising from a given choice of mixer input frequencies. The charts are based on the fact that when the ratio of the two input frequencies, A/B, is also equal to the ratio k/l where k and l are integers and A is the smaller of the two input frequencies, two unwanted components exist capable of coinciding or zero beating with the sum frequency $B + A$. These are $(l + 1)A - (k - 1)B$ and $(k + 1)B - (l - 1)A$. Where the wanted frequency is $B - A$, the corresponding unwanted components are $(l - 1)A - (k - 1)B$ and $(k + 1)B - (l + 1)A$.

Unwanted components up to the 15th order are classified in the charts according to the ratio A/B for which coincidence with the wanted sum or difference frequency occurs.

If coincidence does not exist, notice the components corresponding to ratios not far removed from the ratio being investigated. The frequencies of these components, especially those of low order, should be calculated to determine how difficult a selectivity problem exists.

Example. A frequency of 4.9 mc is mixed with a frequency of 2.1 mc to produce a sum frequency of 7.0 mc. For this case $R = 2.1/4.9 = 0.429$. On chart No. 2 the interfering components for $R = 0.429$ are of the tenth order and have the forms $4B - 6A$ and $8A - 2B$. Since a tenth-order component is probably not very serious, coincidence can be neglected. Other ratios in the vicinity of 0.429 are investigated next. For the ratio 0.500, there are two third-order components, of the form $2B - A$ and $3A$. These, when evaluated, are 7.7 mc and 6.3 mc respectively and may or may not cause trouble, depending on the selectivity of the 7-mc channel employed.

CHART I. Output Frequency $= B - A$

R = A/B	ORDER 1	2	3	4	5	6	7	8	9	10	11	12	13	14	15
0.000	B	B + A	B ± 2A	B ± 3A	B ± 4A	B ± 5A	B ± 6A	B ± 7A	B ± 8A	B ± 9A	B ± 10A	B ± 11A	B ± 12A	B ± 13A	B ± 14A
0.063															15A
0.067														14A	
0.072													13A		
0.077												12A			
0.083											11A				2B–13A
0.091										10A				2B–12A	
0.100									9A				2B–11A		
0.111								8A				2B–10A			
0.125							7A				2B–9A				14A–B
0.133															
0.143						6A				2B–8A				13A–B	
0.154													12A–B		
0.167					5A				2B–7A			11A–B			
0.182											10A–B				2B–12A
0.200				4A				2B–6A		9A–B				2B–11A	
0.214															13A–2B
0.222									8A–B				2B–10A		
0.231														12A–2B	
0.250			3A				2B–5A	7A–B				2B–9A	11A–2B		
0.273												10A–2B			
0.286							6A–B				3B–8A				
0.300											9A–2B				4B–11A
0.308															12A–2B
0.333		2A				2B–4A 3A–B				3B–7A 8A–2B				4B–10A 11A–2B	
0.364													10A–2B		
0.375									7A–2B				4B–9A		
0.400					4A–B				3B–6A			9A–2B			
0.414															11A–4B
0.429								6A–2B				4B–8A			
0.445											8A–2B				
0.455														10A–4B	
0.500	A			3A–B	2B–3A			5A–3B	3B–5A		7A–3B	4B–7A		9A–4B	5B–9A
0.545															10A–5B
0.556												8A–4B			
0.571									6A–3B				5B–8A		
0.600						6A–2B				4B–6A				9A–5B	
0.625											7A–4B				6B–9A
0.667			2A–B					3B–6A	5A–3B			5B–7A	8A–5B		
0.692															9A–4B
0.714										6A–4B				6B–8A	
0.750					3A–B				4B–5A						
0.778												7A–4B		6A–4B	
0.800							4A–2B								
0.833									5A–4B					6A–4B	
0.857											6B–5A				7B–5A
0.875													7A–4B		
1.000				5B–4A		3B–2A		4B–4A		5B–4A		6B–4A		7B–5A	

CHART II. Output Frequency $= B + A$

R = A/B	ORDER 1	2	3	4	5	6	7	8	9	10	11	12	13	14	15
0.000	B	B A	B ± 2A	B ± 3A	B ± 4A	B ± 5A	B ± 6A	B ± 7A	B ± 8A	B ± 9A	B ± 10A	B ± 11A	B ± 12A	B ± 13A	B ± 14A
0.072															2B–13A 13A
0.077														2B–12A 14A	
0.083													2B–11A 13A		
0.091												2B–10A 12A			
0.100											2B–9A 11A				
0.111										2B–8A 10A					
0.125									2B–7A 9A						
0.143								2B–6A 8A							
0.154															3B–12A 14A–B
0.167							2B–5A 7A							2B–11A 13A–B	
0.182													3B–10A 12A–B		
0.200						2B–4A 6A						3B–9A 11A–B			
0.222											3B–8A 10A–B				
0.250					2B–3A 5A					3B–7A 9A–B					4B–11A 12A–2B
0.273														4B–10A 12A–2B	
0.286									3B–6A 8A–B						
0.300													4B–9A 11A–2B		
0.333				2B–2A 4A				3B–5A 7A–B				4B–8A 10A–2B			
0.364															5B–10A 12A–2B
0.375											4B–7A 9A–2B				
0.400							3B–4A 6A–B							5B–9A 11A–2B	
0.429										4B–6A 8A–2B					
0.445													3B–8A 10A–2B		
0.500		2B–A 3A			3B–3A 5A–B				4B–5A 7A–2B			2B–7A 9A–2B			6B–9A 11A–4B
0.545														5B–8A 10A–4B	
0.556												6B–6A 8A–4B			
0.571											3B–6A 8A–3B				
0.600							4B–4A 6A–2B								
0.625													4B–7A 9A–4B		
0.667					3B–2A 4A–B					5B–8A 7A–3B					7B–8A 10A–5B
0.692															
0.714												6B–6A 8A–4B			
0.750						4B–3A 3A–2B								7B–7A 9A–3B	
0.778															
0.800									5B–4A 6A–3B						
0.833											6B–5A 7A–4B				
0.858													7B–6A 8A–5B		
0.875															8B–7A 9A–4B
1.000		2B 2A		3B–A 3A–B		4B–2A 4A–2B		5B–3A 5A–3B		6B–4A 6A–4B		7B–5A 7A–5B		8B–6A 8A–6B	

PROCEDURE: Divide smaller mixer input frequency by larger to get R. If this value of R is on chart applying to case, coincidence exists and components causing it are given somewhere to the right, with their order given at top of chart. If coincidence does not exist, calculate low-order component frequencies for nearest ratios to determine selectivity requirements

Beat-Frequency Interference Chart

By DON BARTON

INTERFERENCE may be present in the output of superheterodyne radio receivers if their input circuits are not selective enough to reject all but the desired incoming signal. These spurious responses will be the result of the combining of the oscillator frequency and/or its harmonics with the fundamental or harmonics of strong stations radiating a frequency differing from that to which the tuned input circuit of the converter is adjusted.

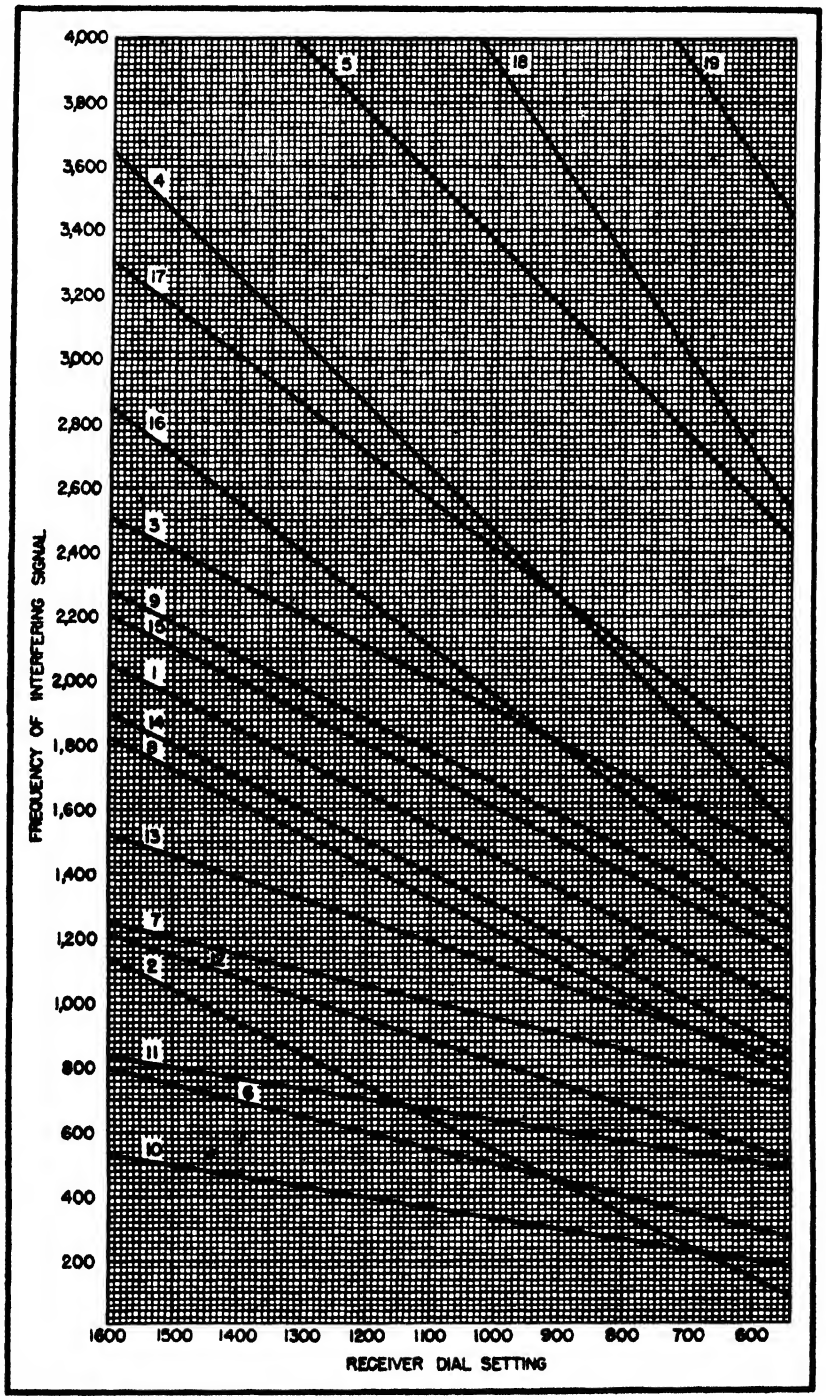

The accompanying chart plots 19 different combinations of signal and oscillator frequencies that can produce interference in a receiver using the RMA standard i-f of 455 kc.

The following examples illustrate several different types of interference. At 660 kc, a vertical line drawn on the chart will intersect all of the curves. Perpendiculars from these points of intersection to the left will give the interfering signal frequency. Thus one objectionable point is determined to be 220 kc from curve 10. A long-wave signal other than that of the i-f may consequently be present in the output of the receiver due to the local oscillator beating with the third harmonic of the interfering signal to produce 455 kc.

The intersection of the 660-kc line with curve 1 indicates an interfering signal of 1115 kc. Although no station operates on this frequency, audible beats would be produced by reaction with either or both the 1110-kc or 1120-kc carriers 5000 cycles away.

Curve number 4 shows that police calls may be received while curves 18 and 19 show that amateur signals can also beat at the same time. By using the formula numbered to correspond to the curve intersected,[1] the exact frequency of the interfering signal can be computed and the audio frequency of the whistle determined, assuming that the station producing the interference is on its assigned wavelength.

REFERENCE

(1) Adams, J. J., Receiver Interference Chart, ELECTRONICS, p 48, Feb. 1941.

Reduction of Heterodyne Interference

Adjacent-channel signals produce both amplitude and phase modulation of the desired carrier. From separate detection of these two modulations, two interference signals are obtained which cancel each other leaving only the desired signal

By H. W. BELLES

REDUCTION of constant-frequency interference such as is caused by heterodyne signals can be accomplished by utilizing the principle that heterodyne waves both amplitude and phase modulate the carrier of the desired signal. This method of interference reduction involves simultaneous detection of amplitude and quadrature modulation components of an interfering wave and subsequent canceling of the two detected outputs by balancing them against each other. The reception of desired signals, which are modulated in only one manner, remains unaffected.

The system is of particular advantage for communications in crowded bands where interference due to carrier heterodynes is objectionable, and increases the number of stations that can occupy a given frequency band without producing cross interference. In operation, the system to be described has attenuated strong interference heterodyne signals to below audibility with no apparent effect on the desired signal.

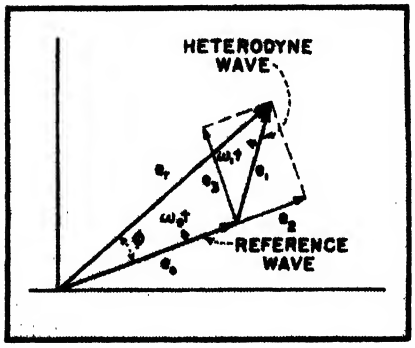

FIG. 1—Vector relations of two waves show phase and amplitude modulation of one by the other

It is an accepted fact[1] that the sum of two waves is a wave which varies in both amplitude and phase. If one of the waves is taken as a reference, the second wave can be said to produce amplitude and phase modulation of this reference wave. In Fig. 1 let e_0 be the reference wave, which may be the carrier wave of a desired signal, and let e_1 be the second wave, which may be an interfering and undesired signal. The combination of these waves can be resolved into a component e_2 which is in phase with the reference wave and produces pure amplitude modulation and a component e_3 which is in phase quadrature and produces pure phase modulation.

A heterodyne interference wave thus produces effects which differ from either those of a pure amplitude-modulated wave in which the resultant modulating vector is always exactly in phase with the carrier, or those of a narrow-band phase or frequency-modulated wave in which the resultant modulating vector may be in phase quadrature with the carrier.

The inherent characteristic of a heterodyne interference wave can be utilized to eliminate the interfering effects of the undesired wave in the reception of amplitude-modulated, or narrow-band phase or frequency-modulated signals, provided that suitable detection circuits as assumed in Fig. 2 can be devised. These detectors must be such that the amplitude-modulation detector responds only to sidebands which are in phase with a carrier, and the phase-modulation detector responds only to sidebands which are in phase quadrature with the carrier.

Detectors devised by Crosby,[2] in which carrier segregation and amplification are utilized, are adaptable for this purpose. Referring to Fig. 3, the carrier, which has been derived from the desired signal by filtering or other means and then amplified, is applied to the balanced detector as shown. Also the entire received signal is applied in a balanced manner to the rectifiers.

In the absence of the carrier, there is no detection of the received signals, and in the presence of the carrier, only those resultant signal vectors which have components directly in phase or 180 degrees out of phase with the carrier are detected. For the a-m detector the segregated and amplified carrier should be in phase with the signal carrier, while for the p-m detector the segregated carrier should be in phase quadrature.

Basic Circuit

A more complete diagram of the system is shown in Fig. 4. The receiver i-f voltage is fed in parallel to a crystal filter for segregation

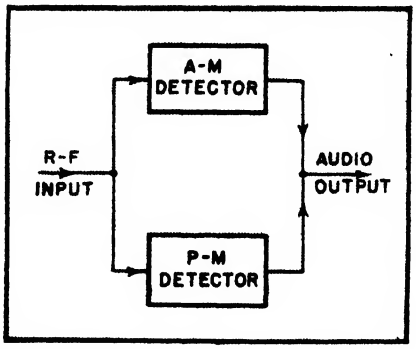

FIG. 2—System by which amplitude and phase modulation components are independently detected

of the signal carrier, and to two detectors through isolating amplifiers. The segregated carrier from the filter is amplified and fed to the two detectors, with the carrier voltage to one detector being shifted 90 degrees in phase.

One of the detectors detects amplitude modulation and the other detects quadrature modulation. For equal applied voltages, the outputs of the amplitude and quadrature detectors are equal. Thus, in the simultaneous reception, for example, of a pure a-m wave and a heterodyne interference wave, the amplitude-modulation detector will respond to both the a-m signal and to the heterodyne signal, while the quadrature detector will respond only to the heterodyne signal. Consequently if the output of the quadrature detector is combined in the proper phase with the output of the amplitude-modulation detector, cancellation of the detected heterodyne signal will result. The output of the quadrature detector must be shifted an additional 90 degrees to bring its output signal into opposition to the heterodyne signal from the other detector. Also the output of the quadrature detector must be shifted an additional 180 degrees when the heterodyne interference wave changes frequency from above to below that of the carrier.

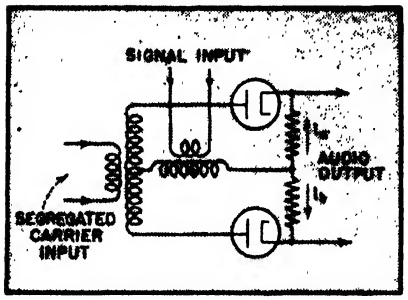

FIG. 3—Balanced rectifier is used to detect either a-m or p-m components of input, but not both

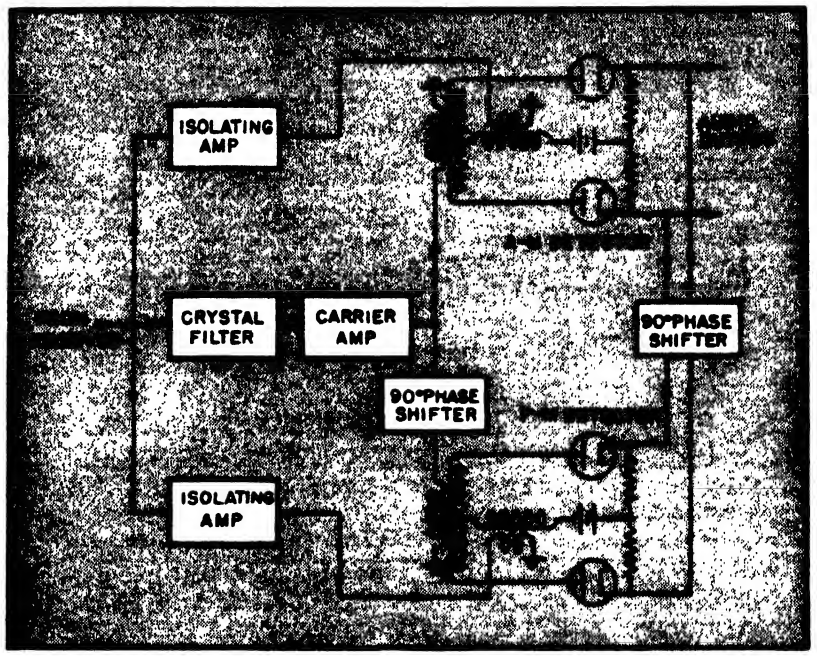

FIG. 4—By means of filters and phase shifters, the interfering carrier heterodyne can be eliminated in the detector stage, leaving only the desired signal

Detecting systems, other than that described, are also usable. For example, a single diode to which the segregated carrier and received signal are applied will detect substantially only those signal components in phase with the segregated carrier, provided that the voltage of the segregated carrier greatly exceeds that of the total signal.

It is interesting to note the effects of the large phase shifts which occur in the crystal filter when the incoming carrier is slightly off resonance. One such effect causes detection of amplitude-modulated signals by the phase-modulation detector, because if the carrier is not at exactly 90 degrees phase difference with the amplitude-modulation components some detection of these components will result. This effect of carrier phase shift can be overcome by biasing the detectors so that the segregated carrier voltage will exceed the bias voltage only when the phase shift in the crystal filter is less than a predetermined amount which should be less than 45 degrees, at which condition the outputs from the two detectors are equal.

References

(1) H. J. Reich, "Theory and Application of Electron Tubes", McGraw-Hill Book Co., New York, 1944, (2nd Ed.), p. 314.
(2) M. G. Crosby, Communication by Phase Modulation, *Proc. I.R.E.*, 27, p. 126, Feb., 1939.

Surge Protection of Pilot and Heater Circuits

By RALPH P. GLOVER

ENGINEERING a satisfactory circuit arrangement for the pilot lights and heater string in transformerless radio receivers and amplifiers has always been a trying problem. Pilot lights flare up when the set is first turned on, ultimately settle down to an illumination level which is frequently either too low for a satisfactory visual effect, or too high for reasonable pilot light life. And when the pilot light burns

out due to oft repeated surges or over-voltage operation, or opens due to mechanical failure, the set either operates at appreciably reduced efficiency or is totally disabled by the resulting subnormal heater voltage.

The growing use of selenium rectifiers has focused attention on these problems, for the rectifier tubes which were displaced had acceptable (though operationally not too satisfactory) means for connecting the pilot light in the form of a tap on the heater.

The falling resistance-temperature characteristics of negative-temperature-coefficient resistors, also known as semiconductors, thermal resistors, or thermistors, make possible an improved solution to the pilot light-heater circuit problem, and resistors of this type have recently been designed into radio receivers for current production.

Figure 1 shows the resistance of typical one-watt Keystone NTC units as a function of temperature. The temperature coefficient of resistance is negative, is much higher than that of ordinary metallic conductors, and depends upon the temperature. The NTC units are produced from rare earth oxides in values ranging from 1.0 ohm to 1 megohm at room temperature. The size and shape of the piece may be varied over a considerable range to achieve suitable electrical and thermal properties.

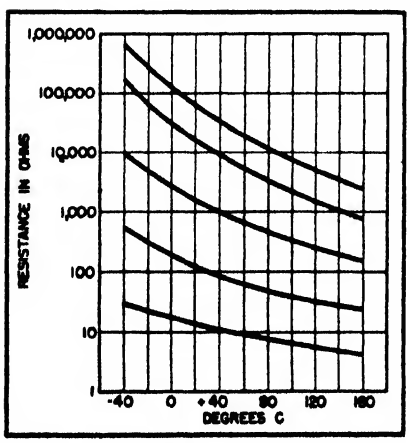

FIG. 1 — Resistance-versus-temperature curves for typical negative temperature coefficient resistors

Circuit Operation

If an NTC resistor is connected in series with other circuit resistance, the initial total resistance will be the sum of those due to the unit at ambient temperature and to the remainder of the circuit. If voltage is applied across the circuit, the initial current will be that corresponding to the above initial resistance. However, the I^2R loss in the resistor unit immediately begins to elevate its temperature and there is an accompanying and corresponding fall in resistance and an attendant increase in current. These changes continue progressively until equilibrium is reached, after which the current and the temperature and resistance of the unit remain at the equilibrium value. This value may be defined as that corresponding to the condition for which the attained temperature rise of the unit above its ambient is sufficient to produce heat loss at the same rate as electrical energy is being supplied.

The cold resistance of vacuum-tube heater circuits is exceedingly low compared with the normal continuous operation value, and hence there is a heavy current surge at switch-on. The pilot light, with its relatively small and fragile filament which is continuously evaporating in service, is less well adapted to withstand surges of the order of three to four times rated current, with the result that conventional series arrangements of pilot light and heater lead to burn-outs much earlier than is the case for more nearly constant voltage operation.

Figures 2 and 3 shows a number of practical circuits for 150 and 300-ma heater strings in combination with one or two type 47 pilot lights and suitable resistor units. Many other circuit arrangements are possible with the indicated NTC units or other values; the particular types shown here, however, are likely to show advantages in cost and ready availability over special units in limited quantities.

Figures 2A and 2B are simple, basic 150-ma circuits in which the resistor unit supplies cushioning

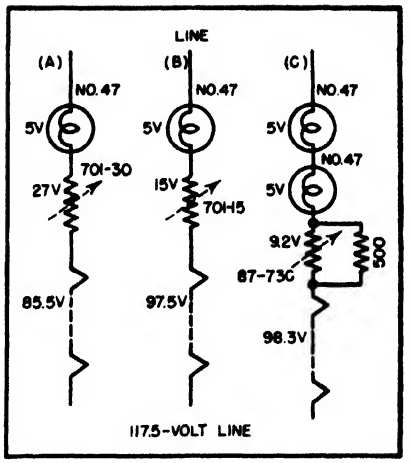

FIG. 2—For 150-ma heater tubes, the negative temperature coefficient resistors act as the only voltage dropping unit

of the initial surge and acts as the sole voltage-dropping resistor. Surge voltages across the pilot light may be limited to peak values of the order of 150 percent or less of rated voltage. Figure 2C uses two pilot lights, and a low-wattage fixed resistor is shunted across the resistor unit to achieve the desired operating characteristics.

Figure 3 shows arrangements for different heater voltage requirements with 300-ma tubes. These circuits employ the same NTC unit for the sake of standardization, the fixed resistance elements being varied to secure the desired result. It does not appear feasible to secure the total voltage drop for most 300-ma applications in the resistor unit alone, since a sufficiently large piece would have an excessively long thermal time constant.

Figure 4 shows simple and inexpensive means for automatically restoring circuit conditions upon failure of the pilot lamp, and the method is applicable regardless of the way in which the operating voltage for the lamp is secured. The resistance of the shunt protective unit is normally high compared with that of the pilot light. When the pilot fails, a substantial proportion of the total circuit voltage appears across the resistor unit, followed by an extremely rapid drop in resistance to a value approximating that of the pilot. This change takes place in a mat-

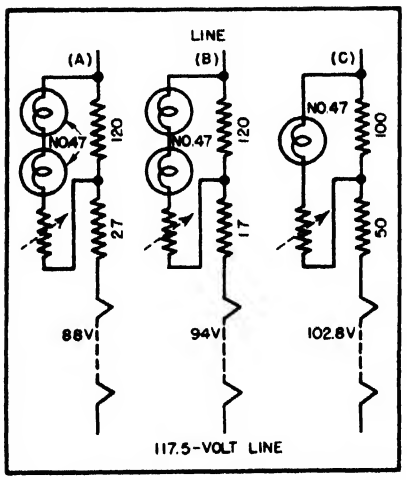

FIG. 3—Circuits for 300-ma heater stringer using type LA-701 NTC resistor units

ter of a few seconds before the operating temperature of the heaters has had an opporunity to change appreciably. In several applications, less than 3 percent change in total heater string voltage has been observed with the pilot light in and out of the socket. The LA-701 resistor for pilot light shunting is the same as that employed for voltage dropping and compensation in Fig. 3.

For these applications, it is inherent that the NTC units attain high final operating temperatures (around 300 F) to bring about the necessary resistance change in a suitable time interval. Moreover, the high operating temperature brings the unit to a point on the characteristic curve where the temperature coefficient is relatively low, and hence the effect of normal changes in ambient room temperature with season and geographical location on operating voltages is relatively small and unimportant.

Locating in Chassis

The high operating temperature presents no special problems to the receiver designer and it is necessary to observe only a few simple precautions in applying the units to production set design. These are: (1) The resistor unit should be suspended in air and should not be in contact with any part or component; (2) Leave the resistor leads as long as is consistent with space and mechanical support considerations, and anchor to large terminal lugs if there is any choice. This will result in the greatest possible temperature drop between the resistor and the supporting insulation; (3) Make sure that operating voltages are checked with the resistor unit in the proposed location after ultimate operating temperatures are reached at the room ambient conditions which are applicable. Some adjustment of operating voltages is possible by relocating the unit in a warmer or cooler position in the set.

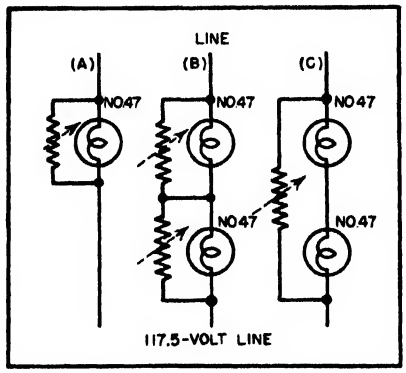

FIG. 4—Pilot lamp shunting circuits for type LA-701 units. About three percent change in total heater voltage occurs when the lamp burns out

For convenience, the resistance characteristics of the NTC units employed in the illustrated circuits are tabulated below. The rating resistance applies to a temperature of 100 F, no current. In production, tolerance is plus or minus 20% of the rating resistance. Voltage drop is measured in open air and allowance for confined space or increase due to other components must be made.

Type	*Resistance*	*Operating Current*	*Voltage Drop*
701-30	912	0.15 amp	27 v
701-15	790	0.15 amp	15 v
87-73C	2,000	0.15 amp	9.2 v
LA-701	250	0.15 amp	10 v

Use of Shunt Diode for Supplying Bias Voltage

IT IS AN UNFORTUNATE fact that radio men in general do not recognize the full potentialities of the shunt diode. In the two bias supplies to be described, shunt diodes are used for rectification with attendant advantages.

The conventional bias supply for amplifier use is shown in Fig. 1. In this circuit, a diode (usually a 6X5) is reversed and used as a half-wave rectifier for negative output. Because the heater-cathode rating will usually be exceeded, it is necessary to use a separate heater winding which frequently means an extra filament transformer. Then, because the voltage across the input filter capacitor is often too high, it must be limited by R_1. If we want only a hundred volts or less of bias (say for 2A3's), we must have an additional dropping resistor R_2. This requires two power resistors, which means power wasted and a lot of heat dissipated.

The circuit of Fig. 2A, uses a shunt diode with the cathode grounded, so there is no problem of heater supply. The load is tied directly across the output filter capacitor and the dropping resistor

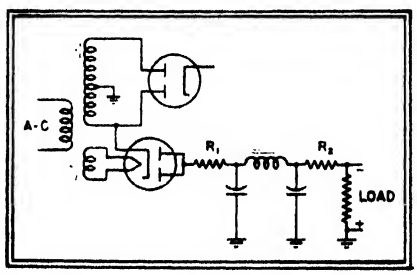

Fig. 1—Conventional method of obtaining bias from the high-voltage winding of the power transformer

is eliminated. The capacitors work at low voltage so their rating need not be high. The entire voltage drop

is accomplished in the input capacitor C with, obviously no loss of power and no heat.

For an output of 100 volts at about eight milliamperes (to 2A3 grid-voltage control potentiometers or other load), C will be of the order of 0.1 μf. It will vary with line frequency and load requirements. If separate bias voltages are not required, the load (which is merely a grid return to ground) may be removed from the output capacitor and placed across the diode as shown in the alternate circuit of Fig. 2B. The grid returns are connected to the filter output. Since the filter is then unloaded, this will provide even better filtering.

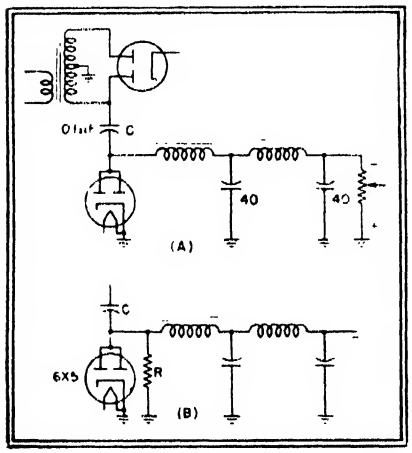

Fig. 2—At *A* is a circuit for obtaining bias with a shunt diode. Capacitor *C* acts in conjunction with the load resistor to form a voltage divider. When only one bias voltage is needed, the circuit shown at B may be used

The circuit of Fig. 2A, with the values shown, delivered 100 volts across four 5000-ohm potentiometers connected in parallel to supply the grids of push-pull parallel 2A3's. The ripple level was 0.01 volt.

Practical Circuit

An adaptation of this circuit is shown in Fig. 3A. This is intended as a source of 3 volts bias for r-f and i-f stages of deluxe receivers, thereby saving cathode bypass capacitors and resistors, and the space they occupy. This circuit will deliver up to 9 volts from a 6.3-volt heater line, depending upon C and R_1. The value of the filter resistor R_2 may be of the order of 50,000 or 100,000 ohms. It is not critical.

Figure 3B shows the circuit applied in a high-fidelity receiver as source of bias and avc delay voltage. The avc diode (also wired in shunt) is fed from the plate of the last i-f stage so that the flywheel effect of the transformer secondary will iron out the peak shunting due to the diode and hence eliminate distortion from this source. The detector is of the infinite-impedance type and will not load the secondary and so reduce the Q. The cathodes throughout the set may be grounded.

Figure 3C shows a half-wave voltage doubler supplied from the 6.3-volt heater line that will provide up to 18 volts (again depending on C and R) to pentode and beam-power tube grids for fixed-bias operation.

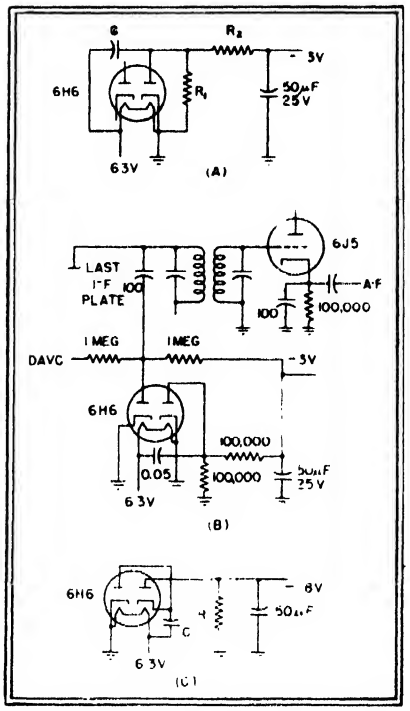

Fig. 3—Bias voltage for r-f and i-f stages is obtained from the simple circuits at A. By supplying the rectifier plate from the heater line, up to nine volts of bias is provided. B is for use in an high-fidelity receiver. Bias for beam-power tubes is provided by the circuit at C, a half-wave voltage doubler whose output is 18 volts at an input of 6.3 volts rms

Diode Contact Potential for Negative Bias

By HOWARD T. STERLING

EVER since the discovery of the so-called Edison effect, contact potential has been a source of interest and frequently of annoyance to workers in electronics. It can, however, serve as a convenient source of bias in high gain audio amplifiers and in the r-f and i-f stages of receivers.

When a diode is connected as shown in Fig. 1 there will be a d-c output voltage of from zero to something over 1 volt depending upon the value of the load resistor. The curve in Fig. 1 shows this characteristic for a typical 6H6 diode. This curve should be taken merely as indicative; the exact voltage developed will depend on several factors, such as heater voltage and the condition of the cathode. Other rectifiers will conform approximately to this characteristic.

In a triode, the grid will demonstrate the same sort of phenomenon, since it acts as a diode plate. It has become common practice to operate high-mu triodes as shown in Fig. 2A, using a high value of grid resistance, and hence permitting the tube to bias itself. A refinement of this system is to use one of the diodes of a tube like a 6SQ7 to provide bias, as shown in Fig. 2B. In this case the audio bypass capacitor C is necessary only

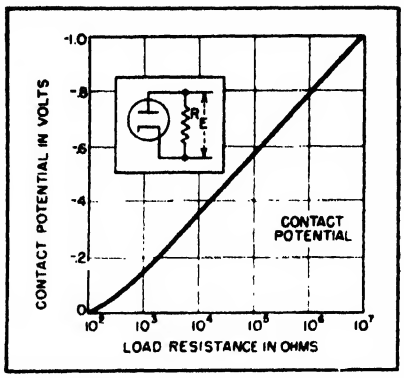

Fig. 1—Diode contact potential increases as value of load resistor is increased

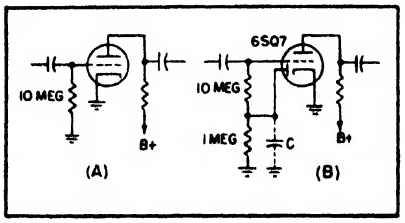

Fig. 2 — Conventional self-biasing circuit used with high-mu triodes (A). Diode section of duo-diode triode is used to furnish bias (B)

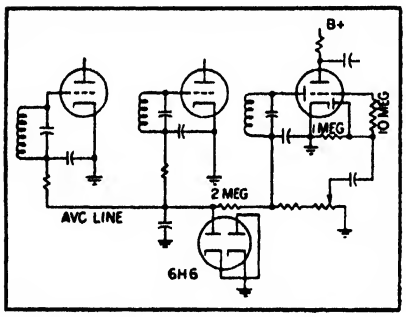

Fig. 3—Initial diode bias on avc line saves capacitors and resistors in r-f and i-f cathode circuits, also provides threshold voltage for delayed avc

when the peak signal approaches the bias voltage.

In a receiver with a number of r-f and i-f stages, considerable saving in cathode resistors and bypass capacitors may be achieved by the use of an initial diode bias on the avc line, as shown in Fig. 3. Two diode sections are shown connected in series across the avc line with an avc decoupling resistor of two megohms. With a load of one megohm per diode, it can be seen from Fig. 1 that there will be an initial bias on the r-f and i-f tubes of 0.8 volt per diode or 1.6 volts total, which is more than enough for most modern tubes. In the circuit shown, the 1.6 volts furnished by the series diodes acts as delayed avc threshold voltage. If more bias and/or more avc delay is desired, a second double diode may be connected in series with the first. It may be noted that one of the diodes of the duo-diode triode is used for triode bias in this circuit.

In a diode detector, the major source of distortion apparently lies in the fact that the d-c load and the audio load on the diode are not equal. In a typical circuit shown in Fig. 4A, the d-c load consists of R_1 and R_2 in series. For audio frequencies, however, there is the additional load of R_3 plus the effect of R_4 in parallel with whatever part of R_3 is in use. Common practice is to make R_4 as high as possible, usually about 10 megohms. This is in keeping with the use of contact potential bias in a high-mu triode. R_3 is made as high as is permissable for use in the grid circuit of the r-f and i-f tubes. This value is usually limited to 2 megohms, representing a somewhat more serious load on the diode. Distortion from this source, that is, the audio load of the avc decoupling resistor, may be eliminated by the use of a separate diode as avc rectifier, as was common practice several years ago.

A simple form of delayed avc may be realized in this manner by biasing this diode so that it will not conduct until the avc threshold has been reached. The disadvantage of this method is that with signals of the same order of magnitude as this threshold, the avc voltage will be dependent upon the modulation. With normal modulation percentages this effect is not too serious.

A separate avc rectifier lends itself to use with contact potential bias as shown in Fig. 4B. In this case, since R_4 is returned to the negative bias voltage, R_3 will have to be returned to a point several volts positive with respect to the cathode so that the diode will not be cut off.

A number of combinations suggest themselves in assembling a practical circuit. The double-diode triode can be used together with another double diode as in Fig. 5A. Here, the triode is conventionally biased and any additional avc delay desired may be achieved by increasing the value of the resistor R.

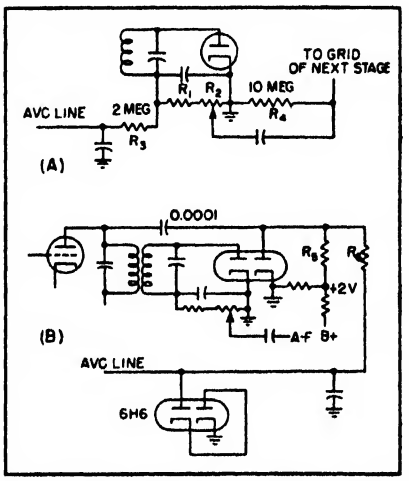

Fig. 4 — Conventional detector-avc circuit uses common diode (A). To minimize distortion, separate detector and avc diode are combined with contact-potential bias circuit (B)

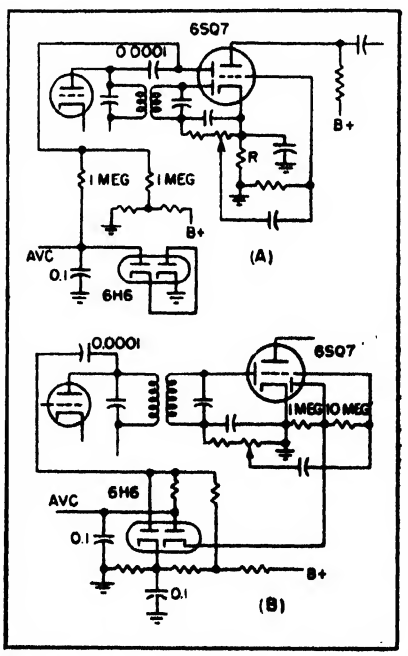

Fig. 5—Additional avc delay may be had by increasing value of R (A). Maximum simplicity and economy of parts are achieved by use of one diode section for both audio grid bias and r-f and i-f bias (B)

A circuit similar to that in Fig. 3 may be used with an additional double diode, of which one section can be the avc rectifier and the other section can be put in series with the bias diodes to provide additional bias and delay voltage. A system using one diode for both audio grid bias, and as part of the r-f and i-f bias, is shown in Fig. 5B. This circuit makes use of all the considerations put forth in this paper, and represents what is probably the maximum in simplicity and economoy of parts.

In using any of these diode biasing systems, it should be remembered that the contact potential will vary widely with change in heater voltage, and should be used for bias in circuits where stability is important only when the circuit is balanced. Examples may be found in some vacuum-tube voltmeters where the contact potential of the diode used as rectifier is balanced by that of a second diode.

Remote Tuning with Reactance Tubes

Remotely-located radio receivers are tuned over a limited band by means of reactance tubes connected across their oscillator tank circuits. The reactance tubes are controlled by direct voltages applied over connecting telephone lines

By H. B. BARD, Jr.

IN MOST radio receiving stations involving remotely controlled equipment it is desirable to be able to exercise at least a limited amount of tuning from the control location. Transmitter frequencies will vary slightly within the permissible tolerance allowed. In order to compensate for such slight variations it is necessary to shift the receiver frequencies slightly to provide optimum reception.

Several means have been utilized in the past, such as motor-driven tuning capacitors, stepping relays which switch in various crystals or capacitors, and the transmission of i-f signals over telephone lines. Each of these systems has its merits but from the constructional standpoint they are complicated mechanically or electrically, or do not provide continous variation of the controlled frequency.

Basic Principle

An electronic, continuous, and simple means of control can be achieved by utilizing a reactance-tube circuit. Such a circuit is one in which a direct-current or voltage variation is converted into a variation in impedance at the output terminals. The impedance variation may be either capacitive or inductive, depending upon the component parts used in the circuit, and is achieved by the use of a tube that draws from its load either a leading or lagging current with reference to the impressed voltage.

The use of reactance tubes is common in the automatic-frequency-control circuits of receivers and in the modulators used in some types of frequency-modulated radio transmitters.

Figure 1 shows a basic reactance tube circuit in which a change in d-c voltage on the control grid, through R_1, produces a reactance change between points A and B. Capacitor C_1 is a blocking capacitor, C_2 is a phase splitting capacitor, and C_3, C_4, and C_5 are bypass capacitors. Resistor R_2 merely drops screen voltage to a desirable value.

Points A and B are attached to the circuit over which control is desired. In the example under discussion in this instance, a receiver oscillator is to be controlled and therefore AB is connected across the oscillator tank circuit. Inasmuch as the impedance presented at AB may have a resistive term, there will be some loading of the oscillator circuit by the control tube. The magnitude of the resistive term diminishes as the phase difference between the grid voltage and the impressed voltage at AB approaches ninety degrees.

C-W vs. Voice Reception

When tuning a receiver by means of the reactance-tube circuit several different methods may be used. Where reception is limited to voice signals, it is necessary to control the high-frequency oscillator, but for the reception of C-W telegraph signals the control may be applied to the beat-frequency oscillator and the high-frequency oscillator may be crystal controlled.

The range of frequency variation at 5 mc when the high-frequency oscillator is controlled may be as high as 30 kc with a 12-volt bias

variation. When the control is applied to the beat-frequency oscillator at 465 kc the available variation in beat note is approximately 10 kc each side of zero beat for a total bias variation of 12 volts. The amount of variation, or control, is largely determined by the amount that the grid bias on the reactance tube is varied and the value of the coupling capacitor C_1; the larger this capacitor the greater the control.

Circuit Variation

Figure 2 shows schematically a typical installation in which two receivers are remotely controlled over two telephone lines. Closing the dpst power switch at the office turns on the office amplifier and also turns on the remote receivers. Closing the tuning switch at the office applies bias to the two remotely located reactance tubes. Variation of the tuning-control potentiometers changes the output reactance of the two reactance tubes and accomplishes the desired tuning. Audio output of the two receivers is fed back to the office over the associated telephone lines and applied to the office amplifier input through potentiometers and spst switches providing individual control.

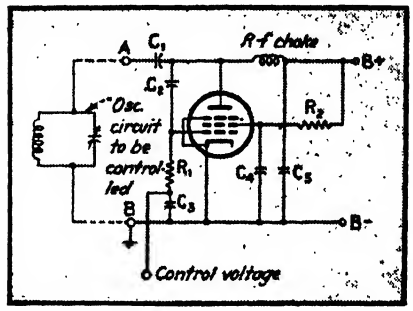

FIG. 1—Fundamental reactance-tube tuning circuit

In this instance one remote receiver is used for c-w reception and the other for voice and therefore one reactance tube controls a beat-frequency oscillator while the other controls a high-frequency oscillator, as previously outlined. Where both c-w and voice are to be received with one receiver it is a simple matter to arrange remote switching of a reactance tube from beat-frequency oscillator to high-frequency oscillator or vice versa. In such instances additional relays are connected in series with the power relay and adjusted to pull up at different currents. An additional potentiometer included in the relay battery circuit permits suitable currents to be selected.

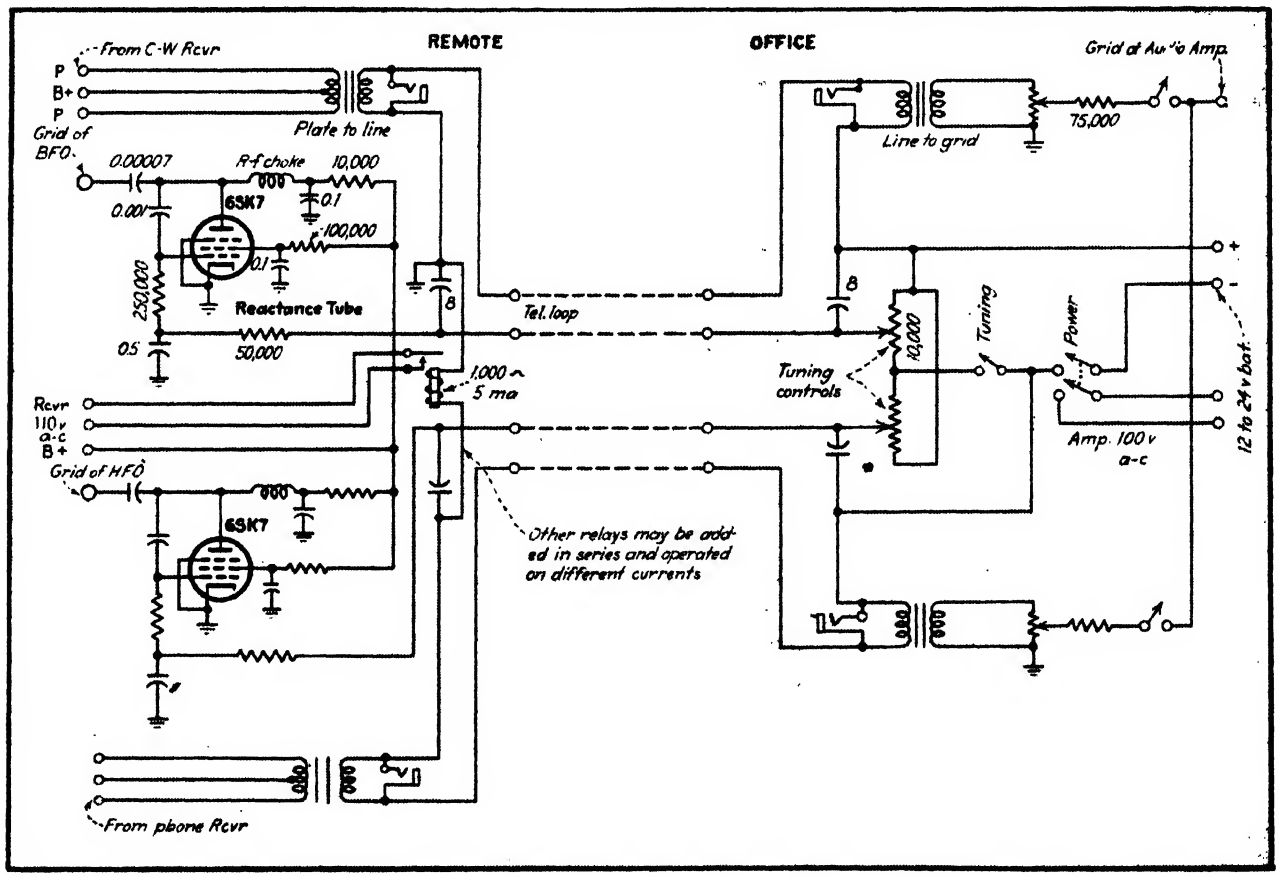

FIG. 2—Remote-tuning arrangement suitable for handling two receivers. Addition of other relays and another potentiometer permits a number of variations discussed in the text

Continuously Variable Radio Remote Control

Phase-shifting properties of a resonant circuit provide automatic self-adjustment of a radio control system. Guided missiles, aircraft, satellite transmitters, and telemetering systems can be radio controlled by the stepless positioning provided

By DAVID W. MOORE, JR.

THE HEART of any type of remotely operated device is the control method used. Its speed of response, accuracy, and ease of operation must all be satisfactory or the efficiency of the controlled object will be impaired. In some applications, such as guided missiles, the equipment for locating the missile with respect to the target may be more complicated than that for effecting control, but the control must be satisfactory to insure the success of the missile.

The basic problem of radio control may be stated as that of definitely positioning a rotating shaft by means of signals transmitted on a radio channel. Many methods have recently been developed for doing this on a step by step basis in which the controlled shaft positions itself in definite increments in response to the control signal. Some systems merely control the direction of rotation of the controlled shaft, the duration of the running determining the ultimate shaft position. In comparison to these control means, a smooth, stepless, and definite positioning device is usually preferable.

The radio control system to be described is this latter type, and its operation is obtained from the phase-shifting properties of an electrical series resonant circuit that consists of an inductance and capacitance in series. The phase of the current flowing through a series resonant circuit is a function of the relation of the resonant frequency of the circuit to the applied voltage frequency. If the resonant frequency of the circuit is the same as the line frequency, the current flowing will be in phase with the line voltage and the series resonant circuit is said to be tuned to resonance with the line.

If the line frequency is varied above or below the resonant frequency of the circuit, the phase of the current with respect to the line voltage will vary as a function of this frequency difference. Figure 1 illustrates graphically this phase-shifting property of the series resonant circuit.

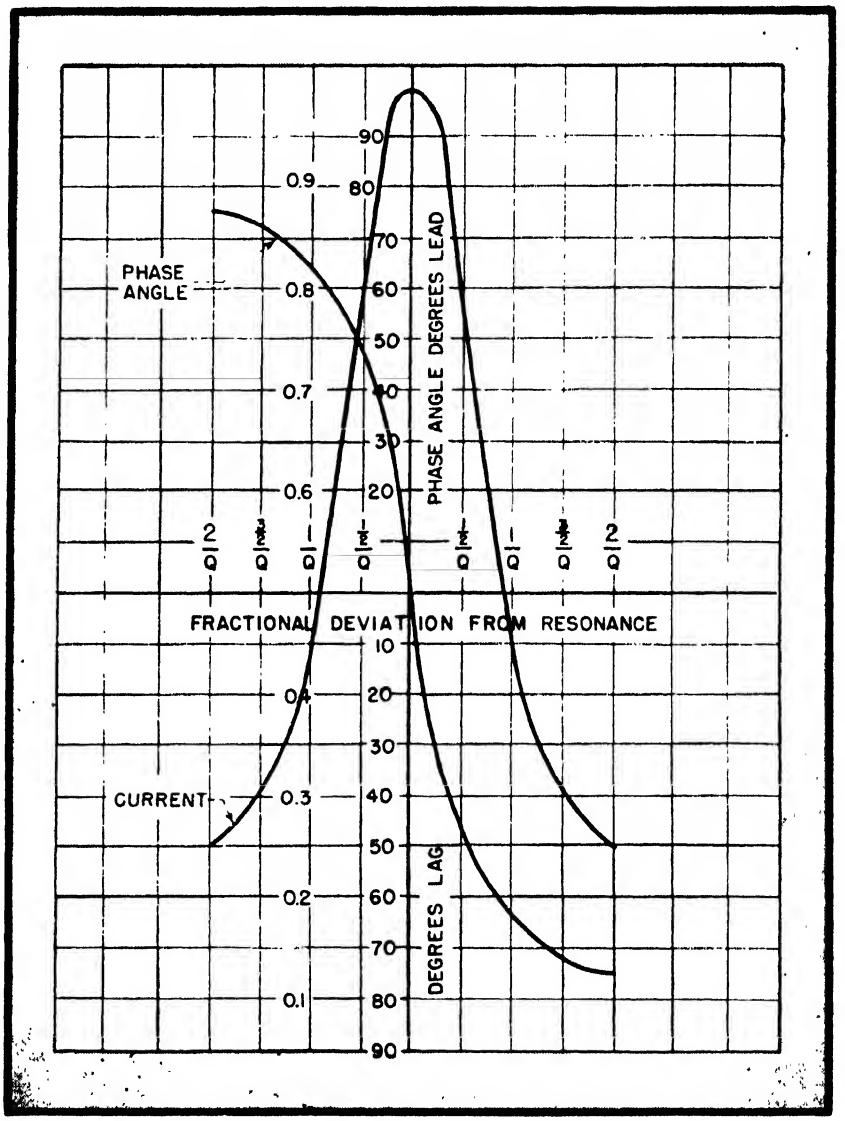

FIG. 1—Near resonance, the phase angle changes rapidly. Advantage of this characteristic is taken in design of the control system

The rate of change of the phase angle close to the point of resonance is particularly interesting and is the characteristic that makes possible a

sensitive-control system. The effective Q, or figure of merit, of the circuit elements used controls the slope near resonance, the higher the Q the greater the rate of change of phase angle. Values of Q of five to ten, which can easily be obtained with commercial inductors, will enable a very sensitive control.

Use of Servo Motor

Figure 2 shows how a circuit of this type may be used in conjunction with a phase-sensitive servo to control the speed and direction of rotation of a shaft. The phase-sensitive servo used is a conventional two-phase motor which is sensitive to small, phase angle shifts. The resonant circuit consisting of C_1 and L_1 is in series with phase 1 of the motor and so controls the phase of the current flowing through that motor winding. Phase 2 is connected directly across the line and, because it is wound to be essentially resistive, the current flowing through it is approximately in phase regardless of the line frequency.

The torque output of a two-phase motor is proportional to the product of the current in phase 1 and phase 2 and the sine of the phase angle between the two currents. Figure 1 shows that the phase of the current through phase 1 can be varied by changing the line frequency. By adjusting this frequency above and below the resonant point of L_1 and C_1, the current through phase 1 can be made to either lead or lag the current through phase 2, thus causing the servo motor to develop torque in either direction.

If the line frequency is equal to the resonant frequency of the tuned circuit, the current in phase 1 will be in phase with the line voltage and also in phase with the current through motor winding 2. This condition will result in zero torque, or a condition of equilibrium.

Because the line frequency can be transmitted by radio, we have a means for remotely controlling the operation of a servo motor. Thyratron tubes can be employed as phase-sensitive servos instead of a two-phase motor, to control large motors by a small amplifier.

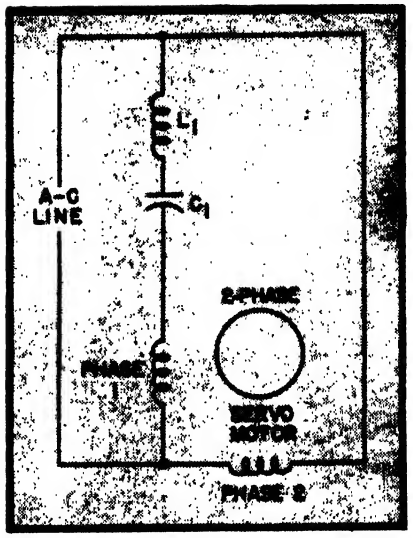

FIG. 2—The reasonant circuit formed by L_1 and C_1 controls the current flowing through the motor winding of phase 1

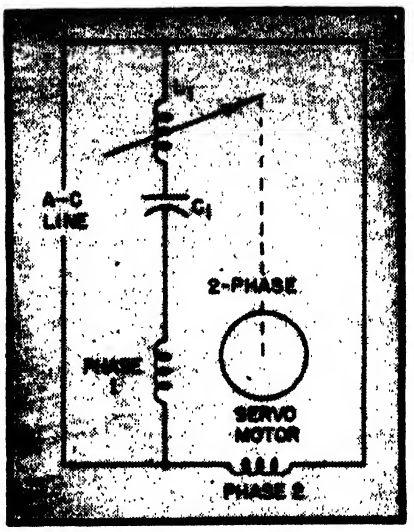

FIG. 3—Coupling the servo motor to L_1 provides automatic tuning of the motor circuit to the line frequency

Motor Controls Inductance

For most control applications, a control which definitely positions the controlled shaft is desired rather than one which only governs the rotation of a servo motor. Figure 3 shows how the servo motor of Fig. 2 can be coupled mechanically to a variable L_1. If the motor is phased correctly, it will automatically tune the circuit L_1 and C_1 to resonance with the applied voltage by varying the value of L_1. The position of the shaft which controls the value of L_1 is a function of the value of L_1 and therefore of the line frequency, because L_1 is automatically adjusted to keep circuits tuned to line frequency.

In appearance, the variable inductance resembles a motor. There are no windings on the rotor, and consequently no brushes or slip rings to wear and deteriorate. The inductance variation is linear for a little more than sixty degrees rotation of the shaft.

Values of Circuit

A range of line frequency is necessary to position the shaft of L_1 throughout its range of some sixty degrees. The magnitude of this frequency band is determined by the inductance value and that of the tuning capacitor. Typical calibrations are shown in Fig. 4 and 5.

Referring to Fig. 4, control throughout sixty degrees of inductance shaft rotation requires a frequency band of from 50 to 80 cycles. In this example the inductance value is 20.5 henrys and the tuning capacitor 0.283 μf. The inductance of the motor winding in series with the resonant circuit is 5.65 henrys.

The control whose calibration is shown in Fig. 5 was adjusted for a different frequency band, seventy degrees of motion being controlled by a frequency variation from 135 to 198 cycles. The value of inductance is 28.2 henrys and the tuning capacitor is 0.033 μf.

Both of these controls could be transmitted on one carrier requiring

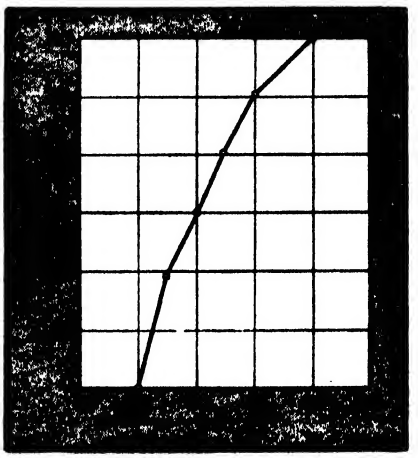

FIG. 4—Operation in the frequency range from 50 to 80 cycles provides 60 degrees of rotation of the inductance shaft

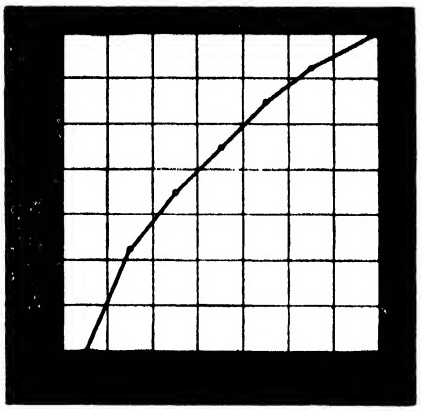

FIG. 5—Seventy degrees of rotary motion were obtained by using frequencies between 135 and 198 cycles

an audio band of from 50 to 198 cycles. More controls at higher frequency bands could be added. For a large number of controls on one carrier, though, a subcarrier frequency system should be employed which would enable a practically unlimited number of controls especially if microwave transmission is employed. The carrier with the numerous subcarriers could be beamed to the controlled unit along with any other necessary intelligence.

Torque-error Data

The relationship between the torque generated by this system of radio control and the error between the control resonant frequency and the frequency of the voltage applied to the control is shown by the graph of Fig. 6 The solid lines illustrate the motor torque for different applied frequencies for three settings of the control. The graph covers a band of 50 to 75 cycles with the control set at 52, 60, and 73 cycles. These control setting frequencies are the frequencies to which L_1 and C_1 are set. Zero torque is not usually obtained when these frequencies are impressed upon the control due to slight phase shifts in phase 2 with changes in frequency.

The dotted lines show the motor torque for various constant displacements between the control setting and applied frequency throughout the bands. For example, it may be seen that for a one-percent deviation, substantially 0.025 inch ounce can be obtained at any place in the band. Five-percent deviation increases this torque to 0.13 inch ounce.

From these charts the operation of a system of this type can be easily predicted. These figures are typical only of the control constructed and more or less torque could be obtained by suitable design. The torque output shown is that obtained at the motor shaft and gearing to bring this up to the required amount must be employed.

The tuned circuits of this radio control method are natural filters and help to minimize any effects due to harmonic content of the applied frequency. However it is best to keep the harmonic content low. If trouble were experienced from this source, additional harmonic filters could easily be included. Phase shifts in the filters would not affect the operation.

Figure 7 is a schematic of a complete single-channel control system which has been designed to permit very close tracking between the position of the transmitting inductance shaft and the position of the controlled inductance shaft. The transmitting inductance is electrically identical to the controlled inductance and, the tuning capacitors are also equal; thus $L_1 = L_2$ and $C_1 = C_2$.

The radio position transmitter is designed to operate in conjunction with a standard type of audio-frequency oscillator and adjusts the tuning control of the oscillator until its output frequency is equal to the resonant frequency of the circuit L_1C_1. The resonant frequency of this circuit is adjusted to the desired value by setting L_1, manually or otherwise. The oscillator frequency is then transmitted by radio to the radio position receiver.

The radio position receiver tunes itself to the oscillator frequency, and, because the tuned circuit constants are identical elements, L_2 is driven by the servo motor to a position corresponding to the position of L_1, effecting the desired control.

The detailed operation is as fol-

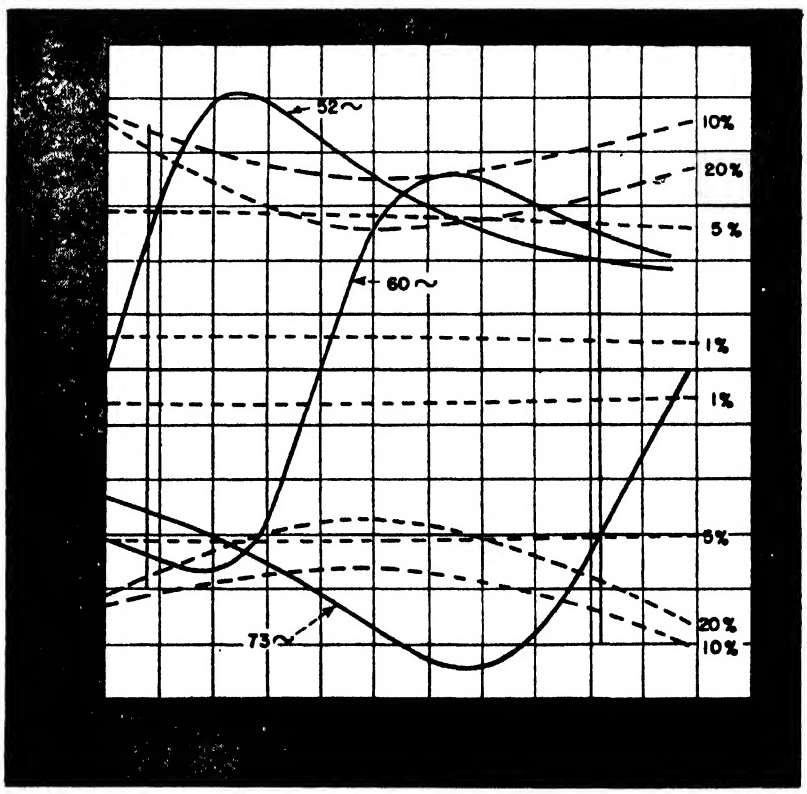

FIG. 6—Torque response curves of the control when set for resonance at frequencies of 52, 60, and 73 cycles. The solid lines indicate the resonant frequency constant; the dashed lines show the constant deviation in percent

lows: First, L_1 is adjusted, setting the resonant circuit L_1C_1 to a definite resonant frequency. The audio oscillator output is impressed across the radio position transmitter circuit which is like that shown in Fig. 3, except that the servo motor adjusts the audio oscillator frequency instead of the inductance L_1. Thus the servo motor tunes the oscillator to the resonant frequency of L_1C_1 instead of adjusting L_1 to tune L_1C_1 to the oscillator frequency.

The radio position receiver is identical to Fig. 3, the servo motor adjusting L_2 to tune L_2C_2 to the oscillator frequency which has been transmitted by radio. The control shafts of inductances L_1 and L_2 are thereby synchronized.

The purpose of this circuit is twofold. It permits a linear response between the transmitting and controlled shafts which makes for ease of control in many applications. It also automatically compensates for frequency drift in the audio oscillator due to temperature or supply voltage changes because the servo motor will retune the oscillator should frequency variation occur.

If a subcarrier system were employed, the desired number of controls would be set up and each oscillator output would modulate a subcarrier. The subcarriers would be transmitted by a high-frequency carrier to the controlled device. The frequency of the carrier would be determined by the number of subcarriers desired.

Small, two-phase, servo motors operating in the type of circuits shown will develop adequate power to set the controls of an automatic pilot in any aircraft to be remotely guided. More power, to adjust the aircraft control surfaces directly, could be easily obtained by having the two-phase, servo motor operate a hydraulic pilot valve or through the use of thyratron tubes. Other interesting variations can be worked out.

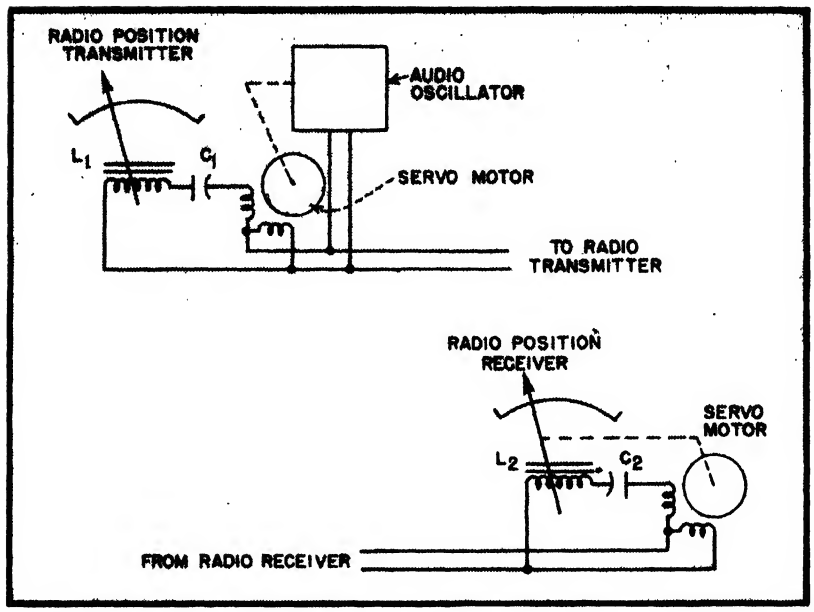

FIG. 7—Essential units of the receiver and transmitter of the radio control system

Radio Control Circuit

MODEL AIRCRAFT AND BOATS can be remotely controlled by radio. A circuit suitable for such applications where economy of space, weight, and battery drain is essential is shown in Fig. 1. The subminiature RK61 thyratron is used in a self-quenching superregenerative detector to operate a high resistance relay upon reception of a radio signal. Sufficient series plate load resistance must be used to limit the anode current to less than two milliamperes; greater tube life will be obtained at lower currents.

In the circuit either a 45-v battery or raw a-c can be used for the plate supply; the filament requires 1.4 v at 50 ma. In the absence of a radio signal the circuit is oscillating at audio frequency. When the r-f is received, a-f oscillations stop with a decrease in anode current from between 1.0 and 1.5 ma to between 0.1 and 0.5 ma. Average anode current can be increased by increasing antenna coupling, decreasing the L/C of the tank circuit, or both. Maximum controllable current can be increased by increasing the anode bypass capacitance, decreasing the grid-leak resistance, or both. If the capacitance of the anode bypass capacitor is reduced and the relay replaced by headphones, the Raytheon RK61 krypton and xenon filled thyratron will operate in this circuit as a conventional superregenerative receiver with an anode supply as low as 30 v. It is not recommended for use above 100 mc.

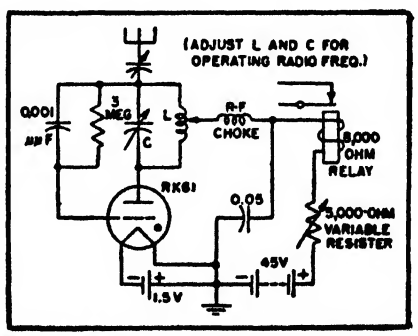

FIG. 1—Remotely controlled radio circuit uses subminiature tube

XIII. TELEVISION

Carrier-Difference Reception of Television Sound

Use of a common i-f amplifier for sight and sound signals reduces costs, eliminates local oscillator tuning and drift difficulties

By R. B. DOME

SEVERAL PROPOSALS have been made in the past for the use of a common amplifier channel for sight and sound in a television receiver. Such a system would simplify the receiver, and render its operation free from the disturbing effects of local oscillator hum frequency-modulation and frequency drift. Most of these proposals are based on some form of multiplex[1, 2, 3] wherein the sound signals modulate the picture carrier during the horizontal blanking interval when no picture information is being transmitted. These methods may be classified as time division systems of transmission of intelligence, since the receiver employs a time-gated amplifier which opens only during that portion of time devoted to the transmission of sound.

Time division methods of sound transmission are weak for two reasons. The first is that the amount of power devoted to sound is relatively small which means that the signal-to-noise ratio will not be adequate over as long a range as if more average power had been used, and secondly, failure of the gated amplifier to synchronize properly in noisy locations means a further decrease in average signal-to-noise ratio.

The disadvantages of time division systems may be overcome by the use of a frequency division system with simultaneous transmission of picture and sound signals exactly as in the manner used today in black-and-white television in the frequency bands between 44 and 216 megacycles. There is nothing very complicated about such transmissions. The video signal modulates continuously one carrier frequency with amplitude modulation while the sound signal modulates continuously another carrier frequency with frequency modulation. A conventional receiver arrangement has been commonly used in the past. The local oscillator beats the two carrier waves down to two intermediate frequencies. Here the receiver is split into two i-f channels, a wide one for the picture, and a narrow one for the sound. Separate second detectors are employed: a simple rectifier for the picture, and a discriminator-detector for the sound.

The objections to this type of receiver are: (1) Frequency modulation of the local oscillator at power frequency rates, if present, will show up in final detection as an unwanted component. (2) If the local oscillator frequency drifts excessively with warm-up or with changes in line voltage, the signal at the discriminator may wander so far away from the balance point that the signal may become noisy or distorted or even entirely lost. (3) The system is subject to microphonics in that the movement of oscillator tube elements or oscillator circuit elements may produce frequency modulation which is detected along with the desired signals.

Another type of receiver, which may be used to receive these simultaneous transmissions, makes use of the frequency difference between the picture and sound carriers. The carrier-frequency-difference receiver does not depend on any precise local oscillator frequency for its successful operation. Instead, the high frequency which is finally to be detected is the difference between the picture and sound carrier frequencies. In black-and-white television in the channels between 44 and 216 mc, this frequency difference is 4.5 mc, as set by the FCC standards.

The receiver is constructed along fairly conventional lines. There is only one i-f channel. This is broad enough to pass both picture carrier and sound carrier plus the necessary sidebands of each carrier. In order that the wave applied to the second detector be dominated by the picture i-f carrier so that it can successfully demodulate the sound i-f carrier, it will generally be necessary to provide some attenuation for the sound i-f. This may be done by means of absorption trap circuits coupled to the i-f coils.

A pair of such circuits with the proper Q's and couplings will result in an i-f response characteristic which is characterized by a shelf several hundred kilocycles in width with its center about the mean sound i-f. Figure 1 shows the frequency response characteristic of a typical i-f. The shelf height should be comparable to the minimum level expected for the picture carrier. If, for example, the picture transmitter does not modulate downward to any point below 15 percent of the voltage difference between peak of the synchronizing signals and zero, the receiver slope will reduce this to 7.5 percent since the picture carrier should be halfway down the slope, and hence, if the sound carrier amplitude is equal to the black level of 75 percent, the shelf should be in the order of 7.5/75 or one tenth of the maximum height of the i-f response.

With this treatment to the input to the second detector, the sound carrier will appear to the picture carrier as just another sideband so that in the detector output there will be found, in addition to the video frequencies, a 4.5-mc signal frequency-modulated with the sound. The 4.5-mc wave will be amplitude-modulated to some extent by picture modulation, but this may be easily removed by the employment of suitable limiter circuits at a later point in the receiver. The amount of amplitude modulation present in the wave depends upon the ratio of the amplitude of the two carriers at the second detector and is given by the following equation to an accuracy of better than one percent

$$e = \frac{a m E_1 E_2}{[m^2 E_1^2 + a^2 E_2^2]^{1/2}}\left[1 + \frac{3 a^2 m^2 E_1^2 E_2^2}{64[m^2 E_1^2 + a^2 E_2^2]^2}\right] \quad (1)$$

where mE_1 is amplitude of picture i-f, and aE_2 is amplitude of sound i-f.

To show graphically how e is affected by the picture modulation factor m, let aE_2 be assigned a value of 1.0 and mE_1 assigned a range of values from 0.1 to 10. The resulting output e is then shown in Figure 2. It will be observed that as mE_1 decreases from 10 to 1 the value of e decreases from 1.0 only to 0.715. Thus the limiter has only to remove some 30 percent total modulation from the wave and not 100 percent.

Figure 3 illustrates this effect in a different way. At Fig. 3A is shown the picture modulated wave with a minimum modulation of 15 percent of the peak of the synchronizing pulses. Figure 3B shows the frequency modulated sound carrier having a level of 7.5 percent of synchronizing pulses. At Fig. 3C is shown what the 4.5-mc wave looks like as a result of the wave at Fig. 3A demodulating the wave of Fig. 3B. It will be noted that there is very little left for the limiter to do.

The whole output of the second detector may then be amplified by the usual video amplifier. Thus the video and sound channels are still common. Separation of sound and picture may be made at the conductor leading from the video amplifier to the picture tube, as shown in Fig. 4. A transformer has its primary 2 connected between the final video amplifier tube 3 and the picture tube 4.

The primary circuit 2 is tuned to the difference frequency of 4.5 mc. This tuning will prevent that frequency from appearing as picture modulation on the cathode-ray tube screen. At the same time it will provide a circulating current of considerable strength in the primary. This current is sufficient to induce a 4.5-mc wave in secondary 5, which is tuned to 4.5 mc. The secondary is connected to a tube 6 which serves as a limiter-amplifier to feed discriminator-transformer 7 and balanced-detectors tube 8 and tube 9. These tubes detect the frequency modulation present on the 4.5-mc wave and the resulting audio output is fed to audio amplifiers and to a loudspeaker for

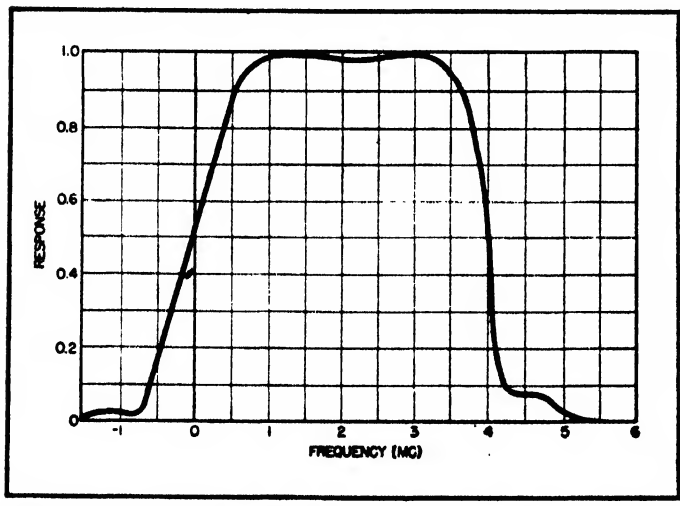

FIG. 1—Typical i-f passband for carrier-difference receiver. The sound carrier at 4.5 mc is attenuated by the plateau at the base of the curve

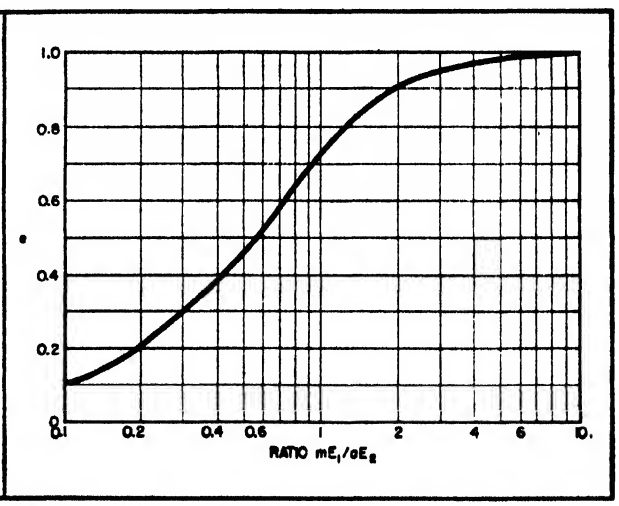

FIG. 2—Ratio of sight and sound carriers at input to second detector, as affected by the amplitudes of both signals. When picture carrier predominates, little limiting is required

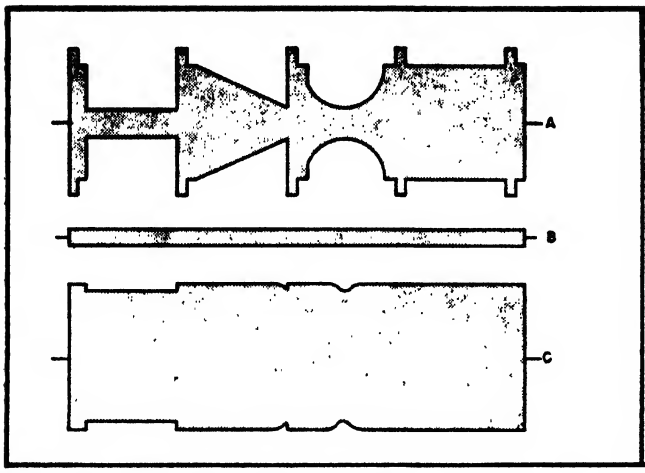

FIG. 3—Modulated sight carrier (A), sound carrier (B), and combined f-m carrier showing slight amplitude modulation (C)

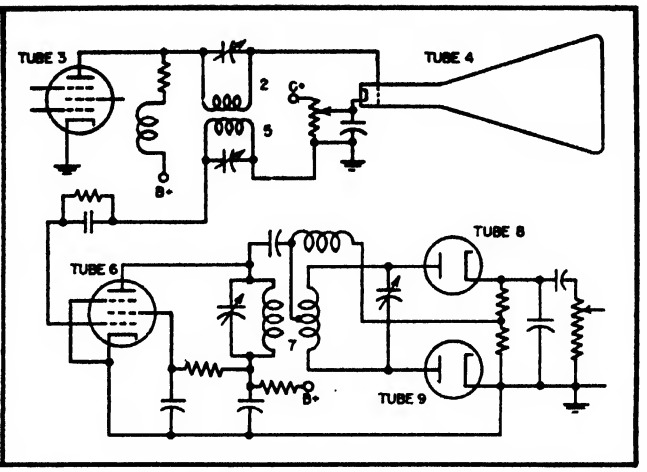

FIG. 4—Schematic of the carrier-difference sound system. The f-m sound carrier is taken directly from the picture-tube grid

translation into sound. Another limiter tube may be added prior to tube 6 if cascade limiters are desired.

Thus a very simple receiver is effected which uses but few tubes and circuit components for sound and which has important improved characteristics over the conventional receiver. A nominal amount of drifting of the local oscillator frequency is of no consequence because the 4.5-megacycle frequency has been determined by quartz crystals at the transmitters and this difference frequency is held accurately to within ± 5 kilocycles. Hum modulation or microphonics in the local oscillator cannot affect the sound signal because any change in the sound i-f is accompanied by an equal change in the picture i-f so that the difference frequency is undisturbed by any variation of local oscillator frequency.

Selector-switch tuning is done without re-adjustment of the local oscillator because of the wide range of permissible variation in local oscillator frequencies. If the receiver is provided with a local oscillator tuning adjustment, it can be operated by unskilled personnel with ease because no special effort is needed to tune in the sound. In actual operation, towards one end of the tuning control the picture fades due to lack of sufficient picture carrier while at the other end of the control the sound fades due to lack of sufficient sound carrier.

Operation of the television picture contrast (gain) control does not appreciably affect the audio signal level because the limiter tends to apply a constant level to the balanced detector. The picture will be considered far too dim for use long before the sound fades to half strength.

Any phase or frequency modulation on the picture carrier in this system is directly transferred to the 4.5-megacycle beat frequency and ultimately detected. It is therefore important to place a limit on the amount of frequency modulation permissible on the picture carrier. Since the peak frequency deviation of the sound carrier frequency has been set at ±25 kilocycles, the limit on the picture transmitter should be about ±100 cps maximum, which corresponds to a modulation of ±0.4 percent or 48 db below 100-percent modulation on the sound transmitter.

Another transmitter requirement is that some picture carrier must always be present. This is necessary in order to detect the sound carrier continuously. The present standards read that the transmitter shall be capable of modulating down to 15 percent of peak synchronizing level on maximum white. The standard may be modified to read "at least to 15 percent but not greater than 10 percent for downward modulation". This change will provide a 10 percent safety zone perfectly adequate for the system's operation.

It is recommended that the peak deviation of the sound transmitter be increased to ±40 kilocycles from the present ±25 kilocycles. This will aid in masking any inadvertent frequency modulation present on the picture carrier.

The signal-to-noise ratio of the system described may be calculated in terms of the conventional system and will be found to vary depending upon the average brightness of the picture. The equation is

$$\frac{S}{N} = \left(1 + \left[\frac{E_2}{mE_1}\right]^2\right)^{-1/2} \quad (2)$$

where E_1 is maximum amplitude of picture carrier, E_2 is amplitude of sound carrier and m is modulation factor of picture carrier. Thus for an all "white" picture, assuming $m = 0.17$, $E_1 = 1$ and $E_2 = 0.707$,

$$\frac{S}{N} = \left(1 + \left[\frac{0.707}{0.17}\right]^2\right)^{-1/2} = 0.234 \quad (3)$$

For an all "black" picture, assuming $m = 0.75$, then

$$\frac{S}{N} = \left(1 + \left[\frac{0.707}{0.75}\right]^2\right)^{-1/2} = 0.73 \quad (4)$$

And for an average picture $m = 0.49$, so

$$\frac{S}{N} = \left(1 + \left[\frac{0.707}{0.49}\right]^2\right)^{-1/2} = 0.566 \quad (5)$$

Thus, assuming optimum tuning of the conventional receiver, on the average the signal-to-noise ratio

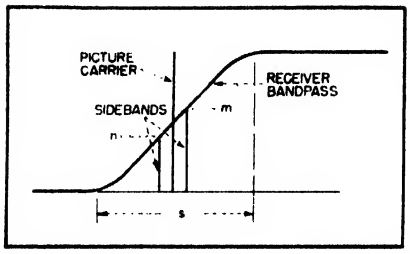

FIG. 5—Symmetrical picture sidebands of unequal amplitude, produced by slope of receiver bandpass characteristic, cause slight phase modulation, but the resulting disturbance is negligible

will run about 5-db lower than the conventional system; but in the long run, it actually may run better than the conventional system because drifting of the local oscillator may easily throw the conventional system well off the balance point on the discriminator characteristic, so that not only noise but audio distortion may be produced in considerable amplitude to degrade the otherwise excellent performance obtainable with precise adjustment.

Picture-Carrier Phase Modulation

Even though the picture carrier is cleared of spurious frequency modulation at the transmitter, reception with the picture carrier on the slope of the receiver i-f response characteristic will cause the picture carrier to take on a modulation of its phase angle as a result of unequal amplitudes of symmetrical sidebands.

In Fig. 5 is shown a carrier wave placed half way down the receiver slope. An upper and a lower sideband are shown for a picture-modulation frequency lying in the audible frequency range. It will be noted that due to the slope, the upper sideband will have an amplitude m and the lower sideband an amplitude n. If the total frequency band of the slope be denoted by s, then it can be shown that the maximum possible phase angle modulation of the carrier wave (when the minimum picture level is 10 percent of the amplitude at synchronizing signal peaks) is

$$\phi_{max} = \tan^{-1}\left[\frac{\frac{1.68a}{s}\sin 2\pi at}{1 + 0.84\cos 2\pi at}\right] \quad (6)$$

where a is the picture modulating frequency.

It is evident that as a approaches zero, negligible phase angle modulation will occur, but as the frequency increases, the phase angle modulation may become significant. The worst possible case occurs at 15,000 cps. If therefore a be assigned a value of 15,000 and s a value of 1,500,000, the phase angle will oscillate between the limits of plus 0.032 radians, when $2\pi at =$ 140 deg, and minus 0.032 radians when $2\pi at = 220$ deg.

On the sound transmitter, the equivalent phase modulation of 25-kc deviation for 15,000-cps modulation frequency is 25,000/15,000 or 1.66 radians. Therefore the spurious signal will be $0.032/1.66 =$ 0.0193 of maximum audio output. But since 75 microsecond deemphasis is used, this spurious 15,000 output is multiplied by a factor of 0.147, and hence the resultant audible level is $0.0193 \times 0.147 =$ 0.00275, which is 51 db below 100-percent modulation. If the sound transmitter deviation is increased from 25 kc to 40 kc, an additional 4-db reduction would be obtained, or the 51-db figure would become 55 db. In a similar manner, phase modulations at other frequencies may be calculated and are summarized in Table I. Since these levels are far below the usual residual hum and noise levels of even a good receiver audio amplifier system, it may be concluded that spurious responses due to incidental phase modulation are quite negligible.

Table I—Noise Introduced by Receiver

Picture Modulating Frequency in cps	Spurious Responses Below 100 percent Modulation in db	
	25-kc Deviation	40-kc Deviation
1,500	76	80
2,500	69	73
5,000	61	65
10,000	55	59
15,000	51	55

References

(1) Kallman, H. E., Audio and Video on a Single Carrier, ELECTRONICS, p 39, May 1941.
(2) Fredendall, G. L., Schlesinger, K., Schroeder, A.C., Transmission of Television Sound on Picture Carrier, *Proc. of I.R.E.*, p 49, Feb. 1946.
(3) Lawson, D. I., Lord, A. V., Kharbanda, S. R., A Method of Transmitting Sound on the Vision Carrier of a Television System, *Institution of Electrical Engineers*, p 251, July 1946.

Timing Action of the Blocking Oscillator

By EMANUEL LAST

TIMING AND TRIGGER circuits are becoming increasingly important with each new application of electronic circuits in industry, television, and allied radio fields. All types of multivibrators, start-stop circuits, and relaxation oscillators have made their appearance as timing devices. One of the lesser known but very useful timing methods is the blocking oscillator.

A typical blocking oscillator circuit is shown in Fig. 1. The transformer shown has a one-to-one turns ratio. Since there is no external or fixed biasing arrangement in this circuit, the tube will conduct with the closing of the switch. When the tube current begins to build up through the plate coil of the transformer, there will be a back emf across the coil, of polarity as shown in Fig. 1, which results in a dropping of plate voltage.

The changing primary current will induce a voltage into the secondary or grid coil of opposite po-

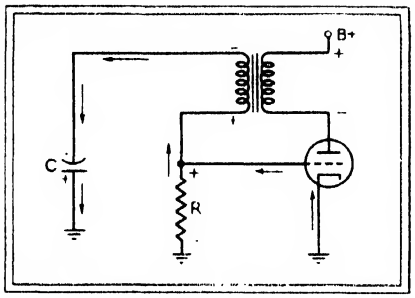

FIG. 1—Circuit of typical blocking oscillator and polarities established when switch is first closed

larity to the voltage in the plate coil. This induced voltage will cause an electron flow in the grid circuit producing a voltage across resistor *R* of such polarity as to make the grid positive with respect to the cathode. At the same time, this grid current will be charging capacitor *C* through resistor *R* until the grid goes positive, when the charging current will flow mainly through the tube from cathode to grid. This charging path being through the cathode-to-grid resistance, which is relatively small, the capacitor will tend to charge quickly to the voltage induced into the grid coil.

The grid of the tube having been driven in a positive direction, the tube will draw more plate current. The increased plate current will produce a further drop in plate voltage and a greater induced voltage into the grid circuit, tending to drive the grid further positive. If this action continues we soon arrive at a point where the increase in grid voltage will not result in an increase in plate current as great as previously. Since the rate of change of plate current thus decreases, the voltage induced into the grid coil decreases.

Effect on Capacitor

The voltage across capacitor *C* has been closely following the voltage induced into the grid circuit. Therefore, a reduction in the induced voltage due to the reduced rate of increase of plate current will result in the voltage across the capacitor being slightly larger than the induced voltage. The resultant reversal of current flow in the grid circuit gives us a slight negative voltage on the grid (voltage across the capacitor less the induced voltage as shown in Fig. 2A).

Condition for Cutoff

The grid voltage going slightly negative would tend to make the tube draw less current. Since there is a coil in the plate circuit, the coil will build up a counter emf to oppose this change in current. The grid coil will have a voltage induced into it 180 degrees out of phase with the plate-coil voltage. Now the voltage across the capacitor and the induced voltage are additive, causing a current flow that gives a large voltage across resistor *R*. (See Fig. 2B.) This voltage makes the grid negative with respect to the cathode by a more than sufficient amount to cut off the tube.

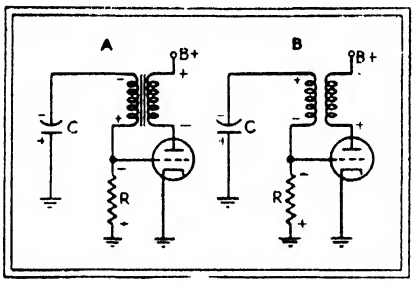

FIG. 2—Changes in polarities that lead to cutoff of plate current

The cutting off of plate current will cause the plate voltage to rise to B + and then rise above this value due to the back emf of the plate coil resulting in a slight oscillation whose extent will depend on circuit constants.

The induced voltage in the grid circuit will be negligible after the fast positive rise in plate voltage. The voltage on the grid will now be due only to the capacitor *C* discharging through resistor *R*. This discharge will give an exponential decay of grid voltage continuing to fall till the grid voltage reaches the cutoff potential of the tube. As soon as the grid voltage rises above cutoff, the tube will conduct and thus the cycle will repeat itself. Figure 3 shows the plate voltage E_p, the grid voltage E_g, and the voltage across the capacitor E_c for a period of three cycles.

The output of this circuit is usually the platevoltage variation. The negative pips or pulses occur each time the tube operates. Thus the frequency of the pulse repetition depends on the amount of time the tube is cut off or the time of discharge of the capacitor in the grid circuit from its charged voltage to the cut-off voltage. This time will depend on three items; first, the voltage to which the capacitor is charged; second, the cut-off value of the tube; and third, the *RC* of the discharge circuit. The first two items will be determined by the applied voltage, the tube, and the transformer. Once these factors have been determined, the *RC* will be the main frequency controlling factor. Thus by varying the resistor and capacitor, we can considerably vary the frequency of the output pulses.

Shape of Pulse

In addition to controlling the frequency of the output voltage, we may also be interested in the output waveshape. The output waveshape can be considered under two aspects; first, the sharpness and time duration of the negative pulses; and second, the oscillation following the negative pulse.

The sharpness and time duration

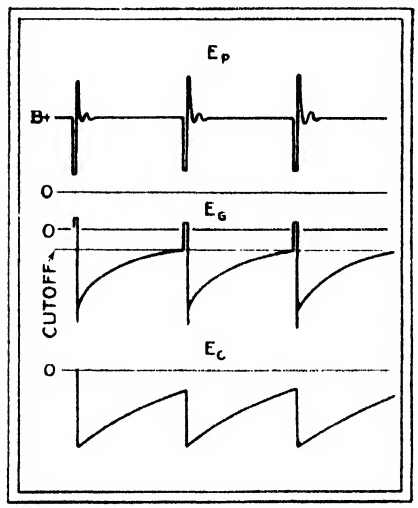

FIG. 3—Voltages produced at the plate, grid, and capacitor by the blocking action

of the pulses will depend largely on the transformer used. For a sharp, short-duration pulse, we must have a transformer that will pass this pulse. This involves the transformer's ability to pass some fairly high frequencies of which the pulse is composed. With an iron-core transformer, this is practically impossible due to eddy current and hysteresis losses at high frequencies. However, with the advent of powdered permalloy cores, the frequency range of these transformers has been considerably increased. With this type of transformer, short-duration pulses can be obtained.

Our second waveshape problem, that of oscillation, can be counteracted in a few ways. One possible way is to load down the plate coil with a shunt resistor which will tend to reduce oscillation. An example of this effect is shown in Fig. 4A.

Another method of reducing the oscillation in the output signal is to place a load resistor between the plate coil of the transformer and B+. The output is then taken off at the point between the plate coil and the load resistor. This results in eliminating most of the oscillation in the output. The value of the load resistor must be large enough to produce a sufficiently large pulse voltage across it, yet it must not be so large as to excessively limit tube current. Figure 4B shows the output with the plate load resistor in the circuit.

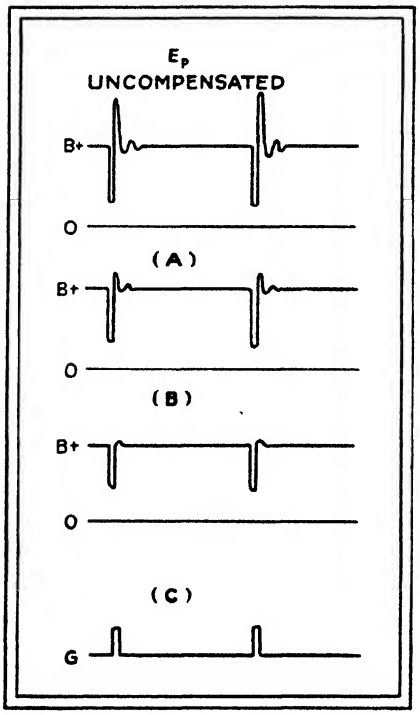

FIG. 4—Uncompensated output from plate compared with output from other points in circuit

A third possible method can be used where a low-impedance output is acceptable and where too large a voltage is not required. This method is to insert an unbypassed cathode resistor and take the output across the cathode resistor. Using this method we obtain positive pulses which have no oscillating component. (See Fig. 4C.) A fourth possibility would be to take the original output and feed it into a limiter circuit that would respond only to the negative pulse.

Design Factors for Intercarrier Television Sound

Large scale production of television receivers employing intercarrier sound has focussed attention on the advantages and disadvantages of the system. This review emphasizes problems facing transmitter and receiver designers

By STUART W. SEELEY

THE intercarrier system of television sound reception, as previously described in these pages[1], amplifies the picture and sound signals together in the picture i-f amplifier. At the output of the picture second detector a beat note between the two signals appears. This beat is in effect a 4.5-mc intermediate frequency, frequency-modulated in accordance with the sound signal and amplitude-modulated (to some extent) in accordance with the picture signal. This intercarrier beat is passed through a frequency-modulation detector which is not sensitive to amplitude modulation. The sound modulation is thus separated from the picture and may be amplified and applied to the loudspeaker, as shown in Fig. 1.

When this system was first proposed the principal advantage appeared to be economy. The picture i-f amplifiers and video amplifiers do double duty in amplifying the sound signal, so a separate sound i-f amplifier is not necessary. Thereafter it became clear that the economic argument is by no means the most important one. There are many pros and cons rooted in the technical performance of the system which outweigh the cost factor.

The principal technical advantage of the intercarrier system is the fact that it is immune to the idiosyncrasies of the local oscillator of the receiver. Frequency modulation of the local oscillator due to hum and microphonics, as well as

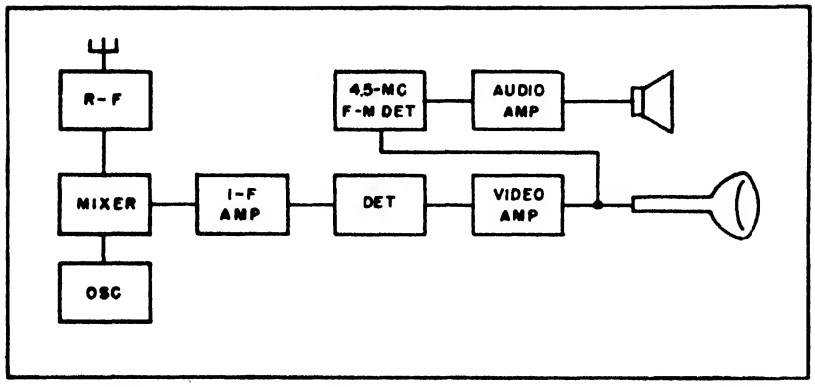

FIG. 1—Typical intercarrier receiver. The i-f, video detector and video amplifiers do double duty, handling picture and sound signals simultaneously

frequency drift, affect both sound and picture i-f signals substantially identically, so the 4.5-mc difference frequency remains unaffected. In a conventional receiver (using a separate i-f amplifier for sound, as shown in Fig. 2) these defects of the local oscillator produce an average effect four times as bad at the highest television channel (216 mc) as in the f-m band (108 mc) at full modulation. With television systen deviation (one third f-m sound broadcast deviation) the effect is emphasized by an additional factor of three.

Secondly, the tuning of an intercarrier receiver is considerably simplified by the fact that the sound is always correctly tuned in when switching from one station to another. Fine tuning of the local oscillator is not necessary to tune in the sound. Moreover, the intercarrier system is somewhat freer from the effects of interference.

Technical advantages related to economy of design include not only the dual use of the i-f and video amplifiers but also the fact that the local oscillator design can be somewhat less expensive. In fact, hum frequency modulation and drift may have values several times those allowable in a conventional receiver. In inexpensive receivers, the i-f passband may be made symmetrical, and this will allow the local oscillator to operate on the high side for the lower channels, and on the low side for the upper channels.

The primary disadvantage of the intercarrier system is the fact that the 4.5-mc beat signal depends on the presence and character of the picture carrier. Any unusual effect present in the picture carrier can have a corrollary effect on the sound output and this possibility exists whether the effect arises in the transmitter or the receiver, or is caused by interference from other sources.

One of the most important examples occurs whenever the picture modulation is so heavy that the picture carrier disappears completely during the transmission of a peak white portion of the picture. When the picture carrier is thus modulated to zero, the 4.5-mc beat note disappears for that instant and no sound signal is received. This causes severe interference in the sound signal, in the form of a 60-cycle buzz or 15,750-cycle hiss, since the loss of sound signal is repeated at the field and line-scanning rates. This possibility requires that the percentage modulation at the transmitter be monitored carefully, so that the minimum picture modulation shall not fall below approximately 10 percent of the peak value. There is at present no regulation requiring such monitoring. Before the intercarrier system can be employed with assurance of high-quality transmission at all times, such a regulation will be required.

A second effect, of nearly equal importance, is that caused by any phase or frequency modulation of the picture carrier. This carrier is nominally modulated in amplitude only, but actually may be modulated in phase or frequency to a slight degree. Such variations in picture phase or frequency are imposed on the 4.5-mc beat note and cannot be separated from the frequency modulation of the sound signal. The result is, again, a 60-cycle or 15,750-cycle note of magnitude depending on the extent to which the picture carrier is phase or frequency modulated. It should be noted that the frequency-modulation detector which converts the 4.5-mc beat signal to audio is in effect a phase detector, for all frequencies above about 2.5 kc, when 75 μsec de-emphasis is used.

There are many possible causes of phase or frequency modulation of the transmitted picture carrier. One is variation in the transit time

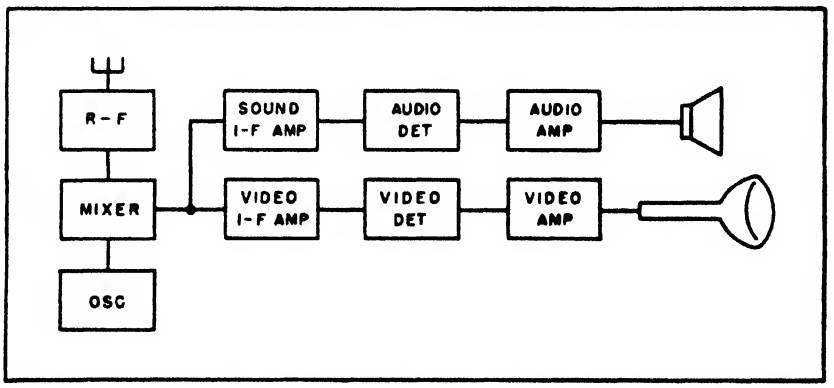

FIG. 2—Typical conventional television receiver. This type of receiver is more susceptible to faults in the local oscillator than is the intercarrier type

(which produces a change in phase angle of the carrier) in any modulated stage of the transmitter. However, this is of negligible magnitude compared with the effects of unsymmetrical tuning or incomplete neutralization. In a 5-kw transmitter, even one-half watt of constant fed-through power can produce as much as a 6-degree total phase shift when the modulation level is at 10 percent of peak carrier. This amount of feed-through can occur even in a properly neutralized stage, and the effect can be identified in the output of an intercarrier sound receiver. For example, 4 degrees peak shift at 15 kc will produce interference only 28 db below average (30 percent) modulation without deemphasis.

Deemphasis improves the situation and the effect is less prominent at lower audio frequencies. But, even with deemphasis, over the range of audio frequencies from 3,750 to 15,000 cps, a 4-degree phase shift will produce interference from 48 to 45 db below average modulation. This would not be considered sufficient for a high-quality sound system. But recent tests have shown that much more than 4 degrees of phase shift can be present without adverse effects on sound quality. At least two additional factors tend to lessen the interference:

1 Since the transmitter's residual frequency modulation is caused by a phase-variation process the corresponding frequency modulation decreases 6 db per octave as the audible frequency of the video modulation causing the phase variation is decreased. Other types of interference (which the FCC specifies must be below a -60 db level in a high-quality aural broadcasting system) have more uniform distribution in the audible spectrum.

2 The second point concerns the distribution of audible energy in a composite video signal. If we examine the amplitude-modulation components between zero and 20,000 cycles derived from a picture-modulated transmitter we find one very strong component at the 60-cycle field frequency and another at the 15,750-cycle line frequency. What occurs in between depends partly upon the number, position and intensity of any horizontal lines in the picture. However, harmonics of 60 cycles up to a rather high order, but with rapidly decreasing level with frequency, are caused by the square-wave nature of the vertical synchronizing and blanking portions of the signal.

Obviously 60 cycles is too low to convert phase modulation to frequency modulation in any important degree, being 48 db below the 15,000-cycle conversion. Also, 15,750 cycles is outside the audible range and can be removed in the receiver if necessary. Therefore, it is apparent that we need only be concerned with audible video components lying considerably above the field frequency and below the line frequency. Observation has indicated that this entire range seldom, if ever, contains components stronger than those which occur at the start and finish of a vertical blanking pedestal transmitted with a white background picture. The latter cause spikes of frequency modulation which plainly delineate the vertical-blanking time when viewed on an oscilloscope.

The energy in those spikes from a transmitter having more than 20 degrees of total phase variation is still next to inaudible in a wide-range sound system even though the spikes are frequently as much as 15 db above the meter reading of the average incidental audible frequency modulation. Experience thus far has indicated that satisfactory performance, at least in receivers which do not offer the full range of audio fidelity, can be obtained without difficulty on all presently operating stations provided they do not overmodulate the picture carrier.

Another difficulty with the intercarrier system is the fact that any drift of the frequency-modulation detector from the 4.5-mc center frequency will introduce distortion, and there is no way to correct this condition except by adjustment of the detector itself. Similar distortion in a conventional receiver can be corrected by adjustment of the fine tuning control.

A final difficulty is that which occurs if the sound carrier, as presented to the second detector, exceeds a certain level relative to the picture carrier. If this occurs, severe distortion of the sound output and picture quality may occur, including possible reversal of the image tones ("negative" in the photographic sense). This effect may be controlled by care in the design of the i-f pass-band curve, as described below.

The first question in the design of an intercarrier receiver is the

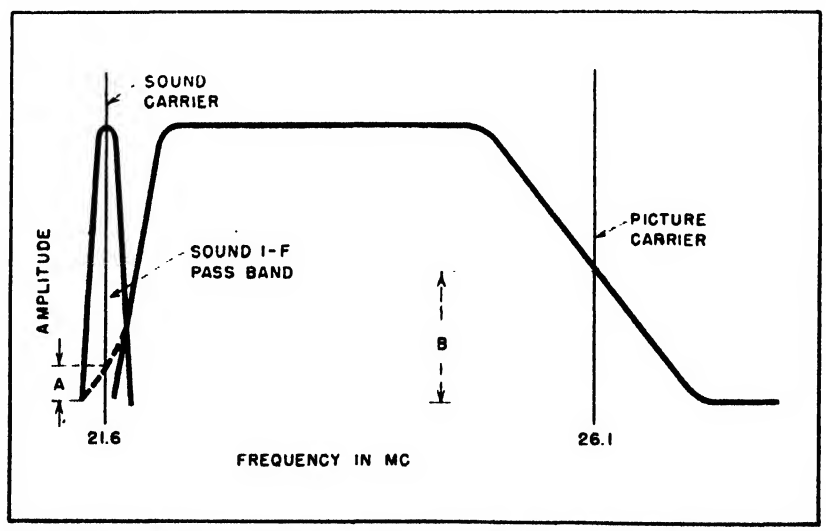

FIG. 3—Intermediate-frequency response characteristics of conventional (heavy solid line) and intercarrier (dashed-line extension) receivers

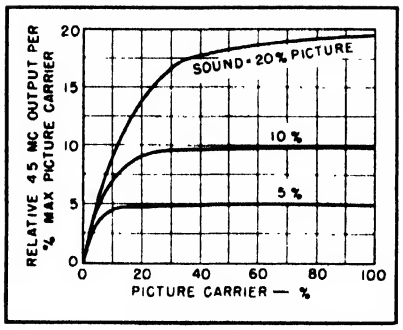

FIG. 4—Amplitude modulation of 4.5-mc beat note as a function of picture modulation, for various amplitudes of sound signal relative to picture signal

method of setting the relative level of the sound and picture carriers at the input to the second (video) detector. In the conventional receiver the pass-bands of the i-f systems are as shown in Fig. 3. The picture i-f amplifier has substantially no sensitivity (on the average 45-db attenuation) at the associated sound channel frequency.

In the intercarrier system, the sound-carrier pass band is dispensed with and the picture i-f pass band is extended slightly to increase slightly the gain at the sound carrier. This is shown in Fig. 3 as a dashed-line extension of the picture pass-band curve. The percentage response of this extended curve at the sound-carrier frequency is indicated by the dimension *A*. This dimension should never be greater than 10 percent of the carrier level (dimension *B*) in linear units. This is on the assumption that the sound and picture carriers are of equal strength as received from the transmitter. But variations in relative signal strength of as much as 10 db, arising from differential attenuation and wave interference effects dependent on the receiver location, are apt to occur so a more conservative figure for dimension *A* is 3 percent of *B*.

One basis for the 10 percent maximum figure may be seen from Fig. 4, which shows the relative output of a linear detector when f-m sound and a-m picture are fed to it simultaneously. So long as the rms level of the sound signal is 5 percent or less of the maximum rms picture signal, as in the lowest curve, the 4.5-mc beat note amplitude remains substantially constant as the level of the picture carrier (abscissas) varies under modulation from 15 to 100 percent of the peak value.

If the sound level is 10 percent of the maximum picture level as in the middle curve, the output remains flat from 25 to 100 percent modulation. At higher relative sound levels (top curve) the output would contain substantial amplitude modulation in accordance with the picture modulation. Also the picture quality would be badly degraded as previously stated.

Much of the residual amplitude modulation may be removed by the use of a limiter or by the use of a balanced discriminator or ratio detector. However, if the residual amplitude variation is too severe an excessive burden is placed on the f-m detector. This is the basis of the previous statement that the amplitude modulation level of the picture transmitter should not normally be allowed to fall below 10 percent of the peak synchronizing level.

The attenuation of the sound signal, to 3 percent or less of the picture carrier, implies a corresponding increase in amplification (relative to that provided in a separate sound i-f amplifier) to bring the sound signal up to the level required for detection and audio amplification. A portion of this extra amplification is provided by the passage of the sound signal through the video amplifiers. Normal peak video level at this point is about 30 volts, so the sound level usually does not exceed one volt. Conservative design suggests that this level be increased before the sound signal is applied to the f-m detector.

An auxiliary amplifier for this purpose also serves an important function in keeping the volume level substantially constant as the picture gain control is varied. Such constancy of gain is also useful in overcoming the tendency of the sound level to increase as the picture is detuned. Otherwise, if fine tuning is provided, the lay user might try to tune for loudest sound, which would produce a poor picture.

Care should be taken to avoid overload in any stage which could remove the picture signal (and its concomitant 4.5-mc sound i-f signal) even momentarily. The diode second (video) detector should be as linear as possible, and the ratio of a-c impedance to d-c resistance of the second detector load should be as near unity as possible. Finally the tuned circuits in the f-m detector should be designed to maintain proper adjustment since drift

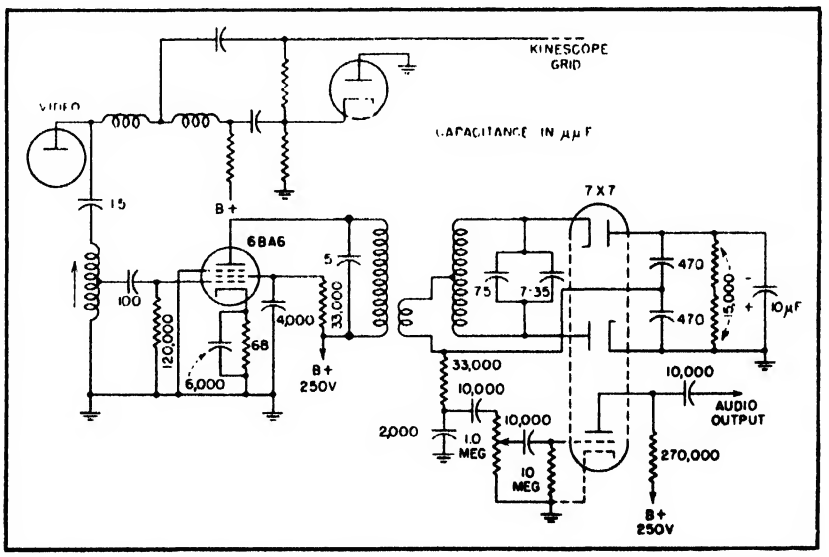

FIG. 5—Typical intercarrier sound circuit using a limiting amplifier and ratio detector for demodulation

in these components cannot be corrected by the user. If these precautions are followed, and if the restrictions on transmitter operation previously mentioned are observed, the intercarrier system can give excellent performance.

A typical example following closely the design criteria mentioned is shown in Fig. 5. The 4.5-mc beat note is taken directly from the last video amplifier plate. The series resonant impedance at this point removes any remaining 4.5-mc beat from the picture tube grid. The first tube (6BA6) serves as a volume-leveling amplifier, or limiter. It is so designed that the tube operates under plate voltage overload when a small signal is applied to its grid. Hence the output does not change when substantially stronger signals are applied. The output of this amplifier is passed to a conventional ratio detector which develops the audio output. The output is about 2.5 volts rms for 25-kc deviation, so a voltage amplifier must precede the audio output stage. In this example, this is provided by a triode in the same envelope with the double diodes, in a 7X7 tube.

REFERENCE

(1) R. B. Dome, Carrier Difference Reception of Television Sound, p 102, ELECTRONICS Jan. 1947.

Stagger-Tuned Amplifier Design

Practical wideband amplifier considerations, limits to overall bandwidth of cascaded stages, and transient response characteristics of stagger-tuned circuits are prevented. Curves and tables give design criteria. Comparisons are made to other coupling circuits

By HENRY WALLMAN

THIS PAPER presents principles of operation and practical design of stagger-tuning schemes, presents curves of step response of certain of these circuits, and discusses practical considerations[1, 2].

Single-Tuned Circuit

The simplest i-f interstage network is a single-tuned circuit the usual connection of which is shown in Fig. 1A, and the equivalent form in Fig. 1B. The effective load resistance R is the parallel combination of the plate resistor R_L, the plate resistance of the first tube, the input resistance of the second tube, and the equivalent parallel loss resistance of the inductance L. The capacitance C is the sum of the output capacitance of the first tube, the apparent input capacitance of the second tube, the self capacitance of L, and the wiring capacitance. With careful wiring and a fixed tuned inductor about the size of a one-watt resistor, the value of C between two 6AG5 tubes is about 12 pf (picofarad is a micromicrofarad).

The bandwidth of the single tuned circuit is $1/(2\pi RC)$ and is independent of center frequency. The voltage amplification at band center is $g_m R$ where g_m is the tube transconductance. The amplification-bandwidth product (figure of merit), denoted by AB, is $g_m/(2\pi C)$. For a g_m = 4,500 micromhos and C = 12 pf, as with conservatively rated 6AG5 tubes, AB is 60. An amplification of 6 with a bandwidth of 10 mc, or an amplification of 15 with a bandwidth of 4 mc is thus attainable in this case. Because the AB product depends only on the tube, being independent of center frequency, it is no easier to build a single-tuned amplifier covering the band from 28 to 30 mc (B = 2 mc) than one from 8 to 10 mc (B = 2 mc) with a given tube (except for the effect of smaller inductor size on interstage capacitance).

Synchronous Single Tuning

The simplest wideband i-f amplifier employs cascaded single-tuned stages all of the same bandwidth and resonant frequency. This synchronous tuning method is simple, noncritical, and has excellent transient response.

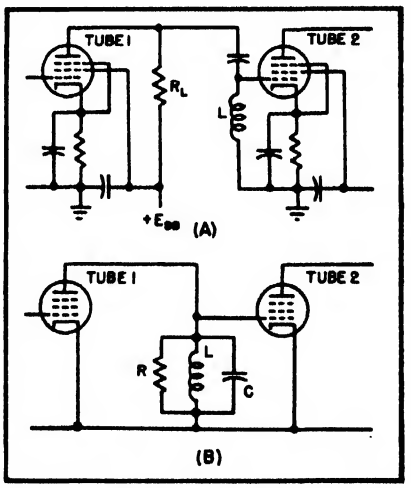

FIG. 1 (A) Single-tuned wideband amplifier coupling, and (B) its equivalent circuit

The disadvantage of the synchronous single-tuned amplifier is its low efficiency, resulting from the rapidity with which overall bandwidth shrinks as stages are cascaded. For example, for an overall amplification of 10,000, a synchronous single-tuned amplifier employing a tube that gives an AB = 60 has a maximum overall bandwidth of 7.1 mc, and requires 18 stages; the use of more stages yields an even smaller bandwidth.

Overall bandwidth for N synchronous single-tuned stages is to a very good approximation

$$\frac{\text{bandwidth of single-tuned stage}}{1.2\,(N^{1/2})}$$

To illustrate this relation, consider a cascade of 5 synchronous 6AG5 single-tuned stages, each of 10-mc bandwidth. If AB is taken to be 60 and the amplification per stage to be 6 (giving a bandwidth per stage of 10 mc), the overall amplification is 7,800, but, from the above expression the overall bandwidth is only 3.5 mc.

This shrinkage of bandwidth can be avoided while preserving the simplicity and low cost of single-tuned coupling by stagger tuning. For an overall bandwidth B, it is possible to stagger tune N single-tuned stages so as to achieve a center-frequency stage-amplification of A with AB still equal to $g_m/(2\pi C)$. Note that here B is the *overall* bandwidth and A the *gain per stage.*

The stagger-tuned passband for which $AB = g_m/(2\pi C)$ has a selectivity characteristic $1/(1 + x^{2N})^{1/2}$ where x is a variable proportional to the deviation of the frequency from resonance.

Staggered Pairs and Triples

As N increases, the curves become squarer and flatter. Stagger-tuned couplings of this sort where $N = 2, 3, 4, \ldots$, are called staggered pairs, triples, quadruples, etc.

In almost all cases, a passband with small dips is substantially superior for either optimum selectivity or optimum AB to a maximally flat passband, while for small overshoot, a more rounded curve is preferable. The only advantage of the maximally flat curve, apart from its mathematical simplicity, is its easily recognized shape when aligning amplifiers with a swept-frequency generator.

Table I shows the center frequencies and bandwidths to which individual coupling circuits should be designed to obtain flat-staggered amplifiers of overall bandwidth B at center frequency f_0. The data are presented in terms of the fractional bandwidth B/f_0. The values shown are valid only when B/f_0 is small, less than 0.3 for practical purposes. The exact case, which holds even for B/f_0 greater than unity, is fully considered elsewhere.[1,2]

Table I—Flat Staggered Combinations

Bandcenter = f_0, overall bandwidth = B, and $B/f_0 < 0.3$

Number of Circuits	Component Single Tuned Circuits	
	Center frequency	Bandwidth
Staggered pair (2)	$f_1 = f_0 + 0.35B$	$0.71(B/f_0)f_1$
	$f_2 = f_0 - 0.35B$	$0.71(B/f_0)f_2$
Staggered triple (3)	f_0	B
	$f_1 = f_0 + 0.43B$	$0.5(B/f_0)f_1$
	$f_2 = f_0 - 0.43B$	$0.5(B/f_0)f_2$
Staggered quadruple (4)	$f_1 = f_0 + 0.46B$	$0.38(B/f_0)f_1$
	$f_2 = f_0 - 0.46B$	$0.38(B/f_0)f_2$
	$f_3 = f_0 + 0.92B$	$0.19(B/f_0)f_3$
	$f_4 = f_0 - 0.92B$	$0.19(B/f_0)f_4$
Staggered quintuple (5)	f_0	B
	$f_1 = f_0 + 0.29B$	$0.81(B/f_0)f_1$
	$f_2 = f_0 - 0.29B$	$0.81(B/f_0)f_2$
	$f_3 = f_0 + 0.48B$	$0.31(B/f_0)f_3$
	$f_4 = f_0 - 0.48B$	$0.31(B/f_0)f_4$

An example will make the use of Table I clear. Suppose a flat-staggered quintuple consisting of an input circuit and four interstage circuits is desired at $f_0 = 30$ mc with an overall bandwidth $B = 10$ mc. Then $B/f_0 = 0.3$, and the quintuple consists of four tubes and five single-tuned circuits that satisfy the following conditions:
(1) the first should have a bandwidth of 19 mc at 30.0 mc, and
(2) the second, a bandwidth $0.81\times0.3\times32.9=8.0$ mc at 32.9 mc
(3) the third, a bandwidth $0.81\times0.3\times27.1 = 6.6$ mc at 27.1 mc
(4) the fourth, a bandwidth $0.31\times0.3\times34.8 = 3.2$ mc at 34.8 mc
(5) and the fifth, a bandwidth $0.81\times0.3\times25.2 = 2.3$ mc at 25.2 mc
If each tube has an AB of 60, the amplification per stage is 6 and the overall amplification is $6^4 = 1{,}296$.

A flat-staggered pair has the same selectivity curve as that obtained with a critically coupled double-tuned circuit. For such circuits, the overall bandwidth shrinks less rapidly as stages are cascaded than for synchronous single-tuned circuits. The overall bandwidth for M flat pairs is

$$\frac{\text{bandwidth of single flat pair}}{1.1\,(M^{1/4})}$$

To illustrate this relation, consider a 6-circuit amplifier consisting of 3 flat-staggered pairs ($M = 3$). For an overall bandwidth of 10 mc, each pair must have a bandwidth of $10 \times 1.1(3^{1/4}) = 14.5$ mc. If AB is 60, the stage amplification is therefore 4.1.

A flat-staggered pair, a flat double-tuned circuit, and a flat inverse-feedback pair have the same transient response, because they are of the minimum phase shift type and have the same amplification-vs-frequency curves.

A flat-staggered triple has the curve of a flatly coupled triple-tuned circuit. For such circuits, the overall bandwidth for M flat triples is

$$\frac{\text{bandwidth of single flat triple}}{1.06\,(M^{1/6})}$$

To illustrate this expression, consider a 6-stage amplifier consisting of 2 flat-staggered triples ($M = 2$). For an overall bandwidth of 10 mc, each triple must have a bandwidth

of $10 \times 1.06(2^{1/6}) = 11.9$ mc. For $AB = 60$ the amplification per stage is therefore 5.1.

Overstaggered Circuits

Appreciable increases in AB result from overstaggering the stages to yield pass bands with slight dips. For example, if a 6-stage amplifier consisting of 2 triples is over staggered so as to have 2 percent dips in the overall passband of the composite amplifier, there results an increase of fully 25 percent in amplification per stage over the flat-staggered triple amplifier of the same overall bandwidth; however, the transient response is degraded.[3] Table II summarizes the characteristics of various coupling combinations, showing, for 5 interstage networks, the effect of overstaggering. (For values of AB other than 60, for which the table is computed, the bandwidths should be multiplied by the ratio of actual AB to 60. Similarly, the overall amplifications for given bandwidth should be multiplied by the Nth power of this ratio, where N is the number of amplifier stages.)

Many variations of overstaggering are possible, but a simple approximate procedure for converting a stagger-tuned amplifier of given bandwidth that has a flat passband into one having the same bandwidth but with small dips is to narrow the individual stage bandwidths all in the same ratio, leaving the individual resonant frequencies unchanged. Considerable narrowing is necessary to produce any effect; thus, in a flat-staggered triple, the individual stage bandwidths have to be reduced 30 percent to produce 1-percent dips.

Practical Considerations

For a given overall bandwidth, a staggered sextuple has somewhat greater amplification than two staggered triples. However, as a practical matter, the combination of two staggered triples is probably preferable because of the smaller overshoot and less critical reaction to misalignment, unless the fractional bandwidth is close to unity.

Table II—Bandwidth vs Amplification

Tube type assumed to have $g_m/(2\pi C) = 60$; listed amplifications do not include effect of input network

Number of Amplifier States	Overshoot (see text) in percent	Bandwidth in mc for Gain of 10^3	Bandwidth in mc for Gain of 10^4	Gain for Bandwidth of 2.5 mc	Gain for Bandwidth of 4 mc	Gain for Bandwidth of 10 mc
Input plus 2 interstages						
3 synchronous single tuned	0	0.9	0.3	150	58	9
flat staggered triple	8.2	1.9	0.6	580	225	36
over staggered triple with 1 percent dips	10.2	2.2	0.7	800	310	50
3 flat double tuned with equal Q loading	7.7	1.9	0.6	580	225	36
3 flat double tuned with one sided loading	7.7	2.7	0.8	1,200	450	72
Input plus 3 interstages						
4 synchronous single tuned	0	2.6	1.2	1,100	290	19
2 flat staggered pairs	6.2	4.8	2.2	7,000	1,700	110
flat staggered quadruple	10.9	6.0	2.8	14,000	3,400	220
4 flat double tuned with equal Q loading	8.4	5.6	2.6	11,000	2,800	180
4 flat double tuned with one sided loading	8.4	7.9	3.7	32,000	7,800	510
Input plus 4 interstages						
5 synchronous single tuned	0	4.2	1.9	7,700	1,200	30
flat staggered pair plus flat staggered triple	10	8.9	5	16×10^4	25,000	630
flat staggered quintuple	12.8	10.7	6	33×10^4	50,000	1,300
5 flat double tuned with equal Q loading	9.2	9.4	5.3	20×10^4	30,000	770
5 flat double tuned with one sided loading	9.2	13.2	7.4	79×10^4	12×10^4	3,100
Input plus 5 interstages						
6 synchronous single tuned	0	5.3	3.3	42,000	4,000	41
3 flat staggered pairs	7.7	10.7	6.8	14×10^5	14×10^4	1,400
2 flat staggered triples	11.2	13.0	8.2	37×10^5	36×10^4	3,600
2 over staggered triples with 2 percent overall dips	14.5	16.1	10.2	11×10^6	11×10^5	11,000
6 flat double tuned with equal Q loading	10	12.6	8.0	32×10^5	31×10^4	3,200
6 flat double tuned with one sided loading	10	17.8	11.2	18×10^6	17×10^5	18,000

For such reasons, most stagger-tuned amplifiers employ pairs or triples, although sometimes quintuples are used.

For reasons of noise figure, it is desirable to have a centered input circuit, and overload considerations suggest a centered circuit driving the detector, if possible; otherwise the order of staggering is unimportant. Gain control can be applied to any stage or combination of stages in the staggered amplifier. Except for detuning resulting from changes in input capacitance with variation of grid bias, which was never serious in Radiation Laboratory experience, there is no reason for applying gain control to pairs.

The plate resistor R_L in a stagger-tuned stage should have whatever value yields the design bandwidth for that stage. Usually R_L is somewhat greater than the effective damping resistance R, but it can be less if the input resistance of the following tube is negative. Because of grid-plate capacitance, a tube having a resonant plate circuit has a negative input resistance at frequencies somewhat below resonance of its plate circuit. This condition occurs for the tube between the low- and high-frequency circuits of a staggered pair.[4]

Where the fractional bandwidth is too large for Table I, exact formulas must be used.[5]

For very low frequencies such as those at the lower end of the audible spectrum, stagger-tuned amplifiers using stages employing selective R-C degeneration with twin-T networks, which have selectivity curves approximating those of single-tuned L-C networks, can be designed to give sharp cut-off without using heavy iron-cored inductors.[6]

Another means for obtaining high-gain wideband amplifiers is to use single-tuned circuits with resistive feedback,[7] the *AB* performance being equivalent to that of stagger tuning, except that the inverse feedback produces a slight reduction in effective transconductance, generally negligible unless the bandwidth exceeds about $0.3g_m/(2\pi C)$.

Comparison of Methods

Table II shows that (1) synchronous single-tuned circuits are extremely inefficient, (2) flat-staggered pairs are slightly less and flat-staggered triples slightly more efficient than flat double-tuned circuits loaded to have equal primary and secondary Q, and (3) flat-staggered combinations are less efficient than flat double-tuned circuits loaded on one side only.

Inverse feedback and stagger-tuned amplifiers have the advantage over doubly-tuned amplifiers of considerably cheaper coil construction, which is their only significant advantage, apart perhaps from the smaller size and smaller capacitance to ground of the single-tuned inductors. The greater ease of aligning singly tuned stages over doubly tuned ones is thought by some to be an advantage favoring stagger tuning. Actually, because of their mechanical complexity and large capacitance, tunable coils are costly and degrade the performance of the circuit. Fixed tuned coils can be wound with sufficient accuracy and the wiring capacitance sufficiently accurately controlled by good mechanical design and layout to make factory tuning unnecessary for either type of coupling, and the amplifier is less subject to subsequent tampering. In addition, because the interstage coils are alike for all stages, inverse feedback and doubly tuned amplifiers have the advantage over stagger-tuned amplifiers.

However, inverse feedback has the disadvantage that gain control cannot be applied to a stage around which there is inverse feedback because it will change the bandwidth. On the other hand, gain control can be applied to any stage in a stagger-tuned or doubly tuned amplifier. Feedback resistors in inverse feedback amplifiers cannot be the ordinary half-watt type, but must be of a sort having considerably smaller end-to-end capacitance (such as the IRC type MPM).

The various coupling networks differ with regard to their sensitivity to the detuning that results from varying interstage capacitance. Doubly tuned circuits loaded on one side only are considerably more critical than doubly tuned circuits having equal primary and secondary Q, which is the principle objection to loading on one side only. In a stagger-tuned combination, the greater the number of different frequencies, the more critical it is.

References

(1) Henry Wallman, Stagger-Tuned IF Amplifiers, M. I. T. Radiation Laboratory Report 524, Feb. 23, 1944.
(2) "Vacuum Tube Amplifiers," Vol. 18, Radiation Laboratory Series, McGraw-Hill, New York, to be published, see esp. Chapter 4.
(3) Reference (2), Chapter 7.
(4) M. T. Lebenbaum, Wideband I-F Amplifiers above 100 Mc, ELECTRONICS, p 138, April, 1947.
(5) Reference (2), Table 4.3.
(6) Reference (2), Chapter 10.
(7) Reference (2), Chapter 6.

Multivibrator Design by Graphic Methods

Simple graphic method permits accurate design of free-running multivibrator circuit, eliminating tedious and repeated calculations. Curves are given for commonly used tubes. All phenomena determining circuit operation are taken into account

By A. E. ABBOT

THE equation for the semiperiod of the free-running zero-bias multivibrator shown in Fig. 1, as derived from its equivalent circuit, is

$$\tau_1 = \left(R_{g1} + \frac{R_L r_p}{R_L + r_p}\right) C_1 \ln\left(\frac{E_b - E_m}{E_x}\right) \quad (1)$$

where τ_1 = semiperiod of multivibrator
R_{g1} = grid resistance
R_L = load resistance
r_p = plate resistance
C_1 = coupling capacitance
E_b = plate-supply voltage
E_m = minimum alternating voltage on the plate
E_x = cutoff voltage corresponding to E_b

The subscript 1 denotes those factors pertaining to tube T_1. The various time and voltage relationships in the wave produced are shown also in Fig. 1. In Fig. 2 is given the output voltage E_o of the multivibrator in peak-to-peak volts as a function of load resistance.

The buildup time of the multivibrator, τ_B, is given on the A scales of the nomograph in Fig. 3. This nomograph is based on

$$\tau_B = 4\,(R_L + r_p)\,C \quad (2)$$

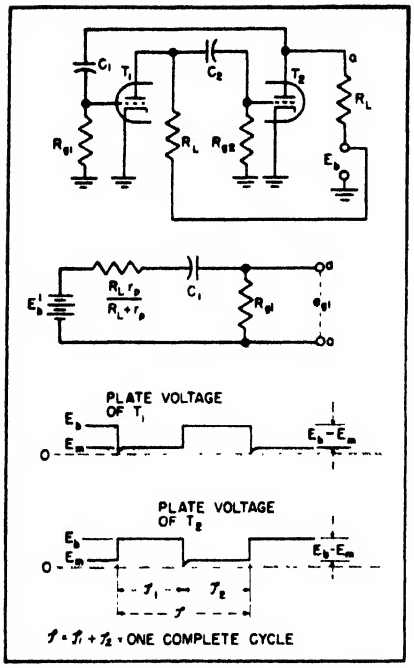

FIG. 1—Basic zero-bias free-running multivibrator, equivalent circuit, and typical time and voltage relations at the plates of the tube

The value of τ_s obtained here covers the period required for the voltage wave to reach 98 percent of its peak value.

In Fig. 4 it is assumed that

$$\alpha = \frac{E_b - E_m}{E_z} \tag{3}$$

and α is plotted in this graph against various values of R_L and E_b. Figure 4, therefore, gives a value of α that can be multiplied by the time constant to give the semiperiod. Therefore, Eq. 1 reduces to

$$\tau_1 = \left[R_{g1} + \frac{R_L r_p}{R_L + r_p}\right] C_1 \alpha \tag{4}$$

Figure 5 is a period-versus-frequency chart, which is included to facilitate the determination of the whole period τ when the frequency is given. This enables a simple calculation of fractional periods in the case of an unsymmetrical multivibrator (Fig. 1):

$$\tau = \tau_1 + \tau_2 \tag{5}$$

where τ_1 and τ_2 are the fractional periods.

In Fig. 6 and 7, it is assumed that

$$\beta = \frac{R_L r_p}{R_L + r_p} \tag{6}$$

Therefore, Eq. 4 further reduces to

$$\tau_1 = (R_{g1} + \beta) C_1 \alpha \tag{7}$$

In Fig. 6, it is also assumed that

$$\gamma = \frac{R_{g1}}{R_{g1} + \beta} \tag{8}$$

When plotted against R_g, the factor γ permits an evaluation of the effect of the load and plate resistances on the grid resistance. For the value of R_L selected, if R_g is made so high that $\gamma > 0.9$, then it can be assumed that $\beta = 0$. When $\gamma > 0.9$, there is approximately a 10-percent error in the calculation of τ_1; this falls to 5 percent when $\gamma = 0.95$.

Equation 7 reduces to a simple equation

$$\tau_1 = R_{g1} C_1 \alpha \tag{9}$$

The B scales of Fig. 3 are a plot of Eq. 9, and enable a simple calculation of the fractional period from the time constant and α.

If the conditions of the problem are such that $\gamma << 0.9$ it will be necessary to include the effect of β and use Eq. 7 rather than Eq. 9.

Figure 7 gives the value of β for different load resistances. The r_p selected in this calculation is an average value. With a given voltage swing, there will be a maximum deviation of 11 percent between any possible r_p and this average value.

Example 1

It is desired to design a multivibrator, using a 6SN7 tube, that will have a peak-to-peak output of 190 volts and will operate at a frequency of 30 kc. The pulse width required for triggering purposes is 10 microseconds. The plate supply is 250 volts.

Then $E_b = 250$ volts, $f = 30$ kc, $E_o = 190$ volts peak to peak, and $\tau_1 = 10$ microseconds.

Step 1 (see Fig. 2): When $E_o = 190$ volts and $E_b = 250$ volts, $R_L = 35$ kilohms.

Step 2 (see Fig. 4): When $R_L = 35$ kilohms and $E_b = 250$ volts, $\alpha = 2.563$.

Step 3 (see Fig. 5): When $f = 30$ kc, $\tau = 34$ microseconds. Then $\tau_1 = 10$ microseconds and $\tau_2 = 24$ microseconds.

Step 4: When $R_L = 35$ kilohms and $R_{g1} = R_{g2} = 0.1$ megohm, $\gamma = 0.93$. Then $\beta = 0$. Using scales B of Fig. 3: When $\tau_1 = 10$ microseconds $\tau_2 = 24$ microseconds, and $\alpha = 2.563$, $R_{g1} C_1 = 10/2.563 = 3.9$ microseconds, and $R_{g2} C_2 = 24/2.563 = 9.35$ microseconds.

Step 5: When $R_{g1} = 0.1$ megohm and $R_{g1}C_1 = 3.9$ microseconds, $C_1 = 40$ $\mu\mu$f. When $R_{g2} = 0.1$ megohm and $R_{g2}C_2 = 9.35$ microseconds, $C_2 = 95$ $\mu\mu$f.

Step 6 (see Fig. 3, scales A): When $R_L = 35$ kilohms and $C_1 = 40$ $\mu\mu$f, $\tau_s = 7$ microseconds.

A multivibrator was constructed according to the above calculations, with resistor and capacitor values accurate to within 1 percent. Calculated and experimental values of the semiperiod were identical, and E_o differed by only 2 volts.

It is desired to improve the buildup time of the multivibrator output in Example 1 at the expense of output voltage. The conditions of the problem remain the same, except that a lower value of R_L is selected.

Example 2

Let $R_L = 10$ kilohms. Then, by consulting the curves in the same order as in Example 1, it is found that $E_o = 132$ volts, $\alpha = 2.205$, $R_{g1} = R_{g2} = 0.1$ megohm, $\gamma = 0.93$, $R_{g1} C_1 = 10/2.205 = 4.54$ microseconds, $R_{g2} C_2 = 24/2.205 = 10.88$ microseconds, $C_1 = 45.4$ $\mu\mu$f, $C_2 = 108.8$ $\mu\mu$f, and $\tau_s = 3.51$ microseconds.

The multivibrator was again constructed, using resistor and capacitor values accurate to within 2 percent; results again were in close agreement.

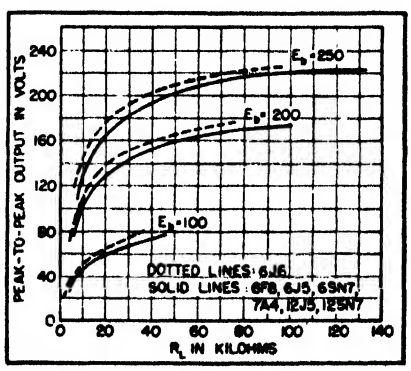

FIG. 2—Variation of output voltage with load resistance for tubes commonly used in multivibrator circuits

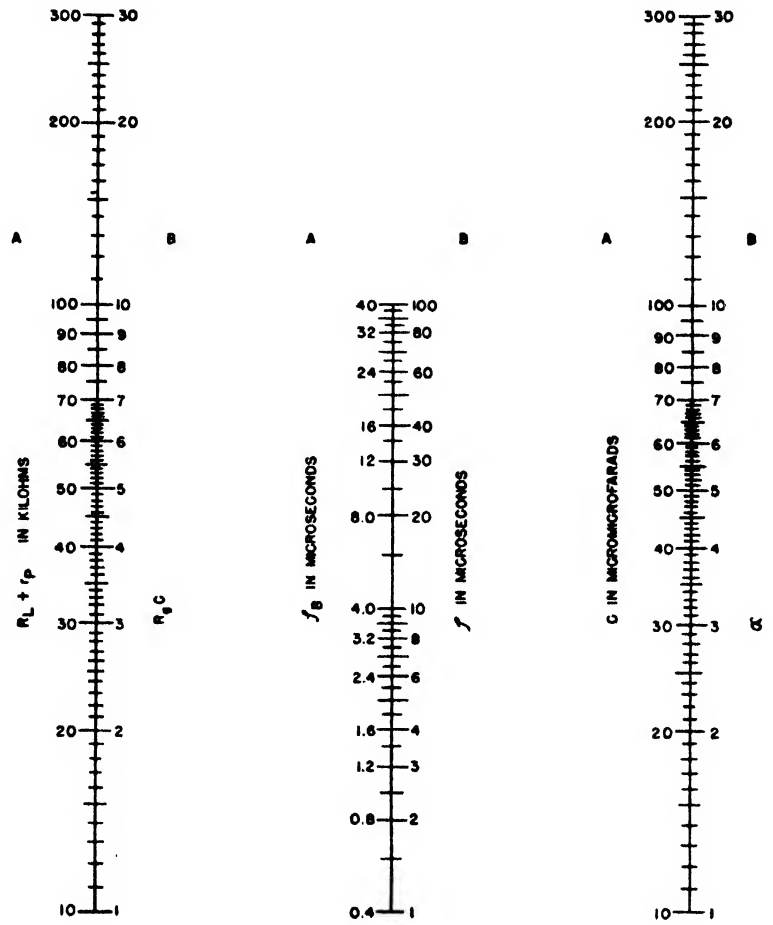

FIG. 3—Nomograph interrelating the various factors involved in multivibrator construction. The plate resistance value may be taken as 9,300 ohms for 6F8, 6J5, 6SN7, 7A4, 12J5 and 12SN7 tubes, as 10,000 ohms for the 6C5, and as 7,100 ohms for the 6J6

Example 3

It is desired to design a 25-kilocycle multivibrator with a buildup time of 2 microseconds and a pulse width of 15 microseconds.

Step 1 (see Fig. 3, scales A): When $C = 31$ $\mu\mu$f and $R_L = 8$ kilohms, $\tau_2 \doteq 2$ microseconds.

Step 2 (see Fig. 2): When $R_L = 8$ kilohms and $E_b = 250$ volts, $E_c = 119$ volts.

Step 3 (see Fig. 4): When $R_L = 8$ kilohms and $E_b = 250$ volts, $\alpha = 2.11$.

Step 4 (see Fig. 5): When $f = 25$ kc, $\tau = 40.1$ microseconds. Then $\tau_1 = 15$ microseconds and $\tau_2 = 25.1$ microseconds.

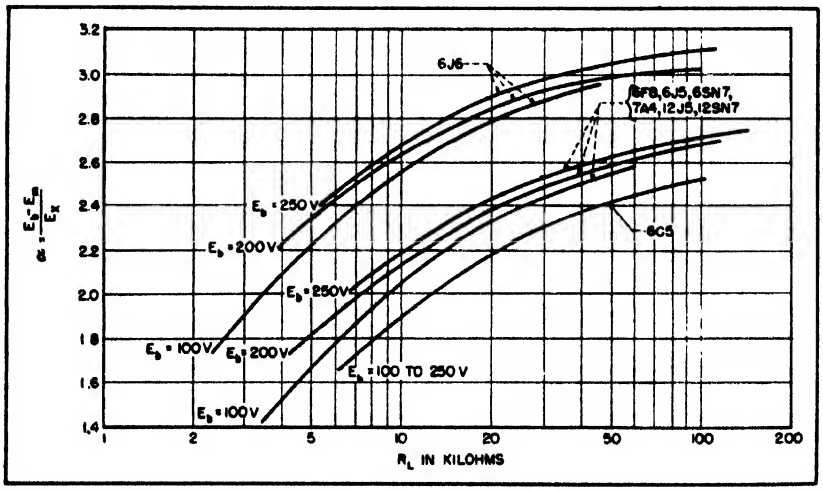

FIG. 4—Curves giving value of α in terms of load resistance and plate voltage for several types of tubes

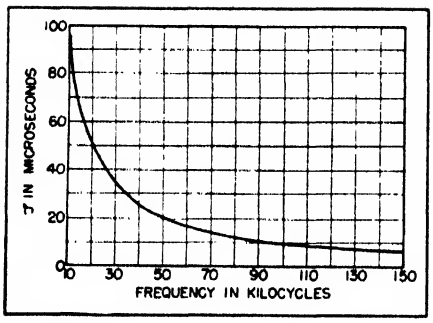

FIG. 5—Time-frequency relationship

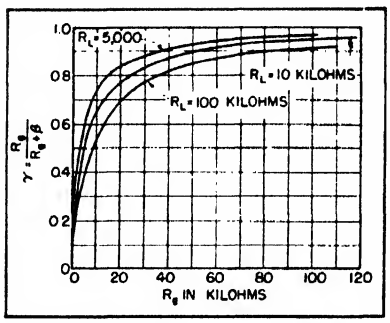

FIG. 6—Load resistance curves

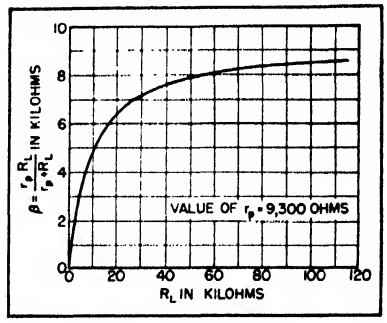

FIG. 7—Effect of load resistance

Step 5 (see Fig. 3, scales B): When R_{g1} C_1 = 15/2.11 = 7.11 microseconds, and C_1 = 31 $\mu\mu f$ R_{g1} = 0.228 megohm. When R_{g2} C_2 = 25.1/2.11 = 11.9 microseconds and R_{g2} = 0.1 megohm, C_2 = 120 $\mu\mu f$.

Limitations

The results of tests on a multivibrator of this design, using resistors and capacitors accurate to within 2 percent, are interesting because they illustrate one of the limitations of the method. The calculated value of τ_1 is 15 microseconds, while the measured value of τ_1 is 13 microseconds. The discrepancy is caused by the low value of coupling capacitance used (31 $\mu\mu$f). At this value, the stray capacitance becomes an appreciable fraction of the total. For extremely accurate results, it would be necessary to subtract the tube and wiring capacitance from the calculated value.

Another solution to the problem would be to use a smaller value of grid resistance, thus permitting a correspondingly larger coupling capacitance. When a high value of coupling capacitance is used, as in the calculation for τ_2, the experimental results are very close to the calculated one.

Another somewhat hidden cause for errors in predicting the semiperiods of a multivibrator is the permanent change in the value of a resistor with temperature. To determine the order of this change, each lead of a ½-watt resistor of 102,600 ohms was heated with a soldering iron for a half minute. The resistor was then cooled and the measured resistance was found to be 148,000 ohms, a change of 45 percent. Each lead of five ½-watt, 0.1-megohm resistors was then heated for fifteen seconds. The average resistance change, after they had cooled for a long period of time, was 17 percent. Thus, the process of soldering resistors into a circuit may change the value of the resistor permanently and, consequently, affect the semiperiod of the multivibrator.

To evaluate the cause of the discrepancy in Example 3, the following experiment was made: The 31-$\mu\mu$f capacitor was replaced by a variable mica trimmer capacitor, which was adjusted until the semiperiod was exactly 10 microseconds. The capacitance value under these conditions was 27 $\mu\mu$f. Thus, a 4 $\mu\mu$f error caused by wiring and tube capacitance is responsible for the 3-microsecond error in the pulse width.

The results obtained with the new value of capacitance were: τ_1 = 10 microseconds, τ_2 = 26 microseconds, τ_B = 3 microseconds, and E_c = 110 volts.

Low-Frequency Compensation for Amplifiers

Two unconventional interstage coupling networks for low-frequency amplifiers are developed. One has a grounded load resistor, thus providing a low impedance output; the other requires very little capacitance, thus decreasing size and cost. Design requirements of the networks are analysed

By KURT SCHLESINGER

MANY MODERN APPLICATIONS of electronics, such as radar, television, electrocardiography, industrial vibration analysis, and electrical gaging, require amplifiers that pass very low frequencies. For example, although in some applications large amplifier distortions may be tolerated because the output can be corrected by clipping and limiting, in television and facsimile where halftone shading must be faithfully reproduced even a little distortion is objectionable. Therefore, the resistance-capacitance coupled amplifiers (used because of their freedom from drift found in directly coupled amplifiers) require

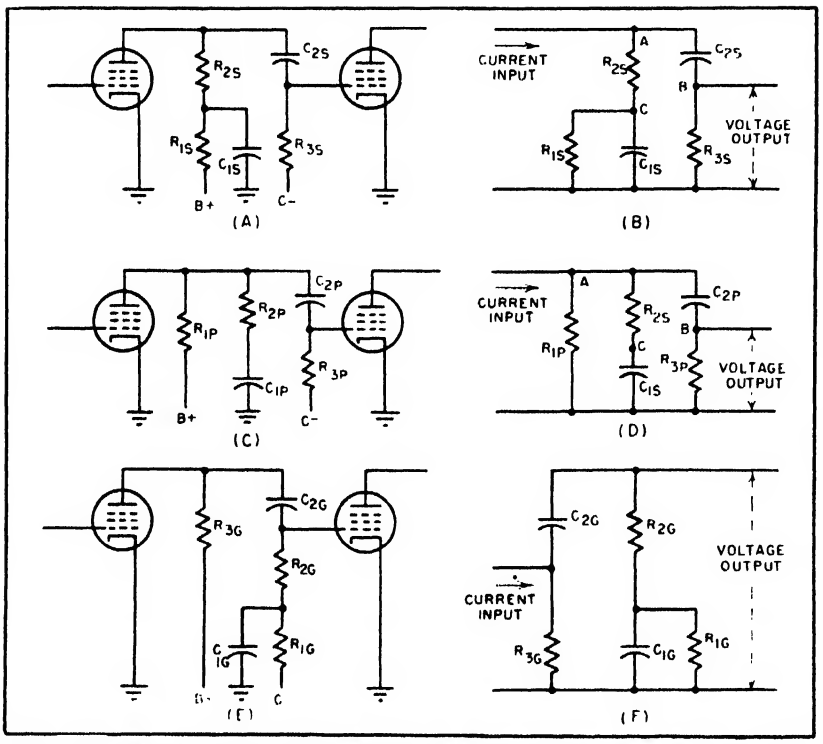

FIG. 1—At (A) is a conventional low-frequency compensating network; (C) and (E) are two other networks that provide the same response but with less compensating capacitance

compensation to pass very low frequencies.

Figure 1A shows the usual type of interstage coupling with low-frequency coupling, called plate series compensation. The equalizing impedance $R_{1S}C_{1S}$ is connected in series with the plate load R_{2S}. Figure 1B shows the equivalent network comprising two resistances and two capacitances, one of which is shunted by R_{1S}. It is this leakage resistance across C_{1S} that causes low frequency cutoff. The limitation could be removed by providing additional leakage across the corresponding capacitor C_{2S} in the other arm. However, the resulting d-c transmission that this resistance would provide excludes this practice in most applications, except perhaps for the final stage of a video amplifier. Obviously the available plate supply voltage limits the maximum value of R_{1S} hence large capacitances are required if coupling is to extend sufficiently into the low frequencies.

These conditions are somewhat improved in the circuit of Fig. 1C. Resistor R_{1P} is in parallel with the load resistor R_{2P}; thus the circuit may be referred to as plate shunt compensation. The equivalent network, shown in Fig. 1D, can be transformed into the equivalent plate series network of Fig. 1B, or vice versa, by the relations

$$R_{1P} = R_{2S} + R_{1S}$$
$$R_{2P} = R_{2S}[1 + R_{2S}/R_{1S}]$$
$$C_{1P} = C_{1S}[R_{1S}/(R_{2S} + R_{1S})]^2$$

Note that the plate filter capacitance C_{1P} for plate shunt compensation is considerably smaller than its equivalent C_{1S} for plate series compensation. The elements R_{2P} and C_{1P} may change places without affecting the low-frequency performance of the signal at B. The circuit then presents a grounded resistor at point C, which offers a convenient source of video signals from a low impedance but without low-frequency compensation.

Figure 1E shows a grid compensation system in which the shunted capacitor combination $C_{1G}R_{1G}$ is located in the grid branch and the plate coupling capacitor C_{2G} is assumed as ideal. The compensation resistor R_{1G} passes only small grid and leakage currents and can therefore assume higher values than its counterpart in the other two circuits. Adequate compensation is obtained with much smaller capacitances, as demonstrated by both theory and practice. If grid compensation is employed, paper capacitors can replace the larger and less reliable electrolytic capacitors.

Figure 1F presents the equivalent grid compensation network. Comparison with Fig. 1B reveals as the only difference the interchange of the points of current input and voltage output. From circuit theory it follows that, with equal elements throughout, both systems are perfectly equivalent. Therefore the following analysis of the pulse response of the series plate compensated stage is applicable to all types of low-frequency compensation.

In the following analysis the tube is treated as a constant-current generator with practically infinite impedance. The effect of screen current is neglected. Grid bias is assumed to be available from an external source and all cathodes are directly connected to ground. A unit step of current is applied at point A of Fig. 1B. The midband load resistance is

$$R = R_{2S}R_{3S}/(R_{2S} + R_{3S})$$

The transfer impedance from A to B is then

$$\frac{Z}{R} = \frac{p(p + c)}{(p + a)^2 - b^2} \qquad (1)$$

where $p = j\omega$, and the transfer impedance is the same in the inverse direction. In Eq. 1, a and b are closely related to the arithmetic and geometric means of two characteristic frequencies ω_1 and ω_2, which are in turn defined by the time constants T_1 and T_2 of the compensating and coupling networks respectively

$$1/\omega_1 = T_1 = C_{1S}R_{1S}$$
$$1/\omega_2 = T_2 = [C_{1S}C_{2S}/(C_{1S} + C_{2S})][R_{2S} + R_{3S}]$$

The mean values of these characteristic frequencies as they appear in Eq. 1 are

$$a = \tfrac{1}{2}(\omega_1 + \omega_2)$$
$$b^2 = a^2 = \gamma g^2$$
$$c = \omega_1/\alpha$$
$$g = (\omega_1\omega_2)^{1/2}$$
$$\gamma = C_{1S}/(C_{1S} + C_{2S})$$
$$\alpha = R_{2S}/(R_{2S} + R_{1S})$$

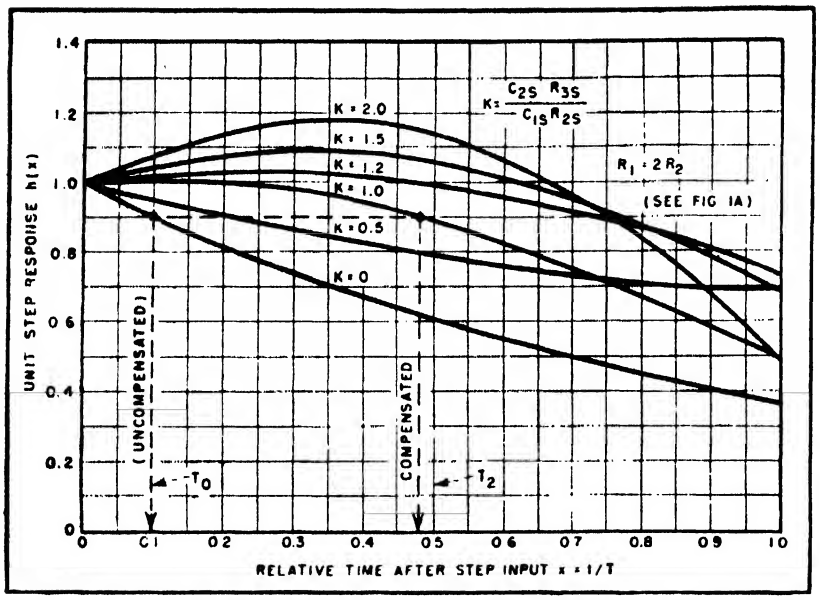

FIG. 2—Network response to a step input for various degrees of compensation is shown against time relative to circuit time constant

Equation 1 gives, by operation, the unit step response of the network (see G. W. Carter, "Calculation of Electrical Transients", p 99, Eq. 11 and 12)

$$h(t) = \epsilon^{-at}[\cosh(bt) + [(c-a)/b]\sinh(bt)] \quad (2)$$

To discuss Eq. 2 in technical terms, expand it into a power series in t so that

$$h(t) = 1 - (c-2a)t + (b^2 + 3a^2 - 2ca)(t^2/2) - \ldots$$

The first order term should vanish because this condition indicates a horizontal tangent at $t = 0$ (step response starts flat). For this condition $c - 2a = 0$ we obtain

Flat top

$$R_{2S}C_{1S} = R_{3S}C_{2S}$$

which condition holds regardless of the value of R_{1S}.

The signal droop at the end of T seconds can now be assessed. Putting the condition for flat top into the power series gives

$$h(t) = 1 - g^2(t^2/a) + ag^2(t^3/3) - \ldots$$

Because the sign of the third order term is positive, the drooping of a compensated stage after T seconds of unit step transmission is smaller than $0.5(gT)^2$. Thus we obtain

Step droop

$$\delta \leq \frac{T^2}{2R_{1S}R(C_{1S} + C_{2S})^2}$$

Note that the droop is determined by such fundamental constants of the network as a-c impedance, d-c leakage, and total capacitance.

Figure 2 presents the unit step response of a stage with plate series compensation for various ratios of time constants in the two bridge arms, and the response of an uncompensated stage for comparison. The compensated stage handles pulses about five times wider than the uncompensated stage with equal droop. In general, the improvement through low-freqency compensation is

$$T_1^2 = 2T_0T_1$$

where T_1 is the duration of pulses handled by the compensated network and T_0 is the duration of pulses handled by the uncompensated one, with equal amounts of drooping. A high value of T_1 for the compensating arm is desirable, hence grid compensation functions much more efficiently than plate compensation. Practical design data are presented in Fig. 3.

Square-Wave Response

Before applying these results to television amplifiers, it must be shown that square-wave response of the network does not exhibit signal distortions in excess of those calculated for unit step operation. Let

$$g(t) = 0.5(-1)^n$$
$$nT \leq t < (n+1)T$$
$$n = 0, 1, 2 \ldots$$

be the expression for a square-wave signal with an amplitude of one volt and a period of $2T$. Heaviside's superposition theorem then relates the square-wave response $H(t)$ to the unit step response $h(t)$ as

$$H(t) = g(t) - [0.5 + \sum_{n=0}^{\infty}(-1)^n h(\theta + nT)]$$

where θ is the time difference between the occurrence of the last unit step and the instant t of the observation. The sum represents the influence on the network of an infinite number of preceding unit steps. Fortunately this series converges to

$$H(t) = g(t) + 0.5\left[1 - \frac{\epsilon^{aT}h(t) + \epsilon^{-aT}h(t-T)}{\cosh(aT) + \cosh(bT)}\right] \quad (3)$$

Figure 4 shows how the square-wave response H can be derived graphically from the unit step response h in accordance with Eq. 3. To obtain H at any time t, take $h(t)$ at that time, as well as a fraction ϵ^{-2aT} of the same function T seconds earlier. Superimposing these two components yields the square-wave response $H(t)$.

In Fig. 4 the procedure is applied

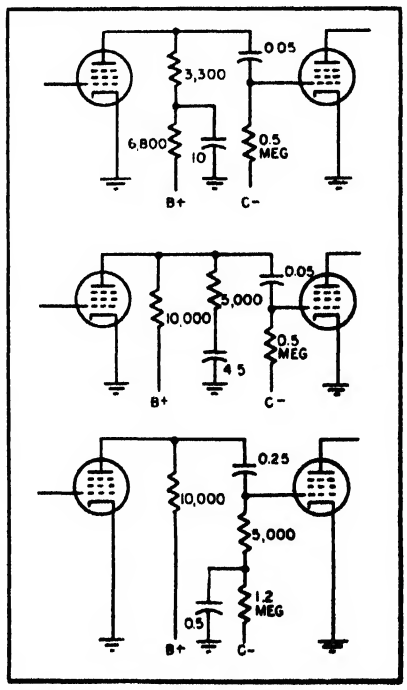

FIG. 3—Typical values of three types of compensating networks giving the same performance

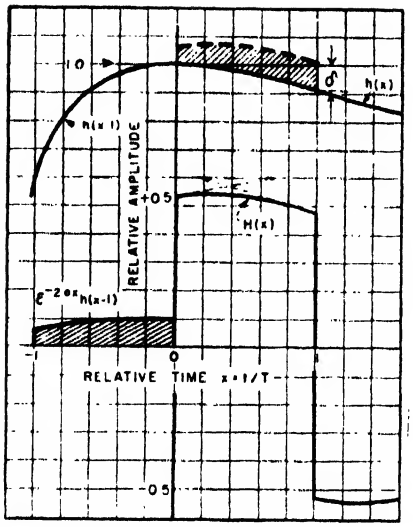

FIG. 4—Development of square-wave response from step response

to a compensated network which has a step response with a horizontal tangent at $t = 0$. The square-wave response of the same network exhibits a slight positive rise at the start of each period. To correct for the rise, the network should be slightly undercompensated. Further, in contrast to the step response, which droops in one direction only, the actual square-wave output shows both positive and negative deviations from the ideal flat. The sum of the distortions, however, does not exceed the ten percent droop of the unit step response during the same time interval. Because this agreement tends to improve for smaller distortions, circuit design based on the conditions for flat top and step droop for the step function seems entirely justified for television.

Practical Conclusions

Figure 3 shows circuits designed by the above approach using the three types of low-frequency compensation. All three circuits were designed to transmit a 1/120 second pulse with a droop of less than 2 percent (1/60 second pulses with less than 6 percent). All circuits have the same d-c plate resistance of 10,000 ohms and the same a-c signal impedance of 3,300 ohms. The value of plate load yields a bandwidth of 4.5 mc if it is used as the termination of a two-section constant-k filter to obtain high-frequency correction.

The conventional plate series compensation needs an electrolytic capacitor of 10 microfarads, the plate shunt circuit uses less than half this capacitance, and the grid compensated circuit requires only 1/20th of the capacitance necessary in the plate series network, or 0.5 microfarad. Because such small capacitors are available with paper insulation, a drastic reduction in size and cost is possible with grid compensation instead of plate compensation. Also the dependability is improved and variations due to aging or overload are minimized.

Whereas the plate compensation capacitor operates at plate voltage, the grid compensation capacitor operates at the small grid bias voltage. These advantages over plate series compensation are realized to some degree by the plate shunt method.

One disadvantage of both plate shunt and grid compensation is that neither offers as much protection against hum and slow fluctuations of plate voltage as does the plate series network. The plate series circuit of Fig. 3 has 28-db attenuation for 60-cps hum between plate supply and grid, while the other two circuits have only 10-db attenuation. This decreased hum attenuation necessitates a somewhat higher investment in power supply filter capacitors, but they are less critical than those in the interstage coupling network. Video amplifiers with two and three stages have been built with the grid compensation network of Fig. 3 and were found to be very satisfactory and stable in operation. By using modern titanium dioxide dielectric capacitors the coupling networks were made unusually small.

Clipping and Clamping Circuits

Performance characteristics of basic circuits for removing that portion of a signal which exceeds a predetermined level or for passing only signals exceeding the clip level, and for restoring or changing average values of signals having level portions

By NORMAN W. MATHER

CLIPPING or leveling circuits are used to perform many useful operations, such as creating square waves from sine waves, removing large noise pulses from audio-frequency signals, and removing portions of signals for special purposes.

Clipping circuits may be arranged either to remove the portion of a signal which exceeds the clip level or to pass only those signals which exceed the clip level. Some of the circuits can be modified so that the signal is clipped only a portion of the time, or so the signal is eliminated except when it arrives at the proper time.

Clamping circuits, also called d-c restorers, are used to restore or change the average value of signals which have level portions in their waveforms. The level portions of the waveforms are necessary if the clamping action is to be accomplished. Signals having random variation (or low-frequency a-c

components) which are passed through a-c amplifiers usually have the low-frequency components badly distorted. Clamping circuits act to restore these components, and also to change the d-c level of the signal if desired, by periodically clamping a level portion of the signal waveform at a specified voltage.

Shunt Diode Clipping

The simple clipping circuit in Fig. 1A uses a diode in shunt with the path of the signal. Circuits of this type can be used only when the load on the circuit is small compared to the load imposed by the diode when it conducts.

This type of circuit clips or levels the signal whenever the plate voltage of the diode becomes positive because its resistance is then much smaller than that of the series resistor, so that a large voltage drop occurs in the series resistor. When the plate voltage is negative, however, the diode is essentially an open circuit and the voltage drop in the series resistor is small. Reversing anode and cathode connections gives positive output pulses.

Copper-oxide, selenium, or crystal rectifiers can be used in place of diodes, depending upon the characteristics of the signal and the circuit in which the clipping circuit is placed. Due to their large shunt capacitance, large dry-disk rectifiers are unsuitable when the signal has high-frequency components.

Application of an adjustable voltage to the cathode as in Fig. 1B makes it possible to set the voltage at which the input signal is clipped. The opposite portion of the signal can be clipped by reversing the diode. The diode and potentiometer resistance must be much smaller than the series resistance.

Series Diode Clipping

With a diode in series with the path of the signal as in Fig. 1C, the circuit can be loaded more heavily than when using a shunt diode. The values of the circuit elements are not critical insofar as the clipping action is concerned but depend upon the application. The diode passes the signal whenever the instantaneous flow of current is in the direction which tends to make the diode plate positive. The signal is clipped when the plate voltage becomes negative. Reversing polarity of diode connections gives negative output pulses.

In the series diode circuit of Fig. 1D the clipping level is set by adjustment of the variable potentiometer. In the circuit of Fig. 1E, the clipping level is determined by a voltage wave applied from an external source. The circuit of Fig. 1F uses a series battery to change the average level of the signal and thus change the clipping level.

Series Capacitor for Bias

Circuits with adjustable clipping levels, in which the average value of the signal is changed by the d-c voltage developed across a series capacitor, appear in Fig. 2A and 2B. This voltage is developed due to the difference of the charging and discharging time constants of the circuit, which includes the capacitor and the diode. The ratio of these time constants can be changed by means of the variable resistance in the circuit, thus changing the voltage across the capacitor and the clipping level. The clipping level also depends upon the average amplitude of the signal, hence these circuits cannot be used with irregular waveforms.

Emission-Saturation Clipping

A clipping circuit which depends upon the emission saturation of a tungsten-filament tube is given in Fig. 2C. Clipping in this circuit occurs when the plate voltage is negative or when the emission limit of the filament is reached. The resistance shown in the circuit represents the load. Tungsten-filament tubes are not commonly available in small sizes; however, the type FP-400 can be used.

Grid and Plate Clipping

With grid circuit clipping as in Fig. 2D, the positive portions of the grid signal are clipped in the same way that signals are clipped in the diode circuits of Fig. 1. The signal is amplified, inverted, and

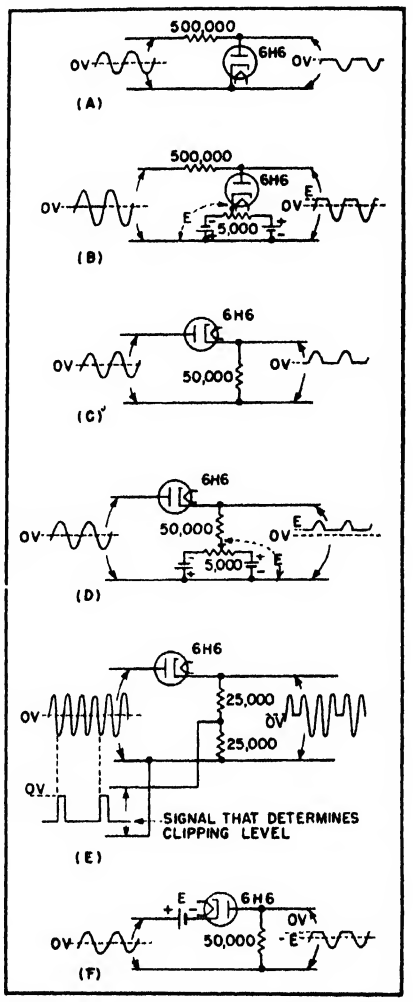

FIG. 1—Basic series and shunt diode clipping circuits

the opposite portion of the signal is clipped if the grid signal becomes negative enough to cause plate current cutoff. A bias voltage may be applied in the grid circuit to change the clipping level.

Clipping in the plate circuit due to plate-current cutoff at one extreme and to space-charge limitation of plate current at the other extreme is utilized in Fig. 2E. The signal is amplified and inverted as well as clipped. A large load resistance is used in the plate circuit so that the path of operation on the plate characteristic will be as indicated. The flow of grid current in this circuit loads the circuit supplying the signal, which therefore must have a low internal impedance.

Clipping in the plate circuit of a pentode, illustrated in Fig. 2F, is

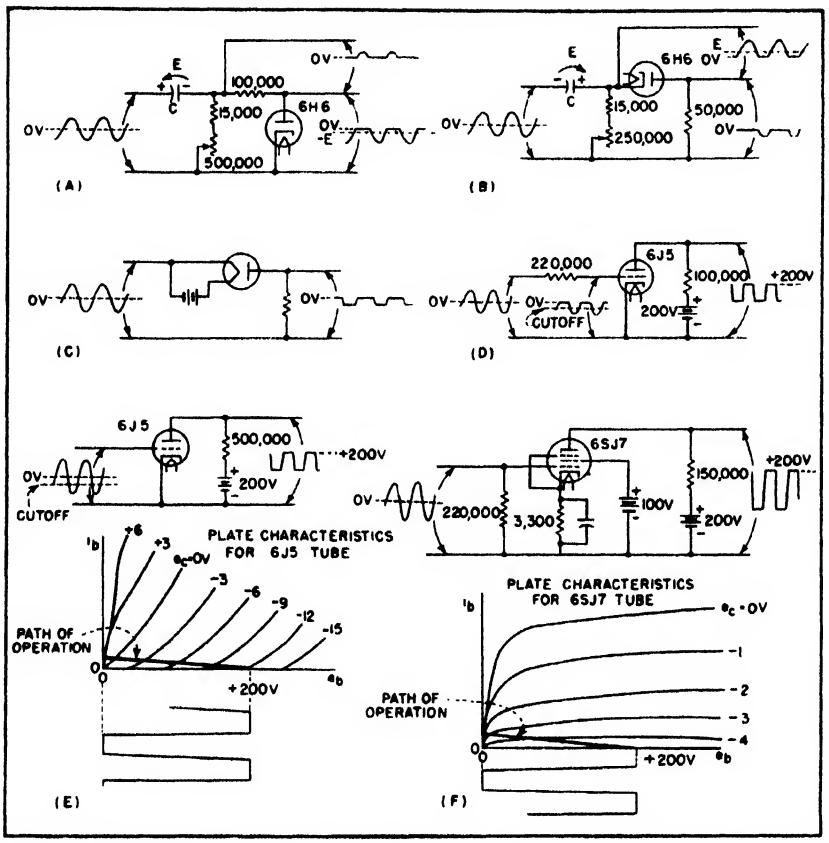

FIG. 2—Special clipping circuits, including arrangements for grid and plate clipping

similar to the action of the triode circuit of Fig. 2E except that the grid is not driven positive and thus the loading of the signal source is eliminated. The signal must not be too large and sufficient cathode bias must be used for proper operation.

Cathode-Circuit Clipping

When clipping in a cathode-follower circuit as in Fig. 3A, the top of the input signal is clipped when grid current flows due to the voltage drop in the resistor in series with the grid. The bottom of the signal is clipped when the grid-to-cathode voltage becomes negative enough to cut off plate current. A relatively large input signal is required if both the top and bottom of the input wave are to be clipped. A potentiometer across the cathode resistor adjusts the average value of the input signal and controls the grid bias voltage.

Clipping in the cathode-input amplifier of Fig. 3B occurs when grid current flows and when plate current is cut off. This circuit requires a low-impedance signal source (such as the output of a cathode follower). It has the advantage of giving voltage amplification and clipping without inverting the signal.

Coincidence Circuit

The signals in Fig. 3C are clipped except when they coincide. Either of the control grids can cut off plate current, and both are biased beyond cutoff in this circuit. When they are both raised above their cutoff potentials, plate current flows and an output signal is obtained. Similar effects can be obtained with ordinary triodes and pentodes by applying one of the signals to the cathode, screen grid, or suppressor grid.

VR and Thyrite Clippers

Neon lamps or VR tubes can be used in the gas diode type of clipping circuit shown in Fig. 3D. The resistor is chosen so that the current conducted by the tubes stays within their ratings. The output voltage has small spikes on the leading edges because the gas tubes require a starting voltage which is greater than their normal voltage drop while conducting.

A clipping circuit using a Thyrite element appears in Fig. 3E. Thyrite devices are often used on power transmission lines to minimize voltage surges due to lightning.

In the diode clamping circuit of Fig. 4A, the upper portion of the input signal is clamped at zero voltage. By reversing the diode

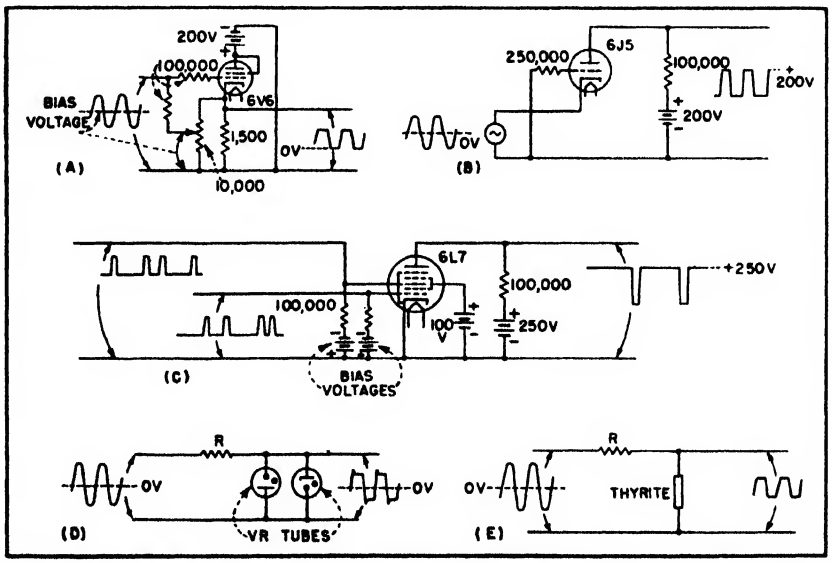

FIG. 3—Examples of cathode-circuit clipping, a coincidence circuit that clips except when two input signals coincide, and special gas diode and Thyrite clipping circuits

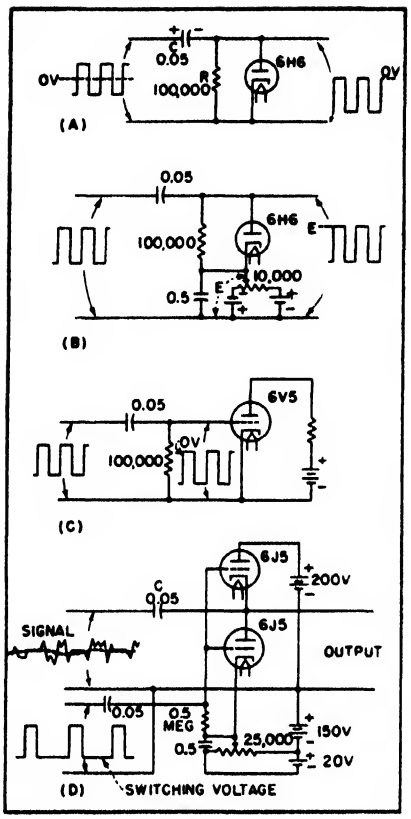

FIG. 4—Diode and triode clamping circuits, also called d-c restorers

the opposite side of the signal can be clamped at zero voltage. Operation depends upon the difference in time constant for charging and discharging *C*. When charging, the diode resistance shunts *R*, but while discharging the diode acts as an open circuit. Selenium, copper-oxide, or crystal rectifiers can be used in place of the diode.

A clamping circuit with an adjustable clamping level is given in Fig. 4B. By placing the diode in a circuit containing an adjustable d-c voltage *E*, the clamping level assumes the voltage *E* instead of zero level. The opposite side of the signal can be clamped by reversing the diode.

Clamping in the grid circuit of a tube as in Fig. 4C involves action of the grid circuit of a tube similar to diode action, hence clamping can be obtained by using the grid in place of the plate of the diode. This operation is merely a special case of grid-leak biasing.

If neither top nor bottom of the wave to be clamped has a suitable level portion, clamping can be accomplished with the synchronized clamping circuit of Fig. 4D if some intermediate portion of the wave is level. Signals which occur at random about such a level portion will cause the signal to have a varying average value as indicated by the dotted line on the input waveform. If the signal has passed through stages having a-c coupling only, these low-frequency components become out of phase with the main signal or are lost entirely. The purpose of the clamping circuit is to restore the signal to its original form.

The switching voltage is synchronized with the signal so that the tubes, which are normally biased beyond plate-current cutoff, are switched on when the portion of the signal to be clamped occurs. The tubes then conduct and cause the output to have the proper value during the clamping period. The coupling capacitor assumes a charge during this period which results in the random signal starting at the right level. Before the capacitor voltage has had time to stray far from the proper value, the circuit again clamps and the capacitor voltage is brought back to the proper value.

Synchronized clamping can also be accomplished by using diodes in place of the triode tubes of Fig. 4D. Instead of a battery or other steady voltage source, switching signals are applied to the cathode of one diode and to the anode of the other. During the time that these two signals have the same voltage, clamping occurs at this voltage, but when the cathode signal is made more positive and the anode signal is made more negative than this voltage, the circuit is free to follow the main signal voltage.

Square-Wave Differentiating Circuit Analysis

From analytical treatment of pulse-generating circuit, generalized circuit design charts are plotted giving pulse amplitude and length. Time constant of the input wave front and stray shunt capacitance of the differentiating circuit are considered

By G. P. OHMAN

IN THIS PAPER the response of a conventional *R-C* differentiating circuit to a square-wave voltage having an exponential rise is to be analyzed. Formulas will be derived and curves given which apply to both analysis and design of this type of differentiating circuit. In particular, these formulas and curves enable one to calculate the shape, length and magnitude of the output-pulse voltage of the differentiating circuit.

Electrical Considerations

Upon sharply differentiating a square-wave voltage it is common experience to find that the magnitude of the output-pulse voltage is only a small fraction of the magnitude of the input. This loss in magnitude is due principally to two things. Firstly, the square wave is never truly square but has a front of finite slope (usually closely exponential in form); secondly, there is always associated with the resistance of the differentiating circuit some stray shunting capacitance which brings about a division of

the input voltage between this stray capacitance and the series capacitance of the differentiating circuit.

Intuitively one can see that the more closely the voltage wave approaches a true square wave and the smaller is the stray capacitance, the greater will be the output of the differentiating circuit. However, it is difficult to say beforehand just what the amplitude and wave shape of the output pulse will be. It is the purpose of this paper to attempt to answer these questions as well as some others.

Mathematical Analysis

Derivation of a mathematical expression describing the behavior of this type of differentiating circuit is simple and straightforward. One has but to set up the Kirchhoff voltage equations for this circuit and solve the resulting first order linear differential equation.

Let the differentiating circuit be as represented in Table 1. Applying Kirchhoff's law to this circuit one obtains the following voltage equations

$$e_i = \left(\frac{1}{C_1} + \frac{1}{C_2}\right)\int i_1 dt - \frac{1}{C_2}\int i_2 dt \qquad (1)$$

$$0 = -\frac{1}{C_2}\int i_1 dt + \frac{1}{C_2}\int i_2 dt + Ri_2 \qquad (2)$$

By differentiating both Eq. (1) and (2) with respect to time and then eliminating i_1 from the two resulting equations, one gets a differential equation in i_2

$$R\frac{di_2}{dt} + \frac{i_2}{C_1 + C_2} = \frac{C_1}{C_1 + C_2}\cdot\frac{de_i}{dt} \qquad (3)$$

But because $e_o = i_2R$ one can convert Eq. (3) into a differential equation in e_o, i.e.

$$\frac{de_o}{dt} + \frac{e_o}{R(C_1 + C_2)} = \frac{C_1}{C_1 + C_2}\frac{de_i}{dt} \qquad (4)$$

Equation (4) is a common first order linear differential equation which may be solved in the conventional way by means of the integrating factor, $\epsilon^{t/R(C_1 + C_2)}$ yielding.

$$e_o = \frac{C_1}{C_1 + C_2}\epsilon^{-t/R(C_1 + C_2)} \times \int_0^t \epsilon^{t/R(C_1 + C_2)}\cdot\frac{de_i}{dt}dt \qquad (5)$$

Equation (5) gives the response of the differentiating circuit to an input voltage of any form. To make practical use of this equation it is necessary to express the input voltage as a differentiable function of time.

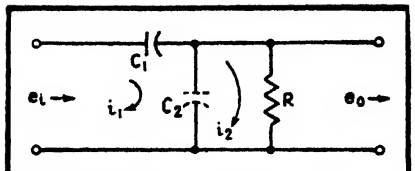

C_1 = Series capacitance, in farads
C_2 = Stray shunt capacitance, in farads
R = Shunt resistance, in ohms
e_i = Applied input potential, in volts
e_o = Developed output potential, in volts
t = Time, in seconds

$e_i = E_i(1 - \epsilon^{-t/\tau_i})$
E_i = Amplitude of square wave, in volts
τ_i = Time constant of input voltage wave front, in seconds
$\tau_o = R(C_1 + C_2)$, time constant of differentiating circuit
$\beta = \tau_i/\tau_o$
$\gamma = C_1/(C_1 + C_2)$
$T = t/\tau_i$

TABLE I—Differentiating circuit and definitions of terms discussed in text

It should be observed that the lower limit of the integral of Eq. (5) is zero. This follows from the assumption that the differentiating circuit is at rest when the input voltage is applied to the circuit at $t = 0$. This assumption also implies that the square wave is longer than the output pulse if the square wave is one of a train of square waves.

Square Wave Input Voltage

In recent applications, television being one of the common and widely known ones, practice is to differentiate the front or back of a square-wave voltage to obtain a sharp-pulse voltage. Because the differentiation of square waves is therefore relatively important, and because of the impracticability of considering all the possible wave shapes only the differentiation of square waves will be considered further.

It was previously pointed out that one never encounters true square waves in practice since their fronts and backs have finite slopes usually approximately exponential in form. A square wave having an exponential front will be assumed. Let this voltage be represented by the expression $e_i = E(1 - \epsilon^{-t/\tau_i})$ where the terms are as defined in Table 1.

This expression gives only the rise of the square wave, not the fall, but this is not a serious limitation because the front and the back of the square wave can be considered separately. If the back of the square wave is similar in form to the front, a pulse similar to that generated in the differentiating circuit by the front, will be generated by the back, but of opposite polarity.

If one differentiates the above expression for e_i with respect to time, substitutes it in Eq. (5) and performs the indicated integration, one arrives at the expression

$$e_o = \frac{E_1C_1}{\tau_i(C_1 + C_2)}\cdot\frac{1}{\frac{1}{R(C_1 + C_2)} - \frac{1}{\tau_i}} \times (\epsilon^{-t/\tau_i} - \epsilon^{-t/R(C_1 + C_2)}) \qquad (6)$$

Equation (6) is unwieldly, but by substituting τ_o, β, γ and T as defined in Table I, it can be simplified to

$$e_o = E_i\gamma(\epsilon^{-\beta T} - \epsilon^{-T})/(1 - \beta) \qquad (7)$$

For the purpose of plotting, however, this expression is unsuitable because it contains too many variables. But E_i and γ appear only as simple multipliers and hence have no effect upon pulse shape other than its amplitude. By letting $e_o' = e_o/E_i\gamma$, one obtains an expression which may be plotted as a family of curves.

$$e_o' = \frac{1}{1 - \beta}(\epsilon^{-\beta T} - \epsilon^{-T}) \qquad (8)$$

Figure 1 is a plot of Eq. (8).

Two other quantities which are of importance are the peak voltage reached by the output pulse and the time interval after the arrival of the square wave at which this occurs. Both of these quantities depend upon the value of β. These quantities may be found by maximizing Eq. (8).

$$\frac{de_o'}{dT} = \frac{1}{1 - \beta}(-\beta\epsilon^{-\beta T} + \epsilon^{-T}) = 0$$

$$\text{or } \epsilon^{-T} = \beta\epsilon^{-\beta T} \qquad (9)$$

Substituting Eq. (9) into Eq. (8) one finds that

$$e_o'_{max} = \epsilon^{-\beta T} \qquad (10)$$

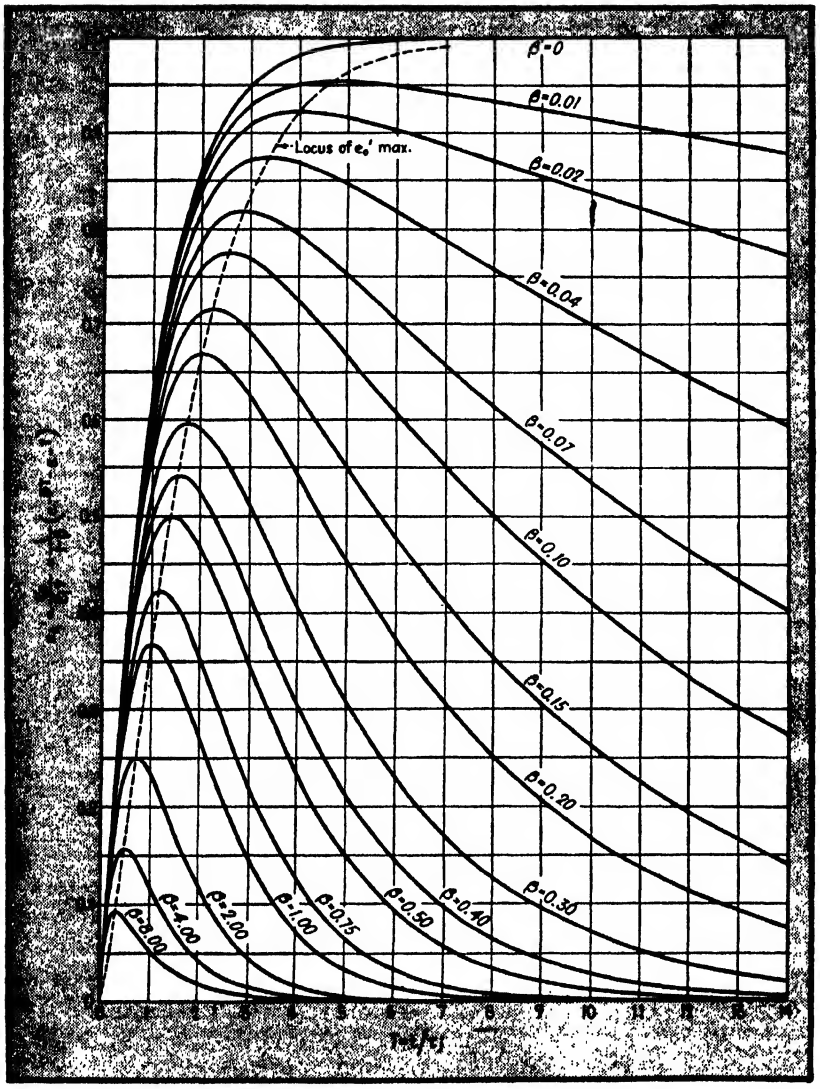

FIG. 1—Family of curves for relative pulse amplitude vs relative time shows the effect on the pulse amplitude and length of the ratio of the input wave-front time constant to the differentiating circuit time constant

Eliminating T from Eq. (9) and (10), one obtains

$$e_o'_{max} = \left(\frac{1}{\beta}\right)^{\beta/(\beta-1)} \qquad (11)$$

Solving Eq. (9) for T

$$T \text{ for } e_o'_{max} = \frac{1}{\beta - 1} \log_e \beta \qquad (12)$$

Equations (11) and (12) are plotted in Fig. 2.

In addition to the curves already mentioned a third set of curves, given in Fig. 3, has been calculated and plotted, which gives an indication of pulse length as a function of β. Pulse length is defined as the time at which the pulse voltage has decayed to a certain percentage of the maximum pulse voltage. Figure 3 gives the T at which the pulse amplitude has decayed to 10 percent and to 1 percent of its maximum value.

Use of Charts

It is tacitly assumed in the derivation of these formulas and curves that the differentiating circuit has negligible loading effect upon the square-wave voltage source. This is not likely to be the case if the source impedance is relatively high compared to the impedance of the differentiating circuit. This should be kept in mind when one chooses the parameters of the differentiating circuit since loading of the voltage source will increase the time constant τ_i of the input wave front. In some cases allowance may have to be made for loading.

On Fig. 1 e_o' and T are pure numerics and do not per se represent voltage and time respectively. e_o' must be multiplied by $E_i\gamma$ to obtain the output voltage, e_o, and T must be multiplied by τ_i to convert the abscissa scale to a time scale. If this is done the curve corresponding to the proper β will be a chart of the output voltage as a function of time. The curve corresponding to $\beta = 0$ will be a chart of the input voltage if the ordinate scale is multiplied by E_i alone and the abscissa scale is multiplied by τ_i.

Frequently one wants to know the maximum voltage reached by the output voltage pulse and the time at which this maximum occurs; Fig. 2 gives this information. Here again e_o' and T must be treated in the same way as on Fig. 1.

It can be seen upon examination of Fig. 1 that no matter how great β is, that is—no matter how sharply one differentiates the input wave, the front of the output pulse never has a slope greater than that of the input wave. However, increasing β has two desirable effects; it shortens the length of the pulse, and it reduces the time necessary for the pulse to reach its maximum value. Increasing β has one very undesirable effect; the maximum pulse amplitude decreases, consequently it is not generally practical to make β very large.

Examination of Eq. (7) shows that one should keep C_2 as small as possible; a large C_2 in comparison to C_1 results in loss in amplitude of the output voltage pulse because γ becomes appreciably less than unity. A large C_2 also increases the time constant of the differentiating circuit.

Illustrative Problem

Response of a given differentiating circuit to a given square wave may quite readily be found using

the formulas and charts that have been derived and plotted. For example, suppose that a square wave of 100 volts amplitude and having a front whose time constant is 0.25 microsecond is applied to a differentiating circuit in which $C_1 = 90\ \mu\mu f$, $C_2 = 10\ \mu\mu f$, and $R = 5000$ ohms, and suppose one wants to answer the questions:

(1) What is the equation of the output voltage pulse?

(2) What is the maximum output voltage?

(3) At what time will the maximum voltage be reached?

(4) What is the pulse length, i.e., when will the pulse voltage decay to 1 percent of its maximum value?

To answer question (1) we calculate τ_0, β, γ, and T from their equations as given in Table I, obtaining

$\tau_0 = 0.50$ microsecond

$\beta = 0.50$ (coincidence that $\beta = \gamma_0$)

$\gamma = 0.90$

$T = 4.0t \times 10^6$

These values are substituted in Eq. (7), giving for the output-pulse voltage as a function of time the equation

$$e_0 = 180(\epsilon^{-2t \times 10^6} - \epsilon^{-4t \times 10^6})$$

This equation corresponds to the curve $\beta = 0.50$ in Fig. 1.

Question (2) is answered by finding the $e_0'_{max}$ for $\beta = 0.50$, in Fig. 1 which is 0.50 coincidentally, and multiplying this value by $E_i\gamma$, or $e_{0_{max}} = (0.50)(100)(0.90) = 45$ volts.

Figure 2 is also used to answer question (3). One finds the T for $e_0'_{max}$ corresponding to $\beta = 0.50$ and multiplies by τ_i, thus t for $e_{0_{max}} = (1.40)(0.25) = 0.35$ microseconds.

The answer to question (4) is found with the aid of Fig. 3 which shows T for decay to 1 percent of the maximum to be 12.1 for $\beta = 0.50$. This T times τ_i gives the pulse length in time, which is 3.78 microseconds.

Design Difficulties

The problem of design, as is usually the case, is more difficult than the problem of analysis. Given a square wave with certain amplitude and rise time it may not be possible to design a differentiating circuit which will produce an output pulse having simultaneously all of the desired characteristics of pulse amplitude, pulse length, and time for pulse to reach its maximum value. It may not be possible even to satisfy the requirement of pulse amplitude alone, although the requirements of pulse length and time required to reach a maximum may usually be met by differentiating sufficiently sharply.

Unfortunately, as was previously pointed out, the more sharply one differentiates, i.e., the greater is β, the smaller will be the magnitude of the output pulse so it is not generally advantageous to differentiate any more sharply than necessary. Because of this close interdependence of pulse characteristics, one is usually forced to design the differentiating circuit to meet the most urgent requirement first and then to try to satisfy the others if possible.

As an example of design, suppose one wishes to design a differentiating circuit which will produce a pulse of at least 40 volts maximum amplitude and that this maximum should be reached as quickly as possible, given a square-wave input voltage of 100 volts amplitude and having a rise whose time constant is 0.25 microsecond.

A number of assumptions will have to be made in solving this problem. One is in regard to C_2. If the differentiating circuit is isolated this stray capacitance C_2 is ordinarily quite small, perhaps 1 or 2 $\mu\mu f$, but if the differentiating circuit is in close physical proximity to other circuits, and especially if the output is connected to a vacuum tube, C_2 is likely to be higher, say in the order of 10 $\mu\mu f$. In this example a C_2 of 10 $\mu\mu f$ will be assumed.

Another assumption is in regard to γ. Ordinarily one would like γ to be close to unity, but this means choosing a large C_1. If C_1 is large, R must be small in order to differentiate sharply. A small R would make the impedance of the circuit low and possibly load the

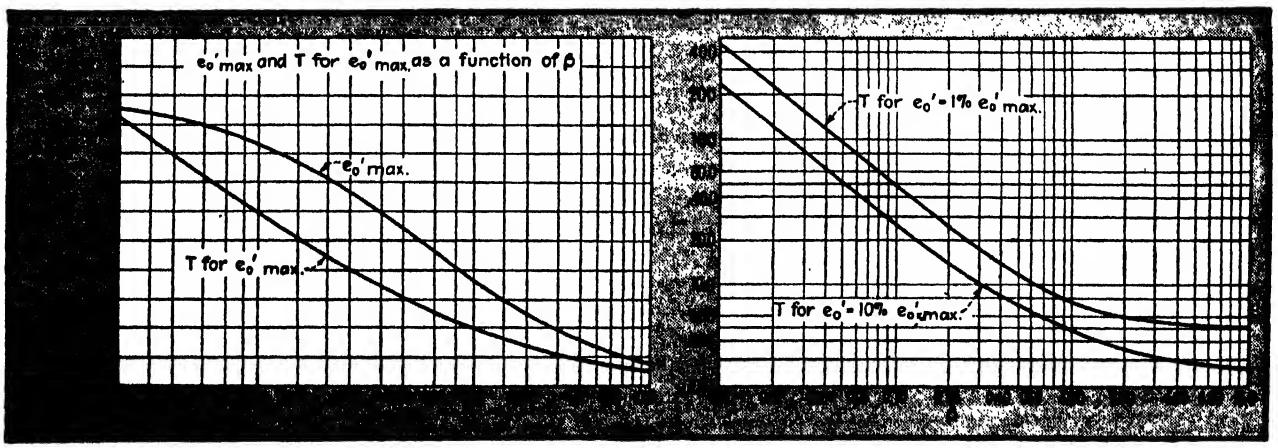

FIG. 2—For use in designing R-C differentiating circuits, these curves give relative amplitude and time for pulse maximum

FIG. 3—Curves, giving relative time for the pulse to decay to a small percent of its maximum, indicate pulse length

voltage source to such an extent that the advantage of differentiating sharply would be lost. Usually it is not practical to make γ much larger than 0.90; often, it has to be made smaller. In this example a γ of 0.90 will be chosen since a relatively high output voltage is the principal requirement. It will be seen subsequently that choosing a γ at this point is equivalent to choosing a C_1 and fixing the value of R.

Now because γ has been chosen as 0.90 and C_2 as 10 $\mu\mu$f, C_1 will have to be equal to 90 $\mu\mu$f as given by $\gamma = C_1/(C_1 + C_2) = 0.90$. Given an $e_{o\max}$ of 40 volts, $e_o'_{\max}$ will have to be $e'_{\max} = e_{o\max}/E_i\gamma = 40/(100 \times 0.90) = 0.45$. On Fig. 2, corresponding to this value of 0.45 one finds that β can not be greater than 0.65. This means that $\tau_o = \tau_i/\beta = 0.25/0.65 = 0.47$ microsecond. But $\tau_o = R(C_1 + C_2)$, hence $R(90 + 10) \times 10^{-12} = 0.47 \times 10^{-6} = 4700$ ohms.

As a matter of interest one can find, using Fig. 2 and 3, that t for $e_{o\max} = \tau_i T$, where T is taken at $e_{o\max}$, is $0.25 \times 1.23 = 0.31$ microsecond, and that the time at which the pulse has fallen to 1 percent of its maximum value is $\tau_i T$, where T is taken at 1 percent, is $0.25 \times 9.9 = 2.25$ microseconds.

As an example of designing a differentiating circuit for a desired pulse length, suppose one wants the pulse to be down to 1 percent of its maximum value in 1.50 microseconds, given the same input voltage as in the previous example; what must the circuit parameters be?

To find the value of T corresponding to the 1-percent time we divide the pulse length of 1.50 microseconds by τ_i, which is 0.25 microsecond, giving 6.00. From Fig. 3, for this value of T we find that β is 1.92 hence $\tau_o = R(C_1 + C_2)$ $= \tau_i/\beta = 0.25/1.92 = 0.13$ microsecond.

Now again an assumption must be made. One can either assume a value for $C_1 + C_2$ and solve for R, or vice versa. In this example a resistance of 3900 ohms will be chosen.

As has been previously pointed out, the minimum permissible value of R is determined by the impedance of the voltage source. If one assumes a value for $C_1 + C_2$ and this assumption results in a value for R which is too low, a smaller value of $C_1 + C_2$ must be assumed. Consequently it is usually advisable to select a value for R and solve for $C_1 + C_2$ if either may be chosen. Sometimes, however, as in the previous example, it makes the solution of the problem simpler if a value for $C_1 + C_2$ is chosen instead. If R is taken as 3900 ohms, $C_1 + C_2 = \tau_o/R = 0.13 \times 10^{-6}/3900 = 33$ $\mu\mu$f.

Current Oscillator for Television Sweep

Electron beam deflection in kinescopes and camera tubes is provided by this saw-tooth current oscillator in conjunction with the horizontal deflection yoke. Full deflection with excellent linearity is obtained in a 12-inch, 38-degree kinescope

By GEORGE CLIFFORD SZIKLAI

THE SUGGESTION of using the output voltage across the horizontal winding of the deflection yoke in a cathode-ray tube for triggering the sweep output tube has been frequently considered in the past. In a conventional television receiver, for instance, a blocking oscillator and a discharge tube may be eliminated if the horizontal output tube is made to oscillate and produce a saw-tooth waveform.

Problem

Saw-tooth current oscillators have been described in the literature[1, 2] and patents.[3-7] Practically all the saw-tooth current generators referred to had four inadequacies in common:

(1) Lack of linearity in the long portion of the saw-tooth wave.

(2) Interdependence of the amplitude and frequency controls, making the adjustment of the device very difficult. In some cases, to permit amplitude variation without falling out of synchronization, a wide locking-frequency range was required, making necessary the use of large synchronizing pulses.[6]

(3) Difficulty of synchronization. Most generators described in the literature require large-amplitude signals for lock-in, and, due to their instability, have to follow the signals over a wide range, tending to make the deflection susceptible to noise disturbances. Farnsworth[4] proposed high-impedance (auxiliary grid) injection of the synchronizing pulses, in a system where the effect of this auxiliary electrode was less than that of the oscillator grid.

In the last few years the superior-operation of automatic frequency-controlled type of deflection has been demonstrated as compared to the more conventional lock-in type of synchronization. This type of operation requires a sensitive reaction of frequency change to a small change of applied direct potential. Such control was not provided in the oscillators referred to above.

(4) Lack of stability. In some applications, such as non-synchronized picture sources, when no convenient stable frequency source is available for locking the oscillator,

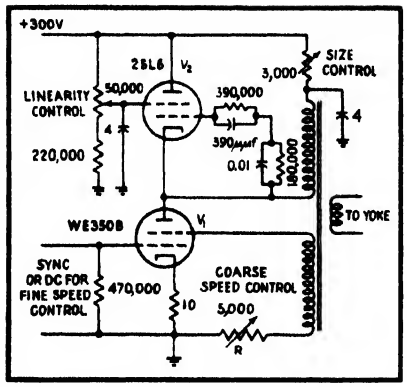

FIG. 1—Circuit of saw-tooth current oscillator used to feed horizontal deflection yoke

it is highly desirable to keep the scanning frequency constant. This requirement is not fulfilled even by conventional pulse generators (such as blocking oscillators and multivibrators) unless stabilizing circuits are provided.

Besides these general faults, practically all the schemes have further disadvantages peculiar to their particular design. For example, Rhea's circuit[6] requires the yoke circuit to have an alternating potential to ground, increasing crosstalk difficulties. In Wheeler's and Bahring's circuits, the tube grids are loaded considerably. In spite of these disadvantages, saw-tooth current oscillators were used in Europe, where tube cost considerations outweighed the shortcomings of these circuits.

The circuit shown in Fig. 1 is practically free from the faults described, and is more economical than most of the prior saw-tooth current oscillators. To fully understand its operation, it may be advisable to review the fundamentals of saw-tooth current generation in electromagnetic deflection circuits.

Basic Principles

A reactive saw-tooth current generator is shown in its idealized form in Fig. 2. The battery symbol E_B represents a power source (which can be replaced by a charged capacitor); S is an ideal switch capable of high-speed operation, able to withstand high voltages in its open position, and having perfect bidirectional conduction in its closed position; L represents the inductance of the yoke, and C the incidental capacitance. For the time being, no resistance is assumed anywhere in the circuit.

When the switch is first closed (Fig. 3, curves, time t_1), the current will increase linearly with time according to

$$di/dt = E_B/L$$

until at time t_2 the switch is opened. The current stored in inductance L will then be discharged through capacitor C in an oscillatory manner. The solution for the equilibrium equation is

$$L\frac{di}{dt} + \frac{1}{C}\int i\,dt = 0$$

$$i = -\frac{E_B}{\sqrt{L/C}} \sin \frac{t}{\sqrt{LC}}\Big)$$

If the switch is then closed at time t_3 at the end of a half period of the self resonance, the inductance returns its energy to the battery again with a current linearly changing with time until t_4, at which time there is a current equilibrium, and from there on the battery will deliver current in a linear manner to the yoke again.

If there were no resistance in the circuit, and a perfect switch could be provided, no external energy would be required to provide a saw-tooth current (which would be a wattless current in that case, and the purely reactive load would behave the same way as zero power-factor loads behave with sinusoidal currents). By deflecting the electron beam periodically, there is actually no work done; the reactance of the yoke acts as a fly-wheel moving the beam bidirectionally.

In Fig. 3, curve *a* represents the voltage that would appear to the left of dotted line *A* in Fig. 2 if no load were applied to the battery-switch combination. Curve *b* shows the current flowing through the inductance, and curve *c* shows the voltage appearing across the inductance,

$$E_L = L\frac{di}{dt}$$

It may be observed that the form of this voltage is substantially identical with the required input voltage. This voltage is, however, far greater than the input voltage, the ratio being

$$E_L = 1.41\,E_B\frac{t_5 - t_4}{t_3 - t_2}$$

Since the yoke always has some resistance, the current going into the yoke has to satisfy the equation

$$iR + L\,di/dt = E_B$$

and it will take the exponential form

$$i = \frac{E_B}{R}\left(1 - e^{-\frac{R}{L}t}\right)$$

spoiling the linearity of the saw-tooth. Greater difficulties are, however, encountered with the resistance of the switch. Normally a grid-controlled electron tube is used for this purpose, with a resistance many times that of the resistance in the yoke. We may resort to impedance transformation, but a limit is found by the fact that the return time is determined by the inductance and the distributed capacitance of the transformer

$$(t_3 - t_2 = \pi\sqrt{LC}).$$

Another difficulty is met by the fact that the electron tube is not bidirectional. It does not conduct until the yoke is discharged, and the voltage across the yoke retains its oscillatory nature until the voltage across it drops below the supply potential, at which time the plate of the tube becomes positive again. In Fig. 3, curve *d* shows the potential across the yoke under this condition, while curve *e* shows the corresponding current flowing through the yoke.

Damping Tube

Blumlein[8] proposed the connection of an inverted diode across the inductance to damp the oscillation and to act as the switch during the period while the amplifier tube is not conducting due to reversed potential on

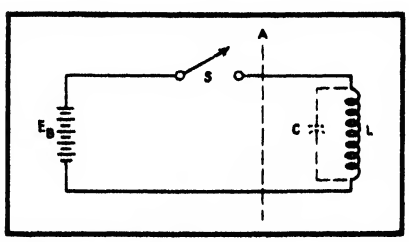

FIG. 2—Basic circuit of a reactive saw-tooth current oscillator

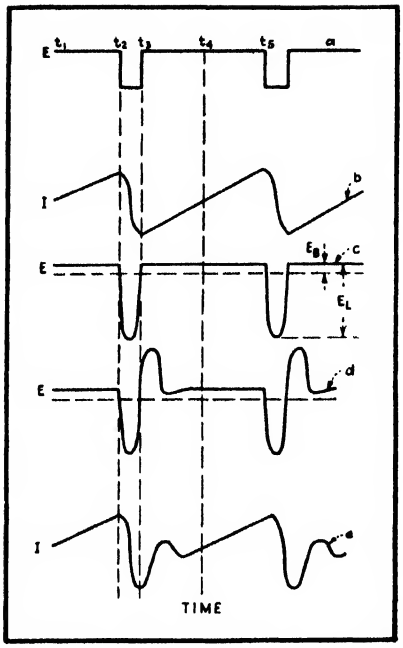

FIG. 3—Current and voltage variations in the circuit of Fig. 2 when the switch is operated

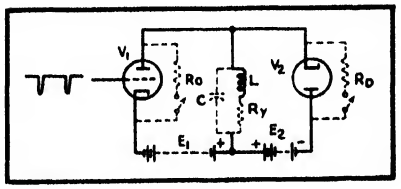

FIG. 4—Elements of basic damping circuit that acts like the switch of Fig. 2

its plate. The analysis of the operation of the damping tube has been described in detail in patent literature.[7-9]

The damped output circuit is shown in its simplest form in Fig. 4. The output tube V_1 is pulsed by a grid voltage as shown, and builds up the current exponentially in the yoke due to its own resistance R_o and the resistance in the yoke R_y until the grid is biased beyond cutoff by the pulse (this pulse must be of considerable amplitude since the plate voltage during the return time assumes a very high value). At this time the yoke current begins its decaying oscillation until the potential across it becomes larger than E_b, at which time the damper tube starts to conduct and maintains a constant potential across the yoke.

Figure 5 shows the currents flowing through the output tube (I of V_1) and the damper tube (I of V_2); it may be seen that they add in the form of a linear total current output. This operation was frequently compared to the push-pull operation of class B amplifiers.

The Tolson and Wheeler patents each show the use of a grid-controlled damping tube[7-9] to change the impedance of the damper, and thereby improve the linearity of the saw-tooth. The damper, while adding to the available saw-tooth a sizeable portion (about 30 percent greater amplitude), is not a perfect counterpart of the ideal switch, since it does not return the stored energy to the battery E_b, but dissipates the power through another battery E_2, which is normally replaced by an R-C circuit.

The plate of the damping tube V_2 must be connected to the positive terminal of E_1 rather than to the cathode of V_1 due to its high impedance. This requires a higher potential than available from the back swing, as shown in curve d of Fig. 3, to pass the current from the yoke back to battery E_b. To provide a damper tube with a lower impedance, larger cathode area has to be provided, with correspondingly higher filament power requirements, making inroads in the overall efficiency. The damping tube must be able to withstand the high voltage generated across the deflecting circuit during the return time.

Oscillator Operation

The type of pulse required to drive the output tube is identical with the voltage wave shape developed across the deflection yoke or any winding of the output transformer. In Fig. 1, a separate winding on the output transformer is used to feed the pulses to the grid. It was found that by feeding this signal to the control grid of a tube, the frequency adjustment made by R-C in the grid circuit will change the saw-tooth output amplitude materially, and in reverse, any change in the amplitude adjustment altered the frequency. Since the grid in that case was drawing current for a considerable time, and appeared heavily loaded, a sizeable signal was required for synchronizing.

By using the screen of a beam power output tube for feed-back, the control grid was made available for synchronizing purposes. Due to the high transconductance of the control grid, a very small synchronizing signal is adequate to lock in the oscillator. By changing the d-c potential of the control grid, the frequency varies approximately 3 percent per volt change, without any noticeable change of the saw-tooth amplitude.

Figure 6 shows the saw-tooth frequency plotted against the voltage

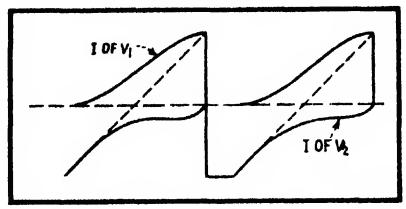

FIG. 5—The combination of the current through the damping tube and the output tube form a linear total current (dashed line)

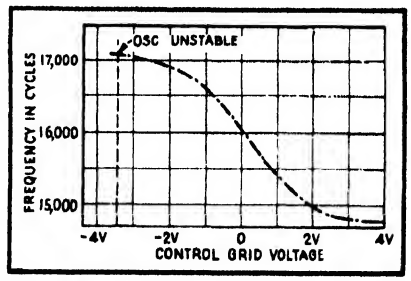

FIG. 6—Saw-tooth frequency and grid voltage for one value of screen voltage

applied to the control grid, at one particular adjustment of the coarse speed control (R in the screen return circuit). The zero-bias frequency may be shifted by the coarse speed control. This sensitivity and behavior make this deflection circuit particularly adaptable for control by automatic frequency control circuits.

The frequency of the saw-tooth current oscillation is determined by the forward and return periods (t_a to t_c and t_c to t_a), but the return time is determined purely by the natural periods of the yoke circuit since during that time the tube is disconnected. The forward period may be determined from the grid voltage developed during that time

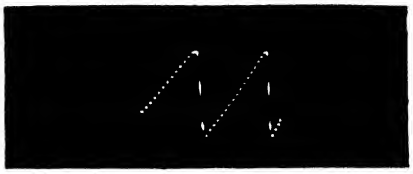

FIG. 7—Saw-tooth current through the deflection yoke

FIG. 8—Linearity of the horizontal deflection

FIG. 9—Voltage across grid winding of transformer

FIG. 10—Cathode current of oscillator tube

$$E_g = E_D + L_g\frac{di_g}{dt} + L_p\frac{di_p}{dt}$$

where E_g is the voltage developed between the screen and the cathode of the oscillator tube, E_D is the voltage drop across the coarse speed control resistance, L_g and L_p are the inductances reflected across the screen grid and plate circuits, respectively, and i_g and i_p are the grid and plate currents.

Since the derivatives of the plate and screen grid currents are constant during the time t_3 and t_4, and the boundary conditions for the forward period are determined by this time and the maximum currents, the value of the last two parts of the above equation may be evaluated as

$$L_g\frac{di_g}{dt} + L_p\frac{di_p}{dt} = \frac{L_g i_{g\,max} + L_p i_{p\,max}}{t_4 - t_3}$$

Substituting this value, and solving for the time, we obtain

$$t_4 - t_3 = \frac{L_g i_{g\,max} + L_p i_{p\,max}}{E_g - E_D}$$

where the denominator is the potential appearing across the grid winding of the transformer, and is therefore equal to the plate voltage multiplied by the transformer ratio. This final equation shows that the period increases as the resistance in the screen grid circuit is reduced, since i_g *max* then increases in contrast with the conventional blocking oscillator.

Due to the resistance in the circuit, the long portion of the saw-tooth follows an exponential curve, unless provision is made to linearize it. This is accomplished by varying the impedance of the damper tube, in accordance with the inverse of the non-linearity of the trace. In addition, the impedance of the damper tube is made to compensate for the nonlinear characteristics of the oscillator tube. The impedance of the damper tube is varied by controlling the grid through an R-C circuit as shown in Fig. 1. The average value of the impedance may be adjusted by the potential of the screen which serves as a linearity control.

The cathode of the damper tube will be several thousand volts above ground during the return time, and it may break down to the filament if the latter is at ground potential. The capacitance of the cathode to ground also must be minimized, since it appears directly across the transformer, and it will influence the length of the return time. This situation can be easily remedied by floating the filament above ground either by using a separate filament transformer with low capacitance for the damper tube, or by connecting the filament to the supply through a double choke so that the cathode-filament capacitance is in series with this inductance. Such chokes can be made very economically, and specifications for one may be found at the end of this article.

Figure 7 is an oscilloscopic picture of the trace of the saw-tooth current through a five-ohm resistor connected in series with the deflection yoke. The beam was modulated by a voltage with a frequency of approximately 300 kilocycles to show the length of the retrace time.

To show the linearity of the deflection, the horizontal deflection frequency of the oscilloscope was lowered to make the dots form lines as shown in Fig. 8; the even distribution of the horizontal lines provides an indication of the degree of linearity obtained.

Figure 9 shows the voltage across the grid winding of the transformer and Fig. 10 shows the current flowing through the cathode resistor of the oscillator tube.

Several tetrodes, pentodes, and beam power amplifier tubes were tried as the oscillator, such as types 6Y6, 6L6, 6V6, 6F6, 6K6, 48, 807, and Western Electric types 339A and 350B. The largest deflection currents were obtained with the last two types. The Western Electric type 350B is very similar to the 6Y6G type, but the screen dissipation is four watts against the 1.75-watt rating of the 6Y6, or 2.5 watts of the 6L6.

The screen potential is approximately 100 volts during the forward trace, and it draws a current of 20 to 40 milliamperes. If this power is permitted to heat the screen excessively during the retrace period, when the screen swings 1,000 or more volts negative, it will emit thermionically, and some of the electrons are collected by the No. 1 grid, charging it negative and increasing the frequency as can be seen from Fig. 6.

Due to the thermionic conduction to the No. 1 grid, the synchronizing input impedance is lowered and the pulse, or d-c control source, will be loaded. It is possible to feed the afc potential through one of the i-f amplifiers and take the d-c variations of the cathode resistor of the same tube. However, this seems to be an unnecessary complication when a tube with proper screen dissipation can be constructed.

In certain applications when no primary synchronizing source is available, it is desirable to have a basic stability, comparable to that of sinusoidal oscillators. It was found that by connecting a high-Q resonant circuit in the control grid circuit, this circuit will be shock excited

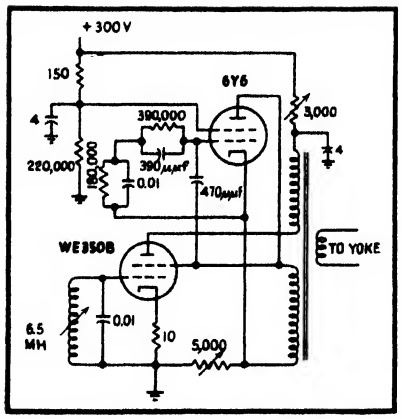

FIG. 11—To stabilize the saw-tooth oscillator, a resonant circuit is introduced into the grid circuit

and produce a sine wave determined by its inductance and capacitance. The oscillator will then lock in on this frequency, and the stability will depend primarily on the constancy of the L-C circuit.

Figure 11 shows the circuit diagram of the stabilized oscillator. In this case the damping tube is connected across the grid winding, thereby placing the cathode near ground potential. This circuit eliminates the necessity of floating the filament, but, due to the leakage inductance, it places slight ripples in the return trace. These are not objectionable unless the pulse is to be used for d-c reinsertion, keyed avc, or like purposes.

SPECIFICATIONS

Oscillator Transformer

Core: 30211-3 and 30211-4
Center leg: 37/64-inch square stack
Window: 37/64 x 17/16 inch
MLMC: 10.6 centimeter
Height: 2-5/16 inch
Width: 1-⅝ inch
Material: 0.003-inch silicon steel P.S. 188
Butt Joint
Coil: Wind yoke winding first, 80 turns No. 24 wire layer wound. Plate winding, 400 turns No. 30 wire, two 3/16 pies, universal winding. Grid winding—same as plate winding. Plate and Grid windings are wound on top of yoke winding side by side.

Dual Filament Choke

Core: 63917-2
Center leg: ½ inch, square stack
Window: ¼ x 13/16 inch
MLMC: 8.4 centimeter
Height: 1-11/32 inch
Width: 1-½ inch
Material: 0.014-inch silicon steel
Air gap: 0.05 inch
Coil: 500 turns each of No. 34 wire wound parallel, 0.002-inch paper between layers
Inductance of one winding: 0.5 henry
Total resistance: 125 ohms

REFERENCES

(1) Somers, F. J., Scanning in Television Receivers, ELECTRONICS, p. 18, Oct. 1937.
(2) Mulert, T., & Bahring, H., Transformer Deflection Unit, *Fernseh AG VI*, 3, April, 1939.
(3) Kobayashi, U. S. Patent 1,913,449.
(4) Farnsworth, U. S. Patent 2,051,372.
(5) Farnsworth, U. S. Patent 2,059,683.
(6) Rhea, H. E., U. S. Patent 2,165,815.
(7) Wheeler, H. A., U. S. Patent 2,250,170.
(8) Blumlein, A. D., U. S. Patent 2,063,025.
(9) Tolson, W. A., U. S. Patent 2,280,733.

Iron-Core Components in Pulse Amplifiers

A discussion of the rate of voltage change in the "leading edge," "flat top" and "trailing edge" portions of square-wave or flat-top pulses when impressed on iron-core reactors

By REUBEN LEE

SQUARE or flat-topped pulses of steep wavefront have come into considerable use of recent years, particularly in television and allied techniques. They may be impressed on iron-cored transformers by a vacuum tube, a transmission line, or even a battery and a switch.

The analysis to follow discusses the rate of rise of the front edge, the extent of the flat top and the rate of decay of the trailing edge as functions of circuit constants. The mathematical expressions for these portions of the wave, which describe the transient conditions producing these waves, are not given, in the interest of economy of space. All the essential data necessary for one to understand these rates-of-voltage change are given, however.

The pulse itself is given in Fig. 1 and a generalized circuit for the amplifier is given in Fig. 2A with the equivalent so far as the transformer is concerned in Fig. 2B.

During the front edge period when the pulse voltage e is rising abruptly to its final value E, the transformer open-circuit inductance presents practically infinite impedance to the voltage change and is omitted in Fig. 2B. The leakage inductance, however, has considerable influence on the wave shape and appears as L. Other quantities are defined on the figure. Quantities in the secondary circuit are all referred to the primary by multiplying them by $(N_p/N_s)^2$ or, if it were more convenient to treat the transformer entirely from the secondary, the primary quantities would be referred to that side by a reciprocal multiplying factor.

Since there are two capacity terms

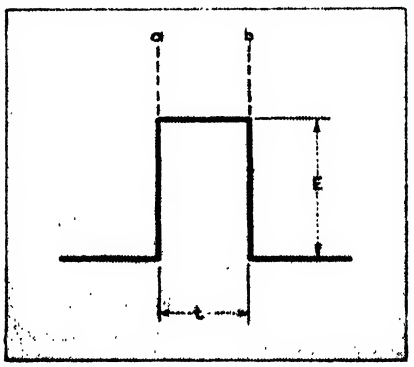

Fig. 1—Square-top pulse to be studied

C_1 and C_2 then for any considerable deviation of the transformer turns-ratio from unity, one or the other of these capacitances will become preponderant. Turns-ratio and therefore voltage-ratio affect these capacitances in such a way that for a step-up transformer, C_1 may be neglected

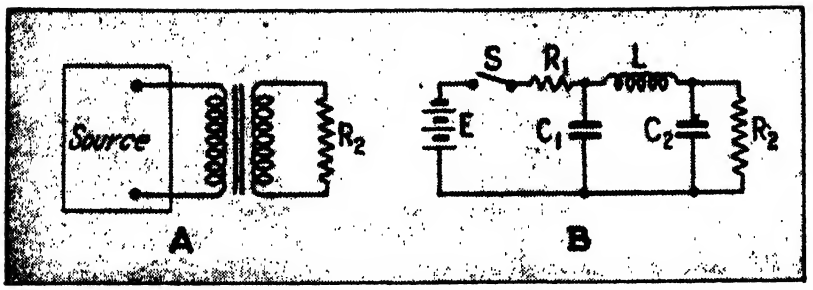

Fig. 2—Pulse amplifier and equivalent circuit. L is transformer leakage inductance. R_1 is the source resistance, R_2 is the load resistance, C_1 and C_2 are primary and secondary winding capacitances

and for a step-down transformer, C_2 may be neglected. The discussion here will be confined to the step-up case, although the step-down and the 1 to 1 ratio cases are not markedly different.

Front-edge Conditions

When the front of the wave is impressed suddenly on the step-up transformer, Fig. 3, as by closing a switch, the initial voltage e and current entering from the battery are zero. The rate at which the voltage rises is given in Fig. 3. The final value $E\left(\frac{R_2}{R_1+R_2}\right)$ indicates that the amplifier will be more efficient the smaller R_1 is. In Fig. 3, R_1 is considered negligibly small. If the value E for the top of the pulse is multiplied by $\frac{R_2}{R_1+R_2}$ the curves are reasonably accurate. Note that the abscissas are not time but percentage of the time constant of the transformer.

The rate of voltage rise is governed by the leakage inductance L, the secondary capacitance C_2 and markedly by another factor, k, which is the product of the decrement and the angular velocity of an oscillatory circuit, but which has the same form for a circuit which is not oscillatory. Other things remaining equal, the greater the transformer leakage inductance and distributed capacitance, the slower the rate of voltage rise. R_1 and R_2 also are important since they affect factor k. Note that if a slight amount of oscillation can be tolerated, the wave rises much faster than if no oscillations are present. If the circuit is far removed from oscillation, the rise is very slow. If the circuit is damped very little, the oscillation may reach a maximum initial value of two times the steady-state voltage E and often such marked peaks would be objectionable. The values for k given on the curve appear to be those which fall within the most practicable range.

Once the pulse top is reached, the value E is dependent upon the transformer open-circuit inductance for its maintenance at this value. If the pulse stayed on indefinitely at the value E, it would require an infinite inductance to maintain it so, and of course this is not practical. Therefore, the top of such a pulse always has a tendency to droop. The equivalent circuit during this time is shown in Fig. 4. Since the rate of voltage change is relatively small during this period, C_1 and C_2 disappear from the picture. Since the leakage inductance is usually small compared to the open-circuit inductance, it is neglected. When the circuit (Fig. 4) is first closed, the e is assumed to be at the steady value E, which is strictly true only when R_1 is negligibly small. Therefore, the curves for the top of the wave need to be corrected the same as those for the front of the wave, in that e should be multiplied by the ratio $R_2/(R_1+R_2)$. Several curves are given, representing several types of pulse amplifiers ranging from a pentode where the source resistance is very high (R_2 is 1/10th of R_1), to an amplifier whose load resistance is infinity or whose output power is zero. In the latter case, e need not be multiplied by any ratio of resistances; its final value is the same as that of the battery. All the curves are exponential, having a common point at 0, 1. The abscissas are not time, but are the product of time and ratio

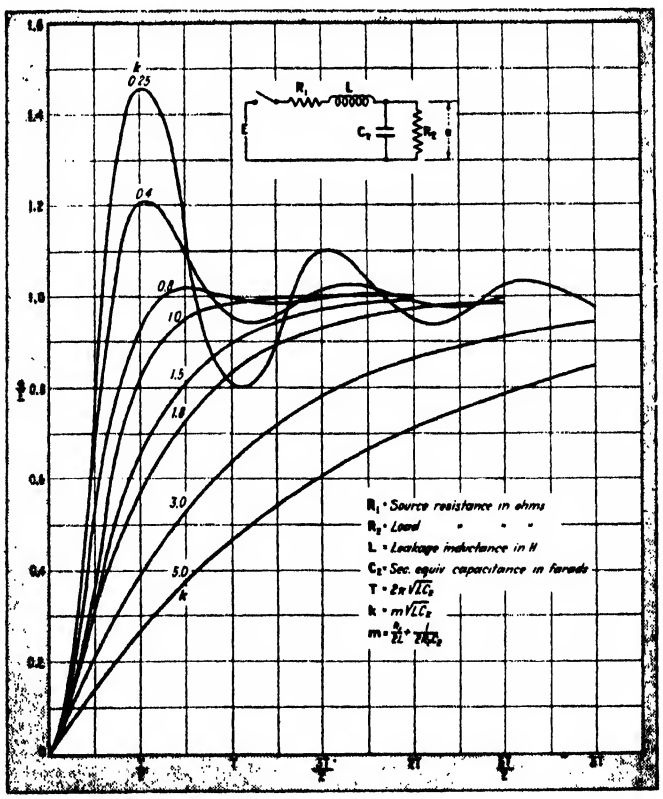

Fig. 3 — Influence of transformer constants on front edge of pulse

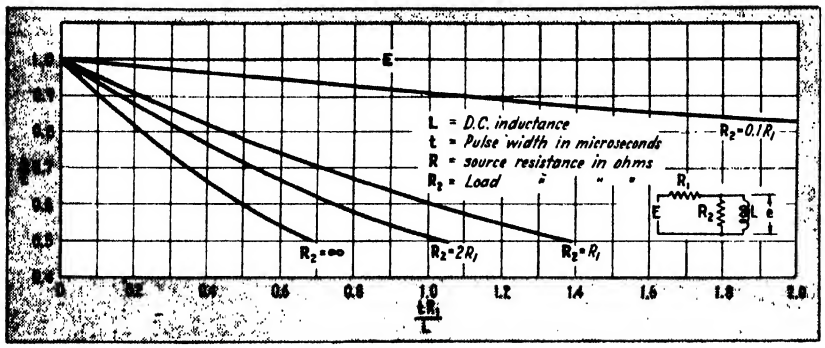

Fig. 4--Influence of transformer open-circuit inductance on flat-top portion of pulse. The inductance in this case is in microhenrys

R_1/L the time being the duration of the pulse between points a and b in Fig. 1. Obviously, the greater the inductance L the less deviation from a flat top pulse there is during this amount of time.

At time instant b in Fig. 1, we will assume that the battery circuit in Fig. 4 is suddenly opened. The circuit now becomes that of Fig. 5, in which L is the open circuit inductance. Secondary capacitance (C), is again present to an appreciable extent. It will be assumed that the current through L has not increased to an appreciable amount, and therefore the flat top wave was practically unimpaired at instant b; but if this is true, it is the same as saying that there is no initial current in inductance L, so when the switch is open, C_2 supplies all the load current momentarily. This is the basis upon which Fig. 5 is drawn. The time constant is now determined by the open-circuit inductance L and capacity C rather than by leakage inductance and capacity C_2 as was the case in Fig. 3. The constant k is again the product of decrement and angular velocity for the oscillatory case, but the decrement now has a different meaning. Lest it be assumed that the time constant is so great in this case that it precludes satisfactory performance, attention is drawn to the fact that higher open-circuit inductance L results in higher values of k, and the curves with higher values of k drop much more rapidly than do the smaller values, but only with reference to the time constant, T.

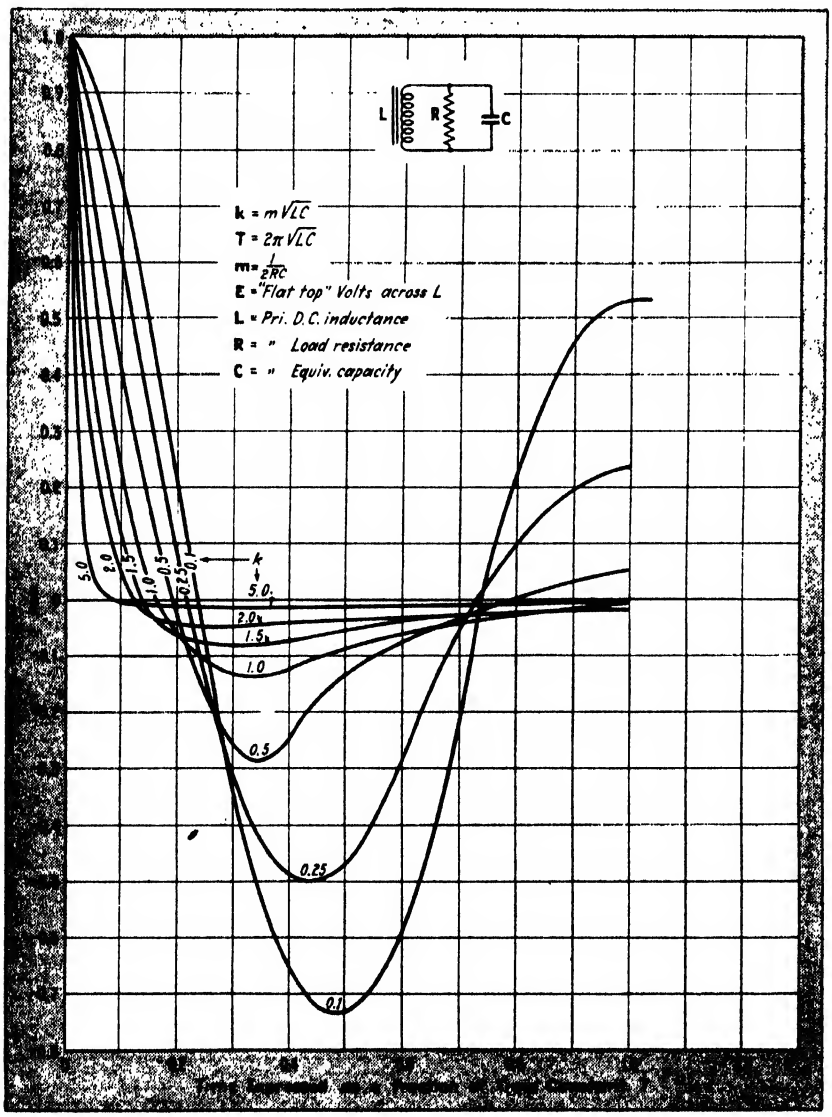

Fig. 5—Effect of transformer constants on trailing-edge of pulse

This does not mean that such a wave will drop more rapidly in time, but only with reference to the time constant which is determined by open-circuit inductance and capacitance. It does mean, however, that the slope of the trailing edge can be kept within tolerable limits, provided the transformer capacitance can be kept small enough. The accurate predetermination of this capacitance is therefore of first importance.

A Numerical Case—a 5Mc I-F Transformer

By means of the three sets of curves we can now construct the pulse shape delivered to load R_2. Suppose a transformer with the following measured constants be required to deliver a flat top pulse of 15 microseconds duration.

Leakage inductance L (secondary short-circuited) $= 1.89 \times 10^{-4} H$

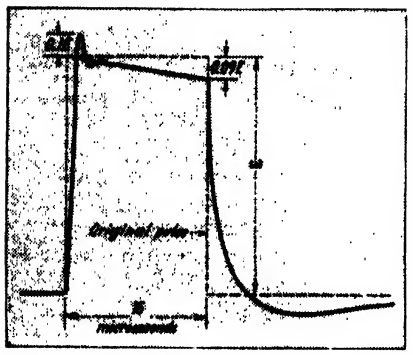

Fig. 6 — (left) — Actual pulse delivered by typical case treated in text

Fig. 7 — (below) — Typical saw-tooth pulse and circuit analyzed in text

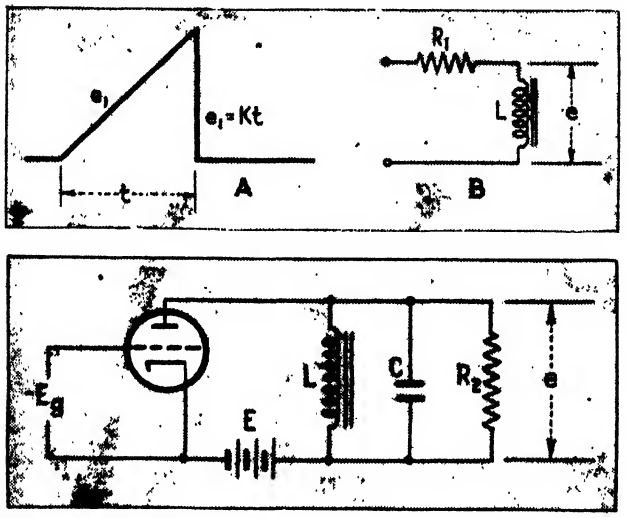

Fig. 8—Circuit for developing high voltages by interrupting a current through a reactor

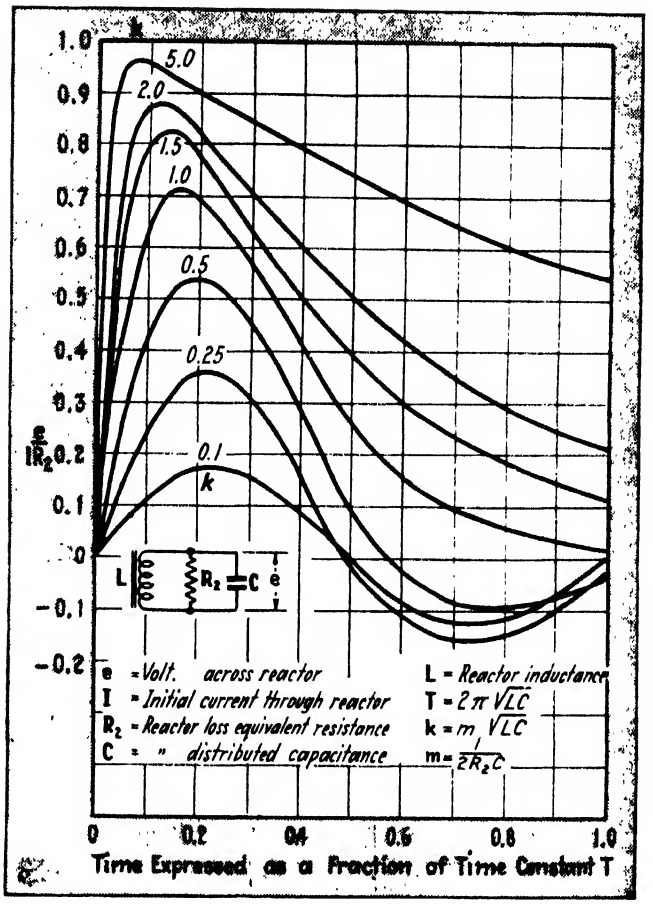

Fig. 9—Curves of voltage rise across a reactor

Primary open-circuit inductance	= 0.1 *H*
Primary secondary turns ratio N_p/N_s	= 1.3
Source Resistance R_1	= 800 ohms
Load Resistance (Primary equivalent)	= 5000 ohms
Capacitance C_2 (calculated)	= 388 $\mu\mu f$

From the expressions given in Fig. 3, we find

$$m = 2.38 \times 10^6$$
$$T = 1.7 \text{ microsecond}$$
$$k = 0.65$$

The front of the wave will follow a curve between those marked $k = 0.4$ and $k = 0.8$ in Fig. 3. The value E will be reached in $0.5T$ or 0.85 microsecond, and a peak of about 10 percent occurs in 1 microsecond.

The top of the wave will slope down to a value determined by the product $tR_1/L = 0.12$, and by a curve between those for $R_2 = \infty$ and $R_2 = 2R_1$ in Fig. 4. The value is evidently $0.91E$.

The trailing edge is given by Fig. 5. Here

$$m = 0.258 \times 10^6$$
$$T = 39.1 \times 10^{-6}$$
$$k = 1.6$$

so that the load voltage reaches zero in $0.115T$ or 4.5 microseconds. There is a slight negative loop of 7 percent at $0.3T$ or 11.7 microseconds beyond the pulse edge *b*.

The pulse delivered to load R_2 as shown in Fig. 6 is a combination of these three curves.

Probably the most common application of saw-tooth transformers is to provide a linear sweep to elements of a cathode-ray oscillograph. In such a circuit, the load on the transformer can be regarded as negligible. Therefore we will assume a linearly increasing voltage as shown in Fig. 7A to be applied to the circuit of Fig. 7B. Analysis shows that the voltage e across the inductance L has the same slope as the applied voltage times an exponential term determined by the resistance R_1 of the amplifier, the open-circuit inductance of the transformer, and the time between the beginning and the end of the linear sweep. Under the conditions assumed, the value of the exponential for any interval of time can be taken from the curve marked $R_2 = \infty$ in Fig. 4. For example, suppose the sweep lasts for 500 microseconds, the tube plate resistance is 800 ohms, and the transformer inductance is 10 henries. The value of the abscissa is 0.04, and since the slope of this exponential curve equals its ordinate, the slope of the voltage applied to the plates of the oscillograph will be, at the end of the time interval, 96 percent of the slope which it had at the beginning of the time interval.

Let us assume that at the end of the time interval *t*, Fig. 7A, the tube is cut off. Then the sweep circuit transformer reverts to that of Fig. 5, in which R includes only the losses of the transformer, which were neg-

lected in the analysis for linearity of sweep. That is, the voltage does not immediately disappear, but follows the curves of Fig. 5 very closely, the same as the trailing edge of the flat-top pulse.

Voltage Rise in Reactors

Numerous circuits have been devised for the development of relatively high voltages by interrupting the current through a reactor. We will here discuss only one, namely, that of Fig. 8 which is typical.

Battery E is supplying current through choke L to the tube, when suddenly a negative voltage $-E_c$ is applied to the grid of the tube. This interrupts the current through L, forcing it to discharge into its own capacity and loss resistance R_2. There is this difference in the assumptions made for choke L compared to those that were made in previous analyses for the open-circuit inductance of transformers: the initial current through L is not negligible, but is the current drawn by the tube itself. We will assume that the series resistance of the choke is zero, so that the initial voltage across C and R_2 is also zero. This analysis, therefore, applies only where the choke is shunted only by a high resistance such as its own losses. The case where a voltage *drop* is produced has already been covered by the analysis for the trailing edge of a flat top pulse transformer.

The performance of this choke is shown in Fig. 9. The ordinates on the curve are the voltage rise divided by the IR drop consisting of the choke initial current and the loss resistance R_2. The effect of high inductance is seen by the fact that for high values of k the voltage rise is quite steep and great. Low capacitance is also important to attain such steep voltage rises. Close observance will show that the choke voltage rises up to its peak value in about the same length of time that the voltage on the trailing edge of the transformer decreased to its minimum value. There is this difference, however, that for small values of k the voltage amplitude is small. Usually in the operation of such chokes, only the relatively linear portion of the voltage rise curve is used. Figure 9 shows that with proper values of k it may be possible to utilize considerably more of such a pulse. For example, where $k = 5$ the pulse could be allowed to continue unchanged up to some value approximately 25 percent of the time constant T, instead of being cut off at much smaller values of T and voltage rise. This again requires low capacitance in the choke, but it has the advantage of requiring less subsequent amplification for the final pulse.

Transformers and reactors designed in accordance with the principles here formulated are entirely practicable; they have been built with fairly small dimensions for pulses of ½ to 2700 microseconds duration.

Capacitances C_1 and C_2 must be evaluated in terms of voltage gradients in the windings; i.e., C_1 and C_2 are not the ordinary measurable capacity between primary and core, or secondary and core, or primary and secondary, but usually exceed these values if the transformer is step-up and are less than these values if the transformer is step-down. In any transformer, regardless of turns-ratio, voltage gradient must be considered for proper evaluation.

For example, in the transformer whose cross-section is shown in Fig. 10 the primary and secondary are each wound in a single layer concentrically, and will be assumed as wound in the same rotational direction, and in the same traverse direction (right to left). It will further be assumed that the right ends of both windings are connected to ground (or core) through large capacitances, as shown dotted, so that the right ends are at substantially the same a-c potential. Capacitance C_1 is composed of many small incremental capacitances C_p and C_s of many small incremental capacitances C_x each of which has a different voltage across it. Likewise, there exist many small incremental capacitances C_a between primary and secondary which have different potentials across them. If the transformer is step-up

$$C_1 = 1/3\Sigma C_p \text{ and } C_2 = 1/3\left[\Sigma C_s + \left(\frac{N_s - N_p}{N_p}\right)^2 \Sigma C_a\right]$$

If the transformer is step-down,

$$C_1 = 1/3\left[\Sigma C_p + \left(\frac{N_p - N_s}{N_p}\right)^2 \Sigma C_a\right] \text{ and } C_2 = 1/3\, C_s.$$

If the ratio is 1:1,

$$C_1 = 1/3\left[\Sigma C_p\right] \text{ and } C_2 = 1/3\left[\Sigma C_s\right]$$

For transformers with opposite angular rotations of primary and secondary windings, or with opposite traverse directions, (but not both), the factor $\left(\frac{N_p - N_s}{N_p}\right)^2$ and $\left(\frac{N_s - N_p}{N_p}\right)^2$ in the foregoing equations become $\left(\frac{N_p + N_s}{N_p}\right)^2$; Add $4/3\Sigma C_a$ to C_1 and C_2 for 1:1 ratio: there is no other change. For transformers with *both* angular rotations and traverse directions opposite there is no change at all in these equations. If there is a shield between primary and secondary, omit terms containing C_a in these equations, and make ΣC_s and ΣC_p include the capacity of secondary and primary to shield, respectively. Note that ΣC_s is the measurable capacity of the short-circuited secondary to ground (or core), and ΣC_p the measurable capacity of the short-circuited primary to ground (or core).

For more interleaving of primary and secondary windings, more elaborate evaluation of capacitance is necessary. This will be illustrated below by the description of an actual transformer (the pulse shape of which is given in Fig. 6.)

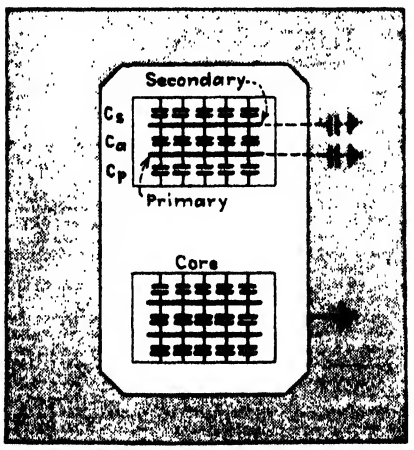

Fig. 10—Cross section of transformer with concentric windings showing interwinding capacitance

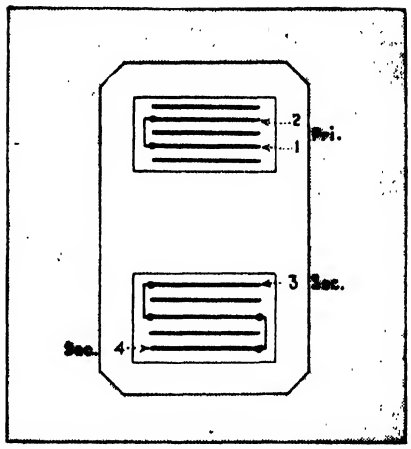

Fig. 11—Placement of primary and secondary windings

As shown in Fig. 11 the primary is wound in two layers, interleaved between three secondary layers. This interleaving is done to reduce leakage inductance. The secondary winding is wound in a 2-layer "bank" fashion, in each of the 3 layers above mentioned. This is done to reduce its own capacitance. The transformer is used to couple a type 2A3 tube to a pair of cathode-ray tube plates. The plates are an open circuit; hence R_L would be infinite, but the transformer has sufficient iron loss to give R_L a finite value. The measurable constants are:

N_p = 112 turns (56 per layer)
N_s = 360 turns (120 per layer)
R_1 = 800 ohms
R_2 = 5000 ohms

The capacitance from secondary to core is 100 $\mu\mu$f. The capacitance (average) between primary and secondary layers is 46 $\mu\mu$f. Leads 1 and 3 are at a-c ground potential. All windings are wound in same direction of rotation, but the directions of traverse are:

Secondary Section			Primary Section	
1st	2nd	3rd	1st	2nd
L to Rt.	Rt to L.	L to Rt.	L to Rt.	Rt. to L

Designate these winding sections, in the order above as, S_1, S_2, S_3, P_1, P_2. The voltage gradients along these windings are as shown in Fig. 12 except that turns are used instead of volts. This is permissible since $e_p/e_s = N_p/N_s$.

In the space between	Turn gradient is
S_1 and core	0 to $N_s/3$
S_1 and P_1	0 to $N_s/3 - N_p/2$
P_1 and S_2	$N_s/3 - N_p/2$ to $2N_s/3$
S_2 and P_2	$N_s/3 - N_p/2$ to $2N_s/3 - N_p$
P_2 and S_3	$2N_s/3 - N_p$ to $N_s - N_p/2$
S_3 and core	$2N_s/3$ to N_s

The transformer is so constructed that there is 10.3 $\mu\mu$f from S_3 to core.

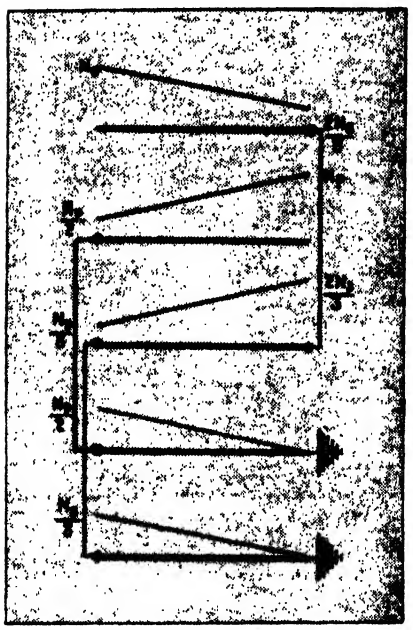

Fig. 12—Voltage gradients along the windings in terms of turns

The secondary-to-core capacitance is mostly S_1 to core. The primary effective value of this capacitance is $\Sigma C_s/3N_p^2 \times (N_s/3)^2$. Putting the $C_s/3N_p^2(\Delta n_1^2 + \Delta n_2^2 + \Delta n_1\Delta n_2)$. Thus numerical values of N_s and N_p in this expression form the above table we have $\frac{(100 - 10.3) \times (120)^2}{3 \times 112^2} = 38$ $\mu\mu$f for the effective value when referred to the primary. For the inter-winding spaces we can use the equation $C_e = C_s 3N_p^2(\Delta_1^2 + \Delta n_2^2 + \Delta n_1\Delta n_2)$. Thus we get for S_1-P_1, $\Delta n_1 = 0$

$$\Delta n_2 = N_s/3 - N_p/2 = 120 - 56 = 64 \text{ turns.}$$

$$Ce = \frac{46 \times (64)^2}{3 \times (112)^2} = 5.0 \ \mu\mu f$$

for P_1-S_2, $\Delta n_1 = 64$
$\Delta n_2 = N_s/3 = 240$

$$C_s = \frac{46}{3 \times (112)^2}\left[(64)^2 + 240^2 + 64 \times 240\right] = 84 \ \mu\mu f$$

for S_2-P_2, $\Delta n_1 = 64$
$\Delta n_2 = 2N_s/3 - N = 240\text{-}112\text{-}128$

$$C_s = \frac{46}{3 \times (112)^2}\left[(64)^2 + (128)^2 + 64 \times 128\right] = 35 \ \mu\mu$$

for P_2-S_3, $\Delta n_1 = 128$
$\Delta n_2 = N_s - N_p/2 = 360\text{-}56 = 304$

$$Ce = \frac{46}{3 \times (112)^2}\left[(128)^2 + (304)^2 + 128 \times 304\right] = 178 \ \mu\mu f$$

for S_3-core $\Delta n_1 = 2N_s/3 = 240$
$\Delta n_2 = N_s = 360$

$$C_s = \frac{10.3}{3 \times (112)^2}\left[(360)^2 + (240)^2 + 240 \times 360\right] = 75 \ \mu\mu f$$

Thus, because of the high voltage across it, the small S_3-core capacity becomes appreciable.

Since the secondary winding intervenes between any primary winding section and the core, $C_1 = 0$. C_2 is the sum of all the layers C_s's plus C_e of S_1-core. It has already been referred to the primary side in the above calculations, and hence the multiplier $(N_s)^2/(N_p)$ is unnecessary.

Hence $C_2 = 75 + 38 + 5 + 84 + 35 + 178 = 415$ $\mu\mu$f. Adding another 25 $\mu\mu$f for tube, load and incidental capacity, $C_2 = 440$ $\mu\mu$f. If it had been referred to the whole secondary winding, this value would have been $440 \times \left(\frac{112^2}{360}\right) = 42$ $\mu\mu$f.

The measured value of capacity from secondary to primary and core is 240 $\mu\mu$f. Contrast this value with 42 $\mu\mu$f, and the importance of the above calculations becomes apparent.

Square-Wave Response

Nomograph correlates tilt of square wave after passage through uncompensated RC-coupled video or audio amplifier with low-frequency response of amplifier and time constant of coupling circuit

By A. J. BARACKET

WHEN USING rectangular or square waves for testing audio and video amplifiers, the output of the amplifier is compared with the input on an oscilloscope. The degree or percent of tilt of the top of the square wave represents the amplifier's deterioration of the lower frequencies.

In the uncompensated RC-coupled amplifier stage shown, the effect of the amplifier on low frequencies is almost completely a function of the value of the RC time constant in the grid coupling circuit. The smaller the time constant, the poorer the low-frequency response and consequently the greater the percent tilt S of a rectangular wave (referred to the peak plate voltage value E, as indicated on the waveform diagram).

The accompanying nomograph is useful in computing the RC value required to give a maximum specified tilt S (expressed as a decimal part of E) for a rectangular wave having a duration t, or conversely it may be used to determine the tilt that will be obtained from a given time constant. The chart also gives the relationship between tilt and low-frequency cutoff of an amplifier coupling circuit (the frequency f_L at which the amplitude—frequency response characteristic is down 3 db).

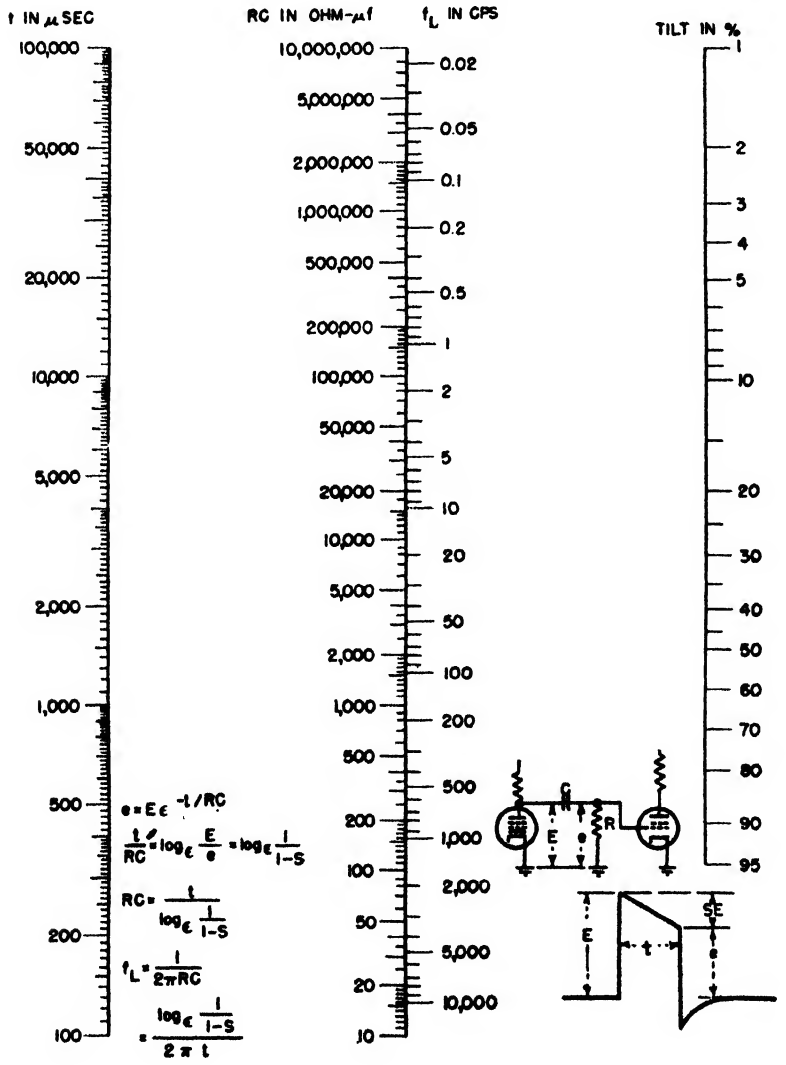

Example of Use

The percent tilt of an uncompensated video amplifier stage is specified as 2 percent maximum on a 60-cycle square wave. What will be the required time constant of the coupling circuit and the corresponding low cutoff frequency?

By means of a straightedge, connect the 2-percent point on the tilt scale with the 8,300-μsec point (corresponding to the half-cycle duration of a 60-cycle square wave) on the t scale. The straightedge will cross the RC scale at approximately 410,000 ohm-μf. The corresponding low cutoff frequency f_L is found to be 0.4 cycle.

Multivibrator Circuits

Basic types presented for convenient reference, with characteristics of each, waveforms at different points, frequency-determining equations, and representative values of components. Three methods of injecting synchronizing signals are shown

By NORMAN W. MATHER

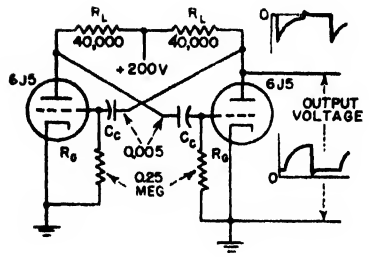

SYMMETRICAL MULTIVIBRATOR — Grid returns are made to the cathodes. This is a basic form of the multivibrator in which corresponding circuit elements used in conjunction with the two tubes are identical. The frequency depends chiefly upon the time constant and in most cases this can be simplified to R_gC_c with little error. For grid returns to the cathodes as shown, the frequency is approximately $0.3/R_gC_c$, but it also depends to a small extent on the tube characteristics and the supply voltage. Connecting the grid returns to the plate supply lead results in a higher frequency, approximately equal to $1/R_nC_c$. Frequency variation can be obtained by connecting the grid returns to an adjustable positive voltage. The amplitude of the generated waves is proportional to the supply voltage, and is only slightly affected by changes in the grid return connection. At high frequencies, distributed capacitances reduce the amplitude and make calculation of frequency difficult

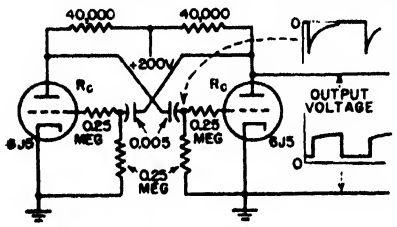

SQUARE-WAVE MULTIVIBRATOR — Addition of resistors R_n to the symmetrical circuit results in a plate-voltage waveform which is approximately a square wave. The frequency of oscillation is affected only slightly by the addition of these resistors

MULTIVIBRATOR WITH ELECTRON-COUPLED OUTPUT—The cathode and first two grids of the pentode operate in the same manner as the second triode in a conventional multivibrator circuit, the screen grid taking the place of the plate. The output waveform of this circuit has a large amplitude and is almost square. Due to the characteristics of pentodes, the plate voltage has little effect on the operation of the multivibrator portion of the circuit and the frequency of oscillation may be estimated in the same way as for conventional multivibrators

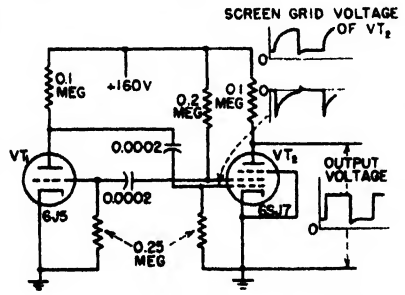

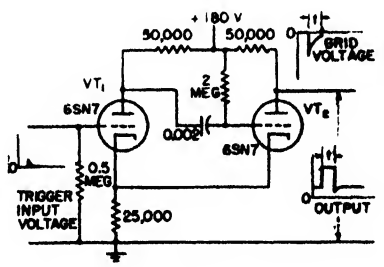

CATHODE-COUPLED ONE-SHOT MULTIVIBRATOR—Circuit values are adjusted so that VT_1 is cut off when VT_2 is conducting. The trigger signal interrupts this stable condition, but after the period t, the circuit automatically returns to the stable condition. If the grid return of VT_2 is made to cathode instead of to +180 volts, a somewhat longer period is obtained. This circuit has the advantage that the triggering circuit is isolated from the multivibrator circuit by VT_1

CATHODE-COUPLED MULTIVIBRATOR—This circuit is particularly adapted to synchronization, and the output voltage can be used without disturbing the circuit operation. As a free-running multivibrator, the frequency tends to be erratic

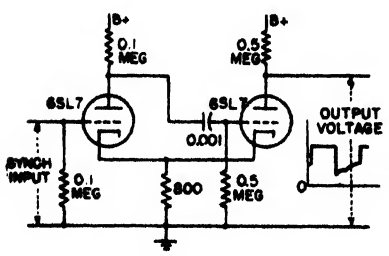

MULTIVIBRATOR WITH CATHODE-COUPLED OUTPUT—This circuit is useful because it has a low-impedance output and a steep wave front on the output signal. The addition of R_K affects the free-running frequency only slightly.

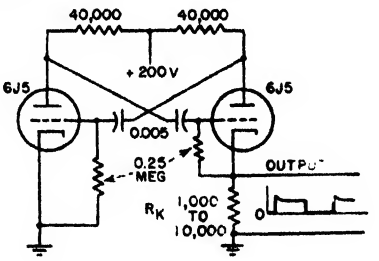

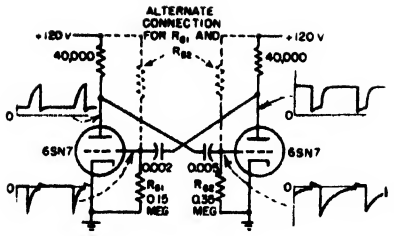

ASYMMETRICAL MULTIVIBRATOR—Same as symmetrical multivibrator except that corresponding circuit elements used in conjunction with the two tubes are dissimilar. One or both of the grid returns may be made to a positive voltage. The tubes used may be of different types. The frequency of oscillation can be estimated by calculating a pseudo frequency for each tube as though the circuit were symmetrical. The approximate frequency of the asymmetrical multivibrator is then $2f_1f_2/(f_1 = f_2)$ where f_1 and f_2 are the pseudo frequencies. Oscillation can be obtained with widely different circuit components, giving considerable design leeway

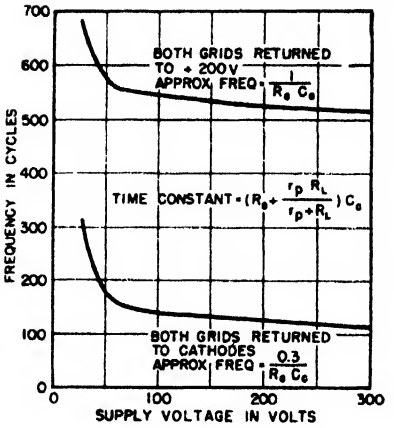

EFFECT OF SUPPLY VOLTAGE ON FREQUENCY OF TYPICAL SYMMETRICAL MULTIVIBRATOR—A multivibrator is relatively insensitive to changes in the supply voltage except when the supply voltage becomes quite low. The increase in frequency obtained by changing the grid returns from the cathodes to the plate supply lead is clearly shown. The amount of increase can be made greater by making the cathodes 2 or 3 volts positive

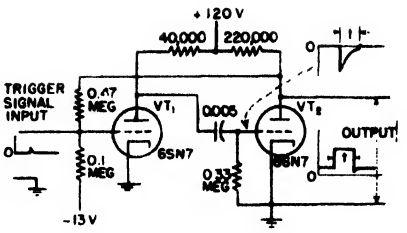

ONE-SHOT MULTIVIBRATOR—Also called one-kick trigger circuit. Feedback from VT_2 is direct coupled to VT_1. Feedback and the plate supply voltage are adjusted so that VT_1 is cut off when VT_2 is conducting. This stable condition can be interrupted by a positive trigger signal on the grid of VT_1. After a short period t the circuit automatically returns to the stable condition. Somewhat more accurate timing can be obtained by making the grid return of VT_2 to +120 volts instead of to the cathode. The period t is approximately half the period of a symmetrical multivibrator having circuit elements corresponding to those used with VT_2 in this one-shot multivibrator circuit

THREE METHODS OF INJECTING SYNCHRONIZING SIGNALS

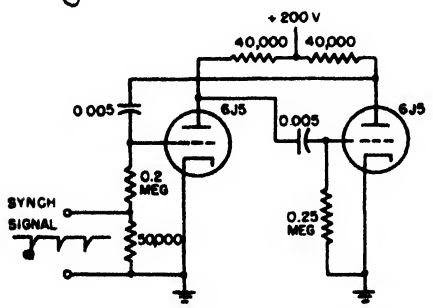

SYNCH INPUT TO ONE GRID—This circuit tends to favor the odd submultiples of the synchronizing frequency when a sine-wave synchronizing signal is used. When pulses are used, synchronization occurs more readily with negative pulses

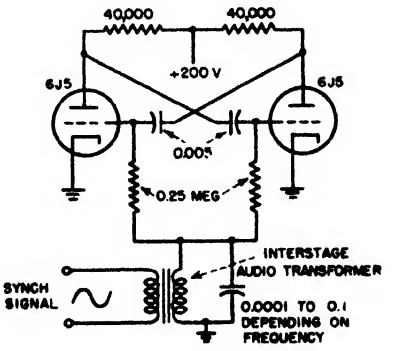

SYNCH INPUT TO BOTH GRIDS—Method of injecting synchronizing signal on both grids with the same phase. This circuit tends to favor even submultiples of the synchronizing frequency and should not be used when frequency ratio is one to one

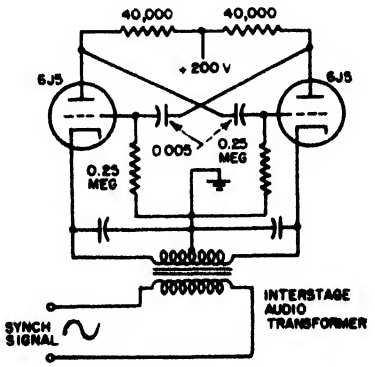

SYNCH INPUT TO BOTH CATHODES—Method of injecting the synchronizing signal so that it is out of phase on the cathodes. This circuit tends to favor odd submultiples of the synchronizing frequency applied through the transformer

Linear Sweep Circuits

Eight methods of correcting nonlinearity in sawtooth sweep-generating circuits for cathode-ray tubes are presented and analyzed, with 60-cycle circuits as examples

By ROBERT P. OWEN

THE CONTINUING REFINEMENT of cathode-ray equipment, particularly for television, has made necessary the generation of almost perfectly linear sweeps. These are most easily obtained by the application of some form of linearity correction to the more or less exponential output of a conventional sweep circuit. Several of the more practicable and effective methods of correcting nonlinearity have been selected for description here, although there are many others that may be equally valuable in a particular application.

The sawtooth waveform of both electrostatic and low-frequency electromagnetic sweeps is almost invariably derived from the charging or discharging of a capacitance through a resistance. The resistance may be that of a simple fixed or variable resistor, or the plate resistance of a so-called constant-current pentode. In either case the rise or fall of voltage will be exponential, for the plate current of an uncompensated constant-current tube is never absolutely independent of the plate voltage. In the case of a variable-frequency circuit the sweep range is determined by the size of charging capacitor, and a fine adjustment of frequency is provided by variation of the charging resistor or of the grid or screen potential of a constant-current pentode.

Discharge of the capacitor after

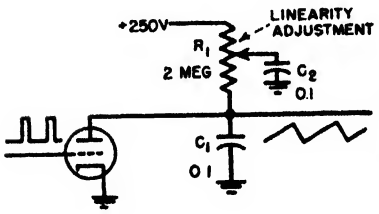

METHOD 1—The simplest means of attaining linearity correction in a fixed frequency sweep is to bypass part of the charging resistor with a capacitor. This gives two *RC* circuits in cascade, which, if it were not for the loading effect of the second upon the first, would result in a perfectly linear output when the two time-constants are equal. In practice, linearity can be definitely improved. The best value of C_2 should be determined experimentally. Input and output waveforms shown here apply to all methods covered

METHOD 2—This circuit, sometimes known as a bootstrap circuit, has been widely used. The sawtooth is fed back through a cathode-follower, which has a gain of approximately one and does not reverse the phase, to the top of charging resistor R_1. In this way a constant voltage is maintained across R_1 and a constant current into C_1. The isolating resistor R_2 may be replaced by a diode, but this is usually of little advantage. As a cathode-follower output is often required after a sweep generator, use of this circuit does not necessarily mean the inclusion of an extra tube. The circuit is especially suitable for use with high-speed sweeps. R_1 and C_1 may be varied without affecting linearity. Almost perfect linearity may often be obtained, although over-compensation is not possible except where constants are such that the combination of R_2 and C_2 acts as in Method 1

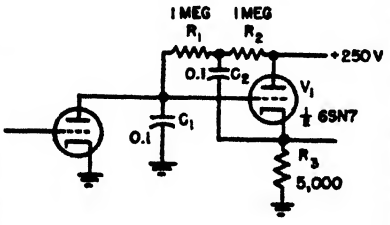

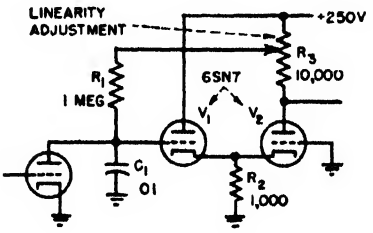

METHOD 3—As in the preceding method, correction is accomplished here by feeding back without phase reversal to the top of the charging resistor. Output is linear when the gain around the feedback loop (from lower end to upper end of R_1) is one, and over-compensation will result as the arm of the linearity adjustment potentiometer is advanced toward the plate of V_2. It should be noted that if a load resistor equal to R_2 is added in the plate circuit of V_2 these two tubes can function as a balanced output amplifier. This method is one of the best available for compensating low and medium-frequency sweeps, either fixed or variable

it has charged (or recharge after it has discharged) is accomplished by means of a thyratron or, in more modern circuits, by an ordinary triode, the grid of which is periodically pulsed from cutoff to near zero bias.

In the data given here the charging resistor and capacitor will be designated R_1 and C_1, respectively, and the discharge (or recharge) will be assumed taken care of by an externally controlled triode. All the methods mentioned are applicable to single or driven sweeps as well as to continuous sweeps. The circuits are shown in their most elementary form, and approximate component values for a 60-cycle sweep are given. Many modifications of each are possible. Adaptation to the particular sweep circuit in use will be necessary.

Most of the circuits discussed here are in actual use, and are covered by U. S. or British patents. Methods 4 and 7 were developed by the writer while a member of the staff of Allen B. DuMont Laboratories, Inc.

References

(1) Puckle, O. S., "Time Bases", John Wiley & Sons, Inc., New York, 1943.

(2) Clarke, A. C., Linearity Circuits, *Wireless Engineer*, June, 1944. (The analysis of Method 6 in this reference is incorrect, as it disregards the fact that the signal fed back to the pentode cathode appears between cathode and control grid.)

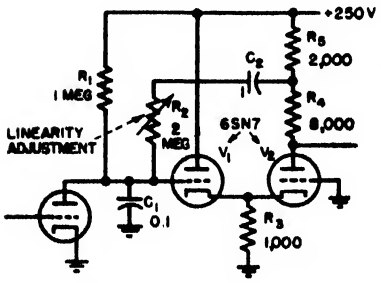

METHOD 4—This circuit is a modification of Method 3 which is useful under certain conditions. Although slightly more complicated, it has the advantage that the linearity-adjusting potentiometer is not the load resistor of V_2. Perfect linearity will result when the ratio of R_2 to R_1 is equal to $A-1$, where A is the gain around the feedback loop

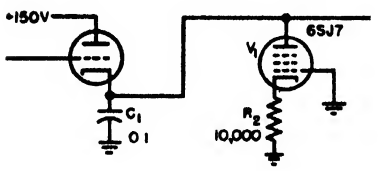

METHOD 5—The output of almost any type of sweep generator can be improved by replacing the charging resistor with a constant-current pentode, but this is easily done only where the capacitor discharges, rather than charges, through the resistor. A pentode having a high plate resistance should be used, and the tube should be operated well out on the flat portion of the characteristic. The screen potential must of course be held constant, as by a fairly heavy bleeder between the positive supply and ground. Constancy of plate current will be much improved by a large cathode resistor, the effective plate resistance being increased by a factor of $1-G_mR_k$

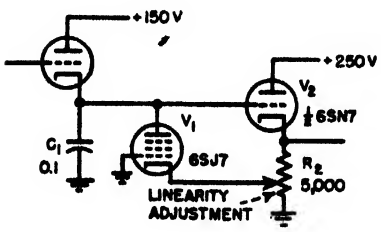

METHOD 6—The use of a constant-current tube may improve linearity though it will never make possible a perfect sawtooth, but by the additional application of feedback even strong overcorrection can be attained. This method utilizes the cathode-follower which often follows such circuits to feed a small part of the output voltage back to the cathode of the constant-current pentode. The circuit is useful both for high-speed sweeps and, because it is direct-coupled, for those of extremely low frequency

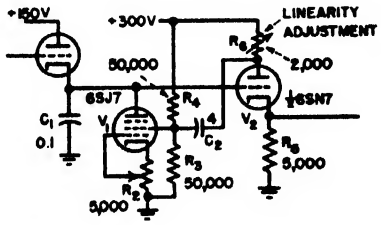

METHOD 7—The preceding method can not easily be applied to some sweep circuits because of their use of cathode degeneration for frequency control. In this case feedback can be to the pentode screen, with equally good results. A variable resistor, R_4, can be inserted in the plate circuit of the cathode-follower with little effect on the output, if it is small compared with the plate resistance of the tube. The screen supply bleeder R_4 and R_3 may be omitted and the screen connected directly to the plate of the cathode-follower instead of through C_2 if operating voltages permit

METHOD 8—Vacuum tubes are not linear devices, in that their e_c-i_p characteristics are seldom straight lines. With careful design, advantage can be taken of this curvature to counteract imperfections of the sawtooth. This is done in many magnetic sweep circuits, with a bias control on the output stage as the linearity adjustment. At present, ordinary tubes are capable of giving definite improvement. In the future, special types designed especially for this purpose may be available

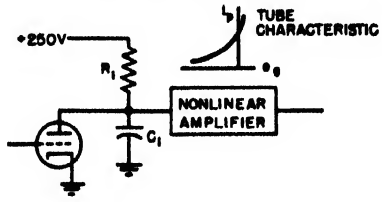

Pulsed Rectifiers for Television Receivers

Brief analysis of pulsed cascade rectifiers used in television receivers indicates that no component is subjected to potentials substantially higher than those encountered per section. In a doubler, this voltage is about half the output voltage from the rectifier

By I. G. MALOFF

TO OBTAIN HIGH VOLTAGES for cathode-ray tubes of television receivers, the pulse produced by flyback of the scanning generator is used to excite a step-up transformer. Under ideal conditions with present television standards, the transformer will deliver a voltage having a waveshape shown in Fig. 1A. The high voltage so developed is usually rectified by cascaded diodes charging a series of capacitors connected as shown in Fig. 1B. To determine ratings for circuit components, it is necessary to first examine circuit operation to ascertain their respective functions.

For analysis, let us consider the simplest pulsed cascade rectifier, the doubler, a schematic diagram of which is shown in Fig. 1C. The time constant of the output circuit, ignoring C_3, is $T_0 = R_L(C/2) = 0.0175$ sec or approximately 300 times the duration of the trace. Therefore, except for regulation, operation of the circuit is unaffected by the load R_L.

During the trace the circuit can be represented as in Fig. 2A and 2B. The drop across R_1 (Fig. 2B) is the full battery voltage at the start of the trace. The time constant of the above circuit for $R_1 = 10^6$ ohms is $R_1(C/2) = 250$ microseconds, which means that in 60 microseconds (trace duration) the battery will change the potential on the two capacitors by 20 percent of the battery voltage, or 70 volts per capacitor. At the end of the trace, therefore, the voltages in the active part of the circuit change to those shown in Fig. 2C.

On retrace, a voltage of 7,000 volts is suddenly applied in the reverse direction by the transformer winding as at Fig. 3A. Rectifier A_1 starts conducting, in effect connecting C_1 across the high-voltage transformer secondary as at Fig. 3B. It also connects C_3 across R_1, thereby isolating the two circuits.

Rectifier A_2, being between C_2 and C_3, has 70 volts more on its plate than on its filament; therefore, it tends to equalize the charges on C_2 and C_3 while the full voltage of C_3 is impressed across R_1. The time constant of this discharge circuit being $R_1C_3 = 500$ microseconds (or approximately 80 times longer than the retrace), the loss of charge through the resistor is of the order of one percent. In other words, the circuit elements tend to come to the same potentials as those given for the beginning of the trace, because the transformer quickly brings the potential of C_1 to the initial 7,000 volts.

The remarkable thing about a cascading pulse rectifier is that the circuit elements have to stand only a few volts more across their terminals than the d-c output voltage per stage as summarized in Table I. Output capacitors C_1 and C_2 have on their terminals only the d-c output voltage per stage plus the ripple, which is of the order of one percent. Coupling capacitor C_3 has only the d-c output voltage per stage plus a small boost in voltage during trace; resistor R_1 has 10 percent of the output voltage per stage on trace and about 101 per cent of it on retrace. The peak inverse voltage on the rectifier tubes is only 10

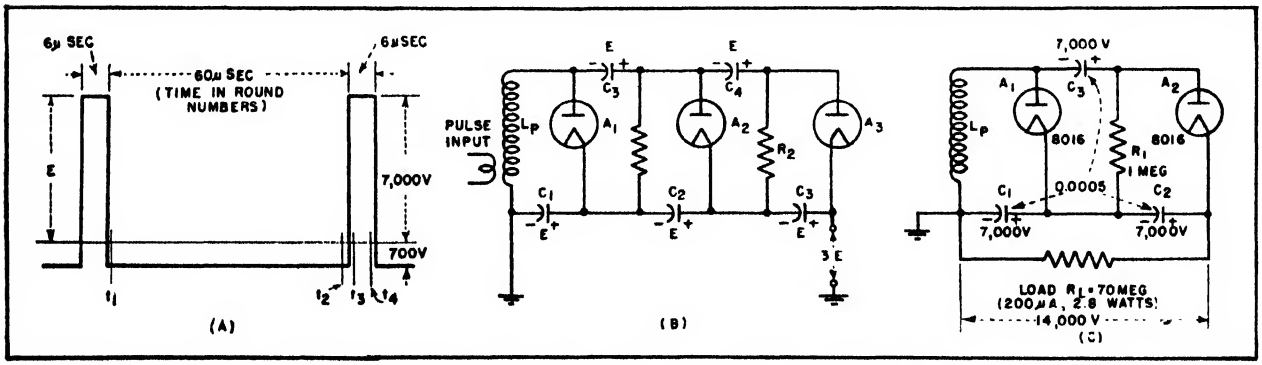

FIG. 1—(A) Pulse delivered by television receiver sweep circuit to rectifier has this idealized waveshape. (B) Pulsed cascade rectifier consists of sequence of diodes charging capacitors in cascade. (C) A typical and simple type of cascade rectifier consists of two sections with a load across the output

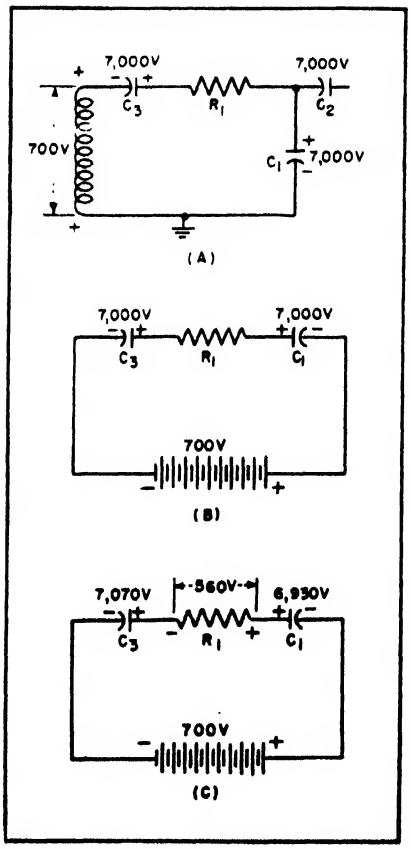

FIG. 2—During the operating cycle, voltages are redistributed about the rectifier. To simplify analysing the action of the pulsed circuit, the input transformer is replaced by a battery

percent higher than the d-c output voltage per stage. (Of course, some components have to withstand the total output voltage between high terminal and ground.)

The above analysis is very elementary but is sufficient to explain the operation of the circuit, which may be summarized as follows: During trace, the coupling capacitors are charged through the resistors to a voltage slightly higher than the d-c voltage per stage; during retrace this excess voltage is transferred to the filter capacitors, except for the first stage which is directly charged by the transformer.

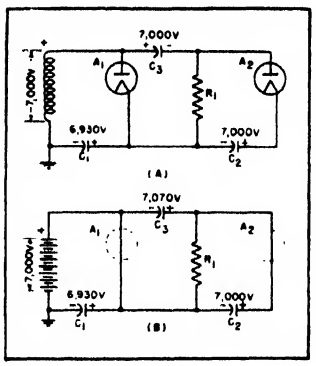

FIG. 3—The diodes act to transfer charges from capacitor to capacitor

L_P	A_1	A_2	C_1	C_2	C_3	R_1	R_L
			Beginning of trace (t_1)				
−700	−7,700	−7,700	+7,000	+7,000	+7,000	−700	+14,000
			Ending of trace (t_2)				
0	−6,930	−6,860	+6,930	<7,000	+7,070	−560	+13,930
			Beginning of retrace (t_3)				
+7,000	+70	+70	+6,930	<7,000	+7,070	+7,070	+13,930
			Ending of retrace (t_4)				
0	−7,000	−7,000	+7,000	+7,000	+7,000	0	+14,000

Polarities of capacitor voltages as shown in Fig. 1C; for others, positive is at top. Times are indicated in Fig. 1A. All voltages approximate.

Table 1—Voltages Across Components During Operating Cycle

Transient Video Analyzer

Cathode-ray test set combining a five-signal transient generator with a wide-band oscilloscope, used for checking accuracy of various types of steep waveforms reproduced by wide-band amplifiers used in television and communications equipment

By CLEMENT MORITZ

AT present considerable work in the communications field is concerned with systems for the transmission of transient waveforms. Especially in television are the requirements severe as to the accuracy of reproduction of steep waveforms without overshoots or ringing.

Testing and design of such equipment customarily involves laborious use of ordinary steady-state signal generators. Sometimes oscillators with continuously swept frequency are used, but in general such methods have two disadvantages: (1) the shape of the transmission (gain)-vs-frequency characteristic is not singly related to the transient performance which is the real objective; (2) the phase characteristic is ignored by such measurements, and even if it were known, the preceding objection would also apply to it.

A step in the right direction is the use of square waves in conjunction with an oscilloscope having excellent transient response and a sweep of adequate speed.[1,2] Such systems give a fairly good direct indication of the quality of transient reproduction.

The instrument described in this article is intended to carry forward the same idea. However, in addition to square waves of certain desirable frequencies, it provides a sharp impulse or spike function for checking

the high-frequency portion of a video system, and a sawtooth wave for checking linearity. The transient generator feeds a signal through the wideband system into an oscilloscope used as an indicator of quality of transient reproduction. The transient generator and the oscilloscope have been incorporated for convenience into a single unit with associated components.

Although an aperiodic transient would be quite sufficient for analysis, periodic transients become necessary for visual observation with an oscilloscope. The transient period is controlled by a stable timing oscillator, also used for timing the horizontal sweep, as shown in Fig. 1. An initiation phase control is inserted into the link between the oscillator and the transient generator to control the timing of the transient test signal with respect to the sweep, and so facilitate the study of the system output.

The transient output of the wideband system under test goes to the vertical deflecting plates of a cathode-ray oscilloscope through an amplifier whose gain can be varied to suit conditions. The complete block diagram of the system is given in Fig. 2.

Five transient signals are available from the generator in the transient video analyzer, as follows:

(1) A 30-cycle square wave primarily used for low-frequency analysis.

(2) A 5-kc sawtooth wave used as a signal for linearity checks. A stepped wave would serve the purpose no better and would only further complicate the completed instrument.

(3) A 10-microsecond pulse keyed at the rate of 5,000 per second, for use in checking middle frequency response (10 to 1,000 kc).

(4) A step function.

(5) A spike function used to determine high-frequency performance. The high-frequency response limitation is primarily in the vertical-channel amplifier of the oscilloscope.

These waveforms appear on the cathode-ray oscilloscope when the output of the generator is connected directly to the input of the analyzer. However, in the instrument the 10-microsecond pulse and 1-microsecond sweep are both used twice; only four signals and four sweeps are generated, but the circuit is arranged for switching from one type of operation to another, as shown in Fig. 2.

All transient outputs are one volt peak-to-peak across 70 ohms except the spike, which can have any height (in this case about 9 volts peak-to-peak). The instrument was designed to operate into and out of coaxial lines matched to television equipment.

This instrument makes use of two transient recurrence frequencies derived from two timing oscillators. Each recurrence-frequency channel has its own horizontal and vertical trigger generators for sweep and transient signal initiation. Although both vertical and horizontal trigger generators are similar to each other in each channel, separate trigger generators are necessary to provide a signal trigger which can be advanced or delayed in time with respect to the horizontal sweep trigger.

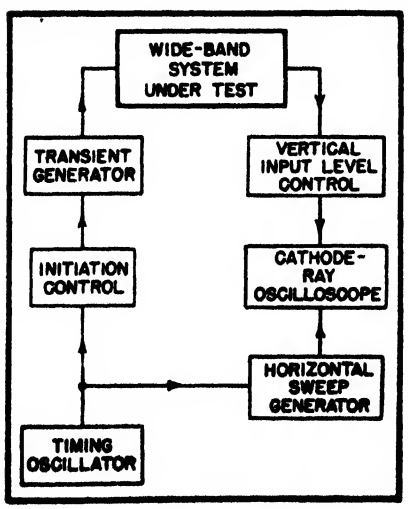

FIG. 1—Essential components of transient video analyzer, shown in relation to wide-band system under test

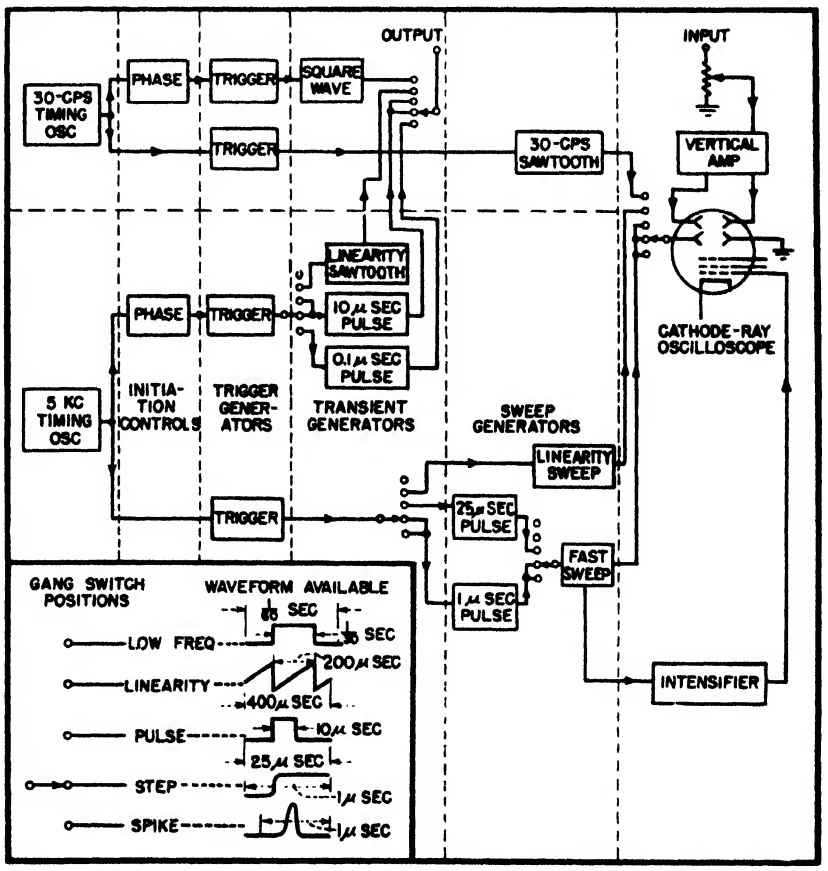

FIG. 2—Block diagram of complete analyzer. Wide-band system under test is connected between output and input terminals

A switch selecting the desired transient signal also selects the correct timing and sweep circuits for proper analyzer operation. Circuits which are not necessary for operation automatically have their high voltages disconnected to decrease the drain on the power supplies. It is necessary only to connect the output of the analyzer to the system to be studied, connect the output of the system back into the input of the analyzer, and set the switch for the transient desired.

The 30-cycle square wave is generated by a multivibrator which must be supplied with both positive and negative triggers for one full cycle of operation. This type of square-wave generator was selected to assure perfectly flat-top square waves. The stage is fed by a negative supply so that the plate returns may be grounded, and the output is then taken from a tap on one of the plate load resistors, ensuring perfect fidelity and freedom from a-c coupling troubles which would be encountered in passing the low-speed square wave. The circuit appears in Fig. 3A.

The trigger generators in the 30-cycle channel employ a double-triode for clipping, with a differentiating network feeding into the grid circuits of the multivibrator and sweep circuits.

The sweep is a conventional gas-tube switch across a capacitor, with a constant-current pentode for charging. This is necessary to give a linear sweep of sufficient amplitude for deflection without amplification.

The timing oscillator is of the phase-shift type. Output is fed into the delay tube circuit (Fig. 3B), which serves as a phase inverter. The delay tube provides, in its cathode circuit, a low-impedance driving source for the first horizontal clipper, and between plate and cathode a source from which phase may be shifted by a resistance-capacitance combination before the 30-cycle sine wave is fed into the first signal clipper. The delay may be varied by varying the resistor in series with the capacitor. Almost 180 degrees of phase shift can be obtained in this manner, with an output having substantially constant amplitude value.

A double-triode bridge oscillator performs more stably at 5,000 cycles and is therefore used for the 5-kc channel in preference to the phase-shift type. Output is fed into the first horizontal clipper and the vertical phase-controlling stage.

This stage operates in the same fashion as the one in the 30-cycle

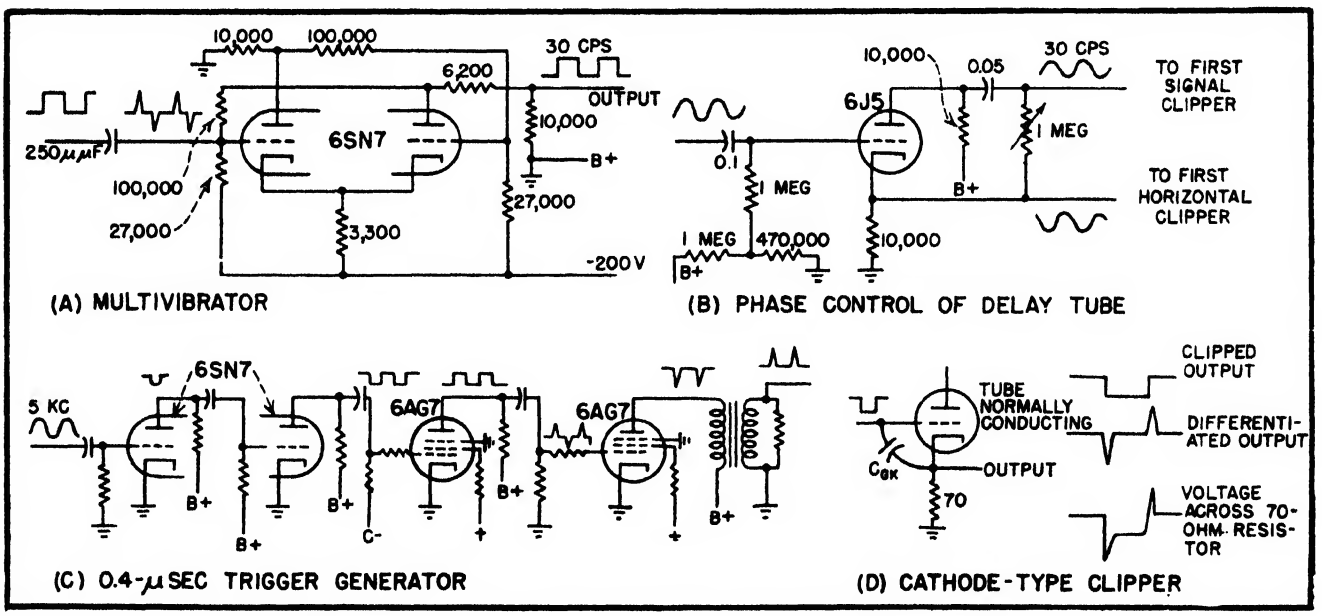

FIG. 3—Waveforms at inputs and outputs of various stages in the analyzer

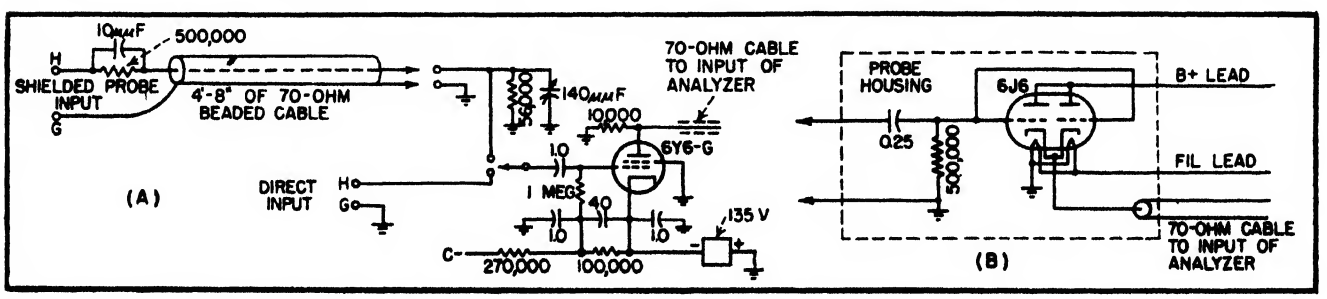

FIG. 4—Plate-loaded tetrode probe circuit (A) with removable input attenuator, and cathode-follower type probe (B) which can also be used with an attenuator

channel but different circuit constants are necessary at the higher frequency. The variable delay resistor is made up of two variable resistors in series, one to be used as a vernier. The other section of the double triode is merely for a fixed delay adjustment which puts zero delay in the middle of the range of delay available, and makes possible initiating the signal transient ahead of the sweep when necessary.

Both trigger generators employ four stages, as in Fig. 3C. The first two are triode clippers. A pentode is necessary in the third stage to prevent feed-through by the grid-plate capacitance, which is much too great in the case of a triode. The clipped wave in the plate circuit is differentiated, and the positive portions are used to drive another pentode as a trigger amplifier. The transformer in the plate circuit of the latter tube reverses the pulse polarity.

By using this rather elaborate trigger generator, a 0.4-microsecond synchronizing pulse has been achieved with a steep front edge which provides a good positive trigger for initiating the succeeding circuits.

Synchronizing accuracy (with time) is quite important in the 5-kc channel when the 1-microsecond sweep is being used. If the error is greater than 0.02 microsecond or 0.01 percent, any vertical lines on the oscilloscope screen would be too wide and too dim to be useful. With the 1-microsecond sweep, the c-r tube face is excited only 0.5 percent of the time.

The linearity sawtooth is generated conventionally, and taken out of a cathode follower to develop the requisite power without loading the sawtooth generator.

The 10-microsecond pulse is generated by a nonoscillating multivibrator. Since the pulse is not perfect, it is shaped by two pentode clippers. Both conditions of amplitude of the pulse are determined by one of the tubes at cutoff to assure flatness. At first a triode cathode follower was tried for the second clipper but satisfactory results were not obtainable, because differentiation of the grid signal feeding through the grid-cathode capacitance of the tube into the cathode load resistor gave a very objectionable overshoot (shown in Fig. 3D). This trouble was eliminated by the use of a plate-loaded pentode stage. Such a stage gave a very good rate of rise (0.07 microsecond) but necessitated the use of a negative supply. Thus this output became good enough to be used also as the step transient with the fast (1-microsecond) sweep.

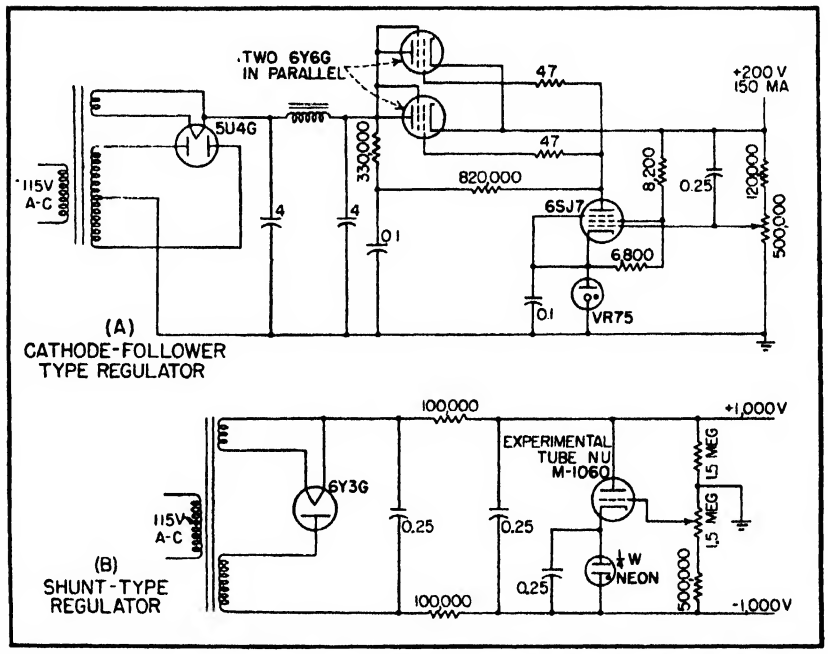

FIG. 5—Basic regulator circuits used in the power pack of the analyzer

The spike pulse is generated by the discharge current of a capacitor passing through a thyratron. This pulse should be as short as possible and of reasonable height.

Spike Pulse

The sawtooth sweep for linearity is similar (except for circuit constants) to the one in the 30-cycle channel. Its base frequency is 2,500 cycles to provide one full sawtooth at 5,000 cps.

The fast sweeps are constructed by pulse integration. Two pulses are available: a 25-microsecond pulse from a nonoscillating multivibrator, and a 1-microsecond pulse from a delay-line thyratron-type pulse generator. The pulse is fed into a pulse amplifier, after which it is integrated in the cathode circuit of a cathode follower. Constant current is supplied meanwhile by a pentode. At 1 microsecond, the wiring capacitance into the horizontal deflecting plates is used as the capacitance for integration; at the slower (25-microsecond) sweep speed, it is necessary to add capacitance for use with the same charging current from the pentode current generator. It was necessary to use a 6AG7 for this pentode stage since with the existing circuit capacitances a large charging current was necessary for integration.

Some of the negative pulse is taken from the pulse amplifier and used to cut off a pentode to provide a pulse for intensifying the cathode-ray tube beam during the usable portion of the fast sweeps. The intensifier does not operate when the linear sawtooth sweeps are being used.

High-Frequency Oscilloscope

Since the oscilloscope must of necessity have greater fidelity than the system which it tests, severe demands are made on the vertical amplifier. The low-frequency cutoff is difficult to measure, but is theoretically one cycle. The 30-cycle square wave is reproduced excellently. High-frequency response is down to 70 percent at 15 megacycles. The maximum available deflection on the cath-

ode-ray tube face is four inches, but some linearity is lost. The maximum linear deflection is two inches.

The amplifier is made up of five stages, all push-pull Class A. Push-pull deflection was used to maintain sharp focus over the cathode-ray tube face. Most of the inversion is performed by the first two stages. The cathode bisector type of inverter has been effective and quite free of phase-shift trouble. The tubes in each stage must be reasonably well matched or one tube will tend to draw more than its share of current and bias its mate to cutoff.

Simple shunt peaking was used since it yields the most linear phase characteristic at the high end of the pass band. Sufficient low-frequency response was realized by the proper selection of grid time constants, and compensation was also applied to the plate circuit of the first stage.

The input to the amplifier is a 70-ohm carbon potentiometer used to terminate a coaxial transmission line. When desired, a high-impedance probe using a cathode follower with the potentiometer in its cathode circuit can be used for circuits having impedances higher than 70 ohms.

Two types of probes have been built which have a high input impedance and can work into the 70-ohm analyzer input impedance. The first probe built used a plate-loaded tetrode connected as in Fig. 4A.

The input of the 6Y6G can be switched either directly to a pair of input terminals or to a circuit probe of the compensated attenuator type, which must be used when freedom from stray fields is needed. The first portion of the attenuator is placed at one end of a piece of 70-ohm transmission line, the other portion being the line capacitance in shunt with a resistor. An auxiliary capacitor serves as an adjustment for perfect performance over the pass band. The voltage gain through this probe is only about 1/30, however, which is a decided handicap where low peak signal voltages (of the order of one volt) are encountered.

In the cathode-follower type probe shown in Fig. 4B, developed for low-voltage applications, the triode sections of a 6J6 have been paralleled and built into a small bakelite tube with an input coupling network. The unit feeds a piece of 70-ohm transmission line to which are laced the filament and anode voltage leads going to the analyzer.

Probes have also been built with compensated attenuators ahead of the 6J6, for use with higher signal voltages.

Because of the heavy load currents and the polarities required, five individual regulated power supplies are used. For the four low-voltage supplies the lowest possible terminal impedance must be realized to eliminate phase-shift trouble in the vertical amplifier and other low-frequency circuits, and therefore cathode-follower type series regulators like that in Fig. 5A have been used. The number of control tubes in parallel is dic-

Complete schematic circuit diagram of transient video analyzer, with the exception of the five power pack circuits which are of the types shown in Fig. 5

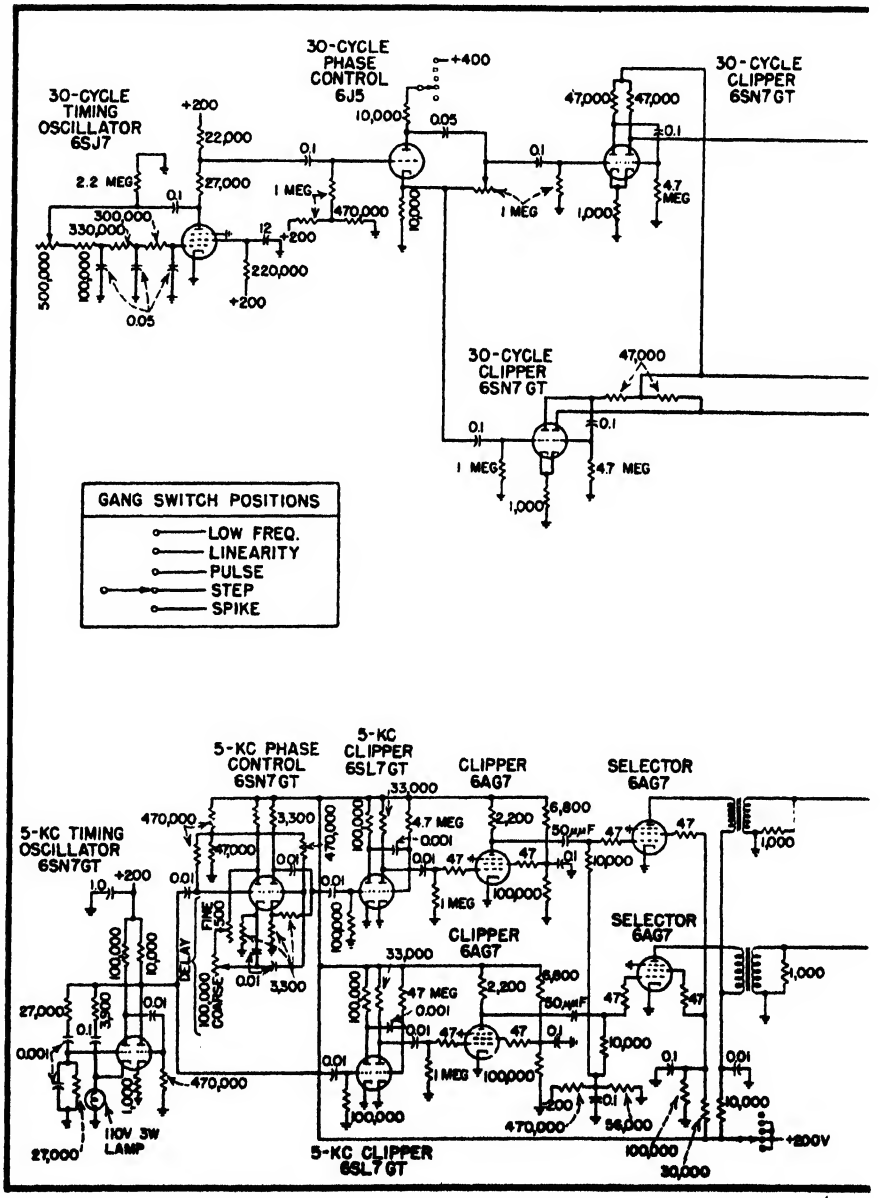

tated by the load current required.

The high-voltage supply for the cathode-ray tube was regulated primarily for freedom from line-voltage trouble, which caused a variation in deflection sensitivity. The simple shunt regulator circuit in Fig. 5B was used, since low supply impedance was not necessary. The special high-voltage triode has an amplification factor of 500 and will pass 2 ma at 10 kv with 5 volts bias.

Much appreciation must be expressed for the encouragement and help given by William E. Bradley and C. T. McCoy, under whose direction the instrument was developed, to F. M. Bowdon who worked on the power supplies and probes, and to Daniel Naidamast and T. Schachat who developed engineering samples.

References

(1) Kullman, H. E., Portable Equipment for Observing Transient Response of Television Apparatus, *Proc. IRE*, p 351–360, Aug. 1940.

(2) Kell, R. D., Bedford, A. V., and Kozanowski, H. N., A Portable High-Frequency Square-Wave Oscilloscope for Television, *Proc. IRE*, p 458–464, Oct. 1942.

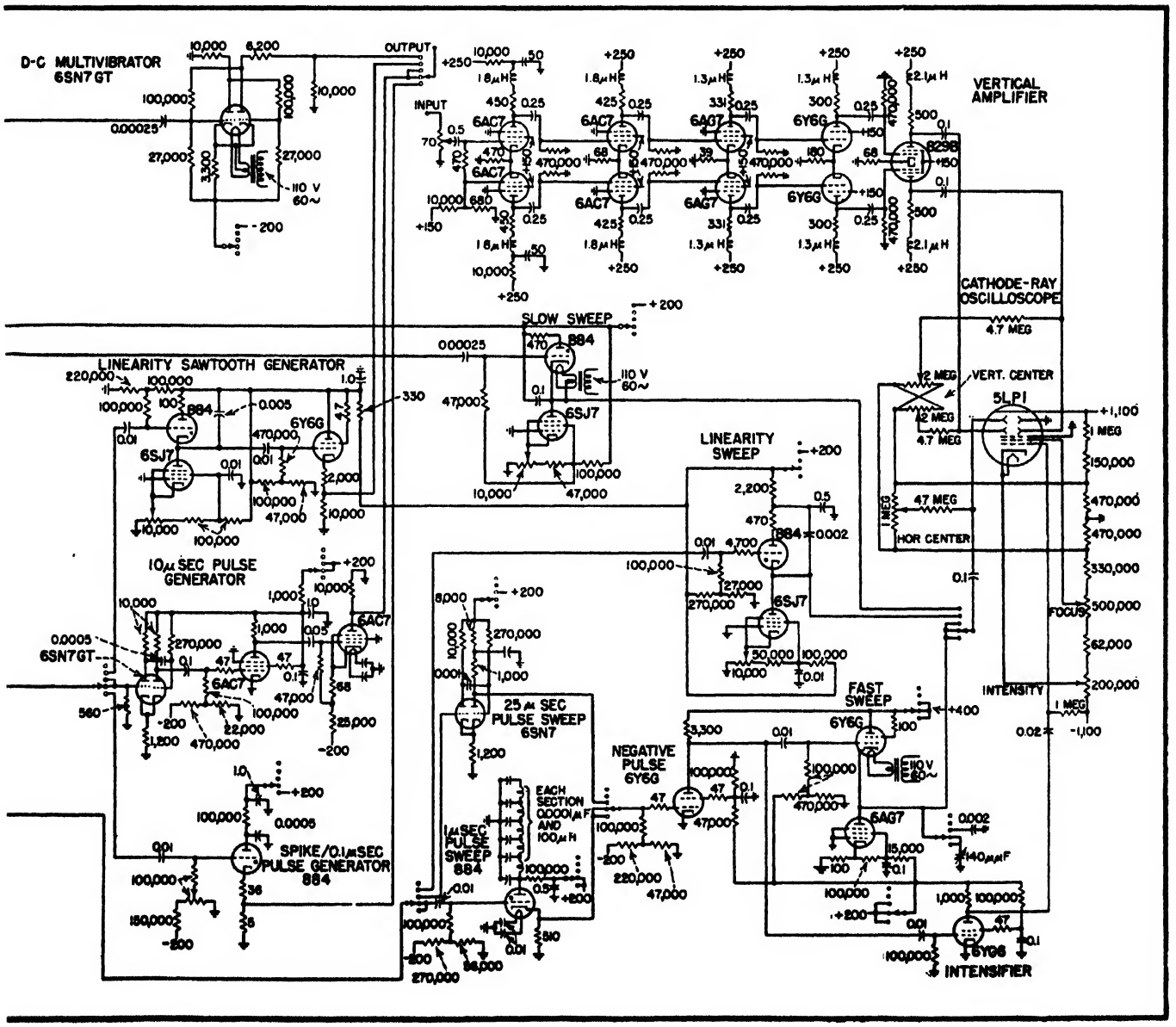

Test Oscilloscope for Television

A modified standard oscilloscope is used to measure television transmitter modulation. Either the radio frequency or a video signal can be used for synchronization. Design and installation of additional circuit elements is discussed

By A. H. BROLLY and W. R. BROCK

THERE has been a definite need for some simple means of checking the modulation of television transmitters quickly and with reasonable accuracy. No commercial equipment suitable for operation at the high carrier frequencies involved has thus far become available.

It is possible to modify a commercial oscilloscope so that the technique of employing a trapezoidal pattern to measure modulation, used in sound broadcasting, may be adapted to television. The equipment provides a convenient means of determining the percent of carrier amplitude devoted to synchronizing pulses and hence compliance with the standard.

The modification necessary consists of providing a linear horizontal sweep at half the line or frame scanning frequency and of adapting the input circuits to the television carrier frequencies. The modified circuit of such an instrument is shown in Fig. 1.

Use of the type 5JP1 cathode-ray tube is advantageous since the deflection plate leads terminate on the bulb. This feature minimizes capacitance coupling between horizontal and vertical plates, and simplifies the r-f circuit. It is desirable to shield the tube electrostatically by wrapping it in a sheet of copper foil.

Provide an aluminum or brass case for the whole instrument. In addition to shielding it is wise to isolate the leads from the horizontal sweep amplifier by some resistance to prevent any possibility of resonance in these lines. For this purpose 1,000 ohms was found satisfactory.

Filament, anode and bias supply

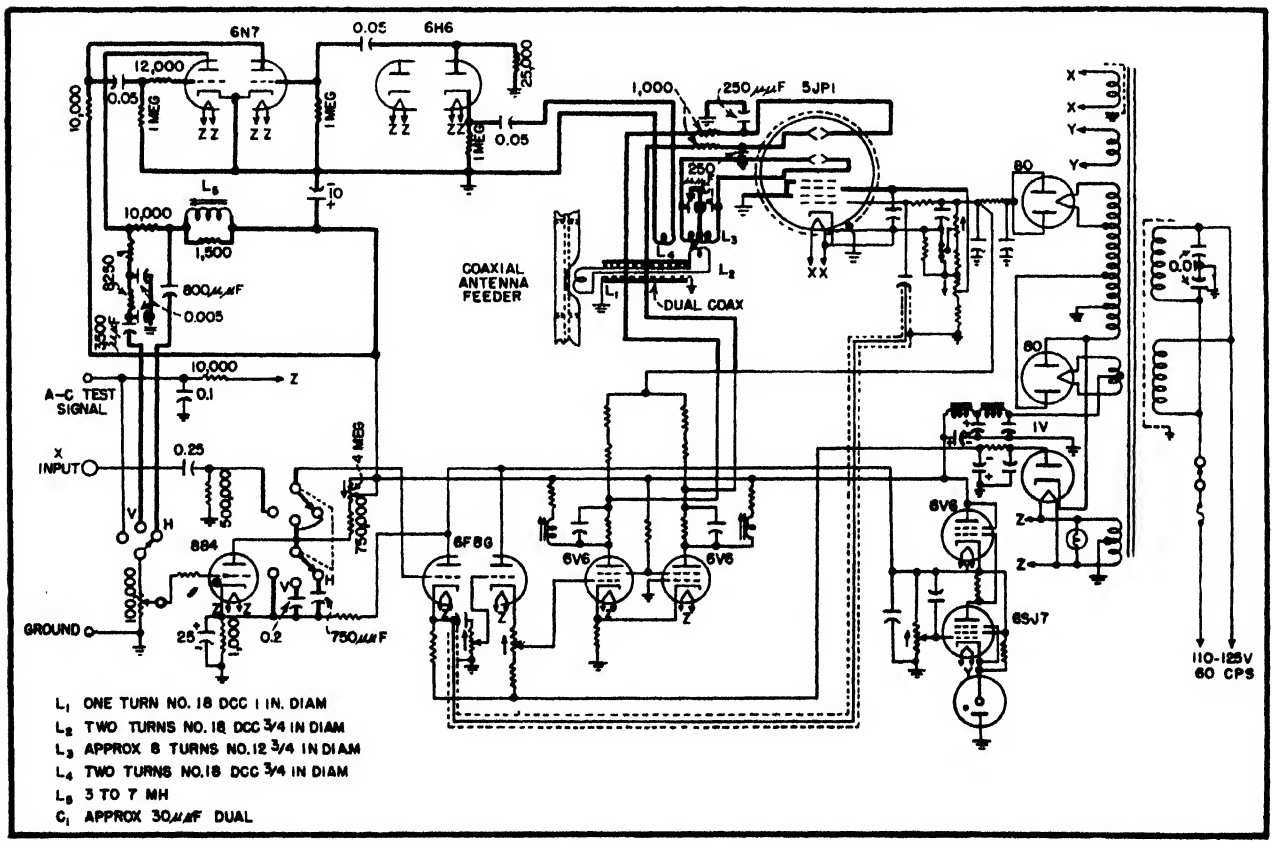

FIG. 1—Circuit modifications, shown in heavy lines, adapt standard oscilloscope for operation at television carrier frequencies

circuits are those commonly employed in most oscilloscopes, with the exception that the high voltage supply should have a positive ground. This feature is important since it permits grounding the center tap of the tuned circuit and the use of low voltage r-f bypass capacitors on the horizontal deflection plates. The plate supply of the critical stages of the sweep amplifier is regulated and the horizontal sweep oscillator and amplifier are similar to those of conventional oscilloscopes with the exception of the synchronizing circuit and sweep-speed control.

The most critical consideration when using very high frequencies for vertical deflection is the tendency of these voltages to stray over to the horizontal deflection plates, causing a curvature of the parts of the pattern that should be vertical. The resulting image distortion can be prevented by symmetrical voltage distribution in the r-f circuit and effective r-f bypassing of the horizontal deflection plate leads. Capacitors must be selected that will have a low reactance at carrier frequency but a high reactance through the tenth harmonic of the horizontal sweep frequency. A 250 micromicrofarad capacitor has a reactance of 10.7 ohms at 60 megacycles and 8,100 ohms at 7,875 × 10 cycles and gives good results. The frequency 7,875 is one half the 15,750 cycles required for horizontal scan in 525-line television. This sweep frequency permits patterns of two scan lines to be shown on the screen.

The vertical deflection plates are driven by a tuned circuit that provides enough voltage at resonance to produce adequate deflection with small power input. In the lower group of television channels, up to 88 megacycles, a split-stator capacitor of 20 to 30 micromicrofarads per section is used for tuning. It is not necessary to load the circuits to pass the wide sideband since the highest frequency components in the extremes of the sideband are not necessary for ordinary measurements.

The center of the coil feeding the vertical deflection plates must be grounded to provide the required d-c potential on these plates. The rotor of the tuning capacitor may also be grounded. This common ground must be connected to the shield on the cathode-ray tube by a strap, ribbon, or wire of large area and as short as is feasible. Such an arrangement assures symmetry of voltage on the vertical deflection plates and reduces coupling to the horizontal plates.

A coil suitable for the lower group of television frequencies can be wound with no. 12 wire on a ¾-inch form. An 8-turn coil of this diameter has been found suitable for the 60- to 66-megacycle channel. One or two turns more or less will be required for other channels of the group.

R-F Pickup

To secure a balanced feed, a dual coaxial line is desirable. The line should be flexible so that it can be run through conduits or wire ducts with ease and its losses are low enough so that almost any reasonable length can be used.

Coupling coils at the input and output of the feed line are connected to the inner conductors and not to the outer sheath. The feed line input coil is a ¾-inch, one-turn loop inserted part way into an opening in the outer conductor of the transmitting antenna coaxial line just outside the transmitter cabinet. Where the coaxial line enters the oscilloscope cabinet the outer sheath must be grounded to the metal cabinet. The cable terminates in a two-turn coil of ¾-inch diameter and is loosely coupled to the tuned circuit of the oscilloscope.

Since such a loop cannot be expected to provide an entirely nonreflecting termination there will be some standing waves in the line, and some degree of unbalance in spite of precautions. Coupling between loop and tuning coil is adjusted by trial, inserting the loop a small distance between the turns of the coil; the most effective point may be found one or two turns above or below center.

Because of the standing waves in the line it is possible for the loop initially to be at a low-current point in the standing-wave pattern, in which case the line can be shortened somewhat.

Synchronizing voltage for the horizontal sweep may be taken from a video line if available or, if more convenient, it may be taken from the r-f signal (Fig. 1). The detector circuit shown is suitable for either method.

A small pickup coil of two turns is loosely coupled to the lower end of the tuned circuit and applies about a volt to the cathode of the 6H6 tube. This tube is located directly below the pickup coil so that the leads are kept short. Peaks of the r-f signal corresponding to the sychronizing pulses are rectified, biasing the cathode of the diode positively so that only synchronizing pulses appear in the plate circuit.

The diode performs the two functions of rectifying r-f and clipping off picture components. Negative impulses appear across the plate load resistor. If video signals are used for synchronizing, they may be applied to the diode that will serve in the same way to separate synchronizing pulses from the picture. If the pulses are negative with respect to ground, the signal is applied to the cathode of the 6H6 tube in the same manner as the r-f signal. If the pulses are positive, they are applied to the plate of the diode through a network consisting of a 0.05 microfarad capacitor and a one megohm resistor. The output is then taken from the cathode across a 25,000-ohm load resistor. In this case the output pulse is

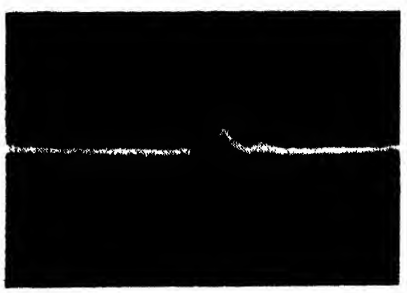

FIG. 2—Integrated vertical synchronizing pulse fed to the type 884 tube

FIG. 3—Horizontal synchronizing pulse taken from L_6 through the *H* position of selector switch

positive. This difference of polarity does not adversely affect synchronism of the sweep for reasons that will be pointed out later.

The output pulses from the detector are amplified by the two-stage amplifier utilizing a type 6N7 tube that operates without external bias since the plate current is sufficiently limited by the 10,000-ohm plate resistors. As long as there is a substantial signal applied to this amplifier, grid rectification provides bias for the tube. The time constants of the grid resistor and coupling-capacitor networks are large enough to permit amplification of the 60-cycle field scanning impulses.

Impulses passing through the amplifier will usually be of both line and field frequencies. It is the function of the two networks in the plate circuit of the left section of the 6N7 tube to separate the two frequencies so that either can be applied to the horizontal sweep oscillator of the scope. The network consisting of two 8,250 ohm resistors and 0.005 microfarad capacitors, separates by integration the vertical pulse from the composite of both pulses. After separation the pulse is partially differentiated by the 3,500 micromicrofarad coupling capacitor and the 884 tube grid resistor producing both a positive and negative pip as shown in Fig. 2 Therefore, the polarity of the pulse from the 6N7 amplifier is unimportant since the 884 tube will always receive a positive impulse on which it synchronizes best.

The horizontal pulses are separated from the vertical by differentiation in L_5. Again a positive and negative swing is produced, as shown in Fig. 3, to synchronize the 884 tube.

Switching circuits are provided to select synchronizing voltage from either the vertical or horizontal separator output or from the 60-cycle line.

Appropriate *RC* networks can be switched into the plate circuit of the 884 tube to generate suitable sawtooth waves at 30 and 7,875 cycles for sweep speeds to show either frame or line patterns. Provision is made for external deflection for special cases. A potentiometer in the plate circuit of the 884 tube permits continuous adjustment of sweep frequency over a range from 3 or 4 lines or frames to one line or frame. The sawtooth output of the sweep oscillator is amplified by a 6F8G and two 6V6 tubes in a conventional circuit before being applied to the horizontal deflecting plates. A back-trace blanking impulse is fed to the cathode ray tube from the cathode circuit of the 6F8 tube.

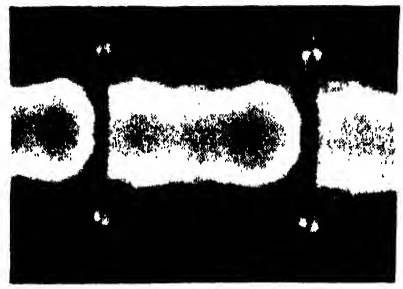

FIG. 4—One frame of a typical television signal as seen on the screen of the modified test oscilloscope

A typical pattern of two frame periods of a television signal as it appears on the oscilloscope screen is shown in Fig. 4 The synchronizing pulse envelope may be seen at the vertical extremities of the pattern. Between these the horizontal line indicates the peaks of the line impulses.

At the base of the synchronizing impulses, the bright line indicates the blanking pulse shoulders or black level. The whole central portion of the pattern is taken up with picture components.

Television Synchronizing Signal Generator

Horizontal and vertical driving pulses, the composite blanking signal and the composite synchronizing signal, all within FCC and RMA specifications, are produced. Linearity test signals can be mixed with blanking for testing picture monitors and receivers; simultaneous cathode-ray monitoring of all frequencies is provided

By A. J. BARACKET

THE instrument to be described provides the means for insuring synchronism between the scanning of a picture at the receiver and the scanning of a subject at the transmitter. Features are provided that are not usually found in a synchronizing generator which are specific aids in television station operation and maintenance.

The generator meets the RMA recommendations for the standard signal, that is, the horizontal and vertical driving pulses, the composite blanking signal and the composite synchronizing signal.

Linearity test signals are provided at 900 cycles and at 157.5 kc

mixed with blanking by means of a switch for use in testing scanning linearity of picture monitors and television receivers. These produce 15 horizontal bars and 10 vertical bars on a raster permitting a rapid check of sweep linearity. In addition, the 157.5-kc test signal serves as an accurate 10 percent H (6.35 μsec), electronic marker for use with an ordinary oscillograph in the precise setting of pulse widths and front porch.

The leading edges of the equalizing pulses are also the leading edges of horizontal and vertical synchronizing pulses, thus insuring perfect interlacing.

Two 3-inch cathode-ray tubes permit simultaneous monitoring (without switching) of all frequencies in the synchronizing generator. Thus, frequency counts may be checked or adjusted without the use of an external oscilloscope.

A crystal oscillator at 157.5 kc or a highly stable self-excited oscillator at 157.5 kc may be selected by a switch for the master oscillator. The self-excited oscillator is used in synchronizing the generator, by means of the provided lock-in circuit to the 60-cycle power line or to a remotely generated synchronizing signal.

Negative feedback is used in many of the circuits to minimize the effect of changes in tube characteristics and variations between tubes. A double-regulated supply is used having an internal impedance of less than 0.15 ohm.

Circuit Breakdown

The generator consists of the following units:

1. Timing generator
2. Blanking-driving unit
3. Sync shaping unit
4. Regulated low-voltage supply
5. High voltage supply for the cathode-ray monitors
6. Power control panel containing switches and fuses.

Figure 1 is a block diagram showing the interrelation of the units in the development of the standard signals. Accurately timed signals at 157.5 kc, 31,500 cycles, 15,750 cycles, 900 cycles and 60 cycles are developed in the timing generator for use in the other units.

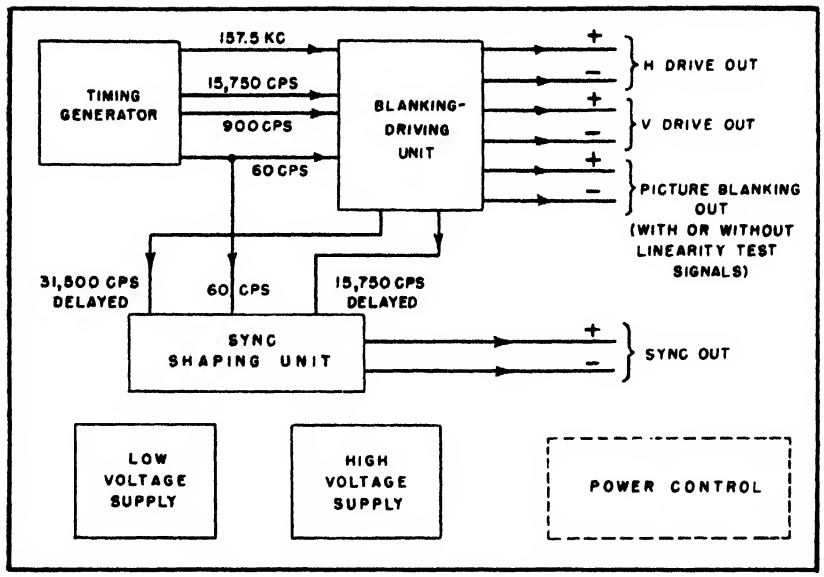

FIG. 1—Interrelation of units forming the sync generator

The blanking unit utilizes the 60-cycle signal and the 15,750-cycle signal in the development of vertical driving and horizontal driving pulses and in the development of the composite blanking signal. It also uses the 157.5-kc signal and the 900-cycle pulses in the development of the composite linearity test signal which becomes available mixed with blanking.

The sync shaping unit utilizes the 31,500-cycle pulses and the 15,750-cycle pulses with suitable delays (for accurate synthesis of the horizontal and vertical sync pulses) in a specially designed delay line contained in the blanking-driving unit for the formation of the high-frequency components of the composite synchronizing signal. The 60-cycle pulse from the timing generator is used undelayed in the development of the low-frequency component of the composite synchronizing signal.

To meet the severe requirements of the RMA-recommended synchronizing signal generator signals, there must be precise time relationship among the pulses developed by the timing generator. This may be obtained by starting at a high frequency and by suitable frequency division deriving the lower frequency pulses. An alternate method is to begin with the lowest frequency and obtain the higher frequency signals by suitable frequency multiplication. In the timing generator shown in Fig. 2, the former method is used because it may be effected by simpler circuits.

In the circuit diagram of Fig. 2, the two basic oscillators are the 6AC7 crystal oscillator and the 7F8 master oscillator, both operating at 157.5 kc. The 6SN7 blocking oscillator frequency dividers are used to derive the lower frequencies required. The first division is by 5 to 31.5 kc, the equalizing pulse frequency. From 31.5 kc there is one division by two to 15,750 cycles, the horizontal rate, and another division by seven to 4,500 cycles. The frequency of 4,500 cycles is divided by five to 900 cycles, one of the linearity test signal frequencies.

Division of 900 cycles is done by five to 180 cycles which is in turn divided by three to 60 cycles, the field repetition rate. Sawtooth wave forms at 60 cycles and at 900 cycles are fed respectively to the deflecting plates of the low-frequency and the high-frequency cathode-ray monitors, to serve as time bases for the presentation of the count-down frequencies on the monitor screens.

Figure 3 shows the presentation on the screens of the cathode-ray tubes. The left-hand screen is that

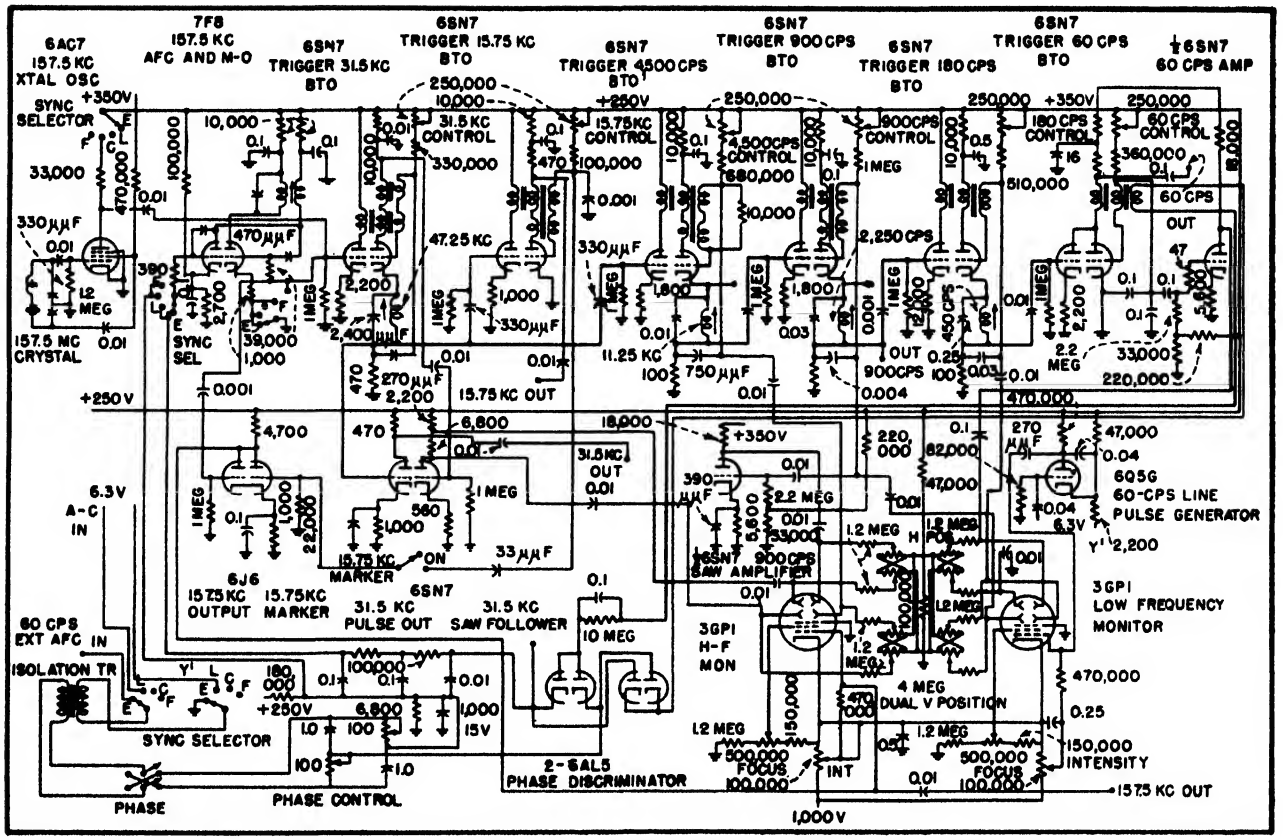

FIG. 2—Timing generator circuits of the Du Mont TA107 A/B sync generator

of the high-frequency monitor whose horizontal time base is 900 cycles. The dots represent the master oscillator or crystal oscillator frequency 157.5 kc. There are five dots along each line or step in the vertical "ladder" indicating a division from 157.5 kc to 31,500 cycles.

The bright dots on the high-frequency monitor correspond to the 15,750-cycle horizontal repetition rate. There are seven steps in each of the ladders, indicating a frequency division from 31,500 cycles to 4,500 cycles; in other words each ladder represents 4,500 cycles. The presence of five ladders for each cycle of the time base points to a frequency division from 4,500 cycles to the time base frequency of 900 cycles.

On the right-hand or low-frequency monitor, the ladder steps represent 900 cycles. Since there are five of them to each ladder, the indication is frequency division from 900 cycles to 180 cycles. The three ladders per cycle of the time base indicate a frequency division from 180 cycles to 60 cycles.

The blanked out section in the middle of the low-frequency scan being derived from the power line further confirms the time base of 60 cycles and indicates synchronism with the line. When the generator is not locked to the 60-cycle power line, the blanked out section moves across the time base. This presentation has been found highly useful in the analysis at a glance of synchronizing generator failures due to improper timing.

The type of blocking oscillator frequency divider circuit used is the cathode - tuned - circuit - stabilized

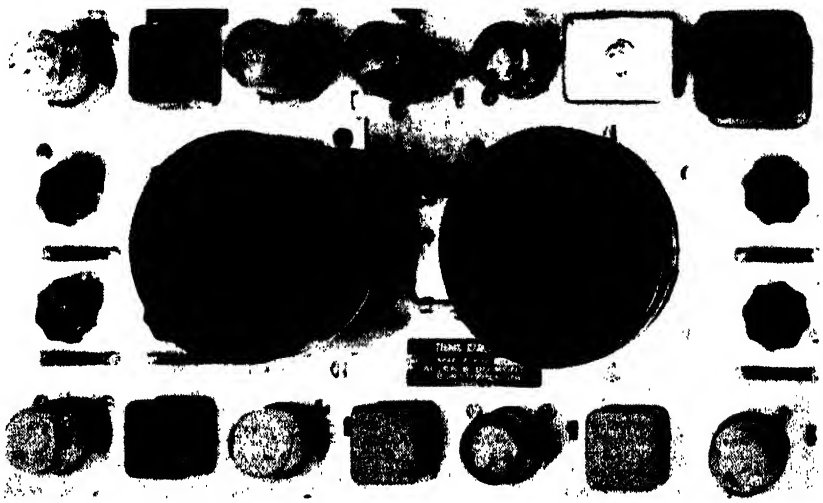

FIG. 3—Presentation of count-down frequencies on cathode-ray monitors

type, Fig. 4. Firing of the blocking oscillator results in a surge of current through the cathode circuit which is normally tuned to a frequency half that of the trigger repetition rate. This results in a ringing of the tuned circuit due to its Q. The cathode voltage wave form is that of a damped sine wave lasting for 2½ cycles (for a 5 to 1 count down) before the blocking oscillator fires again. The grid to ground and the grid to cathode voltage waveforms are shown in the diagram of Fig. 4. As indicated, discrimination is very good against all trigger pulses other than the one producing proper count down.

In the design of the timing circuits, extreme care was taken to minimize any possibility of frequency modulation of the timing pulses. Considerable attention was paid to the chassis layout especially with respect to keeping high level pulse points away from the afc circuit. The blocking oscillator grids are returned to +250 volts giving a steep capacitor voltage discharge waveform and consequently improving freedom from jitter.

The source of B voltage is a double-regulated power supply with an output impedance of less than 0.15 ohm. This eliminates the possibility of extraneous signals modulating the blocking oscillator grid base, a common source of frequency modulation.

The 157.5-kc and 900-cycle outputs of the timing generator are fed directly to the blanking unit for use in the production of a linearity test signal mixed with blanking. The 60-cycle pulse output of the timing generator is routed to the blanking-driving unit and the sync shaping unit for use in the generation of RMA driving pulses, and the low-frequency components of RMA blanking and sync pulses.

To conform to the strict requirements of the RMA recommended synchronizing signal, it is good design practice to use the same signal for the formation of the leading edges of all of the pulses which make up the synchronizing signal. In the synchronizing signal generator under discussion, the leading edges of the equalizing pulses are used to form the leading edges of the horizontal and the vertical synchronizing pulses. This is done by adding a horizontal component and a vertical component, both of which have been delayed a precise time by a lumped LC delay line in the blanking unit, to the equalizing pulses and clipping the result as indicated in Fig. 5.

Two separate delay lines are used, one for the 31,500-cycle signal and the other for the 15,750-cycle signal. Each line consists of 70 π sections with a total delay of 10 percent of the horizontal period or approximately 6.3 microseconds. Provisions are made for tapping connections in any one of the sections in both lines. This permits very accurate shaping of the sync pulses as well as very precise setting of the front porch. Multivibrator stability is in part a function of the trigger pulse rise time. To maintain as short a rise time as practical in the delayed 15,750 and 31,500-cycle trigger pulses, the delay line is designed for a frequency band of over three megacycles. Figure 6 shows the schematic of a single section of the delay line.

Equalizing Pulses

The equalizing pulses shown as *G* in Fig. 5 are generated directly by multivibrator V_{17} in the sync shaping unit, block diagram of Fig. 5. They are amplified and limited by V_{18} and mixed with the other synchronizing signal components in the plate circuits of V_{18}, V_8 and V_9.

Horizontal Pulses

Figure 5 is a timing diagram indicating the synthesis of the composite synchronizing signal from its various components. The horizontal pulses are formed by adding delayed 15.750-cycle pulses to the equalizing pulses, amplifying, limiting and keying-out undesired 31,500-cycle pulses. The result before final clipping is shown at *U* of Fig. 5.

Tube V_1 in Fig. 5 is the horizontal pulse multivibrator whose output (*O* in Fig. 5) is permitted to clear through V_2 only during the horizontal pulse interval.

The 15,750 cycle pulses (*Q* in Fig. 5) are then amplified and limited in V_8 and mixed in the common plate circuit of V_{18} and V_9 with the vertical and equalizing pulse components of the composite synchronizing signal.

The first and last sections of *U* in Fig. 5 show the horizontal component of the mixed signal at V_9. The raised portion of this component indicates the overlap between the equalizing pulse and the delayed horizontal pulse. This is later clipped off in limiters V_9 and V_{10} as

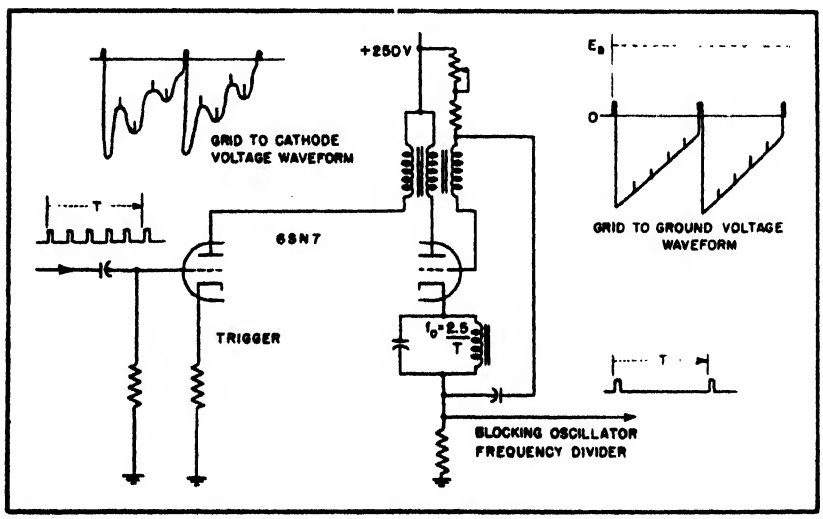

FIG. 4—Cathode-stabilized blocking oscillator frequency divider

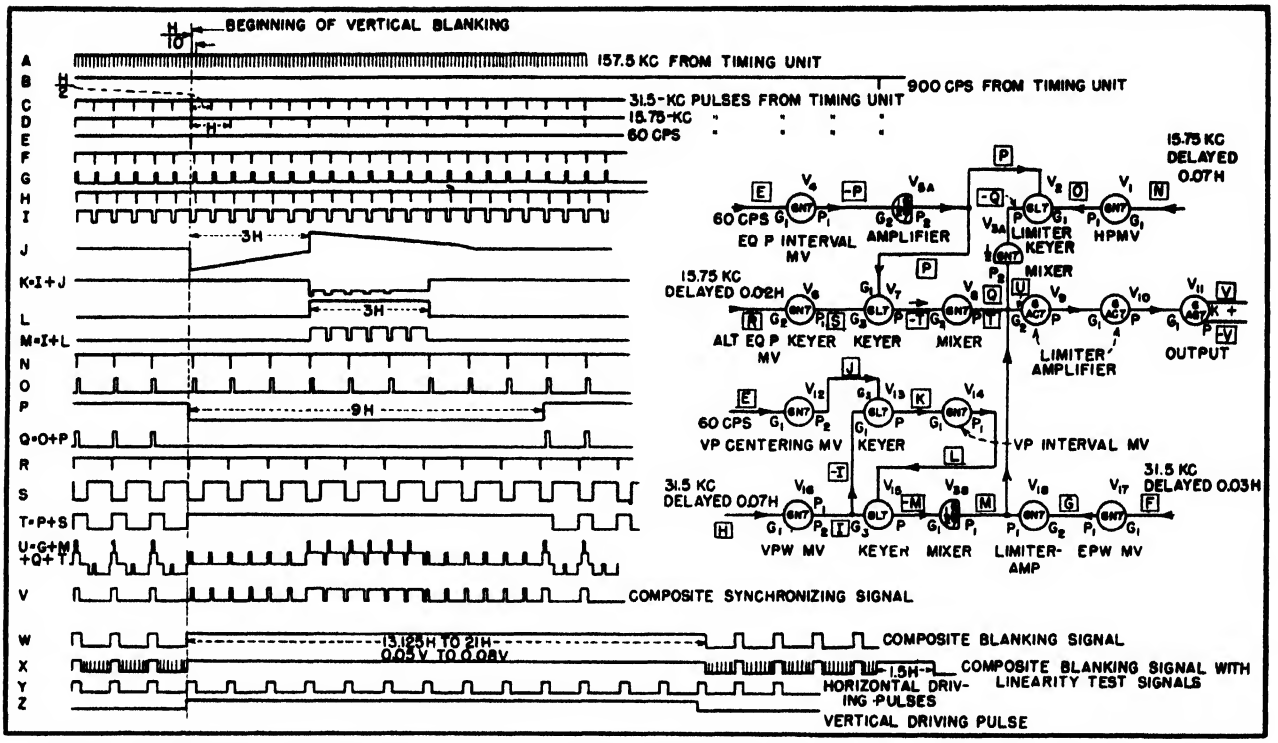

FIG. 5—Timing diagram shows the formation of the composite synchronizing signal and block diagram of sync shaping unit

shown in the first and last sections of V in Fig. 5.

The keying out of the horizontal pulses during the equalizing pulse interval is accomplished by the gating of keyer tube V_3 by pulse P in Fig. 5 derived from the equalizing pulse interval multivibrator V_4 through amplifier V_5. The elimination of unwanted equalizing pulses is obtained by first pushing them down into a region lower than that of the desired horizontal pulses by means of 15,750-cycle pulses shown as T in Fig. 5 and later removing them by clipping. Waveform T is derived from the alternate equalizing pulse keying multivibrator V_6 through keying tube V_7 and amplifier-limiter V_8. The pushed down equalizing pulse is shown in the first and last sections of U in Fig. 5.

The elimination of alternate equalizing pulses must not take place during the equalizing pulse interval. For this reason keying tube V_7 by means of the equalizing interval pulse P permits the alternate equalizing pulse keying signal S to be applied only during the horizontal pulse interval. The output of V_7 is T in Fig. 5. The duration of the horizontal pulses in the output signal V is 8 percent of H ($+0$ -1 percent).

Vertical Pulses

The vertical pulses in the composite synchronizing signal consists of a group of six at a 31,500-cycle rate. The group repeats itself once each scanning field, see center section of V in Fig. 5. The duration of each pulse is 43 percent of H where H is the line period and the group must appear during the vertical blanking interval between the first and second group of six equalizing pulses.

The timing of the vertical pulse interval is determined by the trailing edge of a pulse, J in Fig. 5, three lines wide from the 60-cycle vertical pulse centering multivibrator V_{12}. The vertical pulses are generated at a 31,500-cycle rate in the vertical pulse multivibrator V_{13}. These are shown at I in Fig. 5. One of its pulses, upon coincidence with the trailing edge of the vertical centering pulse K, is permitted by keyer tube V_{13} to trigger the vertical pulse interval 60-cycle multivibrator V_{14} whose pulse width is normally set equal to three horizontal lines or the interval required by six vertical pulses at the 31,500-cycle rate.

Waveform L in Fig. 5 is the output of V_{14}. The vertical pulse interval gate, in turn, permits the vertical pulses to be amplified by keyer tube V_{15} only during the vertical pulse interval. The result is M in Fig. 5. In turn, the six vertical pulses during the vertical pulse interval are amplified and limited by tube V_8 and appear in the common plate circuit of V_5, V_8 and V_{15}. Thus, into a common plate load are fed the horizontal pulses during the horizontal pulse interval from tube V_5, the equalizing pulses during the equalizing pulse interval from tube V_{15} and the six vertical pulses dur-

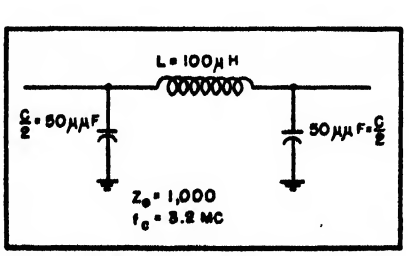

FIG. 6—Single pi section of delay line

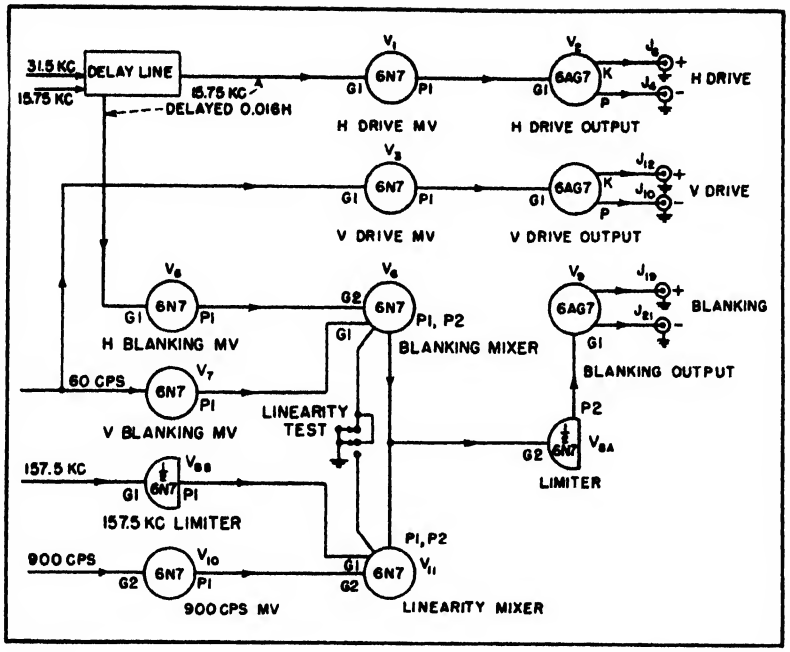

FIG. 7—Functions of stages in the blanking-driving unit

ing the vertical pulse interval from tube V_8. The mixed signal, U, is amplified and limited by V_9 and V_{10} and appears at the cathode and plate of output tube V_{11} as a positive and negative composite synchronizing signal. Figure 5 shows the final sync output signal at V.

The block diagram of the blanking-driving unit is shown in Fig. 7. The 15,750-cycle pulses trigger the horizontal blanking multivibrator V_5 whose output is fed into blanking mixer V_6. The 60-cycle pulses trigger the vertical blanking multivibrator V_7 whose output is fed to the grid of the second triode of blanking mixer V_6. In the blanking position of the linearity test switch, the mixed vertical and horizontal blanking signals are limited and amplified in tube V_{9A} and applied to the grid of blanking output tube V_9. At the cathode and plate of output tube V_9, appear respectively the positive and negative composite blanking signals.

The 157.5-kc signal derived from the timing generator is amplified and shaped in V_8 and mixed in V_{11} with the 900-cycle pulse derived from multivibrator V_{10}. In the *blanking and linearity bars* position of the linearity test switch, these are inserted into the blanking signal in the common plate load of blanking mixer V_6 and linearity mixer V_{11}. The mixed blanking and linearity test pulses are clipped in limiter V_{8A} and applied to the grid of output tube V_9. In this position of the switch the output signals at J_{19} and J_{21} consist of the composite blanking signal mixed with vertical and horizontal linearity signals. In the *linearity bars* position of the selector switch only linearity test signals are permitted to appear at the blanking signal output jacks. Figure 8 shows a test pattern generated by an iconoscope film chain driven by the sync generator. The linearity test switch is in the *blanking and linearity bars* position.

The horizontal driving pulses originate in the 15,750-cycle multivibrator V_1 and are directly applied to the grid of the horizontal drive output tube V_2. They appear as positive and negative horizontal driving signals respectively at J_6 and J_4. In a similar manner the vertical driving pulses originate in the 60-cycle multivibrator V_3; the output is applied directly to the grid of vertical output tube V_4. Vertical driving pulses appear in positive and negative polarity at jacks J_{12} and J_{10}. At Y and Z of Fig. 5 are shown the waveforms of the horizontal and vertical driving pulses produced by the circuits.

Power Supplies

The high-voltage supply is used to provide the accelerating potential for the cathode-ray tube monitors in the timing generator.

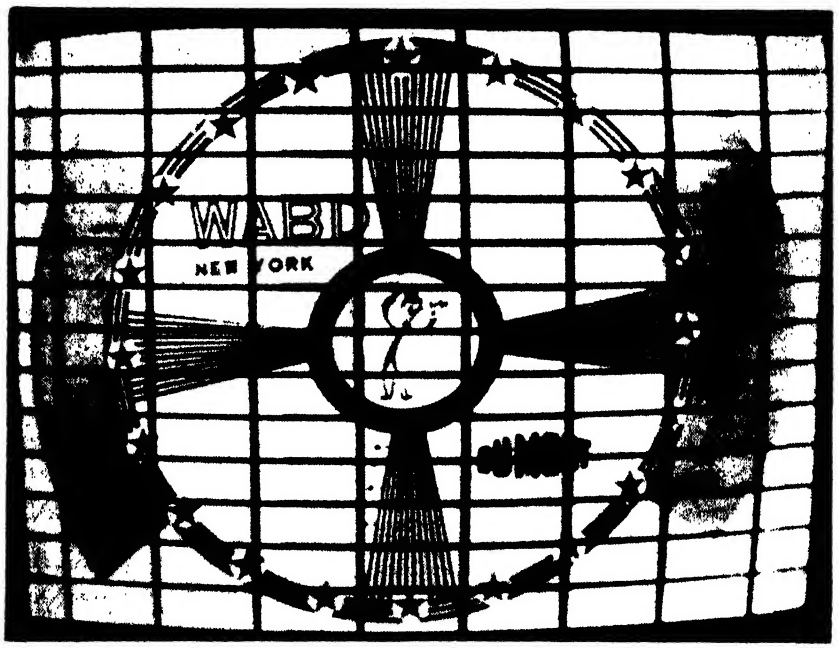

FIG. 8—Camera chain output picture signal with the linearity test switch of sync generator set at blanking and linearity bars for adjustment of monitor sweep linearity

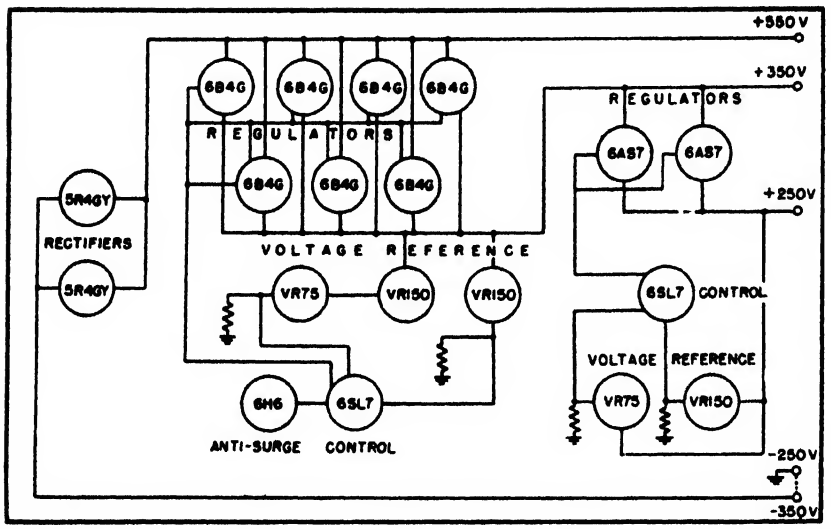

FIG. 9—Block diagram of low-voltage power supply

A double-regulated low-voltage supply is used to provide 250 volts and 350 volts for the three signal units. This supply has an output impedance of less than 0.15 ohm at 1,000 cycles. The change from no load to full load at 400 milliamperes results in a change of only 0.1 volt at the output. A block diagram of the low-voltage supply is shown in Fig. 9. Transients from the ordinary power supply filter circuit are eliminated by use of an "electronic choke" in the form of a first regulator for the 350 volts ahead of the final regulator for the 250 volts.

A number of these synchronizing generators have been in operation during the past two years with excellent results.

Acknowledgment

Acknowledgment is made to the following men of the Du Mont Laboratories who took part in the development and product design of the synchronizing generator: H. Beste, L. Durgin, C. Quirk and L. Spooner, and to N. Accardo and M. Demeyer, who aided materially in the test of models.

Counter Circuits for Television

Basic step-type counter circuit is analyzed to determine design criteria. Its limitations, possible improvements and the relationships between parameters that govern the most stable operation are discussed

By ALLAN EASTON and PAUL H. ODESSEY

STEP-TYPE counter circuits are widely used as frequency dividers in the design of television synchronizing generators where stability of division, accuracy of phase and freedom from jitter are of paramount importance. Mention will be made of some artifices for increasing the stability and frequency-division product.

The basic circuit arrangement of the step-type counter is shown in Fig. 1A. It contains a source of periodic pulses (all of equal height) at a frequency f_o, the step-type counter, and a discharge device operating at a frequency f_o/n. The counter circuit shown consists of two capacitors and two diodes.

When a positive pulse is impressed between terminals *A-O*, capacitors C_1 and C_2 are charged through diode V_1. During this interval V_2 is nonconducting. As the charging time constant is usually very small, both capacitors attain the maximum charge in a relatively short time and the impressed voltage, E_p, is divided between the two capacitors in a definite manner. When the individual impressed pulse decreases in voltage from E_p to zero, capacitor C_1 is discharged through the input circuit by means of diode V_2, while C_2 is prevented from losing its acquired charge by the fact that V_1 is nonconducting during this part of the cycle.

A second impressed pulse will deposit an additional increment of charge on C_2. Thus, corresponding to a regular succession of impressed pulses, the voltage across C_2 builds up step-wise and approaches, asymptotically, the value of the impressed voltage E_p, unless interrupted by the discharge device which discharges C_2 completely and causes the process to begin anew.

The manner in which the voltage builds up on capacitor C_2 is shown in Fig. 2 for three values of the ratio C_2/C_1. Curve *A* illustrates the case where the ratio is relatively low resulting in large steps of voltage initially and then smaller incremental changes as the count approaches the desired order of division, in this instance, five to one. Curve *C* illustrates the case where the ratio is relatively high and indicates an almost uniform, but very small, incremental change in capac-

itor voltage from the first to the n^{th} step. Curve *B* represents the charging curve using optimum parameters, and differs notably from curves *A* and *C* in that the n^{th} or fifth step is much greater than in either of the other cases, and is the maximum value possible.

From the practical point of view, greatest stability of a step-type counter is attained when the voltage increment corresponding to the n^{th} step of capacitor, C_2, voltage is a maximum. Graphically, this corresponds to the point of maximum slope of the charging envelope at the specified order of division. Thus, in curve *B* the last increment of voltage is larger than are those of curves *A* and *C*. This condition of stability arises from the fact that it is the n^{th} increment of voltage which is utilized to actuate or trigger the following discharge circuits.

The conditions for obtaining the maximum increment, the size of that increment, and the magnitude of the voltage across C_2 when the n^{th} increment is reached, are all of importance when the designer wishes fullest utilization of the step-type counter.

In the basic circuit, Fig. 1, the increment of voltage appearing across capacitor C_2 (initially without charge) corresponding to the first of a series of narrow impressed pulses of equal magnitude, is:

$$e_1 = E_p \frac{C_1}{C_1 + C_2} \quad (1a)$$

or $$e_1 = E_p K \quad (1b)$$

where $$K = \frac{C_1}{C_1 + C_2}$$

E_p = magnitude of impressed pulses; e_1, e_2, e_3, . . . = increment of voltage corresponding to first, second, third, . . . pulses.

The second increment of voltage is

$$e_2 = (E_p - e_1)K \quad (2a)$$

or

$$e_2 = E_p K (1 - K) \quad (2b)$$

The third increment of capacitor voltage is

$$e_3 = [E_p - (e_1 + e_2)]K \quad (3a)$$

or $$e_3 = E_p K (1 - K)^2 \quad (3b)$$

Similarly the n^{th} increment of voltage across C_2, corresponding to the n^{th} pulse is

$$e_n = E_p K (1 - K)^{n-1} \quad (4)$$

Curves representing Eq. 4 are shown in Fig. 3 for several values of n and clearly indicate the existence of a maximum value of e_n/E_p for each order of division, and that greatest stability may be realized by employing the optimum value of K.

The maximum value of e_n may be determined in the conventional fashion:

$$\frac{de_n}{dK} = \frac{d}{dK}\left[E_p K (1 - K)^{n-1}\right] = 0 \quad (5)$$

from which is obtained the optimum value of K, that is

$$K = \frac{1}{n} \quad (6)$$

Now since

$$K = \frac{C_1}{C_1 + C_2}$$

Then $$\frac{C_2}{C_1} = (n - 1) \quad (7)$$

$$n > 1$$

Substituting the above criterion for maximum into Eq. 4 results in

$$e_{n(max)} = \frac{E_p}{n}\left(\frac{n-1}{n}\right)^{n-1} \quad (8)$$

The total potential E_T to which C_2 is charged at the end of n pulses of impressed voltage is

$$E_T = \sum_1^n e_n = E_p K [1 + (1 - K) + (1 - K)^2 + (1 - K)^3 \ldots (1 - K)^{n-1}] \quad (9a)$$

From the methods of series summation

$$E_T = E_p [1 - (1 - K)^n] \quad (9b)$$

Equation 9B may be transformed into a more familiar form

$$E_T = E_p (1 - e^{n \ln \left(1 - \frac{1}{n}\right)}) \quad (10)$$

Equation 10 is clearly of the same form as the well-known equation for

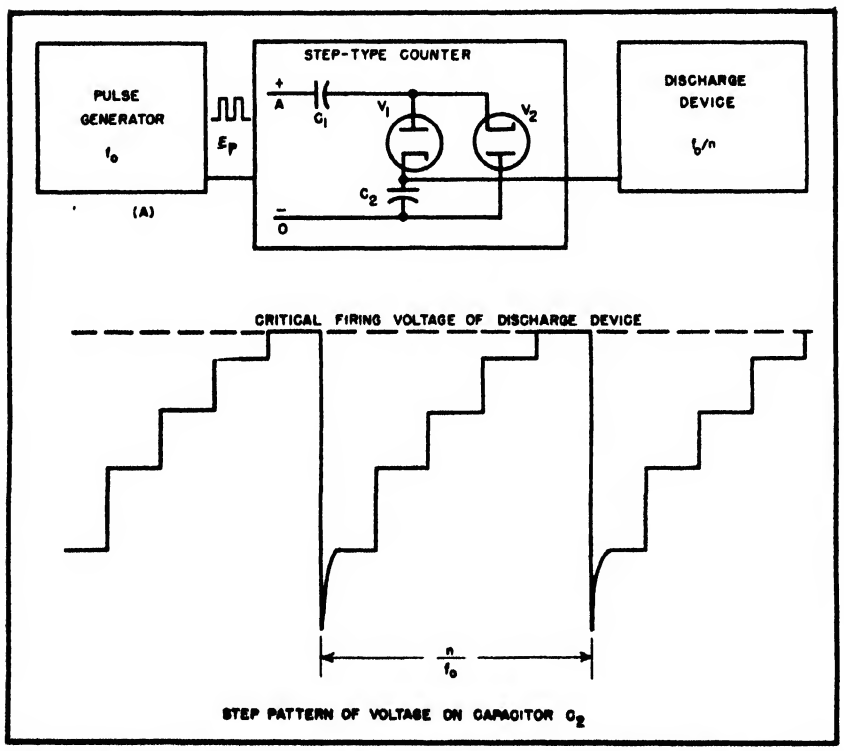

FIG. 1—Elements of the basic counter circuit and output waveforms applied to the discharge circuit

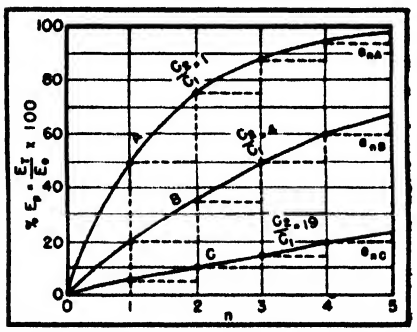

FIG. 2—Charging waveform indicating effect of choice of ratio of C_2/C_1

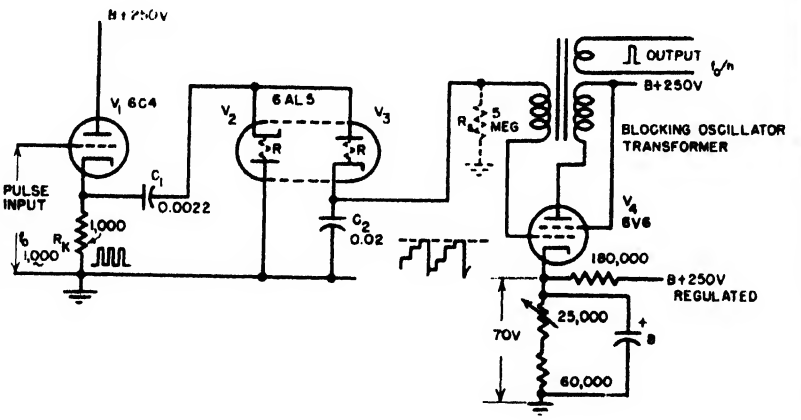

PRACTICAL FREQUENCY DIVIDER CIRCUIT

A typical design of the step-type frequency divider presents the following specifications:

Desired division n	= 10
Initial frequency, f_o	= 1,000 cycles per second
Pulse amplitude, E_p	= 100 volts peak
Pulse width	= 100 microseconds
Critical Firing Voltage	= − 10 volts
Shunt Leakage, R_s	= 5 megohms
Effective series resistance (Source plus diodes)	= 1,000 ohms

A suitable circuit is shown above. Tube V_1 is a cathode-follower pulse source, type 6C4.

Tube V_4 is a 6V6 blocking oscillator.

From Eq. 7

$$C_2 = (n-1)\,C_1$$
$$C_2 = 9\,C_1$$

From Eq. 14

$$\text{Minimum } C_2 = \frac{10n}{f_o R_s} = \frac{10 \times 10}{10^3 \times 5 \times 10^6}$$

$C_2 = 0.02$ microfarad

and $C_1 = 0.0022$ microfarad

With these values, the height of the tenth step will be 3.9 volts and the value of capacitor C_2 voltage about 63 volts. This requires a negative bias of approximately 70 volts on the discharge tube grid. The bleeder circuit in the cathode of tube V_4 can be adjusted to provide the correct bias.

The charging time constant based on an effective series resistance of 1,000 ohms is approximately 2 microseconds.

growth of capacitor voltage in a series R-C circuit, that is

$$E_T = E_p\,(1 - \epsilon^{-\alpha t}) \qquad (11)$$

in which t is replaced by n and minus alpha by the natural logarithm of $1/(1\text{-}K)$.

If the criterion for maximum is substituted into Eq. 10, there results

$$E_T = E_p\left[1 - \left(\frac{n-1}{n}\right)^n\right] \qquad (12)$$

Examination of Eq. 12 indicates that when optimum conditions are employed, E_T is always less than E_p, in fact

$$0.75\,E_p \geq E_T > 0.636\,E_p \qquad (13)$$

The curves in Fig. 4 summarize the relationships derived thus far.

The analysis presented to this point has stated an optimum value of the ratio of C_2 to C_1. However, knowledge of this ratio is not enough, since the magnitudes of the two capacitors have not yet been determined. Practical circuit considerations dictate the maximum and minimum values which may be assigned. The important factors which limit the choice of values are as follows: (1) The leakage resistance shunting C_2; (2) The perveance of the diodes; (3) The effective resistance of the pulse source; (4) The stability of the power supply; (5) The stability and resettability of the discharge device; (6) The recovery time of the discharge device; (7) The stability of the pulse source; (8) The highest and lowest frequency of operation; (9) The width of the impressed pulses; (10) The minimum phase shift permissible between input and output pulse; (11) The minimum jitter permissible between input and output pulses.

Every practical circuit has intimately associated with it leakages, which in this case may be represented as a definite resistance R_s shunting the storage capacitor C_2. The effect of R_s is to partially discharge C_2 in the time between successive steps. If the frequency $f_o/_n$ is low, C_2 must, of necessity, be made large, so that the shunt discharge time constant, R_sC_2, will be sufficient to maintain the charge on C_2. The appearance of the step wave form with a short time constant is shown in Fig. 5. A good rule of thumb is to make C_2 sufficiently large, so that the discharge time constant, R_sC_2, is at least ten times the period of the lowest operating frequency. That is

$$R_sC_2 \geq 10\,\frac{n}{f_o} \text{ seconds} \qquad (14)$$

It was assumed in the earlier analysis that the time for C_2 to acquire an increment of charge is negligibly small. Actually, this may not always be the case, as the series resistance of the pulse source and the perveance of the diodes will slow up the rise time appreciably. Figure 6 shows the wave form during the charging interval at the n^{th} increment.

The finite rise time has two undesirable effects. It prevents the

increment of charge from ever reaching the value predicted by Eq. 8 during the charging interval, especially if narrow pulses are used. This effect reduces the apparent pulse voltage by some definite amount and thereby makes the frequency division somewhat dependent on pulse width and operating frequency. A satisfactory design rule which produces a negligible loss in voltage because of charging time constant is to make the series time constant less than ten percent of the pulse width.

A more important difficulty introduced by the finite rise time is the irreducible phase delay. Phase delay, in itself, may not be objectionable in many designs, but what is troublesome is the jitter resulting from minute fluctuations in pulse height and power supply variations. The net effect is to cause slight shifts in the time of firing of the discharge device. The series charging time constant of the R-C circuit, made up of the source resistance, diode resistance, C_1, and C_2 should be very small. This requirement dictates the use of high-perveance diodes, low-impedance pulse sources and minimum values of C_1 and C_2.

Earlier in this discussion it was stated that periodically capacitor C_1 was discharged by means of diode V_2 through the pulse generator impedance. Consideration of the time intervals involved as well as the circuit constants shows that this statement is only approximately correct. It takes an infinite time to discharge C_1 completely; a finite time to reduce the voltage across C_1 to some predetermined value. The effect of this residual charge is to oppose the pulse voltage which is trying to produce voltage increments on C_2. This effect becomes more pronounced as the pulse width is increased or as the pulse repetition frequency is raised; that is, as the duty cycle is made larger. The cumulative result is to make the stability of division dependent upon frequency and pulse duty cycle. To minimize this phenomenon, C_1 should be chosen as small as possible and the circuit resistance held down.

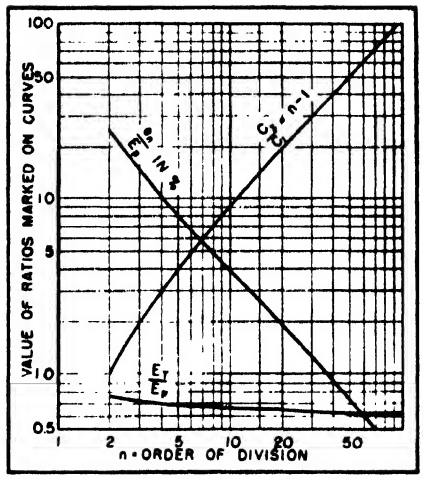

FIG. 4—Set of design curves for diode counters

The recovery time of the discharge circuit places an upper limit on the frequency of operation; but many suitable discharge circuits are known to the art, so that a suitable one can be selected for the particular frequency range.

It has been shown that low-frequency considerations dictate large values of the counter circuit capacitances, whereas high-frequency work requires just the opposite. Evidently, the designer must reconcile the conflicting requirements and effect a suitable compromise.

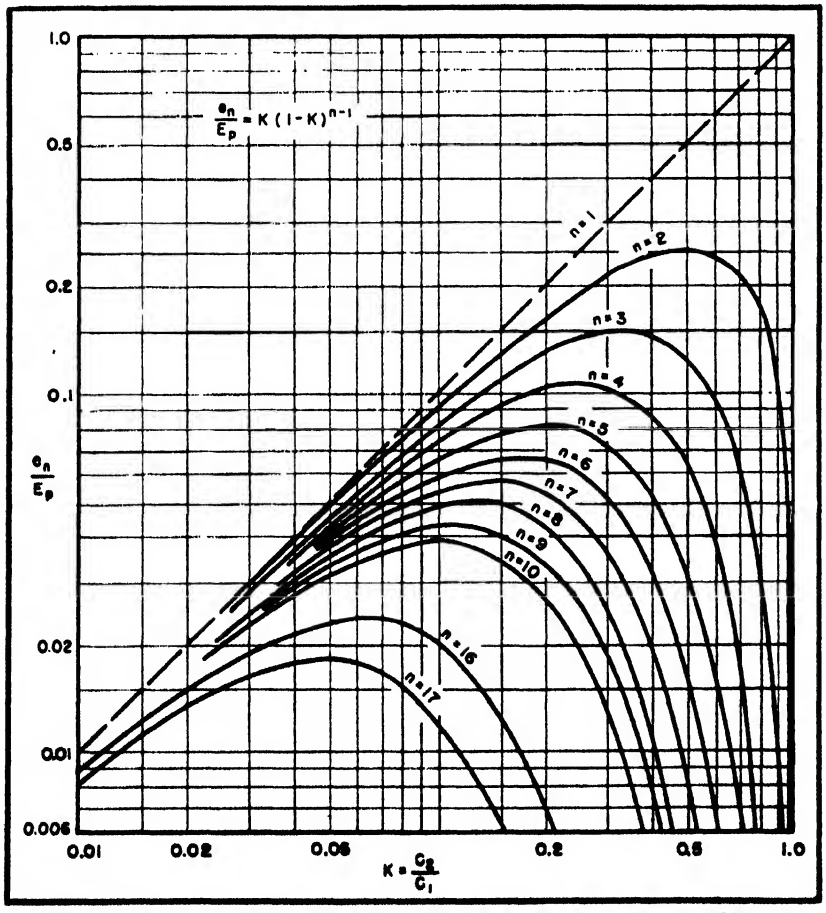

FIG. 3—Curves of various values of n for determining the optimum value of K

Conclusions

Having achieved the optimum choice of circuit parameters, the maximum order of frequency division which may be attained with good stability depends upon the amplitude of the n^{th} increment of voltage on capacitor C_2 and on the nature of the discharge device. The previous analysis has shown that as the magnitude of n is increased, the size of the step decreases to the point where the discharge device may trigger erratically because of noise, line voltage fluctuation, or

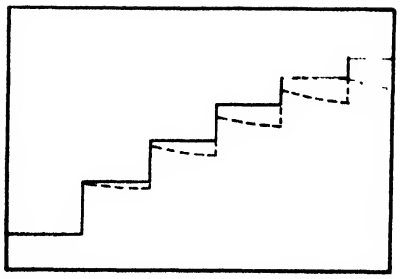

FIG. 5—The solid line represents the normal charging waveform and the dashed line shows the effect of shunt leakage across C_1.

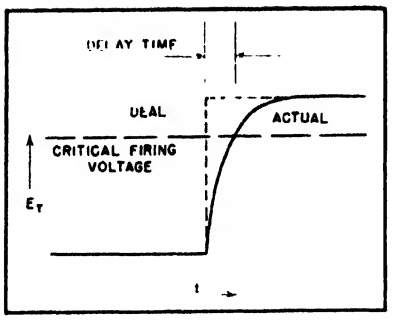

FIG. 6—Effect of finite rise time in producing delays between initiating pulses and output pulses. Small changes in pulse height or of critical firing voltage will cause changes in delay time, causing jitter in the output pulses

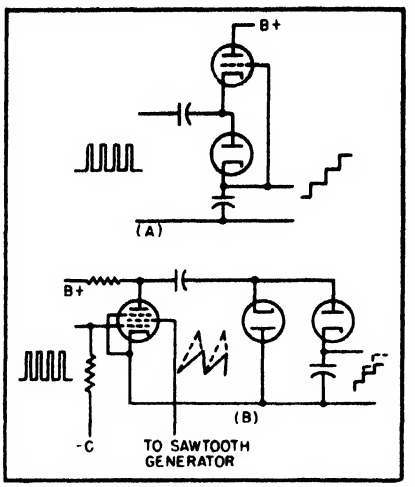

FIG. 7—Two proposed circuits for improving counter stability. Shown at *A* is the Hallmark system using a triode for linearization of the staircase charging curve. In circuit *B*, a sawtooth waveform on the screen grid of a pentode driver tube causes the transconductance of the tube to rise with time, and cause heights of steps to increase instead of decrease. By proper selection of waveform of screen grid voltage, any type of charging characteristic may be obtained

power supply ripple. Thus, the size of the n^{th} step must be sufficiently large to make negligible these inevitable disturbances. Some allowance must also be made for ageing of the circuits which may change the operation and critical firing voltage of the discharge device.

The curves in Fig. 2 show that the envelope of the charging curve of capacitor C_2 voltage is an exponential function of the form

$$y = K(1 - \epsilon^{-\alpha t})$$

where K and α are constants. One of the inevitable characteristics of such a function is that successive increments of y must become progressively smaller as time elapses. As shown for a count of ten to one the size of the n^{th} step cannot exceed approximately 3.9 percent of the impressed pulse voltage. To improve the stability of counter performance, some means for making the tenth step larger than 3.9 percent of E_p is needed. Graphically, the envelope of the charging curve must be made less concave downward, perhaps more closely linear, or best of all, concave upward. At the same time, the charging curve should attain the same or even greater value at the end of n steps than does the normal curve.

Several methods are known for accomplishing the desired distortion of the charging curve. Figure 7 shows some of the possible methods. In a particular design, the availability of auxiliary pulses and waves will suggest other methods of approach.

Television Receiver Laboratory

Design of test facilities, shielding, and filtering for a development laboratory. An oscilloscope adapter, line-isolating amplifiers, safety boxes for c-r tubes and the construction of the shielded room are among the features

By FRANK R. NORTON

The first essential equipment of a television laboratory is a television synchronizing generator, preferably one complying with RMA standards[1]. The second major requirement is a dependable source of picture signals such as those obtained from a monoscope or other test pattern which remains fixed while adjustments are made and which can always be used to observe the geometric distortion, resolution, contrast, focus and general quality of the received picture.

An electrical bar or grating pattern generator is needed to accurately and rapidly adjust sweep linearity. The pattern generator signals provide a grating of horizontal and vertical bars accurately spaced in time. Thus their distances apart on the picture screen show the sweep speed averaged over each time interval between bars. The pattern can be chosen so as to produce squares when the aspect ratio is correct and then the linearity and amplitude of the sweeps can be quickly adjusted.

A monoscope camera includes an amplifier which mixes blanking signals with the picture signal. Either its output or that of some

other camera or picture signal source is then put into a line amplifier where sync pulses are added to produce a standard RMA composite picture signal. This composite video signal should then be monitored by a laboratory picture monitor and a waveform monitor. For complete receiver testing, a laboratory television transmitter is necessary if locally broadcast picture signals are not available.

A noise generator to provide a known and controllable amount of various types of noise, such as thermal noise, but more particularly impulse noise similar to ignition noise, is also needed to permit study of noise limiting and sync interference and other important receiver characteristics.

All the RMA sync generator outputs are made available both on the central racks and at seven line-isolation amplifiers mounted in boxes on the wall above the benches at convenient locations around the laboratory. These locations are connected through RG 59/U coaxial lines to the central racks. The coaxials and d-c power connections for each line-isolation amplifier are run in ducts mounted along the walls near the ceiling with branches down to each box. From each box two coaxial cables run directly to the central panel. Signals can be sent from any part of the room to any other location by making a suitable connection at the jack panel. This saves time and avoids having lines remain on the floor.

A small broadband scope near the racks is used as a waveform monitor and doubles as a test oscillograph. However, it is desirable to have a rack-mounted waveform monitor which is always available when needed.

The test transmitter is crystal controlled for the desired channel. The output stage uses a grid-modulated 832A tube with a 2-inch c-r monitor directly connected to the plate coil. A balanced mutual-inductance type attenuator is used, giving a continuously adjustable output from 100,000 to 1 microvolt with a direct-reading dial. This balanced output appears on two coaxial jacks, at an impedance level of 50 ohms to ground from either side, or 100 ohms from side to side. This is very convenient in receiver testing.

Line-Isolation Amplifiers

The line-isolation amplifiers shown in the schematic of Fig. 1 have five type 6J6 tubes, one for each of the five independent circuits. Both plate and cathode-coupled outputs (either polarity of the applied signal) are available at coaxial jacks on the front of the box. The first three circuits are intended for pulse signals such as sync, blanking, camera driving, and the last two for composite picture signals or camera output signals. Slightly different circuit values were used for convenience.

The polarity of the input signals on the first and last circuits are black negative so the output jacks are marked — on the cathode and + on the plate to indicate the output signal polarity. The middle three circuit jacks are marked with the + on the cathode and — on the plate to indicate whether the output is the same or the opposite polarity from the applied input.

The maximum output level is about 0.5 volt peak-to-peak if compression is to be avoided. This level is often insufficient, but a few booster amplifiers used on the bench as needed have been found satisfactory. Other engineers may prefer to use more distribution amplifiers whose outputs can be patched from central racks to any location desired. This line-isolation amplifier system provides a multiplicity of outputs always available at each location. Larger output tubes were not used because the total B current drain of the isolation amplifiers would become excessive.

The coaxial line to the amplifiers is looped into one after another, the amplifier inputs being simply bridged across the line except at the last amplifier, where the line must be accurately terminated to avoid reflections which may become serious if there is an appreciable mismatch. A small coaxial cable of the length used here has about 3-db loss at 5 mc. The output of the amplifiers is practically flat to beyond 5 mc except for the line loss, which is not serious since the phase response is excellent.

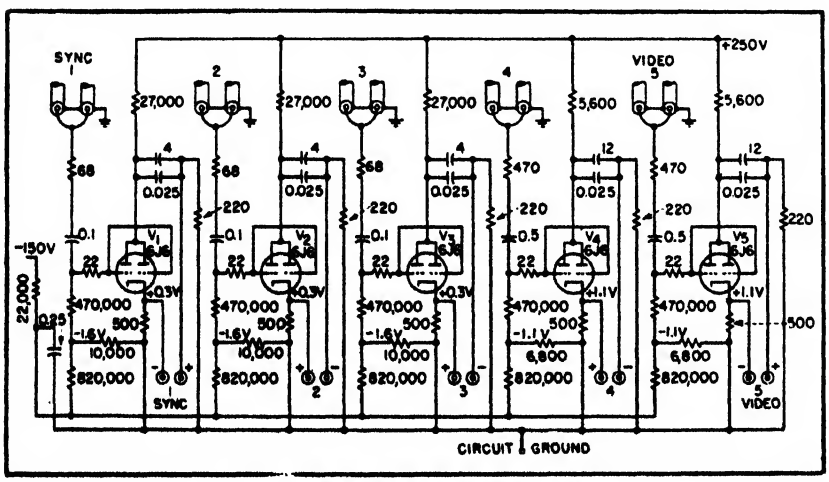

FIG. 1—Circuit of line-isolation amplifier

Oscilloscope Adapter

A scope adapter may be conveniently used with any broad-band oscilloscope to increase its utility in television development work. Its schematic diagram is shown in Fig. 2. The adapter is used to supply a 60-cycle calibrating voltage to the input probe to compare in amplitude with the signal under test, and to supply a variable sweep voltage to provide sufficient sweep velocity to view only a few lines of a television

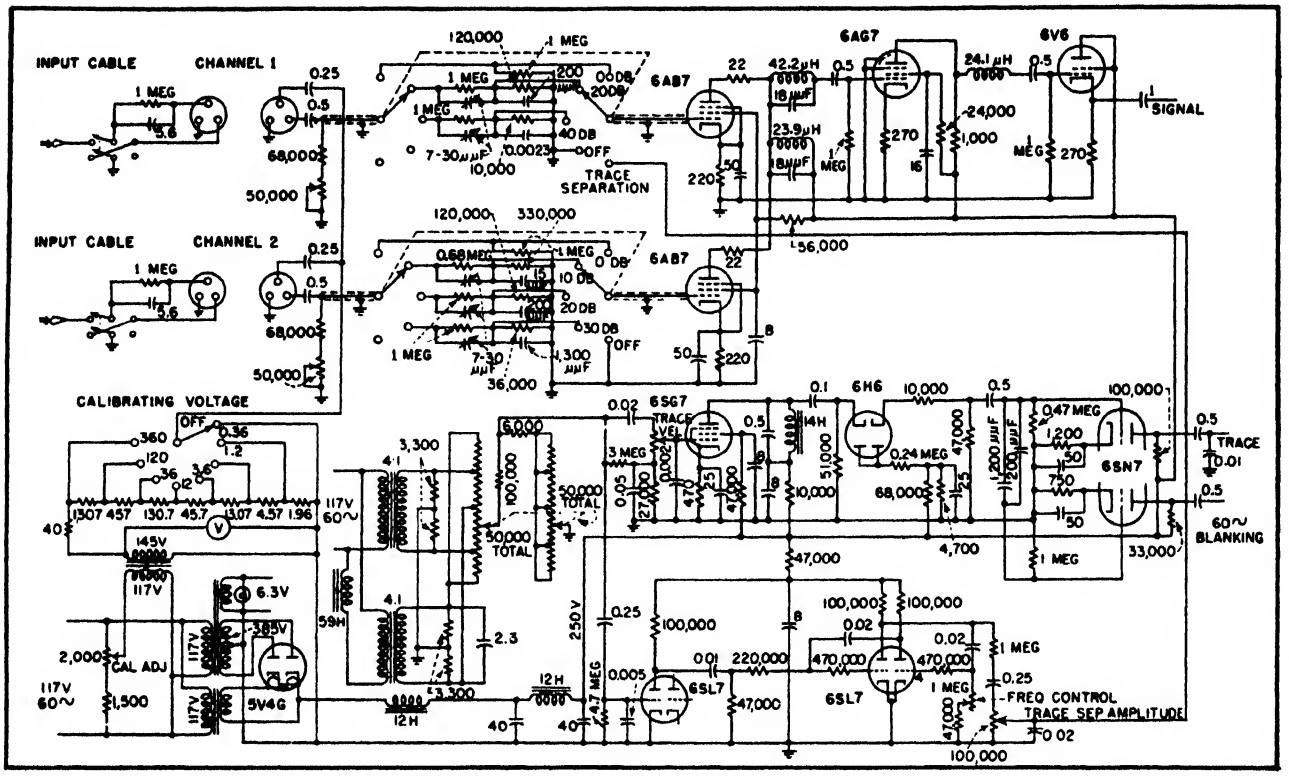

FIG. 2—Circuit of oscilloscope adapter

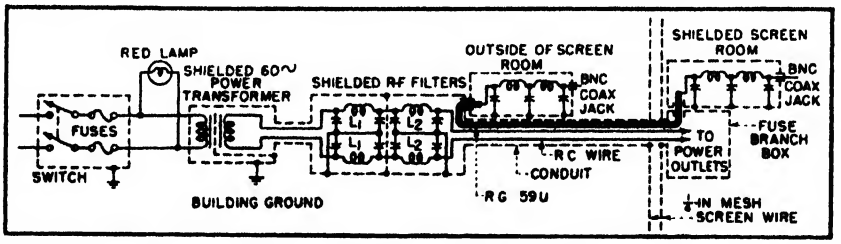

FIG. 3—Power line and video input filters for the shielded room

signal. This is also adjustable in phase; any desired portion of the signal may be expanded for close examination. The unit also provides a double trace on the oscilloscope at a 30-cycle rate for study of the interlace of a television signal, and provides a broadband (6-mc) video mixing amplifier with two inputs.

The sweep-voltage waveform is a trapezoid, produced from a 60-cycle sine wave which is adjustable in phase over about 360 degrees. The slope or velocity may be varied to allow only a few lines of a television signal to be viewed if desired. Blanking for the oscilloscope is produced by differentiating the sweep to avoid bright spots on the screen where the beam would otherwise dwell during the time between the fast sweep intervals.

In using the unit, compression of the positive trace may occur due to nonlinearity in the amplifier if the trace separation is widened too far. The phase shifter is quite satisfactory but an autosyn resolver would give even more constant output amplitude and make it possible to adjust the phase continuously in any direction. The present arrangement is limited to 360 degrees and has a slight variation in amplitude with phase.

The screen rooms are somewhat unusual in that hardware cloth with ¼-inch mesh is used for both the inner and outer screens on the usual wooden 2 × 4 frames. The relatively open mesh permits excellent interior illumination by fluorescent light fixtures suspended just over the enclosure, thus eliminating any radio interference due to them and not loading the special filtered power circuit to the room. The open mesh also permits a free circulation of fresh air from an anemostat over the screen room.

The galvanized steel wires of the hardware cloth are bonded at every intersection, and it is believed that the efficiency of the screen in eliminating radio interference will be higher over a period of years than for a fine mesh copper screen, which is likely to corrode in time and cause poor contact between wires.

In constructing the rooms, care was exercised to solder all joints in the hardware cloth. Joints around the door between the screen on the door and that on the main frame are doubly sealed by bronze weather-stripping on both the door and the frame, on both the inner and outer sides. No connection anywhere between the inner and outer screens was permitted except for the single conduit which carries power wires and coaxial cable circuits.

A schematic of the filters for one

of the screen rooms is shown in Fig. 3. With this arrangement the screen room provides more than 70-db attenuation anywhere within the room with respect to a signal level measured just outside the room, throughout the frequency range from 20 to 250 mc.

The main power fuse and switch box for each room is mounted outside the door, with a red lamp to indicate when the power is on. The 60-cycle shielded transformer and all the wiring are enclosed in metal boxes or conduit. A motor-driven voltage regulator supplies a constant 117 volts.

The two r-f filter sections are made resonant at widely different frequencies, and seem to be quite effective throughout the spectrum. Chokes L_1 and L_2 in the r-f filters are multiple-layer solenoids wound with large rectangular wire to avoid heating and keep the line voltage drop low.

Two coaxial lines into the screen room (only one is shown in the schematic) have 15-mc low-pass filters in small boxes on both the outside and the inside of the room. Thus any video signals (including color picture signals) can be transmitted without distortion of the signal and without any interference being introduced into the screen room at present television i-f or carrier frequencies.

The author wishes to acknowledge the contributions made by many engineers and technicians associated with him, particularly those of W. B. Wilkens and J. E. Mackenzie, and the encouragement and assistance of A. C. Omberg, chief research engineer.

References

(1) Report of Sub-Committee on Studio Facilities of Committee on Television Transmitters, Dec. 4, 1946 and drawing, Recommended Synchronizing Generator Waveforms, Oct. 9, 1946. RMA Data Bureau.

(2) Report of Sub-Committee on Studio Facilities, (above) and drawing, Picture Line Amplifier Standard Output, Oct. 9, 1946. RMA Data Bureau.

Television Resolution Chart

Designed for the purpose of standardizing television resolution measurements, the chart illustrated overpage has been made available to the industry by the RMA

CALIBRATION of the chart illustrated is based on a height of 18 inches and a width of 24 inches, which is the size supplied by the RMA Data Bureau. For transmitter checking, the chart should be televised by the studio equipment and reproduced on a suitable picture monitor.

Resolution is to be read only after equipment has been adjusted to have a minimum of distortion; by checking scanning, shading if system employs shading, low-frequency phase shift, and focus.

Procedure

After these adjustments, note the maximum gray scale reading (for perfect adjustments, reading should be same on all four scales), and then take maximum resolution (horizontal and vertical) readings on the large wedges in the central portion of picture; and on the small wedges in circles at corners. For example, read the horizontal resolution from the wedges located vertically on the chart, and read the vertical resolution from the wedges located horizontally on the chart. A measure of maximum resolution should be accompanied by a statement of the number of the distinguishable gray steps (for example, 400 lines—steps 2, 3, 4, 5 and 6).

The maximum resolution reading will indicate system performance. The least of the maximum resolution readings (usually found in picture corner) will indicate the system degradation due to failure in achieving optimum results for one or more of above adjustments or due to inherent c-r tube distortion.

To Check Scanning

The scanning adjustment involves size, linearity, and aspect ratio.

Focus the chart on the camera tube so that its area (boundaries determined by arrow heads) exactly covers the usable area scanned by the camera.

Check vertical sweep linearity by comparing the spacing of the short horizontal bars at both top and bottom of picture with that of the bars midway between.

Check horizontal sweep linearity in a similar manner by comparing the spacing of the vertical bars in the square at each side of picture with that of the bars in the center square.

Check aspect ratio by measuring the large pattern formed by the gray scales to see if it is a square. If the horizontal and vertical scanning is linear and the above pattern is square, the aspect ratio is correct.

To Check Shading

If camera employs shading, check by visual inspection of the picture monitor to determine if the background is an even gray, or use the waveform monitor and note if the average picture signal axis is parallel to the black level line both at line and field frequencies. As an additional aid in correcting the shading, adjust same until the gray scale reading is the same (and a maximum) for all four scales.

Streaking following either one of the two horizontal black bars at the top or bottom of the large circle is an indication of low-frequency phase shift.

Two checks are required: camera lens focus and cathode-ray beam focus (camera tube and receiving tube). Cathode-ray beam focus adjustments are made for a maximum resolution reading, first of the horizontal scanning and then of the vertical. Due to beam characteristics a maximum adjustment for one may not be the maximum adjustment for the other; in this event a compromise adjustment is used.

Miscellaneous Chart Information

All bars for checking sweep linearity are spaced for 200 lines resolution.

One of the wedges for checking horizontal resolution is calibrated in both lines and megacycles to facilitate equipment checking.

The gray scale is composed of ten steps varying in an approximate logarithmic manner from maximum white brightness to approximately 1/30 of this value. This scale may be used in connection with a waveform monitor to check the transfer characteristic of the system.

The four diagonal lines in the square may be used to check quality of interlacing. A jagged line indicates pairing of the interlaced lines. (Not effective when interlace failure is 100 percent).

The circumference of each of the four small circles is tangent to an imaginary circumference at the point nearest the corner of the chart. The radius of this imaginary circle is 4½ inches (on the full-size chart), and is located along a line bisecting the corner angle of the chart. (This is to indicate the part of corner masked off by some television receivers.) The corner circles should be visible on a receiver whose picture corners are masked.

The resolution circles in the center of the pattern and in the center of the corner resolution wedges are for testing spot ellipticity on cathode-ray picture tubes (useful to tube manufacturers). The resolution of the circles in the corners (150) was made less than the resolution in the center (300) because of added deflection defocusing in these areas.

Table I—Line Calibration of Resolution Wedge. Based on 18-inch Chart Height

No. of Lines	Width per Line	Width of 9 lines	Width of 19 lines
200	0.090″	0.810″	1.71″
250	0.072″		1.37″
300	0.060″	0.540″	1.14″
350	0.051″		0.97″
400	0.045″	0.405″	0.85″
450	0.040″		0.76″
500	0.036″	0.324″	0.68″
550	0.033″		0.62″
600	0.030″	0.270″	0.57″

Example: The 300-line point is located on the large wedge where its total width is 1.14 inch and on the small wedge where its width is 0.54 inch.

Table II—Frequency Calibration of Resolution Wedge. Based on 18-inch Chart Height

$$f_n = A_r n \frac{10^6}{H_a \times 2}$$

Where f_n = fundamental frequency for n number of lines
A_r = aspect ratio = 4/3
n = number of lines
H_a = active time of horizontal trace. (Horizontal time less blanking time. Blanking time is 0.16 H — the average between maximum and minimum allowable time.) Horizontal time = 63.5 μsec and H_a = 63.5 × 0.85 = 53.3 μsec

Substituting given values in the above formula:

$$f_n = \frac{4}{3} \frac{10^6}{53.3 \times 2} n = 0.0125\ n \text{ mc, or } n = f_n/0.0125 \text{ lines}$$

When f_n =	3 mc	4.0	5.0	6.0	7.0
n =	240 lines	320	400	480	560

f_n	No. of lines	Width per line	Width of 19 lines
3	240	0.0750″	1.42″
4	320	0.0562″	1.07″
5	400	0.0450″	0.85″
6	480	0.0375″	0.71″
7	560	0.0325″	0.62″

Locate frequency calibration along wedge by same method employed to locate line calibration (see example in Table I).

An alternate method suggested for locating the line calibrations along the wedge uses the following formula:

$$L_n = L\left(\frac{300}{n} - 1/2\right)$$

Where L_n = distance from end of wedge indicating maximum lines resolution (in this case 600)
L = length of entire wedge (shortest distance between ends)
n = number of lines per picture height

The four crosses (+), positioned one at the center of each side of the chart, are used for alignment of projection kinescopes and the optical system of projection receivers.

The gray background of the chart provides a satisfactory balance with the whites so that a studio system correctly set up by the use of this chart will operate satisfactorily on an average scene without additional adjustments.

The two sections of single-line widths, 50–300 (50–100–150–200–250–300) and 350–600 (350–400–450–500–550–600), provide an accurate means of checking "ringing" in equipment. (The multiple lines in the wedge are confusing in checks of this type.)

Printed copies of the chart, in its original size of 18 by 24 inches, may be obtained from the RMA Headquarters, Wash. D. C.

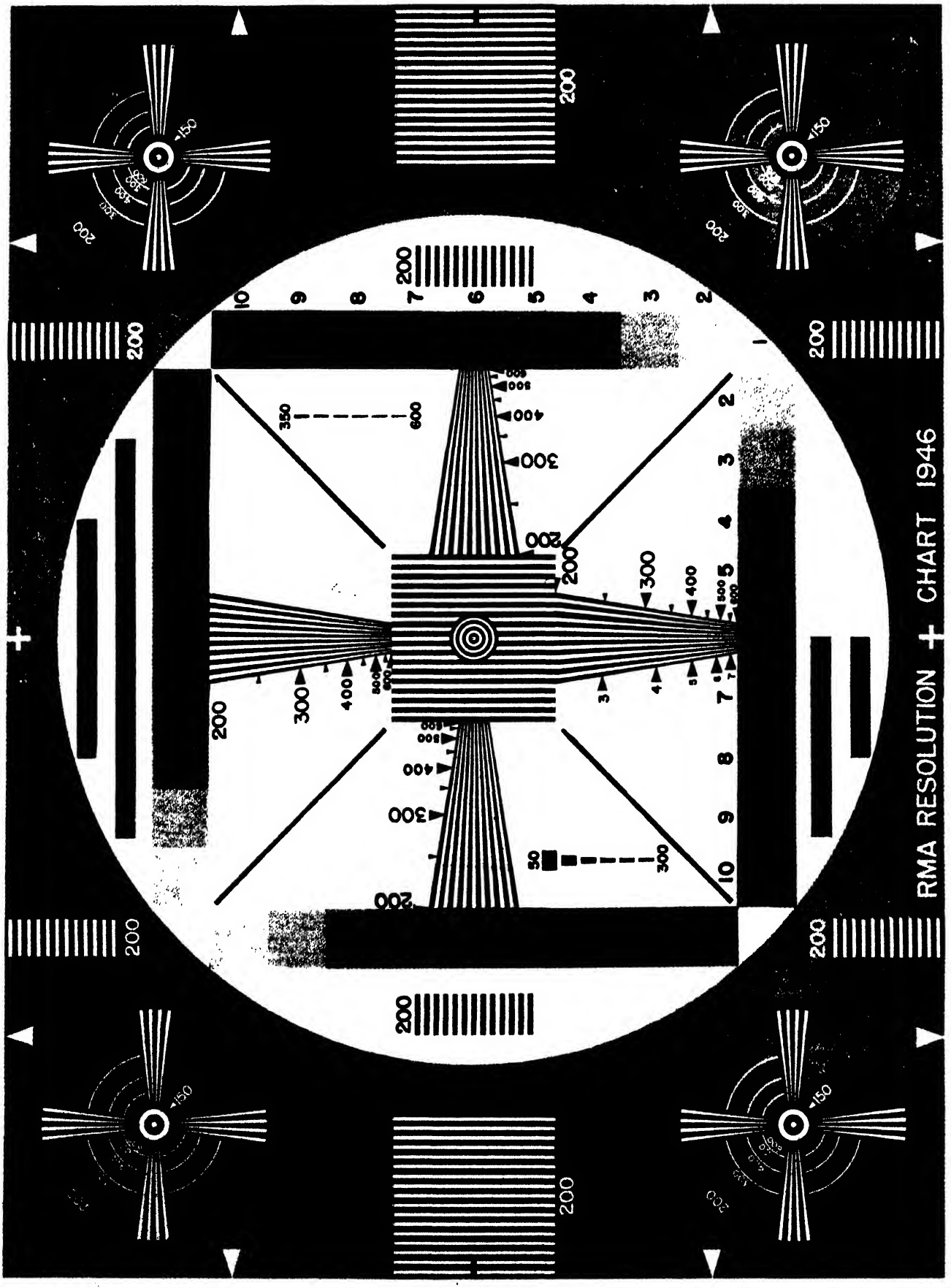
RMA RESOLUTION CHART 1946
200
150
300
400
500
600
350

Television Service Areas

By JOHN H. BATTISON

THE accompanying charts, based upon FCC assumptions and data, provide a quick approximation of television service areas for the 5,000 μv per meter (solid line) and 500 μv per meter (dashed line) contours. Receiving antenna height is assumed to be 30 feet above average terrain.

To determine the distance from a channel 2 20-kw transmitter 2,000 feet above average terrain to the 5,000 μv per meter contour, enter the appropriate chart at the left and follow the effective radiated power line across to its junction with the solid curve for 2,000 feet. Then read off the distance in miles (29 miles, in this case) from the scale at the top of the graph. The 500 μv contour from a similar transmitter would be found at 60 miles, using the dashed line for height and the lower scale of miles.

Power and antenna height necessary for desired coverage can also be determined from the charts.

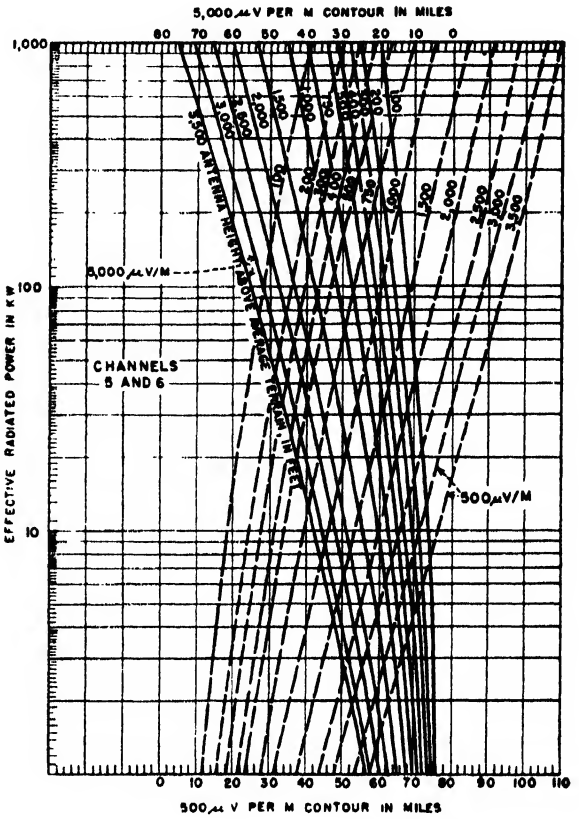

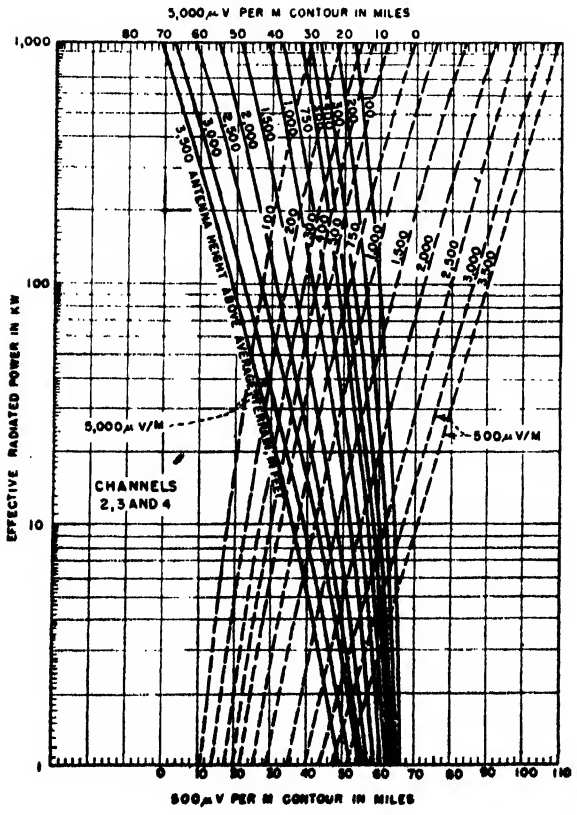

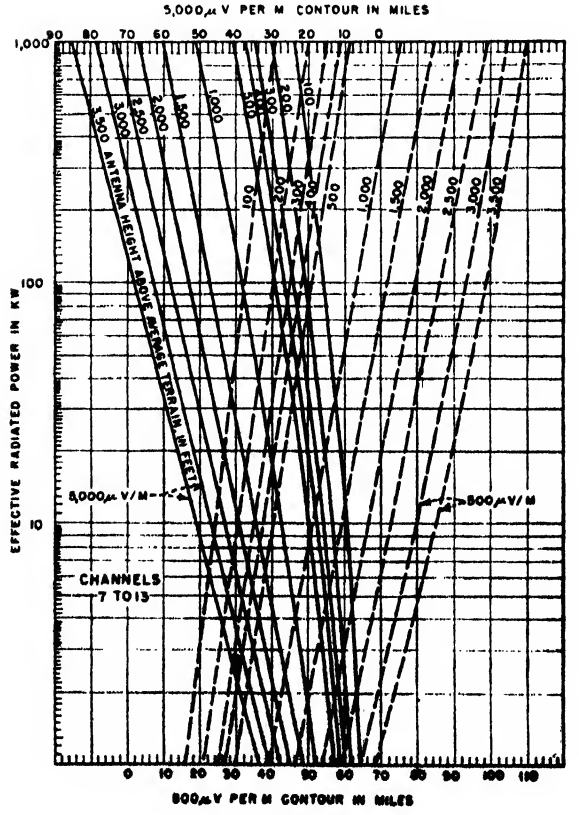

Photometry in Television Engineering

This introduction to fundamental photometric concepts and measurements provides an understanding of principles and methods whereby performance of television receivers may be evaluated. Quantities needing measurement and their interrelations are explained

By D. W. EPSTEIN

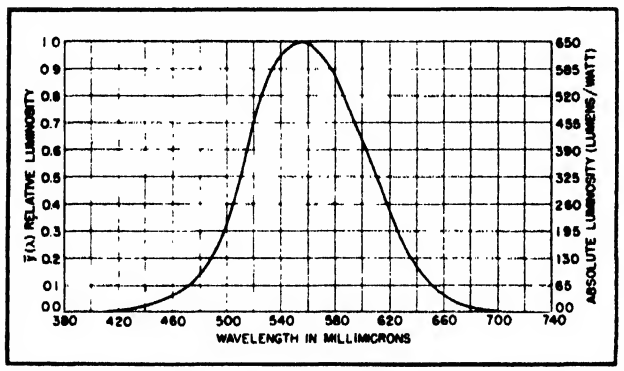

FIG. 1—Relative values (left) of luminosity curve apply to conditions met in television; absolute values (right) are used to determine luminous efficiency

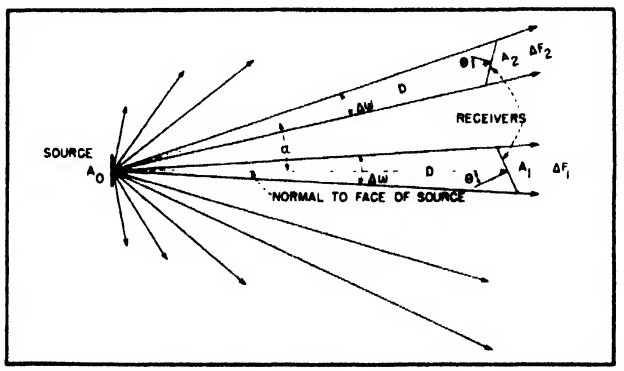

FIG. 2—Luminous intensity of the source is the flux emitted per solid angle. Illuminance of a receiver is the flux per unit area incident on its surface

PHOTOMETRY is of considerable interest to television engineers because the engineering evaluation of television receivers depends to an important extent on photometric measurements. By making these measurements television engineers can accumulate objective data on the distribution of light output over the picture plane on which to base future designs of receivers.

Receiver Performance

Among the factors affecting receiver performance and in which photometry plays an important role are: (1) highlight brightness, (2) brightness range or large area contrast, (3) brightness gradation or gamma, (4) detail contrast, resolution contrast or sharpness, (5) ambient illumination, (6) directional characteristic of the emission, and (7) such other effects on the photometric performance of the receiver as hum and flicker. Although the relative importance of these factors for viewer satisfaction is determined essentially by experience in the field, it is only by possessing photometric data on them that this experience can be converted into specifications.

Photometry is concerned not only with the measurement and computation of the energy relationships in the emission process, propagation, absorption and reflection of radiant energy in the wavelength range of 380 to 765 millimicrons, but also with the quantitative evaluation of this radiant energy with respect to its capacity to stimulate visual sensations.

A luminosity curve shows as ordinates the relative effectiveness (plotted as the reciprocal of the required radiant energy) of various wavelengths of radiant energy to evoke, for a particular observer and under particular conditions, visual sensations of equal brightness. A luminosity curve may thus be considered as the relative response characteristic of the eye.

The difficulties encountered in attempting to make photometry an objective science are that the relative response characteristic of a given individual is different for different conditions of observation and that the relative response characteristics of different observers, under the same conditions of observation, are not identical.

The use of many luminosity curves would, obviously, lead to endless confusion and ambiguity in photometric measurements and specification. To avoid this, the International Commission on Illumination adopted in 1924 a standard luminosity curve. Figure 1 shows the standard I. C. I. luminosity curve which was obtained as an average of a reasonably large number of luminosity curves. It should be realized, that, (because a different average curve would have been obtained if a different group of observers or different conditions of observation have been used), the standard-luminosity curve is essentially an arbitrarily assumed standard for purposes of standardization and specification of photometric data and is not necessarily the response of any normal or average individual. Table I gives the standard luminosity function, $\bar{y}(\lambda)$, at 5 millimicron steps.

Units of Photometry

Photometry has been complicated by nomenclature and systems of units. To alleviate this situation,

Table I—Standard Luminosity Function

λ in mμ	$\bar{y}(\lambda)$	λ in mμ	$\bar{y}(\lambda)$	λ in mμ	$\bar{y}(\lambda)$	y in mλ	$\bar{y}(\lambda)$
380	0.0000	480	0.1390	580	0.8700	680	0.0170
385	0.0001	485	0.1693	585	0.8163	685	0.0119
390	0.0001	490	0.2080	590	0.7570	690	0.0082
395	0.0002	495	0.2586	595	0.6949	695	0.0057
400	0.0004	500	0.3230	600	0.6310	700	0.0041
405	0.0006	505	0.4073	605	0.5668	705	0.0029
410	0.0012	510	0.5030	610	0.5030	710	0.0021
415	0.0022	515	0.6082	615	0.4412	715	0.0015
420	0.0040	520	0.7100	620	0.3810	720	0.0010
425	0.0073	525	0.7932	625	0.3210	725	0.0007
430	0.0116	530	0.8620	630	0.2650	730	0.0005
435	0.0168	535	0.9149	635	0.2170	735	0.0004
440	0.0230	540	0.9540	640	0.1750	740	0.0003
445	0.0298	545	0.9803	645	0.1382	745	0.0002
450	0.0380	550	0.9950	650	0.1070	750	0.0001
455	0.0480	555	1.0002	655	0.0816	755	0.0001
460	0.0600	560	0.9950	660	0.0610	760	0.0001
465	0.0739	565	0.9786	665	0.0446	765	0.0000
470	0.0910	570	0.9520	670	0.0320		
475	0.1126	575	0.9154	675	0.0232		

The commonly used units of wavelength are the micron (μ) = 10^{-6}meter, the millimicron (mμ) = 10^{-9}meter, and the Angstrom unit (A) = 10^{-10}meter.

Table II—Nomenclature and Symbols Used in Photometry

RADIOMETRY			PHOTOMETRY		
Name	Symbol	Unit MKS	Name	Symbol	Unit MKS
Radiant Energy	U	joule	Luminous Energy	Q	talbot
Radiant Flux	P	watt	Luminous Flux	F	lumen
Radiant Emittance	W	watt/m²	Luminous Emittance	L	lumen/m²
Radiant Intensity	J	watt/ω	Luminous Intensity	I	lumen/ω(candle)
Radiance	N	watt/ωm²	Luminance	B	lumen/ωm² (candle/m²)
Irradiance	H	watt/m²	Illuminance	E	lumen/m² (lux)
	m	meter		w	steradian

the committee on Colorimetry of the Optical Society of America has recommended Table II, which gives the names, symbols, and basic mks units of radiometry and photometry. The term luminance in Table II replaces the older term brightness, which led to the confusion between the objective concept of brightness as a measurable quantity and the subjective concept of brightness which refers to the sensation in the consciousness of the human observer. It is recommended that the term brightness be used only in the latter sense.

Any radiometric unit in Table II is converted into the corresponding photometric unit by evaluating it with respect to the standard luminosity function $y(\lambda)$. Thus, if $P(\lambda)$ be radiant flux (in watts per millimicron) distributed over the continuous spectrum extending between λ_1 and λ_2, then the luminous flux in lumens is given by

$$F = 650 \int_{\lambda_1}^{\lambda_2} P(\lambda)\,\bar{y}(\lambda)\,d\lambda \qquad (1)$$

where λ is measured in millimicrons. The ratio of any photometric quantity to the corresponding radiometric quantity in Table II is defined by the ratio

$$K = 650 \frac{\int_{\lambda_1}^{\lambda_2} P(\lambda)\bar{y}(\lambda)d\lambda}{\int_{\lambda_1}^{\lambda_2} P(\lambda)d\lambda} \quad \text{lumens per watt} \qquad (2)$$

and is called the absolute luminosity or luminous efficiency (expressed in lumens per watt) of the radiant energy. Thus one watt of monochromatic radiant flux of wavelength 555 mμ (peak of standard luminosity curve) is equivalent to 650 lumens, whereas one watt at 500 mμ is equivalent to $0.323 \times 650 = 210$ lumens. (The value of 650 lumens per watt has been adopted by the committee on Nomenclature and Standards of the Illuminating Society of America. However, as soon as the new proposed international photometric standard is adopted, this value will probably increase to 685 lumens per watt.

Luminous efficiency K should not be confused with the efficiency of a practical light source, which is the ratio of the total luminous flux to the total power input. The efficiency of a light source is less than K since generally only a fraction of the power input is converted into radiant flux.

Calculations

Referring to Fig. 2, let the small plane source of area A_0 emit P watts or $F = 650 \int_0^\infty \bar{y}(\lambda)P(\lambda)\,d\lambda$ lumens, and let A_1 and A_2 be the areas of two small receivers which subtend the same solid angle $\Delta\omega$ at the center of the source and are located at the same distance D from it. The luminous intensity or candlepower of a source is given by

$$I = \Delta F\ \Delta\omega \qquad (3)$$

and is measured in candles or lumens per steradian. The number of lumens ΔF_1 and ΔF_2 contained in the solid angles $\Delta\omega$ will, in general, be different. Thus the intensity $I_1 = \Delta F_1/\Delta\omega$ measured in the direction normal to the source is different from the intensity $I_2 = \Delta F_2/\Delta\omega$ measured along a direction making the angle α with the normal. In specifying the intensity or candlepower of a source, it is therefore necessary to state the direction in which the intensity is measured or preferably to give a candlepower distribution curve. The directional characteristic of many extended sources, such as a luminescent screen of a cathode-ray tube, obey Lambert's law which states that

$$I_2 = I_0 \cos\alpha \qquad (4)$$

In the case of a uniform point or spherical source, the intensity is independent of direction and is equal to $F/4\pi$. Table III shows the relationship between the three most frequently used units of intensity.

A surface of area ΔA placed in a field of flux F is said to be illuminated with the illuminance in lumens per square meter (in mks units) of

$$E = \Delta F/\Delta A \tag{5}$$

where ΔF is the flux incident on the surface. The illuminance of receiver ΔA_1 (Fig. 2) is

$$E_1 = \Delta F_1/\Delta A_1 = I_0\Delta\omega/\Delta A_1 = (I_0/\Delta A_1)\,(\Delta A_1\cos\theta)/D^2 = (I_0/D^2)\cos\theta \tag{6}$$

The illuminance of receiver ΔA_2 is

$$E_2 = (I_2/D^2)\cos\theta \tag{7A}$$

which, for a source obeying Lambert's law, is

$$E_2 = (I_0/D^2)\cos\alpha\cos\theta \tag{7B}$$

In the case of normal incidence the illuminance of the two receivers

$$E_1 = I_0/D^2;\ E_2 = I_2/D^2 \tag{8}$$

Equation 8 expresses the well known inverse square law of illumination. Equation 6 or 7 expresses the combination of two fundamental laws of illumination; the inverse square law and the cosine law. The inverse square law, which is the basis of most photometers, applies to large extended sources if D is considerably larger than the extension of the source. Thus, Eq. 8 holds to within about one percent if D is at least five times the greatest linear dimension (the diagonal of the raster on a cathode-ray tube screen) of the source. Equation 8, rewritten in the form

$$I_0 = E_1D^2;\ I_2 = E_2D^2 \tag{9}$$

serves as a basis of determining the intensity of candlepower of extended sources if D is again at least five times the greatest linear extension of the source.

The luminance B of the surface A_0 (Fig. 2) in any direction α is the ratio of the intensity I_α in that direction to the area of the projection of A_0 on a plane perpendicular to this direction so that

$$B = I_\alpha/A_0\cos\alpha \tag{10}$$

Luminance is measured in candles per square meter in mks units. If Lambert's law is obeyed, then

$$B = \frac{I_0\cos\alpha}{A_0\cos\alpha} = \frac{I_0}{A_0} = B_0 \tag{11}$$

and the luminance of a surface is independent of α. The brightness sensation depends upon the luminance of the surface. Hence, if the surface obeys Lambert's law, its luminance is the same in all directions, and it will appear equally bright from all angles.

The luminous emittance L of a surface is the total luminous flux the surface emits per unit of area

$$L = F/A \tag{12}$$

Luminous emittance is measured in lumens per square meter in mks units. The luminous emittance of a surface obeying Lambert's law is

$$L = \pi B \tag{13}$$

Thus a perfectly diffusing surface with a luminance of B candles per square meter emits πB lumens per square meter. If the area of the surface is A square meters, then it emits πBA lumens.

Equation 13 is the basis for another unit of luminance called meter-lambert. One meter-lambert (equal to $1/\pi$ candle per square meter) is the luminance of a perfectly diffusing surface emitting, reflecting or transmitting one lumen per square meter. This lambert unit is extremely convenient when dealing with reflecting and transmitting surfaces which are perfectly diffusing. For, if these surfaces do not absorb any light, then the number of lumens incident on them is equal to the number of lumens transmitted or reflected, and the illuminance in lumens per square meter equals the luminance in meter-lamberts.

Besides the mks units given above, there are many others in widespread use. They differ from the mks units only in the fact that different units of area are used. Tables IV and V give the names and the relative magnitudes of the more commonly used units of illuminance and luminance.

Table III—Conversion Factors for Units of Luminous Intensity

UNIT	Int'n'l Candle	New Candle	Hefner Candle
One Int'n'l Candle	1	1.02	1.11
One New Candle	0.98	1	1.09
One Hefner Candle	0.90	0.92	1

Photometric Measurements

The methods of light measurement may be divided into two classes: visual photometry, and physical photometry.

In visual photometry the human eye is used as the detector. Although the human eye is incapable of measuring, it is capable of fairly accurately judging the equality of luminances of adjacent areas. In a visual photometer, two adjacent areas of a screen are illuminated by a calibrated source and an unknown source. The observer adjusts the illuminance on the half-field pro-

Table IV—Conversion Factors for Units of Illuminance

Unit	Lumen/M² or Meter-Candle or Lux	Lumen/Ft² or Foot-Candle	Lumen/Cm² or Phot	Millilumen/Cm² or Milliphot
One Lumen/M² or Meter-Candle or Lux	1	0.0929	0.0001	0.1
One Lumen/Ft² or Foot-Candle	10.76	1	0.001076	1.076
One Lumen/Cm² or Phot	10,000	929	1	1,000
One Millilumen/Cm² or Milliphot	10	0.929	0.001	1

Table V—Conversion Factors for Units of Luminance

UNITS	Candle per sq Cm	Candle per sq In.	Candle per sq Ft	Candle per sq M	Cm-Lambert	Foot-Lambert	Milli-Lambert	Meter-Lambert
One Candle/Cm² or Stilb	1	6.452	929	10,000	3.142	2,919	3,142	31,420
One Candle/In²	0.1550	1	144	1,550	0.4869	452.4	486.9	4,869
One Candle/Ft²	0.00108	0.00694	1	10.764	0.00338	3.142	3.38	33.82
One Candle/Meter	0.0001	0.000645	0.0929	1	0.0003142	0.2919	.3142	3.142
One Cm-Lambert	0.3183	2.054	295.7	3,183	1	929	1,000	10,000
One Foot-Lambert	0.000343	0.00221	0.3183	3.426	0.0010764	1	1.0764	10.764
One Millilambert	0.000318	.002054	0.2957	3.183	0.001	0.929	1	10
One Meter Lambert	0.0000318	0.0002054	0.02957	0.3183	0.0001	0.0929	0.1	1

Intensity (measured along line of sight) per unit of area (measured in plane normal to line of sight)

duced by the calibrated source, (by varying the distance between source and screen) until he judges the two half-fields to be equally bright. The better visual photometers (such as the Macbeth Illuminometer) use a Lummer Brodhun cube to split the field. Relatively accurate measurements may be made with visual photometers only if the chromaticities of the calibrated and unknown sources are approximately the same. Although a series of filters may be used to relieve this limitation, measurements upon sources of different colors (heterochromatic photometry) are generally subject to considerable errors unless a flicker photometer is used.

In physical photometry, the detector is generally a photovoltaic or photoemissive cell. A cell corrected with a suitable filter, so that its sensitivity throughout the spectrum is proportional to the standard luminosity curve will give standard photometric values regardless of the color of the light. The most important error in physical photometry is generally due to the difference between the spectral response of the cell and the standard luminosity curve. Other errors arise from the directional, temperature and fatigue characteristics of cells. Most commercial light measurements are now made using a photovoltaic cell with a correcting filter to give a response typical of the human eye.

Although physical photometry is obviously the ideal, visual photometry will continue to be used because no portable physical photometer has as yet been developed which is as universal a light measuring instrument as the Macbeth Illuminometer. It can be used to measure the light from small or large areas and, with suitable filters, covers a very wide range of intensities. For trained observers, the Macbeth will yield reasonably accurate and consistent results over a wide spectral range. The correct manner of using the Macbeth illuminometer is given in the instruction book issued by the manufacturer (Leeds and Northrup).

However, because of the spectral distribution of the light emitted by cathode-ray tubes and in the case of semiroutine measurements especially by nonspecialists, it is preferable to use a physical photometer. A barrier-layer cell photometer, such as a Weston Photronic cell with a Viscor filter, will, under the circumstances, often yield more consistent and more standard results than those obtained with a Macbeth if as much care is taken in its calibration and reasonable care is exercised in following procedure (such as that outlined by L. E. Barbrow, A Photometric Procedure Using Barrier-Layer Photocells, Jour. of Res. Nat. Bureau of Standards. 25, 703, 1940). However, the barrier-layer cell photometer is not very suitable for the measurement of very low intensities, or of the ratio of luminance of small areas, as is required in measuring contrast gamma and hum. Under these circumstances it may be necessary to use the Macbeth and, whenever possible, calibrated filters to match the color of the light from the luminescent screen should be used.

The measurement of contrast, gamma and hum involves primarily the measurement of light intensity ratios. The absolute value of luminance need not be known and the spectral characteristic of the light stays approximately constant throughout the measurement. It is believed that a physical photometer, such as a well stabilized vacuum photocell arrangement preferably with an optical system, and several field limiting apertures should be developed for the purpose.

The following procedure may be used for measuring with a barrier-layer cell the luminance (brightness) of a uniformly emitting area of a cathode-ray tube screen: (1) Place a good mask with an opening of accurately known area A over the tube face. (2) Locate the cell facing the tube and one foot away.

The luminance in foot-lamberts is then $\pi E/A$ where E is the reading of the meter in foot-candles. If the area (in square feet) of the aperture in the mask is standardized, then the factor π/A can be included in the calibration of the meter and thus the luminance in foot-lamberts may be read directly. The largest linear dimension of the aperture in the mask should be kept below six inches, if the error, due to the assumption that the inverse square law holds for extended surfaces, is to be less than about 0.06.

The same procedure may be adopted in the case of projection receivers, except that here the luminance should be measured at least in two directions: normal and a preassigned value.

Simplified Television System

A new iconoscope makes possible circuit simplification and permits reproduction on the receiving cathode-ray tube screen comparable to newspaper half tones. Complete circuit details are given for the 250-line 60-frame system

By R. E. BARRETT and M. M. GOODMAN

A major step toward reducing the cost of a television system has been made with the introduction of a new two-inch iconoscope, the RCA 5527. It is relatively inexpensive and has been designed so that the equipment associated with it can be compact, simple, and economical. For a satisfactory picture with this pickup tube, only about 1,000 foot-candles of incident illumination are required. This amount of light is roughly the same as that used in present television broadcasting studios and can be obtained with three 200-watt lamps placed four feet from the subject. An outdoor scene televised by the 5527 on a normal sunny day produces a picture, when viewed on a 7GP4 directly-viewed kinescope, comparable in quality to a newspaper reproduction of a photograph.

Although the tube is designed to operate with 800 volts on the accelerator electrode, it will perform satisfactorily at 600 volts with only a slight loss in picture definition. The small area of the mosaic permits the use of a low-cost lens such as the lens of a 35-mm camera having a speed of F:3.5 or greater.

Although the tube uses electrostatic deflection rather than the more expensive and cumbersome electromagnetic deflection system, good picture definition is obtained through the use of the wartime-developed fine-spot cathode-ray gun with balanced deflection. The resolution capabilities of the tube are exceptionally good, and as measured by television standards, (lines per picture height) are 250 lines. The difficulty from non-uniform background signals, or dark spots found in all iconoscopes, is ordinarily not troublesome in industrial applications and, therefore, very satisfactory pictures are obtained without the use of shading signals. In addition, the tube does not require keystone correction.

The system illustrated in Fig. 1 contains all of the components necessary to give a good television picture and can be adapted to a transmitting and receiving system. The sensitivity and resolution of the system, together with the modest cost of components, make it applicable to many uses in both the industrial and educational fields. The adaptability of the system and its excellent performance make the system extremely versatile and provide a wide range of possible applications.

The complete system includes the camera and monitor as illustrated in the block diagram of Fig. 2. The scene to be televised is converted to an electrical signal by the pickup tube. This signal is then amplified and reproduced on the screen of the kinescope. The necessary synchronizing circuits, blanking amplifiers, and power supplies are included.

Camera System

The components contained in the camera are the two-inch iconoscope, a four-stage video preamplifier, and the lens mounting. The entire camera housing is made of 1/16-inch copper and a partition of the same material separates the camera tube from the video preamplifier. This type of shielding is necessary, since the presence of spurious signals on the kinescope can be very annoying and detract from the quality of the picture produced.

Care should also be taken if long cables are used between the camera and the monitor to filter all electrode voltages properly and to carry a good low-resistance ground between the two pieces of equipment. All of the shields for the cables and the camera housing should be returned to the monitor rack and a solid connection made at one point only. This will eliminate possible pickup loops due to nonuniform ground potentials.

It is recommended that the camera tube be operated with its second anode at ground potential

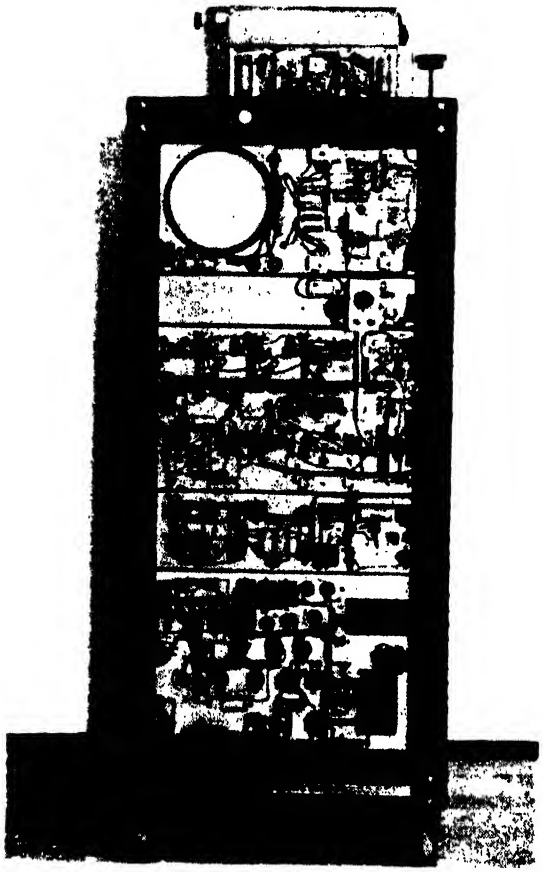

FIG. 1—Television camera and picture system chassis in a 4-foot rack

and its cathode at a high negative potential. This method of operation eliminates the need for a high-voltage input capacitor to the grid of the first preamplifier stage, since the signal plate of the iconoscope operates at second-anode voltage. Operating the iconoscope in this manner also eliminates the possibility of coupling hum from the high-voltage power supply into the input of the video preamplifier.

The video preamplifier, diagrammed in Fig. 3, consists of four stages using the miniature tube type 6AG5. Conventional shunt peaking is used to obtain a flat response over the range from 60 cycles per second to 2.5 megacycles. Because of the shunt capacitance of the iconoscope signal electrode and the input stage of the first video preamplifier, it is necessary to compensate the video preamplifier for the loss of high frequencies. The loss of high-frequency picture intelligence may be observed on the kinescope as a black streak following a black bar on a white background. The action of the compensation stage is to reduce in amplitude the low-frequency response and to amplify the high frequencies, giving an overall linear response with reduced amplitude over the desired bandwidth. Over-compensation of the amplifier, that is, peaking the high frequencies too much, is evidenced by a white streak following a black bar on a white background. The output of the video preamplifier is fed over a 75-ohm coaxial cable, at a level of 0.6 volts peak-to-peak, to the gain control at the input to the video line amplifier.

Optical System

The lens mount and optical focusing system for the camera consist of two pieces of concentric tubing. The smaller tubing has the lens mounted on one end and the inside surface of this tubing is painted a matte black to reduce inside wall reflections. The larger tubing is solidly mounted on the front panel of the camera.

Optical focus is obtained by sliding the smaller tubing back and forth on its axis inside the larger tubing. The two pieces of tubing take the place of a bellows since they are light tight and give a wide range of focus. Because of the small mosaic in the two-inch iconoscope, a physically small lens with a large opening (F:2 or F:3.5) and a short focal length (2 to 3 inch) may be used. A short focal length lens of this type is inexpensive and easy to obtain.

It is also desirable to have an adjustable iris on the lens so that best light conditions can be obtained. With this simple optical system a good picture of about 250-lines resolution can be obtained with about 1,000 foot candles scene illumination.

Video Line Amplifier

The video line amplifier, Fig. 4, uses three 6AC7 type tubes as amplifiers and, like the video preamplifier, uses conventional shunt peaking to obtain a flat response from 60 cycles per second to 2.5 megacycles. The output of the amplifier is a video signal complete with horizontal and vertical kinescope blanking pulses and is capable of producing a 40-volt peak-to-peak signal to drive the grid of the 7GP4 kinescope.

Because this system was not designed for transmitting a video signal, the insertion of synchronizing pulses was eliminated. These synchronizing pulses could be inserted into the line amplifier after the blanking insertion stage. In this case, the output of the video line amplifier would be a composite video signal with the synchronizing pulse superimposed on the blanking pulses. This output could then be coupled into a video modulator for transmission of a televised picture.

The standard method of interlaced scanning for both the kine-

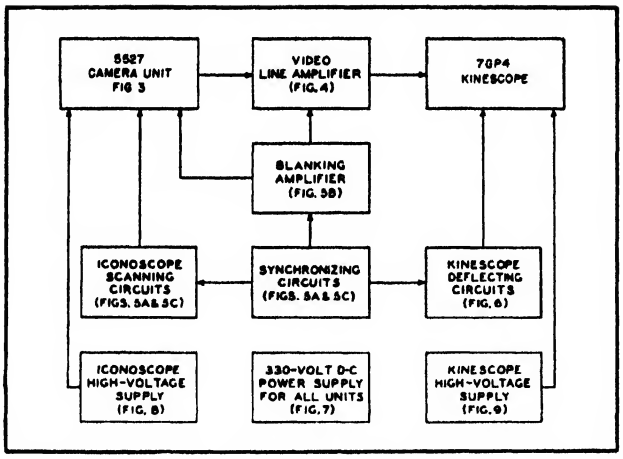

FIG. 2—Block diagram of television camera and complete picture system

scope and the iconoscope was rejected in favor of a simpler method to keep the expense low and physical size of the equipment small. The 60-cycle-per-second relaxation oscillator synchronized to the 60-cycle-per-second power frequency supplies the vertical time base. This simple oscillator synchronized with the power frequency is stable enough to eliminate the need of a speed control. A free-running multivibrator operating at approximately 15,000 cycles per second supplies the horizontal time base. These frequencies give a 250-line, 60-frame noninterlaced scanning raster, which when properly blanked, gives a stable picture.

Vertical and Horizontal Oscillators

A 6AC7 tube is used for the vertical oscillator, as shown in Fig. 5A. The frequency of oscillation is determined by the tube capacitance in conjunction with the RC constants in the screen-grid and suppressor-grid circuits. A 60-cycle saw-tooth voltage is developed in the plate circuits of this oscillator and coupled into a 6SN7-GT phase inverter.

The output of the inverter stage is a push-pull saw-tooth voltage of sufficient amplitude to scan the iconoscope in the vertical direction. The screen circuit of the 6AC7 vertical oscillator produces a straight-sided pulse of approximately 20 volts peak-to-peak which is used as the driving pulse for the kinescope vertical scanning. With this method both the iconoscope and kinescope vertical scanning systems are in synchronization.

The horizontal synchronizing pulses and driving pulses are derived from a free-running cathode-coupled multivibrator utilizing a 6SC7, as shown in Fig. 5C. The cathode of the horizontal multivibrator produces a positive straight-sided pulse which is coupled to a 6J5 discharge tube; this cathode pulse is also used as the driving pulse for the horizontal kinescope scanning. The output of the horizontal discharge tube is coupled to a 6SN7-GT phase inverter and pushpull output tube which produces the horizontal deflection for the iconoscope.

Across the cathode resistor of the vertical oscillator, a straight-side negative pulse of approximately eight volts peak-to-peak is developed. In the plate circuit of

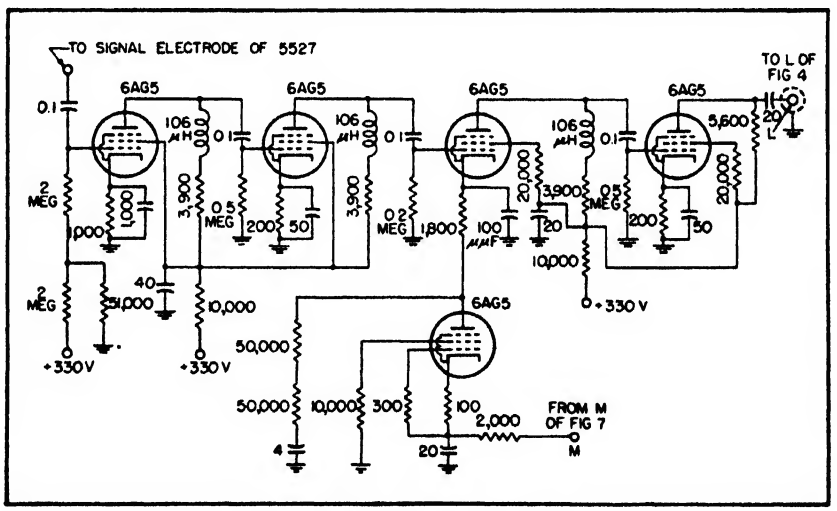

FIG. 3—Video preamplifier circuit

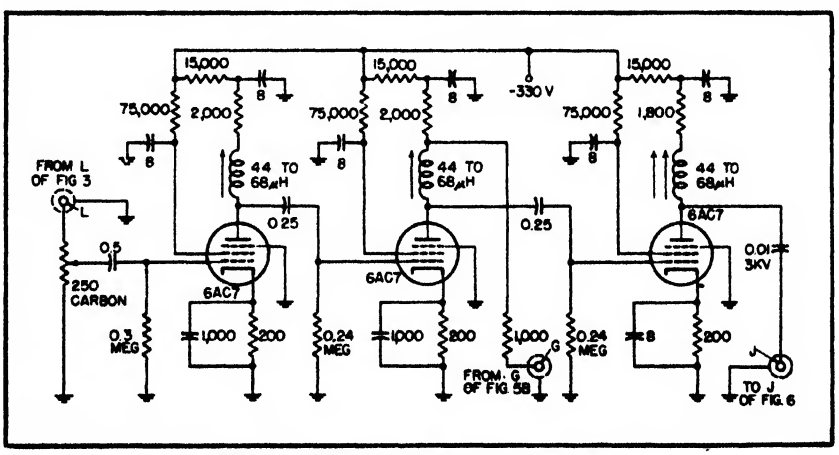

FIG. 4—Circuit of video line amplifier

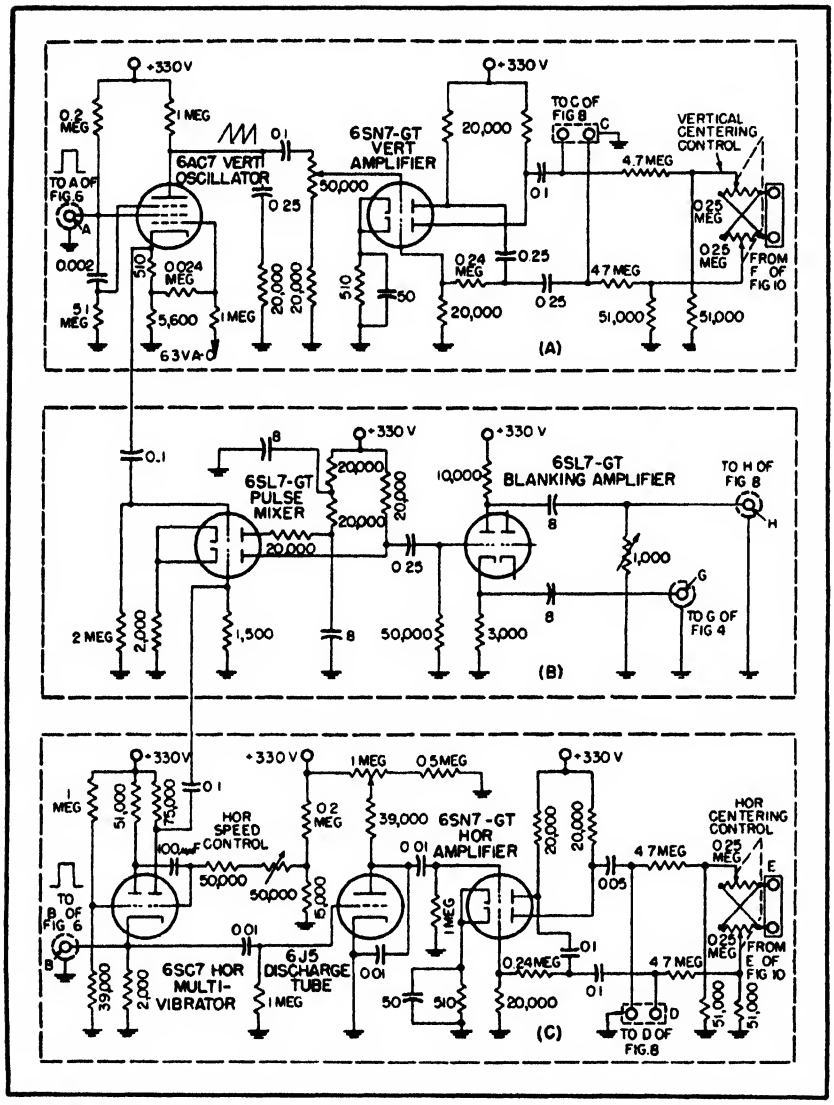

FIG. 5—(A) Vertical oscillator and scanning circuit for the 5527. (B) Mixing and blanking circuits. (C) Horizontal multivibrator and scanning circuit for 5527

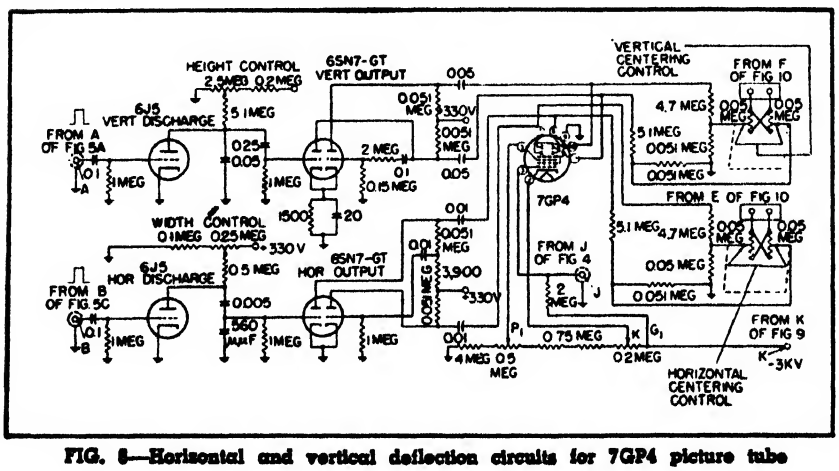

FIG. 6—Horizontal and vertical deflection circuits for 7GP4 picture tube

the horizontal multivibrator, a similar straight-sided negative pulse is produced. These two pulses are combined in the 6SL7-GT pulse-mixer tube, Fig. 5B, and then amplified in the 6SL7-GT blanking amplifier. The kinescope mixed blanking voltage is developed across the cathode resistor of the blanking amplifier and fed into the second stage of the video line amplifier. The iconoscope mixed blanking voltage is taken from the plate of the blanking amplifier and fed to grid 1 of the iconoscope. Since the vertical and horizontal blanking pulses are derived from the same oscillators that produce the driving pulses for the scanning circuits, the blanking time is not sufficient to eliminate the bright edges which appear on the sides of the scanned raster. This effect is not desirable but it does not detract too much from the quality of the picture produced.

Deflection Circuits for Kinescope

The electrostatic deflection for the 7GP4 kinescope is developed from the horizontal and vertical timing oscillators. These driving pulses are coupled into the grid circuits of a pair of 6J5 discharge tubes, Fig. 6, which produces horizontal and vertical saw-tooth voltages. The horizontal and vertical saw-tooth voltages developed in the plate circuits of the 6J5 discharge tube are coupled to a pair of 6SN7-GT phase inverter and push-pull output tubes. The width control is in the plate circuit of the horizontal discharge tube, and the height control is in the plate circuit of the vertical discharge tube.

Power Supplies

The direct-current power supplies for the complete television system consist of a 330-volt, 300-milliampere electronically regulated supply, two r-f operated high-voltage

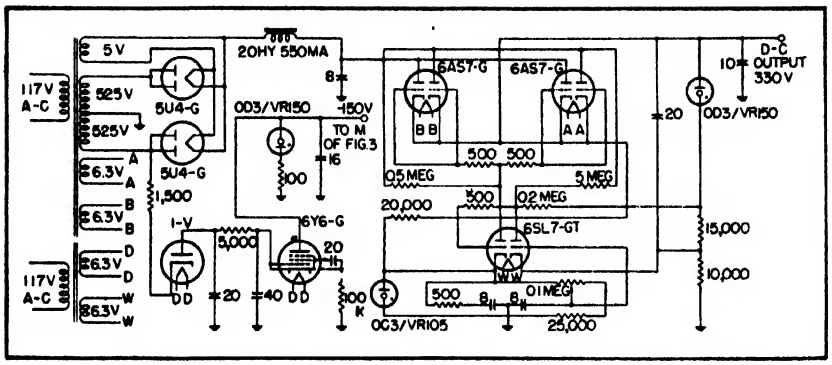

FIG. 7—Electronically regulated d-c power supply

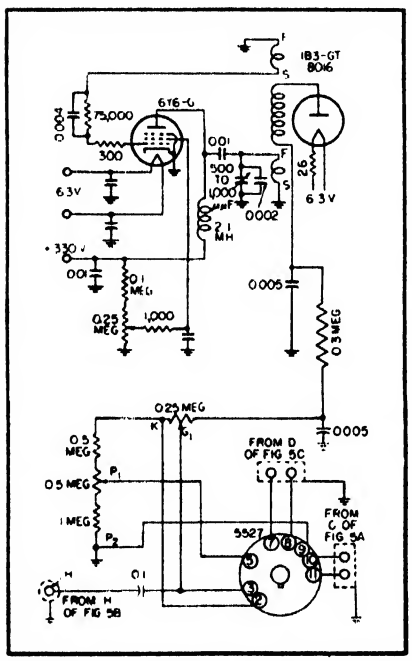

FIG. 8—Circuit of r-f operated high-voltage supply for the 5527

supplies, and two glow tube regulated supplies. The 330-volt d-c supply, Fig. 7, operates the deflection circuits, the video amplifiers, the blanking amplifier, and the oscillators for the high-voltage supply. One r-f high-voltage supply, Fig. 8, operates at −1 kilovolt maximum and is capable of one milliampere current drain. This supplies the focus and P_2 voltage for the iconoscope. The second r-f high-voltage supply, Fig. 9, operates at −three kilovolts and supplies focus and P_1 voltages for the 7GP4 kinescope. The two glow-tube regulated supplies, Fig. 10, operate at −75 volts output voltage and produce electrostatic centering voltages for the iconoscope and kinescope.

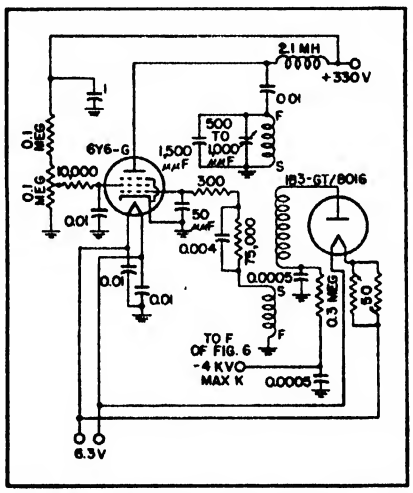

FIG. 9—R-f-operated high-voltage supply for the 7GP4

All of the components in this simplified television system may easily be mounted on a standard rack measuring 22 × 47 × 17 inches. The camera unit, however, may be mounted separately in a small compartment 4 × 12 × 6 inches and cabled to the monitor rack. All of the components may be cabled together by means of Jones plugs or Amphenol connectors. In this way, any components may be removed from the rack for servicing or study without unsoldering any connections.

Operating tests have proved that this television equipment is reliable and stable. Under proper lighting conditions, it is possible to obtain a good television picture with sufficient detail to meet the requirements of most industrial or educational needs. The equipment is small and compact and because of its simplicity, does not require highly trained personnel.

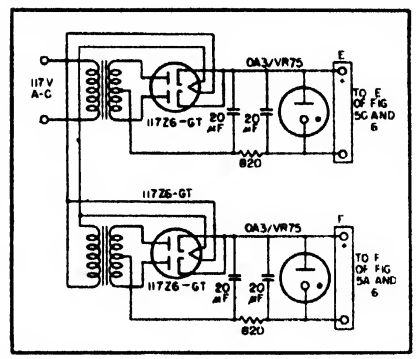

Fig. 10—Horizontal and vertical centering supplies

TRANSMISSION LINES

Design of Transmission Line Tank Circuits

Graphs are presented based on equations for short-circuited lines. From these graphs, dimensions of a concentric or parallel line for a given frequency, impedance, and selectivity can be directly determined, along with conditions for optimum efficiency

By WALTER C. HOLLIS

A STRAIGHTFORWARD procedure is outlined for the design of transmission line tank circuits. At high frequencies, short-circuited transmission lines are often used to replace inductances in tank circuits. This paper discusses tank efficiency, condition for resonance, impedance of tank circuit, conditions for maximum impedance, and selectivity of the tank circuit. Specifically, design charts are given for concentric and shielded parallel line tank circuits having dimensions as shown in Fig. 1.

The purpose of the plate tank circuit of any class-C amplifier or multiplier is to transfer efficiently to the load the power delivered by the plate of the tube[1]. The unloaded impedance of the tank circuit should be 10 or 20 times the loaded impedance. The tank efficiency in percent is then

$$100\,\frac{R_o}{R_o + R_L} \qquad (1)$$

where R_o is the unloaded impedance of the tank, and R_L is the impedance coupled into the tank from the load. This equation can be written in the form

$$100\,\frac{Q_u - Q_L}{Q_u} \qquad (2)$$

where Q_u is the unloaded tank Q, and Q_L is the loaded tank Q. Both equations, of course, yield the same result.

The condition for resonance of a capacitance-loaded transmission line is defined by the equation

$$X_c = Z_o \tan (2\pi l/\lambda) \qquad (3)$$

where X_c is the reactance of loading capacitor in ohms, Z_o is the characteristic impedance of the line in ohms, given in Fig. 2, l is the

Very High Frequency Amplifier—Parallel Wire Tank Circuit

A 823-A beam tetrode is to be used in a push-pull class-C amplifier in the 144 to 148-mc amateur band. Space considerations limit the outside diameter of the shield to 3 in. and the length to 6 in. or 15.2 cm. In the design of a shielded parallel wire tank circuit, using the notation of Fig. 1, c is determined by the spacing between plate leads from the tube, which is 0.848 in. Assuming $\frac{1}{16}$-in. wall tubing is used for the outer conductor, making b = 2.875 in. or 7.3 cm, then

$$q = c/b = 0.848/2.875 = 0.295$$

Using q = 0.3, we find (from Fig. 5) that maximum unloaded tank impedance occurs at r = 18 and $\psi\,(r,q)$ = 9,520. For this value of r, $a = b/r = 2.875/18 = 0.16$ in. which can be approximated by using $\frac{1}{16}$-in. tubing. The characteristic impedance is (from Fig. 4) then 265 ohms. At 146 mc, the wavelength is $(3 \times 10^4)/146 = 205$ cm, l/λ is 15.2/205 = 0.074, and C/λ is (from Fig. 3) equal to 0.04, hence C is $0.04 \times 205 = 8.2$ $\mu\mu$f, which includes the tube capacitance. The unloaded tank impedance is found from Eq. 7, for which $\phi(l/\lambda)$ is (from Fig. 3) equal to 0.23

$$R_o = bf^{\frac{1}{2}}\,\psi\,(r,q)\,\phi(l/\lambda) = 7.3(146^{\frac{1}{2}})9{,}520(0.23) = 194{,}000 \text{ ohms}$$

and the Q (from Eq. 8), for which $\theta(r,q)$ is (from Fig. 6) equal to 17.8, is

$$Q = bf^{\frac{1}{2}}\,\theta(r,q) = 7.3(146^{\frac{1}{2}})17.8 = 1{,}570$$

Assuming that 20 watts are delivered to the load at 900 volts peak to peak plate swing, giving $R_L = E_p^2/2P$ = 20,200 ohms, we find (using Eq. 1) that the tank circuit efficiency is

$$100\,\frac{R_o}{R_o + R_L} = 100\,\frac{194{,}000}{194{,}000 + 20{,}200} = 90.5 \text{ percent}$$

which is quite satisfactory. The accompanying drawing shows the circuit and the construction of the output tank circuit

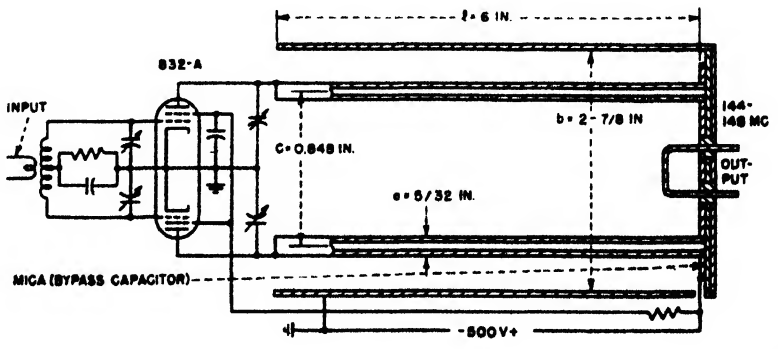

Citizens' Band Class-C Amplifier—Concentric Line Tank Design

A 2C40 disc-seal tube[4] is to be used as a class-C amplifier in the citizens' band at 465 mc. The tank circuit is to be a concentric line with the outer conductor at 2-in. outside diameter by $\frac{1}{16}$-in. wall copper tubing. The loading capacitance is to be $2\mu\mu f$, which includes tube and tuning capacitance. Using the notation of Fig. 1, the diametric ratio r for the optimum Q with fixed loading capacitance is found (from Fig. 6) to be between 3.6 and 9.2. Assume that the outside diameter of the inner conductor a is to be $\frac{1}{2}$ in. or 1.27 cm. The value of b (inside diameter of outer conductor) is $1\frac{7}{8}$ in. or 4.76 cm. Thus

$$r = b/a = 4.76/1.27 = 3.75$$

Using this value of r, we obtain (from Fig. 4 for a concentric line) a characteristic impedance Z_o of 80 ohms, a value (from Fig. 5 for a concentric line) for the function $\psi\ (r)$ of 6,700 ohms, and (from Fig. 6 for a concentric line) a value of 42 for the function $\theta\ (r)$. Furthermore, from the foregoing values, the product fCZ_o appearing in Eq. 4 is, for C in $\mu\mu f$ (not farads)

$$fCZ_o = (465 \times 10^6)\ 2\ (80) = 7.45 \times 10^4$$

Thus (from Fig. 2) $l/\lambda = 0.18$. The wavelength λ is $(3 \times 10^4)/465 = 64.5$ cm, therefore l is $0.18 \times 64.5 = 11.6$ cm or 4.57 in., which gives (from Fig. 3) $\phi\ (l/\lambda) = 0.54$. Then the unloaded impedance of the tank circuit (from Eq. 16) is

$$R_o = bf^{\frac{1}{2}}\ \psi\ (r)\ \phi(l/\lambda) = 4.76(465^{\frac{1}{2}})6{,}700(0.54) = 372{,}000 \text{ ohms}$$

and the Q (from Eq. 17) is

$$Q = bf^{\frac{1}{2}}\ \theta(r) = 4.76(465^{\frac{1}{2}})42 = 4{,}320$$

The drawing shows the mechanical arrangement of the tank circuit. The cathode line can be designed by the same method.

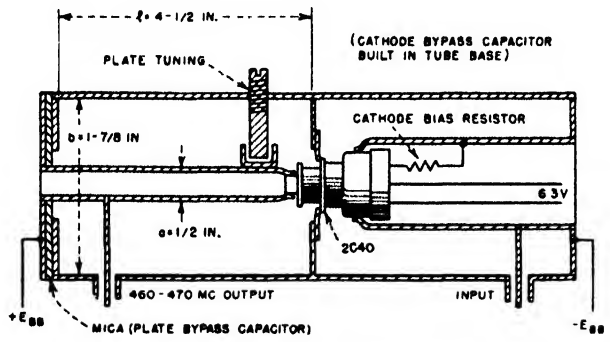

length of line in cm, and λ is the wavelength in cm.

Equation 3 can be rewritten as

$$\frac{l}{\lambda} = \frac{\tan^{-1}(X_c/Z_o)}{2\pi} = \frac{\tan^{-1}(1.59 \times 10^5/fCZ_o)}{2\pi} \quad (4)$$

where f is the resonant frequency in mc, and C is the loading capacitance in $\mu\mu f$. This relation is shown in Fig. 2 together with the relations for length in electrical degrees.

In some cases, the length may be fixed by physical limitations in size. Under these conditions, Eq. 3 can be rewritten as

$$\frac{C}{\lambda} = \frac{5.3}{Z_o \tan(2\pi l/\lambda)} \quad (5)$$

This relation is plotted on Fig. 3, using the lefthand scale, for several values of Z_o.

Impedance and Selectivity of Tank

The unloaded impedance of the tank circuit is given by the equation

$$R_o = \frac{4\pi Z_o^2}{R_s \lambda}\left[\frac{1 - \cos(4\pi l/\lambda)}{(4\pi l/\lambda) + \sin(4\pi l/\lambda)}\right] = 4.19 \times 10^{-4}\ (fZ_o^2/R_s)\ \phi\ (l/\lambda) \quad (6)$$

where R_s is the series resistance of the line in ohms per cm and $\phi\ (l/\lambda)$ is given on Fig. 3 using the righthand scale. The derivation of Eq. 6 is given in Appendix I.

As will be shown later, $R_s = K\ (f^{\frac{1}{2}}/b)$ where K is a function of the line geometry and material, and b is an outside dimension of the line geometry. Equation 6 becomes

$$R_o = bf^{\frac{1}{2}}\ \psi\ (a, b, c, \ldots)\ \phi\ (l/\lambda) \quad (7)$$

where $a, b, c, \ldots$ are dimensions of the line geometry. The function $\psi\ (a, b, c, \ldots)$ is readily determined for any line configuration for which Z_o and R_s can be analytically defined. Later $\psi\ (a, b, c, \ldots)$ will be determined for concentric and shielded parallel lines.

Transmission line reactances vary more rapidly with frequency than lumped reactances; as a result the selectivity expressed as the Q is larger than for an equivalent lumped reactance. The following equation is derived in Appendix II, assuming a lossless loading capacitance

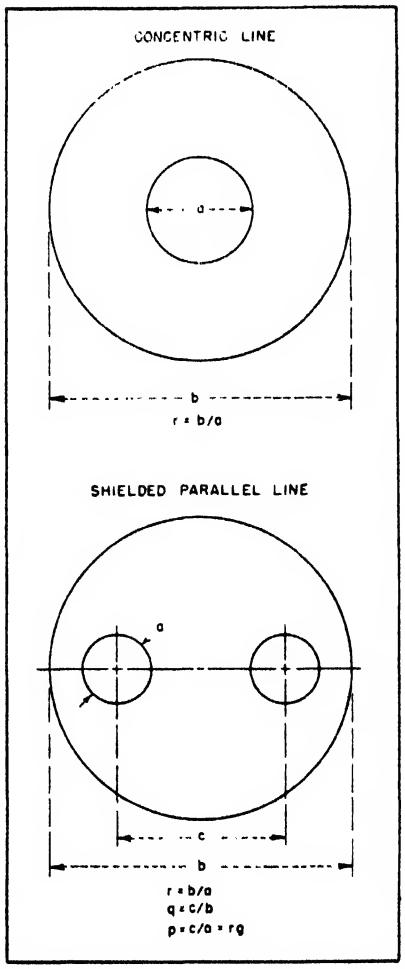

FIG. 1—(A) Size of concentric line is expressed by dimensionless ratio. (B) Size of shielded parallel line is expressed by two dimensionless ratios

$$Q = 2.09 \times 10^{-4} f\,(Z_o/R_s) = bf^{1/2}\,\theta\,(a, b, c, \ldots) \quad (8)$$

Equation 8 shows that the selectivity is independent of the length, a rather unexpected result. Because $\alpha = R_s/2Z_o$, it is readily seen that the condition for maximum selectivity is the same as for minimum attenuation.

Conditions for Maximum Impedance

From the standpoint of tank efficiency, it is desirable that the unloaded tank impedance be as large as consistent with good design. The conditions for maximum impedance are readily determined for two extreme cases. They are (A) length limited by physical considerations of size and (B) loading capacitance fixed at a certain minimum determined by maximum tube capacitance.

(A) Length Fixed—It is readily seen from an examination of Eq. 7 that the maximum impedance occurs at the maximum of the function $\psi\,(a, b, c, \ldots)$, because $\phi\,(l/\lambda)$ is constant.

(B) Loading Capacitance Fixed—Let us start with Eq. 6. From observation of $\phi\,(l/\lambda)$ on Fig. 2 it is readily seen that $\phi\,(l/\lambda)$ is approximately linear to $(l/\lambda) = 0.15$. Using the series expansion for sin $(4\pi l/\lambda)$ and cos $(4\pi l/\lambda)$ and neglecting terms of higher order than two, we obtain

$$\phi\,(l/\lambda) \cong \pi\, l/\lambda \qquad (l/\lambda) < 0.15 \quad (9)$$

But the condition for resonance demands that

$$l/\lambda = \frac{1}{2\pi}\tan^{-1}(X_c/Z_o) \cong X_c/2\pi Z_o \qquad (l/\lambda) < 0.08$$

or

$$\phi(l/\lambda) = X_c/2Z_o \quad (10)$$

Substituting Eq. 10 in Eq. 6, we obtain

$$R_o = 2.09 \times 10^{-4} f\, X_c\,(Z_o/R_s) = b f^{1/2}\,\theta\,(a, b, c, \ldots)\, X_c \quad (11)$$

Equation 11 is seen to be Eq. 8 multiplied by X_c. Thus the maximum impedance occurs at the maximum for the selectivity. This relation is true only for short lines. For longer lines, the condition for maximum impedance increases toward the condition for the maximum for fixed length, because for X_c/Z_o decreasing, l/λ approaches a limit of 0.25, a constant.

All the needed equations have been presented for the general case. Equations 6 and 7 give the relations for unloaded impedance R_o, and Eq. 8 the relation for selectivity or the Q. The proper relations can be determined readily for any line configuration for which Z_o and R_s can be determined.

The remainder of the discussion

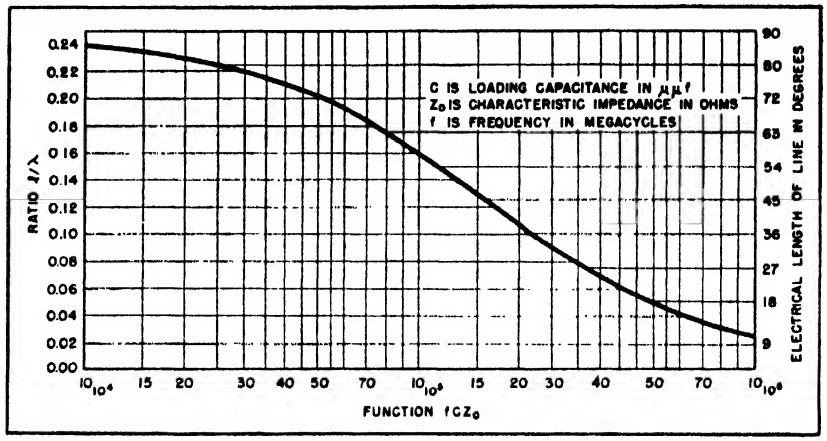

FIG. 2—Length of line relative to resonant wavelength is a function of the capacitance loading and characteristic impedance

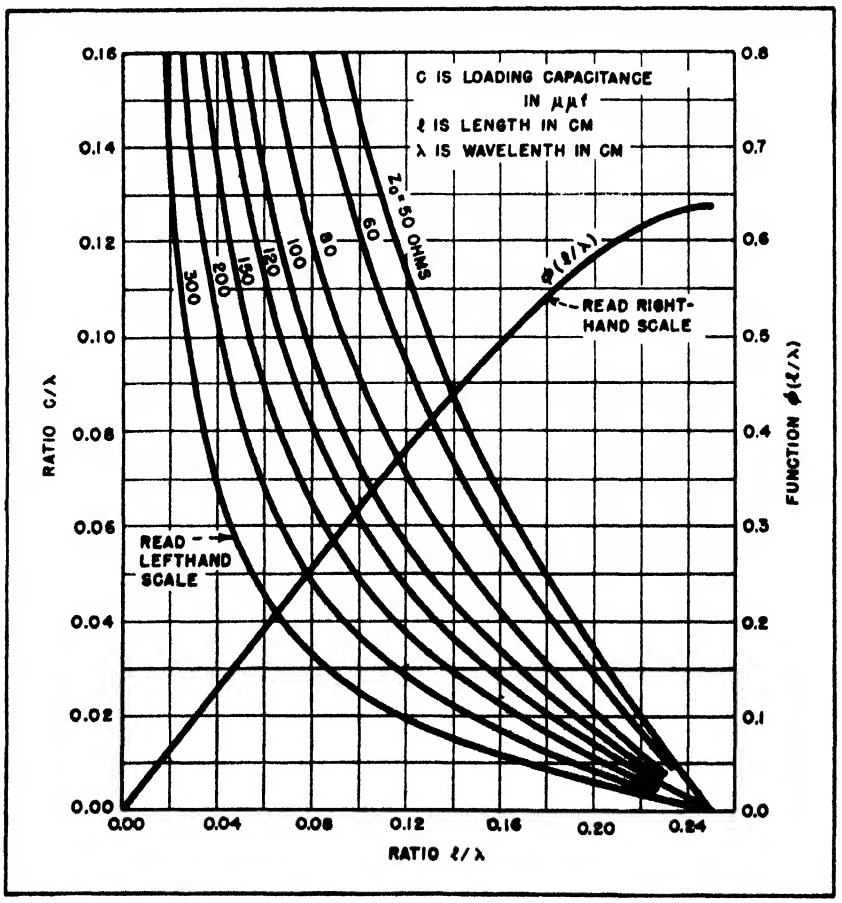

FIG. 3—Left hand scale gives ratio of loading capacitance to wavelength as a function for line length (see Fig. 2) for various characteristic impedances (see Fig. 4). Right hand scale gives unloaded impedance length parameter (see Eq. 6)

will be concerned with the specific relations for concentric lines and shielded parallel lines.

Let us define the following parameters: a is the outside diameter of inner conductor, b is the inside diameter of outer conductor, c is the center to center line spacing in cm, and ρ_s is the skin effect surface resistivity of the conductor in ohms per square cm. These dimensions are shown on Fig. 1.

Let us determine ρ_s, as it enters into the calculation for all line configurations. Resistivity ρ_s, is defined as

$$\rho_s = \rho/\delta \tag{12}$$

where ρ is the specific resistivity of material in ohms per cubic cm and δ is the skin depth in cm. For copper at 20 C, $\rho = 1.724 \times 10^{-6}$ ohms per cm cube, and $\delta = 6.62 \times 10^{-6}$ per $f^{1/2}$ cm. Therefore, ρ_s for copper becomes

$$\rho_s = 2.61 \times 10^{-6} f^{1/2} \tag{13}$$

For other materials, ρ_s is proportional to the square root of the resistivity of the material relative to copper.

Concentric Lines — Using the above notation, Ramo and Whinnery[3] give the following relations for Z_o and R_s

$$Z_o = 60 \ln (b/a) \tag{14}$$

$$R_s = \frac{\rho_s}{\pi}\left(\frac{1}{a}+\frac{1}{b}\right) = 2.61 \times 10^{-6} f^{1/2}(1 + b/a)/\pi b = \frac{8.31 \times 10^{-6} f^{1/2}}{b}\left(1+\frac{b}{a}\right) \tag{15}$$

Equation 6 then becomes

$$R_o = 18{,}150\, b f^{1/2} (\ln b/a)^2 \phi(l/\lambda)/(1 + b/a) = b f^{1/2} \psi(r) \phi(l/\lambda) \tag{16}$$

where $r = b/a$. Substituting Eq. 14 and 15 in Eq. 8, we obtain

$$Q = 151\, b\, f^{1/2} \ln (b/a)/(1 + b/a) = b f^{1/2}\, \theta\, (r) \tag{17}$$

Equations 16 and 17 have been derived independently by Hansen's derivation.[8]

Shielded Parallel Lines—Using the same notation, Ramo and Whinnery[3] give the following relations for Z_o and R_s

$$Z_o \cong 120\left\{ \ln\left[2p\frac{(1-q^2)}{(1+q^2)}\right] - \frac{1+4p^2}{16p^4}(1-4q^2)\right\} \tag{18}$$

$$R_s \cong \frac{\rho_s}{\pi b}\left\{ r\left[1+\frac{1+2p^2}{4p^4}(1-4q^2)\right] + 4q^2\left[1+q^2-\frac{1+4p^2}{8p^4}\right]\right\} = 1.66 \times 10^{-6}\frac{f^{1/2}}{b}\left\{ r\left[1+\frac{1+2p^2}{4p^4}(1-4q^2)\right] + 4q^2\left[1+q^2-\frac{1+4p^2}{8p^4}\right]\right\} \tag{19}$$

where r = b/a, $q = c/b$, and $p = c/a = rq$. Substituting Eq. 18 and 19 in Eq. 6 and 8, we obtain $\psi(r,q)$ and $\theta\ (r,q)$ respectively.

Figure 4 shows characteristic impedance versus r for concentric and shielded parallel lines (the latter for several values of q); Fig. 5 shows unloaded tank impedance

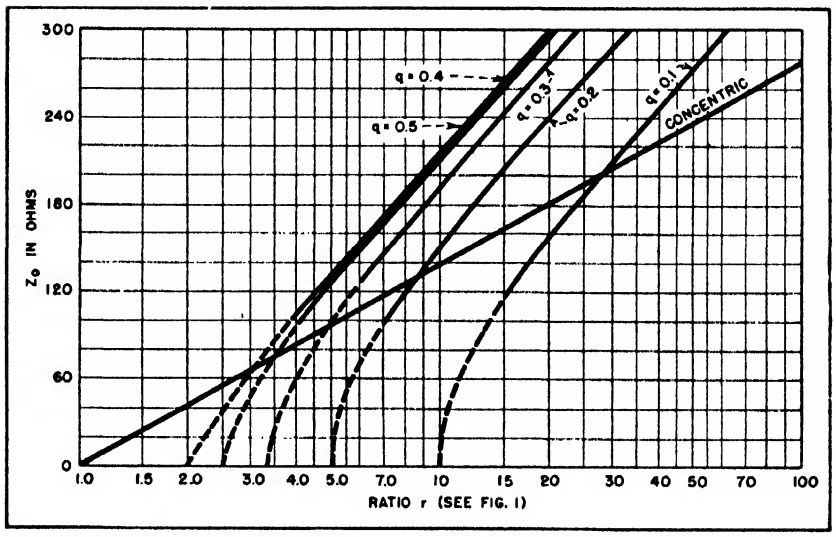

FIG. 4—Characteristic impedance is shown as a function of dimensionless ratios of line size. Using this and the four other curves presented herewith, one can design transmissions line tank circuits. The cross-sectional dimensions of either a coaxial or shielded balanced line (Fig. 1) are used with Fig. 6 (next page) to obtain the optimum proportions. Capacitive loading effects of tube are obtained from Fig. 2 and 3. This (Fig. 4) graph is used to obtain impedance of the line for use with Fig. 3. Figures 3, 5, and 6 give angular functions that are substituted into the appropriate Eq. 4, 5, 7, 8, 16, or 17 as outlined in the two boxes on the opening pages

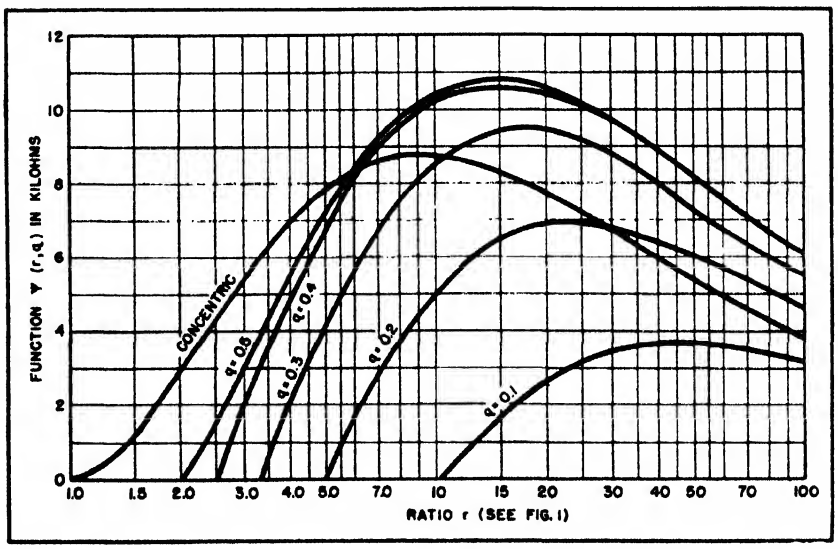

FIG. 5—Unloaded tank impedance cross-section parameter (see Eq. 7) is given as a function of the dimensionless ratios of line size

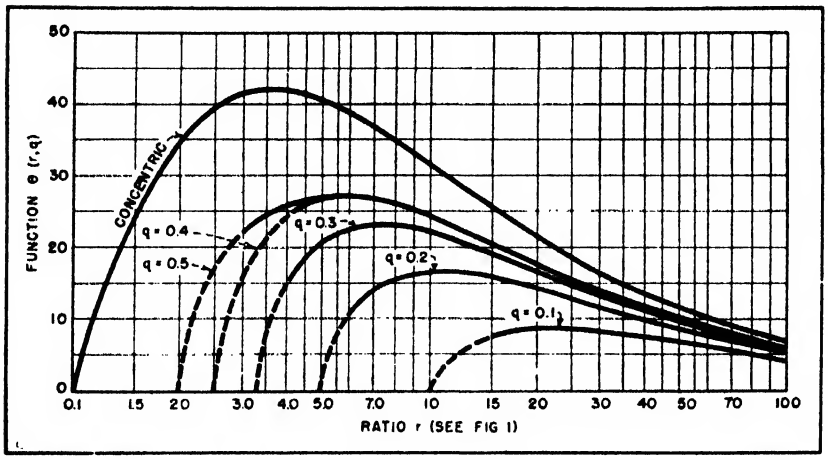

FIG. 6—Selectivity function (see Eq. 8) indicates optimum relative line dimensions for any application. If design is begun with this graph, optimum tank efficiency can be obtained

versus r and q, and Fig. 6 shows Q versus r and q. It should be noted that the curves for the shielded parallel line apply approximately for $q' = 1 - q$. Because relations for shielded parallel lines are only approximate, they do not apply for values of p (Eq. 18 and 19) close to one. As a result, the extrapolated curve in this region is shown as a dotted line.

Appendix I

Although these transmission-line equations are conventional, they need to be re-arranged into forms more useful for graphical presentation.

The formula for the unloaded impedance of a tank circuit can be derived by using the notation of Table I. The sending end impedance of a short-circuited transmission line is given by the equation

$$Z_s = Z_c \tanh \gamma l = Z_c \tanh (\alpha + j\beta)l$$
$$= Z_c \frac{\sinh 2\alpha l + j \sin 2\beta l}{\cosh 2\alpha l + \cos 2\beta l}$$
$$\cong Z_c \frac{\alpha l}{\cos^2 \beta l} + j \tan \beta l \qquad (20)$$

For a well-designed line αl is very small, $\cosh 2\alpha l \cong 1$, and $\sinh 2\alpha l \cong 2\alpha l$.

Next Z_c, α and β must be determined. Both Z_c and $\gamma = \alpha + j\beta$ are defined as follows (transmission line tank circuits are usually made with air dielectric, therefore G_s is zero)

$$Z_c = (Z/Y)^{1/2} = [(R_s + j\omega L_s)/j\omega C_s]^{1/2}$$
$$= (L_s/C_s)^{1/2} [1 - j (R_s/\omega L_s)]^{1/2} \qquad (21)$$

$$\gamma = (ZY)^{1/2} = [(R_s + j\omega L_s)(j\omega C_s)]^{1/2}$$
$$= j[\omega^2 L_s C_s (1 - jR_s/\omega L_s)]^{1/2}$$

But $(R_s/\omega L_s) << 1$, $(L_s/C_s)^{1/2} = Z_o$, and $\omega (L_s C_s)^{1/2} = 2\pi/\lambda = \beta$, therefore

$$Z_c = Z_o (1 - jR_s/2\omega L_s) \qquad (22)$$

$$\gamma = \omega (L_s C_s)^{1/2} [(R_s/\omega L_s) + j]^{1/2}$$
$$\cong (2\pi/\lambda) [(R_s/2\omega L_s) + j]$$
$$= \alpha + j\beta \qquad (23)$$

From Eq. 23, $R_s/2\omega L_s = \alpha/\beta$. Substituting the value in Eq. 22 gives

$$Z_c = Z_o (1 - j\alpha/\beta) \qquad (24)$$

Substituting Eq. 24 into Eq. 20 gives

$$Z_s = Z_o \left[\left(\frac{\alpha l}{\cos^2 \beta l} + \frac{\alpha \tan \beta l}{\beta} \right) + j \left(\tan \beta l - \frac{\alpha^2 l}{\beta \cos^2 \beta l} \right) \right]$$

The term $\alpha^2 l/\beta \cos^2 \beta l$ is negligible compared to $\tan \beta l$, therefore

$$Z_s = Z_o \left[\left(\frac{\alpha l}{\cos^2 \beta l} + \frac{\alpha \tan \beta l}{\beta} \right) + j \left(\tan \beta l \right) \right]$$
$$= R + jX \qquad (25)$$

Now resonate the impedance Z_s with a capacitive reactance of $-jZ_o \tan \beta l$. The parallel impedance presented by this combination is then

$$R = \frac{|X^2|}{|R|} = \frac{(Z_o \tan \beta l)^2}{Z_o[(\alpha l/\cos^2 \beta l) + (\alpha \tan \beta l)/\beta}$$
$$= \frac{Z_o \beta}{\alpha} \left[\frac{1 - \cos 2\beta l}{2\beta l + \sin 2\beta l} \right] \qquad (26)$$

But $\beta = 2\pi/\lambda$, and $\alpha = R_s/2Z_o$, therefore

$$R_o = \frac{4\pi Z_o^2}{R_s \lambda} \left[\frac{1 - \cos (4\pi l/\lambda)}{(4\pi l/\lambda) + \sin (4\pi l/\lambda)} \right]$$
$$= 4.19 \times 10^{-4} (fZ_o^2/R_s)\phi (l/\lambda) \qquad (27)$$

Equation 27 is Eq. 6.

Appendix II

To derive the formula for selectivity, expressed as Q, of a tank circuit, consider that $\Delta X_c = X(\Delta f/f_o)$. For a line Terman[1] gives the equation

$$\Delta X_L = X (\Delta f/f_o) (2\beta l/\sin^2 \beta l) \qquad (28)$$

The total change in reactance with detuning is

$$\Delta X = \Delta X_c + \Delta X_L$$
$$= X (1 + 2\beta l/\sin^2 \beta l) (\Delta f/f_o)$$

where $X = Z_o \tan \beta l$. Let $(\Delta X/Z_o) = (R/Z_o)$, which is the condition for half power, then

$$(\tan \beta l)(1 + 2\beta l/\sin 2\beta l)(\Delta f/f_o) =$$
$$\left(\frac{\alpha l}{\cos^2 \beta l} + \frac{\alpha \tan \beta l}{\beta} \right) \times$$
$$\left(\frac{2\beta l + \sin 2\beta l}{2} \right) \left(\frac{\Delta f}{f_o} \right) =$$
$$\left(\frac{\alpha}{\beta} \right) \left(\frac{2\beta l + \sin 2\beta l}{2} \right) \left(\frac{\Delta f}{f_o} \right) = \frac{\alpha}{\beta} =$$
$$\frac{R_s/2Z_o}{2\pi/\lambda} = \frac{R_s \lambda}{4\pi Z_o} = \frac{3 \times 10^{10} R_s}{4\pi f Z_o}$$

From the definition of the Q

$$Q = \frac{1}{2(\Delta f/f_o)} = \frac{4\pi f Z_o}{6 \times 10^{10} R_s}$$
$$= 2.09 \times 10^{-4} f (Z_o/R_s)$$

which is Eq. 8.

Table I—Symbolic Notation

Z_s	= sending end impedance of line in complex ohms
Z_c	= characteristics impedance of line in complex ohms
Z	= series impedance per unit length of line
Y	= shunt admittance per unit length of line
R_s	= series resistance per unit length of line
L_s	= series inductance per unit length of line
G_s	= shunt conductance per unit length of line
C_s	= shunt capacitance per unit length of line
α	= attenuation constant of line
β	= phase constant of line
γ	= propagation constant of line
ω	= angular frequency

References

(1) Terman, Frederick E., "Radio Engineering Handbook", McGraw-Hill Book Co., Inc., p 449.
(2) Ramo and Whinnery, "Fields and Waves in Modern Radio", John Wiley and Sons, p 382.
(3) On Resonators Suitable for Klystron Oscillators, Hansen, W. W., and Richtmyer, R. D., *Jour Appl Phys*, p 189 March 1939.
(4) McArthur, E. D., Disc-Seal Tubes, ELECTRONICS, p 98, Feb. 1945.
(5) Terman, Frederick E., Resonant Lines in Radio Circuits, *Elect Engr*, p 1046, July 1934.

Characteristic Impedance of Balanced Lines

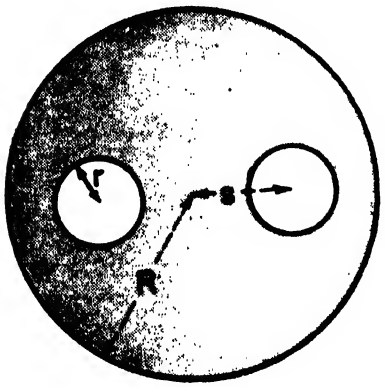

Comparison of three equations for Z_0 of a balanced two-wire transmission line with a cylindrical shield, and expressions for the errors in the equations

By PETER J. SUTRO

CONSIDER a balanced transmission line composed of two inner conductors plus a shield. The inner conductors are circular cylinders of outer radius r whose axes are separated by a distance $2s$. The shield is a circular cylinder of inner radius R, symmetrically placed with respect to the two inner conductors.

If, by definition, $x = r/s$ and $y = s/R$, the characteristic impedance Z_0 in ohms between the inner conductors can be expressed in terms of x, y, and the dielectric constant ϵ of the dielectric filling the line.

Sommer[1] derives an expression for the capacitance between the inner conductors of such a transmission line, following a method used by Kaden[2]. This expression can be transformed into

$$Z_0 = \frac{120}{\sqrt{\epsilon}}\left\{\log_e\left(\frac{2}{x}\,\frac{1-y^2}{1+y^2}\right) - \frac{1}{4}x^2\left(1-\frac{4y^2}{1-y^4}\right)^2 - \frac{1}{32}x^4\left[3+\frac{32y^4(1+2y^2)}{(1-y^4)^2} - \frac{128y^4(1-2y^2-2y^4-3y^6)}{(1-y^4)^4}\right] - \ldots\right\} \quad (1)$$

This is presumably correct as far as the series is carried, the next term being one in x^6. When the shield is removed (that is, as R approaches infinity or as y approaches zero) the formula reduces to the series expansion of the exact expression for the characteristic impedance of the unshielded balanced line

$$Z_0 = \frac{120}{\sqrt{\epsilon}}\cosh^{-1}\left(\frac{1}{x}\right) = \frac{120}{\sqrt{\epsilon}}\left\{\log_e\left(\frac{2}{x}\right) - \frac{1}{4}x^2 - \frac{3}{32}x^4 - \frac{10}{192}x^6 - \ldots\right\} \quad (1a)$$

Thus the error in Eq. 1 always enters in the terms in x^6 and higher powers.

The second formula is transformed similarly from an expression for the capacitance of the line which Sommer, in the same article, attributes to Breisig[3]. The result of this transformation can be written

$$Z_0 \pm \frac{120}{\sqrt{\epsilon}}\cosh^{-1}\left[\frac{1}{x}\,\frac{1-y^2(1-x^2)}{1+y^2(1-x^2)}\right] \quad (2)$$

This formula is a good approximation for large values of R, giving a value which is too small by an amount

$$\Delta Z_0 = \frac{120}{\sqrt{\epsilon}}\left\{\frac{x^2y^2}{(1+y^2)^2} - \frac{1}{16}x^4y^2(10+y^2+\ldots) + \ldots\right\} \quad (2a)$$

The error can be seen to go to zero when the shield is removed ($y = 0$), as is obvious from the fact that Eq. 2 then reduces to the closed form given above for the unshielded line.

It is interesting to compare Eq. 1 and 2 with the formula given by Terman[4], which can be written

$$Z_0 \pm \frac{120}{\sqrt{\epsilon}}\left\{\log_e\left(\frac{2}{x}\,\frac{1-y^2}{1+y^2}\right) - \frac{1}{4}x^2(1-4y^2) - \frac{1}{16}x^4(1-4y^2)\right\} \quad (3)$$

This equation appears to neglect terms in y of higher order than y^2 and terms in x of higher order than x^4. The terms in x^3 and x^4 are incorrect, however, and the expression gives a value which is too small by

$$\Delta Z_0 = \frac{120}{\sqrt{\epsilon}}\left\{\frac{x^2y^2}{(1-y^4)^2}(1-4y^2-y^4) - \frac{1}{32}x^4(1+8y^2-\ldots) + \ldots\right\} \quad (3a)$$

Note that while the error in the x^2 term goes to zero if there is no shield ($y = 0$), the error in the x^4 term does not.

Breisig's expression, Eq. 2, is more useful on the whole than Eq. 3. If y is large, the error in Breisig's equation is very nearly the same as that in Eq. 3, while for small y the error in the second equation is considerably less than that in the third. This may be of importance when x is large.

In general, Eq. 1 is the most accurate. It is better than Breisig's equation everywhere except when y is very small. In most practical cases, it is sufficient to keep only the first two terms of Eq. 1, dropping the term in x^4 (which then gives the error). On the other hand, Eq. 2 is a more convenient form, and is sufficiently accurate for most purposes if x and y are not too large (x and y are always less than one).

This work was done in whole (or in part) under Contract No. OEMsr-411 between the President and Fellows of Harvard College and the Office of Scientific Research and Development, which assumes no responsibility for the accuracy of the statements contained herein.

References

(1) Sommer, F., Die Berechnung der Kapazitäten bei Kabeln mit einfachem Querschnitt, *Elektrische Nachrichten Technik*, 17, p. 281-294, 1940.
(2) Kaden, H., Die Leitungs Konstanten symmetrischer Fernmeldekabel, *Europ. Fernsprechdienst*, 52, p. 174, 1939.
(3) Breisig, F., "Theoretische Telegraphie", Second Edition, p. 68, Braunschweig, 1924.
(4) Terman, F. E., "Radio Engineers' Handbook," McGraw-Hill Book Co., 1943, p. 174.

Vectorial Treatment of Transmission Lines

By representing current and voltage as vectors, and distance along the line as phase displacement, a clearer treatment of transmission lines is obtained than that given by equations. Typical problems are solved

By J. P. SHANKLIN

MOST TRANSMISSION LINE problems can be solved by vectors. The use of vectors makes the action of the line clear and allows visualizations which would otherwise be difficult.

Conditions at Load

Standing waves on a transmission line are caused by two waves, the incident and the reflected waves, traveling in opposite directions. At certain points the two voltages add and at certain other points they subtract. In Fig. 1A let $Z_R = 2Z_0/\underline{0°}$. A 2:1 standing wave ratio will be caused by the mismatch, the maximum value of which will be $E_0 + E_R$ and the minimum value $E_0 - E_R$ and $E_0 + E_R = 2\ (E_0 - E_R)$ or

$$E_0/E_R = 3 \qquad (1)$$

where the symbols are as defined in Table I.

The load is resistive and higher than the line impedance, therefore there is a high of the standing wave at the load or

$$E_R = E_0 + E_R \qquad (2)$$

The voltage vectors of Fig. 1B may be drawn from Eq. (1) and (2).

As to the currents involved, the incident current I_0 is considered to be in phase with the incident voltage E_0 but the reflected current I_R is considered to be 180° out of phase with the reflected voltage E_R. This is because of the sense of direction of flow which has been chosen.

The reflected wave may be considered as negative power because it is returning to the generator. The voltages are considered to have the same direction sense because both are measured across the line. A scale for the currents is chosen which will make the vectors I_0 equal E_0 and I_R equal E_R in length. The ratio of the scales used for voltage and current is dependent on the line surge impedance Z_0 according to the relation

$$\text{Scale Ratio} = Z_0 = E_0/I_0 = E_R/I_R \qquad (3)$$

Figure 2A is a vector diagram of the line voltages and currents for the same load as in Fig. 1 but where l equals 45 electrical degrees of line.

A single vector is used to represent E_0 and I_0. This vector is advanced 45° (counterclockwise) from the position of E_0 and I_0 in Fig. 1B because the incident wave will reach this point earlier. The vector E_R is drawn from the terminal of vector E_0, I_0 and retarded (clockwise) 45° since the reflected wave reaches this point later.

The vector sum of E_0 and E_R results in the line voltage vector E_R. The vector I_R is drawn as before, 180° out of phase with E_R. The vector sum of I_0 and I_R results in the line current vector I_R. This diagram reveals that

$$Z_R = E_R/I_R = Z_0\ \underline{/-37°}$$

and also that the phase angle of E_R and I_R relative to E_R and I_R can be measured.

Figure 2B is the vector diagram

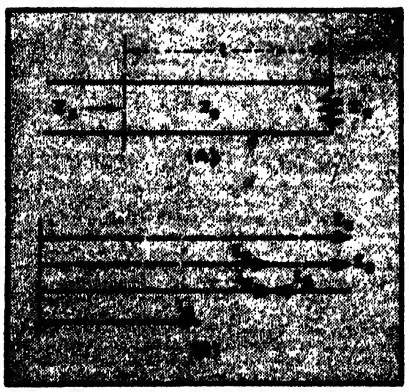

FIG. 1—(A) Transmission line showing relation of point, surge, and load impedances, and (B) currents and voltages at load for a load of $2Z_0$

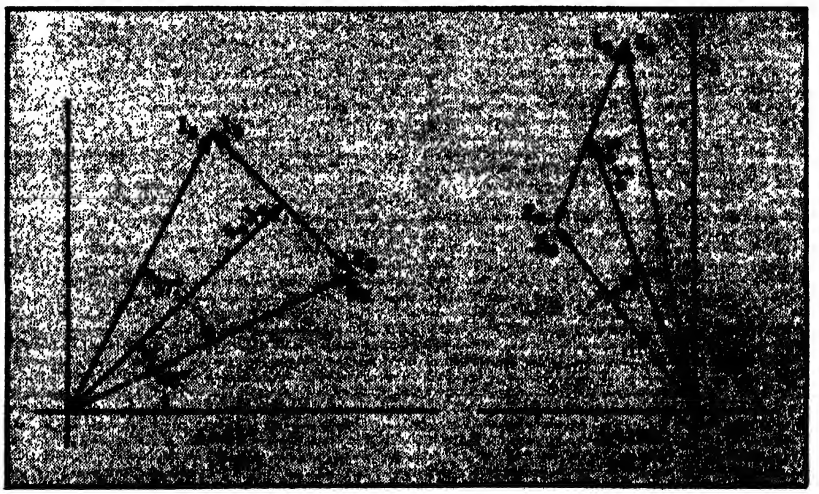

FIG. 2—Current and voltage relations for a line terminated in a resistance of $2Z_0$ (A) 45 electrical degrees from the load, and (B) 110 electrical degrees from the load

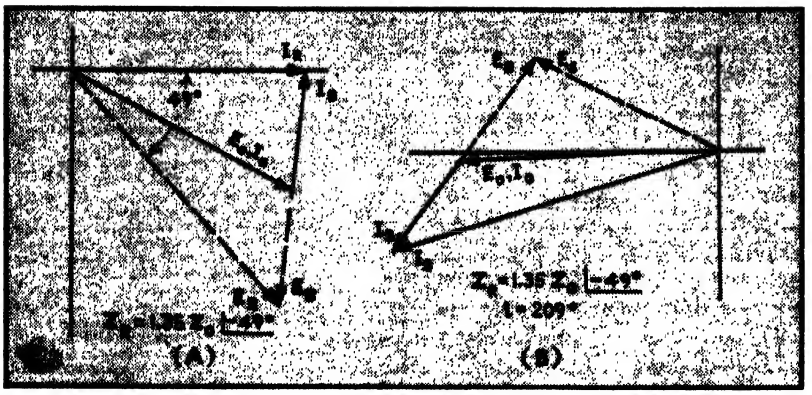

FIG. 3—Vectorial representations of conditions at a complex load (A), and some distance from it (B)

when l is 110° and yields the following data

$Z_R = 0.608\ Z/26°$.

I_R is 100° ahead of load current I_R.

E_R is 126° ahead of load voltage E_R.

Figure 3A is the vector diagram at a complex load 1.35 Z_o /−49°. First the vectors I_R and E_R are drawn, making E_R equal 1.35 I_R and current leading 49°. I_R has been taken on the zero or reference axis although this is immaterial.

Connect the terminals of I_R and E_R and plot a point in the center of this line. This point is the terminal of the E_o, I_o vector. I_R can be seen to be the vector sum of I_o and I_R, and E_R the vector sum of E_o and E_R. The E_o, I_o and E_R, I_R vectors have now been determined so that the vector diagram for any point on the line may be drawn.

Figure 3B is the vector diagram 209° away from the load. The E_o, I_o vector has been rotated 209° counterclockwise from its position in Fig. 3A and E_R and I_R have been rotated clockwise 209° from their positions in Fig. 3A.

TABLE I
DEFINITION OF SYMBOLS USED IN THE TEXT

E_o, I_o	—Incident voltage and current at the load
E_R, I_R	—Voltage and current across load Z_R
E_R, I_R	—Voltage and current reflected by the load
E_s, I_s	—Voltage and current a distance l from the load toward the generator
Z_o	—Surge impedance of the transmission line
Z_R	—Impedance of the terminating load
Z_s	—Impedance at a point on the transmission line
l	—Distance along transmission line measured in electrical degrees from the load toward the generator

For other symbols used in text, see circuit diagrams

Antenna Feeding

A problem sometimes encountered in a high-frequency array is to feed three dipoles in phase, the center dipole to be fed 1.5 times the current of the outer dipoles. This problem is similar to that of feeding the towers of a broadcast transmitter at the necessary current amplitudes and phases to develop a required radiation pattern.

The feeding system is shown in Fig. 4A. Because the end antennas were similar, they were combined reducing the circuit to that of Fig. 4B and impedances expressed in terms of the feed line impedances. Fig. 4C is the vector diagram at the Z_1 load and Fig. 3A the vector diagram at the Z_2 load. Note that the two load current vectors are drawn to satisfy the antenna requirements. That is, they are in phase, and the length of I_R Fig. 4C is scaled two units representing current in both end dipoles, and I_R of Fig. 3A is scaled 1.5 units.

There are three requirements to be met: (1) dipole currents must be in phase, (2) dipole currents must be in a 1.5 to 1 amplitude ratio, and (3) a resistive 50-ohm load must be presented to the 50-ohm line. Using the two variables l_1 and l_2 it is probable that any two of these requirements can be satisfied. The first two have been chosen because they must be satisfied before the lines are joined. The loads must

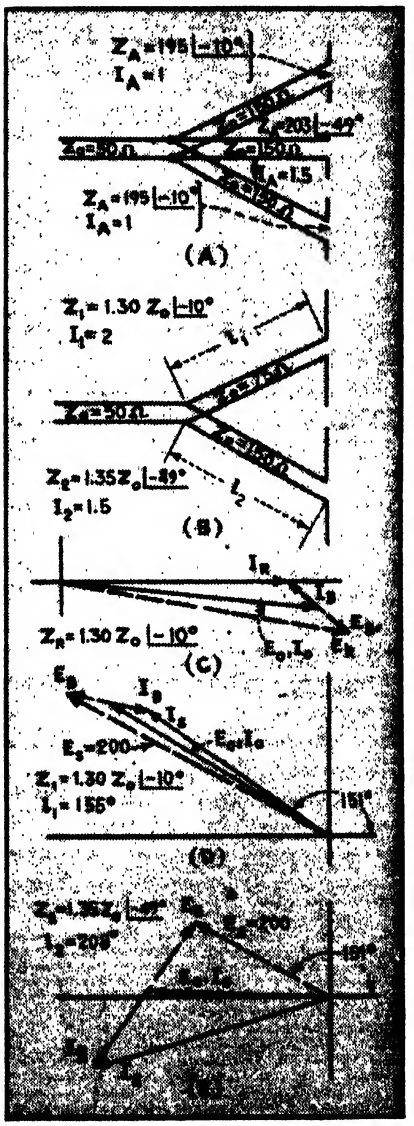

FIG. 4—Determination of feeding condition for a three-element array can be made vectorially. The given conditions are shown at (A), which can be simplified to (B) from which vectors at the upper antenna can be plotted (C). Vectors for the lower equivalent antenna are as at (A) in Fig. 3. The angular distance at which voltages on antenna feed lines are in phase is determined from (D) and (E)

give enough reflection to cause sufficient impedance variations along the lines to make a solution possible.

It is then necessary, by drawing trial vector diagrams for different lengths of l_1 and l_2, to find the lengths which will fill the first two requirements. Because the loads do not greatly mismatch their lines, lengths near even $\lambda/2$ multiples were tried in hopes of also partially satisfying requirement (8). Also, it is apparent that l_1 must be longer than l_2 because the current in Z_2 is to lead the current in Z_1 by 39° and must therefore be retarded.

Figure 4D is the solution. In order to connect the two lines together their voltages must be equal and in phase. The apparent difference in amplitude of the E_2 voltages in Fig. 4D and E is due to 2:1 ratio of scales used for the 150 and 75-ohm lines. The current scales, however, are equal.

Figure 5 is the vector diagram of the input currents and voltage at the juncture of l_1 and l_2. The currents I_1 and I_2 in the two lines are added vectorially to give the 50-ohm line current I_3. The E_2 vector is the same vector as E_2 of Fig. 4D and 4E except that the voltage scale has been changed to conform to a 50-ohm line. The input impedance of 1.1 Z_0 $/\underline{-21.5°}$ would be considered satisfactory for most high-frequency work.

The impedance 55 ohms $/\underline{-21.5°}$ may be matched to the 50-ohm line by the short-stub corrector shown in Fig. 6A. First draw the vector

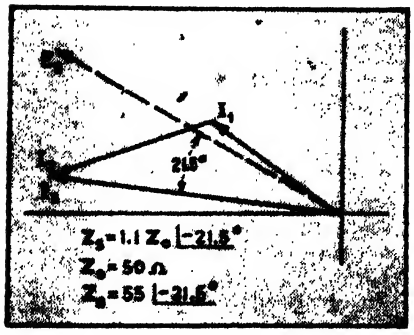

FIG. 5—At the juncture of the feed lines of Fig. 4B the voltages and currents have this relation as determined from Fig. 4D and 4E

diagram of Fig. 6B at the load. As I_R is leading E_R an inductive or lagging current will be needed to bring them into phase. Also, the length of the I_S vector must equal the E_S vector to represent a 50-ohm load.

Next draw the diagram of Fig. 6C. Draw the E_0, I_0 vector of Fig. 6B at any angle (180° in Fig. 6C). From the terminal of E_0, I_0 strike an arc of radius equal to E_R. Draw the vectors E_S and E_R, making the angle between them 90°. Draw I_R and I_S. I_C will then represent the inductive current to be drawn by the correcting stub. Note that it lags 90° behind the voltage E_S across the stub.

The 50-ohm line current I_{50} is the vector sum of I_C and the input current I_S to line l_1. The angle between E_0 and E_R in Fig. 6B is 105.5° and the angle between E_0 and E_R in Fig. 6C is 79°. The difference of 26.5° is caused by their rotation in traveling over the length of line l_1. The electrical length of l_1 will be half this amount or 13.25° because the vectors rotate in opposite directions. If desired, Fig. 6C may be redrawn in proper angular reference to the preceding diagrams. This results in Fig. 6D which is the input diagram for $Z_R = 1.1\ Z_0\ /\underline{-21.5°}$ and $l_1 = 13.25°$.

Figure 6C could have been drawn by calculating the magnitude of E_S first, and drawing E_R at right angles to E_R. The total power on the line will be the same at all points, therefore in Fig. 6B $P = E_R I_R \cos 21.5°$, or scaling E_R and I_R, $P = 200 \times 3.6 \times 0.930 = 670$. In Fig. 6C, $P = E_S^2/Z_0$ or $670 = E_S^2/50$, thus $E_S = 183$.

In determining the length of the stub l_2 of Fig. 6A, first consider the characteristics of a shorted line. There will be 100 percent reflection at the short, therefore E_R will equal E_0 and I_R will equal I_0. There can be no voltage across the short, therefore E_R must be 180° out of phase with E_0 at the short. Since the voltages are 180° out of phase, the currents I_0 and I_R must be in phase and adding. A vector diagram could be drawn representing these conditions at the short.

Now draw Fig. 6E, the vector diagram for the input to the stub.

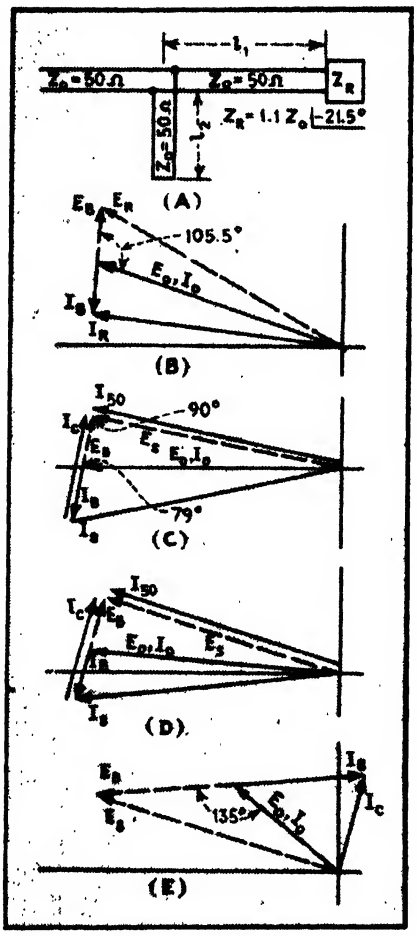

FIG. 6—To match the transmission and feed lines, a shorted stub (A) is required. Conditions at the load are shown at (B), and the inductive current to be drawn by the stub is determined from (C). (D) is (C) reoriented to agree with previous vector positions. (E) represents the input to the stub from which stub length is determined

I_0 and E_R are copied from Fig. 6D. E_0 and E_R are 45° out of phase in Fig. 6E and were 180° out of phase at the short. Since E_0 turns counterclockwise and E_R clockwise, to have reached their position in Fig. 6E they must have moved in relation to each other by the larger angle between them, or 135°. Therefore l_2 of Fig. 6A must then be half this long or 67.5°.

Because a transmission line is linear, the percentage loss to the incident wave will equal the percentage loss to the reflected wave. If the input and output powers are known or can be measured, the line loss can be determined, and apportioned for any length line.

Mismatch Loss Chart for Transmission Lines

Loss due to mismatch between load and line impedance is given directly, in terms of total rated loss of line and standing wave ratio at load end

By J. M. HOLLYWOOD

LEAST loss in a transmission line is obtained when its load impedance is equal to the characteristic impedance of the line, and standing waves are absent. Attenuation figures for lines are usually given on this basis. Since perfection is seldom obtained in practice, it is desirable to know the penalty incurred if a line is not perfectly matched. The accompanying chart shows this in a simple manner for ready use.

Each curve is for a line having a given loss in db when perfectly matched (loss equals attenuation in db per unit length multiplied by the length used). From published or known line data, the appropriate curve is selected or interpolated. If the standing wave ratio (SWR) at the load end of the line is known, the intersection of the corresponding vertical line and the selected curve gives the added line loss or attenuation in db, as shown on the scale at the left. This can be found in the same way for a known ratio of a resistive load R to the line impedance Z_0, using the alternative scale at the bottom.

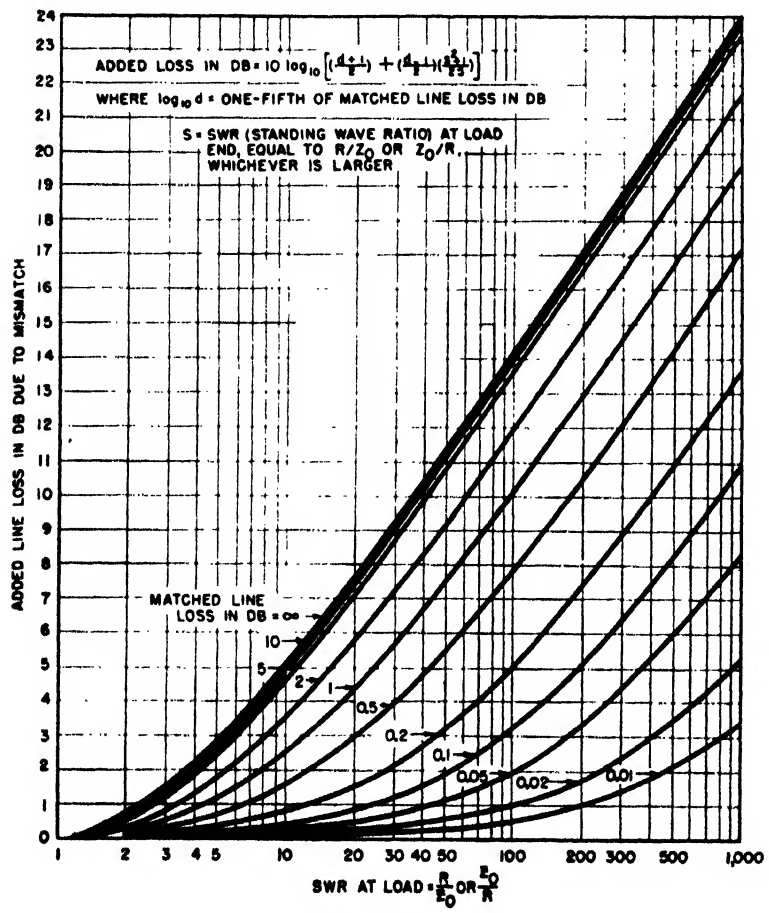

As an example, consider a 500-ohm antenna used with 100 feet of RG-8/U cable at a frequency of 93 mc, having 2 db nominal attenuation, and a characteristic impedance of 52 ohms. R/Z_0 is 9.6; using the 2-db curve on the chart, the added loss due to mismatch is found to be 3.3 db.

As another example, if an antenna has to be used over a frequency range such that the standing wave ratio on a 52-ohm line becomes 5:1 and the line has 5 db attenuation when matched, the chart shows the added line loss to be 2.4 db at the extremes of the frequency range used.

The chart illustrates several points: (1) large SWR introduces little added loss if matched loss is very small; (2) little loss is added even to a large matched loss if the SWR is very small; (3) the added loss is almost the same for any matched loss over 10 db.

The chart and equation apply strictly only to lines of an integral number of quarter-wave lengths, or half-wave lengths for complex impedance loads. A very short line without leakage, for example, would have least loss if operated into an infinitely large load resistance.

Transmission Lines as Tuning Elements

Graph for designing tuning element consisting of a section of transmission line shunted by a capacitor. Values of one or two unknown circuit parameters may be found when values of two or three others are known

By H. E. NEWELL, JR.

SEGMENTS of transmission lines used as circuit elements in present day high frequency work have made desirable a simple, rapid method for solving the equation

$$1/\omega C = Z_0 \tan 2\pi l/\lambda, \; l \gtrless \lambda/4 \qquad (1)$$

The equation gives the wave length λ of the resonant frequency $\omega/2\pi$ of a parallel combination of a capacitance C and a short circuited length l of transmission line of characteristic impedance Z_0, shown in Fig. 1.

The graph on the next page shows two sets of contours, the plots of which are superimposed upon each other in such a manner as to afford a convenient means for solving Eq. 1 graphically. The discussion below contains a brief outline of the construction of the graph, followed by its application to the solution of two typical problems.

Rewrite Eq. 1, by using the relations $\omega = 2\pi f$ and $\lambda = v_0/f$, where f is frequency in cycles per second and $v_0 = 3 \times 10^8$ meters per second, the propagation constant.

$$1/Z_0C = 2\pi f \tan (2\pi fl/v_0) \qquad (2)$$

Equation 2 may be applied to the circuit of Fig. 1 by expressing Z_0 in ohms, C in farads, f in cycles per second, and l in meters.

But if Z_0 is in ohms, C in $\mu\mu f$, f in mc, and l in cm, Eq. 2 becomes

$$\frac{1}{Z_0 \times 10^{-12}C} = 2\pi 10^6 f \tan \frac{2\pi 10^6 f \left(\frac{l}{100}\right)}{3 \times 10^8}$$

or

$$\frac{10^6}{Z_0C} = \frac{2\pi f}{10^6} \tan \frac{2\pi fl}{3 \times 10^4} \qquad (3)$$

$$F_2 (Z_0, C) = F_1 (l, f)$$

where

$$F_1 (l, f) \equiv (2\pi f/10^6) \tan (2\pi fl/3 \times 10^4)$$

and

$$F_2 (Z_0, C) \equiv 10^6/Z_0 C$$

On logarithmic graph paper, plot F_1 (l, f) against l for the various values of f. Upon these contours

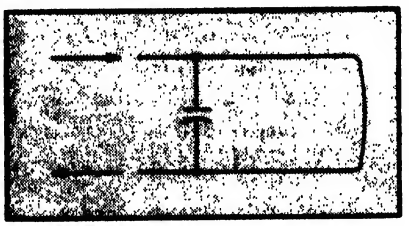

FIG. 1—Short-circuited transmission line of length l, and characteristic impedance Z_0 tuned by shunt capacitance

superimpose those of F_2 (Z_0, C) plotted versus C with Z_0 as a parameter, so that the F_1 and F_2 scales coincide. The C and l scales coincide as do the F_1 and F_2 scales. This, however, is not necessary, and in this case is due merely to the choice of range for the values of C. It is essential that the F_1 and F_2 scales be identical.

The construction of the chart makes evident the general principles involved in its use. A solution is obtained for Eq. 3, by making F_1 $(l, f) = F_2$ (Z_0, C). Suppose that a 10 cm line of 50 ohms characteristic impedance is to be tuned to resonance at 400 mc by shunting a lumped capacitance C across the input and short circuiting the other end.

To find C, the solution is as follows: from the 10 cm point on the l scale of the graph move vertically to the $F_1(l, f)$ contour marked 400 mc. Then move horizontally to the $F_2(Z_0, C)$ contour labelled 50 ohms. From this point move vertically again to the C scale and read off the capacitance, 7.3 $\mu\mu f$.

If any three of the quantities l, Z_0, C, f in Eq. 3 be given, the fourth is obtanied by a procedure similar to that used above. If two of quantities be given, the remaining two can assume infinitely many pairs of values satisfying Eq. 3.

Consider now the problem of a shorted open wire line to be used as a circuit element in a high frequency amplifier. A variable capacitance, ranging from 5 $\mu\mu f$ to 10 $\mu\mu f$, is shunted across the open end of the line and used for tuning. If the frequency range to be tuned is from 150 mc to 200 mc, what should the physical length and characteristic impedance of the line be?

Mathematically this problem is that of solving simultaneously two equations in two unknowns

$$F_1 (l, 150\ mc) = F_2 (Z_0, 10\ \mu\mu f.) \qquad (4a)$$
$$F_1 (l, 200\ mc) = F_2 (Z_0, 5\ \mu\mu f.) \qquad (4b)$$

Using the graph, make a table of solutions of Eq. 4a, alone, and another of solutions of Eq. 4b, alone.

l in cm	Z_0 in ohms from Eq. 4a	Z_0 in ohms from Eq. 4b
10	325	360
15	207	220
20	147	143
25	108	94

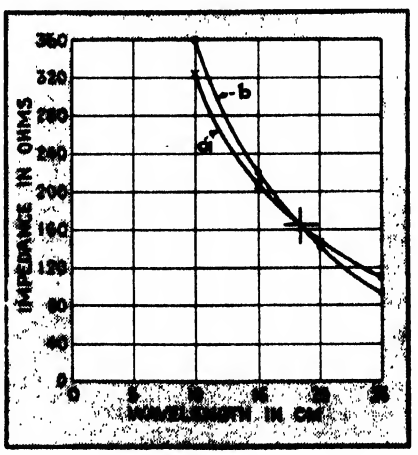

FIG. 2—Graphical solution for Eq. 1, where two quantities are unknown

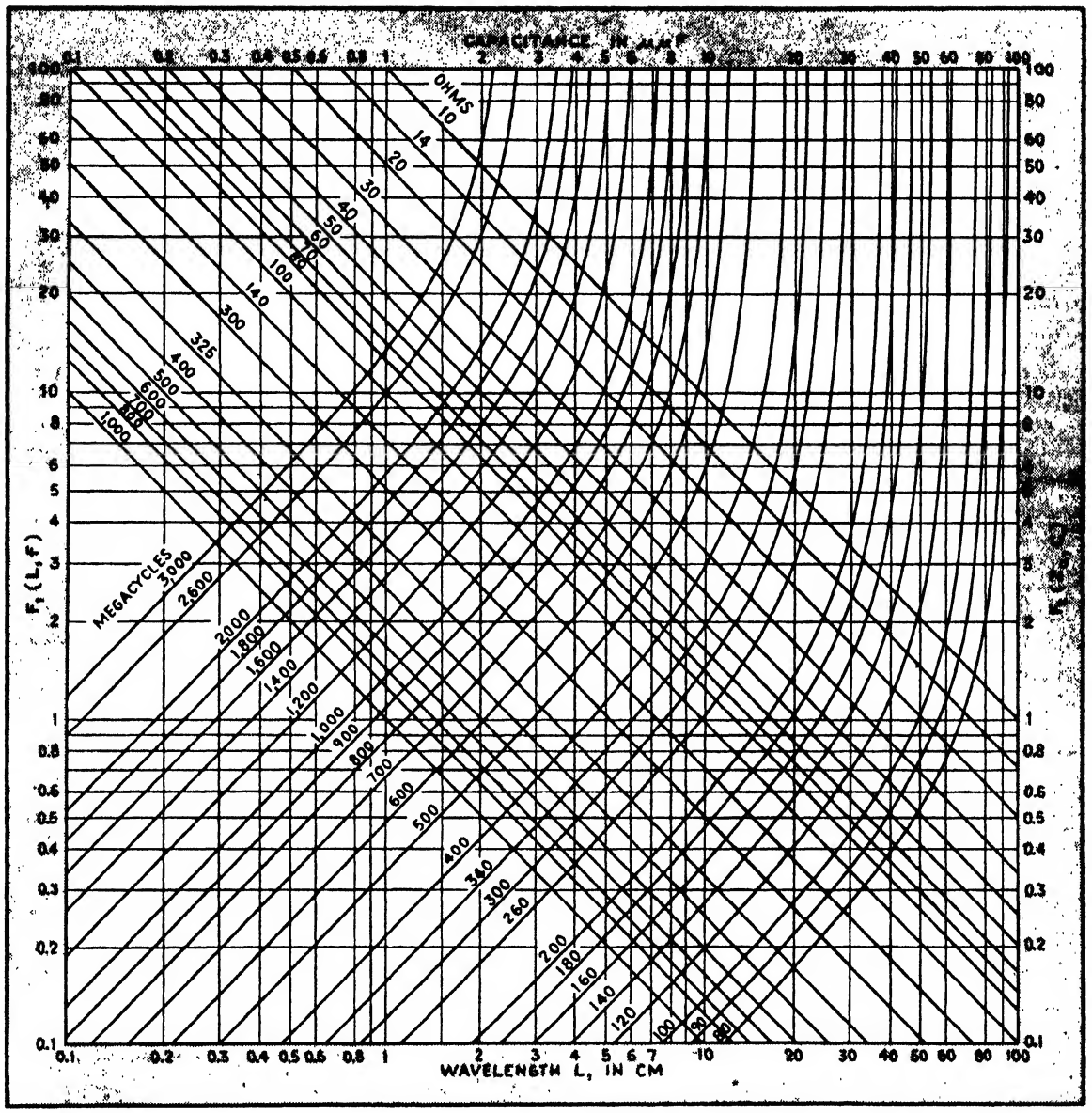

Graphical solution of Eq. 1 for obtaining the value of one quantity when values of three are known or values of two quantities when the other two are known

Draw the curves corresponding to both tables on the same graph, using identical scales for both as in Fig. 2. The intersection of the two curves gives the solution; in the present case: $Z_0 = 164$ ohms, $l = 18.4$ cm.

As a purely mathematical problem, the contours of the graph may be used over the entire ranges of f and Z_0 for the solution of Eq. 3, but the application of such solutions to actual physical circuits is of doubtful validity in the upper ranges of frequency and impedance. At high frequencies a shorting bar on a very high impedance line of less than a quarter wave length must itself form a considerable part of the line. Moreover, the assumption that the total capacitance involved can be lumped into a single element is undoubtedly invalid under these conditions.

High-Frequency Cable Design

Practical design equations and two nomographs facilitate calculation of characteristic impedance, inductance, time delay, attenuation, and power rating for solid-dielectric coaxial and two-conductor balanced lines operating in h-f and vhf bands. A typical polyethylene cable design problem is worked out

By K. H. ZIMMERMANN

At high frequencies (in the megacycle range) the transmission line must be terminated in a load whose impedance is equal to the characteristic impedance of the line, in order to prevent reflections and standing waves that cause excessive power loss. For high-frequency operation, therefore, the characteristic impedance of the cable becomes one of its most important properties.

Characteristic impedance in ohms, usually denoted Z_0, is determined by

$$Z_0 = \sqrt{\frac{R + j\omega L}{G + j\omega C}} \qquad (1)$$

where R is resistance in ohms per unit length, L is inductance in henrys per unit length, C is capacitance in farads per unit length, and G is conductance in mhos per unit length. This reduces to

$$Z_0 = \sqrt{L/C} \qquad (2)$$

since R is very small compared to ωL and G is very small compared to ωC.

The most common type of high-frequency cable is the coaxial cable in which the outer conductor completely surrounds the centrally disposed inner conductor. At high frequencies the internal inductance is negligible due to the skin effect which confines the current to the outer surface of the inner conductor and the inner surface of the outer conductor. The inductance of a coaxial cable then becomes

$$L = 0.140 \log_{10} (D/d) \qquad (3)$$

and the capacitance is

$$C = 7.36\, k/\log_{10} (D/d) \qquad (4)$$

where L is in microhenrys per foot, C is in micromicrofarads per foot, D is the outside diameter of the insulation, d is the diameter of the inner conductor, and k is the dielectric constant of the insulating material.

Substituting Eq. 3 and 4 in Eq. 2 gives the useful design equation for characteristic impedance in terms of the diameters of the conductors and the dielectric constant of the insulating material.

$$Z_0 = \frac{138}{\sqrt{k}} \log_{10} (D/d) \qquad (5)$$

The nomograph in Fig. 1 gives a rapid solution of Eq. 5.

In the foregoing equations, d represents the outside diameter of a solid inner conductor. For the usual concentrically stranded seven-strand conductor, 93 percent of the maximum conductor diameter is used as the effective diameter.

From Eq. 4 and 5 another equation is obtained which is useful in determining the characteristic impedance of a cable from actual measurements of the capacitance C in $\mu\mu$f per foot and the dielectric constant k

$$Z_0 = 1{,}016\, \sqrt{k}/C \qquad (6)$$

Radio waves travel at a speed of 300 million meters per second in free space. The velocity of a wave propagated along a solid dielectric cable is related to the dielectric constant and the velocity in free space by the relation

$$\frac{v}{c} = \frac{1}{\sqrt{k}} \qquad (7)$$

where c is the velocity of propagation in free space and v is the velocity of propagation in the cable. For polyethylene insulated cables the statistical average of the ratio v/c is 0.663. The velocity of propagation and the dielectric constant can be calculated by finding the resonant frequency of a known length of cable open-circuited at the far end.

The time in microseconds per foot for a wave to travel through a cable can be determined from Eq. 3, 4, and 7

$$T = \sqrt{LC} = \frac{1.016 \times 10^{-6}}{v/c} \qquad (8)$$

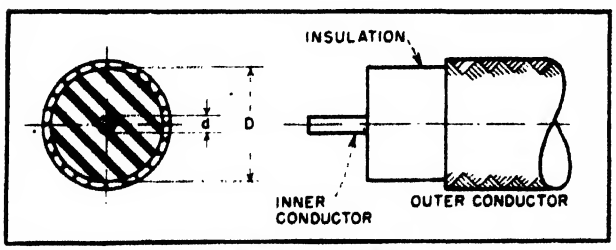

Single coaxial line

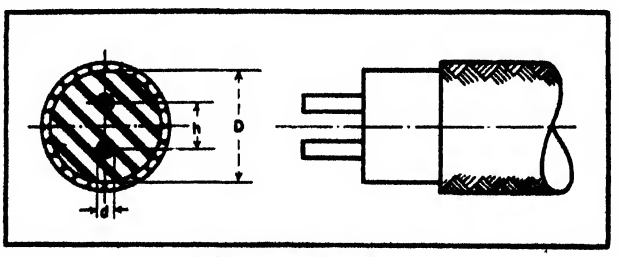

Balanced shielded line

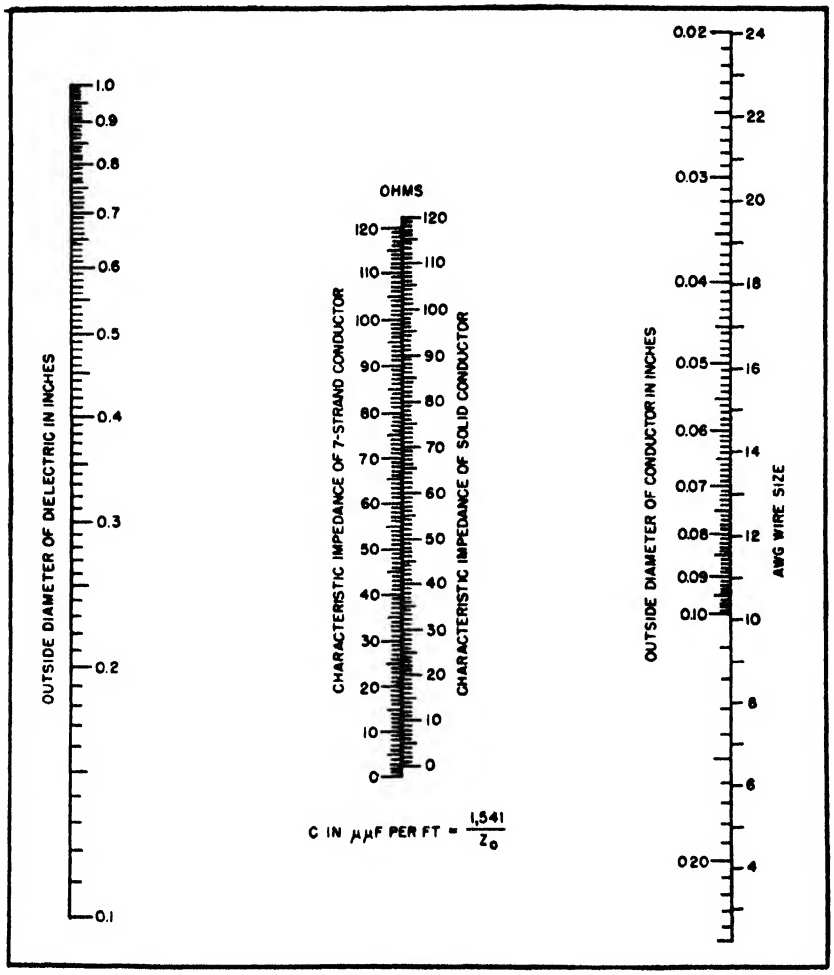

FIG. 1—Nomograph giving characteristic impedance of polyethylene-dielectric single coaxial line. For solid inner conductor, read answer on righthand portion of center scale; for stranded inner conductor, use maximum outer diameter on conductor scale at right and read answer on lefthand portion of center scale

Whenever it is desirable to transmit power from a balanced source, neither side of which is grounded, the balanced line is used instead of the coaxial line.

Two-conductor shielded lines are designed for a specified characteristic impedance in accordance with the following relation

$$Z_0 = \frac{276}{\sqrt{k}} \log_{10}\left(2v\frac{1-Q^2}{1+Q^2}\right) - \frac{120}{\sqrt{k}}\left(\frac{1+4v^2}{16v^4}\right)(1-4Q^2) \qquad (9)$$

where $Q = h/D$ and $v = h/d$, and h is the center-to-center spacing of the conductors. This line has one primary disadvantage in that it is only flexible at right angles to the plane through the two parallel wires. Any attempt to bend it in another direction will damage the conductors or the dielectric. This difficulty has been overcome by separately insulating each conductor to a diameter equal to the desired center-to-center conductor spacing. The insulated conductors are then twisted and another extrusion of dielectric is applied to obtain the final circular cross-section. This not only improves the flexibility of the line but also improves the balance characteristic by providing a closer tolerance on the conductor spacing. Moreover, since the conductors change their positions relative to the shield there is less tendency to unbalance than in the parallel-conductor arrangement where it is possible for one conductor to be closer to the shield for the entire length of the line.

The design of the unshielded twin-conductor parallel transmission line which is used for dipole transmitting and receiving antennas is based upon a certain amount of actual experience. Satisfactory results have been obtained with the relation

$$Z_0 = 120\left(\frac{v}{c}\right)\cosh^{-1} h/d \qquad (10)$$

where h is the center-to-center spacing of the conductors, d is the effective conductor diameter, and v/c is as defined in Eq. 7. The value of v/c was determined from measurements of actual lines as 68, 70, and 81 percent for 75, 100, and 300-ohm lines respectively at 100 mc.

When an extremely high degree of electrical balance is required, two coaxial lines are enclosed in a common braid. The characteristics of each coaxial are determined by precise measurements before the lines are assembled under the common braid and jacket. The characteristic impedance of twin coaxial lines is the sum of the impedances of the individual coaxial units.

Low-Capacitance Lines

For certain applications, capacitance lower than normally possible with solid-dielectric materials is required. Coaxial lines insulated with polyethylene are usually made with impedances ranging from 30 to 150 ohms. The capacitance of a 150-ohm line, obtained from Eq. 6, is 15.6 $\mu\mu$f per foot. The ratio of dielectric diameters, obtained from Eq. 5, is nearly 43 to 1. If No. 22 AWG solid conductor is used for this cable, the dielectric diameter would be 1.08 inches.

If the effective dielectric constant is reduced by replacing part of the dielectric material with air, it is possible to obtain capacitances below 10 $\mu\mu$f per foot. This is accomplished by wrapping a thread of polyethylene or other low-loss material around the inner conductor with a long lay and extruding a tube of polyethylene over the spiral. The polyethylene thread supports the tube and also centers the conductor. A capacitance of 10 $\mu\mu$f per foot can be obtained with a diameter ratio of 11 to 1.

The time delay of solid dielectric lines is often used as a timing or calibrating device in radio applications, especially radar and television. However, when a greater delay than that possible with the usual coaxial line is required, it is necessary to employ especially constructed lines referred to as delay lines.

The delay line is exactly similar in appearance and construction to the usual coaxial line except that the inner conductor consists of an insulating core around which a spiral of insulated wire is wrapped. The inductance of a single-layer coil is then

$$L = 3.06 \times 10^{-2}\, \pi^2\, n^2\, a^2 \qquad (11)$$

where n is the number of turns per inch and a is the diameter of coil between wire centers, in inches. The inductance of the line is thus increased while the capacitance remains essentially the same.

Time delay T in microseconds per foot, which is the reciprocal of the velocity of propagation, can be computed from L and C

$$T = \sqrt{LC} = \frac{4.76 \times 10^{-4}\, \pi\, n\, a\, \sqrt{k}}{\sqrt{\log_{10}(D/d)}} \qquad (12)$$

Since the inductance of the line has been increased, it follows that the characteristic impedance has also been increased. From Eq. 2 the characteristic impedance becomes

$$Z_0 = \sqrt{\frac{L}{C}} = \frac{64.5\, \pi\, n\, a}{\sqrt{k}} \sqrt{\log_{10}(D/d)} \qquad (13)$$

It is possible with this construction to obtain impedances greater than 1,000 ohms without increasing the size of the line beyond practical limits.

A high-impedance line is often required in video-frequency transmission when it is desired to drive a terminated line from a high-impedance source.

Attenuation and Power Rating

Attenuation determines the length of line that can be employed and its power-handling capacity. The total attenuation of a line is due to the losses in the inner and outer conductors and the loss in the dielectric. The attenuation in db per 100 feet due to the copper loss is expressed by the relation:

$$A_c = 4.35\, R_t / Z_0 \qquad (14)$$

where R_t is the total high-frequency resistance of the inner and outer conductors in ohms per 100 feet. For solid copper conductors

$$R_t = 0.1 \left(\frac{1}{d} + \frac{1}{D} \right) \sqrt{F} \qquad (15)$$

where d is outer diameter of inner conductor in inches, D is inner diameter of outer conductor or dielectric in inches, and F is frequency in mc.

For other than solid copper inner and outer conductors, such as stranded inner conductors and braided outer conductors, other factors must be introduced to compensate for the effects of spiralling, proximity, and contact resistance. Equation 15 then becomes

$$R_t = 0.1 \left(\frac{R_1}{d} + \frac{R_2}{D} \right) \sqrt{F} \qquad (16)$$

and the total copper loss in db per 100 feet becomes

$$A_c = \frac{0.435}{Z_0} \left(\frac{R_1}{d} + \frac{R_2}{D} \right) \sqrt{F} \qquad (17)$$

where R_1 and R_2 are multiplying factors that are determined by the construction of the conductors and are also variable with frequency. It is necessary to combine experience with experimental data to estimate their magnitude in connection with actual design of various types of cables.

The attenuation in db per 100 feet due to the dielectric is dependent upon the frequency, dielectric constant, and power factor of the material

$$A_d = 2.78\, \sqrt{k}\, pF \qquad (18)$$

where p is power factor of dielectric, k is dielectric constant of dielectric, and F is frequency in mc. The total attenuation in db per 100 feet is then the sum of Eq. 17 and 18.

$$A = \frac{0.435}{Z_0} \left(\frac{R_1}{d} + \frac{R_2}{D} \right) \sqrt{F} + 2.78\, \sqrt{k}\, pF \qquad (19)$$

The power rating of a cable is a function of the maximum temperature which the insulation can safely withstand. The power-handling capability of the cable is limited by the rate at which the cable can dissipate the heat due to the copper and dielectric losses and the rate at which the heat is generated internally. The first depends upon the diameter of the cable, the color, texture, and materials of the jacket, paint, or armor, and the ambient temperature. The second depends on the dimension and construction of the conductors, the dielectric material, and the frequency, among other factors.

The amount of heat which flows radially from the components, conductors, dielectric, and braid will depend upon the temperature gradient, the thermal resistances of the dielectric and jacket, and the thermal resistance of the jacket surface to air (jacket emissivity). The relation for power input[1] is

$$P = \frac{T_e - T_a}{t_a (2A_c + A_d) + 2A_t (t_j + t_s)} \qquad (20)$$

where P is maximum average power input, T_e is maximum temperature in degrees F that the dielectric can withstand, T_a is ambient temperature in degrees F, t_a is thermal resistance of dielectric, t_j is thermal resistance of jacket, t_s is thermal resistance of jacket surface to air, A_c is attenuation due to inner conductor, in nepers per inch, A_d is attenuation due to dielectric in nepers per inch, and A_t is total attenuation of the cable in nepers per inch.

For accuracy, values used for attenuation should be corrected to include the effects of temperature rise and any mismatch that may occur.

In view of the safety factor that is required in power rating, the following equation[2] for input power P has been found quite useful and easy to handle

$$P = \frac{K_1 (K_2 + 6 D_c)}{A} \qquad (21)$$

where K_1 is 435 for black vinylite jackets and 826 for grey vinylite or armored cables, K_2 is 3 for 50-ohm cables and 2.5 for 75-ohm cables, A is attenuation in db per 100 feet, and D_c is outer diameter of cable in inches. This relation is based on a maximum temperature of 80C at

the surface of the inner conductor and an ambient temperature of 20C.

If the ambient temperature is higher than 20C, the power rating of the cable is reduced; conversely, if the ambient is lower, the rating is increased. The results of Eq. 21 can be corrected by the nomograph shown in Fig. 2.

Typical Design Problem

Required: A 70-ohm coaxial cable to transmit 7.5 kw of 100-mc power at an ambient temperature of 30C. The dielectric material selected is polyethylene with a dielectric constant k of 2.26, and the available jacket material is black vinylite.

Since the characteristic impedance is specified as 70 ohms, the ratio of D/d is fixed and equal to 5.75, as can be determined from Eq. 5 as follows:

$$70 = \frac{138 \log_{10} (D/d)}{1.5}$$

Arbitrarily, a No. 5 AWG solid inner conductor is selected. Here d is 0.182 inch, so that dielectric diameter D becomes 1.05 inch. Using a typical thickness value of 0.225 inch for the braid and 0.05 inch (50 mils) for the jacket, the overall outside diameter D, becomes 1.6 inch. From these values the attenuation and power rating can be calculated by using Eq. 19 and 21, assuming values of 1 for R_1 and 2 for R_2 based upon experience with cables having No. 30 AWG braid at 100 mc, and using a value of 3×10^{-4} for dielectric power factor p

$$A = \frac{0.435}{70}\left(\frac{1}{0.182} + \frac{2}{1.05}\right)(10) + 2.78\,(1.5)\,3 \times 10^{-4}\,(100)$$
$$= 0.584 \text{ db per 100 feet}$$

From Eq. 21 the power rating at 20C is determined as

$$P = \frac{435\,(2.5 + 9.6)}{0.584} = 9{,}013 \text{ watts}$$

The power rating at 30C, obtained from the nomograph in Fig. 4, is then 7,500 watts.

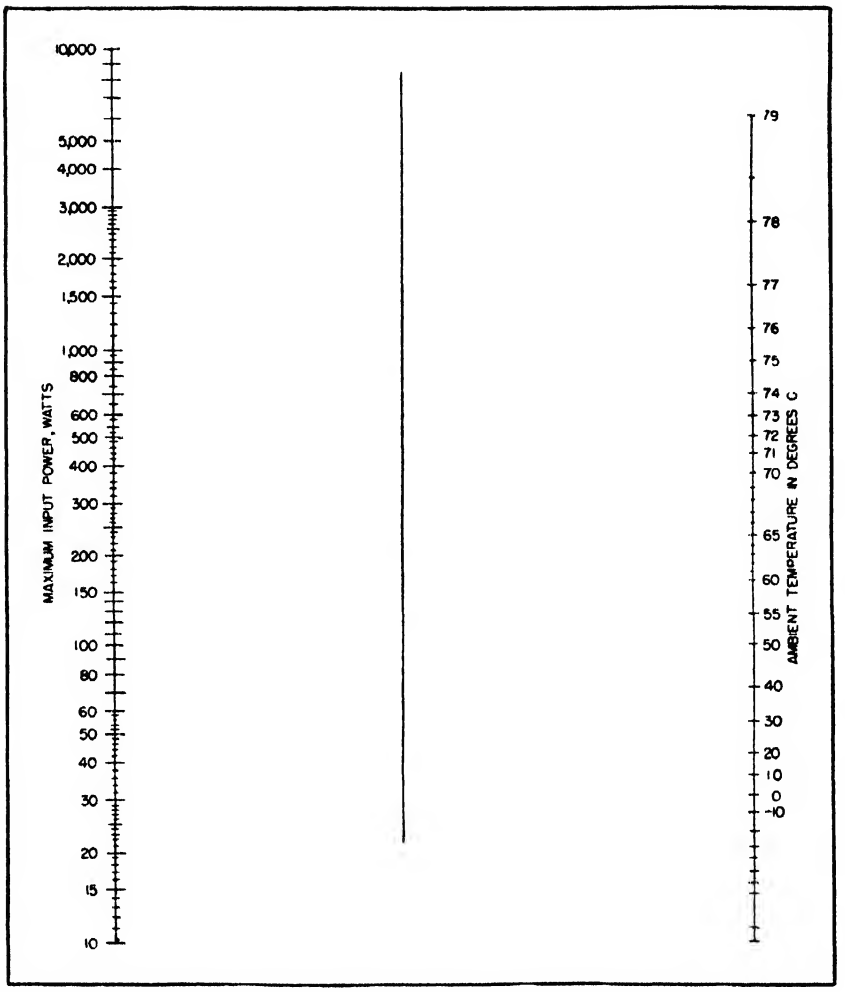

FIG. 2—Nomograph giving power rating at any ambient temperature when rating for one temperature is known. Values are based on maximum inner conductor temperature of 80C. Place straightedge on known values of power and temperature, mark intersection with center vertical scale, rotate straightedge about this intersection to new temperature value, and read new power rating on lefthand scale

References

(1) L. C. Swicker, Recommended Values of Thermal Constants for Use in Estimating the Thermal Characteristics and Power Rating of Various Cables, Navy Report—Case 24893.

(2) Devised by F. A. Muller of Federal Telecommunications Laboratories, R-17.

TRANSMITTERS

F-M Transmitter Performance Measurements

Frequency response, harmonic distortion, a-m and f-m noise in f-m broadcast transmitters must be held within legal limits. Techniques of using standard test equipment in meeting FCC requirements for proper performance are described in detail

By H. P. THOMAS and L. M. LEEDS

THE PERFORMANCE of f-m broadcast transmitters is based primarily on the requirements of the Federal Communications Commission which specify the overall performance of the entire transmitting system from microphone input to antenna output. No definite portion of the total system degradation is assigned to the transmitter proper, although in the case of harmonic distortion it is recommended that the transmitter should not contribute more than half the total.

When the system is made up of studio equipment and some circuit such as a telephone line or radio link between the studio and transmitter it would be desirable to have the transmitter contribute less than one third of the total. The Radio Manufacturers Association has established minimum transmitter performance specifications which approach this degree of system perfection, as shown in Table 1.

Audio Input Signal

The equipment necessary in order to measure the audio frequency characteristics of the transmitter is shown as a block diagram in Fig. 1. The source of audio input must cover the frequency range from at least 50 to 15,000 cycles with low harmonic and hum output, and have an audio output level of at least +20 dbm (7.7 volts rms in 600 ohms). The output should be balanced to ground if a balanced input is to be used in the transmitter.

Following the audio oscillator some method must be provided of measuring input level, such as a calibrated vu meter or vacuum tube voltmeter that will read correctly at all frequencies from 50 to 15,000 cycles. This instrument should read over a voltage range of at least +20 to −10 dbm, or should be used in combination with an adjustable calibrated attenuator to give the same range of input voltages.

A pad of at least 10 db should precede the transmitter input in order to provide isolation between the audio input equipment and the transmitter input.

Output Detector

An f-m detector to convert the transmitter output to an audio frequency signal must be used to monitor the transmitter. This element of the measurement system is of considerable importance as it must have low harmonic distortion, low noise level, and a flat frequency characteristic in order not to affect the measurements of transmitter performance. There also should be sufficient limiting in the f-m detector to prevent small amounts of amplitude modulation of the transmitter carrier from affecting the readings. A minimum of 20-db limiting is considered necessary, and between 30 and 40 db is desirable. Fortunately, f-m station monitors are now available that have sufficiently good performance to meet the needs of this element of the measuring system, and since a station monitor is required equipment at every commercial f-m transmitter, it is normally available for measurement purposes. The use of the f-m station monitor also makes determination of the percent modulation of the transmitter very simple as a calibrated meter is provided which reads this value directly.

A de-emphasis circuit having the standard 75-microsecond time constant is necessary in order to translate back to a flat system. This is normally provided in the f-m station monitor, in which case it does not need to be provided separately.

Noise and Distortion Analyzer

The instrument for reading harmonic distortion and noise level at the output of the de-emphasis circuit should have a response to at least 30 kc so that the second harmonic of 15 kc can be measured. This device should preferably be of the type which balances out the fundamental audio frequency either by an infinite rejection filter or by reintroduction of some of the input signal properly adjusted in magnitude and phase. In both types, the residual signal consists of harmonic distortion and noise, and if the noise level is 60 db or more below the 100-percent modulation level, a reading of the residual signal, made with a vacuum tube voltmeter and

suitable attenuators, is a good measure of the total rms distortion of the system. In all cases the true harmonic distortion is of a value slightly less than the value determined by this measurement.

The block diagram also shows a cathode ray oscilloscope connected to the output of the noise and distortion meter. Although not essential, it is of assistance in analyzing the character of the distortion or noise being measured.

The procedure for measuring frequency response is merely to read the input voltage required to maintain a given percentage modulation as indicated by the station monitor. The input can be read directly in db if an input attenuator or vu meter is used for measuring input level, or voltage readings can be converted to db so that the response can be plotted in db to give a curve as shown in Fig. 2, which is of the form required by the FCC standards of good engineering practice.

Data on harmonic distortion are taken by passing the input signal from the audio oscillator through the system, balancing out the fundamental frequency in the noise and distortion meter, and reading the residual distortion components by means of the vacuum tube voltmeter in the instrument. These readings can be made at various percentages of modulation, as indicated by the station monitor modulation level indicator. An example of one such curve is shown in Fig. 3.

The f-m carrier noise level is read by modulating the transmitter to 100-percent modulation (±75 kc swing) with a tone of any frequency below the point at which the pre-emphasis is appreciable, usually 400 cycles or less, and setting the noise and distortion meter to read any convenient level, say +30 db under these conditions. Then the modulating tone is removed, and a reading of the residual noise taken on the noise and distortion meter. This procedure usually permits a noise level reading to be made down to about −70 db. If readings are to be made of noise levels even less than −70 db, a modulation level 10 or 20 db below 100-percent modulation can be used for the input signal while still setting the noise and distortion meter to +30 db.

Amplitude-modulation carrier ripple is measured by using an ordinary diode detector with a standard 75-microsecond de-emphasis circuit, connected to the transmitter output, and measuring both the d-c and a-c ripple voltages developed across the detector load resistance. The noise level is then the ratio of the square root of two times the rms a-c voltage to the d-c voltage. In db, it will be 20 times the logarithm to the base 10 of this ratio.

Checking Measurement Equipment

There are certain checks on the performance of the measuring equipment which can be made fairly easily. By connecting the noise and distortion meter input terminals across the transmitter input terminals, a reading of harmonic distortion will be obtained that is essentially the harmonic content of the audio oscillator output.

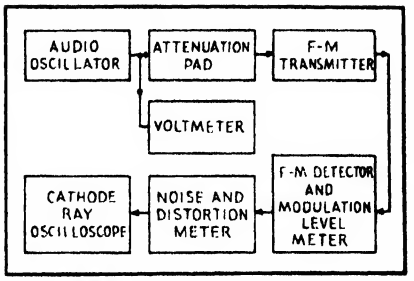

FIG. 1—Block diagram of measuring apparatus used in checking audio frequency characteristics. Pre-emphasis network in transmitter and de-emphasis circuit in monitor are not shown

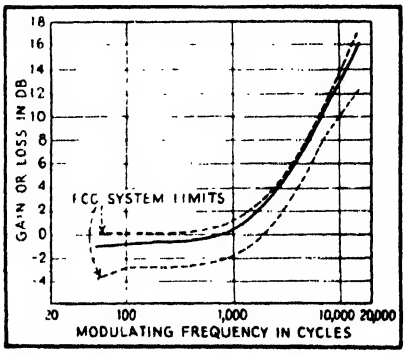

FIG. 2—Frequency response of a typical f-m broadcast transmitter for 100-percent modulation (75-kc deviation)

Measurements on the linearity of the f-m detector are not easily made, but its performance is usually guaranteed within certain limits by the manufacturer. Any very serious misadjustment of the discriminator will usually show up as a large apparent shift of the transmitter center frequency with modulation, as shown by the monitor's center frequency indicator. This indication is a definite sign of discriminator nonlinearity in the case of a phase modulated transmitter where the center frequency is definitely crystal controlled even in the presence of modulation. The Armstrong and Phasitron types of transmitters are in this class. Frequency shifts 200 cycles or less, represent only a very small nonlinearity.

In some cases the ability of the measuring system to measure exceedingly low values of f-m carrier

Table I—Transmitter Performance Requirements

	FCC System	RMA Transmitter
Frequency response (departure from 75 Usec)		
50 Cycles	+0,−4 db	
100–7500 Cycles	+0,−3 db	±1 db
15,000 Cycles	+0,−5 db	
Harmonic distortion		
50–100 Cycles	3.5%	1.5%
100–7,500 Cycles	2.5%	1.0%
7,500–15,000 Cycles	3.0%	1.5%
F-M Carrier noise level	−60 db	−65 db
A-M Carriers noise level	−50 db	−50 db

noise may be questioned. The capability of the system in this regard may be checked by altering the transmitter in such a way as to definitely minimize f-m carrier noise and then noting if the measuring equipment will read this low value. This can be accomplished in most phase modulated transmitters by driving the multiplier stages directly from the crystal oscillator without passing through the modulator stage, and with sufficient signal to minimize noise in the early multiplier stages. In this check a reference level for the measuring equipment must be set up before the modulator is disconnected.

Determining Frequency Deviation

To check the percent modulation readings of the monitor requires the use of a highly selective communication type receiver, preferably one having a crystal filter and an S meter. The receiver is tuned and coupled to the i-f of the monitor. When the transmitter is modulated with a fairly high audio frequency the receiver, if it possesses sufficient selectivity, will pass only the carrier frequency. As the amplitude of the modulating frequency is increased it will be possible to recognize readily the points where the carrier amplitude goes to zero by the almost complete lack of signal. Certain combinations of modulating frequency, percent modulation, and the number of the carrier null are given in Table 2. For example, if we want to check the 100-percent modulation indication, we can modulate with a tone of 5,020 cycles and slowly increase the amplitude of the modulation until the receiver indicates that the fifth point where the carrier disappears has been reached. This will be exactly ±75-kc deviation or 100-percent modulation. Similarly 50-percent modulation will occur when the fifth carrier null is reached with a modulation of 2,510 cycles.

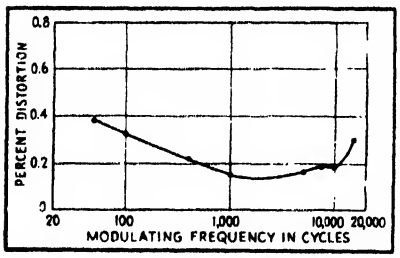

FIG. 3—Harmonic distortion at 100-percent modulation in a typical f-m broadcast transmitter

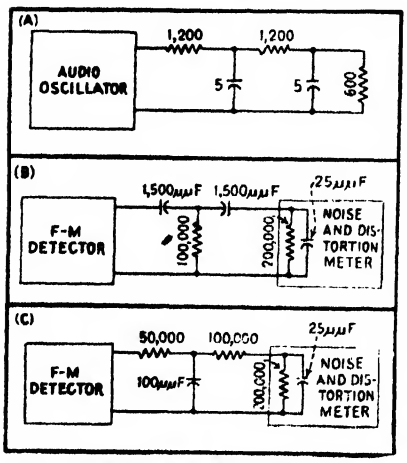

FIG. 4—Easily constructed circuits for facilitating transmitter measurements: (A) 50-cps low pass filter; (B) high pass RC filter for high frequency distortion measurements; (C) low pass RC noise filter

Special Techniques

There are a few methods which can be used to help overcome some of the difficulties encountered in making these transmitter measurements. For instance, when making harmonic distortion measurements, two difficulties are normally encountered. One is that many audio frequency oscillators have a considerable amount of harmonic content, particularly at the low frequency end of the audio range. It is possible to employ such an oscillator in spite of this trouble by using a filter connected between its output and the transmitter input which will pass the fundamental frequency and attenuate the harmonics. A plain low pass filter is suitable for this purpose. In some cases it is possible to improve conditions considerably by using a two section RC filter as shown in Fig. 4A. For example, two sections each consisting of 1,200 ohms and 5 microfarads, feeding a 600 ohm transmitter input will reduce the second harmonic of 50 cycles about 7 db, and the third harmonic about 12 db. Such a filter attenuates the fundamental considerably (in this case about 19 db), but this condition is not serious if the oscillator has sufficient output.

The other difficulty occurs when measuring distortion at high modulation frequencies and low percentages of modulation, when power frequency hum begins to be in the order of magnitude of the distortion being measured. For example, suppose it is desired to measure distortion at 15,000 cycles and 25-percent modulation, and the transmitter is good enough so the actual distortion is in the order of 0.5 percent. The harmonic level will then be 12 db down from 100-percent modulation owing to the modulation level, 46 db farther down if it is 0.5-percent distortion, and 17 db more because of the de-emphasis in the monitor at 15,000 cycles or a total of 75 db. This will be in the order of the noise level of even a good f-m system. It is allowable in this case to use a high pass filter which will attenuate hum frequencies, but which will have no appreciable effect on the higher audio.

In Fig. 4B is shown a simple high-pass RC network consisting of two 1,500 micromicrofarad capacitors in series with the high side of the monitor output, and 100,000 ohms from the center point of these two capacitors to ground.

Table II—Carrier Null Method of Determining Frequency Deviation

Carrier Null	Modulating Frequency for 100 percent Modulation (Cycles)
1	31,140
2	13,580
3	8,660
4	6,360
5	5,020
6	4,150

For modulation percentages other than 100 percent, multiply the modulating frequency in this table by the modulation factor.

This RC network, when working into a noise and distortion meter having about 200,000 ohms input resistance attenuates the hum frequencies sufficiently to allow these high frequency distortion measurements to be made. Numerically this circuit provides less than 1 db attenuation at 5,000 cycles and above, but 45 db at 60 cycles and 34 db at 120 cycles.

High-Frequency Noise

When making noise measurements of f-m transmitters, in which an appreciable part of the noise may be of a random nature, improved readings can be obtained by cutting off frequencies beyond 15,000 cycles. This is allowable since these components are beyond audibility and do not contribute to audible noise although they may add considerably to the reading of a noise and distortion meter which has a frequency response extending well beyond this frequency. A sharp cutoff filter could be used but it is difficult to realize for impedances in the order of several hundred thousand ohms. It is possible to work at low impedance with a filter and then use a transformer to step back up to a high impedance for the input of the noise and distortion meter, but this requires a considerable amount of equipment. We have found that we can use an RC de-emphasis type of circuit, as shown in Fig. 4C, having a time constant of 5 microseconds. This will give less than 1 db attenuation at 15,000 cycles, and will provide sufficient attenuation at the higher frequencies to give an appreciably improved noise reading when the noise is of a purely random type.

Accuracy of Measurements

The accuracy with which the frequency response can be measured depends largely on the accuracy of the attenuators and voltage indicating instruments employed and can be in the order of 0.1 db without great difficulty.

The accuracy of harmonic distortion readings is limited by the harmonic content of the audio oscillator and the distortion in the f-m detector used for demodulating the transmitter. One commercially available audio oscillator gives in the order of 0.1 percent harmonic content. Commercial f-m station monitors have distortion in the order of 0.25 percent, so the normal accuracy of distortion readings may not be better than ± 0.35 percent. In other words, readings less than 1 percent are sometimes open to question, for even a 1 percent figure may actually mean from 0.65 to 1.35 percent, and a figure of 0.5 percent may actually be 0.15 to 0.85 percent. It would be possible to increase the accuracy of these readings by using a filter at the audio oscillator output, which might reduce the harmonic content to about 0.02 percent. By using a counter type discriminator, the f-m detector distortion can be made as low as about 0.1 percent, which would give a total inaccuracy of ± 0.12 percent. However, the counter type discriminator has a very low output, which makes it difficult to avoid running into hum pick-up troubles when making very low distortion readings. This will again decrease the accuracy, although it is not possible to set a definite limit on the possible accuracy of low distortion readings.

Errors From Noise

The errors in measuring carrier noise levels are largely in the direction of making the noise voltages greater than in actuality because any stray hum pick-up, noise in the test equipment, or other introduced noise, all tend to produce an increase in total noise voltage. If these other sources of noise are sufficiently small, the only errors of reading should be inaccuracies in the attenuators and indicating instrument of the noise and distortion meter, and should be less than ± 1 db under normal conditions.

There is a possible source of error in both harmonic distortion and noise readings when using the type of instrument which employs a vacuum tube voltmeter to give rms readings, since the vacuum tube voltmeter actually reads an average voltage, although it is calibrated in rms volts. This error is zero for a single sine wave, as would be the case when reading a distortion that was all caused by a single harmonic. However, even for fairly extreme wave forms, the error is small. In the case of a 50 percent square wave the instrument will read high by 11 percent, and for a triangular wave it will read low by 3.7 percent. In most cases, this error is probably less than 10 percent of the instrument reading, and is therefore relatively unimportant.

Hum-Reducing Circuit

By ALVIN H. SMITH

THE CIRCUIT shown in Fig. 1 can be used to reduce carrier hum in a transmitter if the source of hum is 240 cps. It is particularly useful in transmitters having a Scott-connected two-phase filament supply and has been so applied in a five-kilowatt composite a-m broadcast transmitter at KSCJ.

The a-c output of the circuit in Fig. 1 is approximately 0.5 volt at 240 cps. This voltage may be fed into the audio circuits of the transmitter at any point desirable, observing polarity of leads for cancellation of hum, also ascertaining that other circuits are not adversely affected.

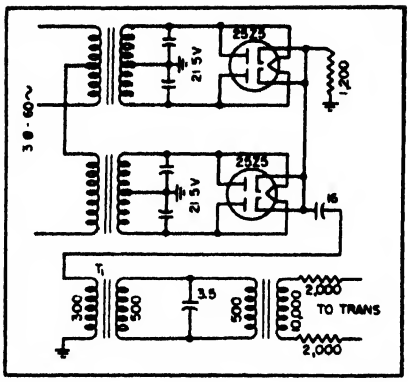

FIG. 1—Heaters and plates of the 25Z5 tubes are supplied by the same winding that feeds the 343A tubes in the transmitter

A bridging circuit across the transmitter a-f input terminals was used at KSCJ to insert the 240-cps a-c into the audio circuit, where after subsequent amplification and modulation, it acts to balance out the 240-cps component generated in the transmitter. This connection is shown in Fig. 1.

It is desirable to experiment with different values of capacitance, as resonance at 250 cps is desired in both the primary and secondary circuits of T_1. The wiring should be kept out of strong r-f fields. The ground connections should be made directly to the center taps on the filament transformers, rather than just any transmitter ground. These precautions are necessary in order to prevent r-f pick up which produces an undesirable a-f output in the 240-cps hum-reducing circuit.

This circuit is largely self regulating as its input is taken from the power amplifier filament supply—both will increase and decrease together. The 25Z5 tubes must be matched for best results.

As pointed out by Loy E. Barton "Hum Compensator for Broadcast Stations," (*RCA Broadcast News*, Feb. 1935), the predominate hum frequency using a 60-cps supply is 240 cps. This fact was verified by the use of a General Radio sound analyzer.

With 14 db of inverse feedback in the KSCJ transmitter, the following readings were obtained, before the hum-reducing circuit was connected: at 60 cps, −68 db below 100 percent modulation; at 120 cps, −56 db; at 180 cps, −67 db; at 240 cps, −47 db; and at 360 cps, −60 db.

Using 14 db of inverse feed-back, the noise reading on a General Radio distortion and noise meter—used by many broadcast stations—was −41.5 db. A carrier noise reduction of 8.5 db was obtained with the hum-reducing circuit, giving a carrier noise level of −50.0 db. Tests indicated that the 240-cps component, for all practical purposes, was eliminated. From a listening standpoint this 8.5-db reduction is very pronounced, as 240 cps is readily passed by most receivers and the ear is fairly sensitive.

Wide-Deviation Reactance Modulator

Operating principle and design procedure for obtaining maximum deviation from reactance tube frequency modulator. Use of cathode follower minimizes shunting of the oscillator. A typical test oscillator is described and a universal design chart is developed

By HARRY D. HELFRICH, JR.

FREQUENCY-MODULATED OSCILLATORS having large deviation are frequently needed for testing. To meet such a requirement, the reactance tube modulator has been modified to provide a larger linear sweep than has heretofore been obtainable from it. Although the reactance tube as a frequency modulator is well known,[1,2] only one report has discussed the problem of obtaining maximum deviation at high frequencies.[3] The equipment for which this modulator was designed required a linear 20-mc sweep at 118 mc. Such systems as beating oscillators and motor-driven variable capacitors were unsuitable due to weight, space, output voltage, and variable sweep-width requirements. With conventional reactance tubes, as well as in this modification, the percent deviation decreases with increasing center freqency. However, in the circuit to be described, the required percent deviation could be obtained at a frequency that could conveniently be multiplied to 118 mc, whereas it could not with the others.

Essentially, a reactance modulator consists of a resonant circuit of constant elements to which a controllable reactance is added in parallel. Thus, if the resonant frequency of the constant elements is f_0, the change of frequency Δf when the inserted reactance is inductive is

$$\Delta f = f_0 [(1 + L_{TANK}/L_{ADDED})^{1/2} - 1]$$

and when the inserted reactance is capacitive, it is

$$\Delta f = f_0 [1 - 1/(1 + C_{ADDED}/C_{TANK})^{1/2}]$$

Either case requires that the fixed reactances be as large as possible (large L and small C) and that the added reactance be as small as possible for maximum $\Delta f/f_0$.

With these requirements in mind, the modulator, shown by heavy lines in Fig. 1, was developed. An electron coupled oscilla-

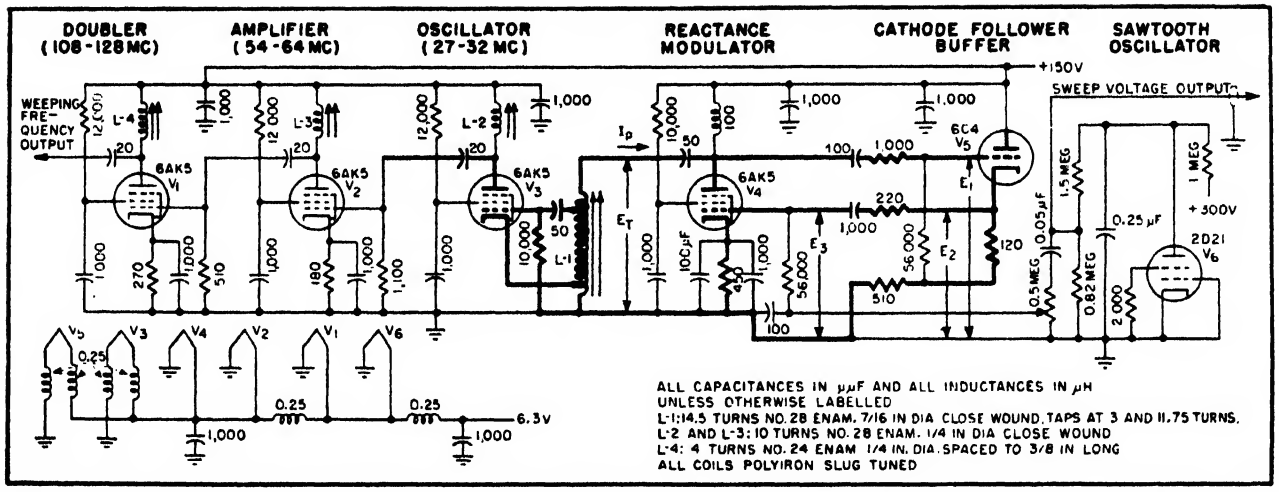

FIG. 1—Heavy lines show a-c portions of reactance modulator. Complete diagram shows basic circuit incorporated in test equipment

tor was employed to permit taking output from the circuit without capacitively loading it. In addition, a cathode follower buffer was inserted between oscillator and reactance tube; the input capacitance of the triode cathode follower could be made appreciably less than that of any high-transconductance reactance tube. Thirdly, an autotransformer connection from the oscillator circuit was employed to reduce the reflected impedance from the reactance tube. Furthermore, all stray capacitances were eliminated from the oscillating circuit, tuning being done by a variable polyiron slug.

Curve B of Fig. 2 shows the deviation obtained by this circuit. However, only 60 percent of the total deviation was in the linear portion of the frequency vs control voltage characteristic, as shown in Fig. 3. By operating the oscillator at a fundamental of 29.5 or 39.3 mc and multiplying, it was possible to obtain the 20-mc deviation at 118 mc. Of course, the necessity of loading or using band pass circuits made multiplication difficult. The electron-coupled oscillator was advantageous because it permitted multiplying in the output.

Two phasing networks, one before and one after the cathode follower, are used, tube input capacitance forming the reactive legs. If the transmission of the cathode follower is assumed to be $0.6/\underline{0°}$, the vector diagram of the voltages is as shown in Fig. 4, so that the reactive modulator plate current I_{PR} is

$$I_{PR} = g_m E_T (0.6/\underline{0°}) \cos\phi_1 \cos\phi_2 \cos\phi_3$$

and the sum of the angles ϕ_1, ϕ_2, and ϕ_3 is $\pi/2$. By partial differentiation, it can be shown that maximum I_{PR} occurs when each of these three angles is $\pi/6$, at which condition I_{PR} is approximately $0.4 g_m E_T$. However, because there is a component of I_P in phase with E_T, resistive loading will occur, which will vary with frequency. By properly proportioning the R-C phasing networks this loading can theoretically be eliminated (when $\phi_1 + \phi_2 = \pi/2$; $\phi_3 = 0$ and $I_P = I_{PR}$).

Due to secondary effects not considered, it is doubtful if this ideal condition can be attained. In practice, cut-and-try was used to obtain the maximum frequency deviation compatible with the permissible resistive loading. To be able to evaluate the closeness with which the optimum condition is approached, the theoretical deviation can be determined prior to adjusting the circuit. Because maximum I_{PR} is approximately $0.4 g_m E_T$, the minimum added reactance is

$$E_T/I_{PR\,MAX} \approx 2.5/g_m$$

and the minimum added inductance is

$$L_{2\,MIN} \approx 2.5/2\pi f_0 g_m$$

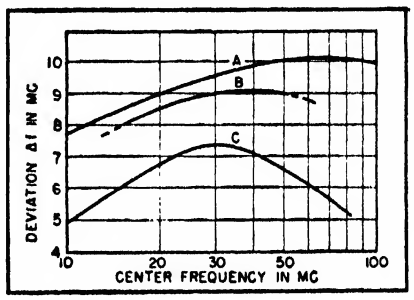

FIG. 2—Comparison of modulator deviations

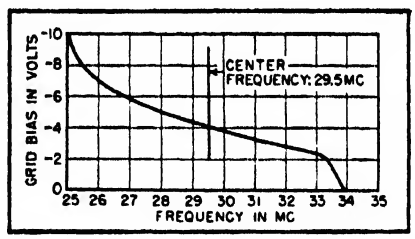

FIG. 3—Curve shows linearity of modulator

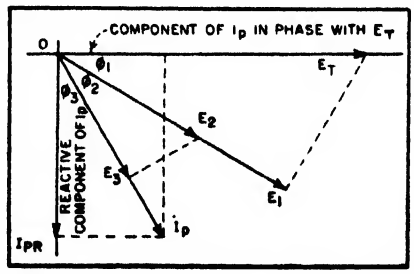

FIG. 4—Voltage vectors; see text and Fig. 1

If we define a constant

$$K = L_{TANK}/L_{2\,MIN} \approx g_m/5\pi f_0 C_{TANK}$$

and suppose g_m to have a range of

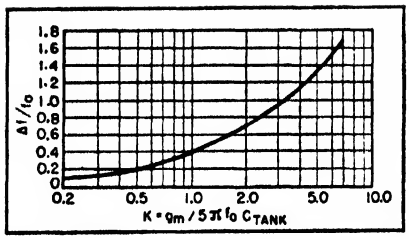

FIG. 5—Knowing circuit constants, one can find maximum deviation from this chart

20 to 1 with variation in reactance tube control voltage, we get by subtracting

$$\Delta f = f_{MAX} - f_{MIN} = f_0 [(K + 1)^{1/2} - (1 + K/20)^{1/2}]$$

From this result the dimensionless ratio $\Delta f/f_0$ has been plotted in Fig. 5 to provide a ready method of computing theoretical maximum deviation for a given center frequency for any type tube.

To verify this theory, operation of a practical adaptation of the circuit was studied. Using g_m = 5,000 μmhos and C_{TANK} = 13.5 pf (checked in actual circuit) for a 6AK5 oscillator, 6C4 buffer, and 6AK5 reactance modulator, curve A for Fig. 2 was obtained; curve B is the actual performance curve. The maximum obtainable Δf from a conventional triode oscillator and reactance tube combination[3] is shown as curve C. These curves represent the maximum Δf, not the range of linear frequency vs control voltage response.

Numerous tests made with this circuit indicate that tube replacement is not critical, although a 6AK5 reactance tube of definitely low g_m does reduce the sweep. Control of the sweep range is easily accomplished by a potentiometer between saw tooth oscillator and reactance tube control grid.

The circuit can be adapted to other uses with or without the multipliers. It has application in a panoramic receiver as the sweep oscillator, as a sweeping oscillator for i-f amplifier alignment, and as a wide band noise generator.

The author is appreciative of valuable criticism and assistance given by numerous engineers of the Airborne Instrument Laboratory. In particular, M. T. Lebenbaum helped during design and construction of the oscillator and by his constructive review of this paper.

REFERENCES

(1) C. Travis, Automatic Frequency Control, *Proc IRE*, p 1125, Oct. 1935.
(2) C. F. Sheaffer, Frequency Modulation, *Proc IRE*, p 60, Feb. 1940.
(3) J. I. Heller, Notes on Oscillators in Connection with Electronic Tuning for Panoramic Reception, Panoramic Radio Corp., Report 1138-1, March 8, 1944.

Extending Linear Range of Reactance Modulators

By FRITZ BRUNNER

LARGE FREQUENCY DEVIATION can be obtained directly from a frequency modulated oscillator by interposing a stage of amplification between the oscillator tank and the grid of the reactance tube.

Principle of Operation

In the basic reactance tube frequency modulated oscillator, a variable reactive current I_R whose magnitude is controlled by the modulating signal is supplied through a reactance tube to the tank circuit. The oscillator tube supplies a constant in-phase current I_P to the tank circuit as shown in Fig. 1. Under these conditions the instantaneous frequency is

$$f = \frac{1}{2\pi[L(C + I_R/2\pi fE)]^{1/2}}$$

where L is the inductance of the tank, C is its capacitance, and E is the voltage across it. If the resonant frequency of the tank circuit is

$$f_0 = 1/2\pi(LC)^{1/2}$$

the deviation frequency approximates

$$\Delta f = f - f_0 \approx -I_R/4\pi EC$$

which shows that the extent of the deviation is directly proportional to the reactive current supplied by the reactance tube.

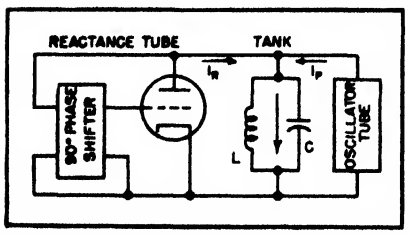

FIG. 1—Basic reactance modulators

In conventional reactance tube f-m oscillators I_R is obtained by shifting the phase of the tank circuit voltage as near as possible to 90 degrees by a resistance-reactance circuit, and using this voltage to control the reactance tube. Unfortunately considerable attenuation is associated with the phase-shifting network, so that the I_R available from the reactance tube is small in comparison to the voltage across the tank circuit. The frequency deviation that can be produced, especially at vhf, despite the greatest possible L/C of the tank circuit, is small. The oscillator must often be followed by several multiplier and converter stages to yield the necessary frequency deviation.

The introduction of an amplifier before or after the phase splitter

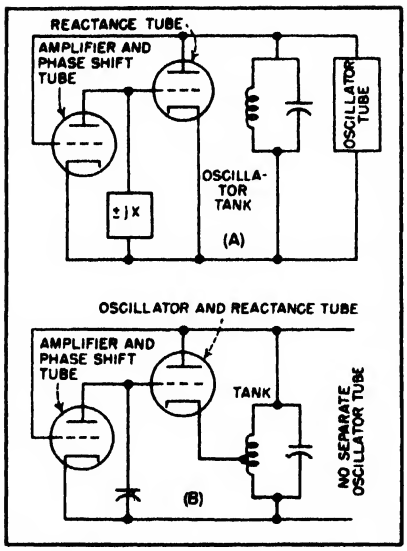

FIG. 2—Improved f-m oscillators

makes possible greater deviation. Because the phases in this amplifier affect the stability of the oscillator, only one stage can usually be used.

Circuit Simplification

The simplest arrangement is to use the dynamic plate resistance of the amplification tube as the resistance of the phase shifter as is done in Fig. 2A. If this tube has a high plate resistance, the voltage appearing across the reactance is shifted nearly 90 degrees. This reactance can be either an inductance or a capacitance. The reactive current delivered to the tank circuit can be modulated by changing the effective mutual conductance of one or more of the tubes associated with it.

At very high frequencies only the tube capacitances need be used for the reactive component of the phase shifter. *At higher frequencies the transit time in the reactance tube can supply the 90 degree phase shift so that a single transit-time reactance tube replaces the two tubes.* Otherwise the effect of transit time can be counteracted by adjustment of the phase shifter.

The circuit can be simplified still further by using the oscillator tube simultaneously as the reactance tube as shown in Fig. 2B.

Practical Execution

To obtain the largest possible frequency deviation with good stability, it is necessary to limit the amplitude of operation to the linear portion of the grid characteristic of the amplifier. A crystal diode can provide this limiting.

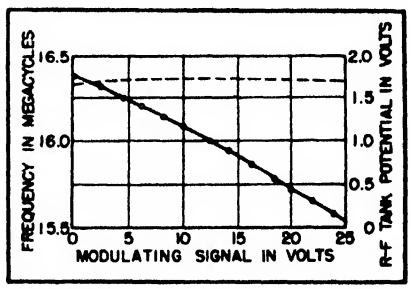

FIG. 3—Typical experimental results

The fact that the tank circuit capacitance is distributed over the several tubes of the system must be taken into consideration. If, at vhf, the inductances of the tube connections are too near that of the tank circuit, and the reactance tube supplies a strong reactive current, oscillation may be unstable. This condition can be avoided by increasing the inductance of the tank circuit, decreasing the tube capacitances, and decreasing the inductances of the connections, possibly by concentrating all the tubes in one envelope.

Using the oscillator tube as the reactance tube also, and using low transconductance tubes, linear deviation and constant amplitude of oscillation were obtained. Figure 3 shows typical experimental results. At frequencies where the reactances are concentrated in the tank circuit, frequency deviations of 10 percent of the mean frequency can be obtained with reasonably magnitude. Even in the uhf range frequency deviations commonly obtained at lower frequencies can be produced, so that the mean frequency can be regulated without inertia in a wide range by superimposing a control voltage on the modulating voltage.

Stability of Crystal Oscillators

Factors affecting crystal oscillator drift and practical means of minimizing them are discussed. Design of a secondary frequency standard serves as an example

By A. J. ZINK, JR.

IN DEVELOPING an ultrahigh-frequency secondary standard, it was decided to use a fixed-tuned crystal oscillator as a frequency base. Use of such oscillators in standard frequency generators and for stabilizing the frequencies of radio carriers is familiar. However, in designing a secondary frequency standard it is advisable to re-evaluate the factors affecting oscillator stability.

In the particular design under discussion, it was considered essential to have a constancy of frequency of ±0.001 percent for long periods of time. A crystal operating at 100 kc was to be used. This stability figure was derived from the fact that a final accuracy of ±0.0025 percent was required of the com-

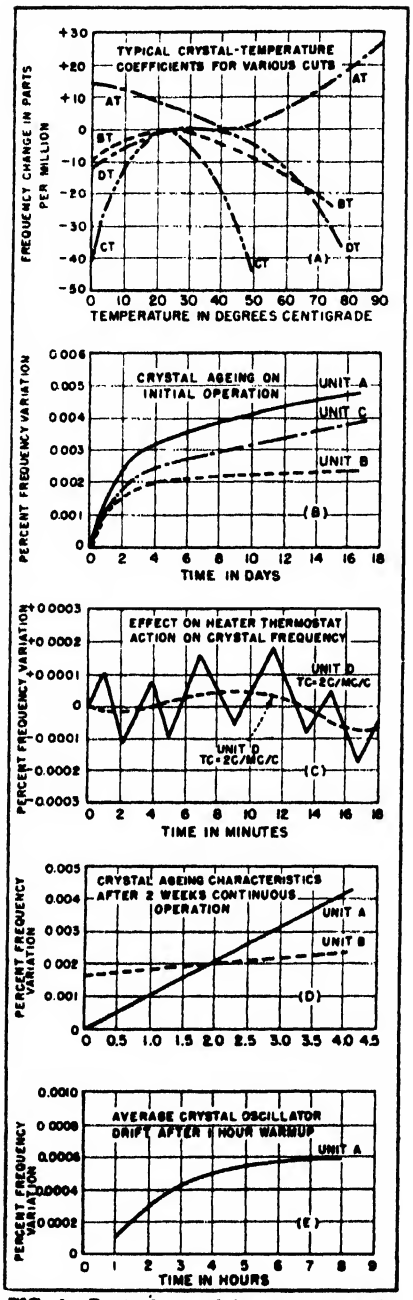

FIG. 1—Typical instabilities of crystals

pleted instrument. Allowable error must be distributed over several factors: stability of the crystal, human error in calibrating the tunable oscillator, tunable oscillator tracking error, and tunable oscillator short-time instability. It would seem entirely proper, therefore, that the crystal be reliable within the stated figure.

We shall consider the factors which will contribute to a satisfactory crystal calibrator of ±0.001 percent accuracy.

CRYSTAL TEMPERATURE COEFFICIENT—All too commonly we accept the crystal temperature coefficient supplied by the manufacturer without seriously considering what it means. A temperature coefficient of one cycle per megacycle per degree Centigrade, for example, does not indicate that we need only multiply our temperature range by this figure to find the maximum frequency change. Figure 1A indicates that temperature coefficients are not linear with temperature. It does indicate, however, that that is approximately true for a relatively narrow range of temperature. If the crystal is operated in an oven at the best portion of its characteristic, we can expect good results. It is important to note that seldom do two crystals, cut from the same slab and processed in the same manner, possess identical temperature coefficients of frequency.

CRYSTAL AGEING—Careful measurements on crystal-controlled oscillators show progressive frequency changes, such as those plotted in Fig. 1B, which are rightly attributed to ageing. It is believed that the grinding process tends to leave a surface accumulation of both the abrasive and pulverized quartz. This material dusts from the surface with a resulting slow change of frequency. Such ageing is noted even with carefully washed and acid-etched plates. It is also believed that microscopic surface fractures left by the grinding process contribute to the ageing effect. A minimum operating period of two weeks seems to be required to reduce ageing to a tolerable value and it is possible that at the end of this period some crystals must be rejected.

TEMPERATURE CONTROL—A relatively simple thermostatically controlled oven will maintain the crystal temperature to within plus or minus one degree Centigrade of some selected temperature. The temperature variation affects the frequency in the manner depicted in Fig. 1C. Experience has shown, however, that the thermostat itself ages, and that the crystal may well run a few degrees cooler after some months of operation.

CRYSTAL MOUNTING — It goes without saying that the matter of properly mounting a crystal is highly specialized and must remain a problem of the crystal manufacturer. Judged by the writer's observations, crystal mounting is perhaps the limiting factor in overall stability. Very few completely assembled ovens and crystals on the market seem entirely satisfactory. Two highly developed commercial units are compared in parts of Fig. 1; ageing is shown at Fig. 1D. Fig. 1E shows warmup. Obviously, unit B is a great improvement over unit A. Because unit A employs a spring mount with crystal contacts which are not located at the nodal points, we would expect both ageing of the springs and shifting of the contact points. Lessening of spring pressure tends to cause ageing to higher frequencies while conversion of the metallic coating to an oxide results in increased crystal pressure and, consequently, shift to a lower frequency. Incidentally, both crystals had directly deposited silver electrodes.

Oscillator Test Circuit

Figure 2 shows a test setup capable of measuring minute frequency shifts in either relative or absolute terms. The 100 kc crystal oscillator, and its associated buffer stage, is contained within a test chamber capable of producing and maintaining known ambient temperatures. The buffer feeds a harmonic amplifier which produces a few millivolt output at 10 mc. This harmonic amplifier is fed to the input of a 10 mc receiver tuned to WWV, and the crystal is purposely detuned to produce a beat note of perhaps 200 cps with the standard signal. The low-pass filter removes the 4,000-cps modulation normally on the WWV carrier but passes the 440-cps modulation plus the 200-cps beat note. The resulting output is fed to one pair of deflection plates of a standard oscilloscope, the other

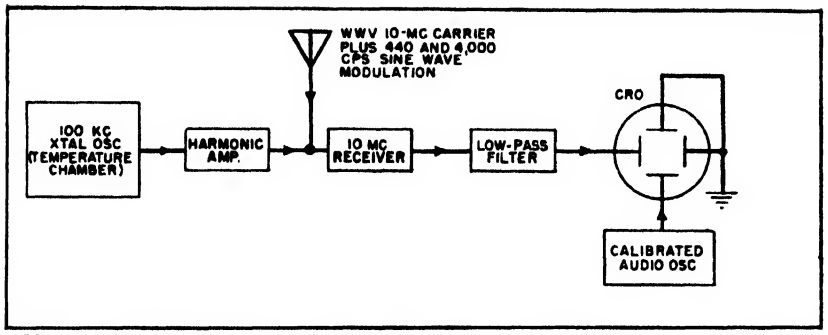

FIG. 2—Block diagram shows technique used in checking stability of crystal oscillators against WWV

pair of plates being fed by a calibrated audio oscillator.

Examination of the test setup indicates that all measurements are made against a 10-mc primary standard accurate to at least one part in ten million. The 100th harmonic of the 100-kc crystal is being compared with this standard, and crystal frequency shifts are thus made 100 times more evident. A shift of one cps at 10 mc is the equivalent of a 0.01-cps shift at 100 kc. The output of the receiver contains two different frequencies, one the normal 440-cps modulation of WWV and the other the 200-cps beat note. When the audio signal-generator frequency is varied, two 1:1 frequency ratio patterns are obtained. The pattern obtained at 440 cps serves to calibrate the audio-frequency generator and the 200 cps pattern is a direct measure of the beat note frequency. The procedure is seen to be entirely satisfactory for our requirements. Shifts of five-cps crystal frequency can be read directly on the audio signal generator. It is easily possible to estimate shifts of one cps. The resulting accuracy of measurement is thus in excess of 0.5 part per million.

Circuit Selection

Reviewing requirements for a secondary standard, we realize that sound engineering is the ultimate aim, and that standard components should be employed insofar as possible. Extremely complex circuits, difficult production testing, and costly special parts should be avoided. Our unit should be: accurate to within ±0.001 percent over periods exceeding one month, stable over ambient temperatures commonly encountered in the United States (32 to 120 F), and reasonably stable under shock.

To satisfy the first two requirements, we recognize the need of temperature control because an accuracy of only about ±0.02 percent is considered normal with uncontrolled low-drift crystals. The oven is also required to combat the wide range in ambient temperature. The third requirement rules out any but rigid crystal mounts.

The circuit used is shown in Fig. 3. In addition to simple construction, it has other attractive features. Many thermostatically controlled ovens with enclosed crystal holder have at least one massive contact plate designed to have high thermal capacity. A circuit such as this one in which this contact can be grounded is desirable. A convenient method of accurately setting the crystal to a frequency standard is also necessary. A small air trimmer C_1 is used in the circuit to make this adjustment. The rotor is grounded, which removes effects of hand capacitance. Crystals designed for this method of tuning are produced about 25 cps high in frequency because wiring capacitance plus the capacitance in C_1 lowers the crystal frequency. An undesirable feature of this circuit is the fact that variations in tube input capacitance, designated C_7, also tune the circuit. A high ratio of C_1 to C_7 is desirable in reducing this effect.

Now, having chosen our circuit, we should apply those means of stabilization which will increase its effectiveness.

Adequate protection against low impedance changes is afforded by lightly coupling a pentode buffer amplifier to the oscillator. If this buffer is run Class A, it will draw negligible grid current and avoid the possibility of reflecting load changes back to the oscillator plate circuit.

Optimum Conditions for Stability

The oscillator plate circuit itself deserves more than casual mention. The crystal is being operated in a shunt resonant condition which requires that the plate circuit be inductive in order that proper phase conditions for oscillation exist. This is simply another way of saying that the plate circuit must be tuned to a frequency higher than 100 kc in order that the crystal oscillate at all. Hight and Willard (Proc. I.R.E., p 549 May 1937) have found that by proper choice of C_2 and C_3, a high degree of protection against frequency changes due to variations in electrode voltages and circuit constants is provided. The tuning procedure is to alternately adjust C_1 and C_3 for the highest oscillator frequency. In the circuit shown, the

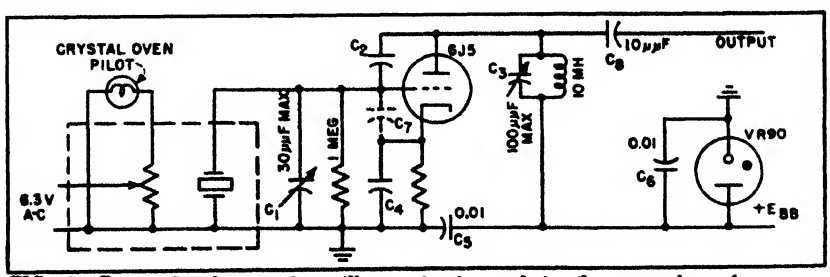

FIG. 3—Conventional crystal oscillator circuit used in the secondary frequency standard

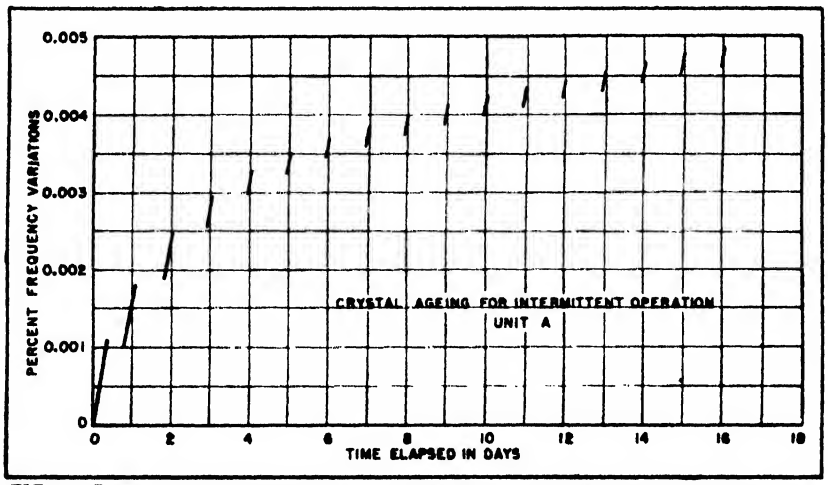

FIG. 4—A typical crystal and oven assembly can be expected to have this ageing characteristic for intermittant operation during its first few weeks of operation

plate circuit is then resonant at about 300 kc.

Figure 4 is a combination of curves from Fig. 1B and 1E, and indicates the ageing trend if the crystal oscillator is operated for eight out of every 24 hours. It is apparent that day-to-day shifts are progressively less, and that the ageing curve is much more prolonged in terms of days although not necessarily in total hours. The difficulty of predicting what would happen under such operating conditions makes it essential to operate the unit continuously for highest stability.

Effects of moderate variations in either filament or plate supplies are not as great as would ordinarily be expected, if the circuit is properly designed. The complete circuit, as shown, has an instantaneous crystal frequency shift of about ±5 cps or one part per million when the line voltage is varied abruptly from 95 to 125 volts. A less rapid shift is also evident after the heater voltage has assumed its new potential. The effects, however, are so slight that they are difficult to identify. During the above check, the VR tube still controls the plate supply voltage. The choice of regulator was made on the basis of its excellence as a regulator plus tube-to-tube uniformity. Experience has dictated that the VR-105, VR-150, VR-90 and the VR-75 are to be preferred in that order.

We are now in a position to judge overall stability if we consider one additional factor, namely, temperature stability under an ambient temperature range from 32 to 120 F or about 50 C. Manufacturers' data indicates a change in frequency of about ±0.0001 percent for a high-quality crystal and a well designed oven. Here are the figures:

Cause of Drift	Percent Drift
Instability due to ambient temperature	±0.0001
Approximate ageing per month	±0.0007
Instability due to line voltage variation	±0.0001
Total	±0.0009

From the tabulation above, it can be seen that the most significant weakness is the comparatively high shift of frequency due to ageing, which is in turn largely attributed to the mounting of the crystal.

Desired accuracy can, however, be attained by careful oscillator circuit design and by thorough production testing. All crystals must be aged at least two weeks and those with high ageing characteristics rejected. Knowing the ageing trend of each crystal, the oscillator itself can be tuned to take advantage of anticipated drift. It should be pointed out that any such detuning would amount to only about 0.1 cps at 100 kc in an average case.

BIBLIOGRAPHY

(1) Heising, Raymond A. and others, "Quartz Crystals for Electrical Circuits", D. Van Nostrand Co., New York, 1946. In addition to describing manufacture of crystals for use in oscillators and filters, this book discusses crystal oscillators and develops a figure of merit for crystals.

(2) Cady, Walter Guyton, "Piezoelectricity", McGraw-Hill Book Co., New York 1946. Physical properties of quartz and other piezoelectric crystals are described, with extensive references.

(3) Mason, W. P., Low Temperature Coefficient Quartz Crystals, *Bell Sys Tech Jour*, p 74 Jan 1940. See also: New Quartz-Crystal Plate, Designated the GT, which Produces a Very Constant Frequency over a Wide Temperature Range, *Proc Inst Radio Engrs*, p 220 May 1940.

(4) Elbl, L. A., Crystal Testing Techniques, ELECTRONICS, p 120 Aug 1944. Production testing techniques and variations of characteristics tested for are described.

(5) Chalfin, Norman L., Temperature Coefficient of Quartz Crystals, ELECTRONICS, p 147 Nov 1943. Two charts are presented for determining temperature coefficients of crystals for which normal operating frequency and frequency change for a given temperature change are known.

(6) Bushby, T. R. W., Thermal-Frequency-Drift Compensation, *Proc Inst Radio Engrs*, p 546 Dec 1942.

Transmitter Breakdown Alarm

By W. K. ANGUS

A device installed on the monitor rack of CFRN gives warning of interruption of program service. A bell rings instantly on failure of the carrier and the same bell also rings, after an appropriate delay of 15 or 20 seconds, if there is any interruption in the audio level from the studio.

The unit has since proved its usefulness. On at least two occasions it gave warning of program interruptions when the operator was talking on the phone with the monitor speaker cut.

The circuit finally employed is given in the diagram. The d-c relay should be adjusted to close at 4 or 5 ma and release at 1.5 ma or better. (A less sensitive relay can sometimes be used by bleeding some additional current through it with a resistor.) This relay is in the plate circuits of the 6J7 and the two 6K7 control tubes which are normally biased to cut-off.

The grid of the input stage is fed with a small amount of r-f from some convenient place, or a short antenna can be used. The output circuit is tuned to the operating frequency and coupled to the first half of the 6H6 rectifier. The voltage so developed across the diode load resistor is applied, with minimum time delay, to the grid of the 6J7 control tube. The relay closes instantly when this tube loses its bias.

The audio component from the same source is amplified by the 6C5 and rectified by the second half of the 6H6, thus providing the cutoff bias for the 6K7's. The two tubes in parallel give more reliable operation than one tube used alone. Two 6J7 tubes were tried here but proved to be somewhat temperamental due to their sharp cutoff characteristics.

A good tubular paper capacitor should be chosen for the delay network. Larger paper capacitors of the block type give erratic operation due to leakage. The network

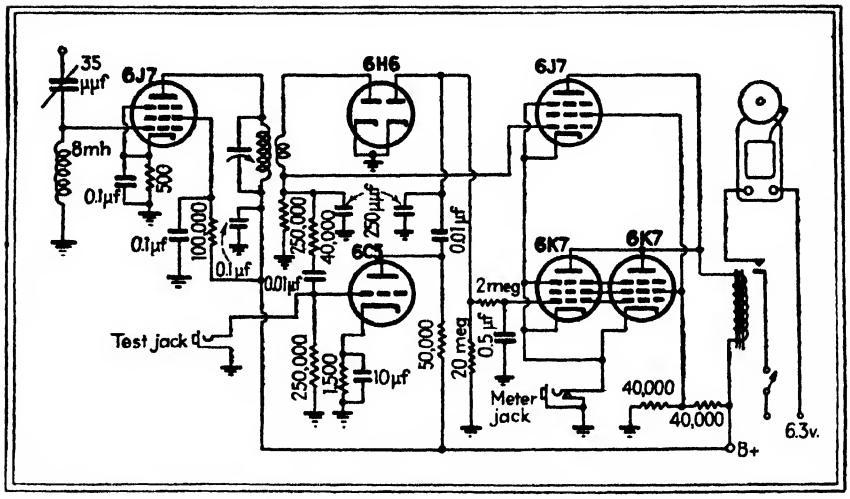

Complete circuit of the transmitter breakdown alarm. The bell rings immediately if the carrier is interrupted, and if the carrier is maintained without modulation for more than about 15 seconds

arrangement results in high bias voltage from the 6H6. The capacitor charges in a second or two which is desirable from the standpoint of uniformity of time constant with varying program conditions.

On failure of modulation, the time that elapses before the bell will ring is determined by the r-f input, the voltages on the control tubes and the setting of the relay, as well as by the constants of the resistance-capacity network on the grids of the 6K7's. The metering jack for watching the performance of the control tubes when adjusting the unit is almost indispensable.

The stand-by switch and the bell itself are the only parts mounted on the front panel. At present we are operating the bell on the filament circuit. This means that the alarm will not function on a power line failure, although the bell will ring about fifteen seconds after the resumption of power if the transmitter does not also come back on.

This condition will be remedied when we obtain another sensitive relay to place in parallel with the first one. Then, with a small bleeder resistor to hold the second relay open and batteries for the bell circuit, the unit will be complete.

Wide-Angle Phase Modulator

Technique for phase modulating a crystal-controlled carrier, whereby two components of fixed phase difference are amplitude modulated and added to give the output, is described. Circuit can be used to give frequency modulation, or modified to give amplitude modulation

By H. K. BRADFORD

A FREQUENCY-MODULATION system was developed concurrently with amplitude-modulation equipment for railroad communication so that its advantages could be made known to the railroads. The equipment was designed so that conversion from one type of modulation to the other would be as simple as possible. While the amplitude-modulation system is conventional, the frequency-modu-

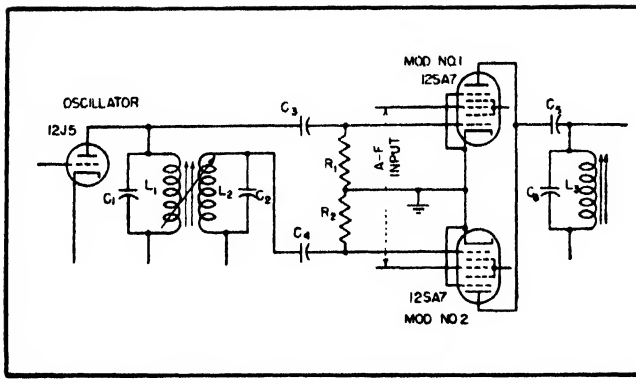

FIG. 1—Basic modulator consists of a phase-shifting network feeding two differential amplitude-modulating tubes. The vector output is phase modulated

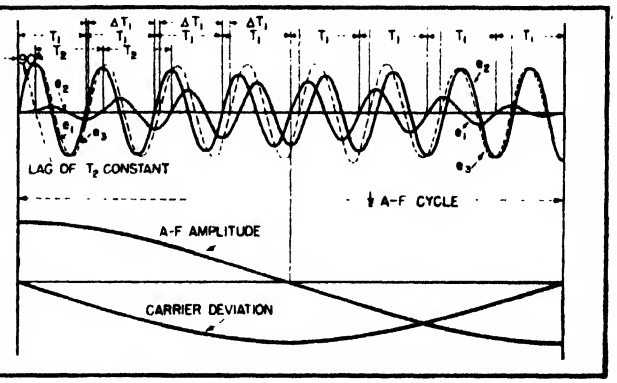

FIG. 2—Addition of two components of varying amplitude and constant phase difference gives a signal of constant amplitude and varying phase position

lation system offers some interesting aspects.

The phase-shift method of modulation was chosen for this mobile equipment so that direct crystal control could be used for the carrier. The use of a master oscillator with correction circuits necessary for the frequency stability required in the vhf band of 152 to 162 mc was regarded as impractical. With phase-shift modulation, the carrier is derived from a crystal oscillator, the frequency of which remains unchanged in the process of modulation.

With reactance-tube frequency modulation the base or oscillator frequency can be changed as much as desired within the circuit capabilities, but with phase-shift modulation we do not change the base or oscillator frequency, we continuously shift the phase of a frequency component derived from the oscillator. The oscillator component is never completely detached from the multiplier-amplifier following it so its component is always part of the driving force. For this reason the phase shift is limited to an amount which will not seriously change the driving amplitude.

For example, if the phase shift becomes as much as 180 degrees, the derived phase component will cancel the normal oscillator component and there will be no output, providing that the amplitudes are equal. This fact restricts the angle of phase shift to an amount which, with the oscillator component, will not seriously affect the total amplitude used to drive the multiplier-amplifier. For a complete discussion of the theory of various forms of angle modulation refer to Frequency Modulation by W. L. Everitt, *A. I. E. E. Trans.*, Nov. 1940, p 613.

For the purpose of this discussion we will regard phase-shift modulation as adding or subtracting increments of time throughout each r-f cycle. If equal increments of time are added to each cycle, the resultant frequency will be lower than before and constant. However if we add increasingly larger increments of time to succeeding r-f cycles, the frequency reduces in accordance with the sizes of these increments. If the increments are proportional to sine functions, those at the beginning of the modulating cycle will be largest, displacing the frequency by the greatest degree, while those toward 90 degrees of the modulating cycle will tend toward zero, at which time the r-f will return to normal frequency. The carrier deviation is proportional to the rate at which these time increments increase or decrease and not to their magnitude.

If the phase between two carriers remains constant they will have the same frequency regardless of the amount by which their phase differs. Thus if time (and hence phase) increments follow a sine-wave form, their rate of change will follow a cosine form. If these increments follow a transient form, their rate will follow as their first differential.

If we define the instantaneous voltage of a sine wave as

$$e = E_0 \sin \omega t \qquad (1)$$

we must realize that the angular velocity ωt is changing in frequency modulation according to one law for the reactance tube and according to another for the phase-shift method. Suppose that we are to phase-shift modulate with another sine wave defined as $E_1 \sin \omega_1 t$, then the angle ωt in Eq. 1 would have to be altered as $\omega t + E_1 \sin \omega_1 t$. However the amplitude here defined as E_1 has the meaning that a maximum number of degrees or radians of angle is to be added to or subtracted from the original angle ω. The circuit analysis to follow will show that the a-f amplitude E_1 produces a proportional phase shift. If it is more convenient to regard ωt as a rotation, then the addition of $E_1 \sin \omega_1 t$ simply means that this rotation is periodically accelerated and decelerated by an amplitude E_1 and a period $\omega_1 t$. If E_1 is actually a maximum angle set by the design of the equipment, it may be designated more properly as an angle ϕ in which case the entire equation for a phase-modulated wave becomes

$$e = E_0 \sin (\omega t + \phi \sin \omega_1 t) \qquad (2)$$

Because we are not immediately interested in the energy distribution in the radio spectrum it is possible to make a very simple analysis of Eq. 2.

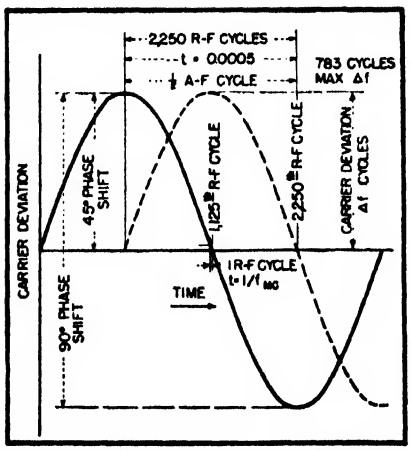

FIG. 3—Determination of frequency deviation produced by modulator

The part of the total carrier angle $\omega t + \phi \sin \omega_1 t$ which accounts for modulation only is $\phi \sin \omega_1 t$. Moreover, we have just found that it is the rate of change of this expression which determines the frequency deviation of the carrier, hence

$$2\pi\Delta f = \frac{d(\phi \sin \omega_1 t)}{dt} = \omega_1 \phi \cos \omega_1 t$$

$$= 2\pi f_m \phi \cos \omega_1 t$$

$$\Delta f = f_m \phi \cos \omega_1 t \qquad (t = 0 \text{ for } \Delta f_{max})$$

$$\Delta f = f_m \phi \qquad (3)$$

where $\omega_1 = 2\pi f_m$
f_m = modulating frequency
ϕ = angle in radians

Circuit Operation

A simple circuit for performing this type of modulation fundamentally is shown in Fig. 1. Elements C_1 and L_1 are the crystal-oscillator plate-tank components adjusted for oscillation in the usual way. The circuit L_2C_2, inductively coupled to the oscillator tank, is adjusted so that it acts capacitively. For example, if the phase shift produced by C_1 and L_1 while loaded with C_3R_1 and the distributed input values of Mod No. 1 could be made plus 45 degrees, and that from L_2C_2 in turn made minus 45 degrees by detuning for higher inductance, then the potential on Mod No. 1 would be 90 degrees out of phase with respect to that of Mod No. 2 (Fig. 1). Now if these tubes (12SA7's) are differentially (push-pull) amplitude modulated at their No. 8 grids by an a-f input indicated so that the r-f in the No. 1 grids can be used in inverse degrees, C_3L_3 will alternately be driven with the r-f component from the grid of one of the 12SA7 modulators and then the other. During one-half of an audio cycle, the utility of the r-f energy in the modulator grid circuits will be transferred from one 12SA7 to the other and 90 degrees of r-f phase will be gained or lost depending on the instantaneous polarity of the a-f. The modulation process will bring about a smooth transition of energy from one source to the other.

The mechanism of this type of modulation is shown in Fig. 2. The designation e_1 refers to the carrier component entering the grid of Mod No. 1 (12SA7) of Fig. 1 and e_2 is the wave entering the other 12SA7 modulator grid. Each cycle of e_1 is marked off and its period T_1 is constant. Likewise e_2 has a constant period T_2 and throughout the entire range of e_2 it is lagging e_1 by exactly 90 degrees.

Now e_1 is decreasing in amplitude due to amplitude modulation, while e_2 is increasing in amplitude. The sum of these two waves is designated e_3. This sum-wave (dotted curve Fig. 2) appears in C_3L_3 of Fig. 1. Note in Fig. 2 that as the amplitudes of e_1 and e_2 change inversely the sum-wave e_3 is actually changing frequency. Its frequency is lowered by the ratio of $(\Delta T_1 + T_1)$ to T_1. It appears to be changing phase with respect to e_1. If this process can be made to take place fast enough, a considerable frequency change can be brought about. To understand how a phase shift amounting to a fraction of an r-f cycle can bring about many hundreds or even thousands of cycles deviation, it is important to note carefully that only one-half of one a-f cycle from positive to negative peak is shown in Fig. 2.

We must produce all of the r-f frequency change or deviation from the carrier in the time consumed by one-half of an a-f cycle just as we must achieve all of the amplitude change from peak to peak of the a-f cycle in this time. An example of the conditions actually used may serve even better to explain the phase modulation.

With a carrier of 4.5 mc and an a-f of 1,000 cycles, in 1/2000th second we must obtain 90 degrees of phase shift between the two carrier components derived from the oscillator. In this time there will occur 4,500,000/2,000 or 2,250 r-f cycles. At the middle or 1,125th r-f cycle the maximum deviation will occur.

There will be 45 degrees r-f phase

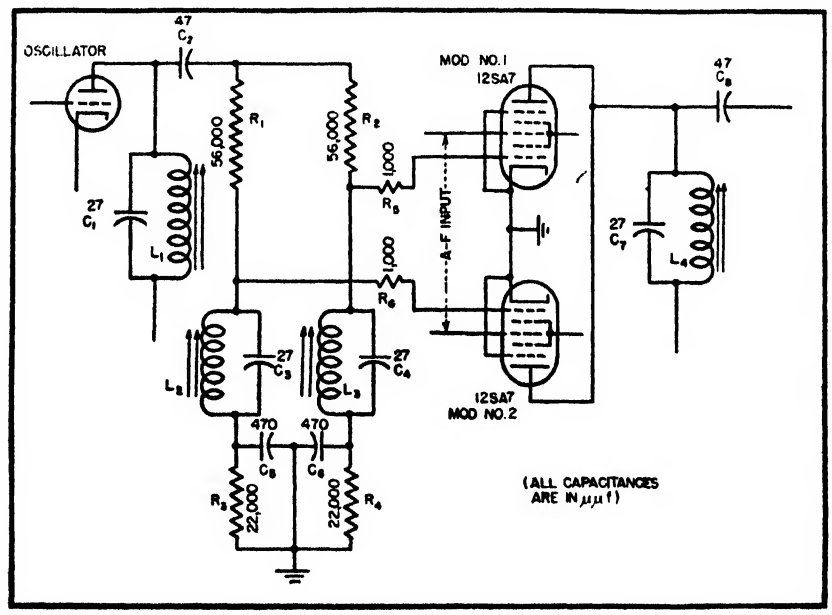

FIG. 4—Actual phase modulator circuit as used in railroad communication equipment

shift at the middle cycle covering 90 degrees of the a-f cycle. Thus the maximum phase shift per r-f cycle to quite a high degree of accuracy will be

$$\Delta_f = 45 \sin (90/1125)^\circ$$
$$= 45 \sin 0.08^\circ$$
$$= 0.06264^\circ$$

Figure 3 shows the conditions involved here. Because these values are given in degrees, it is obvious that if the time of one cycle is measured by 360 degrees that the time of this cycle in question is longer by 0.06264 degrees and the ratio of 360 to 360.06264 is 1.0 to 1.000174. Multiplying 4.5 mc by this figure we obtain 4.500783 mc showing that the carrier has deviated 783 cycles from 4.5 mc. From Eq. 3 it is clear that the deviation is proportional to the a-f times the total angle of phase modulation. For example with 1,000 cycles a-f and a total phase shift of 90 degrees or $\pi/2$ radians, from Eq. 3 we have $1{,}000\pi/2$ or 1,566 cycles total deviation of which 783 cycles or one-half of this is the deviation in one direction from the carrier. Thus by this process of rapidly shifting phase, it is possible to change the frequency considerably.

The method of modulation of the 12SA7 modulators from the amplitude viewpoint in Fig. 1, is not important except that it must be as linear as possible and as near 100 percent as possible if the advantages of total phase shift are to be realized. Grid modulation using converter tubes such as the 12SA7's shown in Fig. 1 provides a good means although 100-percent modulation may not always be realized. Plate modulation would seem effective although more apparatus is required and the circuit is thereby made more complex.

Because the r-f phase-shift rate and hence the deviation of the carrier is dependent upon the a-f, the degree of modulation must be made inversely proportional to the a-f if a constant bandwidth is desired. A network for accomplishing this was found unnecessary however and was not used. Because the transient noise components are largest in the upper part of the a-f band the modulation factor (ratio of carrier deviation to a-f) being constant, the noise will be attenuated more than it otherwise would be. Audio correction can be made easily in the a-f system of the receiver.

Practical Circuit

Although the circuit of Fig. 1 is useful for explanation it is not a practical circuit. Adjustment of the phase-splitting circuit L_2C_2 would affect the operation of the oscillator. Every time the oscillator is adjusted, the phase between the grids of the 12SA7 modulators is altered. Out of several circuits tried, a final design was chosen. It is shown in Fig. 4. In this circuit, the oscillator may have any phase suitable for oscillator tank components C_1 and L_1.

Using the output voltage at C_2 as a reference, components are fed through resistors R_1 and R_2 to two individual tank circuits L_3C_3 and L_4C_4. The shunt impedances of these tank circuits unloaded are approximately 80,000 ohms at resonance and they lose about 30 percent of this value when displaced 45 degrees in phase by tuning. Values of R_1 and R_2 up to 560,000 ohms were found quite successful, but lower values made adjustment of L_3 and L_4 less critical and suitable for a fair degree of oscillator frequency range without readjustment. In addition, the grid driving voltages into the phase modulators were increased to a more practical degree through a more favorable voltage division between the series resistors R_1 and R_2 and the tuned circuits.

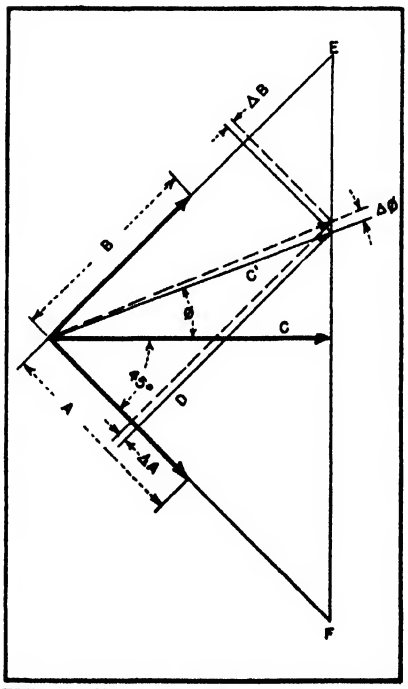

FIG. 5—Vector analysis of modulator linearity

The grid drive must be just adequate to produce a vector sum in the plate circuit C_7L_4 sufficient to drive the following tube. More than this amount of drive makes grid modulation less effective in the limited grid range for a-f. Values of 56,000 ohms for R_1 and R_2 were found satisfactory. Capacitors C_3 and C_4 are large enough (27 $\mu\mu$f) so that the modulator tubes can be replaced without readjustment of L_3 and L_4 and to provide ready compensation for distributed capacitances. Bias and bypass components are conventional.

Because the driving power was more than enough for the purpose, it was found more practical to use grid or plate suppression of self-oscillation than any form of neutralization. Grid suppressors R_5 and R_6 are shown in Fig. 4 and are adequate for the purpose. Inductors L_3 and L_4 can be adjusted with an oscilloscope and set for the life of the equipment. They are set at the r-f grids of the phase modulators for the most perfect circle obtainable (showing 90 degrees phase difference between the r-f components fed to the grids). Phase modulation can be observed and the actual angle of modulation measured by attaching the vertical and horizontal free oscilloscope plates to C_3 and C_4, and adjusting L_4 for a straight diagonal line in the absence of modulation. Modulation will open the line into a family of ellipses the limits of which will be an index of the angle of phase modulation. Ninety degrees phase modulation will be indicated when the major axes of these ellipses are four times the lengths of their minor axes and their major axes

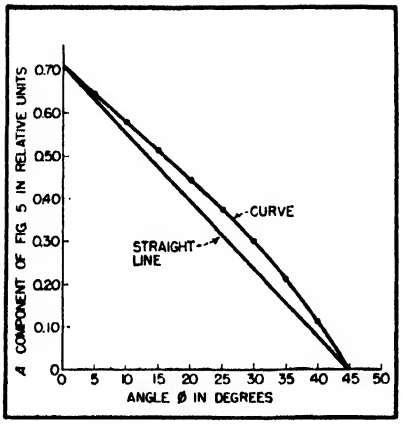

FIG. 6—Curve shows degree of nonlinearity in modulator circuit

are 45 degrees from each other in their limiting positions.

The oscillator frequency was arranged to be multiplied 36 times to the vhf output of 152 to 162 mc to take advantage of the phase modulator and have a deviation of approximately 30-kc total at the carrier output. For overall modulation angles in the neighborhood of a radian, the overall distortion was found to be about 9.5 percent so the following calculations were made to determine the distortion inherent in the phase modulator for 90 degrees total phase shift (approximately 1.5 radians).

Figure 5 shows vector grid components A and B 90 degrees displaced, and a sum vector C. Linear amplitude modulation of A and B will subtract an increment ΔA from the A vector and add an equal increment ΔB to the B vector at any arbitrary point in the a-f cycle simply by definition of linear modulation. These increments will produce a phase shift $\Delta\phi$ of the sum vector. Line EF is the locus of all positions of the sum vector C limit, and by geometry, any increment such as ΔA will intersect proportional increments along EF. The angle $\Delta\phi$ however, will vary throughout the distance EF. From Figure 5, it may be seen that

$$\frac{C}{C'} = \cos\phi \tag{5}$$

and $\frac{A}{C'} = \cos(\phi + 45°)$

or $A = C'\cos(\phi + 45°)$ (6)

Substituting Eq. 5 in Eq. 6

$$A = \frac{C\cos(\phi + 45°)}{\cos\phi} \tag{7}$$

Equation 7 gives us a true expression of A in terms of ϕ and constants. Plotting A in relative units against ϕ (C=1) between zero and 45 degrees for ϕ, we obtain the curve shown in Fig. 6. This curve shows that within 90 degrees total phase shift the proportionality between A and ϕ is fairly good. The distortion resulting from this much curvature is directly related to the area between the curve and the straight line as compared to the total area under the curve. This was roughly estimated at 9 percent which checks well with actual measurement. At the low-level point where phase modulation is accomplished other sources of distortion are very low, less than one percent by measurement.

It is interesting to note that if modulation makes A or B of Fig. 5 more than double, the phase change abruptly stops. An analysis was made on this same basis of the distortion conditions for a total phase shift of 120 degrees and the distortion was estimated at about 43 percent which is of course, prohibitive for intelligibility using ordinary communication techniques.

Cascade Phase-Shift Modulator

Simple new modulator circuit for f-m transmitters is easy to adjust and maintain, requires only standard tubes, and has minimum inherent amplitude modulation. Adding phase shifts of six crystal frequency stages permits low order of frequency multiplication

By M. MARKS

This paper will give a brief general review of phase shift modulators, showing the relationship between phase and frequency modulation, then develop the theory of the new modulator and give performance data.

When the phase of a carrier wave of constant frequency is advanced or retarded, the instantaneous frequency of the carrier also changes; the frequency deviation is proportional to the rate of change of phase.[1] The operation of all phase modulators depends on this important relationship, which may be visualized by considering a sinusoidal voltage of constant frequency. If the phase of this wave is advanced, say by 90 degrees, through insertion of a suitable phase shifting device, it can be seen that during the time taken for the phase to change to the new advanced value, the wave actually has to move faster than it would have moved if no change had taken place. Therefore, while the phase is changing, the effect is the same as if the frequency were higher. In a like manner, delaying the phase results in a lower frequency while the change is taking place. As soon as the shift in phase is stopped, the wave continues on at the original frequency.

From this, it follows that the more rapidly the phase is shifted, the greater will be the resulting

frequency deviation. Thus, if the phase of an r-f signal is shifted by plus and minus 90 degrees at a sinusoidal audio-frequency rate of 100 cycles, the frequency would deviate (in accord with a cosine function) 157 cycles above and below the original frequency; if the audio frequency rate of phase shift is now increased tenfold to 1,000 cycles, the frequency deviation will likewise be increased ten times to give 1,570 cycles deviation. The frequency deviation in cycles, therefore, can be seen to equal the product of the audio frequency (also in cycles) and the phase shift in degrees, divided by a constant (the number of degrees per radian).

Inasmuch as the frequency deviation must be held constant at 75,000 cycles for 100-percent modulation, regardless of the modulating frequency, the number of degrees phase shift must be varied inversely with the modulating audio frequency. This effect is readily accomplished by use of an integrating circuit (also known as an inverse frequency network), consisting of a series resistance and a shunt capacitance, usually placed between the source of modulating signal and the phase modulator. The higher modulation frequencies are thus attenuated in precisely the desired manner for true frequency modulation.

The phase shift obtainable with low distortion from conventional phase modulator circuits rarely exceeds 25 degrees. The resulting frequency deviation for a 30-cycle modulating signal may be readily calculated to be equal to 13.1 cycles. Since this small deviation falls far short of the required 75,000 cycles, it becomes necessary to multiply the original frequency deviation by a factor M approximately equal to 6,000 in order to attain the required final frequency deviation. The well-known fact that multiplication of frequency produces a like multiplication of frequency deviation is used for this purpose to good advantage in practically all phase modulators.

There is a good practical reason, however, for keeping M not much over 1,000. Assuming the lowest usable crystal frequency as 75 kc (5 times the highest audio frequency) and an operating frequency of 100 mc, a factor M equal to 1,333 is obtained. To attain higher multiplication factors than this, it is necessary to resort to the use of heterodyne frequency converters.

In general, frequency converters are undesirable because the spurious beat frequencies present in their output circuits must be carefully discriminated against by means of tuned circuits and adequate shielding. In addition, there is the possible production of additional spurious beats caused by voltages from the low-frequency stages entering one or more of the broad pass bands of the stages following the converter. Hence, if M can be reduced to approximately 1,300 or less, the above difficulties will not materialize.

Addition of Phase Shifts

Large values of M are a direct consequence of the limited phase shift of which conventional modulators are capable. It is possible, however, to increase the useful phase shift of a modulator substantially by adding the individual phase shifts of two or more stages connected in cascade. The block diagram of Fig. 2 illustrates the manner of connecting the phase shift stages in cascade for the transfer of r-f energy, but in parallel as far as the a-f signal is concerned. The progressive increase of frequency deviation from stage to stage is also given for N, the number of cascaded stages, equal to 6, and for a maximum phase shift per stage of 23.9 degrees (required for a 30-cycle a-f signal at full deviation). It should be noted that if only the first stage were used ($N = 1$), the conventional modulator would result for which M must be 6,000 (75,000 cycles/12.5 cycles); if all six stages are used ($N = 6$), M is reduced to 1,000 (75,000 cycles/75 cycles)—the latter condition obviating the need for a frequency converter.

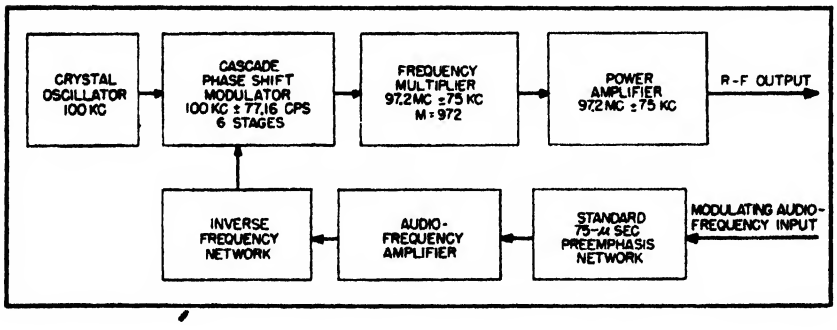

FIG. 1—Block diagram of f-m transmitter using cascade phase shift modulator

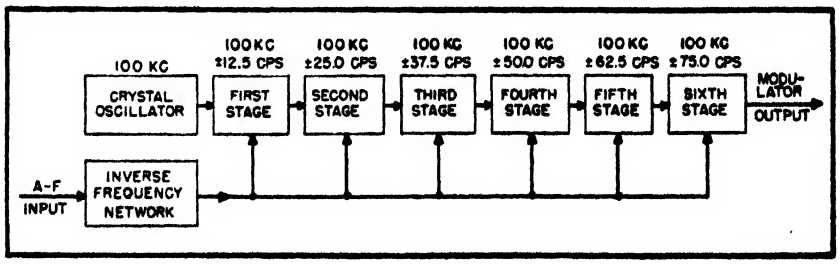

FIG. 2—Block diagram showing individual stages of cascade phase shift modulator. A maximum phase shift per stage of plus or minus 23.9 degrees is required for a 30-cycle signal at full frequency deviation

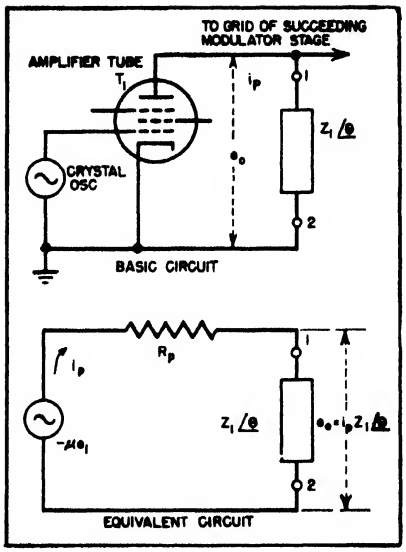

FIG. 3 (left)—Basic phase shift stage operating at crystal frequency, and equivalent circuit

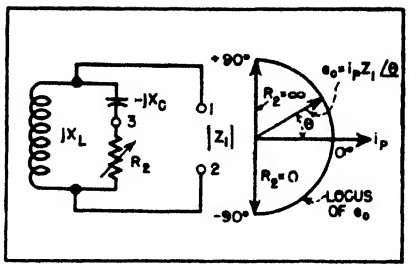

FIG. 4 (above)—Constant-impedance network and corresponding vector diagram

From the preceding discussion it follows that N may be considered as effective as M in producing the final frequency deviation. This relationship may be stated as follows: The frequency deviation at the operating frequency in cycles is equal to the product of the audio frequency in cycles, the phase shift per modulator stage in degrees, the factor M, and the factor N, divided by the number of degrees per radian (57.3).

There is yet another advantage which comes from keeping M relatively low. When an unmodulated r-f signal is passed through a vacuum tube amplifier, it becomes modulated by the random noise voltages which are ever present; one portion produces amplitude modulation of the r-f signal and the other produces irregular fluctuations in its phase.

The amplitude modulation is readily removed by the limiting action of subsequent multiplier stages, but the irregular fluctuations in the phase of the signal represent a noise modulation. The frequency deviation corresponding to these fluctuations increases for the higher audio frequencies because there is no inverse frequency network to attenuate them. The magnitude of the resulting phase shift of the r-f wave due to the noise may be shown[3] to be approximately equal to 57.3 times the value of noise voltage divided by the signal voltage. Hence, assuming a noise of 10 microvolts and a signal of 10 volts, the phase shift would be approximately 0.0000573 degrees.

For $N = 1$ and $M = 6{,}000$, approximately 0.05 degree phase shift is required at 15,000 cycles to produce 100 percent modulation. The ratio, then, of the phase shift for 100 percent modulation to the noise phase shift, expressed in db, should give the f-m noise level at the output frequency. For the above case ($M = 6{,}000$) the noise level is 58.8 db below 100 percent modulation. Performing the same calculation for $M = 1{,}000$ and $N = 1$, the phase shift required is 0.3 degree, and the noise level for this source of noise becomes 74.4 db below 100 percent modulation.

The foregoing calculations considered the case of an unmodulated r-f signal for $N = 1$. The effect on the noise level of adding N modulator stages in cascade will now be taken up. As previously mentioned, the phase shift appearing at the modulator output terminals is equal to the sum of the phase shifts produced in the individual stages. But the random nature of fluctuation noise produced in each modulator stage makes it necessary to take the rms sum of these voltages in order to find the resultant noise voltage at the modulator output terminals. Therefore, N modulator stages will add $\sqrt{N}$ times the noise of one stage. If four stages are cascaded, there will be a fourfold increase in phase shift, but only a twofold increase in the noise of the system. In actual practice, noise is also produced in other parts of the transmitter, so that the relative contribution of the modulator section to the total noise is even smaller.

In order to minimize harmonic distortion under certain conditions of modulation, it is desirable to use a modulator circuit in which the percentage of amplitude modulation produced concurrently with phase modulation is very small. This distortion becomes a maximum when the percentage of phase modulation is such as to produce only the first pair of sidebands.[4] The effect in this case consists of a change in the relative magnitudes of the sideband, and any subsequent limiting action which may remove the amplitude variation will still be powerless to restore the relationship between the carrier and sidebands necessary for low distortion. Therefore, a further requirement for the design of the modulator is that any amplitude modulation produced along with the desired phase modulation be kept at a minimum.

Theory of Cascade Phase Shift Modulator

The basic phase shift stage in Fig. 3 consists of an amplifier tube T_1 and its plate load impedance, the two-terminal network Z_1 connected across terminals *1* and *2*.[4] T_1 serves both as an amplifier which isolates the cascaded phase shift stages from one another and as a source of constant current for Z_1.

From the equivalent circuit it follows that the phase of the output voltage e_o must vary as the phase angle of Z_1. This is so because the load impedance is much smaller than the plate resistance R_p and therefore can have practically no part in determining the plate current i_p. Since the product of the plate current and the vector impedance, $Z_1 \angle\theta$, is equal to the output voltage, any change in phase of this impedance must therefore

result in phase modulation of the output voltage. It also follows that any change in the magnitude of Z_1 will result in amplitude modulation of the output voltage.

The two-terminal network shown in Fig. 4 may be designed to maintain a substantially constant impedance while phase modulation is taking place. The general expression for the impedance of this network is[8]

$$|Z_1| = X_L \sqrt{\frac{1+\left(\frac{1}{b}\right)^2}{1+\left(\frac{1}{b}\right)^2\left(\frac{1}{a}-1\right)^2}} \qquad (1)$$

where

$$a = X_C/X_L \qquad (2)$$

$$b = R_2/X_C \qquad (3)$$

A study of Eq. 1 will show that when the quantity $(1/a)-1$ is set equal to unity, the quantity under the radical sign will also be equal to unity and therefore $|Z_1|$ will remain constant and equal to X_L regardless of any variation of b. This condition occurs when a is set equal to 0.5. Substituting this solution in Eq. 2, it follows that $|Z_1|$ will be constant when

$$X_L = 2X_C \qquad (4)$$

This network is used as the plate load of a vacuum tube whose plate resistance is over 100 times greater than $|Z_1|$, and since the parallel resistance of a coil with a Q of about 30 is also of the same high order of resistance, the effect of these two quantities on the magnitude of Z_1 may be neglected. These two quantities, however, do play a minor part in determining the phase angle of the network. Therefore, the phase characteristic of the network[8], calculated for a coil Q of 30, is shown in Fig. 5 for values of a equal to 0.4, 0.5 (the constant-impedance solution), and 0.6.

A mental picture of the phase shift action to which the output voltage in this circuit is subjected may be obtained by considering the two extremes of resistance, bearing in mind that the inductive reactance is equal to twice the capacitive reactance (Eq. 4). For R_2 open, the current through terminals *1* and *2* of Fig. 4 must be inductive. Therefore, the output voltage will lead the plate current by approximately 90 degrees.

When R_2 is short-circuited, the current taken by the capacitive branch will be twice as great as that taken by the inductive branch, thus making the net current into terminals *1* and *2* capacitive. The output voltage, therefore, will lag behind the plate current by approximately 90 degrees for this other extreme. Intermediate values of R_2 will cause the locus of the output voltage vector to follow the semicircle depicted in Fig. 4.

The most important part of the basic shift stage is the device which converts the a-f modulating signal into a corresponding a-f variation of resistance. This device, which is known as the modulator or resistance tube, replaces R_2 of Fig. 4 in the practical circuit. To obtain low distortion, the characteristic of resistance versus control voltage of this device must be made to approximate the curvature of the phase angle characteristic (Fig. 5). This requirement is important mainly for low-frequency signals in the band from 30 to 50 cycles, where a maximum phase shift of about plus and minus 25 degrees per stage is required for full frequency deviation.

Conventional vacuum tube circuits utilizing the dynamic plate resistance of a tube as a function of control grid voltage cannot be used because the adjustment of bias becomes too critical when the above requirement must be met. Therefore, the circuit shown in Fig. 6 was developed to do the job. With the r-f voltage assumed to be zero, the circuit behaves not unlike a cathode follower. The plate is bypassed to ground through C_2, the a-f modulating signal e_s is applied between control grid and ground (across the shunt capacitance C_1 of the inverse frequency network), and an output voltage (the gain is less than one) appears between cathode and ground. For this condition of operation the resistance looking into terminals *2* and *3* may be given as[7]

$$R = \frac{1}{\frac{1}{R_k}+\frac{1}{R_p}+\frac{\mu}{R_p}} \qquad (5)$$

where R_k is the resistance connected externally between cathode and ground, R_p is the effective plate resistance of the tube at its operating point, and μ is the amplification factor of the tube at its operating point.

Now consider the circuit from the standpoint of the r-f voltage e_o, which is the voltage across the constant impedance Z_1 in Fig. 3.

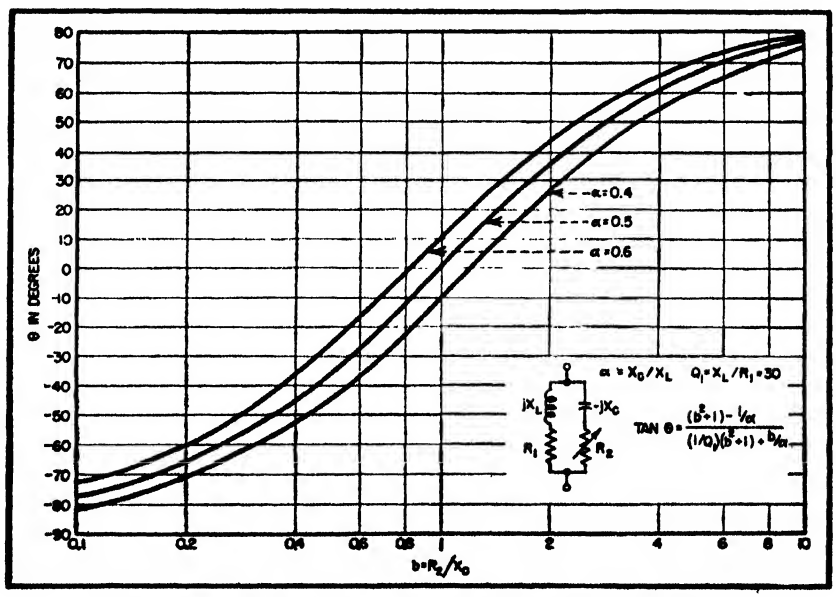

FIG. 5—Phase characteristics of constant-impedance network

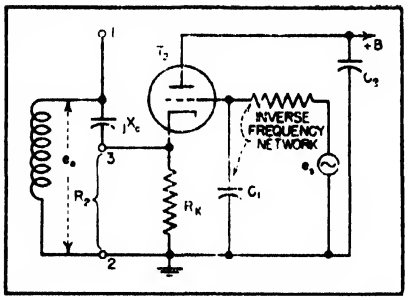

FIG. 6—Basic circuit of resistance-tube stage

Assuming the modulating signal e_s in Fig. 6 equal to zero, the circuit behaves like a grounded grid amplifier because C_1 effectively puts the grid at ground potential for r-f. Thus, any r-f voltage between cathode and ground is also applied between control grid and cathode of T_2. Under normal conditions of operation, the relatively high value of R_k never allows grid current to flow during the positive portion of the r-f cycle. However, if the r-f grid-to-cathode voltage is high enough, tube T_2 will be cut off during some part of the cycle, the point of cutoff being a definite function of the instantaneous grid-to-cathode and plate-to-cathode voltages.

The modulating a-f signal e_s thus determines the fraction of the r-f cycle during which the plate current flows through T_2. In other words, during the time the modulating signal is positive, the angle of flow is increased, and during the balance of the modulating signal cycle, the reverse is true.

During the part of the r-f cycle cycle over which T_2 is cut off, R_2 is equal to R_k. For the remainder of the r-f cycle, R_2 must be equal to R as defined by Eq. 5. By proper choice of r-f voltage level and the value of R_k, the curvature of the resistance tube characteristic can be made to match the curve in Fig. 5, so that no bias adjustment is necessary.

In the final design of the modulator portion of an f-m transmitter using the cascade phase shift modulator, six cascade stages are followed by several frequency multipliers with a factor M of 12, as shown in Fig. 7. The final multiplier provides an M equal to 81, so that the overall M is 972. A built-in tuning meter enables the operator to make adjustments without the aid of external measuring equipment.

Assuming that the crystal oscillator stage is operating normally, the r-f voltage level at the grid of each cascade amplifier (T_1 through T_{11}) is adjusted to a predetermined setting on the tuning microammeter. Although this meter reads the grid current, it acts as a peak-reading vacuum-tube voltmeter. A variable capacitor in each amplifier grid circuit provides the means of adjustment by forming a simple voltage divider with the associated coupling capacitor. This r-f voltage level setting fulfills the requirement for curve matching of the resistance tubes.

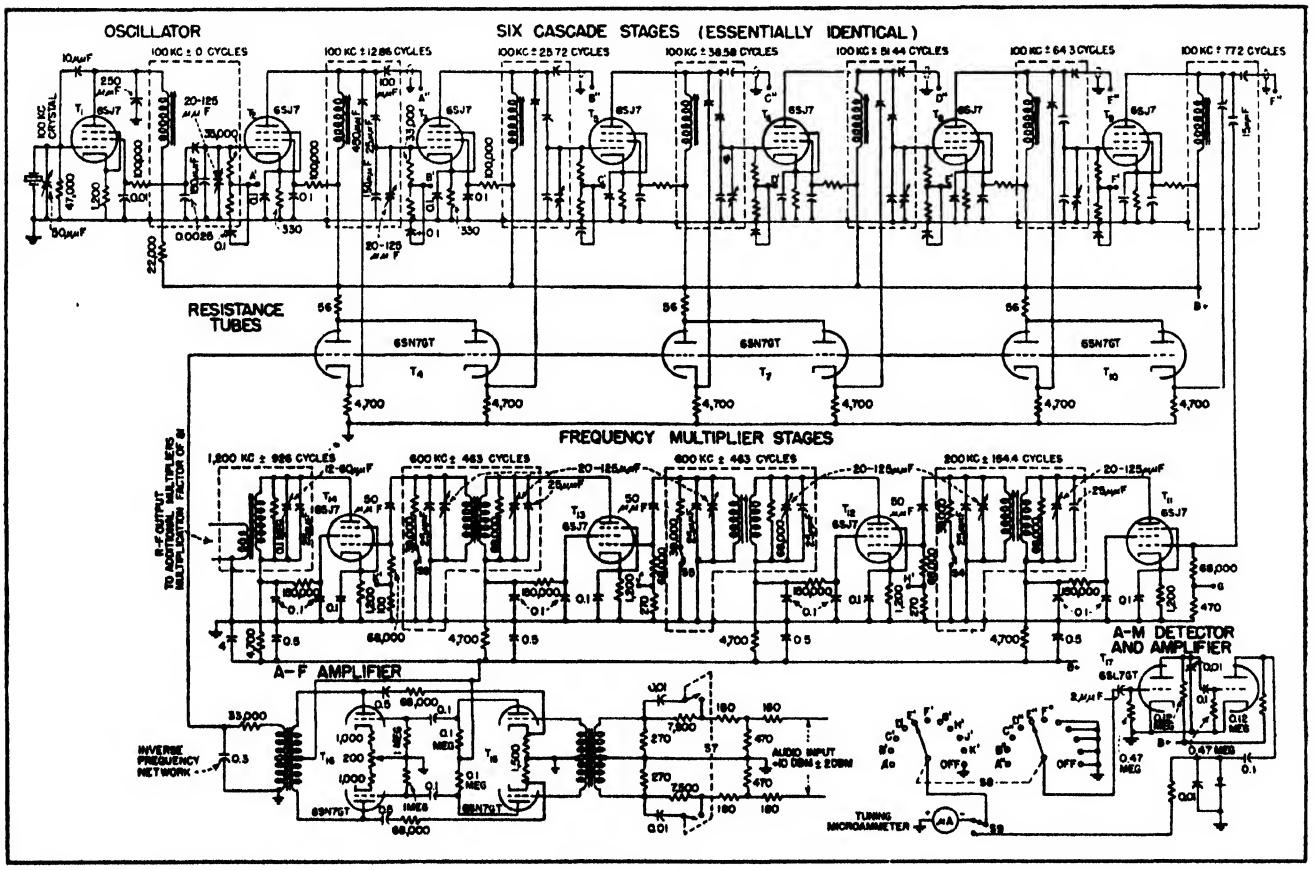

FIG. 7—Schematic diagram of modulator of f-m transmitter using the cascade phase shift modulator

For the next step, the inductance X_L of the constant-impedance network in each amplifier must be adjusted to conform with Eq. 4. Ordinarily this would present a difficult problem because the coil cannot be peaked to the crystal frequency—the actual resonant frequency being the crystal frequency divided by 1.414. However, this lifficulty may be overcome by taking advantage of the theory which states that a minimum of amplitude modulation will be observed at the plate of each amplifier tube when the inductance of its constant impedance network is adjusted correctly (X_L equal to $2X_C$).

Accordingly, an a-f modulating signal is applied through the normal a-f channel, of a level sufficient to bring about full frequency deviation and of a frequency low enough to produce a reasonably large phase shift in each modulator stage. Then use is made of a built-in amplitude modulation detector and amplifier (the double triode T_{11}) which uses the microammeter as a modulation indicator. Sample r-f voltages from each phase shift amplifier plate are piped over to this detector via the meter switch, and thus any plate may be selected at will.

Starting with the first stage, each inductance in turn is adjusted for minimum meter deflection of the amplitude modulation indicator. Of course, if the coils are found to be so far out of adjustment as to materially alter the r-f voltage set up in the initial step, then both steps must be repeated. That is all there is to the adjustment of the modulator proper.

Transmitter Alignment

The only other adjustments are those of the multiplier and amplifier coupling transformers. These transformers are designed so they will pass a band wide enough to accommodate twice the highest modulating frequency, but attenuate the undesired adjacent harmonics produced in the preceding stages. These requirements usually lead to a slightly double-peaked selectivity curve corresponding to a coupling greater than critical.

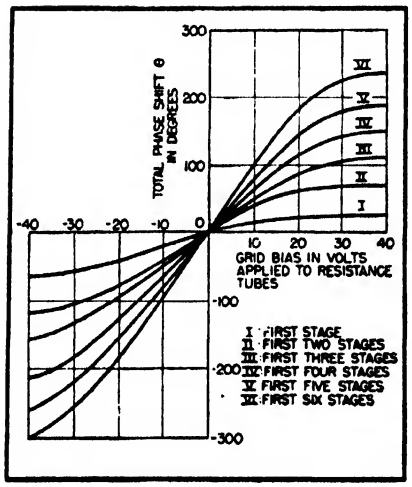

FIG. 8—Operating characteristics of cascade phase shift modulator

Misalignment of such transformers invariably causes asymmetrical selectivity curves, which usually increase the harmonic distortion and may even reduce the frequency deviation for the higher modulating frequencies. It is important, therefore, that overcoupled transformers be properly aligned.

The method of alignment of overcoupled transformers adopted for use in this transmitter is simple, requires no external equipment and gives the right answers in terms of performance. A pushbutton switch is provided on all overcoupled transformers. A damping resistance is permanently connected to the top of the secondary of each transformer, and when the pushbutton switch is pressed, the free end of the damping resistance is grounded. This action has the effect of decreasing the secondary impedance. Because the ground side of the resistance is switched, there is no appreciable change of circuit capacitance due to the switching action.

It is well known that a decrease of secondary impedance in an overcoupled transformer reduces the coupling. Thus, with proper choice of damping resistance, the coupling is reduced to a value below critical and the transformer may be easily and accurately tuned for maximum output at the center frequency provided by the preceding stage.

Upon releasing the pushbutton, the transformer again becomes overcoupled and gives the symmetrical pass band required for high-quality performance. All band-pass transformers are aligned in this manner. Normal transmitter tuning technique is used for the higher-powered portions of the transmitter. It is possible to adjust all tuning elements shown in Fig. 7 in less than ten minutes.

A static characteristic curve giving the total phase shift in degrees as a function of the grid bias applied to the resistance tubes for 1, 2, 3, 4, 5, and 6 cascade stages is shown in Fig. 8. The linearity of the curve for six stages is attested by harmonic distortion measurements, for 75-kc frequency deviation, of 1.25 percent for 30 cycles and less than 0.6 percent for 50 to 15,000 cycles. Distortion for 100-kc frequency deviation is less than 1 percent from 50 to 15,000 cycles. The f-m noise has been measured at 72 db below a frequency deviation of 75 kc.

The author wishes to express his appreciation for the perseverance and help given by W. E. Phillips and S. G. Jones, under whose direction this modulator was developed, and to D. A. Skinrood, G. L. Dufield, L. Schultz, E. A. Andrade, and Y. K. Luk of the Broadcast Equipment Division of Raytheon Manufacturing Co.

References

(1) Hund, August, "High-Frequency Measurements", McGraw-Hill Book Co., New York, p 368, 1933.
(2) Hund, August, "Frequency Modulation", McGraw-Hill Book Co., New York, p 104, 1942.
(3) Reference 2, p 59.
(4) Seeley, S. W., Kimball, C. N., and Barco, A. A., Generation and Detection of Frequency-Modulated Waves, RCA Review, p 276, Jan. 1942. A variation of this circuit is described.
(5) "Reference Data for Radio Engineers", First Edition, Federal Telephone and Radio Corp., New York, p 52, 1944. Eq. 1 may be obtained by proper manipulation of the formula given for magnitude of impedance.
(6) Reference 5, p 53. The phase characteristic equation in Fig. 5 may be obtained by modifying the formula given for phase angle of two parallel impedances.
(7) Pacini, Humbert P., Cathode Follower Calculations, ELECTRONICS, p 187, Oct. 1944.

Serrasoid F-M Modulator

Design data for an improved four-tube phase-shift type modulator that initiates 100-percent modulation with noise 80 db down and 0.25 percent harmonic distortion in broadcast service. Low relative cost suggests potentially greater utilization of the educational frequencies. Variations of the basic circuit open new fields of application

By J. R. DAY

THE development of a simple f-m modulator has been one phase of a broad program to enlarge the technical horizons of f-m broadcasting. In particular, it was aimed at providing one solution to the problems of relay and chain broadcasting. Such service requires that the noise background and distortion be very low in the individual links so that the final signal may still meet the relatively high standards required for any f-m broadcasting system. Such chain systems have been operated satisfactorily using available equipment, but it cannot be said that, in the more extensive chains, the limiting noise rests with the audio facilities at the origin. This latter condition has always been regarded as a minimum requirement of a really good f-m broadcast setup.

Careful examination of the problems in a reasonably extensive chain yields the conclusion that an 80 db ratio of 100-percent modulation to noise in the modulator would be satisfactory. In addition, a maximum figure of 0.25-percent harmonic distortion for 100-percent modulation with single tones from 50 to 15,000 cycles was set as a correlative objective. Since a practical modulator involves accessory circuits such as an audio amplifier, which can be expected to make some definite though small contribution to the numbers above, the actual net requirements on the modulation process are somewhat more severe than the overall figures. It is evident that such performance will also be of significant application in a single f-m broadcast setup, apart from the special question of relaying.

Means of generating frequency-modulated currents fall into two general classes, the reactance-modulated type, and the phase-shift type. In the first, the frequency of an oscillator is caused to vary linearly with modulation through the agency of a reactance tube or its equivalent, which is an integral part of the frequency-determining circuit. Because of the modulation and linearity requirement such an oscillator in general is not stable enough for broadcast service. Automatic frequency control is therefore employed. In the phase-shift type of modulator the frequency of the carrier oscillator is not varied, and therefore a stiff control such as a quartz crystal can be used to secure the desired stability, which then is completely independent of the modulation process. Modulation of the frequency in such a system is secured by varying the phase of the frequency-stabilized wave. The frequency will be deviated from its controlled value only during the time the phase is changing, and the deviation, other things being equal, is proportional to the rate of change of phase.

The Serrasoid is the latter type. Although it is capable of broader application, the numbers involved for the f-m broadcast case provide the clearest illustrative material. As noted above, frequency deviation is proportional to rate of change of phase. For sinusoidal modulation this is simply expressed by saying that the peak frequency deviation is equal to the product of the peak phase shift and the modulating frequency. The new circuit is conservatively capable of a peak phase shift of ±150 degrees, but ±90 degrees or ±1½ radians is used as the basis for 100-percent modulation at 50 cycles. For 1½ radians and 50 cycles the peak deviation therefore will be ±75 cycles. Since 100-percent modulation in f-m broadcasting is a deviation of ±75,000 cycles, a frequency multiplication of 1,000 is indicated. Actually, 972 is used since it can be factored into a convenient assortment of doublers and triplers. In all that follows we shall discuss a modulator for a frequency of 97.2 megacycles which starts at a base frequency of 100 kilocycles.

Figure 1 is a schematic diagram of the essential parts of a complete broadcast Serrasoid. Audio amplifiers and frequency multipliers have been omitted since they are conventional and employ small standard type tubes. Tube V_1 is a pentode oscillator controlled by quartz crystal Y. The crystal operates very close to its series resonant frequency. The net reactance of the crystal arm may be conveniently varied by a series capacitor for fine frequency adjustment of about ±0.005 percent. This crystal is oven controlled in the broadcast case to a net stability of ±0.0002 percent, which is also the stability of the final carrier frequency. The operation of the oscillator is such that plate current is drawn only during a small part of the cycle. Negative going pulses shown in Fig. 2A are generated at the plate of V_1. These pulses are differentiated by C_2, R_4, and grid-cathode conductance of V_{2A} to yield still shorter pulses several times the cutoff voltage of V_{2A}. The corresponding short positive pulses at the plate of this latter tube are bottom clipped (to clean the base line) by cathode follower

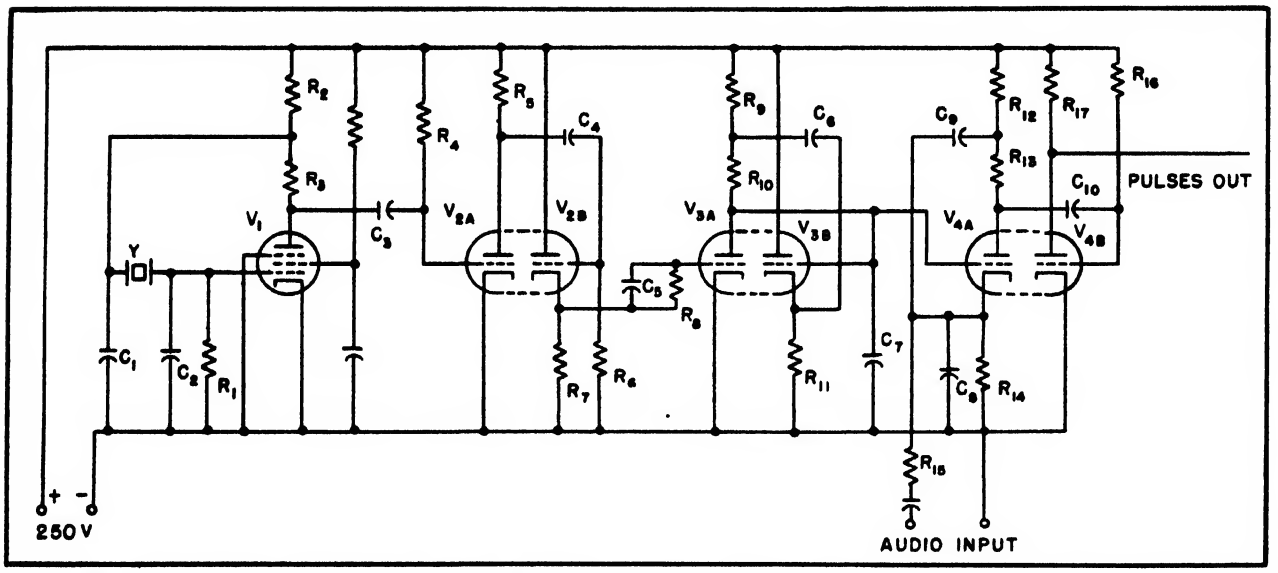

FIG. 1—The modulator proper showing the crystal oscillator, clipper, sawtooth generator and bootstrap cathode follower, and f-m pulse output tubes. The frequency multiplier stages that follow are conventional

V_{2B}. Resistor R_7 is selected so that this tube is biased beyond cutoff between pulses by the automatic grid bias of C_4 and R_6. The pulses at the cathode of V_{2B} appear as shown in Fig. 2B. The two halves of V_2 perform the functions of a single pentode that might have been used in the same place, with the additional advantage that the final waveform is developed in a lower impedance than is practicable with a pentode.

Linear Sawtooth Wave

According to the numbers of the illustrative case these pulses recur at a rate of 100 kilocycles, that is, corresponding points or events on consecutive pulses are 10 microseconds apart. Tube V_{3A} constitutes a nonoscillatory sawtooth generator timed by the pulses from V_{2B}. The slowly increasing portion of the sawtooth has a slope corresponding to the charging of C_7 through R_{10} to the relatively steady voltage at the junction of R_9 and R_{10}. This period coincides with the time between pulses at the grid of V_{3A}, cutoff bias having been developed on C_6 by previous pulses. The quickly decreasing portion of the sawtooth occurs at the time of positive pulses on V_{3A}, when C_7 is discharged nearly to cathode potential by the plate-cathode conductance. In round numbers the discharge point is about 5 volts from cathode or ground potential and R_{10} and C_7 are adjusted to give a rising rate of about 4 volts per microsecond to the increasing portion of the wave. As will be shown the whole linearity of the modulation process depends on the straightness of this sawtooth wave. In its simple form, it would have too much exponential curvature to be useful. This condition is corrected by the bootstrap connection comprising the cathode follower V_{3B}, R_{11}, C_9, and R_9. The normally constant voltage at the positive end of R_{10} has superimposed upon it the rising voltage on C_7 so that the drop on R_{10} and hence the charging current is maintained practically constant. Resistor R_9, as in other bootstrap applications could be a diode with its anode at plate supply potential, but for the voltage magnitudes involved here the resistor is more than adequate. The d-c voltage at the junction of R_9 and R_{10} is about +190 volts for a B+ value of 250 volts.

Pulses are Frequency-Modulated

The sawtooth wave thus developed is directly coupled to the grid of V_{4A}. This tube is cathode biased by its plate current so that conduction begins when the sawtooth is about half way up; the passage from the beginning of plate current flow to grid current consuming about 0.25 microsecond. Because C_8 is large and holds the bias constant during the sawtooth period, grid current stops the charging of C_7, and the latter half of the sawtooth rise is clipped. The resulting waveform is shown in Fig. 2C the dashed line indicating the waveform without the direct coupling to the grid of V_{4A}. Thus, the plate current of V_{4A} flows only during the latter half of the sawtooth wave. If the bias for V_{4A} is varied, the leading edge of this current pulse will vary in time or phase, an advance resulting from a lowering of the bias and a retardation from an increase. It is in this way that phase modulation in the unit is accomplished.

Audio or program is applied at the indicated terminals. Values of R_{12} and C_9 are so proportioned that for constant audio input amplitude versus frequency, the resulting amplitude at C_8 is inversely proportional to audio frequency over the range upward from 50 cycles. This circuit is included so that the peak phase shift shall be inversely proportional to modulating frequency and the resulting frequency response of the frequency modulation shall be flat. The function and the network are the familiar corrector

present in all phase-shift type frequency modulators. In order that at 50 cycles the phase of the pulse edge be shifted $\pm 1\frac{1}{2}$ radians, approximately 50 volts rms is required at the input to the corrector. In the complete modulator a two-stage amplifier provides the gain to raise the standard input of ± 10 dbm to this level. Since feedback is used in this audio amplifier to provide linearity, the effective modulation sensitivity is also stabilized to a marked degree. This sensitivity depends only on the audio gain and the stability of R_{10} and C_7, and ordinarily is stable to within 1 percent for the standard ranges of temperature, line voltage, and tube changes.

Figure 2D illustrates the waveform at the plate of V_{4A}, the dashed lines showing the extreme positions of the leading or negative going edge during 100-percent modulation at 50 cycles. For 100-percent modulation at 100 cycles the excursion is one half that shown, and so on. This wave is differentiated by C_{10}, R_{16}, and the grid cathode conductance of V_{4B} so that the latter is cut off for a short time each cycle beginning at the leading edge. The resulting positive-going pulses at the plate of V_{4B} are shown in Fig. 2E. These pulses are frequency modulated approximately ± 75 cycles at 100-percent modulation. They are applied to the grid of the first of a string of frequency multipliers. The plate loads of this and subsequent multipliers are resonant at the various harmonics, and therefore, involve only sinusoidal c-w currents. In the broadcast version these multiplications are 3, 3, 3, 3, 2, 3, and 2, for a total of 972 times, yielding a carrier frequency in this illustration of 97.2 megacycles with a deviation of ± 75 kilocycles at 100-percent modulation.

Circuit Design Factors

Before proceeding to a discussion of distortion and noise in a system of this sort several salient features may be pointed out. First, in common with all phase-shift modulators, there is no interaction whatever between the functions of modulation and carrier-frequency control, and the final stability is exactly that of well engineered crystal control. Exclusive of the frequency control the modulation process is accomplished in three standard receiving type tubes operating under cutoff to saturation or cathode follower conditions. As a result the process is remarkably independent of tube changes or aging. There are no resonant circuits and no reactances. Largely to eliminate the commercial tolerances of resistors and capacitors, C_3, C_7, C_{10}, and R_{14} are factory adjusted, and thereafter no adjustments even of a maintenance nature are necessary, except after outright component failure. Tubes V_1 through V_4 drain about 20 milliamperes at 250 volts.

Possible Variations

An interesting aspect of the development of this modulator lies in its apparent simplicity. Until certain special factors were fully appreciated performance was indifferent and the simultaneous attainment of low distortion and low noise hardly seemed practical without considerable elaboration. A good many detailed variations from the sample circuit shown are operative, and some yield high performance. But without the observance of certain principles, design can be surprisingly difficult. The important rules affecting linearity and noise are enumerated below.

Having selected the sawtooth waveform as the basic timing or phase-shifting mechanism, it developed that linearity could not be preserved if it was amplified or caused to appear as a current variation in a plate-loaded tube, no matter how attractive such a step may have appeared at first. Other means of straightening the sawtooth beside the bootstrap arrangement shown are entirely practical provided the sawtooth waveshape as such is not amplified. In particular, in the modulation process the tube performing the timing, V_{4A}, cannot carry currents of sawtooth shape and still preserve linearity in the timing process. It was found also that the amplitude of the current pulses in V_{4A} should be constant during the modulation cycle. To insure this condition the plate supply voltage is maintained constant by C_9. The supply voltage is low, about 30 volts, giving a small cutoff voltage.

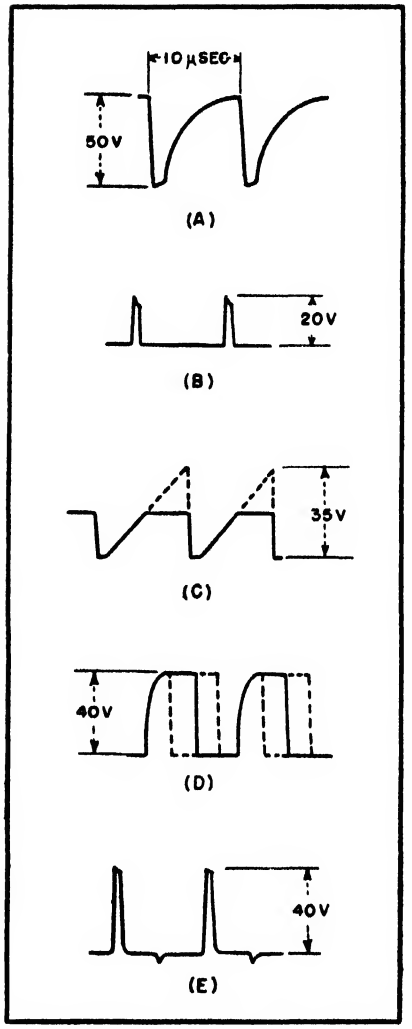

FIG. 2—Waveforms, oscillator to output

Noise arises in such a system in the form of random variations in the time of occurrence of corresponding events in consecutive cycles. Such timing variations ordinarily are the result of superposition of noise voltages on the desired wave-form. The noise voltages originate either in tube current variations or as Johnson noise in resistors. The effects of both kinds of noise are reduced by increasing the time rate of change of voltage in the sides of the pulses.

and by maintaining low circuit impedances at certain points. For instance, impedances controlled by R_8, R_7, and R_{10} are in a position to contribute to the residual modulator noise unless maintained below values appropriate to the pulse amplitudes appearing across them. This is another way of saying that the circuit bandwidth should be as great as possible so that the pulse rise-time is short. Noise originating from uniformly distributed random voltage variations causes frequency modulation noise with a triangular distribution spectrum, extending linearly up from zero at zero modulating frequency. For the band up to 15,000 cycles the integrated noise power from a given resistance is approximately 44 db greater than would be the case for a flat noise spectrum. The 75 microsecond de-emphasis in the f-m receiver reduces this effect by 13 db. The reduction factor is different if the original noise is other than triangular. For instance, Johnson noise in R_{10} is modified in its spectrum by C_7 before it can phase modulate pulses determined by the sawtooth. It is a straightforward matter to show by calculation that if the linearity were secured without the bootstrap or its low-voltage equivalent, that is, by making the supply voltage very high, the noise generated by the necessary large resistor would be excessive by a considerable factor. Thus it comes about that the bootstrap or its low voltage equivalent is uniquely essential to securing simultaneously low noise and low distortion. By similar reasoning it can be shown that the lowest noise is obtained when the corrector capacitor C_8, is directly at the modulator cathode. If the corrector were to be located at a lower level in the audio section, tube and Johnson noise originating after it would have a 31 db handicap and with practical tubes and circuit constants, this effect would be insurmountable. The possibility of noise phase modulation in the first tube after V_4 is minimized by making this a frequency multiplier so that the noise deviations are multiplied by a smaller factor than those originating in V_4 and earlier.

Performance

The general performance of the Serrasoid system in the particular case shown, and following the design rules noted can be summarized as follows. The linearity of the phase-shift process is readily made to be equivalent to less than 0.1-percent f-m distortion for peak phase shifts of ± 135 degrees. It should be noted that nonlinearity in the phase-shift process results in f-m distortion proportional to the order of the harmonic generated. Thus 1 percent third harmonic expressed as distortion of the phase shift is equivalent to 3-percent distortion measured as frequency modulation. In the commercial f-m broadcast modulator the distortion is largely controlled by the included audio amplifier, and the overall figure is held to less than 0.25 percent for 100-percent modulation at 50 cycles. At high frequencies where the peak phase shift is less the distortion falls until it is entirely accounted for in the audio circuits. At the upper end of the audio spectrum, distortion owing to tuned circuits in the frequency multipliers rises slightly, but by reasonable design is held below 0.25 percent, measured without de-emphasis. It is much easier to contrive that the distortion be this low than it is accurately to measure it once secured!

The f-m noise originating in the modulator and in the band from 50 to 15,000 cycles, measured with 75-microsecond de-emphasis is somewhat better than 80 db below 100-percent modulation. This noise is made up of approximately equal contributions from the crystal oscillator plate circuit and the plate circuit of V_{4A}. It can be reduced still farther by designing for greater pulse bandwidth and higher tube currents, and by the special artifices described below. Microphonism is no practical problem at all with non-selected ordinary tubes. Because of the simplicity of the circuits involved shielding and isolation by ordinary means serves to suppress the noise effects of r-f feedback from high-level sections of the transmitter.

Increasing Phase Shift

There are two ways by which the total phase shift can be increased over the practical maximum of ± 150 degrees. One of these is by cascading, or iterated modulation. The pulses at the plate of V_{4B} are similar in form and amplitude to those at the plate of V_{2A}. If, instead of coupling here to the grid of a multiplier, these pulses are fed to a duplicate of the circuit extending from V_{2B} to V_{4B} inclusive, another complete modulation process will have been encompassed. One stage of such cascading doubles the peak phase shift with the same percentage of f-m distortion and yet raises the f-m noise by less than 3 db. Thus the effective signal to noise ratio is improved by at least 3 db. The price paid for this iteration is two and a half additional tubes and a doubling of the audio power required to modulate. The process can be extended beyond two modulations. The other method involves generating two or more interlaced sawtooths at submultiples of the crystal frequency by means of a step-counter frequency divider; separately modulating pulses from each of the proportionately longer submultiple sawtooths; and recombining the sets of modulated pulses. The submultiple frequency, of course, must be more than twice as high as the highest modulating frequency involved.

In general, by the use of cascading and interlacing, as noted, by the use of a modification of the scheme employed in the Armstrong dual channel phase shift modulator, and by several other arrangements too detailed to describe here, the application of this system can be extended to cover a very wide field.

F-M Service Areas

Chart shows approximate distance to 1-mv/m and 50-μv/m contours for effective radiated powers between 1 and 1,000 kw and transmitting antenna heights from 100 to 3,500 feet above average terrain

BY JOHN H. BATTISON

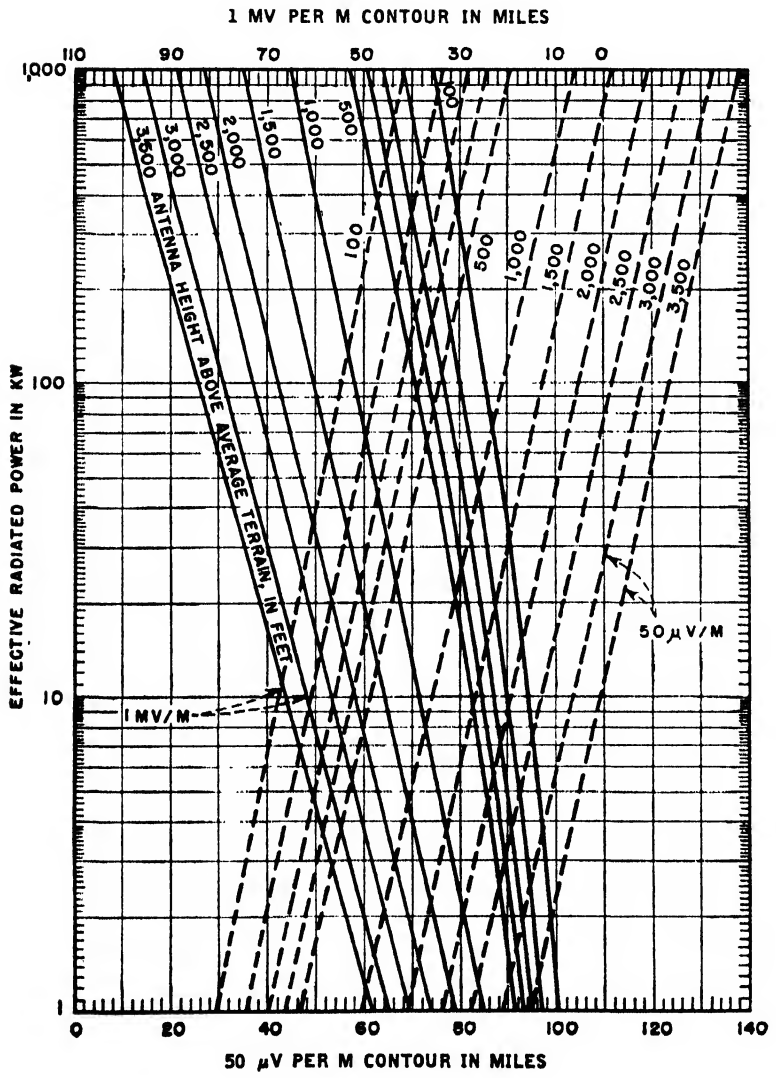

THE accompanying chart, based on FCC data, provides a quick means of determining the approximate service areas of a transmitter operating on any channel between 88 and 108 mc. Distance to the 1 mv-per-meter contour (solid lines) is shown by the upper scale and distance to the 50 microvolt-per-meter contour (dashed lines) by the lower scale, for various effective radiated powers and transmitting antenna heights. Receiving antenna height is assumed to be 30 feet above average terrain.

Using the Chart

To determine the distance to the 1 millivolt-per-meter contour with a transmitting antenna height of 2,000 feet and 20-kw of effective radiated power, enter the chart at the left and, at the point where the 20-kw horizontal line intersects the solid diagonal line labelled 2,000′, read on upper scale 57 miles. To determine distance to 50 microvolt-per-meter contour follow the same procedure but use the dashed diagonal line labelled 2,000′ and read the lower scale.

If coverage is desired at a given distance, with a known transmitting antenna height, the effective radiated power required may be read to the left of the point of intersection of appropriate distance and height lines. Similarly, should it be necessary to determine the transmitting antenna height required to provide a certain contour with a given power the chart may be entered from the left and the bottom, and the height read from the appropriate solid or dashed line.

Overmodulation Without Sideband Splatter

By adding this balanced-modulation circuit to an a-m phone transmitter, modulation in excess of 100 percent can be produced without causing adjacent-channel interference. The technique permits communication modulators to operate at high average level

By OSWALD G. VILLARD, JR.

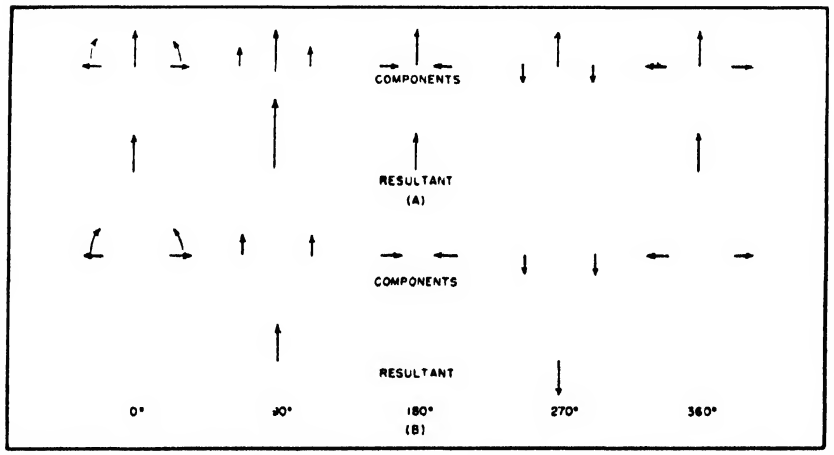

FIG. 1—Vector diagrams for (A) 100-percent amplitude modulation with carrier and (B) 100-percent modulation with fully suppressed carrier show that the resultant signal in the latter case reverses phase as a consequence of the modulation

IN OPERATING an amplitude-modulated radiotelephone transmitter in communications or broadcast service it is always desirable to keep the average percentage of modulation as high as possible in order to increase the energy in the intelligence-bearing sidebands. In this way a louder-sounding and hence more reliable signal is delivered to the receiver. However, the average percentage of modulation may only be increased until overmodulation begins to occur on the program peaks, for the waveform distortion caused by overmodulation clipping is rich in harmonics, and the corresponding sidebands spilling over into adjacent channels may interfere with adjacent-channel services. Yet in the case of speech, when the gain is adjusted to prevent overmodulation on peaks, it is found that the average percentage of modulation is distressingly low.

The circuit described in this article offers a simple means of increasing the average percentage of modulation of amplitude-modulated phone transmitters above 100 percent without causing adjacent-channel interference due to sideband splatter. Accompanying this increase in modulation percentage is a certain amount of distortion which will be noticed in receivers tuned to such a signal. However, it is unlikely that this distortion, occurring as it does only on peaks, will degrade speech intelligibility appreciably unless the percentage of modulation exceeds 100 by a very large amount.

The circuit can be readily incorporated in existing plate-modulated phone transmitters, both single-ended and push-pull, having more audio power available than that required for 100-percent modulation. Installation of the circuit requires relatively few components. For radiophone service where intelligibility rather than fidelity is important, the system makes possible a saving in total primary power consumption and in class-C amplifier tube capacity for a given sideband power output. This advantage is obtained even though the bandwidth required for transmission is maintained at the absolute minimum.

Peak Limiting and Volume Compression

Various ways of increasing the average percentage of modulation have been suggested. One method is to alter the dynamic range of the original program material in such a way that the weak passages are made louder and the loud passages made weaker; known as volume compression. Another method is to introduce peak limiting devices which limit the maximum possible excursion of the audio signal fed to the transmitter. The two systems will increase both the average percentage of modulation and the intelligibility of a signal, at the expense of a certain amount of naturalness which is lost when excessive compression of the dynamic range or distortion due to clipping occurs.

In the case of the peak chopper, there is the disadvantage that the clipped waveform, if allowed to modulate the transmitter directly, contains harmonics capable of causing just about as much adjacent-channel interference as if the clipping had been caused by overmodulation itself. If these harmonics are removed by a low-pass filter, the waveform is no longer clipped at a fixed level, and overmodulation is no longer prevented.

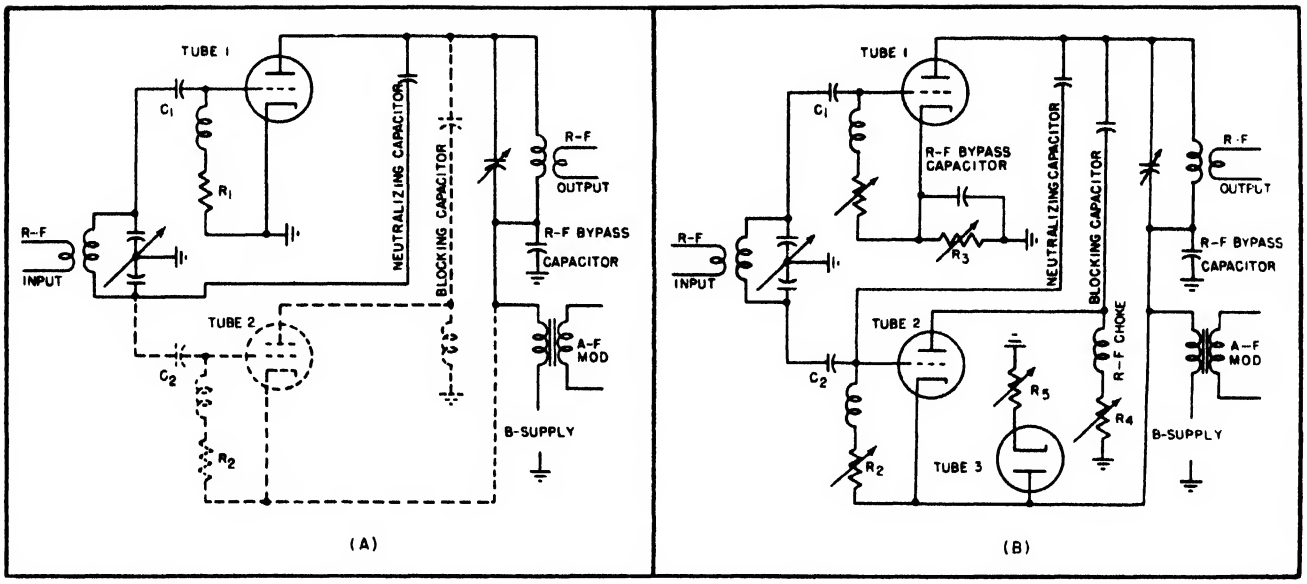

FIG. 2—(A) Additions to conventional class-C modulated amplifier to produce phase reversal of the carrier on overmodulation peaks are shown by dotted line. (B) To bring the two circuits into balance, variable resistors are added. Adjust either R_1 or R_2, or R_3 or R_4, one or the other pair but not both, until equal r-f outputs at a given plate voltage are obtained. Adjust R_5, reversing polarity of tube 3 if necessary, until tubes 1 and 2 present the same load impedance to the modulator

Where splatter and adjacent-channel interference must be avoided, it is clear that peak chopping is not particularly practical.

If proper care is taken in their design, peak-actuated volume compressors can be made to prevent momentary overmodulation on peaks, without perceptibly increasing the bandwidth of the audio signal as a result of the distortion which occurs during the transient changes in gain. The only limit to the advantages to be derived from their use as a means for increasing the average percentage of modulation is the loss in naturalness—and eventually intelligibility—which results when weak sounds are amplified much more than loud sounds (unless, of course, a proportionate volume expansion is introduced at the receiver, but such systems of communications where volume expansion at the receiver is possible will not be considered in this article).

Another method of increasing the average percentage of modulation of an amplitude-modulated radiophone transmitter, which in effect allows the percentage of modulation to exceed 100 without causing any adjacent-channel splatter whatsoever, is to increase the power in the sidebands beyond the level produced by 100-percent modulation. It will be seen that this method, used in conjunction with volume compression, makes possible a still further increase in intelligibility over that obtainable by means of volume compression alone.

Briefly, the proposed system allows the ratio of sideband to carrier power to exceed one-half (the condition corresponding to 100-percent modulation) without permitting any distortion of the sidebands to occur. This condition of operation might be called "double sideband reduced carrier," which would be analogous to the "single sideband reduced carrier" systems now in widespread commercial use.

Figure 1A shows the familiar vector diagram of an amplitude-modulated wave, 100-percent modulated. Figure 1B shows the same wave with the carrier removed but with the sidebands unchanged. It is possible to remove the carrier without altering the sidebands in any way; then, because the sidebands have suffered no distortion, there can be no splatter. Figure 1B could, for example, represent the double sideband output of a balanced modulator in which the carrier had been suppressed.

It is important to note that the resultant of a pair of a-m sidebands taken by themselves is a wave of the same frequency as the carrier, but changing in amplitude and also in phase, as shown in Fig. 1B. During the positive half of the audio-frequency modulating cycle, the resultant varies from zero to a maximum and back again; during the negative half cycle, the resultant follows a similar change in amplitude but with the phase of the carrier voltage reversed. This change in phase may be considered to be part of the normal a-m modulating action. When the resultant of the two sidebands is in phase with the carrier, we have phase addition and upward modulation; when the resultant is 180 degrees out of phase, we have phase cancellation and downward modulation.

Modulator Circuit

If we cause the amplitude and phase of a radio-frequency wave of the carrier frequency to vary in the same manner as the resultant of the two sidebands discussed in the preceding paragraph, we will have

a means for producing a double-sideband carrierless signal. In practice this can be done in the following way. Two class-C amplifiers are fed from the same modulator in such a way that one produces output during positive half cycles of the modulating voltage, while the other produces output during negative half cycles. If one class-C amplifier is excited by a radio-frequency voltage 180 degrees out of phase with the excitation fed to the other, and both amplifiers work into a common output, we have the required condition of operation. The basic circuit is shown in Fig. 2A.

The portion of the circuit drawn in with a solid line is simply a conventional grid-neutralized single-ended class-C amplifier stage. The portion drawn with a dotted line represents the additional equipment needed to convert this stage into a double-sideband generator. For the moment, we will assume that the B-supply is shorted. It will be seen that tube 1 will produce r-f output during the positive half cycles of modulation, while tube 2 will produce r-f output of the opposite phase during the negative half cycles. If the output of the two tubes is properly balanced we will have the desired double-sideband output.

It will be noted that this circuit is nothing more than a species of balanced modulator. If the modulation transformer had been provided with a center-tapped secondary, and if the center-tap of this winding had been bypassed to ground and the ends connected through shunt-feed r-f chokes to the plates of the class-C amplifier stages, the circuit would have been recognized at once as one of the standard variations of a balanced modulator. The only real difference between the two cases lies in the method of connecting the supply voltages to the two class-C amplifier stages.

We are accustomed to think of balanced modulators as consisting of identical tubes or rectifying elements, which is, of course, the normal arrangement when double-sideband carrierless output is desired. But there is no reason why the carrier must be completely suppressed; it can, in fact, be present in any desired amount without disturbing or distorting the sidebands in any way. In order to make our balanced modulator produce double-sideband reduced-carrier signals, it is only necessary to insert d-c in the desired amount by means of the B-supply. In fact, for a given modulator a-c voltage output, which fixes the amplitude of the sidebands, we can make the ratio of sideband-to-carrier voltage (and also the percentage modulation) in the final r-f wave anything we would like—from something much less than one up to infinity—by simply adjusting the amount of injected d-c and thus setting the amplitude of the carrier.

Need for Balancing the Modulator

Of course, when a carrier is added to the sidebands in this way, the tube supplying the carrier will handle more power than its mate, which is called upon only to supply sideband energy. In the application of the circuit of Fig. 2A to over-modulation splatter suppression, tube 2 will not, in general, be identical to tube 1, and consequently it is of interest to consider how a modulator consisting of two dissimilar tubes can be brought into balance. The circuit of Fig. 2A lends itself nicely to a consideration of balanced modulator operation in terms of familiar class-C amplifier concepts.

The curve of r-f output voltage versus plate voltage for a class-C amplifier stage is very nearly a straight line beginning at the origin and possessing a slope slightly less than unity. This characteristic comes about because the peak r-f voltage across the tank circuit of an adequately excited class-C amplifier is always very nearly equal to the plate supply voltage. The difference between these two voltages is, of course, the voltage required to draw the pulse of plate current through the tube. The magnitude of this voltage difference, assuming constant plate load impedance, is controlled to a first approximation by two factors—the angle of plate current flow and the amplitude of the grid driving voltage. Increasing either, within limits, will tend to increase the amplitude of the fundamental-frequency component of the plate current pulse, and thus increase the voltage drop at fundamental frequency across the tuned plate tank circuit.

The amount by which the slope of the r-f output voltage versus plate voltage curve is less than unity is roughly proportional to the magnitude of the instantaneous plate voltage required to draw the plate current pulse, and this magnitude is dependent on the angle of plate current flow and the amplitude of the grid driving voltage.

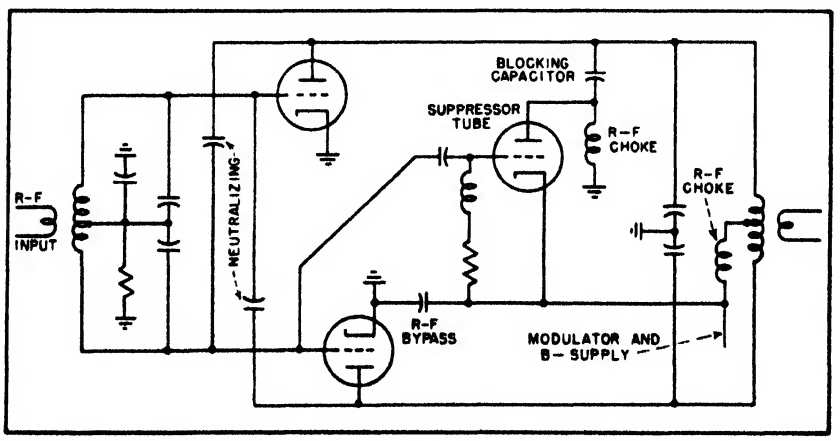

FIG. 3—Addition of splatter suppression circuit to push-pull modulated amplifier can be done simply. Balancing controls are not shown; see Fig. 2B

Consequently, if we have two class-C amplifiers whose r-f output versus plate voltage curves we wish to match, or stating it another way, whose slopes we wish to make equal, to a first approximation it is only necessary to vary the grid bias or the driving voltage of one amplifier until its performance matches the other. This equality is the condition we wish to achieve in the balanced modulator of Fig. 2A. Modulating voltages of from zero to maximum positive should produce r-f outputs of exactly the same magnitude from one amplifier tube as modulating voltages from zero to maximum negative produce from the other.

Another, somewhat more wasteful way of accomplishing the same result would be to add resistance in series with the supply voltage lead of whichever class-C tube is found by experiment to have the r-f output versus plate voltage curve of greater slope.

However, matching the slopes of the output curves does not guarantee that the two class-C amplifier tubes will then each present exactly the same load impedance to the modulator. It is entirely possible that the two tubes may produce equal r-f outputs at the same magnitude of d-c plate voltage, but at the same time draw differing d-c plate currents. The modulator will then be working into one value of load impedance during positive half cycles, and another during negative half cycles. Unless the effective output impedance of the modulator has been reduced by some means (such as negative feedback) to a very low value, positive and negative half-cycles of output voltage will have differing amplitudes and distortion will result.

Method of Producing Balance

A difference in load resistances can easily be eliminated by measuring the d-c voltage-current ratios of the two class-C tubes at a given plate voltage, and then in effect connecting a resistance in shunt with the plate supply leads of that tube having the higher ratio. The added resistance should be of a value such that the parallel combination of this resistance and its associated class-C amplifier presents the same load resistance to the modulator as the other class-C tube considered alone.

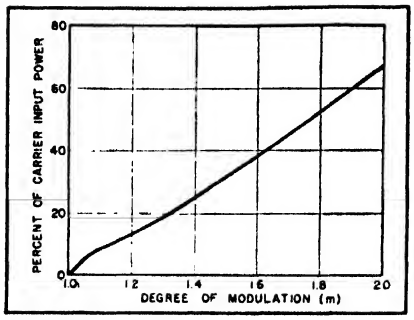

FIG. 4—Average power input to suppressor tube is shown as a function of degrees of sinewave modulation

In the case of the double sideband generator circuit that we have been discussing, both tubes are effectively connected across the output of the modulator at all times; consequently the equalizing resistance must be connected to the circuit through a diode in such a way that this resistance is effectively present in the circuit only during positive or negative half cycles of modulation, as the situation may require.

Figure 2B is similar to Fig. 2A but with various balancing controls included. Resistors R_1 and R_2 are, of course, the grid leak resistors normally present in the circuit. (Use of grid leak bias is desirable from the standpoint of improving the linearity of the modulation characteristic.) Resistors R_3 and R_4 represent two alternative points of connection of amplitude balance controls. Resistor R_5 illustrates a way of connecting the load impedance balancing resistor. It should be emphasized that both R_3 and R_4 will not be needed. Only one resistor will be required, once the proper point of connection has been determined.

So far nothing has been said about the effect of the double sideband generator tube on the neutralization of the original class-C amplifier. Inspection of Fig. 2A will show that if tube 2 has the same grid-plate capacitance as tube 1, the tubes will neutralize each other and no neutralizing capacitor such as the one shown will be needed. If the effective grid-plate capacitances are not exactly equal, as will almost invariably be the case when stray circuit capacitances are taken into account, a neutralizing capacitor may have to be connected between the plate leads, which are in parallel for r-f, and the grid of one tube or the other in order to make the neutralization perfect.

The circuit of Fig. 2A is correct when the effective grid-plate capacitance of tube 2 is less than that of tube 1. For the reverse situation, the plate connection of the neutralizing capacitor remains the same, while the grid connection should be made to the grid of tube 1.

Phase Shift in Grid Circuits

A word needs to be said at this point concerning the possibility of undesirable phase shift in the grid circuits of the two class-C amplifier tubes. Referring to Fig. 2A, note that grid coupling capacitors C_1 and C_2 will normally be so designed that their reactance at the operating frequency is very low compared to the equivalent shunt resistance of the grids of the two tubes at the positive peak of the grid driving cycle. Yet the reactance of these capacitors at the highest modulating frequency should be equal to at least twice the resistance of the grid leaks (neglecting, in the interests of simplicity, the effect of the r-f chokes), for good linearity of modulation.

In view of the extremely low shunt resistance which the grids may represent when driven well into the positive region of operation, it may not always be possible to prevent a certain amount of phase shift in the coupling circuits. If the two tubes are dissimilar, with differing grid driving requirements and differing grid impedance characteristics, the phase shifts in the two grid circuits may not be the same and the two tubes may not be driven exactly 180 degrees out of phase.

Unfortunately, the phase of the

voltage in the grid circuits at the positive crests of the grid driving cycle directly determines the phase of the steady-state r-f voltage across the common plate tank circuit. The remedy is to equalize the time constants of the two grid circuits at the crest of the driving cycles, which can be done by varying the capacitance of one or the other of the coupling capacitors or by connecting a low resistance in series with the grid of whichever tube displays the lowest grid impedance at the positive crest of its driving cycle.

Fortunately, in most practical cases the phase shift through the coupling capacitors will be negligible; phase correction in the grid circuit will only be found to be necessary in the case of low-carrier-frequency, high-fidelity transmitters when widely dissimilar tubes are used.

Exactness of balance, both as regards phase shift and relative amplitude, can be easily checked by applying equal d-c plate voltages to both tubes simultaneously, and noting the presence or absence of r-f voltage of the fundamental frequency in the common plate circuit. This check should be made at a number of different supply voltages.

One other point is worthy of mention. Examination of Fig. 2 will show that tube 2 is shunt fed in both grid and plate circuits, and a low-frequency parasitic oscillation can be expected as a matter of course unless the r-f choke in the plate circuit is given a much larger value of inductance than that in the grid circuit.

Modifying Existing Equipment

On the basis of the foregoing discussion it is not difficult to see how almost any plate-modulated radiotelephone transmitter can be converted into a double-sideband generator for the purpose of suppressing adjacent-channel interference due to overmodulation. When the percentage of modulation is low, we have normal class-C modulated amplifier performance, with only tube 1 conducting. However, when overmodulation occurs, and the instantaneous plate potential of tube 1 becomes negative with respect to ground, tube 2 comes into action and produces an undistorted sideband output corresponding to the negative modulation peaks which would otherwise have been clipped off. Because there is no distortion, no adjacent-channel interference is generated.

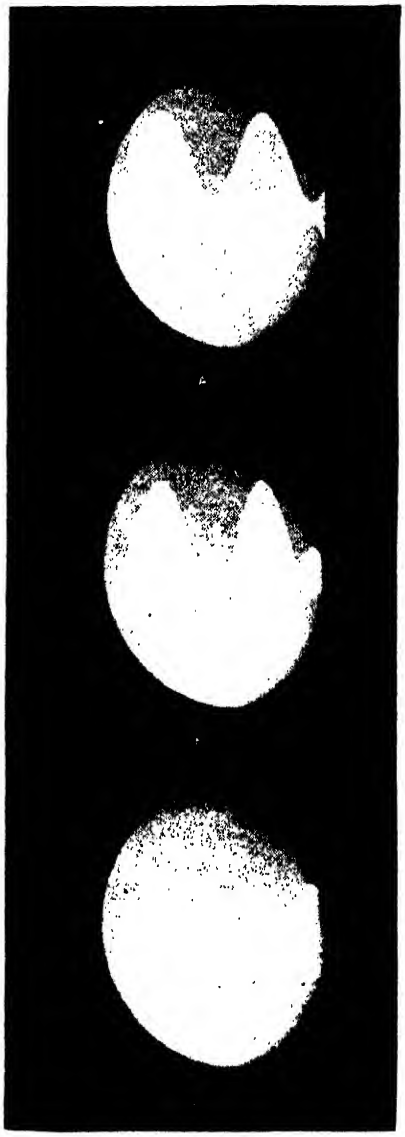

FIG. 5—Oscillograms show various degrees of modulation, including overmodulation, obtained with the suppressor circuit

The splatter-suppression circuit can readily be added to existing transmitters provided, of course, that sufficient reserve audio power is available. It will be seen that the number and the cost of the added components is not very great. The only possible complication is the filament supply for the suppressor tube, which must have high-voltage insulation and a low capacitance to ground. However, standard rectifier filament transformers meeting these requirements are not hard to find.

The splatter-suppression circuit can be added to push-pull class-C r-f amplifiers just as easily as it can be added to single-ended ones. Reference to Fig. 3 will make this clear. The tube labelled Suppressor Tube performs the same functions as tube 2 in Fig. 2. The circuit is in all other respects that of a conventional push-pull amplifier. From the standpoint of r-f, the suppressor tube is connected between the grid of either one of the push-pull tubes and the plate of the other. The main point is that, when overmodulation occurs and the common plate-voltage lead becomes more negative than ground, causing the suppressor tube to come into operation, the suppressor tube must deliver to the tank circuit r-f which is 180 degrees out of phase with that supplied by the push-pull tubes when the common plate-supply voltage lead is at a positive potential.

Splatter-Suppressor Power

The splatter-suppressor tube need not have large plate dissipation capacity. Because tube 2 conducts only during the modulation peaks, the average power dissipated at its plate will be small. Consequently, a small, inexpensive tube can be used, provided one is selected with adequate insulation and adequate peak emission.

For a sinewave modulating waveform, the average power input to the splatter-suppressor tube can be calculated in the following way. Power input to the suppressor tube, expressed as a percentage of the carrier power input, is 0.278 $m\alpha$ for sinewave modulating voltage, where α expressed in degrees is the angle whose cosine is $1/m$, and m is the modulation factor (defined as the difference between the maximum and average envelope ampli-

tudes divided by the average amplitude.)

A plot of this relation is given in Fig. 4. The actual power dissipated at the plate of the suppressor tube is, of course, the product of the total input times the efficiency of the suppressor tube as a class-C amplifier. Especially in the case of complex modulating waveforms, such as speech and music, it will be found that the power dissipated by the plate of the suppressor tube is relatively small for reasonable degrees of overmodulation.

It should be evident that use of the above splatter-suppression circuit will not prevent distortion at the receiver when the transmitter is modulated in excess of 100 percent. Some representative oscillograms will make this clear.

Figure 5 illustrates the patterns obtainable. In all three figures the modulator output voltage is constant, and only the d-c plate input to the larger of the two class-C tubes was varied. Figure 5A shows the familiar modulation envelope pattern obtained when the percentage of modulation is less than 100 percent. In Fig. 5B the effective percentage modulation is now in excess of 100 percent, and the suppressor tube is beginning to make its contribution. In Fig. 5C the d-c or carrier power input has been reduced virtually to zero and we have very nearly a pure double-sideband output. In this particular setup, the two class-C load impedances presented to the modulator were not balanced, and time did not permit of any attempt to reduce the distortion present in the output of the laboratory modulator below the level shown. However, the oscillograms serve to illustrate the basic idea of the system, and the results obtained were in full agreement with expectations.

Figure 6 shows the trapezoidal patterns corresponding roughly to the conditions of adjustment illustrated in Fig. 5.

When a signal as much overmodulated as the one shown in Fig. 5B is demodulated by a wideband conventional receiver using a linear detector, a badly distorted replica of the original sinewave will be obtained. However, it should be borne in mind that any sideband clipping caused by the selectivity of the receiver circuits will reduce the effective percentage modulation of the incoming signal and thereby reduce the distortion.

Sideband clipping will, of course, normally be noticed only on the higher audio frequencies, 1,000 cps and above. In communication circuits where quality of reproduction is not important, it may be possible to put this effect to some practical use. Considerable high-frequency preemphasis at the transmitter could be followed by high selectivity at the receiver, such as that obtainable with the conventional crystal filter. If high-frequency program peaks were then strong enough to overmodulate, receiver selectivity could easily be made sufficient to reject the excess sideband energy, thus leaving a signal at the second detector which was modulated less than 100 percent and hence undistorted. The chief practical difficulty with this arrangement is that most of the energy peaks in speech occur at frequencies below 1,000 cps. However, when overmodulation did occur at any frequency, it would not produce sideband splatter because of the carrier phase reversal of the suppressor tube.

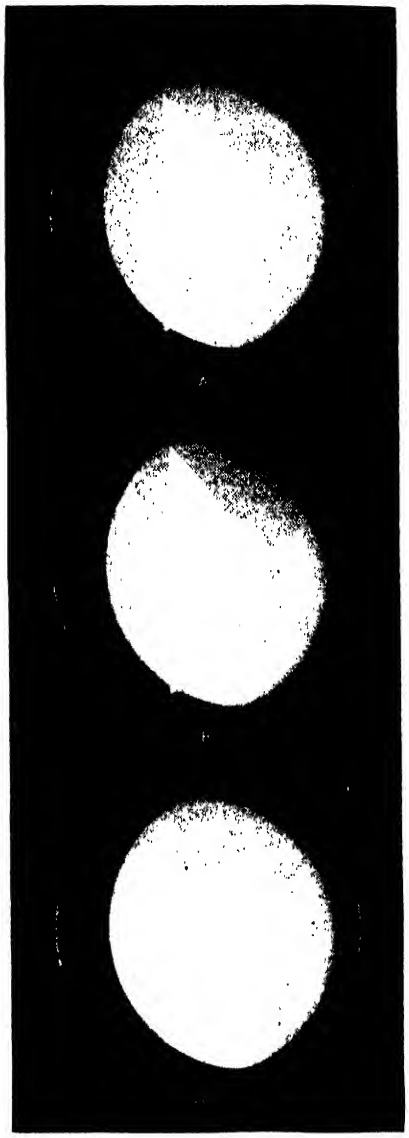

FIG. 6 — Corresponding trapezoidal patterns show the percents of modulation represented by oscillograms of Fig. 5

Bridging Amplifier for F-M Monitoring

Complete data on a monitor amplifier whose signal-to-noise ratio at maximum power output is approximately 80 db. It contains a combination differential amplifier and cathode-coupled phase inverter for balanced line input and a response flat within 0.5 db from 20 to 25,000 cps

BY GEORGE E. BEGGS, JR.

INCREASING DEMAND for higher quality audio transmission requires apparatus capable of gaging the true quality of transmitted programs, especially in frequency modulated radio stations.

The amplifier to be described is capable of 15 watts output at frequencies as low as 20 cycles per second and as high as 25,000 cycles per second, having response flat within better than ± 0.5 decibel between these limits. This is obtained by the use of an all pushpull triode circuit particularly adapted to monitor bridging amplifier use, but also usable with single-ended input sources. Adequate gain for operation from a standard 500-ohm, 0-v-u (0 v-u = 1 mw) line and good signal-to-noise ratio further justify its use in monitor applications.

Components and circuit details are such that the unit can be duplicated at relatively low cost with assurance that good performance will be obtained. The addition of a single-ended preamplifier would make the unit adaptable to applications other than monitor use, such as quality reproduction in homes.

The unit has excellent response, as shown in Fig. 1, low effective source impedance for loudspeaker or cutter operation, differential amplifier, cathode-coupled phase-inverter input in place of a bridging transformer, balanced inverse feedback, low noise level, and adequate gain.

Push-pull triode operation is utilized throughout, as shown in Fig. 2. The input stage, comprised of a 6SC7 dual triode, is employed in place of a standard bridging input transformer. Since it has 500,000-ohm resistors in the grid-return circuits, the load imposed on the standard 500-ohm line is negligible. An input voltage of the order of 0.3 volt rms grid-to-grid will drive the amplifier at full output.

This input stage has several useful features. By utilization of a 25,000-ohm unbypassed cathode resistor in place of the usual 1,000-ohm resistor, a combination differential amplifier[1] and cathode-phase-inversion amplifier[2] is obtained. In normal operation, when a push-pull signal is introduced to the grid, the cathode remains at a fixed potential. However, if an in-phase signal is introduced to both grids, it will tend to drive grid *A* in a positive direction, and the cathode, due to the large value of cathode resistor, will also tend to go in a more positive direction. This is equivalent to grid *B* going in a negative direction. However, since grid *B* is also going in a positive direction, the in-phase signals cancel out, which is the desired characteristic to allow cancellation of hum pickup in balanced lines, etc. In spite of the high value of cathode resistor, full gain of the 6SC7 stage is realized with the circuit outlined.

Single-Ended Input

The amplifier may be supplied with a single-ended input signal by grounding the unused grid. A signal fed to the other grid, the signal voltage being developed between ground and that grid, will appear as a push-pull signal in the plate circuits of the input tube. This is occasioned by a similar action to that outlined above, that is, if grid *A* goes in a positive direction, the cathode follows the grid, giving an equivalent negative signal to grid *B*, thus providing a push-pull signal reproduced in the plate circuits. With the circuit constants shown, a balance of five percent or better can be obtained between the two signals, that is, the ratio of a-c plate signal *A* to plate signal *B*, will be approximately 1.05 or less.

The ratio of the plate signal magnitudes in the two plate circuits is given by the equation[2]: $E_{pA}/E_{pB} = 1 + 1/G_m R_k$ where G_m is the mutual conductance of the tube and R_k is the cathode resistance.

When the amplifier is used with single-ended input, it is important that provision be made to ground the unused grid directly, rather than depend upon the 500,000-ohm, grid-return resistor to furnish adequate ground return. If the grid is left at 500,000 ohms above ground, high-frequency response of the amplifier suffers (curve 3 of Fig. 1 results). Apparently the effective capacitance between grid and cathode causes the unused grid to follow the cathode at frequencies where the impedance of the capacitance approaches the value of the grid resistor, the effect becoming progressively more pronounced at higher frequencies. This decreases the overall gain at these frequencies by decreasing the input to the unused grid, that is, the differential voltage between the two grids is reduced.

In a sense, this effect is similar to the Miller effect[3] in usual triode operation, where the effective input capacitance C_i of a triode is many times the grid-cathode capacitance C_{gk}. The actual value of C_i is given

by: $C_i = C_{gk} + (M + 1)C_{gp}$ where M = stage gain at mid-frequency and C_{gp} = grid-plate capacity.

For a 6SC7 with plate load and plate voltage conditions noted on the circuit, this capacitance is about 90 $\mu\mu$f, which is an impedance of 500,000 ohms at about 3,000 cps.

Driver Stage

The basic circuit of the driver stage is conventional with certain exceptions. The gain control of the amplifier, which might be omitted under certain application conditions, is a push-pull gain control. In the circuit shown, a two-circuit, six points per circuit, switch was utilized to give five steps of gain and an off position, in steps of approximately six db, except for the last step which was made approximately 10 db. It is probable that a standard dual gain control, with a resistance of 250,000 ohms per section, could be used.

The plate circuit of the driver stage and the grid circuit of the output stage can best be described jointly. A UTC type HA-107 interstage transformer having split secondaries is utilized to allow the application of fixed bias, with individual adjustment, to the output tubes. The two secondaries are individually loaded to reflect an impedance of approximately 10,000 ohms per plate to the 6SN7 driver sections. This serves to provide proper operation of the transformer over a wide range of frequencies. In the primary of the transformer, a 22-henry choke is utilized in the plate supply lead, to provide a high a-c impedance to ground from the center point of the driver transformer primary. This insures that the 6SN7 will maintain class A operation, since any tendency for the sum of the two plate currents to depart from a constant value (true class A operation) is offset by the a-c impedance of the choke. Since there is no necessity to drive this tube into the grid-current region to obtain adequate driving voltage for the output tubes, class A operation is to be desired under all circumstances for low-distortion operation, and is assured by the inclusion of this choke.

The output tubes utilized are type 6A5G'. These tubes are similar to the 2A3 triode, but have two advantages over 2A3's. First, since they operate with 6.3 volts on the heater, no 2.5-volt transformer is needed. Secondly, the inclusion of a cathode internally tied to the center tap of the heater makes an equipotential electron source available. This has proved of great assistance in reducing the residual hum level present in the amplifier. The unit was previously constructed with 2A3's but the change was made to reduce hum. The output tubes are operated with a fixed bias of approximately 68 volts derived from the two potentiometers and the voltage divider network supplied by the 5W4 bias rectifier. Individual adjustment of these tubes, so that they draw equal plate current, is accomplished by use of the two potentiometers and the 50-ma meter. The switch allows checking current of either tube independently. Each tube is adjusted to draw 40-ma with no output.

Since the cathodes are grounded, the center-tap ground return for all heaters is accomplished through the internal connection within the 6A5's, a common 6.3-volt supply being used for all three amplifier tubes. The output transformer utilized is an LS-55 UTC type.

Feedback

Monitor amplifier application requires excellent response over a wide range of frequencies. It is

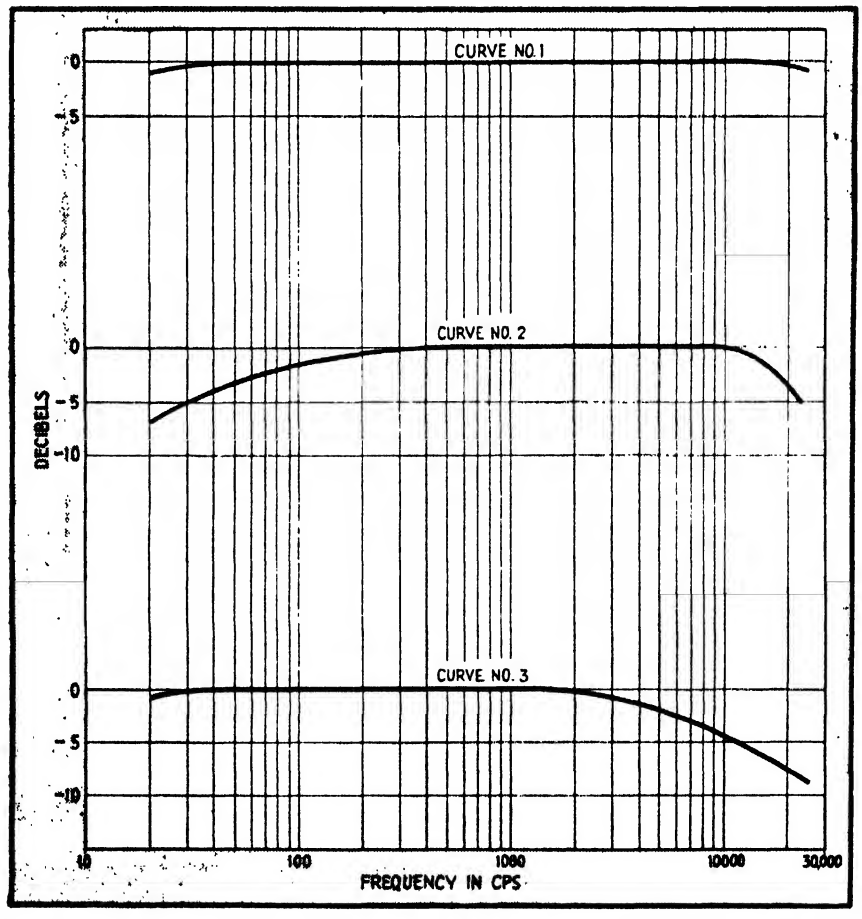

FIG. 1—Curves made at one-volt rms input to amplifier feeding a 500-ohm resistive load. For curve 1, the input was a balanced line and feedback was used in the amplifier. A similar curve was obtained with single-ended input and one grid grounded. Curve 2 resulted when feedback was omitted. Curve 3 was produced with single-ended unbalanced input to one grid and the other grid not directly grounded, with feedback

most desirable to obtain a response curve which is flat over a wide range and which contains no positive slopes within or near the range of frequencies normally supplied to the amplifier. This last characteristic improves transient response.

Feedback is incorporated in the amplifier in a balanced fashion, in keeping with the overall push-pull characteristics, by feeding a portion of the output voltage from each output plate back to the appropriate driver cathode, through a large blocking capacitor, to reduce phase shift in the feedback circuit to negligible proportions. These bypass capacitors are 8 μf electrolytics further bypassed by paper capacitors to reduce the impedance effect of electrolytics at high frequencies. A $\mu\beta$ of 4 is provided [8] (corresponding to about 14-db feedback) without any tendency to oscillate.

Feedback could have included the output transformer under certain conditions but it was thought desirable to leave the output lines entirely independent of any relation to ground so that they could be operated with associated equipment in which one side of the output line might be operated at ground or the output line might be floating or center tapped to ground. The frequency response does not appear to suffer from the omission of the output transformer from the feedback loop.

Frequency Response

The characteristics of the amplifier without feedback, with push-pull balanced line input, are shown in curve 2 of Fig. 1. Under these conditions, the amplifier is flat within $\pm$ 2 db from 40 cycles to over 20,000 cycles, which is reasonably good. However, with feedback, as shown in curve 1 of Fig. 1, response is within better than $\pm$ 0.5 db from 20 cycles to 25 kc. The usual low impedance of the 6A5G's is further reduced by the addition of feedback. Under these conditions, a power output of 20 watts at 1,000 cps may be realized before overloading.

Output capabilities at low frequencies are sufficient to allow 15 watts (+ 42 v-u) to be developed at frequencies as low as 20 cps, while a similar output may be obtained at 25 kc. In addition, the introduction of feedback lowers the overall noise and hum level of the amplifier to a point where the signal-to-noise ratio at maximum power output of the amplifier is approximately 80 db. The actual background noise at full gain, with the input open but shielded, is —40 v-u below zero

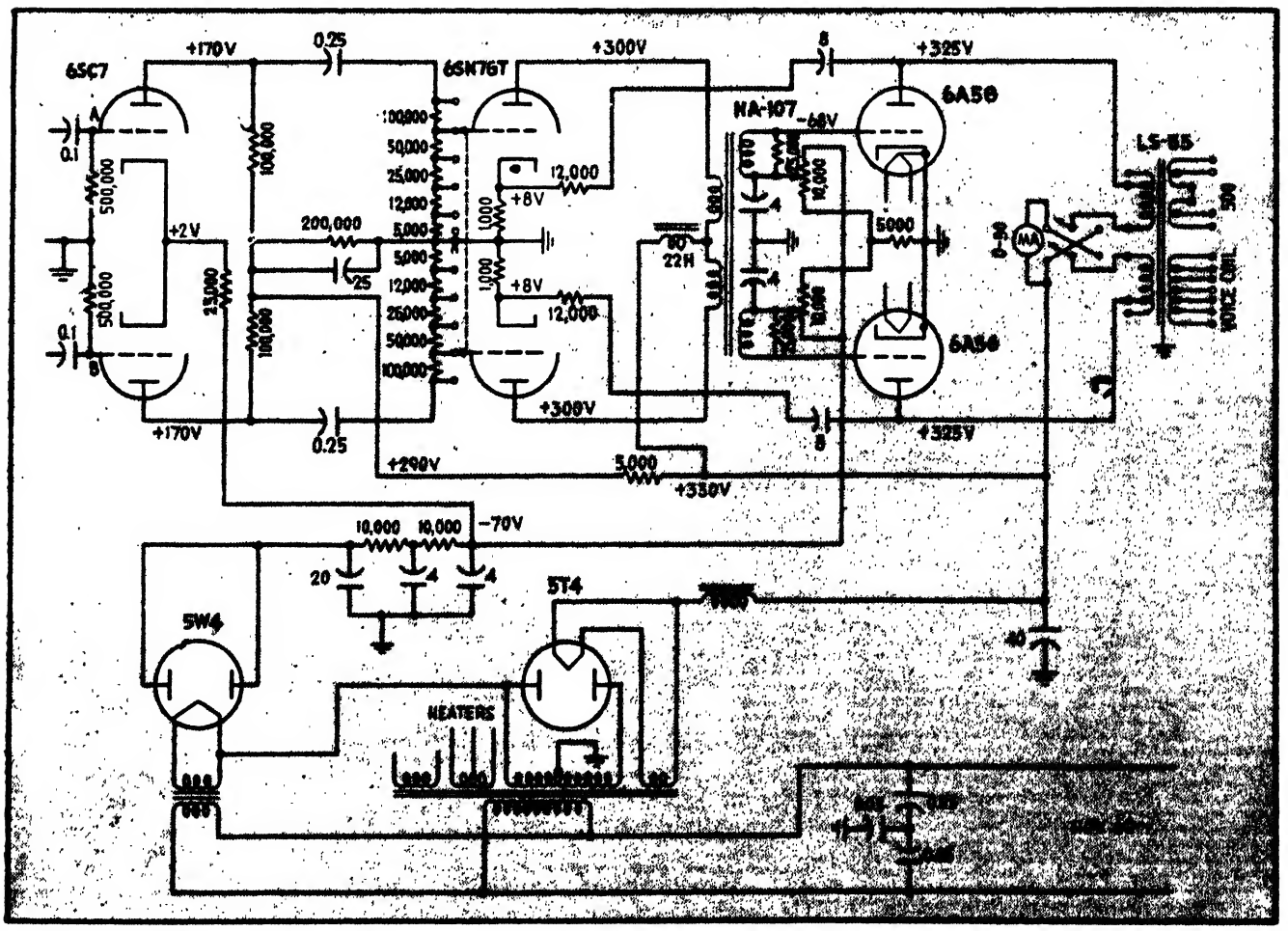

FIG. 2—Complete circuit of amplifier. For single-ended input, the unused grid is connected to ground

(approximately seven mv across the 500-ohm output line), or 82 db below maximum signal. A noise level of this magnitude is practically inaudible even when the amplifier is utilized with speakers capable of excellent wide-band response [6,7,8].

Other Features

The time constant of coupling circuits in the first two stages has been made quite large, 0.05 second, to maintain adequate low-frequency response. Input capacitors are included to allow coupling to sources having d-c components present.

The negative bias supply, in addition to being used to supply bias to the two output tubes, allowing operation as a fixed-bias amplifier, also supplies a point of return for the cathode circuit of the input tube. Since a large voltage drop occurs across the 25,000-ohm cathode resistor (approximately 72 volts), it is desirable to return the cathode to a point at −70 volts, so that the effective bias on the input tube is approximately two volts, the grids being returned to ground. While this is not essential, returning the cathodes to ground through 25,000 ohms would reduce the effective plate voltage on the tube by 70 volts, and necessitate returning the grids to a point above ground, thus reducing the overall gain of the tube and also creating a rather high heater-cathode potential which is not a favorable operating condition.

A study of the circuit diagram will indicate that upon applying power to the amplifier, the output tubes are initially biased practically to cutoff until all the heaters in the amplifier warm up, since the 6SC7 input tube initially does not draw any current, resulting in a smaller drop across the filter resistors in the bias supply, or effectively increasing the bias on the output tubes. This makes for longer life and lack of surge current conditions in the output tubes during heating.

Individual adjustment was provided in an early model for the return point of the 6SC7 cathode but it was found that this was not required despite various tube changes and a fixed value was used which, with the other resistors, gives appropriate potential.

The output transformer is sufficiently well shielded so that it does not pick up appreciable hum from the power transformer. Grounding practice of returning single-stage grounds to a single point, with special care being taken to exclude any portion of the chassis from grid and and grid-return circuits within a single stage, has been followed. This is straightforward r-f and audio practice but is particularly necessary to obtain the noise level realized in this amplifier. The output transformer was chosen to allow use with standard line impedances or voice-coil impedances, adequate match being obtained from 500 ohms down to approximately one ohm. Since triodes are utilized in the output stage, with feedback, the damping characteristics of the circuit are excellent for applications in which the impedance of the driven device may vary over wide ranges. This is the case with almost all electroacoustic devices such as recording cutters and direct-radiator or horn-type loudspeakers. In addition, with direct-radiator loudspeakers, the damping provided by the amplifier tends to reduce distortion present at low frequencies to some degree. This unit has been successfully used with compact horn-type loudspeakers[6, 7, 8]

References

(1) Toennies, J. F., Differential Amplifier, *Rev. Sci. Inst.*, p 95, 9.
(2) Schmitt, O. H., Cathode Phase Inversion, *Rev. Sci. Inst.*, p 548, 12.
(3) Radiotron Designer's Handbook, RCA Mfg. Co., p 46–48, 1941.
(4) Technical Manual, Sylvania Elec. Prod. Inc., 1942.
(5) Terman, F. E., "Radio Engineers' Handbook", McGraw-Hill Book Co., New York, 1943, p 895.
(6) Klipsch, P. W., A Low Frequency Horn of Small Dimensions, *Jour. Acous. Soc. Am.*, 13, No. 2, p 137–144, Oct. 1941.
(7) Klipsch, P. W., Improved Low Frequency Horn, *Jour. Acous. Soc. Am.*, 14, No. 3, p 179–182, Jan. 1943.
(8) Klipsch, P. W., A Note on Acoustic Horns, *Proc. I.R.E.*, 33, No. 7, p 447, July 1945.

Low-Impedance Reactances for VHF

Flat-plate transmission lines make convenient low impedances at vhf. Such reactances are mechanically large enough even at 1,000 mc to be readily fabricated. Design requirements are developed, and applications to an amplifier and to a matching section are described

By E. K. STODOLA and HENRY LISMAN

TRANSMISSION LINE SECTIONS are used in very-high-frequency circuits in the same way that lumped reactances are used at lower frequencies. Although open and coaxial lines are frequently employed, flat-plate lines can conveniently be used in both balanced and unbalanced circuits, especially in the region from 300 to 1,000 megacycles.

Transmission Line Parameters

At the high frequencies, sections of open or short circuited transmission lines are used as circuit elements in place of lumped reactances because of their negligible losses compared to other circuit elements (input conductance of tubes, antenna radiation resistance, and such). The losses are kept small by using line sections longer than 0.1 wavelength and with spacings be-

tween conductors and other dimensions small enough compared to a wavelength so that simple current distributions are maintained.

Reactance of a short-circuited transmission line is

$$X_{sc} = Z_o \tan (2\pi l/\lambda)$$

where l is electrical length of the line, λ is wavelength of the current involved in the same units of length as l, and Z_o is characteristic impedance of the line in ohms. The term $(2\pi l/\lambda)$ is the electrical length in radians of the transmission line.

For lines such as are considered here, using air dielectric, and with negligible lumped capacitance introduced by mechanical supports, the wavelength is practically the free-space wavelength; the electrical length and the mechanical length of the line are equal.

The above relation shows that, if a low value of reactance is desired for a circuit element, either the line section must have a low Z_o or it must be very short. If the line section is not to be too short; for example, at least 0.1 wavelength long, there is a maximum.

With conventional round-conductor open lines it is difficult to obtain a low enough characteristic impedance to be able to use a reasonably long section of line and still produce the low reactance required for circuit elements. However, for a transmission line with a parallel return and perfect conductors, regardless of their shapes, the characteristic impedance is

$$Z_o = V_o/C_o$$

where V_o is the velocity of propagation, and C_o is the capacitance per unit length of line. Substituting the value of V_o for air, and changing units of length to inches yields

$$Z_o = 84.7/C_o'$$

where C_o' is the capacitance in picofarads per inch length of line.

This last relation applies to any parallel-conductor air-dielectric line. It shows that, to obtain a low Z_o, a high capacitance per unit length is required. A flat parallel-plate line affords a more efficient means of obtaining this capacitance than round rods, and therefore such lines are the basis of this approach to vhf circuit design.

Designing Flat-Plate Circuits

The capacitance per inch of length for two parallel plates in air

$$C_o' = 0.225\ (W/D)$$

where W is width of the plates in inches, D is spacing between the plates in inches, and C_o' is in picofarads. The characteristic impedance in ohms of a parallel-plate line is thus

$$Z_o = 377(D/W)$$

neglecting fringe effects. If the width and length of the plates are large compared to their spacing, fringing can be neglected. Because there would be little object in using flat plates unless they were to be closely spaced, the foregoing equation is reasonably accurate for practical applications. The impedance of a shorted parallel-plate line section is thus

$$X_{sc} = 377(D/W)\tan(2\pi l/\lambda)$$

and of an open parallel-plate line

$$X_{oc} = -377(D/W)\cot(2\pi l/\lambda)$$

so that, for a line less than 0.25-wavelength long, the shorted line gives an inductive reactance and the open line gives a capacitive reactance.

Beyond these basic design requirements there are certain practical considerations. To illustrate these practicalities, consider a 600-mc grounded-grid amplifier using a planar triode, such as in a receiver preamplifier. Although these tubes are designed for use with coaxial lines, they lend themselves to flatline construction.

The basic r-f circuit of such an amplifier, with the plate and heater power feeds omitted, is shown in Fig. 1A. Two resonant circuits are required. The inductive element of each resonant circuit is to consist of a section of shorted flat-plate transmission line enough less than 0.25-wavelength long to present an inductive reactance equal to the capacitive reactance of the tube capacitance.

The plate-grid resonant line is designed as follows: The grid-plate capacitance of the tube is 1.4 pf. It is tentatively assumed that an added variable tuning capacitance of about the same value will be used for adjustment of the resonant frequency of the circuit. The total capacitance is then 2.8 pf. At 600 mc this capacitance has a reactance of 95 ohms.

Primarily because of mechanical considerations involving the diameter of the vacuum tube and the spacing between plates and grid discs, a line having a spacing of 0.2 inch and a width of 1.5 inches is chosen for initial consideration. These dimensions give the line a characteristic impedance of 50 ohms. The wavelength in inches is

$$\lambda = 11{,}800/f$$

where f is frequency in megacycles. For 600 mc, λ is 19.7 inches, or a quarter wavelength is 4.93 inches. Use of the previous equation for X_{sc} shows that the length of line to give 95 ohms is slightly less than 3.5 inches, or about 0.2 wavelength.

A suitable length of line has been determined, but no consideration has been given to the feeding of d-c to the plate connection. It is advantageous to have the line plate solidly grounded to the main ground plate of the amplifier. A construction that achieves this goal is shown in Fig. 1B. A sandwich type of line is used in which the plate line consists of the main plate which is grounded, and an auxiliary plate which is bonded to the other

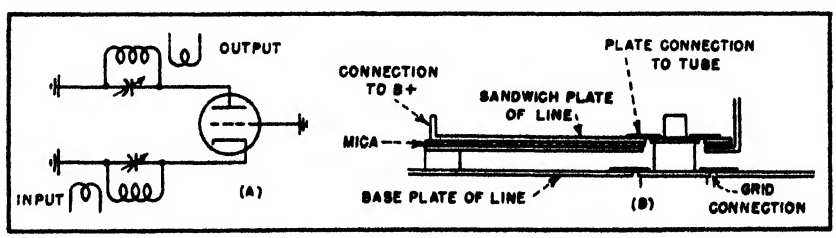

FIG. 1—Basic grounded-grid tuned amplifier (A) for very high frequencies can be made using flat plates (B) one leg of which is built as a sandwich to provide d-c feed

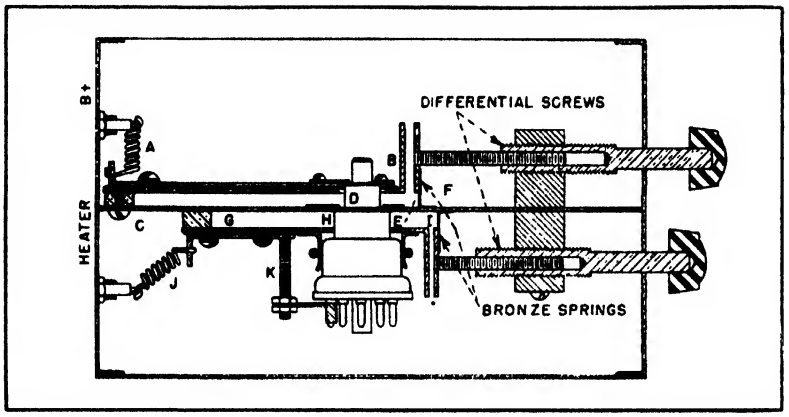

FIG. 2—Cross section of amplifier shows mechanical simplicity of flat-plate construction

plate insofar as r-f is concerned but is insulated for d-c by being separated from the main plate by a thin strip of mica.

Tuning of this system is relatively critical and it is necessary to provide a fine tuning arrangement for the variable capacitor at the end of the line, such as a differential screw shown in Fig. 2. As the knob is turned, the inner shaft moves in opposition to the outer shaft so that the resultant movement of the capacitor plate is the difference of the two axial motions.

Numerically, if there are T_1 turns per inch on the outer shaft and T_2 turns per inch on the inner one, the capacitor plate will move as if driven by a simple screw having T_3 turns per inch where

$$T_3 = T_1T_2/(T_2 - T_1)$$

so that, even with coarse threads for T_1 and T_2, the capacitor is driven with a fine motion. For example, if T_1 and T_2 are 24 and 28 turns per inch, respectively, T_3 is 168 turns per inch.

A flat spring is soldered between the movable capacitor plate and the base plate to serve three purposes. (1) It prevents the inner screw from rotating. (2) It takes up backlash in the differential screw so that precision parts are unnecessary. (3) It provides a low-impedance r-f path to the movable plate.

Size of the capacitor plate that is required for this tuning can be computed from the relation for parallel plate capacitors

$$C = 0.225(A/D)$$

where C is capacitance in picofarads, A is area of one plate in square inches, and D is spacing between plates in inches. The area of the plates should be chosen to given a reasonable spacing.

The cathode-grid line can be designed similarly. By operating with one side of the heater grounded and by mounting the cathode-bias resistor directly on the tube base, the bypass capacitor for this resistor being inside the tube, only a single-layer sandwich plate is required. A multiple layer sandwich could be used to allow using an ungrounded heater or measuring cathode current. In constructing an amplifier using the 2C40, the tube is mounted through a large base plate to which the grid is grounded. On each side of the base are mounted the smaller flat plates that form the other halves of each line, as shown in Fig 2. Figure 3 shows the circuit. Coupling to the plate line is provided by an adjustable loop at the edge of the line. Input coupling to the cathode line is obtained by a sliding clip on the edge of the line.

Two stages of preamplification were built using this amplifier design. They satisfactorily replaced a more complicated coaxial-cavity amplifier. The noise factor of the flat-line preamplifier was 9.7 db, the gain of the two stages between 72-ohm input and 72-ohm output was 28 db, and the bandwidth between half-power points with both stages tuned to the same center frequency was 1.67 mc. Wider bandwidth with some loss in gain could be obtained by slight staggering of the tuning.

Other Applications

While the use of flat-plate lines at very high frequencies has been emphasized, this type of line has applications at lower frequencies where low impedances are necessary. For example, it was necessary to match a 17-ohm generator output to a 250-ohm load at 100 mc. A quarter-wavelength matching section was to be used. The characteristic impedance of such a section must be the geometric mean between the two impedances involved, or

$$Z_{OM} = (Z_{OG}Z_{OL})^{\frac{1}{2}}$$

where Z_{OM} is the characteristic impedance of the matching section, Z_{OG} is the impedance of the genera-

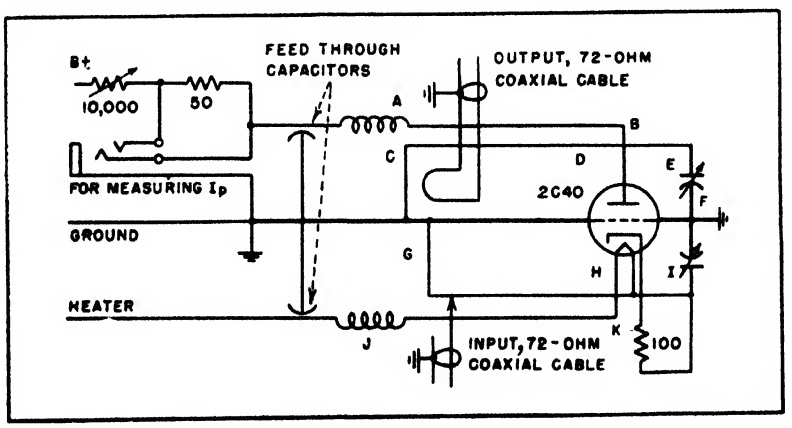

FIG. 3—Points on this schematic diagram are labeled by letters in accordance with Fig. 2

tor, and Z_{OL} is the impedance of the load. In this case the matching section should have a characteristic impedance of 65 ohms. It can be constructed easily with flat plates 1-inch wide, spaced 0.173-inch, and 29.5-inches long. If the spacing of the line is maintained by insulating washers, they should be as small as possible in order to minimize lumped capacitances.

An incidental advantage of the flat-plate line is its power-handling ability. For the same characteristic impedance, the spacing of a flat-plate line, having plates of the same width as the diameter of the elements of a comparable parallel-wire line, is greater. Hence the flat-plate line will withstand higher voltages without flashover. This is an important consideration in lines for transmitting high power or for sections used as tuning elements in high-voltage circuits.

It should also be noted that, particularly for transmitting r-f power, a flat-plate line can be made of a center plate and a plate on each side, in which case the characteristic impedance will be half that given previously. To increase rigidity, or for some other reason, the line can be made from angle metal. The plate-type line can thus be considered, and used, as an intermediate form between the conventional open-wire line and that of the coaxial line.

UHF Repeater Station

Transmissions on 2,726 kc from isolated mountain dams are relayed to flood-control headquarters during noisy daylight hours. The centrally-located and unattended 312-Mc equipment at W6XFE may be turned on or off at any time by radio remote control from KFCD. A clock-switch renders it inoperative after dark

By MAURICE E. KENNEDY

Poor daytime reception from 100-watt medium-frequency stations located at isolated mountain dams led to the development of an ultra-high-frequency repeater for the Los Angeles County Flood Control District. A suitable location was selected on 1900-foot Flint Peak, near the center of the heavily populated area of Southern California. This site is nine miles visual distance from KFCD, the headquarters station in the city of Los Angeles, where transmissions from the various dams must be received.

It was considered desirable to arrange the equipment so that it could be turned on or off at any time by radio remote control from Los Angeles. This was accomplished by means of an auxiliary circuit and selective relays.

Medium - frequency reception was satisfactory at night so it was also desirable to render the repeater inoperative during the hours of darkness. This was accomplished by equipping the station with a clock-switch.

The repeater equipment utilizes a conventional superheterodyne for reception of signals on 2,726 kc.

The receiver incorporates one stage of r-f preselection, two stages of iron-core i-f amplification, a crystal-controlled (Pierce) oscillator for fixed channel reception, and one stage of a-f amplification.

Automatic volume control voltage is obtained from one diode of a 7C6 tube. The output of the triode section of the 7C6 is coupled to the grid of a zero-bias isolating stage operating control relays and to the transmitter modulator tube.

Coupling and filter networks isolate automatic control circuits from normal audio circuits.

One triode section of a 7N7 tube is used as a zero-bias isolation amplifier and the other section of the tube is biased to operate as a grid-controlled d-c rectifier. A band-pass filter network is used to prevent the automatic control from operating on frequencies other than the 1000-cps dial-tone transmitted by a pulsing dial at the Los Angeles station.

A 10,000-ohm sensitive relay is connected in the plate circuit of the 7N7 rectifier section. This relay serves to pulse the stepping relay, which was constructed to permit automatic re-set when the last contact is reached. The filament and re-set relays have holding contacts which lock them in place as the stepping arm passes their contact. All holding circuits are broken when the stepping relay is dropped to its zero position.

A seven-dash dial-pulse from the control desk at the Los Angeles station lifts the stepping arm to the contact which closes and holds the filament relay. Filament current is thus supplied to the oscillator and modulator tubes of the 312-Mc transmitter. After a 30-second pause to permit the tubes to warm up, a second seven-dash pulse is transmitted and plate power is applied. The circuit is in operation as soon as plate power is applied and reception of the repeater channel is available on a loudspeaker in the control room in Los Angeles.

When service from the repeater

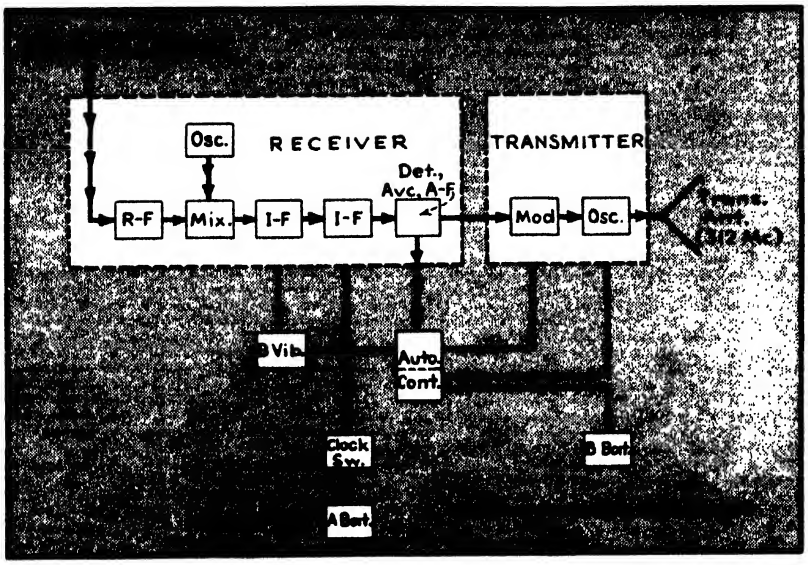

FIG. 1—Block diagram of W8XFE gear, comprising a medium-frequency superheterodyne automatically controlling and modulating an ultrahigh-frequency oscillator. Details are given in the schematic of Fig. 2

channel is not desired, a dial pulse of six dashes on the 2,726-kc carrier of KFCD lifts the stepping arm to the re-set contact and the relay drops to zero. This procedure gives the central station operator control of the unattended transmitter and serves to conserve battery power when the repeater channel is not used.

U-H-F Transmitter

Two type HY615 tubes are used in a push-pull, tuned plate-tuned cathode, oscillator circuit. The heater supply leads are twisted and pulled through the cathode lines to keep heaters and cathodes at the same r-f potential.

Very little difficulty was experienced in obtaining strong oscillations at frequencies up to 325 Mc. A marked reduction in output was experienced above 325 Mc and it was not possible to obtain satisfactory oscillations above 350 Mc.

Frequency drift over a 24-hour period was quite a factor in the operation of the original 312-Mc oscillator. The drift was traced to extreme temperature fluctuations encountered on the unprotected mountain peak. It was necessary to redesign the plate and cathode lines to maintain the all-important constant center-spacing of the copper tubing. Heavy-wall, larger-diameter tubing was used with a single-point tuning-fork type mounting. Flexible leads were provided to connect the open ends of the plate line to the tube connections.

The transmitting frequency is determined by the length of the lines, spacing between the lines and by the setting of the shorting bar at the closed end of the lines. Adjustable "penny size" plates have recently been installed across the tube end of the lines. Frequency is measured by Lecher wires and a General Radio type 758-A wavemeter. Approximately 8 watts output is realized.

The HY615's are plate-circuit modulated by a 6K6G pentode operated from the transmitter power supply and driven by the associated receiver.

Antenna Systems

The receiving antenna for the 2,726-kc receiver is a conventional single-wire type.

The radiating system for the 312-Mc repeater transmitter is a square-corner reflector type with the excited element near the focal point and 0.5 wavelength in front of the vertex of the reflector frame. The 0.6-wavelength reflector elements are spaced 4 in. apart on 4 ft. by 4 ft. frame. The excited element is 95 percent of a half-wavelength. The active element is current-fed by means of a short tuned transmission line and "hairpin" coupling-link placed in inductive relation to the plate line of the transmitter.

All elements and feeder measurements were calculated and later checked by actual operating measurements. The calculations were found to be sufficiently accurate. Standing waves on the feeder lines are checked by moving a metal rod or a finger along in close relation to the line and watching the dips on the plate meter of the transmitter. Insulation problems were greatly simplified by having all points of mechanical contact at ground potential.

The 312-Mc receiving antenna on the roof of the office building in which the Los Angeles station is located is similar in design. Because of the physical proximity of this antenna to the tuning house for the KFCD 2,726-kc transmitting antenna, it was more convenient to voltage-feed the active element to the u-h-f receiver located in the tuning house.

Field strength measurements show a 30-db front-to-back signal difference for the parasitic reflector type of square-corner antenna used.

Power Supply

Power for the mountain-top station is developed by a heavy-duty wind-driven Wincharger and a 600 ampere-hour storage battery. Heavy-duty B batteries are used for plate power on the modulator and u-h-f oscillator. Plate supply for the 2,726-kc receiver and the relay control tube is developed by a vibrator power unit.

Time Switch

A weight-driven time-switch turns the 2,726-kc receiver and relay control tube's plate and filament power on at 8:00 A.M. and off at 5:00 P.M. Satisfactory communication is possible on the regular low-frequency channel during

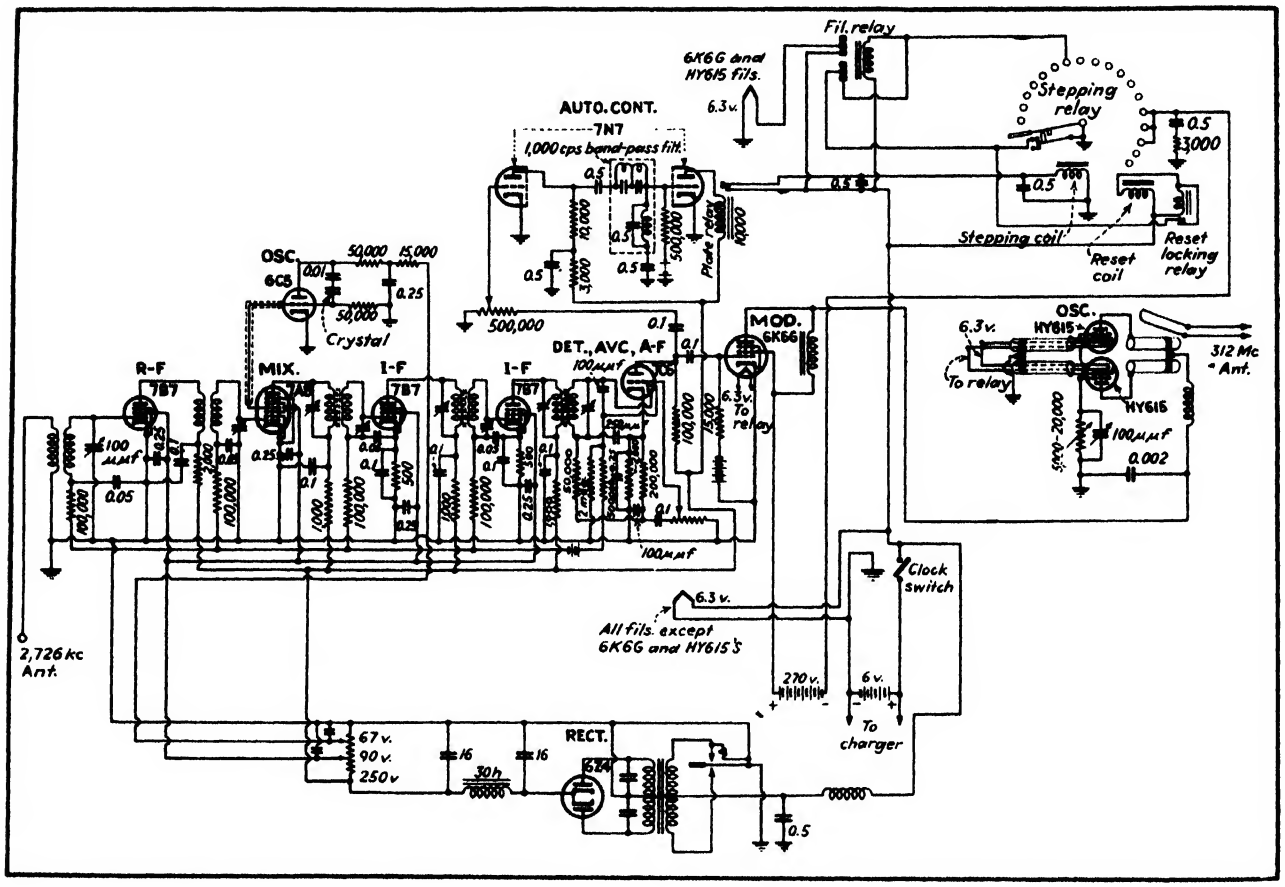

FIG. 2—Schematic of mountain-top radio repeater unit shown on a preceding page in block-diagram form

the balance of the 24-hour day. This procedure conserves battery power at the repeater station.

Battery-Charging Problem

Current consumption of the repeater equipment is 4½ amperes at 6 volts in the stand-by condition and 5½ amperes when transmitting messages to the headquarters in Los Angeles.

The wind-driven charger scheme is not entirely satisfactory during certain months of the year and will ultimately be supplemented with an engine-driven charging system for prolonged periods of calm weather.

The receiver used in Los Angeles is a simple oscillator with a single type HY-615 tube used as a self-quenching super-regenerative detector. Tuning is accomplished by means of a dial-operated copper wedge between the copper tubes forming the resonant circuit, at the tube end.

U-H-F Receiver

One stage of a-f amplification is used at the receiver, on the roof of the building, to feed a 500-ohm audio line running down to the control desk on the fourth floor. An additional amplifier for the repeater channel is mounted on a channel rack in the control room of KFCD.

Filament and plate power are supplied to the receiver by a small a-c power unit located within the antenna tuning house. Relay control from the fourth floor turns the receiver on and off.

An early attempt to locate the u-h-f receiver in the control room, with a concentric feeder to the antenna on the roof, was not successful because of high losses in the transmission line at 300 Mc.

Performance Data

A routine service trip is made to the station on the mountain at 30-day intervals.

Reliable average signal levels over the 9-mile visual signal path have been obtained for a period of more than two years. Short duration fading and signal attenuation of approximately 4 db has been observed during periods of heavy rain.

F-M Short-Range Carrier System

A simple communication system for open-wire lines twenty to thirty miles in length operates in the 100 to 400-kilocycle range. Wide-band frequency modulation and limiting are used to minimize audio gain variations due to climatic changes

By E. H. B. BARTELINK and EDWARD DASKAM

THE USE of carrier systems has become widespread in the telephone industry in the last few decades, and a number of systems are available on the market. In general, these systems are designed to permit the bridging of long distances.

In view of the cost of long-distance lines, it has been desirable to accommodate the largest practicable number of speech channels, which results in a close spacing of the frequency bands used for the different carrier channels. This puts very stringent requirements on the design and manufacture of the filters employed to separate the different speech channels. In addition, it is generally required that a number of such carrier sections can be used in tandem to form parts of transcontinental and other long-distance telephone channels. This requires extremely low distortion.

There are many cases where additional circuits are needed for relatively short toll lines of 25 or 30 miles; where only two or three additional circuits are required, and where the need for using many such systems in tandem does not exist. Such problems are encountered in large numbers by the independent telephone industry, the telephone companies not forming part of the Bell System. These companies operate an appreciable number of toll lines, most of which are restricted to the ranges mentioned.

For use in such applications, the carrier equipment developed for long-haul applications is prohibitive in cost in the majority of cases. It seemed that a much simpler carrier system could be developed if short-range requirements were given full consideration from the start and that the cost of such a system might be low enough to make carrier systems attractive for short-haul applications.

The system to be described will operate over 20 to 30 miles of open-wire line. It permits application of three carrier channels, and the channels are selfcontained so that they can be added or removed without affecting the remaining channels.

Basic Operation

One of the major items in the cost of conventional carrier systems is represented by the filters necessary to separate the different speech channels. As the needs for short-haul carrier systems are as a rule restricted to only a few circuits, it was decided to use large frequency separation (50 kc) between channels; this greatly simplifies the filter design and manufacture. This process is further helped by putting all carrier channels in the 100 to 400-kc range where the required pass bands have been reduced to reasonable fractions of the carrier. As a result, the filters closely re-

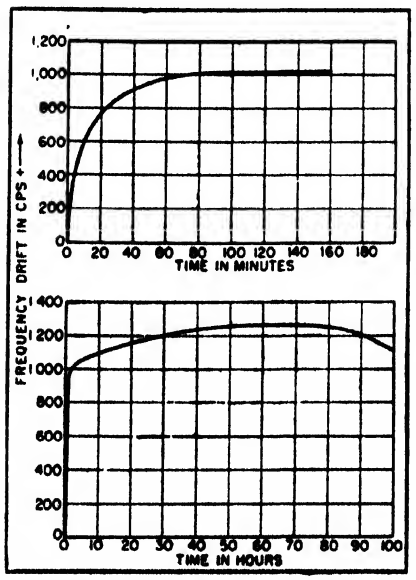

FIG. 1—System frequency change

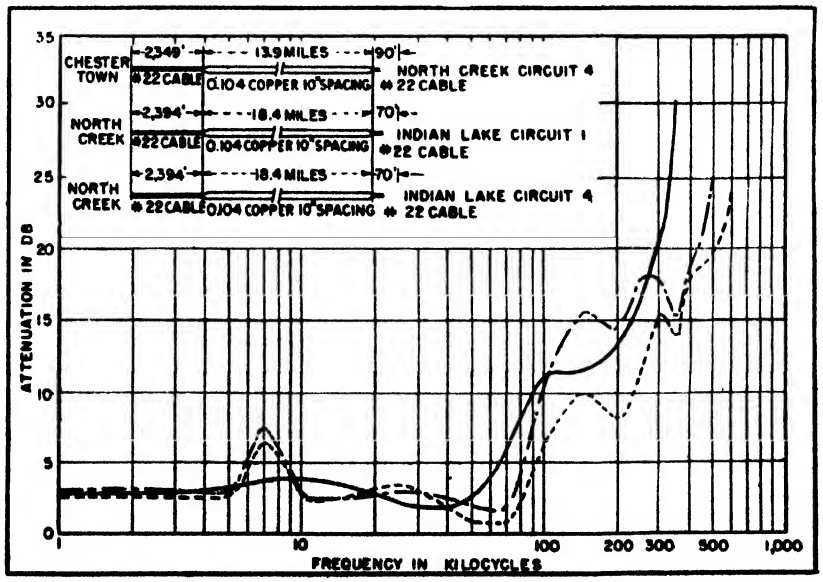

FIG. 2—Attenuation of signal on three open-wire lines and their entrance cables

semble standard double-tuned i-f transformers used in broadcast receivers. In addition, the use of these higher frequencies reduces the equipment for separating the normal (300-3,000 cps) speech channel from the carrier to the most elementary and uncritical components.

Another problem encountered is that of paralleling the filter output circuits for the different channels at the transmitting end and the filter inputs at the receiving end. In conventional carriers, it is necessary to design the filter systems so that the overall impedances of these paralleled structures will meet close tolerances. In this system, a brute-force method was used. Relatively high resistances were inserted between some of the filters and the line. Thus the bridging impedances of these filter branches have been made sufficiently high so that interaction of different carrier channels may be neglected. This involves some transmission loss in the system, but power on the transmitting end and gain on the receiving end can be obtained easily and at low cost. In addition, it is possible to put in additional carrier channels without having to modify any other channels.

Another problem in the design of carrier systems is that of keeping the transmission in the circuit reasonably constant, independent of any climatic and other changes to which the line might be subjected by conditions.

This problem is solved by the use of wide-band frequency modulation which, with proper limiting, will provide an audio-output signal which is independent of the incoming r-f voltages within wide limits. Frequency modulation also helps suppress crosstalk from undesired signals, whether it originates in a neighboring carrier system operating on the same channels or from adjacent carrier channels.

Wide-band frequency modulation is obtained by the use of a positive-bias multivibrator. Such a device was described in an earlier paper,[1] and it was shown that the relation between frequency and positive-bias voltage is a linear one in first approximation. As was described in patent literature,[2] it is possible to apply a modulation voltage in series with the positive-bias supply of such a multivibrator, and such an arrangement will permit frequency modulation corresponding to a large fraction of the carrier frequency.

This is the method used in the new carrier system. Its usability for practical communications purposes depends to a large extent on the ability of obtaining stable average frequencies in the multivibrators because excessive deviations would cause them to drift beyond the filter acceptance bands. Refinements in technique and proper choice of components have made it possible to obtain a high degree of frequency stability in multivibrators. Figure 1 shows that if constructed with proper care, such a circuit can be stable enough to meet the requirements.

Attenuation

The attenuations which occur in a uniform open-wire line can be calculated with reasonable accuracy. However, in most cases the actual lines will have entrance cables at both ends and sometimes at intermediate points. If these are of any appreciable length, mismatch and reflection losses can occur. In the process of determining the attenuations for which the system should be designed, consideration has been given not only to the losses of uniform lines, but also to attenuations existing in some actual operating circuits.

Figure 2 gives a plot of attenuations as a function of frequency for three circuits, each having an appreciable amount of entrance cable. These measurements were made in mid-winter when a considerable amount of snow and ice were deposited on both insulators and cross arms along the line and thus represent rather adverse climatic conditions.

Several irregularities occur in these curves, corresponding to reflections and standing waves. However, for all frequencies under 300 kc, the attenuations do not exceed 20 db, and do not exceed 30 db for any frequencies up to 350 kc. It is possible to eliminate the irregularities and reduce the losses by proper modification of the line, but the carrier system as a whole is most valuable if it does not require any changes in existing lines.

Crosstalk and Noise

In most cases 2-wire operation, using adjacent channels for the east-west and west-east transmission, is desirable. The interfering signals will then reach the receiver without any attenuation, while the desired signal may be down by a maximum of 30 db with respect to it. An interference level of at least 35 db below the desired signal at this extreme condition has been assumed to be satisfactory for service and the filter systems have been designed towards this value.

A high transmission level will simplify the receiver sensitivity problem and reduce the influence of outside interference. Excessive levels may give rise to interference in neighboring radio circuits. On this basis, a maximum transmission level of 50 milliwatts in 600 ohms was assumed. To develop the same output voltage in entrance cable which may have an impedance as low as 100 ohms at these frequen-

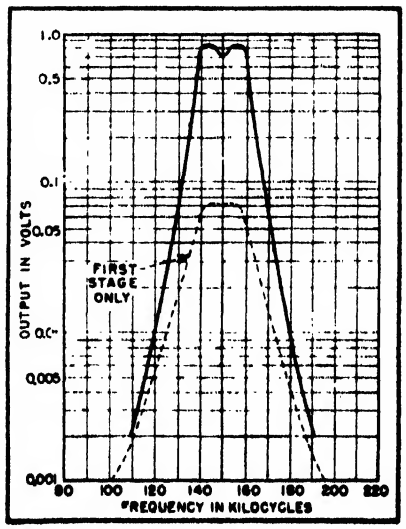

FIG. 2—Selectivity of two stages in the receiver is indicated by solid curve. Output voltage taken from a 500-ohm resistor in each plate circuit

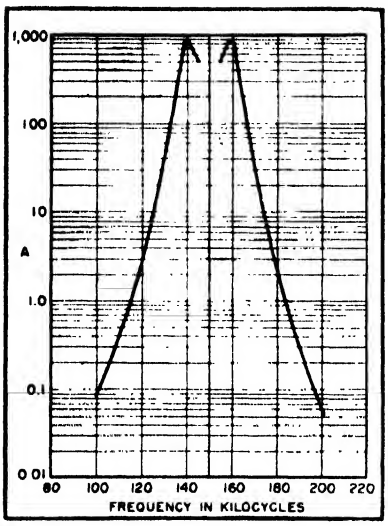

FIG. 4—Selectivity of three stages of the receiver plotted for values of *A*, the d-c voltage from the discriminator divided by receiver a-c input

cies up to six times the power or 300 milliwatts may be required. This level can be obtained for normal circuits without undue requirements on the power output stage.

Bandwidth and Selectivity

The frequency excursion chosen for this system is approximately 6 kc each side of center. As the speech band normally transmitted is 300 to 3,000 cycles, this gives a frequency modulation index of 2.0 on the highest frequencies. On this basis, an interference suppression of approximately 10 db can be expected.

To have a safety factor in the crosstalk, the interference suppression obtainable by the use of frequency modulation has been completely discounted in the determination of the selectivity needed in the receiver. The adjacent channel attenuation requirement was accordingly set at 65 db at frequencies 40 kc removed from the center of the carrier channel.

A selectivity curve for the first two stages of the receiver is given in Fig. 3. It shows that a rejection of 50 db at 40 kc off, is already obtained in the first two of the three filter stages. The third stage, which is connected as a discriminator stage, will raise this selectivity to the desired value, as can be seen in Fig. 4. Because of the discriminator connection, this curve does not have a flat top; the significant item is the steepness of the sides of the curves, which shows an attenuation of 65 db at frequencies 40 kc from the center carrier frequency.

Parallel Filters

The method chosen to connect the receiver filters in parallel is a brute-force one. Between the line and filter systems, some fairly high resistances ($2 \times 3{,}300$ ohms or more) have been connected. As a result, the bridging impedance of these filters is high enough so that they can be connected in parallel without causing undue interaction.

Since entrance cable as well as open-wire line must be fed by the transmitter, it must be capable of developing normal output voltage across a 100-ohm entrance cable as well as a 600-ohm open-wire line. This means more than 50 milliwatts will be put into an entrance cable, but the cable will attenuate it to such an extent that by the time the transmitter output reaches the open-wire line no trouble from excess radiation is expected. To develop this voltage in such a low impedance, the tuning elements in the secondary of the output transformer are series rather than parallel connected to the line. Since the series connection is used, the off-resonance impedance is higher than at resonance, thereby solving the problem of paralleling transmitters 50-kc apart. The transmitter output is adjusted to the desired level for the type of line encountered by a screen voltage control on the power output stage.

The circuit of the transmitter panel is shown in Fig. 5. The audio signal from the termination panel is fed into one triode section of a 6SN7 connected as a cathode follower. This tube modulates the carrier oscillator which is the positive-bias multivibrator comprised of both triode sections of another 6SN7.

The multivibrator frequency, linear with the positive-bias voltage impressed at point *A*, can be changed over wide ranges by changing this potential from zero to B+. Hence wide-band frequency modulation is obtained directly from the output of this multivibrator. The bias potential and thus the center frequency is controlled by a 50,000-ohm potentiometer in a voltage-divider circuit between the plate-supply voltage and ground.

The output from one of the cathodes of the multivibrator is connected to the cathode of the other triode section of the first 6SN7 tube which acts as a cathode fed, grounded-grid buffer stage that feeds the 6V6 output tube. This latter tube is tuned to the center frequency of the carrier channel in its plate circuit. The pass band of the tuned circuit is wide enough to pass the + and − 6-kc carrier swing without too much discrimination, yet is selective enough so that it reduces the harmonic output to a low level and hence provides a fairly sinusoidal output waveform.

If it is desired to reduce any single harmonic in order to suppress interference in other channels, this may be done by adjusting the pulse

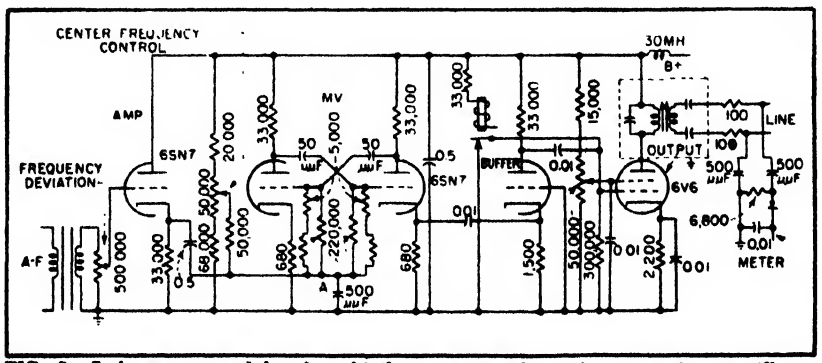

FIG. 5—A frequency-modulated multivibrator is used as the transmitter oscillator

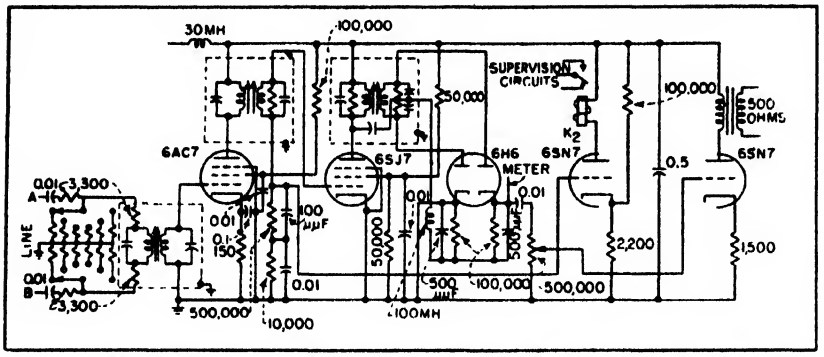

FIG. 6—In the receiver circuit, output of the discriminator feeds both an audio channel and an electronic relay circuit for supervision

width of the multivibrator, so that the amplitude of that particular harmonic is zero, and operating the output 6V6 class A. The selectivity of this circuit also aids in tuning the multivibrator approximately to the desired channel. This tuning is done by adjusting the multivibrator frequency control for maximum r-f output voltage.

A tuned secondary on the transmitter-output transformer provides an inductively coupled r-f output. The secondary tuning capacitors also act as blocking capacitors. This type of connection is used to obtain sufficient output voltage since the line presents such low impedance (100-500 ohms) to the tank circuit. Two 100-ohm resistors are also connected in series with this circuit to help raise the off-resonance impedance for paralleling purposes.

A transmitter-control relay grounds the grid of the output tetrode when it is energized, thus taking the transmitter off the line. Since this relay follows dial pulses and ringing frequencies, it is fast acting.

Receiver Circuit

The circuit of the receiver panel is shown in Fig. 6. The r-f input to the receiver, which comes from the line via the distribution panel, is fed to a simple H-pad resistance attenuator. This attenuator has at least 6,600 ohms input impedance and provides 25-db attenuation in 5-db steps. It is used to set the input to the grid of the first amplifier tube in the receiver just above the point at which the limiting begins. The first stage feeds a 6SJ7 limiting r-f amplifier pentode.

A standard discriminator transformer provides the typical S-curve characteristic of the discriminator; the straight portion of the curve being used for the detection of the frequency-modulation signals. The audio output from the discriminator is fed to one triode section of a 6SN7, which provides the final audio output through an output transformer to the wiring-distribution panel.

When a signal is received, a negative voltage is developed across the grid-leak combination in the grid circuit of the 6SJ7 limiter tube. This voltage is directly applied to the grid of the other triode section of the 6SN7 tube which operates as a d-c amplifier. The sensitive relay K_2 in the plate circuit of this tube is normally held in by plate current flow when no signal is being received. When a signal is received and a negative voltage applied to the grid of the d-c amplifier, the current in its plate circuit decreases below that required to hold the relay and it releases. In this manner the relay provides supervision of the incoming carrier.

In the receiver circuit, the high-impedance attenuator between the line and the input is of the H type. The four series elements consist of 3,300-ohm resistors: the parallel branch is made variable in order to provide a symmetrical control of the incoming carrier level. In all cases, the impedance bridged across the line will exceed 6,600 ohms. This method of coupling and attenuator construction does involve appreciable minimum losses between the line and the first receiver filter circuit, but makes it possible to use extremely simple components. At the same time, it provides some of the necessary damping for the first filter circuit.

Audio-Frequency Characteristics

The requirements for the audio-frequency characteristics are: (1) to have as near a zero loss voice circuit as possible, (2) to have a flat frequency response within 3 db from 300 to 3,000 cps, and (3) to have the distortion at normal operating level low enough so that two or three channels can be cascaded

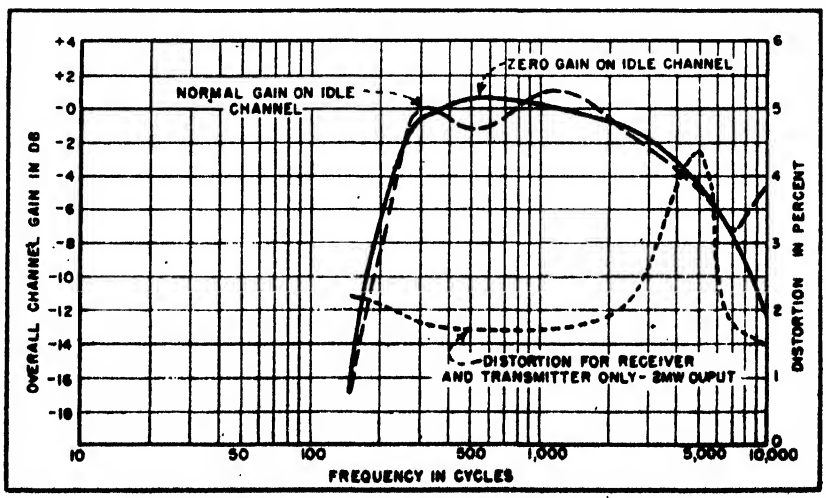

FIG. 7—Audio response of complete channel at 0.5-mw output

without the overall distortion rising to an objectionable level.

The overall audio-frequency characteristics of the system are shown in Fig. 7 as plotted for an output level of 0.5 milliwatt in 600 ohms. The solid curve was plotted for normal gain on the channel in one direction and zero gain on the channel in the opposite direction. This gives the true audio response of a complete channel unaffected by any positive or negative feedback, which results if the impedances of the line and the line balance are not matched perfectly through the frequency range.

The dotted curve was plotted for normal gain on the channels in both directions, with as good a hybrid balance as could be obtained at short notice, and hence is representative of actual operating conditions. The irregular variations of gain with frequency for this curve are partially caused by the fact that the phase of the feedback due to imperfect balance varies with frequency.

With the return channel at either zero gain or normal gain, the midband gain is zero db. This may be slightly higher or slightly lower in practice, depending upon how perfect a balance of the hybrid may be obtained, because the obtainable gain is determined by the point at which the feedback due to unbalance becomes of the proper phase and amplitude to produce oscillations or serious amplitude distortion, rather than because of lack of gain in the transmitter or receiver audio circuits.

The frequency response between 300 and 3,000 cps is flat within − 2 and + 0.5 db with zero gain on the return channel and within − 2 and + 1 db with normal gain on the return channel when a 600-ohm resistive line termination is used.

In the normal transmission band of 300 to 3,000 cps, the total harmonic distortion for the receiver and transmitted alone at a 2-milliwatt output level is 2 percent or less. This is about as high a level as would ever be normally encountered. At 3,000 cps and higher, the distortion rises above this; but since any harmonics of even 3,000 cps would be above the response range of normal telephone equipment, this additional distortion is of little importance.

Signaling

The carrier is switched on and off to transmit supervision signals. Short interruptions in the carrier are used to transmit ringing signals in a manual system and dial pulses if it is desired to dial through the system.

To obtain proper hook-switch supervision, a high voice-frequency tone (3,500 cps or higher) can be superimposed on the transmission channel whenever the reverse battery supervision indicates that the distant subscriber has not yet lifted his receiver or terminated the call —his tone is removed as soon as the distant subscriber lifts his receiver. Thus this supervision does not take up any part of the total available modulation percentage of the system during the transmission of speech.

The carrier-relay is adjusted to operate approximately at the carrier level where effective limiter action starts. The normal adjustment of the receiver level is about 3 or 4 db above this point. The limiter action occurs at approximately 23 db below the reference level of 1 milliwatt in 600 ohms (0.775 volt) or 40 db below the maximum transmitter level of + 17 db, which corresponds to 50 milliwatts in 600 ohms (5.50 volts). These data refer to maximum gain setting of the receiver r-f control.

This method of using the carrier to control the supervision relay makes it possible to obtain extremely fast operation. The system in its present version permits operation of the supervision relays up to speeds of over 100 cps.

Apart from the requirement of proper transmission of speech in either direction, a carrier system must provide suitable termination and supervision facilities. The proper termination can easily be obtained by means of a differential transformer or hybrid which, by proper balancing between the line and an artificial line, prevents the incoming received speech signals from energizing the outgoing transmitter and thus prevents feedback and oscillations.

The supervision signals permit the operator at one end of the line to signal the distant operator when she wants to initiate or terminate a call or when she wants her to come in on an existing connection for further instruction (so called "recall"). They are also needed if 1-way or 2-way dial operation is desired. The problem of providing proper supervision is sometimes more tricky than that of obtaining the proper speech transmission. In the system described here, the presence or absence of the carrier and its interruptions are used for this supervision.

Ringdown Toll Supervision

About the most common method of supervision on the toll lines operated by the independent telephone companies is the ringdown supervision in which an a-c ringing current (generally 20 cps) is used for initiation of a call, for termination, and for recall.

The exact method of obtaining the desired performance differs but in general the method of operation is as follows:

A line relay is attached to both ends of the line when it is idle. Reception of ringing current will energize this relay and light a line lamp or other visual signal. A locking arrangement keeps the lamp lit until it is restored, which happens when the operator plugs a cord into the corresponding line jack. This extinguishes the lamp or releases the visual signal; it also disconnects the line relay from the line by means of additional contacts on the line jack.

The supervision is now taken over by a similar relay attached to the cord circuit. If this supervision relay receives ringing current, it will light a cord lamp or operate a visual signal; another locking arrangement keeps the lamp lit or the signal operated until the operator

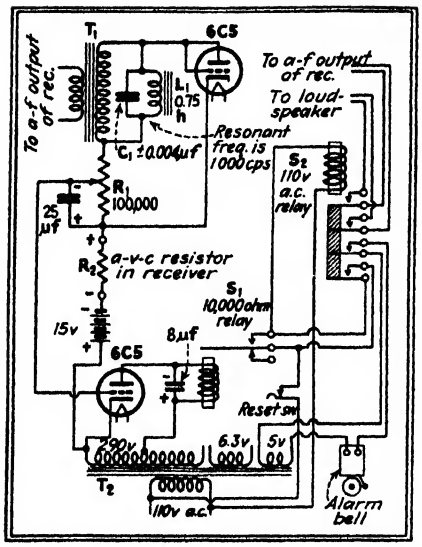

Complete circuit diagram for a carrier-failure and tone alarm system suitable for use at broadcast stations

the receiver, and the other is made to the a-f output of the receiver, as shown in the circuit diagram. When the alarm is set off for any reason, the loudspeaker is automatically connected to the output of the receiver for aural monitoring until such time as the alarm system is reset by means of the reset switch.

The alarm bell circuit is closed by relay S_2 when relay S_1 releases. Relay S_1 is energized by the plate current of the lower 6C5 tube in the diagram, and this current in turn is determined by the net C bias voltage of the tube. Three distinct voltages in series determine the C bias:

(1) A fixed d-c voltage of 15 volts obtained from a C battery, making the grid negative with respect to the cathode.

(2) The d-c voltage across the a.v.c. resistor (R_2) in the monitor receiver, utilized in such a way that it opposes the C battery voltage. When the carrier signal is present, the resulting voltage across R_2 lowers the net C bias voltage, allowing enough plate current to flow through relay S_1 to energize this relay and keep the alarm circuit open. Conversely, failure of the carrier opens relay S_1 and closes the alarm circuit.

(3) The d-c voltage across the lower portion of potentiometer R_1, utilized in such a way that it aids the C battery voltage. When a 1000-cycle tone signal is received, it is rectified by the upper 6C5 tube acting as a diode detector, producing a d-c voltage across R_1. This voltage aids the C battery voltage, increasing the net C bias and lowering the plate current of the lower tube, so that arrival of the 1000-cycle tone releases relay S_1 and sets off the alarm.

Parallel resonant circuit L_1-C_1 is tuned to 1000 cycles, and hence this stage accepts only this one frequency. A 25 μf electrolytic condenser across the lower portion of R_1 provides a time delay of about 5 seconds at this frequency, thus preventing strong 1000-cycle components in a program from setting off the alarm.

The parallel resonant circuit should be tuned quite accurately. This can be done by connecting a d.c. voltmeter across R_1, feeding a 1000-cycle tone to the input of the upper 6C5 stage, and adjusting the value of C_1 above and below 0.004 μf with small mica condensers until a maximum voltmeter reading is obtained.

An ordinary plate-to-grid audio transformer is used for T_1, and T_2 is a standard replacement power transformer providing the indicated voltages.

Relay S_1 can have a coil resistance of about 10,000 ohms, and should operate on a change of about 0.003 amp. Relay S_2 is a 110-volt a-c unit having a four-pole, single-throw contact arrangement.

Adjustment of the system is simple. With a carrier signal present and with the system connected to the receiver as shown in the diagram, turn up control R_1 until the alarm is set off by program peaks. Now lower the setting of this control a small amount and press the reset button, repeating the procedure until the alarm is no longer set off by program peaks.

Frequency Deviation Measurement of F-M Transmitters

The frequency deviation can be determined by noting the constant amplitude modulating frequencies for which the carrier disappears. A graph relating the frequency deviation with the modulating frequency for zero carrier simplifies this calculation

By L. N. HOLLAND and L. J. GIACOLETTO

FROM the theory of frequency modulation it is known that the generation of a frequency-modulated signal produces a carrier and side frequency terms. For a sinusoidal modulating signal, the amplitude of the carrier is directly proportional to $J_0(Z)$ where $J_0(Z)$ is the Bessel function of zero order and argument Z. The argument Z is usually called the modulation index and is defined by

$$Z = mf_0/f_1 \qquad (1)$$

where f_0 is the carrier frequency, mf_0 is the frequency deviation to

either side of the carrier, and f_1 is the modulating frequency. The Bessel function, $J_n(Z)$, goes through variations having a close resemblance to a damped cosinusoidal function as is shown in Fig. 1. For certain values of Z, the carrier goes through zero or null points. The values of Z for which $J_n(Z) = 0$ are denoted by Z_i and are tabulated in Table I.* If the point at which the carrier disappears is known, the frequency deviation can be found because at this point

$$mf_c = Z_i f_1 \qquad (2)$$

There must also be known the order of the zero, that is, the value of i.

In order to use this method of frequency deviation measurement, there is first required an audio signal generator with a calibrated output. This generator is connected to the transmitter a-f input. A selective a-m type receiver capable of receiving c-w signals is used to ascertain the presence of the carrier. In order to make the measurements, reduce the transmitter a-f input to zero and tune in the carrier on the receiver obtaining an audible beat or heterodyne note. Slowly increase the transmitter a-f input (analogous to increasing m in Eq. (1)). The audible beat note should gradually decrease in intensity and finally disappear entirely when the amplitude of the carrier reaches zero. At this point the frequency deviation is $mf_c = 2.405\ f_1$. If the a-f input is again increased, the carrier beat note will return, increase to a maximum, decrease, and again disappear. For the second null point the frequency deviation is $mf_c = 5.520\ f_1$.

TABLE I

i	Z_i	i	Z_i
1	2.4048	11	33.7758
2	5.5201	12	36.9171
3	8.6537	13	40.0584
4	11.7915	14	43.1998
5	14.9309	15	46.3412
6	18.0711	16	49.4826
7	21.2116	17	52.6241
8	24.3525	18	55.7655
9	27.4935	19	58.9070
10	30.6346	20	62.0485

* If additional zeros are desired, note that the difference approaches π units as i increases.

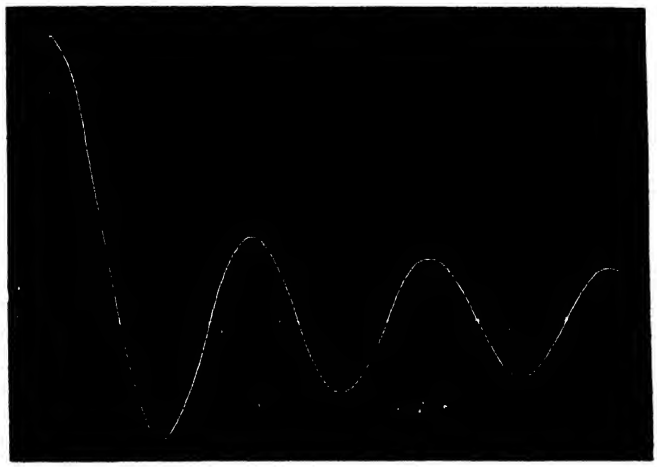

Fig. 1 — Graph of Bessel function, $J_n(Z)$, plotted as function of modulation index, Z

In general, the receiver will not be selective enough to admit the carrier alone, but will admit the carrier and several of the side frequencies. For this case if the receiver is tuned to give an audible beat note, f_c, it is quite possible that there will also be heard the frequencies $f_1 \pm f_c$, $2f_1 \pm f_c$, etc. This may lead to some confusion in determining when the carrier disappears. Considerable improvement can be obtained by introducing a low pass audio filter between the receiver output and the speaker or headset. The filter should be designed to admit f_c and to attenuate the other frequencies. If the cut-off frequency for the filter is chosen as f_c then f_1 must be greater than $2f_c$ in order that the other heterodyne notes fall outside of the filter pass band.

In order to facilitate the measurement of frequency deviation, the chart has been prepared. The radial lines are a plot of Eq. (2) (the dashed curved lines are used with another method of measuring deviation described below). Each radial line when numbered counterclockwise corresponds to the value of i in Table I. As an example of how the chart may be used, suppose that the modulating frequency is 5 kc. The deviation when the carrier disappears for the first time is found by following along the lower edge of the chart to the 5-kc ordinate and moving upward along this ordinate until it intersects the first radial line. The deviation, 12 kc, is read from the scale on the left. For the second null point continue upward along the 5 kc ordinate to the second radial line where the deviation is found to be 27.6 kc. In this manner the deviations may be determined for successive null points.

The above method of measuring deviation follows closely the method described by M. G. Crosby† A slightly different method has been used by the authors with success. For this method the a-f input is held constant and the modulating frequency varied. If this is done, the carrier will disappear for several values of f_1. Any two successive modulating frequencies which cause the carrier to disappear will uniquely determine the frequency deviation. Suppose in this method that a modulating frequency of 7.8 kc gives a carrier null, and the frequency is decreased until another null is obtained with a modulating frequency of 5.0 kc. Then the intersection point of the ordinate at 7.8 kc (upper frequency) and the dashed curve at 5.0 kc (lower frequency) indicates a frequency deviation of 43 kc. The intersection point of the lower and higher frequency must always fall on a radial line. Also the interpolation between the dashed curves for lower frequency values is linear along any radial line.

While these methods of frequency deviation measurement are basic in that they are independent of all circuit parameters, they have certain

† Murray G. Crosby, "A Method of Measuring Frequency Deviation," *RCA Review*, Vol. IV, pp. 473–477, April 1940.

shortcomings which limit their usefulness. First they presuppose a linear relation between input voltage and frequency deviation. A departure from linearity means that the carrier null points are no longer null points but minimum points. If the departure from linearity is very serious, it may be impossible to detect even a carrier minimum point. The carrier frequency must also remain reasonably constant. If the carrier frequency changes considerably as the input level or modulating frequency is changed (depending on which method is being used), no carrier null points will be obtained. Even a small change in carrier frequency may be bothersome in that the carrier heterodyne note will change, possibly to such an extent that the heterodyne note will move outside of the filter pass band. For this reason the filter cut-off frequency should not be too small. Also for this reason the modulating frequency should be kept at as large a value as is feasible so that the carrier heterodyne note will never be confused with the sideband heterodyne notes. In this connection, from the nature of the carrier zeros, it will be necessary to decrease the modulating frequency for measuring smaller deviations. This factor must be given additional attention when making measurements on mobile f-m transmitters where the maximum deviation is usually only 15 kc. A filter with lower cut-off may prove useful in such cases, and the receiver should be returned to the same note if the carrier shifts.

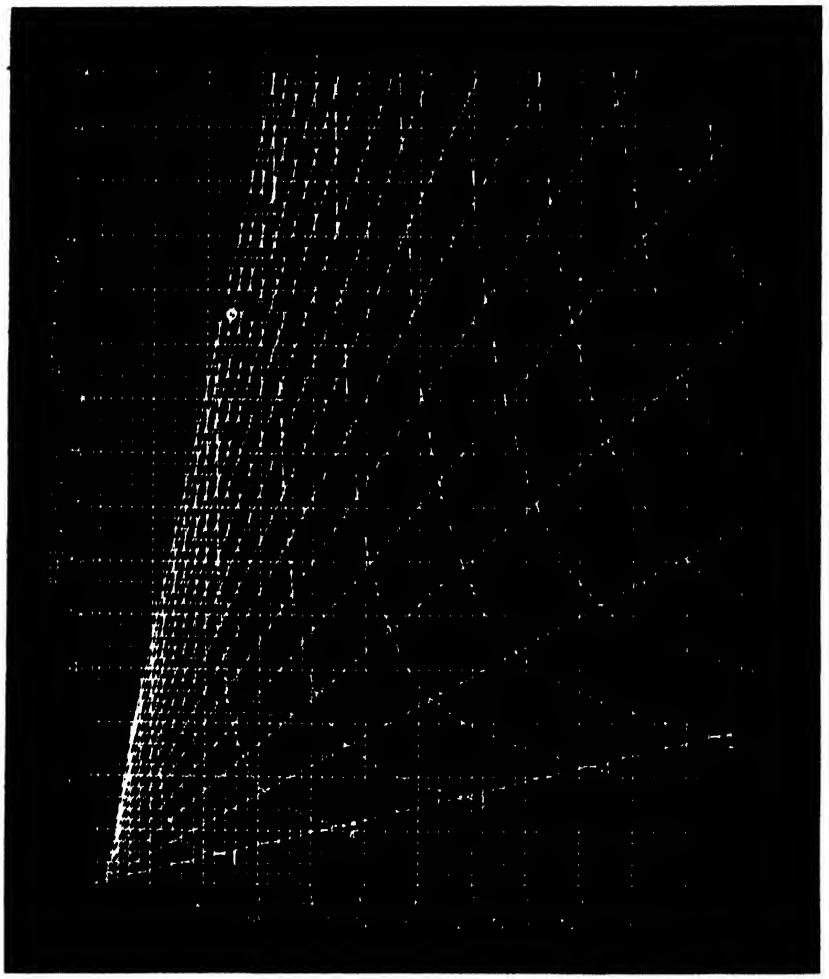

Fig. 2—Graph relating frequency deviation of f-m transmitter and modulating frequency for zero carrier

In using the first method for making deviation measurements, care must be taken to count every null point. If a null point is overlooked the deviation measurements will be incorrect. The second method is an improvement in this respect since the deviation is uniquely determined. On the other hand the second method is useless when there is appreciable variation of deviation with audio frequency. Such a situation will arise in any transmitter if either audio pre-emphasis or uncorrected phase modulation is present.

Using Phone Line for Remote Indication of Overmodulation

By ALVIN LEEMAN

THE SIMPLE CIRCUIT arrangement in Fig. 1 permits one modulation monitor unit to provide indications at both transmitter and studio of a radio station.

The output of the modulation monitor at the transmitter location is fed to a d-c relay arranged to close its contacts on overmodulation. The studio-transmitter order line and ground provide a complete circuit for these relay contacts to the grid circuit of a gas triode at the studio Closing of the contacts lowers the bias on the tube enough to energize

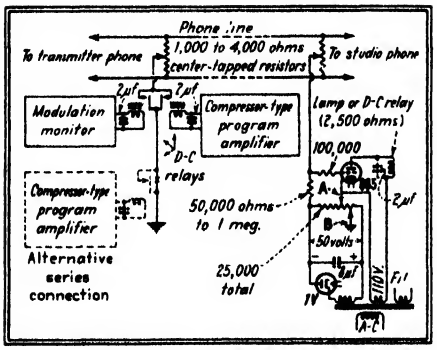

Fig. 1—Overmodulation indicator circuit and phone line connections. Ordinarily only the modulation monitor will be connected to the transmitter end of the line

the relay or lamp in the plate circuit and give the desired indication.

The center-tapped resistor across the phone line at each end should be made high enough in resistance to prevent it from affecting normal use of the telephone line. Satisfactory operation can be obtained with less than 1 ma of relay current in the line circuit.

As some of the compressor types of program amplifiers also have facilities for operating relays at some predetermined level, they can be used in place of the modulation monitor, or the contacts of the relays of each unit can be connected either in parallel or in series to indicate a predetermined program condition. In parallel, either the modulation monitor or the program amplifier can produce an indication at the studio. In series, the relays of both monitor and amplifier must operate to give a studio indication.

In adjusting the device for operation, first see that the relay contacts at the transmitter end of the order wire stay open. Decrease the bias voltage at movable contact *A* until the relay or lamp in the plate circuit of the 885 tube is energized, then increase the bias voltage until the relay or lamp is no longer energized. Increase the bias slightly more so that induced voltage on the telephone line will not operate the indicator.

For the adjustment of *B*, close the relay contacts at the transmitter end of the order wire and move sliding contact *B* toward the negative side of the voltage divider until the relay or indicating lamp is deenergized, then move this contact toward the positive side until the relay or lamp is again energized. Slide the contact a little further in the same direction so that positive operation of the device is assured.

In the circuit as shown in Fig. 1, the relay in the plate circuit of the 885 tube will operate as a buzzer-type indicator. A 2-μf capacitor across the relay coil will cause this relay to operate as a straight relay,

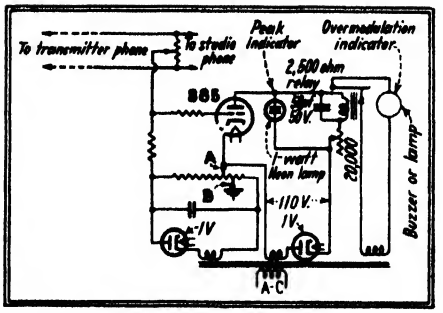

Fig. 2—Alternative studio circuit for providing both peak and overmodulation indications. The 50-μf capacitor prevents the overmodulation relay from operating on momentary peaks

however, and its contacts can then be used to make or break other circuits as desired.

For those desiring to use a neon bulb as a peak indicator and a lamp or buzzer as an overmodulation indicator, the arrangement shown in Fig. 2 can be used. The overmodulation indicator then operates only when the modulation monitor relay remains closed an appreciable period of time due to sustained loud tones, applause or other causes of overmodulation. The 20,000-ohm rheostat is used to vary the period of time between the moment the neon lamp lights and the relay closes. This gives an indication of average peaks and a warning when the program level has been materially increased.

Speech Scrambling Methods

Complete data on a frequency-inverter circuit that scientifically scrambles a human voice for purposes of secrecy in transmission. The same circuit may be used for unscrambling speech at the receiver. Five band-splitting methods that combine with inversion to insure even greater privacy are also taken up

By WILLIAM W. ROBERTS

In communication over ordinary telephone circuits, the instantaneous amplitudes and frequencies of the electric waves transmitted correspond to the instantaneous amplitudes and frequencies of the various sound-pressure waves making up articulate speech. These speech waves are intelligible only when the fundamental frequency components and their associated harmonics or overtones are transmitted so that the correct relative amplitudes and phase relationships are not too greatly changed. Therefore, any operation which alters these conditions materially will make it impossible to detect the transmitted waves as intelligible speech until the approximate correct relationships have been restored.

In straining ordinary speech through the medium of scrambling, the frequencies of each of the components of speech currents are changed in such a manner that, although the changed speech currents will occupy the same frequency

range as that of the original speech, the essential relationship for intelligibility will have been destroyed.

Frequency Inversion

One of the simplest ways of scrambling the human voice is by means of frequency inversion. In this method, a device known as the speech inverter virtually turns a person's voice upsidedown, much as the lens of a camera inverts the image of an object in the field of vision. Everyday English becomes as unintelligible as a strange foreign language, with seemingly no apparent relation to the original speech. Yet this same incoherent jargon may be restored to normal by a similar process of inversion.

In creating inverted speech, normal voice frequencies are caused to modulate in a well known manner a constant audio frequency (inverting frequency) to produce frequencies which are combinations of the speech frequencies and the inverting frequency. These frequencies will include an upper and lower side-band which are, respectively, the inverting frequency plus the voice frequencies and the inverting frequency minus the voice frequencies. If the inverting frequency is just above the highest essential voice frequency, it will be obvious that the lower side-band will be an inverted picture of the original input voice frequencies, so that the low frequencies become highs, and the high frequencies become lows.

Using an inverting frequency of 3000 cycles, as is the case in most apparatus developed before the war, an input frequency of 200 cycles will become 3000 minus 200, or 2800 cycles in the difference frequency band. A 2500-cycle input would become 500 cycles, and all other input frequencies will correspondingly be inverted. The upper side-band is representative of the original input frequencies raised up in the spectrum by the value of the inverting frequency. In actual practice of secret telephony, this upper side-band is attenuated by filters and only the inverse frequency band is used for transmission.

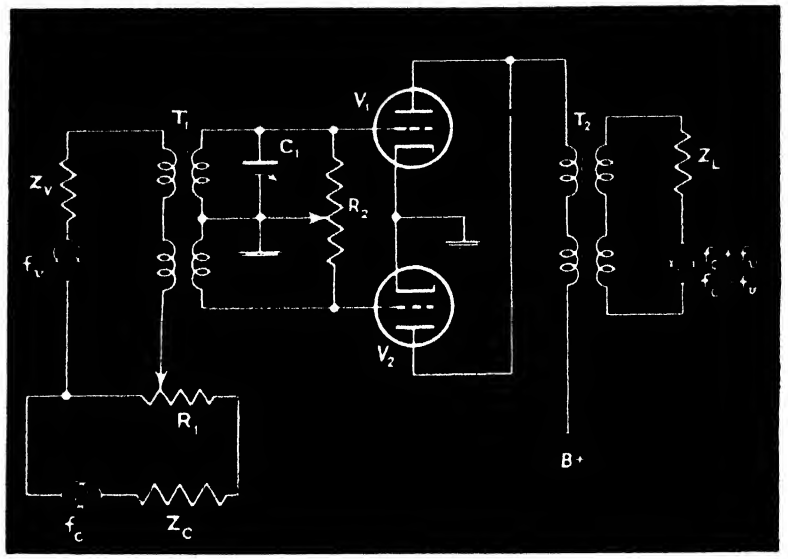

FIG. 1—Fundamental circuit of balanced modulator for speech inversion

It is rather difficult to describe the discordant nature of inverted speech, but anyone who has listened to the confused mumble-jumble of a phonograph disk reversed will get a fair idea of the type of meaningless sounds produced. The low frequencies of speech are transformed into high-pitched squeaks, while the highs and over-tones present in the voice produce a succession of low gutteral noises.

On listening to certain words spoken through the inverter, it is possible in some instances to pronounce them. For example, the words "telephone company" when translated by an inverter sound something like "playafiend crinkanope".

The inversion of music results in a jangling of tones which are particularly amusing. This process will mutilate the most beautiful symphony so that it is completely lacking in structure and composition. Increasing-pitch notes of music become decreasing-pitch notes in the inverse frequency band and vice versa.

Inverted speech has long been employed on the trans-oceanic telephone circuits to provide a limited amount of privacy against eavesdropping by short-wave radio listeners. For a higher degree of secrecy on some of the more important telephone links carrying diplomatic calls and such, a form of garbling more commonly known as band-splitting has been employed.

Speech Inverter Circuit Theory

Figure 1 illustrates a fundamental circuit for one type of speech inverter. The same circuit is applicable for both scrambling and unscrambling. It is essentially a Hartley balanced modulator or demodulator in which a pair of triodes are connected to produce certain frequencies and to suppress certain other frequencies.

The term f_v is representative of voice currents, as from an ordinary telephone set, and represents a band extending from 200 to 3000 cycles, which is considered adequate for good communication, measured in terms of satisfaction given to telephone subscribers. The term f_c indicates a sustained high-frequency carrier or inverting frequency. The impedances Z_v, Z_c and Z_L indicate the voice frequency source, inverting frequency source and the output line impedance, respectively.

Since the inverted speech will occupy the same frequency range as the original speech, but in reverse order, it is essential for complete privacy that these original voice currents f_v do not appear across the out-

put line impedance Z_L. Since the inverting frequency is near but higher than the highest essential voice frequency, it is essential that it, also, does not appear across the output impedance Z_L.

These results are secured to a high degree with the type of balanced modulator shown, producing certain frequencies which are combinations of the voice frequencies f_v and the carrier frequency f_c, but suppressing the unmodified frequencies which are the impressed waves uncombined with each other.

The frequencies produced are the upper and lower side-bands, f_c+f_v and f_c-f_v, which are respectively the inverting frequency plus the voice frequencies and the inverting frequency minus the voice frequencies. It will be seen that the upper side-band f_c+f_v is the original voice frequency band raised up in the spectrum by the value of f_c. The lower side-band f_c-f_v is an inverted version of the original voice frequencies, occupying the same position in the spectrum but in reverse order. High notes then become low notes, and lows become highs.

While the process of modulation is merely a side show in scrambling, an analysis of the interaction of currents to produce sum and difference frequencies will be interesting.

The current in the output of a three-electrode vacuum tube is assumed to be capable of representation by a power series having as an independent variable the voltage impressed upon the input circuit. That is, I_1, the output current from one such tube due to an input voltage v_1, may be completely represented by $I_1 = av_1 + bv_1^2 + cv_1^3 + \ldots$ in which a, b, c, etc., are constants depending on the tube characteristics. If another tube having essentially the same constants, a, b, c, etc., be used, the output I_2 from this tube, due to a similar impressed wave, will be substantially $I_2 = av_1 + bv_1^2 + cv_1^3 + \ldots$

It is found in practice that all terms in this series after the second power term bv_1^2 may be neglected for most purposes. It is also obvious that the first term, which simply represents the amplifying property of the tube without any frequency modification, plays no part in the modulation process. The property represented by the square term bv_1^2, however, is commonly made use of for effecting the modulation of one input wave by another.

Since one object of using a balanced modulator is to suppress unmodified frequencies, the two tubes are connected with respect to the unmodified waves so that the unmodified wave from one tube is neutralized by that of the other tube, as shown in Fig. 1. The unmodified frequencies are fed into the grids of V_1 and V_2 in push-pull. The plates form a parallel output circuit by means of the substantially zero reactance connection. With this arrangement the input wave v_1 impressed on one tube is reversed in sign relative to that impressed on the other, so that the two waves have a phase difference of 180 deg. and the output currents are added. This produces the result desired, as indicated in the following equation in which the relatively unimportant higher power terms are neglected.

$$I_1 = av_1 + bv_1^2$$
$$I_2 = -av_1 + bv_1^2$$
$$I_1 + I_2 = 2bv_1^2$$

The completeness of this action is dependent, however, upon the tubes being identical as to the properties represented by the constants a and b in the equation, and it is also dependent upon the current I_1 being completely added to the current I_2. The addition of the two output currents represents in part really the

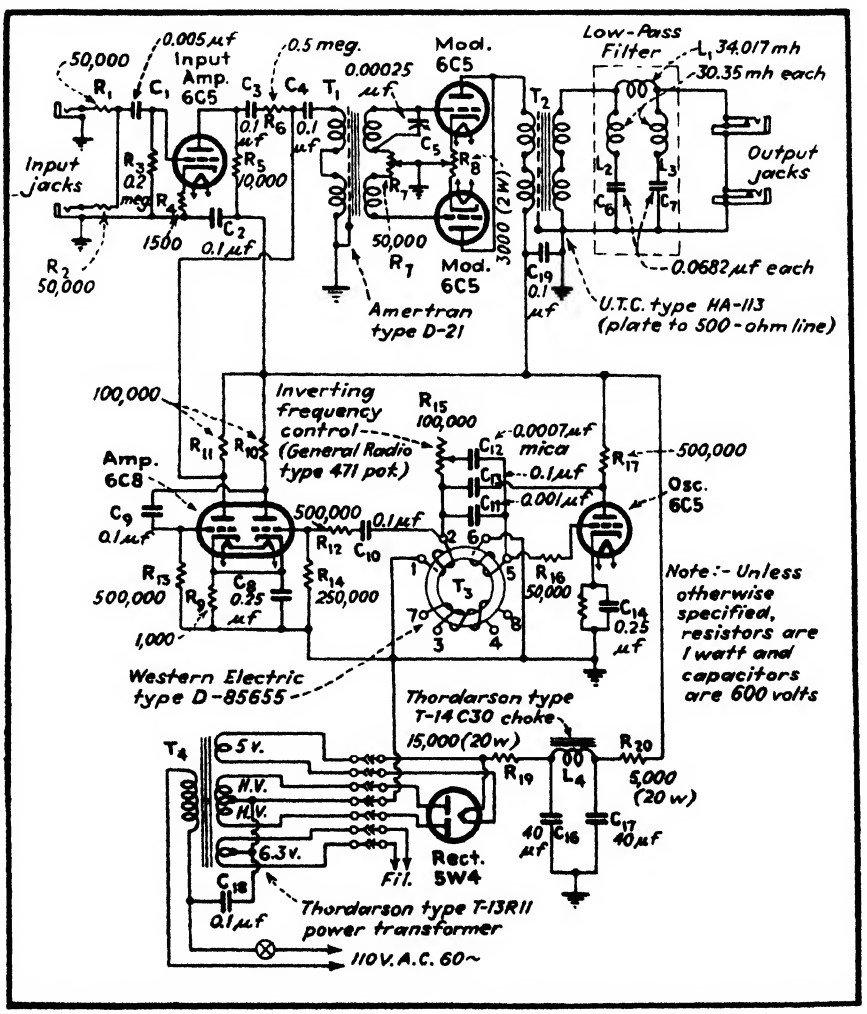

FIG. 2—Complete practical circuit for the speech inverter shown in the photographs. The inverting frequency generated by the 6C5 oscillator is controlled by R_{15}, and is about 3000 cycles with the control at its mid-position

cancellation of the undesired component represented by the first power term av_1; therefore, if the current I_1 from the first tube is exactly equal to I_2 but if the adding function does not completely involve both I_1 and I_2, there will be a residue of the component av_1 appearing across output transformer T_3.

Across the secondary of T_1 is a variable resistance R_2, with the adjustable contact going to the common ground or cathode connection. A variable capacitor C_1 is connected in shunt with one half of the secondary winding. The purpose of this is to compensate for any inequalities in the two halves of the secondary winding and to secure a symmetrical balance of the two sides of the circuit with respect to ground.

The two tubes V_1 and V_2 should be carefully selected to have as far as possible identical characteristics. This is important, as has already been pointed out in connection with the above equations.

Potentiometer R_1 is for adjustment of the amplitude of the inverting frequency f_c, which must be large in comparison with the f_s input voltage.

In actual practice there would be included a suitable wave filter connected to impedance Z_1 for selecting the inverted side-band.

Complete Speech Inverter Circuit

Figure 2 shows a complete schematic of the speech inverter shown in the photographs. The unit is complete with power supply and a low-pass m-derived filter. Two high-impedance input circuits are provided so the unit can be used in conjunction with two short-wave receivers for unscrambling trans-oceanic telephone conversations. Two receivers are necessary if one wishes to hear both sides of a conversation.

The output impedance is 500 ohms looking directly out of the low-pass filter. The two output jacks permit using two pairs of 250-ohm impedance headphones connected in series.

The 6C5 input amplifier is really a mixer stage to couple the outputs of two radio receivers to the modulator input transformer T_1. This transformer plays an important role in the circuit and should be carefully chosen. The Amertran Type D-21 was found to be satisfactory. It can be seen mounted near the top of the panel in the rear-view photograph.

In brief, to supply the grids of the two modulators with voltage at different frequencies that are exactly 180 deg. out of phase and of equal amplitude is an ideal condition but is difficult to attain in practice. A perfect balance obtained for one frequency will not be a perfect balance at another frequency.

The transformer used for T_1 must have low distributed capacitance and low capacitance between windings, and the center tap on the secondary cannot be taken from within a winding. Two leads must be brought out from separate sections of coils to provide magnetic and inductive balance.

Since we cannot have an ideal transformer, the controls R_7 and C_5 are provided to compensate for any inequalities present. The function of R_5 is to provide for balancing the plate currents of the two 6C5 modulators. All these controls are used to balance out of the output circuit the incoming speech waves and the inverting frequency from the 6C5 oscillator. They can be seen as the three small knobs across the bottom in the front-view photograph. Preliminary balancing can be aided by careful selection of the two 6C5 modulators and by interchanging them during the process of balancing. The half of the secondary across which capacitor C_5 must be shunted can only be determined by experiment.

Transformer T_2 is a standard plate-to-line transformer, and any good make will serve the purpose.

The low-pass filter is of the m-derived type to provide for suppression of the upper side-band produced by modulation. The filter is calculated with the following characteristics: $f_c = 2810$; $f_\infty = 3620$; $R_0 = 477$; $m = 0.63$.

The construction of the filter should be undertaken with the following points in mind. It is essential that the a-c resistances of the various coils be kept as low as possible if sharp discrimination between the unwanted frequencies and the pass frequencies is to be obtained. Honeycomb coils may be used for the inductances since the values in this case are not very high. Choose coils of greater inductance than the values given, and remove turns while checking with an inductance bridge, until the desired value is obtained.

The capacitors can be a paper dielectric type because of the relatively low frequencies involved. The odd values given for C_6 and C_7 can be stacked up from a number of standard capacitors in parallel to provide the correct capacitance.

The inductances should be treated with wax or other moisture-resisting material. The individual inductances should be shielded from each other or spaced by their own diameter and placed alternately at right angles.

The 6C8 amplifier is perfectly straightforward and is for amplification of the inverting frequency from the 6C5 oscillator. A fixed value is shown for R_{14}, but it might be well to use a standard volume control instead to provide for relative adjustment of the amplitudes of the inverting frequency and incoming speech frequencies.

The frequency from the 6C5 oscillator is controlled by means of a variable resistance and capacitor in series. The control is the large dial shown on the front of the panel. The values of the various components comprising the oscillator circuit have been chosen so that a frequency of 3000 cycles is provided with the control near the center position. A Wien bridge or any other well-known type of oscillator may be used for supplying the inverting frequency.

Because of the close proximity of the component parts of the inverter, hum pickup is reduced by isolating power transformer T_4. This transformer is mounted externally in a small can and made a part of the line cord.

In operation, the inverter may be used for both scrambling and unscrambling. If desired, two units may be placed at either end of a two-way circuit with the usual balanced hybrid coils, to provide a complete privacy system for two-way telephone communication.

To secure privacy of speech by

means of band splitting, the speech-frequency band is divided as to frequency into a plurality of sub-bands, some of which may be transmitted without modification. Others first have their frequency order inverted and are then transmitted along with the unchanged sub-bands, or, if desired, each of the sub-bands may be inverted before transmission.

It is preferable in this type of secrecy system that the frequency width of each of the sub-bands be kept narrow enough so as to be incapable of reproducing understandable speech by itself. The maximum width of a sub-band must not exceed certain limits because of the large amount of intelligibility that would hundred cycles wide, especially if this portion were chopped out of the spectrum in the neighborhood of 1000 cycles.

The number of sub-bands into which the voice frequency band is divided is dependent on the degree of privacy required. The greater the number of sub-bands, the greater the number of transposition combinations that are possible.

The combination of transposition and inversion of the various sub-bands is accomplished by suitable modulation processes. By using bilateral modulators, the same apparatus may be used for retransposing and reinverting the sub-bands of a speech band that has been rendered unintelligible in the manner described.

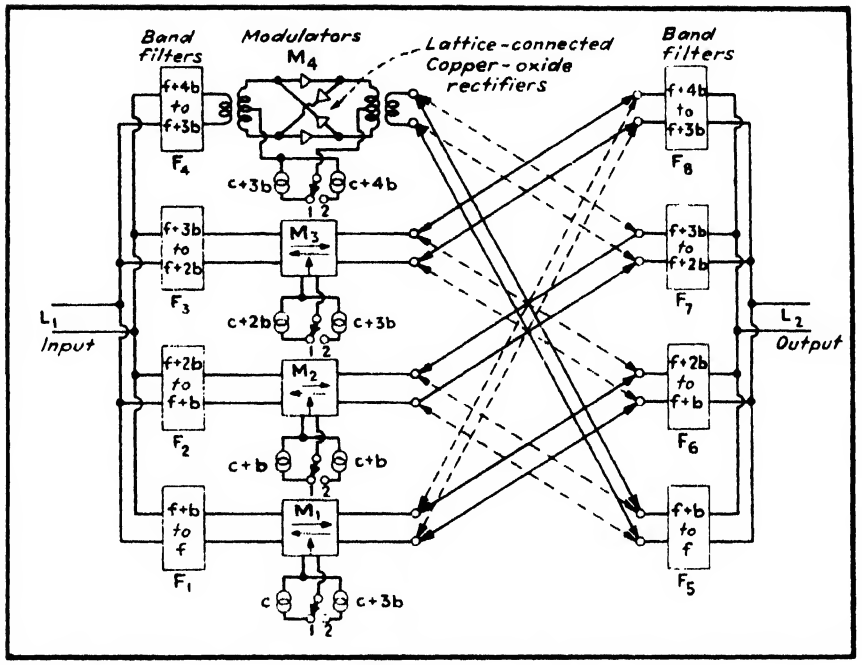

FIG. 3—Basic band-splitting arrangement for increased privacy in radiophone communication. The band filters divide essential voice frequencies into four equal bands of width *b*, with *f* being the lowest essential voice frequency. Two oscillator frequencies are available for each copper-oxide modulator to provide speech inversion. The output of each modulator may be fed to either of two filters, one passing the upper and the other the lower sideband, thus providing many possible arrangements

Band-Splitting Circuit

Figure 3 represents schematically a band-splitting privacy system. The normal speech currents are derived from the line L_1 and impressed on the sub-band filters F_1, F_2, F_3, and F_4. These filters serve to divide the speech currents into four equal sub-bands which may each have a width of b cycles. For instance, filter F_1 will pass a range of frequencies f to $f + b$, where f is representative of the lowest essential voice frequency necessary for transmission.

Each input filter is connected to supply selected voice currents to four separate modulators M_1, M_2, M_3, and M_4. These are bilateral modulators of the double balanced copper-oxide type, shown in detail in the case of M_4. Each modulator is essentially a lattice network having a copper-oxide rectifier unit in each of the series and lattice arms, and two transformers each having two windings, one winding of each transformer being connected across one of the two sets of terminals of the network, and the source of carrier current for modulation with the voice frequencies supplied to the other windings of each transformer being connected across the midpoints of the first two windings. However, any of the other known types of bilateral modulators may be used, such as the balanced modulator shown in Fig. 38, p. 550 of Radio Engineering Handbook*.

The carrier frequencies supplied to these modulators are so chosen that the sub-bands may be transposed with respect to each other in various combinations.

The outputs of each of the four modulators may be variously connected to the output band filters F_5, F_6, F_7, and F_8, as shown in Fig. 3. These output band filters have exactly the same cut-off limits as indicated for the input band filters.

By shifting the connections of the modulators to output filters and employing various carrier frequencies, we alter our different combinations f transposition and inversion of sub-bands.

Transposition in Band Splitting

Transposition of sub-bands with and without frequency inversion is shown in the schematic by the solid-line connections between modulators and output filters. The necessary carriers are provided when the modulator switches are in position 1.

In the case of the dotted-line connections and the carrier switches in position 2, each of the sub-bands is inverted as well as displaced.

With reference to the solid-line connections and the carrier switches in position 1, if a carrier current c is supplied to M_1, with input frequencies of f to $f + b$, there will be produced a lower and upper side-

* Edited by K. Henney. *McGraw-Hill Book Co., New York 18, N. Y.*

band, namely $c-f$ to $c-(f+b)$ and $c+f$ to $c+f+b$. The range of frequencies $c+f$ to $c+f+b$ is the original band f to $f+b$ raised up in the spectrum by the value of c, and corresponds to the sub-band of the original voice band extending from $f+b$ to $f+2b$. This range of frequencies can then be selected by filter F_6 and transmitted to the output circuit L_2. The action of modulators M_3 and M_6 in this case would be similar to that of M_1.

The original voice sub-band $f+3b$ to $f+4b$ from filter F_4 is displaced down in the spectrum to a position occupied by the original voice sub-band f to $f+b$. Here, in addition to being displaced, the frequency orders of the speech components are inverted, as will be seen by the following action.

With input frequencies of $f+3b$ to $f+4b$ and a carrier of $c+3b$ applied to the modulator M_4, there will appear in the output the side-bands $c+3b+f+3b$ to $c+3b+f+4b$ and $c+3b-(f+3b)$ to $c+3b-(f+4b)$.

It will be seen that the lower side-band, $c+3b-(f+3b)$ to $c+3b-(f+4b)$, is an inversion of the original input frequencies $f+3b$ to $f+4b$ which now occupy the position of the original voice sub-band f to $f+b$.

It will be noted in the arrangement of this apparatus that by shifting the connections of the filters and carriers in various combinations from time to time in such a manner that corresponding combinations are simultaneously employed at the two terminals of a receiving circuit at the same time, it will be extremely difficult for an unauthorized listener to obtain an intelligible message.

Shifting from one combination or scheme of interrelation to another can be accomplished by switching relays under control of timing cams associated with an accurately controlled driving means to provide additional secrecy.

The use of bilateral modulators allows the transmitted and received waves to pass in opposite directions through the same privacy apparatus, to produce a scrambled message for transmission or to unscramble a message from a received secret wave.

Attenuation with Band Splitting

Another type of privacy system proposed is an arrangement whereby the speech band is divided into a plurality of sub-bands, as by filters F_1 to F_4 of Fig. 3. Each sub-band is then subjected to different degrees of attenuation before transmission instead of being displaced by modulation. Accordingly, when the voice is transmitted it will be so distorted as to be practically unintelligible. To restore the voice to normal at the receiving station, the sub-bands of the voice are again subjected to unequal degrees of attenuation, so that all of the sub-bands will be attenuated to the same degree and the distortion removed.

Phase Shift with Band Splitting

Still another arrangement for secret telephony is to alter the order of occurrence of the various frequency components of speech. Briefly, this is accomplished by taking the subdivided waves, as from filters F_1 to F_4 of Fig. 3, and producing a phase or time shift in some of the sub-bands with respect to others before transmission. This phase shift is produced by the use of a storage device such as the telegraphone. The various sub-bands are then recombined and transmitted, or they may first be shifted to a different frequency level and then transmitted. At the receiving end employing this system, the various sub-bands are again separated by filters, and such a phase shift is made in the individual sub-bands as is necessary to reproduce the normal speech waves.

Variable Inverting Frequency

Still another arrangement is one that the writer built and patented in 1939*. In this arrangement, the speech was scrambled as in the process of Fig. 3. Then, to destroy the limits or boundaries between the plurality of sub-bands, the combined frequency bands were inverted by a modulator in which the inverting frequency was caused to vary cyclically in an irregular manner. The varying inverting frequency, combined with a complex scheme of variation, provided a high degree of secrecy. It can be seen that in accordance with such a principle, it would be practically impossible for an unauthorized listener to separate the individual sub-bands as their frequency limits would never remain fixed in the spectrum. To separate the individual sub-bands it would be necessary to know the inverting frequency at any instant and the complex manner in which it varied.

Let us assume that the inverting frequency varies cyclically in any desired manner between the limits c and $c+d$, where d varies between zero and a predetermined limiting value. If the speech frequency band as a whole, such as from L of Fig. 3, is represented by s and if the inverting frequency is modulated by these speech frequency currents, the resulting components will be of frequencies $c+d-s$ and $c+d+s$. The lower side-band $c+d-s$ would be the one selected for transmission.

The receiving station cooperating with such a system would use substantially the identical means used for transmitting but in reverse.

* U. S. patent No. 2,301,455

Automatic Control Circuits for Broadcast Transmitters

Four manpower-saving electronic circuits for transmitters, providing protection against arcs during storms, automatic restoration of the carrier after an overload, automatic starting after breakdown, and automatic timing of each carrier interruption

By W. R. SLOAT

It is the purpose of this article to present four automatic devices, three of which were designed by the author and the fourth, the carrier restoring device, by the transmitter staff of WABC under the supervision of Mr. R. W. Newby. All have been in use at KMOX for some time, giving excellent service.

The four devices are independent of one another, and each self-sufficient for its purpose. Collectively they provide comprehensive and measureable improvement in station dependability. All contain only small standard components that are ordinarily at hand.

Under certain conditions, radio-frequency arcs become established at a transmitting antenna by electric storms or static discharges and are sustained by the transmitter output. These arcs may be of insufficient magnitude to operate the transmitter overload relays, although capable of damaging parts of the equipment. Two methods of stopping these arcs are momentarily cutting the carrier or reducing the output of the transmitter to a point where it will not maintain the arc.

Initiating devices to achieve one of these methods fall into several classes. One comparatively complicated type, usually difficult to handle, balances out-of-phase components of the r-f energy in one stage or the transmission line against that in the preceeding stage. Another method, applicable only to a case where the arcs occur repeatedly at the same point, uses a phototube to actuate the system. A third method uses the arc itself as a conducting path for relay current.

A fourth method, in use at KMOX, is one operating directly from a portion of the radiated carrier power. It can be used with low-level modulated transmitters without any restarting equipment. An independ-

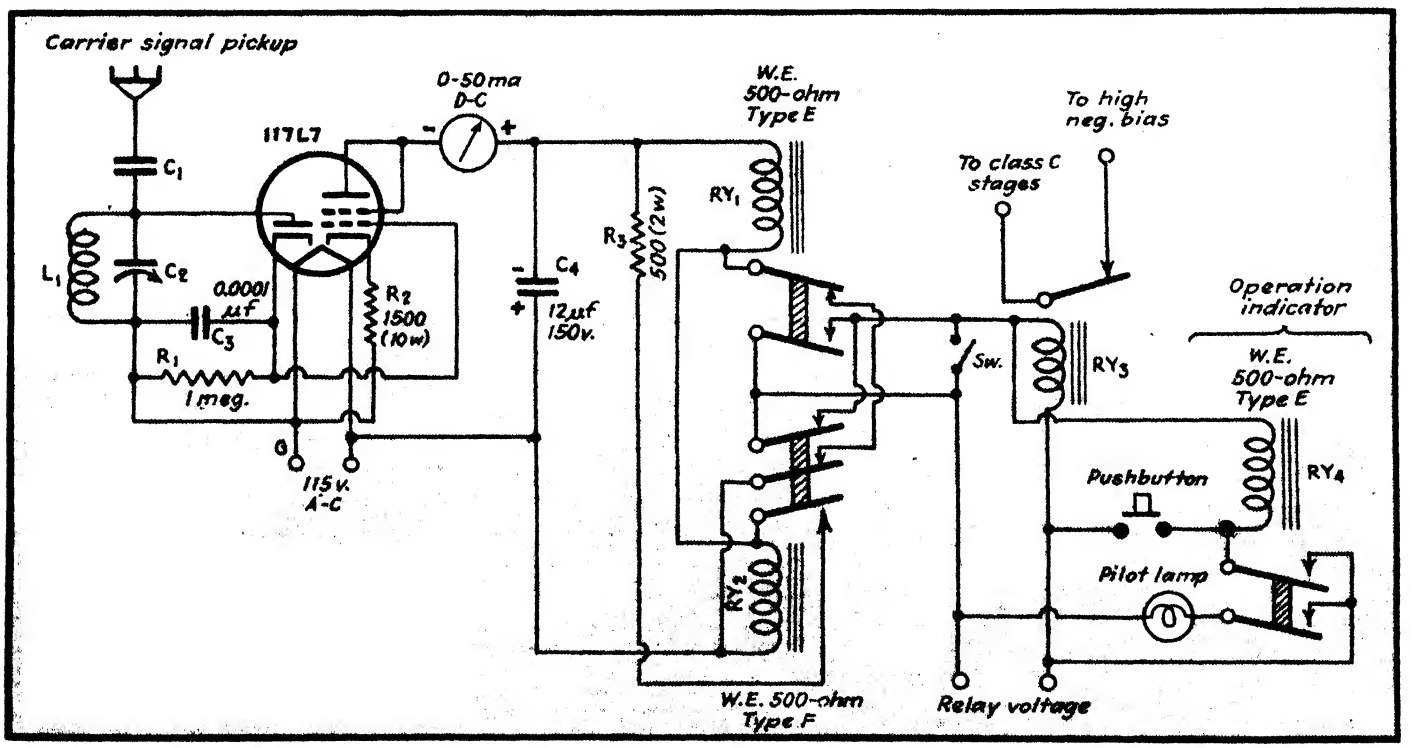

FIG. 1—If an r-f arc becomes established and is sustained by the transmitter output without drawing enough current to trip overload relays, this carrier-actuated protective circuit automatically reduces the transmitter output momentarily to about 15 percent of normal to kill the arc. If RY_2 is inherently slow enough, the interlock with RY_1 may be omitted

ent restarting device, having no tubes and only one relay, can be used in conjunction with the device for protecting high-level systems.

The circuit of the KMOX carrier-protective device for low-level systems is shown in Fig. 1. The instrument is controlled by carrier energy picked up by a short antenna and fed to the diode section of the 117L7. The diode develops positive bias for the tetrode section of the tube, which is also cathode-biased.

When normal energy is radiated, two relays, RY_1 and RY_2, are energized by the tetrode plate current by virtue of positive grid bias from the diode and RY_2 is also energized. Under this condition, the coil of RY_1 is paralleled by R_3, and only a slight drop in plate current will cause RY_1 to open. An abnormal condition anywhere in the transmitter resulting in a moderate drop in radiated energy will cause such a drop in plate current, and RY_1 will release RY_3, applying high negative bias to the buffer and modulated amplifier stages.

RY_3, may, of course, have any contact arrangement desired for the application of this bias, which must be determined to suit the individual transmitter. This bias should be sufficient to reduce the carrier power to about 15 percent of normal, which will not sustain arcs unless there has been some damage to equipment. When the power drops to this low value, RY_2 will not have sufficient current to hold and will drop out, picking up RY_4 through a set of de-energized contacts, removing the high bias and returning the carrier to normal. These de-energized contacts on RY_2 also perform the useful function of protecting the device against tube failure, since the relay cannot pick up without plate current, and these contacts hold in RY_3.

When RY_2 opens two other functions occur: R_4 is removed from its position in parallel with the coil of RY_1, and RY_2 is locked out through its remaining de-energized contact and a similar one on RY_1. Thus, RY_1 is subjected to the full plate current, and will now pick up on a smaller current than is present when it opens, and RY_2 is prevented from picking up until after RY_1 has closed. RY_1 closes at about 25 percent normal power, and RY_2 at about 80 percent when the tetrode plate current is large enough to keep RY_1 energized as the paralleling resistor R_4 is reconnected. The instrument is now recycled. If damage has occurred to the transmitter or other trouble is present to prevent the carrier from returning to full power, the device will remain static, with RY_2 open, RY_1 open or closed, and transmitter bias normal (RY_3 closed).

The contacts of RY_1 should make before break and the springs should have about half the tension of those on RY_2. C_4 is provided to avoid relay chatter on the rectified alternating current in the plate circuit of the 117L7. A switch SW is provided in parallel with the energized contacts of RY_1 in order to hold in RY_3 when adjusting the device or taking it out of service for some other reason. C_1 must be used to isolate the antenna from the power system, so that in the event the power source becomes reversed, the antenna will not be at line potential. C_1 also provides a convenient means of limiting the r-f input to the instrument. Enough r-f energy, however, should be fed to L_1C_2 so that this tank may be operated somewhat detuned from the station frequency, and C_2 used as a control of the tetrode bias and the dropout point of RY_1. When properly adjusted for dropout at 75 percent of full carrier, the plate current should be about 22 ma, and about 7 ma when the high bias is applied to the transmitter during an overload.

For use with high-level systems, where power reduction by means of high bias is more difficult to achieve, the contacts of RY_3 would be placed in series with the plate OFF button or in series with the series-overload circuit of the transmitter, both generally arranged as normally closed circuits. Operation of the device would then result in an interruption of the plate-contactor holding circuit, shutting off the high voltage. As previously pointed out, a carrier-restoring device will be necessary for this method of operation, unless manual restoring of the carrier is to be depended upon.

An operation indicator is a desirable accessory to the carrier protective device. The one in use at KMOX is shown at the right in Fig. 1, and is so simple that very little explanation will be needed. Under normal conditions (RY_1, RY_2 and RY_3 closed), RY_4 is energized by the push button, seals itself in through RY_1, and lights the pilot lamp. When RY_1 is opened, RY_4 will drop out and put out the pilot light, which will remain out until the operator resets it with the pushbutton. The protective device will continue to operate when called upon to do so, regardless of conditions in the indicator.

WABC Carrier-Restoring Device

Overloads are probably the most common cause of carrier interruptions in broadcast stations. These result in operation of the protective relays and removal of the plate voltages. Where a manual operation is necessary to restore plate voltages, there is usually a delay of at least several seconds before the operator can reach the switch to restore the carrier to the air.

The carrier reset to be described cannot be praised too highly. It has been in service at WABC and then at KMOX since 1933, and has proven itself thoroughly dependable. The author does not know of a single case of trouble due to failure of this device. It is probably the simplest gadget yet designed that is capable of performing the standard three-shot and lockout cycle of reclosing devices. This unit, shown in Fig. 2, needs only as many relay contacts as there are protected plate circuits in the transmitter. It will operate within 0.3 second on the first attempt to restore the carrier, and within 0.6 second on the two subsequent attempts. Under these conditions, instead of a definite program interruption, a simple overload results in a momentary break of such short duration that only the most attentive listeners will be aware of it. In addition to its electrical and mechanical simplicity, it has no buttons

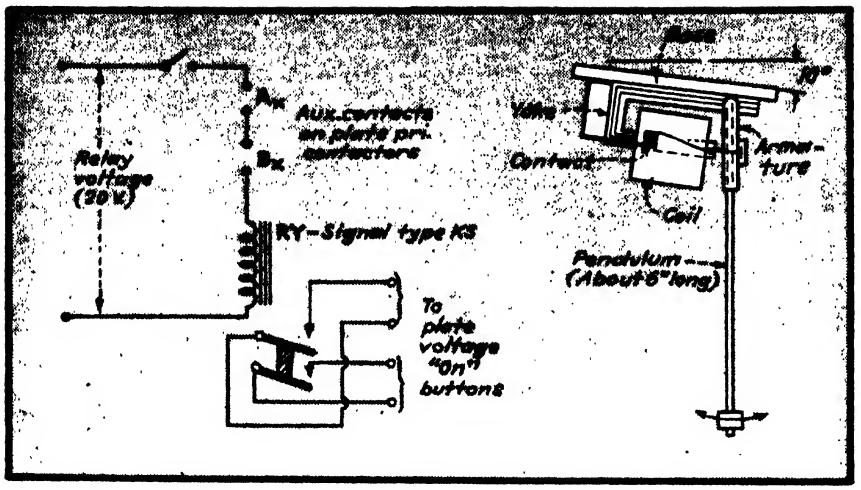

FIG. 2—In the event of carrier failure due to overload, this simple relay arrangement performs the standard three-shot and lockout cycle of reclosing devices. It makes three attempts to restore power, working so fast that listeners are not aware of trouble

to push to recycle it after a lockout. It is completely automatic in every respect. Its contacts never break a circuit and consequently never need attention.

This reclosing device consists essentially of a relay with one set of de-energized contacts for each protected plate circuit, and a pendulum associated with the relay armature. Most transmitters have only two protected plate circuits, a medium voltage for the exciter and driver stages, and a high voltage for the buffer and final amplifiers. This is the case at KMOX, as represented in Fig. 2. The relay contacts are paralleled with the plate ON control buttons, so that the high-voltage circuit breakers are closed by operation of the relay. The relay is energized by current flowing through auxiliary contacts *Ax* and *Bx* on the plate voltage primary contactors. Thus, when either contactor is opened as a result of an overload, the reset relay becomes de-energized and the pendulum-yoke arrangement is released. The contacts will close at the end of the first half swing of the pendulum and the plate voltage will be reapplied.

If the overload has cleared, the contactor will remain closed, energizing the reset relay and restoring conditions to normal. If the overload still exists, the plate contactor will reopen by action of the protective relays, and the reset relay pendulum will continue to swing. If the overload has not cleared by the time the third application of plate voltage has been made, lockout will occur as the reset pendulum has lost its kinetic energy and will come to rest in a neutral position. The carrier must now be restored manually. As soon as the plate contactors remain closed simultaneously long enough to energize the reset relay, the device is ready for another operation cycle.

Nearly any type of clapper relay is suitable for conversion into a pendulum reset device. The relay voltage source may be chosen to fit the relay, or vice versa. The relay used at KMOX is a Signal Electric and Manufacturing Co. type KS, operating from the 20-volt filament supply. Connections are made to the moving contact arms by means of flexible leads. The pendulum is of such a length that three full swings take place, resulting in three contact closures before the arc of the swing has become too short to close the contacts. A complete swing of the pendulum requires about 0.6 second, but the first closure occurs in half that time since only a half swing is required.

A quarter-inch rod of any material will suffice for the pendulum, and several nuts may be threaded on the end to provide weighting for energy storage. The relay is mounted approximately 10 deg. from the horizontal so that the contacts are open when the relay is not energized and the pendulum is at rest.

If no auxiliary contacts are available on the plate contactors, they can usually be installed without great difficulty. However, where this is utterly impossible, auxiliary relays in parallel with the plate transformer primaries could be used.

An automatic time-delay starting device is particularly useful in two ways, for getting back on the air after a breakdown with a minimum

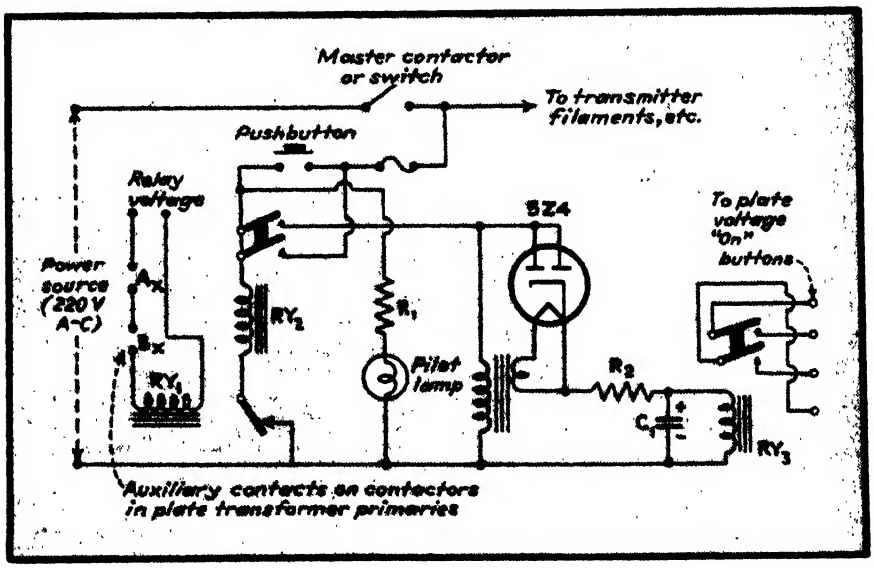

FIG. 3—Automatic starting circuit for getting back on the air after a breakdown with a minimum of lost time

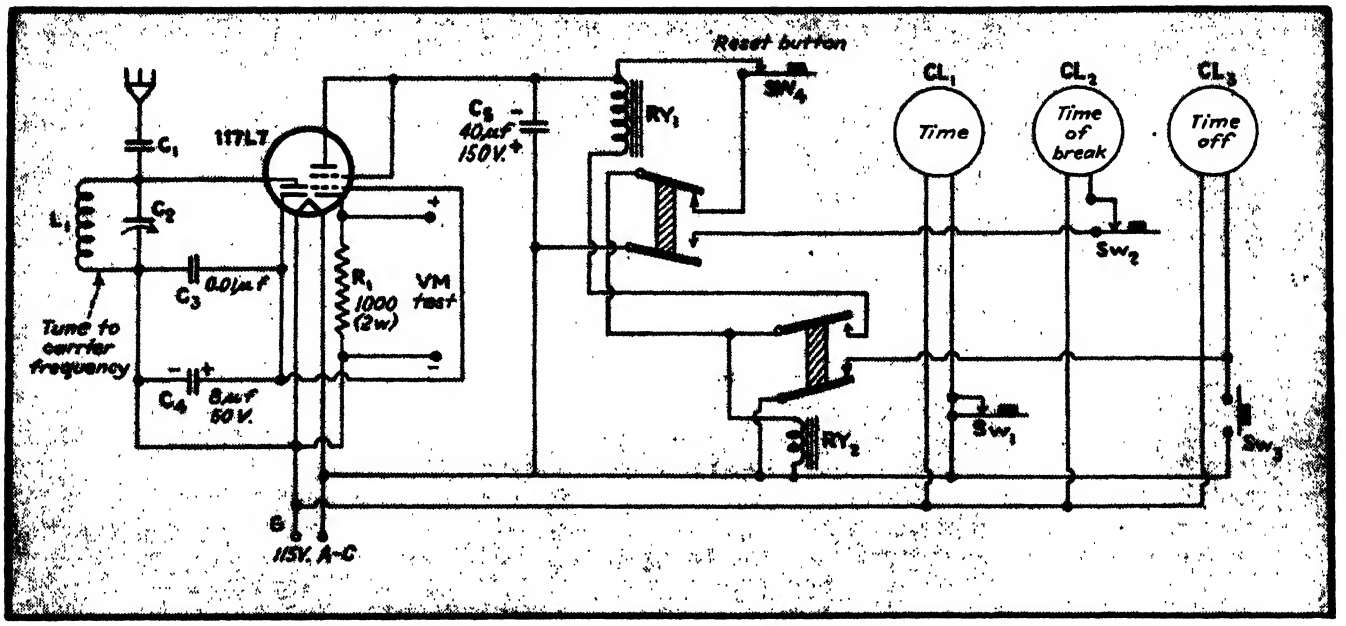

FIG. 4—Arrangement for securing automatically a record of the time that carrier failure occurred and the duration of the failure

of lost time, and for locating trouble where the fault cannot be expeditiously located without the power on and it is impossible to keep it on without damaging equipment.

The device in use at KMOX will give a start in 10 seconds, providing the interlocking grid and filament relays are all clear, otherwise the start will wait until they do clear. This 10-seconds can be utilized by the operator in getting the studio on the order wire, or in proceeding to the point where trouble is suspected, so that he may observe the equipment at the moment the plate voltage is applied. For example, in the latter situation, the operator is enabled to locate readily a bad tube in a parallel installation when the only indication of trouble is a flash inside the tube.

Electrical details of this device are shown in Fig. 3. If either plate voltage is off, RY_1 will be de-energized and its contact closed. The method of energizing RY_1 is the same as for the reset relay. RY_2 may now be picked up by means of the pushbutton, and it will seal itself in through its lower contacts. The pilot lamp will go on and remain on until the starting action is completed. The upper contacts of RY_2 then excite the filament transformer of the rectifier tube, and apply alternating voltage to the plates of the tube. When the cathode has reached conduction temperature, RY_1 will be energized, closing its contacts across the plate ON buttons. As soon as the plate contactors close, RY_1 will operate, opening its contacts and releasing RY_2. Thus the transmitter has been given one starting impulse. Subsequent starts will not require a full 10 seconds if the tube has not fully cooled. Obviously, RY_2 cannot be picked up when the plates are on or the master control off, eliminating the possibility of accident through a "stored up" start.

Resistors R_1 and R_2 are for dropping the pilot lamp and RY_3 voltages to the proper values from the 220-volt relay circuit used at KMOX. C_1 is shown across RY_3 coil for removing the chatter if RY_3 is a d-c relay. It will not be necessary if an a-c relay is used.

Carrier-Interruption Timing Device

This auxiliary device records the time at which a transmitter breakdown occurs, as well as its duration, permitting the operator to give his entire attention to the cause and repair of the failure without having to note the time both before and after the repair period. It is, like most automatic instruments, capable of greater accuracy than can be obtained by mere observation.

The KMOX timer is shown diagramatically in Fig. 0. Its operation is similar to that of the carrier-protective device described above. The control element is the carrier wave, a bit of which is rectified and used to develop positive grid voltage for the tetrode section of the 117L7 tube, also cathode biased. When the carrier is on, RY_1 and RY_2 are energized, and clocks CL_1 and CL_2 are running, while CL_3 is stopped. All three clocks are self-starting. CL_1 keeps correct time, running continuously.

When the carrier is interrupted, RY_1 and RY_2 are de-energized, CL_2 is stopped, and CL_3 is started. CL_2, therefore, determines the time that the interruption occurred. When the carrier is restored, RY_2 is picked up, stopping CL_3. This clock thus determines the duration of the interruption. RY_1 is not picked up by the carrier, for its coil is shorted through its own de-energized contact and the reset button. After the operator has noted the time of the breakdown, the reset button is pushed, allowing RY_1 to become energized and returning the instrument to its original condition.

The clocks may be set by means of switches 1, 2, and 3, at the operator's convenience. CL_2, normally running, keeps correct time until the carrier is stopped, and CL_3 is set at 12:00, ready to time any interruption in terms of hours, minutes, and seconds by direct reading.

Coil is Interlocked

The coil of RY_1 is interlocked through an energized contact on RY_2 to insure simultaneous opening of both relays. This interlock may not be necessary in all cases, depending on the characteristics of the relays used.

The diode circuit is similar to that of the carrier-protective device, with two notable exceptions. C_2L_1 is tuned exactly to the carrier frequency, C_2 being fixed if desired and the tank tuned by removing turns from L_1. The other, and major exception, is the substitution of C_4, an 8-μf capacitor, for the tetrode grid leak. This provides a time delay of about one second, the time required for C_4 to discharge to the point where the bias limits the plate current to the point where it will no longer energize RY_1 and RY_2. The delay is incorporated to keep the instrument from operating on a normal reset due to overload, since this is not considered an interruption.

A grid leak is not necessary because of the conduction through the electrolyte of C_4. Cathode bias resistor R_1, being 1000 ohms, will bias the tube to a value numerically equal in volts to the plate current in ma. This provides a convenient test consideration, and leads are incorporated for measuring the bias with a voltmeter. When properly adjusted, the bias should be about 15 v with the carrier on and about 8 v with no signal. The circuit C_2L_1 may be tuned by adjusting for maximum bias voltage. Capacitor C_1 isolates the antenna and limits the r-f input. The circuit arrangement operates all the clocks on a 117L7 tube failure, and this calls the attention of the operator to the failure.

Foolproof Cuing System for Broadcast Stations

By JOSEPH ZELLE

BROADCAST STATIONS frequently use part of their regular channel equipment in special circuits, for routine tests and other similar operations. Unless precautions are taken temporary circuits may cause embarrassment when programs are placed on the air. The accompanying diagram illustrates a simple changeover circuit which reduce the human error to a minimum. The success of its operation is entirely dependent upon the type of switch used. Among those suggested are the Western Electric type 479 non-locking key and the type 392 push-button key. Where remote control is required a type "E" relay made by the same company can be substituted in conjunction with a push-button, or the relay may be actuated by other conventional means.

A specific application of this circuit is in the control room of a broadcast studio. The studio engineer must frequently "spot" or "cue" records before going on the air. That is, he must set the pickup needle about a half turn ahead of the music to allow the turntable to attain normal speed and must still start playing immediately after the announcer's introduction. In order to cue the record, part of the regular circuit must be used temporarily without placing it on the air. Sometimes the operator blunders when switching.

Circuit Details

The cuing system presented here provides a mechanical safety feature which is practically foolproof. It is simple to install and parts can be salvaged from almost any radio shop. Readily available switches can be easily revamped to make and break the necessary circuits.

With the key in the neutral position the cuing monitor is disconnected. To operate the cue monitor the operator simply holds the key in the cuing position. Since the key (or relay) is non-locking, there will be no danger of putting the pickup on the air as long as the key is held down. Releasing the key will connect the pickup to normal circuits. Thus, once the studio engineer becomes accustomed to "push to cue" it will become second nature with him.

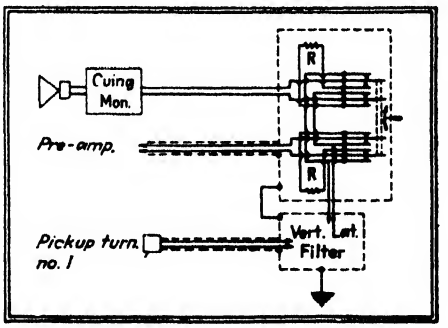

Circuit of foolproof cuing system. The value of input-shorting resistors R is not critical

The system especially proves its worth during moments of confusion or programming error, when time is at a premium. With this system the controlroom engineer can quickly cue the record with perfect confidence, and worry only about the program detail to be aired. The moment he releases the key after cuing, the pickup will be on the air if the regular gain control is open. Furthermore, since the pickup is monitored after the "Vertical-Lateral Filter"

control, the danger of playing transcriptions with the wrong filter is virtually eliminated.

Installation is simple. The shielded leads from the filter and pickup in the turntable cabinet are cut and the switch inserted as shown in the diagram. Then, to prevent accidental open inputs, resistors R are so placed that they short-circuit either the cuing monitor or pre-amplifier when these are not in use.

The cuing monitor can be placed in the turntable cabinet to avoid complicated wiring.

Grounded-Grid Power Amplifiers

Radio-frequency power amplifiers using grounded-grid circuits operate at higher frequencies and can handle wider bandwidths than capacitance-neutralized grounded-cathode circuits. These advantages suit the grounded-grid circuit to television, f-m, and industrial uses

By E. E. SPITZER

There are three practical ways of utilizing a triode as an amplifier. The most common way is to apply the input signal between grid and filament terminals and take output from plate and filament. A second way is to apply input to grid and plate and take output from filament and plate. This type of amplifier is known as a cathode follower. The third way is to apply input to grid and filament and take output from plate and grid. There is no generally accepted name for this type of amplifier. It has been variously called grounded-grid amplifier, inverted amplifier, and common grid circuit because the grid is common to the input and output circuits. According to this terminology, the normal amplifier would be called a common cathode circuit, and the cathode follower would be a common plate circuit. In this article, the designation grounded-grid will be employed since it has been used fairly widely.

Problems of Tube Design

Consider a normal triode circuit with input applied between grid and filament and a tuned output circuit between plate and filament. The filament is grounded. It is well known that such an amplifier will oscillate by itself at some undesired frequency because of feedback through the grid-plate capacitance of the tube. The cure for this difficulty is neutralization. However, as the frequency is increased, neutralization becomes increasingly difficult to handle. Because feedback is caused by capacitance between grid and plate and because any external neutralizing circuit is isolated from the internal capacitance by the inductances of grid and plate leads, the frequency band over which the tube can be neutralized becomes narrower and narrower with increasing frequency and finally vanishes altogether. Another undesirable effect is that capacitance neutralization serves to increase the input and output capacitances of the amplifier. For example a push-pull cross-neutralized amplifier has an output capacitance per tube equal to the plate-filament capacitance of the tube plus twice the grid-plate capacitance. This resultant high capacitance narrows the r-f bandwidth that can be handled or it may reduce the efficiency of the amplifier because of excessive circulating kilovoltamperes.

Tetrodes and pentodes were developed to overcome the foregoing difficulties. In these types of tubes, the screen and suppressor shield the control grid from the plate so that the feedback capacitance is low enough to make neutralization unnecessary. However, as the frequency is increased, self-oscillation may occur if the screen and suppressor leads have appreciable in-

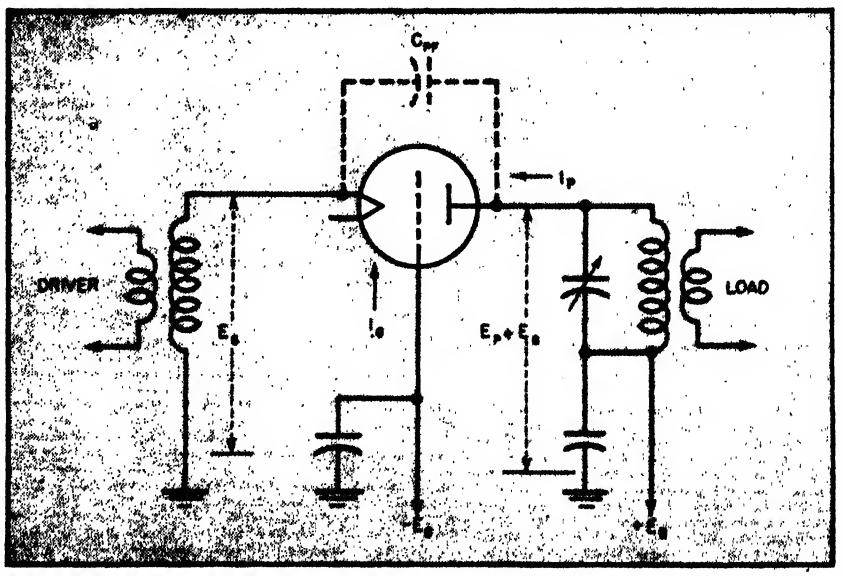

FIG. 1—Circuit and parameters of grounded-grid r-f power amplifier

ductance. Then, these grids cannot be held effectively at r-f ground potential and, as a result, feed-through may occur. Twin tubes such as the RCA-829B were designed to overcome this difficulty. In a twin tube designed for push-pull operation, screen grids and cathodes can be intimately connected within the tube so that practically no inductance is present between these electrodes. Tubes of this design give excellent performance. The only difficulty is that tube cost for a twin-pentode tends to be high compared to the cost of triodes or triodes for equivalent power output capability.

Circuit Characteristics

The grounded-grid circuit is a way of using a triode which reduces the possibility of self-oscillation without the need for neutralization. Figure 1 shows a grounded-grid amplifier circuit, in which the control grid acts as shield between plate and cathode to reduce feedback capacitance C_{PF}. Thus, the control grid performs one function of a screen grid in a tetrode.

A second characteristic of the grounded-grid circuit is that the driver tube and output tube act in series to supply the load. In Fig. 1, the driver produces an r-f voltage E_G across the input terminals of the output tube. The latter has an r-f voltage E_P across its plate and cathode. These voltages are 180 degrees out of phase with respect to the cathode so that the r-f voltage from plate to grid and also across the output circuit is $E_P + E_G$. If I_P is the fundamental component of plate current 180 degrees out of phase with E_P, and I_G is the fundamental component of grid current in phase with E_G, the following relations then hold

Power delivered to load circuit = $(E_P + E_G)I_P$
Power delivered by output tube = $E_P I_P$
Driver power transferred to load circuit = $E_G I_P$
Power delivered by driver circuit = $E_G(I_P + I_G)$
Power absorbed by output tube = $E_G I_G$

It is apparent from these relationships that driver tube and output tube act in series to supply the load circuit. Power output, therefore, is higher than would be expected and the conventional efficiency, based on the input to the output tube, is unusually high.

The foregoing discussion brings out a third characteristic. The driving power of a grounded-grid amplifier is higher than when the same tube is used in a normal triode circuit and may be three to ten times greater. However, this increased power is not lost; it is merely transferred to the plate circuit and appears as output, as explained above.

A fourth characteristic is lower output capacitance. In a grounded-grid circuit, output capacitance is approximately C_{GP}, whereas in a normal capacitance-neutralized amplifier the output capacitance is more than twice this value. This fact is most important at high frequencies because lower output capacitance results in increased r-f bandwidth-handling capabilities and in lower circulating kva in the output circuits.

All of the foregoing characteristics are advantageous with the exception of the increased driving power. The latter is a disadvantage because it may require more or bigger amplifier stages in the transmitter design. Because a pentode or beam tetrode does not have this disadvantage, the field of application of grounded-grid amplifiers is at fre-

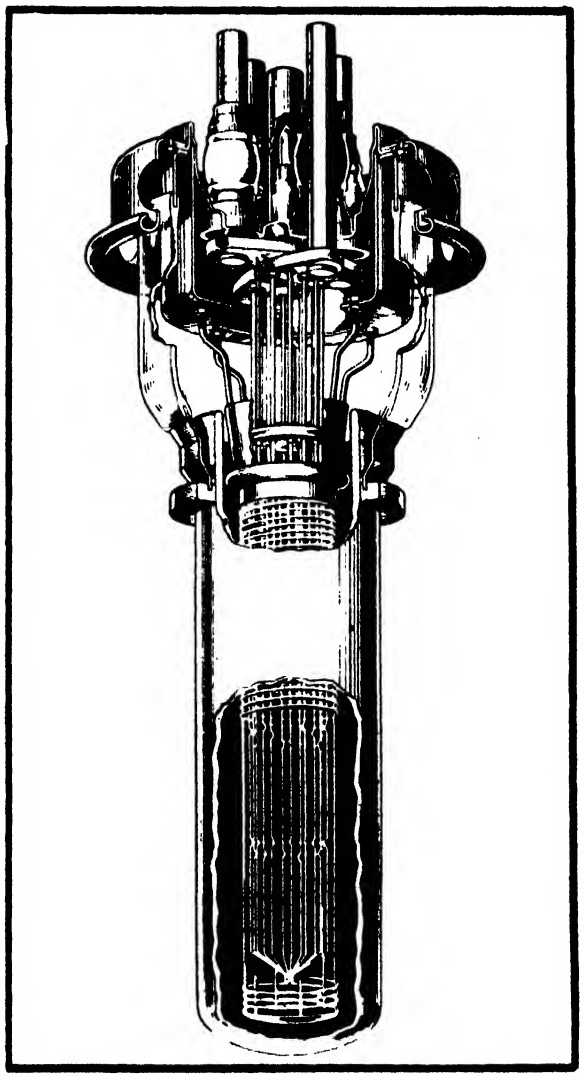

FIG. 2—Cut-away view showing method of extending grid cylinder to complete the shielding between filament and plate circuits in a triode especially designed for grounded-grid circuits

quencies at which pentodes are not available for the desired power, or where the cost of pentodes is greater than the cost of additional driving stages required by the grounded-grid circuit. Present indications are that the frequency and power boundaries are about as follows

Power in Kw	*Frequency in Mc*
0.1	300
25	30
100	10

For the stated power, the grounded-grid circuit becomes desirable at a frequency above that listed.

Most of the characteristics which make a triode desirable in a normal circuit also make it desirable in a grounded-grid circuit. However, there are some additional requirements for a good grounded-grid tube. It has been stated above that the grid and its associated external ground plane should act as a screen between anode and cathode and their respective circuits. Therefore, the tube should be so designed that the anode and cathode connections are on opposite sides of the grid connection. For example, a tube which has an external anode with the grid terminal insulated from one end and the filament terminal insulated from the other end is not at all suited for grounded-grid operation. On the other hand, a tube such as the 9C21 illustrated in Fig. 2 is ideally suited for grounded-grid operation because the grid terminal is a large metal flange which can be connected to a metal shield separating the anode circuit from the cathode circuit. In addition, the grid support of the 9C21 has very low inductance and, therefore, meets the second requirement for a good grounded-grid triode.

Let it be required to design a grounded-grid stage utilizing one 9C21 triode. The tube will be used in the circuit shown in Fig. 1. The manufacturer's data show the following typical operating conditions for normal grounded-cathode circuits

D-c plate voltage = 17,000 v
D-c grid voltage = −1,600 v
Peak r-f grid voltage = 2,200 v
D-c plate current = 7.9 amp
D-c grid current = 0.9 amp
Driving power = 1,800 w
Power output = 100 kw

Amplifier Design

It is first necessary to obtain the r-f plate voltage swing E_p. This can be estimated from the fact that in a properly excited class-C amplifier, the plate voltage will swing down to the value of the peak positive grid voltage. Because the value of the latter is equal to 2,200 minus 1,600 volts, or 600 volts, E_p is

$2^{-\frac{1}{2}}(17{,}000-600) = 11{,}600$ volts rms.

Next, the fundamental components of plate current and of grid current must be obtained using the power output and driving power values given above

$$I_p = \frac{100{,}000}{11{,}600} = 8.63 \text{ amperes}$$

and

$$I_g = \frac{1{,}800\sqrt{2}}{2{,}200} = 1.16 \text{ amp.}$$

The output power and the driving

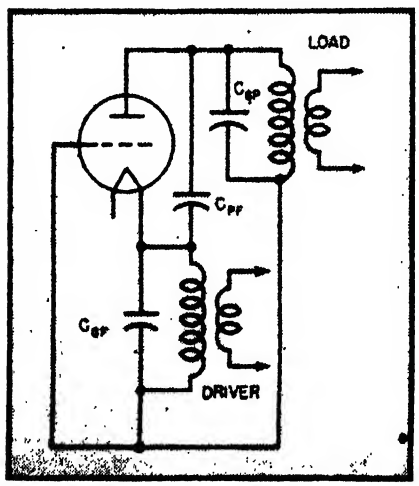

FIG. 3—Rearrangement of circuit of Fig. 1 shows that the grounded-grid amplifier is similar to the Colpitts oscillator

power of the grounded-grid stage can now be calculated from the relations given earlier. We obtain

$$\text{Power output} = (E_p + E_g) I_p$$

$$= \left(11{,}600 + \frac{2200}{\sqrt{2}}\right) 8.63 = 113 \text{ kw.}$$

$$\text{Driving power} = E_g(I_p + I_g)$$

$$\frac{2200}{\sqrt{2}} (8.63 + 1.16) = 15.2 \text{ kw.}$$

It is possible to change the power output to some extent by varying the grid bias and the grid swing. For example, if the bias should be changed from −1,600 to −2,000 volts and the grid swing by a like amount, i.e., to 2,600 volts, the power output would be 116 kilowatts.

A grounded-grid amplifier stage can go into self-oscillation, particularly at high frequencies, because of feedback from plate to cathode through the plate-filament capacitance. This action is more easily understood if the amplifier stage is redrawn as a Colpitts oscillator circuit, as shown in Fig. 3. Because we are dealing with the worst conditions, inductive tuning only is assumed. The output circuit must be inductive at the oscillation frequency, as the following analysis proves.

Conditions for Oscillation

It is well known that circuit reactance between filament and grid must be capacitative and, furthermore, should be at least one-fifth the reactance between plate and filament. This reactance will produce an excitation ratio, that is, a ratio of plate swing to grid swing, of five. In any good grounded-grid tube, the plate-filament capacitance will be so low that its ratio to the grid-filament capacitance will be much less than one-fifth. Thus, to produce oscillation, the input circuit must be inductive so as to reduce the effective capacitance between grid and filament to a value about five times that of the plate-filament capacitance. With tuned input circuits, this condition can easily be fulfilled. Let it be assumed that this condition is exactly fulfilled.

The total tank circuit capacitance is then

$$C_T = C_{pp} + \frac{5\, C_{gp}\, C_{pp}}{C_{gp} + 5\, C_{pp}}$$

In the case of 9C21, this capacitance would be

$$C_T = 1.8 + \frac{48 \times 5 \times 1.8}{48 + 5 \times 1.8} = 9.4 \ \mu\mu f$$

Thus for this 100-kw tube, the tank capacitance for parasitic oscillation is only 9.4 $\mu\mu$f, a value which is quite small. This capacitance will

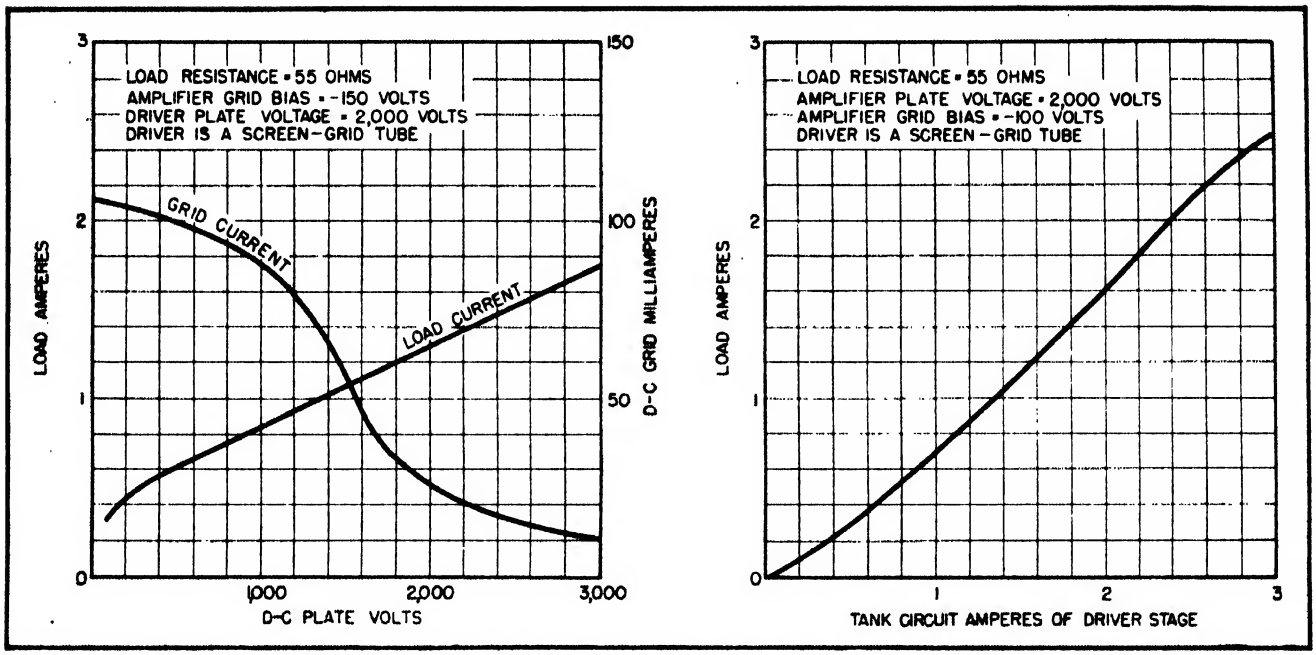

FIG. 4—Plate modulation characteristic of grounded-grid r-f amplifier

FIG. 5—Class-B power amplification characteristic of grounded-grid circuit

store only appreciable amounts of power at high frequencies. Assume operation at a frequency of 20 mc. The reactance of C_T is then 850 ohms. If the tube is operated at 12 kilovolts with a plate swing of 11.6 kilovolts, the reactive power is $(11,600/2)^2/850 = 80$ kilovoltamperes.

We also know that oscillator stability necessitates an operating Q of at least 12. Therefore, in the above case, the circuit could be loaded to 6.7 kw. If all the circuit losses, including driving power and any power delivered to the load, are less than 6.7 kw, the tube will oscillate with certain adjustments of the input and output circuits. If we assume that the normal output circuit loss is five percent of 100 kw, or 5 kw, this value plus the driving power and the normal load coupled to the tube would be sufficient to make the amplifier stable at the assumed frequency.

Modulation Characteristics

When plate modulation of only a grounded-grid amplifier stage is attempted, a characteristic such as illustrated in Fig. 4 is obtained. It will first be noted that grid current varies widely with plate voltage. As the plate voltage increases, the plate current also increases and causes an increasing load on the driver stage. Due to the regulation of the latter, driving voltage decreases and with it grid current. This decrease of grid current is quite large and is characteristic of this type of amplifier.

Over quite a range of plate voltage, the output current is linear with plate voltage as in the case of conventional class C amplifiers. However, at low voltages load current departs from linearity and will not be zero until negative values of plate voltage are reached. This phenomenon is due to the fact that r-f driving voltage and d-c plate supply voltage are in series as shown in Fig. 1. As a result the plate not only has a d-c supply voltage but also simultaneously an r-f supply voltage. Therefore, the plate current and the load current do not drop to zero until a value of negative plate voltage equal to the value of the peak driving voltage is reached. Accordingly, the resultant characteristic of modulating only a grounded-grid stage shows distortion unless one is satisfied with partial modulation. To obtain a modulation characteristic which will permit 100-percent modulation, it would be necessary to modulate simultaneously one or more successive stages.

The above problem is of little practical consequence because amplitude modulation is rarely used at the high frequencies for which the grounded-grid circuit is particularly applicable. The problem does not exist for such services as frequency-modulation, television and industrial power.

When a grounded-grid amplifier is used as a linear, class-B r-f amplifier, quite satisfactory results are obtained, as shown in Fig. 5. Such an amplifier could be used to amplify television signals.

Bibliography

(1) Alexanderson, E. F. W., U. S. Patent 1,696,534, filed May 13, 1927, granted Feb. 7, 1933.

(2) Spitzer, E. E., "Grounded-Grid Operation of Triodes as Class B and C Amplifiers", an unpublished report dated Dec. 22, 1930.

(3) Lindenblad, N. E., U. S. Patent 2,136,448, filed Apr. 14, 1932, granted Nov. 15, 1938.

(4) Romander, H., "The Inverted Ultraudion Amplifier" *Q.S.T.*, p 14, Sept. 1933.

(5) Potter, R. K., U. S. Patent 2,088,722, filed June 12, 1936, granted Aug. 3, 1937.

(6) Strong, C. E., The Inverted Amplifier, ELECTRONICS, p 14, July 1940.

(7) Labin, E., Design of the Output Stage of a High Power Television Transmitter, *Electrical Communication*, 20, No. 3, p 193, 1942.

(8) Gurewitsch, A. M., Cavity Oscillator Circuits, ELECTRONICS, p 185, Feb. 1946.

TUBES

Filament and Heater Characteristics

Mathematical analysis of volt-ampere characteristics of various filament metals. Resulting equations are plotted as a reference chart that gives filament current, temperature and wattage for any electron tube at various operating voltages with good accuracy

By CECIL E. HALLER

FREQUENTLY in the design and application of electron tubes it is necessary to predict the value of filament current and possibly also the filament temperature when the applied filament voltage deviates from the normal or rated value. Such an instance occurs when two or more filaments having different volt-ampere characteristics are operated in series and it is required to predict the voltage variation across each individual filament with respect to the supply voltage variation. The solution of this problem requires a knowledge of the volt-ampere characteristic of each filament. The voltage across each filament can then be determined for any arbitrary assumed current value. If appropriate current values are chosen, a curve of each individual tube voltage versus the supply voltage can be constructed.

A knowledge of the individual volt-ampere characteristics over the required range may not be readily available unless it has previously been experimentally determined. It is the purpose of this paper to indicate a method of constructing the volt-ampere characteristic if the current is known for at least one operating voltage. The knowledge of this point enables the current to be predicted at a new operating voltage with good accuracy providing the change in voltage is within approximately ±25 percent of the known voltage. The same analysis will also permit the determination of the value of watts and temperature in terms of the known operating condition.

Basic Filament Equations

In order to illustrate the method of transposing the operating condition of a filament, the two basic equations involved in the design of filaments and heaters for electron tubes will be considered.

The first equation is:

$$W = K_1 T^{n_w}$$

where

W = power radiated in watts
K_1 = constant of proportionality, which includes the area of the emitter
T = temperature in degrees Kelvin
n_w = an exponent which is reasonably constant for a given metal over a limited range of temperature.

The second equation is:

$$W = E^2/R = I^2R$$

where

E = applied filament voltage
R = resistance of the filament, which is in general a function of temperature
I = filament current

In order to solve Eq. (1) and (2) let

$$R = K_2 T^{n_r}$$

where

K_2 = a constant of proportionality
n_r = an exponent which may be regarded constant over a limited temperature range.

Solutions of Eq. (1), (2) and (3) for W, I, and T in terms of E yield:[1]

$$W = K_1\left(K_1K_2\right)^{\frac{2n_w}{n_w+n_r}}\left(E\right)^{\frac{2n_w}{n_w+n_r}} \quad (4)$$

$$I = \left(\frac{K_1}{K_2}\right)^{\frac{n_w-n_r}{2}}\left(\frac{1}{K_1K_2}\right)^{\frac{2}{n_w+n_r}}\left(E\right)^{\frac{n_w-n_r}{n_w+n_r}} \quad (5)$$

$$T = \left(\frac{1}{K_1K_2}\right)^{\frac{2}{n_w+n_r}}\left(E\right)^{\frac{2}{n_w+n_r}} \quad (6)$$

Thus, when using W_o, I_o, T_o, E_o and W_s, I_s, T_s, E_s as the known and unknown conditions respectively, Eq. (4), (5) and (6) may be written:

$$\frac{W_s}{W_o} = \left(\frac{E_s}{E_o}\right)^{\frac{2n_w}{n_w+n_r}} \quad (7)$$

TABLE I. VALUES OF EXPONENTS FOR FOUR FILAMENT METALS

Material	Temp.	n_w	n_r	$\frac{2n_w}{n_w+n_r}$	$\frac{n_w-n_r}{n_w+n_r}$	$\frac{2}{n_w+n_r}$
Tungsten[1]	1000°K	5.65	1.20	1.68	0.650	0.292
Tungsten[1]	2000°K	4.93	1.19	1.61	0.612	0.327
Tungsten[1]	2500°K	4.66	1.20	1.59	0.590	0.341
Molybdenum[2]	1000°K	5.32	1.15	1.64	0.645	0.309
Molybdenum[2]	2000°K	4.99	1.15	1.63	0.625	0.296
Tantalum[3]	1600°K	4.80	0.785	1.72	0.720	0.358
Tantalum[3]	2800°K	4.80	0.785	1.72	0.720	0.358
Nickel	1000°K	4.65*	0.62**	1.76	0.764	0.379

* Values by different investigators range from 4.65 to 5.29.
** Estimated from experimental data on nickel.

$$\frac{I_2}{I_e} = \left(\frac{E_2}{E_e}\right)^{\frac{n_w - n_r}{n_w + n_r}} \quad (8)$$

$$\frac{T_2}{T_e} = \left(\frac{E_2}{E_e}\right)^{\frac{2}{n_w + n_r}} \quad (9)$$

Use of Average Values for Exponents

Values for n_w have been determined for some of the more common metals, and are given in Table I. The exponent n_w includes the change of total emissivity with temperature. Since the total emissivity of metals increases with temperature,[8] the Stefan-Boltzmann law of radiation requires that n_w be greater than four. For materials having an emissivity independent of temperature the value will be four. The value of n_r for some metals at different temperatures is also given in Table I. These limited data indicate n_r ranges from 0.6 to 1.2.

If W_1 and W_2, the watts radiated at temperatures T_1 and T_2 are known, then

$$n_w = \frac{\log (W_1/W_2)}{\log (T_1/T_2)}$$

In a like manner, if R_1 and R_2 are the resistances at temperatures T_1 and T_2, then

$$n_r = \frac{\log (R_1/R_2)}{\log (T_1/T_2)}$$

These permit an experimental check of the values of n_w and n_r if two sets of operating conditions are known.

Table I also gives the value of $(n_w - n_r)/(n_w + n_r)$. It will be noted that it ranges from 0.59 to 0.76. It is now of interest to see what error results in using an average value of this exponent in Eq. (8). A voltage ratio E_2/E_e of 1.25 will be taken as the maximum voltage for which Eq. (8) is to be used. If the exponents 0.59 and then 0.76 are used, the respective values of current ratio I_2/I_e are 1.140 and 1.185 or a deviation of only ±1.9 percent from the mean value.

It is evident therefore that an average exponent can be chosen which applies to all the metals in Table I, and in general

$$\left(\frac{I_2}{I_e}\right) = \left(\frac{E_2}{E_e}\right)^{0.61}, \quad 0.75 < \left(\frac{E_2}{E_e}\right) < 1.25 \quad (10)$$

is true to sufficient accuracy for most engineering purposes. This equation has been drawn as the current curve for the chart in Fig. 1.

It can further be shown that the accuracy involved in assuming $2n_w/(n_w + n_r) = 1.61$ and $2/(n_w + n_r) = 0.327$ is even greater than for the case just discussed. Then

$$\frac{W_2}{W_e} = \left(\frac{E_2}{E_e}\right)^{1.61} \quad (11)$$

$$\frac{T_2}{T_e} = \left(\frac{E_2}{E_e}\right)^{0.327} \quad (12)$$

These equations are plotted in Fig. 1.

In order to check Eq. (8) and Fig. 1, data were taken for a wide variety of electron tubes. It will be noted from Fig. 1 and Table II that the calculated values of current deviate, in general, by less than ±4 percent from the measured values. We can conclude from this that Fig. 1 is generally applicable to all types of electron tubes for the specified range of (E_2/E_e).[8] Some samples of the use of this curve will now be given.

Example 1. The type RCA-826 has a thoriated-tungsten filament rated at 7.5 volts and 4 amperes. What will be the filament current at 5.62 volts (75 percent of rated voltage)? Tracing up from 75 on the horizontal scale in Fig. 1 to the current curve, and then across, gives 83.8 percent. The new filament curve is then $0.838 \times 4 = 3.35$ amperes. By actual measurement the current was found to be 3.34 amperes. While no temperature measurements were made at this voltage one would expect the temperature to decrease to 91 percent of its rated value in degrees Kelvin.

Example 2. An oxide-coated cathode has a temperature of 1000 deg. K when the heater is operated at 5 volts. What voltage will be required to increase the temperature to 1060 deg. K? From Fig. 1, when $T_2/T_e = 1.06$ one finds $E_2/E_e = 1.19$ or $E_2 = 5 \times 1.19 = 5.95$ volts. The heater voltage was found to be 6.0 volts when determined experimentally. If the voltage had been increased to 7 volts, then $E_2/E_e = 1.4$ and $T_2/T_e = 1.118$ or $T_2 = 1118$ deg. K. Actual measurements indicated the temperature to be 1135 deg. K.

In order to examine the operation of filaments or heaters in series, let two tubes T_1 and T_2, having the same nominal voltage rating, be connected in series to a power supply E_s (see Fig. 2). In general the filaments of tubes T_1 and T_2 may have different volt-ampere characteristics. Such differences may be due to the individual variation of filament current when read at a specified or rated voltage. These variations of filament currents, which are expected and normal, result from the necessary manufacturing tolerances on both materials and processes.

The usual filament current tolerance on receiving and the smaller transmitting tubes whose filaments or heaters might be operated in series is generally of the order of 5 to 10 percent. In order to insure satisfactory operation initially and throughout the expected life of the tube, the tube manufacturer usually specifies the percentage the applied filament voltage may be allowed to deviate from normal. This voltage deviation is usually of the order of ±5 percent for the thoriated-tungsten type emitters and ±10 percent for the oxide-coated filament or heater-cathode types. It becomes apparent that for series operation of the filament or heaters the supply voltage variation needs careful consideration in order to insure that the individual filament voltage tolerances are not exceeded on either T_1 or T_2.

If T_1 and T_2 are both high or both low filament-current tubes, no problem exists since the volt-ampere characteristics are substantially identical (i.e., they have the same currents for the same applied voltage). Only the combination needs to be considered, where one has the higher limit value and the other has the lower limit value of filament current.

As a specific problem, assume the filament-current tolerance to be ±5 percent and let it be required to determine the permissible varia-

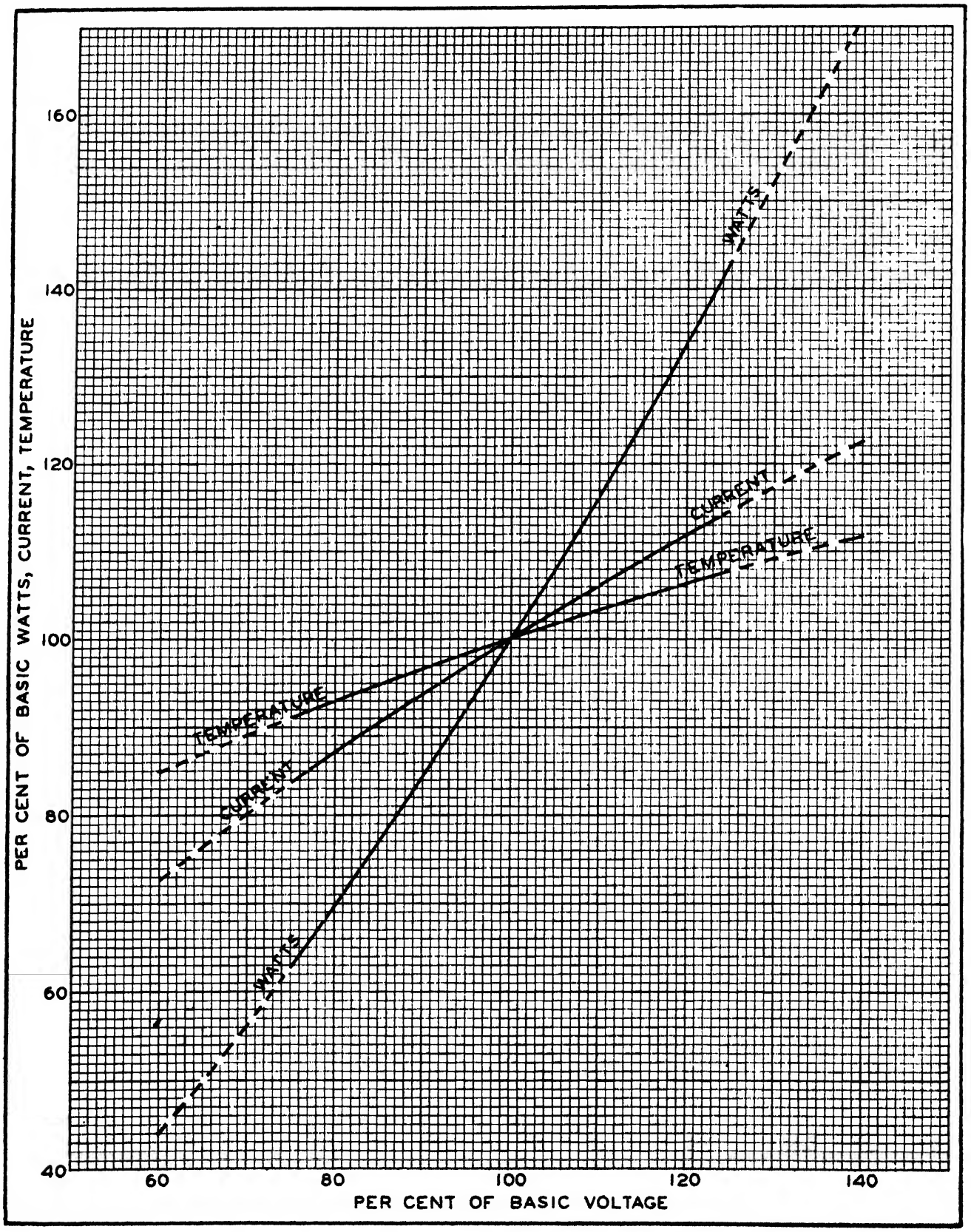

FIG. 1—Chart giving wattage, current and temperature of a filament or heater at operating voltages up to 25 percent above or below basic voltage, with sufficient accuracy for most engineering purposes. Accuracy drops in dotted regions

tion of supply voltage without exceeding an individual tube voltage range of ±10 percent. This problem frequently arises in the design of mobile transmitters when the filament or heaters are operated in series.

The bogie or normal volt-ampere characteristic *BKE* of Fig. 2 may then be constructed from Eq. (10). For T_1, the 5 percent high filament-current tube, the equation of the volt-ampere characteristic is

$$\frac{I_x}{I_o} = 1.05\left(\frac{E_x}{E_o}\right)^{0.61} \qquad (13)$$

Curve *AJD* can be constructed from this equation.

Similarly for T_2, the low filament-current tube, the equation is

$$(I_x/I_o) = 0.95\,(E_x/E_o)^{0.61} \qquad (14)$$

which is represented by the curve *CLF* in Fig. 2.

An arbitrary current may then be assumed in order to determine the individual voltage across tubes T_1 and T_2. The supply voltage is represented by the sum of the voltages across T_1 and T_2. If T_1 (the high filament-current tube) has the minimum permissible voltage 0.9 E_o represented by point *A*, tube T_2 (the low filament-current tube) will have a voltage represented by point *O*. The sum of the two voltages at points *A* and *O* represents the minimum permissible supply voltage consistent with the previous imposed condition of ±5 percent filament-current tolerance and ±10 percent individual voltage tolerance.

In a similar manner the maximum voltage 1.1 E_o that can be applied to T_2, the low filament-current tube, is represented by point *F*, and the voltage on T_1, the high filament-current tube, by point *G*. The sum of the voltages at points *G* and *F* gives the maximum permissible supply voltage. The nominal supply voltage is twice the nominal tube voltage or 2 E_o since it was assumed the nominal voltage ratings of T_1 and T_2 were identical. The maximum permissible percentage of supply voltage deviation may then be calculated directly from the graphical analysis. This solution

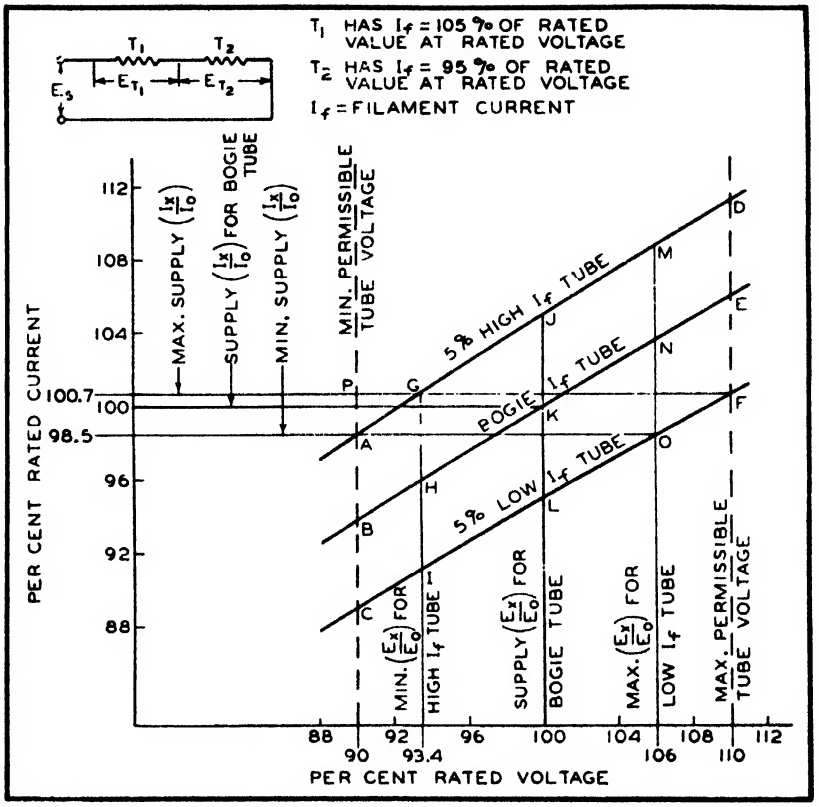

FIG. 2—Volt-ampere characteristics for series operation of filaments or heaters having different characteristics

indicates supply voltage tolerance of +1.7 percent and −2.0 percent.

It is interesting to note that the distance *A* to *P* represents the maximum permissible range of supply current. This suggests that if the supply voltage cannot be maintained within the required limits, a series ballast tube whose current is maintained within the range *A* to *P* might be used to permit a larger variation in the supply voltage. The use of the ballast tube would of course require an increased supply voltage in order to supply the required voltage drop of the ballast tube.

An alternative solution to permit wider supply voltage tolerances consists in shunting the low filament-current tube with a resistor. This resistor is adjusted until both tubes have substantially the same filament voltage. This method is essentially one of shifting the operating point on the volt-ampere characteristic of the low filament-current tube and resistor until at normal supply voltage it coincides with that of the high filament-current tube. This method does not, however, make the volt-ampere characteristics identical and therefore never can permit a percentage supply-voltage change equal to the permitted percentage of individual filament voltages. In order to simplify adjustments, adjustable resistors are frequently used across both filaments.

Generalized Solution for Tubes in Series

The method of the solution of two tubes in series may be generalized for N_H tubes having high filament currents in series with N_L tubes having low filament currents, as shown in Fig. 3. Let

m = percentage filament-current tolerance

p = permissible percentage tolerance of individual applied voltage

The volt-ampere characteristic of a limit tube is expressed by

$$\left(\frac{I_x}{I_o}\right) = \left(\frac{100+m}{100}\right)\left(\frac{E_x}{E_o}\right)^{0.61} \qquad (15)$$

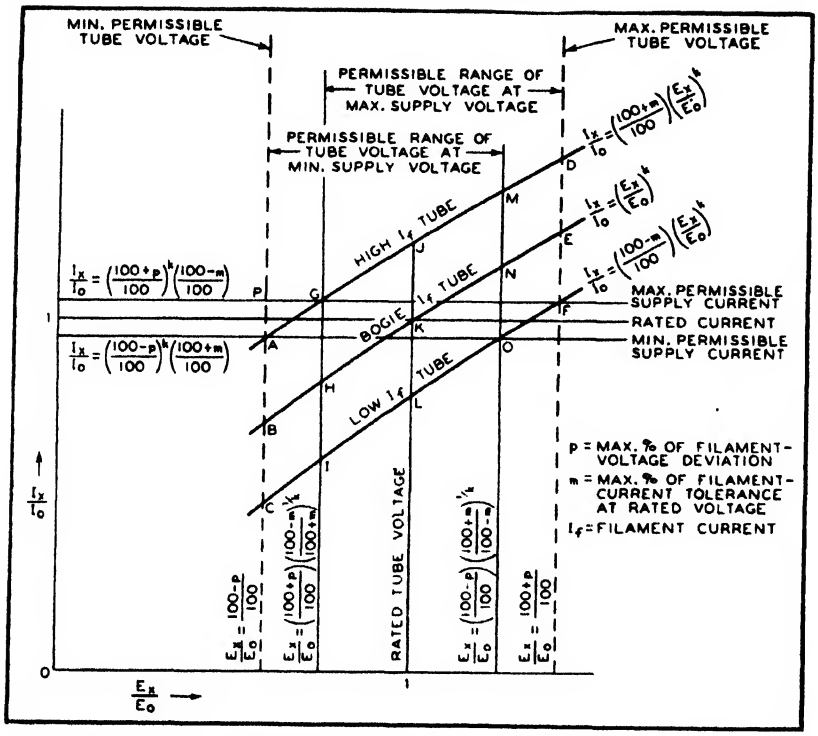

FIG. 3—Generalized solution for any number of tubes in series, some having high and some low filament current

But since E_x/E_o for the limiting condition of maximum voltage on a low filament-current tube is equal to $(100 + p)/100$, Eq. (15) may be re-written for a low filament-current tube as

$$\left(\frac{I_x}{I_o}\right)_{max.} = \left(\frac{100 + p}{100}\right)^{0.61}\left(\frac{100 - m}{100}\right) \quad (16)$$

where I_x/I_o is the maximum permissible supply current when at least one each of limit values of high and low filament-current tubes are operated in series. Similarly, the minimum permissible current is given by

$$\left(\frac{I_x}{I_o}\right)_{min.} = \left(\frac{100 - p}{100}\right)^{0.61}\left(\frac{100 + m}{100}\right) \quad (17)$$

Equations (14) and (15) form the basis for calculating the current requirements imposed upon a series ballast tube should one be used.

The values of current given in Eq. (16) and (17), when substituted in the appropriate equations for the volt-ampere characteristics, give the voltage at points G and O respectively as

$$\left(\frac{E_x}{E_o}\right) = \left(\frac{100 + p}{100}\right)\left(\frac{100 - m}{100 + m}\right)^{1.64} \quad (18)$$

and

$$\left(\frac{E_x}{E_o}\right) = \left(\frac{100 - p}{100}\right)\left(\frac{100 + m}{100 - m}\right)^{1.64} \quad (19)$$

The value of (E_x/E_o) given in Eq. (18) represents the voltage across a high filament-current tube at the maximum permissible supply voltage, while the value given in Eq. (19) represents the voltage across a low filament-current tube at the minimum permissible supply voltage. The sum of N_H voltages given in Eq. (18) + N_L voltages of the value $(100 + p)/100$ gives the maximum supply voltage or

$$\left(\frac{E_s}{E_o}\right)_{max.} = N_H\left[\left(\frac{100 + p}{100}\right)\left(\frac{100 - m}{100 + m}\right)^{1.64}\right] + N_L\left(\frac{100 + p}{100}\right) \quad (20)$$

In a like manner the minimum supply voltage is

$$\left(\frac{E_s}{E_o}\right)_{min.} = N_L\left[\left(\frac{100 - p}{100}\right)\left(\frac{100 + m}{100 - m}\right)^{1.64}\right] + N_H\left(\frac{100 - p}{100}\right) \quad (21)$$

The percentage of supply voltage tolerance becomes

$$\%\ E_s \text{ above normal} = \left\{\frac{N_H\left[\left(\frac{100 + p}{100}\right)\left(\frac{100 - m}{100 + m}\right)^{1.64}\right]}{N_H + N_L} + \frac{N_L\left(\frac{100 + p}{100}\right)}{} - 1\right\}100 \quad (22)$$

$$\%\ E_s \text{ below normal} = \left\{\frac{N_L\left[\left(\frac{100 - p}{100}\right)\left(\frac{100 + m}{100 - m}\right)^{1.64}\right]}{N_H + N_L} + \frac{N_H\left(\frac{100 - p}{100}\right)}{} - 1\right\}100 \quad (23)$$

Equations (22) and (23) were derived on the premise that at least one tube of the group had a filament current $(100 + m)/100$ times rated value and at least one other had $(100 - m)/100$ times rated value. This premise imposes the condition that both N_H and N_L must be different from zero in Eq. (22) and (23). If either N_H or N_L is zero, the solution is simple as all possess the same volt-ampere characteristic. The permissible supply voltage percentage deviation is p.

Application to Universal Receivers

It is common practice in the design of a-c/d-c sets in which the filaments or heaters are connected in series to use tubes that have different values of rated filament voltage. The analysis of this condition can be reduced to an expression similar to Eq. (22) and (23) except that N_H and N_L must include the equivalent number of respective tubes in terms of the lowest nominal voltage tube. For example, a 35-volt tube may be represented by 5.55 tubes of 6.3 volts nominal rating.

Substitution in Eq. (22) and (23) of the conditions of the previously discussed case of two tubes ($N_H = 1$ and $N_L = 1$) with $m = 5$, $p = 10$ and $(n_r - n_r)/(n_r + n_r) = 0.61$ gives +1.8 percent and −2.0 percent for the supply voltage tolerance, which is in good agreement with the graphical solution.

An examination of the case of three tubes in series where $N_H = 2$, $N_L = 1$, $m = 5$, $p = 10$, and $(n_r - n_r)/(n_r + n_r) = 0.61$ gives the tolerance on the supply voltage as −1 percent and −4.7 percent. In other words the supply voltage can never be permitted to rise to normal without exceeding the maximum voltage rating on the low filament-current tube.

The curves given in Fig. 1 enable the transposition of heater or fila-

TABLE II. MEASURED AND CALCULATED DATA ON TYPICAL TUBE SAMPLES

Type Number	Filament or Heater	Type of Emitter	Rated Voltage E_{r_r}	Rated Voltage I_{r_r} Observed	Reduced Voltage E_{r_1}	Reduced Voltage I_{r_1} Observed	Reduced Voltage I_{r_1} Calc. from Fig. 1	Reduced Voltage % Difference	Increased Voltage E_{r_2}	Increased Voltage I_{r_2} Observed	Increased Voltage I_{r_2} Calc. from Fig. 1	Increased Voltage % Difference
203A	Filament	Th-W	10.0	3.28	7.5	2.72	2.74	+0.7	12.5	3.70	3.76	+1.6
801A	Filament	Th-W	7.5	1.22	5.62	1.05	1.02	−0.3	9.38	1.42	1.40	−1.4
807	Cathode	Oxide	6.3	0.87	4.72	0.74	0.73	−1.4	7.88	0.99	1.00	+1.0
813	Filament	Th-W	10.0	5.00	7.50	4.12	4.18	+1.5	12.5	5.80	5.72	−1.4
815	Cathode	Oxide	6.3	1.65	4.72	1.39	1.37	−1.4	7.88	1.88	1.89	+0.5
826	Filament	Th-W	7.5	4.00	5.62	3.35	3.34	−0.3	9.38	4.55	4.58	+0.7
833A	Filament	Th-W	10.0	10.10	7.5	8.50	8.44	−0.7	12.50	11.60	11.56	−0.3
836	Cathode	Oxide	2.5	5.05	1.88	4.22	4.25	+0.7	3.13	5.75	5.78	+0.5
861	Filament	Th-W	11.0	10.05	8.25	8.30	8.40	+0.1	13.75	11.50	11.50	0
866	Filament	Oxide	2.5	5.00	1.87	4.03	4.18	+3.7	3.13	5.80	5.72	−1.4
913	Cathode	Oxide	6.3	0.600	4.72	0.504	0.502	−0.4	7.88	0.685	0.687	+0.3
1616	Filament	Oxide	2.5	4.90	1.87	3.97	4.10	+3.3	3.13	5.73	5.61	−2.1
1624	Filament	Oxide	2.5	1.83	1.87	1.47	1.53	+4.1	3.13	2.12	2.09	−1.4
2050	Cathode	Oxide	6.3	0.575	4.72	0.489	0.481	−1.6	7.88	0.657	0.657	0
2051	Cathode	Oxide	6.3	0.605	4.72	0.515	0.506	−1.8	7.88	0.688	0.693	+0.6
8025	Filament	Th-W	6.3	1.94	4.72	1.65	1.61	−2.4	7.88	2.19	2.22	+1.4
9001	Cathode	Oxide	6.3	0.157	4.72	0.135	1.31	−3.0	7.88	0.177	0.179	+1.1
1T4	Filament	Oxide	1.4	0.0525	1.05	0.043	0.044	+2.3	1.75	0.0613	0.0600	−2.2
6SK7	Cathode	Oxide	6.3	0.310	4.72	2.61	2.59	−0.8	7.88	0.352	0.355	+0.9
6S57	Cathode	Oxide	6.3	0.150	4.72	0.129	1.25	−3.1	7.88	0.170	0.172	+1.2
12A6	Cathode	Oxide	12.6	0.156	9.45	0.134	1.30	−3.0	15.75	0.177	0.178	+0.6
2AP1	Cathode	Oxide	6.3	0.595	4.72	0.508	0.498	−2.0	7.88	0.668	0.680	+1.7

ment operating conditions within the usual desired engineering accuracy for electron tube applications. These curves should not be used when an accuracy within ±3.5 percent for filament current is desired with a ±25 percent change in filament voltage. The percentage of error in all equations converges to zero as the ratio of E_r/E_r approaches unity, or the smaller the percentage change of voltage in the transposition the smaller the degree of error. A limited number of types of filaments and heaters have been examined and found to give good agreement with the curves of Fig. 1. The accuracy of the volt-ampere characteristic can be established by experimentally determining $(n_r - n_r)/(n_r + n_r)$ for the particular application. This determination may be made from the relation

$$\frac{n_r - n_r}{n_r + n_r} = \frac{\log (E_1/E_2)}{\log (I_1/I_2)}$$

where I_1, E_1 and I_2, E_2 are currents and voltages at known operating points.

Once the value of $(n_r - n_r)/(n_r + n_r)$ has been established over the probable application range of voltage the operating conditions of a group of filaments in series may then be predicted for various supply voltages. This permits the supply voltage tolerance to be established such that the applied filament voltage tolerance may not be exceeded.

The solutions given here represent the steady-state conditions and do not indicate what may happen during the initial application of voltage or for short-time voltage transients.

The writer is indebted to Mr. A. C. Grimm for suggestions as to the method of attack in the solution of a group of tubes in series and to Mr. E. E. Spitzer for his criticism and suggestions in the preparation of this manuscript.

References

(1) Jones and Langmuir, The Characteristics of Tungsten Filaments as Functions of Temperature, *General Electric Review*, June, July and August, 1927.
(2) "Temperature—Its Measurement and Control in Science and Industry," American Physical Society, Reinhold Publishing Co., New York, p. 1186.
(3) Worthing, A. G., Physical Properties of Well Seasoned Molybdenum and Tantalum as a Function of Temperature. *Physical Review*, 28, No. 1.
(4) Mellor, Joseph W., "Comprehensive Treatise on Inorganic and Theoretical Chemistry," Longmans and Co., New York.
(5) Forsythe, W. E., "Measurements of Radiant Energy," McGraw-Hill Book Co., New York, p. 82.

Graphical Determination of Operating Point of Self-Biased Tube

By ARTHUR SCHACH

IN CHECKING vacuum tube circuits, the problem of finding the proper operating point on the static characteristic curve frequently arises. The circuit of Fig. 1 shows the data usually given: the supply voltage (E_{bb}) applied across the tube, a plate resistor (R), and a cathode resistor (R_k) in series.

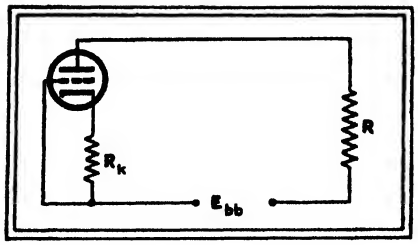

Fig. 1—Essentials of typical self-biased stage

The usual method of solution is one of successive approximations. First the load line corresponding to R (or $R + R_k$, if R_k is not negligible in comparison with R) is drawn on the plate characteristic chart. Then a guess is made at a likely plate current, and the voltage drop that this would produce across R_k is computed. Next, there is read from the load line the current which would result from a bias equal to the computed drop. The whole process is repeated several times until a current is obtained which differs only slightly from the previous approximation.

If an error of several ma may be neglected, we might stop at the second current obtained (i.e., the first computed current), and take the mean of it and the initial guess. The error incurred will depend on the accuracy of the initial guess.

But, quite as expeditiously, we can obtain the true limit of the above process, and hence, the exact solution of the problem, by the following procedure for which an example is worked out in Fig. 2.

(1) Note the intersection of the load line with the zero-bias curve (A, Fig. 2) and mark the point A' vertically below it on the voltage axis.

(2) Choose a convenient plate current, I_a, (preferably less than that corresponding to A) and calculate the drop it would produce across R_k.

(3) Locate the point B, on the load line, which corresponds to a grid-bias equal to the drop just calculated, and mark the point B' vertically above or below B on the horizontal line corresponding to the chosen current.

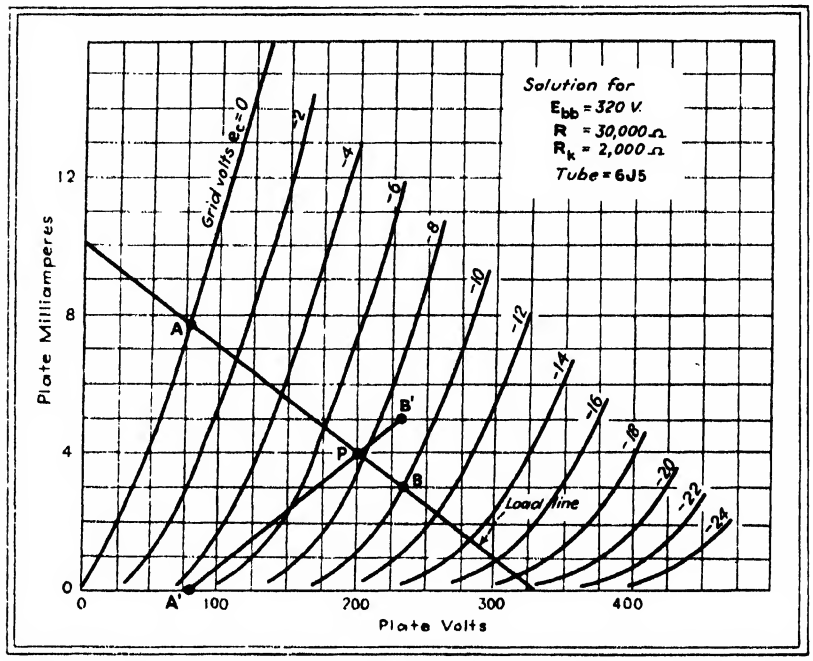

Fig. 2—Graphical solution illustrating the method described in the text. The current, I_{a1} was taken as 5 ma as suggested in step 2

(4) Draw $A'B'$. Its intersection, P, with the load line is the required operating point.

If a constant bias is superimposed upon the self-bias, the method of solution is the same if we allow the grid-bias curve corresponding to the constant bias to play the same role as the zero-bias curve plays in the method as outlined above. That is to say, if the constant bias is e_c, the point A will then be the intersection of the load line with the bias curve for $e_c = e_c$.

The correctness of the method just described rests on the assumption that the constant-grid-bias curves, corresponding to equal increments of grid-bias voltage, cut the load line into equal segments. Within the limits of graphical accuracy, this assumption is nearly always justified.

Figure 3 is a repetition of part of Fig. 2 plus the points B'', P', and Q, whose geometrical relationship to the others is made clear in the figure. Now, if I_a is the plate current chosen in step 2, then the current corresponding to P will be

$$\frac{A'P'}{A'Q} I_a$$

In virtue of the similarity of triangles $A'P'P$ and $A'QB'$ this is equal to

$$\frac{P'P}{QB'} I_a$$

and this would produce in R_k a drop equal to

$$\frac{P'P}{QB'} I_a R_k \qquad (1)$$

But, by construction, the bias corresponding to B is $I_a R_k$. Hence, because of the above-mentioned as-

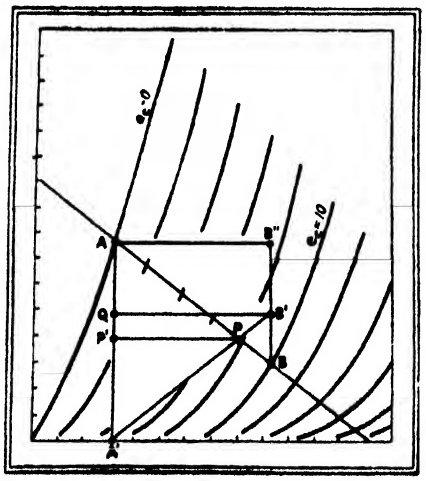

Fig. 3—A portion of Fig. 2 showing the geometrical relationship of the various points discussed in the text

sumption, the bias corresponding to P is

$$\frac{AP'}{AB} I_s R_k$$

which, in virtue of the similarity of triangles $AP'P$ and $AB''B$ and because $AB'' = QB'$, is equal to

$$\frac{P'P}{QB'} I_s R_k, \qquad (2)$$

But the equality of (1) and (2) proves that P is the desired solution; i.e., that the plate current corresponding to P produces a drop in R_k equal to the grid-bias corresponding to P.

Tube Failures in Eniac

Analysis of causes of tube failures in 18,800-tube electronic computing machine during one year of operation shows that open heaters and damaged cathode coatings are chief troubles. An average of two tubes failed each time the a-c supply to the heaters was shut down

By F. ROBERT MICHAEL

The Electronic Numerical Integrator and Computor (ENIAC) provides, after a year of operation, unique life test information in the failures among its 18,800 vacuum tubes and their chronological occurrence during that year. All tubes which failed were opened and examined with a binocular microscope, and all noticeable defects were classified and recorded. The various faults which caused tube failure are illustrated and discussed here, and in several cases their rate of occurrence is plotted against time.

In the ENIAC, numbers are represented by combinations of electrical pulses, and the pulse system is used for the transmission of orders as well. Pulse repetition rate is 100 kc, with rise times of approximately 0.2 and 0.5 μ sec for pulse durations of 2 and greater than 10 μ sec respectively. Pulse amplitudes range from 15 to 50 volts in most cases. The numbers of vacuum tubes used and their general functions are shown in Table I, along with the numbers of failures for each type.

Operating Practices

The vacuum-tube heaters were in operation approximately 80 percent of the time from November 1945 to November 1946, amounting to 7,000 hours. Heater circuits were turned off at night for the first few months, and during this period a comparatively large number of tube failures resulted from heater-to-cathode shorts. It was felt that these failures might be due to initial current surges in the a-c circuit. Investigation showed the transient current to be approximately four times steady state, which agrees well with the hot-to-cold resistance ratio of tungsten heaters at 1,000 to 1,200 degrees K.

It was necessary at that time to allow any corrective circuit change to wait until the scheduled moving of the ENIAC to Aberdeen, Maryland, and to leave the heater circuits on 24 hours a day with the exception of accidental power failures. The rate of failure for a-c shut downs averaged about two tube failures out of 18,800 per heater shut down, which was a small rate but undesirable because of the time required to locate and replace failures.

Meanwhile a series of experiments was started, using 100 tube samples, to determine whether a graduated application of voltage would materially reduce the rate of failure caused when heaters were turned off and on. Such experiments showed no difference between the group of tubes to which full voltage was applied at once and those receiving a gradual application of voltage.

It was the practice to shut off the d-c supply each night and at any time the ENIAC was left unattended except when it was actually working on a problem. No correlation between d-c supply voltage shut downs and tube failure rate was noticed.

Tube life and probability for failure are important considerations when a large number of vacuum tubes is involved; especially when, because of ENIAC's high speed, so much possible work is lost in breakdown time. Design center values were therefore chosen conservatively.

Heater voltages were designed for 95 percent of rated voltage or 6.0 volts $\pm$ 0.1, although they averaged about 5.9 volts. Grid current was limited to 1 ma, with 0.5 ma average current. Grids were swung negative three times the cutoff voltage, but not exceeding 150 volts negative to the cathode.

Plate voltage was set at 50 percent of maximum ccs (continuous commercial service) rating, plate current at 25 percent maximum ccs rating, screen voltage at 50 percent maximum ccs rating, and screen current at 25 percent maximum ccs rating.

Maximum heater-to-cathode po-

tential was limited to ± 50 volts, with one side of all heaters tied to a d-c potential. Power supply voltages were bypassed to cut signal hash and a-c hum to 2 percent (peak to peak) of the d-c magnitude.

Standard commercial receiving tubes with octal bases were purchased throughout 1943 to 1945 from a number of manufacturers and were tested individually for acceptance before use in the ENIAC. Allowance was made for a ± 50 percent cutoff voltage variation and a ± 40 percent variation in r_p for all tubes with the exception of cutoff in 6AC7. This latter was held to a ± 0.5 volt tolerance. Approximately 5 percent of all tubes were rejected except 6AC7, in which case about 40 percent were rejected.

Table I—Summary of Tube Failures in ENIAC

Type	Approx. Number of Tubes	Percent of 18,800	Number of Tubes Removed	Percent of 644 Tubes Removed	General Use
6SN7 Twin Triode	6,550	35.0	200	31.0	Trigger and pulse counting circuits; also normally-on amplifier
6L6 Beam Power	4,200	22.0	175	27.2	Pulse amplifier; transmission normally off, pulsed on
6SA7 Pentagrid Converter	2,600	14.1	50	7.8	Coincidence tube, normally off; turned on by pulsing both grids; called gate
6SJ7 Triple Grid Amplifier	1,500	8.0	20	3.1	Input pulse amplifier; normally off
6V6 Beam Power	1,300	7.0	25	3.9	Pulse-forming circuits; normally on, pulsed off
6L7 Pentagrid Mixer	1,200	6.5	35	5.4	Use similar to 6SA7
6AC7 Television Pentode	500	2.5	110	17.1	Normally on; input amplifier with critical cutoff
807 (Enlarged 6L6)	350	1.8	20	3.1	Power amplifier, high voltage swings; normally off
6J5 Detector Triode	300	1.6	2	0.3	Amplifier; normally on
6Y6 Beam Power	300	1.6	7	1.1	Amplifier; normally on
	18,800	100.0	644	100.0	

Tube Failure Records

It was evident that keeping a record of tube failures would allow anticipation of more troublesome periods in operation. Investigation of causes of failures gave information for possible circuit changes and tube specifications which would permit further reduction of breakdowns, increasing the reliability of operation. An attempt was made to open each tube that failed in a way that would not change the internal conditions at the time of failure.

Figure 1 provides a graphic record of tube failure per month for the 644 tubes removed from the ENIAC. The downward trend from November 1945 to March 1946 is probably marking the decreasing number of tubes at the borderline of acceptability when placed in operation in the ENIAC. This downward trend in rate of failure for the first 1,000 hours or so is normal experience when using large numbers of tubes. The peak in August 1946 is due largely to a complete overhaul given the machine in preparation for a problem which used its facilities to the utmost.

The five major causes of these 644 tube failures were: (1) open heater wire; (2) damaged oxide cathode coating; (3) internal leads and supports dangerously close; (4) open electrode spotwelds; (5) burned-open shorts. Open or damaged heaters accounted for 270 failures and damaged cathodes caused 150 failures, while the remaining three types of faults accounted for between 50 and 100 failures each.

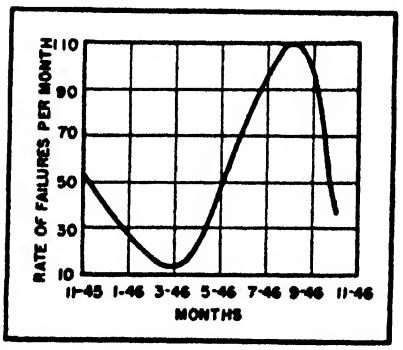

FIG. 1—Rate of failure of all tubes in one year of ENIAC operation

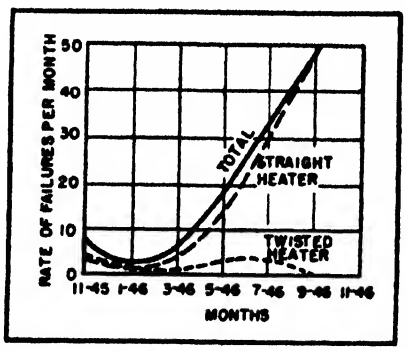

FIG. 2—Comparison of failures of straight and twisted heaters

The 6SA7 tubes (14 percent of all tubes used in ENIAC) were constructed with the twisted type heater, and had no open-heater faults. The 6L6 tubes (22 percent) were constructed with straight or looped heaters and gave 15 percent of all open-heater failures. The 6SN7 tubes (35 percent) were constructed with both types of heaters, and contributed 75 percent of all open-heater failures, of which 15 percent were in twisted heaters and the remainder in straight heaters. The remaining 10 percent of open-heater failures came from tubes having straight heaters.

The fact that 57 percent of all tubes in the ENIAC produced 90 percent of the heater failures indicated possibilities of faults peculiar to these two types (6L6 and 6SN7). It was found that the straight folded-type heaters in these types, combined with certain manufacturing features, were mainly responsible for the failures.

In most of the open-heater faults

of the twisted type, the heater wire had pulled away from the support wire. Such faults in both straight and twisted heaters seem to occur only when the spot weld between the heater and support wire has not imbedded the tungsten heater wire sufficiently in the softer metal (Ni alloy) support.

Examination of straight heaters showed approximately 90 percent of all faulty tubes with straight heaters either had the insulating coating chipped off their bends, baring the tungsten wire with additional circumferential cracks over its length, or appeared to have had their insulating coatings shifted away from the bend while in a semi-liquid state. The latter were probably coated by dipping, and tilted before they were dry. The first condition was the more prevalent. It is common practice in manufacturing to coat the tungsten wire by processing it while being wound from one spool onto another. The coated, spooled wire is then bent into the straight heater folds. In so bending, the coating cracks, baring some bends. A more elastic insulating coating is being sought by tube manufacturers.

Few twisted heaters showed chipped insulating coating and exposed bends. The 6L6 straight heaters gave most of their trouble in cathode-to-heater leaks. Figure 2 shows, for all tubes inspected, the rate of failures per month traceable to chipped or otherwise bared heater faults. Separate curves for twisted and straight-type heaters are included for comparison.

In an attempt to correlate a-c shutdowns with tube failures, a rack of 100 6L6 and 100 6SN7 tubes was tested by applying full heater voltage long enough for tubes to heat, and turning tubes off till cool, with this cycle being repeated continually. In the same rack another 100 6L6 and 100 6SN7 tubes were similarly cycled, but with heater voltage applied in steps to approximate a constant linear expansion in the heaters. This test showed little difference in tube failures between samples over a period of eight months.

One other fault noticed with heaters had to do with their mountings. Figure 3 shows the various types of heater mountings encountered in this investigation. In the case of single-heater tubes, the support wires are cut to the same length and bent into position. The heater wires should be run parallel far

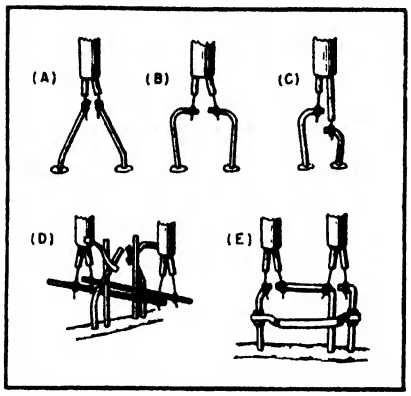

FIG. 3—Types of heater mountings encountered in ENIAC tubes

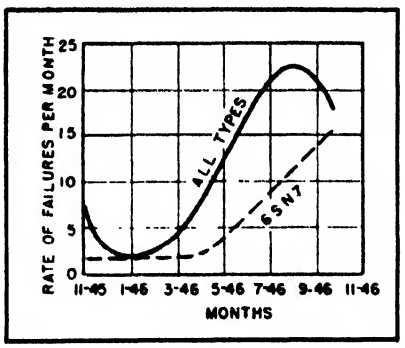

FIG. 4—Failures traceable to blistered oxide cathode coatings, causing low emission

enough apart so that the supports do not touch, and close enough to slip easily into the cathode sleeve. Heaters were observed with the insulating coating worn away by rubbing of the cathode sleeve edge during vibration, expansion, and contraction. For this consideration the construction of Fig. 3A proves better than that of Fig. 3B.

If one support were cut shorter before bending, as in Fig. 3C, the supports could be closer without shorting, providing the heater wire is insulated down beyond the upper support. The heater would not then be spread, and chances of rubbing its insulating coating against the edge of the cathode sleeve would be minimized.

Of the two 6SN7 double mountings, that of Fig. 3E seemed to be the neater and less troublesome in this investigation. The upright posts in Fig. 3D provided more obstruction to the pliable cathode bands, causing the bands to short and burn open; actually, however, this mounting allows closer, more parallel heater wires to enter the cathode sleeve.

Damaged Cathode Coating

With little exception, the main damage to cathode coatings was blistering—an uneven, bubble-like puff of oxide coating which when broken away exposes the bare cathode sleeve. Other damages, noted rarely, were burns or holes adjacent to shorted electrodes.

Rates of failures per month due to damaged oxide coatings are shown in Fig. 4 for all tubes and for 6SN7 tubes individually. The same tendency was noted for each other tube type. The curves turn upward in the vicinity of March, when the ENIAC was being used to capacity. The percentage increase in failures is many times greater than the approximate percentage of additional tubes used in March, which would indicate that blistering involves an aging effect.

As would be expected, most of the tubes with blistered cathodes were removed because of low emission. The most acceptable answer to blistering seems to be that of gas formation between sleeve and coating. This effect would increase with age if the following is assumed. Many cylindrical cathode sleeves, such as 6SN7, are made with seams down their length. During processing, these sleeves are exposed to oil (or some other liquid) baths. If not thoroughly cleaned before the oxide coating is applied, the liquid, if thin enough, will infiltrate the seam and be covered with the oxide coating. In use, the heated liquid would diffuse through the coating along the surface of the cathode sleeve and liberate gas, causing blisters.

Support wires are considered to be those wires which leave the tube

base pins to pass through the glass stem and press into the evacuated envelope. In some cases these support wires are bent and spot-welded directly onto the electrode structure. In other cases a thin, pliable copper or nickel band, here called a lead, is used to connect the support to the electrode structure.

The compromise necessary between the spread of the heater wires entering the cathode sleeve and the closeness of their supports can be responsible for shorted heaters.

The most dangerous of all near-shorts seemed to be those involving the pliable lead bands connecting support wire to electrode post or another support wire. These bands are usually used long enough to provide necessary slack for running them around other supports. In some cases the cathode bands are curved to avoid the control grid supports, only to be curved too close to each other. If the cathodes are at an appreciable voltage difference with respect to each other, their bands may touch from expansion or the electrostatic pull between them. In pentagrid tubes, with numerous electrode posts, the cathode band is very often quite close to a support wire.

Approximately 100 of the tubes removed from the ENIAC had near shorts. Percentages of these failures for each type of tube indicate that near shorts are of general occurrence in all types.

Failures discussed here are those in which tubes investigated showed an internally open connection between support wires and electrode posts. No cases were found in which a lead band had pulled away from another wire.

Open Electrode Spotwelds

With open spotwelds (other than open heater-to-support spotwelds, already covered) it was not possible to identify definite characteristics of the opened spotwelds that might indicate faulty welds, though discoloration from the heat of the weld was seen.

Records of the rate of these approximately 50 failures with time show no significant tendencies, and the distribution among the various tube types is in rough proportion to the relative number of the tubes of each type employed in the ENIAC.

A few cases were found in which the screen support had pulled away from the screen grid post, and consequently touched or nearly touched the plate support. In most cases the size of the bend in the screen support decided whether it shorted or not.

Burned-Open Shorts

Initial reasons for these shorts were usually burned away, hence a separate classification was made even though causes may have been one or more of the faults previously taken up. Tabulation gave a random distribution of failures with time, in rough proportion to the numbers of tubes of each type in the ENIAC.

The author wishes to acknowledge the helpful criticism given by Thomas Kite Sharpless of the Moore School of Electrical Engineering Research Division, University of Pennsylvania, who is chief engineer of the EDVAC project (Electronic Discrete Variable Computor—a faster, more compact, and more versatile successor to the ENIAC). Appreciation is also expressed for the untiring efforts of Viola Andreoni, project worker.

Producing Tube Curves on an Oscilloscope

Stepping circuit switches grid voltage after each characteristic curve is traced on cathode-ray oscilloscope. In this way a complete family of curves is automatically produced. Equipment makes possible rapid and detailed studies of all factors affecting tube operation

By HENRY E. WEBKING

AN EASY and common method of predicting performance of vacuum tubes is by using plate-current versus plate-voltage characteristic curves, commonly called plate characteristic curves, and plate-current versus grid-voltage or transfer characteristic curves. From these curves it is possible to determine, among other things, plate resistance of the tube, amplification factor, transconductance, power output, and percentage of harmonic distortion introduced.

Useful as they may be, ordinarily available curves are subject to limitations. For instance, plate characteristic curves such as are given in tube manuals and electronic books are usually static curves and, for pentodes, are given only for one particular set of screen and suppressor grid voltages. From the designer's standpoint, a set of characteristic curves for each possible combination of these voltages would be very advantageous. With such a set of curves, it would be easy to select the optimum set of conditions under which to operate the particular tube. In the design of audio amplifiers, for example, it would be a relatively simple problem to select the set of operating conditions under which a given output could be obtained with minimum

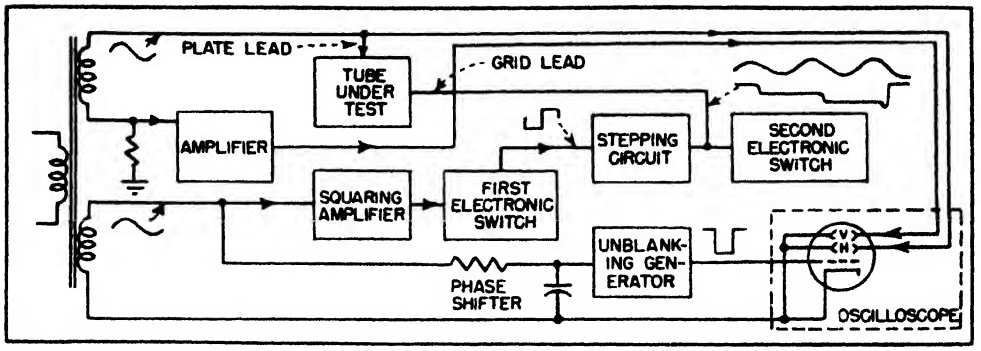

Block diagram relates elements of system

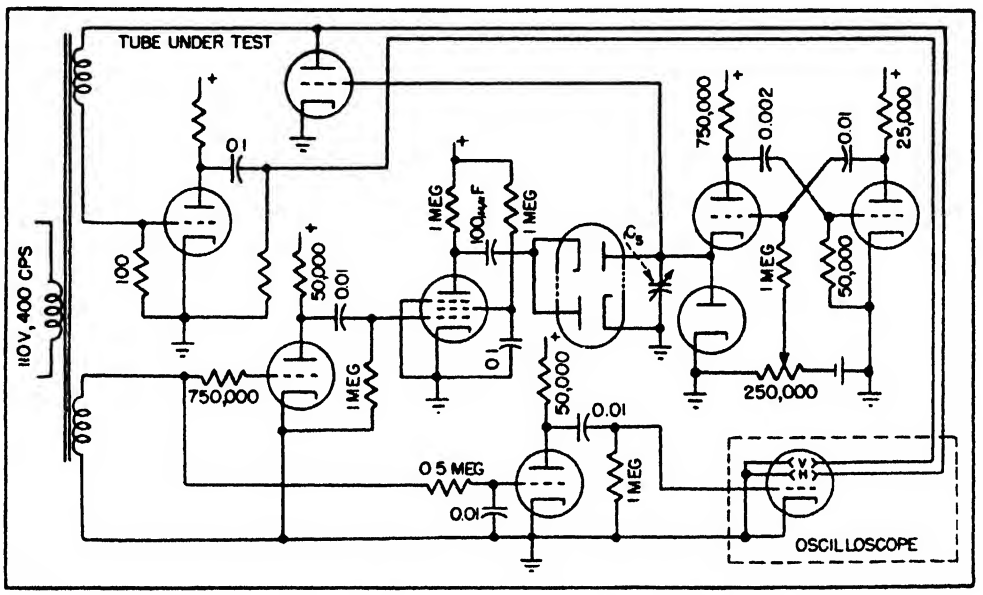

Circuit shows principal components of each stage

distortion. In electronic control systems, where the irregular portions of the characteristic curves are utilized, a complete set of these curves would enable the designer to pick the operating conditions under which these irregularities could be used to greatest advantage.

Desirable as it would be, to include in tube manuals such a set of curves is impractical, because of the vast number that would be required. The designer then has two choices. He may be satisfied with one set of static curves from which to make his calculations or he may actually plot, point by point, a set of curves for each given set of conditions. Such a process is long and laborious and unless an excessive number of readings are taken, small irregularities, such as appear on 6L6 characteristic curves, are not likely to show.

Instead of manually plotting such curves, the circuit given here offers a method of showing these characteristic curves on the screen of a cathode-ray tube.[1] By the use of a few calibrated controls, it is possible to produce practically any combination of operating conditions and to observe the shape of the curves under these conditions, as demonstrated by the accompanying traces obtained with this equipment. These curves offer a visual indication of the changes in such things as amplification and linearity with changes in operating conditions. Additional flexibility is provided by controls on the front panel which vary the magnitude of the grid bias steps as well as the number of steps. Consequently, any number of curves with any desired spacing may be shown on the screen of the cathode-ray tube.

In addition to the plate characteristic curves, this circuit (by changing connections to the tube under test) is capable of producing a dynamic transfer characteristic curve (grid-voltage versus plate-current curve) on the screen of the cathode-ray tube. As with the plate characteristic curves, the operating conditions under which this transfer characteristic curve is produced may be varied, giving a visual indication of the corresponding changes in the shape of the curve. Because this is a dynamic curve, nonlinearity of the curve itself indicates the amount of distortion that will be produced by the tube when oper-

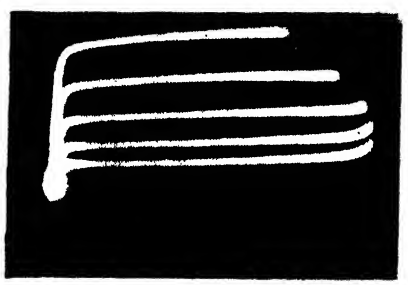

Family of plate curves for 6SK7

Type 6SK7 connected as tetrode

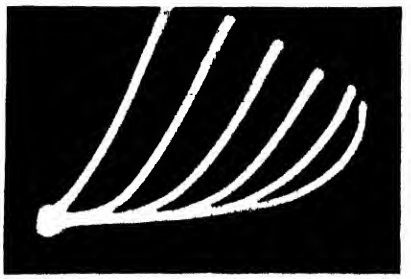

Plate characteristics of 6J5

ated under the given conditions. This fact is utilized a great deal in the design of audio amplifiers even though the usual manner of obtaining such a curve is to plot it with values obtained from the tube's plate characteristic curves. The technique has also been used to measure tube characteristics under extreme conditions.[8]

The equipment is so constructed that any type of tube can be tested. Meters are built in to indicate the various element voltages. A switch located in the middle of the larger panel has five positions and enables the operator to show curves of (1) plate current versus plate voltage, (2) screen current versus plate voltage, (3) plate current versus control grid voltage, (4) screen current versus control grid voltage, and (5) output waveform of the tube with an external signal applied to the grid.

Circuit Operation

The block diagram shows the complete circuit. A 110-volt 400-cps sinewave (readily available from surplus aircraft dynamotors) is fed into the primary of the transformer, producing sinewave voltages across both secondary windings. The high frequency is used to avoid flicker on the cathode-ray tube, which would be noticeable at 60 cps. The 300-volt rms voltage across the upper winding is applied to the tube under test and also provides the horizontal sweep for the cathode-ray tube. Because the plate current of the tube under test flows through the small grounded resistor connected to the upper winding, the voltage across this resistor, when amplified and applied to the vertical plates of the cathode-ray oscilloscope, produces a vertical deflection proportional to the plate current in the tube under test and in synchronism with the corresponding plate voltage independently of waveshape. Thus the curve traced on the screen of the oscilloscope will be a graph of plate current versus plate voltage or a plate characteristic curve.

The output voltage of the lower transformer secondary winding is first fed into a squaring (overdriven) amplifier. (Coming from the common source, this voltage is in synchronism with that applied to the tube under test.) This amplifier changes the sinewave input into a squarewave and changes the phase by 180 degrees. The resultant squarewave is fed into the first electronic switch, which in turn applies voltage on alternate half-cycles to the stepping circuit, the switch being closed during positive half-cycles of its squarewave input and open during negative half-cycles.

The stepping circuit is so arranged that each time voltage is applied, its output voltage will increase by a predetermined amount. Because the first electronic switch applies voltage to the stepping circuit only on alternate half-cycles, the output voltage will correspondingly increase only on alternate half-cycles. Consequently the voltage on the grid of the tube under test, which is controlled by the stepping circuit, changes only during the time that its plate voltage is negative and consequently when it is not conducting. The grid voltage remains constant during the positive half-cycle of the applied sinewave (the time during which the plate characteristic curve is traced on the screen), but has a larger negative value for each successive positive half-cycle of plate voltage. Thus each successive characteristic curve traced on the screen of the cathode-ray oscilloscope will be for a larger value of grid bias, and a complete family of curves is traced.

This process continues until the maximum desired value of grid bias is reached. At this time, the second electronic switch operates long enough to reduce the stepping circuit output voltage to zero. The stepping process is then repeated.

The output of the lower secondary is also fed into a 90-degree phase-shifter ($10X_r \leq R$) and its output in turn is applied to the unblanking pulse generator (squaring amplifier). Its squarewave output, applied to the control grid of the cathode-ray tube, is used to increase the beam intensity during the time that the plate voltage of the tube under test is increasing and thus during the first quarter-cycle of the applied sinewave, or for the time that each plate characteristic curve is being traced on the screen of the oscilloscope.

Stepping Circuit

The second electronic switch, which discharges the grid voltage stepping circuit, is designed so that it remains open until the voltage across it builds up to a predetermined value, at which time it closes and remains closed until the voltage across it decreases nearly to zero. As shown in the circuit diagram, in which all elements are in their same relative positions as in the block

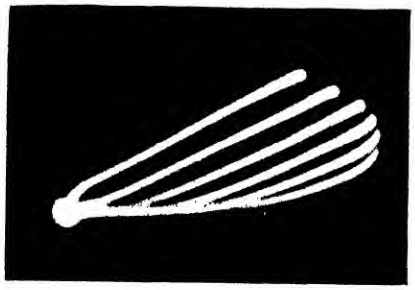

Type 6J7 with cathode degeneration

Nonlinear portion of 6L6 curves

diagram, this second electronic switch can be a one-shot multivibrator with the lefthand tube normally beyond cutoff. The first electronic switch is a gated pentode, while the stepping circuit proper is a variable capacitor having one value of 0.01 microfarad.

During the positive half-cycle of the applied sinewave, the first electronic switch is open (pentode cut off) and the capacitor in its output is charged through one half of the duodiode to approximately the d-c power supply voltage. The R-C time constant of this circuit should be a small fraction (1/20) of the period of the base frequency to permit full charging in the half-cycle. During the negative half-cycle of the input sinewave (squared before being applied to the switch) this switch is closed and its output capacitor discharges through the other half of the duodiode, thereby charging the grid voltage stepping capacitor and making the grid of the tube under test become more negative with respect to ground. The voltage step produced across the stepping circuit depends on the ratio of its capacitor to that in the output of the first switch and the plate d-c supply voltage ($N \simeq CE_{bb}/C_s$, where N is the voltage of each step). The second electronic switch is open during this operation.

The charging of the stepping circuit capacitor continues every alternate half-cycle, maintaining the phase relation to the input sinewave shown in the block diagram. When the voltage across the stepping circuit reaches a sufficiently high value, determined by the potentiometer in the multivibrator circuit, the lefthand triode of the multivibrator conducts and the stepping circuit discharges through the diode in its cathode circuit. Thus this diode is the second electronic switch and the multivibrator is the switch control. After the stepping circuit is substantially discharged, the multivibrator returns to normal.

Versatility of Application

The circuit can be built into a compact unit and arranged so that any ordinary type of tube can be tested. A calibrated switch can be provided for changing the magnitude of grid voltage steps and a potentiometer for varying the number of steps. A small resistor with a shorting switch, placed in the cathode circuit of the tube under test, enables the operator to show the effect of cathode degeneration on the tube characteristic. Similarly, a switch in series with the screen by-pass capacitor will permit showing the effect of screen degeneration. Another potentiometer may be provided to vary the screen grid voltage of tetrode and pentode tubes.

Some interesting observations may be made if a potentiometer is connected between the screen grid and ground with the suppressor grid connected to the movable arm. As the potential on the suppressor grid is varied from a positive value to zero, the characteristic curves change from those of a tetrode to those of a pentode. This effect is shown in the accompanying pictures. There are many possibilities for additional potentiometers and switches which will make the circuit even more flexible.

One of the main applications of this circuit, its use in the design of electronic circuits, has already been pointed out. This application offers the designer a method of easily trying all possible circuit combinations in order to ascertain the best combination for a particular case. It also affords him a method for noting the effects on the characteristic curves of such things as feedback and degeneration.

In addition, an opportunity is provided for making a more detailed study of any portion of the curves by merely increasing the gain of the amplifier in the cathode-ray oscilloscope. Such an enlarged picture would be useful, for instance, in the design of low-level audio amplifiers. These amplifiers are usually operated with such low plate voltages that the portion of the characteristic curves actually required for design purposes is either not given or is too small to be of any practical value.

This circuit can also be used to obtain a full set of characteristic curves and thus check the comparative performance of new tubes during manufacture. These curves can be photographed and used for further study. If small irregularities appear on the curves, that portion of the curves on which they appear can be enlarged on the screen of the cathode-ray tube, making it easier to determine their exact nature.

Another application of this circuit is its use as a lecture-room or laboratory demonstration apparatus. It provides a positive means of demonstrating what happens to a tube's characteristic curves, and consequently to its operating characteristics, when element voltages are varied, when degeneration is used, and when various circuit parameters are changed.

References

(1) Jacob Millman and Sidney Moskowitz, Tracing Tube Characteristics on a Cathode-Ray Oscilloscope, ELECTRONICS, p 86, March 1941.

(2) E. C. Easton and E. L. Chaffee, Pulse-Type Tester for High-Power Tubes, ELECTRONICS, p 97, Feb. 1947.

Disk-Seal Tubes

Altering conventional construction so that the tube elements become part of the electromagnetic circuit improves high-frequency operation. Disk-seal tube design places the electron stream in the high-impedance region of a cavity resonator

By E. D. McARTHUR

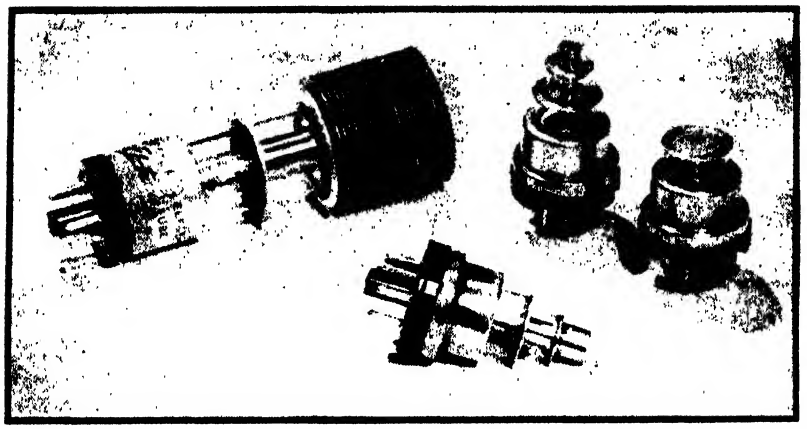

FIG. 1—Commercial disk-seal and lighthouse tubes

THE DEMAND for higher frequency and more power for new services and industries has grown as rapidly as research and development could push back the frontier. One of these outgrowths of research is the disk-seal tube. This new type tube, which includes that group known as lighthouse tubes, is a development that has greatly extended the usable frequency spectrum and introduced a new concept of the relation between the electron tube and its associated circuit.

The Basic Idea

Electronically, the disk-seal tube, or more simply the disk tube, is a multi-electrode tube using the same space-charge control principle as conventional triodes, tetrodes and pentodes.

Geometrically, it is a tube built from simple, smooth-surfaced disks and cylinders into a structure which usually, but not necessarily, has circular symmetry. As we shall see, the ultrahigh-frequency property of any such metal shape is a design factor whose significance is just becoming evident.

Philosophically, the disk tube is an embodiment of the principle that in the microwave field we can no longer speak of tubes and circuits as two distinct entities. It is necessary to think of a microwave oscillator, for example, not as an electron tube with an attached circuit but rather as a single electrical system having one section walled off and evacuated to house the electronic activity.

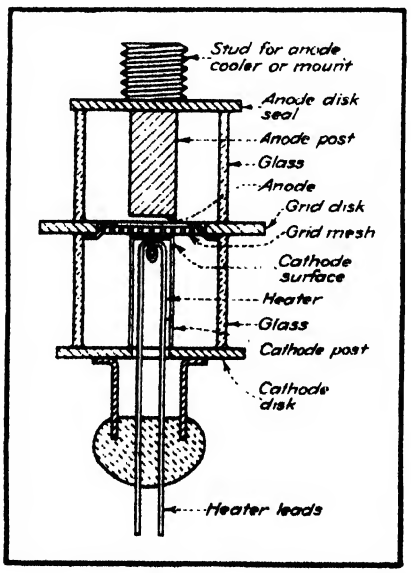

FIG. 2—Basic construction of disk-seal tube

A group of commercial disk tubes is shown in Fig. 1. Figure 2 is a cross-sectional view showing the basic mechanical features common to disk tubes. Figure 3 shows the constructional details of the 2C40 lighthouse tube.

Frequency Limitations of Conventional Tubes

In trying to reach the highest possible oscillation frequency with a given tube one usually starts at a low frequency, using some standard oscillator circuit such as the one in Fig. 4(a). The frequency is raised by decreasing L and C until the circuit looks like that in Fig. 4(b). A point is finally reached where the circuit has been made as small as possible and the tube is being operated at the maximum allowable plate power dissipation and voltage. The tube has reached its apparent maximum frequency.

Let us study the circuit arrangement in Fig. 4(c), which is the same as that in Fig. 4(b) but with the interelectrode capacitances and the lead inductances shown. If the cathode is sufficiently isolated by the chokes, the radio-frequency potential of the cathode will be fixed with respect to the anode and grid by the two interelectrode capacitors C_{gk} and C_{pk}. Thus, the excitation or feedback voltage appears across C_{gk} and is not adjustable. When we include these two capacitors, it becomes clear that Fig. 4(b) is the familiar Colpitts oscillator circuit which we might expect to operate in the usual way if it were not for a number of new factors which creep in as we try to drive the frequency higher.

One reason why the frequency

cannot be made higher lies in the indicated lead inductances and distributed capacitance of the electrode structures. In many cases, the main oscillating circuit is a two-wire transmission line connected to the grid and anode; a line which, in addition to its desirable features, has several serious drawbacks. One is that, although a quarter-wave line in itself is physically large even at very short wavelengths, the line is shortened by the interelectrode and stray capacitance of the tube elements until at some high frequency the part external to the tube vanishes.

Another factor is the increased energy losses due to the electromagnetic radiation from every part of the circuit. This becomes more severe as the tube electrodes and circuit elements become more comparable in size to the wavelength. Usually this tube radiation becomes so large that little or no useful output can be obtained, or it may even prevent oscillations from starting. This radiation is always a major limitation on the impedance which can be developed with an unshielded system.

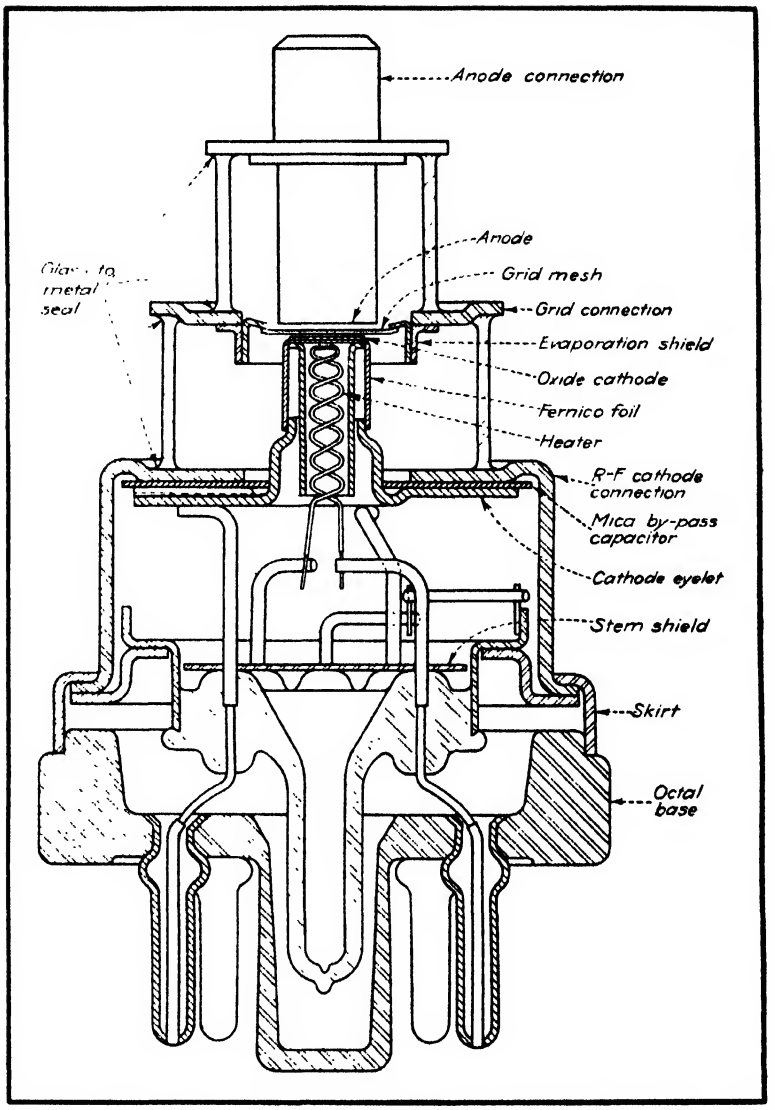

FIG. 3—Mechanical details of the 2C40 lighthouse tube

Electron-Stream Transit Time

Still other difficulties arise from the electron transit time. When the electron transit time becomes comparable with the oscillation period, some properties of the electron stream which were negligible at low frequency become important. This does not mean that an insuperable barrier has been raised. It does mean that the system must be looked at in a far broader sense.

Because of transit time of the electron stream, there will be a dissipative load introduced at the excitation or input terminals of the circuit. There will also be a phase angle between the excitation voltage and the fundamental component of anode current such that the tube input and output voltages will almost never have the 180-degree phase relation common at low frequency. Phase angle as such need not be harmful provided we recognize and meet the added circuit requirements which it imposes. On the other hand, characteristics such as transconductance are adversely affected in comparison with d-c values so that there is an even greater need for efficient circuits than at low frequency.

The feedback circuit in the oscillator must be capable of providing the necessary excitation voltage in spite of the extra driving power, as well as almost any phase angle between its input and output voltages. But, with the arrangement shown in Fig. 4(c) the feedback voltage is almost entirely fixed both in amplitude and phase by the self and mutual reactances of the tube parts. None of these circuit elements can be adjusted and so above the frequency at which the phase relation between input and output becomes appreciably different than 180 degrees, the feedback conditions for sustaining oscillation cannot be met.

Use of Cavity Resonators

The frequency-determining circuit connected between grid and anode of Fig. 4(b) can be reduced to a simple capacitance-shortened quarter-wave line by ignoring all direct-current parts of the circuit. Fig. 5(a) shows the simplified extract from Fig. 4(b) together with

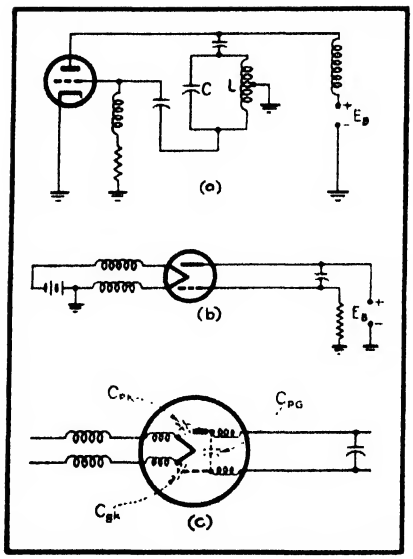

FIG. 4—At low frequencies, the lumped-constant oscillator circuit shown at (a) can be used. At higher frequencies the line oscillator shown at (b) replaces the lumped constant oscillator. At still higher frequencies the important circuit elements lie within the tube as illustrated at (c)

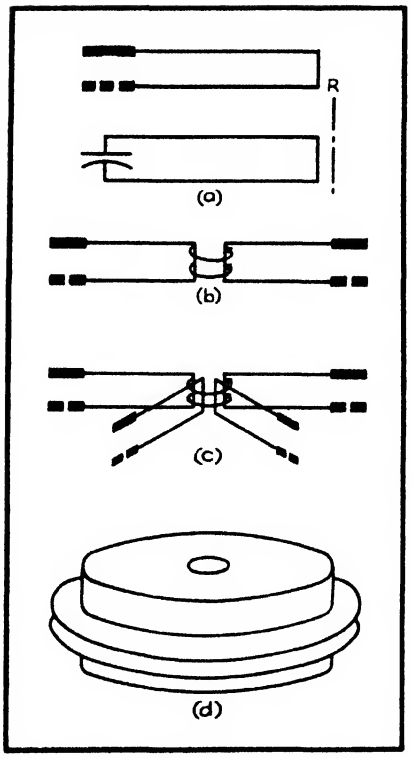

FIG. 5—At (a) the grid and plate are connected to a transmission line. The equivalent high-frequency circuit is shown directly below. (b) Two such circuits can be inductively coupled. Coupling an infinite number of such circuits gives the electrical arrangement shown at (c) and the mechanical arrangement shown at (d) which is in effect a figure of revolution of the equivalent circuit about the axis *R*

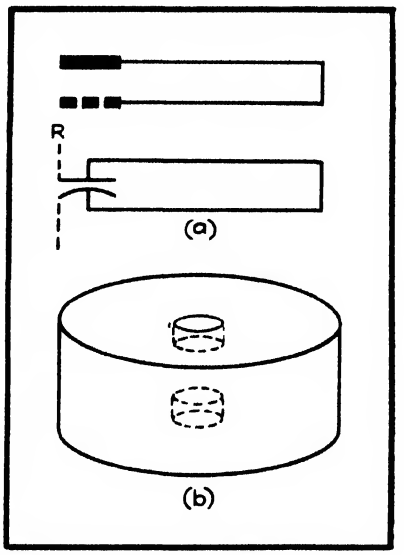

FIG. 6—Choosing a different axis of revolution from that of Fig. 5 for the equivalent circuit at (a) gives the mechanical arrangement at (b) which readily lends itself to use as the electromagnetic basis of the disk-seal tube; the electrodes for the electronic system go at the center

the equivalent circuit. We could have another tube and circuit coupled to this circuit at the high-current point as shown in Fig. 5(b). In fact, many such circuits could be added as at Fig. 5(c), the ultimate being equivalent to the rotation of the circuit at Fig. 5(a) about an axis *R* to give the structure shown in Fig. 5(d). The shortened quarter-wave line in Fig. 5(a) has, by rotation, generated a closed metal structure made of two parallel flat metal disks joined by a cylindrical hub at the center and terminated at the periphery by an annular ring capacitor.

Continuing the same line of thought gives rise to other structures such as that in Fig. 6. Such totally enclosed circuits or cavity resonators are ideally suited to ultrahigh-frequency needs. The one shown in Fig. 6, for example, would be expected to have much the same current and voltage distribution as do the quarter-wave line sections from which it was developed and which make up its radii.

This is a sound physical picture but inaccurate numerically. A more exact analysis must be based on the electrical properties of the geometrical shape. A simple radial resonator and a quarter-wave open line are shown in Fig. 7, together with the current and voltage distribution for each. In the uniform open line, the resonant line length is 0.25 λ, whereas in the resonator the radius is 0.38 λ.

The most important distinction between line and cavity is that the hollow resonator of Fig. 7 is self shielding. The electric and magnetic fields exist wholly within the resonator. If the metal walls of the resonator are made a few times thicker than the skin thickness or depth of field penetration, there will be no appreciable coupling between the space inside and that outside the resonator and, therefore, there will be no energy lost by radiation.

If cavities are to be used to their fullest advantage, the electronic part and the electromagnetic part of the circuit must be considered as a unit. The disk tube brings about this union in a way illustrated by Fig. 8. Fig. 8(a) shows a vertical cross section of a simple radial resonator similar to that developed in Fig. 6. The point of maximum impedance occurs internally between the two surfaces, *S*. It is here that the grid and anode connections would be made if the cavity were to be used in place of the open wire line of Fig. 4(b).

The genesis of the disk tube is obvious from here on, for, if the surfaces *S* are proper for grid and anode connections, it would be even better if they became the actual grid and anode electrodes. Fig. 8(b) shows the development of such electrodes and Fig. 8(c) shows a section of a resonator containing the electrodes walled off and evacuated to form the upper part of the disk tube illustrated in Fig. 2. The electronic circuit element has been coupled directly to the electromagnetic circuit element with very little geometric disturbance to either component. There is no anode- or grid-lead inductance in the ordinary sense. Neither is there un-

wanted capacitance except that due to the active part of the electrodes. All of these metal surfaces help to shape and contain the electromagnetic field. By maintaining substantial continuity of the metal surfaces, the tube elements become an integrated part of the circuit.

Controllable Feedback

The use of a cavity resonator goes a long way toward solving the problems posed by the output circuit of our sample oscillator but some other problems—feedback for example — have not yet been touched.

It was pointed out that one reason why the circuit of Fig. 4(c) fails is that it allows no adjustment of either the amplitude or phase of the feedback voltage. The essentials of this circuit are redrawn in Fig. 9(a) using lumped circuits and showing the interelectrode capacitances which fix the feedback voltage.

A considerable amount of control can be gained by including C_{pk} in a tuned circuit as shown in Fig. 9(b). This tuned input circuit should be a cavity resonator for the same reasons which prescribe a resonator for the output circuit. Frequently C_{pk} is not large enough to provide adequate feedback and, in that case, it is supplemented by an added adjustable link.

Figure 10, which shows two resonators having a common central wall, illustrates the general mechanical combination of a disk tube and a double resonator which has come to be known as the grid-return, grounded-grid or, more properly, the grid-separation circuit.

An important attribute of the disk tube is the physical separation of the input and output circuits which it permits. This is important because physical separation means electrical separation since, even though the central cavity-dividing wall and the grid disk are common to both resonators, the small depth of field penetration into this wall effectively keeps the electromagnetic fields within their own cavities. In other words, C_{pk} is the only coupling reactance left; the dozens of small coupling capacitances and mutual inductances between electrode parts and leads in conventional tube designs are eliminated.

If it is desirable—and it is in some cases—C_{pk} may be made inconsequential by adding a screen grid.

Through these features, the disk tube permits the use of distinct input and output circuits; the feedback circuit between the two is reduced to a known impedance and the various circuit parameters brought under individual control. These circuits have been the subject of much intensive study, both theorectical and physical, and several basic forms have been evolved.

Figure 11 shows a cavity oscillator circuit. The mechanical layout of this circuit illustrates another very important property of the disk tubes. At very high frequencies, the electric field within the resonator and between electrodes penetrates the metal surfaces a distance in the order of only about one thousandth of an inch and therefore the current conduction is entirely confined to those surfaces which are exposed to the electric field. Thus, there will be high frequency electric currents flowing on the inner surfaces of the resonators and none on their outer surfaces. One might say that the inner and outer surfaces are insulated. Heat, on the other hand, does penetrate the resonator walls and is conducted throughout the metallic circuit. These differing laws of behavior are the source of a most advantageous function

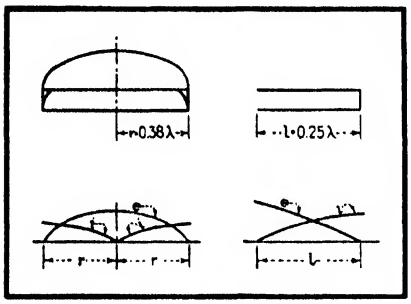

FIG. 7—Resonant dimensions of a cylindrical cavity and a transmission line, and the current and potential distribution of each

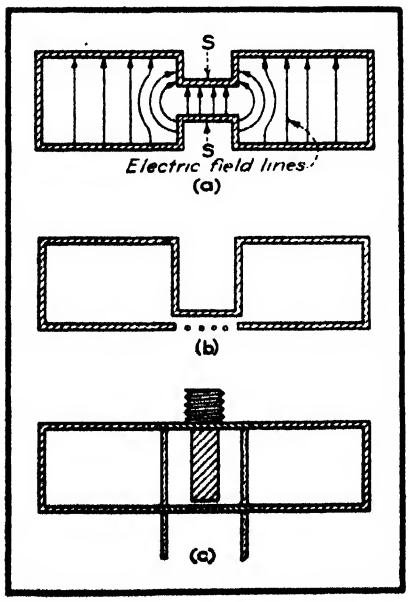

FIG. 8—The evolution of the disk-seal tube from a cavity resonator

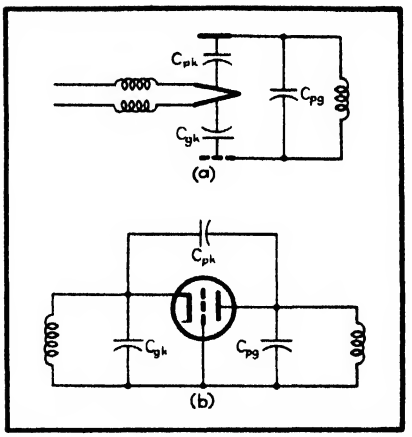

FIG. 9—The circuits used with the disk-seal tube take advantage of the interelectrode capacitances shown in drawing (a) by placing them in the resonant circuits as at (b)

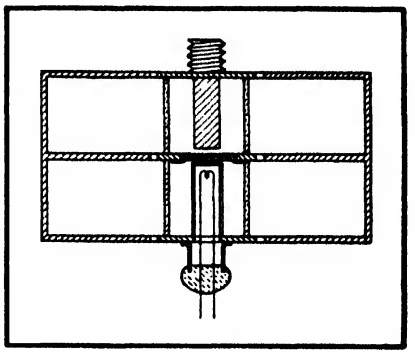

FIG. 10—The disk-seal tube and resonator equivalent of the lumped-constant circuit shown at Fig. 9 (b)

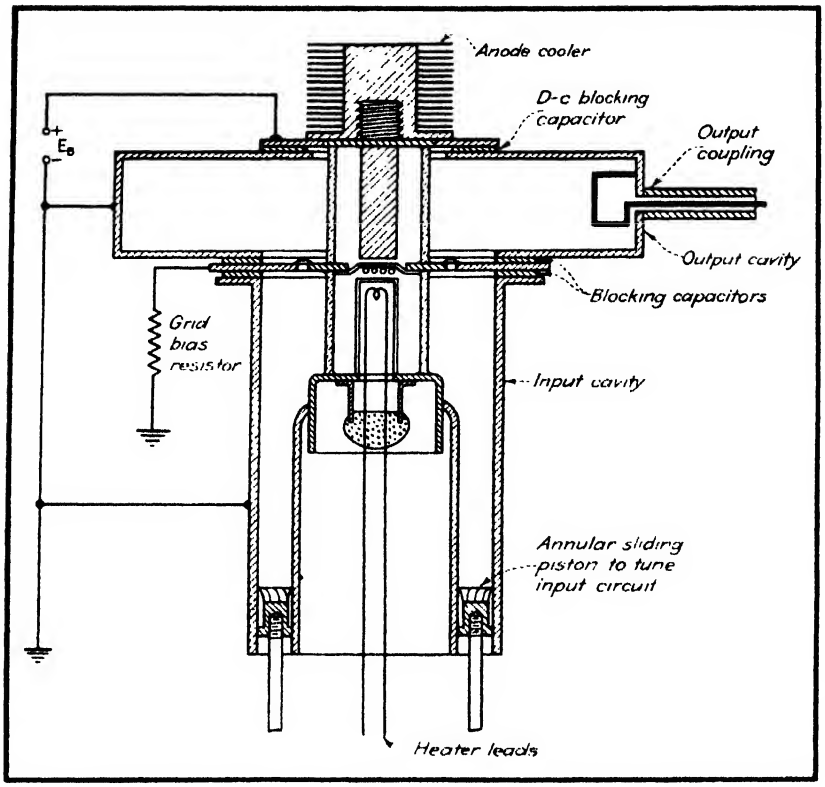

FIG. 11—Mechanical layout of a disk-seal tube circuit shows unity of the tube proper with the wave circuit

which occurs automatically in the disk tubes.

In the disk tube, high-frequency energy flows from its point of origin on the anode surface into the resonator. On the other hand, heat generated at the anode flows through the solid anode rod to the outside of the resonator. This automatic filtering permits anode cooling to be carried out by any appropriate method outside the cavity without interfering in any way with the high-frequency part of the system inside the cavity. The grid is cooled in the same manner so that troubles arising from primary grid emission are greatly reduced.

Since the same reasoning applies in reverse, it is possible to locate the cathode heater together with all its power supply wiring wholly outside the cavities and free of ultrahigh-frequency field.

The same filtering occurs with direct current or low-frequency alternating current and therefore power connections can be made to the cavity system without the use of elaborate isolating chokes.

Mechanically the disk seals in many of these tubes are made of a metal suitable for sealing to glass. High electrical conductivity is preserved by a thin coating of copper or silver which, since it need be only a few thousandths of an inch thick, will not cause dangerous stresses in the vacuum seals. Again we take advantage of the small field penetration to fabricate a composite structure having good electrical conductivity as well as suitable mechanical properties.

The parallel-plane electrodes offer an opportunity as well as pose a problem. To make efficient microwave tubes it is important to use the electron stream efficiently. The degree to which desirable electronic properties are achieved may be judged by one or more of several criteria depending on the type of service considered. For instance, we are always interested in low interelectrode capacitance and yet for a power amplifier we must not sacrifice current-carrying ability. For this application we might use the ratio C/i_c as a figure of merit. For low level amplifiers, where power gain and electron noise are important, we want the highest transconductance possible for a given current. Here we are interested in a large ratio of G_m/i_p. For some jobs, interest will center on power gain and bandwidth. In almost every case, it is desirable that the transit angle be kept small.

Manufacturing Tolerances

When we examine the various criteria, we find generally that they are all improved by decreasing the interelectrode spacing, particularly the grid-cathode spacing. The end-on presentation of plane electrodes is an arrangement uniquely suited to this need. The electrodes require accurate positioning in only one major dimension rather than two as would be the case for cylindrical electrodes. Tube construction and assembly methods enable a tube like the 2C40 to be built with a cathode-grid spacing of 4.0 mils. Developmental tubes have been built with only 1.0 mil cathode-to-grid clearance.

If space-charge control of the usual type is to be retained, the grid-wire size and pitch must be reduced in proportion otherwise it will become so coarse relative to the reduced interelectrode spacing that the electric field will become nonuniform between the grid and cathode. Under this condition, the low-frequency characteristics are poor and the high-frequency characteristics suffer even more severely from the resulting multiplicity of transit angles.

Even more important is the need for keeping the electrodes parallel within rather small limits. The damage due to non-parallelism can be seen if one considers that, in tubes in which the transit angle is fairly large and the electrodes are misaligned, the current from one element of cathode area can have a quite different phase angle from that of neighboring areas. Since the high-frequency components of

current from these elements add vectorially, the resultant alternating current may be quite small and bear no relation to the low-frequency or static characteristics of the tube.

Liberal credit is due the members of the Naval Research Laboratory and the Camp Evans Signal Laboratory who not only expedited the development work by their active interest and early support but helped apply the results with satisfying effect.

Many men have contributed much to many phases of this work but more than ordinary credit is due Mr. R. J. Bondley and Mr. J. E. Beggs, who have been associated with the work almost from its inception and who, through individual effort and contribution, have solved many of the basic design problems in these tubes.

Klystron Oscillators

Operation of velocity-modulation oscillators is explained by correlating the theory of electron bunching with the performance of two coupled tuned circuits. Effects of resonator tuning, feedback and electrode voltages are analyzed and compared with experimental results obtained with a type 410-R/2K30 tube. Similarity to triodes is shown

By A. E. HARRISON

THAT Klystron oscillators and other velocity - modulation tubes utilize electron transit-time effects to convert an electron beam into radio-frequency energy introduces certain characteristics which will undoubtedly be of interest to radio engineers. This dependence upon transit time in a Klystron oscillator causes the frequency of such tubes to be affected by the voltage applied to the tube. Another equally important characteristic which is due to the dependence upon the transit time is the occurrence of voltage modes, i.e., a Klystron oscillator will operate at certain voltages for a given adjustment of the other variables, but is inoperative in the voltage region between these modes.[1] In other respects these newer types of tubes are quite similar to the more familiar triode oscillators, and it will be convenient to use these comparisons in an explanation of the characteristics described above.

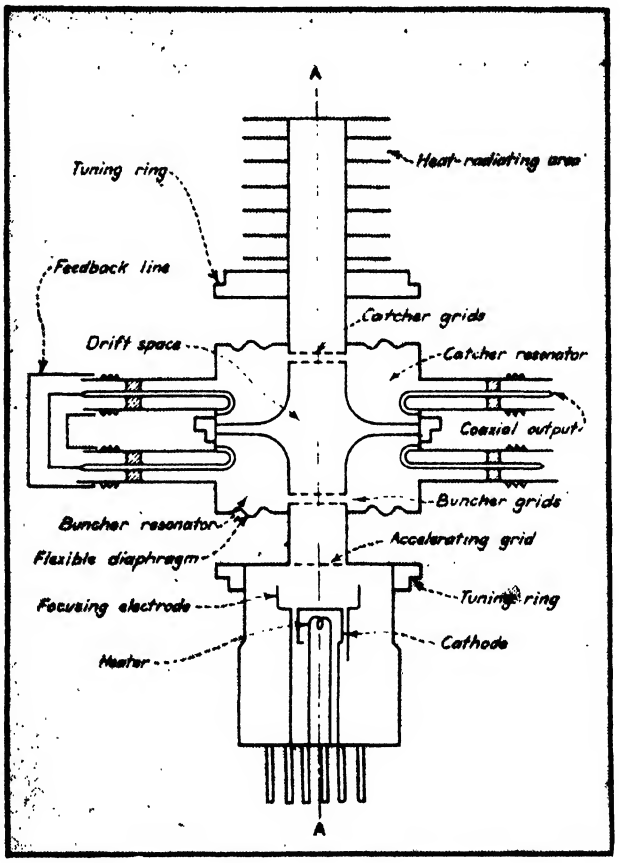

FIG. 1—Sectional view of the double-resonator Klystron of the type discussed in the text

Review of Bunching Theory

A brief review of the principle of electron bunching will be made in order to compare the characteristics of velocity-modulation tubes with the plate current characteristics of more conventional vacuum tubes. The results from an analysis of coupled tuned circuits can then be combined with the tube characteristics obtained from the electron bunching theory to explain the behavior of Klystron oscillators as adjustments are made of the tuning of the resonators, or as the voltage applied to the tube is varied. The effect of the phase and the magni-

tude of the feedback will also be considered, and the theoretical conclusions will be compared with experimental results obtained from the operation of a type 410-R/2K30 Klystron used as an oscillator.

References to the theory of electron bunching have appeared in a number of publications[2-4]. A short review of this material will aid in the understanding of velocity-modulation tubes.

The sectional view of one type of Klystron which is shown in Fig. 1 will be used to explain the theory of electron bunching. The tube is a figure of revolution about the axis AA. An electron gun furnishes a beam of electrons which are accelerated in the space between the cathode and the accelerating grid. The beam continues to move beyond this grid with a high average velocity, and therefore the transit time of the electrons past the resonator grids corresponds to a small fraction of a cycle. The fact that the electrons are accelerated to a high velocity before being acted upon by a radio-frequency field overcomes one of the disadvantages of triodes at ultrahigh frequencies.

A radio-frequency field in the buncher resonator produces an alternating electric field between the buncher grids. This field will speed up certain electrons and slow down other electrons which pass the buncher grids during a different part of the cycle. Consider a group of electrons which pass the buncher grids at the time when the field is changing from a retarding field to an accelerating field. An electron which leaves early in the cycle will be slowed down and will continue along the drift space with less than average velocity. An electron which passes the grids when the field is zero will not be affected and will continue with average velocity. Other electrons which leave later in the cycle will be accelerated and will move along the drift space with greater-than-average velocity. The variation of velocity will be small compared to the average velocity.

As a result of this velocity modulation, electrons which leave later in the cycle travel faster and overtake the slower electrons which left earlier in the cycle. The electron beam is given an alternating component of its electron density as it travels along the drift space. This conversion process requires time; a transit time in the drift space corresponding to several cycles is typical. This transit time is quite important in the analysis of a Klystron oscillator, and the number of cycles corresponding to the transit time in the drift space will be designated by N. The electron bunches center around those electrons having average velocity, and therefore the value of N is determined by the average velocity. The following relations between the frequency f, drift distance s, transit time T, transit angle τ, average velocity v_0 and the acceleration voltage E_0 will be used frequently.

$$N = \tau/2\pi \tag{1}$$

$$N = fT = fs/v_0 \tag{1a}$$

The average velocity is related to the acceleration voltage by

$$v_0 = \sqrt{\frac{2e}{m}E_0} \tag{2}$$

where e and m are the charge and mass of an electron. Therefore Eq. (1a) can be rewritten

$$N = \frac{fs}{\sqrt{\frac{2e}{m}E_0}} \tag{1b}$$

The degree of bunching is directly proportional to the transit time in the drift space and is also proportional to E_1, the peak radio-frequency voltage between the buncher grids. E_1 will also be referred to as the buncher voltage. The degree of bunching is expressed by a bunching parameter which will be designated x, whose value is given by

$$x = \pi N \frac{E_1}{E_0} \tag{3}$$

which with Eq. (1b) gives

$$x = \frac{\pi fs}{\sqrt{\frac{2e}{m}}} \frac{E_1}{E_0^{3/2}} = \sqrt{\frac{m}{8e}} \frac{\omega s E_1}{E_0^{3/2}} \tag{3a}$$

The radio-frequency component of the bunched beam current, frequently called the catcher current, will be designated i_2 and is related to the bunching parameter by the expression

$$i_2 = 2I_0J_1(x), \tag{4}$$

where I_0 is the d-c beam current and J_1 is a Bessel function of the first order and first kind. This relation is illustrated by Fig. 2. The curve will be recognized as the Klystron bunching characteristic which has been described frequently.[2-4] This curve may be considered analogous to an I_p vs. E_g characteristic for a conventional vacuum tube where

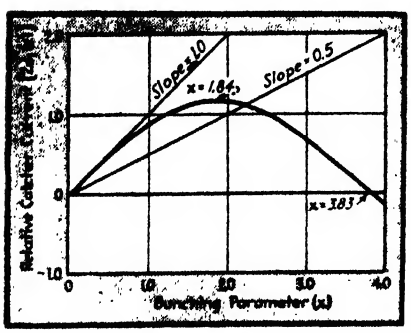

FIG. 2—Klystron bunching characteristic curve, analogous to E_g-I_p curve of ordinary tubes

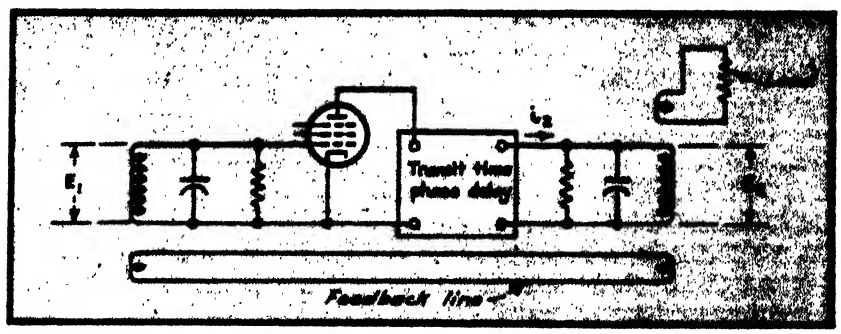

FIG. 3—Equivalent circuit for a Klystron oscillator. The pentode is used to indicate that only electron coupling exists between input and output in this velocity-modulated tube, of which the 410-R/2K30 is a typical example

relative catcher current corresponds to I_2 and the bunching parameter corresponds to E_2, although it differs in appearance because the output reaches a maximum at a bunching parameter of 1.84, and then decreases as the bunching parameter increases. Underbunching refers to values of less than 1.84, usually very small values, and the term overbunching is used to describe the conditions when the bunching parameter is greater than this optimum value.

These principles of electron bunching will now be applied to the analysis of a Klystron oscillator. Any amplifier will oscillate if the gain of the tube is greater than unity and sufficient energy to overcome tube losses is returned from the output to the input in the proper phase.

An equivalent circuit for a Klystron oscillator is shown in Fig. 3. A multiple-grid tube is shown to emphasize the fact that only electron coupling exists between the elements of this type of velocity-modulation tube. The input and output circuits are completely isolated unless a means of feedback is supplied. The voltage between the grids of the buncher resonator is E_1 and this voltage is also indicated as the voltage across the input circuit of the equivalent diagram. A voltage E_2 is shown across the output circuit, and represents the voltage between the grids of the catcher resonator.

A current i_2 is shown flowing into the output circuit. This current represents the radio-frequency component of the bunched beam current, and is related to the input voltage E_1 by Eq. (3) and (4). A four-terminal network is used to represent τ, the transit-time phase-angle. A means of feedback is indicated as a link circuit between the output and input circuits, and an output load is also coupled to the circuit.

Oscillation will occur when the sum of the phase angles around the complete loop is equal to some integral number times 2π radians, provided the magnitude of the feedback is sufficient to maintain oscillation. J. R. Ragazzini has suggested the diagram in Fig. 4 to illustrate these phase angles and the relations between them. The electrons which passed the buncher grids at zero phase (i.e., when E_1 was zero and changing from deceleration to acceleration) become the center of the bunch. These electrons correspond to a maximum value of the electron current and arrive at the catcher grids after a phase delay equal to τ. This phase delay corresponds to slightly less than 2¼ cycles in Fig. 4 and is indicated by an oblique line connecting the zero axes of the E_1 and i_2 curves.

In order to transfer maximum energy to the resonator field, the electrons in the bunch must pass the catcher grids when the resonator field is a maximum and in a direction which will decelerate the electrons. The current in the equivalent circuit must be in phase with the voltage if maximum power is to be transferred. This means that i_2 is a minimum when the electron current is a maximum. The transit phase angle τ corresponds to the phase between a zero value of E_1 and a negative peak of i_2 and there-

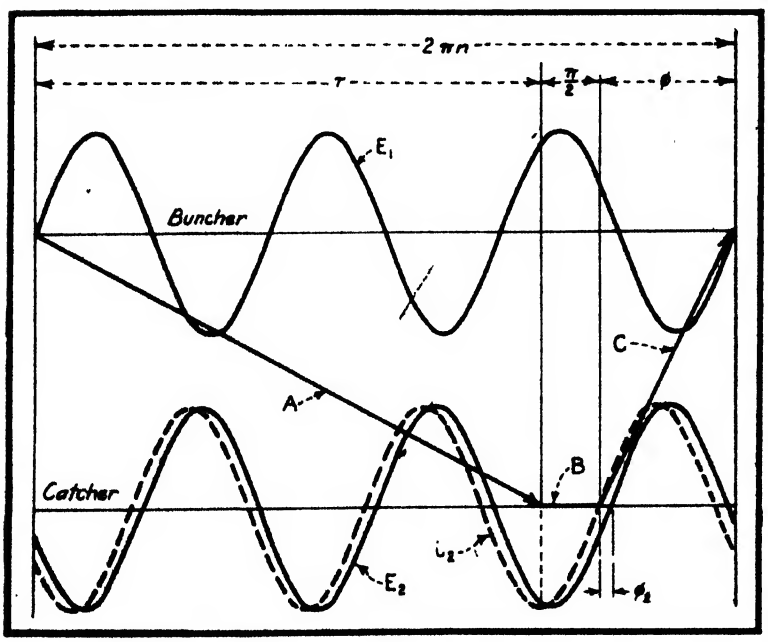

FIG. 4—Phase relations in a Klystron oscillator. The phase change from buncher to catcher along the electron beam drift is represented by vector *A*. The phase shift between the bunched electron stream and the catcher resonator-field current component is represented by vector *B*. The phase shift due to the coupling from the catcher to the buncher is represented by vector *C*. The transit-time phase-angle is represented by the angle

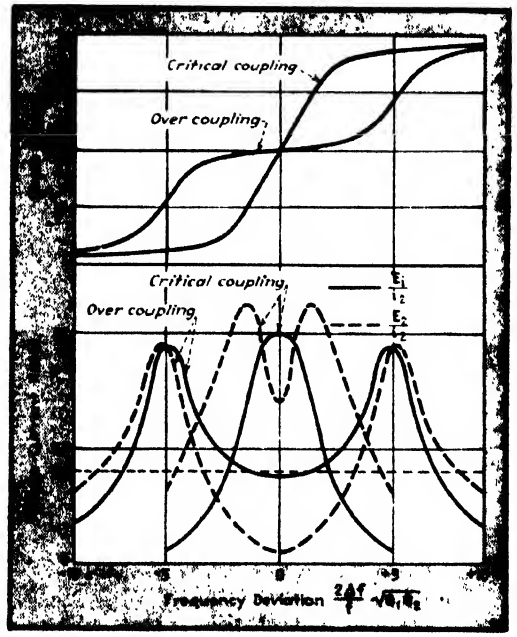

FIG. 5—Phase and voltage relations in coupled circuits where the primary Q is half the secondary Q. The over-coupling condition is for five times critical coupling. The phase angle at the top of the graph is that between primary (catcher) current and secondary (buncher) voltage

fore the phase angle between E_1 and i_b, introduced by the transit time and bunching considerations, is equal to $(\tau + \pi/2)$.

A phase angle ϕ_2 between i_b and the catcher voltage E_2 is shown because E_2 need not be in phase with i_b. However, this phase angle is not used in this analysis of oscillator theory. The angle ϕ represents the phase between i_b and E_1, introduced by the two coupled circuits. The phase relation which must be satisfied for oscillation can be written

$$\tau + \pi/2 + \phi = 2\pi n \qquad (5)$$

where n must be an integer. The value of n in Fig. 4 is 3 cycles. If τ is changed by varying the acceleration voltage, a corresponding change in ϕ must occur.

An analysis[6] of the phase relations in two tuned coupled circuits shows that ϕ will change if the frequency of oscillation is varied. These conditions explain the fact that the frequency of a velocity-modulation oscillator varies when the acceleration voltage is changed, in order to maintain the necessary phase relations.

The equivalent circuit in Fig. 3 shows that a Klystron oscillator may be considered as two parallel resonant coupled circuits, fed by a constant-current source i_b. The analysis of such a circuit to obtain the phase and magnitude of the voltage across the primary and secondary can be obtained, with some slight modifications, from radio engineering handbooks and other sources.[5,6,7] This information about the phase and magnitude of the feedback can then be combined with the bunching characteristic of a Klystron tube, as illustrated by Fig. 2 and Eq. (4), to obtain a prediction of the output characteristics of a Klystron oscillator as the acceleration voltage is varied.

Certain assumptions will be made to simplify the analysis. The resonant frequencies of both circuits will be considered identical; this assumption will make the characteristics symmetrical with respect to frequency. A feedback line of zero length will be assumed so that the analysis for lumped constant circuits at low frequencies can be used. The Q of the two circuits will not be equal because one circuit has been loaded. The Q of the output circuit in Fig. 3, which corresponds to the primary of the two coupled circuits, will be considered half as great as the Q of the input circuit, which corresponds to the secondary. Calculations will be carried out for two degrees of coupling between the two circuits. In one case the coupling will be assumed five times greater than the value for critical coupling, and critical coupling will be assumed for the second case.

Curves of primary and secondary voltage as a function of frequency are usually given in the reference texts[5]. The curves in Fig. 5 will be recognized as typical illustrations of these characteristics for two coupled tuned circuits. Ratios of E_1/i_b and E_2/i_b are plotted so that unit coordinates may be used, and the maximum ratio of E_1/i_b is indicated by a value of unity. Increasing the value of i_b will increase the value of voltage across the circuit but will not affect the ratio. The phase relation between i_b, the constant-current source in the analysis, and secondary voltage E_1 is also shown as a function of frequency.

The form of the curves in Fig. 5 is not ideally suited to the analysis of a Klystron oscillator where the frequency is dependent upon the beam voltage as well as upon the tuning. To examine the behavior of such an oscillator as the acceleration voltage is changed, it will be convenient to replot the frequency as a function of voltage. This step is illustrated by the frequency vs. voltage curves in Fig. 6, which correspond to Fig. 5.

The previous discussion has concerned only the coupled circuit theory. It is necessary to relate these results to the bunching characteristic of a Klystron tube, shown in Fig. 2, in order to complete the analysis and obtain the power output curves shown in Fig. 7.

The Klystron oscillator characteristic illustrated by Fig. 8, which has been obtained by modifying the presentation of the information in Fig. 2, has been used to convert the data in Fig. 6 into the Klystron output characteristics in Fig. 7. Frequency curves have been transferred directly to the corresponding figures, for the values of acceleration voltage which permit oscillation.

Oscillator Characteristics

Calculations for the procedure described briefly in the preceding paragraph are quite simple, and the steps will be outlined in detail. The relation between voltage and frequency is obtained by evaluating τ in terms of E_0, the acceleration voltage, and correlating the values of τ with values of ϕ in Fig. 5. Separate calculations must be made for each value of coupling. Values of τ for chosen values of E_0 are tabulated from

$$\tau = \frac{2\pi f s}{\sqrt{\frac{2e}{m} E_0}} \qquad (6)$$

which is obtained by equating Eq. (1) and (1b). The percent change in frequency is small, and therefore all factors except E_0 may be lumped into a single constant. Corresponding values of ϕ are obtained by substituting the values of τ into Eq. (5). These values of ϕ are used to determine the frequency which corresponds to the acceleration voltage chosen for the tabulation. Then these data are replotted to give the frequency curves in Fig. 6, and the values of E_1/i_b and E_2/i_b are transferred from Fig. 5 to Fig. 6, using this f-vs.-E characteristic.

The necessary correlation between the feedback circuit and the bunching characteristic of a Klystron tube (see Fig. 2), can be obtained by evaluating E_1/i_b in terms of the bunching parameter defined by Eq. (3) and (4). Equation (3), which relates E_1 and the bunching parameter x, can be rewritten

$$E_1 = E_0 x/\pi N \qquad (7)$$

Substitution of Eq. (7) and (4) in the ratio E_1/i_b gives

$$\frac{E_1}{i_b} = \frac{E_0}{\pi N I_0} \frac{x}{2J_1(x)} \qquad (8)$$

The ratio E_0/I_0 may be replaced by R_0, which is known as the beam re-

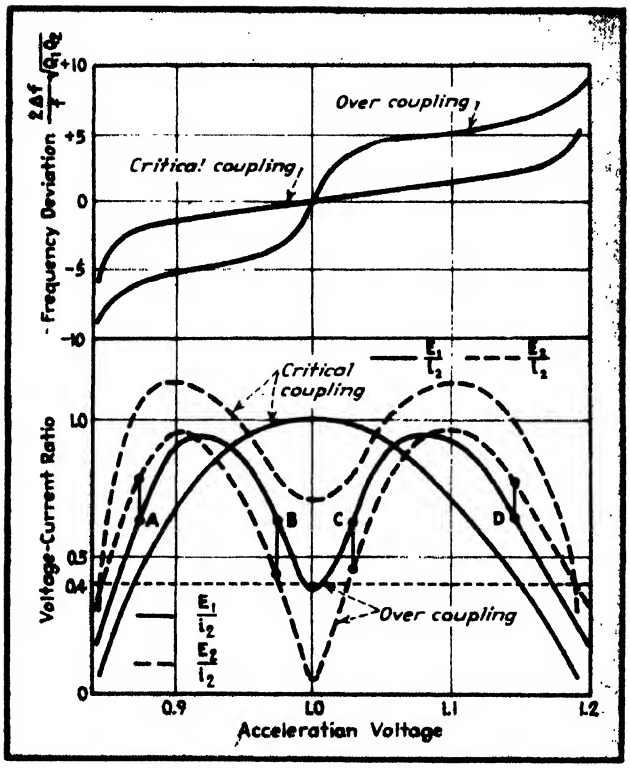

FIG. 6—These curves are for the same conditions as in Fig. 5 but are plotted against accelerating voltage, which is related to frequency by Eq. (5) and (6). The upper curves give the relative frequency deviation vs. accelerating voltage

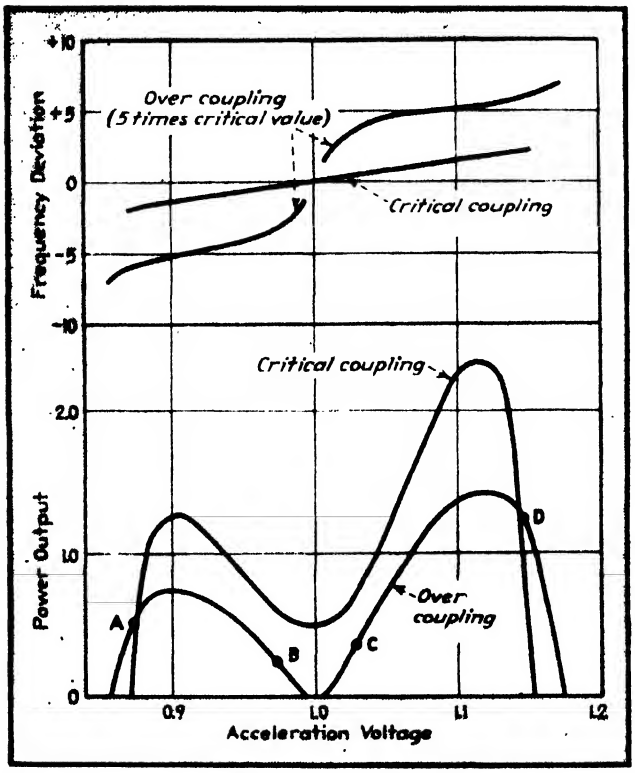

FIG. 7—Taking the power output as proportional to the catcher voltage squared, these curves are obtained from the curves of Fig. 6. Note the linearity between frequency deviation and accelerating voltage for the critical coupling condition

sistance of the tube. Equation (8) can be rewritten

$$\frac{x}{2J_1(x)} = \frac{\pi N I_0}{E_0}\frac{E_1}{i_2} = \frac{\pi N E_1}{R_0 i_2} \qquad (9)$$

These equations furnish the correlation between the feedback circuit characteristic which determines E_1/i_2, and a modification of the bunching parameter.

The significance of the factor $x/2J_1(x)$ can be illustrated by reference to Fig. 2. This factor is merely another form of bunching parameter. Any line from the origin with a slope less than unity will intersect the curve at some point other than zero and less than $x = 3.83$, where the Klystron output again becomes zero. A line with a slope of 0.5 is shown, and this line intersects the curve at a point somewhat beyond the maximum. Another line with a slope of unity is tangent to the curve at the origin. This line does not intersect the curve, and represents the conditions when oscillations start. This starting-characteristic line with a slope of unity corresponds to a unity value $x/2J_1(x)$. Lines with slopes less than unity correspond to values of $x/2J_1(x)$ greater than unity, since the slope of a line is equal to the reciprocal of $x/2J_1(x)$.

Each point on the curve in Fig. 2 corresponds to some operating condition for a Klystron oscillator. It will be convenient to replot $2J_1(x)$, which is proportional to i_2, as a function of $x/2J_1(x)$. This modification of the bunching characteristic makes it possible to obtain the value of i_2 from a value of E_1/i_2, since Eq. (9) shows that $x/2J_1(x)$ is proportional to E_1/i_2. Figure 8 shows such a characteristic, and has been obtained by plotting the ordinate of a point on the curve in Fig. 2 as a function of the reciprocal of the slope of a line drawn from the origin to that point on the curve. The curve in Fig. 8 is used to obtain the value of E_2 from the information in Fig. 6.

Figure 8 is used to obtain data for the curves of power output vs. acceleration voltage in Fig. 7 in the following manner. Typical operating conditions would determine the starting conditions for the Klystron oscillator. We will assume that E_1/i_2 equal to 0.4 corresponds to these starting conditions. For this assumption, Eq. (9) can be rewritten

$$x/2J_1(x) = 2.5\, E_1/i_2 \qquad (10)$$

The dash lines in Fig. 6 represent the starting conditions for the Klystron oscillator. The acceleration voltage corresponding to the intersection of the dash line and the E_1/i_2 curve in Fig. 6 is noted. The output for this value of acceleration voltage is zero. A higher value of E_1/i_2 for a different acceleration voltage is substituted in Eq. (10) to obtain the value of $x/2J_1(x)$, and a corresponding value of $2J_1(x)$ is determined from Fig. 8.

The beam current I_0 is computed from the 3/2 power law and the ac-

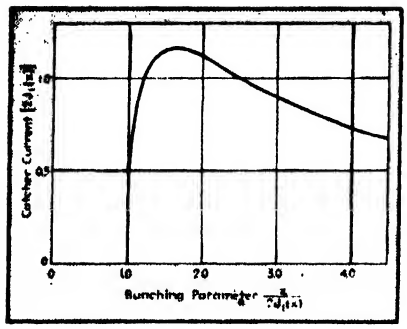

FIG. 8—A change of abscissa converts the bunching characteristic of Fig. 2 to this more convenient form

celeration voltage. The value of i_1 is then obtained by substitution of I_0 and $2J_1(x)$ in Eq. (4). E_2 is calculated from i_2 and the value of E_2/i_2 from Fig. 6 corresponding to the acceleration voltage which was chosen. The power output is proportional to the square of E_2 and is plotted as such in Fig. 7. The frequency curve is transferred directly from Fig. 6 to Fig. 7.

The two sets of theoretical output curves in Fig. 7 are typical of two different types of Klystron oscillators. The curves for five times critical coupling represent a tightly coupled oscillator and exhibit the familiar pair of voltage modes. The maxima of the two modes occur when the frequency has values corresponding approximately to $\phi = 0$ and $\phi = \pi$ in Fig. 5. If these values of ϕ are substituted in Eq. (5), the value of τ is given by

$$\tau \cong 2\pi (n \pm 1/4) \qquad (11)$$

Equation (11) is often stated in the form, "The number of cycles of oscillation during the transit of an electron from the buncher to the catcher is an integer plus or minus one quarter." It should be noted that this statement is a special case which does not apply to all Klystron designs.

The more loosely coupled oscillator illustrated by the critical coupling curves of Fig. 7 has the two modes merged into continuous output. The latter characteristic is typical of the type 410-R/2K30 Klystron oscillator, and differs from overcoupled types which exhibit two separate families of voltage modes.

Experimental curves for a number of voltage modes in a type 410-R/2K30 Klystron oscillator are shown in Fig. 9 and 10. These curves were obtained by a dynamic method which eliminated tuning changes due to thermal variations caused by changing the power input to the tube. The similarity of Fig. 9 to the theoretical curve in Fig. 7 for critical coupling indicates that the assumptions used in obtaining the theoretical curve are reasonably good. The equal height of the two peaks of each mode in Fig. 9 was obtained by purposely detuning the tube to produce the flattest characteristic, and does not represent a deviation from theory. Detuning the tube in the opposite direction emphasizes the higher voltage peak and produces maximum power output and efficiency. This effect is illustrated by Fig. 10.

Note that the frequency deviation characteristic in Fig. 9 is almost linear with accelerating voltage over the useful range of output. This characteristic is gained by some sacrifice in power. (Compare with Fig. 10). Because of this, the type 410-R/2K30 Klystron is quite useful as an oscillator in frequency-modulation circuits. The frequency modulation is obtained by varying the acceleration voltage. However, considerable modulation power is required.

The effect of tuning the Klystron oscillator, as described in the discussion of the output characteristics in Fig. 9 and 10, can be derived from circuit theory but the details will be omitted. Certain important conclusions can be obtained from a qualitative analysis of the overcoupled case, and the general nature of these results applies equally well to the behavior of the type 410-R/2K30 Klystron. However, electron bunching theory must be considered in some detail before returning to a discussion of the effect of tuning.

One of the principal factors in the explanation of Klystron oscillator power output characteristics is introduced by the variation of i_2, the radio-frequency component of the bunched beam current, as the value of E_1 is increased. Figure 2 and Eq. (3a) and (4) illustrate this variation of the radio-frequency current. The term overbunching is applied when the current is decreased from the maximum value because the voltage E_1 is too great. It is more important to analyze overbunching in a diagram similar to Fig. 8, since $x/2J_1(x)$ is more useful than the bunching param-

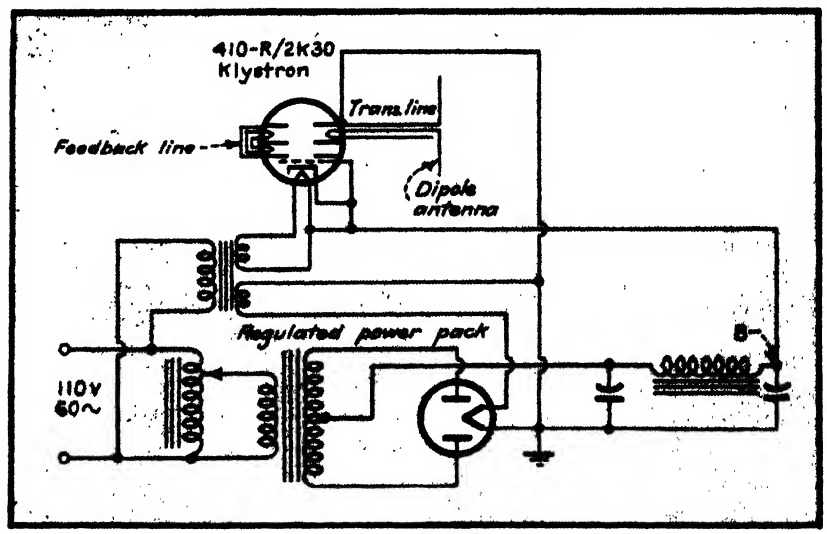

Basic Klystron oscillator circuit, showing the extreme simplicity of the voltage requirements. Like all electron oscillators the frequency is affected by the power pack voltage, but in the case of the Klystron the effect is large (shown in Fig. 9). A coaxial transmission line delivers the uhf energy from the oscillator to the load, which is an antenna in this case

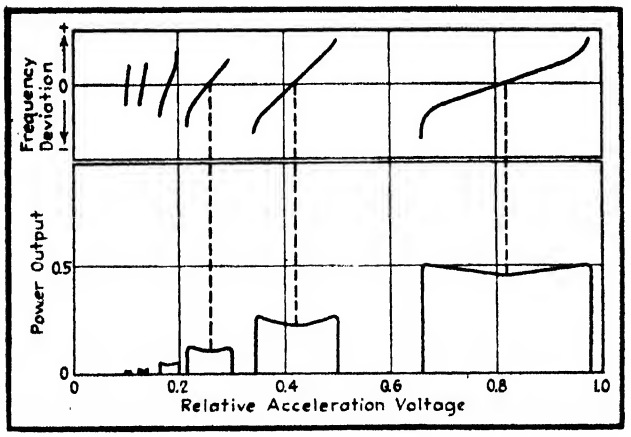

FIG. 9—Experimental characteristics for 410-R/2K30 Klystron oscillator with critical coupling. The tuning was adjusted to give flat output. Compare these curves with the critical coupling curves of Fig. 7

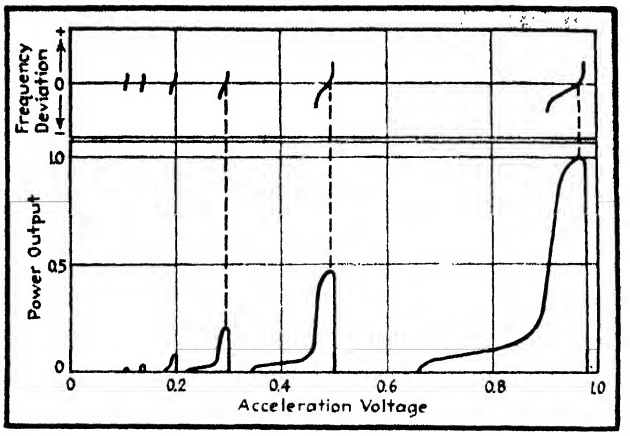

FIG. 10—By adjusting the tuning, the output can be made a maximum. This has been done to obtain these experimental curves. One peak is accentuated at the sacrifice of the other. Operation is more critical of accelerating voltage

eter x in analyzing an oscillator. Optimum bunching in Fig. 8 corresponds to the maximum in the curve when $x/2J_1(x)$ is equal to 1.59, which corresponds to a value of 0.635 for E_1/i_1. Larger values of E_1/i_1 cause overbunching.

Overbunching does not necessarily reduce the output. Note in Fig. 6 that the ratio E_2/i_2 is increasing rapidly at the acceleration voltages corresponding to points A, B, C, and D, which represent the ratio of E_1/i_1 required for optimum bunching. Increasing the ratio of E_1/i_1 above the optimum value does not reduce i_2 very rapidly, since i_2 is proportional to $2J_1(x)$, and Fig. 8 shows that this factor decreases slowly beyond the point of optimum bunching. The increased E_2/i_2 ratio allows the output to increase in the region between A and B, also in the region between C and D. Corresponding points have been marked on Fig. 7 to illustrate this effect.

Any deviation from identical tuning will decrease one peak in the E_1/i_1 curve when the losses in the two resonators are unequal. The other peak may remain approximately the same, or it may increase slightly, depending upon the ratio of the losses in the two resonators. The effect of detuning the buncher resonator to a lower frequency, leaving the catcher resonator tuned to the frequency corresponding to the identical tuning represented in Fig. 5, is illustrated in Fig. 11 for the case when the losses in the catcher resonator are twice as great as the losses in the buncher resonator. Both patterns are moved in the direction of lower frequency and the patterns are no longer symmetrical. The higher-frequency peak in E_1/i_1 is reduced and the corresponding peak in E_2/i_2 is increased.

As a result of the detuning, the degree of overbunching in the high-frequency mode will be less and i_1 will increase. Since E_2/i_2 has also been increased by the detuning, the output of this mode will increase considerably. In contrast, the overbunching remains about the same in the lower-frequency mode but the ratio of E_2/i_1 is decreased, and therefore the output of this mode decreases slowly. However, the ratio of E_1/i_2 for the higher-frequency mode can be reduced to the value corresponding to the starting conditions while the lower-frequency peak in E_1/i_2 remains greater than this value. This relation means that continued detuning of the buncher resonator to a lower frequency causes the higher-frequency mode to increase at first, then disappear before the lower-frequency mode is eliminated. The frequency of the higher-frequency mode approaches the frequency of the tuning of the catcher resonator. The lower-frequency mode can be accentuated by detuning the buncher resonator to a higher frequency than the tuning of the catcher resonator.

Effect of Length of Feedback Line

The previous discussion has been based upon a zero length of feedback line. This assumption obviously does not apply to a type 410-R/2K30 Klystron, since an external feedback line of considerable electrical length must be used. The problem is complicated when the line is not terminated with its characteristic impedance. However, it is fairly satisfactory to assume that the phase shift in the line can be represented by an angle ϕ_L, and rewrite Eq. 5 in the form

$$\tau + \frac{\pi}{2} + \phi + \phi_L = 2\pi n. \qquad (12)$$

The logical conclusion from Eq. (12) would be that the acceleration voltage, which determines τ, could be arbitrarily chosen by adjusting the length of the feedback line. Some choice of the operating voltage is permitted by such an adjustment. However, the feedback line is not usually matched, and certain line lengths prevent operation at the frequency which may be required. Therefore, it is not always possible to correct for changes in the transit time by changes in the length of the feedback line. As a result, there are some regions of acceleration

voltage where oscillation can not be obtained by any simple adjustment of the tube or feedback line.

All of the previous discussion is influenced by the output load which is connected to the tube, but this effect has been included implicitly in the assumption that the losses in the output resonator were twice as great as the losses in the buncher resonator. This assumption is equivalent to the statement that the resonators are identical and that the power transferred to the load is equal to the power losses in the output resonator itself.

Power Output

Data have been obtained which relate the output power which can be transferred from a Klystron oscillator to a given load resistance. These data are shown by the points in Fig. 12. The curve in Fig. 12 represents a constant-current source feeding a parallel resonant circuit with internal losses and a coupled load. The theoretical curve was made to coincide with the observed maximum output from the Klystron oscillator. Zero load resistance in this illustration corresponds to a light load, i.e., the load resistance is an equivalent series resistance. The agreement between the experimental points and the theoretical curve in the region beyond the maximum output fails because the Klystron does not oscillate when the load becomes too great.

It is apparent that the characteristics of velocity-modulation tubes must be considered carefully when equipment is designed to use these tubes. In some respects these tubes are similar to the more familiar types of vacuum tubes. They can be used as oscillators or amplifiers, and when equipped with the proper resonators, they can also be used as frequency multipliers. Klystron oscillators are more dependent upon the voltage applied to them than triode vacuum tubes, and both frequency and output will vary if the voltage is changed. Operation is possible at a number of different voltage modes, but oscillation does not occur in the region between these modes. When these characteristics are either used or circumvented in the design of the equipment, these factors do not limit the application of the tubes and actually make it possible to accomplish results which are difficult to achieve in any other way.

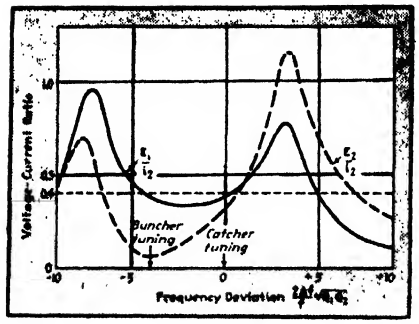

FIG. 11—Detuning the buncher to a lower frequency shifts the peaks to lower frequencies. Except for this detuning of the buncher, these curves represent the same conditions as those illustrated by the over-coupling curves of Fig. 5

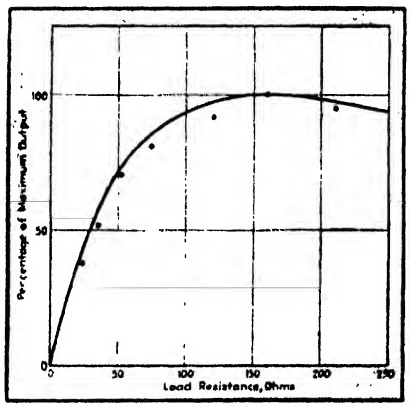

FIG. 12—Theoretical output curve and experimental output points measured for the 410-R/2K30 Klystron oscillator

References

(1) Varian, R. H., and Varian, S. F., A High-Frequency Oscillator and Amplifier, *Jour. Appl. Phys.* 10, No. 5, p. 321-327, May 1939.

(2) Webster, D. L., Cathode Ray Bunching, *Jour. Appl. Phys.* 10, No. 7, p. 501-508, July 1939.

(3) Webster, D. L., The Theory of Klystron Oscillations, *Jour. Appl. Phys.* 10, No. 12, p. 864-872, Dec. 1939.

(4) Harrison, A. E., "Klystron Technical Manual," Sperry Gyroscope Company, Inc., Great Neck, N. Y., 1944.

(5) Terman, F. E., "Radio Engineer's Handbook," McGraw-Hill Book Co., New York, 1943.

(6) Aiken, C. B., Two-Mesh Tuned Coupled Circuit Filters, *Proc. IRE*, 25, No. 2, p. 230-272, Feb. 1937.

(7) Ragazzini, J. R., Ultra-High Frequency Techniques, Lecture Notes, Columbia University Bookstore, 1943.

Testing Cathode-Ray Screens

Equipment for determining the light output of cathode-ray tube phosphors makes possible accurate evaluation of screen materials during development and product sampling to assure adherence to tolerances. Special features of test set are described

By JOSEPH C. TELLIER and JOSEPH F. FISHER

INTRODUCTION of long-persistence cathode-ray tube screens for radar indicators necessitated standardization of characteristics of the screens among all tube manufacturers. Toward this end a group at the Radiation Laboratory of the Massachusetts Institute of Technology under the direction of W. B. Nottingham developed basic specifications, test equipment, and procedures for testing.

Equipment developed by the Philco Research Division was in accordance with the standards and

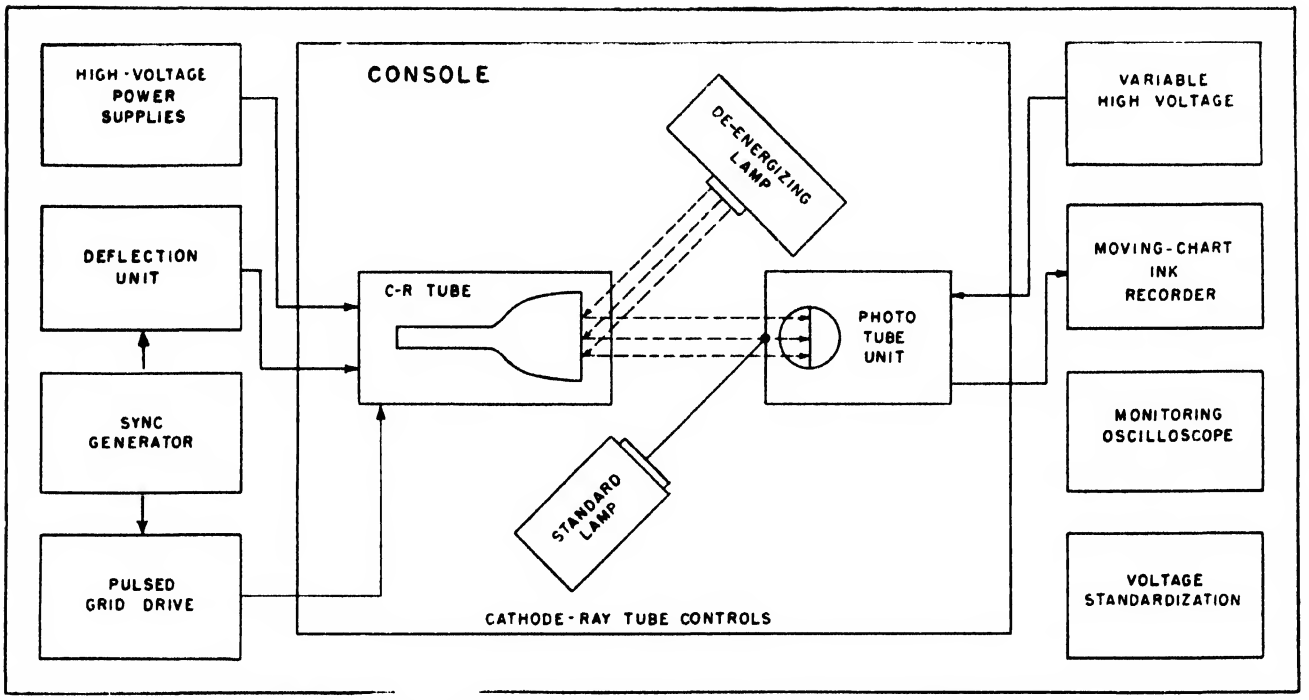

FIG. 1—Block diagram shows interrelation of units of cathode-ray tube test equipment

utilized basic circuits developed by the Radiation Laboratory, but was extended in scope to provide greater versatility. Two complete units were constructed and are now in use as an adjunct to further screen phosphor development.

Functions of Equipment

Broadly, the functions performed by the equipment can be divided into three general categories. All static voltage and current characteristics of a wide variety of cathode-ray tubes can be measured. Steady measurements of light output from tube screens under various test conditions can be made. However the primary function of the equipment is to measure the build-up and persistence of light output from long-persistence screens exemplified by the P7 type.

Physically the equipment consists of 18 standard relay-rack chassis in two six-foot racks, and a light-tight wooden console in which the cathode-ray tube is mounted for test. The several units comprising the equipment, together with the general nature of their functions, are represented in Fig. 1.

CONSOLE—This unit provides for mounting any of a variety of cathode-ray tubes at a standard distance of 30 centimeters from a 931 photomultiplier tube. It also contains provision for making absolute calibration of light intensity, and means for rapidly de-energizing the screen between tests.

CRT CONTROLS—Filament voltage, cathode bias, and other potentials are controllable from a convenient central point.

SYNC GENERATOR — Synchronizing pulses for the deflection unit are provided in this compartment

DEFLECTION UNIT — Horizontal and vertical deflection voltages producing a 200-line, noninterlaced raster at a 60-cycle frame rate are provided for either electrostatically or magnetically deflected tubes.

PULSED GRID DRIVE UNIT—Duration of the raster, repetition rate, and number of rasters applied in total are determined by an electromechanical network incorporated in this chassis.

MOVING CHART INK RECORDER—A record of light output as a function of time is made on the chart of an ink recorder. From this record is obtained all numerical data relating to light output from the crt screen.

VOLTAGE STANDARDIZATION UNIT —Critical voltages from the entire system are brought to this unit and checked against a standard-voltage cell, in a comparison circuit utilizing a 6E5 indicator tube.

PHOTOMULTIPLIER TUBE POWER SUPPLY—This is a variable, regulated high-voltage supply used to adjust the amplification of the 931 tube.

POWER SUPPLIES—These are two conventional low-voltage regulated power supplies.

H-V POWER SUPPLIES — Three supplies provide anode voltages to the crt under test and incorporate a unique, extremely effective regulating system. Multirange current metering is also provided.

MONITORING OSCILLOSCOPE — This unit permits observation of waveshapes throughout the system and facilitates adjustment of the synchronization of various units.

The P7 screen, which is a typical long-persistence type, comprises a double layer, the outer layer being a zinc cadmium sulphide and the inner a zinc sulphide silver activated fluorphor. Under electron bombardment, the inner layer fluoresces brightly and excites the outer layer. The latter phosphor-

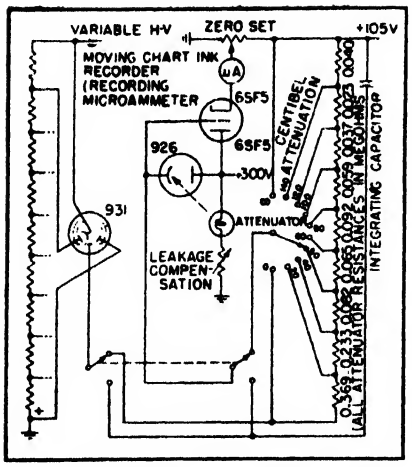

FIG. 2—Basic prototube-unit circuit

esces under this excitation, continuing to glow long after the fluorescent excitation has disappeared. If the excitation is applied periodically, for brief intervals, the light output from the outer screen will take on increments until a saturation condition is reached. This condition represents maximum light output.

To obtain a unique unit of measurement, the centibel was adopted, and defined. This unit is one one-hundredth of a bel, so that the number of centibels corresponding to a given light power ratio is given by $cb = 100 \log_{10} (P_1/P_2)$ where P_1 and P_2 are the two values of light power whose ratio is to be expressed. In addition, the zero level was chosen as 2×10^{-6} foot lamberts, corresponding to the generally accepted zero sound level of one milliwatt.

If, then, the voltages and beam current of a particular cathode-ray tube are set to specified values, the raster size is adjusted to a given area, and the raster is applied to the screen for brief, constant periods, spaced by known time intervals, the light output will vary as a function of time in the following general fashion. Each instant of raster application will produce a bright fluorescent flash from the inner screen, followed by a slowly decaying phosphorescent glow. The glow after each flash will be at a higher level than that after the preceding flash, with the increments gradually becoming smaller.

The light level after a fixed number of flashes is a direct measure of the buildup characteristic of the screen. This measurement is the data actually taken in practice to determine this characteristic.

Test Parameters

Certain values of test parameters were found to give optimum results, and standards of test procedure were consequently based on these. The type 5FP7 tube, as an important example, is tested under the following conditions.

The anode potential is accurately set to 4,000 volts, and the beam current, during raster application, to 60 microamperes. The raster area is 50 square centimeters, and is applied for one sixtieth of a second, at one-second intervals. All of these factors are maintained precisely, some manually in conjunction with self-contained measuring instruments, and some automatically by the equipment itself. The resulting light output as a function of time is plotted on the recorder. From this plot, the light output after the first, fifth, and tenth flashes is measured, the ratio of the fifth to the first and the tenth to the first is calculated, and the corresponding number of centibels derived. These ratios of light output are defined as $cb_{(5:1)}$ and $cb_{(10:1)}$ respectively, and are taken as factors indicative of the build-up and persistence of the screen. On the basis of these factors, tubes can be directly compared, or tolerances can be established on $cb_{(5:1)}$ and $cb_{(10:1)}$ within which production tubes must lie.

Two auxiliary tests are commonly made in conjunction with the build-up measurements. The first of these is the fluorescent measurement and involves applying a steady raster, all other test conditions being the same, and measuring the total light output emanating from the screen. The second of these is a measurement of integrated flash. For this purpose a single raster is applied for one sixtieth of a second, and the phototube output circuit is converted to an integrating network. This technique provides an

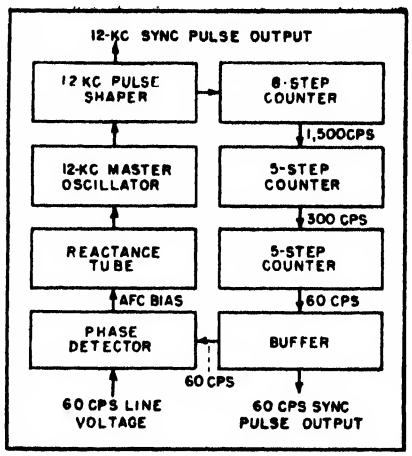

FIG. 3—Elements of sync generator

accurate method of measuring the effect of the initial flash from the inner screen, and is important because the latter is a source of annoyance to the eye of the operator, and must not be allowed to become excessive.

Mounting the tube to be tested presented the first equipment design problem. Several pieces of associated equipment had to be positioned near the tube, light output had to be measured under darkroom conditions, and yet access for changing tubes rapidly had to be provided. The solution to these mechanical problems was to use the console.

In the console, the tube under test is mounted in the righthand section, which is accessible by lifting the hinged lid. In position, the tube faces the lefthand section in which is the phototube chassis and de-energizing lamp. The entire lefthand section can be dropped flush with the table top, leaving the tube face exposed for preliminary adjustments. This section is raised

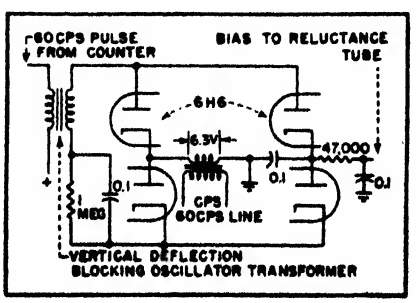

FIG. 4—Circuit of phase detector

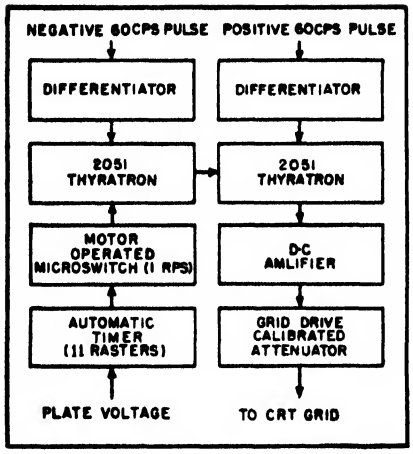

FIG. 5—Pulsed grid drive unit

by means of a foot pedal. Various compartments and drawers provide space for adaptors and other equipment.

In the righthand section is a sliding carriage so arranged that the faces of tubes of any length can be positioned at the standard distance of 30 cm from the phototube. Positioning is accomplished quickly by the use of front and rear sighting wires. A variety of clamping sections, providing for several neck diameters, can be bolted to the base of the sliding carriage. On the rear wall are sockets providing all needed electrical connections.

Phototube Unit

A long, rectangular closed chassis in the lefthand section of the test equipment is the heart of the optical portion of the system. The central point in this chassis is the 931 photomultiplier tube, which provides the basis for making absolute measurements of light output from the screen under test. The tube is mounted on a sliding subchassis, in order that the light-sensitive surface may be set at exactly the correct distance from the sighting wires used to position the cathode-ray tube face. Other auxiliary components of this chassis are the light-leakage compensation phototube, the inner standard lamp, the attenuator, and the cathode-follower output stage, shown in Fig. 2.

By means of the ganged switch in this unit, the plate load impedance of the 931 tube may be made either the centibel-calibrated attenuator or the integrating capacitor. The output voltage developed across either load is directly coupled to the grid of the 6SF5, and the recorder microammeter is connected into the cathode. Initial current in the recorder is adjusted to zero by setting a variable resistor such that the 6SF5 is just cut off, with the grid at +105 volts. There is always a small current flow in the 931 plate, because of dark current in the latter, light leakage into the console, and the crt filament glow. In order to cancel this current, a 926 leakage-compensation phototube is connected in opposite polarity, and the magnitude of the cancelling current is controlled by means of a small lamp. The brilliance of the latter is adjusted by the compensation resistor.

To avoid frequent use of the external standard lamp, an inner secondary standard lamp is provided. The brilliance of this lamp is controlled by a precision attenuator, which is calibrated occasionally by means of the external standard lamp.

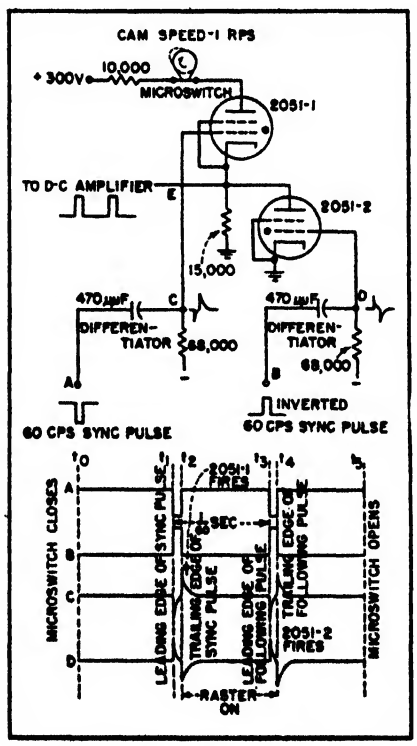

FIG. 6—Thyratron control raster

To the base plate of the phototube unit is mounted a swivel arm on the end of which is placed the external standard lamp. In position, the standard lamp is directly in front of the 931 phototube, and exactly 22.6 cm from it. When the current in the lamp is of such a value as to develop a drop of 1.018 volts (standard cell voltage) across a resistor of 16.75 ohms, exactly +500 cb of light is produced.

In making tube tests, it is necessary to start with a condition of no light output. A P7 screen, however, will glow for at least one half hour after excitation. It has been found, fortunately, that red light at a frequency of about 6,000 angstroms will deactivate a screen in 45 seconds. Light at this frequency will release the electrons momentarily established in trapped energy levels, without raising them to higher energy levels. Hence they fall to the desired neutral level, and the tube face is darkened. A red theater flood light is used for this purpose.

The crt control chassis needs little description. Here, in a central convenient point, are means for controlling and metering filament voltage, cathode bias, and focus-coil current. In addition, the master power switch is located in this chassis. In particular, cathode bias is controlled by a precision step attenuator, operating from an accurately established 300-volt supply.

Deflection Unit

In order to obtain comparable light output readings, a consistent pattern must be applied to the crt screen; this is accomplished by standardizing on a 200-line, noninterlaced raster. In order to maintain such a raster, it is first necessary to derive certain synchronizing pulses, in this case a 12-kc and a 60-cps pulse. The sync generator unit is outlined in Figure 8. Output at approximately 12 kc is first obtained from a master oscillator. This sinusoidal voltage is then applied to an overdriven two-stage

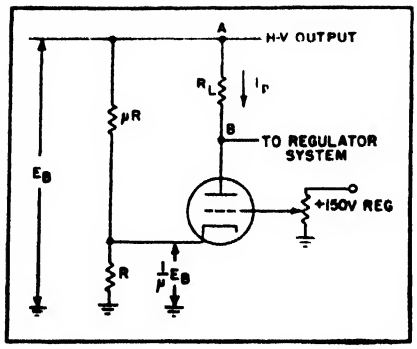

FIG. 7—Improved voltage regulator

amplifier whose output is essentially a 12-kc square wave. The latter signal is next applied to a conventional 8-step diode counter and blocking oscillator, the resulting signal being a 1,500-cps pulse. The procedure is repeated in two 5-step counters, the final output being a pulse at approximately 60 cps. This pulse is then compared with the 60-cps line voltage by means of a phase detector, and the resulting bias applied to a reactance tube which holds the master oscillator frequency at exactly 12 kc. The basic phase detector is shown in Fig. 4.

The deflection circuits utilized to produce the 200-line raster are conventional and need not be elaborated upon. Some complexity of switching is caused by the necessity for providing horizontal and vertical deflection for both magnetically and electrostatically deflected tubes, but individual circuits, neglecting switching, are those commonly found in the literature.

Raster Timer

With the raster-producing voltages available, it is next necessary to apply the raster periodically for brief intervals. This keying is accomplished through the medium of the pulsed grid drive unit—a most important unit upon which the sequence of all operations performed automatically depends. The basic elements of this circuit are shown in block diagram in Fig. 5.

A Microflex automatic timer is so connected as to close a 300-volt circuit for slightly more than eleven seconds after a switch inaugurating the raster pulsing is thrown. A Telechron clock motor drives a cam at the rate of one revolution per second, which in turn is arranged to close a Microswitch for slightly more than one sixtieth of a second, once each revolution. Plate voltage is thus applied through the timer and Microswitch to the thyratrons once a second for an eleven-second interval.

By means of the thyratrons, the grid of the crt under test is raised from below cutoff to a value determined by the calibrated attenuator. During this period, a raster corresponding to a previously determined beam current is thus applied to the screen.

Operation of the thyratrons can be discussed with reference to Fig. 6 where a typical sequence of Microswitch closing and pulse occurrence is illustrated. At time t_0 the Microswitch closes. At time t_1, the leading edges of two pulses, coincident but of opposite polarity, are applied at terminals A and B. The differentiated pulse at C is negative, however, and nothing happens. At a slightly later instant t_2 a positive pulse appears at C corresponding to the differentiated trailing edge of the pulse at A. Thyratron 2051-1 is fired, and a positive voltage appears at E. This voltage is transmitted through the d-c amplifier and the attenuator to the crt grid, and a raster appears on the screen. At time t_3, the pulse at D is negative, because of differentiation, and thyratron 2051-2 remains nonconducting.

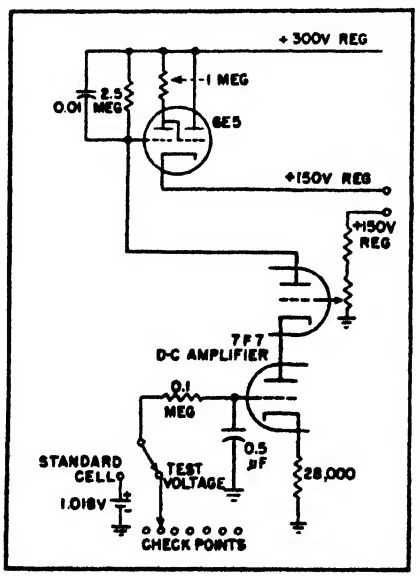

FIG. 8—Voltage and current calibrator

At time t_4, essentially one-sixtieth of a second later, a positive pulse appears at D, firing thyratron 2051-2 and reducing the voltage at E to a sufficiently low value to cut off the crt. Shortly afterward, at t_5, the Microswitch opens, turning off both thyratrons. This cycling continues for eleven seconds, after which the automatic timer removes the plate voltage permanently and the run is completed.

As was noted (Fig. 2) the phototube current developed by the raster is applied through a cathode follower to the sensitive element of an ink recorder. This element has a full-scale sensitivity of 250 microamperes. The recorder chart moves at a rate of approximately 5 inches in 11 seconds.

To provide for testing as many crt types as possible, three high-voltage supplies at nominal outputs of 7, 3.5, and 2 kv are supplied. These supplies contain an unusual feature in the regulating system which makes the latter very effective. Referring to Fig. 7, it will be seen that the grid of the triode is connected to an adjustable bias point, while in the cathode, a voltage equal to the output voltage divided by μ is applied. Under these conditions it is possible to show that I_p is independent of E_b. Therefore, the voltage drop across R_L is constant, and if voltage variations occur at A, the same magnitude of variation occurs at B, but at a lower center value. This behavior is in contrast with a resistive divider wherein the voltage variations are reduced in magnitude by exactly the reduction in center value. Thus the gain of the regulating network is greatly increased by the use of this additional tube.

To establish exactly all critical voltages in the system, a method of comparison with the voltage output from a standard cell is used. These

voltages are obtained from current flow through precision resistors. Knowing the resistance value, the required current flow to produce a given voltage is calculated. Next, the resistance required to produce a voltage of 1.018 volts with this current is determined and obtained. This latter voltage is then compared with a standard cell, and the current adjusted until both are equal.

For the purpose of comparing standard cell and test voltages, a circuit utilizing a magic-eye tube is used, as shown in Fig. 8. The standard cell and test voltages are switched alternately to the grid of a d-c amplifier, whose output is connected to the grid of the 6E5. When no change is observed in the eye angle, the voltages are equal.

The final unit is the monitor, which is a conventional oscilloscope mounted with the rest of the equipment for convenience in establishing correct operating conditions.

Photographing Patterns on Cathode-Ray Tubes

Comprehensive investigation of the photography of transient traces on cathode-ray tubes indicates that writing speeds up to 1,000 km per sec can be recorded. Procedures for obtaining maximum writing speed are outlined, with alignment charts to simplify calculation

By RUDOLPH FELDT

TODAY, cathode-ray equipment is in extensive use for visual observation of both transient and recurrent phenomena in nearly every field of scientific endeavor. But despite the tremendous number of applications in which such equipment is used, and the frequent necessity of obtaining photographic records of the information appearing on fluorescent screens, little information is available concerning the technique of obtaining such records and the maximum speeds of the cathode-ray beam which can be recorded photographically using standard commercial type cathode-ray tubes.

Either the published information is limited to development tubes operated under special conditions by means of which extremely high writing speeds have been recorded (up to 50,000 kilometers per second), or complicated formulas are given which the average user of cathode-ray equipment is unable to employ because of the various factors which are usually unknown and difficult to measure.

It is the purpose of this article to give data on maximum writing speeds which can be recorded photographically with commercial tubes operated at low and medium accelerating potentials. These data are based on the light output of the fluorescent screen, which, in combination with the color of the screen radiation, determines the photographic efficiency of a cathode-ray tube.

Screen brightness can be measured by simple methods which do not require connections to the high-voltage circuits of the oscilloscope. Minimum brightness values of each tube type are usually available from the tube manufacturer and thus the choice of a desirable tube is considerably facilitated.

The information given herein is divided into three parts. First, methods are outlined which lead to the determination of the most suitable film emulsion and of the photographic efficiency of the more common types of standard cathode-ray tube screens. Second, the method of measuring the maximum photographic writing data is described. Finally, a tabulation of the results is given in the form of tables and graphs, with practical illustrations demonstrating the use of the tabulated data for predicting results.

Comparison Procedure

Photographic density (logarithm of opacity) and exposure (product of light intensity and time) are not related in a linear manner, but by the Hurter and Driffield or *D*-log *E* curve, in which the density, plotted against the logarithm of the exposure, results in an *S*-shaped curve. Any satisfactory method of comparing films must employ a method which permits comparison over the entire range of their sensitivity response or *D*-log *E* curve. This evaluation may be accomplished quite simply and accurately by the use of calibrated gray scales, which was the method used in this investigation. Measurements were carried out in the following manner:

(1) The visual brightness of the various cathode-ray tubes was determined in accordance with the RMA recommended procedure, i.e., with a linear raster two inches by

two inches. A 60-cps saw-tooth signal was applied to one pair of deflecting plates and a 3,000-cps signal was applied to the other pair of plates producing a 50-line raster. When compressed to the extent that the line structure merges into a solid block of illumination, such a raster may be considered as a light source of equal brightness over its entire area. The brightness of the raster was measured with a Weston type 603 illumination meter provided with a Viscor filter.

(2) A calibrated photographic gray scale of the transmission type*, mounted in proximity to the fluorescent screen and illuminated by the raster, served as a calibrated attenuator with twenty approximately equal steps of brightness increase at a standard step ratio of $\sqrt[4]{2} = 1.26$. The gray scale was mounted on a protecting glass plate and was covered by a black paper through the scale.

(3) The gray scale illuminated by the raster was photographed with constant lens aperture and exposure time but with various types of fluorescent screens as light sources and different photographic emulsions. The developed negative contained a density scale graduated in successive steps exposed with exposure ratios of $\sqrt{2}$. With constant development conditions, the density of the scale on the negative depends upon the brightness of the tube, the color of the fluorescent screen, and the sensitivity of the photographic emulsion. For any given screen, the films may be compared directly by noting the density of corresponding steps on the density scale. For different screens, the comparison of different films may be made on the basis of equal visual brightness as measured by the illumination meter.

(4) Comparison of various films is easily done by superposing the films in pairs and comparing the recorded scales side by side. One of the scales is moved in a direction parallel with respect to the other until steps of equal density coincide on both scales. The number of values obtained at both ends of the scales are of interest and are presented in Table I. The density of the film base and the residual fog are eliminated by this method and only densities above fog are compared.

* Available from Eastman Kodak Co.

TABLE I—Comparison of Relative Film Speeds at High and Low Densities for Various Emulsions and Fluorescent Screens

FILM	RELATIVE EXPOSURE REQUIRED					
	P1 Medium-persistence green; $B = 7.5$ ft-lamberts		P2 Long-persistence green; $B = 1.55$ ft-lamberts		P5 Short-persistence blue; $B = 0.9$ ft-lamberts	
	Low Density	High Density	Low Density	High Density	Low Density	High Density
Agfa Triple S Ortho	1 0	1.0	1.0	1 0	1.25	1.6
Eastman Ortho X	3.2	1 25	1.6	1.6	2.0	2.5
Eastman Superpan Press	5.0	1.25	1 6	1 6	3 2	3.2
Defender Ortho X-F	3.2	2.0	1.6	1.6	1.6	2 0
Eastman Super XX	3.2	2.0	2 0	1.6	4.0	4 0
Defender X-F Pan	4.0	2.0	2.0	2.0	4.0	4.0
Agfa Triple S Pan	4.0	2.5	2 0	2.0	4.0	4 0
Agfa Fluorapid Blue	40	....	5.0	4.0	1.0	1.0
Eastman X-ray Blue	64	....	5.0	5.0	2.0	1.6

TABLE II—Photographic Light-Producing Efficiency of Common Screens (P5 Screen-Unity)

Type of Fluorescent Screen	P1 Medium-persistence green	P2 Long-persistence green	P5 Short-persistence blue
Visual Brightness (ft lamberts)	7.5	1.55	0.9
Relative Brightness	8.3	1.7	1 0
Relative Film Speed (from Recorded Density Scales)	0.63	0.25	1 0
Test Film	Agfa Triple S Ortho	Agfa Triple S Ortho	Agfa Fluorapid Blue
Photographic Efficiency K	0.076	0.15	1.0
$1/K$ (ft lbt for equal photographic effect)	13.2	6.7	1.0

Table I shows the relative film speeds of nine different film emulsions when exposed by the three most common types of screens employed in cathode-ray oscillography: P1 medium - persistence green, P2 long-persistence green,

and P5 short - persistence blue. The films with a relative speed of 1.0 have the greatest sensitivity and serve as a reference basis. The figures shown, with relation to other film types, are the factors by which the exposure must be increased to produce the same density on the negative as was produced on the emulsion used as the basis of reference. Agfa Triple S Ortho film gives excellent results for all screen colors, while Agfa Fluorapid Blue gives slightly better results for the P5 screen.

Table II presents a summary of the photographic efficiency of the three screens, under conditions usually found in commercial equipment (Du Mont Type 175-A). The steps by which the ends of the scales are displaced is an expression of the difference in sensitivity of the emulsion, or of the photographic efficiency of the fluorescent screen. Since adjacent steps correspond to an exposure ratio of $\sqrt{2}$, a difference of three steps means that the exposure would have to be doubled to obtain the identical negative density.

Comparison of Films

Certain emulsions behave in a very different manner at low and high densities. Therefore, the tubes were operated at medium voltages and brightness. The photographic efficiency K is obtained by dividing relative film speed by relative brightness. Note that for the P1 screen more than thirteen foot-lamberts are required to secure the same photographic effect as is produced by one foot-lambert using the P5 screen.

TABLE III—Ratio of Increase of Photographic Efficiency and Visual Brightness Through Use of Intensifier

Screen	Photog. Eff. Ratio	Visual Brightness Ratio
P1 Medium-persistence green	5:1	4.7:1
P2 Long-persistence green	6.3:1	7:1
P5 Short-persistence blue	5:1	4.5:1

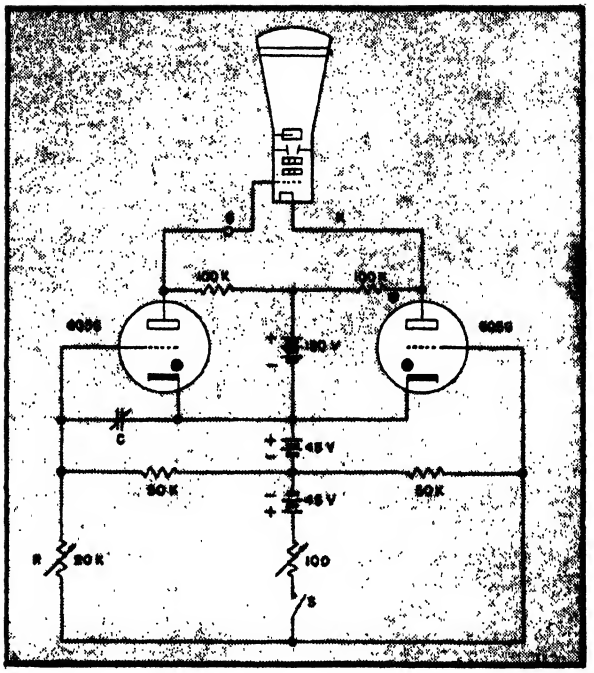

FIG. 1—Schematic wiring diagram of circuit providing modulation of beam of cathode-ray tube for eliminating background light. Values used for C are 500, 5000, 50,000 and 500,000 $\mu\mu f$

Effect of Intensifier Electrode

Table III indicates the extent to which the visual brightness and photographic efficiency can be increased by means of an additional electrode intensifier located between the deflecting plates and the screen. It is held at a positive potential with respect to the second anode so as to impart additional kinetic energy to the electron beam after deflection. Tube types such as the 5CP1 and 5LP1 are constructed with this additional electrode. It can be seen that the increase of efficiency corresponds to the increase of visual brightness.

To summarize the results of the initial investigation it may be concluded:

(1) Agfa Triple S Ortho Film is desirable for recording the radiation from P1, P2 and P5 screens, while Fluorapid Blue gives slightly better results with the P5 screen. For high-speed recording Triple S Ortho is somewhat superior to Fluorapid Blue.

(2) Using the film most suitable for each fluorescent screen, the P1 screen requires more than thirteen times the visual brightness (as measured with the illumination meter) of the P5 screen to produce equivalent photographic effects on the negative.

(3) Blue - sensitive emulsions such as Fluorapid Blue and X-ray Blue are not desirable for recording radiation from a P1 screen.

(4) Comparisons were made using a single standard condition for development. However, once the most suitable emulsion has been selected (from Table I) it is possible to improve results by employing film development procedures which make possible the attainment of maximum speed for the emulsion selected.

(5) Proper use of the intensifier electrode increases visual brightness and photographic efficiency five-fold, compared to results obtained without an intensifier.

These results were obtained using the cathode-ray tube screen as a steady light source. Effects caused by screen persistence characteristics are therefore disre-

garded. It is in order, therefore, to investigate the behavior of the two most suitable film emulsions at high-speed dynamic conditions.

Definitions and Standards

It is essential to use certain definitions and standards as a basis for an easy comparison of photographic results. The standards employed are those used by other investigators.

The maximum photographic writing speed is the maximum speed of the luminescent spot which produces a recording of density 0.1 above fog at an object-image ratio of 1:1 with a lens aperture of $F/1$ on an unspecified high-sensitivity emulsion developed with high-contrast developer.

TABLE IV—Film Sensitivity Rating Under Dynamic Conditions:

Light source: P5 tube on 175-A with intensifier. Maximum brightness B = 0.9 ft-lambert (same conditions as for Table I) Development: D76, 10 minutes. Signal amplitude: ± 1 cm constant.

Emulsion	Photographic Density		
	$f = 1$ kc, $F = 4.5$	$f = 10$ kc, $F = 1.5$	$f = 100$ kc, $F = 1.5$
Agfa Fluorapid Blue	0.36	0.34	0.02
Agfa TSO	0.36	0.37	0.04
Agfa SPP	0.30	0.30	*
Agfa TSP	0.23	0.25	*
Eastman Ortho	0.21		
Eastman Ortho X		0.23	*
Eastman SPP	0.20	0.22	*
Eastman Super XX	0.18		*
Defender KF Panchro	0.06		
Eastman SXX		0.21	
Defender XF Ortho		0.14	

* Too weak to be measured accurately.

The relation between illumination intensity on the photographic film, I', the light radiation of the object, I, the transmission of the lens system, T, the object-image ratio, M, and the lens aperture, F, can be expressed by the formula

$$I' = \frac{I\,T}{4F^2\,(1+M)^2} \qquad (1)$$

The artifice of recording oscillograms reduced in size permits securing higher writing speeds. If V_1 is the writing speed at the screen, recorded for an object-image ratio $M=1$ and V is the writing speed on the screen at any reduction ratio M, it follows that

$$\frac{V}{V_1} = \frac{4}{(1+M)^2} \qquad (2)$$

This equation shows that photographic writing speed cannot be increased by more than a factor of four even with extreme reduction in size. The values appearing in this discussion for maximum writing speeds always refer to $M=1$ and $F=1$.

The manufacture of sensitive photographic emulsions is far from stabilized, and no standard emulsion has been established. The film emulsions and development procedure finally adopted were selected empirically from the most sensitive commercial emulsions and developer.

Determination of Writing Speeds

The pattern which the spot describes on the screen must be a simple geometrical form if calculation of the speed at which the spot moves is to be facilitated. Furthermore, the spot should traverse the screen but once throughout the duration of exposure for any single reading.

A geometrically simple and easily generated pattern which conforms to the above requirements is a sine-wave transient of known frequency f and amplitude A. The writing speed of the spot is then the vector sum of the horizontal and vertical velocity components. If the horizontal component is kept relatively small, as by using a low sweep frequency and a small sweep amplitude, it may be neglected; the vertical component, which follows the cosine function, then gives a close approximation to the writing speed.

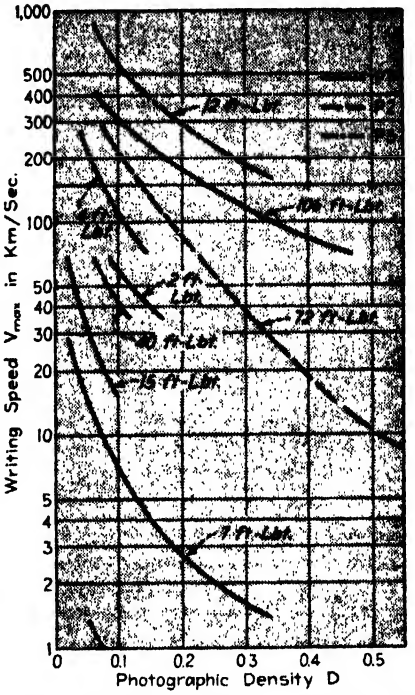

FIG. 2—Graph of writing speed plotted against photographic density for various screens and various screen brightness values in foot-lamberts

The maximum writing speed, S, of the spot describing a sine wave, occurs at the cross-over point on the axis and consequently may be expressed as $S=2\pi fA$. The sweep frequency f_s is maintained at a value of one-tenth f, the sweep amplitude at approximately five cm, and the sine wave amplitude at approximately one or two cm, peak to peak. A single-stroke sweep produced by a circuit using a high-vacuum tube is used to provide axis deflection up to a maximum speed corresponding to 5 Mc.

Elimination of Background Light

The density of the photographic images recorded on the film must remain unchanged by any external influence. Therefore, the exposures are made with the oscilloscope and camera in practical darkness. Furthermore, the light produced by the spot in its stand-by position before the operation of the single sweep must be suppressed by a black mask

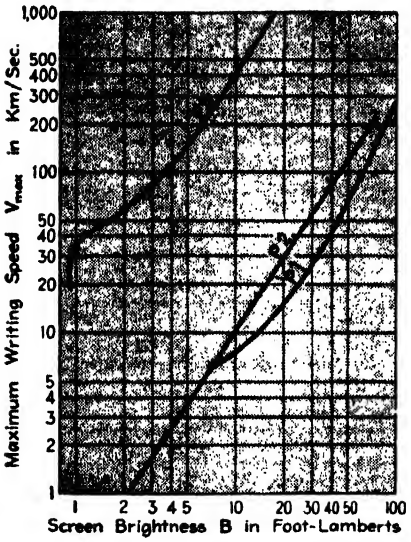

FIG. 3—Maximum photographic writing speed, plotted as a function of brightness of fluorescent screen for three common types of cathode-ray tube screens

on the tube. The influence of the background light is kept small by using a high-speed shutter, synchronized with the single sweep.

This system operates satisfactorily up to approximately 6000 volts total accelerating potential, at which point the fog due to the background light of the screen becomes objectionable (even at shutter speeds of 1/100 second) and danger of permanent damage to the screen by burning becomes imminent. Finally, at high frequencies (above 1 Mc) the adjustment of the equipment becomes difficult, since the signal becomes nearly or completely invisible because of masking by the background light. (It was possible to record on blue screens with satisfactory density high-frequency transients which were completely invisible to the eye.)

Beam modulation permits overcoming background light difficulties. A recurrent sine wave is applied to the deflection plates of a tube which is biased beyond the cut-off point. Previously the tube was focused at zero grid bias, and screen brightness was measured with the two-inch standard raster. Then a single rectangular wave pulse, whose duration is equal to, or less than, one period of beam frequency, is applied to the grid of the cathode-ray tube. The amplitude of signal delivered by the beam modulation circuit shown in Fig. 11 is sufficiently high to permit full modulation of any standard cathode-ray tube up to zero bias.

This pulse amplitude is limited to the zero-bias value by means of a diode which is connected across the cathode-grid terminals of the cathode-ray tube, preventing positive grid potential. As in the case of the single transients, the sweep frequency is generally $f_s = 0.1\ f$, and the maximum writing speed of the spot on the screen is

$$V = 2\pi f A \text{ cm/sec} \qquad (3)$$

where A is measured in centimeters.

Measurement of Recorded Density

According to the definition given previously, we consider, as a maximum writing rate, the speed which produces a density of 0.1 above fog on the photographic emulsion after development in a high-contrast developer. Since the photographic record of the transient occurs as a fine line it is necessary to find a rapid method of measuring accurately the density (above fog) of a large number of thin lines whose thickness ranges from 0.1 to 1 mm.

The method employed is believed to be new and is analogous to the method of calibrated wedges previously described. Briefly, a set of lines of calibrated and constant density is compared visually with the recordings to be measured. It has been found extremely difficult to compare visually the densities of areas whose dimensions are dissimilar, such as the density of a recorded thin line with respect to a calibrated standard wedge. It is even difficult to compare lines of incommensurate width. In such a case, the apparent density of the thin line will appear less than its actual density, especially at low density values. Conversely, lines which are similar may be compared with a high degree of accuracy and ease. Consequently, two sets of lines of 0.3 and 0.6 mm thickness are recorded and their densities calibrated. The density of these reference lines is determined by means of a calibrated densitometer. Since it is difficult to measure the density of the lines directly because of their small width, a larger area exposed under the same conditions and having the same density as to the corresponding line is recorded adjacent to each line.

The comparison of calibrated lines (with densities of longer areas recorded) is done by superposing the reference scale with the record transient, making the linear part of the sine wave pattern parallel

TABLE V—Density Recorded for Different Conditions of Exposure

Screen	Freq.	Lens Aperture	Film	Recorded Density	Total Acceleration Pot.
P5	1 kc	1.5	TSO SPP	0.60 0.75	2.7 kv
P5	1 kc	16	TSO SPP	0.12 0.06	2.7 kv
P5	100 kc	1.5	TSO SPP	0.06 0.03	2.7 kv
Experimental	100 kc	1.5	TSO SPP	0.60 0.75	9.7 kv
Experimental	1 Mc	1.5	TSO SPP	0.26 0.16	9.7 kv

and close to the calibrated lines, until one of these lines matches the transient. By this means, densities above fog are directly compared and the "apparent" density of the recorded lines is taken instead of the integral of density. This method permits measurement of a large number of photographic recordings in a very short time and with sufficient accuracy (density ± 0.01 at low densities.)

Measurement of Tube Parameters

The data concerning the photographic writing rates of cathode-ray tubes should be presented in such a manner that it becomes possible to determine immediately whether a given photographic problem in cathode-ray tube oscillography can be solved through the use of a given tube operated in accordance with given electrical conditions. The writing speed is determined by the brightness and color of the screen, which in turn are determined by the screen material, its thickness and the amount of power dissipated per unit area of the screen.

A simple and logical way to measure the photographic writing speed is to consider it a function of the brightness of the fluorescent screen rather than of the electrical parameters of the tube itself, for brightness can be measured by the user with sufficient accuracy using simple instruments.

Accordingly, the photographic writing speed is measured as a function of the screen brightness at zero grid bias and with the standard two-inch raster in focus. Consequently, the brightness of the tube is measured under the same conditions and with the same spot size which exists for the recording of the pattern. This method results in independence from individual tube characteristics, and the plots obtained result from measurements secured on several tubes of the same screen material. Finally, the results obtained give a figure of merit for the visual efficiency as well as for the photographic quality of the tubes. The electrical characteristics of the tubes are measured and recorded as parameters.

Film development time and temperature must be carefully checked and maintained constant. Fresh developer must be used for each development. By means of these precautions (and others not described) it is possible to develop each negative in a large series of films under practically identical conditions.

Electrical Conditions

Measurements are carried out using a standard commercial cathode-ray oscilloscope providing a total accelerating potential of 2700 volts as a basic power supply for the cathode-ray tube. Once the limit of recordings with the normal accelerating potential was reached, the brightness of the tube screen was increased by applying a variable post-accelerating potential to the intensifier electrode of the tube. The maximum post-acceleration potential was limited by the danger of screen burning, by the astigmatism of the tube, and by the intensity of background light. This limit was about 5 kv with respect to ground or about 6000 volts with respect to cathode.

Recording With Beam Modulation

As it is intended to determine the extreme limit of photographic writing speeds which can be obtained with commercial tubes, it is not undesirable to increase the brightness of the tubes further by increasing accelerating potential and beam current up to the safety limit of the tubes. An obvious method of doing this without damaging the tube is by means of beam modulation, as outlined above. The circuit used is shown in Fig. 1.

This circuit permits producing single rectangular pulses, the durations of which are continuously variable from about 1/30 second to a fraction of one microsecond. As the entire circuit including batteries is at cathode potential, it must be carefully insulated from ground.

TABLE VI—Brightness and Writing Speed Increase from Medium to High Accelerating Potentials (2.7-9.7 kv)

Screen	Brightness Increase	Increase in Writing Speed
P1	14.2	43
P2	46 5	300
P5	13.4	26.5

Development Procedure

From the previous investigation Triple S Ortho Film was found to give the best results for P1 and P2 screens, while Fluorapid Blue was slightly better for P5 screens. Development was carried out for 10 minutes at 65 deg F using Eastman D76 developer. The behavior of these same films at high frequencies must be tested; upon the recommendation of the manufacturer, Superpan Press film was added to this list. Table IV contains a tabulation of the results.

It can be seen that a frequency of 100 kc appears to be the recording limit at low voltages. The best results are obtained with Triple S Ortho film. The density can be further increased by using a more active developer but the fog increases simultaneously with increase of density and a compromise must be made.

A satisfactory compromise can be made by developing films for 8 minutes at 65 deg F in formula D72, other conditions remaining the same. A density D=0.07 was obtained for Triple S Ortho at f=100 kc, which compares to the value of D=0.04 obtained with the former development method under the same development conditions. Fluorapid Blue produces a very high fog and must be eliminated. Consequently Triple S Ortho and development in D72 for eight minutes has been employed for all the following recordings on which the measurement of photographic writing speeds is based.

The problem was therefore considerably simplified, insofar as Agfa Triple S Ortho seems to be the most sensitive emulsion for all the

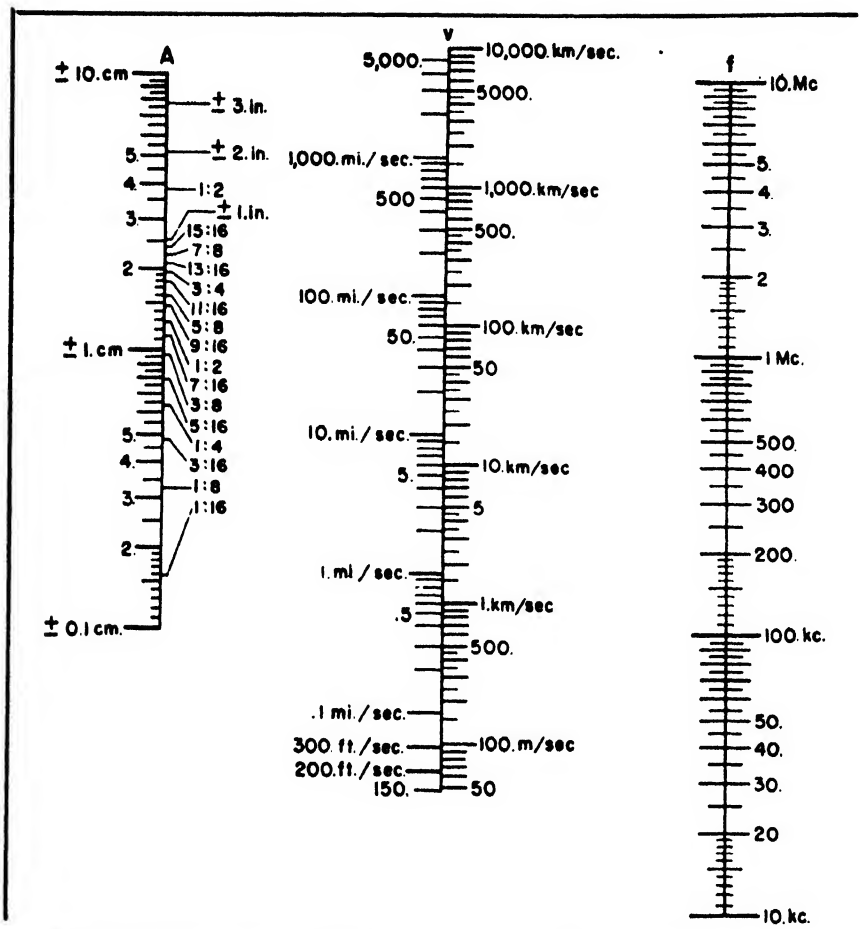

FIG. 4—Alignment chart relating amplitude, frequency, and maximum writing speed for sinusoidal traces

screen materials investigated, so long as low exposures are considered, resulting in a record density less than 0.3 regardless of the duration of the exposure. Table V shows the recorded density for different exposures.

Table V indicates that when the exposure (i.e. the product of light intensity and time) is sufficiently high, Super Pan Press gives higher recorded density and should be substituted for Triple S Ortho. It is shown that this holds true for a range from 1 kc to 1 Mc and probably beyond. It can be seen how the same pattern, recorded by lenses of different aperture, can produce results which are in favor of one or the other of both films, according to the total amount of exposure. The importance of using high-speed lenses is emphasized.

The graph of Fig. 2 has been used to determine the maximum writing speed V_{max} corresponding to density of 0.1 above fog. The values of V_{max} are referred to a lens aperture of $F = 1$ and to an object-image ratio $M = 1$ according to the definitions outlined. The values at highest brightness (9.7 kv) have been obtained with beam modulation.

In Fig. 3 the maximum writing speed, V_{max}, is given as a function of brightness for different screen materials. The lowest values at which the curves start are measured with 2.7 kv accelerating potential and maximum brightness, while the highest values were obtained at nearly 10 kv total accelerating potential and with beam modulation.

It is interesting to note that at low voltages the values of the maximum writing speeds are widely different for the various screens, the minimum being 0.7 and the maximum 20 km per sec, which represents a ratio of about 1:29. At high voltages all the screen materials investigated produced high recording speeds with only slight variations. The maximum speed was 560 and the minimum 210 km per sec, giving a ratio of 1:2.7.

This result obtained for different screens is also valid for individual tubes of the same type. While at low voltages the efficiency of a tube depends to a high degree on the quality of the electron gun, at high accelerating voltages only the total accelerating potential appears important, and a number of tubes of the same type show nearly the same results.

The increase of efficiency with accelerating voltage is shown in Table VI where brightness increase (and corresponding increase of writing speed) are given for the various screens. The figures of the table are based on data plotted in Fig. 3. Table VI shows that, at low voltages, screens with a high photographic efficiency (such as the P5) show relatively little increase in photographic effectiveness as the accelerating voltage is increased. On the other hand the photographic effectiveness of the P2 screen, which has a very low overall efficiency at low voltages, increases rapidly and becomes excellent at high accelerating potentials. The fact that the photographic efficiency increases so much more than the visual brightness can be explained only by a considerable change in color at higher voltages—the light becomes richer in blue actinic radiation.

With this information available and considering the tubes selected

TABLE VII — Photographic Efficiency Rating

Medium Voltage (2.7 kv)		High Voltage (9.7 kv)	
Screen	Relative Photog. Eff.	Screen	Relative Photog. Eff.
P5	1.0	P5	1.0
P1	0.35	P1	0.53
P2	0.035	P2	0.38

as representing each type, the following conclusions are apparent:

(1) The P5 screen produces the highest photographic writing speed.

(2) P2 screens should not be employed at low voltages, but give very satisfactory results at high voltages.

Ratings of photographic efficiency of various screens at medium and high voltages, referred to voltage on the tube using a P5 as reference, are given in Table VII.

Practical Applications

When the brightness of the tube which is to be used for photographic recordings is measured by means of a standard two-inch raster and an illumination meter equipped with Viscor filter, the corresponding maximum photographic writing speed V_{max} can be found on the graph of Fig. 4. Most cathode-ray tube manufacturers are in a position to provide information concerning the minimum screen brightness for any standard type of tube in cases where the user does not have access to a suitable illumination meter. Certain manufacturers have expressed willingness to provide more accurate brightness data on any single tube which is to be used for photographic recording applications. It should be considered that such brightness values will change throughout the life of the tube.

Once the maximum brightness for a tube is known, this data serves as a standard of calibration with which an ordinary exposure meter with photocell may be used to adjust the brightness level to a value desired for any particular application.

For all practical purposes it is advisable to divide the maximum writing speed, V_{max}, by two to provide a sufficient margin of safety and to obtain recordings of higher density than 0.1. The corresponding values of the graph of Fig. 4 are valid for a lens with an aperture of $F=1$, an object-image ratio of 1:1 and for Agfa Triple S Ortho Film with development formula Eastman D72, 8 minutes at 65 deg F.

Figures 4 and 5 are nomographs designed to facilitate solving prac-

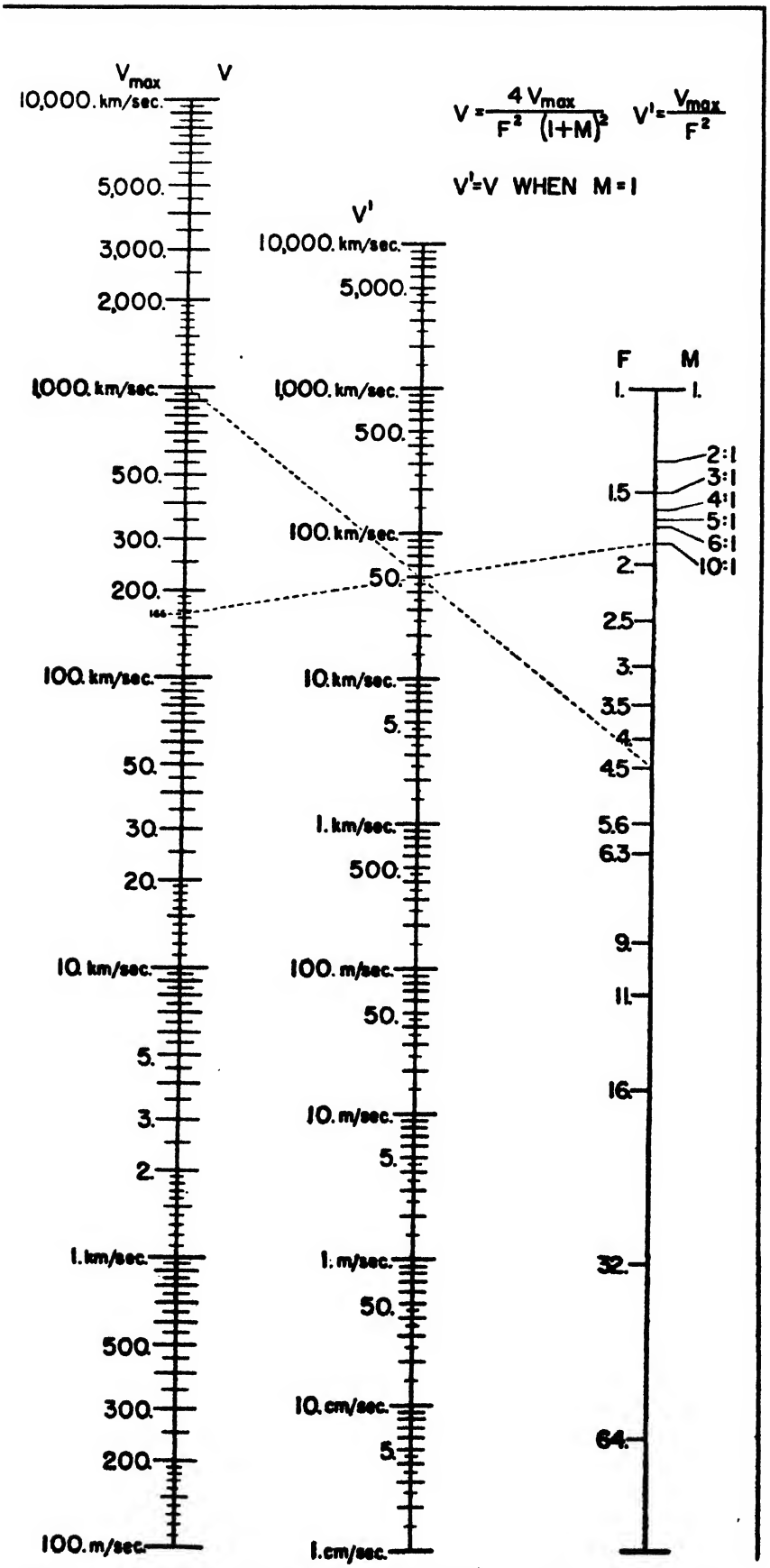

FIG. 5—Alignment chart for determining writing speed in terms of lens aperture F, object-image ratio M and maximum writing speed V_{max}

tical problems. Figure 4 demonstrates the relation between amplitude, frequency and maximum writing speed for sine waves; Fig. 5 gives the photographic writing speed V as a function of V_{max}, lens aperture F, and object-image ratio M.

Nomographs

Suppose it is desired to record a sine-wave transient having a peak-to-peak amplitude of approximately 6 cm ($A = \pm 3$ cm) and a frequency f of 5 kc. The tube may have a P5 screen with a raster brightness of 2 ft-lamberts. From Fig. 2, V_{max} is determined to be 60 km per sec. for $D_1 = 0.1$. Half of this is taken for safety purposes as explained above, so $V = 30$ km per sec.

The speed of the phenomenon which is to be recorded can be found from Fig. 4 by considering a frequency of 50 kc and dividing the result by ten to give the required frequency of 5 kc. A value of approximately 1 km per sec is obtained for V'.

By means of the nomograph in Fig. 5, we find that recording this speed at $V_{max} = 30$ km per sec permits the use of an aperture of $F = 5.6$ for $M = 1$. If a different ratio of object on screen to image on film is desired, perhaps $M = 10:1$, a line drawn from this value to 1 km per sec on the V' scale crosses the V scale at 3.3 km per sec. Use of $M = 10:1$ permits the recording of speeds 3.3 times higher than with $M = 1$. To confirm this, locate 3.3 km per sec on the V' scale and draw a line to the previous determined aperture $F = 5.6$. The cross point on the V_{max} scale establishes the corresponding increase in V_{max} to 102 km per sec. Since the recorded speed is only 1 km per sec, a line can be drawn from 102 km per sec on the V_{max} scale through $V' = 1$ km per sec, which shows an aperture between $F = 9$ and $F = 11$. Consequently, the phenomenon can be recorded either with an aperture $F = 5.6$ for $M = 1$, with $F = 10$ for $M = 10:1$, or with any intermediate values.

Assume a rectangular wave is to be recorded with a maximum rise of 5 cm per microsecond. The maximum speed to be recorded is therefore 5×10^6 cm per sec or 50 km per sec.

Recording of Transient Rectangular Wave

The available lens has a maximum aperture of $F = 1.9$. The nomograph of Fig. 5 shows that $V_{max} = 180$ km per sec. Figure 3 indicates that a P5 screen with $B = 5.6$ ft-lamberts would be satisfactory. Assuming that in this case only 4 ft-lamberts are available from the cathode-ray tube under the given operating conditions, it would probably be advisable to increase the exposure by raising the object-image ratio. For $M = 8:1$ the apparent writing speed is increased threefold and a recording of satisfactory density would be secured.

Recording of Recurrent Phenomena

As another example of the use of data given in this article, assume the exposure time for the recording of recurrent phenomena is to be determined.

Let us assume that an amplitude of ± 2 cm and a sine wave of 1000 cps, with a sweep frequency of 100 cps, appears on a P1 screen yielding a brightness, B, of 7.5 foot-lamberts. If n is the number of images per second appearing on the screen, t is the exposure time, and V is the maximum writing speed of the phenomenon which has to be recorded, then $V = t\ n\ V_{max}$ or $t = V/(n\ V_{max})$. Referred to a lens with aperture F, $t = VF^2/(n\ V_{max})$.

In this case $n = 100$, and $V = 2\pi \times 10^3 \times 2 = 12.6 \times 10^3$ cm per sec. From the graph of Fig. 6, $V_{max} = 6 \times 10^3$ cm per sec, and it can then be calculated that $t = 2.1 \times 10^{-4} F^2$ sec. If an aperture of $F = 7$ is employed, $t = 1/100$th sec.

Conclusions

As a result of a comprehensive survey of the technique of producing photographic records at maximum writing speed, we may draw the following conclusions:

(1) For high-speed recording, Agfa Triple S Ortho film gives the best results of the films tested for P1, P2, and P5 screens. Recommended development procedure: Develop 8 minutes at 65 deg F in D72.

(2) The P5 screen has the highest photographic efficiency.

(3) The maximum photographic writing speed plotted against tube brightness gives an accurate means for determining the exposure time. With standard tubes and high accelerating potentials, phenomena of more than 1000 km per sec have been recorded.

(4) At high accelerating voltages (9.7 kv) all the screens previously mentioned became very efficient for photographic recordings, and the differences, which are quite important at low voltages, become relatively small. At high voltages the brightness differences between individual tubes of the same type seem to diminish.

(5) Type P2 screens, which give very poor results at low voltages, show a tremendous increase in efficiency at high voltages and it is desirable to employ this screen at high voltages.

(6) It has been shown that by using synchronized high-speed shutters (1/100 sec) undesirable fogging of the film by background light of the screen can be minimized up to accelerating potentials of about 6 kv. Beam modulation eliminates the necessity for synchronizing the shutter and permits the use of high accelerating potentials and strong beam currents, without danger of screen burning.

BIBLIOGRAPHY

(1) Ardenne, M. V., "Cathode-Ray Tubes," English edition p. 294–346 (German edition p. 215–250).
(2) Parr, G., "The Cathode-Ray Tube and its Applications," Second edition, Appendix p. 157–160.
(3) Rider, J., "The Cathode-Ray Tube at Work," p. 316–317.
(4) Henney, K., and Dudley, B., "Handbook of Photography," McGraw-Hill Book Co., New York.
(5) Mees, "The Theory of the Photographic Process."
(6) Choosing Film for your Camera, *Film Catalog Edited by Agfa Ansco*, 1941.
(7) Crawford, J. D., Photography of Transients with Cathode-Ray Oscillograph, *General Radio Experimenter*, May, 1934.
(8) Lamson, H. W., A New Moving Film Camera, *General Radio Experimenter*, Nov. and Dec., 1934.
(9) Borries, V. and Knoll, The Blackening of Photographic Emulsions by Electrons and Electron-Excited Fluorescence, Zeitschr. Physik., 88, 1934.

(10) Exposure Meter for Cathode-Ray Oscillographs. *RCA Application Note* No. 70. February 17, 1934.
(11) McGillewie, D. L., The Use of the High-Vacuum Cathode-Ray Tube for Recording High-Speed Transient Phenomena. *Jrl. Inst. Elec. Engineers*, November, 1938.
(12) Kaiser, H., Theory of the Photographic Recording. *Zeitschr. Physik.*, 1938, No. 10.
(13) Bigalke, A., A Post-Acceleration Oscillograph. *Zeitschr. Physik.*, 1938, No. 6.
(14) Blok, L., An Apparatus for the Measurement of the Scanning Speed of Cathode-Ray Tubes, *Philips Technical Review*, July, 1938.
(15) Rogers, T. A., and Robertson, B. L., Cathode-Ray Tube Photography, ELECTRONICS, July, 1939.
(16) Custers, J. F. H., The Recording of Rapidly Occurring Electric Phenomena with Aid of the Cathode-Ray Tube and the Camera, *Philips Technical Review*, May, 1939.
(17) Bigalke, A., Four-Beam Cathode-Ray Tube of High Recording Speed, *Arch. f. El.*, 1939, No. 2.
(18) Rogowski, W., and Thielsen, H., Post-Acceleration in Cathode-Ray Tubes, *Arch. f. El.*, 1939, No. 6.
(19) Kats and Westendorf, Obtaining High Recording Rates by Means of an Electro-Static Cathode-Ray Tube of Constant-Vacuum. *Zeitschr. Physik.*, 1939, No. 7.
(20) Bigalke, A., Electron-Ray Oscillograph, Part I. *Archiv. f. techn. Messen*, J884-27, August, 1939.
(21) Borries, V., and Ruska, E., Proposal for the Standardization and the Objective Comparison of the Measuring Efficiency of Cathode-Ray Oscillographs, *Arch. f. El.*, No. 3, 1940.
(22) Angelini, A. M., Voltage Dividers and Delay Cables for the Oscillographic Recording of Rapid Transient Phenomena, *Bulletin Assoc. Suisse des Electriciens*, July 18, 1941.
(23) Baxter, H. W., A Concise Report on a High-Speed Camera for Simultaneous Photographic Records, *Jrl. Sci. Instr.*, p. 183-184, 1942.
(24) Folkerts, H. F., and Richards, P. A., Photography of Cathode-Ray Tube Traces, *RCA Review*, October, 1941.
(25) Roberts, H. C., An Auxiliary Circuit for Cathode-Ray Photography, ELECTRONICS, September, 1942.

Noise in Gas Tubes

By J. D. COBINE and C. J. GALLAGHER

NOISE FOR visual presentation of filter frequency response and for reverberation can be obtained from gas tubes. High level, wideband noise sources, developed during the war for use in radar jammers, provide greater output than previously obtained.

Characteristics of Gas Tubes

Gas tubes have always had a reputation of being noisy, although the character of the noise has not been clearly defined. Recent investigations have shown that the noise generated in hot cathode arcs consists of oscillations of several hundred kilocycles superimposed on a background of random noise. The random noise contains a continuous band for frequencies extending from the very low audio range to five megacycles. A suitably placed magnetic field greatly increased the noise level and eliminated the oscillations.

The spectrum obtained from a typical gas tube without magnetic field is shown in Fig. 1A for two discharge currents. The noise level is expressed in db above 10 $\mu v/(kc)^{1/2}$ because, if the bandwidth of the spectrum analyzer is sufficiently small, the random noise voltage varies as the square root of the bandwidth.

The two peaks in the curve of Fig. 1A for the higher current represent two distinct oscillations that are not harmonically related. The lower frequency peak is due to plasma ion oscillations; the higher frequency peak is caused by oscillations of positive ions in the potential minimum at the cathode. A summary of the characteristics of a number of hot cathode discharge tubes is presented in Table I. This table gives the frequency and amplitude of the lowest frequency oscillation, as well as the noise level at three selected frequencies. The values are average, there being considerable variation from tube to tube. The last column gives the total rms noise voltage obtained by integrating the spectrum from zero to four megacycles. For comparison, the level of shot noise of a diode for two different currents and with a 3,000 ohm load resistance is presented. The shot noise is much lower than that obtained from the gas tubes.

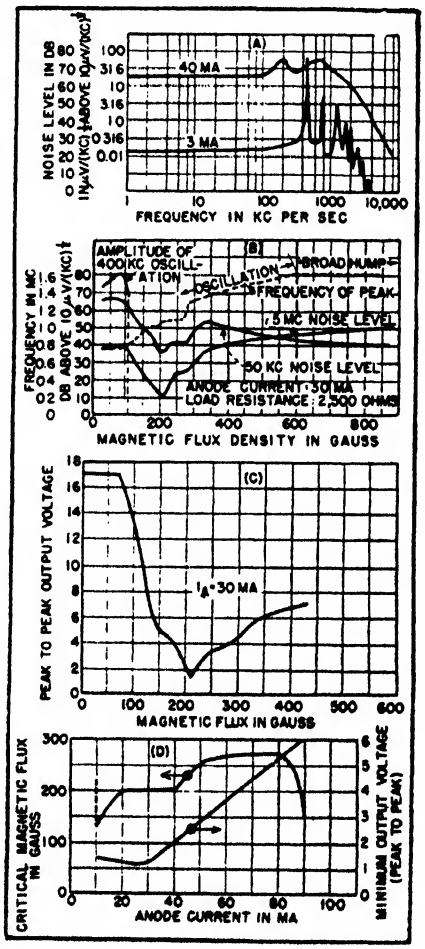

FIG. 1—Noise characteristics of 884 for various operating conditions

The cathode oscillation is differently affected by the magnetic field. The frequency of the peak noise increases with increasing magnetic field, and the spectrum in the vicin-

Effect of Magnetic Field

If a transverse magnetic field is applied across the discharge and the field strength gradually increased, the spectrum of noise undergoes marked changes. Figure 1B shows the change observed in an 884. For this particular tube the amplitude of the low frequency oscillation at 400 kc increased slightly for low magnetic field strengths and then disappeared with no change in frequency as the field was further increased.

ity of the peak broadens so that eventually a distinct oscillation is no longer observed. The noise at 50 kc and 5 mc go through a minimum at 210 gauss and then increase. The ultimate level of the 5 mc noise is about 12 db higher than the zero field level.

It is interesting to note that there is an optimum value of magnetic field for which the total variational voltage is a minimum, as shown in Fig. 1C. This optimum value of field is dependent on the current as is the minimum value of the peak-to-peak voltage, as shown in Fig. 1D. Because of variations between tubes, the exact value of the optimum field must be found experimentally for any given tube. This property of reducing the variational voltage has been very useful in control circuits where other tubes are subjected to undesirable random triggering under the influence of a conducting gas tube.

The general shape of the spectrum obtained from a gas tube depends on the type of tube. Figure 2A shows spectra of several types of tubes with magnetic fields. The noise levels are compared with the noise levels from a 931A electron multiplier phototube and a temperature-limited diode.

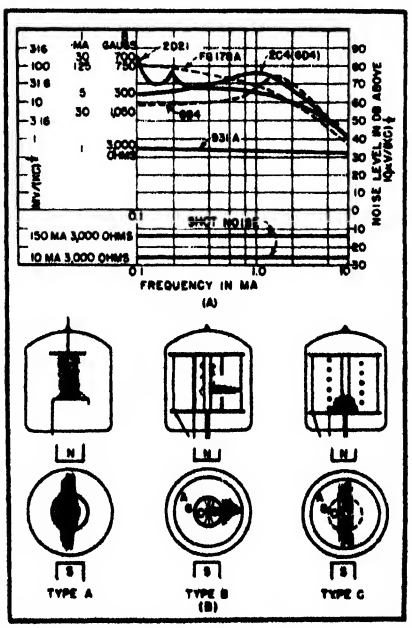

FIG. 2—Characteristic noise from several types of gas tubes

Table I—Noise Characteristics of Gas Tubes

Tube	Current (ma)	Oscillation		Noise Level			
				decibels[a]			volts RMS
		(kc)	(db)[a]	50 kc	1 mc	5 mc	4 mc
Shot	150	——	——	−14	−14	−14	0.00133
Noise[b]	10	——	——	−26	−26	−26	0.00034
884	40	180	76	66	70	35	0.91
	3	440	76	24	22	−8	——
2A4G	100	450	52	50	24	−5	0.06
WL629	40	210	85[c]	44	58	——	——
WE256A	75	120	51	38	40	−4	0.4
RK62	1.5	650[d]	34	——	1	−10	——
2050	90	150	84	60	31	14	——
	3	90	78	36	14	−10	——
6Q5G	40	550	73	45	50	17	——
FG178A	125	100	78	——	38	——	——
2D21	41	85	94	80[e]	54	18	——
816	125	170	67	60[e]	37	9	——

[a] Zero level is 10 $\mu v/(kc).^{1/2}$
[b] Temperature limited diode with 3,000 ohm plate resistor.
[c] Second harmonic amplitude is 90 db.
[d] Probably another nonharmonic peak below 100 kc.
[e] Approximate.

Table II—Noise with Transverse Magnetic Field

Tube	Current (ma)	Flux Density (Gauss)	Noise Level				Type[b]
			(peak volts)	decibels[a]			
				100 kc	1 mc	5 mc	
6D4	5	375	8.2	63	76	38	B[c]
(2C4)	5	720	——	66	76	43	
	20	375	——	70	77	53	
884	45	1,050	5.6	56	62	48	B
2A4G	100	2,000	8.3	60	60	40	A
WL629	40	2,500	4.4	71	69	43	A
WE256A	75	2,000	——	65	58	33	B
RK62	7	620	——	60	57	42	C[d]
6Q5G	40	2,500	——	55	63	37	C[d]
WE323A	100	1,800	——	62	44	8	A
2050	75	500	——	74	47	13	[d]
FG178A	200	960	9.9	82	70	43	A
2D21	41	1,200	5	72	70	47	[e]
	30	700	5	70	64	46	[f]
GL546	13	740	——	68	70	48	

[a] Zero level is 10 $\mu v/(kc).^{1/2}$
[b] See Fig. 2B.
[c] Standard RRL Noise Unit. Maximum is 80 db at 700 kc.
[d] Oscillations not suppressed.
[e] Anode to cathode noise.
[f] Grid to anode noise.

Shape of the spectrum is determined by tube geometry. Three general types of structure are found in commercial tubes as shown in Fig. 2B. Type A, represented in Fig. 2A by the FG178A, has a circular-plate anode with the cathode some distance away on the axis of the anode so that the magnetic field can be concentrated at the cathode. The spectrum of this type structure has high low-frequency noise, with no peak and a steady decrease in level as the frequency increases. The Type B tube, represented in Fig. 2A by the 884 and the 2C4(6D4), has closer spacing and the cathode is surrounded by the anode structure so that both anode and cathode are in a strong magnetic

field. The grid is a solid sheet of metal completely surrounding the cathode except for a small slit which defines the current beam. The spectrum obtained with this structure shows a maximum in the vicinity of one mc. Type C, not represented in Fig. 2A, is similar to Type B except that the grid is an open wire structure. With this type tube (Dumont 6Q5G) it was not possible to eliminate the oscillations for any orientation of the magnetic field. Similar difficulties with the oscillations were found with the 2050 and 2D21 gas tetrodes.

The characteristics of the various types of tubes studied with transverse magnetic field are summarized in Table II. Representative values are given. For most types there is wide variation between tubes. Great uniformity was found in the 6D4 tube, with maximum deviations between tubes of the order of one db or less.

Simple Test Set for Mercury Vapor Rectifiers

By M. J. WEINER

THE USUAL DIFFICULTIES encountered with mercury vapor rectifiers can be held to a minimum if certain operating conditions are maintained. In properly designed equipment the tube temperatures are held within certain prescribed limits to avoid arc-backs. The internal tube drop, however, is a function of the filament emission and load current, and increases with the age of the tube.

Since there has been no readily available measuring equipment to check the filament emission of mercury vapor tubes, it was decided to build one in as simple a form as possible to permit routine tube tests. The test set to be described gives an indication of the tube performance by measuring the tube drop when passing rated current. The parts required are simple and few in number.

The basic circuit is shown in Fig. 1. Being a half-wave rectifier circuit with resistance load, the average voltage drop across the tube and resistor is

$$(E_T + E_{DC})\ \text{av.} = E_{max}/2\pi \int_0^{\pi} \sin \omega t\, d\omega t = 0.318\, E_{max}$$

The a-c voltmeter reads the effective value E, however, so the maximum (peak) applied voltage is

$$E_{max} = 1.414\, E$$

Substituting:

$$(E_T + E_{DC})\ \text{av.} = 0.45\, E$$

$$E_T = 0.45\, E - E_{DC}$$

For the initial calibration procedure, place a new tube in the proper socket for a preliminary warm-up period, with the plate supply off. Next, apply plate voltage and increase it until the d-c ammeter indicates the rated load current for the particular tube under test. This is 1.25 amp for a type 872 tube, and 0.5 amp for a type 866 tube. Read the d-c voltmeter connected across the resistor to get the value of E_{DC}. Read the a-c voltmeter to get the r.m.s applied voltage E. Now, subtract E_{DC} from 0.45 E to get the average tube drop E_T. Repeat for each other type of tube to be tested and record all values. (If it is desired to rate the tube in terms of peak values, multiply this result by π.)

A calibration chart can now be made up, showing the drop across the resistor at rated load current for each type of tube to be tested. The d-c voltmeter across the resistor may then be removed and this chart can be used to find the value of E_{DC} for the tube being tested.

If the tube drop E_T as measured for an old tube exceeds the drop in a new tube by 5 to 10 volts, erratic operation of the rectifier equipment will follow and the tube should be taken out of service. It may still give many hours of useful service, however, in lower-powered equipment, where the load requirements are less.

The complete schematic circuit of the test set is shown in Fig. 2. The filament voltage at each tube socket must be the exact value required for the tube under test.

The tube to be tested is placed in the correct socket and allowed to warm up with plate supply off. Plate voltage is then adjusted until the ammeter reads rated load current for the tube, and the a-c voltmeter is read to get E. Reference to the calibration chart gives E_{DC} for the rated load current, and this subtracted from 0.45 E gives the average tube drop E_T.

The equipment is calibrated in terms of the readings obtained with a new tube because the input voltage required for rated load current will vary according to the position of the d-c return lead with respect to the filament winding. For example, connecting the d-c return to the filament center-tap will not give a value of input voltage which is the means of the values obtained by connecting this lead to either side of the filament.

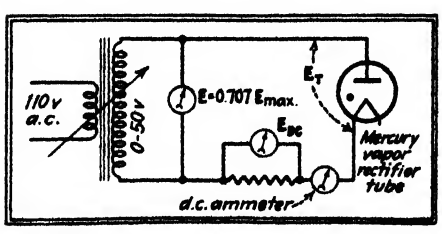

Fig. 1—Basic circuit arrangement for testing a mercury vapor rectifier tube

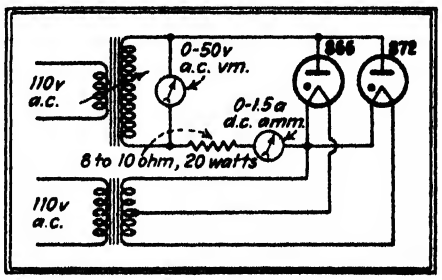

Fig. 2—Schematic circuit diagram of a simple test set for mercury vapor rectifiers. Additional sockets can be provided for other types of tubes if desired

AUTHOR INDEX

A

Abbot, A. E., 685
Adler, Robert, 585
Aiken, C. B., 265
Albers, V. M., 186
Angus, W. K., 774
Anker, H. S., 281
Artst, Maurice, 251
Atwood, H., Jr., 394

B

Badessa, R. S., 659
Baller, H., 278
Bann, J. J., 378
Baracket, A. J., 708, 722
Bard, H. B., Jr., 667
Barrett, R. E., 743
Bartelink, E. H. B., 805
Barton, Don, 660
Bastin, D. H., 100
Battison, John H., 738, 789
Bauer, B. B., 49
Beggs, George E., Jr., 796
Belles, H. W., 661
Blatterman, A. S., 550
Blow, Thomas C., 232
Bowers, Jack L., 292
Bradford, H. K., 775
Bradley, William E., 593, 606
Brailsford, H. D., 239
Brill, Edmund R., 596
Brock, W. R., 720
Brolly, A. H., 720
Bruck, George G., 514
Brunner, Frits, 770
Buchheim, Robert W., 188
Buts, Nelson A., Jr., 79

C

Campbell, R. D., 567
Carnahan, C. W., 598, 604
Chaffee, E. L., 572
Chapman, R., 494
Cheatham, T. P., Jr., 590
Cleckner, D. C., 1
Close, R. N., 174
Cobine, J. D., 869
Coile, R. C., 112
Cole, Larry S., 433
Cooper, George R., 458
Cox, C. Russell, 5, 31
Crane, Richard W., 72
Crosby, Murray G., 218, 365

D

Daniel, George, 115
Daskam, E., 805
Daubendiek, A. W., 575
Day, J. R., 785
Dester, E. L., 545
Dilatush, E., 532
Dome, R. B., 144, 673
Duke, C., 354
Duttera, William S., 11

E

Easton, Allan, 191, 419, 434, 572, 613, 728
Ehrlich, Robert W., 75
Eltgroth, G. V., 221
Epstein, D. W., 739
Espy, Dawkins, 197

F

Faulkner, W. H., Jr., 517
Feiker, G. E., 504
Feldt, Rudolf, 403, 861
Fisher, J. F., 856
Fleming, Lawrence, 103, 276
Frank, Ernest, 289
Frankart, William F., 597
Fundingsland, O. T., 170

G

Gallagher, C. J., 869
Gehres, F., 37
George, L., 653
Giacoletto, L. J., 812
Gilbert, R. W., 416
Ginzton, Edward L., 148, 257
Glover, Ralph P., 662
Goddess, Eugene, 553, 556, 558
Goodman, M. M., 743
Gordon, H., 653
Gottlieb, Irving M., 515
Graber, R. E., 413
Green, A. P., 233
Griffin, Dana A., 547
Grignon, L. D., 80
Gross, Ervin E., Jr., 474
Guenther, J. H., 53
Guillemin, E. A., 295
Gurewitsch, A. M., 466

H

Haller, Cecil E., 830
Hansen, Elmer F., 584
Hanson, Robert M., 312
Harries, J. H. Owen, 462
Harrison, A. E., 849
Haseltine, A., 609
Helber, Carl A., 509
Helfrich, Harry D., Jr., 768
Hellman, R. K., 579
Henry, D. Stanley, 374
Herold, Joseph, 811
Herrick, George Q., 106
Herrick, J. F., 182
Hill, D. M., 365
Hilliard, John K., 116
Hills, E. G., 489
Hings, D. L., 656
Hitchcock, Richard C., 528
Hoag, Oliver, 540
Holland, L. N., 812
Hollis, Walter C., 748
Hollywood, J. M., 757
Hooper, C. K., 544
Hopkins, R. J., 577
Hunter, Dan, 74

I

Iannone, F., 278

J

Javna, Stephen L., 234
Jeffries, Carson D., 501
Jenks, F. A., 479
Johnson, E., 655
Jordan, E. C., 28
Jurek, W. M., 53

K

Kallman, Heinz E., 520
Kalmus, H. P., 598
Karplus, Eduard, 359
Katchky, M., 44
Kearse, George P., 20
Kees, H., 37
Kennedy, Maurice E., 802
Kerr, Donald E., 321
Kiernan, E. F., 32
King, D. D., 517
Kline, Melvin B., 209, 210, 211
Klipsch, Paul W., 85
Koonts, P., 532
Kornei, Otto, 107
Kramer, B., 439
Kraus, John D., 14
Krauss, Herbert L., 131
Kunde, Walter W., 121

L

Lafferty, Raymond E., 201, 311, 519
Last, Emmanuel, 676
Lebenbaum, Matthew T., 174, 620
LeCaine, H., 44
Lee, Reuben, 702
Leeds, L. M., 764
Leeman, Alvin, 814
Lester, John M., 317
Libby, Lester L., 381
Licklider, J. C. R., 387
Lisman, H., 799
Lohr, Lloyd A., 212
Loughlin, B. D., 609
Ludman, Walter W., 404

M

MacIlvain, K. L., 123
Malling, Leonard R., 386
Maloff, I. G., 713
Marchand, N., 494
Marks, M., 779
Maron, William, 379
Mather, Norman W., 691, 709
McArthur, E. D., 844
McComb, C. T., 233
McManus, Lindsay, 26
Meahl, H. R., 504
Mentser, J. R., 537
Menzies, E. B., 652

Merchant, C. J., 291
Meager, G. Robt., 271
Michael, F. Robert, 837
Miller, Fred, 562
Miller, W. E., 28
Miller, William B., 539
Moore, David W., Jr., 669
Moore, John B., 624
Moreno, Theodore, 447, 469
Morita, Clement, 714
Musselman, Glenn H., 345

N

Newell, H. E., Jr., 758
Newlon, Arthur E., 407
Newman, E. B., 387
Norton, Frank B., 732

O

O'Brien, B. C., 9
Odessey, P. H., 728
Ohman, G. P., 694
Olson, Harry F., 66
Owen, Robert P., 394, 711

P

Paine, Robert C., 213
Pappenfus, E. W., 97
Peek, R. L., Jr., 197
Peyser, W. P., 34
Phillips, Edwin N., 455
Pierce, J. A., 331
Pihl, George E., 424
Pine, Cecil C., 430
Pinney, L. E., 385
Plauts, A. C., 545
Purington, E. S., 203

Q

Quirk, Carl J., 113

R

Rankin, J. C., 654
Reyner, J. H., 398
Richman, D., 609
Richter, Walther, 125
Roberts, William W., 815
Robinson, Alfred K., 357
Rosentreter, E. W., 643

S

Sabaroff, Samuel, 87
Sanabury, G. L., 97
Seal, Robert K. F., 199
Schach, Arthur, 835
Schlesinger, Kurt, 688
Schmitt, O. H., 34
Schottland, Frederic D., 301
Schuler, Earl R., 92
Schumann, F., 354
Scott, H. H., 57, 60
Seeley, Stuart W., 678
Shanklin, J. P., 754
Shepard, W. G., 280
Sherbin, Leonard E., 452
Sherwood, F. L., 9
Silverman, M., 583
Simon, A. W., 444, 445, 645, 646
Sloat, W. R., 821
Smith, Alvin H., 83, 767
Smith, Ernest J., 214
Smith, Wilbert B., 348
Smitley, C. R., 413
Soucy, Chester I., 227
Spitzer, E. E., 826
Stephens, W. E., 243
Sterling, Howard T., 377, 664, 665
Stockman, Harry, 617
Stodola, E. K., 799
Stolte, F., 439
Strauss, W. R., 571
Sulser, P. G., 340, 390
Sutro, Peter J., 753
Swan, Arthur G., 432
Saiklai, George Clifford, 698

T

Taylor, John P., 21, 517
Taylor, Paul K., 306
Tellier, J. C., 856
Thomas, H. P., 764
Thomson, R. F., 94
Totah, E. J., 567
Toth, Emerick, 583, 627
Travis, Earle, 4, 379
Tuller, W. G., 590
Tyson, B. F., 423

V

Vandeven, E. O., 428
Villard, Oswald G., Jr., 639, 790
Vladimir, L. O., 16, 647

W

Wagner, H. M., 182
Waidelich, D. L., 441, 524
Wald, Sidney, 39
Wallman, Henry, 682
Webking, Henry E., 840
Weiner, M. J., 872
Wels, W. C., 265
Whale, H. A., 189
Wheeler, G. J., 170, 187, 213, 301
Wheeler, Harold A., 224
Whitehead, J. W., 91
Wilson, Gardner P., 384
Woodward, O. M., Jr., 497
Wolf, L. J., 23

Y

Yu, Y. P., 262, 283

Z

Zelle, Joseph, 810, 825
Zimmermann, K. H., 760
Zink, A. J., Jr., 771

INDEX

A

Absorption, acoustic, 112
Acoustic absorption nomograph, 112
Acoustic devices, testing, 579
Adaptor, single-sideband, 643
Adjustable-bandwidth f-m discriminator, 590
Adjustment of directional antennas, 11
AFC system, microwave, 479
AGC-noise in receivers, 624
Aircraft antenna, cavity, 37
Aircraft antenna pattern plotter, 34
Aircraft antennas, 32
Alarm, transmitter breakdown, 774
All-wave filter, 430
A-M antenna, two-station, 26
A-M tower with f-m antenna, 21
Ammeter, antenna, remote indicating, 31
Amplifier, bolometer, 517
Amplifier, direct-coupled r-f, 379
Amplifier for f-m monitoring, 796
Amplifier low-frequency compensation, 688
Amplifier, pulse, 407
Amplifier response tester, 407
Amplifier, self-switching r-f, 182
Amplifier, stagger-tuned, 682
Amplifiers, d-c, 251 283
Amplifiers, wide-band i-f, 620
Amplitude control, oscillator, 377
Analysis of audio distortion, 87
Analysis of cathode followers, 137
Analysis of full-wave rectifier, 524
Analysis of tube shrinkage, 556
Analyser, audio harmonic, 94
Analyser, intermodulation, 115, 116
Analyser, transient video, 714
Antenna ammeter, remote indicating, 31
Antenna, artificial, 39
Antenna beam evaluator, microwave, 44
Antenna bridge amplifier, 379
Antenna, cavity, 37
Antenna characteristics, aircraft, 32
Antenna coupler, f-m, 21
Antenna coupling to waveguide, 469
Antenna coupling transformer, 16
Antenna impedance measurement, 354, 374
Antenna impedance meter, 381
Antenna, low-impedance loop, 16
Antenna meter, clip-on, 27
Antenna pattern plotter, 34
Antenna pattern recorder, 44
Antenna phase monitor, 9
Antenna phasing networks, 5
Antenna power divider, 4
Antenna radiation patterns, 1
Antenna resistance measurement, 301
Antenna, slotted-cylinder, 26
Antenna, triplex, for tv and f-m, 23
Antenna, two-station cooperative, 26
Antennas, aircraft, 32
Antennas, directional, adjustment of, 11
Antennas, f-m and tv receiving, 20
Antennas, multi-wire dipole, 14
Apertures in cavities, 462
Applications, superregenerative circuit, 617
Approach to waveguides, 447
Artificial antenna, 39
Asymmetrical multivibrator, 709
Attentuation in waveguides, 450, 455
Attenuator, electronic, 80
Attenuator, piston, 819
Audio crossover network, 85, 92
Audio distortion analysis, 115, 116
Audio filter design, 291
Audio frequency meter, 571
Audio generator, high power, 547
Audio harmonic wave analyzer, 94
Audio inductor design, 234
Audio limiters, 627
Audio mixer design, 72
Audio noise reduction circuits, 57, 60, 66, 71
Audio oscillator, thermistor-regulated, 103
Audio phase reverser, automatic, 83
Audio phase-shift oscillator, 121
Audio record noise suppressor, 57, 60, 66, 71
Audio wow meter for recording, 97
Automatic amplitude control, oscillator, 377
Automatic audio phase reverser, 83
Automatic battery charger, 545
Automatic controls for broadcast transmitters, 821
Automatic fader, 74
Automatic gain control, audio, 53
Automatic limit bridge, 567

B

Background noise suppressor, 59, 60, 66, 71
Balanced lines, impedance, 753
Balanced-modulation a-m circuit, 790
Balanced modulator for speech inversion, 815
Bandpass filters, 292
Bandwidth for pulses, 407
Bandwidth vs noise, 140
Battery charging control, 545
Beam blanking, oscilloscope, 394
Beam evaluator, microwave antenna, 44
Beat-frequency interference chart, 660
Beat-frequency oscillator, 370
Beat-frequency tone generator, 91
B-H curve tracer, 585
Bias from contact potential, 665
Bias supply, stabilized, 546
Bias voltage with diode, 664
Bisectable reactance networks, 203
Blanking, oscilloscope, 394
Blocking oscillator, 434
Blocking oscillator, timing, 676
Bolometer amplifier, 517
Bolometer, d-c amplifier, 265
Bolometer, signal-detecting, 34
Bootstrap circuit, 711
Breakdown alarm, transmitter, 774
Bridge amplifier, r-f, 379
Bridge, automatic limit, 567
Bridge-balanced amplifiers, 262
Bridge, comparison, 570
Bridge rectifier, 528
Bridge-type phase shifter, 311
Bridging amplifier, audio, 83
Bridging amplifier for f-m monitoring, 796
Broadcast array phase monitor, 9
Broadcast array phasing networks, 5
Broadcast array power divider, 4
Broadcast array, two-element, 4
Broadcast carrier alarm, 811
Broadcast frequency monitoring, 433
Broadcast receiver loop antenna, 16
Broadcast receivers, permeability tuning, 645, 646, 647, 652
Broadcast r-f bridge, 354
Bridge, r-f, for broadcast stations, 354
Broadcast station antenna ammeter, 31
Broadcast station cuing system, 825
Broadcast station volume compressor, 106
Broadcast studio fader, 74
Broadcast studio mixer design, 72
Broadcast studio noise suppressor, 60, 66
Broadcast transmitter controls, 821
Bursts, measurement of vhf, 352
Butterfly circuit, 359
Butterfly circuits, coaxial, 474
Butterfly oscillator, 501
Buzzer signal generator, 3,000 mc, 508

C

Cable design, high-frequency, 760
Cable propagation velocity, 439
Calculator, db gain-loss, 212
Calibrating laboratory standards against WWV, 384
Calibration, time-base, 404
Calibrator, microphone, 100
Calibrator, oscilloscope, 404
Cancellation of interfering signals, 661
Capacitor testing, 577
Capacitors, resonance in, 233
Carrier-current signal voltmeter, 445
Carrier-difference television sound reception, 673, 678
Carrier-failure and tone alarm, 811
Carrier-frequency voltmeter, 445
Carrier system, f-m, 805
Cascade phase-shift modulator, 779
Cascaded cathode phase inverters, 125
Cathode follower analysis, 137
Cathode follower circuits, 125, 131
Cathode follower coupling in d-c amplifiers, 283
Cathode follower for square waves, 139
Cathode follower nomographs, 131, 209, 210, 211
Cathode follower, very low output resistance, 139
Cathode-coupled half-shot multivibrator, 199
Cathode-coupled multivibrator, 709
Cathode-coupled phase inverter, 796
Cathode-coupled voltmeter, 416
Cathode-driven discriminator, 590
Cathode-follower d-c amplifier, 278, 281
Cathode-follower oscillator, 218
Cathode-loaded power amplifier, 131
Cathode-ray analysis of audio, 87
Cathode-ray curves for tubes, 840
Cathode-ray oscilloscope, 398
Cathode-ray oscilloscope, wide-band, 394
Cathode-ray phase measurement, 428
Cathode-ray Q meter, 403
Cathode-ray screen testing, 849
Cathode-ray television analyser, 720
Cathode-ray tube pattern photographing, 861
Cathode-ray video analyzer, 714
Cavities, apertures in, 462
Cavity aircraft antenna, 37
Cavity oscillator circuits, 466
Central signal generator for production testing, 562
Characteristic impedance of balanced lines, 753
Characteristics, crystals, 243
Characteristics, magnetic recording, 107
Characteristics of cathode followers, 131, 137, 209, 210, 211
Characteristics, tube filament, 826
Charger control, battery, 545
Charging circuits, exponential, 170
Checking uhf oscillator stability, 385
Choke, swinging, 312
Chart, beat-frequency interference, 660
Chart, filter ripple, 544
Chart, f-m service areas, 789
Chart, line mismatch, 757
Chart scanner, 848

Chart, television resolution, 735
Chart, television service areas, 738
Chart, transmission line mismatch, 757
Charts, mixer frequency, 659
Circuits, flat - late vhf, 799
Circuits, multivibrator, 709
Circular sweep generator, 428
Circular waveguide fields, 458
Clamping circuits, 691
Clip-on antenna meter, 27
Clipping and clamping circuits, 691
Coaxial butterfly circuits, 474
Coaxial line adjustments, 497
Coax reactance measurement, 374
Coax-waveguide comparison, 447
Code reception, 656
Coefficients, temperature, 227
Coils, measurement of, 239
Coils, mutual inductance of, 232
Combination antenna, two-station, 26
Combination f-m/a-m receiver, 597
Combination f-m/a-m transmitting antenna, 21
Combination f-m/tv antenna, triplex, 23
Communication system bandwidth vs noise, 140
Communication system noise, 214
Comparator for coaxial line adjustments, 497
Comparison bridge, 570
Compensation, amplifier, low-frequency, 688
Compensation circuits, crystal pickup, 49
Complex components, measuring, 424
Components of uhf field meters, 359
Composite sync signal, 722
Compressor, volume, 106
Concentric coils, mutual inductance of, 232
Concentricity tester, 584
Constant-current circuits, 170
Constant-impedance networks, audio, 80
Construction of shielded room, 430, 432
Contact potential, diode, 665
Continuously variable radio remote control, 669
Conversion chart, impedance-admittance, 213
Conversion from series to parallel impedance, 187
Converter, single-sideband, 612
Cooperative two-station antenna, 26
Correction, diode voltmeter, 419
Correction of sweep linearity, 711
Counter circuits for television, 728
Coupler, f-m antenna, 21
Coupling for telephone recording, 123
Crossover network, audio, 85, 92
Crystal filters, single-sideband, 306
Crystal oscillator stability, 771
Crystal pickup compensation circuits, 49
Crystal rectifiers, 243
Crystal voltmeter, 423
Crystal-controlled multivibrator, 404
Cuing system for broadcast stations, 825
Current oscillator for television sweep, 698
Curve tracer, B-H, 585
Curve-tracer for acoustic devices, 579
C-W reception, noise-free, 656
Cylinder antenna, f-m and tv, 28

D

DB gain-loss calculator, 212
D-C amplifier design techniques, 257
D-C amplifier for bolometers, 265
D-C amplifier for low-level signals, 265
D-C amplifiers, 251–283
D-C voltmeter, high-resistance, 441
Decrement measurement, 403
Delay circuit, phantastron, 174
Delay line, 317
Delay multivibrator, 434
Design, cathode follower, 125, 131
Design factors for intercarrier television sound, 678
Design of dummy antennas, 39
Design of f-m signal generator, 365
Design of loudspeaker dividing networks, 92
Design of phantastron circuits, 174
Design of transmission line tank circuits, 748
Design, parallel-T network, 197
Design, phase-shift oscillator, 121
Detector, high-level, 654
Detector, superregenerative, 606, 609, 613
Deviation measurement, f-m, 812
Diathermy interference suppression, 432
Differential amplifier, f-m, 796
Differentiating circuit analysis, 694
Diode contact potential for negative bias, 665
Diode for bias voltage, 664
Diode noise generator, 390
Diode voltmeter pulse response, 419
Diplexer, antenna, 23
Dipole antennas, multi-wire, 14
Dipoles, f-m and tv, 20
Dipoles, stacked, f-m and tv, 20
Direct-coupled amplifiers, 251–283
Direct-coupled oscilloscope, 398
Direct-coupled r-f amplifier, 379
Direct-current amplifiers, 251–283
Directional antenna phase monitor, 9
Directional antennas, 4, 5
Directional antennas, adjustment, 11
Directly coupled phase inverter, 655
Directors, f-m and tv receiving, 20
Discharging circuits, exponential, 170
Discriminator, f-m adjustable bandwidth, 590
Discriminator, heptode, 593
Disk-seal oscillators, 466, 474, 509
Disk-seal tubes, 844
Distortion analysis, audio, 87, 115, 116
Distortion, audio harmonic, 94
Distortion, harmonic, 188
Distortion, record, correction of, 49
Distributed capacitance measurement, coils, 239
Dividing networks, audio, 85, 92
Doublet antennas, 14
Dummy antenna, 39
Dynamic noise suppressor, 57, 60, 66
Dynamic suppression of phono noise, 57, 60

E

Eccles-Jordan multivibrator, 709
Economical television system, 743
Effective resistance of coils, 239
Electronic heating interference, 432
Electronic relay, voice-operated, 113
Electronic scanner for charts, 348
Electronic switch for pulse production, 413
Elliptical sweep, 434
Enamel film tester, 584
Engineering approach to waveguides, 447
Eniac tube failures, 837
Equaliser, three-band variable, 80
Equivalent series and parallel impedances, 197
Error, tracking, 652
Expander, volume, 75, 79
Exponential charge and discharge circuits, 170
Exposures for c-r tube photography, 861

F

Fader, automatic, 74
Failures, tube, 837
FCC frequency measurement techniques, 357
FCC performance requirements, f-m, 764
Feed, effect on antennas, 1
Field strength meter, uhf, 359
Fields, circular waveguide, 458
Fields, rectangular waveguide, 447
Filament and heater characteristics, 830
Filter chart, R-C, 289
Filter, r-f heating, 432
Filter ripple chart, 544
Filters for electronic equipment, 301
Filters, high and low-pass, 291
Filters, incidental dissipation, 295
Filters, R-C bandpass, 292
Filters, reactance network, 203
Filters, r-f noise, 301
Filters, single-sideband crystal, 306
Flat-plate transmission lines, vhf, 799
F-M and A-M receiver, 597
F-M antenna coupler, 21
F-M crystal voltmeter, 423
F-M detector, single-stage, 593
F-M discriminator, adjustable-bandwidth, 590
F-M impedance measurement, 374
F-M impedance meter, 381
F-M limiter, synchronized, 598
F-M modulator circuit, 775, 785
F-M modulator, serrasoid, 785
F-M phase-shift modulator, 779, 785
F-M reactance modulators, 768, 770
F-M receiving antennas, 20
F-M service areas, 789
F-M short-range carrier system, 805
F-M signal generator, 365
F-M squelch circuits, 604
F-M sweep oscillator, 365, 370
F-M transmitter performance measurements, 764
F-M transmitter power measurement, 379
F-M transmitter wattmeter, 386
F-M transmitting antenna, triplex, 23
Folded dipoles, 14
Folded dipoles, f-m and tv, 20
Foolproof cuing for broadcast station, 825
Foster-Seeley discriminator, 590
Frame analyser, television, 720
Free-field sound room simulator, 100
Frequency comparator, uhf, 385
Frequency control, microwave, 479
Frequency control, oscillator, 186
Frequency deviation measurement, f-m, 812
Frequency divider, half-shot, 199
Frequency divider, television, 728
Frequency drift compensation, 227
Frequency measurement techniques, 357
Frequency measurements, 433
Frequency meter, audio, 571
Frequency meter, grid-dip, 428
Frequency meter, shf heterodyne, 501
Frequency response of magnetic recording, 107
Frequency response recorder, audio, 100
Frequency stability of tuned circuits, 221
Frequency standard, secondary, 771
Frequency standards, calibrating, 384
Frequency-scanning vhf impedance meter, 381
Full-wave doubler rectifier, 528
Full-wave rectifier analysis, 524

G

Gain-loss calculator, 212
Gas tubes, noise, 870
Gas-tube bridge rectifier, 528
Gas-tube coupling for d-c amplifiers, 278
Gate circuit, noise suppressor, 57, 60
Generator, audio tone, 91
Generator, buzzer, 3,000-mc, 508
Generator, crystal, adjustable, 378
Generator, f-m, 365
Generator, high-power audio, 547
Generator, klystron, 370
Generator, noise, 387, 390
Generator, pulse, 413
Generator, television sync, 722
Generator, wide-range, 377
Germanium crystal rectifiers, 243
Germanium diodes for noise reduction, 66
Graphical design of multivibrators, 685
Graphical determination of harmonic distortion, 188
Graphical solutions for cathode followers, 131
Grid-dip oscillator, 428
Grounded-grid power amplifiers, 826

H

Half-shot multivibrator, 199
Half-wave doubler rectifier, 528
Half-wave rectifier, 528
Harmonic distortion determination, 188
Harmonic distortion tests, 116
Harmonic wave analyser, audio, 94
Hartley law, 140
Heater protection from surges, 662
Heptode f-m discriminator, 593
Heterodyne frequency meter, shf, 501
Heterodyne interference reduction, 661
Heterodyne method, 385
High and low-pass filter design, 291
High-accuracy signal generator, 378
High-current d-c amplifier, 276
High-frequency cable design, 766
High-frequency crystal voltmeter, 423
High-gain d-c amplifier, 280
High-impedance crossover network, 85
High-sensitivity d-c amplifier, 281
High-speed resistor tester, 575
Hum-reducing circuit, 767
Hysteresis curve tracer, 585

I

I-F amplifiers, 620
Ignition noise measurement, 393
Imaginary components, measuring, 424
Impedance, balanced lines, 753
Impedance, cathode follower output, 211
Impedance conversion, series to parallel, 187
Impedance measurement, coil, 239
Impedance measurements, 427
Impedance measurements, uhf, 494
Impedance measurements, vhf, 374, 489
Impedance meter, vhf, 381
Impedance nomograph, 213
Impedance-admittance conversion chart, 213
Impedance-matching pi networks, 301
Impedances, equivalent series and parallel, 197
Impedances, stabilized negative, 148
Incidental dissipation in filters, 295
Inductance measurement, 239
Inductance meter, r-f, 224
Inductance tuning, 645, 646, 647
Inductors, iron-core, 234
Instrument for intermodulation measurements, 115, 116
Intercarrier system for television sound, 673, 678
Interference chart, 660
Interference reduction, heterodyne, 661
Interference, r-f heating, 432
Intermodulation measurements, 115, 116
Intermodulation testing, 116
Inversion, speech, 815
Inverter, phase, 655
Ionosphere equipment for field use, 345
Ionosphere measuring equipment, 340
Iron-core components in pulse amplifiers, 702
Iron-core inductor calculations, 234

K

Klystron oscillators, 370, 515, 849

L

Laboratory standards, calibrating, 384
Laboratory, television receiver, 732
Lamination B-H tester, 585
Lattice networks, 144
Lattice-type crystal filters, 306
Lighthouse tubes, 844
Limit bridge, automatic, 567
Limit bridge, resistance, 575
Limiter, f-m synchronized oscillator, 598
Limiter, nonlinear, 596
Limiters, noise and output, 627
Limiting amplifier, audio, 53
Linear sweep circuits, 711
Linearity correction, 711
Line-isolation amplifier, television, 732
Lines, balanced, impedance, 753
Lits wire soldering, 583
Loading, voltmeter, 201
Long-persistence c-r screens, 849
Loop antenna, broadcast, 16
Loss chart for transmission line mismatch, 757
Loudspeaker crossover network, 85, 92
Loudspeaker response recorder, 100
Low-distortion crossover network, 85, 92
Low-frequency compensation, amplifier, 688
Low-impedance crossover network, 92
Low-impedance loop antenna, 16
Low-impedance reactances for vhf, 799
Low-pass filter design, 291
Luminosity, television picture, 739

M

Magnetic characteristics tester, 585
Magnetic recording, response of, 107
Manufacture, tube, quality, 553
Manufacture, tube, quality control, 558
Manufacture, tube, shrinkage, 556
Manufacturing sensitivity limits, 550
Measurement, antenna impedance, 354
Measurement, audio harmonic distortion, 94
Measurement, carrier frequencies, 445
Measurement, decrement, 403
Measurement, frequency, 357, 426
Measurement, frequency deviation, 812
Measurement, frequency, uhf, 501
Measurement, intermodulation, 115, 116
Measurement, noise, 393
Measurement, noise figure, 387, 390
Measurement of velocity of propagation in cable, 439
Measurement of vhf bursts, 352
Measurement, phase, 428
Measurement, Q, 403
Measurement, uhf field strength, 359
Measurement, voltage, of high-resistance source, 441
Measurements, aircraft antenna, 32
Measurements, f-m transmitter, 764
Measurements, impedance, 427
Measurements, uhf impedance, 494
Measurements, vhf impedance, 374, 381, 489
Measurements, vhf power, 379, 386
Measurements, vhf receiver, 653
Measuring antenna R and L, 11
Measuring audio distortion, 87
Measuring broadcast frequencies, 433
Measuring coil characteristics, 239
Measuring complex components, 424
Measuring equipment, ionosphere, 340, 345
Measuring mutual inductance, 444
Measuring pulse characteristics, 434
Memory circuit, audio, 53
Mercury vapor rectifier tests, 872
Metallic-oxide detector, 654
Meter, audio frequency, 571
Meter, clip-on antenna, 27
Meter, frequency, 433
Meter, frequency, grid-dip, 428
Meter, noise, 393
Meter, phase, 428
Meter, Q, 403
Meter, r-f inductance, 224
Meter, uhf heterodyne frequency, 501
Meter, standing wave, 520
Meter, wow, 97
Method, FCC frequency-measuring, 357
Method of plotting tracking error, 652
Methods of correcting sweep linearity, 713
Mica capacitor resonance, 233
Microphone calibrator, 100
Microsecond time delay circuits, 174
Microwave afc, 479
Microwave antenna beam evaluator, 44
Microwave filter, 430
Microwave power supply, 540
Microwave signal generator, 508
Microwave tuning systems, 479
Miller sweep circuit, 174
Minimum attenuation in waveguides, 455
Mismatch loss chart, 757
Mixer design, audio, 72
High-level detector, 654
High-Q iron-cored inductor calculations, 234
High-resistance d-c voltmeter, 441
Mixer for frequency comparison, 385
Mixer frequency charts, 659
Model antenna tests, 34
Modes, waveguides, 447, 456
Modulation booster, 106
Modulator, cascade phase-shift, 779
Modulator, f-m serrasoid, 785
Modulator, high-level a-m, 790
Modulator, reactance, 768, 770
Modulator, wide-angle phase, 775
Monitor amplifier, f-m, 796
Monitor, antenna phase, 9
Monitoring broadcast frequencies, 433
Multivibrator, 433
Multivibrator circuits, 709
Multivibrator, crystal-controlled, 404
Multivibrator design, graphical, 665
Multivibrator frequency divider, 434
Multivibrator, half-shot, 199
Multivibrator, manual delay, 434
Multivibrator, phantastron, 174
Multivibrator switch, 182
Multi-voltage regulated power supplies, 537
Multi-wire dipole antennas, 14
Mutual capacitance measurement, 444
Mutual inductance measurement, 444
Mutual inductance of concentric coils, 232

N

Narrow-band d-c amplifier, 265
Negative impedances, stabilized, 148
Network, audio crossover, 85, 92
Network design, parallel-T, 197
Network, phase-shifting, 311
Networks, crystal pickup compensation, 49
Networks, phase shift, 144
Networks, reactance, 203
Neutralizing tests, 810
Noise and output limiters, 627
Noise figure measurement, 387, 390
Noise filters, 301
Noise generator, 387, 390
Noise in communication systems, 140
Noise in gas tubes, 870
Noise meter, 393
Noise ratios, 214
Noise, receiver, 624
Noise reduction circuits, 57, 60, 66, 71
Noise suppressor, Scott, 57, 60
Noise-free code reception, 656
Nomograph, harmonic distortion, 188
Nomograph, impedance, 213
Nomograph, mutual inductance, 232
Nomograph, phase-shifter, 311
Nomograph, piston attenuator, 519
Nomograph, R-C filter, 289
Nomograph, series-parallel impedance, 187
Nomograph, square-wave response, 708
Nomograph, voltmeter loading, 201
Nomographs, cathode follower, 131, 209, 210, 211
Nomographs, phase-shift oscillator, 121
Nomographs, reverberation time, 112
Nonlinear limiter, 596
Null indicator circuit, 575

O

Olson noise suppressor, 66
One-shot multivibrator, 709
Operating point of self-biased tubes, 835
Oscillator amplitude control, 377
Oscillator, beat-frequency audio, 91
Oscillator, blocking, 676
Oscillator, cathode-follower, 218
Oscillator, crystal, adjustable, 378
Oscillator, current, 698
Oscillator design, phase-shift, 121
Oscillator frequency comparator, 385
Oscillator frequency control, 186
Oscillator, frequency-modulated, 768
Oscillator, grid-dip, 428
Oscillator, pulse-modulated, 191
Oscillator, R-C, 189
Oscillator stability, crystal, 771
Oscillator stability, uhf, 385
Oscillator stabilization reflex, 514
Oscillator, sweeping, 370
Oscillator, thermistor-regulated audio, 103
Oscillator, three-centimeter, 515
Oscillator, two-terminal, 218
Oscillator, variable-frequency, 25-cm, 512
Oscillators, cavity, 456
Oscillators, klystron, 849
Oscillators, synchronized, as limiters, 598
Oscillators, uhf, stability of, 509
Oscilloscope adapter, television, 732
Oscilloscope, direct-coupled, 398
Oscilloscope for pulse studies, 394
Oscilloscope for tube curves, 840
Oscilloscope, phase-measuring, 428
Oscilloscope, television, 720
Output control, signal generator, 377
Output limiters, 627
Output meter, uhf, 359
Output transformer crossover network, 85
Output transformer response, audio, 87
Overmodulation indicator, 814
Overmodulation without sideband splatter, 790
Overvoltage testing of capacitors, 577

P

Parallel-T filter, 292
Parallel-T network design, 197
Pattern photographing, c-r, 861
Pattern plotter, antenna, 34
Peak limiter, audio, 53, 106
Peak-to-peak voltmeter, 419
Pentagrid phantastron, 174
Pentode cathode follower nomograph, 210

Pentode phantastron, 174
Performance tests, f-m transmitter, 764
Permeability tuning, 647
Permeability-tuned circuit tracking, 645, 646, 652
Phantastron time delay circuits, 174
Phase inverter, directly coupled, 655
Phase meter, 428
Phase modulator, wide-angle, 775
Phase monitor for broadcast arrays, 9
Phase reverser, automatic, audio, 83
Phase shift networks, 144
Phase shifter, 434
Phase splitter, 434
Phase-shift oscillator, audio, 103
Phase-shift oscillator design, 121
Phase-shifter nomograph, 311
Phasing networks, antenna, 5
Phonograph noise suppressor, 57, 60, 66, 71
Phonograph record noise reduction, 57, 60, 66, 71
Phono recording wow measurement, 97
Phono record responses, 49
Photoelectric power measurement, 379
Photographing patterns on c-r tubes, 861
Photometry in television, 739
Pi networks as tank circuits, 301
Pickup compensation circuits, 49
Picture quality, 739
Pilot lamp protection from surges, 662
Piston attenuator, 519
Plate-loaded cathode followers, 131
Plotter, aircraft antenna pattern, 34
Plotter, microwave antenna pattern, 44
Plotter, response curve, 579
Plotting tracking error, 652
Polar response plotter, audio, 100
Polyphase measurements, 428
Power amplifiers, grounded-grid, 826
Power divider, antenna, 4
Power factor measurement, coils, 239
Power measurements, vhf, 379, 386
Power supplies, voltage-regulated, 532, 537, 539, 540
Power supply, motor-controlled, 540
Production limit bridge, 567
Production signal generator, 562
Production test bridge, 570
Progar, 53
Propagation of very short waves, 321
Propagation velocity in cable, 439
Pulse amplifier components, 702
Pulse bandwidth requirements, 407
Pulse counter, 434
Pulse delay network, 317
Pulse generator, 413, 428
Pulse generator, triggering, 404
Pulse measurements, 434
Pulse oscilloscope, 394
Pulse response of diode voltmeters, 419
Pulse transformer design, 702
Pulse transmission in amplifiers, 407
Pulse voltmeter, 419
Pulsed ionosphere measurements, 345
Pulsed rectifiers, television, 713
Pulse-modulated oscillator, 191
Pulse-stretching circuit, 419
Pulse-type tube tester, 572
Push-pull cathode follower, 131
Push-pull volume expander, 75

Q

Q measurement, coils, 239
Q meter, 404
Quality control in tube manufacture, 558
Quality engineering in tube manufacture, 553

R

Radiation from r-f heating generators, 432
Radiation meter, antenna, 27
Radiation patterns, antenna, 1
Radio control circuit, 672
Radio manufacturing sensitivity limits, 550
Radio remote control, 669
Radio static generator, 387, 390
R-C bandpass filters, 292
R-C oscillator design, 189
R-C tuning of tone generator, 91
Reactance modulator, 365, 368, 770
Reactance networks with resistance terminations, 203
Reactance-tube remote tuning, 667
Real values, measuring, 424
Receiver, f-m and a-m, 597
Receiver laboratory, television, 732
Receiver measurements, vhf, 653
Receiver mixer frequencies, 659
Receiver noise, 624
Receiver sensitivity limits, 550
Receiver squelch circuits, f-m, 604
Receiver static generator, 387, 390
Receiver testing, television, 739
Receivers, permeability tuning, 645, 646, 647
Receivers, remote tuning, 667
Receivers, remotely controlled, 669
Receiving antennas, f-m and tv, 20
Reception, code, noise-free, 656
Reception, single-sideband, 639
Record noise suppressor, 57, 60, 66, 71
Record response, phono test, 49
Recorder, audio frequency response, 100
Recorder, microwave antenna pattern, 44
Recorder, radiation pattern, 34
Recorder, voice-operated, 113
Recording, magnetic, 107
Recording sky-wave signals, 348
Recording, telephone, 123
Recording, wow measurement, 97
Rectangular waveguides, 447, 450
Rectifier analysis, 524
Rectifier circuits, 528
Rectifiers, crystal, 243
Rectifiers, mercury vapor, 872
Rectifiers, pulsed, 713
Reduction of heterodyne interference, 661
Re-entrant cavity oscillators, 466
Reflectors, f-m and tv receiving, 20
Reflex d-c voltmeter, 441
Reflex klystron oscillator, 370
Reflex oscillator stabilization, 514
Regulated power supplies, 532, 537, 539, 540
Relay, voice-operated, 113
Remote control of receivers, 669
Remote indicating antenna ammeter, 31
Remote overmodulation indicator, 814
Remote tuning with reactance tubes, 667
Remote-controlled uhf repeater, 802
Repeater station, ufh, 802
Resistance comparator, 575
Resistance tester, 575
Resistance-capacitance filter chart, 289
Resolution chart, television, 735
Resonance in mica capacitors, 233
Resonator, uhf, 359
Response, analysis of audio, 87
Response, magnetic recording, 107
Response, phono test records, 49
Response, square-wave, 708
Reverberation time nomographs, 112
Reverser, automatic audio phase, 83
R-F amplifier, direct-coupled, 379
R-F amplifier, self-switching, 182
R-F bridge for broadcast stations, 354
R-F heating interference, 432
R-F inductance meter, 224
R-F power measurement, 379
Ripple analysis, 524
Ripple chart for filters, 544
RMA television resolution chart, 735
Rotobridge, 567

S

Sawtooth sweep circuits, 711
Scale model antenna tests, 34
Scanner for charts, 348
Scott noise suppressor, 57, 60
Scrambler, speech, 815
Screen testing, cathode-ray, 849
Screen-coupled cathode follower, 283
Selectivity, receiver, 653
Selectivity, superregenerative detector, 613
Self-bias, 835
Self-switching r-f amplifier, 182
Semi-conductors, 243
Sensitivity limits in radio manufacturing, 550
Series and parallel impedances, 197
Series-parallel impedance conversion, 187
Serrasold f-m modulator, 785
Service area charts, television, 736
Service areas, f-m, 789
SHF heterodyne frequency meter, 501
Shielded room, 430, 432
Shrinkage analysis in tube manufacture, 556
Shunt diode for bias, 664
Signal generator, buzzer, 508
Signal generator, crystal, 378
Signal generator, f-m, 365
Signal generator, klystron, 370
Signal generator, production, 562
Signal generator, television sync, 722
Signal generator, wide-range, 377
Signal source, noise, 387, 390
Signal-to-noise ratios, 214
Silicon crystal rectifiers, 243
Simplified microwave afc, 479
Simplified single-sideband reception, 639
Simplified television system, 743
Single-sideband adaptor, 643
Single-sideband converter, 612
Single-sideband crystal filters, 306
Single-sideband reception, 639
Single-sideband telephony, 144
Single-signal single-sideband adaptor, 643
Single-stage f-m detector, 593
Sky-wave signals, recording, 348
Sky-wave transmission, 2-mc, 331
Slot antenna, f-m and tv, 28
Slots in cavities, 462
Slotted transmission line, vhf, 489
Slotted-cylinder antenna, 28
Soldering Litz ends, 583
Sound absorption nomograph, 112
Sound reverberation nomograph, 112
Speaker crossover network, 85, 92
Speaker response recorder, 100
Speech scrambling methods, 815
Splatter suppression, 790
Square-wave differentiating circuit analysis, 694
Square-wave multivibrator, 709
Square-wave response, 407, 708
Squelch circuits for f-m receivers, 604
Stable d-c amplifier, 271
Stable voltmeter, 416
Stability of crystal oscillators, 771
Stability of tuned circuits, 221
Stability of uhf oscillators, 385, 509
Stabilization of reflex oscillators, 514
Stabilized bias supply, 546
Stabilized d-c amplifier with high sensitivity, 281
Stabilized negative impedances, 148
Stabilizer for r-f oscillator, 186
Stacked dipoles, f-m and tv, 20
Stagger-tuned amplifier design, 682
Stagger-tuned i-f amplifiers, 620
Standard frequency, secondary, 771
Standard phono record responses, 49
Standard television test chart, 735
Standards, frequency, WWV, 384
Standing wave measurement, 494
Standing wave meter, 520
Static for radio receiver tests, 387, 390
Studio audio facilities, 53
Studio fader, automatic, 74
Studio mixer, broadcast, 72
Superregenerative circuit applications, 617
Superregenerative detection theory, 606, 609, 613
Superturnstile antenna, 23
Suppression, diathermy interference, 432
Suppression of splatter, 790
Suppressor, noise, 57, 60, 66, 71
Surge protection of heaters, 662
Surgeless volume expander, 79
Survey of d-c amplifiers, 251
Sweep circuits, linear, 711
Sweep generator, f-m, 365
Sweep oscillator, television, 698
Sweeping oscillator, 370
Sweeps for high voltage, 713
Swinging filter choke, 312
Switch, electronic, 413
Switch, multivibrator, 182
Synchronised oscillators as f-m limiters, 598
Synchronising signal generator, 722

T

Tank circuit frequency control, 186
Tank circuits, pi network, 301
Tank circuits, transmission line, 748

Tape recorder frequency response, 107
Technique, cable propagation velocity measurement, 439
Technique, FCC frequency-measuring, 357
Technique for distortion analysis, 87
Technique, impedance-measuring, 427
Technique, pulse-measuring, 434
Technique, shielded room, 430, 432
Technique, uhf field strength, 359
Telephone recording, 123
Television clippers and clampers, 691
Television counter circuits, 728
Television crystal voltmeter, 423
Television i-f amplifier, 682
Television impedance measurement, 374
Television impedance meter, 381
Television intercarrier system, 673, 678
Television line-isolation amplifier, 732
Television oscilloscope, 394, 720
Television photometry, 739
Television pulsed rectifiers, 713
Television receiver laboratory, 732
Television receiving antennas, 20
Television resolution chart, 735
Television service areas, 738
Television sweep oscillator, 365, 370, 698
Television synchronizing signal generator, 722
Television system, economical, 743
Television system, simplified, 743
Television transient video analyzer, 714
Television transmitter modulation analyser, 720
Television transmitter power measurement, 379
Television transmitter wattmeter, 386
Television transmitting antenna, triplex, 23
Television, video amplifier, 708
Temperature coefficients in circuits, 227
Terrain-clearance indicator, 381
Test chart, RMA television, 735
Test oscilloscope for television, 720
Test phono record responses, 49
Test set for mercury vapor rectifiers, 872
Tester for enamel film, 584
Tester, resistance, 575
Testing capacitors, 577
Testing cathode-ray screens, 856
Testing, intermodulation, 116
Tests, neutralizing, 810
Theoretical signal-to-noise ratios, 214
Thermionic rectifier circuits, 528
Thermistor-regulated audio oscillator, 103
Three-band variable equalizer, 80
Time constant, volume expansion, 75, 79
Time delay circuit, oscilloscope, 394
Time delay circuits, phantastron, 174
Time delay network, 317
Time-base calibration, 404
Timer, tube-seasoning, 583
Timing action of blocking oscillator, 676
Tone alarm, 811
Tone generator, beat-frequency, 91
Tracer, B-H curve, 585
Tracking error, 652
Tracking permeability-tuned circuits, 645, 646, 652
Transformer design, audio, 234
Transformer response, audio, 87
Transformer, waveguide, 469
Transformers, mutual inductance, 444
Transformers, pulse, 702
Transient delay line, 317
Transient trace photography, c-r tube, 861
Transient video analyser, 714
Transmission line loss chart, 757
Transmission line tank circuit design, 748
Transmission lines as tuning elements, 758
Transmission lines, flat-plate vhf, 799
Transmission lines, vectorial treatment, 754
Transmitter breakdown alarm, 774
Transmitter f-m deviation, 812
Transmitter power measurements, 386
Transmitter protection, arcover in storms, 821
Transmitter protection, breakdown, 821
Transmitter protection, carrier interruption, 821
Transmitter protection, overload, 821
Transport aircraft antennas, 32
Trapezoidal pattern analyser, television, 720
Triggered-tone code reception, 656
Triggering pulse generator, 404
Triplex antenna for tv and f-m, 23
Triplexer, antenna, 23
Tube curves on oscilloscope, 840
Tube failures in Eniac, 837
Tube filament characteristics, 826
Tube heater protection, 662
Tube manufacturing shrinkage, 556
Tube, operating point, self-bias, 835
Tube quality control, 553, 558
Tube tester, pulse-type, 572
Tubes, disk-seal, 844
Tubes, klystron, 849
Tubes, lighthouse, 844
Tube-seasoning timer, 583
Tuned circuits, frequency stability of, 221
Tuned circuits, transmission-line, 758
Tuned circuits, uhf, 359
Tuning, microwave, 479
Tuning with reactance tubes, 667
Turnstile type antenna, 23
Turntable wow meter, 97
Two-element antenna power divider, 4
Two-station antenna, cooperative, 26
Two-terminal oscillator, 218

U

UHF field meters, 359
UHF impedance measurements, 494
UHF low-impedance reactances, 790
UHF oscillator stability, 385, 509
UHF repeater station, 802
UHF signal generator, 474
UHF tuned lines, 758

V

Vacuum-tube voltmeter, 416, 441, 445
Variable equalizer, 80
Variable-frequency electronic generator, 547
Variable-frequency oscillator, 25-cm, 512
Variable-reactance vhf line, 489
Varistor control for r-f oscillator, 186
Vector synthesis of antenna phasing networks, 5
Vectorial treatment of transmission lines, 754
Velocity of propagation in cable, 439
Velocity-frequency characteristics, test records, 49
VHF burst measurements, 352
VHF cable measurements, 439
VHF crystal voltmeter, 423
VHF impedance measurements, 374, 489
VHF impedance meter, 381
VHF power measurements, 379
VHF receiver measurements, 653
VHF shielded room, 430
VHF tank circuits, 748
VHF transmitter power measurements, 386
VHF wattmeter, 386
Video amplifier compensation, 688
Video amplifier response, 708
Video analyser, transient, 714
Voice-operated electronic relay, 113
Voltage supply, diode, for bias, 664
Voltage-regulated power supplies, 532, 537, 539, 540
Voltage-stabilized bias supply, 546
Voltmeter, carrier-frequency, 445
Voltmeter, crystal, 423
Voltmeter, diode, response of, 419
Voltmeter, high-resistance d-c, 441
Voltmeter loading, 201
Voltmeter, peak-to-peak, 419
Voltmeter, stable, 416
Volume compressor for radio stations, 106
Volume expander design, 75, 79

W

Wattmeter, vhf, 386
Wave analyzer, audio harmonic, 94
Wave propagation, 321
Waveguide attenuation, 450, 455
Waveguide characteristics, 447, 450
Waveguide data, 452
Waveguide fields, circular, 458
Waveguide fields, rectangular, 447
Waveguide transmission system, 469
Waveguide-antenna coupling, 469
Wavemeter, direct-reading, 504
Wavemeter, standing wave, 520
Wein bridge oscillator, 189
Wide-angle phase modulator, 775
Wide-band amplifier, 682
Wide-band antenna, slotted-cylinder, 28
Wide-band i-f amplifiers, 620
Wide-band impedance meter, 381
Wide-band noise, 870
Wide-band oscilloscope, 394, 398
Wide-band phase shift networks, 144
Wide-band power amplifiers, 826
Wide-deviation reactance modulator, 768, 770
Wide-range signal generator, 377, 378
Wide-range sweeping oscillator, 370
Wire antenna radiation patterns, 1
Wire enamel tester, 584
Wire recorder frequency response, 107
Wired television, 743
Woofer-tweeter crossover network, 85, 92
Wow meter for turntable testing, 97
Writing speed, c-r tube, 861
WWV for calibration, 384
WWV frequency comparator, 433
Wxx Amplifier, direct-coupled, 398

Z

Z-axis oscilloscope, 394

DATE OF ISSUE

This book must be returned within 3, 7, 14 days of its issue. A fine of ONE ANNA per day will be charged if the book is overdue.